REPORT DOCUMENTATION PAGE

Form Approved
OMB No. 0704-0188

Public reporting burden for this collection of information is estimated to average 1 hour per response, including the time for reviewing instructions, searching existing data sources, gathering and maintaining the data needed, and completing and reviewing the collection of information. Send comments regarding this burden estimate or any other aspect of this collection of information, including suggestions for reducing this burden, to Washington Headquarters Services, Directorate for Information Operations and Reports, 1215 Jefferson Davis Highway, Suite 1204, Arlington, VA 22202-4302, and to the Office of Management and Budget, Paperwork Reduction Project (0704-0188), Washington, DC 20503.

1. AGENCY USE ONLY *(Leave blank)*	2. REPORT DATE	3. REPORT TYPE AND DATES COVERED
	30 April 2003	Final Report, 1 October 2002 – 30 September 2003

4. TITLE AND SUBTITLE
D/B/F 03: FINAL REPORT OF THE AIAA STUDENT AIRCRAFT DESIGN, BUILD & FLY COMPETITION

5. FUNDING NUMBERS
G: N00014-98-1-0493
PR: 97PR04749-00

6. AUTHORS
By Gregory Page, Chris Bovias, Michael Selig and the student participants of D/B/F 2003.
Compiled by Stephen Brock, AIAA Student Programs

7. PERFORMING ORGANIZATION NAME(S) AND ADDRESS(ES)

American Institute of Aeronautics and Astronautics
ATTN: AIAA Foundation
1801 Alexander Bell Dr., Ste 500
Reston, VA 20191-4344

8. PERFORMING ORGANIZATION REPORT NUMBER

2003DBF7630

9. SPONSORING/MONITORING AGENCY NAME(S) AND ADDRESS(ES)

Office of Naval Research
800 North Quincy St (ONR 351)
Arlington, VA 22217-5660

10. SPONSORING/MONITORING AGENCY REPORT NUMBER

11. SUPPLEMENTARY NOTES

12a. DISTRIBUTION/AVAILABILITY STATEMENT

APPROVED FOR PUBLIC RELEASE

12b. DISTRIBUTION CODE

13. ABSTRACT *(Maximum 200 words)*

This report is made up of the combined reports of 38 separate teams of students who entered the 2003 Design, Build & Fly Competition. The objectives of the Design, Build & Fly Competition were to have students teams design, build and fly unmanned remote control electric aircraft designed for two of three specific missions: a Missile EW Decoy sortie, a Sensor Deployment sortie, and/or a Communications Repeater sortie. A "fly-off" took place on the Ridgely Airpark Field near Ridgely, MD, in April 2003. Winners of the contest: 1st place, San Diego State University; 2nd, CA Polytechnic and State Univ.—San Luis Obispo; 3rd, La Sapienza University (Italy). The Design, Build & Fly Competition was supported by Cessna, the Office of Naval Research and the AIAA Foundation.

14. SUBJECT TERMS

Unmanned / Remote / Control / RC / Aircraft / Student / Design / Build / Fly / AIAA

15. NUMBER OF PAGES

2125

16. PRICE CODE

17. SECURITY CLASSIFICATION OF REPORT	18. SECURITY CLASSIFICATION OF THIS PAGE	19. SECURITY CLASSIFICATION OF ABSTRACT	20. LIMITATION OF ABSTRACT
			SAR

20030604 142

INSTRUCTIONS FOR COMPLETING SF 298

The Report Documentation (RDP) is used in announcing and cataloging reports. It is important that this information be consistent with the rest of the report, particularly the cover and title page. Instructions for filling each block of the form follow. It is important to ***stay within the lines to meet optical scanning requirements.***

Block 1. Agency Use Only *(Leave blank)*.

Block 2. Report Date. Full publication date including day, month, and year, if available (e.g., 1 Jan 88). Must cite at least the year.

Block 3. Type of Report and Dates Covered. State whether report is interim, final, etc. If applicable, enter inclusive report dates (e.g., 10 Jul 87 - 30 Jun 88).

Block 4. Title and Subtitle. A title is taken from the part of the report that provides the most meaningful and complete information. When a report is prepared in more than one volume, repeat the primary title, add volume number, and include subtitle for the specific volume. On classified documents enter the title classification in parentheses.

Block 5. Funding Numbers. To include contract and grant numbers; may include program element number(s), project number(s), task number(s), and work unit number(s). Use the following labels:

C -	Contract	**PR** -	Project
G -	Grant	**TA** -	Task
PE -	Program Element	**WU** -	Work Unit Accession No.

Block 6. Author(s). Name(s) of person(s) responsible for writing the report, performing the research, or credited with the content of the report. If editor or compiler, this should follow the name(s).

Block 7. Performing Organization Name(s) and Address(es). Self-explanatory.

Block 8. Performing Organization Report Number. Enter the unique alphanumeric report number(s) assigned by the organization performing the report.

Block 9. Sponsoring/Monitoring Agency Name(s) and Address(es). Self-explanatory.

Block 10. Sponsoring/Monitoring Agency Report Number. *(If known)*

Block 11. Supplementary Notes. Enter information not included elsewhere such as: Prepared in cooperation with . . . ; Trans. of . . . ; To be published in . . . . When a report is revised, include a statement whether the new report supersedes or supplements the older report.

Block 12a. Distribution/Availability Statement. Denotes public availability or limitations. Cite any availability to the public. Enter additional limitations or special markings in all capitals (e.g., NOFORN, REL, ITAR).

DOD - See DoDD 5230, "Distribution Statements on Technical Documents"
DOE – See authorities.
NASA– See Handbook NHB 2200.2.
NTIS – Leave blank.

Block 12b. Distribution Code.

DOD - Leave blank.
DOE – Enter DOE distribution categories from the Standard Distribution for Unclassified Scientific and Technical Reports.
NASA– Leave blank.
NTIS – Leave blank.

Block 13. Abstract. Include a brief *(Maximum 200 words)* factual summary of the most significant information contained in the report.

Block 14. Subject Terms. Keywords or phrases identifying major subjects in the report.

Block 15. Number of Pages. Enter the total number of pages.

Block 16. Price Code. Enter appropriate price code *(NTIS only)*.

Blocks 17. - 19. Security Classifications. Self-explanatory. Enter U.S. Security Classification in accordance with U.S. Security Regulations (i.e., UNCLASSIFIED). If form contains classified information, stamp classification on the top and bottom of the page.

Block 20. Limitation of Abstract. This block must be completed to assign a limitation to the abstract. Enter either UL (unlimited) or SAR (same as report). An entry in this block is necessary if the abstract is to be limited. If blank, the abstract is assumed to be unlimited.

CESSNA/ONR STUDENT DESIGN/BUILD/FLY COMPETITION

An AIAA Student Activity

The 2003 Cessna/ONR Student Design/Build/Fly competition was held at the Ridgely Airpark in Ridgely Maryland over the weekend of 25-27 April. Thirty three teams from the United States, Canada, Italy and Turkey attended the fly-off portion of the contest. Of the 33 teams attending the fly-off competition, 19 made at least one successful scoring flight attempt, with many teams completing the maximum allowed 5 flights during the two days of competition.

The contest was moved from it's traditional east coast home, Webster Field, due to the increased security at military installations resulting from the Iraq war. Mr. Tracy Coleman volunteered the use of Ridgely Airpark so that the contest could continue it's 7 year history without interruption. The facilities at Ridgely provided an excellent contest site with ample setup and flying area. The managers, sponsors, and teams of the DBF competition would like to express their thanks to Mr. Coleman for his generosity.

The competition spanned two days of flying, with the flight queue filled with aircraft waiting for their turn to make a competition flight. A number of the flights on Saturday had to dodge the rain drops, while Sunday provided near perfect flying weather.

The design objective for this years competition was to create an airplane that could be rapidly assembled from a 2 x 4 x 1 foot shipping container and then complete two of the three specified simulated UAV missions: Missile EW Decoy; Sensor Deployment; or Communications Repeater. Each mission was assigned it's own Degree of Difficulty multiplier factor.

The total score for each team is comprised of their flight performance on their best two flights, their score on a written report documenting their aircraft design and selection, and a "Rated Aircraft Cost" representing the complexity and manufacturing costs of their design.

The final results showed a close battle between teams from the San Diego State University and California Polytechnic State University at San Luis Obispo. One of the Italian teams from Università degli studi "La Sapienza" di Roma placed a close third.. The highest score obtained on the written report portion of the competition was from Utah State University with 96.5 of a possible 100 points awarded.

The final positions and scores for all of the competing teams are listed in the table below.

More details on the 2003 competition objectives and rules can be found at the contest web site at http://www.aae.uiuc.edu/aiaadbf.

Position	School	Team	Paper	RAC	Flight	Score
1	San Diego State University	Spirit of Monty	84.5	8.28	1.16	11894.80
2	Calif Poly State Univ SLO	Bareback	85.5	7.91	1.09	11736.63
3	La Sapienza	Galileo IV	89.5	7.99	0.95	10609.09
4	Univ of Southern California	SCyRaider	93.5	10.90	0.97	8365.98
5	Oklahoma State University	OSU Black	91.6	9.86	0.89	8228.28
6	Oklahoma State University	OSU Orange	90.5	10.24	0.83	7331.55

7	USNA	Severn Discomfort	86.0	13.04	1.03	6775.88
8	Mississippi State University	SWAG	90.0	12.09	0.89	6605.70
9	USNA	Yeager Chasers	89.7	12.25	0.86	6263.12
10	Middle East Technical University	Anatolian-Craft	87.0	12.21	0.80	5699.88
11	Uinv of California San Diego	Aerodrone F8273	80.5	9.15	0.61	5380.84
12	Istanbul Technical University	Ucakcilar	74.8	11.24	0.80	5301.99
13	University of Illinois UC	Gas Guzzler	72.0	9.35	0.65	5009.39
14	Washington State University	CAT	46.0	10.01	0.59	2692.87
15	Utah State University	Nyx	96.5	13.34	0.35	2563.83
16	Univ of Texas Austin	7700	93.4	8.70	0.23	2490.02
17	Uinv of California San Diego	Furious Flier	74.0	9.22	0.31	2473.78
18	University of Colorado	Bellwether	68.4	8.41	0.28	2279.43
19	La Sapienza	Leonardo	79.5	6.69	0.19	2264.63
20	*Georgia Tech	Buzzweiser	89.0	7.30	0.01	121.95
21	*University of Maryland	The Stop and Go	89.5	9.71	0.01	92.17
22	*Ohio Northern University	It's Supposed to Fly	59.0	8.08	0.01	73.05
23	*Case Western Reserve	Marsupial Falcon X	61.3	8.92	0.01	68.69
24	*Virginia Polytechnic University	Draggin Fly	77.3	11.81	0.01	65.40
25	*W. Virginia University	Lock-N-Load	79.0	12.65	0.01	62.46
26	*University at Buffalo	Bull Ship	71.0	11.86	0.01	59.87
27	*Queen's University	Some Assembly Required	79.2	13.28	0.01	59.61
28	*Wichita State University	WU Flyer	74.3	12.79	0.01	58.05
29	*Univ California LA	Bruin Bud-E	58.9	10.58	0.01	55.62
30	*Calif Poly State Univ Pomona	Pegasus	47.5	8.78	0.01	54.13
31	*Western Michigan University	Western Flyer	59.3	11.83	0.01	50.17
32	*University of Arizona	AirCat 2003	47.9	10.08	0.01	47.51
33	*Univ of Texas Arlington	Spirit of Arlington	65.0	13.70	0.01	47.45
34	†Turkish Air Force Academy	Haberci	90.0	100.00	0.01	9.00
35	†Syracuse University	The Judge Chaser	73.8	100.00	0.01	7.38
36	†Clarkson University	Knight Riders	73.3	100.00	0.01	7.33
37	†University of Central Florida	K-03 Pegasus	69.9	100.00	0.01	6.99
38	†University at Buffalo	Frier Fly	66.5	100.00	0.01	6.65

* Present at Fly-off, but did not have a successful scoring flight

† Not present at the Fly-off

The success of the competition required the efforts of many individuals. A special thanks goes to the judges who assisted in the operation, technical inspections and scoring of the flight competition; and to the many judges who evaluated and scored the teams written proposal reports. Thanks also go to the Applied Aerodynamics, Aircraft Design, Design Engineering, and Flight Test Technical committees of the AIAA who organized and manage the competition, and the AIAA Foundation for their administrative support. Special thanks is due to the competitions corporate supporters, the Cessna Aircraft Company and the Office of Naval Research.

Overall the 2003 Cessna/ONR Student Design/Build/Fly competition marked another very successful event, allowing the participating students to mix a highly enlightening educational experience with a good dose of fun. Congratulations to all the teams who participated for your great enthusiasm and achievement.

See you next year - Greg Page: Contest Director

2002-2003 Design, Build Fly Competition

Place: Ridgely, MD—Ridgely Airpark

Ranking By Total Score
Order Within this Document

School	Team	Paper Score	RAC	Flight Score	Overall Score	Overall Position
San Diego State University	Spirit of Monty	84.5	8.28	1.16	**11894.8**	1
Calif Poly State Univ SLO	Bareback	85.5	7.91	1.09	**11736.63**	2
La Sapienza	Galileo IV	89.5	7.99	0.95	**10609.09**	3
Univ of Southern California	SCyRaider	93.5	10.9	0.97	**8365.98**	4
Oklahoma State University	OSU Black	91.6	9.86	0.89	**8228.28**	5
Oklahoma State University	OSU Orange	90.5	10.24	0.83	**7331.55**	6
USNA	Severn Discomfort	86	13.04	1.03	**6775.88**	7
Mississippi State University	SWAG	90	12.09	0.89	**6605.7**	8
USNA	Yeager Chasers	89.7	12.25	0.86	**6263.12**	9
Middle East Technical University	Anatolian-Craft	87	12.21	0.8	**5699.88**	10
Uinv of California San Diego	Aerodrone F8273	80.5	9.15	0.61	**5380.84**	11
Istanbul Technical University	Ucakcilar	74.8	11.24	0.8	**5301.99**	12
University of Illinois UC	Gas Guzzler	72	9.35	0.65	**5009.39**	13
Washington State University	CAT	46	10.01	0.59	**2692.87**	14
Utah State University	Nyx	96.5	13.34	0.35	**2563.83**	15
Univ of Texas Austin	7700	93.4	8.7	0.23	**2490.02**	16
Uinv of California San Diego	Furious Flier	74	9.22	0.31	**2473.78**	17
University of Colorado	Bellwether	68.4	8.41	0.28	**2279.43**	18
La Sapienza	Leonardo	79.5	6.69	0.19	**2264.63**	19
*Georgia Tech	Buzzweiser	89	7.3	0.01	**121.95**	20
*University of Maryland	The Stop and Go	89.5	9.71	0.01	**92.17**	21
*Ohio Northern University	It's Supposed to Fly	59	8.08	0.01	**73.05**	22
*Case Western Reserve	Marsupial Falcon X	61.3	8.92	0.01	**68.69**	23
*Virginia Polytechnic University	Draggin Fly	77.3	11.81	0.01	**65.4**	24
*W. Virginia University	Lock-N-Load	79	12.65	0.01	**62.46**	25
*University at Buffalo	Bull Ship	71	11.86	0.01	**59.87**	26
*Queen's University	Some Assembly Required	79.2	13.28	0.01	**59.61**	27
*Wichita State University	WU Flyer	74.3	12.79	0.01	**58.05**	28
*Univ California LA	Bruin Bud-E	58.9	10.58	0.01	**55.62**	29
*Calif Poly State Univ Pomona	Pegasus	47.5	8.78	0.01	**54.13**	30
*Western Michigan University	Western Flyer	59.3	11.83	0.01	**50.17**	31
*University of Arizona	AirCat 2003	47.9	10.08	0.01	**47.51**	32
*Univ of Texas Arlington	Spirit of Arlington	65	13.7	0.01	**47.45**	33
†Turkish Air Force Academy	Haberci	90	100	0.01	**9**	34
†Syracuse University	The Judge Chaser	73.8	100	0.01	**7.38**	35
†Clarkson University	Knight Riders	73.3	100	0.01	**7.33**	36
†University of Central Florida	K-03 Pegasus	69.9	100	0.01	**6.99**	37
†University at Buffalo	Frier Fly	66.5	100	0.01	**6.65**	38

* Present at Fly-off, but did not have a successful scoring flight
† Not present at the Fly-off

2002-2003 Design, Build Fly Competition

Place: Ridgely, MD—Ridgely Airpark

Ranking By Paper Score

School	Team	Paper Score	RAC	Flight Score	Overall Score	Overall Position
Utah State University	Nyx	96.5	13.34	0.35	**2563.83**	15
Univ of Southern California	SCyRaider	93.5	10.9	0.97	**8365.98**	4
Univ of Texas Austin	7700	93.4	8.7	0.23	**2490.02**	16
Oklahoma State University	OSU Black	91.6	9.86	0.89	**8228.28**	5
Oklahoma State University	OSU Orange	90.5	10.24	0.83	**7331.55**	6
Mississippi State University	SWAG	90	12.09	0.89	**6605.7**	8
†Turkish Air Force Academy	Haberci	90	100	0.01	**9**	34
USNA	Yeager Chasers	89.7	12.25	0.86	**6263.12**	9
La Sapienza	Galileo IV	89.5	7.99	0.95	**10609.09**	3
*University of Maryland	The Stop and Go	89.5	9.71	0.01	**92.17**	21
*Georgia Tech	Buzzweiser	89	7.3	0.01	**121.95**	20
Middle East Technical University	Anatolian-Craft	87	12.21	0.8	**5699.88**	10
USNA	Severn Discomfort	86	13.04	1.03	**6775.88**	7
Calif Poly State Univ SLO	Bareback	85.5	7.91	1.09	**11736.63**	2
San Diego State University	Spirit of Monty	84.5	8.28	1.16	**11894.8**	1
Uinv of California San Diego	Aerodrone F8273	80.5	9.15	0.61	**5380.84**	11
La Sapienza	Leonardo	79.5	6.69	0.19	**2264.63**	19
*Queen's University	Some Assembly Required	79.2	13.28	0.01	**59.61**	27
*W. Virginia University	Lock-N-Load	79	12.65	0.01	**62.46**	25
*Virginia Polytechnic University	Draggin Fly	77.3	11.81	0.01	**65.4**	24
Istanbul Technical University	Ucakcilar	74.8	11.24	0.8	**5301.99**	12
*Wichita State University	WU Flyer	74.3	12.79	0.01	**58.05**	28
Uinv of California San Diego	Furious Flier	74	9.22	0.31	**2473.78**	17
†Syracuse University	The Judge Chaser	73.8	100	0.01	**7.38**	35
†Clarkson University	Knight Riders	73.3	100	0.01	**7.33**	36
University of Illinois UC	Gas Guzzler	72	9.35	0.65	**5009.39**	13
*University at Buffalo	Bull Ship	71	11.86	0.01	**59.87**	26
†University of Central Florida	K-03 Pegasus	69.9	100	0.01	**6.99**	37
University of Colorado	Bellwether	68.4	8.41	0.28	**2279.43**	18
†University at Buffalo	Frier Fly	66.5	100	0.01	**6.65**	38
*Univ of Texas Arlington	Spirit of Arlington	65	13.7	0.01	**47.45**	33
*Case Western Reserve	Marsupial Falcon X	61.3	8.92	0.01	**68.69**	23
*Western Michigan University	Western Flyer	59.3	11.83	0.01	**50.17**	31
*Ohio Northern University	It's Supposed to Fly	59	8.08	0.01	**73.05**	22
*Univ California LA	Bruin Bud-E	58.9	10.58	0.01	**55.62**	29
*University of Arizona	AirCat 2003	47.9	10.08	0.01	**47.51**	32
*Calif Poly State Univ Pomona	Pegasus	47.5	8.78	0.01	**54.13**	30
Washington State University	CAT	46	10.01	0.59	**2692.87**	14

* Present at Fly-off, but did not have a successful scoring flight

† Not present at the Fly-off

2002/2003 AIAA

Cessna/ONR Student

Design/Build/Fly Competition

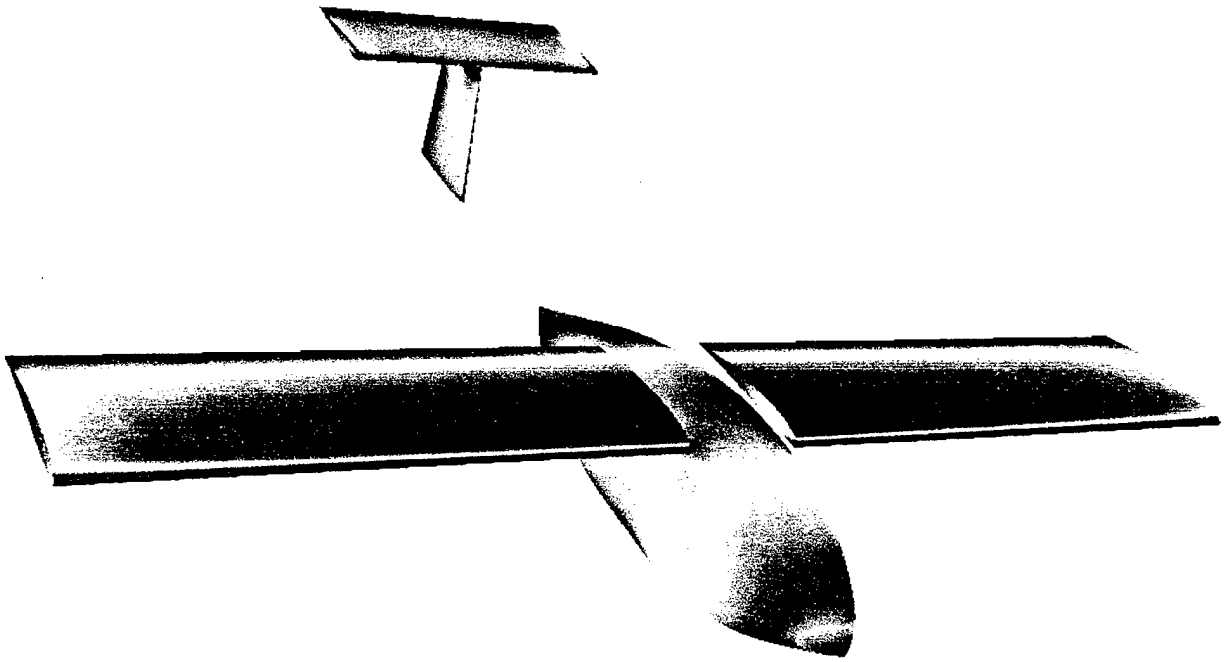

San Diego State University

Spirit of Monty

Table of Contents

1. Executive Summary 1

1.1. Conceptual Design 1

1.2. Preliminary Design 2

1.3. Detail Design 3

2. Management Summary 4

2.1. Architecture and Responsibilities of the Team 4

2.2. Schedule Control 6

3. Conceptual Design 8

3.1. Problem Statement 8

3.2. Assumptions 9

3.3. Trade-offs Between Mission Flights 14

3.4. Design Considerations 15

3.5. Conclusion of Conceptual Design Phase 22

4. Preliminary Design 23

4.1. Configuration Basics 23

4.2. Assembly System 24

4.3. Wings 25

4.4. Fuselage 30

4.5. Tail Options and Sizing 32

4.6. VSAERO Configurations Tested 33

4.7. Wing-Body Lift Curve 35

4.8. Drag Estimation 35

4.9. Power Plant Design 36

4.10. Structural Considerations 37

5. Detailed Design 38

5.1. Configuration Summary 38

5.2. Rated Aircraft Cost 39

5.3. Dynamic Stability Estimation 39

6. Manufacturing Plan 46

6.1. Major Components 46

6.2. Materials 46

6.3. Figures of Merit 46

6.4. Summary of Material Choices 47

6.5. Manufacturing Schedule 48

6.6. Manufacturing Processes 50

6.7. Electronic Components and Payload Deployment System 52
6.8. Structural Integrity 52
6.9. Conclusion of Fabrication Phase 52
7. Testing Plan 53
7.1. Flight Testing Objectives and Checklist 53
7.2. Lessons Learned 54

1. Executive Summary

The following summarizes the development of "Spirit of Monty", an entry from San Diego State University into the Cessna/ONR Student Design/Build/Fly Competition at St. Inigos, Maryland, on 25-27 April 2003. The competition requires that the students design, fabricate, and demonstrate the airplane that best satisfies the required missions. Three different missions are specified, but only two of the three need to be performed. Depending on the mission there are different types of payloads and flight requirements. The goal is to maximize the Total Score, which is accomplished by scoring the best in three areas. One area is to maximize the flight performance of the aircraft and thereby maximizing the Total Flight Score. Another is to achieve the lowest virtual cost of the airplane called the Rated Aircraft Cost (RAC). Finally, the Report Score must be maximized by well documenting the design, fabrication, and testing process. To accomplish this mission, the team "Spirit of Monty" began its exploration from the conceptual design.

1.1. Conceptual Design

First, the problem statement of the competition was made so that the following assessments would be well targeted. Before investigating alternative designs, some assumptions were made according to calculations as well as to the results from last year's competition entry. These assumptions were necessary to determine the core characteristics of the aircraft such as the minimum planform area and the estimated weight. Next, competition requirements, including a choice of three different missions, were assessed in order to create design parameters for each conceptual design consideration. Evaluating alternative designs of the aircraft with the parameters, conceptual design phase led to one configuration for each of five design considerations, with maximum scoring potentials.

1.1.1. Conceptual Design Considerations

Design considerations included the basic aircraft configuration, payload system, wing configuration, type of the landing gear, and assembly systems. Basic aircraft configurations were discussed such as the conventional with T-tail, conventional with V-tail, conventional with twin-boom, canard, flying-wing, and bi-plane. Concepts for the payload system consisted of a vertical-drop, roll-aft, and roll-front. High-, mid-, and low-wing configurations were evaluated for structural and stability aspects. Type of landing gear resulted in one version without competing concepts. Lastly, effective assembly of the aircraft was examined. Alternative designs for each of these five considerations were evaluated by using the design tools.

1.1.2. Conceptual Design Tools

Design tools included visualization tools, calculation tools, and design parameters that worked in the process of calculations. To visualize alternative designs, Pro-Engineer (CAD) was used to create 3-dimensional images. Excel spreadsheets were one of the main calculation tools, providing a qualitative analysis with embedded programs that were constructed by the team. Design parameters were called

Figures of Merit (FOM). FOM are the factors that would either directly or indirectly affect the scoring potential of the aircraft. Effects of the direct factors, such as RAC, were calculated by the spreadsheet, while effects of the indirect factors were interpreted qualitatively to give the numerical value of the scoring potentials of each alternative design.

1.1.3. Results of the Conceptual Design Phase

The first two of the three specified missions, Mission A and B, were selected for further design because of their scoring potential. Spirit of Monty would be a conventional T-tail (or V-tail) plane with high-wings and a tractor-propeller. Payload would be vertically dropped during Mission B, while the cylinder for Mission A would hang below the fuselage. Wings would be split into two parts in order to fit in the assembly box and the landing gears would be a tricycle configuration: one nose and one on either side of the fuselage. An assembly process was also conceived to allow for a rapid assembly time.

1.2. Preliminary Design

To begin with, schematic drawings of the assembly components of the aircraft were made and were placed in a drawing of the storage box to find a suitable position. This was the foundation to designing the assembly mechanisms. The next step was the determination of the wing design, since it would define the upper surface of the fuselage. Airfoil, planform area, wingspan, and chord length optimization was performed. Using the upper surface of the chosen airfoil (SD7043), the outer mold line of the fuselage came next, followed by the analyses on the tail configurations. Drag and stability of the chosen configuration were evaluated. Power plant and structural analyses were also was performed.

1.2.1. Preliminary Design Considerations

Several assembly methods were considered for each component, from which a concept with the quickest connections was selected. Design considerations for the wing consisted of three different airfoils, including the one from Monty's Revenge, last year's airplane. The fuselage design had two competing concepts concentrating on the trailing edge style. Tail considerations focused on the comparison between T-tail and V-tail. Power plant was designed from different combinations of motors and propellers.

1.2.2. Preliminary Design Tools

Airfoil choice began by researching various airfoils and utilizing the 2-D viscous solver X-FOIL for airfoil optimization. Graphs of C_l vs. α and C_d vs. C_l of different airfoils were used to determine which was best for the mission. Planform area, wingspan, and chord length were determined by designing an Excel spreadsheet, which allowed comparison of RAC values for different combinations. For the fuselage design, X-FOIL was used to create the lowest drag-configuration, and Pro-Engineer (CAD) was used to model it into a 3-D shape. VSAERO, an inviscid 3-D solver, was used to integrate the fuselage, wing, and tail configurations to predict the performance. Lift and drag were numerically calculated and

compared with the computer data. MotoCalc and P-calc, two electric power plant optimization programs, were used to design the power plant configuration.

1.2.3. Results of the Preliminary Design Phase

Final decisions were made on the assembly methods and the configurations of the wings, fuselage, and tail. Component optimization was now complete and estimation of the performance gave satisfactory results to proceed into the detail design.

1.3. Detail Design

The final design was created which included detailed drawings of the major and minor components. Component selection and system layout was also completed. Final Rated Aircraft Cost was determined, which was lower than originally predicted during the early design phase. Performance evaluation, including dynamic stability, was performed to determine if any modifications would be necessary.

1.3.1. Detailed Design Considerations

Since the sizing had been performed and all other specifications of the design are known, the stability and detailed weight tracking were now the focus. Battery placement and the actual weight of the composite materials were only estimated during the previous design phases. To ensure a balanced aircraft a team member was assigned the Mass Properties position to keep track of weights and locations.

1.3.2. Detailed Design Tools

Dynamic stability performance was evaluated by utilizing many sources. Advanced Aircraft Analysis (AAA), a computer aircraft design tool was used to evaluate the stability. Used in conjunction with AAA much of the stability calculations were performed by hand. For that to be accomplished, Pro-Engineer was used to obtain the moments of inertia and other needed measurements. Other performance was recalculated such as take-off distance and maximum rate of climb to compare with the earlier estimations.

Pro-Engineer was the most used tool during the final design phase. Codes were obtained to operate the CNC mill in order to machine the fuselage foam cores. Pro-Engineer was also used to create drawings from the models in order for the Manufacturing Team to build the major components.

1.3.3. Results of the Detailed Design Phase

The final design showed that the extensive work during the Conceptual and Preliminary Design phases benefited the project. The airplane was evaluated to be stable using two separate methods. Take-off distances and other performance characteristics were very close to design parameters

Machining of the foam cores saved the Manufacturing team many hours of shaping it by hand. The team was handed the drawings to begin the fabrication process.

2. Management Summary

Design work started with only five members, who participated in last year's competition. The five gathered in August, after the release of a draft of the 2002/2003 Competition Rules. Greg Marien, the Project Manager, would continue to lead the team, and assigned an Assistant Project Manager and some of the team leaders. As the AIAA Student Chapter at San Diego State University grew dramatically in Fall 2002, the team was able to add members to each design group. Assignment areas for each member depended on both skills and wishes. Ultimately, the team was composed of 1 faculty advisor, 1 graduate student, 12 seniors, 10 juniors, and 5 freshmen.

2.1. Architecture and Responsibilities of the Team

As Figure 2-1 below illustrates the architecture of the team followed by the description of the positions.

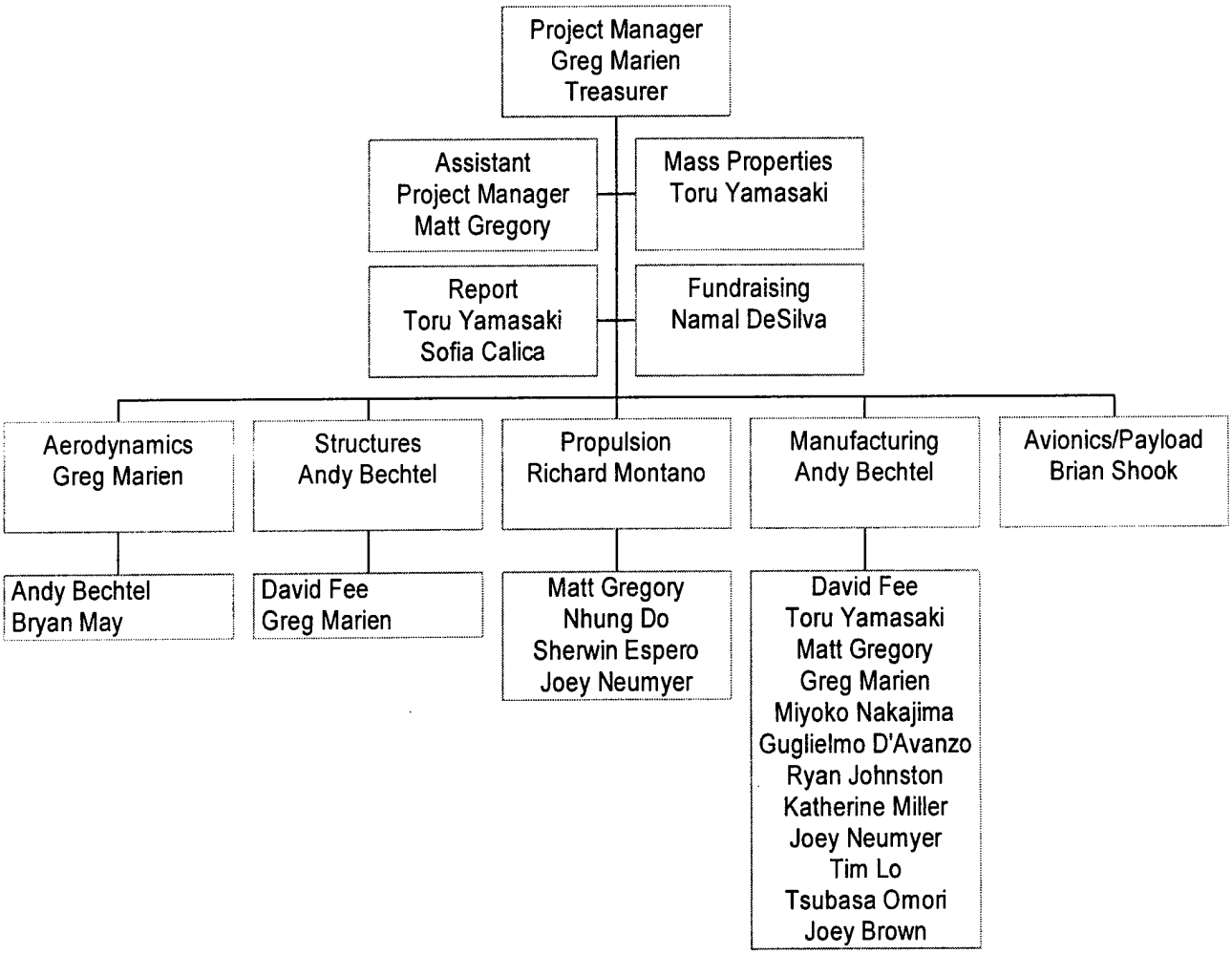

Figure 2-1 Team Architecture

2.1.1. Project Manager

The Project Manager calls the meetings and is responsible for schedule management. Leading the fundraising presentations and approving the budget are also the Project Manager's responsibilities. Important decisions made by the design teams need to obtain recognition from the manager.

2.1.2. Assistant Project Manager

This position was created to train a new Project Manager for the following year. Appointed to the position was a junior member on his second year of Design/Build/Fly participation. The assistant is to be involved with all the aspects of the Project Manager's duties to ensure the transfer of knowledge.

2.1.3. Treasurer

The Project Manager also serves as the AIAA Student Branch Treasurer, so the positions were combined. The treasurer is responsible for the registration of all donors and donations given to the team. The Team Leaders should obtain permission for necessary purchases from the treasurer for reimbursement.

2.1.4. Team Leaders

Responsibilities include organizing each team by assigning duties to individual members, and to report to the Project Manager the status of the group's tasks.

2.1.5. Fundraising

This team organizes fundraising events and presentations. The events include several BBQ's and lunch meetings with permission from the school, and an exposition featuring Monty's Revenge from last year. Also, letters have been sent to alumni, asking for monetary and/or equipment donations. Corporate funding was also received from Northrop-Grumman.

2.1.6. Aerodynamics

This team is responsible for analyzing and aerodynamically optimizing the fuselage, wing, and tail configurations. They are also responsible for stability evaluation.

2.1.7. Power Plant

This team is responsible for wind-tunnel tests on several motor-propeller combinations. Research on the other equipment including batteries is also the responsibility of the group.

2.1.8. Avionics/Payload

This team is responsible for the electrical wiring within the aircraft. The focus is on the security and effectiveness of the connections between assembled parts of the aircraft, as well as the payload interface system.

2.1.9. Structure and Fabrication

This team is responsible for submitting a feasible fabrication plan that met both the budget and skills of the team. Then, the group fabricates the aircraft based on the drawings from the drawing team. Structural analysis and logistics are also assigned to this group.

2.1.10. Drawing

This team is responsible for converting the alternative designs and the final configuration into CAD parts and drawings. This job was a group effort between the Aerodynamics, Structures, and Manufacturing teams.

2.1.11. Report

The Report Team collects the data from the research and development, and compiles it into the final report. The group also provides some design parameters to the other teams, in accordance with the design report requirements from the competition rules.

2.2. Schedule Control

An original milestone plan was made at the first meeting of the team. Table 2-1 on the following page illustrates the comparison between the original plan and actual design processes. Weekly meetings of the Team Leaders along with the Project Manager helped manage the schedule of the design phases. Any changes to the schedule had to be addressed at the weekly meetings and approved by the Project Manager.

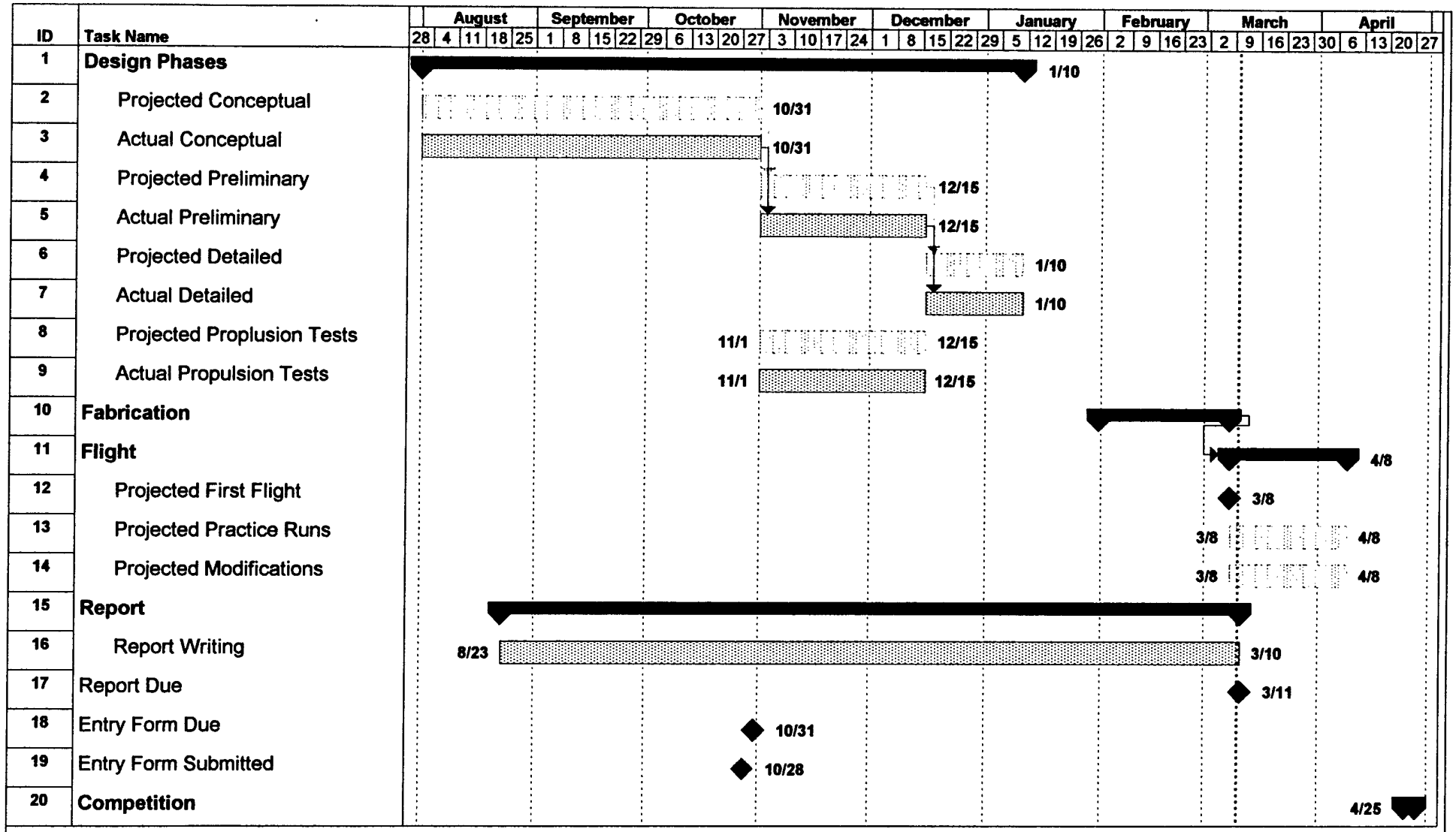

Figure 2-1 Milestones and Schedule

3. Conceptual Design

The conceptual design phase was an investigation of the mission requirements and design considerations, which created the best path to the most competitive design. Alternative designs in each concept competed towards a maximum scoring potential. Design considerations included basic aircraft configuration, payload system, wing configuration, landing gear type, and assembly of the aircraft. For each of the considerations, the best concept was chosen. The remaining structure, shape, sizing, and power plant were evaluated in the preliminary and detail design phases.

3.1. Problem Statement

Total Score of the competition incorporates **Total Flight Score**, **Rated Aircraft Cost (RAC)**, and **Report Score** such that:

$$\text{Total Score} = \frac{\text{Total Flight Score x Report Score}}{\text{Rated Aircraft Cost}}$$

Equation 3-1 Total Score

Report Score was held at 90 (average competition report score) throughout the report for simplicity. Therefore, the conceptual design phase would focus on how **Total Flight Score** and **RAC** affect **Total Score** as they change with respect to alternative design configurations. Following the design analyses, alternatives that offer maximum scoring possibility against the specified missions were selected.

As illustrated in Figure 3-1, the missions would be flown on a specified course to compete toward **Total Flight Score**.

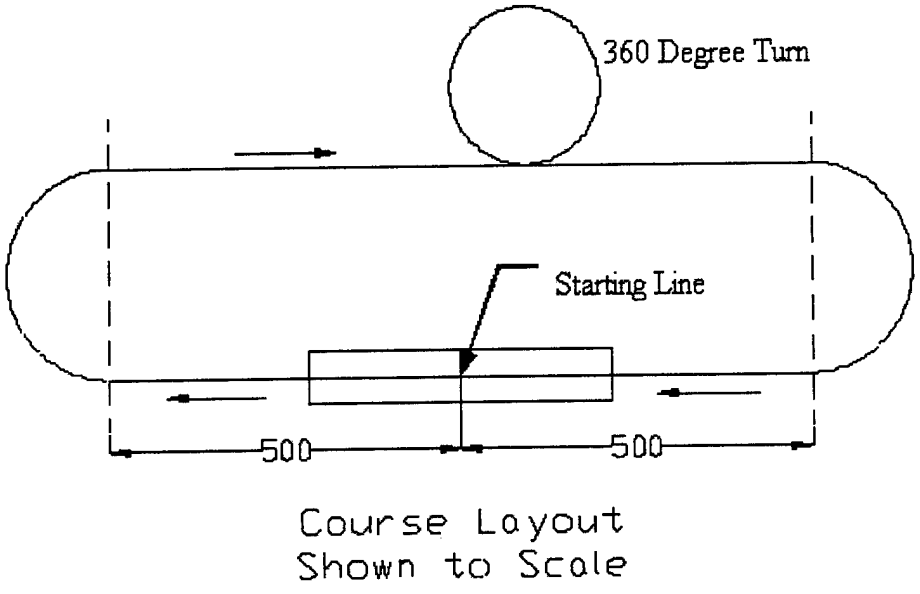

Figure 3-1 Course Description; distances are in feet (reproduced from competition rules)

Total Flight Score is calculated by summing the best **Single Flight Score** (see Equation 3-2) from two of the three missions, A, B, or C. Each of the missions has a numerical difficulty factor of 2.0, 1.5, and 1.0, respectively. Table 3-1 below briefly summarizes the profiles of these missions broken down into its component parts.

$$\text{Single Flight Score} = \frac{\text{Difficulty Factor}}{\text{Mission Flight Time} + \text{Aircraft Assembly Time}}$$

Equation 3-2 Single Flight Score

Mission	A	B	C
Difficulty Factor	2.0	1.5	1.0
Total Laps	4	4	4
# of 180° turns/lap	2	2	2
Total # of 180° turns	8	8	8
# of 360° turns/lap	1	1	3
Total # of 360° turns	4	4	12
Payload	5lb 6"x6"x12" box	5lb 6"x6"x12" box	5lb 6"x6"x12" box
Particular Task	A simulated cylindrical antenna, a section of unmodified 6" PVC pipe 3" tall	Landing and remote deployment of payload after 2 laps	

Table 3-1 Mission Summary

Mission Flight Time is the total time between a "go" signal from the official and the aircraft's complete stop past the starting line after finishing a mission. Included in the **Single Flight Score** is a timed assembly task, which must be performed at least once before the first attempted mission. Prior to the assembly task, the disassembled aircraft must fit in to a 2' X 1' X 4' (inner dimension) box. Three team members are timed on the assembly of the aircraft to make it flight-ready. The wing tip lift test and control system function/orientation test are then performed with a 3-minute penalty added to **Aircraft Assembly Time** for each incorrect operation. This makes the quickness and reliability of assembly an important design parameter.

3.2. Assumptions

Assumptions depended both on calculations and on the data from Monty's Revenge, last year's competition entry. The estimated parameters included the empty/loaded weight, cruising speed, weather conditions, Assembly Time, and RAC. These assumptions were necessary to obtain an estimate of the Total Score on which the design would be based.

3.2.1. Estimated Take-off Weight

Empty weight of the aircraft was set to 12 pounds. This estimation was based upon previous years of fabrication experience. Last year's entry had a 20 pound empty weight and since there is a 4 pound reduction in payload the weight was set to 16 pounds. Furthermore, a reduction in 4 more pounds is achieved from the improved experience in a lighter weight structure and a lighter weight power plant. Therefore, the empty weight was set to 12 pounds and a maximum take-off weight of 18 pounds (5 pounds for box and 1 pound for cylinder).

	lb
Empty weight from last year	20
Payload reduction	4
Structure reduction	4
Estimated empty weight	**12**
Box payload	5
Cylinder payload	1
Maximum take-off weight	**18**

Table 3-2 Estimated Take-off Weight Summary

3.2.2. Estimated Cruising speed

Baseline speed of 100ft/s was used, which was the same speed as last year's competition entry. This speed is only used for initial sizing calculations and estimating flight scores. Further evaluation of the speed is performed in the preliminary design phase. Because this year's design is lighter and more research was to be performed on the power plant, speed was raised to 120 ft/s with the payload box, while the cylinder payload remained at 100 ft/s. The reduction in speed is based on a calculated 2 pounds of cylinder drag from empirical data (Reference 5).

3.2.3. Weather conditions

Historical weather conditions from www.weatherbase.com were used for design considerations. A worst-case scenario of a low atmospheric pressure and a high temperature was used to ensure adequate performance in extreme conditions, shown in Table 3-3 below.

3.2.4. Initial Wing Sizing

Initial wing sizing was based on weather conditions, estimated take-off weight, cruising speed, turn performance and take-off distance (<120 ft). Evaluating different families of possible airfoils (low drag/high lift), a C_{lmax} of 1.6 was used for estimations.

Temperature (T)	100	F			
Pressure (P)	28.75	in Hg	Loaded weight (W)	18.00	lb
Density (ρ)	0.00212	slugs/ft^3	Average velocity (V)	100	ft/s
Viscosity (μ)	3.97E-07	lb-s/ft^2	Takeoff velocity (V)	50	ft/s
Kinematic viscosity (ν)	0.00019	ft^2/s	Dynamic pressure (q)	10.59	lb/ft^2

Table 3-3 Sizing parameter assumptions

Table 3-4 below shows the results of the initial sizing of the wing using the assumptions from Table 3-3 above. The limiting factor was the 4.5-g turn performance; therefore the planform area was set to 5.5 ft^2

Turns	g-loading	4.5	
	ϕ (bank angle)	77.16	degrees
	Turn radius	71.23	ft
	Required planform area	5.50	ft^2
Cruise	Required planform area	3.40	ft^2
Take off	Required planform area	4.86	ft^2

Table 3-4 Planform area requirement to meet the mission

3.2.5. Rated Aircraft Cost (RAC)

The initial working concept must be designed to reduce the RAC as much as possible for the maximum Total Score. There is a limit to the amount of reduction since the concept must still be a stable and flyable design. The following RAC equation is used to simplify the theoretical cost of each team's airplane.

$$RAC = \frac{100 \times MEW + 1500 \times REP + 20 \times MFHR}{1000}$$

Equation 3-3 Rated Aircraft Cost Calculation

Where:

MEW = Manufacturers Empty Weight

REP = Rated Engine Power

MFHR = Manufacturing Man Hours

Table 3-5 below shows a breakdown of the RAC for one conceptual concept.

	RAC	8.71	
	MEW	12.00	
	REP	2.84	
	MFHR	163	
# of cells	24		Sanyo 1700 SCR
weight per cell	1.89	oz	weight includes extra hardware
total battery weight	2.84	lb	

WBS[1]	**Value**	**Hours**	**Multiplier**
1.0 Wings			
wing span (ft)	5.50	44	8 hr/ft Wing Span
chord (ft)	1.00	8	8 hr/ft Max chord
# of control surf	2	6	3 hr/control surface
2.0 Fuselage			
Max length (ft)	5	50	10 hr/ft max length
3.0 Empennage			
# of vertical-nc	0	0	5hr/vertical-no control
# of vertical-ac	0	0	10 hr/vertical-active control
# of horizontal	0	0	10 hr/horizontal-see wing rule
V-tail only		15	v-tail-15 hr
4.0 Flight Systems			
# of servos/control	6	30	5 hr/servo (Note 1)
5.0 Propulsion			
#of engines	1	5	5 hr/engine
#of propellers	1	5	5 hr/propeller

Note 1: 2 ailerons, 2 stabilizer, 1 nose wheel, 1 payload release

Table 3-5 RAC Calculation

3.2.6. Propulsion Configuration

Early in the conceptual phase, use of an Excel spreadsheet shown in Table 3-5 above allowed the removal of a two-motor concept. Using only one motor reduced the RAC by almost 15%, which is significant enough to affect the Total Score.

Using a tractor configuration instead of a pusher was decided early on due to the interference of the pusher propeller and the released payload during Mission B.

[1] WBS is the Work Breakdown Structure. The summation of the WBS is equivalent to the Manufacturing Man Hours

3.2.7. Landing Gear Configuration

Landing gear configuration had two options, tricycle or a tail wheel. First, the released payload would interfere with the tail wheel during the take-off. Second, if the payload release concept was to drop from the fuselage then the payload should be parallel to the ground for ease of deployment. Therefore, the tricycle landing gear was chosen.

3.2.8. Assembly Time

Another assumption was that for the assembly task each step would take 10 seconds; for example, it took roughly 10 seconds to assemble the wings of last year's competition entry, which had a plug-in type design. Three personnel are allowed on the assembly team and therefore up to three steps could be done simultaneously. For example, the time of assembly would be 10 seconds for three parallel tasks. The tasks considered were, assembly of the landing gear, connection of the wing parts, connection of the tail, and connection of the wing to the fuselage. The first three steps would be done in parallel while one person would perform the final step. Total Assembly Time by this estimation is 20 seconds, but 10 more seconds were added for the unforeseen circumstances factor. The final estimated Assembly Time was set to 30 seconds. Further sizing and configuration will reduce this time to a minimum.

3.2.9. Estimated Total Score

Total Score predications were made based on the three types of missions using the assumed flight speeds and estimated RAC. Results are in Tables 3-6 through 3-9 below.

Mission A	**4 laps/ 8-180° turns/ 4-360° turns**		
1 lap	**distance (ft)**	**velocity (ft/s)**	**time of flight (s)**
Straight cruise	2000	100	20.00
2-180° turns	157	80	1.96
1-360° turn	157	80	1.96
Total distance (4 laps)	9256		95.70
	Flight Time (min)	1.60	
	Single Flight Score	0.95	

Table 3-6 Mission A Estimated Flight Performance

Mission B	**4 laps/ 8-180° turns/ 4-360° turns /one landing**		
1 lap	**distance (ft)**	**velocity (ft/s)**	**time of flight (s)**
Straight cruise	2000	120	16.67
2-180° turns	157	100	1.57
1-360° turn	157	100	1.57
Landing			30.00
Total distance (4 laps)	9256		109.23
	Flight Time (min)	1.82	
	Single Flight Score	0.65	

Table 3-7 Mission B Estimated Flight Performance

Mission C	4 laps/4 turns/4-360's		
1 lap	distance (ft)	velocity (ft/s)	time of flight (s)
Straight	2000	120	16.67
2-180° turns	157	100	1.57
3-360° turn	471	100	4.71
Total distance (4 laps)	10512		91.79
	Flight Time (min)	1.53	
	Single Flight Score	0.49	

Table 3-8 Mission C Estimated Flight Performance

Aircraft assembly time	30 seconds	0.50 minutes	
Mission	A&B	A&C	B&C
Report Score	90	90	90
Total Flight Score	1.60	1.45	1.14
RAC	8.71	8.71	8.71
Total Score	16.54	14.95	11.77

Table 3-9 Estimated Total Flight Score

Initial observation shows the best strategy for obtaining the highest Total Score is to design around Mission A and B. But, changing the design to fit only specific missions may improve RAC enough to justify a reduced difficulty flight routine. The next section deals with this exact concern.

3.3. Trade-offs Between Mission Flights

A trade study was performed on whether neglecting Mission B can result in a higher Total Score. Exclusion of Mission B meant an improved RAC due to one less servo, since there would be no payload deployment, and subsequently less weight for the release mechanism. Assembly Time was assumed to not improve, since it is not related with deploying of the payload. Cruising speed may increase by a small amount due to weight reduction.

Figure 3-2 shows how the combination of Mission A & C compares to that of Mission A & B. Even if the aircraft acquires 10ft/s more cruising speed in the first combination, it is apparent that for Missions A & C to beat the Total Score of A & B, a 0.3 decrease in RAC is needed. However, one less servo contributes to only a 0.1 decrease, and negligible weight decrease, which is only 1/3 of what is needed. Hence it is concluded that Mission B is to be accomplished. Mission B & C scoring would be so low that the design would no longer be competitive. The conclusion is to design around Mission A and B; Mission C will still be able to be flown if needed by designing around Missions A & B.

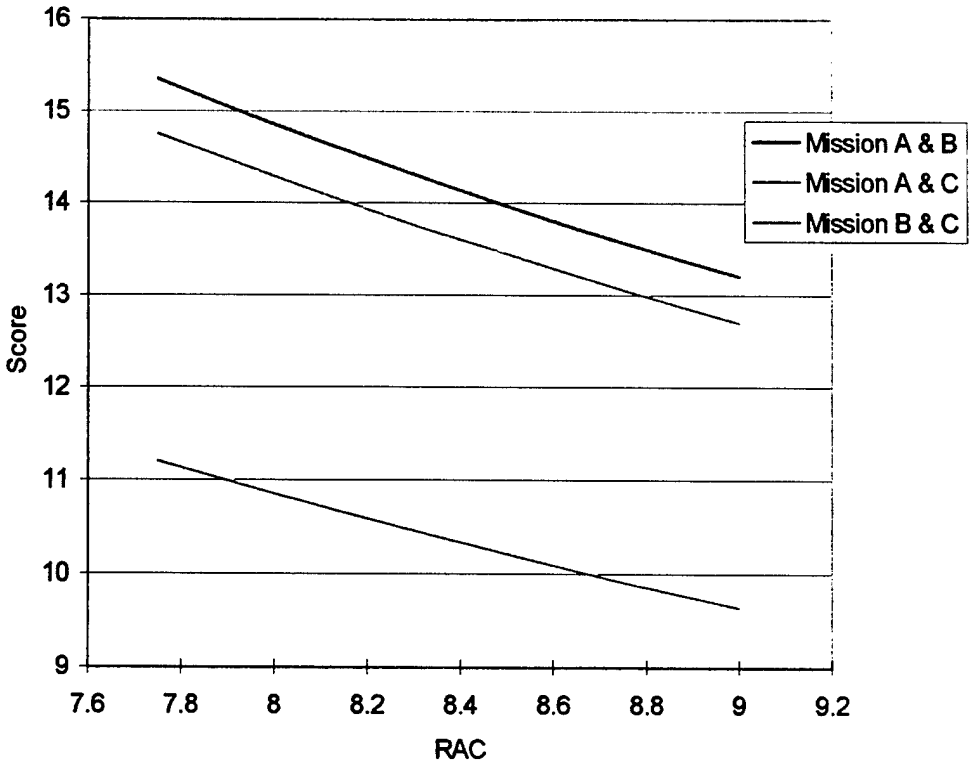

Figure 3-2 Comparison of Total Points for Different Missions

3.4. Design Considerations

Five different areas were considered in the conceptual design phase. The following is a list of the design areas along with the reasons why it was felt necessary to discuss them.

1. **Basic Aircraft Configuration:** The most fundamental characteristics of the aircraft were decided at the beginning. This decision induced restrictions on the other aspects of the design.
2. **Payload System:** Method of deployment affects both internal and external structure of the aircraft, especially that of the fuselage. For instance, if the payload would roll aft for deployment, structure would be required at and around the opening of the fuselage. Landing gear interference was another concern. Along with the payload deployment system is the simulated antenna, which must be mounted externally at least 3" away from the airplane's structure. The location of the antenna must also be in the air stream with no obstructions (not including the tail and the landing gear).
3. **Wing Configuration:** High-, mid-, and low-wing configurations were discussed. While the natural tendency was to choose a high-wing for a cargo plane, the discussion justified the choice. This concept led to detailed assembly methods and fuselage structure, as well as restrictions on landing gear locations.
4. **Type of Landing Gear:** Since the payload deployment system had to be finalized before choosing the landing gear configuration, there were few considerations. A tricycle configuration

was already decided upon, nevertheless, the landing gear configuration led to further exploration in the conceptual design phase for rapid assembly.

5. **Assembly Systems:** Several assembly methods were evaluated for the wings, tail, and landing gear. Reducing the number of parts needed to be assembled and simplifying the way the parts are assembled shortens the time of assembly.

For each design consideration, design parameters are defined as Figures of Merit (FOM), which include Rated Aircraft Cost (RAC). FOM, which vary from one design consideration to another, are the parameters that affect scoring potential. One example of FOM is stability, because poor stability can prevent a design from being competitive. A definition and calculation of RAC is summarized in Section 3.2.5 above.

FOM, which cannot affect Total Score numerically, are rated individually. The ratings range from -0.2 to +0.2 with an increment of 0.1; 0 represents normal. The reason for the small values of the ratings is that the ratio of change to the Total Score has to be small in order to emphasize the significance of its effect. An Effective Score is then calculated by summing Total Score with the sum of the FOM. Effective Score is a numerical equivalent to the potential scoring capability of the design.

$$\text{Effective Score} = \text{Total Score} + \text{Sum of FOM}$$

Equation 3-4 Effective Score Calculation

3.4.1. Basic Aircraft Configuration

Basic designs of the fuselage, wing, and tail were determined during this step. Each configuration with the highest Effective Score was carried through to the next design consideration. Basic aircraft configuration was evaluated using the following Figures of Merit:

I. **RAC:** a numerical value was calculated accordingly.

II. **Ease of Assembly:** each advantage or disadvantage was accounted for by a difference in Assembly Time.

III. **Drag Performance:** increasing or decreasing the cruising speed by 10 ft/s accounted for each predicted increase or decrease in drag.

IV. **Take-Off and Landing Performance:** 3 seconds were either added or subtracted for an advantage or disadvantage in the performance.

V. **Flight Performance:** Flight performance including stability and control is a significant factor since it affects the ability to complete the missions.

VI. **Experience:** The team's ability to design a competitive aircraft affects all design configurations. If the experience does not exist, this could affect the overall competition outcome.

One (I) through four (IV) above were first numerically evaluated for Total Score. FOM V and VI were then used to evaluate six alternative configurations. An Effective Score was calculated to allow a decision to be made of not only the best design, but to help the team decide which one could be more

easily fabricated. Summary of the evaluations are in Table 3-10 below. Pictures of the conceptual configurations are in Figure 3-3.

1. **Conventional with T-tail:** A Total Score of 14.26 set the standard for other configurations. Rating for both FOM V and VI was 0.2 because this was the configuration in which the team had the most experience. Effective Score is 14.46.
2. **Conventional with V-tail:** RAC decreased by 0.1 for the V-tail compared to the T-tail. This change made Total Score 14.75. FOM V dropped to –0.1 because the V-tail has effective area losses and therefore requires a bigger tail to attain the same stability and control. This results in a possible increase in RAC due to the 25% contest rule with the tail versus the wingspan. FOM VI dropped to –0.2 because of the lack of v-tail design experience. Resultant Effective Score is 14.45.
3. **Conventional with twin boom/H-tail:** H-tail increases RAC by 0.1 and an additional boom weighs roughly 0.25 lb more increasing RAC by 0.02. Alignment of two tail booms during assembly is more complicated than one boom; therefore, Assembly Time is increased by 3 seconds to accommodate this resulting in a Total Score of 14.12. Two-boom support gave an improved stability due to the more rigid tail structure resulting in a FOM V of 0.1. Less experience with this design results in a -0.1 rating. The result is an Effective Score of 14.12.
4. **Canard:** First three Figures of Merit were evaluated as the same as conventional because the only fundamental difference between a canard and conventional is the location of the wings and horizontal stabilizers. The result is a Total Score of 13.96. Better stall performance of the canard made the rating of stability 0.1, and since the team has no experience with canard, FOM VI is set to –0.2. Effective Score is 13.86.
5. **Flying wing:** RAC decreased by 0.3 due to removed tail weight and control surfaces. Assembly Time also improved by 3 seconds for not having to assemble the tail. Worse take-off and landing performance added 3 seconds per event. Calculated Total Score is 14.72. Marginal stability of the flying wing resulted in a stability rating of -0.2. Experience was moderately lacking resulting in a rating of -0.1. Effective Score is 14.42.
6. **Bi-wing:** Since layering the wings would require a 6-inch longer combined wingspan due to lower aspect ratios, RAC increased by 0.08. It might be possible to shorten Assembly Time by 3 seconds, assuming that two wings would be attached and fit in the box (1-foot box height), but the wings would also be too close together for proper airflow, which reduces lift. Calculated Total Score is 14.82. Parasitic drag is also a common problem with a bi-wing design. Lack of experience is also a factor, thus ratings for the last two FOM are both -0.2. Effective Score is 14.42.

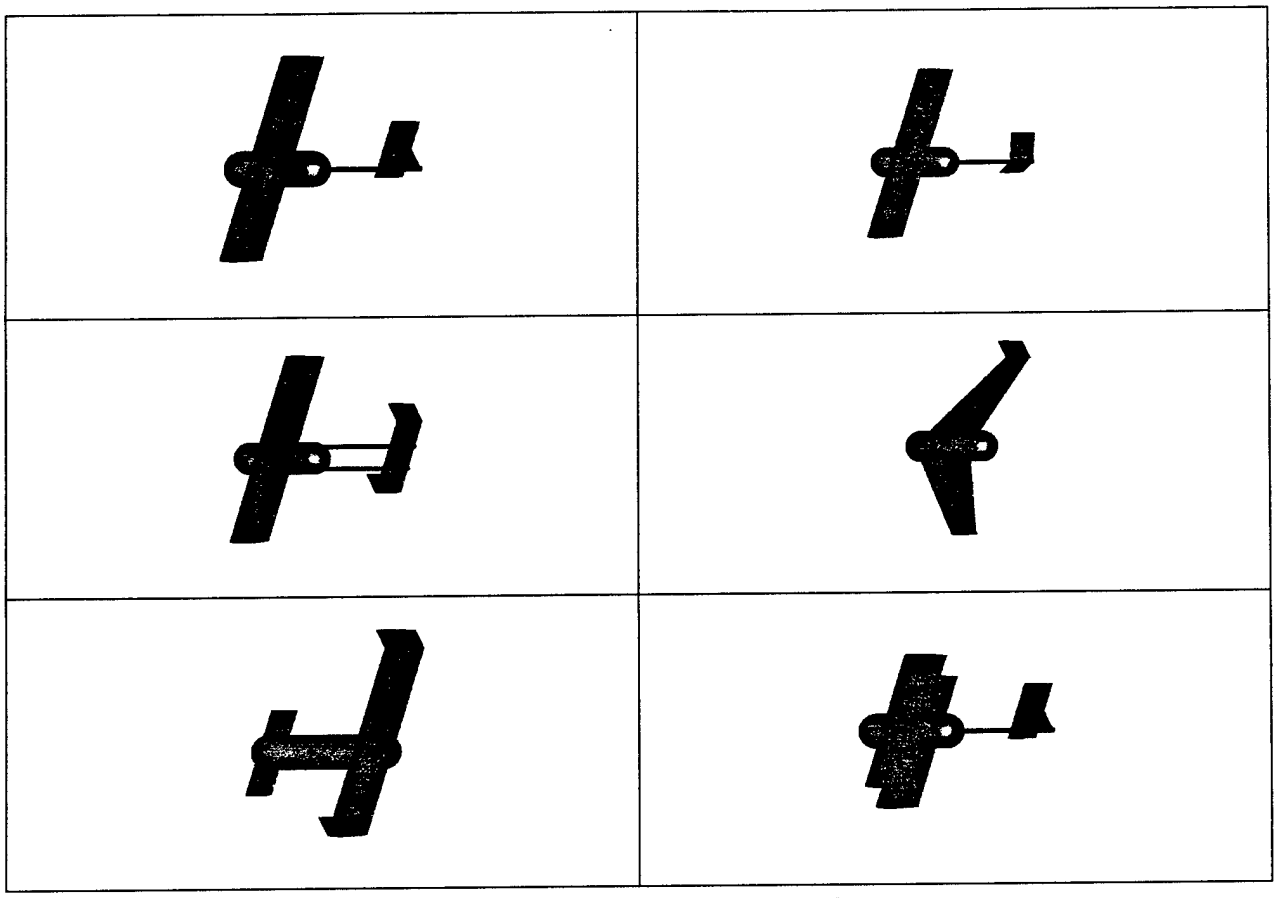

Figure 3-3 Conceptual Configurations

		FOM Ratings		
Configurations	**Total Score FOM I-IV**	**V**	**VI**	**Effective Score**
Conventional w/T-tail	14.26	0.2	0.2	14.46
Conventional w/V-tail	14.75	-0.1	-0.2	14.45
Conventional w/H-tail	14.12	0.1	-0.1	14.39
Canard	13.96	0.1	-0.2	13.86
Flying Wing	14.72	-0.2	-0.1	14.42
Bi-plane	14.82	-0.2	-0.2	14.42

Table 3-10 Configuration Summary

Conventional configuration with T-tail was chosen over the other configurations. The choice was reasonable in the sense that this configuration was balanced in potential Total Score, stability & control, and experience. Because the V-tail configuration also scored high, both designs would be further evaluated in the preliminary design.

3.4.2. Payload System

Remote deployment of the payload is critical to Mission B. The concepts that were presented and discussed include vertical drop, roll-front, and roll-aft. Figures of Merit (FOM) for the system are the following:

I. **Total Score:** This contains estimated flight time, RAC, time of assembly, and drag performance of the components. Values were calculated in the same manner as Table 3-5.

II. **Landing Gear Interference:** Deployed payload should not interfere with the landing gear to ensure the second take-off during Mission B.

III. **Complication:** Complication of the mechanism results in an increase in weight and/or payload deployment reliability problems.

Summary of the evaluation is in Table 3-11 below.

1. **Vertical Drop:** To set a standard, FOM III has rating of 0. The landing gear interference is not anticipated for this concept because the payload would be on the ground between the main gears; therefore, FOM II rating is set at +0.2. Total Score is 14.43, and Effective Score is 14.63.
2. **Roll-front:** Rolling would increase deployment time by at least 3 seconds because a mechanism would be needed to help the deployment instead of using gravity. Necessary space in the fuselage for the rolling would make the body longer by about 3", which increases the weight and therefore increasing the RAC by an estimated 0.05. Total Score is now 14.22. Landing gear might be an interference problem since the deployed payload would be in front of them. A complicated mechanism would also be required to roll the payload while keeping the surface of the fuselage in the same shape after deployment (faired payload doors). Therefore, each FOM was assigned a –0.1 rating. Effective Score became 14.02.
3. **Roll-aft:** In this concept, a longer fuselage was unnecessary because the edge of the payload might be exposed at the back end of the body. However, this increases drag during flights, which would decrease cruising speed by 10ft/s. Total Score calculated is 13.98. Rolling-aft would not interfere with the landing gear, so the rating was 0.2. Mechanism may be as simple as the vertical drop; therefore, the FOM III is set to 0. Effective Score becomes 14.18.

		Ratings of FOM		
Alternatives	**Total Score FOM I**	**II**	**III**	Effective Score
Vertical Drop	14.43	0.2	0.0	14.63
Roll-front	14.22	-0.1	-0.1	14.02
Roll-aft	13.98	0.2	0.0	14.18

Table 3-11 Summary of Payload Release Configuration

The decision process showed that the vertical drop has significant advantage in the Total Score; therefore, vertical drop is the winning concept.

There are two locations to mount the antenna, above the airplane or below the airplane. Above the airplane may cause instability due to an upward shift of the CG. Also, the concern of the wake interfering with tail surfaces prompted the decision for mounting the cylinder under the fuselage.

3.4.3. Wing Configuration

Before a landing gear design or assembly method could be created, wing location had to be determined. Keeping assembly times constant, high-, mid-, and low-wing configurations were evaluated for the following considerations:

I. **Weight:** This FOM was considered since it affects Total Score due to the structural weight. Increased weight of the vehicle results in a higher RAC and slower flight speeds, which reduce Total Score.

II. **Landing Gear Interface:** Mounting location of the landing gear will be affected by wing location. Normal mounting location beneath the fuselage has been removed from consideration because of the payload deployment method.

III. **Stability:** This quantifies the ability of the aircraft to complete the mission flights.

Evaluation of the alternatives is as follows; a summary is in Table 3-12 below:

1. **High-wing:** For high-wing, it is possible to mount the wing on top of the fuselage in which a through-type structure could be attached to the fuselage. Because of the reduced weight, Total Score result is 14.75. Disadvantage of the high-wing is that a retractable landing gear system would not be able to be deployed from it; therefore, a FOM II rating of –0.2 was assigned. On the other hand, a high-wing allows for good roll stability resulting in an assigned FOM III rating of 0.2. Effective Score becomes 14.75.
2. **Mid-wing:** Total Score is 14.43. It is lower than the high-wing because a through-type spar structure cannot be designed due to the payload; therefore, increasing structural weight. Both landing gear interface and stability are average, so their ratings are 0 each. Effective Score stays 14.43.
3. **Low-wing:** Total Score is 14.43. It is low for the same reason as the mid-wing. Low-wing provides an excellent landing gear interface, which makes FOM II rating 0.2. Roll stability is lower, so FOM III rating is –0.1. Effective Score is 14.53.

		Rating of FOM		
Alternatives	**Total Score FOM I**	**II**	**III**	Effective Score
High-wing	14.75	-0.2	0.2	14.75
Mid-wing	14.43	0.0	0.0	14.43
Low-wing	14.43	0.2	-0.1	14.53

Table 3-12 Summary of Wing Location

3.4.4. Landing Gear Type

Tri-cycle landing gear configuration was chosen as stated previously in Section 3.2.7. Since the high-wing was chosen the main landing gear could not be reliably deployed from wing hard points. A simple one-piece type gearing mounted to the centerline was also discounted because of the payload deployment method. The only alternative for the main landing gear is to separate the two and integrate them as part of the fuselage structure.

3.4.5. Assembly System

With the conceptual design mostly complete, an assembly method was needed to place the airplane in a flight-ready condition in the least amount of time. Restriction in the size of the 4' X 1' X 2' assembly box forced a partition of the wing into two pieces, which has been conceptually sized to a 5-½ -foot span. For the same reason, the tail boom needs to be disassembled from the fuselage. Fuselage shall remain untouched to avoid a complicated assembly task. Both nose gear and main landing gear also need to be either detached from or tucked into the body. Mechanically retractable gears are yet another consideration, but desired to be avoided due to their unreliability. The goal is to assemble the entire airplane in the least amount of time, thus improving the Total Score. The following is a summary of decisions made during the conceptual design meetings and why.

- **Wing interface:** Last year's wing interface was a rod and socket assembly which worked very well. In addition to this method, it must include a provision for quick disconnect wiring for the aileron servos.
- **Main gear:** Since the main gear had to be split due to the payload deployment, two concepts were discussed. One was a hinged gear that would fold back. The disadvantage of this concept is that there would be a complicated interface with the fuselage structure. The other concept was a plug-in type. The landing gear would have a flat upper portion, which would lock in place. This was the simplest of the concepts.
- **Nose gear:** This was the most difficult part to devise a concept for since the steering mechanism must be a single unit. The complex interface with the servo and the nose gear shaft required it to be permanently installed in the aircraft. Since the landing gear would be too tall for the assembly box, the shaft would have to be cut and have an interface that would allow for quick assembly. The two choices were a threaded assembly or a hinged assembly. The threaded assembly concept was thrown out since there would be possible alignment problems. Although requiring more parts, the hinged method was chosen for it reliability. The hinge would also allow for a rapid deployment of the nose wheel.

3.5. Conclusion of Conceptual Design Phase

In summary, Spirit of Monty shall have:

- Conventional configuration with a T-tail or a V-tail
- Complete Missions A and B
- Vertical-drop payload deployment system
- Simulated antenna mounted below the fuselage
- Plug and socket main gear
- Single tractor power plant configuration
- High-wing with a plug and socket interface
- Tri-cycle gear with separate main landing gear on either side of the fuselage
- Hinged nose wheel

4. Preliminary Design

Preliminary design phase began with using the conclusions from the conceptual design phase to develop the most competitive aircraft to meet the mission requirements. Choosing the best airfoil, designing the best wing planform, and optimizing the fuselage shape are the major factors. Along with these factors the airplane must still be able to fit in the assembly box and be able to be made flight ready in a very short period of time, the goal is 20 seconds. Every design decision was made with these factors in mind.

4.1. Configuration Basics

To create the baseline fuselage shape known components had to be used to ensure proper sizing. Design began by working around a Graupner and an Astro Flight motor. Both types of motors were used to ensure the airplane could be easily modified to accept either motor once the motor and propeller configuration testing was complete. Other components included batteries (main and control), receiver, empennage, landing gear, payloads and wing. A right-handed global coordinate system was first set up as follows: X-axis named Fuselage Station (FS), Y-axis named Butt Line (BL), and the Z-axis named Water Line (WL). Numbers after the WL, BL, or FS abbreviation described the distance in inches from the origin. For example, anything in the YZ plane would be at FS0.

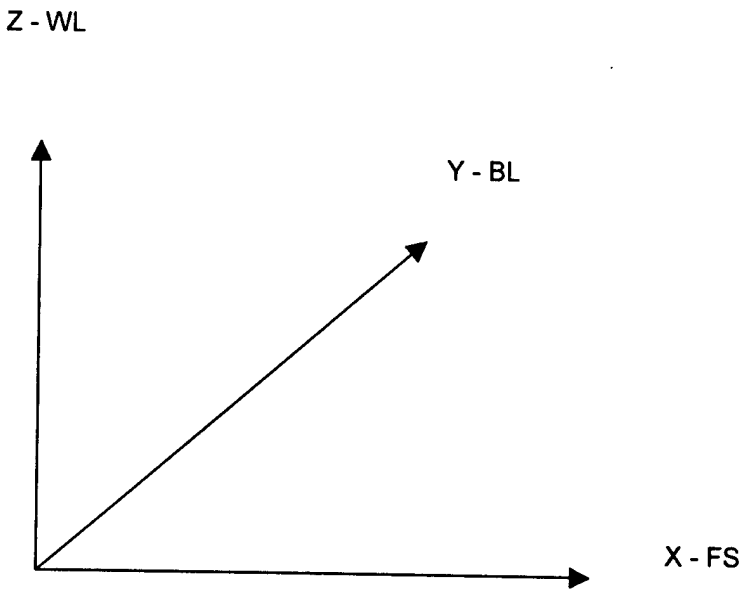

Figure 4-1 Global Coordinate System Used for Design

Two-dimensional components were sketched on a drawing board using the X-Z plane of the above coordinate system and manipulated to determine the best location. The payload's center of gravity (CG) was set at FS15/WL15, which was also the defined CG for the entire airplane; this was to ensure there would be no CG travel concerns after deploying the payload. The high wing was set above the payload with the ¼ chord directly above the CG. Motor placement put the thrust line directly through the CG. Battery packs were placed in the space between the payload and the motor. A tail boom was added passing through the fuselage aft of the payload. An aerodynamic shape was then sketched around the internal components, resulting in a glider-type cockpit area shape. Landing gear locations were added to ensure structure would be included to support them. Some preliminary bulkheads were added for structure including the motor mount bulkhead. A provision for longerons and stiffeners in strategic areas were also included. A horizontal and vertical stabilizer was then drawn to approximate size. The sketch was set as the baseline for the preliminary design and was instrumental in creating the best possible airplane. In addition to the drawing, a weight balance was performed using each of the components approximate weight to ensure there was no extreme nose-heavy or tail-heavy situation.

4.2. Assembly System

With the configuration laid out on the drawing, a method of assembly could be designed. First, a full-scale side-view and top-view drawing was made for the fuselage, wings, and empennage (including the tail boom). Another full-scale drawing was made for the assembly box. The separate parts were then set in the box outline to examine how they would fit. Example side and top views are shown in Figure 4-2 below (not to scale).

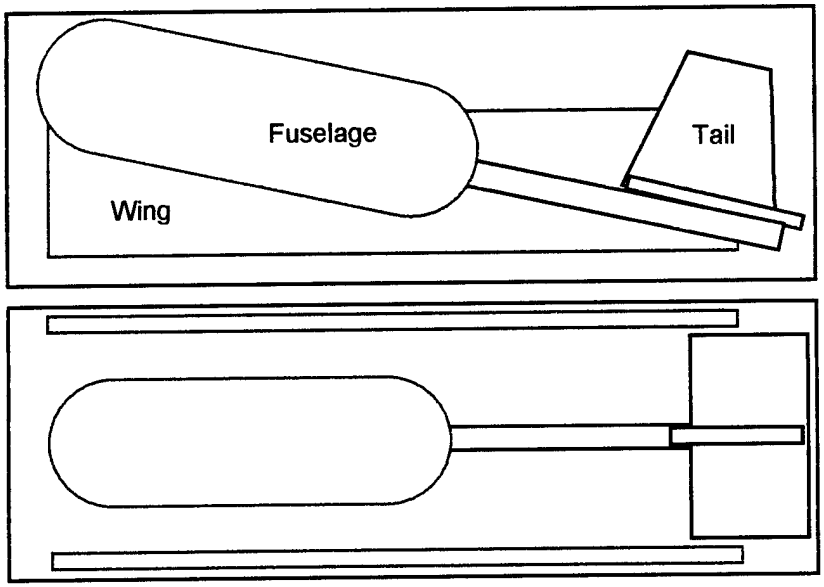

Figure 4-2 Side and Top Views of Assembly Box

1. **Wings:** During the conceptual design, the wings were projected to be too long for the box; therefore, they would consist of a two-piece assembly. The assembly of the wings would be a plug-in type, which would include connectors for the wiring for rapid assembly. This was the method used last year, which was reliable.
2. **Fuselage:** Fuselage had been originally sized to fit in the box in one piece, so no special assembly system was needed.
3. **Empennage:** This was the most difficult part because the tail would have to extend past the box to be effective as stability and control surfaces. A possibility was to size the tail to fit in the box and attach it to the tail boom. Upon the timed assembly, the tail boom could be slid into the fuselage and secured. The problem with this configuration is that the wire connection for the tail servos becomes difficult, a lesson learned from last year's airplane. Another option was to have a retractable tail boom. Since the payload will not be in the fuselage at the time of the assembly task, the boom can be shifted forward into the fuselage. It could then be retracted and secured, with the servo wiring already connected. This would enable a compact design and rapid assembly.
4. **Landing gear:** For adequate propeller, payload drop, and antenna clearances, the main landing gears must be long and have a wide stance. The wide stance is to maintain the 3" distance from the simulated antenna. Since the retractable landing gear had been observed to be unreliable in previous year's designs (demonstrated by the failure cases at the competitions) a method of quick assembly still needed to be devised. The answer was to make a plug-in, screw-in, or hinged type gearing, which would tie into the structure.

4.3. Wings

With the high-wing configuration the goal was to blend the wing into the upper outer mold line of the fuselage. Before fuselage design could continue, an airfoil had to be chosen to accomplish this.

4.3.1. Airfoil determination

Many airfoils were evaluated to determine suitability for the mission. Since this competition requires high-speed turns and fast level flight, the evaluation concentrated on high lift and low drag airfoils. This would also allow for a smaller planform area, which would improve the RAC. NACA 65 and 66 series, RG, Selig-Donovan (SD), and last year's G8-AR high-lift airfoil were compared.

NACA 65 and 66 series were dropped from further consideration because of their higher drag with no advantage of lift. RG airfoils were too low in lift and were also dropped from consideration. The search was narrowed down to 3 airfoils, the SD7037, SD7043, and the G8-AR. Comparison of the Selig-Donovan (SD) airfoils to the G8-AR showed a lower C_{lmax} for the SD airfoils, but a higher α_{stall} (see Figures 4-3 and 4-4). The stall was also not as abrupt as the G8-AR. At this point the choice of the airfoil was heading more toward the Selig-Donovan type.

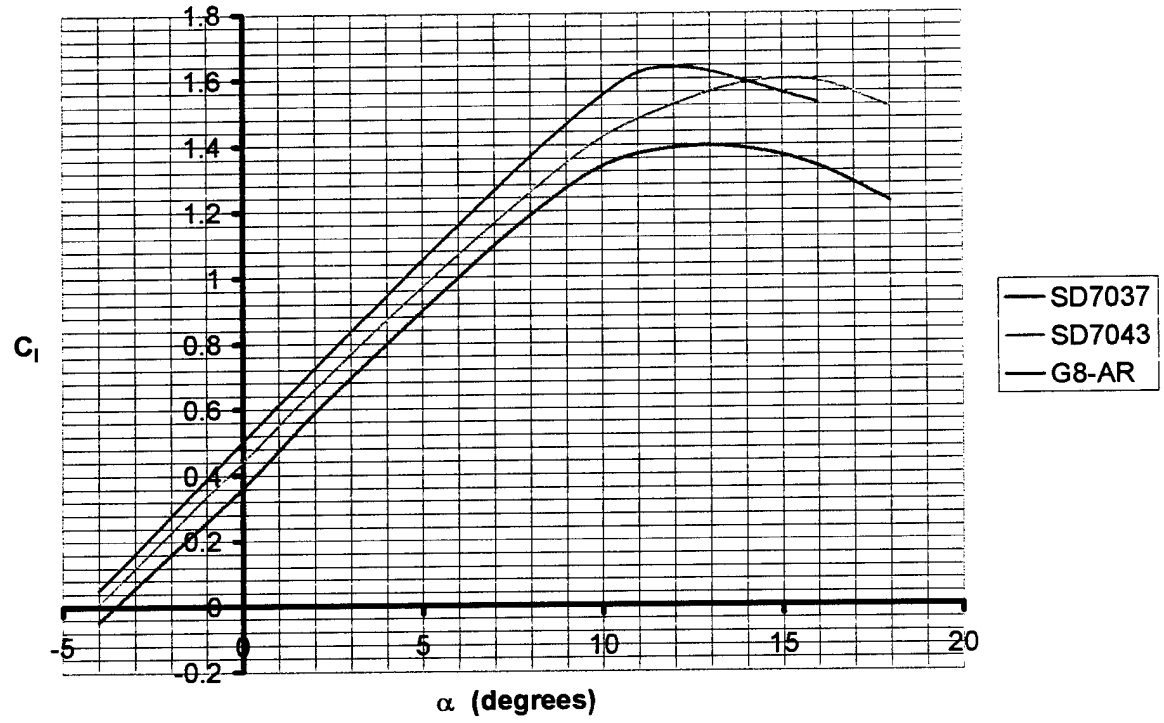

Figure 4-3 Lift versus Angle of Attack for Various Airfoils

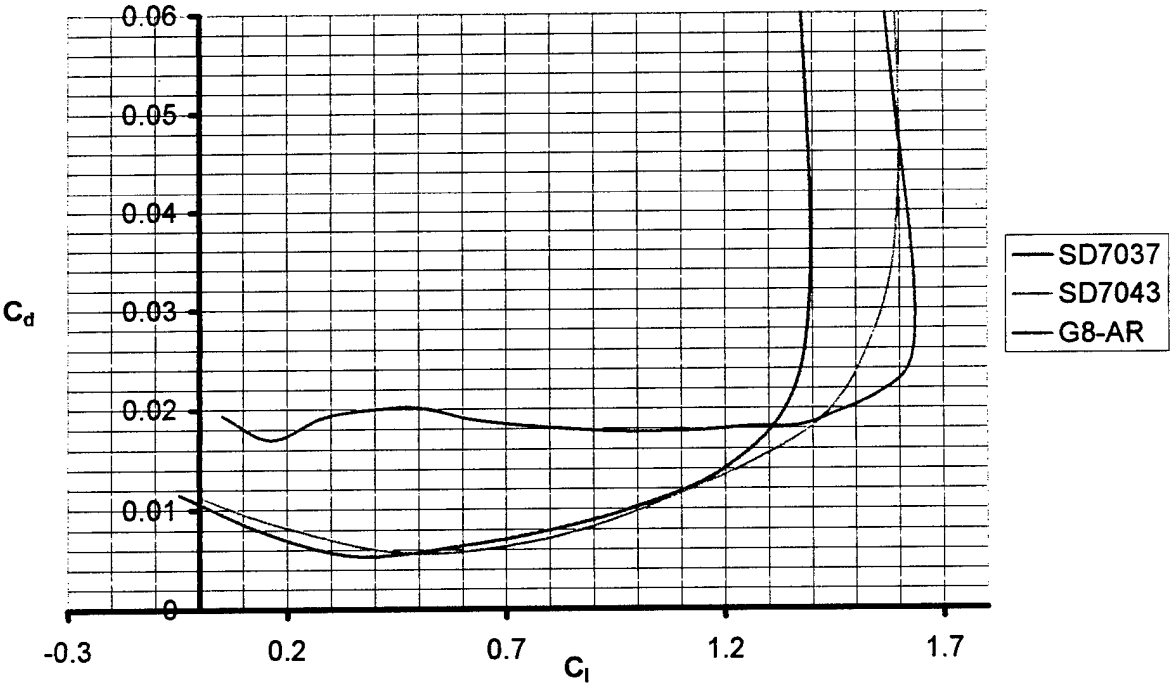

Figure 4-4 Drag versus Lift for Various Airfoils

Since a low drag airfoil was also a goal, the C_d vs. C_l curve for all three airfoils were evaluated. Both SD airfoils were relatively equal in drag, but the G8-AR had twice as much drag (see Figure 4-4). Although the G8-AR had more lift, high-speed demand of the competition led to the decision that this airfoil would not be used.

The choice was now between the SD7037 and the SD7043. To ensure the best turn and take-off performance, the airfoil with the highest C_{lmax} was chosen, SD7043. XFOIL was used to try to improve upon the airfoil, but this airfoil type was already at its peak performance, therefore it was maintained as the original.

Reading from Figure 4-3 and 4-4, minimum drag for the SD7043 is 0.055 at a C_l of 0.525. The respective angle of attack is approximately 1 degree. Design of the wing would ensure a provision for a 1-degree cruise angle of attack.

4.3.2. Planform Shape

Based on turn performance (4.5-g turn) and take-off distance (120 ft), required planform area was calculated to be 5.52 ft^2, turn performance being the limiting factor.

The RAC dictated the decisions on the planform shape. Every foot of wing span increases the RAC; therefore, the wingspan should be minimized. Minimizing the wing span increases chord size, which also increases the RAC, but not as much for a given area; Figure 4-5 illustrates this effect. Span can only be minimized to the point where the chord increases to 1 foot since anything larger would have trouble fitting in the required assembly box. A maximum root chord of 11 inches was chosen to reserve the ability to have some growth if necessary. Changing the taper ratio toward a more efficient (elliptical) planform shape would cause a significant increase in the RAC, as shown by the dashed curves in Figure 4-5. To minimize RAC, taper ratio was fixed at 1, resulting in a rectangular planform.

Increasing the Aspect Ratio (AR) to increase the lift slope of the wing was limited by the increased structural requirements and the increased RAC. Increasing AR would also decrease the drag of the wing, summarized in Table 4-1. Decreasing the AR would not only decrease the lift slope, but would result in the increasing of the chord size, causing a storage issue with the assembly box, as illustrated in Figure 4-6. Applying the range of appropriate aspect ratios from Figure 4-6 to the allowable chord sizes in Figure 4-5, the wing span becomes 6 ft, chord 0.92 ft, and AR 6.5. This allows for the minimum RAC while still accomplishing the mission.

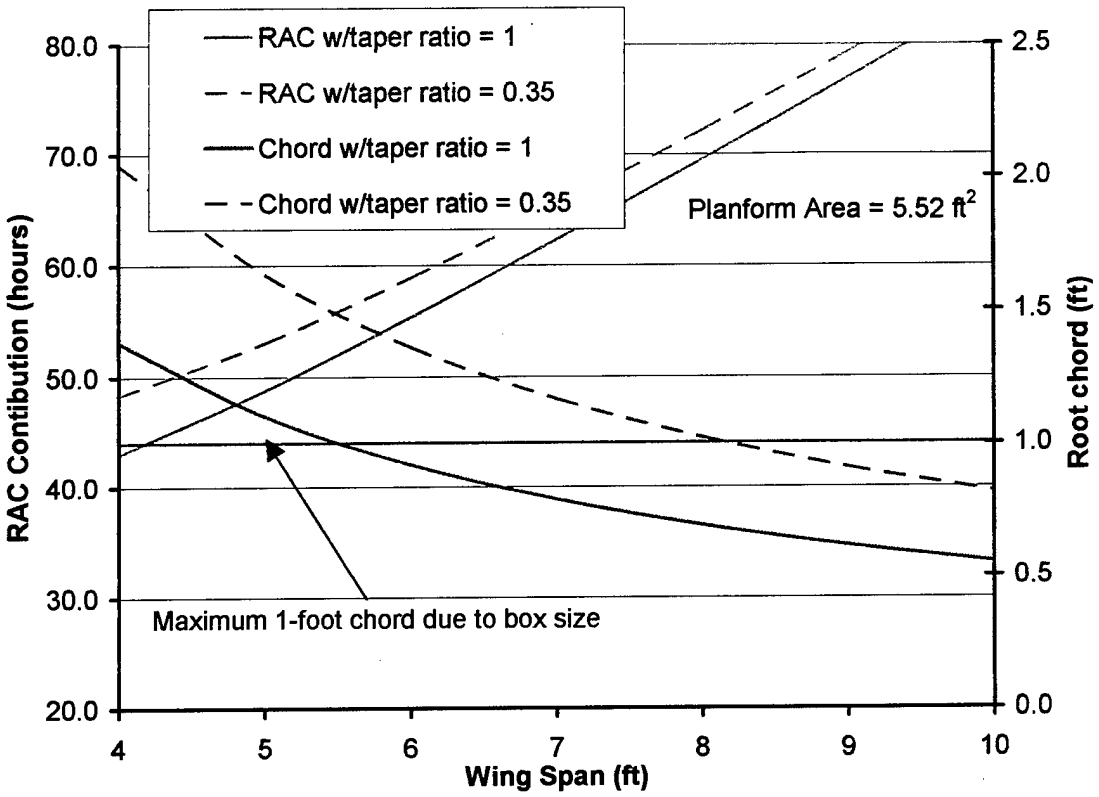

Figure 4-5 Rated Aircraft Cost Contribution from Wing Span

S	AR	b	c	c	b/2	C_D	Drag	RAC
ft^2		ft	ft	in	ft		lb	
5.5	5.5	5.50	1.00	12.00	2.75	0.01252	0.729	52.00
5.5	6.0	5.74	0.96	11.49	2.87	0.01236	0.720	53.62
5.5	6.5	5.98	0.92	11.04	2.99	0.01215	0.708	55.19
5.5	7.0	6.20	0.89	10.64	3.10	0.01203	0.701	56.73
5.5	7.5	6.42	0.86	10.28	3.21	0.01186	0.690	58.23
5.5	8.0	6.63	0.83	9.95	3.32	0.01167	0.679	59.70

Table 4-1 Summary of AR Versus Drag and RAC

With an aspect ratio of 6.5, C_L will be lower than the C_l due to finite wing effects. Calculated C_L due to finite wing effects for various aspect ratios at 1° angle of attack are shown in Figure 4-7 below.

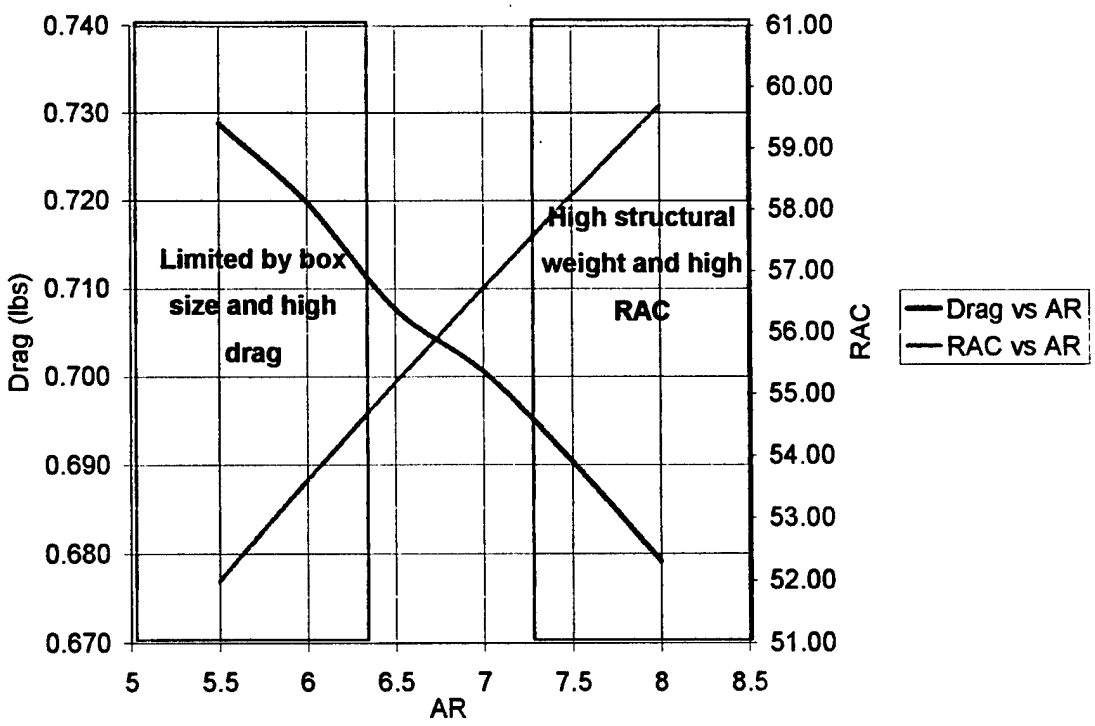

Figure 4-6 Drag and RAC Comparison with Aspect Ratio

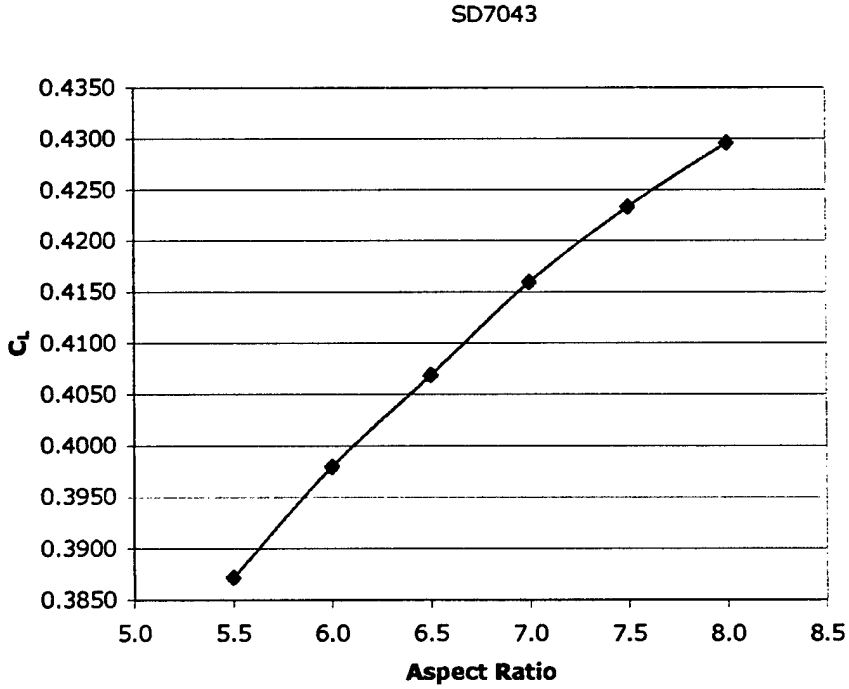

Figure 4-7 Lift Coefficients for Various Aspect Ratios at 1° alpha

Applying the same calculation for the entire lift curve results in Figure 4-8. C_{Lmax} and stall angle were calculated by methods in Reference 7.

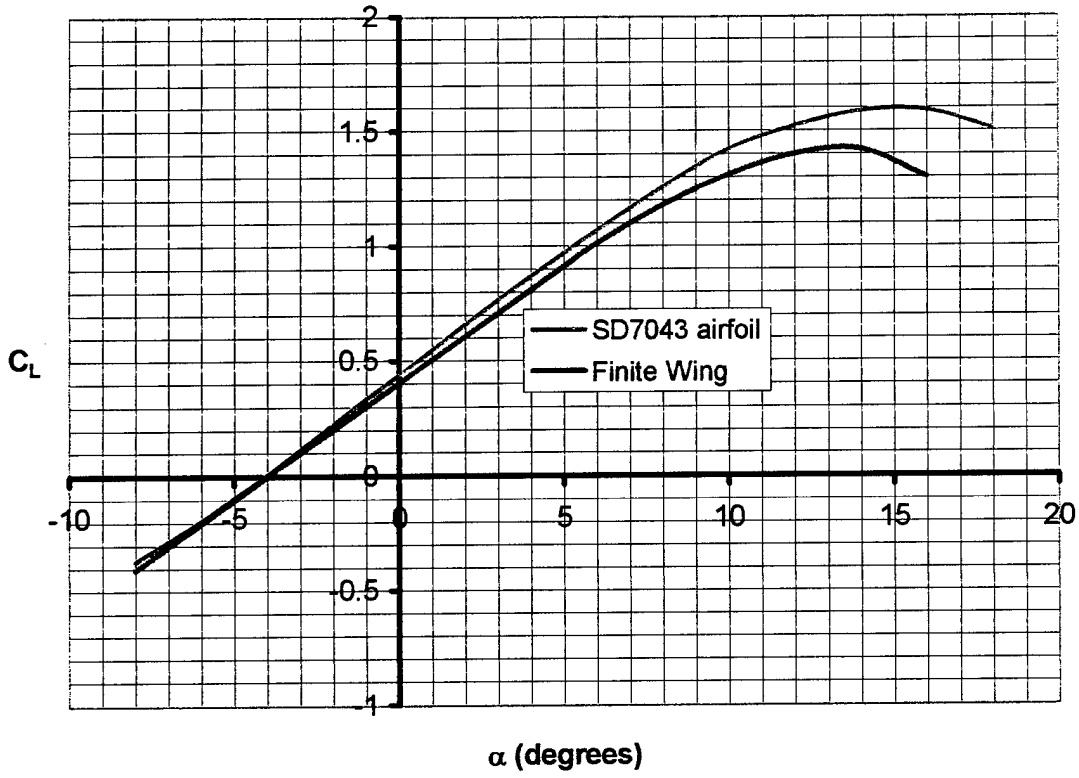

Figure 4-8 SD7043 Airfoil Compared to Finite Wing with an AR of 6.5

4.3.3. Wing Sizing Summary

- Rectangular planform
- Planform area 5.52 ft^2
- Span 6 feet
- Chord 0.92 feet (constant)
- Aspect Ratio of 6.5

4.4. Fuselage

Weight savings had to be considered when evaluating the aerodynamic shape of the fuselage. The first step was to design an aerodynamic type shape around the payload box. A 2-D shape was drawn around the box payload. The points were then used as an input file for XFOIL. Using XFOIL, the shape of the pressure coefficient curve was modified to reduce drag to a minimum. The final shape is shown in Figure 4-9 below. By varying the angles of attack, drag was found to be minimum at 0 degrees.

The final points were then used to reproduce the shape in PRO-Engineer as a 3-D form. Two concepts were designed; one with a pointed trailing edge, and the other with a flat trailing edge (see Figure 4-10). The cross-sections were modified to minimize the size of the body and therefore reducing overall weight, but still able to carry the required payload.

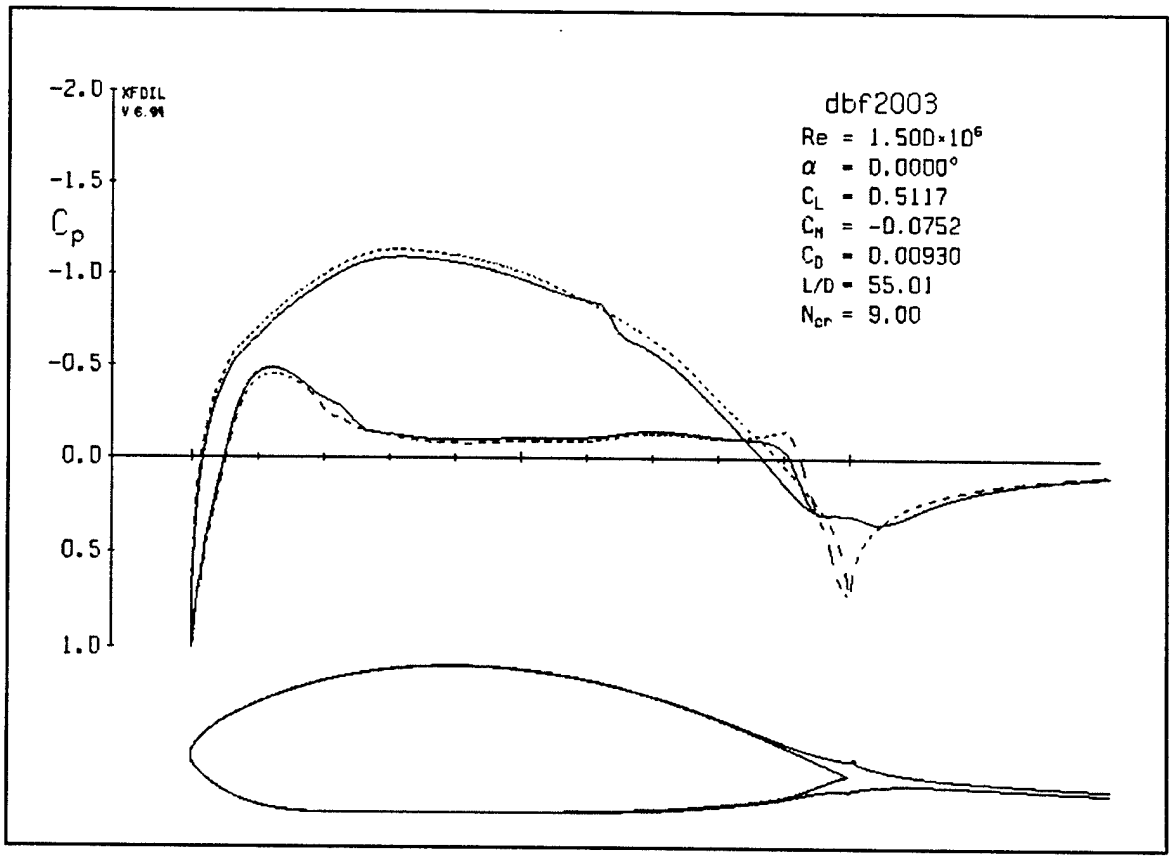

Figure 4-9 XFOIL Pressure Coefficient Diagram of Fuselage

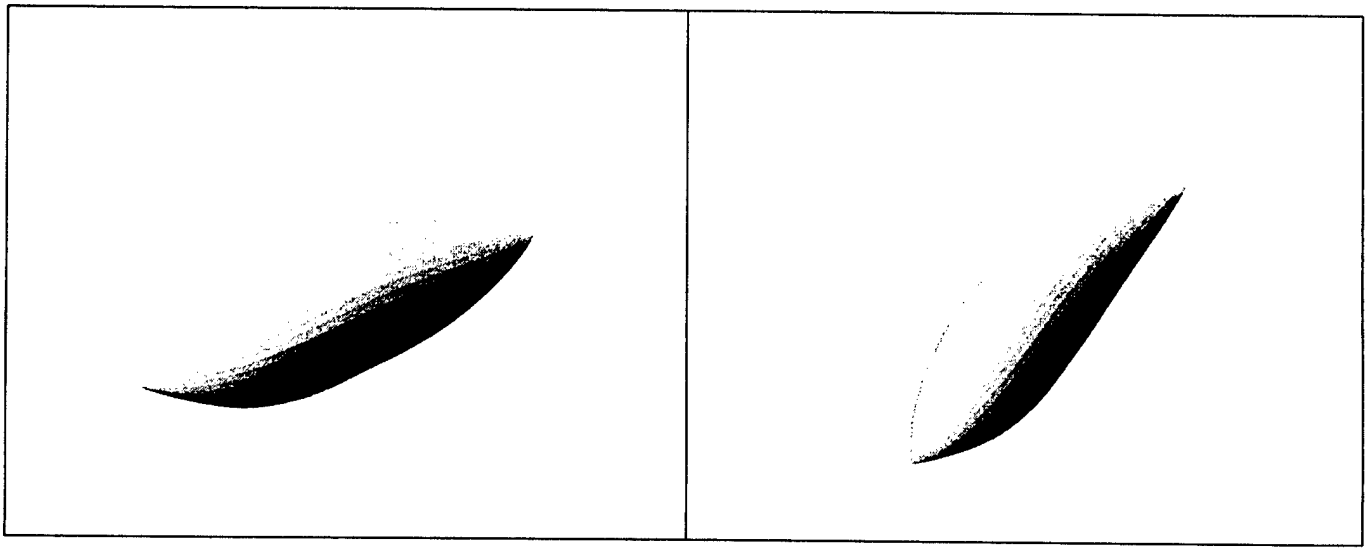

Figure 4-10 Fuselage Concepts

Comparison of the weights, as shown in Table 4-2 below, illustrates a significant difference between the flat trailing edge and the pointed trailing edge; there is a 10% weight savings with the pointed trailing edge. This result shows that the pointed trailing edge version has a significant advantage. Aerodynamic performance (lift, moments, and drag) was then evaluated to screen any advantage for the flat trailing edge. Weight was based on the assumption that the fuselage skin was the same carbon composite as last year's competition entry.

	Surface Area	Weight/Area	Weight
Concept	in^2	lb/in^2	lb
Flat	830.8	0.00168	1.40
Point	750.5	0.00168	1.26

Table 4-2 Weight Comparison of Fuselage Concepts

4.5. Tail Options and Sizing

Tail design had to be evaluated through multiple considerations. First, the concept had to be evaluated by the RAC to determine its pre-sizing competitiveness. It also had to be evaluated for its simplicity to allow for a more rapid assembly time and a higher Total Flight Score. Lastly, it must provide for static and dynamic stability. RAC scoring does not directly penalize for the tail surface area unless its span is larger than ¼ span of the main wing. However, it does penalize for the overall length of the airplane; therefore, the length should be shortened while increasing the tail surface area. A further evaluation in the next section is aimed for sizing the tail to fit in the storage box, shortening the longitudinal length of the tail to minimize the RAC, but still maintaining stability.

4.5.1. T-tail

Using a T-tail is the most conventional approach. As discussed in the conceptual design, it has a lower RAC, but the highest Effective Score. The problem is that the vertical stabilizer may need to be assembled, reducing the Total Flight Score. If a quick assembly could be devised, or if the tail sizing shows that the tail will fit in the box without disassembly, then this type of tail will work. An advantage of this tail is that the pilot has experience flying T-tail aircrafts; also, the fabrication team preferred to have a T-tail. If there is no notable advantage found from the stability evaluation then the T-tail would be the best choice.

Horizontal tail span was set at 18 inches to keep it within ¼ of the main-wing span in order to take advantage of the lower RAC. By assuming a large tail volume ratio of 0.6, the resulting chord is 8 inches. The reason for the higher-than-normal tail volume was to overcome the moment of the cylinder payload. A tail this size would still fit in the assembly box (based on initial packing concepts).

Vertical tail sizing began with the 1-foot maximum dimension of the assembly box, resulting in a vertical ratio of 0.034. This is a reasonable ratio for this type of aircraft. Final vertical tail size has a root chord of 8 inches, tip chord of 6 inches, and a span of 9 inches.

4.5.2. V-tail

A V-tail configuration results in a lower RAC. It also simplifies the assembly phase, if sized correctly. The disadvantage is the loss of effective surface area, resulting in a larger tail. If the tail is too large it may cause the RAC to rise significantly and thereby negating the advantage of the V-tail. More evaluation had to be performed to determine the effectiveness of the concept.

Sizing of the V-tail used the combined planform areas of the T-tail. Angle of the V-tail was set at 110°. The size would allow it to fit in the assembly box without being disassembled.

4.6. VSAERO Configurations Tested

Both of the tail concepts, T-tail and V-tail, along with each of the fuselage concepts were evaluated in VSAERO to determine their effectiveness for static stability. Figure 4-11 shows each of the concepts evaluated, including an inverted T-tail. The inverted T-tail had been removed from consideration due to the concerns of wing and cylinder wakes.

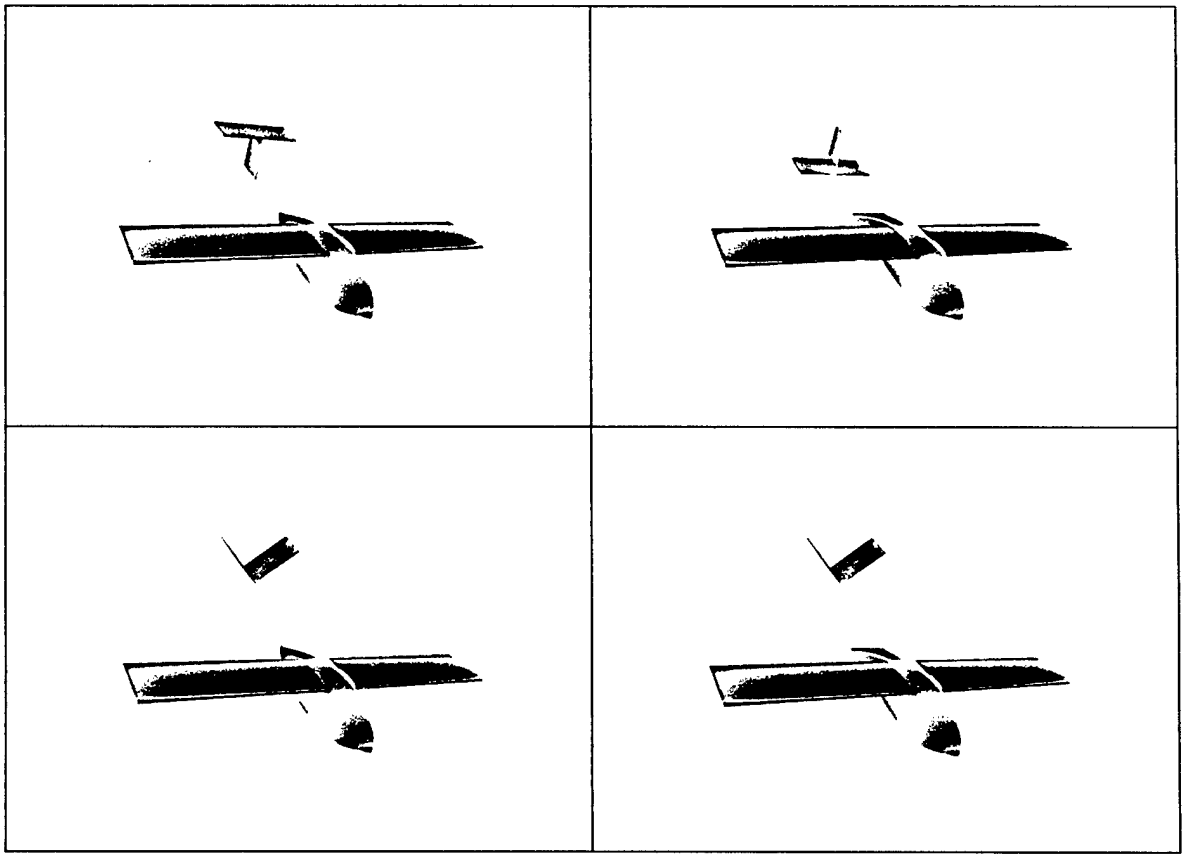

Figure 4-11 VSAERO models

4.6.1. Tail incidence angle optimization

To optimize the tail placement, its incidence angle first had to be found at various distances (as measured by l_t). Placing the body at its cruise angle, 0 degrees, and adjusting the tail incidence angle to achieve a C_M of zero, optimum tail incidence angles were found. This was done to minimize the trim drag during level flight, because last year's airplane suffered from an extreme amount of trim drag. Figure 4-12 was produced using data from VSAERO; it is a summary of tail incidence angles. Once dynamic stability is complete as a function of l_t, the length of the airplane can be reduced to a minimum, then the tail incidence angle (i_t) can be set to the minimum trim drag angle.

4.6.2. Fuselage Static Stability Comparison

Placing the tail at the minimum trim drag incidence angle, static stability was evaluated for each of the concepts. First, the fuselage concepts were compared to see if any static stability advantage is gained from the different trailing edges. The comparison presented a negligible advantage as shown in Figure 4-13. Each concept demonstrated a positive C_{M_o} with a negative C_{M_α} slope, requirements for static stability.

Each tail and fuselage concept was then evaluated to obtain the static margin (K_n); static margin ranged from 0.20 to 0.50. The data shows the expected trend, as l_t increases so does static margin. Slightly higher static margins were achieved by the lifting-tail fuselage concepts.

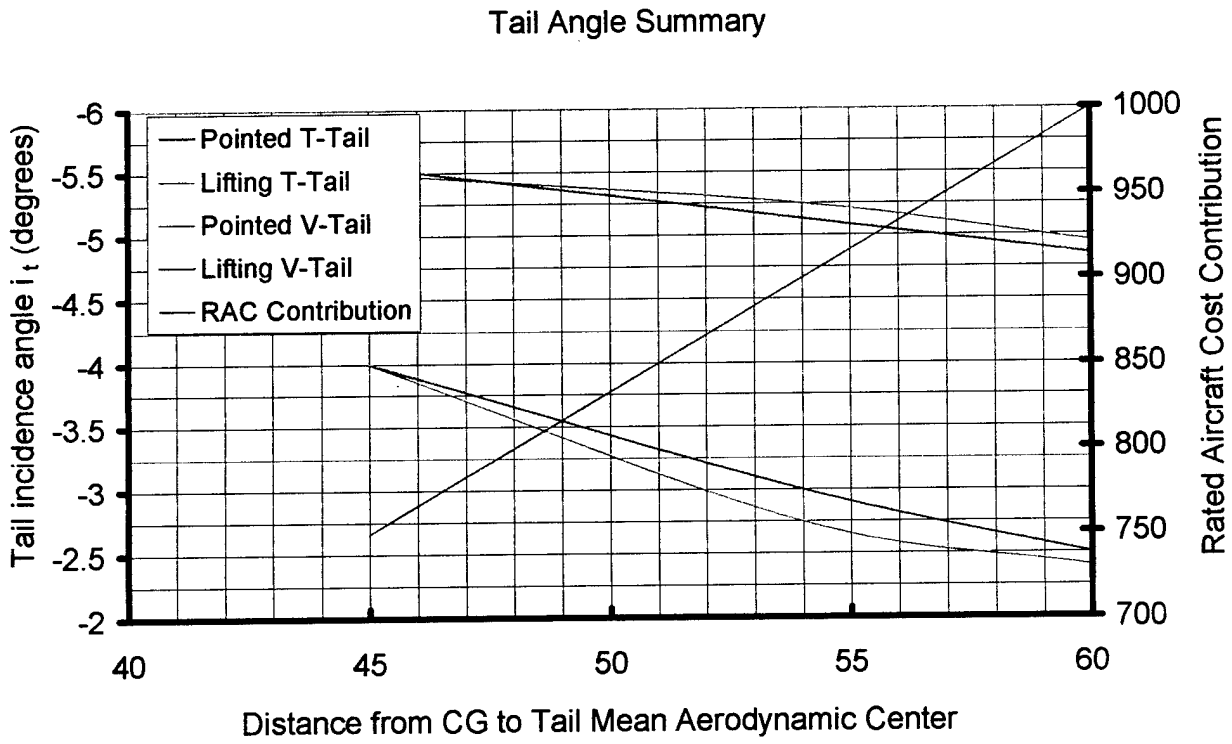

Figure 4-12 Tail Angle Summary

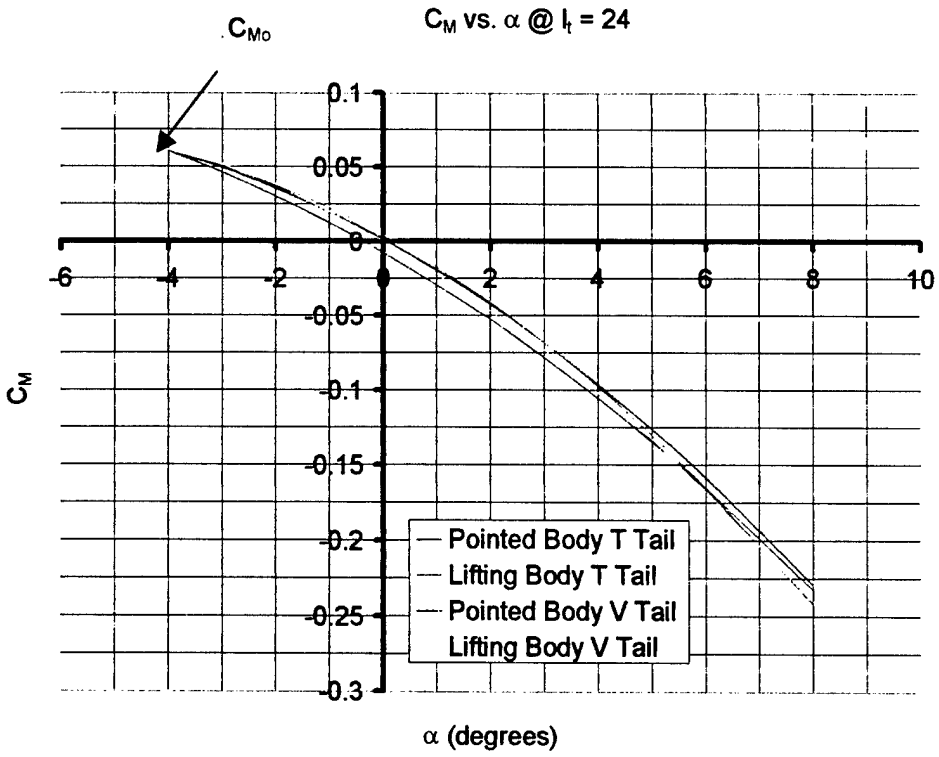

Figure 4-13 Static Stability of Fuselage Concepts

4.6.3. Tail and Fuselage Conclusion

There was little advantage in stability or lift of the flat trailing edge fuselage over the pointed fuselage. Choosing the pointed fuselage as the final design was due to the fact there was a significant weight savings. The V-tail provided no significant advantage and therefore was dismissed.

4.7. Wing-Body Lift Curve

VSAERO was used to find the wing-body lift curve for the final configuration. C_{Lmax} and α_{stall} was determined by the methods of reference 7. The curve did not change significantly from the finite wing curve in Figure 4-8 and therefore is not reproduced here.

4.8. Drag Estimation

Breaking the final configuration down into four component parts, namely the wing, fuselage, empennage, and landing gear, C_{Do} was calculated by the methods in Reference 8. The results are as follows:

C_{Do} =	$C_{Do\ (wing)}$	$+C_{Do\ (fuselage)}$	$+C_{Do\ (empennage)}$	$+C_{Do\ (gear)}$
0.0253849	0.01578482	0.006471667	0.003092458	3.5952E-05

Table 4-3 C_{Do} results

Applying the C_{Do} to the 3-term drag polar equation results in Figure 4-14 below.

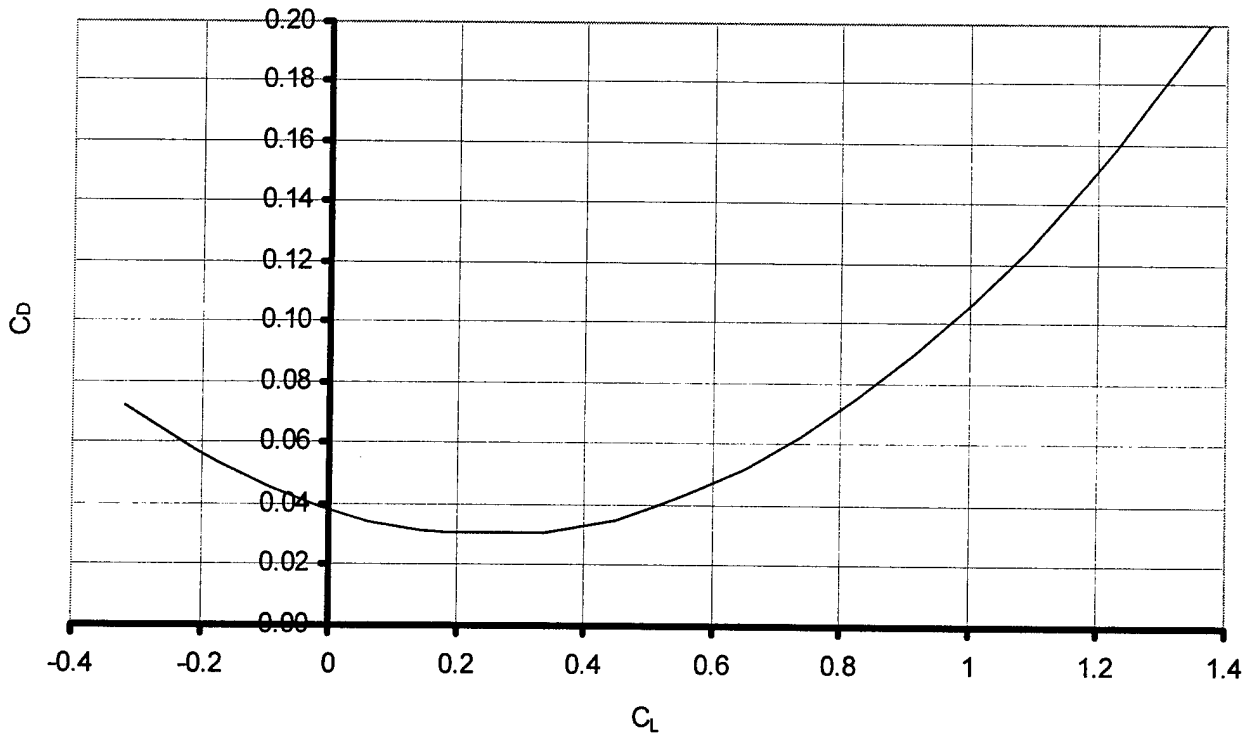

Figure 4-14 Three-Term Drag Polar

4.9. Power Plant Design

Initial investigations suggested that the Graupner Ultra 3300-10 motor would give better performance than the Astro 60, which had been used for last year's design. The Graupner motor was purchased and tested against the Astro, and the Graupner showed a higher efficiency.

Computer simulation using P-Calc and MotoCalc suggested that maximum performance with the 10-turn Ultra 3300 would be obtained from high voltage battery packs with more than 28 cells. In order to investigate lower voltage (lighter weight) systems, the 3300-7 motor was selected. The results from calculations suggested that maximum performance would be obtained from approximately 22 cells. Further calculations predicted that the 3300-5 motor would yield even higher thrust and pitch speed than the 3300-7 on as few as 18 cells. In order to allow for some flexibility in the power system, both the 7-turn and 5-turn Graupner Ultra 3300 motors were purchased.

MotoCalc and P-Calc were used to model the power systems using a number of propeller sizes. The resulting parameters of major interest were a predicted thrust and pitch speed. While the 18x16 propeller was near optimum for the 3300-7, a smaller propeller of 15x16 yielded even more encouraging results for the 3300-5. The 3300-7/18x16 combination yielded 102.7 oz of in-flight thrust, with a pitch speed of 74.6 MPH. The 3300-5/15x16 gave only 68.2 oz of in-flight thrust, but at a pitch speed of 87.6 MPH.

Total battery weight is a very significant factor in the payload carrying ability of any aircraft; therefore, the decision was to keep battery weight to the minimum required to complete the flight missions. Minimizing the battery weight also reduces the RAC considerably. Because the 24% higher in-flight thrust of the 22-cell 3300-7 power system required a 50% increase in battery weight, the 18-cell 3300-5 system was chosen for initial flight testing. For enough duration to finish one mission the Sanyo CP-2400 was chosen.

In conclusion the initial power system is as follows: Graupner Ultra 3300-5 motor, Kruse 2:1 gearing, RFM 15x16 propeller, 18 Sanyo CP-2400 cells, SWN Super 120 speed controller.

4.10. Structural Considerations

Conceptual Design defined a requirement such that the aircraft must be able to sustain a 4.5-g turn. Landing may also cause high loading due to rough conditions. To ensure structural integrity, a skeletal structure was designed with proper load paths between the wings, motor, tail boom, and landing gear. A model was created in Pro-Engineer and evaluated with Pro-Mechanica. Any high stress areas, which were marginal, were redesigned to reduce these stresses.

Although there was a major concern for the wing base, results showed no significant structural problems in this area. Since the fuselage skin is a carbon fiber composite, it will provide enough extra strength to accommodate the high stress areas shown in Figure 4-15 below.

The split-wing interface loading was calculated to have a bending moment of 600 in-lbs at a 4.5-g turn. This translates to a bending stress of about 50,000 psi using a ½ in. solid-carbon rod, which can take four times that amount (safety margin of 4).

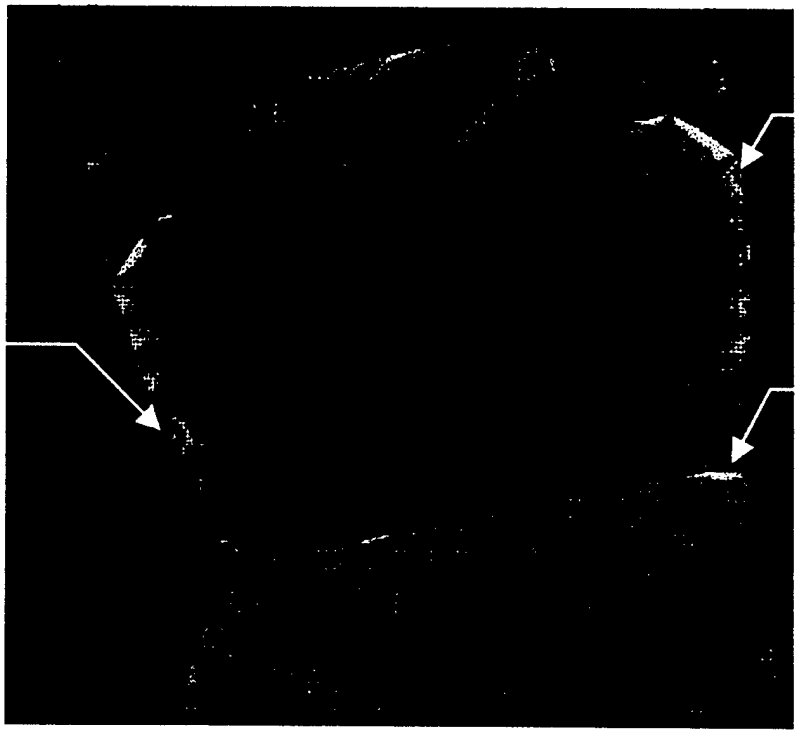

Figure 4-15 Pro-Mechanica Structural Analysis

5. Detailed Design

The detail design was the final step before fabrication could begin. Drawings were created and performance was estimated.

5.1. Configuration Summary

The following table contains all the configuration data as required by the report. Performance was calculated using the methods in Reference 7.

Geometry		Performance	
Length	4.5 ft	C_{Lmax}	1.41
Wing span	6 ft	L/D_{max}	11.0
Height	1.7 ft	Maximum rate of climb	15 ft/s
Wing: root chord	0.92 ft	Stall speed	44.2 ft/s
Wing: tip chord	0.92 ft	Maximum Speed	118 ft/s
Wing area	5.52 ft^2	Take off field length (empty)	50.6 ft
Aspect Ratio	6.5	Take off field length (gross)	119 ft
Horizontal area	1 ft^2	**Systems**	
Horizontal volume ratio	0.58	Radio	Hitec Prizm 7X
Vertical area	0.44 ft^2	Servos	Hitec HS-225BB
Vertical volume ratio	0.034	Battery	18 Sanyo CP-2400
Weight Statement (lb)		Motor	Graupner 3300-5
Airframe	7	Propeller	15x16 RFM
Propulsion	4	Gear Ratio	2 to 1
Control System	0.5		
Payload System	0.2		
Payload	6		
Empty Weight	11.7		
Gross weight	17.7		

Table 5-1 Final Component Selection, Geometry, Performance, Weight Statement, and Systems

5.2. Rated Aircraft Cost

Final RAC is 7.81, based on the following table.

	RAC	7.81	
	MEW	11.7	
	REP	2.34	
	MFHR	156.36	
# of cells	18		Sanyo 2400
weight per cell	2.08	oz	weight includes extra hardware
total battery weight	2.34	lb	
WBS	**Value**	**Hours**	**Multiplier**
1.0 Wings			
wing span (ft)	6.00	48	8 hr/ft Wing Span
chord (ft)	0.92	7.36	8 hr/ft Max chord
# of control surf	2	6	3 hr/control surface
2.0 Fuselage			
Max length (ft)	4.5	45	10 hr/ft max length
3.0 Empennage			
# of vertical-nc	1	5	5hr/vertical-no control
# of vertical-ac	0	0	10 hr/vertical-active control
# of horizontal	1	10	10 hr/horizontal-see wing rule
V-tail only		0	v-tail-15 hr
4.0 Flight Systems			
# of servos/control	5	25	5 hr/servo (Note 1)
5.0 Propulsion			
#of engines	1	5	5 hr/engine
#of propellers	1	5	5 hr/propeller

Note 1: 2 ailerons, 1 elevator, 1 nose wheel, 1 payload release (no rudder)

Table 5-2 Rated Aircraft Cost of Final Configuration

5.3. Dynamic Stability Estimation

Section 4.6 showed that the airplane would be statically stable, but dynamic stability still had to be confirmed. A combination of sources was used to accomplish this task. Pro-Engineer provided the moments of inertia, Advanced Aircraft Analysis (AAA) supplied some information, and the rest was hand calculated using References 4, 7, and 8. The derivatives had to be performed for the vehicle's stabilities in the longitudinal and lateral directions.

Based on an average speed of 100 ft/s the phugoid period is 13.8 seconds, which is enough time for the pilot to make corrections.

Longitudinal and lateral stability derivatives are as follows:

Conditions			Longitudinal		Lateral	
θ_o	0	(degrees)	C_{Xu}	-0.1	$C_{y\beta}$	-0.3826
g	32.2	(ft./sec.^{2})	C_{Zu}	-0.1	C_{yp}	0.0015
M	0.09	(Mach #)	C_{Mu}	0.0015	C_{yr}	0.0846
W	18	(lbs.)	$C_{X\alpha}$	0.2	$C_{l\beta}$	0.0800
I_y	771	(slug*ft.^{2})	$C_{Z\alpha}$	-5.76	C_{lp}	-0.4680
alt	100	(ft.)	$C_{M\alpha}$	-0.7953	C_{lr}	0.3886
a(h)	1117	(ft./sec.)	C_{Xq}	0	$C_{n\beta}$	-0.1059
ρ	0.00237	(lbs.*sec.^{2}/ft.^{4})	C_{Zq}	-6.63	C_{np}	-0.1451
S_w	5.52	(ft.^{2})	C_{Mq}	-10.76	C_{nr}	-0.0863
$c_{bar\ w}$	0.92	(ft.)	$C_{X\alpha}^{dot}$	0		
			$C_{Z\alpha}^{dot}$	-2.056		
			$C_{M\alpha}^{dot}$	-3.27		

Table 5-3 Stability Derivatives

Using the characteristic equation coefficients and Routh's criteria for stability, the aircraft has no unstable modes for this flight condition. An evaluation was performed for takeoff, landing, and different load conditions and no stability problems were found.

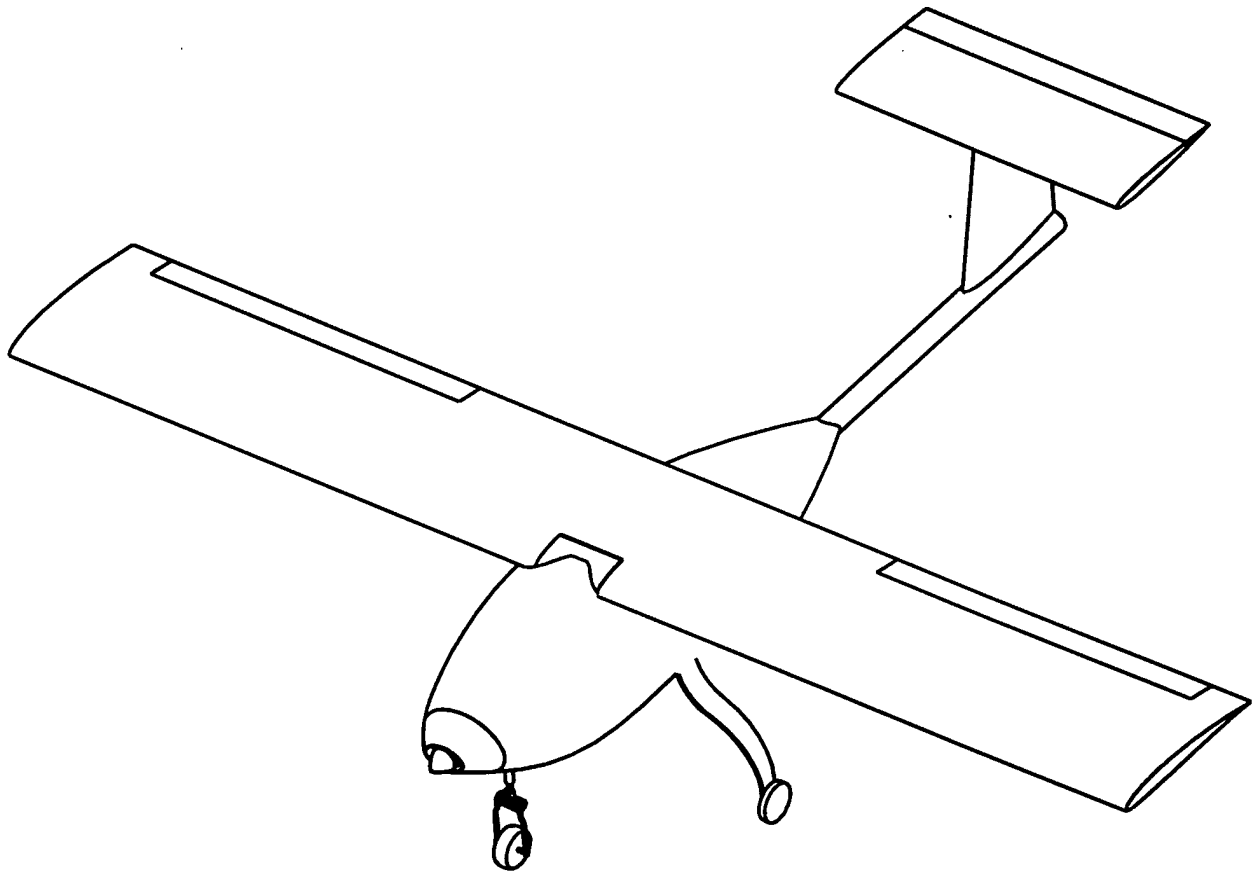

SCALE 0.100

SDSU AEROSPACE ENGINEERING	
DRAWN BY	DATE
SIZE A	DWG NO DBF2003
SCALE	SHEET OF 5

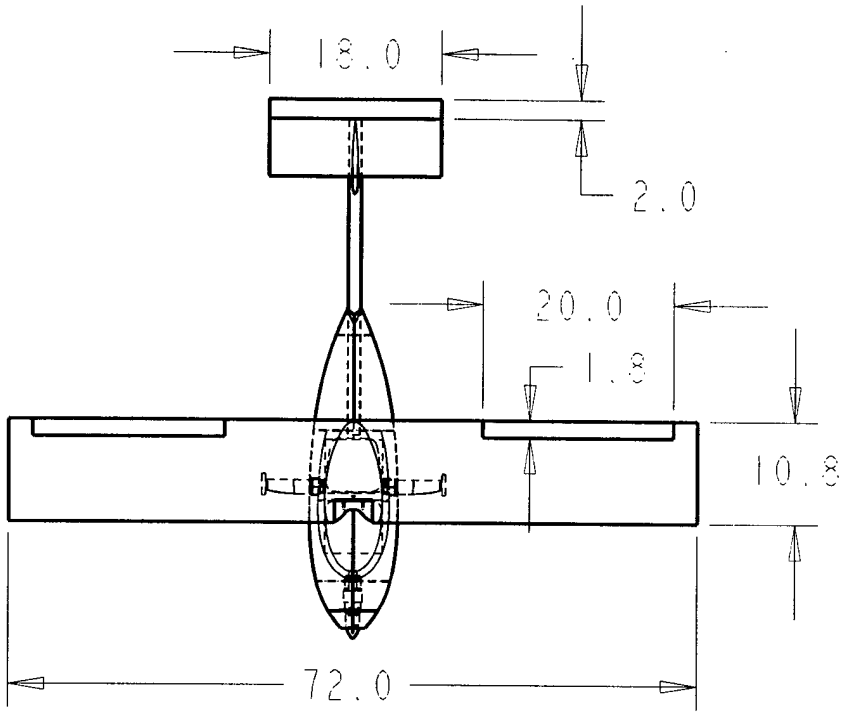

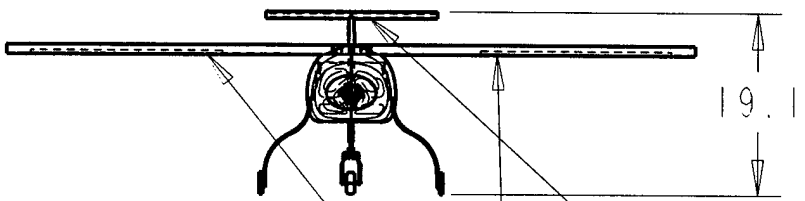

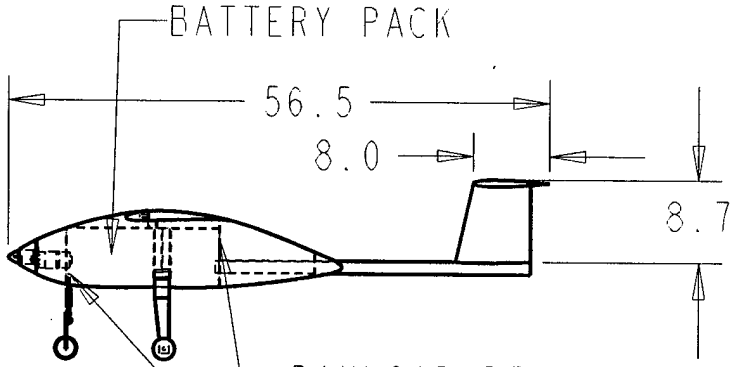

ELEVATOR SERVO

AILERON SERVOS

PAYLOAD RELEASE SERVO

NOSE WHEEL SERVO

SIZE	DWG NO	REV
A	3-VIEW	
SCALE		SHEET 2

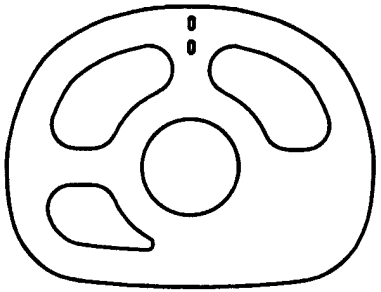

FS 6 BULKHEAD

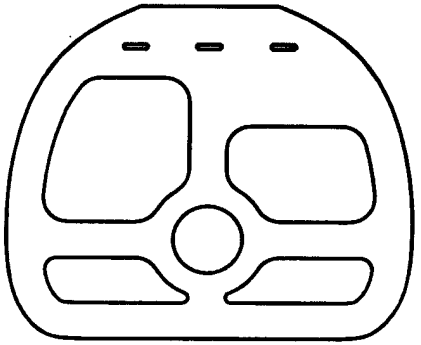

FS 22 BULKHEAD

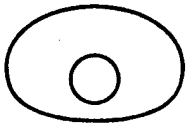

FS 32 BULKHEAD

ALL PARTS SCALE .250

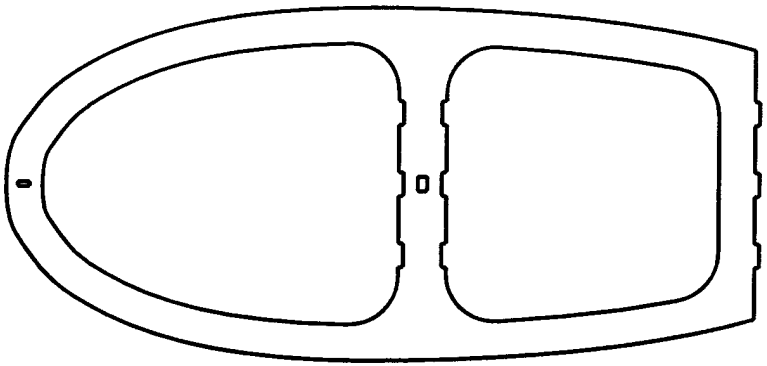

UPPER FRAME

ALL PARTS ON THE SHEET ARE
CARBON/FOAM SANDWICH PLATES

SIZE	DWG NO	REV
A	FOAM CORE CARBON PARTS	
SCALE		SHEET 3

ALL PARTS ON THE SHEET ARE MADE WITH A 7-PLY CARBON/ KEVLAR COMPOSITE

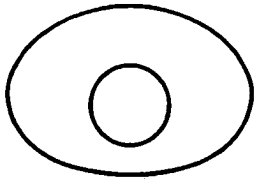

MOTOR MOUNT BULKHEAD

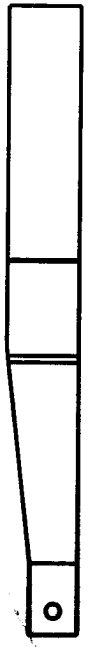

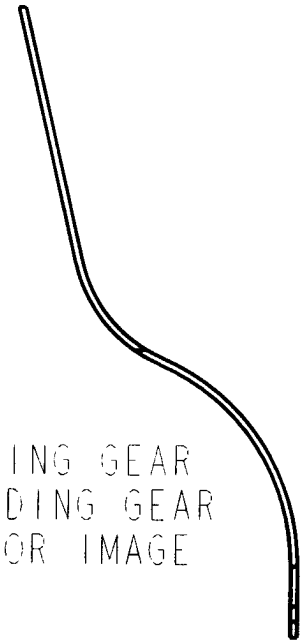

LEFT LANDING GEAR
RIGHT LANDING GEAR
IS A MIRROR IMAGE

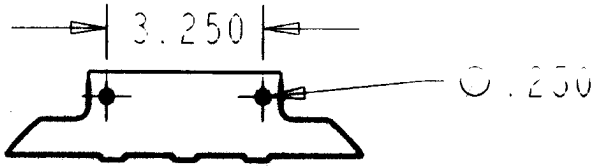

WING MOUNTING BRACKET

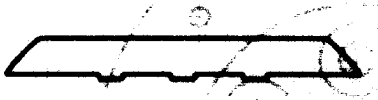

STIFFENER

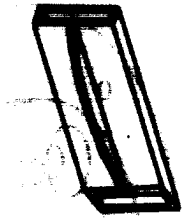

LEFT LANDING GEAR SOCKET

ALL PARTS SCALE 0.250

4

SIZE	DWG NO	REV
A	CARBON/KEVLAR PARTS	
SCALE		SHEET 4

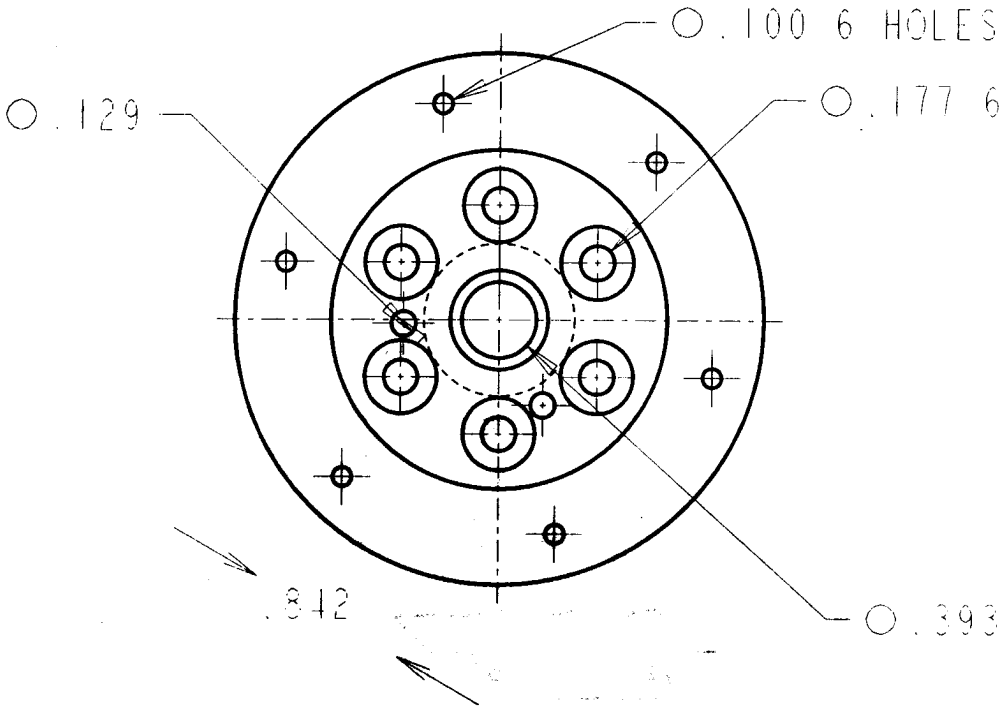

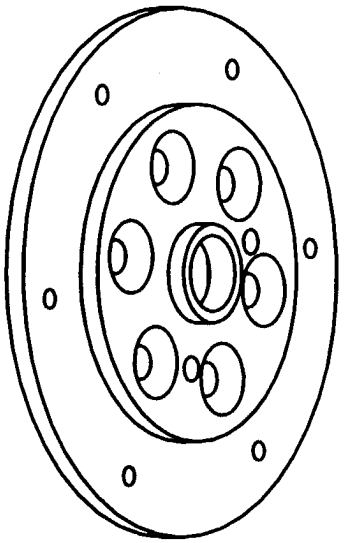

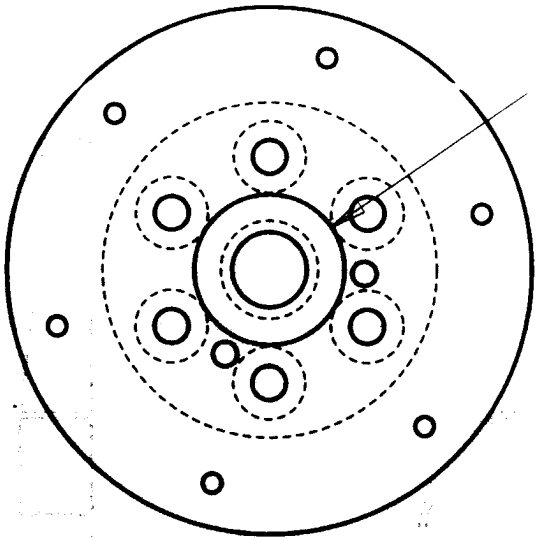

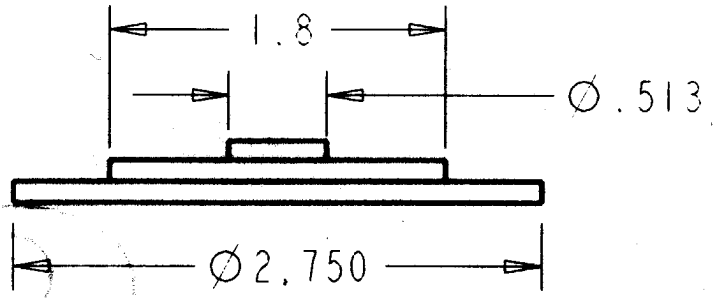

SCALE 1.000

SIZE	DWG NO	REV
A	MOTOR MOUNT PLATE	
SCALE		SHEET 5

6. Manufacturing Plan

Evaluating all the major components with respect to the choices of the materials resulted in choices of fabrication methods. Each process was rated on a number scale in which high numbers were desirable characteristics and low numbers were undesirable characteristics. After the evaluation a manufacturing schedule was created.

6.1. Major Components

Major components were defined as the parts of the aircraft that needed to be fabricated before the propulsion system, assembly systems, and electronic components were installed. The major components were the fuselage, wings, tail, bulkheads, tail boom, motor mount, nose/ main landing gear, and wheels. They also included the interfacing mechanisms with each other. Other parts such as assembly systems were produced in parallel with the major components.

6.2. Materials

Materials that were considered for the major components included carbon fiber, fiberglass, plywood, aluminum, and plastic, and one other commercially available material (steel) in a pre-manufactured form for the nose gear. The materials were rated for each component by using Figures of Merit (FOM). Minor components were made either of the above materials or of brass, Kevlar composite, or balsawood. Because minor components required less lead-time, they were fabricated in various ways and allowed choices to be made based on the component performance.

6.3. Figures of Merit

Figures of Merit (FOM) were used to evaluate the materials for the availability, required skill levels, cost, time to manufacture, and strength to weight ratio.

6.3.1. Availability

Scaling ranged from 0 to 2. If the materials or the components were on hand, it received a 2. If they had to be purchased or they required machining, it received a 1. If the material was not available due to reasons beyond the team's control, it received a 0.

6.3.2. Required Skill Levels

Easy to fabricate materials, which required no previous or limited experience, were issued 5 points. A prohibitively difficult process or an unavailability of the manufacturing equipment received a 1. Skills of the team members were also used in order to make an informed decision about the manufacturing process within each of the categories. Table 6-1 is a summary of number of personnel with the appropriate skills.

	Skills						
	Model plane building	Wood working	CNC	lathe	composites	hotwiring	electric motor power plants
Number of personnel	4	4	2	2	5	5	3

Table 6-1 Skills Matrix

6.3.3. Cost

A value of 1 was assigned if the cost of the material was beyond the means of the project's budget. Inexpensive material received a 5. If the material was already on hand or if it was to be donated in sufficient amount, it was given a rating of 5; carbon fiber and fiberglass were in that category.

6.3.4. Time to Manufacture

This parameter was added as a FOM because the team needed to fabricate the major components in time for flight-testing. Composite materials received the low rating of 1 because the team had to fabricate bulkheads and cut them to size. Material or components available in their final form received the high rating of 3.

6.3.5. Strength to Weight Ratio

A qualitative approach was taken to determine the strength to weight ratio for each material since many of the materials such as some of the carbon fiber fabrication techniques are not readily calculated. Experience and experimental techniques were used to determine the capability of the material properties.

6.4. Summary of Material Choices

Table 6-2 shows the evaluation of the materials for different components of the aircraft. Highlighted numbers are the highest scoring material and therefore chosen for the fabrication method for the specified component. Most components would be fabricated using a carbon fiber composite with only a few exceptions. The motor mount plate is to be made of aluminum and both the wheels and nose gear were obtained commercially; modifications were made to optimize the commercial products to fit the design.

		Availability	Required Skill Levels	Cost	Time to Manufacture	Stregth to Weight Ratio	Average
Fuselage	carbon-fiber	2	3	5	1	5	3.20
	fiberglass	2	3	5	1	3	2.80
	balsawood frame	1	5	3	2	2	2.60
Wing	carbon-fiber (foam core)	2	3	5	1	5	3.20
	fiberglass (foam core)	2	3	5	1	4	3.00
	balsawood frame	1	5	3	2	2	2.60
Tail	carbon-fiber (foam core)	2	3	5	1	5	3.20
	fiberglass (foam core)	2	3	5	1	4	3.00
	balsawood frame	1	5	3	2	2	2.60
Bulkheads	carbon-fiber (foam core)	2	3	5	1	5	3.20
	fiberglass (foam core)	2	3	5	1	4	3.00
	plywood	1	5	3	2	3	2.80
Tail Boom (commercial)	carbon-fiber	2	2	5	1	5	3.00
	fiberglass	0	2	1	1	5	1.80
	wood	2	3	5	1	2	2.60
	aluminum	1	4	3	2	3	2.60
Motor Mount	aluminum	1	3	3	1	4	2.40
	plastic	2	1	0	2	2	1.40
Nose Gear	commercial						
Main Gear	carbon-fiber	1	3	5	1	5	3.00
	aluminum	1	4	4	2	3	2.80
Wheels	commercial	2	5	2	3	4	3.20
	aluminum	1	5	4	1	4	3.00
	plastic	0	3	2	2	1	1.60

Table 6-2 Figures of Merit Summary for the Manufacturing Process

6.5. Manufacturing Schedule

The manufacturing team leader created the schedule to complete fabrication and test fly a prototype before the report was due. Both projected and actual schedules are shown in Figure 6-1 below.

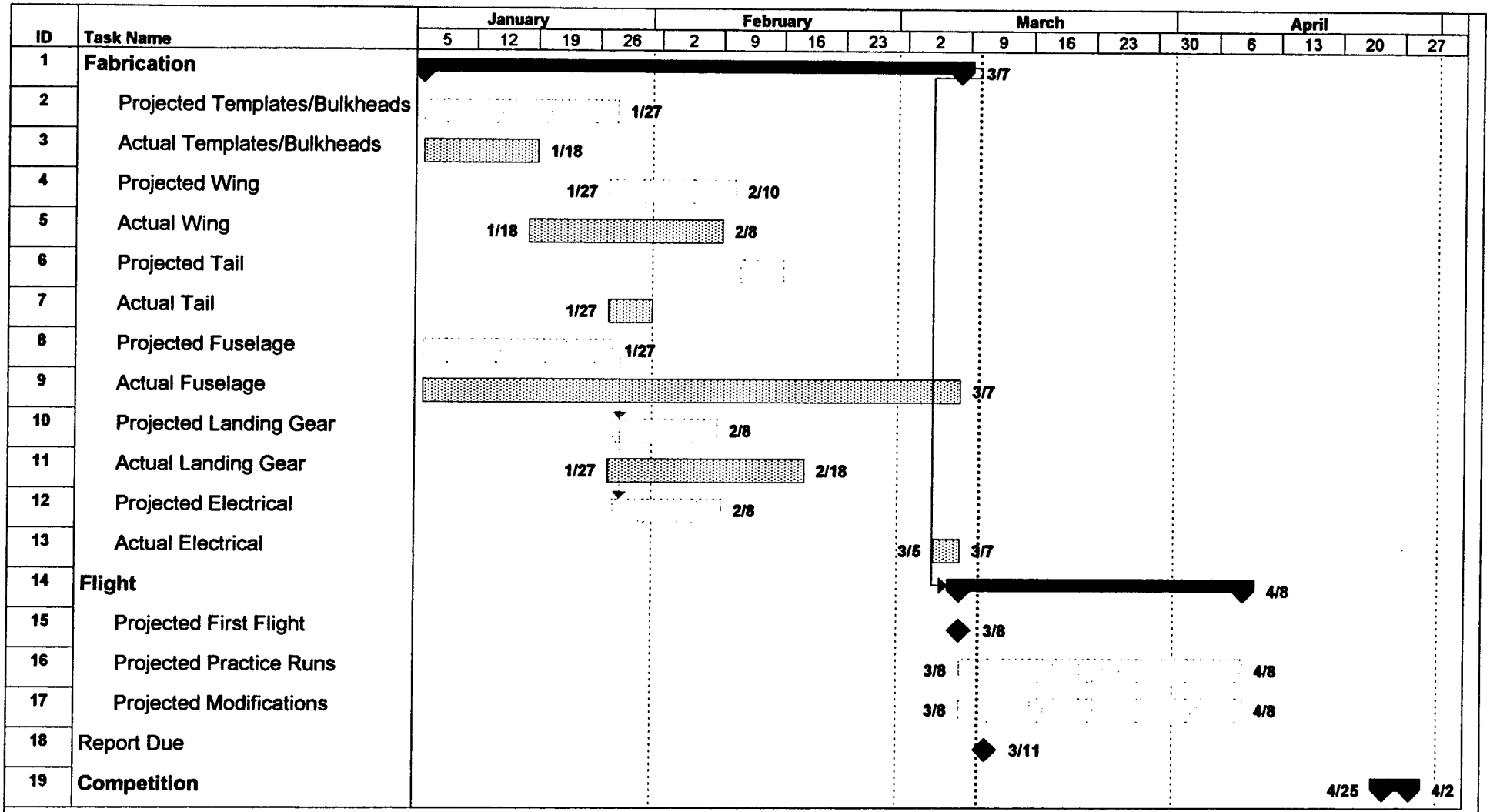

Figure 6-3 Manufacturing Schedule

6.6. Manufacturing Processes

Fabrication sites were at the Aerospace Lab at San Diego State University and at the shop of the Manufacturing Team Leader. Safety during the manufacturing processes was maintained by following the team leader's instructions.

Choices of the materials led to a definitive process of fabrication for each component. Alternative processes investigated were to use a foam core or a female mold for the fuselage fabrication. These two processes were evaluated with respect to the following FOM:

I. Time to Manufacture: With the projected date of the flight-testing approaching, this was the most significant of any other factors; the foam core required less time to manufacture.
II. Expected Product Performance: The foam core would create a rougher finish on the outer surface of the composite skin. Female molds could be smoothened out to reproduce a close shape to the drawings.
III. Required Skill Level: Team lacked the experience in manufacturing the molds.
IV. Cost: The foam was considerably less expensive than the materials required for making the molds.
V. Repeatability: A high repeatability would ensure easy reproduction in case of failure in fabrication or damaged to the finished product. The use of foam core is an irreversible process, whereas the female molds could be used repeatedly.

The alternative with an advantage in each FOM was awarded a 1. Summation of the points led the decision to use the foam core. This evaluation is summarized in Table 6.3 below.

	Time to Manufacture	Expected Product Performance	Required Skill Level	Cost	Repeatability	Sum
Foam Core	1	-	1	1	-	3
Female Molds	-	1	-	-	1	2

Table 6-3 FOM Summation for Fuselage Manufacturing Technique

The following describes the processes of the major component fabrication. Pictures of some of the manufacturing processes are shown in Figure 6-1 below. The processes for each component are chronologically ordered.

Figure 6-1 Manufacturing processes used (clockwise from upper left: basic internal structure with payload, CNC milling, vacuum bagged wings, foam core prior to sanding)

6.6.1. Structural Framework

Structure framework was first created using carbon fiber/foam sandwich composite sheets. Other parts such as the motor mount bulkhead used a multiple layer of carbon composite including Kevlar. Templates were used to cut the bulkheads to size.

6.6.2. Fuselage

Codes (m-code) were obtained from Pro-Engineer (CAD) of the fuselage outer-mold-line (OML) and then transferred to the CNC for an autonomous milling of the foam core. The foam core was combined with the bulkheads and finished sanded to a smooth surface. Lay-up consisted of carbon fiber and epoxy, using a flexible vacuum bag. Upon curing, the foam was removed and interface areas prepped for the final assembly.

6.6.3. Wings and Tail

The first step was to hotwire the foam cores by using a fabricated endplate template. To obtain a smooth finish and accurate sizing carbon fiber and epoxy lay-up was used along with a vacuum bag and Mylar sheets.

6.6.4. Main Landing Gear

Landing gear shape was designed using Pro-Engineer. The drawing was used as a template to create a wood mold. Landing gear was then fabricated in the same multi-layered method as the motor mount bulkhead.

6.6.5. Nose Gear

A commercially obtained nose wheel had to be modified for the assembly system. The upper shaft was cut and threaded to accept the hinged adapter. The hinged adapter was designed and then machined in the school's lab by the manufacturing team.

6.6.6. Motor Mount

An adapter plate between the reduction gear and the motor was substituted for a motor mount plate designed and machined by the manufacturing team. It was needed to interface the motor to the motor mount bulkhead.

6.6.7. Tail Boom

A wrapped carbon fiber tube was obtained for the tail boom. Because of the expense of the tail boom, a lightweight aluminum was purchased as a standby.

6.7. Electronic Components and Payload Deployment System

The final steps of the fabrication were the installation of electronic components and the payload deployment system. Electronic components, namely wires and servos, were installed in such a way that they would require the shortest length of the connections while reducing the possibility of failure. The payload release system was then placed into the structure. Finally, the fuse was mounted on a relatively flat surface on the side of the fuselage.

6.8. Structural Integrity

Dropping the body with a 15 lb load from one-foot high tested the landing gear interface. The load simulated a rough landing during the actual missions; the test was conducted more than 10 times. Although a large amount of flex occurred on the main gear, the structure did sustain the load.

Based on wing loading during a 4.5-g turn, the wings were tested to ensure they could handle the load. Wings were assembled to the body and an extra 45 lb box payload was hung from the CG. The wings were then lifted from 1/4 span to test the wing body interface; the test was successful.

6.9. Conclusion of Fabrication Phase

Installation of the electronic components and payload deployment system marked the end of the fabrication phase. The propulsion system, namely the motor and the batteries, would be placed into the reserved spaces without affecting the structure. Now the Spirit of Monty was ready for the flight-testing.

7. Testing Plan

Completion of the fabrication phase was in time for flight-testing on March 9, 2003 at Lakeside, California.

7.1. Flight Testing Objectives and Checklist

The objectives were set to simulate the competition, to evaluate the general performance of the prototype, and to obtain information for optimization. Simulation of the competition would be achieved by conducting a safety inspection and by attempting the three mission flights. A completed checklist for first-flight is shown in Table 7-1 below. Results of the testing and lessons learned are described in Section 7.2.

Security Inspection checklist

Check	Order to be followed
x	1. Secure connection of the aircraft components
x	2. Propeller structural and attachment integrity
x	3. Adequate electronic connections and confirmation of the maximum current draw
x	check
x	4. Structural verification to include: lifting with one point at each wing tip, cg location
x	5. Radio range check with motor off and on. Radio fail-safe check
x	6. Control surfaces operations
x	7. Integrity of the payload system
x	8. Static propulsion test

Flight performance checklist

rating	checklist
C	1. Take-off performance.
A	2. Near-stall performance after the take-off.
A	3. High-g turn performance.
A	4. Altitude.
N/A	5. Endurance.
F	6. Landing performance.

rate as follows:
A --- No major/minor problems
B --- Minor problem(s)
C --- Major problem(s)
F --- Failing

	misison A	mission B	mission C
AH used			
Flight time			

AH = Amp-Hour

Table 7-1 Testing Worksheet

7.2. Lessons Learned

Testing began in the late afternoon. As Table 7-1 indicates, the security inspection was completed without problems. However, the flight was limited for one lap without payload, due to the sunset; the aircraft made its first flight with glow-lights attached. The measured take-off distance was approximately 110ft. Time of flight, including the times of take-off and landing, was 44 seconds. The aircraft stumbled and flipped up side down at the end of the landing. The payload box was not installed. Power usage was not measured.

Although the flight was brief, the post-testing conference addressed some key issues in power plant, control surfaces, and landing gear performances. According to these results, recommendations were made for modifications and further optimizations.

7.2.1. Power Plant

A considerably longer take-off distance, compared to the estimated distance in the detail design, indicated that the aircraft was underpowered. The analyses of the combination of the propeller and battery, or the pitch of the propeller, should be reviewed. In the analyses, effects on static performance may need to be emphasized against dynamic performance, so that the take-off thrust is sufficient. Power plant was expected to be a limiting factor since the configuration was the minimum required, which saved on RAC. Steps will be done to try to improve this power plant while marinating a low RAC.

7.2.2. Control Surfaces

The landing-run required more than 200ft, at the end of which the aircraft lost control. This was due to a lack of yaw control, as the pilot alluded to in the conference. The aileron-only-landing provided less than necessary control than expected. A provision was already included into the vertical stabilizer to add a rudder if needed. Although the extra servo will increase the RAC, the team wanted to first attempt flight without it. In addition, the sensitivity or the effect of the elevator was observed to be too profound. Adjustment on the transmitter can be done to accommodate this for the next flight.

7.2.3. Landing Gear

The aircraft was observed to tend sideways during the take-off and landing. Insufficient rigidity of the nose gear and/or main gear could cause this issue. The aluminum socket for the nose gear was spotted as one of the possible causes; a modification will be made on the joint. Also, the placement of the nose gear with respect to the servo structure may need to be assessed whether it was aligned to the direction of take-off with the controller deactivated.

References

1. Abbott and A.E. Von Doenhoff. Theory of Wing Sections, New York: Dover, 1959
2. Anderson, John. Fundamentals of Aerodynamics. New York: McGraw-Hill, 1991
3. Drela, Mark. XFOIL 6.94 User Guide. Boston: MIT, 1986
4. Etkin, Bernard. Dynamics of Flight. New York: John Wiley & Sons, 1996.
5. Katz, Joseph, and Allen Plotkin. Low Speed Aerodynamics. New York: Cambridge, 2001
6. Nathman, James. VSAERO User's Manual Version 6.2. Redmond: Analytics Methods Inc., 1982
7. Nicolai, Leland. Fundamentals of Aircraft Design. San Jose: Mets, 1984.
8. Roskam, Jan. Airplane Design: Part VI. Lawrence: DARcorporation, 2000.

2002/2003 AIAA

Cessna/ONR Design/Build/Fly Competition

Design Report

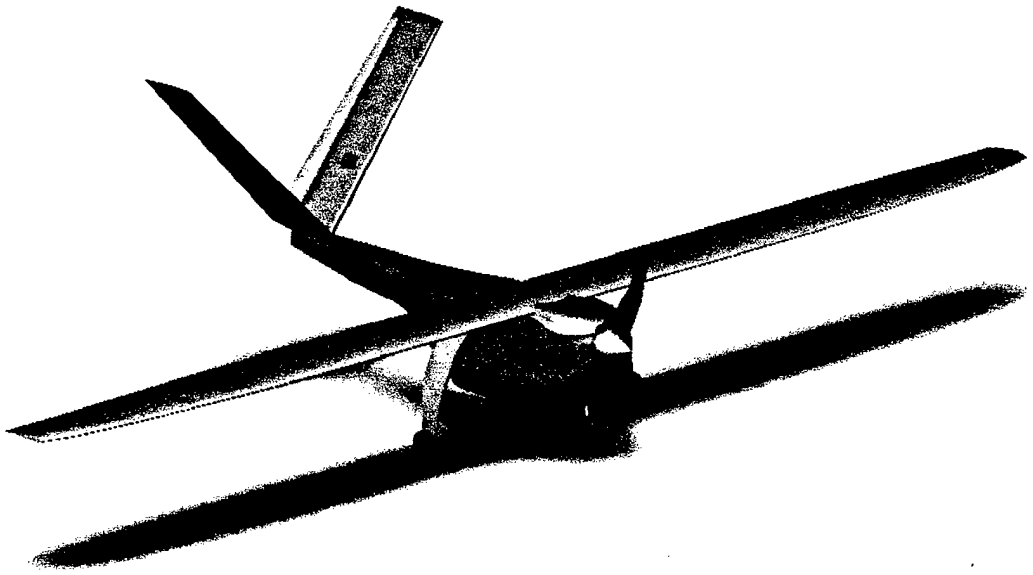

California Polytechnic State University

"Bareback"

Table of Contents

1.0 EXECUTIVE SUMMARY 1

1.1 Conceptual Design 1

1.1.1 Conceptual Design Alternatives 1

1.1.2 Conceptual Results 2

1.2 Preliminary Design 2

1.2.1 Preliminary Design Alternatives 2

1.2.2 Preliminary Design Results 2

1.3 Detail Design. 3

1.3.1 Detail Design Alternatives 3

1.3.2 Detail Design Result 3

1.3.3 Detailed Design tools 3

2.0 MANAGEMENT SUMMARY 4

2.1 Design Team Architecture 4

2.1.1 Schedule Control 5

3.0 CONCEPTUAL DESIGN 7

3.1 Mission Selection 7

3.2 Payload Configuration 10

3.2.1 Antenna Location 11

3.2.2 Electronics Box Deployment 11

3.3 Airframe Configuration 12

3.3.1 General Configuration 12

3.3.2 Wing Placement 14

3.3.3 Fuselage Configuration 15

3.3.4 Engine Configuration 16

3.3.5 Landing Gear Configuation 17

3.3.6 Empennage Configuration 18

3.4 Material Selection 19

3.5 Conceptual Design Results 19

4.0 PRELIMINARY DESIGN 20

4.1 Aerodynamic Preliminary Design 20

4.1.1 Wing Planform Design 21

4.1.2 Wing Aspect Ratio Design 22

4.1.3 Final Wing Configuration 22

4.1.4 High-lift Devices 24

4.1.5 Airfoil Selection 24

4.1.6 Tail Type selection 27
4.1.7 Tail Size Selection 28
4.2 Fuselage Components Preliminary Design 29
4.2.1 Antenna Payload 29
4.2.2 Retraction Mechanism 29
4.3 Propulsion Preliminary Design 30
4.3.1 Battery Selection 30
4.3.2 Motor Selection 33
4.4 Analytical Tools 35
4.4.1 Spreadsheet Application 35
4.4.2 Other Simulation Methods 39
4.4.3 Weighted Decision of Motors 37
4.4.4 Investigation of Astro FAI Series Motors 37
4.4.5 Motor Selection 38
4.5 Conclusion 40
5.0 DETAIL DESIGN **41**
5.1 Power System Optimization 41
5.2 Aircraft Flight Characteristics 41
5.2.1 Center of Gravity Calculation 45
5.3 Rated Aircraft Cost 45
5.4 Wing Strength Calculation 46
5.5 Aircraft Assembly 46
5.6 Payload Extraction Mechanism 47
6.0 MANUFACTURING PLAN AND PROCESSES **48**
6.1 Manufacturing Concepts 48
6.1.1 Competing Concepts 48
6.1.2 Downselect 48
6.2 Manufacture of Primary Components 49
6.2.1 Fuselage 49
6.2.2 Wing 49
6.2.3 Tail 50
6.2.4 Keel 51
6.2.5 Landing Gear 51
6.2.6 Release Mechanism 51
6.3 Manufacturing Milestone Chart 51
7.0 TESTING PLAN **53**
7.1 Testing Objectives 53

7.2 Testing Schedule 53
7.2.1 General Testing 53
7.2.2 Static and Dynamic Testing 54
7.2.3 Flight Testing 55
7.3 Testing Results 55
7.3.1 Component Static Testing Results 55
7.3.2 Completed Aircraft Static Testing Results 56
8.0 REFERENCES **57**

Table of Figures

3.1 Antenna and Sting Balance Strut in Cal Poly's 3'x4' Wind Tunnel 7
3.2 Floworks Antenna Drag Estimation 8
3.3a Configuration Score vs. Wing Loading 9
3.3b Configuration Score vs. Cruise Speed 10
3.4 Possible Configurations 13
4.1 Effects of Aspect Ratio on Score 22
4.2 Wing Planform 23
4.3 Local Lift Distribution 23
4.4 Lift Distribution and Elliptical Approximation 24
4.5 JA161 Airfoil Profile (Clean and 10° Flap Deflection) 25
4.6 C_L versus C_D at Different Cambers 26
4.7 Airfoil Comparison (No Flaps) 27
4.8 Retraction Mechanism Operation Schematic 30
4.9 Typical NiCd Discharge Rates 32
4.10 A Small Portion of the Input-Output Interface of DBF03 37
4.11 The RAC Component Breakdown 38
4.12 Time Breakdown of Mission A 39
5.1 Moment coefficients vs. Cl 42
5.2 finalized aircraft configuration from DBF03 43
5.3 Aircraft Datasheet 44
6.1 Manufacturing Milestone Chart 52
7.1 Destructive Testing of the Tail 56

Table of Tables

2.1 Team Members and Assignment Areas 5
2.2 Milestone Chart: May 2002 – April 2003 7
3.1 Deployment Mechanism Figure of Merit 12

3.2 Figures of Merit for General Configurations 14
3.3 Figures Of Merit For Wing Placement 15
3.4 Fuselage Length Figures of Merit 16
3.5 Number of Engines Selection 17
3.6 Landing Gear Configuration Figures Of Merit 18
3.7 Material Selection 19
4.1 Wing Planform Design 21
4.2 Wing Planform Design 22
4.3 Empennage Configuration 28
4.4 Battery Cell Comparison 31
4.5 Candidate Motors 34
4.6 Propulsion Systems Evaluated in MotoCalc 35
5.1 Center of Gravity Calculation 45
5.2 RAC Calculations 45
5.3 Wing Weight/Spar Cap Thickness Calculations 46
5.4 Retraction Mechanism Operation 47
7.1 Testing Check List 53
7.2 Static Testing Schedule 54
7.3 Dynamic Testing Schedule 55

1.0 Executive Summary

In response to the AIAA's Design Build Fly 2002/2003 challenge, California Polytechnic State University at San Luis Obispo (Cal Poly SLO) assembled a small group of aerospace students consisting of both upper and lower classmen to design, build, and fly a radio-controlled aircraft in the Cessna Office of Naval Research Student competition. The goal was to create an aircraft designed for optimum performance within the contest rules and requirements. The competition total score was comprised of a written report score multiplied by the flight score, divided by the rated aircraft cost. The flight score was a result of two chosen flight missions and a timed assembly task. The design process of this aircraft consisted of a conceptual design stage, a preliminary design stage, and a detailed design stage.

1.1 Conceptual Design

Cal Poly's DBF team began this year's design by evaluating the three possible missions and picking the two that had the highest potential total scoring potential. Manufacturing methods and basic aircraft configurations which satisfied the mission profiles were discussed and selected, based on data obtained through research, spreadsheet applications, and previous student experience with the DBF competition. Basic configuration components and the payload deployment mechanisms were all researched and selected. In addition, the team continued the development of the design tools that were used for determining the optimum configuration and approximate dimensions.

1.1.1 Conceptual Design Alternatives

The mission profiles were selected by defining figures of merit, and analyzing how each profile met these requirements. The effect that the difficulty factors had on flight score as well as the feasibility of the aircraft was considered. The team also calculated the outputs of a simplified performance estimation program that predicted the score of an aircraft operating in a set of two missions. Having made the mission selection, possible aircraft configurations could then be tailored to meet the requirements. Basic aircraft configurations were chosen. In order to design a fuselage to best house and deploy the payload while having the smallest cost possible, the tradeoffs between a four foot fuselage, which required no assembly, and one with a plug-in tail boom were discussed.

For the wing configuration, the aerodynamics group studied the conventional wing, biplane, canard, flying wing, and blended wing/body. The aerodynamic group analyzed different shapes of fuselage and tail configurations. The conventional tail, cruciform tail, T-tail, V-Tail, and inverted V-tail were all analyzed. The propulsion group discussed and analyzed the number and type of engines to be used. The structures group studied landing gear and keel placement along with assembly choices.

1.1.2 Conceptual Design Results

Mission profiles A and B were selected. Simulation of mission profiles on DBF2003, a program written in Visual Basic consistently showed higher scores for this set of missions. A large portion of the design would be spent on the payload compartment and deployment system. The deployment system chosen was a gravity drop system due to its perceived mechanical simplicity and low weight. Because of the high-keel design of the aircraft, a conventional high wing was chosen to attach to the keel and avoid interference with the payload deployment. For easy ground handling, takeoff characteristics and strength, a tricycle non-retractable landing gear was chosen.

1.2 Preliminary Design

After the mission profiles were chosen and the basic configuration of the aircraft was finalized, the approximate aircraft size, component placement, landing gear, motors, and control surfaces were decided upon. The aircraft was to have 33 ounces per square foot wing loading, and be powered by a Graupner 930-6 motor operating from the power provided by a 12-cell Sanyo CP-1700SCR battery pack.

1.2.1 Preliminary Design Alternatives

Many of the options that were ruled out were based on the assembly time of the aircraft. Wing planform alternatives investigated were swept, elliptical, rectangular, tapered, and a modified Schuemann. The optimum aspect ratio was determined from the outputs of the DBF2003 performance simulation program and practical considerations. Tails such as the T-tail, the cruciform tail, and the canard configuration were discarded early since their disadvantages in complexity outweighed any benefits. Propulsion system components were selected to allow the optimum performance in the missions chosen. Motors from Graupner and AstroFlight product lines, different types of NiCd batteries and propellers of various diameter and pitch were compared in order to come up with the final configuration. One of the important topics for preliminary design was the payload deployment. The gravity deployment system discussed in conceptual design was also expanded upon.

1.2.2 Preliminary Design Results

The modified Schuemann wing planform was used in this design because it posed the best compromise between all of the concepts reviewed. After weighing the benefits of the 3 possible tails, the V-Tail empennage was chosen to decrease the aircraft rated cost, provide for maximum control authority and to simplify construction and operation. The size of the selected tail was calculated using tail volume coefficients equations from Raymer (Ref.1). The optimal landing gear for the mission was finalized as a non-retractable tricycle configuration for reasons of stability and simplicity. The landing gear was designed to have a steering front wheel with brakes. A one-piece conventional fuselage with the V-tail positioned at the end of an upswept tail boom was designed to enable easy payload deployment.

1.3 Detailed Design

After the basic configuration of the aircraft was laid out, the group developed more detail to the design and was able to perform more analysis of the chosen aircraft components. At this point the materials and manufacture processes were finalized. Finally, solid carbon joiner tubes for plug-ins, Velcro, and nylon bolts were chosen for the assembly.

1.3.1 Detailed Design Alternatives

Locations of all secondary components were investigated for aircraft balance requirements. The geometry of the payload deployment system was analyzed and improvements on the design were studied.

1.3.2 Detailed Design Results

At the conclusion of the detail design phase all aircraft dimensions, system components, and materials were decided on, aircraft performance and control characteristics determined and manufacturing processes selected. The estimations conducted by the design team predicted an RAC of 6.29, and an ideal final competition score of 18.75, with a flight time of 3.2 minutes for mission A and 3.1 minutes for mission B. Assembly time was estimated at 30 seconds.

1.3.3 Detailed Design Tools

The tools used in the detailed design process were X-foil and the DBF 2003 performance simulation program. A solid model of the aircraft used for visualization and balancing was created in Solid Works 2001 Plus. Many of the other estimates and design methods used by the team originated from the experience gained in Cal Poly's previous DBF entries.

2.0 Management Summary

Cal Poly's DBF team was organized to maximize productivity. Team members were assigned to areas based on experience and interest. Each person assigned to a specific topic worked continuously in concert with team members who were working in other areas of the design, facilitating immediate integration of parts and compatibility checks. In addition, a timeline was constructed to keep the project on task and on time.

2.1 Design Team Architecture.

Cal Poly's DBF team started its organization by choosing a team leader who had the responsibility for overall team direction as well as completion of each task in the allotted timeframe. After the demands of the project were ascertained, the team broke up the project assignments into four main groups: configuration, aerodynamics, propulsion, and structure. Team members were assigned to one or more groups depending on experience and demand.

The configuration group was responsible for the overall design of the aircraft, for using the simulation program to establish component requirements and calculating the initial dimensions of the aircraft. The simulation program itself was also developed further to be more accurate. This group was also responsible for the design of the deployment mechanism. At all times, this group was responsible for keeping the overall design optimized for maximum score.

The aerodynamics group was responsible for wing planform and airfoil selection and worked together with the structures group to design the fuselage and wing components of the aircraft to best fit the performance requirements. This group was also responsible for the stability and control of the aircraft, and had to integrate with the other groups with regards to location, size and type of empennage chosen, and the means of driving its control surfaces. Similarly, the flaperons had to be integrated into the wing and actuated.

The propulsion group had the responsibility of selecting the motor and batteries requirements to be used along all other radio gear that would be required for mission demands. Research on an optimum gearbox and propeller combination was conducted in parallel with motor and battery selection, and an integrated propulsion system was designed.

Finally, those in the structure group examined the aerodynamic and point loads to be taken, examined the load paths, sized the structural members and chose the best materials and manufacturing methods for the proposed design. The structure group was also responsible for the purchase of the materials chosen, and the construction of the aircraft and all systems involved. In order to carry out the construction of the aircraft, agreements were made with the Aerospace and Manufacturing departments at Cal Poly concerning use of their facilities, and established the 'Cal Poly DBF Shack.'

Few of the problems encountered were completely independent to a specific group, developing an awareness of the overall state of the project necessary for all team members. Having a small team kept the lines of communications shorter and more direct, therefore, there were less opportunities for misunderstandings. While each group member was responsible for a separate part, the group was integrated

into all parts of the project and constant communication between the members was maintained. Modifications to the design were reported to the team leader and the solid model of the airplane was modified accordingly and checked for possible integration problems with other areas of the design.

All team members contributed to the writing of the report in their specific expertise areas. Responsibility for public relationships and funding was equally split. These areas were crucial to securing the funds necessary to complete the project.

Table 2.1 – Team Members and Assignment Areas

Design Personnel	Assignment Areas
Yevgeniy Gisin/AE/SR	Team Leader, Configuration, Aerodynamics, Propulsion, Structure
Francesco Giannini/AE/SR	Configuration, Aerodynamics, Propulsion, Structure
Erin Clare/AE/SR	Aerodynamics, Propulsion, Structure
Matt McCue/AE/SR	Configuration, Aerodynamics, Propulsion, Structure
Nick Christiansen/AE/SR	Configuration
Torrey Smith/AE/JR	Configuration, Structure
Mike Radin/AE/SR	Structure
Renee Pasman/AE/JR	Aerodynamics, Propulsion, Structure
Eric Naess/AE/JR	Structure

2.1.1 Schedule Control

Once the competition rules had been published, the team members evaluated them and a schedule was set up immediately. The timely completion of the various tasks that comprise the construction of an airplane is key to producing a winning DBF aircraft. In order to assure this, a tight schedule had to be adhered to. The team produced a calendar with all the projected deadlines for the different phases of the competition including conceptual, preliminary, and detailed design as well as the manufacturing process, testing and the report write-up. As the project progressed, the actual time of completion was recorded and entered into the milestone chart versus the projected time (Table 2.2). In case of one of the tasks lagging, extra resources could be re-directed to keep the team on track.

Table 2.2 - Milestone Chart: May 2002 – April 200

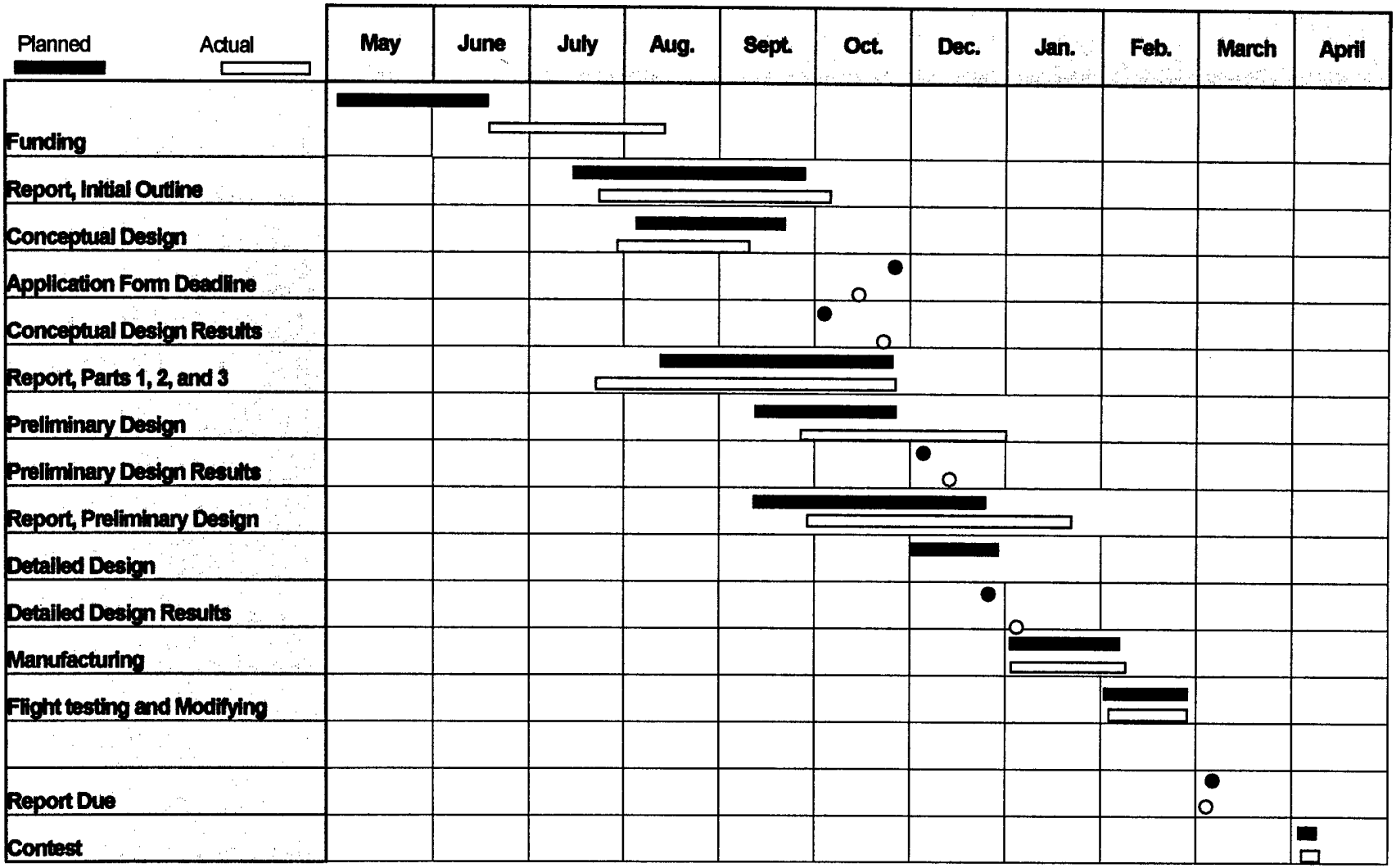

3.0 Conceptual Design

The conceptual design process of CalPoly's2003 DBF aircraft was a difficult task due to the selection of two of the three possible mission tasks specified in the RFP. In the previous years of DBF competition, the aircraft design had to be focused on optimizing a configuration for a specific mission. This year, the first choice that had to be made was the selection of two missions with the highest scoring potential.

The deployment mechanism was identified as the primary concern. This heavily influenced landing gear design, fuselage design, and wing placement. In order to accurately predict mission performance in mission A, the additional drag of the antenna had to be found. This was accomplished through independent methods whose results were matched closely enough for a reasonable confidence level in the predictions.

The final configuration chosen was best suited for the contest rules and mission, providing the greatest scoring potential.

3.1 Mission Selection

In order to initiate the conceptual design, the team first had to determine the two missions that the aircraft would be optimized for. Both the aircraft weight and drag would change from mission to mission, affecting aircraft performance and controllability. It was easy to estimate weight changes that the "electronics payload" container would cause; however, the team did not have any estimation of how the "antenna" would increase the drag of the aircraft. Knowing this amount of drag increase would be crucial in calculating aircraft performance in mission A enabling the down selection to two missions. The antenna model was placed in the Cal Poly open-circuit low speed wind tunnel and drag measurements at a number of airspeeds were taken (Figure 3.1 and 3.2).

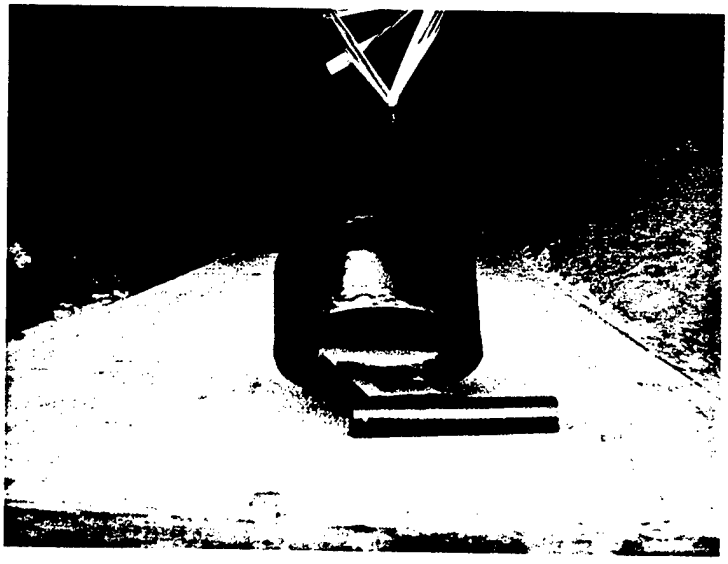

Figure 3.1- Antenna and sting balance strut in CalPoly's 3'x4' wind tunnel

The antenna, because of its shape and size, would constitute a considerable addition to the overall drag of the aircraft. The coefficient of drag of the antenna that was calculated from the test data was later used to predict the total drag of the aircraft during the "missile decoy" mission task. This number was compared to

results of a Floworks simulation of a solid model of the antenna at the predicted cruise speed (Fig. 3.2). The numbers obtained were closed enough that the wind tunnel results were confirmed.

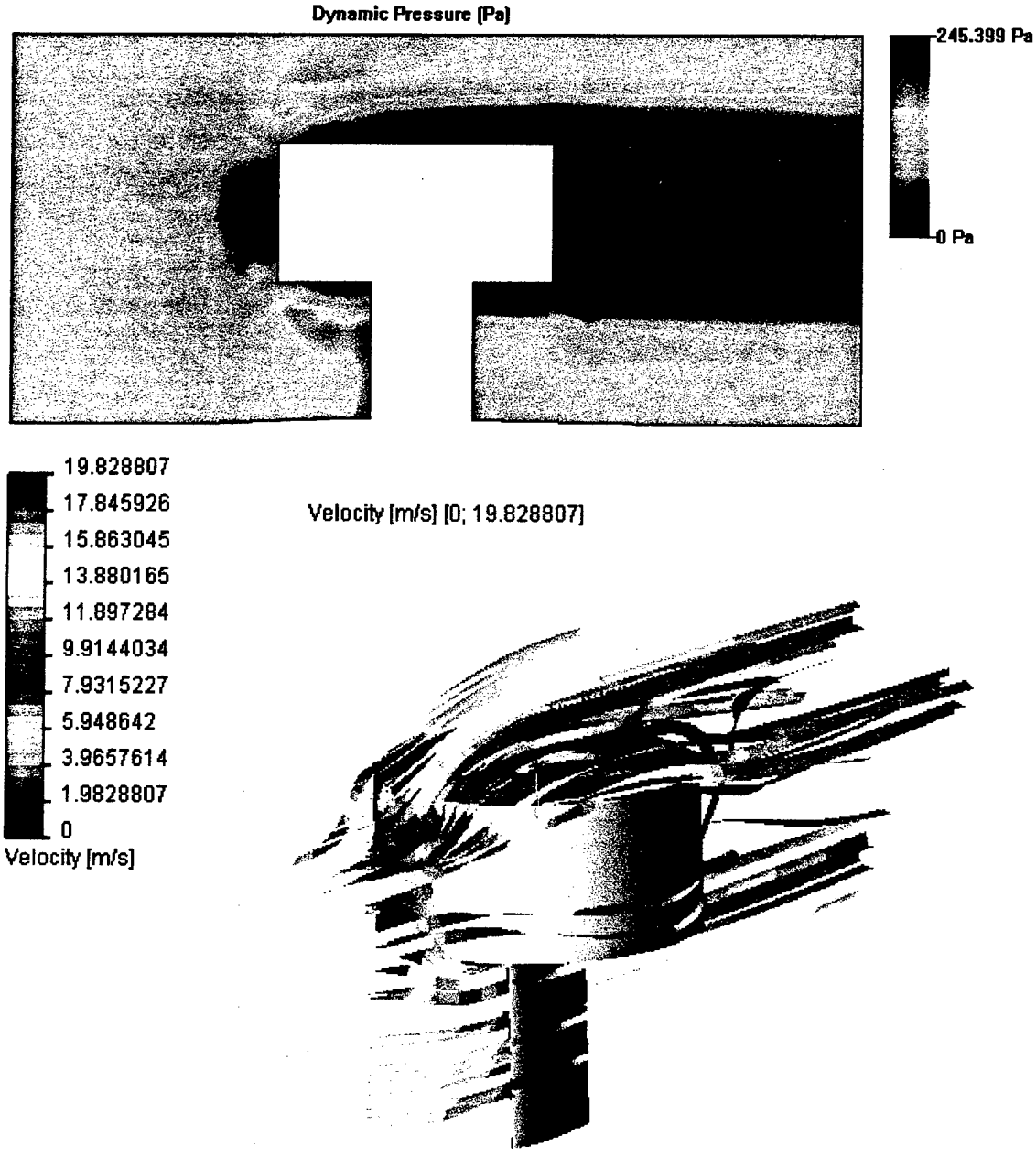

Figure 3.2- Floworks antenna drag estimation (V_∞ = 10m/s)

Having acquired all the necessary data to correctly estimate the effects the different missions would have on the aircraft performance, the selection of the two aircraft mission tasks could begin. The selection process was performed using the DBF2003 program that is described in detail in Section 4.5.1. Using the

program, three different aircraft configurations were optimized, each focusing on a set of two different missions. An important configuration driver was wing loading since it affects every aspect of aircraft performance. Power required on takeoff, C_L required in cruise, most efficient speed and a score of other parameters all depend on wing loading. Because of its importance, it was chosen as the independent variable for the results of the mission merit investigation to be portrayed against. Figure 3.3a&b shows the relative maximum score trend lines that would be attained by the three airplanes, each data point optimized for one of the three possible mission combinations.

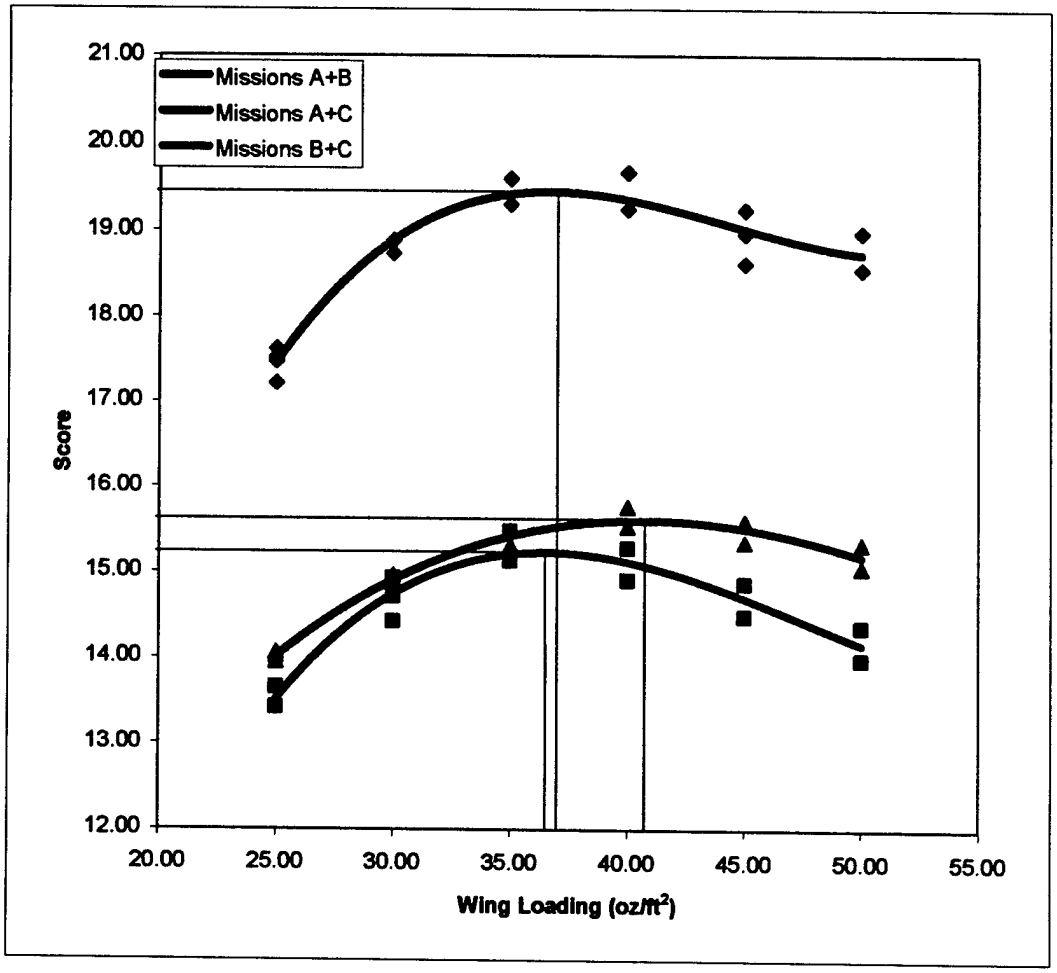

Figure 3.3a – Configuration Score vs. Wing Loading

Due to the definite correlation among score and mission optimization, missions A and B are the two missions that an aircraft should be designed for. For missions A and B, the peak score is significantly higher than the other mission combinations, directly pointing to the optimum mission combination.

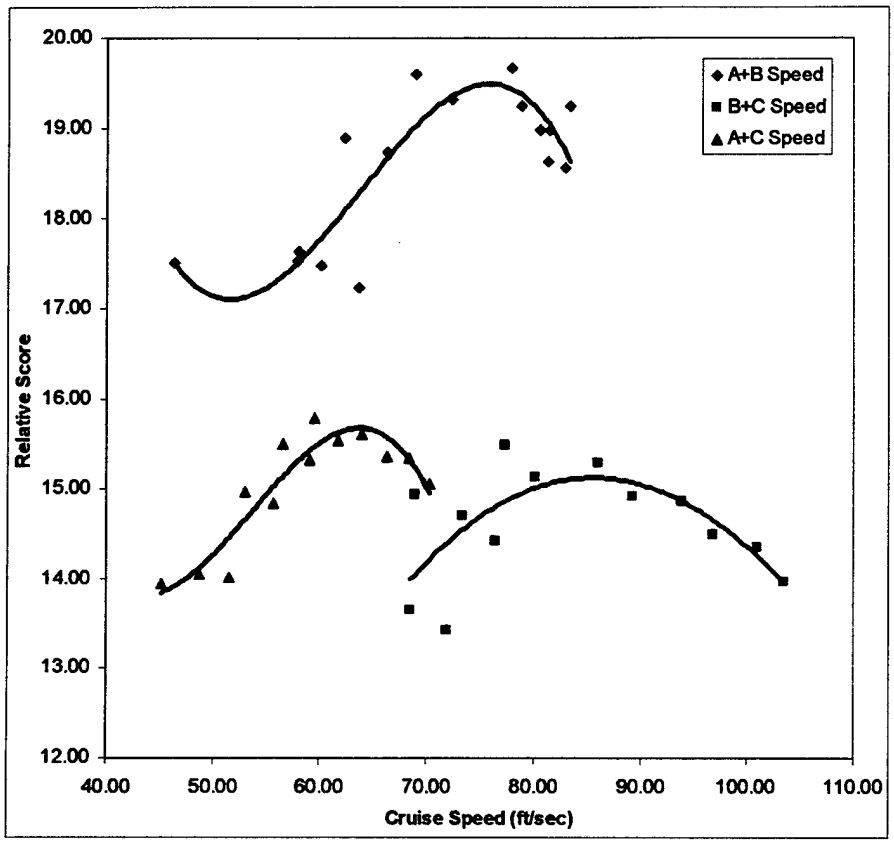

Figure 3.3b – Configuration Score vs. Cruise Speed

Although an aircraft designed for missions A and B would be more complex to construct and also be more challenging to operate due to the inclusion of the weight and complexity of a payload deployment system, and the extra landing-takeoff included in mission B, it was concluded that the demonstrated gain in configuration score would justify the risk taken.

3.2 Payload Configuration

A malfunction of the payload deployment system is an event that is sure to nullify the result of an otherwise successful mission. It was felt that compromising the reliability of the deployment system in order to allow operation from a conventional airframe configuration was the wrong approach to acquire. Selecting an airframe configuration prior to selecting the payload deployment method would automatically rule out many deployment mechanisms. Although the configuration of the airframe certainly has a significant effect on the performance of an aircraft, it was felt that a more conservative approach should be taken.

First, the method by which the payload would be deployed was established, and only then was an aircraft configuration chosen, based on how well it integrated with the deployment method selected. Due to the rigid limitations that the competition rules placed on the antenna mounting, the team could not come up with an innovative way to mount it (a way that would act to increase the performance of the aircraft in a noticeable manner). Therefore it was decided to concentrate on mounting the antenna simply and securely.

3.2.1 Antenna Location

The team was not able to identify an antenna location that would both adhere to the competition rules and have a beneficial effect on the performance of the aircraft as well. Since the rules specify that the antenna must have an unobstructed 360° horizontal field of view, it could not be placed either in front of the aircraft or behind the fuselage in the aircraft wake, a location from which a reduction in parasite drag could be achieved. Therefore it was decided to locate the antenna on top of the fuselage, in a position that would mitigate adverse effects on performance. Two locations were studied: one in front of the CG and one on the same vertical plane as the CG. The former would be calculated so that the moment generated by the drag of the antenna in cruise would cancel out the moment generated about the CG. The latter would not shift the CG location from one mission to the other, when the antenna is not flown. The choice of antenna location was left to later stages of design, when more certitude about the weight and balance would be acquired.

3.2.2 Electronics Box Deployment

Having selected to operate the airplane in mission task A, the issue of payload deployment method was the next to be addressed. Desirable attributes of the deployment mechanism were reliability, serviceability, ease of extraction, weight, and ease of manufacture. After much deliberation, the team decided to investigate the following four deployment methods.

Method 1 – This method involved a single servo rotating an arm in the horizontal plane to which the payload box would be constrained. After sliding on the surface of the cargo hold, the box would be pushed out onto the ground. Such a setup would be heavy, complex and would raise doubts regarding its reliability.

Method 2 – This method involved a simple drop mechanism, similar in action to those used on modern-day bombers. The downside of this method would be that it would theoretically require at least 6 inches of clearance between the bottom of the aircraft and the ground. An aircraft with such a high landing gear would not be able to fit into the storage container without being disassembled. Furthermore, the shackle mechanism must be strong enough to constrain the payload under all conditions, including potentially hard landings.

Method 3 – This method was a modification of the "drop" mechanism described earlier, differing in having a split bottom payload bay door that would split through the upsweep on the rear portion of the aircraft, therefore allowing the dropped payload container to pass through the back of the aircraft. This modification would allow an aircraft with a shorter gear stance to be built, one that could fit into the storage container without being disassembled. One potential disadvantage is that the payload might get stuck in the clamshell doors, preventing the departure of the aircraft.

Method 4 In this case, the payload would be pushed out the back of the fuselage, in a fashion similar to cargo transports. A servo would wind a wire loop constrained by pulleys, causing a plate to push the payload towards the back of the fuselage. This system would be complex and slow, but the payload would cause little interference with the departing aircraft once it is dropped.

Table 3.1- Deployment mechanism figure of merit

Description	Reliability	Serviceability	Manufacturability	Weight	Payload Extraction	score
Weighting factor	.3	.1	.1	.2	.3	1.0
Rotative deployment	1	1	0	1	1	.9
Bomb Drop	3	2	3	3	2	2.6
Bomb drop, clamshell	3	2	3	3	3	2.9
Ramp deployment	1	2	1	1	2	1.4

3.3 Airframe Configuration

Decision matrices were used to determine the alternatives that best met the mission requirements for each component. Figures of merit were chosen and a weighting factor was applied to the rating of each component, yielding a final score. For each alternative, the final score was compared and the highest was chosen.

3.3.1 General Configuration

Configurations considered during this early phase of design included flying wing, canard, biplane, conventional, twin fuselage, and blended wing/lifting body. Significant figures of merit in the selection of the configuration were ease of manufacture, rated aircraft cost, performance, payload ease of extraction and weight.

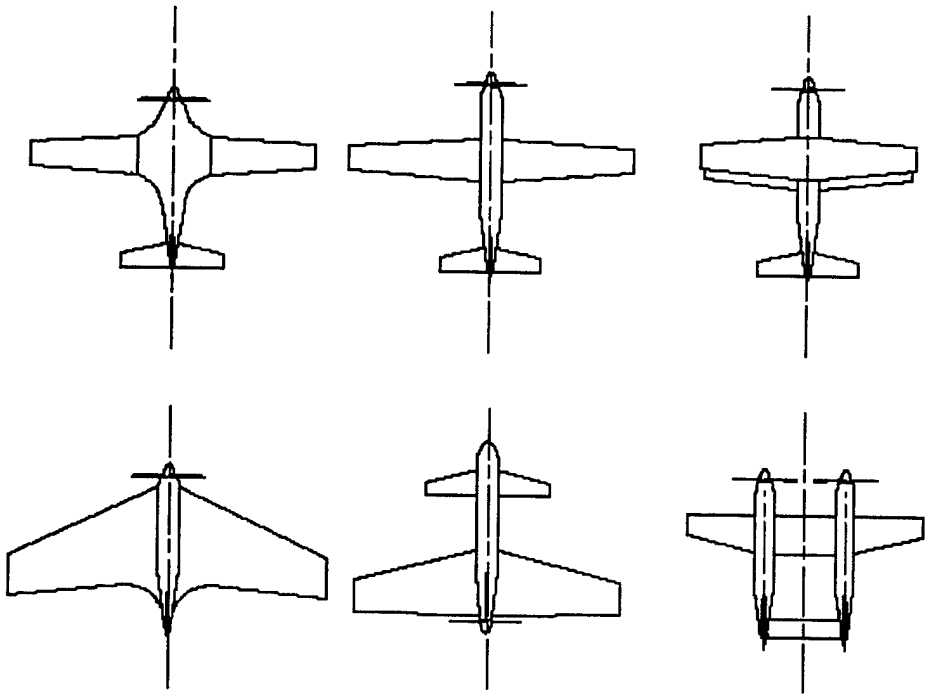

Figure 3.4- Possible Configurations

Flying wings require airfoils with reflexed mean camber lines near the trailing edge. This produces a positive pitching moment that obviates the need for a tail. Unfortunately, the maximum trimmable coefficient of lift for that airfoil is adversely affected, largely negating the benefits of this configuration. Flying wings make the installation of high lift devices problematic; their high pitch-down moment created upon deployment cannot be offset by the limited trim capabilities of a tailless airplane. A quick estimate of development time showed that too much time would be required to fine-tune this configuration.

Biplanes achieve a greater total lift by increasing the wing area and the wing can be made lighter if externally braced, albeit at the expense of drag. The relative closeness of the sets of wings leads to interference drag and a reduction of efficiency. A monoplane with the same reference area but greater aspect ratio achieves greater efficiency. Since this year's rules place no real limit on the wingspan, the biplane configuration was discarded.

The team also investigated the canard configuration. This concept seemed promising because both foreplane and main wing act as lifting surfaces, and a smaller, more compact airframe can be built. On the other hand, the particular lift distribution between the two surfaces requires special consideration. At high angles of attack, the foreplane must stall before the main wing to ensure that an unrecoverable departure does not result. In attempting a dive, however, the main wing must arrive at its angle of zero lift before the foreplanes achieve zero lift. If the foreplanes were to cease to lift while the main wing still lifts, a violent dive

would result. These and other complications involved with fine-tuning this configuration prompted the design group to decide against the canard.

The twin fuselage configuration proves attractive only if a twin-engine solution is chosen. The mass of the fuselages is far from the centerline, which results in high moments of inertia and sluggish lateral handling. The added expense of a second engine makes this arrangement unattractive. Furthermore, the electronics payload would have to be mounted asymmetrically. The blended wing/lifting body configuration was rejected early-on, because of many reasons: at the comparatively low speeds and Reynolds numbers at which the model operates, lifting bodies (basically low-AR wings with a low C_L/C_D) do more harm than good. Given the particular shape of the electronics box, the volume afforded by a blended wing-body configuration could not efficiently be put to use. A blended wing-body would also be much more difficult to manufacture and operate.

A conventional layout presents no technical challenges. It is easy to manufacture, its handling characteristics are well understood, and the design team generally felt that it conformed well to this year's set of rules. Thus a conventional configuration was selected for further study.

Table 3.2- Figures of merit for general configurations

Description	Manufacture	Performance	Rated cost	Weight	Extraction	score
Weight Factor	.1	.2	.3	.2	.2	1.0
Flying Wing	1	1	3	1	2	1.8
Biplane	2	2	2	1	2	1.7
Conventional	3	3	2	2	2	2.3
Canard	3	2	2	2	1	1.9
Blended Wing/Body	1	3	2	2	1	1.9

3.3.2 Wing Placement

In terms of wing/fuselage arrangement, the wing can be classified in three categories: high wing, mid wing, low wing. Figures of merit include: lateral stability, ease of manufacture, interference drag, and serviceability. Cost remains unchanged from one configuration to another. Having selected the deployment, the team proceeded to evaluate the wing placement that hindered operations the least while possessing

adequate performance. A mid-wing is desirable from a drag standpoint; a low wing would keep landing gear height small. However, both interfere with payload positioning, which has to be necessarily close to the center of gravity. The wing placement that allowed for the simplest payload drop was the high-wing design, which was favored throughout the design process.

Table 2.3- Figures of merit for wing placement

	Figures of Merit	Manufacture	Serviceability	Lateral Stability	Payload Deployment	Drag	Score
	Weighting Factor	0.1	0.2	0.1	0.4	0.2	1.0
Low Wing	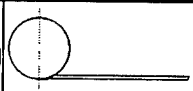	3	3	2	1	2	1.9
Mid Wing	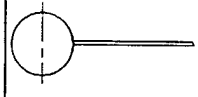	1	1	2	0	3	1.1
High Wing	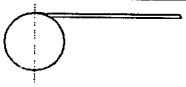	2	3	3	3	2	2.7

3.3.3 Fuselage Configuration

The fuselage had to be sized to carry the payload box, due to the fact that there was not a set of two missions that did not include it. The team also attempted to keep the total length of the airplane below 4 feet, although this would necessitate a large tail in order to obtain the tail volume coefficients required for good control characteristics, it was felt that this would be more preferable then having a plug-in tail arrangement that would both add to weight, complexity and assembly time of the aircraft.

When sizing the fuselage, many variables were considered, namely wetted area, frontal area, total length, and ease of access to internal components.

Because of the mission requirements, the aircraft was essentially molded around the payload. The fuselage was designed as a one-piece structure to minimize assembly time, with the highest possible fineness ratio while encompassing the payload box and fitting in a four-foot long container.

During the mission, aircraft weight will change as a result of the payload being deployed. To keep the payload from destabilitizing the aircraft by shifting the center of gravity location relative to the mean aerodynamic quarter-chord, the center of gravity of the payload was made to coincide with the center of gravity of the airplane.

The size of the tail is influenced as well; the length of the tail moment arm is determined in large part by the distance from the center of gravity of the aircraft to the aerodynamic center of the tail surface.

An important factor that severely affected the preliminary design of the fuselage was the length of the container box that the airplane had to fit in. Length of the fuselage is an important factor, it increases the

moment that the empennage can exert, thereby aiding to the controllability of the aircraft. However a fuselage length of more than four feet would require a plug-in tail arrangement, be more expensive and add to the timed assembly score of the aircraft. Because the control surfaces do not have cost assigned to their areas, it was decided that it would be cheaper and simpler to build an aircraft with a short fuselage and a large empennage to compensate for the short moment arm that would result. Although this configuration decision did not necessarily minimize the drag of the aircraft, it was thought that considering the relative poor aerodynamic characteristics of the fuselage designed to carry the 5lb payload, the extra drag added by the tail surfaces would not add up to a big performance penalty. The larger tail surfaces also increase control authority when functioning in the disturbed air behind the "dirty" fuselage and the antenna.

Table 3.3 – Fuselage Length Figures of Merit

FOM	Construction	Weight	Drag	Complexity	Control	score
Weighting factor	.1	.2	.15	.3	.2	1.0
4ft long body	3	3	2	3	1	2.3
Plug-In Tail Boom	1	1	3	1	3	1.65

The results of the analysis performed on fuselage configuration indicated that overall, the benefits of a one-piece construction would outweigh the disadvantages, and would be preferable to a longer, plug-in fuselage.

3.3.4 Engine Configuration

During the conceptual design of the aircraft it was calculated that a single engine operating with the expected battery pack voltage would be able to provide the takeoff power required while not exceeding the 40 ampere limitation dictated by the rules on the engine current. Since large engines are generally more efficient than smaller ones and the stringent takeoff constraint did not drive the design towards the use of multiple engines, a single large engine would be used instead.

Both single motor and twin motor configurations were considered. It was determined universally that for a given power requirement, the single motor solutions outperformed the twins in final score. This was caused by the additional cost of having more than one motor and speed controller, because for a given power level, two smaller motors, gearboxes and propellers weigh more than a single (increasing empty weight), and because larger motors generally have higher efficiency. It was decided that unless no single motor of sufficient size was available, the aircraft would not have two motors.

Table 3.4- Number of engines selection

Description	Weight	Efficiency	Rated cost	score
Weighting Factor	.3	.4	.3	1.0
Single Engine	3	3	3	3.0
Twin Engine	2	2	2	2.0

3.3.5 Landing Gear Configuration

The landing gear of a propeller driven airplane serves two major functions. The first is to provide adequate clearance between propeller tips and the ground. The second is to permit the plane to rotate on both takeoff and landing so that the wing's angle of attack comes close to the stall angle of its airfoil. At this angle of attack, the wing is near the airfoil's maximum C_L. This permits the aircraft to achieve the lowest allowable landing and takeoff speeds. The configurations considered where realistically limited to taildragger and fixed or retractable tricycle.

A taildragger configuration affords more propeller clearance and low drag. Unfortunately, it would also make the implementation of the deployment method used in mission task A extremely difficult if not impossible. The tail-dragger gear configuration also exhibits inferior ground handling characteristics compared to those of a tricycle gear setup.

For the reasons above it was decided to build the aircraft with a tricycle landing gear system. While exhibiting higher drag than a taildragger configuration, the tricycle gear permits a flat fuselage bottom and wide separation for optimum payload deployment. It also makes landings possible at sideslip angles and is generally more forgiving of rough ground handling.

A retractable landing gear eliminates a major source of parasite drag, but adds considerably to the complexity of the aircraft. An additional set of servos would be required, and it is doubtful that typically delicate retractable systems could cope with hard landings.

Table 3.6 Landing gear configuration figures of merit

	Description	Ground handling	Propeller clearance	Manufacturability	Weight	Payload Extraction	Score
	Weighting Factor	.3	.2	.1	.1	.3	1.0
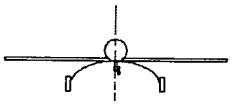	Taildragger	1	3	3	3	1	1.8
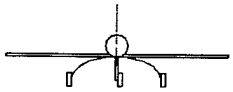	Tricycle	3	2	3	2	3	2.7
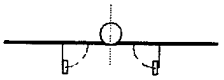	Retractable	3	2	0	1	1	1.7

3.3.6 Empennage Configuration

For an airplane in level flight at its selected cruise speed, the sum of the positive and negative pitching moments must be zero. Four major moment sources must be compensated. The main source is center of gravity location. A CG that is ahead of the mean aerodynamic chord's quarter chord causes a nose down moment and results in a longitudinally stable airplane. Locating the CG further back decreases static pitch stability. The other sources of pitching moments are the wing's drag moment, the thrust moment and the airfoil pitching moment. The balancing is achieved in a conventional and canard design by the use of a horizontal tail or foreplane. The horizontal tail's angle of attack, relative to the wing's downwash, should be sufficient to provide lift or most often, down force required to provide equilibrium.

The H-tail configuration was considered as having a set of benefits for the particular mission that this airplane would be designed for. An inverted H-tail has the benefits of not requiring assembly after removal from the storage box and at the same time not being blanketed with turbulent air from the payload or the fuselage. However, the H-tail might cause ground clearance issues and is also more expensive, requiring two servos for control and being counted as two vertical surfaces with control. On other hand, the aircraft rated cost formula showed a small cost break for a V-tail compared to all other tail plane configurations. As a result of conceptual design, conventional, V, and H-tails were both considered to have enough merit to be deliberated upon further in the design process.

3.4 Material selection

Three material and construction methods were considered: conventional buildup of lightweight wood skeleton and Monocote skin, conventional buildup of carbon fiber skeleton and skin, and composite skin with foam core. The figures of merit that were selected for the conceptual material selection were: ease of manufacturing, repairability, and durability

Table 3.7- Material Selection

Description	Manufacture	Reparability	Durability	Score
Weighting Factor	**.3**	**.3**	**.4**	**1.0**
Mixed Carbon/glass with foam core	**3**	**3**	**2**	
Wood with Monocote	**2**	**2**	**2**	
Molded composite	**2**	**2**	**2**	

3.5 Conceptual Design Results

As a result of the conceptual design stage, a gravity retraction (clamshell) system in a one-piece conventional fuselage was selected. This configuration, together with a high-set wing and tricycle landing gear, promises trouble free payload deployment operations, which was a key concern in this design phase.

4.0 Preliminary Design

During the preliminary design stage, the team studied and made a variety of design choices that shaped the configuration of all of the aircraft components. One of the overall goals that the team had for the preliminary design of the airplane was to ensure a quick and simple assembly of the aircraft. This would both simplify the operation of the aircraft and increase the final score. The team believed that a quickly assembling aircraft could be created without detrimental effects to either weight or complexity.

4.1 Aerodynamics Preliminary Design

Building on the analysis performed during the conceptual design phase, further analysis of the aircraft was performed to refine the design. The areas examined included: wing aspect ratio, airfoil and high lift devices, tail type and sizing. The concepts for each aspect were evaluated in a decision matrix and a down selection was performed on the basis of the highest scoring concept.

4.1.1 Wing Planform Design

Planform is the shape of the wing as viewed from above. The wing planform is important in defining the performance of the aircraft. It may be swept, elliptical, straight, tapered, or a combination of both. Swept wings were ruled out immediately because they only offer disadvantages at the expected flight conditions.

- Elliptical wings: This is the ideal wing planform. It has the lowest induced angle of attack and induced drag, and stalls evenly across its span. These factors increase for rectangular and tapered wings. Structurally, the elliptical wing is difficult to manufacture, especially using some of the methods likely to be used on this type of an airplane.
- Rectangular wings: Rectangular wings are the easiest to design and build. All chord sections are the same, and wing skins have a single chordwise curvature. While it suffers in comparison with an elliptical wing, for small models, it maintains a constant Reynolds number across its span. A tapered wing of the same area could have tip Reynolds numbers in the high drag/ lower lift and stalling-angle range of low Reynolds numbers, leading to premature tip-stalls at low speeds. Structurally, the wing roots need reinforcing, owing both to narrower root chords and higher bending moments that are generated as a result of the center of lift of each wing being farther from the centerline than an elliptical or tapered wing.
- Tapered wings: A tapered wing with a tip chord of 40 percent of the root chord closely approximates the ideal elliptical planform both in induced angle of attack and induced drag. For wings of model aircraft, this taper ratio results in narrow tip chords and undesirably low Reynolds numbers at low speeds. Increasing the taper ratio produces larger tip chords. Lift is lost at the tips; the wider the tip chord, the greater the loss. The resulting loss in efficiency isn't great and is the lesser of the two evils. Structurally, the tapered wing has lower root bending moments, and the wider, deeper root chord provides the greatest strength where it's needed most- at the root. A tapered wing can be lighter yet stronger than a rectangular wing of the same area.

- Modified Schuemann wings: This planform has an elliptical leading and trailing edge for 70% percent of the semispan and a sheared wingtip. It comes close to the elliptical wing in efficiency and is more easily produced than an elliptical wing. The rectangular inner portion is wider in chord, which provides a strong root, and bending moments are lower than for a rectangular wing.

The design team chose the Modified Schuemann wing because it represents the best compromise in terms of performance.

Table 8- Wing Planform Design

	Figures of Merit	Ease of Manufacture	Efficiency	Strength to Weight	Stall	Score
	Weighting Factor	0.3	0.4	0.1	0.2	1
Elliptical	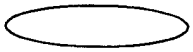	1	3	3	2	2.2
Rectangular	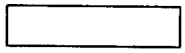	3	1	1	3	2
Simply Tapered		2.5	2	2	2.5	2.25
Modified Schuemann		2	2.5	2.5	2.5	2.35

4.1.2 Wing Aspect Ratio Design

The aspect ratio of the aircraft's wing was determined by using the DBF03 performance simulation program to produce data points based on aircraft configurations of maximum performance at a range of aspect ratios. The conclusion of this trade study can be seen in Figure 4.1, which shows a light peak in score at the aspect ratio of 9. The graph also shows that relative to the score difference that is provided by picking Missions A+B, the effects of aspect ratio on the aircraft final score are close to linear. Before making the final selection, some of other advantages that high-aspect ratio wings possess were considered. It was realized that the efficiency of a high aspect ratio wing also has benefits that could not be simulated by the Oswald's efficiency approximation in DBF03 program. First benefit of the high-aspect ratio wing is to increase the rolling moment of the aircraft, making it more "stable" in the roll axis. A high aspect ratio wing also allowed the designers to have a higher span horizontal tail surface (span of which is constrained by the rules to 25% of the wing span). A shorter-chord empennage can be mounted further back on the fuselage, effectively increasing the tail moment arm. Both from the team's experience with the composites construction technologies used by the previous years' DBF teams, it was concluded that wings of aspect ratios up to 12 could be easily built without incurring a weight or strength penalty. Thus a wing with an aspect ratio of 12 was picked for this year's aircraft.

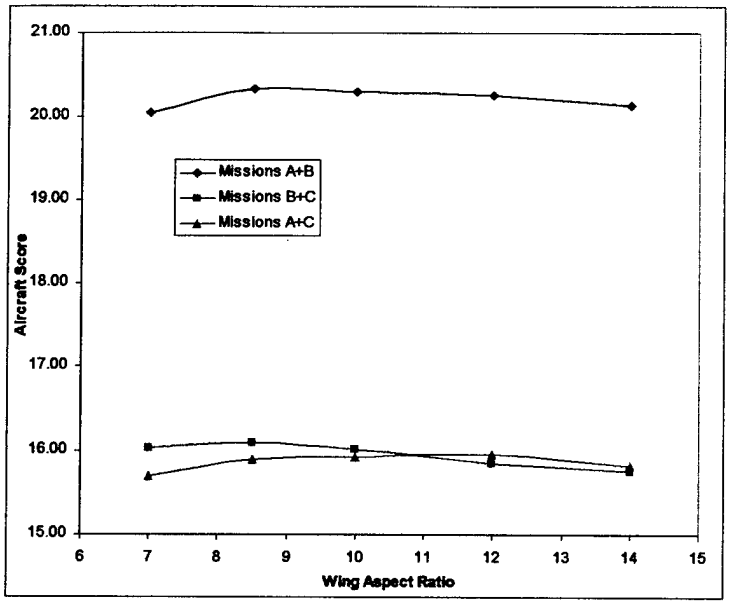

Figure 4. 1 – Effects of Aspect Ratio on Score

Table 4.1- Wing Planform Design

	Figures of Merit	Efficiency	Horizontal Tail Span	Strength	Roll Rate	Score
	Weighting Factor	0.4	0.3	0.2	0.1	1.0
High		1	1	-1	1	0.6
Medium		0	0	0	0	0
Low		-1	-1	1	-1	-0.6

4.1.3 Final Wing Configuration

When determining the final configuration of the wing, the team was trying to achieve a very difficult goal. The wing needed to produce high levels of lift when operating during the high-lift laps, but had to produce as little drag as possible when generating low levels of lift (when flying the empty laps).

The planform finally adopted was a modified Schuemann wing as seen in Figure 4.2. The wing has elliptical leading and trailing edges for the inner 70% of the span and a sheared wingtip design. This closely approximates the ideal span wise lift distribution (Figures 4.3, 4.4), without incurring the low Reynolds numbers at the tips that can lead to the stall occurring at the tips earlier than at the roots. More specifically, the wing was designed so that at a given angle of attack, the outer section of the wing would be operating at a CL

that is .1 lower than that of the root section. All the span wise sections of the wing can thus fly near peak efficiency while still preventing the tip-stall characteristic.

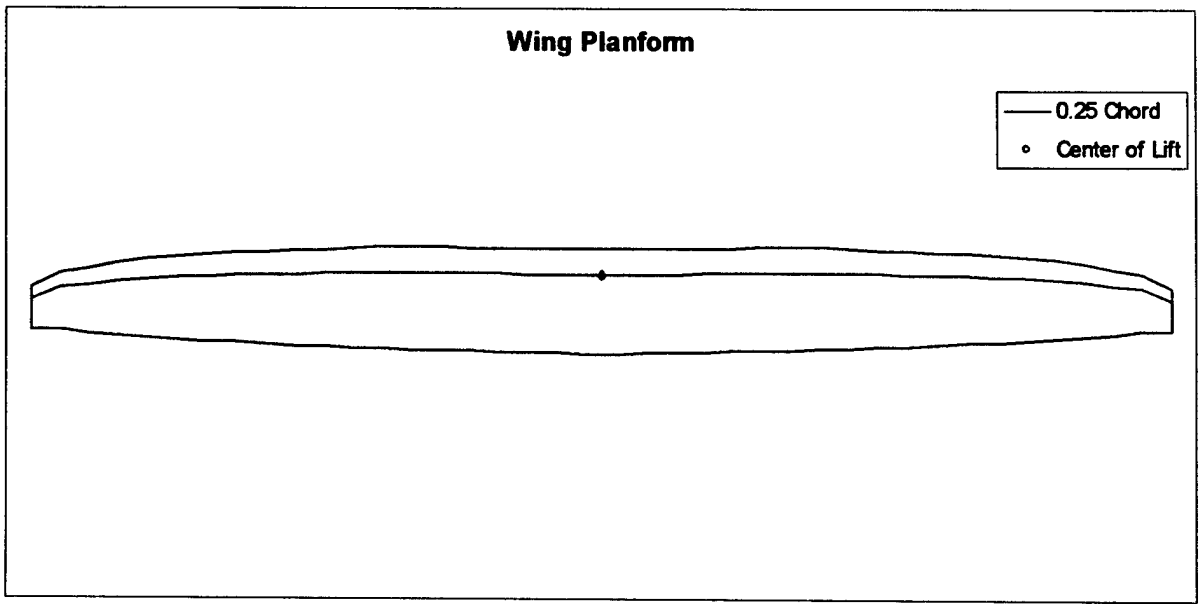

Figure 4. 2 – Wing Planform

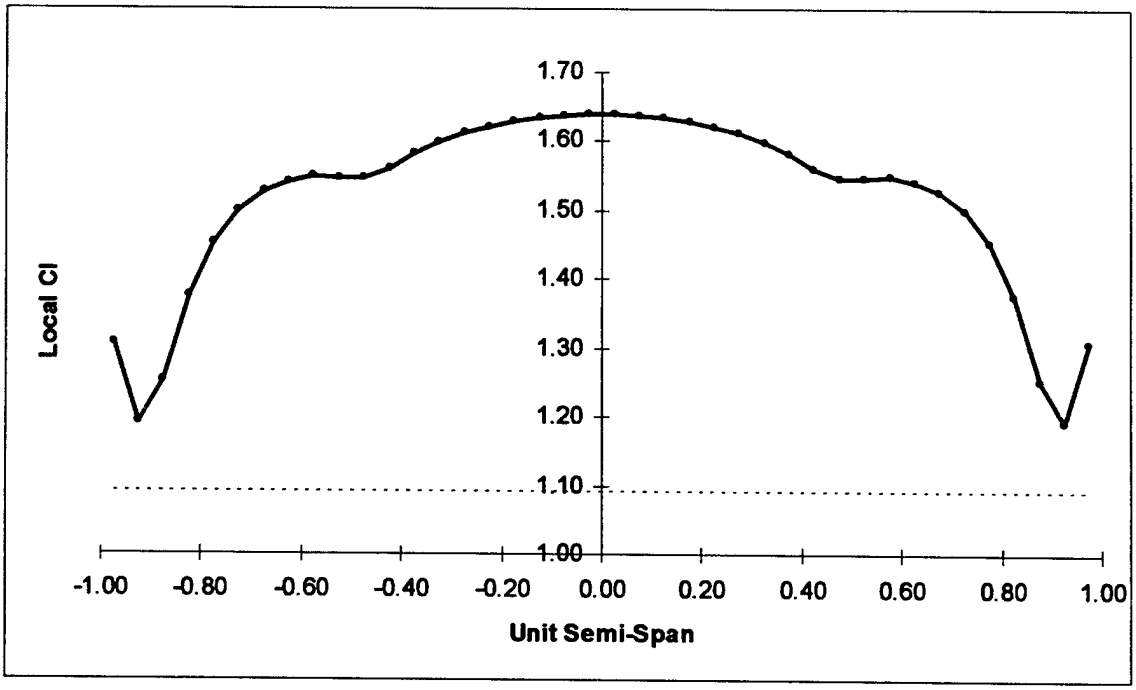

Figure 4. 3 – Local Lift Distribution

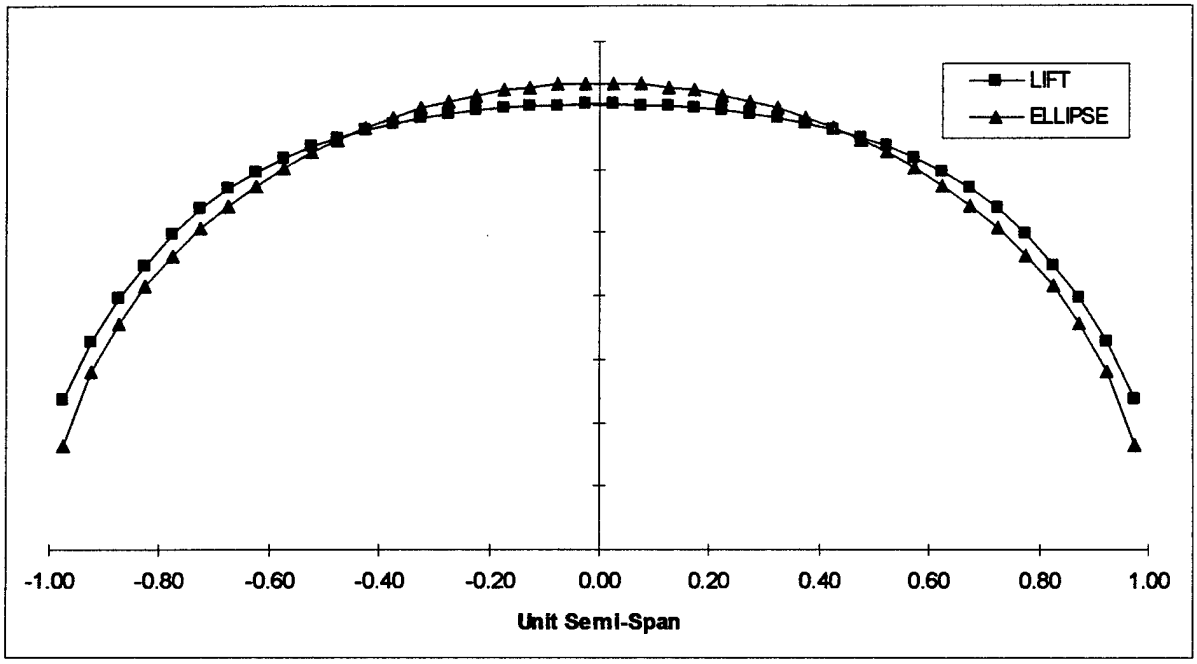

Figure 4. 4 – Lift Distribution and Elliptical Approximation

4.1.4 High-Lift devices

In order to meet the takeoff constraint, and to attain efficient climb, the team investigated different ways to increase the maximum wing C_L. Simple leading and trailing edge devices were the most obvious choice in this situation, with wing tilting, area increase devices (fowler flaps), and thrust vectoring deemed too complicated and not overly efficient on this type of an airplane. Keeping in mind the penalty that the competition rules assign for extra servos (which would be required to power separate control surfaces), flaperons seemed to be the most obvious choice.

The flaperons extend for the inboard 80% of the wingspan and 20% of the chord, and are used for roll control. Model airplanes with moderate-chord flaps fully extended, and reduced throttle tend to porpoise upward. In order to prevent this behavior, elevator down trim must be applied. The sharp increase in angle of downwash from the flaps forces the tail-plane down and creates a greater force than the increase in nose-down pitch. Increasing the flap size to 20% of the chord produces a balance between nose-down and nose-up forces, producing little change in pitch trim.

4.1.5 Airfoil Selection

Early in the design phase, it was recognized that the cost of the wing represented 20-40% of the total cost of the airplane. Wing cost was largely dependent on wing area, so in order to reduce cost as much as possible, the wing was designed capable of operating efficiently at high lift coefficients. This was a function mainly of the airfoil selected for the design. The wing planform was also considered in the design because of its impact on handling, aerodynamic efficiency, and the maximum lift achievable given a constant wing area.

In sizing the aircraft, many different airfoils were compared to find the airfoil and wing configuration that would maximize score and performance. It was recognized early on that the majority of flight time in the missions picked was spent in low-speed high-CL cruising flight. Likewise, the sizing software results favored thick, highly cambered high lift airfoils for the payload carrying laps. Out of the 8 laps flown in the course of the two missions, only two were flown with the airplane unloaded. With the lightly loaded airplane, a high lift airfoil is not desirable because of the lighter wing loading and the relatively low efficiency at low CL (0.3-0.4). During these two laps, a thinner, lower camber airfoil is optimal. These different lift requirements were very difficult to meet with any single, commonly used model aircraft wing section. In attempt to achieve both, an adjustable trailing edge camber changing airfoil was investigated.

JA-161, the airfoil chosen for the 02-03 Cal Poly DBF airplane is an excellent example of such an airfoil. JA-161 is a high-lift airfoil especially when coupled with a 10° flap deflection used to achieve a maximum CL of 1.9. With the flap set to an angle of 0° the airfoil operates efficiently during the relatively high-CL cruise.

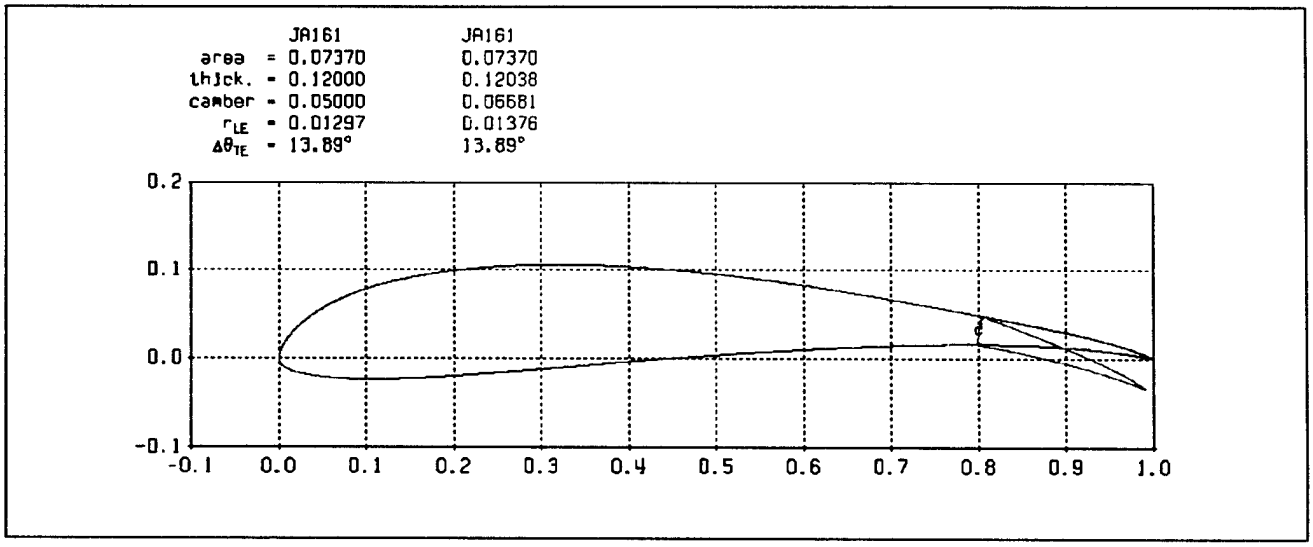

Figure 4. 5 – JA161 Airfoil Profile (Clean and 10° Flap Deflection)

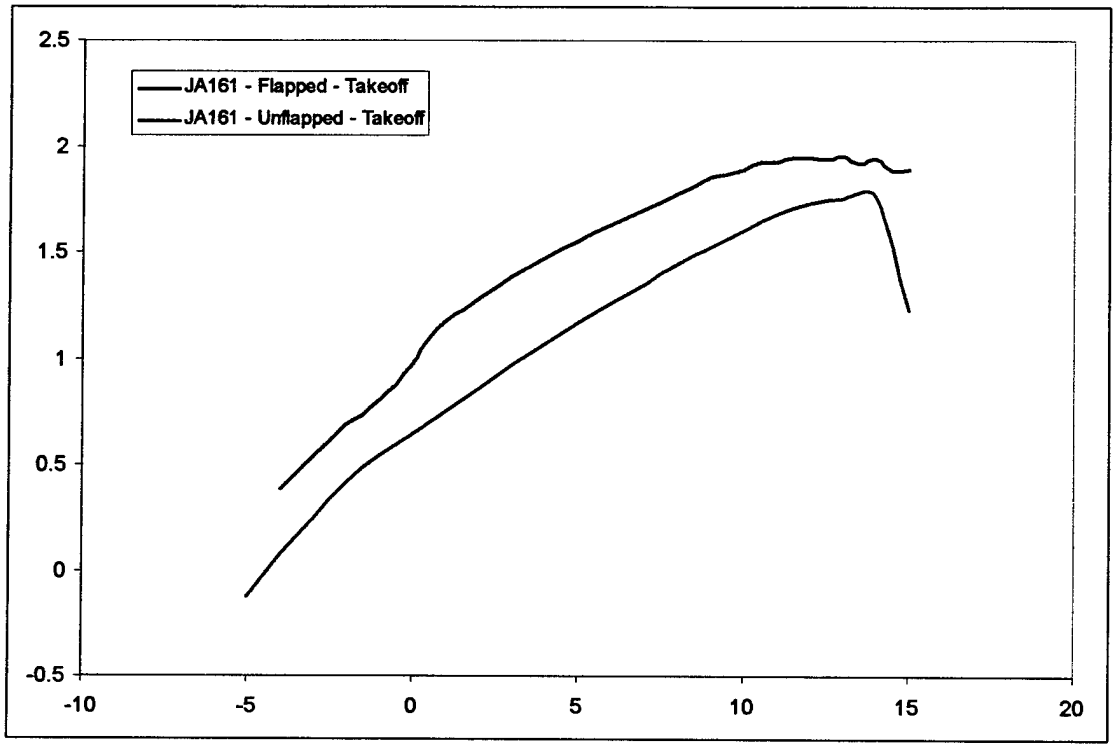

Figure 4. 6– Cl versus CD at Different Cambers

The design team investigated the camber changing airfoil concept using the same tool used to evaluate the commonly available model aircraft sections, X-foil. The design goal was to create an airfoil able to reach a CL of approximately 1.9 at the takeoff Reynolds number (~100,000) and to provide higher efficiency than the other candidate airfoils during both the payload and ferry missions. Maximum lift coefficient, drag at loaded cruise (CL 0.5-1.0), usable CL range, unloaded fast cruise (CL 0.3-0.4), and behaviors near stall were all considered. The design Reynolds number range for the final configuration was Re(CL)^0.5 = 180,000. After much iteration, JA161, the final design of the airfoil was far more capable and well suited for the aircraft than any of the other considered airfoils. Figure 4.7 shows the other candidate low Reynolds number airfoils considered for the design compared to the composite polar of the camber changing section. The Ja-40 is the airfoil used on the 01/02 DBF aircraft, the LA202 is an airfoil used in the past by the University of Southern California DBF team, the RAV is the AeroVironment Raven airfoil, and the SD7032 is a Selig-Donovan low Reynolds number airfoil. From Figure 4.7 it can be seen that the JA161 airfoil used on the 02/03 DBF aircraft outperforms all of the competitor airfoils in the loaded cruise CL range.

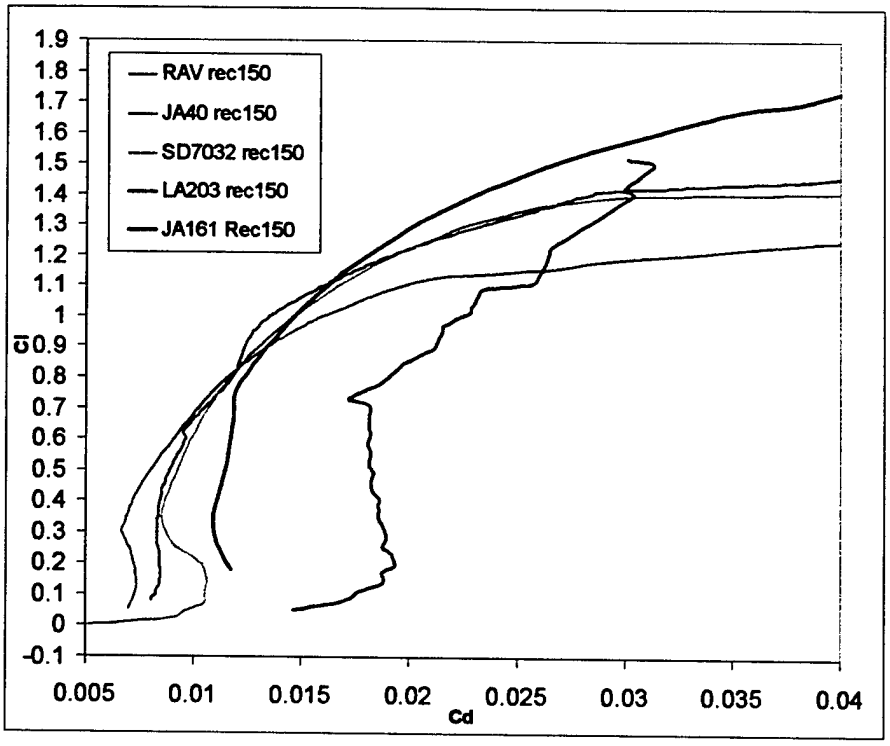

Figure 4. 7 – Airfoil Comparison (No Flaps)

The airfoil thickness is a moderate 12%, which is not optimum for drag reduction, but since most mission time is spent in comparatively low-speed flight this is acceptable. In addition to increasing the stiffness for a given weight of wing structure, the high thickness also tends to keep the efficient CL level quite broad.

4.1.6 Tail Type Selection

Although technically there are many different tail configurations that could have been used, only three ended up being a point of serious deliberation. Configurations such as the T-tail, the cruciform tail, the canard configuration, and other unorthodox configurations were quickly discarded. The team weighted the moderate performance advantages offered by some of these configurations versus the increases in systems complexity and the amount of time required to build, test and fine-tune these advanced configurations and decided against using any of them.

The three configurations that the team deliberated between were the H-Tail, the conventional tail and the V-tail. In order to not increase the assembly task time, the team hoped to spend as little time as necessary on tail assembly. If the horizontal tail were to be permanently mounted to the fuselage, it would have to be less than two feet in span in order to fit into the payload box, therefore not using up the entire span allowed by the rules. If the vertical and the horizontal tail were to be made as a "single piece", it could be made of a higher span, but then would be difficult to store in the box when removed. Since the team did not want to include the assembly of the horizontal surface in the timed assembly task, and it would be quite difficult to "package" an appropriately-sized tail in the box it was decided to investigate other options.

Both the V-tail and the H-tail have the advantage of being affected less by the air disturbed by the antenna payload, however, the two tails greatly differ in cost. With the servos, the V-tail has a RAC cost of only 35 hours, while the H-tail would drive the cost up to 60 hours. The H-tail's high cost was unlikely to have been recouped by its virtue of having a zero assembly time, but "the final nail in the coffin" for the configuration was the minimum upsweep (for "rotation" clearance) requirement that made the vertical tail volume coefficient too low for stable flight.

Table 4.3 – Empennage configuration

	Figures of Merit	Manufacture	Assembly	Rated Aircraft Cost	Handling Qualities	Score
	Weighting Factor	0.1	0.3	0.4	0.2	1
Conventional/ Cruciform		3	2	2	3	2.3
H-Tail		1	3	1	2	1.8
T-Tail		2	2	2	3	2.2
V-Tail		2	2	3	2	2.4

After considering the above arguments and comparing their numerical figures of merit, it was decided to build an aircraft with a V-tail empennage.

4.1.7 Tail Size Selection

Vertical and horizontal tail sizes were calculated using tail volume coefficient formulas on page 124 of Aircraft Design[1]. The conversion of the appropriate horizontal and vertical tail areas to V-tail areas was done using the following equations:

$$S_{VT} = c_{VT} b_W S_W / L_{VT}$$

$$S_{HT} = c_{HT} \check{C}_W S_W / L_{HT}$$

where L is the moment arm taken to be the length from the tail's quarter chord to the wing's quarter chord. S_W is the wing area, b_W is the wing span, and $\check{C}_W$ is the wing mean chord. The vertical and horizontal tail volume coefficients are c_{VT} and c_{HT}, respectively. The tail volume coefficients were chosen based on experience gained from the past three Cal Poly DBF aircraft. The handling qualities of these airplanes were very good and the tail volumes were chosen using them as a model.

The Charles River Radio Controllers' website provided a conversion equation to convert the horizontal and vertical tail area components into the V-tail area.

$$S_{V\text{-}tail} = S_{VT} + S_{HT}$$

$$\theta = \arctan[\sqrt{(S_{VT} / S_{HT})}]$$

$$S_{HT} = S_{V\text{-}tail} \cdot [\cos(\theta)]^2$$

$$S_{VT} = S_{V\text{-}tail} \cdot [\sin(\theta)]^2$$

"$S_{V\text{-}tail}$" is the area of both halves together, rotated flat. "θ" is the V-tail's dihedral angle from the horizontal. The formulas taken from the Charles River Radio Controllers' website are only to be used for large tail aspect ratios. These formulas do not account for the local interference and lift cancellation at the V-tail roots during yaw or "rudder" application. Using the equations above, the V-tail panel sizes were calculated to be 20 in. in length with an average chord of 8 inches, set at an included angle of 80°.

4.2 Fuselage Components Preliminary Design

Building on the analysis performed during the conceptual design phase, further analysis of the aircraft was performed to refine the design. The areas examined included: antenna payload and retraction mechanism. The concepts for each aspect were evaluated a down selection was performed on the basis of the highest scoring concept.

4.2.1 Antenna Payload

The mounting of the antenna on the aircraft is going to be accomplished by a simple airfoil-shaped 3-in. long strut positioned on the center of gravity of the aircraft. Mounted to the rules' minimum of 3 inches, the antenna is not in a position to minimize drag – in order to decrease interference drag, pods are usually placed at least a diameter away from the surface of the aircraft. This aspect of antenna mounting was investigated in some detail – the decrease in interference drag was compared to the increase of trim drag to cancel out the higher moment generated by the drag. As a result of this comparison, it was concluded that the increase in trim drag produced was higher than the decrease in interference drag.

4.2.2 Retraction Mechanism

The implementation of the general concept picked for the payload retraction mechanism deserved a lot of discussion. Because of the payload retraction concept chosen, the fuselage needed to have a large amount of upsweep immediately following the cargo compartment. This was necessary in order to minimize the length of the payload hatch, which negatively affects the torsional stiffness of the fuselage. A step-by-step diagram of the operation of the payload retraction mechanism is presented in Figure 4.8. Having been released, the payload box falls to the ground, forcing the spring-loaded aerodynamic fairing doors of the compartment to split open. As the plane powers away, the five pound box forces the doors to swing out further, letting the plane pass the box through the cutout in the back. As soon as the box is no longer pushing

on the doors of the compartment, they spring back closed. The exact method for restraining the electronics payload container in the fuselage of the aircraft was left to be determined during detailed design.

Figure 4. 8 – Retraction Mechanism Operation Schematic

4.3 Propulsion Preliminary Design

Fabricating on the analysis performed during the conceptual design phase, further analysis of the aircraft was performed to refine the design. The areas examined included: battery selection and motor selection. The concepts for each aspect were evaluated in a comparison matrix and a down selection was performed on the basis of the highest scoring concept.

4.3.1 Battery Selection

The contest rules specify that the propulsion system must be powered by a nickel cadmium battery pack no more than 80 oz in weight. Numerous types and sizes of NiCd batteries were available. Approximately 30% of the rated aircraft cost of most configurations was due to the battery cost, which is directly related to battery weight. Because of this, battery selection heavily drove the design. Choosing a battery that just met the energy and power requirements was vital in fielding a competitive aircraft. Depending on the characteristics and type of NiCd cell used, there are limits to the maximum power and efficiency to the rate of discharge. Research on the characteristics of NiCd cells was conducted to choose the best battery to fulfill both the aircraft's energy and maximum power requirements. The 40amp fuse restriction and the voltage requirements/maximum current capabilities of the available motors were all considered during the search.

Two styles of NiCd cells were investigated in detail, the high capacity Sanyo KR series, and the NiCd cells typically used for electric powered R/C models, the fast charge Sanyo R series. Table 4.1 shows the characteristics of each cell type.

Table 4.4- Battery Cell Comparison

Nicad Cell	mAh	Weight (oz)	Package	mOhm/cell	Amps @ 1.0V	Watts/oz	Watt-hr/oz
KR-1100AAU	1100	0.85	AA	20	10	11.8	1.55
KR-1500AUL	1500	1.09	4/5A	16	13	11.5	1.65
KR-1700AU	1700	1.25	A	14	14	11.4	1.63
N-1250SCR	1250	1.50	4/5sub C	4.5	44	29.6	1.00
RC-2000	2000	2.00	sub C	3.8	53	26.3	1.20
RC-2400	2400	2.15	sub C	3.6	56	25.8	1.34
CP-2400SCR	2400	2.1	sub C	3.6	56	26.5	1.37
CP-1700SCR	1700	1.65	4/5 sub C	4.5	44	26.9	1.24
CP-1300SCR	1300	1.25	½ sub C	6.5	31	24.6	1.25

The fast charge cells are designed to handle high maximum current and therefore are well suited for typical electric aircraft motors. The specific power density of these cells is on the order of 25 Watts/oz. These cells have a specific energy density of approximately 1.2 Watt-Hours/oz. The new Sanyo "CP" series cells have the highest energy density and excellent power density compared to all of the fast charge cells. Table 4.4 shows the different NiCds considered for the design.

The high capacity KR cells were considered because of their higher energy density (1.6 Watt-hours/oz). The compromises in the cell design that give them the high capacity also hurt the cells' internal resistance – affecting their maximum discharge rate. Therefore, the power density is only half that of the fast charge cells, approximately 11 Watts/oz. Unfortunately, most of the design concepts required nearly 600 Watts of peak power to meet the take off constraint and minimum climb requirement, making the high capacity cells unsuitable. NiCd cells delivering power at their maximum rate are not operating efficiently which significantly reduces their delivered energy.

Charge or discharge comparison of batteries is done using the term "C" or "C rate". The term "C" is numerically equivalent to the rated capacity of a cell discharged at the "C" rate will expend its minimum capacity in one hour, while taking only 15 minutes if discharged at a rate of 4Cs. The resistance of the cells is extremely important when one considers that the energy lost to the resistance is mainly converted into heat. With the C discharge rate for the 2003 aircraft approaching the value of 15, the team was extremely

concerned with the cooling of the battery pack – both construction of the pack and its location had to be optimal in order to allow for the best possible air circulation.

Every nickel-cadmium cell or battery has a specific rated capacity, discharge voltage, and effective resistance. Individual cells are rated at 1.2 volts and voltage for batteries are multiples of the individual cell nominal voltage of 1.2 volts. Twelve cells connected in series would result in a 14.4-volt battery. As can be seen, however, the discharge voltage will exceed 1.2 volts for some portion of the discharge period (during the takeoff and climb segments). Most manufacturers rate cell capacity by stating a conservative estimate of the amount of capacity that can be discharged from a relatively new, fully charged cell.

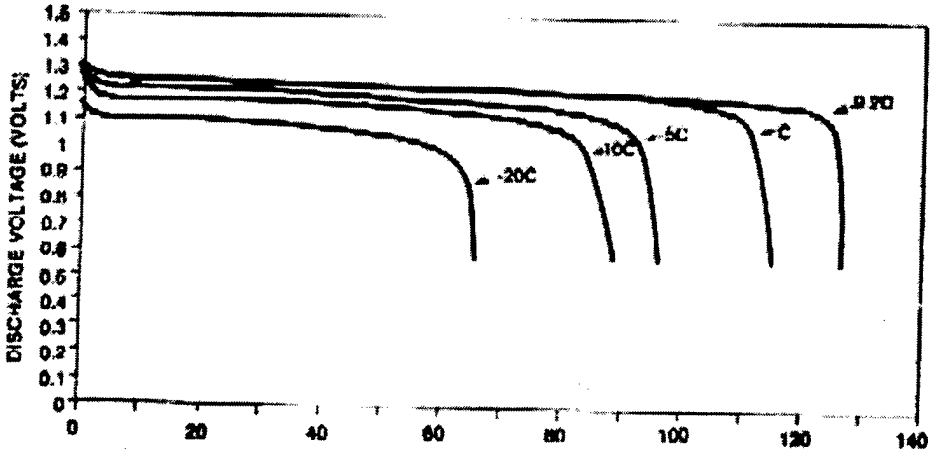

Figure 4.9 – Typical NiCd Discharge Rates

This graph shows that when rates of discharge are increased the available capacity becomes more dependent on the discharge rate. Therefore, at a discharge rate of approximately 15C, the battery efficiency will drop below 80%. When rates of discharge increase, the available capacity decreases as the discharge rate increases. The above trends were also very important for the application in this year's aircraft – working to decrease the C rating would result in higher battery energy available.

Most electric motors available for powering a 12 lb aircraft require 10-15 Volts input instead of the near 100 Volts that a series pack of high capacity cells would be. A combination parallel-series pack was considered to reduce the voltage and increase the current capabilities, but the difficulties in charging and maintaining balance between the cells eliminated this idea.

The energy requirement for the battery was approximately 15 Watt-hours. The aircraft was sized to use 12 CP-1700SCR cells because they provided the highest energy density, allowing the lightest, least costly battery pack. This pack potential is approximately 13.8 volts under load. Factoring the 40amp maximum current allows 600Watts for takeoff and climb. The Sanyo CP-1700SCR cells were chosen because of their high performance, availability, and suitability for the design.

4.3.2. Motor Selection

After initial sizing, it was determined that the aircraft needed a propulsion system able to run on approximately 11-12 NiCd cells, and be capable of handling 550-650 watts to attain the necessary takeoff and climb performance.

To evaluate the performance of the motors available for the aircraft, a Visual Basic subroutine modeling electric motors was written. This model uses motor parameters including Kv (RPM/V), idle current, armature resistance, RPM and thermal limits to calculate output power and efficiency for DC motors. This program was used in conjunction with a propeller model and the mission simulation to compare the various motors offered by Astro Flight and Graupner.

Although during the 2002 DBF year the team intended to use Astro Flight motors, after testing of sample motors from both AstroFlight and Graupner, it was discovered that the Graupner motor (290-8) tested was more efficient than a comparable size AstroFlight motor (Astro 40). Even though the 2003 aircraft carries about half the payload of the 2002 aircraft, it has a much shorter takeoff constraint, which drives up the peak power required. Using the output from the performance calculation program, the peak power requirement for this year's aircraft was determined to be about 90% of that required last year. Learning from the conclusions reached the year before, the team decided to select motors from the Graupner product line.

The power requirements of the design limited our selection to two motors in the Graupner line: the Graupner 290-30 and the Graupner 290-20. Table 4.2 shows the available winding configurations of the two Graupner motors that were considered in the propulsion configuration of the 2003 aircraft. With the battery pack picked from the endurance requirements of the missions flown, the motors were expected to handle 600Watts of electric power input at a voltage of 11 volts that would be provided by a 12 cell CP1700SCR battery pack under load. Generally the motors with lower turn armatures were more efficient at full takeoff power while suffering in efficiency during the relatively low powered cruise. The higher turn motors showed lower efficiency at full power while being much more efficient during cruise. Most of the propulsive energy during the mission is used during cruise so the decision was made to optimize cruise efficiency. Another constraint to consider, however was the fact that a high-winding motor would not be able to function at the current it has to operate at during the takeoff segment.

Table 4.5 – Candidate Motors

Motor	Weight (oz)	Max Watts	RPM/V	Ohms	Idle Current	Gear
Graupner Ultra 920-4 7V	11.3	420	3298	0.016	3.480	5.1:1
Graupner Ultra 920-5 7V	11.3	450	3422	0.02	3.91	5.1:1
Graupner Ultra 930-6 8V	13	500	1975	0.04	2.0	3.7:1
Graupner Ultra 930-7 10V	13	630	1667	0.0463	2.0	3.7:1
Graupner Ultra 1300-6 12V	12	1200	1511	0.052	5.6	1:1

All of the motors come available with various gear reductions. Although the gear reduction reduces the mechanical efficiency of the motor, the larger, lower disk-loading propeller usually makes up the difference in efficiency while also providing significantly higher static thrust for takeoff. Another advantage of the high-diameter propeller is that, with the fuselage being at least 6x6 inches in frontal area, a large propeller is needed to avoid thrust loss due to the effects of fuselage interference. The Graupner motors are capable of producing more power using a gear reduction because they can be run at higher voltages. Because of the above reasons and using numerical output of the motor efficiency program (Figure 4.10, in the end of chapter), the decision was made to use a motor with gear reduction.

The Graupner (Ultra 1300) is capable of running at 1200 watts of input power, but is oversized for this mission. This motor was nonetheless considered in the preliminary motor selection stage as a possible direct-drive solution. The Graupner 920 and 930 motors can operate at power levels up to 800 watts, which is higher than the takeoff power level projected for the aircraft in takeoff. The mission profile calls for short periods at full power for takeoff and climb followed by extended cruise periods well within the normal power limits of both of the Graupner motors. The Graupner 930 motor possesses a comfortable "safety margin" that would allow extra power to be input to the power system in case of the built aircraft having takeoff performance inferior to that of the predictions. The 930 motor is also projected to be very efficient at the cruise level of operation. The 920 motor, although lighter in weight is also smaller, which negatively affects the torque it can output – this torque limitation is something that is quite important during the stringent heavy takeoff segment of the mission. Since the 920 is lighter, it has a smaller magnet, causing the 920 to not have as much peak torque as the larger 930. The 920 motor also has a low "safety margin" when compared to the 930 motor. During the takeoff segment, the 920 motor would be operating at very high power levels. The disadvantage of running the motor at such high power levels is premature erosion of the brushes and

commutator, and loss of efficiency due to increased resistance and demagnetizing of the permanent magnets.

After considering all the alternatives, the team decided to use the 930-6 motor because of the safety margin provided and the high efficiency during cruise. This motor choice provides the aircraft with a good power to weight ratio, high cruise efficiency and improved scoring potential, along with its larger armature spinning causes the 930 produce more torque which is needed to use a large diameter propeller.

The propeller performance model indicated propellers 14 to 17 inches in diameter with 10 to 13 inches of pitch would load the selected motor to the required 550-650 watts. The relatively high pitch of the propeller was chosen because of the aircraft's high cruise speed (60ft/sec). This pitch was a compromise between the advance ratio required for efficient cruise, and for good full throttle takeoff and climb performance. Because of variation in efficiency and power absorption between different propeller manufacturers, the propeller model was calibrated using data gathered from the motor manufacturer and with testing performed with the Graupner 930-6.

The finalized drive system combinations were also evaluated using the MotoCalc software, with the propulsion systems evaluated presented in Table 4.6.

Table 4.6 – Propulsion Systems Evaluated in MotoCalc

Motor	Reduction	Propeller	Max. Efficiency	Weight (g)
1300-6	3.71:1	16x13	40	420
1300-6	1:1	11x6	28	340
1300-6	1:1	12x7	29	340
930-6	3.71:1	16x12	55	370
930-6	3.71:1	17x13	55	370
920-5	5.1:1	14x13	50	320
920-6	5.1:1	16x12	50	320

4.4 Analytical Tools

Several analytical methods were used in design analysis, including tools used by previous Cal Poly DBF teams, and additions in both Visual Basic and Microsoft Excel.

4.4.1 Spreadsheet Application

Throughout the past years of the DBF competition, the performance design of the DBF airplane was analyzed using an interactive spreadsheet program in Microsoft Excel. Although extremely simple, this program provided good indication of the parameters driving the design.

During the summer of 2002, a new performance design program (DBF03) was created from the ground up using the Microsoft Visual Basic programming language. This program used a Microsoft Excel front end similar to that used by the previous version of the design software, but was more powerful and provided a much higher ease of expansion than the previous version. This software simulated the

performance of the aircraft through all the stages of the mission, iteratively calculating thrust, drag and other characteristics of the aircraft performance. For example, DBF02 used a simple approximation formula to calculate takeoff distance. DBF03 iterated through increments of 0.1 second, calculating thrust, drag, lift, power input to the engine and other parameters in order to output an answer with a higher degree of precision.

The program estimated the overall performance of the airplane by combining many specific performance calculations and estimation methods.

- Weight – This estimate was created from weight/area constants that were obtained from weighing model parts created via different traditional RC-model construction methods. Multiplying these weight/area constants by their respective areas created the weight estimate of the airplane.
- Drag – A flat-plate drag estimate was created based on CD estimates and experience compiled by the previous year's DBF teams.
- Thrust –The curve predicting thrust was derived using a combination of two methodologies – using momentum methodology to predict the decline of thrust with increase in forward speed and using static thrust equations from Chuck Gadd's Electric Electric Motor Calculator.(Ref 7).
- Energy accounting – A propulsion system efficiency constant (efficiency in converting electric energy into volts – motor + propeller + drive efficiencies) was used to estimate the amounts of current/energy that will be drawn out of the batteries during the duration of the contest.
- Mission time – This parameter was created by adding together the following separate mission segments: Takeoff, Climb, Turns, Cruising, Landing, Payload Drop. Constant acceleration on takeoff and constant-G turns were assumed to simplify the calculation.
- Cost – A cost estimate was easy to create by simply applying the given rules to the airframe parts, the dimensions of which were estimated by the simulation components described above.
- Mission score – This result was obtained by using the preceding estimates in the context of the competition rules.

The 4 main variables that were systematically modified in order to achieve the highest possible flight score were Airplane Weight, Wing Loading, Aspect Ratio, number of batteries. A load of other assumptions and initial values were used, but those did not vary when trying to select an optimum airplane configuration.

The program DBF03 was the main software package used in the design of the aircraft. This performance estimation program could take as input any of the 7 following mission segments: Accelerate, Climb, Land, Brake, Cruise, Turn180, Pause. The user would then proceed to enter a distance or quantity for each mission and the aircraft parameters (Δ drag, Δ weight, speed, turn G) during the mission. A set of required parameters for the general aircraft to be simulated would also be entered – based on those aircraft and mission parameters the simulation would be run. The program would output a variety of relevant data for each segment, examples of which are listed below:

Energy Used	CL	L/D
Peak Power	Distance in segment	Stall Speed
Battery Efficiency	Energy Left	Total time

A comprehensive set of data was output to show the performance of the aircraft in the entire mission, allowing educated design choices to be made and new designs to be evaluated.

Being written in Visual Basic, the program could be made modular, having different functions and subroutines that would execute the same calculation using data inputs from different sources. For example, the drag calculation functions IDragCalc and PDragCalc needed inputs of current speed, current Cl and a set of general airplane characteristics to calculate drag for any of the 5 mission segments simulated: Accelerate, Climb, Land, Brake, Cruise, Turn180. Because of the program's modularity, new functionality could be added with minimum effort, or effects of different methods of calculation could be compared against each other. Presented in Figure 4.10 is a small portion of the input-output interface of the program.

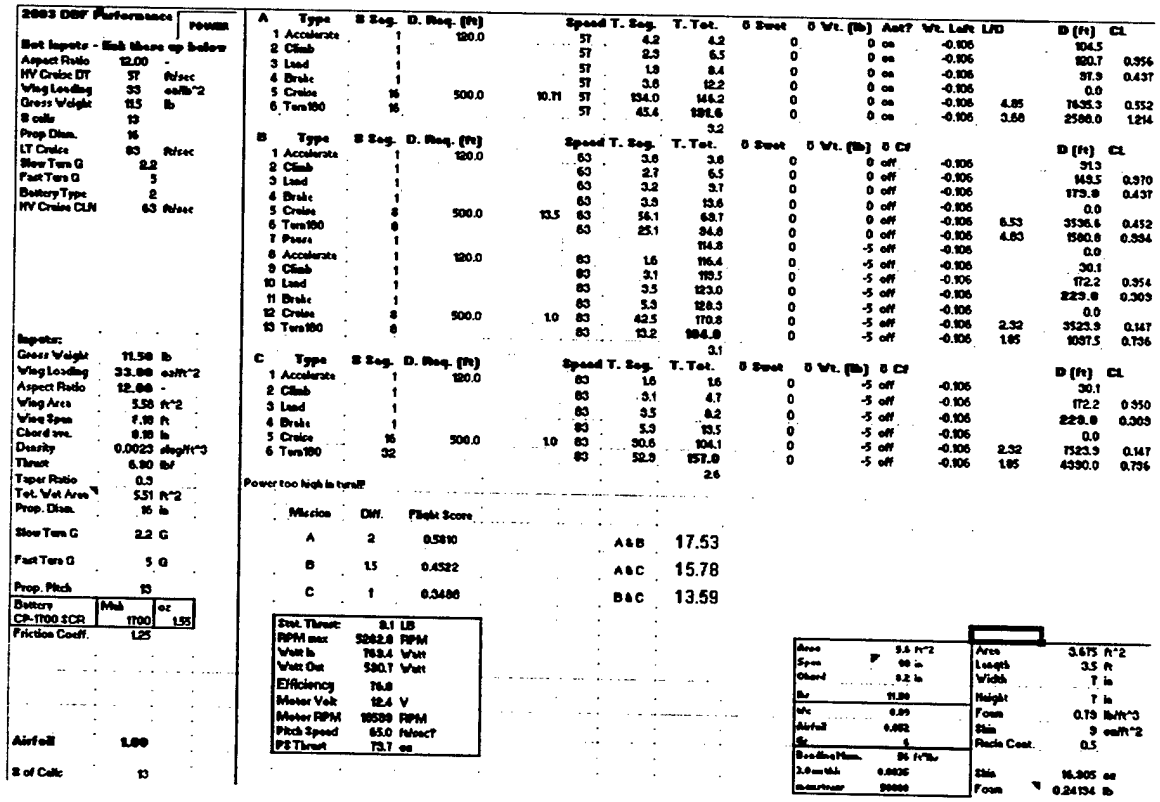

Figure 4.10 – A Small Portion of the Input-Output Interface of DBF03

Besides doing performance estimation for the aircraft, the program evaluated many other variables, all of which affected the preliminary design decisions made.

- Estimation of the effects of aspect ratio on weight (because of the varying strength required from the spar cap) and on wing efficiency (induced drag).
- Estimation of wing root bending moment and output of necessary spar cap thickness.
- Estimation of weight breakdown of the aircraft's components based on configuration.
- Effects of wing planform on efficiency
- Effects of tail area increase vs. fuselage length increase
- Aircraft longitudinal static stability
- Wing lift distribution depending on the planform picked
- Wingtip deflection

The price breakdown output of the spreadsheet enabled the team to visualize which components of the aircraft were of the most impact on the final score, therefore allowing the optimization process to focus on addressing those significant score drivers.

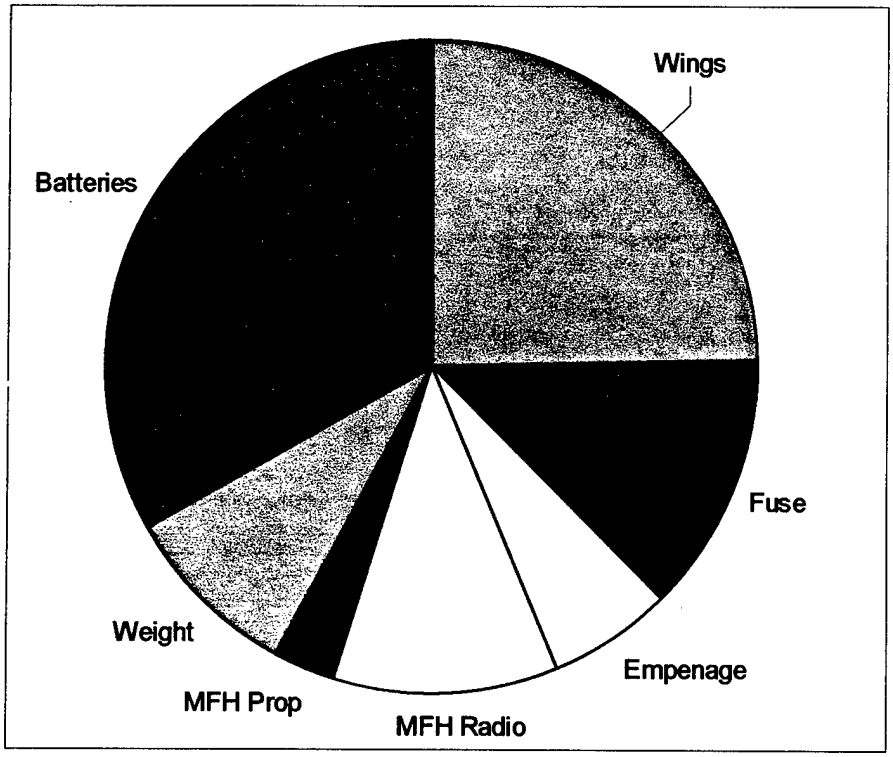

Figure 4.11 – The RAC Component Breakdown

The breakdown of the mission segment time allowed the team to visualize which segments took the longest, and thus allowed us to see the which segment's power needs had most effect on the total mission

energy consumption. This data allowed us to both make a better choice in propeller/motor combination selection (correct pitch speed, power level for the longest task).

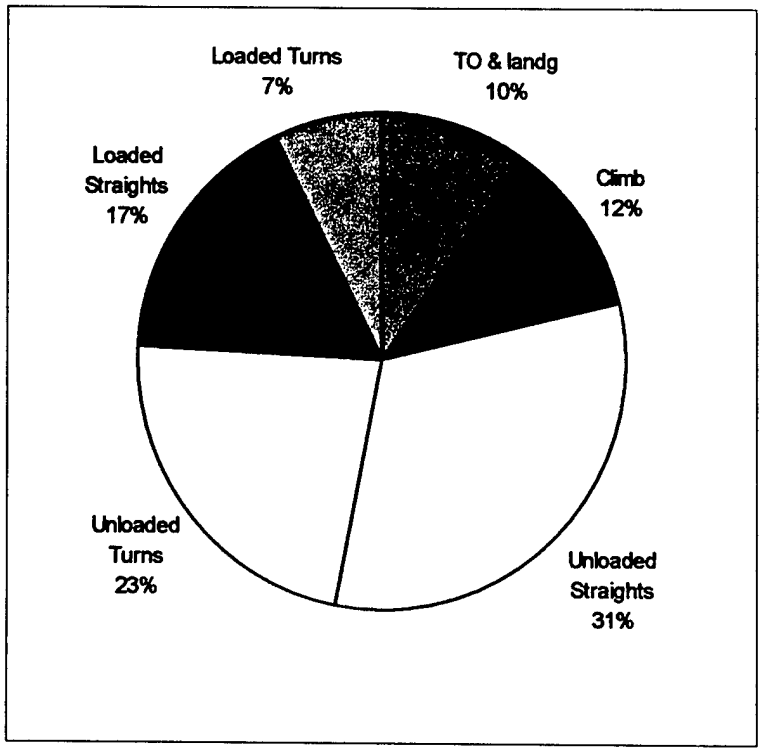

Figure 4.12 – Time Breakdown of Mission A

The simulation program helped to define some of the directions on which the development of the airplane should focus.

4.4.2 Other Simulation Methods

Besides the DBF03 program, the team also created numerical figures of merit in order to choose the design components best suited for this year's mission. After evaluating the combined effects of the characteristics inherent to each design choice with the figures of merit, more educated decisions could be made. Figures of merit were used in the decisions made in/on the following components: Deployment mechanism, general configuration, wing placement, fuselage length, number of engines, landing gear configuration, empennage configuration, materials, wing planform, and aspect ratio.

Many of the tools used in the design process were created by the team members using Visual Basic or in Microsoft Excel. Nearly all the programs were written some time before work on the 02/03 Design/Build/Fly aircraft began and had been already well tested and validated. These programs include an electric motor/ propeller model, an aerodynamic model, a weight estimation spreadsheet, a longitudinal static stability model, takeoff and climb simulation, and a lift distribution spreadsheet. These tools were incorporated

into a 02/03 DBF mission simulation model that included a cost model. To check validity, aircraft with known performance from the 99/02 competition years were also run through the simulation successfully.

One tool not developed by the team members was X-foil, written by Mark Drela of the Massachusetts Institute of Technology. After learning to use X-foil, results from low Reynolds number wind tunnel testing performed at University Illinois Urbana Champaign were compared with data produced by X-foil. At the relatively high Reynolds numbers that this aircraft will fly at, the correlation between test data and predicted performance was excellent. Experience gained with these correlations and the good results obtained with the JA40 airfoil designed using X-foil and flown during the 01/02 DBF contest gave the team confidence in the design tool. The X-foil predictions for the performance of the JA-161 airfoil can be seen in figure 4.9 below.

The MotoCalc electric flight performance prediction program available at www.motocalc.com was also used to evaluate and fine-tune the final propulsions systems configurations output from the VisualBasic software.

4.5 Conclusion

At the end of the preliminary phase, the primary components of the configuration were all sized and placed according to the figures of merit. Based on the scores obtained in the decision matrices, the aerodynamic characteristics of the airplane were defined. The aircraft now sported a high aspect ratio wing with a modified Schuemann planform, and a custom-designed airfoil. The propulsion system was agreed upon and consisted of a Graupner 936, battery pack size of 12 Sanyo CP-1700SCR cells. The fine-tuning of the less general details of the aircraft was left to be performed during the detailed portion of the design process.

5.0 Detailed Design

After all of the preliminary aircraft characteristics had been established, design leading up to the manufacturing of the aircraft could be undertaken. Motor performance characteristics were evaluated and the correct batteries for the propulsion system were selected. With a more definite knowledge of the aircraft configuration and components, the simulation model could be modified to provide a detailed prediction of the mission performance of the completed aircraft. The aircraft center of gravity and control characteristics were calculated, and components were adjusted in order to move the CG to the desired location. The methods by which to secure airframe components together were picked.

5.1 Power System Optimization

The performance of the final selection Graupner 930-6 motor was evaluated in more detail when coupled with the RFM 17x13 propeller. After constructing a detailed solid model of the aircraft, it was discovered that the ground clearance of the 17-inch diameter propeller was not satisfactory – it is possible that during strut compression a ground strike would occur. Because of this, the team investigated lower-diameter propeller solutions, stopping at a 16x13 diameter propeller. Although the efficiency of this propeller is slightly lower, it enables the plane to fly faster and lowers the chance of a ground strike.

The battery pack underwent modification during detailed design. In order to receive maximum power output from the cell bank, a technique termed "cell matching" was used – each cell was selected to have the same exact voltage and resistance before being assembled into a pack. This allowed for better use of every cells' internal capacity and for higher overall energy to be recovered from the battery pack. After being discharge tested, the battery pack performance compared favorably to the spreadsheet predictions.

Some other modifications were made to the standard battery pack design. First off, the battery pack used "end-to-end" soldering as much as possible, thus decreasing unnecessary weight and resistance in the pack – therefore reducing the voltage losses that a high resistance leads to in a high current drain situation. Rather than keeping the standard long battery leads, the connectors were soldered straight onto the battery pack, reducing the pack weight.

5.2 Aircraft Flight Characteristics

A detailed design of the wing was undertaken – relative twist of wing panels was implemented to modify the aircraft's moment coefficient in the pitch axis. The resultant figure below shows that the wing is designed to have a zero-moment coefficient the aircraft's cruise CL of roughly 0.5. This allows for better control authority and trim drag reduction during the longest flight times (cruise section of the mission). The team will avoid induced drag from the fuselage by setting the wing relative to the fuselage such that the fuselage is at a 0° angle of attack during cruise. Figure 5.1 also shows that the moment coefficient at the takeoff lift coefficient is relatively low; this requirement being taken into account during the design of the elevator control surface.

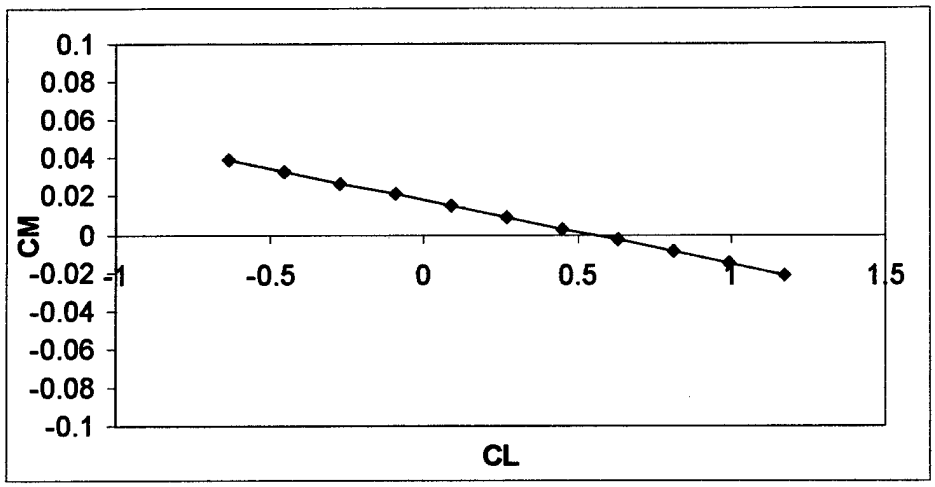

Figure 5.1 – Moment coefficients vs. Cl

5.2 Simulated Aircraft Mission Performance

The performance of the finalized aircraft configuration could be predicted using the DBF03 program, and can be seen in Figure 5.2.

A	Type	# Seg.	D. Req. (ft)	Speed	T. Seg.	T. Tot.	Δ Wt. (lb)	Antenna	D (ft)	CL	kJ used	kJ left	EPower	Vstall.	η Batt.
	Accelerate	1	120.0	57	4.7	4.7	0	On	117.3		3.53	88.28	600.00	38.00	0.8
	Climb	1		57	2.7	7.4	0	On	141.1	0.956	2.03	86.25	600.00		0.8
	Land	1		57	2.0	9.4	0	On	102.5	0.437		86.25			
	Brake	1		57	3.8	13.2	0	On	0.0			86.25			
	Cruise	16	500.0	57	133.3	146.5	0	On	7597.8	0.552	56.33	29.92	375.00		0.8873
	Turn180	16		57	45.4	**191.9**	0	On	2588.0	1.214	25.99	**3.93**	485.00		0.84737
						3.2	minutes					**87.87**	KJ Total Used		
B	**Type**	**# Seg.**	**D. Req. (ft)**	**Speed**	**T. Seg.**	**T. Tot.**	**δ Wt. (lb)**	**Antenna**	**D (ft)**	**CL**	**kJ used**	**kJ left**	**Power**	**Vstall.**	**B. Eff.**
	Accelerate	1	120.0	63	4.2	4.2	0	Off	100.8		3.15	88.65	600.00	37.72	0.8
	Climb	1		63	3.0	7.2	0	Off	164.9	0.970	2.25	86.40	600.00		0.8
	Land	1		63	3.2	10.4	0	Off	**179.8**	0.437		86.40			
	Brake	1		63	3.9	14.3	0	Off	0.0			86.40			
	Cruise	8	500.0	63	55.7	70.0	0	Off	3512.0	0.452	18.67	67.73	305.00		0.91069
	Turn180	8		63	25.1	95.1	0	Off	1580.8	0.994	11.92	55.81	415.00		0.87327
	Pause	1				115.1	-5	Off	0.0			55.81			
	Accelerate	1	120.0	83	1.8	116.9	-5	Off	34.3		1.35	54.46	600.00	29.50	0.8
	Climb	1		83	3.3	120.2	-5	Off	181.1	0.954	2.47	51.98	600.00		0.8
	Land	1		83	3.5	123.7	-5	Off	**229.0**	0.309		51.98			
	Brake	1		83	5.4	129.1	-5	Off	0.0			51.98			
	Cruise	8	500.0	83	42.3	171.4	-5	Off	3509.2	0.147	34.24	17.74	635.00		0.78402
	Turn180	8		83	13.2	**184.6**	-5	Off	1097.5	0.736	15.13	**2.61**	795.00		0.69494
						3.1	minutes					**89.19**KJ Total Used			

Figure 5.2 - finalized aircraft configuration from DBF03

Aircraft Datasheet

School: California Polytechnic State University

Name: Bareback

Aircraft Parameters	
Maximum Length:	4.08 ft
Wing Span:	8.33 ft
Height, Assembled:	2.17 ft
Wing Area:	5.7 ft^2
Aspect Ratio	12 -
Control Volumes	
Vertical tail	0.9 -
Horizontal tail	0.8 -
CL max	-
No Flaps	1.75
10° Flaps	1.9
L/D max	15 -
Maximum ROC	4 ft/sec
Stall Speed	
Empty Weight	29 ft/sec
Gross Weight	38 ft/sec
V Max	85 ft/sec
Takeoff Field Length	
Empty Weight	80 ft
Gross Weight	105 ft

Component Weights		
Component	Weight (oz)	Weight (lb)
Wing	20.8	1.3
Tail	7.2	0.45
Body	17.6	1.1
Gear	16	1
Motor	7.68	0.48
Batteries	20.8	1.3
Nose Gear	4	0.25
Propeller	2	0.125
Reciever/Servos	9.6	0.6
Hardware	3.2	0.2
Total Empty Weight	**108.88** oz	
	6.8 lb	

Systems	
Radio:	Airtronics 7ch Rx
Servos:	Hitec HS-85M
Battery:	12-cell Sanyo S-P1700SCR
Motor:	Graupner Ultra 930-6
Propeller:	RFM 16x13 Carbon Folder
Gear Ratio:	3.7:1 Planetary

Figure 5.3 – Aircraft Datasheet

5.2.1 Center of Gravity Calculation

Using the detailed solid model and the estimated component weights, a center of gravity calculation could be undertaken, in order to enable the design team to locate the aircraft components with respect to each other. This also allowed the team to make some specific design decisions regarding the components yet to be manufactured. For example, the keel could be reinforced in thickness with extra plys of carbon fiber in the location where the landing gear and the wing attachment points were calculated to be. Likewise, the tail strike angle could be calculated with more precision, the position of the landing gear now accurately determined.

Table 5.1 Center of Gravity Calculation

Component	Weight (oz)	Arm (in)	Moment (oz-in)
Wing	20.8	13	270.4
Tail	7.2	43	309.6
Body	17.6	15	264
Gear	16	15	240
Motor	7.68	4	30.72
Batteries	20.8	6	124.8
Nose Gear	4	6.8	27.2
Propeller	2	3.2	6.4
Total Moment (oz-in)			1273.12
Total Weight (oz)			94.08
CG Location (in)			**13.53**

5.3 Rated Aircraft Cost

The rated aircraft cost was calculated using the contest supplied cost model. The total cost was found to be $6,210 dollars.

Table 5.2 – RAC Calculations

Component	Value		Multiplier	Result	WBS Section
Wing Span	8.3	Ft	8	66.4	WBS 1.0
Max Exposed Chord	0.8	Ft	8	6.4	
Control Surfaces	2	#	3	6	
Max Body Length	4.00	Ft	10	40	WBS 2.0
No Act. Cont. Vert. Surf.	0	#	5	0	WBS 3.0
Act. Cont. Vert. Surf.	1	#	10	10	
Horizontal Surfaces	1	#	10	10	
Servo/Controller	6	#	5	30	WBS 4.0
Propellers	1	#	5	5	WBS 5.0
Engine Number	1	#	5	5	
MFHR TOTAL				**178.8**	

Rated Aircraft Cost, $ (Thousands) = (A*MEW + B*REP + C*MFHR)/1000

MEW = 6.8lb REP = 1.3lb

A=$100 B=$1500 C=$20

RAC = (100*6.8+1500*1.3+20*178.8)/1000 = **6.21**

5.4 Wing Strength Calculation

Using the DBF03 program, the wing strength and weight could be easily calculated. Both the bending moment at the root and the thickness of the carbon-fiber spar cap necessary to resist the loads taken during flight were included in this estimate. The results can be seen in Table 5.3.

Table 5.3 – Wing Weight/Spar Cap Thickness Calculations

Area	5.7ft^2	Root Thickness	5.7	in
Span	99Ft	Spar Cap Area	0.0164	in2
Chord	8.3In	Spar Cap Width	4.7	in
		Total Area	373	in2
Aircraft Weight	11.8Lbs			
		Skin	3	oz/ft2
T/c	0.09	Resin Content	0.5	
Airfoil	0.052	Foam	1.6	lb/ft3
G's	6			
		Caps	1.7	Oz
Bending Moment	59Ft*lbs	Skins	8.8	Oz
3.0 oz thickness	0.0035	Foam	6.0	Oz
max stress	50000ksi	Misc	5.5	Oz

Total	**22.0 Oz**
	1.4 Lb

5.5 Aircraft Assembly

Although most of the aircraft components would be secured together using quick plug-in connections, some had to be connected permanently. Since the aircraft could fit into its storage container with these components on, the main landing gear and the wing root were both attached with bolts. In order to lessen the damage that would be taken in a crash, both the wing and the landing gear used nylon bolts that would shear in a crash, reducing the damage taken by the actual airframe components. The V-tail was attached using a quick "pin" connection, utilizing a set of carbon fiber tube plug-ins.

5.6 Payload Extraction Mechanism

Although the preliminary design of the aircraft ended up selecting a method for the retraction of the electronics payload box, the exact method by which the box would be restrained in the fuselage was yet undetermined. The design of this deployment system was one of the most important tasks the team accomplished during detailed design. The goal for the payload deployment system design was simplicity and reliability of operation. The system that resulted from the detailed design stage was a simple one – it consisted of a thin aluminum "plate" in which a Y-shaped pin moved by a servo could slide. This moveable pin would go through tabs on the top of the payload box, and be pulled out for retraction. The schematic of the retraction mechanism can be seen in Figure 5.3.

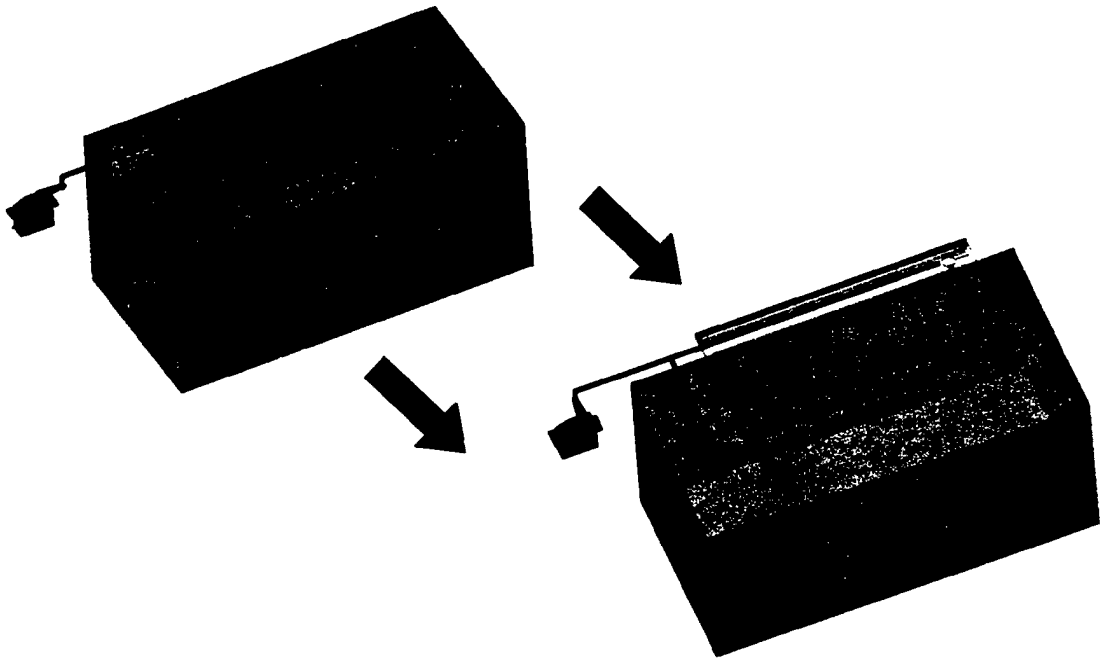

Figure 5.4 – Retraction Mechanism Operation

Once the pin was pulled, the payload box would fall out of the fuselage, pushing the payload doors open as it slid out. The payload doors were designed such that there was a substantial moment arm about the door hinges for the points of contact between the payload box and doors, to insure that the payload doors did not get stuck during deployment. After deployment, the aircraft could be taxied away, with the doors closing via springs upon clearing the payload box.

6.0 Manufacturing Plan and Processes

In constructing the aircraft, different manufacturing techniques were used to manufacture the primary components. While several different concepts were considered, composite construction was used extensively on the aircraft for its relatively high strength and low weight characteristics.

6.1 Manufacturing Concepts

As the team completed the detailed design, the construction method had to be determined. Several construction methods we available at the team's disposal and using figures of merit, the team rated each of the methods. First, the team considered the traditional balsa-hardwood construction with heat shrinking plastic covering such as Monocoat. This method was found to be heavier then other methods and much more rudimentary. Next, the team considered foam core composite construction. This method used a foam core material which was cut or sanded into the desired part geometry and then applied a composite cloth with resin along with heat and pressure. This method was found to have great strength to weight characteristics and moderate durability. The final method considered was a hollow mold composite method in which a negative mold was created, then adding a composite cloth with resin, or using pre-impregnated resin composite (prepreg) material with the application of heat and pressure. This method was found to have the highest strength to weight characteristics, but a much lower durability than the foam core due to lack of a core material providing compression resistance.

6.1.1 Competing Concepts

After thinking about the options, the team found that balsa-hardwood built up construction, has many benefits. It is cheap, requires little skill, and few pieces of equipment. The dilemma is that it would not have the desired strength, especially in shear stress and is heavier than the composite methods therefore eliminated. The hollow-core composite method had many benefits. It is the lightest method, but required a high level of expertise, time, and effort. The part required a negative mold which was laid up into using conventional wet layup techniques or prepregnated composites. Using this method the aircraft would be more prone to compression damage due to handling and assembly which would be more difficult to repair.

6.1.2 Downselect

Due to the high strength to weight ratio, along with simpler manufacturing procedures, the foam-core composite process was selected to be used as the primary construction technique. The foam core method permitted the part to be cut or sanded out of foam and then laid up using the desired orientation and thickness of composite material. The foam core allowed a much quicker final part compared to the hollow-core parts while much stronger parts than that of a balsa build up. If the aircraft were to be mass-produced, the long-term benefits of the hollow-core method would out weigh that of the foam core in particular areas of the aircraft, producing an ultimately lighter aircraft.

6.2 Manufacture of Primary Components

After the manufacturing concepts were narrowed down to a mostly foam-core composite construction, the team drew on experience gained in past years to determine the proper manufacturing techniques for the individual components. Different techniques and materials were utilized depending on the part be manufactured. The team selected this comparatively advanced method of construction despite of its higher level of complexity because of the potential it offers to builders experienced enough to utilize it. Although the method of construction is complex to learn; once learned, it delivers results that are superior in most respects to the alternatives.

6.2.1 Fuselage

Fuselage construction began with the general cross section of the fuselage cut out of white foam using templates generated from a solid model. The entire form was then sanded to bring out the detailed shapes, such as the nose and rear of the payload area tapering to the tail. Once the fuselage was sanded, a cutout was made on the top surface, into which the keel was set into. The entire surface was then filled with a light weight spackle to reduce the number of imperfections on the surface. With this step completed, the fuselage was ready for the composite lay up.

The composite lay up began with a layer of fiberglass, which was laid down on the foam surface "on the 90" after being coated with a light layer of spray adhesive. Next, unidirectional carbon fiber strips were applied to parts of the fuselage that were load-carrying. These parts were the underside of the tail boom, the hinge and cutout lines of the payload doors, and the nose of the aircraft. Over this layer of carbon fiber, two more layers of fiberglass were applied. After these layers were adhered with spray adhesive, the entire fuselage was brushed with epoxy. The excess epoxy was then removed by "squeegeeing" in order to reduce weight. The entire assembly was then cured in an oven at 135 °F for 12 hours. After the curing cycle, the fuselage was further sanded, and the doors were cut out. The fuse was then hollowed out where payload and propulsion items were to be located.

One would think that the keel and shell method of construction compromises strength when compared to a fiberglass fuselage with load-bearing walls. In fact, the choice to not build the fuselage using a construction with load-bearing walls was made because of the big hole that was to be cut out of the fuselage. The doors would have seriously compromised the structural integrity of a fuselage built without a load-bearing keel. Another advantage of the keel-shell configuration is that it is much lighter and easier to modify, making it more aerodynamic therefore giving the airplane higher performance.

6.2.2 Wing

Due to the fact that the wing must be able to fit into the 4'x2'x1' shipping container, the team decided that the wing should be broken into three pieces, a 2 foot center section that will have two 3 foot tip panels. The tip panels are to be adjoined with the center section with a solid joiner tube comprised of a 3/8" OD carbon tube that is to be inserted into the 3/8 ID wrapped carbon tube. The use of ribs and sub-ribs made of ¼" aircraft plywood at the faces of both the adjoining surfaces of the wing panels and center of tip panels will

allow the transfer of flight loads from the wing into the hollow-wrapped carbon tubes and the solid carbon joiner tubes. The joiner tube will not only carry the flight bending load of the wing, but also allow quick and easy assembly of the wing panels onto the aircraft.

Then the wing will be manufactured using standard vacuum bag foam core construction, wrapping a foam core with thin sheets of fiberglass and layers of carbon fiber arranged in the spanwise direction to act as the spar cap along with the carbon joiner tubes. Unidirectional carbon fiber will be placed on the quarter chord to resist bending moment in the wing. The wing core will be constructed out of 2.3 lb density white spyder foam, commonly used for surfboard cores.

A unidirectional carbon fiber spar cap laid up on top of the foam core will take up the bending loads in the tip panels. The direction of the fibers in the spar cap will be placed from the root to the tip of the wing because this is the direction of the bending force and the fibers only have strength lengthwise. The fiberglass has fibers placed ninety degrees to each other and will be placed at a forty-five degree angle with respect to the leading edge of the wing. The fiberglass will provide strength for the wing in torsion.

After the carbon fiber and fiberglass are attached with epoxy, the wing is placed in a vacuum bag. The vacuum bag is very convenient. It provides uniform pressure around the part while curing holding everything together and producing consistent parts.

6.2.3 Tail

The tails were constructed in the same manner as the wing. Again, the tail must be detached from the fuselage to fit inside the shipping container utilizing the the plug-in approach as described with the wing. The tail will plug together with the keel using carbon fiber joiner tubes.

The tail consists of a foam core, with carbon fiber spar caps, a fiberglass skin. The cores were cut out of spyder-foam, using templates created from the solid model program. The skin consists of one layer of two-ounce fiberglass. The spar caps were constructed out of two layers of unidirectional carbon fiber. Mylars were used to achieve a smooth surface finish, and to transfer the paint pattern to the tail. The paint pattern was selected to provide pilot visibility. After the tail is laid-up, it is vacuum bagged and cured in the oven for the prescribed curing cycle.

When the basic construction is completed, the control surface and spars are placed. The control surfaces were controlled by a servo, which was placed in a cavity dug out of the lower surface of the tail. Wires were run through the wing up to the servo. To construct the actual control surface, a cut was made in the fiberglass skin from the underside of the tail, up to the surface of fiberglass. This allowed the fiberglass to serve as the hinge for the control surface, eliminating additional complexity. The servo attachment was located at the heel of the control surface. The wires connected from the receiver to the servo were run through the fuselage.

6.2.4 Keel

Since the keel carries most, if not all, of the bending load in the fuselage, extra care was taken with its construction. Rohacell ® foam was cut into the shape of the keel. It was treated with a wet lay up of several layers of both uni and bi-directional carbon fiber, to provide stiffness and strength. After vacuum bagging and curing in the oven for the prescribed cycle, the keel was ground to the final dimensions. The engine mount was created in the same manner, and then attached using more Rohacell ® foam and carbon fiber. The entire assembly was then placed in the fuselage.

6.2.5 Landing Gear

The landing gear was constructed using a dry composite lay up. The landing gear went through several iterations, and the final gear was created using 30 layers of prepregnated unidirectional carbon fiber, placed at both 90 and 45 degree orientations. The gear was vacuum bagged over the gear form before being cured in the oven. After the cure was complete, the landing gear was ground to its final dimensions, and holes were drilled into the mounting part to attach it to the keel. The tires were attached using collets and 5/16" axles.

6.2.6 Release Mechanism

The release mechanism construction began with the fuselage. The doors were cut out of the fuselage and shaped to properly fit the payload. Additional fiberglass and carbon fiber was applied to strengthen the doors. The interior of the payload area was hollowed out, and further smoothed to provide a proper fit for the payload. The mounting plate was attached to the keel, and the servo was placed in the rear end of the payload area. The servo could be freely moved in the tail and could be used to fine-balance the aircraft.

6.3 Manufacturing Milestone Chart

When building the aircraft, it was not unusual to have several components under construction at the same time. The primary difficulty in scheduling the construction, especially for the composite materials, was the difference in curing cycles for the different materials used. Because of this constraint, it was vital certain parts were constructed in the correct order. Figure 6.1 shows the manufacturing milestone chart illustrating the scheduled event timings.

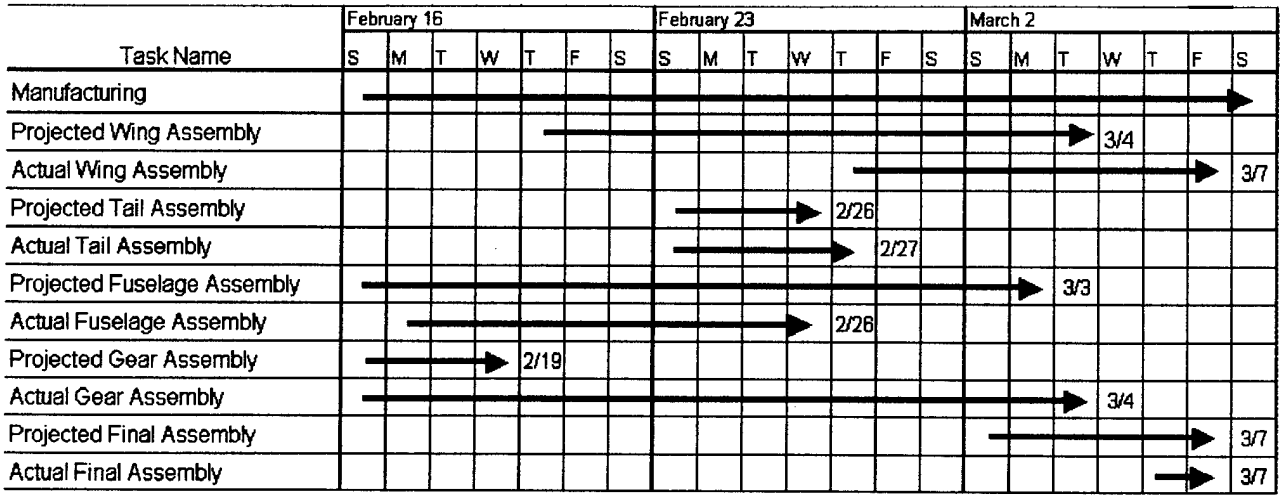

Figure 6.1 – Manufacturing Milestone Chart

7.0 Testing Plan

When designing the aircraft, several factors remained unknown, including structural capabilities and proper manufacturing techniques. By testing components before and after final installation, the aircraft's final configuration was confirmed to be strong enough to withstand the design loads, and controllable enough to fly the selected missions.

7.1 Testing Objectives

The static tests conducted on the components as well as the full aircraft confirmed the structure was capable of handling the design loads. The testing processes also afford the team opportunities to test the ease of assembly for the aircraft, and helped improve the manufacturing techniques used for the components. The dynamic testing will help gain valuable experience relating to the real-life handling qualities of aircraft, as well as gain pilot experience. Overall, the testing allowed the team to ensure the aircraft was fit for competition, and functioned in the way that was expected. It also allowed for validations of the assumptions made in the early stages of the design.

7.2 Testing Schedule

In order to ensure all the required testing was completed before the competition, a testing schedule was created. The schedule allotted time for general testing of components, static testing of the entire configuration, and dynamic, or flight, testing of the final aircraft.

7.2.1. General Testing

The testing schedule was largely dictated by the manufacturing schedule, since components were tested as they were produced. Table 7.1 shows the basic checklist used to ensure uniform testing for each component.

Table 7.1- Testing Check List

Testing Check List		
Component		
	Pass	Not Pass
Dimensions Surface defects		
Stresses (if applicable)		
Torsion Bending Normal Axial		

The actual testing was conducted by a combination of visual inspection and force application. The surfaces and dimensions were visually inspected for any problems that might cause undesirable effects such

as stress concentrations. The stress testing was done by placing predetermined weights on the components in such a way as to produce torsion, bending, normal or axial stress, depending on the component being tested. The weights used were chosen in such a way to simulate the maximum design load the given component would have to withstand. Yielding was taken as the criteria for failure – even small plastic deformations would cause a part to fail the stress test. Since fiber reinforced composites do not generally allow for a large plastic deformation before yielding, this was a good estimate of the maximum strength of the parts manufactured.

Due to the large amount of composite construction used on the aircraft, surface defects such as de-lamination were important indicators of weak components. In some cases, such as the landing gear, having surface de-lamination caused a part to fail.

Another component of the aircraft that had to be tested extensively was the engine. Its testing cycle was dictated primarily by its arrival date. Before mounting the engine on the aircraft, its static thrust was tested, to ensure our initial assumptions were reasonable.

7.2.2 Static and Dynamic Testing

In order to better organize the time allotted for testing, a schedule was drawn up. Figure 7.2 shows the static testing schedule, which was largely adhered to.

Table 7.2- Static Testing Schedule

First Round 3/01	Horizontal Tail	
	Vertical Tail	
	Fuselage (foam)	
	keel	
	Landing Gear	
Second Round 3/02	Fuselage (full)	
	Cargo Doors	
	Wing	
Third Round 3/03	Connections	
	Release Mechanism	

After all the static testing was completed, the separate components were assembled for a final static test. At the time of writing, the entire model has not been flight tested because of a delay encountered with motor shipment. Once the motors arrive, the entire model will be flight tested – this will allow for "real-life" testing of the deployment system, as well as testing of controllability of the aircraft. This process was also scheduled, as shown in Figure 7.3.

Table 7.3 – Dynamic Testing Schedule

Test Flight #1 TBA	Takeoff Requirement Release Mechanism Release Mechanism (2) Correct Flight Path Landing Visual Inspection	
Test Flight #2 TBA	Takeoff Requirement Release Mechanism Release Mechanism (2) Correct Flight Path Landing Visual Inspection	
Test Flight #3 TBA	Takeoff Requirement Release Mechanism Release Mechanism (2) Correct Flight Path Landing Visual Inspection	

7.2.3 Flight Testing

After each test flight the aircraft will be visually inspected for any surface damage or weak parts. The deployment system will be tested sufficiently to ensure the mechanism works reliably. The flight path used in the test flights will be the same as that used in the competition.

7.3 Testing Results

While the testing the individual components and the full aircraft, several discoveries were made. The component testing showed problems with pre-preg carbon construction, while the full aircraft static testing showed no problems.

7.3.1 Component Static Testing Results

No major problems were encountered during the testing phase. Several lessons were learned, mainly dealing with the composite construction methods employed. Several landing gears failed their initial test due to delamination before the proper pressure and temperature levels for curing were determined. The gear was fairly strong in bending, but the sections that delaminated plastically deformed during the normal stress test. After the correct curing procedure was determined, the component passed all the stress tests, and was ready to be installed on the aircraft.

Test Flight #1 TBA	Takeoff Requirement Release Mechanism Release Mechanism (2) Correct Flight Path Landing Visual Inspection	
Test Flight #2 TBA	Takeoff Requirement Release Mechanism Release Mechanism (2) Correct Flight Path Landing Visual Inspection	
Test Flight #3 TBA	Takeoff Requirement Release Mechanism Release Mechanism (2) Correct Flight Path Landing Visual Inspection	

Figure 7.3 – Dynamic Testing Schedule

7.2.3 Flight Testing

After each test flight the aircraft will be visually inspected for any surface damage or weak parts. The deployment system will be tested sufficiently to ensure the mechanism works reliably. The flight path used in the test flights will be the same as that used in the competition.

7.3 Testing Results

While the testing the individual components and the full aircraft, several discoveries were made. The component testing showed problems with pre-preg carbon construction, while the full aircraft static testing showed no problems.

7.3.1 Component Static Testing Results

No major problems were encountered during the testing phase. Several lessons were learned, mainly dealing with the composite construction methods employed. Several landing gears failed their initial test due to delamination before the proper pressure and temperature levels for curing were determined. The gear was fairly strong in bending, but the sections that delaminated plastically deformed during the normal stress test. After the correct curing procedure was determined, the component passed all the stress tests, and was ready to be installed on the aircraft.

Another part that experienced problems due to construction was the horizontal tail. The tail's fiberglass coating had not properly cured the first time it was put in the oven. This caused its ability to take bending stresses to be compromised to such a degree that it was no longer usable. In order to test the sample structure, the unusable tail was destructively tested for the normal stress case. This test showed that even the weakened tail was able to withstand the design normal load. This test is illustrated in the photo shown in Figure 7.4 below:

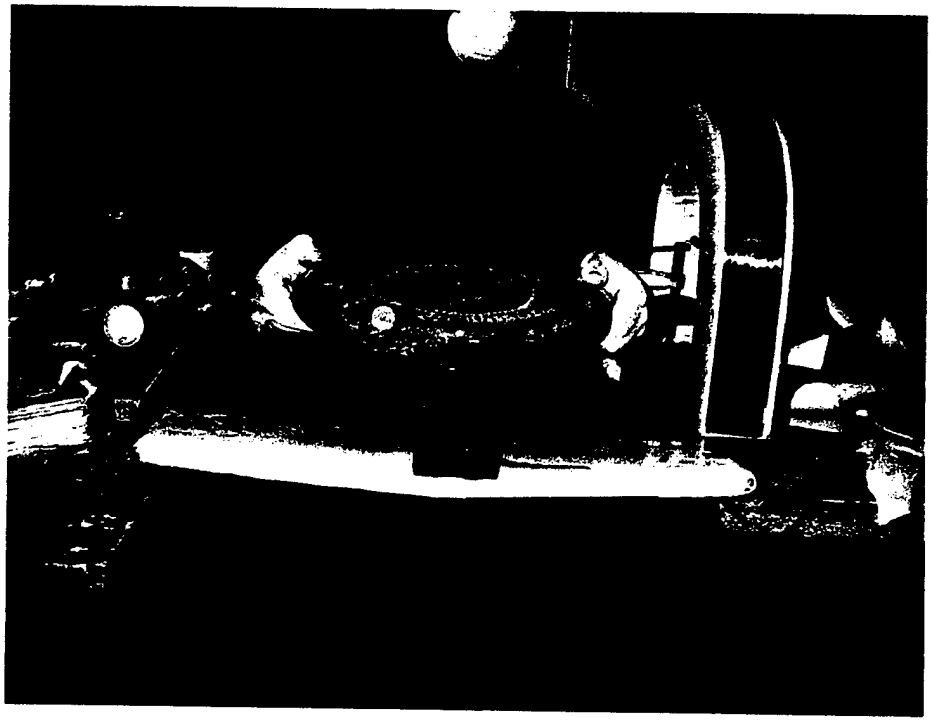

Figure 7.1 – Destructive Testing of the Tail

Other than these two components, no other problems were encountered. Due to the composite construction used, all the components were strong enough to withstand the design loads. The engine testing proved our original assumptions were reasonable. With all the parts statically tested, they were assembled into the final configuration for the full aircraft static and dynamic tests.

7.3.2 Completed Aircraft Static Testing Results

The full aircraft static test was conducted in much the same way as the individual components' static tests. One of the most important tests was the wing-tip test that the aircraft is expected to pass after assembly at the competition. Special attention was paid to any vital connectors, such as wing plugs, tail plugs, and servo connections. The aircraft was loaded to the maximum design load, and inspected for signs of stress or strain. Due to the careful component testing, none were found.

References

1. Raymer, Daniel P., Aircraft Design: A Conceptual Approach, AIAA Education Series, 2001.

2. Lennon, Andy. Basics of R/C Model Aircraft Design: Practical Techniques for Building Better Models, Motorbooks International, September 1996.

3. Abbott, Ira H., and Von Doenhoff, Albert E., *Theory of Wing Sections* Dover editions, 1956.

4. Simons, Martin. *Model Aircraft Aerodynamics,* Motorbooks International, 2000.

5. Randolph, Randy. *R/C Airplane Building Techniques* Motorbooks International, 1997.

6. Roskam, Jan. *Airplane Design Part I : Preliminary Sizing of Airplanes*, DAR Corporation; June 1989.

7. http://www.csd.net/~cgadd/eflight/calcs_motortest.htm

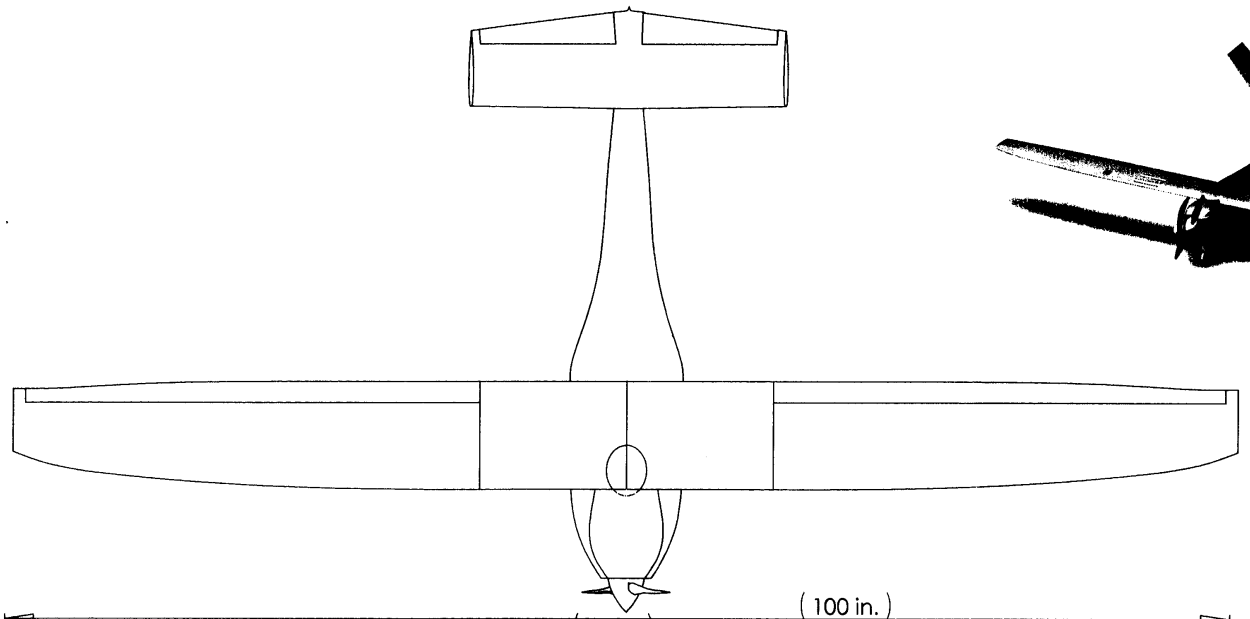

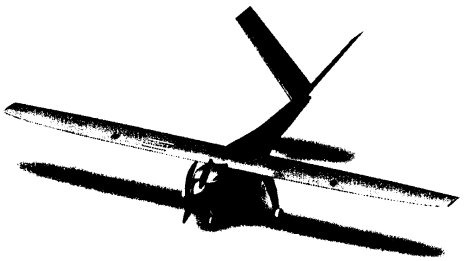

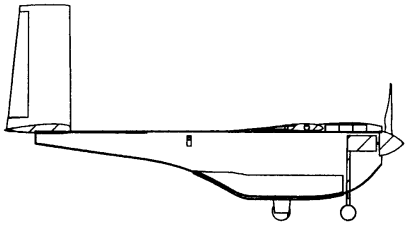

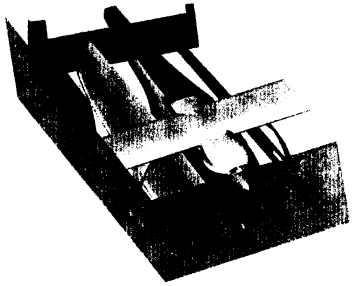

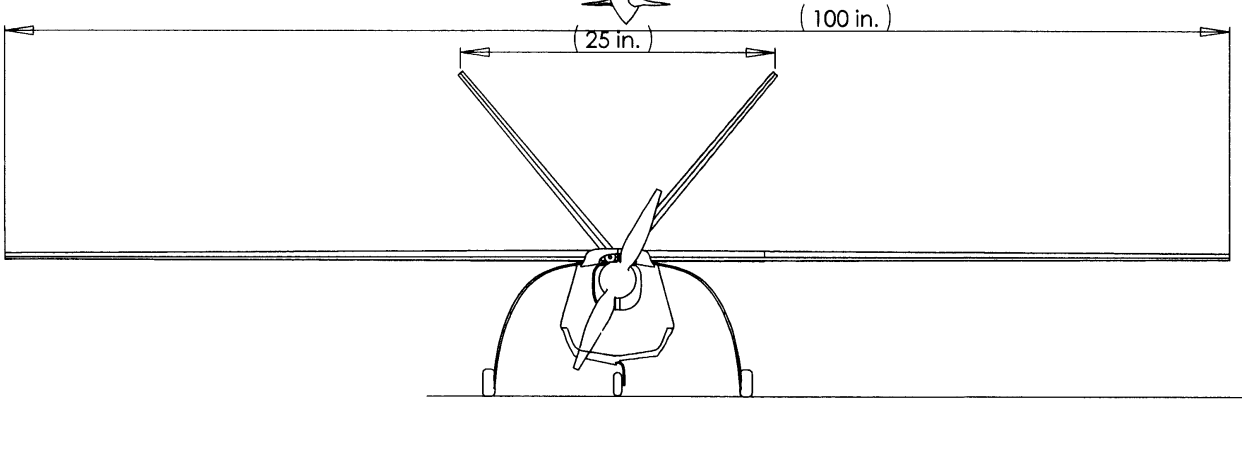

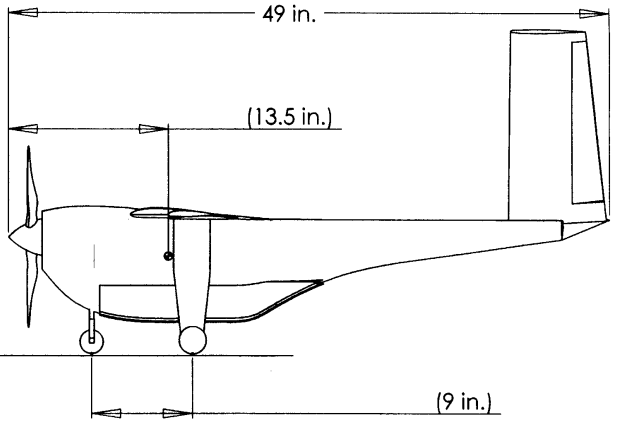

olidWorks Educational License
Instructional Use Only

	DATE	NAME
DRAWN	03/01/03	Gene Gisin
CHECKED	03/01/03	Matt McCue
COMMENTS:		

Cal Poly DBF Team

TITLE: "Bareback"

SIZE B | DWG. NO. 1 | REV

SCALE: 1:10 WEIGHT: SHEET 1 OF 1

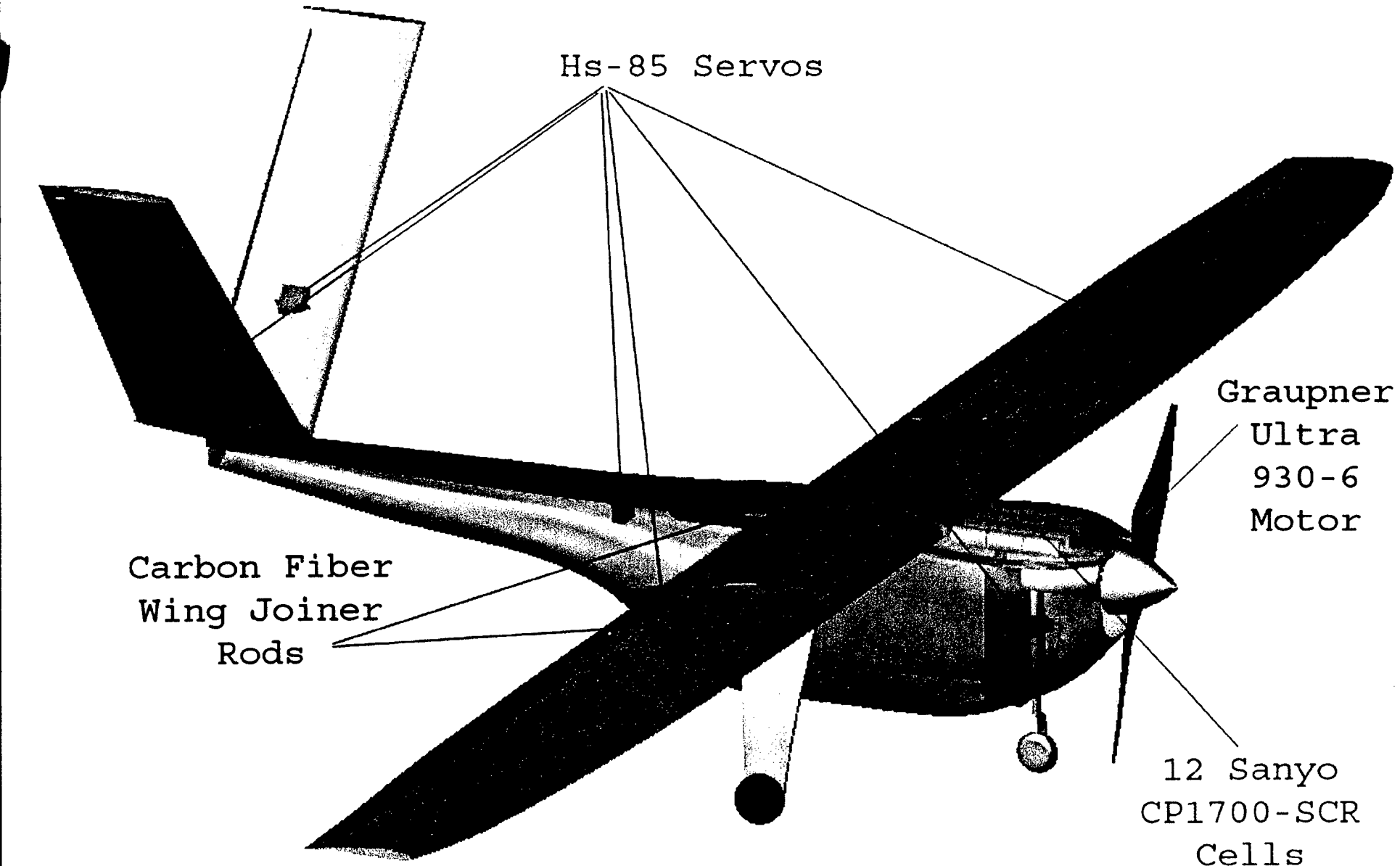
Hs-85 Servos
Graupner
Ultra
930-6
Motor
Carbon Fiber
Wing Joiner
Rods
12 Sanyo
CP1700-SCR
Cells

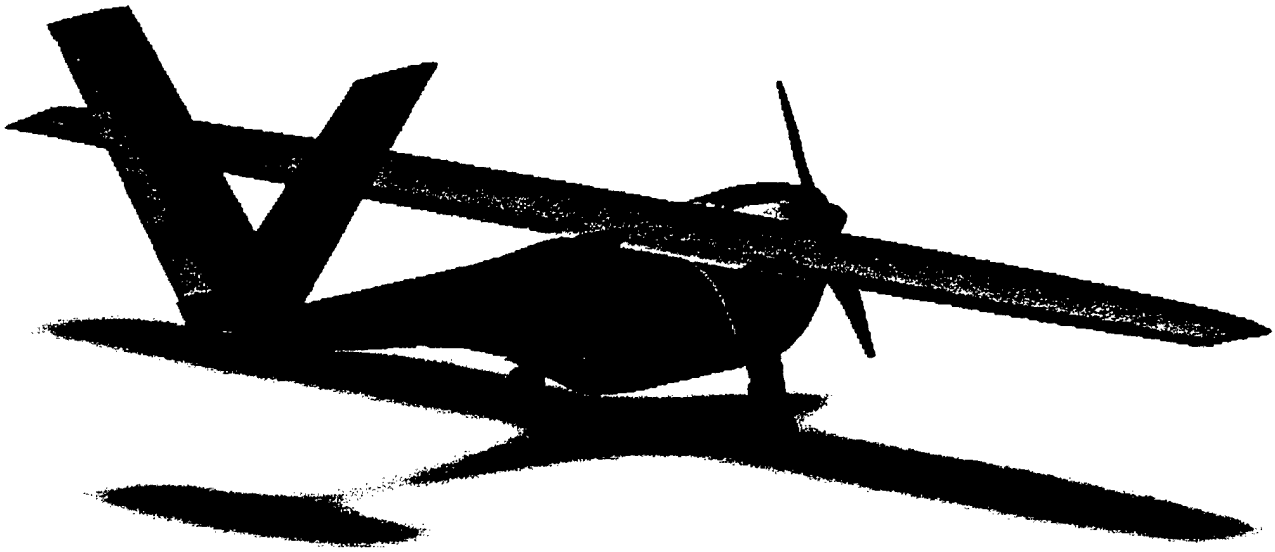

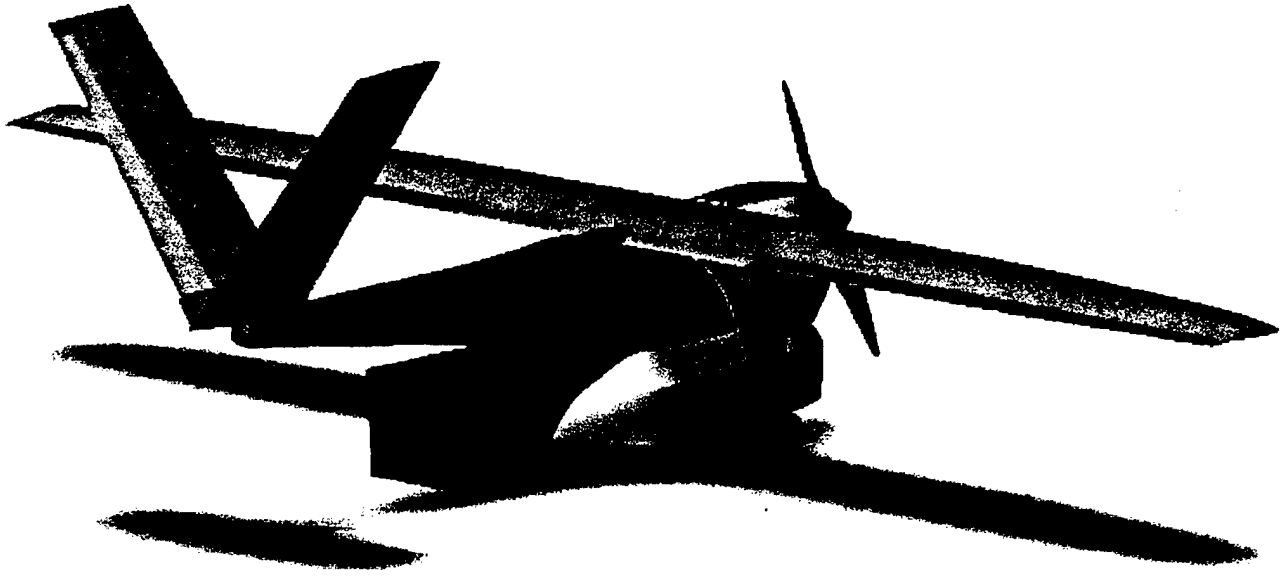

AIAA / CESSNA / ONR Student Design / Build / Fly Competition 2002/03

Università degli studi di Roma "La Sapienza"

Design Report :

[redacted]

The Flying Centurions

... saggi, tranquilli e combattivi

Table of Contents

1	**Executive Summary**	pag 1
1.1	Introduction	pag 1
1.2	Conceptual Design	pag 1
1.3	Preliminary Design	pag 1
1.4	Detail design	pag 2
1.5	Manufacturing Plan	pag 2
1.6	Testing Plan	pag 2
2	**Management Summary**	pag 3
2.1	Team Organization	pag 3
2.1.1	*The first step: Organization and "Pre-Conceptual" Design*	*pag 3*
2.1.2	*Driving lines in Team Management*	pag 3
2.1.3	*Team Architecture*	pag 3
2.1.4	*Design Area*	pag 4
2.1.5	*Building Area*	pag 4
2.1.6	*Testing Area*	pag 4
2.1.7	*Report Area*	pag 4
2.1.8	*Logistic Area*	pag 4
2.2	Milestone Chart	pag 5
3	**Conceptual Design**	pag 7
3.1	Problem Statement	pag 7
3.2	Design Parameters	pag 7
3.3	Mission Concepts	pag 7
3.4	Alternative Configuration Concepts	pag 8
3.4.1	*Aircraft Configuration*	pag 8
3.4.2	*Wing Configuration*	pag 9
3.4.3	*Fuselage Configuration*	pag 12
3.4.4	*Tail onfiguration*	pag 13
3.4.5	*Motor and Propeller position*	pag 14
3.4.6	*Lancding gear configuration*	pag 16
3.4.7	*Structural Configuration*	pag 17
3.5	FOMs Analysis Results	pag 19
4	**Preliminary Design**	pag 20
4.1	Introduction	pag 20
4.2	First Sizing Trade Studies	pag 20
4.2.1	*Main Assumptions*	pag 20
4.2.2	*Known Parameters*	pag 22
4.2.3	*Major Design Parameters*	pag 22
4.2.4	*Standard Mission*	pag 22
4.2.5	*Cost Function*	pag 23
4.2.6	*Analysis Methods*	pag 23

4.2.7 Analysis Results pag 25
4.3 Fine Trade Studies and design Optimisation pag 25
4.3.1 Aerodynamic Considerations pag 25
4.3.2 Propulsion Analysis pag 28
4.3.3 Performances & Flight Mechanics pag 29
4.3.4 Structural Analysis pag 33
5 Detail Design pag 39
5.1 Introduction pag 39
5.2 Flight Dynamic and Control pag 39
5.2.1 Control Surfaces pag 39
5.2.2 Handling Qualities pag 40
5.3 Structures pag 43
5.3.1 Fuselage Structural Details pag 43
5.3.2 Wing Structural Details pag 44
5.3.3 Tail Structural Details pag 44
5.3.4 Landing Gear Structural Details pag 44
5.3.5 Radome Structural Details pag 45
5.4 Propulsion System pag 45
5.5 Final Aircraft Table pag 45
5.6 Rated Aircraft Cost pag 46
5.7 Drawing Package pag 46
6 Manufacturing Plan and Processes pag 51
6.1 Manufacturing Processes Selecte pag 51
6.1.1 Fuselage Manufacturing and Tooling pag 511
6.1.2 Wing Manufacturing and Tooling pag 51
6.1.3 Tail Manufacturing and Tooling pag 51
6.1.4 Landing Gear Manufacturing and Tooling pag 51
6.2 Analytic Methods pag 51
6.3 Manufacturing Milestone Chart pag 52
7 Testing Plan pag 53
7.1 Structural Tests pag 53
7.1.1 Testing ASTM standard specimen pag 54
7.1.2 Static and Dinamic Wing Tests pag 54
7.2 Aerodynamic Tests pag 55
7.2.1 Tests on the semi-model pag 55
7.2.2 Testing the propeller mounted on the fuselage pag 55
7.3 Propulsive Tests pag 56
7.3.1 Instruments and Tests Organization pag 56
7.3.2 Measurements Procedures and Results pag 56
7.4 Flight –Tests pag 57

1 Executive Summary

1.1 Introduction

This report documents the complete study carried out by the Flying Centurions team from University of Rome "La Sapienza", to realize the UAV Galileo IV for attending to the AIAA/Cessna/ONR Student Deign/Build/Flying 2003 Competition. Beginning by accurately analyze the contest rules, we tried to develop a design able to best meet mission requirements and to be competitive in the final phase of the contest, i.e. the fly-off held at Webster Field in April 2003. The rules for this edition keep the same layout of previous year, regarding the scoring and the RAC calculation scheme, but include different kinds of missions. The aim of the team, dealing with this new experience, was to improve the results achieved in the previous editions of the contest. To reach this target, we focused the main attention to improve those aspects of the design process that penalized teams from our University during previous editions. We sought from the beginning to optimise the RAC function and to give our new aircraft the proper aerodynamic, structural and propulsive solutions. Particular attention was paid to the model assembly procedure, because the need of a fast way to mount the plane is the real new for this year.

1.2 Conceptual Design

At the beginning of the design process, four main areas of interest were identified. The team was split into four design groups: each one performed a study aimed to identify the configuration with could gain the highest potential score. A first group (aerodynamic) attended to the aerodynamic branch of the design; a second one (flight mechanics) developed methods to predict aircraft performances, and to find a way to optimize them. A third one (structures) focused its attention to the structural solutions and the problems related to the assembly; the fourth one (propulsion) studied how to give the plane the proper propulsive system. For each choice each group would deal with, figures of merit had been introduced. This is a way to take into account how each option affects the final score and how this option can be implemented. After each group had proposed the solutions it judged the best from its own point of view, brainstorming within the groups' leader allowed us to define the final aircraft configuration, tooling and material to be used for manufacturing, and the kind of propulsive scheme. Aerodynamics and Flight Mechanics considerations had been esteemed the most important for shaping the configuration (monoplane with high wing, axis symmetric fuselage and H tail), while structural and manufacturing requirements drove the selection of self-made composite materials to build nearly all the structural components. The propulsive group selected the motors number (one), gave a rough estimation of the number of cells needed and proposed the location of each component of the propulsive subsystem.

1.3 Preliminary Design

The first objective of this stage of the design process was the implementation of an optimization program which could lead to size the configuration able to reach the maximum total score. The study started by summarizing configuration data previously obtained. Then, we had to take into account each phase of the possible flight missions. A "standard mission" was identified to this purpose. Then we identified the main design parameters we wanted to be determined by running this program, and a broad range of possible

variation for them (wing airfoil, wing area, cruise speed, turn loading factor, cells number, propulsive subsystem). These parameters, input in the program with a large range of values, were linked to the global performances of the virtual plane, and to the global score it could reach performing the standard mission. By running the program, we could narrow the range of variation of design parameters, but we could not identify yet a unique solution for each of them. So, groups had to focus their attention upon the possible choices left, trying to extrapolate the best one. The aerodynamic group studied different airfoil types and found out an approximation of lift and drag for each surface and for the whole aircraft. The flight mechanics group studied the static stability and developed models to predict the flight performances of the aircraft. The structural group used analytical and numerical methods to find the stress field in the main components and sized them, selecting for each the most suiting material. The propulsive group selected the motor model, the most opportune reduction and a set of propellers. At this point the first components were sized, and we could find out the performances of the plane in term of range, speed in the various flight phases and mission time. A 1:2 scale moke-up was carried out to visualize the choices and to take familiarity with the whole project. We could produce the first CAD model.

1.4 Detail design

After the preliminary sizing, we led a detail analysis of each component, each subsystem, and their integration in the global project. So doing we became able to build the first prototype to test the choices we had maiden. The aerodynamics and flight mechanics group studied the dynamic stability, by calculating the stability derivatives. A more precise estimation of the aerodynamic loads allowed sizing the servo controls and their location. The structural group completed the sizing of all the parts; particularly it defined the payload release system and the assembly. Then the locations of receiver and cables were defined. A final solution for the manufacturing process was identified. By using opportune software, the propulsive group tested several propellers and cells with the motor selected. At the end of this study, we could produce final CAD drawings of each component of Galileo IV, and the assembly schemes.

1.5 Manufacturing Process

The production phase was the benchmark to value the goodness of the choices carried out. In some cases building difficulties or non-satisfying results (most of all about the preparation of composite materials) led us to introduce little changes on the earlier design. In other cases we felt the need of further studies on some components or alternative solutions.

1.6 Testing Sessions

To check our choices, and to identify the way to optimize the whole design, experimental analyses were performed in each design area. Mechanical tests on standard specimens allowed us to evaluate the properties of the material to be used. Testing entire half-wings till their failure provided us the confidence about their actual loading capabilities. Wind tunnel tests of a semi-model 1:2 scaled gave the whole aircraft polar drag and important indications on the shape of the aerodynamic fairings of the fuselage. At last, the propulsive group tested the motor-propeller set, obtaining experimental data on thrust at various flight speeds. Finally, flight test have been planned to indicate the way for further optimization.

2 Management Summary

2.1 Team Organization

2.1.1 The first step: organization and "pre-conceptual" design

When our team was born, at the end of July 2002, it was immediately clear it would have to solve two main problems: to organise into an engineering team a big number of students (there were 58 of us at the beginning!) and to supply them with enough funds, tools and items to reach the targets. More over, our main suppliers, the Rector of University of Rome La Sapienza, wanted us to prepare a didactical project, which could engage so many students. Only in this way it could be possible to receive the aid of University to carry on a new experience in DBF competition. The first step of the organization process was to split the team into 5 littler groups. The work they had to do along the summer was mainly didactical: the students with previous DBF experience had to lead the junior ones into the major areas (technical an logistical) the competition affects. The objective of this session was to perform a pre-conceptual design: each group had to take confidence with the rules and to propose one or more possible concepts.

2.1.2 Driving lines in team management

At the end of this first stage, back home from holiday, we reorganized the entire team trying to realize a well-ordered structure. We knew that to design, build and fly an aircraft best fitting the requirements of the competition it is necessary to coordinate the work of many people, in such a manner that any decision affects the work of anyone. In this way, a group of students can produce what no one within them could on his own: this is the aspect of a teamwork we have learned to appreciate most of all. But it is quite evident that this work has to be properly coordinated. So, we organized the architecture of the team on the basis of the following principles of management: 1: to clearly identify people who would have the responsibility of leading the team along the design process; in particular, there should be a person, the team manager, able to make decision, schedule work-packages, assign tasks and check for they are performed. 2: tasks must be shared to specialized groups, each one with its own leader; the latter should play inside his group the same role the team manager plays within the team. 3: the authority should be delegated to the groups' leader who organize their group's work to make specific, "local" decisions, in such a manner that the flow of tasks assignation goes from up to bottom, and problem resolution goes from bottom to up. 4: "global" decisions must be made by the team manager with the help of technical "staff tables", masters in the subject is being discussed.

2.1.3 Team architecture

Driven by such considerations, we organized the team trying to meet the requirements of the competition: designing / building / testing / flying /documenting a little plane. Figure 1 outlines the architectural structure of the team, and displays individual contributions. Note that the direct implication of our official advisor, prof. G. De Matteis, has been very precious: he has furnished to us his suggests in any phase of the design process, and has vested the student leaders with the authority needed to drive the team along the way to Maryland. The team manager was responsible for overall team direction, both technical and logistical. He had to identify the major areas of the work, to assign tasks and check for they were performed, to supply the different groups with the items, tools and information they needed to reach their targets. He had to control the development of the design process by marking deadlines and scheduling timings. In such a charge of coordinating the teamwork, he was supported by a "seniors council", composed by students taking part to previous DBF competitions. He could also count on the help of two graduate students who has played an

important role in precedent contest. At the subsequent level, the team was divided in three main areas, including 6 groups of study, each one with its own leader who drove the work within the group. Another task of each group leader was to observe the didactical aspects of the studies to be conducted. There have been a few studies the various group leaders carried on together with the team manager; that concerned multi-subject studies as the conceptual design stage and the realization of the optimisation algorithm to analyse overall performances of the plane.

2.1.4 Design Area

Aerodynamic Group: tasks of this group, along the entire process of design development, were the shaping and sizing of external surface of the aircraft and the evaluation of aerodynamics loadings. Tools used were analytical, numerical an experimental ones. Flight Mechanics Group: it concentrates on the study of aircraft performances, stability and handling qualities, identifying the solutions to best design the plane answering the mission requirements. Its work based most of all on analytical and experimental tools. Structural Group: this group was responsible for sizing of main structural elements, choice of materials and integration methods. It was also its task to supply the building group with the drawings needed for manufacturing process. During the different phase of the design process, the group used analytical, numerical and experimental tools to reach the goal of design lightweight, reliable structures fast to assembly. Propulsive Group: it was responsible for the selection of the system motor-propeller-batteries. It used analytical and experimental tools to narrow the possible combinations to a few solutions to be tested directly during the prototype flight test session.

2.1.5 Building Area

The leader of the group of buildings had to implement in real things the input he received about the shape and the internal structure of the plane. He had to coordinates building activities and to control the work so to answer the design requirements. Nearly all the students had to partake in the manufacturing process of the moke-up, prototype, or final model since we felt this experience would teach us what academic courses could not.

2.1.6 Testing Area

The activities of this area regarded three main fields: aerodynamic, structural, propulsive and flight test. Since the results of such tests were extremely useful for the design process, their organization and planning was strictly linked with the design process. Leaders of the Design Area's groups were also responsible for test activities regarding the subjects of their studies.

2.1.7 Report Area

Students who took a part in last year team of our University in DBF competition know very well how report preparation is important to reach a high overall score! That is because since the beginning of the work we started to think to report and selected a report group, with each own leader. Along the process of designing, building and testing each group of study, also the ones of the pre-conceptual phase, had to produce papers documenting the work they produced and the results they achieved. Those documents have been collected, organised and revised by the report group so to produce an organic review fitting the requirements of the competition.

2.1.8 Logistic Area

This area collected activities not properly connected to the design or building process, but fundamental for the progress of the work. In fact, to carry on the work the team should be supplied with funds, tools, facilities,

hardware and software instruments, and any item to improve the configuration sizing, realizing, testing. In particular, we felt the need to identify 2 people responsible for the management of funds, one person for looking for and deliver materials and components, 2 persons for dealing with the laboratories; 1 person for external relationships and contact to AIAA organisation.

2.2 Milestone Chart

To meet the requirements of the competition it was also necessary to consider its deadlines. So, we identified early in the design process a series of scheduled timings for the major activities we had to do, and marked some deadlines representing the main milestones we would have to meet along the work. An overall summary of main timings and deadlines is represented in figure 2. Many more detailed monthly plans were produced during the work, so to guarantee not to disagree with the dates imposed AIAA organisation.

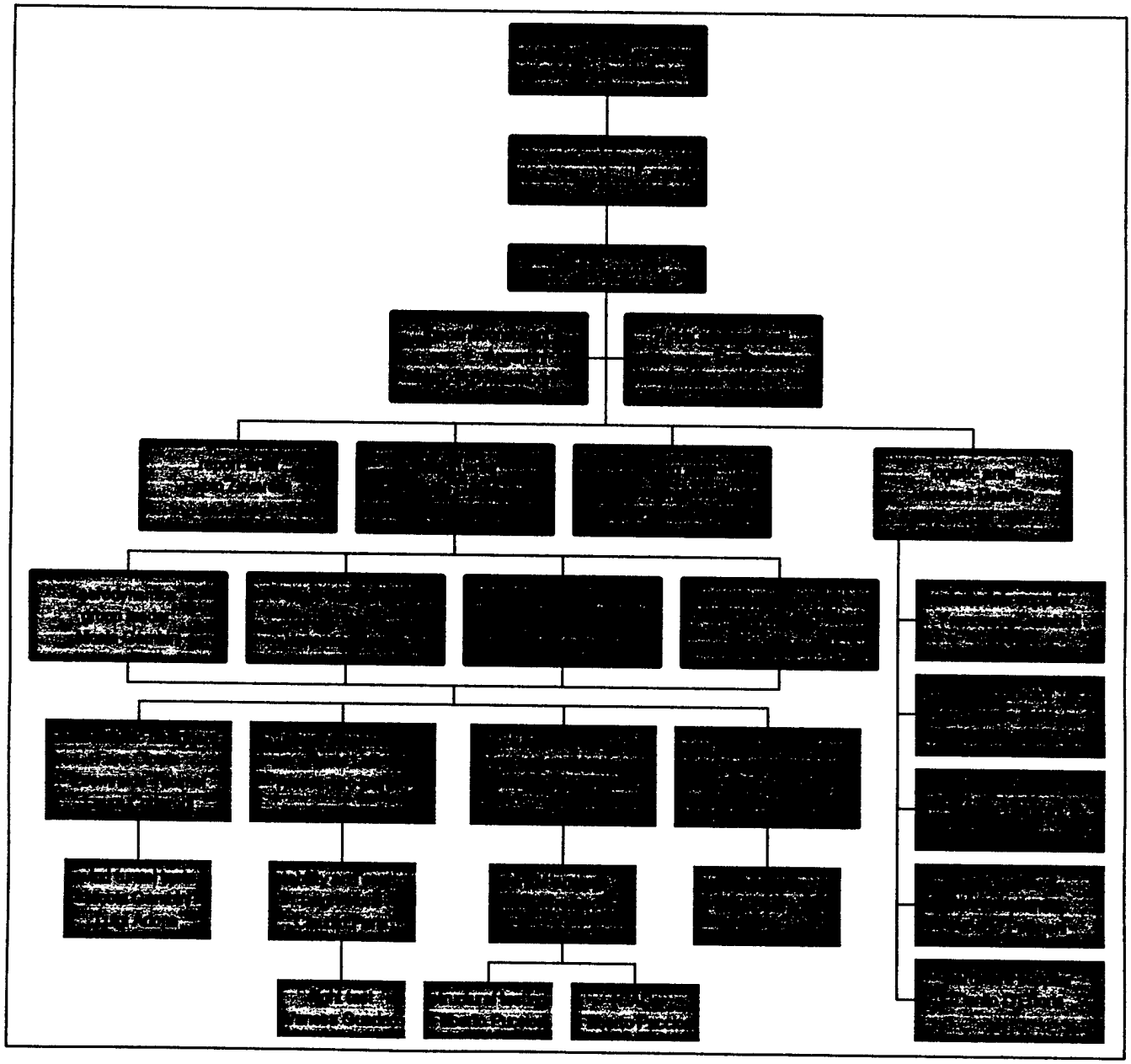

Figure 2.1: team architectural structure

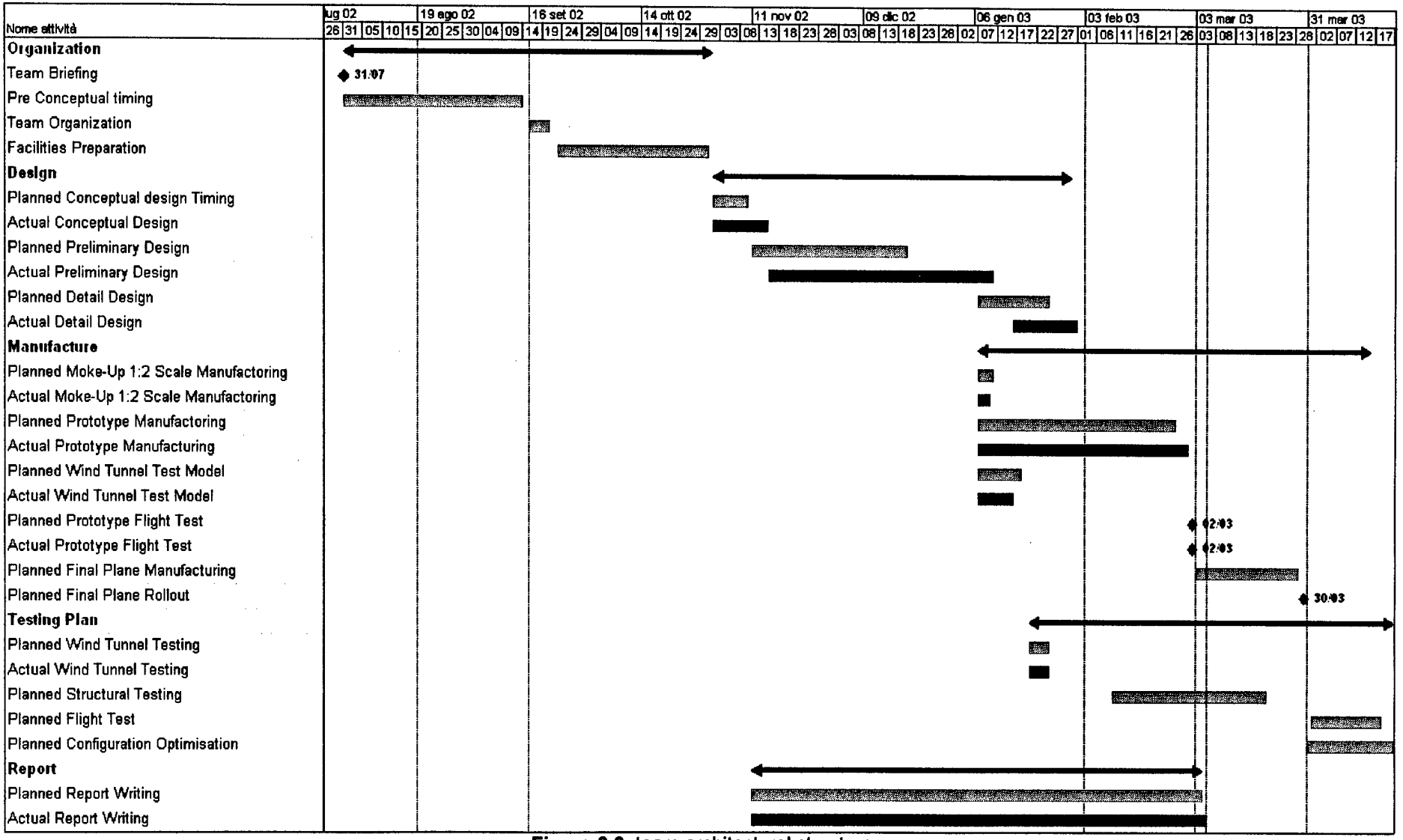

Figure 2.2: team architectural structure

3 Conceptual Design

3.1 Problem Statement

The rules request to design an aircraft able to fit the following major requirements: 1) it must be stowed in a box with defined sized, 2) it must be assembled in the shortest possible time, 3) it must take off in assigned run space, 4) it must be able to perform at least two out of the three missions, 5) it must earn a high total score, then it must have a low RAC and be fast and efficient. So we have defined some primary design parameters whose optimization led us to the final configuration.

3.2 Design Parameters

Constraints on the dimensions of the aircraft have been considered because the aircraft must fit in the box and must be fastly assembled. Next, since the beginning of the design process we have assigned a maximum value for the fuselage length and the wing span. We have investigated different configurations according to the following design parameters: missions to perform, number and location of lifting surfaces, wing planform, tail configuration, propulsive system location and configuration, structural solutions.

3.3 Mission Concepts

The rules allow only 5 flight attempts. In the final score only the best scores achieved in each of two different missions are taken into consideration. For this reason we felt important to select in this early stage the missions we will fly to achieve the highest final score. Indeed, the mission selection affects the final design. For example in mission A a housing for the antenna is needed; in mission B an unloading system for the payload is required. In mission C a greater range is necessary, and an optimisation of the aerodynamic and propulsive performances is important. To select the mission to perform we have introduced the following Figures of Merit (FOMs):

- RAC: this parameter is strongly linked with the final score. It is affected by the mission because it depends from the propulsion system (mission C) and from the number of servos (one more for the mission B).
- Flight distance: this parameter is linked with the flight range. To obtain a larger range, a greater aerodynamic and propulsive efficiency is needed.
- Difficulty factor: it multiplies the single flight score.
- Mission time: the shorter time mission the higher single flight score.

		ALTERNATIVE MISSIONS		
FOMs	***Weighting Factors***	**Mission A**	**Mission B**	**Mission C**
FACTOR	0.50	4	3	2
TIME	0.25	5	3	2
RAC	0.15	5	4	3
DISTANCE	0.10	5	5	3
Tot	1	**4.5**	3.35	2.25

Table 1: mission selection: weighted decision matrix

The most scoring missions are mission A and mission B. This is good, because it does not prevent us from adapting the design, born for mission A and B, to the mission C (back-fitting the following preliminary

design), simply enhancing the propulsion system (cells #, motor-propeller coupling).

3.4 Alternative Configuration Concepts

Once the design parameters were selected, we evaluated the different possible solutions introducing adequate FOMs. The problem of choosing the configuration consists in selecting, among every possible configuration, the one that best suits the design requirements. We found two ways to solve this problem:

- The first one is to consider at one time all the variables and create a single global decision matrix,
- The second one is to consider a set of "sub problem", each with a reduced number of variables; the configuration selection goes on in a cascade of solutions of these local problems.

We found this second "modus operandi" more efficient because it permits to unveil, by suitable FOMs, the influence of each parameter on a reduced set of design targets,.

3.4.1 Aircraft Configuration

The first and more general sub system concerned the choice of number and location of lifting surfaces. The investigated configurations were:

- The canard solution was considered because it is globally more efficient, due to the absence of trim drag and the higher global Cl_{max} at take-off with respect to a conventional configuration. This allows, at the same thrust level, a reduction of the wing area, compared with the conventional configuration. Considering that in a canard the gravity center is usually backward and the gear is aft, there are no take-off rotation problems. This leads to a smaller landing gear and a simpler stowing of the pieces in the box. Drawback: the longitudinal stability is worst, either for the fore position of the elevator, or for the lack of tolerance in the mass distribution. Yet, in spite of the advantage of a short gear, there is the problem of unloading the payload: selecting this configuration probably would lead to discard mission 2.
- The conventional solution is very well known, allows an accurate prediction of performances and flight characteristics, especially for stability and flight qualities. For these reasons it requires a faster and easier research and development program, suiting the requirements of the contest. It is used as a standard to evaluate the other concepts. Although its drawback is in the absolute performances, a bit worst than the other concept, the reliability is a significant advantage.
- The fling wing has a very low RAC, having no tail, control surfaces and associated servos. Also, it usually has a very low drag. Drawbacks: very poor flight and handling qualities, due to the low number of control surfaces, high airfoil thickness, which gives low Cl_{max} and, therefore, requires a larger wing surface and/or take-off thrust. This leads to a higher RAC. Another drawback is that we have no reference for the design.

To evaluate the configuration which best fitted the requirements of the contest we considered the FOMs in table 1, with adequate weighting factors:

- RAC: rated aircraft cost was considered as the main figure of merit for screening the concept, since it is directly related to the final score and it is a method for quantifying the cost of different solutions. It was therefore heavily weighted.

- Mission: this FOM shows how a configuration is able to perform different missions as stated by the rules. A configuration providing the same level of performance in all the missions would give a wider choice; on the other hand, every configuration investigated seems to be able to perform at least two of the three missions. For this reason the weighting factor is low.
- Drag: a configuration with a low aerodynamic drag needs less power, then allows us to reduce the number of cells and use a lighter motor. This point heavily affects the single flight score, because variations of both the RAC and the flight speed are involved.
- Handling qualities: The evaluation of stability and maneuverability is another considered parameter. An aircraft with good handling qualities allows a more accurate tracking of the flight profile, reducing flight time, and, above all, take-off and landing times. Yet, the weighting factor is low because expected wheatear conditions on the site are rather calm.
- Easy to build: the need to build the aircraft in a short time, with somewhat limited resources led us to consider this important FOM, also if it is non directly linked to the contest score. This FOM has the second higher weighting factor.

The values assigned to the FOMs for the different configurations were evaluated in a qualitative way. Being the RAC the most important parameter among the FOMs, it was calculated for the different configurations using a first quantitative sizing.

Table 2 shows the weighted decision matrix used to chose the configuration considering the previous FOMs. Even if RAC is the parameter with the greater weight, the winning configuration is not the one with the lowest RAC, that is the flying wing. In fact this configuration presents several problems concerning maneuverability, construction and assembly. The canard also has a good RAC, but has the same maneuverability problems as the flying wing. It appears that the conventional solution is the best option, as it suits very well the requests of the FOM.

		ALTERNATIVE CONCEPTS		
FOMs	**Weighting Factors**	**Canard**	**Conventional**	**Flying wing**
RAC	0.40	4	3	5
EASY TO MOUNT	0.20	4	5	3
DRAG	0.15	4	3	5
EASY TO BUILD	0.15	3	5	1
MISSION	0.05	2	5	4
HANDLING QUALITIES	0.05	2	5	1
Tot	1	3.65	3.9	3.75

Table 2: aircraft configuration: weighted decision matrix

3.4.2 Wing Configuration

The second addressed problem was the selection of the shape and location of the wing. The FOMs adopted in this screening are:

- Unloading: it evaluates how the unloading of the payload is simple, fast and reliable. Its fundamental importance for the mission B, explains the high weighting factor assigned.

- Mountability: a solution simple and fast to be mounted allows to obtain a higher score. Therefore, the assigned weighting factor is high.
- RAC: it was considered as a very important FOM, since it is directly related to the final score. The number of surfaces, their extension, and the weight of the required structures all affect this FOM. As a result, RAC was heavily weighted, even though not as high as the two above.
- Structure: it measures the difficulty of the process of sizing and building a tough and reliable fuselage-wing junction. We did not consider this parameter very critical, so it was given a low weighting factor.
- Stability: it quantifies the roll stability contribute; also in this case the weighting factor is low because we can correct the instability with other wing parameter (ie. dihedral, sweep...).
- Aerodynamics: indicates the aerodynamic efficiency of the wing-fuselage system. Once the wing span is fixed, a lower wing is more sensitive to interference between the boundary layers of wing and fuselage, and therefore requires greater attention in designing appropriated aerodynamic fairings. It was given a medium weighting factor because it affects cruise speed and mission time.
- Landing gear interface: provides a measure of the easiness in designing and building the main landing gear in the different cases. Our target was a configuration with the gear already mounted, and then the study of the interface system was quite important.

		WING CONFIGURATIONS		
FOMs	***Weighting Factors***	**High wing**	**Bi-wing**	**Low wing**
UNLOADING	0.25	5	1	2
MOUNTABILITY	0.25	5	2	5
RAC	0.20	5	2	4
AERODYNAMICS	0.10	5	2	3
LANDING GEAR	0.10	2	4	5
STRUCTURES	0.05	4	3	4
STABILITY	0.05	5	4	2
Tot	1	**4.65**	2.1	3.65

Table 3: wing configuration: weighted decision matrix

For the wing, the following solutions were considered:

- The mid-wing was discarded immediately due to the difficult solutions necessary, in designing and building the aircraft, to avoid interference between the carrying structures and the payload.
- The high-wing is the best solution for the unloading problem. It has good efficiency without fairings if compared to a low-wing. It also provides a positive contribution to the roll-stability. Finally it is easy to connect to the fuselage, but not with the gear system.
- The low-wing needs greater attention in designing the unloading system. Compared to the high-wing, it has a lower aerodynamic efficiency and a negative contribute to the roll-stability. These problems can be solved introducing supplementary devices (fairings, wing twist, ...) that have a negative effect on the RAC. The low wing can be easily coupled with the landing gear.

- The biplane-wing was also considered to celebrate the 100th anniversary of the first flight of the Wright brothers. It allowed obtaining a good aspect ratio with a short wing span, clearing more room (longitudinally) available in the box. Unfortunately, this solution is ruled out by high RAC, low aerodynamic efficiency, mounting and unloading difficulties.

Table 3 shows the decision matrix that led to the select in the high wing. Once a high-wing configuration was adopted, the problem of wing planform was addressed. The proper FOMs for this screening are:

- RAC: considering that the RAC depends from the wing span and the maximum chord, we felt important to find how the planform, keeping unchanged the area, affects this parameter. We gave to this parameter the highest weighting factor because it affects the final score more than the others.
- Drag: measures, at a fixed wing area and flight C_L, the aerodynamic drag produced by the wing. It has a double influence on the flight mission. Also, it affects the flight speed and, consequently, the mission time. Moreover, it affects the RAC through the battery consumption. For these reasons it has an high weighting factor.
- Construction: this parameter measures the difficulties related to the wing construction, from the point of view of the requested tools, the complexity and the time of assembling the parts. This is less important than the previous two.
- Stall behavior: this FOM measure how the different planforms affect the behavior of the aircraft in incipient stall conditions. The considered effects are the Cl spanwise distribution and the Reynolds's number at the wing tip. These considerations, very important from a theoretic point of view, were considered less important with respect to the problems introduced so far.

The considered planforms are:

- Elliptic wing: this is the best shape from the aerodynamic point of view because the induced drag is minimum. The RAC value is between rectangular and tapered wings and the wing has a quite good stall behavior. The main drawback is the higher complexity in realization.
- Rectangular wing: keeping unchanged the area, this solution presents the minimum RAC value. Moreover it can be built very easily leaving aside the building techniques used. However it has a poor efficiency from the aerodynamic point of view.
- Tapered wing: has a quite good aerodynamic efficiency, but lower than the elliptic wing. The building difficulties of this solution is intermediate between those of other two planforms but the RAC is higher. The stall behavior of this configuration is particularly critical. In fact, considering for example a taper ratio 1:3, which minimize the induced drag, the Reynolds number decreases from the root to the tip of the wing. Considering the typical sizes of our model, this would lead to a very low tip Re (about 70'000), with a negative effect on airfoil performances (for an elliptic wing this fact is less important because the part of wing with reduced chord has a far smaller surface). Another problem for the wing tip is due to the spanwise Cl distribution of the tapered wing, where Cl grows from the root to the tip. A negative twist angle would solve these problems realizing a good stall behavior. However, this would significantly increase the building complexity.

Table 4 shows the decision matrix that led us to select the rectangular planform.

		WING PLANFORM		
FOMs	***Weighting Factors***	**Elliptic**	**Rectangular**	**Tapered**
RAC	0.4	4	5	2
DRAG	0.3	5	3	4
CONSTRUCTION	0.2	1	5	3
STALL BEHAVIOR	0.1	4	5	2
Tot	1	3.7	4.4	2.8

Table 4: wing planform: weighted decision matrix

3.4.3 Fuselage configuration

The FOMs for the analysis of the fuselage configuration are:

- RAC: the fuselage configuration affects the RAC through the structural weight
- Aerodynamic efficiency: measure the global aerodynamic efficiency of the configuration.
- Lengthenability: this FOM evaluates the possibility of realizing a fuselage with an overall length greater than the box size, without compromising the assembly time.

		FUSELAGE SHAPE		
FOMs	***Weighting Factors***	**Axial sym.**	**Lifting**	**Pod-like**
EFFICIENCY	0.5	5	3	3
RAC	0.4	4	5	5
LENGTHENING	0.1	1	1	5
Tot	1	4.2	3.6	4

Table 5: fuselage shape: weighted decision matrix

In order to choose the fuselage configuration we required that total length is lower than the maximum box size. In this phase of the project we did not want to freeze the fuselage length yet, but this constraint makes easier the screening process. Once the length and the cross size of the fuselage (equal to the payload size) were grossly specified, there were few possibilities for fuselage shape. So the analyzed solutions were:

- Axial sym: the axial symmetric is the worst solution from the RAC viewpoint, because the larger volume leads to heavier structures. Nevertheless this solution has a good aerodynamic behavior, with a low drag.
- Lifting body: the lifting force produced by this configuration allows a reduced wing span, reducing the total structural weight. This leads to a lower RAC compared to the other configurations. During the cruise, which represents the larger part of the mission, this configuration has a higher drag; this affects both flight time and propulsive sub-system and therefore the RAC.
- Pod-like: this configuration has an axis symmetric section, carrying only payload and propulsive system; tail surfaces are connected to the fuselage by a boom. It has the advantage of using less material than the conventional axial symmetric solution, and then it is lighter, with a lower RAC. The aerodynamic efficiency is not very good, because the limited length of the fuselage does not

allow the realization of fairings in the aft region. On the other hand, this solution permit to build a fuselage the length of which is over the 4' limit. It is possible to build an extendable boom to achieve the required tail-fuselage distance.

Table 5 shows the decision matrix that led to the selection of the axial symmetric configuration.

3.4.4 Tail configuration

The FOMs considered for the analysis of the tail configurations were:

- RAC: the RAC directly affects the overall score, and so the weight of this FOM is high. The tail parameters that influence the RAC are the number of surfaces and the number of controls.
- Control moment: this parameter is strongly dependent on the tail configuration. It affects the take-off and cruise performance of the aircraft. It should ensure a high global value of Cl, a high control power at take-off, and low drag and good longitudinal stability during cruise. Control moment contribution to the final score was estimated less important than that of the RAC.
- Efficiency: an aerodynamically efficient tail produces a low drag, requiring less thrust for take-off and cruise, and making less critical the sizing of the propulsion system.
- Mountability: this FOM evaluates the time necessary to mount the tail once the box is open. In particular we gave the maximum score (5) to the configurations that can have the tail connected to the fuselage in the box. A weight equal to the RAC was assigned to this FOM because a fast and simple assembly was regarded as a key factor to earn a high score.

The considered alternatives are:

- H-tail: after the definition of the wing and fuselage configuration, similar considerations led us to introduce the H-tail like a potentially high-scoring solution. The box dimensions with the requirement of an easy assembly lead to a horizontal surface with no more than 2' span. It is also to be considered that the expected wing span should be less than 8' (twice the length of the box) and that the RAC rules states a limit to the size of the tail. On the other hand the maximum size of the box calls for a very short fuselage, so that the maximum distance of the tail from the center of gravity is somewhat limited. Furthermore, due to fuselage shape and wing position (high wing), the horizontal surface is expected to be in the wake flow, particularly at take-off, when the tail is more important. As a result a highly efficient horizontal surface is necessary. The H-tail solution, with the two fins acting like winglets, was a way to increase the effective aspect ratio of this surface, without a significant penalty on the RAC, particularly when the use of vertical control surfaces is ruled out. Also, this configuration can be stored in the box, already mounted on the fuselage. Note that a single vertical surface (cross-tail), fitting the box dimensions, that would be undersized.
- Conventional tail: this configuration has the advantage of a reduced RAC. However, as explained before, it would give an aircraft with lower performances, due to the low efficiency of the horizontal surface. We felt that a conventional tail already mounted (in the box) was less convenient because the fin would be undersized for the directional stability requirements.

- Cross-tail: compared to the conventional tail, this solution would solve the "accountancy" problem, allowing a double size of the vertical surface. As a disadvantage, with the same number of controls, the RAC would be higher.
- T-tail: the great advantage of this solution is to be immune from the wake effects of wing and fuselage. The efficiency is higher than the conventional tail, but lower than the H-tail. The RAC is similar to that of the conventional tail. However the mountability is penalized: for a really efficient T-tail, the vertical surface should be realized in two sections, to be assembled outside the box.
- V-tail: apart from the great advantage of optimizing the RAC, this solution has lower scores on the other FOMs. It has to be assembled outside the box, has a low aerodynamic efficiency since the equivalent horizontal surface would be undersized, giving insufficient longitudinal stability and control.

Table 6 shows the results of weighted decision matrix. The winning configuration is the H-tail.

		TAIL CONFIGURATIONS				
FOMs	***Weighting Factors***	**T**	**V**	**H**	**Conv.**	**Cross**
RAC	0.35	4	5	3	4	3
MOUNTABILITY	0.35	2	3	5	4	5
CONTROL MOMENT	0.15	5	2	5	2	2
EFFICIENCY	0.15	4	2	5	3	3
Tot	1	3.45	3.4	4.3	3.55	3.55

Table 6: tail configuration: weighted decision matrix

3.4.5 Motor and Propeller position

Excluding configurations with more than two motors because too complicated, we analyzed advantages and drawbacks of three alternatives:

- One motor with one battery pack: it has the advantage of a weight lower than the bi-motor configurations, and of being less penalized by the RAC. With the same number of cells this configuration has an intermediate shaft power, but has the advantage of allowing the mounting of nearby motor and batteries, which results in short supply cables.
- Two motors with one shared battery pack: it is the typical solution for a wing-mounted bi-motor and allows the highest power to be obtained, because the full voltage powers both motors. Yet, it has the great drawback of high energy loss due to the long supply cable connecting the centrally mounted battery pack with the far motors.
- Two motors, each with its own battery pack: this is the perfect solution for push-pull configuration; it has low power loss, but shows its limits in term of RAC and maximum available power.

For this selection we considered the following FOMs:

- RAC: this parameter is directly affected by the number of motors and by the weight of the battery; among the bi-motor configurations the one with two battery packs gives a little advantage.
- Power: measures the maximum available power, strictly connected with the take-off performances.

- Weight: is affected by the configuration; it has a small influence on RAC but it is also a very important parameter for the aircraft performances (take-off, mission time...).

Table 7 shows the results of weighted decision matrix. The winning motor configuration is 1M-1BP.

		MOTOR CONFIGURATIONS		
FOMs	***Weighting Factors***	**1 Motor 1 Battery Pack**	**2 Motors 2 Battery Packs**	**2 Motors 1 Battery Pack**
RAC	0.4	5	3	2
Energy loss	0.3	5	4	2
Power	0.2	4	3	5
Weight	0.1	4	3	3
Tot	1	4.7	3.3	2.7

Table 7: motor configuration: weighted decision matrix

Once the number of motors and battery packs was decided, we examined the relative positions of the three components of the propulsion system: motor, battery pack and propeller.

The related FOMs were:

- Center of gravity: it quantifies the possibility of balancing the aircraft. This is highly affected by the position of the propulsive system, because it has the heaviest components (motor, batteries). Furthermore, it would be better that motor and batteries were as near as possible, to avoid energy loss in too long cables.
- Rotation: this FOM measures the problems in the take-off rotation, critical for the pushing aft propeller.
- Propulsion efficiency: this FOM measures the thrust loss due to the interaction of the propeller flow with the surfaces in the wake. It is strongly affected by the relative position of propeller, fuselage, and wing. The propulsion efficiency has a double effect on the global score. An higher efficiency allows limiting the number of cells for the same range, reducing the RAC, and increasing the thrust of the same propulsion system, so that the flight time is shorter. Therefore, the weighting factor of this parameter is the highest considered.
- Structures: this FOM quantifies the structural difficulties of integrating the propulsion system with the aircraft fuselage. The effect of a weight increase was considered less important with respect to the other parameters.
- Energy loss: this FOM measures the loss of electric energy due to the length of the supply cables. The weight of this FOM is quite important.
- RAC: it is affected by the configuration propulsive efficiency (higher efficiency leads to fewer cells) and by the weight of the structures containing the different propulsive systems (motor housing, transmission shafts).
- The fore position of the motor-propeller system is poorly efficient, because the fuselage is in the propeller wake. Nevertheless, it is the configuration that best fits the design requirements.
- The aft position is the most efficient; but generates the issues of rotation at take-off and aircraft balancing. The latter problem can be solved by putting the batteries in a forward position, but this

would require long cables. The use of a long shaft, leaving motor and batteries in front, would cause greater structural complexity.

Table 8 shows that the wining configuration is the one with fore motor, propeller and batteries.

		PROPULSION CONFIGURATIONS		
FOMs	***Weighting Factors***	**Fore Motor Fore Propeller Fore Batteries**	**Aft Motor Aft Propeller Fore Batteries**	**Fore Motor Aft Propeller Fore Batteries**
EFFICIENCY	0.25	3	5	5
ROTATION	0.20	5	2	2
RAC	0.20	3	4	3
ENERGY LOSS	0.15	5	1	5
CENTER OF GRAVITY	0.10	5	3	4
STRUCTURES	0.10	5	4	1
Tot	1	4.1	3.3	3.5

Table 8: propulsion configuration: weighted decision matrix

3.4.6 Landing gear configuration

The study of the landing gear configuration considered four options, using the following FOMs:

- RAC: it takes into account the effect on the RAC of the structural weight and the number of servos, needed for the considered configuration. The weighting factor is the lowest, for the little effect of the landing gear configuration on the RAC.
- Aerodynamic efficiency: it measures how configuration affects the aircraft aerodynamic performances, in terms of additional drag. This FOM is very important, because it directly affects the aircraft range and speed and, therefore, the weighting factor is high.
- Unloading interference: it measures the difficulty of implementing the unloading system, in terms of volume and limitations of the mechanics of the cargo bay door. To this FOM the highest weighting factor was assigned.
- Reliability: this is an estimation of the landing gear reliability. It penalizes the retractable configurations, because a possible failure of the deploying system during the landing, would be fatal for the whole aircraft. For this reason this FOM has an high weighting factor.

Considered landing gear configurations are:

- The fixed fore tricycle configuration has the drawback of an additional drag during the cruise flight, penalizing the aerodynamic efficiency. It has an excellent reliability and offers several solutions for the unloading system.
- The fixed aft tricycle configuration has an aerodynamic drag and structural weight a little lower than the previous one, but presents great limitations for the unloading system solutions, due to the short distance from the ground. It is hardly possible to produce a ventral payload unloading.
- The retractable fore tricycle configuration, compared to the fixed one, improves the aerodynamic behavior. But it has a negative effect on the RAC, because of an additional servo and of higher weight. It could have reliability problems.

- The retractable aft tricycle configuration has the advantage of producing low additional aerodynamic drag, but is penalized in term of RAC, reliability and unloading interference.

Table 9 shows how the fixed fore tricycle configuration better meets the requests of the selected FOMs.

		LANDING GEAR CONFIGURATION			
FOMS	***Weighting Factor***	**Fixed Fore Tricycle**	**Retractable Fore Tricycle**	**Fixed Aft Tricycle**	**Retractable Aft Tricycle**
EFFICIENCY	0.30	2	5	3	5
CARGO	0.30	5	5	2	2
RELIABILITY	0.25	5	3	5	3
RAC	0.15	4	1	5	2
Tot	1	3.95	3.65	3.5	2.9

Table 9: landing gear configuration: weighted decision matrix

3.4.7 Structural Configuration

At this point the different building technologies to implement the main parts of the aircraft were analyzed: wing, fuselage, tail, and landing gear. The FOM used for each study were:

- RAC: it is affected by the weight of the structures, as a function of the used building technology.
- Cost: it measures the economical resources needed to realize the component with the selected building technology.
- Reparability: it measures how simple is to recover the strength of the damaged structure, in the shortest possible time.
- Know how: it measures the experience and the skill of the team to use the selected technologies.
- Technologies: it measures the availability of the tools required to implement the selected production technology (i.e. machines as lathes for the moulds, pressurized vat, vacuum bags, ...).
- Strength: it is an estimation of the strength to weight ratio.
- Unloading: it is a FOM for the fuselage, and measures the easiness of realize the unloading system (cargo bay door).
- Payload interference: it evaluates the landing gear interference with the payload release system.

The structural configuration technologies are:

- The traditional wooden structure with ribs and spars (frames and spars for the fuselage) is the cheapest and lightest, and requires simple technologies; however, it also requires a long and complicated building process and is very difficult to repair after an accident.
- The shell configuration has important advantages in terms of weight, strength, volume (and then frontal area) and has a maximum assembling easiness; but this configuration requires a good knowledge-base and expensive techniques.
- Skin + core configuration, i.e. a structure with a core of a light material (nomex, polystyrene, aerogel) covered with a composite skin (glass fiber, Kevlar, carbon). Compared with the shell structure, has a lower structural strength and required technologies and skills intermediate between the two preceding solutions.

- The sandwich box configuration, for the fuselage, has the advantages of the assemblability and reparability of the traditional configuration, coupled with the strength of the skin + core structure, from which also inheres the higher technological and building complexities.

		WING STRUCTURE		
FOMs	***Weighting Factors***	**Traditional**	**Shell**	**Composite skin + core**
KNOW HOW	0.25	4	2	5
TECHNOLOGIES	0.20	5	2	4
STRENGTH	0.20	3	4	5
REPARABILITY	0.15	1	2	4
RAC	0.10	5	1	3
COSTS	0.10	5	1	3
Tot	1	3.75	2.2	4.25

Table 10: wing structure: weighted decision matrix

		FUSELAGE STRUCTURES			
FOMs	***Weighting Factors***	**Traditional**	**Shell**	**Composite skin + core**	**Sandwich box**
KNOW HOW	0.20	4	2	5	5
TECHNOLOGIES	0.20	5	2	4	5
STRENGTH	0.20	3	5	4	4
RAC	0.15	4	1	3	4
UNLOADING	0.15	1	5	4	5
COST	0.10	5	1	3	4
Tot	1	3.65	2.8	3.95	4.55

Table 11: fuselage structure: weighted decision matrix

		LANDING GEAR STRUCTURES			
FOMs	**Weighting Factors**	**Aluminum bow**	**Aluminum single leg**	**Composite bow**	**Composite single leg**
STRENGTH	0.4	4	3	5	4
RAC	0.3	1	2	4	5
REPARABILITY	0.2	3	2	1	2
COST	0.1	5	4	1	2
Tot	1	3	2.6	3.5	3.7

Table 12: landing gear configuration: weighted decision matrix

		TAIL STRUCTURES		
FOMs	***Weighting Factors***	**Traditional**	**Shell**	**Composite skin + core**
KNOW HOW	0.25	4	2	5
TECHNOLOGIES	0.20	5	2	4
STRENGTH	0.20	3	4	5
REPARABILITY	0.15	1	2	4
RAC	0.10	5	1	3
COST	0.10	5	1	3
Tot	1	3.75	2.2	4.25

Table 13: tail structure: weighted decision matrix

Tables 10-11-12-13 show that a sandwich solution and a composite solution are required, respectively, for wing and fuselage structures, and for tail and landing gear structures.

3.5 FOMs Analysis Results

At the end of the conceptual study we found a high potential score configuration. The axial symmetric fuselage gives a reduced front area, and then a low shape drag. The high wing, gives a good behavior in term of stability with cross wind (the worst condition), and the interaction between wing and fuselage gives advantages during the take off run. The H-tail increases the horizontal surface efficiency; being the vertical surfaces both over and below the horizontal one, it causes a better behavior in spin recovery. The ventral unloading offers high reliability and an easy construction. The selected missions are the ones with the highest score coefficients.

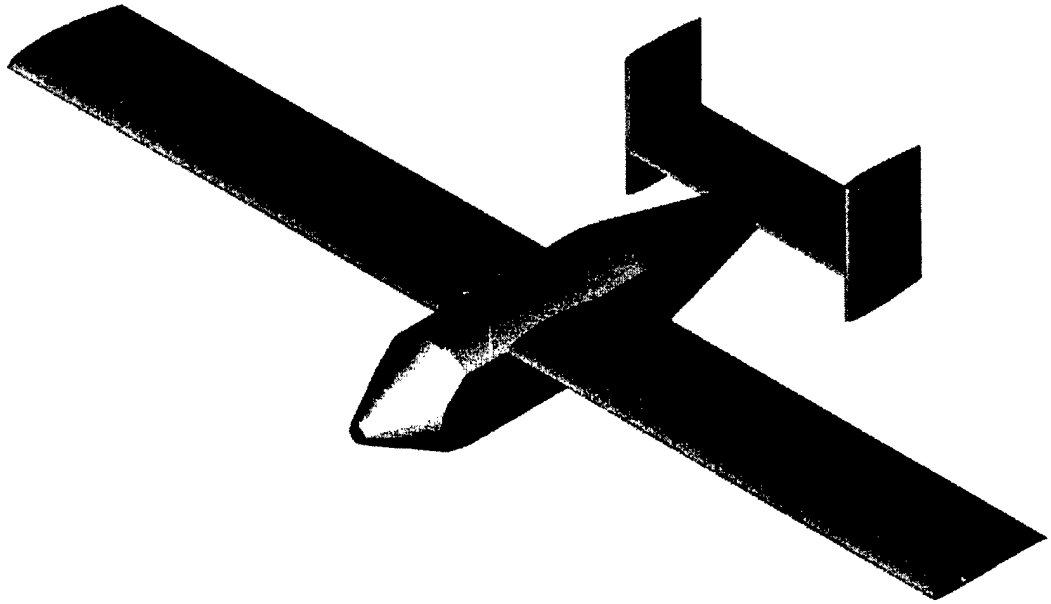

Figure 1: final concept

4 Preliminary Design

4.1 Introduction

At the end of the conceptual design phase, the concept configuration of our aircraft was stated, and the technological solutions necessary to realize the different subsystems were found. The adopted analysis methods had a statistic-qualitative character, and the actual aircraft performance was not accurately determined. The aim of the next study phase was the sizing of the main subsystems, so that their integration would give an aircraft able to gain the highest contest score. To this end, we needed to find out suitable criteria to deal with this problem. We needed to lay out an optimization method able to evaluate the global efficiency of the possible set of design parameters. It required analysis and calculation tools able to faithfully estimate the actual performances of the various subsystems, and how these affect the behavior of the whole aircraft. To reduce the problem complexity, due to the large number of variables, we proceeded with two level of study. The first goal was carry out sizing trade studies able to evaluate the influence of the various parameter sets on the overall score and to reduce the range of the design variables. Then, we executed fine trade studies in major design areas, refining the solutions pointed out by the first study phase. At the end of the preliminary design phase, the sizing of the main aircraft subsystems was done.

4.2 First Sizing Trade Studies

In the first phase of the sizing process, we implemented an optimization algorithm capable to evaluate the effects on the score of the various sets of the design variables investigated, and to give the optimum configuration as output, that is the one with the highest score. Yet, a computation with the design parameters varying in a discrete way gives results suffering from intrinsic limits (the iteration steps of each variable have a finite space, while the relative optimum could fall in one of the gaps). More, an algorithm dealing with a problem with a high number of variables, unavoidably introduces approximations and simplifying hypotheses. As a consequence, we decided not to take into account every factor, leaving the more detailed analyses, regarding the particular aircraft subsystems. For these reasons, the results given as output by the optimization program, were not considered as the unique and definitive solution for the configuration sizing problem. Instead they reduced the range or variation of the considered design parameters. In particular, each set of parameters, gaining a score within 15% of the maximum, was considered for the following fine trade studies.

4.2.1 Main assumptions

To formulate the optimization algorithm some simplifying hypotheses were introduced:

1. In the optimization algorithm we needed to know the aerodynamic parameters of the whole aircraft. For the sake of simplicity, we chose to link these parameters to the adopted airfoil: known the characteristics of an airfoil and the actual dimensions of a finite wing, is possible to find out the lift, the drag, and the pitch moment of the wing. In addition, we need to sum the contribution of the tail, the fuselage, the landing gear, and the antenna. These contributions can be considered as known parameters in agreement with the following assumptions:

- the geometry of the horizontal tail (span, chord, planform, and airfoil) was fixed because the most important effects on the performance of the whole aircraft are the reduction of the maximum take off C_L and the increase of the cruise C_D. These effects can be easily found from the wing geometry (chord and airfoil). In fact, chosen the airfoil, from the pitch balance, the angle of attack of the horizontal tail during take off and cruise can be found, and so we can evaluate which % of C_L and C_D must be added or subtracted to those developed by the wing. A more accurate study on the parameters of the horizontal tail (airfoil, chord, coupling angle, % of elevator, maximum elevator deflection) will be also conducted.
- We considered that the effect of vertical tail, fuselage, and landing gear was to increase the C_D with respect to wing and horizontal tail. During the conceptual design the fuselage shape and dimension were determined, together with maximum dimensions of the tail vertical surfaces and landing gear (mainly for the needs to fit in the box).

As a consequence, the variables for the aerodynamic design were reduced to the coefficients of the selected airfoil: Cl_{MAX}, Cm_{AC}, k e Cd_0. So we identified five families of low Reynolds airfoils (about 10e5). For each one of them, we considered only an airfoil, in order to represent the main characteristics of its family. The optimization process analyzed these airfoils and pointed out which one was the best. That meant to select for further studies the family it belonged to.

2. For the stability and handling qualities, we set the aerodynamic center of the wing (i.e. the 25% of the chord) about half an inch aft the center of gravity (c.g.). The latter, due to the mission with the payload deployment, was located in the middle of the cargo-bay, 0.42 m (16.5") from the aircraft nose. Therefore, the distance among c.g. and tail remained fixed, equal to about 0.63m (24.8").
3. An analytic relation between propulsive configuration and thrust was introduced in the optimization algorithm. We found this relation by extrapolating the data of maximum thrust, as a function of the number of cells and of the system motor/propeller/reduction-gear, obtained from a set of analyses performed with commercial software, MotoCalc. This software uses a database with the characteristics of several electric motors and other components and, for a set motor/cells/reduction/propeller gives useful data on:
    - Available thrust at various airspeeds.
    - Shaft power.
    - Voltages e currents.
    - Temperatures reached by the motor and the cells.

    The latter two data allow to exclude some options of propeller diameters or cells numbers, which lead to excessive temperatures or currents higher than the 40 A limit imposed by the rules. The results were filtered with the following criteria:
    - Current < 40 A
    - Power loss < 100 W
    - Discharge time > 5 min

A preliminary analysis allowed us to limit the possible motor-propeller-reduction configuration to 5 options, which gave the best results in term of shaft power, efficiency, and cell discharge time (table 1). For each configuration the T_{MAX} vs. #cells curve was found. Then, the parameters in the optimization process were the number of cells (8 to 24) and the motor/propeller/reduction set (out of 5 selected).

4. In the conceptual design phase a maximum take-off weight of 8 kg (17.6 lbs) was considered. We found that this value is slightly affected by the change of the design parameters, in particular by the wing surface and the number of cells: increasing the first, for the take-off requisites, the second decreases.

4.2.2 Known parameters:

Hence, as stated before, and by the conceptual design results, the following parameters are known:

- W gross take-off weight: 8 kg (17.6 lb)
- bw wing span 2.4 m (8 ft) (due to maximum box dimension)
- bt horizontal tail span: 60 cm (2 ft) (=25% bw)
- ct horizontal tail chord: 20 cm (8")
- μ friction coefficient: 0.05
- Cd fuselage + vertical tail + landing gear = 0.03 + 0.008 + 0.04 = 0.042
- Tail distance from the center of gravity = 0.63 m (25")
- Wing planform (selected in the conceptual)

4.2.3 Major Design Parameters

The variables considered in the optimization algorithm were reduced to the ones shown in table 4.1. For any of them, the table indicates the lower and upper limits of the considered range of variation.

		Range	
variable	**description**	**minimum**	**Maximum**
Sw	Wing surface	0.5 m^2 (5.4 sq ft)	1 m^2 (10.8 sq ft)
Ncell	Number of cells	8	24
"motor"	Motor-propeller-reduction set	ULTRA 920,930,1800,2000,3300; propeller: 18" to 23"; reduction set: compatibles.	
Vc	Cruise speed	15 m/s (49 ft/s)	30 m/s (98 ft/s)
Nv	Turn loading factor	1	2
"airfoil"	Clmax, Cm, k, Cd0	families: SD, FX, Eppler, NACA 4 digit , CH.	

Table 4.1: First Sizing Trade Studies: Major Design Parameters

4.2.4 Standard mission:

The standard mission introduces, among the possible flight missions, the most critical conditions from the energetic point of view. This standard mission consists in flying the course of mission A, always with the full payload and the antenna, without landing and deploying the payload. Therefore the mission phases are:

- take-off run; starts with the aircraft motionless and ends when the take-off speed, that is 1.1 times the stall speed, is reached;

- climb: from the end of the take-off, till an altitude of 30 m (about 100 ft); the analytic model used to describe this phase is the one for the maximum rate of climb at the maximum excess power;
- cruise: this phase sums up the 7 straight parts (about 7000 ft);
- turn: sums up the 2 turns at the pylons and the 360° turn in the downwind leg for each lap, in a total of 16 180° turns; the analytic model used is the one for the correct turn at the cruise speed; the loading factor is a variable;
- landing: a glide from the cruise altitude to ground and braking: from landing speed to zero.

4.2.5 Cost function:

For each set of design variables, the algorithm calculates the RAC and the time spent to perform the standard mission. The target function to be maximized by the optimization tool is:

Final Score = 100/ (Flight Time*RAC)

4.2.6 Analysis Methods

The "skeleton" of the optimization algorithm is described (figure 4.1) with a block diagram. This was implemented in the Optim program (written in Matlab 6.5), which carries out the computations sketched in the figure, varying input sets and selecting the one that provides the higher overall score. In the **OPTIM 5.4** final version, the program calls the following Matlab subroutines:

- **TAKEOFF**: from the thrust vs. speed law, it integrates the motion equation (from zero to the take-off speed) considering the aircraft aerodynamic characteristics, the weight, and the effect of the wheels-runway friction.
- **CLIMB**: finds analytically the fastest-climb speed, depending on the wing loading and the parameters of the polar curve for the whole aircraft, namely C_{D0} and K. It integrates the aircraft motion equation, from the take-off speed to the climb speed; finds out the time spent to reach this speed, and then the time to reach the cruise altitude of 30m (100 ft). The flight path angle is found analytically; so that it is possible to have in output the horizontal range flown.
- **CRUISE**: finds out the length of the path flown in this condition, subtracting from the sum of straight segments the horizontal length run in take-off and climb. From the cruise speed, it gives the elapsed time.
- **TURN**: uses a bonded turn model with constant speed (equal to the cruise speed). From the turn loading factor, it finds out the required thrust, C_L and the turn radius, and then the length flown, the time and the energetic expenditure.
- **LANDING**: it uses a descent model of glide with turned-off motor and at angle of attack for maximum efficiency. It integrates the motion equations from cruise altitude to ground in these conditions and finds out the residual horizontal speed. Then, the motion equations are integrated from this speed to zero speed, considering the braking action of the wheel friction on the runway and of the aerodynamic drag. It gives as output the distance run and the time for the descent and braking phases.

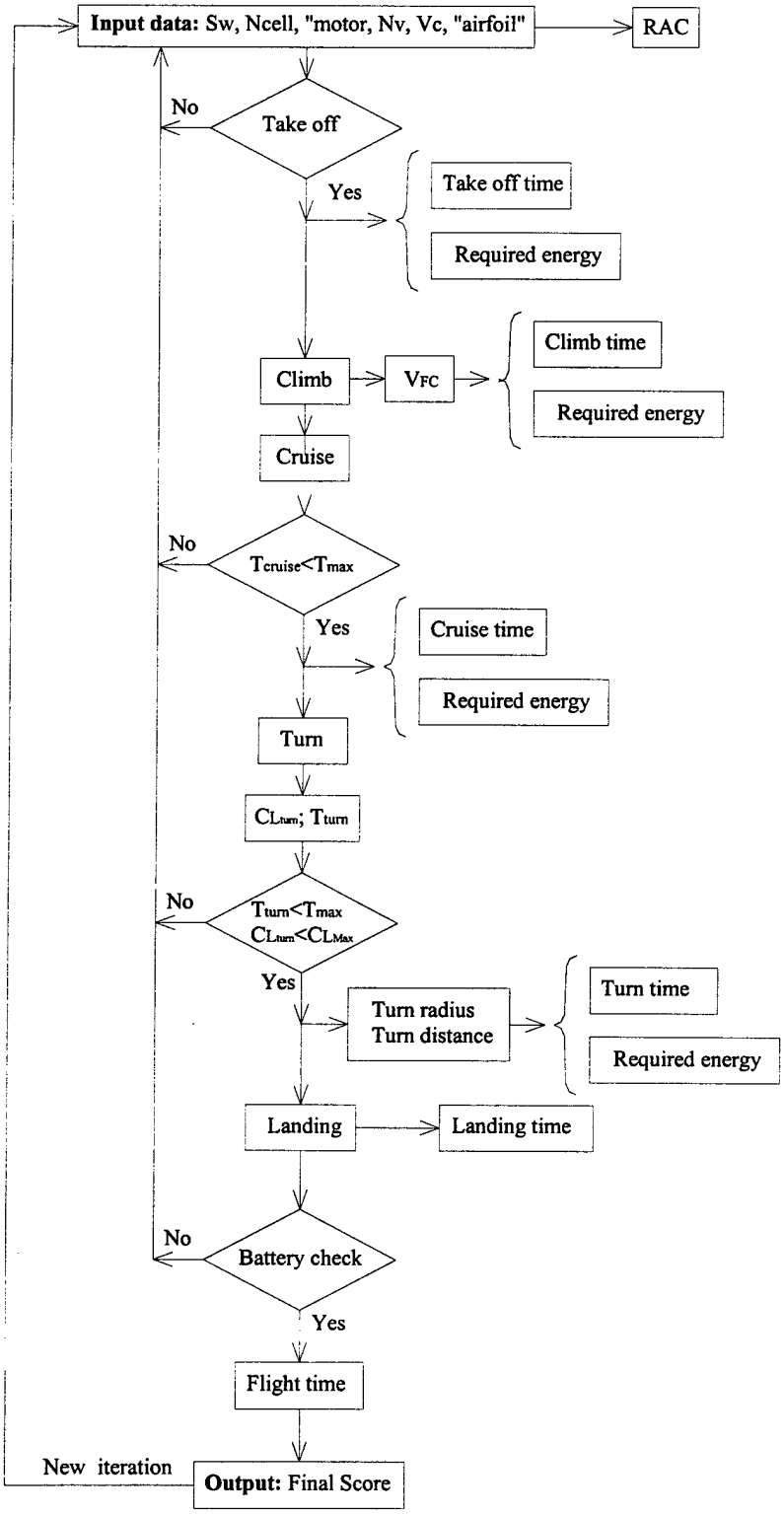

Figure 4.1: optimization algorithm

The OPTIM 5.4 executes as follows: it takes as input a set of design variables, from which the RAC is calculated. Therefore, considering the particular relation Maximum thrust vs. Speed of the selected propulsion system, the TAKEOFF subprogram is run. Then it performs a check on the lifting equation at the end of the runway. If the requirement is not satisfied, the execution stops and a new set of design variables is considered. Now the elapsed time and the energetic expenditure for take-off are calculated. Next, the CLIMB subprogram is executed, and the time and the energetic expenditure for this flight phase are found. From the cruise speed it is possible to find the cruise thrust. At this point the program checks if the cruise thrust is lower than the maximum thrust available for the adopted propulsion system. If the requirement is not satisfied, the execution stops and a new set of design variables is considered. Then the CRUISE subprogram is called. It takes as input the cruise speed and gives as output the time and the energetic expenditure. In the turn analysis a double check is performed: on the turn thrust, lower than the maximum one, and on the C_L, lower than C_{Lmax} (to be sure than the aircraft does not stall during this maneuver). The TURN subprogram works like the preceding ones, computing turn time and energetic expenditure. Next, the LANDING subprogram is executed, giving the same data as output. Now it is possible to perform the "battery check", to verify that the mission energetic demand is lower than the battery configuration supply. Finally, in this case the total flight time and the Final Score are calculated.

4.2.7 Analysis Results

The results of the program, when the final score is within 15% of the maximum overall score, indicate, for each design parameter, the following range:

Sw:	from 0.66 to 0.75 m^2 (7.1 – 8.1 ft^2)
Tmax:	from 26 to 30 N (5.8 – 6.7 lbf);
Cells:	from 11 to 17;
Motor:	Ultra 930-8 12V, Ultra 1800-3 10V, Ultra 3300 -3 10 V.
Propeller:	19" to 21";
Airfoil:	SD family;
Vc:	from 20 to 25 m/s (65 – 82 ft/s);
nv:	from 1,4 to 1,7;
Vto:	from 12 to 15 m/s (39 – 49 ft/s);

4.3 Fine Trade Studies and design Optimisation

4.3.1 Aerodynamic Considerations

The airfoil more advantageous in term of overall score belongs to the "SD" family; now there is the problem of choosing the exact airfoil to be used on the aircraft. Out of the nine airfoils analyzed from this family, we disregarded those with a very low Cm_{ac}, because the double camber on the upper surface makes too hard to build the wing with sufficient accuracy. We also discarded the laminar ones, because the cusp on the trailing edge causes the same building problems. The other six airfoils are very simple to produce (no sharp trailing edge, no high camper or cusp), and don't have moment coefficient too high (no more than –0.1), condition that our OPTIM 5.4 shows to be particularly penalizing. At this point we

compared the polar and C_l curves. Once wing surface and geometry, weight and flight speed (and then the whole aircraft C_L) are defined, the cruise C_l of the airfoil is determined. Comparing the polar for various family SD airfoils, we found out that the difference in the C_d at C_l near the cruise value is quite small, also considering the trim drag. By focusing on the curves with the higher maximum C_l (always taking into account the trim loss), in its two versions, "S" and "D" we concluded that the SD 7032 airfoil has superior characteristics. Among these, we selected the "D" variant, for the higher maximum C_l (but only some %) and for the smoother stall. The wing dimensions, allowing us to take-off safely and with an high cruise efficiency, are 240 cm (8 feet) in span (as previously fixed) by a chord of 30 cm (about 1 foot). A NACA 0012 airfoil was used for the tail, because the high H tail efficiency does not make necessary a cambered airfoil, more difficult to build and with a worse behaviour when the camber is changed by the deflection of a control surface. The most efficient tail, for the requested control moments, has a span of 60 cm (2 feet) (25% of the main wing span) and 20 cm (8") chord. The aerodynamic characteristics were found with software, developed by us in Excel which, from the aircraft geometry, generates the curves of lift, drag, efficiency and the polar for the single components and for the whole aircraft, considering the interference between the parts regarding the wakes and the induced speeds. To deal with the stall, the program finds the spanwise lift distribution using the Shrenk method. It considers only the linear part of the lift curve, and the related polar, using experimental data to update the curves and foresee the behavior of the non-linear parts.

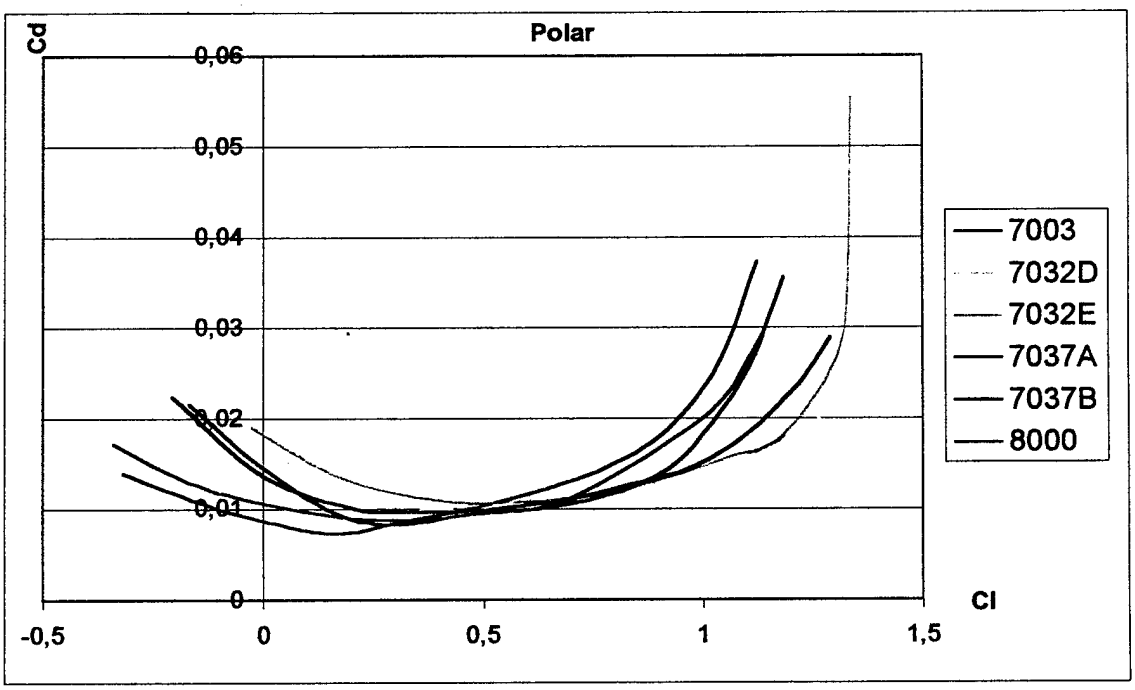

Fig

Figure 4.2: SD family polars

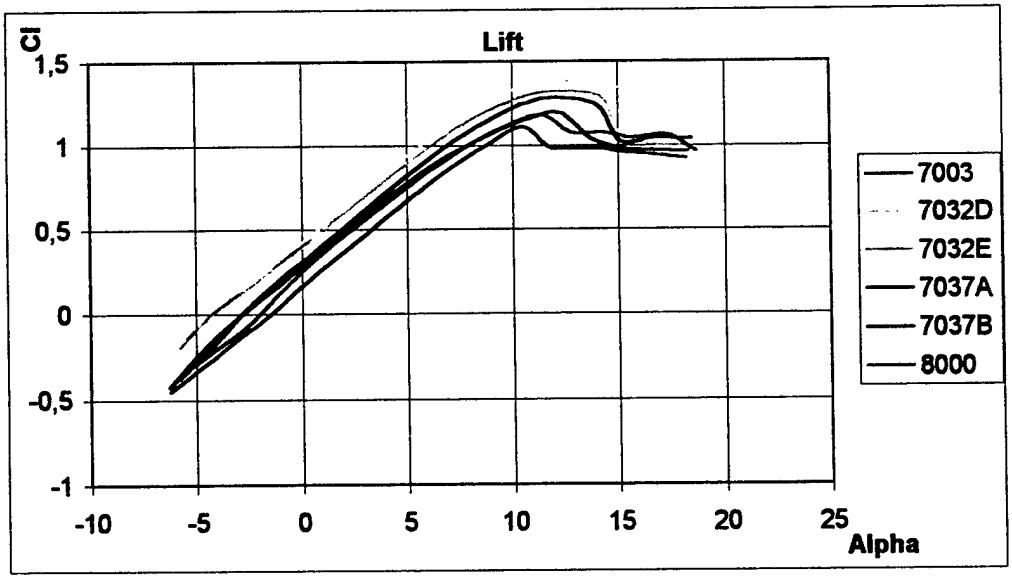

Figure 4.3: SD family lift

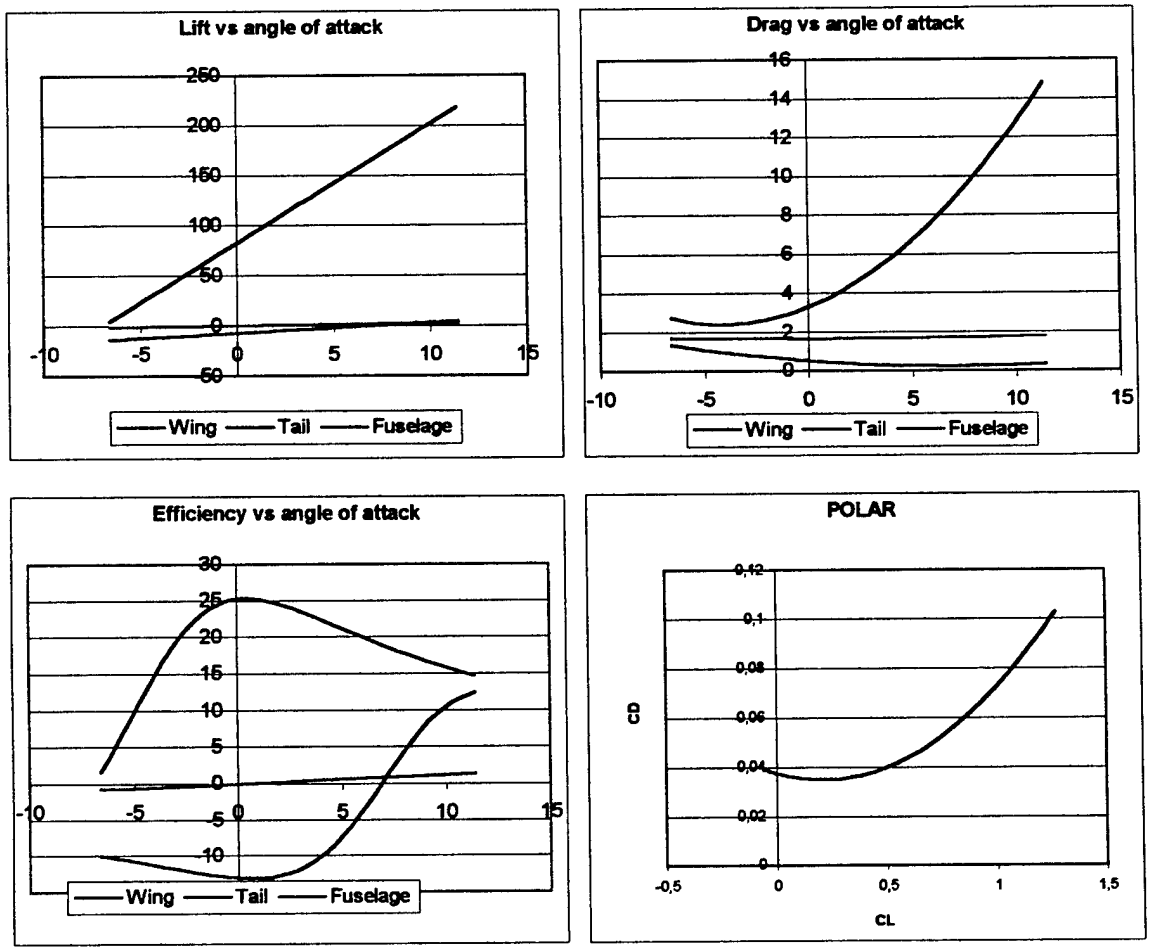

Figure 4.4: Whole aircraft

The angle of attack of the fuselage was used as reference. As a result, the cruise is at 0° angle of attack, with the minimum of the fuselage drag. From the efficiency curves it can be seen that, for the design angle of attack, the efficiency of each aircraft component is very near to the maximum, (minimum for the tail because with negative lift) which is proof of a good design. For the choice of the fuselage shape, stated the axis-symmetric shape, which minimizes the form-drag, we looked for the best trade-off between shape and cross-section, but we did not trust completely in the results, being impossible to model the rotating flow induced by the propeller. Then we postponed to a following phase the final choice.

4.3.2 Propulsion Analysis

The optimisation program OPTIM 5.4 shows that we need a thrust of 26-30 N at zero speed. Suitable motors are the three Graupner models: Ultra 930-8 12V, Ultra 1800-3 10V and Ultra 3300 -3 10 V. These models have low values of both the torque constant, Kt, and the speed constant, Kv. At this point we tried to use these motors without a reduction, (changing only diameter and pitch of the propeller) to limit weight and cost; but the simulations with the program "Motocalc" and the Matlab code "Motor1_testprop", gave us non acceptable results: it is necessary to use a reduction. Among the models fitting the Ultra series, we choose the HP 3.7:1. Each motor was considered working at zero speed and full throttle. We considered number of cells from 11 to 17, and the coupling motor-reduction-propeller, with propellers form 18" to 23" of diameter. For each value of the number of cells we found the performances (thrust, input power, RPM etc) and the propeller diameter giving the highest global efficiency.

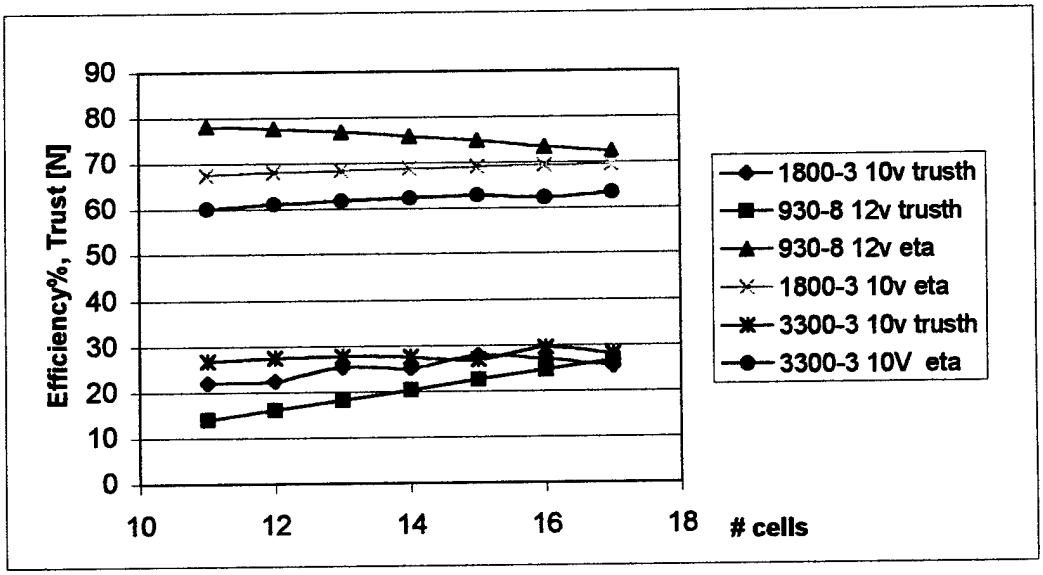

Figure 4.5: motors comparison

It can be seen from figure 5 that the 930-8 has the highest efficiency, but the lowest thrust. On the other side, for some cells numbers, this motor can produce the same thrust, with higher efficiency values. From these studies the best set is Ultra 930-8 12V, HP 3.7:1 reduction, 20" x 10" propeller, 17 cells; this configuration allows the generation of a zero speed thrust equivalent to 28 N (6.3 lbf).

4.3.3 *Performances & Flight mechanics*

Steady level flight: The first considered condition was the steady level flight at an altitude of 30 m (about 100 ft). From the aerodynamic analysis we knew the polar of the complete aircraft, and from the propulsive analysis the thrust as a function of the flight speed. Then, considering the balance of forces and pitch moment, we found out a cruise speed for the full payload case (with a total weight near 8 kg, 17.6 lb) of 20 m/s (65 ft/s). For this condition we studied the fixed command longitudinal static stability. For zero elevator deflection and angle of attack, we found the pitch coefficient of the whole aircraft, given the static margin and the tail distance, and considering the wing, tail and fuselage contributes, and the downwash effect on the tail. With an iterative method we found coupling angles of wing and tail that would make the aircraft stable, i.e. with $Cm_0>0$ and $Cm_\alpha<0$. It results: $i_w = 2.2°$; $i_t = -2.5°$.

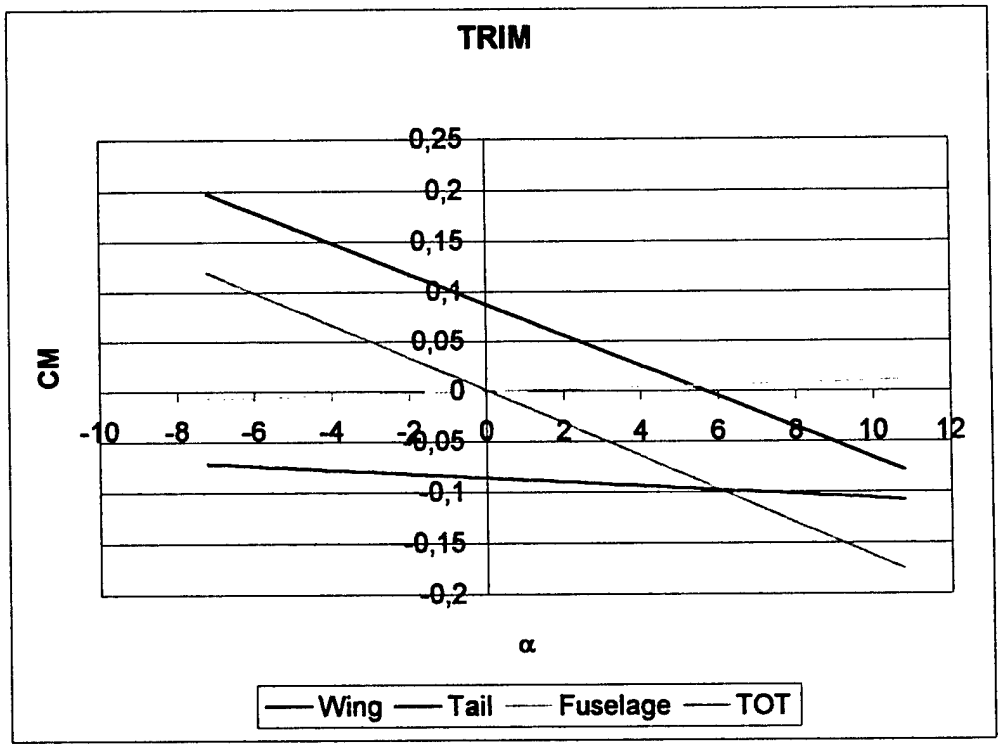

Figure 4.6: trim analysis

Thrust and Power: From the propulsive analysis we obtained the maximum shaft power, the available power and the thrust as functions of the flight speed. The required power and thrust were easily found form the aerodynamic parameters. The graphical analysis of the power shows the excess power at different flight speeds: at the higher speed flown for the largest part of the mission and at the lower ones, which represent the speeds of second regime. The required power curves were determined for the maximum aircraft weight, with payload and antenna, and for the unloaded aircraft, and are put into evidence the stall speed for both the conditions. Indeed, the stall speed deeply affects the take-off and climb phases analysed in the following points. The other characteristic speeds were also calculated too, and they will be utilised further during the mission analysis. The stall speed is $V_S = 11.5$ m/s (38 ft/s) at full

load and 10m/s (33 ft/s) empty. The minimum required power speed coincides with horizontal tangent to the curve and is equal to $V\pi$ = 12 m/s (39 ft/s); the maximum efficiency speed, which can be found tracing the tangent curve from the origin of the axes, is V_E = 17 m/s (56 ft/s).

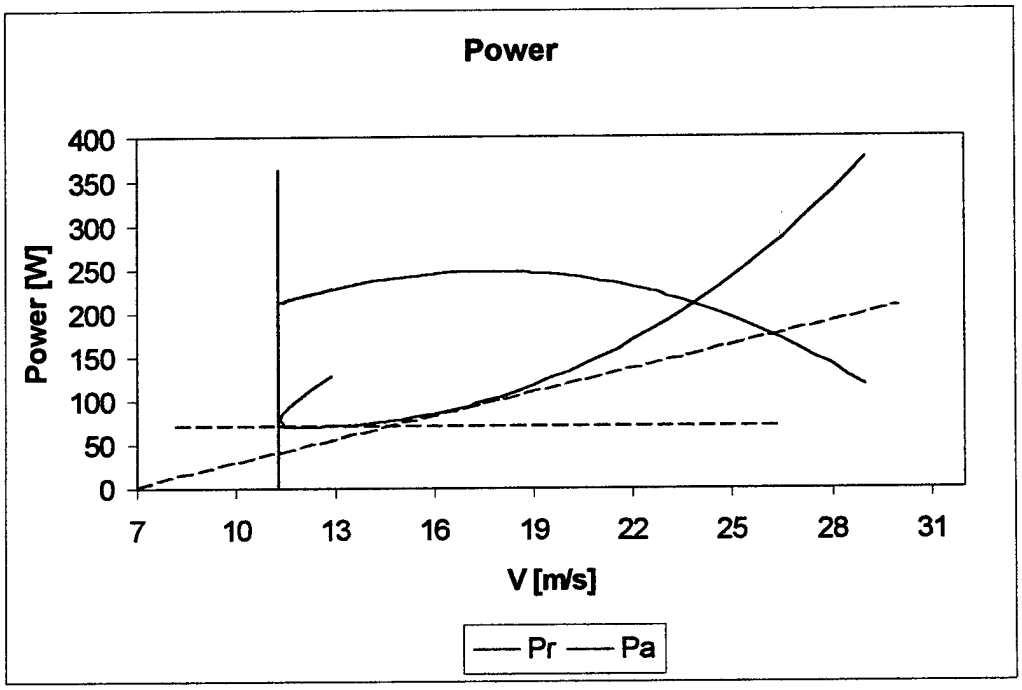

Figure 7: power analysis of loaded configuration

Take-off analysis: the take-off analysis in the optimisation algorithm indicated the take-off speed range: Vto=12-15 m/s (39-49 ft/s). In the previous point we determined the stall speed, setting Vto=1.1 V_S, we had Vto_{load}=12.65 m/s (41 ft/s), Vto_{empty} = 11 m/s (36 ft/s). Then, it was possible to calculate the take-off distance in the two conditions: loaded and empty weight. It is:

- T/W_l = 0.36; T/W_e =0.52; the thrust to weight ratio, with the take-off thrust equal to the maximum;
- W_l/S: =109 N/m^2 (2.28 lbf/ft^2); W_e/S = 69.55 N/m^2(1.45 lbf/ft^2); the wing loading;

from the force balance we calculated the acceleration during the run from zero to take-off speed, which is function of the two above parameters and of the aerodynamic data. Then we calculated the take-off distance integrating from zero to the take-off speed, as shown:

$$S_G = \frac{1}{2g}\int_0^{V_{TO}} \frac{d(V^2)}{K_T + K_A V^2} \quad ; \quad \text{where } K_T = \left(\frac{T}{W}\right) - \mu ; \; K_A = \frac{\rho}{2(W/S)}\left(\mu C_L - C_{D0} - K C_L^{\,2}\right)$$

The aerodynamic coefficients were taken at the ground angle of attack, measured with respect to the zero lift angle. These are the obtained distances:

S_{Gl} = 27.57 m (90 ft) ; S_{Ge}= 12.53 m (41 ft).

Climb: for a constant speed climb, it is possible to follow a graphical approach, considering that the rate of

climb (RC), i.e. the vertical speed, is $RC = V\sin\gamma = \frac{\Pi_a - \Pi_r}{W}$. From the previous analyses, we knew the powers as function of the speed and for the weight in two loading conditions: empty and full load. Then, it is simple to compute the RCs, for both conditions, as function of the flight speed, and the maximum RC, corresponding to the maximum excess power flight speed. Then, we can find the fastest climb speed and the flight path angle. The obtained values are:

$RCmax_{empty}$ = 7.217 m/s (23.7 ft/s); $RCmax_{load}$= 4.456 m/s (14.7 ft/s);

Vfc_{empty} = 13 m/s (42.7 ft/s); Vfc_{load} = 15 m/s (49.2 ft/2);

γ_e = 33.72° γ_l=17.28°.

In both the considered conditions, the fastest climb speed is higher than the stall speed. It is then possible to perform the climb with the maximum excess power. For this condition we easily found out the thrust to weight ratio, from the level flight efficiency and the flight path angle:

$T/W_e=(1/(L/D)e)+\sin\gamma_e$= 0.672; $T/W_l=(1/(L/D)g)+\sin\gamma_l$ = 0.385;

On the other hand, it is impossible to perform the climb at the steepest climb speed, i.e. at the maximum flight path angle, because it is lower than the stall speed.

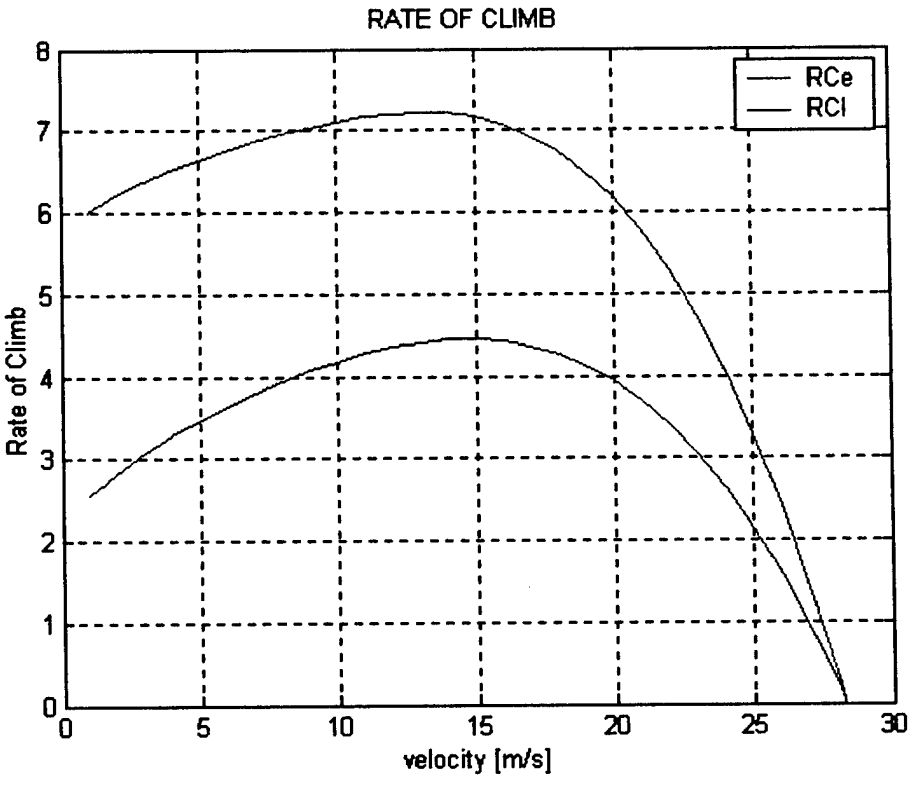

Figure 4.8: rate of Climb vs. flight speed

Level turning flight: we decided to perform the turn at the maximum efficiency speed, which is near to the cruise speed, as shown in the aerodynamic analysis. We calculated the loading factor, and then the bank

angle ϕ and the turn radius rt. These are the results for the two configurations, empty and loaded:

nv_e= 1.53;	nv_l= 1.34;
Rt_e= 19.73m (64.7 ft);	Rt_l= 33m (110 ft);
ϕ_e= 49.32°.	ϕ_g= 41.83°

Gliding flight: this flight condition was considered because the landing is carried out without thrust, to optimise the cell consumption and/or in the case of a propulsion system failure. The basic parameters we need to know are: the (negative) flight path angle γg, which, from the force balance with zero thrust, has the trigonometric tangent equal to the inverse of the efficiency, and the glide speed Vg. These parameters were determined in the case of a glide from the altitude of 10 m (33 ft), when the aircraft exits from the last turn. The results are:

γg_l = 5.05°;	γg_e = 6.6°;
Vg_l= 20.31 m/s (66 ft/s);	Vg_e = 24.83 m/s (82 ft/s);
time=5.6 s	time= 3.52 s

Analysis of the two missions: in this analysis the mission time as function of the energetic consumption is determined for A and B.

- Mission A: the weight remains constant and equal to the maximum (payload + antenna), the aircraft performs four laps, with a 360° turn on each downwind leg, one take-off and one landing.
- Mission B: there are two different phases: in each one the aircraft has a different weight (payload + antenna and only antenna) and performs 2 laps, with a 360° turn on each downwind leg, one take-off and one landing.

In splitting the course into sections, we took into account the short part of cruise the aircraft flies after the climb and before the pylon turn. This section is the *semi-cruise*, in dark green.

	MISSION A		MISSION B			
FLIGHT SEGMENT	# Segments	Time	# Segments		Time	
			Loaded	Empty	Loaded	Empty
Take-off run	1	4.6	1	1	4.6	2.5
Climb	1	7.7	1	1	7.3	5.4
Cruise	7	15.2	3	3	15	14.5
Semi-cruise	1	0.9	1	1	0.9	1
Turn	8	6.3	4	4	5.5	4.1
360°	4	12.5	2	2	11	8.2
Descent	1	5.6	1	1	5.6	3.5
Brake	1	6	1	1	6	8
Mission time	**231.6**		**210.1**			

Table 4.2: mission analysis

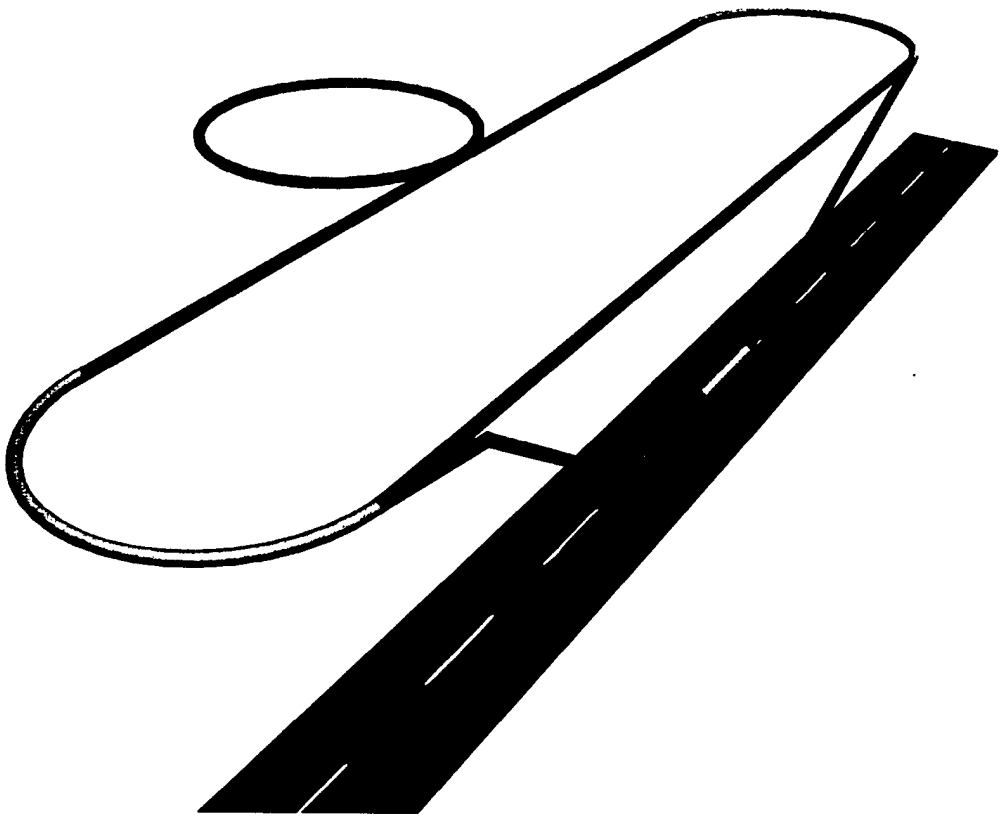

Figure 4.9: flight path segments

4.3.4 Structural Analysis

The structural design group investigated all the main components of the vehicle: wing, fuselage, tail and landing gear. We performed an analytical study followed by a numeric validation of the obtained results. The numerical analysis was developed using the MSC Nastran software and it reached a growing reliability, year by year, thank to accurate tests on mechanical property of the utilized composite materials.

Wing structural analysis

Designing the wing means to identify the critical operating conditions: structural test verification the aircraft will sustain corresponds approximately to a load factor of 2.5. The load diagram of our UAV predicts a maximum load factor equals to 2. The most critical condition for a wing is gust load. Considering such situation we designed the wing to resist a load factor equal to 3.6. We modelled the half wing as a cantilever beam, fixed to the root and loaded with elliptic lift and constant drag and momentum. Thanks to previous years experiences, the lightest and the most suitable choice appeared to integrate a single sandwich spar (polystyrene core + composite caps) in the maximum airfoil thickness. It will sustain the whole bending moment of the wing. Bending stresses versus spar caps thickness along the half wing span led us to laminate the spar caps with

two ply of the carbon ribbon for a total thickness of 0.5 mm (0.02")(figure 4.10). It is sufficient to resist to the maximum stresses (230 MPa) on the root section. Twist analysis verified that a single ply of glass fiber 0.25 mm thick (0.01"), weighting 80 g/m^2, is generously resistant. The half wing critic element is the cylindrical tube joining the fuselage. We were not able to find or built carbon tubes with the correct diameter and thickness, so we looked for commercial glass fiber tube with a diameter of 25 mm and a thickness of 3 mm. They suited our strength request but they were too much heavy. A lime wood pole with a diameter of 25 mm provided the necessary strength with a lesser weight, so that we decided to use it unless we will find a correct composite tube. The pole runs into the core of the half wing for 39 cm, from the root balsa rib to the inner balsa rib, both 10 mm thick. It extends itself out of the root rib for 85 mm to join with the fuselage. A finite element (FE) analysis confirmed our analytical results; figure 13 shows the half wing deformation under structural test load conditions.

Fuselage structural analysis loaded

The fuselage is basically made up of 5 composites plates (nomex honeycomb + carbon skins); it must bear the load sent by the half-wings, the tail planes and the landing gear, coupled to it with cylindrical connectors (wing and tail) or directly laminated on it (gear). The sandwich thickness was analytically determined for the most loaded plates, i.e. the lateral ones where are connected the half-wing. Were available nomex core of two different thicknesses, 6 mm and 8 mm (0.24" and 0.32"), while for the skins we used one layer of carbon fabric weighting 100g/m^2. Then a whole fuselage FE model was developed to check the analytic study and, above all, the shear strength of the glued zones of the landing gear legs.The primary structure has been modeled with different properties laminate elements, dividing it in the following three parts: a front portion, putting up the motor-battery group; a middle portion, putting up the payload; a tail-cone rear portion, connecting to tail surface. Both of the front and rear portions have been realized in carbon fiber reinforced plastic (CFRP) laminate, instead of the middle portion is sandwich, Nomex-CFRP made. The connections between fuselage and tail and between fuselage and motor-case have been simulated using DOF spring elements with fitted stiffness. The resultant model consists of 2262 elements and 1845 knots. Two load conditions were considered: first, the static load acting on the fuselage when the aircraft is on the ground; in this case the fuselage has been considered fixed to the landing gear constrains. Second, the aerodynamics loads in the worst flight condition; in this case the fuselage has been considered pinned to joint of the wing. The considered loads are:

- the propellers reaction couple;
- the loads (forces and moments) transmitted from the tail;
- the loads (forces and moments) transferred from the wings;
- the motor-group weight;
- the body accelerations due to the worst flight condition.

The result of the static analysis showed the most stressed elements and permitted to size them suitably. Figure 4.10 shows maximum stresses of the laminate. The 8 mm core was elected as the most satisfying for the required strength in the wing connector area. The overall sandwich thickness is 8.6 mm (0.34").

Tail structural analysis

The tail H configuration was thought as a single structural element, mounted on the fuselage by the carbon boom, to which the horizontal tail spars, also made of carbon, are linked. The boom sizing was performed on the basis of the maximum bending stress, transmitted by the tail during the maneuvers; a 40 mm (1.6") diameter pipe, 1 mm (0.04") thick, made of carbon fiber, and with a button lock system, was elected as the optimum solution; the maximum stress it has to bear is a little higher than 50 Mpa (7'250 psi) (See figure 4.11). For the horizontal tail plane, two 8 mm (0.32") diameter, 1 mm (0.04") thick carbon spars were chosen. This solution was preferred to the single-spar one, for the small airfoil thickness (t_{max} = 20 mm, 0.79"). The two spars are located the first at the maximum thickness and the second 8 cm (3.15") aft of it. The vertical planes are linked directly to the two horizontal plane spars by two other identical spars. The maximum bending stress is lower than 200 MPa (29'000 psi). (See figure 4.12).

Landing gear structural analysis

The landing gear was sized on the basis of the maximum bending and shearing stresses generated during the landing phase. It was modeled as a beam with a kwon initial warp, fixed on the lateral fuselage plate for 8 cm (3.15") of its length. The need that the aircraft fits partially mounted in the box, pones a one-foot-limit to the wheel distance. This leads to a low warp, and then to poor flexibility, useful to absorb the impact energy by bending deformations; on the other hand, the legs are mainly loaded axially, and then arise the buckling problem. Therefore, an analytic study was performed to investigate the buckling behavior of the landing gear structure. The results of this study, suggested us to laminate 10 layers of Carbon+Kevlar fabric + 2 layers of unidirectional CFRP. A numerical FE analysis verified this decision. The structure has been simulated with120 elements and 150 nodes FEM model. The Hoffman fracture criterion has been used because of non isotropic material property in 1 and 2 principal directions. In order to simulate the ground impact condition, the connection between the landing gear and the wheel has not been considered infinitely rigid, DOF spring elements with appropriate stiffness but have been used. The load conditions considered in the landing gear sizing, are referred to a landing at a vertical speed of 2 m/s (6.6 ft/s), widely in the range of vertical speed found for the gliding flight phase. The maximum stress, produced in the external carbon layers are nearly 100 Mpa (14'500 psi), while the max failure index is abundantly under 0.06 value. (See figure 4.15).

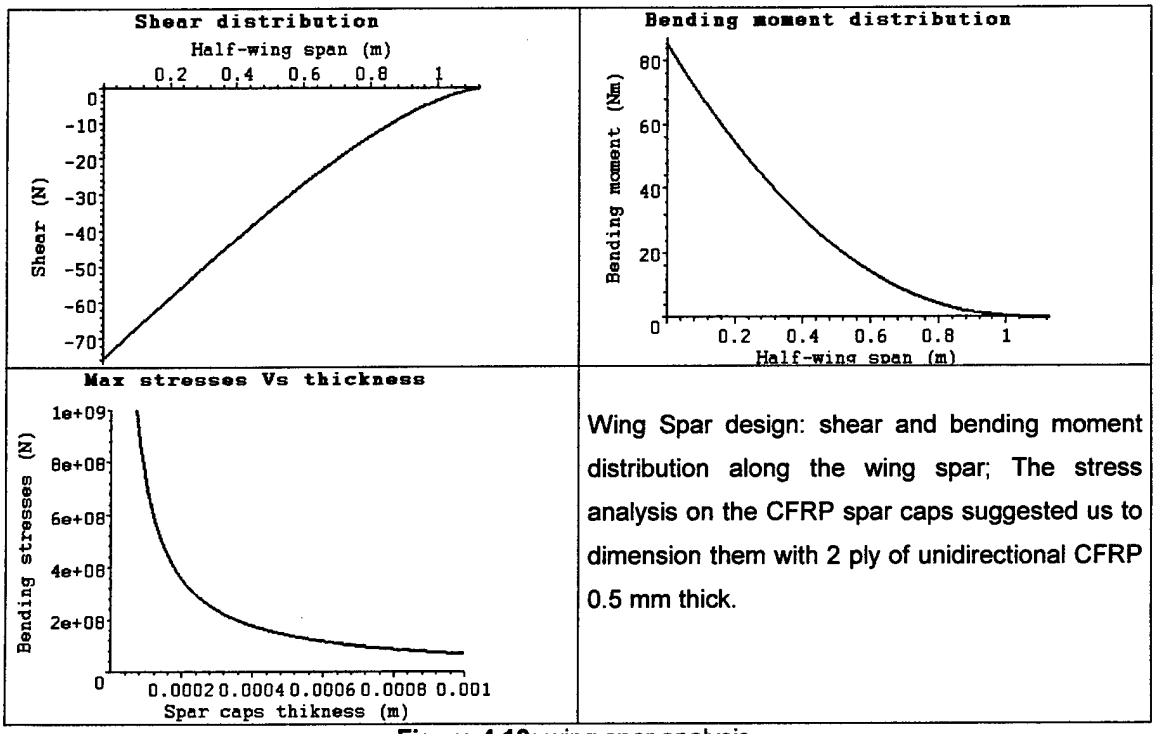

Wing Spar design: shear and bending moment distribution along the wing spar; The stress analysis on the CFRP spar caps suggested us to dimension them with 2 ply of unidirectional CFRP 0.5 mm thick.

Figure 4.10: wing spar analysis.

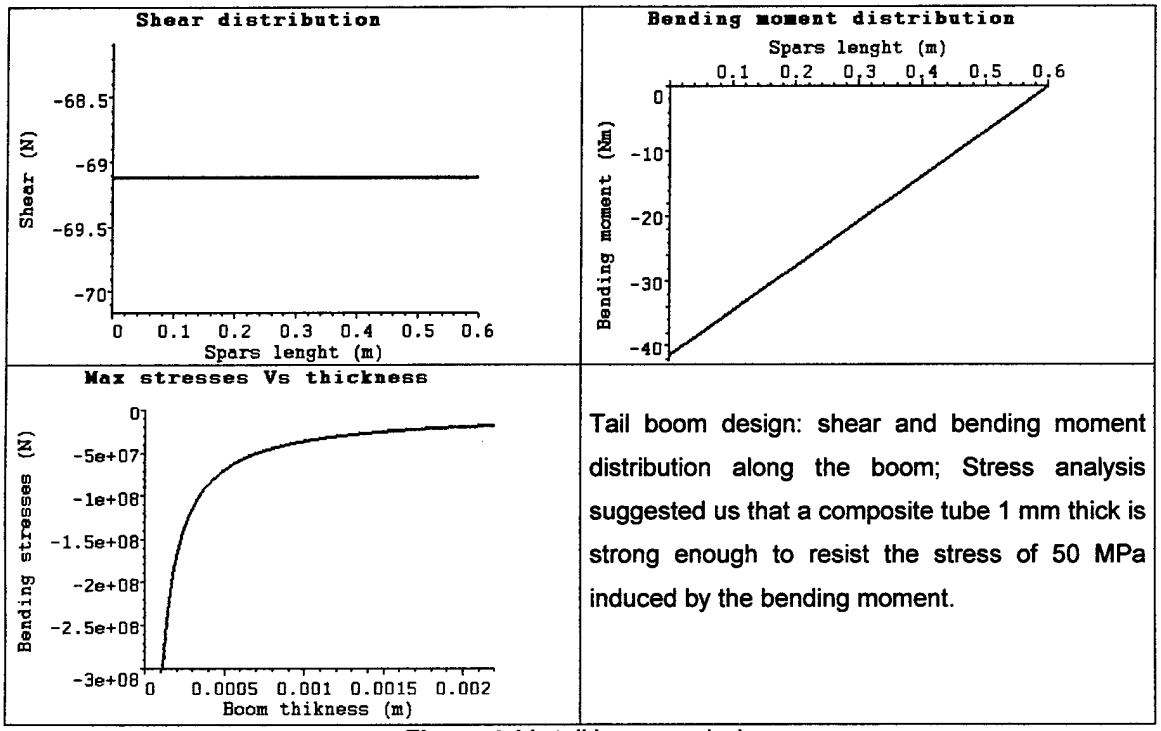

Tail boom design: shear and bending moment distribution along the boom; Stress analysis suggested us that a composite tube 1 mm thick is strong enough to resist the stress of 50 MPa induced by the bending moment.

Figure 4.11: tail boom analysis

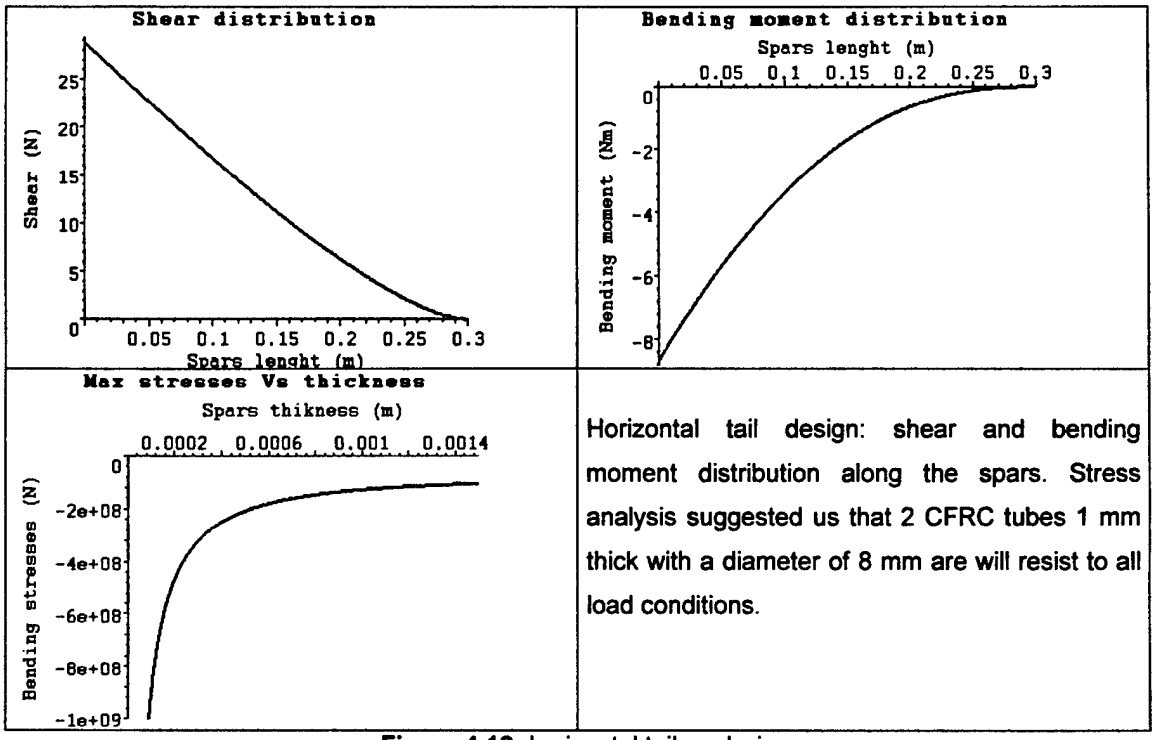

Figure 4.12: horizontal tail analysis

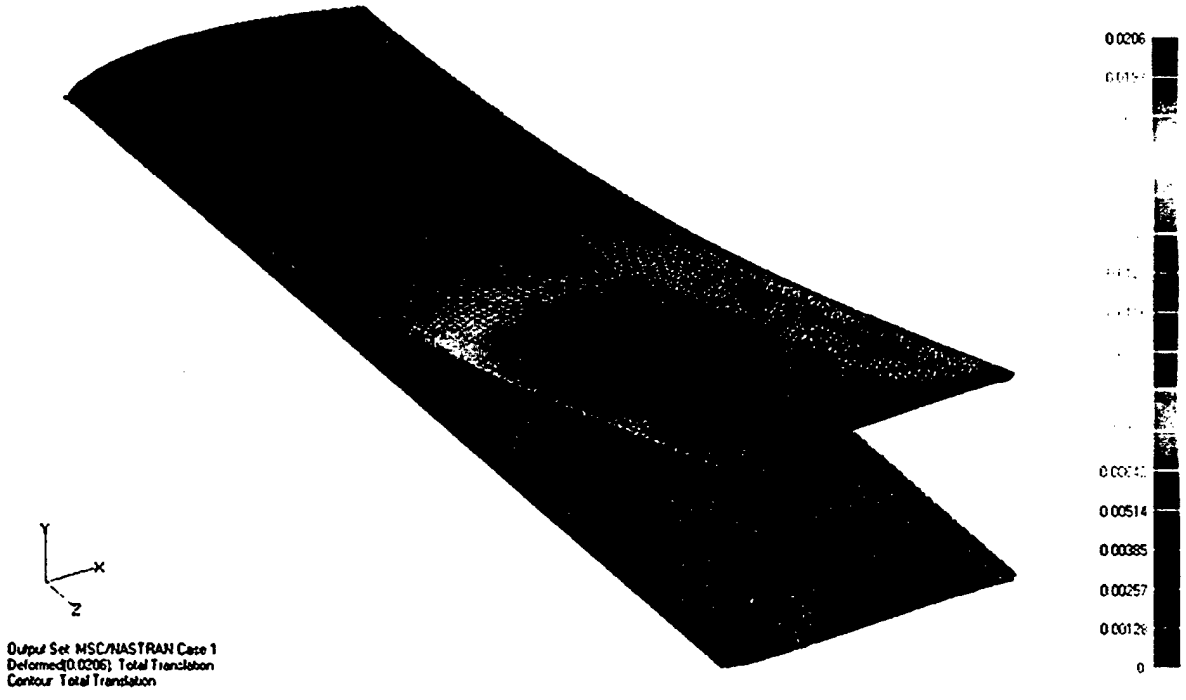

Figure 4.13: half wing: total traslation

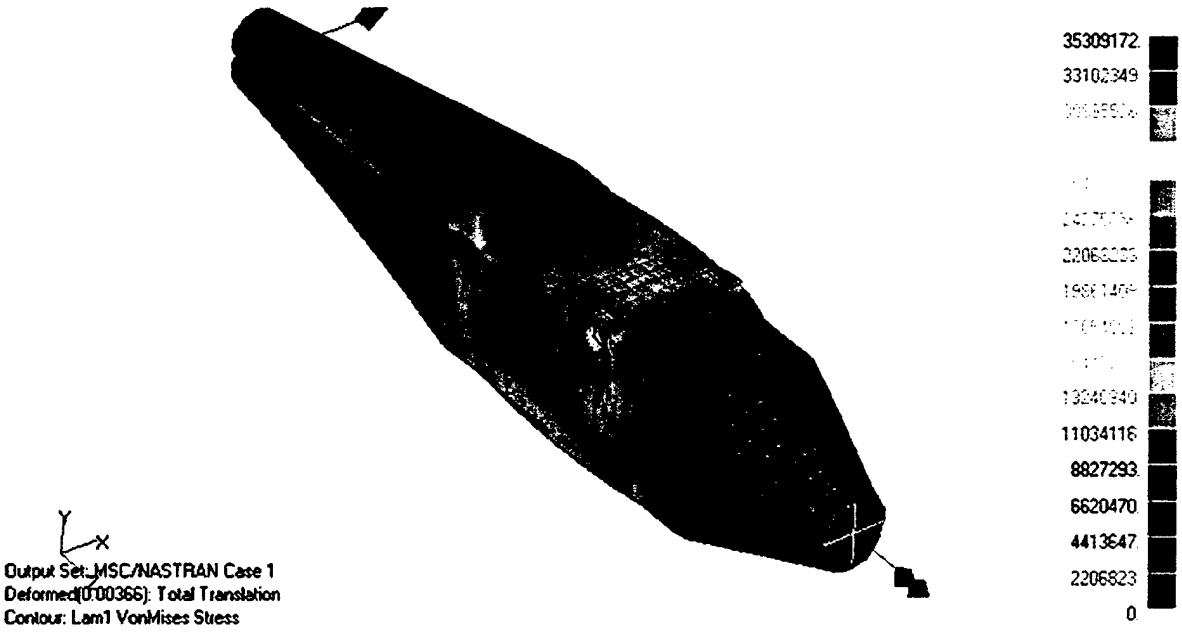

Figure 4.14: fuselage: max Von Mises stresses

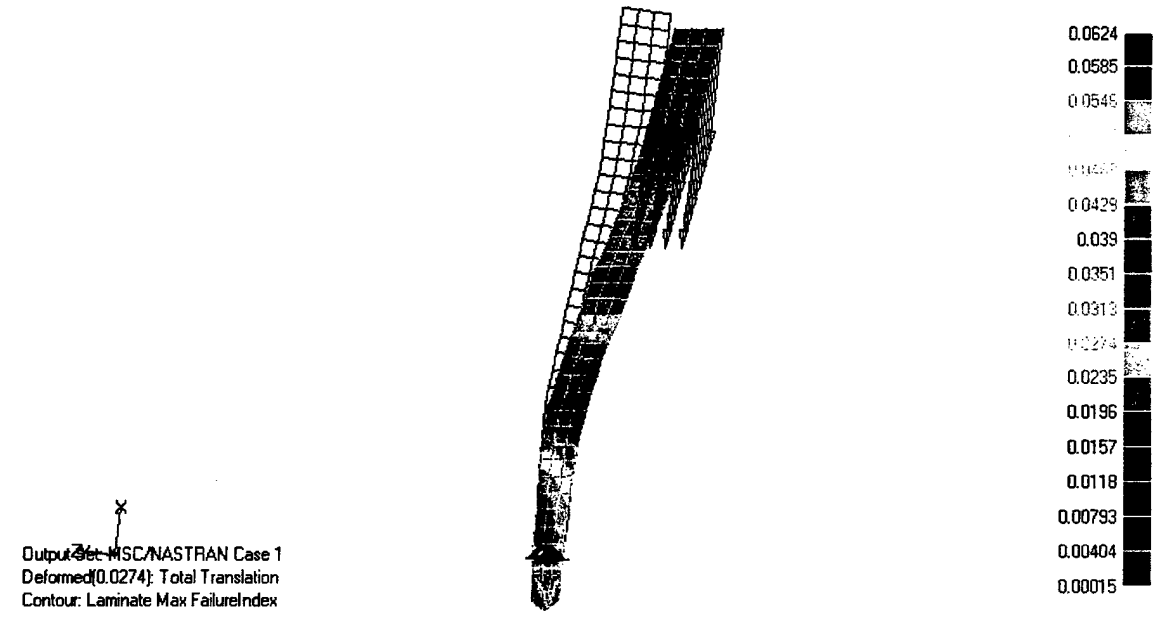

Figure 4.15: maximum failure index distribution, using Hoffman fracture criterion.

5 Detail Design

5.1 Introduction

At the end of the preliminary design stage, we had already sized the main components of our plane. It was known the concept shape, as well as the structural and propulsive subsystem. Moreover, we had identified its predicted performances in various flight conditions. In the next phase of the design process we had to focus attention on that elements we did not have studied yet, and to evaluate with more accuracy the performances we could not estimate in detail before, such as the dynamic behaviour of the plane. Therefore, we proceeded with the sizing of control surfaces, and the analysis of the systems to join the main structural elements. Next we tried to find solutions for the problem of the extendable door for the payload disposal. Finally, we addressed the problem of the cooling system of the propulsive group and the best way to arrange servos and wires.

5.2 Flight Dynamics and Control

5.2.1 Control Surfaces

We had to size the elevator and ailerons mobile surfaces. We decided not to have rudder, because the missions do not include acrobatic manoeuvres and the weather in the contest site should be calm, without wind. For the ground directional control, we introduced a steering nose gear. We sized the control surfaces using the procedure suggested by Raymer.

Elevator: It was sized to produce enough tail load to achieve the take-off rotation at the maximum payload condition. The elevator effect can be considered as the one of a wing flap; then the rotation of this surface does not change the Cl_α but reduces the zero-lift angle. In particular:

$$\Delta\alpha_{0L} = -\frac{\Delta C_L}{C_{L\alpha}} = -\frac{1}{C_{L\alpha}}\frac{\partial C_L}{\partial \delta_E}\delta_E$$

With an iterative method and using empirical curves, giving $\frac{\partial C_L}{\partial \delta_E}$ as a function of the ratio between elevator and the tail chords (c_e/c_t), it was possible to determine the c_e/c_t ratio for the maximum deflection in the range 15-20°. The obtained result is c_e =0.06 m (2.4") for a span b_e =0.48 m (19"), for a maximum deflection of 18°.

Ailerons: For the ailerons sizing we used the same procedure seen for the elevator. The ailerons do not occupy the whole wing span, as the elevator, then we used the balance between the roll moment produced by the ailerons and the roll damping at steady-state roll rate p_{ss}. For p_{ss} =100 deg/sec and maximum deflection δ_A = 17°, from:

$$\frac{p_{SS}b}{2} = \frac{C_{l,\delta A}}{C_{l,p}}V\delta_A$$

we found out: b_a=0.50 m by a chord, c_a =0.07.

Pitching-moment equation and Trim: The pitch moment, about the center of gravity, has to be equal zero. This moment is the sum of the contributes produced by the various aircraft components: wing, fuselage, tail. For a given flight condition, is possible to calculate the single contributes and check if the sum is zero. If this condition is not met, it is possible to vary the tail lift, changing the elevator deflection or the tail incidence, so that the moment vanishes. The change of the tail lift produces a change of the total lift of the aircraft, which should balance the weight. Then, the change of the tail lift causes a change of the angle of attack. To solve the problem an iterative method can be used, or better the graphical solution proposed by Raymer: once the angle of attack α and the elevator deflection δ_E are arbitrarily chosen, we calculate the total pitch moment coefficient:

$$C_{mcg} = C_L(\overline{X_{cg}} - \overline{X_{acw}}) + C_{mw} + C_{mfus} - \eta_h \frac{S_h}{S_w} C_{Lh}(\overline{X_{ach}} - \overline{X_{cg}})$$

where C_{Lh} is the tail contribute, function of the downwash angle and the zero lift angle due to the elevator deflection, found out in the previous elevator sizing. Under the considered hypotheses, it is possible to calculate the total lift coefficient, where the wing and tail lift coefficients are summed, considering the change of the dynamic pressure on the tail. For different angles of attack we calculated the total lift coefficient and C_{mcg}. For C_{mcg} =0, it is possible to find the trim conditions for different elevator deflections.

5.2.2 Handling Qualities

At this point we encountered the problem of studying the dynamics stability of the designed aircraft. That means to predict how the aircraft motion evolves following a perturbation of its equilibrium state. As trim condition we considered a steady state level flight at cruise speed and full weight. The equations of motion were then linearized using the theory of little perturbations. In so doing we obtained, as usual, two sets of decoupled equations for longitudinal and lateral dynamics. The linear equations were written in the space-state. So, we could calculate eigenvalues, damping, and therefore, coefficients and natural frequencies and to analyse the stability of the system. Then we studied the response of the system to inputs of 1 deg for elevator (longitudinal dynamics) and for ailerons (lateral dynamics). To follow this procedure we needed to calculate stability and control derivatives (non dimensional and dimensional). To this end, the method proposed by Roskam was used.

$C_{L,\alpha}$	$C_{D,\alpha}$	$C_{M,\alpha}$	$C_{L,q}$	$C_{M,q}$	$C_{L,\dot{\alpha}}$	$C_{M,\dot{\alpha}}$
4.6261	negligible	-0.8298	4.5669	-5.3245	negligible	negligible

Table 5.1. Longitudinal non-dimensional derivatives

C_{L,δ_E}	C_{D,δ_E}	C_{M,δ_E}
0.9704	negligible	-2.0935

Table 5.2. Longitudinal control derivatives

$I_{yy}[kgm\text{^}2]$	X_α	M_α	$M_{\dot{\alpha}}$	M_q
1.8318	5.7115	-23.95272	0	-2.30543

Table 5.3 Longitudinal derivatives and moment of inerzia about Y body axis

$C_{y,\beta}$	$C_{l,\beta}$	$C_{n,\beta}$	$C_{y,p}$	$C_{l,p}$	$C_{n,p}$	$C_{y,r}$	$C_{l,r}$	$C_{n,r}$
-0.4918	-0.0125	0.2907	-0.0035	-0.4710	-0.0444	0.6127	0.1237	-0.5649

Table 5.4 Lateral-directional non-dimensional derivatives

C_{l,δ_A}	C_{n,δ_A}	C_{y,δ_A}
1.82178	-1.40612	negligible

Table 5.5. Lateral control derivatives

$I_{xx}[kgm\text{^}2]$	$I_{zz}[kgm\text{^}2]$
1.2983	3.0745

Table 5.6 Moment of inertia about X and Z body axes

Y_β	L_β	N_β	L_p	N_p	L_r	N_r
-4.3341	-5.28768	3.1102	-11.95439	-1.1269	3.1396	-28.6753

Table 5.7 Lateral-directional dimensional derivatives

Once the aerodynamic derivatives and the reference flight condition were calculated, we had the components of the state and control matrices. Then, two simple codes were developed in commercial software Matlab to calculate eingenvalues, damping coefficients and frequency for the longitudinal (phugoid and short period) and lateral-directional modes (roll, spiral and ducth roll).

Longitudinal dynamics

From table 5.8 we observe that the real part of the eingenvalues is negative, positive damping so that both modes are stable. Furthermore, the results show how the short period damping is nearly ten times that of the phugoid. The same frequencies, calculated with the approximate models (second-order) of phugoid and short period, are respectively: ω_{PH} = 0.6937 rad/sec, e ω_{SP} = 10.21rad/sec.

Mode	**Eingenvalue**	**Damping**	**Frequency [rad/sec]**
Phugoid	-0.0348 ± 0.611i	0.0569	0.612
Short Period	-5.22 ± 9.87i	0.471	11.1

Table 5.8. longitudinal modes

These values are quite close to the ones obtained as output of the Matlab program.

Next we evaluated the response of the plane model to a single nose down impulse command of 1 deg elevator. By analysing figure 5.1, we can deduce that in the first seconds, when the short period is excited, we find the biggest variation of angle of attack and pitch rate. Then, at later time, when the phugoid mode is the dominant one, we can see the biggest variation of airspeed and pitch attitude.

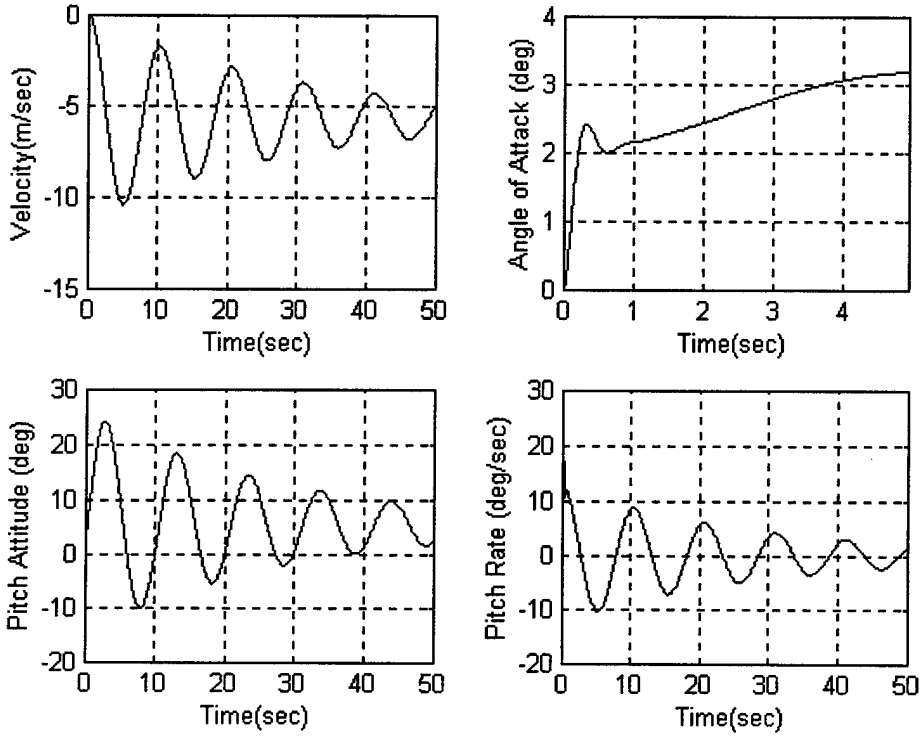

Figure 5.1. longitudinal response to a 1-deg elevator impulse input

Lateral-directional dynamics:

The Matlab program gave the eingenvalues, damping coefficients and frequencies shown in table 5.9 for the roll, spiral and dutch roll modes.

Mode	Eingenvalue	Damping	Frequency [rad/sec]
Spiral	0.00202	-1	0.00202
Dutch Roll	-2.6 ± 5.84i	0.407	6.4
Roll	-14.6	1	14.6

Table 5.9. lateral-directional modes

Results show a slightly unstable spiral mode. It is associated with a real eingenvalues which mainly represents the variations in roll attitude $\Delta\phi$ and depends mostly on the $C_{l,\beta}$. Anyway, spiral mode is typically associated with a slow dynamic. This is our care, actually: in fact the time constant is low so that the pilot has time to react. The dutch-roll is an oscillatory mode with significant component in the yaw Δr and the roll $\Delta\phi$ variables. Table 5.10 shows that it is stable. The roll mode is associated with a real root and the motion is predominantly in roll rate Δp .Next we analysed the response to a single 1 deg impulse on the ailerons, positive (i.e.: right aileron upwards).

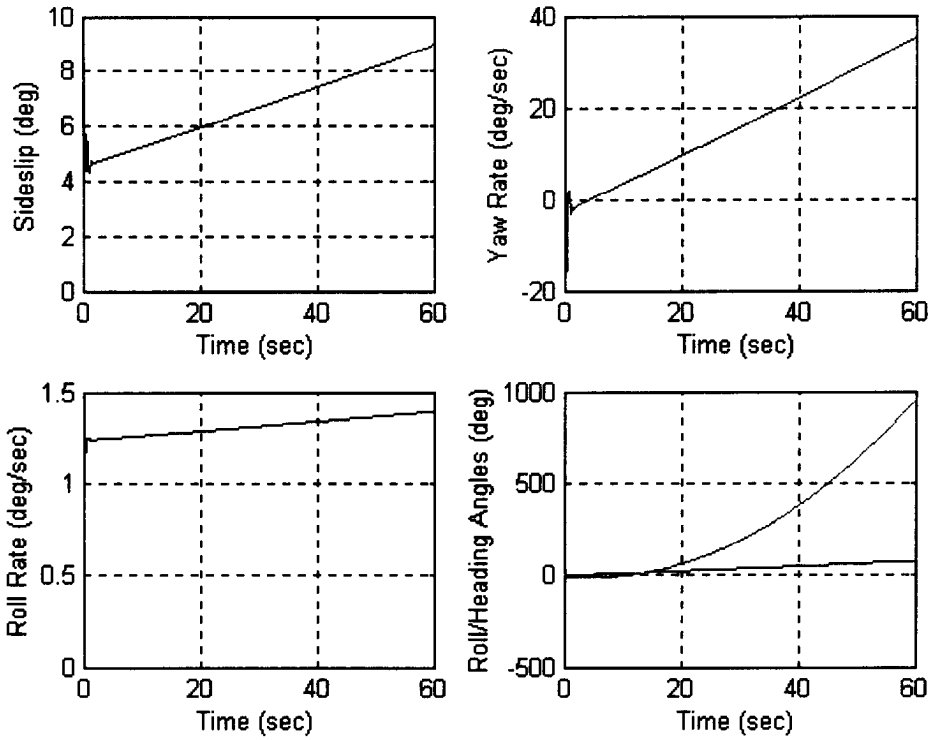

Figure 5.2. lateral-directional aircraft responses to a 1-deg aileron impulse input

5.3 Structures

After the structural sizing of the major elements of the UAV we performed in the preliminary phase, their integration and detailed description was faced in detail design. This aspect of the design process has a strategic role for the entire project. New rules ask to contain the airplane in a specific size box that makes expected to disassemble the model in different parts. Besides, the time needed to extract and to assemble the model will influence the final score. Few elements and easiness to join is a prior task .

5.3.1 Fuselage Structural Details

Fuselage was designed around the payload to limit the frontal surface, caring to not expose sharp angles to the flow of the propeller. It consists in two volumes between three bulkheads and two longitudinal plates sandwich made where all other structures join. The main bay contains the payload, while a smaller volume behind contains the receiver and its cell and a tube to join with the tail section. An opening ensures access to it. Cargo bay has two doors on the bottom where payload is expelled from. The doors open for the weight of the payload and after the deployment it close for the action of two torsion spring. A servo placed outwardly in one of the doors commands the opening. It acts on a pin that works as a bolt. Wing junction is realized by an hand made CFRP T tube where wing booms and antenna join. Wings are prevented to slip from tube thanks to two screw fixed on the aligning little spars. The tail section is fixed to the central section of the fuselage by a CFRP tube constrained between the two aft bulkheads. A blocking

system prevents the tail section to rotate or translate. On the front bulkhead a GFRP pocket is glued to contain the cells' pack. Polystyrene fairings bring the desired aerodynamic shape.

5.3.2 Wing Structural details

The wing is formed by two parts, joining the fuselage. Each half wing is shaped on a polystyrene core and covered with a single ply of GFRP skin. A spar with two caps of CFRP integrated in the maximum airfoil thick provides the required bending strength. The polystyrene core transmits loads to the composite structures. Two balsa ribs are placed at the root and wing tip. A third rib 39 cm far from the root rib allows to align the wing boom joining the fuselage. The ailerons' servos are drowned into the core and fixed to the wing skin by a lime wood thin plate.

5.3.3 Tail Structural Detail

The H tail follows the same building philosophy of the wing: polystyrene core with composite strength element. Loads resistance is provided by two carbon tubes drowned into the core; with the GFRP skin, they constitute the tail structure. The tail's aerodynamic surfaces are glued on the boom that joins with the fuselage main section. The fuselage tail section is a polystyrene shell covered by a thin GFRP and it smooth the shape of the fuselage from the largest section of the cargo bay by an axialsymmetric low drag geometry. The disassembled configuration of the model in the box expected the tail to be set in the fuselage, but it is rotated by 90° to get the horizontal surface to be parallel to the two feet long side of the box. Assembling is obtained by spinning the tail until a blocking system forbid further movements.

5.3.4 Landing Gear Structural Details

The tricycle landing gear consists of a fore leg and a couple of after legs positioned behind the center of gravity of the plane. The froe leg is made of a carbon fiber reinforced plastic tube jointed with a couple of hinges to the foe frame of the fuselage. The main gear is constituted by a couple of legs realized by a manual lay up of carbon-kevlar fabric with epoxy resin cured at environmental conditions and controlled pressure. The latter are jointed directly to the lateral frames of the fuselage box. A servo is positioned on the upper side of the fuselage and moves directly the fore leg to allow driving the plane while on the ground (taxi, rull-out). The need to place the fuselage inside the box with the landing gear already mounted imposed a severe limit to the wheel-truck; in fact the distance within the wheels must be lower than the minimum dimension of the box, that is 1 foot. As a result the curving slope of the two main legs is very little, and its sizing calculations had to considered the possibilities that buckling phenomena would occur. The junction of the main legs to the sandwich frames of the fuselage has been realized using epoxy resin as structural glue. Locally the junction has been reinforced with a manual lay up of carbon fiber reinforced fabric. In fact this junction is severely loaded by huge shear stresses given by the legs at touch down, because of the little energy dissipation the leg can provide with its little flexural deformability. At the moment of sending this paper we have already performed some flight tests on the prototype. As a consequence of that, we are valuating the possibility to adopt a different solution for the after legs. In fact the very little wheel-truck comport stability problems at landings. So we are considering to realize a demountable carriage which would be more reliable, even if it would comport a bigger time for assembly.

5.3.5 *Radome Structural Detail*

Radome is made with polystyrene foam covered with CFRP. The enclosed volume contains the motor and the cells' pack. It transmits the trust to the plane by a connection on each of the two longitudinal plates of the cargo bay. The connections are obtained by two slides of aluminum and four screws for each slide. The junction is intended to be permanent because the two section of the UAV will lay joined into the container box. Two frontal inlets will supply the right cooling of the motor and cells pack.

5.4 Propulsion System

The propulsion system had already been fully designed at the end of preliminary design phase. The propulsive group had selected the proper motor and gear-box. It planned to perform a series of wing tunnel and flight test to choose the propeller and number of cells which would enhance aircraft performances. At this stage of the design the propulsive group considered the various possible cooling systems. It decided a simple air intake would be enough just properly disposing motor, controller and cells inside the radome. The inlet was sited so to guarantee a sufficient airflow not to cause the temperature of the system reaching values so high to endanger the safety of the system.

5.5 Final Aircraft Table

Geometry		
Length	1.18 m	3.87 ft
Span	2.4 m	7.87 ft
Height	0.52 m	1.71 ft
Wing area	0.72 m^2	7.75 ft^2
Aspect ratio	8	
Control volume	0.35	

Weight Statement		
Airframe	2.937 kg	6.475 lb
Propulsion System	1.575 kg	3.472 lb
Control System	0.698 kg	1.539 lb
Payload System	2.268 kg	5 lb
Antenna	0.522 kg	1.151 lb
Empty Weight	5.21 kg	11.4 lb
Gross Weight	8 kg	17.637 lb

Performances			
C_{LMax}		1.14	
L/D Max		14.32	
Static Margin		0.16	
Rate of Climb	Empty	7.22 m/s	23.7 ft/s
	Gross	4.46 m/s	14.7 ft/s
Stall Speed	Empty	11 m/s	36 ft/s
	Gross	12.65 m/s	41 m/s
Max Speed	Empty	29	95
	Gross	25	82
Takeoff Run	Empty	12.53 m	41.11 ft
	Gross	27.57 m	90.45 ft

System	
Radio	Futaba FP8 UPS
Servos	Futaba S9402
Battery Configuration	17 cells, serial
Motor	GraupnerUltra 930-8 12 V
Propeller	20" x 10"
Gear Ratio	3.7:1

Table 5.10: final aircraft table

5.6 Rated Aircraft Cost

In the following table the final competition aircraft RAC is determined according to the supplied cost model: RAC=(A*MEW+B*REP+C*MFHR)/1000 = **8.017** thousand $

Coefficients calculation

Coefficient	Description						Value
A	Manufacturers Empty Weight Multiplier						**$100**
B	Rated Engine Power Multiplier						**$ 1500**
C	Manufacturing Cost Multiplier						**$20**/hour
MEW	Manufacturers Empty Weight						**11.46** lb
REP	Rated Engine Power	# of Motor	# of Cells	Battery Weight			**2.24**
		1	17	2.24 lb			
MFHR	Manufactoring Man Hours	***Wing***	Span	Man Hours/Unit	WBS	***76.87***	**175.57**
			7.87 ft	8 hour/ft	63		
			Chord	Man Hours/Unit	WBS		
			0.98 ft	8 Hour/ft	7.87		
			# of control Surface	Man Hours/Unit	WBS		
			2	3 Hour/ft	6		
		Fuselage	Lenght	Man Hours/Unit	WBS	***38.7***	
			3.87	10	38.7		
		Empenage	# of vertical Surface with no control	Man Hours/Unit	WBS	***20***	
			2	5	10		
			# of Horizontal Surface	Man Hours/Unit	WBS		
			1	10	10		
		Flight System	# of servos	Man Hours/Unit	WBS	***30***	
			6	5	30		
		Propulsion System	# of motor	Man Hours/Unit	WBS	***10***	
			1	5	5		
			# of propeller	Man Hours/Unit	WBS		
			1	5	5		

Table 5.1: final RAC

5.7 Drawing Package

The following pages contain the CAD drawing package.

5.6 Payload Extraction Mechanism

Although the preliminary design of the aircraft ended up selecting a method for the retraction of the electronics payload box, the exact method by which the box would be restrained in the fuselage was yet undetermined. The design of this deployment system was one of the most important tasks the team accomplished during detailed design. The goal for the payload deployment system design was simplicity and reliability of operation. The system that resulted from the detailed design stage was a simple one – it consisted of a thin aluminum "plate" in which a Y-shaped pin moved by a servo could slide. This moveable pin would go through tabs on the top of the payload box, and be pulled out for retraction. The schematic of the retraction mechanism can be seen in Figure 5.3.

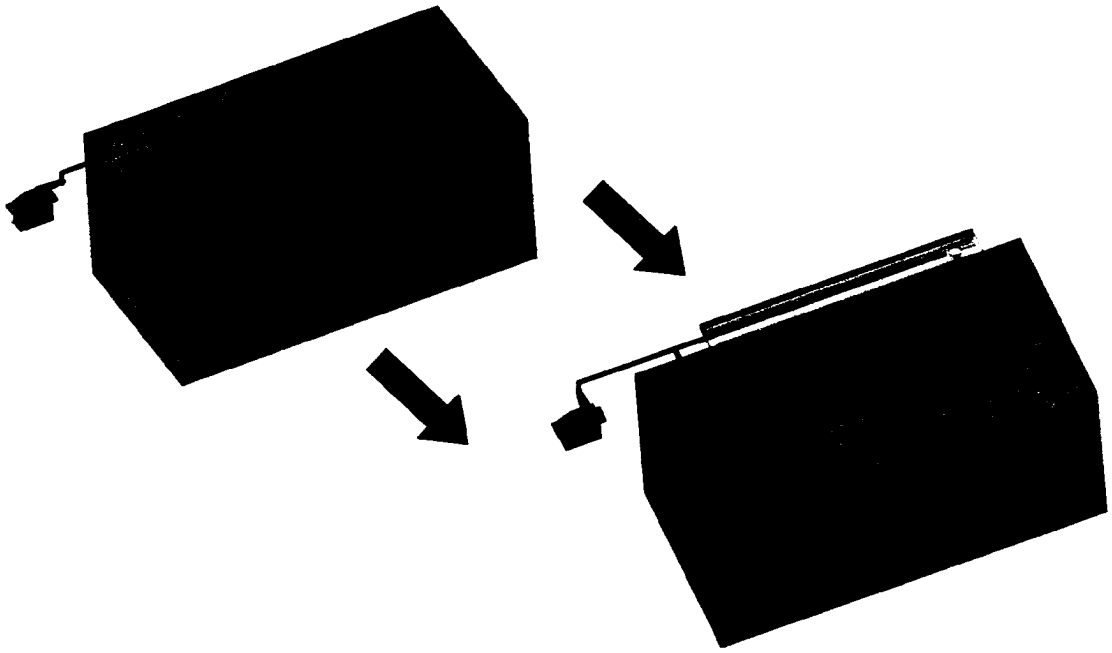

Figure 5.4 – Retraction Mechanism Operation

Once the pin was pulled, the payload box would fall out of the fuselage, pushing the payload doors open as it slid out. The payload doors were designed such that there was a substantial moment arm about the door hinges for the points of contact between the payload box and doors, to insure that the payload doors did not get stuck during deployment. After deployment, the aircraft could be taxied away, with the doors closing via springs upon clearing the payload box.

6.0 Manufacturing Plan and Processes

In constructing the aircraft, different manufacturing techniques were used to manufacture the primary components. While several different concepts were considered, composite construction was used extensively on the aircraft for its relatively high strength and low weight characteristics.

6.1 Manufacturing Concepts

As the team completed the detailed design, the construction method had to be determined. Several construction methods we available at the team's disposal and using figures of merit, the team rated each of the methods. First, the team considered the traditional balsa-hardwood construction with heat shrinking plastic covering such as Monocoat. This method was found to be heavier then other methods and much more rudimentary. Next, the team considered foam core composite construction. This method used a foam core material which was cut or sanded into the desired part geometry and then applied a composite cloth with resin along with heat and pressure. This method was found to have great strength to weight characteristics and moderate durability. The final method considered was a hollow mold composite method in which a negative mold was created, then adding a composite cloth with resin, or using pre-impregnated resin composite (prepreg) material with the application of heat and pressure. This method was found to have the highest strength to weight characteristics, but a much lower durability than the foam core due to lack of a core material providing compression resistance.

6.1.1 Competing Concepts

After thinking about the options, the team found that balsa-hardwood built up construction, has many benefits. It is cheap, requires little skill, and few pieces of equipment. The dilemma is that it would not have the desired strength, especially in shear stress and is heavier than the composite methods therefore eliminated. The hollow-core composite method had many benefits. It is the lightest method, but required a high level of expertise, time, and effort. The part required a negative mold which was laid up into using conventional wet layup techniques or prepregnated composites. Using this method the aircraft would be more prone to compression damage due to handling and assembly which would be more difficult to repair.

6.1.2 Downselect

Due to the high strength to weight ratio, along with simpler manufacturing procedures, the foam-core composite process was selected to be used as the primary construction technique. The foam core method permitted the part to be cut or sanded out of foam and then laid up using the desired orientation and thickness of composite material. The foam core allowed a much quicker final part compared to the hollow-core parts while much stronger parts than that of a balsa build up. If the aircraft were to be mass-produced, the long-term benefits of the hollow-core method would out weigh that of the foam core in particular areas of the aircraft, producing an ultimately lighter aircraft.

6.2 Manufacture of Primary Components

After the manufacturing concepts were narrowed down to a mostly foam-core composite construction, the team drew on experience gained in past years to determine the proper manufacturing techniques for the individual components. Different techniques and materials were utilized depending on the part be manufactured. The team selected this comparatively advanced method of construction despite of its higher level of complexity because of the potential it offers to builders experienced enough to utilize it. Although the method of construction is complex to learn; once learned, it delivers results that are superior in most respects to the alternatives.

6.2.1 Fuselage

Fuselage construction began with the general cross section of the fuselage cut out of white foam using templates generated from a solid model. The entire form was then sanded to bring out the detailed shapes, such as the nose and rear of the payload area tapering to the tail. Once the fuselage was sanded, a cutout was made on the top surface, into which the keel was set into. The entire surface was then filled with a light weight spackle to reduce the number of imperfections on the surface. With this step completed, the fuselage was ready for the composite lay up.

The composite lay up began with a layer of fiberglass, which was laid down on the foam surface "on the 90" after being coated with a light layer of spray adhesive. Next, unidirectional carbon fiber strips were applied to parts of the fuselage that were load-carrying. These parts were the underside of the tail boom, the hinge and cutout lines of the payload doors, and the nose of the aircraft. Over this layer of carbon fiber, two more layers of fiberglass were applied. After these layers were adhered with spray adhesive, the entire fuselage was brushed with epoxy. The excess epoxy was then removed by "squeegeeing" in order to reduce weight. The entire assembly was then cured in an oven at 135 ^{o}F for 12 hours. After the curing cycle, the fuselage was further sanded, and the doors were cut out. The fuse was then hollowed out where payload and propulsion items were to be located.

One would think that the keel and shell method of construction compromises strength when compared to a fiberglass fuselage with load-bearing walls. In fact, the choice to not build the fuselage using a construction with load-bearing walls was made because of the big hole that was to be cut out of the fuselage. The doors would have seriously compromised the structural integrity of a fuselage built without a load-bearing keel. Another advantage of the keel-shell configuration is that it is much lighter and easier to modify, making it more aerodynamic therefore giving the airplane higher performance.

6.2.2 Wing

Due to the fact that the wing must be able to fit into the 4'x2'x1' shipping container, the team decided that the wing should be broken into three pieces, a 2 foot center section that will have two 3 foot tip panels. The tip panels are to be adjoined with the center section with a solid joiner tube comprised of a 3/8" OD carbon tube that is to be inserted into the 3/8 ID wrapped carbon tube. The use of ribs and sub-ribs made of ¼" aircraft plywood at the faces of both the adjoining surfaces of the wing panels and center of tip panels will

sandwich fabrication and propulsion equipment. Particular emphasis is to be set to the high costs of team travel to USA that reduces the funds available for the materials and construction, so cost is the mean FOMs we considered to select the manufacturing and tooling processes.

Skill Matrix

The skill matrix is a mean to select team members to assign to each manufacturing processes. It evaluates the skill required to perform tasks needed to complete the selected manufacturing processes, so that the most efficient members could work on their specific tasks. High values means high skills required.

Aircraft Components	Foam cutting	Wood working	Mould preparation	Composite layup	Radio and electrical installation	CAD Modelling
Fuselage	3	1	0	1	2	3
Wing	2	2	0	3	2	2
Landing gear	0	0	2	2	1	2
Tail	2	2	0	3	2	2
Radome	3	0	2	3	2	3
Propulsion	0	0	0	1	2	1

Table 6.1: skill matrix

6.3 Manufacturing Milestone Chart

Aircraft consists in six separate sections: radome, main fuselage section, tail fuselage section, tail, wing and landing gear. A milestone chart was developed to plan and to coordinate the construction.

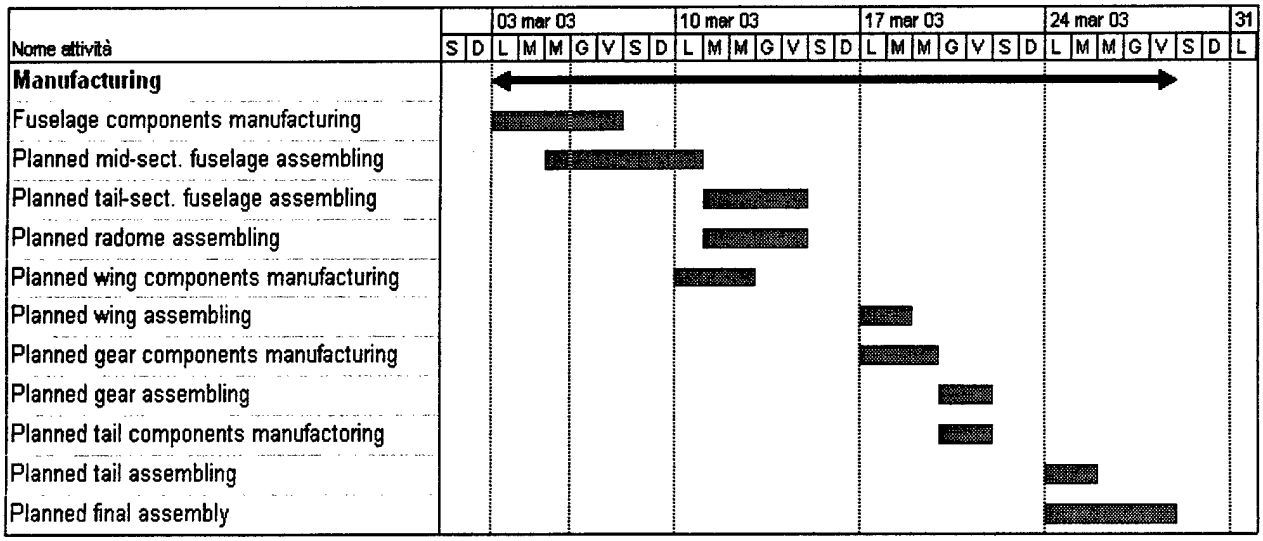

Figure 6.1: manufacturing scheduled timings

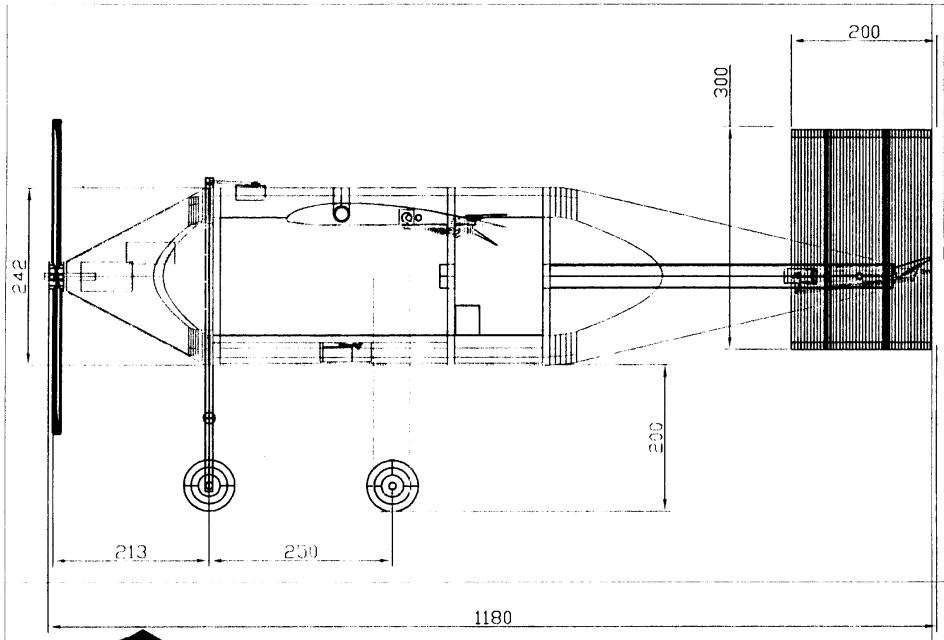

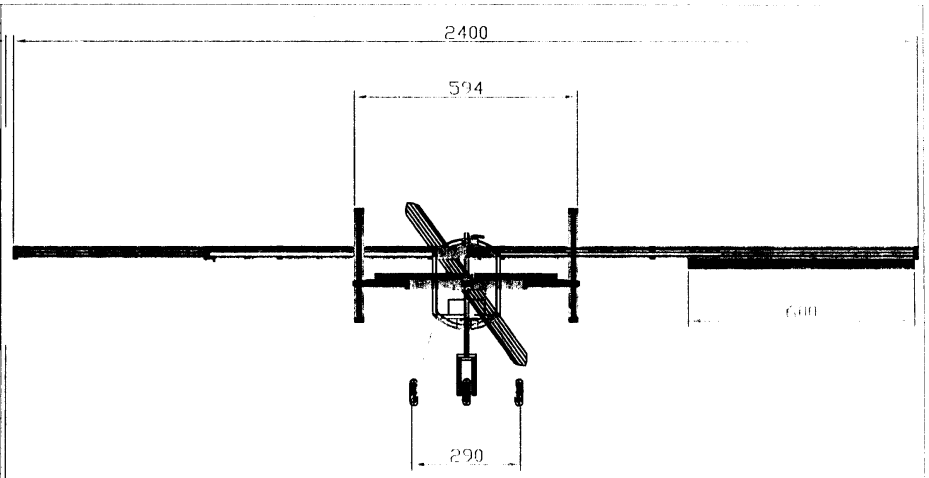

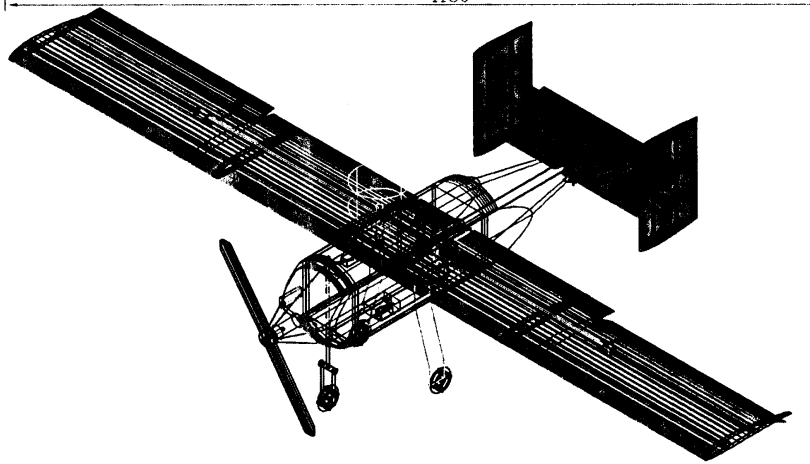

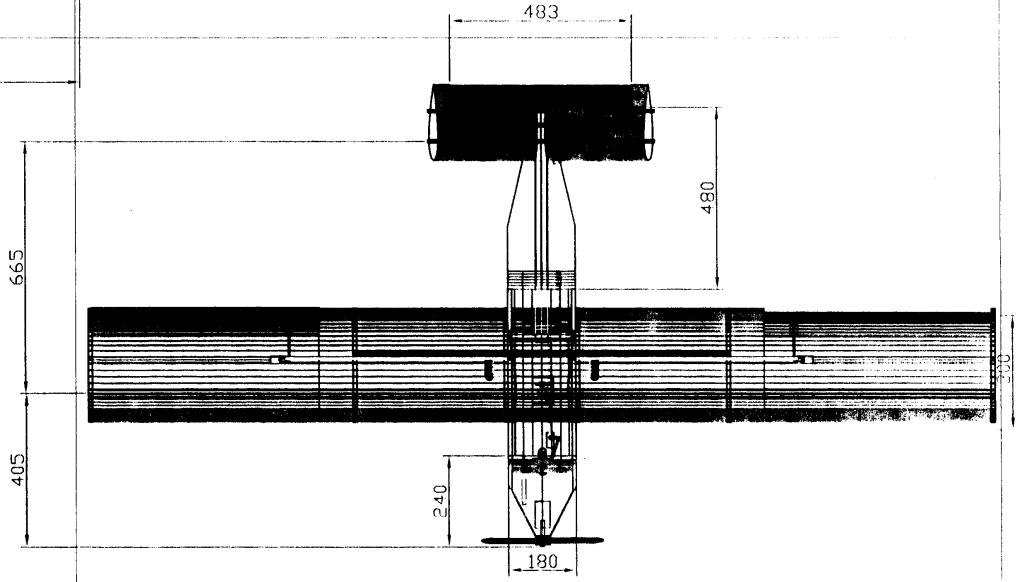

1/03	1	3 view of final concept and assonometry			Article No.54/01
Designed by F_PUCCICA		Checked by F_ZAVARELLA	Approved by - date P_GRECO_03/07/03	File name 3VIEWS.DWG	Date 03/07/03

Galileo IV
final concept

University of Rome La Sapienza

TFC Studium LIV

Edition 1

Sheet 1/5

"A" type rib

"B" type rib

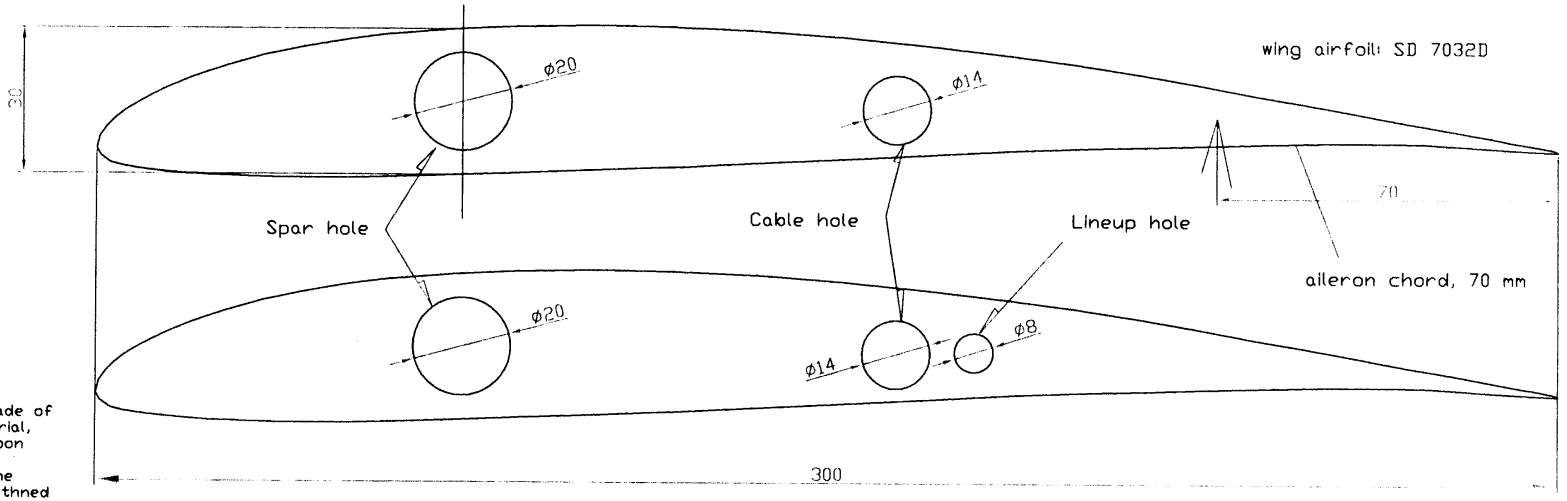

Both the rib types are made of a sandwich composite material, witha nomex core and carbon fiber skins.
Where there are holes, the honeycomb must be strengthned with other resin before applying the skins.

Rib thickness is 10 mm.

Spar and lineup

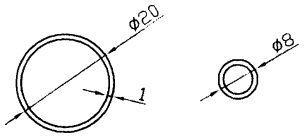

Spar and lineup are carbon fiber pipes of indicated dimentions.

Ribs, spars and lineup are fixede together with epoxy glue.

Assembly scheme of the wing structural components

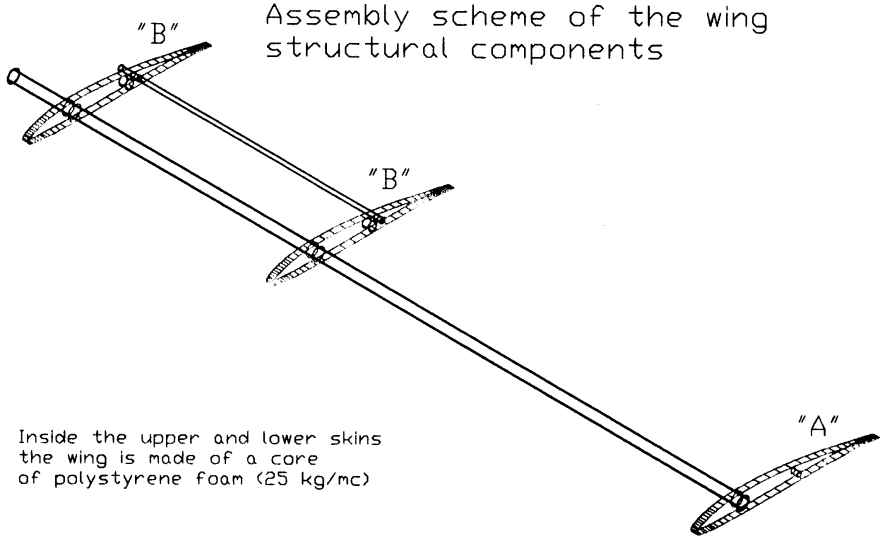

Inside the upper and lower skins the wing is made of a core of polystyrene foam (25 kg/mc)

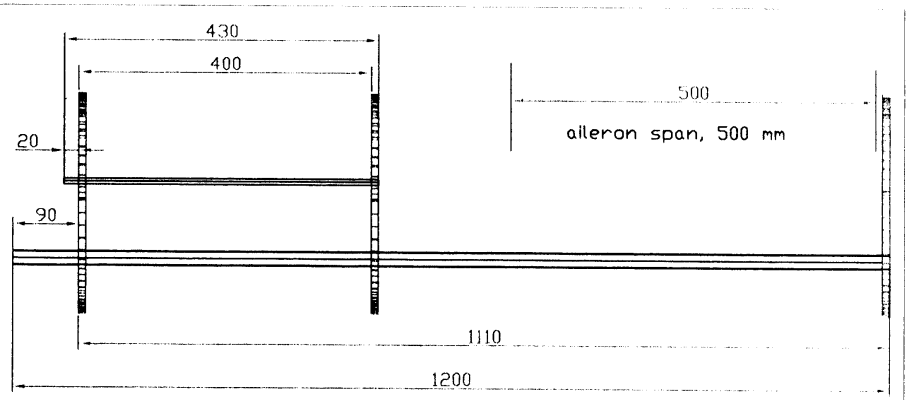

2	1	Wing components and assembly scheme			Article No.54/02	
Designed by F_PUCCICA		Checked by V_GUARINO	Approved by - date P_GRECO_21/01/03	File name FUSEEXE.DWG	Date 09/02/03	Scale 1:1
Galileo IV executive drawings for wing construction and assembly		University of Rome La Sapienza				
		TFC Studium LIV			Edition 1	Sheet 2/5

Fuselage frame # "1" and "3"

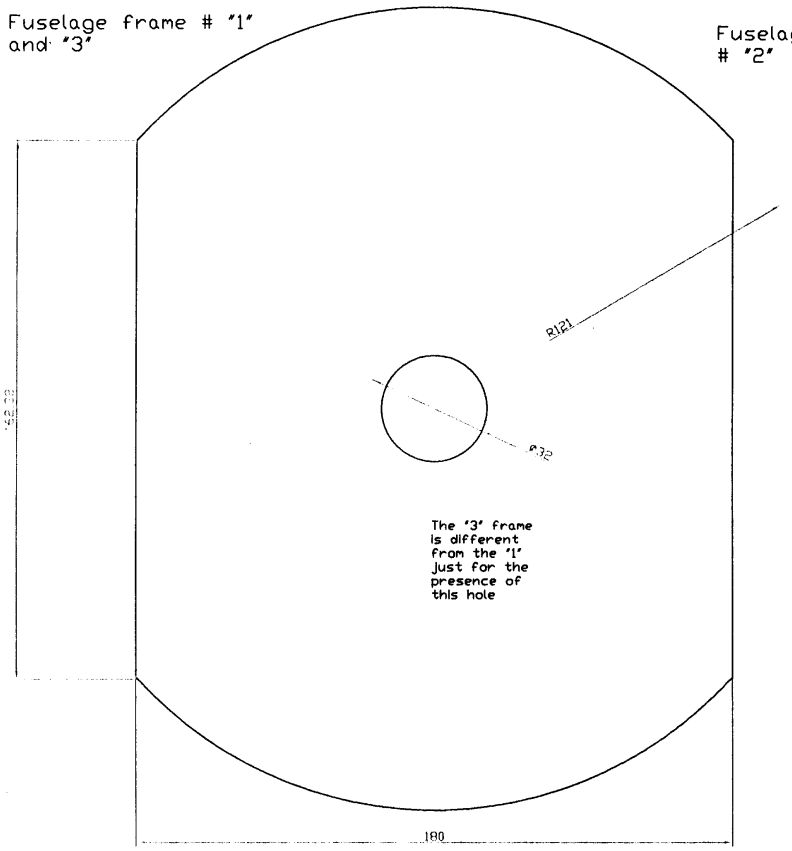

The '3' frame is different from the '1' just for the presence of this hole

Fuselage frame # "2"

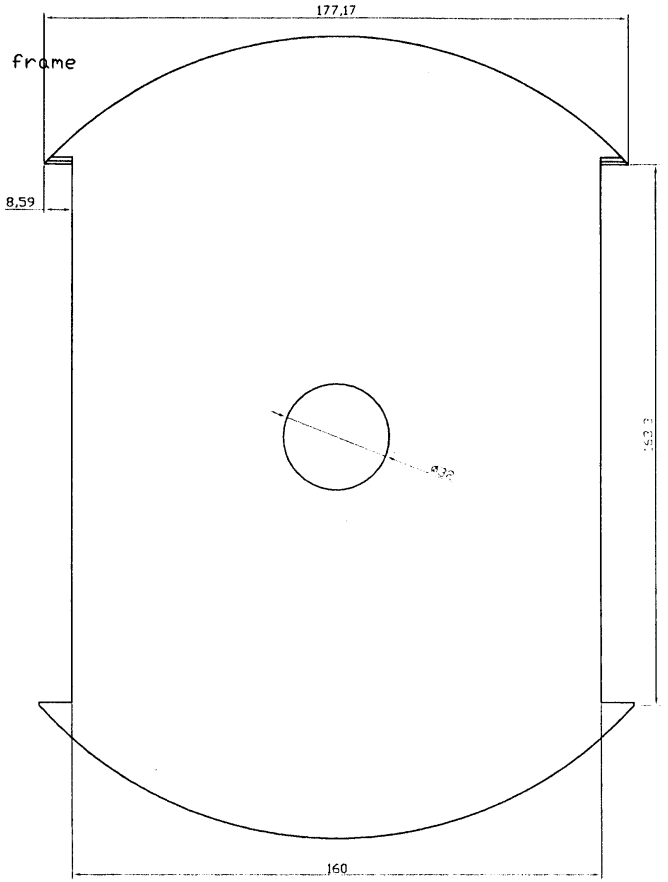

device for the coupling within the fuselae and tail boom . It is made by carbon fiver freinforced plastic filamnet wound ontu on the tub of the spar

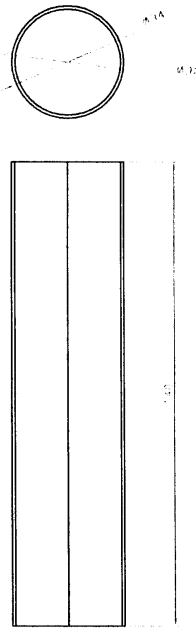

Assembly scheme of the fuselage

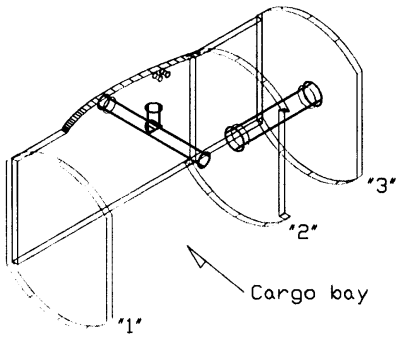

The fuselage frames are made of a sandwich composite material, with a nomex core and carbon fiber reinforced plastic skins.
Where there are holes, the honeycomb must be strengthned with other resin injected before applying laying up the skins.

The frame thickness is 10 mm.

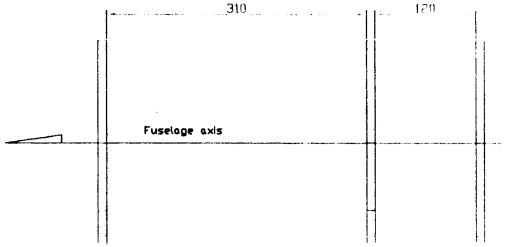

3 | 1	fuselage components and assembly scheme				Article No. 54/03	
Designed by F_PUCCICA	Checked by F_ZAVARELLA	Approved by - date P_GRECO_03/07/03	Filename WINGEXE.DWG		Date 01/15/03	Scale 1:1
Galileo IV executive drawings for fuselage construction and assembly	University of Rome La Sapineza					
	TFC Studium LIV				Edition 1	Sheet 3/5

The horizontal and vertical tail planes have the same airfoil

NACA 0012 airfoil

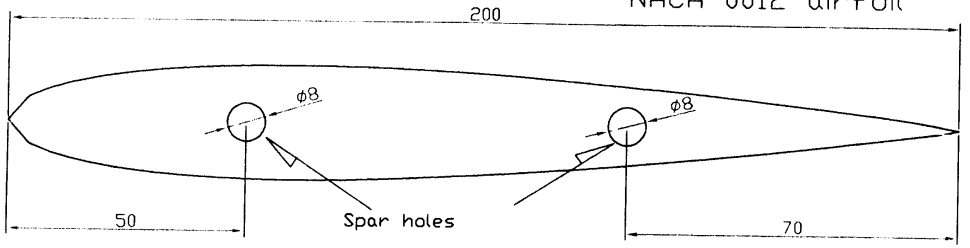

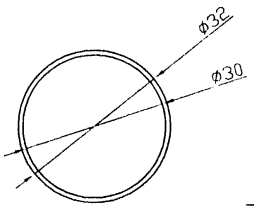

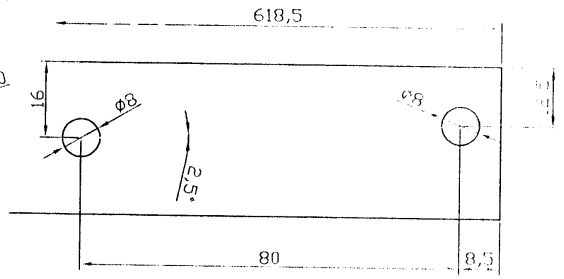

The tail is conneted to the fuselage with CFRP boom

The 4 ribs are made of a sandwich composite material, witha nomex core and carbon fiber skins. Where there are holes, the honeycomb must be strengthned with other resin before applying the skins.

The rib thickness is about 10 mm.

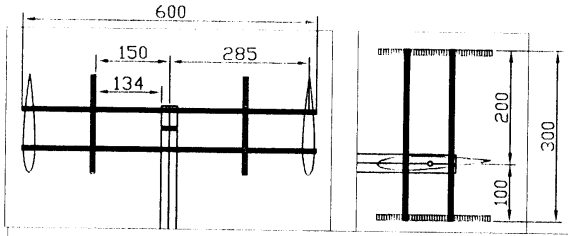

Tail structure assemply scheme

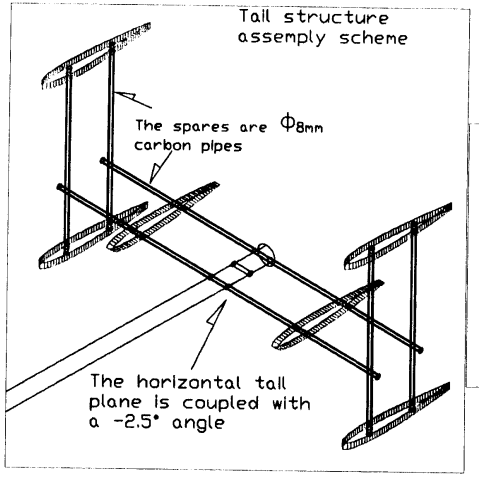

The 'B' type core must be cut in to parts with its symmetry plane

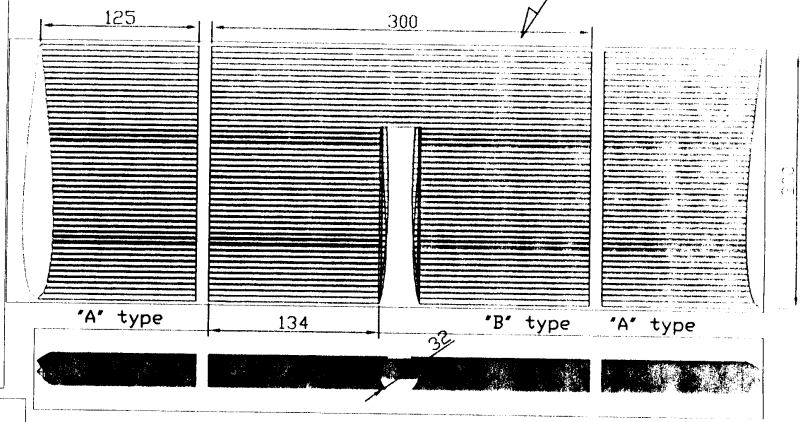

Horizontal tail assembly

1) Spars fixing to the boom
2) Frames fixing
3) 'A' type core inserting
4) 'B' type core inserting

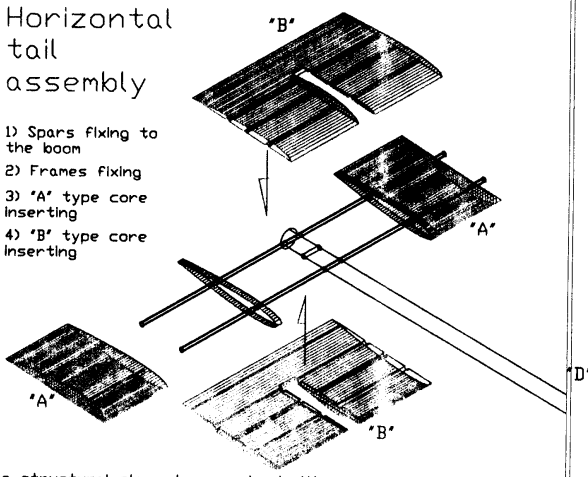

the structural elements are glued with epoxy resin, the cores with vinylic glue

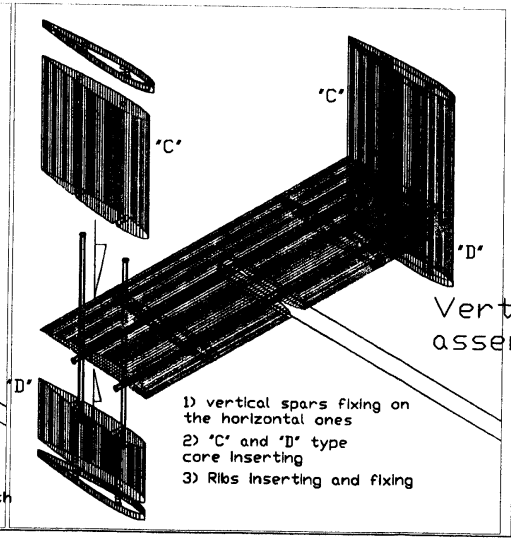

1) vertical spars fixing on the horizontal ones
2) 'C' and 'D' type core inserting
3) Ribs inserting and fixing

Vertical tal assembly

The cores, both vertical and horizontal, have the same airfoil of the ribs, and with the same spares holes

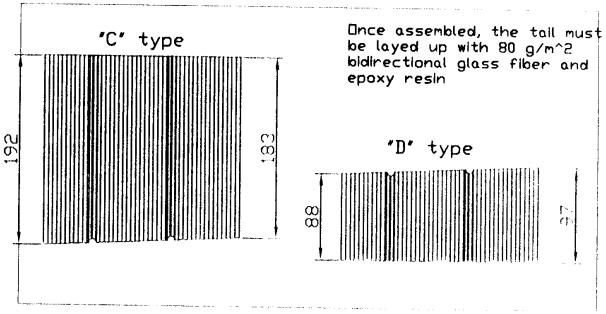

Once assembled, the tail must be layed up with 80 g/m^2 bidirectional glass fiber and epoxy resin

4	1	tail components and assembly scheme			Article No./54/04
Designed by F_PUCCICA		Checked by E_ARGENTINI	Approved by - date P_GRECO_03/07/03	File name TAILEXE.DWG	Date 11/02/03
Galileo IV executive drawing for tail construction and assembly		University of Rome La Sapienza			
		TFC Studium LIV		Edition 1	Sheet 4/5

7 Testing Plan

Since the first stage of the work, we planned to perform several testing sessions. They would have run parallel to the design process, supplying designers with the needed information about the actual behavior of the various subsystems, and to verify the goodness of the choices made. More, they would have supplied the basis for an iterative optimization process of each single subsystem and of the integrated aircraft.

7.1 Structural Tests

Despite the successes of FE methods, limitations with the constitutive material models available in the numerical codes, particularly for composites, has meant that the days of conducting experimental tests are far from over. Instead, a shift in emphasis such that the experimentalist can maximize the usefulness of a single test has been promoted. It is therefore essential that both numerical and experimental disciplines be used to promote and support each other. This was the driving idea we had to follow in planning our work. In fact, to build our model, we identified a technology that could allow us to produce in a little time several prototypes of each structural element, but we did not have enough confidence with it. It means the results we could have from a numerical design could be very far from the actual characteristics of the structure we could realize. The first step in assessing the performance of any new material/structure normally involves the testing of standard coupons. Although coupon data is a valuable starting point, the results obtained may not be representative of the final structure, due to the actual conditions it will experiment in its life. Better, it is essential to understand how the individual components behave within a complex structure. Resolution of this situation can be limited to the production of sub-structures which can give the designer confidence in using new materials / technologies in a given configuration. We could early produce some benchmarks of our sub-structures (wing, fuselage, ...), and test them by carefully reproducing the boundary and loading conditions of the given configuration, without the problem of the scalability involved in testing scaled structures. So, we thought that by integrating the disciplines of numerical and experimental analysis it was possible to enhance the FE modeling further, whilst reducing the number of experiments that need to be performed. In so doing, we could bridge the gap between coupon testing and the real structure in a time enough short as the one of this competition. So, quite early in the design process we planned a series of structural tests, beginning with the ones on standard coupons and ending by testing entire sub-structures to characterize their performances in the real condition.

7.1.1 Testing ASTM standard specimen

For engineering design purpose it s important to know the mechanical properties of the materials used to manufacture the real object. We said we early thought to use composite materials to manufacture many structural components of the aircraft. After last year experience, we had a sufficient know-how in a self-made technology consisting in a manual lay-up of fiber fabric and a resin curing process in ambient temperature and controlled pressure. However, lesson learned last year suggested extremely care must be taken to secure maximum degree of uniformity in details preparation, treatment an handling, since the method of preparation is directly linked to the final properties of a composite material. Because of the high degree of sensitivity exhibited by many plastics to rate of straining, environmental conditions and - most of all - preparation procedure, data furnished by the product sellers often could not be considered satisfactory in a design process. This is particularly true for our applications involving a self-made technology of curing composites. Thus, to predict the behavior of structural components realized with our method of lay-up and curing, we needed to directly test the materials as they actually appears after the manufacturing process, in

the real condition of operation. So, quite early in the design process we planned a series of test to characterize a few materials we would produce with the dry fabric and resins we could find from our suppliers. We considered the standard test methods as they are described by ASTM rules. In particular, we referred to the rules ASTM C 393-94 for flexural properties of sandwich construction, ASTM D 638M-84 for tensile properties of plastics; ASTM D 790-86 for flexural properties of unreinforced and reinforced plastics.

7.1.2 Static and Dynamic Wing Tests

If standard coupon tests were important to supply the structural design process with the data about materials properties, testing the various structural elements of the real plane would be essential to evaluate the performances of the actual structure in the operation conditions. In particular, we planned to perform experimental analyses on the wing, to establish its load carrying capabilities and its dynamic behaviour. We planned also to perform tests on the structural subsystems which are located within the fuselage, such as the bayonets for joining wing and tail booms and the carriage. Testing the assembled half-wing had the scope to estimate the real stiffness and strength with respect to the nominal data obtained with analytical and numerical studies. We manufactured 3 half wings and collocated an electric strain-gauge (S/G) near the root section, at the point of maximum airfoil thickness (where is the spar), to measure strains on the skin. Then we simulated the static inspection condition, i.e. we fixed the root section of the wing as a cantilever beam and applied to the tip an increasing load. The S/G works like a Wheatstone bridge. It uses the variation of the resistivity of conductor when it is deformed by mechanical stress. We used a half-bridge configuration to obtain bridge amplification on the signal, to avoid the effects of temperature and of unwished tensile or compressive forces applied on the wing. The S/G was glued by a phenolic resin on the wing upper surface, 8 cm from root section upon the upper spar cap. We managed data acquisition and setting of the device by the HBM software supplied with the SCOUT 55 amplifier. To load the wing we used weight of different sizes; analysis data for the three specimens are summarized in table 7.1. An unexpected result was the difference within the loads breaking the wings. Inspecting the wing 1 fracture area, we could notice in the crack region (on the lower surface) that carbon fibres were not properly impregnated of resin. So the failure was due to the buckling of those fibres. On the other side Wing 3 broke showing a clear delamination within the fibres and the core (fig. 7.1). We noticed that this delamination began from servo seat, a point of stress concentration. By plotting the experimental diagram σ–ε for the first wing, we deduced a value of the elastic modulus equals 20 GPa, exactly the one we used in the sizing study, averaging the results supplied by standard coupon tests we had performed. This result validate our first impression about the flexural strength of the broken wing: the offset from nominal behaviour of the material is certainly due to local manufacturing faults. Testing the dynamic behaviour of the half-wing has been performed to compare experimental data, upon natural frequencies and mode shapes, with the ones output by numerical FE codes. We felt useful to compare also this kind of data, to estimate the correspondence within predicted and actual behaviour of the structure. We could predict the actual wing would show lower frequencies with respect to the ones found by using FEM codes, because of the imperfect manufacture and the difficulty of simulating a proper constraint condition. We used an impact hammer. An accelerometer (shock limit of 500 g) was placed on the hammer's head (PCB 356B18), while the measurement accelerometer (PCB333B30) had a 50g shock limit with a voltage sensitivity of 100 mV/g. The acquisition system was made of a 16 bit National board NI DAQ Card AI 16XE 50, with 16 channels and a scan rate of 20000 samples per second. To properly constrain the wing at

its root, trying to represent its real condition of operation,: we clamped the cylindrical spar to a steel support. Along the wing span (1,110 mm) we identified 11 key-points of measure (with a step of 100 mm).

Applied load	Wing 1	Wing 2	Wing 3
[kg]	strain[μm/m]	strain[μm/m],	strain[μm/m]
1	64,2	63,2	59,6
2	143,1	129,5	135,6
3	197,6	188,7	190,9
3,5	229,9	212,4	222,1
4	the wing broke	240,9	243,8
4,5		259,9	263
5		296	294
5,5		325	319
6		the wing broke	331

Table 7.1: static test on the half-wing

	FEM analysis output	Experimental results
ω1	25,04	9,9 Hz
ω2	69,17	72,7 HZ
ω3	130,77	138,4 Hz

Table 7.3: dynamic test

Data recording and processing was done by software we developed in ambient LabVIEW™. We could identify the first 3 natural frequencies of the structure. Table 7.3 shows the comparison between experimental and numerical results. Figure 7.1 illustrates a typical FRF (frequency response function) acquired and the comparison between experimental and analytical calculation of the first modal shape.

7.2 Aerodynamic Tests

We perform two sessions of aerodynamic tests. First we studied a complete semi-model (i.e. a model of the whole airplane, split up by its plane of symmetry) to estimate the interaction among the parts of the airframe (wing, fuselage, tail). Then we tested the assembled fuselage, to measure the effect of the propeller twisted airflow. While the first session was planned to be performed after the end of the preliminary design phase, for testing the interaction propeller-aircraft body we had to wait the the prototype had been realized.

7.2.1 Tests on the semi-model

The model is in 1:2 scale, so to work in dynamic similitude at a wind speed of about 40 m/s (130 ft/s). It is 60 cm (23.6") wide and 60 cm long, made of polystyrene foam and wood, with reinforces in aluminum and glass fiber. (figure 7.2). There are also weights to make the models more stable in the airflow at the higher speeds. In the tests on the half-model, one screen were used to achieve the symmetry condition. In the first day spent at the tunnel we calibrated the balance, i.e. we weighted note masses to find the constants of the linear law that link the output voltage with the load. Then we mounted the half-model, with its screen, and measured drag and lift at various angles of attack. The results, shown in figure 7.2, display a very good match with the analytical data used in the preliminary and detail design. This year we did not consider necessary to test a wing section, to achieve real data on the selected airfoil, because in previous years we already led test on this airfoil, finding a very good match between the experimental data and the ones the ones supplied by Selig (see figure 7.2, lower line).

7.2.2 Testing the propeller mounted on the fuselage

We led test on the assembled fuselage to measure the effect of the propeller twisted airflow. It was not possible to simulate in the wind tunnel the propeller induced velocities (we should mount a complete model with motor and propeller, all in dynamic similitude!). So we performed the test outside the tunnel. With a load

cell we measured the global force on the fuselage. Being known the propeller traction, the difference in the acting force, was the additional drag due to the interference between fuselage and propeller wake.

7.3 Propulsive Tests

In order to estimate the real performances of the propulsive configuration we chose, we planned a second wind tunnel session to test the adopted system motor-gear box-propeller We need to know propulsive performances at various air speed values, so we thought to perform experiments at the bench (in motionless air) and inside a wind tunnel. Tests' results would also be important as comparison data with the output of the numerical simulation codes we used in the design phase. So to eventually update the simulation algorithms, enhancing their capabilities to predict performances in that operation ranges we could not test directly. For the reasons mentioned, it was important to test the motor with a series of different propellers. In so doing we would have enough data to optimise the propulsive configuration to best fit the requirements of the competition. Since we did not have the possibilities to dispose of many motors to be tested, we planned to perform this kind of experiment once the motor had already been chosen.

7.3.1 *Instruments and tests organization*

The measurement system is composed by two blocks linked together by wires for signal transmission and electrical supply. The first block (figure 7.2) includes structures and tools which stay inside the wind tunnel (sensors, structures needed to carry the whole system and a dynamometer connected to the motor). The second block is completely outside the wind tunnel. It includes the power pack for supplying energy, the signal acquirer "Keithley" and the PC that manages it. Figure 7.2 shows an overview of the system.

- Tests' conditions: tested propellers: Menz 17x10, 18x10, 18x12, 19x10, 19x12, 20x10
  tested airspeed: 0, 5, 8, 12, 16, 21 m/s.
  measured data: thrust, propellers' rounds per minute, power absorbed
- Wind tunnel airspeed measures: even if the wind tunnel controls are well calibrated, we decided to put in the flow a Pitot tube to measure the exact air speed. The Pitot tube was put in front of the propeller, immediately after the beginning of the measure room.
- Thrust and propeller RPM measures: the motor was able to roll by its axis (horizontal) thanks to an axial bearing; it was mechanically connected to a vertical cantilever beam. The latter was subjected to a bending moment caused by the tensile loading of the propeller. Measuring the strain near the constraint point of the beam allowed determining thrust. To measure such strain we used electrical strain-gauges. Double precision has been achieved using a variable electrical resistance to evaluate the horizontal displacement of the beam tip. The propeller angular speed was measured with a little invasive optical tachometric probe. The system was calibrated before starting testing.
- Motor input power measures: it was obtained measuring separately voltage and current supplied.

7.3.2 *Measurements procedures and results*

Once fixed the wind tunnel airspeed (v) and the supply voltage at a constant value (16V), we changed the supply current until the RPM measured by probe (n) gave the desired value of the propeller's working ratio. $\gamma = v / (n*D)$. After a time interval, when the system reaches a steady state regime, we could record values of voltage an current input to the motor, thrust and RPM. Varying current and airspeed we could measure, for each propeller, the values of thrust, absorbed power and torque as functions of the working ratio. The results we obtained were comparable with the ones predicted by the softwares Motocalc and Motor1-testprop. It seemed the design of the propulsion system had been performed on the base of reliable data and tools. Only

a real flight test would have said if it could guarantee the performances needed to best fit mission requirements. Table 7.2 reproduce the work sheet used to record data related to a measurement session in the wind tunnel. The software used to manage data recorded by the Keithley system is XLINX 2700.

Propeller size		19x10		
Shunt resistance [W]		0,0008		
Airspeed	Current	Voltage	Thrust	RPMx1000
[m/s]	[A]	[V]	[N]	
0	39,36722	15,72153	28,456	3,992
5	39,14729	15,72211	25,345	3,975
8	38,26821	15,71335	23,543	3,982
12	37,14954	15,71458	19,623	4,198
16	33,7544	15,71824	14,715	4,56
21	24,56729	15,72437	10,115	5,037

Table 7.1: wind tunnel test of motors and propeller

7.4 Flight Tests

We had planned to build quite early a prototype, and fly it, so to directly verify the actual behavior of the selected configuration and so to have enough time to optimize it on the basis of an exact estimation of its performances. When the prototype flew we implemented on it a system able to detect some flight parameters. The scope was to verify actual performances, in comparison with the ones predicted by earlier analyses. We mounted the following items: an altimeter, a Pitot tube to detect the speed in the different phases of the flight, a couple of inclinometers to measure roll and pitch angles. We monitored the values of the control surfaces angle and of the motor throttle. We used commercial sensors connected to a system for data managing realized for embedded acquiring of tension signal. The architecture of the system basis upon a controller (8 bit) which manage a real time clock; a 12-bit analog-digital converter, with a sample time of 10 μs; an eight channels multiplexer; an internal voltage reference generator, for the AD conversion; a coupling circuit for the serial line; an E^2PROM rewritable, non volatile memory; four conditioning modules (one for each channel connected to the sensors). This system, is capable to acquire on four channel, with a scan rate up to 0,1 sample/sec. To program the acquisitions and read the data, it has to be connected to a PC by the serial port. The system is managed by means of programs realized in LabVIEW™ ambient. Since we wanted to acquire 7 signals (altitude, speed, pitch, roll, throttle, elevator and ailerons), we needed to load in the aircraft cargo bay two acquisition systems. The overall instruments weight and volume was not higher than the contest payload, figure 7.4. About the data collected during the flight, the most interesting fact is that speed in the various flight phases is higher than the predicted one. Particularly, the maximum predicted speed was about 20 m/s, while the actual one is 22 m/s. Figure 7.3 show the prototype during flight.

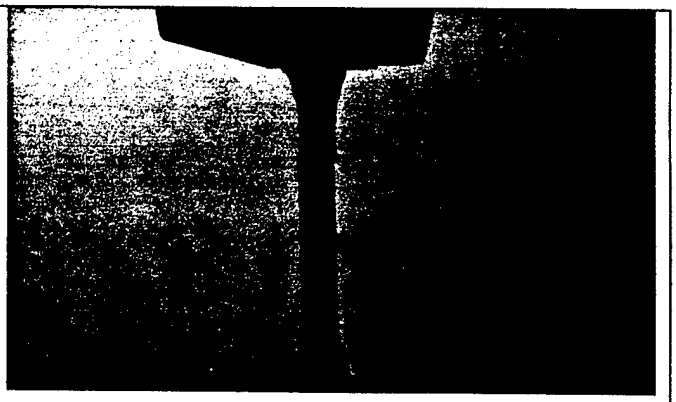

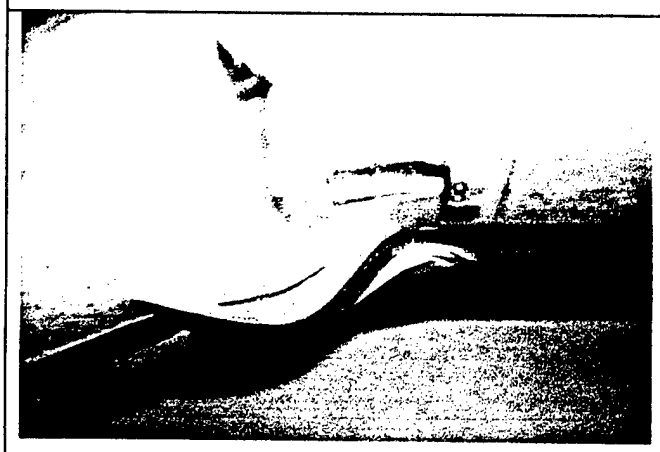

static test on the half-wing: zoom on the failure area

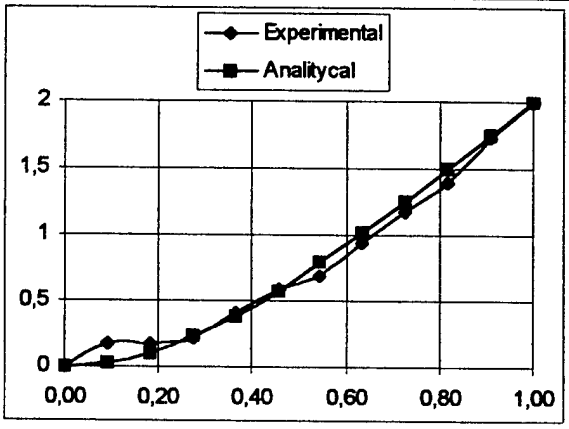

dynamic tests on the half wing: first mode shape

dynamic tests on the half wing: FRF modulus

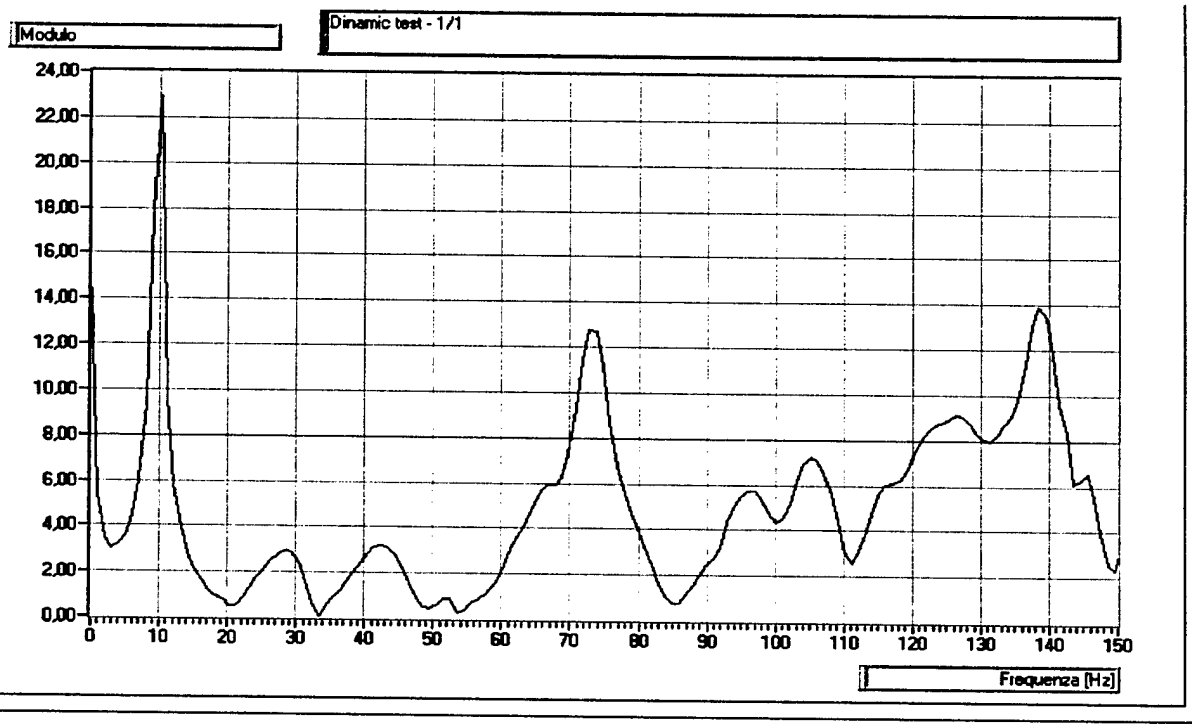

Figure 7.1 structural tests

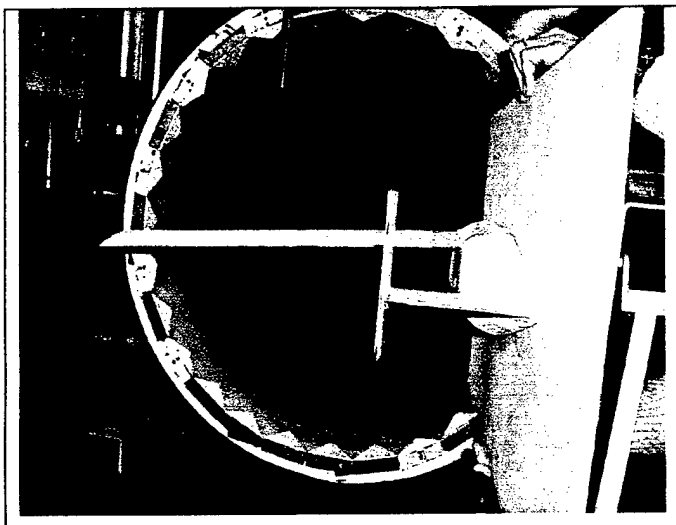

7.2.A: the semi-model in the wind tunnel

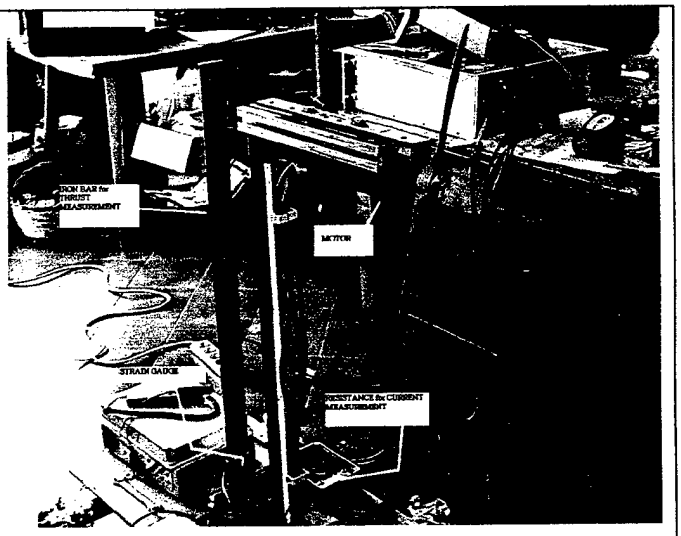

7.2.B: measure system for propulsive tests

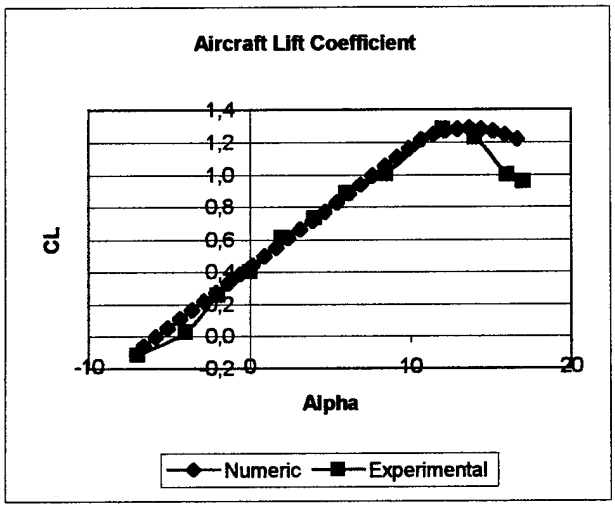

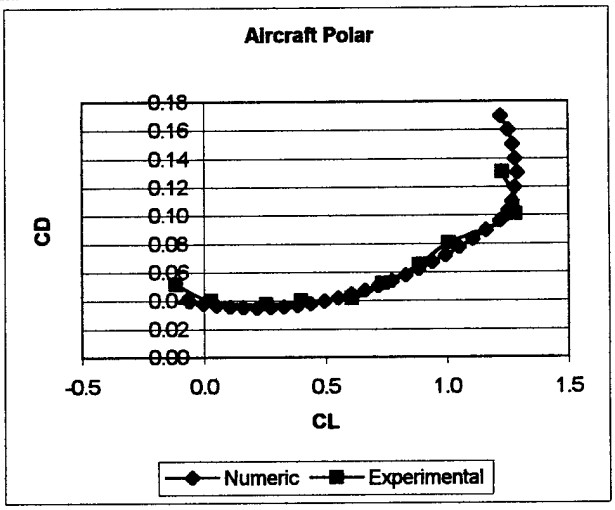

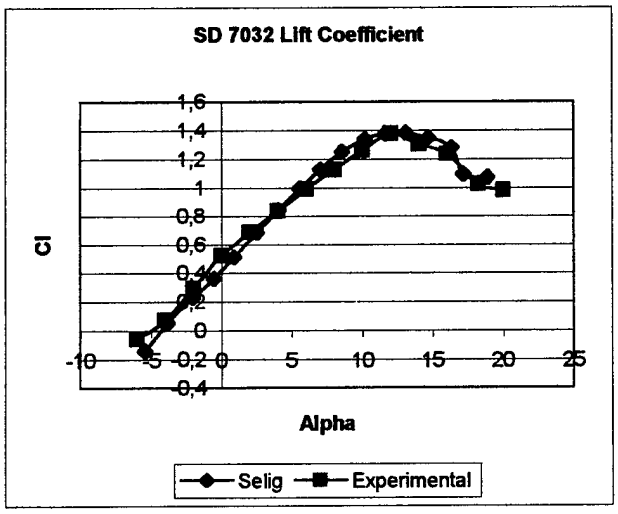

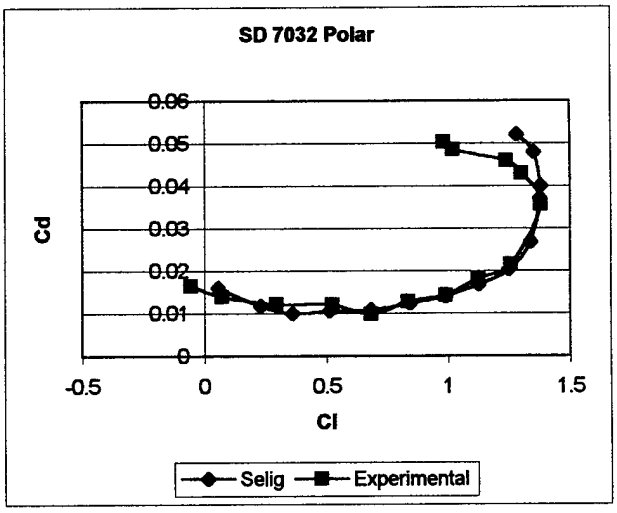

Figure 7.2: wind tunnel and propeller tests

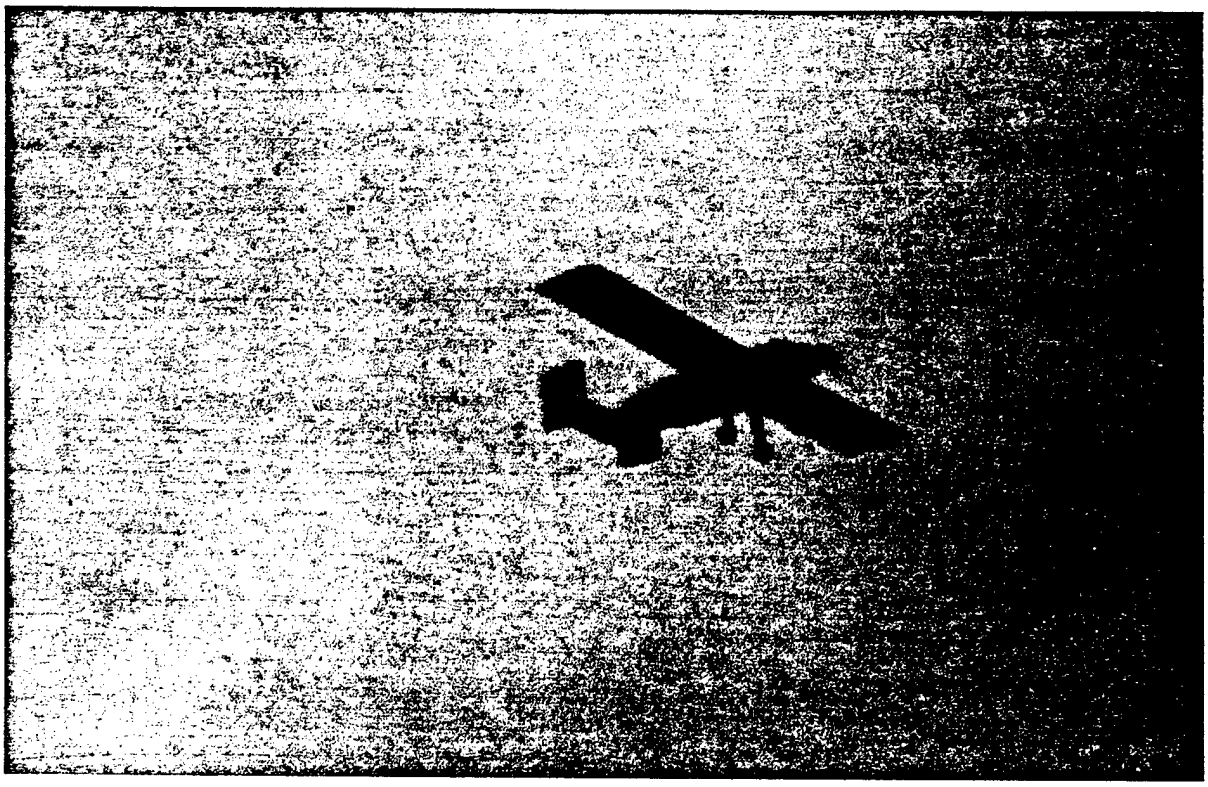

Figure 7.3: the flight of the prototype

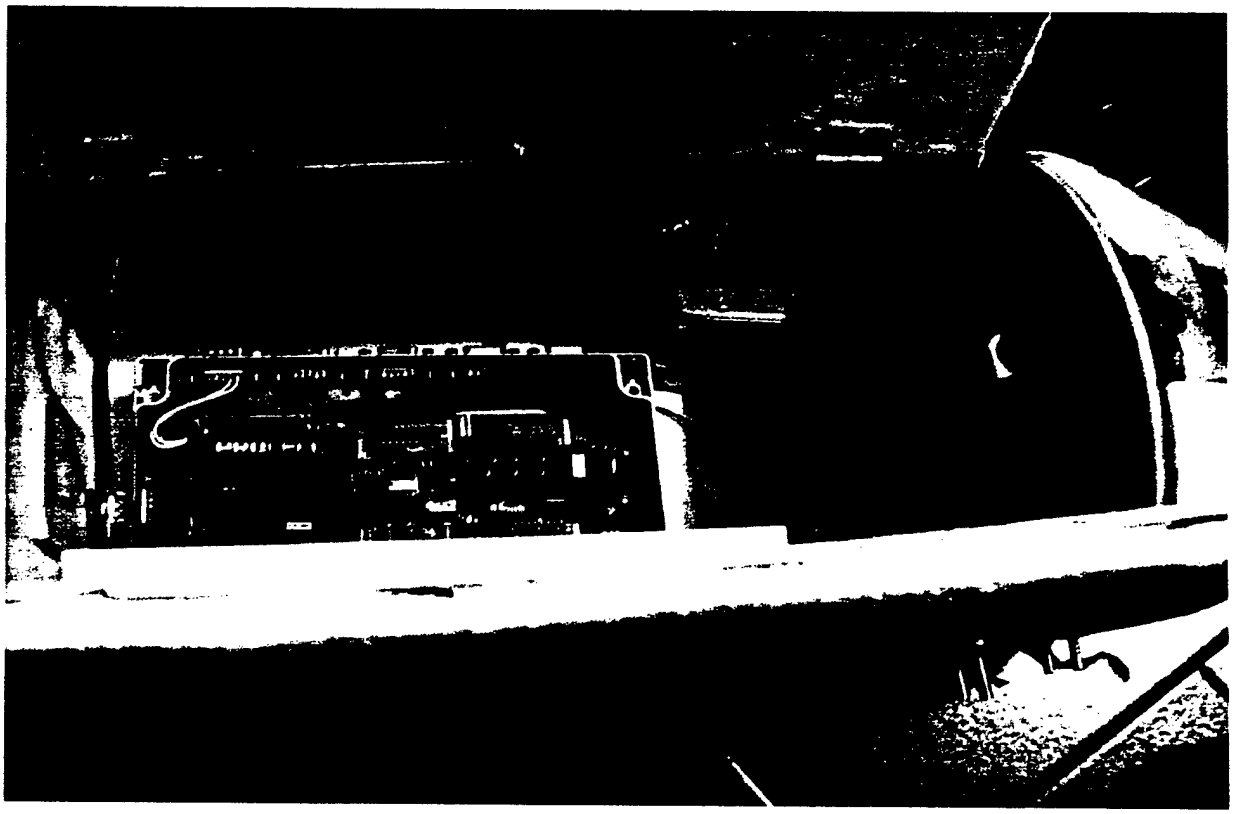

Figure 7.4: measure system inside the fuselage of the prototype

University of Southern California

SCyRaider

AIRCRAFT DESIGN REPORT

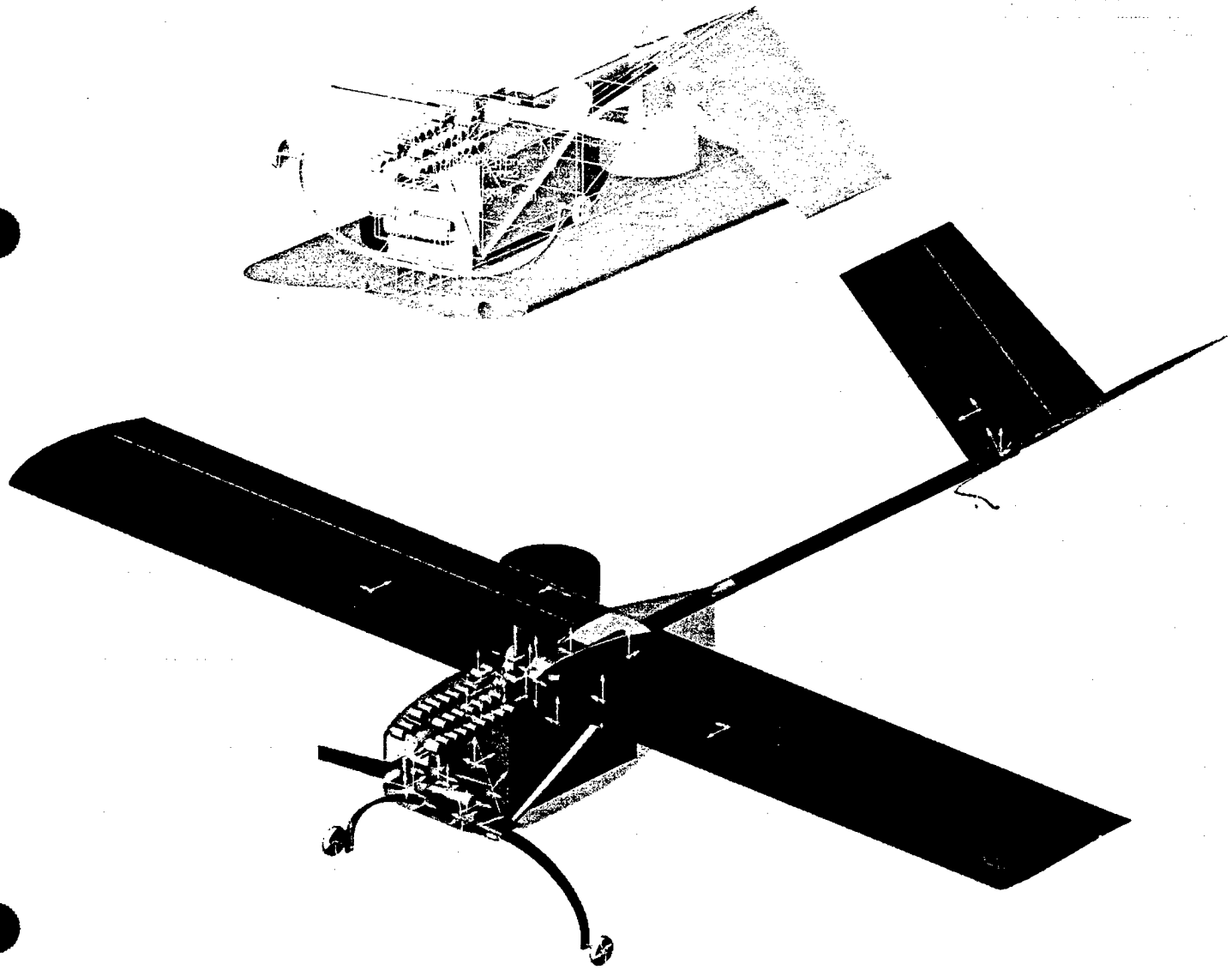

2002/2003 AIAA Cessna/ONR Design/Build/Fly Competition

On behalf of the USC AeroDesign Team, we would like to thank our faculty advisor, Dr. Ron Blackwelder, and our industry advisors Mark Page, Wyatt Saddler, Jerry Chen, Nathaniel Palmer and Jacob Evert, for their inexhaustible efforts to support and encourage the team every year. Your knowledge and teaching has made the AeroDesign team an invaluable experience.

TABLE OF CONTENTS

1.0 EXECUTIVE SUMMARY 1

2.0 MANAGEMENT SUMMARY 3

2.1 TEAM STRUCTURE 3
2.2 GROUP AND PERSONNEL ASSIGNMENTS 3
2.3 CONFIGURATION AND SCHEDULE CONTROL 6

3.0 CONCEPTUAL DESIGN PHASE 8

3.1 ASSUMPTIONS AND JUSTIFICATIONS 8
3.2 ALTERNATE CONFIGURATIONS 9
3.3 FIGURES OF MERIT 11
3.4 DESIGN PARAMETERS QUANTIFYING THE *TOTAL FLIGHT TIME* FIGURE OF MERIT 12
3.5 DESIGN PARAMETERS QUANTIFYING THE *STRUCTURAL ROBUSTNESS* FIGURE OF MERIT 12
3.6 DESIGN PARAMETERS QUANTIFYING THE *RATED AIRCRAFT COST* FIGURE OF MERIT 13
3.7 CONFIGURATION DOWNSELECT 13
3.8 *RAC* COMPARISON WITH CONCEPTUAL DESIGN RANKINGS & FINAL DESIGN FEATURES 14

4.0 PRELIMINARY DESIGN PHASE 16

4.1 MISSION MODEL 16
4.2 DESIGN PARAMETER & SIZING TRADES 17

5.0 DETAILED DESIGN PHASE 33

5.1 NEW ASSUMPTIONS FOR SPECIFIC SUBSYSTEMS 33
5.2 COMPONENT SELECTION & SYSTEMS ARCHITECTURE 33
5.3 ESTIMATED MISSION PERFORMANCE 36
5.4 WEIGHT, BALANCE AND RATED AIRCRAFT COST WORKSHEETS 38

6.0 MANUFACTURING PLAN 45

6.1 FIGURES OF MERIT 45
6.2 ANALYTIC METHODS USED TO SELECT FINAL SET OF MANUFACTURING PROCESSES 45
6.3 PROCESSES SELECTED FOR MAJOR COMPONENT MANUFACTURE 47
6.4 MANUFACTURING SCHEDULE 51

7.0 TESTING PLAN 52

7.1 COMPONENT AIRCRAFT TESTING 52
7.2 FULL AIRCRAFT TESTING 57

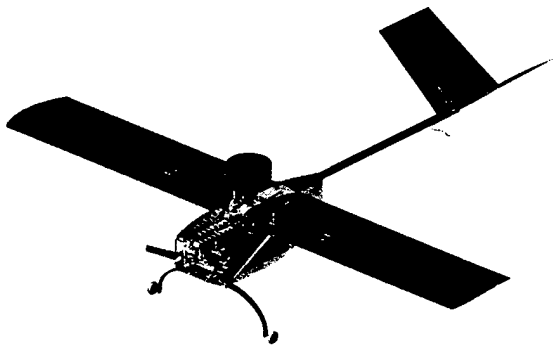

1.0 EXECUTIVE SUMMARY

The University of Southern California AeroDesign Team (ADT) has participated in the Cessna ONR AIAA Design Build Fly competition for several years with consistently high results. The nature of the competition is to design, build and fly an electric radio control aircraft for a specific mission that changes every year. For the 2002/2003 competition, the rules varied by specifying three different types of missions with a difficulty factor assigned to each one of them. Each team had to pick two of the three possible missions and complete them with the same aircraft. The missions were: Missile Decoy (A), Sensor Deployment (B) and Communication Repeater (C). The goal of the AeroDesign team was to develop a solid configuration that would complete the two missions chosen in the most efficient way. To accomplish this goal, the time frame was divided into 3 sections; Conceptual design, Preliminary design and Detail design.

1. *Conceptual Design:* During this phase, the team looked into the feasibility of the different missions; especially mission A. Different methods were used to calculate the drag increase due to the mission characteristics as well as to determine if the propulsion system was able to perform due to the increased drag of the radome. Once the results where analyzed, missions A and B were chosen as the two flying missions. Also during this stage, alternative configurations were looked upon for the general layout of the plane. Tail, backbone and wing configurations were the main parameters used when comparing the different planes proposed. A constraint of packing the plane into a 1'x2'x4' box drove the design towards a classical mono plane, single boom and tail dragger with a V-tail as the most efficient configuration to fulfill the missions chosen.
2. *Preliminary Design:* During this stage the MiniMission code was created to improve the iteration process of sizing the plane. By suggestion from one of our sponsors, the analytical code used in the past was discarded and a new analytical tool, coded by current students was developed to improve the learning experience of the team. This new code, characterized by a main page called "Frontpage", was designed to be easy to use with different libraries for different parts, divided into logical subsections and with the ability of performing different trade studies. The code would perform the iterate part of the design, outputting the plane's sizing and configuration. By using MiniMission, the different batteries, motors and propellers could be matched for the optimal propulsion system as well as selecting the best airfoil. During this stage the deployment group looked at different configurations for the doors and release mechanism needed for mission B. One of the major challenges was to develop a platform that would satisfy the needs of both missions. To facilitate the process, the CG location was decided to be the same for all missions.
3. *Detail Design:* During this phase the team froze the design layout, sized the plane's components and began some preliminary manufacturing of the different parts. Sizes and configurations were obtained from this stage based on initial assumptions and given

parameters plus the iteration process. Table 1.1 and 1.2 summarizes the contest rules with the design criteria.

Rule Constraints		
Parameter		
Battery Weight	<=	5lbs
TOFL	<=	120ft
Storage Box	<=	1' x 2' x 4'
Max Current	<=	40 Amps
Payload Weight	=	5lbs
Flight Time	<=	10min
Assembly Time	=	As quick as possible

Table1.1 *2002/2003 DBF constraints*

Design Criteria			**Reference/Reason**
Design TOFL	=	75%Rules TOFL	Flight test derived
Battery Energy	=	60% rated energy	Bench testing
Cell voltage	=	1.1 volts average	Bench testing
Flight Load Factor	=	5.5g's	(70%CLmax @ Cruise speed)
Hard-Landing LF	=	Flight LF	designed softened main gear
Hard-Landing LF	=	2g's aft on landing gear	
Hard-Landing LF	=	1g aft at wing tip	
Safety Factor	=	1.50 for structure	
Prop Efficiency	=	90% of Theoretical	Flight test derived
Pitch Stability	~	25% static margin	
Yaw Stability	>	0.0016/deg	Flight test derived
Tipover Limit	>=	1g braking & 1g cornering	Flight test derived
Tip Stall @ Taper Ratio=0.6	=	2deg washout	
Tip Stall @ Taper Ratio=1	=	0deg washout	
Min ROC @ Vcrz	>=	400 fpm for mission	Balances altitude loss in turns
Servo Hinge-Moment	>=	50% □max @ Vcruise	
CG location	=	Same CG for all payloads	Flight test derived
Max Elevator Deflection	=	Required to stall wing	Carefree maneuvering
Max Aileron Deflection	<=	7.5deg(25%c)- full-span	Flight test derived

Table1.2 *USC AeroDesign team criteria in sizing SCyRaider*

2.0 MANAGEMENT SUMMARY

2.1 Team Structure

The AeroDesign Team consisted of a faculty advisor, Dr. Ron Blackwelder, and several industry advisors from Aerovironment Inc, Boeing, Raytheon and Swift Engineering as well as student members organized into groups as seen in Figure 2.1. Our advisors served as a resource of experience and supervision over the project. The industry advisors used their expertise to help with design and construction techniques. The student leader of the team, George Sechrist, was responsible for scheduling, setting an agenda for the weekly meetings, overseeing the design and construction phases, and making sure each deadline was met accordingly. Communication between groups occurred primarily at the team meetings were held weekly for typically two hours. Specific groups met as needed to accomplish their specific goals in design and construction.

2.2 Group and Personnel Assignments

Each group of Fig. 2.1 was assigned a captain based on experience and interest and, where possible, a resource person that had previous background and was able to advise the captain. To promote learning, underclassmen volunteered to help each group. The captains were responsible for organizing the group and making sure all deadlines and goals were achieved. Since our team used an Excel program to optimize the design of the plane, most captains had to develop an Excel spreadsheet that would be able to reiterate their calculations. With the help of our advisors, the analysis for each spreadsheet was completed and integrated into the "MiniMission" design tool. Additional captain meetings were held several times to discuss and solve any issues with the integration process. The development was then carried further into the three design phases where intense analysis and optimization was performed to obtain the final configuration of the aircraft. Each group was responsible for planning and building the components under the supervision of industry advisors and more experienced team members.

1. *Aerodynamics Group*: The main responsibility of this group was to estimate the total airplane drag given initial parameters that could be changed later for optimization. This included calculating vortex and airfoil drag using independent variables such as geometry and airfoil data. Other responsibilities were to determine the efficiency factor "e", C_{Lmax}, $C_{Lcruise}$, flap deflection, and L/D at different flight conditions.
2. *Propulsion Group*: The Propulsion Group was in charge of finding the available brands of batteries, motors, propellers and gearboxes. A library of different manufacturers and specifications was built and integrated within MiniMission. Matching these parameters to model the mission for this year was a critical aspect of performance, hence testing of the top choices of each of these components was done to further complete the analysis.
3. *Stability & Control Group*: The S&C group was responsible for analyzing the various tail configurations proposed during conceptual design. They also created a spreadsheet containing the multiple parameters and equations for different types of tails. Further analysis

was performed to determine the hinge lines and moments for each control surface as well as the sizing for servos and actuators on both the empennage and primary lifting mechanism.

4. *Structures Group*: The structures group was in charge of proposing and analyzing different types of wing spars, fuselage and landing gear configurations both for static and dynamic loads. They were also responsible for the wing and landing gear attachments constrained by the 1'x2'x4' packing box required in the 2002-2003 rules.
5. *Weights Group*: This group was charged with measuring the specific weight of each component that might be part of the plane, such as the radome, actuators, payload, etc. An estimate of the take off gross weight (TOGW) was calculated, and the CG locations of both the light and heavy airplane in different flight conditions specified by the three missions proposed this year
6. *Performance Group*: The Performance group was responsible for the MiniMission integration process of each team's spreadsheet. A user friendly Frontpage was created with all the inputs and important outputs that should be checked at every iteration to be within the limit assigned, such as take off field length (TOFL), maximum weight of batteries, current draw, etc. They were also in charge of optimizing the plane configuration to produce the best flying score possible. Each aircraft system was then sized accordingly and passed down to the individual groups.
7. *Flight Test Group*: This group was in charge of assigning and accomplishing specific goals for each flight test as well as collecting the necessary data. After each flight, the group was responsible for further analysis and conclusions that would be presented to the rest of the team.
8. *Systems Deployment Group:* The deployment group had the responsibility of devising a mechanism that would eject the payload box from the aircraft without any intervention from the ground crew. The system had to be compatible with the rest of the plane in completing the mission and fitting in the transportation box.
9. *Configuration Group*: This group had to determine the overall design and architecture of the plane making sure it falls within the given parameters. They also had to integrate the ideas and changes made during Conceptual, Preliminary and Detail Design by providing updated CAD drawings. Further, they were responsible for insuring that sizing within each group was done appropriately for the configuration to fit in the carrying box.
10. *Design Report Group*: They were in charge of gathering the information for each part of the report and writing it in a coherent technical voice. All the requirements and guidelines provided by the 2002-2003 rules had to be met. They also had to assign deadlines to each captain that needed to provide the information necessary for each section.

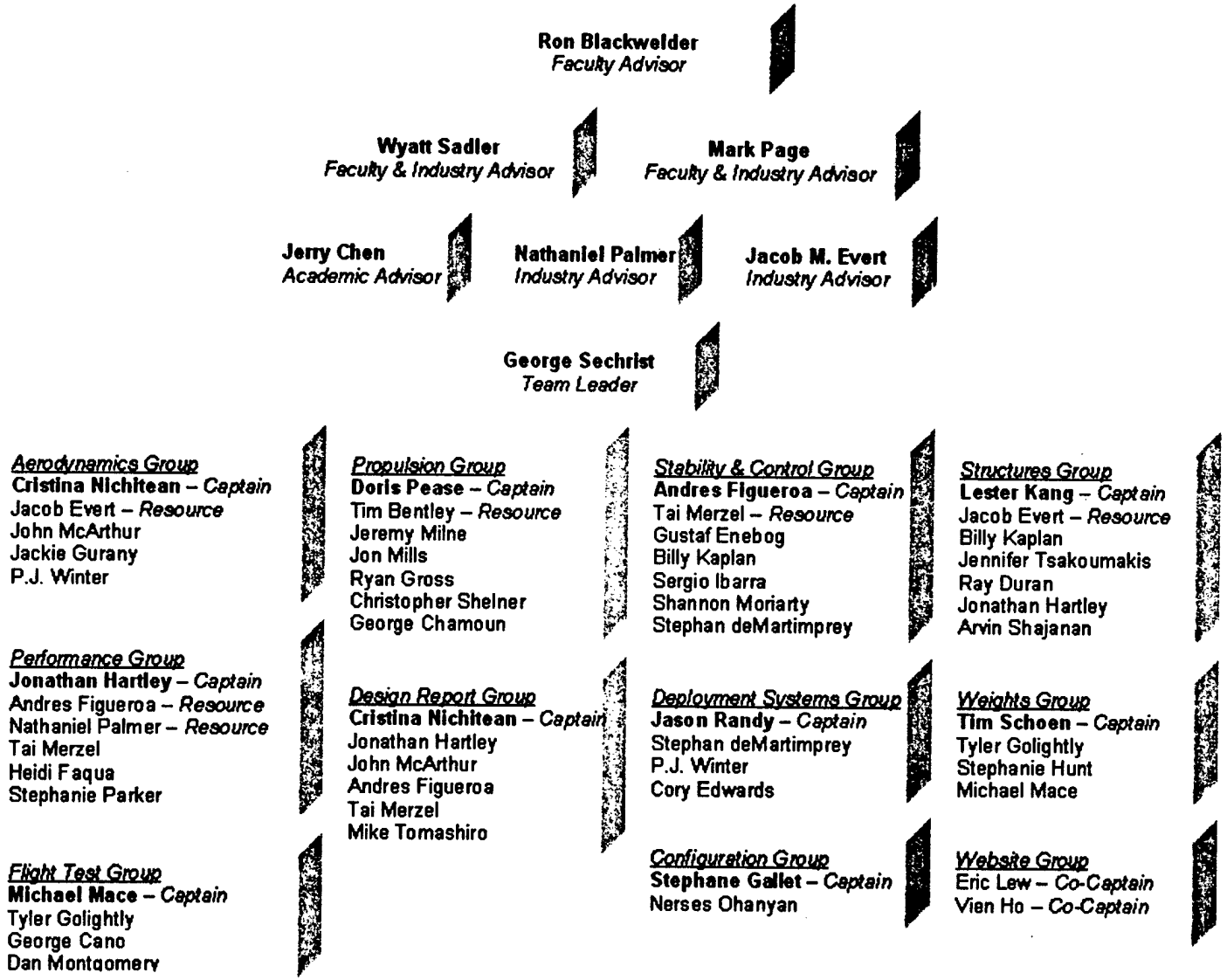

Figure 2.1 *USC AeroDesign Team Structure showing advisors and different groups with their captains*

11. *Website Group*: The website group was responsible for creating a webpage containing the team's description and progress as well as history. They had to collect the appropriate information and present the team with the final product. Maintaining it by frequent updates and changes was their essential role for the rest of the year.

2.3 Configuration and Schedule Control

A schedule of important dates and deadlines was created at the beginning of the year so that time management could be easily visualized and changed in case of need. For example, each phase of the design process was assigned a definite period of time so that construction and testing would not be suppressed. The schedule allowed for change where needed and certain processes overlapped for efficiency. Figure 2.2 shows the final schedule with planned and actual dates.

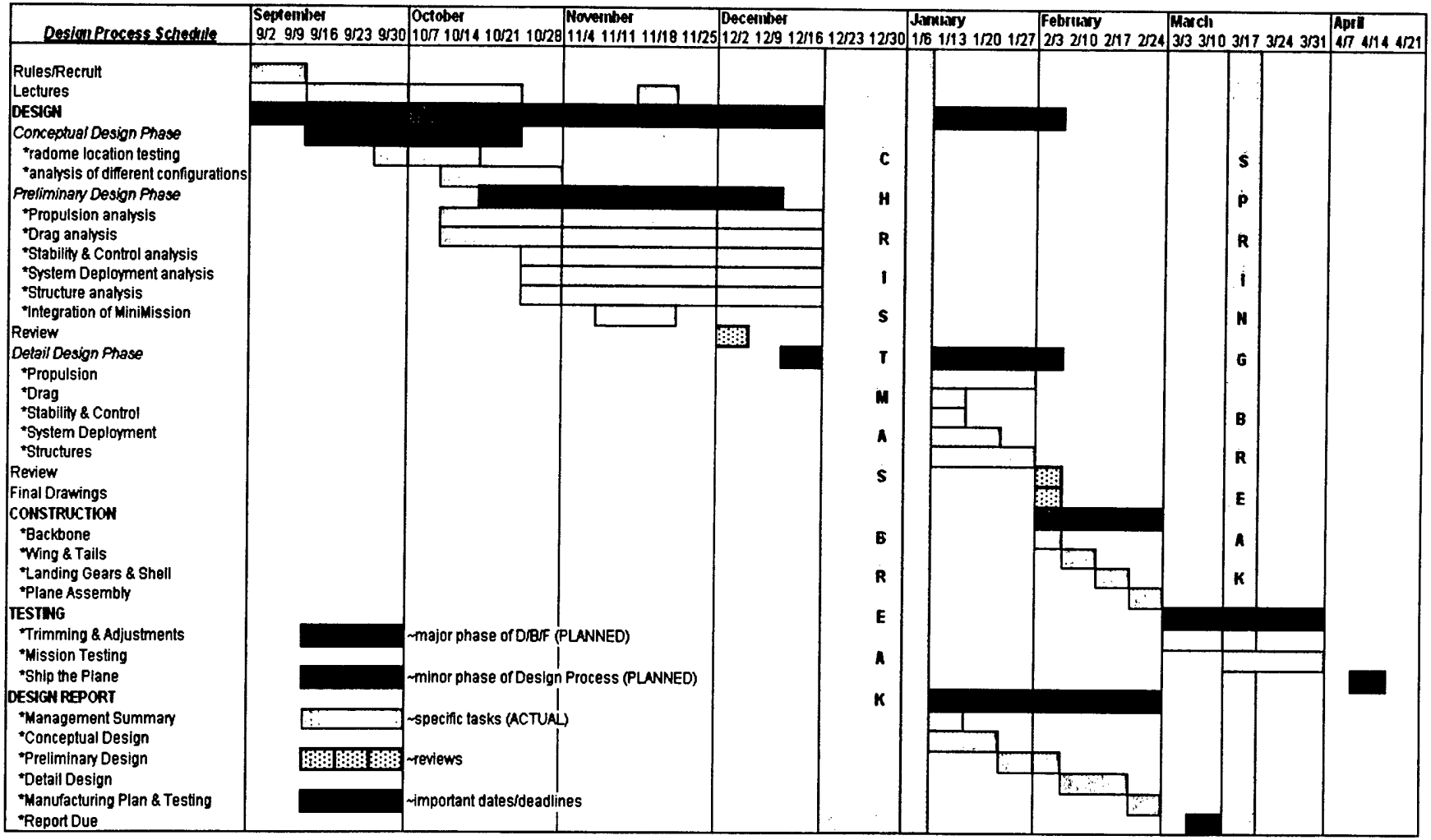

Figure 2.2 *USC AeroDesign Team Schedule*

3.0 CONCEPTUAL DESIGN PHASE

For the 2002/2003 Design/Build/Fly contest there will be three missions to choose from, out of which only two will be scored. Each mission entails different tasks: *Missile Decoy*, which provides an increased drag and has the highest difficulty factor, requires the plane to carry a completely un-faired radome simulating a cylindrical antenna together with a 5lb payload. The second mission, *Sensor Deployment*, requires the plane to fly two laps, land, deploy a 5lb simulated avionics payload, take off and fly two additional laps. The third mission, called *Communications Repeater*, has the lowest difficulty factor and requires the plane to complete four laps each with three 360-degree turns on the downwind leg of each lap, which poses an energy challenge.

There were six configurations proposed to tackle these requirements. The main differences between the configurations were found in the structural backbone, wing and tail types; single vs. twin boom, monoplane vs. biplane, and standard vs. V-tail. No H-tail was considered for simplicity of design. Three primary *Figures of Merit* (FOM's) were applied to each plane configuration; Total Flight Time, Structural Robustness and Rated Aircraft Cost (RAC). For each FOM a rating of 1 to 6 was awarded. Regarding the general and specific mission rules, there were several assumptions made and justified below. A final ranking chart provided the best airplane configuration for this year's contest.

3.1 Assumptions and Justifications

The following conditions were applied to all six candidates, shown in Figure 3.1 for a fair comparison.

1. *Plane has to fit in a 4'x2'x1' Box:* The contest rules specify that the whole plane had to be sized to this box, which drove the configuration to be small and flexible enough to allow folding parts. There was also an assembly time to be considered, which included taking the airplane from the box and preparing it for flight.
2. *Backbone Structure:* The simple single or twin booms fuselages were assumed for the plane's backbone in all configurations. This was based on the boom's ability to fit in the box by telescoping for quick assembly. It also allowed for major components such as motor and batteries to be easily attached.
3. *90ft. Take Off Field Length (TOFL):* A Safety Factor of 30 feet was added, which meant the plane was designed for a 90ft TOFL to insure that 120ft would not be exceeded. This criteria was determined from flight testing in 2000 and was incorporated into the Excel Spreadsheet, "MiniMission" designed by the 2002/2003 AeroDesign Team to calculate the performance and design parameters of the plane for an optimum solution to the different missions required this year.
4. *Only One Motor Used:* Because of the expense that an additional motor would add to the Rated Aircraft Cost (RAC), only one motor was assumed for all configurations. From the MiniMission calculations, one AstroFlight motor provided enough power to meet the TOFL. Studies were later conducted to confirm this assumption.

5. *5lb Battery Weight Capacity:* All configurations were to have provisions for the maximum 5lb battery weight limited by the 2002/2003 rules. This condition ensured that each configuration would have sufficient energy to complete each mission. Although the first two missions of the 2002-2003 contest do not require a long mission time, the configurations proposed took this into account in case the third mission would prove to be advantageous.
6. *55lb Maximum Take Off Gross Weight (TOGW):* Each candidate was assumed to fit this requirement given by the contest rules, implying light, simple structures.
7. *Carry a 5lb Payload:* All three missions for the 2002/2003 contest required a 6"x6"x12" payload, simulating an avionics package that was placed at the C.G. of the plane (the wing's center of lift located at the root quarter-chord). The coincidence of the C.G. with and without the payload minimized variations between heavy and light missions for ease of handling.
8. *Use of Composite Materials for Construction:* The high strength-to-weight ratio of composite materials, such as carbon fiber and fiberglass reduced the weight and provided enough strength to withstand the applied loads. The backbone (boom) and wing spar were essential structures that supported a substantial load, and therefore were made of composite material.
9. *Mission A, Missile Decoy Requirements (2.0 rank):* The 2002/2003 rules requires two out of three mission types to be flown. The USC team chose the first and second missions because of their high-ranking scores. The first Mission entailed flying a radome with 3in of clearance to the nearest airframe structure driving the other configurations to accommodate the extra drag and weight as well as a possible change in the C.G. location.
10. *Mission B, Sensor Deployment Requirements (1.5 rank):* This mission involved a self-deployment mechanism to release the avionics package and take off again to complete the final two mission laps. The conceptual configurations had to provide the structural means for deployment and allow the plane to clear the dropped payload.
11. *Standard Configurations Considered:* Due to the complexity of design, assembly time, structures and manufacturing, configurations such as canards, flying wings, blended wing bodies and others, exotic aircraft types were ruled out making classical configurations the safest and most efficient to consider.

3.2 Alternate Configurations

Six configurations were considered for the Conceptual Design Phase. As presented in Figure 3.1, variations of three main structures were selected: Backbone, Wing & Tail types. Aircrafts A, C, D & E had in common a single wing that had to be jointed in order to fit the box, while the biplane configurations, B & F, had the potential of a short span for a one piece wing. Landing gears remained to be assessed later in the design phase because of their complexity.

A. *Monoplane with a Low Wing, a Single Boom & Standard Empennage:* This design was selected for its conventional features that involved known building methods. In order for this configuration to fit into the box, the wing as well as the vertical and horizontal tails would have

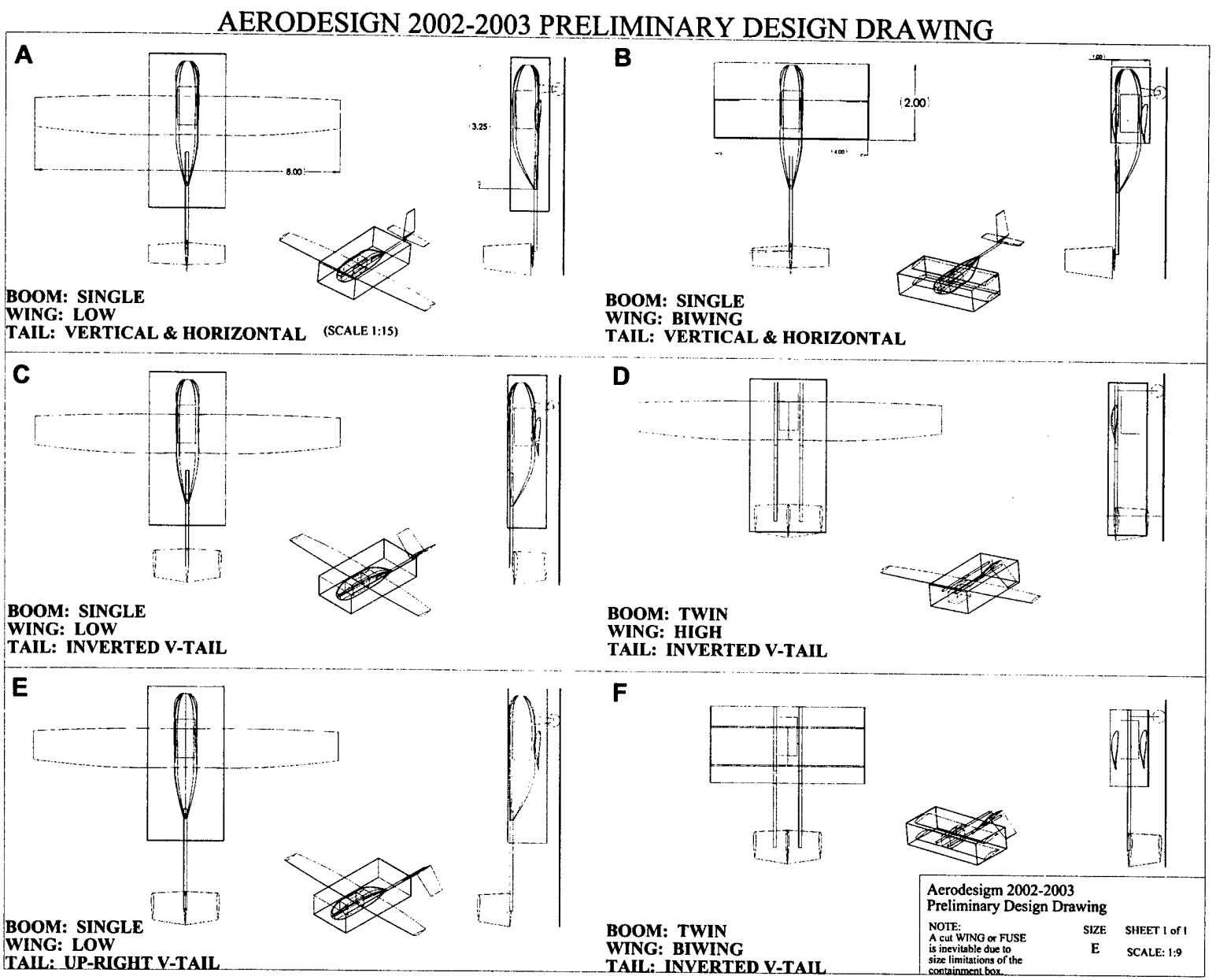

Figure 3.1 *Conceptual Configurations considered for Downselect and optimization of design*

to contain joints to maintain the proper sizing for stability and control. This would increase weight and assembly time. The low wing required special attachments to the backbone and restricted the payload deployment to a complicated action of sliding it through the back of the fuselage, as opposed to simply dropping it.

B. *Biplane with a Single Boom & Standard Empennage:* The structural advantage of the biplane, compared with the aircraft A, was its ability to fit in the box without any hinges in the wing. The disadvantage would be the increase of the rated aircraft cost due to a penalty for a second wing and extra control surfaces. It also increased drag and required more constructed parts.

C. *Monoplane with a Low Wing, a Single Boom & Inverted V-Tail:* The inverted V-tail was considered because it cleared the deployed avionics package, was not in the wake of the radome and fit in the box without any junctions in the tails. The structural robustness of the inverted V-Tail would have to match that of a landing gear, which implied a complex and heavy structure. The low wing caused the same problems as aircraft A.

D. *Monoplane with a High Wing, Twin Booms & Inverted Split V-Tail:* The Twin Boom Configuration was considered because of the absence of a fuselage, which decreased weight and the number of parts to build. The twin booms and the high wing allowed the payload box to be dropped without the need of a sliding mechanism. The disadvantage was there were two telescoping tail booms instead of one.

E. *Monoplane with a High Wing, Single Boom & Up-Right V-Tail*: This aircraft varied from configuration C by reversing the V-Tail from Inverted to Up-Right. This eliminated the problem of structural robustness needed for landing. It still fit into the box because the telescoping tube could be rotated 180° during assembly to allow stowage of the tail in an inverted position. In addition, the V-tail would reduce the assemble time.

F. *Biplane with a Twin Boom & Inverted Split V-Tail:* As aircraft B, the biplane provided an easy method to fit the wing without any junctions, but the twin booms would have to be removed to fit the box as opposed to configuration D.

3.3 Figures of Merit

To analyze the conceptual configurations with performance, fabrication, reliability, etc. the following three primary Figures of Merit (FOM's) were selected.

1. *Total Flight Time*: The 2002-2003 contest rules specified that the total flight time was composed of the actual mission performance plus the assembly time. Since minimum flight time maximizes the flight score, a high velocity and low C_D were required. The timed assembly task was important and needed to be performed accurately and efficiently. The conceptual configurations could accomplish this by having parts that are easy to assemble such as telescoping tubes or biplanes with a short wingspan.

2. *Structural Robustness*: Structural integrity was important for the conceptual aircraft in order to survive possible crash scenarios with minimal damage. Especially critical were structures such as deployment mechanism and the tubular backbone. This consideration would lead to a minimal number of joints and parts as well as simplicity of design and construction.
3. *Rated Aircraft Cost (RAC)*: The formula for the total contest score uses RAC to penalize complex designs. From last year's competition, the team realized that other teams had similar results with lower RAC's. Trying to minimize this parameter was an important goal for this year's design. The RAC is a function of the number and size of components used to accomplish the different missions such as motors for propulsion, batteries for energy, wing area for lift, and the number of actuators for aircraft control. A minimum cost would result in a maximum score for a given report and flight scores.

To further analyze each configuration, the primary FOM's were further broken down into components that contributed to each design requirement and specification.

3.4 Design Parameters Quantifying the *Total Flight Time* Figure of Merit

The *Total Flight Time* FOM was influenced greatly by the following important design parameters:

1. *Minimum Total Aircraft C_D*: Parasite and vortex drag had to be lowered to obtain the minimum aircraft drag. This results in a lower required power at a fixed velocity or in an increased maximum speed for a fixed available thrust.
2. *Minimum Assembly Time*: This requirement was determined by the time it will take to unload the aircraft from the carrying box and assemble it to ready flight conditions. Simple unfolding mechanisms and automated assembly could reduce the time. Mechanisms considered were the telescoping backbone, the spring loaded joints in the wing, a folding landing gear and a folding V-Tail to eliminate assembly of the empennage.

3.5 Design Parameters Quantifying the *Structural Robustness* Figure of Merit

1. *Minimum Number of Structural Discontinuities*: All the design loads for the different missions were taken into account for the conceptual aircraft. Fewer junctions result in fewer fasteners, less reinforcements, simplicity of design and a fewer number of parts. This also affects the total weight and cost. Composite materials increased the robustness of the plane as well as reduced weight. These materials used in the spars and telescoping backbone could be manufactured with fewer discontinuities thus improving the integrity of the aircraft.
2. *Fitting the Aircraft into the Shipping Box*: The mission profiles required a 5lb-deployable 6"x6"x12" payload box. This requirement, together with the propulsion system, roughly determined the aircraft fuselage dimensions. All of the aircraft components had to be designed to fit the 4'x2'x1' shipping box. This dictated the need for structurally sound junctions in the wing and flexibility in resizing, such as the telescoping boom.
3. *Simple Deployment Mechanism*: Because Mission B was chosen as one of our team's sorties, the deployment system was extremely important in the design of the aircraft. The

challenge was to keep the deployment system without interfering with other airplane components that might prevent it from taking off again for the last two laps of the mission profile. Several types of doors were considered, such as bomb bay door, clamshell doors, etc. in the conceptual design stage. Integration of a release mechanism with the different types of doors was an important consideration, as well as the placement of bulkheads and reinforcements for attaching the payload.

3.6 Design Parameters Quantifying the *Rated Aircraft Cost* Figure of Merit

The *Rated Aircraft Cost* FOM is designed to penalize configurations for complex geometry and the size of the plane. Minimizing these parameters can improve performance and substantially increase the overall score of the plane since the flight score is divided by RAC to obtain the final score. The following represent the most important factors that affect the *Rated Aircraft Cost*.

1. *Propulsion System*: The number of motors and the total battery weight had a large effect on the *Rated Aircraft Cost* because its weighted value was one order of magnitude larger than other parameters in the cost formula. It is also weighted twice, first as the rated engine power and then as the manufacturing man hours. Since sufficient energy is a factor to meet the mandated TOFL, a balance between penalties and performance had to be attained.
2. *Primary Lifting Mechanism and Empennage*: In this section the number of wings and therefore wing area, control surfaces, vertical and horizontal tails were penalized substantially in the RAC. Careful decisions had to be made to weigh the cost versus the advantages gained through adding additional components. For example, brakes provide an advantage in reducing ground handling time but at the cost of weight and an extra servo. These considerations account for approximately the same percentage of the RAC as the propulsion system cost.
3. *Manufacturers Empty Weight*: This section penalized the excess materials used in construction and rewards the efficiency of the structure. Relative weight was depended on use of high strength-to-weight ratio materials, simple designs, and simple mechanisms. Another aspect considered was the battery weight vs. energy, and gearbox vs. direct drive, since once again the propulsion system counts in the airplane's empty weight.

3.7 Configuration Downselect

To validate the down-select assumptions, tests were performed on critical mechanisms and aerodynamic features. The emphasis was on wing-joint assembly time, radome drag, payload deployment, and payload doors.

1. *Wing Joints*: Four types of joints were considered and tested on old wings from previous years competitions before an optimum solution was obtained. The first configuration consisted of a wing with two 45° hinges, folding inward and aft toward the tail of the plane. A 2ft center wing was attached to the fuselage. The hinges were located on the underside of the wing and the spar-joiners were spring loaded. This mechanism worked well and showed

that the servo wiring and alignment of the spars would not be a problem. But the wingspan did not fulfill the aerodynamics requirement for TOFL. To compensate for that, a 70° cut was tested, with wings folding upward and hinges on the top surface. The design became more complicated and weight increased. Next, a three-piece wing was considered with a middle 2ft long section attached to the fuselage and two 3ft pieces sliding into the center spar. It was simple and decreased assembly time, but servo wiring was difficult as well as spar alignment. The last configuration was a two-panel wing that fit into a center tube spar. This minimized wiring connection problems and optimized the alignment. This wing was chosen because of its potential for quick assembly time, simplicity of design, and its ease of manufacture. Sizing details were performed later in the preliminary phase, taking into consideration the high shear and bending stresses at the fuselage.

2. *Radome Drag*: The team wanted to know the effects of the radome on drag and stability in flight. Therefore a model radome was analytically analyzed, tested in the wind tunnel, and flight-tested on last year's airplane. Results, presented later in the testing section, were the same for all three approaches producing a radome C_D of about 0.72, which was reasonable enough to estimate its performance. The radome placement was also tested in flight to reduce its drag by finding an optimum mounting location. The tested locations chosen were above and below the CG, as well as on the aft part of the fuselage. The highest flight speed, corresponding to the lowest drag, was found above the CG.
3. *Deployment Mechanism*: For mission B, a mechanism was required to self-deploy the simulated avionics package. Initially, a balsa replica of the aft fuselage was constructed with clam doors. To promote the learning experience, some of the underclassmen were taught to use carbon fiber to build a fuselage by a wet lay-up and vacuum bagging techniques. This fuselage became the prototype for testing the release mechanism and doors. Three different door types were tested; clap doors with vertical hinges and a rubber band for pushing the payload out the rear, clam doors with horizontal hinges and clam doors with diagonal hinges. Both the clam door prototypes allowed the payload to fall directly under the fuselage. This method worked the best and was further analyzed in the preliminary design phase. Different release mechanisms were also considered such as rubber bands and an actuating servo. The pin system released by a servo proved to be more secure in holding the payload as well as keeping the doors closed. The wing position affected the payload drop since a low wing would interfere with the drop path when released from the fuselage. A high wing was needed to allow the package to drop out by gravity.

3.8 *Rated Aircraft Cost* Comparison with Conceptual Design Rankings and Final Design Features

A final ranking chart for each FOM was constructed to select the best configuration (Table 3.1). Each aircraft was rated on a scale from 1 to 6, 1 being the best, and therefore the minimum score resulted in the optimum configuration. Note also that each FOM was assigned an importance factor to

weigh the score appropriately. After this analysis, the monoplane fit the closest description of the aircraft that would best perform in the missions for the 2002-2003 contest. The foregoing studies and tests confirmed that flying the extra drag in Mission A and the deployment device in Mission B were both achievable. A single motor configuration with a high, 2-panel wing was then considered for configuration E. This allowed for clearance for the payload release and provided ease of manufacturing as well as structural ability to handle required loads. The chosen tail was an upright V-tail due to its ability to fit into the box by rotating the backbone at its joint. This tail configuration also reduced the area affected by the wake of the radome when mounted above the CG, and reduced the cost of an inverted V-tail since the structure would be less complex. The telescoping backbone was selected for its multifunction ability to minimize assembly time, provide sufficient structural robustness to support the other components of the airplane and reduce cost by simplifying manufacturing

	Monoplane				**Biplane**	
	A	*C*	*D*	*E*	*B*	*F*
Total Flight Time **FOM (1.5)**	**9**	**4**	**9**	**4**	**9**	**7**
• Minimum Aircraft C_D	*3*	*2*	*4*	*1*	*5*	*6*
• Minimum Assembly Time	*6*	*2*	*5*	*3*	*4*	*1*
Structural Robustness **FOM (2)**	**6**	**9**	**11**	**5**	**15**	**17**
• Minimal Discontinuities	*1*	*3*	*5*	*2*	*4*	*6*
• Fit within Carrying Box	*4*	*2*	*3*	*1*	*6*	*5*
• Simple Deployment	*1*	*4*	*3*	*2*	*5*	*6*
Rated Aircraft Cost **FOM (1)**	**5**	**9**	**13**	**5**	**13**	**18**
• Propulsion System	*3*	*2*	*4*	*1*	*5*	*6*
• Primary Lifting Mechanism	*1*	*3*	*4*	*2*	*5*	*6*
• Manufacturer's Empty Weight	*1*	*4*	*5*	*2*	*3*	*6*
Section 1.01 **TOTAL WEIGHTED SCORE**	**30.5**	**33**	**48.5**	**21**	**56.5**	**62.5**

Table 3.1 *Final Conceptual Design Rankings and Rated Aircraft Cost Summary*

4.0 PRELIMINARY DESIGN PHASE

This phase further developed the conceptual design studies by breaking down the different disciplines and analyzing them thoroughly. Four main design subject areas were examined: Aerodynamics, Propulsion, Stability & Control, and Structures. Parametric models were created for each area including; Aerodynamics, Stability and Control, Propulsion and Batteries, Performance, Weights and Cost which were then integrated into a single analytical tool called "MiniMission. Once MiniMission was created, sizing studies were performed to optimize the configuration for the different missions. From the initial trade studies, missions A and B appeared to be the most rewarding, so these were used for all subsequent trade studies. Later, the sized airplane showed promising results for mission C also.

4.1 Mission Model

The goal of any analytical tool used by the USC Aero-Design team was to provide the means necessary for simple calculations focusing on the results rather than on the tedious calculations and to provide a learning experience to its members on the impact of the different parameters that size a plane. For several years the USC Aero-Design team has used its own code based on a Microsoft Excel spreadsheet called MISSION to fulfill this goal. Unfortunately most of the members that fully understood the coding and functions of MISSION were no longer on the team, leaving the lower classmen with a powerful software package but with inadequate understanding of its complexity. For this reason, the team decided to start a new program that would perform the same function as MISSION but developed by current team members. The result was called MiniMission. It is also an Excel spreadsheet in which each group captain was assigned the responsibility of coding a module that would facilitate that group's calculations. The completed modules were then given to the performance team who linked all the modules together. This resulted in a spreadsheet with multiple sub-sheets categorized by their function. Some of them were composed of data libraries while others did actual calculations. To facilitate the use of the software package, a front page was created that incorporated all the required inputs for the mission as well as the most relevant outputs. Table 4.1 shows some of the different sub-sheets and their function.

With MiniMission, the team had the tools necessary to perform several iterations for different variables and compare their results. Each sizing iteration adjusted wing area for target take off field length (TOFL), sized the tail for pitch and yaw stability, and adjusted cruise velocity to achieve a specified rate of climb. Once this process concluded, the tail was checked to see if it fit in the box. If it didn't then the tail aspect ratio was reduced and the process restarted. Some early results from MiniMission yielded cruise speeds of 70 to 90 mph optimized to the SD7032 airfoil. Because MiniMission was a new code, the team's industry advisor compared the values of MiniMission with a secret version of MISSION modified for this year's competition to make sure the information obtained was reliable. In order to analyze the results, a "Best Flight Score" was predicted in order to compare one configuration to the other. This best flight score took into account missions A, B and C as well as heavy and light laps. In the trade study graphs below, a circle represents the optimized parameter.

Sheet Name	Function
Propulsion	Battery, Motor, propeller & Gearbox libraries, and Thrust solver
Configuration	Airplane sketch as well as component location
Cost	Cost calculation for each mission
S & C	Tail Sizing as well as S & C Characteristics
Weights	Weight & C.G. bookkeeping
Performance	Calculate plane characteristics; e.g. thrust, TOFL, Rate-of-Climb, Prop Efficiency, Flight Time and energy consumption for all 3 missions
Shotgun	Single variable Trade Study utility

Table 4.1 *Description of some of MiniMission modules.*

Other programs were used by the structures group to calculate the sheer and bending moments of the landing gear, interactions between the tube spar and the telescoping backbone and other components of the plane. These programs could also calculate the schedule of layers of pre-preg carbon fiber needed to make individual components.

4.2 Design Parameter & Sizing Trades

4.2.1 Aerodynamics

The goal of the aerodynamics groups was to insure that the aircraft would meet all of the main constraints of the competition including the take off field length, provide sufficient lift, minimize the drag, etc. The L/D ratio and C_{Lmax}, were the most important figures for this year's competition.

1. *Drag*: To calculate the total airplane drag, vortex and parasite drags were computed using relations derived from "Fluid Dynamic Lift" and "Fluid Dynamic Drag" by S.F.Hoerner, with airfoil polars from XFOIL. Vortex drag due to lift is accompanied by strong wingtip vortices whose influence can be minimized by using high aspect ratio wings to separate the vortices. Elliptical span-loading and winglets also reduce the vortex drag. Most wings don't have a perfectly elliptical span-load, efficiency factor "e" accounts for this inefficiency, which is typically 0.89 for an un-tapered wing. Other types of drag considered in the Aerodynamics model are junction drag formed at the intersection of two aerodynamic bodies, such as the wing and the fuselage; gap drag at the control surface hinge lines that can be sealed; base drag that occurs at the aft part of the fuselage and can be eliminated by bringing the tail cone to a point or blade; step drag which can be prevented by using flush brackets; trim drag which is a result of download trimming of the tail and can be minimized with a long tail arm l_H/c and aft C.G. position; and profile drag caused by the 2-D airfoil type. These were all analyzed and

incorporated into the MiniMission spreadsheet with resulted in the drag polar shown in Figure 4.1.

2. *Airfoils*: Airfoil lift and drag was calculated using the "X-Foil" program developed by Dr. Mark Drela of MIT (http://raphael.mit.edu/xfoil/). By employing a panel method calculation of the pressure distribution plus a boundary-layer model, plots for C_L vs. α and C_{MO} vs. α for a given airfoil at a Reynolds's number (Re) of 500,000 can be obtained. SCyRaider (this year's plane) employs geared flaps to optimize L/D across the C_L range. To simulate the geared flaps, a single airfoil polar was obtained by fitting a curve to a range of flap deflections from -5 to +20 degrees. Elevator settings are adjusted to achieve this polar in-flight. The locus of minimum C_D's created the single polar as seen in Figure 4.2 below. A library of different airfoil types was developed including: SD8020, SD800, LA203a, RG15, RG15+flap, NACA4414, NACA4414+fla-p, NACA2214, SD7032+flap, SD7032+12% increased thickness+flap, SD7032+14% increased thickness+flap. These were selected either for their high C_{Lmax}, capability to meet the TOFL requirements, or low C_D at cruise velocity. On some of these airfoils the 10% thickness was too thin for the sized spars to fit at the quarter chord of the wing, so increased thickness cases were analyzed in XFOIL and incorporated into MiniMission.

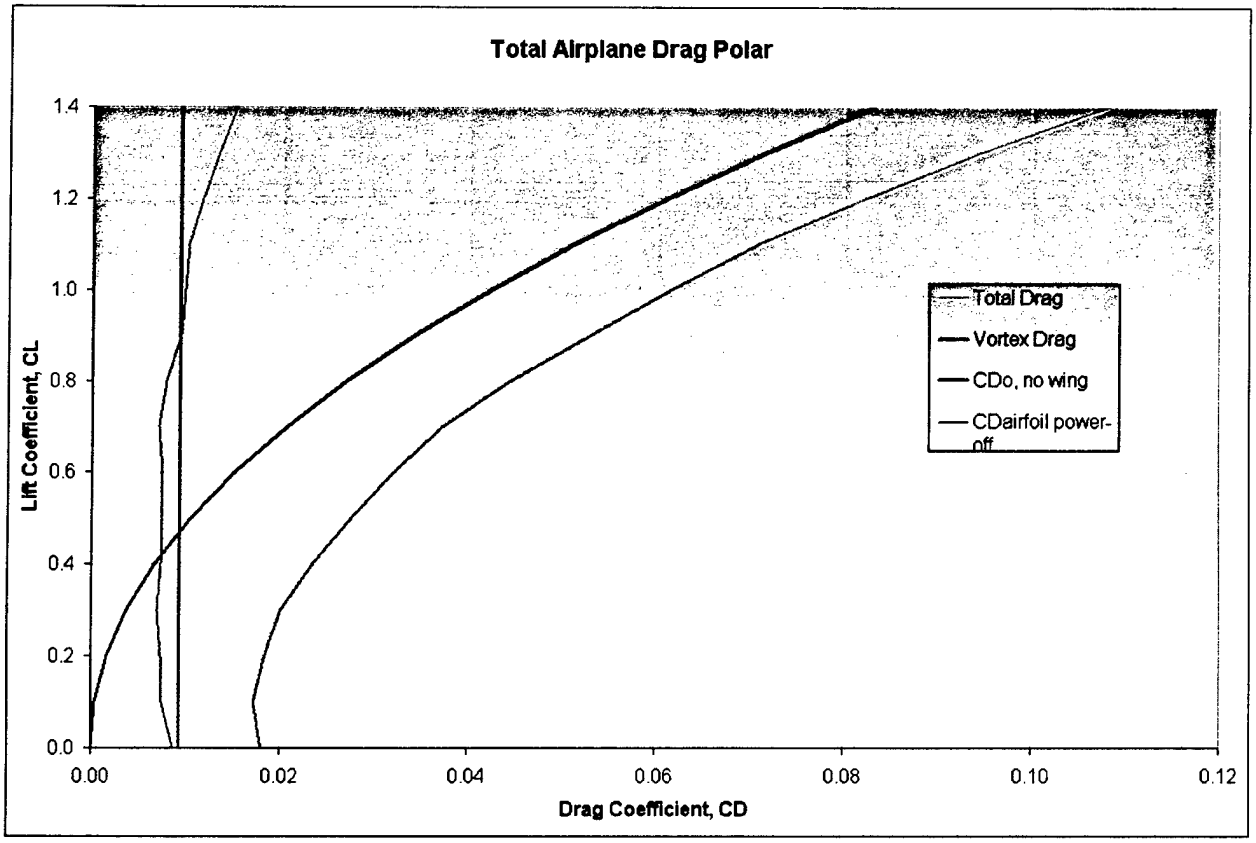

Figure 4.1 *Example of Total Airplane Drag for the SD7032+12% increased thickness+flap. Note the Vortex and Parasite Drags are also depicted*

3. *Wing*: The wingspan was constrained by the 4'x2'x1' box and the timed assembly task. To minimize the assembly time, a minimum number of wing sections was desired. This constraint and the box size restricted the wingspan. The wing had to also deliver the appropriate lift for take off and fulfill the two missions chosen, Missile Decoy (A) and Sensor Deployment (B). Trade-studies were performed one parameter at a time. Mini-Mission optimized both the wing area for TOFL, and cruise speed for Rate-of-Climb. One of these studies is shown in Figure 4.3 where the wingspan of a SD7032+12% airfoil is varied from 5 to 9ft. The figures of merit, such as best flight score, mission time, rated aircraft cost, available/required energy, TOFL, etc. are plotted versus wingspan. The 7ft wing provided the highest score with better excess energy and a smaller wing area than shorter wingspans. A 9ft. wingspan had the slightly better V_{cruise}, but it also had a higher cost and lower mission score. It would have been difficult to fit a nine-foot wing into the box without more junctions and structural complications, which compromises the structural robustness FOM. Estimated aerodynamic characteristics for the plane with a seven-foot wingspan are given in Table 4.2.

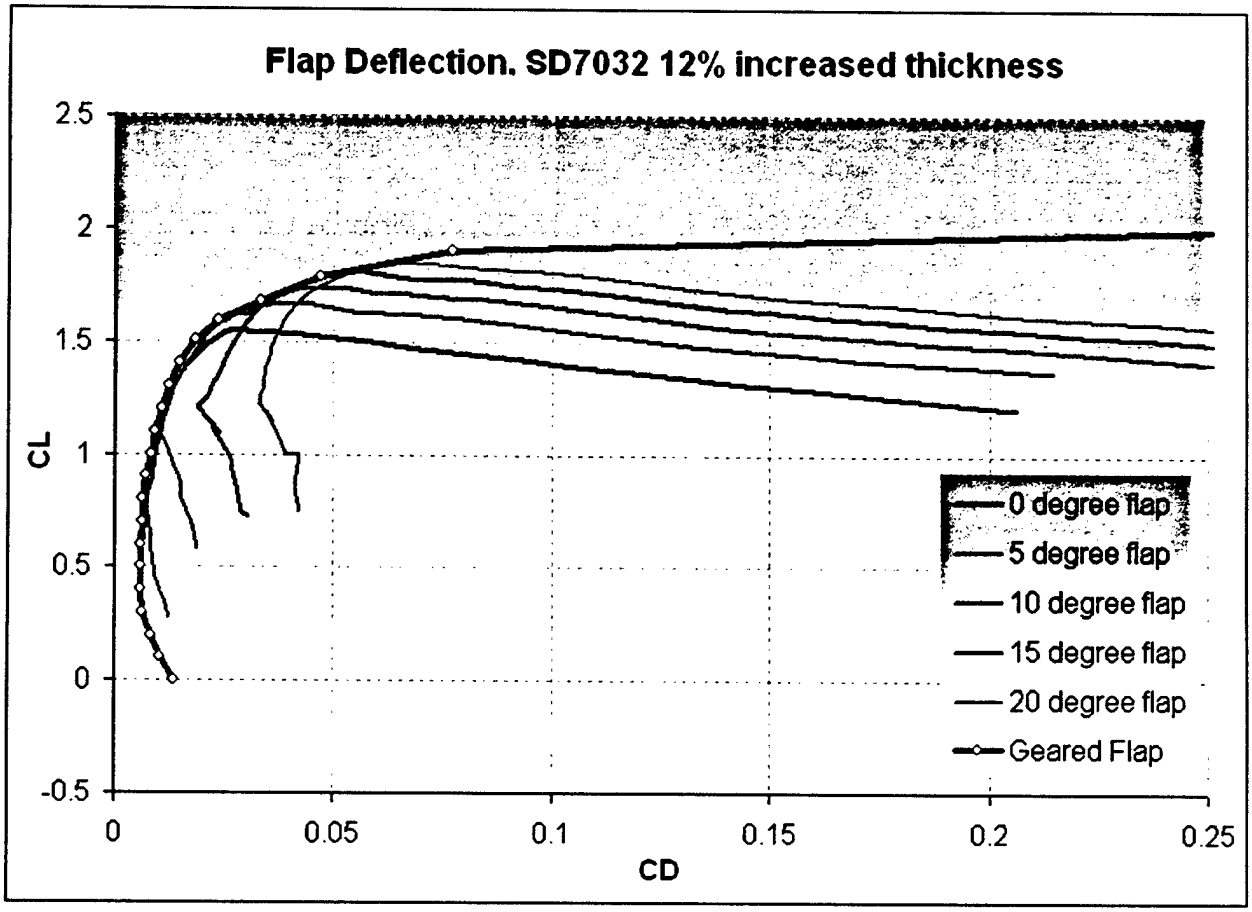

Figure 4.2 *Geared Flap Deflection Example for the SD7032+12% increased thickness airfoil with flap varying from -5 to 20 degrees*

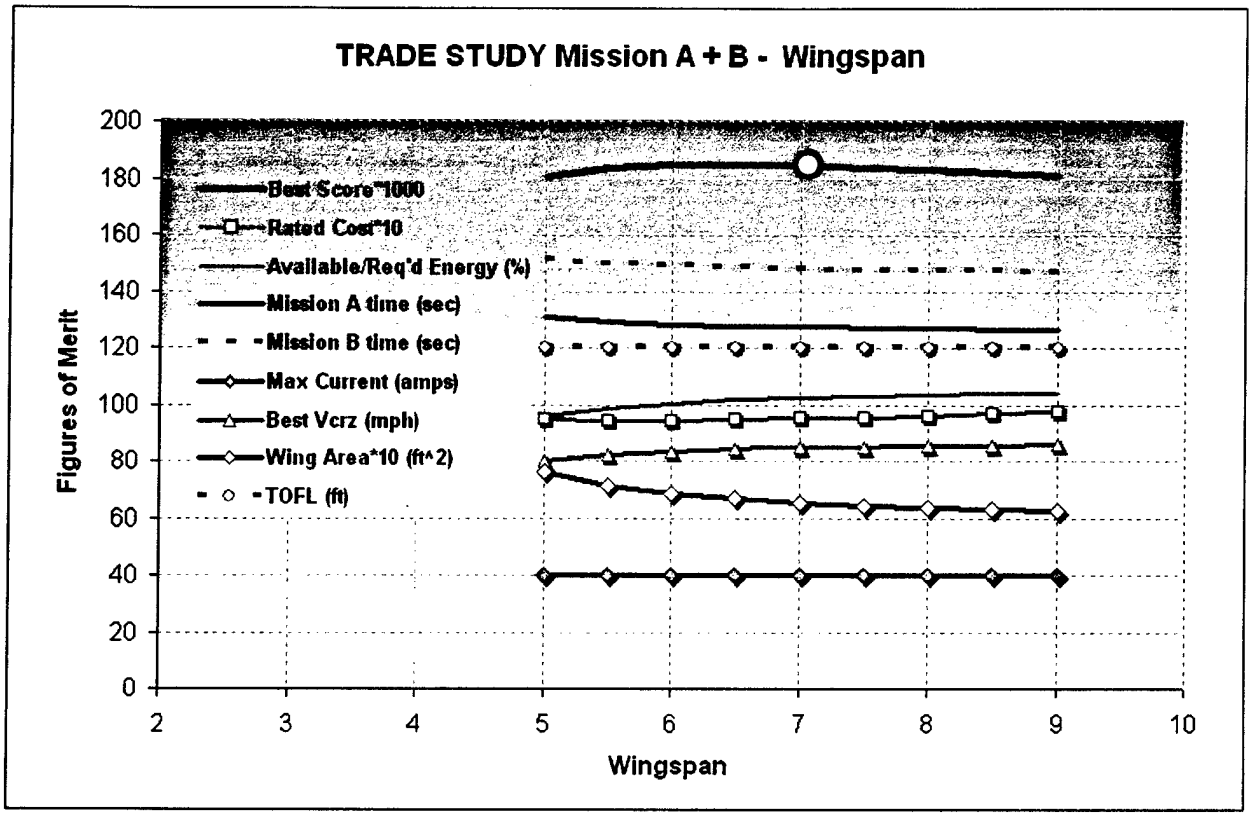

Figure 4.3 *Trade Study for a wingspan range of 5 to 9ft on a SD7032-12%.*

	Section 1.02 Interpolated Drag Values at Cruise				General Aerodynamic Characteristics	
		C_{L1g}	C_D	L/D	e	0.94
A	Heavy Cruise	0.224	0.030	7.425	C_{Lmax}	1.88
B	Heavy Cruise	0.161	0.017	9.390	t/c	0.12
C	Light Cruise	0.108	0.016	6.565	C_L at V_{cruise}	0.2
	Airfoil: SD7032 12% thickness + flap				C_L in turns	1.0

Table 4.2 *Estimated Aerodynamic properties of SCyRaider with the selected airfoil*

4.2.2 Propulsion

The propulsion system consisting of batteries, motors, gearboxes and propellers was the most important factor in determining the aircraft performance. It was analyzed by using MiniMission and optimized until the final propulsion configuration was obtained. The software calculated the total resistance of the circuit by summing the internal resistance of the individual components such as batteries, cables, speed controller and motor. An initial *assumed current* was run through the circuit to calculate a voltage drop across each component in the circuit. The voltage across the motor was used to

calculate the motor's rpm. The propeller model took this rpm and computed the torque required for the specified prop, yielding a *required current*. The process was repeated until the *required current* matched the *assumed current*.

1. *Batteries*: The main constraints on batteries and power were a 5 lb maximum weight limit, which influenced the rated aircraft cost significantly, and a 40 amp maximum current draw. The available energy stored in each cell was needed to provide efficient conversion to kinetic energy. Tests conducted by the team indicated that the advertised energy content of the batteries was not available primarily due to the heavy current draw by the motor. This produced temperature effects resulting in increased resistance in the motor, the controller, the wiring and other power losses. The tests suggested that the batteries produced only 60% of the manufacture's listed storage capacity. This factor was incorporated into the Mini-Mission spreadsheet analysis. For the analytical model, a library of Sanyo batteries was compiled with six different types: KR-1400AE, RC-2000, RC-2400, CP-1400, CP-1700 and CP-1300. They were selected due to their easily accessible data, the 2002-2003 rule constraint of using only over the counter NiCad's and the past performance experienced with a number of these batteries. A trade study documented in Figure 4.4 showed the optimum solution for the battery type was Sanyo CP-1300 for its ability to lower the RAC significantly because of decreased weight. These batteries had slightly smaller energy efficiency; but since this year's contest didn't require long periods of flight time, there wasn't a shortage of energy for completing the missions. The major consideration in this case was the energy required to meet the TOFL requirement. To optimize this battery type, the number of cells trade study was performed and shown in Figure 4.5. 36 cells provided a high overall score and high velocity at cruise conditions, a lower cost and didn't exceed the 40amp limit. The total battery weight including solder was 2.9 Lbs.
2. *Motors*: The competition rules stated that the motors had to be from the Graupner or AstroFlight families of brushed electric motors. A library of motors was constructed that included parameters such as the torque and speed constant, internal resistance, etc. These parameters were important for efficient battery usage consistent with the maximum power delivered to the propeller. Out of the six motor types documented in the analytical model, Cobalt 60 was the only one found to fulfill the two mission conditions. By carefully mating it with the battery pack, the gearbox could be eliminated. This saved weight and also reduced the rated aircraft cost.
3. *Propellers*: The propeller diameter and pitch had to be mated properly with the motor and battery pack to insure the aircraft could meet the 120 foot TOFL constraint as well as maintain sufficient cruise velocity. Large pitch propellers required more current draw whereas large diameter gave a slower velocity, but improved TOFL. Propeller libraries were built and trade studies for these two parameters were performed (Figures 4.6 & 4.7).

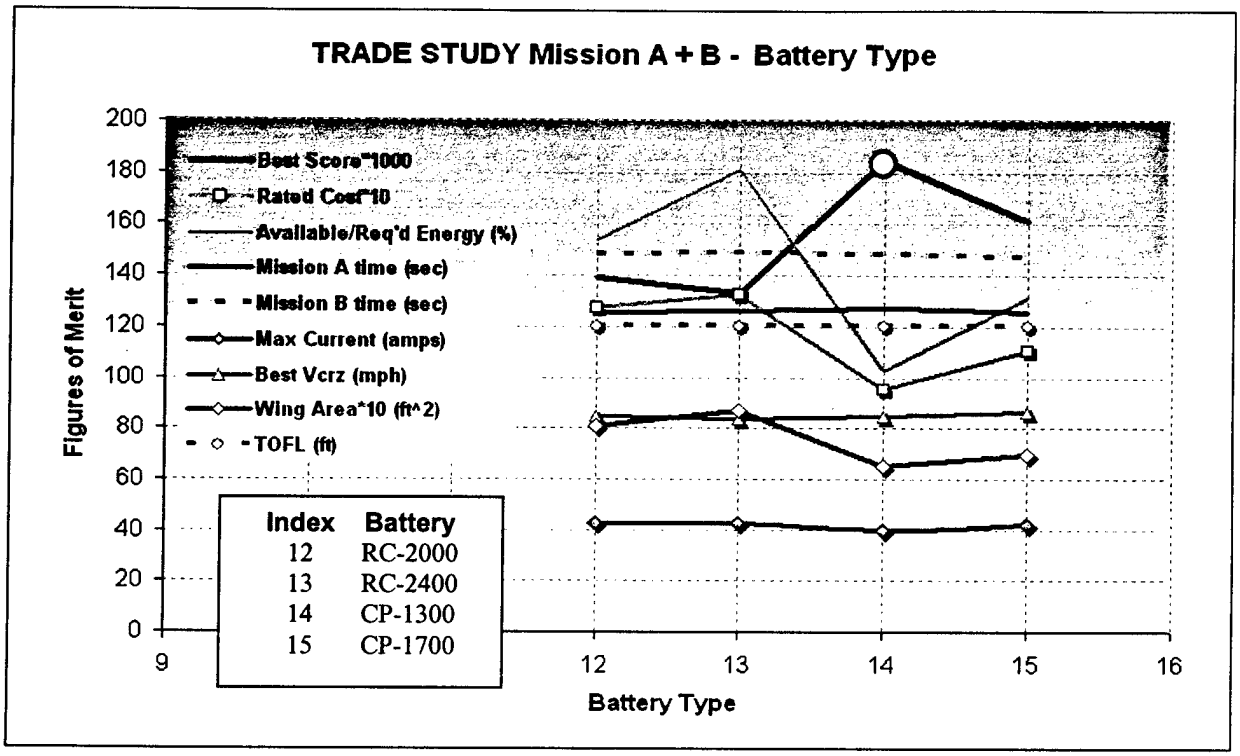

Figure 4.4 *Trade Study for different types of batteries considered*

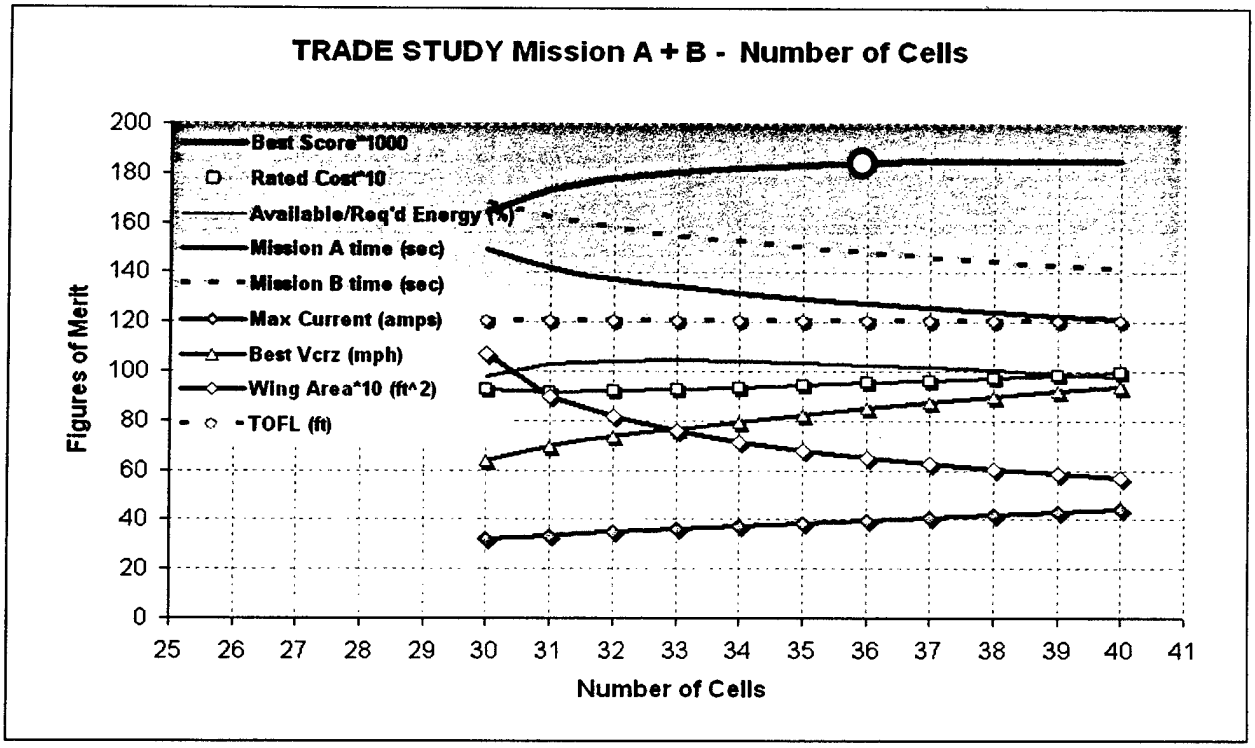

Figure 4.5 *Trade study performed on the Sanyo CP-1300 battery type, to optimize the number of cells*

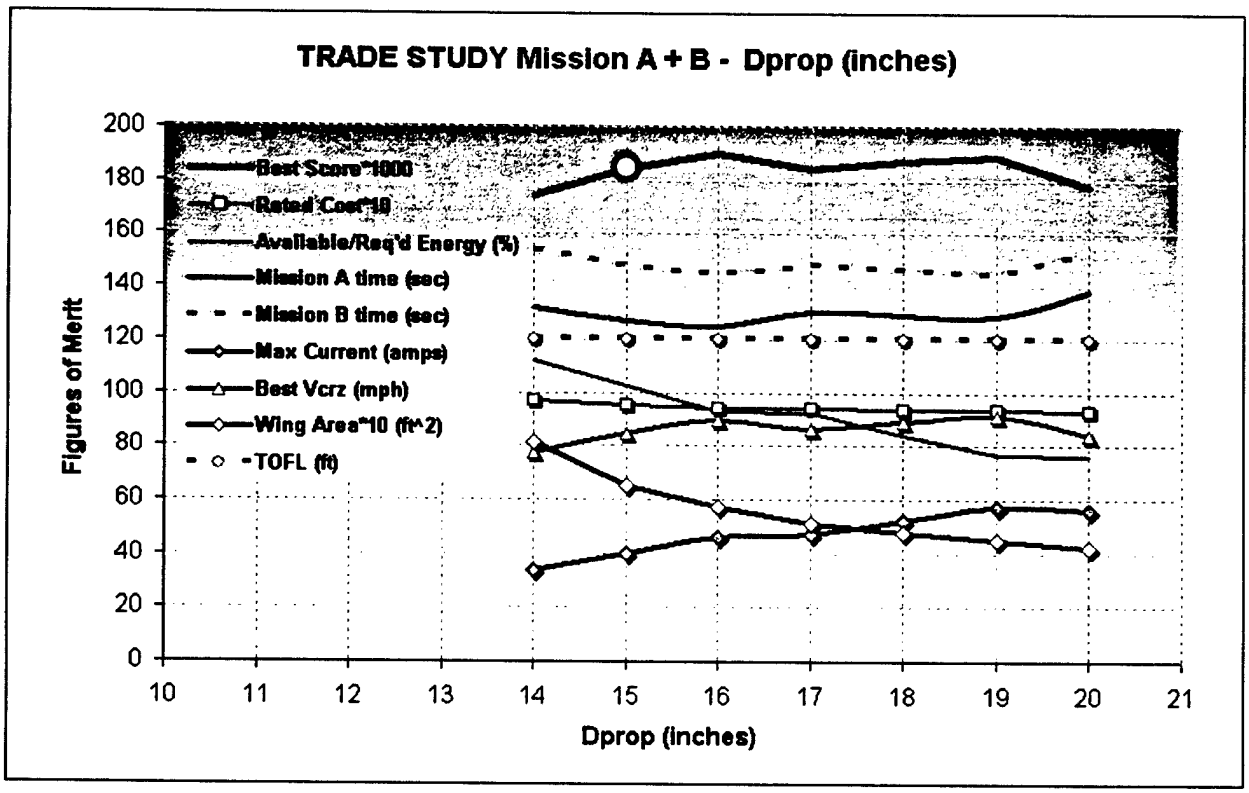

Figure 4.6 *Trade Study on propeller diameter (14'-20')*

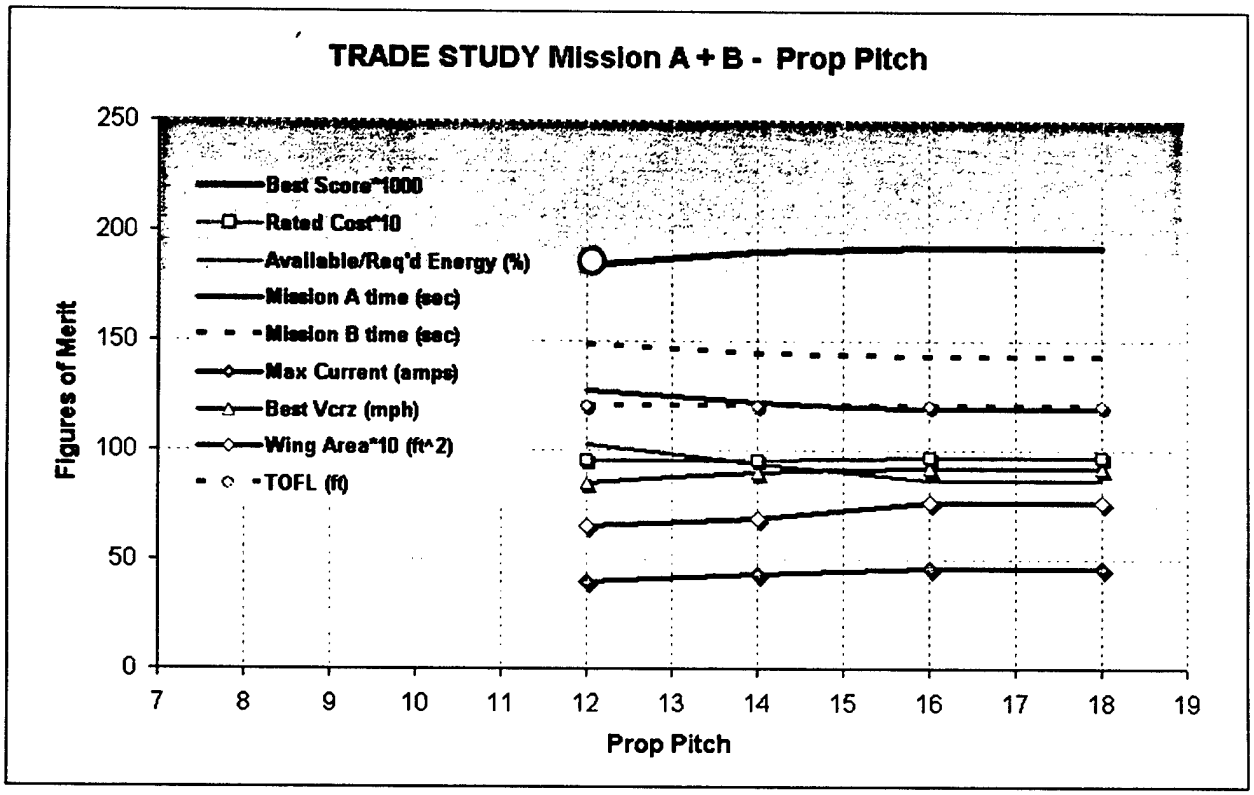

Figure 4.7 *Trade Study on propeller pitch (6-18)*

As the diameter increased, at a fixed pitch, some figures of merit presented two peaks. The second peak had a higher score, but the available energy decreases substantially and the current draw exceeds the max allowable; therefore a diameter of 15 inch was chosen. For a given propeller diameter, the prop pitch was varied from 6 to 18 and the optimum found at 12 by available energy and current draw.

4.2.3 Stability and Control

The goal of the stability and control group was to provide a stable and maneuverable plane with the least tail area for low drag. In addition, the team did not want the tail panels to require assembly. This reduced assembly time and constrained the tail to have a limited span. Initial studies showed a V-Tail to be best suited for packaging. In order to implement this tail, different design parameters had to be considered in sizing the V-tail as well as the control surfaces of the wing. The most important ones were the horizontal tail's level arm, the tail aspect ratio, tail stall characteristics, as well as the frequency and the damping ratio of the plane. Each one of these parameters was directly related with other sub-components of the plane. For this reason the whole sizing process had to be performed in parallel with the rest of the aircraft. In MiniMission, the tail area was varied until the required static margin was satisfied, then tail dihedral was adjusted to satisfy the directional stability ($C_{n\beta}$) requirement. The process was repeated until both conditions were met.

1. *Inputs*: The input parameters were based on known values from the literature or historical sources as well as from different tests conducted. The handling characteristics like the static margin and the yaw moment coefficient of the plane were embedded into the code, which sized the V-tail so that these characteristics would match the ones specified. The output was the geometry of the tail as in chord, span and dihedral angle. Once the geometry of the tail was known, the ability of fitting it into the box could be determined and corrected if necessary.
2. *Static Margin*: The static margin was initially assumed to be 25% based on test flights in previous years. In these tests, the horizontal tail size was varied until the pilot complained of insufficient stability. The S & C group for that year then reverse engineered the design process and concluded that a static margin of 25% was ideal for the AIAA DBF plane. In a similar manner this year, the minimum allowable directional stability ($C_{n\beta}$) was determined by testing last years DBF plane. Several test flights were performed with the height of the vertical tail reduced by 2 inches in each successive flight. This process continued until the pilot complained of insufficient stability. The minimum allowable $C_{n\beta}$ was found to be 0.0016/degree.
3. *Frequency Response & Damping Ratio*: Other important S&C characteristics were the frequency response and the damping ratio of the plane. These parameters would determine how well the plane would return to its initial conditions once it was perturbed. Ideally the frequency should be as large as possible, minimizing the time required to return to initial conditions. In reality, frequencies above 1 Hz are deemed acceptable to avoid sluggish

handling. The damping ratio specifies how much overshoot the oscillations have and how rapidly the plane will return to its initial conditions. Damping ratios of 70% are considered ideal. Anything above 90% was considered too sluggish, and below 50%, the plane would oscillate excessively. Stability and packaging constraints required a significant tail volume of about 1.5. The payload was also compact leading to low pitch inertia. Both effects cause high damping ratios meaning SCyRaider would have more than 70% damping ratio.

4. *Stall Characteristics*: Stall characteristics of the aircraft were also analyzed to make sure that in the event of stall, the plane would behave in a predictable way. The tail was designed so that it would stall later than the wing to prevent any loss of control. The wing's taper ratio was selected prevent that wingtip stall. An un-tapered wing was selected so the wing roots would stall earlier than the tips to prevent sudden rolling and provide an upwash at the tail resulting in a pitch down moment for recovery.

4.2.4 Structures

The main aircraft structural components were the wing spars, the fuselage's telescoping backbone, a joiner that connects these two items, bulkheads, and the landing gear. Robustness, ease of manufacture and reparability were considered in the design of each of these items. Each component was sized for different loads that would occur either in flight, during a hard landing or in the event of a crash. Studies were conducted to fulfill mission A, carrying the radome and payload, as well as Mission B which required ejecting the payload. Figure 4.9 shows the loads estimated on the plane for maximum turn (a) and for a hard landing (b).

1. *Wing Structure*: The wing was composed of two sections joined together at the fuselage so that a seven-ft wingspan (required for take off) could fit into the 4'x2'x1' box. This implied only one junction on each side for quick assembly. Each section contained a tube-spar, which was able to slide into a center spar (16 inch long) extending outward from the fuselage. This allowed an overlap between the tubes of ½ ft. on each wing side. Several spar designs were considered, such as I-beams, live spars with carbon fiber spar caps, C-beams and square-beams; but for ease of assembly and simplicity of design, tube spars were chosen. They were designed for a 5.5G maximum (Figure 4.9a) maneuvering load, (70%C_{Lmax} @ cruise) with an added safety factor of 1.5. The shear and bending diagrams for these conditions are shown in Figure 4.10. Other calculations for determining spar caps sizing were performed. Overlap was a necessity since the shear close to the junction becomes larger in magnitude. No skin rupture, shear failure, core crushing or skin buckling were allowed.
2. *Fuselage Structure*: The main structural components of the fuselage were the telescoping backbone, the two bulkheads, and the door mechanism (for mission B, payload drop).
   a. *Telescoping Backbone:* The backbone had several essential roles; first it's ability to extend quickly during assembly, second to support the motor, batteries and payload, and third to carry the wing load. A circular cross section as opposed to rectangular or

oval shapes was chosen during the preliminary design phase because of its ease of construction and its ability to satisfy the above requirements. The spar and the backbone were analyzed and manufactured in a similar way. The Shear and Bending Moment diagrams are shown in Figure 4.11-12, for each section of the backbone. Pre-preg uni-directional carbon was used, because it provided a high strength to weight ratio. The layers were bonded at 45° and -45° on the mandrel in order to take the torsional forces on the plane. The orientation took into account a margin of safety (MOS) of the ultimate load that was greater than zero. The backbone was also equipped with extra carbon hoops at the points where the motor and other structures were hung to provide the needed stiffness. Aeroelasticity of the boom was neglected because the tube diameter was large relative to the length.

b. *Tube Spar and Backbone Joiner:* Another advantage of the backbone and tube spar was the simplicity of joining them together. The design basically entailed two carbon fiber saddles oriented at 90 degrees from each other, with the backbone along one direction and the 16 in. spar centerpiece aligned perpendicular in the other direction simplifying the manufacturing process. The two saddles were joined together by four nylon bolts that were sized to shear during a 1G wingtip strike. That is, a 1G aft wingtip loading would shear the nylon bolts so that the wing would easily separate and sustain minimal damage during a crash (Figure 4.8).

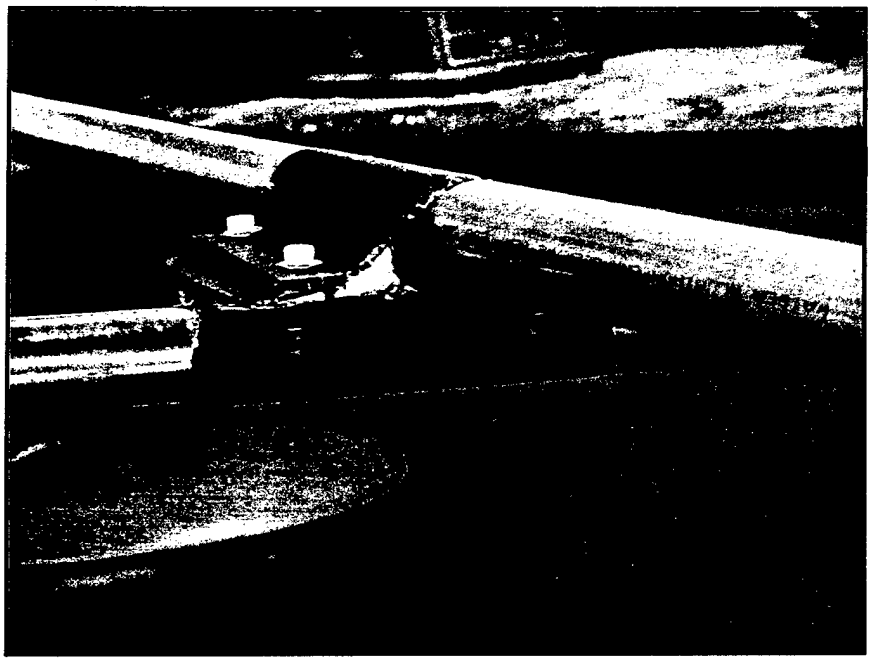

Figure 4.8 *Tube Spar and Backbone joiner picture during shear testing (The photo was taken after the joiner had failed)*

c. *Bulkheads:* Two bulkheads were designed to carry the loads of the landing gear and to support the payload and the clam doors. The main bulkhead was perpendicular to the flight direction and carried the loads between the landing gear and the backbone. The secondary bulkhead was at an inclined angle from the bottom of the main bulkhead aft toward the backbone along the hinges of the clam doors. This orientation allowed it to support part of the landing gear loads as well as the door structure. The payload pins and support mechanism for the payload were also attached to the inclined bulkhead.

3. *Doors and Release Mechanism:* Sensor Deployment in Mission B required the self-deploying of the simulated avionics package. This required a well-engineered and novel system of doors and ejection mechanism (Figure 4.13). There were three types of doors considered: a vertically, horizontally, and diagonally hinged door (Figure 4.14a, b & c). While a vertical seam between the closed doors would minimize the surface area over which airflow might force the doors open in flight, the doors would need to travel through a greater angle to provide clearance for deployment. Horizontal hinges would have minimized the area of the door seams in the closed position but would require careful manufacture to insure the closed doors mated well during flight and did not have a gap between them. The need to secure each of these seams with added carbon layers would drive up the weight and therefore the cost. The final door design (Figure 4.14c) had diagonal hinges along the secondary bulkhead in the fuselage that opened directly beneath the avionics payload. The diagonal motion required less travel distance than the vertical hinges, and prevented airflow along the fuselage from forcing the doors open. Two systems were considered for releasing the payload. The first utilized a rubber band and push-pull cables activated by a servo as seen in Figure 4.14d. This simple design utilized a large rubber band that would be tension loaded around the unit and restrained by a latch connected to a servo. A second set of rubber bands would hold the doors closed during flight. At activation the large rubber band would force the box rearward forcing the doors open and ejecting the box out the rear of the plane. The doors would be tensioned to close shut after its deployment. The second deployment mechanism is shown in Figure 4.14e. This mechanism uses a set of pins allowing deployment through the bottom of the plane. Horizontal pins passing below tabs protruding from the payload box were fitted into slots drilled into brackets attached to the plane's diagonal bulkhead. The tabs fit snuggly into these brackets to restrain the unit's motion in all directions, while the pins prevented it from falling downwards. The servo would open and close the fuselage doors and when fully extended, the servo would pull the pins allowing the payload to fall by gravity. This latter system was adopted because it was more reliable and provided a more secure attachment of the payload.

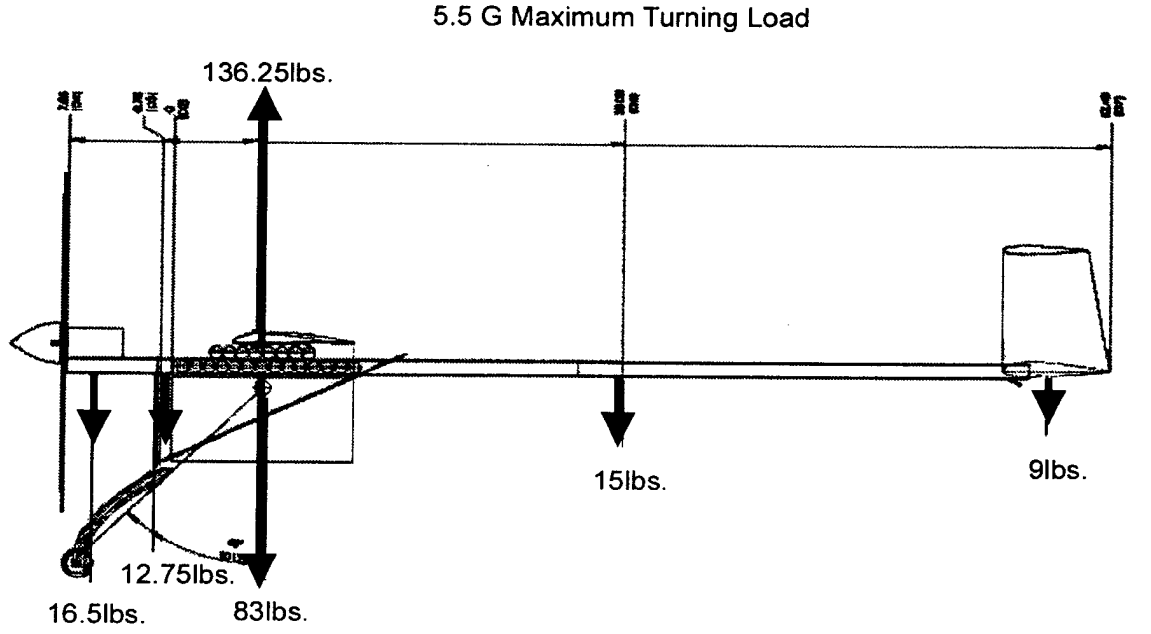

(a)

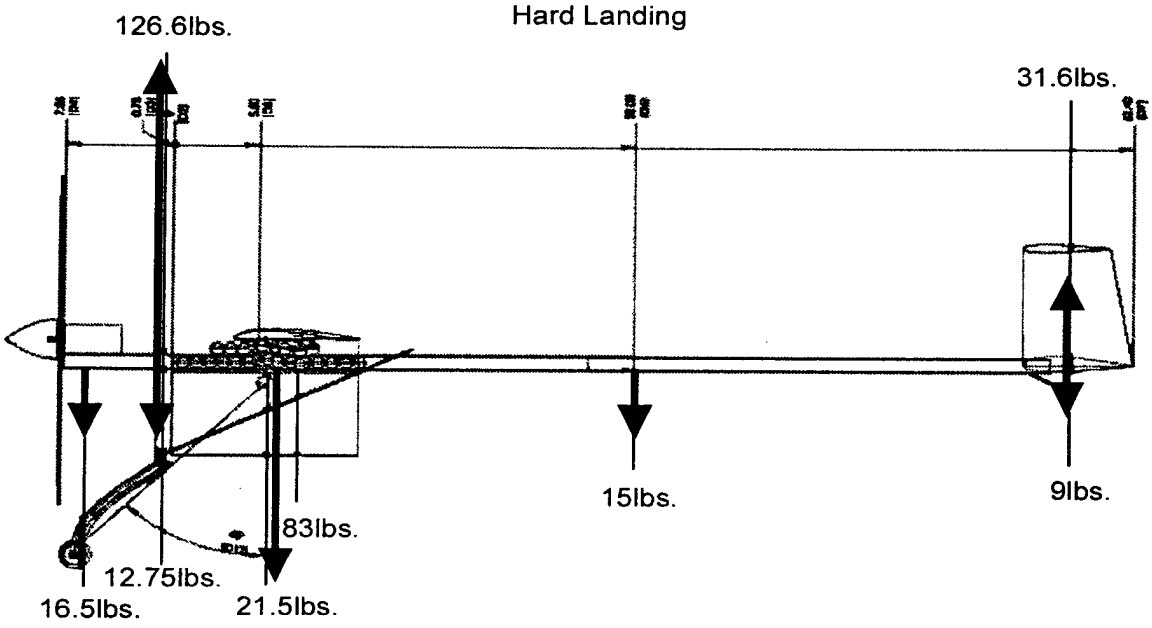

(b)

Figure 4.9 *Loads taken by structural components in two different situations: (a) maximum turning loads and (b) hard landing.*

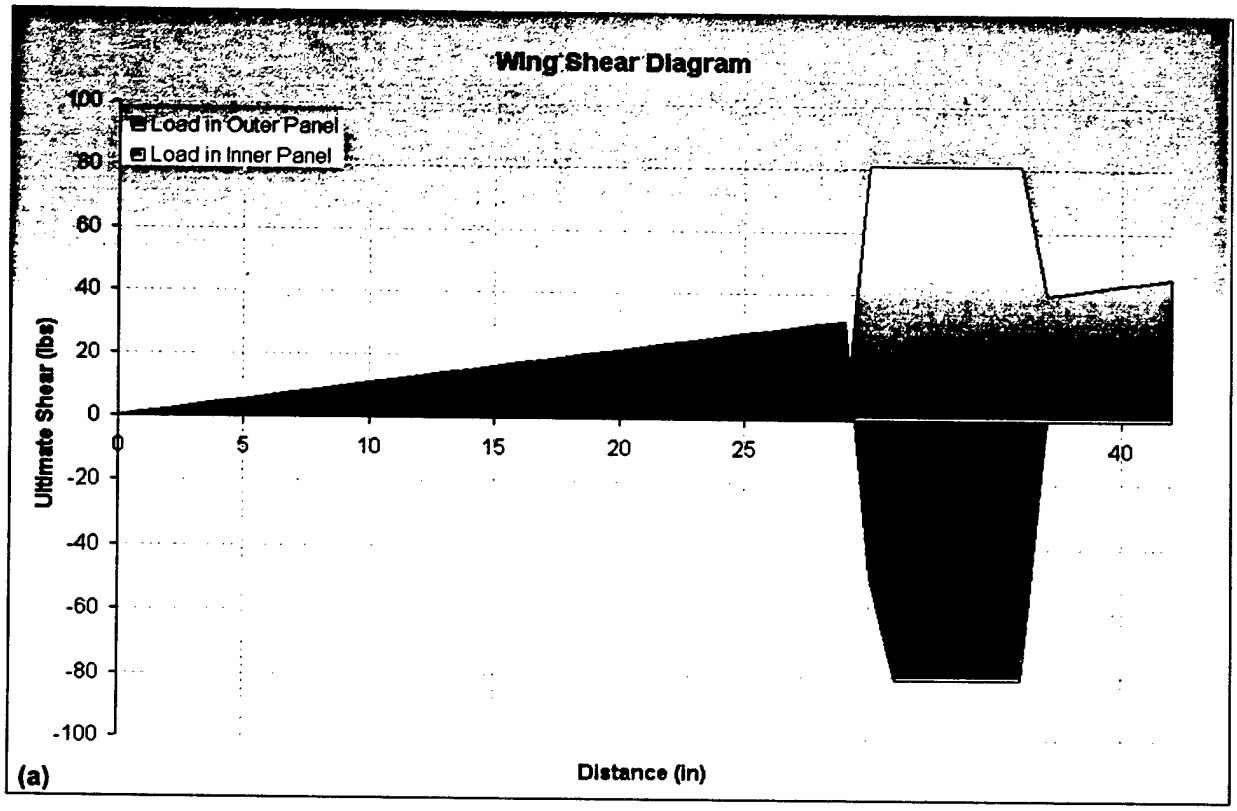

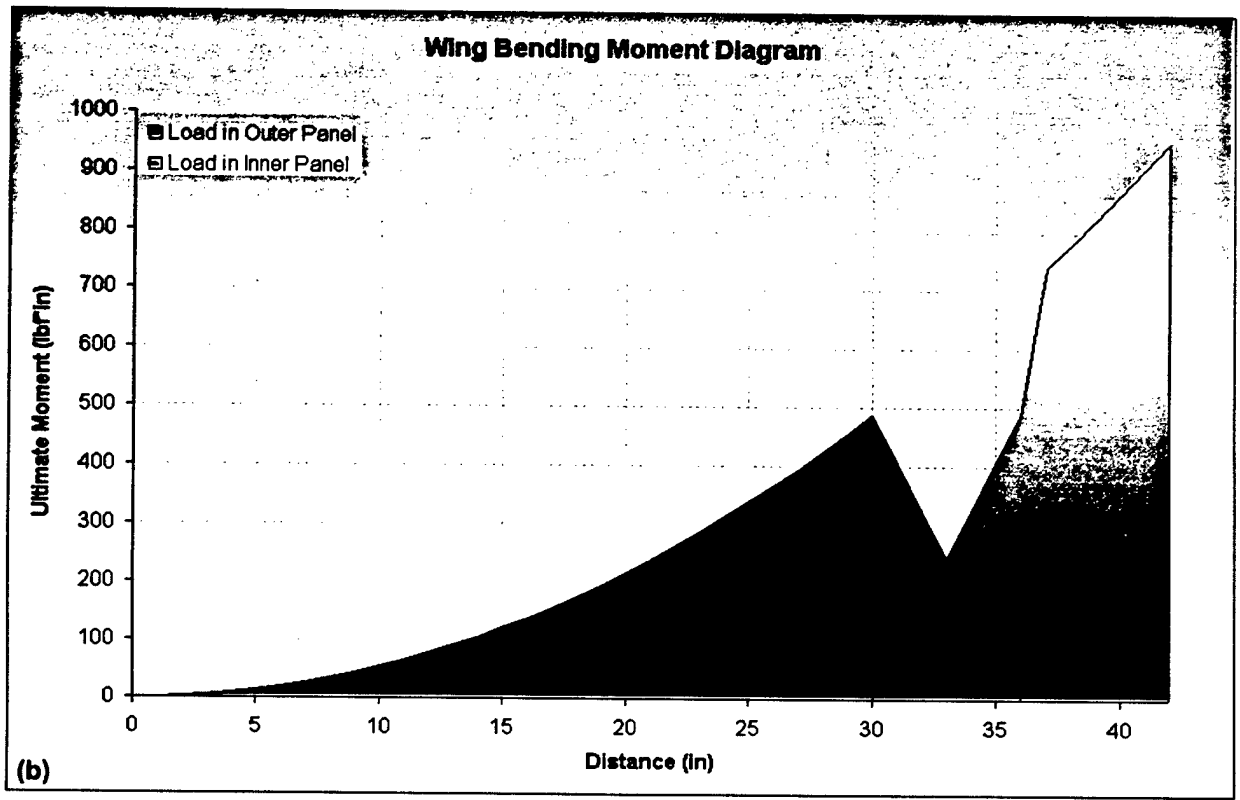

Figure 4.10 *Sizing Diagrams for Shear (a) and Bending Moment (b) for one side of the wing. The blue area represents the 16 in. center spar with overlap*

4. *Landing Gear Structure*: Two types of landing gear were considered, tricycle and tail-dragger. The tricycle advantages were ease of payload deployment, sufficient ground clearance, and decreased loads on the backbone. However, this system would require a heavier structure for the nose wheel thus increasing the cost. The tail-dragger was considered and chosen for its simplicity and substantial weight reduction. The disadvantage was that the clearance for the payload deployment could be compromised. To accommodate for that aspect, a raked tailskid, which can be upgraded with a wheel if necessary, was attached to the aft part of the backbone so that the tail assembly could slide over the deployed payload package. To reduce the assembly time, the main gear was designed to fold over the fuselage with an aft hinge at the vertical bulkhead. To prevent the landing gear from folding while trying to land a tab was designed to keep it in place. The main gear was also angled forward to counteract the initial impact.

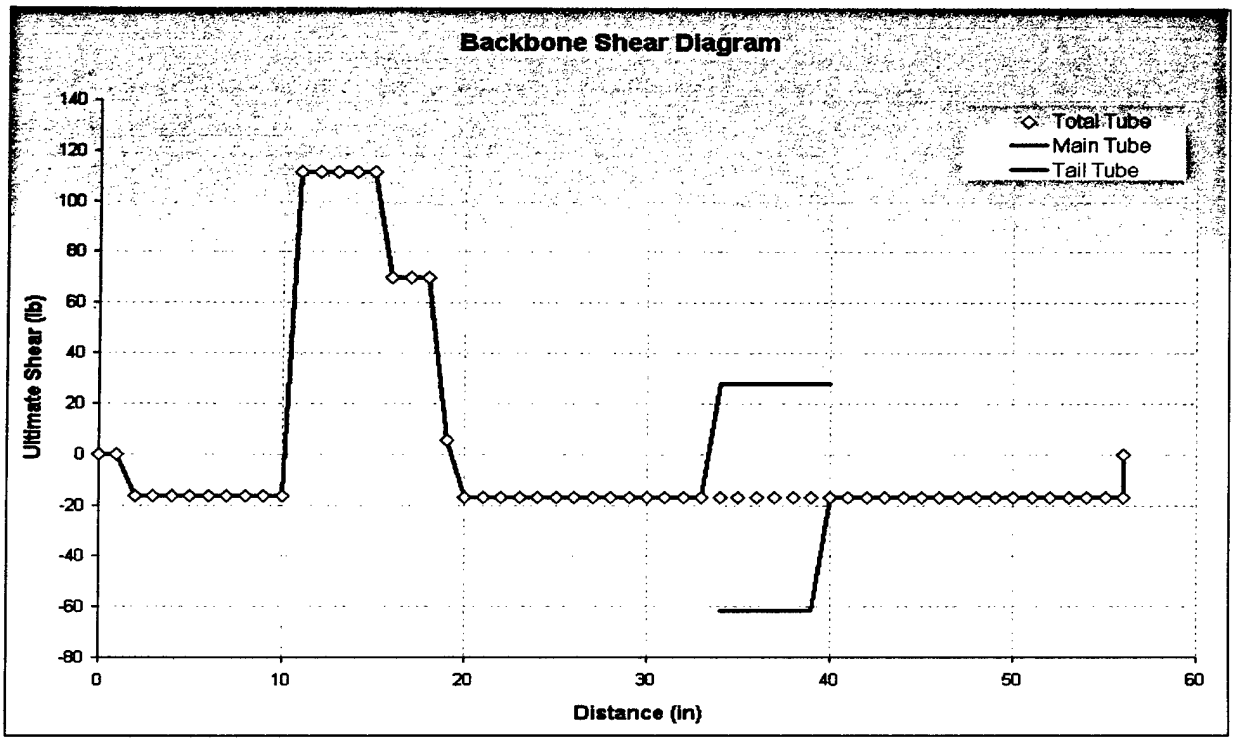

Figure 4.11 *Shear diagram for the telescoping backbone. The red lines denote the main section of the backbone and the violet line shows the shear on the extension*

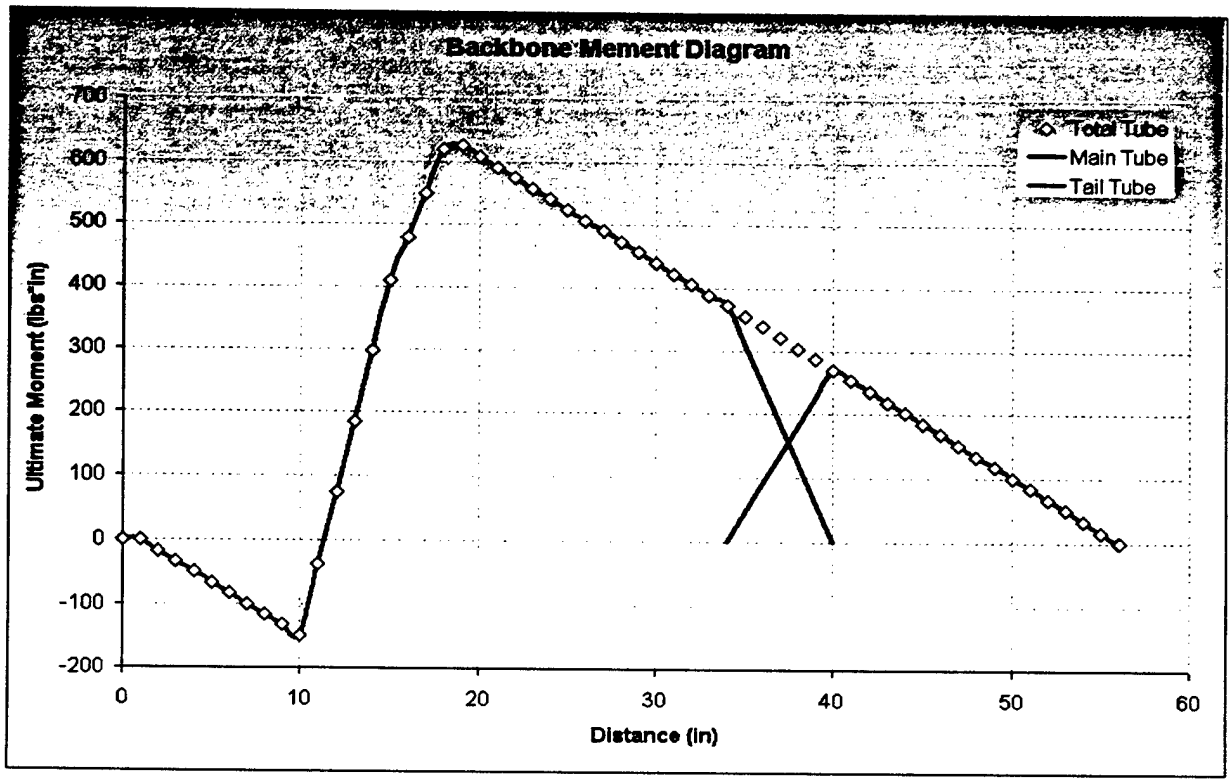

Figure 4.12 *Bending Moment Diagram for the telescoping backbone. The red lines denotes the main section of the backbone and the violet line shows the moment on the extension*

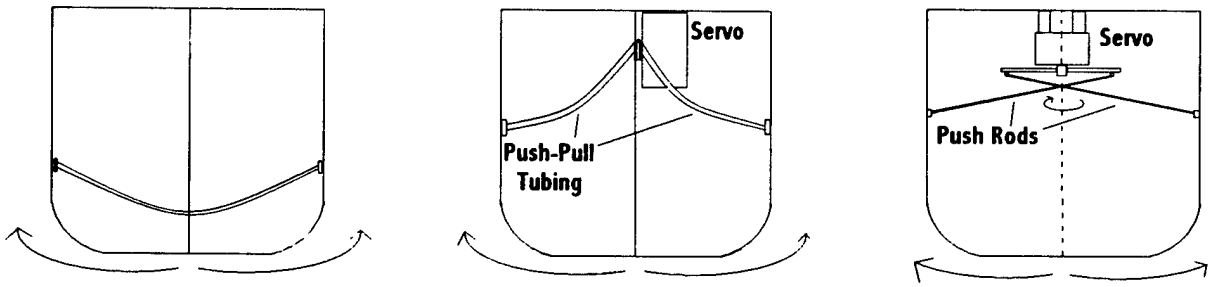

(a) Rubber Band Restraint **(b) Push-Pull Tubing** **(c) Fixed Servo Arm**

Figure 4.13 *Rear view of doors with (a) rubber band restraint, (b) push pull tubing and (c) fixed servo arm mechanism*

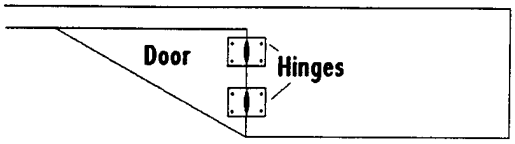

(a) Vertically Hinged Doors

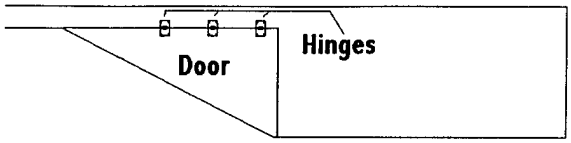

(b) Horizontally Hinged Doors

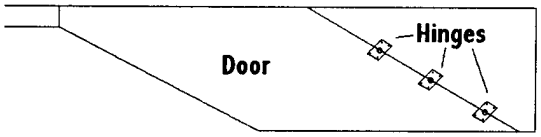

(c) Diagonally Hinged Doors

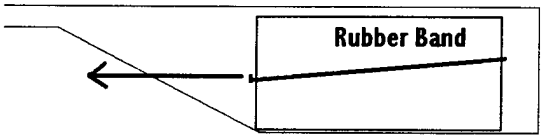

(d) Rubber Band Deployment

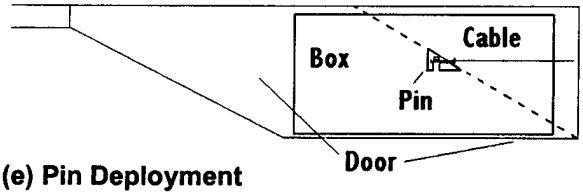

(e) Pin Deployment

Figure 4.14 *Side view of different door configurations and release mechanisms (the forward fuselage is on the right): (a) vertical hinge for minimum surface area that can be open during flight (b) horizontal hinge for minimum area of door seams (c) diagonal hinge for less payload travel distance (d) rubber band system for simplicity (e) pin deployment for security*

5.0 DETAILED DESIGN PHASE

This design phase continued and finalized the configuration of the aircraft by further developing the analysis performed during the preliminary phase. New assumptions were incorporated within the design that focused on detailed aspects of certain systems. Component selection and architecture of the aircraft were also decided based on testing and analytical iterations within the MiniMission tool.

5.1 New Assumptions for Specific Subsystems

The following new assumptions were necessary to simulate the contest mission with realistic flight conditions:

1. *100% Throttle Setting*: Full throttle setting was assumed and used throughout MiniMission calculations to enable highest cruise velocity and obtain best propulsion efficiency.
2. *20 sec. Average Assembly Time*: Aircraft assembly time was determined by the performance obtained for the wing joints and two panel assembly tests as well as design intuition.
3. *CP1300 Battery Type Used*: Because data on this battery type was hard to obtain for the purpose of the two missions and model aircraft flying, the CP1300's were found to accomplish the mission requirements by static testing.
4. *Direct Drive Capabilities*: It was found that smaller diameter and pitch propellers combined with direct drive produce a better performance than a geared motor with large pitch and diameter propeller combinations. This was due to a substantial decrease in cost since the energy required to complete the mission is low allowing the use of smaller and lighter batteries.
5. *2.9 lb Battery Weight*: As mentioned above the battery weight could be reduced from 5 lbs. because direct drive is more efficient for the high flight speeds needed this year, and eliminates losses through the gearbox. This was also possible because the energy required to complete each mission this year was not a problem due to a decreased flight time. The maximum time calculated by MiniMission was found to be 2.5 min. for Mission C, which had the lowest difficulty factor.

5.2 Component Selection & Systems Architecture

5.2.1 Propulsion System

The radio used to drive the propulsion system was a Futaba 9CA model. For the system final configuration the Cobalt 60 motor with direct drive, CP1300 NiCad batteries and a 15x12 inch foldable propeller were chosen. The motor as explained in the Preliminary Design Phase was the best choice that fulfilled the Figures of Merit requirements such as TOFL, V-cruise, 40amp current draw limit, etc. analyzed through trade studies and MiniMission. The battery pack was composed of 36 cells to ensure there was enough excess energy to complete missions at the highest cruise velocity. Direct drive was a major improvement in the performance of the aircraft allowing smaller pitch and diameter propellers to be used such as the 15"x12", which produced the best results in different trade. A foldable propeller was chosen because it prevents damage to the motor and other components of the aircraft in the event of a

crash. Also, an AstroFlight 204D speed controller was used because it could handle the current and voltage required to fly.

The propulsion system was organized around the front end of the backbone with the motor hanging from it using an aluminum motor mount and a faceplate that bolted to the plug in the tube to constrain the motor in the vertical direction and help it resist torque. The aluminum was wide enough to distribute the loads over a large area and bent to the dimensions of the backbone and motor forming two hoops. A bolt was placed between them to adjust the clamping force. The mount was designed to protect the motor in case of crashing by having it snap out of the saddle under certain loads. For this purpose the hoop around the motor was cut into two tabs that slid into each other and could come apart during impact. A detailed picture is shown in the subsystem figures of the drawing package. The batteries were configured to fit horizontally on the sides of the backbone, on top of the motor in front of the wing, where cooling was determined to be most advantageous because of the vacuum pressure on the top of the wing. Because temperature greatly affects the performance of the motors and batteries cooling was a major design consideration. Hence aluminum fins were fit around the motor to provide more surface area for conduction of heat to the air. Also, internal ducting was formed to ensure proper airflow for cooling by convection making a $12in^2$ inlet area sufficient for this purpose.

5.2.2 Stability & Control

The empennage consisted of a V-tail with geometry parameters as presented in Table 5.1. Control surfaces utilize 40% of the tail area and are driven by two Micro (MG) servos. The wing flaperon area was sized to 25% chord with an option of two S11CL (MG) or Micro (MG) servos. The breaks and deployment actuators were sized as shown in Table 5.2.

The V-tail was sized considering two main factors; the aspect ratio of the tail and the horizontal moment arm. These two parameters had direct effects on constraints such as the required static margin, directional stability and the ability to fit in the box. A symmetric SD8020 at 8% t/c was used as the tail airfoil with a decreased thickness to reduce parasite drag. Last year, the team learned that having different CG locations for each flight required excessive trimming before reaching the first pylon. Although stability was good, Pilot workload was excessive. This year it was decided to have only one CG location for every mission, thus easing the pilot's workload as well as providing a more stable and reliable aircraft. This allowed the critical static margin requirement to reduce from 35.8% last year to 23% this year, simplifying tail fit into the box. Several tail-sizing iterations were performed in parallel with wing-sizing for TOFL using MiniMission. The pitch frequency calculated was sufficient to avoid sluggish handling although the high damping ratio prevented the plane from overshooting or returning to its original state. There were several ways of correcting the damping ratio such as decreasing the size of the horizontal tail arm but this would not guarantee the tail would fit in the box. The team decided to test fly the current tail configuration first before making any changes.

Full span flaperons were used on the wing. This decision reduced the number of servos, lowered the cost and simplified the design. It also provided a new trim for landing maneuvers due to increase in

C_{Lmax} at low speeds. The flaperons extended from the root chord at the fuselage to 1.5in from the tip chord. This padding was designed to prevent hanger rash or infield accidents that would damage the control surface. The drawback to this configuration was the increased stiffness needed over the area of the control surface to guarantee the same deflection angle at the root as well as the tip. Also, the size and weight of the actuators increased the torque required to move these control surfaces.

Stability Parameters	*Units*	*Value*
Tail Area	(ft^2)	2.60
Tail Span	(ft)	2.60
C_{root}	(ft)	1.11
C_{tip}	(ft)	0.89
Tail Dihedral	degrees	38.00
Pitch Frequency (@ Cruise)	Hz	4.92
Yaw Frequency (@ Cruise)	Hz	2.30
Pitch Damping Ratio (@ Cruise)	n.d	102%
Static Margin	n.d	23%
Directional Stability	1/deg	0.002

Table 5.1 *Stability and Control final parameters computed*

Brand	**Model**	**Dimensions (*in*)**	**Weight (*oz*)**	**Torque @ 6V (*oz-in*)**	**Application**
GWS	Micro (MG)	1.1x0.55x1.17	0.98	89	Wing+Tail Control Surfaces
GWS	S11CL	1.7x0.85x0.86	1.52	111	Deployment
GWS	Naro +	0.87x0.43x0.98	0.35	28	Brakes

Table 5.2 *Servo Specifications for the final aircraft configuration*

The servos were sized taking into consideration the control surface area, the maximum deflection angles in both directions and max cruise velocity multiplied by a safety factor. The maximum deflections used to size the servos for the tail control surfaces was $\pm 10^{\circ}$ at V-cruise of 90mph while the max deflections of the flaperons was $\pm 25^{\circ}$ at the same speed. The servos were located at the center of each wing and tail section for even distribution of the loads. The tail was permanently attached to the backbone and swiveled upside down for packaging in the required box. This provided maximum efficiency between

tail volume and assembly time. Also in the carrying box the two wing panels were placed under fuselage/backbone configuration with an opposite orientation from each other to provide a balance.

5.2.3 Braking System & Deployment

The pneumatic braking system was composed of an air bottle fit below the motor beside the vertical bulkhead and a proportional release valve that was servo controlled. The pressure required to activate the brakes was determined by past experience with ground testing. The main gear was placed far forward of the CG to avoid tip-over and propeller strike when brakes were applied.

The 5 lb simulated avionics payload was suspended on tabs attached to the diagonal bulkhead (see figure of subsystems in drawing package). An actuator was used to open the doors and release the pins holding the payload in place. The actuator was an S11CL (MG) servo sized to open and close the doors. It was lightweight as seen in Table 5.2 and was hung from the backbone behind the payload inside the fuselage.

5.2.4 *Landing Gear & Joiner*

The main landing gear was hinged along the bottom of the fuselage to optimize the assembly time. The main gear was able to freely rotate 170 degrees upward to facilitate storage in the carrying box. After rotating the main gear during assembly, a ¼ turn nylon bolt locks the gear in place and is designed to shear in a crash to protect the fuselage frame as well as the landing gear itself. Stress analysis of the landing gear indicated 32 layers of carbon fiber were needed to provide the strength and flexibility needed during hard landing. Flexibility was set by strut thickness and strength by strut chord. The raked tailskid was attached to the aft backbone underneath the V-tail.

The joiner consisted of two saddles created to attach the backbone to the wing spar at 90°. Each saddle was wrapped around the tubes and was joined with nylon bolts to fail in crash conditions. This would protect the wing from receiving major damage that can't be fixed within 30 min, which would result in a non-scored flight attempt. The joiner was made of eight layers of uni-directional pre-preg carbon fiber and was tested to withstand a tensile load greater than 200 lbs. Its design entailed a simple U-bolt concept that weight less than 2% of the wing. Often wing mounts account for 10% of the wing weight, hence this design proved cost effective as well as structurally robust for carrying the required loads.

5.3 Estimated Mission Performance

MiniMission was used to predict the plane characteristics as well as its flight performance. The different modules built by the group captains calculated the required parameters that allowed for optimization. Final configuration data is tabulated below including geometry, performance factors and weight statements.

1. *Geometry*: The estimated geometry based upon the aerodynamic calculations is found in Table 5.3. The wingspan was set to 7ft by the constraint imposed by the carrying box and the control surface was sized as 25% of the chord.
2. *Performance Factors*: Table 5.4 shows different velocities for the three missions, where mission B has two stages: heavy and light. Table 5.5 shows the important flight

characteristics such as the TOFL, maximum current draw and total energy for different missions. Note that the rules mandate a 40amp max current and the mission model shows a 39.8 amp draw, but considering the multiple safety factors and the conservative nature of MiniMission, this value is considered acceptable. Table 5.6 shows the lift and drag coefficients during cruise.

Calculated Geometry	*Units*	*Wing*	*H.Tail*	*V.Tail*
Total Area S_w, S_H, S_v	ft^2	6.51	2.22	2.22
MAC	ft	0.92	0.93	0.93
Y MAC	ft	1.77	0.45	0.37
Projected Span	ft	7.08	1.86	0.76
Root Chord	ft	0.92	1.03	1.03
Tip Chord	ft	0.92	0.82	0.82
Root Incidence	deg	-1	1	-
Tip Incidence	deg	-1	1	-
Fuselage Height, Width, Length (including spinner)	ft	0.58	0.58	6.17

Table 5.3 *Airplane main geometry*

Parameter	*Unit*	*Mission A*	*Mission B1*	*Mission B2*	*Mission C*
V_{cruise}	fps	114.3	132.5	136.4	133.3
V_{stall}	fps	37.8	37.8	32.6	36.8
V_{LO}	fps	45.4	45.4	39.1	44.2
$V_{climb\&\ Landing}$	fps	49.2	49.2	42.3	47.9

Table 5.4 *In flight velocity breakdown*

Parameter	*Unit*	*Mission A*	*Mission B1*	*Mission B2*	*Mission C*
TOGW	lbs	19.8	19.8	14.7	18.7
TOFL (incl safety pad)	ft	110.5	103.5	60.6	98.7
Total Flight Time	sec	125	93	54	144
Total Flight Energy	ft-lbs	93780	41189	37119	89063
Max Current	amps	39.8	39.8	39.8	39.8
Takeoff Thrust	lbs	8.14	8.14	8.14	8.14
Thrust @ V_{crz}	lbs	4.24	3.29	3.09	3.25

Table 5.5 *Performance characteristics*

Parameter	*Unit*	*Mission A*	*Mission B1*	*Mission B2*	*Mission C*
$C_{Lmax3\text{-}D}$	n.d.	1.60	1.60	1.60	1.60
$C_{Lcruise}$	ft	0.18	0.14	0.10	0.13
$C_{Dcruise}$	n.d.	0.029	0.017	0.016	0.017
L/D_{crz}	n.d.	6.22	8.14	5.85	7.66

Table 5.6 *Aerodynamic characteristics*

5.4 Weight, Balance and Rated Aircraft Cost Worksheets

1. *Rated Aircraft Cost*: From last year's competition, the group realized that other planes from other teams performed similarly with a smaller RAC. For the 2002/2003 competition, the team focused in reducing this parameter to be more competitive. By investigating alternatives for different power plant configurations, the RAC was reduced from 12.26 last year to 9.62 for this year. This reduction of 21% was achieved by looking at the main contributor to the RAC, the propulsion system. It was realized that by using a smaller propeller in direct drive, the capacity of the batteries needed diminished, allowing the use of smaller, lighter batteries. Table 5.7 shows the cost breakdown of the plane for this year's competition
2. *Weight Budget*: The predicted weight of the plane was calculated through the model in MiniMission using measurements of the aircraft's dimensions from the design and library sheets. The weights and densities of purchased materials were taken from manufacture's specifications and from lab test data. The lab data was very important because the manufacture's claimed weights were often inaccurate, especially in composite densities. For instance, the manufacture's claimed density for different composite materials was up to 30% less than the densities that were measured in lab. Lab results were also used to create data correlations; for example the relation between propeller diameter and propeller weight.

Cost Table			Manuf.	Hours	Cost	Total Cost	Rated Cost
Rated Aircraft Cost		Dims	Hours	sub-total	sub-total	**$9,617**	**9.62**
MEW (Manufacturers Empty Weight)				**13.63**	1363 19		14.2%
REP (Rated Engine Power)	= (1+.25*(#Motors-1))*BattWt			2.91	4358 8		45.3%
	# of Engines	1					
	Total Battery Weight (lbs)	2.91					
MFHR (Manufacturing Man Hours)				194 75	3894 9		40.5%
WBS1.0	# of wings	1	71.2			14.8%	
	Wing Span	7.08					
	Max Wing Chord	1.07					
	# of control surfaces	2					
WBS2.0	Fuselage Length (ft)	5.85	58.5			12.2%	
WBS3.0	Number of Vertical Surfaces	0	0.0			4.2%	
	Number of Vertical Tails	1	10.0				
	# of Horizontal Tails	1	10.0				
WBS4.0	# of Servos and Motor Controllers	7	35.0			7.3%	
WBS5.0	# of Motors	1	10.0			2.1%	

Fixed Parameters

A (MEW Mulitiplier) ($/lb.)	**100**
B (REP Multiplier) ($/Watt)	**1500**
C (MFHR Multiplier) ($/hour)	**20**

Table 5.7 *Rated Aircraft Cost calculation and results*

Weights for complex shapes were calculated by estimating their volume with simple rectangular approximations, and then multiplying by material density. The weight of the outside skin of the wing and tail was calculated by finding the area of the exposed surfaces of and then multiplying by the thickness of the coating material and its density. The spar of the wing was treated as a separate tube and its weight was calculated using its thickness, length and density. The weight build-up model is shown if Table 5.8 with the break down of different systems and the K_{Fudge} parameter (weights safety factor). Empty and Heavy Gross weights are given at the bottom of the table.

3. *Balance Distribution*: The CG for both light and heavy planes was set at the same location for ease of handling and flying. A CG balance sheet was created in MiniMission and linked to the configuration sheets. Since the plane was geometrically symmetrical about the center plane, and the vertical CG location had negligible effects on the handling of the plane, these vertical CG calculations were not performed. The individual components of the plane were then moved for and aft to position the CG so that it aligned with the desired value at 30% of the wing chord. Since the length of the plane was fixed, the batteries, receiver, wing and payload placement were the items primarily reconfigured to achieve the desired CG.

WEIGHT BUILD-UP

System	KFudge	Sub-Component	Weight Breakdown	% of Heavy Weight
PROPULSION	1.0	Sub-Total (incl Kfudge))	**7.955**	**51.9%**
		Motor(s)	1.563	10.20%
		1 Motor Mount / Heatsink	0.138	0.90%
Recommend 1.0		Battery wt incl. solder & jack	4.953	32.33%
"good historical data"		All Wiring	0.100	0.65%
		1 Speed Controller	0.150	0.98%
		1 Propeller	0.480	3.13%
		1 Spinner & Prop Nut	0.102	0.67%
		1 Motor Mount	0.46875	3.06%
WING	1.0	Sub-Total (incl Kfudge))	**1.570**	**10.2%**
		Wing Spar	0.041	0.27%
Recommend 1.0		Wing Core	0.405	2.64%
		Wing Skin	1.124	7.33%
TAIL & Winglets	1.0	Sub-Total (incl Kfudge))	**0.457**	**3.0%**
		HTail Skin	0.384	2.51%
Recommend 1.5		HTail Core	0.072	0.47%
for joints & adhesives		VTail Skin	0.000	0.00%
or 1.0 depending on skill level		VTail Core	0.000	0.00%
		Winglets	0.000	0.00%
RADIO	1.0	Sub-Total (incl Kfudge))	**1.750**	**11.4%**
		Receiver	0.125	0.82%
Recommend 1.0		Servos	1.125	7.34%
"good historical data"		Battery Pack	0.500	3.26%
LANDING GEAR	1.0	Sub-Total (incl Kfudge))	**1.794**	**11.7%**
		Main Gear Struts & Bolts	1.152	7.52%
Recommend 1.0		Main Wheels	0.343	2.24%
"good historical data"		MG Axle Hardware	0.063	0.41%
Retracts use a 2.0		Nose Wheel or Tail Wheel	0.077	0.50%
multiplier on strut weights.		Nose Gear Strut & Mount	0.063	0.41%
		Brakes, Tubing, Air Tank	0.094	0.62%
FUSELAGE	1.00	Sub-Total (incl Kfudge))	**1.797**	**11.7%**
		Fuselage Skin	1.797	11.73%
Recommend 1.0		Bulkheads	0.000	0.00%
since bulkheads are now in.				

Airframe Weight =	**5.52**	
Flying Empty Weight =	**15.32**	
Radome Weight =	**1.05**	
Heavy Payload =	**6.05**	Avionics package + Antena
Light Payload =	**5.00**	Avionics package only
Heavy Gross Weight =	**21.37**	
Light Gross Weight =	**20.32**	

Table 5.8 *Weight Breakdown of the plane (in Lbs)*

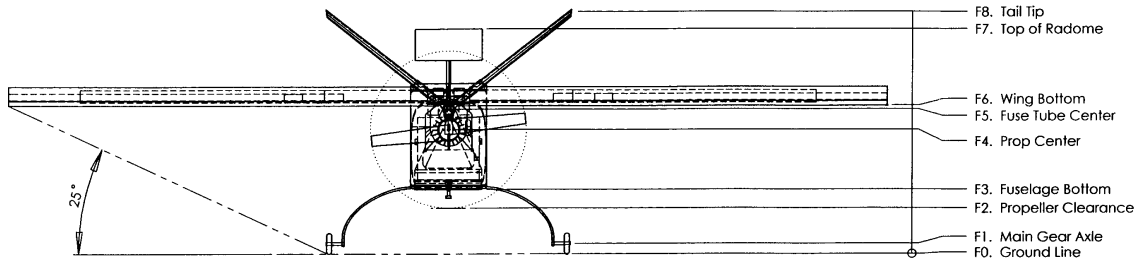

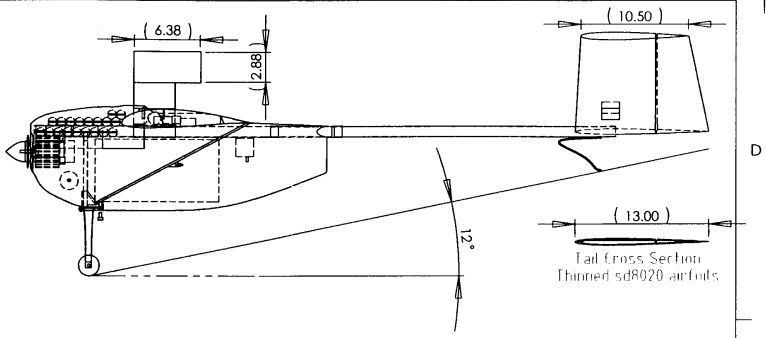

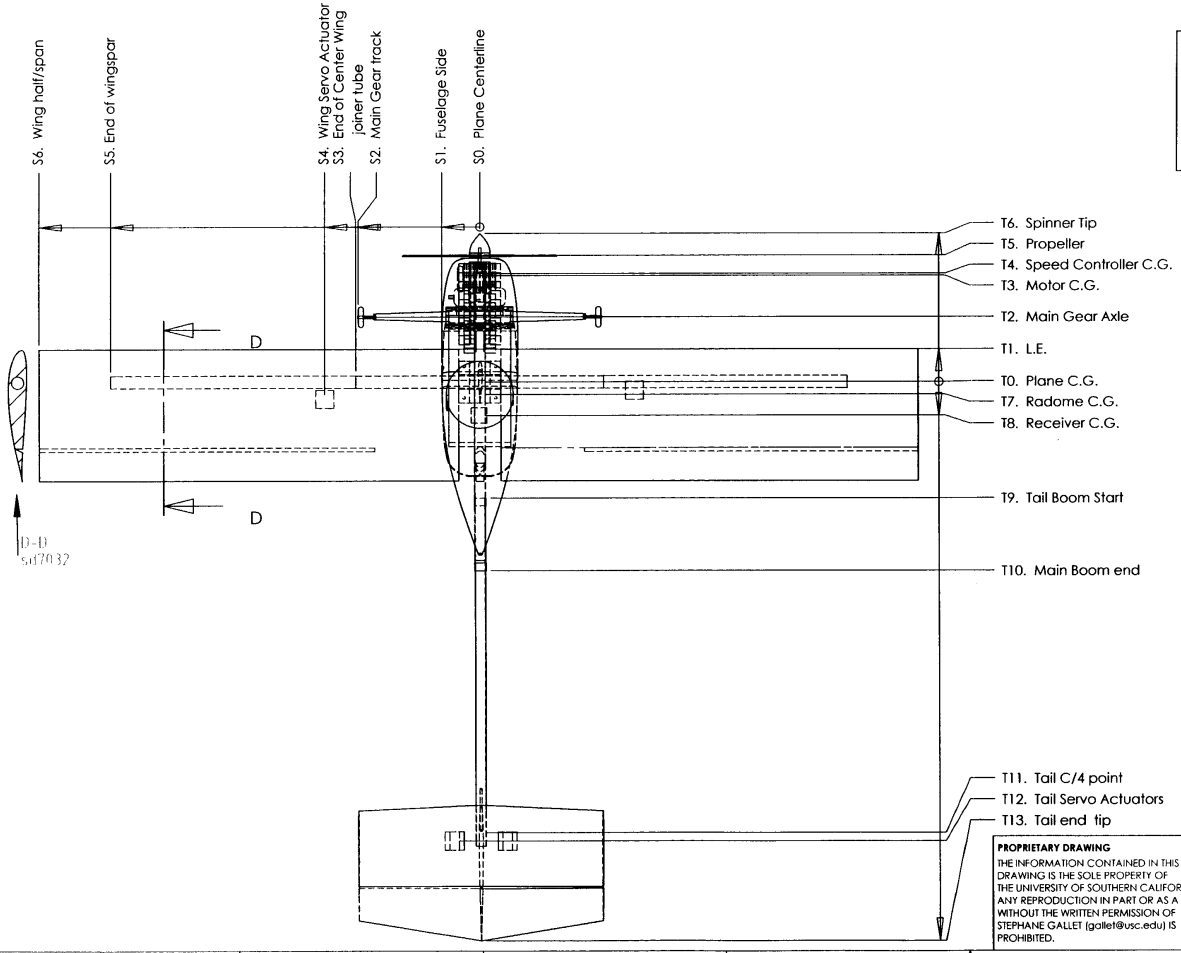

Wing		
Span	(ft)	7.00
Wing Area	(ft^2)	6.30
Aspect Ratio	(n.d)	7.77
Ctip	(ft.)	0.90
Sweep	(deg)	0.00

Tail		
AR	(n.d.)	3.00
Sweep	(deg)	0.00
Taper Ratio	(n.d.)	0.80
Hor. Tail Arm	(ft)	3.50
Horizontal Area	(ft^2)	2.02
Horizontal Span	(ft)	2.46
Horizontal macH	(ft)	0.82
Croot	(ft)	0.91
Ctip	(ft)	0.73
Tail Dihedral	(deg)	39.49

Component Location
Dimensions Relative to T0, F0 and S0

Dim	(in)
T1	3.19
T2	6.31
T3	10.31
T4	10.50
T5	12.28
T6	14.41
T7	-1.22
T8	-3.25
T9	-11.25
T10	-18.25
T11	-43.45
T12	-44.25
T13	-53.81

Dim	(in)
F1	1.00
F2	4.41
F3	6.21
F4	11.97
F5	13.93
F6	14.26
F7	21.63
F8	23.29

Dim	(in)
S1	3.68
S2	11.75
S3	12.00
S4	15.00
S5	35.65
S6	42.55

PROPRIETARY DRAWING
THE INFORMATION CONTAINED IN THIS DRAWING IS THE SOLE PROPERTY OF THE UNIVERSITY OF SOUTHERN CALIFORNIA GW. ANY REPRODUCTION IN PART OR AS A WHOLE WITHOUT THE WRITTEN PERMISSION OF STEPHANE GALLET (gallet@usc.edu) IS PROHIBITED.

UNLESS OTHERWISE SPECIFIED:
DIMENSIONS ARE IN INCHES
INTERPRET GEOMETRIC TOLERANCING PER: .01
MATERIAL -- Composite

	NAME
DRAWN	Stephane Gallet
CHECKED	P.T. BlackWelder
ENG APPR.	Mark A Page
MFG APPR.	Geoff Sechrist
Q.A.	
COMMENTS:	

USC Aerodesign

TITLE: 2002-03 Cessna/ONR DBF
SkyRaider

SIZE	DWG. NO.	REV
B	/8	

SCALE: 1:12 | WEIGHT: | SHEET 1 OF 4

Flight Ready Plane

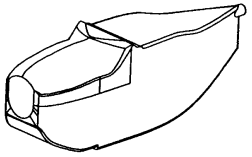

Carbon Composite Shell Removed for Clarity

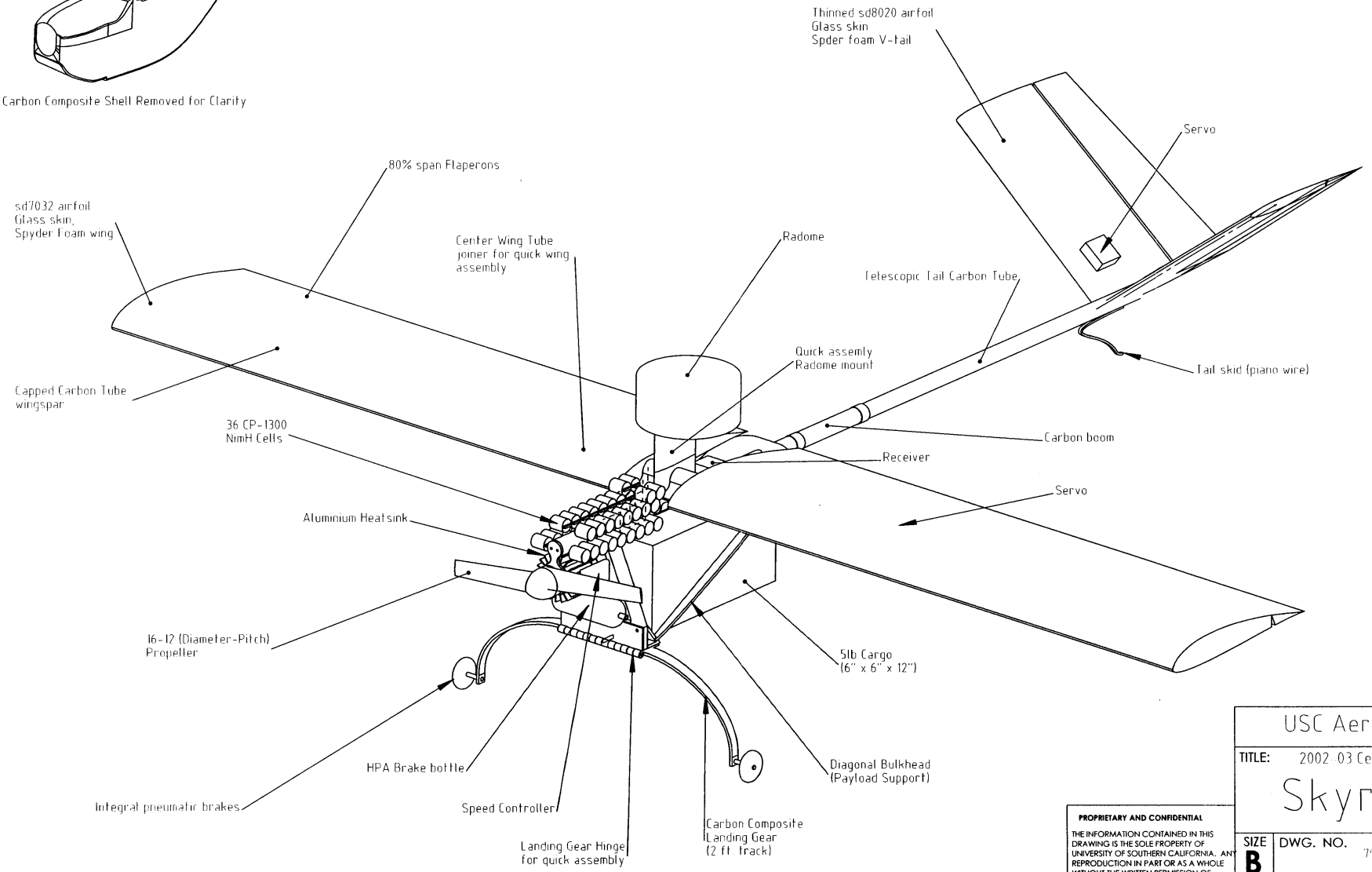

PROPRIETARY AND CONFIDENTIAL

THE INFORMATION CONTAINED IN THIS DRAWING IS THE SOLE PROPERTY OF UNIVERSITY OF SOUTHERN CALIFORNIA. ANY REPRODUCTION IN PART OR AS A WHOLE WITHOUT THE WRITTEN PERMISSION OF STEPHANE GALLET (gallet@usc.edu) IS PROHIBITED.

USC Aerodesign

TITLE: 2002-03 Cessna/ONR DBF

Skyraider

SIZE	DWG. NO.	REV
B	79	

SCALE: 1:12 | WEIGHT: | SHEET 2 OF 4

Packaged Plane (1x2x4 ft)

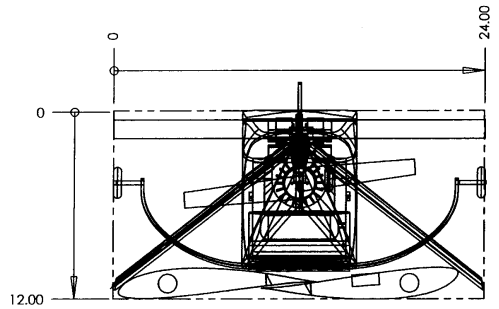

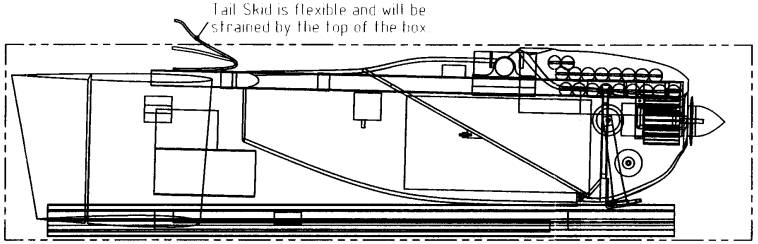

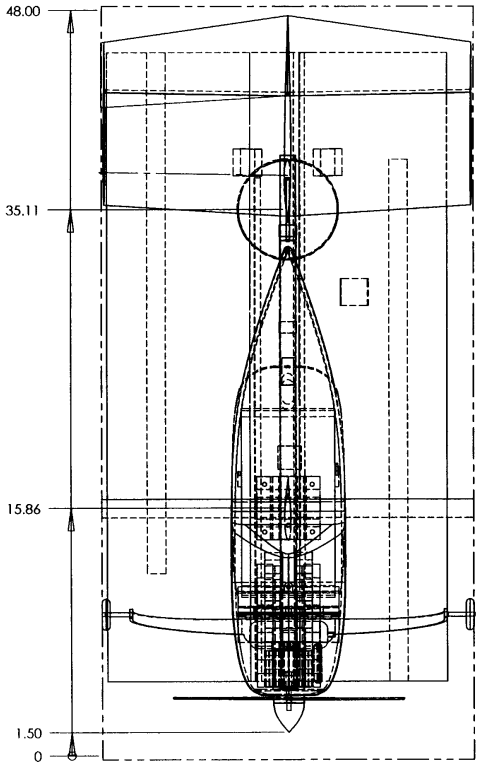

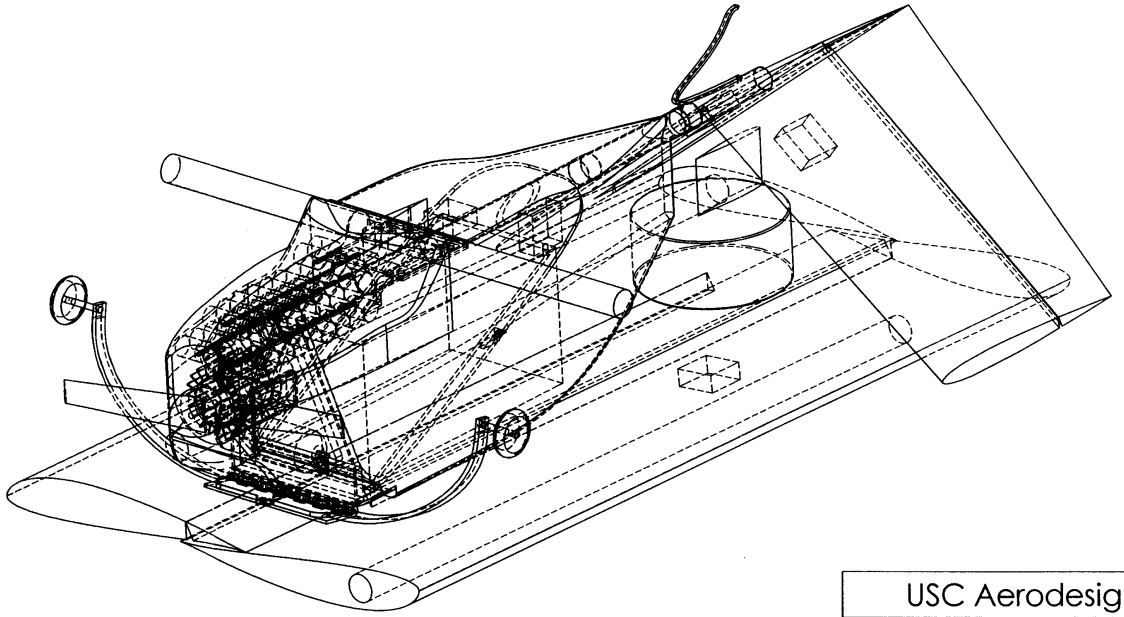

Assembly Procedure
- Slide wing halves into main joiner tube (2 steps)
- Rotate and slide tail boom (2 steps)
- Fold back landing gear and lock with 1/4 turn bolt (2 steps)
- Pop Radome onto radome-mount (1 step)

Estimated Assembly time <= 20s

PROPRIETARY
THE INFORMATION CONTAINED IN THIS DRAWING IS THE SOLE PROPERTY OF THE UNIVERSITY OF SOUTHERN CALIFORNIA. ANY REPRODUCTION IN PART OR AS A WHOLE WITHOUT THE WRITTEN PERMISSION OF STEPHANE GALLET (gallet@usc.edu) IS PROHIBITED.

USC Aerodesign

TITLE: 2002-03 Cessna/ONR DBF

Skyraider

SIZE	DWG. NO.	REV
B	80	

SCALE: 1:8 | WEIGHT: | SHEET 3 OF 4

Motor Mount provides ejection of motor and prop without breakage at crash.

Expendable pieces are:
-motor faceplate
-Balsa plug
-aluminium motor mount
-heat sink

Non-expendible components:
-main tube
-motor
-propeller

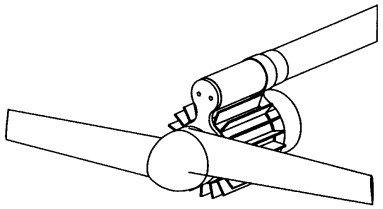

Propulsion System -- Scale (1 : 4)

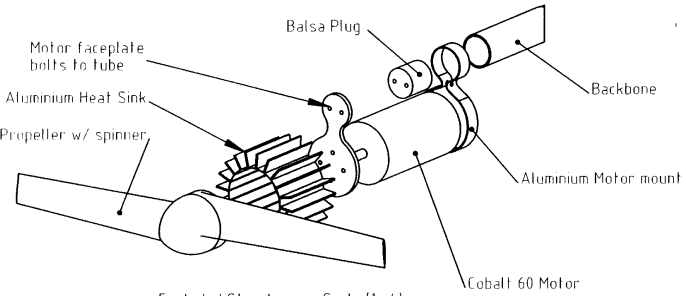

Exploded Structure -- Scale (1 : 4)

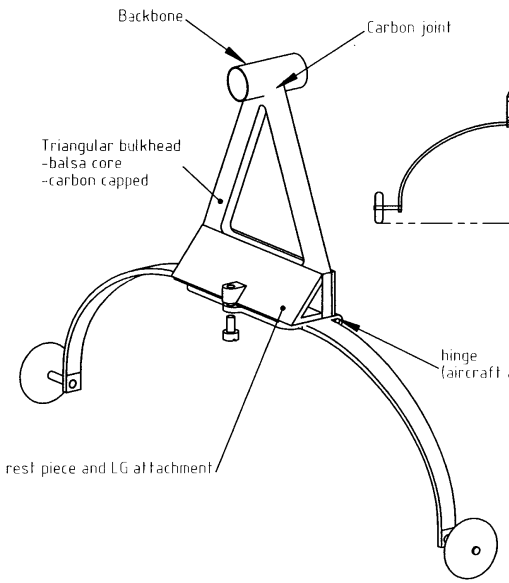

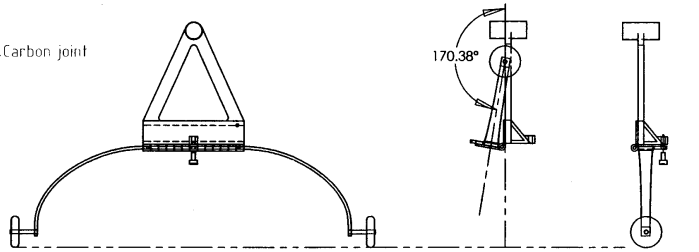

The landing gear/firewall structure is designed to fail in crash, at all bolt locations (nylon).
The 1/4 turn nylon bolt provides quick assembly.

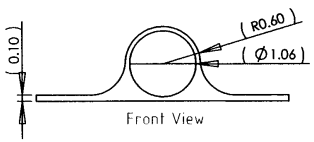

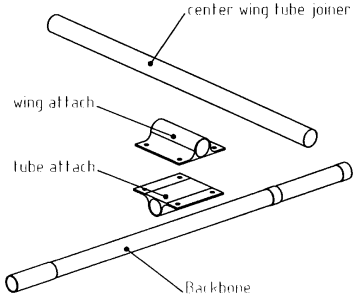

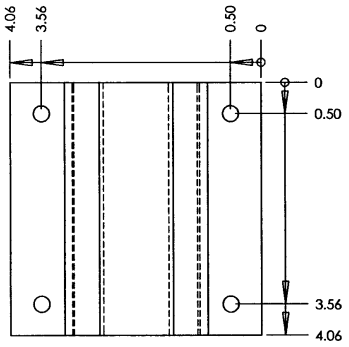

The wing attachments are carbon-balsa composite, bonded to the tubes. Both are identical.
They are joined by nylon bolts, which have been designed to shear at a lg drag loading at the tip of the wing.

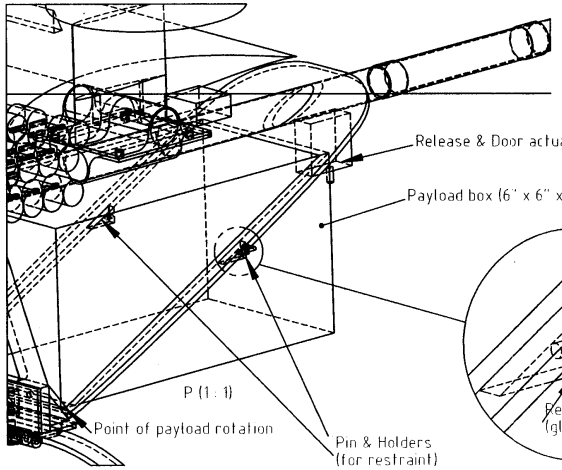

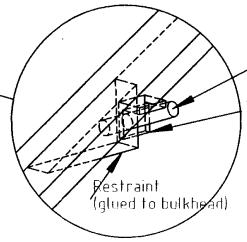

Release Procedure:
-Actuator opens clam-shell doors which rotate about the diagonal bulkhead.
-At the the end of servo travel, the actuator releases the pins, holding the payload.
-The pin frees the payload, which drops as it rotates about the triangular support.
- Reverse action closes the doors and redies the plane for flight.

THE INFORMATION CONTAINED IN THIS DRAWING IS THE SOLE PROPERTY OF THE UNIVERSITY OF SOUTHERN CALIFORNIA GW. ANY REPRODUCTION IN PART OR AS A WHOLE WITHOUT THE WRITTEN PERMISSION OF STEPHANE GALLET (gallet@usc.edu) IS PROHIBITED.

Subsystems

M (1 : 4)

6.0 MANUFACTURING PLAN

The building and manufacturing techniques employed were of great concern because of its weight implications. To better determine the optimal solution to key components, different figures of merit were created to quantify the analysis.

6.1 Figures of Merit

1. *Material Cost and Availability:* Materials that are difficult to obtain could increase construction time. Hence, more consideration was given to materials that were readily available for purchase and relatively inexpensive. Standard graphite and fiberglass were within our budget, and were available from the Aircraft Spruce and Specialty Company at anytime.
2. *Required Level of Workmanship*: Many methods can be used to create the same component for the aircraft. Some of these methods had the potential of making better parts but required a high level of experience. Table 6.1 lists the team's skill with certain materials and methods. Although the team opted to use more common methods of construction like balsa built up R/C planes, the option of using advanced manufacturing methods was frequently discussed due to the composite material advantages of high strength to weight ratio, its ability to survive crashes with less damage and easiness to repair. If use of an advanced method for a part was considered necessary, the more experienced members carried out the task while teaching the less experienced.
3. *Repeatability and Crash-worthiness*: The idea of being able to create a part easily and quickly became an important factor for the manufacturing plan. Should a part fail during flight-testing due to a crash or other reasons, the ability to make a new one or repair the damaged component was an essential element in choosing a manufacturing process. For this FOM, the key factor was to reduce the amount of downtime between flight tests.

6.2 Analytic Methods Used to Select Final Set of Manufacturing Processes

The manufacturing skill of the team members was considered during the design process to assure that the team had the capability of building this year's design. A chart was constructed that ranked the team members building skills so we could determine where the team stood and who could head up different construction areas of the airplane (Table 6.1).

This year the team received a donation of pre-preg unidirectional carbon fiber. The use of this material was assumed in the design of our structural components although the risks of experimenting and relying on initial results were very high. To accelerate the learning curve, our industry team advisors were crucial and provided guidance and experience for building the composite tube spar and other components. An estimate of the time required to make a 1" diameter 40" length tube with 2 students was about 6 hours. This was time consuming, considering the fact that there where 4 tubes to build. Commercially available composite tubes were then considered, but the specific dimension and ply orientation needed for SCyRaider could not be found.

Member Name	Team Experience (Yrs)	Composite Workmanship	Machining Workmanship	Wood Workmanship
George Sechrist	6	5	5	5
Stephane Gallet	3	4	4	4
Tyler Golightly	3	3	4	4
Jonathan Hartley	3	4	3	4
Tai Merzel	3	2	3	3
Michael Mace	3	1	3	3
Andres Figueroa	2	1	3	3
Billy Kaplan	2	1	3	3
Cristina Nichitean	2	1	2	2
Doris Pease	2	1	2	2
Tim Schoen	2	1	3	3
Lester Kang	2	1	1	1
Jason Randy	1	1	2	2
John McArthur	1	1	1	1
Heidi Faqua	1	1	1	1
Stephanie Parker	1	1	1	1
Dan Montgomery	1	1	1	1
Jeremy Milne	1	1	1	1
Stephan deMartimprey	1	1	1	1
Shannon Moriarty	1	1	1	1
Jennifer Tsakoumakis	1	1	1	1

Table 6.1 *Skill Matrix for ADT Workmanship rated on a scale from 1-5, with 5 defining a very high level of workmanship*

Other components of the plane, e.g. wing, landing gear, and fuselage shell, utilized more familiar methods of construction such as wet lay-ups, female molds, foam cores etc. which relied on the experience acquired through previous years. This gave the opportunity for the team's traditional techniques to be taught to younger members and required less manufacturing time.

6.3 Processes Selected for Major Component Manufacture

For the following components, a summary of the manufacturing processes used for construction is given, as well as any alternatives investigated.

1. *Tube Backbone & Wing Spar*: With extensive work and analysis done on shear and moment forces, the backbone & wing spar where both designed to take a maximum crash loading of 5.5Gs. In case these parts could not be made from the pre-preg material, alternative methods where investigated to meet the structural demand. These included aluminum and composite tubes that could be purchased, however they would not be as efficient as our designed tubes using a specific lay-up schedule. The manufacturing of the tubes was documented to improve the time and repeatability of subsequent tubes. A simplified version of the process follows:
   a. *Strip Cutting:* Dimensions and layout of the pre-preg are calculated to see how much pre-preg must be cut off the main roll. This involves calculating the strip width, so at 45 degrees the strip will wrap evenly around the tube.
   b. *Mandrel Preparation:* Mandrels of different lengths were de-burred in order for the tubes to slide out easily. Wet sanding with 400 & 800-grit sandpaper was used to remove any scratches. After wet sanding, the mandrels were cleaned with acetone. From this point on, it was crucial to keep the mandrel clean to prevent contamination and bonding problems. The mandrels were then polished with turtle wax until they became black, and were buffed out lightly with cotton rags. The polishing was repeated 3-4 times. Acetone was then used again to clean the mandrels, which were brought into the exhaust room. Freekote44 was applied onto the mandrels using a lint cloth until a continuous, smooth wet film was apparent. This process required eye protection, respirators and gloves to handle Freekote44. Using a heat gun, the mandrels were heated for 10 minutes at 150F and the release agent was then buffed out. This procedure was repeated 3 times. After applying the third coat, a generous amount of Miller-Stevenson mold release was sprayed on. Protection for eyes, lungs and gloves were also needed during this procedure. The mandrels were then heated again for 5 min at 150F and were finally ready to be laid-up with strips of pre-preg. These steps were required to insure that the carbon tubes would release properly from the aluminum mandrels after they were autoclaved.
   c. *Strip Layout:* Shear strips were then laid-out on the mandrel. The strips were laid out and stretched by hand so that no bubbles or wrinkle marks were formed which would have caused imperfections. After the 1st layer of shear strips was done, the tube was wrapped with a 1" stretch tape with a hand-held tension regulator. While one team member would turn the mandrels, the other member could wrap it with three even overlaps using the tube wrap machine. This procedure ensured the elimination of any remainder bubbles and wrinkles formation. The wrap was kept on for 10 minutes and

the next layer of shear ply was then applied over the first layer. This procedure was repeated four times for four layers of shear plies. After the shear plies were laid out, the caps were taped onto the top and bottom of the tube by measuring equal distances along the circumference. By using the heat gun the adhesive properties of the caps were increased so that they could stick better onto the mandrel. After laying out all the caps, two layers of 90 degree strips were added to create hoops; i.e. hard points at the joints. This was to strengthen the tube and prevent it from splitting or crushing.

d. *Curing & Removing:* After laying out all the caps and hoops, the tubes were wrapped for the final time and placed into the oven to cure at 260F for approximately 2 hours. The mandrels were then taken out of the oven and placed into the freezer to allow the aluminum to contract so that the pre-preg tube could slide out easily.

2. *Wing Attachment Mount*: Wing mounts have been a significant source of unanticipated weight growth in the past; up to 10% of total wing weight. This was due to the reliability and robustness the aircraft needed to achieve. Frangible links in past designs sometimes broke at either higher loads than specified to save the wing or under lower loads preventing scoring flights. This year, the design required the wing spar and backbone to be joined together at a 90 deg angle. Hence, the team developed a 'U bolt' like design under the guidance of industry advisors that tied the two manufactured tubes together in a very simple way (Figure 6.1). The load from the wing was transmitted to the mount through compression (A) and was

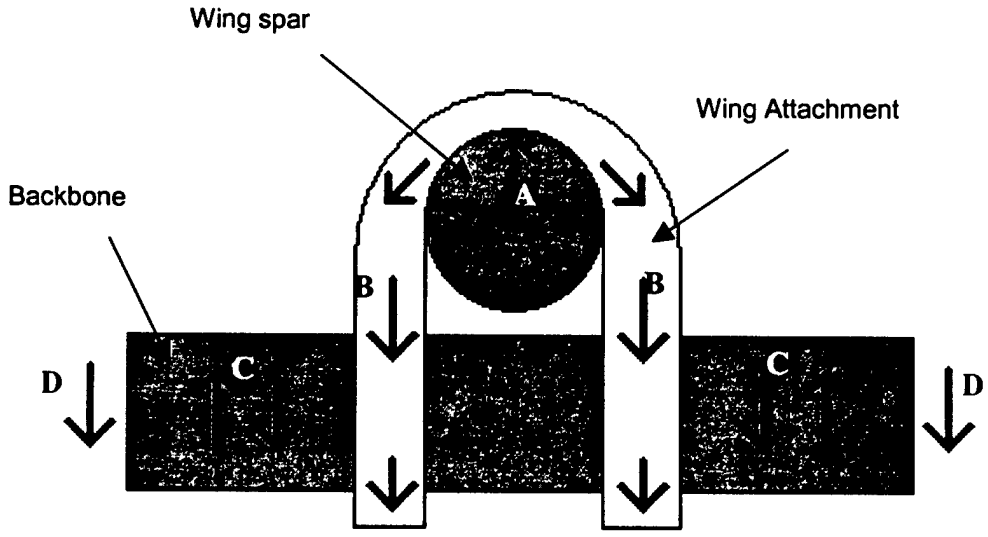

Figure 6.1 *Force analysis on the wing attachment (viewed from the side of the plane)*

reacted by the mount and mounting bolts through tension (B). The bolts transmitted the load to the backbone by compression (C). As designed, the backbone also supported the shear forces. The initial design used a wet lay-up carbon fiber as the plank and the 'U' shaped saddle. Later iterations used pre-preg carbon fiber to reduce weight and increase strength. The mount also had to be movable along the backbone to accommodate the airplane's CG uncertainty during design and construction. The final design included a carbon fiber cap and panel for fastener attachment. Ply orientations over the tubes were primarily perpendicular to their axis. This provided added strength in the direction of the load path vs. a balanced lay-up. To transmit tip-drag loads from the wing spar to the mount, plies were applied at 45 degrees. To account for our designed frangible wing, nylon bolts were used as fasteners to sheer off in case of a 1G-lateral tip loading (20 lbs) and must withstand a 5.5G-turn load (120lbs). The first parts tested weighed approximately 40 grams and could not handle the 1G tip load. Once redesigned with an additional layer of bi-directional pre-preg carbon, the joiner weighed only 25.1 grams and met all the specifications required.

3. *Motor Mount*: The motor mount was designed to fail in the event of a crash. This feature has proved very effective in the past to protect the motor, gearbox and propeller. The initial design for this year's plane was made of unidirectional carbon tape molded around the motor and the backbone forming two joined loops. The team also discussed using an aluminum bracket along with a plastic face plate that attaches the motor to the end of the backbone to react to the torque. This method was adopted because of the lack of reliability of the carbon fiber system especially in reacting the torque loads of the motor (see Figure 6.2 and the drawing package).
4. *Fuselage Shell & Hatch Doors*: Because last year's fuselage two ply shell performed so well, the team decided to use the same method for this year's plane. This allowed the younger team members to take charge and have more responsibilities in the manufacturing process. Using the buck-to-female mold method, the shell was shaped by hand from blue tooling foam using CAD drawn templates for guidance. The foam was covered in MonoKote and laid up in fiberglass to form the female mold. After some stiffness testing, the fuselage shell was laid up in the female mold using two plies of bi-directional carbon skin plus additional plies at the weak points (i.e. hinge line). All details such as cooling vents and the hatch doors were cut into the shell after it was fabricated. The blue foam master could have been used as a male mold, eliminating the female mold step. However, this process was used in previous year resulting in poor surface quality, which increased drag.
5. *Landing Gear*: The main gear was designed to flex under high stress acting as a shock absorber in the event of a hard landing. The strut's spring rate was set to 55lbs/inch to limit vertical acceleration in a no-flare landing to 5.5g's. Of all the materials available for construction, carbon fiber was by far the best choice for the gear. It has a very high strength

to weight ratio, and is easy to mold into the shape desired. The two techniques used to make landing gears are pre-preg and wet lay-up. Both techniques where used to build different landing gears in order to compare and optimize the system.

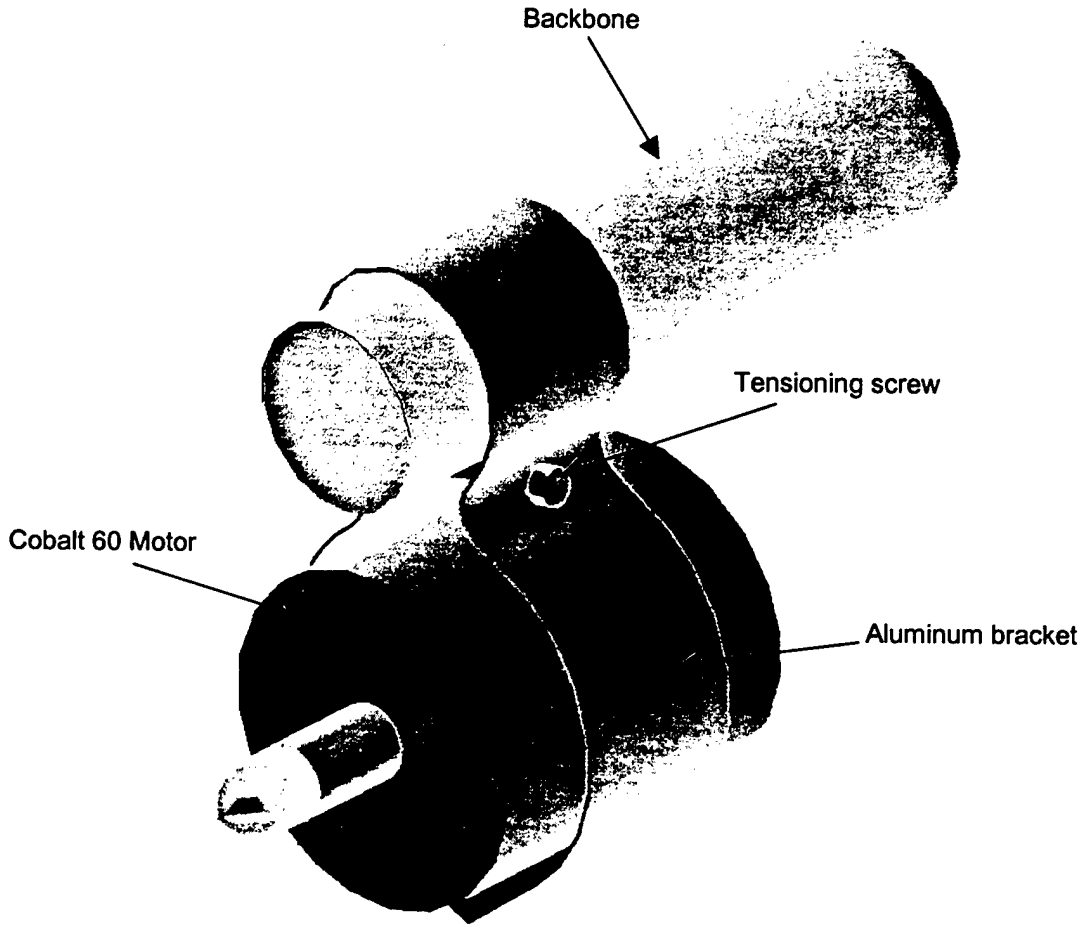

Figure 6.2 *Engine Motor mount attaching a Cobalt 60 with the backbone by an aluminum bracket (plastic restraint not depicted for clarity. Refer to drawing package)*

6. Wing: The wing was constructed out of Spider foam (Surfboard foam) because of its high resistance to crushing. Using wood templates cut to the desired airfoil shape, the wing cores were cut from the foam sections using a hotwire. The holes for the spar tubes were cut out with the hot wire and then the composite spars were glued in place. To cover the skin of the wing, 3oz fiber glass at $\pm$ 45° was chosen to counter the twisting moments of the wing and to reduce any dimpling of the core due to hanger rash. The control surface utilized a 'live hinge' meaning the wing skin was used as the hinge. Kevlar was used in the hinge area since it is flexible. The live-hinge allowed for a better airfoil end product. In the past, control surfaces were cut off the wing core section, prepped and re-attached. Attaching them with no

ridge between the cut is almost impossible. The wing cores were finally covered using a wet lay-up process, and vacuum bagging procedure, to insure a smooth surface.

7. Empennage: The 'V' Tail sections were built in the same wet lay-up and vacuum bag method as the wing, however they did not require a complex spar design. In place of a 'tube spar', 'Live Spar' uni-directional carbon caps were used to give the tails additional stiffness. 3 oz fiberglass was also used to cover the skin surface and give some additional stiffness but most importantly to increase the robustness of the foam core and protect it from handling. Again, Spider foam was used as the core material because it allowed for a stiffer control surface with a small increase in weight versus using lighter Styrofoam that would require a more complex structure.

6.4 Manufacturing Schedule

Table 6.2 shows the manufacturing schedule, which details the build times for each component.

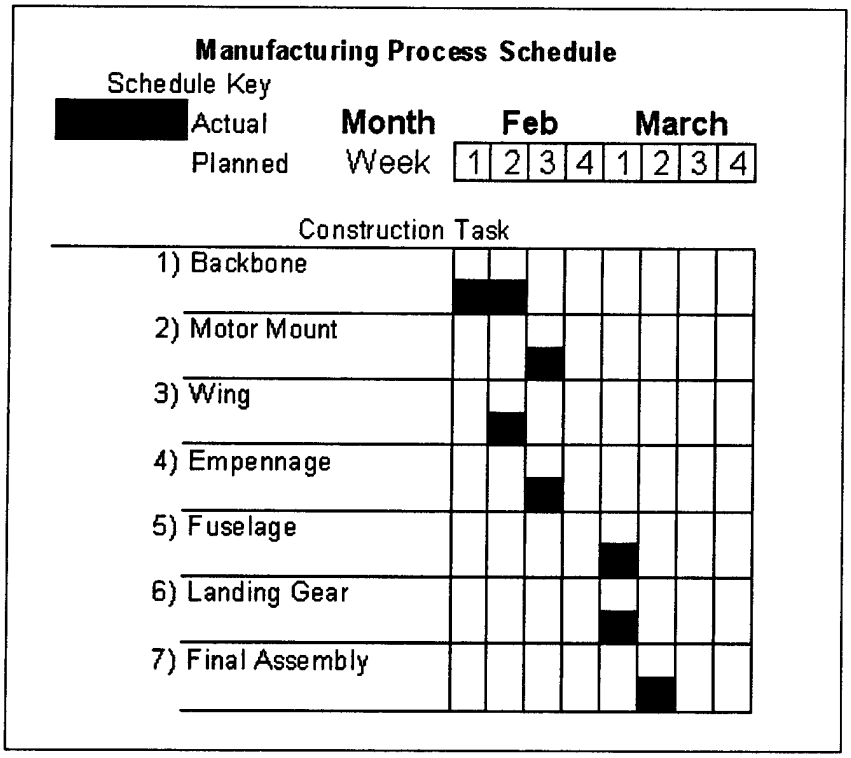

Table 6.2 *The Manufacturing Milestones Chart, showing planned and actual timing of construction events*

7.0 TESTING PLAN

Throughout the different design phases as well as construction, testing was performed on different components and sections of the aircraft to prove the ability of the design to perform as desired and improve the configuration. Full aircraft testing was also planned to facilitate handling during contest flying as well as verify the model's design strengths and possible weaknesses that could be improved.

7.1 Component Aircraft Testing

Testing of different designs proposed for individual components of the plane was important in providing physical proof for mechanisms that worked and ones that didn't. Some of the aircraft component testing included radome locations, drag estimation for mission A, different joints & hinges proposed for the wings, spar & backbone joiner testing, payload deployment mechanisms for Mission B and propulsion system testing. They are described as follows.

1. *Radome Testing*: The first question posed by the team at the beginning of the design phase was which mission to choose to fly. Since A & B had the highest difficulty factor, the incremental drag caused by the radome was required and a working model of the deployment system was deemed desirable to study its structural requirements. Hence, radome testing was performed, first through an analytical method, second by wind tunnel testing and third by actual test flying using last year's model airplane. Analytically, a fluid dynamic formula for a short cylinder was used to approximate the coefficient of drag resulting in a C_D of 0.72. To test the validity of this solution, the radome was built and tested in a wind tunnel. Knowing the velocity of the airflow in the wind tunnel, the air density, the drag force and frontal area of the radome, the C_D was calculated using the equation:

$$C_D = \frac{D}{.5\rho v^2 S}$$

The drag increase with velocity can be seen in Figure 7.1 including the strut that the radome was attached to. Also, the drag vs. the square of the velocity was plotted to obtain a linear function from which C_D can be easily calculated. The wind tunnel tests gave a C_D of 0.7, which agreed with the analytical solution. To determine the optimal location of the radome, last year's plane was used for test flights. The radome was mounted in three different positions: above the CG, below the CG, and on the top rear of the plane, in front of the vertical tail. Then, the plane was flown 1000 ft. straight-aways at full throttle. By timing each of these upwind and downwind legs the average speed was calculated at the different radome locations. The results are shown in Table 7.1. The highest velocity, which was assumed to coincide with the lowest drag position, was found when the radome was mounted above the CG. Note that without the radome the speed was higher as expected. Another advantage to this mounting position was the location of the CG, which stayed the same with and without the radome for consistent trim and handling.

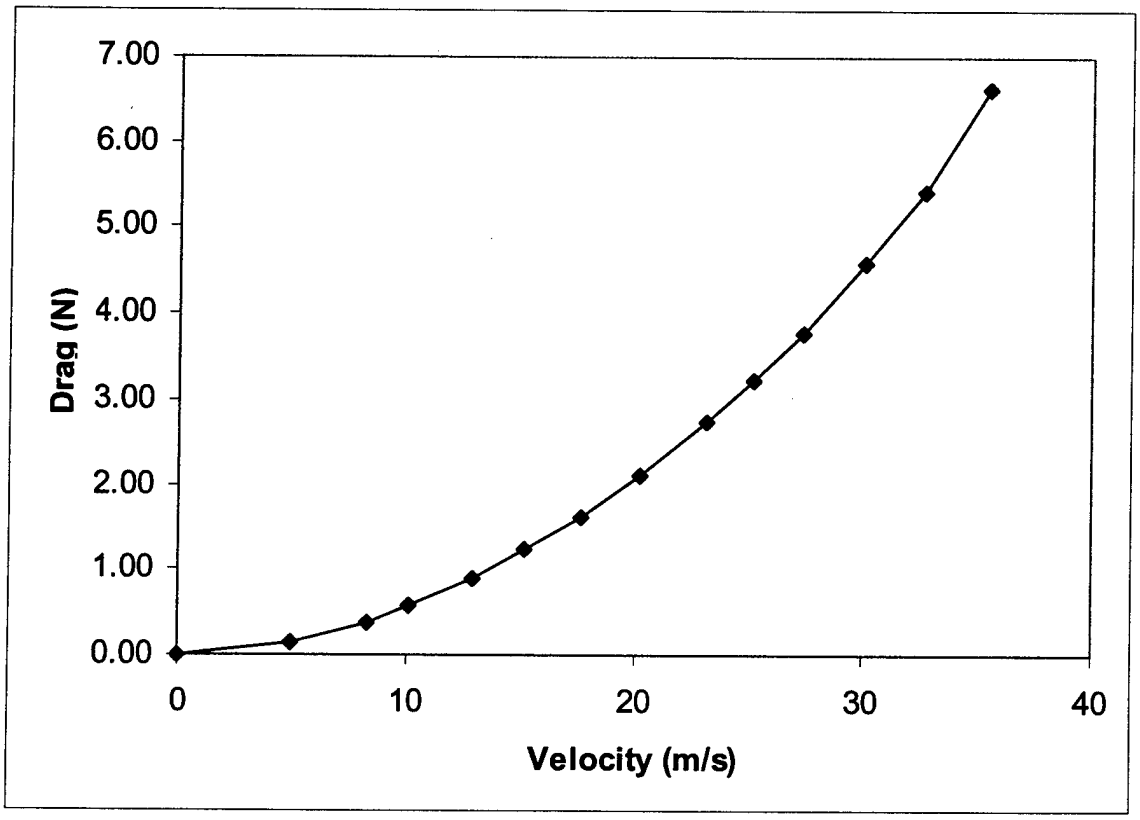

Figure 7.1 *Wind Tunnel Test results shows drag increase as velocity increases*

Location	Speed (Mph)
No Radome	67.0
Above C.G.	64.8
Above Back	62.6
Below C.G.	62.0

Table 7.1 *Results of Radome location testing*

2. *Stability Model Verification Testing*: Another series of flight test were conducted to verify last year's stability and control design characteristics. The plane was flown over the pylon course, but each successive flight had two inches of the vertical tail removed to test the aircraft stability and observe handling during flight. The tail had been deliberately overbuilt last year due to probability of high crosswinds at the contest site. The results showed that the aircraft's yaw stability was still in good shape with 35% (8 in) of the vertical tail removed. Therefore the coefficient of moment in yaw, $C_{n\beta}$, for this year was significantly reduced to 0.002/deg.

3. *Tests for Flow Separation*: Concerns about regions of separation on the radome were studied using oil drops. . This procedure was performed with white oil drops placed over the fuselage (Figure 7.2a), wing, landing gear and radome. During flight, the oil moved along the surface streamline before drying. This provided a visual image of laminar and turbulent regions of flow as well as areas of separation. When the radome was mounted on the bottom of the fuselage, underneath the CG, reversed flow could be observed indicating an increase in drag due to separation (Figure 7.2b). Other areas of the plane generally showed attached flow as expected. .

(a) (b)

Figure 7.2 *Oil dot testing on last year's plane (a) flow over the fuselage (b) reversed flow over the radome and landing gear*

4. *Wing Joints & Hinges Testing*: Since the 2002-2003 rules required the aircraft components to fit in a 4x2x1ft box the wing had to be cut at certain points to meet this requirement. Two types of joints were proposed; hinged and slide in panels. Both these were tested to find the best alternative to biplanes. The joints had to be structurally sound, require little assembly time and still be within the team's ability to manufacture. The hinged joint was made by cutting the wing at a 45° angle from the leading-edge, and attaching the two pieces together with an aluminum hinge. This design made the wing tip point 90-degrees back from the wing root when folded. Aluminum tubes were bored into each half of the wing and aligned so that a spring loaded rod in one tube would move halfway into the other tube to lock the hinge. The second joint type, the slide-in joint, was made by cutting the wing 90-degrees from the leading edge and placing thin aluminum tubes in one section and thin protruding rods in the other. The rods would slide into the tube to connect the wing. Though both proved to be

structurally sound, the folding wing posed problems fitting it into the box. The folding wing also took nearly twice as long to assemble, was heavier due to the weight of the spring and the hinge, and was much more complicated to manufacture. The final design incorporated the slide-in joint.

5. *Spar & Backbone Joiner Testing*: The joiner was a connector used to hold together the tube spar of the wing and the backbone of the aircraft, both made of composites for high strength to weight ratios. The joiner consisted of two identical parts assembled at 90 degrees from each other to accommodate each of the tubes (see drawing package subsystem figures). Nylon bolts, holding the two saddles together, had to be sized to shear at 1G lateral tip loading. Testing was performed to ensure the bolts would fail in shear at an applied torque of 70 ft-lbs, at the same time being capable of holding a tensile load of more than 150 lbs. Using two 10-24 nylon bolts at opposite corners of the flat plates, the part failed at 32 ft-lbs of torque. With four 10-24 nylon bolts, the bolts failed at the desired 70 ft-lbs. These four bolts were also able to support a 150 lb tensile load, tested by hanging weights that act in the vertical direction. Thus, the final design used four 10-24 nylon bolts.

6. *Deployment Mechanism Testing*: Tests were also performed with the payload deployment device and payload doors. Several mock-ups of the fuselage were built with different hinge designs and deployment methods. Vertical, horizontal, and diagonal hinges were all constructed and tested; the diagonal hinge seemed to be the best design because it opened directly beneath the avionics payload unit, required less travel distance than the vertical hinges, and prevented airflow along the fuselage from forcing the doors open. The devices tested for the deployment of the box were rubber bands and pins. Push-pull cables and fixed servo arms were tested for opening the payload doors. The rubber band design consisted of a rubber band wrapped around the avionics box; when the band was released, it would eject the box through the open payload doors. This design proved simple and easy to build; however it was not reliable and it required an extra servo to release the rubber band. The pin design featured horizontal pins passing below tabs protruding from the avionics box that were then fitted into slots drilled in brackets attached to the plane's diagonal bulkhead. The pins were tied to the servo that opened the payload doors. After the doors were opened to their full extent, the last bit of traverse on the servo pulled the pins and the payload dropped out. This eliminated the need for the extra servo and took the weight of the box off the doors; hence it was chosen as the final design. The two methods tested for opening the payload doors were push-pull cables and fixed servo arms. The push-pull design allowed the doors to remain securely closed during flight, but required a complex system to act at the middle of the doors where they would be most effective. Also, the rigidity of the system necessitated the addition of a large pulley affixed to the servo to direct its motion. The fixed servo arm design secured both the doors and acted at the desired location. In addition, crossing the arms over

the servo axis caused any force attempting to open the doors to be directed against the servo support rather than causing the rotation of the servo. Fixed servo arms were therefore decided for the final release mechanism design.

7. *Motor Mount Testing*: Several designs for the motor mount were built and tested. The designs consisted of a combination sling and tube plug; the sling was designed to resist translational motion and the tube plug torsional motion. The first sling tested was built of carbon fiber that was molded to the shape of the backbone and the motor underneath. A slit was cut in the bottom of the carbon fiber to release the motor in the event of a hard landing or crash. This sling was tested with the gearbox bolted to a tube plug so that the tube plug would resist the torque and the sling would hold the motor in the vertical direction. Unfortunately, the carbon fiber was not elastic enough and failed during testing. The next sling was made of aluminum bent to the dimensions of the backbone and motor. The saddle, the part of the sling in contact with the backbone, was wide enough to distribute the loads from the motor over a large area. From the saddle, two arms extended around the motor to attach to each other underneath the motor using tabs. The tabs were designed to spring apart if the plane landed hard enough. A bolt was placed between the saddle and the arms to adjust the tension of the sling. Like the previous carbon fiber sling, the aluminum sling could not resist torque. A final design change during this phase of testing called for no gearbox, so a plastic faceplate was made to connect the tube plug directly to the motor (the tube plug had connected to the gearbox in the previous test). The faceplate was made of plastic so it would break in shear but would resist torque; therefore, the motor would be released from the backbone in the event of a crash. Tests showed that this combination worked well, since both the sling and the faceplate would release the motor for a hard landing but hold all other loads (see drawing package subsystem figures).

8. *Propulsion Testing*: Since the CP1300 and CP1700 batteries didn't have data that could be trusted for the purpose of the missions, and our team didn't have experience with these battery types, bench testing was performed and set up as seen in Figure 7.3. Note the instrumentation is depicted in red and the system components in blue. The RPM was measured with an optical tachometer, the current by an induction amp meter, the voltage was converted to a digital signal by an ADC (analog to digital converter) card and sent to the computer and the thrust was read from a spring scale attached to a sliding plate upon which the motor and propeller were mounted. The voltage was measured across the battery terminals. The first test was on 36 CP1700 cells with direct drive and a 16.5x15 Aeronaut propeller. This revealed that these cells provided more power than necessary for the mission goals (Figure 7.4a). The second test involved the same set-up with 36 CP1300 cells which performed as desired and had sufficient energy to complete the missions (Figure 7.4b). Since these batteries had less weight, they were used for the final configuration.

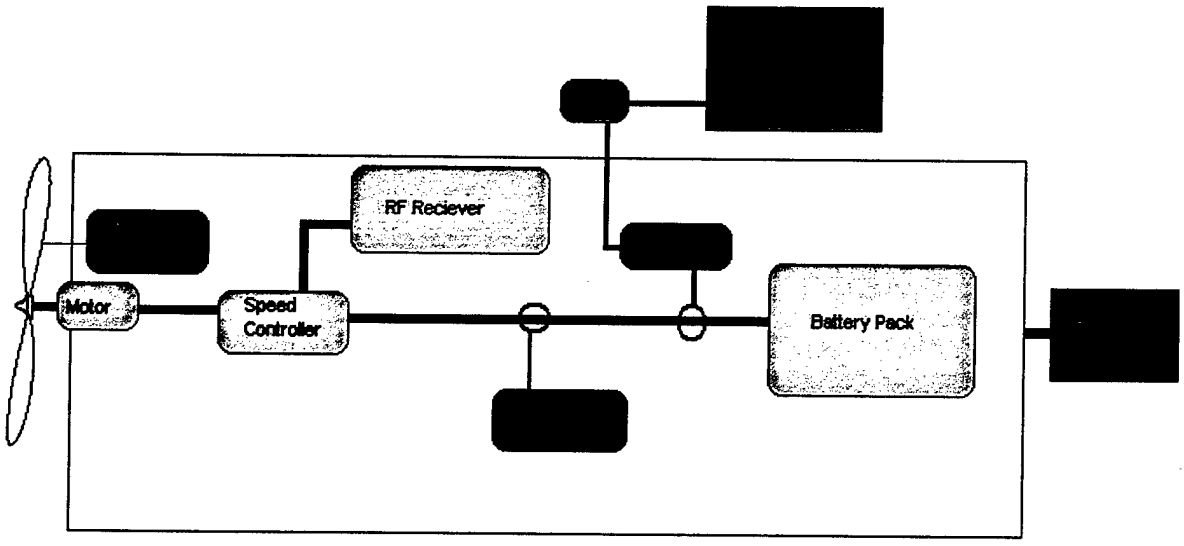

Figure 7.3 *Propulsion System with Batteries, Motor and Propeller testing bench set-up*

For a better comparison between these two battery types, a time trace of the voltage life of the CP-1300's and CP1700's was plotted during discharge (Figure 7.5). The maximum mission time required was 120 seconds, so the CP1300 cells satisfied this constraint. This result is conservative since the voltage increases during dynamic testing as opposed to static testing as presented here. From the graph it may seem that the CP1700's would perform much better, but they are also 1lb heavier adding to the Rated Aircraft Cost and becoming an over designed parameter. A 16x12 APC propeller was also tested to compare performance, but was discarded due to its increased weight.

7.2 Full Aircraft Testing

Full aircraft test flights are scheduled to begin March 15, 2003. Prior to the first flight, several functional tests will be performed. The CG of the plane will be adjusted until it occurs at the designed point; the plane will be lifted at the wingtips to simulate a 2.5-g loading; control surfaces, the transmitter, and the receiver will be range-checked, control deflections will be verified static thrust, rpm, current, and voltage will be measured. Once the functional tests are complete, actual flight tests will begin. For the first flight, the pilot will take the plane into the air and trim the control surfaces. For the next flights, he will perform some basic maneuvers, such as S-turns, power-off and power-on stalls, control doublets, and steady-heading sideslips. This will allow us to verify that the plane handles the way it is expected. After these initial flight tests—which may be repeated several times to accommodate necessary improvements— contest missions flying will start.

When flying the missions, a major concern will be the speed of the aircraft and determining its limits. These sorties will be timed, takeoff field length will be measured, and battery as well as cooling performance will be closely monitored. Real time voltage and temperature will be down-linked.

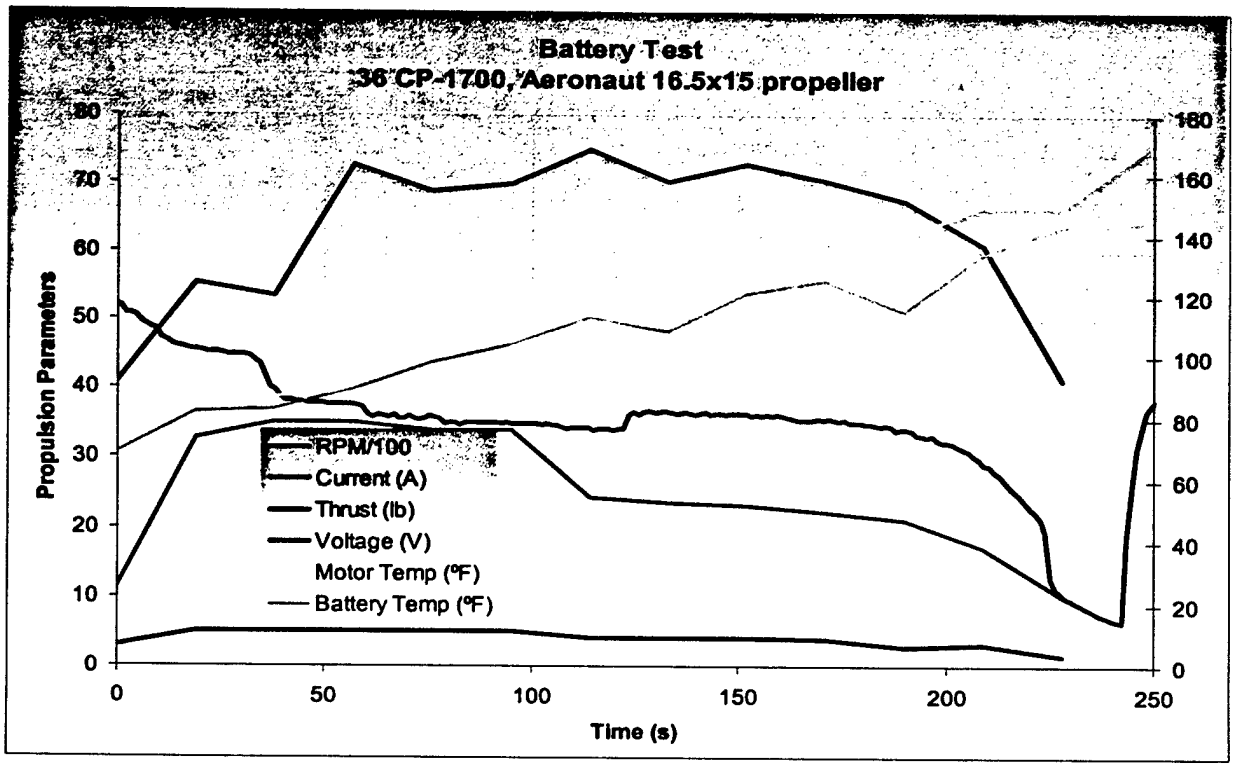

(a)

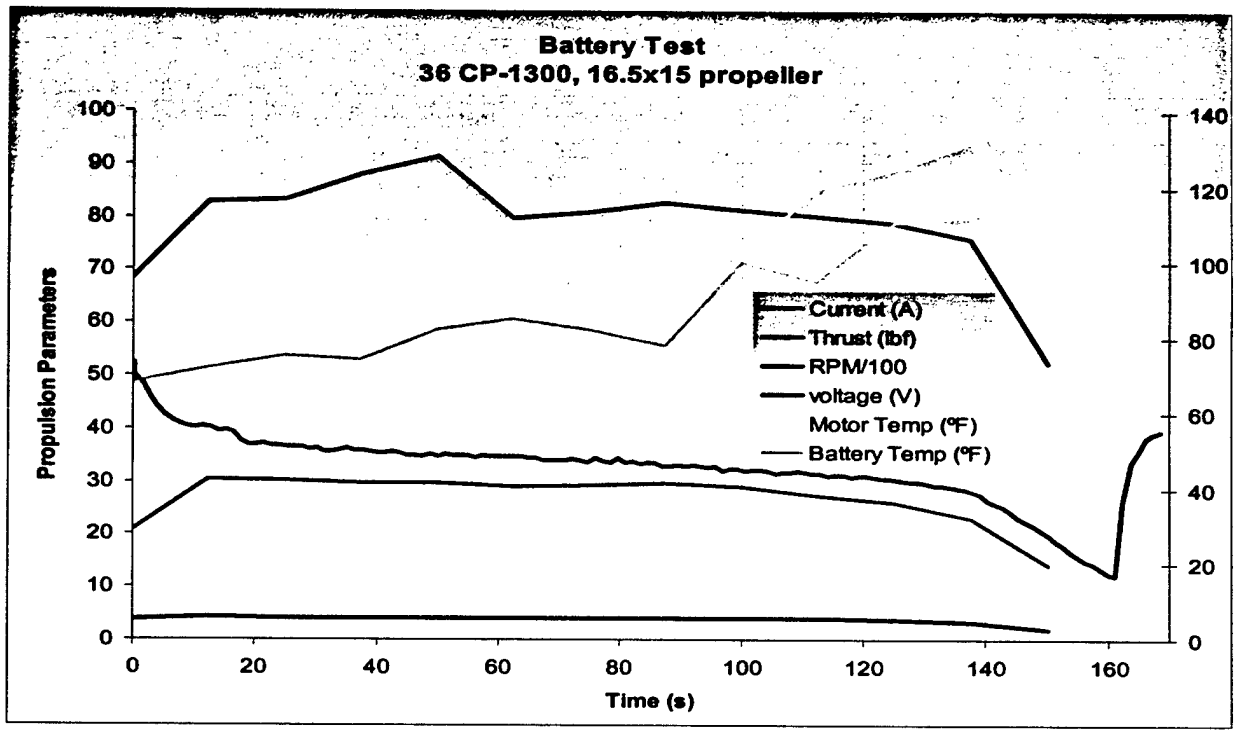

(b)

Figure 7.4 *Battery Testing for (a) CP1700's and (b) CP1300's*

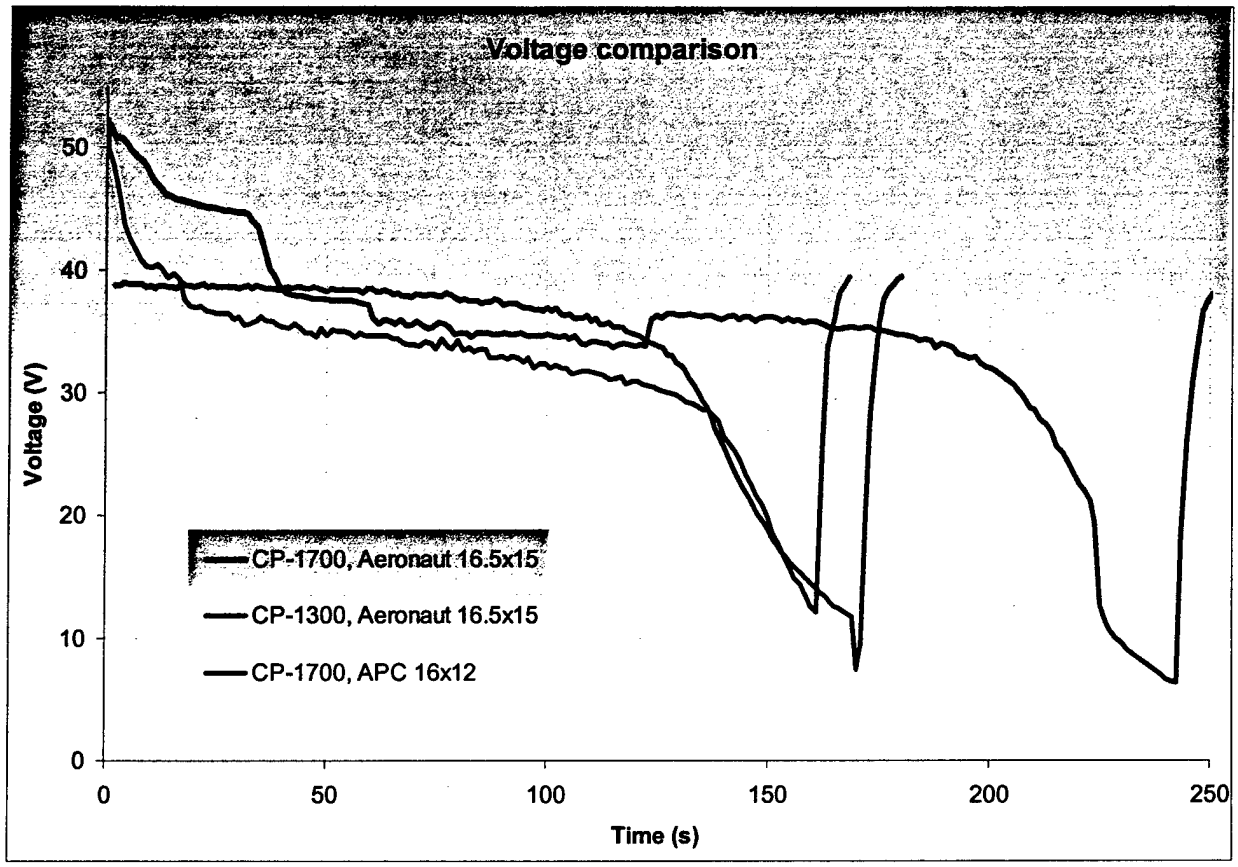

Figure 7.5 *Voltage Comparison between different battery and propeller types*

SCyRaider will fly with different propellers to observe which one provides the best performance. The pit crew will practice taking the plane out of the box and perform the timed assembly as quickly as possible. In addition to making sure the plane is ready for the contest, the testing will also prepare the pilot and pit crew for the competition. The last day available for test flights is April 12, 2003. This date was chosen because it is two weeks before the contest, giving the team one week to improve and/or repair the aircraft in case of crash or major defects, plus one week to ship the plane to the contest.

Conclusion:

The 2002/2003 USC AeroDesign Team made a conscious effort to document criteria and lessons-learned from prior years, but retired all tools developed in past years. This required each design Captain to create their own design tools from scratch, enhancing team competence. Design emphasis was focused on reducing RAC, which has been a weakness at USC. In particular, the propulsion system underwent extensive testing and analysis to validate the gear-less system by a team led by advisor Jerry Chen. New team members made significant contributions in prototyping the payload and wing stowage systems. This will be the first year USC has used significant amounts of pre-preg materials (donated). The team would like to thank advisor Wyatt Sadler for teaching the tube-making process and other processes necessary for this material. This has led to a substantial improvement in component quality.

2003 Cessna/ONR Design Build Fly Competition Design Report

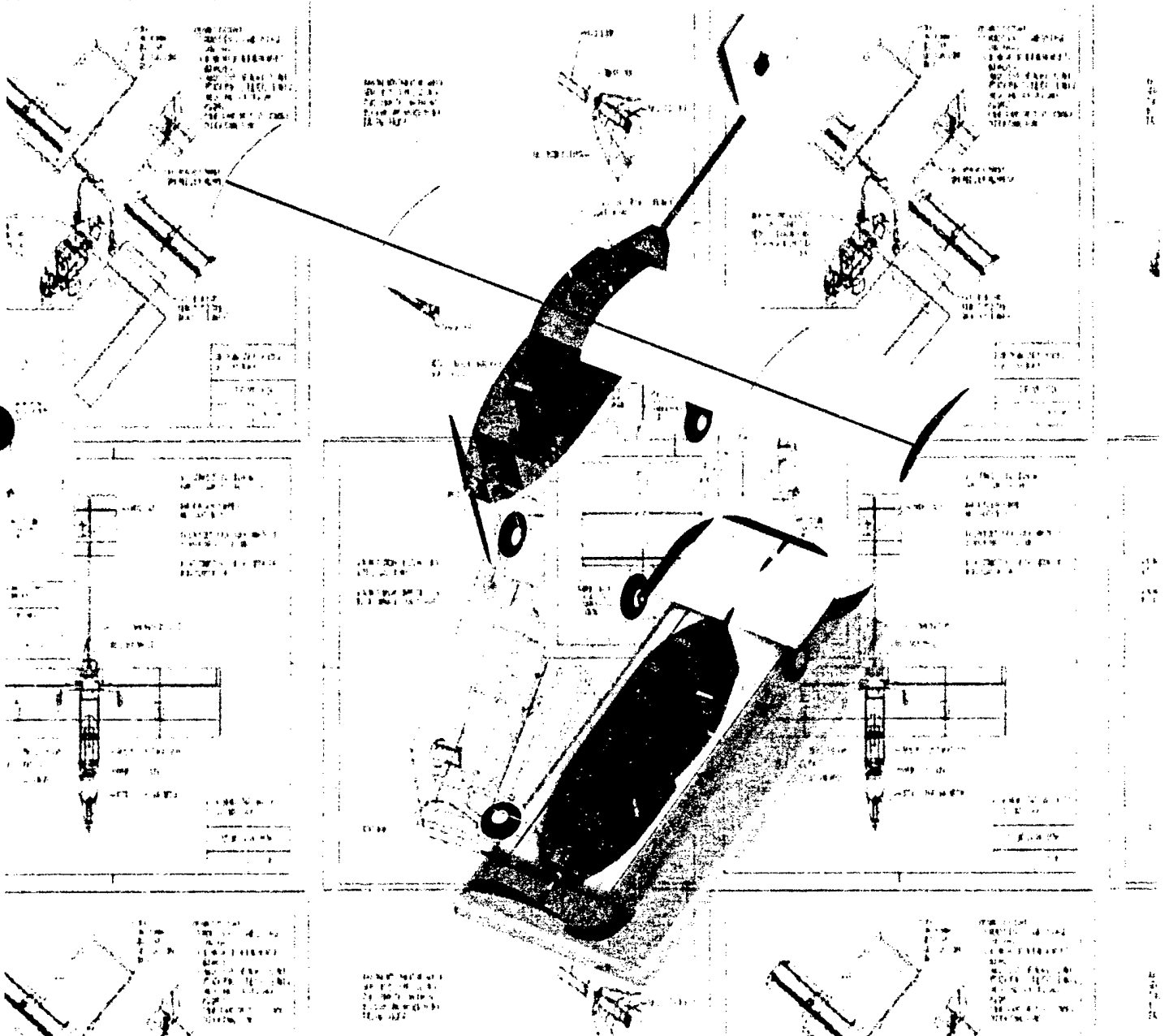

Oklahoma State University Black Team

Table of Contents

1 Executive Summary 1

1.1 Conceptual Design 1

1.1.1 Conceptual Design Alternatives 1

1.1.2 Conceptual Design Tools 2

1.1.3 Conceptual Design Results 2

1.2 Preliminary Design 2

1.2.1 Preliminary Design Alternatives 2

1.2.2 Preliminary Design Tools 2

1.2.3 Preliminary Design Results 3

1.3 Detail Design 3

1.3.1 Detail Design Alternatives 3

1.3.2 Detail Design Tools 3

1.3.3 Detail Design Results 4

1.4 Manufacturing and Testing Plans 4

2 Management Summary 4

2.1 Design Team Structure 4

2.2 Project Scheduling and Milestone Identification 6

3 Conceptual Design Phase 7

3.1 Contest and Mission Requirements 7

3.2 Mission Selection 7

3.3 Aircraft Configurations Investigated 8

3.3.1 Overall Aircraft Configurations 8

3.3.2 Wing Configurations 9

3.3.3 Tail Configurations 11

3.3.4 Fuselage Configurations 11

3.3.5 Landing Gear Configurations 12

3.3.6 Propulsion Configurations 12

3.4 Figures of Merit and Weighted Decision Matrices 13

3.4.1 Overall Aircraft Configurations 13

3.4.2 Wing Configurations 14

3.4.3 Tail Configurations 14

3.4.4 Fuselage Configurations 15

3.4.5 Landing Gear Configurations 15

3.4.6 Propulsion Configuration 16

3.5 Final Aircraft Summary 16

4 Preliminary Design Phase 17

4.1 Design Parameters and Sizing Trades Investigated 18
4.1.1 Aerodynamics Design Parameters and Sizing Trades Investigated 18
4.1.2 Propulsion Design Parameters 19
4.1.3 Structural Design Parameters 20
4.2 Analysis Methods 21
4.2.1 Airfoil Analysis 21
4.2.2 Drag Analysis 22
4.2.3 Aircraft Stability Analysis 22
4.2.4 Aircraft Control Sizing Analysis 23
4.2.5 Motor Analysis 23
4.2.6 Battery Analysis 24
4.2.7 Propeller Analysis 24
4.2.8 Main Gear Analysis 24
4.2.9 Nose Gear Analysis 25
4.2.10 Wing Analysis 25
4.2.11 Analysis of the Wing/Fuselage Connection 25
4.2.12 Tail Boom Analysis 25
4.2.13 Tail Stabilizer Analysis 26
4.2.14 Fuselage Analysis 26
4.3 Mission Modeling 26
4.3.1 Mission A 27
4.3.2 Mission B 27
4.4 Optimization Trade Studies Performed 27
4.4.1 Study of Number of Battery Cells Required 27
4.4.2 Study of Power Required for Takeoff and Climb 27
4.4.3 Study of Cruise Velocity Required 28
4.4.4 Study of Wing Area Required 28
4.4.5 Study of Wingspan Required 29
4.5 Analysis Results 29
4.5.1 Aerodynamic Analysis Results 29
4.5.2 Propulsion Analysis Results 32
4.5.3 Structural Analysis Results 33
4.6 Predicted Aircraft Performance 35
5 Detail Design Phase 35
5.1 Systems Architecture and Component Selection 35
5.1.1 Main Gear 36
5.1.2 Nose Gear 36

5.1.3 Wing 36
5.1.4 Wing/Fuselage Connection 36
5.1.5 Boom 37
5.1.6 Tail Stabilizers 38
5.1.7 Fuselage 38
5.1.8 Payload Release System 40
5.1.9 Antenna Mounting System 40
5.1.10 Motor 40
5.1.11 Propeller 41
5.1.12 Batteries 42
5.1.13 Radio 42
5.1.14 Servos 42
5.2 Final Rated Aircraft Cost 43
5.3 Aircraft Performance Parameters and Details 43
5.4 Drawing Package 45
6 Manufacturing Plan 45
6.1 Manufacturing Processes Investigated and FOM Considered 46
6.1.1 Landing Gear 46
6.1.2 Wings 46
6.1.3 Tail Stabilizers 46
6.1.4 Fuselage 47
6.2 Analytic Methods Used 47
6.2.1 Cost 47
6.2.2 Skills Matrix 48
6.2.3 Manufacturing Schedule and Milestones 48
6.3 Manufacturing Processes Selected 48
6.3.1 Main Landing Gear 48
6.3.2 Wings 49
6.3.3 Tail Stabilizers 49
6.3.4 Fuselage 50
7 Testing Plan 50
7.1 Brake Testing 50
7.1.1 Testing Objectives and Procedures 50
7.1.2 Testing Results and Conclusions 51
7.2 Breakaway Connection Testing 51
7.2.1 Testing Objectives and Procedures 51
7.2.2 Testing Results and Conclusions 51

7.3 Propulsion Testing 52
7.3.1 Testing Objectives and Procedures 52
7.3.2 Testing Results and Conclusions 52
7.4 Taxi Testing 52
7.4.1 Testing Objectives and Procedures 53
7.4.2 Testing Results and Conclusions 53
7.5 Flight Testing 53
7.5.1 Testing Objectives and Procedures 53
7.5.2 Testing Checklists 54
7.5.3 Testing Results and Conclusions 54
8 References 55

List of Figures

Figure 2-1: Team Structure and Personnel Assignments 5
Figure 2-2: Project Gantt Chart 6
Figure 3-1: Aircraft Design Configurations 9
Figure 3-2: Conceptual Design Sketch 17
Figure 4-1: Optimization Trade Study of Score Versus Design Parameters 28
Figure 4-2: Drag Polar Comparison for Eppler 423 30
Figure 5-1: Wing and Landing Gear and Boom Connection to Fuselage 37
Figure 5-2: Fuselage Design Details 39
Figure 5-3: Final Rated Aircraft Cost Breakdown 44
Figure 6-1: Manufacture Gantt Chart 49

List of Tables

Table 3-1: Overall Aircraft Configuration Decision Matrix 14
Table 3-2: Wing Location Decision Matrix 14
Table 3-3: Tail Configuration Decision Matrix 15
Table 3-4: Fuselage Configuration Decision Matrix 15
Table 3-5: Gear Configuration Decision Matrix 16
Table 3-6: Propulsion Configuration Decision Matrix 16
Table 4-1: Aircraft Drag Estimates 30
Table 4-2: Stability Moment Coefficients 31
Table 4-3: Predicted Aircraft Performance 35
Table 5-1: Motor Properties and Cost 41
Table 5-2: Aircraft (a) Geometry, (b) Weight, (c) Performance, (d) Systems 45
Table 6-1: Skills Matrix 48

1 Executive Summary

The report outlines the methodology used by the 2003 Oklahoma State University Black Team to design and construct an aircraft that meets the required mission profile established by the contest rules. The overall goal of the contest is to achieve the highest score by designing, building, and flying an unmanned-aerial vehicle around a closed course. To accomplish this goal, the design team used followed a design process beginning with the conceptual phase, the preliminary phase, then the detail design phase.

1.1 Conceptual Design

Based on contest rules and restrictions, the design team identified the major tent poles required for successful completion of the missions. These tent poles are required to complete the missions and obtain a flight score. For the contest, the aircraft must:

- fit into a 4-by-2-by-1 foot box.
- takeoff within 120 feet.
- carry a five-pound payload box.
- finish two of the three assigned missions.
- assemble quickly and easily.
- use no more than five pounds of Ni-Cad batteries.
- use specified electrical motors for power.
- be propeller driven.
- not draw more than 40 amps of current.
- not be a rotary wing or a lighter-than-air design.

These tent poles were analyzed by the three technical groups: aerodynamics, structures, and propulsion. Each group determined design parameters based on the tent poles to determine which factors influenced the scoring potential the most. Performance analysis optimized the design parameters. Results of the optimization assisted in developing figures of merit (FOM) to determine the concepts that exhibited the highest scoring potential.

1.1.1 Conceptual Design Alternatives

The aerodynamics group investigated different aircraft, wing and tail configurations. The final configuration was based on the advantages and disadvantages of each. The structures group investigated different fuselage and landing gear configurations. The group also investigated methods for fitting the aircraft in the storage box, where the minimum amount of connections was desired in order to reduce assembly time. Propulsive configurations included combinations of engines, propellers and battery cells. The final concept was based on initial optimization of the aircraft performance.

1.1.2 Conceptual Design Tools

The design team first investigated the contest and mission requirements. These were used to finalize the selection of the missions. Next, the aerodynamics group investigated possible aircraft, wing and tail configurations. The propulsion group determined configurations based on the number of engines and propellers used. The structures group evaluated possible configurations for the fuselage and landing gear. Each configuration considered was evaluated using weighted figures of merit. Decision matrices were used to finalize the aircraft configurations.

1.1.3 Conceptual Design Results

At the completion of the conceptual design phase, the team selected the aircraft configuration with the highest scoring potential. The aircraft chosen was a high-wing conventional configuration with a conventional tail. The fuselage houses the propulsive and payload systems. Certain wing components and aircraft characteristics were determined. The wings are designed in two sections, which are secured together and assembled on top of the fuselage. The main landing gear is also removable and is secured between the fuselage and wings. In order to accommodate a fuselage length greater than four feet, the tail boom is removable. Bomb-bay doors are used to deploy the payload for Mission B. These features reduce the time for assembling the aircraft, which is critical to reduce the flight time for each mission.

1.2 Preliminary Design

After determining the configuration, the design groups began sizing trades, aircraft analysis and performance, and optimization trade studies. The aerodynamics group focused on airfoil selection and sizing considerations for stability and control. The structures group performed structural analysis and identified load-bearing members. The propulsion group, using analysis data from the aerodynamics group, selected the appropriate motor, propeller and number of battery cells for the required power outputs. Gearboxes were matched to the selected motor in order to provide necessary efficiency and power.

1.2.1 Preliminary Design Alternatives

The design team identified and investigated design parameters and sizing trades that affect the performance of the conceptual aircraft configuration, aircraft components, and propulsion system. The aerodynamics and propulsion groups utilized analysis programs to determine aircraft performance. The structures group used analysis methods to analyze components based on strength characteristics. The trade studies involved the optimization of the score with respect to the design parameters. The mission performance of the aircraft was also estimated.

1.2.2 Preliminary Design Tools

The aerodynamics and propulsion groups used analysis programs that modeled the aircraft and missions.

These programs optimized the aircraft and determined propulsive efficiencies of the propulsion system. An airfoil analysis program analyzed different airfoils in actual flight conditions. A drag prediction model analyzed the total drag on the aircraft. In order to accurately locate the center of gravity (c.g.) determined by the aerodynamics group, the structures group used 3-D modeling software. With this computer-drafting tool, the weight and exact location of each component could be mapped according to actual scale. These drawings also modeled the aircraft within the storage box.

1.2.3 Preliminary Design Results

At the conclusion of the preliminary design phase, the aircraft components were properly sized. The aerodynamics group calculated the hinge moments of each control surface and provided all aircraft measurements to the structures team. The structures team analyzed the aircraft components based on flight loads and structural loads. After studying connection joints, the group selected the quickest methods of assembly. The propulsion group analyzed the motor and propeller and optimized for the number of batteries required to complete the missions.

1.3 Detail Design

Detail design phase determined the component selection and systems architecture for the aircraft. All components were ordered and lead times were identified for initial and restocking purposes. The final rated aircraft cost was determined as well as the aircraft performance parameters and details. A drawing package was assembled that outlined the aircraft components and systems.

1.3.1 Detail Design Alternatives

The structures group investigated different alternatives for component material selection. The decision to use expanded Polypropylene foam and fiberglass construction for the wing and tail surfaces was based on cost, ease of construction, weight, and strength characteristics. The group selected a carbon fiber/nomex sandwich construction for the fuselage components and carbon fiber layers for the landing gear. In addition, breakaway connections and seams were selected to reduce damage to the fuselage. Carbon fiber tubing was selected for the wing spars, tail spars and the boom based on strength-to-weight characteristics. The propulsion group selected an Astro Flight 640S motor, a 14-inch propeller and 22 battery cells for use in the propulsion system.

1.3.2 Detail Design Tools

The propulsion analysis program was invaluable for optimization of the propulsion system. Many computer analysis tools were utilized to simulate mission flights using the sized components of the aircraft. Score optimization was accomplished by taking advantage of earlier sensitivity studies and continually striving for a lower rated aircraft cost. Component testing of the landing gear and payload deployment system was conducted to identify any re-engineering requirements.

1.3.3 Detail Design Results

At the completion of the detail design phase, the design team finalized the selection of all aircraft components. From the selections made, a final rated aircraft cost was determined and aircraft performance parameters and details were calculated. A drawing package was assembled that showed the details of the entire aircraft.

1.4 Manufacturing and Testing Plans

In order to complete the manufacturing process, different construction methods were analyzed to determine the most efficient manufacturing plan. Each manufacturing process used certain figures of merit to analyze the construction method. Analytic methods were used to determine the cost, skills required to construct the part, and scheduling of the process. Based on these criteria, the final manufacturing process was determined for the landing gear, wings, tail stabilizers, and fuselage. Reusable construction molds were designed along with component mass production techniques to facilitate possible reconstruction. At the completion of the manufacturing phase of design, the team developed a prototype aircraft ready for flight-testing.

A testing plan was developed to determine the reliability of the aircraft and component systems. A full-scale prototype aircraft was constructed to test the performance of the breakaway connections, braking system, propulsion system, and aircraft during taxi and flight. The overall objective of the testing is to determine if improvements or change is necessary for the design. Observation and results of the aircraft testing were recorded to form conclusions of the prototype aircraft. Based on the conclusions, changes and improvements will be performed on the final aircraft design to ensure mission success. Overall, the design team determined that pneumatic brakes, quarter-inch nylon bolts, and a 15-inch propeller would be used on the aircraft design. Based on the results of the taxi and flight-testing, the aircraft performed exceptionally both on the ground and during flight.

2 Management Summary

In order to efficiently complete the design project, a management summary was completed. The summary detailed the team structure, which was divided into three technical groups: aerodynamics, structures, and propulsion. To further divide the design tasks, certain duties were assigned to each design group member. The completion of each task in the design process was managed by a Gantt chart, which was strictly followed.

2.1 Design Team Structure

The team structure was broken down according to the major components required for the accomplishment of the project. An organizational chart is shown in Figure 2-1. The chief engineer is responsible for the planning and scheduling of events for the entire team. Another critical task is the development of good communication between all group members and to keep everyone informed of the

direction of the group. The chief must completely understand the contest rules and ensure that no element of the design violates the rules. All financial matters are the sole responsibility of the chief as well. Overall, responsibility for the project rests with the Chief Engineer; however, those responsibilities are shared with the project group leads.

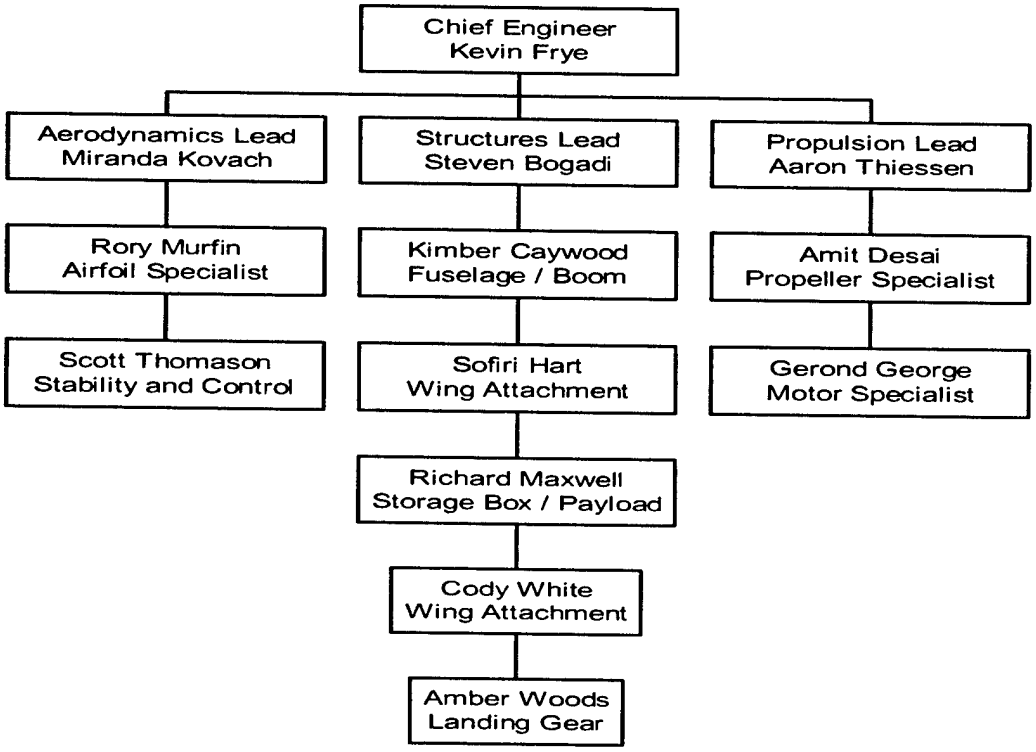

Figure 2-1: Team Structure and Personnel Assignments

The aerodynamics group responsibilities include all matters concerning the initial aircraft configuration. The group investigates airfoil selection and wing design and utilizes historical data to finalize the design. Flight mission optimization is a collaborated effort with the propulsion group, and critical for enhancing the overall score. Finally, handling qualities are considered using stability calculations, control surface sizing, and effects of aircraft center of gravity (c.g.).

The propulsion group is responsible for the optimization and development of the propulsion system. This includes motor, propeller, and battery cell selection as well as the configuration of the propulsion system. Engine maintenance, modifications, and propulsion tests are critical to mission success. Close work with the aerodynamics group determines the optimal configuration of power requirements.

The structures group is responsible for the integration of all aircraft elements. Stress analysis and sizing of structural members are important to the strength of the design. Test mock-up sections of wing and fuselage validate that construction methods meet the anticipated loading conditions. The aircraft is further

sub-divided into major components with a specialist assigned to develop solutions to these unique problems. Therefore, the design team was further divided into individual or group assignments.

2.2 Project Scheduling and Milestone Identification

To ensure rapid and efficient project completion, development of a Gantt chart served as a visual reference tool. The Gantt chart is shown in Figure 2-2. The chief engineer identified six milestones:

- completion of the conceptual design phase.
- completion of the preliminary design phase.
- completion of detail design phase prototype rollout.
- design report due to AIAA.
- final design freeze.
- final flight tests.

The milestones were documented on the Gantt chart with start dates and ending dates for all major aspects of the design. The Gantt chart highlights the important parts of the design process. Progress reports were used in writing the final AIAA design report and were compiled by the chief engineer.

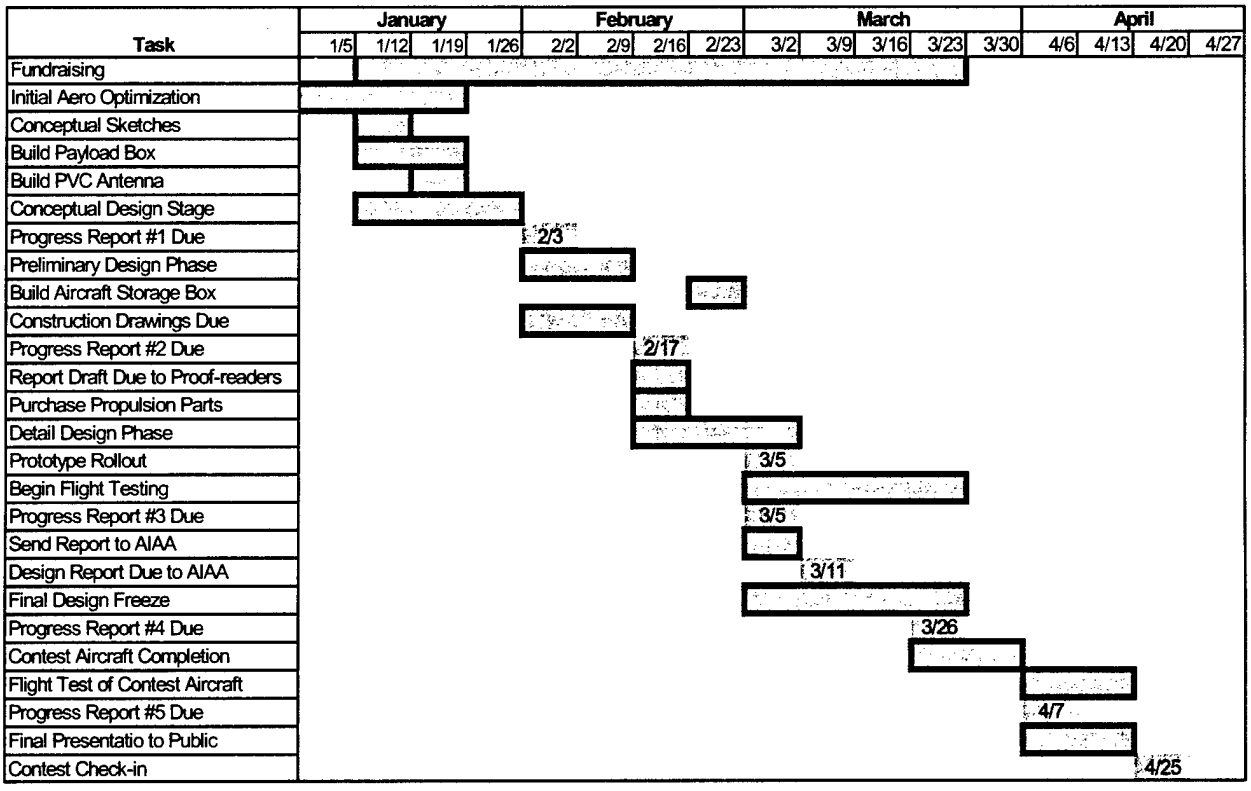

Figure 2-2: Project Gantt Chart

3 Conceptual Design Phase

The conceptual design phase included understanding the contest requirements and restrictions, evaluating different design configurations, and modeling initial optimization analysis programs. The design team investigated different design configurations based on contest requirements and past history. The aerodynamics and propulsion groups used initial optimization programs to analyze the aircraft performance of each design. The optimization analysis programs determined the figures of merit (FOM), which finalize the conceptual configuration.

3.1 Contest and Mission Requirements

Contest requirements state that the team is to design, build, and fly an aircraft for two missions. The design team must select two of the three mission options. Each of the missions is flown around a closed oval course. For each of the three missions, four laps must be completed to receive a flight score. In Mission A, the aircraft must internally carry a five-pound payload box and externally carry a one-pound antenna throughout the mission. A 360-degree turn must be completed for each lap. For Mission B, the payload box is carried for two laps. The aircraft must then touchdown, deploy the payload, and complete the remaining two laps. Again, the aircraft must complete a 360-degree turn for each lap. For Mission C, the aircraft must carry the payload box for the duration of the mission and complete four-360° turns for each lap. Missions B and C do not require the antenna. The score of each mission attempt is based on the time it takes to complete the mission.

The contest also requires each team to fit the aircraft inside a storage box and complete an aircraft assembly task. The storage box must have dimensions of 4-foot by 2-foot by 1-foot. The time it takes for the team to remove the aircraft from the storage box and fully assemble the aircraft is included in the total flight score. Electrical connections must also be complete on the aircraft; control surfaces are tested and penalized due to an inaccurate actuation.

Each team must also provide a rated aircraft cost (RAC) for the aircraft design. The RAC is based on the manufacturer's empty weight, the rated engine power, and the manufacturing cost. The manufacturer's empty weight is the airframe weight including all flight and propulsive batteries, but not the payload. The rated engine power is based on the number of engines used and the total battery weight. The manufacturing cost is a breakdown of the number of hours spent on each structural component. The RAC is a divisor in the total score of the aircraft.

3.2 Mission Selection

In order to determine the conceptual design of the aircraft, two of the missions are selected. The design team compared the requirements and modeled the performance of each mission. The model estimated the total time and the scoring potential. The RAC was varied to determine a range of scores.

Mission A included the weight of the payload and antenna and estimated the drag produced by the antenna. The scoring potential was calculated between 3.5 and 5.0. Mission B was modeled by doubling the time for takeoff, climb, decent, and landing. Mission B has a scoring potential between 2.5 and 4.0. The time during the 360° turns was quadrupled for Mission C. Therefore, Mission C has a scoring potential between 1.0 and 2.0.

Based on the estimated scoring potentials for each mission, Missions A and B were selected. Mission C was eliminated since there is substantial energy lost during the turns, which increases the time and decreases the score. This was a low-risk decision since an aircraft optimized for Missions A and B will be able to perform Mission C.

3.3 Aircraft Configurations Investigated

To optimize the aircraft performance, careful consideration was taken to determine the aircraft configuration. The aerodynamics group considered the configurations of the overall aircraft, wing and tail. The structures group considered fuselage and landing gear configurations. The propulsion group considered the number and configuration of the engines and propellers.

3.3.1 Overall Aircraft Configurations

In order to optimize score, the aerodynamics group investigated several configurations. After reviewing the contest and mission requirements and restrictions, some configurations were easily eliminated. The remaining choices were given more consideration and are discussed as follows:

- **Canard:** The aerodynamic advantage to the canard configuration shown in Figure 3-1 (a) is due to the stall characteristics. Since the canard is forward of the wing, this surface would stall before the wing, which allows for correction during the stall. The disadvantage is that a canard requires more takeoff distance than a single, high-lift wing. There is also an RAC penalty due to the extra horizontal surface.
- **Flying wing:** As shown in Figure 3-1 (b), this configuration requires no horizontal tail, which lowers the RAC. Due to fewer surfaces and a streamlined fuselage design, a flying wing has less drag than a conventional configuration. According to past contest history, teams using this configuration had pitch-damping difficulties.
- **Bi-wing:** As shown in Figure 3-1 (c), the extra wing in this configuration provides an increase in the maximum lift, which is desirable for takeoff. There is an additional RAC penalty for the extra wing. This design also produces excess drag compared to a mono-wing aircraft, which is due to the additional wing and struts used to connect the wings.
- **Conventional:** A conventional configuration, shown in Figure 3-1 (d), is reliable and has good performance qualities at subsonic, low Reynolds number conditions. This is based on past

contest history. The number of surfaces required is beneficial to RAC. A conventional aircraft is also favorable due to the ease of construction.

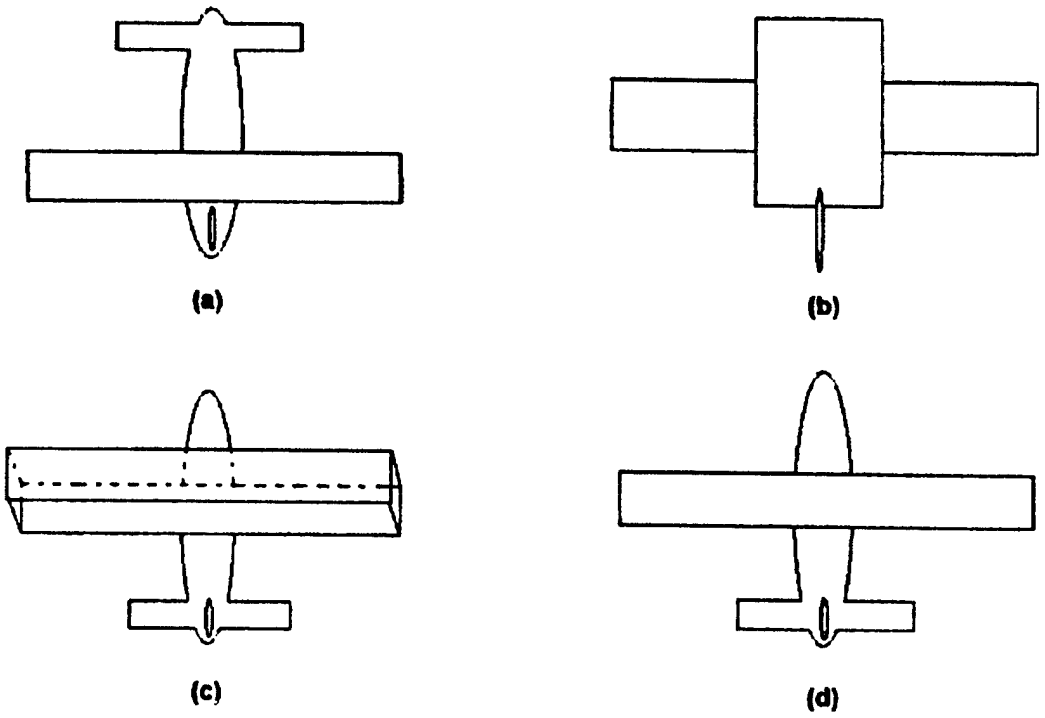

Figure 3-1: Aircraft Design Configurations

3.3.2 Wing Configurations

Several factors affect the decision for wing location and wing characteristics. The decision for wing location is primarily based on the mission requirements and ease of construction; the decision for wing characteristics is based on ease of construction, handling qualities, and aerodynamic performance.

Due to the mission requirements, payload deployment is a significant factor. The location of the payload provides the most difficulty in deciding the wing location. Since the payload must be located at the c.g. of the aircraft, there is possible interference with the wing structure. Three wing locations were investigated as follows:

- **Low wing**: Locating the wing below the fuselage produces a destabilizing roll moment created by the flow around the fuselage (Nelson 1998). To overcome this, dihedral angle must be added, which increases the construction difficulty. Additionally, the wing would interfere with the payload deployment required in Mission B.
- **Mid wing**: For this design, the payload interference with the wing location is critical. In a mid-wing configuration, the carry-through structure of the wing goes directly through the center of the

fuselage, which is the location of the payload release system. Based on construction, a mid-wing configuration still requires some dihedral angle to provide roll stability.

- **High wing**: This design does not require dihedral angle due to the dihedral effect of the fuselage and wing interaction (Nelson 1998). Additionally, the height of the landing gear can be shortened, which reduces the structural weight. There is a tradeoff, though, since the fuselage must be strengthened to support the landing-gear loads (Raymer 1999). Since the wing is above the fuselage, there is no interference with the payload deployment system.

The aerodynamics group also examined wing characteristics. These characteristics include taper ratio, sweep angle, aspect ratio, twist, and dihedral angle, discussed as follows:

- **Wing taper:** Wing taper affects the lift distribution along the span of the wing. For a highly tapered wing, the lift distribution is higher at the wing tips than at the wing root. Therefore, the stall pattern occurs at the tip and progresses to the root, which provides little warning to correct for the stall. For an untapered (rectangular) wing, the lift distribution is parabolic. Thus, the stall pattern begins at the root and generates outward toward the tip. Since the stall occurs slowly, there is enough warning to correct for it. Due to these considerations, the aerodynamics group chose a rectangular wing.
- **Sweep:** A swept wing is primarily used on aircraft traveling at transonic and supersonic speeds. Since the missions are flown in subsonic, low Reynolds number conditions, this characteristic is not advantageous (Raymer 1999). One major advantage to sweeping the wing is to place the wing carry-through at a different location along the fuselage, which avoids the payload deployment system. Since a high-wing configuration doesn't interfere with the payload, wing sweep is unnecessary.
- **Aspect ratio:** Aspect ratio also determines the stalling characteristics of the wing. For a given wing area, a high aspect ratio wing stalls quicker than a low aspect ratio wing due to the lift distribution. For a rectangular wing, when the low aspect ratio wing stalls, the stall is gradual from the root to the tip. For a high aspect ratio, once the wing stalls at the root, the entire wing becomes stalled quickly. For a high aspect ratio wing, there is less loss in lift (as compared to a low aspect ratio wing) due to the reduced effective angle of attack at the tips. Thus, a high aspect ratio wing has less drag for a given lift, which is favorable in this design.
- **Twist:** The twist in a wing changes the airfoil angle of attack along the wingspan. This is used to prevent stall at the tips. Twist is also used to optimize the lift distribution over the wingspan. An important factor to remember is that for an applied twist, the lift distribution is only valid at one coefficient of lift; the benefit of the twist is not seen at other coefficients of lift. Since twist is difficult to construct, the aerodynamics group eliminated this characteristic.
- **Wing dihedral:** Wing dihedral is affected by the position of the wing. The disadvantage to a low-wing configuration is the destabilizing roll moment created by the flow around the fuselage, which

produces a negative dihedral effect. To gain a positive dihedral effect, a low-wing configuration requires a greater dihedral angle in the wing. The high-wing configuration is advantageous due to the dihedral effect of the fuselage/wing interaction. For a high-wing configuration, the relative flow around the fuselage produces a stabilizing roll moment. Therefore, the high-wing position does not require dihedral.

3.3.3 Tail Configurations

The aerodynamics group investigated the following tail configurations: conventional, cruciform, T-tail, V-tail, and inverted V-tail. The decision for tail configurations is based on ease of construction and contest restrictions. The tail characteristics were discussed as follows:

- **Conventional:** This design is most commonly used due to the stability and control characteristics. A conventional tail is also lightweight and easy to manufacture.
- **Cruciform:** The benefit of the cruciform tail is that it lifts the horizontal tail above the turbulent downwash from the wing. This makes the elevator controls more effective. However, extra weight must be added to provide the structural integrity required to support the horizontal tail within the vertical tail.
- **T-tail:** The same benefits of a cruciform tail apply to a T-tail. With the horizontal tail mounted at the top of the vertical tail, the entire rudder becomes exposed to a less turbulent airflow and is therefore more effective than the rudder of a cruciform tail. Like the cruciform tail, additional structural weight must be added to the vertical tail.
- **V-tail:** One advantage to this configuration is that RAC is lowered. However, a great deal of concern lies in the ability to fit this design in the storage box when appropriately sized. Additionally, the V-tail produces an undesired adverse yawing tendency.
- **Inverted V-tail:** Like the non-inverted V-tail, this configuration performs well in RAC. In addition, the inverted V-tail has a proverse yawing tendency. There is still a concern with fitting this design in the storage box.

3.3.4 Fuselage Configurations

The structures group examined some fuselage configurations. These include conventional, single boom, and twin boom configurations. The decision for fuselage configurations is based on ease of construction, drag qualities, structural weight and fitting in the box.

- **Conventional:** This design is easy to construct and provides reduced drag if streamlined properly. Due to the size of the box, the length is restricted to four feet. Based on stability requirements, the fuselage must be long enough to provide adequate pitch stability, which is difficult to fit inside the storage box.
- **Single-boom:** This design allows an increased fuselage length to provide pitch stability. The boom can disassemble from the main fuselage and easily fit in the storage box. Assembly of the

boom to the main fuselage only requires one motion. There is no construction required since the boom can be purchased.

- **Twin-boom:** A twin-boom fuselage extension also provides adequate pitch stability and disassembles to easily fit in the storage box. The assembly requires attachment at two points and is less efficient than a single-boom connection. Additionally, the boom results in additional weight, which increases RAC. Again, there is no construction required since the component can be purchased.

3.3.5 Landing Gear Configurations

Landing gear configuration considered by the structures group included tripod, bicycle, quad-wheel, and tail dragger. The decision for landing gear is based on stability and steering characteristics, drag qualities, and structural weight.

- **Tripod:** The tripod configuration provides a large amount of variability for aircraft implementation. The arrangement places the nose gear beneath the power train and the main gear just behind the center of gravity. This distributes the gear loads evenly, which provides adequate stability on the ground. A tripod gear arrangement provides good steering and takeoff stability.
- **Bicycle:** The bicycle configuration has reduced weight compared to the tripod and quad wheel configurations. The stability and steering characteristics are less desirable, though. This configuration has reduced drag since there are only two wheels. This configuration does not provide good steering characteristics and takeoff stability.
- **Quad Wheel:** For a quad-wheel configuration, the ground stability is overall more effective. Due to the additional wheels and legs, the drag and weight increases. Therefore, this configuration is least desirable.
- **Tail dragger:** The disadvantage to the tail dragger is based on the contest mission requirements. For Mission B, the tail has to maneuver around the payload after deployment, which is difficult with this configuration. This increases the amount of time spent on the ground. Steering and stability characteristics are also a concern.

3.3.6 Propulsion Configurations

The propulsion configurations included number and location of engines and propellers required for the propulsion system. The propulsion group performed initial propulsive optimization to determine the combination of engines and propellers necessary to complete each mission. One and two engine/propeller configurations were considered. Based on performance, the propulsion group determined that only one engine and propeller is necessary to successfully complete the mission.

Through research, the propulsion group investigated several propeller locations for the aircraft. The group discussed various arrangements of the propeller on the aircraft. Each of the configurations can be placed into two major groups:

- **Tractor:** The tractor configuration has the propeller and motor located in the front of the fuselage and pulls the aircraft through the air.
- **Pusher:** The pusher configuration pushes the aircraft through the air, since the propeller and motor are located at the rear of the fuselage.

3.4 Figures of Merit and Weighted Decision Matrices

In order to determine the conceptual configuration, each of the configurations discussed earlier are assigned figures of merit (FOM). The FOM are based on contest requirements and restrictions, ease of construction, and aircraft performance. Once these FOM are assigned, they are weighted according to their importance. Numerical values of –1, 0 or 1 are assigned to each configuration. These numerical values are used as a rating system, where the lowest rating determines the worst performance. After researching the FOM for each configuration, the design team used weighted decision matrices to determine the final aircraft configuration.

The rated aircraft cost is an important parameter for success in this contest. In several aspects, the RAC determines the design of the aircraft. RAC is determined in the analysis of the aircraft, tail, and propulsion configurations. For these configurations investigated, the aerodynamics group assumed a constant wing area, wingspan, fuselage length, and number of battery cells and servos. To accurately determine the effects of RAC, initial sensitivity tests compared score to RAC. For a 10% increase in RAC, there is approximately a 10% decrease in score. This reference helps to determine the effect of the RAC for a certain configuration over another. The RAC was calculated using a spreadsheet method.

3.4.1 Overall Aircraft Configurations

To determine the overall aircraft configuration, certain FOM are used for screening. Takeoff distance and the ability to fit inside the storage box are considered the critical FOM. For this competition, these criteria are important for the success of the aircraft. The aerodynamics group also considered RAC as an important FOM due the affect on the overall score. To determine the RAC for the overall configuration of the aircraft, the aerodynamics group assumed a single propeller/motor assembly and a conventional tail for the canard, bi-wing, and conventional aircraft. The RAC for each configuration is as follows: Canard 9.48; Flying wing 9.28; Bi-wing 10.00; and, Conventional 9.48.

Handling qualities for each configuration were also considered. This FOM is important to consider for the pilot and overall performance of the aircraft. The figures of merit are weighted in a decision matrix given in Table 3-1. Takeoff distance and the ability to fit in the box are weighted more than the other FOM since the aircraft must complete these requirements. RAC and handling qualities are rated based on the importance of success of the aircraft. Based on the overall rating, a conventional configuration was selected for this competition.

Figures of Merit	Weighting Factor	Conventional	Flying Wing	Canard	Bi-Wing
Takeoff Distance	0.30	1	0	-1	1
Fit in Box	0.30	0	1	-1	-1
RAC	0.25	0	1	0	-1
Handling Qualities	0.15	1	-1	1	1
Total	**1.00**	**0.45**	**0.10**	**0.15**	**-0.10**

Table 3-1: Overall Aircraft Configuration Decision Matrix

3.4.2 Wing Configurations

FOM for the wing location are based on stability, payload interference, and the ease of construction. The aerodynamics group placed equal weight on each FOM since all qualities are important to the success of the aircraft. The decision matrix for the wing location is given in Table 3-2. Due to payload interference, the high-wing configuration outperformed low- ad mid-wing configurations. Overall, a high-wing configuration has better stability and construction qualities than a low- and mid-wing configuration.

Figures of Merit	Weighting Factor	High Wing	Low Wing	Mid Wing
Stability	0.33	1	-1	0
Payload Interference	0.33	1	-1	-1
Ease of Construction	0.33	1	0	-1
Total	**1.00**	**1.00**	**-0.66**	**-0.66**

Table 3-2: Wing Location Decision Matrix

3.4.3 Tail Configurations

The aerodynamics group considered the ability to fit inside the box, controllability, RAC, and ease of construction as the FOM to decide a tail configuration. Fitting in the storage box and controllability are given the most weight since both are critical to compete. RAC is important since it affects the overall score; therefore, it is also weighted highly. RAC values for the different tail configurations are determined by assuming a conventional aircraft configuration and a singe propeller/motor assembly. The RAC results are as follows: Conventional 9.48; Cruciform 9.48; T-tail 9.48; V-tail 9.38; and, Inverted V-tail 9.38.

Construction is also an important FOM since it determines the quality of the tail surface and how quickly the design can be manufactured. The decision matrix for the tail configuration is given in Table 3-3. The final decision of a conventional tail is primarily based on ease of construction.

Figures of Merit	Weighting Factor	V-tail	Conventional	T-tail	Inverted V-tail	Cruciform
Fit in Box	0.30	-1	1	1	-1	-1
Controllability	0.30	0	1	0	1	0
RAC	0.25	1	0	0	1	0
Ease of Construction	0.15	0	1	0	0	-1
Total	**1.00**	**-0.05**	**0.75**	**0.30**	**0.25**	**-0.45**

Table 3-3: Tail Configuration Decision Matrix

3.4.4 Fuselage Configurations

For the fuselage configuration, the most important figure of merit is the ability to fit inside the storage box, which is given the greatest weight. If the components do not fit inside the box, the team is penalized. Other important FOM include assembly time and ease of construction. Assembly time is critical since it determines the overall score. This FOM considers all attachments to the fuselage, which must be efficient and quick. Construction determines the quality of the fuselage and the time to manufacture the parts. Cost is important since it determines the quality of the material used. Connections of the tail to the fuselage are also considered since this determines the amount of weight needed to support the structure. To determine the fuselage configuration, the structures group constructed the decision matrix in Table 3-4. Based on the FOM, the single-boom fuselage received the best rating and was therefore selected.

Figures of Merit	Weighting Factor	Full Fuselage	Fuselage with Boom	Fuselage with Twin Boom
Fit in Box	0.50	-1	1	0
Assembly Time	0.20	-1	1	0
Ease of Construction	0.20	0	1	1
Cost	0.05	0	0	-1
Tail Attachment	0.05	1	0	0
Total	**1.00**	**-0.65**	**0.90**	**0.15**

Table 3-4: Fuselage Configuration Decision Matrix

3.4.5 Landing Gear Configurations

While selecting the appropriate landing gear configuration, the structures group considered drag and steering as the critical FOM. Reduced drag is important since it affects the performance of the aircraft, which could affect the scoring potential. Steering is important especially during Mission B after deploying the payload. Ground stability and weight of the landing gear are also important FOM. The main gear must provide enough stability to the aircraft during takeoff to prevent the aircraft from rolling. The weight of the landing gear affects the overall weight of the aircraft, which is penalized in the RAC function. The final considerations include cost and cargo clearance. The cost of the materials determines the quality of the materials. For Mission B, the landing gear must provide enough height and width to avoid the cargo

after deployment. Table 3-5 shows the decision matrix used to select the landing gear configuration. Based on these FOM, the tripod gear was selected.

Figures of Merit	Weighting Factor	Tripod	Bicycle	Quad-Wheel	Tail Dragger
Steering Ease	0.25	1	-1	0	-1
Drag	0.25	0	1	-1	1
Weight	0.15	0	1	-1	1
Stability	0.15	1	-1	1	0
Cost	0.10	0	1	-1	1
Cargo Clearance	0.10	1	-1	1	-1
Total	**1.00**	**0.50**	**0.00**	**-0.25**	**0.15**

Table 3-5: Gear Configuration Decision Matrix

3.4.6 Propulsion Configuration

The propulsion group considered RAC, power, and weight as the FOM to determine the propulsion configuration. RAC is important since it affects the overall scoring potential. The RAC is based on a conventional aircraft and conventional tail configurations. The RAC results are as follows: Single motor/propeller: 9.48; and, Dual motor/propeller: 9.68.

Power is a critical FOM since it determines whether the aircraft completes the missions. Weight is also considered since it affects the performance of the aircraft. Table 3-6 shows the decision matrix to determine the propulsion configuration. Due to the impact of RAC and weight, a single motor/propeller configuration is selected.

Figures of Merit	Weighting Factor	Single Motor/ Propeller	Dual Motor/ Propeller
RAC	0.40	0	-1
Weight	0.30	1	-1
Power	0.30	0	1
Total	**1.00**	**0.30**	**-1.00**

Table 3-6: Propulsion Configuration Decision Matrix

3.5 Final Aircraft Summary

The final aircraft design selected by the design team includes a conventional aircraft configuration with a single boom for the aft portion of the fuselage. A conventional tail and high-wing configuration is used on the aircraft. The propulsion system consists of a single-motor and single-propeller. The landing gear is a tripod design. A sketch of the final conceptual configuration is provided in Figure 3-2.

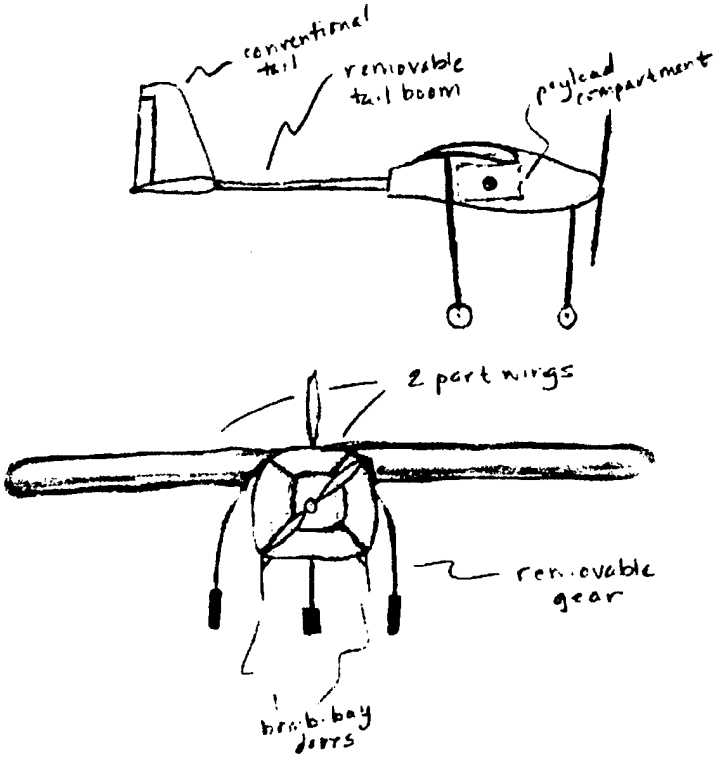

Figure 3-2: Conceptual Design Sketch

In order to decrease assembly time, the design team incorporated component features into the design of the aircraft, which include two-part removable wings, removable landing gear, removable tail boom, and bomb-bay doors to release the payload.

The wings are designed in two sections, which are secured together and assembled on top of the fuselage. The main landing gear is also removable and is secured between the fuselage and wings. In order to accommodate a fuselage length greater than four feet, the tail boom is removable. Bomb-bay doors are used to deploy the payload for Mission B. These features reduce the time for assembling the aircraft, which is critical to reduce the flight time for each mission.

4 Preliminary Design Phase

After selecting a conceptual aircraft configuration, the preliminary design phase began. The design team identified design parameters that affect the performance of the aircraft, aircraft components, and propulsion system. Sizing trades of the design parameters were also investigated by the design team. The aerodynamics and propulsion groups utilized analysis programs to determine aircraft performance. The structures group used analysis methods to analyze components based on strength characteristics. The trade studies involved the optimization of the score with respect to the design parameters. The mission performance of the aircraft was also estimated.

4.1 Design Parameters and Sizing Trades Investigated

In order to optimize the design of the aircraft, the design team investigated several design parameters and performed sizing trades. The aerodynamics group investigated the number of battery cells required, the power required for takeoff and climb, cruise velocity, wing area and wingspan. The propulsion group investigated the number and type of battery cells, the motor and propeller types. The structures group investigated the design of the landing gear, wing, boom, tail stabilizers and fuselage. These parameters were used during analysis to determine aircraft performance and features.

4.1.1 Aerodynamics Design Parameters and Sizing Trades Investigated

In order to optimize score, the aerodynamics group identified five design parameters: the number of battery cells required, power required for takeoff and climb, cruise velocity, wing area, and wingspan. The group investigated the sizing trades of these design parameters based on contest restrictions, mission requirements, and aircraft performance.

The number of battery cells was considered an important design parameter based on RAC restrictions and score optimization. Optimum power is critical in order to complete a mission. Using the maximum amount of batteries (five pounds) would give the optimum amount of power; however, the maximum battery weight does not optimize score. The score is reduced due to the RAC penalty on battery weight. Selecting an efficient motor and propeller optimizes power, reduces the number of battery cells, and reduces the RAC, which increases the score.

The second design parameter considered is the power required for takeoff and climb. Due to the runway restriction of 120 feet, a large amount of power is required during the takeoff and climb phases of the mission. Since the team must complete the mission to obtain a flight score, there must be enough power remaining after these phases. Thus, the power required to takeoff and climb must be monitored and optimized to ensure that enough energy remains to complete the mission.

Cruise velocity is another crucial design parameter investigated. The power remaining from the takeoff and climb phases must be managed during the cruise phase in order to complete the mission. This is difficult to monitor since there is substantial energy lost during the turns. Based on initial optimization, cruise velocity is sensitive to score. Therefore, it is important to determine the throttle setting that manages cruise velocity without sacrificing score.

Wing size is an important design parameter for both the aerodynamics and structures groups. Due to the runway restriction, the aircraft must have either excessive power or a substantial wing area to takeoff. Based on initial optimization, increasing the battery weight obtains a greater RAC penalty compared to

increasing the wing area. Due to the size of the storage box, the maximum size of the wing is restricted. Therefore, the RAC must be optimized between the number of battery cells and wing area.

The final design parameter investigated by the aerodynamics group was the wingspan. This parameter directly affects the aspect ratio of the wing based on a fixed wing area. A long wing has a high aspect ratio, which has a better lift distribution compared to a low aspect ratio wing. For a fixed wing area, as the wingspan decreases the RAC decreases. With a shorter wingspan, there is less difficulty fitting the wing in the storage box.

4.1.2 Propulsion Design Parameters

In order to optimize propulsive efficiency, the propulsion group investigated four design parameters: number and type of battery cells, motor and propeller types. The group investigated the sizing trades of these parameters based on contest restrictions, mission requirements, and aircraft performance.

The number of battery cells was considered an important design parameter based on RAC restrictions and power optimization. Optimum power is critical in order to complete a mission. Using the maximum amount of batteries (five pounds) would give the optimum amount of power; however, the maximum battery weight is penalized in the RAC function. Selecting an efficient motor and propeller optimizes the power and reduces the number of battery cells, which reduces the RAC.

The type of battery cells is limited to nickel-cadmium (ni-cad) cells. Battery type is an important design parameter based on the current discharge and the energy produced. Ni-cad batteries are characterized by a high current discharge. High current discharge is necessary to produce the power required for the motor. The battery cells are sized by the energy, which is rated in milli-amp hours (mah). The size is a measure of the energy produced by the battery, which determines the battery endurance and power produced.

The motor is another crucial design parameter investigated by the propulsion group. Since the group is limited to the Astro Flight or Graupner motors, the motors are investigated based on the manufacturing characteristics. The motors are characterized by the power output ranges. The power output is determined by the potential chemical energy delivered by the batteries, which is converted to kinetic energy by the motor. The motor uses the kinetic energy to provide torque to the propeller. Selecting the motor based on the power output optimizes the efficiency of the propeller. The size of the motor affects the overall RAC.

The final design parameter investigated was the propeller type. The propeller is an important design parameter based on the amount of thrust produced. The torque provided by the motor is converted into

thrust by the propeller. Therefore, propeller selection determines the thrust of the aircraft, which is used to overcome the weight and drag. The size of the propeller determines the amount of optimum thrust produced.

4.1.3 Structural Design Parameters

In order to optimize the structural design of the aircraft, the structures group investigated five design parameters: landing gear, wing, boom, tail, and fuselage. The sizing trades of these design parameters are investigated based on aircraft performance and mission requirements.

The design of the landing gear is important due to the loads it must overcome upon landing. It is important for the gear to absorb the majority of the impact, which reduces the stress at the connection to the fuselage. To absorb the impact, the landing gear must also be flexible. Since the landing gear provides stability on the runway and at takeoff, the main gear must be wide at the base.

The wing is a crucial design parameter due to the lifting characteristics. In order to produce lift, wind loads must be applied to the wing. The structure of the wing must support the wind loading and transfer it to the wing/fuselage connection. Therefore, the design of the spars is crucial for surface support. The size of the wing determines the wind loading acting on the surface. A larger wing area produces more lift based on a constant wingspan.

The boom is important since it supports the loads acting on the tail stabilizers. Based on weight penalties in RAC, the boom must be designed light in weight. It is also crucial for the boom to be rigid, which prevents drastic deflection of the tail. The boom is also crucial to the pitch stability of the aircraft. The length of the boom determines the moment arm required to overcome a destabilizing pitch moment.

The design of the tail is important due to the lifting characteristics. Lift acting on the tail determines the controllability of the aircraft. In order to produce lift, wind loads must be applied to the tail. The structure of the tail must support and transfer the loads to the boom. The design of the spars within the tails determines the strength of the surface to support the loads. The tail sizing determines the stability of the aircraft. The horizontal tail must be sized properly to overcome a destabilizing pitch moment, whereas the vertical tail overcomes a destabilizing yawing moment.

The final design parameter investigated is the fuselage. The fuselage is an important design parameter since it supports all loads transferred from other aircraft components. The fuselage must be reinforced to withstand all loads at all locations along the structure. The fuselage also houses the aircraft components and systems. The fuselage is sized based on the area needed to house the internal systems and support the aircraft components.

4.2 Analysis Methods

In order to optimize the score and analyze the propulsion system and the aircraft performance, the aerodynamics and propulsion groups used optimization codes that utilized the conjugate gradient method of analysis. Modeling the missions in these programs allowed the groups to understand the sensitivity of design parameters within each mission, thereby predicting the mission performance. Additionally, the use of an airfoil analysis program allowed the characteristics of the wing and tail to be studied. The structures group used structural analysis methods to determine the structural strength of the aircraft components. Stress estimations determine the material selection for the aircraft, which ultimately determines the construction methods.

The programs were based on the missions selected for completion at the competition. The programs maximized the scoring potential, determined aircraft performance, and optimized the propulsive system. These factors were used to develop optimization trade studies to compare the design parameters to the final score, which determined the detail design of the aircraft.

4.2.1 Airfoil Analysis

The aerodynamics group used the airfoil analysis program to determine the characteristics of the wing and tail airfoils. Due to the runway restriction, either a high-lift wing airfoil or excessive battery cells is required for the aircraft to takeoff. In order to avoid an RAC penalty due to the additional battery weight, the aerodynamics group investigated different airfoil types. Although the drag coefficient decreases for a lower-lift airfoil, the wing area must be large to meet takeoff requirements. The large area required for a low-lift wing has approximately the same total drag as a small, high-lift wing. Since a smaller wing fits inside the storage box, and a high-lift airfoil avoids excessive battery cells, the aerodynamics group decided to employ a high-lift airfoil.

The group considered several different airfoils, including the Selig 1210, Selig 1223, Wortmann FX 76MP-140, and Eppler 423. The two Selig airfoils provide excellent high-lift capabilities, but their profiles are difficult to construct due to the trailing-edge angles. The Wortmann FX 76MP-140 airfoil provides slightly less drag with decreasing lift. Therefore, the group eliminated this airfoil. The Eppler 423 provided the best compromise of high-lift capability and ease of construction.

The drawback of the Eppler 423 is the increase in the drag coefficient at lower lift coefficients. Due to the highly cambered shape, this airfoil produces high drag and pitching moments during the cruise phase. An increase in the pitching moment adversely affects the stability and stall characteristics of the aircraft. An increase in drag has two possible consequences: the propulsive power must be increased to overcome the drag, which is penalized in RAC; or, the time to complete the missions is increased, which decreases the scoring potential.

To eliminate these problems, the ailerons are designed to operate as flaps during the cruise phase. To be effective, the flaperons are analyzed to run the full span of the wing and are 25% of the wing chord. Using the airfoil analysis program, the aerodynamics group investigated the effects of the flaps during cruise. The aerodynamics group also determined the airfoil used for the horizontal and vertical stabilizers. The horizontal tail was analyzed to provide sufficient lift at a zero-degree angle of attack. Since the main wing produces a large nose-down pitching moment, the aerodynamics group needed a tail to counteract the moment. The group analyzed vertical tails that produce no lifting force. This avoids a yawing moment that acts on the aircraft.

4.2.2 Drag Analysis

Using the performance and airfoil analysis programs, the aerodynamics group estimated the drag forces acting on the aircraft. The performance analysis program is a drag prediction model that estimates the parasitic and induced drag of the aircraft. The model uses a component build-up method to estimate the drag coefficient of the aircraft.

The airfoil analysis program determined the drag coefficients for the wing and tail stabilizers. The drag polar for the Eppler 423 airfoil used on the main wing is input into the performance analysis program to account for the parasitic drag of the main wing. A flat-plate skin-friction coefficient and a form factor estimate the separation drag for the fuselage. Miscellaneous drag coefficients for the landing gear, fuselage upsweep, and interference drag are also estimated. The drag acting on the antenna is estimated by calculating the drag acting on a cylinder. Frontal area of the antenna is then normalized to the wing area.

4.2.3 Aircraft Stability Analysis

Using the stability analysis program, the aerodynamics group estimated the stability characteristics of the aircraft. The stability characteristics determine the performance of the aircraft and size the aircraft components. Longitudinal, directional, and roll stability characteristics were investigated.

First, the longitudinal stability of the aircraft was estimated. From the stability analysis program, the aerodynamics group determined the stability based on the contributions by the wing, fuselage and horizontal tail. The stability analysis program helped determine the curve slope of the pitching moment coefficient with respect to angle of attack ($C_{m\alpha}$). For longitudinal stability, $C_{m\alpha}$ must be negative. The longitudinal stability analysis was used to estimate the trim point of the aircraft. Increasing or decreasing the angle of attack at trim increases the drag on the aircraft during the cruise phase. Therefore, the group determined that a trim angle of approximately zero degrees angle of attack is desired.

The static margin for the aircraft is also determined in the stability analysis program. The static margin determines whether the aircraft produces a restoring moment when perturbed from a stable condition. Therefore, the aerodynamics group determined that a positive static margin was necessary.

Stability analysis was used to determine the directional stability of the aircraft. Contributions by the wing, fuselage, and vertical tail were determined in the analysis. The stability analysis program was used to determine the curve slope of the yawing moment coefficient with respect to the sideslip angle ($C_{n\beta}$). In order to have directional stability, $C_{n\beta}$ must be positive.

Roll stability analysis was also determined for the aircraft. The major contribution to roll stability is the dihedral effect of the wing. Due to the high-wing configuration of the aircraft, some dihedral effect is present without adding a dihedral angle to the wing. Using the stability analysis program, the dihedral effect due to the wing placement is calculated to determine the roll stability of the aircraft.

4.2.4 Aircraft Control Sizing Analysis

Based on the stability analysis results, the aerodynamics group used the stability analysis program to size the control surfaces. The control characteristics determine the volumes of the control surfaces. If the control surfaces are properly sized, the aircraft demonstrates good stability characteristics.

In order to provide longitudinal stability and control, the horizontal tail and elevator require proper sizing. The stability analysis program sized the horizontal tail and elevator to counteract any destabilizing pitch moment. The airfoil analysis program also calculated the hinge moment produced by the elevator upon deflection. The aerodynamics group also sized the vertical tail and rudder to provide directional stability and control for the aircraft. The stability analysis program sized the vertical tail and rudder to counteract any destabilizing yaw moment. The hinge moment of the rudder was calculated using the airfoil analysis program. To provide adequate roll stability and control, the wings and the flaperons require proper sizing. Using the stability analysis program, the aerodynamics group sized the wings and flaperons to counteract any destabilizing roll moment. Using the airfoil analysis program, the hinge moment acting on the flaperons is estimated.

4.2.5 Motor Analysis

The propulsion analysis program was used to evaluate the most efficient motor. Using information gathered from the manufacturers, the propulsion group included the following motors in the selection process: Astro Flight Cobalt 640, 640G, 640S; Astro Flight Cobalt 661, 661S; and, Graupner Ultra 3450-7. Each motor is capable of operating at the higher-performance levels necessary to complete the selected missions. These motors provide a sufficient amount of power to the propeller in the single-

engine, single-propeller configuration. In order to achieve an optimum selection, the propulsion group compared performance, size, weight, and economic feasibility.

In order for the aircraft to complete the mission and achieve an optimum score, the aerodynamics group required a takeoff and climb battery power between 790 and 1100 Watts with a takeoff thrust of five pounds. Using this information as a foundation, the propulsion group commenced its selection process by placing each motor's respective operating characteristics into the propulsion subroutine. The subroutine then furnished the group with the current and shaft power produced by each motor.

4.2.6 Battery Analysis

The next component of the propulsion system analyzed was the batteries. The batteries require a high energy density along with a high current discharge to accomplish the mission. Three different battery providers were researched including SR Batteries, Panasonic, and Sanyo. Battery selection was based on the type used by past teams, turnaround time, optional pack shapes, and matched and packaged packs. The next consideration included the number of battery cells to ensure the best possible score on both missions. The contest rules allow up to five pounds of batteries. Analysis was used to determine the best possible score in conjunction with the optimum propulsive performance. The propulsion group also considered the capacity of the batteries. The two viable options from SR Batteries are the 2400 and 3000 milliamp-hour (mah) classes. Performance was based on optimization analysis performed by the aerodynamics group. Analysis was based on estimates using the 2400 class, adjusted for losses.

4.2.7 Propeller Analysis

Finally, the propulsion group analyzed propellers for use in the propulsion system. The group modeled different propeller types in the propulsion analysis programs. The program determined propeller efficiencies, which estimated the performance of the propellers in the optimization program. Based on performance estimates using the Astro Flight motor, the group narrowed the propeller choices.

4.2.8 Main Gear Analysis

To analyze the stress and deflection, the main gear was modeled as a cantilevered beam. Using this method, the necessary loads and appropriate gear geometry was calculated (Raymer 1999). Gear geometry facilitates the functional needs of other aircraft components, including the clearance of the aircraft to accommodate the payload deployment, the propeller, and the tail upon landing.

The height of the landing gear is based on an estimated angle of attack on landing of 13°. The main gear must be far enough behind the center of gravity (c.g.) that the aircraft does not lose stability after takeoff. The gear placement was found by assuming a 15° angle of takeoff. The wheel spacing was then found based on the overturn angle in order to allow adequate ground control (Raymer 1999). The forces that

the landing gear must withstand were also calculated. The vertical load was found by multiplying the weight of the aircraft (approximated as 20 pounds) by the loading safety factor of 3. The largest horizontal load that the gear sees is due to the spin-up on the wheels when the aircraft first touches down. This force is estimated as half the vertical force.

4.2.9 Nose Gear Analysis

The nose gear was also analyzed using cantilever beam analysis. Based on theory, the nose gear is designed to support no more than 20% of the weight of the aircraft. Upon landing, the height of the nose is designed shorter than the main gear to prevent the nose gear from touching down before the main gear. The type and diameter of the nose gear tires is determined by the brakes selected.

The structures group analyzed four possible braking methods, including pneumatic, hydraulic, electro-mechanical, and mechanical. These choices were analyzed in a decision matrix based on weight, size, braking force, cost, ease of attachment, and balance of force. Weight is an important FOM based on the penalty of aircraft weight in the RAC. The size of the brakes is also important since it dictates how the aircraft fits inside the storage box. Braking force is necessary to determine the benefits of time reduction affecting the scoring potential. The cost of the brakes is considered due to the overall quality of the brakes. Construction of the brakes is important to consider for the manufacturing time. Balance of force is the last FOM, which considers the distribution of the force and how it affects the braking force.

4.2.10 Wing Analysis

The design of the wing and wing spars is based on the wing loading due to takeoff. To support the bending loads of the wing, various sizes of spar tubing were analyzed. The deflection of the spar was limited to one inch. The structures group analyzed one- and two-spar configurations at the quarter chord of the wing.

4.2.11 Analysis of the Wing/Fuselage Connection

Design of the wing and fuselage connection is based on a shear-stress analysis. Upon landing, the connection of the wing and landing gear to the fuselage incurs the most stress. Due to the rotation of the landing gear, a shearing force is applied at the connection joint.

4.2.12 Tail Boom Analysis

The boom was analyzed to ensure that it withstands certain applied stresses. The external forces on the tail boom include a gravitational force, hinge moments acting on the control surfaces, and normal wind forces acting on the boom, tail stabilizers, and control surfaces. The size of the boom is based on a maximum vertical deflection of no more than one inch.

The connection of the boom to the fuselage is analyzed to determine the stress at the connection points. A connection of one and two bulkheads was analyzed to determine which method was more effective. If only one bulkhead were used, the loads would be applied on the bulkhead, which would induce stress at that location. Inserting the boom through two bulkheads provides additional structural support against the loads applied on the boom.

4.2.13 Tail Stabilizer Analysis

The design of the tail stabilizers was based on the stress analysis of the spars. Since most of the loading on the stabilizers occurs during landing, the spars are design for these loads. To support the bending loads of the stabilizers, various sizes of spar tubing were analyzed. The deflection of the spars was limited to one inch. The majority of the stress is concentrated at the location where the spar intersects the boom. The structures group analyzed the connection of the spar at this location. Wind and lift loads and moments created by the deflection of the control surfaces were estimated and used in the analysis.

4.2.14 Fuselage Analysis

In order to determine the design of the fuselage, analysis of the structure must be investigated. The analysis was based on six bulkheads placed throughout the fuselage interior. One bulkhead is placed at the most forward and aft locations of the fuselage. Two bulkheads surround the c.g. location, identified by the aerodynamics group. This surrounds the payload and payload system. One bulkhead is placed both six inches behind the nose and six inches ahead of the aft section.

The assumed loads acting on these bulkheads are analyzed. The forward-most bulkhead supports the loading of the propeller and motor, whereas the second bulkhead supports the nose gear. The center bulkheads provide support for the wing and landing gear mounting and payload deployment system. Here, the ultimate loading is concentrated in the fuselage. The aft two bulkheads carry the loading transmitted from the boom.

4.3 Mission Modeling

The aerodynamics group used an optimization program to model each of the three missions, which determined the scoring potential for each. The propulsion group used a propulsion analysis program to model the propulsion systems during the missions. Based on mission performance of the aircraft from the aerodynamics group, the necessary power and time of each flight phase is modeled in the program. This determines if the motor, propeller, and battery configurations can complete the missions. The necessary power for each phase also determines the throttle setting required to overcome the drag in the cruise phases.

4.3.1 Mission A

To model Mission A, the following inputs are used in the aerodynamic optimization program: payload weight including the weight of the antenna and an estimation of the additional drag caused by the antenna. The Eppler 423 airfoil is also modeled in the program with and without flaps to determine its effect on the scoring potential. Takeoff, climb, and cruise are crucial flight phases due to the additional weight and drag.

4.3.2 Mission B

To model Mission B within the aerodynamic optimization program, the time to takeoff, climb, descend, and land is doubled. After two laps are complete, the weight of the payload is removed due to payload deployment. The Eppler 423 is also modeled in this mission to determine the effect on scoring potential. The obstacle in this mission is to manage the power during takeoff and climb, which are most critical flight phases for this mission.

4.4 Optimization Trade Studies Performed

After analyzing the aircraft performance and modeling the missions, the aerodynamics and propulsion groups used the optimization program to evaluate the sensitivity of score and RAC with respect to the design parameters. Since the optimization program only outputs the local maximums for the aircraft performance, the global maximum was solved graphically. As shown in Figure 4-1, the score and RAC are plotted versus the individual design parameters.

4.4.1 Study of Number of Battery Cells Required

The number of battery cells is investigated to determine the effects of battery weight on the aircraft performance and propulsive efficiency. Figure 4-1 shows the range of battery cells compared to score and RAC. As demonstrated, RAC increases linearly as the number of cells increase. Due to this factor, the score decreases as cell number increases. Based on the required power approximated from the propulsion analysis program, an initial range of 18 to 24 battery cells is required to complete the mission. After further analysis the propulsion group, determined 22 cells account for any losses and are sufficient to complete the missions. Since this cell range does not greatly affect the scoring potential or aircraft configuration, the final selection of 22 battery cells was justified.

4.4.2 Study of Power Required for Takeoff and Climb

The power required during takeoff and climb is investigated to determine the maximum power available for these flight phases. As shown in Figure 4-1, the power range required is compared to the score. Further analysis compared the scoring range to the optimal power and number of batteries required. Overall, there is a 19% change in score over the entire range of required power for takeoff and climb. The scoring potential for the number of battery cells compared to the scoring potential for the power required is only a 4% difference. Since the scoring loss is negligible, the propulsion team justified the use

of the highest power output from the propulsion system. Based on the optimization program, the aerodynamics group determined the maximum power available is 968 Watts.

4.4.3 Study of Cruise Velocity Required

Cruise velocity is investigated to determine the optimal thrust setting during the cruise phase. For all missions, it is necessary to regulate the thrust in order to decrease the time and optimize score. Figure 4-1 shows the relationship between score and cruise velocity. There is an optimum velocity based on score, where exceeding 70 ft/s decreases the score. This velocity does not necessarily indicate the optimum velocity. Based on the optimization analysis program, cruise velocity determines the amount of power used during the cruise phase. If the cruise velocity exceeds the amount of energy allowed for the cruise phase, the aircraft cannot complete the mission, which results in a flight score of zero. Comparing the cruise velocity to the available cruise power determines an optimum cruise velocity of 60 ft/s for Mission A and 65 ft/s for Mission B.

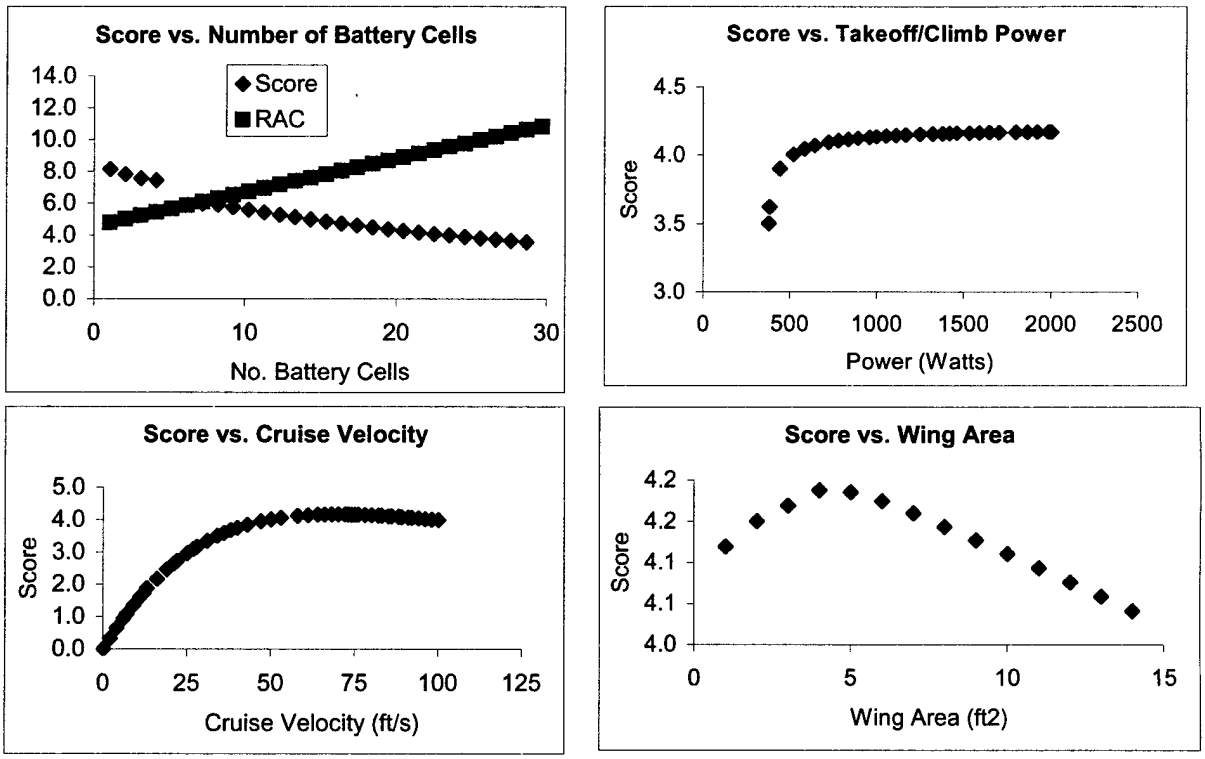

Figure 4-1: Optimization Trade Study of Score Versus Design Parameters

4.4.4 Study of Wing Area Required

The wing area is investigated to determine the size of the wing required to complete the missions and fit inside the box. Using the optimization analysis program, initial optimization showed a wing area range of 8 to 12 square feet. Figure 4-1 shows the score compared to wing area. There is an optimization

tradeoff between wing area and number of batteries. Since there is only a 2% change in score over the range of wing area compared to a 62% change in score over the range of battery cells, then optimizing for the number of battery cells and compromising wing area is justified. Based on the number of battery cells required to complete the missions, a wing area of 8.75 square feet is justified.

4.4.5 Study of Wingspan Required

The wingspan is investigated to determine the size of the wing required to complete the missions and fit inside the box. Since there is negligible change in score and RAC due to wingspan, the wingspan is based on the optimum number of battery cells. Due to the 22 battery cells required to complete the missions, a wingspan of 7.75 feet is justified.

4.5 Analysis Results

The performance of the aircraft in each mission is based on the analysis performed and the optimization of the design parameters. First, the aerodynamics group estimated the airfoil and stability performance based on the optimum wing area and wingspan. The propulsion group predicted the performance of the optimum number of battery cells with the optimum motor and propeller configuration. These parameters determined the final design of the aircraft.

4.5.1 Aerodynamic Analysis Results

Using the airfoil analysis program, the aerodynamics group investigated the effects of the flaps during cruise. When deflected upward 10 degrees, the flaperons provide a change in angle of attack of approximately 5 degrees, a drag coefficient reduction from 0.040 to 0.013, and a moment coefficient reduction from –0.23 to –0.14. Therefore, the flaperons provide a 67.5% reduction in drag during the cruise phase, which is desirable. Based on the performance analysis, the power required during the cruise phase is reduced by 9%. Therefore, the aircraft cruises 10 ft/s faster at the same power setting. Figure 4-2 shows the drag polars for the Eppler 423 with flaps up and flaps down.

Based on data from the airfoil analysis program, the aerodynamics group also selected a horizontal and vertical tail airfoil. For the horizontal tail, the NACA 1409 cambered airfoil was selected. This airfoil provides sufficient lift at a zero-degree angle of attack compared to a symmetric airfoil, which requires a negative angle of attack. Since the main wing produces a large nose-down pitching moment, the aerodynamics group decided to invert the airfoil. This provides a downward force on the tail, which counteracts the nose-down pitching moment created by the wing. For the vertical tail, the group decided to use a NACA 0006 airfoil. This airfoil is a symmetric airfoil, meaning it has no camber. Since this airfoil is symmetric, there is no lifting force acting on the airfoil, which could produce a yawing moment.

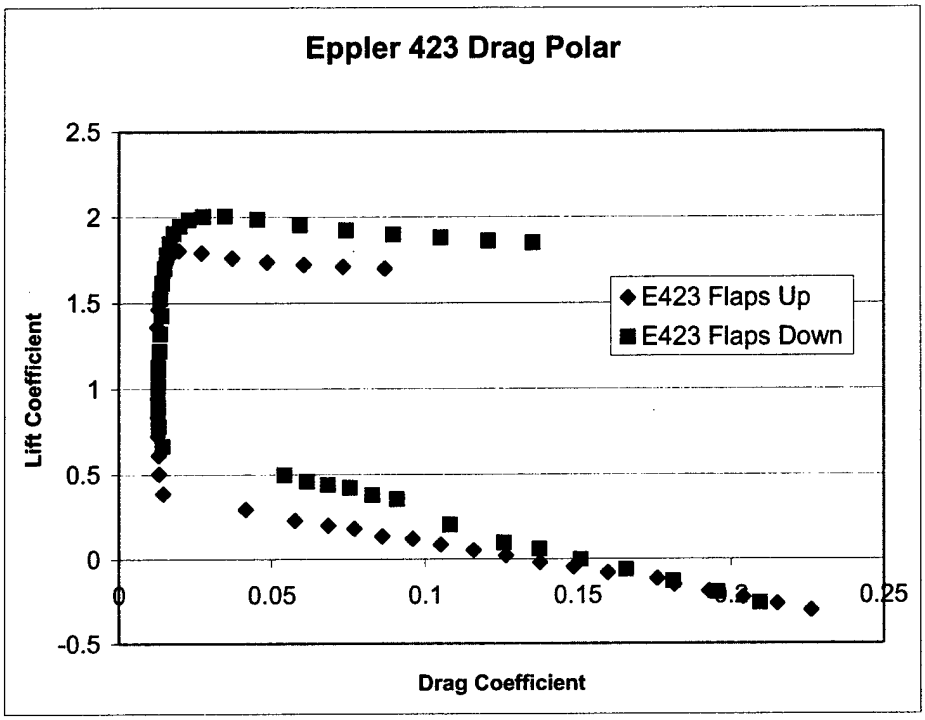

Figure 4-2: Drag Polar Comparison for Eppler 423

Using the performance and airfoil analysis programs, the aerodynamics group estimated the drag forces acting on the aircraft. Table 4-1 shows the contribution of each component to the total parasitic drag of the aircraft. Based on the drag analysis, the drag for Mission B is less than the drag for Mission A. This is due to the additional drag provided by the antenna in Mission A. Analysis of the drag governs the optimal analysis of the propulsion system.

Skin Friction Drag					
	Horizontal Tail		**Vertical Tail**		**Fuselage**
Characteristic Length (in)	12		12		60
Skin Roughness (in)	2.04E-05		2.04E-05		2.04E-05
Reynolds Number	400000		400000		2000000
Wetted Area (ft^2)	3		1.5		10
Skin-Friction Drag Coeff.	0.007		0.0058		0.0064
Form Factor	0.942		0.942		1.628
Interference Factor	1.05		1.05		1
Reference Area (ft^2)	8.75		8.75		8.75
Normalized C_d	0.0024		0.00099		0.00731
Miscellaneous Drag					
Wing	**Nose Gear**	**Fuselage Upsweep**	**Wheels**	**Antenna**	**Main Gear**
1.00E-02	8.90E-04	1.23E-02	1.80E-03	2.00E-02	1.80E-04
Total Parasitic Drag					
Mission A:	**0.056**			**Mission B:**	**0.036**

Table 4-1: Aircraft Drag Estimates

Using the stability analysis program, the aerodynamics group estimated the longitudinal, directional, and roll stability characteristics of the aircraft. Based on the analysis of the longitudinal stability, the aerodynamics group determined that the aircraft was inherently longitudinally stable. The stability analysis program estimated the wing and fuselage contribution to be overall destabilizing, whereas the horizontal tail is stabilizing. Since the horizontal tail contribution is greater than the wing and fuselage contribution, the aircraft is longitudinally stable.

The stability analysis program helped determine the curve slope of the pitching moment coefficient with respect to angle of attack ($C_{m\alpha}$). Table 4-2 shows the individual contribution of $C_{m\alpha}$ for wing, fuselage and horizontal tail, and the overall longitudinal stability of the aircraft. The longitudinal stability characteristics of the aircraft also determined the static margin of the aircraft, which was estimated as 18%. The aerodynamics group estimated the trim point of the aircraft at just over zero degrees angle of attack. Trimming at zero degrees angle of attack eliminates any excess drag on the aircraft during cruise.

Analysis of the directional stability determined that the aircraft was directionally stable. Based on the stability analysis program, the wing and fuselage contributions are overall destabilizing. Since the vertical tail provides directional control, the stabilizing contribution is greater than the wing/fuselage contribution. The stability analysis program determined the curve slope of the yawing moment coefficient with respect to the sideslip angle ($C_{n\beta}$). Table 4-2 shows the overall directional stability of the aircraft based on the individual contributions from the wing/fuselage interaction and vertical tail.

Stability Moment Coefficients					
	Wing	**Fuselage**	**Horizontal**	**Vertical**	**Aircraft**
$C_{m\alpha}$	0.149	0.002	-0.77		-0.619
$C_{n\beta}$	-0.014			0.053	0.039
$C_{l\beta}$	-0.033				-0.033

Table 4-2: Stability Moment Coefficients

Analysis of the roll stability determined that the aircraft is inherently roll stable. Due to the high-wing configuration of the aircraft, some dihedral effect is present without adding a dihedral angle to the wing. Using the stability analysis program, the dihedral effect due to the wing placement is calculated and found to be adequate for roll stability without any added dihedral angle. Table 4-2 shows the roll moment coefficient of the overall aircraft with respect to dihedral angle, $C_{l\beta}$, which is based primarily on the contribution of the wing dihedral.

Based on the stability analysis results, the aerodynamics group used the stability analysis program to size the control surfaces. The stability analysis program sized the horizontal tail and elevator to counteract any destabilizing pitch moment. The airfoil analysis program also calculated the hinge moment produced

by the elevator upon deflection. Assuming a velocity of 90 ft/s at a Reynolds number of 300,000, the elevator is deflected twenty degrees. The resulting hinge moment was 49.1 oz-in.

The aerodynamics group used the stability analysis program to size the vertical tail and rudder, which provides directional stability and control for the aircraft. The size the vertical stabilizers counteracts any destabilizing yaw moment. The airfoil analysis program was used to calculate the hinge moment of the rudder, assuming a velocity of 75 ft/s at a Reynolds number of 300,000. Deflecting the rudder twenty degrees results in a hinge moment of 13.54 oz-in.

To provide adequate roll stability and control, the wings and the flaperons require proper sizing. The flaperons are sized large since they operate during the cruise phase, which provides enough roll control. Using the airfoil analysis program, the hinge moment acting on the flaperons is estimated. Assuming a velocity of 82 ft/s at a Reynolds number of 300,000, the flaperons are deflected upward ten degrees. Due to the large size, the resulting hinge moment is 141 oz-in.

4.5.2 Propulsion Analysis Results

Based on the optimization trade studies performed, the propulsion system is optimized for the number of battery cells. The aerodynamics group determined the best score with the minimum amount of power comes from 18 battery cells. Propulsion analysis indicated that the 18 cells do not provide the four pounds of takeoff thrust required by the aerodynamics group, which results in no score if the aircraft cannot complete the mission. It was decided that up to a 10% reduction in score was acceptable between 20 and 22 battery cells; the difference is a 4% reduction. Using 22 battery cells is therefore justified since it provides the additional performance necessary to complete the missions. For the propulsion system, the batteries require a high-energy density along with a high-current discharge to accomplish the missions.

The propulsion analysis program was used to evaluate the most efficient motor. Motor analysis was based on the Astro Flight 640 and 661 series and the Graupner 3450-7 motors. In order to complete the missions, the group observed that the shaft power must be between 650 and 750 Watts. From the published power ratings, each motor is capable of producing a sufficient amount of power or more, except the Cobalt 640 with a power rating of 600 Watts. Even though the Astro 661 and 661S have power rating ranges from 900 to 1200 Watts, the subroutine demonstrated that these two motors did not operate near the power rating since the power ratings for these motors are greater than what is necessary for the missions. Each motor operated near or below the maximum current allowed by the fuse, except the Astro 640. The Astro 640 exceeded the 40-amp rating of the fuse with a current of 75 amps. This current burns the fuse in a matter of seconds, which results in the aircraft not completing the missions. The Astro 640G operated nearest to the 40-amp rating.

Finally, the propulsion group analyzed propellers for use in the propulsion system. Based on performance estimates using the Astro Flight motor, the group narrowed the propeller choices. The possible propellers demonstrated enough takeoff thrust, power for cruise, and a reasonable flight velocity. Other propellers required more battery cells to increase efficiency and performance. Currently, the propeller analysis includes theoretical modeling in the propulsion analysis program. The propulsion group will initiate testing with the different propellers to establish actual performance constraints.

4.5.3 Structural Analysis Results

The main gear was analyzed based on cantilever beam analysis. The height of the landing gear (measured from the ground to the top of the fuselage) needed for tail clearance was approximated as 11.5 inches. However, this height does not allow enough clearance for the payload. The height needed for payload deployment is estimated as 14.5 inches with an 8-inch tall fuselage. The estimated distance behind the c.g. is 3.5 inches. A wheel spacing of twelve inches was within the 63° limit based on theory. The forces that the landing gear must withstand were also calculated. The vertical load was calculated as 60 pounds. The largest horizontal load that the gear sees is a 30-pound horizontal force.

The nose gear was also analyzed as a cantilever beam. To prevent support of 20% of the weight of the aircraft, the nose gear is placed 13 inches ahead of the c.g. of the aircraft. The height of the nose gear extends 6.5 inches from the bottom of the fuselage. Upon landing, this prevents the nose gear from touching down before the main gear. The type and diameter of the nose gear tires is determined by the brakes selected. The tire size ranges from a 2.5- to a 3.5-inch diameter; the types of tires are either solid or inflatable.

The possible braking methods analyzed included pneumatic, hydraulic, electro-mechanical, and mechanical. The choices were analyzed based on weight, size, braking force, cost, ease of attachment, and balance of force. These FOM are weighted to determine the most reliable and efficient option. Based on the analysis of the FOM, the pneumatic and electro-mechanical brakes scored equally. The strongest advantage to these options is the quick assembly time. The configuration of the plane is designed such that either pneumatic or electro-mechanical brakes can be placed on the aircraft. Further analysis and testing was performed to determine the final braking method. Based on the time to stop and the braking force the pneumatic brakes were selected.

The design of the wing and wing spars is based on the wing loading due to takeoff. To support the bending loads of the wing, various sizes of spar tubing were analyzed. The deflection of the spar was limited to one inch. The structures group analyzed one- and two-spar configurations at the quarter chord of the wing. A two-spar configuration provided added resistance against wing rotation and deflection. The group also noted that a two-spar design weighed less than a one-spar design for the same deflection

load. This is due to the reduction in diameter size for the two spars compared to one. Based on this analysis, the tubing for these spars has an outer diameter of 0.440 inches and an inner diameter of 0.375 inches.

Design of the wing and fuselage connection is based on a shear-stress analysis. Upon landing, the connection of the wing and landing gear to the fuselage incurs the most stress. Due to the rotation of the landing gear, a shearing force is applied at the connection joint. Based on the analysis, a breakaway connection is used at the junction of the wing and fuselage to prevent damage to either component. Based on the testing of the breakaway connection, which simulated the force acting at the connections, this method is justified. At the connection point, the wing is reinforced with several ribs and the fuselage is reinforced with extra plies.

The boom was analyzed to ensure that it withstands certain applied stresses. Based on the analysis, a lightweight tube with a 0.8-inch outer diameter was selected as the tail boom. The size is based on a maximum vertical deflection of no more than one inch. The connection of the boom to the fuselage is analyzed to determine the stress at the connection points. Since two bulkheads would provide additional structural support against applied loads, using two bulkheads at the boom connection is justified.

The design of the tail stabiiizers was based on the stress analysis of the spars. The spars were analyzed at the location where the spar intersects the boom. Based on a limited deflection of one inch, a 0.25-inch diameter spar provides enough strength and resistance against deflection.

The design of the fuselage was based on the analysis of the structure. In order to provide support, the use of six bulkheads placed throughout the fuselage interior is justified. One bulkhead is placed at the most forward and aft locations of the fuselage. Two bulkheads surround the c.g. location where the payload and payload system is located. Two bulkheads are located 6 inches from the front and aft sections of the fuselage.

Based on the weight of the propulsion system and ultimate thrust provided by the system, the forward-most bulkhead provides the structural support for this loading. Since the nose gear is designed to support no more than 20% of the aircraft weight, the second bulkhead for the gear is designed to support the load. The center bulkheads provide support for the wing and landing gear mounting and payload deployment system, where the ultimate loading is concentrated in the fuselage. Therefore, these bulkheads are reinforced to withstand the forces. Based on the analysis of the boom, two bulkheads must be used to support the loading on the boom.

4.6 Predicted Aircraft Performance

Based on the aerodynamic, propulsive and structural results of the analysis and optimization, the aircraft performance is predicted. The performance is based on aerodynamic and propulsive parameters, such as the sizing of the aircraft and the efficiency of the propulsion system. These parameters are provided by the aerodynamic and propulsive groups. The predicted performance is shown in Table 4-3.

Performance Parameters	Mission A	Mission B	Units
Takeoff Thrust	8.5	8.5	lbf
Takeoff Distance	113	45	ft
Climb Velocity	42	40	ft/s
Rate of Climb	7.3	12.5	ft/s
Climb Angle	9.8	17.4	degrees
Cruise Velocity	60	65	ft/s
Cruise Power	341.9	349.5	Watts

Table 4-3: Predicted Aircraft Performance

The aerodynamics and propulsion groups estimated the takeoff and climb parameters including the takeoff thrust, takeoff distance, climb velocity, rate of climb, and the climb angle. These parameters were estimated using an Astro Flight 640 series motor, a 15-inch propeller, and 22 battery cells. The cruise velocity and power was estimated to determine the final motor and propeller needed based on propulsion testing.

5 Detail Design Phase

The detail design phase was used to determine material selection for the aircraft components. Material selection was based on the aircraft analysis performed in the preliminary design phase. The final rated aircraft cost was determined based on the component selection. The aircraft geometry, performance data, weights, and systems used were determined.

5.1 Systems Architecture and Component Selection

Systems architecture determines the final design of the component or system based on preliminary analysis. Component selection establishes the required materials for the manufacturing of the aircraft. The structures group designed and selected materials for the landing gear, wings, wing/fuselage connection, boom, tail stabilizers, fuselage, payload release system, and antenna mounting system. Based on propulsion analysis, the propulsion group determined the component selection of the batteries, motor, propeller, and radio controller. The aerodynamics group selected servos for the control surfaces.

5.1.1 Main Gear

The main gear is constructed as a bow extending down from the top of the fuselage. The gear is connected below the wing through bolts protruding from the fuselage, which also connects the wing down onto the landing gear. In order to prevent the main gear from rotating about the plane of the bolt connections, the landing gear has a tab located between the two bolts. This tab transmits the loads from the landing gear into the fuselage, instead of the wing. Therefore, the fuselage location underneath the tab is reinforced to withstand the compression load.

5.1.2 Nose Gear

Based on this analysis, a typical mousetrap configuration is selected for the nose gear. Research of previous teams showed that either spare nose gear were used or it was purchased from a manufacturer. Based on the intricacies of constructing nose gear, the structures group decided to purchase the gear. Overall, this selection saves time during manufacturing.

5.1.3 Wing

Based on the analysis of the wing, the aircraft requires a total wingspan of 7.75 feet and wing area 8.75 square feet. Structurally, the wingspan is divided into two sections, each 3.875 feet in length, which allows the wing sections to fit inside the storage box. Structural support against bending and twisting is provided by the spars. The spars also double as a connection for the two wing sections. For each wing, an outer spar is fitted along the span. In order to connect the wings, a second shaft inserts inside the existing spar. A tab is attached to the inner shaft to prevent it from sliding too far into the spars.

The hinge system for the flaperons is provided by two arrow shafts. The outer shaft is placed along the hinge line of the flap except at the location of the flap. A smaller shaft is used as the pin on the hinge, which is attached to the flaperon. This hinge system was selected for its strength, which is necessary since the flaps are raised during cruise. The movement of the flap is driven by a servo mounted on a rib at the center of the wing section, which prevents uneven deflection of the control surface. Since the servo is more effective using a pulling force, it is mounted on the topside of the wing. An access hatch approximately 2-inches by 2-inches is constructed to mount and access the servo. Quick-connect plugs are used to connect the wiring from the servos to the battery supply.

5.1.4 Wing/Fuselage Connection

Ensuring precision of assembly means utilizing techniques that only allow proper alignment of components. In order to accomplish the alignment of the wing and fuselage, the wing airfoil shape is cut into the top and side panels of the fuselage molds. The fuselage forms a lip over the leading edge of the wing, which reduces drag at the connection. The lip is made separate from the fuselage to prevent damage from perpetuating throughout the fuselage.

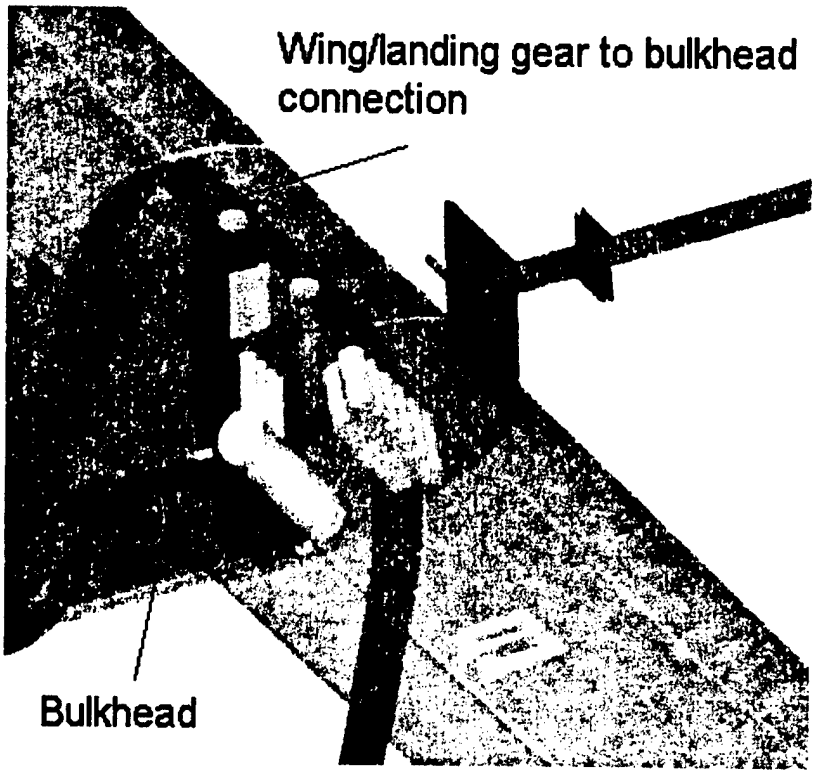

Figure 5-1: Wing and Landing Gear and Boom Connection to Fuselage

The leading edge of the wing is fitted with two nylon bolts that fasten inside the fuselage. This connection secures the front of the wing sections. Another set of nylon bolts is anchored to the bulkhead behind the payload and extrudes from the top panel of the fuselage. During assembly, the landing gear and wing section slide over these bolts, which extrude on the topside of the wing as shown in Figure 5-1. A pin is inserted through holes aligned in the bolts, which secures the wing sections to the fuselage. Based on the bending analysis of the wing connections, the inboard wing sections require reinforcement with several ribs and strengthened skin. The bolt connections are sized based on testing performed with the landing gear.

The structures group considered electrical connections that would not increase assembly time. Therefore, electrical plug-ins between the wing and fuselage were considered. Wires from the servo in each wing lead to a plug-in connection at the bottom of the wing. When the wing is placed onto the fuselage, the plug-in connects to a jack receiver on the fuselage. The jack is connected to the receiver and batteries. This connection is reliable and easy to assemble.

5.1.5 Boom

The material selected for the boom was based on the flight loads acting on the tail stabilizers and ease of construction. Since the tail stabilizers and boom are connected permanently, attaching the tail was important. In order to accomplish this, the structures group determined that the spars for the stabilizers

could be integrated into the boom, which doesn't jeopardize the connection to the boom. In order to support the flight loads on the stabilizers, the boom material was selected as a carbon fiber tube.

In order to attach the tail boom to the fuselage, a "twist-lock" method is used. This method uses a loose tube-within-a-tube interference fit. Based on the structural analysis, the boom has an outer diameter of 0.8 inches. To connect to the fuselage, the outer diameter of the boom shaft slides within a tubular receptacle with an inner diameter of 0.8 inches located at the rear of the fuselage. The tube receptacle is held secure by two bulkheads.

The inner bulkhead has two opposing one-sixteenth-inch diameters, with ¼-inch long pins protruding into the receptacle tube. The bulkhead has a spring mechanism that opposes the axial motion of the boom into the fuselage receptacle. The boom shaft has a one-sixteenth-inch diameter "J" notched into the tube wall at the insertion end; the pins of the bulkhead slide into the notch of the boom. The boom is then twisted to lock its axial and rotational motion.

5.1.6 Tail Stabilizers

Based on the bending analysis, the horizontal and vertical tail stabilizers use carbon fiber tubing for the spars. In order to carry the loads acting on the stabilizers and control surfaces, the spars are located at the quarter chord of the airfoil sections. A 0.25-inch by 24-inch long spar passes horizontally through the boom to provide support for the horizontal tail; a second spar passes vertically through the boom to support the vertical tail. The servos for the control surfaces are mounted to ribs at the center of the stabilizers. Quick-connect plugs are used to connect the wiring from the servos to the battery supply.

5.1.7 Fuselage

Drag was considered when deciding between a rectangular or round cross-sectional fuselage. The fuselage drag estimated by the aerodynamics group was based on a conventionally shaped fuselage design. The group determined that the potential differences in drag between the two cross-sectional styles were negligible. Thus, the decision was based on ease of construction. A rectangular cross-section was selected for the fuselage to improve the ease of construction and reparability.
After completing the analysis, the aerodynamics group determined the sizing of the fuselage based on stability. The main fuselage was 36 inches in length with the c.g. 18 inches from the nose of the aircraft. Based on preliminary sizing of the payload release system, the frontal dimensions of the fuselage body were 7-inches wide by 8-inches tall. In order to size the fuselage and place the components, Pro-Engineer drawings were rendered, which determined the final sizing of the fuselage dimensions based on internal component sizing. Pro/E was also used to estimate the weight and c.g. of the aircraft.

Since the payload is the dominant component of the aircraft, this system drives the fuselage design. In order to retain the same c.g. location before and after payload deployment, the payload is placed at the c.g. Therefore, the cargo bay is placed in the middle of the fuselage. The fuselage is designed to be wider in the middle and tapers both forward and aft. A bulkhead is placed on either side of the payload to reduce the stresses caused by aerodynamic and landing gear loading and structural weight.

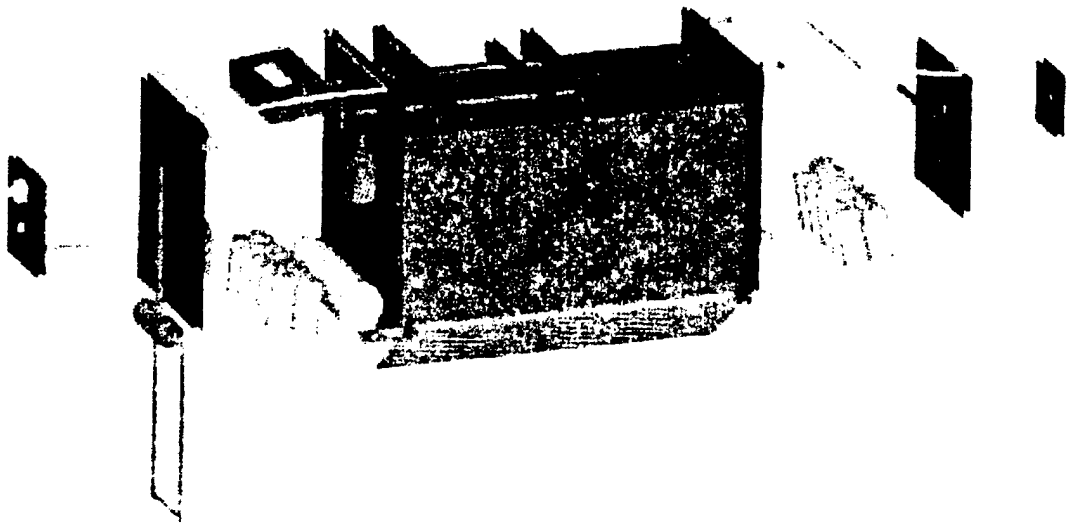

Figure 5-2: Fuselage Design Details

The exterior shape of the fuselage is defined by the propulsion system, payload system, and tail boom connections, based on preliminary sizing. For support, the motor needs a 3-inch by 3-inch mounting surface, the payload system needs two 8-inch by 7-inch bulkheads surrounding the c.g., and the boom needs a 2-inch by 2-inch bulkhead for support. Figure 5-2 shows the preliminary fuselage design, which displays the interior bulkheads.

Based on the placement of the propulsion system, payload system, and boom, the placement of the surrounding bulkheads was determined. One bulkhead was set five inches back from the nose of the aircraft to provide a mounting surface for the nose landing gear. The last bulkhead is positioned four inches from the rear of the fuselage based on calculations of the bending moment created by the boom. The remaining bulkheads surround the interior systems. The space forward and aft the payload compartment is reserved for propulsion batteries. This arrangement adjusts the c.g. if necessary to trim the aircraft. The remaining components are placed on bulkheads or the fuselage ceiling as necessary. Figure 5-2 shows the fuselage assembled with the interior components.

5.1.8 Payload Release System

The payload release system was designed based on the size of the payload and restricted fuselage size. The payload is restrained at the c.g. of the aircraft by two bulkheads forward and aft of the payload location. These bulkheads are designed to provide minimal clearance around the sides of the payload, which reduces payload shifting in flight and aids in payload deployment.

In order to eject the payload, a quick and simple trigger system was necessary. Different trigger systems include floor-, side- or top-mounted. Since the payload is deployed from the bottom of the fuselage, a top-mounted design was selected. This type of mounting is space efficient and locates the deployment system above the payload and at the center of gravity.

Two tabs are mounted to the top of the payload. Two one-fourth-inch rods slide into the payload-mounted tabs to vertically support the payload. Frame-mounted tabs directly in front of the payload tabs also support the two rods. The payload-mounted tabs are enclosed on both the forward and aft side by frame-mounted tabs. This assembly ensures an unintended deployment does not occur. The support rods extend forward through each of these tabs and through the bulkhead. To release the payload, a trigger is actuated by a servo that pulls the support rods one-fourth inch horizontally out of the payload-mounted tabs. Nylon is placed on sliding surfaces to prevent frictional forces.

Cargo-bay doors are used to secure the payload in the vertical direction. The doors are hinged on the interior side of the fuselage and are spring-loaded in the closed position. When the payload is released, it deploys against the doors, which causes them to open. Once the payload deploys, the doors return to the closed position by spring force.

5.1.9 Antenna Mounting System

Mounting the antenna used in Mission A became a critical issue. The structures group decided to mount the antenna below the payload area. The cargo-bay doors are removed to connect the antenna to the aircraft for Mission A. The antenna-mounting plate uses the same mounting locations as the doors. To remove the door, the hinge pins slide out of the guides. The antenna is mounted using the hinge guides to secure it in place.

5.1.10 Motor

Motor selection was based on component weight, price, technical service availability, and gear ratio used. Component weight is considered due to the adverse impact of weight on the RAC. The price of the motor determines the quality and reliability of the motor performance. Technical service is required to efficiently correct any problems with the motor performance. Gear ratio must be properly sized to prevent over-driving the motor. As determined by the aerodynamics and propulsion teams, the Astro Flight 640S

provided the required power to complete the missions. The price of the motor was acceptable based on the performance output. Since the manufacturer is within the United States, technical service for the motor is satisfactory. The gear ratio was rated as a 3.1-to-1.0 ratio.

The design selection was based on producing a sufficient amount of power while keeping the overall size and weight of the motor at a minimum. A comparison of the size and weights of each motor is shown in Table 5-1. If only basing the selection on size and weight, the table shows that the size and weight of the Astro 640 series are far below that of the Astro 661 series and Graupner 3450. Since the Astro 640 does not produce the sufficient amount of power, the Astro 640G and 640S prevail in this comparison. Another aspect of the design is the cost of each motor, also provided in Table 5-1. From the information shown, the Astro 640 prevails over its counterparts but it does not produce the amount of power necessary for the mission; therefore, the Astro 640S is desirable. In addition, the Astro 661 series and Graupner incur an elongated lead-time compared to that of the Astro 640 series.

	Length (in.)	Diameter (in.)	Volume ($in.^3$)	Weight (ounces)	Power Rating (Watts)	Cost ($)	Delivery Time (weeks)	Tech Support
Astro								
640	2.75	1.68	6.1	15	600	149.95	4 to 6	California
640G	3.75	1.68	8.31	15	750	199.95	4 to 6	California
640S	3.75	1.68	8.31	16	1000	209.95	4 to 6	California
661	3	1.68	6.65	22	900	249.95	4 to 6	California
661S	4	1.68	8.87	25	1100	309.95	4 to 6	California
Graupner								
3450-7	3.93	1.96	11.93	28	672	450	4 to 6	Germany

Table 5-1: Motor Properties and Cost

By comparing the data, the optimum motor selection for the propulsion group is the Astro 640S, as shown in Table 5-1. The 640S provides the shaft power necessary for thrust during takeoff, weighs much less than most of the other motors in the field, and has a cost much less than the other models.

The propulsion system contains other components necessary for proper function. The aircraft speed is managed using a speed controller. Fuses are needed to regulate current through the motor. In order to measure the power expended from the battery, the propulsion group will use a wattmeter during the prototype testing. The team is also using no-loss connectors and high-gauge wire to prevent energy loss through heat. Extra pinion gears are required for the gearbox, since gears strip-out on occasion.

5.1.11 Propeller

Based on performance estimates using the Astro Flight motor, the group narrowed the propeller choices. The possible propellers demonstrated enough takeoff thrust, power for cruise, and a reasonable flight

velocity. Other propellers required more battery cells to increase efficiency and performance, which were therefore eliminated. Based on propulsion testing, the propulsion group selected 15-inch propeller, which provides the power and thrust to complete the missions.

5.1.12 Batteries

The propulsion group also selected the type and configuration of the batteries based on the number of batteries required in the propulsion analysis. Three different battery providers (SR Batteries, Panasonic, and Sanyo) were researched and SR Batteries was chosen for the following reasons:

- **History:** Previous teams have been satisfied with the performance of both the batteries and the company.
- **Quick turn-around time:** Orders placed with the company arrive quickly, making it less critical that all of necessary battery packs be ordered at once.
- **Versatile pack shapes:** The company offers various battery shapes, and they are willing to work with OSU teams to achieve the optimum shape.
- **Matched and packaged packs:** The cells are tested, matched, and packaged at the factory, which eliminates the need for exhaustive testing here in the lab to form matched packs.

The propulsion group also considered the capacity of the batteries. The aerodynamics group performed optimization estimates using the 2400 class, adjusted for losses, and were able to meet the mission objectives. The 2400 class also has a higher energy density, smaller size and weight, and costs less per mah. Due to these factors, the SR 2400 class of batteries was chosen.

Based on the number of battery cells required by optimization, the 22 cells were divided into two packs of 11 cells. Space was designed in the fuselage to allow movement of the propulsion battery packs, which adjusts the c.g. of the aircraft. The battery packs are placed on either side of the payload box to balance the aircraft. The SR 2400 batteries are packaged in the required number of batteries for easy handling and charging. The battery packs are secured with Velcro to facilitate repositioning needs.

5.1.13 Radio

To control the aircraft, a Futaba 8UAPS radio controller is selected. This controller offers the versatility of eight control ports. Flaperon control is also possible with the Futaba through programming of the signals. Since the RC pilot is familiar with this controller, there are fewer control mistakes.

5.1.14 Servos

After estimating the hinge moments produced by the control surfaces, the aerodynamics group determined the servos necessary. Servo selection is based on torque rating, manufacturer, response speed, size, and weight. It is important to match the torque rating of the servo to the required torque of

the control surface. For convenience and cost reduction, the design team preferred purchasing all servos from the same manufacturer. Response speed for a servo is critical to consider. A servo with a smaller response speed rating is preferred. Size and weight are considered due to aircraft performance.

For the flaperons, a 200 oz-in servo was selected, primarily based on response speed and weight. Compared to a servo with a torque rating of 150 oz-in, the 200 oz-in servo had a greater response speed and weighed 0.05 ounces less. The servos for the elevator and rudder were primarily selected based on manufacturer, response speed, size and weight. It was preferred to purchase these servos from the same manufacturer as the flaperon servos. The torque ratings for the elevator and rudder were 55 and 32 oz-in, respectively. These servos offered the smallest size and reduced weight compared to other servos of comparable torque ratings.

5.2 Final Rated Aircraft Cost

Configuration decisions finalized in the preliminary and detail design phases determine the final RAC of the prototype aircraft. The pie chart of Figure 5-3 shows the RAC breakdown of the aircraft based on each contributing component. It is observed that the majority of the RAC is based on battery weight, which is 46%. Another contributor to the overall RAC is empty weight (15%), which also includes the weight of the batteries. Since battery weight greatly affects RAC, it adversely affects the overall scoring potential. Therefore, optimizing for the battery weight is crucial. The RAC value is determined by each aircraft component and tabulated in Figure 5-3. It is observed that the RAC is governed by the battery weight and empty aircraft weight. Based on this data, optimizing for the battery weight is justified.

5.3 Aircraft Performance Parameters and Details

For the final aircraft design, the sizing, weight and performance of the aircraft, including the systems used, is provided in Table 5-2 (a) through (d), respectively. The aircraft geometry and performance is based on aerodynamic, stability, and propulsive analysis and optimization. The weight of the aircraft is based on structural composition of components and component systems. The systems used in the aircraft are based on weighted FOM used during component selection.

The aerodynamics group sized the aircraft geometry in conjunction with the propulsion group. Based on the number of batteries used in the propulsion system, the aerodynamics group optimized the wingspan and area. Stability and control analysis was used to size the fuselage and control volumes. The group also determined the aircraft performance parameters based on the propulsion system and some aerodynamic parameters. The maximum lift coefficient was estimated using the performance analysis program, as well as the maximum lift-to-drag ratio. The maximum rate of climb is based on the propulsive thrust available during the climb phase. Stall speed occurs at the maximum lift coefficient. Therefore, stall speed was estimated during the landing phase of flight. Maximum speed was determined as the

MANUFACTURERS EMPTY WEIGHT					
Aircraft empty weight with batteries (lbs)				Multiplier	Weighted MEW
15.09				0.1	**1.509**
RATED ENGINE POWER					
Total Battery Weight (lbs)	**Number of engines**		**REP**	**Multiplier**	**Weighted REP**
2.9	1		2.9	1.5	**4.35**
MANUFACTURING MAN HOURS					
Component	**Hour/unit**	**Aircraft Value**	**Aircraft MFHR**	**Multiplier**	**Weighted MFHR**
Wing WBS					
Span (ft)	8	7.750	62.000	0.02	1.24
Chord (ft)	8	1.129	9.032	0.02	0.18
Control Surface	3	2.000	6.000	0.02	0.12
Fuselage WBS					
Maximum length (ft)	10	5.25	52.5	0.02	1.05
Empennage WBS					
Vertical surface w/o controls	5	0	0	0.02	0.00
Vertical surface w/controls	10	1	10	0.02	0.20
Horizontal surface (less than 25% wing span)	10	1	10	0.02	0.20
V-tail	15	0	0	0.02	0.00
Flight System WBS					
Servo or motor controller	5	7	35	0.02	0.70
Propulsion System WBS					
Engine	5	1	5	0.02	0.10
Propeller or fan	5	1	5	0.02	0.10
TOTAL WEIGHTED MFHR					**3.89**
RATED AIRCRAFT COST					**9.749**

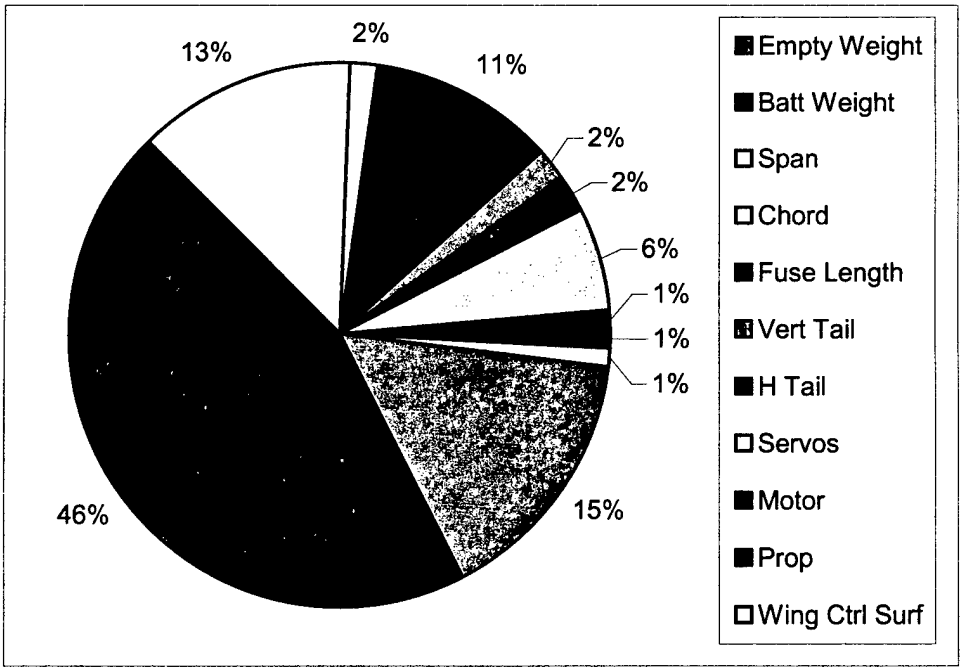

Figure 5-3: Final Rated Aircraft Cost Breakdown

fastest velocity for either mission, where the aircraft still completes the mission. Takeoff distance was estimated in the optimization program.

Aircraft Geometry		
	Fuselage	
	Length	5.25 ft
	Height	8 in
	Wing	
	Span	7.75 ft
	Area	8.75 ft^2
	Aspect Ratio	6.86
	Control Volumes	
	Flaperons	0.485 ft^3
	Elevator	0.175 ft^3
	Rudder	0.047 ft^3

(a)

Weight Statement		**Pounds**
	Airframe	1.55
	Propulsion System	4.13
	Control System	0.91
	Payload System	0.25
	Payload	5.00
	Empty Weight	10.96
	Gross Weight	21.09

(b)

Aircraft Performance		**Empty Weight (15.09 lb)**	**Gross Weight (21.09 lb)**
	C_{Lmax}	1.22	1.22
	L/D_{max}	7.176	7.176
	Maximum Rate of Climb	14.55 ft/s	7.34 ft/s
	Stall Speed	27.93 ft/s	33.71 ft/s
	Maximum Speed	65.00 ft/s	62.25 ft/s
	Takeoff Field Length	33.38 ft	106.91 ft

(c)

Systems	**Component**	
	Radio	Futaba 8UAPS
	Servos	Airtronics
	Battery Configuration	22 Cells
	Motor	Astro Flight 640S
	Propeller	Bolly 15
	Gear Ratio	1.31:1

(d)

Table 5-2: Aircraft (a) Geometry, (b) Weight, (c) Performance, (d) Systems

The weight of the aircraft was based on the airframe, component systems, and payload. Due to the structural complications, the weight of the aircraft was more than expected for the prototype. The design team determined that weight could be decreased in several components for the final aircraft. The propulsion, control, and payload systems will remain the same approximate weight for the final aircraft. Based on the component selection, the aircraft systems were selected based on weighted FOM.

5.4 Drawing Package

Detail drawings are provided in the last five pages of this document.

6 Manufacturing Plan

In order to complete the manufacturing process, different construction methods were analyzed to determine the most efficient manufacturing plan. Each manufacturing process used certain figures of

merit to analyze the construction method. Analytic methods were used to determine the cost, skills required to construct the part, and scheduling of the process. Based on these criteria, the final manufacturing process was determined for the landing gear, wings, tail stabilizers, and fuselage.

6.1 Manufacturing Processes Investigated and FOM Considered

The design team investigated manufacturing processes for the landing gear, wings, tail stabilizers, and fuselage. Certain figures of merit were used to evaluate the most efficient manufacturing plan for each component.

6.1.1 Landing Gear

Based on the analysis, the structures group determined that main gear constructed of carbon fiber provides strength and durability. Therefore, the group considered two options for the selection of the landing gear, which included purchasing or manufacturing the gear. Purchased gear does not require any time to manufacture, whereas manufactured gear is custom fit to the design. Research of previous teams showed that the main gear was manufactured by the design team.

6.1.2 Wings

Different construction materials were investigated for the manufacturing of the wing sections. Historically, previous teams used carbon fiber with a blue foam core due to the strength characteristics. However, this competition places more emphasis on weight than in the past, which eliminates blue foam that increases the weight. To select a wing construction, the design team used weight, strength-to-weight ratio and ease of construction as the FOM.

To determine strength-to-weight characteristics, several mock wings were built and tested. Of the construction materials tested, the structures group preferred either the white foam with fiberglass or the balsa sheet with Monokote. Based on the testing results, there is only an 8% increase in structural wing weight using a white foam wing with fiberglass instead of a balsa wing with Monokote. Using the balsa/Monokote construction method requires more construction time due to the numerous ribs required to provide structural support. The strength-to-weight ratio for the white foam with fiberglass is greater than the balsa/Monokote construction.

6.1.3 Tail Stabilizers

The selection of the tail stabilizer material was based on the selection of the wings, since the structures group wanted to use the same construction material. Therefore, the same FOM are used to analyze the construction methods.

6.1.4 Fuselage

For the construction of the fuselage, there were three material possibilities: carbon fiber/nomex sandwich, fiberglass, and balsa wood. The FOM considered for material selection was weight, strength, and availability of materials. Researching past competitions, teams used a carbon fiber/nomex sandwich process, which requires less internal structure to support flight loads than the fiberglass or balsa wood construction materials. The strength-to-weight ratio for the carbon fiber/nomex also outperforms fiberglass and balsa wood. The material is available to the design team since the design studio has carbon fiber in stock. Balsa wood and fiberglass would need to be purchased.

6.2 Analytic Methods Used

Based on the FOM used to select the construction method, other analytic tools were used such as cost, skills required to construct the component, and scheduling of the process.

6.2.1 Cost

Cost was considered when selecting a manufacturing plan for the aircraft components. Cost is an important FOM since it determines the finished quality of the component. Cost was considered initially when the design team chose to manufacture the landing gear. Based on past competitions, teams designed and constructed the landing gear to meet the aircraft design. Due to these considerations, it is more expensive to have a manufacturer produce custom-made landing gear. Therefore, cost was based on the material needed to manufacture the gear. Since the team had carbon fiber already in stock, there was no cost associated with construction. Based on cost, the design team selected to manufacture the gear.

The cost of the wings was considered based on the required materials. The team first determined which materials were available at the design lab. In order to construct the white foam wings with fiberglass, all materials would need to be purchased, including the spars. For the balsa/Monokote wings, both construction materials would also need to be purchased. Therefore, the cost of the materials is considered. The white foam/fiberglass wings would cost more due to the quality of the foam; balsa sheets are relatively inexpensive and can be purchased in bulk. Therefore, the balsa/Monokote construction method is cheaper. The cost of the tail stabilizers is considered in the same manner as the wings.

The cost of the fuselage is determined by the materials available. As discussed above, the design lab had carbon fiber and nomex available in the lab; the fiberglass and balsa wood would need to be purchased. Therefore, it is most cost effective to use a carbon fiber/nomex sandwich for the fuselage.

6.2.2 Skills Matrix

The design team evaluated the complexity of the various construction methods. The skills matrix shown in Table 6-1 was developed to analyze the construction process and scheduling. Each manufacturing process was rated by the skills required to complete the operation. The more highly skilled operations are scheduled early in the construction process to allow time for completion.

The skills matrix shows that the fuselage and wings are the most crucial components for manufacturing. Therefore, more time is needed to complete these components. The skills matrix determined which design team members would construct certain parts based on previous experience.

Major Aircraft Components	Mold Preparation	Foam Cutting	Composite Lay-up	Electrical Work	Pro/E Drawings
Landing Gear	1	0	1	1	2
Wing	1	1	2	2	2
Tail Stabilizers	1	1	2	2	2
Fuselage	2	1	2	2	2

High Skills = 2 Average Skills = 1 No Skills = 0

Table 6-1: Skills Matrix

6.2.3 Manufacturing Schedule and Milestones

In order to complete the manufacturing of the prototype, a manufacturing schedule and milestone chart was assembled. The first major milestone was to identify supplies needed and available suppliers. Next, a planned work schedule was identified with start and completion dates for each aircraft component. The manufacturing schedule was based on the skills matrix, which determined the most crucial construction components. Therefore, the wings and fuselage are scheduled first to allow time for completion. The deadlines were charted using a Gantt chart as seen in Figure 6-1. The major components were assigned to personnel capable of completing each task. The figure also documents the actual completion dates of each milestone required for the prototype.

6.3 Manufacturing Processes Selected

Based on the FOM and analytic methods used for screening, the manufacturing processes for the aircraft components were selected.

6.3.1 Main Landing Gear

Since carbon fiber material was available, the design team chose to manufacture the main gear. The main landing gear was constructed of several plies of carbon fiber. The bow-type arrangement was shaped from a foam mold using a hot-wiring method and Masonite templates. Historically, teams have used a lay-up of approximately 25 layers with equal layers in the 90° and 45° directions. Therefore, this same lay-up process was used for the main landing gear. The landing gear is cured and holes are drilled

to mount the wheels. Commercially available tires were purchased based on shock absorption and friction coefficients.

Task	Duration (days)
Identify Needed Supplies	4
Identify Suppliers	4
Build Foam Molds	1
Cut Foam	1
Construct Fuselage	5
Construct Main Wings	3
Construct Tail Section	3
Construct Landing Gear	5
Install Electrical Components	1
Install Propulsion System	1
Prototype Construction	16

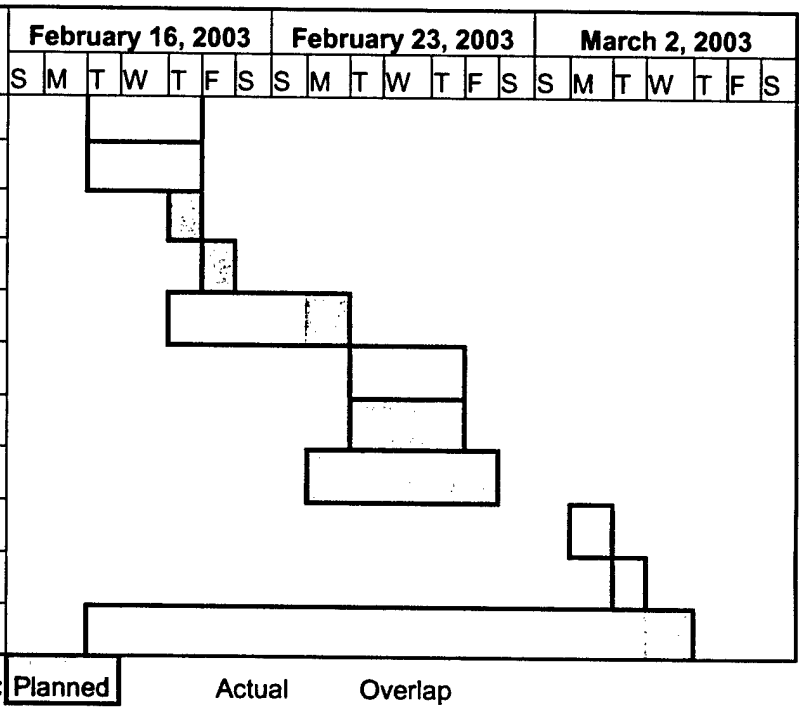

Figure 6-1: Manufacture Gantt Chart

6.3.2 Wings

The wing sections were constructed from a foam hot-wiring method using Masonite templates to outline the airfoil shape. Balsa wood is cut into the complementary airfoil shape and placed at the wing tips, center of the half span, and at the connection to the fuselage. The inboard portion of the wing is constructed of several ribs bonded together, which provides strength at the connection. Spars are imbedded into the foam before the fiberglass is added. A wet lay-up process is used to bond the fiberglass to the foam. This process requires a 24-hour curing time. After curing, the location of the servo is cut out of the wing. The servo is then mounted to the center rib.

6.3.3 Tail Stabilizers

The tail surfaces were constructed in a similar manner as the wings utilizing white foam and fiberglass. Carbon fiber arrow shafts acting as spars were imbedded in the foam before the fiberglass was added and cured. The spars are secured by placing the spars through the boom and applying Epoxy adhesive to the location.

6.3.4 Fuselage

The fuselage was constructed using carbon fiber skin with a nomex core. The actual manufacturing process consisted of female foam molds that were hot-wired using Masonite templates that outline the desired shape. The carbon fiber was layered over the nomex in a sandwich. The desired surface finish was obtained using surface coatings and vacuum pressure during curing times. The molds produced four panels that were mated together to form the rectangular fuselage structure. The bulkheads internal to the fuselage were also constructed of a carbon fiber/nomex sandwich. The bulkheads were notched, plugged into the exterior walls, and secured by epoxy adhesive. This forms the solid structure that supports the wing and landing gear.

7 Testing Plan

In order to determine the reliability of the aircraft and component systems, a testing plan was developed. The objective for testing the design and component systems was to determine if the aircraft and component systems were designed accurately and were reliable. A full-scale prototype aircraft was constructed to test the performance of the braking system, propulsion system, and aircraft during taxi and flight. The overall objective of the testing is to determine if improvements or change is necessary for the design. Observation and results of the aircraft testing were recorded to form conclusions of the prototype aircraft. Based on the conclusions, changes and improvements will be performed on the final aircraft design to ensure mission success.

7.1 Brake Testing

In order to determine the necessity of a braking system for the aircraft, brake testing was performed. Two braking systems were tested, which determined if pneumatic or electro-mechanical brakes were necessary. The objective was to determine the differences in stopping time and braking force.

7.1.1 Testing Objectives and Procedures

Two braking systems were tested to determine if pneumatic or electro-mechanical brakes were optimal for the aircraft. The objective of the testing was to determine the differences in stopping time between the two braking systems. To perform the tests, a wooden mockup of the fuselage was constructed with the nose and main gear installed. A series of tests were performed including pneumatic brakes on the main gear, pneumatic and electro-mechanical brakes on the nose gear, and no brakes on either gear. The testing procedure was conducted by pushing the rig, actuating the brakes, and measuring the time to stop. This procedure is repeated several times for each braking method at various weights. Based on this procedure, the velocity and braking force are estimated, which is used to select the braking method. Brake testing was scheduled during the prototype construction.

7.1.2 Testing Results and Conclusions

The braking method is selected based on the time to stop and the braking force. Table 7.1 shows the percent reduction in time, percent change in RAC and the estimated score reduction for each braking method tested. Based on the testing results, the design team determined that pneumatic brakes are more beneficial than electro-mechanical brakes. The pneumatic brakes were selected for the main gear instead of the nose based on the added reduction in time, which decreases the score, and the percent change in RAC, which is less than the other braking methods.

7.2 Breakaway Connection Testing

In order to determine the effectiveness of the breakaway nylon bolts connecting the wing and landing gear to the fuselage, the design team performed testing. The objective of the breakaway testing is to determine if the nylon bolts can withstand the force upon landing. The bolts should be designed to fail if a loading is applied that is greater than the loading during landing.

7.2.1 Testing Objectives and Procedures

The objective of the breakaway testing is to determine if the nylon bolts can withstand the force upon landing. The bolts should be designed to fail if a loading is applied that is greater than the loading during landing. The nylon breakaway connections used for the wing, landing gear and fuselage connection point are tested by mounting the landing gear to a mock-up of the fuselage. Two tests are performed to simulate the loading on the connection pins. For the first test, weight is steadily applied to simulate the force acting at the connection. The weight where the connection fails is the ultimate strength of the breakaway connection. The connections must support the ultimate force upon landing before failing. The second test is a drop test where the landing gear is dropped from a height of four inches. For each drop test, weight is added to simulate the structural weight, the empty weight, and the gross weight of the aircraft. The breakaway connections must support the impact upon landing of the gross aircraft weight, but should shear away with an applied load greater than the expected landing load. The nylon bolts are tested at quarter- and half-inch diameters.

7.2.2 Testing Results and Conclusions

The nylon breakaway connections were tested until failure. The first test steadily applied weight until the bolts failed. The half-inch diameter bolts did not shear until 60 pounds were applied. The quarter-inch diameter bolts sheared at an applied loading of 45 pounds. Since the bolts must withstand a loading of 40 pounds upon landing, the quarter-inch diameter bolts performed to the advantage of the breakaway design. The second test dropped the landing gear from a height of four inches. For each drop test, weight is added to simulate the structural weight, the empty weight, and the gross weight of the aircraft. Both bolts withstood the gross weight of the aircraft upon landing. Since the bolts performed to the

advantage of the design for both tests, the design team selected quarter-inch nylon bolts to use as the breakaway connections.

7.3 Propulsion Testing

Propulsion testing included static and dynamic wind tunnel testing on different propeller sizes, the Astro Flight 640S motor and on the endurance of 22 battery cells. The objective of the propulsion testing was to determine the selection of the propeller, optimize the motor performance, and estimate the battery endurance.

7.3.1 Testing Objectives and Procedures

The objective of the propulsion testing was to estimate the battery endurance, determine the selection of the propeller, and optimize the motor performance. The testing procedures were performed in the wind tunnel laboratory. A test stand set-up the propeller into the oncoming flow with the motor and batteries connected. Estimations of the mission times at the specified velocities were used to evaluate the performance of the batteries, motor and propellers. The testing evaluated the battery endurance needed for the cruise phase to successfully complete the missions. Twenty, twenty-two and twenty-four battery cells were tested. Testing of the motor and propeller determined the efficiency of the propulsion system. The performance of the different propellers was measured in combination with the motor to determine the most efficient thrust based on the number of battery cells selected. The propulsion team investigated three propeller sizes including 14-, 15-, and 20-inch propellers.

7.3.2 Testing Results and Conclusions

Based on the number of battery cells selected in the preliminary phase, the propulsion group determined that 22 battery cells provided enough power to complete the missions. The batteries were also tested for endurance and observed that more power was available than originally estimated in the analysis. Therefore, the batteries were supplying enough power for the cruise phase. The Astro Flight 640S motor showed excellent performance to produce enough torque for the propeller. Based on the performance of the different propellers with the motor, the results of the testing showed that a 15-inch propeller was suitable to provide enough thrust based on the number of battery cells selected.

7.4 Taxi Testing

Taxi testing was important to check system responses and ground stability before flight-testing. The objective was to ensure that the system controls were responding appropriately. Propeller mounting and ground stability was also tested.

7.4.1 Testing Objectives and Procedures

The objective of taxi testing was to check system responses and evaluate the ground stability before flight-testing. The remote control responses were tested by deflecting the control surfaces. This ensures accurate remote responses by the system. Next, the response of the servos was tested. This determines the response speed of the servos due to a remote command. Accurate deflection of the control surfaces during flight is desired. Proper mounting of the propeller is also tested by setting the motor the full throttle and checking the stability of the propeller rotation. Finally, the aircraft was tested during taxi. This was performed to determine if the aircraft had enough ground stability for maneuvering. Taxi testing was scheduled the day before flight-testing. This ensured that all systems were operational before flight and allowed enough time to correct any problems.

7.4.2 Testing Results and Conclusions

The remote control responses of the aircraft were tested by deflecting the control surfaces. Based on the accurate deflection of all control surfaces, the remote control responses were determined to be functional. The response of the servos was also tested. A problem was discovered with the rudder servo, which the design team assumed was a stripped ball bearing. Accurate deflection of the control surfaces was observed by the design team during the servo testing. The stability of the propeller was properly mounted based on the stability of the propeller during full throttle testing. After checking the functionality of the aircraft systems, the aircraft was tested during taxi. The results showed that the aircraft demonstrated excellent ground stability during taxi. Based on the taxi testing results, the design team concluded that the rudder servo would be replaced to ensure proper control.

7.5 Flight Testing

Flight-testing was utilized to determine the performance of the propulsion system and aircraft and evaluate the stability and control characteristics of the aircraft. The objective was to determine the stability of the aircraft after takeoff, during flight and upon landing and the efficiency and endurance of the propulsion system.

7.5.1 Testing Objectives and Procedures

The objective of the flight-testing was to determine the stability of the aircraft after takeoff, during flight and upon landing. Aircraft flight-testing was also used to determine the efficiency of the propulsion system. A wattmeter was installed to determine the power used during a single lap. The stability characteristics were observed during flight and control characteristics were determined by the pilot. Based on these tests the design team could determine any refinements necessary for the final aircraft. The testing was scheduled to begin immediately after the prototype testing of the braking system, breakaway connections, propulsion system, and taxiing. The objective of flight-testing was to determine the flight capabilities of the aircraft and refine components as observed.

7.5.2 Testing Checklists

In order to prepare for the flight-testing, a checklist was developed to outline necessary items for the design team. A departure and arrival checklist was used to organize the design team before and after the flight-testing. Prior to leaving the design studio, the design team developed a departure checklist for flight-testing to ensure that all components and tools necessary were available. The structures and propulsion groups assembled specific toolboxes with specialized tools and parts for the individual systems. The aerodynamics group prepared analysis sheets to record performance characteristics of the aircraft during flight-testing. The departure checklist was detailed as follows:

- Fully charge propulsion batteries and spare packs.
- Fully charge radio and flight-control batteries.
- Perform flight control operational check.
- Ensure braking system is fully charged.
- Bring cones and flags for course.
- Bring toolboxes and spare parts.
- Bring performance analysis sheets.

In order to prepare for flight-testing, an arrival checklist was developed. Upon arrival at the runway, the following tasks must be completed by the design team before flight-testing commences:

- Check that connections are secure.
- Connect battery packs.
- Perform flight-control operational checks.
- Set up course and station observers around the course.

7.5.3 Testing Results and Conclusions

Flight-testing was utilized to determine the performance of the propulsion system and aircraft and evaluate the stability and control characteristics of the aircraft. The testing determined that the stability of the aircraft after takeoff, during flight and upon landing was exceptional. The pilot reported that the aircraft was well balanced and easy to control. The efficiency of the propulsion system was also determined during flight-testing. The wattmeter was inspected after each flight to determine the power used and available power. After successfully completing one lap, the wattmeter displayed enough power to complete mission and perform more competitively. The stability characteristics were observed by the design team and pilot during flight. The design team observed good stability characteristics. The pilot reported excellent stability and control. Based on these tests, the design team determined that the analysis and design of the aircraft was successful.

8 References

Boucher, Robert J., "Electric Motor Handbook," Astro Flight, Inc., Los Angeles, CA, 1994.

Nelson, Robert C. Flight Stability and Automatic Control, Second Edition. McGraw-Hill, Boston, 1998.

Raymer, Daniel P. Aircraft Design: A Conceptual Approach, Third Edition. AIAA Education Series, Reston, VA, 1999.

Sribnick, Larry, "SR R/C Techniques," SR Batteries, Inc., Volume R-2, Bellport, NY, 1997.

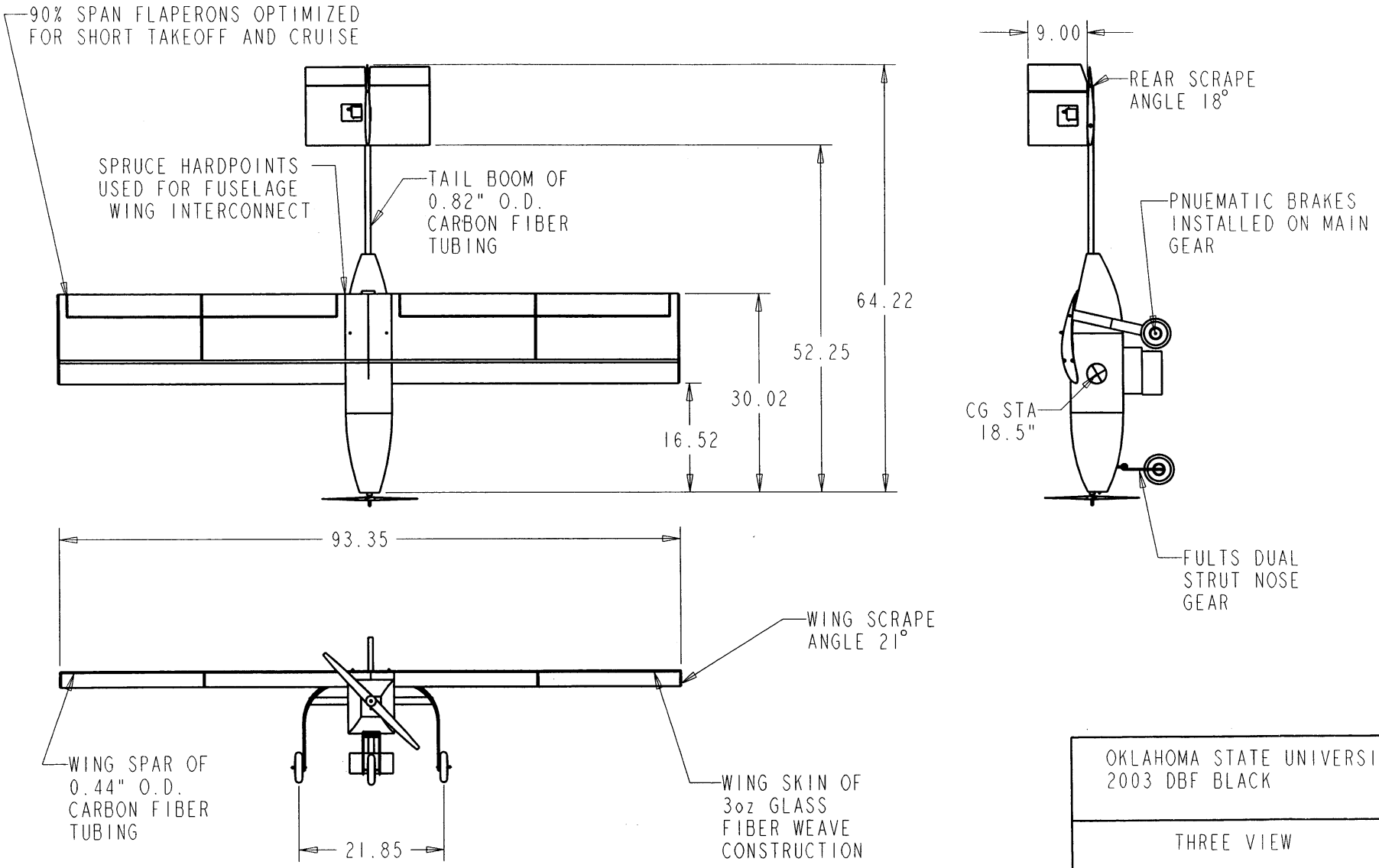

OKLAHOMA STATE UNIVERSITY
2003 DBF BLACK

THREE VIEW

3-10-03

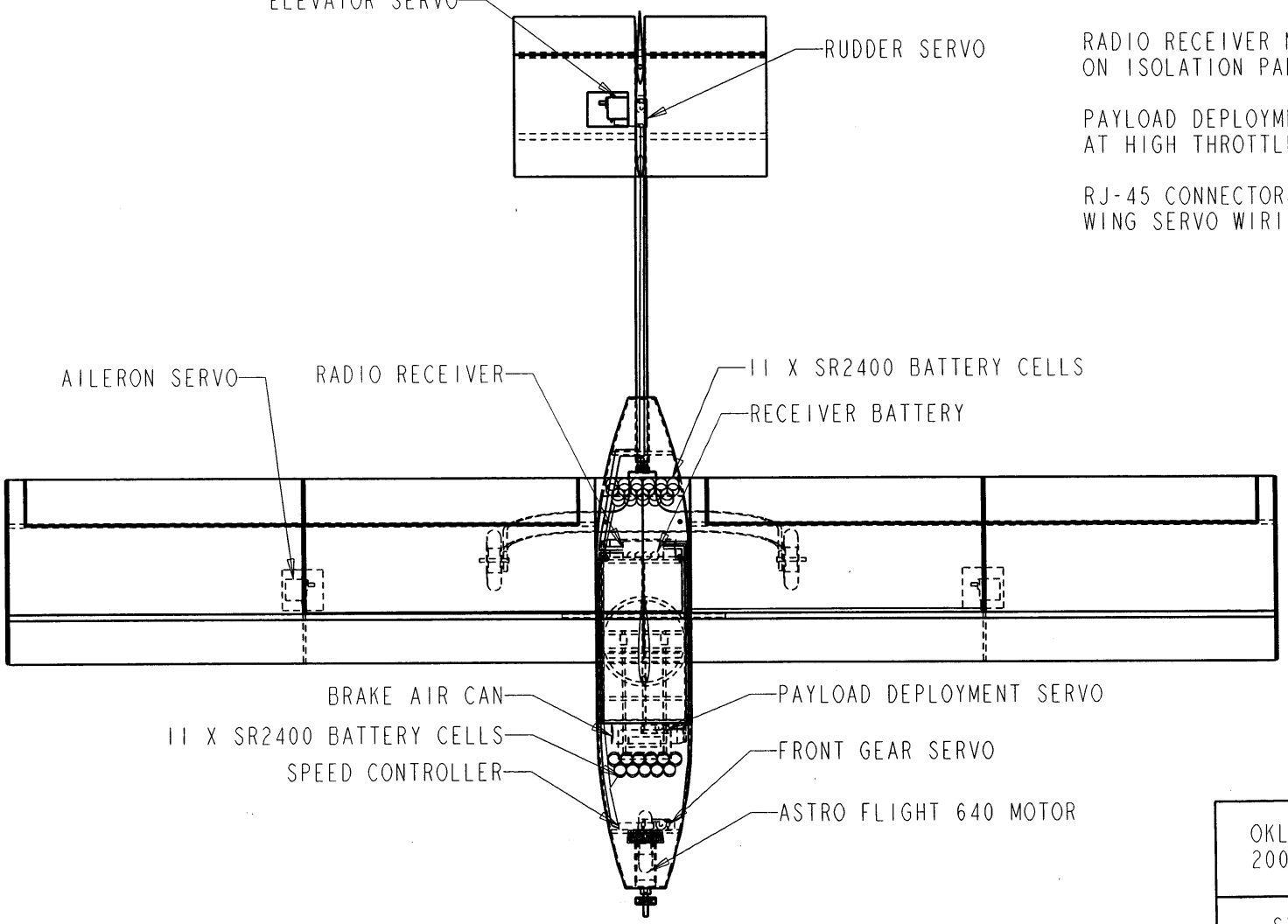

ALL SERVOS OF BALL BEARING CORELESS CONSTRUCTION

RADIO RECEIVER MOUNTED ON ISOLATION PAD

PAYLOAD DEPLOYMENT SERVO INHIBITED AT HIGH THROTTLE SETTING

RJ-45 CONNECTORS FOR TAIL BOOM AND WING SERVO WIRING

OKLAHOMA STATE UNIVERSITY 2003 DBF BLACK
SYSTEMS LAYOUT DETAIL
3-10-03

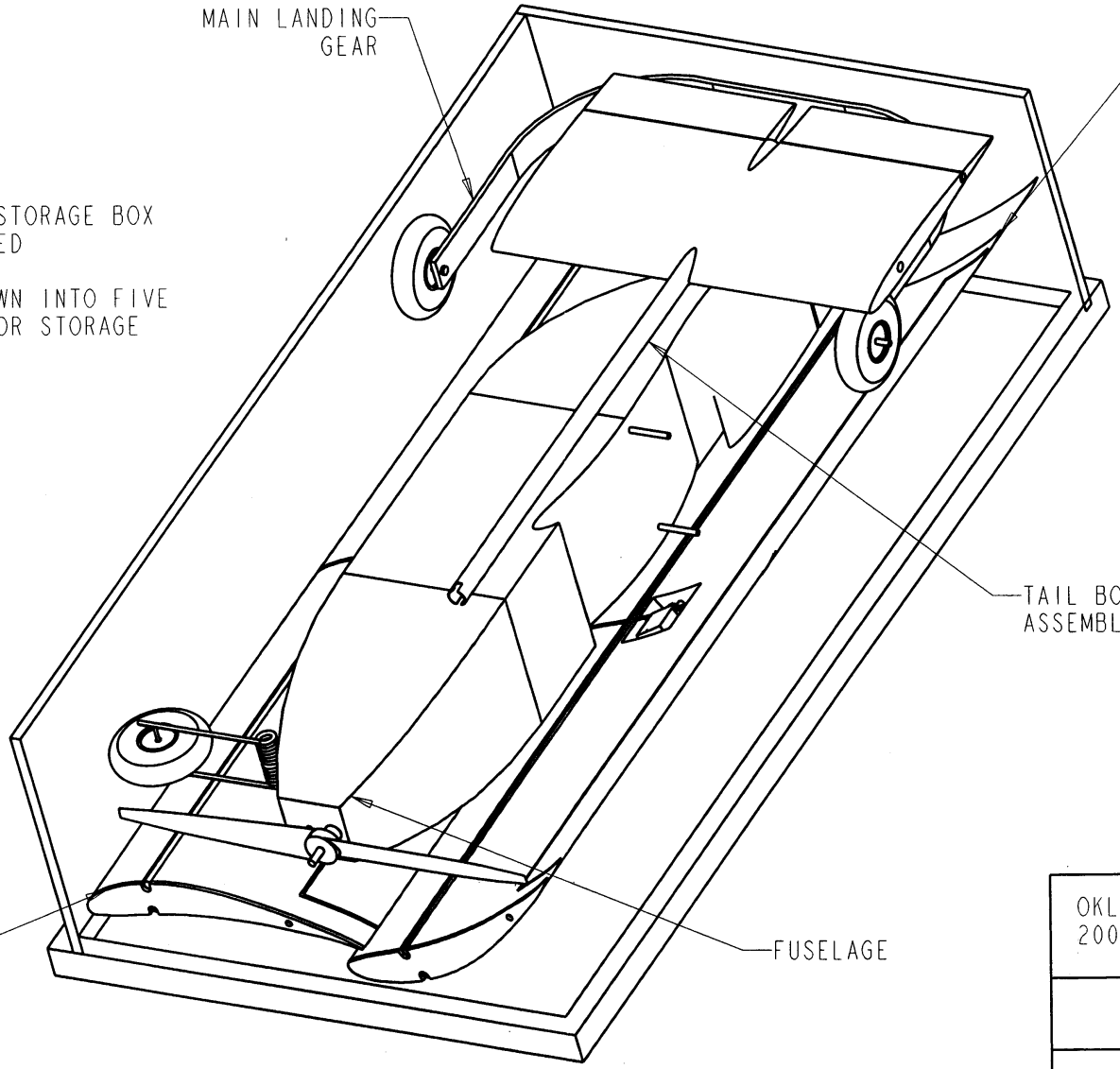

AIRCRAFT SHOWN IN STORAGE BOX WITH 3 FACES REMOVED

AIRCRAFT BREAKS DOWN INTO FIVE MAJOR COMPONENTS FOR STORAGE

OKLAHOMA STATE UNIVERSITY 2003 DBF BLACK	
STOWED VIEW	
	3-10-03

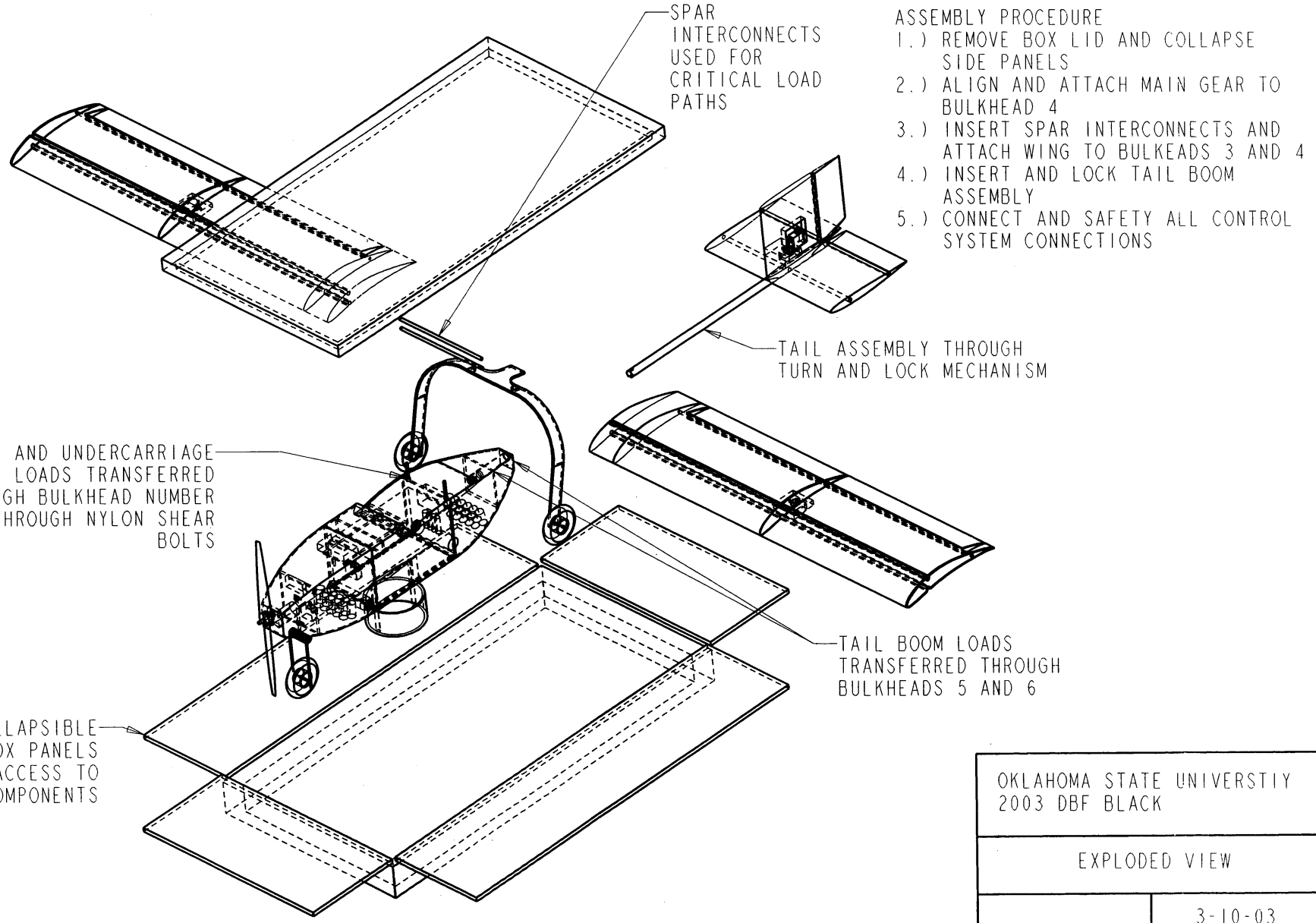

ASSEMBLY PROCEDURE

1.) REMOVE BOX LID AND COLLAPSE SIDE PANELS
2.) ALIGN AND ATTACH MAIN GEAR TO BULKHEAD 4
3.) INSERT SPAR INTERCONNECTS AND ATTACH WING TO BULKEADS 3 AND 4
4.) INSERT AND LOCK TAIL BOOM ASSEMBLY
5.) CONNECT AND SAFETY ALL CONTROL SYSTEM CONNECTIONS

OKLAHOMA STATE UNIVERSTIY 2003 DBF BLACK
EXPLODED VIEW
3-10-03

PAYLOAD DEPLOYMENT MECHANISM
SERVO USED TO PULL SECURING
PINS FROM TABS ON PAYLOAD
BOX DOORS ARE OPENED BY BOX
FALLING THROUGH

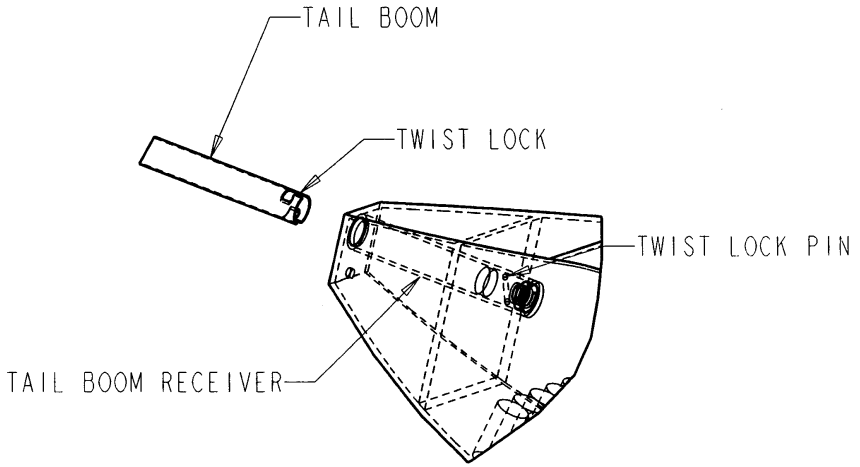

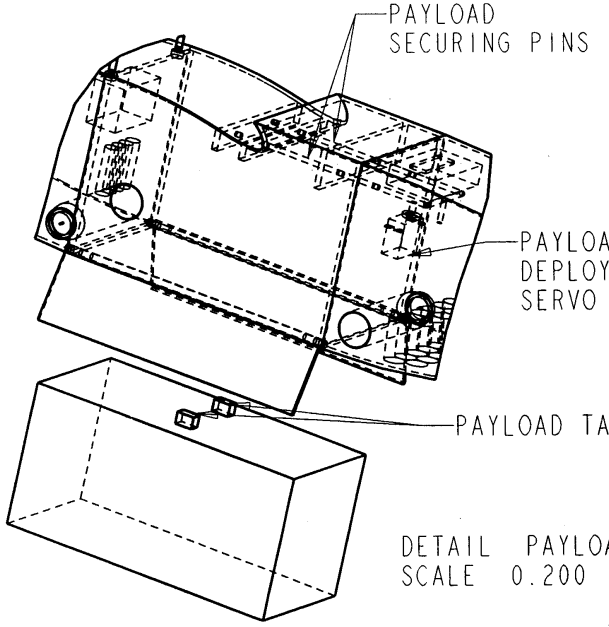

DETAIL PAYLOAD DEPLOYMENT
SCALE 0.200

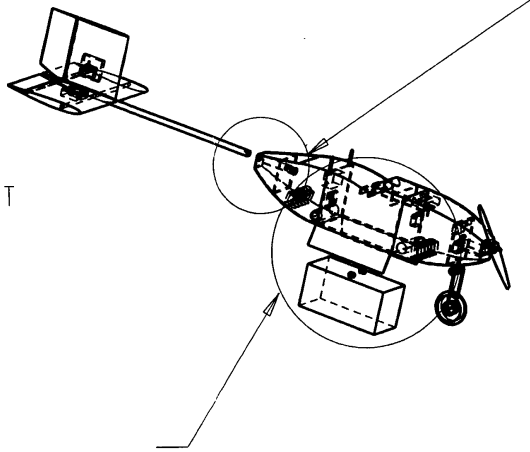

DETAIL TAIL BOOM ATTATCHMENT
SCALE 0.300

TAIL BOOM RECEIVER
TAIL BOOM IS
INSERTED INTO
RECEIVER AND TWISTED
THE SPRING SECURES
THE TAIL BOOM TWIST
LOCK AGAINST THE PIN

OKLAHOMA STATE UNIVERSITY 2003 DBF BLACK
FUSELAGE DETAIL
3-10-03

2003 Cessna/ONR Design-Build-Fly Competition Design Report

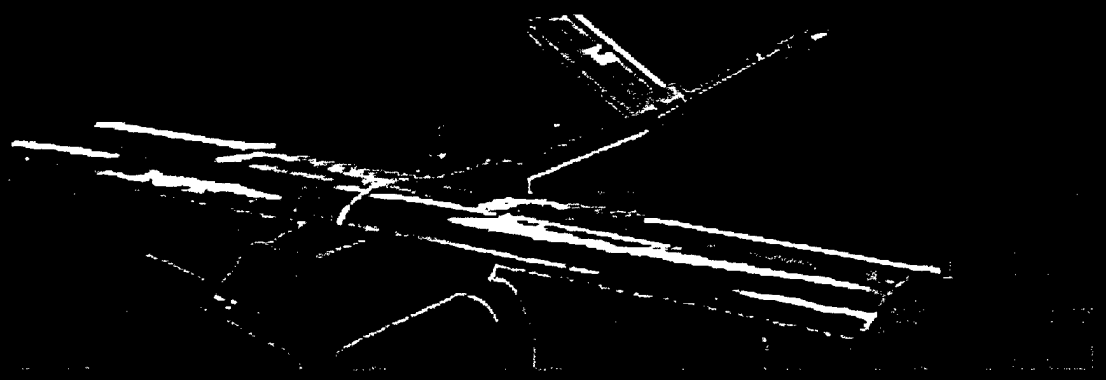

OSU

Oklahoma State University Team

Table of Contents

1 Executive Summary 1
1.1 Conceptual Design 1
1.1.1 Major Areas of Development for Final Configuration 1
1.1.2 Range of Alternatives Investigated 1
1.2 Preliminary Design 2
1.2.1 Major Areas of Development for Final Configuration 2
1.2.2 Range of Alternatives Investigated 2
1.3 Detail Design 2
1.3.1 Major Areas of Development for Final Configuration 2
1.3.2 Range of Alternatives Investigated 2
1.4 Manufacturing Plan 3
2 Management Summary 3
2.1 Team Architecture 3
2.2 Technical Groups 3
2.3 Project Schedule 4
3 Conceptual Design 5
3.1 Mission Requirements 5
3.1.1 Mission A: Missile Decoy 6
3.1.2 Mission B: Sensor Deployment 6
3.1.3 Mission C: Communications Repeater 6
3.1.4 Conceptual Mission Selection 6
3.2 Figures of Merit Analysis 7
3.3 Aircraft and Component Configurations Studied 7
3.3.1 Aircraft Configuration 7
3.3.2 Fuselage Configurations 9
3.3.3 Wing Configurations 11
3.3.4 Tail Configurations 12
3.3.5 Landing Gear Configurations 13
3.4 Structural Configurations 15
3.4.1 Main Fuselage Configurations 15
3.4.2 Boom Configurations 16
3.4.3 Wing Configurations 16
3.4.4 Mission Specific Component Configurations 18
3.5 Propulsive Configuration 19
3.5.1 Figures of Merit 19
3.5.2 Power Plant Configurations 19
3.5.3 Battery Configuration 20
3.5.4 Propeller Configuration 21
3.6 Conceptual Design Summary 21
4 Preliminary Design 22
4.1 Analytical Tools Used 22
4.1.1 Aerodynamic Analysis Methods 22
4.1.2 Propulsion Analysis Methods 24
4.1.3 Structures Analysis Methods 24
4.2 Design Parameters and Sizing Trades 24
4.2.1 Wing Area 25
4.2.2 Wing Span 25
4.2.3 Battery Power in Takeoff and Climb 25
4.2.4 Battery Weight 25
4.2.5 Cruise Velocity 26
4.2.6 Optimal Design Parameter Configuration 26
4.3 Stability and Control Analysis 26
4.3.1 Initial Approximations and Assumptions 26
4.3.2 Longitudinal Static Stability 28
4.3.3 Directional Static Stability 28

4.3.4 Roll Static Stability 28
4.3.5 Neutral Point and Static Margin 28
4.4 Mission Models 29
4.4.1 Mission A: Missile Decoy 29
4.4.2 Mission B: Sensor Deployment 29
4.4.3 Mission C: Communications Repeater 29
4.5 Optimization Trade Studies 29
4.5.1 Aerodynamics Trade Studies 29
4.5.2 Structures Trade Studies 33
4.5.3 Propulsion Trade Studies 34
4.6 Optimization Results 35
4.6.1 Design Parameter Results 35
4.6.2 Stability Characteristics 37
4.6.3 Lift and Drag Predictions 38
4.6.4 Aerodynamic Optimization Analysis Estimates 38
4.7 Predicted Mission Performance 38
5 Detail Design 39
5.1 Structures Components 39
5.1.1 Fuselage 39
5.1.2 Boom 40
5.1.3 Wing 40
5.1.4 V-Tail 42
5.1.5 Payload Drop Mechanism 42
5.1.6 Landing Gear 42
5.2 Propulsion Components 44
5.2.1 Motor Configurations 44
5.2.2 Final Propulsive Configuration 44
5.3 Final Rated Aircraft Costs 45
5.4 Aircraft Sizing 45
5.4.1 Geometric Data 45
5.4.2 Performance Data 46
5.4.3 Weight Statement and Systems Data 46
5.5 Aircraft Assembly Procedure 46
5.6 Final Aircraft Configuration 46
6 Detail Design Drawing Package 48
7 Manufacturing Plan 48
7.1 Manufacturing Processes Figures of Merit 48
7.2 Component Manufacturing Process 49
7.2.1 Main Fuselage Section and Boom 49
7.2.2 Wing 50
7.2.3 Tail 50
7.2.4 Landing Gear 50
7.2.5 Payload and Deployment 50
7.3 Construction Costs 51
7.4 Construction Skill Matrix 51
7.5 Manufacturing Schedule 51
8 Testing 52
8.1 Testing Plan 52
8.2 Test Objectives and Schedule 52
8.2.1 Drag Tests 52
8.2.2 Propulsion Tests 53
8.2.3 Brake Testing 54
8.2.4 Wing Construction Methods 54
8.2.5 Future Testing 54
8.2.6 Testing Schedule 55
8.3 Flight Check-List 55

9 References 55

List of Figures

Figure 2-1: Orange Team Organization 4
Figure 2-2: Project Schedule Milestone Chart 5
Figure 3-1: Conceptual Design Configuration 22
Figure 4-1: Score Sensitivity Trends 25
Figure 4-2: Mission Score Potential 30
Figure 4-3: Manufacturing Man Hours and Rated Aircraft Cost Breakdown 31
Figure 4-4: Aerodynamic Trade Studies 33
Figure 4-5: Structures Trade Studies 34
Figure 4-6: Propulsion Trade Studies 36
Figure 5-1: Spar Connection Assembly 41
Figure 5-2: Aircraft Component Configurations 43
Figure 5-3: Aircraft Assembly Procedure 47
Figure 5-4: Final Aircraft Configuration 47
Figure 7-1: Manufacturing Milestone Chart 52

List of Tables

Table 3-1: Rated Aircraft Cost for all Aircraft Configurations 10
Table 3-2: Aircraft Configuration Decision Matrix 10
Table 3-3: Fuselage Configuration Decision Matrix 11
Table 3-4: Wing Location Decision Matrix 12
Table 3-5: Tail Configuration Decision Matrix 13
Table 3-6: Landing Gear Decision Matrix 14
Table 3-7: Fuselage Cross-Sectional Shape Decision Matrix 15
Table 3-8: Boom Configuration Decision Matrix 16
Table 3-9: Wing Assembly Decision Matrix 18
Table 3-10: Payload Deployment Decision Matrix 19
Table 3-11: Power Plant Decision Matrix 20
Table 3-12: Battery Configuration Decision Matrix 20
Table 3-13: Propeller Selection Decision Matrix 21
Table 4-1: Optimal Design Parameter Configuration 26
Table 4-2: Stability Estimates 38
Table 4-3: Lift and Drag Predictions 38
Table 4-4: Aircraft Optimization Results 38
Table 4-5: Predicted Mission Performance 39
Table 5-1: Astro Flight Motor Comparison 44
Table 5-2: Final Rated Aircraft Cost 45
Table 5-3: Aircraft Dimension Data 45
Table 5-4: Control Surface Dimensions 46
Table 5-5: Performance Data Tables 48
Table 5-6: Aircraft Weight Statement and Systems Data 48
Table 7-1: Wing and Tail Manufacturing Decision Matrix 49
Table 7-2: Fuselage Manufacturing Decision Matrix 49
Table 7-3: Skills Matrix 51
Table 8-1: Flight Check List 55

1 Executive Summary

This report documents the strategy and design process used by the Oklahoma State University Orange Team to achieve the best design for the highest score possible in the 2003 AIAA Design-Build-Fly Competition. This year, competition requirements include that the aircraft be electrically powered, not lighter than air, and without vertical take-off capability. Also, no rotary aircraft are allowed. In addition to these general constraints, the aircraft must arrive at the competition in a box with interior dimensions of 4 feet x 2 feet x 1 foot. The aircraft's assembly time from box to flight ready status is included in the overall score. To commemorate the Wright brothers' first flight, the takeoff distance must be within 120 feet. Also, the maximum battery weight is limited to five pounds. Each team is required to perform two out of three prescribed missions. All three missions four laps around the course, and one 360-degree turn on the downwind leg of the course, and a five-pound payload box measuring 6 inches x 6 inches x 12 inches. Mission A also requires the addition of a simulated cylindrical antenna, made of six inch diameter Schedule 40 PVC pipe three inches long and mounted a minimum of three inches away from the fuselage. The antenna must also have an unobstructed 360-degree horizontal view. Mission B requires the aircraft to complete two laps, land, remotely deploy the payload box, and fly two more laps. Mission C only requires two additional 360-degree turns.

1.1 Conceptual Design

The conceptual phase of the design process began with understanding the mission requirements and their affect on aircraft design. Many conceptual ideas were generated and evaluated. These ideas, corresponding to aircraft configurations and component configurations, were explored and compared to each other using relative figures of merit (FOM). The configurations satisfying the FOM best were initially chosen for further development in the preliminary design phase.

1.1.1 Major Areas of Development for Final Configuration

The first step in the design process involved the generation of numerous conceptual sketches. These sketches were then reviewed and compiled to create several different conceptual configurations. The next step was an initial mission analysis to determine the basic aircraft component requirements to complete the missions. That information was used to select a conceptual design. Another task in the conceptual design phase was determining how the aircraft would fit in the box.

1.1.2 Range of Alternatives Investigated

The Orange Team investigated numerous alternatives during the conceptual design phase. This included configuration of the aerodynamic, structural, and propulsion designs. The chosen configuration consists of a high wing, conventional with boom aircraft design. The aircraft has a V-tail mounted onto the aft end of the boom, tricycle landing gear, and is designed for Mission A and B capabilities. To fit in the box, the wings were removed completely, the main landing gear is rotated 90 degrees, half of the V-tail rotates closed, and the boom retracts into the fuselage.

1.2 Preliminary Design

In the preliminary design phase, the aircraft was analyzed and studied extensively. Analytical tools were used to make initial approximations and assumptions necessary for the stability and control analysis. Specific mission models were created for further analysis and the predicted mission performances were determined as well the lift and drag in cruise and flight. Finally, multiple optimization trade studies were performed over a wide range of the aircraft parameters.

1.2.1 Major Areas of Development for Final Configuration

The first phase of preliminary design was to determine the necessary component sizing. During component sizing, it was critical to ensure that the components fit within the box as required by the competition rules. This was a determining factor in many decisions. Another important design challenge involved determining the deployment method for the payload in Mission B. The incorporation of this system into the overall aircraft design was also a major concern.

1.2.2 Range of Alternatives Investigated

The alternative component sizing was investigated during the preliminary design. This included optimization of the configuration and components selected in the conceptual design phase.

1.3 Detail Design

All of the main aircraft components were decided upon from the optimization analysis in the preliminary design phase. In the detail design phase, all of the sub-components and sub-systems necessary to make the entire aircraft design come together were designed. Upon completion of all sub-components and sub-systems, the final RAC for the prototype was calculated and a detailed list of all of the aircraft sizing parameters created. The Structures Group then created all necessary construction drawings and documents.

1.3.1 Major Areas of Development for Final Configuration

The detail design phase mainly consisted of determining how all of the components and subcomponents would fit together to create the entire aircraft. This included determining necessary structural reinforcement for the attachment of components to the fuselage. The team decided upon the use of five bulkheads to reinforce the fuselage and the use of hard points in the fuselage to reinforce where the components would be attached. Filling the honeycomb with epoxy created the hard points. It was also decided how the components would be attached to the fuselage. The wings attached using four nylon bolts, the main gear attached with one nylon bolt and two spring loaded pins to lock it in place, the boom and tail assembly attached also using spring loaded pins.

1.3.2 Range of Alternatives Investigated

The alternatives investigated during the detail design phase concentrated on construction material selection. Both conventional wood and composite material were investigated for the wing and tail construction. The wood construction would consist of mainly balsa wood with Monokote to give the

surfaces the necessary streamlined shape. A white foam core covered with fiberglass and a blue foam core covered with carbon fiber were the composite materials investigated. Members of the Structures Group conducted research previously on this topic. They discovered that by using carbon fiber on the shear web of the conventional balsa wing, balsa had a greater strength to weight ratio than that of the composites. An added benefit to the wood wing is that it costs much less than the composites. For these reasons, the Orange Team decided to construct the wings and tail using a conventional balsa wood structure covered with Monokote. Several materials were also investigated for the fuselage. These included carbon fiber, a carbon fiber and honeycomb sandwich, a wood truss structure covered with Monokote, and wood construction. Due mainly to the increased strength and durability, the Orange Team used the carbon fiber and honeycomb sandwich to construct the fuselage.

1.4 Manufacturing Plan

The manufacturing plan determined how the aircraft components were made. The fuselage was made using a female mold for the sides, while the top and bottom were laid up flat on a piece of glass and then trimmed to fit. The main landing gear made using foam male mold and twenty layers of carbon fiber. The wings and tail were built using a wing jig. Holes were drilled in the ribs so they could be slid onto the wing jig and properly aligned. The spars were then inserted and glued in place. The wings and tail were then removed from the wing jig and the leading and trailing edges were then attached and the skin was glued in place. The wing was then covered with Monokote.

---

2 Management Summary

2.1 Team Architecture

The Orange Team is divided into three main technical groups: aerodynamics, structures, and propulsion. Each group has a lead engineer, while all share the same chief engineer. The organizational structure is shown in Figure 2-1.

The chief engineer is responsible for the overall management of the team and project. Her duties include keeping the project on schedule, organizing meetings, meeting budgetary and fundraising needs, facilitating necessary communication between the technical groups, as well as other logistical tasks. The group leads are responsible for and direct the activities of their technical groups. They are responsible for their group's quality of work. They assign tasks and deadlines to their members, communicate with the other group leads to ensure that each groups' work will fit together and identify all obstacles. The group leads are also responsible for providing timely and detailed advice to the chief engineer.

2.2 Technical Groups

The Aerodynamics Group is responsible for the sizing and configuration of the aircraft and all sensitivity studies. They are also responsible for flight performance analysis and mission selection. Additionally,

the Aerodynamics Group conducts any necessary aerodynamic testing.

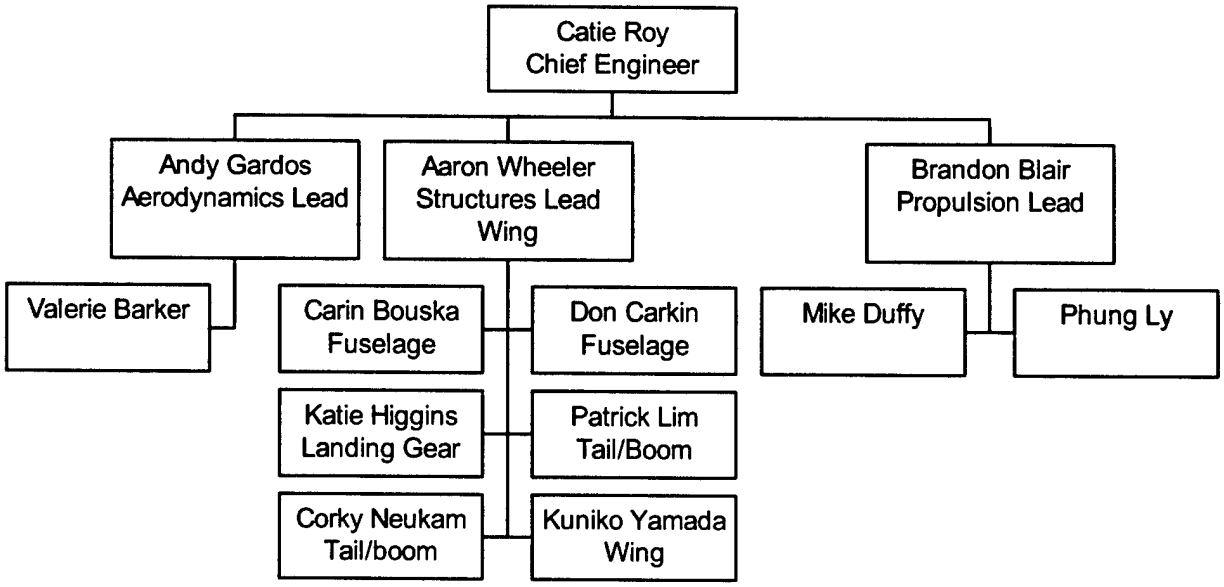

Figure 2-1: Orange Team Organization

The Structures Group is primarily responsible for the structural design, analysis, and construction of the aircraft. This year, they are also responsible for determining how the aircraft will fit in the required box. This group performs all stress analyses and designs the internal layout of the aircraft. They are responsible for material and construction method selections. The Structures Group conducts all testing of the structural components and creates the construction documents and drawings.

The Propulsion Group is responsible for powering the aircraft. This includes all testing and analysis of possible propulsion components and relaying all of the pertinent information back to the Aerodynamics Group for collaboration. They are also responsible for the selection of the propulsion components including the motor, batteries, and propeller. Maintenance, upkeep, and installation of the propulsive and electrical systems are also the responsibility of this group.

2.3 Project Schedule

To ensure successful completion of the design process, official bi-weekly team meetings are held. The chief engineer and the group leads meet weekly to plan the upcoming week and identify any problems that need to be resolved. The group leads meet with their respective groups as often as necessary to complete that week's goals. This requires careful scheduling to ensure that all tasks are completed on time, keeping the project running smoothly. The overall project schedule is shown in Figure 2-2.

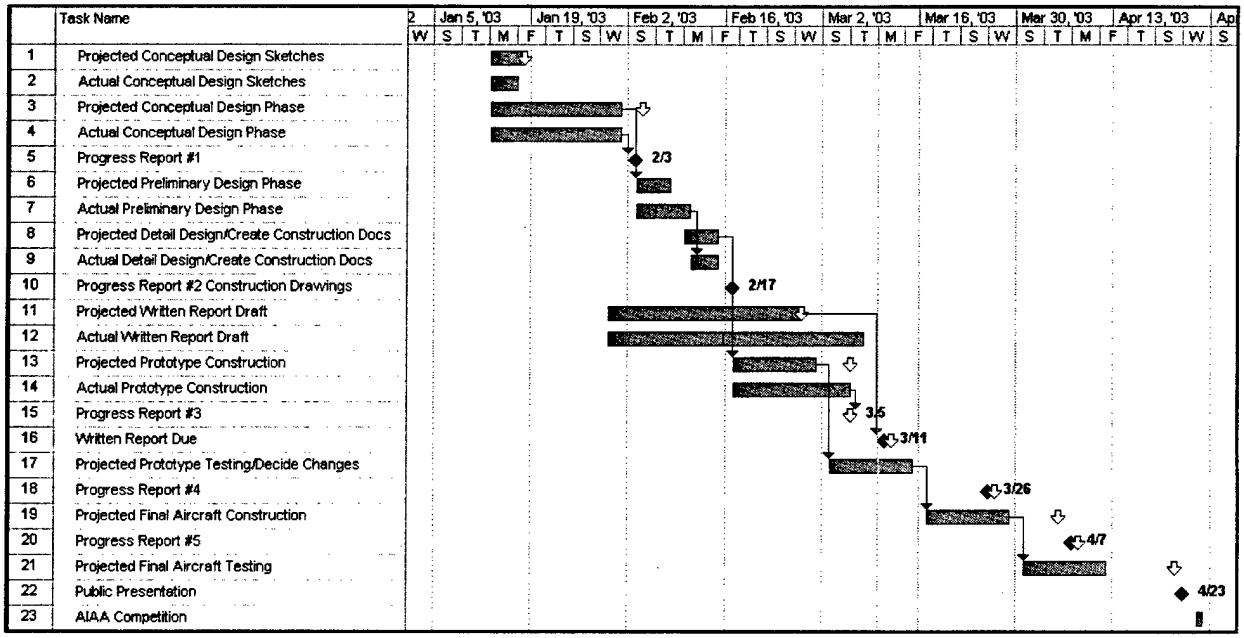

Figure 2-2: Project Schedule Milestone Chart

3 Conceptual Design

The conceptual phase of the design process began with understanding the mission requirements and their affect on aircraft design. Many conceptual ideas were generated and evaluated. These ideas, corresponding to aircraft configurations and component configurations, were explored and compared to each other using relative figures of merit. The configurations satisfying the figures of merit best were initially chosen for further development in the preliminary design phase.

3.1 Mission Requirements

This year's competition has specific requirements and constraints that govern the design of the aircraft. The aircraft must be electrically powered, not lighter than air, and have no vertical takeoff capability. Additionally, no rotary aircraft are allowed. The aircraft must have a maximum gross weight of less than fifty-five pounds and use no more than five pounds of batteries.

In addition to these general constraints, the aircraft must arrive at the competition in a box with interior dimensions of 4 feet x 2 feet x 1 foot. The aircraft's assembly time from storage in the box to flight ready status is factored into the overall score.

There are three flight missions to select from. Each team selects two different missions to complete with time-based scores. The missions have difficulty factors of 2.0, 1.5, and 1.0 for Missions A, B, and C,

respectively. All three missions require a payload box with dimensions of 6 inches x 6 inches x 12 inches ballasted about its geometric center, weighing at least five pounds. Additionally, all missions require a takeoff distance within 120 feet. All contest missions are flown on the same course.

3.1.1 Mission A: Missile Decoy

For mission A, the aircraft must take-off, complete four laps, and land. On the downwind leg of each lap, the aircraft must complete a 360-degree turn in the direction opposite of the final turns. The aircraft must have a simulated cylindrical antenna, a section of "6-inch" Schedule 40 PVC pipe, three inches tall with the ends sealed flush by 1/16-inch plywood sheets. The antenna must be completely exposed on the exterior of the aircraft and standoff from the nearest airframe structure by a minimum of three inches. The antenna may not be faired in any manner and may only be obstructed by structural members.

3.1.2 Mission B: Sensor Deployment

Mission B is divided into three main tasks. First the aircraft must take off, complete two laps, and land. Upon landing, a simulated sensor package will be remotely deployed and the aircraft will take off again. Finally, two additional laps are flown and the aircraft will land. As described in Mission A, the aircraft must complete one 360-degree turn for each lap flown.

3.1.3 Mission C: Communications Repeater

Mission C is a modification of Mission A in that there is no antenna and instead of completing one 360-degree turn each lap, there are a total of three-360-degree turns per lap. The payload and takeoff requirements are identical.

3.1.4 Conceptual Mission Selection

To maximize the score, the Orange Team wanted to design the aircraft such that it performs the two highest scoring missions. Since all scores are based on mission completion time, the total estimated mission times as well as the difficulty factors were considered in a conceptual evaluation of the missions.

Missions A and B seemed to require a similar amount of time to complete and have the two highest difficulty factors, increasing their scoring potential. Mission C has the benefit of less drag than Mission A and less complexity over Mission B, however it must complete two additional 360-degree turns per lap. Having the smallest difficulty factor (half of mission A's), the aircraft would have to fly two times as fast in Mission C to score the same as in Mission A.

Since it is almost unreasonable for the aircraft to fly a speed for one mission and twice that for the other, Mission C was eliminated. Thus, initially, Missions A and B were selected for the designing process. An additional advantage in designing for Missions A and B is that if necessary, the aircraft is able to perform Mission C as well. If the aircraft was designed for mission combinations involving Mission C, it would not be able to perform the unselected mission, thus limiting the aircraft's versatility.

3.2 Figures of Merit Analysis

All of the considered aircraft configurations were evaluated through comparison of benefits and disadvantages. Figures of merit (FOM) were developed from the most important characteristics for the configurations. The best aircraft and component configurations based upon the mission requirements were numerically determined using the FOM. Each of the FOM were given a weight factor based on its relative importance. Each configuration possibility was given an FOM rating. A scaling system from one to five ranked the configuration possibilities: five corresponding to the best selection. With the weight factor of the FOM and the ranking of the concept possibility, an overall score was calculated for each configuration. The relevant FOM for each of the components are listed in their respective sections.

3.3 Aircraft and Component Configurations Studied

The conceptual design of the aircraft and all main components were evaluated using figures of merit related to the mission requirements. The configurations investigated included the following: overall aircraft, fuselage, wing, tail, and landing gear.

3.3.1 Aircraft Configuration

When determining the best type of aircraft configuration for the competition missions, the Orange Team narrowed the selection down to the four main configurations: canard, flying wing, biplane, and conventional. The mission requirements necessitate a high lift-to-drag ratio to allow for takeoff within the required distance, a manageable aircraft size in order to fit within the designated box, and good handling qualities for the pilot. Most importantly, the aircraft configuration selected should provide the highest potential for score.

- Figures of Merit:

The reliability of the aircraft is very important. In order to complete the selected missions, the team requires an aircraft that performs well, repeatedly. The next highest weighted FOM concerns the stability and control. Aircraft performance is heavily based on the natural tendencies of the aircraft. For this reason, inherent stability is required so that less time and resources are focused on the complexity of the design. Additionally, if the aircraft does not possess natural stability, the control would be greatly complicated for the pilot. The purpose of aircraft control is for ease in maneuvers and basic flight.

The Rated Aircraft Cost (RAC) is considered an important FOM due to its involvement with overall score calculation. It is important to keep the RAC as low as possible in order to maximize the mission scores. For this reason, it is assigned a relatively high weighting factor. The convenience for box storage is another FOM considered. Since the entire aircraft must fit within the contest regulation size box, this FOM is deemed highly important. Not only is this FOM concerned with size, it considers the ease of assembly and disassembly for the designs in consideration. The final FOM considered regards the ease of construction. Even though this FOM has the lightest weight factor associated with it, it is still an important consideration since the Structures Group must be able to build all of the designed components.

If this FOM was neglected and the decisions based on solely the others, the Structures Group could possibly struggle through the construction phase. This would more than likely result in a less than perfect design, making it a less desirable selection after all.

- Canard Configuration:

The canard configuration offers increased lift due to the additional horizontal surface. To benefit from the increased lift, the canard surface must be precisely located, causing it to stall before the wing. The short takeoff distance requires a high useful lift coefficient on the main wing. However, the stall limitations of the canard configuration limit the wing lift coefficient. Additionally, the span of the canard must be less than twenty-five percent of the span of the main wing to prevent it from being counted as another lifting surface in the RAC calculator. With an additional lifting surface, the RAC will greatly increase.

- Flying Wing Configuration:

The main advantage of a flying wing lies in the diminished RAC. This configuration eliminates the need for tail surfaces and associated servos. The flying wing configuration also allows for an overall reduction in drag due to the streamlined shape of the aircraft without the tail protrusions. However, this design presents assembly complications, making it difficult to fit into the required dimensions of the box. Additionally, the stability and control issues of the flying wing design present a large challenge.

- Biplane Configuration:

The biplane configuration offers increased lifting capability due to the extra set of wings. With an additional set of wings, the overall wingspan can be reduced allowing for more convenient storage. However, the addition of another wing greatly penalizes the RAC, increasing it eight hours per foot of wingspan and exposed wing chord. The aircraft weight also increases and causes additional RAC penalties. Additionally, the initial conceptual estimates of the required wing area do not necessitate the use of two wings. The wing area and span are both manageable for a single wing, while still allowing the structure to fit inside the box.

- Conventional Configuration:

A major advantage with a conventional design is in its simplicity. Due to the design reliability, the majority of aircraft utilize this design. The wing may be adequately sized in order to provide the necessary lift for a short takeoff, while still satisfying the transportation box requirements. Several different tail configurations are available to provide adequate handling, stability and control of the aircraft. Additionally, the RAC of a conventional plane is comparable to the other configurations.

- Rated Aircraft Costs:

The Rated Aircraft Cost is a model, in thousands of dollars, representing a simulated cost for the entire development and construction of the aircraft. The contest provides this model as shown in the following equation. The coefficients A, B, and C represent cost multipliers with values of $100, $1,500, and $20 per hour, respectively. They are coefficients for the parameters: MEW, REP, and MFHR.

$$\text{Rated_Aircraft_Cost} = \frac{(A \cdot MEW + B \cdot REP + C \cdot MFHR)}{1000}$$

The parameter MEW represents the Manufacturer's Empty Weight and is the actual aircraft empty weight, measured in pounds. This weight includes all flight and propulsion batteries but excludes the payload. The second parameter, REP, represents the Rated Engine Power. The quantity of engines and total battery weight govern this parameter. The total battery weight is defined as the weight of the propulsion battery packs, not to exceed five pounds.

The final parameter, MFHR, represents the Manufacturing Man-Hours. The MFHR is dependant on the WBS (Work Breakdown Structure), which takes into account the wings, fuselage, empennage, flight systems, and the propulsion system. Each of the parts to the WBS is measured in hours per feet, surface, control surface, servo, engine, or propeller/fan.

The RAC for each of the designs was an important FOM. RAC calculations were performed for each of the possible design configurations in order to evaluate this FOM. Several parameters were held constant for all of the aircraft configurations in order to make them comparable. These constraints included: wing area, wing chord, fuselage length, number of engines, total battery weight, and the number of propellers.

The values used to normalize the designs were ten square feet for the wing area, twelve inches for the wing chord, and six feet for the fuselage length. An additional assumption was that all of the planes have a single engine and propeller with four pounds of batteries. The airframe weights are assumed to be equal to twelve pounds for all of the designs except for the biplane. The biplane is assumed to be two pounds heavier due to the extra wing surfaces.

The results show that the flying wing has a value of 10.1, giving it the smallest RAC. The conventional, canard, and biplane configurations have RACs of 11.1, 11.2, and 11.9, respectively. The exact breakdown for the RAC evaluations is shown in Table 3-1.

- Decision Matrix and Selection:

From the overall FOM analysis, the conventional aircraft design proves to be the best configuration for mission requirement satisfaction. It has a score of 4.55 out of 5.00. The biplane, canard, and flying wing configurations had trailing scores of 3.85, 3.45, and 2.90, respectively as shown in Table 3-2.

3.3.2 Fuselage Configurations

The fuselage is the building block of the aircraft. Not only does it connect all of the main components together, it houses all necessary equipment and payload. For the overall configuration, two designs were considered: conventional and conventional with a boom.

	Canard	Flying Wing	Biplane	Conventional
Actual Airframe Weight	10	10	12	10
Wing Span	10	7	12	8
Maximum Wing Chord	1	1	1	1
Num.Control Surfaces on Wings	2	2	2	2
Fuselage Length	6	6	6	6
Num. Vertical Surfaces	1	0	1	1
Num.Vertical Surfaces w/ Controls	1	0	1	1
Num. Horizontal Surfaces	0	0	1	1
Num. Servos	6	3	6	6
Num. Engines	1	1	1	1
Num. Propellers	1	1	1	1
Total Battery Weight	4	4	4	4
Rated Aircraft Cost	11.2	10.1	11.9	11.1

Table 3-1: Rated Aircraft Cost for all Aircraft Configurations

F.O.M.	Weight Factor	Canard	Flying Wing	Biplane	Conventional
Reliability	0.30	4	3	5	5
Stability & Control	0.25	3	2	5	5
Rated Aircraft Cost	0.20	3	5	2	4
Storage (Box)	0.15	4	2	2	4
Construction Ease	0.10	3	2	4	4
Score		3.45	2.90	3.85	4.55

Table 3-2: Aircraft Configuration Decision Matrix

- Figures of Merit:

The most important FOM regarding the fuselage is the convenience for storage in the box. Since the entire aircraft must fit within the contest regulation box, this FOM is heavily weighted. This FOM is not only concerned with size, but also considers the ease of assembly and disassembly for the design in consideration. In order to eliminate potentially complex designs, simplicity of the design is used as an FOM evaluation tool. With additional complexity comes more opportunity for accidents and problems. The RAC is considered an important FOM due to its involvement with the calculation of score. It is important to keep the RAC as low as possible to maximize the mission scores. The final FOM concerns the ease of construction. Even though this FOM has the lightest weight factor associated with it, it is still an important consideration since the Structures Group must build all of the designed components.

- Conventional Configuration:

A conventional fuselage consists of a single piece structure that spans from nose to tail of the aircraft. Historically, this single piece design is sturdy and reliable. However, it may prove difficult to fulfill the stability requirements of the aircraft with a single piece fuselage since the fuselage length is limited by the size of the transportation box.

- Conventional with Boom Configuration:

The conventional with boom configuration divides the fuselage into two sections: a main conventional fuselage and a boom extension. The forward main section of the fuselage must be large enough to house the motor, payload, batteries, and necessary servos. The boom extends out of the main fuselage, housing the tail at the end. The boom provides overall weight reduction of the aircraft while maintaining adequate fuselage length to position the tail for sufficient control. The boom section is retractable into the main fuselage section. This feature allows for conservation of space inside the transportation box.

- Decision Matrix and Selection:

The FOM analysis on the fuselage shows that a conventional with boom design is the optimal choice. This configuration scored twenty-eight percent higher than the conventional alone configuration. The decision matrix is shown in Table 3-3.

F.O.M.	Weight Factor	Conventional	Conventional with Boom
Storage (Box)	0.35	2	5
Design Simplicity	0.30	4	5
Rated Aircraft Cost	0.20	3	4
Construction Ease	0.15	5	4
Score		3.25	4.65

Table 3-3: Fuselage Configuration Decision Matrix

3.3.3 Wing Configurations

The selection of the vertical location of the wing on the fuselage is very important in the conceptual phase of the design process. The vertical location will dictate overall features designed into the wing for stability later in the design process. This selection may also limit or restrict payload and landing gear options. The Orange Team considered placing the wing in the low wing, mid-wing and high wing positions.

- Figures of Merit:

The highest weighted FOM is the stability and control since performance is heavily based on the natural tendencies of the aircraft. The wing is the main lift-generating component of the aircraft and has a highly exposed surface area to the airflow. Thus, stability and control issues are very important. To eliminate potentially complex designs, the design simplicity is used as an FOM evaluation tool. The RAC is considered an important FOM due to its involvement with score calculation. Since the Structures Group must be able to build the wing, the ease of construction is an additional FOM considered.

- High Wing Configuration:

The high wing location allows for payload deployment from the bottom of the fuselage without interference from the wing structure. This option is advantageous if Mission B is selected. The high wing also has characteristics of reduced landing gear weight, little dihedral requirement, and "floating tendency" prevention, which reduces ground run requirements. However, a high wing usually requires a greater fuselage weight due to necessary reinforcement to support the wing load (Raymer 69).

- Mid-Wing Configuration:

A mid-wing design offers the lowest drag for circular fuselage geometries; however, this configuration requires some dihedral for stability. Structural carry through is a problem and usually eliminates the possibility for a payload with this type of wing design.

- Low Wing Configuration:

A low wing aircraft usually has the fuselage mounted higher off of the ground and requires the highest dihedral angle of the three configurations. Wing structure carry through can also cause interference with the payload deployment. With the low wing design, the landing gear and wing can both fasten to the fuselage at the same attach points. This allows for a reduction in concentrated reinforced areas.

- Decision Matrix and Selection:

The wing vertical location FOM analysis shows that a high wing design is optimal for the mission requirements. The high wing scored 4.60 points, which is greater than the mid and low wing designs, having scores of 3.55 and 3.35, respectively. The decision matrix is shown in Table 3-4.

F.O.M.	Weight Factor	High Wing	Mid-Wing	Low Wing
Stability & Control	0.35	5	4	3
Design Simplicity	0.30	5	3	3
Rated Aircraft Cost	0.20	3	4	4
Construction Ease	0.15	5	3	4
Score		4.60	3.55	3.35

Table 3-4: Wing Location Decision Matrix

3.3.4 Tail Configurations

Selecting an appropriate tail for the aircraft involved determining which type best meets the FOM requirements. The Orange Team considered many types of tail configurations; however, the final candidates were narrowed down to include the conventional, T-tail, and V-tail.

- Figures of Merit:

Once again, the reliability of the aircraft is very important and was given the highest FOM weight for the tail analysis. Stability and control was also a big consideration since the tail supplies stability in both the longitudinal and directional modes. As with all other major design considerations, the RAC, box storage, and construction ease played a major role in determining the tail component selection.

- Conventional Configuration:

The most widely used tail is the conventional configuration. It is estimated that more than seventy percent of aircraft in service use this proven configuration. The conventional tail consists of a horizontal and vertical stabilizer. This configuration provides adequate stability and control at a relatively light weight (Raymer 77).

- T-Tail Configuration:

The second tail configuration considered was the T-tail. This design consists of a vertical stabilizer supporting a horizontal tail on top. Since the horizontal tail is above the vertical stabilizer, it is clear of the wing wake and the propwash. Buffet on the horizontal tail is also minimized; therefore the overall structural fatigue is reduced. This increases the horizontal surface efficiency, allowing for a reduction in size. The benefits of a T-tail configuration lie in the increased efficiency of the horizontal tail. Due to this, both it and the vertical stabilizer are usually smaller. However, since the vertical stabilizer must support the loading seen by the horizontal tail, it must be additionally strengthened. For this reason, the T-tail configuration is usually heavier than the conventional tail design.

- V-Tail Configuration:

The final configuration considered was the V-tail. This design uses approximately the same area as the conventional; however, it has the advantage of reducing interference drag. The V-tail design "feels" the projected forces resulting from the horizontal and vertical stabilizer exerted upon the "V" surfaces. Due to the stabilizers configuration, the traditional rudder and elevator are not possible. However, these control surfaces are combined into "ruddervators" that act as both through a mixing device. The ruddervators on the V-tail require the same number of servos as a conventional tail, thus is no RAC penalty. While adds complexity in the controls, a mixing device should eliminate this concern. A disadvantage of the V-tail is that the ruddervators may produce a rolling moment in the left direction (adverse roll-yaw coupling) when the aircraft is initiated in a turn to the right. Test flights and experienced piloting should account for this problem, making it insignificant.

- Decision Matrix and Selection:

From the tail configuration FOM analysis, it was determined that the V-tail is the optimal design. The V-tail scored 4.20 out of 5.00, which was the highest of the three configuration possibilities. The T-tail and conventional scored a 3.70 and 4.00, respectively. The tail FOM analysis is shown in Table 3-5.

F.O.M.	Weight Factor	Conventional	T-Tail	V-Tail
Reliability	0.25	5	4	4
Stability & Control	0.25	5	4	4
Rated Aircraft Cost	0.20	3	3	5
Storage (Box)	0.20	3	4	4
Construction Ease	0.10	3	3	4
Score		4.00	3.70	4.20

Table 3-5: Tail Configuration Decision Matrix

3.3.5 Landing Gear Configurations

The landing gear is an important component of the plane, allowing for taxi, take off, and landing. All missions require dependable landing gear. Four different types were considered: bicycle, tricycle, quad-wheeled, and tail dragger.

- Figures of Merit:

The speed of assembly is an important FOM for the landing gear. The assembly time is added to each of the individual mission scores. Additionally, the storage of the landing gear in the box is a major concern. The strength of the landing gear is a critical FOM. If the gear lacks sufficient strength in any way, the integrity of the overall aircraft is compromised. The cost of the landing gear is also a considered FOM, but it is not heavily weighted. Finally, the ease of construction is also considered.

- Bicycle Gear Configuration:

Bicycle landing gear is difficult to balance with wings that sit on the top of the fuselage. Since this type of gear requires wheels at each wing tip, excessive drag and airflow disturbances may result. The location of the payload poses a problem since the main bicycle gear is housed inside the fuselage. Additionally, modifications may be necessary for Mission B package deployment if selected.

- Quad-Wheel Gear Configuration:

Compared to the other possibilities, quad-wheeled landing gear adds increased stability but requires additional parts. The addition of more components increases cost and makes it harder to fit the gear into the required box dimensions. Additional drag will result from a four-wheel configuration due to the increase of structural members exposed to the airflow.

- Tail-Dragger Gear Configuration:

The tail-dragging configuration complicates the design possibilities for Mission B, forcing the ejection to occur on top or out the side of the fuselage. Using the tail dragging method, there is not adequate clearance to allow payload deployment from the bottom of the fuselage without driving over it.

- Tricycle Gear Configuration:

Tricycle gear allows for the height of the rear gear to adequately clear the payload drop from the bottom of the fuselage for mission B. The possibility of locating the antenna for Mission A underneath the fuselage is also reserved with this configuration.

- Decision Matrix and Selection:

The tricycle landing gear appears to be the best configuration for the aircraft based on the FOM analysis. This configuration allows for the most design possibilities for all three missions. The resulting decision matrix is shown in Table 3-6.

F.O.M.	Weight Factor	Bicycle	Quad-Wheeled	Tail Dragger	Tricycle
Assembly Speed	0.35	5	1	3	4
Storage (Box)	0.25	3	1	4	5
Strength	0.20	2	5	3	4
Cost	0.10	3	2	4	3
Construction Ease	0.10	3	4	1	4
Score		3.50	2.20	3.15	4.15

Table 3-6: Landing Gear Decision Matrix

3.4 Structural Configurations

The Orange Team considered alternative methods for structural configurations of all necessary main aircraft components. Specifically, structural configurations were considered for the fuselage, boom, wing, and for performance of Missions A and B.

3.4.1 Main Fuselage Configurations

The cross-sectional shape of the main fuselage determines the necessary fuselage size to hold the payload and other internal components. The geometrical cross-sectional shapes considered for the fuselage included circular, pill-shaped, and rectangular.

- Figures of Merit:

The main fuselage geometrical shape was also evaluated for drag production on each geometrical shape. The available internal volume for housing all of the necessary internal components such as the motors, batteries, and payload was also considered.

- Circular Cross-Section:

A fuselage with a circular cross-section requires several days to manufacture. Manufacturing a cylindrical fuselage with flat areas on the bottom for possible payload deployment requires the production of a male mold. A female mold is created from this male mold and is used to lay-up the final part. A cylindrical fuselage has less internal volume in comparison to a rectangular or pill shape with the same internal diameter requirements.

- Pill-Shaped Cross-Section:

A pill-shaped cross-sectional fuselage has more internal volume than a cylindrical fuselage. The manufacturing process is comparable to that for a cylindrical fuselage, requiring several days to complete.

- Rectangular Cross-Section:

A rectangular fuselage has the best ratio of used to unused volume with the rectangular payload requirement. Additionally, it has a simpler manufacturing process than the other two alternatives and requires less time to build.

- Decision Matrix and Selection:

The FOM show that the optimal main fuselage cross-section is rectangular shape.. The rectangular shape had the highest ranking of 5.00 out of 5.00. The pill-shaped and circular shapes ranked 3.35 and 2.70, respectively. The decision matrix is illustrated in Table 3-7.

F.O.M.	Weight Factor	Pill-Shaped	Circular	Rectangular
Volume	0.35	4	2	5
Storage (Box)	0.30	3	3	5
Drag	0.20	3	4	5
Construction Ease	0.15	3	2	5
Score		3.35	2.70	5.00

Table 3-7: Fuselage Cross-Sectional Shape Decision Matrix

3.4.2 Boom Configurations

The Orange Team considered three geometries for the cross-sectional shape of the boom: square, triangular, and circular.

- Figures of Merit:

The boom construction FOM included assembly speed, box storage, component strength, and the construction ease. The construction ease FOM is based on the assumption that the Structures Group will manufacture the boom "in-house". The assembly speed is weighted the heaviest of these FOM since this time directly affects the score of each mission.

- Square Cross-Section:

A square boom cross-section fits in the box equally as well as the other possible configurations, however it offers a slower assembly speed. The slower assembly speed arises from the necessity of pulling out the boom fully and then rotating it if necessary. A square shape also has a low construction ease since all four sides must be perfectly aligned. This shape also adds increased weight over the other possibilities having similar diameters. Since the boom will experience large torsional loads, the square cross-section is not as strong in the torsional mode as other shape configurations.

- Triangular Cross-Section:

The triangular cross-section shape offers greater construction ease than the other configurations. This shape also has a relatively similar assembly time as compared to the square section since it must be fully extended before rotation. However, a triangular cross-sectional boom has lower strength properties.

- Circular Cross-Section:

The circular cross-sectional shape has the greatest torsional properties and the quickest assembly speed. However, it is the most difficult shape to manufacture and thus has low construction ease.

- Decision Matrix and Selection:

The optimal cross-sectional area for the boom is circular according to the FOM analysis shown in Table 3-8. Not only does a circular cross-sectional boom reduce weight over the other designs, it also allows for easy rotation for storing the aircraft in the box.

F.O.M.	Weight Factor	Square	Triangular	Circular
Assembly Speed	0.35	3	3	5
Storage (Box)	0.25	4	4	4
Strength	0.20	3	4	5
Construction Ease	0.20	4	5	3
Score		3.45	3.85	4.35

Table 3-8: Boom Configuration Decision Matrix

3.4.3 Wing Configurations

Four main concepts were considered for the wing construction design. These concepts included a single

piece wing attached to the fuselage at mid-span, a wing that folds parallel to the fuselage, two wing sections joining inside the fuselage with pin or bolt between two hard-points in the fuselage, and two wing sections joined with a long bar or rod inserted into a hollowed region of the spar.

- Figures of Merit:

The figures of merit used to judge the wing configurations included the reliability, storage, construction ease, strength, and assembly speed. Reliability is highly weighted since the wing is a main governing component for the entire aircraft design. If the wing is not dependable, the scoring potential is minimal.

- Single Piece Wing:

The first concept considered was a single piece wing joined at mid-span to the fuselage. The actual logistics of this concept prove to be very difficult due to the wingspan limitation of four feet imposed by the longest dimension of the box. The small wingspan would not meet the size requirements necessary for flying the missions at the optimal efficiency for scoring potential.

- Folding Wing:

An ideal aircraft for this competition has no detachable parts, but rather components that fold to fit into the box. Inspired by the example of folding wings on the Grumman F4F aircraft of World War II, the Structures Group further investigated this method. The F4F uses a Grumman Fold to rotate the wing ninety degrees to face the leading edge down, and then folds the wing ninety degrees again, aligning them parallel to the fuselage. A small model was constructed using a ball-socket joint. This apparatus created a similar effect. However, even with a folding wing, the pivot point does not allow enough room in the box for the necessary wingspan.

- Wing Sections Joined Within Fuselage:

The third concept developed involves creating two wing sections joined inside the fuselage and pinned or bolted in place along the vertical axis. The fuselage would have a rectangular slot with rigid plates on each side; wood or plastic could be used to reduce weight. The wings would have male rectangular pieces protruding from the root and cut with finger joints to lock together inside the fuselage. This concept fulfills the size requirements and fits inside the box, however, it proves difficult for construction. Additionally, due to the fact that each male piece of the wing is considerably short due to the restrictions of the fuselage sizing, the stresses at the wing root would be too large due to the induced bending moment applied during the wing tip test.

- Wing Sections Joined with a Connecting Spar:

The final concept involves inserting a rod into a hollow section of the spar joining the wings together. This method fulfills the size and construction requirements while being fairly reliable. Since the wings are identically designed, the construction method is simple. This reduces the need for separate molds, thus reducing design complexity. By inserting a long rod into the spar, the stresses imposed on the wing by the induced bending moment seen in the wing tip test will be distributed over the length of the rod.

- Decision Matrix and Selection:

According to the FOM analysis, the wing should be constructed in two sections that connect together with an internal spar. This method scored the highest ranking of 4.20 out of 5.00, as shown in Table 3-9.

F.O.M.	Weight Factor	Single Piece	Parallel Folding	Double Piece with Inside Connection	Double Piece with Spar Connection
Reliability	0.25	5	2	3	4
Construction Ease	0.20	5	1	2	4
Storage (Box)	0.20	1	2	4	5
Strength	0.20	4	3	3	4
Assembly Speed	0.15	5	5	3	4
Score		4.00	2.45	3.00	4.20

Table 3-9: Wing Assembly Decision Matrix

3.4.4 Mission Specific Component Configurations

In addition to the conventional aircraft components, mission specific components were considered for Missions A and B. Mission A requires the addition of an antenna that may not be faired in any manner; however, it may be located behind a structural component, such as the landing gear. Mission B requires remote deployment of a simulated sensor package (the payload) following a full stop on the runway. The main considerations regarding mission specifics included the location of the antenna for Mission A and the payload deployment mechanism for Mission B.

- Figures of Merit:

In addition to the reliability, construction ease, and design simplicity, two specialized FOM were considered in the analysis of the payload drop mechanism. The deployment time of the payload is included in the time required to complete the mission and thus affects score. Safety is another high-ranking FOM in the selection process. If a component proves potentially dangerous, not only may the success of the mission be sacrificed, but the safety of the participants at the competition as well.

- Mission A: Simulated Antenna:

Since the antenna in Mission A must have an unobstructed 360-degree horizontal view about, its location is limited to the top or bottom of the fuselage. Locating the antenna on top creates a pure drag-creating object, which is undesirable. Locating the antenna underneath the fuselage takes advantage of any benefit the nose gear may provide in drag reduction.

- Mission B: Payload Drop Mechanism:

Several locations were considered for payload deployment: out of the rear, side, top, and bottom of the aircraft. All of these methods considered that the payload needed to be near the CG of the aircraft for stability issues. The rear ejection concept requires the payload to be located near the rear of the aircraft, causing the CG to shift after deployment. If the payload is placed on the CG location at takeoff, a mechanism would be required to move the payload to the rear. This imposes design complications

resulting in excess weight that must be avoided. Topside ejection is nearly infeasible for this competition. Designing a spring-loaded mechanism able to throw the five-pound payload out the top of the fuselage is very difficult, complicated, and detrimental to the weight and RAC. The payload would also be turned into a projectile and may pose a threat to the aircraft as well as spectators. This type of ejection system also eliminates the possibility of a high wing design, which has already been selected. Side ejection makes the storage and deployment of the payload at the CG easy, however the reliability of this ejection method is less than desirable. The payload may damage the wing structure when ejected if it is not done precisely. The bottom ejection method takes advantage of the gravitational force when dropping the payload out of the aircraft. This method also allows for convenient payload storage near the CG of the aircraft. Overall, the bottom ejection method provides simplicity, safety, and reliability.

- Decision Matrix and Selection:

The optimal method for the payload deployment in Mission B is through the bottom of the fuselage, as determined by the decision matrix in Table 3-10. This method outranks the next closest method by thirty-seven percent according to the FOM analysis. Bottom ejection is the safest and most reliable method and does not require extremely complicated construction procedures.

F.O.M.	Weight Factor	Rear Ejection	Top Ejection	Side Ejection	Bottom Ejection
Reliability	0.25	2	1	3	5
Safety	0.25	3	1	2	5
Construction Ease	0.20	3	3	2	4
Design Simplicity	0.20	2	4	3	4
Deployment Time	0.10	1	2	4	4
Score		2.35	2.10	2.65	4.50

Table 3-10: Payload Deployment Decision Matrix

3.5 Propulsive Configuration

The aircraft's propulsion system consists of several main components. The power for the system comes from un-modified, over-the-counter, nickel cadmium (NiCad) batteries. The batteries are linked in series with a 40-amp fuse limiting the maximum system current. The Whattmeter measures the remaining battery power. The speed controller regulates the power drawn from the batteries, which is controlled by the pilot. A motor provides the torque, via gearbox, to turn the propeller.

3.5.1 Figures of Merit

The FOM used to rate the propulsion components included, performance, RAC, reliability, safety, cost, and stability and control. Performance was the main propulsive issue due to the fact that if the selected configuration was unable to perform as required, the aircraft would be unable to complete the missions.

3.5.2 Power Plant Configurations

Three different propulsion configurations were considered during the conceptual design phase: one motor with one propeller (single), one motor driving two propellers (single-shared), and two motors with two

propellers (double). The single configuration consists of one motor and propeller mounted near the nose of the fuselage. This is considered to be a traditional design for this type of aircraft application. This design offers the smallest penalty in RAC and reduces the cost of the propulsion system due to fewer necessary components. The single-shared configuration consists of a single motor driving two propellers, one on each wing, using a chain or belt drive mechanism. This design has the most complexity due to the addition of the chain drive connecting the two propellers. The double configuration consists of two motors, each turning one propeller, mounted on each wing. This design has the greatest cost and the highest penalty in RAC. This design also has increased complexity over the single configuration.

- Decision Matrix and Selection:

From the FOM analysis, the single motor and propeller configuration is the optimal configuration. This configuration scored 3.85 points out of 5.00, which outscores the nearest choice by eighteen percent. The resulting decision matrix is shown in Table 3-11.

F.O.M.	Weight Factor	Single	Single-Shared	Double
Performance	0.40	4	4	5
Rated Aircraft Cost	0.25	5	3	1
Cost	0.20	5	3	1
Reliability	0.15	5	3	4
Score		4.60	3.40	3.05

Table 3-11: Power Plant Decision Matrix

3.5.3 Battery Configuration

Several factors affected the choice for the propulsion system battery configuration. The most important was the internal volume limitation imposed by the fuselage shape. The battery configuration fit inside of the aircraft's main fuselage section. The NiCad batteries must deliver a high rate of discharge for the aircraft to be competitive. Several configurations of batteries, such as those placed end to end, did not allow sufficient discharge rates to be reached so they were avoided. Cooling the battery pack was another consideration. The batteries need to be arranged to provide as much convective cooling as possible. Increasing the amount of battery surface area exposed to air will aid in the cooling process.

- Decision Matrix and Selection:

The FOM analysis shows that the side-by-side arrangement is optimal as illustrated in Table 3-12.

F.O.M.	Weight Factor	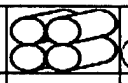	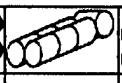	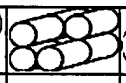		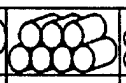	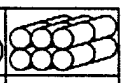
Performance	0.40	3	2	1	4	1	1
Stability & Control	0.30	1	4	1	4	2	2
Safety	0.30	1	4	2	5	1	1
Score		1.80	3.20	1.30	4.30	1.30	1.30

Table 3-12: Battery Configuration Decision Matrix

3.5.4 Propeller Configuration

Choosing the right propeller is a very complicated process. The Propulsion Group investigated two major categories of propellers: traditional fixed propellers and folding propellers. The folding propellers provide for easier storage in the box, have a lighter weight, and are less expensive over the traditional fixed design. In addition to the propeller category, the ratio of pitch to diameter plays a significant role in the propulsion system performance.

- Decision Matrix and Selection:

The FOM analysis for the propeller configuration shows that the traditional propeller is optimum for the aircraft, as shown in Table 3-13.

F.O.M.	Weight Factor	Folding	Traditional
Performance	0.40	2	5
Storage (Box)	0.25	5	3
Weight	0.20	4	3
Cost	0.15	5	4
Score		3.65	4.00

Table 3-13: Propeller Selection Decision Matrix

3.6 Conceptual Design Summary

From the FOM analyses, the optimal configuration consists of a high wing, conventional with boom aircraft design. The wings on the aircraft are manufactured into two pieces and are detachable. A boom with a circular cross section is attached out of the aft end of the main fuselage section to house the tail. The main fuselage section has a rectangular geometry and is sized to hold the payload box and all other necessary internal equipment.

The aircraft has a V-tail mounted onto the aft end of the boom. One of the V-tail sections is fixed stationary to the boom while the other rotates for storage purposes in the box. The boom rotates and is retractable for storage reasons.

The landing gear has a tricycle configuration and is located on the aft section of the main fuselage. The aircraft is designed to be able to perform Missions A and B, which allows for the possibility of Mission C as well.

The sketch shown in Figure 3-1 illustrates the conceptual design of the Orange Team's aircraft. All of the key features are marked for convenience.

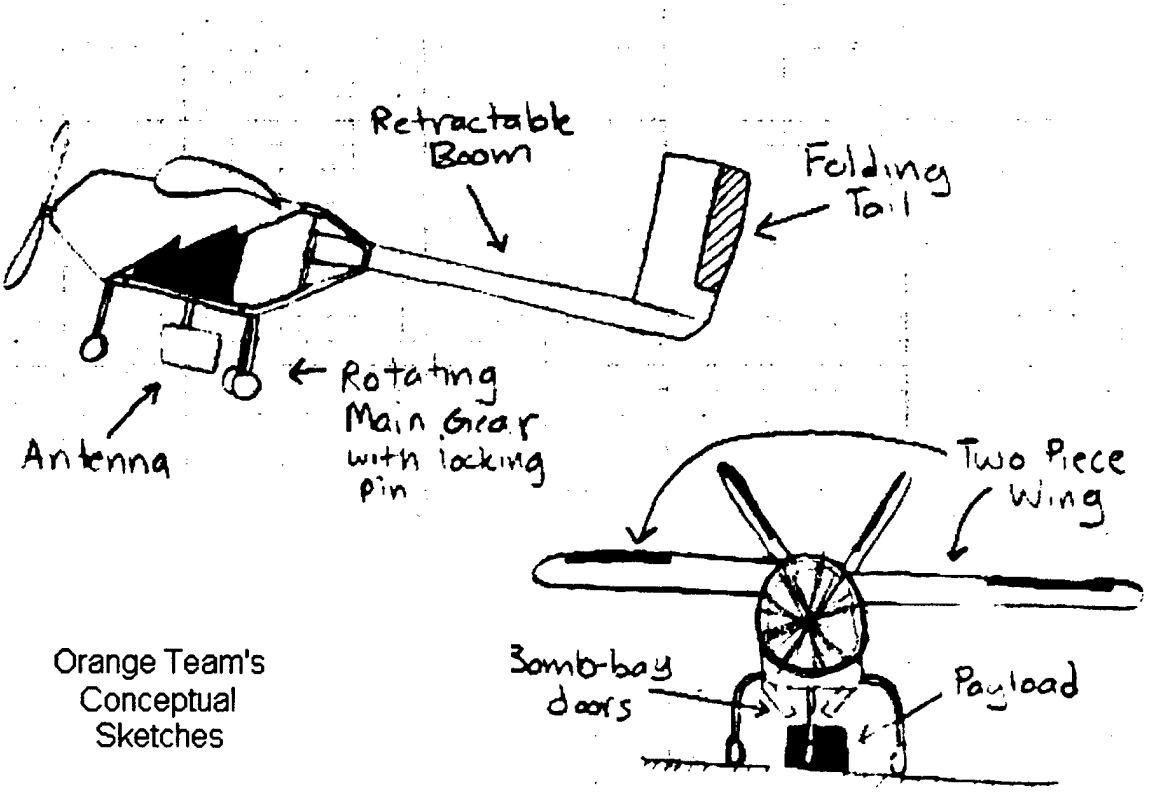

Figure 3-1: Conceptual Design Configuration

4 Preliminary Design

In the preliminary design phase, the aircraft design was analyzed and studied extensively. Analytical tools were used to make initial approximations and assumptions necessary for the stability and control analysis of the aircraft design. Specific mission models were created for further analysis and the predicted mission performances were determined as well the lift and drag in cruise and flight. Finally, multiple optimization trade studies were performed over a wide range of the aircraft parameters.

4.1 Analytical Tools Used

Extensive analysis and optimization were performed in the areas of aerodynamics, structures and propulsion. Optimization in these three areas played a key role in the maximization of scoring potential.

4.1.1 Aerodynamic Analysis Methods

The Aerodynamics Group developed several software programs to perform their analysis: an optimization analysis program, an airfoil analysis program, and a stability and performance analysis program.

The optimization analysis program utilized the conjugate gradient method to calculate the necessary design parameters. These parameters included the wing area, wingspan, cruise velocity, battery weight, and required power for takeoff and climb. Additional parameters corresponding to each phase of the

flight were also evaluated in this program. These initial estimates were used to make additional approximations with historical and statistical data concerning airplanes. The main purpose of this optimization analysis program is to calculate initial possible aircraft configuration sizing optimized for highest scoring potential. Then, using this information conjointly with the other analysis programs, a refined aircraft design is modeled and evaluated for its scoring potential.

The airfoil analysis program was used to size the control surfaces. The hinge moments produced by control surface deflections during various phases of flight were also calculated.

Finally, the stability and performance analysis program calculated the stability derivatives for the aircraft as well as other variables analyzed during critical phases of flight, such as lift, drag, and velocities.

- Structural Weight Model:

In the optimization analysis program, a model was necessary to calculate the empty weight of the aircraft. Additionally, the weight model was needed for CG estimations necessary for stability calculations.

To develop an accurate model, the materials being used as well as other necessary component weights were required. The material choice selection was narrowed in order to reduce the complexity of the model. Two weight models were developed based on the different material combinations for the wing. The first model consisted of a balsa wood wing with a Monokote skin, having spars made of spruce, balsa, and carbon fiber. The second model consisted of wings created from a white foam core with a fiberglass skin having spars made from spruce and carbon fiber.

The weight model for the fuselage was designed using a carbon fiber – honeycomb sandwich frame. All of the additional weights consisting of servos, propulsion equipment, landing gear, and the payload were included in a bulk estimation.

The tail contribution to the weight model was developed using the same material selection as for the wing. It was given a certain percentage of the wing contribution less the contribution from the spars.

- Initial Drag Model:

An initial aircraft drag model in the optimization analysis program was constructed using data from Oklahoma State University's historical database. This database provided information for the drag contribution due to the main components of the aircraft. Additionally, through historical airfoil testing, an accurate contribution from the wing was included in this drag model.

Additional drag contributions must be considered as a result from the antenna drag device in Mission A. The drag contribution from the antenna was initially estimated by calculating the drag on a cylinder with the same dimensions. This drag coefficient was then corrected for wing area so that it could be

integrated into the overall drag model in the optimization analysis program.

With results from wind tunnel tests, as described in the testing section, a more accurate drag model was created. Using a full-scale prototype model, the parasite drag for the entire aircraft less the wing was experimentally determined and used in the analysis.

- Additional Mathematical Models:

The optimization analysis program also included calculations of dozens of other important parameters vital to different phases of flight. These parameters were calculated using modifications for the specific missions as well as using models developed from the Oklahoma State University historical database.

4.1.2 Propulsion Analysis Methods

The Propulsion Group developed a mathematical analysis program using constraints from the mission requirements as well as information from Oklahoma State University's historical database. This propulsion optimization analysis was used conjointly with the aerodynamic optimization analysis for comparison of key parameters and possible configurations.

The main parameters investigated in the propulsion optimization include the amount of power and thrust required at the designed takeoff and cruise velocities. From the analysis, the most efficient propulsion system was determined in terms of cost, propulsive efficiency, and RAC.

4.1.3 Structures Analysis Methods

Many of the structural components were analyzed using basic strength of material and stress-strain calculations. The Structures Group also utilized several smaller analysis programs and spreadsheets specifically developed for stress and deflection calculations.

4.2 Design Parameters and Sizing Trades

With the aid of the aerodynamic optimization analysis program, several sizing trades were performed to find out which parameters had the greatest effect on the score. Initially, five key sizing parameters that were determined to have the most significant effect on the actual performance, RAC, and score included: wing area, wingspan, battery power required in takeoff and climb, battery weight, and cruise velocity. The aerodynamic analysis outputs local maximums for possible combinations of these parameters. To find the actual trends of the data, hundreds of trials were performed. Graphs of these sizing parameters were plotted versus their corresponding score and are shown in Figure 4-1.

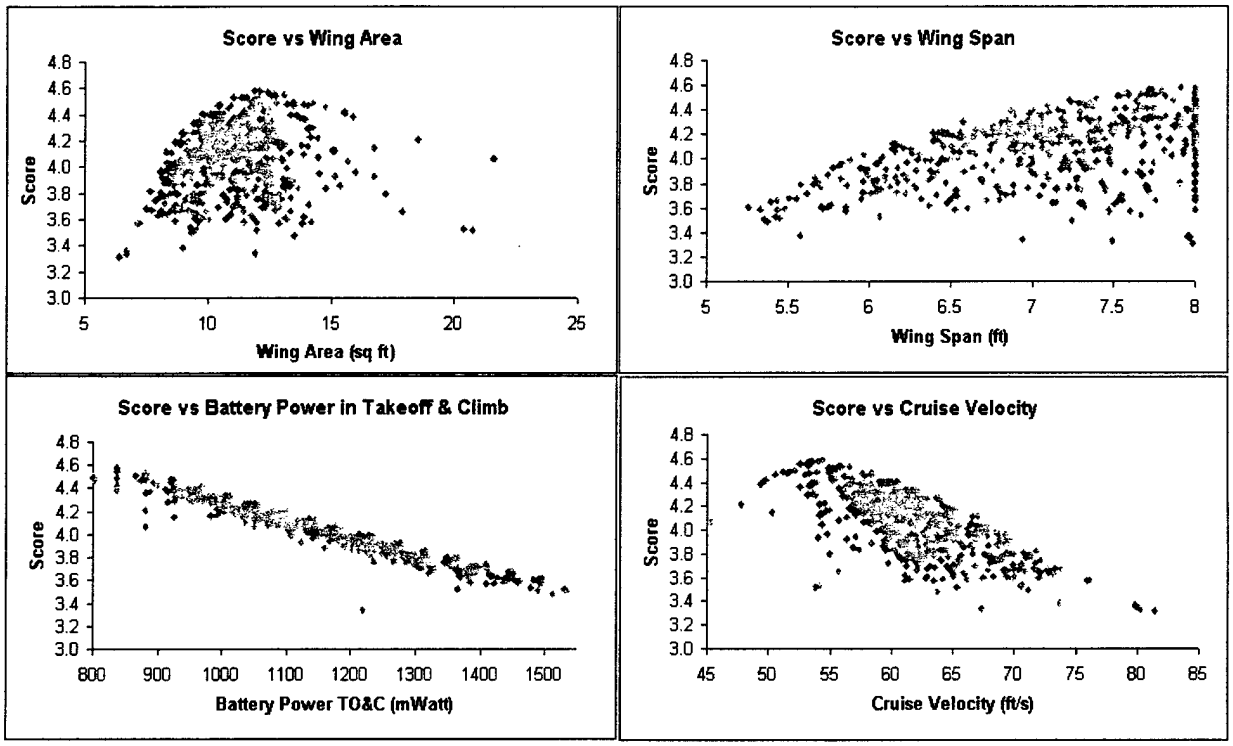

Figure 4-1: Score Sensitivity Trends

4.2.1 Wing Area

From the wing area versus score plot in Figure 4-1, an optimal peak occurs. A wing area of 11.35 square feet corresponds to the greatest score of 4.58. From the plot, it is evident that even if the optimal wing area is used, other parameters must also be chosen wisely to get the optimal score. Otherwise the same wing area may correspond to any number of decreasing values for the score.

4.2.2 Wing Span

The score is maximized with an eight-foot wingspan as shown in the plot of Figure 4-1. In the initial optimization analysis, the maximum wingspan was limited to eight feet, since that corresponds to twice the value of the longest dimension of the storage box.

4.2.3 Battery Power in Takeoff and Climb

The trend of the battery power required in take off and climb versus the score as seen in Figure 4-1 seems to be obvious. The score is maximized when the required power is the least. The optimal required battery power in takeoff and climb is 836 watts. The required battery power is minimized when the wing area and span are at their maximums. This is due to the great lifting ability of larger wings that require less power from the motor due to increased surface area.

4.2.4 Battery Weight

The score appeared to be a linear function of the battery weight. As the battery weight increased, the

score decreased, as with the required battery power in takeoff and climb. A battery weight of 2.49 pounds produced the optimal score.

4.2.5 Cruise Velocity

The last of the five key parameters varied was the cruise velocity. Its plot versus score in Figure 4-1 shows the optimal velocity peaking at 54.31 feet per second. Any variation in the velocity (positive or negative) resulted in a decreased score.

4.2.6 Optimal Design Parameter Configuration

The plots in Figure 4-1 suggest that the best configuration for score maximization has the values listed in Table 4-1. However, the optimal values for these parameters were determined based on mission requirements as summarized in section 4.6.1.

Wing Area	Wing Span	Takeoff & Climb Power	Battery	Cruise Velocity	Score
(ft^2)	(ft)	(Watt)	(lb)	(ft/s)	
11.85	8	836	2.49	54.31	4.58

Table 4-1: Optimal Design Parameter Configuration

4.3 Stability and Control Analysis

To perform the stability analysis, several initial approximations and assumptions were necessary. These estimates were used to approximate the location of the aircraft's CG. Once the CG location was approximated, enough information was available to perform stability calculations.

Stability calculations were performed to calculate the longitudinal static stability, directional static stability, and roll static stability. Static stability is the initial tendency of the aircraft to return to its equilibrium point after a disturbance of any kind.

Dynamic stability calculations were not performed based upon the assumption that the aircraft is of conventional design and should be dynamically stable if all of the static stability criterions are met.

4.3.1 Initial Approximations and Assumptions

The Aerodynamics Group calculated initial estimates for fuselage length, tail size, control surface sizes, and the wing dihedral angle using the takeoff weight estimates from the analysis (Raymer 122).

- Fuselage Length:

Using the estimated 19.27 pounds of takeoff weight from the aerodynamic optimization program, an initial fuselage length was approximated. Using statistical data and assuming that the aircraft is in the homebuilt-composite category, the fuselage length was approximated to be 6.9 feet long (Raymer 122).

- Tail Sizing:

For initial size estimations, the tail was assumed to be of conventional design. The main purpose of an

aircraft's tail is to counteract the moments produced by the wing. Thus, initial tail approximations can be made using the size of the wing and the tail moment arms.

The vertical and horizontal tail moment coefficients were found from historical data, assuming that the aircraft was in the "homebuilt" category (Raymer 125). The tail size equations were based off of wing area, span, chord, and tail moment arms. For the analysis, the vertical tail moment arm was assumed to be equal to the horizontal tail moment arm. An aircraft with a front-mounted propeller has a tail arm around sixty percent of the fuselage length. This corresponds to 4.14 feet (Raymer 124).

With these estimations, the vertical and horizontal tail areas are approximated as 0.721 square feet, and 1.33 square feet, respectively. Although these estimations are for a conventional tail, a "V-tail" is similarly approximated. The surfaces of the V are sized such that they provide the same total surface area as the conventional tail, thus the total area is approximately 2.051 square feet.

- *V-Tail Dihedral*

The dihedral angle of the V-tail was determined using the projected areas of the horizontal and vertical tails. The two areas were summed together and divided by two, one for each of the "V" control surfaces. From the area, the chord was determined and the span of each V-tail segment was calculated. The dihedral angle was found to be 30.6 degrees from the arctangent of the square root of the ratio between the required vertical and horizontal tail areas (Raymer 125). This resulted in a 118.8-degree angle between the two "V" surfaces.

- Control Surface Sizing:

The ailerons were estimated to be from about fifty to ninety percent of the wingspan. These are the primary control surfaces used for roll movement about the longitudinal axis. The ailerons only span outward to ninety percent because the vortex flow over the wing tips provides little control effectiveness at full span. With the ailerons spanning approximately forty percent of the wingspan, they should have a chord of about twenty-five percent of the wing chord to be effective.

Since the aircraft uses a V-tail, the rudder (yaw control surface) and elevator (pitch control surface) are combined into one, a "ruddervator." Elevators and rudders usually extend ninety percent of the tail span and are typically twenty-five to fifty percent of the chord.

- *Hinge Moment Analysis*

The control surfaces were sized based upon historical and statistical data. The elevator was sized to trim at the maximum lift coefficient of the wing. The Aerodynamics Group used the airfoil analysis program to determine the hinge moments on each control surface (ruddervators and ailerons).

The hinge moment approximations were calculated using overestimates of deflection angles and a "never

expected to exceed" velocity. A twenty-degree control surface deflection was used for the ruddervators and a ten-degree deflection for the ailerons. The hinge moments were also evaluated at a velocity of seventy feet per second. The ruddervators were designed using only the elevator calculations since the elevator is the most governing of the two control surfaces for the tail.

- Wing Dihedral Angle:

The airplane has a high wing; this design is inherently stable without any dihedral from the wings. Due to the conventional design and the lack of roll-destabilizing contributions to the aircraft, the Aerodynamics Group set the wing dihedral angle equal to zero.

4.3.2 Longitudinal Static Stability

The tail contribution to the static longitudinal stability was determined assuming that the V-tail may be modeled as a conventional tail by using the horizontal and vertical projections. The projections were constrained to have the same chord for both the vertical and horizontal tails.

The fuselage contribution was calculated with the Multhopp method. In this method, the fuselage section is divided up into many small sections so that the geometry of the fuselage is more accurately analyzed.

The overall static longitudinal stability was found by summing all of the individual components' contributions. For static stability and balance, C_{m0}, the derivative of the pitching moment coefficient at zero angle of attack, must be positive. This ensures that the aircraft is able to trim at positive angles of attack. Conversely, $C_{m\alpha}$, the derivative of the pitching moment coefficient with respect to angle of attack, must be negative. This is necessary since the aircraft must generate opposing moments to counteract any change in the angle of attack in order to return to its equilibrium point (Raymer 486).

4.3.3 Directional Static Stability

The wing and fuselage contributions to directional stability were calculated as one term. This was due to the relatively small magnitude of the wing's contribution at small angles of attack. The total directional static stability was calculated by summing the contributions of the wing-fuselage and the vertical tail.

4.3.4 Roll Static Stability

Roll static stability is the tendency of the aircraft to return to its equilibrium position after it has been disturbed from a wings-level attitude. Roll static stability was calculated from historical data based solely upon the wing contribution (Nelson 78).

4.3.5 Neutral Point and Static Margin

The neutral point and static margin are calculated once the longitudinal stability of the airplane is known. As mentioned, the pitching-moment derivative must be negative for stability. This occurs when the CG is in front of the neutral point, giving the aircraft a positive SM (static margin). One of the constraints in the calculations included maintaining a positive SM greater than fifteen percent (Raymer 487).

4.4 Mission Models

To more accurately determine the optimal geometry, performance, and characteristics of the aircraft, the aerodynamic optimization analysis program was modified. The analysis was divided into three separate codes, each specialized for one of the three missions. All three codes have commonalities in the takeoff distance and completion of at least one 360-degree turn per lap.

4.4.1 Mission A: Missile Decoy

For Mission A, the optimization code was modified to include the additional drag and weight produced by the antenna. An approximation of one pound was given for the antenna weight.

4.4.2 Mission B: Sensor Deployment

The Mission B model was modified to include additional time for taking off and landing twice. Additional time was also allowed for the package deployment. For initial estimations, the deployment time was estimated to be twenty seconds.

4.4.3 Mission C: Communications Repeater

The model for Mission C was similar to Mission A, however the antenna considerations were neglected and two additional 360-degree turns were added for each lap. This gives a total of three turns for each of the laps flown.

4.5 Optimization Trade Studies

Sensitivity studies were used to determine which variables in the optimization codes affected the critical parameters the most. The Aerodynamics, Structures, and Propulsion Groups performed trade studies specific to their technical divisions.

4.5.1 Aerodynamics Trade Studies

The Aerodynamics Group performed sensitivity studies on many different design and stability parameters. Through their variation, observations were made on parameters such as score, RAC, and takeoff distance.

- Study of Mission Score Sensitivity and Mission Selection:

The missions were selected through hundreds of trial runs of the optimization code. Using the collected data, a graph of score versus trial run was plotted for each mission as shown in Figure 4-2. Missions A and B were selected due to their increased potential for score over Mission C. This data confirmed the initial mission selection done in the conceptual design phase.

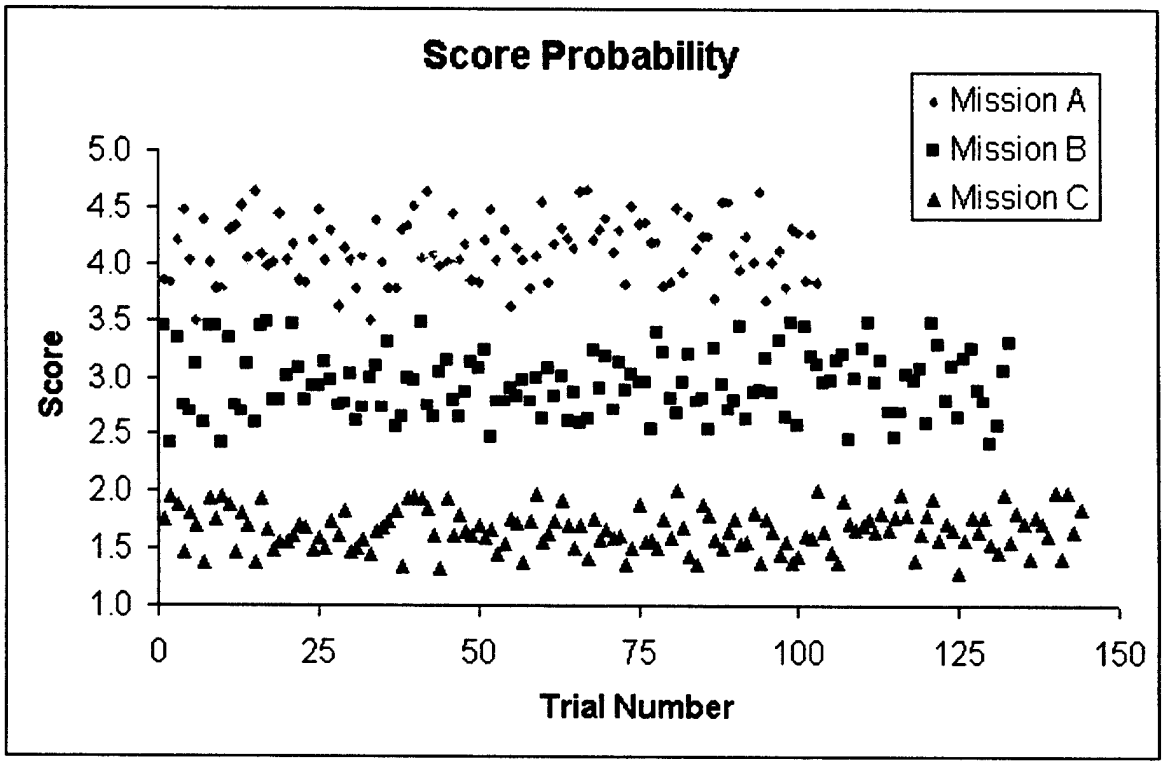

Figure 4-2: Mission Score Potential

- Study of Rated Aircraft Cost:

The overall breakdowns for the MFHR and RAC are shown in Figure 4-3. The RAC is an important parameter since it is used to calculate the score. Since the score is divided by it, it is desirable to keep the RAC as low as possible without compromising the design of the aircraft.

- Study of Design Parameters:

Not all of the design parameters had a great effect on the score. Some of the parameters such as the wingspan, and wing area did affect the score by lowering the RAC. However, it was only by a magnitude less than three percent of a point.

  - *Battery Weight*

As the battery weight was increased, the score decreased in a linear manner. This trend seemed reasonable due to the fact that RAC increases with increasing battery weight. From the battery trend, it was determined that the aircraft should have the least amount of batteries possible.

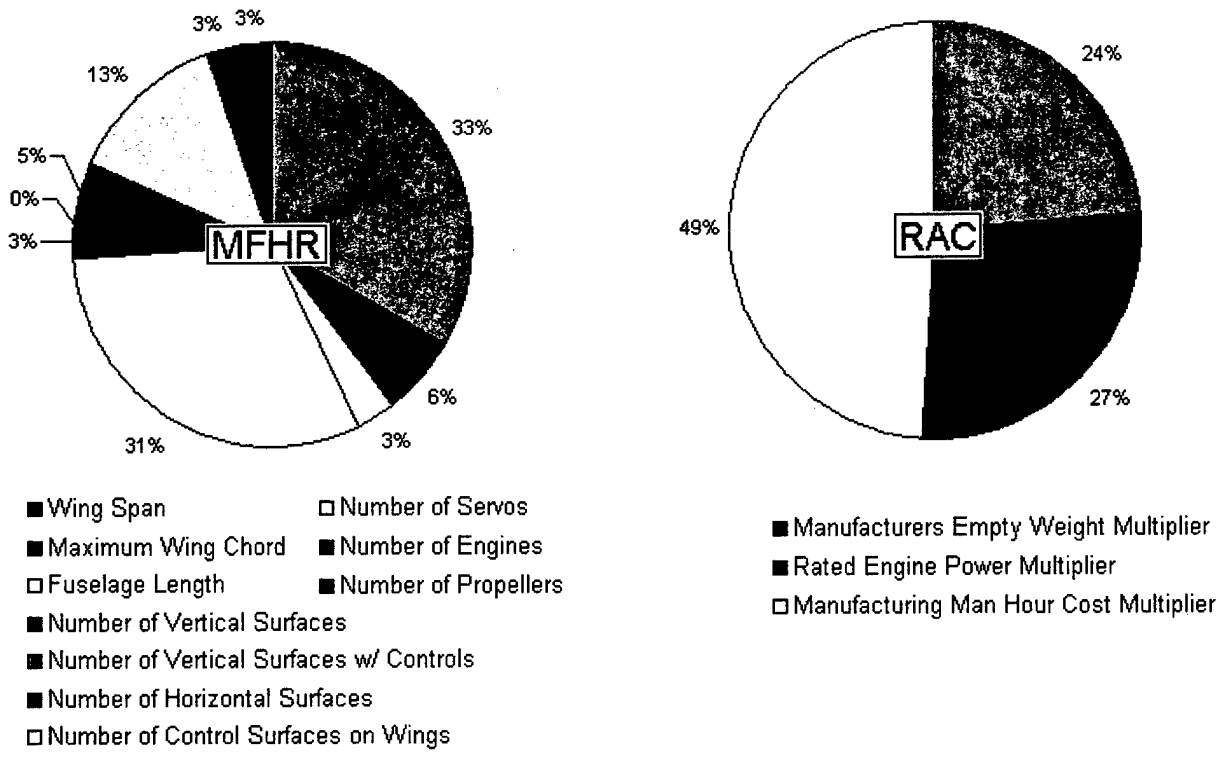

Figure 4-3: Manufacturing Man Hours and Rated Aircraft Cost Breakdown

- *Cruise Velocity*

The cruise velocity has a maximum score occurring at approximately seventy feet per second. However, the aircraft motors would have to produce a large amount of power to produce a cruise velocity of seventy feet per second. Therefore, the cruise velocity was decreased to fifty-seven feet per second, resulting in a score reduction of approximately one percent.

- *Wing Span and Wing Area*

The score decreased linearly with increasing wingspan. However, the necessary wing area and box dimensions restricted the wingspan from changing. An increase in wing area resulted in a decrease in score. This was attributed to the increased RAC caused by the larger wing area. However, the decreases in score were small, resulting in only a 0.3-point reduction in score over the range of the sensitivity study (seven to sixteen square feet). Therefore, the wing area was kept at a value that allowed for good performance and box storage requirements.

- *Study of Wind Speed*

The wind speed did not affect the score. However, it affected the takeoff distance tremendously. A headwind of five miles per hour decreased the takeoff distance by forty feet. The effect of wind speed from zero to thirty miles per hour was analyzed, and the results are shown in Figure 4-4.

- *Wing Taper Ratio*

The score increased with increasing wing taper ratio. However, the increasing wing taper ratio complicated the construction of the aircraft and it was determined that the score increases did not provide enough benefits to warrant the construction difficulty increase.

- o *Cruise Altitude*

The score decreased linearly as cruise altitude was increased. From the study, it was determined that the aircraft should fly as low as possible and still allow for the safety of the observers.

- Study of Stability Parameters

To determine the affects of various parameters on the aircraft stability, the Aerodynamics Group conducted a sensitivity study with the stability and performance analysis program. The following parameters were varied: tail incidence angle, horizontal and vertical tail spans, CG location, wing incidence angle, fuselage length, and boom diameter. The results were plotted to find trends in the data.

- o *Longitudinal Stability*

Longitudinal stability was affected by a number of parameters, but most significantly by the CG location. The CG needed to be located near the aerodynamic center in order to stabilize the aircraft without having to greatly increase the tail size. Locating the CG near the aerodynamic center also allows for a simple symmetric tail airfoil, a NACA 0009. In addition, the more foreword the CG is of the aerodynamic center, the greater the positive SM, as illustrated in Figure 4-4.

The wing provides an overall statically unstable contribution to the longitudinal stability. Therefore, that instability has to be balanced with the tail. The fuselage contribution was found to be insignificant when compared to the contributions of the wing and tail and was ignored in subsequent calculations for trim and elevator sizing.

The sensitivity studies show that the fuselage length could be reduced to accommodate the assembly of the aircraft by slightly increasing the tail. The tail contribution was the stabilizing factor in the longitudinal stability calculations. The static stability was very sensitive to the horizontal tail projection size.

- Directional Stability

The directional stability sensitivity studies indicated that the aircraft was inherently directionally stable. Through analysis, it was found that the vertical tail size could be reduced to zero without having the directional stability coefficient become negative.

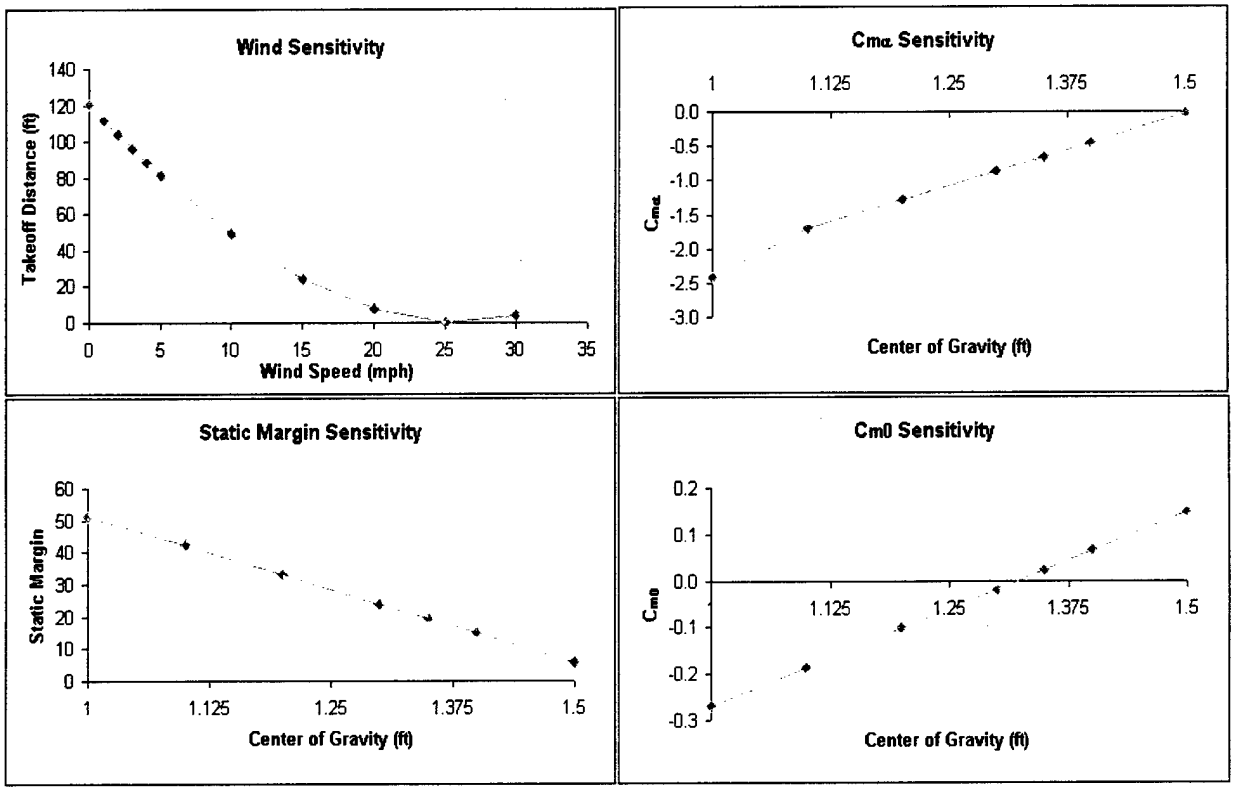

Figure 4-4: Aerodynamic Trade Studies

4.5.2 Structures Trade Studies

The Structures Group performed sensitivity studies regarding drag, assembly and deployment times, and construction materials.

- Study of Parasite Drag

The variation of parasite drag resulted in some interesting conclusions. By increasing it 250 percent in the optimization code, the takeoff distance still remained less than 120 feet. These results are shown in Figure 4-5. With this information, the antenna for Mission A seemed to provide less of a threat as far as takeoff distance is concerned, however drag reduction on the aircraft was still a priority.

- Study of Fuselage Drag

Through wind tunnel testing, fuselages of circular and rectangular cross-sectional shapes were compared with equivalent hydraulic diameters. It was found that the circular fuselage had slightly less drag. However, once correcting for necessary wing area to provide adequate lift to carry the payload box, the rectangular fuselage had lower drag. These results are shown in Figure 4-5.

- Study of Assembly and Deployment Time

The assembly and deployment time greatly affect the score. The score decreased linearly with increasing time. The values range from a score of six with no assembly and deployment time to a score of 4.32 with ninety seconds of combined assembly and deployment time. From the study, it was determined that the

assembly and deployment times needed to be kept as low as possible. These results are graphically displayed in Figure 4-5.

- Study of Wing and Tail Construction Materials

The Structures Group found through testing and research that the material selection for the wings and tail had a big effect on price and weight. Carbon fiber with blue foam, fiberglass with white foam, and balsa wood materials were all evaluated. It was discovered that using carbon fiber on the shear webs of the wing spar with unidirectional tape increased the strength-to-weight ratio of a conventional balsa wing beyond that of a composite wing. The strength-to-weight of the balsa with carbon fiber shear webs was found to be as high as 255, while the strength-to-weight ratio of a composite wing was 200. Additionally, the cost of a balsa wing was dramatically less than that of a composite. These results are graphically represented in Figure 4-5.

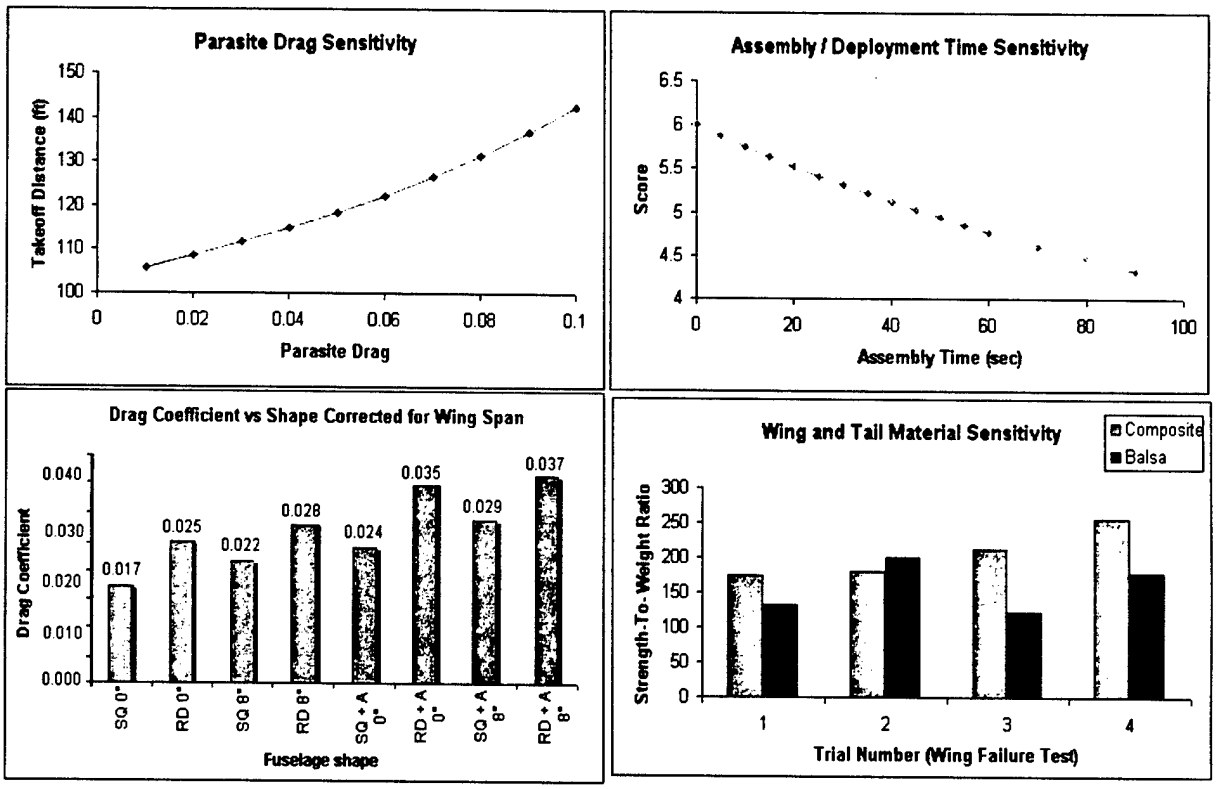

Figure 4-5: Structures Trade Studies

4.5.3 Propulsion Trade Studies

The Propulsion Group performed trade studies regarding the overall propulsive efficiency, power required in takeoff and climb, thrust, and current. All studies used an Astro Flight 640S motor with a super gearbox of ratio 1:3.1 with twenty-two NiCad battery cells at full throttle conditions.

- Study of Propulsive Efficiencies

Another parameter that greatly affected the takeoff distance was the propulsive efficiency. Through

variation of the propeller efficiency, it was shown that an increase of ten percent reduced the take off distance by more than twenty-two feet. Similar trends for the controller, motor, and thus the overall propulsive efficiency were found as well. These trends are shown in Figure 4-6.

It was found that the overall propulsive efficiency; consisting of the propeller, motor, and battery efficiencies increases as the cruise velocity increases. This trend was found by varying the pitch on a twenty-inch propeller. By testing different pitch over diameter (P/D) ratios, the Propulsion Group was able to match a propeller with the optimal cruise velocity. The twenty-inch propeller with a pitch over diameter ratio of 0.7 gives the optimal efficiency at the aircraft's cruise speed, as shown in Figure 4-6.

- Study of Thrust Sensitivity

Thrust is a very important propulsive consideration due to takeoff and cruise requirements. For Mission A, the most restrictive of the missions, the aircraft requires 5.57 pounds of thrust. Using three P/D ratios with a twenty-inch propeller, the available thrust was plotted versus cruise velocity. It was found that using the same twenty-inch propeller with a P/D ratio of 0.7, there is relatively more thrust available for takeoff, which may reduce the necessary takeoff distance. The results are shown in Figure 4-6.

- Study of Current Sensitivity

With the competition requirement of a forty-amp fuse, it was necessary to see which propeller best suits the mission requirements. On a fixed motor with a fixed gearbox, the current nonlinearly increases with an increase in the propeller diameter. From the results in Figure 4-6, it was found that by decreasing the P/D ratio to 0.7, the amp range was within the forty-amp limit while still providing maximum thrust.

- Study of Power in Takeoff and Climb

The power required in takeoff and climb produced a scoring trend similar to the battery weight trend, with the score decreasing linearly with increased power requirements. This is due to the increased amount of battery cells required to produce the increased thrust. From this sensitivity analysis, it was determined that the power requirements should be kept as low as possible.

4.6 Optimization Results

From the sizing trades investigated, the five main design parameters were selected. The stability and performance analysis program calculated all of the stability and control characteristics. Additionally, the lift and drag estimates for key phases of flight such as takeoff and cruise were calculated.

4.6.1 Design Parameter Results

- Wing Area

The optimal wing area was found to be 11.85 square feet. However, this large amount of wing area makes it extremely difficult for the aircraft to fit efficiently inside of the box. Thus, a compromise was made to fulfill the aircraft requirements as well as meet the box sizing limitations.

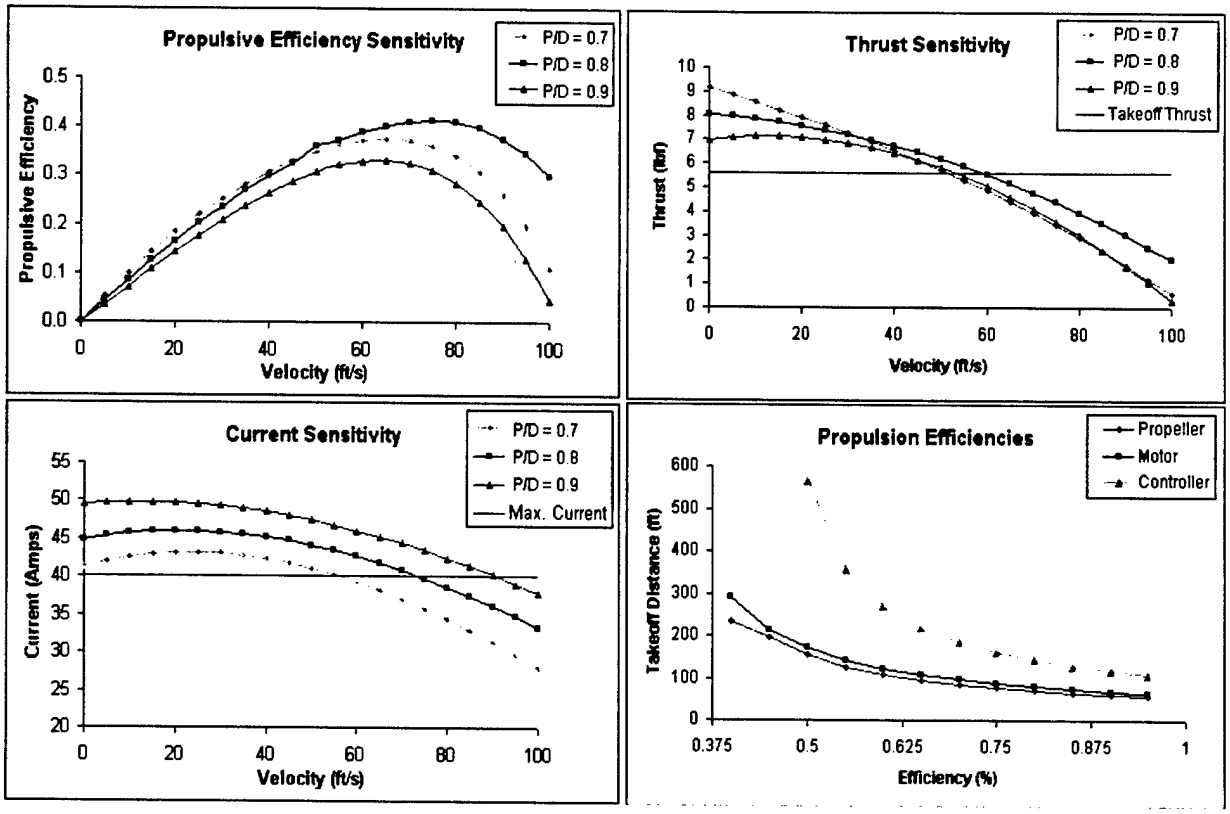

Figure 4-6: Propulsion Trade Studies

From the wing area plot in Figure 4-1, it was determined that the wing area could be reduced without drastically affecting the score. Reducing the wing area by twenty-one percent (2.471 square feet) caused a reduction of the score by only by 5.5 percent (0.251). Thus, the optimal wing area for the aircraft was determined to be 9.379 square feet, giving a score of 4.333.

- Wing Span

The optimization analysis was performed with an eight-foot wingspan limit. If a span of eight feet were exceeded, the wing would require more than two sections. Since the addition of aircraft attachments is undesirable, the Structures Group determined that the wingspan should not exceed this imposed limit.

To allow for manufacturing imperfections and slight tolerances for the box, the wingspan was reduced by half an inch to 7.96 feet. This modification did not affect the score by more than a thousandth of a point, however it increased the takeoff distance by an estimated half foot (110.84 feet to 111.34 feet). Once the wing area and span were both known, the wing chord was calculated. Since the aircraft has a rectangular wing, the chord equals the wing area divided by the span, giving a chord of 1.179 feet.

- Battery Power Required in Takeoff and Climb

The battery power corresponding to the selected wing area and span for the aircraft is approximately 1060 watts in the takeoff and climb phase and 657watts for the cruise portion.

- Battery Weight

From the battery weight, the optimal number of batteries was twenty-three cells. However, due to the arrangement of the batteries in the aircraft, an even number was needed for symmetry. This raised the number of batteries to twenty-four, corresponding to a weight of 3.24 pounds, decreasing the score approximately 2.3 percent (0.10) to 4.24.

- Cruise Velocity

As with the other design parameters, the set wing area dictated the values of the cruise velocity. To satisfy all of the aircraft requirements, the optimal cruise velocity was found at fifty-seven feet per second.

4.6.2 Stability Characteristics

As with the lift and drag predictions, the stability characteristics calculated are based on the performance values associated with Mission A.

- Longitudinal Static Stability

The longitudinal static stability, $C_{m\alpha}$, is determined from the wing, tail, and fuselage contributions. $C_{m\alpha}$, is necessary for the aircraft to perform well if pitching perturbations occur. In the analysis, the wing was found to have a destabilizing effect since the CG is aft of the aerodynamic center. The fuselage contribution, using Multhopp's method, was found to be of a magnitude two times less than that of the wing and thus did not contribute much to the overall longitudinal static stability. Since the tail contribution is stabilizing and much greater (nearly eighty percent) in magnitude to that of the wing, the tail provides the necessary stability, giving the aircraft longitudinal static stability. With a positive total coefficient of pitching moment with respect to zero angle of attack, C_{m0}, the aircraft also possesses balance.

- Neutral Point and Static Margin

From the analysis, the neutral point was found to be 1.64 feet behind the nose of the airplane. This makes the neutral point lie aft of the CG giving a positive SM of 24.6 percent, well above the desired limit.

- Directional Static Stability

The directional static stability, $C_{n\beta}$, was found by summing the contributions from the wing-fuselage and vertical tail. The aircraft must possess directional static stability to recover from yaw disturbances. The wing-fuselage contribution to the directional static stability was found to be destabilizing. However, the contribution from the vertical tail was calculated to be over 10,000 percent larger than the wing-fuselage contribution. This gave the overall yawing moment coefficient with respect to the sideslip angle a positive value, providing ample directional static stability for the aircraft.

- Roll Static Stability

The roll static stability, $C_{l\beta}$, was calculated to be zero based upon the wing contribution. This was caused by the lack of dihedral in the wings, mainly Γ_{wing} equaling zero. However, due to the high wing design, the airplane should be stable in roll without any wing dihedral. Additionally, the dihedral of the V-tail provides stability to the aircraft as well. All of the static stability estimates are summarized in Table 4-2

C_{mo}	0.066
$C_{m\alpha}$	-0.843
$C_{n\beta}$	0.055
$C_{l\beta}$	0

Static Margin	24.60%
Aerodynamic Center	1.295 ft (¼ chord)
Center of Gravity	1.350 ft
Neutral Point	1.579 ft

Table 4-2: Stability Estimates

- Hinge Moments

The hinge moments for both the ailerons and ruddervators were calculated using takeoff and cruise conditions. For the takeoff conditions, a Reynolds number of 282,019 was used, while 455,175 was used in the cruise calculations. After unit conversion, the hinge moments of the ailerons were found to be: 99.0 ounce-inches at takeoff, and 85.6 ounce-inches in cruise. The hinge moments for the ruddervators were found to be: 28.4 ounce-inches at takeoff, and 25.8 ounce-inches in cruise.

4.6.3 Lift and Drag Predictions

The predictions for the lift and drag of the wing and the tail during takeoff and cruise are shown in Table 4-3. These estimates are based upon Mission A performance. The additional drag created by the antenna is included in these estimations.

	Takeoff	**Cruise**
Lift on Wing	31.330 lbf	25.231 lbf
Lift on Tail	-0.653 lbf	-2.121 lbf
Lift on Aircraft	19.110 lbf	18.923 lbf
Drag on Aircraft	2.036 lbf	2.803 lbf
Drag on Antenna	0.157 lbf	0.350 lbf

Table 4-3: Lift and Drag Predictions

4.6.4 Aerodynamic Optimization Analysis Estimates

The results of the aerodynamic optimization analysis are shown in Table 4-4.

Wing Area	Wing Span	Weights			Takeoff Distance	Cruise Velocity	Total Time	Score	RAC
		Empty	Loaded	Battery					
(ft^2)	(ft)	(lb)	(lb)	(lb)	(ft)	(ft/s)	(min)		
9.379	7.958	10.03	19.27	3.24	109.95	57	3.87	4.24	9.92

Table 4-4: Aircraft Optimization Results

4.7 Predicted Mission Performance

Using the final prototype design (consisting of the previously calculated data), the Aerodynamics Group ran the optimization programs for Mission A and Mission B to determine their predicted mission performances. Table 4-5 shows all of the important results of these optimizations for both missions.

Prediction	Mission A	Mission B
Score	4.24	3.01
Mission Time to Complete	3.82 minutes	4.11 minutes
Takeoff Distance	111.34 feet	90.09 ft
Power Used	95%	76%
Cruise Speed	62.12 ft/s	62.12 ft/s
Takeoff Speed	38.29 ft/s	37.27 ft/s
Aircraft Weight	19.18 lb	18.18 lb

Table 4-5: Predicted Mission Performance

5 Detail Design

All of the main aircraft components were decided upon from the optimization analysis in the preliminary design phase. In the detail design phase, all of the sub-components and sub-systems necessary to make the entire aircraft design come together were designed. Upon completion of all sub-components and sub-systems, the final RAC for the prototype was calculated and a detailed list of all of the aircraft sizing parameters created.

5.1 Structures Components

Each major structural component of the aircraft was analyzed to achieve the desired strength. The major components of the aircraft were separated into: fuselage, tail/boom, payload mechanism (for use in Mission B), wing, and landing gear.

5.1.1 Fuselage

In addition to the FOM discussed for the fuselage in the conceptual design phase, the fuselage was designed with three additional major goals. The first goal was to have enough size and strength to attach all of the external components. These components included the tail and boom, wings, landing gear, and propeller. The next goal was to have enough space to accommodate the internal components. The internal components included the motor, batteries, collapsible boom, payload, and dropping mechanism. The final goal was to have the lowest amount of drag possible.

A tapered, rectangular-shaped fuselage was ultimately chosen for the final design. It was constructed with eighth-inch honeycomb, sandwiched with carbon fiber. The NOMEX® honeycomb is a very strong and lightweight fiber material used to increase the moment of inertia. Additional structural reinforcement is gained from five bulkheads; two near the nose end and three in the aft end of the main fuselage section. The front most bulkhead was riveted to the fuselage and is used as the motor mount. The second bulkhead has two holes at the top for ram air being blown off of the motor to pass through into the main fuselage section to cool the propulsion batteries. The third bulkhead has an "L" shape that helps reinforce the area where the main gear is mounted. The fourth and fifth bulkheads are used to cradle the spine used for boom support.

The fuselage has several hard-points built into it for attachment of other components. Filling epoxy into the honeycomb in key areas created these hard points. These key areas included the location of the nose gear, main gear, and wing attachments as well as the front bulkhead.

5.1.2 Boom

In the conceptual design phase, it was decided to have a boom with a round cross-sectional area that elongates to flight ready status in a short period of time. This choice had the worst FOM rating regarding ease of construction. To alleviate this problem, the Structures Group decided to purchase pre-made carbon fiber tubes instead of manufacturing them "in-house".

The structural integrity of the boom was paramount to the overall success of the airplane. The boom needs to withstand any loadings that might hinder the flight mission or controlled landing. The boom was analyzed not only for the extreme cases that result in total failure of the flight mission but was also analyzed for the ease of control during flight.

The boom needed to house a snap-locking device and the necessary wiring for the tail servos, while being as lightweight as possible. The Structures Group decided on a hollow carbon fiber tube, since the material is light and has relatively good deflection characteristics as compared to aluminum and stainless steel. An iterative process was used to decide the optimal cross-sectional shape was optimum for the boom. This process involved calculating the bending and shear forces at extreme points of the tube as well as the deflection of the farthest point of the tail. The maximum stresses felt by the boom were then compared to the manufacturer's specification stresses to see if the material selection could withstand the loadings. Upon completion of the structural analysis of the boom, the Structures Group chose a carbon tube with an outer diameter of 1.5 inches and a thickness of 0.09 inches.

Structurally, the boom was used to support the tail at the aft end. After the boom was extended, there was a five-inch overlap into the main fuselage where it was held in place with a spine. The spine was a carbon fiber tube with a diameter slightly larger than the boom, and was used for stability and alignment.

5.1.3 Wing

The wings of the aircraft were constructed primarily from balsa wood. This decision was made based on strength-to-weight ratio research conducted by members of the Structures Group.

- Spar and Rib Design

The wing's spar connection assembly consists of two mating spar tubes with extremely close tolerances. The female tube was permanently inserted into the ribs of the wing a span of two feet. The male connector extends two feet into each wing. The male tube is removable with a 0.009-inch clearance. The removable male tube was designed to withstand the bending moment experienced during the wing tip test as well as in the wing during flight. The wing's spar connection assembly is shown in Figure 5-1.

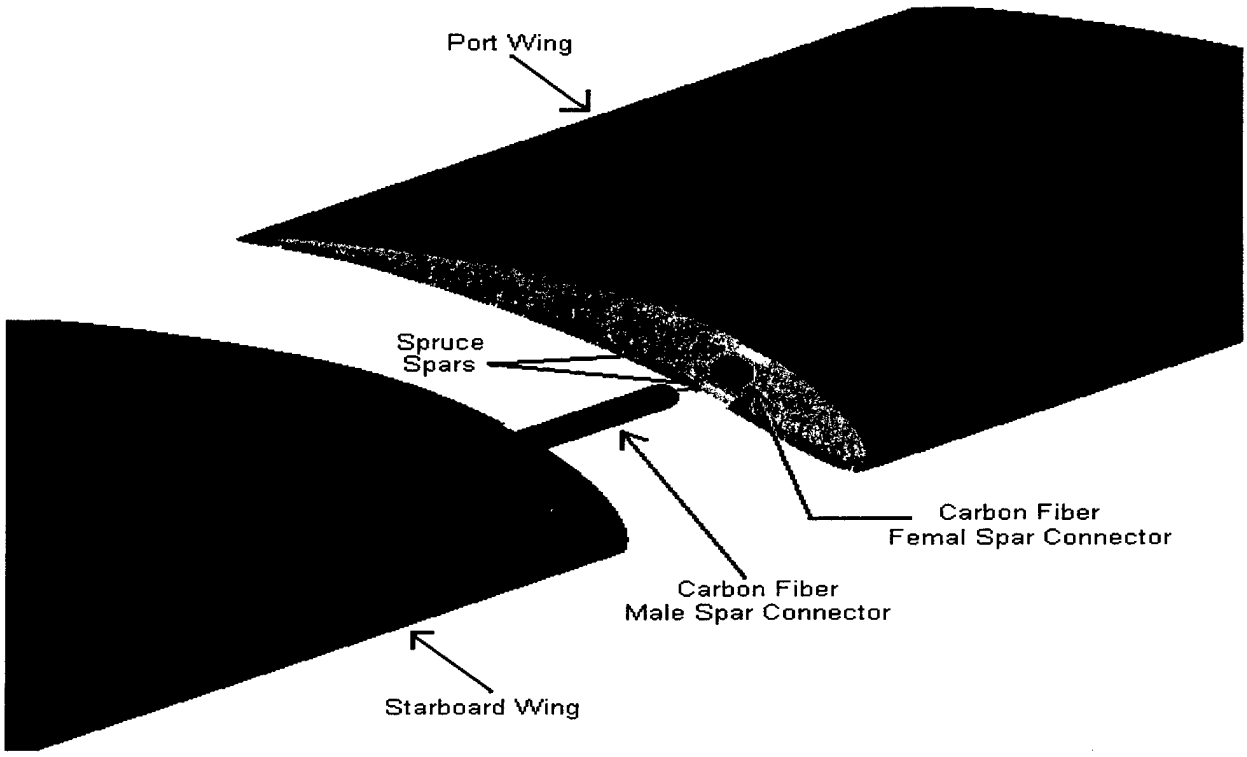

Figure 5-1: Spar Connection Assembly

The female tube is located at quarter-chord of the airfoil, centered vertically in the rib. The ribs in this section are constructed from eighth-inch model-aircraft plywood to resist the shear stress from the spar tube, and are spaced 2.5 inches apart. The control surfaces are located from two feet outward from the mean fuselage reference line to a half-inch from the wing tip. The outboard ribs were constructed from eighth-inch balsa. Using the plywood ribs only on the inboard section of the wing provides sufficient bending load distribution, as well as overall weight reduction.

In addition to the female spar in the inboard two feet of the wing, a spruce spar with a shear web runs the entire span of the wing. The shear web was constructed using a single ply of carbon fiber to stiffen the spruce. The wing was covered approximately two thirds from the leading edge with 1/16-inch balsa skin. The ribs were covered with end caps made from the same skin material to even up the surface of the wing. Monokote film was used to cover the wing and give it a streamlined shape.

- Wing Bolt Design

The wing was designed to be removable for box storage requirements. The wings attach to the fuselage with four nylon bolts housed inside cutoff arrow shaft sections protruding through the top fuselage section. The cutoff arrow shafts were permanently fixed into the honeycomb hard point on the top of the fuselage. Epoxy was used to secure the bolts to the inner side of the fuselage through the arrow shafts so that only nylon bolts need to be threaded. The wing bolts connect to the wing through a hard point constructed

from short plywood ribs stacked together to fill the 2.5-inch gap in the ribs. The bolts are evenly spaced on each side of the spar. The required diameter of the bolts was determined using bending stress equations. This resulted in using quarter inch diameter bolts, providing a safety factor of two.

5.1.4 V-Tail

The Structures Group decided to construct the tail similarly to the wing using balsa wood ribs and spruce spars. Space constraints dictated by the box require that one side of the tail folds. The folding mechanism, constructed similar to a door hinge, must lock in place with snap-locking pins. For manufacturing purposes the snap-locking pins are made identically to the boom's locking pin. Torsional shearing forces will affect the tail during flight, thus the snap-locking mechanism as well. The torsional shear felt by the snap-locking pin was calculated to be 6,926 pounds per square inch (psi). The two locking pins will divide this torsional shear; therefore they need to withstand a shearing force of about 3,500-psi, which is less than the 11,000-psi aluminum yield strength. The V-Tail and boom combination are illustrated in Figure 5-2.

5.1.5 Payload Drop Mechanism

The Structures Group investigated several possible configurations for the payload drop mechanism. The best alternative used a double trap door release system that opened parallel with the fuselage. The cargo was held in the ready position on the dividing line between the doors. The doors are held in the locked-shut position by an overlap at the dividing line with locking tabs. Once the payload is deployed, the doors automatically retract. The doors are constructed from a carbon fiber-honeycomb sandwich.

The payload drop mechanism is made out of aluminum components, and consists of several small pivoting tabs and a rod. A servo is used to push in on one end of the tabs, which causes two ears (one on each of the payload doors at opposite ends) to retract into the unlocked position. This allows the cargo to drop under the force of its own weight.

After the payload has successfully been deployed, the bay doors automatically retract by the tension created by rubber bands located at each outer center corner on the doors. The payload release mechanism is illustrated in Figure 5-2.

5.1.6 Landing Gear

The nose gear consists of a Fults dual strut nose gear, standing an overall height of 11.75 inches with a 2.25-inch diameter tire. The dual strut connects to a reinforced area in the fuselage, created using a mixture of epoxy with micro balloon filler poured into the honeycomb. The dual strut is angled forward two degrees to ensure that the moment on the tail does not make the nose contact the ground during landings. The nose gear is placed 7.5 inches back from the nose of the aircraft, as close to the front of the aircraft as possible.

To ensure that the dual strut does not buckle under the loads, a factor of safety equal to five was used. Buckling equations were used to calculate the maximum force applied to the nose gear. This analysis showed that the lower part of the dual strut would buckle first. However, this buckling does not occur until the predicted loadings are far exceeded. The steering strut buckles under four times the loading that causes the dual strut to buckle. This analysis shows that the nose gear will not buckle during landings.

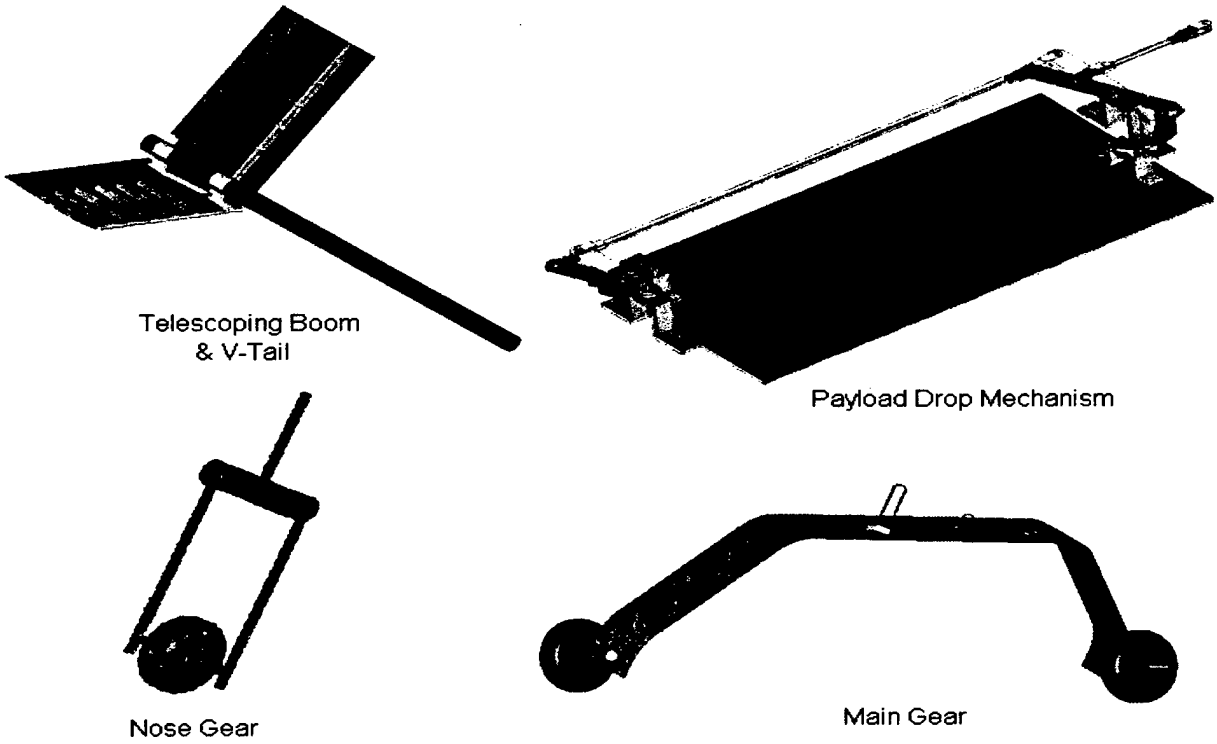

Figure 5-2: Aircraft Component Configurations

The main landing gear was manufactured from carbon fiber. Carbon fiber withstands great amounts of force and shear through layering. Historical data shows that carbon fiber contains the necessary strength and rigidity for the main gear. The main gear bow was made with multiple layers of carbon fiber using a foam male mold. The design of the main gear allows only for a half-inch deflection during landing, with an overall 7.5 inches of ground clearance. The main gear is attached twenty-two inches aft from the nose of the fuselage. This puts the landing gear approximately five inches behind the CG, allowing for the operation of the payload doors. The main gear wheels, each 2.625 inches in diameter, are located sixteen degrees back from a line perpendicular to the ground passing through the center of gravity (Raymer 275). This adds stability to the plane during landings and assures that the tail does not scrape the ground upon rotation. The wheel span, as measured from the center of each tire, was set to equal two feet. This distance is equivalent to one-fourth of the wingspan. The main gear connects to a reinforced area of the fuselage at a pivot point, allowing for rotation during assembly. The rotation joint consists of a nylon rod with two threaded ends, locked into place by nylon nuts locking on either side.

This allows the gear to rotate about a smooth central region. Two spring-loaded pins pop into place as the gear is rotated into the correct position. Both the main and nose gear are illustrated in Figure 5-2.

5.2 Propulsion Components

The Propulsion Group analyzed each component of the propulsion system and developed a system configuration with the best overall efficiency for the mission requirements. While the propulsion system configurations were selected in the conceptual design phase; all of the specific components were selected in this detail design phase.

5.2.1 Motor Configurations

A Graupner motor was used on the winning aircraft in the competition last year. This gives them a significant amount of credibility; however, a disadvantage with selecting one of these motors lies in the order lead-time order. With the only supplier located in Germany, all orders take a significant amount of time for shipping due to demand. Waiting for the motor shipments to arrive hampers the team's ability to perform early flight-testing, which is very important.

Astro Flight motors also have a history of great performance and reliability. The motors have a several week lead-time, however, they cost less than half of that for a comparable Graupner motor. Based on the lead-time and cost comparisons, the Propulsion Group decided to purchase motors from Astro Flight, Inc.

After selecting the motor manufacturer, the Propulsion Group needed to select a specific engine model best suited for the mission requirements. Based on early estimates of required power, the Astro Flight Cobalt 625, 640, and 661 size motors were considered. Through preliminary propulsive analysis, it was found that the Cobalt 625 would be inadequate to handle the amount of necessary power. The size and power specifications for the Cobalt 640 and 661 series motors are shown in Table 5-1.

Motor	640	640G	640S	661	661S
Weight (oz)	13.5	15.0	16.0	22.0	25.0
Power (Watts)	600	750	1000	900-1100	1100-1200
Batteries (# Cells)	18-21	18-21	21-24	28-32	32-36
Length (in.)	2.75	3.75	3.75	3.00	4.00
Cost ($)	150	200	210	250	320

Table 5-1: Astro Flight Motor Comparison

5.2.2 Final Propulsive Configuration

Due to extensive wind tunnel testing and optimization analysis, it was determined that a slightly different propulsion configuration was necessary than that determined in the conceptual design phase. The final propulsive configuration included an Astro Flight 640S motor with twenty-two NiCad battery cells and a twenty-inch propeller. This reduction of two batteries was made to increase the scoring potential since installed thrust testing by the Propulsion Group estimated adequate thrust for takeoff constraints due to the changed gearbox. This setup provides the best overall performance while meeting the requirements

of the Aerodynamics and Structures Groups. This configuration also allows the pilot flexibility in flying the aircraft on the edge of its performance envelope.

5.3 Final Rated Aircraft Costs

With the selection of all aircraft components and performance estimations, the final aircraft RAC is calculated to be 9.78. The composition of the RAC estimate is found Table 5-2.

Manufacturers Empty Weight	$1,003
Empty Weight	10.03 pounds

Rated Engine Power	$4,528.50
Rated Engine Power	3.019

Manufacturing Cost	$3,842
Wing Span (8 feet)	64 hours
Maximum Wing Chord (1.2 feet)	9.6 hours
Number of Control Surfaces on Wings (2)	6 hours
Fuselage Length (5.75 feet)	57.5 hours
V-tail	15 hours
Number of Servos (8)	40 hours
Number of Engines (1)	5 hours
Number of Propellers (1)	5 hours

Total Cost	$9,373.50
RAC	9.78

Table 5-2: Final Rated Aircraft Cost

5.4 Aircraft Sizing

The overall aircraft sizing is represented by three main categories resulting from the analyses. These three categories include data pertaining to geometry, performance, and weight and aircraft systems.

5.4.1 Geometric Data

The final aircraft dimensions are shown in Table 5-3, while the control surface data is shown in Table 5-4. These values were determined mainly from the aerodynamic and airfoil analyses.

Aircraft Dimensions			
Wing Airfoil	Eppler 423	Tail Airfoil	NACA 0009
Wing Span	7.958 feet	V-Tail Span	2.833 feet
Wing Area	9.379 feet^2	V-Tail Span (tip-to-tip)	2.438 feet
Wing Chord	1.179 feet	Tail Area	2.419 feet^2
Wing Aspect Ratio	6.753	V-Tail Chord	10.25 inches
Total Fuselage Length	5.75 feet	Boom Length	2.75 feet
Main Fuselage Length	3.0 feet	Wing Incidence Angle	0°
Main Fuselage Height	7.5 inches	Tail Incidence Angle	0°
Main Fuselage Width	7 inches	Wing Dihedral Angle	0°
Fuselage Angle	3 degrees	Tail Dihedral Angle	30.6°
Boom Diameter	1.5 inches		

Table 5-3: Aircraft Dimension Data

5.4.2 Performance Data

The performance properties of the aircraft are summarized in the multiple tables of Table 5-5. These results were primarily determined with the stability and performance analysis performed by the Aerodynamics Group.

Control Surface Dimensions			
Ailerons	3.5 inches chord	Ruddervators location	10% span to 100% span
	24 inches span	Ruddervator Flap Effectiveness	0.76
	84 in^2 area	Aileron Flap Effectiveness	0.292
Ruddervators	3.25 inches chord	Ruddervator hinge moment	32.67 oz-in.
	14.5 inches span	Aileron hinge moment	190.34 oz-in.
	47.125 in^2 area	Elevator angle to trim at cruise	2.414°
Aileron location	45% span to 95% span	Elevator angle to trim at takeoff	10.203°

Table 5-4: Control Surface Dimensions

5.4.3 Weight Statement and Systems Data

The weights of the different components of the aircraft are summarized in Table 5-6. The aerodynamic optimization analysis as well as the information provided by the Structures Group was used to determine the information regarding the weights of the aircraft and components.

Through their analysis, the Propulsion Group primarily determined the information regarding the selection of the aircraft systems. The data in Table 5-6 includes the electrical systems as well as the propeller and gear ratio used for the final aircraft design.

5.5 Aircraft Assembly Procedure

One of the main considerations in all of the phases of the design process was the aircraft's assembly time and procedure. All of the aircraft's major components were designed so that it takes minimal time and effort to get the plane into the flight ready position from storage in the box. With the exception of the wing, all of the main components use snapping-pins to lock into place.

Only the wings completely detach from the aircraft, however they are easily fastened to the top of the fuselage with four nylon bolts. The boom is collapsible and extends out into the flight position. One of the V-tail sections is fixed to the aft end of the boom while the other rotates outward into position. In the box, the landing gear is aligned with the length of the fuselage and rotates ninety degrees to the correct position. The process from box storage to flight ready is shown in Figure 5-3.

5.6 Final Aircraft Configuration

The final configuration of the Orange Team's aircraft is illustrated in Figure 5-4. This figure illustrates the modeled aircraft design as compared to the final prototype design.

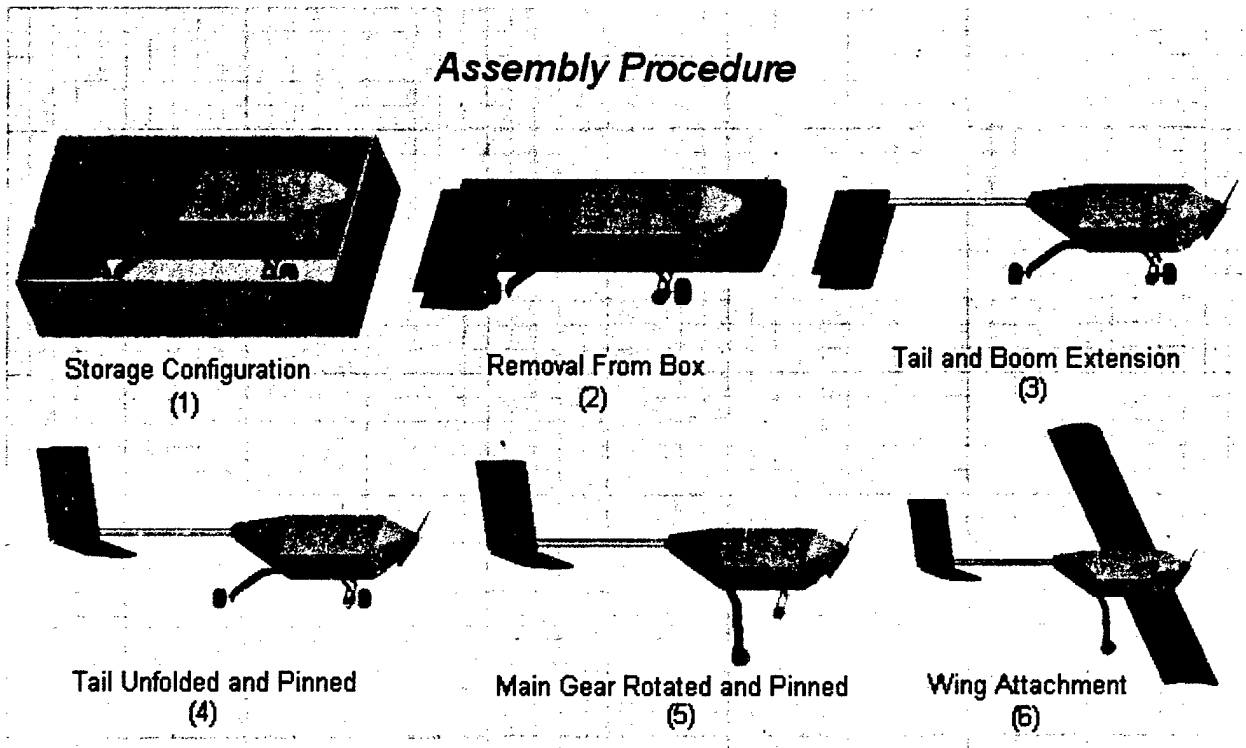

Figure 5-3: Aircraft Assembly Procedure

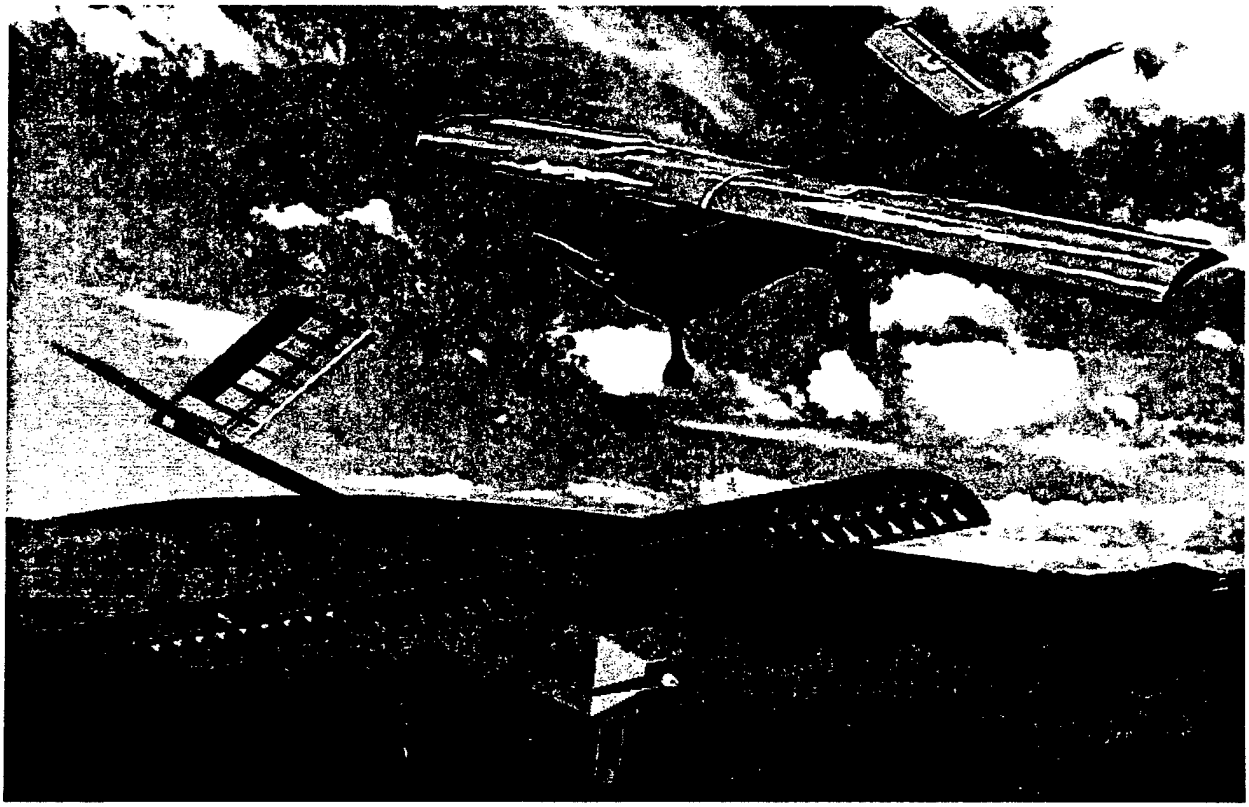

Figure 5-4: Final Aircraft Configuration

Performance Properties	
Mission A Takeoff L/D (with payload)	8.643
Mission B Takeoff L/D (with payload)	9.308
Mission A Cruise L/D (with payload)	5.667
Mission B Cruise L/D (with payload)	6.375
Stall Speed	
Mission A with payload	33.338 ft/s
Mission B with payload	32.457 ft/s
Mission A without payload	31.089 ft/s
Mission B without payload	27.636 ft/s
Drag	
Mission A with payload	2.471 lb
Mission B with payload	2.294 lb
Mission A without payload	3.379 lb
Mission B without payload	3.004 lb

Maximum Rate of Climb	
Mission A with payload	6.13 ft/s
Mission A without payload	10.83 ft/s
Mission B with payload	7.24 ft/s
Mission B without payload	12.96 ft/s
Takeoff Length	
Mission A without payload	46.13 feet
Mission B without payload	36.78 feet
Mission A with payload	120.2 feet
Mission B with payload	98.11 feet
Lift	
Takeoff: Mission A	18.995 pounds
Takeoff: Mission B	18.995 pounds
Cruise: Mission A	18.923 pounds
Cruise: Mission B	17.872 pounds

Table 5-5: Performance Data Tables

Weight Statement	
Component	Weight (lbs)
Airframe	10.38
Payload	5
Payload System	0.41
Control System	0.56
Propulsion System	4.21
Gross Weight	20.56
Empty Weight	12.56

Systems Data	
Radio Used	Futaba 8UAPS-8 channel
Servos Used	S3003,S9602, HS-925MG
Battery Configuration	2-24 side by side sticks
Motor	Astro Flight 640S
Propeller	20 inch
Gear Ratio	01:03.1

Table 5-6: Aircraft Weight Statement and Systems Data

6 Detail Design Drawing Package

The detail design drawings are located at the end of this report. The drawings include schematics of the aircraft three-view, systems layout, safety of flight checks, telescopic V-tail, and payload deployment mechanism.

7 Manufacturing Plan

7.1 Manufacturing Processes Figures of Merit

The manufacturing method for each major component was investigated using four important FOM. The FOM were rated on a scale from zero to two, two being the best choice. These FOM included: cost, strength and durability, ease of construction, and weight. Carbon fiber lay-up, conventional wood construction, and fiberglass lay-up were all considered for manufacturing methods. The FOM were evaluated using a weighted decision matrix. The decision matrix used for the wing and tail, shown in Table 7-1 states that the optimal manufacturing process is that of conventional wood construction.

F.O.M.	Weight Factor	Carbon Fiber Lay-Up	Conventional Wood Construction	Fiberglass Lay-Up
Weight	0.30	1	2	0
Cost	0.25	0	2	1
Ease of Construction	0.25	1	2	0
Strength & Durability	0.20	1	0	1
Score		0.75	1.60	0.45

Table 7-1: Wing and Tail Manufacturing Decision Matrix

The same FOM used for the wing and tail applied to the fuselage construction decision matrix. However, there were different weighting factors involved. The highest weighted FOM for the fuselage was the strength and durability since all other components rely on the fuselage for support and attachment points. The FOM analysis, as shown in Table 7-2 resulted in a carbon fiber lay-up manufacturing process being optimal for the fuselage.

F.O.M.	Weight Factor	Carbon Fiber	Carbon Fiber & Honeycomb	Solid Wood	Wood Truss & Monokote
Ease of Construction	0.25	4	4	4	2
Weight	0.25	3	4	3	4
Strength	0.23	5	4	3	2
Durability	0.2	5	5	3	3
Cost	0.07	2	3	5	4
Score	1	4.04	4.13	3.39	2.84

Table 7-2: Fuselage Manufacturing Decision Matrix

7.2 Component Manufacturing Process

Different manufacturing processes were evaluated for all of the major structural components of the aircraft. These major structural components included: the fuselage, wing, tail, landing gear, and the payload deployment mechanism.

7.2.1 Main Fuselage Section and Boom

The fuselage is made of multiple layers of carbon fiber with a honeycomb core. Although this is a relatively expensive process, the honeycomb increases the strength by thirty-seven percent while only increasing the weight by six percent. Since a lightweight aircraft is optimal, this is a very attractive construction method for the fuselage design. The fuselage is constructed by epoxying four main sections together: top, bottom, and the two sides.

The fuselage requires a mold for the two side-pieces. Since the sides are symmetrical, they are simultaneously produced as one large section and later cut to size following the curing process. The top and bottom of the fuselage are fabricated in flat sections. This flat lay-up only requires the use of glass and a cut piece of foam to place on the top segment to cradle the wing structure. The fuselage receives additional structural reinforcement carbon fiber-honeycomb sandwich bulkheads. These methods are

time and labor efficient. After fuselage assembly, all rough edges are smoothed down with a grinder and the payload hatch is cut out of the bottom section. The payload doors are made of layered carbon fiber composite and honeycomb and attached to the fuselage by hinges.

An independent manufacturer designed and created the boom. The Structures Group purchased it from Maclean Quality Composites located in Sandy, Utah. Aluminum standoffs were made from aluminum stock and epoxied onto the rotating cuff and fixed sections on the boom's aft end for the tail attachments.

7.2.2 Wing

The majority of the manufacturing process for the wing was done through hand-craftsmanship. Rib templates were made and used to cut out the plywood and balsa ribs. The plywood ribs were used for the inboard part of the wing while the balsa ribs were used outboard. A wing jig was assembled using two wooden bars so that the ribs could be aligned during their assembly. While held in place in the jig, the spruce spars and the carbon fiber spar were inserted into the ribs.

After the spars were inserted, the shear webs were created from a template. They consisted of a sheet of balsa supported by a sheet of carbon fiber for strength. They were installed onto the wing structure. Finally, the leading edge and trailing edges for the wing were formed from balsa stock by hand. The balsa stock was sanded down to the appropriate shape and bonded onto the wing. The ailerons were created similarly to the process for the wing, just on a smaller scale.

Monokote is finally applied to the wing surface to give it the final streamlined shape. This process involved heating the Monokote so that it adhered to the ribs and skin of the wing. All air bubbles and ripples were carefully taken out of the Monokote with an iron. The ailerons were coated with white Monokote to provide visibility to the pilot during flight. The wing tips were also coated with white Monokote for similar visibility reasons.

7.2.3 Tail

The tail was manufactured using the same materials and techniques as used for the wings. As with the wings, the tail was coated with Monokote conform to its final shape. For visibility reasons, the control surfaces on the tail, ruddervators, were coated with white Monokote.

7.2.4 Landing Gear

The main landing gear was constructed from multiple layers of carbon fiber. A male mold cut from blue foam serves as the foundation for the carbon fiber lay-up procedure. The wheels, brakes, and front gear struts were all purchased directly from the manufacturers using the desired specifications developed through the analyses.

7.2.5 Payload and Deployment

The payload box was required to weigh a minimum of five pounds and measure 12 inches x 6 inches x 6

inches. This was achieved using three pieces of foam, each measuring 12 inches x 6 inches x 2 inches glued together with two 2.5 pound dumbbell weights in the center of the middle foam piece. The final payload box weighed 5.07 pounds, fulfilling the dimension requirements.

The cargo release mechanism was constructed from pieces of aluminum. Several small aluminum bars (two with ears for holding the payload bay shut) were joined with pivots on either side of the payload doors, connected by an aluminum rod. A servo pushes on a linkage segment that opens and closes the doors. No tooling is required for this system, just detail drawings for the Structures Group to follow.

7.3 Construction Costs

A large consideration for construction of the aircraft involved the cost of materials. These estimations were based on information from Oklahoma State University's historical database. The greatest foreseen costs involved the necessary components for the mechanical and propulsion systems at $991.70. The aircraft construction materials account for about $871.33, a large portion as well. Consumable materials account for $293.11, giving a total estimated manufacturing cost of $2,159.14.

7.4 Construction Skill Matrix

It took many skills to design and construct the Orange Team's aircraft. Some of these construction skills included composite lay-up, computer aided modeling, radio equipment installation, and woodworking. To evaluate the different components' skill requirements for construction and assembly, a skill matrix was created. The skill matrix assigned difficulty factors from zero to two. The rating of two corresponded to a component or system requiring a high level of skill while one and zero corresponded to a medium and zero skill level, respectively. The skill matrix is shown in Table 7-3 for the primary aircraft systems.

Primary Aircraft Systems	Foam Cutting	Composite Lay-Up	Mold Preparation	Radio Equipment Installation	Electrical Work	Computer Modeling	Wood Working
Wing	0	1	0	2	1	2	2
Fuselage	2	2	2	2	2	2	0
Landing Gear	1	2	1	2	1	2	0
Tail/Boom	0	1	0	2	2	2	2
Propulsion System	0	0	0	2	2	1	0
Antenna	1	0	0	0	0	1	0
Payload System	0	1	0	1	1	2	0

Table 7-3: Skills Matrix

Since the Orange Team had members with many different skill specialties and experience, there were no major problems with any of the required skills listed in the matrix.

7.5 Manufacturing Schedule

A schedule was created to maintain progress throughout the aircraft-manufacturing phase. This schedule documented the manufacturing progress of all the necessary systems and components for the aircraft. Major milestones, such as the prototype and final aircraft roll out dates were noted in addition to other

important construction dates. Even with the schedule, unforeseen diversions occurred, forcing slight deviations from the schedule. The planned and actual manufacturing schedules are shown in Figure 7-1.

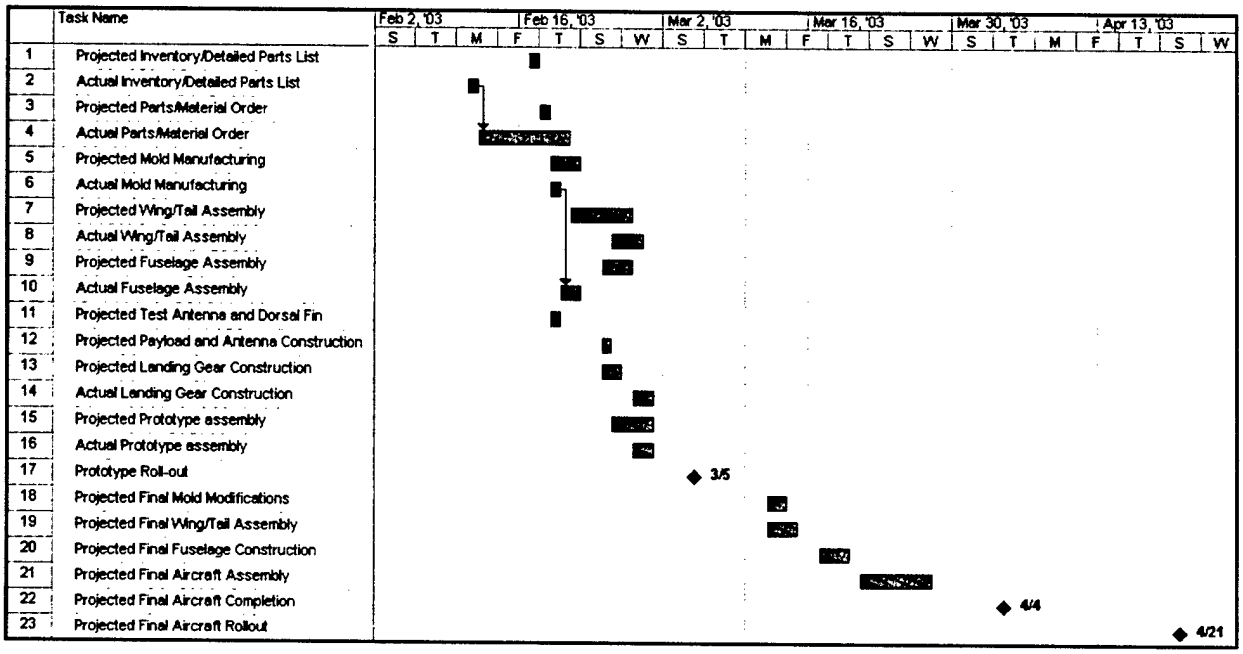

Figure 7-1: Manufacturing Milestone Chart

8 Testing

8.1 Testing Plan

In addition to all of the analyses performed, the Orange Team decided to do extensive testing regarding many different aspects of the aircraft performance and configuration.

8.2 Test Objectives and Schedule

The Orange Team decided to perform tests in the following areas: drag analysis, propulsion system analysis, brake performance, wing construction techniques, and flight-testing.

8.2.1 Drag Tests

Both the Structures Group as well as the Aerodynamics Group did drag testing. Their tests included evaluation of different fuselage cross sectional shapes as well as full aircraft and antenna drag.

- Fuselage Cross-Sectional Drag Tests

Using a force balance mounted in the Oklahoma State University wind tunnel, the Structures Group tested the drag forces on fuselages with different cross-sections. The tests were performed at a zero and eight degrees angle of attack to represent cruise and takeoff, respectively. The drag produced by a circular cross-section was compared to that from a rectangular cross-section with similar hydraulic

diameters. It was found that the rectangular cross sectional fuselage produced less drag than the circular when considering the cross-sectional area required to hold the payload.

- Aircraft Drag Tests

The Aerodynamics Group performed drag tests on a full-scale aircraft prototype. Since the Oklahoma State University wind tunnel is not large enough to house the wingspan of the aircraft, the drag was measured for the entire wingless aircraft. Tests were performed at two angles of attack. First, the tests were done at zero degrees, representing flight in cruise. Then, the tests were repeated at an angle of ten degrees to represent takeoff as closely as possible with the drag stand's angular restraints. Additional tests were performed using a teardown method. This involved removing the main components of the aircraft piece by piece until only the fuselage remained.

During the teardown drag tests, the airflow behind the nose gear and tapered back end portion of the fuselage seemed to be the most turbulent. An aerodynamic faring placed in front of the nose gear was created to see if better airflow could result. However, through the analysis of the data, the addition of this faring created an increase in drag on the aircraft. For this reason, further development into nose gear fairings was not pursued.

However, this estimate is based on a velocity of 55.35 feet per second, which is slightly less than the optimal fifty-seven feet per second. This and additional results from the analysis of the data were used to update the aerodynamic optimization analysis program.

8.2.2 Propulsion Tests

The Propulsion Group will expand its knowledge of the propulsion system with continued experimental testing and evaluation. Completed tests include performance analysis on folding propellers and installed thrust tests using various propellers. Future testing includes endurance testing, installed thrust testing, and flight-testing.

- Propellers

The performance of Graupner and Aeronaut 16 inches by 10 and 18 inches by 10 folding propellers was tested in the Oklahoma State University wind tunnel. The propellers were mounted on an Astro Flight 640G motor and tested over a large range of airspeeds. Thrust and torque data was collected using a force balance mechanism. Traditional propellers were also tested in the wind tunnel using an Astro Flight 640S motor.

The data from the propeller tests was analyzed to plot the curves of the thrust and power coefficients versus the advance ratio. This information was analyzed to determine the overall propeller performances and efficiencies. It was determined from the plots that the folding Aeronaut propeller outperformed the folding Graupner propeller by 6.6 percent. However, it was discovered that the overall propulsion efficiency is lower with the folding propellers in comparison to the traditional propellers previously tested.

- Battery Endurance

Extensive battery endurance tests were performed in the wind tunnel. The tests were conducted using the aircrafts actual propulsion system: Astro Flight 640S motor, twenty-two cell NiCad battery packs, and a twenty-inch traditional propeller. It was found that the thrust provided by the system was adequate for the aircraft and mission selections. In fact, the system provided forty seconds of additional cruise time on average. This additional power will allow the aircraft to utilize additional thrust in takeoff if necessary.

8.2.3 Brake Testing

Performance tests were conducted on pneumatic and electromagnetic brakes. The tests used a tricycle gear mounted sled with the addition of variable weights placed on it. The air pressure to the pneumatic brakes and the voltage to the electromagnetic brakes were continuously applied in varying proportions until the brakes no longer locked-up and skid. The forces used to move the sled were documented. The pneumatic brakes were tested both on the nose and main gear. The electromagnetic brakes only work on the nose gear so their location was not varied. Although both the electromagnetic and pneumatic brakes had similar results in braking distances, the pneumatic brakes seemed to be more reliable. Since the comparison was relatively close, the pneumatic brakes were selected for use on the aircraft.

8.2.4 Wing Construction Methods

Members of the Structures Group investigated wing construction methods from June to December of 2002 as independent research. This research investigated the strength-to-weight ratios of various methods of wing construction for conventional balsa and foam core with a fiberglass skin. The foam wings were studied with and without spars.

The tests of the wing construction techniques showed that a conventional balsa wood wing has a higher strength-to-weight ratio than one with a fiberglass skin and a foam core. These results are shown in Figure 4-5 in the preliminary design phase section.

8.2.5 Future Testing

The future testing for the Orange Team includes extensive flight-testing as well as additional propulsion and drag testing.

- Flight-Testing

The Orange Team plans to spend a large amount of time flight-testing. This testing will begin upon completion of the aircraft prototype. The prototype flight-testing will uncover any problems with the flight handling qualities and the maneuverability of the aircraft. It will also test the compatibility of the aircraft components and systems to ensure that everything is functional. Any necessary changes will be incorporated into the final aircraft design. The final aircraft will be tested in flight extensively to ensure that all of the problems have been fixed. This will also give the pilot ample time to practice the missions before the competition.

- Propulsion Testing

Flight-testing will be a continual process of measuring and evaluating the amount of power consumed by the propulsion system during each lap of the missions. This stage will be the most extensive testing phase since it will be an ongoing process. Eventually, the Propulsion Group will have collected enough test data to accurately predict the remaining power in the batteries at any point of the flight.

- Drag Testing

Future drag testing is planned for the aircraft prototype. The entire prototype will be tested during simulated critical phases of the flight missions by mounting it to a force balance located in the bed of a truck. The force balance will allow us to measure the drag of the aircraft in simulated flight. These measurements will assist the team in refining the final design.

8.2.6 Testing Schedule

The Orange Team devised a testing schedule to keep all of the testing on track. The schedule was made so that any testing data necessary for analysis was completed on time and could be used throughout all of the phases of the design process. The majority of the future testing will involve the functional prototype and the finished aircraft. The weekly breakdown for testing is as follows:

- Week of February 23: Brake Testing
- Week of March 2: Propulsion Endurance Testing, Drag Wind Tunnel Testing, and Structural Testing
- Week of March 9: Flight-Testing of Prototype
- Week of March 16: Flight-Testing of Prototype
- Week of April 6: Flight-Testing of Final Aircraft
- Week of April 13: Flight-Testing of Final Aircraft

8.3 Flight Check-List

The Orange Team developed a flight check-list to make sure that the aircraft was always ready before each flight. All of the tasks listed in Table 8-1 must be checked before each flight.

Motor Mount Secure		Starboard Aileron Secure	
Propeller Nut Tight		Payload Installed and Secure	
Front Landing Gear Secure		Payload Doors Locked	
Wing Wires Connected		Perform Wingtip Test	
Wing Bolts Secure		Radio Test all Control Surfaces	
Boom and Tail Locked into Position		Brakes Work	
Main Gear Locked into Position		Nose Gear Steering Works	

Table 8-1: Flight Check List

9 References

Nelson, Robert C. Flight Stability and Automatic Control. McGraw Hill: Boston, MA 1998.

Raymer, Daniel P. Aircraft Design: A Conceptual Approach. American Institute of Aeronautics and Astronautics, Inc.: Reston, VA 1999.

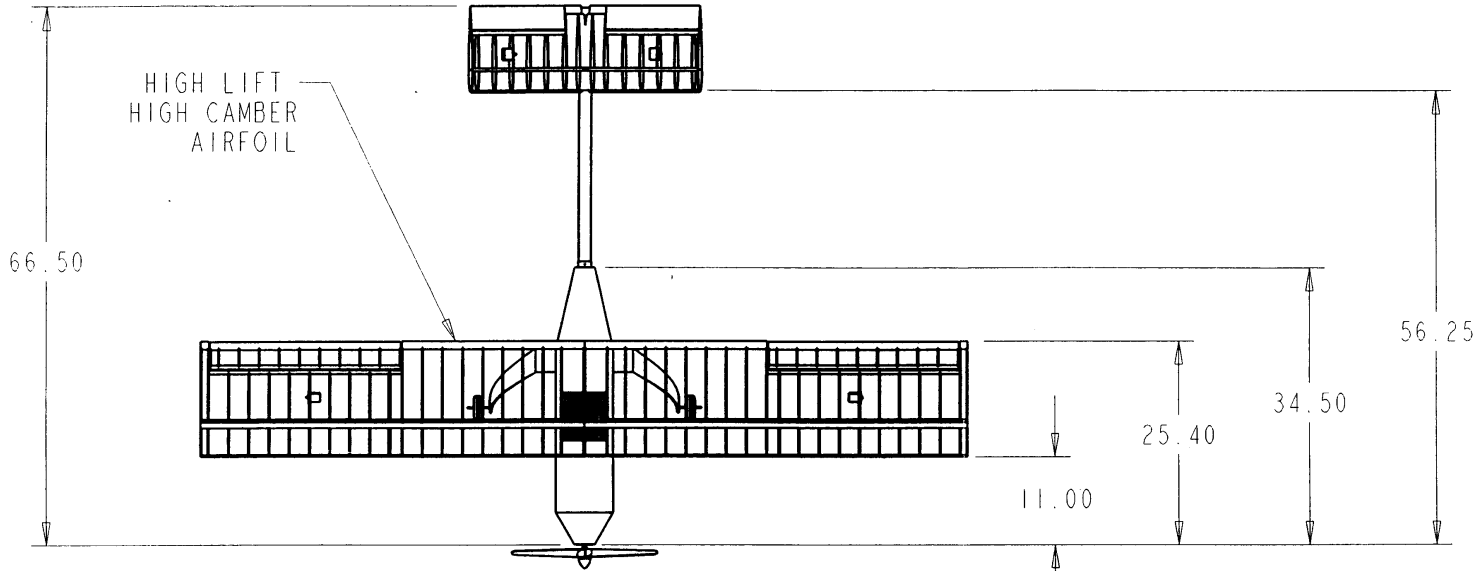

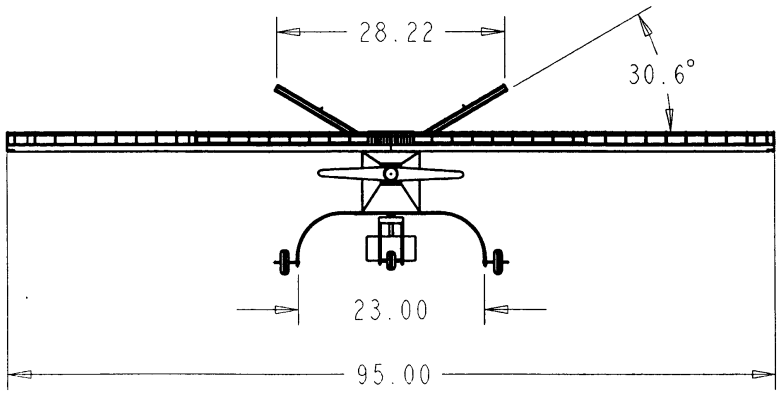

DUAL STRUT NOSE GEAR
MAIN GEAR CARBON
FIBER SANDWICH

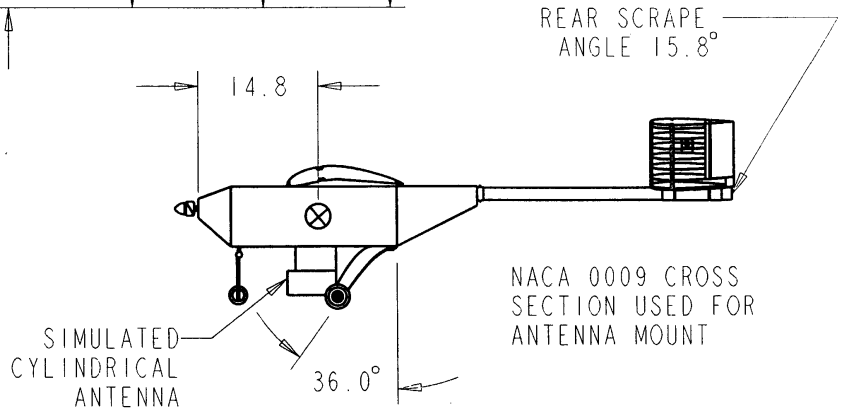

ENGINEERED BY: A.W.	OKLAHOMA STATE UNIVERSITY - ORANGE TEAM
PREPARED BY: D.C.	THREE - VIEW
CHECKED BY: C.R.	
SCALE: 0.065	DBF 2003 DRAWING PACKAGE
UNITS IN INCHES	DATE: 2-26-03 PAGE 1 OF 5

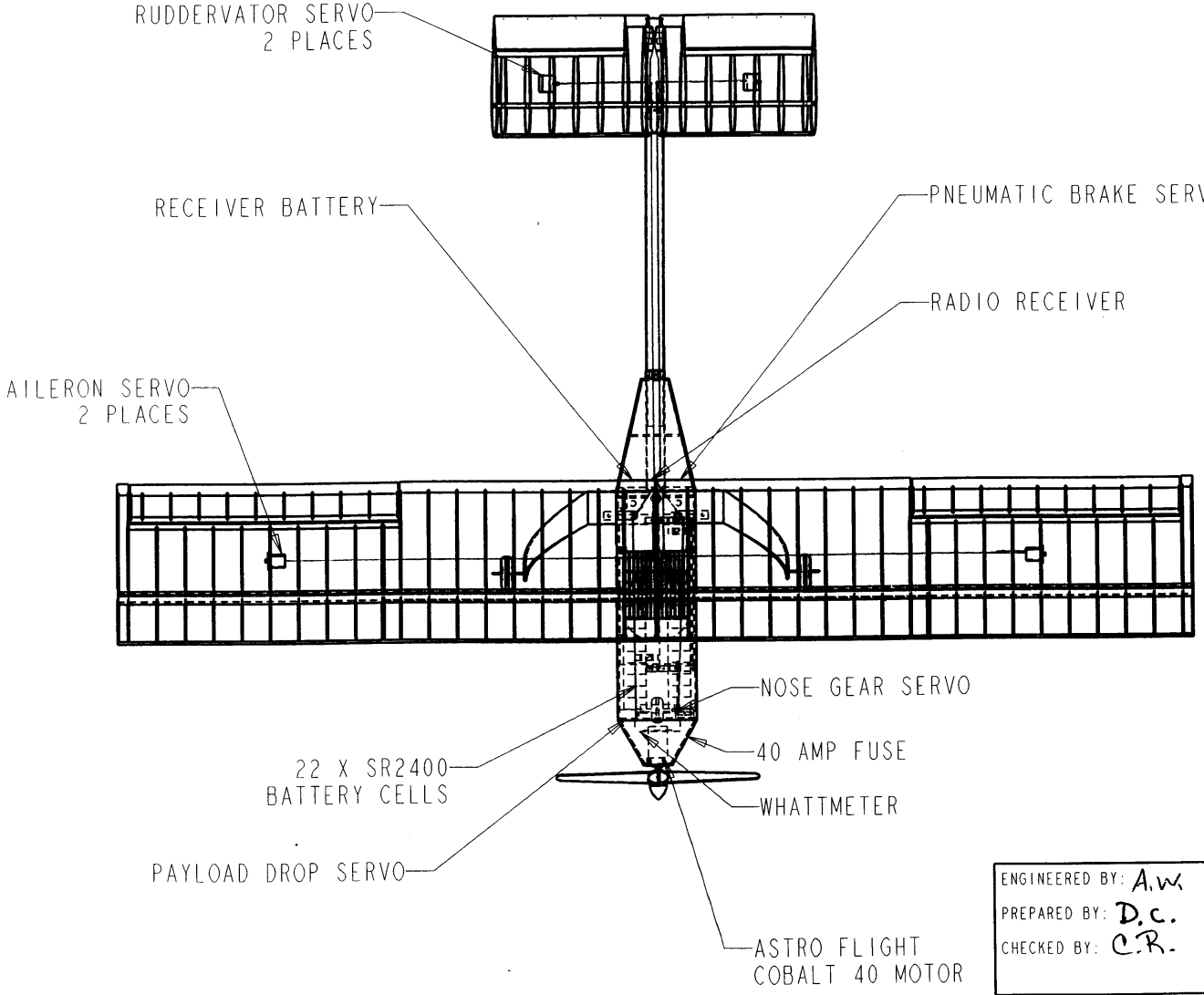

ALL SERVOS TO BE OF HIGH-QUALITY, CORELESS, HIGH-SPEED, METAL GEAR CONSTRUCTION

ALL SEVO CONNECTIONS TO HAVE SAFETY CLIPS

WHATTMETER TO BE INSTALLED FOR FLIGHT TEST PURPOSES ONLY

FUSE CLIP USED TO SAFETY DURING GROUND MAINTENANCE

ENGINEERED BY: A.W.	OKLAHOMA STATE UNIVERSITY - ORANGE TEAM
PREPARED BY: D.C.	SYSTEMS LAYOUT
CHECKED BY: C.R.	
SCALE 0.10	DBF 2003 DRAWING PACKAGE
UNITS IN INCHES	DATE: 2-26-03 PAGE 2 OF 5

PERFORM RADIO TRANSMITTANCE TEST WITH ANTENNA DOWN

CHECK RECEIVER ANTENNA MOUNT

CHECK SERVO CONNECTIONS AND HORN HARDWARE

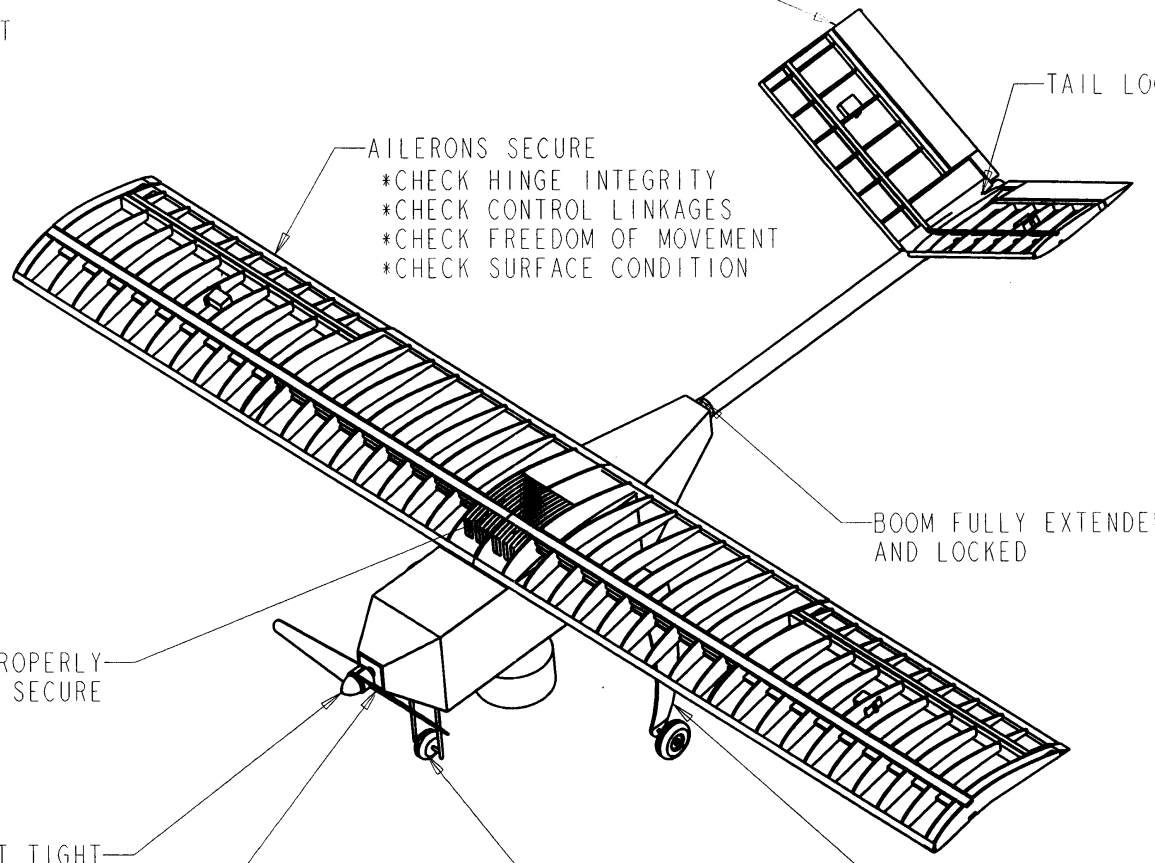

ENGINEERED BY: A.W.	OKLAHOMA STATE UNIVERSITY - ORANGE TEAM
PREPARED BY: D.C.	CRITICAL SAFETY OF FLIGHT CHECKS
CHECKED BY: C.R.	
SCALE: 0.11	DBF 2003 DRAWING PACKAGE
UNITS IN INCHES	DATE: 3-8-03 PAGE 3 OF 5

SPRING LOADED PINS ALLOW FOR QUICK EXTENSION OF BOOM AND UNFOLDING OF THE V-TAIL

ALUMINUM PINS INSERTED IN CARBON FIBER SLEEVES TO ALLOW FOR ADDITIONAL STRENGTH AND LESS FRICTIONAL RESISTANCE

STARBOARD TAIL SECTION AFFIXED TO PERMANENTLY ATTACHED CARBON FIBER COLLAR

PORT TAIL SECTION AFFIXED TO ROTATABLE CARBON FIBER COLLAR

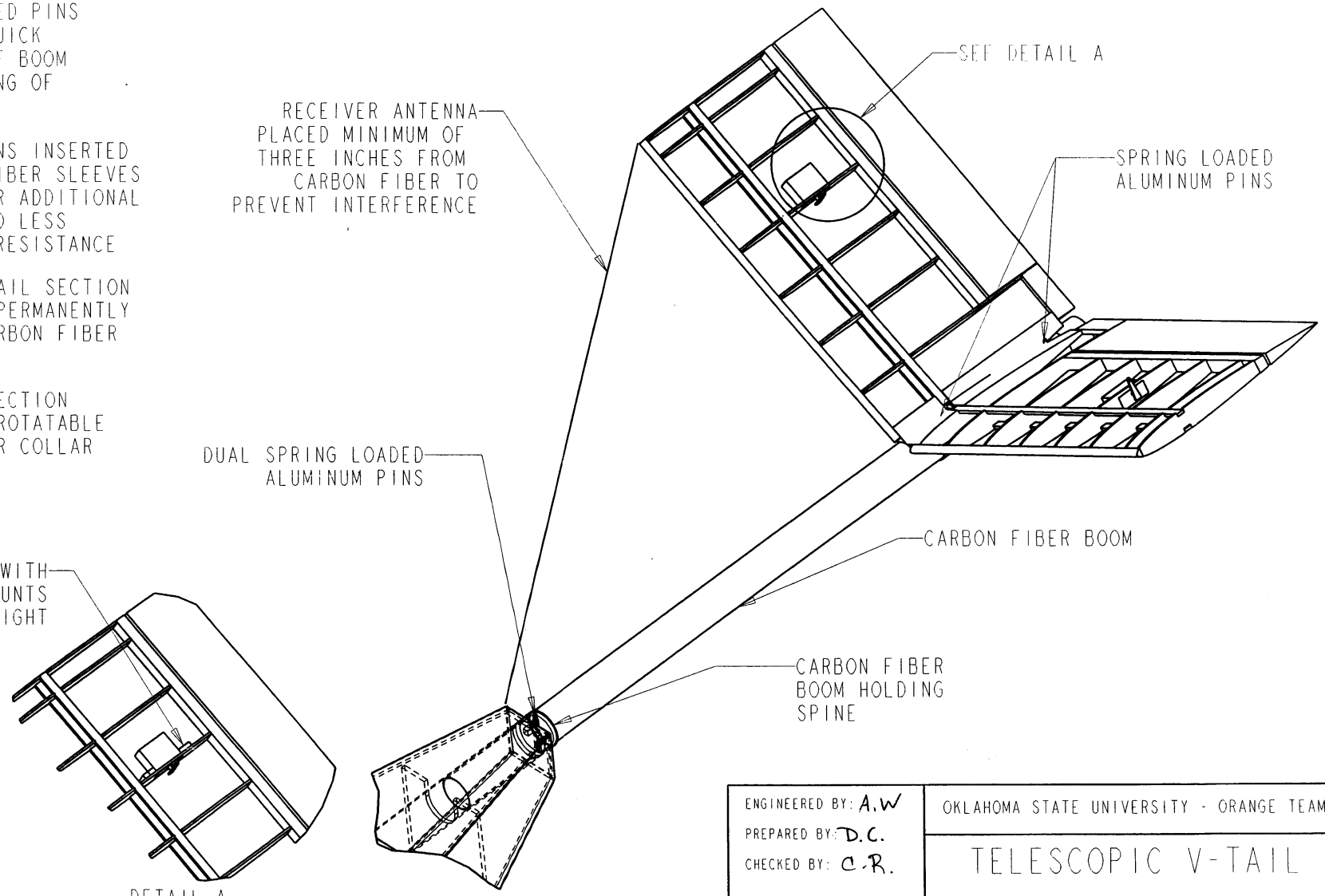

ENGINEERED BY: A.W PREPARED BY: D.C. CHECKED BY: C.R.	OKLAHOMA STATE UNIVERSITY - ORANGE TEAM TELESCOPIC V-TAIL
SCALE: 0.25 UNITS IN INCHES	DBF 2003 DRAWING PACKAGE DATE: 3-7-03 PAGE 4 OF 5

DISTANCE BETWEEN LATCHES AND PIVOT POINT HELD CONSTANT TO ENSURE UNIFORM VELOCITY OF LATCHES

DISTANCE BETWEEN MECHANISM LINKAGE AND PIVOT POINT HELD CONSTANT TO ENSURE UNIFORM VELOCITY OF LATCHES

SPRING LOADED DOORS FOR RAPID RETRACTION

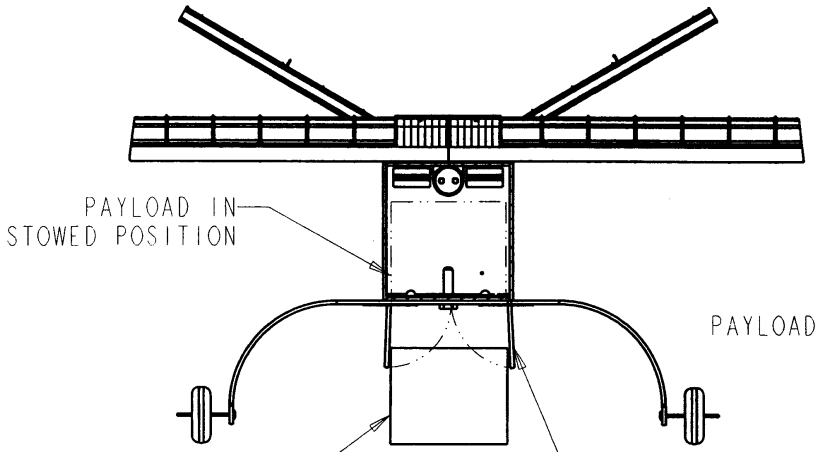

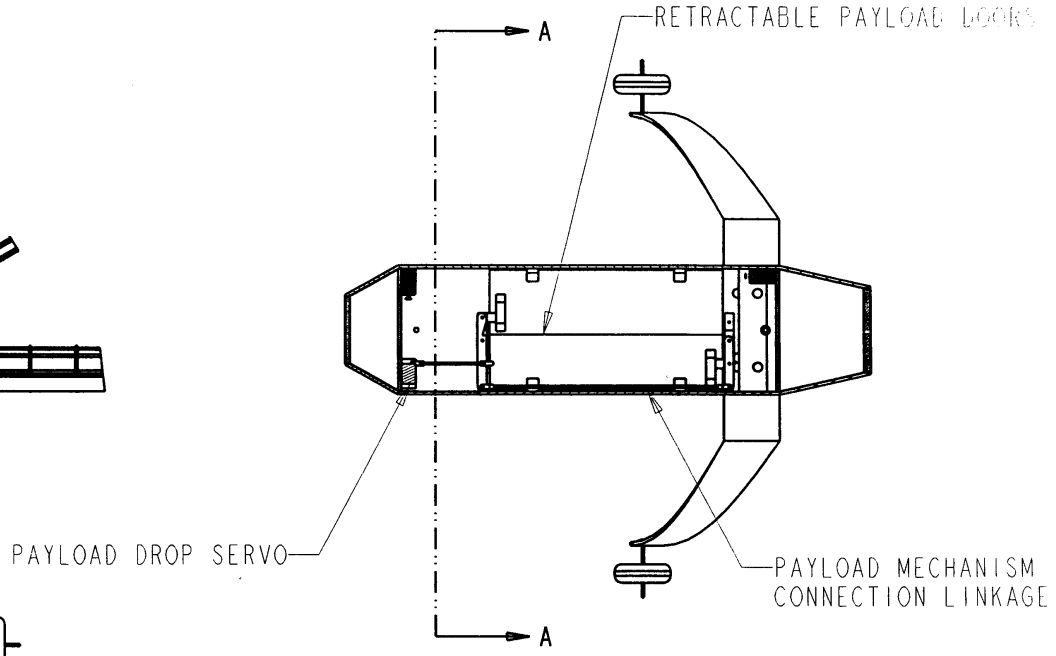

ENGINEERED BY: A.W. PREPARED BY: D.C. CHECKED BY: C.R.	OKLAHOMA STATE UNIVERSITY - ORANGE TEAM	
	PAYLOAD DEPLOYMENT MECHANISM	
SCALE: 0.15	DBF 2003	DRAWING PACKAGE
UNITS IN INCHES	DATE: 3-7-03	PAGE 5 OF 5

2003 AIAA Foundation/Cessna Aircraft/ONR Undergraduate/Graduate Student Design/Build/Fly Competition Report

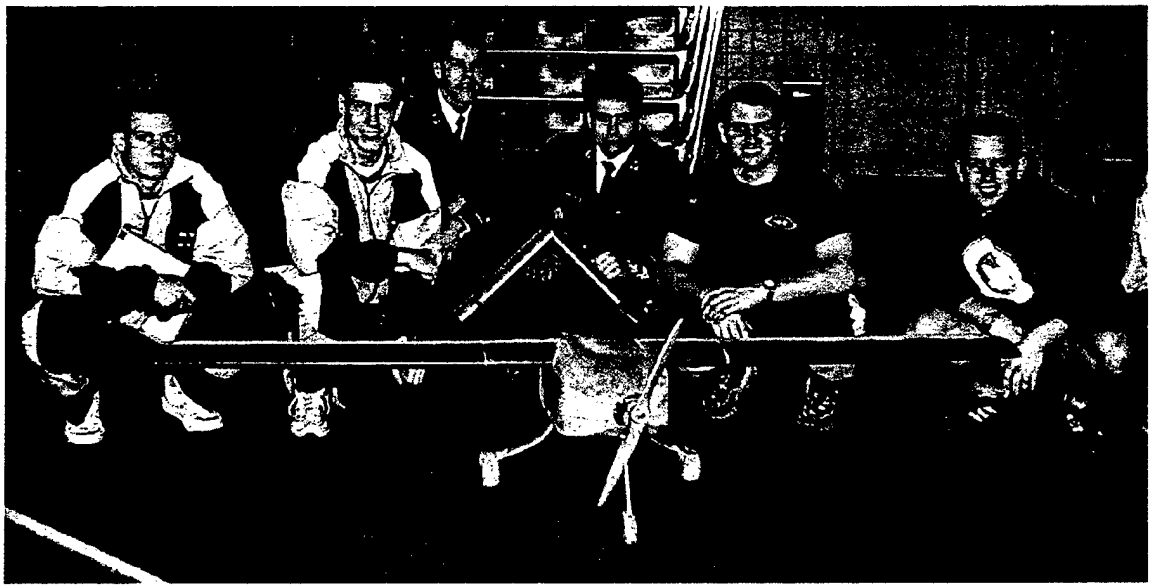

Submitted by:
United States Naval Academy
Team SEVERN DISCOMFORT

March 6, 2003

Contents

1 Executive Summary 1

1.1 Conceptual Design 1

1.2 Preliminary Design 2

1.3 Detail Design 3

1.4 Manufacturing Plan and Processes 3

1.5 Testing Plan 3

2 Management Summary 4

2.1 Team Positions 4

2.2 Program Plan 5

3 Conceptual Design 7

3.1 First Look 7

3.2 Individual Conceptual Designs 9

3.3 Sensitivity Analysis 10

3.4 Conceptual Design Assessments 14

4 Preliminary Design 19

4.1 Wing Construction Techniques 19

4.2 Wing Attachments 21

4.3 Tail Boom Torsional Analysis 22

4.4 Payload Deployment Techniques 23

4.5 Initial Propulsion Testing and Calibration 24

4.6 Astro Cobalt 90 Endurance Test 26

4.7 Landing Gear Wind Tunnel Test 27

4.8 Landing Gear Assembly 28

4.9 Airfoil Selection and Wind Tunnel Test 28

4.10 Radome Wind Tunnel Test 30

4.11 Improved Propulsion Validation 32

4.12 Drag Build up and Thrust Required 33

4.13 Preliminary Weight and Balance 33

4.14 Performance 34
4.15 Stability 35
4.16 Preliminary Design Wrap Up 36

5 Detail Design 38
5.0.1 Wing 38
5.0.2 Fuselage 38
5.0.3 Gear 39
5.0.4 Empennage 39
5.1 Final Geometry Determination 39
5.2 Final Weight Statements 39
5.3 Performance 41
5.4 Systems and Components 42
5.5 Rated Aircraft Cost 43
5.6 Drawing Package 43

6 Manufacturing Plan and Processes 45
6.1 Manufacturing FOMs and Material Selection 45
6.2 Components 46
6.2.1 Fuselage 46
6.2.2 Gear 47
6.2.3 Wing 47
6.2.4 Empennage 48
6.3 Manufacturing Plan 48

7 Testing Plan 50
7.1 Flight Testing Schedule 50
7.2 Ground Testing Results 51

8 References 54

List of Figures

2.1 Detailed Program Plan 6

3.1 Variables Affecting Rated Aircraft Cost and Final DBF Score 12
3.2 Aircraft Configuration Decision Matrix and Selected Planforms 15
3.3 Tail Configuration Decision Matrix 16
3.4 Conceptual Design 18

4.1 Composite Spar Strength and Stiffness Test, Standard Layup 20
4.2 Composite Tube Bending Moment Test Setup and Results 21
4.3 Composite Tube Torsional Test Setup and Results 23
4.4 Deployment Technology Demonstrator 24
4.5 Wind Tunnel Propulsion Test Setup and Advance Ratio vs Efficiency (Astro 40, 1.63:1, 12 X 8 propeller) 25
4.6 Landing Gear Wind Tunnel Test Components and Drag Results 27
4.7 Preliminary Internal Structure Design 29
4.8 Eppler Airfoil Construction, and Lift and Drag Results 30
4.9 Radome and Splitter Plate Test Apparatus and Results 31
4.10 Thrust vs Velocity: Trends in Pitch 32
4.11 Thrust Required and Optimum Thrust Available 34
4.12 Preliminary Design: Component Packaging and Assembly 37

6.1 Fuselage, Landing Gear, and Internal Structural Details 47
6.2 Wing and Empennage Construction 48
6.3 Manufacturing Schedule 49

7.1 Final Production Aircraft Assembled for Ground Testing and the Payload Deployment Test . 53

List of Tables

2.1 Team Position Breakdown 4

3.1 Estimate of Critical Performance Parameters 8
3.2 Conceptual Design Ranking Chart 10
3.3 Baseline Values for Sensitivity Analysis 11
3.4 Mission Selection Decision Matrix 14
3.5 Empennage Selection Decision Matrix 16
3.6 Gear Configuration Decision Matrix 16
3.7 Gear Integration Decision Matrix 17
3.8 Wing Orientation Decision Matrix 17
3.9 Power Plant Selection Decision Matrix 17
3.10 Fuselage Selection Decision Matrix 18

4.1 Results of Wing Construction Testing 20
4.2 Preliminary Weight and Balance 35
4.3 Preliminary Design Stability 36

5.1 Aircraft Parameters and Sizes 40
5.2 Aircraft Weight Statement 40
5.3 Aircraft Balance Statement 41
5.4 Aircraft Performance 42
5.5 Systems and Components 43
5.6 Final Rated Aircraft Cost 44

6.1 Manufacturing FOMs and Selection Criteria 46

7.1 Preflight Checklist 50
7.2 Flight Testing Plan 52

Chapter 1

Executive Summary

The following document contains a summary of the design process for the United States Naval Academy (USNA) SEVERN DISCOMFORT team entry submitted to the 2003 Design/Build/Fly competition. It discusses all relevant analysis, design, and testing conducted by the team. Additionally, it provides a detailed documentation of the team's thought process and how decisions were made at each stage of the design from the conceptual to the preliminary to the detailed design phase. Finally, it serves as a guide to the aircraft's component manufacturing and fabrication, as well as system integration and flight testing.

1.1 Conceptual Design

The conceptual design phase began with a study of the competition requirements and rules. The biggest change to rules this year were that the aircraft must be designed to be assembled from a 4 X 2 X 1 foot box and fly 2 of 3 missions. The missions each carried a different weighting factor and varied slightly from the baseline mission requirements, which required the aircraft to take off carrying a 5-pound payload, complete four laps on the course with one 360-degree turn per lap, and land. Mission A required a "radome" to be carried externally, mission B required the internal payload to be deployed, and mission C required 2 additional 360-degree turns per lap.

This study was followed by a period of research on previous year's DBF designs, conventional radio-controlled aircraft, and modern unmanned aerial vehicles. The focus of this study was to find available technologies, analyze potential design considerations, and match capabilities to the 2003 DBF missions.

An initial weight and performance estimate was then conducted to serve as the first draft for the team's design. Estimates for wing loading, maximum lift coefficient, thrust-to-weight ratio, and lift-to-drag ratio were set to meet the necessary mission requirements.

Individual conceptual designs were then developed by each team member to provide the greatest possible range of ideas in the initial design phase. After the completion of the individual designs, the team organized into disciplines - aerodynamics, propulsion, performance/stability and control, structures, CAD, and systems analysis with a program manager and systems engineer. A sensitivity analysis was the next order of business, conducted to steer the conceptual design development and focus the development on the most significant parameters. From this, a series of decision matrices were constructed based on

figures of merit derived from the sensitivity study and the individual conceptual designs.

Several different configurations and design possibilities were initially examined. The prefered missions, overall configuration, tail type, landing gear configuration, wing placement, and fuselage type were all selected after assigning weighted figures of merit in a decision matrix. The baseline configuration taken into the preliminary design phase was a high wing, twin tail boom, inverted V-tail aircraft, with a single motor and prop, and a conventional fuselage, designed for missions A and B.

1.2 Preliminary Design

The preliminary design phase began with a look at wing construction. 16 potential composite layups were tested for strength and stiffness to better understand the loads on the aircraft and develop a design robust enough to deal with these loads. An additional experiment provided axial and torsional data on several carbon fiber tubes for potential use as wing spars or tail booms because of both their strength and ease of assembly. A mockup deployment mechanism was then designed to iron out compatability and integration issues, and to check the reliability of the design itself.

Numerous propulsion experiments were conducted during the preliminary design phase in order to produce a viable propulsive combination with adequate power to takeoff, sustain flight, and complete the missions as fast as possible. Computer analysis and wind tunnel testing were both used extensively to produce accurate, reliable data. A full range of motor and prop combinations was analyzed from a direct drive Astro 40 spinning a small 12 inch propeller, to an Astro 90 geared at 2.73:1 turning a 20 inch propeller. Looking at a host of parameters ranging from static thrust, to top speed, to maximum current draw, to endurance, the best combination tested was the Astro 60, geared at 2.73:1, with an 18x18 APC propeller.

Several aerodynamic tests were conducted during the preliminary design phase, as well. Different landing gear setups were tested with varying wheel sizes and fairings to provide drag data and validate the decision not to use a retractable gear. From the results, a design for the aircraft's internal structure and gear assembly was developed. The wing airfoil section was selected based on historical data and wind tunnel testing of an NACA 4412 and an Eppler 67. The 4412 had both favorable lift data through the stall region and less drag through the majority of the flight regime. The radome was also tested in the wind tunnel for drag data, with special attention payed to critical Reynolds number and a reduction of drag with turbulent flow over the body.

A detailed drag build up was developed based on the aircraft design and the subsequent drag polar was plotted against the power available curve to develop some initial performance estimates for the aircraft. Additionally, the weight and balance analysis was refined for a more accurate static stability estimate. With all the major components defined in the preliminary design phase, only a few unresolved issues were carried forward into the detailed design phase of the aircraft.

1.3 Detail Design

In the detail design phase, the team resolved all remaining open design issues and prepared to fabricate components and manufacture the aircraft. This process included selecting specific components for the aircraft, finalizing the sizing for all the major aircraft component groups and parts, and refining the performance estimates. Specific attention was paid to component mating and integration, including: the payload box attachment and deployment system, the landing gear attachment and folding mechanism, the propulsion system integration, servo selection and placement, all aircraft wiring, final structural estimates, and quick assembly techniques. Also included in this section is the drawing package, detailing the final production model aircraft. It contains complete 3-view dimensioned drawings, and a systems layout.

1.4 Manufacturing Plan and Processes

Aircraft fabrication began with an analysis of the different potential construction methods for the various aircraft components evaluated against several figures of merit: durability, repairability, availability, difficulty, timeliness, integration, weight, and cost. A manufacturing plan was then developed relying extensively on composites for the bulk of the load carrying structure of the aircraft. The fuselage, wing, empennage, and gear assemblies were subsequently fabricated according to the program plan and detailed design drawings.

1.5 Testing Plan

Flight testing was scheduled for five separate dates throughout the months of March and April. The testing plan initially called for a series of simple check flights in the middle of the aircraft's predicted performance envelop to determine basic aircraft handling qualities, flying characteristics, stability, and performance. Additional flights over the course of the testing program were planned to expand the aircraft's functional envelop and set limits for its safe flight regime. The last two flight tests, consisting of three flights each, were planned to simulate real competition missions for pilot practice and also to provide an accurate flight score estimate. A preflight checklist was developed to ensure full functionality prior to every test flight.

Chapter 2

Management Summary

The Severn Discomfort team was organized into functional units where all eight senior members were assigned a position within the team structure. Table 2.1 shows the personnel chart for each of the lead positions on the team. Underclass team members were assigned to one of the discipline leads and tasked through him. The underclassmen on the design team were Adam Cohen, Benjamin Hartly, Jonathan Powell, and Scott Sterling.

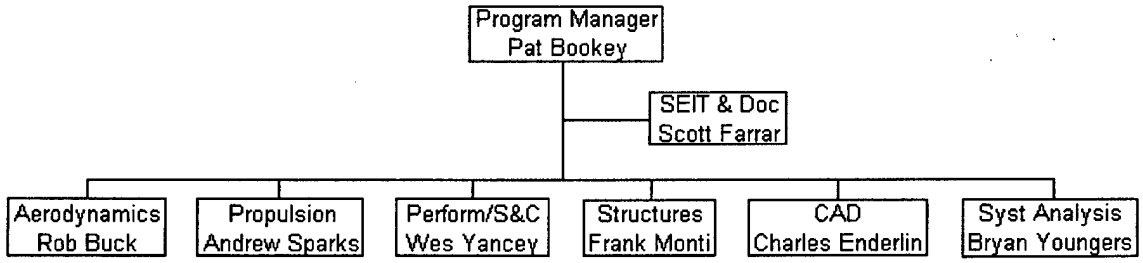

Table 2.1: Team Position Breakdown

2.1 Team Positions

The Program Manager was ultimately responsible for all team activities and products. He worked with each team member to establish a schedule and priorities, set assignments, and insure quality. He also worked directly with the SEIT and Documentation Lead to identify deadlines and produce a quality report. The program manager was tasked with maintaining the overall program schedule, keeping weekly progress reports, and managing daily team activities - modifying schedules and assignments as necessary.

The Systems Engineering, Integration, Test and Documentation Lead worked closely with the program manager and all team members to identify SEIT requirements and priorities, develop schedules, and insure timely execution and proper documentation. He was responsible for maintaining the SEIT plan, insuring thorough documentation of all program activities, maintaining all versions of the DBF report, and providing inputs to the PM that impact the overall schedule and weekly progress.

The Aerodynamics Lead was responsible for all aerodynamic analysis, test, design, and documentation

activities. He worked with other discipline leads to analyze and resolve all aerodynamic issues associated with the evolving design and conducted independent aerodynamic analysis, studies, and tests. Areas of focus included the overall wing, empennage, and configuration development; drag estimation and reduction activities; and mission performance and optimization efforts. He was specifically responsible for the Eppler airfoil testing, drag testing on the radome, and drag testing on the landing gears.

The Propulsion Lead was responsible for all propulsion analysis, test, design and documentation activities. He worked with the other leads to resolve any propulsion issues in support of mission performance and optimization; propulsion system optimization, selection, and design integration; and wind tunnel and flight test validation and risk reduction activities. He was tasked with validating the computer propulsion program called ECalc, conducting all propulsion testing in the wind tunnel, all completing battery and endurance testing.

The Performance/Stability and Control Lead headed up the performance and stability and control analysis, testing, design, and documentation efforts. He worked with the various leads to deal primarily with: the mission performance phases (take off, cruise, turning, and landing); the configuration development, control surface sizing, stability augment, and detailed design; and wind tunnel and flight testing. Tail sizing for both the V-tail and conventional tail, all performance estimates and mission requirements, and all stability estimates were specifically tasked to this lead.

The Structures Lead was in charge of all structures analysis, testing, design, and documentation. Throughout the design, he worked with the discipline leads advising on structural matters in support of the overall configuration development and design optimization; the detailed structural analysis and the development of rapid assembly and payload deployment techniques; and ground and flight validation of air vehicle structural and assembly and deployment designs. The Structures Lead handled the payload box deployment design and the wing attachment and tail boom bending moment and rigidity testing.

The Computer Aided Design Lead was tasked with all CAD analysis and documentation. He worked with the other leads to develop detailed drawings throughout the evolving design, specifically tracking the overall system development and design; the assembly and deployment techniques; and the detailed documentation of all preliminary and final designs. The CAD Lead offered integration support throughout the design, ensuring proper component mating and that all the components fit in the storage crate properly.

The Systems Analysis Lead handled all of the systems analysis tool development and documentation. His main responsibility was working with the other leads to develop a sensitivity study and required figures of merit. His focus was on overall system development and optimization regarding the final scoring, figures of merit assessments, and configuration trades; sensitivity analysis and cost/benefit analysis; and detailed documentation of all design decisions.

2.2 Program Plan

Based on the competition deadlines, each lead laid out an initial schedule of all forseen analysis, design, fabrication, testing, and documentation tasks. The SEIT and PM then complied and edited the individual submissions in a final program plan. This detailed program plan is presented in Figure 2.1.

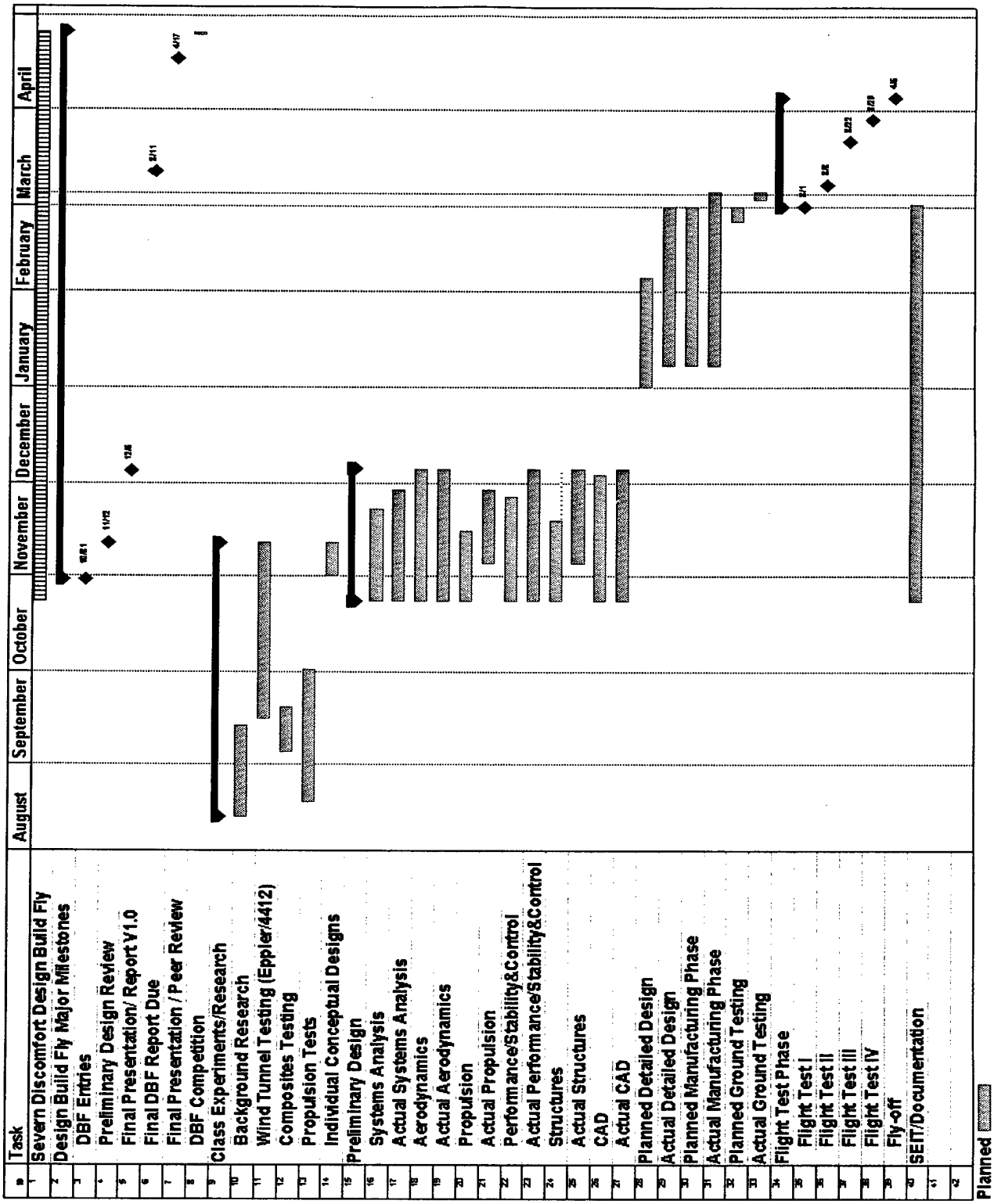

Figure 2.1: Detailed Program Plan

Chapter 3

Conceptual Design

3.1 First Look

For the 2003 Design/Build/Fly competition, "students must design, document, fabricate, and demonstrate the aircraft they determine as best capable of achieving the highest score." The aircraft must carry a five pound payload internally; use an Astro Flight Cobalt or Graupner brushed electric motor limited to five pounds of NiCad batteries, 40 Amps, and a commercially available propeller; be able to fit into, and be assembled from a 4 x 2 x 1 foot crate; be able to take off in 120 feet; and be able to complete 2 of 3 specified missions. For each of the three missions, the aircraft must take off, complete 4 laps around a 2000 foot course (1000 feet between each of 2 pylons), complete 1 360-degree turn on the downwind led, and land successfully. Each mission, however, provides its own twist on the basic mission requirement. Mission A (difficulty factor 2.0) requires that a 6-inch PVC radome be carried external to the aircraft exposed to the slip stream. Mission B (difficulty factor 1.5) requires the 5-pound internal payload to be deployed upon landing following the completion of 2 of the 4 laps. Lastly, Mission C (difficulty factor 1.0) requires an additional 2 360-degree turns on the downwind leg.

Scoring for the competition is based on three things: a written report score, a rated aircraft cost (RAC) based on assigning a representative dollar value to the aircraft; and a total flight score as follows:

$$DBFSCORE = \frac{(WrittenReportScore)(TotalFlightScore)}{RatedAircraftCost}$$

The total flight score is calculated from the sum of the best 2 single flight scores, each from a different mission. An aircraft's single flight score is based on the mission difficulty factor, the mission flight time, and the aircraft assembly time from the crate:

$$SingleFlightScore = \frac{DifficultyFactor}{(MissionFlightTime + AircraftAssemblyTime)}$$

The conceptual design process for Severn Discomfort's 2003 DBF entry began as an individual effort. The eight senior team members each spent time going over the rules and design requirements. Then, individually conducted research on current RC and UAV technologies and designs. This background search provided a foundation to build a conceptual design upon, both in terms of what has been done previously and what is available. It also prompted initial thoughts on sizing, weights, and construction

techniques. Following this study, each member produced an initial weight estimate based on historical data from similarly sized and similarly manufactured aircraft, and the estimated weight of known key aircraft components including the payload and battery weight. Estimates for the initial aircraft weight ranged from 18 to 23 pounds.

Following the weight estimate, each team member developed initial performance estimates for their aircraft design, which were developed to accommodate the various mission requirements. The maximum lift coefficient, wing loading, minimum required thrust to weight ratio, and maximum lift to drag ratio were the four main performance parameters examined. Inherent in the calculations for these, however, were the aspect ratio, drag polar, wing area, stall speed, and static thrust. Table 3.1 summarizes the results of the group's initial findings. These estimates provided a set of parameters through which conceptual designs were framed.

	Low End	High End
Weight (lb)	18	23
$C_{L_{max}}$	1.7	2.2
$\frac{W}{S}$	2	4
$(\frac{T}{W})_{min}$	0.2	0.4
$\frac{L}{D}$	13	19
S (ft^2)	6.5	9
V_s (mph)	22	28
T_o (lb)	4.0	9.0
AR	6	9
k	0.07	0.08
e	0.6	0.9
C_{D_o}	0.015	0.022

Table 3.1: Estimate of Critical Performance Parameters

Based on the performance estimates, viable propulsion systems were subsequently examined. Each of the eight team members selected and analyzed up to three different motor-prop-gearbox combinations using Bob Bucher's *ElectricMotorHandbook* and ElectriCalc2.0. This study provided each team member a familiarity with different combinations of single and twin motors, prop sizing in both pitch and diameter, gearing combinations, and different types of available Ni-Cd batteries. Concurrent with this individual study was a series of wind tunnel tests where 6 different propulsion combinations were wind tunnel tested at 0, 20, 40, and 60 mph; at 10, 20, and 30 Amps for each speed. This was conducted as a validation to check the accuracy of the ElectriCalc program. It was determined to be accurate enough for initial design considerations. Additional testing and the adjustment of several parameters would provide more accurate approximations later in the design process.

With this information, each team member produced his own conceptual design selecting missions, identifying performance parameters, constructing a configuration layout, selecting a power plant combina-

tion, developing a detailed wing design, providing a weight and balance build up, and computing RAC, flight time, and final score estimates. This was done prior to beginning group work on the design. Each member presented their individual conceptual design to the group on 08 October 2002.

3.2 Individual Conceptual Designs

The goal of the individual design efforts was to create a large brainstorming session where each team member's ideas on how to create a competitive aircraft could come out without initial criticism from other team members. This allowed a wide variety of ideas to appear on configurations, power plants, wing and tail designs, and other areas. These conceptual designs included the following aspects. First, each member defined the missions that they hoped to accomplish with their aircraft. All eight members opted to concentrate on Missions A and B, while still leaving Mission C as a viable option. The main justification for choosing Missions A and B was because of their greater potential for a high flight score based on their difficulty factors of 2 and 1.5. This unanimous decision on mission selection is reflected in the final design.

After choosing missions, team members came up with configurations for their aircraft. There were many different configurations ranging from a canard pusher combination to a tractor high-wing with twin tail booms. However, there were many similarities in the designs that are reflected in the final design.

Nearly all team members opted to have a small main fuselage with either a single or twin tail booms to push the tail away from the wing and main body. The high wing configuration was most prevalent in the designs due to the need to deploy the payload. The high wing made the most sense to move the wing out of the way of the deployment mechanism. The deployment mechanism had the most variety, with all team members coming up with very different ideas for unloading the payload box. These ranged from simply dropping it out the bottom to rocket propelled ejection. The complexity of deployment was the main driving factor in the configuration of the aircraft - the box has to deploy or the rest of the contest doesn't matter.

After finding a configuration, the team members sized the aircraft using basic equations for take-off roll, thrust to weight ratio, lift to drag ratio, and lift coefficient estimates. From these parameters, the wings were sized and shaped. Most members opted for a simple rectangular wing, although there was some slight taper in two of the designs. Each design incorporated a detailed weight build-up of all necessary components to include servos, battery packs, wheels, wires, and all other required items. With these estimates, the critical performance parameters of thrust to weight, maximum lift coefficient, lift to drag ratio, stall speed, drag polar, and take-off ground roll were re-examined.

Also calculated in each of the conceptual designs was the location of the center of gravity. This not only ensured that each design was balanced but gave a reference for sizing the tail. All designs used a tail volume ratio of between 0.5 and 0.7. This enabled the team members to find the length of their booms and the location and size of their tails. Each member then verified that the static margin of their aircraft was within acceptable limits, no further than 10 percent of the chord behind the center of gravity. Nearly all aircraft met this requirement.

Finally, each member estimated their Rated Aircraft Cost and calculated a potential final DBF score. The following chart, Table 3.2, ranks each individual design based solely on the Figures of Merit (FOM)

of RAC and Final Score:

FOM	Weighting	Bookey	Buck	Enderlin	Farrar	Monti	Sparks	Youngers	Yancey
RAC	0.25	-1	0.25	0.75	-0.75	-0.25	-0.5	0.5	1
DBF Score	0.75	1	0.25	-0.5	-0.75	-1	0.75	0.5	-0.25
	Score	0.5	0.25	-0.1875	-0.75	-0.8125	0.4375	0.5	0.0625

Actual RAC	15.34	12.68	11.27	15.05	12.99	14.57	12.24	11.27
Actual DBF Score	5.39	4.69	4.65	4.39	4.04	5.13	4.86	4.66

Table 3.2: Conceptual Design Ranking Chart

The end state of these individual conceptual designs was for each team member to brainstorm ideas on what they think would make a good aircraft to accomplish the required missions. Each of the aircraft designed in this conceptual phase were plausible designs, capable of accomplishing the mission requirements. From this point, the team came together with their individual designs in order to develop a composite conceptual design. Work on the final group conceptual design began with an analysis of all the individual efforts. From this, it was determined that no one design was exactly the right way to approach to problem as all of the designs had merit in some areas and were deficient in others. Therefore, the group set about identifying key Figures Of Merit (FOMs) for the various aircraft considerations and components, and evaluated the alternative approaches against these FOMs. All team members agreed that simplicity and robustness were the keys to success. The final approach represented a conglomeration of all eight individual designs. It contains the best combination of the ideas present, and the result was a conceptual design that the team felt had great scoring potential.

3.3 Sensitivity Analysis

Before the group started piecing together an initial conceptual design, however, a sensitivity analysis was conducted on several parameters that factor into both the rated aircraft cost (RAC) and the final score. The systems analyst did this in order to prioritize the various design parameters and focus the conceptual design efforts on the areas with the highest payoffs. Based on the competition scoring algorithm, a computer program was written which evaluated how mission time, assembly time, wing span, chord length, fuselage length, battery weight, propulsion setup, and cruise velocity affected the RAC and final score. Initial estimates for all the parameters were held constant based upon a set of baseline assumptions from initial performance estimates, historical precedence, and the box size limitations. Then, one variable was varied along an acceptable range of values to produce data depicting how a change in one specific variable affected the RAC and overall score. Plots were also generated in order to see the generalized trends in the sensitivity analysis. These results were then prioritized from high to low, based on which variables had the greatest effect on the final score. The relevant variables were initially set at the baseline values shown in table 3.3.

Using these baseline variables, a RAC of 11.85 was achieved along with an overall score of 6.30. These baseline scores were established using an estimated flight time of 3 minutes for both Missions A

Variable	Initial Value
Report Score	85
Assembly Time (min)	1
Mission Flight Time (min)	3
Battery Weight (lb)	4.5
Engines	1
Propellers	1
Wing Span (ft)	7.0
Wing Chord (ft)	1.0
Aircraft Length (ft)	5.5
Vertical Surfaces	1
Vert Surf w/ Control	0
Horizontal Surfaces	1
Contral Surfaces	4
Servos	6

Table 3.3: Baseline Values for Sensitivity Analysis

and B. The three minute flight time was estimated using an average velocity of 45 mph with the radome attached and 55 mph with a clean aircraft, a course length of 2000 ft with an additional 1000 ft to account for the 360-degree turns, and 30 seconds for each takeoff and landing or deployment.

Initially, the relationship between the RAC and the overall score was examined by varying the RAC from the baseline values. It is evident from the scoring algorithm that the DBF score varied inversely with the changing RAC. In particular, an increase of .60 from the baseline RAC was found to produce a 5.7 percent decrease in the overall score. Since these results demonstrated that the RAC was a major factor in the DBF score, the component variables affecting the RAC were next observed.

First, total battery weight values were varied from 0 to 5 lbs, the maximum battery weight allowed. It was determined that the relationship between the RAC and the battery weight was linear, as shown in Figure 3.1. An increase in the battery weight from 4.5 lbs to 5 lbs caused the RAC to increase by 6.3 percent from the baseline - a relatively significant increase.

Next, the effect of the wingspan on the RAC was studied - Figure 3.1. Unlike the total battery weight, the wingspan proved to be a much less significant factor in the score. An increase in the wingspan of 6 inches produced only a .75 percent change in the RAC, which translates to a small effect on the overall score.

Then, the effect on the RAC caused by varying the body max length was observed. The values for the body length ranged from 1 to 6 feet. Figure 3.1 shows the RAC to be directly proportional to the maximum body length. A 6-inch increase in the body length was found to increase the RAC only .84 percent.

The final variable analyzed that directly affected the RAC, was the maximum wing chord, seen in Figure 3.1. The wing chord values varied from 6 inches to 18 inches. As with the other variables affecting the RAC, the relationship between the max wing chord and the RAC was linear. When the wing chord was increased by six inches, the RAC only experienced a .68 percent increase.

Based on the analysis, the greatest effect on the RAC was caused by the variation of the total battery

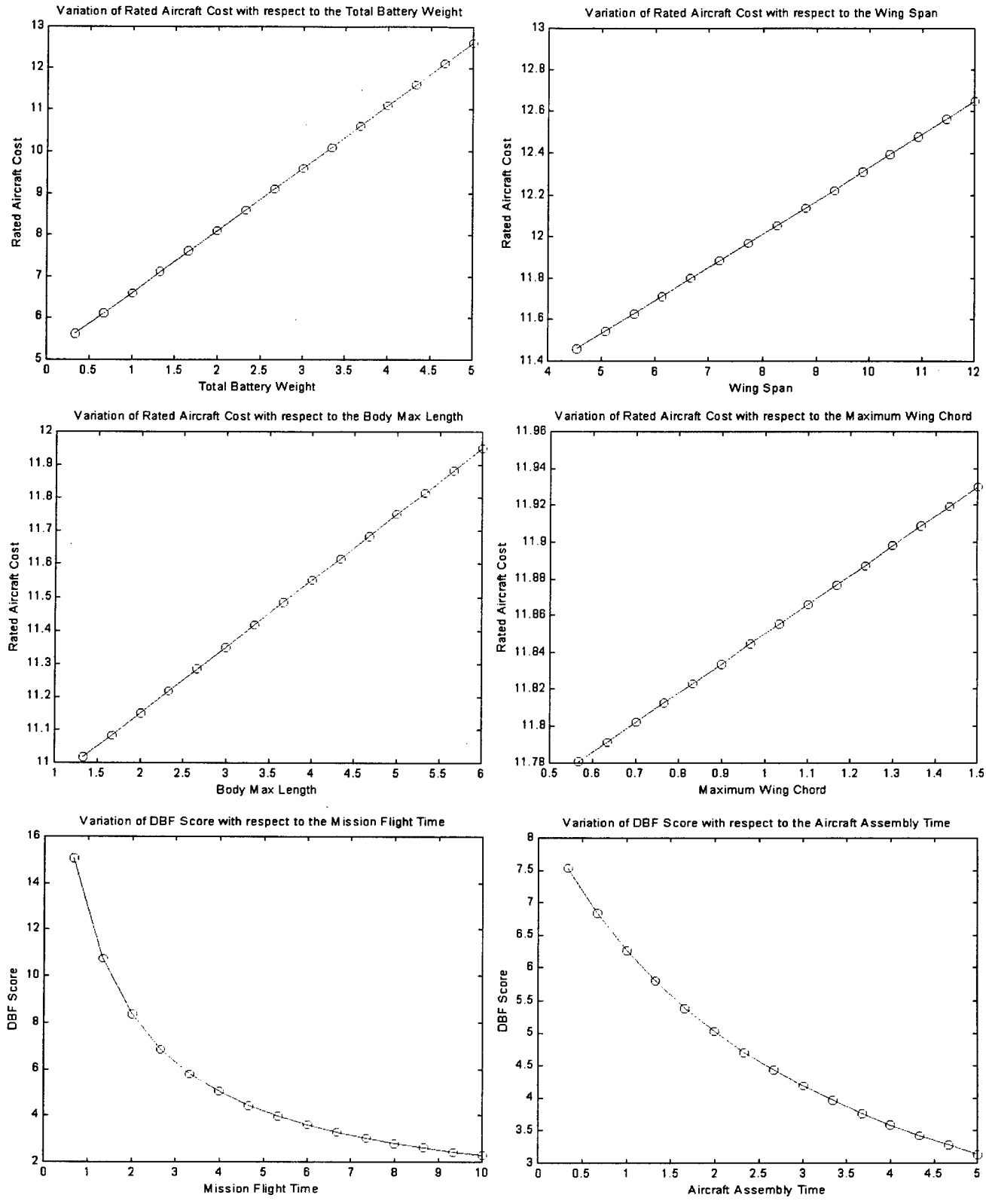

Figure 3.1: Variables Affecting Rated Aircraft Cost and Final DBF Score

weight, while the lengths of the wingspan, chord, and fuselage proved to have a relatively small effect on the RAC and subsequent score.

Once the analysis on the key variables affecting the RAC was completed, a sensitivity analysis on the flight score variables was carried out. The first variable to be analyzed was the mission time, which correlated directly to the cruise velocity of the aircraft. The effect of the mission flight time was observed over a range from 0 to 10 minutes, as 10 minutes is the maximum time allowed for a score. Figure 3.1 shows that the DBF score is inversely proportional to the flight time. At higher values of the flight time, the overall score experienced a less dramatic change. However, when the mission flight time was decreased from 3 to 2.5 minutes the DBF increased from the baseline score by 9.1 percent.

Next, the aircraft assembly time variable was observed as it varies with the final score - Figure 3.1. The assembly time ranged from 0 to 5 minutes. The relationship between the DBF score and the assembly time is shown to vary as $\frac{1}{x}$. Like the mission flight time, the higher values of the assembly time had less of an affect on the total score. However, an increase in the assembly time of 30 seconds (from 1 to 1.5 min) produced an 11.0 percent decrease in the DBF score.

Once the sensitivity analysis on the variables was completed, it was easy to determine the driving factors for the design. The assembly time was shown to have the most significant impact on the total DBF score, and therefore, a significant amount of attention was devoted to the design of the assembly system and quick attachment techniques. The second most important variable was found to be the mission time or flight speed; therefore the design was also focused on producing the maximum amount of speed possible. Although the total battery weight was found to be fairly significant with respect to the RAC and consequently the total score, it was less significant than the mission flight time. A linear relationship between the airspeed and battery weight in the ranges examined was determined from initial propulsion analysis. Therefore, for initial design considerations, the maximum amount of batteries allowed was selected to increase the airspeed as much as possible.

The effects of the wingspan, chord, and body length were found to be of secondary importance to the design. Therefore, the design should be focused on sizing these values based on the size of the box and achieving the best aircraft performance.

In order to determine the effect of a twin tail configuration as opposed to an inverted V-tail configuration, each design was analyzed with respect to the total DBF score. The rules state that a V-tail will be treated as one horizontal surface with control and one vertical surface without control. Furthermore, an inverted V-tail was found to require one less servo, which also affected the overall score.

The baseline configuration incorporated a V-tail. Therefore, in order to determine its effect on the overall score, a twin tail configuration was considered as an alternative to the baseline V-tail configuration. When the new values for the number of control surfaces and servos required of a conventional tail were evaluated through the DBF analysis code, the RAC increased by 3.6 percent and the DBF score decreased by 3.9 percent. This is a significant amount and the analysis supported the incorporation of a V-tail configuration in the preliminary design phase.

Finally, the number of engines used in the design was analyzed in order to determine if it would be more beneficial to use two engines with the hopes of increasing the velocity of the aircraft. The baseline

configuration incorporated one engine. Therefore, in order to analyze the effect of the number of engines on the total score, the program was varied in order to allow for an extra motor and propeller. With these new values for the engine and propeller, the RAC increased by 11 percent from the baseline score. This large increase in RAC and subsequent decrease in score confirmed the initial single engine configuration selected.

In summary, assembly time, mission flight time, and propulsion configuration are the key drivers in the score and were set as the focal points for the design. Some of the other factors affecting the RAC were found to not have as significant an influence on the total score and were left to be optimized for aircraft performance. These variables included wing span, chord length, and fuselage length.

3.4 Conceptual Design Assessments

The wide array of conceptual design approaches were examined using decision matrices. Figures of merit for the assessments were chosen based on three things: design approaches which directly impact the score such as assembly time, component integration, and construction issues; vehicle performance; and pilot flying issues.

The first area assessed was the mission selection, primarily because it was the most significant driver for the design. The figures of merit chosen to select the missions were the weighting factor of each mission, the inherent RAC of flying that mission, the difficulty placed on the pilot of flying that mission, and potential hazards while flying the mission. Breaking these down in terms of the three main issues, the first two FOM's directly affect the score, the last two deal with performance and flight. Weights were assigned to the different FOM's based on how important the group decided each factor was in the final assessment. For each decision matrix, the sum of all the weighting factors was one. In assigning scores to each category, a +1 to -1 scale was implemented. The final score was the sum of each category's weighted figure of merit scores. The highest scores were then selected as the best options, and if several were close, further analysis was conducted prior to making a selection. Based on the assessed parameters, missions A and B have the highest scoring potential and were selected to drive the design as shown in Table 3.4.

FOM	wt factor	Mission A	Mission B	Mission C
Weighting	0.3	1	0.5	0
RAC	0.25	0	-0.5	0
Pilot Ease	0.3	0.5	0	-0.5
Hazards	0.15	0	-0.5	-0.5
Score		0.45	-0.05	-0.23

Table 3.4: Mission Selection Decision Matrix

The range of potential configurations examined came primarily from the individual conceptual design review, with some additional designs that had not been previously considered. Included in Figure 3.2 are planforms of some of the configurations analyzed: a conventional single tail boom design, a flying wing,

a conventional twin tail boom design, a conventional monoplane design, a canard configured design, and a bi-plane design.

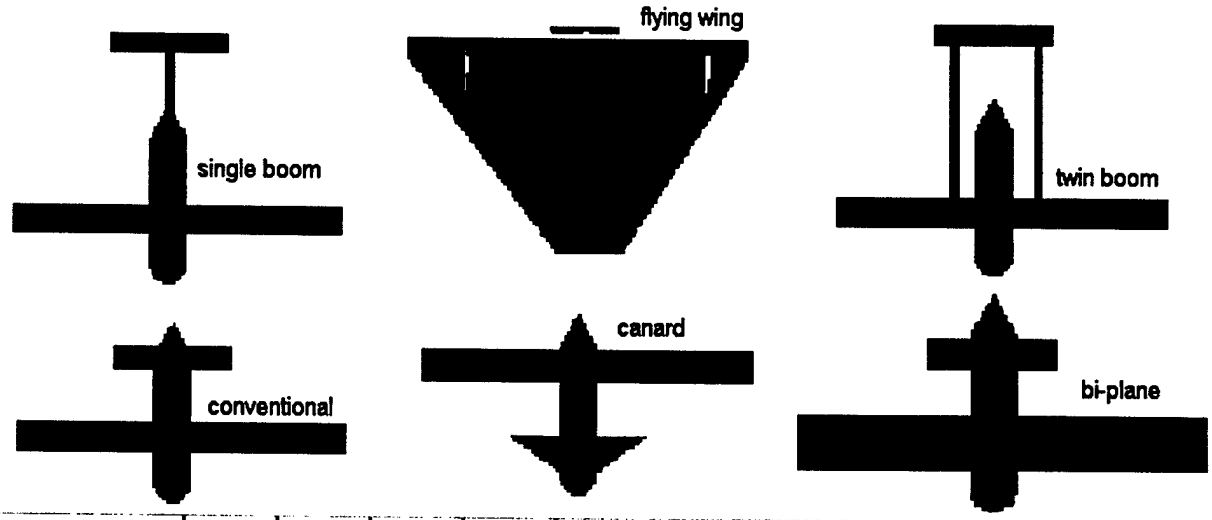

FOM	wt factor	Low Wing V-tail	High wing Twin tail	Canard	High Wing V-tail	High Wing Conventional	Twin tail Pusher	Flying Wing	Bi-plane	Conventional
RAC	0.3	1	-0.5	0	1	0	-0.5	1	-1	0
Assembly	0.2	-0.5	0.5	-1	-0.5	0	0.5	-1	1	0
Drag	0.2	0.5	0	0	0.5	0	0	1	-1	0
Handling	0.15	0.5	0.5	0	0.5	1	0.5	-1	-1	0
Deployment	0.15	-0.5	0	-1	0.5	0	-1	-1	-0.5	0
Score		0.36	0.18	-0.3	0.5	0.2	-0.125	-0.15	-0.65	0

Figure 3.2: Aircraft Configuration Decision Matrix and Selected Planforms

A total of nine different aircraft configurations were analyzed in terms of the following FOM's: RAC, assembly time, drag, handling qualities, and deployment compatability. The revised possible configurations included a low-wing V-tail, a high-wing twin tail, a standard canard, a high-wing V-tail, a high wing conventional design, a twin tail pusher, a flying wing, a conventional bi-plane, and a conventional monoplane. The standard conventional monoplane was set as the control from which all other configurations were compared against. Figure 3.2 shows that the high-wing V-tail outscored the other possibilities.

Possible tail configurations were also examined based on the RAC, drag, ease of construction, deployment flexibility, and assembly time FOM's. Configurations examined included a single-boom V-tail, a twin-boom inverted V-tail, a conventional tail, a T-tail, and a tail with twin-vertical stabilizers. Assuming that if each is sized and implemented correctly, the V-tails were found to be preferential because they reduce the RAC the most without any significant adverse effects. Figure 3.3 presents the results.

Different empennage approaches were reviewed next. Three possibilities were looked at: a conventional fuselage, a single tail boom, and a twin tail boom. Each was reviewed based on assembly time and box storage, structural rigidity, deployment integration, weight, and ease of construction. Because of its rigid, lightweight, box friendly design, the twin-tail boom design came out on top. This data is presented in Table 3.5.

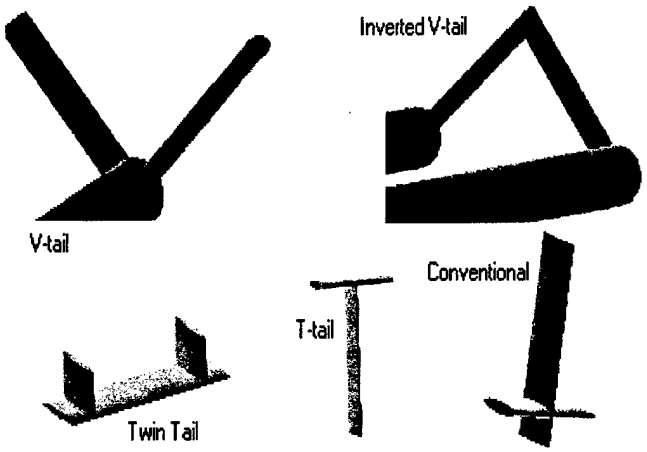

FOM	wt factor	V-tail	inverted V	Twin tail	T-tail	Conventional
RAC	0.3	1	1	-1	0	0
Drag	0.1	1	1	0	0	0
Construction	0.2	-0.5	0.5	1	-0.5	0
Deployment	0.1	0	0.5	0.5	0	0
Assembly	0.3	0.5	0.5	0.5	-1	-0.5
Score		0.45	0.75	0.1	-0.15	-0.25

Figure 3.3: Tail Configuration Decision Matrix

FOM	wt factor	Conventional	Single Boom	Twin Boom
Deployment	0.2	0	0.5	1
Weight	0.2	0	1	0.5
Construction	0.1	0	0.5	0
Assembly	0.3	-1	0	0
Rigidity	0.2	1	0	0
Score		-0.1	0.35	0.4

Table 3.5: Empennage Selection Decision Matrix

Gear configuration was the next big decision. The tail-dragger, bicycle, and tricycle landing gear configurations were each evaluated against the FOM's of landing, taxiing, deployment compatability, drag, and RAC. Table 3.6 shows that the tricycle gear was clearly the best option based on all of the parameters except drag. Drag, however, can be reduced in many ways. One way would include a retractable landing gear.

FOM	wt factor	Tail Dragger	Tricycle	Bicycle
Landing	0.2	-0.5	1	-1
Steering	0.2	0	0.5	-0.5
Deployment	0.2	-0.5	1	-1
Drag	0.2	0	0	-0.5
RAC	0.2	0	-0.5	-0.5
Score		-0.2	0.4	-0.7

Table 3.6: Gear Configuration Decision Matrix

A separate decision matrix, Table 3.7, was constructed to determine if a retractable gear was worth the effort. FOM's concerning this decision included drag, durability, integration and assembly, and RAC. Based on all these factors, no clear winner existed between the two. Each had advantages and disadvantages. This allowed the design to be flexible as it progress into the later design stages.

FOM	wt factor	Retracts	Fixed
RAC	0.2	0	1
Drag	0.2	1	0
Durability	0.3	0	0
Integration	0.3	0	1
Score		0.2	0.5

Table 3.7: Gear Integration Decision Matrix

Wing position with respect to the fuselage was another important consideration. Assembly, payload deployment, construction, stability, and drag were the key factors here. The simplicity of assembly and deployment provided by a high wing aircraft was significantly better than both low and mid-wing designs, as shown in Table 3.8.

FOM	wt factor	High Wing	Mid Wing	Low Wing
Stability	0.05	1	-1	0
Construction	0.15	0	0	-1
Deployment	0.3	1	-1	-1
Gear	0.15	0	1	0
Assembly	0.3	0	0	-1
RAC	0.05	-1	1	0
Score		0.3	-0.15	-0.75

Table 3.8: Wing Orientation Decision Matrix

Another consideration which had significant design implications was the power plant selection. RAC, weight, power, and integration were the driving factors concerning this aspect of the design. Twin Astro 40's, twin 60's and a single 90 were the main power plant considerations. Based on the figures of merit, a single Astro 90 was the best setup, as seen in Table 3.9. Selecting the prop and gearbox combination to maintain the necessary ground clearance and fit in the box was accomplished with the ElectriCalc program and was supplemented with wind tunnel testing.

FOM	wt factor	1 90	2 40's	2 60's
Weight	0.5	1	1	0
RAC	0.2	1	0	0
Integration	0.1	1	0	0
Power	0.2	1	0	1
Score		1	0.2	0.2

Table 3.9: Power Plant Selection Decision Matrix

Table 3.10 summarizes the groups decision concerning fuselage selection. Initially, two competing

camps existed. One that favored a conventional fuselage, with the box oriented lengthwise supporting a hoop style landing gear. The other was leaning toward a blended lifting body with the box oriented widthwise using either retractable or recessed landing gears. Figures of merit were selected to evaluate each and determine which direction to take for entering the preliminary design phase. Consideration for either direction was weighed against assembly time, component integration (landing gear, tail, and wing), payload deployment, and drag FOM's. In the end, a conventional fuselage was determined the better way to go.

FOM	wt factor	Conventional	Lifting Body
Construction	0.05	1	0
Deployment	0.4	1	-1
Tail Integration	0.1	0	1
Motor Integration	0.15	0.5	0
Gear Integration	0.3	0	0.5
Score		0.525	-0.15

Table 3.10: Fuselage Selection Decision Matrix

The conceptual design taken forward into the preliminary design phase is shown in Figure 3.4. It was a high wing, twin tail boom, inverted V-tail design, with a single motor and prop, and a conventional fuselage.

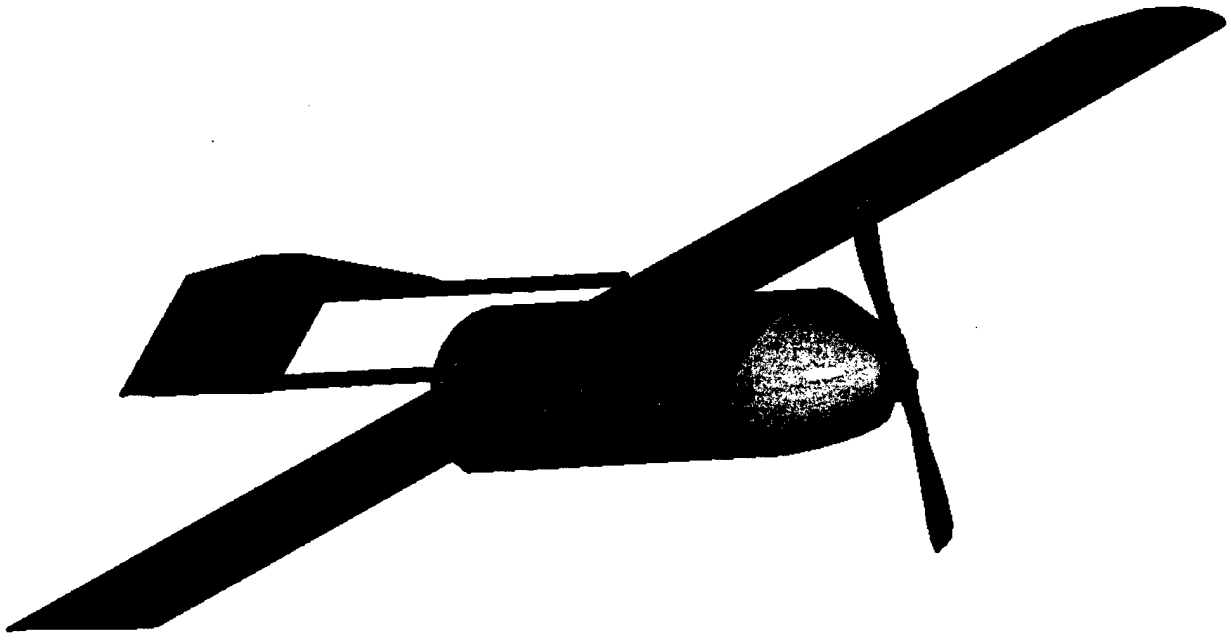

Figure 3.4: Conceptual Design

Chapter 4

Preliminary Design

4.1 Wing Construction Techniques

With the conceptual design completed and the baseline aircraft configuration locked down, discipline leads set about conducting further analysis and testing of key design components. Wing design and construction was one of the first areas looked at. The group initially decided on foam and composite construction vice a traditional balsa buildup because of the ease, speed, durability, and repairability of the construction technique, with comparable weight.

Polystyrene foam was considered as a core material because it is cheap, easy to work with, and can be molded to any shape. The foam by itself does not, however, provide sufficient strength for a wing so a study was conducted using 16 different types of composite/foam layups. Each represented a possible wing spar configuration. Each of the layups was then statically loaded to failure to determine its specific strength and specific stiffness. Figure 4.1 shows one of the samples being tested and the standard layup.

Each sample wing spar was based on a deviation from the standard layup (Figure 4.1), which consisted of: 4 carbon tows on the compression surface and 2 tows on tension side, 2-ounce bi-axial glass oriented at 0/90 on either side of a 1.0-inch polystyrene core acting as the skin, and 6-ounce bi-axial sheer web oriented at +/- 45 acting as a spar.

The test was conducted using weights hung at the center of a 20 inch section of each sample and deflections were measured at 40 pounds. A brief description of each layup and the results of the test are available in Table 4.1.

From this test, a number of key conclusions were reached about the potential wing design for the aircraft. Data shows that samples tested with stringers carried considerably more load than those without stringers. Increased strength in the wing spars was achieved by applying strips of uni-carbon along the length of the beam, most notably on the side of compression. It is important to note that all 16 samples failed on the compression side. Overall, composites work well in tension, but have some limitations in compression.

Despite having superior strength for their weight, the standard lay-ups with additional uni-carbon strips failed to show improvements in stiffness, however. The thicker 1.5 inch samples were the stiffest, but also weighed the most because they had 50 percent thicker cores. Material selection also proves to be

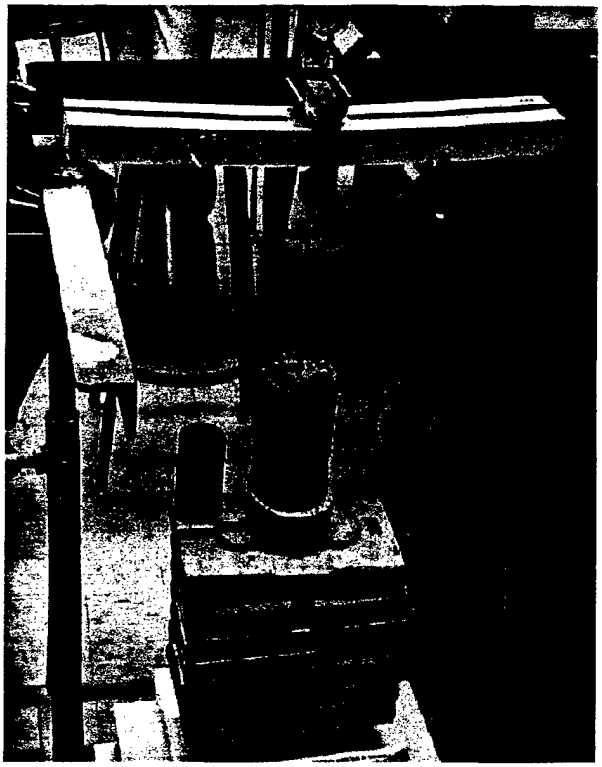

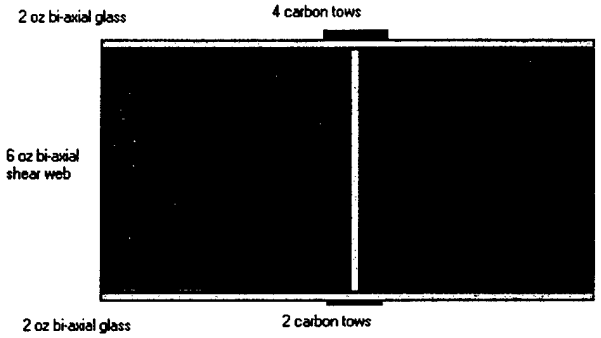

Figure 4.1: Composite Spar Strength and Stiffness Test, Standard Layup

Description	Weight (lbs)	Deflection @ 40 lbs (in)	Load @ Failure (lbs)	Specific Stiffness	Specific Strength
Standard Lay-up (no stringer)	0.121	---	27	---	223
Standard Lay-up (1/8" Balsa Stringer)	0.164	0.215	65	1.31	396
Standard Lay-up (1/8" end grain Balsa Stringer)	0.147	---	30	---	204
Standard Lay-up (Divinicell Stringer)	0.176	0.244	73	1.39	415
Standard Lay-up	0.175	0.204	65	1.17	371
Standard Lay-up (2 Glass Stringers)	0.225	0.186	96	0.83	427
Standard Lay-up (2 Glass Stringers)	0.239	0.17	120	0.71	502
Standard Lay-up (1.5" Core no Stringer)	0.177	0.178	45	1.01	254
Standard Lay-up (1.5" Core)	0.267	0.098	176	0.37	659
Standard Lay-up (w/50% More Compression Carbon)	0.173	0.213	91	1.23	526
Standard Lay-up (w/50% Less Compression Carbon)	0.154	0.34	40	2.21	260
Standard Lay-up (w/2 oz. Glass at +/- 45)	0.176	0.25	61	1.42	347
Standard Lay-up (w/100% More Compression Carbon)	0.176	0.194	111	1.10	631
Uni Glass Lay-up	0.236	0.13	71	0.55	301
Uni Glass Lay-up at +/- 45 on Compression Surface	0.228	0.197	91	0.86	399
Carbon Layup	0.213	0.119	140	0.56	657
1.5" Foam no Stringer 100% more Compression Carbon	0.178	0.166	70	0.93	393

Table 4.1: Results of Wing Construction Testing

important as the standard carbon layup performed significantly better than the standard glass layup with only a marginal increase in weight. For construction, a standard carbon layup was chosen, but to save

weight, only the leading edge to the carbon tows was covered with the carbon fiber composite because of the structural integrity of the "D" shape.

4.2 Wing Attachments

In addition to wing layups, commercially available carbon tubes were evaluated as possible wing attachments for quick assembly out of the storage box. Testing was conducted on two different types of tubes purchased from MacLean Quality Composites. The first carbon tube was a piece of .75-72-6P, which had an outer diameter of 0.82 inches, was 0.035 inches thick and weighed 0.058 lbs per foot. The second sample was a piece of OVRR-.680, which had an outer diameter of 0.745 inches, was 0.033 inches thick and weighed 0.049 lbs per foot. The manufacturer did not provide any strength data on the tubes, so an experiment was set up to test the axial and torsional properties of each. Figure 4.2 shows the experimental setup and test results for the bending moment tests done on the commercial composite tubes.

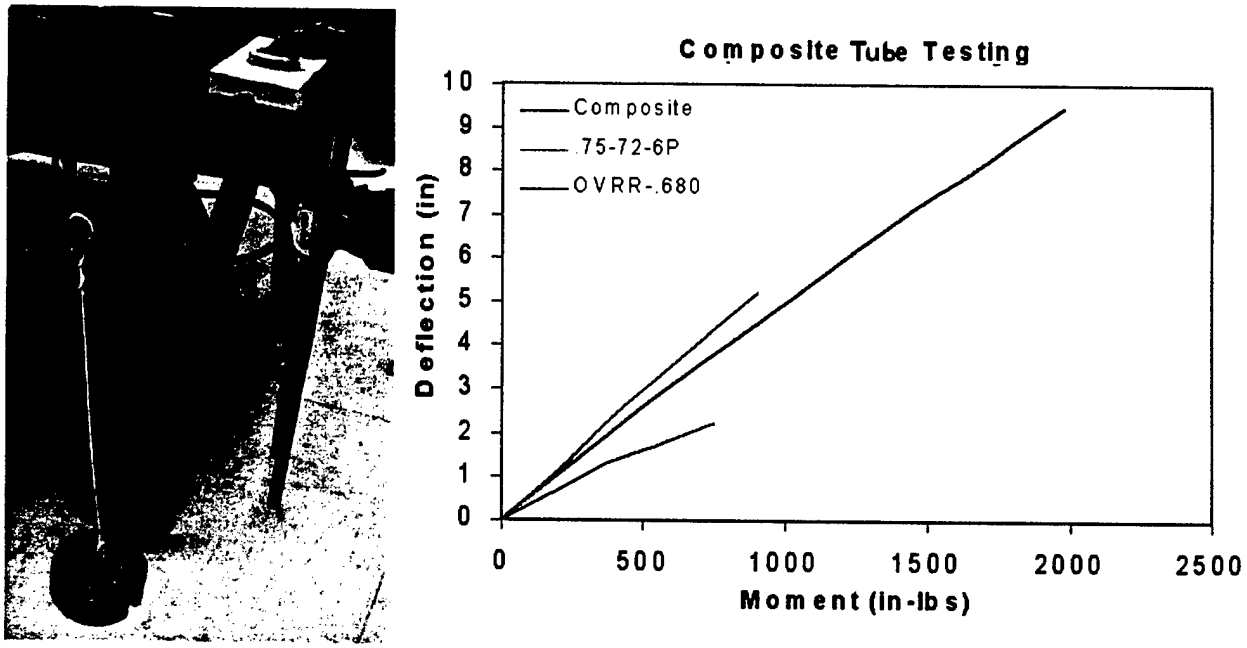

Figure 4.2: Composite Tube Bending Moment Test Setup and Results

Based on an estimate of the root bending moment on a 20 pound aircraft, with an 7-foot wingspan, able to support and instantaneous maximum load 5 g's for robustness, the connections will have to support 850 inch-pounds. Testing on the samples was conducted by using the unidirectional tube as a sleeve. 4

inches of the smaller sample was inserted into the larger diameter tube and tested by incrementally adding 5 lbs weights to a moment arm of 25 inches. The tube ultimately failed at 750 in-lbs on the compressive side of the tube. The unidirectional tube was similarly tested using a steel pipe as a sleeve for testing purposes only. Again, 4 inches of the rod was inserted into the sleeve, however, this time a moment arm of 36 inches was used. The tube failed at 900 in-lbs, a satisfactory strength based on the initial bending moment estimates. Further testing was conducted, however, in an attempt to determine the combined structural strengths of both tubes (labeled "composite tubes" in Figure 4.2). The small diameter tube was glued into the unidirectional tube, and after inserting 4 inches of the composite tube structure into the steel pipe, loads were gradually applied using a 36 inch moment arm. Failure occurred with a root bending moment of 1980 in-lbs, but this increase in strength came at weight penalty. Figure 4.2 shows the results of three tests.

During each test, the carbon tube failed at the end of the sleeve, meaning that the section running immediately from the wing to the fuselage is the section that fails. As such, this is the section of the attachment that needed to be built up with the unidirectional tube. Plans were subsequently developed to connect the tube to a wing spar of the previously discussed composite layup variety.

4.3 Tail Boom Torsional Analysis

Preliminary design concepts called for twin tail booms, therefore it was necessary to have tubes stiff enough to withstand twisting from the aerodynamic forces generated by the tail surfaces. A simple analysis was performed on the same unidirectional carbon tubes used in wing attachment analysis in order to get a rough estimate of the material's torsional strength. A piece of tube measuring 50.9 inches in length was clamped down at one end with a 12 inch moment arm fastened at the opposite end. Loads were then applied in 100 gram increments and the amount of twist was measured. After plotting the amount of twist as a function of the applied load, a linear relationship was obtained. Using the equation for angular twist, the Modulus of Rigidity, G, was found to be approximately 610 kpsi. Figure 4.3 shows the experimental setup and results for this test.

From this experiment, the amount of twist measured in the piece of unidirectional tube seemed too high to serve as a single tail boom. With an estimate of the material's modulus of rigidity, the combined stiffness and separation offered by a twin tail boom, however, appeared adequate for use in the design's construction. A simple change in fiber orientation could, nevertheless, further improve the rigidity. It was concluded after the experiment that by using a unidirectional tube with fibers running in one direction, the level of stiffness was reduced. As a result the decision was made to use composite tubes with carbon woven in a pattern with half of the fibers running +45 degrees off of the longitudinal axis with the other half running -45 degrees off of the longitudinal axis.

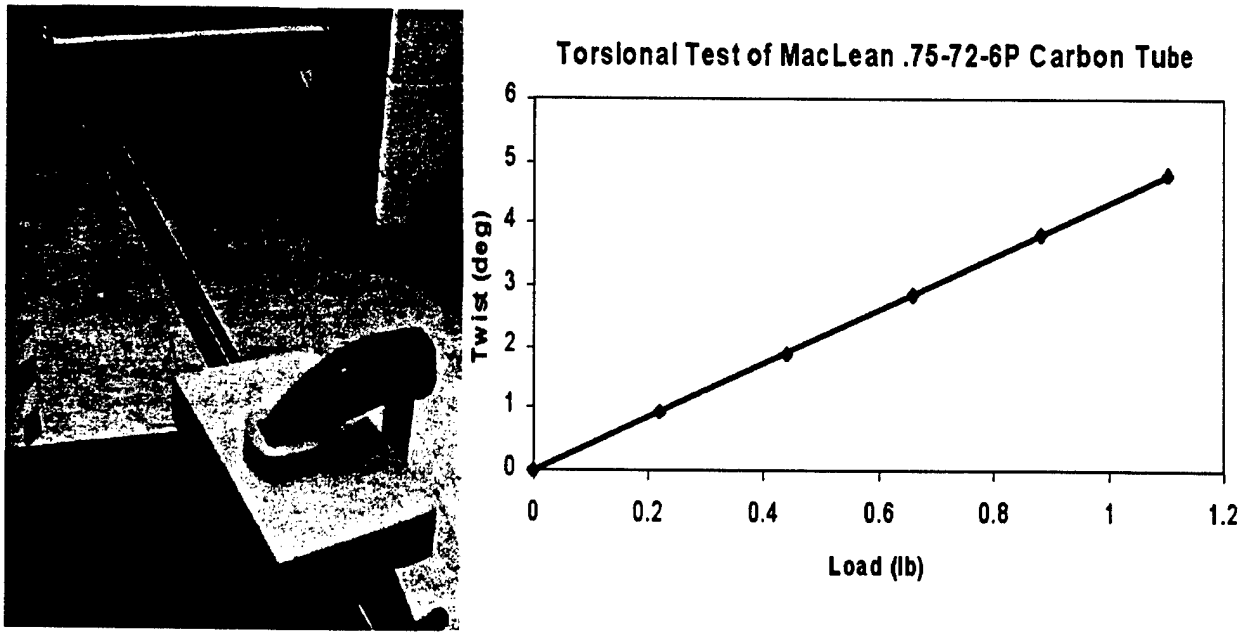

Figure 4.3: Composite Tube Torsional Test Setup and Results

4.4 Payload Deployment Techniques

To accomplish mission B successfully, the five pound payload box must be deposited onto the runway, from a complete stop, unassisted. Because deployment must take place completely by remote, the system was designed to be as simple as possible. It was decided that the box would drop out the bottom of the aircraft, instead of employing other complex design alternatives like using a ramp, rods, or springs to push the box out of the back or off to the side. Furthermore, the box would serve as the bottom of the fuselage until dropped, to avoid the complication of bay doors. After being dropped, a single panel hinged to one side of the box will serve to cover the gap in the fuselage. The panel will be fixed into place possibly by strips of Velcro or magnets. A simple mockup of the release system is shown in Figure 4.4.

An attachment platform suspended from the main wing spar runs through the top of the fuselage. A tab riveted to the top of the payload box with a hole drilled through it fits through the attachment platform. To drop the box, the rod is retracted from the tab by a single servo mounted aft of the payload. By using a single securing point, less chance exists that the box will fail to deploy. The payload will be secured by the addition of foam blocks on all four sides and the top to prevent excessive movement. Construction and testing of the proto-type device shown in Figure 4.6 demonstrated that this type of arrangement was practical and reliable.

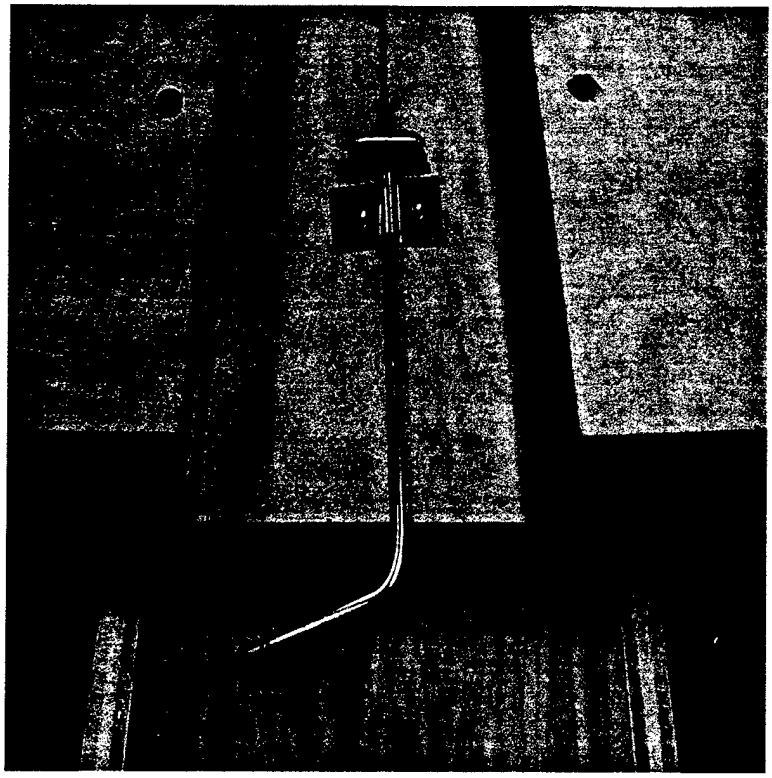

Figure 4.4: Deployment Technology Demonstrator

4.5 Initial Propulsion Testing and Calibration

During the early part of the design process a propulsion lab was conducted to familiarize the design team with all aspects of propulsion and evaluate candidate propulsion systems. Six different motors, propellers, and gear box combinations were tested in the USNA Eiffel subsonic wind tunnel. A photo of the test setup and a sample of the data from this testing is shown in Figure 4.5.

In addition to the lab tests, different candidate considerations were run through the computer program ECALC, a tool that theoretically predicts the performance characteristics of different propulsion combinations. Once validated, this computer program would save time testing multiple combinations in the wind tunnel and money required to purchase parts for testing. As a result, a significant amount of effort was spent calibrating the program to match the actual experimental results.

The initial group consensus on propulsion was that the best possible design would incorporate a single Astro Cobalt 90 motor. Since the testing was completed with only the available Astro Cobalt 40 and 60 motors, this presented one of the first possible sources of error in trying to extrapolate the results for a Cobalt 90. After doing additional research on astroflight.com it was determined that the 60 and the 90 were very similar motors, with each motor having the same diameter, motor RPM, and max amperage. The Astro 90 was just 0.7 inches longer, leading to a slight increase in weight, and it also had a greater power output. Since there was no penalty in the RAC for using a single 90 over a single 60, this was

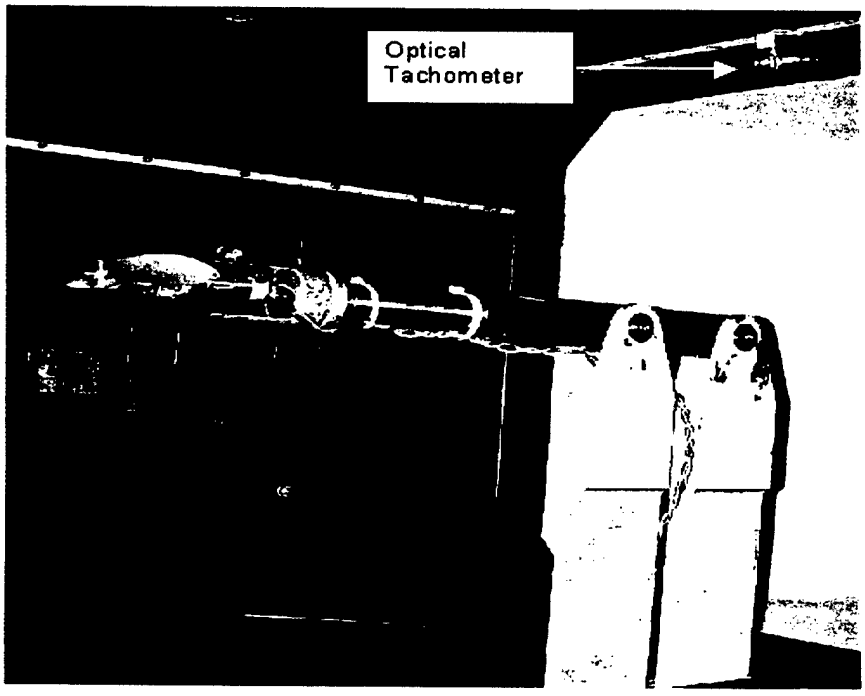

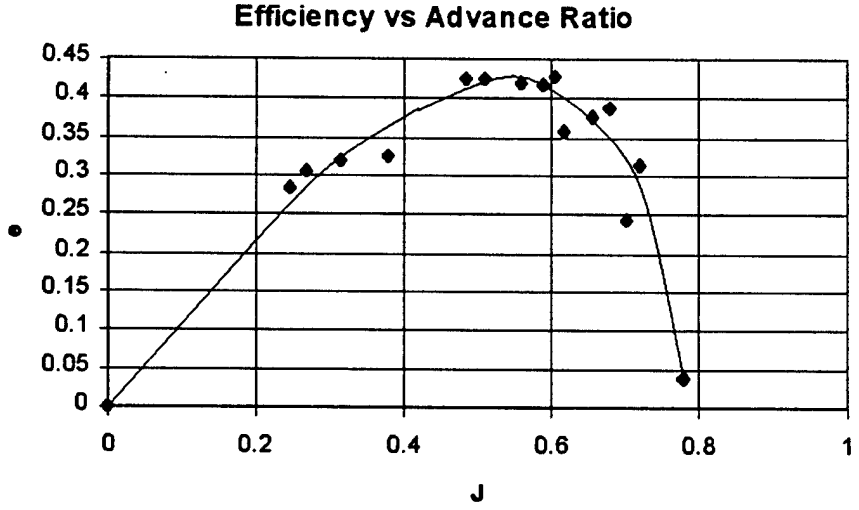

Figure 4.5: Wind Tunnel Propulsion Test Setup and Advance Ratio vs Efficiency (Astro 40, 1.63:1, 12 X 8 propeller)

determined to be the best motor for the design.

Based on the similarity between the Astro 60 and the Astro 90, the 60 data from the initial propulsion testing was used to attempt to validate ECALC. To begin the validation process, the known inputs were loaded into the program. The motor was an Astro 60 geared at 2.73:1. The batteries used were 36 Sanyo N-1700 SRC NiCads. The first propeller tested was a wooden 22 inch diameter with a pitch of 12 (22x12). Since speed is indirectly factored into the score as part of mission flight time, the group was most interested in higher flight speeds of between 55 and 75 mph. The first data matched was taken with the wind tunnel running at its highest tested velocity of 60 mph. At this speed, the propeller was pulling a maximum of just over 20 Amps, producing 43 ounces of thrust, and drawing just over 800 watts of power from the batteries. Several efficiency parameters in the program were varied until three key parameters - Amps drawn, Watts drawn, and thrust - were matched as closely as possible to the actual wind tunnel data. Once this was accomplished, the speed on the program was dropped to 50 mph and minor adjustments were made to the variables to match the data taken from the wind tunnel running at 50 mph. This procedure was followed again at 40 mph. At each stage, the efficiencies were adjusted to match the experimental data for the 20x12 and the 22x12, which proved to be fairly accurate.

While these efficiency values proved the validity of ECALC for the performance ranges the group was most interested in, they also revealed some of the limits of the program. The output data clearly broke down for low amperages (less than 20 A) and low speeds (less than 40 mph). One of the key conclusions reached in the validation of ECALC was the relationship between the propeller efficiency of the program and that obtained in the wind tunnel testing. There was no practical way to isolate the propeller efficiency from the motor efficiency in the wind tunnel. As a result, the propeller efficiency in ECALC had to be adjusted to account for the motor and prop efficiencies obtained by experimentation. With these adjustments, subsequent ECALC approximations were significantly more accurate, though additional wind tunnel testing was conducted on the final propulsion selections for more reliable results.

4.6 Astro Cobalt 90 Endurance Test

The initial decision to use the single Astro 90 was based on an aggressive estimate of the endurance provided by the five pound battery limit. To test this assumption, an Astro 90 was tested for endurance. Two 18 packs (4.8 pounds) of SRC-2400 NiCad batteries were used. The propeller of choice was an APC 30x15. This was chosen because the only available Astro 90 was geared at 2.73:1 and to draw near the 40 Amps with this gear ratio, a larger propeller was necessary. The experiment was conducted statically in a test stand. The procedure was simple, apply throttle and time how long the motor operated at full power. The results were somewhat unexpected. After only thirty seconds the propeller noticeably changed rotation speed, indicating a loss in power. This was significantly less than the two minutes predicted. Based on these results, the Astro 60 looked to be a more economical option, not draining the batteries as quickly. Additional testing of the Astro 60 and the Astro 90 validated this decision and also confirmed the previously obtained results on the 90 - five pounds of batteries was not sufficient power to complete a mission flying the larger 90.

4.7 Landing Gear Wind Tunnel Test

In order to further refine the aircraft's configuration, additional testing was required on potential landing gear designs. Several different possibilities were tested in the wind tunnel in order to obtain drag data and determine whether or not a retractable landing gear would benefit the design. A composite hoop style main landing gear was manufactured for the test and was run in the tunnel with three different wheel combinations and two different wheel and fairing combinations. Additionally, a straight fork style nose gear was tested. Figure 4.6 shows the various gear and wheel combinations tested and the drag results.

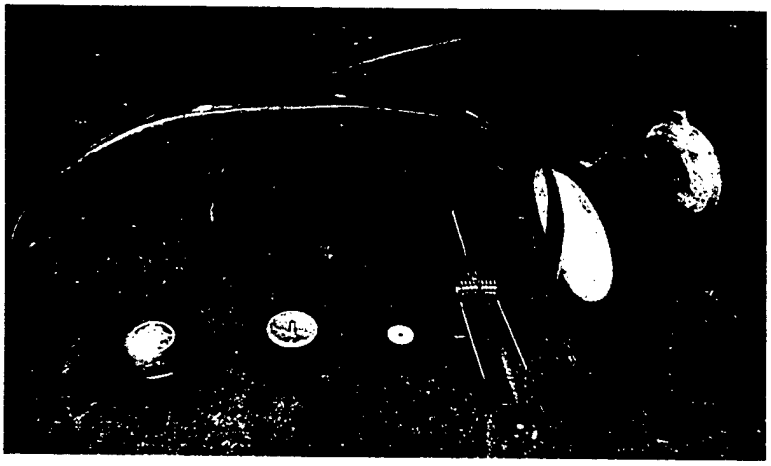

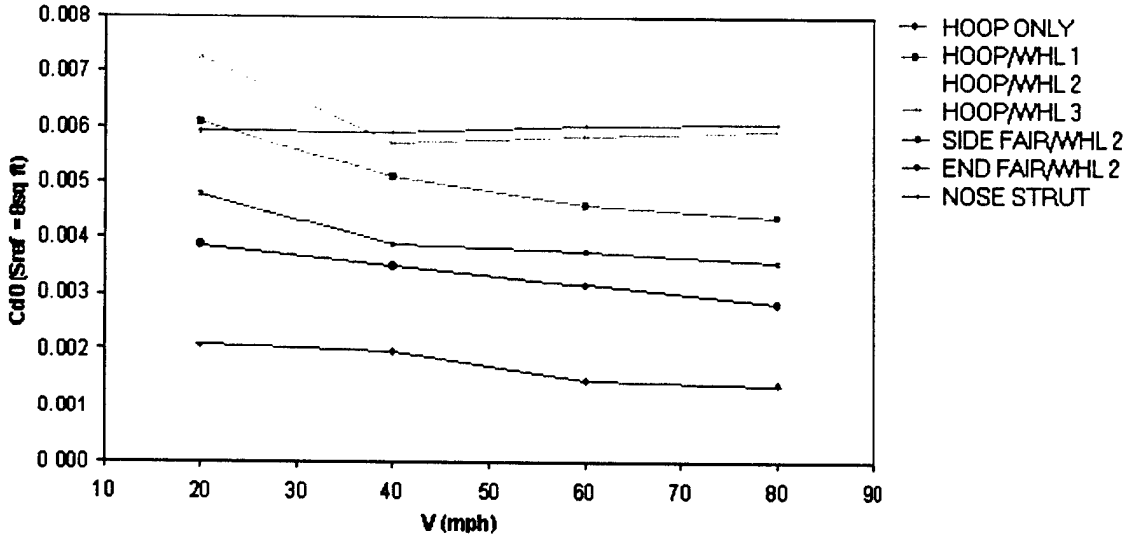

Figure 4.6: Landing Gear Wind Tunnel Test Components and Drag Results

The results of the test confirmed expectations. A wing reference area of 8 feet was used to calculate the drag coefficients based on the initial conceptual wing design for the aircraft and plotted against the tunnel velocity. Notice, there was a significant difference with the advent of fairings and how the fairings were attached. The side mounted fairings showed an 11.6 percent reduction in drag from the naked wheel combinations, and the end mounted fairings showed a 30.1 percent reduction in drag. The actual

fairings used on both the end mounted and side mounted tests where the same. The differences in drag between the two faired wheels were caused by the differences in the interference effects between the fairing approaches and the hoop. This difference was a sizable 20 percent with respect to the naked wheels. These results show that a properly faired main gear provided a viable design.

The nose gear, however, netted more drag than any combination of main gear. For this reason a retractable nose gear was seen as the best choice. A faired nose gear, however, would provide a viable option, as well.

Another issue to consider before deciding on a final gear design was the deployment of the payload out the bottom of the aircraft. For purposes of storing and assembling the aircraft out of the box, the nose gear would have to be either detachable or retractable. The final assessment of this study left the group with several possible gear combinations to carry forward in the design process: a fully retractable landing gear, a faired main gear and retractable nose gear, or a faired main gear and a retractable/detachable nose gear.

4.8 Landing Gear Assembly

Based on the tunnel test results, the hoop gear strut seemed to be a promising design for the aircraft's main landing gear. By shaping the strut to resemble an airfoil, the amount of drag created was significantly reduced - an attractive design considering the ease of construction. Because of the need to have an opening under the fuselage to allow for the payload to be deployed, a continuous hoop run under the fuselage was not a viable option. To resolve this, a split hoop strut, or a similarly shaped strut could be bolted to the sides of the fuselage. Besides the obvious functionality of giving the clearance needed to deploy the box and swing a sizeable propeller, bolting the main gear on allows the struts to swivel for ease in storage and setup of the aircraft. Thus, the only obstacle limiting the design development of the main gear was how to lock the gear into place for assembly out of the crate. A preliminary sketch of this arrangement is shown in Figure 4.7.

4.9 Airfoil Selection and Wind Tunnel Test

To select the airfoil for the aircraft, several different possibilities were considered using available published data and a computer program called ModelFoil. Airfoils examined included various NACA 4, 5, and 6 series airfoils, and several different Eppler airfoils. In order to best fit the design, airfoils were sought out that had solid low Reynolds number performance, a fairly high maximum lift coefficient, and gentle stall characteristics. The airfoil's stall characteristics were especially important because an analysis of last year's competition demonstrated that the vast majority of flight mishaps and crashes were the result of stalling either in the turns or during landing.

Out of this analysis the NACA 4412 and Eppler 67 emerged as the two most viable candidates. For several reasons, the decision was made to test both in the wind tunnel. Goals of the tunnel test included validating existing published data with experimental data at the low Reynolds numbers of the design,

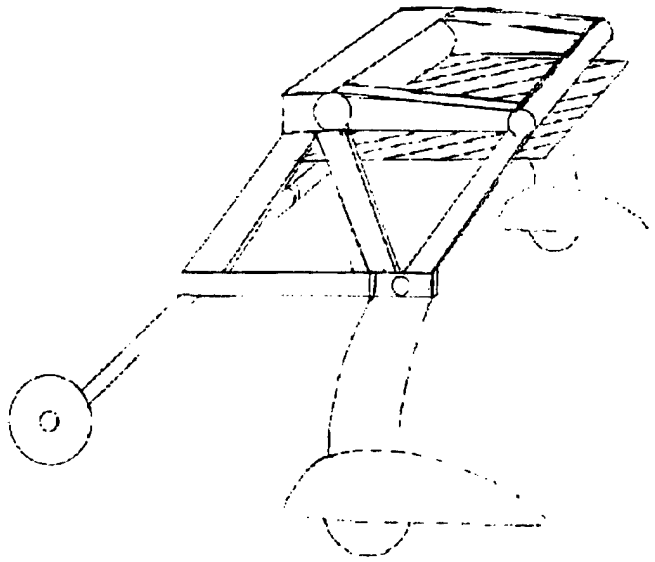

Figure 4.7: Preliminary Internal Structure Design

determining which airfoil exhibited more of the qualities sought by the design team, and determining the accuracy of the wing construction techniques at reproducing known airfoil performance.

For the experiment, the 4412 used was a prefabricated solid wood airfoil with a 9 inch chord, available from the USNA Aerospace Engineering Department. The Eppler 67 had to be manufactured using a hot-wiring technique on polystyrene foam, with the addition of wing spars, and a ceconite skin. The test was run at 20, 40, 60, and 80 mph at angles of attack from -2 to 19 degrees. Figure 4.8 shows the Eppler airfoil construction and the lift and drag for the Eppler and NACA 4412 airfoils.

Results of the experiment indicate that the foam and glass Eppler airfoil produced slightly more lift than the "clean" NACA 4412. An example is given at 40 mph where the lift curve slope for the Eppler was .647 per degree, while the 4412 was .611 per degree. In the region of stall, however, the trend shifted to favor the 4412. Again at 40 mph, the Eppler stalled rather abruptly at 14 degrees absolute angle of attack, while the NACA airfoil leveled off into a gentle stall at 15 degrees.

One of the noted features of the Eppler airfoils is the drag bucket where reduced drag is expected in certain flight regimes. As shown in Figure 4.8, data from the testing indicated that the Eppler did not achieve these results at the design Reynolds numbers. The drag on the Eppler 67 was actually 2 counts higher than on the 4412. This result can be attributed to either the construction techniques employed lacking the ability to produce accurate results, or the low Reynolds number effects. Based on the results of the experiment, the 4412 appears to be the more consistent and benign performer. In the design, a thicker NACA 4415 section was used at the root to support the wing structure.

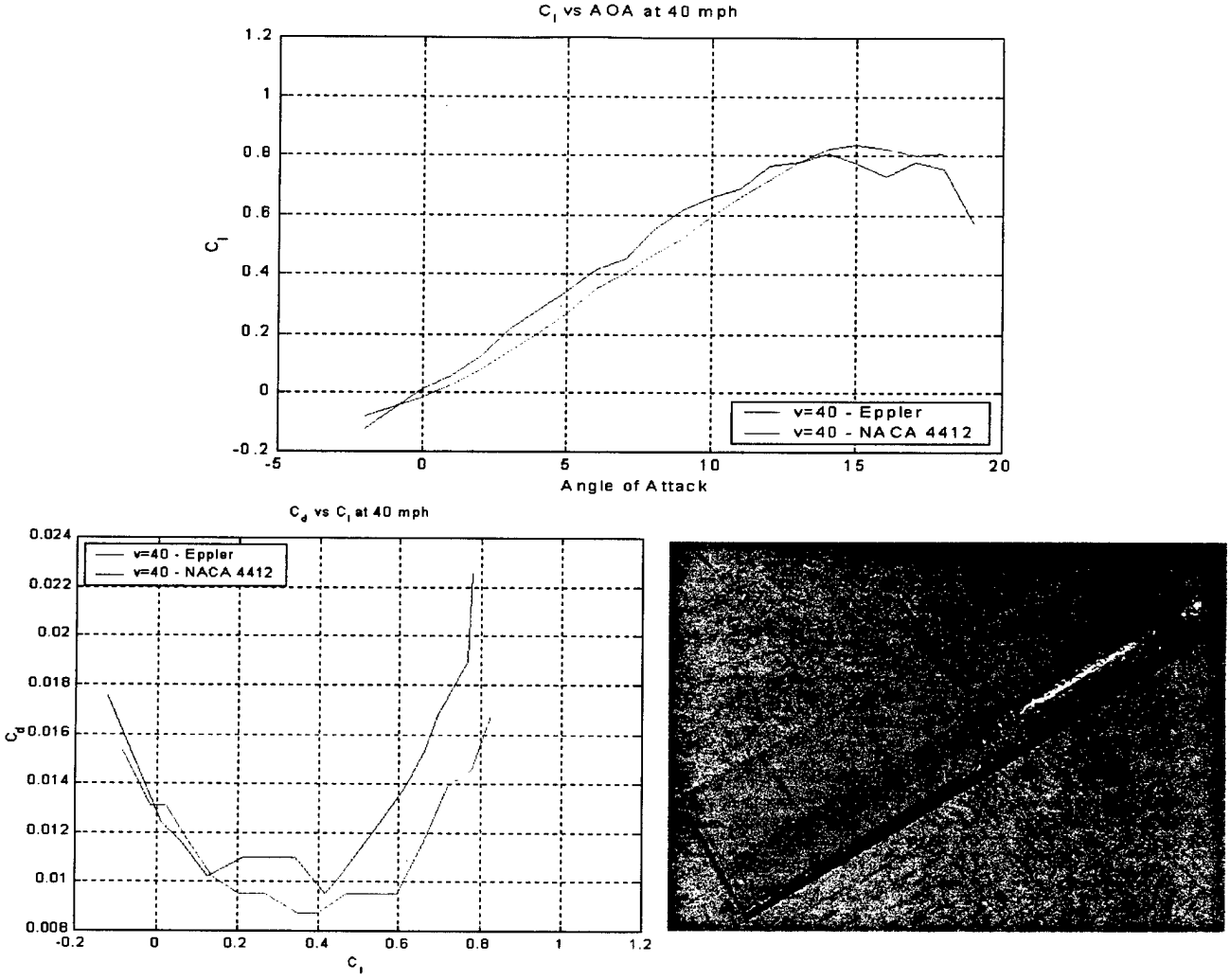

Figure 4.8: Eppler Airfoil Construction, and Lift and Drag Results

4.10 Radome Wind Tunnel Test

The team elected to design the aircraft around missions A and B because of the high difficulty factors. Mission A requires that a cylindrical antenna be carried externally to the aircraft. In order to get an accurate estimate of the how the vehicle will behave carrying the simulated radome, a wind tunnel test was conducted on a full sized model to determine its aerodynamic effects.

There is a certain Reynolds number at which the drag coefficient of a sphere drops dramatically. The same is true of a cylinder. At subcritical Reynolds numbers, the drag coefficient for a cylinder is estimated to be 1.2. At supercritical Reynolds numbers, the drag coefficient drops to as low as 0.3. The critical Reynolds number at which this drop is expected to occur has been shown to be between 2 and 4 hundred thousand. For a 6-inch diameter cylinder this translates to velocities between 63 and 125 miles per hour. The higher value is clearly unattainable, but the lower value is within the predicted speed of the team's

aircraft. The tunnel test was conducted to validate these approximations.

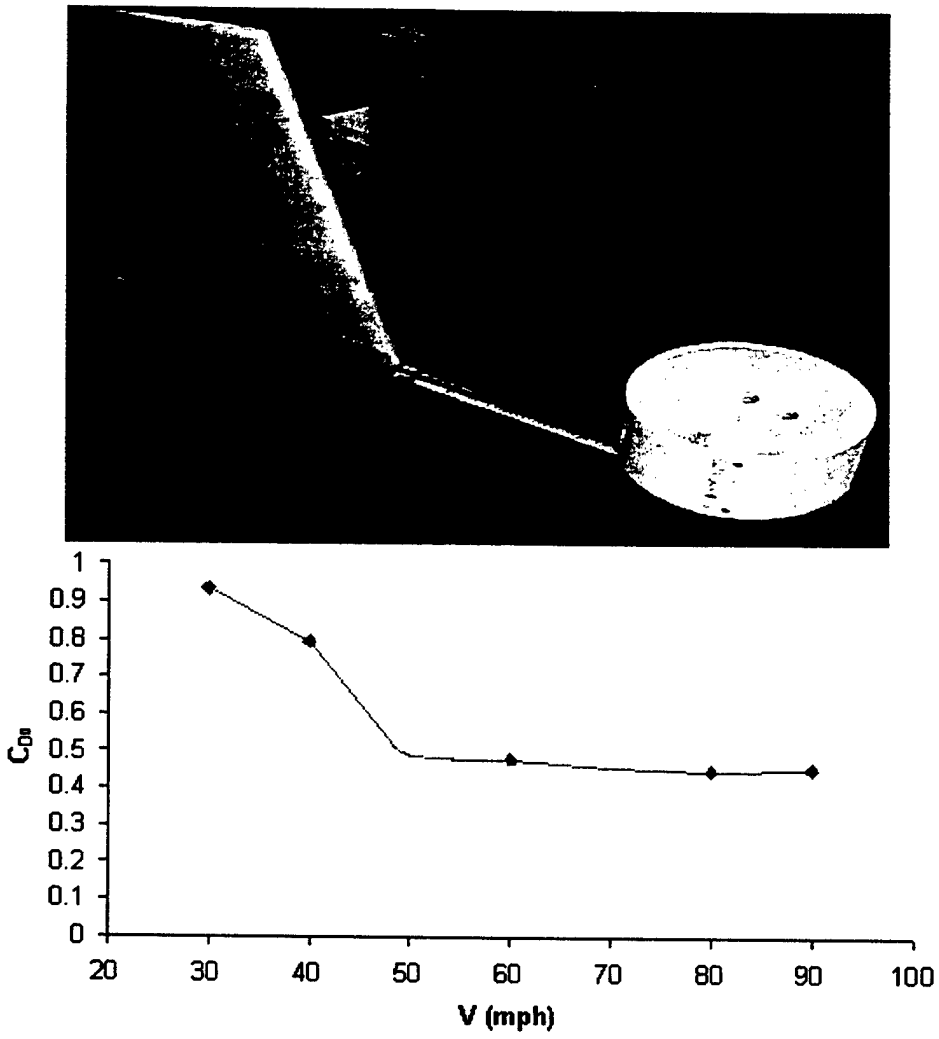

Figure 4.9: Radome and Splitter Plate Test Apparatus and Results

In addition, the rules state that the cylinder must have a 360-degree unobstructed view, except for the vertical tail. A simulated vertical tail was constructed for the experiment and was used to act as a splitter plate. The idea being that at a certain distance, the tail would smooth the separation wake behind the cylinder reducing the drag. Figure 4.9 shows the test apparatus and drag results.

As can be seen, the test results were mixed. The splitter plate did not produce any significant reduction in drag outside the required standoff distance of three inches as specified in the rules. Concerning the cylinder itself, the drag was higher than predicted. However, the critical Reynolds number was lower than expected and the flow transitioned to turbulent at 50 mph - a speed definitely within the predicted performance envelope of the aircraft. This unexpected result was likely due to the flow transitioning from laminar to turbulent on the cylinder, a transition that may have been influenced by the plywood cap attachment screws on the cylinder's surface.

4.11 Improved Propulsion Validation

After determining that the Astro 60 would be the motor of choice, the ECalc program was reevaluated with a better approximation of the earlier test results. The exact parameters of the batteries used in the test were programmed into ECalc and more accurate efficiencies were tabulated. With the new data, the Astro 60 motor was looked at in detail with both available gearing ratios (2.73:1 and direct drive). From this, three viable propulsive options were determined: a 2.73:1 ratio with a two-bladed propeller, a 2.73:1 gear ratio with a three-bladed propeller, and a direct drive two-bladed propeller.

The best option based on the ECalc results was a two-bladed 19 x 18 propeller, geared 2.73:1. This also accounted for additional parameters including fitting in the assembly box, and the required ground clearance. This combination gave six minutes of cruise at 70 mph and a static thrust of 8.3 pounds. The results were calculated using a weight of 20 pounds, 7 square feet of wing area, and a total cruise drag coefficient of 0.0406.

In order to validate this selection, several additional tests were run in the wind tunnel. Three 12-Volt car batteries were connected together to provide a near constant voltage source of 37.0 Volts to eliminate the necessity of recharging the actual competition batteries. Three different 20 inch propellers were tested: a 20x12, 20x14, and 20x16 to look more closely at the trends resulting from changes in pitch. Figure 4.10 shows the results of this testing.

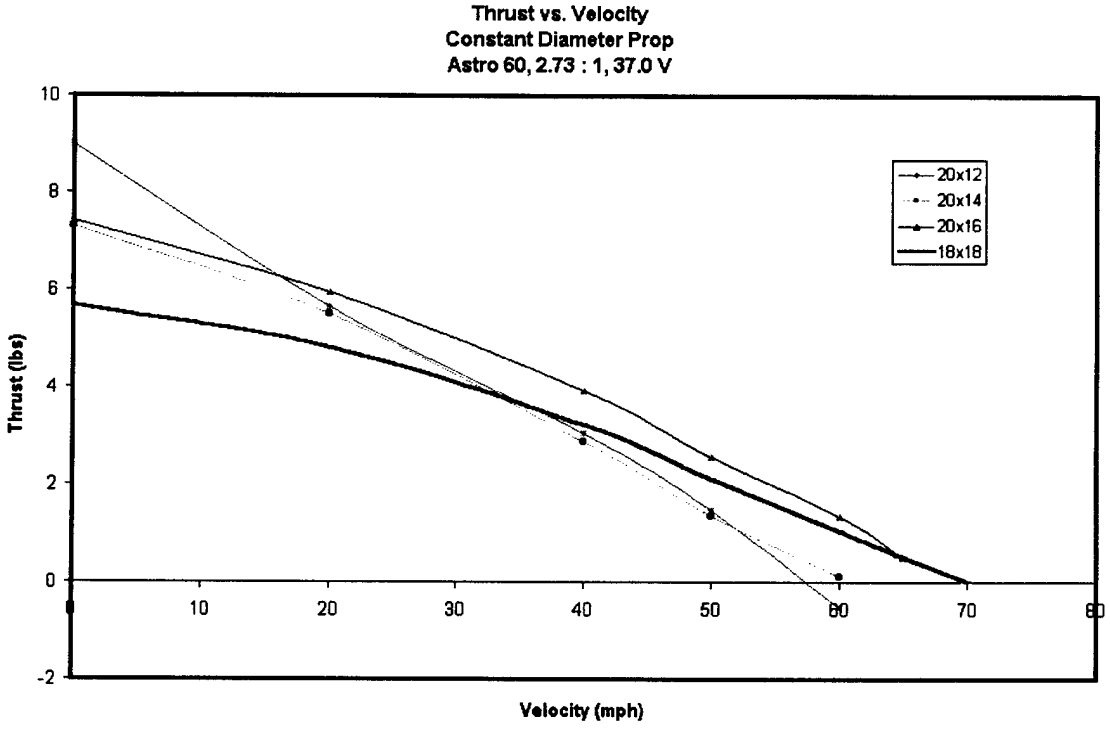

Figure 4.10: Thrust vs Velocity: Trends in Pitch

To reach the higher top end speeds, a slightly smaller diameter with more pitch was determined to be the best approach. An 18x18 APC propeller gave the most promising results in the wind tunnel. At 37.0 volts, it produced 5.67 pounds of static thrust and a top speed of 70 mph. The top end speed was in the predicted region, however, the static thrust fell short of the 7.0 pounds predicted for the takeoff requirement. The reason for this was that the voltage from the constant source was nearly 10 volts less than what a full 5.0 pound battery load could provide. As a result, another test was performed using the competition batteries at 45.8 volts. This test simulated an actual mission from take off to landing and not only provided data on the propeller's static thrust and maximum velocity, but also on the endurance of the batteries. At the higher voltage, the 18x18 produced 6.8 pounds of static thrust with a top speed of 67 mph accounting for the 2 pounds of drag on the aircraft at that speed. In the cruise regime, 17 amps through the motor at 55 mph produced enough thrust to sustain flight for 4.5 minutes - significantly longer than the predicted mission times of between 3.0 to 3.5 minutes.

4.12 Drag Build up and Thrust Required

In order to obtain a good estimate of the maximum speed, and take-off and cruise performance, an extensive drag build up of the preliminary design aircraft was calculated. This included estimating the individual zero lift drag coefficients of each component; wing, tail, tail-booms, fuselage, landing gear, and the radar dome. Two calculations were made from which the drag polar was obtained for the aircraft in a clean configuration and with the addition of the radar dome. The induced drag factor (k) was calculated based on an aspect ratio of 7 and an estimated efficiency of 0.55. The resulting drag polar for the clean aircraft was approximated to be:

$$C_D = .0318 + .075C_L^2 \tag{4.1}$$

Wind tunnel testing was conducted to find the drag coefficient of the radar dome. The results showed an addition of 0.5 lbs of drag, which corresponded to an increase in parasite drag coefficient of about 0.01. The drag polar with the addition of the radar dome is:

$$C_D = .0416 + .075C_L^2 \tag{4.2}$$

These drag polars were then used to calculate the thrust required through the flight velocity regime of the aircraft. This is shown in Figure 4.11. The thrust available curve shown in the figure depicts the optimum thrust available based on the ECalc data for an Astro 60, geared at 2.73:1, and a 19 x 18 propeller.

4.13 Preliminary Weight and Balance

From the established preliminary aircraft design, a theoretical performance analysis was conducted with the goal of ensuring that the competition criteria were being met and ultimately optimized. The starting point for this was the preliminary weight build up and refinement of initial estimations.

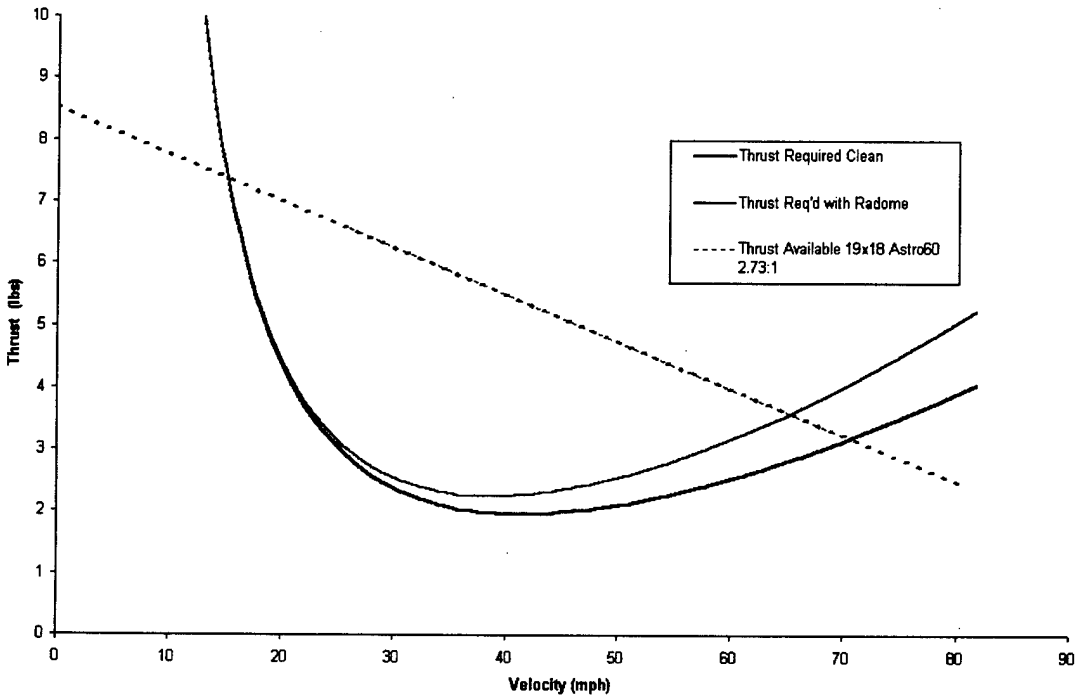

Figure 4.11: Thrust Required and Optimum Thrust Available

Based on measured weights of known components, estimated weights of the unfabricated components, and on established aircraft dimensions, the center of gravity was determined. As depicted in Table 4.2, a complete listing of the scheduled loading is categorized by fixed and variable items, which pertains to the flexibility of their positioning in the detail design. The final center of gravity was desired to be located at the centroid of the payload box so deployment would not change the aircraft's center of gravity. This was accomplished through evaluation of the preliminary design weight distribution and management of component position to best fix the c.g. with respect to the box. Design flexibility was afforded through the movement of the variable items which were adjusted as required.

4.14 Performance

The refined weight and aircraft dimensions were used to update the preliminary design performance predictions. Of particular interest in the performance of the aircraft was the required takeoff distance. The takeoff roll is limited to a maximum of 120 ft based on competition criteria. A 100 ft takeoff was taken as the baseline objective to ensure the aircraft design was well within the required boundary.

A value of 91.5 feet was calculated based on a lift coefficient at takeoff of 1.4 with the contribution of flaperons, without flaperons, the lift coefficient was calculated to be 1.1. Additionally, this distance did not account for any headwind which is likely to be present for the competition. Further evaluation of the full envelope, ensuring mission accomplishment throughout all potential flight conditions, was conducted in

Weight and Balance	Moment Arm Position (in)	Unit Weight (oz)	Unit Weight (lbs)	Index Moment (in*lbs)
Factors				
Datum point (located at most forward point on nose/propeller)	0	0	0	0
Basic Aircraft Empty Weight				
Propeller and gear	1	3.520	0.22	0.22
Motor (Astro 60)	2.5	29.600	1.85	4.625
Nose wheel landing gear	2.5	8	0.5	1.25
Wing	14	32	2	28
Fuselage	15	40	2.5	37.5
Wing servo controls	20	12	0.2	4
Main wheel landing gear	22	16	1	22
Tail booms and assembly	32	4.8	0.3	9.6
Empennage	49	11.2	0.7	34.3
Tail servo controls	56	6	0.375	21
Receiver	21	1.28	0.08	1.68
Receiver batteries	21	4	0.25	5.25
Watt meter	9	3.84	0.24	2.16
Battery package	10	64	4	40
Payload				
Box + deployment equipment	15	88	5.5	82.5
Antenna	15	25.6	1.6	24
Totals			21.315	318.085
C.G. Location			14.92306 in	

fixed/nonmovable
variable/movable

Table 4.2: Preliminary Weight and Balance

the detailed design phase. Nevertheless, initial performance estimates were conducted to ensure mission accomplishment. Based on the estimated drag polars for the aircraft and the powerplant data from ECalc and the propulsion testing, the maximum velocity of the aircraft without the radome was estimated to be 70 mph, and with the radome it was 65 mph. A load factor of 2.5 at 50 mph was estimated for the 360-degree turns, giving a radius of 73 ft and a turn rate of 56 degrees per second.

4.15 Stability

The initial stability and control of the aircraft was determined based on preliminary aircraft dimensions established through a historical examination of aircraft with V-tail configurations. Light weight Unmanned Air Vehicles with inverted V-tail configurations were specifically considered. Although a range of pusher and tractor propulsion configurations were among those considered, the data did not indicate any major deviations from a general trend of tail sizing.

The advantages to employing a V-tail design were primarily related to a reduction of the rated aircraft cost, although a V-tail would also have slightly less interference drag, compared to a conventional tail. An additional benefit of an inverted V-tail configuration was is the favorable rolling moment which accompanies rudder deflections in rolls and decreases the effects of adverse yaw. There are also advantages to V-tail designs during spin recovery; however, this is somewhat mitigated by the fact that the aircraft is

susceptible to abrupt negative pitching moments if placed in a sideslip. The primary concern posed by the V-tail configuration was how to size it properly to provide adequate control power, especially in yaw. For this reason, a V-tail and a more conventional H tail were both fabricated with the aircraft for the flight testing phase. Table 4.3 shows the values determined for tail sizing.

Stick fixed neutral point (h_n)		
h_n	0.458333	
Factors		
(l_sf)	Required static margin, stick fixed	2.50 in
(c_bar)	Mean aerodynamic chord (MAC)	12.00 in
(hc_bar)	Leading edge to C.G.	3.00 in
Tail volume ratio V_Hn @ h=h_n		
V_Hn	0.615111	
Factors		
(h_nwb)	Wing/Body aerodynamic center	0.17
(a_wb)	Lift curve slope (wing/body)	0.08 /degree
(a_t)	Lift curve slope (tail)	0.05 /degree
de/da	Change in downwash depsilon/dalpha	0.25
Area of the tail S_t		
S_t	1.44 ft^2	
Factors		
V_Hn	Tail volume ratio	0.62
S	Wing area (ft^2)	7.00
	S = b*c	
	b_span (ft) 7	
	c_chord (ft 1	
(c_bar)	Mean aerodynamic chord (MAC)	1.00 ft
l_t	Distance between C.G. and tail MAC	3.00 ft
Lift curve slope (aircraft) a		
a	d(C_L)/d(alpha) 0.087689 /degree	
Factors		
(a_wb)	Lift curve slope (wing/body)	0.08 /degree
(a_t)	Lift curve slope (tail)	0.05 /degree
S_t	Area of horizontal tail	1.44 in^2
de/da	Change in downwash depsilon/dalpha	0.25

Table 4.3: Preliminary Design Stability

Initial estimates for the static margin placed it at 10 percent, however, the preliminary weight and balance and aircraft sizing placed it at a slightly more stable 15 percent because of the requirement that the payload box be at the aircraft center of gravity. This value is within the range of acceptable static margins based on historical data for similarly sized unmanned aerial vehicles.

4.16 Preliminary Design Wrap Up

Figure 4.12 shows the final aircraft configuration and accounts for assembly out of the storage crate.

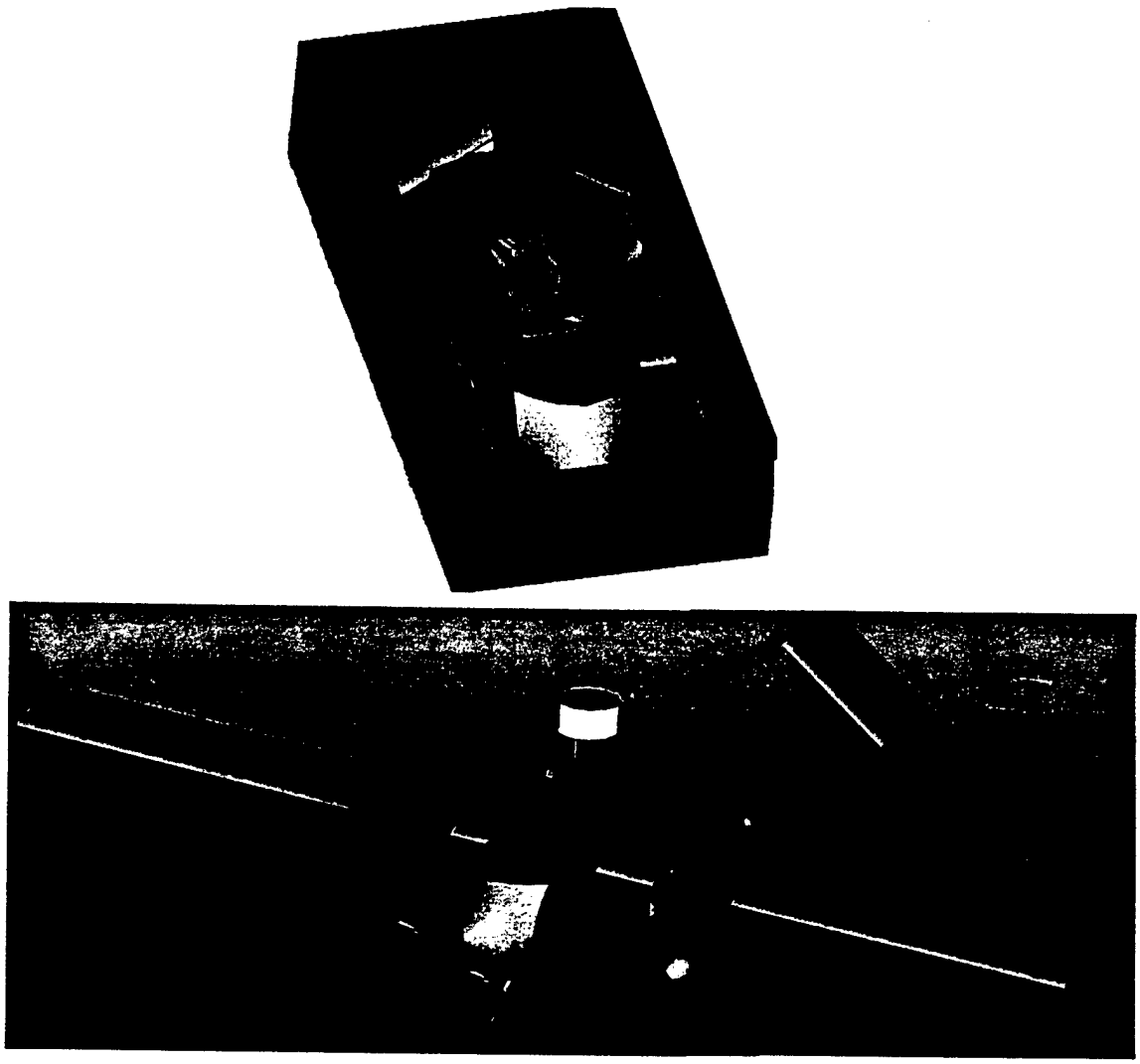

Figure 4.12: Preliminary Design: Component Packaging and Assembly

Chapter 5

Detail Design

In the detail design phase, team Severn Discomfort sought to close any open issues in the iterative design process, finalize all component sizing and construction, lock down the configuration and layout, complete a detailed weight and balance of the aircraft, select the specific component systems, and revisit the aircraft stability.

5.0.1 Wing

The final wing was an NACA 4415 at the root, tapering out to a 4412 at the tip. It had a 7.0 foot span with a 1.0 foot chord from root to tip, providing an aspect ratio of 7.0. The incidence angle was set at 1.5 degrees with respect to the fuselage, washing out to 0 degrees at the tip. The wing was divided into three sections: an internal section permanently mounted to the fuselage, measuring 22 inches across, and two external sections each spanning 31 inches. These external sections were attached by protuding tubes (a main spar at the quarter chord and an anti-torque spar at 60 percent chord), that plugged into receivers in the internal wing section. On each side of the internal wing section was another receiver for the tail boom tubes set 18 inches apart. One inch outboard from each of the tail boom receivers was one submerged servo used to drive the flaperons. Each flaperon spanned 30 inches with a 2.4 inch chord. Since the servos were on the inboard wing section and the flaperons were on the outboard wing section, a mechanical sleeve was designed to fit over a portion of the control surface on the inboard section of the wing. This was done so that all wiring was internal to main fuselage assembly.

5.0.2 Fuselage

The fuselage was designed as two parts: an internal cage structure that housed all the systems and hardware, and an a thin aerodynamic shell. The cage was designed to fit snuggly around the payload box. It was mearly a top and two sides, with internal dimensions allowing for a 0.25 inch clearance on all sides of the payload. A slit in the top of the cage was designed for the deployment tab to slide though, while a servo mounted on the aft end of the cage pulled the connecting rod. Atop the cage sat the permanently mounted internal wing section and receiving tubes for the wings and empennage. The batteries were mounted in horizontal stacks to the two sides of the cage. Tubes connected the front of the cage to the

motor mount and nose gear assembly 6 inches in front of the payload box. The entire structure was 7.5 inches tall, 22 inches long, and 9.5 inches wide (22 inches wide including the wing section). All wiring was neatly secured to the outside of the cage with tape. The aerodynamic shell was designed as a single piece that fit over the cage and wing section. It was 30 inches long, 10 inches wide, and 8 inches tall with a 12 x 6 inch hole in the bottom for the payload deployment.

5.0.3 Gear

The main landing gear was two separate struts bolted to the fuselage cage 2 inches aft of the center of gravity. Each was designed as an aerodynamic shape to reduce the drag of a fixed gear. Wheels and end-fairings were mounted on the end of the struts. The clearance from the ground to the bottom of the fuselage was 8 inches to allow for deployment. In order to fit in the storage crate, the gears were designed to pivot on the attachment bolt with a mechanical stop to lock them in place for flight. The nose gear was a simple single strut and wheel design. An aerodynamic fairing was also designed for the nose gear and strut. The steering servo and gear mount were positioned just aft of the motor mount. In order to fit in the storage box, the nose gear strut was designed to be detachable, capable of being screwed on.

5.0.4 Empennage

The Empennage was connected to the fuselage by two tail booms, set 18 inches apart, that plugged into receivers in the wing section. The wiring for two servos, semi-submerged in both surfaces of the V-tail, was run through the tail booms to a plug in connection attached to each servo. This was done for assembly purposes because a long mechanical connection was not feasible. The V-tail itself was 21 inches wide and 12 inches tall providing 1.63 square feet of horizontal area and 0.65 square feet of vertical surface area. The vertical and horizontal tail volumes associated with the tail were 0.04 and 0.70 respectively. Control surfaces had a 3.18 inch chord and spanned the length of the V-tail.

5.1 Final Geometry Determination

Table 5.1 summarizes the parameters and sizes for the final aircraft design. It also provides sizing details on the tail section and wings. All major components (wings, empennage, fuselage, and gear) were designed to fit within the storage crate for easy and efficient assembly.

5.2 Final Weight Statements

Table 5.2 shows the final aircraft weight detailed for the four different aircraft configurations: conventional tail without radome, convectional tail with radome, V-tail without radome, and V-tail with radome. Table 5.3 details the aircraft balance and center of gravity location for the competition V-tail configurations. These tables changed only slightly from the preliminary estimation, but accounted for the final fixed positioning of the initial variable items. It also provided an accurate weight estimate because construction techniques

Aircraft Sizing	
S	7.0 sqft
b	7.0 ft
c	1.0 ft
AR	7
L	5.5 ft

Tail Sizing	
lt	3.0 ft
St	1.63 sqft
Sv	.653 sqft
Vh	0.7
Vv	0.04
c	.88 ft
Ruddervators	.3c (3.18")

Wing	
incidence	1.5 deg
washout	1.5 deg
taper	0
airfoil	
root	NACA 4415
tip	NACA 4412
flaperons	2.4 x 30 in

Table 5.1: Aircraft Parameters and Sizes

	Mission A		Mission B		Mission A		Mission B	
	C Tail		C Tail		V Tail			
Internal	(oz)	(lbs)	(oz)	(lbs)	(oz)	(lbs)	(oz)	(lbs)
Battery package	80.0	5.00						
Reciver battery	4.0	0.25						
40 - Amp Fuse	1.6	0.10						
Watt meter	3.8	0.24						
Reciver	1.3	0.08						
Motor, propeller, gear	33.9	2.12	w/o box					
Box	80.0	5.00	0.00	0.00			0.00	0.00
Box deployment servo	4.8	0.30						
Wing servo controls	3.2	0.20						
Tail servo controls	3.2	0.20						
External	(oz)	(lbs)						
Fuselage	22.4	1.40						
Wings	16.0	1.00						
Vertical tail	10.0	0.63						
Horizontal tail	10.0	0.63			V Tail			
Empenage (V tail)					15.0	0.94		
Tail boom	4.8	0.30						
Nose landing gear	6.4	0.40						
Main landing gear	12.8	0.80						
Antenna w/mount	27.2	1.70	0.00	0.00			0.00	0.00
Totals			w/box				w/box	
			298.2	18.64			293.3	18.33
			w/o box				w/o box	
	325.4	20.34	218.2	13.64	320.5	20.03	213.28	13.33

Table 5.2: Aircraft Weight Statement

were concurrently decided in the detail design phase. This allowed for weighing actual materials and components to give highly accurate weights for the final weight and balance statements.

	Mission A				Mission B			
	Unit Weight		Moment Arm Position	Index Moment	Unit Weight		Moment Arm Position	Index Moment
	V Tail				V Tail			
Internal	(oz)	(lbs)	(in)	(in*lbs)	(oz)	(lbs)	(in)	(in*lbs)
Battery package	80.0	5.00	12	60				
Reciver battery	4.0	0.25	21	5.25				
40 - Amp Fuse	1.6	0.10	8	0.8				
Watt meter	3.8	0.24	9	2.16				
Reciver	1.3	0.08	21	1.68				
Motor, propeller, gear	33.9	2.12	1.5	3.18				
Box	80.0	5.00	14.62	73.1	0	0	0	0
Box deployment servo	4.8	0.30	22.6	6.78				
Wing servo controls	3.2	0.20	20	4				
Tail servo controls	3.2	0.20	51	10.2				
External	(oz)	(lbs)	(in)	(in*lbs)				
Fuselage	22.4	1.40	14.125	19.775				
Wings	16.0	1.00	14	14				
Empenage (V tail)	15.0	0.94	51	47.94				
Tail boom	4.8	0.30	32.6	9.78				
Nose landing gear	6.4	0.40	4.2	1.68				
Main landing gear	12.8	0.80	17.125	13.7				
Antenna w/mount	27.2	1.70	15	25.5	0	0	0	0
Totals	320.5	20.03		299.525	293.3	18.33		274.025
C.G.	14.95382	in			14.94954	in		
					213.3	13.33		200.925
					15.07314	in		

Table 5.3: Aircraft Balance Statement

5.3 Performance

The review of critical performance factors which significantly affect competition score indicated a strong dependence on flight time. The two variables with the greatest impact on this time were found to be the maximum velocity and the turning capability. Performing well in both of these areas would allow the team to complete the course in the minimum amount of time. With respect to the flight speed, the final propulsion configuration provided a maximum velocity of 65 mph without the radome and 60 mph flying in the mission A configuration with the radome. Cruise velocity was set at 55 mph, pulling 20 Amps without the radome and 23 Amps with, in order to provide adequate endurance to complete each mission as safe and efficiently as possible.

Based on a cruise configuration under nominal flight conditions, the turn radius was determined to be

95 feet at a turn rate of 44 degrees per second. This is a slight change from the preliminary prediction due to a more conservative load factor of 2.0 vice 3.0. This was set because problems last year indicated that most mishaps occured as a result of stall and departure while turning. Flight testing the aircraft with a more conservative estimate will allow for a sequential expansion of the flight envelop.

Without consideration for wind or flap configuration, the climb performance was determined to be 2.1 feet per second. This was based on a climb velocity of 45 mph, 10 mph higher than the takeoff value of 35. This conservative value makes for a steady, but safe climb profile with little chance of stall in no head wind. Again, the full envelop will be tested and expanded in the flight testing phase. Table 5.4 provides the complete design performance parameters for the aircraft.

Performance				
Velocity (freestream)		V	50	mph
			73.33	ft/s
Gravity constant		g	32.174	ft/s
Load factor		n	2	
Lift w/load factor			Weights	Dyanmic Weight
	V Tail		lbs	lbs
	Mission A		19.69	39.4
	Mission B w/box		18.49	37.0
	Mission B w/o box		13.49	27.0
	C Tail			
	Mission A		19.84	39.7
	Mission B w/box		18.64	37.3
	Mission B w/o box		13.64	27.3
Turn Radius			96.50219	ft
Turn Rate			0.759914	rad/s
			43.53985	deg/s
Time for 360 degree turn			8.268288	s
Bank angle			1.047198	rad
			60	deg

Climb rate	2.1 fps
Take off roll (min)	45.7 ft
Take-off roll (max)	91 ft
Stall Velocity	29 mph
Take-off Velocity	35 mph
Vmax clean	65 mph
Vmax antenna	60 mph
T0/W	0.39
W/S	3
(L/D)max clean	9.67
(L/D)max antenna	8.57
CLmax	1.4 (1.1)
Drag Polars	
CD = .0318 + .075CL2	clean
CD = .0416 + .075CL2	antenna

Table 5.4: Aircraft Performance

5.4 Systems and Components

The systems selected for incorporation into the final design were chosen based on availability, compatibility, and performance. The propulsion system was selected after identifying and testing numerous combinations in both the ECalc program and the wind tunnel. The best theoretical design was an Astro 60 with a 2.73:1 gearbox spinning a 19x18 APC propellor. APC does not make a 19x18 propellor, however, and after several tests their 18x18 was selected as the best alternate. The Sanyo 2400 MAH batteries were selected because they were already in stock, available for use, and proved during testing to provide

both the necessary power and endurance for the propulsion combination selected. The radio controller, receiver, and speed controller were all selected based on pilot preference and compatability. The 3.25 inch rubber wheels were selected because they were large enough to conduct initial flight testing on a grass runway, were easily faired into an aerodynamic shape, and provided the necessary damping to land a twenty pound aircraft with a semi-rigid, fixed landing gear. Servos were selected by size, power, and ease of integration into the various components. A detailed discussion of the construction for the modular sub-assemblies (wing, empennage, fuselage, and gear) is conducted in the chapter on manufacturing. Table 5.5 details the systems and components selected for the Severn Discomfort aircraft.

System or Component	Material/Brand/Model/Type
Motor	Astro Cobalt 60
Gearbox	Astro Cobalt 2.73:1
Propellor	APC C-3 18x18
Batteries	36 Graupner Sanyo RC-2400, 1.2-Volt, sealed, rechargeable, Ni-Cd
Radio Controller	Futaba T8UHPS Digital Proportional R/C System
Receiver	Futaba Dual Conversion FP-R138DP, 8-channel receiver
Speed Controller	Astro Model 204 Digital A/C Speed Controller, (60 V max, 50 A max)
Servos	Hitec Miniprecision Servos (HS-225MG, HS-5245MG, HS-562MG)
Wheels	Great Planes, threaded rubber (3.25x2.5 in)
Carbon Tubes	MacLean Unidirectional Carbon Tubing (0.82 , 0.75, and 0.50 in)
Foam	Polystyrene
Fiber	0/90 and +/- 45 2-ounce fiberglass, and +/- 45 6-ounce Carbon

Table 5.5: Systems and Components

5.5 Rated Aircraft Cost

Table 5.6 establishes the final rated aircraft cost of the production model.

5.6 Drawing Package

All 11x17 technical drawings for the Severn Discomfort design are contained in the last five pages of the design report.

Coef	Description	Formula	Quantity	Value
A	Manufaturers Empty Weight Multiplier			$100
B	Rated Engine Power Multiplier			$1,500
C	Manufacturing Cost Multiplier			$20 / hour
MEW	Manufacturers Empty Weight			15 lbs
REP	Rated Engine Power			5 lbs
Wings				
WS	Wing Span	8hr / ft	7 ft	56 hours
MWC	Max Wing Chord	8hr / ft	1 ft	8 hours
CS	Control Surface	3hr / Control Surface	2 control surfaces	6 hours
Fuselage				
BML	Body Max Length	10hr / ft	5.5 ft	55 hours
Empenage				
VSC	Vertical Control Surface	5hr / Vertical Surface	1 vertical surface	5 hours
VSC	Vertical Control Surface with Control	10hr / Vertical Surface with Control	0 vertical surface with control	0 hours
HS	Horizontal Surface	10hr / Horizontal Surface	1 horizontal surface	10 hours
Flight Systems				
S	Servo	5hr / Servo	6 servos	30 hours
Propulsion Systems				
N	Number of Engines	5hr / Engine	1 engine	5 hours
P	Number of Propellers	5hr / Propeller	1 propeller	5 hours
MFHR	Manufacturing Man Hours			**180 hours**
RAC	Rated Aircraft Cost	RAC (thousands) = (A*MEW+B*REP+C*MFHR)/1000		**12.6**

Table 5.6: Final Rated Aircraft Cost

Chapter 6

Manufacturing Plan and Processes

6.1 Manufacturing FOMs and Material Selection

Several figures of merit were used as screeners before team Severn Discomfort selected specific manufacturing techniques to begin component fabrication and aircraft construction. Table 6.1 shows the weighted figures of merit selected and the different construction techniques considered. Two of the most important FOMs were durability and repairability. This was a design goal because should a mishap occur, it was important that the aircraft be built to withstand damage and be repaired easily.

Availability of materials was another concern. The USNA shop had a large supply of different materials available, but some had to be special ordered. Difficulty of construction was used to screen viable techniques that were too complicated or intricate for the needs of the aircraft. This was done because simplicity of design also an original team goal. Similarly, timeliness, or how long a specific technique was expected to take, was weighed in the manufacturing decision making. Weight issues inherent in the manufacturing process were also considered and screened for.

Cost was practically a non-issue because of the supply stock and capabilities of the USNA shop. Nevertheless, inexpensive methods were preferred, and overly expensive construction techniques and materials were discouraged.

Integration was possibly the most important factor in selecting the manufacturing techniques. The design was modular with several different independent components and sub-assemblies. The ability to manufacture these various parts in such a way that they mated well with the complete design was of the utmost importance because of the timed assembly requirement.

Three different material groups were initially considered for all of the manufacturing phases: wood, metal, and composites. Analysis of the properties of each based on the manufacturing figures of merit showed some general trends in the feasibility of their selection for construction. Balsa wood, a common RC building material provides good strength and is light. Construction with Balsa, however, is tedious and intricate, and Balsa is difficult and time consuming to repair. Lightweight Aluminum was also considered as one of the key manufacturing components. It is strong, readily available, easy to use, and easy to repair. Aluminum had several integration issues in the design, though, primarily because of the modular nature of the design. The composite materials considered for construction were strong, lightweight, quick

FOM/weight		Fuselage		Al truss	composite		Al tube	composite		frame/skin	glass/skin	Wing		wood/skin	foam layup		wood	composite		Al tube	composite	Empennage		Al tube	composite		wood/skin	foam layup	Gear		Al strut	composite		stock	Al tube	composite
			cage				mount			shell			wing section				spar			attachment				tail booms			tail section			main			nose		
durability	0.2		1	1			1	1		-1	0		0	1			0	1		1	1			1	1		0	1			1	1		0	0	0
reparability	0.1		1	1			1	1		0	1		-1	1			1	1		1	1			1	1		-1	1			1	1		0	0	0
availability	0.1		1	1			1	1		0	1		1	1			1	1		1	1			1	1		1	1			1	1		0	1	1
difficulty	0.1		1	1			1	1		-1	1		-1	1			1	1		1	1			1	1		-1	1			1	1		0	-1	-1
timeliness	0.1		0	1			0	0		-1	1		-1	1			1	1		0	0			0	0		-1	1			0	0		1	0	0
integration	0.2		0	1			0	1		-1	1		-1	1			0	1		0	1			0	1		-1	1			0	1		0	-1	-1
weight	0.1		0	1			0	1		0	0		0	0			0	0		0	1			0	1		0	0			0	1		0	0	0
cost	0.1		0	0			0	0		0	0		0	1			0	0		0	0			0	0		0	1			0	0		0	1	1
FINAL RANK			.5	.9			.5	.8		-.5	.7		-.5	.9			.5	.8		.5	.8			.5	.8		-.5	.8			.5	.8		.1	-.1	-.1

Table 6.1: Manufacturing FOMs and Selection Criteria

and easy to work with and shape. They are also easily repaired. Many of the aircraft components tailored themselves well to the use of composites and with the vast majority of parts made from composite materials, component integration and mating was simplified.

The skills necessary for the component construction and various phases of aircraft development were not a major consideration as all skills required of the team members for constructing the aircraft were learned concurrently throughout the course of the design phase of the project. Additionally, the team pilot had an extensive background in RC aircraft and assembly, and was able to advise the team on matters including wiring, systems integration, and preferred handling qualities.

6.2 Components

6.2.1 Fuselage

The cornerstone to the aircraft was the dense foam and carbon composite cage that served as the central structure for the entire airframe. Rigidly fixed to this were the motor mount, root wing sections including the main spar assembly and anti-torque rods, the tail boom receivers, landing gear mounts, battery mounts, and the deployment system. The wing spars, tail boom receivers, and motor mount were all manufactured from commercially available carbon fiber tubes. To provide an aerodynamic flow over the fuselage body, a removable fiberglass composite skin was manufactured. It did not support any of the structural load on the plane, but because it was removable, allowed for work on the vital aircraft components. Figure 6.1 shows the completed fuselage structure.

6.2.2 Gear

The main landing gear was fixed on pivoting joint to the internal cage structure. It was composed of a foam and carbon layup giving it an aerodynamic shape. The wheels were end-faired by a thin fiberglass skin to reduce the drag. The structure and servo for the nose gear were fastened to the motor mount. The nose gear itself was a commercially available wire gear assembly that plugs into a receiver in the mount. It was also faired with a thin fiberglass skin for aerodynamic purposes. The complete gear assembly is presented in Figure 6.1.

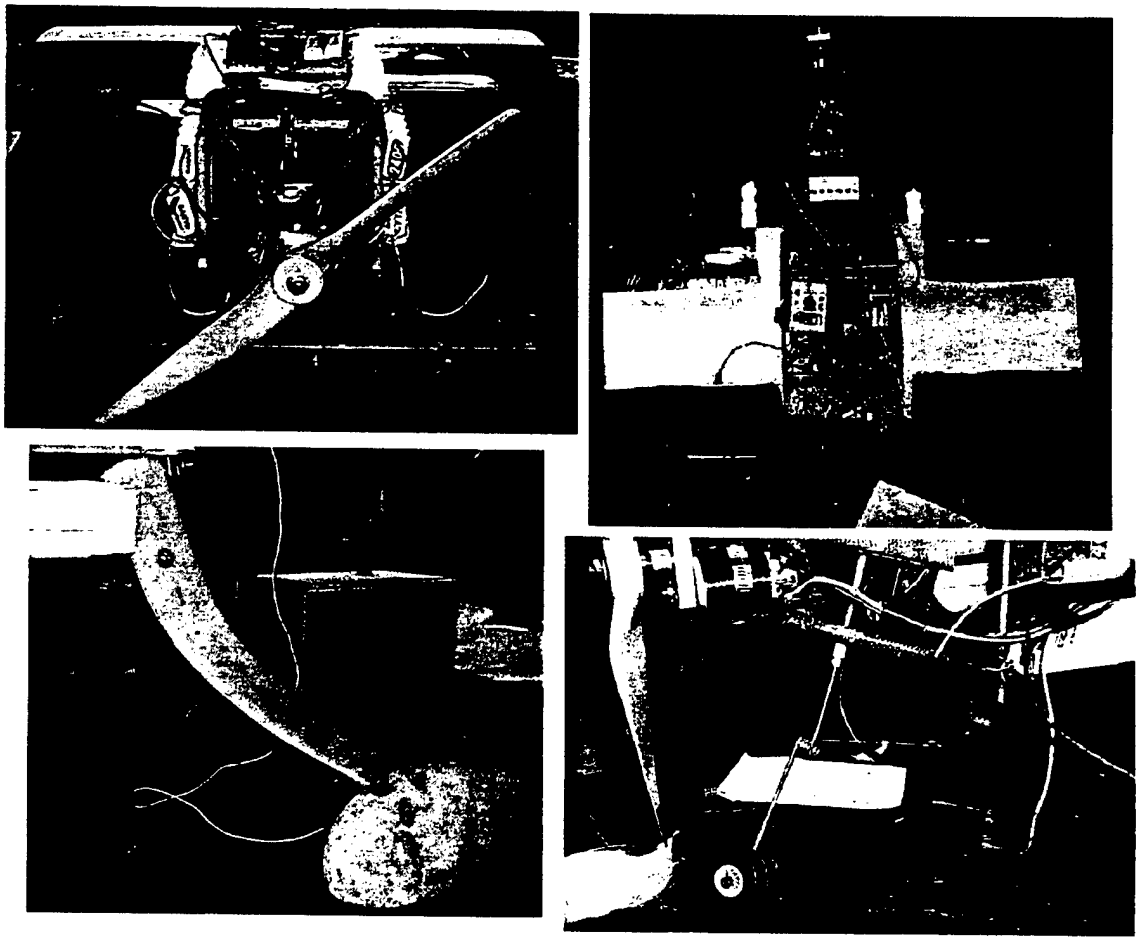

Figure 6.1: Fuselage, Landing Gear, and Internal Structural Details

6.2.3 Wing

The wing was constructed of a hot-wired foam core, with a carbon spar running the span of the quarter chord. It was divided into three sections, a middle section rigidly fixed to the fuselage frame, and two outer sections. The two outer sections contained prepreg carbon strips over the quarter chord spar, twice as much on the compression upper surface. They also contained a leading edge carbon composite layer along the length of the span. The control surface was mechanically fastened to the internal wing section,

where the servo was mounted. The hinges for the control surfaces were carbon composite. The wing attachment was two carbon rods, one at the quarter chord and the other at sixty percent chord, that fit snuggly into the root section and were pinned in place with tapered Aluminum pins. Figure 6.2 shows the final assembled wing.

6.2.4 Empennage

The tail booms were manufactured similarly to the wing attachments. Two carbon fiber tubes rigidly attached to the tail section fit snuggly into receivers in the internal wing section and were also pinned in place with tapered Aluminum pins. The tail itself was a hot-wired foam core with a fiberglass composite skin. The servos were semi-submerged in the tail section, and the control surfaces used a fiberglass composite hinge. Figure 6.2 shows the empennage construction and attachments.

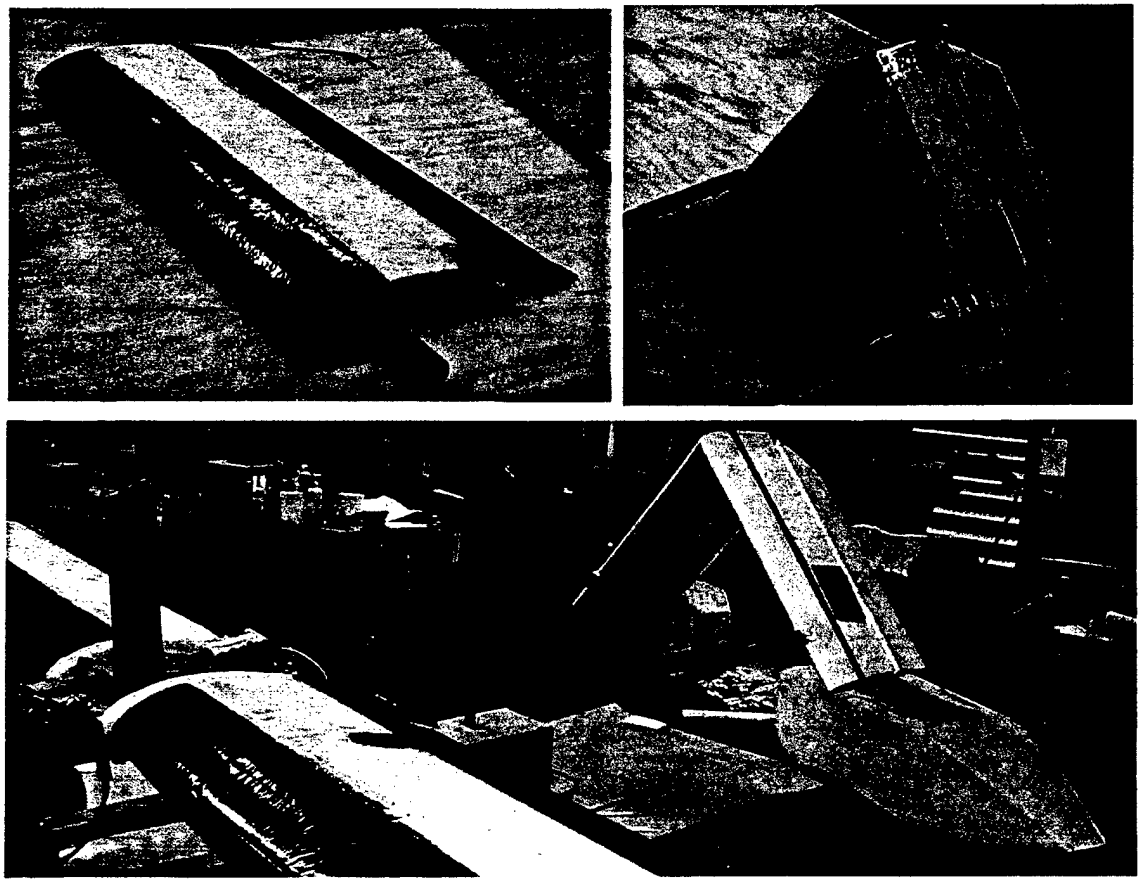

Figure 6.2: Wing and Empennage Construction

6.3 Manufacturing Plan

Figure 6.3 is a team milestone chart showing a breakdown of the planned and actual manufacturing schedule.

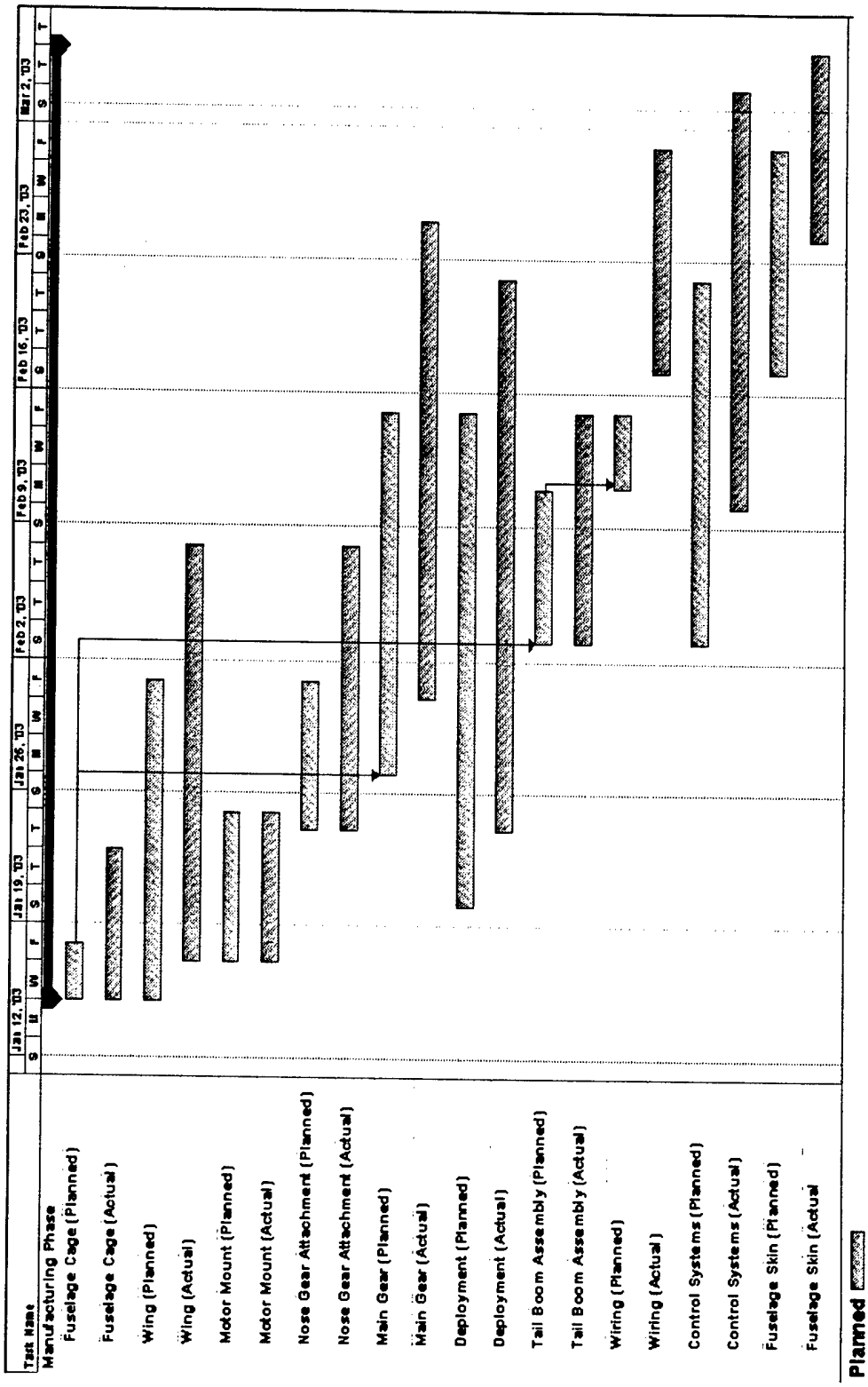

Figure 6.3: Manufacturing Schedule

Chapter 7

Testing Plan

7.1 Flight Testing Schedule

A total of five tests were scheduled for the aircraft beginning with the first flight on 01 March 2003. Each flight test was developed to check specific aircraft handling characteristics, flying qualities, performance, and stability. Prior to each flight test, extensive ground testing was conducted on each sub-assembly, flight critical components, and all electrical wiring. A complete preflight checklist is available in Table 7.1.

Component	Method
Charged Batteries	Volt meter
Motor Installation	By hand
Pin Connections	By hand
Battery Connections	By inspection
Fuse Connection	By inspection
Motor Connection	By inspection
Flap Deflection	Controller
Aileron Deflection	Controller
Elevator Deflection	Controller
Rudder Deflection	Controller
Nose Steering	Controller
Deployment Connection	By Inspection
Deployment Test	Controller
Propellor Spin-up	Controller

Table 7.1: Preflight Checklist

Four flights were scheduled for the first flight test. Both a conventional tail and a V-tail were constructed for the aircraft for its initial flights. The twin-vertical conventional tail was manufactured because of its inherent stability, and to insure that enough control power was available to maneuver the aircraft. The four flights scheduled were, in order; conventional tail/no payload box, conventional tail/with payload box, V-tail/no payload box, and V-tail/with payload box. During each flight, performance in several areas was sequential evaluated. The order of testing for each flight was takeoff and landing, takeoff and climbout, cruise performance including pitch/yaw/roll stability, and finally some slow-rate turning performance. The main goals of flight test one were to determine the overall flyabilty of the aircraft and the feasibility of the

V-tail configuration.

Two flights are scheduled for flight test two, to be conducted on 22 March. Flight one will be with the conventional tail, the payload box, and the radome mounted. Flight two will be with the V-tail, payload box, and radome mounted. The focus of flight test two will be in the middle of the flight envelop evaluating takeoff and landing, climbout, cruise performance, and turning performance. The specific focus of the test will be on how the radome affects the flying qualities, handling, and stability of the aircraft.

Flight test three on 29 March will encompass three flights. Its purpose is to expand the envelop of the aircraft. Flight one will be the empty plane, flight two will be with the payload box, and flight three will be with the payload box and radome. These will all be conducted in the competition V-tail configuration. Testing will be conducted from 20 percent above the stall speed up through the maximum velocity of the aircraft checking stability, handling, and flying qualities in 10 percent power increments. Sustained turning performance will also be evaluated during these flights.

Flight tests four and five, 05 April and 19 April respectively, will contain three flights each. Each flight will be a simulated mission. Flight one will be mission B with the payload box deployment, flight two will be mission A with the radome, and flight three will be the alternate mission, mission C, with three 360-degree turns per lap. These flights are an opportunity for the pilot to focus on specific mission requirements within the safe envelop of the aircraft. It is important that the pilot feel comfortable performing the difficult parts of all three missions. Landing and taking off with the radome, landing and deploying the payload box, sustained turning with the radome, and completing three 360-degree turns are all hazardous maneuvers for the aircraft. In addition, actual times for each mission will be measured during these two flight tests and both compared with initial estimates, and converted into a flight score representative of what can be expected at the competition. Table 7.2 summarizes the complete flight testing plan.

7.2 Ground Testing Results

Team Severn Discomfort was unable to meet the 03 March date for the first flight test due to several weeks of inclement weather in the Annapolis area. The date has been rescheduled to take the place of the second flight test on 22 March. Ground testing and systems checks were performed, however, on 05 March during the first fully assembled operational testing of the aircraft.

All wiring, connections, and control linkages were given a final inspection before assembling the aircraft from its core components. The aircraft's balance was also inspected. It was determined to be within the acceptable margin around the quarter chord with the payload box, both installed and deployed. Once in the testing area, the 40 Amp fuse was installed and a preflight check was conducted according to the check list. All systems on the aircraft were determined to be fully functional following this test.

A major milestone was met when the first operational test of the deployment system was successful. The team was pleased with both how secure the payload box was when fixed internally and with how smoothly it deployed from the aircraft. The next step in the process is to develop the hatch cover that will fill in as the bottom of the fuselage when the box is deployed during the mission.

The motor spin-up was also successful. The static thrust provided by the motor and prop looked

FLIGHT TESTING PLAN				
Flight	Date	Configuration	Flight Test Objectives	Measurements
1	01MAR		t/o, land, climb, cruise, and turn	t/o distance
a		H-tail	aircraft flying qualities, pitch/roll/yaw stability	time to turn
b		H-tail, box	general handling	V-tail go/no go
c		V-tail		
d		V-tail, box		
2	22MAR		t/o, land, climb, cruise, and turn (radome)	t/o distance
a		H-tail, box, radome	aircraft flying qualities, pitch/roll/yaw stability (radome)	time to turn
b		V-tail, box, radome	general handling (radome)	V-tail performance (radome)
3	29MAR		expand and define envelop for each configuration	maximum velocity
a		V-tail		maximum endurance
b		V-tail, box		minimum time to turn
c		V-tail, box, radome		
4	05APR		fly mission profiles, pilot practice, timing	timed assembly
a		V-tail, box	assembly practice	mission A, B, C flight times
b		V-tail, box, radome		
c		V-tail, box		
5	19MAR		fly mission profiles, pilot practice, timing	timed assembly
a		V-tail, box	assembly practice	mission A, B, C flight times
b		V-tail, box, radome		
c		V-tail		

Table 7.2: Flight Testing Plan

promising, however, no static thrust was measured for the aircraft because the necessary equipment was unavailable at the time. Several full power run-ups were conducted with the aircraft held stationary to ensure the pilot had a proportional range of power settings through the radio controller.

Taxiing was another major milestone in the testing process. The lateral strength of the nose gear initially posed a concern when it was first installed on the airframe due to the magnitude of estimated side forces. Any unexpected side force, especially on a landing could result in a nose gear failure. In order to stiffen the strut, a modified unidirectional, carbon fiber, aerodynamic strut was manufactured instead. Initial taxi tests proved it much more suited to take side loads. Taxi tests for the aircraft also showed remarkable tracking and controllability on the ground. One problem encountered during the taxi tests, however, was the rolling resistance of the wheels. This could affect the take off distance of the aircraft, as well as drain unnecessary power while accelerating to the take off velocity. To fix this problem, the wheel fairings and struts need to be pulled away from all contact with the wheels, and the axles need to be lubricated.

The biggest concern that developed from the ground testing was the longitudinal placement of the main gear. The necessity of the gear to fold for placement in the storage crate caused it to be placed slightly further aft than was initially designed. The concern from this is that the elevator power required to rotate the aircraft on takeoff was more than originally intended. Compounding this potential problem is the fact the maximum up elevator deflection mixed into the radio controller was only 15 degrees for the first test. Increasing the maximum elevator deflection and moving the main gear forward stand as the two biggest hurdles prior to the first flight test.

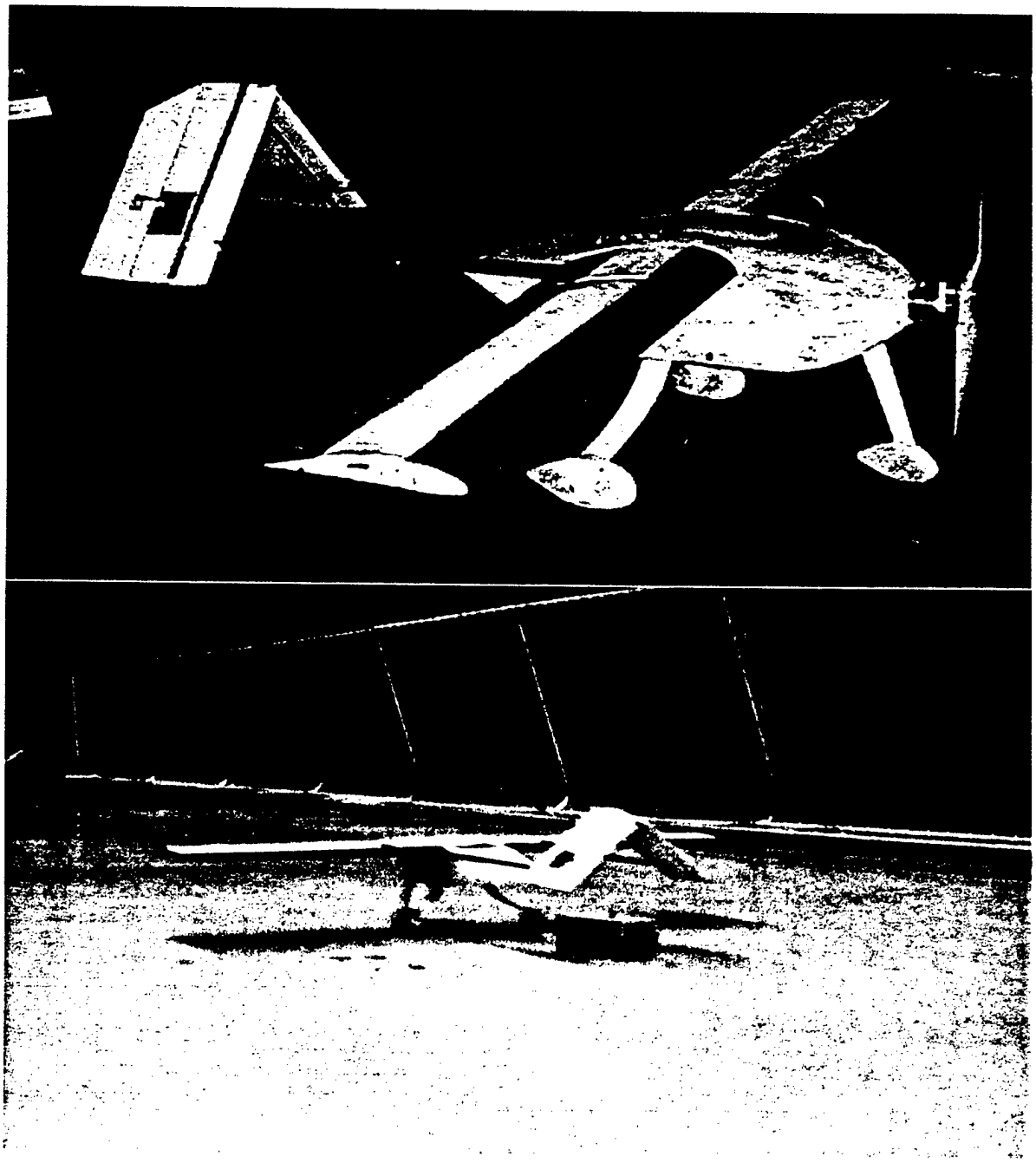

Figure 7.1: Final Production Aircraft Assembled for Ground Testing and the Payload Deployment Test

Chapter 8

References

Anderson, John D., *Aircraft Performance and Design*, McGraw-Hill, New York, 1999.

Birkelbaw, Larry, *DBF Team Positions*, Annapolis, 2002.

Boucher, Robert J., *The Electric Motor Handbook: The Complete Handbook of High Performance DC Motors*, Astro Flight Inc., 1994.

Campbell, John P., *NASA Report No. 823: Experimental Verification of A Simplified Vee-tail Theory and Analysis of Available Data on Complete Models With Vee-tails.*

Perkins and Hage, *Airplane Performance, Stability and Control*, Wiley, 1949.

Raymer, Daniel P., *Aircraft Design: A Conceptual Approach*, AIAA, 1999.

Roskam, John, *Airplane Flight Dynamics and Automatic Flight Controls*, Roskam Aviation and Engineering Corp., 1979.

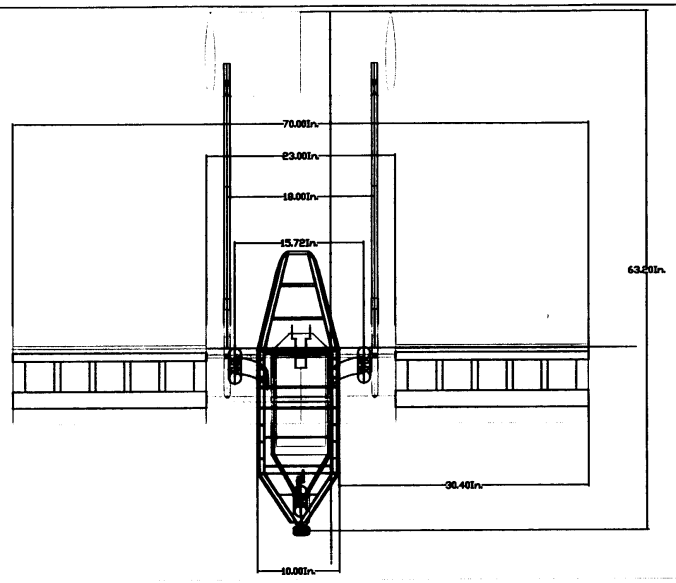

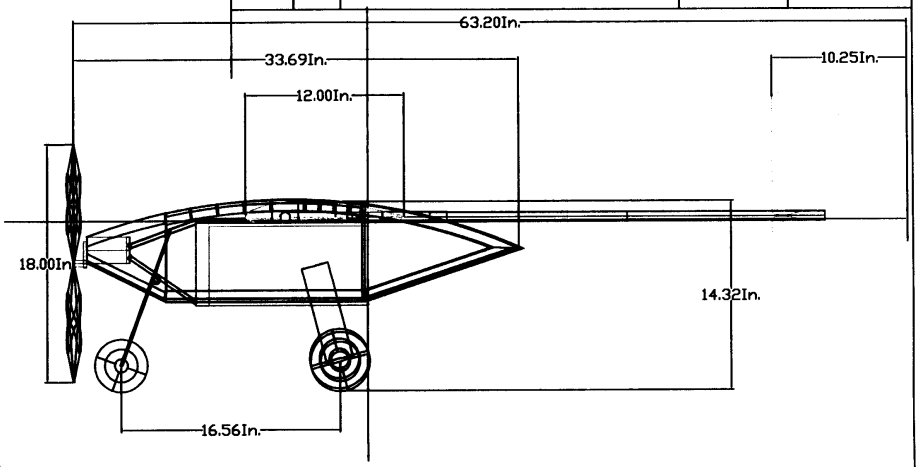

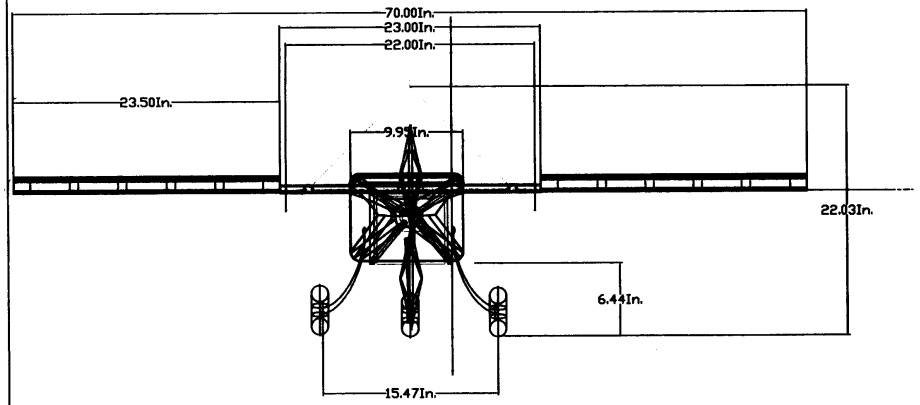

REVISIONS				
ZONE	REV	DESCRIPTION	DATE	APPROVED

USNA	Severn Discomfort		
	Three View		
Page 56	SIZE	FSCM NO.	DWG NO.	REV
	SCALE		SHEET	

REVISIONS				
ZONE	REV	DESCRIPTION	DATE	APPROVED

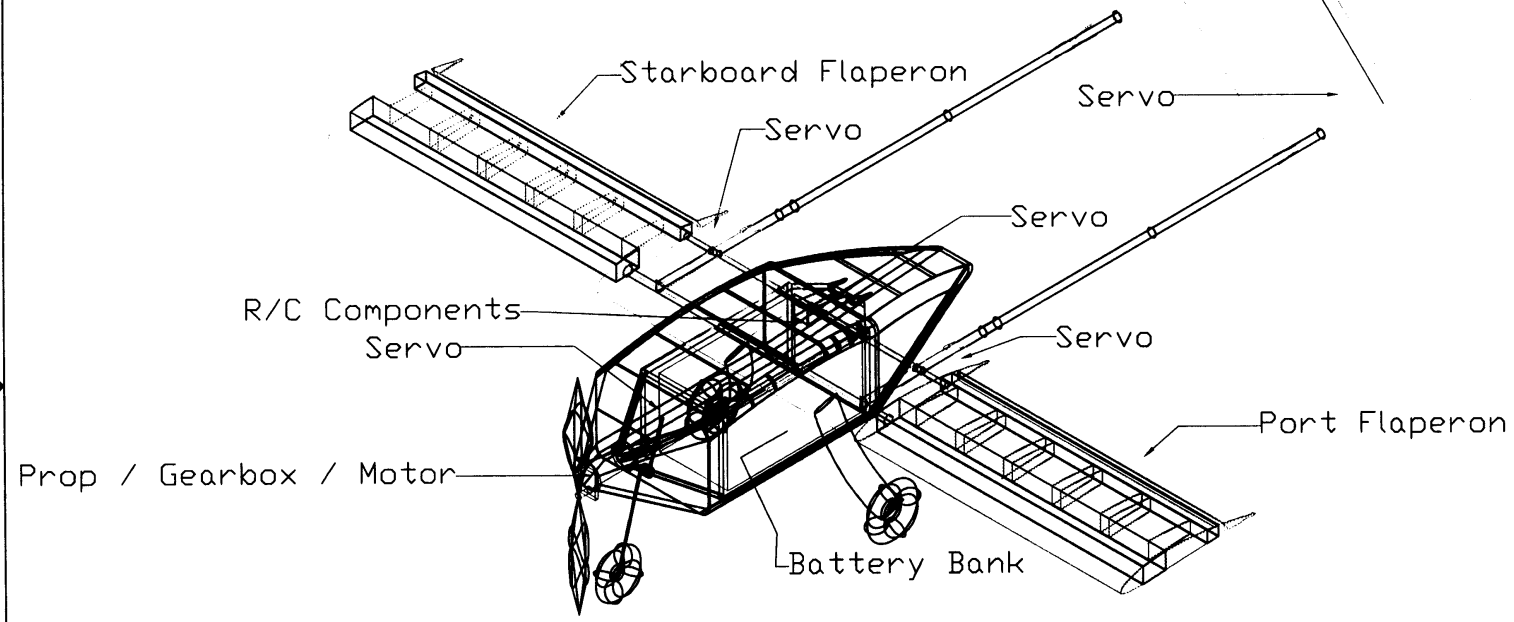

USNA	Severn Discomfort	
	Control Systems	
Page 57	SIZE / FSCM NO. / DWG NO. / REV	
	SCALE / SHEET	

REVISIONS				
ZONE	REV	DESCRIPTION	DATE	APPROVED

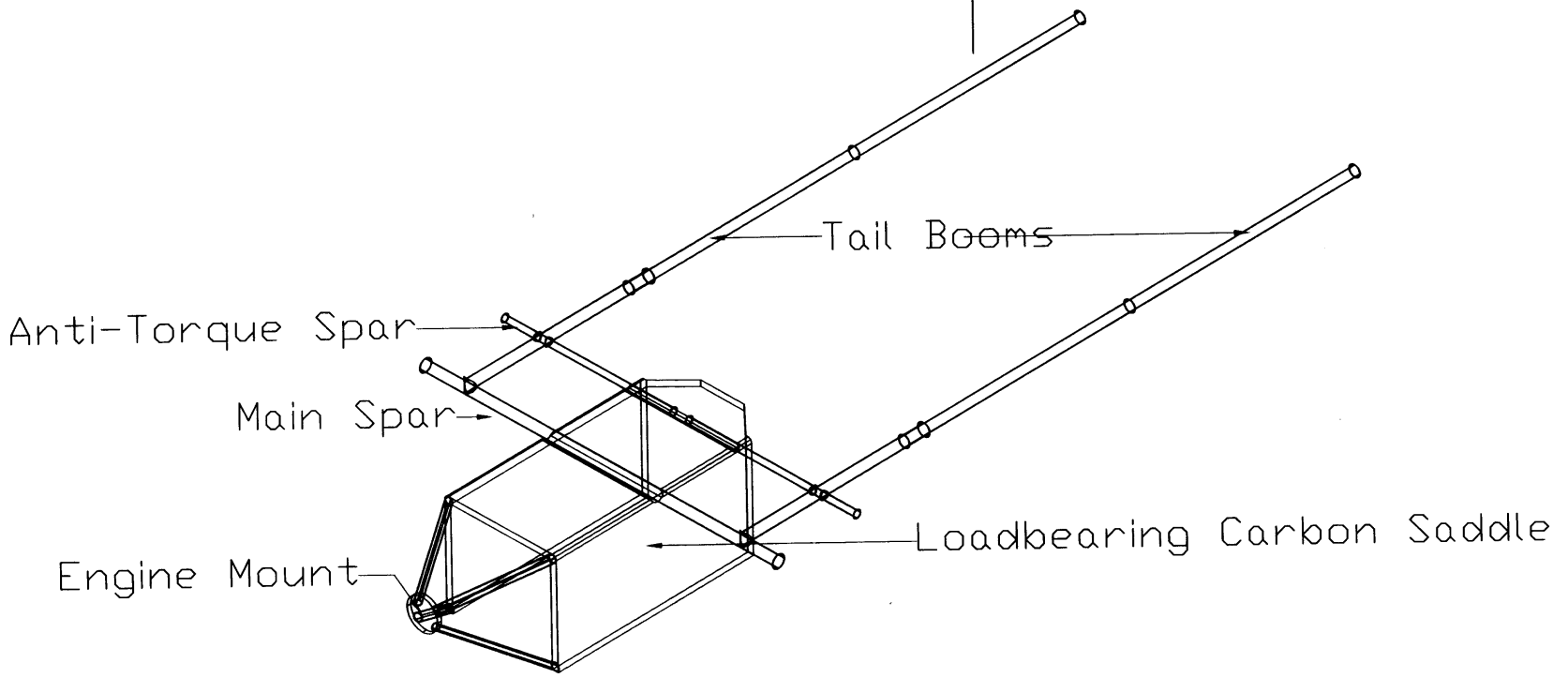

USNA	Severn Discomfort Structural / Loadbearing Components			
Page 58	SIZE	FSCM NO.	DWG NO.	REV
	SCALE		SHEET	

REVISIONS				
ZONE	REV	DESCRIPTION	DATE	APPROVED

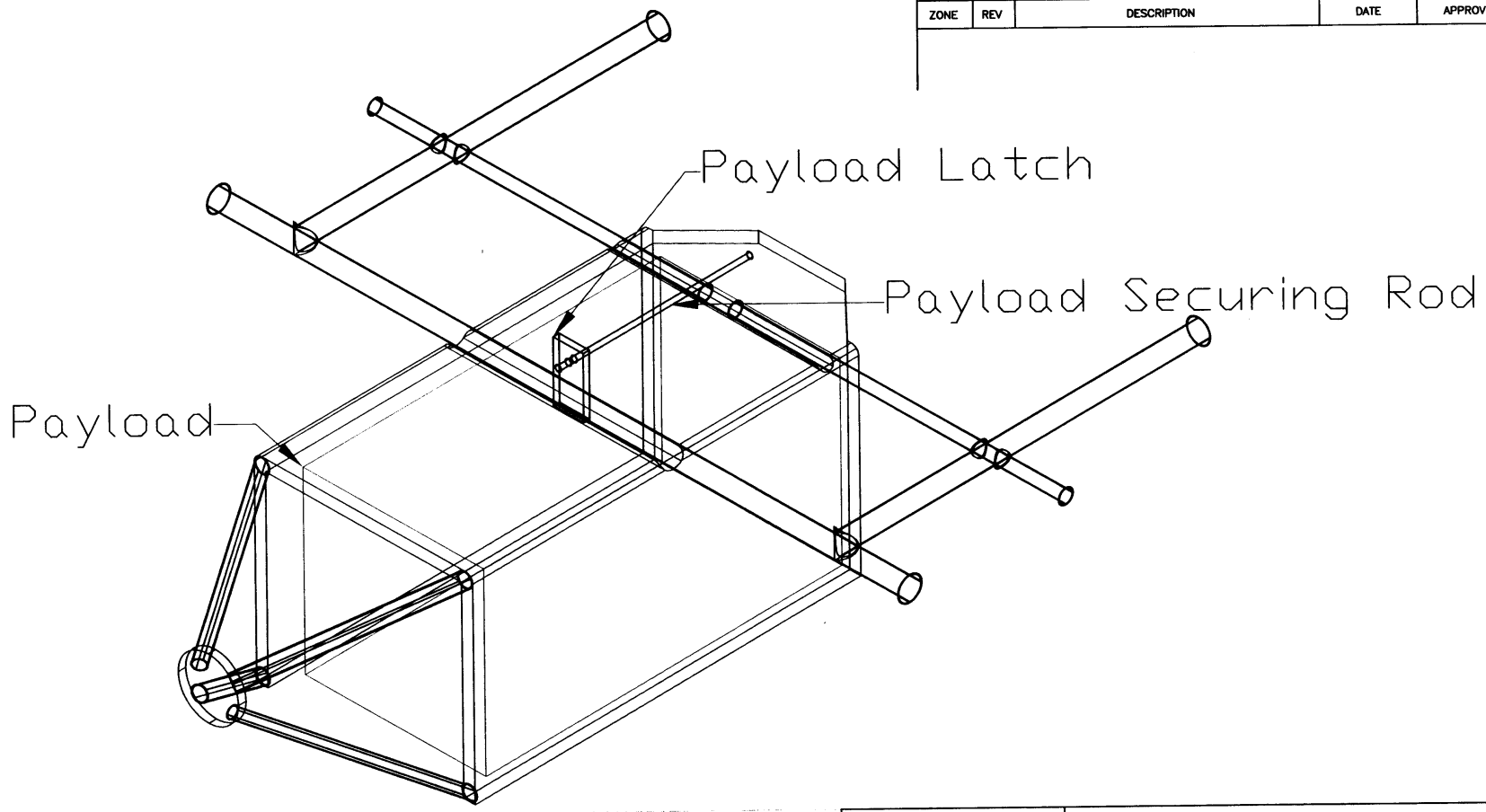

USNA	Severn Discomfort			
	Payload Deployment			
Page 59	SIZE	FSCM NO.	DWG NO.	REV
	SCALE		SHEET	

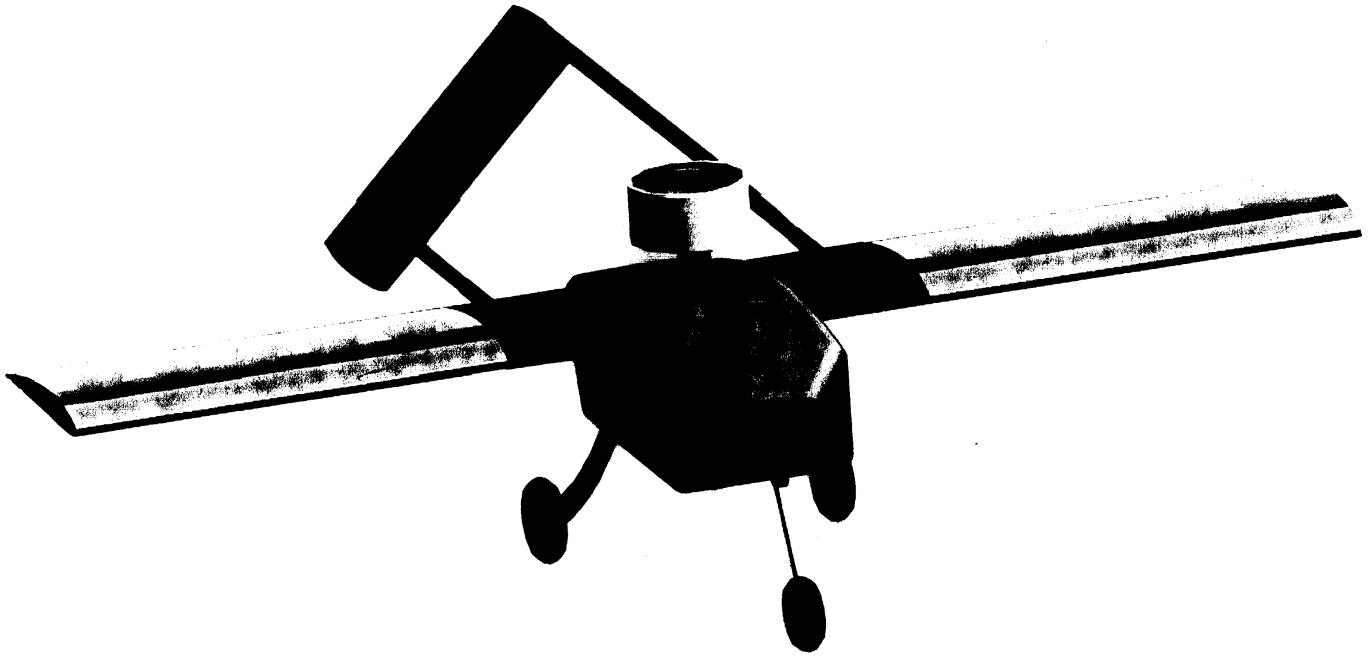

APPROVED	
USNA	Severn Discomfort
	Rendered Image
Page 60	SIZE / FSCM NO. / DWG NO. / REV
	SCALE / SHEET

2002/2003 AIAA Foundation

Cessna/ONR Student Design/Build/Fly Competition

DESIGN REPORT
MARCH 11, 2003

Department of Aerospace Engineering

Mississippi State University

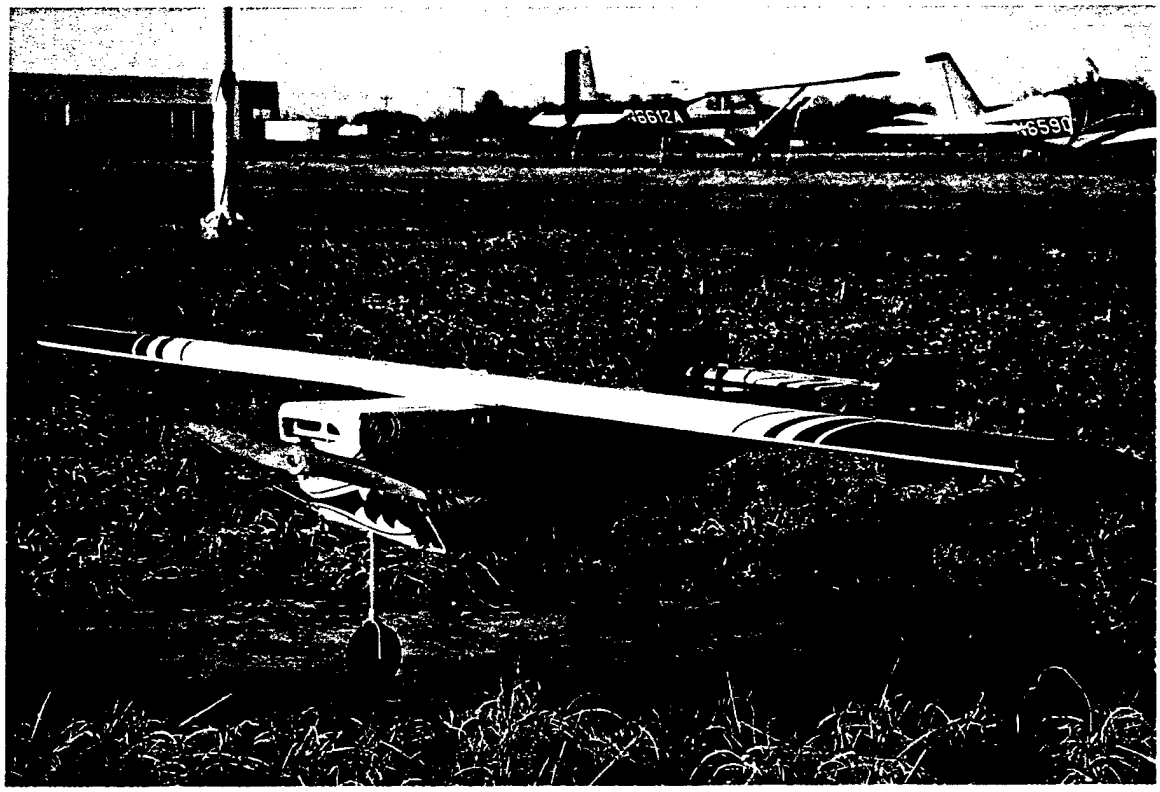

"SWAG"

TABLE OF CONTENTS

Table of Contents i
1.0 Executive Summary 1
1.1 Conceptual Design 1
1.1.1 Conceptual Design Alternatives 1
1.1.2 Conceptual Design Results 2
1.2 Preliminary Design 2
1.2.1 Preliminary Results 2
1.3 Detail Design 4
1.4 Manufacturing 4
1.5 Flight Testing 4
2.0 Management Summary 5
2.1 Organization of the Team 5
2.2 Assignment Areas 5
2.3 Milestone Timeline 5
3.0 Conceptual Design 9
3.1 Mission Requirements 9
3.2 Conceptual Design Concepts 10
3.2.1 Airframe (Fuselage) Configuration 11
3.2.2 Wing Design 11
3.2.3 Empennage Configuration 12
3.2.4 Engine Configuration 12
3.2.5 Landing Gear Configuration 13
3.2.6 Storage Considerations 13
3.3 Figures of Merit 13
3.3.1 Description of the Figures of Merits 14
3.3.2 Scoring of Design Concepts 15
3.4 Rated Aircraft Cost Factors 16
3.5 Conceptual Design Selection 17
3.6 Conceptual Design Summary 17
4.0 Preliminary Design 18
4.1 Airfoil Selection 18
4.2 Zero Lift Drag Prediction 20
4.3 Antenna Wake Avoidance 20
4.4 Thrust Loading and Wing Loading Study 22
4.5 Structural Analysis of the Spar 23

4.6 Engine Selection 24
4.7 Available Thrust Model at Speed 27
4.8 Wind Tunnel Results 27
4.9 Weight Model 28
4.10 Results from Optimization Code 29
4.11 Sizing of the Horizontal Tail 30
4.12 Sizing of the Vertical Tail 34
4.13 Performance Data 35
4.14 Estimated Mission Times 37
4.15 Summary of Preliminary Results 38
5.0 Detail Design 40
5.1 Weights and Balance Sheet 40
5.2 Component Selection 40
5.3 Systems Architecture 41
5.3.1 Wing 41
5.3.2 Fuselage 42
5.3.3 Empennage 42
5.3.4 Landing Gear 42
5.3.5 Engine Mount 43
5.3.6 Payload Deployment 43
5.3.7 Antenna Attachment 44
5.3.8 Storage Box 44
5.4 Drawing Package 45
6.0 Manufacturing Plan 50
6.1 Construction Methods Investigated 50
6.2 Construction Materials Investigated 50
6.3 Figures of Merit 51
6.4 Results 51
7.0 Testing Plan 54
7.1 Schedules and Check Lists 54
7.2 Results 54
7.3 Lessons Learned 56
References 57

1.0 EXECUTIVE SUMMARY

This report documents the efforts of a select group of aerospace engineering students at Mississippi State University to design, fabricate, and flight test an unmanned, electrically powered, aerial vehicle. The UAV offers a simple manufacturing platform while not sacrificing mission capability. Flight tested as being very stable and having good performance with a take off distance of less than 120 feet, *SWAG* represents a well-rounded design that carries a six-inch diameter dorsal antenna measuring three inches in length and a five-pound payload measuring six inches by six inches by twelve inches that is deployable. SWAG can be disassembled and stored in a box measuring four feet in length, two feet in width, and one foot in height.

1.1 Conceptual Design

During the first meeting, members were assigned to one, or more, of six major sub-teams. The sub-teams include aerodynamics, flight mechanics, flight-testing, optimization, propulsion, and structures. During the early team meetings, a sub-team would present an idea for a conceptual design that would meet the requirements specified in the rules of the Cessna/ONR Design/Build/Fly (DBF) Competition for 2003. Also, each member was given the opportunity to submit individual designs. After all conceptual ideas were presented; the sub-teams were instructed to meet each week, separate from the team meetings, to discuss how their subdivision was affected by the conceptual ideas and how to improve on each idea.

1.1.1 Conceptual Design Alternatives

The conceptual ideas, presented by the sub-teams, were categorized as a canard, a conventional, or a twin boom airframe. The canard was presented for its take off capabilities. The conceptual idea was to put the canard on a conventional type fuselage. The conventional airframe was presented for its stability and recognized success. Traditionally, Mississippi State's team has chosen to go with this concept. The idea, in the past, has been to build a conventional airframe around the mission profiles. The twin boom was presented for several reasons. The twin boom was desirable for its potential lightness. The booms would conceptually be constructed with carbon to reduce weight while retaining structural integrity. The booms would also allow space for the deployment of the payload box with an A- or H-tail. Many ideas were developed from the original A-tail, twin boom concept. Originally, the team intended to position the cylinder between the booms. This was eventually found to be illegal according to the rules.

The three conceptual ideas were expanded and improved upon. From three conceptual ideas, a total of fourteen conceptual designs were considered. These designs differed in airframe configuration, payload placement, wing placement, and empennage configuration.

1.1.2 Conceptual Design Results

Based on the Figures of Merit placed on each design, the fourteen conceptual designs were narrowed to three designs to be further considered. In the end, the final configuration chosen was a conventional fuselage incorporating an H-tail with a "Hershey Bar" high wing and a tricycle landing gear. The propulsion system chosen was a single AstroFlight motor with an APC propeller. To decrease assembly time from the storage box, the UAV would have "snap together" linkages for the wing and for the tricycle landing gear.

1.2 Preliminary Design

During the preliminary design phase, the sub-teams communicated and shared information to produce the sizing of the UAV. The sizing of the UAV was optimized from a performance standpoint; utilizing information from the aerodynamics, propulsion, and structures sub-teams. The rated aircraft cost (RAC) was to be minimized. Using the information from the sub-teams, the design space was reduced to two variables, wing span and wing chord, and was constrained using the performance requirement for the take off roll. If the velocity at take off for 120 feet was less than the stall speed, the RAC was assigned a value of zero. Also, side constraints were placed on the design variables based on the storage box dimensions. Once the dimensions of the wing were calculated from the optimization program, the flight mechanics team sized the H-tail to produce a UAV with a positive static margin and good stability characteristics. The constraints placed on the flight mechanics team were that the fuselage length must be less than 48 inches, the span for the H-tail must be less than 24 inches, but greater than 12 inches and the vertical distance of the H-tail must be less than 12 inches.

1.2.1 Preliminary Results

The results from the wing sizing showed that the optimum design coincided with the take off constraint. During the first year that Mississippi State University entered this competition, the design point was chosen close to this constraint. The weight of the UAV increased by five pounds from its predicted value and caused undesirable take off and climb performance. For this year, the design point was chosen such that the best design was away from the side constraint but still possessed a high score.

To acquire accurate data for the propulsion system, the AstroFlight 60 Cobalt engine with gear reduction and a 22x14 propeller were analyzed both statically and dynamically in the Mississippi State wind tunnel. The results of the wind tunnel testing on the motor and propeller showed a static thrust of 11 pounds with a pitch speed of 85 mph.

The final airframe was designed for completing the two most difficult missions. The payload and antenna placement coincided with the empty weight center of gravity. The design was estimated at a weight of approximately twelve pounds and was predicted to attain a RAC of 12.35. The sizing and the performance data of the UAV are presented in Table 1.1 and Table 1.2.

Table 1.1 Preliminary Component Sizing

Preliminary Component Sizing	
Fuselage Length (ft)	4
Wing Span (ft)	7
Wing Chord (ft)	1
Wing Aspect Ratio	7
Horizontal Tail Span (ft)	1.7
Horizontal Tail Chord (ft)	0.75
Vertical Tail Span (ft)	0.75
Vertical Tail Chord (ft)	0.75
Engine Selection	AstroFlight FAI Cobalt 60 Size
Gear Box	2.75:1
Propeller Selection (in)	22x14
RAC (Predicted)	12.35

Table 1.2 Preliminary Performance Results

Preliminary Performance Results		
	Loaded	Unloaded
C_{LMax}	1.5	1.5
L/D Max	12.1	12.1
Stall Speed (mph)	28.3	24
Maximum Rate of Climb (ft/min)	574.5	913.7
Neutral Point Location (% chord)	40	
C.G. Location (% chord)	33	
Take-off Distance (ft)	115	85
Maximum Speed (mph)	59	61
RAC	12.35	

1.3 Detail Design

The purpose of the detailed design was to select components for the UAV and to model the UAV in a graphics program that would indicate UAV size and configuration, storage configuration of disassembled parts, and payload location and deployment. Using the "Analysis" section of the graphics program, a detail of the component weight and location was collected, and the center of gravity was located. Using this information, a RAC table was constructed. A detail of the construction of the UAV was done. This description includes the wing, fuselage, empennage, and landing gear. A description of the payload deployment is also detailed.

1.4 Manufacturing

The construction of the UAV was considered from the beginning of the design. There were many methods of construction suggested by the team, ranging from off the shelf components to a molded design. The team concluded that the construction of the UAV must not be time consuming, must offer a low material weight, and must be low in cost. Based on these Figures of Merit, the team decided to construct the UAV using a built-up approach, utilizing laser cut parts and incorporating composite materials for areas of high concentrated loads. Wood was decided on as the major material based on skill and labor simplicity.

1.5 Flight Testing

Flight testing was a new area added to this year's design analysis. SWAG I was to be built based on the detail design. A second UAV, SWAG II was to be built with modifications based on flight testing of SWAG I. Flight testing would allow the team to analyze performance based on actual mission flights. A group leader was selected from the experienced pilots. The flight testing leader presented a schedule of flights, detailing the timeline of missions to be performed. The flight testing leader was assigned a group of students to help analyze and present the results from flight testing. The results and analysis were to be used in the modification of the second and third set of parts ordered for SWAG II. The third set of parts was considered the contingency plan and would be used for necessary improvements or repairs on either plane.

Flight testing had to be carefully planned and executed. Pre-flight briefings were scheduled before each proposed flight. These briefings allowed the students to gain perspective from actual flight testing personnel. Any problems encountered during flight testing were reported to the team and resolved accordingly.

2.0 MANAGEMENT SUMMARY

The 2003 Mississippi State University DBF team consists entirely of aerospace engineering students. This year's team is large, but contains mostly underclassmen and very few veterans of previous Design/Build/Fly teams. With only 2 seniors, 10 veterans, and a total of 24 students, the group would have to be organized according to experience and skills.

2.1 Organization of the Team

During the first meeting, a chief engineer and a project manager were nominated and elected by team members. With a team of 24 students, mostly underclassmen, leadership would have to be shared. Using the experience of 10 veterans and the skills of four R/C pilots, the team was broken into four sub-teams. The four basic divisions of the team were aerodynamics, flight mechanics, propulsion, and structures. Each of the sub-teams would have a veteran team leader and a pilot as a consultant. This would give all teams the experience from previous DBF teams and also the skills related to experience with building and piloting remotely controlled airplanes. In addition to the major sub-teams, there are several sub-teams which consist of a few team members. Two veterans from previous DBF competitions compose an optimization team in charge of sizing the UAV. There also a team composed of pilots in charge of construction and flight testing. In addition, sub-teams are created to help with administrative activities. An organization table, Table 2.1, presents groups, personnel, and responsibilities.

2.2 Assignment Areas

Each sub-team was assigned the task of contributing to the design and construction of the UAV. Also, on a weekly basis, other tasks were assigned to insure timely satisfaction of goals. Team leaders were responsible for distributing workload in the respective groups and reporting to the entire team. Each team contributed to the overall design and brought forward the major decisions to be made. The team as a whole voted on necessary improvements or changes. Table 2.2 illustrates individual involvement in each process. A maximum rating of 5 is given to those that contributed the most.

2.3 Milestone Timeline

An initial timeline was set to insure that work was done on a consistent basis. The team held weekly meetings, and the chief engineer and project manager met with the faculty advisor weekly to assure that the schedule was maintained. There were delays in propulsion testing due to a backorder of AstroFlight engines. The engine was received in February with testing conducted immediately. Further delays were encountered in construction due to miscommunication between the company making the laser cut parts and the comptroller office at the university. Figure 2.1 shows the milestones and respective timelines.

Table 2.1 Team Architecture and Responsibilities

Group	Chief Engineer: Viva Austin Project Manager: Erin Wahlers Faculty Advisor: Bryan Gassaway Members	Responsibility
Finance and Accounting	Erin Wahlers (GL), Viva Austin, David Bodkin, Nikki King, Jordan Haines, Mark VanZwoll, Cedric Gould	Maintaining and tracking of funds and the purchasing of materials.
Public Relations	Erin Wahlers (GL), Viva Austin, David Bodkin, Nikki King, Jordan Haines	Generating press releases to the university and soliciting funds.
Documentation	Viva Austin, Erin Wahlers	Taking notes during meetings and collecting any material deemed necessary for documentation.
Aerodynamics	Amar Amin (GL), Alex Allan, Nikki King, Robert DiGiacomo, Joel Konkle-Parker	Analysis of UAV components and the interaction of the components with the airflow around them
Construction	Consultants: Cedric Gould, William Lott, Mark Van Zwoll (This activity included entire team participation.)	Scheduling of manufacturing and supervise the construction of the UAV
Flight Mechanics	Kerry Beck (GL), Jason Hopper, Ryan Smith, Travis Klima – Consultant	Sizing the UAV specifications based on stability and control issues.
Flight Testing	Cedric Gould (GL), Viva Austin, David Bodkin, William Lott, Mark VanZwoll	Developing a flight plan for testing the flight envelope of the UAV, and obtaining an airfield to perform testing.
Optimization	Chris Cureton, Allen Hammack	Sizing the UAV based on performance issues as well as optimizing for score.
Propulsion and Systems	David Bodkin (GL), Vanessa Aubuchen, Joshua Jacobs, Alexander Szymamski, Cedric Gould - Consultant	Researching the subject of thrust models for electric engines and experimental testing of potential motor/propeller combinations.
Structures and Design	Jordan Haines (GL), Brent Buckner, Maribeth Davidson, Jennifer Esper, William Lott - Consultant	Taking the sizing of the UAV from the optimization group and putting in structure that would carry the loads.

GL – Group Leader

Table 2.2 Involvement of Each Member

	Alex Allen	Amar Amin	Vanessa Aubuchen	Viva Austin	Kerry Beck	Brent Buckner	David Bodkin	Chris Cureton	Maribeth Davidson	Robert DiGiacomo	Jennifer Esper	Cedric Gould	Jordan Haines	Allen Hammack	Jason Hopper	Joshua Jacobs	Nikki King	Travis Klima	William Lott	Joel Konkle-Parker	Ryan Smith	Alexander Szymanski	Mark VanZwoll	Erin Wahlers
Finance & Accounting:																								
Budget	0	0	0	4	0	0	0	0	0	0	0	0	0	0	0	0	0	0	0	0	0	0	0	5
Purchasing	0	0	0	2	0	0	0	0	0	0	0	0	0	0	0	0	0	0	0	0	0	0	4	5
Manufacturing:																								
Wing Assembly	2	2	3	4	3	3	1	1	1	2	2	5	5	1	3	3	2	2	5	0	3	3	5	1
Fuselage Assembly	0	3	1	2	0	0	1	1	0	3	2	5	0	1	0	2	1	0	5	0	0	0	5	0
Horizontal and Vertical Tail	4	2	1	0	0	0	1	0	1	2	2	5	1	0	0	1	1	1	5	0	0	1	5	0
Systems Integration	5	0	1	2	0	5	3	0	0	1	2	5	1	0	0	0	4	0	5	0	0	0	5	3
Report:																								
Executive & Management	0	0	0	5	0	0	4	0	0	0	0	3	0	0	0	0	0	0	0	0	0	0	0	3
Conceptual Design	3	3	0	5	0	0	5	1	0	3	2	3	2	1	0	0	3	0	0	0	4	0	4	3
Preliminary Design	3	3	0	5	4	0	5	2	0	3	2	3	2	2	0	0	3	0	0	0	0	0	4	2
Detail Design	3	3	0	5	4	3	5	3	0	3	2	2	2	3	0	0	3	0	1	0	3	0	3	1
Manufacturing Plan	0	0	0	0	0	3	5	0	0	0	2	0	2	0	0	0	0	0	2	0	0	0	0	0
Flight Testing:																								
Pilot	0	0	0	0	0	0	0	0	0	0	0	4	0	0	0	0	0	0	5	0	0	0	3	0
Ground Crew	0	5	0	0	0	0	5	0	0	0	0	4	5	0	0	0	0	0	0	0	0	0	5	0
Propulsion:																								
Thrust Model	0	0	0	0	0	0	5	1	0	0	0	3	0	0	0	0	0	0	0	0	0	0	0	0
Motor/Propeller testing	3	3	3	3	1	3	5	0	0	3	0	4	1	0	0	3	3	1	1	0	0	3	3	0
Performance:																								
Sizing and Optimization	2	2	0	0	0	0	0	5	0	2	0	0	0	4	0	0	2	0	0	0	0	0	2	0
CG and Neutral Point Analysis	0	0	0	3	3	0	5	0	1	0	1	0	2	0	0	0	0	0	1	0	0	0	0	0
CAD:																								
Components	0	0	0	0	0	0	5	0	0	0	0	3	0	0	0	0	0	0	0	0	0	0	0	0
Engine Mounts	0	0	0	0	0	0	5	0	0	0	0	0	0	0	0	0	0	0	0	0	0	0	0	0
Wing	0	0	0	0	0	0	5	0	0	0	0	0	2	0	0	0	0	0	0	0	0	0	0	0
Fuselage	0	0	0	0	0	0	5	0	0	0	0	0	2	0	0	0	0	0	0	0	0	0	0	0
Horizontal , Vertical Tail	0	0	0	0	0	0	5	0	0	0	0	0	2	0	0	0	0	0	0	0	0	0	0	0
Stability & Control:																								
Horizontal and Vertical Tail Sizing	3	3	0	0	3	0	2	0	0	3	0	0	0	0	3	0	3	3	0	2	3	0	3	0
Servo Selection	0	0	0	0	0	0	0	0	1	0	1	5	2	0	0	0	0	0	1	0	0	0	0	0
Control Surface Sizing	1	1	0	0	3	0	5	0	0	1	0	0	0	0	3	0	1	3	0	1	3	0	1	0
Administration:																								
Scheduling	0	3	0	5	3	0	3	0	0	0	0	0	3	0	0	0	0	0	0	0	0	0	0	4
Soliciting Funds	0	0	0	5	0	0	0	0	0	0	0	0	4	0	0	0	4	0	0	0	1	0	4	4
Documentation	2	2	0	5	0	0	5	0	0	0	4	0	1	0	0	0	3	0	0	0	0	0	3	5

0 – No Involvement 5 – Maximum Involvement

Task Name	Start	Finish	Sep	Oct	Nov	Dec	Jan	Feb	Mar	Apr
Conceptual Design										
Planned	10-Sep	24-Sep								
Actual	10-Sep	8-Oct								
Propulsion Model and Testing										
Planned	16-Sep	26-Nov								
Actual	26-Sep	12-Feb								
Submission of Entry Form		31-Oct								
Performance and Sizing										
Planned	24-Sep	08-Nov								
Actual	24-Sep	08-Nov								
Obtain Half Funding										
Planned	24-Sep	22-Oct								
Actual	04-Oct	11-Oct								
Detailed Design										
Planned	15-Oct	30-Nov								
Actual	22-Oct	03-Dec								
Manufacturing										
Planned	06-Jan	28-Jan								
Actual	06-Jan	28-Feb								
Flight Testing										
Planned	03-Feb	22-Feb								
Actual	28-Feb	March								
Report										
Planned	27-Jan	28-Feb								
Actual	10-Feb	03-Mar								
Submission of Report		05-Mar								
Design/Build/Fly Competition		26-Apr								

Figure 2.1 Milestone Chart of Major Events

3.0 CONCEPTUAL DESIGN

The conceptual design phase of the UAV design process defines the rough layout of the UAV. Each sub-team is given the challenge of presenting a conceptual idea that meets the mission requirements of the competition. Also, team members are given the opportunity to present individual ideas. From these ideas, conceptual designs are presented, and Figures of Merit are applied. The ideas are narrowed to a conceptual design for *SWAG*. The selection for the conceptual design represents a configuration that will accomplish the mission requirements with little sacrifice in rated aircraft cost (RAC).

3.1 Mission Requirements

The UAV was designed to complete three mission profiles. Each profile is given a difficulty factor based on the complexity of the mission. The higher the difficulty factor, the better the team's score. Competing teams will be allowed five flight attempts, choosing any of the three mission profiles, and will be judged on the best two flight attempts from two separate mission profiles. Adding to the complexity of the design, the UAV must fit into a box two feet wide by one foot high by four feet long. Each team will be judged on assembly time of the UAV from the storage box. Also, each mission profile will be timed based on completion.

Each mission profile shares common characteristics. The UAV must takeoff within 120 feet to commemorate the 1903 Wright Brother's flight and must carry a simulated sensor package. The simulated sensor package measures six inches by six inches by twelve inches and weighs five pounds, ballasted at the centroid of the box. The flight profile consists of a closed traffic pattern with the direction of travel decided based on wind conditions. The upwind and downwind legs measure 1,000 feet with no set distance for the base and crosswind legs. The contest director determines the altitude for the pattern during the competition. From past experience with this competition, the altitude ranges from 100 feet to 200 feet above the ground.

The communications repeater is the least difficult mission. The UAV must take off, complete four laps/patterns, and land. During three out of the four downwind legs, the UAV must complete a 360 degree turn opposite of the base and final turns.

The sensor deployment is the next mission in difficulty. During this mission, the UAV must take-off, complete two laps/patterns, and land. When at full stop, the simulated sensor package must be deployed from UAV. The UAV must take-off again, complete two more laps/patterns, and land. During each downwind leg, the UAV must complete a 360 degree turn opposite of the base and final turns.

The missile decoy mission is the must difficult of the three. In addition to the common characteristics shared by all missions, the UAV must carry a simulated antenna. This simulated antenna is a cylinder measuring six inches in diameter and three inches in height and must be placed three inches from the nearest UAV structure with a 360 degree non-obstructed view. The UAV will take-off, complete four laps/patterns, and land. During each downwind leg, the UAV must complete a 360 degree turn opposite of the base and final turns.

3.2 Conceptual Design Concepts

Individual sub-team concepts were presented during team meetings each week. The number of conceptual designs presented was fourteen. Upon examination of each design, it was determined that four major features defined each of the design concepts presented: airframe configuration, payload placement, wing design, and empennage configuration. Open suggestions taken from the entire team resulted in the following table.

Table 3.1 Concept Descriptions

Concept Number	Airframe	Payload Carriage		Wing	Empennage
		5 lb Box	Antenna		
1	Twin Boom	Under Wing	Above Wing	High AR	V-Tail
2	Twin Boom	Under Wing	Between Booms	High AR	V-Tail
3	Twin Boom	Under Wing	Above Wing	Low AR	V-Tail
4	Twin Boom	Under Wing	Between Booms	Low AR	V-Tail
5	Twin Boom	Under Wing	Above Wing	High AR	H-Tail
6	Twin Boom	Under Wing	Between Booms	High AR	H-Tail
7	Twin Boom	Under Wing	Above Wing	Low AR	H-Tail
8	Twin Boom	Under Wing	Between Booms	Low AR	H-Tail
9	Conventional	Inside Fuselage	Above Wing	Low AR	V-Tail
10	Conventional	Inside Fuselage	Below Fuselage	Low AR	V-Tail
11	Conventional	Inside Fuselage	Above Wing	High AR	H-Tail
12	Conventional	Inside Fuselage	Below Fuselage	High AR	H-Tail
13	Canard	Inside Fuselage	Above Wing	High AR	N/A
14	Canard	Inside Fuselage	Below Fuselage	High AR	N/A

3.2.1 Airframe (Fuselage) Configuration

The twin boom airframe was chosen for two basic reasons. The UAV would be lightweight and therefore conceivably fast, and the antenna could be carried between the booms. Before it was found to be illegal, according to the rules, it was a major part of the team's design concept. Allowing the booms to be far enough apart to comply with the structural three inch rule, the drag caused by the antenna would be greatly reduced. The booms will be constructed of foam with carbon socking. This construction would allow the UAV to be lightweight and structurally sound.

The conventional airframe was chosen for its stable reputation, ease of analysis and construction. It would be heavier than the twin boom, but more stable and reliable in analysis. Being able to analyze data on a well known structure would allow for more trust in theoretical results. Traditionally, Mississippi State University has chosen this configuration. Since attending the competition for the past two years, this airframe has been a consensus for the majority of universities attending this competition.

The canard airframe was chosen for its effective take-off capacity. The essential design of the lifting-canard was to provide lift during flight. If some of the lift from the canard was used during take off in conjunction with the lift from the wings, the ground roll would be less than that of the twin boom and conventional airframes. Using the canard would allow more freedom in areas that would have to be compromised for short takeoff with the other designs such as storage box constraints. The canard would be heavier than the twin boom but comparable in weight to the conventional UAV.

3.2.2 Wing Design

The design of a wing depends largely on the aspect ratio (the ratio of the wing span squared to the wing platform area). For this design, aspect ratios of eight or lower were considered low, and aspect ratios higher than eight were considered high. High aspect ratio wings have the advantage of creating less induced drag. However, high aspect ratio wings do not perform or handle as well as low aspect ratio wings due to the extra inertia, roll damping and tendency to tip stall. Also, a high aspect ratio wing will be difficult to design considering the design constraints of the storage box.

Tapered wings were briefly discussed and dismissed. Although there was quite an advantage to tapering the wings, the skill and time required to design, analyze and build a tapered wing outweighed the advantage. The basic rectangular wing was proven effective in the past was easily analyzed and

manufactured. For stability reasons for a rectangular wing with no dihedral, the placement of the wing would be on top of the fuselage.

3.2.3 Empennage Configuration

The empennage was used for stability and control. Therefore, the airflow hitting the empennage must be unaffected by the payload or antenna for it to be effective. Because the mission profile calls for one of the missions to carry the six inch diameter cylinder (antenna), special consideration was made for the tail configuration. This design would allow for that mission to be flown. Therefore, along with the canard configuration, an H- and V-tail were considered.

The canard, tail surface ahead of the wing, would allow for less wing or propulsion flow interference. It would also lessen the nose-down pitching moment caused by high-lift devices by producing lift that adds to the wing lift. However, canards can be destabilizing if the center of gravity (CG) is not properly located.

The "V"-tail has less wetted area compared to conventional tails. However, it is less efficient in pitch inputs and requires radio mixing. Nonetheless, it moves more of the effective control surface out of the possible antenna wake.

The "H" tail may also remove the control surfaces from the possible wake. It is less efficient in the rated aircraft cost but is simple in design. The span can be adjusted for the width needed to clear the antenna wake.

3.2.4 Engine Configuration

Even though not listed in the table, two engine configurations were analyzed, tractor and pusher. Of the two configurations, tractor and pusher, the latter was chosen. A pusher propeller was decided against because the configuration would put a lot of weight at the tail causing trouble in locating the CG in the correct position. Also, the UAV would disrupt the flow seen by the propeller and thus reduce its efficiency. A tractor prop was decided upon since most props available are made for this kind of operation and it does not face any of the problems faced by the pusher. The next decision was how many motors would be needed. Obviously, the more motors on the plane the greater weight. It would be in the team's best interest to reduce the weight as much as possible. Also, conversing with the optimization group revealed that a single motor would reduce the RAC score. So a single engine, tractor propeller configuration was chosen.

3.2.5 Landing Gear Configuration

Two landing gear configurations were considered, tricycle and tail-dragger. Based on the payload deployment requirements, the tricycle gear was chosen as the landing gear configuration. Incorporating a tail-dragger in the UAV would not allow a successful deployment of the payload box.

3.2.6 Storage Considerations

The UAV would be disassembled and stored in a box measuring four feet by two feet by one foot. The assembly of the plane from the box will be timed until completion. The greater the time, the lower the overall score will be. Therefore, the suggestion was made to make all connections "snap together". The "snap together" pieces would include the main and nose landing gear and the wing panels. Caution was taken on this idea during the construction, but the "snap together" pieces passed the 2.5g structural test as mentioned in the rules of DBF.

3.3 Figures of Merit

Figures of Merit were chosen to identify how each concept compares to the others in the overall selection. Figures of Merit were decided based on the RAC, mission profiles and other scoring qualities and were weighted according to how important it is to the overall score. The weights were assigned a value from one to five, with five being the highest. The RAC has a large value because it is vital to the total score and was negative because it would count against the total score. The Figures of Merit and the weight factors are detailed in the following table.

Table 3.2 Design Parameters and Weighted Value

Design Parameter	Weight Factor	Mission Feature
Performance and Handling	3	Handling qualities of UAV, ease of piloting on closed course
Speed	4	Time to complete entire airborne portion of mission
Takeoff Performance	5	Ease of takeoff within 120 ft
Assembly Time	4	Ease of assembling out of the box
Repair ability	1	Ease of repair upon structural damage
Simplicity	3	Simplicity of design, structure and components
Center of Gravity (CG)	3	Necessity to control CG location
Rated Aircraft Cost	-4	Rated Aircraft Cost

3.3.1 Description of the Figures of Merits

Performance and handling is given a three in weight. It is important that the UAV be controllable in the air. Although the pilot must feel comfortable with the UAV, he does not need a UAV so stable that performance is compromised. The team decided with the advice of the pilot and other consultants, that the UAV must be stable, but not to compromise other merits with the perfection of this one. The pilot states that he will be comfortable with having to "work" the UAV somewhat.

Since the missions are timed, speed is a necessity and is given a four in weight. In order to maximize speed, we must consider weight, drag and propulsion. The weight of the UAV must be kept as low as possible for speed and RAC. The drag produced by the UAV and its payload must also be minimized. This means optimizing placement of the payload.

Because takeoff must be within 120 feet, or the flight is void, this became our most important figure of merit hence, given a five in weight. The plane will have to be light enough and generate enough lift for this parameter to be successful. A design consideration with this parameter is the induced drag during takeoff. Because the UAV is operating at relatively low speeds, the induced drag will be high.

The UAV must be assembled on site while being timed on completion. Therefore, the UAV must be designed for ease of assembly, as it is a major portion of each flight score and is given a four in weight.

Repair ability is given a low rank of one. The reasoning behind this is that the UAV will be designed around the other parameters first and crash worthiness will have to be compromised. The idea is to build a second UAV and have parts for a third. If the UAV is compromised in flight and is lost, there is the

option of replacing parts or the entire UAV. This keeps the ability to design for rated aircraft cost and simplicity more likely.

The last quality, RAC, is considered to be an important design criterion. The objective in any competition is to win, and to win, the overall score must be greater than the opponents'. The RAC is a penalty in the overall score. The higher the rated aircraft cost, the less the overall score will be. This is the reason why the weighing factor is negative. It acted as a penalty in the ranking of the design concepts.

3.3.2 Scoring of Design Concepts

Based on the design parameters discussed, each design concept was evaluated by giving a score of five (excellent) to one (poor). The scores from these design parameters were multiplied by their corresponding weighting factor and summed to obtain the overall score for each concept. In other words,

$$\text{TOTAL} = \sum_{i=1}^{8} s_i \cdot WF_i \quad \textbf{Equation 3.1}$$

where,

s is the score of each figure of Merit for each conceptual design and

WF is the weighted factor of each figure of merit.

Evaluating each configuration, the following table was generated. The top total scores were further considered.

Table 3.3 Scoring of Design Concepts

Concept	Takeoff	Perform.	Speed	RAC	Assembly Time	Repair Ability	Simplicity	CG.	TOTAL	Action
1	5	3	4	-4	8	2	6	3	27	E
2	10	3	8	-8	8	2	6	3	32	E
3	5	3	4	-8	8	2	6	3	23	E
4	10	3	8	-8	8	2	6	3	32	E
5	5	6	4	-4	8	2	6	3	30	E
6	5	6	4	-4	8	2	6	3	30	E
7	5	6	4	-8	8	2	6	3	26	E
8	10	6	8	-8	8	2	6	3	35	FC
9	5	3	4	-4	8	3	6	6	31	E
10	5	3	4	-4	8	3	6	6	31	E
11	10	6	4	-8	8	3	6	6	35	FC
12	10	6	4	-8	8	3	6	6	35	FC
13	5	6	12	-4	4	1	3	6	33	E
14	5	6	12	-4	4	1	3	6	33	E

E - Eliminate FC - Further Consideration

3.4 Rated Aircraft Cost Factors

Rather than discussing individual designs, we will describe the effect of different types of components. These effects are presented in the following table.

Table 3.4 Rated Aircraft Cost Factors

Component	Type	Effect on RAC
Fuselage	Twin Boom	Either a very small fuselage or none. Less cost to RAC. Added structure to wing and boom joiner would add to RAC cost.
	Conventional	Longer than other two types, so costs more. Added length required additional structural weight.
	Canard	More "wing" area but less empennage; about same RAC as conventional except, additional cost expected due to weight.
Wing	High AR	Higher cost per square foot due to cost formula Greater structural weight
	Low AR	Lower cost per square foot Reduced structural weight
Tail	V	Slightly reduced cost from formulas
	H	Slightly higher RAC cost due to increased control area.
	Canard	Increased cost due to necessity to score as a wing.

3.5 Conceptual Design Selection

The end of the conceptual design phase saw three configurations to be elaborated on for further discussion. The canard was eliminated from further consideration because of the stability issues and experience with seeing canards in the past competitions. Although it was known that a correctly designed canard would show the desirable features, the concern with little canard experience overwhelms the possibilities. Since the rules state that the antenna must have a non-obstructed, 360 degree view, concept eight was eliminated. Other reasons which led to this decision were stability and control issues. The conventional UAV has qualities desirable in a payload carrying UAV. Further, concept twelve was eliminated because of clearance issues with the deployment of the payload. Therefore, the conceptual design chosen to be considered for preliminary analysis was concept eleven.

3.6 Conceptual Design Summary

Based on the Figures of Merit placed on each design, the fourteen conceptual designs were narrowed to three designs to be further considered. In the end, the final configuration chosen was a conventional fuselage incorporating an H-tail with a "Hershey Bar" high wing and a tricycle landing gear. The propulsion system chosen was a single AstroFlight motor with an APC propeller. To decrease assembly time from the storage box, the UAV would have "snap together" linkages for the wing and tricycle landing gear.

4.0 PRELIMINARY DESIGN

The preliminary design phase is to size and/or modify the conceptual design for a more detailed analysis. In designing a UAV, many variables must be considered. Engine selection, propeller selection, wing area, chord length, airfoil sections, and aspect ratio are some design parameters of importance. There are many combinations of these variables that will produce a flying UAV. The sizing of the UAV is optimized from a performance standpoint, utilizing information from the aerodynamics group, propulsion group, and structures group. Once the dimensions of the wing were calculated from the optimization program, the flight mechanics group sized the H-tail and the fuselage length to produce an UAV with a positive static margin and good handling characteristics. Once the sizing of the UAV was completed, a performance analysis was done. This included investigations into maximum lift-to-drag ratio, maximum rate-of-climb, power available and power required, and estimated mission times.

4.1 Airfoil Selection

The factors in determining which airfoil section would be used for *SWAG* were: low Reynold's number, high lift coefficient (C_L), and low drag coefficient (C_D). Airfoils such as NACA, Selig/Donovan, and Eppler were evaluated by the Aerodynamics team. Out of the airfoils that fit the criteria, the Selig/Donovan 7062 airfoil was chosen. This decision was based on past experience with this airfoil, simplicity of construction and analysis and fulfillment of requirements.

Historically and from past competitions, symmetric airfoils were chosen for a tail structure. The NACA 0009 airfoil section was selected for the empennage section. This airfoil section has been common in use for tail surfaces and offered predictable performance.

A Reynolds number was predicted for both the wing and empennage airfoil sections. The aerodynamic data from these two airfoils was plotted in Figures 4.1 and 4.2. The software used to generate the data is *XFOIL*. *XFOIL* is an interactive program for the design and analysis of subsonic isolated airfoils.

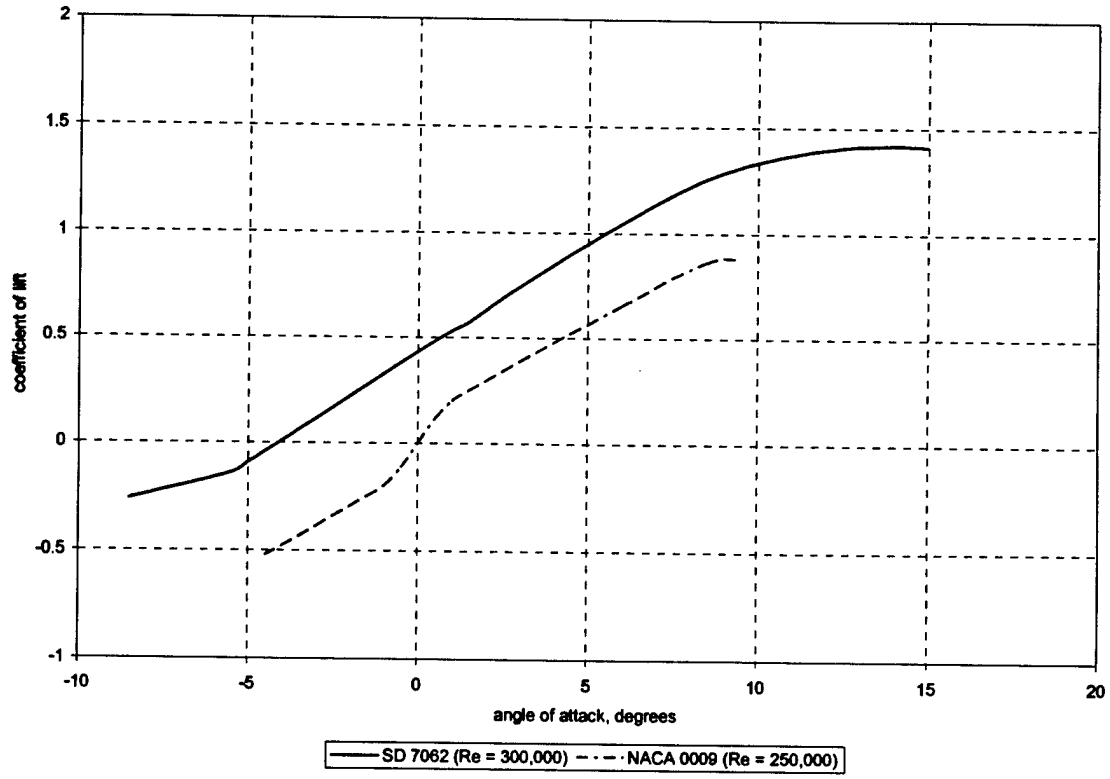

Figure 4.1 Coefficient of Lift for Varying Angle of Attack

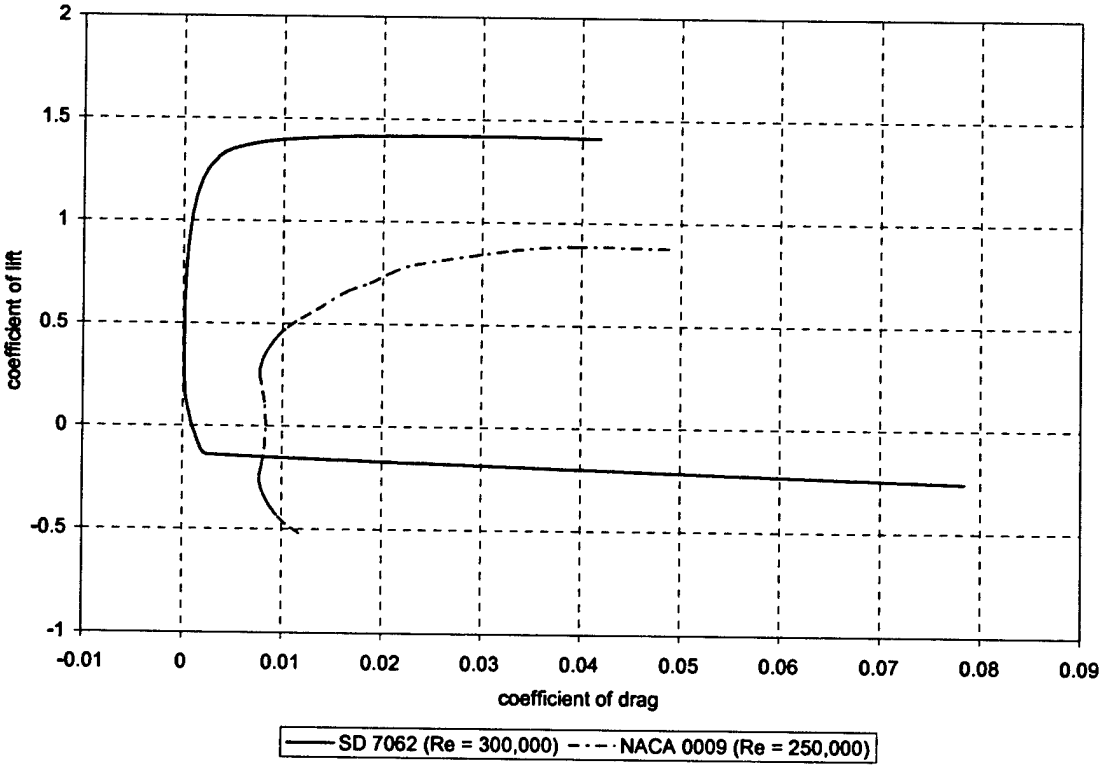

Figure 4.2 Coefficient of Lift for Varying Coefficient of Drag

4.2 Zero Lift Drag Prediction

The zero-lift drag was predicted using Raymer's data and an estimation of the wetted area of the UAV. The estimated wetted area of the UAV was divided by the surface area of the wing. A scaling factor of 0.0065 was chosen from Raymer's data and multiplied by the area ratio previously found. The scaling factor was chosen based on subsonic flight and the UAV's geometry. The result is a zero-lift drag of 0.03.

4.3 Antenna Wake Avoidance

A major concern with the antenna was the wake produced on the tail during flight. Sources from websites and professors within Mississippi State University's Aerospace Engineering Department provided information on cylinder wake analysis. The most critical information to determine was the characteristics of the wake of air behind the antenna. The wake would gradually increase with distance from the antenna to the tail, and concerns arose over blanking out of the tail surfaces during flight. Dr. Keith Koenig provided an understanding of how air flows around a cylindrical antenna and the factors that should be considered. Using this information, an equation was derived to express the width of the wake in terms of the distance from the antenna to the tail surfaces.

$$\frac{w}{d} = \left(\frac{x + n \cdot d}{2 \cdot d} \right)^{0.5} \qquad \textbf{Equation 4.1}$$

where,

d is the width of the antenna,

w is the width of the wake,

x is the distance from antenna to tail,

n is a constant equal to 2, and

n·d is the distance to the virtual origin of the wake.

Equation 4.1 is plotted for several distances between the antenna and tail. At the time of testing, it was estimated that SWAG would have a two-foot distance between the antenna and tail. At a distance of two feet, the distance of the wake was 10.5 inches. If the vertical stabilizers lie more than a foot apart, it was determined that the wake should lie well in between the width of 10.5 inches. Figure 4.3 shows the plotted equation.

The next concern was blanking out the horizontal stabilizer. The structures team determined that the horizontal stabilizer would lie directly on top of the fuselage. Since the antenna was supported at least 3 inches from structure, the wake of the antenna would not affect the horizontal. Since the antenna has flat end-caps, the wake profile will be in the shape of the antenna, even as the wake increases with distance.

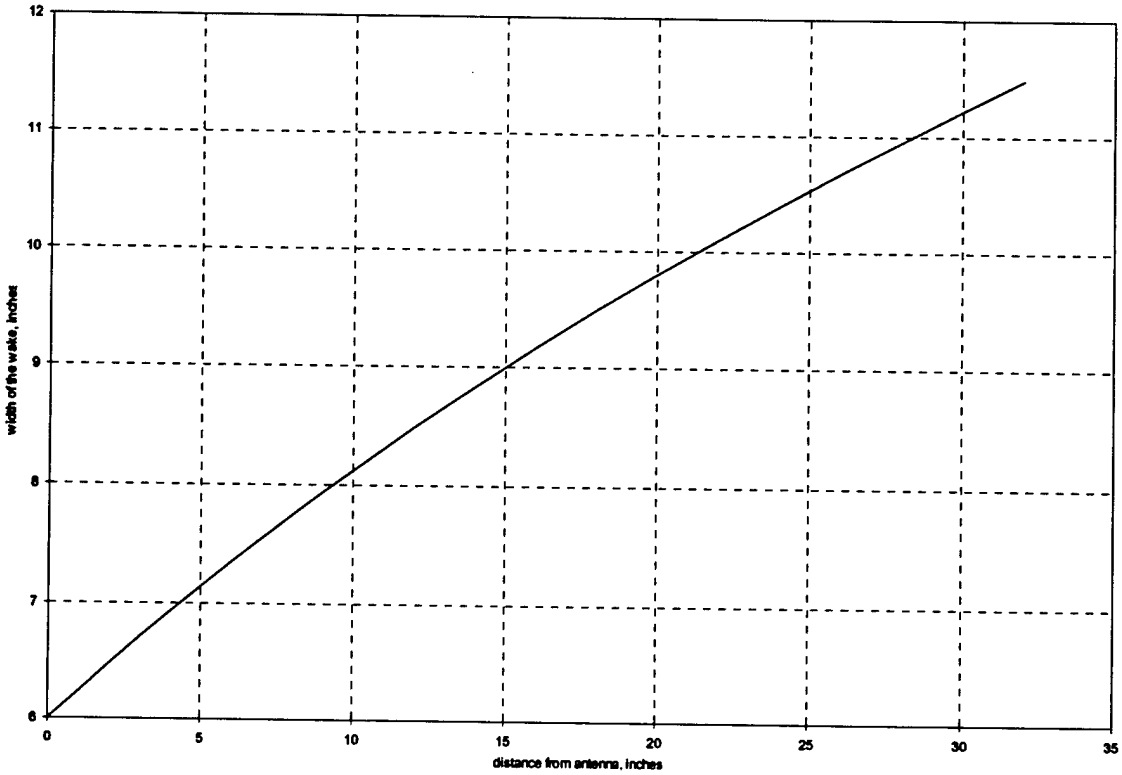

Figure 4.3 Wake vs. Distance

Given the theoretical data, a further investigation of the airflow about the antenna was performed by running wind tunnel tests with the antenna mounted on a fuselage. The UAV that Mississippi State University built for a DBF competition two years ago was used as the fuselage in the wind tunnel testing. The idea was to put the UAV in a subsonic wind tunnel, with the antenna on top of it. Tufts were placed around the UAV from the antenna to the tail at every square inch. The original UAV's four bolts, used to hold down the wing, were used to bolt a one-quarter inch piece of plywood made to match the wing's lower profile. A piece of foam, three inches long, was cut into the approximate shape of an airfoil for the stand and glued to the plywood using epoxy. Epoxy was also used to glue the antenna to the stand. During the test, the free stream velocity was varied from 30 ft/s to 100 ft/s in intervals of 5 ft/s and a digital camera and video recorder were used as recording devices. A visual inspection was used to determine the antenna characteristics.

The horizontal stabilizer was not affected by the wake because it is located three inches below the antenna. With the use of tufts, the effect of the wake on the vertical tail was observed. Observing the sixth row of tufts, the airflow was very disturbed. After that, normal airflow resumed. In the test, the sixth row corresponded to six inches, which meant that the wake was about twelve inches wide. The

experimental data agreed well with theory. For a distance of two feet from antenna to tail, the wake was measured with a probe to be twelve inches. With the theoretical data showing 10.5 inches, the difference was only 1.5 inches.

A final interesting note was in the method of construction. The team had been concerned on how to mount the antenna. Using a foam stand with two layers of Kevlar and epoxy to bind the components, the antenna mount held at speeds up to 100 ft/s with no problems observed.

4.4 Thrust Loading and Wing Loading Study

To obtain a general idea of what type of engine would be needed to take off within 120 feet, an investigation was performed on how wing-loading and thrust-loading affected the take off roll. If the assumption that the aerodynamic forces, namely drag, were much smaller than the mechanical forces, such as thrust, and that the thrust was constant throughout the take off roll, the equation for take off can be simplified as a function of wing-loading and thrust-loading.

$$Take\ off\ roll = \frac{1}{2 \cdot g} \cdot \frac{1}{\frac{T}{W} - \mu} \cdot \frac{2}{\rho \cdot C_{L\max}} \cdot \frac{W}{S} \qquad \textbf{Equation 4.2}$$

where,

g is acceleration due to gravity,

T is the thrust,

W is the weight,

S is the wing platform area,

ρ is the air density, and

μ is the coefficient of friction for the runway surface

The results from this equation are presented in Figure 4.4. Since this is an approximation of the take off distance, a take off distance of 100 feet will be used instead of 120 feet. This will allow a factor of safety. For a take off distance of 100 feet and for a wing loading around 3 lbf/ft^2 the minimum thrust loading needed to take off must be greater than 0.5, which means that the amount of thrust needed must be greater than half of the weight of the UAV.

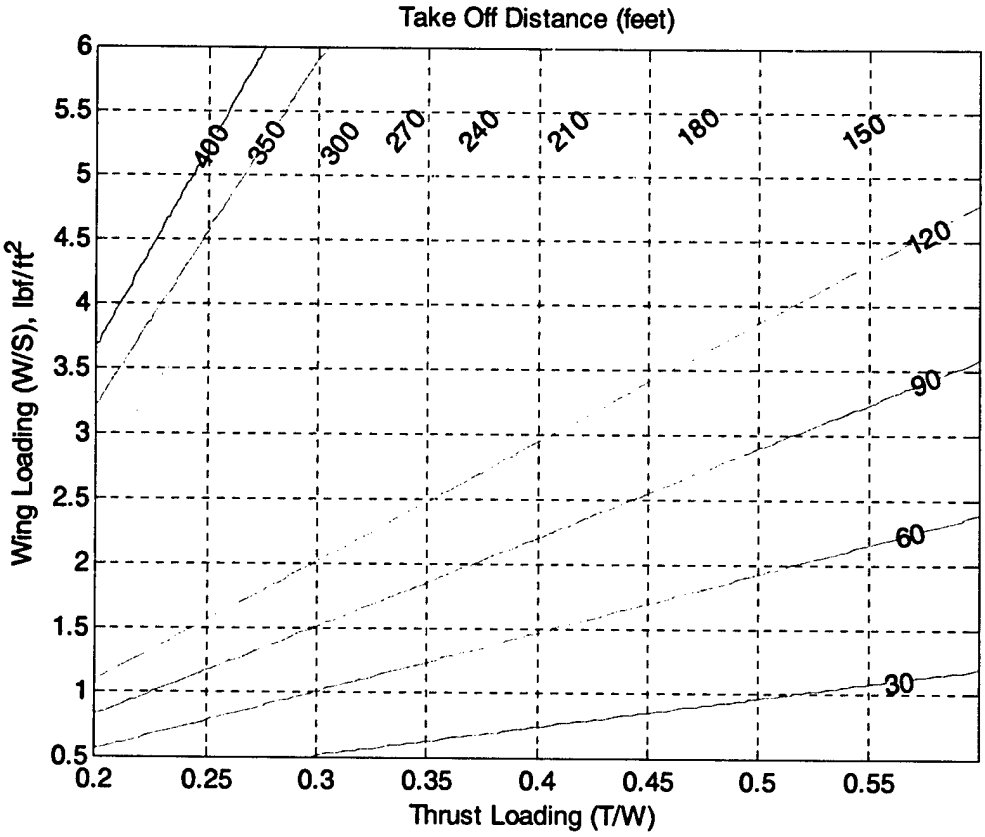

Figure 4.4 Thrust-Loading and Wing-Loading Requirements for Take Off

4.5 Structural Analysis of the Spar

Three main spar setups were examined. To examine the spars, it was assumed that the semi span behaved as a cantilever beam. Also, the loading was modeled after the tip-loading test that will have to be preformed for technical inspection. Using Castigliano's method for pure bending in beams the deflection was expressed as:

$$y = \frac{-p * l^3}{E * I} \qquad \textbf{Equation 4.3}$$

The first spar setup consisted of two quarter-inch square beams of balsa laid into grooves in the wing ribs. This particular spar, while very light, 0.06 lbs, could only support 7.06 pounds at the tips before yielding. The second setup was geometrically identical to the previous spar, but the balsa was replaced with spruce. This spar weighed 0.14 lbs and could support 13.50 lbs from the tips before yielding. Finally, a spar made of carbon fiber caps and balsa was analyzed. This spar weighed 0.27 lbs and could support 117.95 lbs at the tips before yielding. This weight was equivalent to a 5.49G loading. However,

other parts of the wing such as ribs and shear webs would fail at a lower loading. The corresponding theoretical tip deflection of this beam was 1.387 inches.

4.6 Engine Selection

There were two brands of engines that are legal for DBF competitions, Graupner and AstroFlight. AstroFlight electric motors were chosen for consideration because Graupner motors were too small to be effective. The thrust needed was based on the takeoff roll analysis which showed that the thrust loading must be greater than 0.5. For a single engine and 20.5 pound UAV (fully loaded), the only engines that could produce that amount of thrust would be the FAI Cobalt 60 and the FAI Cobalt 90 with a gear reduction ratio of 2.75:1. Using the *MotoCalc* software, a series of propeller and motor combinations were considered.

MotoCalc is a program for choosing and predicting the performance of an electric model UAV power system, based on the characteristics of the motor, battery, gearbox, propeller or ducted fan, and speed control. You can specify a range for the number of cells, gear ratio, propeller diameter, and propeller pitch, and *MotoCalc* will produce a table of predictions for each combination.

The initial results indicated an AstroFlight 90 engine would be a better choice since it is more efficient than the AstroFlight 60 engine. The results of the *Motocalc* analysis are shown in Figure 4.5. A *MotoCalc* analysis was also run on the AstroFlight 60 for the sake of comparison. The results from this analysis are shown in Figure 4.6.

The charts are composed of three data series: static thrust, maximum speed, and static run time. Static thrust is a measurement of the thrust created by the motor and propeller on a stand at 100% throttle at zero velocity. Maximum speed was the top speed that the plane could reach given the UAV model in *Motocalc*. Finally, static run time is the amount of time the motor can run at 100% throttle on a test stand.

Examining the charts revealed that an AstroFlight 90 produces more thrust, better run time, and a higher top speed. With the given results it was decided that an APC 24x18 prop would offer a sufficient static runtime, excess thrust and a high maximum speed. Motor performance for this configuration is shown in Table 4.1.

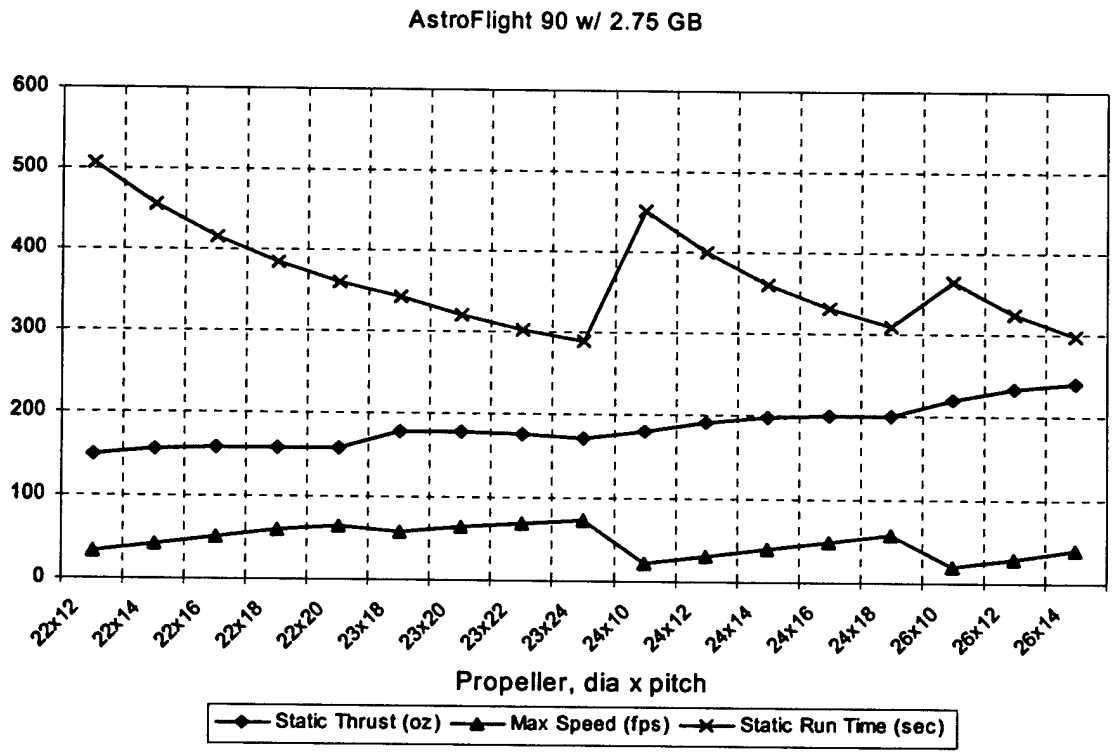

Figure 4.5 *Motocalc* analysis of the AstroFlight 90

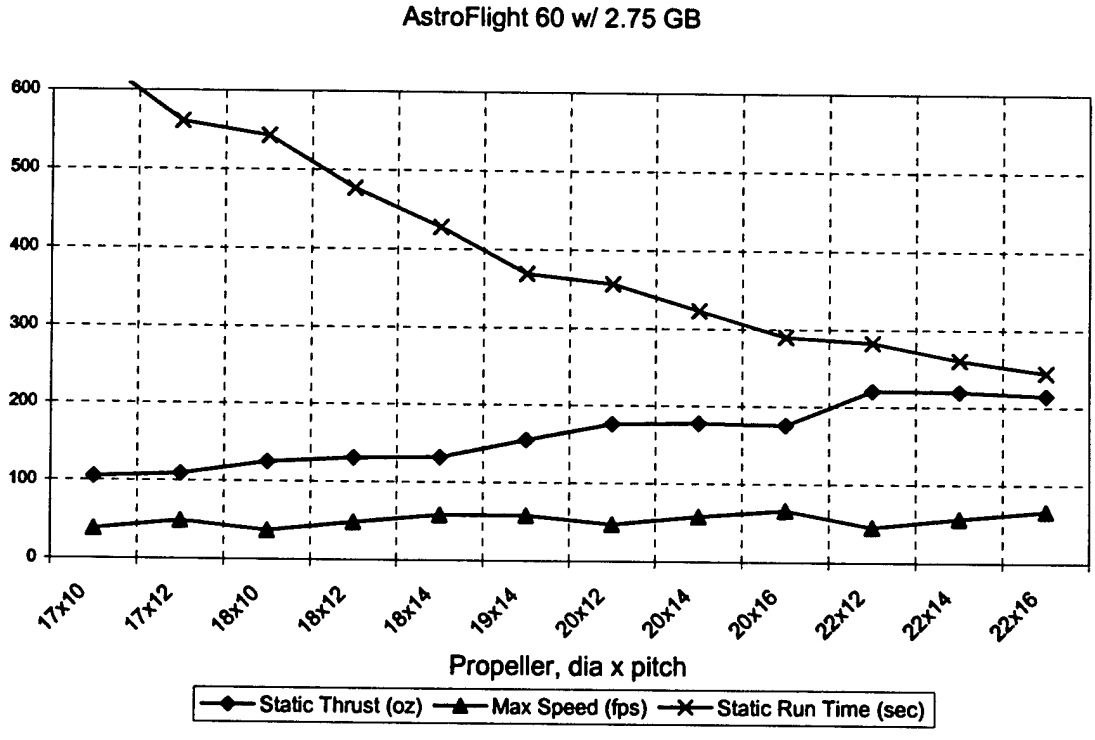

Figure 4.6 *Motocalc* analysis of the AstroFlight 60

Table 4.1 Astro 90 Motor Performance

Static Performance								Performance at 55 mph			
Propeller	Current (Amps)	Input Power (W)	Electrical Efficiency (%)	Input Power Loading (W/lbf)	Output Power Loading (W/lbf)	Prop RPM	Thrust (lbf)	Current (Amps)	Electrical Efficiency (%)	Thrust (lbf)	Time (m:s)
24x18	28.1	1126.5	73.4	59.3	46.9	3306	12.53	17	74.1	3.88	8.27

It is important to note that the amperage is less than the 40 Amp limit mandated by the rules of competition. Another quantity of interest is the input power loading, which is about 59.3-W/lbf. A common rule of thumb among electric modelers is that an input power loading of 55-W/lbf is necessary for an aerobatic UAV. Because the input power loading for *SWAG* is over 55-W/lbf, superb flight performance is expected. The last quantity of interest is the endurance at 50-mph. A rough estimate of the flight distance is around 4000 ft including a few 360 deg turns, which equates to 50 seconds per lap. Four laps at 50 seconds a piece equates to 3 minutes and 20 seconds total time. Therefore, the UAV should have excess duration.

After the parts were ordered, it was apparent that the propeller weighed one pound more than advertised. Nevertheless, the combination was tested to determine its performance. The results matched well with the *Motocalc* predictions in RPM, Amps, Volts, and Power. The thrust did not meet the predictions. This was later attributed to a mechanical problem in the thrust load cell. The problem was fixed and a calibration was done.

Unfortunately, the problem was not detected until later and a change in motor and propeller was determined. It was decided that an AstroFlight 60 with a smaller propeller would save weight. The chart in Figure 4.6 was consulted and an APC 22 x 14 propeller was picked. Table 4.2 details the expected performance of the new motor combination.

For the competition this year, SR 2400 mAh batteries were chosen. It was determined that 36 cells weighed less than five pounds and would provide the most thrust and top speed. The speed controller chosen for the competition was an Astro 204D. The Astro204D can handle the current and has worked well in the past

Table 4.2 Astro 60 Motor Performance

	Static Performance							Performance at 50 mph			
Propeller	Current (Amps)	Input Power (W)	Electrical Efficiency (%)	Input Power Loading (W/lbf)	Output Power Loading (W/lbf)	Prop RPM	Thrust (lbf)	Current (Amps)	Electrical Efficiency (%)	Thrust (lbf)	Time (m:s)
22x14	33.3	1316.7	72	69.3	54.55	4246	13.81	20.2	77.4	4.812	7:09

4.7 Available Thrust Model at Speed

The thrust available from the engine was approximated by the observation of the engine's characteristics. With a given engine/propeller selection, the engine will have its highest thrust, T_{static}, when the UAV is not moving. When the free stream velocity is equal to the velocity off the propeller, V_{max_eng}, thrust will be zero. From this relationship, the thrust available from the engine was assumed to be linear with velocity and was dependant on the number of engines and engine/propeller selection. This assumption, while not exact, resulted in an error of less than 5% for engine/propeller cases evaluated by last year's DBF team. In addition, this error was on the side of caution, as the actual thrust curve is concave downward. In any case, this linear relationship can be expressed as

$$T_{avl}(V) = N_{engines} \cdot \left(T_{static} - \frac{T_{static}}{V_{max_eng}} \cdot V \right) \qquad \textbf{Equation 4.4}$$

4.8 Wind Tunnel Results

In order to get accurate performance numbers for this UAV, the AstroFlight 60 cobalt engine geared at 2.75:1 turning a 22x14 APC propeller was tested in the Mississippi State University wind tunnel. The goal of the experiment was to obtain dynamic properties of the engine/propeller combination at full power. The velocity was varied from 10 mph to 80 mph collecting data from the thrust load cell, and these values would be compared to *MotoCalc* and the thrust available estimate described in the previous estimate.

As shown in Figure 4.7, the *MotoCalc* data over predicted the experimental data collected from the wind tunnel. The thrust available estimate, however, under predicted the experimental data. The conclusion was to use the thrust available estimate in the optimization program because it is better to under predict than to over predict the value for thrust. The reason why *MotoCalc* might have over

predicted was because the engine used in *MotoCalc's* analysis may not have the exact timing as the actual engine obtained.

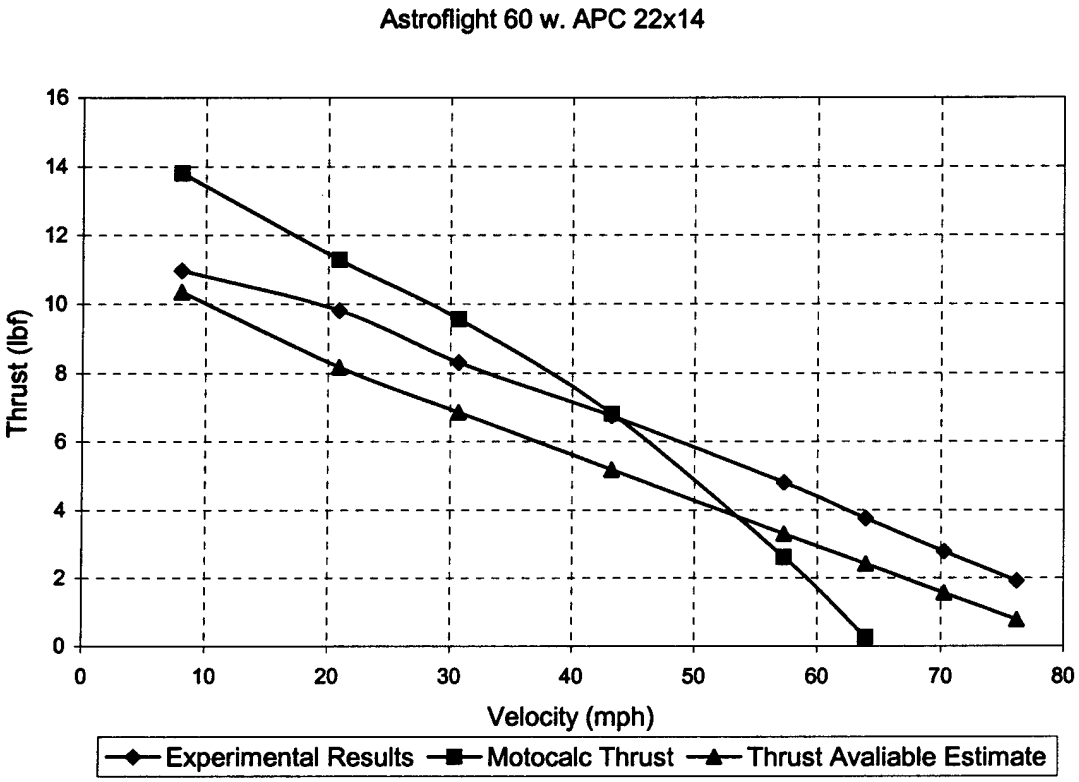

Figure 4.7 Results from AstroFlight 60 Engine Test

4.9 Weight Model

The accuracy of the values for all calculations are directly related to how close the weight model was to the actual weight of the UAV. The weight model was formed by adding all the expected weights of all the components together. In order to calculate the expected weight of each part, the volume of the part and the material selected for the part must be known. After all materials have been selected, the densities can be found. From here, the weights from each part were calculated and the weight model for the entire UAV was calculated. Using a weight model derived by last year's team; it was shown that the empty weight can be expressed as a function of the number of engines, engine/propeller selection, wing surface area, and wing aspect ratio.

$$W_{empty} = f(N_{engines}, Engine_{type}, S, AR) \quad \textbf{Equation 4.5}$$

Further, the above expression can be expanded to include terms for UAV components, i.e. fuselage, empennage, wing, landing gear, electrical equipment, and engines.

$$W_{empty}(N_{engines}, Engine_{type}, S, AR) = W_{fuselage} + W_{empennage}(S) + W_{wing}(S, AR) + W_{gear} + W_{electrical} + W_{engines}(N_{engines}, Engine_{type})$$

Equation 4.6

The cargo consists of a five-pound box and a one-pound cylinder. By adding the cargo weight to the empty weight of the UAV, the takeoff-gross weight, TOGW, of the UAV can be calculated.

$$W_{TOGW}(N_{engines}, Engine_{type}, S, AR) = W_{fuselage} + W_{empennage}(S) + W_{wing}(S, AR) + W_{gear} + W_{electrical} + W_{engines}(N_{engines}, Engine_{type}) + 6\,lbs$$

Equation 4.7

4.10 Results from Optimization Code

Using the models and information described in the previous sections, an optimization code was written using MathCAD to calculate the optimum sizing of the wing based on the RAC.

The design space was reduced to two variables, wing chord and wing span and was constrained using the performance requirement for take off roll. If the velocity at take off for 120 feet was less than the stall speed, the modified score was assigned a value of zero representing the lowest possible score. Also, size constraints were placed on the design variables based on the storage box.

The results from the wing sizing showed that the optimum design coincided with the take off constraint. This result is very similar from previous Mississippi State entries to DBF. During the first year that Mississippi State entered this competition, the design point was chosen close to the take off constraint. The weight for this UAV is increased by three or five pounds from its predicted value, causing undesirable take off and climb performance at full payload. For this year's design, the design point was chosen such that the best design was away from the take off constraint but still possessed a low rated aircraft cost. The results are shown in Figure 4.8.

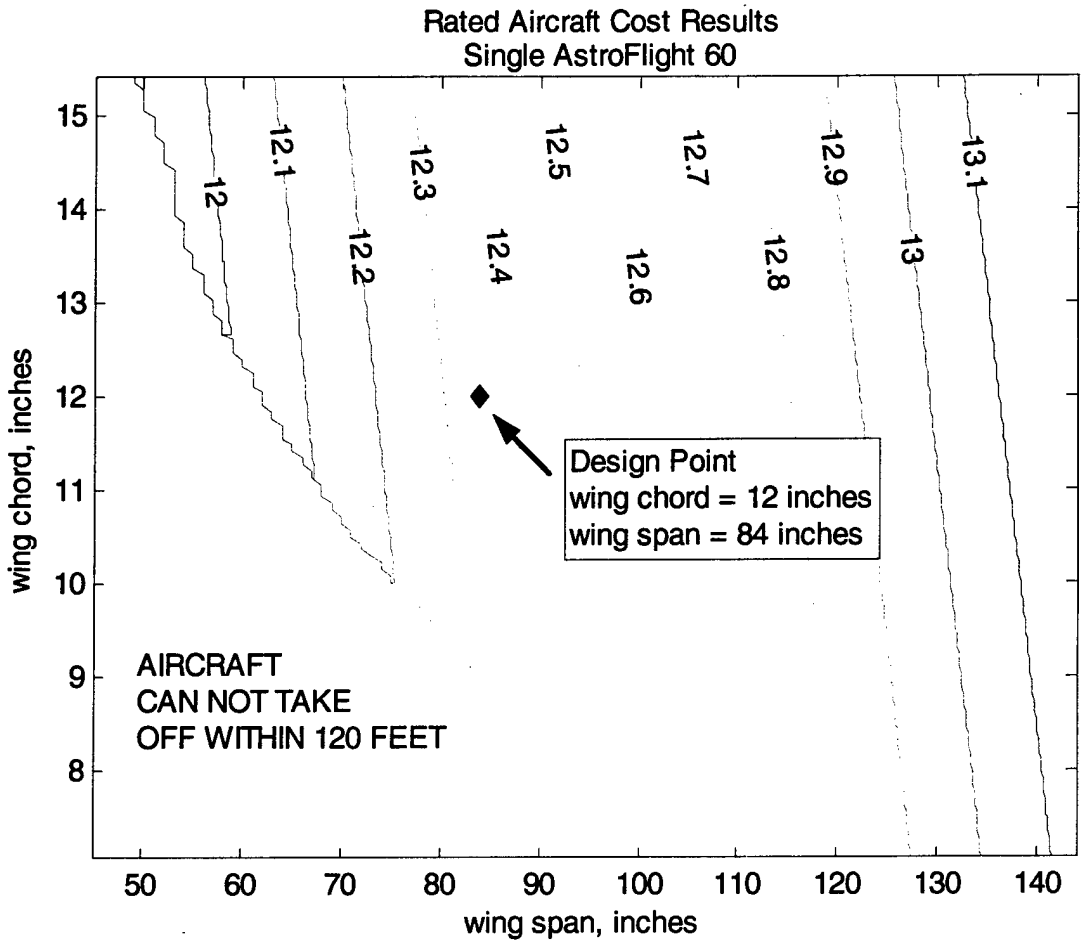

Figure 4.8 Results from Optimization

4.11 Sizing of the Horizontal Tail

Once the dimensions of the wing were calculated from the optimization program, the H-tail was sized to produce a UAV with a positive static margin and good stability characteristics.

In order for the plane to be longitudinally stable, the partial derivative of pitching moment with respect to angle of attack must be less than zero.

$$Cm_\alpha = \frac{\partial C_m}{\partial \alpha} < 0 \qquad \textbf{Equation 4.8}$$

In order for the plane to trim about the pitch axis, the coefficient of pitching moment at an angle of attack of zero must be greater than zero.

$$Cm_0 = Cm_{\alpha=0} > 0 \quad \textbf{Equation 4.9}$$

From these inequalities a force and moment balance was performed with each component of the UAV with and without the antenna. The moment coefficient expressions are

With Antenna

$$Cm_0 = Cm_{0\,wing} + Cm_{0\,fuselage} + Cm_{0\,tail} + Cm_{antenna} \quad \textbf{Equation 4.10}$$

$$Cm_\alpha = Cm_{\alpha\,wing} + Cm_{\alpha\,fuselage} + Cm_{\alpha\,tail} \quad \textbf{Equation 4.11}$$

Without Antenna

$$Cm_0 = Cm_{0\,wing} + Cm_{0\,fuselage} + Cm_{0\,tail} \quad \textbf{Equation 4.12}$$

$$Cm_\alpha = Cm_{\alpha\,wing} + Cm_{\alpha\,fuselage} + Cm_{\alpha\,tail} \quad \textbf{Equation 4.13}$$

The individual terms in these equations were solved for using charts from Nelson and Raymer. Before proceeding, an assumption had to be made. Given no method for calculating the change in moment coefficient with angle of attack for the antenna, it was assumed to be negligible. This is reasonable because Cm_α of the antenna should be less than that of the fuselage and, as can be seen by Table 4.3, the fuselage contributes very little to the overall Cm_α. Flight testing will be the deciding factor for whether or not changes need to be made to the final design.

Table 4.3 Moment Coefficient with Respect to Angle of Attack

Component	$C_{M\alpha}$ Contribution
Wing	0.379
Tail	-0.809
Fuselage	0.09

The individual terms for the Cm_α and Cm_0 equations were composed of sizing parameters such as the incidences of the wing and tail, the surface area of the horizontal tail, the center of gravity for the UAV and the moment arm from the aerodynamic center of the wing to the aerodynamic center of the horizontal

tail. These variables were varied subject to the wake and storage box constraint such that the horizontal tail span was greater than 12 inches but less than 24 inches to produce a longitudinal statically stable UAV that has a trimmed condition for flight. The results for the coefficient of pitching moment curves with varying angle of attack are presented in Figures 4.9 and 4.10. The results from the sizing are presented in Table 4.4.

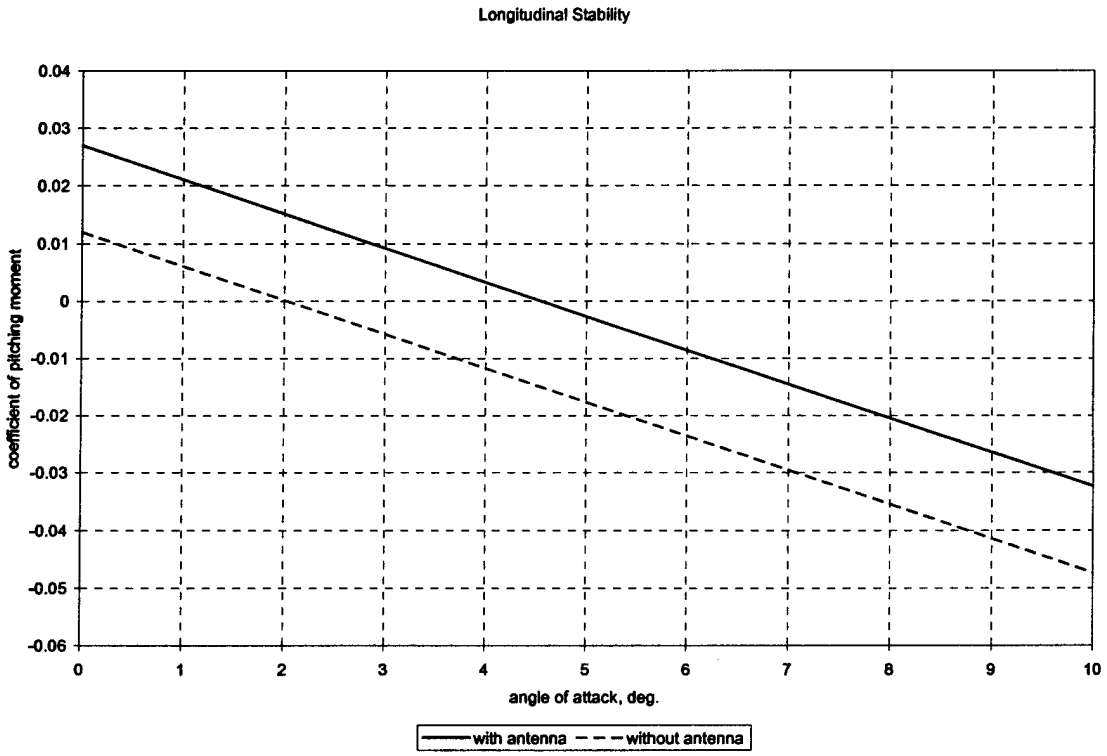

Figure 4.9 Longitudinal Stability Characteristics

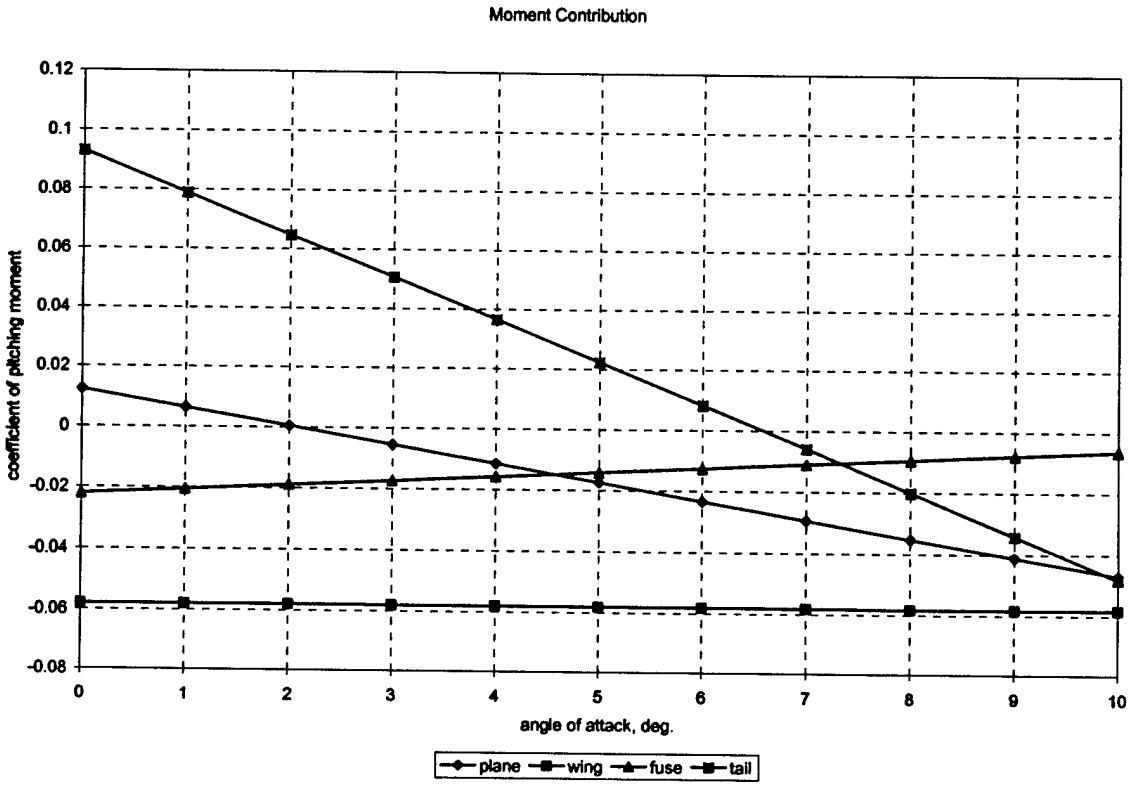

Figure 4.10 Longitudinal Stability Characteristics for UAV Components

Table 4.4 Longitudinal Stability Geometries

Longitudinal Stability Geometries	
Tail Moment Arm	28.57 inches
Incidence of Wing	2.00 degrees
Incidence of Tail	-0.25 degrees
Span of Horizontal Tail	20.5 inches
Chord Length of HT	9.00 inches
Center of Gravity (Xcg/c)	0.26
Trim Condition (antenna)	4.50 deg
Trim Condition (w/o antenna)	2.08 deg
Static Margin (percent)	14.2
Neutral Point (Xnp/c)	0.402

4.12 Sizing of the Vertical Tail

For the plane to be statically stable along the yaw axis it must meet the criteria

$$Cn_\beta = \frac{\partial C_n}{\partial \beta} > 0 \quad \textbf{Equation 4.14}$$

Raymer and Nelson recommend a value for the stability coefficient between 0.05 and 0.1. Using the exact expression for $C_{n\beta}$ found in Nelson, the span of the vertical stabilizer is varied subject to the storage box constraints of one foot. The results are plotted in the figure and tabulated below.

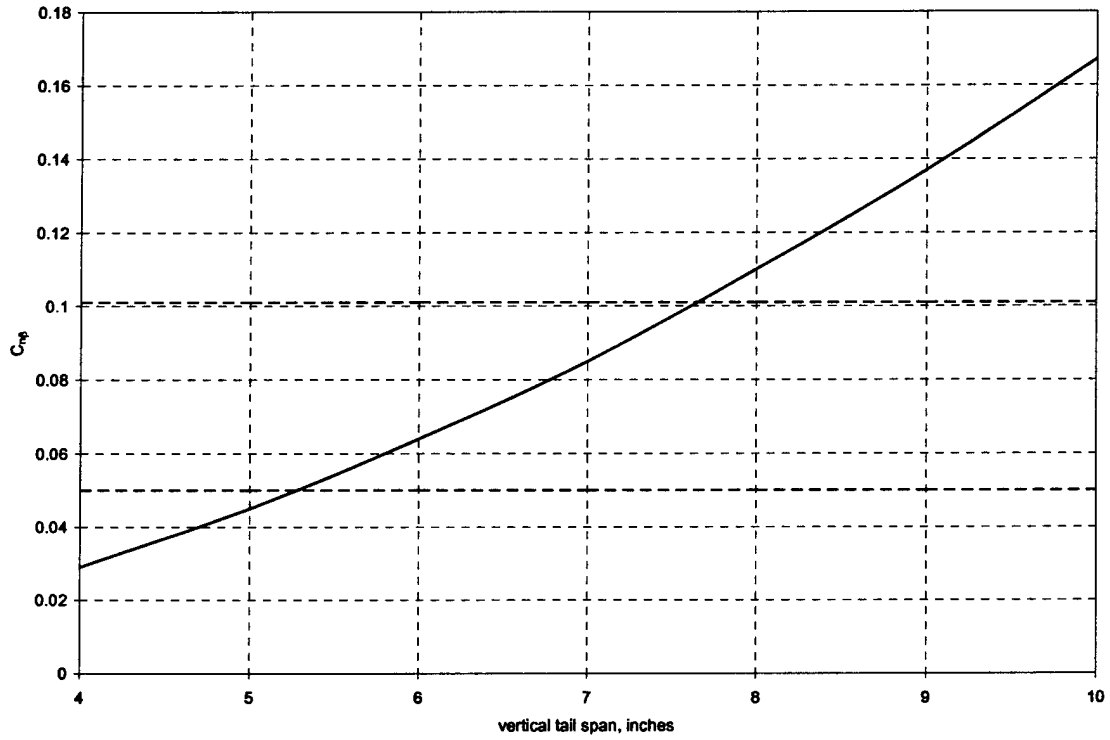

Figure 4.9 Analysis of Vertical Stabilizer Size

The decision was made to size the vertical tail span to nine inches. The tail was oversized for two reasons. This would allow plenty of rudder authority and show good "weathercock" properties. Also, the over sizing would allow the tips of the rudder to be tapered.

Table 4.6 Directional Stability Geometries

Directional Stability Geometries	
Tail Moment Arm	27.6 inches
Span of Vertical Tail	9 inches
Chord Length of HT	9 inches

4.13 Performance Data

Before analyzing the steady flight performance of the UAV, it is necessary to review the geometry of the UAV along with relevant weights.

Table 4.6 Sizing for Performance Calculations

Sizing Numbers for Performance Calculations	
Weight Loaded (payload + antenna) lbs	20.5
Weight Unloaded (lbs)	14.5
Span (inches)	48
Chord (inches)	12
Surface Area (square feet)	7
Aspect Ratio	7
Oswald Factor (Assumed)	0.8
Zero Lift Drag Coefficient (See p. 21)	0.03

The performance numbers of interest to the team were the lift-to-drag ratio, power required, power available, and rate of climb for the velocity ranging from 0 to 80 mph. The following figures illustrate the results of the performance analysis.

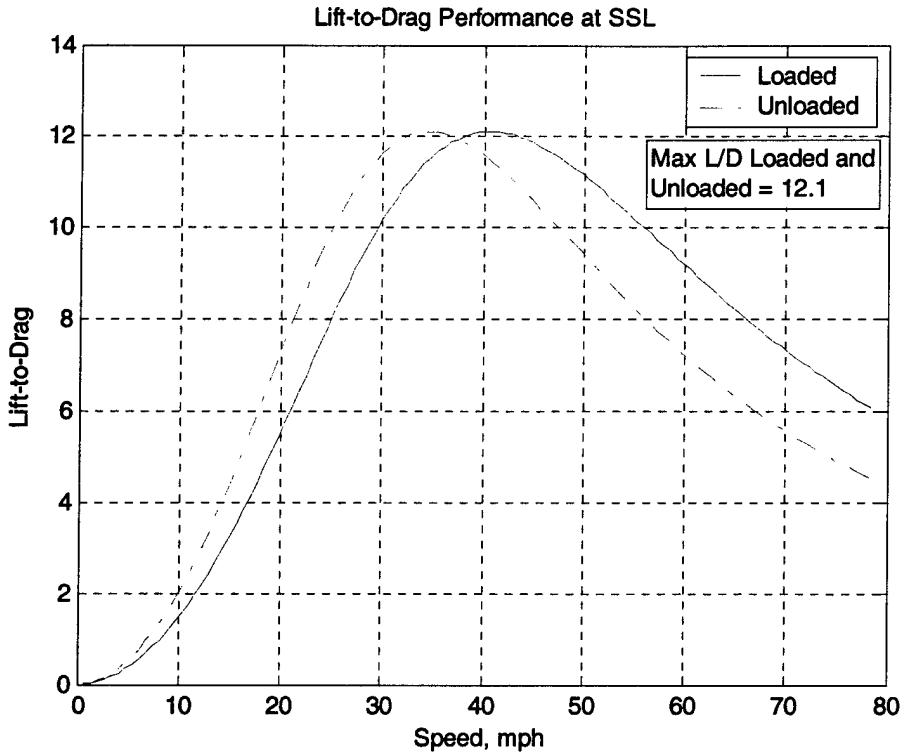

Figure 4.12 L/D Performance

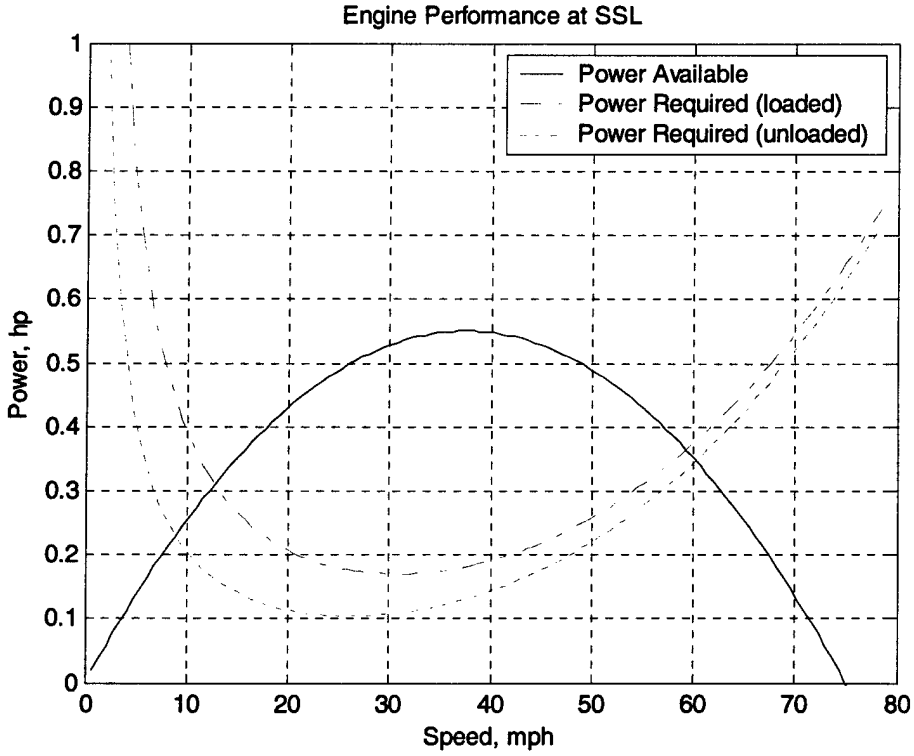

Figure 4.13 Engine Performance

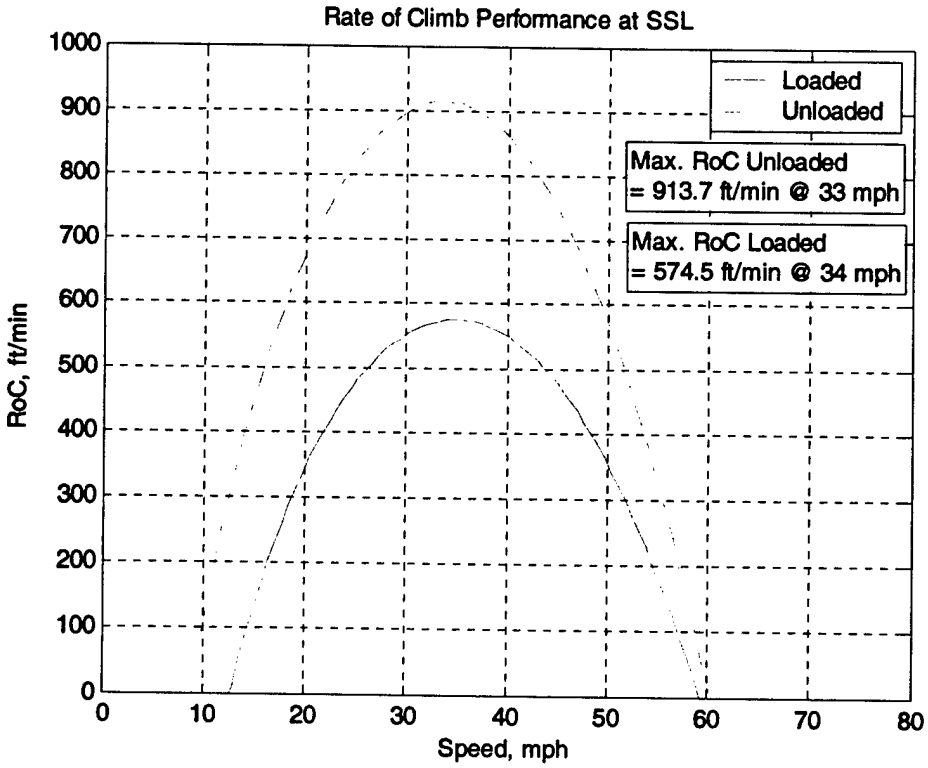

Figure 4.14 Rate of Climb Performance

4.14 Estimated Mission Times

The mission times were estimated using the assumption that the UAV was flying at a speed of 60 mph and with wind conditions being light and variable. The take off/climb and descending/landing times were estimated. The time to complete the 360 degree turns were estimated by finding the circumference of the turn radius and multiplying that number by 60 mph. Time was allotted for turns around the pylon. The results are presented in Table 4.7.

Table 4.7 Mission Times

Mission 1	Time to Complete (min:sec)
Take off, and Climb to Pylon	0:45
3.5 Laps, Payload (Box and Antenna) with four 360 deg. turns	2:30
Landing	0:45
Total Time for Mission 1	**4:00**
Mission 2	
Take off, and Climb to Pylon	0:45
1.5 Laps, Payload (Box) with two 360 deg. turns.	1:10
Landing	0:45
Take off, and Climb to Pylon	0:30
1.5 Laps, No Payload with two 360 deg. turns.	0:55
Landing	0:30
Total Time for Mission 2	**4:35**
Mission 3	
Take off, and Climb to Pylon	0:45
3.5 Laps, Payload (Box) with three 360 deg. turns.	2:00
Landing	0:45
Total Time for Mission 3	**3:30**

4.15 Summary of Preliminary Results

The sizing of the UAV was done using performance equations constrained by RAC and storage box dimensions. The results from the sizing show a stable UAV with a positive static margin and a short take off roll of less than 120 feet. Table 4.8 and 4.9 present a summary of the sizing numbers and the performance values of the UAV.

Table 4.8 Directional Stability Geometries

Sizing Results for SWAG	
Wing (SD 7062)	
Span (inches)	48
Chord (inches)	12
Aerodynamic Center (% chord)	25
Center of gravity (% chord)	33
Neutral Point (% chord)	40
Surface Area (square feet)	7
Incidence (degrees)	2
Aspect Ratio	7
Fuselage Length (inches)	47.5
Empennage (NACA 0009)	
Horizontal Tail Span (inches)	20.5
Horizontal Tail Chord (inches)	9
Vertical Tail Span (inches)	9
Vertical Tail Chord at Root (inches)	9
Incidence (degrees)	-0.25
Tail Moment Arm (inches)	27.6

Table 4.9 Performance Values

	Unloaded	Loaded
CL max	**1.5**	**1.5**
L/D max	**12.1**	**12.1**
RoC max (ft/min)	**913.7**	**574.5**
Stall Speed (mph)	**24.0**	**28.3**
Maximum Speed (mph)	**61**	**59**
Take Off Distance (ft)	**85**	**115**

5.0 DETAIL DESIGN

5.1 Weights and Balance Sheet

Table 5.1 Weights and Balances

	x (in)	W (lb)	x*W (lb*in)
Empennage w/ Servos	40.98	0.36	14.75
Wing w/ Servos	12.29	1.60	19.66
Fuselage w/ Servo	14.13	1.56	22.04
Main Gear w/ Mount, Wheels, & Brakes	19.00	0.81	15.39
Nose Gear w/ Mount, Wheels, & Servo	4.34	0.93	4.04
Motor	0.02	2.79	0.06
Motor Batteries	13.55	4.98	67.48
Receiver	13.55	0.10	1.36
Receiver Battery	13.55	0.25	3.39
W (lb) + 8% to account for electrical wiring	**14.5**		
Aero. Center of Wing %chord	**25**		
Neutral Point % chord	**40.2**		
CG (in)	**26.25**		

5.2 Component Selection

Table 5.2 Component Selection

Component	Selected Part	Comments
Motor (1)	Astro Flight FAI Cobalt 60	Selected by preliminary design optimization
Speed Control (1)	Astro Flight 204D	Appropriately sized for selected motor It can handle the current and has worked well in the past
Battery Packs (3)	SR 2400 mAh 36 cells	Offer best available energy density in a moderate-resistance cell
Servos	JR Mini Digital Servos	Offer both high speed and high torque
Main Landing Gear	Graphtech CLG-109	Relatively light, properly sized for payload deployment
Nose Landing Gear	Robart Nose Strut 664	Spring loaded straight oleo strut
Propellers	APC 22x14	Selected through *Motocalc* analysis and wind-tunnel testing.
Brakes	Kavan Magnetic Brakes	Allow braking without use of extra servo

5.3 Systems Architecture

5.3.1 Wing

SWAG is a high wing UAV that incorporates removable wings. The wing is in three sections, two outboards and one center section. The center section of the wing attaches to the top of the fuselage using four nylon bolts and blind nuts. The outboards are joined to the center section using a light ply tongue joiner on the front and rear spars. The outboard tongue joiners for the front spar are joined to the center section using a spring-loaded pin. These pins constrain the outboard sections from moving in the lateral direction. The placement of the wing was chosen for several reasons. The main reason is payload position. To be structurally sound, the spar of the wing must be continuous or utilize a slot/tongue joining mechanism. The payload must be deployable, and therefore a continuous spar or a slot/tongue joining mechanism cannot be used to carry through the payload housing. The incorporation of a high wind also added stability.

Each outboard section contains an aileron. The aileron is controlled using a JR mini digital servo. If needed, the transmitter that controls the servo can be programmed to incorporate flaperons for assisted take off. The servo is accessible through removable hatches on the bottom surface of the wing.

The internal structure of the wing was constructed of balsa wood, light ply, and carbon caps. The ribs were spaced one-third the distance of the wing chord and were constructed using balsa wood with lightening holes. The lightening holes were positioned to save weight and for use as slots for the wing jig. The spar, a composite sandwich, was constructed of carbon caps and balsa. The carbon caps were glued using 30 minute epoxy to a quarter inch by quarter inch balsa stock on two opposite sides. With the carbon caps pointing to the top and bottom surface, the composite sandwich was glued using 30 minute epoxy to slots cut into the ribs at the quarter chord on the top and bottom surface. Shear webs were placed between the ribs on both sides of the composite sandwich. Using CA, the shear webs were glued to the ribs and the composite. The rear spar consisted of one-eighth inch by one-eighth inch balsa placed in slots cut into the rib at the three-quarter chord on the top and bottom surface. The balsa was glued into place using CA. Shear webs constructed of balsa were placed between the ribs on each side and glued into place using CA. The tongue joiner was constructed using one-quarter inch thick light ply and placed between the composite sandwich of balsa and carbon. The joiner was glued to the composite using 30 minute epoxy. The center section was constructed very similar to the outboards except that the shear webs for the main spar were made using light ply and glued using 30 minute epoxy to the composite. The attachment block for wing to the fuselage was constructed using light ply. The leading edges and trailing edges of the wing were sheeted with one-sixteenth inch balsa. MonoKote was used to cover the wing.

5.3.2 Fuselage

For most aircraft, the fuselage must be designed around the payload. The payload for SWAG, a five pound box of set dimensions, was a major design condition. The skin of the fuselage was constructed using one-eighth inch thick light ply panels with one-quarter inch balsa stock to join perpendicular panels. The panels contained lightening holes which decreased their weight. Care was taken in the locations and shapes of the holes so as not to sacrifice structural integrity. Above the payload compartment, a plywood tray was attached to the sides of the forward fuselage panels. Electrical components for the servos and engine were housed in the tray. Another removable hatch was constructed on the top of the fuselage for access to the electronics bay. Coplanar panels were joined using a piece of one-eighth inch thick light ply and 30 minute epoxy. The wall thickness at the location of the main landing gear was doubled with another piece of one-eighth inch light ply. Monkote was used to cover the fuselage.

5.3.3 Empennage

Even though the empennage is not a major load bearing structure, care was taken to transfer the loads to the fuselage without sacrificing additional weight or structural integrity. The ribs are made from one-eighth inch thick balsa with one-quarter inch thick balsa for the front and rear spars. The ribs were spaced at one-third the distance of the horizontal chord and the leading and trailing edges were capped with balsa and sanded to match the profile of the airfoil section. The spars for the horizontal and vertical sections were joined and glued using CA. Also, the ribs were glued to the spars using CA. Three servos were used in the empennage section with each servo rotating one control surface of the tail. The empennage was attached to the fuselage using two nylon bolts and two blind nuts inside the fuselage. The servos may be accessed through removable hatches incorporated into the tail sections. Monokote was used to cover the empennage.

5.3.4 Landing Gear

Landing gear was researched and analyzed based on two criteria. The two criteria were selected with the missions that the UAV must carry out. The landing gear is a vital component which must comply with the storage box and payload requirements. The gear must be able to disassemble from the UAV easily for storage and also be light in weight but structurally sound for landings with both payloads.

The tricycle landing gear configuration consisted of a main gear and a nose gear. The landing gear was purchased off-the-shelf from TNT landing gear. The main gear was a composite structure made by Graphtech. It is sufficiently wide to allow the deployment mission to be carried out and strong enough

for the heaviest loaded landings. The width from the right to left wheel is 18 ¾ inches and the height is 6 ½ inches. The nose gear is a straight strut that can take advantage of wheel diameters up to 3 ¼ inches. It is made by Robart.

The attachments for the landing gear were machined such that the main gear and nose gear were attached using "snap together" linkages. Using these linkages will decrease the assembly time of the UAV by not utilizing bolts or screws. A member of the team is skilled using a mill and lathe, and he was assigned the task of machining the aluminum pieces that allow the landing gear to be "snapped together" with the fuselage. The schematics for these parts are detailed in the drawing package.

5.3.5 Engine Mount

The original idea for the engine mount was to use sheet metal shaped such that the engine would be secured to the mount and the mount secured to the fuselage. During engine run up, a propeller whirl was noticed. The mount was redesigned such that the motor was mounted to a light ply firewall block that was glued to the electronics tray and the light ply side walls using 30 minute epoxy. This configuration showed no propeller whirl, but was heavier than the sheet metal.

5.3.6 Payload Deployment

A simple servo system is used for payload deployment. A small diameter rod is attached to the payload through holes in an aluminum harness. The harness is two inches in width and follows the payload box lengthwise along the bottom. The rods fit through the holes at the top of the harness for payload carriage. When the landing gear switch is activated using the transmitter, the servo rotates, pulling the rods free from the harness and therefore dropping the payload.

5.3.7 Antenna Attachment

The four nylon bolts, used to hold down the wing, were used to bolt a one-eighth inch piece of balsa wood matching the wing's upper profile. A piece of foam, three inches long, was cut to an airfoil shape and glued to the plywood. The antenna was glued to the foam piece which was glued the antenna to the stand. The antenna pieces were all glued with five minute epoxy.

5.3.8 Storage Box

The disassembly of the UAV occurs in three steps. The spring loaded pins holding the outboard wing section are released with a pull on a metal loop located just inside the center section. Once released, the spring loaded pins allow the outboards to be easily pulled from the center section. The spring loaded pins holding the landing gear are detached by releasing a "catch" between the gear and the structure of the plane. Once pulled, the nose and main landing gear are easily freed. The antenna mount is unscrewed from the center section of wing and a similar shaped piece minus the stand and antenna is replaced. The fuselage, outboard wing panels, main gear, nose gear, and antenna are placed in the box for storage.

Table 5.3 Rated Aircraft Cost Worksheet

	Measurement	Scale		Cost:
Manufactured Empty Weight (lb)	14.5	100		1450
Number of Engines	1			
Battery Weight (lb)	4.86			
Rated Engine Power	4.86	1500		7290
MFHR: Manufacturing Hours				
Item			Hourage	
Wing Span (ft)	7	8	56	
Wing Chord (ft)	1	8	8	
Wing Control Surfaces	2	3	6	
Fuselage Length (ft)	4	10	40	
Vertical Surface Active Control	2	10	20	
Horizontal Surface	1	10	10	
Servos and Motor Controllers	8	5	40	
Engines	1	5	5	
Propellers	1	5	5	
TOTAL MFHR		20	190	3800
TOTAL RAC				**12.54**

Table 5.4 Geometry Data for the Sized UAV

Geometry		
Length (in)	47.31	
Span (in)	84	
Height (in)	18.65	
Wing Area (in^2)	1008	
Performance		
	Unloaded	Loaded
CL max	1.5	1.5
L/D max	12.1	12.1
RoC max (ft/min)	913.7	574.5
Stall Speed (mph)	24.0	28.3
Maximum Speed (mph)	61	59
Take Off Distance (ft)	85	115
Weight Statement		
Airframe (lbf)	4.46	
Propulsion System (lbf)	8.39	
Control System (lbf)	1.02	
Payload System (lbf)	0.13	
Payload (lbf)	6	
Empty Weight (lbf)	14.5	
Gross Weight (lbf)	20.5	
Systems		
Radio Used	JR 8103 w/ 3 Digital Trims	
Servos Used	JR Mini Digital Servo	
Battery Used	SR 2400 mAhr	
Battery Configuration	3 x rectangular pack arrangement (3x4)	
Motor	AstroFlight FAI Cobalt 60	
Propeller	APC 22 x 14	
Gear Ratio	2.75:1	

5.4 Drawing Package

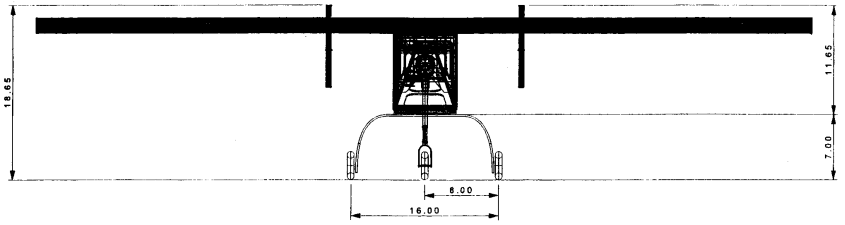

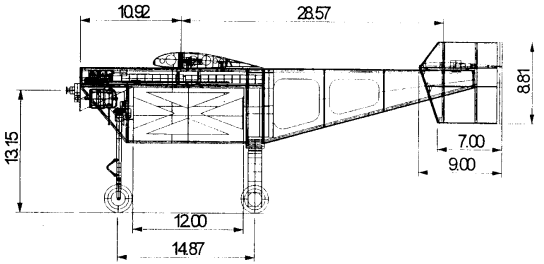

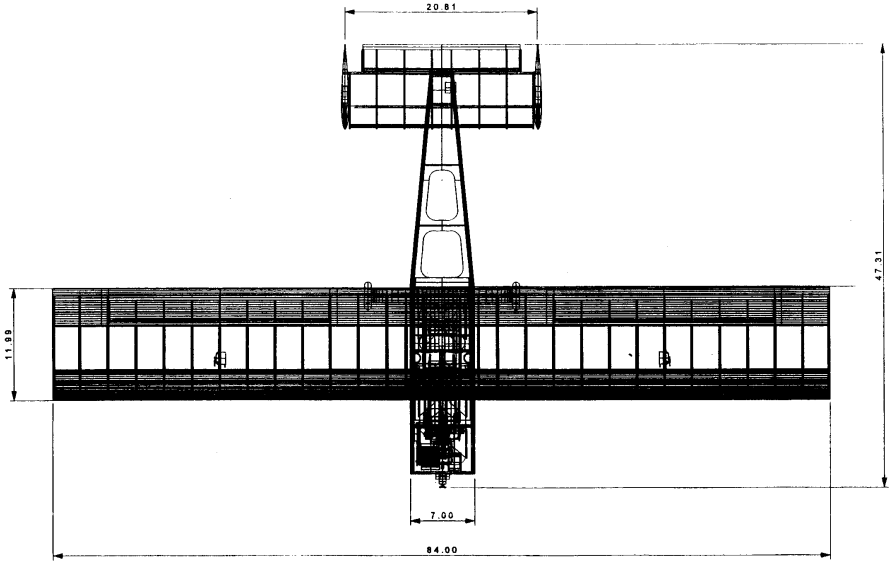

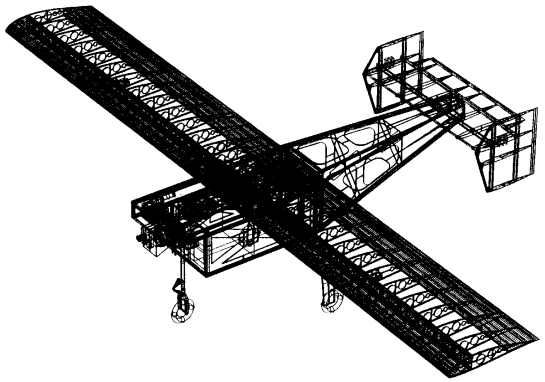

DEPARTMENT OF AEROSPACE ENGINEERING MISSISSIPPI STATE, MS. 39762		
DESIGN/BUILD/FLY 2003 SWAG - THREE VIEW		
Dr. By: D. Bodkin	Prj.Head: V.Austin	
Ck. By: B. Gassaway		SIZE B
SCALE: NTS	04 MARCH 2003	SHEET 1

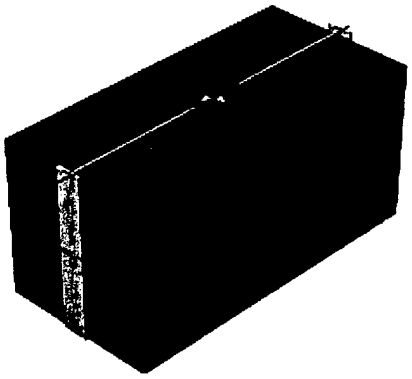

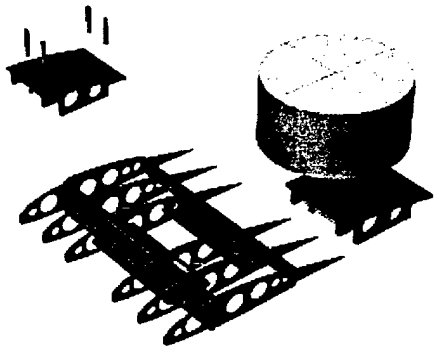

Avionics Package

- **Length:** 12 in
- **Width:** 6 in
- **Height:** 6 in

Antenna

- **Height:** 3 in
- **Diameter:** 6 in

Payload (Avionics Package with Deployment System & Dorsal Antenna)

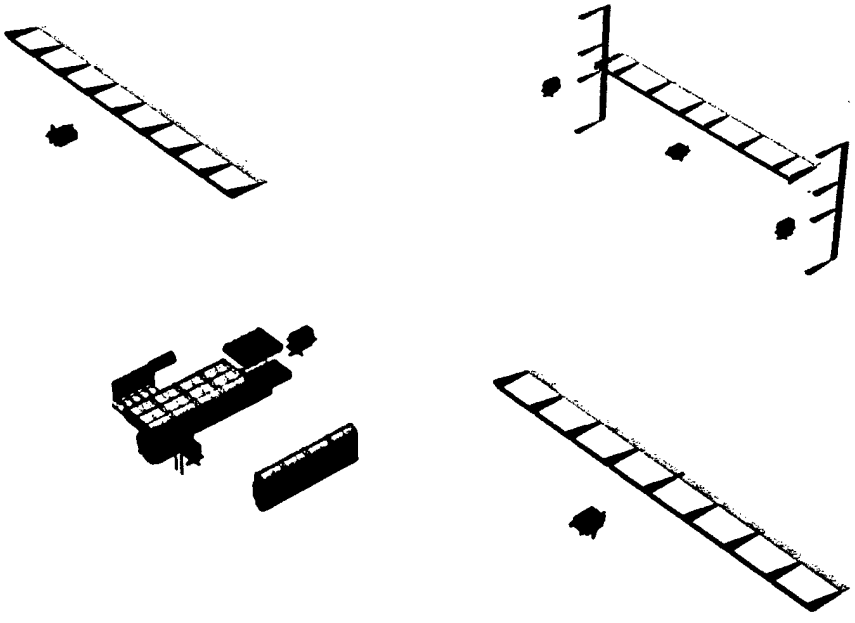

Control Surfaces and Propulsion System

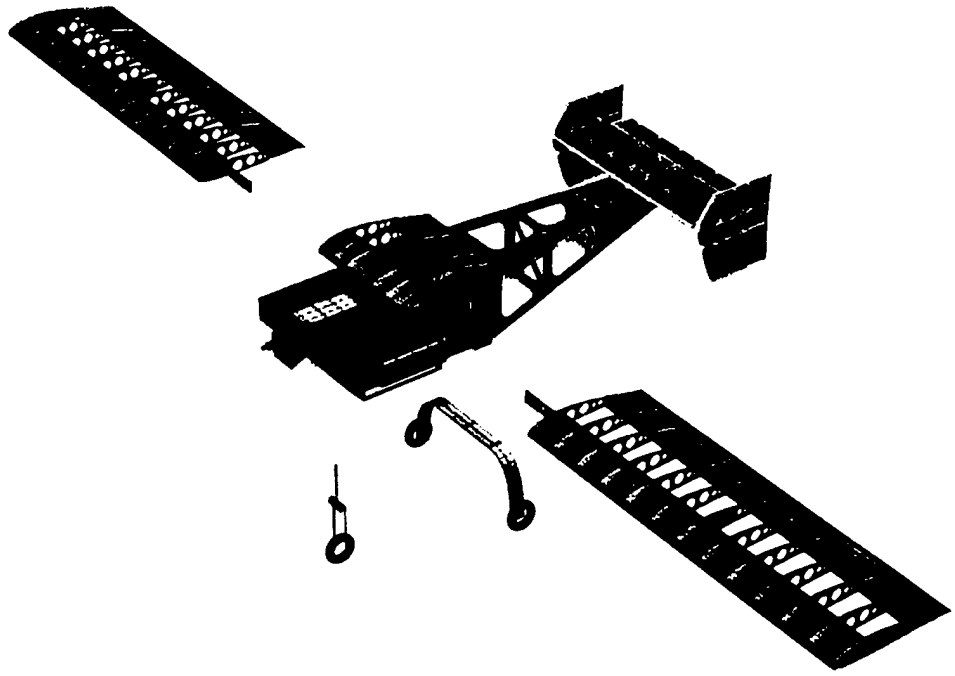

Detachable Wings and Landing Gear

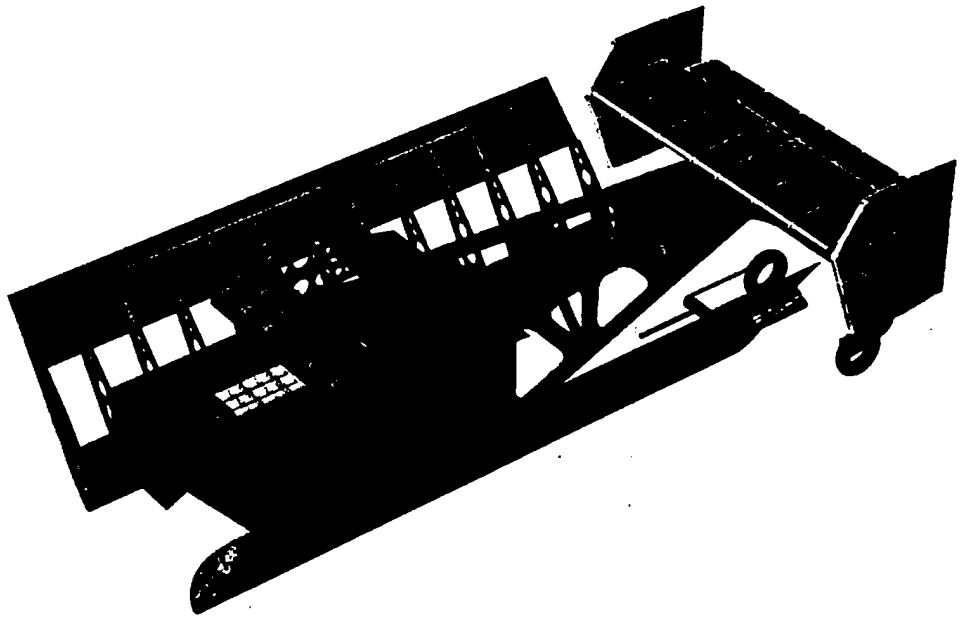

- **SWAG In The Box (UAV must fit in 2'x 1'x 4' box)**

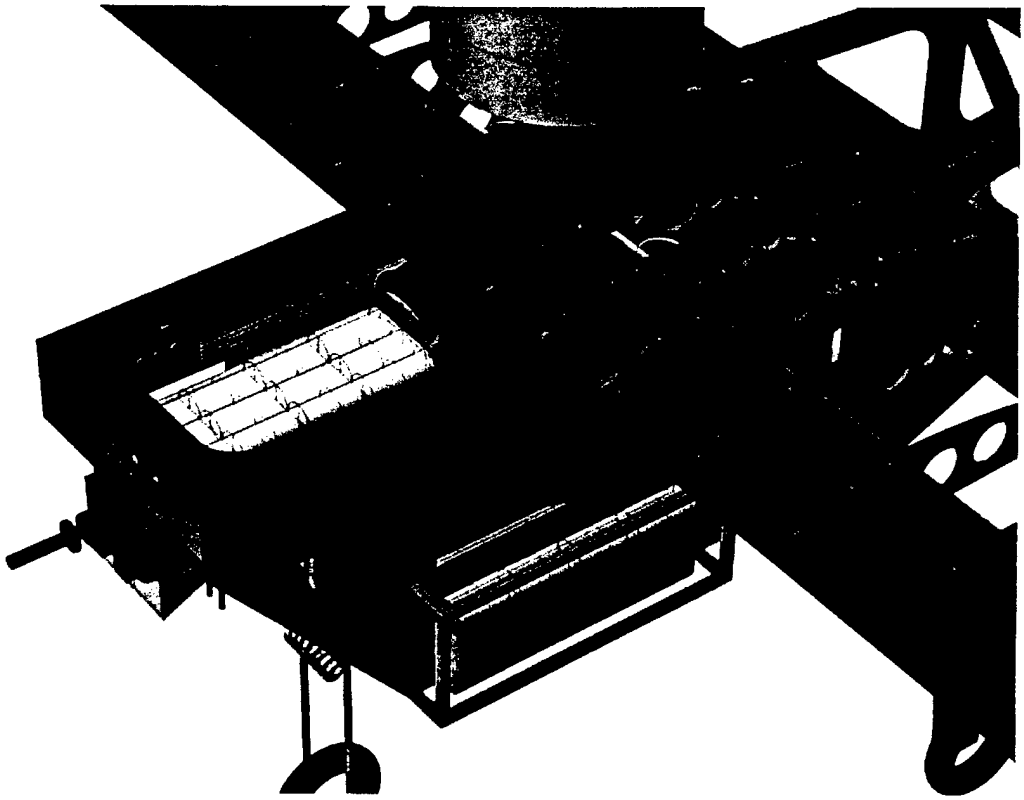

Close View of Battery Placement and Fuselage Components

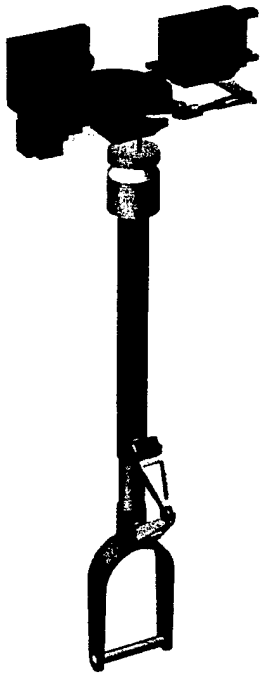

Strut Modified for Quick Attachment to Nose Gear Mount

6.0 MANUFACTURING PLAN

Developing a manufacturing plan requires analysis of options and a manufacturing schedule. An analysis of several methods of construction are investigated and analyzed. From these methods, the team applied figures of merit to decide which would most benefit the design. A schedule was developed to guide construction and modification of major and minor components of the UAV.

6.1 Construction Methods Investigated

Table 6.1 Construction Methods Investigated

Method	Description
Off-the-shelf (OTS)	Components that can be purchased from hobby stores (only applicable to certain structures).
Moldless	Refers to solid-core structures in which skins (if any) are applied directly to the underlying core.
Built-up	Refers to structures that are assembled from individual components that may be either hand- or machine-cut. Skins, if any, simply conform to the underlying structure.
Molded	Internal structures may be built-up or solid-core, but skins are pre-molded to exact shapes before assembly to structure.

6.2 Construction Materials Investigated

Table 6.2 Construction Materials Investigated

Materials	Skill	Description
Advanced Composites	4	Refers to glass-epoxy, Kevlar-epoxy, and carbon-epoxy. Skills associated may include: composite layouts, mold construction, and vacuum bagging techniques.
Foam	3	Includes low- and high-density EPS, as well as 1-lb white foam. Skills associated may include: template construction and hot wire cutting.
Metal	2	Refers to aluminum construction. Skills associated may include: cutting, bending, and drilling.
Wood	1	Includes balsa, light-ply, aircraft plywood, and hardwoods such as spruce and basswood. Skills associated may include: gluing, cutting, and sanding.

6.3 Figures of Merit

The figures of merit applied to the manufacturing plan were developed based mostly on the skills and time of team members. The important factors affecting the plan were decided on by the team and voted on.

Availability of the product is important in two ways. If the product is completely inaccessible, it gets a very low score. However, if the product is accessible but time to receive is prolonged, it may still receive a low score. A good example of this is anything ordered from AstroFlight.

Most underclassmen do not have high skill levels in operating machinery. No one on the team was familiar with advanced composites. Although composites are very lightweight and strong, the skill level required far exceeds the benefits obtained from composites. However, a skilled machinist makes up for what the team lacks in composite skills. The team member with machining skills was able to build landing gear attachments with little trouble. Also, most members of the team are familiar with wood working tools.

The time required to complete component construction is also a vital part of analysis on the manufacturing options. Obviously, no matter the cost of other merits, time is of importance.

Repair ability is considered for select components. The plane is not built for repairability in most senses. However, a second plane is being built and it should be able to use the same landing gear. Hard landings and hangar rash may also lead to the need for some repair ability. Therefore, it is considered.

Cost is always an issue in building an aircraft. The manufacturing plan considered cost from the beginning. Spending a lot of money in one place, may assure cut backs in other places. Considering the need to take twenty-four students to competition this year, cost was a major consideration of the plan in manufacturing.

6.4 Results

The results of the analysis and scoring are detailed in Table 6.3. A score of one is the worst and five, the best. The milestone chart can be found in Figure 6.1. One may notice from the milestone chart that much less time is given to the construction of the second plane. This assumption is made based on modifications and lessons learned during the original construction.

Table 6.3 Selection of Major Component Construction Methods and Materials

Description			Figures of Merit					
			Availability	Skill Level	Time Required	Repairability	Cost	Results
Structure	Method	Material	2	4	5	1	3	
Fuselage (internal)	built-up	wood	5	5	3	2	3	56
		foam	3	4	4	2	2	50
Fuselage (skin)	molded	adv. comp.	2	2	1	4	2	27
	built-up	wood	5	4	4	3	3	58
Wing (spar)	built-up	wood	5	4	3	2	3	52
	moldless	adv. comp.	3	4	2	3	2	36
	OTS	metal	3	3	4	2	1	43
Wing (other internals)	built-up	wood	5	3	3	3	3	49
		foam	3	3	4	2	2	46
		adv. comp.	2	2	1	3	2	26
Wing (skins)	built-up	wood	5	4	4	3	3	58
	molded	adv. comp.	2	2	1	4	2	27
Empennage (internals)	built-up	wood	5	5	3	2	3	56
		foam	3	3	4	2	2	46
		adv. comp.	2	2	1	3	2	26
Empennage (skins)	built-up	wood	5	3	4	3	3	54
	molded	adv. comp.	2	2	1	4	2	27
Landing Gear	OTS	metal	3	4	4	3	3	54
		adv. comp.	4	4	4	4	2	54
	built-up	metal	4	2	2	3	3	38
Wing joiner	OTS	metal	3	3	3	3	2	42
		adv. comp.	2	3	3	3	2	40
	built-up	metal	4	3	2	3	3	42
		adv. comp.	3	2	2	3	2	33
		wood	5	4	3	3	4	56

Manufacturing Timeline

Task Name	Start	Finish	Dec	Jan	Feb	Mar	Apr
SWAG I	01/13/03	02/27/03					
Fuselage Assembly							
Planned	01/26/03	02/03/03					
Actual	01/31/03	02/06/03					
Wing Joiner							
Planned	01/13/03	01/16/03					
Actual	01/20/03	01/22/03					
Wing Spar Assembly							
Planned	01/06/03	01/13/03					
Actual	01/13/03	01/20/03					
Wing Internals							
Planned	01/06/03	01/13/03					
Actual	01/13/03	01/20/03					
Empennage Internals							
Planned	01/16/03	01/23/03					
Actual	01/22/03	01/24/03					
Empennage Skins							
Planned	01/23/03	01/25/03					
Actual	01/24/03	01/31/03					
Landing Gear Integration							
Planned	02/04/03	02/11/03					
Actual	02/03/03	02/21/03					
Final Assembly							
Planned	02/11/03	02/18/03					
Actual	02/15/03	02/27/03					
SWAG II (Predicted)	03/17/03	04/11/03					

Figure 6.1 Milestone Chart of Major Events

7.0 TESTING PLAN

The objective of flight testing is to familiarize the pilot with the UAV and to simulate competition missions for score optimization. In late January, the flight-testing team met with Dr. Tom Edwards and Mr. Calvin Walker at the Raspet Flight Research Laboratory to discuss a test schedule both similar to a full-scale testing plan and that applicable to an unmanned air vehicle (UAV). In order to complete the testing needed to modify the second SWAG, a schedule needed to be developed. The structure of the schedule would allow the team to find problem areas and make necessary adjustments in a timely fashion. Results from each test would be recorded and analyzed for further improvements on the UAV.

7.1 Schedules and Check Lists

Due to the limited amount of time available to accomplish certain landmarks, it was decided to break up flight-testing into five segments. The first four segments would consist of four flights each, while the last segment would continue until competition. The first four segments of testing were to familiarize the pilot with the UAV. Slow speed and stall characteristics, power-off glide, and a simulated competition flight would give the pilot familiarization with UAV handling abilities and mission profiles. The last test segment was intended to simulate competition missions for increased individual flight scores.

Several considerations were noted during the meeting with Dr. Edwards and Mr. Walker. Before flight testing at the airport, a certificate of authority was needed to waive Federal Aviation Regulation (FAR) Part 91 requirements for the UAV, and proper authorities working at the airport had to be notified. Because of the short duration of the flights, the airport board did not find reason to issue NOTAM's during flight testing days. A pre-flight briefing was needed before each test to ensure facility requirements were followed. Some of these requirements were that communication must be made with other aircraft in the pattern, that flight testing would occur only when visual flight rules were issued, and that a Raspet employee would monitor the tests.

7.2 Results

SWAG was ready for flight-testing on February 28. The first flight was scheduled ahead with Raspet, weather permitting. The weather was cloudy and cold with light and variable winds. A pre-flight briefing was held with Mr. Walker and Dr. Robert King. The pre-flight briefing included a summary of flight and payload intentions. A pre-flight report was developed and checked by the team's faculty advisor. The report laid out specifics of the flight tests to be completed. The pre-

flight briefing was intended to oversee and suggest any additional ideas specific to a first flight, as well as, to advise on any regular activity scheduled to occur at the airport.

The first flight attempted the 120-foot takeoff distance without pushing the limits of the UAV. While accelerating to takeoff speed, the UAV lifted off the ground without any elevator input. After turning downwind, down elevator trim on the transmitter was necessary to achieve level flight. The time to accomplish three patterns and a landing setup was approximately three minutes. Upon landing, it began to oscillate from one side to the other on its main landing gear and eventually turned on its nose. After a post-flight meeting, the flight testing group believed the main cause was due to the relatively high landing speed. The pilot stated that the landing could have been slower, but did not want to risk stalling on the first landing. After charging the main battery packs, a second flight was attempted only to discover that the previous landing had loosened the steering clevis, making the nose gear steering non-functional. A second flight was not attempted at this time.

After repairing the nose gear steering clevis, another flight was attempted on March 2. Unlike the previous flight, weather conditions were much colder with stronger winds. Soon after starting the takeoff roll, the tail picked up and caused a propeller strike. Due to the extreme conditions, the pilot and test director decided to postpone testing for the day.

March 3 presented much more favorable weather conditions and another test was attempted. Before flight testing began, taxi testing was requested by the pilot to ensure straight tracking with a replaced steering pushrod. The flight of March 3 was a second pilot familiarization test with no pay load. Takeoff was again achieved in less than 120 feet. The UAV then climbed to a safe altitude for testing slow speed and stall characteristics. After turning upwind, throttle was cut and elevator input was slowly increased to maximum. No tip stalling tendencies were evident. This flight was flown in a pattern prescribed by the competition. The landing approach was much slower, and rollout proved to be less violent. Afterwards, the pilot believed more control in elevator deflection was needed for maximum handling capabilities. After charging the main battery packs, a second flight proved as successful as the first, and it was learned by the pilot that takeoff and landing rolls are much more controllable with up elevator input. It was then decided that ground-handling performance depends greatly on how much weight is placed on the nose-wheel, and the only way to alleviate that pressure is by counter-acting it with the elevator. Also a large amount of down-elevator trim was noticed in the horizontal stabilizer, which is known to increase trim drag. In order to compensate for the down trim, the main wing incidence was lessened.

Flight-testing continued March 4. The objectives for the first four segments had been achieved with the first three flights, so it was decided to continue with the fifth flight-testing segment of carrying payload. With the simulated deployable sensor package onboard, the ground roll for the UAV was within the 120-foot competition limit. It climbed to a safe altitude to again test slow speed and stall characteristics, which resulted in no tip stalling and a steeper glide angle. The test concluded with a smooth landing. With the payload onboard, less elevator input was necessary to attain good ground handling characteristics and static stability was improved. With increasing confidence in the design, a mission pattern was attempted and flown successfully. In post-flight discussion, the elapsed time of the mission flight, five minutes, 16 seconds, was attributed to the exaggerated pattern length. Mission time is expected to decrease with practice and familiarization.

7.3 Lessons Learned

A major lesson was learned during the flight testing of *SWAG*. Previous to and during flight testing, it was noticed that SWAG was inclined to tip forward. Although care had been taken to place the CG in the correct position, the static stability in ground handling had problems. After considering options, the team decided that weight had to be moved away from the top of SWAG. Two of the motor batteries were placed in cargo bays located on either side of the fuselage, close to the ground. By moving the batteries closer to the ground, the CG was moved closer to the ground. This change improved ground handling during turns. *SWAG II* will incorporate this design change.

Figure 7.1 Proof of Flight

REFERENCES

Anderson, John D. Introduction to Flight. 4th Edition. WCB/McGraw-Hill, New York. 2000.

Bruhn, E.F. Analysis and Design of Flight Vehicle Structures. Jacobs Publishing, Inc. Indiana. 1973.

Nelson, R.C. Flight Stability and Automatic Control. 2nd Edition. WCB/McGraw-Hill, New York. 1998.

NASG (*Nihon univ. Aero Student Group*). College of Science & Technology Nihon University. 11 November 2000. http://www.nasg.com/index-e.html .

Raymer, Daniel P. Aircraft Design: A Conceptual Approach. 2nd Edition. American Institute of Aeronautics and Astronautics, Washington, D.C. 1992.

Vinh, Nguyen X. Flight Mechanics of High-Performance Aircraft. 4th Series. Cambridge University Press, New York. 1993.

XFOIL. Massachusetts Institute of Technology. 11 December 2000. http://raphael.mit.edu/xfoil/ .

2003 AIAA Design/Build/Fly Competition Report

Submitted by
Team Yeager Chasers

United States Naval Academy
06-MAR-03

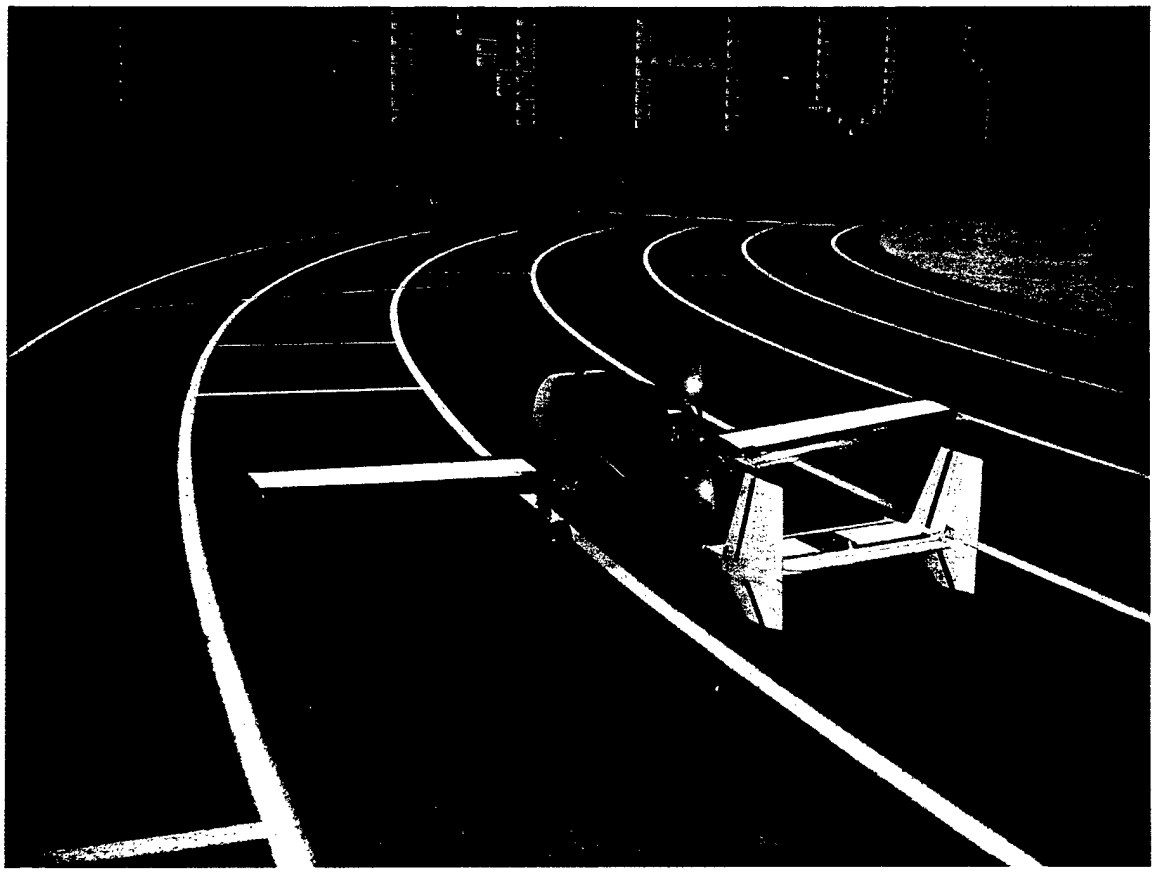

Table of Contents

1.0 Executive Summary..... 1
1.1 Conceptual Design Summary 1
1.2 Preliminary Design Summary 2
1.3 Detail Design Summary 3
1.4 Aircraft Manufacture 4
1.5 Flight Testing 4
2.0 Management Summary..... 4
2.1 Organization of the Design Team 4
2.2 Areas of Responsibility 5
2.3 Scheduling and Documentation 7
3.0 Conceptual Design..... 8
3.1 Mission Requirements 8
3.2 Background 9
3.3 Individual Conceptual Design Summary 10
3.4 Alternate Configurations Considered 11
4.0 Preliminary Design 19
4.1 Methods of Analysis 19
4.2 Sensitivity Analysis 20
4.3 Rated Aircraft Cost Sizing Trades 23
4.4 Trade Studies and Component Analysis 24
4.5 Aerodynamics Preliminary Design 33
4.6 Propulsion Preliminary Design 35
4.7 Preliminary Stability and Control Characteristics 37
4.8 Preliminary Performance Estimates 38
5.0 Detailed Design 41
5.1 Wing 41
5.2 Final Propulsion System 42
5.3 Detailed Structural Design 43
5.4 Stability and Control 45
5.5 Landing Gear 49
5.6 Tables - RAC / Geometry / Performance / Weight Statement / Systems Data 50
5.7 Drawing Package 51
6.0 Manufacturing Plan 51
6.1 Alternate Manufacturing Processes Investigated 51
6.2 Analytic methods 52
6.3 Construction Processes for Major Components 53
7.0 Testing Plan 55
7.1 Test Objectives 55
7.2 Test Results / Lessons Learned 56
8.0 References 57

List of Figures

Figure 2-1 Architecture of the design team. 5
Figure 3-1 Layout of DBF competition course (dimensions in ft) and scoring formula. 9
Figure 3-2 Individual conceptual designs and rankings. 11
Figure 3-3 Decision matrix for fuselage configuration. 13
Figure 3-4 Decision matrix for the tail configuration. 15
Figure 4-1 Mission performance curves. 21
Figure 4-2 Initial propulsion testing. 26
Figure 4-3 Composite wing spar strength test. 27
Figure 4-4 Carbon fiber tube moment arm test. 28
Figure 4-5 Foam and fiberglass Eppler 67 airfoil, lift curves, and drag polars. 30
Figure 4-6 Experimental setup and results for antenna splitter plate study 32
Figure 4-7 Landing gear components tested and wind tunnel drag results 33
Figure 4-8 Drag comparisons for alternate configurations and missions. 35
Figure 4-9 Thrust vs. Drag (Mission C) above, and (Mission A) below. 36
Figure 4-10 Energy Maneuverability Diagram 39
Figure 4-11 Constraint plot. 40
Figure 5-1 Thrust available and efficiency curves for the 14x12 43
Figure 5-2 Wing and flapperon attachment technique. 45
Figure 5-3 Vertical and Horizontal Tail Dimensions 47
Figure 6-1 Wing, empennage, fuselage, and landing gear manufacture. 55
Figure 7-1 Yeager Chaser 1 during ground tests. 57

List of Tables

Table 2-1 Milestone chart 7
Table 3-1 Decision matrix for engine mount location. 16
Table 3-2 Wing Position Decision Matrix. 17
Table 3-3 Landing Gear Decision Matrix 18
Table 4-1 Performance design goals. 22
Table 4-2 RAC components and goal configuration. 24
Table 4-3 Preliminary wing specifications. 34
Table 4-4 Preliminary performance calculations. 38
Table 5-1 Detailed weight and balance 46
Table 5-2 Control surface sizing and effectiveness. 48
Table 5-3 Flaperon Dimensions/Effectiveness 48
Table 5-4 Table of aircraft geometry and aircraft weight statement. 50
Table 5-5 Table aircraft performance data and aircraft systems data. 50
Table 5-6 RAC table. 51
Table 6-1 Skill matrix. 52
Table 6-2 Manufacturing milestone chart. 53
Table 7-1 Flight test schedule. 56
Table 7-2 Test and flight checklists. 56

1.0 Executive Summary

This report details the efforts of the United States Naval Academy (USNA) team Yeager Chasers in the 2003, joint AIAA Cessna/ONR sponsored, Design/Build/Fly (DBF) competition. For the competition, each team must assemble their modular aircraft from components fitting into a transport box and fly two of three designated missions. The missions are weighted by difficulty and designed to simulate current unmanned aerial vehicle (UAV) applications. Mission A is representative of a missile decoy mission with an assigned difficulty factor 2.0. Mission B simulates a sensor deployment vehicle with an assigned difficulty factor 1.5. Mission C simulates a communications repeater with an assigned difficulty factor 1.0. The final competition score is determined by the aircraft's assembly time, flight time, rated aircraft cost, mission difficulty factors for the two missions, and the written report score. To produce a successful design the team would have to create an aircraft that best optimized the scoring criteria.

1.1 *Conceptual Design Summary*

Students in the senior design class began the conceptual design process by conducting a literature search and background survey of UAV's and RC aircraft. Additionally, the results of last year's competition were closely analyzed. Then each student created their own conceptual aircraft design, focusing primarily on aircraft performance, rated aircraft cost, and final DBF score. After teams were selected, the individual conceptual designs and alternate configurations were evaluated with respect to numerical figures of merit. This yielded a baseline conceptual design for an in depth analysis in the next phase of the design process.

1.1.1 Conceptual Design Development Processes

The development process to focus the eight individual designs down to a single conceptual design relied on the use of decision matrices. Decision matrices were a way to organize and visually represent the screening process for potential design configurations. Using figures of merit related to specific mission requirements, the decision matrices accurately weighed the benefits and risks of various alternative configurations. The decision matrices were an evolutionary process that became more specific as the baseline conceptual design solidified.

1.1.2 Conceptual Design Alternatives

The eight individual conceptual designs formed the starting point for range of design alternatives investigated by the team. Configurations from the individual designs along with additional configurations deemed viable by the group were ranked through the numerical screening process of the decision matrices. The group evaluated three different fuselage configurations, four tail configurations, and a tractor vs. a pusher motor configuration. Wing design parameters such as placement, dihedral, and taper were also investigated along with two landing gear configurations.

1.1.3 Conceptual Design Findings

At the conclusion of the conceptual design phase, the decision matrices yielded a baseline configuration, consisting of slender body fuselage with tail booms and pusher motor and tricycle landing gear. The aircraft had a low straight wing with 3° of dihedral. The team's design would employ either a V-tail or a twin conventional tail based on the outcome of more detailed studies in the preliminary design phase.

1.2 *Preliminary Design Summary*

The preliminary design was a stepping-stone between a general conceptual design and a detailed version designed explicitly for specific missions. The configurations decided on in the conceptual design phase were modeled using computer programs and tested experimentally in the preliminary design phase. A sensitivity study resulted in the selection of a mission model. Numerous sizing and trade studies were performed on all aspects of the aircraft. This yielded the components and dimensions of the preliminary design. With accurate dimensions, initial performance calculations were performed in an attempt to optimize design parameters.

1.2.1 Preliminary Design Development Processes

The team first conducted a sensitivity study to establish the impact various design parameters had on the final score. Using a computer program written by the team, the sensitivity study modeled two mission approaches and predicted performance based on inputted aircraft parameters. This allowed the team to select two missions to optimize the design towards. A sizing trade was performed to identify the most heavily weighted components in the rated aircraft cost equation. A number of trade studies and component tests were run during this phase of the design process including an airfoil comparison study, an antenna drag study, landing gear drag evaluations, structural tests, and propulsion studies. These trade studies allowed the team to develop a preliminary aircraft design. Once dimensions and components were locked down, preliminary performance calculations were made with respect to aerodynamics, propulsion, and flight characteristics.

1.2.2 Preliminary Design Alternatives

The preliminary design phase weathered an incessant battle over missions selection. Two mission models were identified that would yield radically different design approaches. These alternate designs would center around either a deployment approach (Missions A and B) or a performance approach (Missions A and C). The deployment approach was selected by the Naval Academy sister team, Severn Discomfort. However, the Yeager Chasers chose the alternative performance approach. Since an aircraft designed for these two missions would not have to deploy a box, significant reductions in rated aircraft cost and flight time could be made. Obviously the greatest factor to overcome would be the mission difficulty factors of the deployment approach. Nonetheless, at the end of the preliminary design

phase, all the members of Team Yeager Chasers were confident that their design, independent from constraints associated with deploying the payload, would win the DBF competition.

1.2.3 Preliminary Design Findings

Based on the analysis and testing conducted during this phase, the baseline preliminary design incorporated a 4412 airfoil with no taper ratio, the most efficient use of wing surface area with respect to rated aircraft cost. Propulsion studies selected an Astro 60 motor with a 14 x 11 propeller for the aircraft's power plant. Structural studies yielded potential construction techniques and attachment methods. The antenna would be mounted above the center of gravity because it the simplest configuration with regards to stability and control. The performance design also relied on the clean configuration manifesting itself both in retractable landing gear and the recessing of servos under the surface of the aircraft. A twin conventional tail was decided on for the final tail configuration after a v-tail's rated aircraft cost benefit proved unfeasible. The Computer Aided Design (CAD) Lead drafted a model, in three-dimensions, of the aircraft in the program AutoCAD 2000. Other leads consulted the model to ensure physical dimensions were accurate; propeller clearance was sufficient for both the ground and the tail booms; fuselage, wing, and empennage were integrated; the landing gear retracted completely into the fuselage and wing, as well as ensuring the unassembled aircraft would fit properly into the box.

1.3 *Detail Design Summary*

The Detail Design was the final process in designing the aircraft. In this phase, measurements and configurations of the aircraft itself, as well as its internal components were designed and finalized. A well thought-out integrated design was the goal, where ease of construction with respect to the composites structures technique chosen, was emphasized. To facilitate this process, the lab technician overseeing the composites layout of USNA's two entries, Mr. Bill Beaver, provided invaluable inputs. As the detailed design of each component was completed, full-scale construction drawings were produced.

1.3.1 Detail Design Development Processes

The tools used in the detailed design consisted mainly of the AutoCAD 2000 program and detailed full-scale drawings. As ordered parts arrived at the laboratory, they were tested. The propulsion plant was run in the wind tunnel with the desired propeller. More exact performance ratings, from experiment rather than modeling, were collected to gain a more accurate prediction of the aircraft's performance, prior to the maiden flight.

1.3.2 Detail Design Findings

The integration of the gear, wing root and fuselage base as well as the configuration of the radio equipment, batteries, nose gear, and "hydraulics" bottle in the nose of the aircraft were the main problems solved in the detailed design of the final configuration.

1.4 *Aircraft Manufacture*

The aircraft manufacture started immediately upon return from the winter leave period. Initially major structures were first cut out of foam. The fuselage was cut out of foam by hand, while the wing surfaces were cut out using a hotwire technique. Strength was added to the foam using composite glass and resin. Spars were built into the ¼ chord and the leading and trailing edges were reinforced with carbon fibers. Carbon fiber tubes were used to join the outboard wing sections to the fuselage/wing center body. The fuselage was laid up out of fiberglass and graphite composites in two pieces: the nose tray was built rigidly around space for a retracted nose wheel and four pounds of batteries; and the main body was laid up using a thinner, lighter construction technique using a male mold. The twin tail empennage was built from hotwired foam sections and fiberglass. The retractable landing gear struts were made from ¾ inch carbon fiber tube, machined aluminum pieces and three commercially available shock absorbers. The landing gear retract devices were embedded in the wing root so that they could be removed and inserted without affecting the structural integrity of the wing. The trailing edge glass on the wings was used as a hinge for control surface movement and servos were embedded for drag reduction.

1.5 *Flight Testing*

The flight test portion of the competition was scheduled for after construction on the 1st of March. A rigorous flight test phase will ensure the airworthiness and competition readiness of the airplane. All aspects of the Radio Control systems including radio control range and system response will be tested. Various performance parameters, including takeoff distance, flight times on turns and straights, landing distances, retractable gear operation, and power plant endurance and performance will be measured and cataloged. This phase will be instrumental in ensuring our pilot's familiarity with the craft well before the competition.

2.0 Management Summary

2.1 *Organization of the Design Team*

This year's United States Naval Academy entry "Yeager Chasers," is primarily composed of a select group of eight fourth year aeronautical engineering students. The team has been augmented by third year, underclass Midshipmen who have opted to share in the design process. While their wind tunnel research was accomplished during class hours, their help towards construction and flying of the model was accomplished outside the classroom. The Advisor of the design class, Dr. Birckelbaw, chose the team's Program Manager, Midshipmen First Class Michael Kingen. He and the other USNA entry's Program Manager, Midshipmen First Class Patrick Bookey, selected teams and discipline leads. First Class leads within the Yeager Chasers along with the Second Class teammates are shown in Figure 2-1.

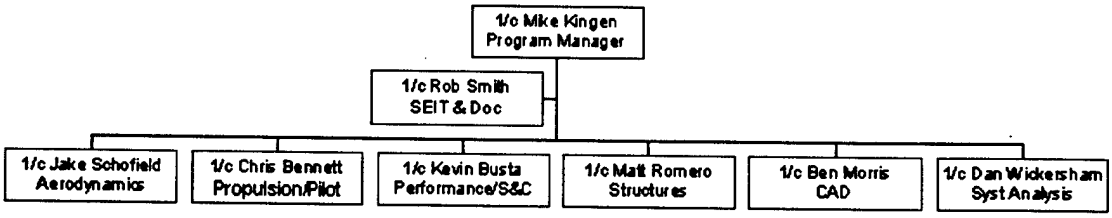

Underclass Team Members
MIDN 2/C Michael Bernard, Aerospace Engineering
MIDN 2/C John Fitzpatrick, Aerospace Engineering
MIDN 2/C Michael Kessler, Aerospace Engineering
MIDN 2/C Jonathan Powell, Aerospace Engineering

Figure 2-1 Architecture of the design team.

2.2 *Areas of Responsibility*

2.2.1 Program Manager

The Program Manger was responsible for the overall product of the team. His primary concern was the scheduling and coordination of tasks amongst team members in order to meet deadlines. He worked closely with SEIT & Doc Lead to ensure a quality design report and thus a quality finished project. In the construction phase, he coordinated among the different leads to develop a single material product and ensured group adherence to the schedule. He was ultimately responsible for everything produced.

2.2.2 Systems Engineering, Integration, Test and Documentation Lead

The SEIT & Doc was responsible principally for the paper side of the design. He ensured the team members submitted progress reports on a timely basis in order to meet deadlines and presented material to Dr. Birckelbaw on a weekly basis. He was the principle architect of this design report, integrating individual reports from team members into the final product. He worked closely with the Program Manager and provided a second opinion on final design decisions.

2.2.3 Aerodynamics Lead

The Aerodynamics Lead was responsible for all research, testing and ultimate aerodynamic characteristics of the design. He worked closely with other members of the team in an integrated fashion to guarantee mission performance goals. This included wing and empennage design, drag build up calculations, optimization efforts, and propulsion plant integration. In particular, he led the team's experimentation on wing sections, landing gear drag, and antenna drag.

2.2.4 Propulsion Lead

The Propulsion Lead was responsible for all propulsion analysis, testing, and design. He worked closely with other team members to resolve propulsion issues including, mission performance, optimization efforts, power plant selection, wind tunnel and flight test validation, and risk management activities. His principle contribution to the design was the selection, ordering, and testing of the power plant.

2.2.5 Performance/Stability and Control Lead

The Performance S&C Lead was primarily responsible for the analysis, testing, designing, and documentation of the aircraft's static and dynamic stability and performance. He worked closely with other team members, especially the aerodynamics lead and the propulsion lead, in integrating design concepts into a single model with the proper balance and control for flight. He concentrated on all phases of the mission, ensuring proper sizing of control surfaces and the desired performance characteristics.

2.2.6 Structures Lead

The Structures Lead was responsible for all structures analysis, testing, and. His primary focus was on weight reduction of the aircraft while maintaining the necessary strength. He led the team in testing wing spar strength and torsion loading of the tail booms. His design of the quick assembly techniques was crucial in optimizing the final DBF score.

2.2.7 Computer Aided Design Lead

The CAD Lead was responsible for all Computer Aided Design analysis and documentation activities. His dimensional layout on the computer documented the physical aspects of the design. He worked closely with other members of the team to produce an integrated design, building conceptual computer designs for integration of systems in the fuselage, aircraft components and their organization in the transport box, and retractable landing gear system. He kept detailed documentation of all preliminary and final designs.

2.2.8 Systems Analysis Lead

The Systems Analysis Lead was responsible for all systems analysis development and documentation. He carried the primary burden of system development and optimization, including DBF score optimization, aircraft performance optimizations, figures of merit assessment, configuration tradeoffs, and rated aircraft

cost studies. He worked the sensitivity analysis, decision matrices, and more advanced figures of data such as the energy maneuverability diagram and constraint plot.

2.2.9 Underclass Team Members

The underclass team members were tasked with running basic wind tunnel tests. They received requests from the primary design team, gathered data, and reported to the Aerodynamics Lead on their findings. In addition, they supported the team during the construction and flight test phases of the program.

2.2.10 Pilot

The Pilot was responsible for ensuring safe passage of the prototype through the competition in April. He advised in the practical "RC" aspect of the competition, ensuring the design was capable of remote operation. He will run the flight tests and be the primary consultant for any final modifications.

2.3 *Scheduling and Documentation*

One of the first tasks accomplished by the team was to create a schedule that encompasses the entire design, build, and fly phases (Table 2-1).

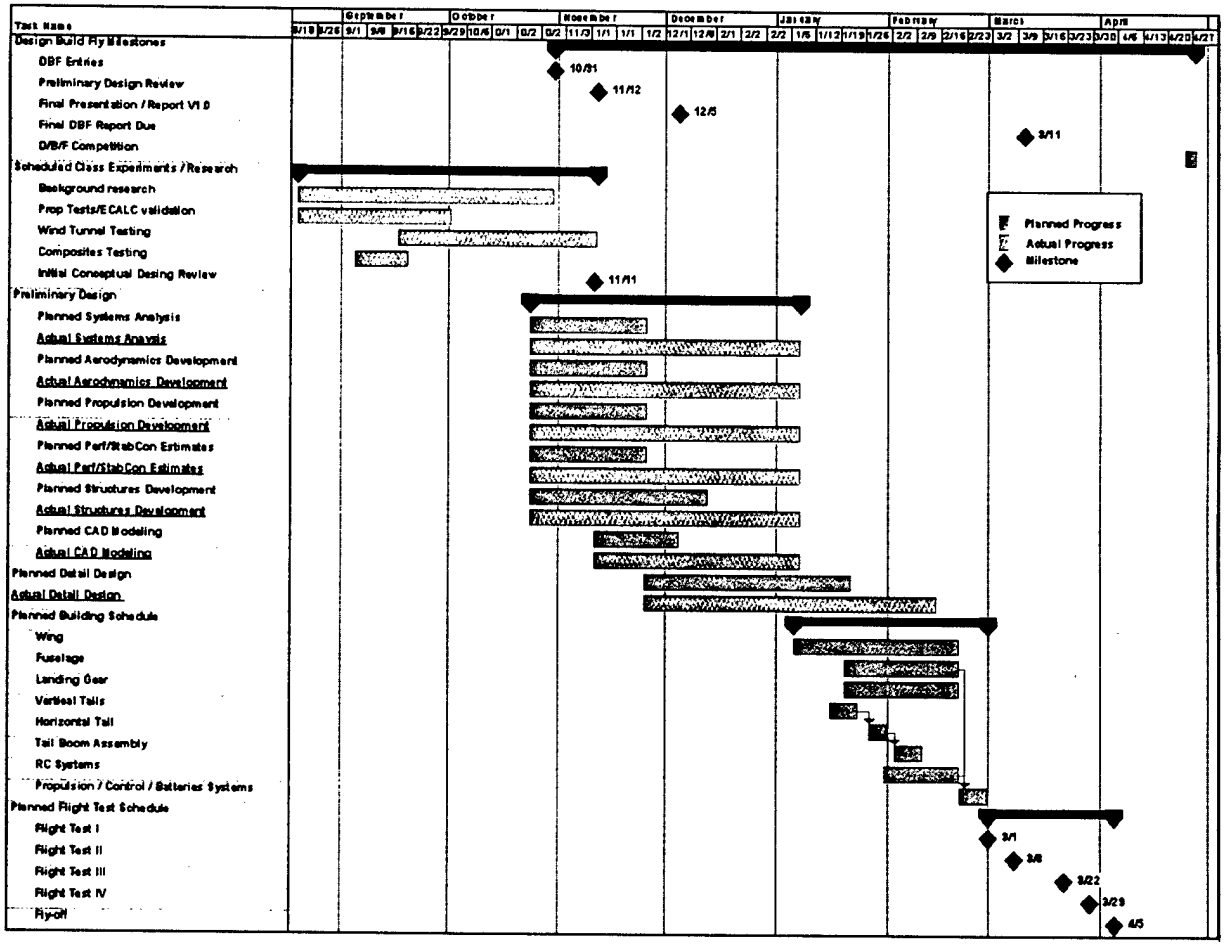

Table 2-1 Milestone chart

Microsoft Project was used to accomplish the daunting task of organizing all required tasks in chronological order, culminating in the April competition. This Gantt chart, encompassing the entire year, is simply a broad outline of tasks. The "preliminary" and "detailed designs" include actual and planned progress, where the "D/B/F milestones" and the "scheduled class experiments / research" were not dependent upon the group's progress. Detailed manufacture and flight test schedules are displayed in the respective sections. The team's design work, including reports, test data, and other important documents, were recorded in the "Yeager Chaser's Notebook" in order to monitor progress. Competition information, updated rules, fabrication work orders, and eventually flight test documents were also collected in the notebook.

3.0 Conceptual Design

3.1 *Mission Requirements*

For the 2003 Design/Build/Fly competition, teams must design a battery-powered, propeller-driven unmanned aircraft. Teams must assemble their aircraft on site from all its components transported in a 2 ft by 1 ft by 4 ft box. For all three missions, the aircraft must complete four laps around a 1000 ft course, carrying a 6 in by 12 in by 6 in payload box, with a weight of 5 lbs. The teams must complete two of three missions weighted by difficulty as follows:

Mission A (Difficulty Factor 2.0) – In the missile decoy mission, the aircraft will be fitted with a simulated cylindrical antenna constructed of six inch PVC pipe three inches in height. The aircraft must execute one 360° turn on the downwind leg of each lap.

Mission B (Difficulty Factor 1.5) – For the sensor deployment mission, the aircraft must take off with the five-pound payload box, fly two laps with one 360° turn per lap, and then land. Upon landing the aircraft must self-deploy the payload box. After a successful deployment, the aircraft must take off again and fly two additional laps with one 360° turn per lap.

Mission C (Difficulty Factor 1.0) – In the communications repeater mission, the aircraft must simply carry the five-pound payload box for four laps. However, the aircraft must perform three 360° turns on each of the downwind legs.

The final score is a function of the grade on the written report, rated aircraft cost (RAC), mission difficulty factors, assembly time, and flight times, where total flight score is the sum of the two best mission scores as given by the relationships in Figure 3-1.

Rated aircraft cost relates the overall dimensions and complexities of the aircraft to an associated price, simulating project budgets in the aircraft industry. The price is determined by the man-hours assigned to various aspects of the aircraft.

The Manufacturer's Empty Weight includes the weight of the aircraft without the mission payloads. The Manufacturing Man Hours are assigned via contest rules. Each component of the aircraft is given a

designated man-hours value per some dimension or weight of that component. The "hours" used to build the aircraft are then compiled and the cost is determined by the $20 multiplier. With this in mind, teams must design an aircraft that optimizes mission flight times without sacrificing assembly time or RAC.

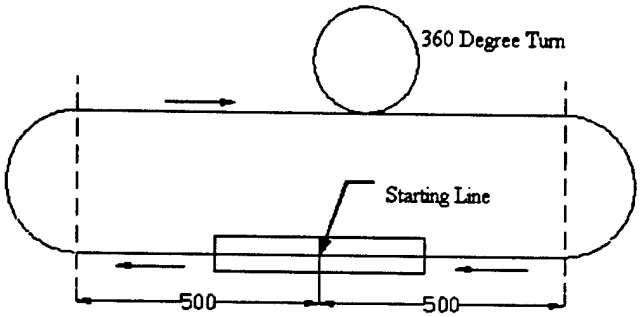

Course Layout
Shown to Scale

$$DBF\ \ Score = \frac{Report\ \ Score * Total\ \ Flight\ \ Score}{RAC}$$

$$Total\ Flight\ Score = \sum \frac{Mission\ Difficulty\ Factor}{Flight\ Time + Assembly\ Time}$$

$$RAC = \frac{\left[\$100 * MEW + \$1500 * REP + \frac{\$20}{hour} * MFHR\right]}{1000}$$

MEW = Manufacturer's Empty Weight (lbs) MFHR = Manufacturing Man Hours

REP = Rated Engine Power $= (1 + .25(\#engines - 1)) * Total\ Battery\ Weight$

Figure 3-1 Layout of DBF competition course (dimensions in ft) and scoring formula.

3.2 *Background*

Before beginning any design work, extensive background research was conducted on the subject of unmanned aerial vehicles and radio-controlled aircraft. This consisted of a thorough literature search of the Internet and library resources, along with an in depth analysis of the previous two year's DBF competitions. Information on the performance parameters of small UAV's was collected to provide a baseline for the initial 2003 DBF design. Specifically, the ratio of empty weight to total gross weight for a number of small UAV's was calculated and used in initial weight estimates for the design with respect to the required payload. An analysis of previous USNA team designs along with the other DBF competitors was performed. Of particular interest was video footage of last year's competition taken by Dr Birckelbaw. With respect to the other competitors, two main conclusions were drawn. Overly unconventional designs such as canard configurations or flying wings usually resulted in disastrous failures. Additionally, failure to consider environmental conditions, such as high winds, prevented a

number of teams from completing a single mission. In light of the competition results, the successes and failures of last year's two USNA teams were more closely studied.

Successful attributes of last year's entries included their high degree of stability and control, along with a number of innovative construction techniques. However, both teams failed to perform a thorough optimization and sensitivity analysis indicated by their high rated aircraft costs. An additional lesson learned from last year's efforts was the need for durable landing gear. Last year's teams broke their landing gear several times after hard landings. A priority in this year's design will be structurally sound landing gear. After the background research was completed, the USNA students began the conceptual design process.

Before the two USNA teams for this year's DBF competition were formed, each individual in the senior design class created their own conceptual design according to the rules outlined in the competition. This was done for two main reasons. By constructing an individual conceptual design, each prospective team member gained a better understanding of the design process and an appreciation for the interdependencies between the different design disciplines. In addition, the eight conceptual designs produced a wide range of approaches to solving the engineering problems presented by the competition. This familiarized everyone with the rules and requirements of this year's competition and provided a solid starting point for optimizing the various score components and aircraft parameters.

3.3 *Individual Conceptual Design Summary*

In September of 2002, each student was tasked with developing an individual conceptual design and presenting it to Dr. Birckelbaw and the class. From the individual designs, teams were selected based on similar design concepts and the input of the program managers. Team Yeager Chasers was selected primarily on a willingness to pursue Missions A and C, but also out of an enthusiasm for optimization. Once the teams were formed, each individual was assigned a lead position in a specific design discipline.

Once the individual designs were completed and the team formed, the first task was to develop a computer code, using Matlab that would tabulate RAC and DBF Score to standardize the individual designs for the purposes of ranking. These individual design rankings would be the basis for deciding how the group would move forward in the conceptual design phase. The logic behind this was to normalize each person's individual conceptual design based on the common assumptions of an assembly time of one minute and a report score of 90%.

Figure 3-2 shows the rankings with respect to RAC and DBF score of the eight individual conceptual designs developed by the Yeager Chasers team members. As shown, Jake and Dan's designs rated the best on both the RAC and DBF score.

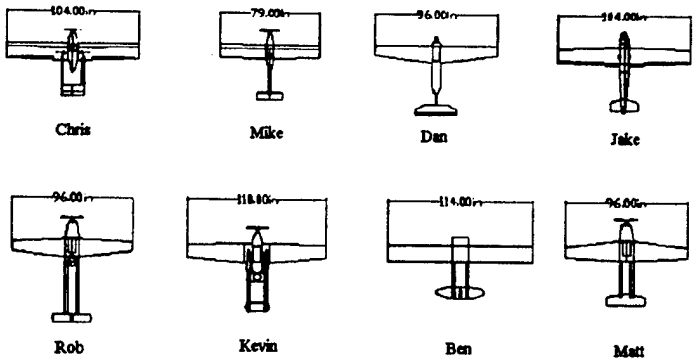

RAC		DBF Score	
Rob	12.5	Jake	7.1
Jake	13	Dan	7.1
Dan	13	Kevin	6.8
Mike	13.3	Rob	6.6
Ben	13.3	Ben	6
Chris	13.3	Chris	5.9
Kevin	13.7	Matt	5.8
Matt	13.8	Mike	5.3

Figure 3-2 Individual conceptual designs and rankings.

As evident from the individual conceptual design CAD drawings, twin tails booms were common to five of the eight designs. Wing area was fairly constant between individual conceptual designs at 8 ft^2. Each design also utilized one engine. Most designs favored fixed tricycle landing gear while others favored retractable landing gear. The next step in the process determined which designs performed well along with the feasibility of each design. Individual conceptual designs that scored high were more closely studied for incorporation into the team design. With these results in hand, a design for the Yeager Chasers Team began.

3.4 *Alternate Configurations Considered*

Before developing the team's conceptual design, a range of alternate configurations was considered. Although the individual team members already developed eight conceptual designs, some configurations appeared in multiple designs and others were overlooked all together. The team wanted to ensure that these additional configurations were examined in more detail along with the individual conceptual designs. Additionally, the best design would most likely represent a combination of components from the eight individual designs and alternate configurations. To facilitate this decision making process, the variations in fuselage, tail, wing position, and motor placement from the original eight conceptual designs

along with additional configurations the team wanted to explore were placed in decision matrices for review.

Decision matrices were the visual representation of the design team's thought process. They were used to make decisions on mission selection, performance characteristics, construction techniques and various other design parameters. Decision matrices were based on figures of merit (FOMs). FOMs were all the key factors necessary for consideration in making decisions. In the decision matrix, each FOM was given a weighting factor. The weighting factors were percents, which represent the significance attributed to each FOM. The weighting of the FOMs was based on theoretical data, experimentation, or the subjective thoughts of the group. For example, flyability of an aircraft for a pilot was not easily calculated, therefore that part of the decision matrix was more subjective than wind tunnel drag data. Once the FOMs and weighting factors were established, each configuration in the decision matrices was rated against each of the FOMs on a scale of negative two (least desired) to positive two (most desired). The highlighted columns represented configurations advancing to next stage of the design process. In decision matrices with close scores, both were highlighted for further review. These were then tested and resolved into a single selection during the preliminary design phase.

3.4.1 Fuselage Shape

The fuselage shape was a key feature of the design. Major design considerations such as the storage box, the payload integration, and room for internal systems drove the design. The fuselage configuration was evaluated based on the following FOMs:

Aerodynamics: Aerodynamics represented the effects of fuselage drag and in the case of a lifting body any beneficial lift produced by the fuselage. This was given the highest weighting factor for two reasons. Traditionally the fuselage is the most significant contribution to aircraft drag. Drag directly affects the speed of the aircraft and flight time. Although the fuselage design is usually mission driven, any lift that can be obtained from it will aid in the wing design.

Assembly: Assembly represented how easily the configuration leant itself to fitting in the box and how quickly it could be assembled at the competition. Since assembly time factored directly into the DBF score, it was given the second highest weighting.

Weight: Weight is simply how much the proposed fuselage configuration will weigh in comparison to other configurations. This was based on the size and supporting structure required by each configuration. Weight is a significant factor in RAC and will also influence the size of the power plant.

Construction: Construction represented the ease in which the proposed configuration could be constructed. Complicated design features would most require more time to design and build. However, since the team felt these complications could be solved if necessary, construction was given a small weighting factor.

From the individual conceptual designs, three distinct fuselage configurations emerged. It was assumed that tail sizing would dictate the length of the fuselage, resulting in similar RAC contributions of each configuration. Based on the FOMs above, the team evaluated the following three fuselage configurations:

Full-Length: The full-length fuselage would be the simplest configuration to construct. However, this design would seriously hamper quick assembly at the competition.

Slender Body with Tail Booms: This configuration consisted of a small fuselage body, containing the payload, batteries, and other aircraft systems with a single or twin tail booms extending to the aircraft's tail surfaces. The use of tail booms would greatly aid in the assembly time and reduce the overall weight of the aircraft.

Lifting Body with Tail Booms: In this configuration a lifting body replaces the slender body. The lifting body would produce an added lift benefit, but would be more difficult to construct.

The results of the team assessment are presented in Figure 3-3.

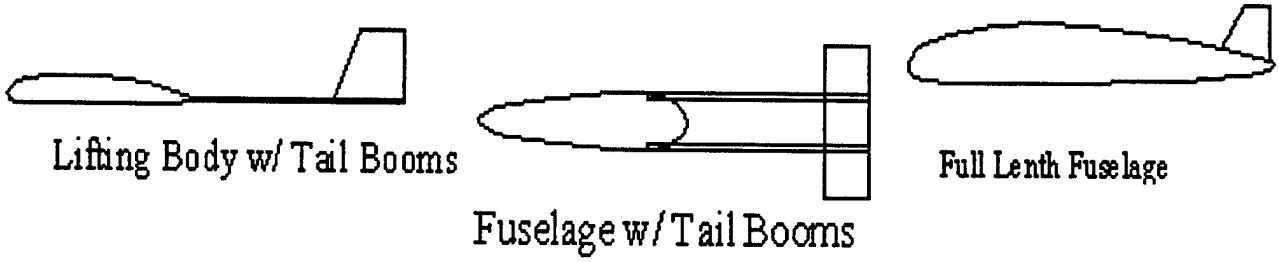

FIGURES OF MERIT	Weighting Factor	Full Length Fuselage	Slender Body/Tail Booms	Lifting Body/Tail Booms
Aerodynamics	0.5	-1	1	2
Assembly	0.2	-2	2	2
Weight	0.2	-1	2	0
Construction	0.1	2	1	-2
Score		-0.9	1.4	1.2

Figure 3-3 Decision matrix for fuselage configuration.

The full-length fuselage was not received well by the team. A single piece full-length fuselage that could fit into the box would be limited to four feet in length, which would restrict the control of the tail surfaces. Therefore, to be a viable competitor, the full-length fuselage would have to be somewhat longer than the four-foot storage box, hindering assembly time. Although, the aerodynamics of the lifting body would be beneficial, the group felt that it would be outweighed by construction and weight issues. For a lifting body, the airfoil section rather than the size and shape of the payload would drive the shape of the fuselage.

This would most likely result in a larger and heavier fuselage than the slender body. As a result, the slender body fuselage with tail booms beat out the lifting body with tail booms configuration, becoming the focus of the team's design.

3.4.2 Tail Configuration

Selecting the appropriate tail configuration was essential for the overall stability and control of the aircraft. To evaluate possible tail concepts, the team used the following FOMs:

Aerodynamics: Aerodynamics was weighted highly, since drag affects flight time and lowers the overall DBF score.

Control Effectiveness: Control effectiveness is unique to the tail evaluation and represents the stability and controllability of the tail configuration. This will have the most significant effect on turn performance and is important in the execution of the 360° turns. Time to turn will factor directly into flight time and DBF score. Control effectiveness was weighted highly because it directly affected the aircraft's ability to sustain controlled flight.

Assembly: Assembly was weighted highly since it is a direct factor in the score equation.

Rated Aircraft Cost: The number of control surfaces is a factor in determining the aircraft's RAC. Since these factors have a small effect on total rated aircraft cost, RAC was not given as much significance as the previous FOMs.

Construction: Since construction does not directly affect DBF score, it was not weighted highly.

The individual conceptual designs yielded configurations consisting of a conventional tail with a single vertical surface, a conventional tail with twin surfaces, and a V-tail. The team also wanted to explore the canard configurations as part of the screening process. The advantages and disadvantages of these configurations are described below:

Conventional Tail: The conventional tail represents a baseline configuration with average drag values and adequate control effectiveness. For the other configurations, RAC was evaluated with respect to the conventional tail.

Twin Tail: The twin tail's main advantage was added control with its two vertical surfaces. However, it paid a penalty in drag and RAC for these additional surfaces.

V-Tail: The inherent RAC bonus for the V-tail in the DBF rules, made it an attractive design component. However, the V-tail's control effectiveness was questionable.

Canard: The canard had the advantage of using positive lift to control upward pitch. However, this configuration posed serious stability and control issues with respect to stalls. No apparent RAC benefit could be seen in using a canard over a conventional tail.

These four tail configurations were evaluated against the FOMs as shown in Figure 3-4.

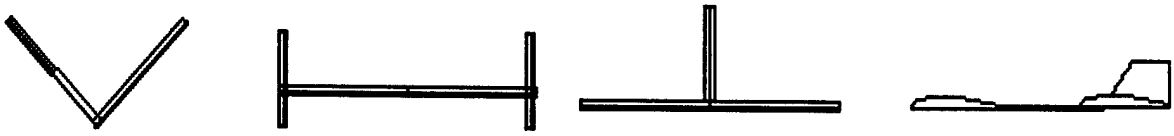

V-tail Twin Tail Conventional Tail Canard Configuration

FIGURES OF MERIT	Weighting Factors	V-Tail	Twin Tail	Conventional	Canard
Aerodynamics	0.3	1	-1	0	2
Control Effectiveness	0.3	-1	2	0	-2
Assembly	0.2	1	1	1	-2
RAC	0.1	2	-2	0	0
Construction	0.1	1	1	0	-1
Score		0.5	0.4	0.2	-0.5

Figure 3-4 Decision matrix for the tail configuration.

The conventional scored close to 0 as expected for a baseline configuration. Although the canard configuration has the potential benefit of increased lift, it is notoriously difficult to fly, as was proven at last year's competition. The twin tail and V-tail came very close in the final score. The V-tail had advantages in reduced drag and lower RAC, but suffered in control effectiveness. On the other hand, the twin tail had the best control effectiveness, but produced more drag and had a higher RAC. In optimizing the DBF score, RAC and drag are important, but these parameters matter little if the aircraft cannot be controlled in flight. At this stage, it was too early to select a final tail configuration without more concrete data.

3.4.3 Motor Configuration

A single engine configuration was selected early on based on the large penalty for multiple engines and props in the RAC. With this in mind, the position of the motor on the aircraft was of substantial importance. Motor position was evaluated with the following FOMs:

Aerodynamics: Aerodynamics represents the motor's effect on airflow over the aircraft and any increased drag it might produce. It was weighted highly as a result of the effect of drag on flight time.

Ground Clearance: Ground clearance represents any interference effects the configuration might present to a large prop. This was given significant weighting since a ground strike in the competition would cause major damage and prevent the aircraft from completing the mission.

Payload Deployment: Payload deployment measures any complications the location of the motor and prop position might have in deploying the 5 lb box. This was given a low weighting since it only applies to mission B and could be solved if necessary.

All of the individual conceptual designs had tractor configurations, but the group wanted to evaluate a pusher configuration as well. As long a single engine was used, both configurations would have identical RACs. The strengths of the two configurations are listed below:

Pusher: The pusher configuration has the advantage of cleaner flow over the fuselage and wing but would complicate the box deployment out of the bottom or back of the aircraft.

Tractor: The tractor exposes the fuselage and wing to the prop wash increasing drag. However, it has better ground clearance and leaves payload deployment options open.

Table 3-1 shows the results of the team's evaluation of the two motor configurations against the FOMs.

FIGURES OF MERIT	Weighting Factors	Pusher	Tractor
Aerodynamics	0.5	2	1
Ground Clearance	0.4	1	2
Payload Deployment	0.1	-2	1
Score		1.6	1.4

Table 3-1 Decision matrix for engine mount location.

The pusher configuration beat out the tractor configuration even with a large penalty in payload deployment. The tractor configuration allows for a more ground clearance, but positions the prop wash directly over the wing and fuselage. The pusher prop would theoretically provide a cleaner, unperturbed flow over the wings and fuselage. Cleaner flow was considered to be most important for mission A flights with the 6-inch cylinder atop the fuselage.

3.4.4 Wing Configuration

The wing position affects many aspects of the design including structures, aerodynamics, and stability. The following FOMs were used to evaluate wing configuration:

Construction: Unlike the other components, construction was weighted highly in the wing placement because the wing-fuselage attachment is an aspect of both rapid assembly and structural integrity. The spar or wing box must transfer the aerodynamic loads of the wings to the fuselage while

withstanding the multiplying effects of g forces. This region will be of even more importance to our design since the wings must be broken at some point to fit in the box.

Stability: Stability was given the next highest weight and is used to recognize that high wings are inherently stable and low wings inherently unstable in roll.

Landing Gear Integration: Gear integration is a measure of how easily landing gear can be installed given the wing placement.

Payload Deployment: Payload deployment was weighted least as it would factor in mission B.

The following wing placement configurations were evaluated against the FOMs:

High Wing: The high wing has the benefits of stability and payload deployment since the wing will be on top of the box. However, landing gear integration would be a problem since gear would most likely be attached somewhere in the wing root area and require a long strut.

Mid Wing: The mid wing represented a compromise on the stability and gear integration issue, but would be the most difficult of the three to construct.

Low Wing: The low wing is inherently less stable in roll, but would be the easies to construct and integrate landing gear. The low wing also presents several structural problems for payload deployment.

Table 3-2 shows the results of wing placement evaluation.

FIGURES OF MERIT	Weighting Factors	High	Mid	Low
Construction	0.4	-1	-2	1
Inherent Stability	0.3	1	0	-1
Gear Integration	0.2	-2	0	2
Payload Deployment	0.1	1	0	-1
Score		-0.2	-0.8	0.4

Table 3-2 Wing Position Decision Matrix.

The ease of construction and integration of landing gear made the low wing configuration the best choice for wing placement. Stability in roll was recognized as a problem, but could be solved by placing dihedral in the wing.

Additional decision matrices were developed for wing dihedral and taper ratio. The amount of dihedral was evaluated with the following FOM's: stability, assembly, and construction. As often seen in model RC aircraft, a slight dihedral was chosen as a compromise. Dihedral exists for stability to aid the pilot in controlling the aircraft. The pilot for this team preferred more control of the aircraft. The addition of slight dihedral provided adequate stability without sacrificing significant control. Therefore a baseline of 3° was chosen. Obviously, the absence of inherent stability could make mistakes unrecoverable. However, the pilot felt this was unlikely. Wing taper was evaluated with the following FOMs: lift distribution, RAC, and

Construction. The team decided that the aerodynamic benefits of taper were outweighed by a straight wing's RAC bonus and ease of construction. The taper ratio of 1.0 or straight wing was ultimately chosen for its simplicity, its historical effectiveness in past competitions, and its wide-spread use in general aviation. Here the RAC benefit was determined to contribute more towards the overall score than small reductions in induced drag. Furthermore, construction would be straightforward, and with the wing would be easily reproducible in the event of damage.

3.4.5 Landing Gear Configuration

The team evaluated two possible landing gear configurations with respect to the following FOMs:

Control: Control represents the ease to which the landing gear tracks on the runway. This was weighted highly since the pilot requires sufficient steering control on the ground to meet the take off requirement of 120 ft. This is especially important in the case of crosswind landings and take-offs.

Weight: Weight was given significance as it affects the take-off performance and RAC.

Retract Integration: This is a measure of how easily retractable landing gear can be integrated with the proposed configuration. At this point of the design phase, the team wanted to leave the retract option open, as it had the potential to greatly decrease flight time.

Payload Deployment: Payload deployment would only be a factor in mission B and was weighted the least as a result.

From the individual conceptual designs two landing gear configurations emerged:

Tricycle: A tricycle configuration has a front nose wheel and the advantage of increased control. However, this comes at the cost of increased weight and added complexity in integrating retractable landing gear.

Tail Dragger: A tail dragger configuration uses a tail wheel too save the weight of an additional strut. The rear wheel of a tail dragger could be steered with the rudder servo, giving a small RAC benefit. To do this, the tail dragger sacrifices control. This configuration could pose a problem for the payload deployment mission.

Table 3-3 shows the results of the landing gear evaluation.

FIGURES OF MERIT	Weighting Factors	Tricycle	Tail Dragger
Control	0.4	2	-1
Weight	0.3	-1	1
Retract Integration	0.2	-1	1
Payload Deployment	0.1	1	-1
Score		0.4	0

Table 3-3 Landing Gear Decision Matrix.

The tricycle landing gear came out ahead primarily as a result of its control benefits. The team felt that the weight and retract integration issues could be addressed if necessary. In addition, the team's pilot felt more comfortable with the tricycle configuration.

4.0 Preliminary Design

At the conclusion of the conceptual design phase, the team had finalized mission selection and screened possible aircraft configurations based on their advantages and disadvantages. Since the preliminary design phase should yield a more specific design, it is important to note that as the design was refined, the need for decision matrices decreased. The subjective decision matrices were replaced with computer models as a means of comparing alternate design approaches. The preliminary design phase made a shift from a reliance on historical data and decision matrices to experimental data and computer analysis as evident in the numerous trade studies and component tests conducted. The careful decisions made earlier on in the conceptual design phase process naturally drove the specific design considerations in the preliminary phase.

4.1 *Methods of Analysis*

In the early stages of the preliminary design phase, a number of different computer programs were used to investigate key design parameters and conduct initial sizing trade studies. These programs were used in conjunction with wind tunnel tests and other experimental trade studies.

DBF Code: The Design/Build/Fly code was written by the team, using the computer programming tool Matlab. This in depth code was developed in several versions and allowed the completion of a design parameter sensitivity study. The code was instrumental in the team's selection of a mission model and RAC optimization efforts.

ECALC: ECALC is a commercially available computer program that predicts electric motor performance for RC aircraft. It was used in sizing trades to select the initial power plant components. It also proved useful in evaluating key design parameters including thrust and cruise velocity.

MFOIL: This computer program is a potential flow analysis tool designed to evaluate 2-D airfoils at low Reynolds numbers. ModelFoil Version 2.0 was used extensively in the wing sizing trade to identify possible airfoils. It allowed design parameters such as lift and drag to be quickly estimated and compared between different airfoils.

Drag Build-Up Program: The team wrote the drag build-up program, using Matlab to estimate the drag polar of the aircraft. The code was designed using a combination of theoretical and experimental data. Theoretical methods were used to estimate the drag on the fuselage, wing, and tail surfaces. In addition, experimental data from the wind tunnel experiments was incorporated to give accurate results for drag on landing gear and drag on the antenna at various speeds. This code aided in the selection of key design components and allowed preliminary estimates of performance.

4.2 *Sensitivity Analysis*

Studies of the Design/Build/Fly rules and regulations and the aircraft's adaptability to those regulations were vital in the optimization of the aircraft. To accomplish this, Version 1.0 of the DBF code was developed to gain a rough perspective on the most influential factors of the total score, namely flight time and rated aircraft cost. This initial version of the code allowed the input of general design parameters such as estimated landing time, takeoff time, deployment time, cruise velocity, mission difficulty factor, assembly time, and RAC. The first version of the DBF code used estimates based on last year's competition for the flight times and RAC. This allowed the program to identify the most heavily weighted components of this year's scoring equation.

4.2.1 Mission Models

Results of Version 1.0 revealed two possible mission models for a winning score: the deployment model, a design for missions A and B, and the performance model, a design for missions A and C. The deployment model has the potential to score high by making use of the two highest difficulty factors. However, mission B, the sensor deployment mission, involves several driving design restrictions such as a fail-safe deployment mechanism (no deployment, no score) and the necessary placement of the box at the plane's center of gravity. These restrictions would most likely result in a slightly heavier and slower aircraft with a higher RAC.

On the other hand, the performance model relies on faster flight times and a lower RAC for its scoring potential. Although the mission difficulty factors put this approach behind at the start, the code showed that a design driven by flight performance and optimized RAC could in the end outscore a design driven by the deployment mission. These results were the reason for seriously considering the performance design over the deployment design.

4.2.2 Predicted Mission Performance

A more accurate model of the aircraft was developed in the second version of the DBF code with more specific design parameters. It was used to model a single design flying the missions for both the performance approach and the deployment approach. This time more specific design parameters such as wingspan, thrust, weight, and stall speed were inputted into the program. The program used basic performance equations such as ground roll, time to turn, and time to climb along with the RAC formula to calculate the effect of these parameters on DBF score. From this code, an important conclusion was observed. The exact same aircraft flying the deployment model would always outscore the performance model, despite the additional take off and landing time for mission B, the only inherent advantage of mission C over mission B. However, the team felt that an aircraft designed for performance could be significantly different than one designed for deployment. Based on this fact, the code was used to gauge the margin of performance and optimization needed for the performance design to outscore the deployment design.

To better observe this margin, the program was used to generate sensitivity curves for predicted mission performance for the two models with respect to specific design parameters. Since the team's goal was to win the DBF competition, final DBF score was used as the measure of mission performance. Figure 4-1shows the mission performance curves for four key design parameters:

RAC: Rated aircraft cost was found to have a significant affect on final score.

Weight: Weight was deemed crucial design parameter as affected flight performance.

Cruise Velocity: Higher cruise velocities were found to substantially decrease flight times for all missions as a result of the 1000 ft straight-aways on the course.

Thrust Available: Thrust available affected take-off times, turn performance, and maximum velocity.

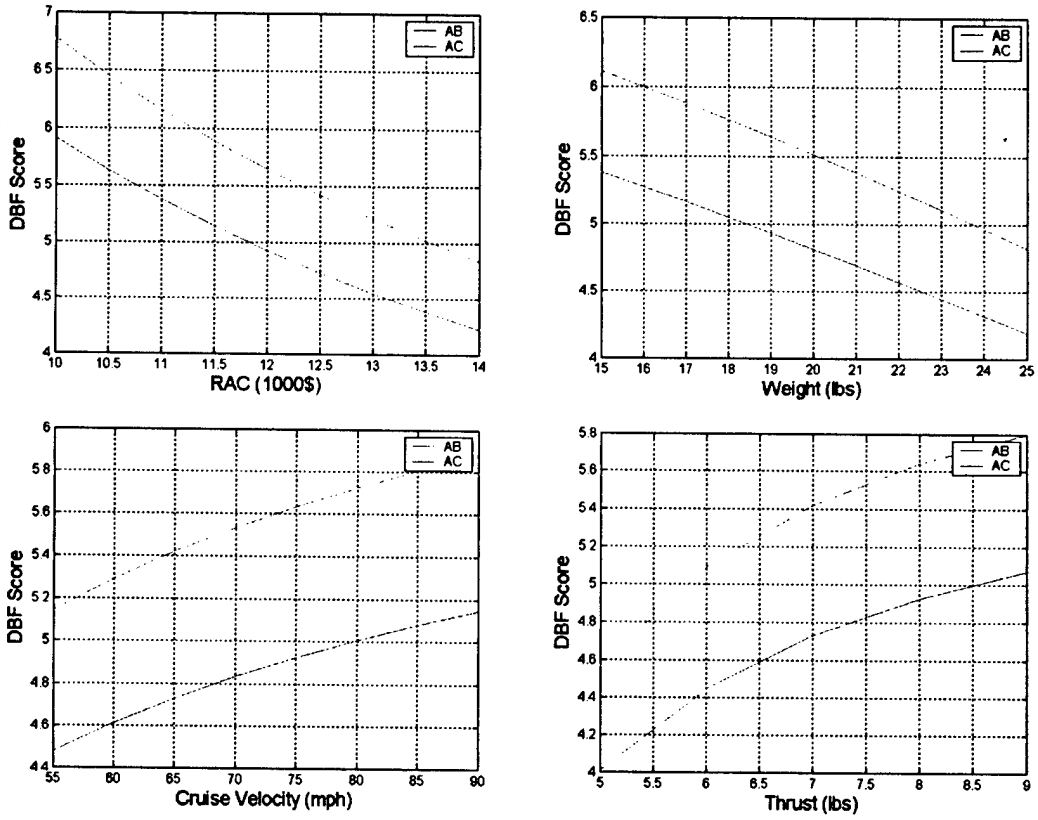

Figure 4-1 Mission performance curves for RAC, weight, cruise velocity, and thrust available.

The weight margin between the two aircraft was the most crucial driver to our design. The weight vs DBF score graph shows the performance design "AC" must weigh at least 5 lbs less than the deployment design "AB" to obtain the same score, holding all other variables constant. Although a 5 lb decrease in weight was unlikely, in combination with other design parameters, the scoring gap rapidly shrunk.

The cruise velocity margin graph showed a large discrepancy in velocity required for the two mission models to achieve the same score. To fly an RC aircraft, on average, 30 mph faster in one mission model

than in the other was recognized as somewhat unrealistic even with the added benefits of a performance design.

As shown in the static thrust sensitivity curve, at low thrusts, the margin between the two mission models was small, but increased dramatically at higher thrusts. However, a static thrust of six to seven pounds on average was predicted and thus the margin, at this point, seemed manageable. While it would be difficult to overcome this thrust margin through a larger or more efficient power plant alone, the performance design had an advantage over the deployment design in the area of drag reduction. With significantly lower drag, the performance design should have more thrust available than the deployment design. This translated into better turn performance, faster take-offs, and a higher top end speed despite similar power plants.

The RAC was the most encouraging with a margin of only 1.5 between the two approaches. Without the constraints of the box deployment mission, the performance approach could be more aggressively optimized with respect to RAC.

Based on the results of this sensitivity study, the performance design was deemed to have a great potential for a winning score. The DBF Code was then used to determine how much better an entry designed for the performance model would need to perform. To illustrate this, the program was altered to calculate single DBF scores based on the key design parameters for an estimated baseline deployment design flying Missions A and B and a goal performance design flying Missions A and C. Thus, Table 4-1 accounts for the discrepancy in mission factors between the two approaches, the advantages in drag, speed, and RAC of the performance model, while holding all other parameters constant (including written report, and assembly time).

	Baseline Deployment Model (Flying Missions A and B)	Goal Performance Model (Flying Missions A and C)
Weight (lb)	22	18
Cruise Velocity (mph)	60	70
Static Thrust (lb)	6.5	7.5
RAC	12	11
DBF Scores	5.4	5.8

Table 4-1 Performance design goals.

The performance model could potentially overcome the deployment model's difficulty factor, through higher cruise velocity and smaller RAC. Furthermore, by eliminating the complexity of a successful payload deployment, the danger of a center of gravity dilemma, as well as an extra take-off and landing, were eliminated. From a competitive design standpoint, it was felt that it would be more effective to eliminate these unknowns and optimize the design for flight. Obviously, focusing on different missions

causes significant design changes that are not easily measured, but the DBF code provided a good starting point. It illustrated that changes in all areas were necessary to outperform a design configured for the deployment model. This proved to be a highly insightful exercise in the ability of design optimization to yield a winning score.

4.2.3 Final DBF Code

In an effort to further optimize the aircraft design a more detailed sensitivity analysis tool was required for sizing trades. This was developed using the same DBF code from the former analysis, adjusted to evaluate a single performance design aircraft. This final version of the DBF code focused on the effect that specific design parameters had on aircraft performance as it impacts the final DBF score. The written code accepted aircraft specifications, calculated flight performance, and outputted the final score. In this manner, it is possible to see the net effect of a change in any aircraft design parameter. Initially, the DBF code was developed primarily for mission selection and rough performance calculations. However, the final version of the code was improved to include an analysis of key performance parameters such as turn performance and load factor. Turn performance was of particular importance, as nearly 70% of Mission C would be flown in a turn. Maximum load factor was also of great importance as the fabrication phase drew near. The impacts of design changes were evaluated using the code before the design was finalized, saving the team a great deal of time and effort.

4.3 *Rated Aircraft Cost Sizing Trades*

The initial sensitivity study showed that RAC was a significant driving factor in total DBF flight score. Minimizing the RAC was therefore necessary to optimize the aircraft design for the highest total DBF score. Due to the complex nature of this design parameter, a separate sensitivity analysis was conducted for the RAC. Using the DBF code, a sensitivity study for all the design components composing the RAC was performed. Using a standard baseline aircraft configuration, the percent effect of each component of the RAC was determined. From this, the most significant drivers with respect to RAC were identified. Included below in Table 4-2 is a breakdown of the RAC study.

The RAC baseline configuration was chosen to represent a conservative estimate for potential competitors at the competition. Assumptions were made as to wingspan and fuselage length, while systems numbers were referenced from a standard configuration aircraft chosen to be a mono-wing, single engine, conventional tail design. Furthermore, the maximum load of five pounds of batteries was used.

As shown in Table 4-2, for the baseline configuration, the driving factors were battery weight, number of engines, aircraft empty weight, wingspan, and total aircraft length. These driving factors represented 87% of the total RAC. Battery weight alone is over 43% of the Rated Aircraft Cost while aircraft empty weight alone is nearly 12%. Together, battery weight, number of engines, and aircraft weight comprised

almost 70% of the total RAC. For this reason, these weights would be a constant focus in designing the aircraft.

RAC Component	Baseline	% Effect	Goal
Battery Weight (lbs)	5	43.50%	4
# of Engines * Battery Weight	5	14.50%	4
Empty Weight (lb)	15	11.60%	13
Span (ft)	8	9.90%	6
Length (ft)	5	7.70%	4
Servos (#)	6	4.60%	5
Control Surfaces (#)	5	2.30%	4
Vertical Surfaces with contols (#)	1	1.50%	1
Horizontal Surfaces (#)	1	1.50%	1
Maximum Chord (ft)	1	1.20%	1
Engines (#)	1	0.80%	1
Propellor (#)	1	0.80%	1
Vertical Surfaces w/o controls (#)	0	0.00%	0
total RAC	12.94	100.00%	10.56

Table 4-2 RAC components and goal configuration.

Also included in the RAC table is a goal configuration. The goal configuration represented the results of the sizing trade study for each design component with respect to RAC. The group adopted the results of the sizing study as the starting point for all preliminary design work. Each lead was instructed to comply with the goal dimensions and component numbers unless a compelling aerodynamic or structural reason could be made. Any deviation from the RAC goals would require the program manager and SEIT lead's approval. The original goal of this group was to build an aircraft with a RAC of ten. Unfortunately, a RAC of 10 did not look feasible, but 11 seemed like a more realistic goal.

The RAC sensitivity study supported the decision for selecting the performance model. By eliminating extra weight for the deployment mechanism package, center of gravity issues with deployment, and one extra servo, the team believed eliminating Mission B would better optimize the aircraft's RAC.

4.4 *Trade Studies and Component Analysis*

Before a final configuration was locked down, a number of trade studies were performed on possible design components. The original design matrices provided a foundation for the investigation of

competing design ideas. However, the decision matrices were too subjective in nature to rely solely on for the final design. More concrete information was needed to substantiate and access the feasibility of the proposed design configuration. These tests provided a wealth of experimental data to support decisions throughout the preliminary design process. The trade studies directly affected the team's choices with respect to propulsion, structures, and aerodynamics.

4.4.1 Initial Propulsion Trade Study / ECALC Validation

The initial testing for the propulsion system was implemented in order to validate the accuracy of ECALC. Program inputs included battery size and weight, prop pitch and diameter, motor make and size, and results included thrust available and thrust required curves along with predicted duration and wattage. Since actual propeller pitches sometimes do not agree with printed specifications, the results of this experiment also calibrated the tested props.

For this open-loop experiment, different candidates of motor, gearbox, and prop combinations were tested as shown in Figure 4-2. Both the Astro-40 and Astro-60 electric motors were tested in the wind tunnel with different pitch and diameter propellers at wind tunnel velocities from 0 to 60 mph. From the experimental data, propulsive system efficiency curves along with thrust available curves were generated. These results were used as the basis with which to compare ECALC's results. Figure 4-2 shows static thrust and propulsive efficiency curves from the tests. As expected, larger props produced more thrust, but drew more current. Additionally, higher pitched props reached their max efficiency at higher advance ratios, signifying a higher available cruise speed.

A small disparity was immediately identified between ECALC and the wind tunnel results. To calibrate the program, efficiency values were adjusted to match the test results. This efficiency corrections account for losses associated with transferring rotational power to thrust along with losses associated with transferring electrical power to mechanical power in the motor.

After ECALC was calibrated for both motors, it agreed closely with the experimental results. The adjusted efficiency value for ECALC was consistent enough to model the 60-size motor, which was the most likely size of motor for this aircraft. However, this corrected value only validated 2-bladed propellers. The 3-bladed propeller, a possible option for reducing propeller diameter at this point, would need to be tested experimentally if it were to be employed. In conclusion, ECALC was verified as a useful tool for comparison purposes and initial power plant selection. However, after a final motor, gearbox, and propeller were selected, wind tunnel tests would be required to obtain accurate thrust data for final performance estimates.

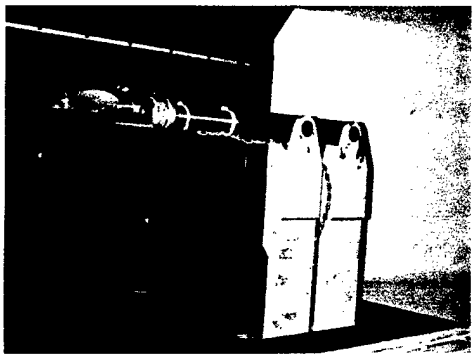

Motor	Gear Ratio	Propeller Size
Astro 40	1.63:1	12 X 8
Astro 40	1.63:1	12 X 10
Astro 40	1.63:1	13 x 10
Astro 60	2.73:1	22 x 12
Astro 60	2.73:1	22 x 10
Astro 60	2.73:1	20 x 12

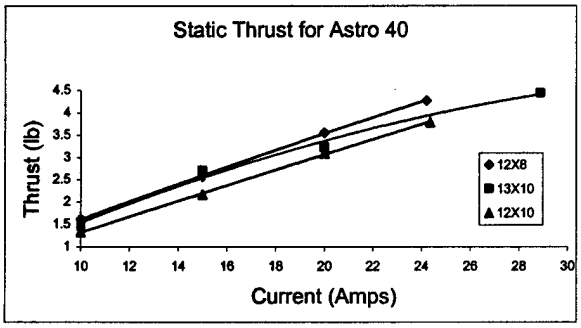

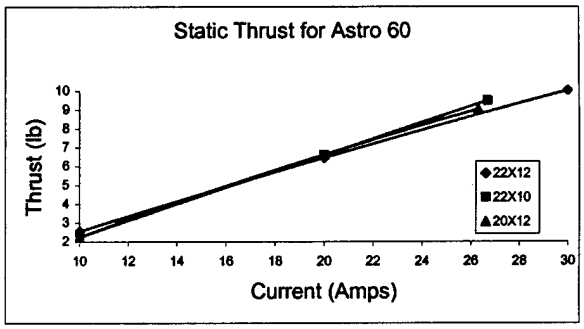

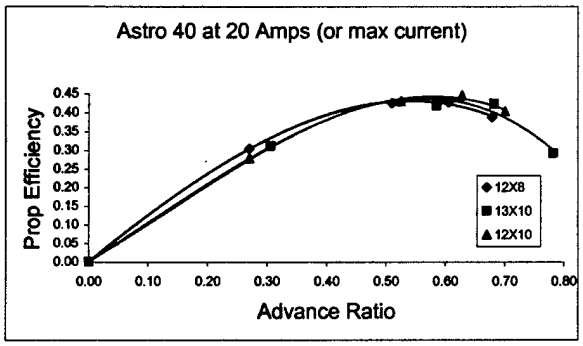

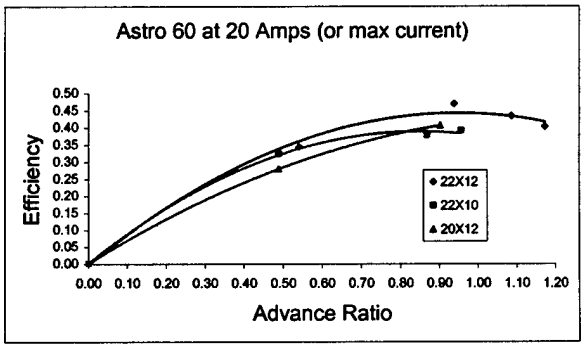

Figure 4-2 Wind tunnel setup, test matrix, static thrust, and propulsive efficiency curves from initial propulsion testing.

4.4.2 Composite Wing Spar Trade Study

Three factors drove the structural design of the wing. They were the wing strength, stiffness, and weight. Strength was most easily quantified by the maximum load factor the aircraft must survive. Stiffness represented the allowable degree of deflection allowed while still maintaining stability and control. Requirements for both of these design parameters were easily achieved, but the design tradeoff came when minimizing weight.

From a construction standpoint, Polystyrene foam was one of the easiest and most available core materials to work with. It could be cut using a hotwire technique, allowing the quick production of multiple

airfoils. Polystyrene by itself was an inadequate core. In efforts to find the best structural design for the wing spar, the team created a matrix of sixteen potential wing-spar lay-ups. Each of the sixteen test beams was a variation of the standard lay-up shown below in Figure 4-3. From the standard lay-up, variations in the orientation of the fiberglass, number of carbon tows, and thickness of the foam core were explored. Each of the two inch wide by 20 inch long samples were destructively tested using the composite test setup show in Figure 4-3.

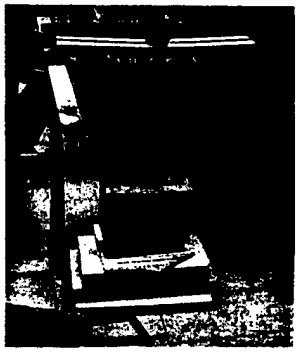

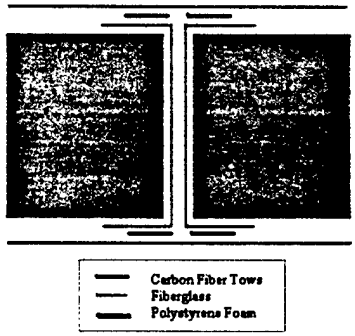

Description	Weight (lb)	δ at 40 lb (in)	Fail Load (lb)	Sp Stiffness (in/lb)	Rank	Sp Strength (lb/lb)	Rank
SL Thick core	0.267	0.098	176	0.37	1	658.13	1
Carbon Layup	0.213	0.119	140	0.56	3	656.11	2
SL 100% more compression carbon	0.176	0.194	111	1.1	8	629.96	3
SL 50% more compression carbon	0.173	0.213	91	1.23	10	526.87	4
SL 2 stringers	0.225	0.186	96	0.83	4	427.38	5
SL Divinicell stringer	0.176	0.244	73	1.39	12	415.29	6
Uni-glass layup +/- 45 degrees on comp	0.228	0.197	91	0.87	5	399.82	7
SL 1/8" balsa stringer	0.164	0.215	65	1.31	11	396.91	8
Thick foam no stringer 100% more carbon	0.178	0.166	70	0.93	6	392.65	9
SL	0.176	0.204	65	1.16	9	368.71	10
SL w/ 2 oz glass @ +/- 45 degrees	0.176	0.25	61	1.42	13	346.06	11
Uni-glass layup	0.236	0.13	71	0.55	2	300.62	12
SL 50% less carbon	0.154	~.34	40	~2.20	14	259.04	13
SL Thick core no stringer	0.177	0.178	45	1.01	7	254.85	14
SL no stringer	0.121	-	~27	-	-	~223.77	15
SL?? 1/8" End grain balsa	0.147	-	~30	-	-	~204.62	16

Figure 4-3 Composite wing spar strength test setup, standard lay-up (SL), and ranked test results.

The samples without stringers performed below the group of beams with stringers. The no-stringer-beams almost always failed due to skin buckling on the compression side. If it resisted the buckling, the skin delaminated from the foam. It was discovered that putting strips of unidirectional carbon on the compression side added the most strength without significantly adding weight. Increasing the thickness of the beam greatly increased the strength. By increasing the thickness by 50% the strength was increased 200% to 300%. However, this added strength came at a high cost of weight gain. The Polystyrene, though seemingly light, added weight quickly with volume. A way to reduce weight was

demonstrated in last year's designs by cutting out excess foam and laminating the wing with mono-coat wing covering.

4.4.3 Wing Attachment Technique Trade Study

In an attempt to find an attachment method for the wing, the team considered using carbon fiber tubes at the quarter chord point to form a spar. At the joining portion of the wing a carbon fiber tube was sandwiched four inches deep into the wing and protruded four inches as shown in Figure 4-4a. The protruding portion of the tube will fit into a sleeve mounted on the fuselage. The carbon rod will then be able to transfer the load from the wing to the fuselage.

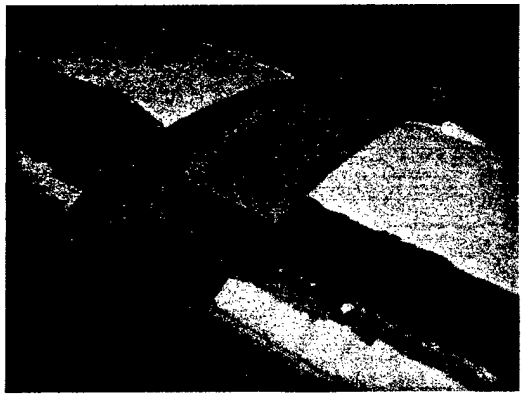

(a)

(b)

(c)

Figure 4-4 Wing attachments(a), Moment arm test setup(b), and Carbon fiber tubes after failure(c).

Two sections of composite carbon fiber tube were purchased from MacLean Quality Composites. The first tube had an outer diameter of 0.82 in, an inner diameter of 0.75 in, a thickness of 0.035 in, and weighed 0.058 lbs per foot. The second sample tested had an outer diameter of 0.745 in, an inner diameter of 0.680 in, a thickness of 0.033 in, and weighed 0.049 lbs per foot. Since the company did not provide any strength data on the tubes it was necessary to test a sample as shown in Figure 4-4b.

With initial estimates of the aircraft weight and wing design, the root moment of the aircraft could be calculated using the Glauert A_n method. This method takes into account many variables of the wing design to model the lift distribution. With an 18 lb aircraft the root bending moment was found to be 172 in-lbs at steady level flight, based on a wingspan of almost seven feet. Initial performance estimates established that the maximum instantaneous load factor the aircraft was likely to encounter would be between 4 and 5 g's. To ensure an adequate factor of safety, it was decided that the aircraft should be designed to structurally withstand loading up to 5.5 g's. In a 5.5 g turn the bending moment would be 946 in-lbs, which was used as a minimum strength requirement for the carbon rod.

A four-inch length of smaller diameter tube was inserted four inches deep into a sleeve, and weight was added 25 inches from the sleeve in five pound increments, to test the sample tubes. The small tube ultimately failed at 750 in-lbs. This was short of the design goal of the aircraft. The larger diameter tube was tested next in the same manner, except this time a 36-inch moment arm was used. It failed at 960 in-lbs, marginally meeting the design goal. For a final test the small rod was glued inside the larger rod, and as before a bending moment was added. By joining the two, the tube failed at 1980 in-lbs. This greatly exceeded the required strength.

4.4.4 Airfoil Trade Study

The initial sizing trade performed with MFOIL produced the Eppler 67 and the NACA 4412 as possible wing airfoil sections. The Eppler 67 was proposed as a low drag wing section that would support higher speeds and still provide sufficient lift to fulfill the mission profile, as compared to the NACA 4412, the baseline airfoil used by last year's USNA teams. Therefore, in order to test the relative benefit of using an Eppler 67 section for the aircraft, a 2-D wing was built out of foam and fiberglass for testing in the Naval Academy's Eiffel Wind tunnel alongside the NACA 4412 airfoil (Figure 4-5). The underclass team members conducted wind tunnel tests for both wings at speeds ranging from 20 to 70 miles per hour.

Figure 4-5 compares the lift curves and drag polars for the two airfoils. It is important to note that the 4412 outperformed the Eppler airfoil in lift throughout the range of angles of attack. The data shown in Figure 4-5 was taken at 50 mph, slightly lower than the intended cruising speed of our aircraft. However, similar results were obtained throughout the range of test velocities. The performance of the Eppler in the stall region was not as bad as we expected, but the overall performance of the airfoil failed to measure up to the 4412.

Although the drag polars for the two aircraft were comparable, the stall region of the 4412 appeared to have less drag. Additionally, at higher speeds (60 and 70 mph) the drag polars separated further, with the 4412 having less drag across the board. Based on these tests, it was decided that the 4412 would serve the team better than the Eppler 67 section.

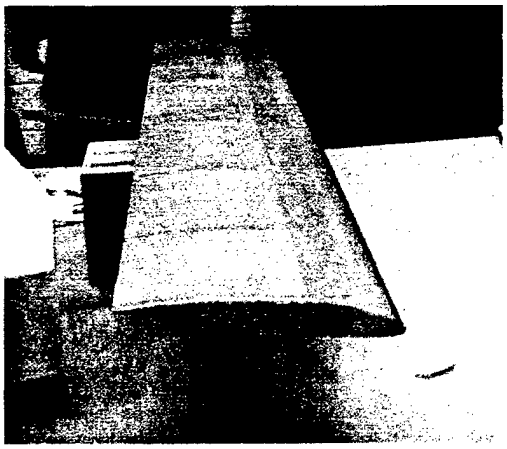

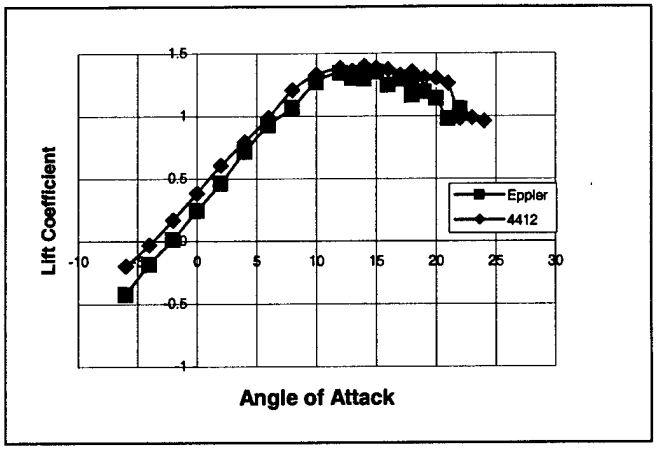

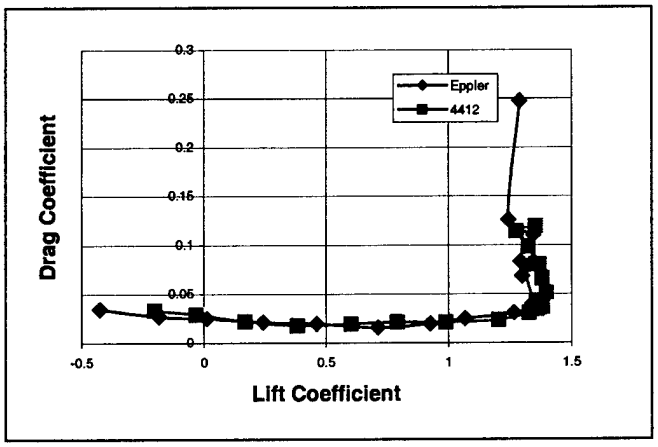

Figure 4-5 Foam and fiberglass Eppler 67 airfoil, lift curves, and drag polars at 50 mph.

4.4.5 Aerodynamic Analysis of the Antenna

A cylinder-mounted perpendicular to an air stream causes enormous amounts of drag proportional to its size. Since the team selected Mission A with the cylindrical antenna due to the high point multiplier, it seemed prudent to examine the drag behavior of the cylinder and potential drag reduction techniques.

There is a certain Reynolds number at which the drag coefficient of a cylinder drops dramatically. According to experimental data in Horner's *Fluid Dynamic Drag*, the cylinder's drag coefficient is estimated to be 1.2 at sub critical Reynolds numbers. At supercritical Reynolds numbers, the drag coefficient could drop to as low as 0.3. The critical Reynolds number at which this is expected to occur has been shown to be between 200,000 and 400,000. For a six-inch diameter cylinder this translated to velocities between 63 and 125 miles per hour. The higher value was clearly unattainable, but the lower value was within the predicted speed of the team's aircraft.

The flow about a cylinder at sub critical Reynolds numbers is characterized by aerodynamic turbulence known as a "vortex street." The rotational motion in this vortex street causes the momentum loss that is

responsible for the excessive drag on a cylinder at a sub critical Reynolds number. Since the rotation of this vortex street causes so much drag, controlling the rotation may result in reduced drag.

The team researched various methods for managing the vortex street while keeping the contest rules in mind. The cylinder cannot be fared in any way, but the vertical tail of the aircraft does not count as a faring. From Horner's *Fluid Dynamic Drag,* it was found that the drag on a cylinder could be reduced using a splitter plate placed downstream of the cylinder. If the vertical tail were to be used as a splitter plate, some drag reduction might be accomplished. The contest rules state that the cylinder must be separated from the rest of the aircraft by three inches, so this limited the distance between the cylinder and the tail splitter plate. By testing the splitter plate at various positions relative to the cylinder, a relationship could be established, allowing the team to decide on the appropriate placement of the vertical tail on the aircraft.

In order to test the drag characteristics of the antenna an apparatus was built to extend the sting balance in the Naval Academy's Eiffel Tunnel. On this extension was mounted an antenna built to the specifications required by the contest rules. Behind this was mounted a splitter plate modeled as a vertical stabilizer. The underclass team members conducted tests without the splitter plate in order to find the critical Reynolds number of the cylinder and with it at distances ranging from 3" to 15" behind the antenna to get a complete picture of splitter plate effectiveness as a function of position. Figure 4-6 shows the set-up for this study in the USNA Eiffel Wind Tunnel.

The results of this experiment were mixed. The splitter plate was shown to have negligible effectiveness as shown in the C_{D0} plot in Figure 4-6, while the velocity at which the flow about the cylinder went turbulent was lower than theoretically predicted. However, the supercritical drag coefficient was not as low as was hoped.

The ineffectiveness of the splitter plate was of particular importance. Had the splitter plate worked, the team would have used a conventional tail with a single vertical stabilizer and placed the antenna near the rudder. This would have caused several design complications, including the stability and control concerns of having disturbed flow over the rudder, mounting issues with regards to the tail boom, and center of gravity problems because of the aft location of the antenna weight. Since the splitter plate was ineffective, the team was able to place the antenna further forward, easing the anticipated control and center of gravity problems. In addition, the test results clearly showed the effects of supercritical flow and a significant drop in drag at velocities greater than 50 mph

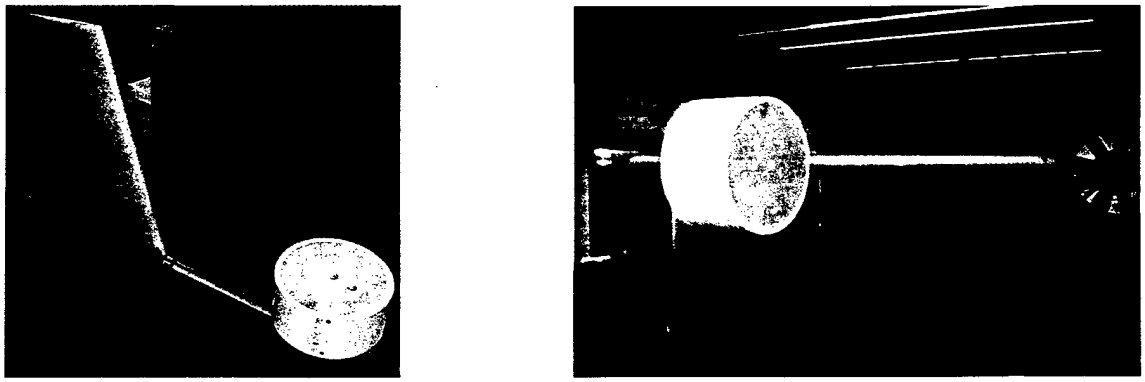

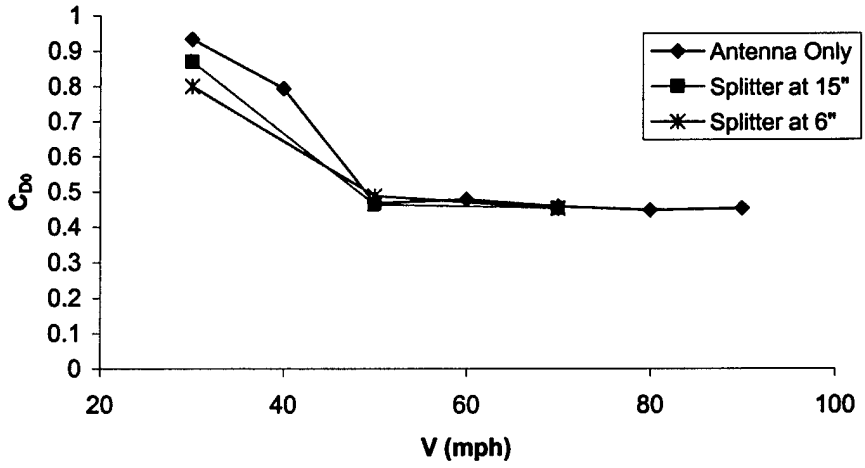

Figure 4-6 Experimental setup and results for antenna splitter plate study.

4.4.6 Landing Gear Trade Study

Since the team's design approach was counting on significant drag reduction, the feasibility of retractable landing gear was explored. However, because of the added complexity and weight of the retracting system, a clear benefit from the system had to be shown to secure its place in the design. To this end, an experiment was performed in the U. S. Naval Academy's recirculating wind tunnel on a variety of landing gear arrangements. Three different wheel shapes and sizes (Figure 4-7a) were first tested by attaching them without fairing to the outboard sides of a simple fiberglass hoop (Figure 4-7b). Two kinds of wheel pants were then added and tested to measure their effect on drag. The first set of pants was attached to the outboard sides of the hoop, while the second was attached by fitting the pants and wheels onto the end of the hoop (Figure 4-7c). A commercially built nose gear assembly designed for a 25 lb. plane was also tested to measure its drag contribution (Figure 4-7d). Furthermore, Figure 4-7shows the experiment results for each configuration tested. This chart shows the contribution to the minimum drag coefficient based on an 8 ft wing reference area.

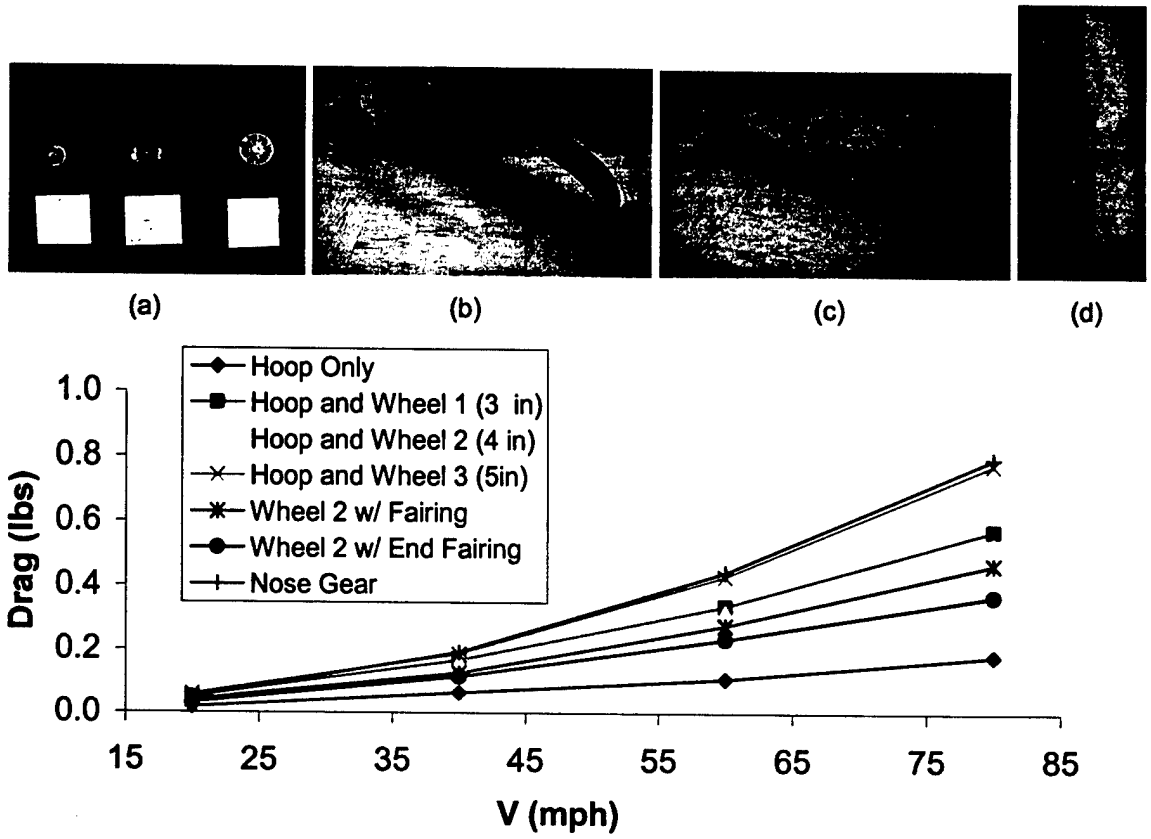

Figure 4-7 Landing gear components tested and wind tunnel drag results.

As expected, the lager wheels produced more drag, while the fairings reduced drag. The end fairing produced the most drag reduction and was the most likely choice of fixed landing gear. However, the commercially available nose gear was obviously not designed with drag in mind. These tests served to show that retractable landing gear is a very attractive option. Further analysis conducted as a part of the drag buildup would confirm the necessity of retractable gear.

4.5 *Aerodynamics Preliminary Design*

4.5.1 Wing Design

The wing design chosen for the aircraft was quite simple. Based on work from the conceptual design phase and wind tunnel tests, it was decided to use an untapered NACA 4412 wing as the baseline configuration at this phase of the design. The dimensions established for the wing were as follows:

Area:	6 ft^2
Taper Ratio:	1
Wing Loading	3 lb/ft^2
C_{Lmax}	1.5
Stall	13°
Flaps	20 % flaperons
Flaps Deflection	15°

Table 4-3 Preliminary wing specifications.

The decision to use a NACA 4412 section was made based on the proven nature of the airfoil, wind tunnel tests that illustrated its gentle stall characteristics, and its performance against the Eppler 67 with respect to drag. RAC was the driving factor in the decision to use an untapered wing. In order to taper the wing, the root chord along with the wing span must be increased to obtain the same area, incurring a double RAC penalty. It was decided that the efficiency benefit of taper was less than the RAC benefit of an untapered wing. The wing area was selected to provide an appropriate wing loading for takeoff roll, stall speed, and turn radius. The predicted maximum coefficient of lift was calculated using MFOIL. Since this program is based on a 2-D analysis, corrections were made to obtain an estimate for the maximum lift for the 3-D wing. Flaperons were added to increase lift for take-offs and drag during landing.

4.5.2 Drag Buildup

Since the team intended to build an aircraft that would optimize the flight time to overcome a mission score multiplier deficiency, estimates of the drag polar were essential. In particular, an examination of the effect of the antenna on drag, as well as an assessment of retractable landing gear as an effective drag-reduction mechanism was required.

To accomplish this, the team developed and used the drag build-up program. Based on preliminary design dimensions, the drag polar for our aircraft with retracted landing gear and without the antenna was estimated to be: $C_D = 0.021 + .05*C_L^2$.

Required coefficients of lift for speeds ranging from 20 to 100 mph were calculated and used to create Figure 4-8, which predicts the drag for four potential configurations.

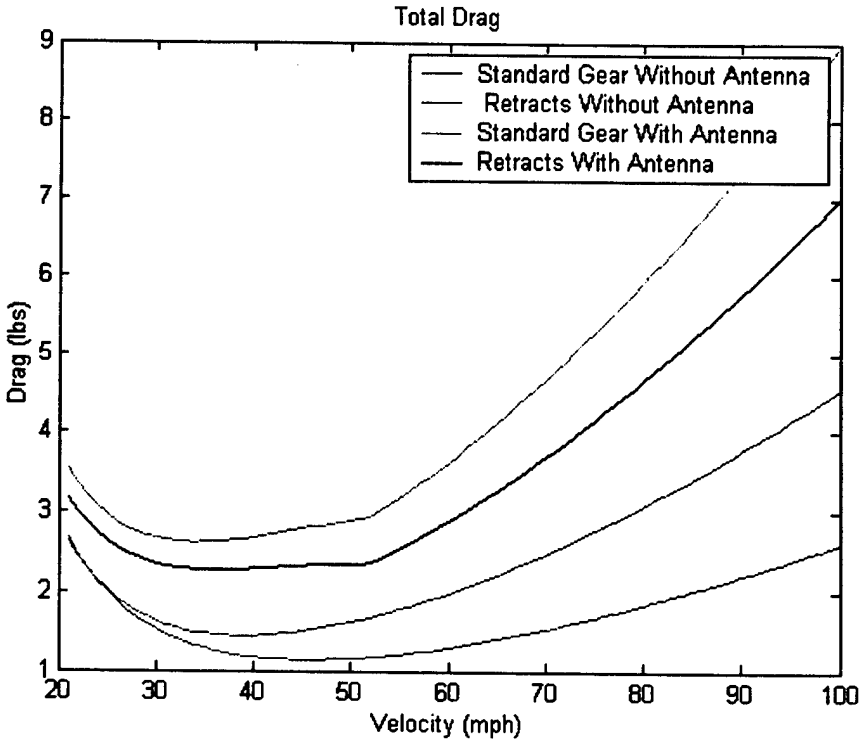

Figure 4-8 Drag comparisons for alternate configurations and missions.

This plot clearly demonstrates the benefit of retractable landing gear, and gave the team a good idea of the impact of flying with the antenna. Using this estimation, a more accurate score estimate was made, and the motor/propeller combination optimized.

4.6 *Propulsion Preliminary Design*

4.6.1 Selection of Power Plant Components

The power plant chosen for the aircraft was an Astro-60 sized motor. It was determined that the Astro-40 size motors could not output the power and thrust needed for a 20-pound plane to stay airborne, for the duration of the competition. An Astro 90 motor would output more than enough power but was almost a half-pound heavier than the 60. The Astro 60 represented a compromise between performance and weight for the baseline aircraft design. Using the 60-sized motor would also reduce any tendency to overheat, which could be a factor in long endurance runs.

The two Astro 60 motor configurations available for consideration were the direct drive setup or gearbox configuration. The gearbox configuration allowed the motor to spin a larger propeller producing more static thrust. This might be necessary for the required take off distance of 120 feet. Additionally, the higher thrust would help climb performance, but losses in the gearbox would sacrifice higher top speeds.

An appropriate propeller selection was considered vital to the completion of the course with enough power left over for contingency.

The computer program ECALC was used extensively in the selection of the power plant. A 14 X 11 propeller with the Astro 60 size motor in direct drive was identified to provide higher speed capabilities as well as adequate thrust during turns. Bassed on estimates from ECALC, this combination would require 28 RC-2400 batteries and produce 7.5 lbs of static thrust. With only 28 of these batteries used, the final weight of the power source was 3.93 lbs. This combination substantially decreased the overall RAC and increased the aircraft's final predicted DBF score by over a point.

4.6.2 Predicted Propulsion Performance

The required endurance and power with respect to the mission requirements and the anticipated aircraft drag were analyzed to confirm that the selected power plant would successfully finish each mission. Using ECALC, thrust available was plotted against the expected drag polar in Figure 4-9.

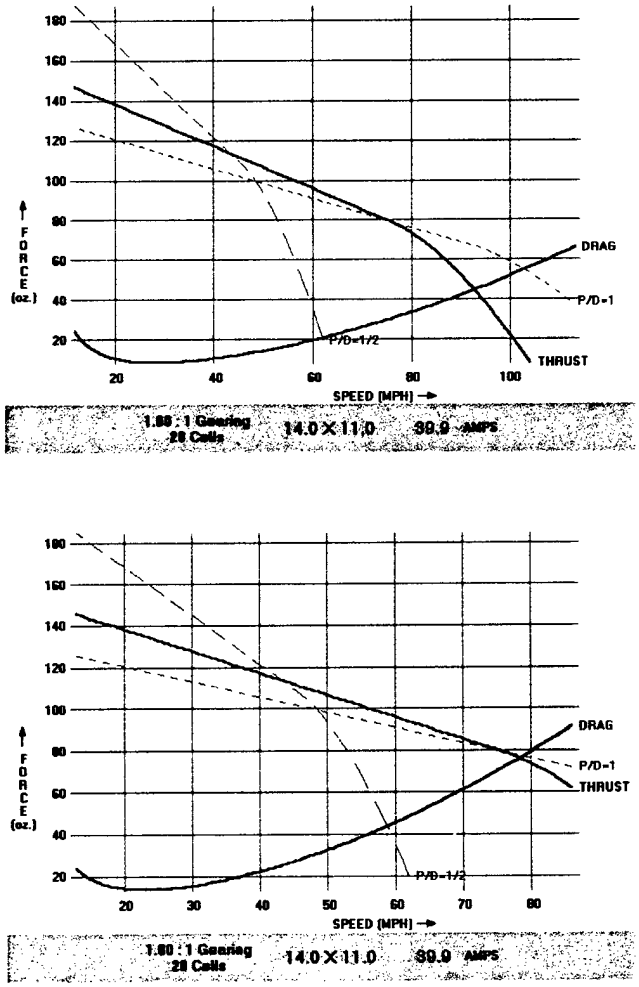

Figure 4-9 Thrust vs. Drag (Mission C) above, and (Mission A) below.

The top portion of Figure 4-9 displays the results for Mission C without the antenna while the bottom portion of Figure 4-9 displays the results for Mission A with the antenna for the selected power plant. The difference between the two is the added weight of the antenna and its increased drag as calculated in the drag build-up. ECALC calculated the endurance time for this configuration as 5.3 minutes at cruise speed (72mph) and 3.4 minutes at full power going an estimated 82 mph. This should be more than enough time to complete 4 laps of the course. Although the earlier trade study showed ECALC provided valid results, the final power plant would be tested in the wind tunnel for both endurance and thrust. This ensured the needed thrust and endurance requirements were met and provided a set of accurate thrust available and propulsive efficiency curves for performance predictions.

4.7 *Preliminary Stability and Control Characteristics*

An analysis of the stability and control parameters of the aircraft was performed to establish the required control surface sizing. Weight estimates and center of gravity analysis were first conducted to verify that a longitudinally stable aircraft was feasible with the preliminary design arrangement. Based on this, preliminary tail sizes were also determined to feedback into the initial balance and drag calculations. Once the design was finalized with set dimensions, a full stability analysis was conducted on the aircraft to predict the final flying qualities and performance.

4.7.1 Weight Estimate and Center of Gravity Calculation

An initial weight estimate of the aircraft was made by weighing the its known components and making estimates for the wings, fuselage, and tail-surfaces. Predictions of the locations of the components were also made for an initial center of gravity (cg) analysis. The initial cg location was deemed to be 0.69 inches behind the datum (the forward bulkhead of the fuselage) and the total weight to be just less than 19 pounds. The vertical cg was then estimated via the same process, for both gear-up and gear-down configurations. The vertical cg was determined to be 2.91 inches above the bottom of the fuselage for gear down, and 3.41 inches above the bottom of the fuselage for the gear-up configuration. In the initial design phase, some concern was expressed about the thrust line of the pusher not being through the vertical cg of the aircraft. However, this analysis allayed those fears.

4.7.2 Tail Sizing

To determine the appropriate dimensions for the tail, Raymer and Anderson were consulted to find historical values for the vertical and horizontal tail volumes. Using predetermined wing dimensions and a set value for the tail boom length based on the box dimensions, the necessary horizontal and vertical tail areas were calculated for the conventional and twin tails. These values were then used to calculate the corresponding dimensions for the desired inverted V-tail configuration.

4.7.3 Conventional Tail

Historical information in Raymer and Anderson indicate that the horizontal tail volume and vertical tail volume should be on the order of 0.7 and 0.04 respectively. The design of the tail was an incessant weighing of the advantages of a short tail and the advantages of a long tail. In the end the constraint was determined to be the size of the transport box. Using the definition of tail volumes and a maximum l_t of 43 inches, the area of the horizontal tail was found to be 1.04 ft^2 and the area of the vertical tail 0.46 ft^2. For twin vertical tails the area would be halved between the two vertical stabilizers.

To convert conventional tail surfaces to a V-tail configuration, the projected area of the V-tail should be equal to the total area of the vertical and horizontal tails combined. However, during the initial tail sizing calculations it was discovered that the projected area of the V-tail would require an increased span. In the RAC rules, a V-tail was counted as a horizontal surface (10 hr) and vertical surface without control (5 hr) for a total of 15 hrs vs. 20 hrs for a conventional tail. However, the horizontal span of the V-tail would be greater than 25% of the wingspan, requiring the horizontal surface to be counted as a "wing" in the RAC calculations. Without this RAC advantage, the team had no reason to keep the V-tail as a design option. As a result, the twin vertical tail design advanced to the detailed design phase.

4.8 *Preliminary Performance Estimates*

At this point, basic performance parameters were calculated for the baseline preliminary design to verify the basic aspects of the aircraft design would meet their objectives. Based on a baseline gross weight without the antenna of 19 pounds, a wing area of 6.5 square feet, static thrust of 7.5 pounds, and a free stream velocity of 70 mph, Table 4-4 lists the key performance results.

Ground Roll (S_g)	78 ft
Stall Velocity (V_{stall})	30 mph
Minimum Turn Radius (R_{min})	26 ft
Maximum Turn Rate (ω_{max})	76°/s

Table 4-4 Preliminary performance calculations.

Per competition rules, the aircraft must have a ground roll no more that 120ft. With flaps the ground roll was found to be 78 ft, well within this mission requirement. The stall speed of the aircraft was critical in predicting the overall performance of the aircraft in the competition. The stall speed determines how tightly the turns can be made and was calculated to be 43.5 feet per second, or 30 miles per hour. Since a large portion of the flights are during the 360° turns on the downwind leg of the course, it is important to determine how quickly and tightly these turns can be made. The minimum turn radius was determined to be 26 ft and a maximum turn rate of 76°/s could be achieved with a 4.75 g or 78 degree

bank turn. However, these represented only the theoretical instantaneous turn radius and rate. Turn radius and rate are limited by thrust available, loading on the aircraft, and the aircraft's stall speed. To develop a more accurate picture of sustained turn performance an energy maneuverability diagram was constructed. In addition, a more careful analysis of turn performance will be conducted during flight testing to establish pilot familiarity with optimal turn procedures.

4.8.1 Energy Maneuverability and Constraint Plot

The energy-maneuverability diagram presented in Figure 4-10 illustrates the turn performance capability of the aircraft. The blue curves are lines of constant load factor. As velocity increases, the turn rate must decrease in order to have the same load factor. Similarly, the green curves represent lines of constant turn radius and as velocity increases turn rate will increase to keep a constant turn rate. The accelerated stall boundary shows the speed at which the aircraft will stall in a turn. For example, in a 2 g-turn the accelerated stall boundary intersects the load line at 37 mph. If the airplane were to slow below this speed it would stall and lose controlled flight. The green turn radius lines can be used to the determine turn rate necessary at a given velocity. For example, to make a 50 mph turn in 200 ft, the turn rate would be 21°/s.

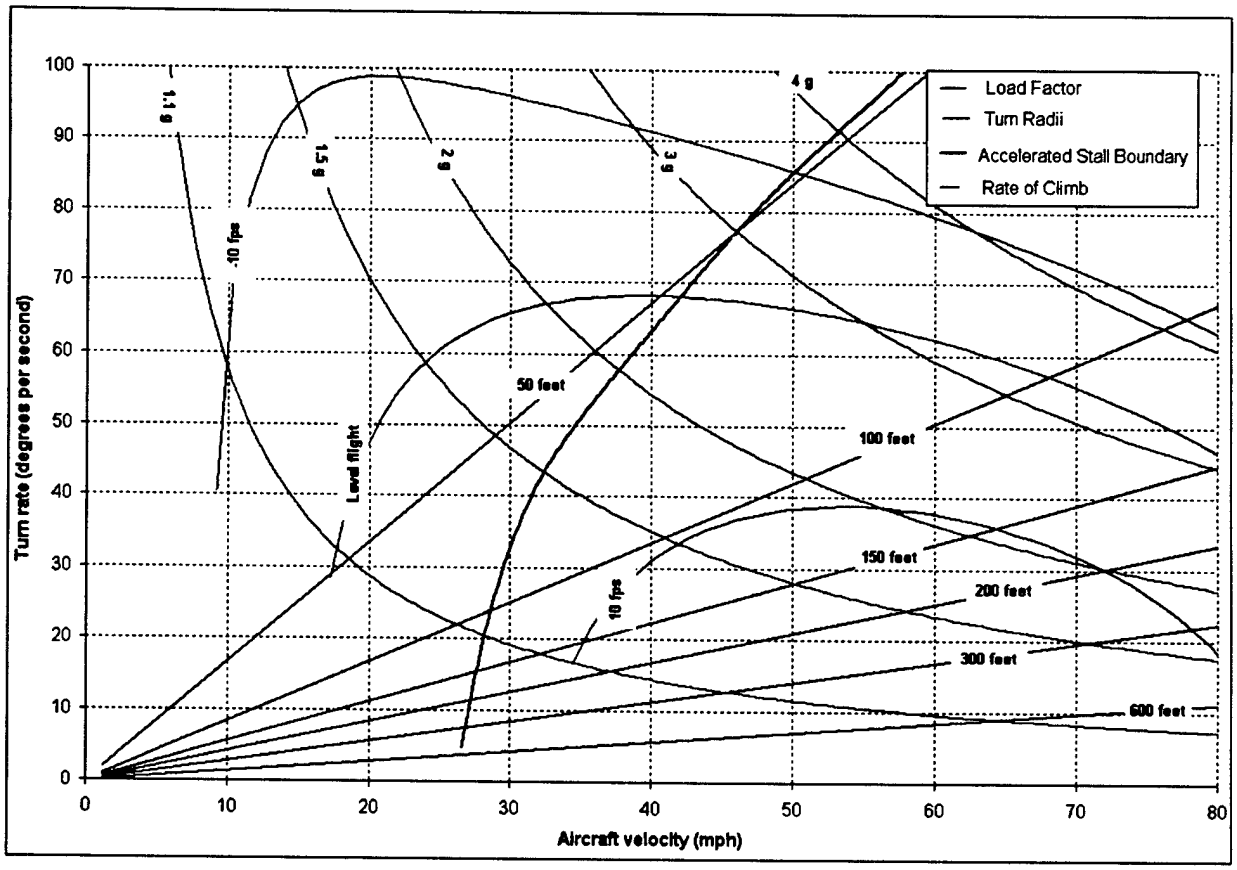

Figure 4-10 Energy Maneuverability Diagram

The three red curves represent the aircraft's vertical speed. This is important to Mission C because it shows the variation in turn rate of the aircraft as it climbs or descends in a turn. To maintain level flight, the maximum turning rate is 67°/s. However, if the aircraft descends at ten feet per second and turns on its stall line, then the turning rate increases to 86°/s. Conversely, if the aircraft must climb in a turn the turning rate dramatically decreases to under 38°/s. Turning rate will dictate time in turn, and for Mission C a large piece of the total flight time. For a 360° turn, the above turning rates correspond to six seconds for level flight, four seconds for descent, and almost ten seconds for climb.

The constraint plot typically comes before an aircraft is designed. The team chose to create one at this stage in the design process as an illustration that aircraft's wing loading and thrust to weight ratio would allow it to meet the performance requirements. The data is shown on the constraint plot in Figure 4-11.

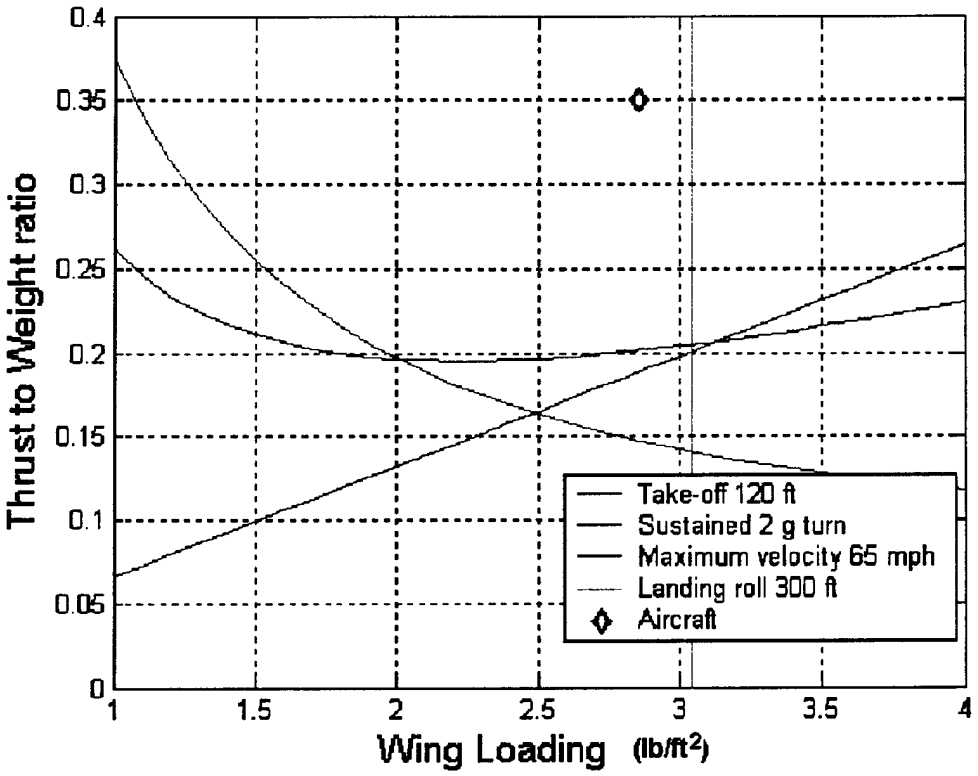

Figure 4-11 Constraint plot.

There was only one performance constraint given in the DBF rules. In commemoration of the 100th anniversary of the Wright Brothers' flight, the DBF entries must be capable of taking off in 120 feet. To meet this constraint the aircraft must be above the dark blue line. There were three other constraints added to this aircraft by the team. Since speed was a large part of optimization, the team added a maximum speed constraint of at least 65 mph, indicated by the area above the red line. Since mission

time is such a driving factor in the final score, landing distance was set at no more than 300 ft, and is represented by the area to the left of the light blue line. The final constraint was a sustained turn of at least 2 g's shown as the area above the green line. The aircraft's thrust to weight ratio and wing loading place it well within these constraints. This was encouraging and indicates the aircraft would not be thrust or lift limited with respect to these constraints

5.0 Detailed Design

The optimization and trade studies of the preliminary design phase resulted in a solid baseline aircraft configuration. Once the overall configuration was locked down detailed design work began. Working closely together, the team made final selections for all design components. During the detailed design process, the program manger and the SEIT lead ensured that the architecture for control and flight systems was properly integrated into all aspects of the aircraft.

5.1 *Wing*

The wing design consisted of six aspects: area, taper, airfoil section, twist, dihedral, and incidence angle. These were all defined in detail before construction was begun.

The wing area was selected to give an appropriate wing loading for the design. From the beginning, the team desired to build an airplane that weighs no more than 18 lbs. Therefore, a six square foot area wing provided a wing loading of three pounds. This wing loading was used in performance calculations including turn radius and most importantly takeoff distance. Although a lower wing loading would allow shorter takeoffs and tighter turns, it would also result in more drag. Because the design was centered on speed, the additional drag would be unacceptable. The final wing design was set at 6'6" long (6 inches covered by the fuselage) with a chord of 12 inches.

The decision to use an un-tapered wing was based primarily on RAC. The efficiency benefits of a tapered wing would not be worth the added cost for an increased root chord and an increased wingspan. Additionally, the tapered wing was heavier because it required a longer main spar and more leading edge structure. Whatever efficiency was lost because of the un-tapered wing was compensated for with twist.

The NACA 4412 section was the final chosen wing section based on wind tunnel tests. The NACA section outperformed the Eppler 67 section by a small margin, and it was chosen for its reliability. However, it was found while creating full-scale drawings that for a 12-inch chord, the 4412 was not thick enough to hold the retracted landing gear. Therefore, the root airfoil was changed to a 4415, slightly thicker but essentially the same airfoil.

The final wing design incorporated three degrees of washout (i.e. twisted, so that the leading edge of the wing tip is three degrees down) in each wing. This geometric twist was added for two reasons. The first reason was stall stability. Because the aircraft will operate very near the stall in turns, it was imperative that the stall be moved as close to the wing root as practicable. The second reason for the wing twist was efficiency. Once the team decided to use an un-tapered wing, it was felt that the addition of twist would yield a more efficient downwash distribution.

Given that the aircraft had a low-wing for the final design, a certain amount of dihedral was desired to promote roll stability. Three degrees was chosen based on historical data. Many low wing general aviation aircraft including the Beechcraft Bonanza have dihedrals on the order of six degrees. In the team's design, this value was halved for two reasons. First, remote-controlled aircraft are traditionally very controllable in roll. Many sport R/C aircraft have no dihedral at all, and pose only a small challenge to a reasonably experienced pilot. Secondly, it was desired by the pilot to have an aircraft that was easy to roll into turns and hold there, given the majority of Mission C would be spent in turns.

The wing was mounted on the fuselage at a two-degree angle of incidence. Based on an average cruising speed of 70 mph the theoretical angle of attack for the 4412 to provide the required lift was two degrees above the zero-lift angle. The zero lift angle on the NACA 44—series of sections is negative four degrees. Therefore, mounting the wing at a two-degree angle of incidence results in a six-degree angle of attack (above zero-lift) at the root, and a three-degree angle of attack at the tip. Although these are above the required cruising value of two degrees, it was decided that it would be preferable to have the aircraft cruise slightly nose-up rather than nose-down.

5.2 *Final Propulsion System*

For the final propulsion system, an APC 14 x 12 propeller driven by an Astro 60 direct drive motor and powered by Sanyo AC2400 NiCd batteries was chosen. The initial propeller selection made using ECALC was a 14 x 11. To gain more accurate performance data, the initial propeller along with a number of similar sized props including a 13 x 13, 13 x 12, and 14 x 12 were tested in the USNA Eiffel wind tunnel. The experimental test data revealed better performance could be obtained from the 14 x 12. The final results for the 14 x 12 are shown in Figure 5-1.

As show in the Figure, the 14x12 produced over six pounds of static thrust, which should be enough to take off in the required distance. The prop produced more thrust at higher speeds than predicted by ECALC. At maximum amperage, the prop still produced 2.5 lbs of thrust at 100 mph. Since the prop blades did not stall at these high speeds, the aircraft's maximum speed will be limited by drag rather than the prop's pitch. The props maximum efficiency occurred at an advance ratio between 0.6 and 0.7, corresponding to approximately 60mph to 80mph. This range of max efficiency should aid endurance since cruise velocity was predicted to occur in this window.

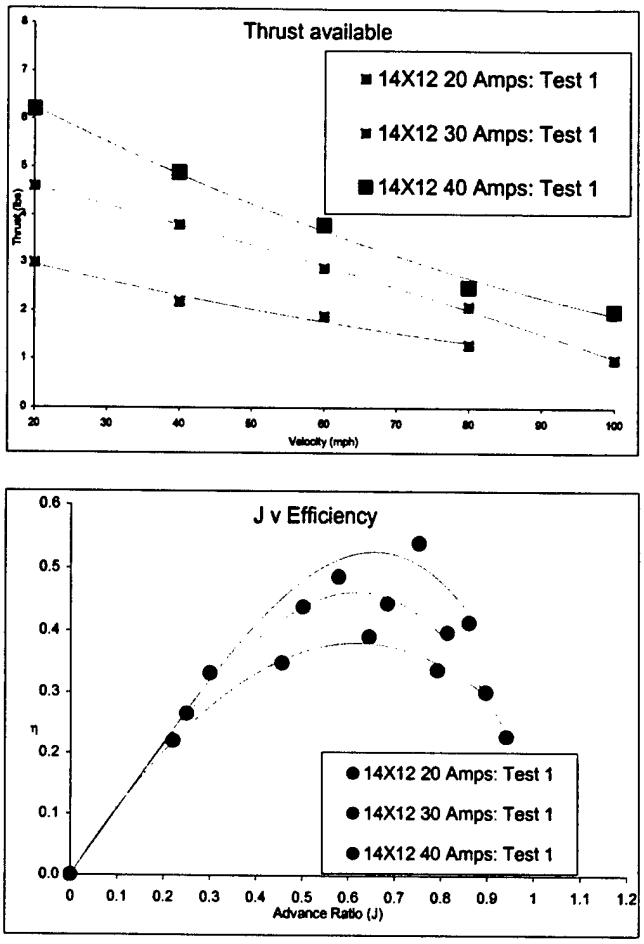

Figure 5-1 Thrust available and efficiency curves for the 14x12 at various amperages.

5.2.1 Endurance Testing

The endurance test on the battery packs was conducted in the wind tunnel at a predicted cruise velocity of 60 mph. The throttle was set for 35 amps and steadily increased over the course of the trial until the throttle was full and the amperage and RPMs started decreasing. Results showed the present battery pack produced about 3.5 lbs of thrust at 60 mph for about three minutes. This amount of time is close to the predicted competition times of 150 seconds for Mission A and 180 seconds for Mission B. In addition, the plane would most likely not be flown at full throttle over the entire course. Flight test will show whether or not the power plant can successfully fulfill each mission.

5.3 *Detailed Structural Design*

5.3.1 Fuselage

The majority of the aircraft's detailed structural concerns involved the fuselage and wing root section. The fuselage was built to permanently attach to the wing root to facilitate fast assembly times. The fuselage and wing sections would have to be constructed separately and connected together. This

created concern since this area of the aircraft experienced the major structural loads including the wing moment, the tail boom moments, and the impact associated with landing.

The detailed design for the fuselage had four main focal points with regards to its structural stability: holding the front nose gear, batteries, and components; securing the five pound payload; mounting of the antenna; and mounting of the motor. The final fuselage design was divided into two separate compartments, which would be constructed separately. The front compartment held the batteries and provided the structural support for the nose gear. The rear compartment held the payload box, with reinforced areas on the top and rear bulkhead. A reinforced strip of graphite composite was attached along the top of the rear compartment and screwed into the front and rear bulkheads to secure the payload box and allow for the attachment of the antenna. The pusher motor mount was placed on the reinforced area of the rear bulkhead.

5.3.2 Wing Structural Design

The detailed structural design of the wing consisted of the main spar and control surfaces. The design of the main spar was based on the composite trade studies conducted in the preliminary design phase. The final design of the wing spar was based on the standard lay-up with fiberglass stringers and carbon fiber spar caps on both the top and the bottom. However, more carbon was added to the compression side since all the test beams failed in this mode. The final design for the carbon spar caps was tapered since the wing tips experience less loading than the wing roots. Sections of the polystyrene foam would be cut out in non-load bearing areas to save weight.

The trailing edge of the wing surfaces was constructed entirely of carbon fiber to ensure strength. The carbon fiber was additionally employed as the hinge line for the flaperons.

5.3.3 Attachment Design

In order to meet the goal of a 30 second assembly time, quick attachment techniques needed to be developed. If designed correctly, the aircraft could be broken into as little as four pieces. These pieces included the fuselage, each side of the wing, and the empennage. The attachment method of choice consisted of the carbon fiber tubes tested in the preliminary design. The carbon fiber tubes were used as twin tail booms, which slide into the wing root section of the fuselage. In this manner, the empennage would quickly attach to the fuselage. The carbon fiber tubes proved more than adequate in strength tests. The twin tail booms would adequately resist torsional forces and provide prop clearance for the pusher configuration.

Carbon fiber tubes placed along the main wing spar would transfer the wing loads across the wing-fuselage connection while providing a quick attachment mechanism. Along the attachment line, a small

diameter carbon fiber tube was embedded along the three quarter chord to provide an anti-torque spar. This spar also passed through the wing root to secure the tail booms in place. The carbon fiber tubes provided a tight fit, but the wing attachment line may also be taped as a precaution to prevent the wing from sliding out in flight.

To eliminate having to connect any electrical control wires while attaching the wing, a sleeve setup inside of the wing-fuselage center body was designed for flaperon control. The flaperon servo was connected to a sleeve at the root of the wing section that was permanently attached to the fuselage. The remaining outboard portions of the wing plugged into the center body via the carbon rods and an extension of the flaperon plugged into the sleeve at the root of the wing. Figure 5-2 illustrates the concept.

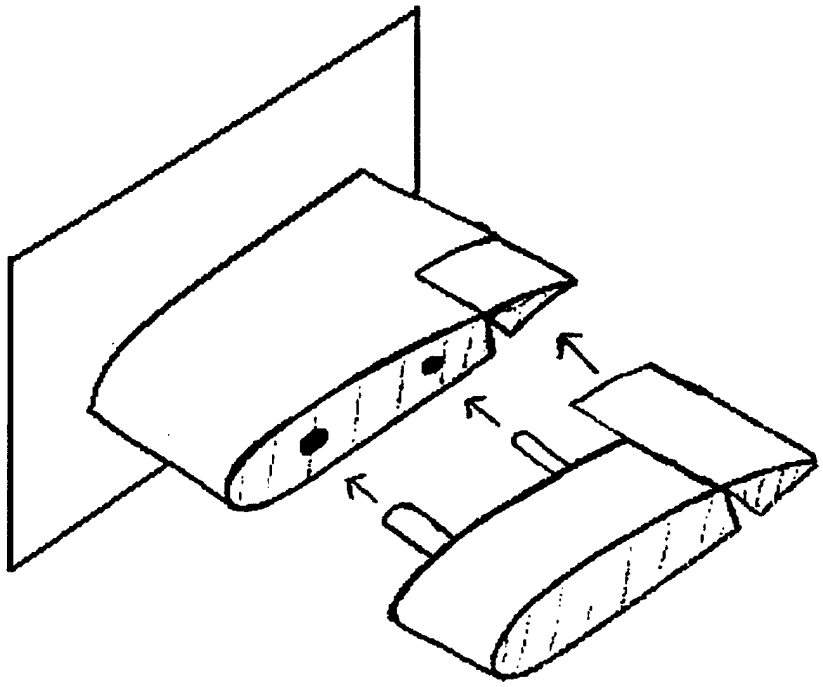

Figure 5-2 Wing and flapperon attachment technique.

5.4 *Stability and Control*

5.4.1 Detailed Weight and Balance Estimation

To determine the center of gravity of the aircraft a full-scale drawing was made depicting the placement of all the critical components. Each component was then either weighed or estimated to the nearest hundredth of a pound and its location relative to the front edge of the forward bulkhead was determined. Using Excel, the moment contributions of each component was calculated, and then divided by the total weight of the aircraft to determine the location of the center of gravity. Table 5-1 below presents the detailed weight and moment contributions of each component.

Item	Weight	Location	Moment
Nose Tire	0.14	-2	-0.28
Nose Gear	0.27	-7.25	-1.96
Batteries	4.2	-3.73	-15.68
Receiver Battery	0.32	-3.88	-1.24
Watt Meter	0.24	-0.5	-0.12
Air Canister	0.08	16.88	1.35
Speed Control	0.12	19.5	2.34
Gear Servo and Valve	0.08	19.5	1.56
Motor	1.7	23.25	39.53
Prop	0.26	25.25	6.57
Main Gear	1.5	10	15
Payload	5	9.5	47.5
Wing (w/servos)	1.5	9	13.5
Fuselage	2.23	7	15.61
Tails (w/servos)	1.06	45	47.7
Totals	Weight		18.7
	CG Location		9.16
	Moment		171.37

Table 5-1 Detailed weight and balance.

5.4.2 Final Tail Surface Sizing

The final sizing of the tail surfaces was conducted, and the same values for the tail volumes were used as during the preliminary design phase. A fixed tail length l_t of three feet was now chosen both because of the reasonable associated chord length it yielded for the horizontal tail, and because it left adequate room to pack the tail assembly in the storage box. For the vertical tails, there was concern about having adequate directional authority; therefore the tail area was intentionally oversized by a factor of 1.5. The fixed dimensions for the tail surfaces and the corresponding tail volumes are presented in the Figure 5-3 below.

The vertical tails are designed with a portion of the tail above the tail booms, and a smaller portion below. Without the lower portions the vertical tail volume matches the recommended value in Raymer. Flight tests will determine whether or not the lower extensions will be included or removed for the final competition design.

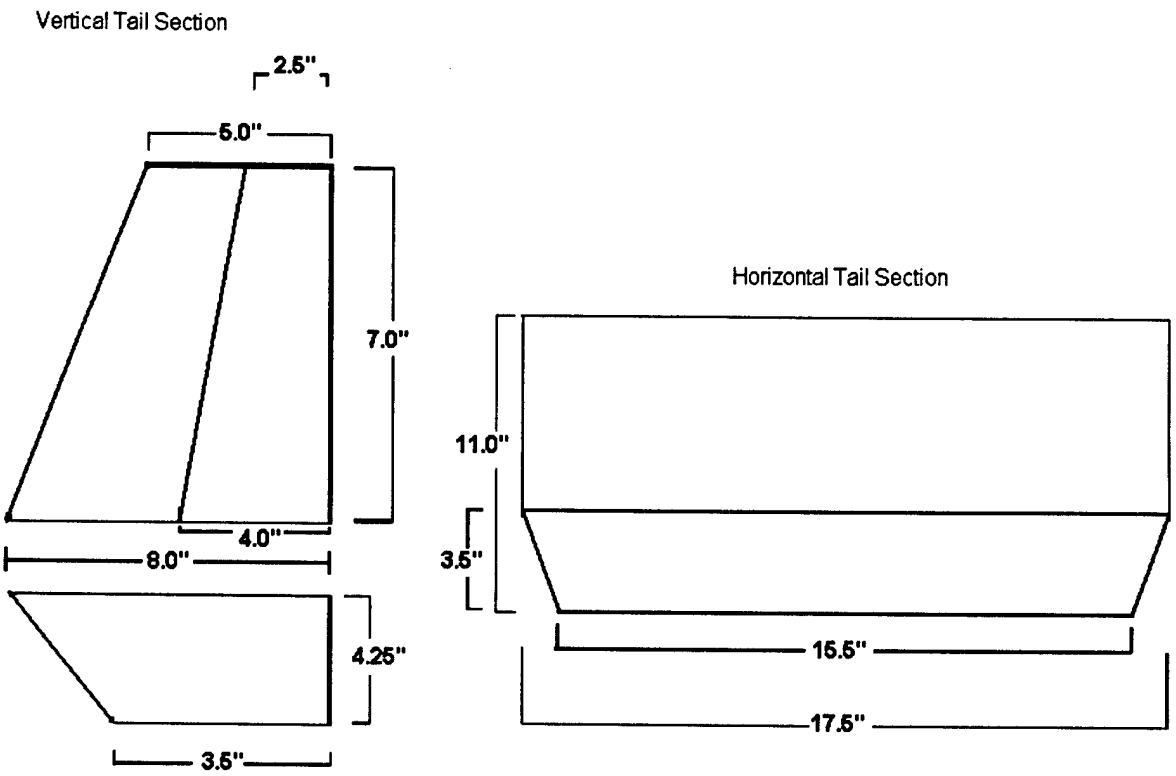

Figure 5-3 Vertical and Horizontal Tail Dimensions

5.4.3 Tail Control Surface Sizing and Control Power/Effectiveness

The tail control surfaces were initially designed using recommended ratios in Raymer of 50% of the area for the rudders and previous radio control aircraft construction experience for the elevators. The effectiveness and power of the control surfaces were then calculated using the following relationships:

$$C_{m_{\delta_e}} = -V_{HT}\eta C_{L_{\alpha_t}}\tau \qquad C_{n_{\delta_r}} = -V_{VT}\eta C_{L_{\alpha_{vt}}}\tau$$

where τ is the flap effectiveness parameter corresponding to the area ratios between the control surface and the tail surface and η is the ratio between the free stream and tail velocities.

Once the needed dimensions and aerodynamic data were known, the values were entered into an Excel spreadsheet. This spreadsheet calculates the body, tail, and wing components' contributions to the various directional stabilities of the aircraft. This validated that the control surface areas provided enough power to correct for the inherent instabilities of the design. Estimates for the drag on the deployed landing gear and its contribution to the nose down pitching moment of the aircraft, in addition to the increased nose down moment resulting from flap deployment, were used to verify that the elevator had the necessary authority to trim and control the aircraft while on landing approach. For all calculations, the

dynamic pressure ratio between the wing and tail surfaces was assumed to be unity. While in powered flight, the tail surfaces would actually have more authority than calculated due to the prop-wash off the pusher configuration. In gliding flight, the unity ratio should be a reasonable assumption.
The control surface dimensions and control effectiveness values are listed in Table 5-2.

Tail Control Surfaces	
Rudder	
Root Chord	4 in
Tip Chord	2.5 in
Height	7 in
Area	22.75 in^2
Rudder Control Power/Effectiveness	-0.06286
Elevator	
Chord	3.5 in
Span	15.5 in
Area	54.25 in^2
Elevator Control Power/Effectiveness	-0.814

Table 5-2 Control surface sizing and effectiveness.

The deflection angles of the surfaces are plus / minus 30 degrees for both the rudders and elevator. This is the recommended value in Raymer and should provide more than enough power for our flight envelope.

5.4.4 Flaperon Sizing and Power/Effectiveness

The flaperon dimensions of the aircraft were determined by the required flap areas to get the appropriate lift for landings. It was ensured that the deflection angles of the ailerons, plus/ minus ten degrees in addition to the flap deployment, were adequate for control of the aircraft. Flaperon dimensions and control power are listed in Table 5-3 below.

Flaperons		
Inner Limit	11.5	in
Outer Limit	39	in
Chord Length	2.5	in
Area	68.75	in^2
Control Surface to Wing Area Ratio	0.073	
Aileron Control Power/Effectiveness	0.204	

Table 5-3 Flaperon Dimensions/Effectiveness.

5.4.5 Control System

The motor includes a 60 size-Astro motor, a 50-amp speed controller, a 40-amp inline fuse, and 28 RC-2400 mAh batteries. A wattmeter was employed during flight testing and established reserve power requirements.

The radio used was an 16-channel JR Computer Radio. This radio has the ability to mix in functions for the flaperons. The servos plug into the receiver, powered by a separate battery 6.0-volt battery pack inline with a 6.0-volt voltage regulator to drive the servos faster with response times and more power. A total of six servos were used in conjunction with the radio system: one in each wing for flaperons; two for the tail; one to actuate the retractable landing gear valve; and one to steer the nose wheel. The servos used for the wings were the HS-5625MG digital super torque servos with 130 oz of torque and a response time of 0.14 seconds. The servos used for the tail surfaces were the HS-5245MG digital mini servos. They output 76 oz of torque and the response time was 0.12 seconds. The HS-225MG Mini servo was selected for the steerable nose wheel and outputs 67 oz of torque at 4.8 volts. For the retractable landing gear actuating valve, a HS-81MG servo with an output of 36 oz of torque at 4.8 volts was selected. An MPI on-board battery monitor was installed to test the battery voltage. The flight control system incorporated an FMA Copilot system. This device employs the infrared signature of the sky and earth in order to keep the roll and pitch level. This greatly reduced the error involved with depth perception while the plane was flying toward the pilot and away from the pilot. Also, it helped a great deal on landings allowing the pilot to concentrate on descent rate rather than roll. In order to use the flaperon functions with this device, a Grauper mixer was obtained to plug in line with each of the channels. Also, a digital inline filter was employed to keep the servos free from noise. Lastly, a century piezo gyro was used on the rudders to control yaw in crosswind landings.

5.5 *Landing Gear*

The landing gear struts for the aircraft were designed to maximize durability and flexibility, while conserving weight. The struts would be built out of half-inch carbon fiber tubes with aluminum joints and oil-filled shock absorbers. They were designed to absorb high impact landings, characteristic of RC model aircraft. Typically, winds are high for the competition and survivability upon landing was considered a key issue. A lesson learned from previous years was to make the landing gear strong but absorbent. Furthermore, the landing gear was designed so that the moment about the strut upon landing was corrective and thus the aircraft would track straight as it settles. Each gear would be slightly compressed when the aircraft was static in order to allow the fullest absorption of impact and ensure the effect of the spring did not overcome the damping effects of the shock absorber. The force upon impact would be lessened by the damping effect of the shock absorbers, while the springs would provide a restoring force.

Each landing gear retracts pneumatically into the aircraft. The retract units were manufactured by Spring Air and are made of T-6 Aluminum. They were designed for an aircraft of 20 pounds and support a half-inch strut. Actuation is achieved by means of air pressure contained in two 120 psi rated aluminum canister. The canisters have enough pressure to cycle the gear at least ten times. Two fail-safe mechanisms are built in to the units, such that if air pressure is lost, all three landing gear will automatically drop. In addition, the retract units have an anti-collapsing mechanism, which makes it virtually impossible for a gear to collapse on take-off or landing.

5.6 *Tables - RAC / Geometry / Performance / Weight Statement / Systems Data*

This section details the aircraft dimensions, weight, predicted performance, systems data, and RAC. Dimensions and weights were measured from the constructed aircraft. The performance data was drawn from the estimates in the preliminary design phase. For the calculations, lift coefficients were estimated from MFOIL while thrust values were taken from wind tunnel tests of the power plant.

LENGTH (ft)		5
SPAN (ft)		6.5
HEIGHT (ft)		1.5
WING AREA (ft^2)		6.5
ASPECT RATIO		6.5
CONTROL VOLUMES	Vv	0.04
	Hv	0.7

	WEIGHT
AIRFRAME (lbs)	6
PROPULSION SYSTEM (lbs)	6.37
CONTROL SYSTEM (lbs)	0.64
PAYLOAD SYSTEM (lbs)	0
PAYLOAD (lbs)	5
EMPTY WEIGHT (lbs)	14.34
GROSS WEIGHT (lbs)	19.34

Table 5-4 Table of aircraft geometry and aircraft weight statement.

	EMPTY	GROSS
C_{LMAX} (no flaps)	1.2	1.2
C_{LMAX} (flaps)	2	2
L/D_{MAX}	10	10
ROC_{MAX} (ft/s)	13	11.5
V_{STALL} (mph)	26	30
V_{MAX} (mph)	68	66
Take-off Dist (ft)	42	78

Radio	JR-10X
Servos Used:	6
Flaperons (2)	HS-5625MG (130 oz)
Tail (2)	HS-5245MG (76 oz)
Steerable Nose Wheel	HS-225MG (67 oz)
Retractable Gear	HS-81MG (36 oz)
Battery Configuration	2-15 cell bundles
Motor	Astro 60-direct drive-pusher configuration
Propeller	14X11 & 14X12
Gear	Spring Air Retractable Landing Gear
	Struts - Midshipmen manufactured

Table 5-5 Table aircraft performance data and aircraft systems data.

RAC Component	Aircraft Input Parameters	Intermediate RAC Contribution
Battery Weight (lbs)	4	4500
# of Engines * Battery Weight	4	1500
Empty Weight (lb)	14	1400
Span (ft)	6.5	1040
Length (ft)	5.67	1134
Servos (#)	6	600
Control Surfaces (#)	5	300
Vertical Surfaces with contols (#)	2	400
Horizontal Surfaces (#)	1	200
Maximum Chord (ft)	1	160
Engines (#)	1	100
Propellor (#)	1	100
Vertical Surfaces w/o contols (#)	0	0
Total RAC / $1000		11.43

Table 5-6 RAC table.

5.7 *Drawing Package*

The drawing package is attached in pages 58-60.

6.0 Manufacturing Plan

6.1 *Alternate Manufacturing Processes Investigated*

Throughout the manufacture process, two figures of merit drove the design of all components. The final component represented a compromise between the following FOM's:

Strength: Strength was essential for structural integrity, but came at the cost of added weight.

Weight: Low weight was essential for performance, but sacrificed strength.

A number of different manufacture processes were investigated and were evaluated with respect to the above FOM's and ease of construction. The selected process for each component generally represented the best compromise of strength and weight. However, the team relied heavily on the USNA Model Shop technician Mr. Bill Beaver for his experience in composite materials. Composites were selected for the construction of all aircraft components based on the high strength, low weight, and ease of manufacture of these materials. Other construction materials such as aluminum framing and balsa wood were explored, but could not match the advantages of composites. Mr. Beaver steered the team in the right direction with respect to accepted composite manufacture techniques. Whenever possible, ease of construction was considered in manufacture. The following two composite construction processed were employed throughout the manufacturing phase:

Hot Wire Technique: In this process, an electrically heated wire is guided over templates to cut components from polystyrene foam. The foam gives the design component its shape while

composite materials are laid up on top of the foam to provide strength. Precise shapes such as airfoils are easily constructed with this method.

Molds: The use of male and female molds was another technique employed for the construction and replication of design components. Molds were useful for modular or structurally significant components such as fuselage compartments.

6.2 *Analytic methods*

6.2.1 Manufacturing Costs

After the preliminary design was completed, and inventory of all existing supplies from the two previous teams was performed. This enabled the team to manage their project budget and place orders for needed parts. The majority of the composite materials including carbon fiber, fiberglass, polystyrene foam, and epoxy were readily available in the USNA model shop. The team placed an order for a direct drive motor, since all the motors in inventory were compatible only with gear boxes. Along with the motor, the team's retractable landing gear device represented the largest single cost components of the design.

6.2.2 Skill Matrix

Before a schedule was developed for the manufacturing phase, a skill matrix (Table 6-1) was created to evaluate the amount of time each component's construction would require. Although the skill matrix cannot predict exact times or unforeseen delays, it allowed the team to gauge the construction times of components relative to each other. The four major components were ranked from 0 to 3 against the various steps in the construction process. A zero indicates that step is not needed for the particular component while three represents significant time and resources required to complete the process.

Aircraft Component	Hot Wire Foam Cutting	Mold Creation	Composite Lay-up	Systems Integration
Fuselage	0	2	2	1
Wings	1	0	1	3
Empennage	2	0	2	2
Landing Gear	0	0	0	3

Table 6-1 Skill matrix.

6.2.3 Manufacturing Scheduling

Based on the projected time required for each component, a manufacturing schede was developed. The manufacturing milestone chart (Table 6-2) shows the groups planned and actual progress in the manufacturing phase.

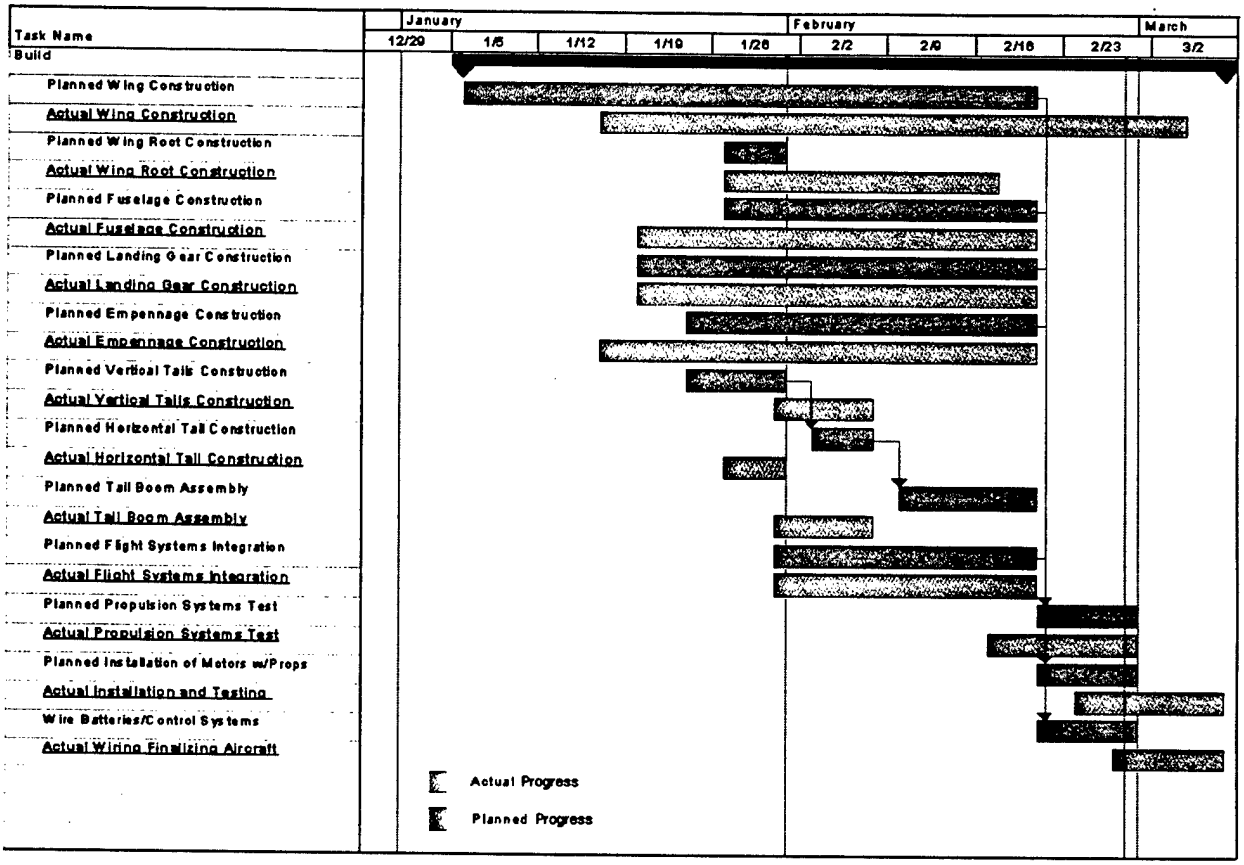

Table 6-2 Manufacturing milestone chart.

6.3 *Construction Processes for Major Components*

6.3.1 Wing

The wing was cut out of polystyrene foam using a hot wire device that cut a 4415 root section and 4412 tip section with three degrees of washout. It was made in two halves and then each wing section was cut along the quarter chord. The spar was laid up with a fiberglass stringer along the quarter chord and carbon fiber spar caps were laid above and below the spar into recessed grooves. The carbon fiber strips were tapered to save weight since less structural support would be needed at the wing tip than the wing root. The manufacture of the wing spar closely resembled the standard lay-up tested in the preliminary design trade study. For efficient attachment purposes a section of the wing would be attached to the fuselage, forming a permanent wing root. Three quarter inch carbon fiber tubes were laid up co-axially with the spar over the wing-tip/wing-root divide. Each wing was then cut along the chord 11 inches from the root side (across the carbon fiber tube) and the male tube wing connection was glued into the wing-tip portion of the carbon fiber tube. The leading edges of both wings were then covered with carbon fiber material. The trailing edges were similarly laid but the carbon extended further on the upper surface than the lower surface and a groove into the foam was cut out of the lower surface to provide a hinge line for the control surfaces. The two center wing root sections were bonded together covered completely with

carbon fiber to provide the necessary structure to support both the wing tips and the tail booms. This center section was permanently attached to the fuselage, with the desired three degrees of dihedral.

6.3.2 Fuselage

The front compartment of the fuselage was fabricated in two parts. The base was made from thick layers of carbon to accommodate the front landing gear and impact loads associated with it. The nose of this base was formed into a u-beam to house the retracted front gear with room to fit batteries on the sides. This piece was taped and bonded to the front bulkhead of the fuselage. A second nosepiece was made from a thin sheet of fiberglass and was designed not to carry any load but to simply act as a fairing over the components and batteries.

The main compartment was constructed of carbon fiber to hold the payload box. The compartment was designed around the box with a recessed airfoil shape in the bottom to allow the integration of the wing root sections. Front and rear bulkheads were constructed from carbon fiber laminate and a balsa wood core to separate the payload bay from the aircraft's internal systems. A single beam spanned the two bulkheads and was bonded to the frame, creating solid points for mounting the antenna. The beam also clamped down on the top of the payload box, acting as the primary payload restraint method. The motor mount was attached to the rear of the main compartment and was reinforced with additional carbon.

6.3.3 Landing Gear Struts

The landing gear struts were fabricated in the Naval Academy machine shop. The main structure of the struts was ¾ inch carbon fiber tubing with an aluminum joint and an end cap machined to fit inside the carbon fiber tubing. Aluminum clamps were manufactured to fit around the carbon fiber tubing to mount the shock absorbers on the strut. Each shock absorber was fitted with a spring to return the absorber to its extended length after the weight was removed. The nose gear was also fitted with a control horn to attach the servo.

6.3.4 Empennage

The empennage and twin tail was built from five pieces: one horizontal stabilizer, two vertical stabilizers with rudder control, and two carbon fiber tail booms. Before glassing the foam, control horn mounts were glued into each of the three control surfaces, recessed into the foam. The servo placements were bored out of the horizontal stabilizer and a flexible vertical stabilizer control rod was also buried into the surface of the horizontal stabilizer. This allowed both rudders to be moved from one servo. The horizontal stabilizer was glassed between the two tail booms, and the four vertical pieces were glassed to the twin tail booms. Figure 6-1 below show the manufacture of the empennage and other major components.

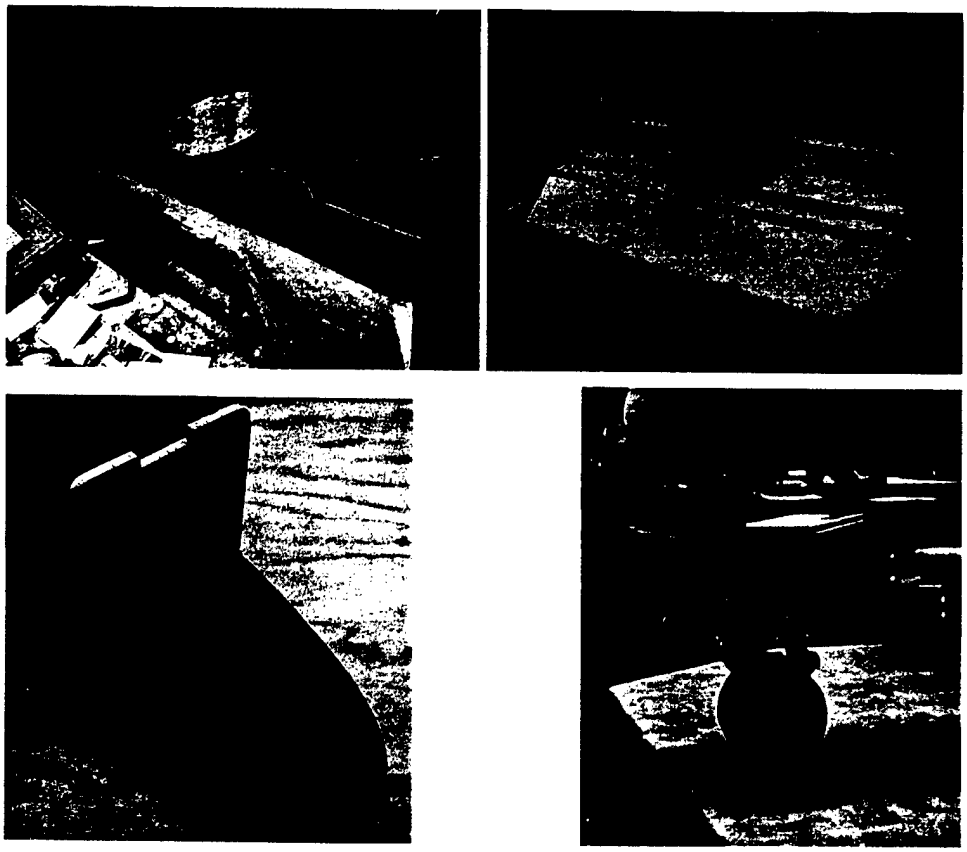

Figure 6-1 Wing, empennage, fuselage, and landing gear manufacture.

7.0 Testing Plan

7.1 *Test Objectives*

The teams who fly their aircraft before the competition do well. This is because a rigorous flight test plan yields both pilot familiarity with the aircraft and an opportunity to fix any deficiencies before the competition. This leads to lower flight times and the opportunity to optimize the design, which will lessen the risk of an accident during the competition. Because of the importance of flying the aircraft before the competition, the team has completed construction two months before the competition, and has planned an array of flight tests to ensure success.

There are two areas that the team intends to center its flight test plans around. The first, performance, will require tests of take of distance, stall speeds, landing performance, max speed, etc. The second area will be reliability, testing the radio range, battery endurance, and retractable landing gear cycles. The objectives for flight tests are as follows:

Flight Test 1: Radio tests, take off, airworthiness, control authority, and landing.

Flight Test 2: Glide performance, climbing flight, 360° turns, and stall recovery.

Flight Test 3: Flight with the antenna attached, including take off, stalls, turns, and landing.

Flight Test 4: Maximum speed, and battery endurance tests.

Flight Test 5: Turn performance optimization.

The scheduled dates for each of these tests are shown in Table 7-1and the test/flight checklist is provided in Table 7-2.

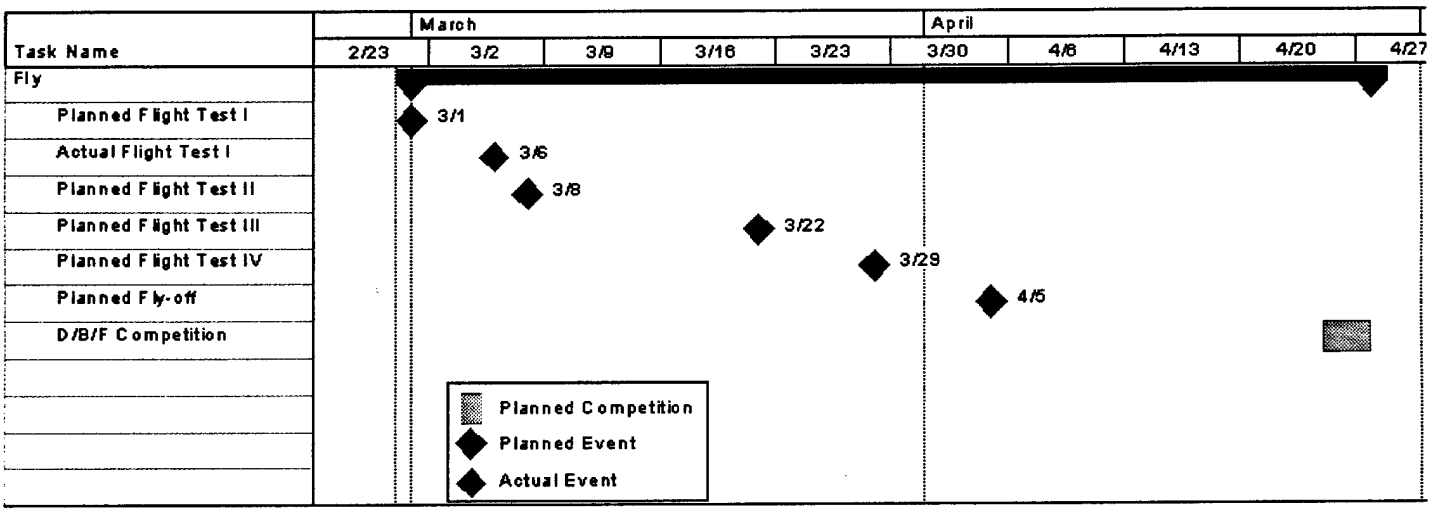

Table 7-1 Flight test schedule.

Pre-Flight Checklist:	Pre-Competition Testing Checklist:
- Center of gravity placement / check	Radio test
- Radio battery / range check	Take off under 120 ft
- Normal control surface functioning	Control Authority
- Gear operation / air pressure check	Slow flight and stalls
- Wings / tail locked	Flap operability and effectiveness
- Main power battery check	Retractable landing gear
- Remove fuseotor run-up	360-degree turn (downwind)
- Motor run-up	180 degree turn
	Landings
	Repeat Procedures with Antenna

Table 7-2 Test and flight checklists.

7.2 *Test Results / Lessons Learned*

Throughout the flight test phase the team learned the importance of patience and flexibility as unforeseen weather conditions complicated the original flight test schedule. A snow storm which dumped more than 2 feet of snow on the east coast prevented the team from completing the first flight test. Although the plane could not be flown due to snow cover on the test site, the team was able to perform initial radio tests, motor run-ups, and ground taxi tests inside the USNA field house. Figure 7-1 below shows Yeager Chaser 1 during the indoor taxi tests. From the tests, the aircraft was found to good control response and

ground handling. Test results indicated more than expected installed static thrust and rapid acceleration. In addition, the team successfully performed a static test of the retractable landing gear.

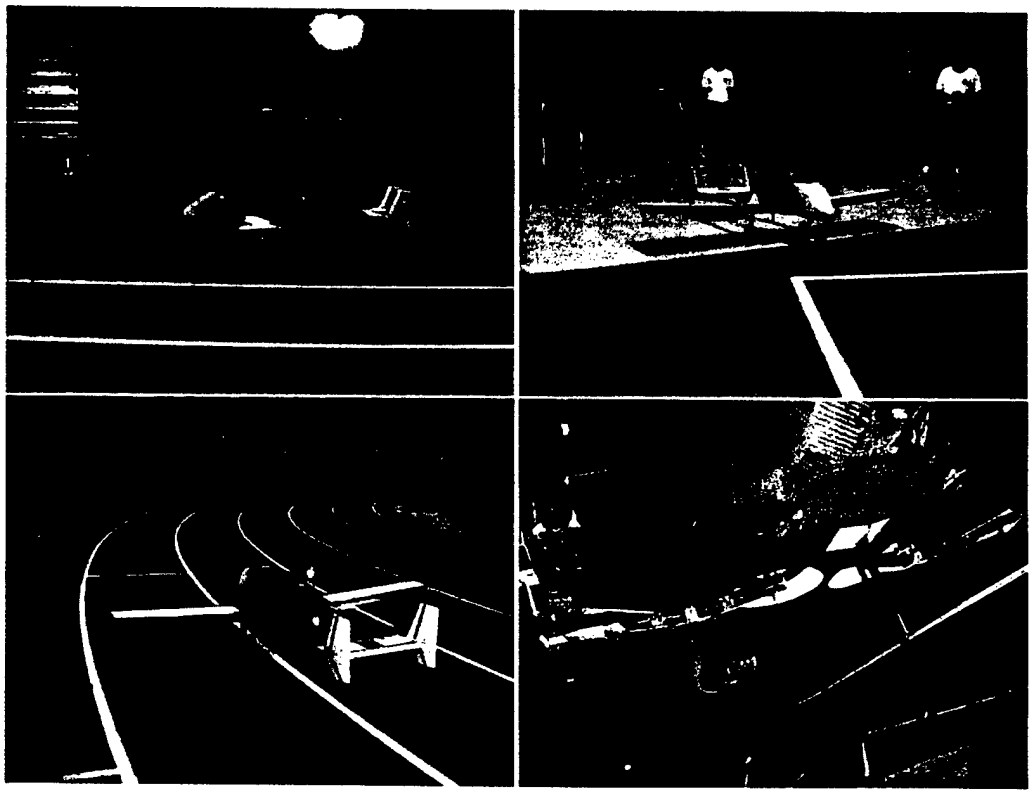

Figure 7-1 Yeager Chaser 1 during ground tests.

8.0 References

Anderson, John D. *Aircraft Performance and Design*. New York: WCB/McGraw-Hill, 1999.

Boucher, Robert J., *The Electric Motor Handbook: The Complete Handbook of High Performance DC Motors*, Astro Flight Inc., 1994.

Etkin, Bernard. *Dynamics of Flight: Stability and Control*. New York: John Wiley & Sons, 1959.

Hoerner, Sighard F. *Fluid-Dynamic Drag*. Published by the Author, 1965.

Koskam, Jan. *Airplane Design: Part VII*. Published by the Author, 1988.

Nelson, Robert C. *Flight Stability and Automatic Control*. New York: McGraw-Hill, 1998.

Raymer, Daniel P., *Aircraft Design: A Conceptual Approach*, AIAA, 1999.

PROPULSION SYSTEM
FLIGHT CONTROL SYSTEM
LANDING GEAR SYSTEM
RESTRAINT SYSTEM

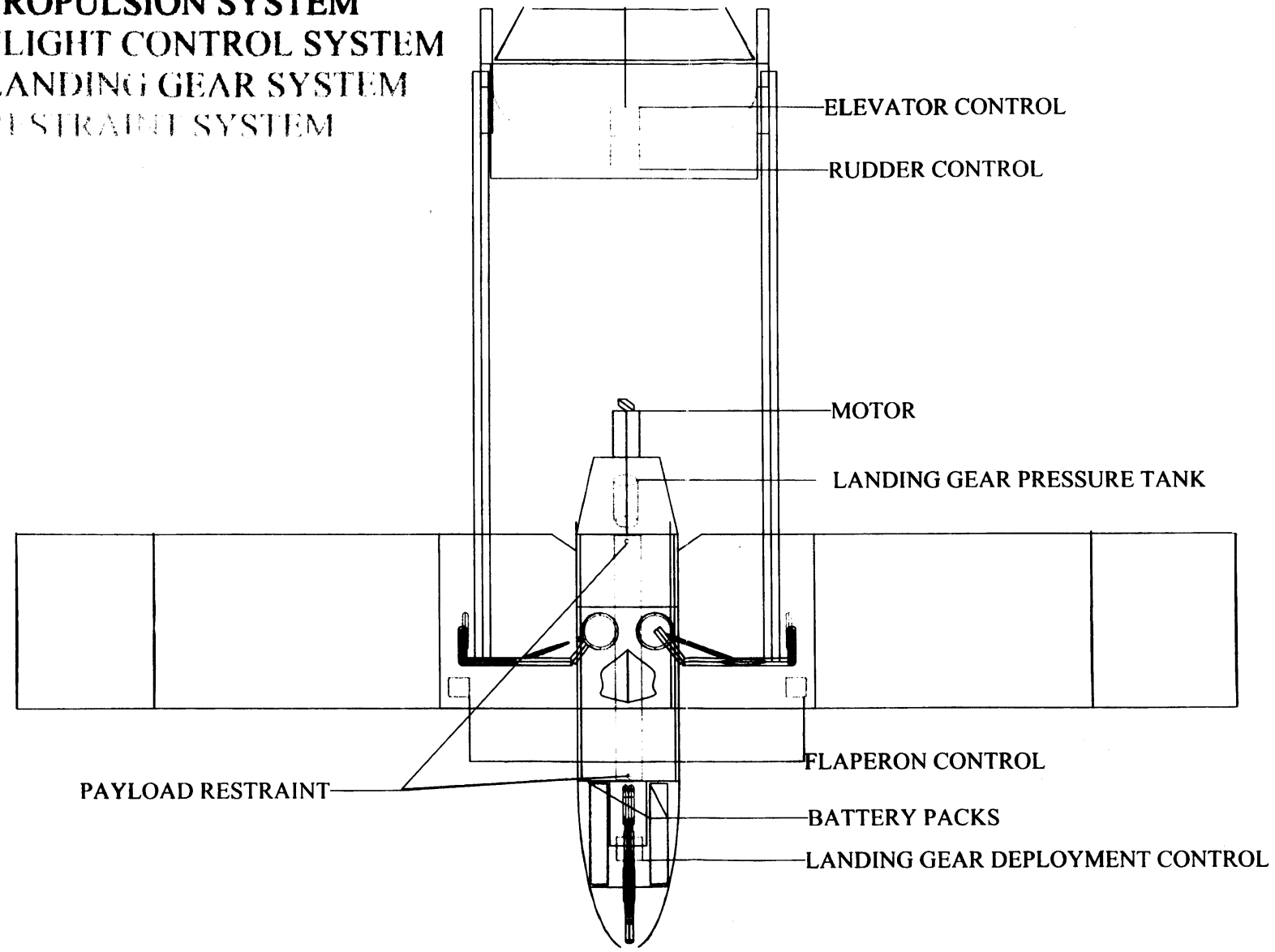

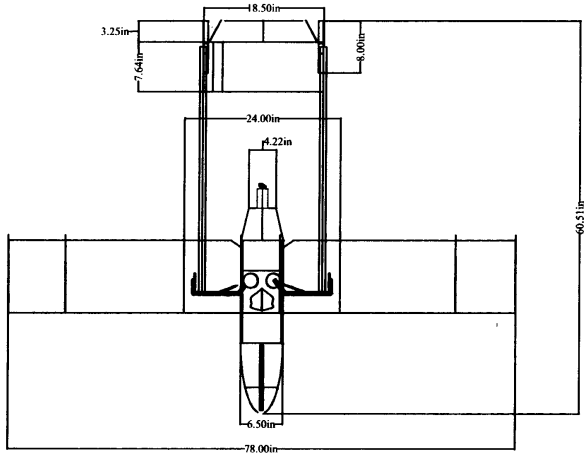

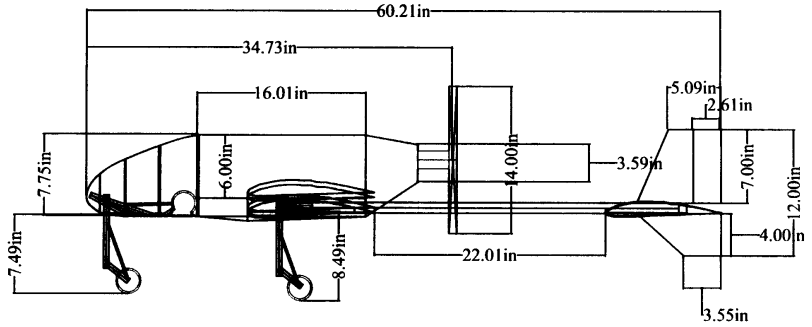

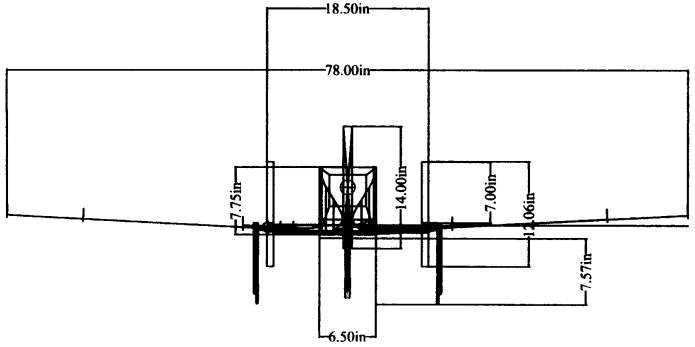

Yeager Chasers
3-View Drawings

YEAGER CHASERS
STRUCTURAL DESIGN

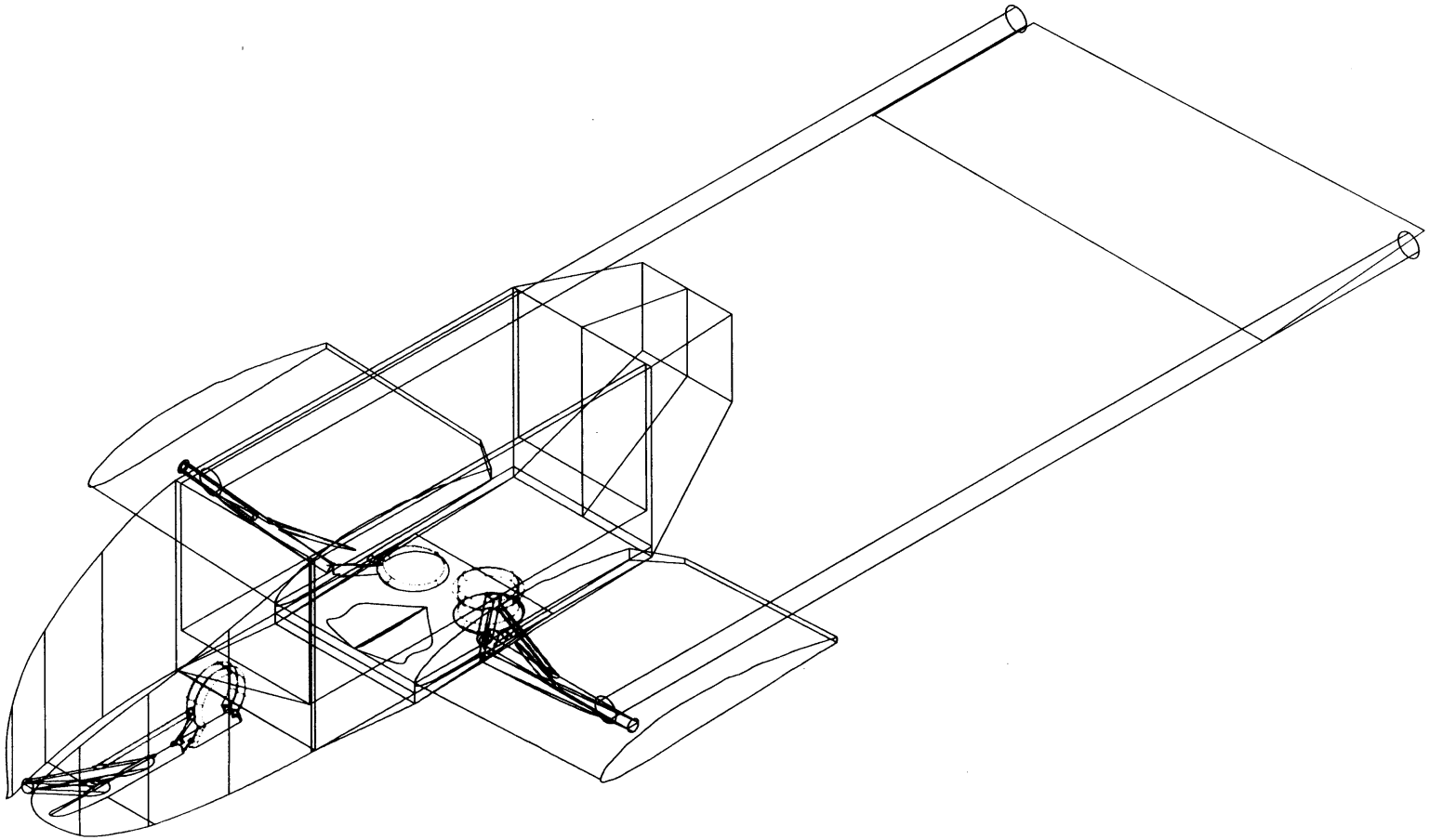

2002/2003 AIAA Foundation
Cessna/ONR Student Design/Build/Fly Competition

DESIGN REPORT

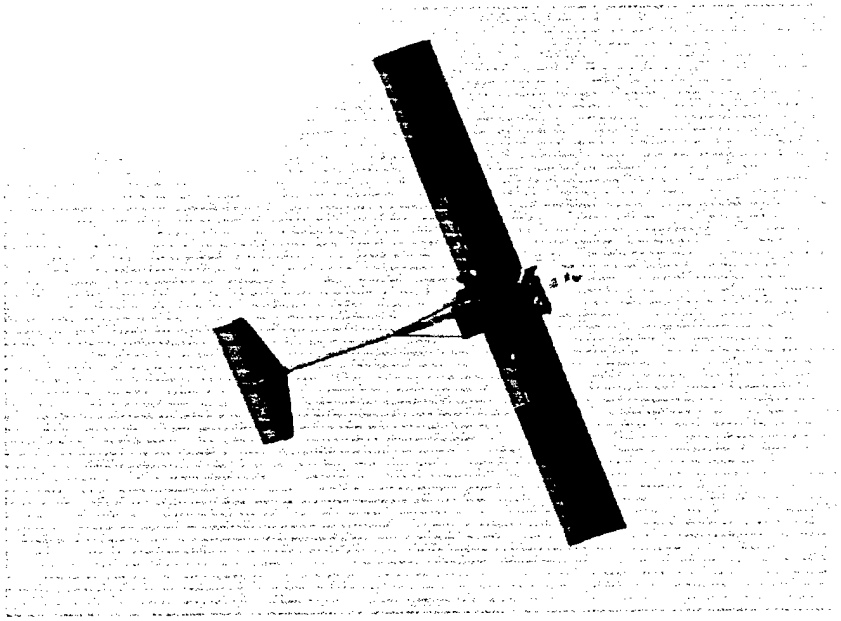

"BASiT"

MIDDLE EAST TECHNICAL UNIVERSITY

DEPARTMENT OF AEROSPACE ENGINEERING

TABLE OF CONTENTS

CHAPTER 1 - EXECUTIVE SUMMARY

1.1 Principles of Design 1

1.2 Development 2

1.2.1 Conceptual Design 2

1.2.2 Preliminary Design 3

1.2.3 Detail Design 3

1.2.4 Manufacturing 3

1.2.5 Testing 3

CHAPTER 2 - MANAGEMENT SUMMARY 5

2.1 Organization of the Design Team: Organization and Assignment Areas 5

2.2 Work Areas of Technical Groups 5

2.2.1 Aerodynamics Group 5

2.2.2 Propulsion Group 6

2.2.3 Stability and Control Group 6

2.2.4 Structure Group 6

2.3 The Milestones Chart 7

CHAPTER 3 - CONCEPTUAL DESIGN 8

3.1 Mission Requirements 8

3.2 Configuration Alternatives 8

3.2.1 The Wing 8

3.2.2 The Tail 9

3.2.3 The Fuselage 10

3.2.4 The Landing Gears 11

3.2.5 Propulsion System 11

3.3 The Value System 11

3.3.1 Figures of Merit (FOM) 12

3.3.2 Results of the Trade-Off Analysis 12

3.4 Payload Mounting & Deployment System Concepts 13

CHAPTER 4 - PRELIMINARY DESIGN 15

4.1 Selection of Wing Loading and Estimation of Maximum Lift Coefficient 15

4.2 Initial Weight Estimation 16

4.3 Aerodynamic Sizing and Geometry Selection 17

4.3.1 The Wing 17

4.3.2 Empennage Group & Stability 19

4.4 Propulsion System 20

4.5 Structural Design Analysis 24

4.5.1 Figures of Merit 24

4.5.2 Fuselage 24
4.5.3 Wing 25
4.5.4 Landing Gear 25
4.5.5 Empennage 26
4.6 Sensitivity Analysis 26
4.6.1 Mission Models & Mission Performance Prediction 26
4.6.2 Detailed Aerodynamic & Stability Analysis 28
CHAPTER 5 – DETAIL DESIGN **31**
5.1 Structural Design Analysis 31
5.1.1 Fuselage 31
5.1.2 Wing 31
5.1.3 Landing Gears 32
5.1.4 Empennage 32
5.1.5 Payload Deployment Mechanism 32
5.2 Propulsion 33
5.3 Rated Aircraft Cost Analysis 34
5.4 Sized Aircraft Data 35
CHAPTER 6 – MANUFACTURING PLAN AND PROCESSES **42**
6.1 Figures of Merit 42
6.2 Wings and Empennage 43
6.3 Tail Boom 44
6.4 Fuselage 44
6.5 Landing Gears 44
CHAPTER 7 - TESTING PLAN **46**
7.1 Static Tests 46
7.1.1 Spar test 46
7.1.2 Landing Gear 46
7.1.3 Tail Boom 46
7.1.4 Tip Test 46
7.1.5 Payload Deployment Mechanism 47
7.2 Flight Tests 47
7.2.1 Ground Testing 48
7.2.2 Airborne Testing 49
REFERENCES **52**

CHAPTER 1 - EXECUTIVE SUMMARY

The aim of this project is to design, manufacture and fly an unmanned, electric powered, radio controlled aerial vehicle which will accomplish the mission profiles specified by the rules of the 2003 Cessna/ONR Student Design/Build/Fly Competition. As in any design process, the given specifications and mission profiles do not describe a unique aircraft configuration. Instead they yield to many possible design concepts and solutions. Therefore, the design should be based upon some major principles.

1.1 Principles of Design

The guiding principles for the design followed in this project are:

- As simple as possible
- As light as possible
- As efficient as possible
- As available as possible
- As cheap as possible

The first principle in the list is about the simplicity of the design. Unnecessary complications in the design must be avoided in order to minimize the difficulties faced during the production and operation phases of the aircraft. These complications will further cause corresponding increases in the manufacturing cost of the design. The best thing to do is not to impose any properties to the concept other than which are strictly required to meet the given specifications.

The second principle is in deed the tendency of every aerospace designer. Any 'too safe' structural member, any excessive aerodynamic surface area, any excessive thrust introduces 'dead weights' to the airplane. The aim of design is to have a 'critical' aircraft that is just capable of performing the specified missions but not more.

The third principle describes how perfectly the design performs its mission. That is, it should meet the mission specifications with appreciably high scores at a low cost.

The fourth aspect describes the availability of the components of the aircraft. Upon any failure, the component or the equipment on the aircraft could easily be replaced and supplied from the market.

The last principle is indeed a measure of how well the first three principles are applied. That is, if a simple, lightweight, available and efficient design is assured then it is also the cheapest one. Indeed, the cost of the aircraft is directly apparent on the scoring procedure of this year's design.

Meeting the above principles guarantees an optimal design. The results of the design process following these principles are given in the following chapters of this report.

1.2 Development

There is no general rule about just where the design process begins. It can be thought to begin with a new aircraft concept. However the concept can best be formed by a competitor study and requirements of the customer or the organization.

The design process is started at June 13th, 2002 when the rules of the competition have not been announced yet. This forced the design team to begin with a deep competitor study. The parameters like the wing loading, power loading, tail volumes are stored for future statistical analysis. The configurations that had achieved good ranks are distinguished.

Meanwhile, development of tools such as codes, spreadsheet programs and a wide database of material weights and properties are initiated.

The announcement of the DBF-2003 competition rules at July 11th, 2002 started the design sequence beginning with conceptual design phase followed by preliminary and detail design phases as summarized below.

1.2.1 Conceptual Design

This stage of design is based on concept sketches of different aircraft configurations that are to be tested for minimum cost and maximum flight score.

Compromises between the arrangement and geometry of the aerodynamic surfaces, possible propulsion system arrangements and production techniques and materials formed a large matrix of configurations. The configuration having the highest score is selected using a value system developed by the design team.

The Value System:

This system evaluates the design alternatives corresponding to each component of the aircraft in the aspects of aerodynamics, structure, weight, manufacturability, cost, assembly and flight times and mission profile. Different aspects have different weighted scores for each different component of the aircraft. At the end, all of the design alternatives are scored separately and the optimum configuration in terms of the described aspects obtained.

Conceptual Design Results:

The resultant configuration is a high wing monoplane with a conventional tail and single tractor engine. The wing is foam/balsa rib construction that is the wing is to be produced by covering the foam with balsa sheets and locally removing the foam/balsa to approach rib construction. The wing is reinforced with a single channel profile aluminum spar. The fuselage is rectangular with thin walled aluminum construction and fiber-glass/film skin (not stress-carrying). The tail is balsa/foam construction and attached to the fuselage by a tail boom instead of lofted fuselage.

1.2.2 Preliminary Design

In the preliminary design phase, the sequence has started with initial weight estimation. Then the iterative sizing procedure was initiated with collaborative work of the design groups formed as aerodynamics, stability and control, structures and propulsion. In proceeding step of the iterations, the design tools have shifted from statistical ones towards analytical ones.

Software programs were developed in this stage. The programs developed were called "PreSize" and "WeiSt", which were mainly used for aerodynamic calculations and structural analysis. When the iterations have been converged to a sized aircraft configuration, the results were validated with 2-D viscous and 3D potential flow models in order to obtain aerodynamic parameters such as lift, drag and pitching moment characteristics.

A loop between all of the groups was created which built up the design cycle. The preliminary design phase was initiated using the data generated at the conceptual design phase. First the wing section was selected followed by the wing geometry and size. Following the calculation of required empennage areas and moment arms, the fuselage was designed. In the mean time, the weight estimations were continuously updated. Propulsion system was selected during preliminary design phase after the aircraft geometry and weight estimation were done.

1.2.3 Detail Design

Almost all of the aerodynamic, propulsion and stability characteristics have been determined in the preliminary design, detail design focused more on the structural aspects including joints, assembly points etc. to be used further in the manufacturing phase. Control surface sizes and travel amounts were refined and the final configuration of the aircraft was fixed. Corresponding drawings and tables including final aircraft data were done accordingly. In case of any inconsistency encountered, the team led back to previous analysis to modify the design.

1.2.4 Manufacturing

During this phase the processes required to manufacture the aircraft were designated. Blue prints for the parts were prepared. For manufacturing the aircraft, team members were organized in such a manner that certain processes were assigned to particular members of the team to increase time efficiency. This organization was also helpful, since members engaged with particular processes gained experience, which in turn increased the quality of the parts manufactured.

1.2.5 Testing

During testing of the aircraft manufactured, resultant work is compared with the expected estimations. Major modifications were done in order to assure "safe" operation of the aircraft and to optimize mission performances.

The team envisaged the use of a GPS system, a 3-axis solid-state gyro and various displacement sensors to indicate the deflection of the control surfaces. The main purpose of installing these on board sensors was to base the flight test results on quantitative data rather than qualitative observations.

It was started as a joint interdisciplinary activity between this project team and a group formed from the Electrical and Electronics Engineering Department of METU.

CHAPTER 2 - MANAGEMENT SUMMARY

Engineering projects are based on teamwork rather than individual contributions. It is the output of the team which constitutes the integrity of multi-disciplinary projects. Of course, a team is composed of individuals and the output of each individual comprises a part of the final product. It is like solving a puzzle, each member of the team fulfils a certain task. Almost all design processes are interdisciplinary in nature and this is why all the design teams should be organized in such a way to maximize the collaboration between the individual team members to increase the efficiency of the groups or members of different disciplines.

The design team of METU has set up an organized process by planning/scheduling the milestones of the design as described in the following sections of this chapter.

In order to realize this, our team formed a joint project with a group of undergraduate students from the Electrical and Electronics Engineering department of METU to perform the flight-testing of the current aircraft with integrated sensors and instruments onboard.

2.1 Organization of the Design Team: Organization and Assignment Areas

The design team of METU, which is named as 'Anatolian-Craft Team', consisted of 11 members. Under the leadership of the team advisor, the team was divided into four major technical groups as aerodynamics, stability & control, structure and propulsion. However the formation of the groups was not rigid. Based upon his/her interest and abilities, every individual member selected one or more groups to participate. Moreover, one member of the team was assigned for avionics systems installation and harness.

There was not a hierarchical structure within the four groups. Instead, all of the group members were under the supervision of the team advisor. The role of the team leader was to maintain the coordination of the team and track the processes to be completed within the planned time frame. Figure 2.1 illustrates the team's organizational structure.

2.2 Work Areas of Technical Groups

Although the members were not strictly assigned to specific technical groups, the task to be accomplished by each technical group was well defined. Since a design process cannot be thought as separate disciplines, weekly meetings were conducted to discuss the design objectives and the achievements to foresee any possible problems. The work areas of each technical group are described under the corresponding subtitles given below.

2.2.1 Aerodynamics Group

The aerodynamics group was mainly involved with the aerodynamic aspects of the design namely, providing the maximum lift and minimum drag to the airplane. Every component of the aircraft, which is

immersed into the airflow, is in the interest of the aerodynamics group. Among the tasks of the group, sizing and shaping the wing is of particular importance. The other tasks can be stated as shaping the fuselage, drag reduction of structural members immersed in the flow, and cooling of the engine and batteries. However, none of these tasks can be accomplished without the consensus of other technical groups.

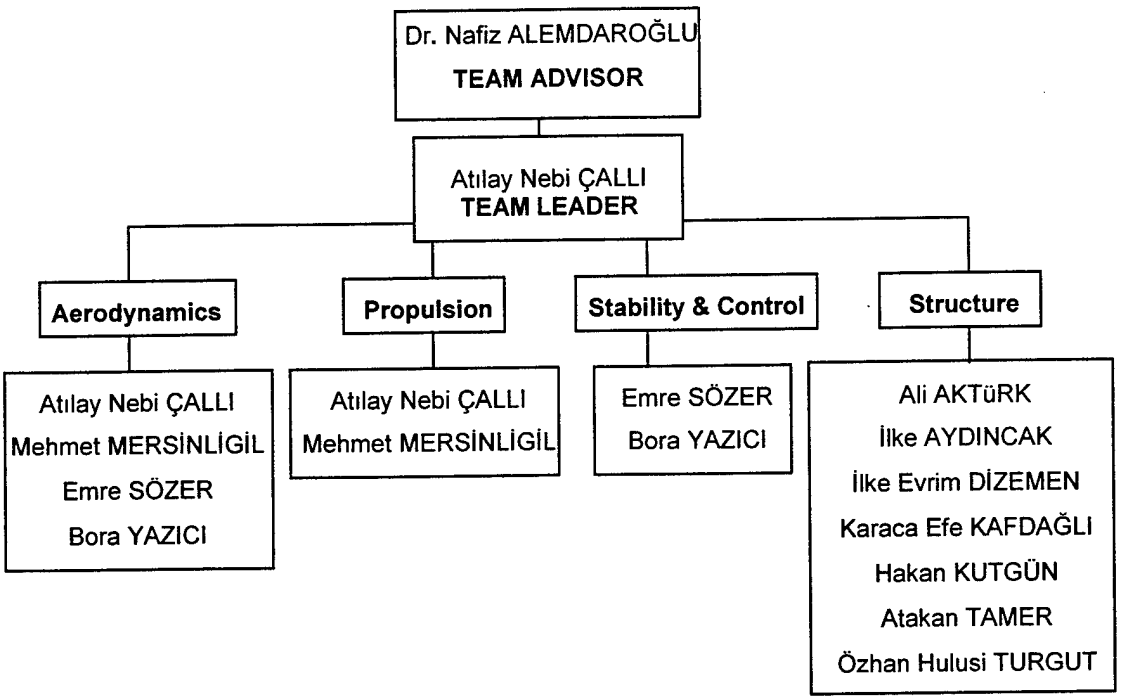

Figure 2.1 METU DBF Team architecture including design personnel and their assignment areas

2.2.2 Propulsion Group

Analysis, optimization and verification of the propulsion system performance were the sole responsibility of the propulsion group. The major task of the group is to perform a trade-off analysis for the determination of the best motor/propeller/battery system configuration.

2.2.3 Stability and Control Group

To 'fly' does not only mean to be lifted-off by the air but also to have full control of the vehicle while in the air. So, after the aerodynamics group ascertains that the aircraft to be lifted-off, the stability and control group tries to 'fly' it. The group is responsible of sizing the tail and the control surfaces in order to provide the adequate stability and controllability about all three axes of the aircraft. Although it is not quoted in the group's name, the group is also responsible for the performance analysis of the aircraft.

2.2.4 Structure Group

The focus of the structure group is to build the aircraft as light as possible while maintaining sufficient structural strength of its members. Design and analysis of the structural members and selection of the

most efficient materials for the construction of the aircraft are in the scope of this group. Moreover, creating the production charts of the structural members and organizing the manufacturing process are planned to be accomplished by this group.

2.3 The Milestones Chart

The efficient use of time has a great importance in this contest. Since the time for the entire design process is very much limited, one needs to be very efficient. Hence, right from the start of the project, time scheduling is done in order to assure the timely completion of the project. Since the completion of the design does not only mean completing the construction of the aircraft but assuring its safe flying and handling qualities, our team decided to allocate a significant time frame to perform sufficient amount of flight testing of the aircraft. This is also an efficient means of correcting the failures and the drawbacks of the design. The time chart for the whole design process is given in Figure 2.2. The sequence of actions are planned in such a way that they reflect the particular logic of the flow-chart of the design procedure. It is not usually allowed to overlap the stages of the project and the milestones chart was followed as closely as possible under the control of the team leader.

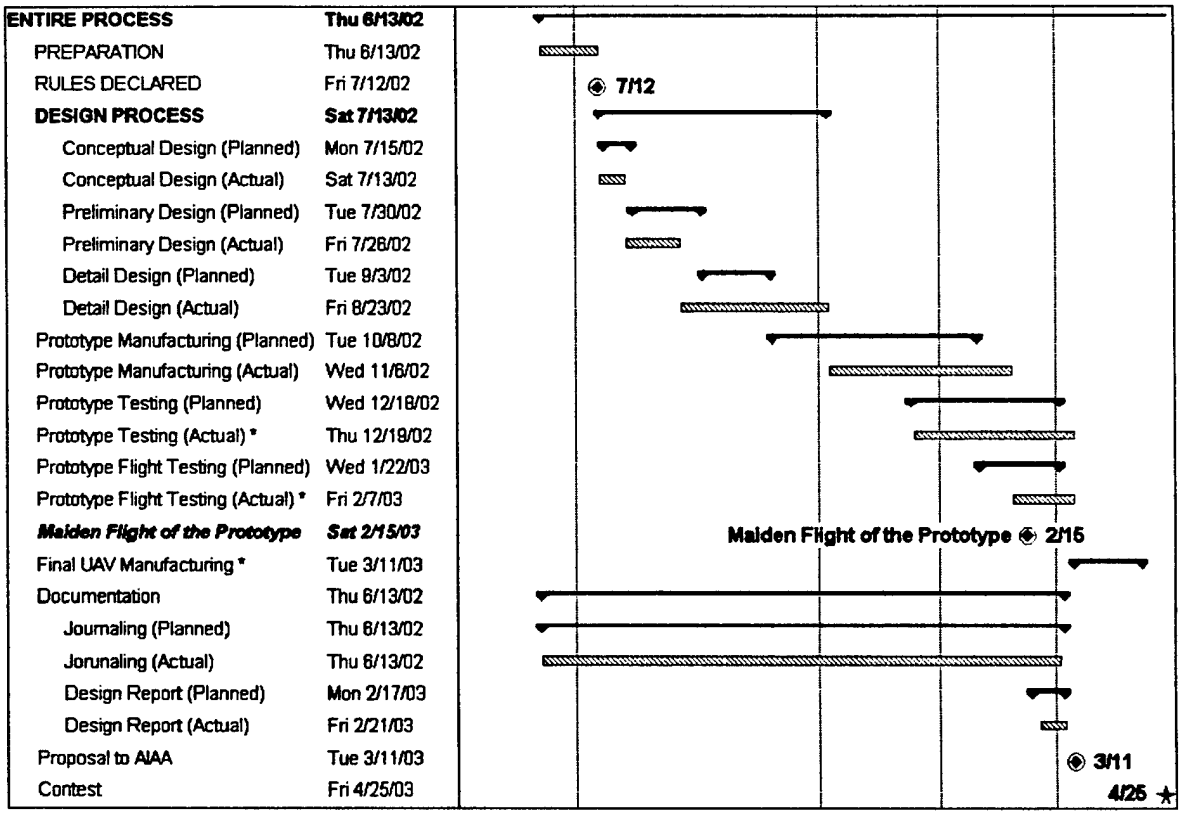

Figure 2.2 METU DBF Project Schedule Chart. **Red** lines illustrate major groups, where **Black** lines illustrate planned and **Green** lines illustrate actual dates. Red marks indicate important events.

CHAPTER 3 - CONCEPTUAL DESIGN

The aim of the conceptual design phase is to come up with a concept sketch of the configuration. Since many design alternatives exist for each component of the aircraft, a tool for quantitative trade-off analysis between different alternatives is needed to be developed. The team started the process of trade-off analysis by determining the figures of merits and continued with developing a scoring procedure to obtain an aircraft concept which best suits to the specified mission requirements.

3.1 Mission Requirements

The key elements of mission requirements can be roughly stated as:

- The aircraft must fit into a box having dimensions of 2 feet wide by 1 foot high by 4 feet long (interior dimensions).
- The aircraft must be electrically powered with a maximum total battery weight of 5 lbs.
- The aircraft must be able to carry and remotely deploy a payload which is a box 6 inches wide by 6 inches tall by 12 inches long and must be ballasted about its planform centroid to weigh at least 5 lbs.
- The aircraft must be capable of carrying a simulated cylindrical antenna with a section of (unmodified) "6-inch" Schedule 40 (white) PVC pipe three inches tall, with the top and bottom sealed flush with flat 1/16" Plywood sheets. The antenna must be completely exposed on the exterior of the aircraft and stand-off from the nearest airframe structure by a minimum of 3 inches. The antenna (cylinder) may not be faired in any manner.
- In any mission type, the aircraft should be able to take-off from a maximum ground roll distance of 120 ft.

3.2 Configuration Alternatives

The design of each component of the aircraft involves many trade-offs among the alternatives associated with them. However, in many cases, this spectrum of alternatives can be narrowed down with a prior competitor study or the mission profile may inherently restrict some of these alternatives.

The competitor study is the investigation of the properties of aircrafts that have similar mission profiles to the current design concept. The aircraft produced for the past AIAA DBF competitions form a perfect set of competitors. Therefore, the most successful DBF aircraft of the past are taken as models when determining and scoring the configuration alternatives.

The key elements of design for each component of the aircraft are described below.

3.2.1 The Wing

The geometrical design parameters that almost totally describe the wing performance of a low subsonic airplane are the aspect ratio, taper ratio and wing orientation on the fuselage.

For a rectangular wing, the taper ratio basically determines how close the lift distribution of the wing is to the elliptical one which in turn minimizes the induced drag of the wing. Actually, the exact elliptical lift distribution can only be achieved with an elliptical planform wing. However, the elliptical lift distribution can be closely approximated with a taper ratio selection of about 0.45.

The aspect ratio is a measure of how much the flow over the wing is influenced by the generation of tip vortices. The higher the aspect ratio, the less the flow over the wing is influenced by the tip vortices. Aside, almost every improvement in the aerodynamics of the wing tends to cause difficulties in production and requires a more complicated structure.

The possible production techniques for wing are foam core with composite or balsa skins, the foam rib structure with balsa skin and the balsa rib structure. In the foam core applications, a block of foam is shaped to a desired wing shape and then covered with a skin of either balsa wood or fiber-glass/carbon composite. Another alternative is described as foam rib covered with balsa wood, that is to say, the foam core is blanketed at certain sections of the wing in order to approach a rib structure which is advantageous in terms of its weight. The balsa rib structure is the classical rib structure application with the material being balsa wood. Note that, each wing structure alternative is considered to include at least a spar spanning the whole wing or a part of it. Also, a film coverage will be applied in order to ensure a smooth surface finish.

3.2.2 The Tail

The use of a tail on an aircraft is to stabilize and/or trim the aircraft in the pitch and yaw axes. This can be accomplished with different configurations of aerodynamic surfaces. Some configurations that are in common use are roughly illustrated in Figure 3.1.a

Each of the illustrated configurations has different characteristics in terms of aerodynamics, stability and control. The conventional tail is mostly preferred because it has a fairly simple and strong structure (Thus weighting less). However, it requires a careful sizing and arrangement of horizontal and vertical surfaces in order to avoid the recovery characteristics. The second most preferred tail configuration is the T-tail. It has a more effective vertical tail because of the end plate effect of the horizontal tail and the rudder is not in the wash of the horizontal tail even at high angles of attack. Therefore, the T-tail takes the advantage of well spin recovery characteristics. However, since the horizontal tail is not generally in the slipstream of the propeller, the take-off distance may be longer compared to the one with conventional tail. Also, horizontal tail may be ineffective of control in the case of stall because of the wake of the wing. V-tail seems advantageous because of the less wetted area and weight. But, the coupled controls in the yaw and pitch axes may cause problems in the handling qualities of the aircraft. For a longitudinally stable aircraft, the canard configuration is efficient in the manner that, the horizontal tail is also contributing to the lift rather than producing a down force in order to null the pitching moment of the wing. However, it is not that simple to adjust the center of gravity of the aircraft to its correct location for longitudinal static

stability. Also the stability and control of the aircraft in the yaw axes require the use of a larger vertical tail and rudder.

3.2.3 The Fuselage

The choices of fuselage geometry and the structure are the most critical parts of the design. The alternatives concerning the geometry of the fuselage are illustrated in Figure 3.1.b. A 3x2 matrix of alternatives is formed by different combinations of tail boom, tail boom with aft fairing and lofted fuselage configurations with the rectangular or circular/elliptical fuselage cross sections. In terms of aerodynamics, the fully lofted fuselage with circular/elliptical cross section stands as the ideal one.

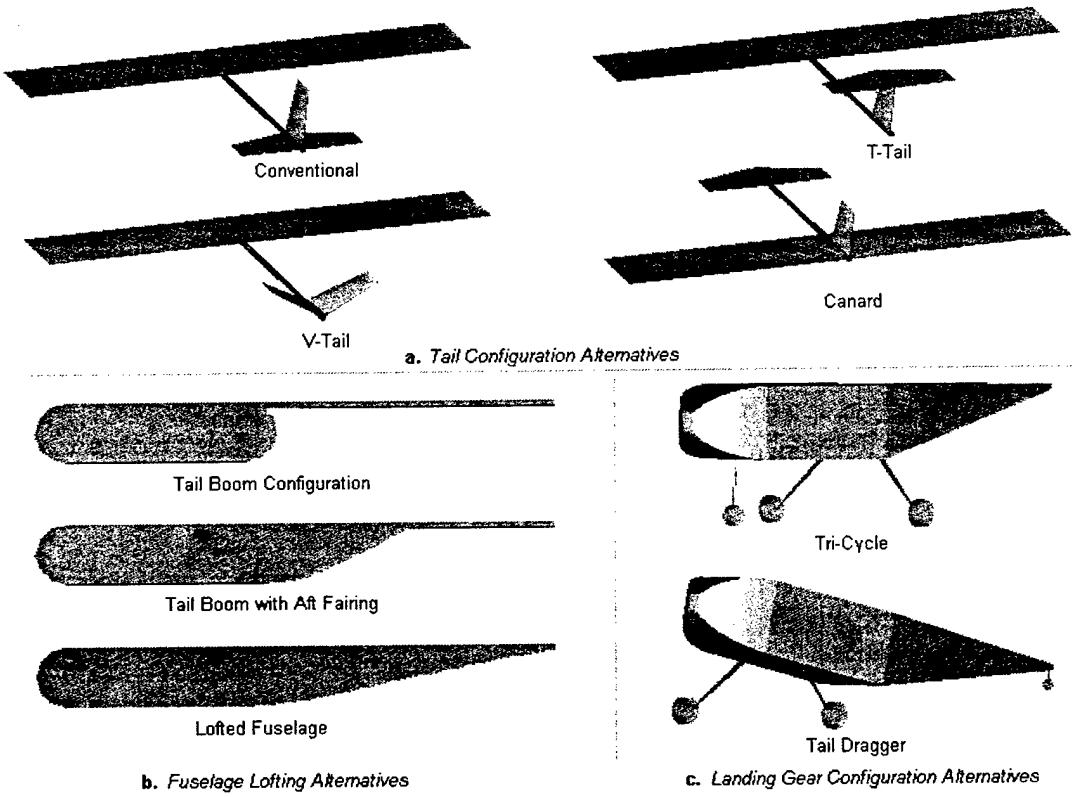

Figure 3.1 The Configuration Alternatives Considered for the Tail, Fuselage and the Landing Gears

However, it is the heaviest one among the alternatives. At the other extremity the tail boom type fuselage represents the lightest solution at a cost of more drag. Another alternative is to reduce the drag by employing a fairing at the aft part of the fuselage where the tail boom joint exists. Obviously, a circular/elliptical cross section offers better aerodynamic characteristics than the rectangular one.

However a rectangular cross-section fuselage is much easier to produce and offers flat surfaces for

easy assembly of various components of the aircraft. Note that, in all alternatives of the fuselage geometry, the fuselage is upswept in order to safe the tail from touching the ground during take-off.

3.2.4 The Landing Gears

The landing gear configuration greatly affects the ground handling qualities, take-off and landing performance of an aircraft. There are many variations in arrangement of landing gears. However, the two types which are named as tail-dragger and tri-cycle (Figure 3.1.c) are preferred for almost all small-scale aircrafts. The design team has not contradicted to this fact and considered only these two alternatives. Also, the mount point of the main landing gear constitutes another trade-off. The alternatives are to mount the main landing gear to the fuselage or to the wing. The former is usually used for high wing configurations whereas the latter is usually used for low wing configurations in order to have a light weight main landing gear. However special purpose designs may differ from this approach.

The landing gears are the strongest structures in an airplane. Since they weight much, it is essential to have a 'critical' design of the landing gears. That is to say, they should not be too oversafe. Usually aluminum or steel is used for the construction of the landing gears. The aluminum is relatively light but not as stiff as the steel. Also, the elastic characteristic of steel is more suitable for use in landing gears.

3.2.5 Propulsion System

Apart from optimizing engine type and number of batteries a conceptual trade-off for the propulsion system was carried on. The options to be considered were the location and number of the engine(s). The option of multi-engine concept provides a safe landing in case of engine failure during flight. But aspect ratio range determined by the end of conceptual design was safe enough to provide sufficient landing by gliding. Also the more propulsive components one has, the more one diverges from the simplicity approach violating the design principles. Furthermore an attempt of mounting engines on the wing (which may be quite necessary) would require additional stiffening of the wing in addition to the aerodynamic consequences it might possibly cause. A more detailed numerical evaluation of multi-engine considerations is taken into account more detailed in the Table 3.1

Although a pusher-prop configuration was also taken into consideration, it was found to be unnecessarily complicated and contradicting to the simplicity principle. Therefore, pusher-prop configuration was eliminated.

3.3 The Value System

The value system is a tool for scoring the configuration alternatives with the predetermined figures of merit (FOM) for each component. It provides a quantitative description of major advantages and disadvantages gained by each choice. Since it separately analyzes each choice of the design, it is not limited to certain aircraft concepts. The scoring procedure is a combination of analytical and statistical evaluations. For analytical evaluations, a critical parameter (like bending moment for the influence of

aspect ratio on the structural stiffness of the wing) is selected for each evaluation and a rough estimation of the parameter for different choices is done. On the other hand, the competitor study is used as the main resource for developing statistical evaluations.

The key design alternatives associated with each major component of the aircraft is scored over 12 for each figure of merit with a corresponding weighted multiplier to obtain a weighted average score. A score of 1 is given for a very low contribution to design performance whereas a score of 12 is given for an apparent superiority over the other alternatives.

Each team member is asked for his/her individual scoring. When averaged, the evaluations of all the team members formed the common choices of the concepts.

3.3.1 Figures of Merit (FOM)

Aerodynamics: For lift producing components, the criteria of scoring is lift to drag ratio, whereas for non-lift-producing components, it is directly the drag caused by that component.

Stability&Control: The effect of individual choices to the overall stability and controllability of the design concept is measured by this FOM.

Structural Stiffness: This FOM is a measure of a member's load carrying capacity. A member gets a high score if it successfully combines sufficient stiffness with enough elasticity.

Weight: Obviously, a design alternative weighing less gets the highest score for this FOM.

Cost: Each design alternative is scored for its cost which is calculated by the given rated aircraft cost model.

Producibility&Maintenance: Although an alternative seems to be very appreciable in the other FOMs, production capabilities may restrict the use of it. So, each alternative is scored for its ease of producibility and maintenance properties.

Assembly Time: Assembly time is one of the major contributors to the total score of the aircraft in this configuration. So, the penalties and gains introduced to the assembly time with the selection of each alternative should be accounted for. Hence the choices suggesting more modularity gets the highest score for this FOM.

3.3.2 Results of the Trade-Off Analysis

The scores of each design alternative corresponding to the prescribed figures of merit are tabulated in Table 3.1. The alternatives with the highest weighted scores are selected to form the initial concept of the aircraft. The selections are listed as:

- A non-tapered wing with aspect ratio between 6 to 9 and located at the top of the fuselage.
- A conventional tail configuration
- Tri-cycle type non-retractable landing gears without a suspension system. Main landing gear is mounted on the fuselage.
- A single tractor engine.

As promised at the beginning of this chapter, the initial concept sketch of the airplane is included in Figure 3.2

CONCEPTUAL DESIGN ALTERNATIVES		Aerodynamics	Stability&Control	Structural Stiffness	Weight	R.A.C.	Producibility	Maintenance	Assembly Time	WEIGHTED AVERAGE
Wing Geometry	*Multiplier*	5	4	4	5	3	3	-	2	
Aspect Ratio	*High (9-12)*	12	8	4	8	4	-	-	5	6.54
	Mid (6-9)	**10**	**10**	**8**	**12**	**7**	**-**	**-**	**8**	**8.42**
	Low (3-6)	3	12	12	9	12	-	-	12	8.31
Taper Ratio	**None (1)**	**7**	**-**	**10**	**12**	**12**	**12**	**-**	**-**	**7.96**
	High (0.7-0.9)	8	-	10	10	11	6	-	-	6.96
	Mid (0.35-0.7)	12	-	12	9	9	6	-	-	7.62
	Low (0-0.35)	8	-	10	8	7	4	-	-	5.88
Wing Position wrt Fuselage	**High**	**8**	**12**	**12**	**12**	**12**	**11**	**-**	**12**	**11.12**
	Mid	10	9	8	10	11	6	-	7	8.96
	Low	12	6	10	11	11	12	-	10	10.31
Tail Configuration	*Multiplier*	5	5	3	4	2	3	-	4	
	Conventional	**10**	**12**	**12**	**11**	**12**	**12**	**-**	**12**	**11.46**
	T-Tail	11	6	11	9	12	10	-	9	9.38
	V-Tail	10	4	11	12	11	8	-	10	9.12
	Canard	12	2	12	12	12	12	-	12	10.08
Landing Gears	*Multiplier*	2	-	5	4	2	3	1	5	
Configuration	**Tricycle**	**12**	**-**	**12**	**10**	**-**	**11**	**-**	**11**	**11.16**
	Tail Dragger	8	-	10	12	-	12	-	12	11.05
Main LG Position	**Under Fuselage**	**12**	**-**	**12**	**11**	**-**	**12**	**-**	**9**	**11.00**
	Under Wing	10	-	7	12	-	10	-	12	10.16
Retractable	Yes	12	-	6	5	4	6	8	12	7.64
	No	**2**	**-**	**12**	**12**	**12**	**12**	**12**	**2**	**8.82**
Suspension	Oleo	12	-	12	3	-	4	6	12	8.70
	Spring	4	-	10	10	-	8	11	10	8.32
	None	**10**	**-**	**10**	**12**	**-**	**12**	**12**	**12**	**11.30**
Number of Engines	*Multiplier*	2	3	5	4	2	3	1	-	
	Single	**12**	**10**	**12**	**12**	**12**	**12**	**12**	**-**	**11.7**
	Double	6	12	8	9	9	5	6	-	8.15

Table 3.1 FOM analysis for the conceptual design

3.5 Payload Mounting & Deployment System Concepts

Any means of electric or hydraulic actuated systems to accelerate the payload are avoided for the sake of simplicity and a low cost aircraft. Instead, gravity driven systems are considered.

The mechanism of deployment is highly dependent on the landing gear and the fuselage configurations. Thus, the tri-cycle configuration landing gear and the tail-boom type fuselage with an aft fairing is assumed upon the FOM analysis which is presented in the previous section.

It is desirable to have an aircraft center of gravity (cg) position essentially independent of the payload configuration. That implies planform centroid of the payload to be close to the aircraft cg. The main landing gear is also located slightly aft of the aircraft cg as a rule of thumb. That necessitates the placement of the payload through the section of the fuselage that the main landing gear is also mounted upon.

Mainly two types of deployment systems are considered. One is the vertical deployment and the other is the inclined deployment with rail guidance. The vertical deployment is the simplest solution of the deployment mechanism. However, it requires the corresponding bottom surface of the fuselage to be free of any structural elements. Since the main landing gear is also to be mounted on the same section, some structural problems would appear. The inclined deployment system prevents these problems at the cost of increased complexity. The design team agreed to use the vertical gravity driven deployment system in order to maintain the simplicity principle.

Another problem was the location of the simulated cylindrical antenna on the aircraft. Since the antenna must have an unobstructed view of 360 degrees, it is almost for sure that it should be mounted somewhere over the fuselage. Since the location of cg of the aircraft is desired to be independent of the antenna configuration (whether mounted or not) it is decided to be mounted on the wing close to the aircraft cg.

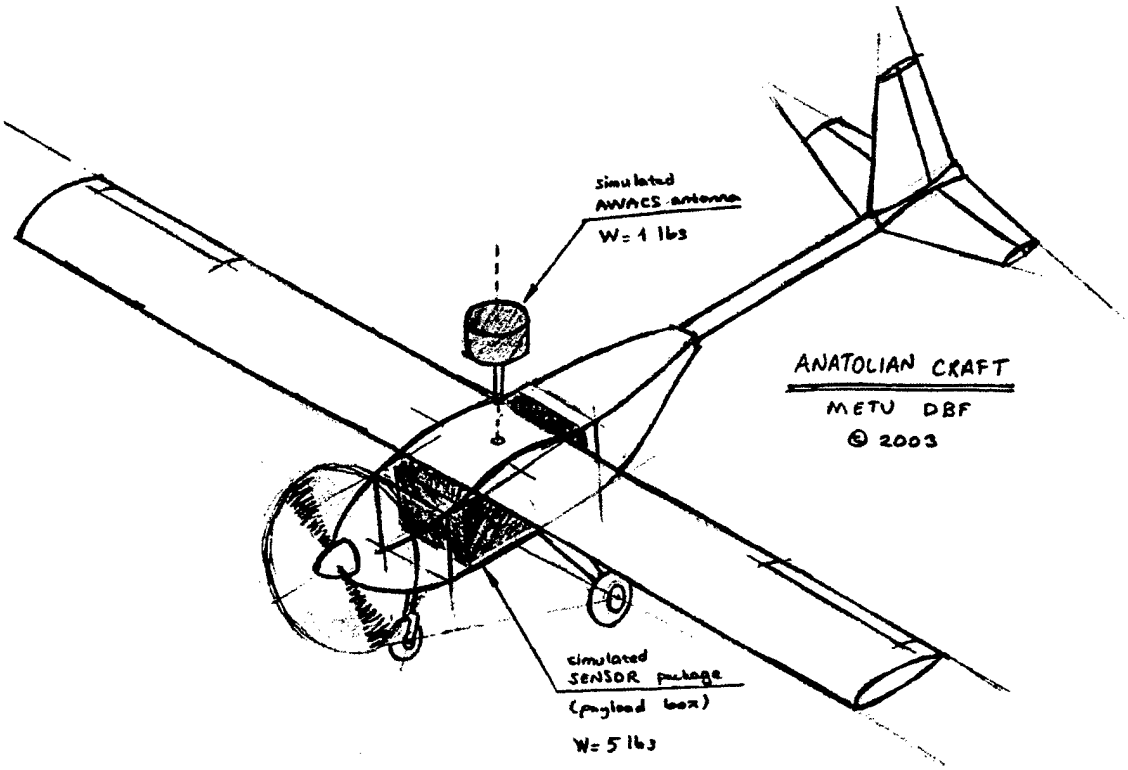

Figure 3.2 Conceptual Sketch of the Aircraft

CHAPTER 4 - PRELIMINARY DESIGN

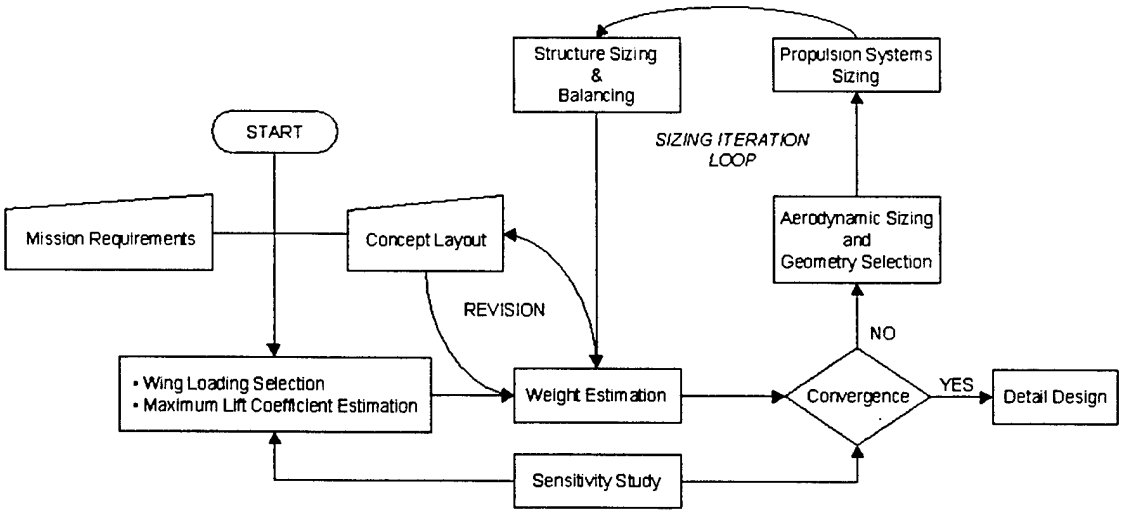

Figure 4.1 Preliminary Design Cycle

There are many different approaches of sizing an airplane. Usually a parameter, which is critical to the mission requirements, is selected as the basis for the sizing. In our case, the design team agreed to employ 'sizing to wing loading' method. This sizing sequence starts with a selection of the wing loading and immediate estimates of the take-off gross weight and maximum lift coefficient. This is followed by sequential sizing of aerodynamic surfaces, propulsion systems and structural elements. With the use of these initial sizing values, the weight estimation is refined and a revision of concept layout is done when necessary. This is in fact an iterative procedure, which is expected to converge after a sufficient number of cycles.

The remaining sections of this chapter are organized in the sequence as shown in the Figure 4.1, which is an illustration of the preliminary design cycle followed.

4.1 Selection of Wing Loading and Estimation of Maximum Lift Coefficient

Wing loading is nothing but the weight of the airplane divided by the wing planform area. A low value of wing loading is desirable in terms of take-off and landing performance of the aircraft. However, this requires a larger wing, which may greatly increase the rated aircraft cost of the aircraft. This constitutes a trade-off problem between aircraft weight and rated aircraft cost vs. wing loading. However, at this stage of design neither an initial weight estimation nor the estimation of maximum lift coefficient is available yet. Therefore, this trade-off analysis is left to the sensitivity studies, which is to be conducted before finalizing the preliminary design phase. Instead adaptation of the history is considered to be a convenient method for this step.

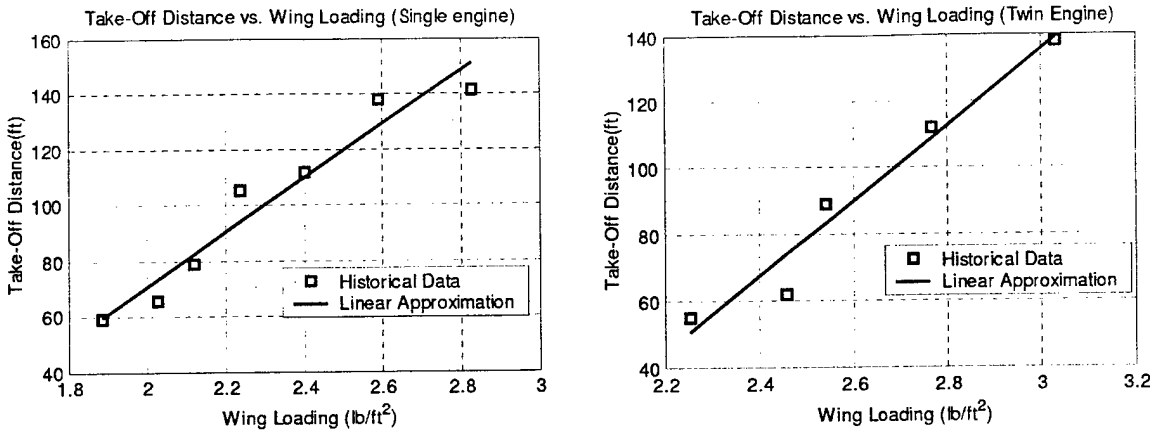

Figure 4.2 Historical Trend Curves for the Selection of Wing Loading

The historical trend curves concerning the take-off distance versus the wing loading values of different aircraft are constructed using the data obtained by the competitor study. Please note that the presented data is the result of a filtering of original data by statistical analysis. That is to say, the data points, which are outside the three standard deviations, are rejected.

This year, contest rules restrict the take-off ground roll distance to maximum 120 ft. The Figure 4.2 suggests a convenient way to select the wing loading value corresponding to 120 ft. of take-off ground roll distance. Aside, if the additional drag caused by the cylindrical antenna which is required for missile decoy mission is taken into account, sizing for a lower value of take-off ground roll distance would be more reasonable. As a first estimate, the team agreed to select the wing loading corresponding to 80 ft. of take-off ground roll distance. Hence, a wing loading value of 2.1 lb/ft^2 is selected referring to the trend curve for single engine aircraft on Figure 4.2.

Another input parameter to the design cycle is a rough estimation of maximum lift coefficient of the wing, which is to be revised in preceding steps of the cycle. A value of 1.8 is selected as a first estimation of the maximum lift coefficient as suggested by Reference [1].

4.2 Initial Weight Estimation

Various methods of getting an initial weight estimation of the aircraft concept exist in the literature. Since the preliminary sizing of an R/C controlled airplane involves relatively simple and quick methods of iterations, one may not need a very close approximation of the actual weight at the beginning but may start with a crude approximation and improve it within the sizing iterations. Reference [2] suggests a quick way of performing an initial weight estimation by assuming the take-off gross weight of the aircraft being equal to four times the payload weight. Knowing that the payload weight is specified as 5.9 lbs (5 lbs simulated sensor package + 0.9 lbs simulated antenna), the initial estimation of the take-off gross weight turns out to be 23.6 lbs.

4.3 Aerodynamic Sizing and Geometry Selection

Aerodynamics mainly concerns the lift, drag and moment created by the components of the aircraft that are immersed to the airflow. The intention of this phase of design is to form and size the aerodynamic surfaces and the fuselage so as to maximize the lift-to-drag ratio of the aircraft at a reasonable range of rated aircraft cost. The analysis and selection of individual components of the aircraft is presented in the following sections.

4.3.1 The Wing

Sizing: Having estimated the wing loading and the take-off gross weight of the airplane, the wing area can easily be calculated based on these estimations. In every sizing cycle (*See* Figure 4.1), the wing area is recalculated using the refined estimation of the aircraft weight. After a sufficient number of iterations, only minor changes are observed in weight estimation between successive steps.
Meanwhile, propulsion system configuration of the aircraft had already been fixed by the propulsion group.

Airfoil Selection: One of the major challenges of this competition seems to be fulfilling the mission requirements with minimum propulsive power. This can be accomplished either by an airfoil with high lift-to-drag ratio or by a high lift class airfoil which minimizes the wing weight and possibly compensates for its relatively high drag.

The other criteria on airfoil selection are the design Reynolds number and the development group. Development groups with high reputation are preferred because they have validations of their airfoil designs with experiments and common uses in existing aircraft. Design Reynolds number describes the operating flow conditions for which the airfoil is designed/optimized. If an airfoil, which is designed for laminar flows, is used at high Reynolds numbers', it will probably fail to achieve the desired performance. The Reynolds number corresponding to UAV's for this size and speed is in the order of 3E5.

Upon a literature survey, the team came up with two alternative airfoils. The first one is Selig/Donovan-7062 which is a relatively thick airfoil designed by UIUC LSATs "Selig Group" for low Reynolds Number flight. The second one is Eppler-423 that produces very high lift even at small angles of attack due to its high camber ratio.

The comparison of these two airfoil sections from several aspects is given as Figure 4.3. Eppler 423 airfoil produces a very high lift compared to Selig at the same angle of attack values but the price for this lift is its high drag. Bearing in mind that the short take off distance requirement and seeing the efficiency (CL/CD) character of this airfoil in high lift coefficient range, Eppler 423 seems to be a reasonable choice for the airfoil section although it produces significantly more drag.

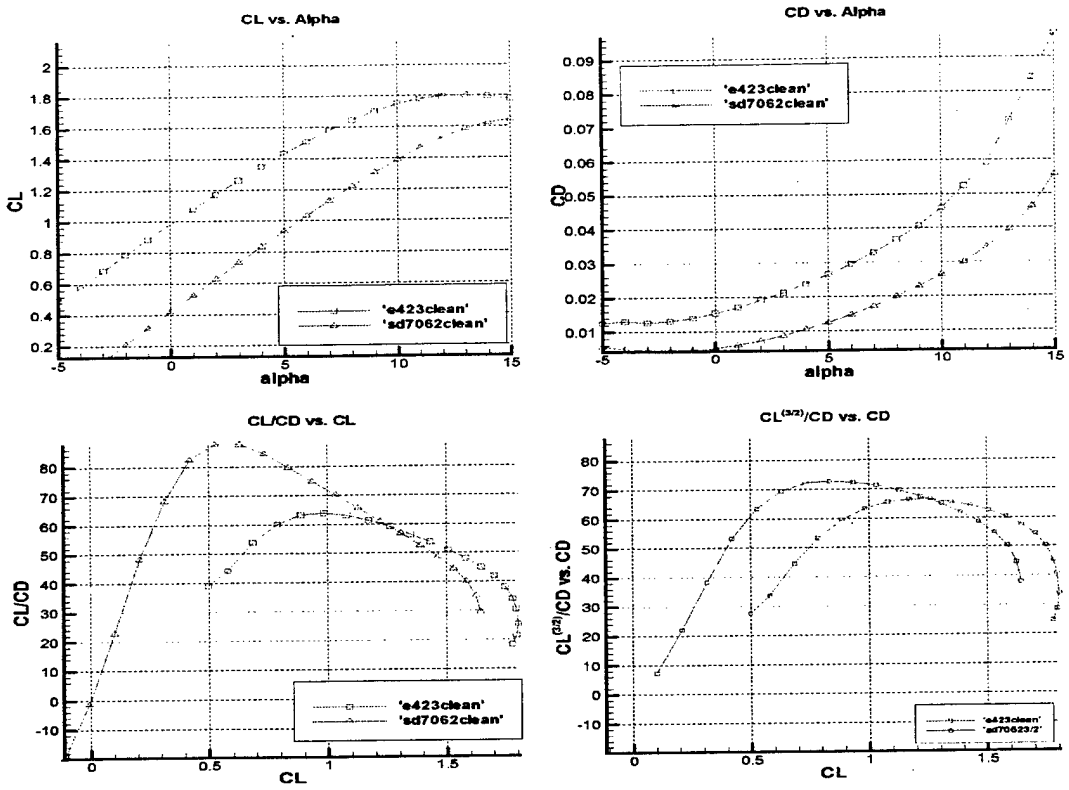

Figure 4.3 Comparison of the e423 and sd7062 airfoils

Geometry: The key geometric parameters of a wing to be flown at low subsonic speeds are its aspect ratio, taper ratio, dihedral angle and section geometry.

In order to stabilize the aircraft laterally, either the wing is located at the top of the fuselage (high wing configuration) or the wings are given a positive dihedral angle. In the conceptual design phase, it was already decided to have a high wing configuration in the light of figures of merit.

In the conceptual design phase, ranges of values for the aspect ratio and taper ratio were scored and selected. According to these choices, a straight wing with an aspect ratio ranging between 6 and 9 was considered as advantageous in terms of the prescribed figures of merit analysis.

The above considerations significantly narrow down the spectrum of alternatives concerning the wing planform geometry. In fact, the only parameter left to be determined is the aspect ratio. Ideally, the greater the aspect ratio, the higher the efficiency of a wing. However, the limiting factor of the aspect ratio is the increased bending moment of the wing, which in turn increases the structural weight of the wing. This constitutes a trade-off problem to be solved by collaborative work of aerodynamic and structure groups. After a few steps of iteration loops (*See* Figure 4.1), the structure group has gained an idea of the wing structure and developed a model for wing weight at different aspect ratios. According to this model, the wing weight is calculated for different aspect ratios and presented in Figure 4.4. The figure reveals that the aspect ratio, which minimizes the weight of the wing, is estimated as 8.

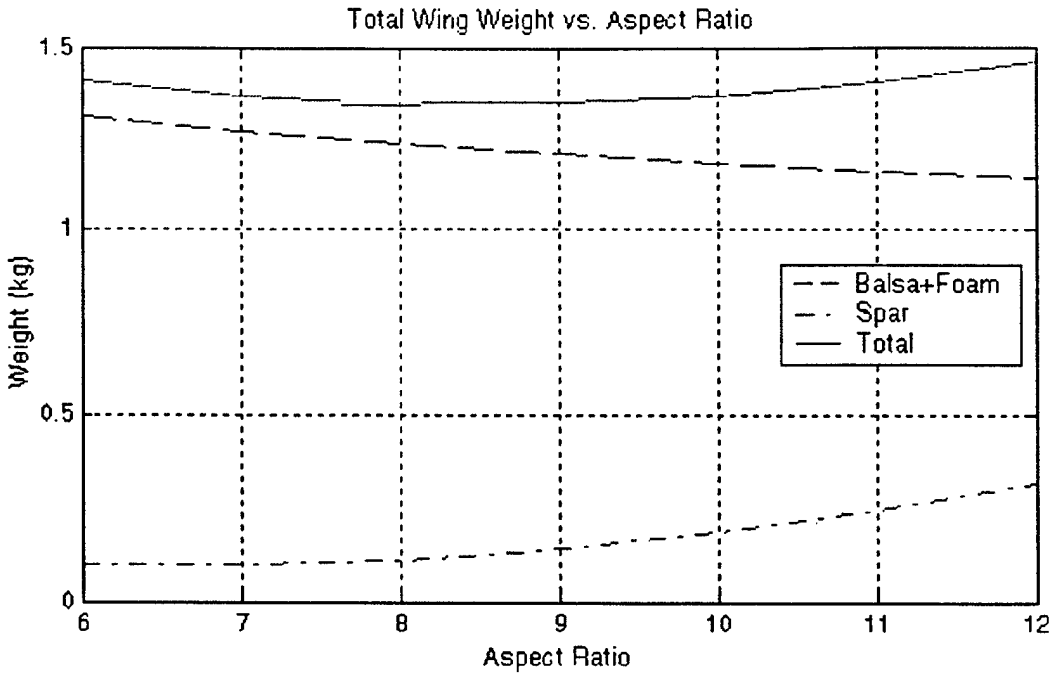

Figure 4.4 The variation of wing weight with aspect ratio

4.3.2 Empennage Group & Stability

The sizing of the tail surfaces is a very complicated and problematic procedure. Lots of problems needs to be solved like, the restriction on the horizontal tail span that it can not exceed the quarter length of the wing span, the designed tail have to overcome the high moment produced by the wing, because the length of the fuselage directly effects the Rated Aircraft Cost and the requirement of fitting all parts of the aircraft into a box which has specified dimensions. These coupled and confusing problems can be solved with iteration on the design. Therefore, a program is developed to gain speed while making routine calculations. The program takes the center of gravity location of the aircraft and the data related with wing as input and calculates the tail boom length, the required tail incidence, tail surface area and the static margin of the aircraft.

Also the effect of the cylindrical antenna has to be taken into account while sizing the empennage.

In the conceptual design phase, the cylindrical antenna was decided to be assembled over the wing near the mid chord. This may have a negative effect on the rudder control and lateral stability. Therefore, during the mission that an antenna is carried a bigger vertical stabilizer is needed compared to the vertical tail that is used for the other missions to stabilize the aircraft.

The effect of loaded and unloaded cg locations and the cylindrical antenna on both lateral and longitudinal stability is another problem. To get rid of the unwanted effect of payload on stability of the aircraft, basically the cg location of the payload has to coincide with the cg location of the empty aircraft. However, the negative effect of the cylinder antenna on the stability cannot be avoided.

At table 4.1 one can see the results of iterations done and the major sizes of the horizontal and vertical tail and the location with respect to the fuselage, the incidence and the airfoil used for both stabilizer surfaces.

Empennage Specifications	
Distance from Wing ac to horizontal stabilizer ac	4.06(ft)
Horizontal stabilizer area	1.45 (ft2)
Vertical stabilizer area	0.81 (ft2)
Horizontal tail angle of incidence	0 deg
Airfoil section used for horizontal stabilizer	NACA0009
Airfoil section used for vertical stabilizer	NACA0009
Stability	
Static margin (empty)	0.17
Static margin (with payload)	0.14
Static margin (with payload and antenna)	0.13

Table 4.1 Estimated Empennage Specifications and the stability characteristics of aircraft for three different conditions.

Depending on the static margin values obtained from Table 4.1, the aircraft seems to be stable but when it is unloaded large static margin may cause a decrease in maneuverability capability of the aircraft. Although static margin changes a lot between loaded and unloaded configurations, the values are in the range of limits.

4.4 Propulsion System

For the propulsion system selection major criteria to be satisfied was the static pitch speed to stall speed ratio, which roughly describes the ability of the aircraft to accelerate near the stall speed. Where a static pitch speed to stall speed ratio of 2 corresponds to a critical flight regime and lack of thrust at typical flying speeds, a ratio of 2.5 is described as ideal for modeling purposes, whereas a static pitch speed to stall speed ratio of 3 is a value which is quite suitable for aerobatic flight characteristics.

In the preliminary design phase, the team decided not to risk the flight performance and preset this ratio to be near 2.5 providing a thrust loading resembling a trainer model aircraft. On the other hand for propeller synchronization and rated aircraft cost considerations, team decided to use a single motor.

The team analyzed and tested combinations of motors/propellers/batteries, which were available in the inventory using commercially available "MotoCalc" software. Table 4.2 summarizes these results.

Propeller	Number of cells	Static pitch speed to stall speed ratio	Static thrust to weight ratio	Excess thrust to weight ratio at stall speed	Full throttle motor current at best L/D airspeed (Amps.)	Motor steady state temp. [°C] at best L/D airspeed	Static pitch speed to stall speed ratio	Static thrust to weight ratio	Excess thrust to weight ratio at stall speed	Full throttle motor current at best L/D airspeed (Amps.)	Motor steady state temp. [°C] at best L/D airspeed
		Graupner Ultra 3450-7 2.75:1					Graupner Ultra 3450-7 1:1				
16x8	30	2.08	0.34	0.08	9.6	0	-	-	-	-	-
	32	1.86	0.28	0.01	5.6	0	-	-	-	-	-
	36	1.75	0.25	0	11.2	0	-	-	-	-	-
18x12	30	2.47	0.41	0.23	21.3	0	-	-	-	-	-
	32	2.61	0.45	0.27	23.8	0	-	-	-	-	-
	36	2.87	0.53	0.35	28.9	0	2.02	0.26	0.11	35.9	106
20x14	30	2.68	0.55	0.35	32.6	0	-	-	-	-	-
	32	2.79	0.5	0.4	35.8	101	1.62	0.2	0.05	29.5	0
	36	-	-	-	-	-	1.1	0.09	0	15.9	0
22x14	30	-	-	-	-	-	1.25	0.17	0.03	26.9	0
	32	-	-	-	-	-	1.02	0.11	0	19.7	0
	36	-	-	-	-	-	-	-	-	-	-
		Astro Cobalt 60 11T#23 2.75:1					Astro Cobalt 60 13T#24 2.75:1				
16x8	30	1.44	0.17	0	7.7	0	1.23	0.12	0	5.2	0
	32	1.53	0.19	0	8.4	0	1.3	0.14	0	5.6	0
	36	1.71	0.23	0	9.9	0	1.46	0.17	0	6.6	0
18x12	30	2.07	0.29	0.11	12.6	0	1.78	0.21	0.04	7.3	0
	32	2.19	0.32	0.14	14.3	0	1.89	0.23	0.06	8.5	0
	36	2.42	0.38	0.21	17.6	0	2.11	0.28	0.1	10.7	0
20x14	30	2.28	0.41	0.22	20.1	0	2	0.3	0.12	12.5	0
	32	2.41	0.45	0.26	22.4	0	2.11	0.3	0.15	14.2	0
	36	2.64	0.52	0.33	36.9	116	2.33	0.39	0.2	17.4	0
22x14	30	2.17	0.52	0.27	24.5	0	1.91	0.39	0.15	15.1	0
	32	2.27	0.57	0.32	27.3	111	2.02	0.43	0.19	17.3	0
	36	2.45	0.64	0.4	32.4	146	2.21	0.5	0.26	21.2	0

* Null values stand for non-critical steady state temperatures at best lift to drag ratio airspeed

** Null values denote configuration is unable to supply the thrust for level flight

Table 4.2 Results obtained from analysis of different motor/propeller/battery pack configurations

From the analysis, two combinations were selected as candidates for final propulsion system configuration. The first candidate was 32x2400 mAh cells in series feeding a Graupner Ultra 3450-7 motor with 2.75:1 gear ratio driving a 2 blade wooden 18"x12" propeller and the other one was again 32x2400 mAh cells in series feeding an Astro-Flight Cobalt 60 11T#23 Motor with 2.75:1 gear ratio driving a 2 blade APC 20"x14" propeller. The first one was not selected at the end of static testing since the gearbox adapted to the original direct drive configuration by the team created some noise and hence

transmission losses. In addition, the motor was not certified for the voltage applied and the team had no functional spares.

After deciding for the second configuration, further analysis and tests were done in order to fix the number and capacity of battery cells and propeller to be used. For selecting the number of cells, our analysis showed that less than 32 cells were not sufficient for supplying the thrust "enough" for climb, and more than 32 cells was not suitable since the steady-state motor temperature was higher than allowed, that is above 100 degrees Celsius.

Endurance was the main parameter in the selection of cell capacity. The most energy demanding flight mission of the present competition to be completed was simulated by a 6-minute static run at full throttle. From the results of the analysis carried out (see Figure4.5-a), 2400 mAh batteries were selected to be the optimum choice for this particular configuration. Besides the limit on maximum battery weight, increasing capacity of cells yielded less flight time when compared to the theoretical value due to their effect on gross weight, whereas choosing a lower capacity was better when compared to the theory, yet unable to meet the 6-minute static run at full throttle condition.

Finally, propeller selection was optimized. For optimizing static pitch speed to stall speed ratio, possible solutions were investigated, among which one can name increasing the pitch, decreasing the diameter, increasing the rpm of the propeller or increasing the voltage supplied to the motor. Team also analyzed various configurations and obtained the curves for three different pitch values against various diameters ranging from 18 to 24 inches as shown in Figure 4.5-b A general criterion for propeller selection used by the modelers is to choose a value of propeller diameter to pitch ratio of 1.5:1. Choosing a diameter to pitch ratio below 1.5:1 results in reduced propeller efficiency at low speeds due to propeller stall. Although this is not likely to affect the flying characteristics, it may cause difficulties during take-off.

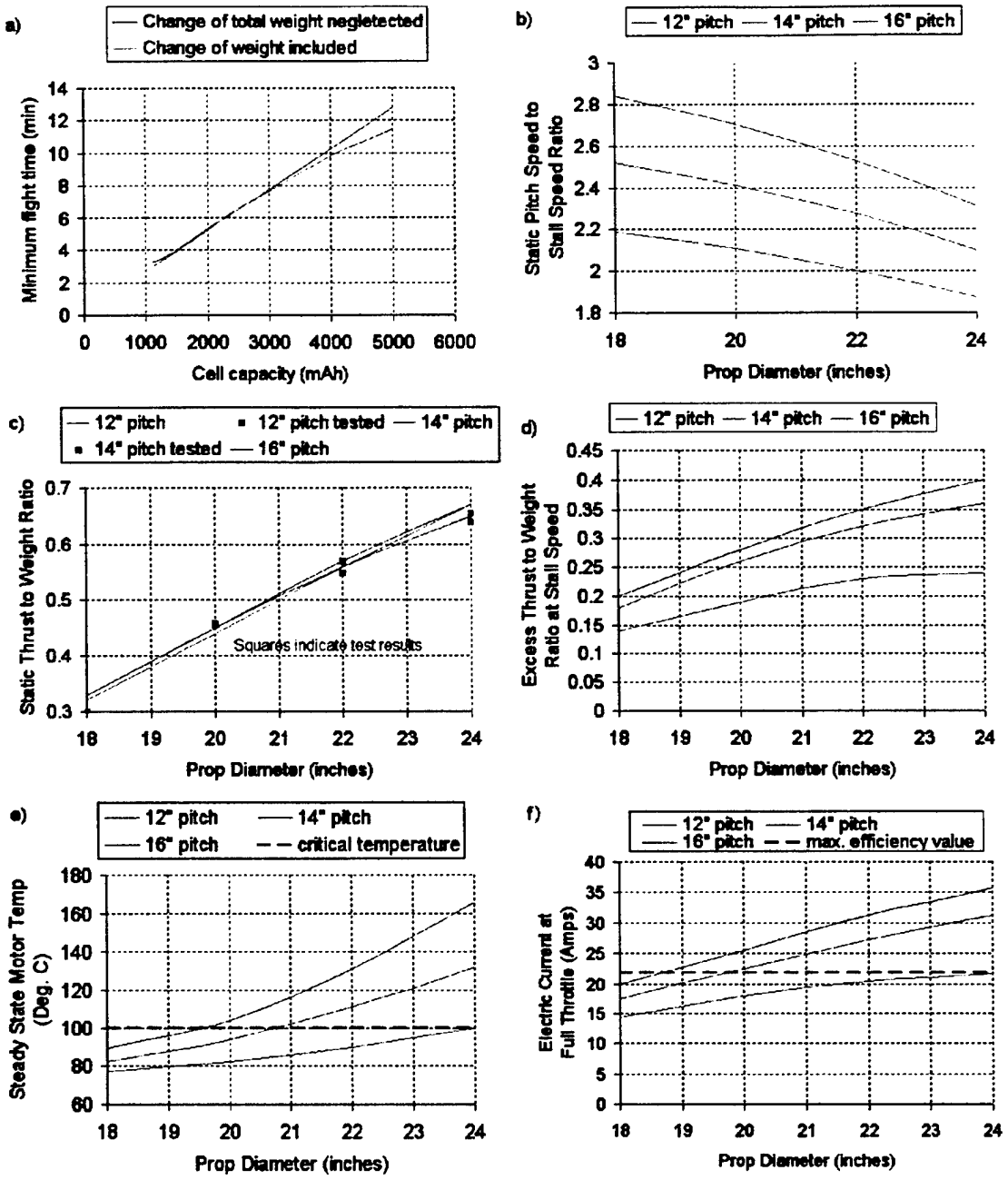

Figure 4.5 Propulsion system optimization curves.

As far as selecting the propeller pitch is considered, it is observed that the propeller pitch has no significant effect on the static thrust values as shown in Figure 4.5-c since the motor has a limiting effect and the propeller pitch is inversely proportional to static rpm. For determining the static thrust to weight ratio, the propeller diameter is determined to be the dominating parameter. It is observed that choosing a static thrust to weight ratio above 0.4 improves the take-off distance and the energy consumed during the

take-off since the ground friction is decreased. On the other hand, increasing the diameter for higher static thrust yields considerably lower flight times.

Considering the thrust available at flight conditions, stall speed was taken as a basis and it was observed that choosing a pitch of 14 inches and above is eminently better in terms of the thrust supplied (see Figure 4.5-d) but endangering the flight in terms of steady-state motor temperature if a propeller diameter above 20 inches was chosen. This is shown in Figure 4.5-e.

Taking into consideration the electrical efficiency of the motor as shown in Figure 4.5-f, it is observed that a current of 22.4 Amperes is the best efficiency current. Under these conditions, a propeller having a diameter of 20 inches and a pitch of 14 inches was chosen as the best choice satisfying all the requirements of the team resulting from the foregoing analysis.

4.5 Structural Design Analysis

In the structural part of the preliminary design phase of the aircraft, various methods were discussed to stiffen the structure of the aircraft, which was designed during the conceptual design phase.

Most of the structural parts of the aircraft are open-section beams. Therefore, the stress analysis methods used contains open-section beam analysis including flat plate buckling under combined loading using Euler stresses. Moreover compression, bending, transverse and shear loading analysis were made on each member of the aircraft. In addition, unit-load method was applied to determine the deflections of the wing spar, the main landing gear and the tail boom.

Besides taking special considerations into account of certain components of the aircraft, technique of FOM's is used to determine the most suitable structural design concepts for the fuselage, landing gear, empennage and the wing.

4.5.1 Figures of Merit

The figures of merit used during this evaluation are the same as the ones used and depicted explicitly in the conceptual design chapter (see Chapter 3).

4.5.2 Fuselage

As discussed in the conceptual design chapter, box profile for the fuselage was selected because of its simplicity in production and maintenance.

First of all, the construction material for the fuselage was selected. Possible options were wood, metal, carbon composite and e-glass composite. Due to the fact that a carbon composite manufacturing facility cannot be found this year, is option is eliminated right from the beginning. E-glass when used to construct a monocoque fuselage came out to be much heavier than either wood or metal stiffened frame structures. Considering that the fuselage is to carry only a very small amount of shear loading, the use of stressed skin is decided to be useless with the help of the FOM's. Since the skin is not expected to carry

a significant shear load much lighter options, like balsa sheeting and heat film, than e-glass skin are considered for further analysis.

The question then was whether to use wood or metal for the construction of the fuselage frame. Although woodworking option seemed easier than the metal working option, wood could not sustain sufficient rigidity at the assembly joints. For an improved assembly time, providing an easy and reliable assembly system is a must. Using the FOM evaluation the frame is decided to be built up from metal. Among the metal options there were two materials; steel and aluminum. Despite its ease in manufacturing as welding, steel came out to be unnecessarily strong and heavy when compared to aluminum. Apparently tempered aluminum 2024-T3 was chosen as the metal construction material for the fuselage.

During the construction phase two approaches arose; first was to use a multi-rib frame which was more elastic and lighter in comparison and the second was the main rib approach which was reducing the assembly time by combining all joints in one and providing a simpler structural analysis. Although in the first approach the stress is distributed more uniformly throughout the whole frame, the assembly time was significantly longer. Therefore the second option seemed to be more sensible.

4.5.3 Wing

It is clear that the wing must be partitioned at least into three segments in order to fit inside the given box dimensions. This also provided the advantage of having no joints at the mid section of the wing where bending stresses due to the wing loading is maximum. Employing the FOM procedure the optimized wing structure was obtained to be the foam rib structure with balsa skin. After carrying out the torsional analysis, the mentioned sandwich structure proved to withstand the corresponding shear stress values. Hence a single spar through the whole span at the quarter chord location is found to be safe enough.

To decide on what type of cross section to be used in manufacturing of the spar, several alternatives were taken into account among which were: C beam, I beam, and the circular profiles. Before starting with a stress analysis, a FOM evaluation is again employed and as a result "C" profile beam is selected for the manufacturing of the spar. Due to its proven structural efficiency, again the tempered aluminum 2024-T3 is used for the production of the wing spar. After this point a detailed stress and buckling analysis are performed. The maximum state of stress at the mid-section of the wing was found to be lower than the estimated buckling stress.

4.5.4 Landing Gear

The result from the conceptual design chapter showed that it is more convenient to place the main landing gear to the fuselage. Since the main rib is the only load-carrying member in the aircraft frame, the main landing gear should necessarily be attached to it. In addition, since the payload is deployed from the bottom of the fuselage, the position of the main landing should not block the payload.

In this case, there were two main options, in which the landing gear is either positioned adjacent to the inside or outside of the fuselage wall. The outside option was eliminated because of the additional drag it will cause, plus some problems in fixing which had a negative effect on the assembly time and the need for more stiffening that would cause an overall increase in weight. Therefore, the inside option was selected. Since producing the landing gear in two pieces, as left and right separately, would require twice as more fasteners while not providing a net superiority in strength, it was decided to have the landing gear as a single piece.

Two materials were considered for its manufacturing, steel and aluminum. In the analysis, both of them were taken into account with different beam profiles. Regardless of the profile shape used, steel provided more strength and stiffness than aluminum. Sufficient strength is obtained from a "T" profile, which was the lightest, however in critical regions, it is modified to an "I" and box profile for safety. These choices are graded in the FOM.

4.5.5 Empennage

According to the calculated aerodynamic loads and initial estimated weight of the empennage, foam and balsa skin was found to provide the required strength. Therefore in the vertical and the horizontal stabilizer no spar is used, which in turn lead to a significant reduction in weight.

To assemble the horizontal and the vertical stabilizers perpendicular to each other, an aluminum box is fixed in the middle of the horizontal by means of adhesion. The cross sectional dimensions of the box are chosen such that the circular tail boom fits into it. By means of the box concept, vertical stabilizer, horizontal stabilizer and tail boom could be assembled easily, which also improved the assembly time.

The tail boom must be sufficiently stiff to ensure that the tail incidence should not be changed due to tail loading. To maintain its stiffness, two different cross sections were considered for the construction of the tail boom: a box beam and a circular cross section. Since the circular cross section had improved torsional rigidity, and is readily available, circular cross section is selected. By looking at the results of the stress analysis of the tail boom, it was decided that a thin-walled circular 2024-T3 aluminum tube is the best material for this design.

4.6 Sensitivity Analysis

4.6.1 Mission Models & Mission Performance Prediction

There are three types of missions at least two of which are forced to be performed as described in the contest rules. Correct determination of the mission types to be performed is the path to obtain a high rank in the contest. Therefore, all of the possible combinations of mission types to be selected were compared quantitatively in terms of associated flight score predictions.

There are three different possibility of combinations exist as described below.

1) A & B: This couple of missions can be described as 'heavy' missions. The cylindrical antenna has an effect of slowing down the airplane greatly. That is to say, the aircraft has to have a lower wing loading in order to be able to produce lift at lower speeds and take-off without violating the 120 ft. take-off distance restriction. The payload deploy mission is 'heavy' because of additional weight of deployment mechanism and has the same low wing loading requirement as a consequence. A reduction in the wing loading means a greater wing thus a higher wing weight and rated aircraft cost. However, this combination of missions has the highest overall difficulty factor.

2) A & C: These couple of missions has a major advantage of the possibility of making a closed structure fuselage without any payload deployment hole and payload deployment mechanism. This results in an ease of stiffening the fuselage structure and a gain in weight and rated aircraft cost. Also with this combination of the missions, the aircraft is free of one extra landing and a deploy job. That is to say, it is a safer combination. However, in terms of difficulty factors, this combination is has an average ranking.

3) B & C: A combination without a cylindrical antenna job significantly reduces the required power of the aircraft. Bearing in mind that the propulsive power is the main contributor to the rated aircraft cost, this mission profile combination yields a 'cheap' aircraft whence having the lowest overall difficulty factor among the possible combinations.

Table 4.3 includes a comparison of mission combinations in terms of predictions of the assembly time, the mission time, the rated aircraft cost and the total flight score.

Mission Couple		Difficulty Factor	Estimated Flight Time (sec)	Estimated Assembly Time (sec)	Single Flight Score	Total Flight Score	Rated Aircraft Cost	Total Score
1	A	2	250	180	0.279	0.49	12.1	4.12
	B	1.5	230	180	0.219			
2	B	1.5	190	180	0.243	0.40	10.5	3.9
	C	1	180	180	0.166			
3	A	2	230	150	0.315	0.48	11.8	4.0
	C	1	210	150	0.166			

Table 4.3 Mission profile combination trade-off analyses

As can be seen from Table 4.3, all of the total scores of the three mission couples are close to each other. But in the competition, the aim of the team is to get as high total score as possible, therefore the first mission couple, which is A&B, is preferred.

4.6.2 Detailed Aerodynamic & Stability Analysis

After determining roughly the aerodynamic characteristics, structural analysis and propulsion system analysis of the aircraft and at previous parts, it is time to analyze the aerodynamic & stability performance of the aircraft in details. For this purpose, a very simple three-dimensional potential flow solver program (VS-AERO) is used. The grid was built at CFDRC-GEOM. The solutions are done at Reynolds Number 300,000 and Mach=0.07. The aircrafts lift and drag coefficients are plotted with respect to angle of attack. And to investigate the stability characteristics of the whole aircraft, moment coefficient is calculated for various angles of attack values. After obtaining reasonable results for static margin values, in the previous parts, once again a negative value of $C_{M\alpha}$ on the C_M vs. alpha graph proves that the aircraft is longitudinally stable.

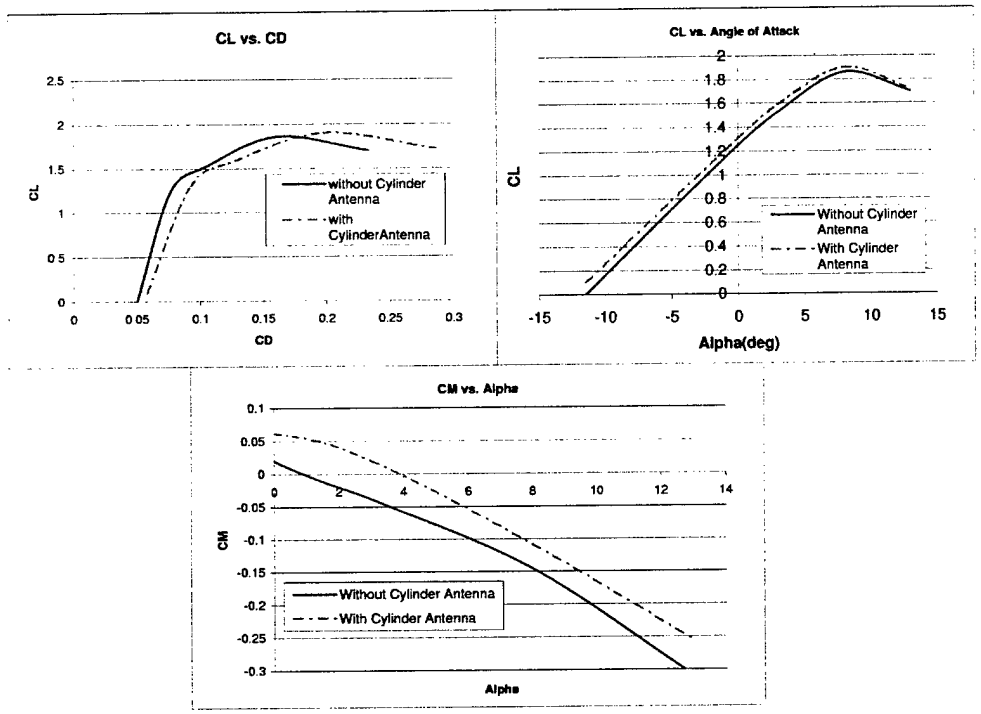

Figure 4.6 C_L vs. alpha, C_D vs. C_L, C_M vs. alpha graphs

In this contest year, the main difficulty in term of aerodynamics is the cylindrical antenna. Therefore, the flight with antenna and without antenna is solved and the lift, drag and moment coefficients are compared with each other. In Figure 4.7-a, Mach distribution is shown. As the color changes from violet to blue, the flow Mach number increases. The pressure distribution is displayed in Figure 4.7-b, red color shows the minimum pressure. Figure 4.7-c and Figure 4.7-d show the skin friction distributions using streamlines; the blue color represents the maximum skin friction.

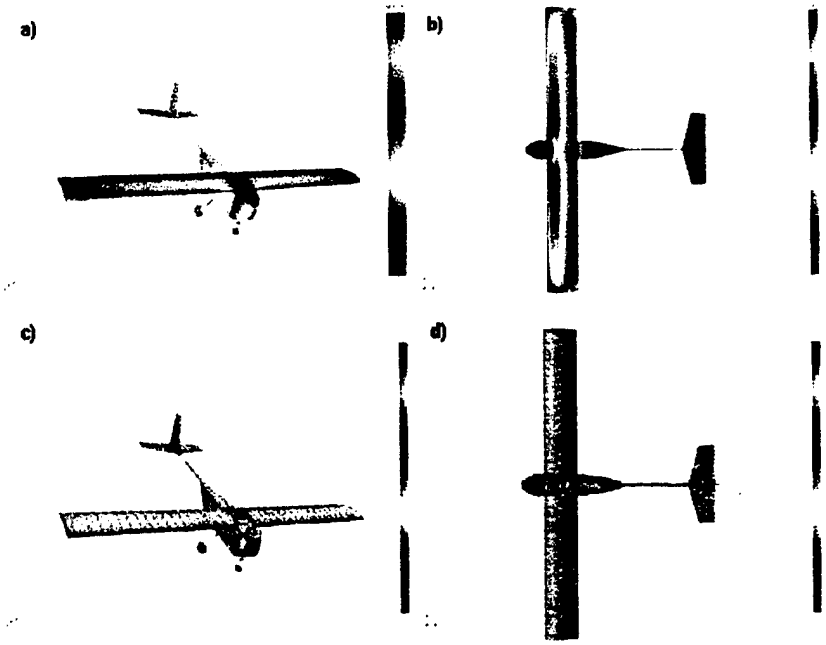

Figure 4.7 CFD Solutions. a) Mach contour; b) Pressure distribution; c & d) Skin friction distribution (3°aoa)

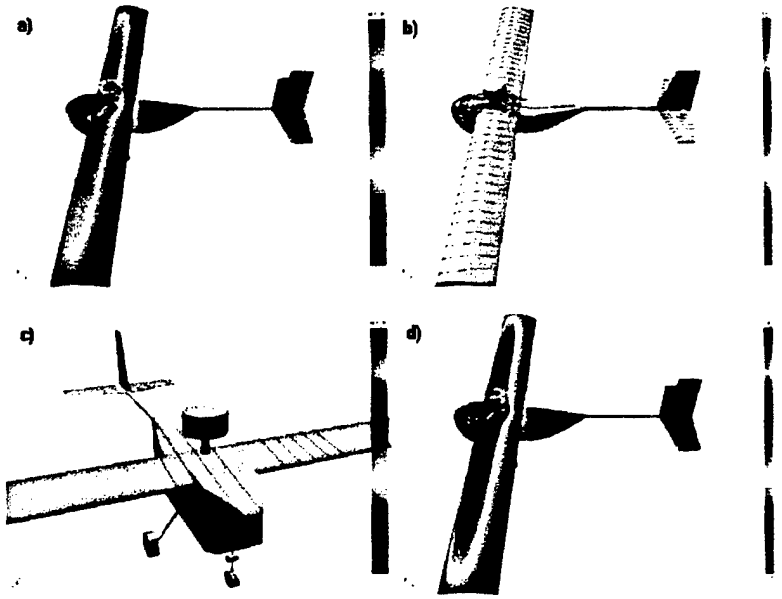

Figure 4.8 CFD Solutions. a) Mach contour; b) Pressure distribution; c & d) Skin friction distribution (3°aoa)

The above solutions was used for improving the aircraft's performance like reducing the drag and increasing the lift. The most visible change was done on the upper part of the aft fairing; at the both solutions, with and without antenna, the flow on this portion of the fuselage is separates from surface and causes additional drag. Also the effect of the cylindrical antenna on rudder and the aft fuselage can be seen clearly with.

CHAPTER 5 – DETAIL DESIGN

The main concern of the detail design chapter is of the documentation of the component and the systems architecture selection including the rated aircraft cost. Geometry, performance, weight and flight systems data of the sized aircraft were given as a table. In addition, drawings of the final configuration, size, structure and the system layout of the aircraft are included in this section.

5.1 Structural Design Analysis

Detailed design of the structural system is investigated in the light of two main considerations; these are the construction and the assembly of the aircraft. Since assembly time had an exceptionally important role in the scoring of the aircraft this year, all design considerations were done to avoid complications in the assembly.

5.1.1 Fuselage

Previously, in the preliminary design phase, the main rib approach was preferred for the body frame. Because of the exceptional design of the main landing gear that must fit inside the rib structure the most appropriate cross-section of the main rib was decided to be a **U** cross-section. The **U** profile rib structure supports the main landing gear from outside and prevents any further deflection under impact forces. Furthermore **U** profile was strong enough to withstand additional loadings.

Since the main rib was the main load carrying member of the fuselage, the wing was also attached to the main rib by two bolts, extending through the main landing gear as a support. In order to prevent the undesired swinging of the payload during the flight, main rib served also as a side support for the payload.

The engine was mounted by an aluminum support to a channel cross section beam in front of the fuselage as shown in Figure 5.1-a. The torsional effect of the engine was avoided by this construction. The battery pack was placed between the engine mount and the payload section. The bottom plate on which the batteries are placed is drilled allowing the circulation of cooling air in order to prevent the excess heating of the battery pack.

The fuselage had a box shaped beam extension that is supported by two stringers to make the connection between the tail boom and the main frame. This box is produced in such a way that the circular tail boom tightly fits into it. The tail boom can be pinned in and out of the box, thereby adjusting its length for stability considerations.

5.1.2 Wing

An aluminum spar was placed at the quarter chord of the wing where the aerodynamic loads are known to be maximum. To maintain the continuity of the spar all along the span, the spars of the side-wings were connected to the mid-wing using an additional, smaller cross section spar segment.

Considering the assembly time, two bolts were used for each connection. To avoid torsional failure at the wing joints where balsa and foam continuity is disrupted an 8mm circular wooden rod was placed near the trailing edge as a secondary extension as shown in Figure 5.1-b.

The metal plate behind the battery pack was extended on top of the fuselage and bent over the leading edge. The mid-wing had two rod protrusions coming out of the leading edge which pass through the spar inside the wing. After inserting the rods into their corresponding holes, assembly of the wing to the fuselage was done by two bolts passing through the main rib and holding the main landing gear.

Two wing servos were embedded in the foam ribs at the mid-locations of the flaps and ailerons. The pushrods of the flaps are mounted outside the wing whereas the pushrods of the aileron servos are passing inside the wing to reduce the aerodynamic drag. The movement of the control surfaces was provided by using commercially available small plastic hinges. To improve the aerodynamic efficiency of the wing, transparency papers are used to seal the gaps between the control surfaces and the wing.

5.1.3 Landing Gears

The main landing gear fits into the main rib and fastens together with the wing by means of two bolts as discussed earlier. Moreover, to prevent the torsional deflection, it is fixed to the main rib from two sides. A special consideration is given to the nose landing gear so that it can be adjusted in length using a set-screw. The rotation of the nose landing gear is provided by two distinct ball bearings.

5.1.4 Empennage

To assemble the horizontal and the vertical stabilizers perpendicular to each other, an aluminum box is used which has a length same as the root chord of the horizontal stabilizer. The cross section of the box is chosen such that the tail boom fits into the box. It is located between the two horizontal tail parts as shown in Figure 5.1-c. The assembly sequence of the empennage is that first the tail boom fits into the tail box then the vertical stabilizer is attached through both the tail box and the tail boom.

5.1.5 Payload Deployment Mechanism

In the payload deployment system a servo switch is used. A push-rod, controlled by this servo, passes through the hole on the main rib. A hook is attached on the upper surface of the payload and it is hung from the push-rod. When the servo is activated the push rod releases the payload. To prevent the swinging of the payload, extensions on both sides of the payload are attached to main rib. They also serve as guidance during the deployment.

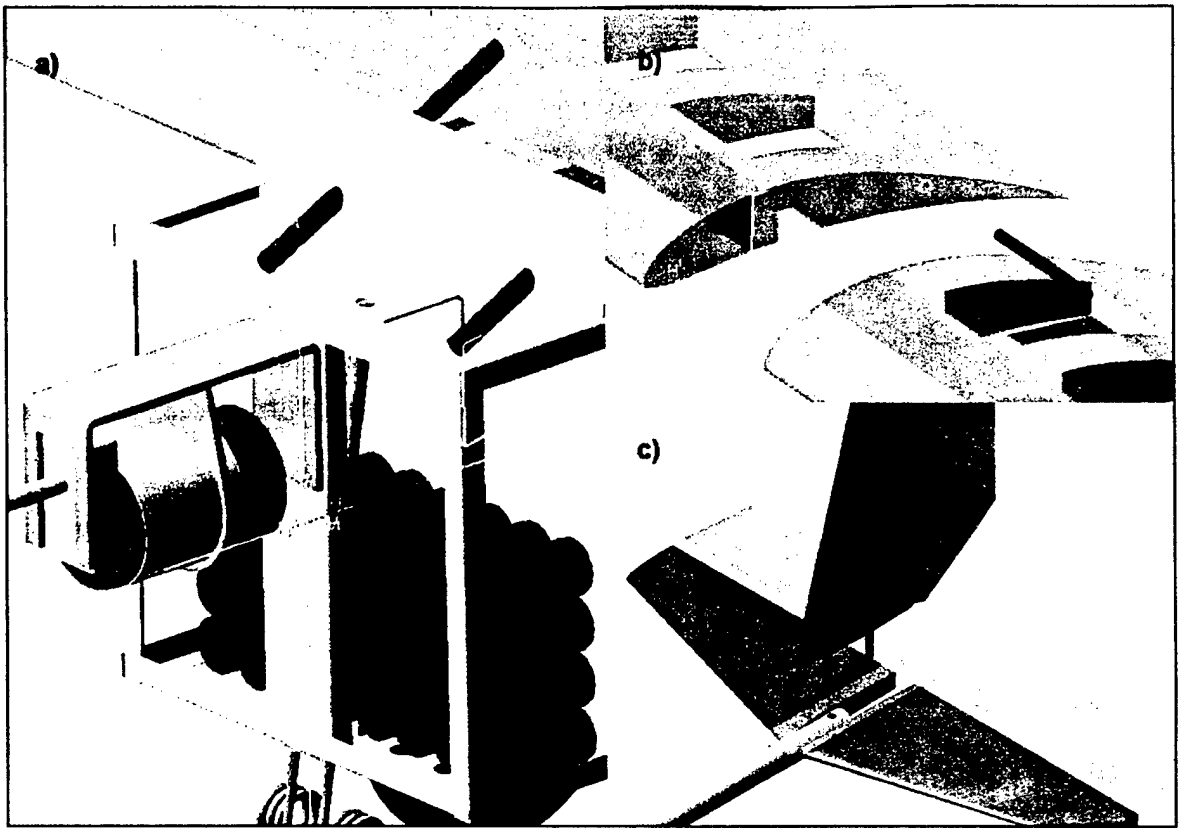

Figure 5.1 Detailed Drawings

5.2 Propulsion

In the preliminary design phase, the propulsive system was designed according to the required parameters of the aircraft. Firstly, the team selected to use the engine from Astro Flight families among the two alternatives of engine selection that are Graupner and Astro Flight. Then, by the use of MotoCalc Electric Flight Performance Prediction Software the team calculated the results of different configurations of the engine and the propeller. During testing the engine, the team observed that the results of the tests did not differ more than 5% of the software results. After all, the team decided to use the Astro Flight Cobalt 60 11T#23 (The optimum engine for the designed aircraft). With the selected engine, a 20 X14 APC two bladed composite propeller was used. To produce the required level of thrust, the team needed 32 Ni-Cd cells. During take-off, the thrust available for the aircraft with this engine was 7.27 lb and the power consumption was 830 W, whereas for the cruise, these values were 1.98 lb of thrust and 250 W of power consumption.

5.3 Rated Aircraft Cost Analysis

According to the final configuration of the aircraft, the rated aircraft cost was calculated. Table 5.1 shows the result given with the intermediate calculations. Contribution of each component to the total RAC is given in percentage as a bonus.

Component	Base	Manufacturing Man-hours	Multiplier	Cost ($)
Empty Weight	16.358 *lb*	-	Empty Weight Multiplier ($100)	1635.8
Rated Engine Power	4.32 *lb*	-	Rated Engine Power Multiplier ($1500)	6481
Wing Span	8.20 *ft*	8 *hr./ft*	Manufacturing Cost Multiplier($20 / hour)	1312.3
Wing Chord	1.05 *ft*	8 *hr./ft*		167.9
Wing Control Surfaces	2	3 *hr./control surface*		120
Fuselage	5.77 *ft*	10 *hr./ft*		1154.9
Vertical Surface (With active control)	1	10 *hr./vertical surface*		200
Horizontal Surface	1	10 *hr./horizontal surface*		200
Flight Systems	7	5 *hr./servo or motor controller*		700
Engine	1	5 *hr./engine*		100
Propeller	1	5 *hr./propeller*		100
			RAC	**12.17**

Table 5.1 Rated Aircraft Cost Table

5.4 Sized Aircraft Data

According to final configuration of the aircraft, geometry, performance, weight and system parameters are shown in Table 5.2 below.

GEOMETRY	Length	5.77 *ft* = 1.76 *m*
	Span	8.20 *ft* = 2.50 *m*
	Height	0.57 *ft* = 0.17 *m*
	Wing Area	8.61 ft^2 = 0.80 m^2
	Aspect Ratio	7.81
	Control Volumes	Horizontal Tail = 0.659 Vertical Tail = 0.047
PERFORMANCE	$C_{L,max}$	1.8
	L/D_{max}	14.2
	Max. Rate of Climb	893 *ft/min* = 272 *m/min*
	Stall Speed	30.87 *ft/s* = 9.41 *m/s*
	Max. Speed	65.62 *ft/s* = 20 *m/s*
	Take-off field length (empty weight)	59 *ft* = 18 *m*
	Take-off field length (gross weight)	98 *ft* = 30 *m*
WEIGHT	Airframe	8.82 *lb* = 4 *kg*
	Propulsion System	6.69 *lb* = 3.03 *kg*
	Control System	0.88 *lb* = 0.4 *kg*
	Payload System	0.12 *lb* = 0.054 *kg*
	Payload	5 *lb* = 2.27 *kg*
	Empty Weight	16.51 *lb* = 7.49 *kg*
	Gross Weight	22.48 *lb* = 10.2 *kg*
SYSTEMS	Radio	Futaba T9ZHP transmitter RI29DP receiver
	Servos	→Futaba S-3001 for Rudder and Payload Deployment System →Futaba S-3102 for Ailerons →Futaba S-9202 for Nose Landing Gear →Futaba S-9204 for Flaps and Elevator
	Battery Configuration	32xSR Batteries 2400 Max NiCd batteries (2400 mAh, 1.2V) in series
	Motor	Astro Flight Cobalt 60 11T#23
	Propeller	APC 20"x14"
	Gear Ratio	2.75:1

Table 5.2 Final Aircraft Data

DRAWING PACKAGE

Drawing Number: METU03 - 001B

Item no:	Item Name	Material	Quantity Per Assembly
1	Wing	Foam+Balsa Rib structure	1
2	Fuselage	Aluminum 2024T3	1
3	Main Landing Gear	IS301 Stainless Steel	1
4	Nose Landing Gear	Steel 1040	1
5	Tail Boom	Aluminum 2024T3	1
6	Tail Box	Aluminum 2024T3	1
7	Horizontal Tail	Foam+Balsa Rib structure	1
8	Vertical Tail	Foam+Balsa Rib structure	1

Drawing Number: METU03 - 002

Item no:	Item Name	Material	Quantity Per Assembly
1	Engine Mount	Aluminum 2024T3	1
2	Nose C-Beam	Aluminum 2024T3	1
3	Frontal Landing Gear	Steel 1040	1
4	Second Rib	Aluminum 2024T3	1
5	Body Stringers	Aluminum 2024T3	4
6	Engine Mount - 2	Aluminum 2024T3	1
7	Payload Rod House	Aluminum 2024T3	1
8	Main Landing Gear	IS301 Stainless	1
9	Main C-Rib	Aluminum 2024T3	1
10	Tail Boom Box	Aluminum 2024T3	1
11	Third Rib	Aluminum 2024T3	1
12	Tail Boom Stiffeners	Aluminum 2024T3	2

Drawing Number: METU03 – 003

Item no:	Item Name	Material	Quantity Per Assembly
1	Central Wing	Foam+Balsa Rib Structure	1
2	Fitting Pins	Wood	2
3	Lightning Holes	-	12
4	Lightning Holes	-	2
5	Spar	Aluminum 2024T3	3
6	Torsion Pins	Wood	2
7	Side Wing	Foam+Balsa Rib Structure	2
8	Ailerons	Balsa Rib Structure	2

Drawing Number: METU03 - 004

Item no:	Item Name	Material	Quantity Per Assembly
1	Tail Boom	Aluminum 2024T3	1
2	Tail Box	Aluminum 2024T3	1
3	Vertical Tail	Foam+Balsa	1
4	Elevator	Foam+Balsa Rib structure	1
5	Horizontal Tail	Foam+Balsa	1
6	Rudder	Foam+Balsa Rib structure	1

Drawing Number: METU03 - 005

Item no:	Item Name	Material	Quantity Per Assembly
1	Payload	Wood	1
2	Payload Rod House	Aluminum 2024T3	1
3	Deploy Pushrod	Stainless Steel	1
4	Deploy Servo	Futaba 9204	1
5	Payload Hook	Stainless Steel	1

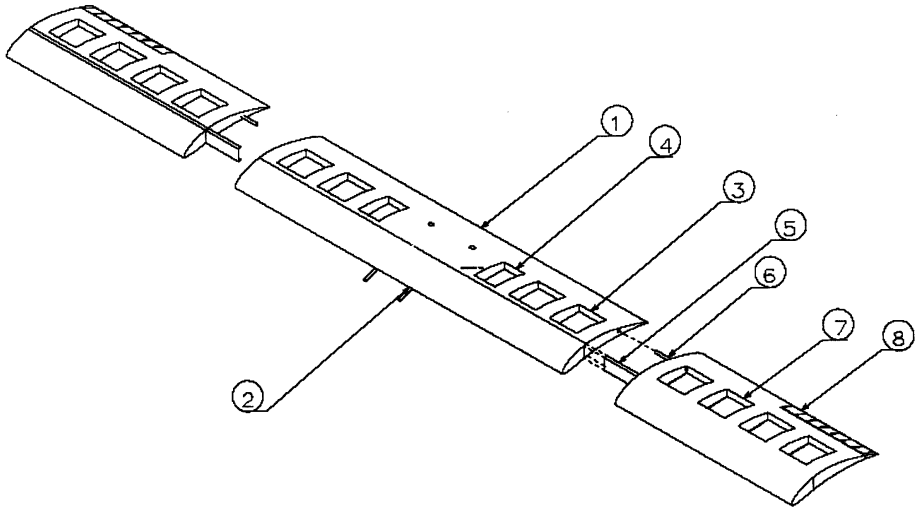

Isometric view

MIDDLE EAST TECHNICAL UNIVERSITY AEROSPACE ENG. DEPT. ANATOLIAN CRAFT DESIGN TEAM			
DRAWING TITLE: WING			
SIZE A4	DRAWING NUMBER: METU03 - 003		REV 2
SCALE 1:10	DATE 19.12.2002	ALL DIMENSIONS IN METRIC	SHEET -

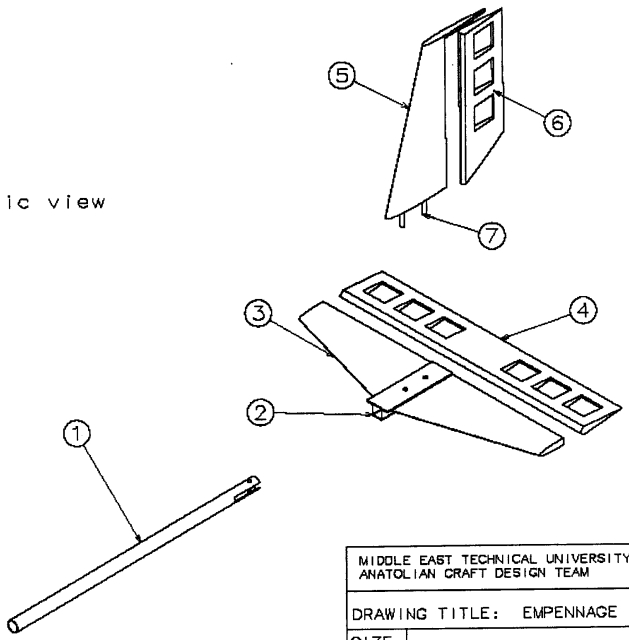

Isometric view

MIDDLE EAST TECHNICAL UNIVERSITY AEROSPACE ENG. DEPT. ANATOLIAN CRAFT DESIGN TEAM			
DRAWING TITLE: EMPENNAGE			
SIZE A4	DRAWING NUMBER: METU03-004		REV 2
SCALE 1:7	DATE 19.12.2002	ALL DIMENSIONS IN METRIC	SHEET -

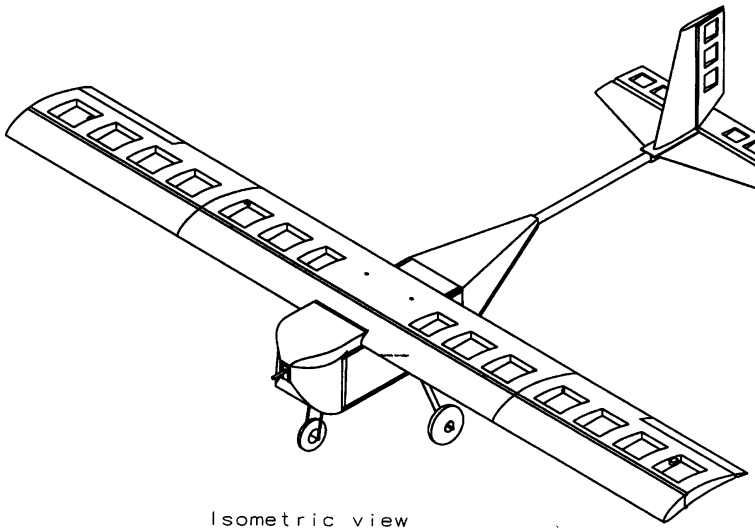

Isometric view

MIDDLE EAST TECHNICAL UNIVERSITY AEROSPACE ENG. DEPT. ANATOLIAN CRAFT DESIGN TEAM			
DRAWING TITLE: MAIN ASSEMBLY			
SIZE A4	DRAWING NUMBER: METU03 -001A		REV 2
SCALE 1:10	DATE 24.01.2003	ALL DIMENSIONS IN METRIC	SHEET -

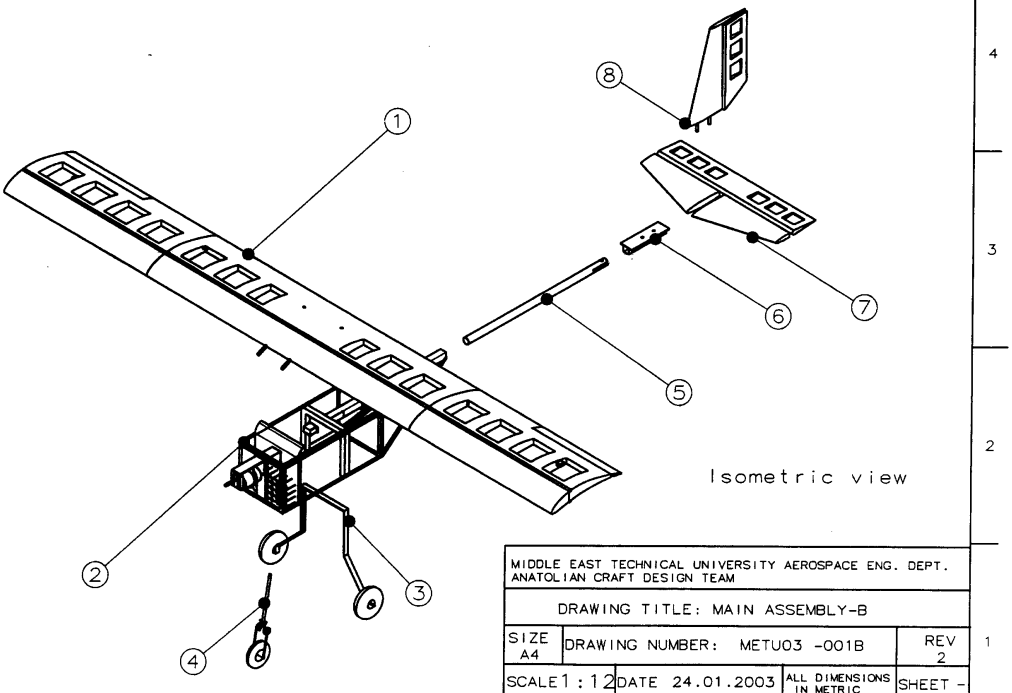

Isometric view

MIDDLE EAST TECHNICAL UNIVERSITY AEROSPACE ENG. DEPT. ANATOLIAN CRAFT DESIGN TEAM			
DRAWING TITLE: MAIN ASSEMBLY-B			
SIZE A4	DRAWING NUMBER: METU03 -001B		REV 2
SCALE 1:12	DATE 24.01.2003	ALL DIMENSIONS IN METRIC	SHEET -

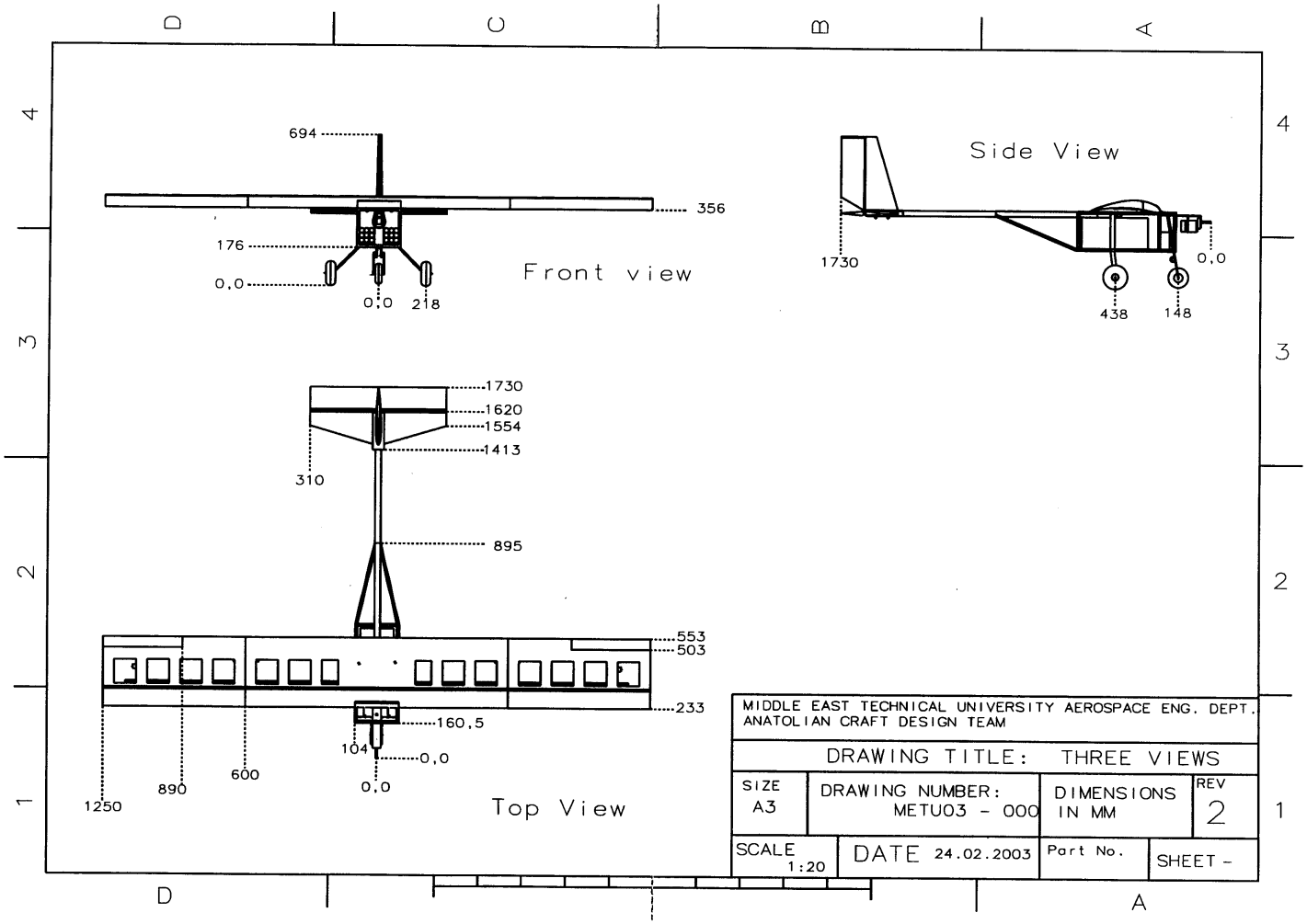
694
356
176
0,0
0,0
218
Front view
Side View
1730
0,0
438
148
1730
1620
1554
1413
310
895
553
503
233
160,5
104
0,0
0,0
1250
890
600
Top View
MIDDLE EAST TECHNICAL UNIVERSITY AEROSPACE ENG. DEPT.
ANATOLIAN CRAFT DESIGN TEAM
DRAWING TITLE: THREE VIEWS
SIZE A3
DRAWING NUMBER: METU03 - 000
DIMENSIONS IN MM
REV 2
SCALE 1:20
DATE 24.02.2003
Part No.
SHEET -

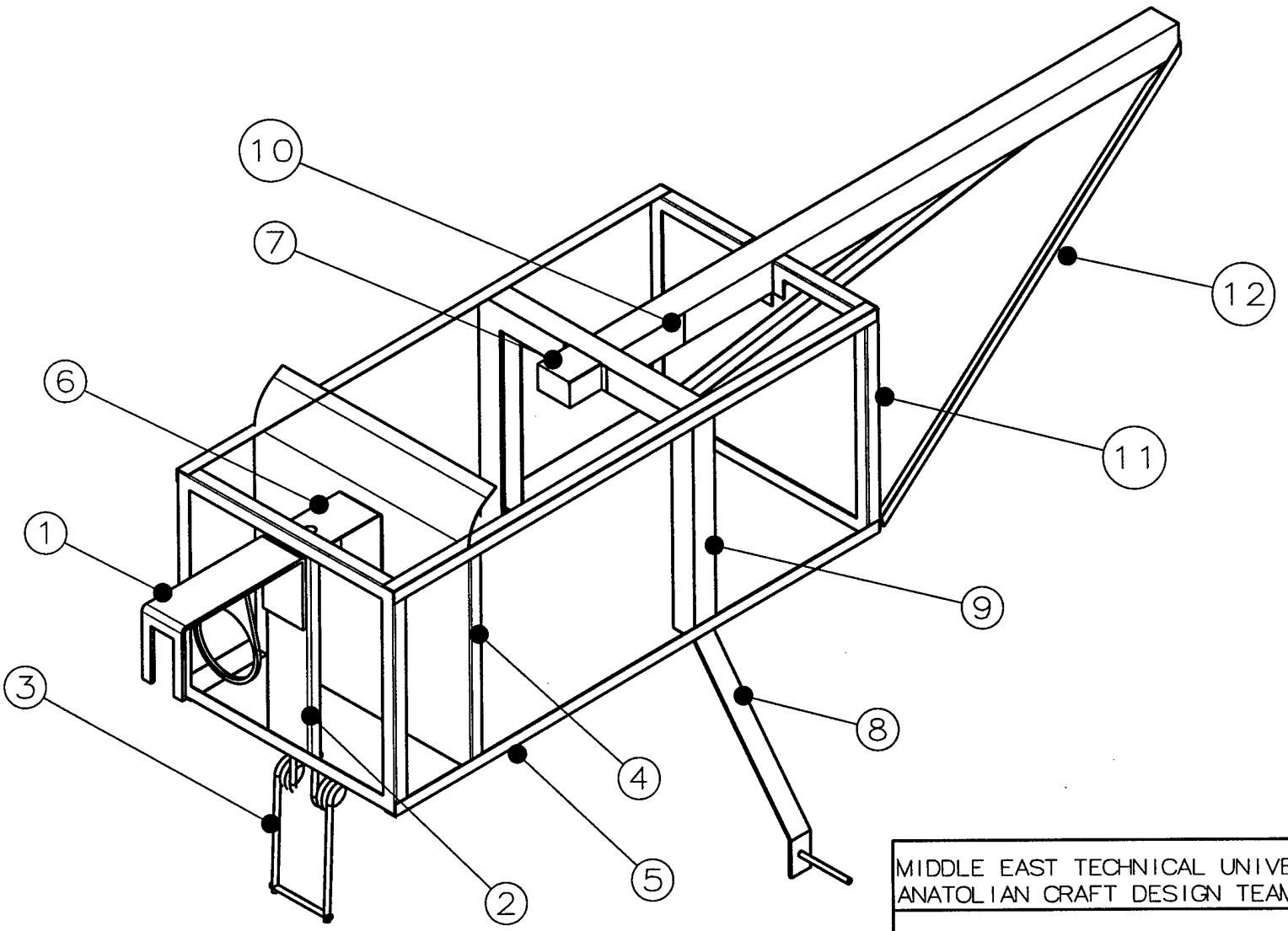

Isometric view

MIDDLE EAST TECHNICAL UNIVERSITY AEROSPACE ENG. DEPT ANATOLIAN CRAFT DESIGN TEAM			
DRAWING TITLE: FUSELAGE			
SIZE A4	DRAWING NUMBER: METU03-002		REV 2
SCALE 1:4	DATE 19.12.2002	ALL DIMENSIONS IN METRIC	SHEET -

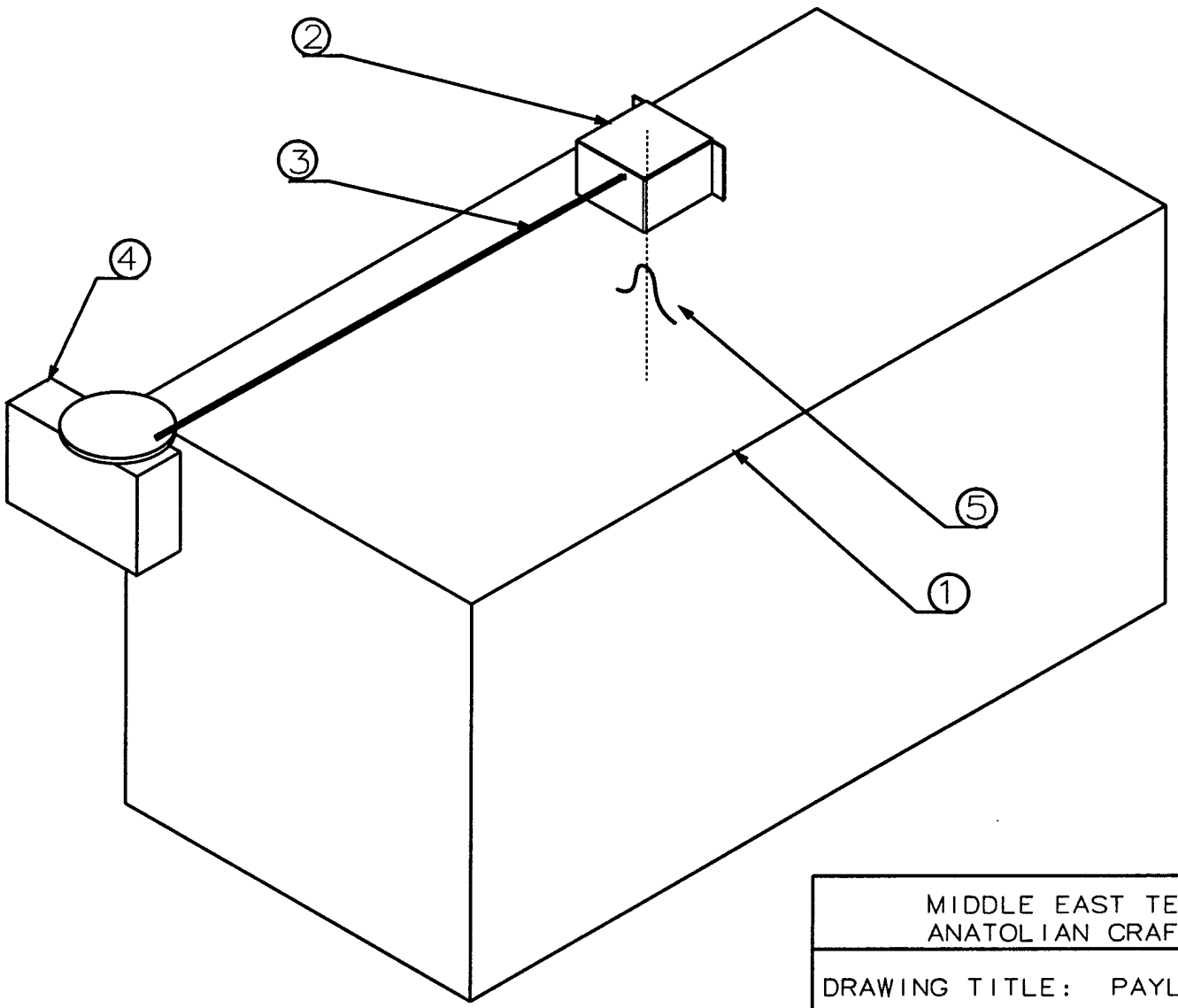

MIDDLE EAST TECHNICAL UNIVERSITY ANATOLIAN CRAFT DESIGN TEAM			
DRAWING TITLE: PAYLOAD			
SIZE A4	DRAWING NUMBER: METU03-005		REV 2
SCALE	DATE 12.11.2002	ALL DIMENSIONS IN METRIC	SHEET -

CHAPTER 6 - MANUFACTURING PLAN AND PROCESSES

After completing the design phase, several manufacturing techniques are investigated to produce the components of the aircraft, then the most efficient and suitable techniques are selected. In addition, to help the manufacturing plan, the "Skill Matrix" is constructed and manufacturing schedule is done. During the investigation, the following parameters were considered; availability of the manufacturing processes, required skill level, required time, reliability and cost of the process.

The availability of the manufacturing process is an important limiting factor. Some process techniques can not be available for the team. Some of the manufacturing processes may require extensive skills which mean that the team should consist of trained and skilled members. Hence a "skill matrix" is constructed as shown in the Table 6.1.

	Wood working skills	Foam hot wiring	Balsa Sheeting	Fiberglass Sheeting	Servo Systems consulting	R/C Modelling	Metal Manufacturing Techniques	Heat Film Application	NUMBER OF TEAM MEMBERS
Number of Members	8	7	6	4	2	1	6	4	11

Table 6.1 Skill Matrix

Team followed a schedule in order to build and test the aircraft before the competition. This helped the team work in a more organized and efficient manner. Due to budget limitations, the team had to select the cheapest available procedure for manufacturing the components. However, this does not affect the accuracy and the quality of the production. Weight of the components is also another important criterion for an aeronautical product. Therefore the most light-weight materials were chosen due to the fact that this is to be an aircraft to fly.

6.1 Figures of Merit

The figures of merit were built-up to help the team to choose the most efficient techniques for the production of each component. The figures of merit consist of availability of production, required skill

level, required time, precision, strength, cost and weight of the process. The final figures of merit were obtained by weighted average with respect to multipliers which implies priority of a figure of merit upon others, scored as 1 up to 5. Scoring of each FOM is held as 1 up to 12 in which higher score implies better characteristics of the corresponding option.

		Availabity of Production	Required skill Level	Time Required	Precision	Strength	Cost	Weight	WEIGHTED AVERAGE
	Multiplier	5	3	2	5	4	2	5	
Fuselage	Bolting	12	12	11	11	7	11	10	10.50
	Welding	10	6	9	7	9	8	9	8.38
	Riveting	**10**	**10**	**12**	**12**	**12**	**12**	**12**	**11.38**
Wing Foam	**CNC Hot Wire**	**8**	**10**	**12**	**12**	**-**	**9**	**-**	**10.12**
	Hand Made Hot Wire	12	12	6	7	-	12	-	9.82
Landing Gear	**Welding Formed Profile**	**12**	**8**	**10**	**8**	**11**	**12**	**11**	**10.27**
	Pre-formed Profile	4	12	12	12	12	7	12	10.08
Fairings	Balsa Wood	11	8	9	12	10	10	11	10.46
	E-glass Composite	**10**	**10**	**12**	**10**	**12**	**12**	**12**	**11.00**
Control Surface Hinges	**Commertial Plastic Hinges**	**12**	**12**	**12**	**12**	**10**	**10**	**12**	**11.54**
	Co-axial Tubes	10	9	10	11	12	9	9	10.12
	Fabric Hinges	11	8	8	9	8	12	11	9.65
Wing Control Surfaces	**Foam with Balsa Skin**	**-**	**12**	**12**	**12**	**12**	**12**	**8**	**11.05**
	Balsa Rib	-	10	8	9	11	11	12	10.33
Tail Control Surfaces	**Foam Rib with Balsa Skin**	**-**	**12**	**12**	**12**	**12**	**12**	**9**	**11.29**
	Balsa Rib	-	10	8	9	10	11	12	10.14

Table 6.2 Figures of Merit

6.2 Wings and Empennage

The wing and the empennage are the most difficult components to manufacture. Foam with a density of 25 kg/m^3 was used for the manufacturing of the wing. The foam was cut to the shape of the chosen airfoil with a CNC hot wire cutting machine. The foam is also cut along the span-wise direction at its 25% chord location to place the channel profile spar. To further increase the strength of the wing and to retain the outer shape, the foam is covered with a 1mm thick sheet of balsa wood. Epoxy is used to glue the balsa wood to the surface of the foam. After the completion of the wing, flaps and ailerons are cut from it. To further reduce the weight of the wing, new ailerons and flaps are constructed using balsa rib structure. The leading edge carrier rods are made of wood and fixed to the wing spar.

For the construction of the empennage, lower density foam (13 kg/m^3) is used. The shaping of the foam is done by using a hand held resistance-wire cutter. After cutting the tail, some foam is removed to place the servo motors. The surface of the foam is again covered by 1mm thick balsa wood to increase its strength and to protect its shape. Detailed final shaping of the tail is done by hand finishing. The two rods are used to connect the horizontal tail pieces to the tail box. Moreover in the connection of the vertical stabilizer, two rods extends from inside of the vertical tail and enters to the tail box.

6.3 Tail Boom

When the tail boom is on the main frame, the length of the fuselage is not short enough to fit into the carrier box therefore it is needed to be easily removable. The boom was fixed into the tail box with one of the rods of the vertical tail.

6.4 Fuselage

Rivets are used to join the parts instead of welding because of the unavailability of qualified aluminum welding technology. High stressed areas were strengthened by additional aluminum sheets. Moreover, the box, that the tail boom is fixed to the main frame, is constructed and attached to the main rib by rivets.

6.5 Landing Gears

The front landing gear is manufactured from steel by forming two springs. It is fixed to the fuselage by a steel rod and two rollers. The main landing gear is produced from stainless steel. Welding is used to form the required **T**, **I** and box profiles.

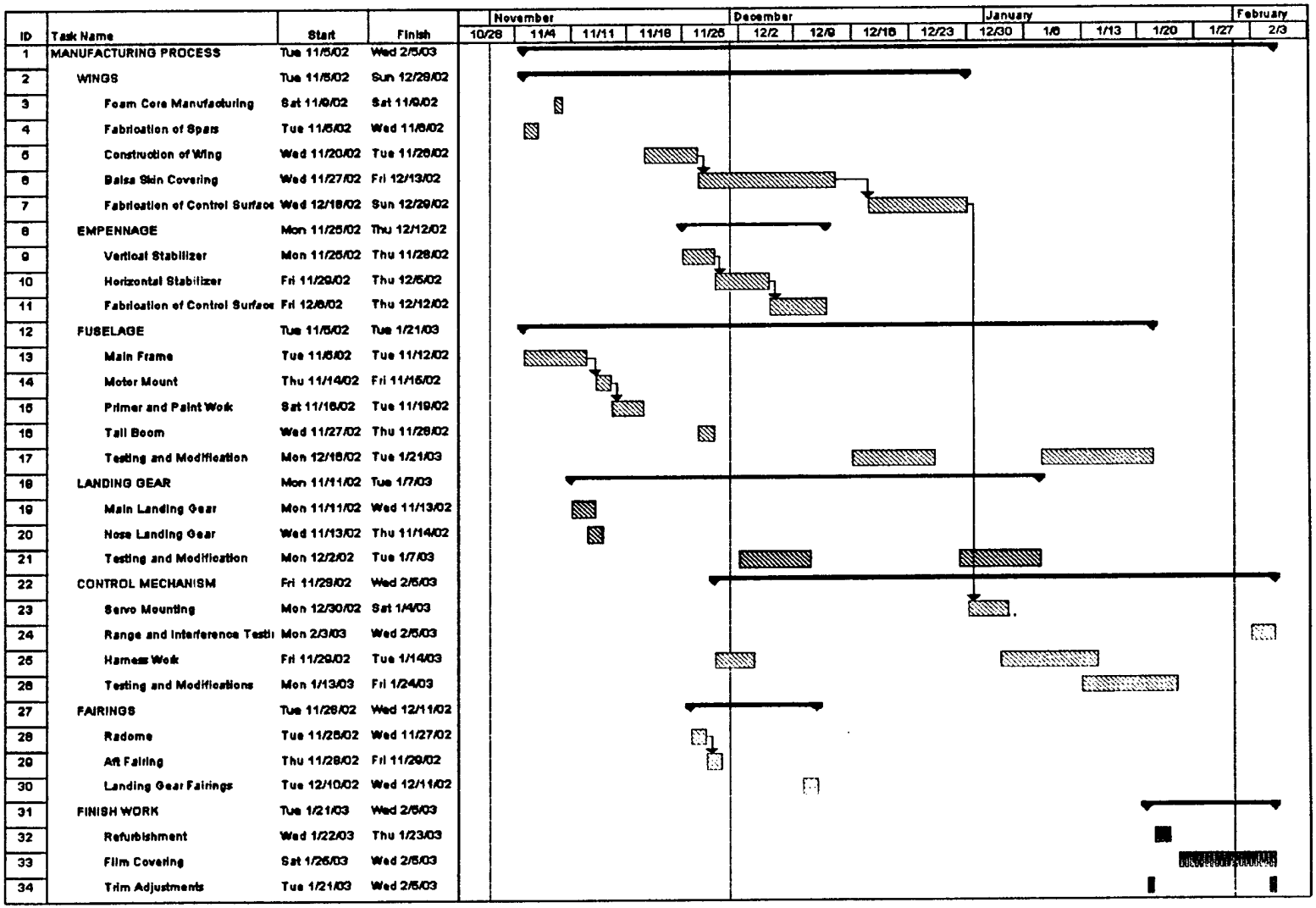

ID	Task Name	Start	Finish
1	MANUFACTURING PROCESS	Tue 11/5/02	Wed 2/5/03
2	WINGS	Tue 11/5/02	Sun 12/29/02
3	Foam Core Manufacturing	Sat 11/9/02	Sat 11/9/02
4	Fabrication of Spars	Tue 11/5/02	Wed 11/6/02
5	Construction of Wing	Wed 11/20/02	Tue 11/26/02
6	Balsa Skin Covering	Wed 11/27/02	Fri 12/13/02
7	Fabrication of Control Surface	Wed 12/18/02	Sun 12/29/02
8	EMPENNAGE	Mon 11/25/02	Thu 12/12/02
9	Vertical Stabilizer	Mon 11/25/02	Thu 11/28/02
10	Horizontal Stabilizer	Fri 11/29/02	Thu 12/5/02
11	Fabrication of Control Surface	Fri 12/6/02	Thu 12/12/02
12	FUSELAGE	Tue 11/5/02	Tue 1/21/03
13	Main Frame	Tue 11/5/02	Tue 11/12/02
14	Motor Mount	Thu 11/14/02	Fri 11/15/02
15	Primer and Paint Work	Sat 11/16/02	Tue 11/19/02
16	Tail Boom	Wed 11/27/02	Thu 11/28/02
17	Testing and Modification	Mon 12/16/02	Tue 1/21/03
18	LANDING GEAR	Mon 11/11/02	Tue 1/7/03
19	Main Landing Gear	Mon 11/11/02	Wed 11/13/02
20	Nose Landing Gear	Wed 11/13/02	Thu 11/14/02
21	Testing and Modification	Mon 12/2/02	Tue 1/7/03
22	CONTROL MECHANISM	Fri 11/29/02	Wed 2/5/03
23	Servo Mounting	Mon 12/30/02	Sat 1/4/03
24	Range and Interference Testi	Mon 2/3/03	Wed 2/5/03
25	Harness Work	Fri 11/29/02	Tue 1/14/03
26	Testing and Modifications	Mon 1/13/03	Fri 1/24/03
27	FAIRINGS	Tue 11/26/02	Wed 12/11/02
28	Radome	Tue 11/26/02	Wed 11/27/02
29	Aft Fairing	Thu 11/28/02	Fri 11/29/02
30	Landing Gear Fairings	Tue 12/10/02	Wed 12/11/02
31	FINISH WORK	Tue 1/21/03	Wed 2/5/03
32	Refurbishment	Wed 1/22/03	Thu 1/23/03
33	Film Covering	Sat 1/26/03	Wed 2/5/03
34	Trim Adjustments	Tue 1/21/03	Wed 2/5/03

Table 6.3 Manufacturing schedule

CHAPTER 7 - TESTING PLAN

Following the successful completion of the design phase of the competition aircraft, during the manufacturing phase, the team started to perform both static and dynamic tests for the components as well as for the whole aircraft. Reasoning, methodology and results of each one of these static experiments are listed below:

7.1 Static Tests

7.1.1 Spar test

Aim: Observing the ultimate loading behavior.

Testing Method: The aluminum spar having length of 80 cm (2.62 ft) was simply supported at two ends. The load was applied at the center of the bar and it was gradually increased up to 35 kg (approximately 77 lb).

Results: There existed buckling at 35kg on the aluminum spar due to applied loading. However, the deflection amount was in the calculated design limits.

7.1.2 Landing Gear

Aim: Landing gear static test.

Testing Method: The main landing gear was mounted on the body. 40 kg (88.2 lb) load was applied which corresponded to 4-g landing load.

Results: It was seen that the calculated stress values were not exceeded. There was no plastic deformation on the landing gear and elastic deflections were observed as expected.

7.1.3 Tail Boom

Aim: To simulate the loading on the tail boom due to aerodynamic forces on the empennage and impact loading during a 4-g landing.

Testing Method: The tail boom was mounted to the fuselage and from the tip of the boom 26.7N (6.6 lb) load was applied.

Results: It was observed that there were no plastic deformations on the boom, showing that the stress generated was below the yield stress.

7.1.4 Tip Test

Aim: To examine whether the wings satisfy the requirement of overcoming the 2.5 g loading.

Testing Method: Initially, the three wing components were plugged into each other, but not mounted on the fuselage. The wing was simply supported from the tips. Considering the weight of the wing, a 7.5 kg (16.5 lb) load was applied at the geometric center to approximate the actual loading on the wing. Afterwards, the wing was mounted on the fuselage, and an actual "tip-test" was performed. This test aimed at both observing the deflection of the wing and to test the strength of the joints.

Results: The deflection of the wing was as expected and the joints were strong enough to hold the wing in place.

7.1.5 Payload Deployment Mechanism

Aim: To test the proper functioning of the payload deployment mechanism, and simulated testing for an impact loading of a 4-g landing.

Testing Method: In the first test the payload deployment mechanism was tested for proper "locking" and "unlocking". In the preceding test, 10 kg of weight was applied to the payload support to simulate a 4-g landing.

Results: The mechanism proved to be properly operating. Also the guides mounted on the side surface of the payload box were properly functioning so that the payload was sliding without any problems.

7.2 Flight Tests

After completing the static testing, team proceeded for dynamic testing which can be divided into two sub-categories as ground and airborne testing. A checklist was prepared in order to assure that the aircraft was flight-worthy before each flight. This checklist included bolts used to fix tail-boom, wing and landing gear, empennage locks, radio system operation, control surface operations, propulsion and receiver battery voltage check, center-of-gravity location and wing tip-test. Before each flight battery voltages and propulsion battery temperature, ambient temperature and wind-speed were recorded. During the flight-testing, starting time, take-off time and take-off distance together with lap completion times were recorded. After each landing, the propulsion battery temperature, battery voltages, total flight time and pilot comments were recorded. After the maiden flight of the aircraft, subsequent flight tests were scheduled for each Saturday morning.

For flight-testing of the aircraft designed, team designed a test-instrumentation system with the help of senior students from Electrical and Electronics Engineering department of METU. The components building this system up can be listed as two wireless modem devices, one differential GPS, one 3-axis gyroscope, five angular deflection sensors and a portable computer with the software developed.

When this report was published, active work on the instrumentation of the aircraft with the above-mentioned sensors was still going on and the instrumented flight tests were about to start.

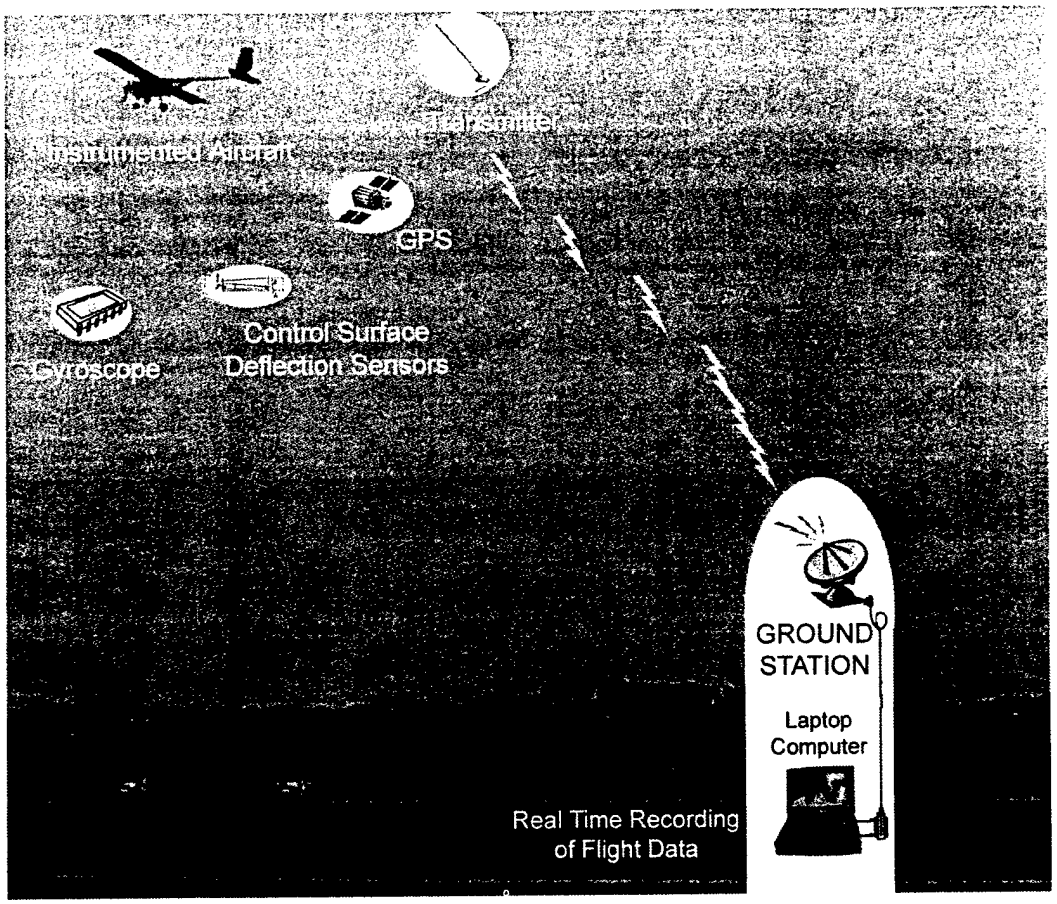

Figure 7.1 Schematic view of the test-instrumentation system

7.2.1 Ground Testing

For the first ground test, it was aimed to examine the landing gear vibrations due to ground friction and to observe landing gear behavior on a "smooth" paved runway, which is still rough for the aircraft. During the test a small bumper on the taxi way used for testing caused the failure of the nose landing gear. Team decided to produce a more flexible, therefore "softer" nose landing gear in order to avoid the brittle fracture experienced. However, no critical case for the main landing gear was observed yet a consensus was established about "clamping" the main landing gear to the fuselage at both sides in order to avoid excessive vibrations of the wheels.

In the next ground test on February 6th, 2003, besides the aims of the first one, it was intended to qualitatively test for the overturn angle. After a 5-minute run on the taxiway, strength of both the nose and the main landing gears were found to be satisfactory. For testing the overturn angle, aircraft was accelerated to stall speed and full rudder deflection was applied in order to test the ground handling and to test the aircraft against tumbling. Finally, the landing gears were found to be satisfactory.

7.2.2 Airborne Testing

On February 15th, 2003, the maiden flight of the aircraft was accomplished without any significant problems. During the maiden flight, it was aimed to observe the stability characteristics of the aircraft. During this test, it was observed that the aircraft was stable. Other problems that were observed can be listed as follows:

- Flaps-down stability of the aircraft was unacceptable,
- Excessive lift was observed which caused the aircraft to climb during cruise,
- Ailerons and elevator controls were very sensitive which were preventing smooth operation of the aircraft during maneuvers.
- Main landing gear was critically loaded during harsh landings, which caused its buckling.
- Tail boom mount was loose which caused low frequency longitudinal oscillations.

For preventing the excessive lift, and therefore increasing cruising speed, flaps were reversed during the test. Reversing the flaps solved the problem temporarily for the loaded configuration. However, characteristics of the aircraft with empty configuration were not satisfactory. An exponential curve was applied to both of the aileron and the elevator controls in order to obtain a less sensitive range near trim positions, which satisfied the pilot. In order to avoid buckling at the main landing gear, new plates were welded on the structure, which transformed the "T" section beam to an "I" beam at certain regions of the main landing gear assembly. To avoid variations of incidence angle caused by oscillations of the tail boom, it was bolted to the fuselage, which increased the assembly time.

During the second flight test scheduled on February 22nd 2003, the simulated antenna was tested for the first time together with an endurance test. Stability of the aircraft with the simulated antenna and the prescribed payload was found to be satisfactory. Also the endurance of the aircraft for the same configuration was long enough to complete the required mission. To prevent torsional buckling of the main landing gear assembly, its structure is modified such that at some locations the "I" beam structure us converted to a box structure. This modification was found to be satisfactory. Since the main landing gear was nearly rigid, tire pressure was reduced in order to reduce the impact loading during touchdown. For empty configuration, two take-off and landing were done successively. For the first flight, the aircraft took-off from 32.8 feet and after a flight, which is 4 minutes and 14 seconds long, and landed safely. Without recharging the battery pack a second take-off was performed and the aircraft took-off after 65.6 ft of ground roll and stayed airborne for 2 minutes and 21 seconds. For missile decoy mission, the take-off distance was 90 ft and the total flight time was 6 minutes and 15 seconds.

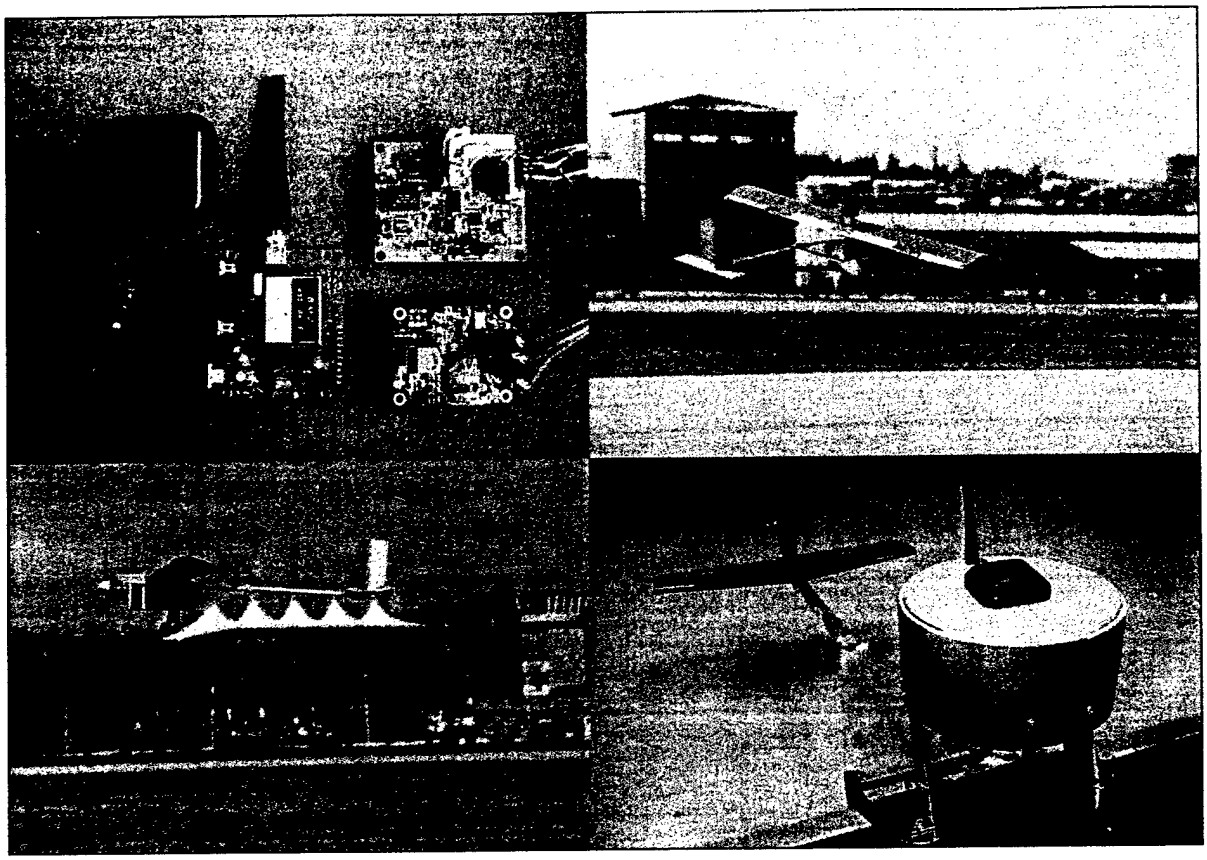

Figure 7.2 *Upper left:* Material to be used for instrumentation of the aircraft during tests. *Upper right:* First missile decoy mission flight. *Lower left:* Maiden flight photo. *Lower Right:* Test-instrumentation system assembled on the aircraft.

Team decided to undergo a reduction of wingspan for 0.3 meters (approximately 1 foot) in order to reduce the lift and consequently the lift-induced drag. Also considering the feedbacks from the pilot suffering from the high-sensitivity of the elevator and the rudder, a reduction in tail-boom length was also considered. The analysis showed that a reduction of 0.15 m (approximately 6") from the tail boom length would shift both the center of gravity location and the neutral point forward in such a manner that the neutral point would shift more which in turn result in a reduction in stability. This would be beneficial for the team since the aircraft had a large static margin, which was causing excessive trim drag. Therefore, reduction of trim drag could be possible by decreasing the static margin, which directly determines longitudinal static stability. Finally, the planned changes were made in a reversible manner such that the pieces cut could easily be replaced back.

During the third flight test on March 2, empty and loaded flight configurations were tested and significant improvements in handling qualities and cruising speed of the aircraft were observed as a result of reducing the span and the tail boom lengths. The aircraft took off with the payload in 86.6 ft, stayed airborne for 4 minutes and 30 seconds and landed. After deploying the payload, took off within 59.05 ft,

stayed airborne for 2 minutes and 30 seconds and landed. On the other hand, this new configuration hardened the missile decoy mission, due to changes in aircraft behavior. During the first trial of the new configuration with the simulated antenna, the aircraft experienced stall since the pilot did not accelerate and climb the aircraft to a sufficient altitude before proceeding for a 180-degree turn. The lesson learned from this crash was not to risk the aircraft before it climbs to a "safe" altitude and reaches a "safe" speed. After replacing the parts that have been damaged, the aircraft took off within a maximum of 98.5 feet, performed a successful flight with the simulated antenna and stayed airborne for 2 minutes and 34 seconds before landing.

After the reducing the span and the tail-boom lengths, new flights are scheduled to optimize the flight scores for missile decoy and sensor deployment missions.

Task Name	Start	12/9	1/6	2/3	3/3	3/31	4/28
static testing	**Thu 12/19/02**						
landing gear	Thu 12/19/02	◆ 12/19					
payload deploy mechanism	Tue 12/24/02		◆ 12/24				
spar test	Sat 1/4/03		◆ 1/4				
wing tip test	Mon 1/13/03		◆ 1/13				
tail boom test	Mon 1/20/03		◆ 1/20				
flight testing	**Tue 1/28/03**						
first ground test	Tue 1/28/03			◆ 1/28			
first ground roll test	Thu 2/6/03			◆ 2/6			
maiden flight	Sat 2/15/03			maiden flight ★ 2/15			
first missile decoy mission	Sat 2/22/03				◆ 2/22		
first flight after modifications	Sun 3/2/03				◆ 3/2		
mission time improvements	Sat 3/8/03						
contest	**Sun 4/27/03**						★ 4/27

Table 7.1 Test schedule

REFERENCES

1. Roskam, j., Airplane Design, Roskam Aviation and Engineering Corp., Ottawa, KS, 1985.
2. Stinton, D., The Design of the Aeroplane, Granada, London, England, UK, 1983.
3. Raymer, Daniel P., Aircraft Design: A Conceptual Approach, Second Edition, AIAA Education Series, USA, 1992.
4. Torenbeek, E., Synthesis of Subsonic Airplane Design, Delft Univ. Press, Delft, The Nederlands, 1982.
5. Megson. T. H. G., Aircraft Astructure for Engineering Students, Second Edition, Edward Arnold, UK, 1990.
6. Bruhn, E. F., Analysis and Design of Vehicle Structures, Tri-state Offset Company, USA, 1973.

University of California

San Diego

Design Report

Submitted March 11, 2003

Aerodrone F8273

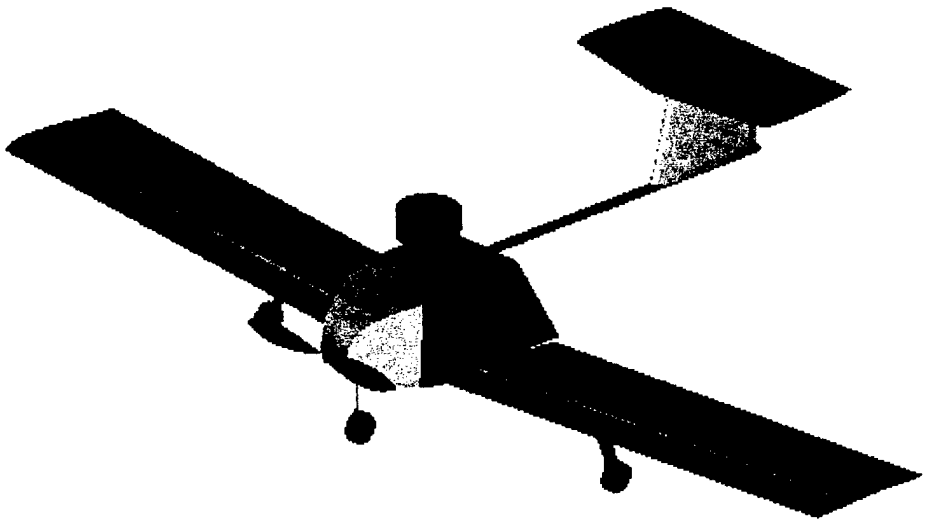

Table of Contents

1.0 Executive Summary 1

1.1 Conceptual Design 1

1.2 Preliminary Design 2

1.3 Detail Design 2

2.0 Management Summary 4

2.1 Architecture of Design Team 4

2.2 Aerodynamics 5

2.3 Structures 5

2.4 Propulsion 6

2.5 Task Scheduling 6

3.0 Conceptual Design 8

3.1 Competition Parameters and Aircraft Configuration 8

3.1.1 Aircraft Requirements 8

3.1.2 Mission Profiles 8

3.1.3 Rated Aircraft Cost 9

3.2 Aerodynamics 9

3.2.1 Aircraft Configurations 10

3.2.2 Wing Placement 11

3.2.3 Wing Shape 11

3.2.4 Tail Design 12

3.3 Structures 13

3.3.1 Wing and Tail Structures 13

3.3.2 Fuselage Structure 14

3.3.3 Automated Payload Delivery System (APDS) 15

3.3.4 Landing Gear 16

3.4 Propulsion 17

3.5 Final Aircraft Configuration 17

4.0 Preliminary Design 18

4.1 Aerodynamics 18

4.1.1 Wingspan 18

4.1.2 Wing Chord Length 19

4.1.3 Airfoil Selection 20

4.1.4 Tail Design 21

4.1.5 Fuselage Shape 21
4.2 Structures 22
4.2.1 Factor of Safety 22
4.2.2 Wing Structure 22
4.2.3 Wing Joiner 24
4.2.4 Tail Configuration 24
4.2.5 Fuselage Structure 25
4.2.6 Aircraft Weight and Center of Gravity 27
4.2.7 Automated Payload Delivery System (APDS) 28
4.2.8 Motor Mount 29
4.2.9 Landing Gear 30
4.3 Propulsion 31
4.4 Final Aircraft Configuration 32

5.0 Detailed Design 33
5.1 Aerodynamics 33
5.1.1 Mission Profile and Flight Performance 33
5.1.2 Takeoff Distance 34
5.1.3 Stability and Control 34
5.2 Structures 35
5.2.1 Wing Structure 35
5.2.2 Tail Configuration 36
5.2.3 Fuselage Structure 36
5.2.4 Automated Payload Delivery System (APDS) 38
5.3 Propulsion Performance 40
5.4 Final Aircraft Configuration 40
5.5 Final Aircraft Configuration Calculations 41
5.6 Rated Aircraft Cost 42
5.7 Detailed Drawings 43

6.0 Manufacturing Plan 49
6.1 Wings 49
6.2 Spar 49
6.3 Wing joiner 50
6.4 Wing sleeve 50
6.5 Rails 50
6.6 Bulkheads 50

6.7 Skin 51
6.8 Motor-mount 51
6.9 Landing Gear 51

7.0 Research and Testing Plan 52
7.1 Objectives 52
7.2 Schedules 52
7.3 Testing Procedures 52
7.4 Check-lists 53
7.5 Results 54
7.5.1 Antenna and Airfoil Results 54
7.5.2 Motor Testing Results 55
7.5.3 Automated Payload Delivery System (APDS) Testing Results 55
7.6 Lessons Learned 56

8.0 References 57

List of Figures

Figure 2.1: Aerodrone F8273 Design Personnel 4
Figure 2.2: AERODRONE F8273 Team Milestone Chart 7
Figure 4.1: Wing Section Configuration 19
Figure 4.2: Effects of Chord Length on RAC 19
Figure 4.3: Drag Polar and Lift Curve for S4083 Airfoil at Re ≈ 300,000 20
Figure 4.4: Distributed and point loads 23
Figure 4.5: Illustration of spanwise profile of the spar 23
Figure 4.6: Tail Boom Load Model 25
Figure 4.7: Location of Bulkheads 26
Figure 4.8: Bulkhead Worst Case 27
Figure 4.9: Latching Mechanism 29
Figure 4.10: Landing Gear Placement 30
Figure 4.11: Main Landing Gear 31
Figure 5.1: von Mesis Stress and Displacement of Spar 35
Figure 5.2: Integrated Tail Assembly. 36
Figure 5.3: Structural Integration 37
Figure 5.4: von Mesis Stress and Displacement of Bulkhead #5 38
Figure 5.5: von Mesis Stress and Displacement of a Rail 38
Figure 5.6: Force Balance on Door 40
Figure 7.1: Research and Testing Schedule Task 51
Figure 7.2: Testing Checklist 52
Figure 7.3: Assembly Checklist 52
Figure 7.4: Pre-Flight Checklist 52
Figure 7.5: Post-Flight Checklist 53
Figure 7.6: Antenna drag 53
Figure 7.7: Airfoil data 53
Figure 7.8: Graupner motor data 54
Figure 7.1: APDS rubber band testing data 54
Figure A.1 11 X 17 Three View Drawing A.1

List of Tables

Table 2.1: Aerodrone F8273 Members' Skills and Contributions 5
Table 3.1: Figures of Merit for Wing Configurations 10
Table 3.2: Figures of Merit for Wing Placement 11
Table 3.3: Figures of Merit for Wing Shape 12
Table 3.4: Figures of Merit for Tail Sections 13
Table 3.5: Figures of Merit for Wing and Tail Structure 14
Table 3.6: Figures of Merit for Fuselage Structure 14
Table 3.7: Figures of Merit for Automated Payload Delivery System 15
Table 3.8: Figure of Merit for Landing Gear Configurations 16
Table 3.9: Figure of Merit for Propulsion 17
Table 4.1: FOM of Cross Section Selection for Tail Beam. 25
Table 4.2: Graupner Motor 3300 series 31
Table 5.1: Evaluation of the mission times and flight modes 33
Table 5.2: Rubber Band Analysis. 39
Table 5.3: Final Aircraft Configuration Calculations 41
Table 6.1: Fabrication processes and their estimated relative costs 48

1.0 Executive Summary

This report outlines the steps taken by the student members of the American Institute for Aeronautics and Astronautics (AIAA) at the University of California, San Diego, (UCSD) to design and construct an unmanned remote aircraft to compete in the 2002/2003 Design/Build/Fly (DBF) competition. The objective of the competition was to design an aircraft that operates at optimum performance while meeting all competition and mission requirements set forth by the Cessna/ONR DBF Committee. This aircraft must be able to complete mission profiles consisting of carrying/deploying a five pound 6x6x12 inch sensor package (payload) and maneuver with a six-inch diameter by three inch tall simulated cylindrical antenna while completing four laps over a closed course.

1.1 Conceptual Design

The conceptual design phase began by first analyzing the competition rules and requirements. The rules stipulate that the aircraft must complete two of three possible missions. An evaluation of several different components was undergone in order to determine the missions that offered the optimum scoring potential. Through a complex analysis, the missile decoy and sensor deployment missions provided the best opportunity for obtaining points.

Once the mission objectives were understood the team was divided into three technical groups: aerodynamics, structures, and propulsion. Each group produced figures of merit to represent mission objectives for each component of the aircraft that fell within their technical area. Concepts and ideas were studied in terms of feasibility, adherence to contest and mission requirements, conformance with all technical areas, and scoring potential.

The aerodynamic group sought an aircraft configuration that had an optimal rated aircraft cost, low manufacturing cost, stability, and aerodynamic efficiency. During the conceptual design, various aircraft configurations were considered: the bi-plane, canard, conventional, and flying wing. Moreover, the aerodynamic group was responsible for the general shape and placement of the wing in regards to the fuselage along with researching various tail designs.

Ensuring the structural integrity of the aircraft was a crucial part of the structural conceptual design process. The structures group took into consideration ease of manufacture, Rated Aircraft Cost (RAC), strength, and weight savings when deciding upon the structural components of the aircraft. Various design concepts for the fuselage, wing, and tail structures along with the Automated Payload Delivery System (APDS) and landing gear were discussed.

The propulsion group examined motor and battery combinations to find the optimal configuration, which maximizes thrust while minimizing the rated engine power. Four motor/battery configurations were considered in regards to their effects on the RAC, battery and motor weight, thrust, and number of fuses.

The conceptual design phase produced a primary aircraft configuration consisting of a conventional monoplane with a rectangular under wing and T-tail with a rear ejection APDS. A single motor with a 2 pound battery pack proved to best optimize the propulsion system.

1.2 Preliminary Design

With a complete general aircraft configuration, the preliminary design phase determined the design parameters and conducted trade studies.

The aerodynamic group performed trade studies to determine the wingspan, chord length, airfoil, and tail area that would optimize the design. Three wingspan configurations were considered along with various chord lengths and tail dimensions. Moreover, the aerodynamics group discussed and researched numerous airfoils before coming to a decision.

The structural preliminary design, included determining the wing, tail, and fuselage structures, along with the motor mount and landing gear configurations. The aircraft's weight, applied loads and location of the center of gravity affected the overall structural design and fuselage layout. The structural group also created a prototype of the selected APDS in order to determine the minimum amount of force required to propel the payload from the rear of the aircraft.

From the information gained by the aerodynamic and structures groups, propulsion requirements were determined by utilizing the stipulated maximum take off distance and aircraft weight. The minimum required thrust to complete the missions was calculated and the optimum propulsion system configuration was found.

The preliminary design determined the sizing of the wing and tail geometry, primary structure dimensions, and propulsion configuration. The wingspan and chord length were calculated to be 8.7 feet and 14 inches, respectively. The S4083 airfoil was selected for the wing, while the NACA0009 was chosen for the tail. The most efficient shape for the spar was found to have a spanwise taper. The aircraft's takeoff weight was found to be approximately 20 pounds and the center of gravity was determined to be 1.5 inches behind the leading edge of the wing. It was determined that eight pounds of force from four, #64 rubber bands would provided adequate force for the APDS. An 18 inch diameter propeller with a 15 inch pitch along with the Graupner 3300-7 motor and 19 Sanyo 2400 cells compose the propulsion system.

1.3 Detail Design

With the information gained from the preliminary design phase, a foundation was provided for finalizing component and system architecture selection.

The aerodynamics group analyzed the mission. The total theoretical flight scores and RAC costs were calculated determining the desired flight mode and predicted possible scoring potential. They also calculated the takeoff distance and stability of the aircraft.

The structures group finalized the component integration and architecture of the structural design. They designed a lightweight spar that best met the load requirements while performing a detailed analysis of four main bulkheads that supported the fuselage. Local strength requirements were established through finite element analysis to be implemented during manufacturing and incorporated into the

engineering drawings. The boom mounting and wing joining details were determined and incorporated into the final design.

The propulsion system was finalized and static tests were performed in order to ensure optimal performance. Wire routing and servo placement for control surface movement was determined and updated into the drawings.

The final configuration of the airplane is a conventional wing-fuselage-tail design. The low-wing configuration requires a dihedral of 2°. The rectangular wing geometry includes a span of 8.7 feet, a chord of 14 inches for an aspect ratio of 7.46. The main wing uses the S4083 airfoil and the T-tail is comprised of the NACA0009 airfoil for both the vertical and horizontal stabilizers. The semi-monocoque fuselage houses the payload that is deployed using a rubber band harness and servo controlled door release. The internal structure of the fuselage consists of bulkheads and rails. All structural members are composed of fiberglass, carbon fiber, and plywood, with blue or white foam used as the core material in sandwich structure members. With the known materials and component size, the CG was able to be placed 1.5 inches in front of the quarter chord by locating the 2.5 lb battery pack on the carbon/foam mounting plate 7.6 in. in front of the quarter chord. The airplane uses a Graupner 3300-5 motor with 19 Sanyo 2400 cells.

The results of the three design phases produced an aircraft to complete two of the required missions with the highest scoring potential. The aircraft performance capabilities and control characteristics were found to met the competition's objective.

2.0 Management Summary

2.1 Architecture of Design Team

The Aerodrone F8273 Team consists of twelve undergraduate UCSD students from various engineering disciplines. Before work commenced, three technical groups were formed: aerodynamics, structures, and propulsion (Figure 2.1). A lead engineering student supervised each technical group, delegating specific tasks and areas of interest to each of their group members. In so doing, they were responsible for directing and managing their groups progress in their specialized areas. A project manager monitored the performance and advancement of the overall team; making sure each group had all the necessary information to complete their assigned tasks. Together the project manager and the lead engineering students kept the team on task and assured the efficient progress and development of the project.

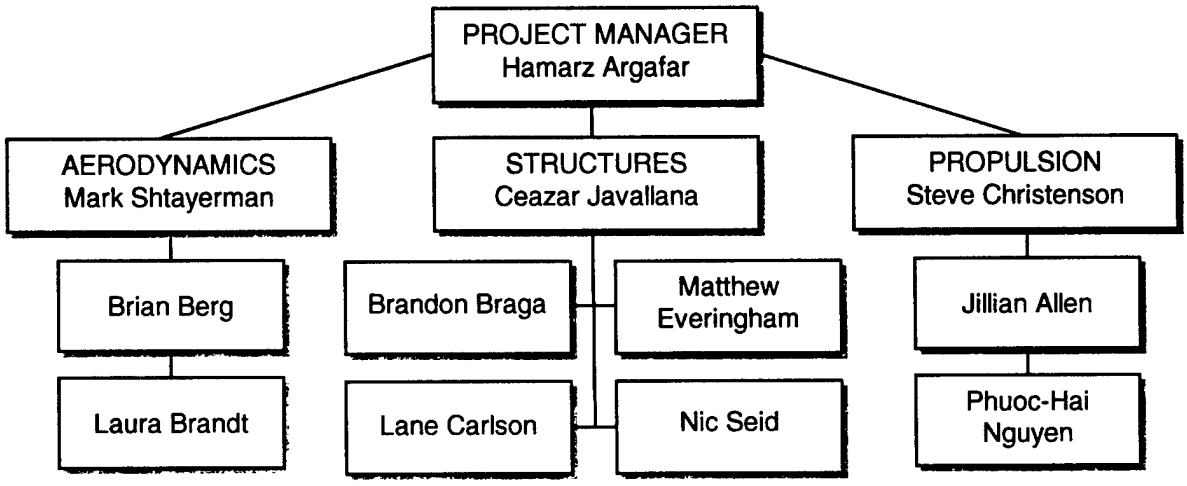

Figure 2.1: Aerodrone F8273 Design Personnel

The consolidation of each groups' efforts into one solid finalized design took a great deal of collaboration and compromise. Since the design concepts of one group places restraints on the other groups, weekly meetings were set up to discuss the integration of the different modules. During these weekly meetings, compatibility issues were resolved, new ideas were generated, and updated assignments were given. This management style allowed for a reliable, secure, and steadfast design process, while considering all aspects of aerodynamics, structures, and propulsion.

Team Members	Major	Year	Pro-Engineer	AutoCAD	PRO-MECHANICA	Technical Writing	Machining	Fabrication
Jillian Allen	BE	SR	X	X				X
Hamarz Argafar	AE	JR	X	X				X
Brian Berg	AE	SO		X				X
Brandon Braga	ME	JR		X				X
Laura Brandt	AE	JR	X	X		X		X
Lane Carlson	ME	JR		X				X
Steve Christenson	AE	SR	X	X	X	X	X	X
Mathew Everingham	AE	SR	X	X	X	X	X	X
Ceazar Javallana	AE	SR	X	X	X	X	X	X
Phuoc-Hai Nguyen	AE	FR						X
Nic Seid	AE	JR	X	X			X	X
Mark Shtayerman	AE	SR	X	X	X	X	X	X

Table 2.1 Aerodrone F8273 Members' Skills and Contributions

2.2 Aerodynamics

The aerodynamics group is responsible for the shape of the aircraft. The group's primarily focus is the analysis of forces acting on the body of the aircraft. These forces are a result of the relative motion between the body and the air (relative wind). In order to accomplish this goal, the aerodynamics group generated a static stability model, based on initial weight estimations, to determine the aircraft lift requirements. Figures of merit and competition regulations were taken into account while performing lift surface sizing. Airfoil selection along with wing, tail, and control surface sizing were conducted with the information gathered from this model. Control surface deflection and servo sizing were also studied using this model to determine control stability and maneuverability. Further aircraft configurations were examined to optimize take off distance, lift-to-drag (L/D) ratio, cruise, and velocity.

During weekly meetings, the structures and propulsion groups conveyed their estimates concerning aircraft weight, sizing, and power requirements, giving rise to the production of updated lift requirements and the refinement of aerodynamic components.

2.3 Structures

The structures group is accountable for determining the structural requirements to support the loads applied on the aircraft; these requirements consist of designing the component configuration of the aircraft, selection of the materials, and the manufacturing techniques needed to produce the aircraft. Various design considerations for the Automated Payload Delivery System (APDS), landing gear, and wing joiner were evaluated in regards to figures of merit and competition regulations in order to obtain an optimum design. The group's analysis focused heavily on hand calculations and CAD modeling to implement their design ideas. Information was exchanged during the weekly meetings with the

aerodynamics and propulsion groups, which aided in the decision of the primary structural components of the fuselage, wing, tail, landing gear, APDS, and other aircraft related components.

2.4 Propulsion

The propulsion group is primarily responsible for providing enough energy and thrust to complete the mission profiles. They were responsible for analyzing different types of motor, propeller, and battery combinations that would provide the most thrust with an efficient Rated Aircraft Cost (RAC). Figures of Merit (FOM) and competition regulations greatly impacted the propulsion group's criteria. The competition guidelines limited the propulsion group's selection of technical equipment: motors, batteries, and propeller selection. Analytical and experimental means were developed to achieve the best combination of the propulsion systems' three main components in order to create an efficient and stable aircraft. Every change in the aerodynamics or structure of the aircraft called for an adjustment in the propulsion system, which called for collaboration and compromise between the groups during the weekly meetings.

2.5 Task Scheduling

In order to meet the deadline a project milestone chart was created. Following this guideline allowed for a quick and efficient design and manufacturing process. Between mid-September and early October, the team set a schedule of completion dates of each phase of the aircraft development. The chart below (Figure 2.2) depicts the intended and actual dates of completion of eight milestones: design team assembly, conceptual design, preliminary design, detail design, design review, report, aircraft construction, and aircraft testing:

- Assembly of Design Team: The returning 2001 DBF members collaborated on how many new members the project would need to compete in this year's competition. During the first week of classes, a meeting was held and a new team began to form. The final team had twelve members.
- Conceptual Design: During the conceptual design phase mission requirements were defined, alternative configuration concepts were discussed, and a final design was constructed.
- Preliminary: With the completion of the conceptual design, an investigation into design parameters was initiated.
- Detail Design: The detail design process was composed of component and system architecture selection.
- Design Review: A presentation of the aircraft's detailed design, plans for fabrication, and a cost brake down to General Atomics (Aeronautical Systems). With the funding from our sponsor General Atomics and the support of the Jacobs School of Engineering (UCSD), our team was able to participate in this year's competition.

- Report: The process of the conceptual, preliminary, and detail designed phases were recorded in order to maintain an organized and efficient project progression.
- Construction: The manufacturing process is the most time consuming and lengthy. Therefore, a substantial amount of time was devoted to this phase of the aircraft development.
- Flight Testing: Having completed construction, test flights were undergone to ensure flyability, structural integrity, and stability. A sufficient amount of time was given to the flight test in order to give our pilot enough time to become comfortable with the aircraft and to fix any problems encountered.

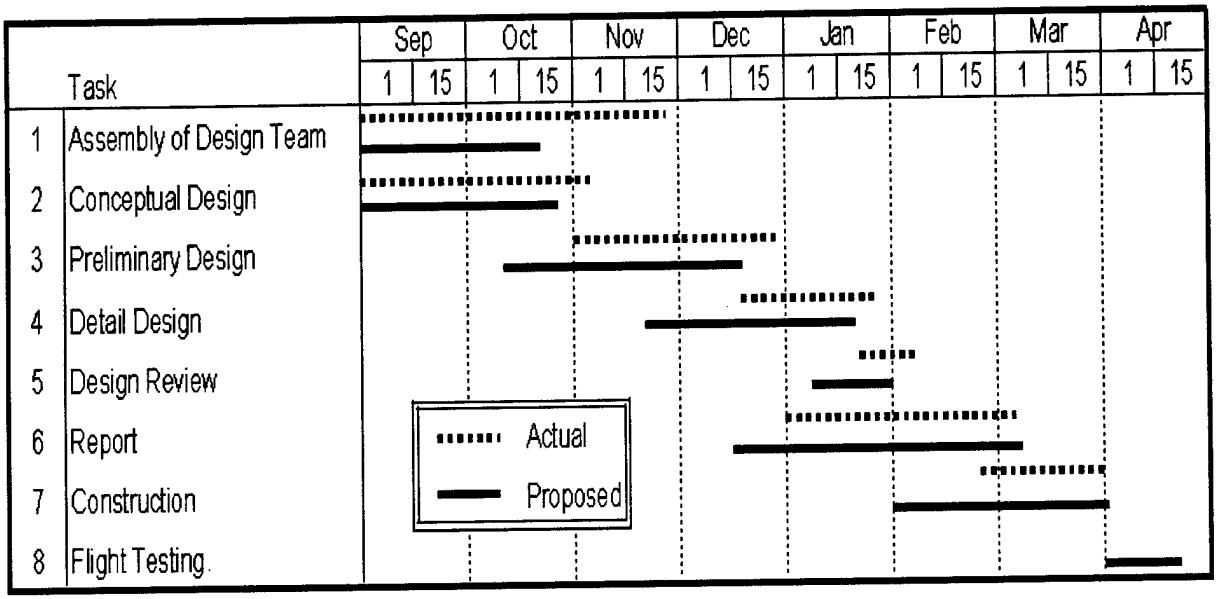

Figure 2.2 AERODRONE F8273 Team Milestone Chart

3.0 Conceptual Design

Four factors dominated the design of the aircraft: competition requirements, aerodynamic effects, structural integrity, and propulsion systems. The competition rules, mission profiles, and rated aircraft cost (RAC) guided the conceptual design phase. The aircraft was considered within three technical areas: aerodynamics, structures, and propulsion. During the conceptual design, the aerodynamic group considered various aircraft configurations, wing shapes, and tail designs while also determining the placement of the wing in regards to the fuselage. The structural group focused on ensuring the structural integrity of the aircraft. They analyzed numerous design possibilities for the fuselage, wing, and tail structures along with the automated payload delivery system (APDS) and landing gear. The propulsion group examined four motor and battery combinations to find the optimal propulsion configuration. Within each group, ideas were generated, concepts were collaborated, and compromises were made in order to optimize the design and fulfill mission requirements in order to achieve the best possible score.

3.1 Competition Parameters and Aircraft Configuration

The conceptual design phase commenced with a study of the competition requirements. Within each technical area, a focus was placed on the parameters set by the competition. These constraints affected the aircraft weight and size and in turn affected the RAC.

3.1.1 Aircraft Requirements

The Cessna/ONR Student Design/Build/Fly Competition Committee provided guidelines for the overall size and weight of the aircraft. The contest rules dictated that the unassembled aircraft must fit in to a 1x2x4 foot container. Using solid modeling analysis, maximum dimensions were determined by placing each component into a 3-D model of the box. These dimensions limited the ultimate aircraft size. Dimensions were estimated so that the maximum wing length was four feet, the maximum fuselage height was under one foot and width less than two feet, and the vertical tail size was less than 1 foot tall. Moreover, the competition requires the aircraft to be less than 55 pounds, which limits the choice of component selection.

3.1.2 Mission Profiles

The aircraft must complete two of three possible sorties. During each lap of the sortie, the aircraft must complete a 360-degree turn on the downwind leg of the flight path.

A. Missile Decoy; Difficulty Factor 2.0. The aircraft must take-off and fly four laps with a 6x6x12 inch, five-pound simulated avionics package and a simulated antenna. The antenna is a six-inch diameter, three-inch tall PVC pipe with capped off ends. It must stand off the aircraft structure a minimum of three inches and cannot be faired in any manner.

B. Sensor Deployment; Difficulty Factor 1.5. The aircraft must take-off complete two laps and land. The payload must be automatically deployed and take-off again and fly two additional laps before landing.

C. Communications Repeater; Difficulty Factor 1.0. The aircraft must take-off, complete four laps, and land. The payload is the 6x6x12 inch, five-pound simulated avionics package. Also, the aircraft must complete three 360-degree turns on the downwind leg of the flight course.

An evaluation of several different components was undergone in order to determine the missions that offered the optimum scoring potential. Because of the different degrees of difficulty, each mission offered a different scoring potential. For instance, mission A requires the aircraft to overcome extra drag because of the additional pitching moment caused by the antenna; while mission B has a more complex design with additional servos and weight penalties. Furthermore, the power requirements for mission B were substantially higher due to the fact that the aircraft must experience two take-offs. Through a complex analysis of comparing the aircraft configurations required by each mission, scoring potential, and RAC, it was found that missions A and B (missile decoy and sensor deployment) provided the best opportunity for obtaining points. Therefore, the team decided on these particular missions.

3.1.3 Rated Aircraft Cost

The RAC is a mathematical cost function relating all of the aircraft design parameters. The battery and aircraft weight, numbers of wings, size and span, number of servos and control surfaces, fuselage length and tail size all contribute to the RAC. The Rated Aircraft Cost is defined by the following equation:

$$RAC = (\$100*MEW + \$1500*REP + \$20*MFHR) / 1000$$

- MEW = Manufactures Empty Weight. (Actual airframe weight without batteries or payload)
- REP = Rated Engine Power. (Defined as (1 + .25*(# Engines)) *Total Battery Weight)
- MFHR = Manufacturing Man Hours. This parameter is the sum of the following:
    1. Wing span and chord length: 8 hr/ft. with 3 hr/control surface
    2. Maximum fuselage length: 10 hr/ft
    3. Each vertical surface with active control: 10 hr/surface
    4. Each vertical surface with no active control: 5 hr/surface
    5. Horizontal stabilizer, no more than 25% of the greatest span: 10 hr/surface
    6. Flight systems: 5 hr/servo or motor controller
    7. Propulsion system: 5 hr/engine and 5 hr/propeller or fan

In order to achieve a high competition score, the RAC must be minimized. Therefore, the wingspan and chord length, fuselage size, and propulsion systems are limited.

3.2 Aerodynamics

The aerodynamics primary components were assessed after the design parameters of the missions were established and the missions with the maximum score potential were chosen. By evaluating past team

experiences and the competition guidelines, suitable Figures of Merit (FOM) were established for aerodynamic analysis. For each aircraft component, alternative configuration concepts were placed in FOM matrices. The FOM considered were: RAC, ease of manufacture, stability, and aerodynamic efficiency.

- RAC effects: The RAC is the most influential component of the final score.
- Weight: Any weight changes associated with a specific configuration will affect flight characteristics and battery requirements.
- Ease of Manufacture: Manufacturing takes materials, time, and resources, which are limited.
- Stability: Any configurations that will render the aircraft unstable will be heavily penalized because of the increased risk of loss of control and possible destruction of the aircraft.
- Aerodynamic Efficiency: The aerodynamic efficiency accounted for the increase of drag and thus decreases in performance of the aircraft.

3.2.1 Aircraft Configuration

Various aircraft shapes were researched, including: bi-wing, canard, conventional, and a flying wing. These aircraft shapes are compared in the FOM matrix in Table 3.1. This FOM matrix exposes the advantages and disadvantages of each design idea. The following are the descriptions of each design:

- Bi-plane: A bi-plane generates extra lift, however, it also generally weighs more, includes more work hours, and the servos associated with a second wing greatly increase RAC.
- Canard: A canard has built-in anti-stall characteristics. However, it requires additional thrust to take off because the main wing cannot reach its maximum angle of attack.
- Conventional: A conventional aircraft has a standard fuselage, tail, and wings, along with well-documented flying capabilities.
- Flying wing: A flying wing has great weight savings, however, the lack of tail surfaces renders the plane unstable. This concept was easily eliminated.

(R) – Rejected (S) – Selected	Figures of Merit (x weighting)					
	Ease of Manufacture (x1)	RAC effects (x1)	Stability (x2)	Weight savings (x1)	Sum of Ratings	Decision
Bi-Plane	-1	-1	0	-1	-3	R
Canard	-0.5	-0.5	1	-1	0	R
Conventional	0	0	0	0	0	S
Flying Wing	-0.5	1	-1	1	-0.5	R

Table 3.1 Figures of Merit for Wing Configurations

Given the relative ease of manufacture, stability, and proven performance, the conventional configuration was chosen, having an RAC of 7.9. The bi-plane had a weight penalty of 2lbs and RAC of 10.7, while the

canard design was rejected because of the 0.2 RAC penalty. The flying wing was abandoned, because it was found highly unstable even though the RAC was 7.1.

3.2.2 Wing Placement

Once the shape of the aircraft was decided, the wing placement relative to the fuselage was taken into consideration. High, mid, and low wing placements were considered and evaluated using the FOM in Table 3.2.

- High: A high wing has better roll stability because of the placement of center of gravity in relation to the wing. While the high wing does not interfere with the payload deployment mechanisms, it does, however, interfere with the landing gear placement.
- Mid: A mid wing is very difficult to construct. This is because they require a transfer of loads through the middle of the fuselage, which would require strengthening the structure and hence adding weight. Furthermore, blending the fuselage body to the wing, to reduce drag, will be almost impossible because of the nature of the payload and relative size of the fuselage to the wing thickness.
- Low: A low wing will require dihedral for roll stability. However, the landing gear is easy to attach and manufacture. Therefore, the landing gear is relatively small in comparison to the landing gear required for a high wing and, thus, lower weight and drag.

(R) – Rejected (S) – Selected	Figures of Merit (x weighting)					
	Ease of Manufacture (x1)	RAC effects (x1)	Stability (x2)	Weight savings (x1)	Sum of Ratings	Decision
High	0	-0.5	1	-0.5	1	R
Mid	-1	-0.5	0	-0.5	-2	R
Low	1	0	0.5	0.5	2.5	S

Table 3.2 Figures of Merit for Wing Placement

Due to the ease of manufacture, stability, weight savings, and the RAC effects, a lower wing seemed ideal. The mid wing placement was discarded because of the difficulty to manufacture. The high wing placement was feasible according to the FOM matrix; however, it required large, strong landing gear in order to eject the payload. The high wing also requires more distance from the fuselage to the ground in order to deploy the payload, thus making a short wheelbase, decreasing landing and take-off stability.

3.2.3 Wing Shape

With a lower wing aircraft in mind, several designs for the wing shape were taken into consideration: elliptical, rectangular, tapered and swept wings. When comparing these different wing designs an additional FOM was included, aerodynamic efficiency (Table 3.3).

- Elliptical: An elliptical wing has the highest efficiency factor, thereby, having the lowest drag. However, the elliptical wing has a complex shape, which is difficult to manufacture.
- Rectangular: A rectangular wing is the easiest to manufacture and has the lowest RAC score per wing area. However, the efficiency factor is low and, therefore, the drag is high.
- Taper: A taper wing is more efficient than the rectangular wing; however, a larger root cord is required to achieve the same wing area.
- Sweep: A sweep wing provides significant benefits at high speeds. However, manufacturing a sweep wing has significant difficulties, the wing-joiner is not as strong, and it increases the effect of Dutch-rolling for a low wing aircraft.

(R) – Rejected (S) – Selected	Figures of Merit (x weighting)						
	Ease of Manufacture (x1)	RAC effects (x1)	Stability (x2)	Weight savings (x1)	Aerodynamic Efficiency (x1)	Sum of Ratings	Decision
Elliptical	-1	-0.5	0	0	1	-0.5	R
Rectangular	1	0	0	0	0	1	S
Tapered	0	-0.5	0	0	0.5	0	R
Swept	-1	0	-0.5	0	-0.5	-2.5	R

Table 3.3 Figures of Merit for Wing Shape

A rectangular wing was chosen because of the ease of manufacture and the RAC score. This was because, an elliptical wing was almost impossible to manufacture without the proper machinery, while a tapered wing was only 4% more efficient than a rectangular wing given an aspect ratio of 8 (Abbot 17). The tapered wing was also disregarded because it had a higher RAC by 0.1. The swept wing was eliminated because of the increased possibility of the effects of Dutch-rolling with a low-wing configuration.

3.2.4 Tail Design

In order to stabilize the aircraft in the pitch and yaw directions, designs for a tail section were considered: V tail, H tail, and T tail. A tail was crucial for the stability of the aircraft. Therefore, the stability FOM was considered the most substantial when it came to selection (Table 3.4).

- V tail: This tail provides stability; however, it is difficult to manufacture compared to other designs.
- H tail: This design is ideal for twin fuselage planes, because it provides additional stiffness to the structure; however, extra controlled vertical surface and extra weight must be considered.
- T tail: This is a conventional tail section design that is highly stable and easy to manufacture.

(R) – Rejected (S) – Selected	Figures of Merit (x weighting)					
	Ease of Manufacture (x1)	RAC effects (x1)	Stability (x2)	Weight savings (x1)	Sum of Ratings	Decision
V – Tail	0	0.5	0	0	0.5	R
H – Tail	0	-0.5	0	-0.5	-1	R
T – Tail	1	0	0	0	1	S

Table 3.4 Figures of Merit for Tail Sections

A T-tail was selected, because it has proven stability and ease of manufacture. A V-tail design was rejected because of the increased complexity of manufacturing, despite the fact that it had a lower RAC by 0.1. The H-tail design was discarded because of the 0.2 RAC penalty.

3.3 Structures

Ensuring the structural integrity of the aircraft is a crucial part of the design process. Therefore, the structural conceptual design phase began with setting up FOM to ensure a high-quality aircraft. The FOM for the fuselage, wing, and tail structures along with the payload delivery mechanism and landing gear configuration are ease of manufacture, RAC, strength, and weight savings.

- Ease of Manufacture: This FOM deals with the manufacturing feasibility and difficulty level. This FOM is important because time, materials and resources are limited.
- RAC Effects: The RAC is an important aspect of the overall score.
- Strength: Each component is evaluated in terms of how well it will behave given general loading conditions.
- Weight Savings: Any weight change associated with a specific configuration will affect flight characteristics. A low weight aircraft is desirable because weight affects the amount of lift, thrust required, and overall RAC.
- Durability: The aircraft must repeatedly be able to withstand heavy loads.

3.3.1 Wing and Tail Structures

The wing and tail structural design requires strength, rigidity, and durability. From past experience, the wings and tail are often subjected to harsh handling conditions and must therefore be able withstand heavy loads. Therefore, durability is considered a figure of merit for the wing and tail designs. Three different ideas were considered for the internal structure of the wing and tail: white foam core, blue foam core, and balsa.

(R) - Rejected (S) - Selected	Figure of Merit (x weighting)						
	Ease of Manufacture (x1)	RAC Effects (x2)	Strength (x1)	Durability (x1)	Weight Savings (x1)	Sum of Ratings	Decision
White Foam Core	1	2	0	0	1	4	S
Blue Foam Core	1	0	1	1	0	3	R
Balsa Frame	-1	-2	-1	-1	-1	-6	R

Table 3.5 Figures of Merit for Wing and Tail Structure

White foam core was selected for both the wing and tail sections because of the ease of manufacture, RAC, and weight. Compared to white foam, a balsa wood structure seemed impractical. The manufacturability of a balsa frame structure is very complex and time consuming; the RAC, strength, weight, and durability costs are also high. Furthermore, white foam is less dense and lighter than blue foam, yielding weight savings and a lower RAC value. White foam is less durable and weaker than blue foam. However, for the predicted loads these components undergo, the white foam should suffice.

3.3.2 Fuselage Structure

The initial conceptual phase of the fuselage structure was centered on the carrying and delivering of the payload. Therefore, an additional FOM is considered, storage capacity. The aircraft must be able to house the payload, batteries, and flight control servos. Two concepts concerning the fuselage dominated the conceptual design phase: a semi-monocoque fuselage and a thin keel fuselage.

- Semi-monocoque fuselage: This design would house the payload and release it using a hatch at the rear of the aircraft.
- Thin keel fuselage: A thin keel would connect the wings, boom, motor and payload to one structural member.

(R) - Rejected (S) - Selected	Figure of Merit (x weighting)							
	Ease of Manufacture (x1)	RAC Effects (x2)	Strength (x1)	Weight Savings (x1)	Storage Capability (x1)	Durability (x1)	Sum of Ratings	Decision
Semi-Monocoque	1	2	0	1	1	0	5	S
Thin Keel	0	-2	-1	-1	0	1	-3	R

Table 3.6 Figures of Merit for Fuselage Structure

The semi-monocoque fuselage structure proved to be the better design. The keel design was heavy and difficult to fabricate. In contrast, the conventional semi-monocoque design provided a balance between the strength, weight and manufacturability. Also, this type of fuselage provides storage room for batteries and motor controller while the keel design does not inherently have extra space.

3.3.3 Automated Payload Deployment

Mission B requires the payload be ejected from the airplane via radio-control with no human intervention or movement of the airplane on the ground. A brief description of three Automated Payload Delivery Systems (APDS) is outlined below:

- Bomb-Bay Drop: This concept entailed dropping the payload from the bottom of the aircraft with bomb-bay-style doors. After deploying the payload, the doors shut and the mission continues.
- Ramp: Another idea was a ramp and door system where the box would slide out the rear of the fuselage assisted by gravity. The cargo ramp would be latched at the top, then pivot and drop down to allow the box to slide out, and then close again with a spring, sealing the fuselage.
- Rear Ejection Method: This idea entails an ejection-style launch mechanism that would use rubber bands or springs to discharge the box out the rear of the aircraft allowing the payload to land under the tail boom.

Each APDS concept was considered using the structural figures of merit (Table 3.7). When considering the APDS, additional FOM were discussed: reliability, required servos, and testing data.

- Reliability: Reliability was the most important design criterion for the APDS. The payload must eject flawlessly every time. Possible APDS systems were examined to uncover any possibilities of the payload becoming jammed in the fuselage.
- Servos Required: Additional servos are expensive and add complexity to the design. It was desirable to keep the number of servos to a minimum and keep the design simple.
- Testing Data: A simple model of each system was generated to examine how feasible each was and determine possible problems.

(R) – Rejected (S) – Selected	Figure of Merit (x weighting)									
	Ease of Manufacture (x1)	RAC Effects (x2)	Strength (x1)	Weight Savings (x1)	Durability (x1)	Reliability (x2)	Servos Required (x1)	Testing Data (x2)	Sum of Ratings	Decision
Bomb-Bay Drop	-1	-1	-1	0	-1	1	-1	0	-2	R
Ramp	1	0	0	0	1	-1	1	-2	0	R
Rear Ejection	0	1	0	0	0	1	1	2	5	S

Fig. 3.7 Figures of Merit for Drop System

The ejection method was deemed the most reliable and had the highest RAC. Therefore, this APDS was selected. Tests and analysis of the rear ejection model showed that the payload exited the fuselage cleanly and completely. Also, only one servo would be required for the rear door. In addition, this design allows for short landing gear and does not limit its selection, thus giving the airplane a lower profile and greater landing stability.

In order for the Bomb-Bay Drop system to deploy the payload successfully, a tricycle-type landing gear must be used. This landing gear must be used to ensure that the payload would clear the tail as the

aircraft taxied away from the deployment site. However, this landing gear would have to be at least six inches tall for the sensor box to clear the aircraft. Another factor taken into consideration is the opening in the bottom of the fuselage would reduce the torsion resistance ability and compromise the structural integrity of the fuselage. The drop system also may require two servos for two bomb-bay doors. This might be avoided by engineering a mechanical linkage between the two doors, but this adds complexity to the design. Since this APDS received low ratings in the FOM matrix and it required tall landing gear, this APDS was rejected.

During the testing of the ramp system, it was found that this APDS requires a steep ramp incline for the box to freely slide down the ramp. Also, an initial force was required to displace the payload in order to overcome the static friction. Without this initial force, the box tended to stop halfway down the ramp. The low scores received for the testing results and reliability FOM caused this APDS to be rejected.

3.3.4 Landing Gear

Three landing gear configurations were studied in the conceptual phase of the design: tricycle, tail wheel and quad. Because of the landing gear's role, three additional FOM were considered: landing performance, fuselage attitude, and ground tracking.

- Tricycle design: The tricycle design has one strut and tire under the nose of the aircraft and two other strut and tire configurations under each wing. This design is ideal for ejecting a payload from the rear of the aircraft.
- Tail Wheel (tail dragger): A tail wheel design is comprised of a strut and tire being placed under each wing and a wheel under the tail boom. This design allows for a wider wheel base and ground directional control.
- Quad: A quad configuration is composed of four tires under the fuselage. This design is unstable at landing and increases weight and drag.

(R) - Rejected (S) - Selected	Figure of Merit (x weighting)									
	Ease of Manufacture (x1)	RAC Effects (x2)	Strength (x1)	Durability (x1)	Weight Savings (x1)	Landing Performance (x2)	Fuselage Attitude (x1)	Ground Tracking (x1)	Sum of Ratings	Decision
Tricycle	1	0	0	0	0	0	1	1	3	S
Tail Wheel	1	0	0	0	0	1	-1	-1	1	R
Quad	0	0	0	0	-1	0	1	-1	-1	R

Table 3.8 Figure of Merit for Landing Gear Configurations

The tricycle configuration was selected because of its advantages in the areas of manufacturing, fuselage attitude, and ground tracking. The tricycle design ensures the tail and boom will clear the payload if it is dropped out of the rear. The tail wheel design was rejected because of interference with payload deployment and the quad design was rejected because of increased weight and ground tracking.

3.4 Propulsion

The goal of the propulsion conceptual design phase was to maximize thrust while minimizing rated engine power (REP). The FOM considered were: RAC, battery and motor weight, thrust, and fuses.

- RAC: The RAC is a substantial part of the overall score.
- Battery and Motor Weight: Battery and the motor weight were separated in the FOM because the addition of each motor directly adds to the manufacture's empty weight (MEW) and REP.
- Thrust: Thrust is important because it is the force required to overcome the drag.
- Fuses: Fuses are vital for safety reasons.

Four motor battery configurations were analyzed to optimize performance: 1 motor/1 (2 pound) battery pack, 1 motor / 1 (3 pound) large battery pack, 2 motors / 1 (3 pound) large battery pack, and 2 motors / 2 (1.5 pound) battery packs.

(R) – Rejected (S) – Selection	Figures of Merit (x weight)						
	RAC (x3)	Thrust (x2)	Fuse Rating	Motor Weight	Battery Weight	Sum of Rating	Decision
1 Motor / 1 (2lbs) Battery Pack	1	-1	1	1	1	3	S
1 Motor / 1 (3lbs) Large Battery Pack	0.5	0	0	1	0	1.5	R
2 Motors / 2 (1.5lbs) Battery Packs	-1	1	1	-1	0	0	R
2 Motors / 1 (3lbs) Large Battery Pack	0	0	-1	-1	0	-2	R

Table 3.9 Propulsion FOM

The setups with two motors received low RAC scores (over 10.7). The RAC is penalized for multiple motors and additional motor weight. Therefore, the systems with more than one motor were discarded.

As seen in Table 3.9, the single motor propulsion systems give favorable RAC values (7.9 and 9.4 respectively for 2 pounds and 3 pounds battery packs), fuse ratings, motor weight, and battery weight. From previous experience and competitions, a 2 pounds battery pack is estimated to be the most efficient and to provide the power required to fulfill the missions. However, in order to formally decide between the two remaining systems, the thrust must be calculated. This calculation is performed in the preliminary and detail sections.

3.5 Final Aircraft Configuration

With the collaboration of concepts from the aerodynamic, structure, and propulsion technical groups, a final aircraft configuration was produced. The final design had a conventional configuration with a rectangular lower white foam wing and T-tail. The fuselage structure was a semi-monocoque configuration and a tricycle configuration was chosen for the landing gear. The propulsion system was comprised of a single motor with a 2 pound battery pack.

4.0 Preliminary Design

With a complete general aircraft configuration, the preliminary design phase focused on design parameters and trade studies. The aerodynamic group performed trade studies to determine the wingspan, chord length, airfoil, and tail area that would optimize the design. While, the structures group determined the configuration of the wing, tail, and fuselage, along with the motor mount and landing gear. The minimum amount of force required for the APDS to perform at maximum efficiency was calculated. Moreover, the propulsion group calculated the optimum propulsion system configuration by determining the minimum thrust required to complete the missions.

4.1 Aerodynamics

Once the conceptual design phase was completed, the parameters obtained by the generated primary aircraft configuration were used in the preliminary design phase to further narrow and refine and design. Trade studies were conducted to determine the wingspan, chord length, airfoil, and tail area that would optimize the design.

4.1.1 Wingspan

During the conceptual phase, the wingspan was limited by the competition rule that the aircraft must fit into a 4x2x1 foot box. Therefore, each wing section length was limited to 4 feet. Furthermore, the competition rules also stipulate that the maximum take off distance is 120 feet. In order to minimize thrust and still take off within the required distance, a large wingspan is desired. Taking this into account, three different wing section configurations were considered:

- First Configuration: The first configuration contained two four-foot sections attached at the sides of the fuselage giving a wingspan of 8.7 feet.
- Second Configuration: The second configuration considered two four-foot sections joined at the bottom of the fuselage, providing an eight-foot wingspan.
- Third Configuration: The third configuration had three four-foot sections joined together yielding a wingspan of 12 feet.

An aircraft with a large wingspan and low thrust typically has a large aspect ratio, which yields a lower induced drag. However because of the competition size restraint that the whole aircraft fit into a predetermined size box, the chord must be reduced in order to allow room for all aircraft components. By decreasing the chord length, the wing thickness must also be decreased, which inadvertently requires a heavier wing structure. For this reason, Configuration 3 was rejected and a two-section wing was chosen. Both configurations one and two have the same sectional size limits placed upon them and will, therefore, offer the same chord length. Since Configuration 1 offered a larger wingspan without compromising the chord length or aircraft's weight, it was selected.

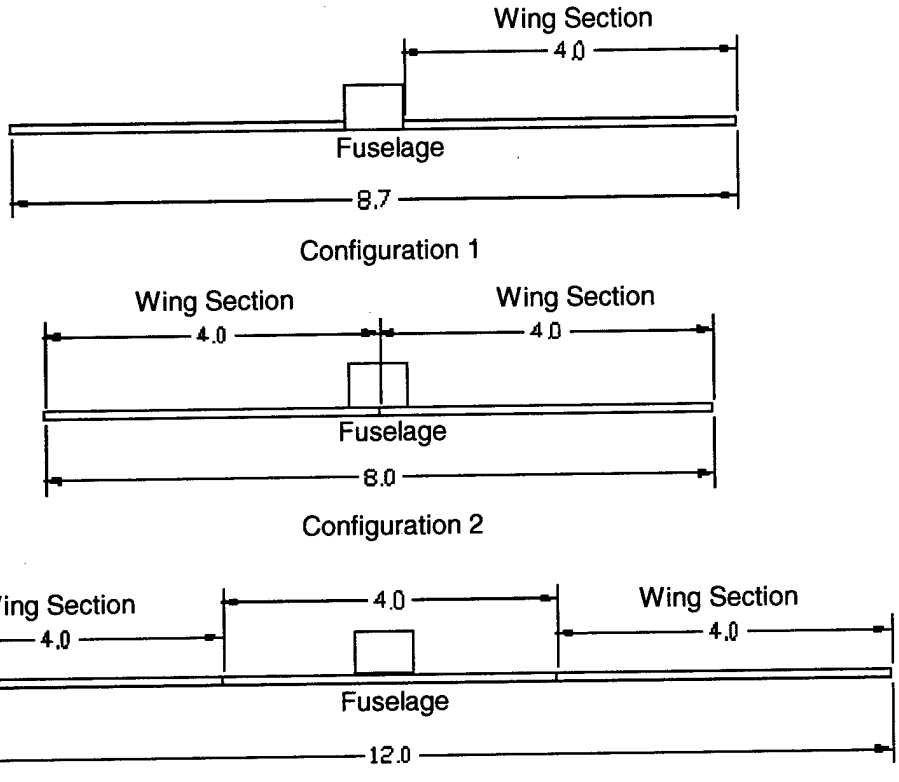

Figure 4.1 Wing Section Configuration

4.1.2 Wing Chord Length

With a fixed wingspan of 8.7 feet, a chord length was determined to minimize the thrust required for takeoff. Because of size limitations, the maximum chord length calculated to fit within the dimensions of the box was 14 inches. The following chord lengths were then considered: 8, 10, 12, and 14 inches. Holding the wingspan constant, the thrust and number of battery cells were calculated for each proposed chord length. The thrust calculations included changes in the empty weight, aspect ratio, and wing area associated with each selected chord length. In Figure 4.2, the RAC was plotted as a function of chord length. It was observed that the larger the chord length, the smaller the RAC. Therefore, a 14 inches chord length was selected.

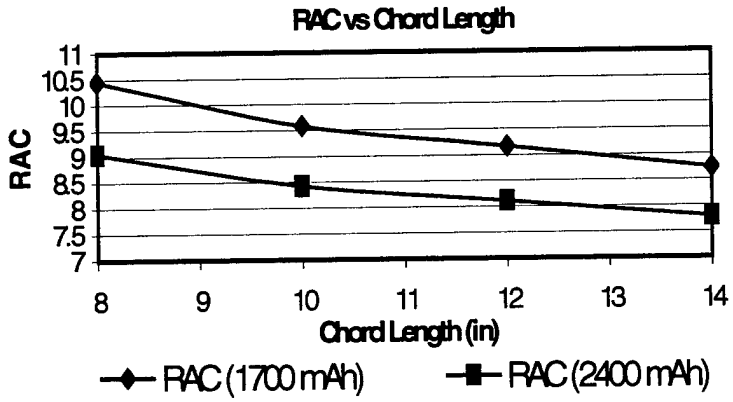

Figure 4.2 Effects of Chord Length on RAC.

4.1.3 Airfoil Selection

In order to optimize the takeoff distance and maximize the lift to drag ratio of the wing, numerous airfoils were considered. Visual Foil software was used as a tool to narrow the airfoil selection. Using this software, theoretical coefficients of lift and drag for the Reynolds number of 300,000 were calculate for over 50 airfoils. In order to verify these computer generated theoretical calculations, a comparison was done between selected airfoil calculations and actual wind tunnel results from research performed by Michel Selig. From those airfoils deemed plausible, calculations were performed to determine the total take off distance and the lift to drag ratio. The selection of the airfoil was a process of reducing the take off distance and optimizing the lift to drag ratio, thereby minimizing required thrust.

The remaining airfoils were divided into two groups: high lift and low drag. Airfoils such as the S1210, S1223, and E423 belonged to the high lift group. These airfoils had lift coefficients greater than 2.0, however their drag coefficients were also high, averaging around 0.020. Therefore, excess lift exists while at cruise, requiring negative trim, which risks the possibility of stalling the wings via flow separation. Furthermore, additional drag at cruise requires greater motor power thereby increasing required thrust. This conflicts with the desired goal to minimize required thrust at both takeoff and cruise. Therefore, the high lift airfoils were abandoned.

Low drag airfoils such as the E210, E214, and S4083 were then considered. The E210 and E214 offered moderate lift coefficients of 1.1-1.3 and low coefficients of drag of 0.010. These airfoils were considered good candidates because of their lift to drag ratio and their proven performance in previous competitions. However, the S4083 airfoil was found to have better drag and lift characteristics in comparison to the Eppler 21x series. This airfoil provided a moderate coefficient of lift of 1.35 and very low coefficient of drag of 0.008. Therefore, the S4083 was chosen because it minimized the power required for takeoff and cruise (Figure 4.3).

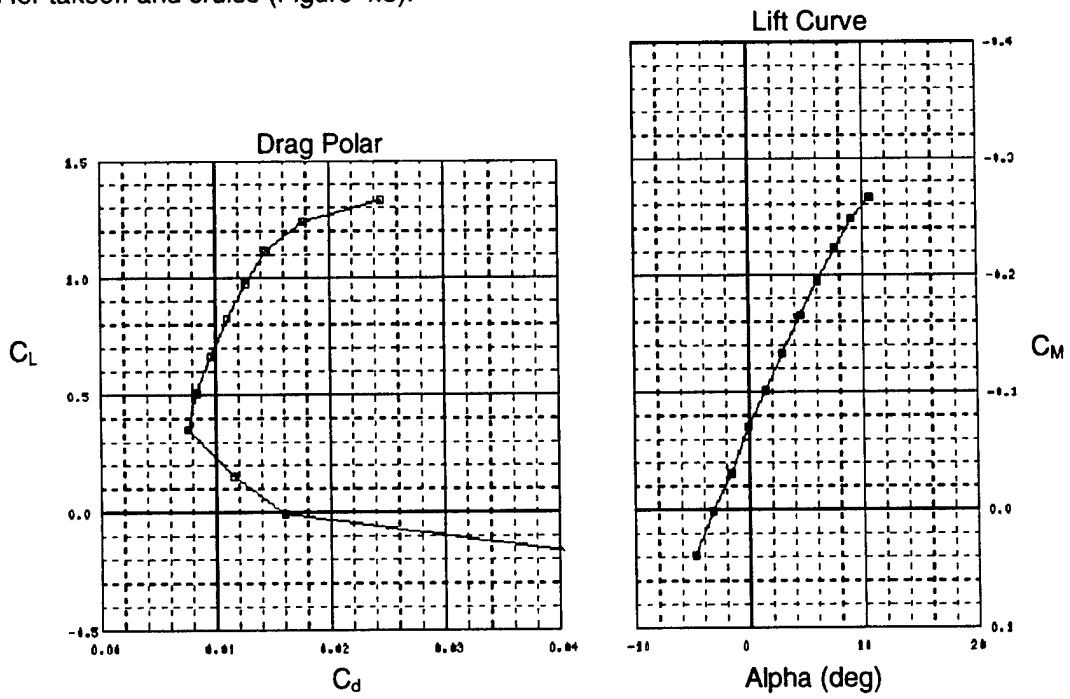

Figure 4.3 Drag Polar and Lift Curve for S4083 Airfoil at Re ≈ 300,000.

4.1.4 Tail Design

Once the wing dimensions were calculated and the airfoil was selected, calculations were preformed to obtain the desired dimensions for the tail. Since the RAC takes into account assembly time, the dimensions of the tail were based on the ability of fitting the entire assembled tail section in the predetermined size box. This factor limited the height of the vertical stabilizer to 10 inches and the horizontal stabilizer to 24 inches. This coincides with the competition rules, which stipulates that the horizontal stabilizer cannot exceed a quarter of the wingspan.

In order to optimize the tail effectiveness, a boom 42 inches long was used. Numerous symmetric airfoil designs were made available. However, the NACA 0009 airfoil was immediately selected for the horizontal stabilizer because of it reduced drag and produced zero lift at cruise. This selection improved the theoretical stability characteristics.

The stability of the aircraft was further enhanced, by optimizing the tail section area. The area was calculated with the following formulas. The volume coefficients of 0.52 and 0.04 were used for the horizontal and vertical stabilizers, respectively.

$$\text{Area}_{\text{HorizontalStabilizer}} = (\text{Coefficient}_{\text{HorizontalVolume}})*(\text{MAC}_{\text{MainWing}})*(\text{Area}_{\text{MainWing}})/(\text{Arm}_{\text{HorizontalStabilizer}})$$

$$\text{Area}_{\text{VerticalStabilizer}} = (\text{Coefficient}_{\text{VerticalVolume}})*(\text{Span}_{\text{MainWing}})*(\text{Area}_{\text{MainWing}})/(\text{Arm}_{\text{VerticalStabilizer}})$$

Using these empirical equations, the horizontal stabilizer and vertical stabilizer areas were calculated to be 317 inches squared and 130 inches squared, respectively.

The mean aerodynamic chord (MAC) for each tail section was determined using the vertical stabilizer's height, horizontal stabilizer's span, and the respective surface areas. Using a taper ratio of 0.85 (Raymer 85), a 12 inch tip and 14 inch root chord were calculated for both the horizontal and vertical stabilizers.

4.1.5 Fuselage Shape

An important concern of the aerodynamic group was to find a fuselage shape that would reduce the zero-lift drag. In order to accomplish this, several fuselage profiles were considered. A fuselage with an airfoil shape would streamline the body and reduce the zero-lift drag. Therefore, an airfoil with a large thickness-to-chord ratio was selected for the fuselage. However, to incorporate this into the design, the fuselage would extend to the tail adding unnecessary weight to the aircraft and increasing labor costs. In turn, the extra weight and fuselage length would adversely affect the RAC. This fairing would also interfere with the automated payload deployment system (APDS). Therefore, this design was abandoned. A modified smooth, well-rounded bullet shaped fuselage with a blunt end was chosen because of its low weight, lack of interference with the APDS, and ease of manufacture.

4.2 Structures

During the conceptual design phase the mission parameters and FOM were used to create a basic structure of the aircraft. In the preliminary design more focus was placed on the aircraft's structural requirements:

- Feasibility of primary structure locations.
- Load paths of primary structural components.
- Materials selection for said components.
- Sizing of components with a safety factor of 1.5 for yield and 2.0 for ultimate.
- Practicality of structural weight to lift available.
- Survivability of structure in respect to impact loads from hard landings and assembly.
- Manufacturability, maintenance and life cycle cost were estimated.
- Fit into the shipping container described in the mission profile.

Trade studies were conducted on these design requirements. These studies provided the necessary tools to investigate structural alternatives in location, applied loads, material selection, sizing, and weight of each component. They also played a part in deciding on the overall assembly of the aircraft. Estimates for the aircraft weight and center of gravity were determined. The information gained from these studies produced an aircraft structure that was sound and efficient.

4.2.1 Factor of Safety

The preliminary analysis used factors of safety to produce initial sizing. The analysis conducted to determine the aircraft's structural components optimal thicknesses were subject to factors of safety of 1.5 for yield and 2.0 for ultimate. If sizes were deemed to thin for practical purpose a margin of safety was added in the detailed design.

4.2.2 Wing Structure

The wing structure consists of two main portions, the spar and skin. Since the spar mainly resists bending and the skin torsion, these two structural elements are individually analyzed in the preliminary design.

The two loading cases determined the tapered shape of the spar: distributed aerodynamic loading and a point load applied at the tip during the wing test. These two cases generate different bending moments, as seen in Figure 4.4. The incorporation of these resulted in the tapered pattern shown in Figure 4.5.

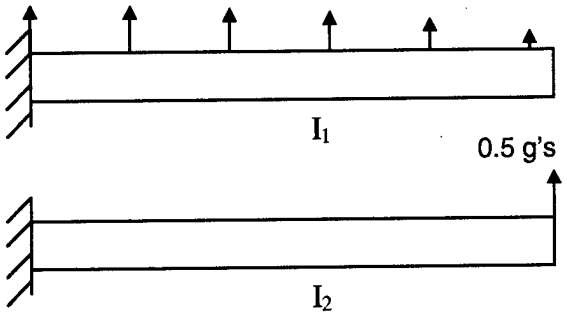

Figure 4.4 Distributed and point loads.

The spanwise taper of the spar gives a better strength to weight ratio for the given loading cases. During the preliminary analysis of the spar structure, the bending moment due to the point load of the landing gear was considered to be insignificant compared to the bending moment of the distributed load, and is not considered separately.

The preliminary thickness needed for the composite spar was calculated by modeling the minimum thickness needed for the spar while retaining a factor of safety of 2.0 is 0.0045 inches for the top and bottom layer.

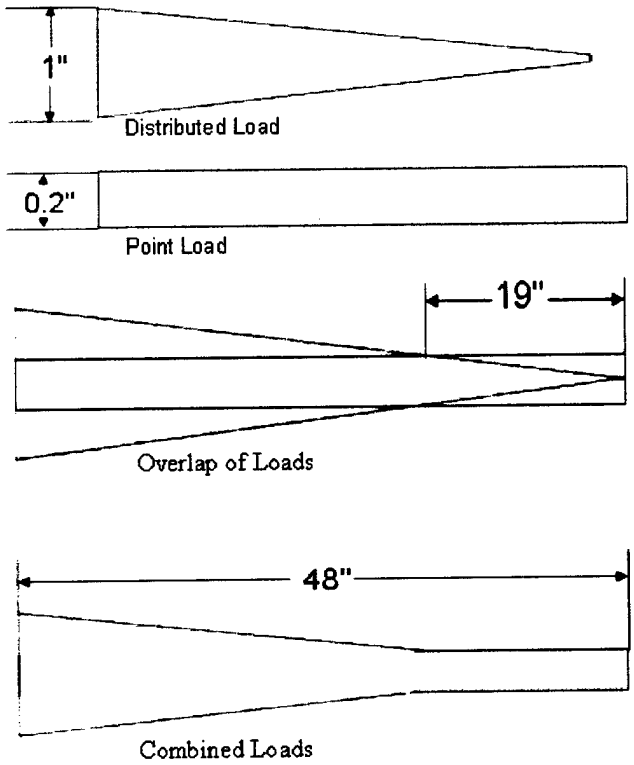

Figure 4.5 Illustration of spanwise profile of the spar.

The primary requirement of the skin is to provide the smooth surface designed by the aerodynamics group and also serve as a platform for the control surfaces. The skin also needs to be as light as

possible for overall aircraft performance, while still transferring the torsional loads to the wing joiner. A fiberglass resin matrix was chosen to build the skin. This would give a hard and smooth aerodynamic surface, has an acceptable strength to weight ratio, and is easy to manufacture to the shape of the airfoil.

The wing skin was analyzed using a MATLAB script. The worst case aerodynamic loading was assumed in sizing the thickness of the skin. The wing skin was considered a closed single cell web in torsion. The shape of the actual airfoil was used in the analysis. The preliminary thickness required with a factor of safety of 2.0 is 0.021 inches. The preliminary thickness being very small requires that a larger thickness be used so that the skin can be manufactured accurately. This will increase the factor of safety and should not have a great effect on the final weight of the wing.

4.2.3 Wing Joiner

The wing joiner, being found at the root of the wing, experiences both torsion and bending, therefore, it is required to analyze this element for both types of loading. The wing joiner is responsible for transferring all wing loads to the main structure.

Once the wing span and configuration was determined, it became necessary that the wing joiner be used as the method by which the wings attach to the fuselage. The wing joiner slips into a sleeve upon assembling the aircraft out of the box. This quick slide-together action enables rapid assembly of the aircraft. A tight fit between the sleeves and wing joiner is needed to ensure that the wings will not slide out during flight.

The wing joiner is the main structural link between the wings and the fuselage. It transfers both bending and torsional forces. The wing joiner therefore is constructed of both bi-directional and uni-directional carbon fiber layers with a blue foam core. Blue foam was used for the core of the wing joiner for maximum strength.

4.2.4 Tail Configuration

The primary purpose of the tail is to act as a platform for control surfaces and enhance stability. Three load paths were assumed critical in the design: boom, vertical and horizontal stabilizer. As shown in Figure 4.6, forces were transferred from the stabilizers causing bending and torsion forces, which were the main forces acting on the boom. The loads applied to these stabilizers were similar to the main wing loads and, therefore, were modeled in a similar fashion.

Two designs were considered for the boom, a truss and a beam. Due to manufacturing limitations, the truss was deemed too complicated and unreliable. Therefore, a beam design was chosen. Several beam cross-sections were considered: square and solid, square and hollow, circular and solid, and circular and hollow. These cross sections were analyzed using the figures of merit: ease of manufacture, plane bending to weight ratio, out of plane bending to weight ratio, torsion to weight ratio, and durability (Table 4.1).

(R) – Rejected (S) – Selected	Figure of Merit (x weighting)						
	Ease of Manufacture (x1)	Plane Bending to Weight Ratio (x2)	Out of Plane Bending to Weight Ratio (x2)	Torsion to Weight ratio (x2)	Durability (x1)	Sum of Ratings	Decision
Square Solid	1	1	-2	-2	1	-1	R
Square Hollow	1	2	-1	-1	0	1	R
Circular Solid	-1	-2	1	1	1	0	R
Circular Hollow	-1	-1	2	2	0	2	S

Table 4.1 FOM of Cross Section Selection for Tail Beam.

After the analysis was complete, the circular hollow tube design was considered the most efficient because of its weight and ability to handle the predicted loads. With forces acting in different directions, a circular tube is desirable because it has uniform behavior. The hollow configuration was chosen instead of the solid configuration in order to lighten the aircraft structure and move the inertial mass away from the neutral axis. The radius arm of the cross section is responsible for the ability of the hollow tube to take torsion loads without weight penalty associated with the solid tube. This produced greater bending and torsion stiffness in reference to a minimized cross sectional area.

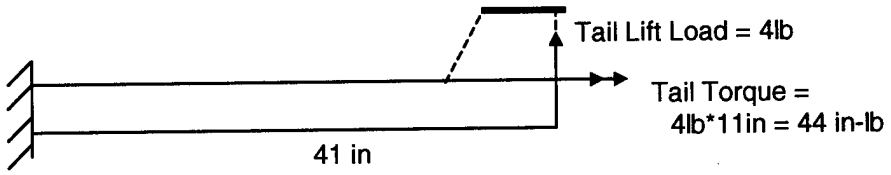

Figure 4.6 Tail Boom Load Model.

Due to availability of material, a boom with an outside diameter of 0.5 inches was selected, while the inner diameter was found through calculations. Using Figure 4.6, two case studies were performed in order to determine the inner diameter of the boom. The first case study investigated bending. The bending of the boom was modeled as a cantilever beam with a 4 pound point load 41 inches from a fixed end. By analyzing the stresses through the cross section of the loaded member, the minimum inner cross sectional diameter was found to be 0.4966 inches. The second case study focused on torsion loads. The torsion of the boom was modeled as a 4 pound side load located at the top of the rudder 11 inches away from the tail boom. By studying the torque applied at the tail, the resulting minimum required inner diameter was found to be 0.4985 inches. Since the inner diameter found in the first case study is smaller than that found in the second, it is deemed the critical inner diameter.

Trade studies conducted on model aircraft tail structures led to the selection of a single vertical and top mounted horizontal stabilizer, T-tail, structure. The studies showed that most tail structures do not contain a spar and are usually comprised of a foam core with fiberglass skin. However, performance aircraft increased bending stiffness by adding a small amount of carbon fiber tow to the top and bottom of the quarter chord. Due to the nature of the competition, the performance aircraft tail structure was

selected. The skin thicknesses of the stabilizers were determined by the same modeling as the main wing. The required thickness was calculated to be 0.015 inches of +/- 45 degree fiber glass.

4.2.5 Fuselage Structure

The fuselage is considered the primary load bearing structure, housing the payload, batteries, wing joiner, tail boom and motor mount. The main components that were loaded consist of bulkheads, rails and skin. The internal structure of the fuselage is shown in Figure 4.7. Using the aerodynamic load paths generated by the aircraft in flight, the placement and number of components were determined.

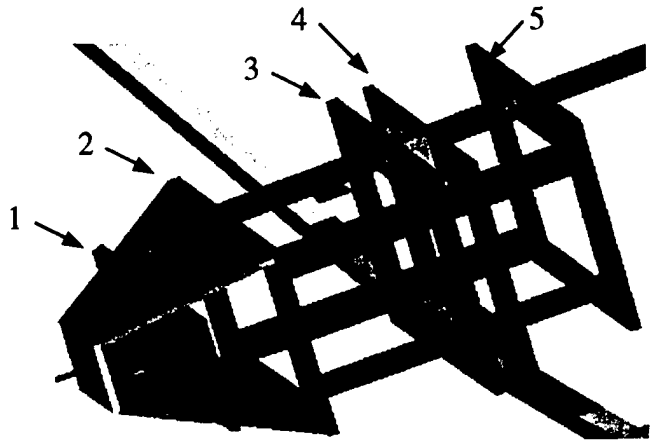

Figure 4.7. Location of Bulkheads

In order to obtain structural rigidity, five bulkheads are distributed about the cargo compartment. The bulkheads are numbered one through five in Figure 4.7. Bulkheads two through four are used for the APDS with three and four assigned to assist in the load transfer from the main wing. The tail boom is kept fixed by the last three bulkheads. The first bulkhead manages front landing gear loads and also acts as the firewall.

The bulkheads are comprised of composite plywood and high-density foam. Plywood was selected primarily for its resistance to shearing at the holes; while high-density foam was selected because of its lightweight and load transfer capabilities. The critical thickness of the bulkheads was determined by two case studies. These case studies took into consideration bulkhead 5, because it experienced the largest applied forces. The first case study focused on the forces the APDS applied to bulkhead 5. The APDS rubber bands are anchored to the bulkhead's midpoints. The APDS produces 8 pounds of force, thereby applying 4 pounds of force on each side of the bulkhead. The model, Figure 4.8, shows a 4 pound point load applied to a beam with two fixed ends. For a conservative estimate, the distance of the beam was taken to be the height of the bulkhead. By applying this point load and determining the yield, the ultimate bending of the bulkhead was found. Through this analysis, the critical thickness of the bulkhead was found to be .006 inches.

The second case study focused on the shearing of bulkhead 5. Bulkhead 5 experiences shearing because of the 4 pound load transfer from the tail. By calculating the shearing force applied on the bulkhead, critical thickness of the bulkheads was found to be .004 inches. Both case one and two

estimate very small critical thicknesses. The chance of using thicknesses this small was highly unlikely due to the availability of material. Therefore, the bulkheads' thickness is substantially larger than the calculated critical thickness. This was seen as a benefit due to the increase in the margin of safety.

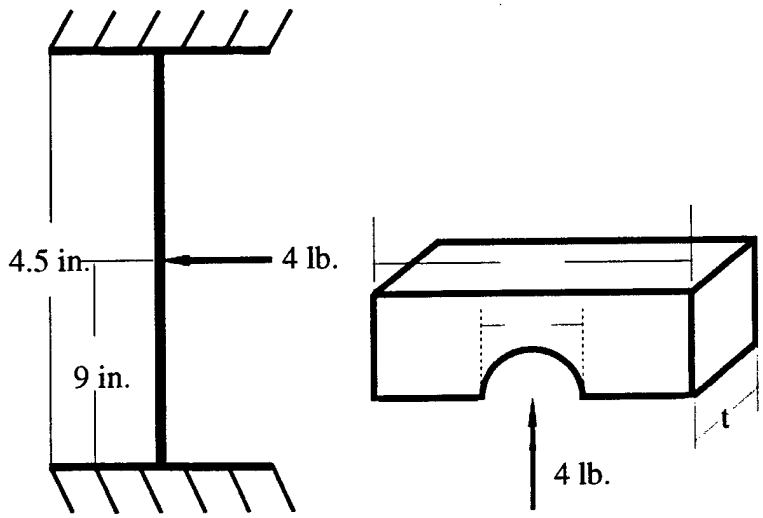

Figure 4.8 Bulkhead Worst Case.

Four 'L' shaped rails run fore and aft through the bulkheads to hold the payload in place and resist bending in the fuselage. The rails are required to be stiff and light weight. Therefore, they are composed of a sandwich structure with unidirectional carbon fiber and high-density foam core. The unidirectional carbon fiber provides strength, while the foam core distributes the applied loads between the top and bottom carbon fiber layers.

The material selection for the skin of the fuselage was critical because of the need for strength. The skin of the fuselage is designed to withstand torsion loads, provide rigidity to the airframe, and resist the tendency to twist. Both fiberglass and carbon fiber were considered for the fuselage skin. However, a sandwich structure comprised of bi-directional carbon fiber and white foam core was selected because of gains in strength. The skin coupled with the bulkheads is able to withstand loads along the length of the fuselage.

4.2.6 Aircraft Weight and Center of Gravity

After the fuselage structural components were initially sized, Pro-Engineer was used to create a solid model. By inputting the material properties of each element into this computer-generated model, the mass and density of each component was determined. With the calculations provided by the aerodynamics group regarding the weights of the wing and tail sections and the information gained using the solid model, the aircraft's weight and center of gravity was determined.

The estimated empty weight of the aircraft was 12 pounds. This value does not include the five pound sensor package, two pound battery pack, or the one pound antenna. The fully loaded aircraft

weight was estimated to be 20 pounds and the center of gravity was found to be approximately 1.5 inches in front of the wing quarter chord.

4.2.7 Automated Payload Delivery System (APDS)

During the preliminary design phase, a prototype of the ejection system was built. A scaled model of the fuselage along with the 5-pound, 12x6x6 inch payload was constructed from reinforced cardboard. These prototypes were used to test potential energy devices, latching mechanisms, door styles, and estimate the friction the box experiences as it slides from the fuselage.

Determining how to eject the box was the first concern during the APDS preliminary design phase. Possible ejection design methods with various types of springs and rubber bands were considered. Springs were determined to be unreliable, because under load, plastic deformation could occur and they would not return to their original shape.

Rubber bands were chosen to propel the payload because they are easy to work with and are very inexpensive. In terms of reliability, multiple rubber bands could be used for a harness so if one breaks, there will still be enough potential energy in the rubber bands to eject the box out.

Four rubber bands are designed to be bunched together into two clusters, one on each side of the payload. The ends of each cluster are designed to be fastened to the aft bulkhead and looped around the payload. This will create a slingshot-type ejection device so when the box is pushed into the fuselage, the rubber bands will be stretched approximately 8.25 inches, thus storing potential energy. A door on the aft of the aircraft, hinged at the top, will hold the payload in the fuselage with a latch and servo mechanism. Thus, the payload will be pushing against the door with the rubber bands in tension. When the latch is released, the door will open swing upward and the rubber bands will transfer their potential energy into kinetic energy of the box. After the box has exited the airplane completely, a rubber band on each side of the door will pull it closed again and the latch can be returned to the locked position by reversing the latching servo.

The inner compartment in which the cargo box is designed to rest inside the fuselage is composed of four 1x1x12 inch L-shaped rails made of carbon fiber-sandwiched quarter inch foam. These rails give both structural rigidity between the bulkheads and serve as guides for the cargo. The four rails are located at the edges of the payload with enough clearance so it can easily slide in and out. The reason for having four rails is to hold the payload securely in place on all four edges. There should be very little independent movement of the cargo during flight.

The rear of the fuselage was eventually designed to be equipped with a cargo door hinged on top with a latching mechanism on the bottom. During the preliminary analysis, a smooth, aerodynamic tapered fairing at the rear of the fuselage was thought to be essential to best keep the airflow attached to the fuselage and keep the drag reduced. However, numerous design problems came up. The gradual taper most beneficial for clean aerodynamics would require a long fairing. The fairing would either have to drop down, be raised up, or split in two, similar to a clamshell. It could not be raised because it would

interfere the tail boom. The shell could not easily be lowered like a ramp since this would involve a hinge at the bottom of the fuselage that would hinder with the clean ejection of the box. Another idea was proposed to make the shell in two pieces so each side could swing open to allow for the payload to exit freely. This idea was eventually rejected because of the complexity of the design and excess weight. This increase in weight would not be justified to offset the increase in performance from the smooth aerodynamic shape. Therefore, it was decided to simply use a door on a hinge that would latch at the bottom. Further, it was resolved that the door does not have to completely cover the rear of the fuselage. The drag and turbulence created by the lack of an enclosed rear door will not affect the aerodynamics of the airplane significantly since it will be flying at relatively low speeds.

Various types of latching devices were considered to find one that would use a single servo, be able the handle the load caused by the rubber bands, and release quickly and reliably without binding. The prototype fuselage was used to build different latches into the door and simulate a servo pull under load. Some latches were found to be putting too much force on the servo pin and therefore binging occurred since the servo did not have enough torque to pull the pin out. The latch that was selected consists of a small C-shaped piece of metal with a hole drilled in the top and bottom halves as shown in Figure 4.9. A pin will be attached to a servo arm at one end and go through the two holes at the other end. The door also has a pin sticking down from the bottom center. This pin will be inserted into the open end of the C-piece while the servo pin holds it into place through the two holes. When the servo pin is pulled, the door is free to swing out and up, releasing the payload. If required, more pins can be integrated into the door if the load on a single pin is too great.

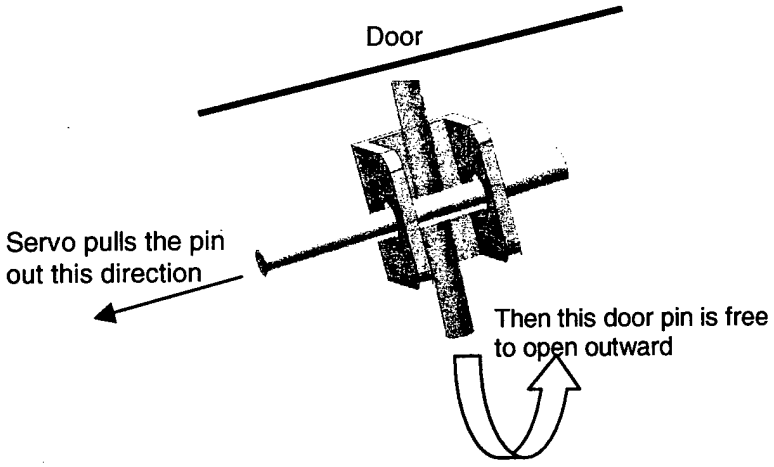

Figure 4.9 Latching Mechanism

4.2.8 Motor Mount

A trade study was preformed taking into account the thrust and landing loads that were transferred to the primary structure. It was found that these loads should be transferred through carbon/foam mounting plates in order to assure the durability of the aircraft. The motor is attached to pre-impregnated Kevlar as

seen in Figure 4.7. The material was chosen for its thermodynamic properties and resistance to shear from load bearing holes in its structure. It is also believed that the mount is an aircraft saving device due to its ability to fail at high impact loads. This quality would theoretically save the motor in the event of a low speed nose impact.

4.2.9 Landing Gear

During the conceptual design analysis, the tricycle landing gear was selected. By selecting this type of landing gear, interference with the APDS was nullified. However, the penalty for using the tricycle landing gear is that it creates a short wheelbase. To optimize minimum take off distance, the CG should be placed over the main wheel causing the plane to achieve a desired angle of attack with minimal required lift. In order to resolve the drawbacks of a short wheelbase and still take off within the required maximum distance of 120 feet, the landing gear was set at an angle back form the CG, thereby increasing the wheelbase. The optimal angle calculated was 15 degrees. This angle is determined from the main landing gear wheel hub to the perpendicular line of the CG with the ground (Figure 4.10). Therefore, the resulting distance of the main landing gear hub from the CG was 2.479 inches.

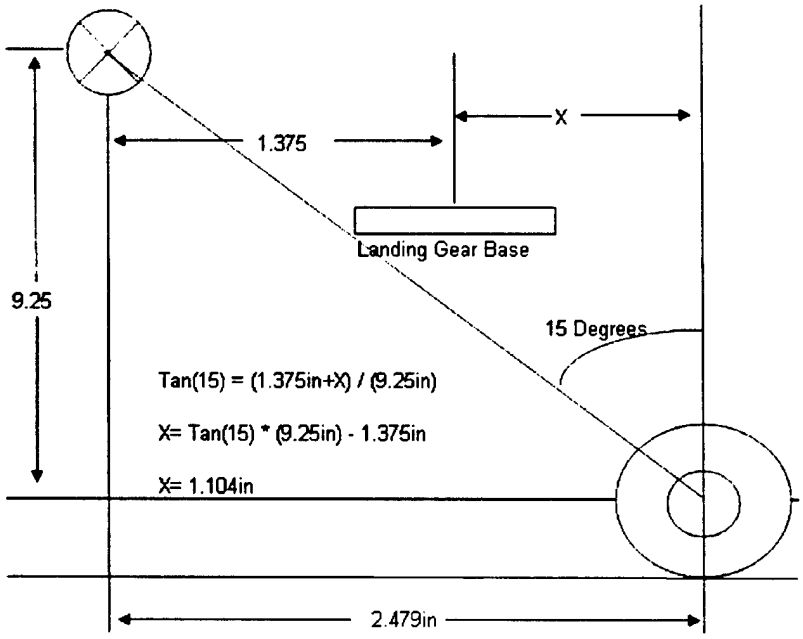

Figure 4.10 Landing Gear Placement (not to scale).

Trade studies were conducted concerning the impact loads applied on the landing gear. However, these types of loads are difficult to predict because of stability issues. In order to account for hard landings, a manufactured solid spring bow gear was selected for the front landing gear. To transfer the nose landing loads to the mounting plates and skin, the gear is mounted to the first bulkhead. The main gear (Figure 4.11) consists of pre-impregnated non-sandwich carbon fiber. An equal number of composite layers of 90 and 45-degree plies were used to handle the various torsion and bending loads caused by impact and breaking. This lay-up produces a spring effect favorable to hard landing conditions. The gear is rated for

impact loads far above those of the primary structure and would subsequently be unexpected to fail in the event of a hard landing.

Figure. 4.11 Main Landing Gear

4.3 Propulsion

During the preliminary design, the minimum required thrust to complete the missions was calculated and the optimum propulsion system configuration was found. Since, takeoff requires the most power throughout the missions, it was used to establish the minimum required thrust. The required thrust of 6.7 pounds was calculated using the aircraft's weight and wing geometry combined with the maximum takeoff distance. It was imperative to find a propulsion system configuration that would provide a minimum of 6.7 pounds of thrust and draw less than 40 amps of current, which was stipulated by competition guidelines.

In the conceptual design, the propulsion system was determined to have a single motor with a two pound battery pack. According to competition rules a Graupner or Astro motor must be used. From past experience and success, a motor from the Graupner 3300 series was chosen. These motors are known to be reliable and demonstrate high performance.

The Graupner 3300 series offer motors with different numbers of windings, which allow peak efficiencies at different voltages. MotorCalc software was used to determine the best combination of propeller geometry, battery cells, and engine windings. Each systems pitch speed, flight time, and current were calculated. These calculations are found in Table 4.2.

Motor and Battery Configuration					
# of Winding	# of cells	Pitch Speed	Flight Time	Propeller Geometry	Current (Amps)
4	15	48	3:40	18x12	59
4	16	51	3:25	18x13	62
5	18	35	3:25	20x11	44
5	19	49	3:25	18x13	43
5	20	50	3:20	18x13	44
7	19	58	4:05	18x15	36

Table 4.2 Graupner Motor 3300 series

The optimum propulsion system has a high static thrust, high pitch speed, long flight time, and minimal battery weight while abiding by competition regulations. A way to increase static thrust without increasing

battery weight is to increase the propeller's diameter. However, by doing so the pitch speed is decreased. Therefore, to overcome this drawback, the propeller's pitch is augmented. By increasing the propeller's pitch, the pitch speed increases while only slightly decreasing static thrust. Thereby, increasing the maximum velocity of the aircraft. By analyzing the MotorCalc results (Table 4.2), the Graupner 3300-7 motor with a two to one gearbox coupled with 19 Sanyo 2400 mAh cells and 18x15 inch propeller was chosen to achieve the desired thrust of 6.7 pounds resulting in a pitch speed of 85.1 feet per second. This configuration offered a reasonably high static thrust, high pitch speed, and long flight time while drawing less than 40 Amps; therefore, it offered the optimum overall theoretical performance.

4.4 Final Aircraft Configuration

At the conclusion of the preliminary design, the design parameters and sizing trades had all been investigated and the final aircraft component selection and systems architecture was ready to be selected. The preliminary design determined the sizing of the wing and tail geometry, primary structure dimensions, and propulsion configuration. The wingspan and chord length were calculated to be 8.7 feet and 14 inches, respectively. The S4083 airfoil was selected for the wing, while the NACA0009 was chosen for the tail. The most efficient shape for the spar was found to have a spanwise taper. The aircraft's takeoff weight was found to be approximately 20 pounds and the center of gravity was determined to be 1.5 inches behind the leading edge of the wing. It was determined that eight pounds of force from four, #64 rubber bands would provide adequate force for the APDS. An 18 inch diameter propeller with a 15 inch pitch, Graupner 3300-7 motor, and 19 Sanyo 2400 cells compose the propulsion system.

5.0 Detailed Design

With the information gained from the preliminary design phase, a foundation was laid for finalizing component and system architecture selection. The aerodynamics group calculated final wing and tail geometry while the structures group finalized the design of the spar. The structures group also conducted a detailed analysis of the internal architecture of the fuselage and the propulsion group determined the propeller, motor, and battery cell optimal configuration.

5.1 Aerodynamics

Based on the design parameters and sizing trades investigated during the preliminary design phase, performance characteristics were determined and modified to achieve the mission specifications.

5.1.1 Mission Profile and Flight Performance

The aerodynamic detailed design focused on the mission profiles, which were determined during the conceptual design phase. The most difficult missions were initially selected since they yielded the highest scoring potential. In order to verify that these missions optimize the final time and flight score, and hence, the final score, each mission was analyzed for both conventional and performance flight modes:

- Conventional mode: The conventional mode focuses on flight efficiency, minimizing the number of batteries used.
- Performance mode: The performance mode was dominated by the concept of maximizing airspeed in order to minimize flight time.

In order to calculate flight time, each mission was profiled by the aircraft's cruise speed, maximum velocity, turn rate, and clime rate, which were determined from the wing geometry, weight, and thrust. Performing numerous calculations (Raymer 27-110), the cruise and maximum velocities were found to be 54.3 and 86.1 feet per second, respectively. Similarly the turn and climb rates were calculated to be 77 degrees per second and 14.2 feet per second, respectively. Each mission flight time was then calculated from these numbers.

The estimated flight times and resulting scores are found in Table 5.1. All of the missions were evaluated with no wind conditions at Standard Temperature and Pressure (STP) and all flight scores included an estimated one-minute assembly time.

Mission Profiling Matrix					
	Conventional		Performance		
Mission (x difficulty factor)	Time	Flight Score	Time	Flight Score	Δscore
Missile Decoy (2x)	3:15	0.472	2:26	0.583	0.111
Sensor Deployment (1.5x)	3:19	0.348	2:46	0.389	0.041
Communications Repeater (1x)	3:10	0.240	2:21	0.299	0.059

Table 5.1 Evaluation of the mission times and flight modes

The three mission flight scores were compared in both conventional and performance modes. In each case, the Missile Decoy and Sensor Deployment flight scores received the highest flight score.

Therefore, the initial assumption that the missions with the most difficulty offered higher scoring potential. This is true whether the aircraft flies in conventional or performance mode.

As shown in Table 5.1, each mission's flight score increased while flying in performance mode. The Missile Decoy mission's flight score increased over 20% with the implementation of high performance maneuvering. While not to the same degree as the Missile Decoy mission, the Sensor Deployment mission and Communications Repeater mission flight scores also increase while flying in performance mode. Therefore, it was deemed that the performance mode increases the flight score. However, this does not automatically mean that the performance mode will optimize the final score.

The RACs of the two different flight modes were calculated for the missions. While the performance mode reduced flight time, it also required high battery capacitance and weight, thereby penalizing the RAC. The conventional flight and performance modes yielded RACs of 8.08 and 9.19, respectively. However, although the RAC yielded by the conventional flight mode is better than that yielded by the performance mode, the final scores received by these modes with RAC effects were determined to be 10.68 and 10.04, respectively. Therefore, it was determined that high performance mode would increase the overall final score.

5.1.2 Takeoff Distance

Calculations were preformed to determine the aircrafts takeoff distance. Using an estimated stall speed of 39.1 feet per second, the takeoff speed was found to be 43 feet per second. For low Reynolds numbers, (300,000 based on mean chord), induced drag is neglected. Therefore, by integrating the ground acceleration (Raymer 565) into Newton's second law, the takeoff distance was found. In order to account for the ground roll, the takeoff distance was increased by 10 percent. A ground-roll distance of 115 feet was achieved with an estimated 6.5 pounds of thrust calculated by the propulsion group.

5.1.3 Stability and Control

An aircraft's stability is defined by its ability to return to equilibrium after experiencing a small disturbance. Static stability is a prerequisite for dynamic stability. Dynamic stability analysis requires wind tunnel testing of a scaled model. Due to the resources at hand, this was considered impossible to complete. Thus, determining the static stability of the aircraft was imperative.

Pitch stability corrects pitch deflections through a relationship between the main wing and the horizontal stabilizer. For an aircraft to be considered stable the calculated static margin is required to be between 0.30-0.35. This relationship, determined by the positions of the center of gravity and the aerodynamic center, was found to be 0.35. Therefore, the airplane could prove to be overly stable requiring the location of the center of gravity to change. Roll stability was achieved by implementing a 2° dihedral in the wing design.

The stability was also evaluated with the antenna in place because of the possibility that it has adverse effects on the stability of an aircraft. The effects on the rolling stability can be neglected since

the antenna is placed on the centerline of the aircraft. However, there was a concern on effects of drag on pitching stability. The static margin of the aircraft with the antenna was found to be 0.31, which was lower then the clean model but still within the recommended range.

5.2 Structures

The structural detailed design focused on the component and systems architecture selection. Integrating and sizing dimensions in order to obtain a proper aircraft load distribution dominated this phase. The main parameter was limiting the competition requirement that the aircraft fit within a 4x2x1 foot container.

5.2.1 Wing Structure

The two load carrying components of the wing are the spar and skin. For analysis, the spar was modeled as a cantilever beam, while the skin was modeled as a shear web. The foam, not being directly in the load path, was not separately modeled, but was integrated into the finite element analysis of the spar.

The spar is designed to transfer the bending forces applied to the wing to the wing joiner. The loading of the spar was broken into two cases, a distributed load approximating the maximum aerodynamic loading during flight, and a point load representing the load seen during the judge's wing test. This load is taken into separate consideration since the wing will deflect differently than it will during natural distributed aerodynamic loading. Pro-Mechanica was used to create a finite element model (Figure 5.1). The smallest thickness that could be fabricated without any flaws was 0.031 inches. The modeling of the spar was, therefore, based on this thickness. The increased thickness used for the spar increased the factor of safety from 2.0 to 28, giving a margin of safety of 13.

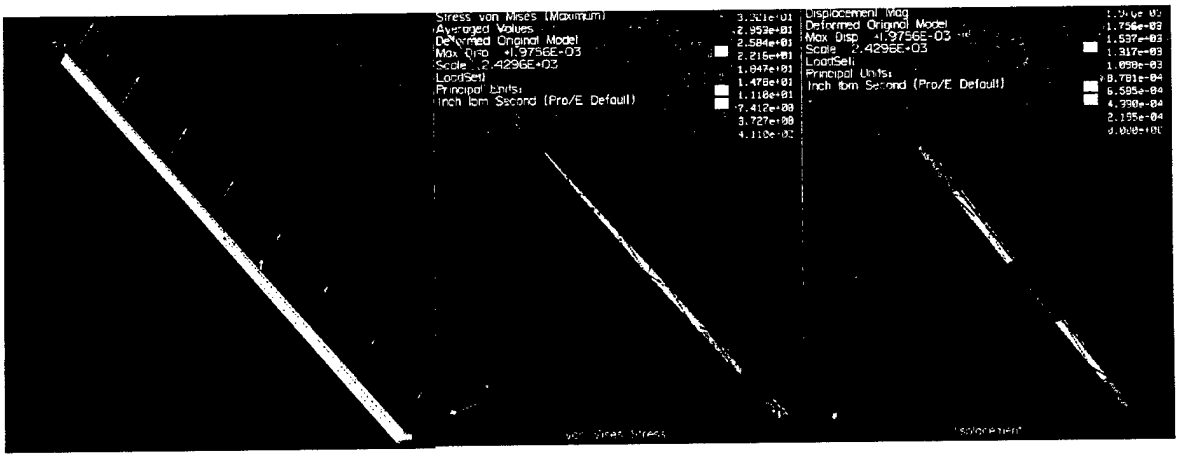

Figure 5.1 von Mesis Stress and Displacement of Spar

The wing skin thickness required for a factor of safety of 2.0 was too small to be manufactured properly. Using MATLAB script with the actual manufactured thickness of 0.05 inches, analysis of the torsional strength of the wing skin was found to have a factor of safety of 23, giving a margin of safety of 10.5.

5.2.2 Tail Configuration

The structural detailed design of the tail section was focused on the component integration of the fuselage, boom, and tail and sizing dimensions.

The boom is designed to attach in a key-like fashion to a sleeve hard mounted to bulkheads 3, 4 and 5 located in the fuselage. The sleeve transfers bending loads while the key is designed to transfer torsion from the tail to the fuselage. Axial loads are transferred through a steel bolt used to keep the boom mounted to the aircraft; a hole was made in the bolt as an attachment point for the antenna in Mission A. A detailed sketch of the integrated tail assembly is depicted in Figure 5.2.

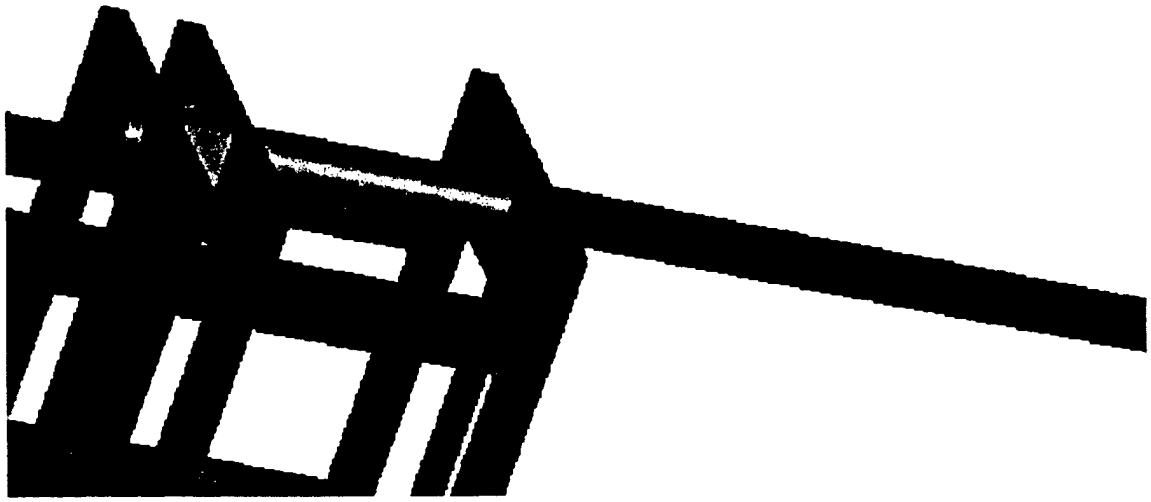

Figure 5.2 Integrated Tail Assembly.

As described in the preliminary structural design, a boom was designed with a 0.5 inch outer diameter and a 0.4966 inch inner diameter. However, a pre-made shaft was selected because of the complexity of manufacturing one from carbon fiber. Unfortunately, a shaft with these dimensions could not be obtained. Therefore, a 0.9 inch shaft with an inner diameter of 0.8 was chosen. The geometry of the boom was verified by applying the estimated loads to the model discussed in the preliminary design. The resulting factor of safety is order of magnitudes greater than that required.

While deciding on how the tail should attach to the boom, concerns were addressed about the possibility of a crash damaging the structure. Therefore, nylon screws that shear in the event of a crash were selected in order to absorb damaging kinetic energy.

Two servos were used to power the control surfaces; one was used for the rudder and the other for the elevator. They are connected to the batteries via a wire harnesses also designed to shear.

5.2.3 Fuselage Structure

The detail design of the fuselage focuses on the placement of the CG and the dimensioning of its internal components. The placement of the CG is affected by the placement of each component of the aircraft. Therefore, the placement of the aircrafts internal components must be placed with precision and

accuracy. However, the internal components of the fuselage must also be able to withstand the applied loads. Within the fuselage, the main internal load bearing structures are the bulkheads and rails. These structures are configured to receive load transfers from the spar, boom, payload, nose gear and motor mount. The integration of the fuselage with the wing and boom is described in Figure 5.3.

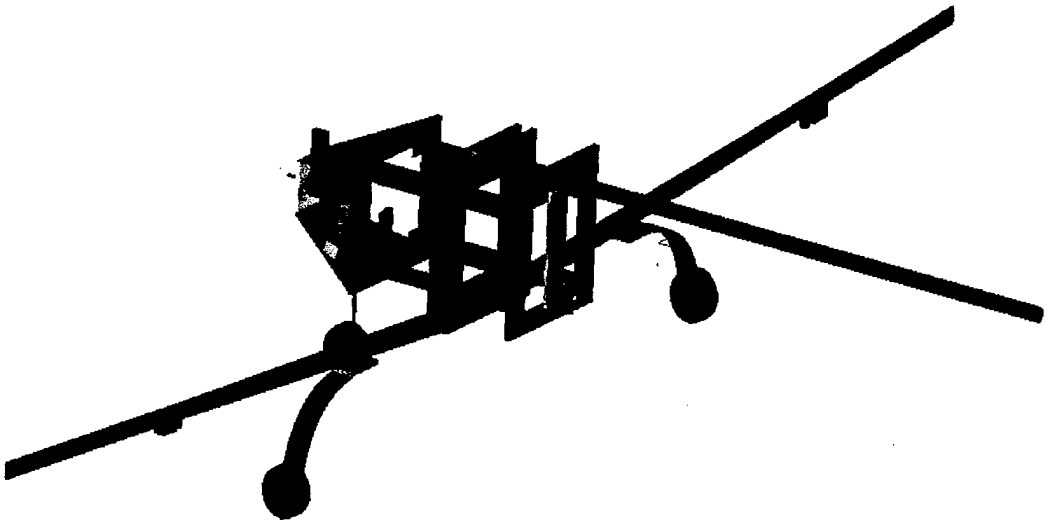

Figure 5.3 Structural Integration

There is ample room for the placement of the batteries, receiver and APDS within the fuselage. With the receiver and APDS locations fixed, the CG was able to be placed 1.5 inches in front of the quarter chord by locating the 2.5 lb battery pack on the carbon/foam mounting plate 7.6 in. in front of the quarter chord. However, if the actual CG location is inconsistent with the theoretical location due to liberties taken in manufacturing, the batteries can be adjusted shifting the CG to its proper location. This CG takes into account all components of the aircraft including other internal components of the fuselage, such as the bulkheads and rails.

As described in the preliminary structural design, the bulkheads were specifically located in the areas with extreme loading. The bulkhead thicknesses were found to be very thin. However, due to material availability, it was decided that the bulkheads were to be composed of two layers of plywood 0.125 inches thick with a 0.25 inch piece of high-density foam in the center. In order to verify these thicknesses, a model of the number five bulkhead was generated with Pro-Mechanica software (Figure 5.4). The model, however conservative, encompasses the loads generated during a high speed jerk pull up maneuver. By applying the proper loads to this model, the desired material thickness was verified. The model produced an ultimate factor of safety of 1.36 with a negative margin of safety of 0.32. Due to the likely chances of this maneuver being performed and the fact that the rails connected to the bulkhead are not entirely rigid as shown in Figure 5.4 it is assessed that the bulkhead geometry is sufficient and the factor of safety is acceptable.

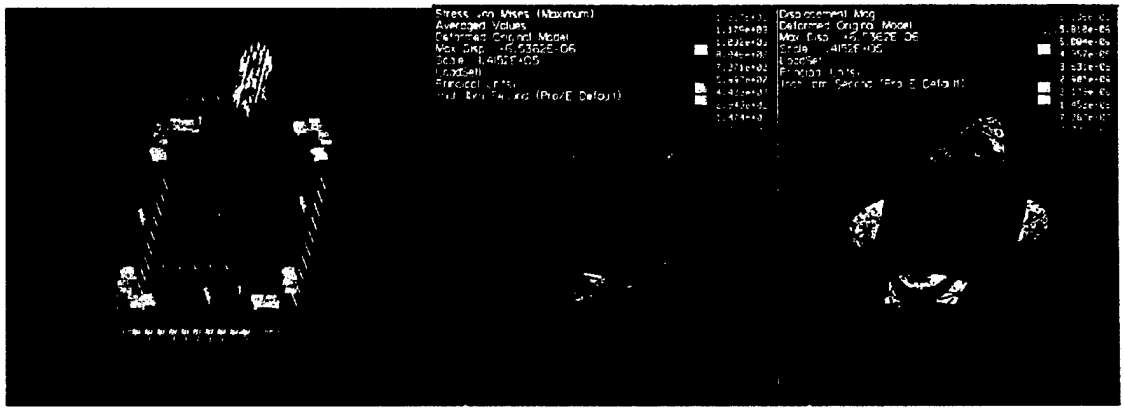

Figure 5.4 von Mesis Stress and Displacement of Bulkhead #5

As with the bulkheads, the available material size selection for the rails was limited. Therefore, it was decided that the rails were to be constructed of two layers of carbon fiber unidirectional applied to the top and the bottom of 0.25 inch foam. Pro-Mechanica rail models were then used to verify these thicknesses (Figure 5.5). The overall thickness of the rails was .3125 inches. This produced a factor of safety of 1.25 and a subsequent margin of safety -0.375. Confidence in the model prompted an increase of unidirectional carbon fiber to the rail structure increasing the factor of safety to 2.15 and subsequent margin of safety of 0.15. One layer of carbon fiber was laid on the inner and outer sides of each rail.

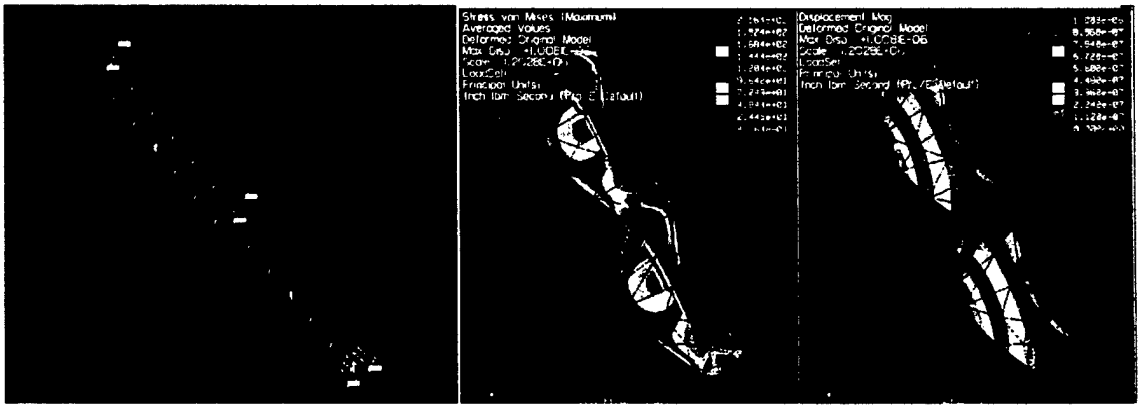

Figure 5.5 von Mesis Stress and Displacement of a Rail

5.2.4 Automated Payload Delivery System (APDS)

The detailed design phase of the APDS constituted of determining the correct sized and number of rubber bands required to propel the payload from the fuselage. Several differently sized rubber bands were considered and their corresponding spring constant were found (Table 5.2).

(R) – Rejected (S) – Selected	Rubber Band (Spring) Selection			
	Size (inches)	K (pounds/ inch)	Force (lbs) when stretched 8.25 inches	Decision
#32	3 x 1/8	.13	1.1	R
#62	2-1/2 x 1/4	.24	2.9	R
#64	3-1/2 x 1/4	.24	2.0	S
#73	3 x 3/8	.50	4.1	R

Table 5.2 Rubber Band Analysis.

While under load, the bands would be effectively stretched 8.25 inches from the rear bulkhead to the front of the box. Rubber band #62 was rejected because of it does meet this requirement. Rubber band #32 stretches 8.25 inches, however, it was considered too thin and fragile to be deemed reliable. The larger #73 rubber band was rejected also because one rubber band did not offer sufficient redundancy. With reliability being the primary objective, #64 rubber bands were an ideal selection because they can easily stretch 8.25 inches and still effectively deploy the payload in case of a band failure.

By using the #64 band spring constant of .24 pounds per an inch, it was calculated that each band produced 2 pounds of force. The calculated friction force of the box was calculated to be 1.5. Therefore, these bands were able to overcome the friction force. The required velocity to eject the payload from the fuselage was calculated to be 30 inches per second. This velocity can theoretically be achieved by two #64 rubber bands. With a factor of safety of two, this number was doubled and it was decided that four rubber bands would be used to eject the payload.

Tests were preformed using a full-scale reinforced prototype in order to verify that this number was correct. It was found that two rubber bands could easily eject the payload. However, after numerous tests the bands began to brake. This was seen as a potential risk, since one stretched rubber band does not have enough potential energy to propel the box. Tests preformed with four rubber bands proved to eject the payload completely clear of the fuselage with no binding or catching.

By using four #64 rubber bands, 8 pounds of force was made available to propel the payload. A static force diagram was used to find the loads applied to the hinge and door latch. Since the force of the system was distributed uniformly on the payload door, the hinge and latch experience the same loads, 4 pounds (Figure 5.6).

Tests were preformed on two types of hinges: a medium-duty nylon hinge and a metal hinge the width of the door. These tests proved that both hinge types would be able to with stand the applied loads. Therefore, due to weight savings the a nylon hinge was selected.

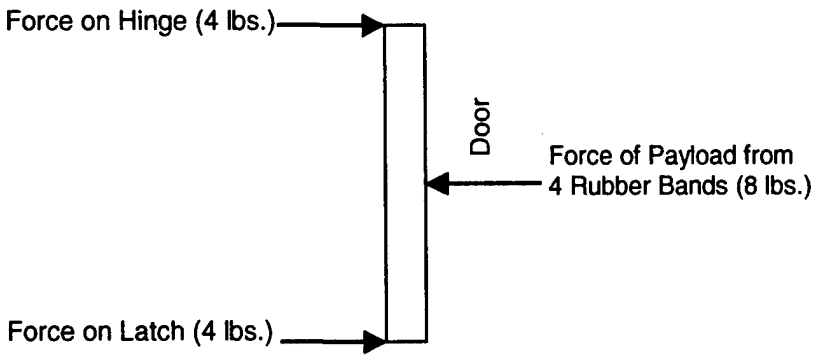

Figure 5.6 Force Balance on Door

5.4 Propulsion

The final propulsion system was selected from comparing both actual and analytical results. There were discrepancies in the dynamometer results and those calculated using MotorCalc software. The MotorCalc efficiency of the Graupner 3300-5 motor was near 50% when the dynamometer efficiency results were over 85%. With the actual efficiency being higher, the thrust output is expected to increase. There was only a minor discrepancy in the motor efficiency results for the Graupner 3300-7. Thus, it was found that the initially chosen Graupner 3300-7 produced less static thrust at the lower voltages then the Graupner 3300-5. Therefore, in order to optimize the propulsion system by reducing battery weight and maintaining maximum thrust, the Graupner 3300-7 was abandoned, and the Graupner 3300-5 was adopted. The final propulsion configuration employed in the aircraft had an 18-inch diameter propeller with 15 inch pitch with a two to one gearbox to provide the required speed and thrust. From these configurations, the power consumption was found to be 830 watts for takeoff and 420 watts for cruise.

5.5 Final Aircraft Configuration

The final configuration is an aircraft with a low-wing, a 2° dihedral, and a moderate aspect ratio of 7.46. Additionally the wings contain no sweep or taper because of the increased cost with only a slight increase in performance. The aircraft has good gliding capabilities because of high 14.7 lift to drag ratio. The fuselage is shaped like a modified bullet out of considerations for weight savings and payload geometry with a reasonable drag penalty. The tail section is a conventional T-tail with span of 24 inches and height of 10 inches. The landing gear is a tricycle configuration with the main wheels 2.479 inches behind the CG with an aircraft ground clearance of 5.451 inches. This configuration was considered optimal for the APDS to deploy the 5 pound payload. The launching mechanism produces an exit velocity of 30 feet per second. The propulsion system is made up of a Graupner 3300-7 motor, 18x15 propeller, and 19 Sanyo cells. The aircraft breaks down into four individual parts when placed in shipping mode; two wings, fuselage and tail boom. Assemble time is estimated at one minute or less.

5.5 Final Aircraft Configuration Calculations (Table 5.3)

Geometry

Aircraft Length	56 in
Aircraft Span	104 in
Aircraft Height	15 in
Main Wing Configuration	Low Mono-Wing
Main Wing Airfoil	S4083
Main Wing Area	1456 in^2
Taper Ratio	1
Aspect Ratio	7.46
Main Wing Control Area	90 in^2 per wing
Horizontal Stabilizer Area	317 in^2
Vertical Stabilizer Area	130 in^2
Tail Airfoil	NACA 0009
Horizontal Stabilizer Control Area	78 in^2
Vertical Stabilizer Control Area	41 in^2

Performance

CL max (actual)	1.07
L/D max (actual)	14.7
Maximum Rate of Climb	14.2 ft/sec
Stall Speed	39.1 ft/sec
Takeoff Speed	43.0 ft/sec
Cruise Speed	54.3 ft/sec
Maximum Speed	86.1 ft/sec
Takeoff Speed Loaded	115 ft
Takeoff Speed Unloaded	52 ft

Weight Statement

Airframe Weight	8.43 lbs
Manufacturer's Empty Weight	13.62 lbs
4x2x1 Payload	5.00 lbs
Antenna	1.00 lbs
Battery Weight	2.54 lbs
Motor Weight	1.90 lbs
Control System	0.75 lbs
Takeoff Gross Weight	19.62 lbs

Systems

Motor	1 x Graupner 3300-5
Propeller	18x15 thin carbon prop
Gear-ratio	(2:1)
Batteries	Sanyo 2400 (19 cells)
Servos	HS-225MG (2), HS-545BB (2)
Reciever	HPD-07RB (PCM)
Handset	Prism 7X (PCM)

5.6 Rated Aircraft Cost

Rated Aircraft Cost (RAC) = (A * MEW + B * REP + C * MFHR) / 1000 = 9.17

Manufacturers Empty Weight Multplier (MEW) A = $ 100

Total Weight w/o Payload =	13.64	lbs	
		MEW =	13.6

Rated Engine Power Multiplier (REP) B = $ 1500

# of engines =	1		
Battery Weight =	2.54	lbs	
		REP =	2.54

Manufacturing Cost Multiplier (MFHR) C = $ 20

WBS 1.0 Wings					
Wing Span=	8.7	ft	*	8 hrs/ft	
Max Chord=	1.17	ft	*	8 hrs/ft	
# of Control Surfaces =	2		*	3 hrs/c.s.	
				WBS 1.0 =	85 hrs
WBS 2.0 Fuselage					
Fuselage Length =	6	ft	*	10 hrs/ft	
				WBS 2.0 =	60 hrs
WBS 3.0 Empenage					
# of Vertical Surfaces w/o cntrl =	0	v.s.	*	5 hrs/v.s.	
# of Vertical Surfaces w cntrl =	1	v.s.	*	10 hrs/v.s.	
# of Horizontal Surfaces w cntrl =	1	v.s.	*	10 hrs/v.s.	
				WBS 3.0 =	20 hrs
WBS 4.0 Flight Systems					
# of Servo or Motor cntrler =	5	ser	*	5 hrs/ser	
				WBS 4.0 =	25 hrs
WBS 5.0 Propulsion Systems					
# of engines	1	eng	*	5 hrs/eng	
# of propellers	1	prop	*	5 hrs/prop	
				WBS 5.0 =	10 hrs
				MFHR	200
				RAC	**9.17**

5.7 Detailed Drawings

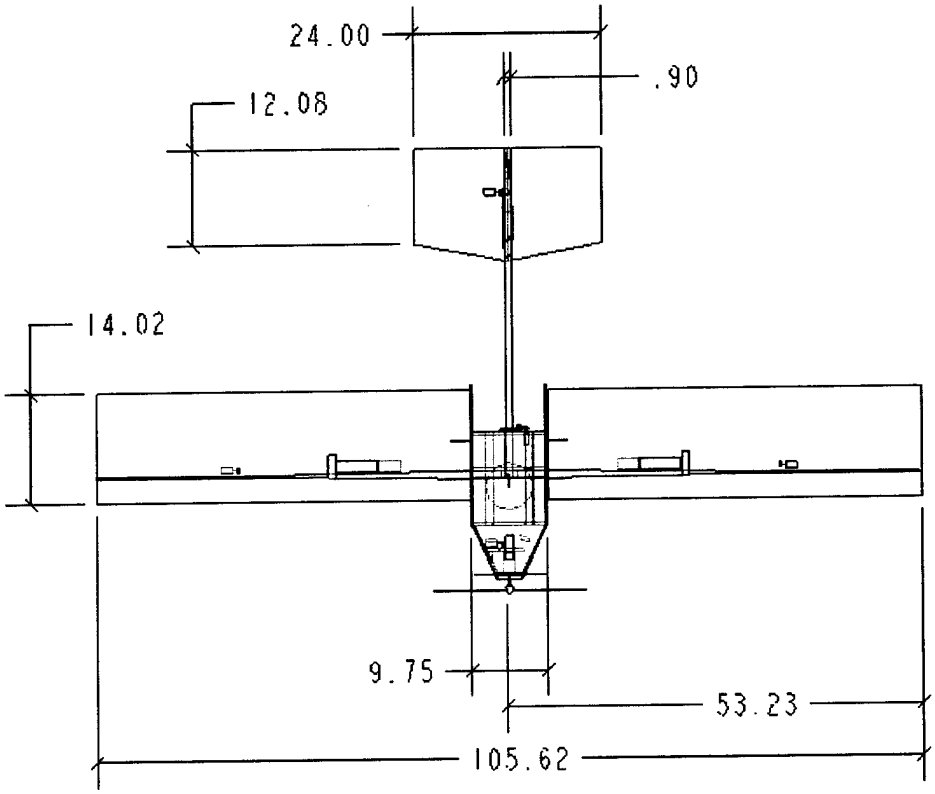

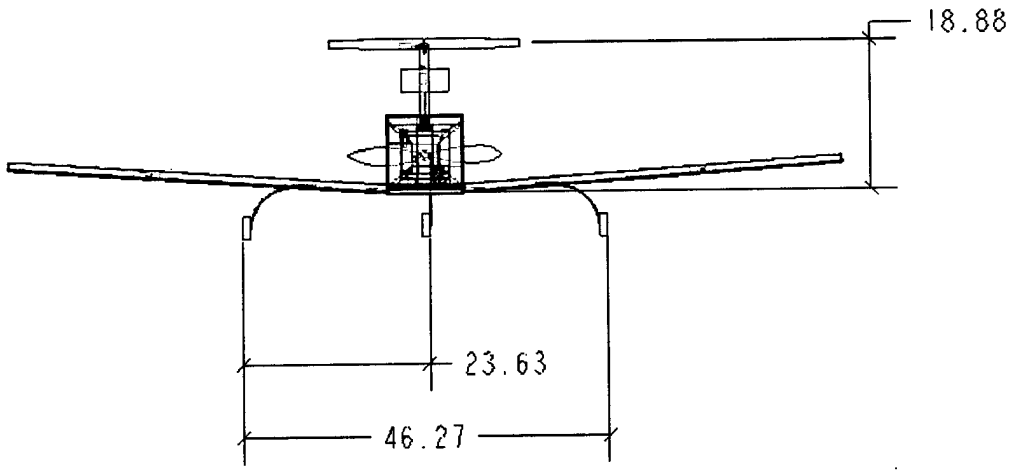

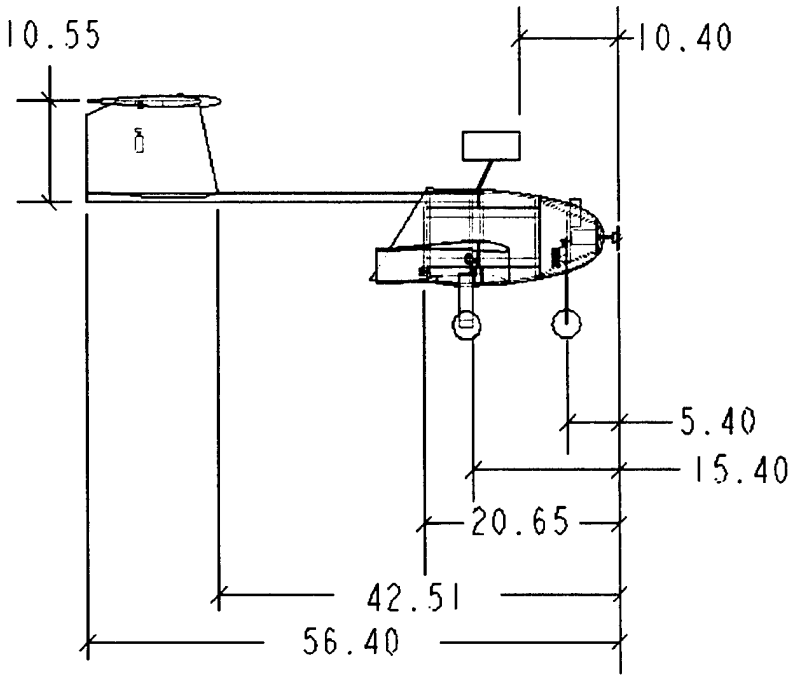
10.55
10.40
5.40
15.40
20.65
42.51
56.40

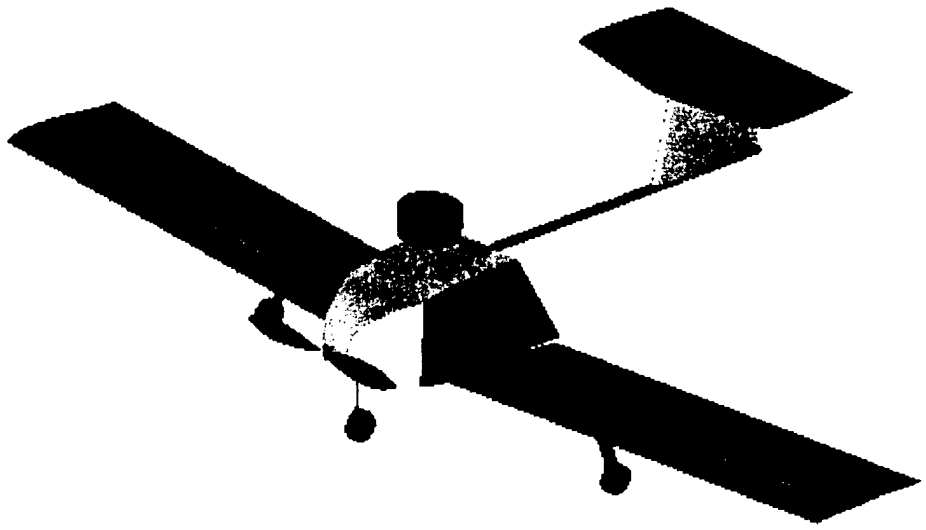

Aircraft Detail

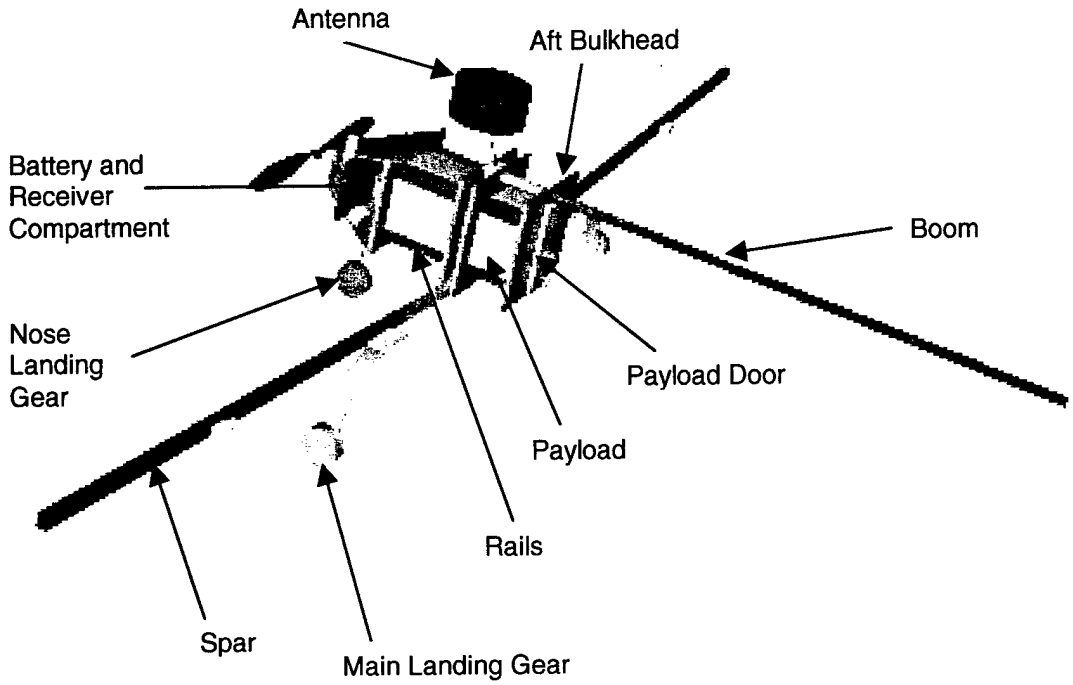

Rib Detail

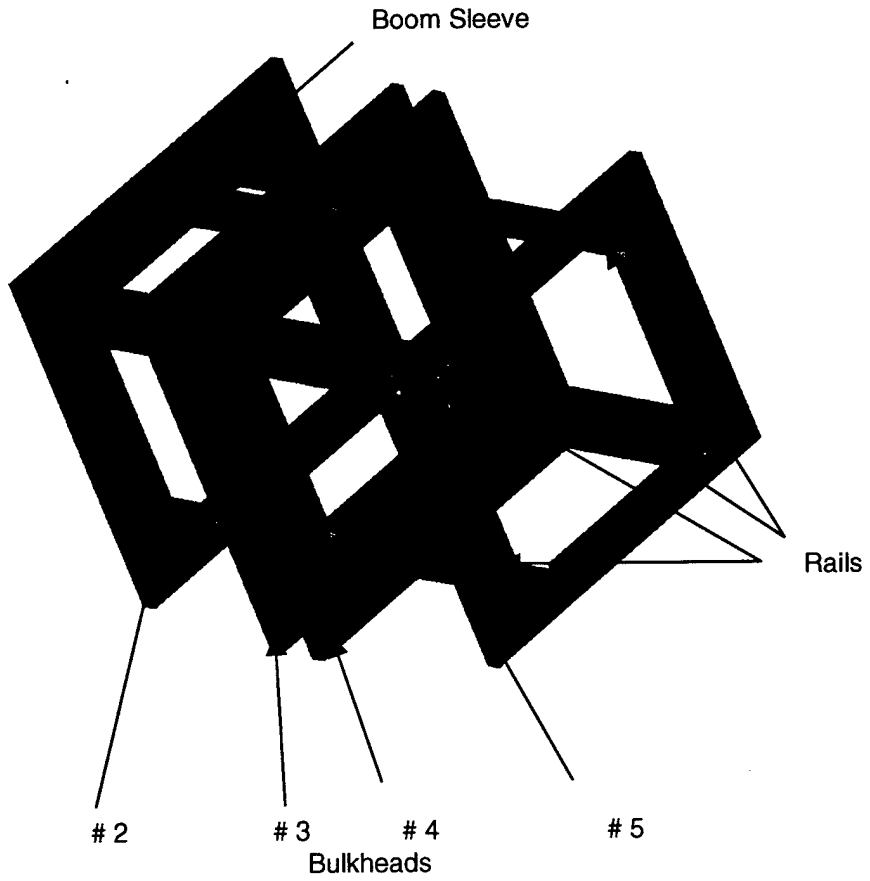

Automated Payload Delivery System Latching Mechanism

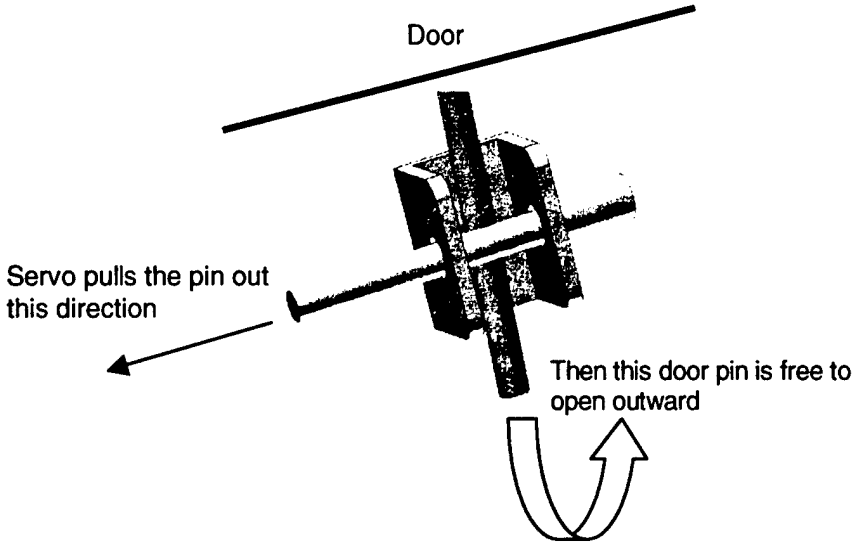

Payload (6 x 6 x12 inch)

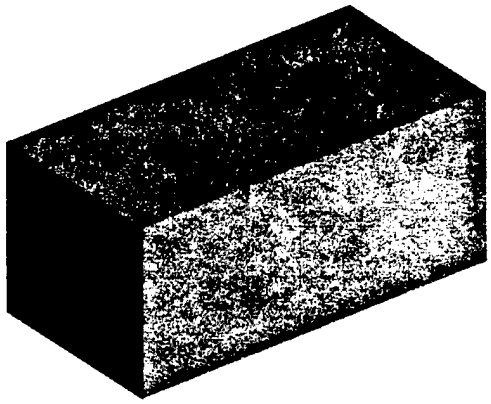

Wing Detail

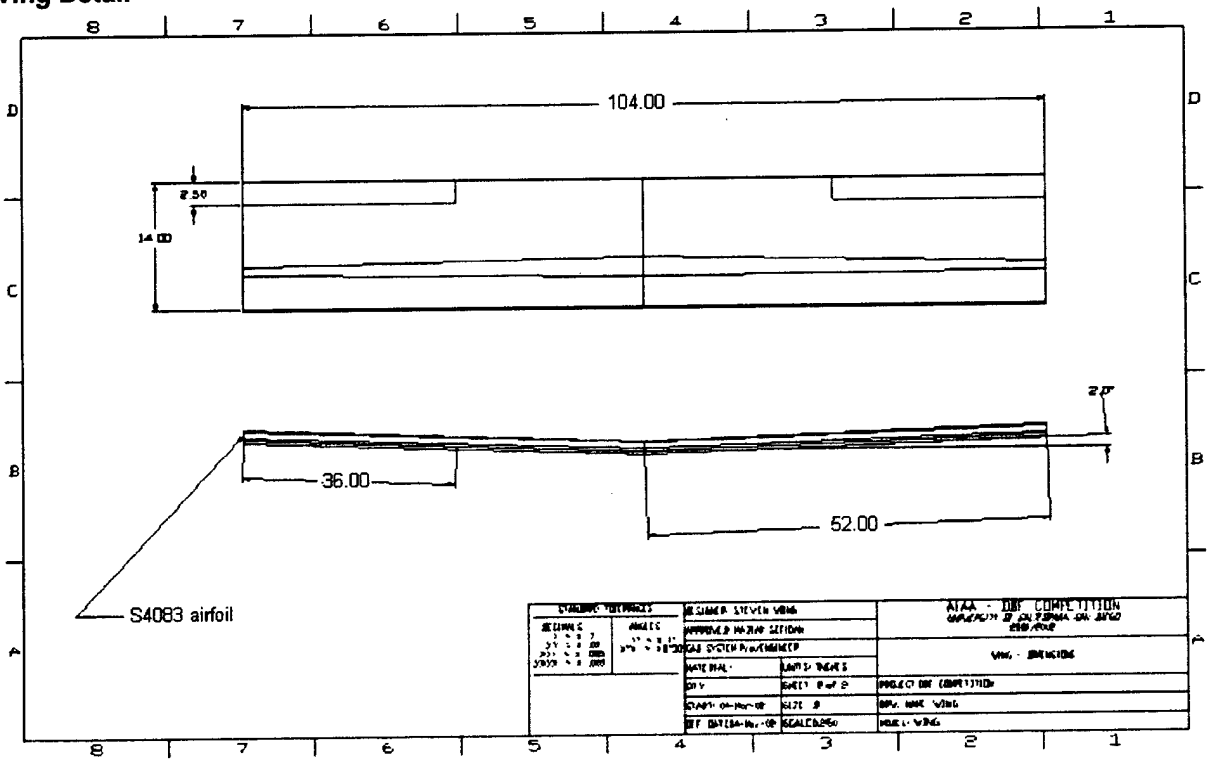

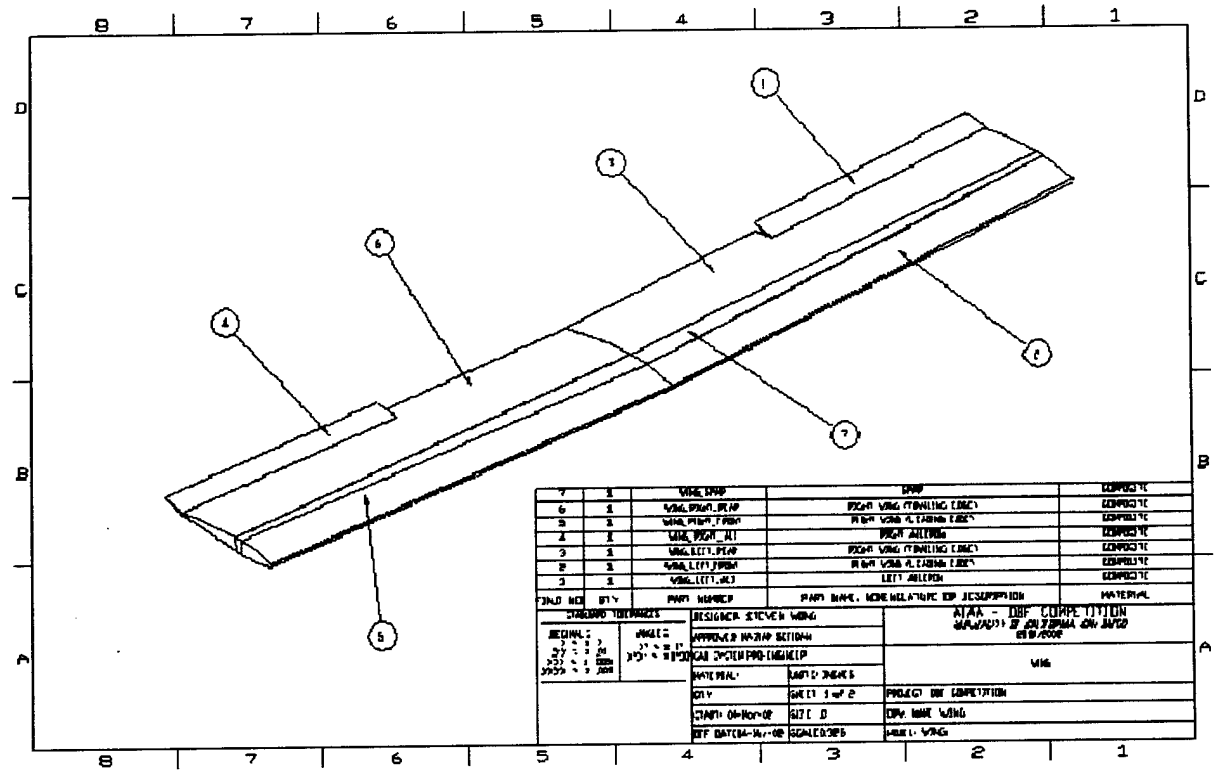

Tail Detail

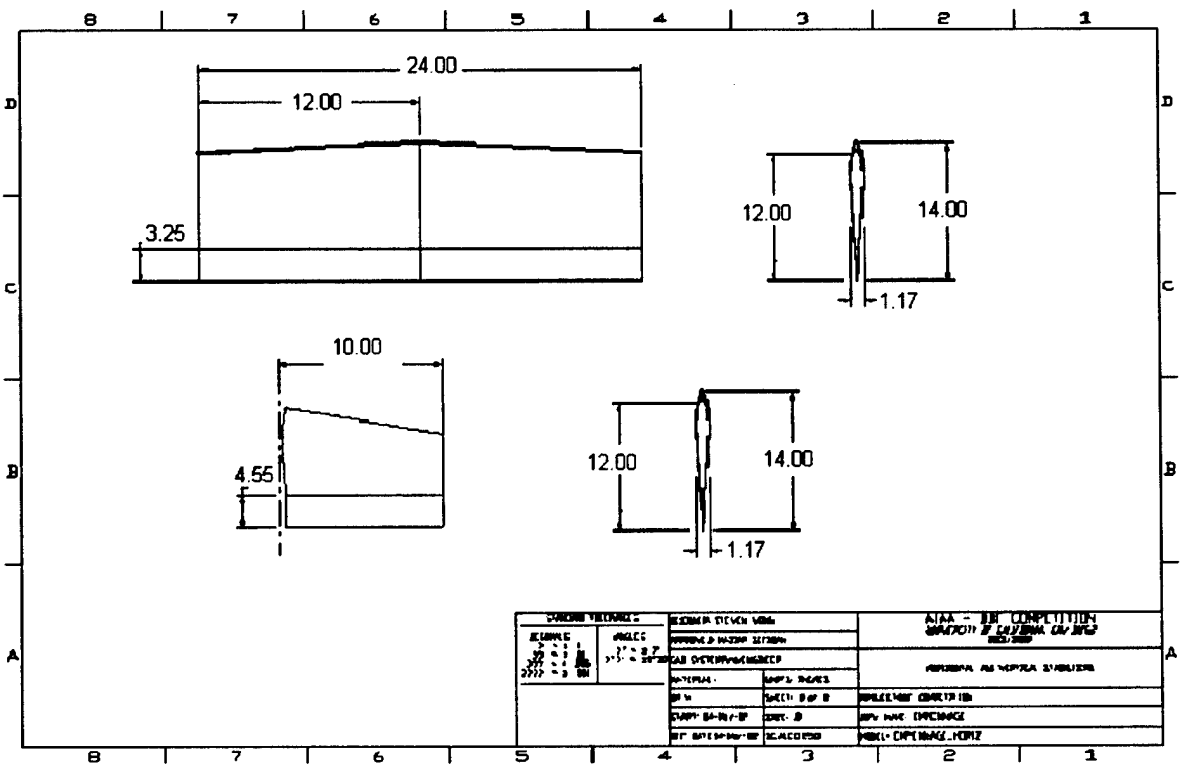

Most of the aircraft is made of carbon fiber or fiberglass and epoxy resin. The techniques to manufacture each individual part vary in order to create the shapes with the level of precision required.

Depending on the requirements for each part, the most efficient fabrication method is selected to give the level of precision needed and minimize the cost, time, materials, and tooling. An estimation of the relative costs of each manufacturing technique is shown in Table (6.1) below.

	Material Use	Training	Difficulty	Tools/ Equipment	Tooling	Time	Total
Hot Wire	0	1	2	1	1	1	6
Vacuum Bag	0	1	0	1	0	2	4
Mold	2	0	0	2	2	2	8
LaserCamm	1	1	0	2	0	1	4
Autoclave	0	1	1	2	0	2	6

Table 6.1 Fabrication processes and their estimated relative costs

Some parts require more precise dimensions than others, therefore the technique with the lowest cost that can still deliver the accuracy required for the part to be useful is selected.

6.1 Wings

The most critical property of the wings is the airfoil designed by the aerodynamics group. The wings must accurately portray the shape of the chosen airfoil or the aircraft would not perform as expected. Templates of the airfoil were cut using a LaserCamm and a hot wire was used to cut the wings. This method was inexpensive and readily available.

Space for the spar was cut out and the foam sanded. Wooden hard points were added for landing gear attachment points. Small slots cut lengthwise hold servo and brake wires. Bi-directional fiberglass was bonded to the top and bottom of the wings to provide the torsional stiffness. Painted mylar enclosed the wing and then the assembly cured in a vacuum bag.

6.2 Spar

The spar must fit inside the wing and connect to the wing sleeve. The critical dimension of the spar is the thickness and is ultimately determined by the number of layers of unidirectional carbon used.

A section from the wing cores was cut for the spar. Unidirectional carbon was laid on the top and bottom to increase the bending stiffness and then wrapped with fiberglass. The spar was then vacuum packed and allowed to cure. After curing, this component was sanded to fit into the wing.

6.3 Wing joiner

The wing joiner is a crucial element of the structure and determines the dihedral of the wings. The dihedral shape improves the stability of an aircraft, thus high manufacturing costs were justified. Given an angle of 2 degrees, a machining mold was chosen to accurately fabricate the wing joiner.

An aluminum mold was created using a CNC machine. A blue foam core was cut using the hot wire technique. Unidirectional carbon fiber was laid on the top and bottom and wrapped with wetted bi-directional fiberglass. It is then molded and allowed to cure. Any excess epoxy was later sanded to ensure a secure fit.

6.4 Wing sleeve

The wing sleeve wraps around the spar and the wing joiner, thus it require high tolerance manufacturing. Therefore, the wing sleeve was fabricated with a level of precision equivalent to the wing joiner and rails. However, instead of creating a new mold, the wing joiner is used to determine the shape of the wing sleeve directly; thereby, reducing the manufacturing costs.

Mold release is applied to the wing joiner and unidirectional carbon fiber is laid on all sides. It was wrapped with the bi-directional fiberglass and cured in a vacuum bag. After curing, balsa wood rectangles are glued to the sides of the fiberglass. The sleeve is then taken off of the wing joiner and sanded down to shape.

6.5 Rails

The rails are an important structural component and have to fit into slots in the bulkhead. This fit required high tolerances for the flat surfaces. Again, the importance of the parts guided the decision to fabricate them using a machined mold.

An aluminum mold was made using a CNC machine. Foam cores were assembled, by bonding two thin flat pieces of foam together at a 90-degree angle. Unidirectional carbon fiber was laid on top and bottom of the foam and placed in the mold to cure. Excess carbon and epoxy are later sanded off to ensure a tight and accurate fit into the bulkheads. Lastly, the edges were capped by epoxy to prevent de-lamination.

6.6 Bulkheads

The bulkheads are structural elements designed to undergo several loading cases. The accuracy of the bulkhead dimensions is also critical for the interference fit with the rails.

The 1/8-inch thick plywood pieces were cut using LaserCamm and ¼-inch pieces of white foam were cut using the hot wire technique. Epoxy is then used to fasten the two-ply wood pieces to either side of the foam. The excess foam is cut off and all sides are sanded. The slots for the rails are carefully trimmed to ensure accurate assembly.

6.7 Skin

The purpose of the skin is to provide additional structural stiffness and streamline the fuselage. The performance of the skin only depends on the thickness of the material used, which is determined by the number of layers of carbon and fiberglass. Therefore, there is no critical dimension requiring high precision fabrication techniques.

The side skins were made with carbon fiber and foam core and cured in a vacuum bag. The top and bottom pieces were cured while in the shape of the fuselage. Once cured, the excess areas were trimmed and sanded. The skin was then fastened to the fuselage using epoxy mixed with cavacil and micro balloons.

6.8 Motor-mount

The fabrication method for the motor-mount was determined to be the vacuum bag because the tight dimensions obtained through creating a mold was not needed for the motor-mount to be functional. Therefore the method with the smallest cost is to use the vacuum bag.

A piece of circuit board was cut to the required size. Next, a thin layer of foam is made using a hot wire. Unidirectional carbon fiber is laid on the foam, followed by bi-directional carbon. The carbon foam sandwich structure is vacuum packed and cured.

6.9 Landing Gear

The landing gear must withstand impact loads and be symmetrical so that the aircraft rolls down the runway straight. These requirements mean that precise and durable parts are needed, negating the importance of low cost fabrication techniques. Therefore, it was decided to make the landing gear with a mold and autoclave.

A mold was created using sheet metal rollers. Cork tape was laid on the mold to create the taper in the components. Preimpregnated unidirectional carbon fiber was placed in the mold and placed in an autoclave for curing. Holes were later drilled for mounting to the aircraft and wheel attachment.

7.0 Research and Testing Plan

7.1 Objectives

The research and testing plan objectives were to gain insight into the drag and lift values of the cylindrical antenna and airfoil types, determine the optimum motor and battery configuration, and validate detailed finite element computer analysis by simplified solid mechanic model calculations.

7.2 Schedules

A research and testing schedule was organized. However, because of the availability of outside resources, some scheduled tests were not performed. Due to the abundant data from Michael Selig's research (Selig) airfoil wind tunnel testing was deemed unnecessary.

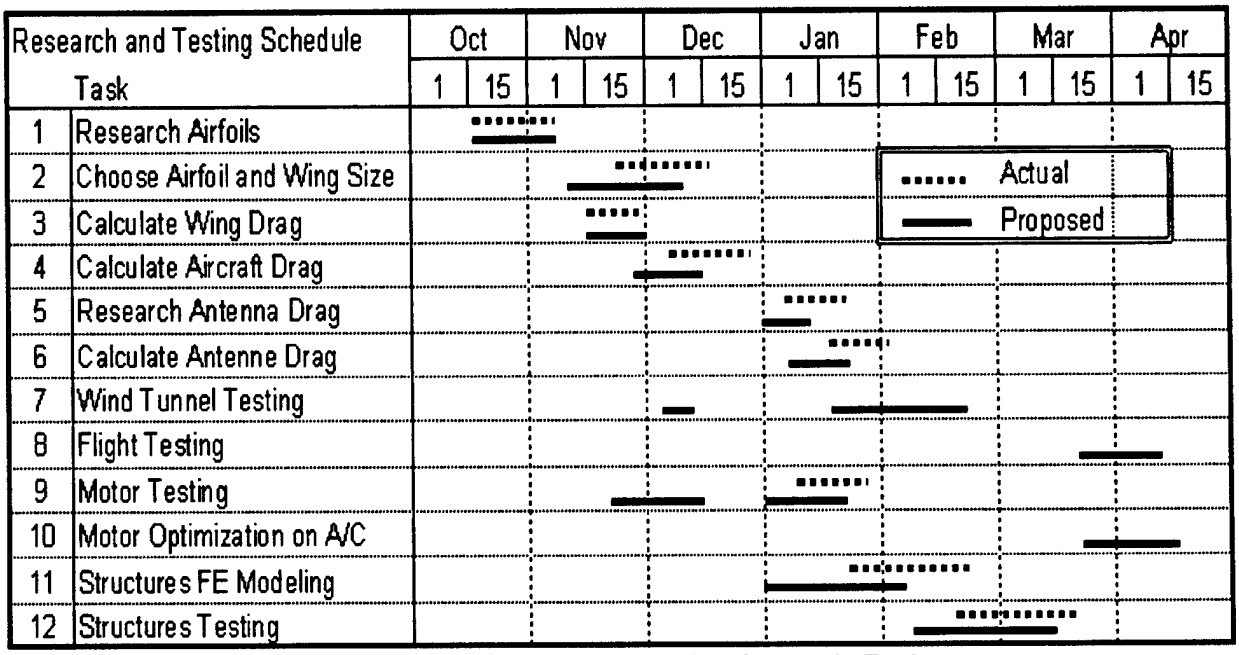

Figure 7.1 Research and Testing Schedule Task

7.3 Testing Procedures

The landing gear is tested for static load bearing ability, as well as for its dynamic properties. The rear landing gear is secured in a cantilever position and 20 pounds of weight is attached to the end of the landing gear. This test is to ensure that the part will be able to hold the entire weight of the airplane. Next, the impact performance of the landing gear is tested by tying the test weight to the end of the landing gear with a string, and the load dropped from a small distance. This will simulate the landing impact of the aircraft on the landing gear. If the landing gear bounces too strongly, damping will be needed to keep the airplane from bouncing back into the air while trying to land.

The structural proof test of the spar is conducted in a similar fashion. This test is to learn whether the spar will withstand the loading being placed on it, as well as to find the deflection of the spar under point loading at the tip of the wing.

The first step of flight testing is to recreate the judges wing test. The aircraft is lifted by the wing tips for a short period of time. This step is important for safety. Next, the motor is throttled up to full speed while holding the aircraft tail. A series of very simple and gentle maneuvers are performed to check for the general stability of the aircraft. After the flight worthiness and stability have been established, the airplane is then put through some more advanced maneuvers. It is important to know how the aircraft will handle.

7.4 Check-lists

Testing, assembly, pre-flight and post-flight checklists were developed to track testing milestones and ensure safety of flight and personnel.

Testing Checklist

	Airfoil wind tunnel testing
	Flight testing
X	Static motor testing
	Dynamic motor testing
X	Structures testing

Figure 7.2 Testing Checklist

Assembly Checklist

	Install and connect battery pack
	Attach wings and servo connections
	Insert boom fully and install locking pin
	Connect tail servos
	Insert payload with rubber bands for ejecting
	Close payload door and ensure pin is installed
	Install fuse

Figure 7.3 Assembly Checklist

Pre-Flight Checklist

	Ensure all batteries are fully charged: motor, receiver and controller
	Check electrical connections and wires for integrity and abrasion
	Inspect fuselage, wings and tail for obvious damage
	Ensure boom and pin are installed properly
	Inspect landing gear for attachment rigidity
	Ensure wheels spin freely
	Check all flight controls respond to given commands
	Check propeller for cracks, dents and dings
	Check forward fuselage area near motor for FOD
	Ensure payload is installed and door securely latched
	Install fuse and check for correct rating
	Start and rev motor; listen for unusual vibrations

Figure 7.4 Pre-Flight Checklist

Post-Flight Checklist

	Check wing attachment points for damage
	Inspect wings for structural integrity and skin for ripples
	Inspect motor mount and firewall for cracks or delaminations
	Inspect motor connecting bolts for tightness
	Check motor, motor speed control and battery pack for overheating damage
	Inspect internal bulkheads and rails for any cracks or delaminations from payload deployment
	Inspect internal bulkheads for any cracks or delaminations at boom connection locations
	Check boom connecting pin for wear and structural integrity
	Ensure vertical and horizontal tail sections are firmly attached and no loosening has occurred
	Check electrical connections for abrasion or overheating
	Check fuse is not blown
	Inspect propeller for cracks, dents or dings

Figure 7.5 Post-Flight Checklist

7.5 Results

7.5.1 Antenna and Airfoil Results

The results from the antenna drag research and airfoil data are shown in Figure 7.5 and 7.6.

Antenna Drag

Velocity	[ft/s]	Re	Density [slug/ft^3]	Drag [lb]
-	32.6	1.00E+05	0.002377	0.074
Vtake-off	43	136076	0.002377	0.129
Vcruise	54.3	171835	0.002377	0.206
Vmax	86.5	273734	0.002377	0.524

Drag Coefficient, Cd: 1.2

Note: Values calculated at 60 deg F and standard sea level pressure

Calculations neglecting end effects

Figure 7.6 Antenna drag

Airfoil Data

Airfoil	Cl	Cdo	Wing L/Dmax	Aircraft Drag [lb]
S4083	1.3	0.008	14.7	1.82
E214	1.3	0.01	13.6	2.00
E423	1.95	0.017	13.1	2.64
S1210	1.8	0.015	12.9	2.45
S1223	2.1	0.02	11.7	2.91

Reynolds number 300,000

Figure 7.7 Airfoil data

The difference in drag values between the S4083, the chosen airfoil for Aerodrone F8273, and the S1223 is 1.09 pounds. This 60% increase in drag is substantial because it would require additional thrust. In attempts to keep the battery weight low, the choice of the S4083 airfoil was prudent because less thrust is required, which corresponds to less battery weight.

7.5.2 Motor Testing Results

Static testing was performed on a dynometer and data collected using Labview software. A relevant portion of the Graupner Ultra 3300-5 motor data is shown below.

Graupner Ultra 3300-5 (5-winding) Motor Data

	# Cells	Volts	Motor RPM	Motor Eff [%]
MotorCalc Data	18	18	7955	52.5
Test Data	18	18	5700	87.0

Figure 7.8 Graupner motor data

It was clear that actual static testing must be performed to validate MotorCalc software results.

7.5.3 Automated Payload Delivery System (APDS) Testing Results

A full-scale prototype mockup of the fuselage's rear ejection APDS, including a 5 pound, 12x6x6 inch cargo box, was constructed out of reinforced cardboard. The objectives were to test different ejection methods, rail schemes, door and latching designs, as well as to estimate the friction the payload experiences as it deploys from the fuselage. The mockup has the same fuselage dimensions, however, the top is removed for access to the inside rails.

Three sets of tests were performed using the prototype fuselage and payload to determine the minimum of bands to completely and reliably deploy the payload.

Rubber Band Testing

	Requirements/ Limitations	Number of Rubber Bands Required	Results
1st Test	Found force required to overcome friction (1.5 pounds)	1	Payload moves approximately two inches and does not exit
2nd Test	Calculated minimum velocity for payload to eject (30 inches/second)	2	Payload deploys with the minimul velocity
3rd Test	Four rubber bands (Test 2 with a factor of safety of two)	4	Payload ejects completely and cleanly with no binding on the rails

Figure 7.9 APDS rubber band testing data

- A first set of tests was conducted to show that only one rubber band was needed to overcome the frictional force. It was concluded that one rubber band does not have enough force to pull the box out completely.
- A second set of tests was conducted to demonstrate that a minimum of two rubber bands will deploy the box but with very low velocity. Binding occurred during 60% of the tests. Further testing with an increased number of rubber bands was required.

- A third set of tests was conducted to confirm that four rubber bands had enough force to cleanly eject the payload. No binding occurred in any of the tests.

7.6 Lessons Learned

The drag on a cylinder is well documented in fluid mechanics and aerodynamics textbooks so no wind tunnel data was necessary. The drag coefficient, Cd, is documented as 1.2 as was used in the above calculations. Edge effects were neglected to give a 'worst case' scenario. The actual drag values are less than reported above, but these theoretical values were used in aerodynamic calculations.

The airfoil data and resulting calculations for the total drag on the aircraft varied. Choosing an airfoil because of its high coefficient of lift (Cl) value is not always the best choice. Comparing the S4083 and S1223 airfoils, it is clear that the latter Cl is much higher. However, the additional drag associated with the S1223 airfoil creates more than a pound of additional drag.

The main lesson learned from the motor testing was the actual test data varied greatly from MotorCalc software calculations. In the case of the Graupner Ultra 3300-5 motor, the motor speed and efficiency with 18 volts is grossly in error. MotorCalc predicts a motor speed of 7955-rpm and 52.5% efficiency while actual static test data gave 5700-rpm and 87% efficiency. Results from the actual test data were used in determining the best motor-battery configuration.

The rubber band testing proved that very few bands were needed to propel the payload with sufficient force to expel it from the aircraft. It was the intuition of the designers that many more rubber bands would be needed to accomplish this.

8.0 References

1. Abbot I.H., Theory of Wing Sections, Dover Publications Inc, 1949.
2. Nelson, R., Flight Stability and Automatic Control, McGraw Hill, 1989.
3. Nicolia, L..M., Fundamentals of Aircraft Design, METS Inc, 1984.
4. Peery, D.P., Aircraft Structures, McGraw-Hill Inc., 1982.
5. Raymer, D.P., Aircraft Design: A Conceptual Approach, AIAA Education Series, 1989.

Figure A.1: Three View Sections of Areodrone F8273:

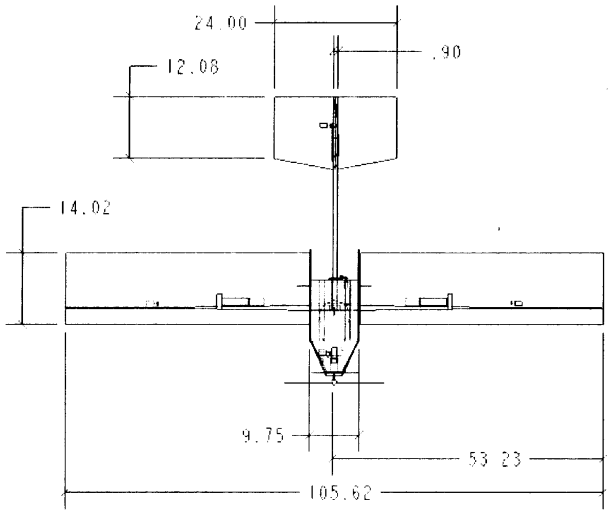

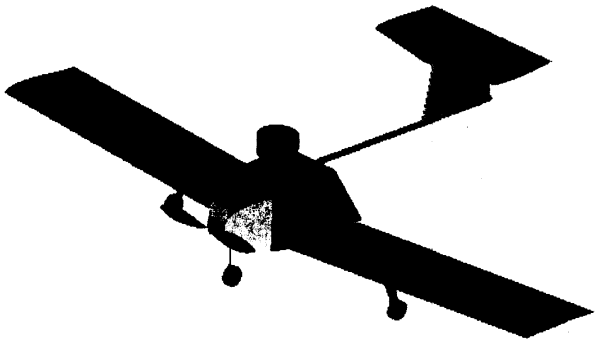

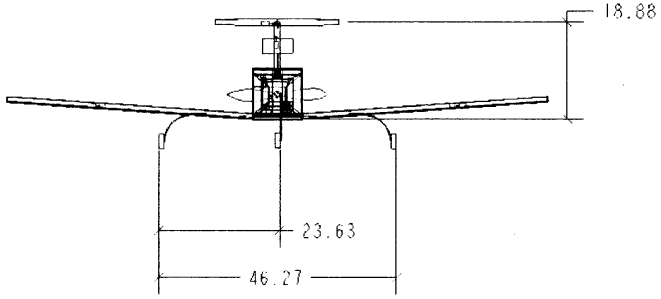

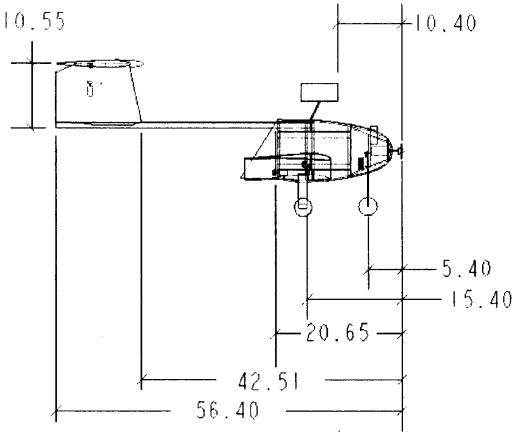

2002/2003 AIAA Foundation

Cessna/ONR Student Design/ Build/ Fly Competition

Design Report

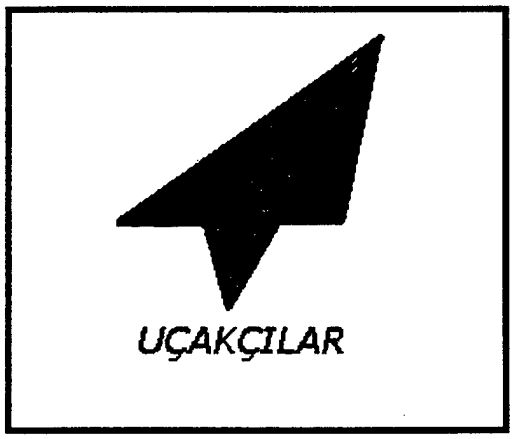

Istanbul Technical University

March 2003

INDEX

INDEX OF TABLES V

INDEX OF FIGURES V

1. EXECUTIVE SUMMARY: 1

1.1. OVERVIEW 1
1.2. FINANCE 1
1.3. DESIGN 1
1.3.1. Design Alternatives 2
1.3.2. Design Tools 3
1.4. MANUFACTURING 3
1.5. TESTS 3

2. MANAGEMENT SUMMARY: 4

2.1. EXPERIENCE 4
2.2. ARCHITECTURE OF THE TEAM 4
2.3. LIST OF PERSONAL AND ASSIGNMENT AREAS 8
2.4. SCHEDULE 9
2.5. COMMUNICATION WITH OTHER COMPETITORS 9

3. CONCEPTUAL DESIGN: 11

3.1. INTRODUCTION 11
3.2. REQUIREMENTS 11
3.3. DESIGN PARAMETERS 11
3.3.1. Mission Selection 11
3.3.2. Assembly Facilities 12
3.3.3. Flight Time 12
3.3.4. Sensor Deployment 12
3.3.5. RAC 12
3.4. AIRCRAFT CONFIGURATION 12
3.4.1. Fuselage and Tail 12
3.4.2. Wing 14
3.4.2.1. Position of Wing 14
3.4.2.2. Wing Planform 15
3.4.3. Power Plant 16
3.4.4. Propeller 16
3.5. DEPLOY MECHANISM 17
3.6. CONCEPTUAL DESIGN RESULTS 17

4. PRELIMINARY DESIGN: 19

4.1. INTRODUCTION 19
4.2. OPTIMIZATION 19
4.2.1. Mission Model 19
4.2.2. Constant Parameters 20
4.2.2.1. Structural Weight 20
4.2.2.2. Airfoil Parameters 20
4.2.2.3. Flap Effects 23
4.2.2.4. Atmospheric Parameters 23
4.2.2.5. Friction Coefficients and Braking 23

4.2.2.6. Body Drag 24
4.2.3. Variable Parameters and their Intervals 24
4.2.3.1. Power Plant (Motor –Battery) 24
4.2.3.2. Wing (Span, Taper, Chord...) 24
4.2.4. Effect on RAC 24
4.3. OPTIMIZATION PROCESS 24
4.4. RESULTS OF OPTIMIZATION 26
4.5. DESIGN OF MAJOR ITEMS 26
4.5.1. Systems Design 26
4.5.1.1. Deploy System 26
4.5.1.2. Assembly system 27
4.5.2. Fuselage and Tail Design 28
4.5.3. Wing Design 28
4.5.4. Power Plant Design 29
4.6. PREDICTED PERFORMANCES 30
4.7. FINAL PRELIMINARY DESIGN RESULTS 31

5. DETAIL DESIGN: **32**

5.1. DESIGN OF ACTUAL PIECES 32
5.1.1. Propulsion System 32
5.1.2. Structural System 34
5.1.3. Fuselage 34
5.1.4. Wing 35
5.1.5. Empennage 35
5.1.6. Landing Gear 36
5.2. TESTS OF MAJOR ITEMS 36
5.2.1. Aerodynamic Analysis 36
5.2.2. Test of Landing Gear 36
5.2.3. Test of Structure 37
5.3. FINALIZED DESIGN RESULTS 37
5.4. ESTIMATION OF RATED AIRCRAFT COST 38
5.5. DRAWING PACKAGE 39

6. MANUFACTURING PLAN AND PROCESSES: **43**

6.1. INTRODUCTION 43
6.2. MANUFACTURING PROCESS SELECTION DESIGNING TOOLS 43
6.2.1. Figures of Merit 43
6.2.1.1. Availability: 43
6.2.1.2. Cost: 43
6.2.1.3. Strength: 43
6.2.1.4. Weight: 43
6.2.1.5. Required Manufacturing Time: 43
6.2.1.6. Required Skill Level: 44
6.2.1.7. Repair ability: 44
6.2.1.8. Manufacture Flexibility: 44
6.3. Manufacturing Method 46
6.3.1. Wing & Tail: 46
6.3.2. Fuselage & Motor mount: 46
6.3.3. Fuselage Nose & Back 46
6.3.4. Landing Gear 47
6.4. SCHEDULE 47

7. TESTING PLAN: 48
7.1. DETAIL TESTING OBJECTIVES 48
7.1.1. STATIC TESTS 48
7.1.1.1. G- LOAD TEST 48
7.1.1.2. CG LOCATION TEST 48
7.1.1.3. LANDING GEAR TEST 48
7.1.1.4. ASSEMBLY TEST 48
7.1.2. FLIGHT TESTS 48
7.2. SCHEDULES 49
7.3. CHECKLISTS 50
7.3.1. ASSEMBLY CHECK LIST 50
7.3.2. THE FLIGHT CHECKLIST 50
7.4. RESULTS 51
8. CONCLUSION 52
9. REFERENCES 53

INDEX OF TABLES

TABLE 1: LIST OF PERSONAL AND ASSIGNMENT AREAS 8
TABLE 2: WING AND BODY CONFIGURATION 13
TABLE 3: POSITION OF THE WING 15
TABLE 4: WING PLANFORM 15
TABLE 5: POWER PLANT 16
TABLE 6: CONCEPTUAL DESIGN RESULTS 17
TABLE 7: RESULTS OF THE OPTIMIZATION 26
TABLE 8: PREDICTED PERFORMANCES I 30
TABLE 9: PREDICTED PERFORMANCES II 30
TABLE 10: STABILITY PARAMETERS 30
TABLE 11: FINAL PRELIMINARY DESIGN RESULTS 31
TABLE 12: FINALIZED DESIGN RESULTS 37
TABLE 13: ESTIMATION OF RAC 38
TABLE 14: MANUFACTURING METHOD DECISION MATRIX 45
TABLE 15: YELLOW CHECKLIST 50
TABLE 16: GREEN CHECKLIST 50

INDEX OF FIGURES

FIGURE 1: DESIGN ALTERNATIVES 2
FIGURE 2: MANAGEMENT PLAN 5
FIGURE 3: SCEDULE 9
FIGURE 4: CONCEPTUAL SKETCH 18
FIGURE 5: CHOSEN AIRFOIL ALTERNATIVES 21
FIGURE 6: CL/ALPHA AND CD/CL GRAPHICS 22
FIGURE 7: FLIGHT OPTIMIZER 25
FIGURE 8: DEPLOY MECHANISM 27
FIGURE 9: ASSEMBLY MECHANISM 28
FIGURE 10: TRUST TEST SYSTEM 33
FIGURE 11: ELECTRIC STSTEM OF THE AIRCRAFT 33
FIGURE 12: DRAWING I 39
FIGURE 13: DRAWING II 40
FIGURE 14: DRAWING III 41
FIGURE 15: DRAWING IV 42
FIGURE 16: DRAWING V 42
FIGURE 17: MANUFACTURING SCHEDULE 47
FIGURE 18: TEST SCHEDULE 49

1. Executive Summary:

The AIAA through the Applied Aerodynamics, Aircraft Design, Design Engineering and Flight Test Technical Committees and the AIAA Foundation invited all university students to participate in the Cessna/ONR Student Design/Build/Fly Competition. 7 students from İstanbul Teknik Üniversitesi formed the team "UÇAKÇILAR" in late May 2002 in order to attend the 2003 Competition. The mission of the contest is building a radio controlled unmanned aircraft, which carries a payload, an avionic packet and an antenna, in various combinations, in the minimum time. The aim of UÇAKÇILAR is to design an aircraft, which can reach the highest total score. In this report UÇAKÇILAR will explain their approach to achieve this aim.

1.1. Overview

AIAA's Design, Build and Fly Competition are getting difficult year by year. The main objective of the competition, carrying a payload in a determined course, is remaining same. The payload was last two year various balls, this year it became a well-defined box and an antenna. The flight course remains same but the missions are renewed. Also difficulty factors for missions are added so competitors have to decide which missions they are going to choose. The most challenging part for this year is that the aircraft must fit in a defined box. While the competition is getting harder, it is accepted that teams are getting experienced. UÇAKÇILAR is a follower of previous ITU Teams, Bosphorus Blue and Ata-4. The transfer of technology and know-how is accomplished in most possible ways.

1.2. Finance

Before any progress in design, UÇAKÇILAR has to attach importance in the budget. There were two main reasons. Firstly, there are very little substructure possibilities in the university and secondly the transportation cost for the fly off in USA was remarkably high. Also after two years' experience UÇAKÇILAR realized that analytical work methods learned at school is not enough for a design, especially for an UAV. UÇAKÇILAR planned to make some experiments, which also required some expenses. For all of these reasons as the first step UÇAKÇILAR defined their budget and expenditure plan accordingly.

1.3. Design

Announcement of the 2003 Rules defined mission profile and general rules. UÇAKÇILAR analyzed this rules and formed the design requirements. There were necessary requirements like "Aircraft must fit in a 2 foot wide by 1 foot high by 4 foot long (interior dimensions) box" or "take-off must be within 120 ft" and optional requirements like RAC calculations. Basis for UÇAKÇILAR was necessary requirements and its restrictions. Those drive UÇAKÇILAR to focus on a simple plug and fly aircraft. Accepting those conditions restricted the variety of design alternatives. In this narrowed design alternatives the aircraft has to achieve the highest possible score. Making an analysis for optimizing the score was possible after all these steps.

1.3.1. Design Alternatives

Design alternatives are investigated under topics of fuselage and wing configuration, position of the wing, wing planform, power plant and propeller. Airfoil selections, landing gear selection, payload location, deploy mechanism, mounting location of landing gear and other components are discussed separately. Many alternatives are evaluated. Fuselage and wing configuration alternatives were conventional, canard and flying. Biplane is considered as a wing position together with high wing, mid wing and low wing alternatives. The most valuable wing planforms to investigate were the rectangular, tapered and twin tapered designs. One and two motor options and different battery configurations were investigated as power plant and puller and pusher options were investigated as propeller. Some design alternatives like empennage and landing gears are almost designated regarding to major design decisions and mission requirements. Therefore other options are easily left behind. The payload, both avionics box and simulated antenna, should locate in the vertical center of gravity. It is an easy task for conceptual design but later it interferes with other decisions like material selection or stability.

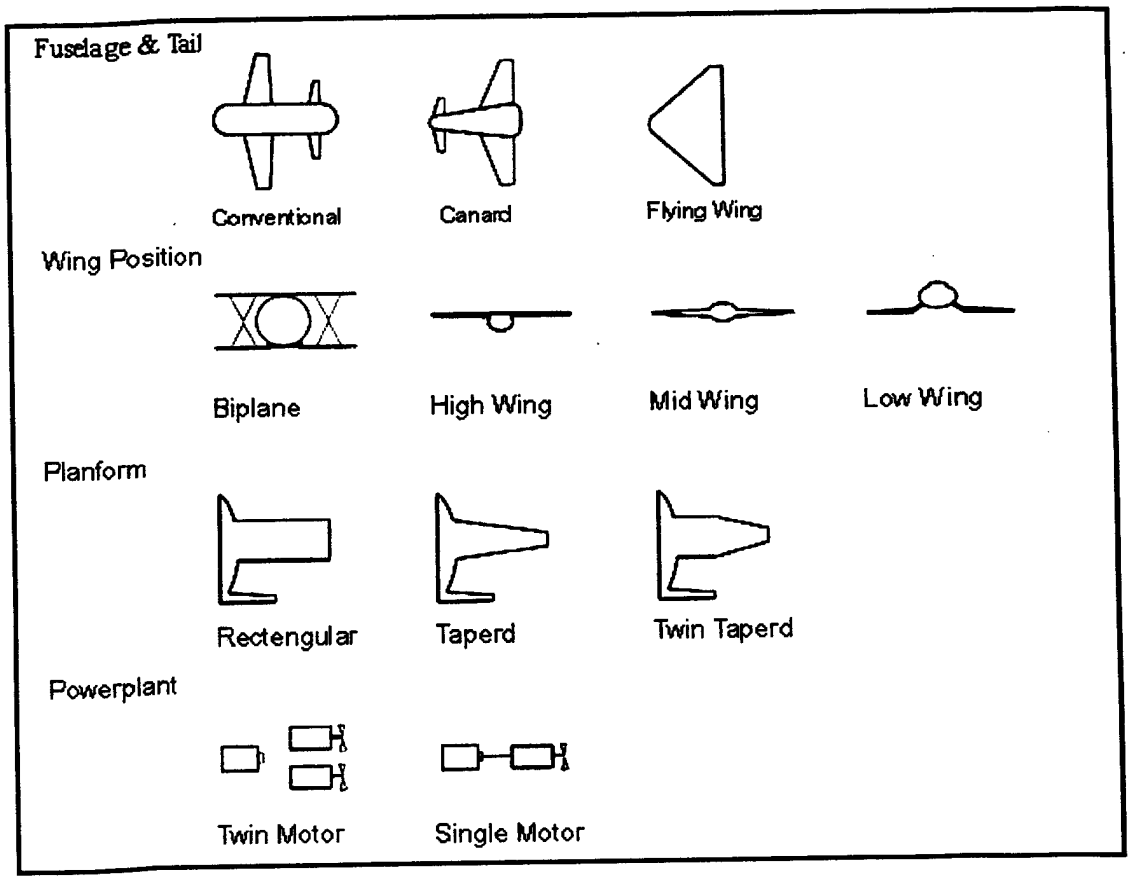

Figure 1: Design Alternatives

1.3.2. Design Tools

Simple EXCEL tables are used for conceptual decisions and for investigating the change rates of dependent variables. For more complex decisions FORTRAN codes are written. An optimization program is needed to reach minimum RAC and maximum flight score simultaneously, so a Visual Basic program "Mission Optimizer" is written. DRAG ESTIMATOR makes some calculations, where no experiment possibilities exist. MOTOCALC is also used to obtain the initial value for calculations since thrust experiments are not completed. Drawings are made both in AutoCAD and CATIA. These programs are also used in a broad spectrum from analysis to manufacturing. Other than tools in computer, some experiments and their tools are designed and manufactured by our team members.

1.4. Manufacturing

Manufacturing was a very important stage for us. Through last years experiences we were familiar with some materials and techniques but other techniques has to be evaluated to achieve the best possible airplane. Therefore many manufacturing processes are evaluated. Sometimes we aren't contented with analytical results; we tested some pieces of products of different techniques. Wing structure is produced with foam – balsa – fiber and also foam – fiber. So the decision is made after testing both pieces. Similarly main landing gear is planned to be manufactured from carbon fiber – Kevlar. But an aluminum main landing gear is also produced to make a comparison. For the mean structure conventional balsa, fiber with foam and hybrid manufacturing processes are examined. Materials, manufacturing processes and tools are decided after some analysis and experiments. All the experiments were planned to be done during the preliminary and detail design, but financial and bureaucratic factors caused some delays. Therefore some experiments are done in manufacturing phase while some didn't.

1.5. Tests

Tests and experiments are designed to increase the validity of analytical work. Many tests are planned, but some of them couldn't be finished until the first week of March. G-load, Landing gear, and assembly tests have been done and presented in this report. Assembly, Cg-location and Flight tests couldn't be done.

2. Management Summary:

2.1. Experience

Since three years student groups from Istanbul Technical University are attending Design, Build and Fly Competitions. Former teams' experiences were the most important input for this year's project. The know-how transfer is made by design reports of previous years. UCAKCILAR members who had attended previous competitions have also been an important advantage for know-how transfer among the team.

2.2. Architecture of the Team

As the members of the ATA-4 group and people who have been outside support to the group, we (five of us) have founded the "Uçakçılar Takımı" right after the DBF-2002 contest. Our first task came to be deciding upon the procedures and the number of members of the team. At first, the idea was to form a rather crowded team and then divide into subgroups with some of us as the head members of these groups, in order to proceed with the tasks of designing, producing, testing and so on, and helping the members of the sub-groups get trained and experienced as well as informed. However, we knew from our experiences of the past years that the personal irresponsibility of a member who has undertaken a particular task, or the disco ordination among groups could disrupt the team. In order to avoid such problems and defects, we would have to spend most of our energy and concern on the management and coordination of these groups. We thought it would be a mistake if the most experienced and trained five people who are most likely to enter the team were to work on such matters to try to get people with uncertain capacities in the group. Also, diving into subgroups would bring forth isolation, and each member would only be working on matters concerning his/her own groups alone- the rest of the team would not benefit from his/her contributions. The individual works of the groups would cause too much trouble no matter how hard we tried to avoid such isolation. For example, the isolated works of the design and the production groups would be beneficial in terms of aerodynamics; however, it could also lead to the creation of a plane that is impossible to make. These problems we foresaw played a major role in our sticking with a more familiar distribution of duties.

Instead of increasing our number of members and dividing into subgroups, we decided to work as one team of little number of members and dividing the tasks into groups.

Surely, the little number of members had its disadvantages too. Firstly, everyone would have to undertake a lot more duties and responsibilities. The unproductive work of even one member could lead to a major decrease in the total productivity of the whole group. Yet the members were totally absorbed in the matter, and so highly concentrated individuals, which brought into the team more safety, completed each task. So, two experienced members, whose abilities we were sure of, entered the team. It was also agreed upon that, if necessary, the team would also take a couple of members from lower classes.

The team took each task in a certain order as a whole, and matters such as the planning of design-production were carried out simultaneously. This approach towards the total of tasks as a whole lead to the contributions of all members and their sharing of experiences. But still, we did at

times divide responsibilities in small degrees with respect to the suggestions and experiences of our members. The team listed the tasks that would take about a week, and the members shared them. When these tasks were completed, new ones were shared. The advantage of this kind of a system was that if any member needed to spend lesser time on the tasks because of personal responsibilities or school matters, another member could easily take on his/her duties with a simple shifting of members. A technique that could not be carried out with a large group worked very well with our team of seven people who were constantly in touch with each other. We never had to deal with the problems of isolation and disco ordination. The "Ucakcilar" team members and their seniorities are shown below:

1. H. Murat Yuksel — Graduate
2. Gokhan Koyuncu — Senior
3. Mehmet Kesler — Senior
4. Altug Tufekcioglu — Junior
5. Serkan Kale — Junior
6. Ozgur Omeroglu — Junior
7. Firat Muslular — Bachelor

Below is the chart, which displays the grouping of the tasks:

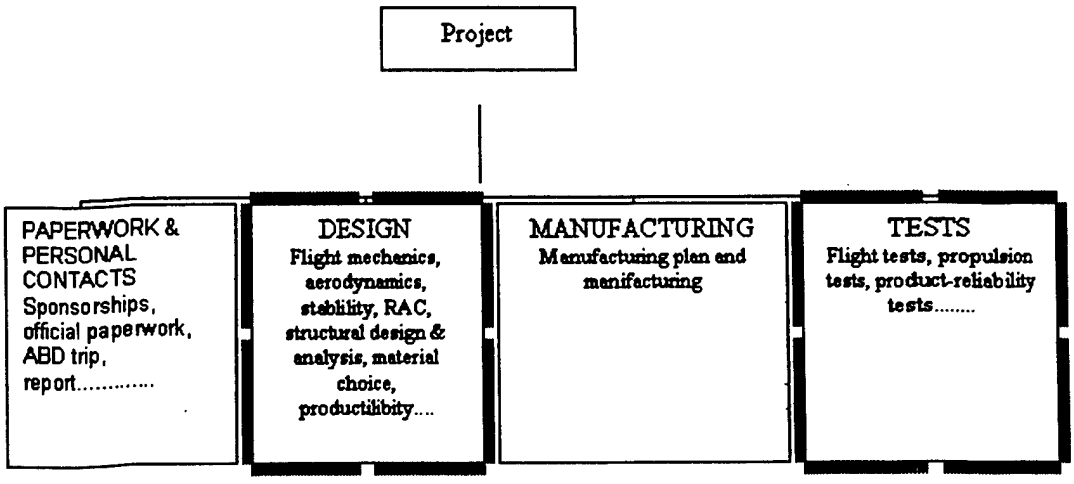

Figure 2: Management Plan

PAPERWORK & PERSONAL CONTACTS:

We required sponsorship, for we are coming from an overseas country and we do not have the necessary structural basis for the atelier. For a need like that, we needed to search for qualified sponsorships and for that we required a detailed budget outline. The sponsorship should have covered all of our expenses including the ones at the United States and for extra pieces. In addition to that according to our experiences from previous years we were aware of the fact that we had to attend the contest as a large group of people. Our budget was extremely high because the crew of nine people which included our own pilot and counselor. Also, because it was hard to have an access to the raw materials we decided to get them and the tickets from our sponsors in addition to the money we would get. We started our search-taking place at the stand of a sponsor in Istanbul, AIREX2002 fair. Because the rules of the contest were not known, all the group members worked in order to design a sponsor file and find a sponsor that suited our approaches above. Unfortunately we could not find enough support and we had to keep searching until the day of the contest. Arrangement of the tickets and getting the supplies are also mentioned here because they are counted as individual contact.

Since we were a team of a government school we had to get involved with bureaucratic issues. All these works, correspondence with AIAA and writing a report are included in this group because of the structural similarities.

DESIGN:

Except for the general airplane design such as the wing, body, control surfaces and landing gear, the structural design of these components, including manufacturing, style were included under this heading. For example, the aerodynamic efficiency of the wing was not presented as the first thing; everything about the wing design including the production method of such a wing, the material to be used and the production period, was handled at the same time. The advantage of this was the fact that the productivity had an effect on the design right from the beginning. As a result, the out coming design was the most efficient wing for the project. The same approach was applied for all parts of the plane. Such comprehensive task was established as a result of collective work and brain storming of the group rather than the efforts of a single member.

MANUFACTURING:

Under the title of manufacturing only constructing the manufacture plan and one to one production were included. Since it was a design-build-fly contest the group members other than the ones that are off the shelf made all the apparatus.

TESTS:

Particular tests had to be carried out because some of the techniques and the materials were very new, and so unfamiliar to the group. According to the results of these tests, they were decided to be worked on or abandoned. The plane's test groups and propulsion system were also carried out.

Below is the chart, which displays tasks completed by the members. The chart shows the contributions and concentration of each member to the tasks. Members appear in alphabetical order of last names. On a scaling of 5 points, the amount of contributions increases from 1 to 5.

Shown below also is how much of his/her own concentration each member had on a particular task with a scaling of percentage.

2.3. List of Personal and Assignment Areas

	Kale Serkan	Kesler Mehmet	Koyuncu Gokhan	Muslular Firat	Omeroglu Ozgür	Tüfekcioglu Altug	Yüksel Murat
PAPERWORK	***3***	***4***	***5***	***0***	***0***	***4***	***5***
Sponsorship	3	3	5	1	1	4	5
Scheduling	1	3	5	0	0	5	3
Sponsorship Documentation	1	1	5	0	0	4	4
Budget Planning with bill of materials	1	1	5	0	0	5	5
Sponsor Search	3	3	5	1	1	4	5
Bureaucracy	**2**	**5**	**5**	**1**	**1**	**4**	**4**
AIAA contact	0	0	**0**	0	0	5	0
University contact	2	5	5	1	1	5	5
USA-Maryland Trip	0	2	5	0	1	5	4
Report Writing	5	**5**	**5**	0	**0**	**5**	5
Material Supply	**3**	1	5	**3**	1	5	5
Tools supply	**2**	**0**	**5**	**0**	**0**	**4**	**5**
Raw-material supply	4	2	3	3	1	5	4
Treasury (Bookkeeping)	**0**	0	0	0	0	0	5
DESIGN	*2*	*2*	*5*	*1*	*2*	3	5
Aerodynamic Design	**3**	**3**	**5**	**0**	**0**	**3**	**5**
Wing	3	3	4	0	0	3	**5**
Fuselage	4	2	4	0	0	1	5
Tail	2	3	3	0	0	3	5
Landing Gear	4	2	2	0	0	5	3
Structural Design	4	3	3	2	0	5	5
Wing	5	2	3	3	0	5	3
Fuselage	5	3	3	0	0	3	4
Tail	2	3	4	0	0	3	2
Landing Gear	4	3	1	3	2	5	3
MANUFACTURING	***5***	***5***	***4***	***5***	***1***	***5***	***5***
Wing	5	5	3	5	2	5	5
Fuselage	4	3	4	5	0	**2**	5
Tail	4	**3**	**3**	**5**	0	4	5
Landing Gear	**4**	5	3	5	**0**	5	**2**
Control Surfaces	5	4	3	5	2	1	3
Electronics	4	3	3	4	5	2	5

Table 1: List of Personal and Assignment Areas

2.4. Schedule

UCAKCILAR started to work just after the DBF-2002 competition. However the rules of the competition weren't announced yet. Also some members of the team were out of city during the summer. Therefore the rest of the team spent all of their time to find money. It did work and the team found a full sponsorship, covering all expenses.

Unfortunately, the sponsorship was canceled because of irrelevant reasons. This effected all plans and the whole schedule changed. All manufacturing and testing plans were shifted. Also, spending extra time for new sponsors caused delay in other plans like report writing.

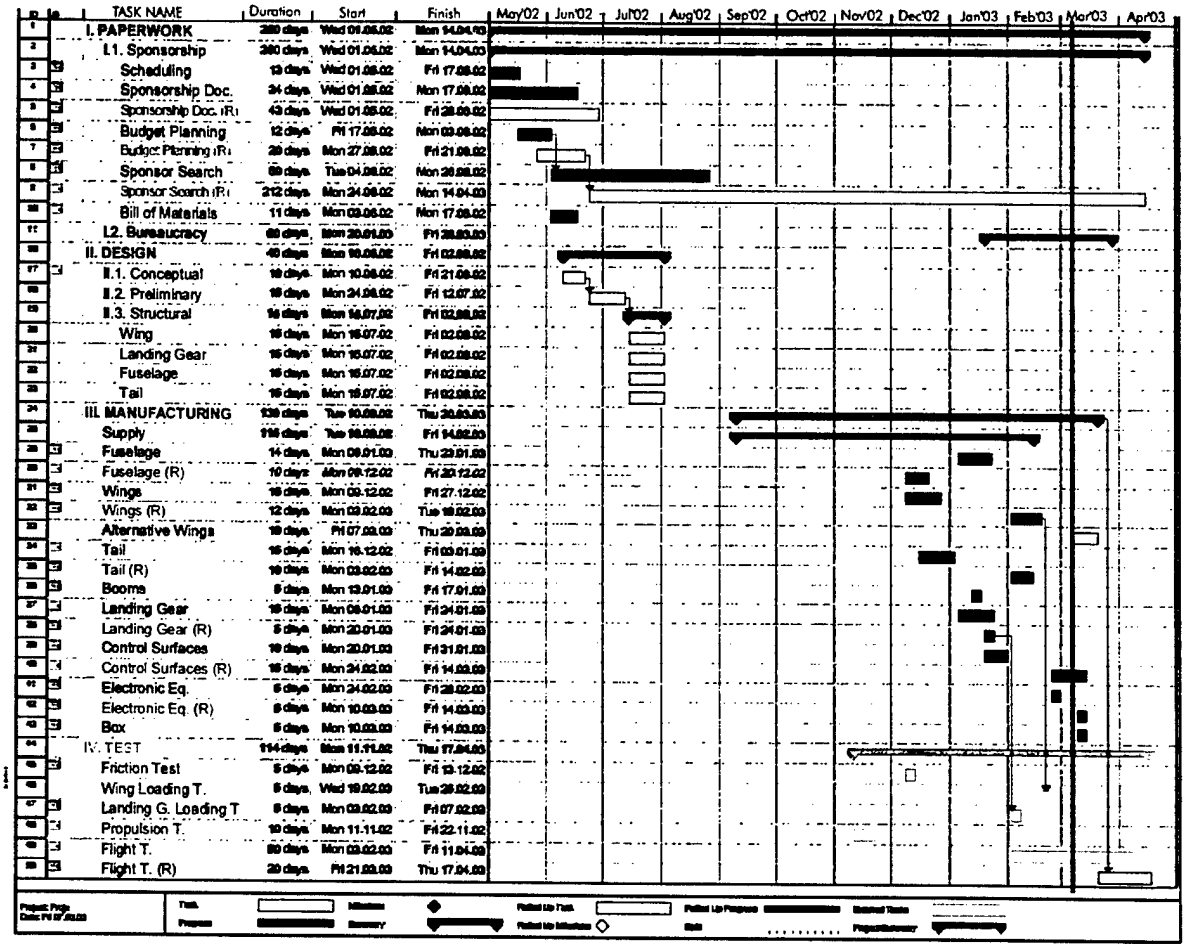

Figure 3: Schedule

2.5. Communication with other competitors

UCAKCILAR attached importance on communication and we tried to build a network between competitors. Some competitors supported this idea and a mail list under yahoo groups is created. However the result has not been as effective as expected. After a little conversation in the beginning there was no more communication. However teams in our region were more interested in this subject.

We had intensively contact with the Turkish Air Force Academy, Middle East Technical University and La Sapienza.

Thanks to our Affiliated Society of EUROAVIA (EUROAVIA Istanbul) we also announced this contest in Europe through EUROAVIA's (the European Association of Aerospace Students) international meetings. There were interested members of different Affiliated Societies but they couldn't be ready for this year's competition. For next year it is possible to expect some more participants from Europe.

3. Conceptual Design:

3.1. Introduction

The conceptual design determines the outline of the aircraft. Mainly this section is based on two elements; requirements and cost. Since this aircraft is designed for a competition, another element occurs; the score. Therefore the aim is to design an airplane, which fulfills all the requirements, stays within our budgets and gets the highest score.

3.2. Requirements

The contest committee has some restrictions on the airplane. They are about its size, power plant, and performance. First of all the airplane can't be a rotary wing or lighter then air. It should carry a payload of 5 lb, whose outer dimensions are 6" x 6" x 12". The payload must be carried in the fuselage, which is defined to be the inner most 18" of span for blended-wing configurations. The disassembled airplane must fit into a box, which has interior dimensions of 1 foot x 2 feet x 4 feet. The power plant must be an electric motor of Graupner or Astro Flight families. The batteries must be NiCad and the maximum pack weight is 5 lb. The structure of the airplane must be strong enough to resist a force of 2.5 g and it must be able to take off in 120 ft. considering these requirements the first ideas of the conceptual design took form.

3.3. Design Parameters

3.3.1. Mission Selection

There are three missions with different scores and it mandatory to perform two of them. First mission is "Missile Decoy" and its difficulty factor is 2. The airplane must complete 4 laps making a 360-degree turn for each lap with the sensor package and the antenna. Second mission is "Sensor Deployment" and its difficulty factor is 1.5. The airplane must complete 4 laps making a 360degree turn for each lap. After the first two laps the airplane must land, deploy the sensor, take off again and perform the remaining two laps. The last mission is "Communications Repeater" and its difficulty factor is 1. The airplane must complete 4 laps making three 360degree turn for each lap with the sensor package and the antenna.

When the results of the calculations are considered it is decided to design an airplane which can perform the first and second missions, because the third mission doesn't give the same flight score as the first one even if the plane flies two times faster. The second mission seems to be more complicated, but it only needs an additional servo and deploy door. These additions affect the RAC negatively, but the higher difficulty factor will compensate it. On the other hand an airplane, which is capable of performing the first two missions, can also perform the third one. During the test flights the third mission will also be experimented and compared with the others.

3.3.2. Assembly Facilities

The airplane has to be disassembled, for it will be carried in a box of a certain size. The team members will do assembly just before the flight and this assembly period will be added to the flight time. Therefore one of the most important aims is to achieve simple and quick assembly.

3.3.3. Flight Time

According to the calculations the plane must fly fast and the landing should be as quick as possible in order to get a high flight score. So the designed plane will be a very fast one with small wings, a powerful engine, heavy batteries, and landing gears with a break system.

3.3.4. Sensor Deployment

To perform the second mission "Sensor Deployment", the plane must have a deploy mechanism. There can be many other systems working with springs, pneumatic actuators etc., but the simplest way to deploy the simulated sensor is using the gravitational force. For this system an electrical servo is needed. This servo will hold the sensor by a handle and when the plane stops for the deployment, it will release the sensor. The simulated sensor will open the deploy door with its own weight.

3.3.5. RAC

In the contest, rated aircraft cost is one of the evaluation factors. High RAC means low score. Empty weight, battery weight, wingspan, number of control surfaces, motors, and servos affect this rated cost. Mostly RAC is a Figure of Merit but sometimes there are more important variables.

3.4. Aircraft Configuration

Good flight performance and assembly facilities increase the score whereas high RAC decreases it. These three concepts should go through an optimization process in order to find the best configuration.

3.4.1. Fuselage and Tail

The only duty of the fuselage is to carry the payload, which is the 6" x 6" x 12" sized box, the battery pack, and the motor. To cause the minimum drag and to have the minimum weight and minimum RAC the fuselage should be as small as possible. Figures of Merit (FOM) of fuselage and wing selection are fitting into the box, flight characteristics, RAC and manufacturing.

Fitting in the box: The size and shape of the airplane should be designed in a way so that the disassembled plane can easily fit into a box of previously established size. This is the most important FOM.

Flight characteristics: This FOM includes take off and landing quality, aerodynamic efficiency, stability, and handling quality. It is a positive situation when these characteristics are accomplished.

RAC: Every Fuselage and Wing configuration has a different RAC interval, which is determined according to the number of control surfaces and the lengths of the body.

Manufacturing: Some Fuselage and Wing configurations require manufacturing with high precision. Those configurations won't be preferred. The effect of manufacturing is minor when compared with the others.

Considering these Figures of Merits and assuming that all the other characteristics are equal, three configurations were compared; conventional, canard and flying wing.

Conventional: A conventional configuration can fit in the specified box without any complication, provide good flight characteristics, has an average RAC and is relatively easy to manufacture.

Canard: A canard configuration has no significant disadvantage in fitting in the box, has some restrictions in flight characteristics, has average RAC and average manufacturing specialties.

Flying wing: A flying wing has advantages in RAC but is very hard to fit in the box. For this configuration delicate handling is essential during manufacturing.

		Configurations		
Figures of Merit	**Weighting Factor**	**Conventional**	**Canard**	**Flying Wing**
Fit in the box	0,4	1	1	1
Flight characteristics	0,3	1	0	0
RAC	0,2	0	0	1
Manufacturing	0,1	0	0	-1
Score	1	0,7	0,4	0,5

Table 2: Wing and Body Configuration

As shown in the figure the conventional configuration is the best choice for fuselage and body configuration. Relating to this configuration, empennage and landing gear are developed. Because of the box's size limitation, the empennage must be separate. Separate empennage means that the rudder and the elevator servos must be on the tail, not in the body. In this case having a steering nose wheel will be a problem, for it will need a separate servo. Another servo means more weight and higher RAC. On the other hand tail wheels are always lighter then nose wheels with their struts. So UÇAKÇILAR has chosen the tail wheel. To have the minimum weight and shortest assembly time the empennage should consist of tubes and tail surfaces. To fit in the box it should be able to be folded. So the best choice is having a V-tail, which has a hinge between two parts and is connected to the fuselage with two tubes, one for each part. The V tail can be a normal V or inverted V. The normal V-tail is selected, because in this case only one tail wheel is needed. If the inverted V was selected, two tail wheels would be needed. In that case the tail would be heavier and wheel control would be more complicated.

3.4.2. Wing

3.4.2.1. Position of Wing

Figures of Merit in the analysis of wing configurations are fitting in the box, flight characteristics, deploy mechanism, assembly time and structure.

Fitting in the box: A wingspan of 4 feet is not enough for any kind of aircraft except a biplane. So, all configurations have to be in two pieces. This is the major point of our decision.

Flight characteristics: This FOM focuses on take-off, landing and stability.

Deploy Mechanism: The wing should neither interfere with the deploy mechanism nor with the simulated sensor.

Assembly Time: Assembly Time is a very important factor since assembly time is added to all flight times. As the wing must be in two pieces and separate from the fuselage for all configurations this FOM must be taken into consideration.

Structure of Wing: Structure of the wing has to resist the bending moment caused by itself. Longer spans need stronger contractions, which makes them heavier.

Structure of Fuselage: Structure of the fuselage has to resist the bending moment caused by the wing. Some parts of the wing need more structural strength.

Considering these Figures of Merits and assuming that all the other characteristics are equal, four configurations were compared; biplane, low wing, mid wing and high wing.

Biplane: Biplane configurations are able to produce large amounts of lift with a smaller span. Because of this, the bending moment they must resist is less. They don't need to be as strong as they are in the other configurations, so they may have light constructions. Biplanes make up a very good solution for fitting in the box.

Low wing: Low wings cannot fit in the box in a single piece. It must be in two pieces at least. The joint between the pieces of the wing will interfere with the deploy mechanism. Take off distance decreases; landing distance increases because of the ground effect. Low wings affect lateral stability negatively.

Mid wing: Mid wings cannot fit in the box in a single piece, too. The joint between the pieces of the wing will interfere with the simulated sensor. Lateral stability is moderate in mid wings.

High wing: High wings don't interfere with any system. High wings don't require dihedral for stability.

			Position of The Wing		
Figures of Merit	Weighted Factor	Biplane	Low	Mid	High
Fit in the box	0,1	1	0	0	0
Flight Characteristics	0,2	0	-1	0	1
Deploy Mechanism	0,25	0	-1	-1	1
Assembly Time	0,2	-1	0	0	0
Structure of Wing	0,15	1	0	0	0
Structure of Fuselage	0,1	1	-1	-1	-1
Score	1	0,15	-0,55	-0,35	0,35

Table 3: Position of the Wing

As shown in the figure the high wing configuration is the best choice for the position of the wing.

3.4.2.2. Wing Planform.

Figures of Merit in the analysis of wing taper are manufacturing, aerodynamic efficiency, RAC.

Manufacturing: Complicity of the wing geometry makes manufacturing harder. This has a minor effect compared to the other FOMs.

Aerodynamic Efficiency: Aerodynamic efficiency is related with wing geometry. This is the most important FOM for a wing.

RAC: Wing chord and span are directly affecting the RAC. Wing affects RAC also through number of control surfaces and servo controllers.

Three types of wing plan forms are investigated. Rectangular, tapered and twin tapered.

Rectangular: This type of construction offers manufacturing advantages but reduces the aerodynamic efficiency.

Tapered: Tapered wing increases aerodynamic efficiency, reduces manufacturing advantages.

Twin Tapered: This plan form offers high aerodynamic efficiency. Cutting control surfaces in the middle causes separate aileron and flaps, so RAC will be higher.

			Wing Planform		
Figure of Merit	Weighted Factor	Rectangular	Tapered	Twin Tapered	Elliptical
Manufacturing	0,3	1	0,5	0	-1
Aero Efficiency	0,4	-1	0	0,5	1
RAC	0,3	1	1	-1	0
Score	1	0,2	0,45	-0,1	0,1

Table 4: Wing Planform

As shown in the figure above the tapered wing configuration is the best choice for plan form of the wing.

3.4.3. Power Plant

The function of the power plant is to carry the payload in defined course. To achieve the minimum time the power plant has to give enough thrust. Weight of the batteries should be considered as well. Figure of Merits for power plant are RAC, weight and efficiency.

RAC: Number of engines and propellers are affecting RAC directly.

Efficiency: Motors are converting electrical energy to kinetic energy. During this process certain amount of the energy is lost. Simplicity of electrical system will reduce this lost.

Weight: Weight is affecting RAC indirectly. The number of motors determines the number of speed controllers, battery packs and motor mounts. Therefore an increase in the number of motors increases the weight.

Possible power plant alternatives are single and twin motor.

Single Motor: Single motor has lower RAC. There is no loss in efficiency.

Twin Motor: Twin motor allows using a smaller propeller. The aircraft's fuselage can stay nearer to the ground and landing gears can be shorter and lighter.

		Power Plant	
Figure of Merit	**Weighted Factor**	**Single Motor**	**Twin Motor**
RAC	0,4	1	-1
Efficiency	0,4	1	0
Weight	0,2	0	-1
Score	1	0,8	-0,6

Table 5: Power Plant

As shown in the figure single motor is a better choice for power plant of the airplane.

3.4.4. Propeller

After it is decided to use a single motor, conventional body, high wing configuration and empennage with tube construction there are two options for a propeller. It can be either puller or pusher. Both choices seem suitable for the design until now, but a pusher propeller has a disadvantage. If using a pusher propeller was chosen, the two tubes of the empennage had to be separated for a distance at least equal to the diameter of the propeller. In this case the tubes have to be fixed to the wings, as a result that part of the wing has to be strengthened. If pusher propeller was

used the decision of making a V tail would be disturbed, because that kind of propeller needs inverted V tail for its tubes' positions.

3.5. Deploy Mechanism

The deploy mechanism consists of a servomotor above the simulated sensor, a small tab on the sensor, and the deploy door down side the fuselage. When the servo releases the load, it falls down and the doors will be closed with the help of their spring mechanism. This is the simplest way of deploying a load.

3.6. Conceptual Design Results

UCAKCILAR decided to design an aircraft with conventional body with short fuselage and extend it with two booms until empennage. This option has remarkable effect on structure strength and the weight of it will be less than any other alternative. RAC is affected through two ways, fuselage length and weight. In this configuration fuselage is not shorter than any other options but the less use of material cause lighter structure and a reduced RAC. Use of V – tail is reducing RAC directly, allow using tail dragger landing gear, causing less aerodynamic drag. But most important is its relation with deploys mechanism. Similarly high wing has many advantages; structural benefits, aerodynamic stability effects and easy assembly. It's more important, that it is also reconciled with deploy mechanism. Wing Planform is selected tapered, this will obtain easy manufacturing and uses of flaperon. Single motor is the best choice both for RAC calculations and energy losses. Each motor and propeller has penalties in RAC and efficiencies are very likely to reduce. Puller propeller is chosen so a clean wind for it is provided. Through this decision the distance between two tubes is free to decide and we decided to attach these to the fuselage alternatively from wing. This reduced the need of strength for the wing and increased the strength of the fuselage. The cutting zones are also considered for a minimum assembly time and a self deploy mechanism for simulated sensor is designed.

Conceptual Design Results	
Systems	**Selection**
Body – Wing	Conventional
Empennage	V - Tail
Landing Gear	Tail dragger
Position of the Wing	High Wing
Wing Planform	Tapered
Power Plant	Single Motor
Propeller	Puller
Deploy Mechanism	Gravity

Table 6: Conceptual Design Results

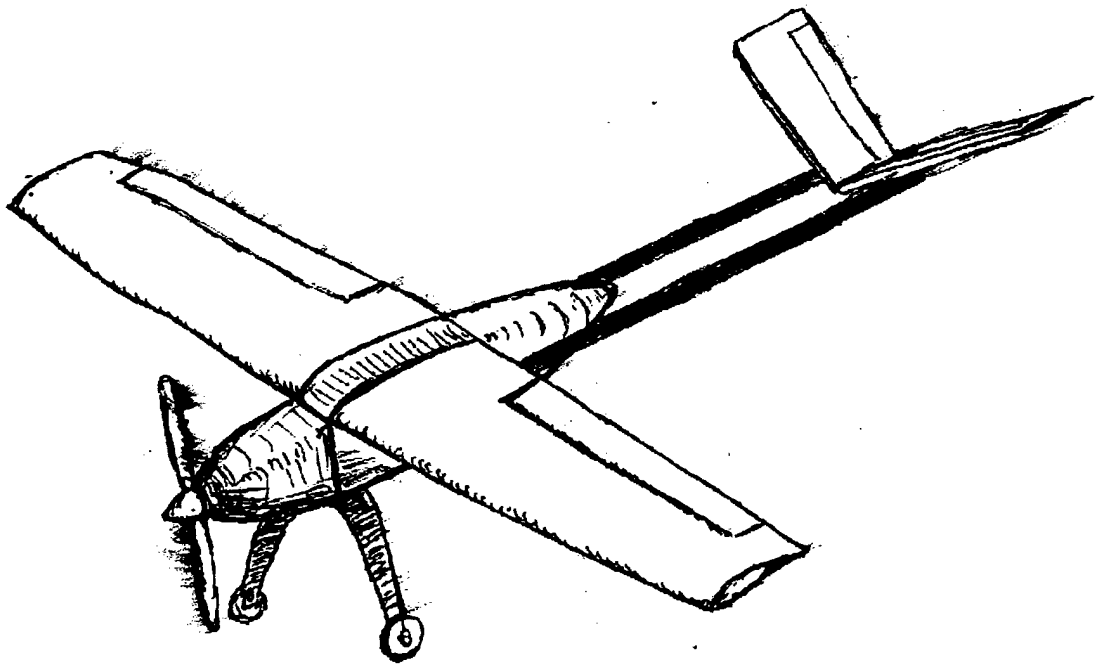

Figure 4: Conceptual Sketch

4. Preliminary Design:

4.1. Introduction

Regarding to conceptual decisions in preliminary design phase we optimized the actual sizes of aircraft and related parameters. The flight course is divided into several zones. They are evaluated with their different specialties and a mission model is shaped. The velocities in these zones are expected different and optimization code is used to decide these speeds. During this process Rated Aircraft Cost is dependently changed. This process includes both airplane sizing and RAC optimization. Therefore main optimization criterion was total score.

4.2. Optimization

The process of optimization the flight score and RAC together was made step by step. First a mission model is defined. Through this model we managed to input data of mission matrix in the optimization program. Then parameters for optimization are defined and their intervals are discussed. Some of these parameters were taken as constants. There were various reasons for this. It was sometimes traditional reasons, other times was a result of an experiment. But these were not only reasons. Sometimes we foresee a value considering different factors. We also examined the effect of various variables on RAC. Changing rates of these variables with RAC determined their importance.

4.2.1. Mission Model

Flight course is divided in 6 zones regarding to aircraft performance needs and grouped. Take off and landing zones are unique ones and computed specially. All turns including turn backs in each lap and 180 grad turns are accepted as same. The cruise flight is defined apart. It is accepted that turn velocities and cruise velocities for best flight score can be different. Two phase, acceleration and deceleration, are considered in order to allow such conditions. These are the bases for evaluating each mission's flight course. Each course is redefined with these bases. Missile Decoy Mission include 4 laps with one 360 degree turn for each that is redefined as one take off and one landing, 16 half turns. Sensor Deployment Mission includes two laps with one 360 degree for each, then a landing, sensor deployment, take off and two more laps as previous. This mission is redefined as two take offs, two landings, sensor deployment and 16 half turns. Communications Repeater Mission includes four laps with three 360-degree turn for each. This last mission is redefined as one take off, one landing and 32 half turns. Two other points should be considered while mission modeling. Each mission has its own difficulty factor and the payloads differ in missions. These conditions are also included in the optimization process.

4.2.2. Constant Parameters

Some parameters are considered as constants. These are as fallows.

4.2.2.1. Structural Weight

After conceptual design the size of the airplane structure has appeared approximately. Structural weight of the aircraft consists of fuselage framework, front – back cowling, landing gear, wing fixing mechanism, tubes to empennage, the wing and the tail. Expectations from each part were considered and material alternatives were investigated. Afterwards by using historical data and previous years' experience we estimated the structural weight as 30N (6.616lb).

4.2.2.2. Airfoil Parameters

Unsuspectingly, the most important element for determining the main flight characteristics of the aircraft was the airfoil. We have chosen one airfoil for optimization. It has aerodynamic constants. Therefore these values are accepted constants for airfoil for the program. An optimization for another airfoil is also done, with its new constants. For choosing the best airfoil we made a general selection. With estimation, the aircraft would be approximately 90N and the flight time would have to be short airfoil has to provide the flight velocity would have to be fast enough. Moreover, influences of the span to the RAC were kept in mind. The criteria according to these restrictions were; the cruise conditions should have to be at maximum $\frac{C_l}{C_d}$, the wing had to support a lift while it had low angle of attack, for providing the aircraft to take off in 120 ft., the $C_{l_{max}}$ of the airfoil would have to be as higher as it could be, in cruise flight, the lift force would have to equal to the approximate aircraft weight, a lift would have to be provided although the aircraft has higher angle of attack.

First of all the Reynolds number was calculated approximately to decide the airfoil with respect to the criteria above. The approximate Reynolds number according to the aircraft's estimated velocity and approximate chord was calculated by using the formula $\mathrm{Re} = \frac{\rho.V.D}{\mu}$ where ρ= 1, 2256 kg/m^3 and μ= 1,714 10^{-5} m^3/s. According to this, while the velocity was nearly 25 m/s and the chord was 0, 30 m. The Reynolds number was 500 000. However the flight velocity could be increase to 35 m/s. For that reason, the airfoils that has Reynolds number lower than 700 000 were searched. Because the Mach number was M= $\frac{U}{\sqrt{\gamma.RT}}$ < 0, 1 compressibility effects weren't kept in mind and the Mach number wasn't thought as a criteria. However, only a few results could be reached about the airfoils that have Reynolds number below the 500 000. Furthermore there was experimental data of many airfoils at the Reynolds number of 300 000. For that reason, by using the criteria above, 12 airfoils were selected for Reynolds number of 300 000 as a primary approach. Furthermore, data of these

airfoils for Reynolds number of 400 000 and 500 000 were compared with the data for Re= 300 000. The characteristics of these 12 airfoils were given below in graphics:

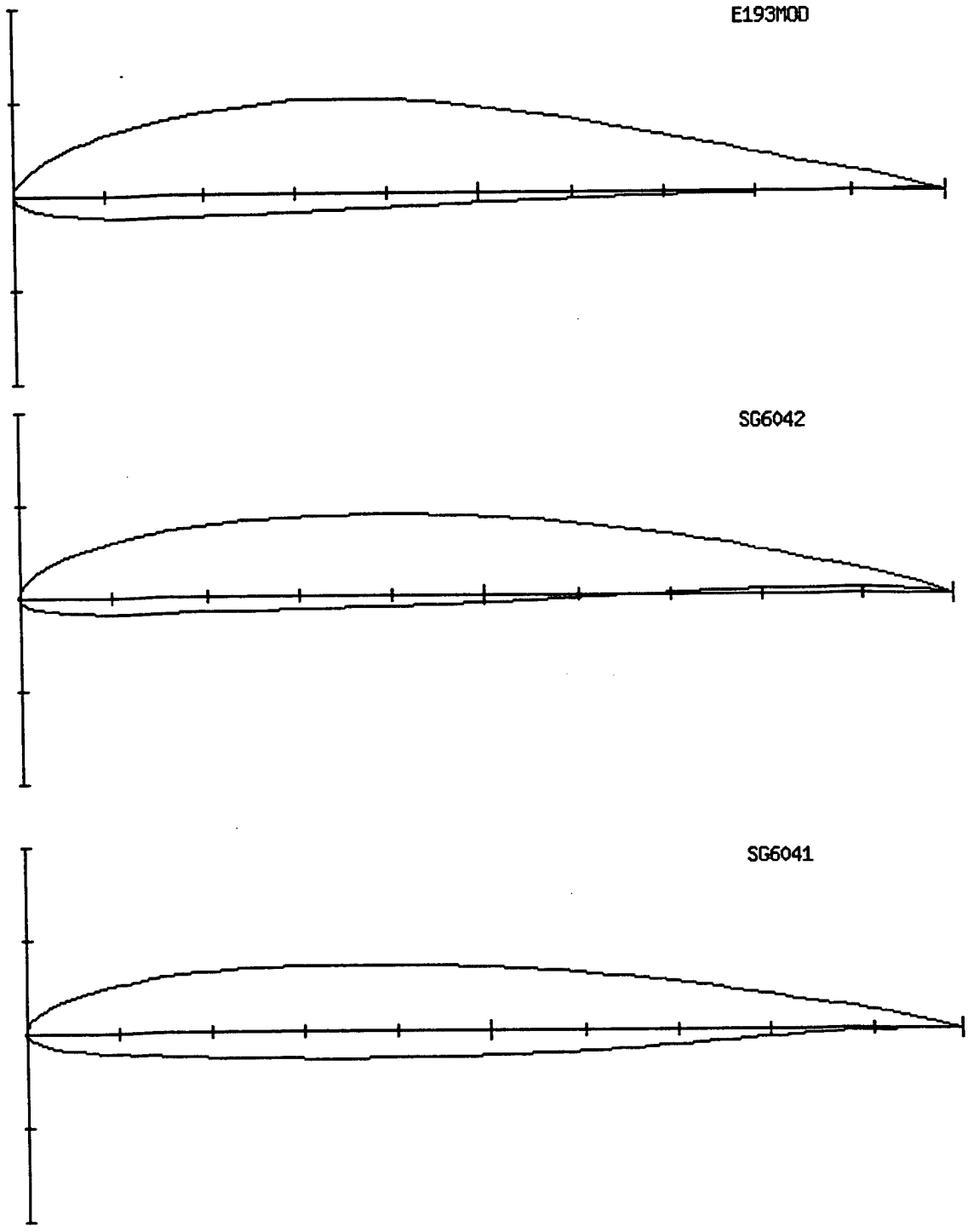

Figure 5: Chosen Airfoil Alternatives

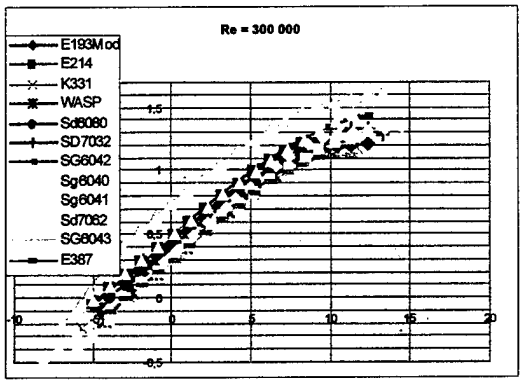

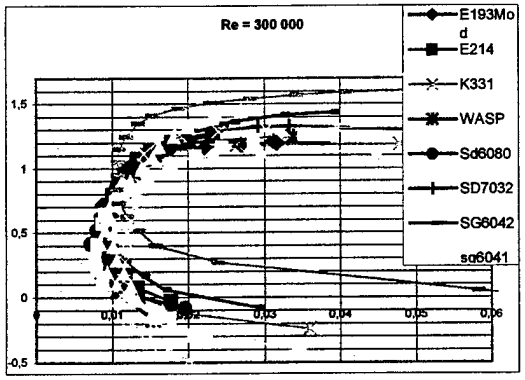

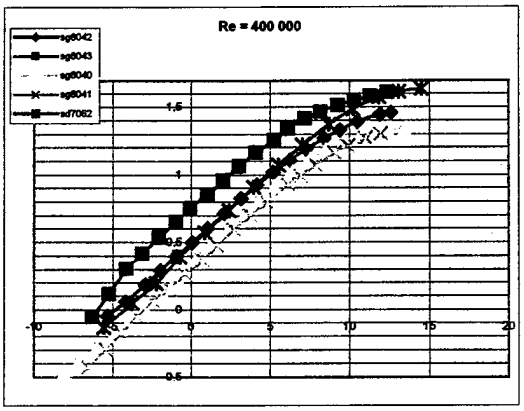

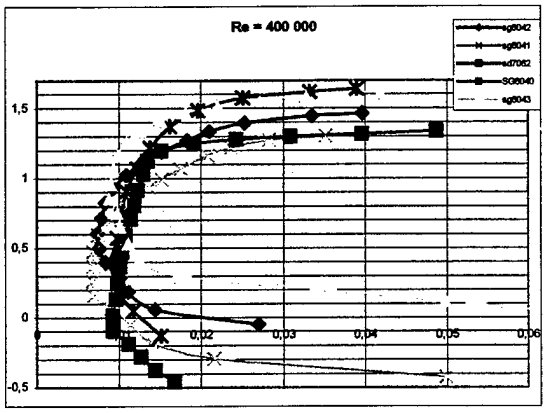

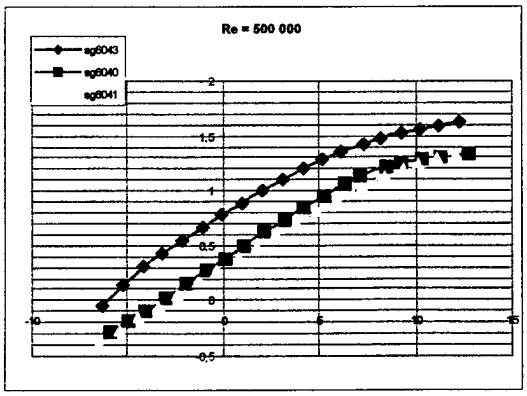

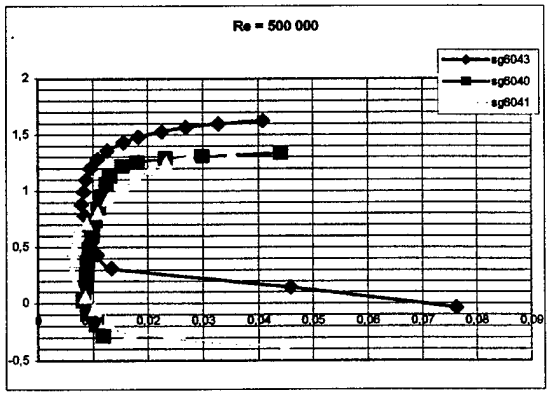

These Graphics are for Re= 300 000, 400 000 and 500 000

Figure 6: Cl/alpha and Cd/Cl Graphics

According to the graphics above, the airfoils SG6043 and E387 were not appropriate the criteria above relatively. The results obtained from the rest of 7 airfoils was approximate the each other. As a result of this, the airfoil SG6041 was realized as the most suitable one. However there was some difference between the airfoils SG6041 and E193 MOD. Moreover the airfoil E193 MOD had been tried in the university, in the past years. With the results of the effects of manufacturing methods that could be used, some of the characteristics of airfoil could be change. As a conclusion, the effects of the changed characteristic weren't provided by the graphics above. Because the experimental knowledge like this was recognized for only the profile E193 MOD, the real flight characteristics of it, was known better. This also provides the reliability of the airfoil E193 MOD. As a result of this, using the airfoil E193 MOD was decided to use for the manufacturing prototype. Meanwhile the wings were not fixed to the fuselage permanently, they were changeable. As a result of this, manufacturing a wing that has different airfoil, and using it could be possible. At the end, after the first flight tests with the wings that had airfoil E193 MOD, because of known flight characteristics of it, manufacturing and testing the other wings that have airfoil SG6041 and SG6040 was decided. As a result of these decisions, the airfoil would be used according to which was the most efficient for the aircraft.

4.2.2.3. Flap Effects

Flight time is a very important parameter and should be reduced as possible. This will result a fast airplane with small wing planform area, but small wing will increase the wing loading and will be problematic in take off and landing. The take off and approach speeds are higher than expected. In this point flaps are important devices to reduce required field length. Different flap systems are investigated and trailing edge flaps are accepted as best fitting alternative. There were two similar alternatives ; plane and split flap. Effects of these kinds of flaps are similar. We tend to choose second because of its high contribution to drag, which is needed during landing as a kind of break. But the possibility of having no flaps but using ailerons in this manner leads us to decide both of these alternatives. This decision is also related with number of servomotors. Separate flaps mean additional servo needs, but flaperons are used as much servos as ailerons.

4.2.2.4. Atmospheric Parameters

There are two atmospheric conditions, which has to be considered. Theses are open-air pressure and air viscosity constant. Assuming minor changes in altitude because of the low flight level and considering the weather conditions of contest site we assumed open-air pressure rho as 1.225 kg/m^3 and the air viscosity constant is taken as $1.714x10^{-5}$. Calculations were maid with no wind assumption and then modified.

4.2.2.5. Friction Coefficients and Braking

Two friction coefficients exist for landing gear. Brakeless friction coefficient and brake friction coefficient are computed after tests in the workshop. These parameters are affecting on take off and landing distances. If decided to use, a break system will cause some drag during landing. The force produced by brake is limited with maximum value to prevent tumbling while landing.

4.2.2.6. Body Drag

The best way of determination of the drag of a body is having wind tunnel tests. Unfortunately we couldn't have the chance to use the wind tunnels because of the bureaucracy. The drag coefficient of the body is calculated as 0.00397 in the computer program "Drag Estimator". Results were satisfactory to input to the optimization program.

4.2.3. Variable Parameters and their Intervals

4.2.3.1. Power Plant (Motor –Battery)

Under title power plant two factors appear, motor and battery. There are a couple options for motor but many choices for battery. We considered Astro Cobalt 90 and Astro Cobalt 60 motors, both are geared with a 2.75 ratio. These were only suitable options for our requirements. The differences between these motors are given in the table below. With these motor choices we are allowed to use 28 to 40 batteries. This means a variety of electrical potential of 31 to 44 Volts. The limit of current use is 40 Ampere. According to wind tunnel tests and historical data, we estimate that the required current is about 35 Ampere. The batteries output is about 1000 to 1500 Watt and the calculated power to be used is going to be 850 to 1400 Watt. Another feature to decide for batteries is the mAh capacity. There are three SR Batteries alternative; 1500, 2000 and 2400 mAh. These batteries have different durability and weight. The calculated mission completion time is going to show which one should be used. Flight time is multiplied with a safety factor multiplier and the lightest one of these batteries with this endurance is going to be chosen.

4.2.3.2. Wing (Span, Taper, Chord...)

The wing is the most variable parameter. Span, chord and taper ratio are parameters, which are independent with each other but together form the shape of wing. Span length is limited by two factors, fit into box and wing loading limit. The interval for span is 2m to 2.6m with steps of 10cm.The cord varies between 0.3m and 0.4m, in order to keep an aspect ratio around 7. Taper ratio increases aerodynamic efficiency of the wing. The taper ratio is traditionally between 0.5 and 1. The values of 0.5, 0.7 and 1 are used for optimization process.

4.2.4. Effect on RAC

The variables contributing to RAC are studied and the importance of these variables is determined. These variables were fuselage length, wingspan, mean cord, taper ratio, weight, number of servos, total battery weight, empennage number of engines and propellers..

4.3. Optimization Process

Optimization Program is coded with Visual Basic in order to be user friendly, which is also more capable of filing excel matrixes. An interface is designed to input the data. In one frame all constant parameters of the airplane are input. In another one all variables with their first and last values of their interval and increase steps are input. Entering these data is the first step of the optimization process. Computers work begins with reading this data. Logical examination is made to

prevent absurd inputs. Such inputs can cause too many unnecessary calculations or can be out of range of some used empirical formulas. Next step is the calculation of all the parameters, which are only functions of the constant parameters. Then the loops begin in the order; number of batteries, span, root chord, taper ratio, and turning speed. In the innermost loop all the other variables and all time periods; acceleration on ground, acceleration on air, cruise, deceleration for turn, turn, acceleration after turn, deceleration for landing, deceleration on ground times are calculated. Summing this time periods the totals flight time is obtained and afterwards RAC is computed. Using this values score is obtained. In this process written report score and assembly time are assumed to be independent on the variable parameters of the optimization. All the results of these loops are stored in a excel document and arranged in an order of the score.

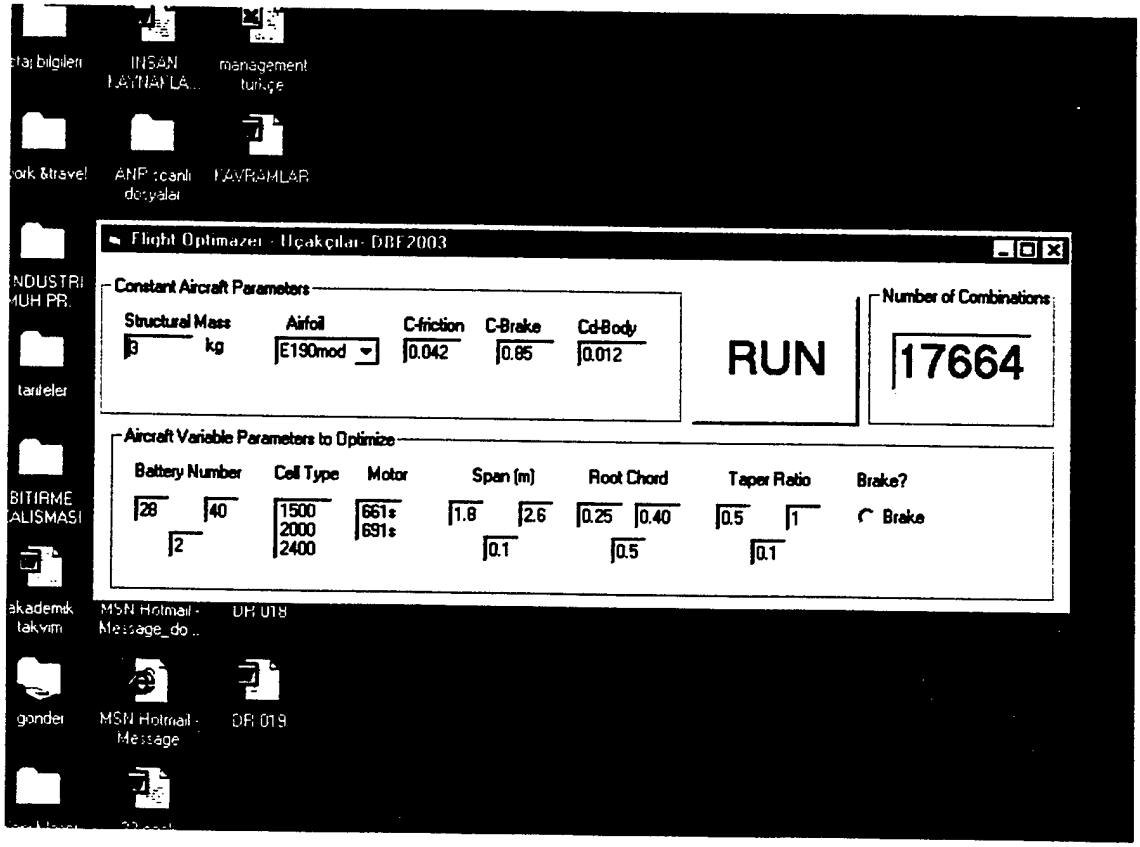

Figure 7: Flight Optimizer

4.4. Results of Optimization

The results of the optimization in the excel table are investigated, the top scores are refined and others are eliminated. All of these refined cases were similar configurations and there were minor changes in their scores. Regarding to our senses we chose one of them.

	Results of the Optimization							
	Num of Batt	Type of Batt	Type of Motor	Span	Root Chord	Taper Ratio	Brake	
	36	1500	691s	2.20	0.35	0.7	Yes	

Table 7: Results of the Optimization

4.5. Design of Major Items

4.5.1. Systems Design

4.5.1.1. Deploy System

The aircraft must have a deploy mechanism, because one of its two missions is "Sensor Deploy". In the conceptual design it's decided to hold the simulated sensor in the deck with a servomotor at flight and release it in the right time. This servo is located between the two parts of the wing in the body. A thin steel rod is connected on it and works in plastic bearings. This rod holds the simulated sensor at its tab. The sensor is located in the center of gravity of the airplane, so this center of gravity doesn't move after the deployment. Four L- profile aluminum bars are placed at its corners to provide an easy slide. These bars also strengthen the framework of the fuselage. There are two deploy doors down side the fuselage, which are closed by their springs. These springs are not strong enough to resist the weight of the simulated sensor, so they open when the sensor is released.

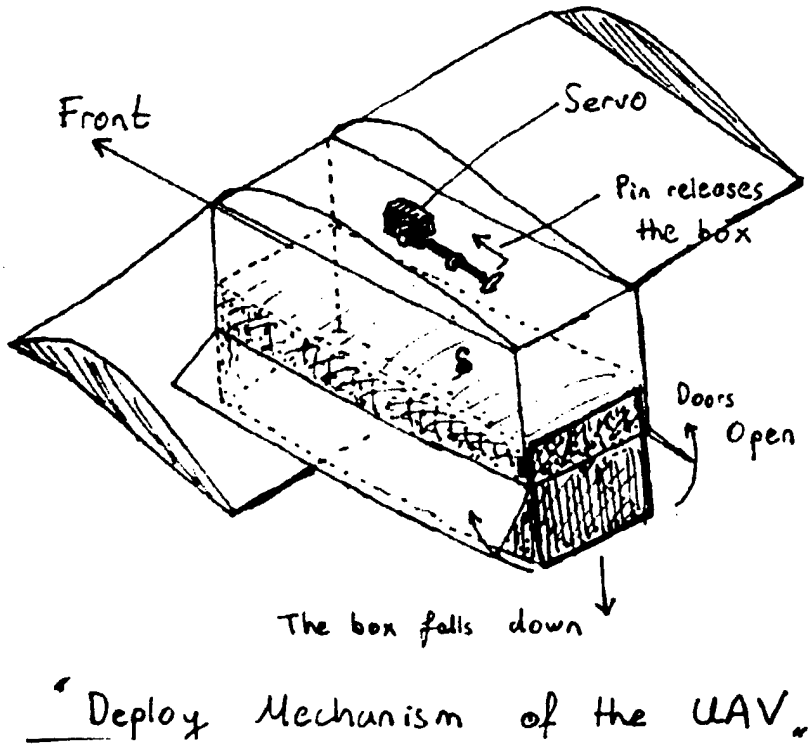

Figure 8: Deploy Mechanism

4.5.1.2. Assembly system

The box, the disassembled aircraft has to fit in, limits the length of the span. Because of this, the wing is divided into two parts. At the assembling these parts has to be fixed to the fuselage. This fixing must be very quick and junction must be very strong, because it resists the bending moment of the wing. The simplest and most common way is using tubes. There is an aluminum tube passing trough the fuselage. There are also paper tubes in the wing parts.

The empennage must be folded to fit into the box. After got out of the box it must be fixed to the fuselage. The fuselage has two wooden sticks and the tubes of the empennage are fitting these precisely. There is also a self-locking mechanism, which prevents separation on air.

The landing gear is also separated from the fuselage. Four bolds and blind nuts make the connection between these.

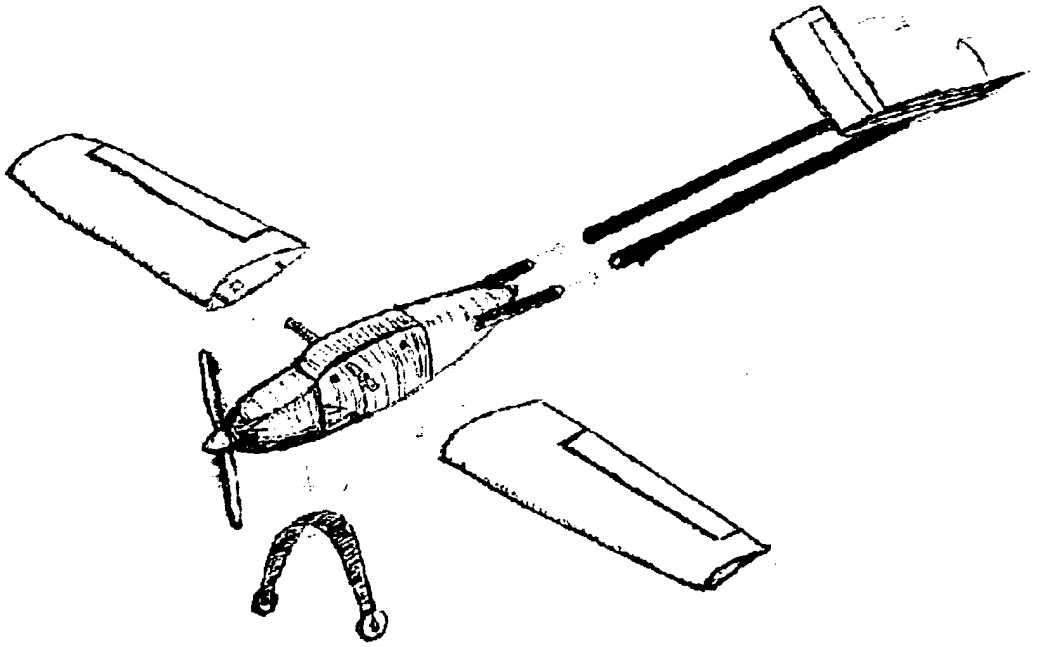

Figure 9: Assembly Mechanism

4.5.2. Fuselage and Tail Design

There are two main functions for the fuselage. One of them is carrying payload and the other one is combining wing, power plant, tail and landing gear. For the carrying function, there is no need for the fuselage to be longer than its payload. Combining other elements of airplane is also positively affected with a short fuselage, because of structural loads over it. Only stabilization effects direct to require a longer fuselage, because of the location of the empennage. Using tubes to fix the location of the empennage is a solution for a short empennage. Other effects on fuselage shape are aerodynamic forces and center of gravity. For aerodynamic reasons shape of the nose, bottom and top of the fuselage is to be curved. The slope of the coverings is limited. For center of gravity reasons the location of the motor and batteries are to be calculated and fuselage has to include those. Therefore a shape for fuselage is to be determined. Another point to consider is harmony with payload. A self deploy mechanism has to be inserted to the body and a pod for simulated antenna should be presence. The conjunction points with all other parts are to be determined and these conjunction systems should let easy assembly conditions.

4.5.3. Wing Design

Wing has three main parameters. These parameters, span, cord and taper ratio, are calculated for achieving best score. Other considerations for wings are discussed afterwards.

Parameters are calculated as fallows. Span wide is calculated as 2.2m, cord length as 0.35m and taper ratio as 0.7. These three parameters are exposing the wing area, aspect ratio on the other hand dihedral and aileron sizes are evaluated separately. An angle of dihedral is not necessary since this combination is a high wing airplane. Ailerons and flaps are assumed to be used together, since the airplane has tapered wing. There were some manufacturing ideas for the wing but these are discussed in manufacturing stages. The wing assembly is also very simple and other alternative wing designs can be tested after manufacturing.

4.5.4. Power Plant Design

The best alternative for power plant is found single motor and a battery pack of 36 with series 1500. This motor is the most powerful one in the range of alternatives and it is chosen for the need for speed. It is slightly heavier than other options but the power it can produce is more important for us. The most important parameter for this competition is battery pack choice. It is contributed in RAC calculations with its weight. So the pack should be lighter but considering the needed power number of batteries should be higher. Assuming the airplane flies fast, the battery pack is considered. The need for power is accepted as it is but the weight is reduced without reducing the number of batteries. This is achieved by using series 1500 SR batteries. These batteries are 1500mAh and their duration is shorter than others. Calculating estimated flight time let these batteries to be used, because these are not completely empty at the end of flight.

4.6. Predicted Performances

Considering these design parameters the predicted performance of the aircraft is calculated.

The times of take off, landing and cruise, which turns are also included in, are calculated for all conditions. These conditions are no load, with simulated sensor and with sensor + antenna. The results of these calculations are shown in table below.

Aircraft Condition	Speed (m/s)				Time (s)			Distance (m)	
	Stall	Takeoff	Cruise	Landing	Takeoff	Cruise	Landing	Takeoff	Landing
Empty Aircraft no load	9,76	11,71	33,52	10,74	2,73	23,65	4,03	15,96	21,64
Only With Sensor	11,38	13,66	31,20	12,52	3,89	25,03	4,23	26,56	26,47
With sensor and antenna	12,03	14,44	25,63	13,23	4,22	29,39	4,39	30,48	29,02

Table 8: Predicted Performances I

	Missions	
	Missile Decoy	Sensor Deployment
Flight Time	126,15	112,23

Table 9: Predicted Performances II

The maximum wing loading occurs in take off with full load and it is 162.4 N/m^2. The stability and control analysis are investigated in two parts. These were longitudinal and lateral directional analysis. For dynamic stability, the first order derivatives of pitching and yaw damping for level flight are calculated.

Lateral Stability	
Yawing Moment due to	
Aileron Deflection	-0,0041
Sideslip	-0,0201
Wing	-0,0503
Derivates with Respect to sideslip	
Yaw Moment.	0,0276
Pitching Moment	0,0287
Roll Moment Coefficient	-0,0014
Yaw Moment Coefficient	-0,0026

Longitudinal Stability	
Derivatives	
Pitching moment	-0,042
Wing pitching mom.	0,084
Fuselage pitching mom.	0,0031
Mom. Coef. About Cg	0,286

Damping Derivates	
Pitching damping derivates	-0,0061
Yaw damping derivates	-0,0037

Table 10: Stability Parameters

4.7. Final Preliminary Design Results

Fuselage					**Wing**			
Length (m)			2,2		Airfoil			E193MOD
Max. Width (m)			0,2		Span Length (m)			2,2
					Root Chord Length (m)			0,35
Tail					Tip Chord Length (m)			0,25
Airfoil			NACA009		Area (m2)			0,66
Span Length (m)			0,9		Incidence Angle (deg)			0
Root Chord Length (m)			0,2		Taper Ratio			0,715
Tip Chord Length (m)			0,2		Flaperon Area (m2)			0,051
Projected Horizontal Area(m2)			0,163					
Projected Vertical Area (m2)			0,076		**General**			
Taper Ratio			1		Center of Gravity location (m)			0,036
Incidence Angle (deg)			0		Maximum Weight (N)			93,195
Angle of the V			130		RAC			10970,6
Ruddervator Area (m2)			0,045		Score(written score=100)			12,1395

Table 11: Final Preliminary Design Results

5. Detail Design:

The main shape of the airplane had been formed in conceptual design phase. After that, in the preliminary design phase, according to aerodynamic performances estimated by programs and experiments, and structural calculations an optimization code is written.

In detail design phase aerodynamic and propulsion performances were tested by experiments to check previous assumptions. To do these experiments some tools were designed and were built. For the aircraft structures CAD data of the aircraft's component were prepared and some of them were tested. The materials of the main body components were selected. Also the equipments used in assemble of the aircraft were selected. Furthermore some of them were designed and built. Before the building, the whole body, some of the main components and equipments were tested. During these studies, the conformity of the items was examined continuously. At the end, to see the results of these studies and to test the prototype was begin to construct.

5.1. Design of Actual Pieces

In this part specially focused on the structural components. For the structural components, main materials were decided. As a difference to this decision, some elements were built and other was selected to conformity of the whole aircraft.

5.1.1. Propulsion System

In the detail design phase some experimental studies had done for propulsive system analysis. According to experimental studies, the final propulsion system was decided. In this section, for controlling and adapting the theoretical results obtained in preliminary phase, an experiment tool was designed and built. The final motor was assembled to a platform moving on rails, and connected to a dynamometer from back. The other propulsive system components were also located on the platform. This tool was used for experiments in wind tunnel for different flight velocities. The CAD data of the tool is below in figure below. According to outputs of several experiments, first, the final motor and propeller combination was decided and second, number of batteries required for this combination and for estimated flight conditions were selected. The output of these experiments verify the results in optimization, the motor and propeller combination was; with the motor AstroCobalt 691S with gearbox,2.75 and 24x14 propeller. Also the required number of batteries was 36. Moreover, as an output of experiments, the static thrust of the system was 5.2 kg. For the take off conditions the thrust was maximum value and for the cruise conditions the thrust was lesser.

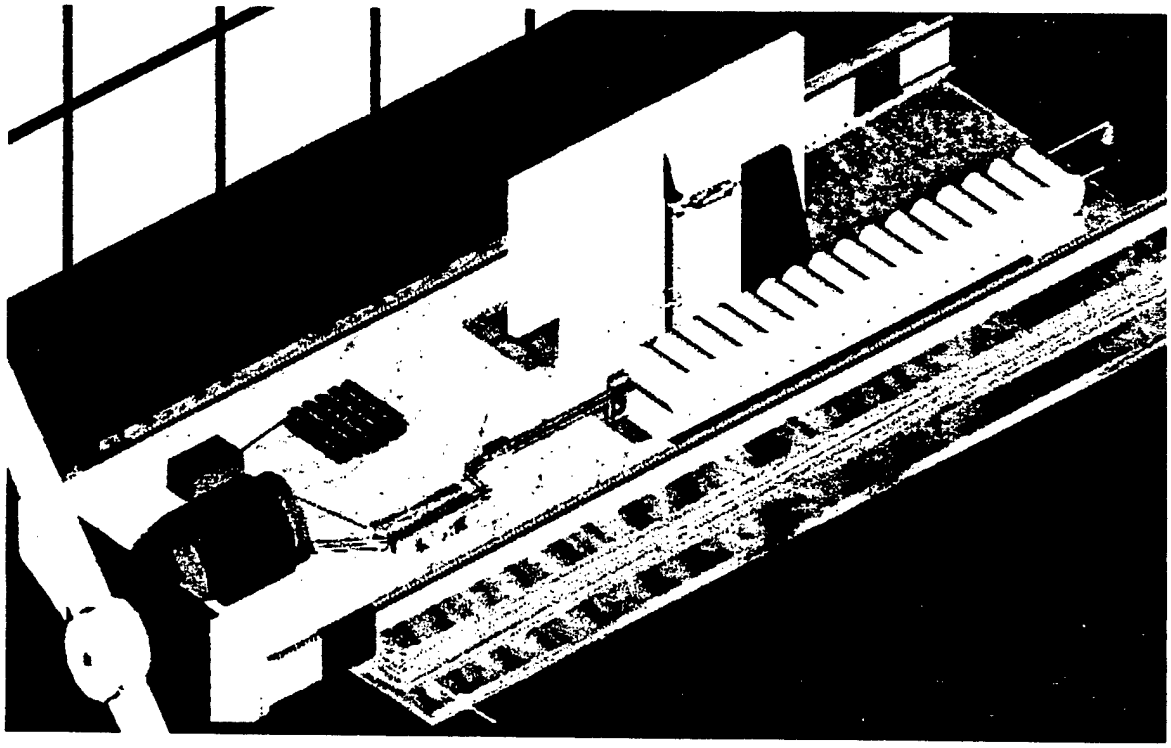

Figure 10: Trust Test System

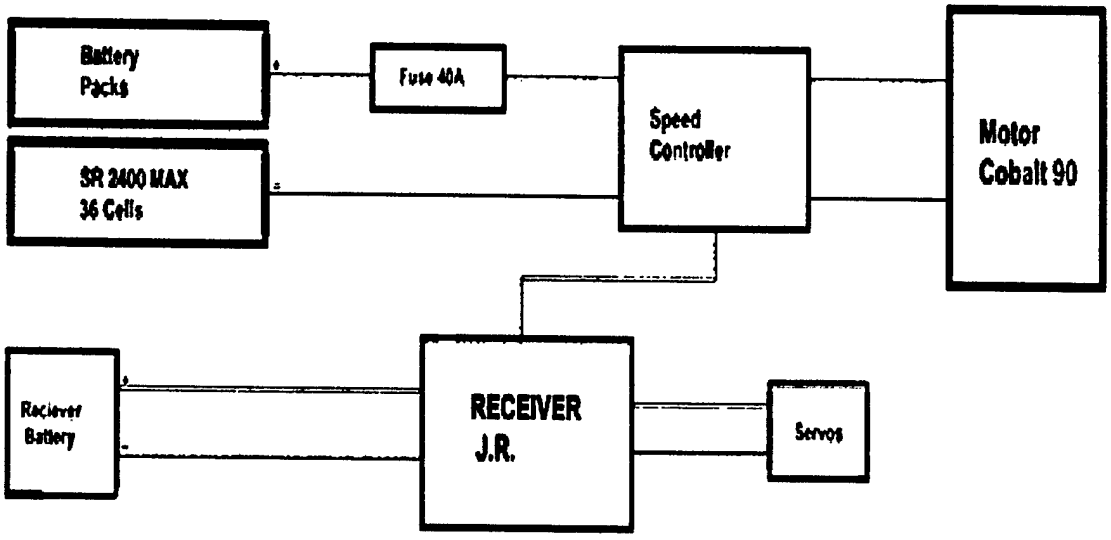

Figure 11: Electric System of the Aircraft

5.1.2. Structural System

The aim of the structural detailed design was assembling the major components of the aircraft that were wing, fuselage, and empennage group, landing gear and propulsion system in the easiest way in the shortest time. Nevertheless there wouldn't be any integration problems. Moreover the components and the conjunction point elements had to provide the transferring the static and dynamic loads without any structural problems.

5.1.3. Fuselage

A general form of the fuselage was designed in preliminary design phase, to have minimum wet surface area with considering the payload sizes. The main missions of the fuselage were to carry the payload and to be a junction element for transferring the loads from other components. The fuselage was designed to perform these two missions and also for having smooth, aerodynamically efficient surface. To have these specifications, it had two parts; first, the inner construction part and the second, outer aerodynamically efficient shell. The main goals of the inner - also can be said "main"- construction was to be a reference component for others, transferring the loads and carrying the payload package. The material of the main construction was decided to be wood. Moreover, the connection points of wings, tail, landing gear and the motor supported with the fiberglass resin. Lightening holes were decided on the whole construction. As a result of this, the main construction began nearly acting as a lattice construction.

The propulsion system deck was supported with extra, thicker wood for not to allow buckling for the reason of torsion of the propeller. The battery pack is placed in front of the payload for cg conditions. There is also a back battery compartment designed. As a result shorter cable could be used and interference the place of the center of gravity was easy by changing the number of batteries. Also for connection of the tail boom, a cylindrical wooden material placed both sides of the main fuselage construction. The wooden aerofoil shaped elements was placed on upper of the both sides. The main wing connection element was cylindrical aluminum tube. This tube is located between the aerofoil shaped elements.

The payload deploying mechanism located at the bottom of the construction as two doors. These doors were closing by the helping of spring and locked by the servo. When the aircraft wanted to deploy the payload, the servo has opened the lock and the weight of the payload opened the doors and simulated sensor was deployed.

Because payload mechanism was on the bottom of the fuselage, landing gear had to locate in front of the deploy doors. Junction materials of the landing gear were four screws having fixed nut in the fuselage. The goal of this decision is shorten the assembling time by screwing easily. The second part of the fuselage was light and smooth shells. One of these shells was placed over the propulsion system deck and the other was placed over the backside battery deck. These components were decided not to support any loads except aerodynamic loads.

5.1.4. Wing

The whole wing was designed as two parts; left and right wings. The aim of this decision was fitting the aircraft in the box specified in the rules and assembling in the minimum time. The structure of the wings decided a sandwich system. Inner part was foam. This foam was providing the aerofoil shape. The surface of the foam was plated with balsa. Balsa plates supported the static and dynamic forces and supported rigidity. Also the important mission of the balsa plates was obtaining the smooth surfaces on the wing to minimize the friction forces. Moreover to support the balsa plates over the wing, during the supporting the forces, balsa layer was cored by fiberglass. The both layer worked together and allowed the supporting forces. Also fiberglass was protecting the balsa. This kind of combination, although it was strong, allows the lightening the wings. Furthermore damaging the whole aircraft in the crash was prevented. Both wings were connected to the fuselage by the aluminum tube located on the fuselage main construction. The aluminum tube provided to insert to the hole in the foam for the junction. For providing the aluminum tube not to damage the foam insert the hole, a fiberglass tube was placed into the hole in the foam. Moreover two small pins were located on to the face of the each wing which, the wings connecting to the fuselage. The goal of these pins was prevent the rotation of the wings around the aluminum tube. For the movement of the both ailerons, small, plastic hinges were used. So that lighter and easier control surfaces were obtained. One servo for each wing is used. These will actuate flaperons. Cable holes are made for servo cables for maintenance. The servomotors are chosen as strong ones because of the size of flaperon surfaces. A self-locking assembly system for wing is designed, which locks both wing and servo cables at once.

5.1.5. Empennage

The concept of tail group consisted two parts; one of them was tail surfaces and the other was tail booms. Tail surfaces were connected to the fuselage by the tail booms. Function of the tail booms here was providing enough pitch moment length for the tail surfaces. As a result of this reason there was no need to extend the fuselage as continuous form to the tail surfaces. Only two booms were enough. This approach resulted lighten the total weight of aircraft and decreased the total friction force of the tail. According to this result strong, rigid, but also light booms had to be use.

For the connection of booms, two wooden cylindrical elements on the fuselage were used. These elements inserted the holes in the booms and screwed by two small screws. Moreover the booms were connected to tail surfaces by small apparatus. However to assembly the aircraft in shortest time, booms were fixed to the tail surfaces.

The structure of the tail surfaces was same as the wing. Again the inner foam provided the airfoil shape and balsa was plated to have smooth surface and supporting the loads. Also balsa plate was coated by fiberglass resin too. This coating worked together with the balsa to support the loads and prevent the balsa from surface deformation. Left and right tail surfaces connected each other with the hinge in one piece. As a result tail surfaces could be collapsible with fixed booms. During assembly, when the booms were connected to the fuselage the collapsed tail surfaces was separated and had design angle between each other again. For the control surfaces of tail, again the same plastic hinges were used like on the wing. For controlling the control surfaces two servo had to be

used. However, here thickness of the tail airfoils was not enough for the servos. So that the servos are placed on the booms.

5.1.6. Landing Gear

The landing gear system enclosed the main gear and the tail wheel. To have minimum drag, main landing gear junction point was located at the bottom of the fuselage. This concept yield a shorten structure. Main mission was to support the landing loads. Also the main gear had to absorb the landing loads of the aircraft. The goal of this approach was building a bit elastic gear. As a result of these, the gear had to be strong and sufficiently elastic. At the end some composite structure were used. Especially the shape of the gear was also important. Providing the elasticity also with the shape, the landing gear designed in bow shape. Four screws obtained connection of the gear to the fuselage. The nuts of the screw were fixed to the fuselage, so the gear could be connected to fuselage easily and in minimum time. Moreover two wheels were screwed to the gear. Before the start of the take off and at the end of the landing, for not loosing a time a brake system integrated to the main landing gear. Controlling of the brake system was provided by a servo. The brake servo was placed in front of the payload and its accurate position is determined regarding to cg of the airplane.

5.2. Tests of Major Items

During the detail design phase, all of the components and elements of the aircraft were designed. However some of the major component had to be built and tested. The reason for this was deciding the suitable item at the correct time. In this section mainly landing gear and wings were tested.

5.2.1. Aerodynamic Analysis

The optimization program Mission Optimizer calculated aerodynamic performances for two missions. The aim of this was to decide which mission would be selected. The general input data was obtained from the preliminary design. With these approximate data, for the each mission the performance of aircraft was obtained. Main performance criteria were velocity and time for each flight stages and also take off distance. The landing distance and time weren't considered because of using the brakes. The performance results data were used to obtain the approximate flight scores for each mission.

5.2.2. Test of Landing Gear

In the detail design the concept of the landing gear was agreed to be a composite material. However other materials were also used and tested. Four landing gear test object was built. One of them was sandwich system with inner part was foam and outer was fiberglass resin. This gear was a bit strong but its elasticity was a bit larger. The other type of landing gear was built from spring steel. Although it was strong and had suitable elasticity, the weight of that was exceeded the limitations that obtained. Third of the landing gear constructed from a carbon fiber and Kevlar. Again this kind of composite material was strong. Also its elasticity was in limitations. However, handwork was a bit difficult with the instruments that in the workshop. The last one was wooden gear. Although it was

strong and had elasticity in limitations, wood was fragile. The grades of all gear test equipments respect to the some characteristics is shown below in figure 5...

5.2.3. Test of Structure

For the structural test especially wing was tested. For the wing, mainly the supporting load capability was considered. The general approach was constructing the wings from composite. From previous experience that was known, using foam and only fiberglass for coating, doesn't have smooth surfaces. To overcome this problem, only balsa plate was used for coating and gave acceptable results. To experiment the load support capability, the test object was applied 3g load. The results of an experiment were in limitations. Moreover another test object that coated balsa plate and fiberglass over the balsa was used. According to surface quality, it was nearly same with the first object. However under the same load, behavior of the second experimental object was better.

5.3. Finalized Design Results

Geometry:	
Length (m)	2,2
Span (m)	2,2
Height (m)	0,55
Wing Area (m2)	0,66
Aspect Ratio	0,7
Control Surfaces	4

Performance:		
Clmax	1,5	
L/Dmax	12,3	
	Empty	Gross Weight
Max. Rate of Climb	10	6,2
Stall Speed (m/s)	9,76	12,3
Max. Speed (m/s)	33,52	25,63
Take-off length (m)	15,96	30,48

Weight Statement (kg)	
Airframe	3,050
Propulsion	2,724
Control	0,420
Deploy System	0,100
Payload	3,268
Empty Weight	6,294
Gross weight	9,562

Systems:	
Radio	Futaba CHP-9(PCM)
Servos	Futaba 9001 BB
Battery Conf.	36 x 1500 mAh SR
Motor	Astro Cobalt 691s
Propeller	Zinger 24 x 14
Gear ratio	2,75

Table 12: Finalized Design Results

5.4. Estimation of Rated Aircraft Cost

At the end of the detail design phase, the data from the preliminary phase improved. These improved data is shown below. According to these data estimated rated aircraft cost was formed.

Manufacturing Man Hours				
Aircraft Components	Man hours/Unit	Aircraft Parameter (Actual)	Aircraft Parameter (Transformed)	Individual Hours
Wing WBS				
Wing Span	8hr/ft	2,35m	7,71ft	61,68
Maximum exposed chord	8hr/ft	0.35m	1,15ft	9,2
Control surface	3hr/surface	2 surfaces	2 surfaces	6
Empennage WBS				
"V" tail	15hr	1 surface	1 surface	15
Fuselage WBS				
Maximum body length	10hr/ft	2,2m	7,22ft	72,2
Flight Systems WBS				
Servo/motor controller	5hr/servo	7 servos	7 servos	35
Propulsion System WBS				
Engines	5hr/engine	1 engine	1 engine	5
Propeller/fan	5hr/propeller	1 propeller	1 propeller	5
		Total Individual Hours		209,08
		Total MMH (20$/hour)		4181,6

Description	Multiplier	Aircraft Parameter (Actual)	Aircraft Parameter (Transformed)	Man Hours	RAC
Manufacturing Man Hours (MMH)	$20/hour	------	------	209.08	4181.6
Rated Engine Power (Rep)	$1500	1.632kg	3.6lb	NA	5400
Manufacturers Empty Weight (MEW)	$100	6.294kg	13.89lb	NA	1389
			Rated Aircraft Cost		10970.6

Table 13: Estimation of RAC

5.5. Drawing Package

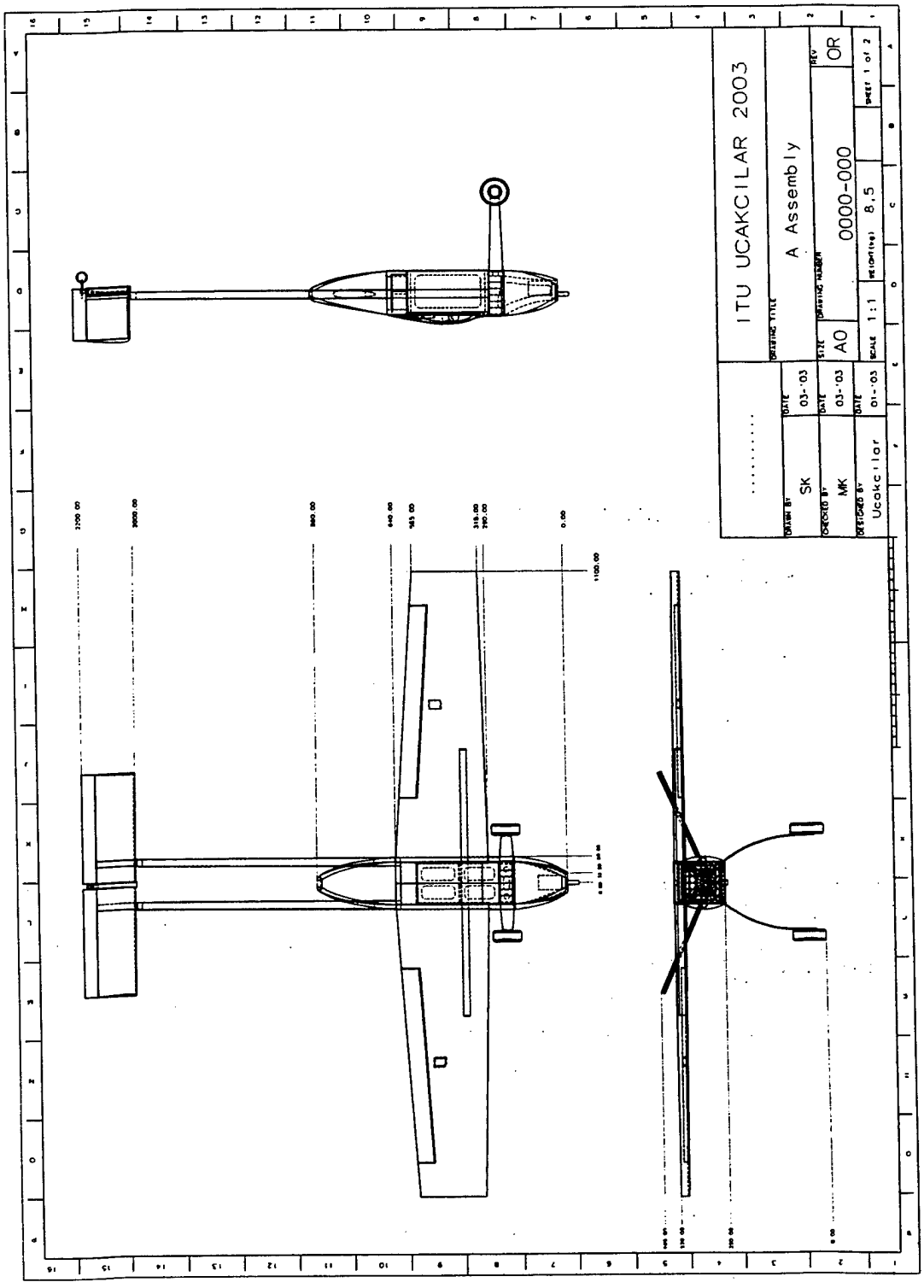

Figure 12: Drawing I

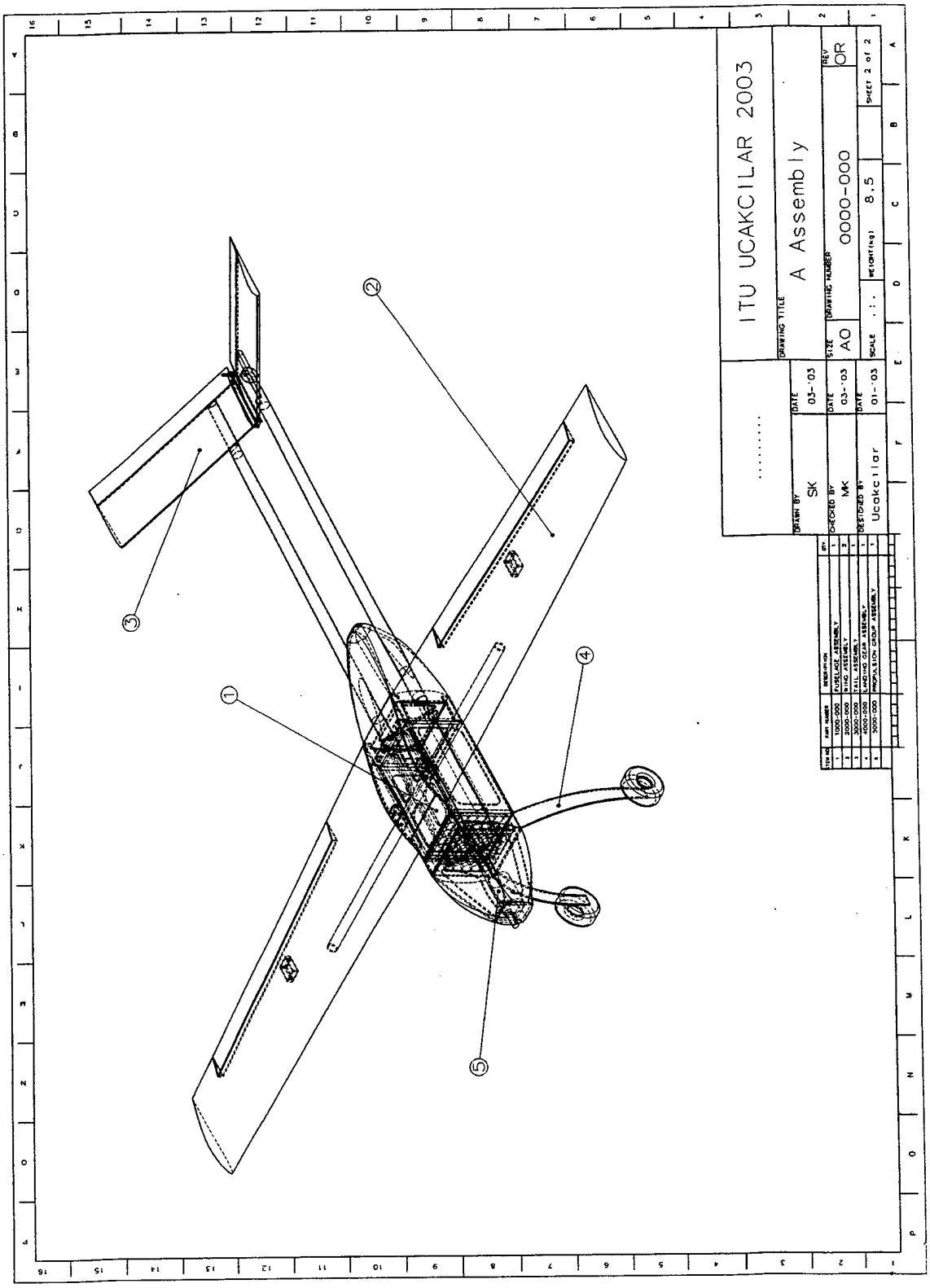

Figure 13: Drawing II

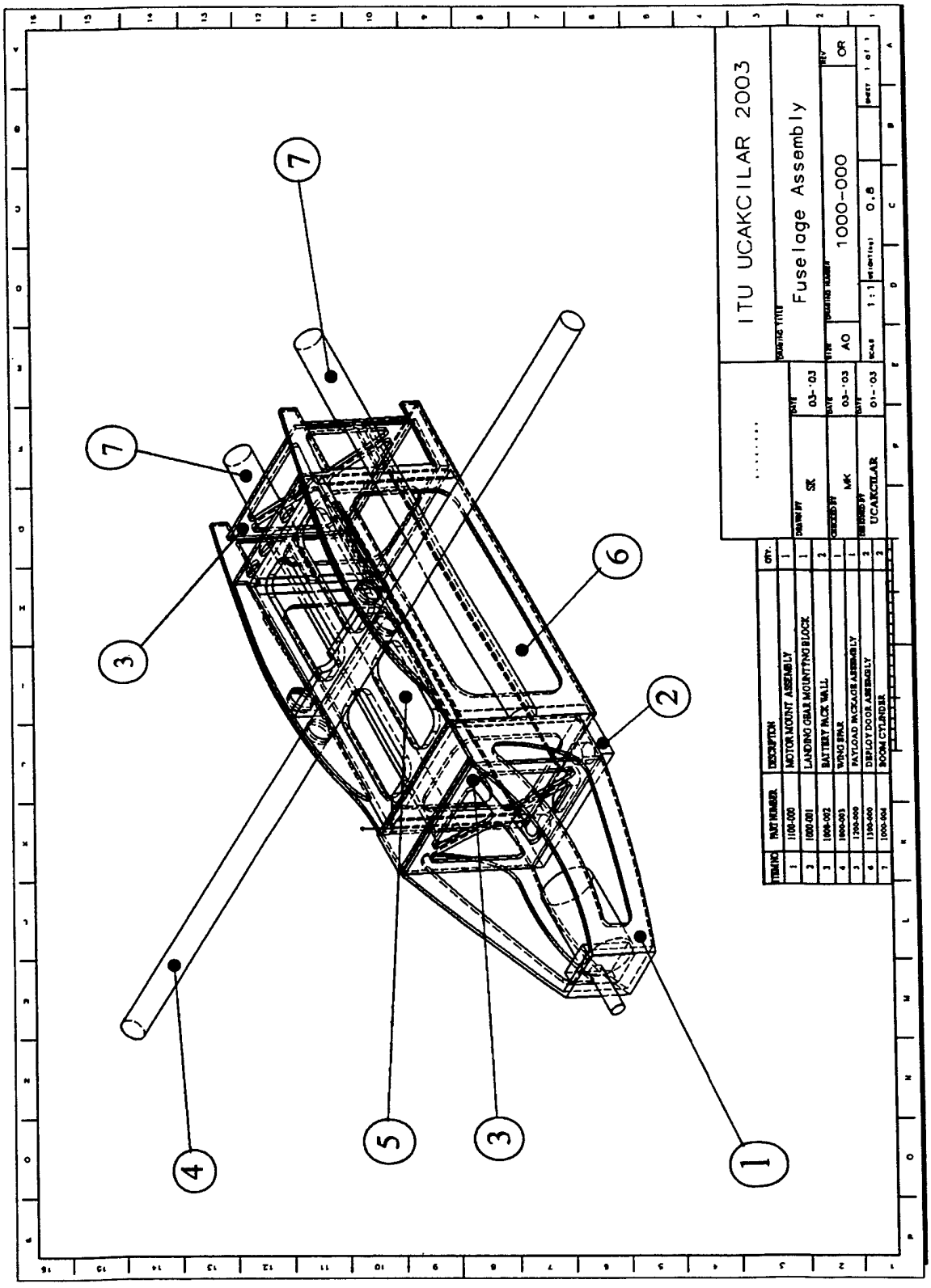

Figure 14: Drawing III

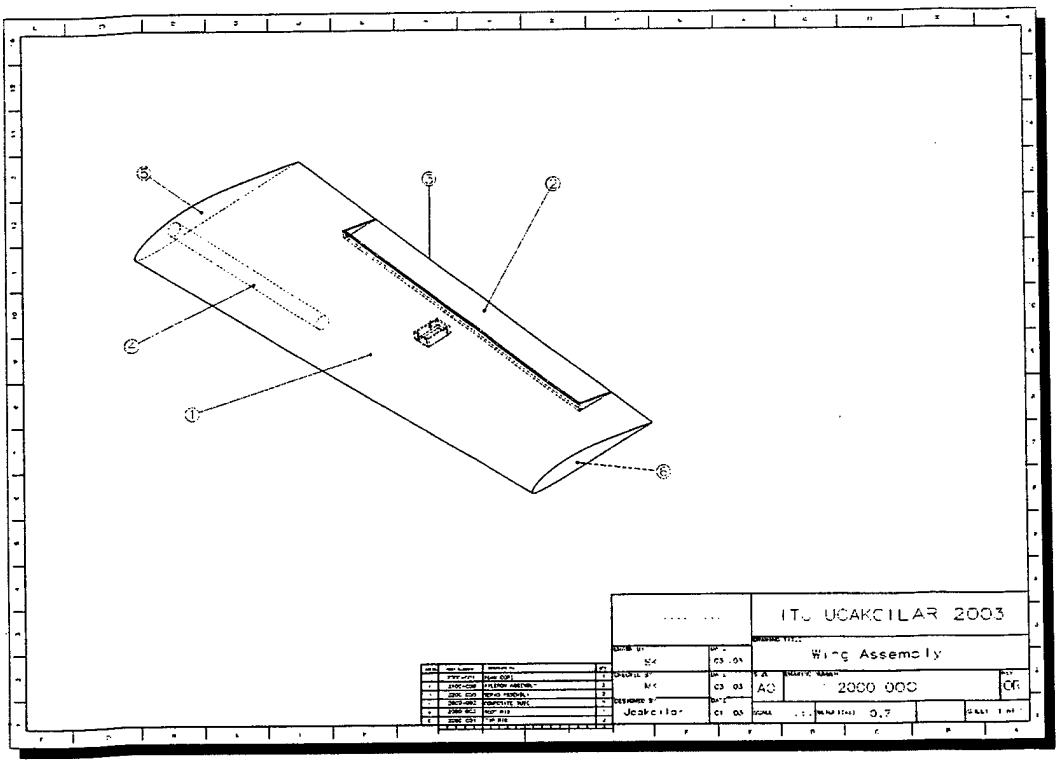

Figure 15: Drawing IV

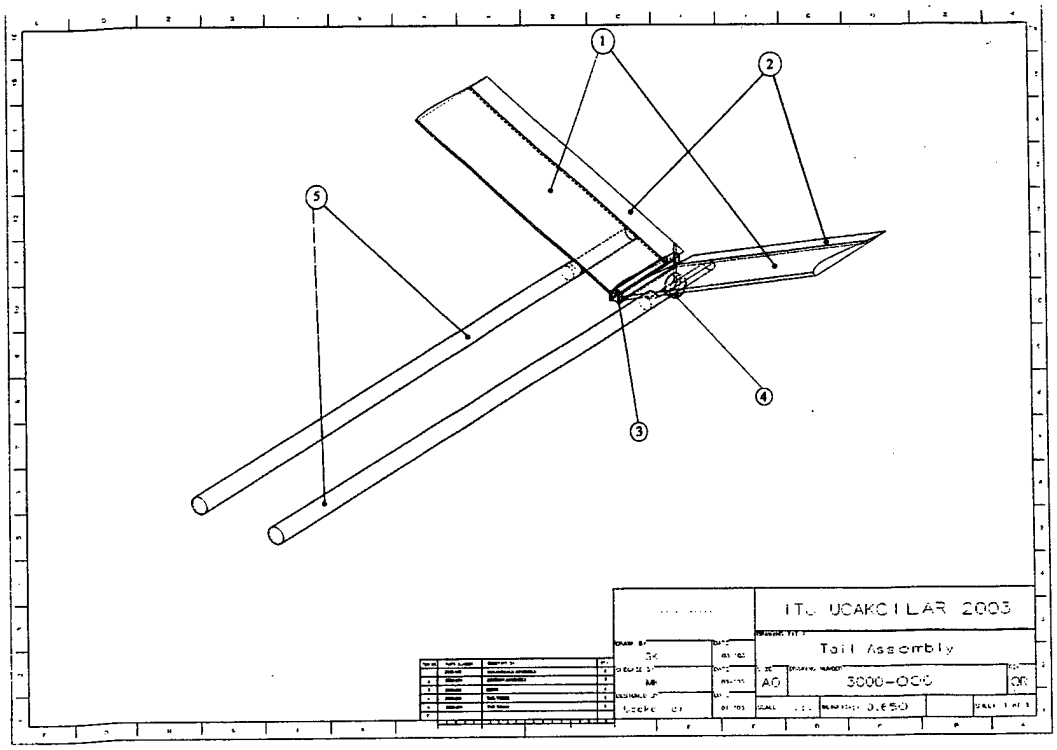

Figure 16: Drawing V

6. Manufacturing Plan and Processes:

6.1. Introduction

Design phase and manufacturing phase of the airplane are evaluated simultaneously, therefore there are less complications occurred. One of its reasons is the work of design, analysis, experiments and manufacturing is planned and done by same persons. During the brainstorm and other conceptual design step, any kind of doubt in manufacturability of a component is discussed fastidiously and the deign changed immediately

6.2. Manufacturing Process Selection Designing Tools

6.2.1. Figures of Merit

6.2.1.1. Availability:

Availability of both raw materials and specific modeling equipment was one of the biggest problems for UCAKCILAR team. It's a result of being in Istanbul – Turkey: Modeling is not a common sector in Turkey. It's not possible to find whatever is necessary for UAV. As an example we could reach only a few different types of epoxy. Thus, it becomes an obligation to produce an UAV according to the materials you reach. It seems possible to import but it gets ultimately expensive to import many things. That's why we ordered only high priority necessary or light stuff from other countries. This situation gives this FOM a special situation: If it's not available, it's not possible to use.

6.2.1.2. Cost:

As we mentioned above, modeling stuff in Turkey is hardly found. And when it's found, it's too expensive (more than 100%). Moreover; most of the prizes are fixed to $ in the market. Those two situations become very important especially because of the nonexistence of the required sponsors.

6.2.1.3. Strength:

Strength of materials is various and a decision has to make. The relation of material weight and strength are very important. Another factor is materials interaction, where more than one type is used. Considering using composite materials these factors are more evident. This is a very important Figure of Merit for all decisions.

6.2.1.4. Weight:

It is obvious that weight is significantly important in aviation. In this competition, it becomes more and more important. Unnecessary weight not only increases the RAC, but also it reduces the flight score. For this reason Ucakcilar spent great effort in reducing the aircraft's empty weight.

6.2.1.5. Required Manufacturing Time:

This year UCAKCILAR decided to try some manufacturing techniques, which are new for us. Nevertheless, manufacturing techniques, which requires too much time, isn't suitable even to be tried.

Instead of spending time on long processes, we tried several short ones. Also, reserves of all parts of the final design should have produced before the competition. Some part could have broken during the final flying tests too. By personal experience we knew the manufacturing schedule could have some delays. That's why we preferred to design a fast building UAV.

6.2.1.6. Required Skill Level:

Experience in manufacturing is not a quantitative specification but has significance in construction. The raw materials are not always homogenous, their specifications have minor differences. These cause miscalculation in design phase and results as problems in manufacturing. An experienced manufacturer has to find a solution in these cases. It is also hard to work with a new material. Some exercises have to be done before manufacturing the actual piece. Some of manufacturing phases require more experience than others.

6.2.1.7. Repair ability:

Accidents may happen any time. Sometimes wrecked parts can be replaced, but it's an insufficient method in the meaning of cost and time. Besides, some parts cannot be removed during the competition. So the chosen material should be available to be fixed easily and without too much extra weight. Also parts should be designed which makes it hard to break down and easy to repair.

6.2.1.8. Manufacture Flexibility:

As we explained in the management part, different tasks will affect the final design. It means the design of any part may be needed to be modified. The table below shows the scores of all manufacturing processes we considered. In scoring, the advantage of the process increases from 0 to 5. Some FOM's are much more important then the other for this project. In order to make this difference effective, we multiplied their marks by two. These are strength, weight and req. man. time.

UAV PART	MANUFACTURING METHOD	AVAILABLITY	COST	STRENGTH x2	WEIGHT x 2	REQ: TIME x 2	REQ: SKILL LEVEL	REPAIRIBILITY	MAN. FLEXIBILITY	OVER ALL
WING & TAIL CORE	White polyethylene 10kg/m^3	5	5	1	5	3	3	2	4	3,4
	White polyethylene 15 kg/m^3	5	5	2	4	4	4	3	4	3,7
	White polyethylene 20 kg/m^3	**5**	**5**	**4**	**3**	**4**	**5**	**3**	**4**	**4,0**
	White polyethylene 25 kg/m^3	5	4	4	2	4	5	3	4	3,7
	DOW type Foam 28kg/m^3	0	4	5	2	4	5	4	5	3,6
WING & TAIL COVER	Balsa Sheet	5	5	2	5	4	5	3	3	3,9
	Balsa Sheet + 25g/m^2 glass fiber	0	3	4	5	3	5	2	4	3,5
	Balsa sheet + 45g/m^2 glass fiber	**5**	**4**	**5**	**4**	**3**	**5**	**3**	**4**	**4,1**
	Balsa sheet + 135g/m^2 glass fiber	5	5	5	1	3	5	3	4	3,6
	25g/m^2 glass fiber	0	3	2	5	4	3	3	4	3,2
	45g/m^2 glass fiber	4	3	3	4	4	4	4	4	3,7
	135g/m^2 glass fiber	5	4	4	2	4	5	4	4	3,8
WING & TAIL	Construction	5	5	3	2	1	4	1	2	2,6
FUSELAGE & MOTOR MOULD	Foam with fiberglass cover	5	4	3	2	2	3	4	4	3,3
	Plywood construction	**4**	**5**	**4**	**3**	**4**	**4**	**4**	**4**	**3,9**
	Balsa construction	4	4	3	4	4	4	3	4	3,7
NOSE & BACK	Foam with no cover	5	5	1	4	4	4	1	3	3,3
	Foam with fiber cover	5	4	5	2	3	4	4	3	3,6
	Mold preparation	**5**	**5**	**4**	**5**	**5**	**4**	**3**	**4**	**4,5**
LANDING GEAR	DurAliminium	1	2	4	2	2	2	1	2	2,2
	Glass fiber	3	3	3	1	5	4	4	4	3,3
	Glass fiber + Carbon fiber	3	3	4	3	5	3	3	4	3,6
	Carbon fiber	5	4	5	4	5	4	3	4	4,4
	Aramid Fiber + Carbon fiber	**5**	**5**	**5**	**5**	**5**	**4**	**3**	**4**	**4,6**
	Steel	4	5	3	0	3	3	4	4	2,9

Table 14: Manufacturing Method Decision Matrix

6.3. Manufacturing Method

6.3.1. Wing & Tail:

Once the wing is design as two parts, a spar, which connects wings and the fuselage together, got necessary. It meant the wing's structure didn't have to carry most of the loadings. So, the weight got more important because the strength FOM has lost its priority.

As shown in the table, construction wing needs too much time and doesn't have any advantage versus foam-core wings. So, the problem was to chose the best core-cover configuration. The lowest density foams wasn't suitable because they wear out too easy when sanding and they emission too much epoxy. Med-density DOW foam would be an alternative, if it's possible to find some. As a result, 20kg/m^3 white polyethylene foam was the best choice.

The balsa cover provided a better surface quality then only fiber covers. However, balsa sheets wouldn't be strong enough. But a thin fiber coating over a balsa sheet layer could give both good surface and good strength. Also, fiber cover was able to be painted, while balsa had to be covered only by film.

We used hot-wire cutting process to give the shape to the wing. However, the tools we had were hand controlled (not cnc) devices and it resulted bad quality in leading and trailing edge. Adding these parts balsa wood and sanding them resulted a good surface quality, low tolerance and more strong structure – balsa acted as a second and third spar). This well-known system was used.

6.3.2. Fuselage & Motor mount:

The fuselage and the motor mould were designed as mono-block. This kind of construction was more rigid and easier. Balsa could be used, but it needed to be strengthened by fiberglass coating. Besides, screws cannot be attached to balsa well. Fuselage pieces were cut from a plywood sheet and attached to each other with epoxy. To provide more strength, we also bonded L- shaped bars to the major inner corners. An other item to strengthen the body was coating the motor mount part with fiberglass. Two wooden cylinders were bonded to the sides of the fuselage. They are the junction points of the empennage and they also provide more stiffness to the body.

6.3.3. Fuselage Nose & Back

Both nose and back of the fuselage was going to be under only aerodynamic loads and may be simple crashes. A block of foam is shaped by hot-wire and hand sanding. This was a long procedure resulting a good shape but a slender part: a little crash would corrupt it. Laying up fiberglass on the foam would be extra strong but too heavy. That's why we considered to use molding. A thin skin cover was going to light and strong. Also getting a new product would be a fat process. A plaster mould decreases the expense of the mould. Besides, a plaster mould result faster then a composite one.

The formed foam covered by a few layers of fiberglass and polished in order to produce the male model. It was plunged into a bucked full of plaster. The female mould was made. Two layers of fiberglass and epoxy applied into the mould. A bag filled with water is put into the mould for pressure.

6.3.4. Landing Gear

The landing gear has two missions: To preserve the propeller from touching ground – even when the plain touches down hard – and to emission the shock of the touchdown. These require a long stiff but not too stiff landing gear. It's hard to produce such gear light and it was the biggest manufacturing problem of the past ITU teams. Firstly we planned a gear of bended Dur-Aluminum profile, but it's not available for a while. Then we routed to glass-fiber gear with or without a wooden core. Fortunately we got some uni-directional Aramid and carbon fibers from our sponsor for free. Such a landing gear would afford desired stiffness with a quiet low weight.

We shaped a 7-cm wide male mould by hot-wire. We lay-up the fibers with epoxy, carbon at the outer and the Aramid in the middle. Product was stronger then we needed. So we thinned and shaped the gear until it got the desired stiffness. It resulted much more lighter then the planned Dur-Aluminum one, so we omit that plan.

6.4. Schedule

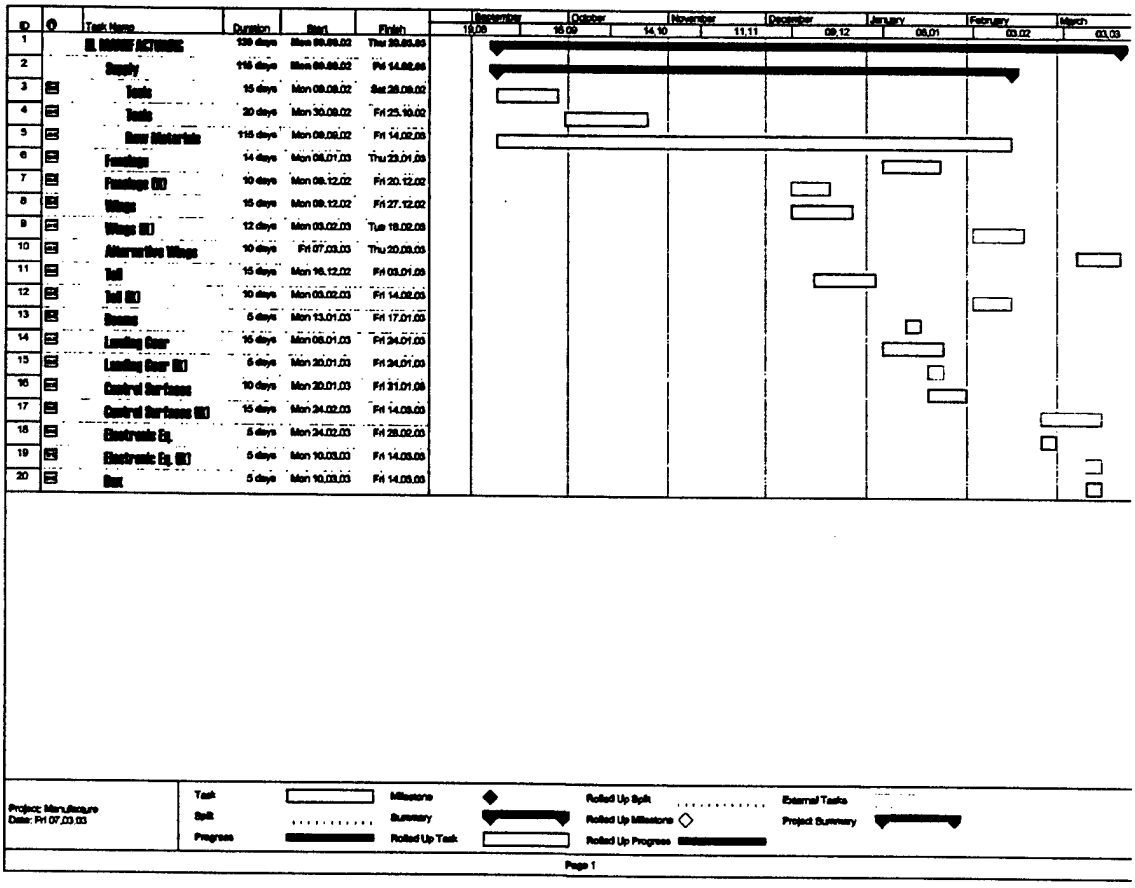

Figure 17: Manufacturing Schedule

7. Testing Plan:

7.1. Detail testing objectives

The performance of the actual components of airplane and itself are calculated and some parts are tested. Component test are maid during detail design and manufacturing, but all mechanism together has to be tested as soon as airplane is completed. Therefore some test procedures are intended.

7.1.1. Static Tests

These test are to be made before flight to check if the airplane is manufactured as it's planned, all components are strong enough and work properly.

7.1.1.1. G- Load Test

A g-load test is necessary as soon as a prototype is produced and this is also an obligation of contest rules. According to these rules, all airplanes have to be strong enough to stay undamaged over a load of 2.5 g. Lifting the airplane at each wing tip makes this test. For our turning maneuver the needed load factor is 4, so an extension to experiment has to be made. The airplane is set upside down and small marble pieces are put on the wing to simulate the air pressure, which comes in question in this load factor.

7.1.1.2. Cg Location Test

Another test is for determining cg location is also necessary to find out any miscalculations or wrong manufacture and a calibration is to be done. The cg has to locate in the designed point, in order to prevent any displacement of center of gravity in various payload combinations. A displacement of the cg from its designed location will cause stability problems.

7.1.1.3. Landing Gear Test

The airplane has to resist harsh landings. The maximum load for the landing gear is defined as 5 g. in this test the landing gear is loaded with 45 kg.

7.1.1.4. Assembly Test

A test for assembly is prepared. The joining pieces have to fit without any problem. The servo cables don't have any contact problem after assembly. The assembly time is also an important parameter for flight and it is also measured.

7.1.2. Flight Tests

The flight tests are done to determine the real flight performance of the aircraft. In this tests, takeoff time, takeoff distance, cruise time, landing time, landing distance, endurance of the batteries, maximum speed and minimum speed are to be measured. Flying a known distance and measuring the flight time will determine the speed.

7.2. Schedules

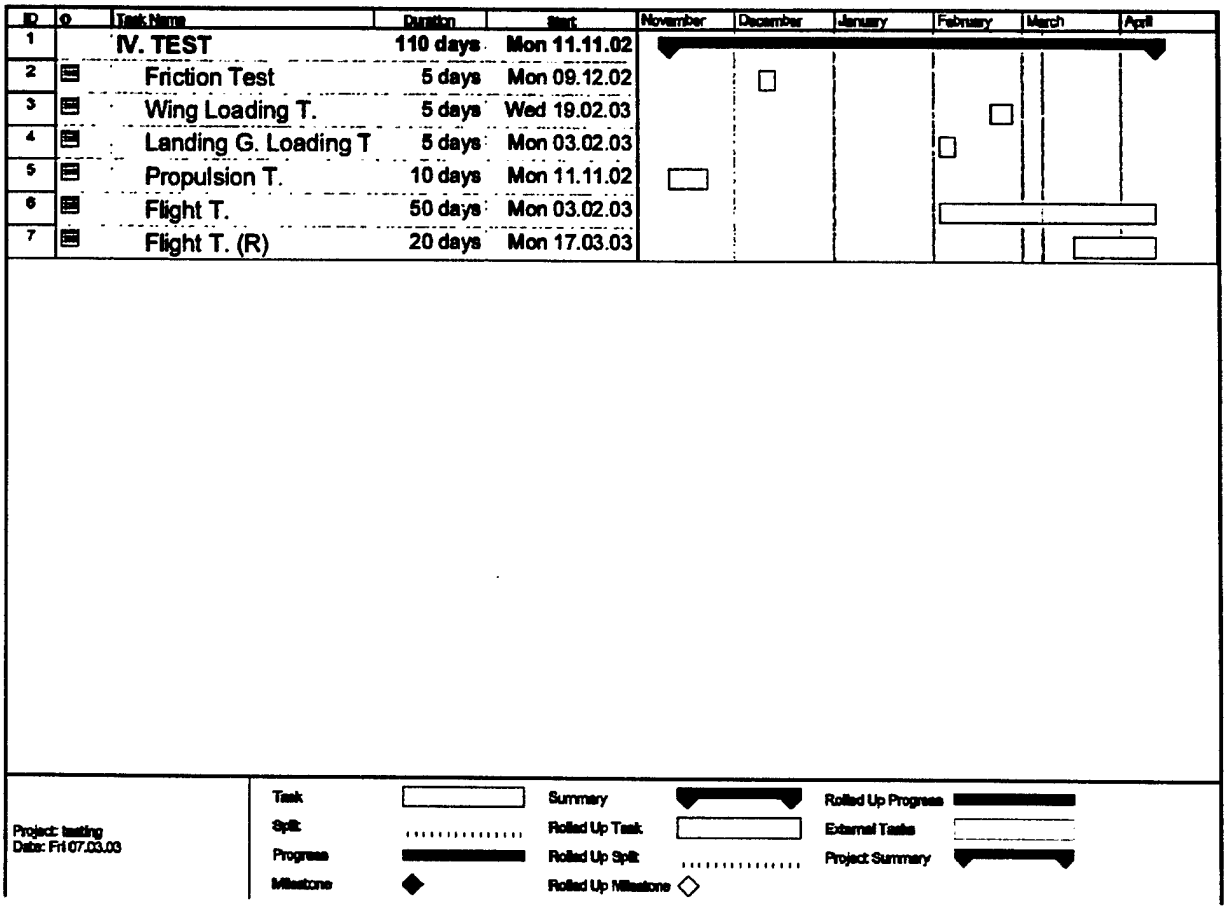

Figure 18: Test Schedule

7.3. Checklists

Two checklists are papered for assembly and flight.

7.3.1. Assembly Check List

Assembly Check List	response	check
open box	ok	
take tail	ok	
take landing gear	ok	
take fuselage	ok	
unfold tail	ok	
plug landing to fuse	ok	
plug tail to fuse	ok	
take wing right and tube	ok	
take wing left	ok	
plug right to fuse	ok	
plug left to fuse	ok	
Done	done	

Table 15: Yellow Checklist

7.3.2. The Flight Checklist

Flight Check List	response	check
Check junction	checked	
Transmitter	opened	
Check program	ucak	
Receiver	opened	
Right Aileron	right	
Left Aileron	left	
Flaps half	half	
Flaps full	full	
Rudder right	right	
Rudder left	left	
Elevator up	up	
Elevator down	down	
Fuse	affixed	
Thrust full	full	
Brake	ok	
Deploy	ok	

Table 16: Green Checklist

7.4. Results

After the g-load test we see that the wings are strong enough and the structural design and the manufacturing process were successful. Landing gear test proved us our final landing gear could resist to a load of 45 kg (441.5 N). Assembly, Cg- location and flight tests could not be done because of the manufacturing delays caused by bureaucratic difficulties.

8. Conclusion

The period between May 2002 to March 2003 was tiring and amusing at the same time. We have experienced many things from manufacturing details to bureaucracy. As designers and manufacturers of an unmanned air vehicle, we are now ready to design and build more sophisticated aircrafts. At the end, we believe that we designed and built a very appropriate airplane. At the fly-off in April we'll have the chance to compare our airplane with the others and to see if we are right.

9. References

Asselin, M., *An Introduction to Aircraft Performance,* American Institute of Aeronautics and Astronautics, Reston, Va, 1997

Anderson, J. D., *Aircraft performance and design,* WCB/McGraw-Hill, Boston, 1999.

Anderson, J. D., *Fundamentals of aerodynamics,* McGraw-Hill, Boston, 2001

Etkin, B., Lloyd D. R., *Dynamics of flight : stability and control,* John Wiley and Sons, New York,1982

Hacker, T., *Flight stability and control,* American Elsevier, New York, 1970.

Megson, T. H. G., *Aircraft structures for engineering students,* Edward Arnold, London,1999

Nelson, R. C., *Flight stability and automatic control,* McGraw-Hill, New York, 1989

Pamadi, B. N., *Performance, stability, dynamics, and control of airplanes,* American Institute of Aeronautics and Astronautic, Reston, VA, 1998.

Perry, D.J.,.Azar J.J., tr. Tolun S, *Uçak yapıları*, Anadolu Universitesi, Eskişehir, 1991

Raymer, D.P., *Aircraft Design: A Conceptual Approach,* American Institute of Aeronautics and Astronautics, Washington, 1992.

Chambana Belle

Final Design Report

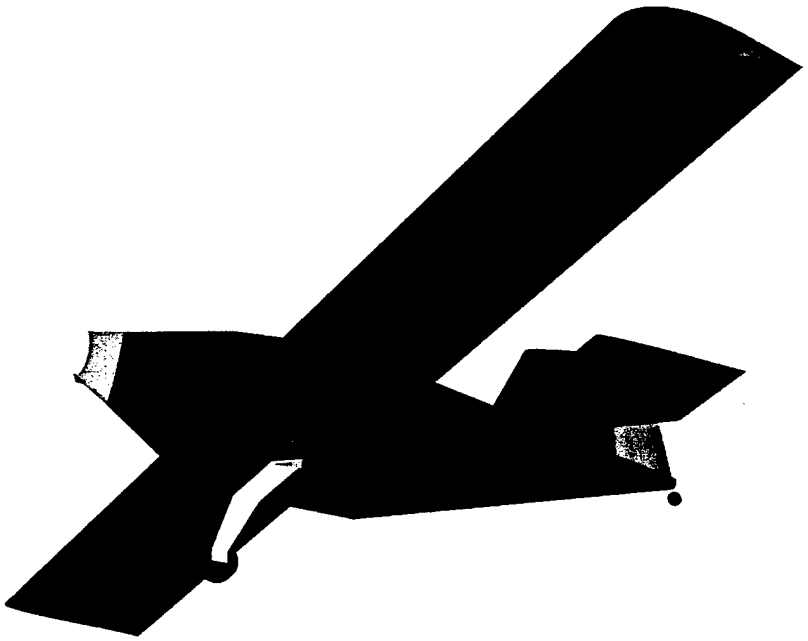

AIAA Design/Build/Fly Competition

Webster Field, Navy Patuxent River Flight Test Center Complex
St. Inigos, Maryland

Submitted by

Department of Aeronautical and Astronautical Engineering
University of Illinois at Urbana-Champaign

on

March 11, 2003

University of Illinois Project Team

Edward A. Whalen
Project Manager

Jeremy M. Sebens
Chief Design Engineer

Christopher M. LaMarre
Chief Manufacturing Engineer

Geoffrey C. Bower
Chief Manufacturing Engineer

Joseph W. Zimmerman

Karl R. Klingebiel

Sung Hyun Kim

Michael J. Koob

Ethan S. Chew

Keven J. Joye

Dr. Kenneth R. Sivier
Faculty Advisor

Dr. Andy P. Broeren
Staff Advisor

Jason M. Merret
Graduate Advisor

Mike Cross
Jeremy Sebens
Pilots

Acknowledgements

Several sources contributed to the success of this year's team and we would like to acknowledge their help and express our appreciation. We thank Jim Schmidt and Hobbico, Inc. for their continued and incomparable support through their generous donation of building materials, tools, supplies, and pilots. Thanks go to Mike and AnnMarie Cross for their donation of time and their skills. Our continued success would not be possible without these great pilots. We would also like to thank Professor Michael Bragg and the department of Aeronautical and Astronautical Engineering for providing space for a workshop and monetary support. We express thanks to the College of Engineering at the University of Illinois at Urbana-Champaign, the Illinois section of the AIAA, and AIAA Region III for their continued financial support. We would also like to thank the University of Illinois SORF Board for its financial assistance.

Finally, we are indebted to our advisors for their encouragement, suggestions, and assistance in operation. We thank Dr. Andy Broeren and Jason Merret for taking the time to assist different subgroups in their work. Above all, we would like to thank Professor Kenneth Sivier for his continued involvement. Our deepest gratitude goes to him for his continued guidance and endless encouragement.

Table of Contents

1.0 Executive Summary 1
2.0 Management Summary 2
3.0 Prototype Aircraft 5
3.1 Prototype Design 5
3.1.1 Configuration Selection 5
3.1.2 Prototype Component Design 6
3.1.3 Materials and Construction 7
3.2 Prototype Testing 9
3.3 Lessons Learned 10
4.0 Conceptual Design 11
5.0 Preliminary Design 15
5.1 Weight Model 15
5.2 Wing Sizing 15
5.3 Motor Selection 17
5.4 Stability and Control 18
5.5 Fuselage Length Study 19
5.6 Payload Deployment 20
6.0 Detail Design 22
6.1 Performance 22
6.2 Aerodynamics 26
6.2.1 Airfoil Selection 26
6.2.2 Wing Detailed Design 26
6.2.3 Total Airplane Aerodynamic Results 27
6.3 Propulsion 33
6.3.1 Motor Selection 33
6.3.2 Propeller Selection 34
6.3.3 Battery Selection 34
6.4 Stability and Control 36
6.4.1 Weight and Balance 38
6.5 Structures 39
6.5.1 Spar Sizing 39
6.5.2 Wing and Empennage 40
6.5.3 Fuselage 40
6.5.4 Landing Gear 42
6.6 Final Airplane Design 42
7.0 Manufacturing Plan 48
7.1 Manufacturing Techniques Available 48
7.2 Major Airplane Components Construction 48

7.3 Airplane Assembly 49
7.4 Payload Deployment 49
7.5 Construction Method Selection andFigures of Merit 49
8.0 Manufacturing Processes 54
8.1 Fuselage 54
8.2 Wing and Empennage 54
9.0 Testing Plan 55
References 56

1.0 Executive Summary

This report presents the design process and results of the University of Illinois' entry for the seventh annual AIAA Student Design/Build/Fly Competition. The final design, Chambana Belle, was the result of detailed aerodynamic, performance, and structural analysis. The processes discussed in this report were based on experimental data as well as analytical data and numerical modeling. The airplane was designed to satisfy all of the competition requirements, including all three missions, while maximizing the total competition score.

The design process involved both a prototype and a competition airplane. The prototype airplane was designed as a concept demonstrator and test bed. It was necessary to build a prototype because there were multiple new mission requirements that required experimental investigation. The results of the prototype testing had a significant effect on the final design, altering the philosophy of the design process as a whole. The initial goal of focusing on minimizing the assembly time was found to result in unacceptable performance degradation. Therefore, the design of the competition airplane focused on reexamining what were the greatest contributors to the competition score and how best to maximize it.

Chambana Belle satisfies all of the requirements set forth by the 2002/2003 Rules and Design Specifications. During the design process the team determined that flying the Missile Decoy and Sensor Missions maximized the competition score. Chambana Belle is expected to complete the Missile Decoy Mission in 130.8 seconds and the Sensor Mission in 130.1 seconds. It also is expected that the assembly time will be less than 20 seconds.

The University of Illinois team is proud to submit this design for the 2002/2003 AIAA Design/Build/Fly Competition.

2.0 Management Summary

This year's DBF team went through a major management change midway through the design process. The change was made due to the relatively small number of students participating and the fact that once the Spring semester began, the competition airplane needed to be designed and built in only three months. Both the management structure and ideology were altered by this change, with spectacular results. Participation increased, including the addition of new members, and productivity skyrocketed. The team was able to meet or exceed all deadlines (Table 2.1) established by the new management plan and, in the process, produced an excellent competition airplane.

The management structure was changed so that there was a veteran team member heading up each major component of the team. A Project Manager, Chief Design Engineer and two Chief Manufacturing Engineers were appointed. The duties of these positions are further explained in Table 2.2. Structuring the management in this way allowed decisions to be made rapidly and streamlined communications between the design and construction team departments. This also left the project manager free to oversee the team and keep the project on track. Other members of the team were assigned design tasks and reported results to the Chief Design Engineer. All team members also contributed to the building process.

Table 2.1 Deadline Calendar

Date	Action	Remarks
January 10th	Configuration Freeze	Basic configuration, layout and general building techniques selected.
January 25th	Preliminary Design Freeze	Sizing of airplane, internal layout and performance prediction complete. No going back, unless a failure mode is discovered.
February 20th	Detailed Design Freeze	Component selection, detailed part design and final manufacturing plan complete. Parts manufacture should begin before this date with approval from executive committee.
March 1st	Report Draft Complete	
March 9th	Final Report Mailed	
March 31st	Flight Test Deadline	First flight should occur no later than this date.

Table 2.2 Leadership Structure

Position	Description	Duties
Project Manager Ed Whalen	Holds ultimate responsibility for team operation and decision making.	Recruitment, budgeting, external relations, participation, oversees engineering staff, keeps design on track, report completion.
Chief Design Engineer Jeremy Sebens	Concerned with big picture. Manages the airplane design.	Assigns tasks, signs off on designs, creates engineering drawings, coordinates with manufacturing, completes any unfinished tasks.
Chief Manufacturing Engineers Geoff Bower Chris LaMarre	Responsible for getting the airplane built.	Schedules work, modifies parts if necessary, approves parts for integration.

3.0 Prototype Airplane

New and unfamiliar mission requirements led to the decision to design and build a prototype airplane. The impact of the radome on performance and stability could be estimated, but its overall effect on handling qualities required a flight test. Furthermore, releasing the payload from the airplane was a challenge that required, at the very least, a model of the payload bay and release mechanism. Finally, the size restriction initially led to plans for a substantially smaller airplane than had been built in the previous years. Battery packs with fewer cells and lower capacity as well as a direct drive propulsion systems seemed feasible, but were mostly untested and outside the design experience of the team.

3.1 Prototype Design

An important first step in the design process was to establish a design philosophy. Minimizing weight and assembly time were the primary design drivers. Low weight is always a focus of the team, but the addition of the assembly time requirement created a scoring variable that could be nearly eliminated by careful design. Therefore, the prototype design effort focused on creating an airplane that could fit in the "box" in the minimum number of pieces, preferably in only one piece. Beyond that the goal was to take advantage of each weight saving feature afforded by a smaller airplane (i.e. fewer batteries, smaller motor, etc.).

3.1.1 Configuration Selection

Candidate configurations were selected during the summer so that those members available during the break could begin the design process early. Two configurations were chosen as candidates for the prototype design. The first candidate was a flying wing configuration. The flying wing would be less efficient aerodynamically than a conventional airplane, because it would operate at a lower L/D. However, it offered the possibility of fitting in the box fully assembled. The characteristically low C_{Lmax} of flying wing designs made the takeoff constraint difficult to satisfy. Other concerns included sufficient ground clearance to deploy the payload, whether to incorporate vertical surfaces and propeller clearance for a pusher design. The second configuration was a conventional one. The conventional configuration had to be at least a two-piece airplane. In order to minimize the assembly time, it was desired that this configuration have only two subassemblies. These could consist of a wing/fuselage subassembly and a tail subassembly or a wing subassembly and a fuselage/tail subassembly.

A rudimentary drag buildup was performed for the two configurations. Propulsion systems were then chosen. Both configurations used the Astroflight 60 motor, but used different gear ratios and propellers. Due to the lower C_{Lmax} of the flying wing design, it required more takeoff thrust than the conventional design. To achieve more thrust and maintain comparable power a lower pitch and higher diameter propeller was used. Because of this it had less thrust at high speed and was much slower. The lower rated cost of the flying wing was outweighed by its higher mission time. Therefore a conventional configuration was chosen for the prototype design.

3.1.2 Prototype Component Design

Once a conventional configuration was chosen for the prototype, the details of the design were determined. The prototype was designed to test assembly techniques, payload deployment mechanisms and the flying qualities of a small airplane. In order to test assembly techniques, the prototype disassembled into three subassemblies: wing, tail, and fuselage. This allowed for either of the two aforementioned combinations of subassemblies: a wing/fuselage and a tail or a wing and a tail/fuselage. Each of these subassembly combinations fit within the prescribed box.

The main wing was designed using a low drag S8036 airfoil because it provided the required C_{Lmax} to meet the takeoff distance requirement. An Astroflight 60 direct drive system was incorporated into the prototype because it was capable of providing the required takeoff thrust, while also achieving a higher top speed than a geared system. The batteries used were 1300mAh Sanyo CP's. The horizontal tail was sized using tail volume coefficients and the incidence angle was set using a cruise trim calculation. All control surfaces on the airplane were sized on a percentage basis from established conventions. A photograph of the prototype is included as Fig. 3.1. Performance estimates revealed promising numbers that indicated that the two piece airplane was actually possible. (Table 3.1) The true test was in the flight tests that followed.

Table 3.1 Estimated Prototype Performance

Mission	Takeoff (ft.)	Time (s)	Energy (mAh)
Sensor	112.3	126.5	826
Missile Decoy	121.5	133.94	978.68
Communications	112.3	171.34	1255.43

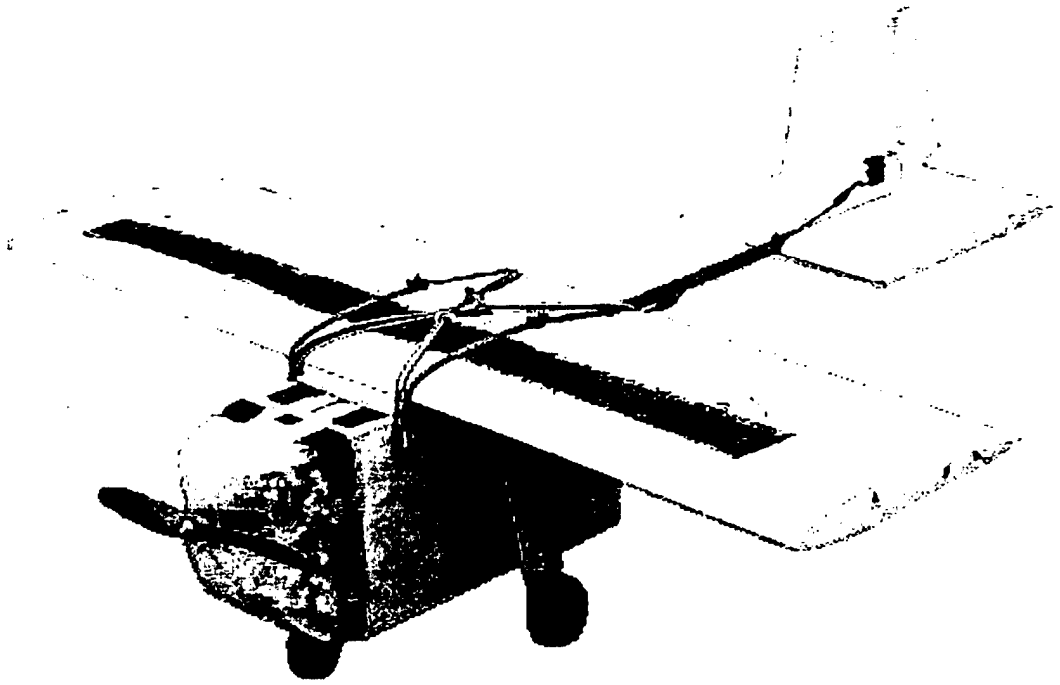

Figure 3.1 Prototype Airplane

3.1.3 Materials and Construction

Many construction techniques were investigated for the primary components of the prototype airplane. The techniques included traditional built-up, wood to fiberglass construction and other composite lay-ups. The primary options for the fuselage were a built-up plywood fuselage or a carbon-fiberglass shell. Hybrids were also considered that included plywood bulkheads within a composite shell. The methods considered for the wing included the traditional built-up balsa wood skeleton, the traditional built-up with composite reinforcements, fiberglass on foam (with and without a spar), a carbon shell and a carbon D-box with traditional coverings on the rear portion of the wing. Elastic bands and nylon bolts were considered for attaching the wing to the fuselage. The primary choices for the construction of the empennage were fiberglass on foam or built-up with balsa wood. The empennage was designed to be removable to allow the airplane to fit into the "box". Methods for achieving this included using a carbon fiber tube as a boom or using a completely removable tail cone that was secured at multiple locations. Composite, aluminum and wire landing gear were considered to include a wide range of strength to weight ratios, failure modes and complexity. The nose cowl was built using a fiberglass shell laid-up over a foam core. Velcro and mechanical latches were considered to attach the cowl to the airplane.

A Figure of Merit ranking system was employed to determine the construction method to be used on the prototype. The FOMs were:

- Strength to Weight Ratio: High strength to weight materials led to the lightest possible airplane that could sustain the necessary flight loads.
- Speed of Construction: Building the prototype in a timely manner was very important in order to complete testing before the winter months.
- Durability: It was important that the airplane was able to stand up to a rigorous flight test program.
- Ease of Construction: The manufacturing techniques needed to be within the skill level of the team.
- Material Cost and Availability: The airplane should be constructed of affordable materials that are easily obtained.

Based on the FOM's, construction techniques were chosen for the various components of the airplane. The fuselage design consisted of a primary plywood box structure that surrounded the payload. Above the payload bay, two channels were created for the batteries. Between these two channels a plywood and foam sandwich was incorporated around an aluminum tube to receive the empennage structure. The front of the payload bay consisted of a firewall with two carbon fiber rods that extended forward to form a motor mount. The nose gear steering servo and speed controller were also mounted on the firewall. The radio receiver and receiver battery were mounted at the rear of the fuselage. Split payload doors were incorporated on the bottom of the payload bay so that the payload could be released. The doors were open when the payload was in the airplane and closed after the payload was released. The payload release servo was never incorporated into the prototype airplane, although it would have been installed between the battery channels.

Fiberglass skin vacuum-bagged on a foam core was chosen for construction of the wing both for its airfoil fidelity and ease of construction. The short span of the wing made it possible to construct in a single piece. To increase the compressive strength of the skin, a carbon fiber skin spar was incorporated into the upper surface of the wing. The wing was attached to the fuselage using elastic bands. Ailerons were cut out of the finished wing, beveled and packing tape was used for the hinge. One micro-scale servo was used per aileron, with the wires running through a small hole bored in the wing core.

The empennage consisted of one layer of fiberglass on a foam core. Polyurethane was used as the matrix for the fibers, instead of epoxy, in order to save weight. This method resulted in extensive delamination of the skin from the foam. However, the foam core was able to sustain the loads. A wound, 0.625" carbon fiber tube was used as the structural component of the boom. The boom was inserted into a hole bored in the horizontal stabilizer. The vertical stabilizer was attached by way of two small diameter carbon fiber rods inserted through the boom. The rudder and elevator were constructed similarly to the ailerons. A bolt was inserted through the boom and the aluminum tube in the fuselage to secure the empennage to the fuselage. After the first flight test, a foam tail cone that fit over the boom was shaped to fair the fuselage back to the empennage.

In order to simplify and speed up construction, an aluminum landing gear was selected. It was manufactured from a 2" by 0.125" bar. The landing gear was inserted through the side of the payload box and bolted to the top of the payload bay.

The cowl was constructed by laying fiberglass and carbon fiber over a foam mold. The mold was compound curved to obtain good aerodynamic characteristics. In order to prevent stress fractures, carbon fiber was added to the high stress regions of the cowl. After the mold was removed, the cowl was finish sanded and holes were cut in it for the propeller shaft and for cooling intakes.

3.2 Prototype Testing

Prototype testing included flight tests as well as static thrust tests. A total of six flight tests and two static thrust tests were completed during the testing phase. Important lessons were learned from these tests that contributed significantly to the design of the competition airplane.

The flight test program aimed to explore the effect of the radome as well the possibilities of direct drive and smaller motors. The first two tests revealed major aerodynamic interaction problems that resulted in "porpoising" during level flight. Because the horizontal tail was unusually close to the main wing some problems were foreseen, but what was observed was entirely unexpected. After some discussion, it was determined that the wake of the fuselage had to be reduced and the tail boom had to be lengthened in order to solve the problem. Six inches were added to the tail boom, a foam fairing was added behind the payload bay and rounded tips were added to the wing and horizontal tail. The problems were eliminated by these changes. It was clear that, in order to locate the tail so close the main wing, the airplane wake would have to be minimized and the size and position of the horizontal tail would have to be scrutinized.

The impact of the radome was the next item investigated. It was found that the drag of the radome had very little effect on stability, but did have a significant effect on time and energy. The drag generated by the radome was actually equivalent, in terms of energy usage, to the additional turns required by the Communications Repeater mission. This result had direct implications on the decision of what missions to fly in the competition. The Missile Decoy and Communications Repeater used similar amounts of energy and took similar amounts of time. However, the difficulty factor for the Missile Decoy mission was twice as much as the Communications Repeater mission. The Missile Decoy mission was an obvious choice to maximize the total score.

Simulated competition flights were flown to evaluate the performance of the direct drive propulsion system as well as the possibility of using a smaller motor. Takeoff distance and total energy were worse than expected, even with the airplane only partially loaded. In fact, the energy usage was high enough that the airplane was only able to complete half of a mission. Both of these problems were attributed to the small wing area and thrust losses, which are described below. In cruise these effects caused the airplane to operate at a high C_L, resulting in high drag. During takeoff the thrust loss resulted

in poorer acceleration than expected. Furthermore, attempting to make parts interchangeable for experiments resulted in an aerodynamically "dirty" airplane.

Static thrust tests were conducted in the team's building shop by suspending the entire airplane from the ceiling and using a force transducer to measure the thrust. MotoCalc™ (Ref. 1) predictions estimated the static thrust of the propulsion system to be approximately 8 pounds. The tests showed that the maximum thrust was only 6 pounds, approximately a 25% reduction. The thrust loss was due to the low fineness ratio of the nose cowl, which coupled with the fact that the direct drive system used a 13" diameter propeller, created significant solid blockage. That result motivated serious consideration of the fineness ratio of the nose during the detailed design process of the competition airplane.

It should be noted that some problems were encountered during the testing phase due to poor preflight preparation. Jammed wheels and not resetting trim are two examples of problems that could have easily been identified by a preflight inspection, but instead led to potentially hazardous situations during the flight. In the future, more attention must be paid to developing and following preflight procedures in order to eliminate unnecessary risk during flight tests.

3.3 Lessons Learned

Many valuable lessons were gained during the design, construction and testing of the prototype airplane. These lessons included:

- Measures would have to be taken to make the competition airplane aerodynamically clean in order to minimize the wake and its effects.
- Polyurethane does not create a sufficiently strong bond between fiberglass and foam.
- The drag of the radome was nearly equivalent, in terms of expended energy, to the extra turns in the Communications Repeater mission.
- Installed static thrust would have to be increased in order to achieve take off in less than 120 feet.
- Drag and solid blockage would have to be minimized in order to reduce energy consumption.
- Pre-flight checklists are essential to guaranteeing the safety of the airplane.

4.0 Conceptual Design

In addition to completing the contest courses and meeting the takeoff requirement the airplane had to perform other tasks that strongly affected the design. The airplane had to be able to eject its payload and carry a radome. The payload deployment created both mechanical complexity and structural issues. The radome interference could affect the handling qualities of the airplane. Finally, the airplane had to be assembled and ready to fly in a minimal amount of time. Taken individually, these requirements suggested very different configurations. In order to be successful, individual features of each of these configurations had to be combined into one airplane. This process required investigations of the design tradeoffs needed to integrate these individual features into one airplane that could efficiently complete all of the missions.

Conceptual design of the competition airplane began by assembling all of the possible configurations and reviewing the positive and negative attributes of each using figures of merit. The primary figures of merit considered were: manufacturability, drag, RAC, assembly time and payload release/integration. Table 4.1 presents the down-selection process that resulted in four candidate designs (Conventional, Canard, Tandem and BWB(tail)). Sketches of each of the configurations considered in the process are included as Figures 4.1a and 4.1b.When the major aerodynamic components of each of these configurations were considered, it was realized that they could be generalized into two groups. The BWB and the Conventional were generalized into a conventional configuration and the Canard and Tandem Wing were generalized into a lifting tail configuration.

An aerodynamic study was then performed on these two configurations in order to determine if the lifting tail had a significantly discernable advantage over the conventional configuration to warrant the added difficulty that would come from the detailed design of this unfamiliar configuration. A drag build up was performed for each configuration and the mission times were calculated using the performance code. Because the lifting-tail configuration would be constrained to a smaller wingspan and therefore lower aspect ratio because of assembly time considerations, it suffered a severe penalty in induced drag. At the level of detail used during this phase in the analysis, the lifting tail configuration proved aerodynamically inferior to the conventional configuration. It was therefore decided to design the more familiar conventional configuration to meet the contest requirements.

Table 4.1 Conceptual Design FOM Study

	1	2	3	4	5
RAC	high				low
Ground Handling	poor				good
Structural Complexity	complex				simple
Aerodynamic Performance	poor				good
Payload Deployment	difficult				easy
Assembly Time	slow				fast

Configuration	RAC	Ground Handling	Structure	Aerodynamic Performance	Payload Deployment	Assembly Time	Total
Weighting (%)	30	5	20	25	10	10	100
Conventional	4	4	4	4	4	3	3.9
Flying Wing	5	3	3	3	3	5	3.8
Canard	4	3	4	4	4	3	3.85
Tandem Wing	2	3	3	4	4	2	2.95
Biplane	2	4	3	2	2	2	2.3
BWB(tailless)	5	3	3	3	3	4	3.7
Joined Wing	2	3	2	3	4	2	2.5
Ring Wing	3	2	1	2	3	3	2.3
Loop Wing	3	3	1	3	3	3	2.6
BWB(tail)	4	4	3	4	4	3	3.7

Conventional	Flying Wing
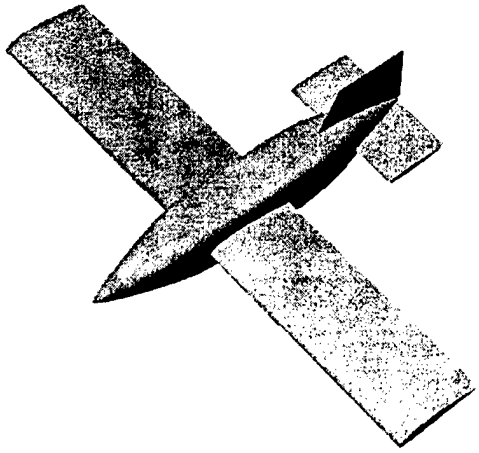	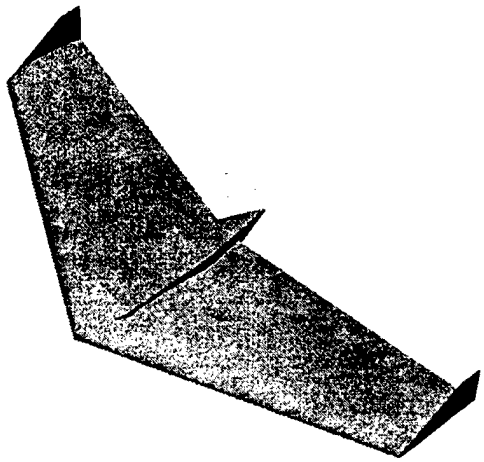
Tandem Wing	**Canard**
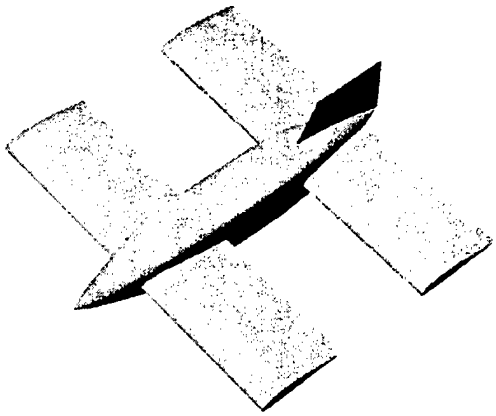	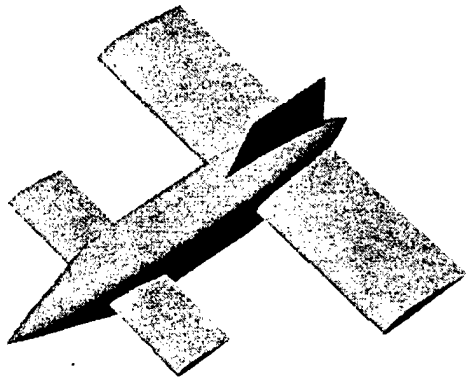

Figure 4.1a Conceptual Design Configurations

BWB (Tailless)	Joined Wing
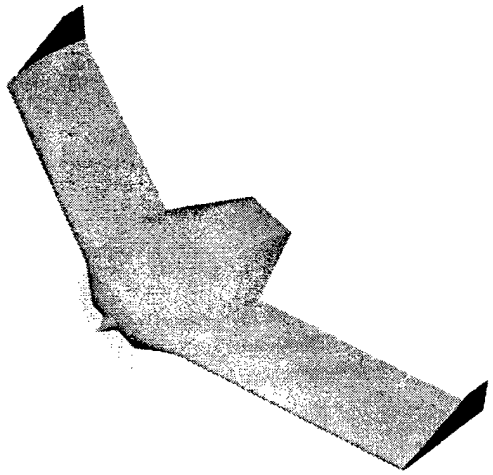	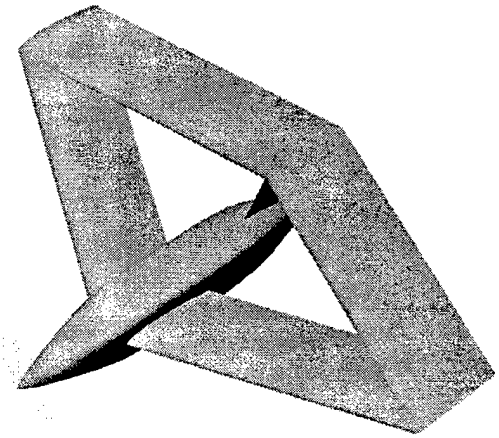
Loop Wing	**Ring Wing**
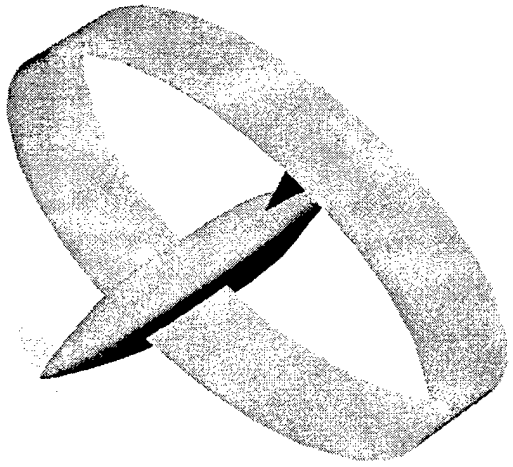	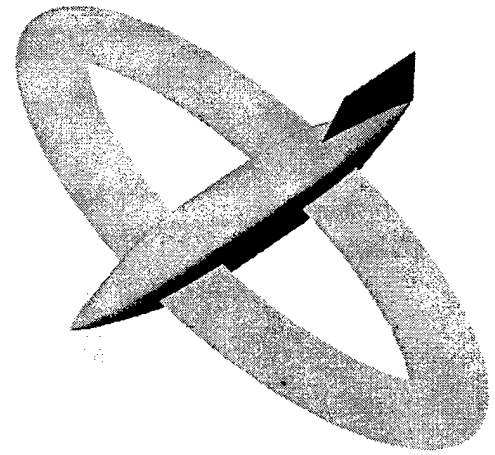
BWB with tail	
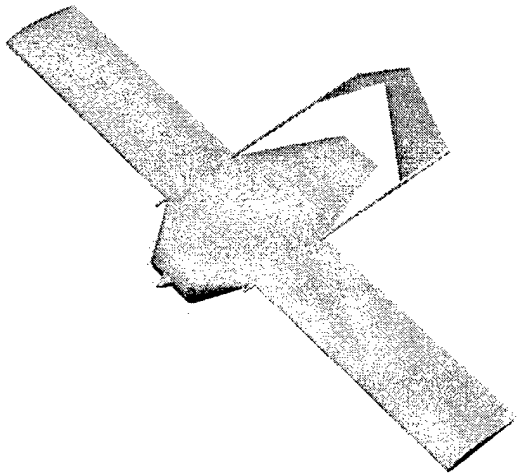	

Figure 4.1b Conceptual Design Configurations

5.0 Preliminary Design

It was apparent from the experiences with the prototype that minimizing assembly time, by using a two-piece design, was outweighed by the resulting performance loss. For the preliminary design of the competition airplane the design philosophy was, therefore, slightly altered. Instead of eliminating the assembly time, the airplane was first developed to fulfill the mission requirements and then the quickest way to assemble it was explored. However, the assembly time was always considered.

It was known from the prototype that a 4-foot wing would not be sufficient to meet the takeoff requirement, and therefore a minimum two-piece wing would be needed to fit in the box. Since the maximum span attainable by a two-piece wing would be 8 feet, this was used as a baseline wingspan.

Both the Astroflight 40 and 60 Cobalt motors were considered in preliminary design. The performance analysis determined which of these motors was optimal.

5.1 Weight Model

In order to evaluate the performance of the airplane, it was necessary to accurately estimate its weight using a detailed weight model. Major components (fuselage, wings, etc.) were modeled using their geometries and materials, while minor components (landing gear, servos, etc.) were modeled based on known weights of off-the-shelf components. For the chosen configuration, weight proved to be a weak function of both wing and tail area, but most other design parameters had negligible effects. This weight model was developed using airplane data from past competitions and had exhibited good predictive capabilities in the past.

5.2 Wing Sizing

The takeoff constraint and the dimensions of the payload drove the sizing of the airplane. Figure 5.1 presents the results of a takeoff analysis that included C_{Lmax}, T, S and W. to provide a safety margin the maximum allowable takeoff distance was set at 100 feet. From Fig. 5.1 it was determined that the baseline airplane, with an 8' x 1' wing, would require eight pounds of static thrust and a C_{Lmax} of at least 1.2 in order to takeoff in less than 100 feet. Note that the plot showed that takeoff in less than 100 feet was possible with seven pounds of thrust, but required a C_{Lmax} that was unlikely for a wing that would also operate efficiently in cruise. The combination of the 8' x 1' wing, a C_{Lmax} of 1.1 and an Astroflight 60 producing seven pounds of thrust offered the best compromise between these parameters to achieve a reasonable chance of success and efficiency. Figure 5.2 presents the next stage in the takeoff analysis, which incorporated a safety margin study. Applying a two-pound weight gain to the airplane tested the extent of the safety margin. The airplane produced eight pounds of static thrust and had eight square feet (8' x 1') of wing area. The results showed that the minimum acceptable C_{Lmax} for that configuration was 1.1. Choosing to use the 8' x 1' wing provided a rather large safety margin, as was seen in Fig. 5.2, however it did offer certain advantages. The greatest advantage was the use of a horizontal stabilizer with a two-foot span, which was the largest that would fit in the box and still be counted as a tail in the

RAC calculation. Furthermore, the added wing area had a negligible impact on the RAC, while insuring takeoff in less than 120 feet in the face of any unforeseen performance losses.

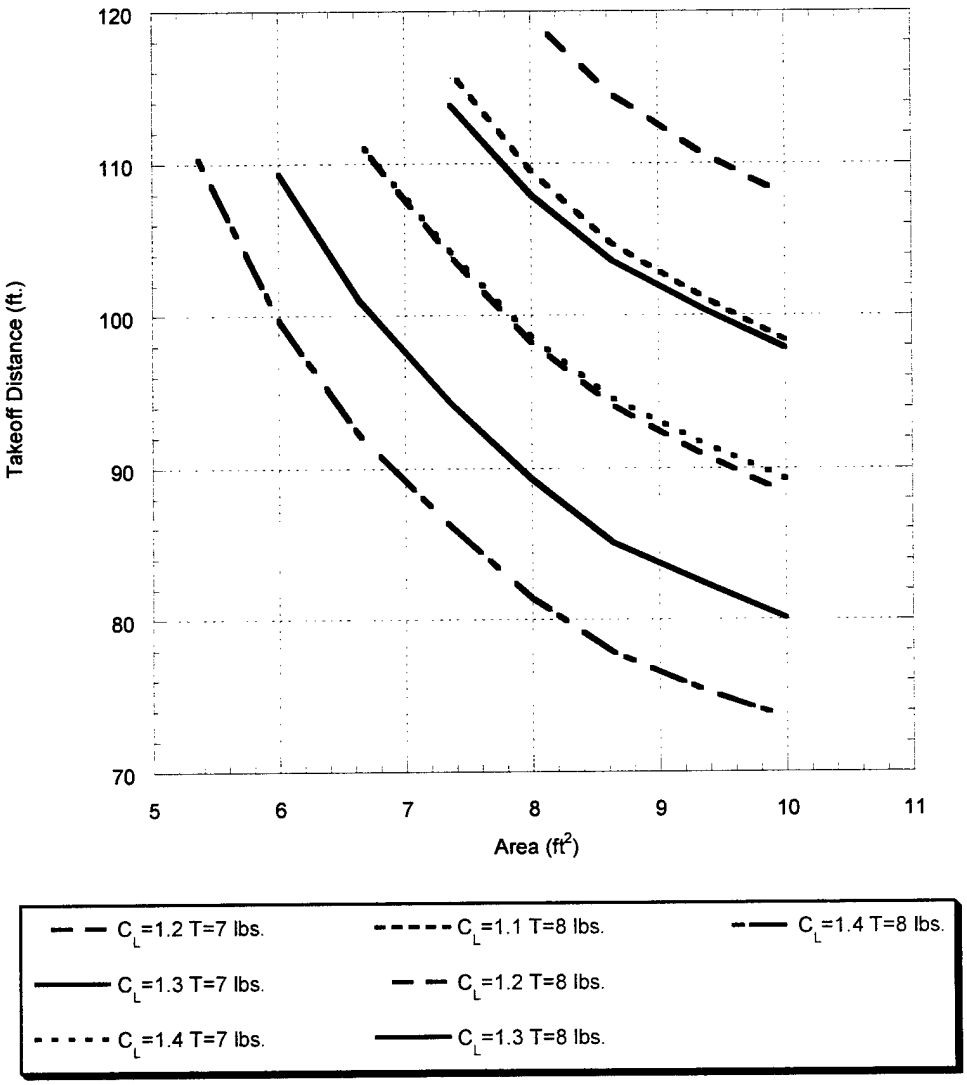

Figure 5.1 Generic Takeoff Analysis

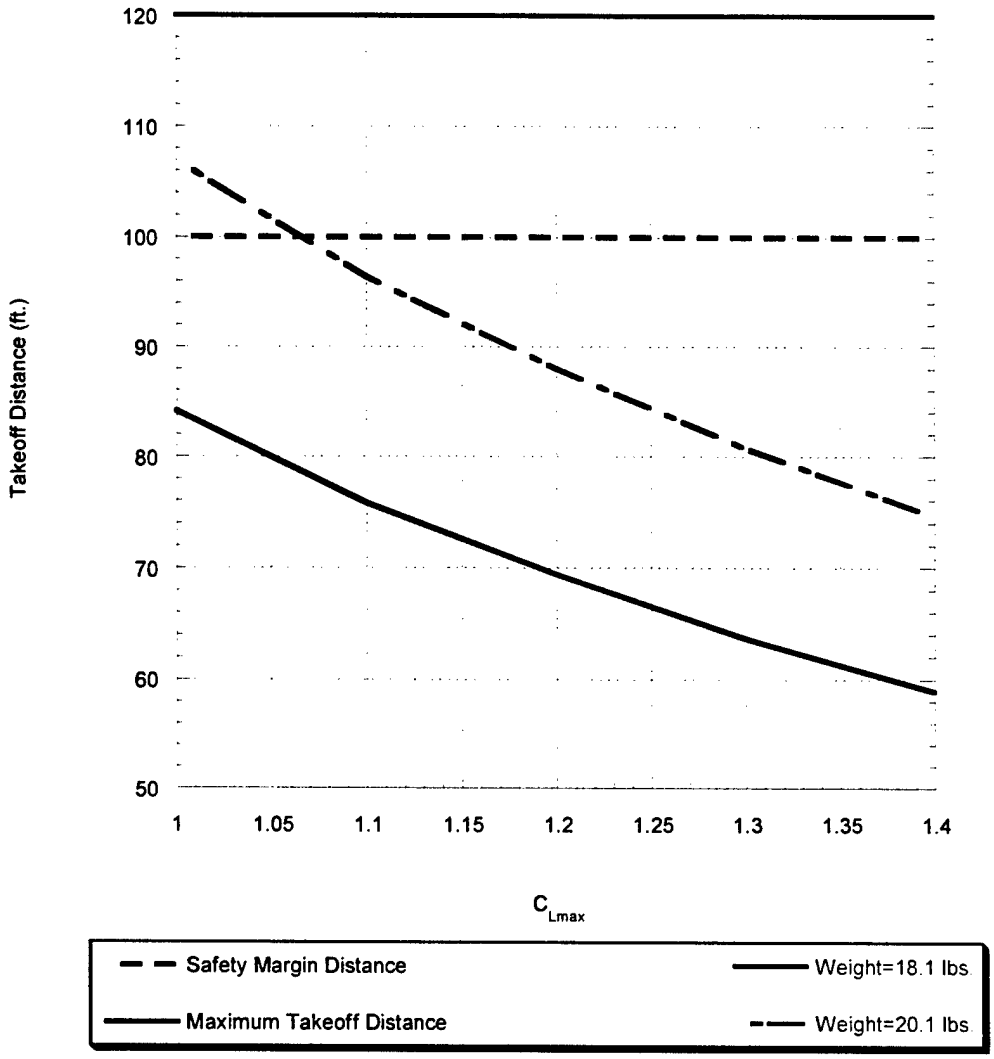

Figure 5.2 Takeoff Estimate with and Astro60 and 18x18 propeller

5.3 Motor Selection

The possibility of using either an Astroflight 40 or 60 was considered. The Astroflight60 was known, from past experience, to have a high pitch speed and produce sufficient thrust for takeoff. Alternatively, the Astroflight 40 produces less thrust, but offers reduced motor weight and battery cell count. It was possible that the lower gross weight would outweigh the slower flight speeds.

Examining the RAC for the two configurations revealed that the Astroflight 60 equipped airplane would have to fly 1.3 times faster than the Astroflight 40 equipped airplane to achieve the same total score. Performance calculations showed that, for the Sensor Deployment mission, the Astroflight 40 equipped airplane had a mission time of 173.2 seconds while the Astroflight 60 equipped airplane had a

mission time of 130.4 seconds, which is approximately 1.3 times faster. However, the Astroflight 40 required 1175 mAh to complete the mission, while the Asroflight 60 required only 870 mAh to complete the mission. Battery weight would have to be added to the Astroflight 40 configuration, clearly making the Astroflight 60 the best choice for the motor.

5.4 Stability and Control

During the preliminary design phase, stability and control analysis was limited to the longitudinal modes of the airplane. Because the fuselage was constrained to 48 inches long, the airplane was extremely short-coupled. This raised some concern, so a detailed longitudinal stability study was performed in order to verify that the configuration was viable from a stability perspective.

As an initial design point, the tail was sized to 2 feet in span by 1 foot in chord, which yielded a tail volume ratio of 0.48. While this volume ratio was on the large side, it was considered appropriate because of the tail's short moment arm and its proximity to the wing.

A complete set of longitudinal stability and control derivatives was produced from the airplane's geometry, using the methods presented in Nelson. (Ref. 2) The static margin was set at 10% to balance good handling qualities with aerodynamic performance. With that done, a state space model of the airplane was constructed, and the longitudinal modes were examined. Level two handling qualities were required for all phases of flight, with level one handling qualities desired. (Ref. 2) Tail size was varied and flight qualities reexamined, but no viable configuration proved to have better characteristics than the initial design point. A summary of the periods and time to double/half of the dynamic modes are presented for several flight speeds in Tables 5.1 and 5.2.

The divergent phugoid for the landing condition is a concern, but when the period of 12 seconds and doubling time of 250 seconds are compared with the time spent in the actual approach, this behavior becomes acceptable in the context of this airplane and its mission.

Also conspicuous is the absence of an oscillatory short period mode, it was replaced by two very fast non-oscillatory modes. This was again due to the short coupling, since it was what drove the required tail area to 2 ft^2.

It should also be noted that the short-coupled tail incurred a penalty on the $C_{L,max}$ of the airplane, as the trim force required to hold the airplane at high angles of attack was non-negligible. The total C_L loss when the wing was at $C_{L,max}$ was 0.08, or approximately a 7% loss.

Table 5.1 Longitudinal Response Modes in Cruise

Mode	Period (s)	Time to double or half (s)
Aperiodic alpha mode	N/A	0.19
Aperiodic q mode	N/A	0.08
Phugoid	12.3	28.3

Table 5.2 Longitudinal Response Modes in Takeoff/Approach

Mode	Period (s)	Time to double or half (s)
Aperiodic alpha mode	N/A	0.30
Aperiodic q mode	N/A	0.41
Phugoid (divergent)	9.4	84

5.5 Fuselage Length Study

Due to the requirement that the disassembled airplane fit within the designated 4'x2'x1' box, a one-piece fuselage was desired to minimize assembly time. Therefore, it was necessary to determine the fuselage drag as a function of length and identify any drag penalties associated with using a 48-inch fuselage. The fuselage drag as a function of length was obtained using the method given in Raymer (Ref. 3), where the drag coefficient of a fuselage shape is calculated from an experiment-based form-factor equation. The fuselage drag coefficient based on the wing reference area is given by

$$C_{D_{0,fuselage}} = \frac{C_f FFQS_{wet}}{S_{ref}}, \text{ where } \quad FF = (1 + \frac{60}{(f)^3} + \frac{f}{400}),$$

f is the fuselage fineness ratio, Q is the interference factor for the fuselage (set to 1 in this case), S_{wet} is the wetted surface area of the fuselage and C_f is the flat-plate skin friction coefficient, a function of Reynolds number. The above relations dictated that minimization of fuselage drag was a tradeoff between fineness and wetted area; a more slender fuselage had a lower form factor, FF, but also a higher surface area. Assuming fully turbulent flow at 100 ft/s, a maximum fuselage cross-sectional area of 6.25"x7.25" and estimating the surface area as a function of length, the fuselage drag coefficient as a function of length was determined. The results of this study, shown in Figure 5.3, indicated that the minimum drag fuselage for the given maximum cross-section and conditions used was achieved with a

fuselage length of approximately 4 ft. This meant that a fuselage fitting in the box length-wise would be roughly the length required for lowest drag.

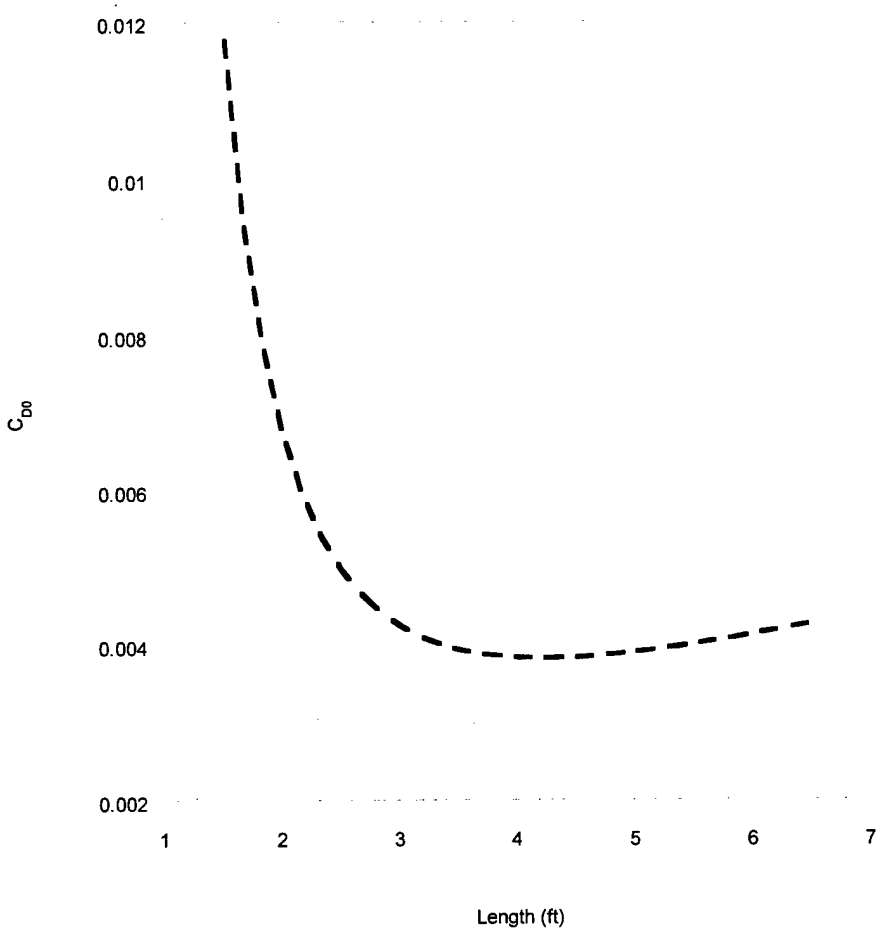

Figure 5.3 Fuselage Length Study

5.6 Payload Deployment

Several payload deployment schemes were considered during the development of the airplane. These included a simple "bomb bay" style release, a C-130-style rear door, and side ejection. Each of these has advantages and disadvantages. The "bomb bay" method required the use of extremely long landing gear, because the bottom of the fuselage had to be at least 6 inches off the runway. Furthermore, the landing gear components could not cross under the payload, meaning that they had to attach to the wing or fuselage sides. The rear door approach was more complex, and required extensive mechanics. The side ejection system created an asymmetric structure in the most critical region of the fuselage, and required careful design to achieve the proper kinetics. It did, however, allow for the use of

very short gear, as well as a tail dragger design. The tail dragger configuration is desirable for its ground handling characteristics and low drag. For these reasons, this method was chosen for the airplane (Fig. 5.4).

In order to eliminate the need for a separate door that opens and closes, the fuselage was planned with the payload forming the side when it was onboard. A panel, which was spring-loaded to eject the payload, sealed the opening once the payload was deployed. This payload deployment method was tested and proven before it was ever implemented on the competition airplane, using a mock-up of the fuselage.

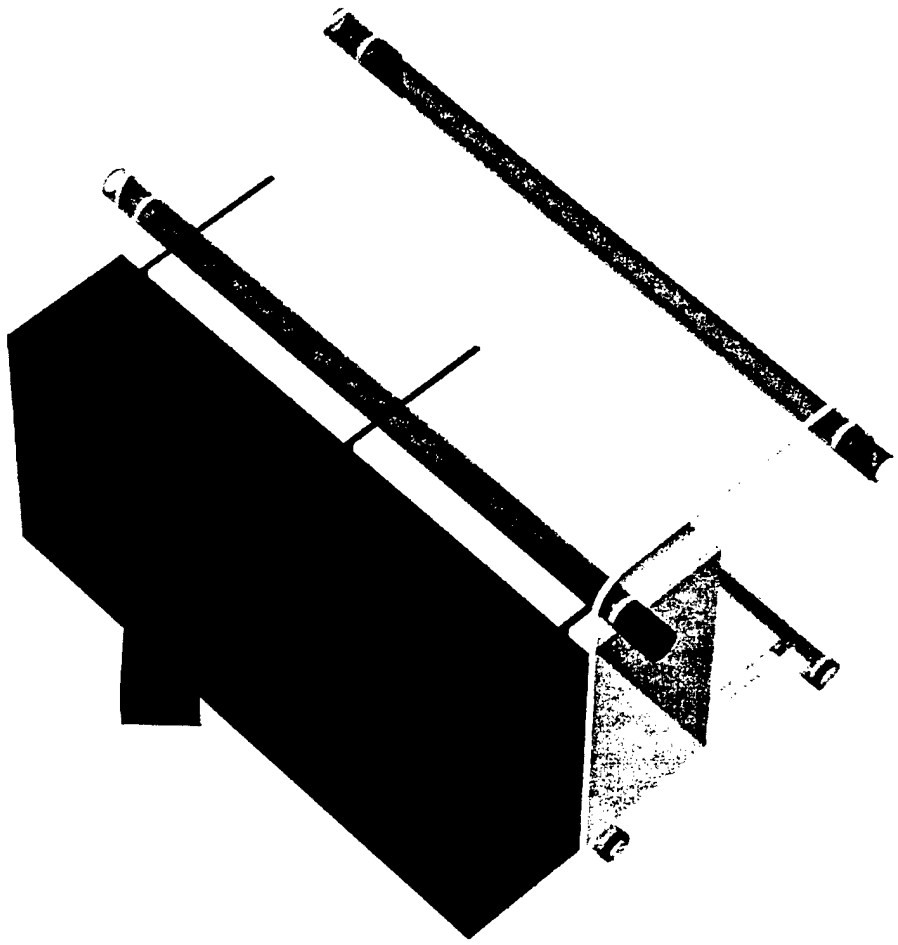

Figure 5.4 Payload Ejection Mechanism

6.0 Detailed Design

6.1 Performance

Performance focused on optimization during the detailed design of the competition airplane. During this phase, airfoil selection was completed based on takeoff distance and performance. Score optimization was of particular interest since the effects of various parameters on the total score were not well known.

In order to choose the best airfoil, the aerodynamics group provided drag polars that were then used in the performance code. The two best performers were the SD7062 and the Clark Y. The Clark Y required a substantially longer takeoff distance (Table 6.1) due to the fact that its C_{lmax} is over 20% less than that of the SD7062. However, it was thought that, due to a lower drag bucket, the Clark Y would perform better in flight. The performance code showed that was not the case and, in fact, the SD7062 potentially could perform better because it allowed for a tighter turn diameter. Furthermore, the Clark Y required a takeoff distance slightly greater than the safety margin of 20 feet established during the preliminary design.

Parameter sensitivity of the total score was of particular interest during the detailed design because it revealed the most significant aspects of the design. Figure 6.1 shows the variation of total score due to multiple variables being changed independently, except in the case of those parameters that also affect weight (e.g. number of battery cells). In the figure, the baseline configuration is at the intersection of the curves. It was apparent that minimizing the airplane weight and parasite drag would have the greatest effect on total score.

The next sensitivity study conducted, two parameters were varied simultaneously in order to further explore the most influential variables and establish the best and worst case scenarios. Figures 6.2a and 6.2b present the effect of weight and parasite drag on mission energy for the Missile Decoy and Sensor Missions. These missions are presented because they were selected as the primary missions to maximize score. These figures also showed that the maximum energy consumption, with a 20% increase in weight and parasite drag, was estimated to be less than 1000 mAh. They also showed that there was relatively little variation in energy usage over the range of variables used. In addition, the score (Fig 6.2c) was predicted to range between approximately 12.5 and 14 min^{-1}.

The effect of assembly time on the total score was also investigated. As expected, when the assembly time is on the order of the mission flight time it has a significant effect on the total score. The mission time is estimated to be approximately 2 minutes and the assembly time is expected to be less than 20 seconds. Therefore, if assembly required the entire 20 seconds it reduced the total score, as measured from the zero assembly time value, by 17%.

Table 6.1 Airfoil Study

Airfoil	Turn Diameter	Takeoff Distance	Energy	Time	G-Loading
	ft	ft	mAh	s	g's
ClarkY	133.0	105.0	870.2	117.2	5.0
SD7062	100.0	79.8	820.0	113.2	6.7
SD7062	130.0	79.8	867.4	117.5	5.0

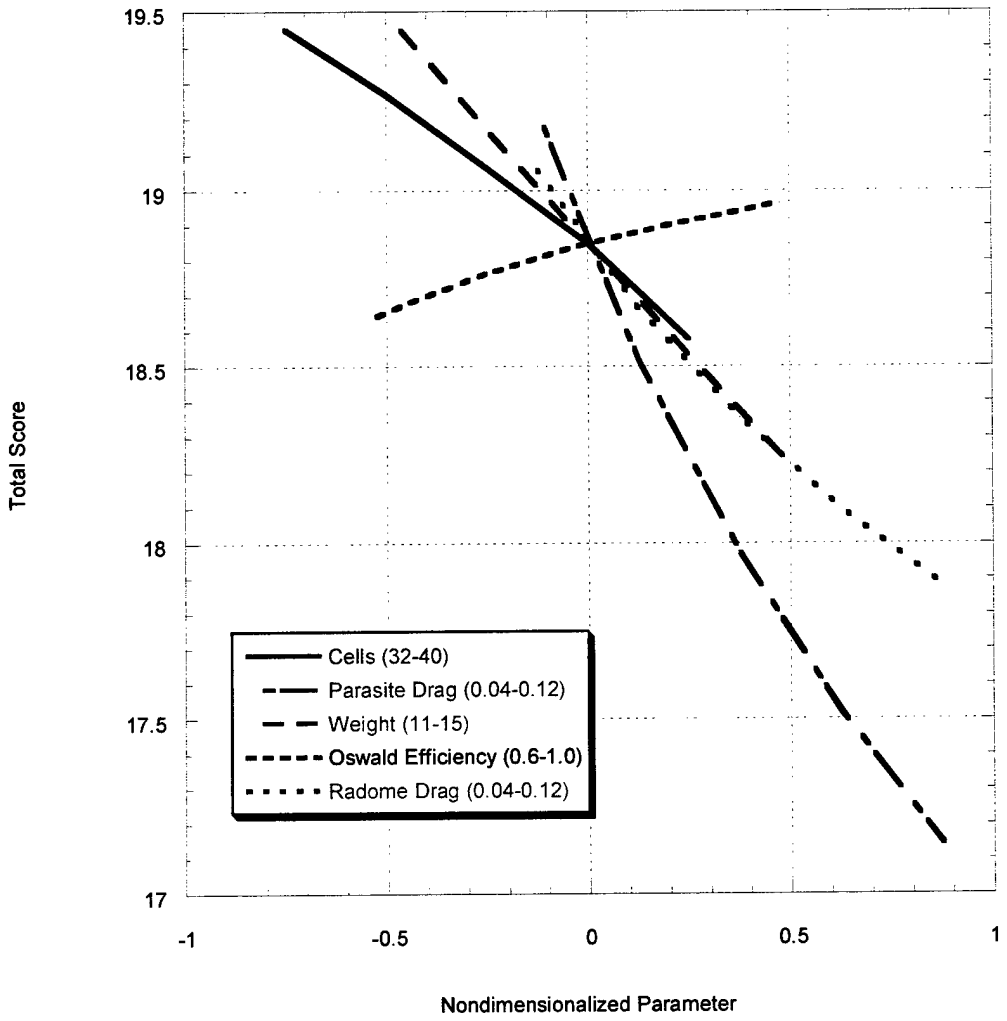

Figure 6.1 Total Score Sensitivity

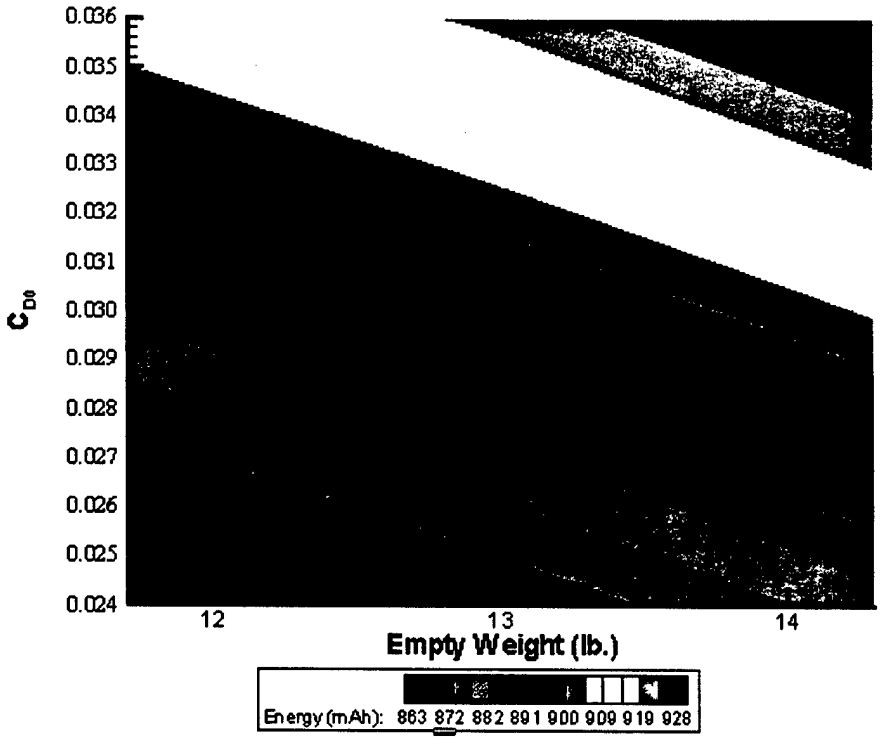

Figure 6.2a Missile Decoy Mission Energy Sensitivity

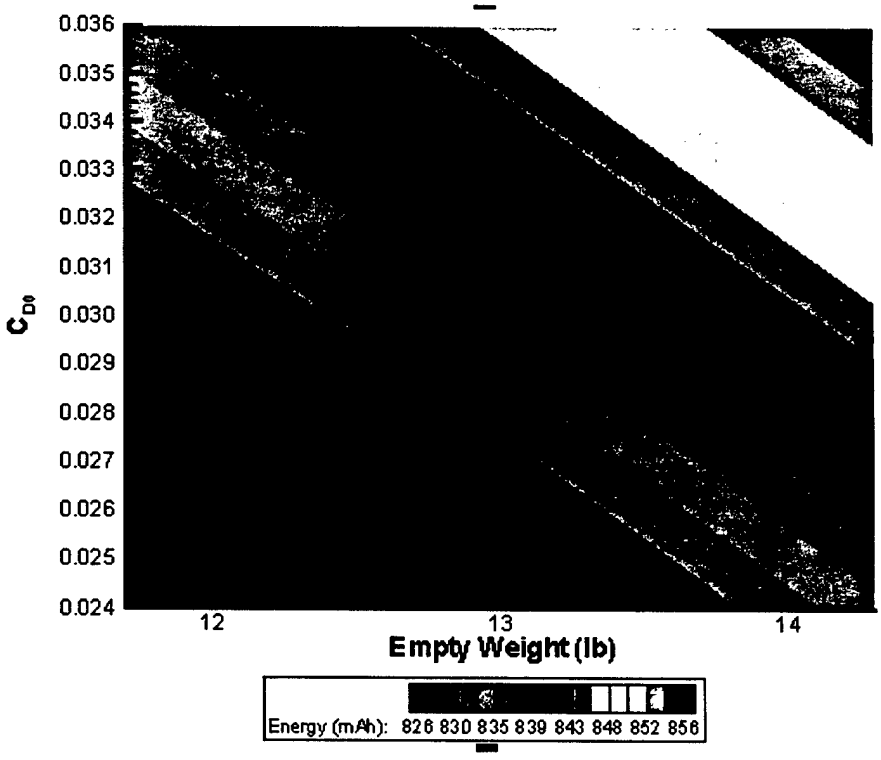

Figure 6.2b Sensor Mission Energy Sensitivity

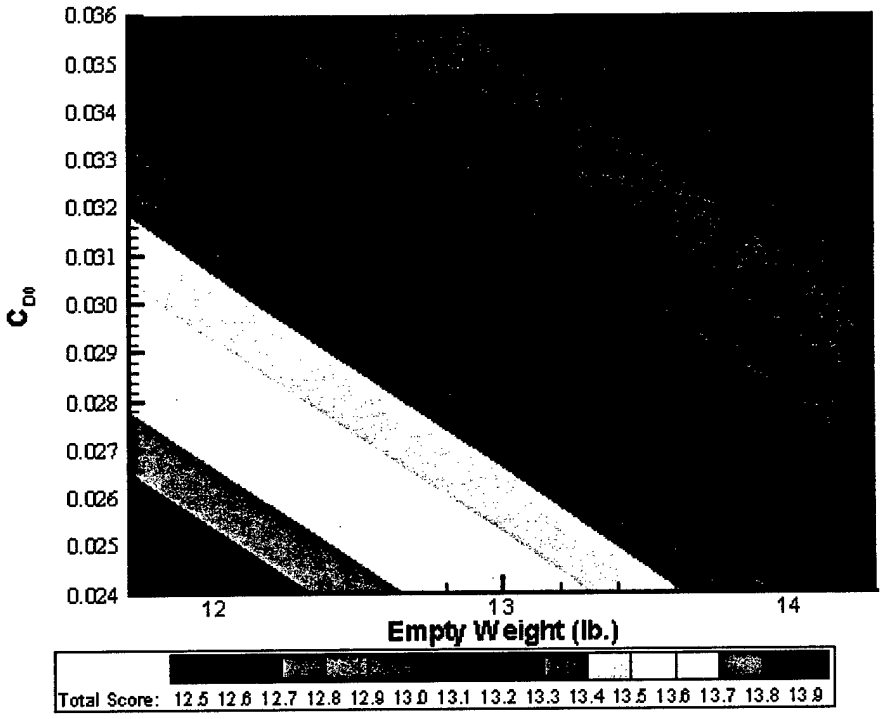

6.2c Refined Total Score Sensitivity

6.2 Aerodynamics

6.2.1 Airfoil Selection

Airfoil selection was made based on low Reynolds number data from Lyon (Ref. 4). Five candidate airfoils were selected and compared at a Reynolds number of 400,000 corresponding to 65 ft/s at sea level and a C_L 0.45 for an 18-lb. airplane. The five airfoils investigated were the Clark Y, S8036, S8037, S8052, and SD7062. The lift curves and drag polars for these airfoils are given in Figures 6.4 and 6.5a respectively. Three-dimensional drag polars for each airfoil as an 8'x1' un-tapered, un-twisted wing (Fig. 6.5b) were calculated using LinAir lifting-line software. (Ref. 5) Clearly, the Clark Y and S8052 had the lower drag than other candidates over the ranges indicated in mission C_L profiles generated by performance. This profile indicated that most of the mission time was spent at a C_L between 0.1 and 0.3. (Fig. 6.6a and 6.6b) However, the C_{Lmax} achieved by these airfoils resulted in marginal takeoff performance for the selected planform. Therefore, the SD7062 was selected due to it having marginally higher drag in the desired C_L range and the best C_{lmax}.

6.2.2 Wing Detailed Design

Once the SD7062 airfoil had been selected, it was necessary to optimize the wing twist for optimal performance over the C_L ranges determined by the performance code. Preliminary performance calculations for the Sensor Deployment and Missile Decoy missions indicated that the airplane would

spend 50-60% of the flight time within the C_L range of 0.1 to 0.3. The airplane also spent 13-26% of the flight time between a C_L of 1.0 and 1.2. The wing twist was therefore, optimized for best performance using Oswald's efficiency, $e = C_L^2/(\pi C_{Di} AR)$. Due to the planned foam core construction and foam-cutting equipment, the wing was designed in 2-ft. linearly twisted sections. So, different combinations of twists over each panel were investigated (example: no twist on 2-ft. inner panel, 2 degrees washout on the outer panel). This analysis was completed in LinAir, and the results are given in Figure 6.7. It can be seen that optimizing the wing twist for high C_L results in poor performance at low lift coefficients. However, optimizing the wing twist for low C_L results in acceptable performance at higher lift coefficients. The combination that performed best in this respect had 0 degrees of twist in the inner panel and 1 degree of washout in the outer panel. In addition, this combination moved the center of pressure inward as compared to 0.5 degrees of washout in each panel (1 degree washout from root to tip), which reduced the bending moment at the root.

6.2.3 Total Airplane Aerodynamic Results

With the airfoil and wing twist selected, a trimmed drag polar was constructed using LinAir to model the wing and horizontal tail and the parasite drag equations from Raymer (Ref. 3) to model the fuselage, vertical tail and landing gear. Points on the trimmed polar were determined by setting a c.g. location (to take the moment about), sweeping through airplane angle of attack for varied tail setting angle, and determining the C_L (and therefore C_D of the wing-tail combination) required to trim. The parasite drags of the other components were then added to the wing-tail trimmed polar. The resulting total airplane drag polar is given in Fig. 6.8. This corresponds to an airplane $(L/D)_{max}$ of ~15. The total C_{Lmax} of the airplane was predicted to be ~1.3 given that the calculated total airplane lift slope is 0.079 per degree and that the airfoil begins to stall at approximately 17 degrees referenced to the zero-lift angle of attack (0.079*16 = 1.343). For performance calculations, the radome was assumed to add 0.02 to the total aircraft drag coefficient.

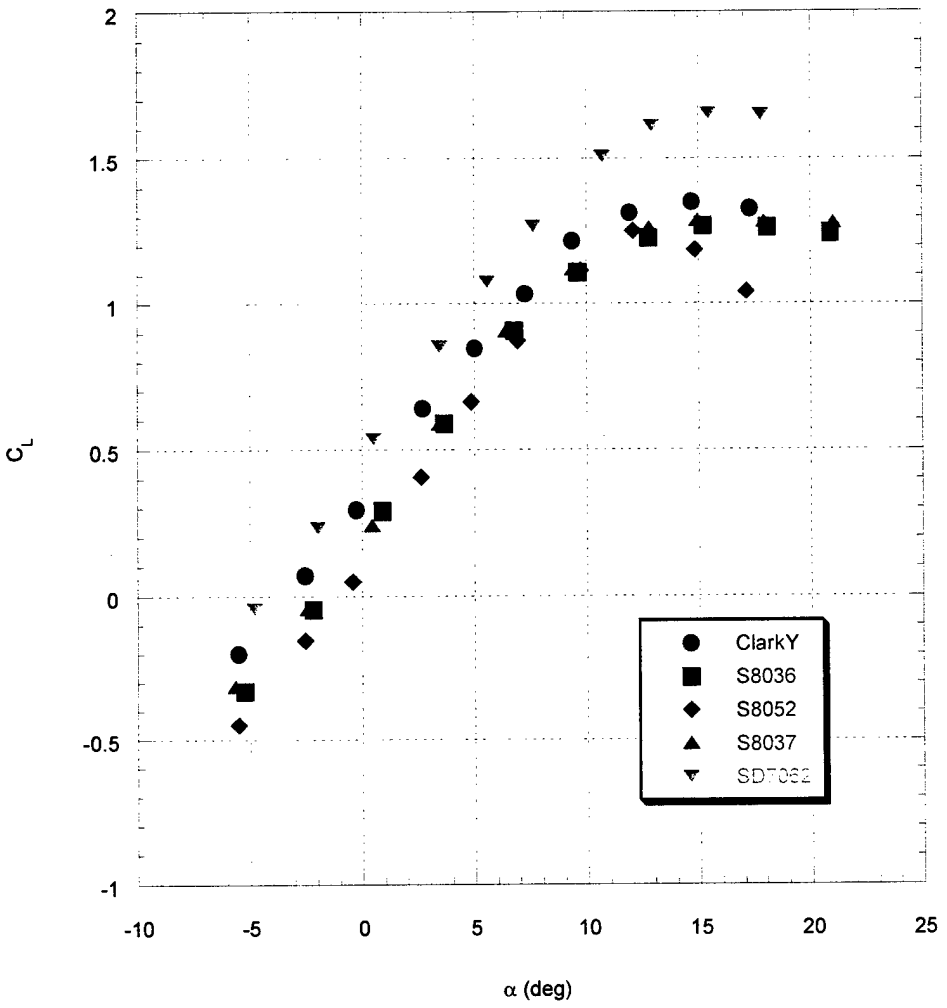

Figure 6.4 Lift Curves of the Candidate Airfoils

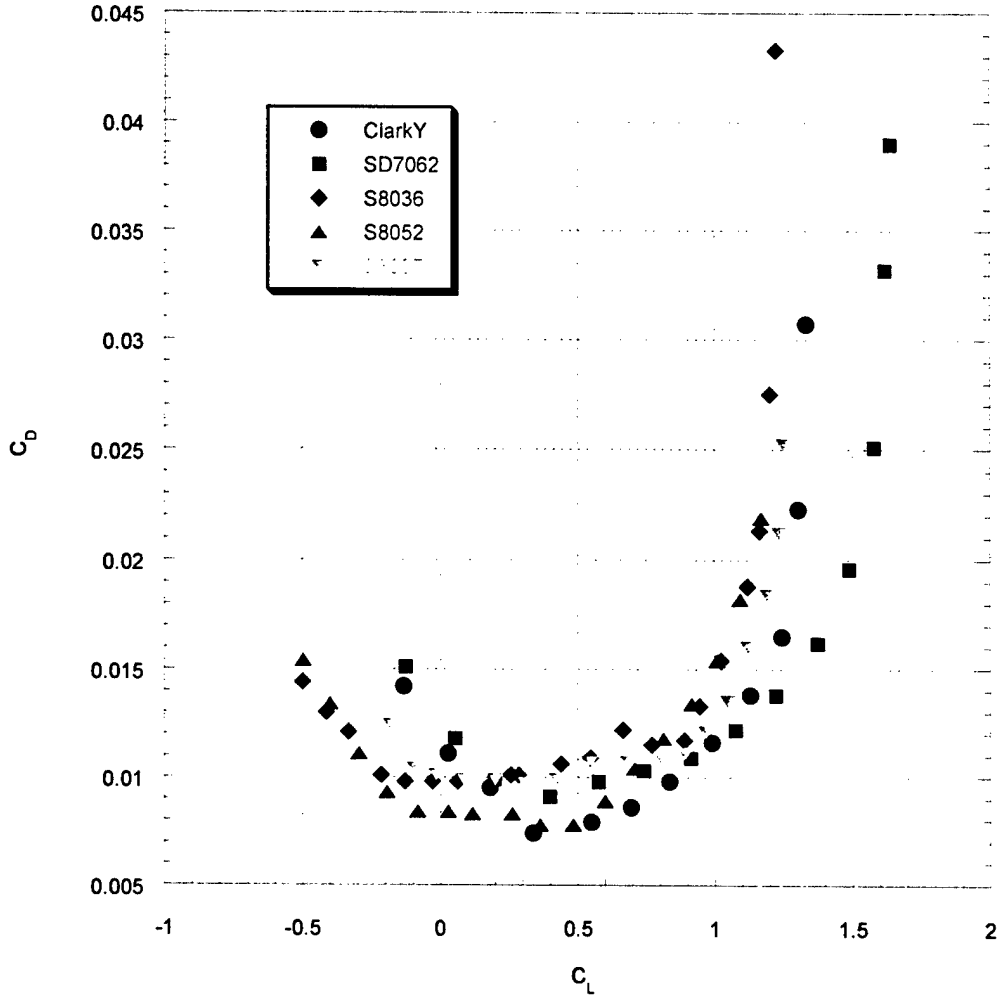

Figure 6.5a Sectional Drag Polars of the Candidate Airfoils

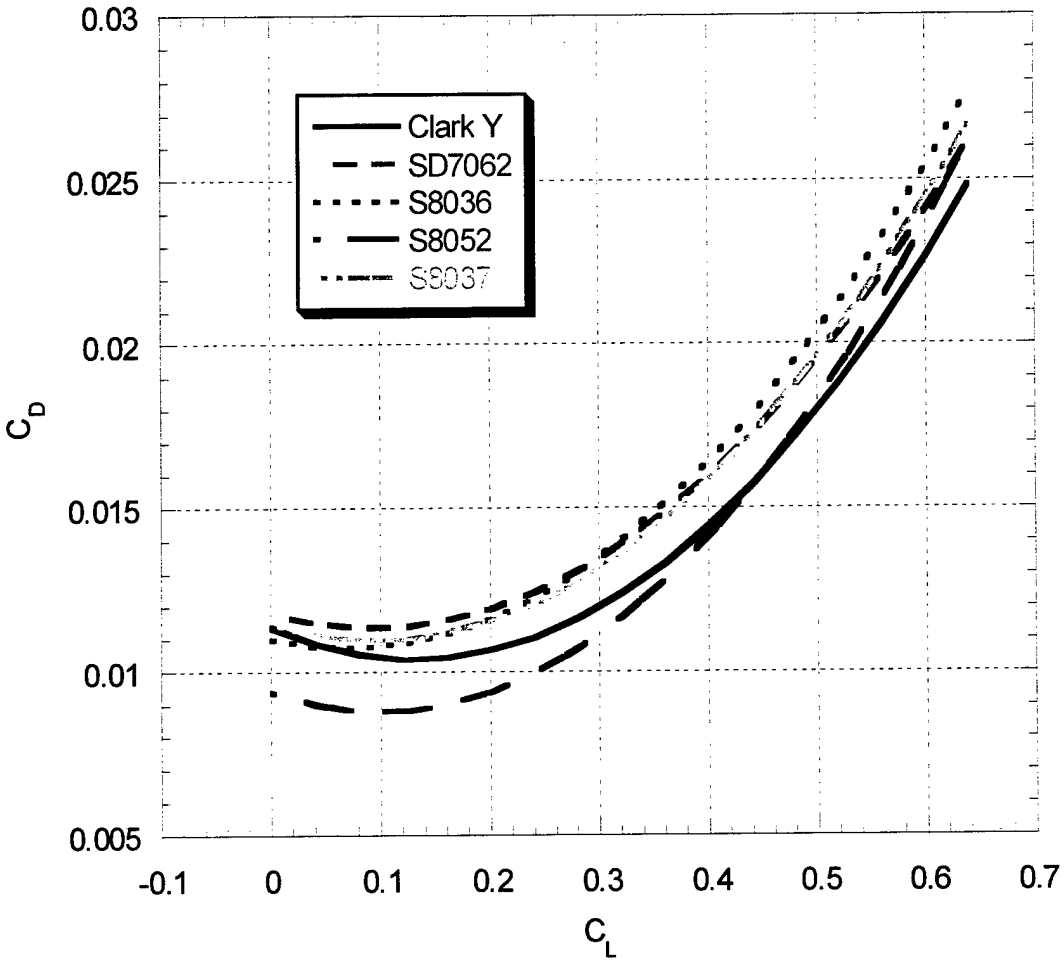

Figure 6.5b Three Dimensional Drag Polars of the Candidate Airfoils

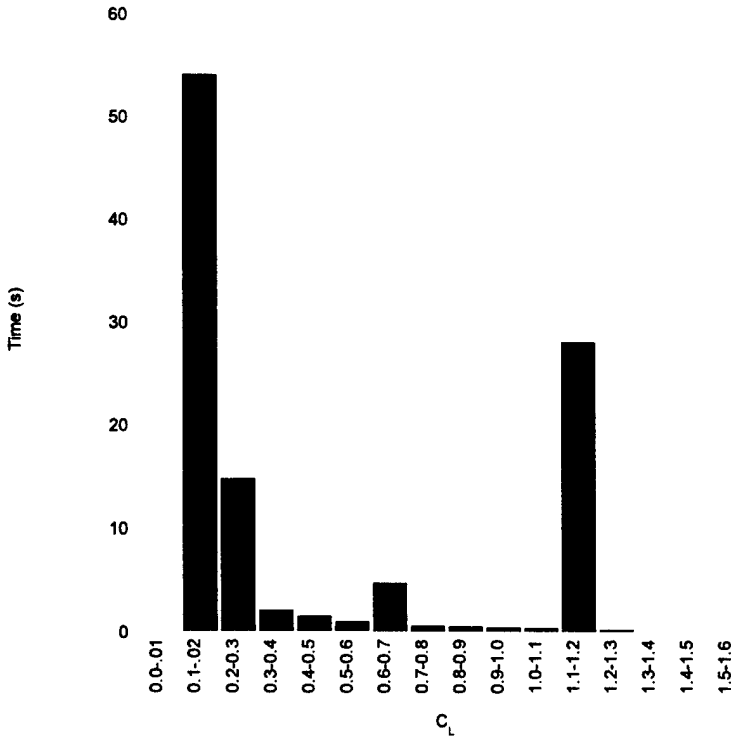

Figure 6.6a Missile Decoy C_L Histogram

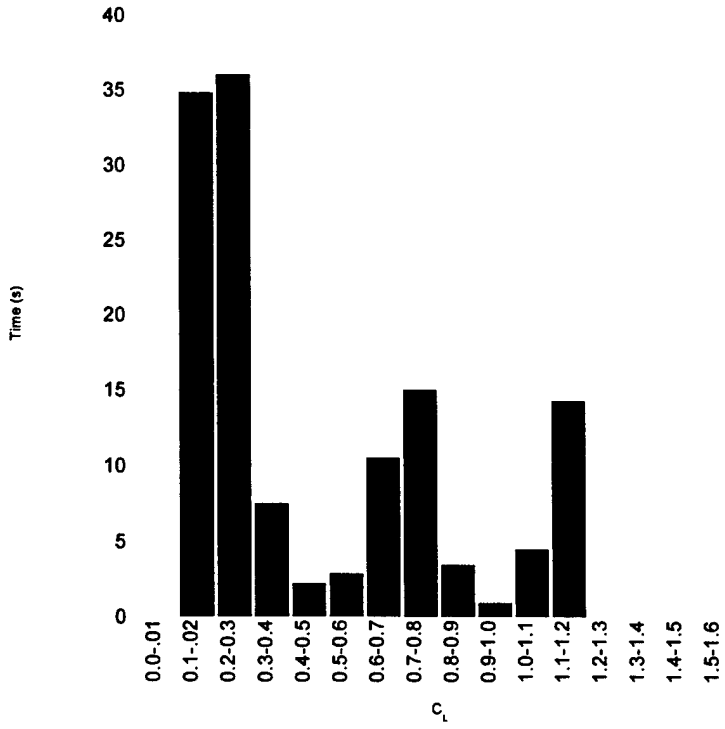

Figure 6.6b Sensor Deployment C_L Histogram

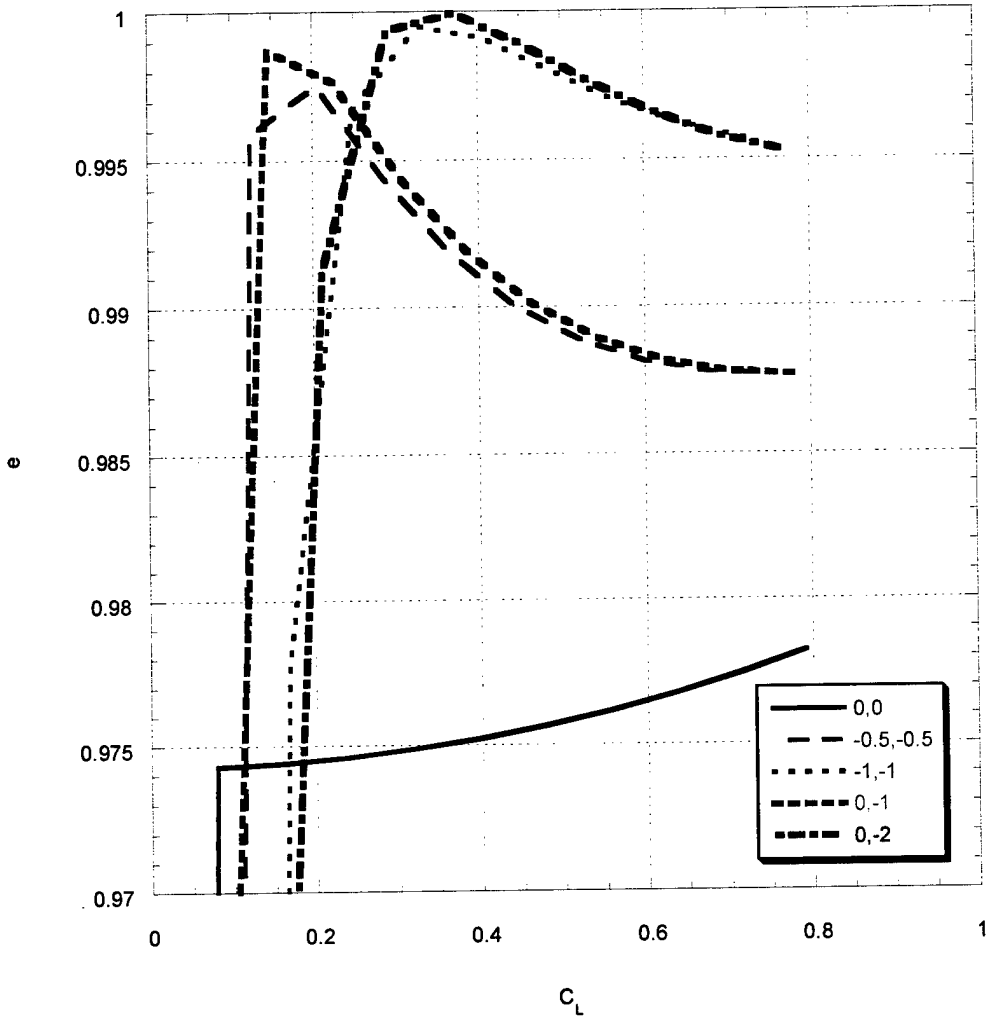

Figure 6.7 Wing Twist Study (inner panel twist, outer panel twist in degrees)

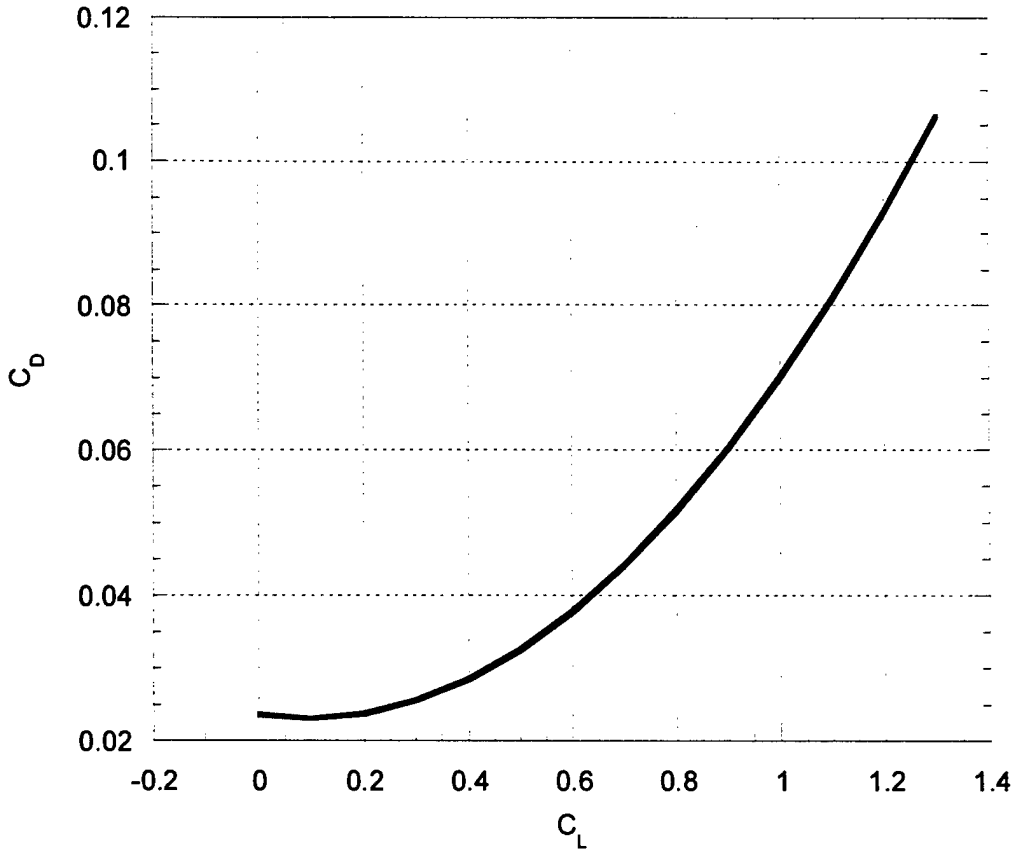

Figure 6.8 Final Aircraft Drag Polar

6.3 Propulsion

The sizing of the airplane and selection of the propulsion system were interdependent. Based on the wing sizing and predicted weight, a static thrust between seven and eight pounds was desired, while keeping runtime as high as possible and battery weight as low as possible. Low static thrust experienced with the prototype prompted an experiment with propeller blockage to determine the loss in thrust due to the presence of a cowl. The Cobalt 60 with a 2.75:1 gearbox was tested on a thrust stand with and without a cowl of geometry similar to that expected on the competition airplane. The test was run using an APC 18x18 propeller, Astroflight 204D speed control and a battery pack of 40 Sanyo 1300CP cells. As shown in Table 6.2, the presence of the cowl caused a loss in maximum static thrust of approximately 7%, or one half pound.

6.3.1 Motor Selection

The set of possible motors was limited to the Astroflight Cobalt 40 and Cobalt 60 due to cost effectiveness and availability. In addition, the team had amassed both static and wind tunnel data on Astroflight motors and had prior experience with both motors. MotoCalc predictions of thrust and current

draw were produced for the Cobalt 40 with 3.1:1 gearbox on 24 cells as well the Cobalt 60 with 2.75:1 gearbox on 40 cells. These predictions were then utilized with the performance code. The result showed that despite the weight savings due to the smaller motor and the drop from 40 to 24 cells, the airplane flew at a significantly lower speed and achieved a lower overall score. Using the Astroflight 40 also reduced the takeoff distance safety margin. Due to the higher overall score and larger safety margin the Astroflight 60 was chosen to power the airplane.

6.3.2 Propeller Selection

The 18x18 and 20x16 propellers were considered for the propulsion system. Previous experience has shown that APC propellers offer good performance for and are easily obtained. Static test results from previous years (Figures 6.9 and 6.10) were used in the propeller selection. Accounting for 7% blockage losses, the 18x18 propeller was capable of producing adequate thrust and also a higher pitch speed than the 20x16 propeller, while drawing less current. As a result the APC 18x18 propeller was selected.

6.3.3 Battery Selection

Based on the proposed competition airplane weight and geometry, the performance code predicted that the capacities needed to complete certain missions ranged from 800 to 1000 mAh. Manufacturer data led to the selection of the Sanyo 1300 CP due to its small size, high energy density and ability to maintain high voltage throughout the desired discharge currents and throughout a large percentage of its capacity. The smaller size and higher impedance of this cell results in a lower voltage under load when compared to the Sanyo 2400 mAh batteries that the team had used in the past. To ensure adequate thrust over the entire mission 40 "zapped" cells were selected for the battery pack. The "zapped" cell maintains a higher voltage throughout its capacity as compared to a standard cell.

Table 6.2 Averaged Results of Propeller Blockage Experiment

Throttle	Configuration	Battery Voltage (V)	Battery Current (A)	Thrust (lbs)
50%	Without Cowl	47.2	8.8	2.84
50%	With Cowl	47.1	8.6	2.59
100%	Without Cowl	40.1	23.7	7.21
100%	With Cowl	40.4	23.7	6.72

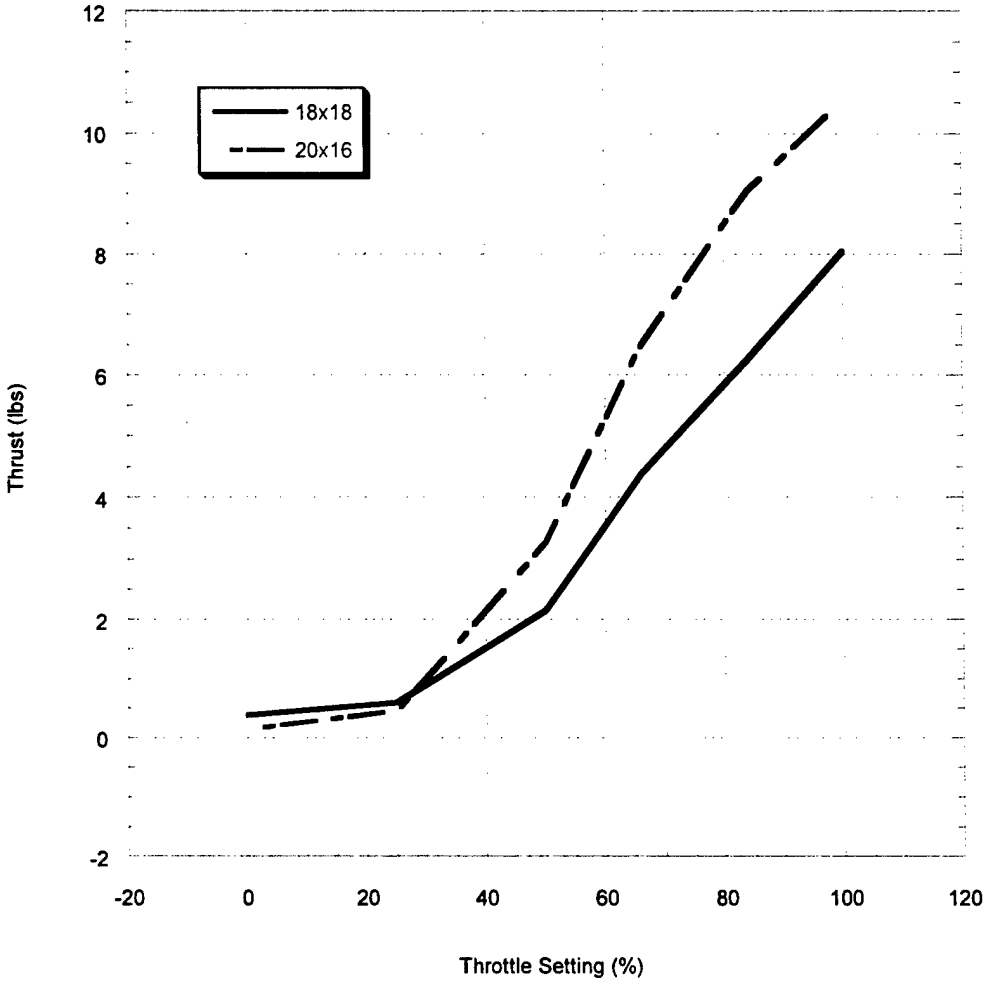

Figure 6.9 Static Thrust Versus Throttle Setting

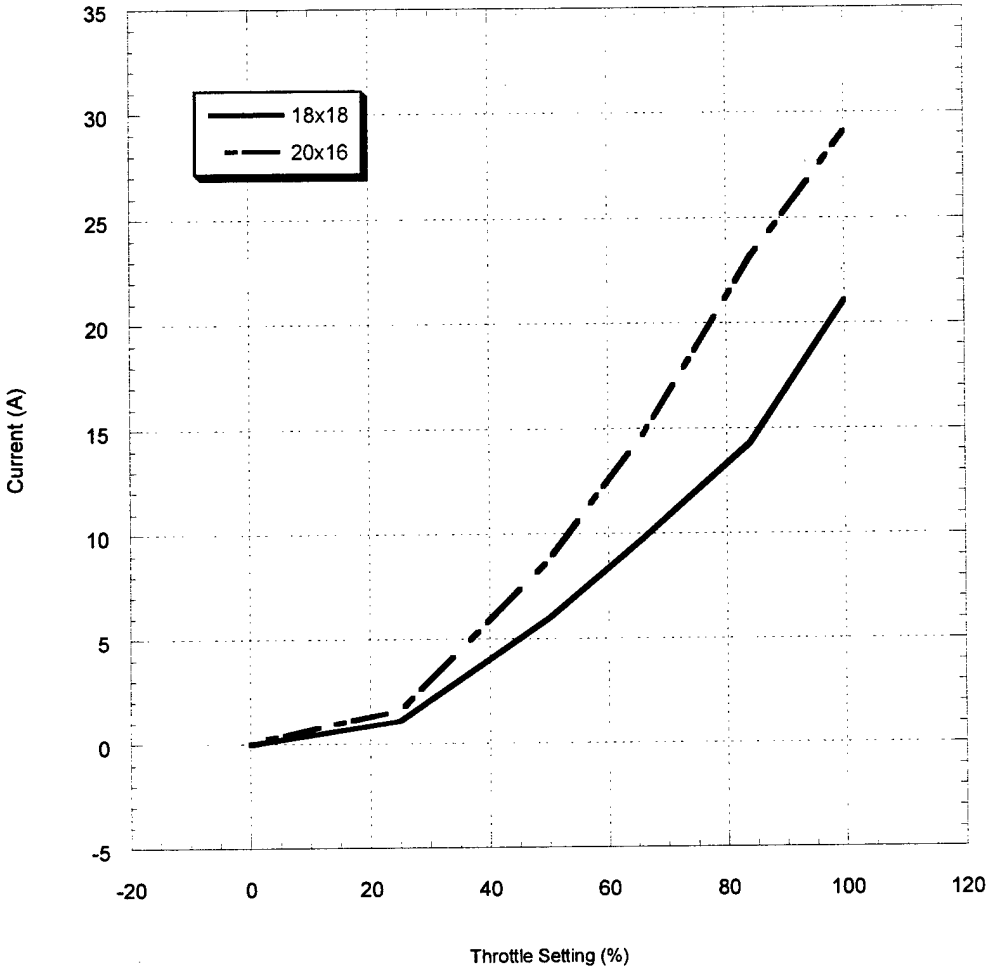

Figure 6.10 Motor Current Draw (Static)

6.4 Stability and Control

The detailed design required that the stability and control analysis, which began in preliminary design as a purely longitudinal study, be finalized. The first task in this requirement was the development of a complete lateral-directional stability model of the airplane. A complete summary of the lateral-directional derivatives was assembled, and a state-space model of the airplane was constructed. In this case, it proved necessary to scale the vertical tail up somewhat from the original 0.5 ft^2 tail. The final tail had an area of 0.7 ft^2, which corresponded to a volume ratio of 0.03. This tail provided good tradeoffs between spiral instability at low speeds and a lightly damped Dutch Roll at high speeds.

It was then necessary to size the control surfaces. Since the law of diminishing returns activates on the flap effectiveness parameter, τ, at 30% chord (which gives approximately 50% of the effectiveness

of an all-moving surface), this chord percentage was selected as an initial value. It was found that 14 degrees of elevator travel were needed to achieve $C_{L,max}$, and that a 20 degree aileron deflection required 1.93 feet of outboard aileron span to achieve 180 degrees per second of steady-state roll rate. For the actual airplane, this was rounded off to 2 feet for manufacturing ease. Finally, the rudder proved more than adequate in authority, capable of achieving 24 degrees of sideslip with 30 degrees deflection.

With the complete stability and control of the airplane modeled, a Simulink™ model was constructed, and the airplane subjected to a series of disturbances. Response in all cases was acceptable, and in most cases, excellent. Sample time histories are plotted in Fig. 6.11 and 6.12.

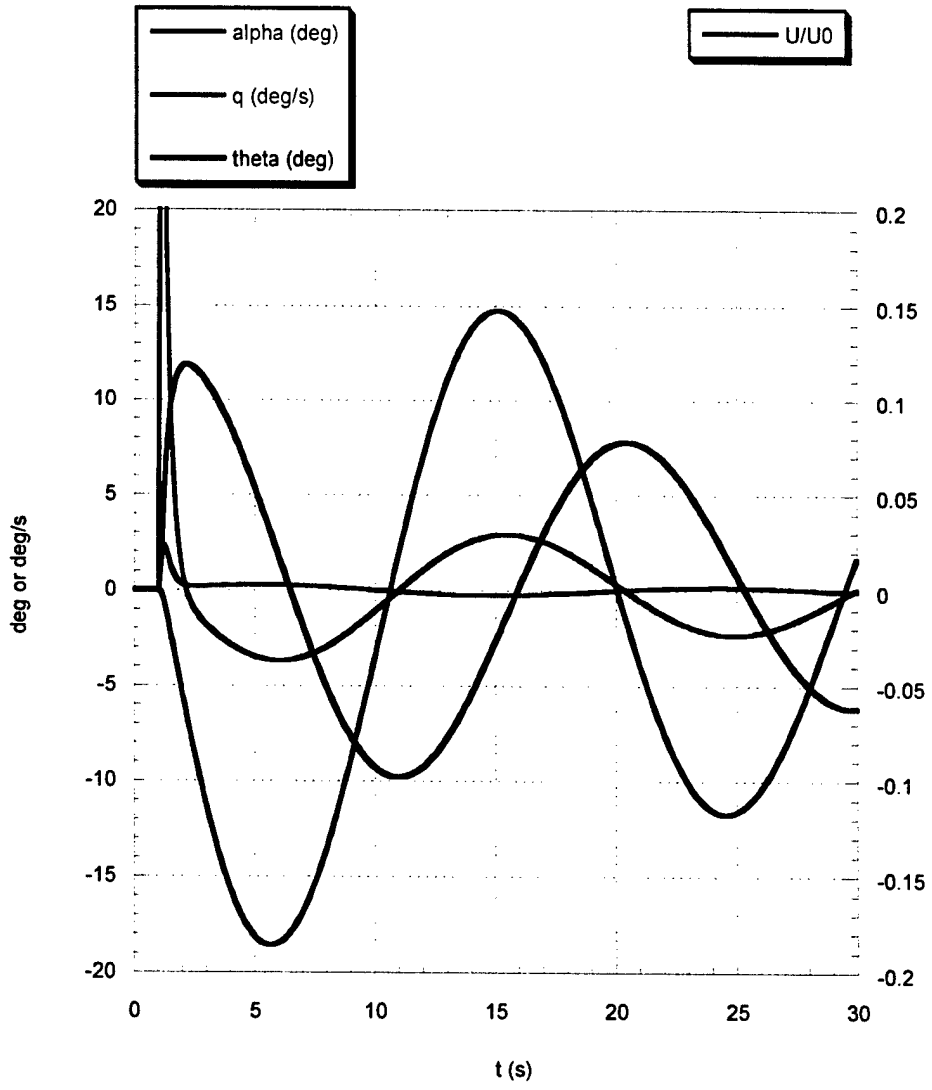

Figure 6.11 Airplane Longitudinal Response to Elevator Impulse

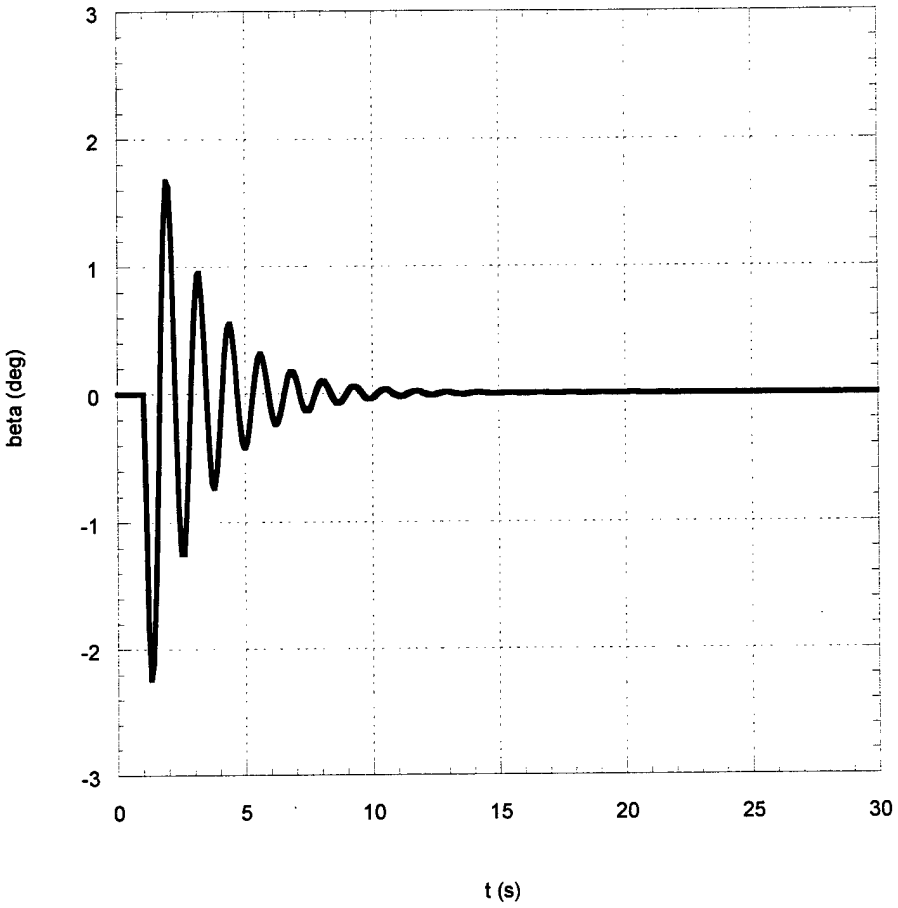

Figure 6.12 Beta Response to Rudder Impulse

6.4.1 Weight and Balance

In order to achieve the static margin of 10% specified by stability and control in the preliminary design phase, it was necessary to place the c.g. at the quarter-chord of the wing. A code was generated based on the initial weight model – slightly refined to account for structural variations – and the longitudinal locations of the various parts of the aircraft. This code was used to place the movable items in the aircraft, with the battery location being the most important contributor to balance. It was quickly found that because of the long moment arm of the motor, it was necessary to place the battery centroid at the planned c.g., as the plane balanced nearly perfectly without the batteries on board. This posed a problem, as the payload bay occupied all available space in this vicinity. This was resolved by breaking the battery pack into 2 sub-packs, with half mounted to the forward bulkhead opposite the payload, and the other half mounted to the rear bulkhead.

With the battery position set, the remaining small parts were placed to finalize the balance of the airplane. Recognizing the possibility of error in the c.g. calculations due to inaccuracies in the component weights, the team postponed battery pack construction until after final assembly and balance of the aircraft was complete.

A list of the major assemblies and their moment arms, along with the final projected weight and c.g. location is presented in Table 6.3.

Table 6.3 Weight and Balance Sheet

Component	Weight (lb)	Centroid Distance from proposed C.G. (in)
Fuselage	1.24	-4.3
Wing	2.88	-1.8
Vertical Tail	0.3	-22
Horizontal Tail	0.57	-22
Landing Gear	1.1	3
Radio Gear	0.54	-8
Motor	1.5	3.5
Batteries and wiring	3.5	0
TOTAL	17.5	-0.1

6.5 Structures

For all primary structures on the airplane, a moldless composite-over-foam method of construction was selected. To finalize the structural design of the airplane, the materials for the cores and skins were selected. For toughness and economics, it was decided that the skins would be primarily composed of fiberglass with carbon fiber and aramid reinforcement in certain key areas. Since the cross-sectional areas involved were so large, it was decided that standard lightweight white EPS foam was adequate for nearly all cores on the airplane. The wing was devised as a skin-spar type structure, with carbon caps laid into the upper and lower surface and the core itself serving as a shear web.

6.5.1 Spar Sizing

The spar caps were sized by developing a moment distribution for the two critical loadings of the airplane: a 6g turn and the structural tip test. The 6g turn proved to be the larger load, so analysis was performed for this case. An expression was developed for the required moment of inertia and the cap widths were determined. Bending load transfer was maintained through the bonds between the caps and the receiver tube. It was necessary to use higher-stress blue foam for the inboard panels in order to achieve adequate shear transfer.

6.5.2 Wing and Empennage

The wing and tail surfaces were designed in a similar manner. First, the flight loads were calculated. Then, the core material and skin material were chosen. Finally, the skin lay-up order and direction were designed to handle the particular directions and magnitudes of the loads on that surface.

The tail structures were designed to carry all the necessary loads in the fiberglass skins. Both tail surfaces were laid up with one layer of 1.6 oz./yd.^{2} ±45 degree biased fiberglass to handle shear loads, followed by another layer of 1.6 oz./yd.^{2} fiber on a 0-90 degree orientation to handle bending moments. For protection and smoothness, these were covered with a layer of tight-weave, 0.6 oz./yd.^{2} fiberglass. Additionally aramid "live hinges" were integrated into the lay-up, allowing the skin to form a gapless hinge once the part was completed and a slot was cut in the opposing skin and core. Finally, an aramid leading edge was used to provide toughness on the most commonly damaged area of these structures.

The vertical tail is joined to the fuselage by means of two carbon rods that attach to both the upper and lower skins of the fuselage. These rods were then inserted into holes drilled in the vertical fin and were glued into place. The horizontal tail uses a similar pair of rods that attach to the two rods in the vertical tail in order to provide a contiguous load path to the fuselage.

The wing was designed such that the skin was the primary load-bearing member. The loads on the wing were much greater than those experienced on either tail section. This was especially true in bending, which required the addition of carbon fiber skin spars along the upper and lower surface of the wing. The carbon fiber spars consisted of unidirectional 0.007-inch carbon fiber cloth: two layers on the upper surface and one on the lower surface. The spars are tapered because the bending moment decreases to zero at the wing tip. The foam core of the wing acts as a shear web for the spar. Additionally, a joiner mechanism was incorporated into the wing so that the wing panels could be easily and quickly attached to the fuselage. The joiner mechanism consists of a 1.5" aluminum tube with a cardboard sleeve.

6.5.3 Fuselage

The fuselage structure of the payload box was problematic. That area is the point of maximum bending in along two principal axes, and yet is missing nearly all of its cross section, as can be seen in Fig. 6.13. In order to better understand the loads generated in that area of the fuselage it was entered into SAP 2000™. A unit torque was applied to the nose of the structure and a one-degree rotation was permitted at the tail. The results was a 200 unit load on the cross braces between the bulkheads. Therefore, the shear loads that the payload bay area experienced were 200 times the torque applied. To handle this load a 0.625-inch diameter carbon fiber tube is positioned at each corner of the payload box. These tubes are secured through bulkheads fore and aft of the payload, which then transfer the loads to the skin of the airplane. Figure 6.14 shows the structure of the payload box. This method also creates a hard-point for the attachment of the aluminum wing joiner tube.

The nose and tail cones were constructed of solid foam with cavities removed for components and cooling ducts. These structures were then covered with two layers of 1.6 oz./yd.^{2} ±45 degree fabric, two layers of 0-90 degree 1.6 oz./yd.^{2} fabric, and one 0.6 oz./yd.^{2} 0-90 degree layer.

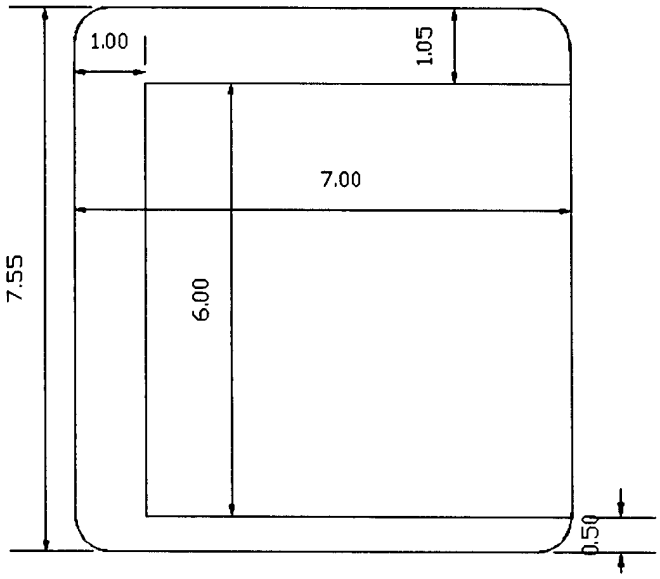

Figure 6.13 Payload Bay Cross Section (all units are in inches)

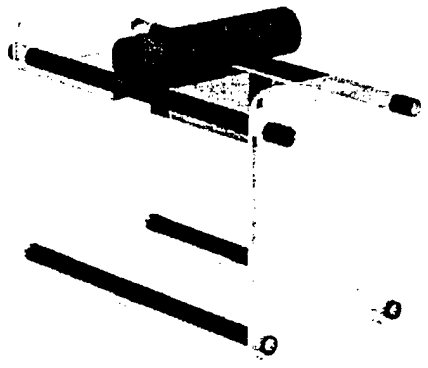

Figure 6.14 Fuselage Structure Drawing

6.5.4 Landing Gear

The landing gear was designed by analyzing the loads it had to endure to allow only 1.5 inches of deflection when the airframe experienced a 2.5g load. This constraint was established to prevent a propeller strike in the even of a hard landing. A model of the landing gear was analyzed in FTOOL™. The model was subjected to 8.3 lb./in.*unit width along the upper surface as seen in Fig. 6.15, which simulated a 2.5g load on the airplane. In order to simplify the analysis the cross sectional area was set to 1 $in.^2$, the modulus of elasticity (E) was set to 10000 psi and the moment of inertia (I) was set to 1 $in.^4$. The modulus of elasticity was then varied to allow a total deflection of 1.5 in. The necessary value of E was found to be 2800 psi. Therefore, the material properties and geometry of the landing gear material were selected such that E*I was equal to 2800 $lb.\text{-}in.^2$. Aluminum provided the required stiffness and low weight, while also yielding under stresses higher than the design stress rather than fracturing like a composite. Accordingly, aluminum was chosen for the landing gear.

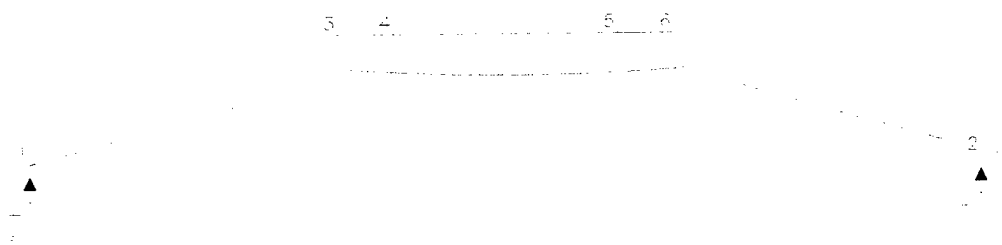

Figure 6.15 Landing Gear Model

6.6 Final Airplane Design

The final performance estimates for the competition airplane are presented in Table 6.4. Figure 6.16a through 6.16d contain complete drawings of the competition airplane. The estimated RAC is included as Table 6.5 and a summary of the final design is included in Table 6.6.

Table 6.4 Expected Airplane Performance

Mission	Takeoff Distance (ft)	Time (s)	Energy (mAh)
Sensor Deployment	76.8	130.1	715.5
Missile Decoy	91.9	130.8	808.0
Communication Repeater	78.7	147.5	928.3

Table 6.5 RAC Sheet

Multiplier	**Equation**	**Breakdown**	**Cost**
MEW*100	MEW=Empty Weight	11.5	1150
REP*1500	(1+.25*(# of engines-1))*Total Battery Weight	(1+.25*(0))*3.2	4800
MFHR*20	MFHR=(8*Span)+(8*Chord)+(3* # of control surfaces)+(10*Length)+(10*Vertical surfaces with active control)+(10*Horizontal surfaces)+(5*Controllers)+(5*#of engines)+(5*# of propellers)	(8*8)+(8*1)+(3*2)+(10*4)+(10*1)+(10*1)+(5*6)+(5*1)+(5*1)	3560
	Total Rated Aircraft Cost	Cost/1000	**9.51**

Table 6.6 Airplane Design Summary

	Parameter	Units	Value/Comments
Geometry:	Length	ft	4.0
	Wing Span	ft	8.0
	Height	in	13.5
	Wing Area	ft2	8.0
	Aspect Ratio	N/A	8.0
	Horizontal Tail Volume Coefficient	N/A	0.48
	Vertical Tail Volume Coefficient	N/A	0.03
Performance:	C_{Lmax}	N/A	1.3
	L/D_{max}	N/A	15.0
	Maximum Rate of Climb (Empty)	ft/min	1900
	Maximum Rate of Climb (Max. Gross Weight)	ft/min	1200
	Power Off Stall Speed (Empty)	ft/sec	30.0
	Power Off Stall Speed (Max. Gross Weight)	ft/sec	37.0
	Maximum Speed (Empty)	ft/sec	126.0
	Maximum Speed (Max. Gross Weight)	ft/sec	125.0
	Takeoff Length (Empty)	ft	39.0
	Takeoff Length (Maximum Gross Weight)	ft	92.0
Weights:	Airframe	lb	4.5
	Propulsion System	lb	2.0
	Batteries	lb	3.9
	Control System	lb	0.75
	Payload System	lb	0.25
	Payload	lb	5.0
	Empty Weight	lb	11.5
	Maximum Gross Weight	lb	17.5
Systems:	Radio	N/A	Futaba 8AU
	Receiver	N/A	R148DP PCM
	Servos	N/A	HS-81MG
	Battery Cell	N/A	Sanyo 1300CP
	Battery Configuration	N/A	End-to-end Brick
	Motor	N/A	Astroflight 60
	Propeller	N/A	APC 18x18
	Gear Ratio	N/A	1:2.75

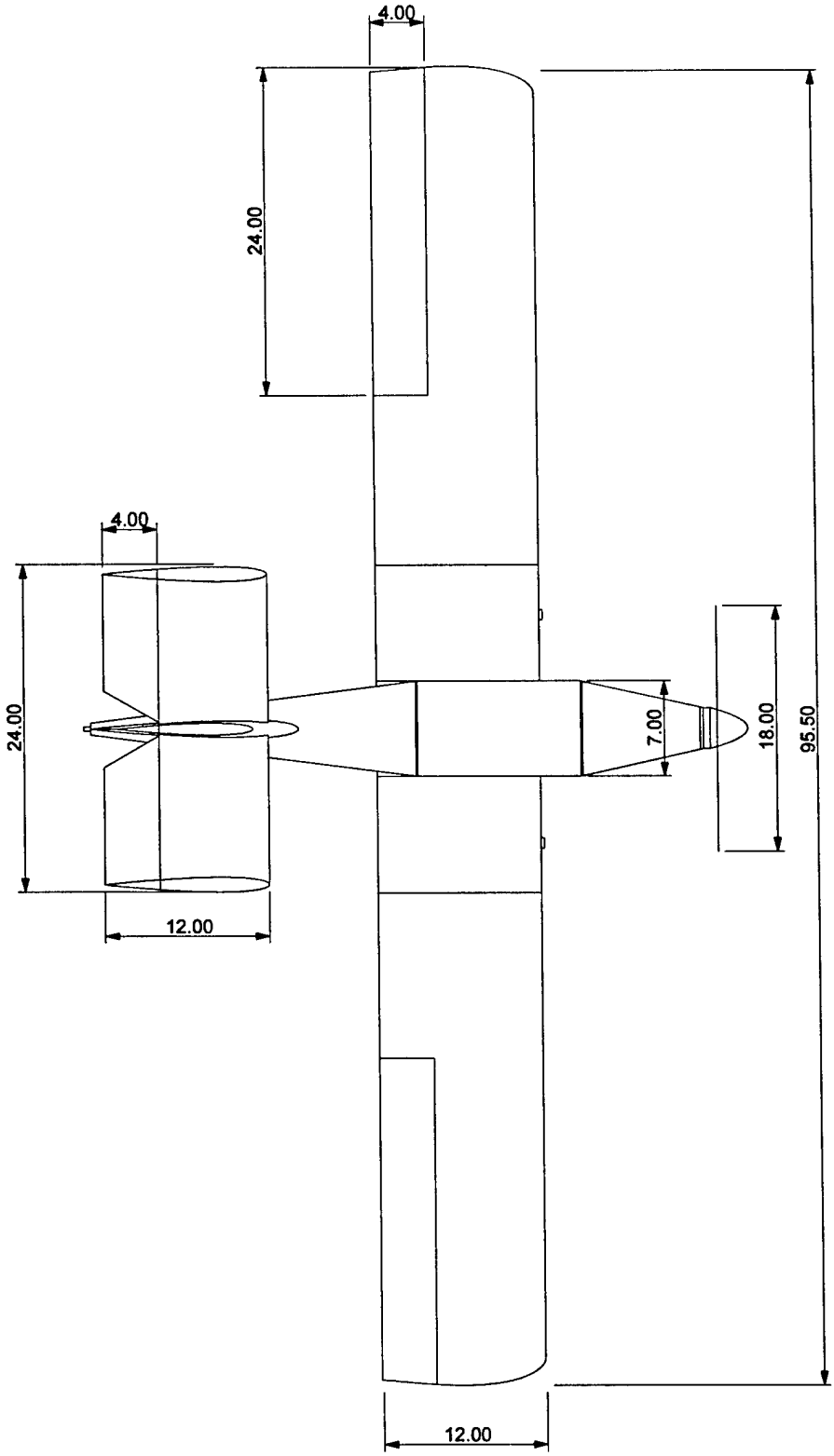

Figure 6.16a Top View (all dimensions in inches)

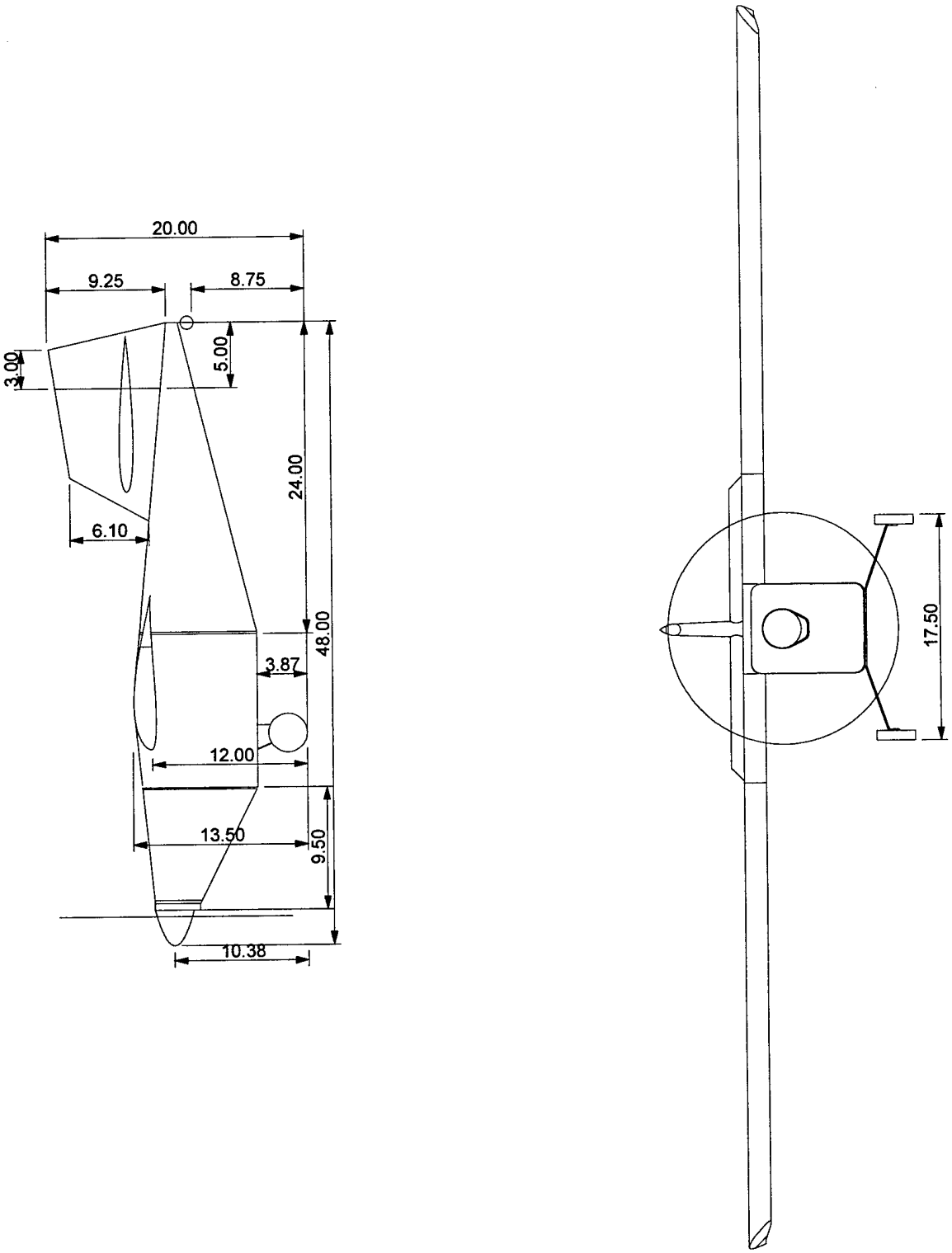

Figure 6.16b Side and Front Views (all dimensions in inches)

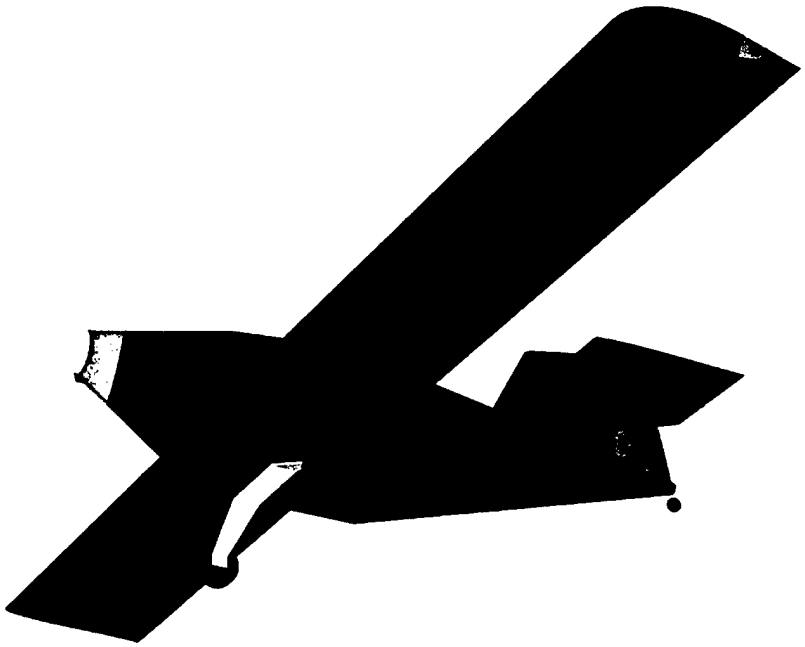

Figure 6.16c External Configuration

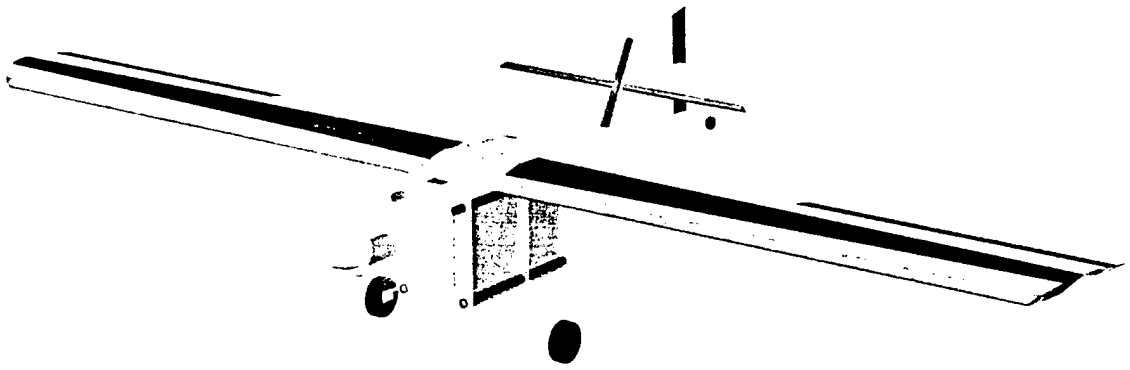

Figure 6.16d Internal Configuration

7.0 Manufacturing Plan

The planned and actual dates for beginning and completing manufacturing tasks are presented in Table 7.1.

Table 7.1 Manufacturing Schedule

	Wing	Empennage	Fuselage	Landing Gear	Integration/ Wiring
Projected Start	19-Feb	12-Feb	26-Feb	28-Feb	6-Mar
Actual Start	21-Feb	12-Feb	1-Mar	8-Mar	9-Mar
Projected End	26-Feb	19-Feb	5-Mar	3-Mar	9-Mar
Actual End	28-Feb	21-Feb	9-Mar		

7.1 Manufacturing Techniques Available

Two possible basic construction methods were considered for the airplane components: built-up and composites. Each basic method utilizes different materials could be accomplished in various manners. In addition to the construction of the major subassemblies of the airplane, the tasks of overall airplane assembly and payload deployment also had to be considered.

7.2 Major Airplane Coponents Construction

The first basic construction method considered was the built-up method. The traditional built-up method consists of hardwood longerons and plywood bulkheads as the primary fuselage structure. The wing and empennage possibilities consists of carbon fiber or hardwood spars and balsa ribs. Variations of this method include sheeting the previously mentioned structures with mylar covering, a balsa skin, or a balsa and fiberglass skin. Structural skin has the advantages of having excellent shape fidelity and adding torsional strength to the structure. Disadvantages of a structural skin include increased susceptibility to handling damage, increased repair difficulty, increased weight, and increased complexity.

The second basic construction method considered was composite construction. This method includes a wide variety of materials and methods. The basic structure consists of a foam core covered with fiberglass, carbon fiber, aramid, or a combination of these. Variations in the wing structure included the possible addition of a spar. Variations in the fuselage included removing some or all of the foam core and inserting plywood bulkheads.

7.3 Airplane Assembly

In order for the airplane to fit inside the "box", it had to consist of at least two subassemblies. Options included having a fuselage with removable outer wing panels or a fuselage with a fully removable two-piece wing or and the possibility of a removable tail. Other assemblies such as the landing gear and empennage had to be removable, or otherwise stowed, if they did not fit inside the box.

The final airplane disassembles into three parts. The main subassembly is the fuselage, including the landing gear and empennage. The main landing gear folds forward to allow the bottom of the fuselage to rest on the bottom of the box. The landing gear is hinged with a spring that deploys the gear and holds it in place. The other two assemblies are the right and left wing panels. Each of the wing panels contains its own radio receiver so that no wires need to be plugged in when the wings are attached.

7.4 Payload Deployment

It is feasible to eject the payload from the airplane in one of three directions: out the bottom of the airplane, out the back of the airplane, or out the side of the airplane. Ejecting the payload out the side or rear of the airplane allows the weight of the payload to be carried by the floor of the fuselage, making the fuselage structure simpler. Ejecting the payload out the rear of the airplane requires that the rear fairing of the fuselage open, adding complexity. Ejecting the payload out the bottom of the airplane requires a stronger latch to secure the payload and requires that the entire fuselage sit at least 6 inches off the ground. Asymmetric fuselage structure is a concern when ejecting the payload out the side of the airplane.

The final release method ejects the payload out the right side of the fuselage. Rubber bands provide the necessary force to push the payload out of the airplane. A servo activates a cam mounted on the outside of the fuselage below the wing that secures the payload in flight. While the payload is stowed, the side of the payload box is flush with the exterior of the airplane. When the payload is deployed, a plywood hatch closes the payload bay opening. A wire guide is used on the exterior of the airplane to ensure that the payload does not damage the landing gear while the payload is being deployed. The payload box is constructed of EPP (expanded polypropylene) foam with a steel weight to ballast it to the specified weight.

7.5 Construction Method Selection and Figures of Merit

Figures of Merit were used to determine the construction method that would be the most desirable for each of the three components: fuselage, wing and empennage. The Figures of Merit used were strength to weight ratio, manufacturing complexity, speed of construction, cost of construction, durability, reparability, and shape fidelity. Each Figure of Merit also had a weighting factor that gave an indication of its relative importance. The Figures of Merit were ranked from 1 to 5, with 5 being the most desirable and 1 being the least desirable. As an example, for speed of construction a 5 would indicate

the fastest construction but for cost of construction a 5 would indicate the least expensive. Figures of Merit with weighting factors of 5 are the most important, while those with weighting factors of 1 are the least important. For example, shape fidelity is more important in wing construction than in the fuselage construction, while durability is more important in the fuselage construction than the empennage construction. Tables 7.2 through 7.4 present the FOM process for the component manufacturing techniques.

Based on these Figures of Merit, the fuselage would be constructed using a foam core fiberglass skin method. The wing would use a foam core and fiberglass skin with a carbon spar. The empennage would also be of a foam core and fiberglass skin construction.

Table 7.2 Fuselage Manufacturing FOM Study

	Fuselage Component				
Construction Method	**Weighting Factor**	**Foam Core Fiberglass Skin**	**Built-up Mylar Skin**	**Built-up Balsa Skin**	**Built-up Balsa and Fiberglass Skin**
Strength to Weight	4	5	3	4	4
Manufacturing Complexity	4	3	5	4	4
Speed of Construction	5	5	4	3	3
Cost of Construction	2	2	5	4	3
Durability	3	5	2	3	4
Reparability	3	2	5	4	3
Shape Fidelity	2	5	2	3	4
Totals		**92**	**87**	**82**	**82**

Table 7.3 Wing Manufacturing FOM Study

	Wing Component					
Construction Method	**Weighting Factor**	**Built-up Mylar Skin**	**Built-up Balsa Skin**	**Built-up Fiberglass Skin**	**Foam Core Fiberglass Skin Carbon Spar**	**Foam Core Fiberglass Skin**
Strength to Weight	3	2	3	3	5	4
Manufacturing Complexity	4	5	4	4	4	4
Speed of Construction	5	4	3	3	5	5
Cost of Construction	2	5	4	3	1	2
Durability	4	2	3	4	5	5
Reparability	3	5	4	3	3	3
Shape Fidelity	5	2	4	4	5	5
Totals		**89**	**92**	**91**	**112**	**111**

Table 7.4 Empennage Manufacturing FOM Study

	Empennage Components			
Construction Method	**Weighting Factor**	**Foam Core Fiberglass Skin**	**Built-up Mylar Skin**	**Built-up Balsa Skin**
Strength to Weight	3	5	3	4
Manufacturing Complexity	4	3	5	4
Speed of Construction	5	5	4	3
Cost of Construction	2	3	5	4
Durability	2	5	3	4
Reparability	2	3	5	4
Shape Fidelity	4	5	2	4
Totals		**94**	**83**	**83**

8.0 Manufacturing Processes

8.1 Fuselage

The first step in constructing the fuselage was to cut the foam cores using the bulkheads as guides. Next, the wing receiver tube and carbon fiber tubes were placed in the foam core. Ducts and the payload opening were then cut into the foam. The foam removed in these steps was left in place during the glassing process. This entire structure was then glassed and cured in a vacuum bag. Next, the access panels were cut and the underlying foam removed. The fuselage surfaces were then finished. Once the fuselage structure was complete, the landing gear, motor, electronics and batteries were installed.

8.2 Wing and Empennage

Firstly, the wing cores were cut. Then the receiver tube was bonded in place. During the glassing process, the aramid leading edges were first attached to the cores, followed by the carbon fiber spars and aramid hinges, and lastly, the fiberglass skin. This entire lay-up was then allowed to cure under vacuum.

After the wing was removed from the vacuum bag, it was finished and hinges were freed. Next electronics were installed. Fuselage attachment mechanisms were then added.

The empennage was constructed in a similar manner, with the exclusion of the receiver tube and carbon spars. The empennage was then secured to the fuselage.

9.0 Testing Plan

Before approving the aircraft for flight, the aircraft must be fully tested on the ground. Planned testing includes verification of static thrust and current draw, load testing of airframe with the required "tip" test, and low-speed taxi testing. High speed taxi testing will be reserved for after the first flight, as the airplane may inadvertently take off if this test is performed with an untrimmed aircraft. Table 9.1 shows the necessary preflight checks that must be performed prior to each flight. The proposed flight test program is outlined in Table 9.2.

Table 9.1 Preflight Checklist

	Verify motor NOT armed (fuse removed)
	Verify integrity of wing attachment
	Verify integrity of all control surfaces
	Landing gear intact, wheels freely rolling
	Tail wheel intact, wheel freely rolling
	Verify that the payload is secured
	Verify all receivers ON
	Test radio range
	Verify tail wheel steering operation
	Verify proper operation, deflection range and neutral position of all control surfaces
	Insert arming fuse (no personnel forward of propeller after completion)
	Verify correct direction of motor rotation
	Verify full power available

Table 9.2 Flight Test Program

Flight	Payload	Radome	Maneuvers
1	No	No	Takeoff, Climb, Coordinated stall testing, Approach, Landing
2	No	No	Takeoff, Climb, Uncoordinated stall testing, Approach, Landing
3	Yes	No	Takeoff, Climb, Uncoordinated and coordinated stall testing, Approach, Landing
4	Yes	Yes	Takeoff, Climb, Uncoordinated and coordinated stall testing, Approach, Landing
5	Yes	No	Communications Repeater Mission
6	Yes	No	Payload Deploy Mission
7	Yes	Yes	Missile Decoy Mission
Cont.			Repeat Missions for Practice and Times
TBD			Envelope Testing (Stall Speed, Max Speed, L/D, Turn Radius, etc.)

References

1 MotoCalc™. Version 6.03, Capable Computing Inc., 2001.

2 Nelson, Robert C., **Flight Stability and Automatic Control**, McGraw Hill, New York, NY, 1986.

3 Raymer, Daniel P., **Airplane Design: A Conceptual Approach**, 3rd Edition, American Institute of Aeronautics and Astronautics, Reston , VA, 1999.

4 Lyon, C.A., Broeren, A.P., Giguere, P., Gopalarathnam, A. and Selig, M.S., "UIUC Low-Speed Airfoil Tests," http://www.aae.uiuc.edu/m-selig/uiuc_lsat.html.

5 LinAir™ for Microsoft Windows™. Version 1.4, Desktop Aeronautics Inc., 1996.

Cougar Air Transport

2002-2003 DBF Team

Washington State University AIAA

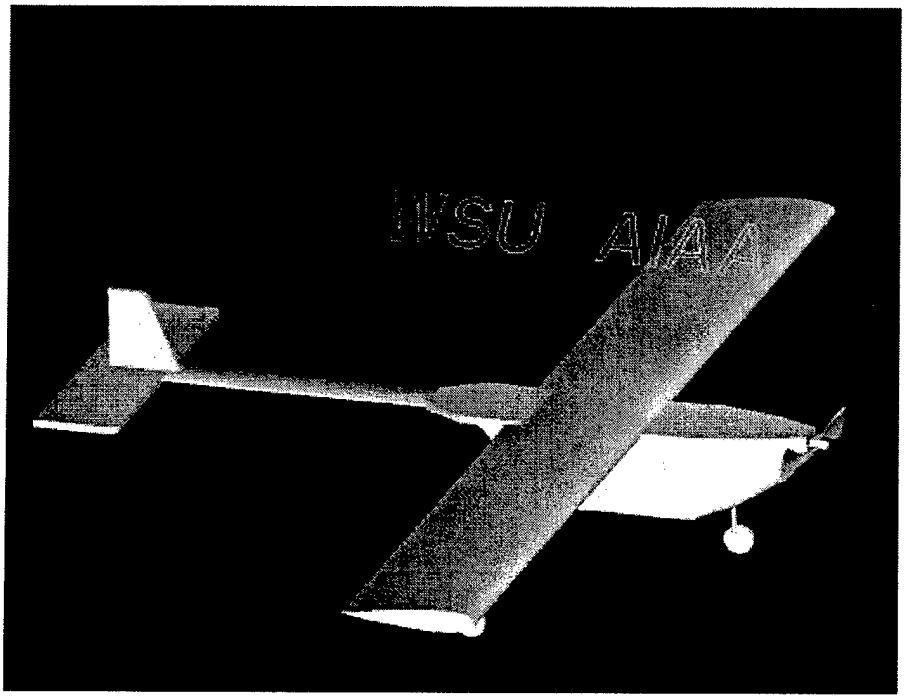

Contents

1 Executive Summary 1

1.1 Design Development Summmary 1

1.2 Design Alternatives Investigated 1

2 Management Summary 2

2.1 Team Organization 2

2.1.1 Chief Engineer 2

2.1.2 Structural Engineer 2

2.1.3 Propulsion Engineer 3

2.1.4 Manufacturing Engineer 3

2.1.5 Aerospace Engineer 3

2.2 Schedule 3

3 Conceptual Design 3

3.1 Problem Statement 3

3.2 Airplane Configuration Study 5

3.2.1 Tractor 5

3.2.2 Biplane 6

3.2.3 Pusher 6

3.2.4 Canard 6

3.3 Materials Study 6

3.3.1 Balsa 7

3.3.2 Fiber Glass 7

3.3.3 Balsa/Composite 7

3.3.4 Carbon Fiber 8

3.4 Rated Aircraft Cost Study 8

4 Preliminary Design 8

4.1 Design Methodology 8

4.2 Fuselage Sizing 9

4.2.1 Fuselage Constraints 9

4.2.2 Fuselage Analysis 9

4.3 Wing Sizing 10

4.3.1 Wing Constraints 10

4.3.2 Wing Analysis 10

4.4 Drag Analysis 11

4.5 Power System Analysis 12
4.5.1 Free Body Analysis 12
4.5.2 Propeller Analysis 12
4.5.3 Motor Selection 12
4.5.4 Battery Analysis 13
4.6 Stability Analysis 13

5 Detail Design **13**
5.1 Component Selection 13
5.1.1 Power System 13
5.1.2 Landing Gear 14
5.1.3 Controls and Servos 14
5.1.4 Radio Gear 14
5.2 Wing Spar Strength Evaluation 14
5.2.1 Aircraft Specification Tables 15

6 Manufacturing Process **18**

7 Flight Testing Program **19**
7.1 Objective and Methods of Testing 19
7.2 Check List 19

List of Figures

1 WSU AIAA Schedule 4
2 Wind Tunnel Data for Eppler 205 11
3 Building Schedule 20

List of Tables

1 Design Administration 2
2 Airplane Configuration Decision Table 5
3 Materials Decision Table 7
4 Rated Aircraft Cost Decision Table 8
5 Rated Aircraft Cost Decision Table 16
6 Aircraft Configuration 17
7 Materials Decision Table 18

1 Executive Summary

1.1 Design Development Summmary

The development of the conceptual design for the aircraft began in September 2002. The WSU AIAA Team started off the year with 6 of last years members and gained a few new members. The design team comprised of most of the student members of the club. The first task the design team completed was the outline of the project goals of based on the requirements. These requirements helped in developing our conceptual designs. The conceptual designs must meet the design competition requirements, and be simple enough to construction. Keeping the conceptual design simple was important due to inexperience of the design team. The team's addtional design constraints were the design must have a simple construction method, aerodynamic stability, and a moderate flight speed of 35 to 45 mph.

1.2 Design Alternatives Investigated

The design process was continued by specifing the aircraft configurations, material selection, and the evaluation of the RAC. The four aircraft configurations that were considered constisted of a biplane, canard, pusher, and tractor designs. The configuration choosen as the best concept for the competition was the tractor design, with its ease of construction, ability to fit within the required dimension, and relatively large amount of data available.

The design team considered carbon fiber, fiberglass, balsa, and balsa composite as the materials in construction the aircraft. Balsa was chosen as the main construction material due to its low weight, low cost, high availability, and simplicity of construction. It decided that balsa had limitations due to its overall low strength. To make the wing spars strong enough to withstand the loads and small enough to fit in the box. It was decided that carbon fiber strips would be required to meet the calculated strength requirements. The final design ended up being a comprising of a hybrid balsa/composite.

The RAC evaluation used attributes of our aircraft design that most affected the RAC, with weighted attributes the determined by the team. The RAC attributes were made up of simplicity of construction, flyability, lower mission time, and higher success rate. The analysis of the attributes found that by adding engines the RAC was most affected, and by the addition of more servos least affected the RAC.

Our preliminary design began with the finalized conceptual design. The design team began defining the shape and size of the fuselage. The specifications for a suitable airfoil were determined and its related dimensions such as span and csrtationhord. With the wing and fuselage was defined, the drag force of the aircraft could be estimated through calculation. The drag force calculations allowed the team to determine the size the propulsion system required for the aircraft. By calculating a suitable factor of safety the team could be reasonable sure that the aircraft will fly. With all the aircraft parameters defined, the numerical flight analysis could being by estimating our aircraft performance. After the analysis, changes were made to the aircraft to improve the overall performance.

2 Management Summary

2.1 Team Organization

The WSU AIAA design group employed five different job assignments. A team member was assigned to a position that he/she was most knowledgeable. Once assigned, that member was responsible for conceptual design input, preliminary design and detailed design related to that position. Table 1 shows the task that each member was assigned to. A description of each position is given in the following sections.

Club Administration	
President	Zak Valentine
Vice President	Brian Schneider
Secretary	Peter Wiseman
Tresurer	Tom Osmundson
CEACC Rep	Colin Merriman
Advisors	Dr. William E. Johns, Dr. B.R. Ramaprian
Design Build Fly Administration	
Chief Engineer	Matt Donovan
Structural Engineers	Peter Wiseman, Jennifer McKamey
Propulsion Engineer	Zak Valentine
Manufacturing Engineer	Tom Osmundson
Aerodynamicists	Brian Schneider, Colin Merriman

Table 1: Design Administration

2.1.1 Chief Engineer

The Chief Engineer is responsible for the synthesis of the design. He drafts the master building plans and makes sure that other engineer's ideas are heard and implemented into the design harmoniously. Quality control and system performance are also ensured by the Chief Engineer.

2.1.2 Structural Engineer

The roll of Structural Engineer is to design the structural support for the vehicle. The type, size and performance of spars, ribs, joiners and control surfaces are decided by this assignment area. Structural engineers research designs that optimize the strength to weight ratio of the final aircraft. Structural Engineers also design the payload release system.

2.1.3 Propulsion Engineer

This engineer designs the vehicles propulsion system. Comparison between multiple power configurations and aircraft power to weight ratios are conducted by the Propulsion Engineer. Optimization of battery capacity and motor performance for a range of flight conditions is also done by the Propulsion Engineer.

2.1.4 Manufacturing Engineer

The Manufacturing Engineer explores the materials that are possible for a given device. Decisions are made based on weight and strength considerations, as well as difficulty to manufacture. Additionally, the Manufacturing Engineer develops a manufacturing process for a device, such as a spar, so that part can be made consistently by any member of the team.

2.1.5 Aerospace Engineer

The Aerospace Engineer handles aerodynamic aspects of the design. By using key mission requirements and constrains, this engineer decides what the wing parameters (airfoil, chord, length) will be. Control surface areas and RAC effects are also considered by the Aerospace Engineer.

2.2 Schedule

Figure 1 shows the actual and anticipated timing of key events during the competition year. Each horizontal bar represents the time span of the task listed in the Tasks column.

3 Conceptual Design

3.1 Problem Statement

The goal of the 2003 Design Build Fly competition is to perform 2 of 3 flight missions with an electric powered RC aircraft. Mission elements range from completing 4 laps, flying in a 360 degree circle, transporting a 6"x6"x12" 5lb payload, deploying the payload on the ground, and flying with a 3" tall 6" cylindrical antenna. Additional requirements for the aircraft include taking off within 120ft, must fit in a 2' wide by 4' long by 1' tall box in disassembled form, and completing each flight mission within 10 minutes. The aircraft must also be less than 55lbs takeoff weight, have a battery pack that weighs at most 5 lbs, the motor must draw at most 40 amps, use Graupner or Astro flight families of brushed electric motors, have a low Rated Aircraft Cost (RAC) and use over the counter nickel cadmium batteries. With these constraints in mind, ideas were developed for the configuration of the aircraft.

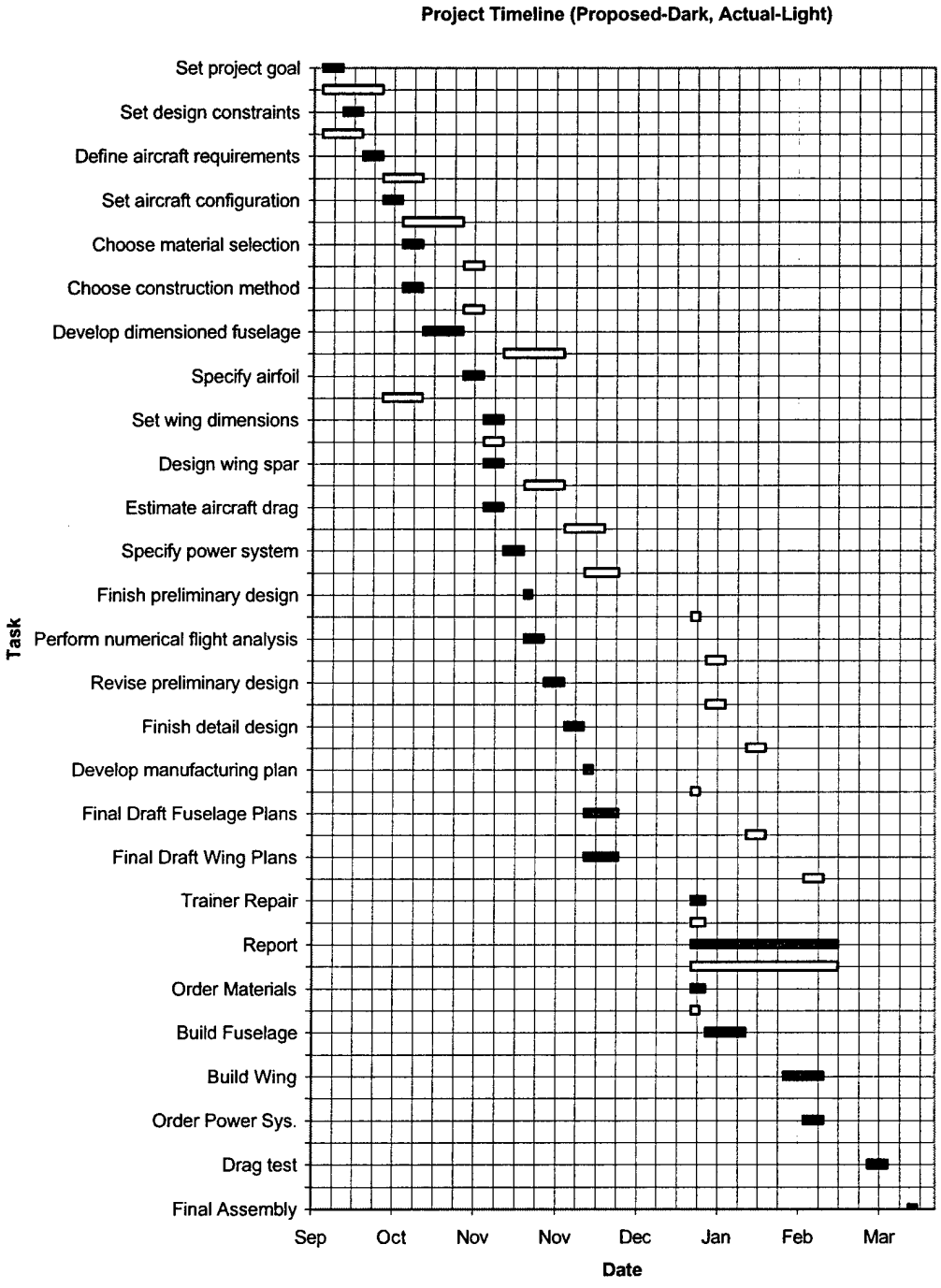

Figure 1: WSU AIAA Schedule

First, the design team came up with a project goal and added some additional requirements. The project goal was to build a plane that would meet all of the competition requirements and be simple enough to design and build for an inexperienced design team. Our additional design constraints include simple construction, aerodynamic stability, and a moderate flight speed of 35 to 45 mph.

The task is to design an aircraft to meet the requirements of three different tasks. Additional constraints are given as measures of safety for competition participants. Due to the complexity of the tasks, a task matrix has been developed to develop design criteria.

The screening process was meant to determine the primary design for competition. This process had three main steps. Each step used a decision Table to decide the best way to continue developing the aircraft. The three steps were broken into the airframe, material used, and the general specifications such as how many engines to use. The screening process has allowed the team to develop an airplane that optimized the Rated Aircraft Cost (RAC) and allowed the plane to fit within the allotted box size. The Decision Tables were essential with many design elements in each stage in the screening process.

3.2 Airplane Configuration Study

The airframe or alternative configuration concepts consisted of four concepts, each with their different advantages and disadvantages. The four designs were made up of Biplane Canard, Pusher, and Tractor. With each having distinct qualities decision had to be made on which design best fit our criteria laid out the rule. An example would that since the flying wing is most likely is going to be built in to a solid piece it would be difficult to meet the requirement of lifting a five pound box and fitting within the limiting dimensions of the box.

Benefits	Low Weight	Simple Construction	Low RAC	High Speed	Easy to Fly	
Weight	0.2	0.2	0.3	0.1	0.2	
Choices						Value
Biplane	50	60	50	50	40	50
Canard	80	70	90	90	50	76
Pusher	90	50	90	90	70	78
Tractor	90	90	90	80	100	91

Table 2: Airplane Configuration Decision Table

3.2.1 Tractor

The tractor design scored the highest in our ranking in the Decision Table. By having the best overall score, it showed that it best met the weighted criteria. By scoring high in all categories such as; low

weight, simplicity of construction, low RAC, high speed, and easy to fly, it was decided to continue to screening process using this design. The tractor design was considered because of the large number amount of data available and it ability to be broken down to fit in the box. The weight of each of the five categories was determined through their relative importance. The scores for the categories for each design were based on research and past experience.

3.2.2 Biplane

The biplane design scored the lowest relative score because of its inability to meet the requirements. With the increased drag and RAC due to the high surface area helped screen out the design. With a low RAC, the most heavily weighted of all the categories, the biplane was singled out as being a poor design. The biplane was initially considered because it increased maneuverability in flight due control surfaces on both wings and its small wing span.

3.2.3 Pusher

The pusher design scored nearly the same as the tractor design because of how similar the designs were. The major scoring difference was based on the simplicity of construction. With by having the motor in the back of the airplane the tail would need to spilt or have two engines. Also with having the power in back, the deployment of the package would difficult without damaging the propeller. The pusher design was initially considered because it minimized the propeller drag and the turbulence created by the propeller.

3.2.4 Canard

The canard design scored the second highest among the four designs. The only category it scored poorly in was in "easy to fly" due the fact the main control surfaces are in the front of the airplane rather then the back. With the control surfaces in the front, the pilot would need to learn a new flying technique. All other categories such as low RAC it scored quite high make it a good choice, but not the best. The canard design was initially considered it would be easily collapsible allowing it to fit in the box.

3.3 Materials Study

The next stage in the screening process involved deciding which material to build the tractor design out of. After doing some research it was found that materials such as carbon fiber, fiber glass, balsa, and balsa composite would be the most like candidates for the construction of the airframe. As with the airplane, there were weighted categories used in a Decision Table to decide on the best material to be used in the construction of the airplane. The categories consisted of low weight, simplicity of

construction, strength, versatility, and cost. The Decision Table allow the team to decide on the best material for construction.

Benefits	Low Weight	Simple Construction	Strength	Versatility	Cost	
Weight	0.3	0.2	0.2	0.2	0.1	
Choices						Value
Carbon Fiber	90	50	90	60	50	72
Fiberglass	60	50	60	50	60	56
Balsa	90	70	65	70	100	78
Balsa/Composite	90	50	70	80	90	76

Table 3: Materials Decision Table

3.3.1 Balsa

The material that ranked the highest was the Balsa due to how to meet all of the categories. With its low weight, simplicity of construction, versatility, and low cost it was the material chosen in the second stage of the screening process. Balsa allowed the team easily construct and modify parts throughout the construction of the airplane. Balsa was initially considered because of its ease of use and the large amount of data that could be found on balsa construction.

3.3.2 Fiber Glass

Fiber glass scored the lowest among the four material chosen. With only minor advantages in each category, it showed that there were no distinct advantages in choosing glass over any of the other fibers. With past experience in constructing an air plane with fiberglass the team understood the many difficulties in the constructing such an airplane. The fiber glass design was initially considered mainly because the team had experience with material in the construction of an airplane.

3.3.3 Balsa/Composite

Balsa/Composite, as a construction material was the second highest in the ranking. With proper design the weight to overall strength could be improved by using balsa the as the main platform for construction and reinforcing with carbon fiber. The balsa/composite design was initially considered because it brought together the advantages of both balsa and carbon fiber.

3.3.4 Carbon Fiber

Carbon fiber ranked very closely with the Balsa composite, but ranked lower mainly because of how expensive the carbon fiber is. As with fiber glass, the construction of such a design would difficult due the molding tools and complex curves. With lack of experience pure carbon fiber construction, this material would have difficult to of optimize the strength without making the plane to heavy. The carbon fiber design was initially considered because it had such high anisotropic strength and its strength to weight ratio.

3.4 Rated Aircraft Cost Study

The Rated Aircraft Cost (RAC) played a major in understanding which aspects of the airplane would have the most affect on our calculated RAC. Each category was then compared by weighted attributes. Each of the four attribute was considered critical to manufacturing a successful aircraft. The four attribute were made up of; the simplicity of construction, flyability, lower mission times, and higher success rate. The category that scored the highest was having more servos was the most beneficial. The lowest scoring category was the addition of engine to the airplane. By adding engines, the RAC would be most affected compared to the other categories. The four categories that score basically even were the increase in battery weight, greater wingspan, increased fuselage length, and higher control surface area. By maximizing these four categories and comparing those to the conceptual designs a primary design could be later determined.

Benefits	Simple Construction	Flyability	Lower Mission Times	Higher Success Rate	
Weight	0.2	0.3	0.1	0.4	
RAC Penalties					Value
More Engines	30	50	70	10	32
Increase Battery Weight	50	90	100	60	71
More Servos	80	100	70	90	89
Greater Wingspan	20	90	40	100	75
Increased Fuselage Length	30	80	60	90	72
Higher Control Surface Area	50	70	60	90	73

Table 4: Rated Aircraft Cost Decision Table

4 Preliminary Design

4.1 Design Methodology

To begin the design of our aircraft a design methodology was established to break the numerous aspects of aircraft design into manageable pieces. The five step process developed is as follows:

1. Develop a dimensioned fuselage design based on all of the constraints.
2. Specify a suitable airfoil and its dimensions.
3. Estimate the drag force of the aircraft.
4. Specify a sufficient power system with a suitable factor of safety.
5. Perform a numerical in-flight analysis to verify and improve the previous steps.

4.2 Fuselage Sizing

4.2.1 Fuselage Constraints

Sizing of the fuselage was based upon the given constraints and existing aircraft. Since the aircraft has been determined in the conceptual design phase to be a single engine tractor with a high wing, only 4 fuselage parameters must be defined; length, width, height and shape. Fuselage length was defined as the length from the tip of the nose structure to the end of the fuselage structure. Width is the width of the average cross section and height is the height of the average cross section. Constraints that affect the final shape are:

- Battery pack dimensions
- Payload Dimensions
- Payload Release Mechanism
- Motor and Landing Gear
- Electronics
- Prop to ground clearance

4.2.2 Fuselage Analysis

Height and Width were based upon the minimum required to surround the payload with adequate structural support using balsa. In addition, space must be allotted to allow for a ramp style release mechanism. This set the height and width to 10" x 8" respectively. This leaves adequate space for electronics and a payload release system. The battery pack would be placed forward of the payload and its dimensions would be limited to 9.75" high and 7.75" wide.

All parts were assumed to be placed in-line with the length of the fuselage. Length was assumed then to be the summation of the lengths of the pay load and all of the other components. Since the battery pack now has its width and height constrained, its length would be varied as power requirements

increase. This results in the length of the fuselage being a function of power, and would be further developed as the power system is defined.

The release mechinism was key because it too needs to fit within the fuselage. With the release mechinism being a rotating arm controlled by a servo, the package can be released easily. With the payload being deployed through the rear of the airplane, it was important that nothing could interfear the deployment. To prevent the jamming problem, ramps of a smooth material were placed inside the aircraft to prevent torsion or pitching. By designing in the deployment features the fuselage's shape had to come under consideration.

To reinforce the fuselage sqare ribs were designed in to help in torsion and add strength. With the five main ribs the ourside panels could be attached to complete the main fuselage structure. The main structure which extends to the tail attaches to these ribs tying the entire structure together. The ribs in the fuslage are key in improving strength and making structure more rigid.

Shape was to be based on ease of construction and aerodynamics, in that order. As a result, the shape of the main fuselage was decided to be square, and the nose would be smoothly curved from the motor to the bulk of the fuselage. To maximize propeller clearance, the motor was placed at the top of the nose, which results in an entirely flat top surface. The nose would be gently curved downward to meet with the rest of the fuselage.

4.3 Wing Sizing

4.3.1 Wing Constraints

To define a wing, a chord, span and cross section must be defined. Constraints that control these variables are as follows:

- Good Flyability.
- 35-45 mph airspeed.
- Take off distance less than 120 ft.

4.3.2 Wing Analysis

Since flyability is essential and speed is low, a low wing loading was chosen. About 1.25 lb/ft^2 is considered a low wing load for an RC model. With the weight of the airplane approximated to be 12 lb., the calculated wing area is $9.6ft^2$. An aspect ratio of 6.7 was chosen so that the wing halves would fit into the length of the box, while maximizing wingspan. Next, an airfoil cross section was defined. Tradeoffs between thickness and camber were compared by researching RC models of similar characteristics. An Eppler 205 was chosen based on this simple analysis, which fully defined the wing geometry.

4.4 Drag Analysis

To specify a power system, it is necessary to know the drag forces exerted on the aircraft during flight. Now that geometry of the aircraft has been defined, an estimate of the drag forces on the wing and fuselage can be accomplished. Ideally, a wing tunnel model would be constructed and drag data would be derived from the testing. Finite Element Analysis (FEA) is another method for developing drag information, however a wind tunnel of sufficient size was not available at the time of analysis and lack of experience with FEA meant that a more general approach must be developed to estimate drag.

Three of the most influential forms of drag were considered in this study, form, induced and parasite drag. Form drag can be determined from wind tunnel data from the Eppler 205 ,as shown in Figure 2. Induced drag was approximated numerically and is essentially a correction for the infinite aspect ratio assumed in a wind tunnel test situation. It was found to contribute very little to the total drag coefficient. Finally, parasite drag was derived. Parasite drag is the contribution made by the fuselage, for a smooth fuselage a typical Cd is 0.01, since the WSU AIAA fuselage has sharp corners and a flat cargo door, it was approximated from past experience that parasite would be at least 2 times higher. Landing gear and the antenna were also added to the total drag coefficient, which totaled to 0.04.

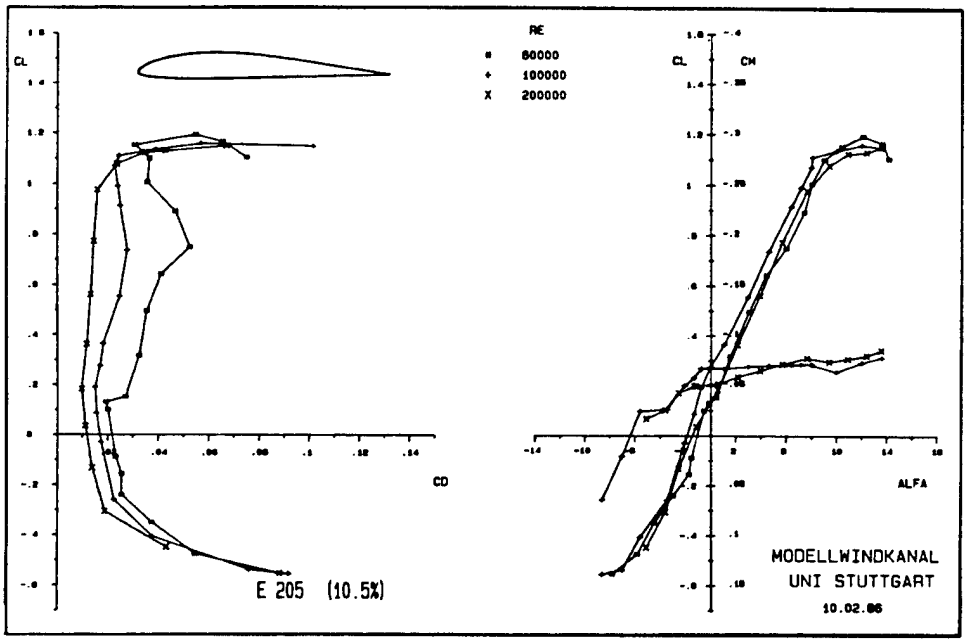

Figure 2: Wind Tunnel Data for Eppler 205

4.5 Power System Analysis

A proper assessment of the power system needs to be made to assure mission success and minimal wasted energy. Energy not used in the batteries is simply dead weight, lowering this valued will decrease mission times, but could increase the likelihood of failure should the unexpected happen. A qualitative analysis is the best way to successfully balance these conflicting demands and is presented in the following sections.

4.5.1 Free Body Analysis

To determine an adequate power system, a free body analysis of the aircraft must be performed at maximum velocity. Four force vectors are prevalent at any given time in flight, but for level flight at constant velocity, only thrust and drag are of concern. From the previous analysis, Cd can be applied to Bernoulli's Equation to find the maximum drag force. At 45 mph, this force was found to be 3.3 lbf.

4.5.2 Propeller Analysis

To maintain flight at 45 mph, a thrust of equal value must be applied. For an electric motor, power required is dependant on the load applied. The load applied is dependant on propeller pitch and diameter. Froude efficiency for a propeller suggests that a larger diameter propeller would provide greater efficiency than a smaller one. This is not true if the propeller tips exceed the speed of sound. The Mach number was calculated for an 18" propeller, and it was determined that the motor couldn't exceed 14000 rpm. None of the electric motors available could turn the propeller at this rate, so the limiting factor was ground clearance, which set the propeller diameter. Next, a motor was chosen. Only two manufacturers were allowed, Graupner and AstroFlight. The decision was made for AstroFlight due to lack of technical and historical data found during research for Graupner motors. AstroFlight's motors were found to have high reliability and served the past WSU AIAA teams well, which is critical to completing the mission.

4.5.3 Motor Selection

To complete the motor choice, comparison between different models in the Cobalt line were made. Going back to the drag force calculated earlier, power required was calculated assuming a rather low efficiency of 65% to provide an adequate safety factor. The result of the power calculation was 400 watts. This number is not an entirely realistic value, since adequate rate of climb and flight performance are not considered. To get trainer like handling, a fly-ability of 40Watts/lb is commonly used. The power system must now exceed 500 watts for acceptable rate of climb and performance. This would suggest using an Astro 25 geared, which has an output of 600W, but does not drive the 18" propeller. The minimum motor to drive the propeller is the Astro 40, with a 3.1:1 ratio gear drive. The efficiency lost by

using a gear system is approximately 3% per mesh, but efficiency lost in using a smaller propeller far exceeds this value, so the Astro 40 is a good choice thus far. The final value to consider is the motor choice's effect on RAC. The only factor that affects RAC directly when using a fixed number of motors is the weight of the battery system. The Astro 40 requires only 20-24 1.2 V NiCad cells, while larger motors require up to 40 cells. Although a decrease in flight times would be noticed, our fixed flight speed does not justify further increase in battery weight and RAC penalty.

4.5.4 Battery Analysis

Since the power requirements were fixed from the previous section, a choice of a battery system can be made. To ensure a successful flight can be made under any given condition, flight time was calculated at maximum speed and thrust. At maximum thrust, 1000 watts of power is being drawn from the 24 1.2 V array of cells, thus current draw equals 35 amperes. The course length was approximated to be 14000 ft for 4 laps, which at 45 mph would be completed in 4:00 minutes, including liftoff and landing. This means that the batteries must have an ampere-hour rating in excess of 2.33. This assumes however that the power into the motor is 1000 watts, but only 500 watts should be required. By choosing 2400 ampere-hour cells, a factor of safety of 2 will insure that the plane can be landed safely if the runway is missed or heavy winds are encountered.

4.6 Stability Analysis

By choosing a high wing tractor design, aircraft stability should be quite high. By placing the wings at 3 degrees of dihedral, additional roll stability is built into the design. To ensure pitching stability, a boom of adequate length must be chosen. By comparing the values for aircraft with similar characteristics and purpose, estimates of boom length and tail surfaces were made. The tail analysis constisted main of finding what rudder and elevator would work best for the size of the aircraft we wish to build. By understanding the size of the aircraft and the cruzing speed the optimal air control surface area could be calculated. Most of the data on the control surface size was based on other aircraft we found with similar specifications. With both sets of data, the design for the tail and it attaching boom could be calculated and drawn up.

5 Detail Design

5.1 Component Selection

5.1.1 Power System

The power system consists of Motor, Batteries, Motor Speed Controller and related wiring. The Motor selected from the previous section was the Astro 40 with 3:1 gear ratio. Batteries selected had to be

at least 2.4 ampere-hour capacity, so 2400mAh batteries were selected. The intended supplier will be SR batteries due to their high quality of service and matched/tested cells. 24 cells will be used, but the number of cells may decrease if power is to high. The Speed controller will be the recommended controller for our current rate and will be purchased from AstroFlight. The wiring will be sufficient to handle the high current of the system, and a fuse will be placed in the circuit as per safety regulations.

5.1.2 Landing Gear

Two possibilities for front landing gear were considered. Split fork gear was eliminated due to excessive weight and increased manufacturing difficulty. Single strut gear was chosen based on simplicity, despite the wheel being offset from centerline. The strut wire was chosen to be 5/32", which proved to be the best balance between weight and strength. Possibilities for rear landing gear were aluminum tapered plate or 5/32" paino wire. Wire was chosen based on ease of manufacturing and higher stiffness. The higher stiffness was necessary due to the extreme length to ensure runway roll stability. Wheel diameters will bee approximately 3" to minimize rolling resistance.

5.1.3 Controls and Servos

The landing gear will be controlled with a single servo. The aeilerons, rudder and tail will be controlled by micro-servos to minimize weight. Additionally, the use of micro-servos will allow them to be installed in narrow structures, such as between the wing and internal to the tailboom. aircarft specifications developed throughout the design process

5.1.4 Radio Gear

The transmitter used for competition flight will be a JR 8 channel PCM fully programmable. This will allow for customization of handling to increase stability of the aircraft. A reciever with a built in failsafe will be used to meet the safety requirements of the competition. An additional requirement of the radio system is to lock out the release mechanism servo while the aircraft is airborn. This will be accomplished by putting a touch switch on the front landing gear sensor. Immediately after take-off, the switch will open the release circuit to eliminate accidental deployment.

5.2 Wing Spar Strength Evaluation

To specify how large the wing spar needs to be, the Materials and Manufacturing Engineers used the structural verification test of the aircraft for the competition as a model for the maximum wing load, which is approximately 2.5 g's. The wing spar was modeled as a simply supported beam with a central load equal to the weight of the aircraft (13 lb.). Using the proposed basswood spar with shear webs, the

moment of inertia was calculated for the basswood, since balsa webs wouldn't be taking the bending load in the wing. Since the basswood was .375" square set apart so it was a 1.7" tall beam, the moment of inertia was calculated as .1267 in^4 The wing is 96 inches long with a 15 pound load in the center. This meant that there were 7.5 pound reactions at the wing tips. The maximum moment in the beam was found to be 360 in-lbs. The distance from the centroid of the beam to the outermost fibers of the spar was half the height, or .85 inches. Using the following bending equation:

Stress = (Moment x Outermost Distance) / Moment Of Inertia

The stress at the top fibers in the spar was calculated to be 2414 psi. This stress exceeds the allowable design stress for basswood which was found to be 1640 psi. Graphite was suggested to reinforce the root of the wing spar. A .5 inch wide .015 inch thick strip of uniaxial graphite would be placed on the top and bottom of the spar. Considering that carbon fiber is much stiffer than the basswood, the moment of inertia for two strips of carbon fiber 1.7 inches apart was calculated it was assumed that it carried all of the bending stress. The moment of inertia was calculated to be .005419in^4. Using the moment of inertia for the carbon fiber in the same bending stress equation used for the basswood spar, the stress in the carbon fibers was calculated to be 28234 psi. This was well below the maximum stress of 135000 psi. Considering that 192 inches of .5x.015 carbon fiber is of low weight, it was decided to use the basswood spar originally conceived with carbon fiber on the top and bottom. Using the composite carbon fiber basswood spar would give a high factor of safety to pass the structural verification test. Using the ratio of allowable stress of the basswood and carbon fiber, a 1:82 ratio, the width of the basswood equivalent to a 0.5 inch wide strip of carbon fiber was 41 inches. Combining the theoretical top and bottom basswood sheets to the basswood spars originally considered, the moment of inertia was calculated to be .4459 in in^4. Using the revised moment of inertia in the bending stress equation, the stress at the outer fibers was calculated to be 686 psi, well below the 1640 psi allowable for basswood. This results in a factor of safety of 2.39 plus the factor of safety built into the allowable stress value for the basswood. Thus the wing spar is rated to a 6g load.

5.2.1 Aircraft Specification Tables

The following Tables shows all aspects of the Aircrafts development. Since the actual aircraft has not been flight tested, the values are approximations and are subject to change. Table 5 shows the final RAC values calculated. Table 6 lists the completed aircraft specifications.

Aircraft Cost Model	
RAC	**$9.76**
A	$100.00
B	$1,500.00
C ($/hour)	20
MEW (lb)	8
REP (lb)	3.3
MFHR (hours)	200.36

Input Parameters	
battery weight (lb)	3.3
airframe weight (lb)	8
wing span (ft)	8
exposed wing chord(ft)	1.17
# of control surfaces	4
fuselage length (ft)	5
vert. surface	0
vert. surface w/control	1
horiz. surface	1
# of servos	6
motor controller	1
# of engines	1
# of propellers	1

MFHR (Manufacturing Man Hours)		
variable name	variable discription	hours
WBS wing	8*wing span + 8*wingcord	85.4
	+ 3*control surface	
WBS fuselage	10*body length	50
WBS empenage	5*vertical surface w/no control +	20
	10*vert surf w/control +10*horiz surf	
WBS flight systems	5*servo or motor controller	35
WBS propulsion systems	5*engine + 5*propeller	10
MFHR Total		200

Table 5: Rated Aircraft Cost Decision Table

Aircraft Specifications		
Lengths	*Meters*	*Inches*
span	2.29	90
height	0.30	11.9
length	1.52	60

Areas	*Square Meters*	*Square Inches*
Wing	0.72	1120

Volumes	*Cubic Centimeters*	*Cubic Inches*
Controls	To be determined	To be determined

Dimensionless Quantities	
Asepct Ratio	6.45
Cl Max	1.1
L/D Max	7
Gear Ratio	3.1:1

Velocities	*Meters per Second*	*Feet per Second*
Rate of Climb Max	2.8	9
Stall Speed	6.5	21
Flight Speed Max	20.2	66

Distances	*Meters*	*Feet*
Takeoff Length Empty	6	20
Takeoff Length Gross	11	36

Weights	*kg*	*lbm*
Unloaded	3.18	7
Loaded	5.90	13
Airframe	1.35	3
Propulsion	1.63	3.625
Controls	0.11	0.25
Payload Release System	0.05	0.1
Payload	2.66	5.9
Propeller	0.06	0.125

Table 6: Aircraft Configuration

6 Manufacturing Process

Choosing a construction method for our aircraft was a simple process. The team considered what types of materials that could be used and what type of structure they are best used in. Considered was how much each material would cost, how long it would take to build, the availability of such materials, and what skills were needed to construct an airframe using those materials. The group spent the previous semester experimenting with lost foam manufacturing, but could not create a high enough quality surface finsish or low enough weight. The group did have some experience with balsa and had the tools needed to build a balsa aircraft. Due to additional delays in order processing and the difficulty and expense with molded composites, balsa and composite reinforcement provided optimum performance. This is reflected in decision matrix shown below.

Benefits	Low Weight	Simple Construction	Strength	Versatility	Cost	
Weight	0.3	0.2	0.2	0.2	0.1	
Choices						Value
Carbon Fiber	90	50	90	60	50	72
Fiberglass	60	50	60	50	60	56
Balsa	90	70	65	70	100	78
Balsa/Composite	90	50	70	80	90	76

Table 7: Materials Decision Table

Balsa is cheap, simple to work with, and very light. Construction is as simple as obtaining or cutting balsa to the correct dimensions and glueing together. Full scale plans were printed and sheeted with plasting on 2 inch foam to provide a straight and pinnable surface. This was useful for duplicating parts of common sizes. However, there were a few situations where it was necessary to concentrate strength in a smaller area than balsa would allow, such as wing spars or the tail boom. In this situation, WSU AIAA used basswood. Basswood is denser than balsa but with a similar strength to weight ratio. In the case of the wing spar, the strength of basswood alone was insufficient. Graphite was used as additional reinforcement, making the structure a composite. Manufacturing this one composite piece was far simpler than typical composite molding. The strip of uniaxial carbon is simply bonded onto the wood surface with epoxy and a light pressure.

For the surface of the wing and fuselage, a smooth and lightweight material must be chosen. Since molded composites were ruled out, only one choice was known to remain, using a mylar coating. Mylar coatings with a heat activated adhesive are available in variable densities and colors specifically designed for model aircraft. This material will be adhered to the sanded balsa surface once completed.

Additionally, the mylar allows easy placement of decals.

Following is a timeline describing details of the building process.

7 Flight Testing Program

7.1 Objective and Methods of Testing

The objective set for testing constisted mainly of the maximum velocity, total drag of the aircraft, diration of flight, and the take off distance. To measure this the team plans on setting up markers set apart at known distance and measure the time it takes to complete the length at maximum speed. With the use of the length and time taken the velocity may calculated. To test the total drag of the aircraft the team concluded that without a wind tunnel it would be needed to measure the drag in the field. To accomplished this the team plans on mounting the aircraft on car to find the total drag force at the team's desired flying speed. The duration of flight is mainly a ground test where the team can simulate the loading on the battery to determine their battery life. By mounting the aircraft to a solid mount there is no chance of moving around in this process. Known the take off distance is very important due to the restricted runway length. To measure the take off distance the team plans to have spotters along the runway to determine the exact point the plane leaves the ground. By knowning the intial takeoff postion and the point in which the plane leaves the ground the takeoff distance can be calculated. Flight testing will occur on dates according to Figure 1.

7.2 Check List

To minimize the cause of mishap, a mandatory preflight checklist will be conducted to ensure safety of the flight crew, bystanders and property. The following list will be used:

- Verify all components are securely fastened, especially fastenters.
- Verify propeller is in good shape.
- Inspect wiring and batteries for corrosion, leakage or damage.
- Check range of radio and speed control operation.
- Check motion of controls to ensure proper sense.
- Make sure load is securely fastened.
- Check runway for debris.
- Make sure bystanders are clear.

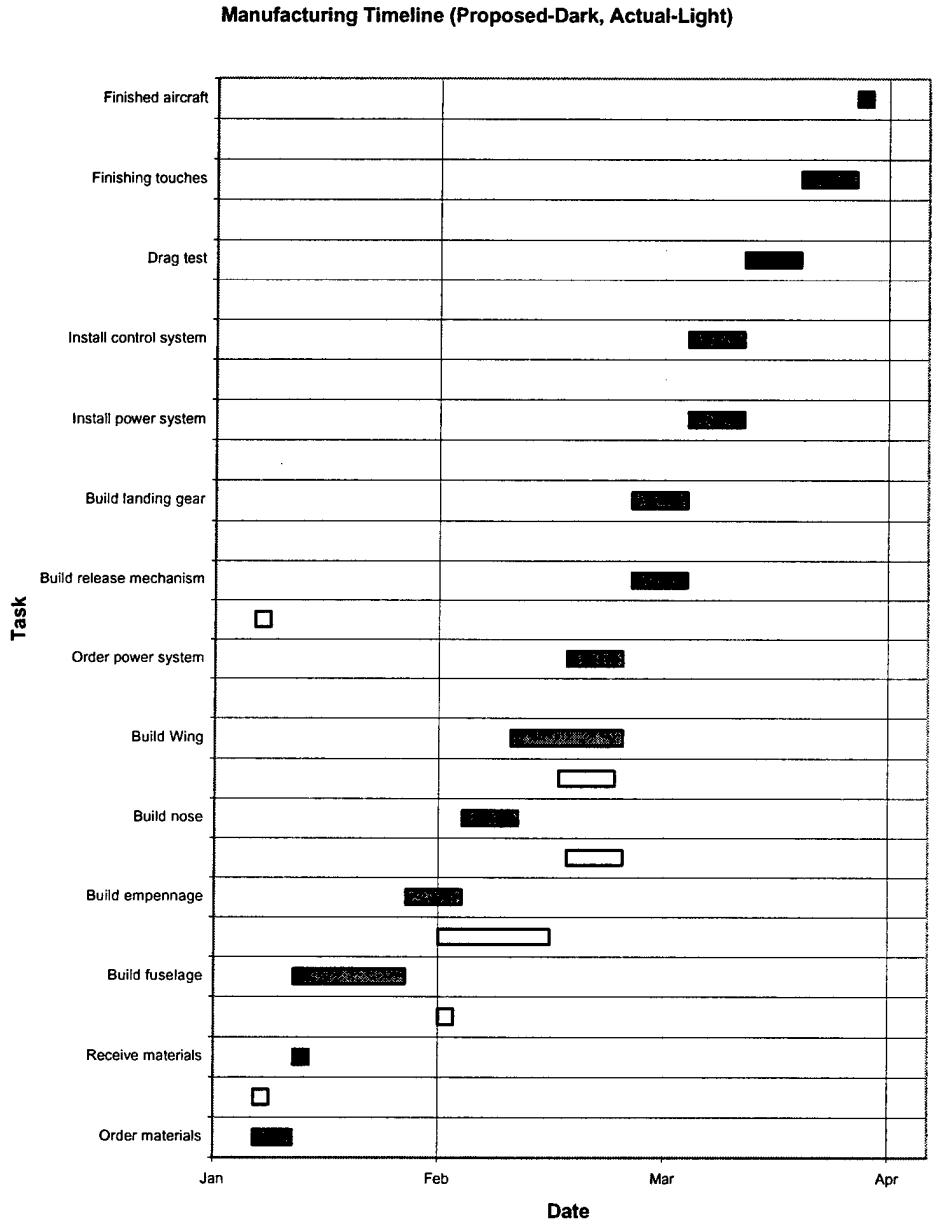

Figure 3: Building Schedule

JAVA USM

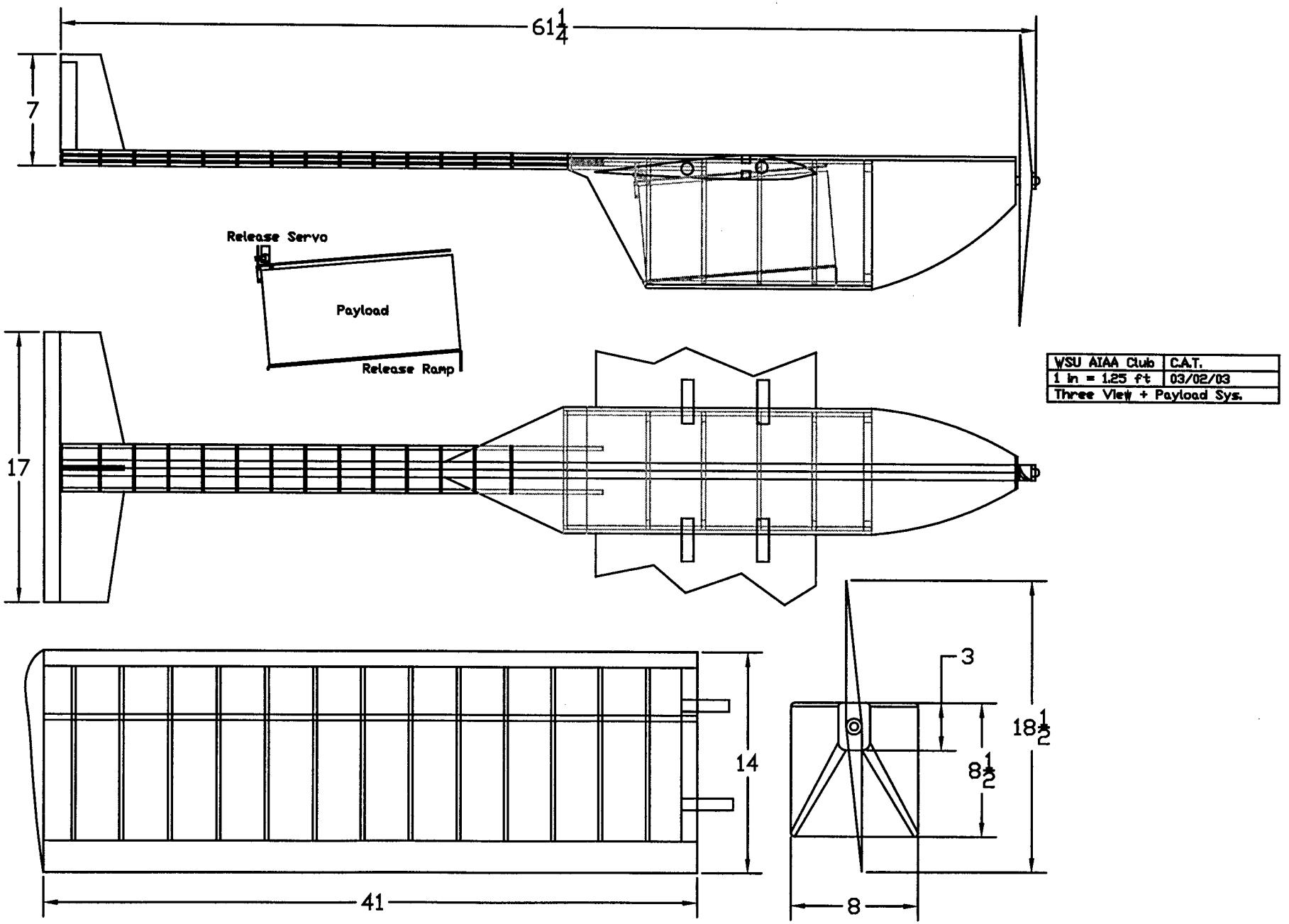

WSU AIAA Club	C.A.T.
1 in = 1.25 ft	03/02/03
Three View + Payload Sys.	

2002/2003 AIAA Foundation Cessna/ONR Student Design Build Fly Competition

DESIGN REPORT

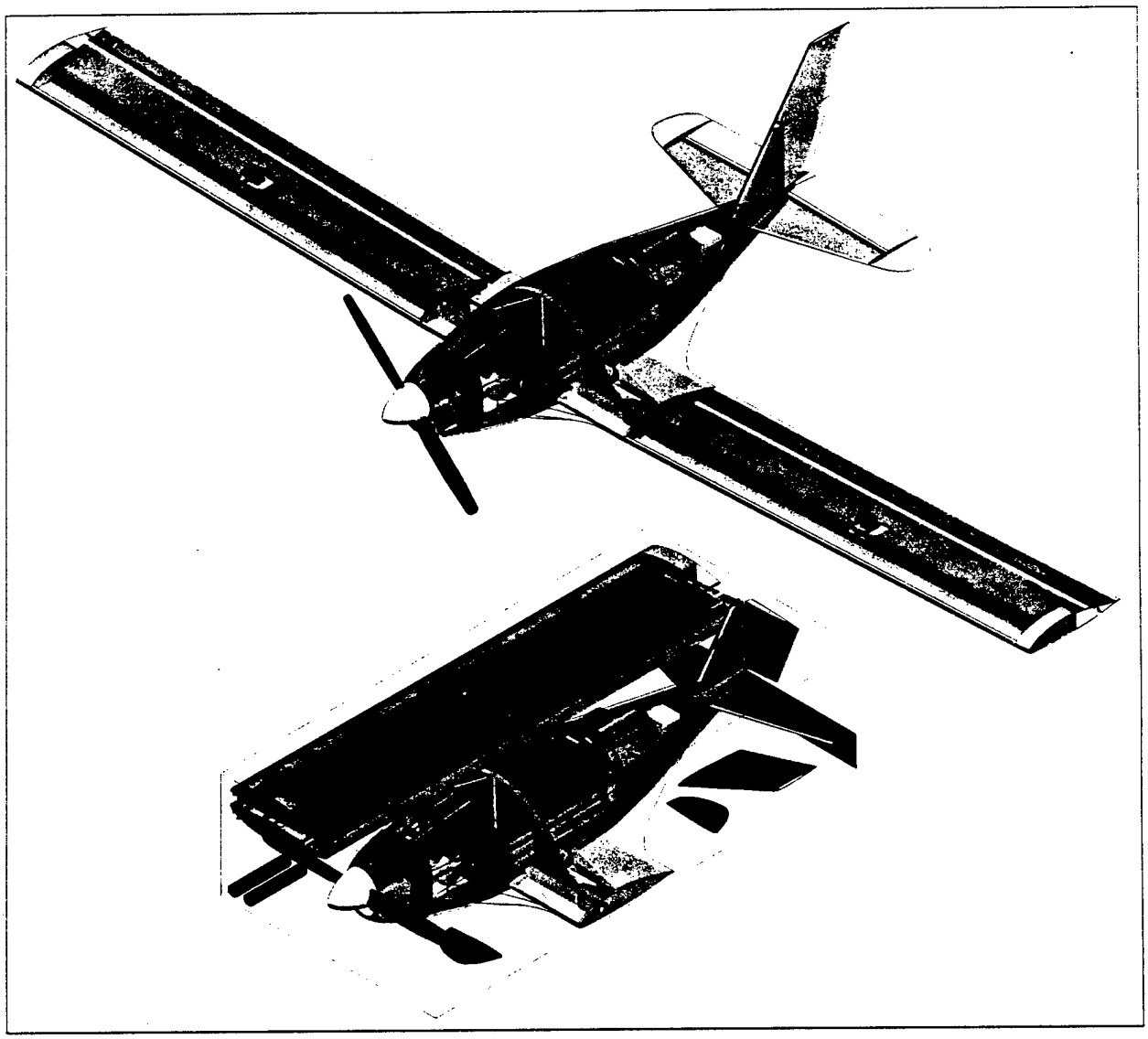

"Zephyr"

Utah State University

March 2003

TABLE OF CONTENTS

1. Executive Summary 1
1.1. Overview of the Design Development 1
1.2. Design Alternatives Investigated 1
1.3. Highlights of the Development Process 2
2. Management Summary 3
2.1. Architecture of the design team 3
2.2. Configuration and Schedule Control 3
Chart of Design Personal and Assignment Areas 4
Milestone Chart, Planned and Actual 5
3. Conceptual Design 6
3.1. Mission Requirements 6
3.1.1. Aircraft Storage and Timed Assembly 6
3.1.2. Takeoff 6
3.1.3. Missile Decoy Mission (MDM) 6
3.1.4. Sensor Deployment Mission (SDM) 6
3.1.5. Communication Repeater Mission (CRM) 6
3.1.6. Aircraft Cost-Effectiveness 6
3.2. Aircraft Configurations Studied 6
3.2.1. Initial Configuration Parameters Studied 7
3.2.2. Critical Configuration Parameters Studied 7
3.3. Numerical Figures of Merit (FOM) used for Screening 7
3.3.1. Takeoff Distance Rating (TDR) 7
3.3.2. Missile Decoy Rating (MDR) 7
3.3.3. Sensor Deployment Rating (SDR) 8
3.3.4. Communication Repeater Rating (CRR) 8
3.3.5. Rated Aircraft Cost (RAC) 8
3.3.6. Total Figure of Merit (TFM) 8
3.3.7. Relation between Mission Requirements and FOM 8
3.4. Mission Modeling and Analysis 9
3.4.1. Total Aircraft Weight 9
3.4.2. Parasitic Drag 10
3.4.3. Induced Drag 11
3.4.4. Takeoff and Accelerated Climb 11
3.4.5. Steady Level Fight 12
3.4.6. Turning 12
3.4.7. Descent and Landing 13
3.4.8. Uncertainty 13
3.5. Results 13
3.6. Conclusions 14
4. Preliminary Design 15
4.1. Critical Design Parameters and Sizing Trades 15

4.1.1. Wing Area 15
4.1.2. Wingspan 15
4.1.3. Overall Aircraft Length and Empennage Size 15
4.1.4. Motor Size and Number 15
4.1.5. Propeller Pitch and Diameter 15
4.1.6. Battery Weight and Number of Cells 16
4.1.7. Load Factor Limit 16
4.1.8. Range of Critical Design Parameters Studied 16
4.2. Improved Mission Modeling and Optimization Analysis 17
4.2.1. Overview of Mission Modeling and Optimization Program 17
4.2.2. Estimating Aircraft Gross Weight 18
4.2.3. Estimating Aircraft Drag 18
4.2.4. Estimating Aircraft Maximum Lift Coefficient 18
4.2.5. Estimating Power Plant Performance 18
4.2.6. Static Stability Analysis 21
4.2.7. Mission Modeling Equations 21
4.2.8. Takeoff Analysis 22
4.2.9. Accelerated Climb Analysis 22
4.2.10. Steady Level Fight Analysis 22
4.2.11. Turning Analysis 22
4.2.12. Descent and Landing Analysis 22
4.3. Optimization Results 23
4.3.1. Configuration Parameters for Optimized Aircraft 23
4.3.2. Aerodynamic and Stability Characteristics of Optimized Aircraft 25
4.3.3. Predicted Mission Performance for Optimized Aircraft 26
4.4. Conclusions 26
5. Detail Design 27
5.1. Engineering Requirements 27
5.2. Component Selection and Systems Architecture 27
5.2.1. The Main Wing 28
5.2.2. The Stability and Control System 34
5.2.3. The Propulsion System 35
5.2.4. The Aircraft Structural System 38
5.2.5. The Payload Support and Deployment System 41
5.2.6. Landing Gear 42
5.3. Final Aircraft Specifications 43
5.3.1 Drawing Package 43
Zephyr Top Assembly 44
Fuselage Frame Assembly 45
Fuselage Assembly 46
Left Wing Assembly 47
Stowed Configuration 48
5.3.2. Rated Aircraft Cost Calculation 49

5.4. Final Aircraft Performance Analysis **49**
5.4.1. Aerodynamic Coefficients and Derivatives 49
5.4.2. Static Stability 49
5.4.3. Dynamic Stability 49
5.4.4. Predicted Performance 51
6. Manufacturing Plan **52**
6.1. Figures of Merit **52**
6.1.1. Availability of Materials (AOM) 52
6.1.2. Required Skill Level (RSL) 52
6.1.3. Time Required (TMR) 52
6.1.4. Strength and Reliability (SAR) 52
6.1.5. Actual Component Cost (ACC) 52
6.1.6. Estimated Component Weight (ECW) 52
6.2. Manufacturing Processes Investigated **53**
6.2.1. Wings 53
6.2.2. Empennage 53
6.2.3. Fuselage 53
6.3. Analytic Methods Used **53**
6.3.1. Critical Path 54
6.4. Processes Selected for Manufacture of Major Components **55**
6.4.1. Wing 55
6.4.2. Empennage 56
6.4.3. Fuselage 56
6.5. Manufacturing Milestones **56**
7. Testing Plan **57**
7.1. Test Objectives and Schedules **57**
7.2. Flight Testing Checklists **58**
7.3. Summary of Test Results and Lessons Learned **59**
References **60**

1. EXECUTIVE SUMMARY

This report provides an overview of the design, manufacturing, and testing procedures used in the development of the Utah State University entry in the 2003 Design, Build, and Fly competition. The aircraft was designed to complete two of three predefined missions; the "Missile Decoy Mission" (MDM), the "Sensor Deployment Mission" (SDM), and/or the "Communication Repeater Mission" (CRM).

1.1. Overview of the Design Development

During the conceptual design phase of the development process, energy approximations and Figures of Merit (FOM), based on mission requirements, were used to identify the two most cost-effective missions and narrow the range of design parameters to be studied in later design phases. Over 5,000 aircraft configurations were studied by varying critical design parameters. Computer code was written to analyze mission profiles and predict FOM. Some important conclusions were drawn from the results. First, the CRM always results in scores that are lower than the SDM or MDM. Second, there are possible optimums in battery weight, turn load factor, and aspect ratio.

In the preliminary design phase, more detailed analysis and experimental testing were used to further investigate potential optimums revealed during conceptual design. A computer program was written to iterate through millions of configurations and compute flight times, airspeeds, and Rated Aircraft Cost (RAC), and total score. The parameters that were investigated were wing area, wingspan, turn load factor, number of battery cells, and motor/propeller combinations. Tests were also performed to get better estimates for important aircraft parameters. This analysis and testing verified many of the trends discovered during conceptual design. High aspect ratio gave improved mission-effectiveness, despite the higher RAC. High load factors were verified to increase mission scores. In contrast to conceptual design results, it was found that including more battery cells in the power plant increased the maximum total score and speed capabilities of the aircraft, despite the higher RAC for increased weight and power.

During the detail design phase, computational aerodynamics, finite element structural analysis, dynamic stability analysis, mission flight simulation, and additional experimental testing were used to finalize geometry, component selection, system architecture, and mission performance predictions. Since overall score is inversely proportional to the flight time, the performance was enhanced by structural analysis and testing to produce an airplane that could perform high-g turns. The lift-to-drag ratio was also an area of focus and was dramatically improved by the use of full-span twisting flaps. Additional analysis and testing also aided in power plant selection and performance prediction. The final result was a stable, high-performance aircraft, which is quick to assemble and should score well.

1.2. Design Alternatives Investigated

Many different aircraft configurations and individual components were considered and evaluated. Three general aircraft configurations were examined early in the design process. These were the conventional aft tail, V-tail, and canard configurations. The conventional tail configuration was chosen based on takeoff, mission effectiveness, and RAC. The dimensions of the payload required a teardrop shaped fuselage instead of a lifting body. Retractable landing gear with brakes were chosen over fixed gear. To accommodate the gear, a low wing, instead of mid or high wing was chosen. The wing was constructed of a foam core and carbon fiber spar covered with balsa, after considering both a foam core with a composite skin and a balsa build-up method. This choice was based on manufacturability and weight constraints. Two antenna mount configurations were considered for the MDM. Based on trim considerations, a top mount was chosen over a bottom mount. One and two-motor designs were analyzed, resulting in a single-motor solution. An air cooling system was chosen, because tests showed

that complex liquid cooling is not beneficial. Two battery types were also considered, 36-cell, 2400-mAhr and 48-cell, 1700-mAhr packs. The latter was chosen based on power versus total energy tradeoffs.

1.3. Highlights of the Development Process

Since the design competition rules only allow two of the three missions to count toward the final team score, it was important to identify the two most cost-effective missions. By creating energy models for all three missions and comparing the resulting scores for thousands of different aircraft configurations, it was discovered that the CRM always generates the lowest scores. Therefore, design efforts were directed toward optimizing an aircraft for the MDM and SDM.

Antenna drag in the MDM was found to have a very significant effect on mission performance. Thus, a full-scale PVC model of the antenna was built and tested in a wind tunnel to obtain an improved estimate for the antenna drag coefficient. Results from this test indicate antenna drag that is 67% higher than that predicted by the relation for finite cylinders presented by White (1999). The measured value was used in all subsequent optimization studies, so that more realistic results would be obtained.

It was found in past years that manufacturer-published efficiency for DC motors does not match the realized efficiency. For the power plants tested, it was found that motor efficiency was at best 70%, whereas manufacturer's published values were 78-80%. Measured battery resistance per cell was found to be 0.015 ohms, compared with a published value of 0.005 ohms. Measured values were used for analysis.

During preliminary design, an effort was made to verify results found in conceptual design dealing with the possibility of an optimum wing aspect ratio. The analysis software written partly for this purpose iterated on different combinations of wing area and wingspan. It was found that an aspect ratio of approximately 11 produced the best mission scores, in spite of the increased RAC.

The effect of maximum load factor in the turns was studied during the conceptual and preliminary design phases. Conceptual design revealed a trend for increasing score with increasing load factor. This was verified using methods developed for preliminary design. A design load factor of 7 was found to be a near optimum solution based on the tradeoff between wing weight and mission flight times.

A static stability analysis was performed to optimize the size and placement of the tail surfaces on the aircraft. Optimum placement of the tail was found to be relatively close to the wing. Another advantage of the short tail was that it made possible a one-piece fuselage that is the length of the 4-ft long box. Overall score increases with decreased aircraft assembly time. Thus, speed and ease of assembly are of high merit and out of the box assembly is greatly simplified with a one-piece fuselage design.

Full-span twisting flaps called *twisterons*, Phillips, Alley, and Goodrich, (2003) were introduced on the aircraft. Twisterons are flaps used to produce variable aerodynamic washout. This reduces induced drag and overall pitching moment produced by the wing. The use of twisterons instead of ailerons and flaps showed improvements in the lift-to-drag ratio of 10 to 20%, in some mission phases. This significantly decreased mission flight times and increased mission effectiveness as measured by total score.

In order to characterize the handling qualities of the aircraft more accurately, a complete dynamic stability analysis was performed. All calculations included the contribution of the propeller and fuselage to the stability derivatives. It was found that the aircraft had divergent spiral and phugoid modes. The spiral mode had a short doubling time of about 2.5 seconds on takeoff. This was initially a concern, but it was decided that a pilot in visual reference flight should be able to easily handle the aircraft. However, the dynamic stability analysis revealed possible problems with the sizing of the vertical stabilizer. The chosen solution was a vertical surface that could be modified during the flight-testing phase of development.

2. MANAGEMENT SUMMARY

The Utah State University design team for this year's competition is composed of eleven Mechanical and Aerospace Engineering students. In order to efficiently utilize the teams various skills and produce a quality aircraft on time, an effective management plan was devised.

2.1. Architecture of the Design Team

In order to ensure that each design task was accomplished and that the workload was distributed as evenly as possible among the team members, the team was divided into three sub-groups; aerodynamics, propulsion, and structures. The aerodynamics team was responsible for generating the aerodynamic models and iterating through various aircraft configurations to be studied. They were also responsible for the stability and control analysis of the aircraft. The propulsion team was responsible for investigating possible motor/battery/propeller combinations. They also studied the effects of battery resistance and motor heating on power plant performance. The structures team was charged with the structural design and analysis of the aircraft. This included the structural testing and finite element analysis of the major aircraft components.

A project manager was chosen along with three sub-team leaders. The project manager addressed concerns that affected the team as a whole and was responsible for making sure the team stayed on schedule. The sub-team leaders were responsible for delegating work to their team members. Three other team members were chosen to keep track of the team's budget, order necessary materials and testing equipment, and arrange the shipping and travel accommodations for the competition. Table 2.1.1 lists the design personnel and their assignment areas.

Project manager: Nick Alley		
Treasurer: Mark Anderson;	*Procurement:* Tristan Young;	*Logistics:* Mike Oksness
Aerodynamics	**Propulsion**	**Structures**
Leader: Wayne Goodrich	*Leader:* Nate Bunderson	*Leader:* Adam Spinner
Mark Anderson	Mike Oksness	Tristan Young
Kyle Barton	Underclassmen	Nick Alley
Mike Oksness		Underclassmen

Table 2.1.1. Team architecture, design personnel and their assignment areas.

Table 2.1.2 shows how each team member was involved in the design, analysis, and construction of the airplane. A rating of 5 indicates that 100% of that team member's work time was devoted to the given phase and a 0 indicates no involvement.

2.2. Configuration and Schedule Control

Early in the design process, the team identified the major design milestones and the dates by which they were to be achieved (see Fig. 2.2.1). Each week thereafter the team met with faculty advisor Dr. W.F. Phillips to discuss the progress and setbacks of the previous week and set goals for the following week. At other times during the week the sub-teams met individually to discuss design goals or to work on tasks as a group.

	Nick Alley	Mark Anderson	Kyle Barton	Nate Bunderson	Wayne Goodrich	Mike Oksness	Adam Spinner	Tristan Young	Underclassmen
3. Conceptual Design									
3.1 Mission Requirements	1	5	5	0	5	5	0	0	1
3.2 Study of Aircraft Requirements	1	5	5	0	5	5	0	0	1
3.3 Screening of Numerical FOM	0	5	5	0	5	5	0	0	1
3.4 Mission Modeling and Analysis	5	5	5	0	5	5	0	0	0
3.3.1-3 Aircraft Weight and Drag	5	5	5	0	5	5	0	0	0
3.3.4-5 Takeoff, Climb, Steady-Level Flight	5	5	5	0	5	5	0	0	0
3.3.6-7 Turning, Descent, and Landing	5	5	5	0	5	5	0	0	0
3.3.8 Uncertainty	0	0	5	0	0	0	0	0	0
4. Preliminary Design									
4.1 Study of Design Parameter and Sizing Trades	1	5	5	1	5	5	4	0	1
4.2 Improved Mission Modeling and Optimization	1	5	5	5	5	5	0	0	1
4.2.2-5 Weight, Drag, Lift and Thrust Estimation	1	5	5	5	5	5	0	0	1
4.2.6 Stability Analysis	1	5	5	0	5	5	0	0	1
4.2.7-10 Takeoff, Landing, Turning, Flight Analysis	0	5	5	0	5	5	0	0	1
5. Final Design									
5.2 Component Selection/System Architecture	2	5	5	5	5	3	5	0	5
5.2.1 Main Wing (Airfoil, *Twisterons*, Flaps)	0	5	1	0	5	1	0	0	0
5.2.2 Stability and Control Surface Sizing	1	1	5	0	5	0	0	0	0
5.2.3 Propulsion (Motor/Battery/Prop Tests)	0	0	0	5	0	2	0	0	5
5.2.4 Structural Design	2	0	0	0	0	0	5	5	0
5.2.5 Payload Support and Deployment	2	0	0	0	0	2	5	5	0
5.3 Final Aircraft Specifications	0	5	5	3	5	5	5	5	0
5.3.1-3 Aircraft Geometry/Weight and Balance	0	5	5	3	5	5	5	5	0
5.4 Final Aircraft performance Analysis	0	5	5	3	5	5	0	0	1
5.4.1 Aerodynamic Coefficients and Derivatives	0	0	0	0	5	5	0	0	0
5.4.2 Static Stability	0	5	5	0	2	5	0	0	0
5.4.3 Dynamic Stability	0	0	1	0	5	5	0	0	0
5.4.1 Predicted Mission Performance	0	5	5	4	5	5	0	0	1
A. Documentation of Design									
A.1 Journal	1	5	5	4	2	2	2	2	1
A.2 Letter of Intent	0	0	0	0	5	0	0	0	0
A.3 Final Report	3	5	5	5	5	0	0	5	2
6. Manufacturing									
6.2 Manufacturing Process Detail	5	0	1	0	0	0	5	5	0
6.3 Manufacturing Processes Selection	5	0	1	0	0	0	5	5	0
6.3 Detail Manufacturing Plan	5	0	1	0	0	0	5	5	0
Final Airplane Construction	5	5	5	5	5	5	5	5	2
B. Drafting Package	0	0	0	0	5	0	5	2	0

Table 2.1.2. List of design personnel and assignment areas. This table summarizes the major design phases and each member's contribution to those phases. A rating of 5 indicates 100% of design time devoted to a given phase and a rating of 0 indicates no involvement.

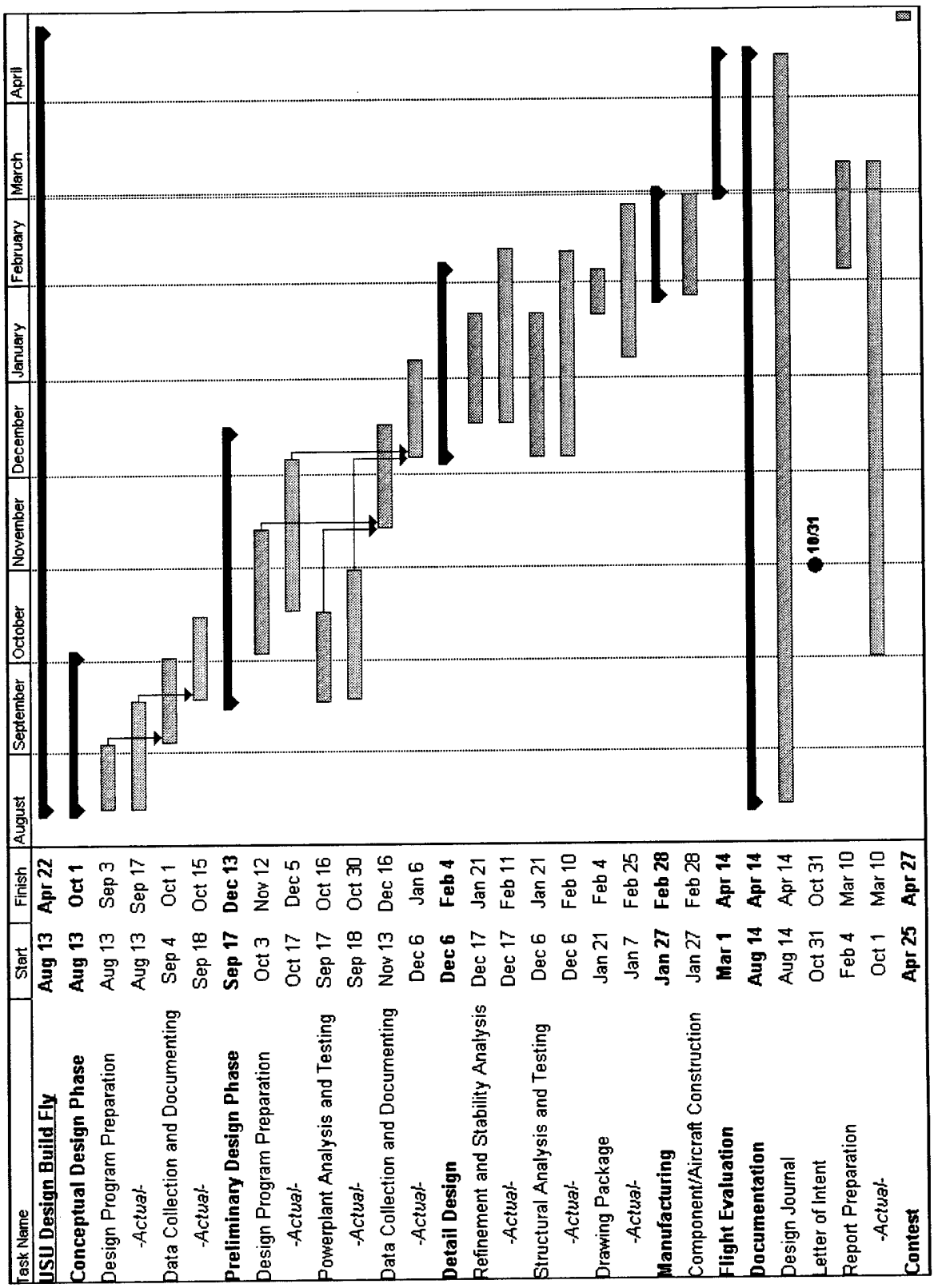

Figure 2.2.1. Project Schedule/Milestone Chart. This schedule illustrates the project milestones and time periods designated for each design phase. The blue bars represent the planned schedule while the pink bars show the time periods over which the events actually occurred.

3. CONCEPTUAL DESIGN

An aircraft was to be designed to complete two of three predefined missions. The goal for the conceptual design process was to eliminate one of the three mission sorties and allow a more focused approach to the design process by narrowing the range of design parameters to be studied in the later design phases. Energy approximations were used along with estimated aircraft parameters to determine the rated aircraft cost and mission flight time, for each aircraft configuration studied. Figures of merit, based on mission requirements, made the best missions and aircraft configurations discernable.

3.1. Mission Requirements

The three possible competition missions were named "Missile Decoy", "Sensor Deployment", and "Communications Repeater". Each mission flown will be scored using a degree of difficulty factor divided by the sum of the mission flight time and the aircraft assembly time. The required mission tasks for each of these three missions are described below.

3.1.1. Aircraft Storage and Timed Assembly. It was required that the aircraft be disassembled and fit into a 4 ft x 2 ft x 1 ft box. One task in the competition will be the timed assembly. This assembly will take place directly from the box and the time required to make the aircraft flight ready will be measured and recorded. The assembly time will be added to the flight time for each mission. This requirement placed certain limitations on the design of the aircraft. However, it was decided that consideration of this requirement would be left for the later phases of design, because the focus of conceptual design was on choosing the most effective missions and narrowing general aircraft parameters, not on specific aircraft structure and construction. An assembly time of 30 seconds was assumed for conceptual design.

3.1.2. Takeoff. For all missions there is a maximum takeoff distance requirement of 120 feet. The wheels must be off the runway within this distance. If the aircraft is unable to meet this constraint, a zero score will result for that sortie.

3.1.3. Missile Decoy Mission (MDM). For this mission, the aircraft must carry a five-pound rectangular payload, 6 inches in width and height, and 12 inches long. A simulated cylindrical antenna created from a 3-inch tall, 6-inch diameter PVC pipe section must be attached to the aircraft and suspended at least three inches from any other aircraft structure. The aircraft must fly four laps with a 360-degree turn on the downwind leg of each lap. This mission was given a difficulty factor of 2.0.

3.1.4. Sensor Deployment Mission (SDM). This mission requires the aircraft to carry the same five-pound payload box as the MDM. The aircraft must land after the second lap, stop completely, remotely deploy the payload, then takeoff again and complete two more laps. Each lap has one 360-degree turn on its downwind leg. This difficulty factor for this mission is 1.5.

3.1.5. Communication Repeater Mission (CRM). This mission requires the aircraft to carry the same five-pound payload box as the MDM, while completing four laps with three 360-degree turns on the downwind leg of each lap. A difficulty factor of 1.0 was assigned to this mission.

3.1.6. Aircraft Cost-Effectiveness. The final competition score will depend on a Rated Aircraft Cost (RAC), which is a function of the complexity and technology of the design. It is essential that the RAC be as low as possible, since the competition score is inversely proportional to RAC. Rated Aircraft Cost is discussed further in Sec. 3.3.5.

3.2. Aircraft Configurations Studied

Aircraft design parameters were selected based on experience and general aircraft knowledge. These were used as a basis for selecting the aircraft configurations studied. Parameters such as

empennage configuration, wing design, battery weight and landing gear were considered in the conceptual design phase. Initial configuration parameters were analyzed to limit the number of aircraft configuration to be studied in detail. The critical configuration parameters were then further analyzed to optimize the aircraft for each mission.

3.2.1. Initial Configuration Parameters Studied. In order to narrow the range of aircraft configuration parameters to be considered for further study, three different main configurations were investigated in the initial phase of conceptual design. These were the conventional aft tail, V-tail, and canard configurations. The method of Phillips and Snyder (2000) was used to compare the mission suitability of the three configurations. All three aircraft configurations were analyzed using the same weight, speed, wing area, planform, aspect ratio and fuselage length. The conventional aircraft configuration was found to have the most efficient distribution of lift, while the V-tail produced counteracting lift, which decreased tail performance. The canard's downwash and upwash on the main wing disrupted the lift distribution, thereby increasing the shed vorticity and induced drag. The canard also had a longer takeoff distance. Based on these results, the conventional configuration was found to have the best overall L/D and a shorter takeoff distance. This configuration was chosen for further analysis.

Mission flight time is a major contributor to total score and shorter mission flight times give higher scores. This meant that drag minimization was critical. For this reason, retractable landing gear was chosen for all aircraft configurations investigated in the critical configuration parameter study. This eliminated a major component of drag.

3.2.2. Critical Configuration Parameters Studied. For the purpose of conceptual design, the aircraft parameters considered to be critical to mission effectiveness were wing area, wingspan, battery weight, and turn load factor. Remaining parameters were estimated through functional relations with these parameters. Over 5,000 conventional aircraft configurations were studied by varying the critical parameters within ranges and by increments shown in Table 3.2.1.

Critical Parameter	Minimum	Maximum	Increment
Wing Area, S_w (ft^2)	2	10	1
Wingspan, b_w (ft)	4	10	1
Battery Weight, W_b (lbf)	1	5	0.5
Turn Load Factor, n_t (g)	2	10	1

Table 3.2.1. Critical aircraft configuration parameters used for conceptual design.

3.3. Numerical Figures of Merit (FOM) used for Screening

A numerical rating system based on FOM, described below, was developed to evaluate each aircraft's performance with respect to critical mission requirements. For each mission, 30 seconds were added to the flight time to account for the timed assembly.

3.3.1. Takeoff Distance Rating (TDR). If the airplane is not able to takeoff within the required distance of 120 ft, the sortie will be disqualified. However, there is no significant advantage to shorter takeoff distances. For this reason, TDR was defined by the relation

$$\text{TDR} = (0.0, \text{if estimated takeoff} > 120\text{ ft}) \text{ or } (1.0, \text{if estimated takeoff} < 120\text{ ft}) \qquad (3.3.1)$$

3.3.2. Missile Decoy Rating (MDR). This FOM reflects the weighted score for the Missile Decoy Mission. This mission has a difficulty factor of 2.0 and is defined as

$$MDR = 2.0/(\text{estimated mission flight time} + 30\,\text{sec}) \tag{3.3.2}$$

3.3.3. Sensor Deployment Rating (SDR). This FOM was used to rate aircraft effectiveness for the Sensor Deployment Mission using its difficulty factor of 1.5. Thus, SDR was

$$SDR = 1.5/(\text{estimated mission flight time} + 30\,\text{sec}) \tag{3.3.3}$$

3.3.4. Communication Repeater Rating (CRR). Suitability for the Communication Repeater Mission was rated based on the mission difficulty factor of 1.0, so CRR was defined as

$$CRR = 1.0/(\text{estimated mission flight time} + 30\,\text{sec}) \tag{3.3.4}$$

3.3.5. Rated Aircraft Cost (RAC). This FOM was specified by the contest rules and is used to estimate the cost of the aircraft based on its components and structures. The RAC was included both as a contest requirement and as a method of quantifying the cost of the concepts studied. It is defined as

$$RAC = (100 * MEW + 1500 * REP + 20 * MFHR)/1000 \tag{3.3.5}$$

where MEW is the Manufacturers Empty Weight, defined as the actual airframe weight with all flight and propulsion batteries but without payload; REP is the Rated Engine Power defined by

$$REP = [(1 + 0.25 * (\#\,\text{engines} - 1)] * (\text{total battery weight}) \tag{3.3.6}$$

and MFHR is the Manufacturing Man Hours, defined as

$$\begin{aligned} MFRH = {} & 8\,\text{hr} * [\text{wingspan (ft)} + \text{maximum exposed wing chord (ft)}] \\ & + 3\,\text{hr} * (\#\,\text{wing control surfaces}) + 10\,\text{hr} * [\text{maximum body length (ft)}] \\ & + 5\,\text{hr} * (\#\,\text{vertical surfaces without control}) + 10\,\text{hr} * (\#\,\text{vertical surfaces with control}) \\ & + 10\,\text{hr} * (\#\,\text{horizontal surfaces}) + 5\,\text{hr} * (\#\,\text{servo/controllers} + \#\,\text{engines} + \#\,\text{propellers}) \end{aligned} \tag{3.3.7}$$

3.3.6. Total Figure of Merit (TFM). The TFM was calculated from the best two mission scores, the TDR, and the RAC according to the relation

$$TFM = TDR * \text{max2}(MDR, SDR, CRR)/RAC \tag{3.3.8}$$

where max2 is a function that returns the sum of the largest two of three arguments.

3.3.7. Relation between Mission Requirements and FOM. Table 3.3.1 describes how the mission requirements are related to the FOM used for conceptual design. Note that aircraft storage and timed assembly were not considered in the conceptual design phase. It was decided that consideration of this requirement would be left for the later phases of design.

Mission Requirement	FOM
Aircraft Storage and Timed Assembly	Not Considered in Conceptual Design
Takeoff	TDR
Missile Decoy Mission	MDR
Sensor Deployment Mission	SDR
Communication Repeater Mission	CRR
Aircraft Cost-Effectiveness	RAC

Table 3.3.1. Relation between mission requirements and figures of merit used for conceptual design.

3.4. Mission Modeling and Analysis

In order to analyze each mission, a program was designed from fundamental equations that were derived to be functions of wing area, wingspan, battery weight, load factor, and payload weight. It was desired to obtain the FOM for all three missions for a range of these characteristic parameters. Over each segment of flight, the total energy available was used to determine the maximum flight velocity attainable, and from this, the time required to complete the mission was estimated.

3.4.1. Total Aircraft Weight. To estimate the weight of the aircraft, every component was assigned a specific weight and summed into an overall weight. Where possible, actual components were weighed. Equations had to be formed for the empennage and main wing weight estimates. A list of the measured component weights and equations is listed in Table 3.4.1.

Main Wing Weight. The weight of the main wing was estimated by finding an average wing weight per area for typical RC aircraft and multiplying by the wing area of the aircraft.

Fuselage Weight. For the conceptual analysis it was assumed that the entire fuselage would be constructed out of balsa. The fuselage was assumed to have 5 cross-sections; 3 in the center section, 1 in the nose, and 1 in the tail. The nose and tail cross-sections were assumed to be half the diameter of the center sections. The skin (outer covering) was assumed to be 1/16 inch thick while the cross-sections were assumed to be 1/4 inch thick. The density of the balsa was found to be 10 pounds per cubic foot. A pound was added for extras, including motor mounts, control rods, epoxy resin, covering, and payload mounting system.

Landing Gear Weight. To determine a reasonable weight for landing gear, Robart Mfg. Incorporated was contacted for weight estimates. For tricycle landing gear rated for a 12-24 pound aircraft, a weight range of 1.6 to 1.8 lbf was given. The weight of the three wheels was 0.31 lbf. A conservative total weight of the gear was used.

Empennage Weight. The main purpose of an empennage is to stabilize the forward pitching moment inherent of any cambered wing. For this reason the empennage was sized according to the main wing area. The 2001 Design Build Fly report was consulted to get a ratio between the weight of the empennage and the area of the main wing.

Component	Weight (lbf)
Motor (lbf) , W_m	0.93
Propeller (lbf), W_p	0.44
Speed Controller (lbf), W_{sc}	0.12
Servo (lbf/servo), W_s	0.1
Fuselage (lbf) W_f	1.62
Landing Gear (lbf)	1.7
Propulsion Battery (lbf)	Input Variable
Receiver (lbf), W_r	0.058
Receiver Battery (lbf) , W_{rb}	0.31
Cylinder (lbf) W_{cyl}	1.75
Empennage (lbf), W_{emp}	$W_{emp} = 0.255*(lbf/ft^2)*S_w$
Main Wing (lbf), W_w	$W_w = 0.238*(lbf/ft^2)*S_w$

Table 3.4.1. Aircraft weight estimates.

Final Weight Equation. Assuming a design requiring 5 servos and 1 motor controller, the total weight of the aircraft was estimated as

$$W = W_m + W_p + W_{sc} + 5W_s + W_b + W_r + W_{rb} + W_{cyl} + W_{emp} + W_w \quad (3.4.1)$$

3.4.2. Parasitic Drag. As with the weight, the drag of the aircraft depended on its many drag components. These components were analyzed and combined into an overall drag equation. For conceptual design, the zero-lift drag slope, $C_{Do,L}$, was assumed to be zero in all calculations.

Tail Boom Drag. Turbulent, axial flow with no separation was assumed, so the drag associated with the tail boom was only due to skin friction and was approximated using an equation for drag on a flat plate. As depicted in White (1999) the skin friction drag coefficient is defined as

$$C_{Dotb} = 0.031/(\mathrm{Re}_L^{1/7}) \quad (3.4.2)$$

The tail boom length was a function of wing area since the size and location of the empennage combine to stabilize the main wing. As the wing area increases, the tail boom must be lengthened for the aircraft to remain stable. To find a relation for the tail boom length as a function of wing area another ratio was developed based on the DBF2001 aircraft. Using this relation the tail boom length is defined as

$$L_{tb} = 0.627 * (1/ft) * S_w \quad (3.4.3)$$

This length was used in calculating the Reynolds Number, thus making the drag coefficient for the tail boom a function of the main wing area.

The equation for tail boom drag was based on the area of a flat plate, so the reference area used to predict the drag created by the tail boom was its surface area. To get this surface area another ratio based on the DBF2001 aircraft was developed in order to find an estimate for the diameter of the tail boom. With this ratio, the diameter of the tail boom is defined as

$$d_{tb} = 0.0147 * (1/ft) * S_w \quad (3.4.4)$$

Equations (3.4.2)-(3.4.4) can be combined with the equation for the surface area of a cylinder to give an area relation based on the wing area.

$$S_{tb} = \pi d_{tb} L_{tb} \quad (3.4.5)$$

Tail Feather Parasitic Drag. The tail feathers were assumed to have NACA 0009 airfoil cross-sections, giving them a parasitic drag coefficient of 0.005, according to Abbot and Von Doenhoff (1959). To estimate the reference planform area, a ratio of the area of the tail feathers to the main wing was found based on the DBF2001 aircraft. Using this ratio the tail feather area was estimated as

$$S_{tf} = 0.0825 * S_w \quad (3.4.6)$$

Main Wing Drag. For conceptual design purposes, the main wing was assumed to have a NACA 2412 airfoil cross-section. These airfoils have a parasitic drag coefficient, obtained from Abbot and Von Doenhoff (1959), of $C_{Dow} = 0.006$. The reference area for this drag coefficient was the planform wing area.

Fuselage Drag. A streamline teardrop shape was chosen for the fuselage in order to accommodate the payload and operational equipment while creating the least possible amount of drag. This fuselage had a parabolic shaped nose, a cylindrical center section, and a parabolic shaped tail. The center section was sized to 8.5 inches in diameter and 12 inches long so the rectangular payload would easily fit inside. The nose and tail sections were sized according to a percentage of the remaining length with the nose containing 25% and the tail 75%. The fineness ratio (d/l) of the complete fuselage was considered to be the largest diameter of 8.5 inches divided by the total length.

An empirical equation from Hoerner (1965) was used to estimate the parasitic drag of the fuselage from the fineness ratio and skin friction coefficient. It is defined by

$$C_{Dwet} = C_f\left(1+1.5(d/l)^{3/2}+7(d/l)^3\right) \tag{3.4.7}$$

where d is the maximum diameter of the fuselage and l is the total length of the fuselage. The skin friction coefficient C_f is defined by Hoerner (1965) to be

$$C_f = 0.427/(\log(R_e)-0.407)^{2.64} \tag{3.4.8}$$

For any given diameter there exists a fuselage length that will produce the minimum amount of drag. With a diameter of 8.5 inches, the minimum drag length was 2.835 feet.

Substituting a Reynolds number based on the length of the fuselage into equation (3.4.8) gave a skin friction coefficient that was substituted into Eq. (3.4.7) along with the fineness ratio to produce a parasitic drag coefficient. When the optimum fineness ratio and a conservative Reynolds number of $2.5\text{x}10^6$ was used, a parasitic drag coefficient of C_{Dof}= 0.0049 based on the fuselage surface area was calculated.

Cylinder Drag. The MDM required the addition of an antenna. A conservative estimate of C_{Dcyl} = 1.0. The reference area for the cylinder was estimated as the fontal area to be S_{cyl} = 0.375 ft^2.

Landing Gear Drag. The drag on the gear is mainly due to pressure drag. The frontal area of the struts, S_s, came from detailed drawings on Robart Mfg. Inc.'s website. The struts have a diameter of 0.5 inches and a length of 5.4 inches. The wheels had a diameter of 3.0 inches and a thickness of 1.0 inch. The coefficient of drag for the strut was approximated for a finite cylinder with an aspect ratio of 10. This was found in White (1999) to be C_{Dos} = 0.82 based on frontal area for laminar flow at Reynolds numbers above 10000. From Hoerner (1965), the wheels could be approximated as supercritical spheres for their drag coefficient. This coefficient (based on frontal area) had a value of C_{Dowh} = 0.1.

Final Coefficient of Drag Equation. When the product of all the previous drag coefficients and areas are summed, the resulting drag coefficient is defined by

$$C_{Do} = \frac{C_{Doth}S_{th}+C_{Doff}S_{ff}+C_{Dow}S_w+C_{Dof}S_f+C_{Dos}S_s+C_{Dowh}S_{wh}+C_{cyl}S_{cyl}}{S_w} \tag{3.4.9}$$

where C_{Do} is the coefficient of drag on takeoff and rotation. It was important to note that the landing gear chosen for conceptual design was retractable. Therefore, during flight, the drag coefficients of the struts and the wheels were set to zero. For missions other than the MDM, the cylinder drag is neglected.

3.4.3. Induced Drag. It was decided to estimate the aircraft's Oswald efficiency factor to predict induced drag. For an aircraft with elliptical wings, a conservative approximation for the Oswald efficiency factor was given by using the span efficiency factor for a rectangular wing with the same planform area and aspect ratio as the elliptical wing. Data for the span efficiency factor of a rectangular wing were computed using a numerical lifting-line method and fit by a least squares polynomial equation.

3.4.4. Takeoff and Accelerated Climb. The total energy required to accelerate from a standing start to the liftoff velocity was the sum of the change in kinetic energy and the energy dissipated by drag and rolling friction divided by the efficiency of the power plant. The equation for takeoff energy used an approximation that neglects the change in net force with airspeed. All forces were evaluated at 70% of the liftoff airspeed as recommended by Phillips (2003) for initial estimates for takeoff.

The total energy required to rotate the aircraft to the takeoff angle of attack was the sum of the energy dissipated by drag and rolling friction divided by the efficiency of the power plant. The equation for rotation energy used an approximation that neglected the change in net force with angle of attack.

The energy required to climb to altitude and accelerate to flight velocity was the sum of the change in kinetic and potential energy and the energy dissipated by drag divided by an average efficiency of the power plant between liftoff and cruise velocity. The drag during accelerated climb was approximated with the induced drag evaluated at the average lift coefficients of the start and finish velocities.

The ground distance of the accelerated climb (s_{ac}) was calculated using an effective net force (F_{ac}) during transition, which was an average of the thrust available and thrust required at the liftoff (V_{LO}) and cruise velocities (V_C). This relation is found in Phillips (2003) to be defined as

$$s_{ac} = W / F_{ac}\left(h + (V_C^2 - V_{LO}^2)/(2g)\right) \tag{3.4.10}$$

where

$$F_{ac} = 0.5 * (T_{ALO} - T_{RLO} + T_{Ac} - T_{Rc}) \tag{3.4.11}$$

$$T_{ALO} = P_A / V_{LO} * (\eta_{ac} / \eta_c) \tag{3.4.12}$$

$$T_{Ac} = P_A / V_C * (\eta_{ac} / \eta_c) \tag{3.4.13}$$

$$T_{RLO} = D_{LO} \tag{3.4.14}$$

$$T_{Rc} = D_C \tag{3.4.15}$$

T_{ALO}, T_{Ac} are the thrust available at liftoff and cruise velocity, respectively. T_{RLO}, T_{Rc}, D_{LO}, and D_C are the thrust required and drag at liftoff and cruise velocity, respectively.

The propulsive efficiency ratio, η_{ac}/η_c, was defined to be the ratio of the efficiency at an instantaneous speed divided by the efficiency at the cruise speed. The power available (P_A) throughout the accelerated climb was assumed to be the greater of either the power required at the cruise velocity or at takeoff. The total time required for the accelerated climb was computed using the average velocity of the climb.

3.4.5. Steady Level Flight. The total energy required for cruising flight was the energy dissipated by drag divided by the efficiency of the power plant at cruise velocity given by

$$E_f \cong s_f \, D_f / \eta_f \tag{3.4.16}$$

where s_f is the flight distance not used in takeoff, climbing, turning, landing or braking over the four laps. η_f is the efficiency computed at the cruise airspeed. D_f is the induced drag given by

$$D_f = \tfrac{1}{2}\rho V^2 S_w C_{D_f} = \tfrac{1}{2}\rho V^2 S_w \left(C_{D_0} + C_{D_{0,L}} C_L + C_{Wf}^2 / \pi e R_A\right) \tag{3.4.17}$$

3.4.6. Turning. The total energy required for a steady, level coordinated turn was estimated to be the energy dissipated by drag divided by the efficiency of the power plant. The equation is defined by

$$E_t \cong s_t \, D_t / \eta_t \tag{3.4.18}$$

where s_t is the distance the aircraft flies during a 360 degree turn calculated by

$$s_t = 2\pi \frac{V_C^2}{g \, Tan(\phi)} \tag{3.4.19}$$

and η_t is the efficiency computed at the turning airspeed, which was assumed to be the cruise airspeed. D_t is found in Phillips (2003) to be the total drag as a function of the bank angle, ϕ, and is given by

$$D_t = \tfrac{1}{2}\rho V^2 S_w C_{D_t} = \tfrac{1}{2}\rho V^2 S_w \left(C_{D_0} + C_{D_{0,L}} C_L + (C_{Wt} / Cos(\phi))^2 / (\pi e R_A)\right) \tag{3.4.20}$$

Three different bank angles were considered for the turning analysis; the stall limited, load limited, and minimum energy bank angle. The smallest bank angle of the three was used to compute the total energy of the turn. The stall limited, minimum energy, and load limited bank angles are defined by

$$\phi_{Stall} = ArcCos\left(2W/(\rho V_C^2 S_w C_{L\max})\right) \tag{3.4.21}$$

$$\phi_{MinE} = ArcTan\left(\sqrt{1+(e\pi(\rho V_C^2)^2 S_w^2 R_A^2 C_{D_0})/(2W^2)}\right) \tag{3.4.22}$$

$$\phi_{ll} = ArcCos(1/n_{\max}) \tag{3.4.23}$$

3.4.7. Descent and Landing. The total energy required for descending flight is the energy dissipated by drag divided by the efficiency of the power plant. In the case where the energy required was negative, a value of zero was assumed since energy cannot be returned to the batteries. The energy required to descend is defined to be

$$E_D \cong (\sqrt{s_D^2+h^2}\,D_D + \Delta KE_D + \Delta PE_D)/\eta_D \tag{3.4.24}$$

where ΔKE_D is the change in kinetic energy defined as

$$\Delta KE_D = \tfrac{1}{2}W/g(V_{LO}{}^2 - V^2) \tag{3.4.25}$$

and ΔPE_D is the change in potential energy defined by

$$\Delta PE_D = W\,h \tag{3.4.26}$$

D_D is drag during decent, which is given by

$$D_D = \tfrac{1}{2}\rho V^2 S_w C_{DD}/2 \cong \tfrac{1}{2}\rho V^2 S_w\left(C_{Do} + C_{Do.L}C_L + (C_{W_C}^2 + C_{W_{TD}}^2)/(2*\pi e R_A)\right) \tag{3.4.27}$$

and η_D is the efficiency during decent evaluated at the average airspeed between cruise and touchdown. The length s_D is the distance from the exit of the last turn to the finish line less the distance needed for braking. Where the braking distance s_b is defined as

$$s_b \cong V_{TD}^2/(2\,g\,\mu_r) \tag{3.4.28}$$

where V_{TD} is the touchdown velocity and assuming the special case of the lift coefficient being equal to the drag coefficient divided by the coefficient of rolling friction. This is a valid, simplifying assumption in the case of no wind and no thrust reversal. The total energy required for stopping was assumed zero because the motor was off. The time required to come to a complete stop is defined by

$$t_b = 2s_b/V_{TD} \tag{3.4.29}$$

3.4.8. Uncertainty. Initially the maximum lift-to-drag ratios for the SDM and CRM were above 35. This was a concern since manufacturing an aircraft with this high of a lift-to-drag ratio would be difficult. It was decided that a "worst case" lift-to-drag ratio would be 20. The drag coefficient for the fuselage was increased until the maximum lift-to-drag ratio of the airplane for these two missions was approximately 20.

The main uncertainty in the mission model was associated with the power plant. It was assumed that there was always enough power to perform the required maneuvers for any given configuration and flight pattern. This assumption was justified in that the main objective in this phase of design was to observe trends that would help in determining which missions would produce the best overall score.

3.5. Results

Due to the number of aircraft configurations studied, it is not possible to show all of the results here. Instead, a representative set was chosen for depicting some general trends. Table 3.5.1 gives the critical configuration parameters for the representative aircraft along with the computed FOM. For every

configuration, the MDR and SDR are always higher than the CRR. Low wing areas, battery weights, and RAC ratings as well as high load factors typically produce larger TFM values.

S_w (ft^2)	W_b (lbf)	n_t	b_w (ft)	TDR	MDR	SDR	CRR	RAC	TFM
4	2	7	6	1	0.9	0.6	0.3	7	0.07
4	2	2	8	1	0.9	0.6	0.3	8	0.07
4	2	7	8	1	0.9	0.6	0.4	8	0.07
6	2	7	6	1	0.9	0.6	0.3	8	0.07
6	2	7	8	1	0.9	0.6	0.4	8	0.07
4	2	7	12	1	0.9	0.6	0.4	8	0.07
6	2	7	12	1	0.9	0.6	0.4	9	0.06
10	2	7	8	1	0.9	0.6	0.4	9	0.06
10	2	7	12	1	0.9	0.6	0.4	9	0.06
10	5	7	6	1	0.9	0.6	0.3	13	0.04
10	2	7	6	1	0.9	0.4	0.4	9	0.04
4	5	7	6	1	0.9	0.6	0.3	15	0.03
6	2	2	8	1	0.5	0.4	0.2	8	0.02
4	2	2	12	1	0.5	0.4	0.2	8	0.02
6	2	2	12	1	0.5	0.4	0.2	9	0.02
10	2	2	8	1	0.5	0.4	0.2	9	0.02

Table 3.5.1. Select random sample of aircraft configurations and example FOM calculation.

3.6. Conclusions

After considering results from conceptual design, some important conclusions were drawn. First, the CRM results in scores that are lower than both the SDM and MDM. For this reason, future design efforts will not consider the CRM. Second, as the battery weight is reduced, the score improves due to the reduction of RAC. Third, as the maximum load factor of the wing increases, the overall score increases due to the aircraft being able to turn at larger bank angles and thus lower turn times. These trends will be taken into consideration in future design phases.

The airplane configuration at the end of conceptual design is summarized in Table 3.6.1. Because of power plant inaccuracies, critical parameter ranges were left fairly large and will be narrowed down in the preliminary design phase.

Geometry	Value	Performance	Value	Weight Statement	Value
S_w (ft^2)	4 ~ 10	C_{Lmax}	1.6	Airframe (lbs)	3.5 ~ 4.7
b_w (ft)	6 ~ 12	$(L/D)_{max}$	20 ~ 35	Propulsion System (lbs)	5.4
W_b (lbs)	1~ 5	Stall Speed (mph)	29 ~ 37	Control System (lbs)	0.5
n_t (g)	3 ~ 10	Max Speed (mph)	105 ~ 135	Payload (lbs)	5 ~ 6.75
		Take-off Field Length (empty) (ft)	80	Empty Weight (lbs)	9.4 ~ 10.6
		Take-off Field Length (Gross Weight) (ft)	110	Gross Weight (lbs)	14.4 ~ 16.35

Table 3.6.1. Aircraft data summary.

4. PRELIMINARY DESIGN

The focus of preliminary design was to determine approximate dimensions, weight, power, load limit, and other physical characteristics for an optimum aircraft, which would best meet objectives for the two missions selected in conceptual design, namely MDM and SDM. The main areas of concern were wing area and span, empennage size, battery weight, motor/propeller combination, and wing strength. The entire aircraft flight routine was modeled more accurately than in the conceptual design phase and motor/propeller performance was modeled in much greater detail. For empennage optimization, the stability of the aircraft was estimated with algorithms that computed static margin and the yaw stability derivative.

4.1. Critical Design Parameters and Sizing Trades

Based on results obtained in the conceptual design phase, the critical design parameters were revised to reflect the performance parameters considered most influential to the overall score. These included main wing dimensions, power plant, empennage dimensions, battery weight, and load factor.

4.1.1. Wing Area. Trends found in conceptual design indicated that an optimum wing area may exist. For a fixed gross weight, decreasing wing area increases wing loading and raises the minimum drag airspeed. This results in higher flight speeds and reduced mission flight times. However, increasing wing loading also increases the stall speed, which increases takeoff distance. Since mission requirements call for short takeoff and high flight speed, wing loading must be a compromise.

4.1.2. Wingspan. The wing contribution to RAC is proportional to the sum of the wingspan and the maximum chord. Thus, minimum RAC per unit wing area is realized with a rectangular wing of aspect ratio 1. This places a penalty on high aspect ratio wings and an even greater penalty on efficient wing planforms, such as elliptic and tapered wings. For a given wing area, a higher wingspan produces a more efficient, faster wing while increasing the RAC. This means that wingspan must be a compromise between cost and efficiency. Other limitations on wingspan were manufacturability, storage of the wing in the aircraft storage box, and speed of assembly.

4.1.3. Overall Aircraft Length and Empennage Size. The main goal in designing an empennage for any aircraft is to stabilize the aircraft both statically and dynamically as efficiently as possible. For the purposes of preliminary design, efficiency was defined in terms of RAC and total drag. Due to the interaction and influence of these parameters, an optimum empennage was known to exist. The RAC increases with overall aircraft length and weight. For a very short aircraft, the total drag can usually be decreased by increasing the empennage length and decreasing empennage area. Thus, aircraft length and empennage size will also be a compromise between cost and efficiency.

4.1.4. Motor Size and Number. Motor selection was based on several criteria; the effect of motor weight and number on the RAC, the power output of the motor, and the maximum current draw. An increase in motor size or increase in the number of motors will increase the power output thereby decreasing takeoff distance. A more powerful motor can produce higher rpm's for a given propeller, which increases the maximum possible velocity. Increasing motor size increases the RAC due to increased weight. Using multiple motors induces a double penalty by increasing weight and rated engine power. Here again, motor selection must be a compromise between cost and mission effectiveness.

4.1.5. Propeller Pitch and Diameter. It is known that for best overall propulsive efficiency, a large air mass should be accelerated over a small incremental velocity. This warrants a large diameter propeller. However, ground clearance and compressibility effects limit allowable propeller diameters. Furthermore, propellers with low pitch-to-diameter ratios have greatest propulsive efficiency at low airspeeds, while

high pitch-to-diameter ratios result in greater propulsive efficiency at higher airspeeds. Since variable-pitch propellers are not available in the sizes required, a fixed-pitch propeller must be used. Due to the large range of velocities encountered in the missions, propeller pitch must be a compromise between takeoff performance and maximum airspeed.

4.1.6. Battery Weight and Number of Cells. As noted in conceptual design, the weight of batteries carried in the aircraft contributes to the RAC, the maximum airspeed, and the maximum time the aircraft can remain in flight. According to trends from conceptual design, there is possibly an optimum battery weight that would maximize the overall score attained by the aircraft. As more batteries are carried the aircraft has the potential to complete a mission in less time. On the other hand, as battery weight increases, the RAC and induced drag increase. Using lower capacity batteries allows more cells to be used within the weight constraint, which produces higher voltage and rpm. The tradeoff for decreasing battery capacity is reduced total available energy.

4.1.7. Load Factor Limit. The conceptual design phase also revealed a potential optimum load factor for the aircraft well above the competition's required 2.5 g's. As the design load factor increases the maximum allowable bank angle increases, thereby reducing the turning radius to use less energy and time in the turns. However, this requires increased power, wing strength, and wing weight, resulting in higher RAC.

4.1.8. Range of Critical Design Parameters Studied. In an attempt to optimize an aircraft for mission cost-effectiveness, a very large number of aircraft configurations were analyzed in greater detail using a computer program written by the design team. Each of the critical design parameters was varied over some range in an attempt to expose the optimum aircraft configuration. Table 4.1.1 shows the range and increments for each of the critical design parameters studied.

In addition to the iterations listed in Table 4.1.1, a data file of approximately 100 Astroflight motors was created along with each motor's associated critical constants. These were iterated through one at a time for each of the possible combinations of critical design parameters defined by Table 4.1.1. The largest horizontal stabilizer span allowed by the RAC was also the most efficient and was fixed at a constant 25% of the main wingspan.

Critical Design Parameter	Minimum	Maximum	Increment
Wing Area (S_w), ft^2	4	10	0.25
Wingspan (b_w), ft	6	12	0.25
Horizontal Stabilizer Area (S_h), ft^2	0.8	2.2	0.2
Vertical Stabilizer Area (S_v), ft^2	0.8	2.2	0.2
Empennage Horizontal Offset (l_h), ft	0.5	4.5	0.4
Motor Number	1	2	1
Propeller Diameter (d_p), in	8	26	1
Propeller Pitch (λ), in	8	24	1
Battery Cells	24	48	1
Battery Capacity (b_c), mAh	1700	2400	700
Turn Load Factor (n_t), g's	3	10	1

Table 4.1.1. Critical design parameters studied during the preliminary design phase.

4.2. Improved Mission Modeling and Optimization Analysis

The preliminary design phase focused on the development and use of computer programs called DBF2002 and DBFEMP. The purpose of these programs was to iterate through the critical design parameters listed in Table 4.1.1. The programs' outputs were the important aerodynamic properties, RAC, and total score. This made it possible to determine which range of aircraft would attain the best overall score and directed detail design efforts toward an optimum range of aircraft.

4.2.1. Overview of Mission Modeling and Optimization Programs. Figure 4.2.1 is a block diagram of the DBF2002 program operation. First, the variables were initialized and data files opened for reading and writing. The data files contained the motor database along with limits and increments for each aircraft parameter. The thrust and power curves of the motor were then calculated. The program iterated through all combinations of motors, battery cells, and propellers that drew a maximum current less than 50 amps. An airplane was then modeled using the geometric parameters listed in Table 4.1.1. along with the chosen power plant. Approximations for the drag, lift, and weight were then computed. Each aircraft configuration was cycled through the two mission flights at the slower of either the maximum possible flight velocity or the velocity that would fully deplete the battery energy. If, at some point during the flight routine, the program determined that the aircraft and mission combination was impossible, a new aircraft was drafted and the cycle repeated. If the missions were completed, the RAC, mission scores, and overall score were then calculated and sent with other important parameters to an output file. The entire process was repeated until all critical design parameters had been stepped through and the results recorded in the output file.

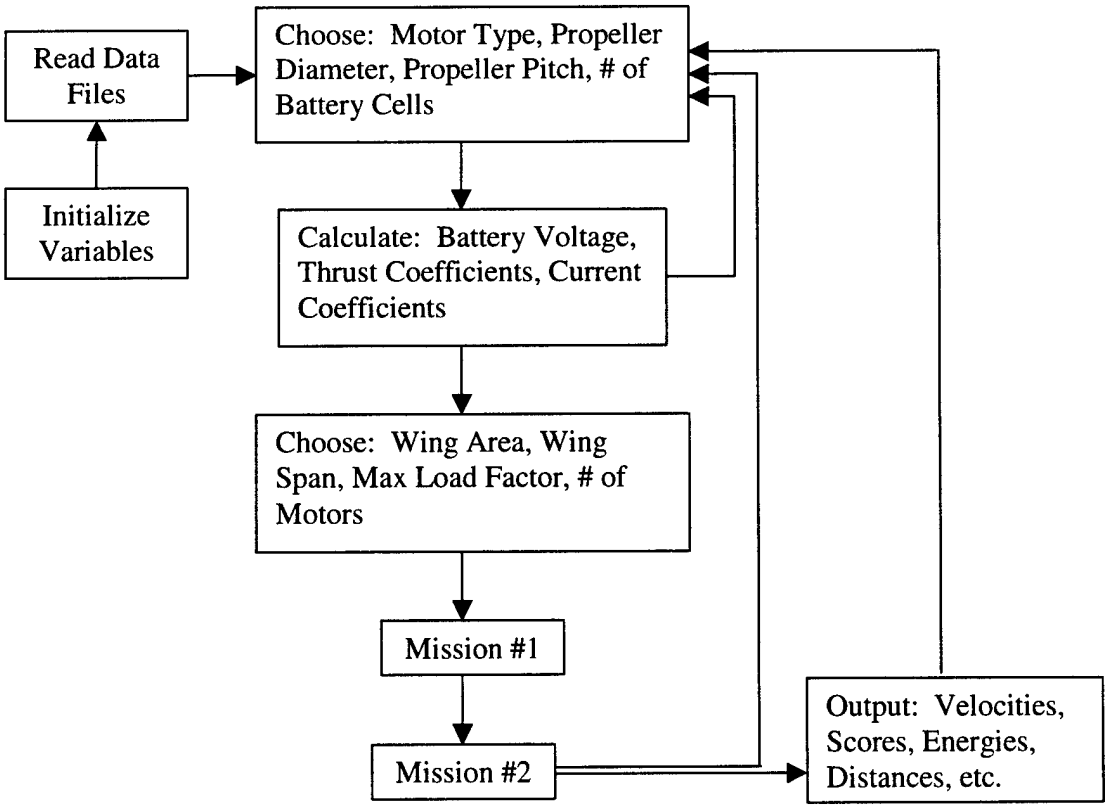

Figure 4.2.1. Block diagram of the DBF2002 optimization program.

After initial runs of the program, data files were created containing many thousands of aircraft configurations along with their respective scores and other characteristics. A spreadsheet program was used to sort the data with respect to score to determine where the maximums occurred. Based on the highest scoring aircraft configurations, a more polished range of aircraft parameters was chosen with higher resolutions set to narrow the search for an optimum aircraft. This refinement process was repeated many times and thus millions of aircraft configurations were simulated.

The DBFEMP program was written to determine the empennage needed to stabilize the aircraft by iterating on the critical empennage parameters located in Table 4.1.1. Stability was quantified by specifying a static margin and a yaw stability derivative. Based on rule of thumb values obtained for conventional aircraft, these were chosen to be 10% and 0.06 respectively. Once a stable configuration was found, the program calculated the RAC of the entire aircraft with the new empennage. The program then simulated the tail being flown through critical flight conditions that the aircraft would encounter such as takeoff, steady flight, and turning. For each flight condition, the program iterated on elevator size and computed the elevator deflection needed to trim the aircraft. It then computed the drag associated with that deflection.

4.2.2. Estimating Aircraft Gross Weight. Several approximations were refined to produce a better model of the overall aircraft weight. The predicted wing weight is not only a function of the wing area, but also a function of the wing design load factor. Wing weight increases proportionally with wing area, span, and design load factor. The model considered the dimensions and weight of a wing spar needed to withstand bending forces, ribs and webbing needed for torsion loads, and non-structural weight. The weights of the empennage surfaces were based on the same formula used for the main wing. The manufacturer's listed weight was used for each motor considered.

4.2.3. Estimating Aircraft Drag. The source of parasitic drag that was of most concern during the preliminary design phase was that of the mock antenna for the MDM. This mission required that a simulated cylindrical antenna be attached to the exterior of the aircraft. Contest rules state that the cylinder must be mounted 3 inches away from any aircraft surface and be entirely exposed to the free stream. Since this structure will create a significant drag force, an accurate prediction of this force was desired. Figure 4.2.2 shows a full-scale model of the cylinder, constructed of competition materials, that was tested in a wind tunnel. A force measurement device was designed and known weights were used to calibrate the setup. Strain and pressure differential data were recorded for velocities up to 80 ft/s. The resultant drag coefficient was found to be a constant for velocities between 30 and 80 ft/s. In this region, the drag coefficient was 0.9 ± 0.15 for a confidence level of 95%. As shown in Fig. 4.2.3, this is significantly higher than the value predicted from the relation presented by White (1999). Drag estimates from conceptual design were used for the other aircraft components.

4.2.4. Estimating Aircraft Maximum Lift Coefficient. For the purposes of preliminary design, the estimate of the aircraft maximum lift coefficient was taken to be the maximum lift coefficient of a NACA 2412 airfoil. This gave a resulting maximum lift coefficient of 1.6.

4.2.5. Estimating Power Plant Performance. The motor-propeller combinations were modeled in a subroutine called GPROPS, which uses principles from Phillips (2002). This program uses Goldstein's vortex theory along with electric motor theory to predict the thrust and current draw for a particular motor-propeller combination. It also uses the propeller geometry of a particular propeller manufacturer to further increase the accuracy of the results.

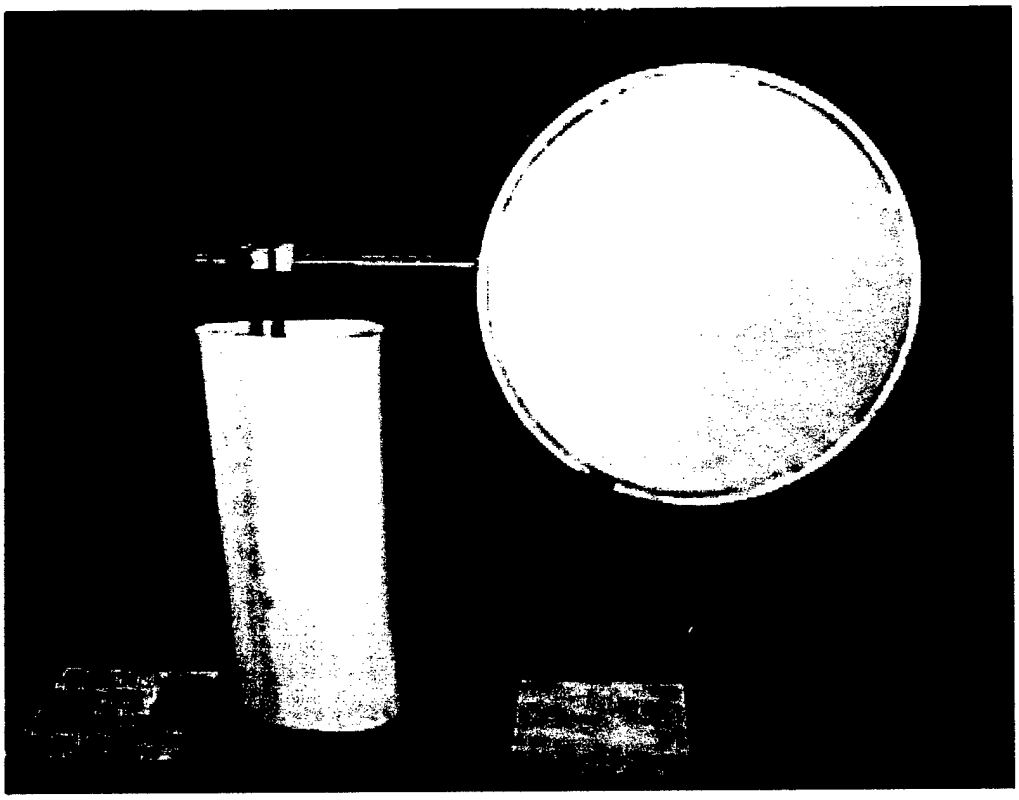

Figure 4.2.2. Wind tunnel setup for cylinder drag measurements.

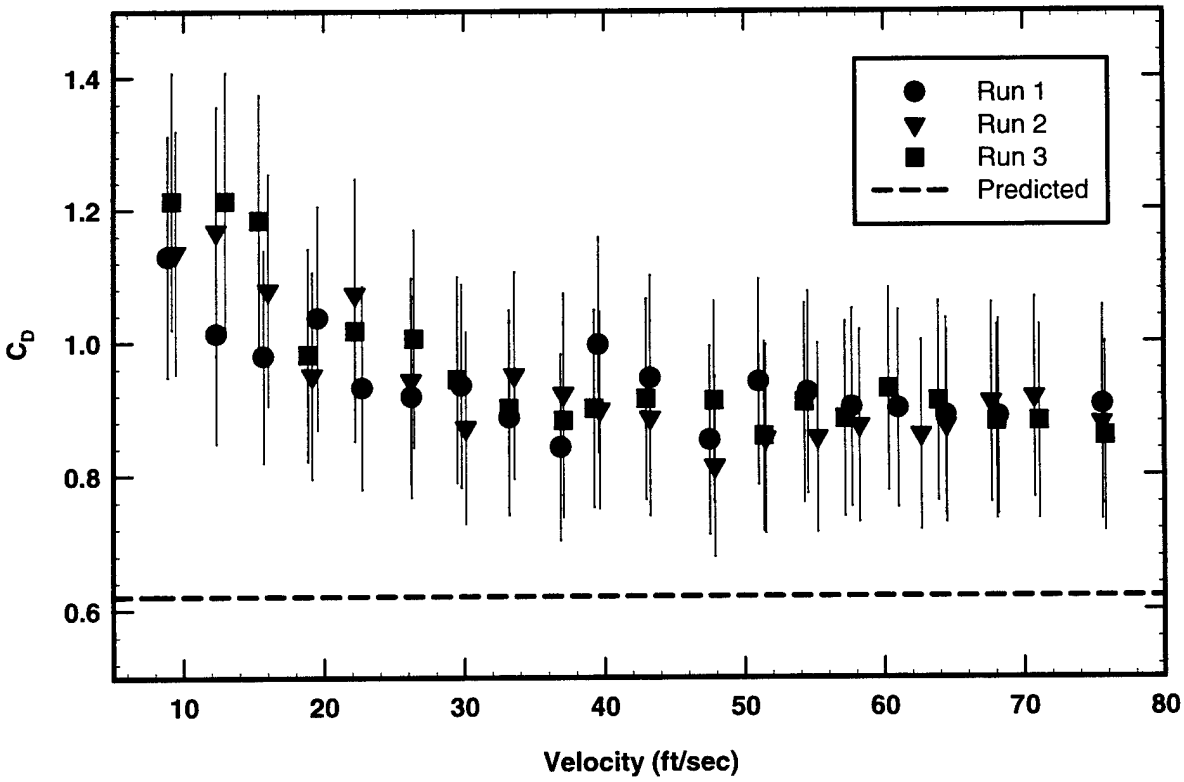

Figure 4.2.3. Results of cylinder wind tunnel testing with confidence level of 95%.

Given a motor and propeller, the GPROPS subroutine would sample thrust data points at six different velocities for each of six different throttle settings. Velocities ranged from 0 to 200 ft/sec in steps of 40 ft/sec while throttle settings ranged from 0.5 to 1 in steps of 0.1. The same was done for current draw. A quadratic least squares fit was used to approximate thrust and current as a function of velocity at each throttle setting. Once these coefficients were obtained another least squares fit was used to fit quadratic functions to these sets of coefficients as functions of throttle setting to yield two 9X9 matrices of coefficients. These two matrices represented the thrust and current as a quadratic function of both throttle setting and velocity. This was done so that the computationally intensive GPROPS subroutine needed only to be called once for each motor and propeller combination thereby greatly reducing the run time of the main program.

It is common to overestimate the performance of batteries and motors by using efficiencies and energy capacities given by the manufacturers of these products. Manufacturers often use the best-case test scenarios and not actual flight conditions. To remedy this problem, tests were designed to monitor power plant component characteristics based upon the conditions that would be expected during an actual flight. These tests gave an estimate of the expected energy output of a possible competition motor and battery pack. These estimates were used in the GPROPS subroutine to aid in the determination of an accurate optimal aircraft range.

Figure 4.2.4 shows general trends in battery voltage, current and motor speed. However, due to the large uncertainty in the torque measurement, a new load cell had to be obtained. Also due to errors in the current measurement, large sections of data had to be removed to provide an accurate picture. Still, sufficient information was gathered for the GPROPS subroutine as seen in Table 4.2.1.

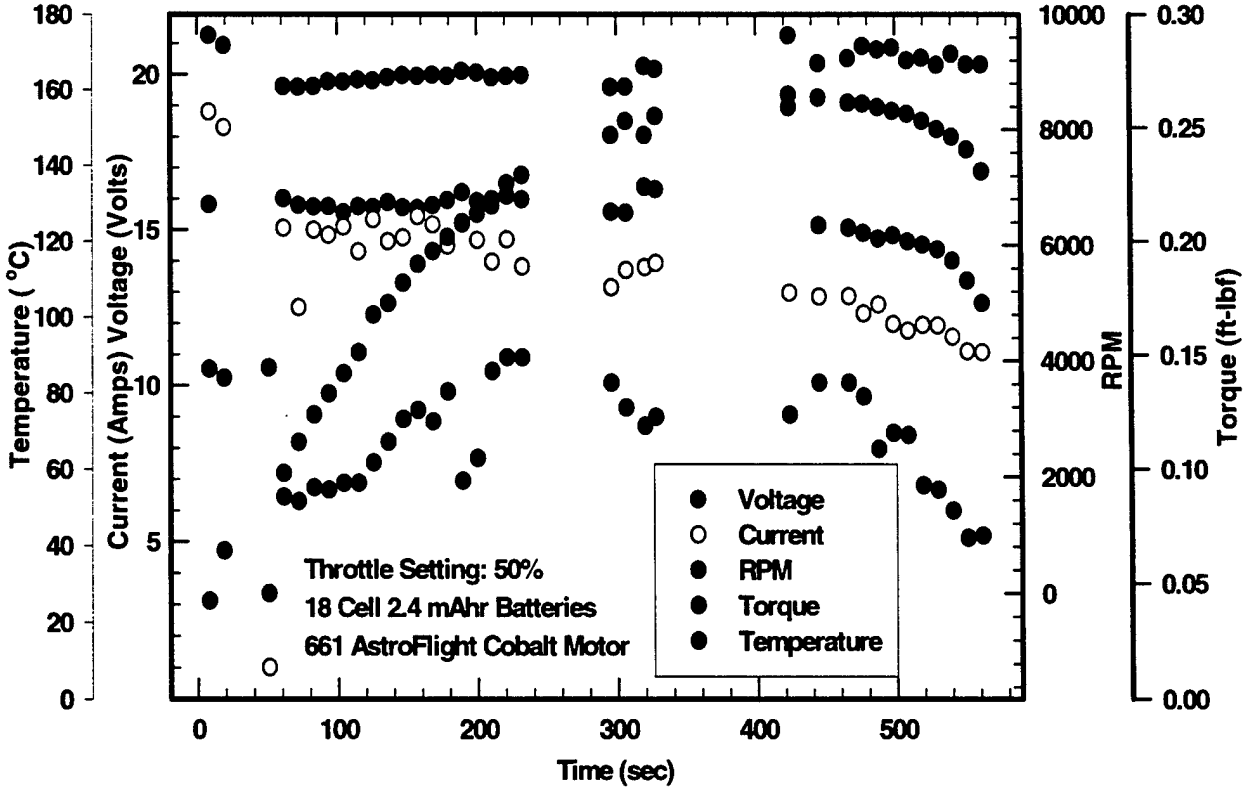

Figure 4.2.4. Test run of AstroFlight 661 cobalt motor.

	Battery Resistance	Battery Capacity	Torque	Speed	Efficiency
Manufacturer	0.005 ohms	2400 mAhrs	0.26 ft-lbf	8400 rpm	80%
Test	0.015 ohms	1800 mAhrs	0.15 ft-lbf	8500 rpm	75%

Table 4.2.1. Comparison between actual tests and manufacturer's battery specifications.

4.2.6. Static Stability Analysis. Both the static margin and yaw stability derivative equations that were used in the DBFEMP program were based on the moment distribution of the aircraft along the fuselage reference line. The aerodynamic centers of all surfaces and the thrust line were allowed to be offset and rotated from the fuselage reference line. Main wing flap, and elevator deflections, along with the destabilizing effects of a tractor propeller and fuselage were accounted for, along with downwash and sidewash effects from the main wing on the stabilizer surfaces.

4.2.7. Mission Modeling Equations. Conceptual design predicted cruise speeds well above takeoff speeds. This meant that a considerable portion of each mission would be spent in accelerating flight. Three options were available to model the accelerated portions of flight; full numerical integration using time steps, closed form approximations assuming a linear change in force and small climb angles, or a closed form integral solution with an approximation for the thrust, drag, and current distributions. Since minimal program run times were critical due to a tight design schedule, the first option was not feasible. The second option used assumptions that were inaccurate due to the nature of the missions, which exaggerate nonlinearities in drag and lift forces. The thrust and current draw curves are well behaved and closely follow the form of a quadratic curve. It was therefore possible to develop, in closed form, the integrals of the time, distance, and energy equations, with respect to velocity. These equations are respectively defined

$$t = \int_{V_o}^{V} \frac{m}{c_1 + c_2 V + c_3 V^2} dV \tag{4.2.1}$$

$$s = \int_{V_o}^{V} \frac{V m}{c_1 + c_2 V + c_3 V^2} dV \tag{4.2.2}$$

$$Energy = E \int_{V_o}^{V} \frac{m(i_1 + i_2 V + i_3 V^2)}{c_1 + c_2 V + c_3 V^2} dV \tag{4.2.3}$$

where t, and s, are the values of time and distance respectively, m is the mass, E is the battery pack voltage. V_o and V are the initial and final velocities, and i and c are the coefficients for the quadratic functions.

The classical form of the drag equation made a closed form solution to the integral impossible. To overcome this, the best approximation theorem, Greenberg (1998), was used to find a quadratic equation that accurately modeled the drag over the velocity interval from liftoff to cruise velocity. There were two advantages associated with using the best approximation theorem as opposed to a curve fit of the data. First, the resulting equation was robust enough to be used for any aircraft configuration and second, it was only necessary to recalculate the coefficients for each V^2 term to acquire the three coefficients for a quadratic. This was faster computationally than having to use a curve fit routine coupled with a Gaussian matrix solver. Figure 4.2.5. shows the original function and the best approximation function curves for the optimal aircraft configuration.

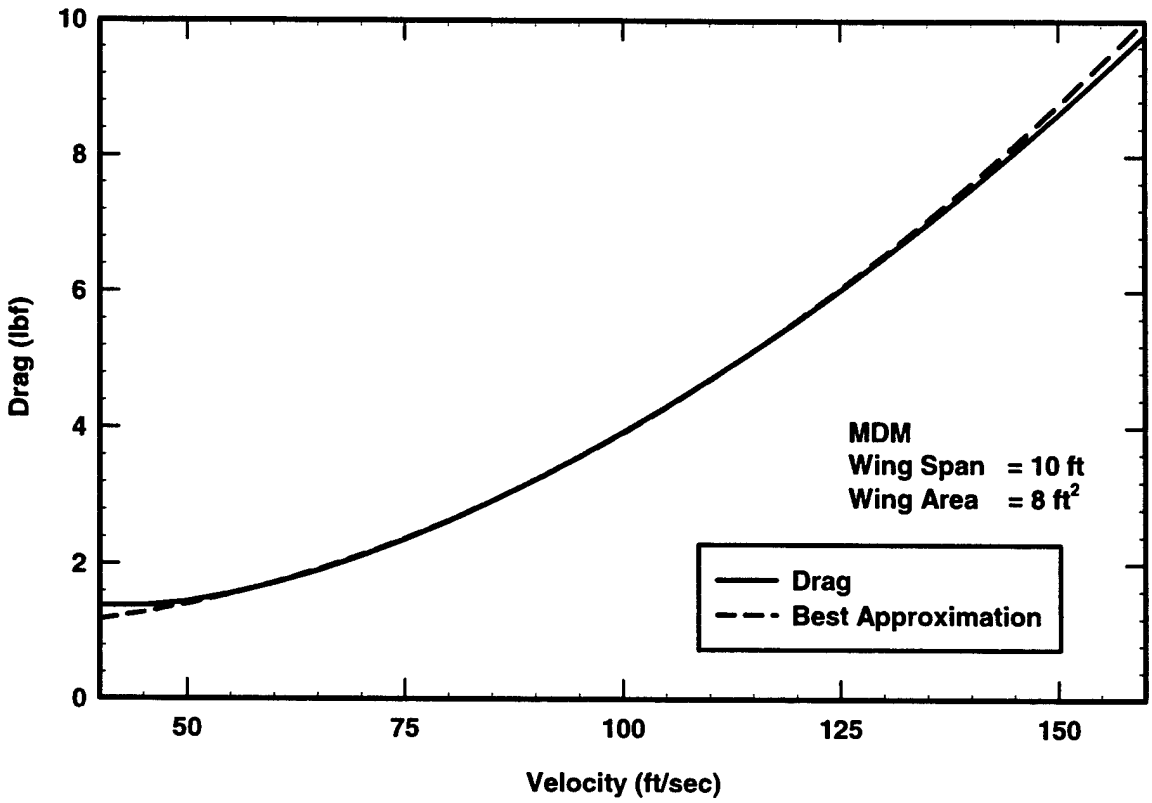

Figure 4.2.5. Aircraft drag and best approximation quadratic function.

4.2.8. Takeoff Analysis. The takeoff portion of the flight routine used the acceleration model along with a rotation time estimate of one second and a liftoff speed equal to 110% of the aircraft's stall speed. The time, energy and distance needed to accelerate to takeoff speed and rotate at a constant velocity were then obtained and sent back to the main routine. Aircraft configurations that exceeded a 120 ft takeoff distance were discarded.

4.2.9. Accelerated Climb Analysis. Given a height to climb, initial velocity, and velocity objective, the accelerating climb portion of the flight was modeled with the same equations developed in Sec. 4.2.7. The required horizontal distance was calculated from the flight distance obtained from Eq. 4.2.2. The climb angle was the tangent of the height to climb and the available horizontal distance of each straight section of the lap. If the required distance exceeded the available distance before the upcoming turn, the velocity that could be attained was evaluated with a root finder and returned to the flight routine. If the distance required to reach the velocity objective was less than that available, then a steady climb, which is a special case of the acceleration equations, was used over the remaining distance.

4.2.10. Steady Level Flight Analysis. The steady level flight portions of the missions were modeled using the same equations of acceleration, but without elevation or velocity change.

4.2.11. Turning Analysis. Accelerated turning was prohibited by the high induced drag caused by large load factors. Instead, a constant speed turn was used that allowed for a loss in altitude to balance the kinetic energy lost due to drag being greater than thrust. The time, energy, and height loss during the turn were computed and returned to the flight routine.

4.2.12. Descent and Landing Analysis. Descent and landing were modeled using the same algorithms but assumed zero thrust or power usage from the motor. A bisection method was used to

determine the point in the last lap of the sortie at which the motor should be shut off to allow the aircraft to touchdown and stop at the start/finish line of the course. This method used decelerating forms of the time and distance equations to calculate losses in potential and kinetic energy of the aircraft through level decelerating turns, the downwind leg straightaway, the decelerating decent from the end of the last turn to touchdown and the ground roll.

4.3. Optimization Results

Data obtained from the optimization programs was sorted and maximum overall scores identified. It was found that an optimum score is given for high aspect ratio wings, despite the fact that RAC increases with aspect ratio. Figure 4.3.1 shows how score is affected by the aspect ratio of the main wing for the MDM and SDM missions. The MDM score increases with aspect ratio while the SDM score decreases. The combined total score has an optimum with an aspect ratio of approximately 11 (see Fig 4.3.2).

High load factor limits also gave better scores due to the ability to turn at higher bank angles, producing higher turns rates. The tradeoff is increased aircraft weight and the associated increase in RAC and induced drag.

Increasing the number of battery cells was found to increase the score despite the penalty of added weight. This results from putting a higher voltage drop across the motor, which increases the power output and maximum flight velocity.

4.3.1. Configuration Parameters for Optimized Aircraft. After analysis of the program outputs, the 10 best airplanes were selected. Table 4.3.1 shows the parameter ranges for these 10 aircraft. These were approximate values to be finalized in detail design with more accurate models and analysis.

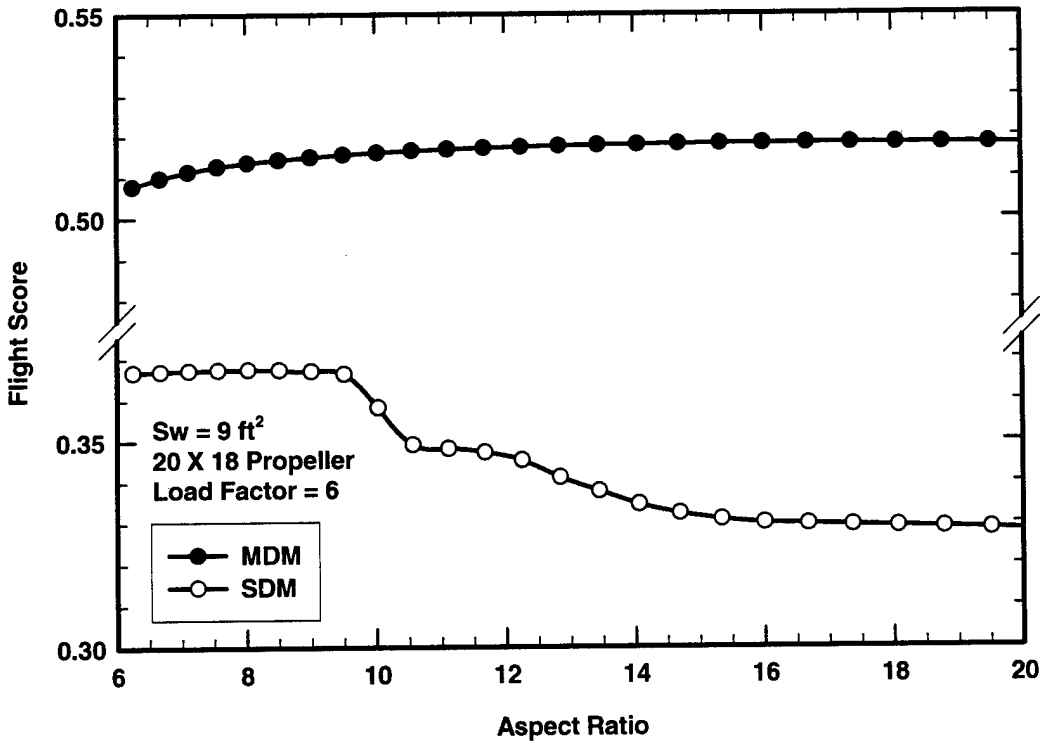

Figure 4.3.1. Flight score with respect to aspect ratio.

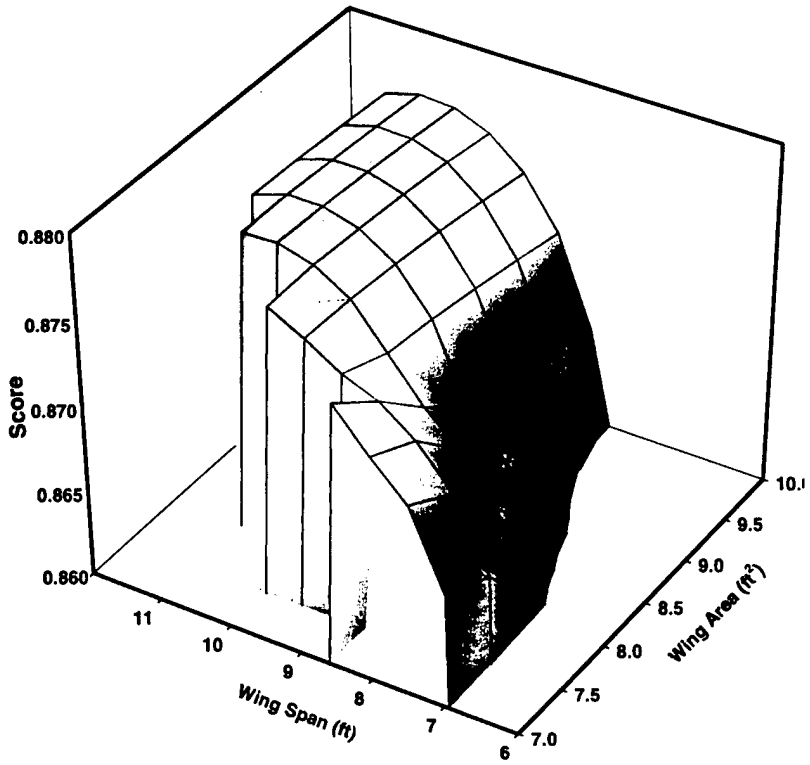

Figure 4.3.2. Combined flight scores as a function of wing area and span.

Design Parameter	Approximate Value
Wing Area (S_w), ft^2	8~9
Wingspan (b_w), ft	9~10
Horizontal Stabilizer Area (S_h), ft^2	1.5707~1.7
Horizontal Stabilizer Span (b_h), ft	2.5
Vertical Stabilizer Area (S_v), ft^2	1.5707~1.7
Vertical Stabilizer Span (S_v), ft	2.5
Elevator Width (% chord)	40~50
Empennage Horizontal Offset (l_h), ft	1.6~1.7
Battery Weight (W_b), lbf	5
Turn Load Factor (n_l), g's	7~8
Number of Motors	1
Motor	Astroflight 691
Propeller Pitch and Diameter (MDM) (λ_p) (d_p), in	21X19 ~ 17X19
Propeller Pitch and Diameter (SDM) (λ_p) (d_p), in	21X19 ~ 17X19
Rated Aircraft Cost (RAC), k$	13.5

Table 4.3.1. Optimized ranges of aircraft design parameters.

4.3.2. Aerodynamic and Stability Characteristics of Optimized Aircraft. Plots were made to evaluate the performance characteristics of aircraft in the optimal range. Figure 4.3.2 is an example of one these plots. They were analyzed to determine the best performance characteristics. This evaluation aided in further narrowing the optimal configuration ranges. Table 4.3.2 gives approximate values for the predicted performance.

The empennage was sized according to a static margin of 10% and a yaw stability derivative of 0.06 at mission flight velocity. These stability derivatives were then plotted over a range of lift coefficients to ensure stability for all operating conditions to be encountered. Figure 4.3.3 shows an example of one of these plots. These plots helped the team decide which aircraft configurations would not only be the most efficient, but also be the most stable through the range of operating conditions.

Performance Parameter	Approximate Values
Maximum Lift Coefficient (C_{Lmax})	1.6
Maximum Lift-To-Drag Ratio (*L/D*)	20
Maximum Takeoff Distance, ft	115
Maximum Takeoff Distance (Loaded), ft	100
Maximum Takeoff Distance (Empty), ft	75
Static Margin, %	10
Yaw Stability Derivative	0.06

Table 4.3.2. Predicted performance characteristics.

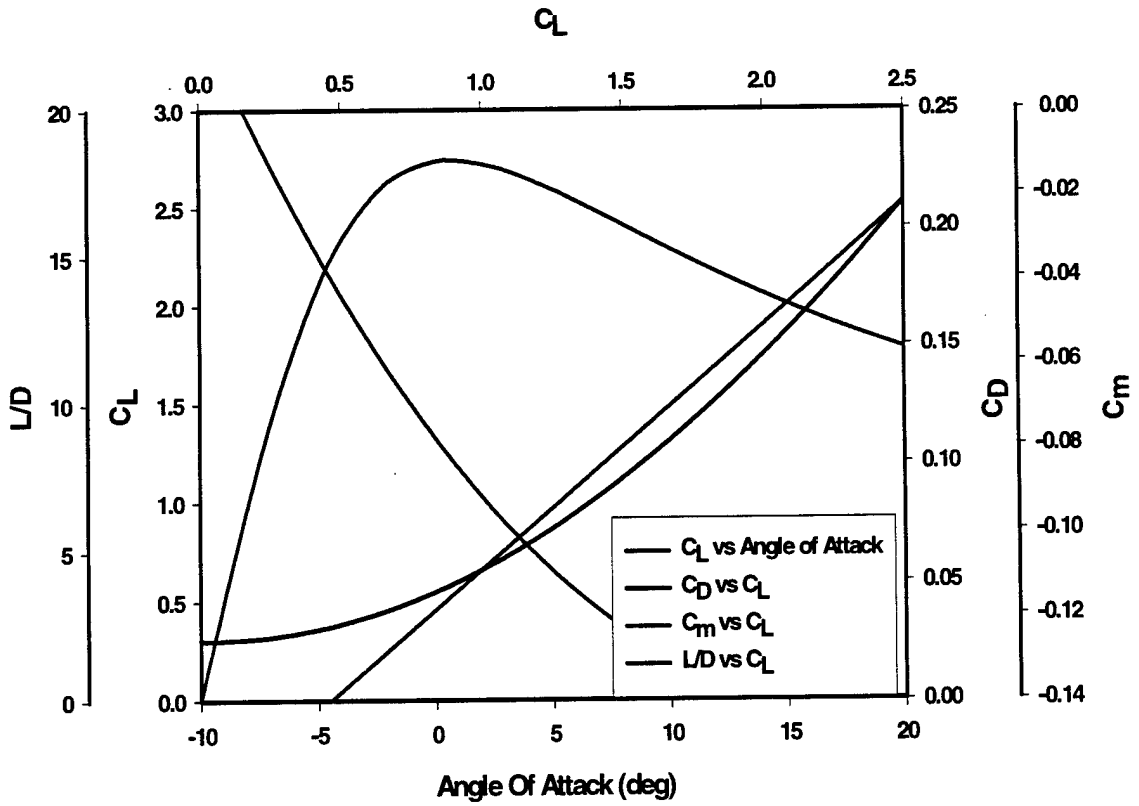

Figure 4.3.2. Graph of some performance parameters at 110 ft/sec.

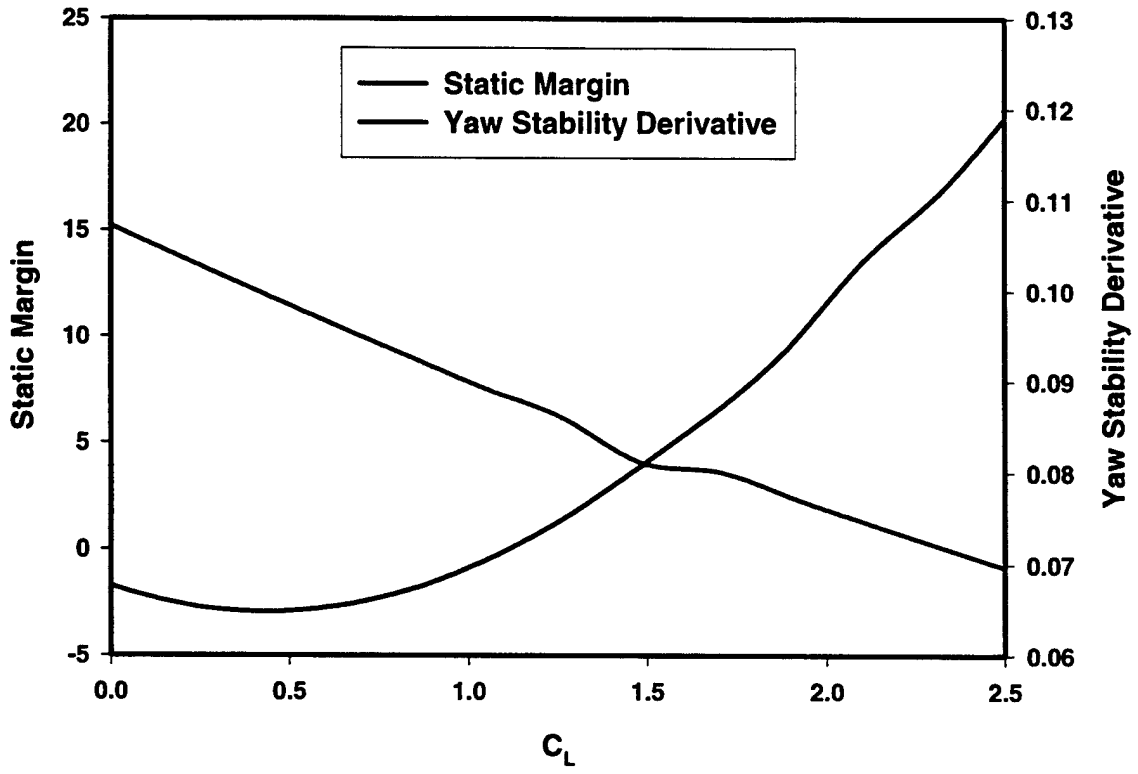

Figure 4.3.3. Graph of stability parameters at 110 ft/sec.

4.3.3. Predicted Mission Performance for Optimized Aircraft. Table 4.3.3 shows the approximate mission performance values typical of the 10 best aircraft, selected from thousands of configurations that were considered during preliminary design.

Performance Parameter	Approximate Value
RAC, k$	13.5
Time MDM, min	2.15
Time SDM, min	2.38
Score MDM	0.482
Score SDM	0.342

Table 4.3.3. Predicted mission performance for the optimized aircraft.

4.4. Conclusions

The results predicted from the preliminary design program showed significant differences from optimal velocities and aircraft sizes predicted during the conceptual design phase. This was due to the introduction of improved estimates for power plant efficiencies, current limits, and more accurate algorithms for predicting drag and thrust. Some trends found in conceptual design were verified, such as the increase in score with aspect ratio and load factor. Unlike results predicted during conceptual design, the preliminary design program predicted that adding cells to the battery pack would increase the total score, up to battery weights beyond the 5-lbf limit.

5. DETAIL DESIGN

With the major aircraft components determined in preliminary design, the final task before manufacturing was to maximize design performance. This was accomplished by shaving off weight and reducing drag while still meeting the stringent demands of strength and stability. This final optimization was done by detailed analysis and design of the airframe's aerodynamics, power plant, and structure.

5.1. Engineering Requirements

The final aircraft design has basic engineering requirements that must be met to guarantee safe and successful flying. These requirements fall under three major categories; contest rules, strength, and flight performance. Most requirements have basic values that must be met or the aircraft design is not viable. The requirements for the detail design phase are listed in Table 5.1.1. All aspects of detail design are aimed at meeting or exceeding these requirements.

Engineering requirements	Required	Goal
Mission Rules		
Gross Weight (lbf)	< 55	< 22
Takeoff Distance (ft)	< 120	110 ~ 120
Flight Time (min)	< 10	2 ~ 3
Radio Fail Safe Mode	Yes	Yes
Disassembled Dimensions (ft)	4 X 2 X 1	4 X 2 X 1
Assembly Time (sec)		15
Rated Aircraft Cost ($1000)		13
Strength		
Load Factor Limit (g)	>7	9
Lift Limit (lbf)	>154	198
Payload Support (lbf)	35	45
Flight Performance		
Maximum Lift Coefficient	1.6	2
Maximum Lift-To-Drag Ratio	20	30
Maximum Speed Empty (ft/sec)	110	140
Stability (Static & Dynamic)		
Static Margin (%)	5 ~ 20	12
Divergent Mode Doubling Time (s)	>1	>3

Table 5.1.1. Engineering requirements for final aircraft configuration.

5.2. Component Selection and Systems Architecture

To optimize the aircraft and meet engineering requirements, the aircraft was divided into subsystems that were analyzed in greater detail. These subsystems were the main wing, empennage, flight control system, propulsion system, structural system, payload support and deployment system, and the takeoff and landing system. The main wing and empennage were optimized with the use of numerical programs such as JAVAFOIL, Hepperle (2002), and code developed by the team. These codes computed the lift, drag, and stability characteristics among other mission performance parameters. The flight control system was chosen to meet the complex flight operations encountered in the different mission profiles. Due to the high structural loadings predicted during flight, high strength-to-weight materials and structures were used. Structures were analyzed using SDRC I-DEAS finite element analysis package and tested to

failure in a laboratory. In order to support and deploy the payload, the mechanism and support structure were optimized for weight, reliability and strength. The takeoff and landing system was optimized to reduce drag, weight, and mission flight time while maintaining good ground handling characteristics, and strength.

5.2.1. The Main Wing. Throughout the conceptual and preliminary phase of the aircraft design, all wing performance was based on the NACA 2412 airfoil section. In order to improve upon the NACA 2412 and the main wing performance, a new airfoil and the use of washout were investigated.

Airfoil. In an effort to improve on the overall performance of the wing, extensive analysis was done on over 200 different airfoils using an application based on the well-used PROFIL code developed by Eppler, called JAVAFOIL, Hepperle (2002). This program uses basic boundary layer theory to predict the viscous drag over an airfoil, the transition from laminar to turbulent flow, and stall of the airfoil based on laminar and turbulent flow separation. Of the over 200 airfoils analyzed, 150 of them were based on various combinations of the NACA 5 and 6 digit camber lines. The remaining 50 airfoils were taken from the University of Illinois, Urbana Champagne 1500+ airfoil database. The airfoils selected were based on their application and thickness greater than 12%, to make room for the retractable landing gear.

The criteria to select the "best" airfoil out of the 200 analyzed, were based upon the following parameters for both the takeoff and cruise speeds; maximum lift coefficient > 1.6 without flaps, maximum lift coefficient > 2.0 with flaps, maximum L/D > 40 without flaps, maximum L/D > 50 with flaps, and moment coefficient about quarter-chord > -0.1 without flaps. The airfoil that had the best overall performance based on these criteria is the Eppler 584, originally designed as a low Reynolds number airfoil for sailplanes (Eppler, 1990). The airfoil polars are plotted in Fig. 5.2.1 for the cruise Reynolds number.

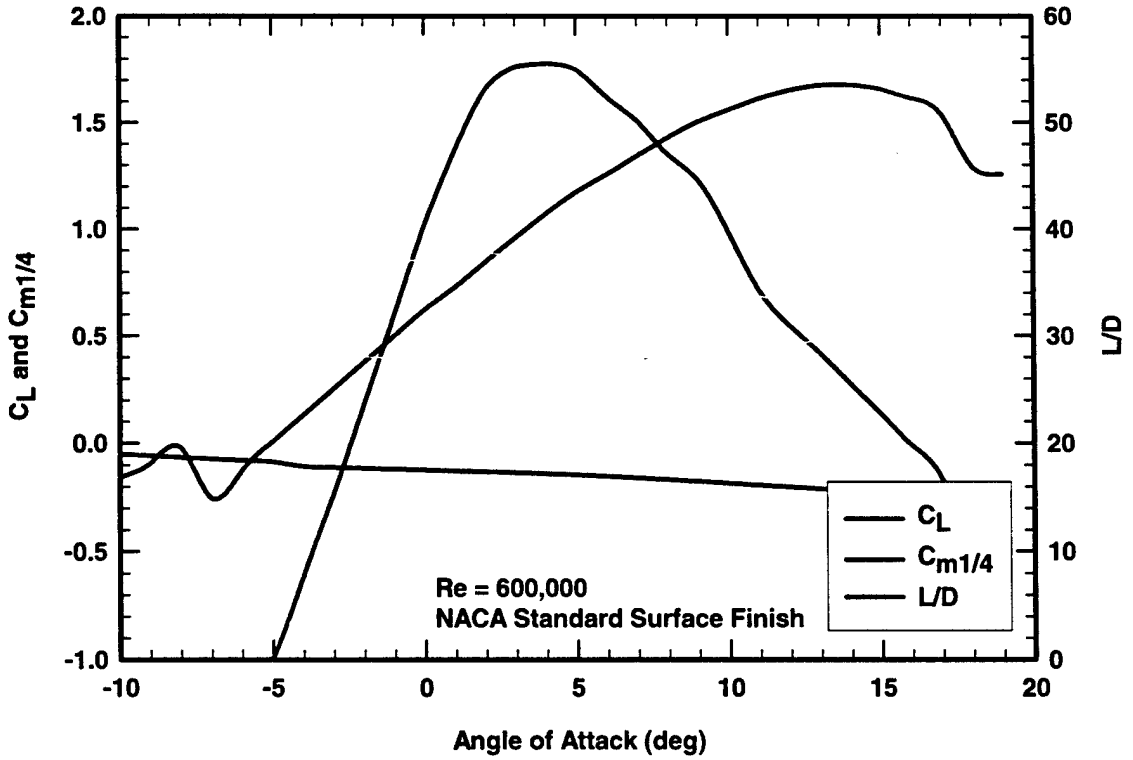

Figure 5.2.1. Polars for Eppler 584 airfoil at a Reynolds number of 600,000.

Washout. With an airfoil and planform shape decided upon, the next option considered was that of using washout to reduce the induced drag of the wing. With the use of an elliptic washout distribution the induced drag of a wing can be reduced to that of an elliptic planform for a given lift coefficient, Phillips (2003). A wing with optimum washout will always produce less induced drag than that of a wing without washout at all lift coefficients above one-half the design lift coefficient. Using the numerical solution for optimum washout presented by Phillips (2003) the effects of washout for a finite wing were studied. Figure 5.2.2 shows the maximum decrease in induced drag that can be obtained for a finite wing for a given aspect ratio. All values are calculated for the Eppler 584 airfoil. For the wing chosen in this design with an aspect ratio of 10.9, the potential performance increase is 8%.

With two possible means of implementing washout, geometric or aerodynamic twist, the simplest is to use geometric twist. To determine the amount of twist needed at the wingtip a program was written using the aforementioned algorithm to iterate on design lift coefficients and compare the reduction in induced drag across the entire range of expected lift coefficients. Figure 5.2.3 shows the optimum drag reduction over the lift coefficient range. One disadvantage of using this fixed twist is shown by the narrow peak at low lift coefficients with reduction in benefit at higher lift coefficients. Since nearly half of the flying will be at the high end of the lift coefficient range due to takeoffs, landings, and high load factor turns, a fixed twist gives relatively little advantage. Other difficulties encountered in using this type of washout were the problems in manufacturing. The washout presented in Fig. 5.2.3 represents only 1.5 degrees of maximum twist at the wingtip. Considering the relatively crude manufacturing methods used in building R/C aircraft, the quality control for such a small amount of twist would be prohibitive to the cost and time required to complete the design.

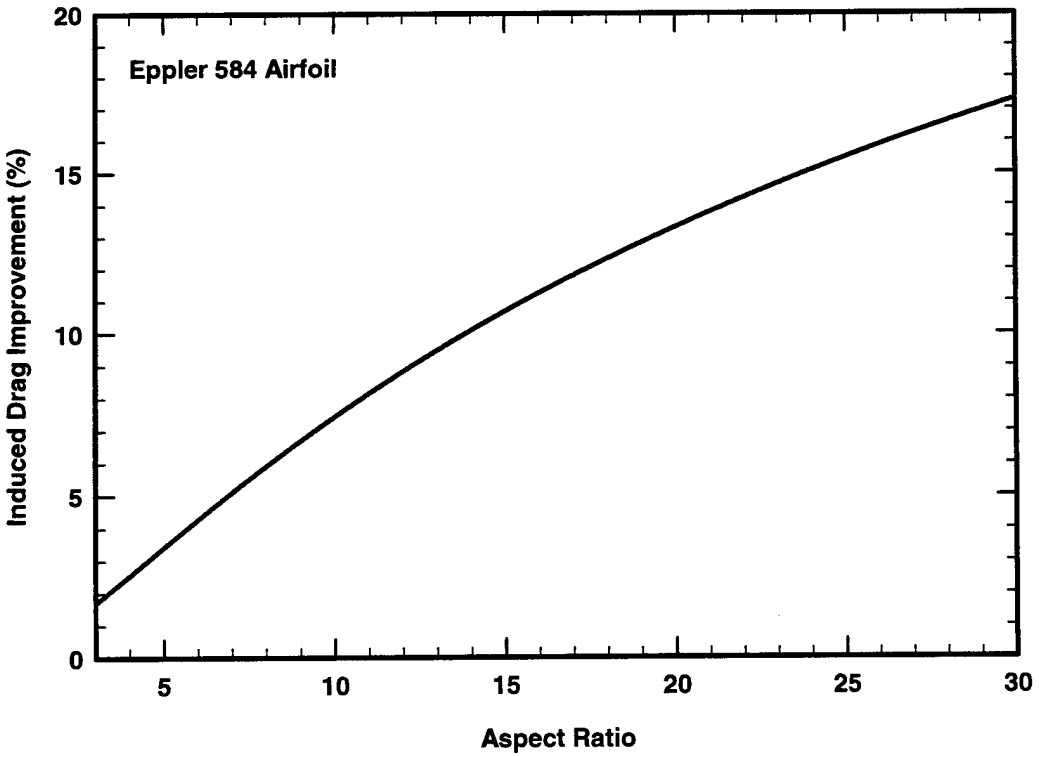

Figure 5.2.2. Reduction of induced drag versus aspect ratio for a wing with optimum washout.

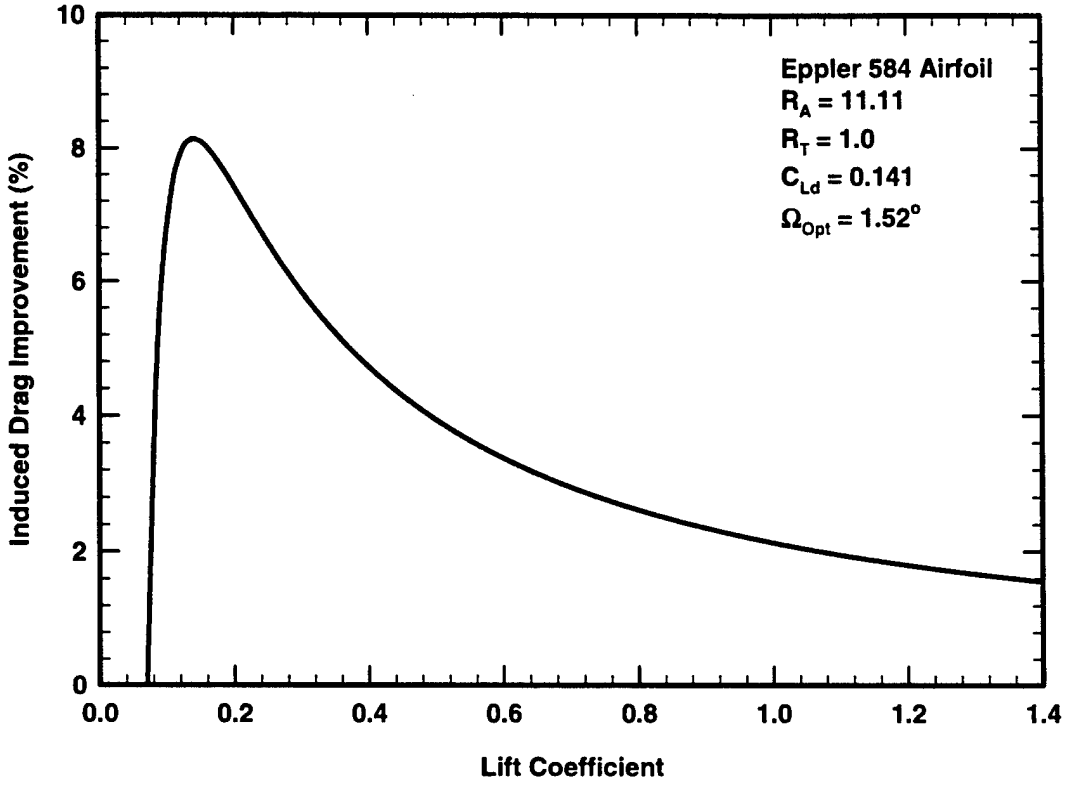

Figure 5.2.3. Reduction of induced drag versus lift coefficient for a wing with optimum washout.

The use of aerodynamic twist presented a more complex problem than that of geometric twist since the washout is implemented by twisting the local zero lift angle of attack along the wing. This would require a very time intensive manufacturing process that uses numerous different airfoil templates, each with the correct zero lift angle of attack. The design of a minimum number of modified airfoils alone would prove too daunting for the time and manpower available. For these reasons, the use of fixed aerodynamic twist was not considered further.

A third option for introducing wing twist is the use of *twisterons*, Phillips, Alley, and Goodrich (2003). This idea utilizes the flaps to produce aerodynamic twist in the wing. The greatest single advantage of using the flaps to produce aerodynamic washout is that the optimum washout can be maintained over the entire range of lift coefficients. Another potential advantage of using flap washout is the reduction in overall pitching moment produced by the wing. This would reduce the negative lift produced on the conventional aft tail in trimmed flight. Because of its potential influence on other surfaces of the aircraft, the method of Phillips and Snyder (2000) was used to analyze the effects of flap washout, or twisterons, on the aircraft lift-to-drag ratio. Since the benefit of twisterons would be best realized in the high-g turns, all computations were done for a lift coefficient of 1.4. Parameters iterated on were; the width of the flaps in percent chord, deflection of flaps in degrees, and twist angle of the flaps at the tip.

Figure 5.2.4 depicts the elliptical twist generated on the flaps along the span. In order to determine which flap percentage should be used for the final design, several more performance criteria were considered. The first considered was the total L/D improvement that the flap washout could produce for the aircraft. Based on these results shown in Fig. 5.2.5, the range of flaps considered for further analysis were the 25, 30 and 35% flap widths.

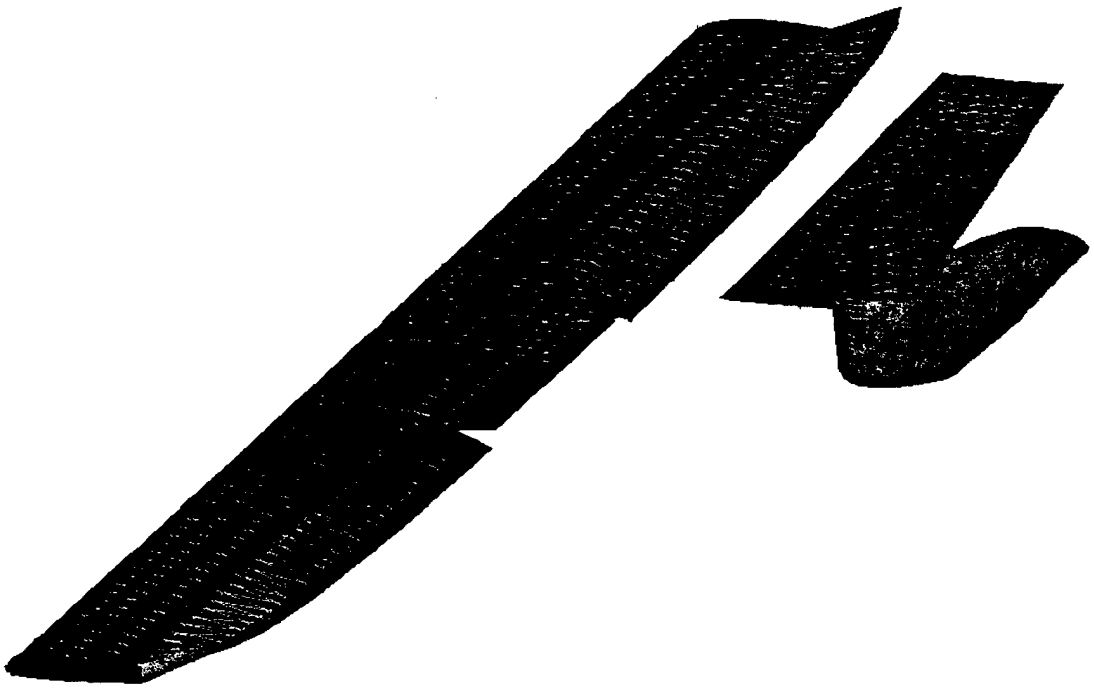

Figure 5.2.4. Representation of twisteron deflection with elliptic washout distribution.

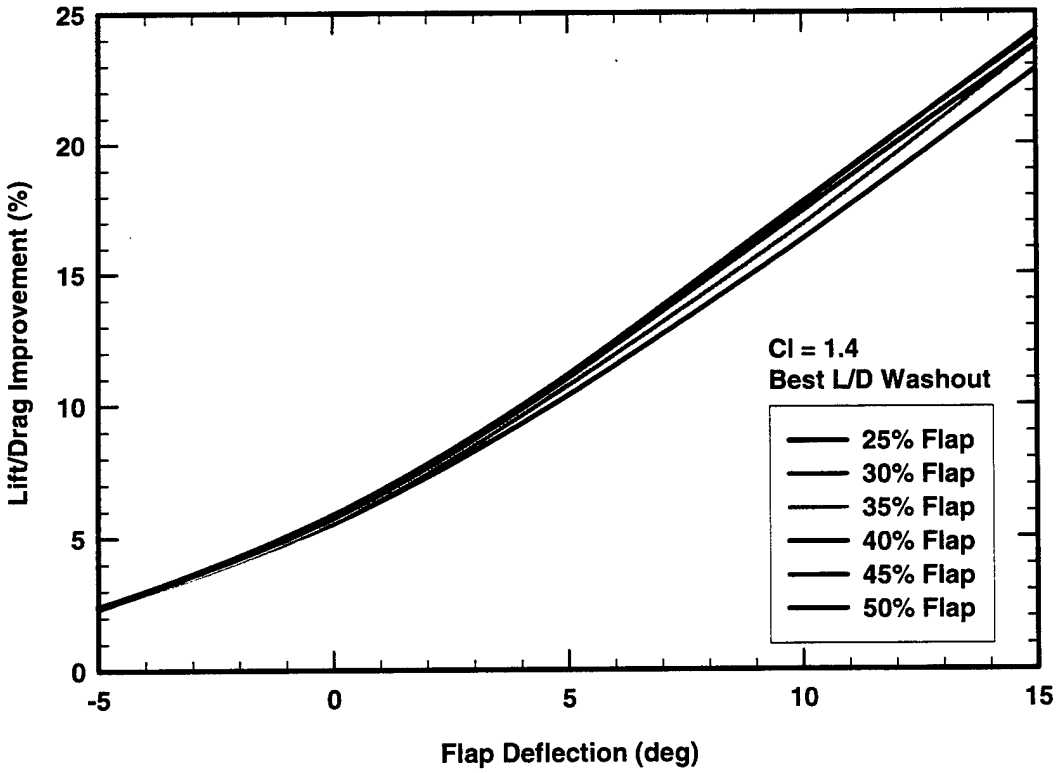

Figure 5.2.5. Best possible lift-to-drag ratio improvement as a function of flap width.

The effect of flap width on the maximum lift coefficient for a given flap deflection was analyzed using JAVAFOIL. Figure 5.2.6 shows the maximum lift coefficient for the three flap percentages. With the 25 and 30% flaps having very similar characteristics, the final criterion considered was that of manufacturability. The 25% flaps are the best choice considering that it would be easier to twist a shorter and thinner flap while sacrificing very little performance over the range of flight conditions to be encountered. Figure 5.2.7 shows the improvement in lift-to-drag ratio that the use of flap washout can provide, for the 25% flaps. As shown in Fig. 5.2.7, increases in lift-to-drag ratio from 10 to 20% can be realized with this flap modification. An improvement of this magnitude with a single modification is unheard of beyond the fairing of bluff bodies. Based on these results, the best configuration is a wing with 25% flaps. The flaps would be deflected 15 degrees with 35 degrees of washout at the tip for turning and takeoff, and the flaps would be deflected –1.5 degrees with 6.5 degrees of washout at the tip for level flight.

In order to address the problem of manufacturing this design, the use of multiple control points along the span are necessary. This can be accomplished with the use of one servo per wing attached to three bellcrank/control horn assemblies and one stationary control point. In order to create the elliptic washout distribution on the flap, the control points are clustered toward the tip with a cosine distribution. Figure 5.2.8 shows the position of each control point along the span at both the cruise and turning flap deflections. With each dynamic control point needed different degrees of rotation and direction, the pushrods connecting each bellcrank assembly must have the correct lever arm length relative to the servo rotation. The servo is placed in the wing at the 60% semi-span with pushrods going to the bellcranks at the root and tip of the wing section. This arrangement minimizes the length of the pushrods

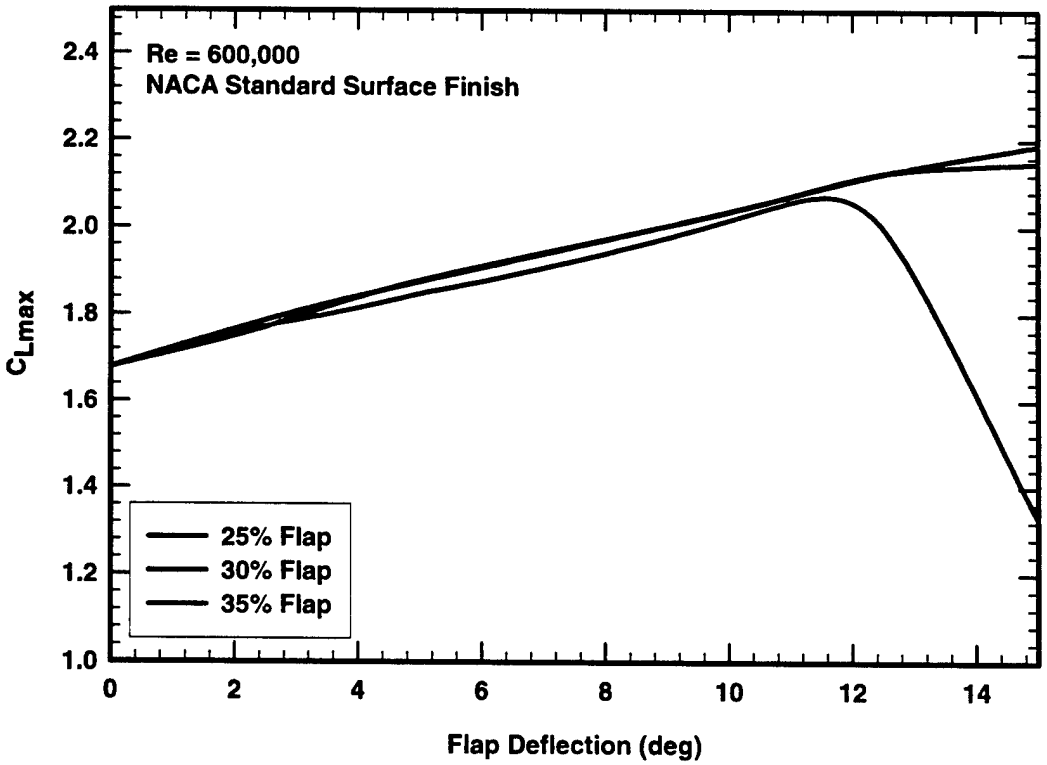

Figure 5.2.6. Maximum lift coefficient for a given flap deflection and flap width.

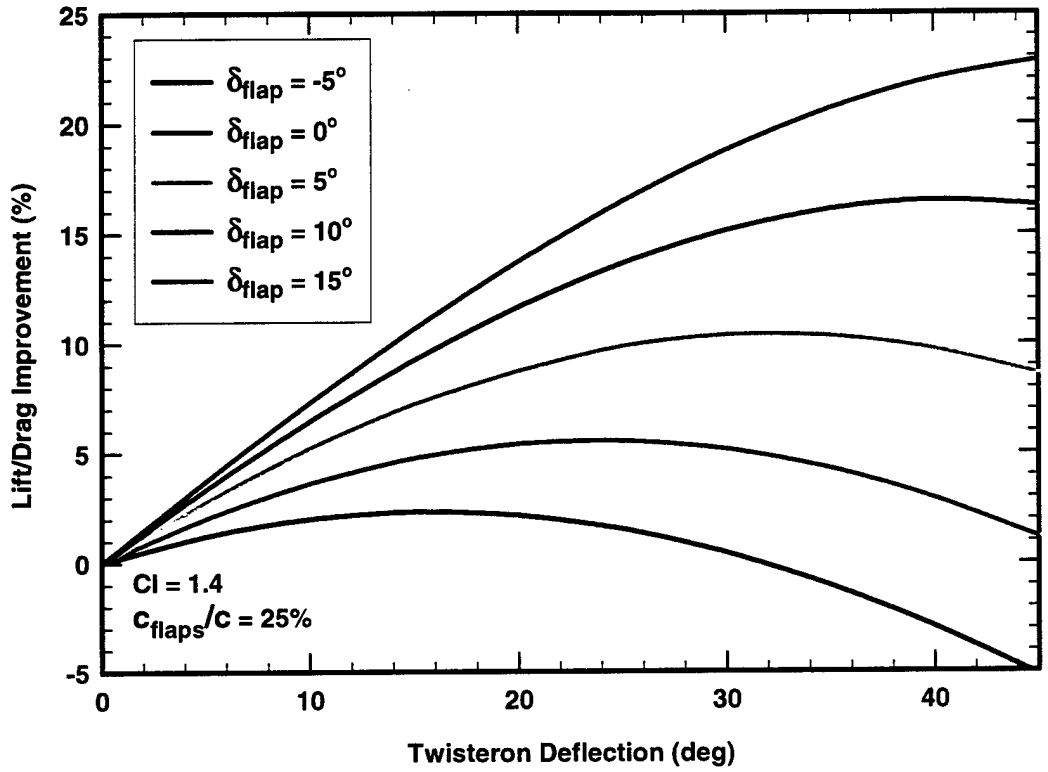

Figure 5.2.7. Lift-to-drag improvement as a function of twisteron deflection.

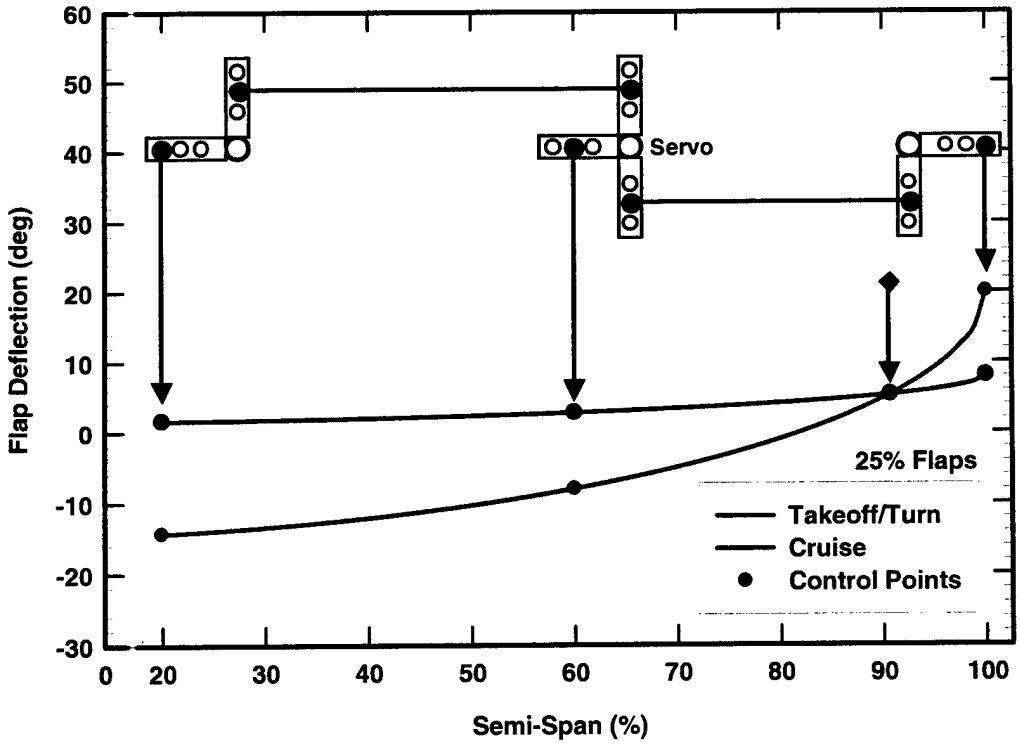

Figure 5.2.8. Flap washout over operating range with control linkage schematic.

and limits the amount of twist between the closest control points. For a flap 2.7 inches wide, the most severe relative twisting that would be experienced is 15 degrees over 6 inches. The rotation of the root bellcrank is 148% of the servo bellcrank and the tip rotation is –111% of the servo bellcrank. By implementing washout, the lift-to-drag ratio of the aircraft can potentially increase by 20%.

5.2.2. The Stability and Control System. The results that were obtained from preliminary design combined with the most recent wing properties, were used to finalize the design of the empennage and its control surfaces.

Empennage. In the detail design phase, more accurate models of the aerodynamic forces and moments were needed to finalize the design of the empennage. For this, the method of Phillips and Snyder (2000) was utilized. The first task was to model the optimal aircraft from preliminary design and analyze its stability. The results were within 5% of those found from the DBFEMP program, giving confidence in the results found in preliminary design. From this optimal empennage geometry it was noticed that the total length of the aircraft was close to the length of the aircraft storage box. This shifted the focus of the team to not only optimize the empennage in terms of RAC, drag, and manufacturability, but also in terms of assembly time. If the empennage could be made to fit into the box, this would greatly reduce assembly time.

Geometry. Elliptical planform lifting surfaces are the most efficient in terms of lift and drag. However, they are extremely difficult to manufacture. Due to the time constraints of this design process, it was decided that elliptical surfaces would not be feasible to manufacture. A tapered lifting surface is a good compromise between elliptical and rectangular shapes. A planform with a taper ratio of 0.4 and some degree of washout approximates an elliptic lift distribution reasonably well, however a planform with a taper ratio of 0.6 fitted with elliptical tips is more accurate. The tradeoff again was manufacturability, the wing with a taper ratio of 0.4 and washout would be easier to manufacture than the wing with a taper ratio of 0.6 fitted with elliptical tips. The final decision was that, because of the high lift carried on the tail during some mission phases, the aerodynamic advantages associated with the elliptic wingtips overcame the increase in manufacturing difficulty.

Control Surface Sizing, Location and Hinging. Once the possibility of storing the fuselage and empennage as one piece was recognized, design efforts were directed toward sizing the empennage to fit within the box. The empennage optimization problem iterated on the empennage parameters of horizontal offset, the tail feather size, and the hinge location.

It was determined that a tape hinge across the bottom of the horizontal stabilizer would facilitate an elevator deflection of 90 degrees. With total aircraft length constrained by the length of the box, an elevator deflection of 90 degrees would allow the empennage to be moved aft a distance equal to the elevator width less the airfoil thickness. This would slightly increase the RAC, while increasing stability and aircraft efficiency. The stability gain outweighed the increase in RAC. Results from preliminary design suggested that an elevator chord of 50% would be within the optimal range. Because the box is only 2 feet wide and the span of the horizontal stabilizer is 2.5 feet, it was decided that the elliptic tips would have to be attached during assembly. A 50% elevator would give a good mounting surface for these elliptical tips.

The same tradeoffs between efficiency and manufacturability were considered for the vertical stabilizer. The rudder was also hinged to deflect 90 degrees. This allowed for a larger vertical tail surface to fit inside the box. Since the vertical stabilizer carries little lift, manufacturability overcame the efficiency considerations and the vertical stabilizer was designed with a taper ratio of 0.4. To increase the

yaw stability for such a short aircraft, the vertical stabilizer was swept aft 41 degrees to increase its effective moment arm. This produced a slight increase in the RAC based on length.

The upper portion of the vertical stabilizer was designed to be removable in order to fit in the box. This removable section attaches to, and acts as an extension of the rudder. The rudder will be hinged on one side with a tape hinge giving it 90 degrees of travel in one direction. This hinge had to be perpendicular to the fuselage in order to fit it into the aircraft storage box.

A 50% elevator chord was in the optimal range from preliminary design. Having an elevator this size offered good control and allowed reasonable surface area to attach the tips. In designing the hinge line of the elevator, two possibilities were considered; one with a straight quarter-chord and one with a straight trailing edge. At cruise speeds, these two designs were modeled using the method of Phillips and Snyder (2000) and had lift-to-drag ratios of 5.9 and 6.1, respectively. Based on these results, the horizontal stabilizer has a swept quarter-chord and a straight trailing edge.

Flight Electronics. The electronic control system for the aircraft was chosen to be a 10 channel JR 10X radio and receiver package. Seven of the channels are used to power the Astroflight speed controller and 6 Hitec servos. To facilitate ease of assembly and allow a single control surface on each wing to serve as both flaps and ailerons, a separate servo was used in each wing. Three more servos were used for the rudder and nose gear, elevator, and retractable gear. One more servo was used to actuate both the wheel brakes and payload release mechanism. This arrangement of servos maximized aircraft control while minimizing the RAC.

5.2.3. The Propulsion System. Optimization of the propulsion system was focused on characterizing the motor and battery packs and implementing them into the power plant program to more accurately predict the best propeller for each mission.

Motor. Motor efficiency tests were performed in order to determine motor characteristics and optimize the motor and batteries with the specific mission requirements. The tests serve several purposes; they show the relationship between motor efficiency and temperature, provide an independent verification of the manufacturer's characteristic curves, and give accurate battery-life profiles under expected flight conditions. Efficiency tests required measurements of battery voltage, current, motor torque, and shaft speed. Measurements provided all the necessary data to effectively analyze the motor/battery combination. The temperature of the motor was also measured in order to monitor thermal effects. The measurements were sampled on a PC using a National Instruments 604xE board and LabVIEW data acquisition software. The test setup is shown in Fig. 5.2.9 with an early test motor. A hysteresis brake with a load cell serves as a dynamometer. Changing the current flow through the brake varies the load applied to the motor.

The uncertainty of the motor efficiency is a function of the uncertainty of each of the four measurements. An error propagation analysis was performed to quantify this uncertainty and was found to be 6% for nominal current, voltage, torque, and speed values. Figures 5.2.10 through 5.2.12 show test results using an Astroflight 691 Cobalt motor with a 24-cell, 1700-mAhr battery pack. This motor was chosen for the final aircraft configuration.

System efficiency. System efficiency is the power put into the motor from the batteries divided by the power output from the motor. The efficiency and temperature of the motor test are plotted in Fig. 5.2.10 with the computed uncertainty. As can be seen, efficiency is basically independent of temperature even after significant heating. This allowed the team to save the added weight of a complex cooling system, which was originally contemplated. A simple air intake was designed to cool the motor.

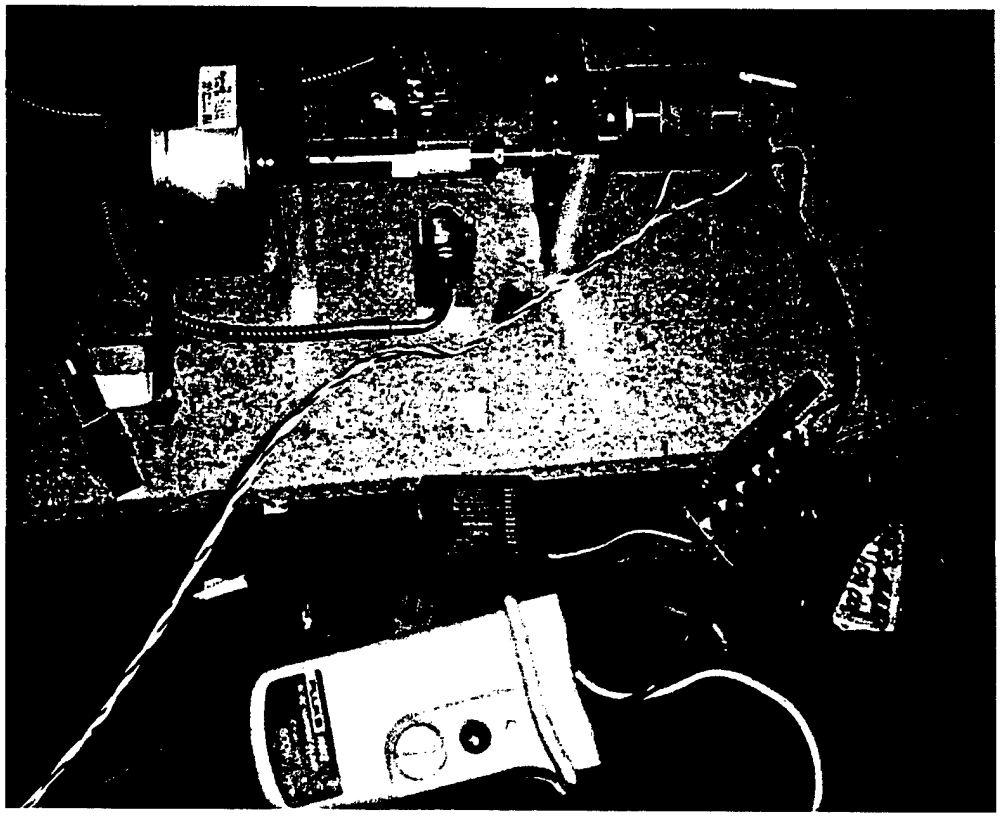

Figure 5.2.9. The motor test setup.

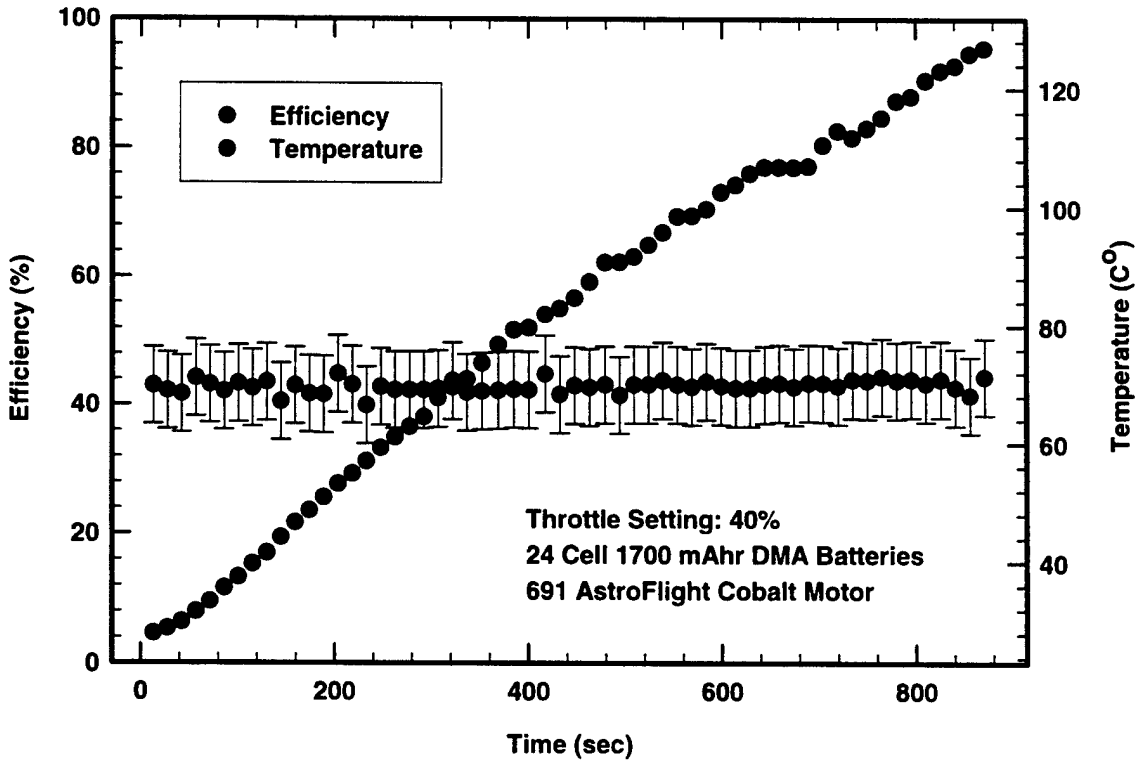

Figure 5.2.10. Temperature dependence of efficiency.

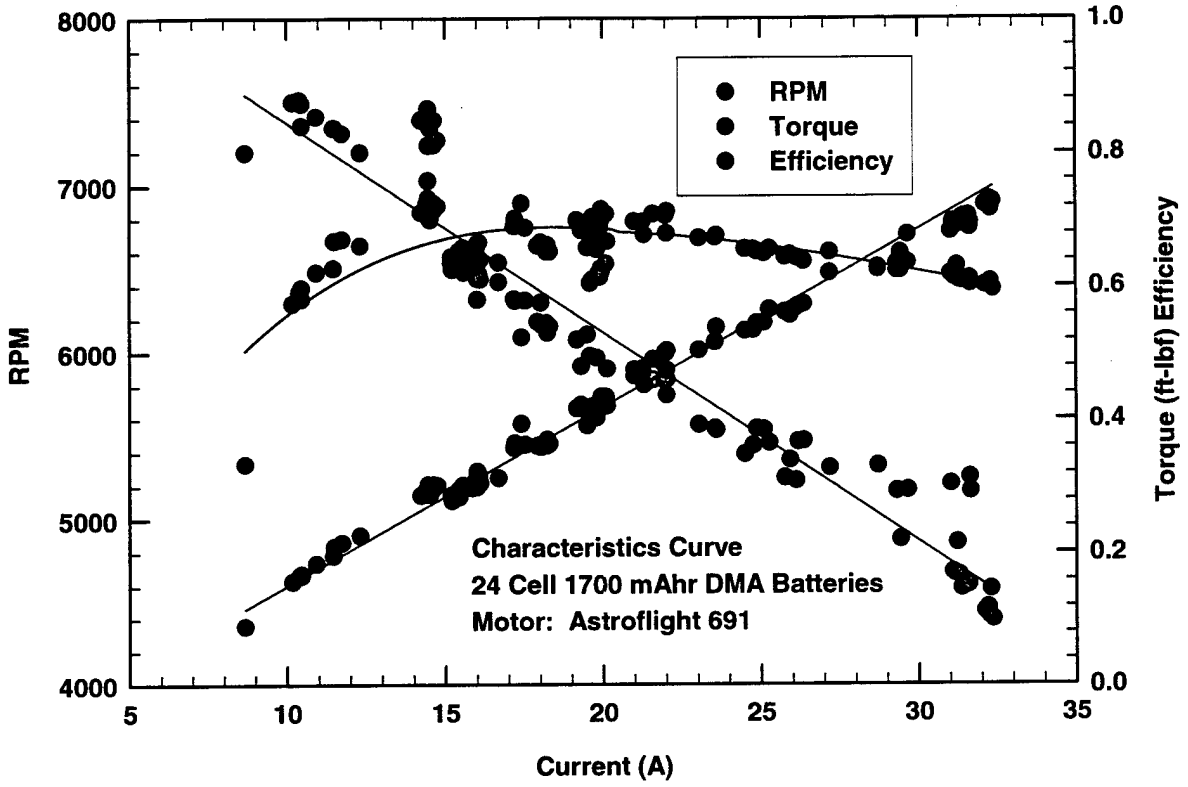

Figure 5.2.11. Characteristic curves of Astroflight 691 motor.

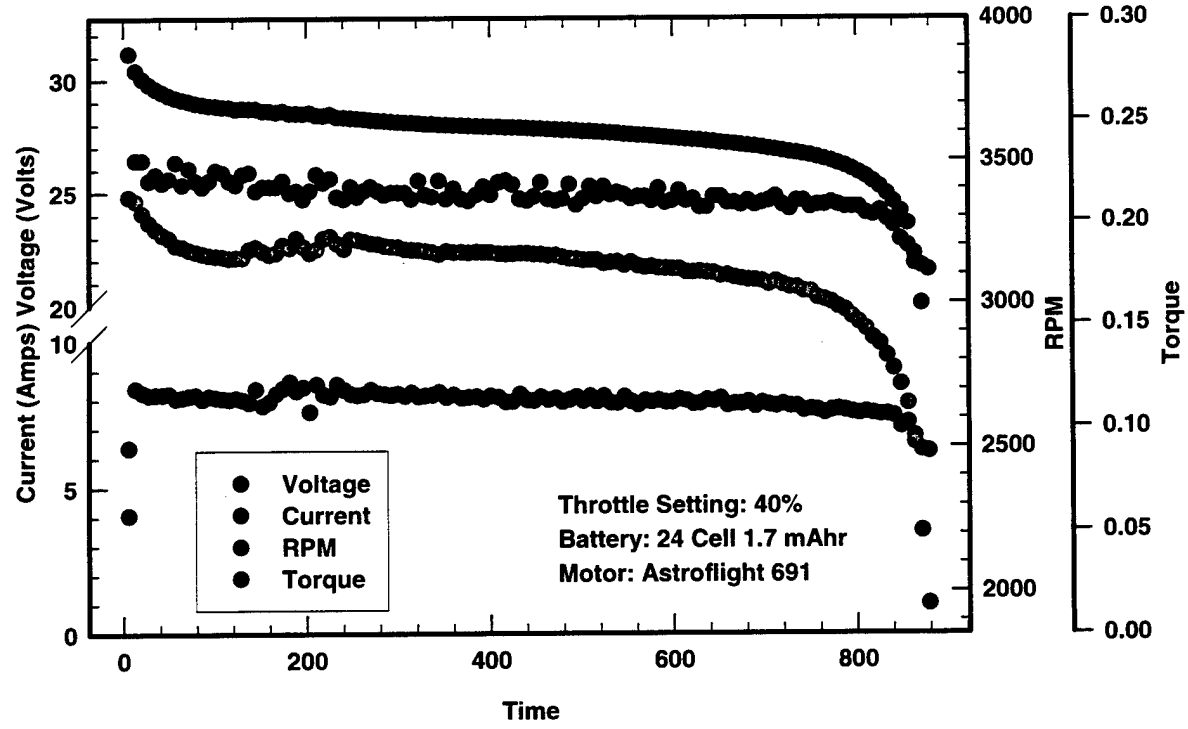

Figure 5.2.12. Motor/Battery performance characteristic curves.

Characteristic Curves. Characteristic curves were generated from these tests showing torque, speed, and efficiency as a function of current draw. Figure 5.2.11 shows samples taken at discrete loads for the same motor/battery combination at full throttle. It can be seen that for this scenario, a peak efficiency of 70% occurs at approximately 20 amps of current. The motor produces 0.4 ft-lbf of torque at this point and is operating at 6000 rpm. It is at this maximum efficiency location that we wish to operate the motor. However, it can also be seen that the efficiency penalty for increasing the current by 10 amps is less than 10%. Based on these curves, a propeller can be selected to give the desired thrust at these conditions.

Batteries. The batteries were selected based on the requirement that a minimum amount of energy, with a reasonable factor of safety, remain in the batteries at the conclusion of each mission. The pack must also provide adequate power to meet mission requirements. Internal battery losses are a major contributing factor in maximum power output. For this reason, a balance was sought between the number of cells and power output of the battery pack. For a given weight of batteries, a tradeoff between capacity and voltage was made. The FOM for battery selection in Table 5.2.1 were based on the flight program and test results. With the 40 amp current limit, a 48-cell, 1700-mAhr battery pack provides more power for a shorter period of time than a 36-cell, 2400-mAhr battery pack, yet still meets the mission requirement for total flight time.

Battery Pack	Power	Weight	Energy*	Resistance	Total
36 cells, 2400 mAhr	0	1	0	0	1
48 cells, 1700 mAhr	1	1	1	-1	2
* Excess energy left over after mission completed.					

Table 5.2.1. Figures of merit for flight battery pack.

In addition to temperature/efficiency profiles and characteristic curves, the motor tests provide information regarding the useful life of the flight batteries. Figure 5.2.12 shows the voltage and current of the flight battery and the torque and speed output of the flight motor. By integrating the area under the current curve for the one battery cycle the total charge in the batteries can be determined. In the same way, total useful output motor energy is obtained by integrating the product of the torque and shaft speed over time. Another useful battery parameter that can be obtained from these tests is the internal battery resistance, which is given by

$$R_b = (E_b - E_m)/(I_m \cdot \#ofcells) \qquad (5.2.1)$$

Figure 5.2.12 shows that the voltage immediately decreases 2 volts from the no-load voltage for a 24 cell battery pack. With the motor drawing 8 amps, equation 5.2.1 yields an internal resistance of 10 mΩ.

Propeller. With the motor and battery pack performance characterized, these values were put into the power plant program used in preliminary design to reiterate on the propellers used for MDM and SDM. Based on best flight score, the optimal propellers dimensions for MDM and SDM are 18X18 and 20X18, respectively.

5.2.4. The Aircraft Structural System. The aircraft's structural design was divided into four major categories for focus during detail design. These are as follows; wing structure, fuselage main support, fuselage secondary support, and aircraft assembly attachments. Each subsystem design involved the input of experts in R/C aircraft, machining, and composites. Along with component testing, this interaction of engineers and manufacturing experts helped minimize costs and redesign.

Wing. Based on the potential for very high accelerations in the turns of every flight, the wing structure needs to support aerodynamic loads in excess of 140 lbf. In order to attain the strength needed for such loads, a very strong, light, and stiff wing was required. The FOM used to select the final wing structure are listed in Table 5.2.2. Based on the selection criteria listed in Table 5.2.2, the best choice for a wing support structure was that of a carbon composite I-beam running through a very light foam core sheeted with balsa. The geometry of the I-beam was engineered to provide the necessary tensile, compressive and shear strength for the flight and wingtip test loads. The I-beam webs were initially sized using a model based on isotropic beam theory. The design was then analyzed using the I-DEAS finite element package to determine the stresses encountered at the transition region between the I-beam and the mounting fixture. The I-beam was modeled with thin shell elements having isotropic properties for the shear web and orthotropic smeared properties of zero degree layers for the flanges. The model was clamped at the attachment point and loaded with a uniform spanwise distributed load of 17.5 lbf/ft. The finite element model results were then verified with component testing. Figure 5.2.13 shows the finite element model, test article setup, and stress plots. The test article withstood an acceptable point load of 80 pounds and failed in the same mode as predicted by the finite element model.

Wing Main Support Structure	Strength to Weight	Total Weight	Manufacturability	Cost	Total		Fuselage Main Support Truss	Strength to Weight	Total Weight	Manufacturability	Cost	Total
Geometry							**Geometry**					
Monocoque Shell	1	0	-1	-1	-1		Monocoque Shell	1	0	-1	-1	-1
Tube	-1	-1	1	0	-1		Tube	-1	-1	1	0	-1
I-Beam	1	1	0	-1	1		I-Beam	1	1	0	-1	1
Box Beam	0	-1	1	0	0		Box Beam	0	-1	1	0	0
Material							**Material**					
Carbon Composite	1	1	0	1	3		Carbon Composite	1	1	0	1	3
Balsa	1	0	-1	-1	-1		Balsa	1	0	-1	-1	-1
Spruce	0	0	-1	0	-1		Spruce	0	0	-1	0	-1
7075-T6 Aluminum	-1	-1	1	-1	-2		7075-T6 Aluminum	-1	-1	1	-1	-2

Table 5.2.2. Design selection matrix for wing and fuselage main support structures.

Fuselage Spar. To meet the desired low wing configuration combined with a vertical drop deployment mechanism a straight spar could not be used. The payload must be located at or slightly aft of the planform center of gravity of the aircraft to maintain stability after deployment. A spar that curves over the payload was designed to meet these requirements. During maximum projected loading the spar will need to support a 190 ft-lbf moment. Aluminum spar designs were discarded because of a small Young's modulus and expensive manufacturing costs. A carbon fiber composite box beam spar was tested using Rhoacel™ foam as the center. This spar failed under relatively light loading because the compressive strength of the foam was exceeded. Carbon fiber I-beam designs were tested with better results. The basic design for the I-beam spar was found using curved beam theory presented in Boresi, et.al. (1993). The web was built using eight layers of 0.010-inch unidirectional carbon fiber laid at 0, 90, 45, and -45 degree angles. The flanges were each made from six layers of the same material laid in the spanwise direction. The figures of merit for the final design of the fuselage spar are listed in Table 5.2.2.

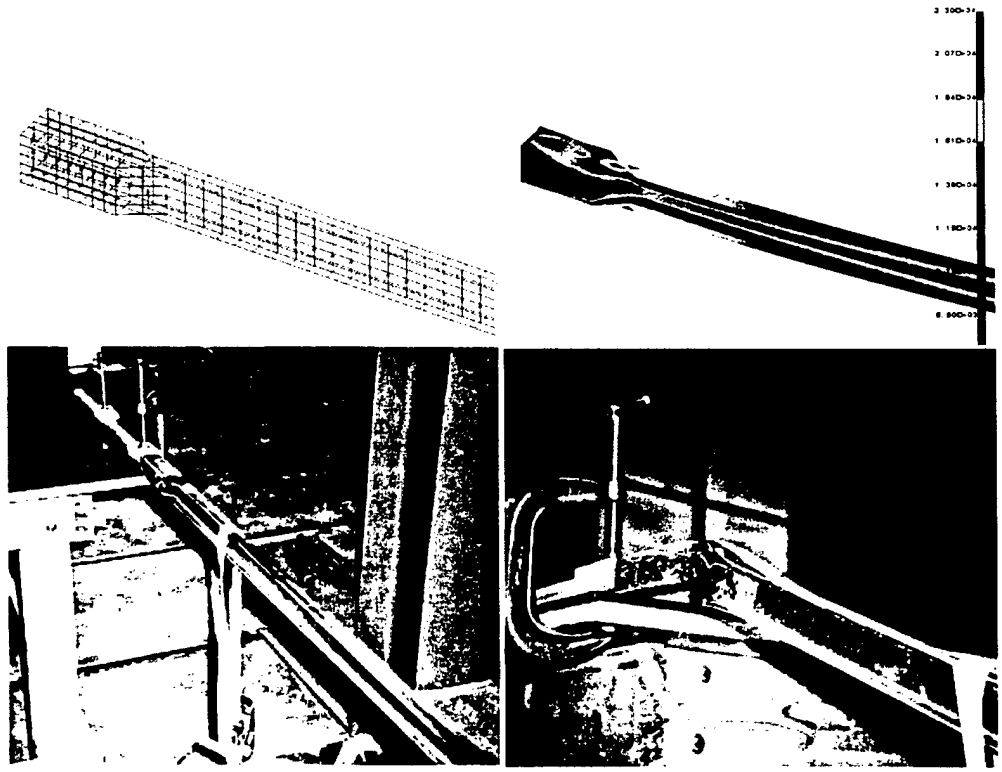

Figure 5.2.13. Clockwise from top left; finite element model, Von Mises stress results, test article failure at 80 lbs, and test article setup.

A finite element analysis of the curved spar was performed using thin shell elements in I-DEAS. The flanges were modeled with orthotropic elements having smeared lamina properties. The web was modeled with isotropic elements, and the model was restrained with plane symmetric boundary conditions. A point load of 80 lbf was placed 26 in out from the plane of symmetry. This point corresponds to the wing center of lift. Stiff beams were used to transfer the applied point load to the end of the spar. The finite model predicted a buckling failure at a 116-lbf load and the test specimen failed at 125 lbf (Fig. 5.2.14). This is less than the required load, so the flanges will be widened in the transition region to provide greater torsional stiffness and increase the buckling factor of safety.

Fuselage Structure. The fuselage structure design is based on the need to provide attachments for the many components required to complete the mission and provide adequate strength to support them throughout the entire flight with a minimum weight penalty. Another important consideration is the access that the structure provides to critical components, such as batteries and servos, for repair or replacement. The fuselage selection matrix in Table 5.2.3 shows the criteria used to determine the general structure of the fuselage. The best choice for the fuselage design is a blended body.

Aircraft Assembly Attachments. The aircraft must fit inside a 4 ft X 2 ft X 1 ft box and be assembled in as little time as possible. This requires that the airframe be modular and easily assembled. Because of the short empennage, the only parts of the aircraft that need to be assembled at the competition are the tips of the tail feathers and the wings.

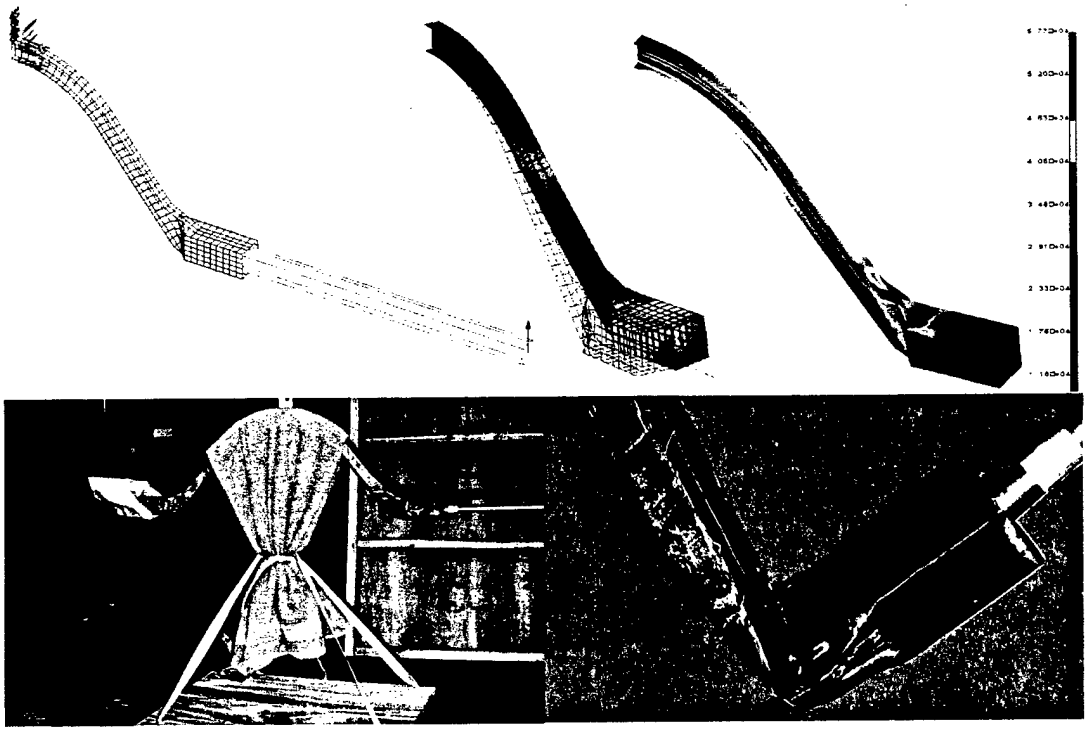

Figure 5.2.14. Clockwise from top left; Finite element model, buckling failure mode, stress plot, buckled truss at transition to mounting block, test setup.

Fuselage Geometry	Drag	Weight	Manufacturability	Cost	Total
Blended Body	1	1	-1	0	1
Lifting Body	0	0	-1	0	-1
Rectangular	-1	-1	1	1	0
Material					
Balsa Builtup	1	1	-1	0	1
Glass Shell	1	0	-1	-1	-1
Foam Core/Balsa	0	-1	0	1	0

Table 5.2.3. Design selection matrix for fuselage structure.

5.2.5. The Payload Support and Deployment System. In order to meet the requirements for MDM and SDM, methods for carrying the missile decoy cylinder and deploying the five pound payload are necessary. To carry the missile decoy cylinder, a small sting attaches the cylinder to the top of the aircraft at the center of gravity. The advantage of this location is that the positive pitching moment it creates reduces the negative lift needed by the horizontal stabilizer to trim the airplane. The possible disadvantage is the turbulent wake that it produces, which shadows a portion of the vertical stabilizer. Because of the unpredictable nature of the wake, test flights will help address the influence of the cylinder on handling characteristics. As for the payload deployment, Figure 5.2.15 shows how the payload is captured by pushrods going thru bearing plates attached at the front and rear of the payload. When released, the payload slides down an attatched rail through a spring-loaded trapdoor.

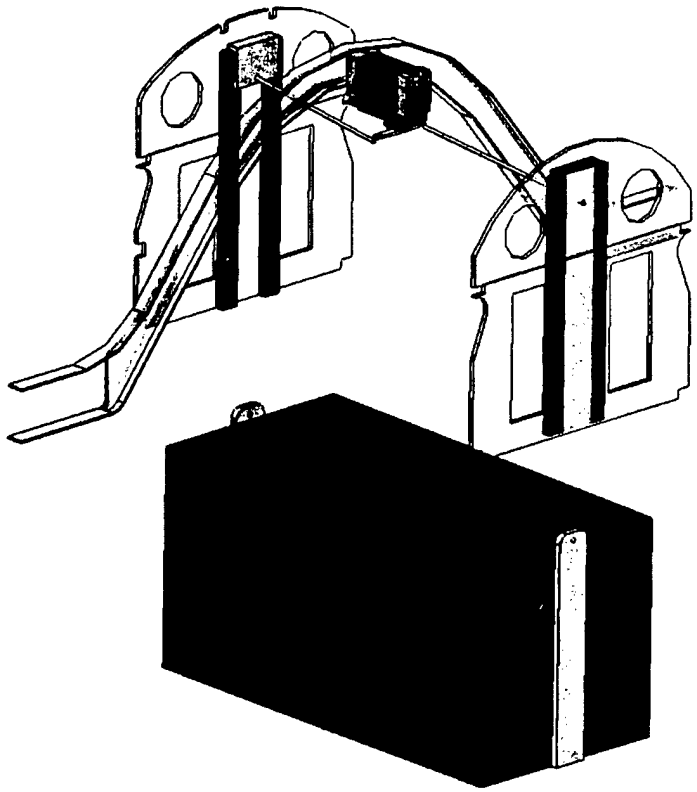

Figure 5.2.15. Deployment mechanism.

5.2.6. Landing Gear. Considerations for the landing gear design were based on drag, ground handling, weight, stopping ability, and compatibility with a rapid payload deployment system. Both stopping ability, and compatibility with a rapid payload deployment system have an effect on mission-effectiveness through the time required to stop and deploy the payload during the SDM. Table 5.2.4 shows the decision matrix used for choosing the landing gear. Based on these results, Robart retracts with BVM Jets proportional brakes were selected.

Landing Gear	Drag	Handling	Weight	Time	Cost	Total
Weighting Factor	3	1	1	2	1	
Fixed Tail Dragger, no brakes	0	-1	0	-1	1	-2
Fixed Tail Dragger, brakes	0	-1	0	0	-1	-2
Retractable Tail Dragger, no brakes	1	-1	-1	-1	0	-1
Retractable Tail Dragger, brakes	1	-1	-1	0	-1	0
Fixed Tricycle, no brakes	-1	0	-1	0	1	-3
Fixed Tricycle, brakes	-1	0	-1	1	-1	-3
Retractable Tricycle, no brakes	1	0	0	0	0	3
Retractable Tricycle, brakes	1	0	0	1	-1	4

Table 5.2.4. Landing gear selection matrix.

5.3. Final Aircraft Specifications

Given the detail design decisions laid out previously, the final design for Utah State University's competition aircraft is given in Table 5.3.1.

Geometry	**Value**
Length, (ft)	4.58
Span, (ft)	9.83
Height, (ft)	1.5
Wing Area, (ft^2)	8.85
Aspect Ratio	10.92
Horizontal Stabilizer Volume, (ft^3)	3.06
Elevator Volume, (ft^3)	1.35
Vertical Stabilizer Volume, (ft^3)	1.01
Rudder Volume, (ft^3)	1.09
Ailerons Volume, (ft^3)	5.4
Main Wing Airfoil, (ft)	Eppler 584
Horizontal/ Vertical Stabilizer	NACA 0009
Weight Statement	**Value**
Airframe, (lbf)	9.6
Propulsion System, (lbf)	7.5
Control System, (lbf)	0.75
Payload, (lbf)	5 & 5.75
Manufactures Empty Weight (MEW), (lbf)	17.85
Gross Weight, (lbf)	22.85 & 24.35
Systems	**Details**
Radio	10 Channel JR 10X
Servos	6 X Hitec NES 517
Speed Controller	1 X Astroflight 204D
Battery Configuration	48X1700-mAhr Diversity Model Aircraft
Motor	1 X Astroflight 691
Gear Ratio	1:1
Propeller(s) (nominal)	Bolly 18X18 or 20X18
Brakes	BVM Jets #5688
Landing Gear	Robart #630, #640

Table 5.3.1. Geometry and weight statement.

5.3.1. Drawing Package. The following assembly drawing package does not include the full set of manufacturing prints that was used to build the aircraft. The assembly drawings include:

Zephyr Top Assembly ..... page 44
Fuselage Frame Assembly..... page 45
Fuselage Assembly ..... page 46
Left Wing Assembly..... page 47
Stowed Configuration ..... page 48

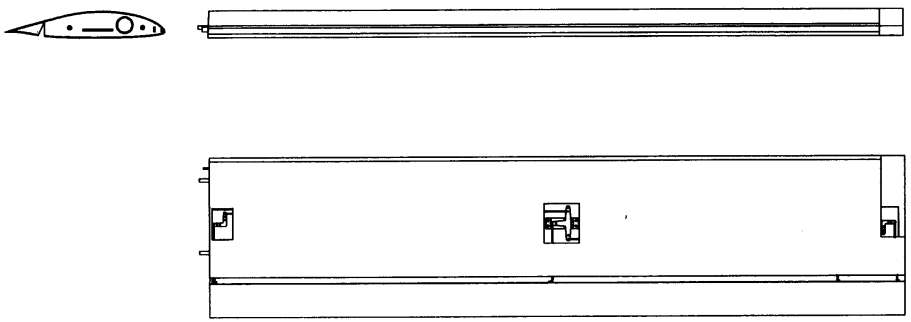

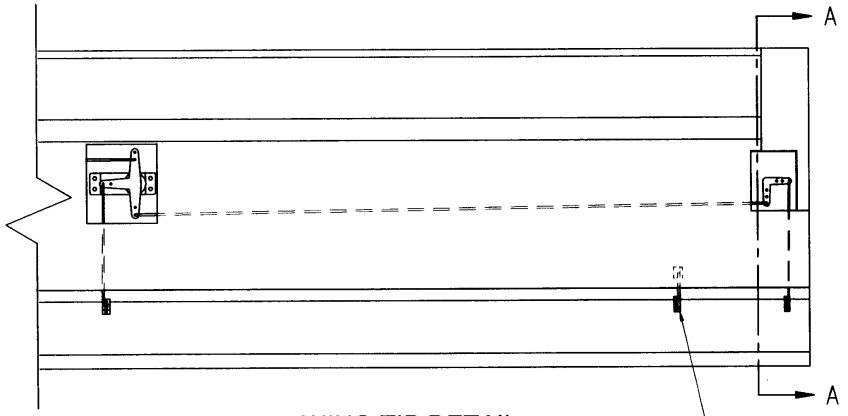

WING TIP DETAIL

BOTTOM WING SKIN REMOVED FOR CLARITY

CONTROL HORN NUMBER THREE IS RIGIDLY CONNECTED TO MAIN WING BODY

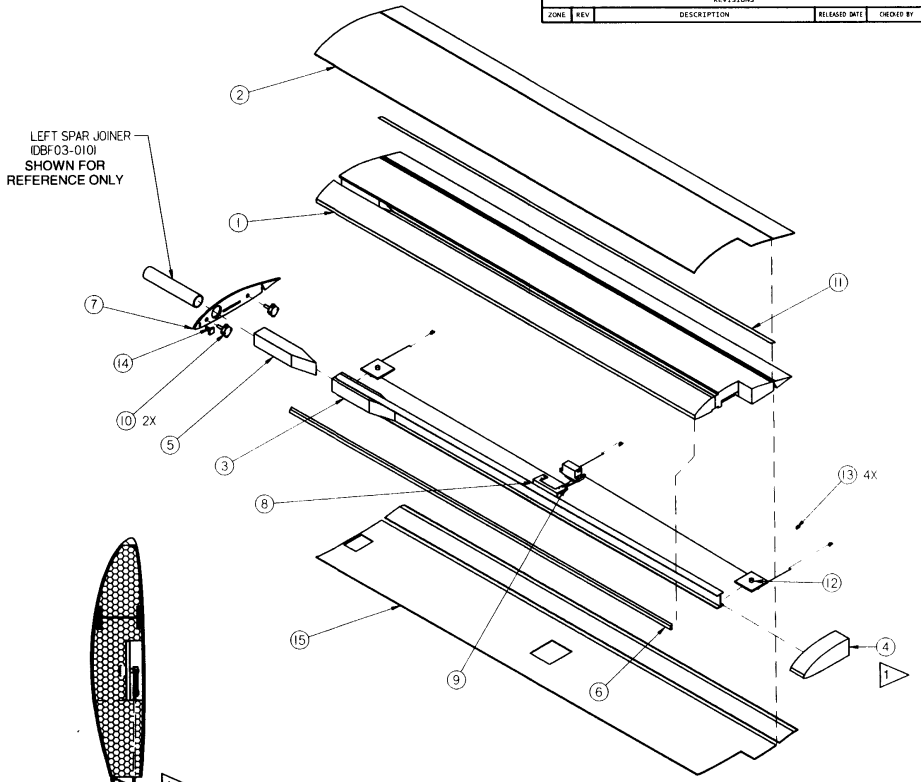

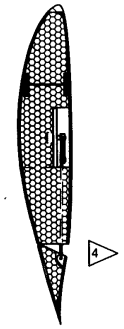

SECTION A-A

NOTES:

1. WING TIP BLOCK HAND SHAPED AFTER COMPONENT ASSEMBLY
2. ASSEMBLY TO BE COVERED WITH TOP FLITE MONOKOTE
3. COVER LINKAGE ACCESS CUTOUTS WITH MONOKOTE HATCHS
4. FLAPERON CONTROL HORNS MOUNTED INSIDE OF FLAPERON
5. AIRFOIL : EPPLER 584

ITEM NO	QTY	PART OR IDENTIFYING NO	NOMENCLATURE OR DESCRIPTION	MATERIAL SPECIFICATION
15	1	DBF03-113	WING SKIN BOTTOM	
14	1	DBF03-112	WIRING HARNESS	
13	4	DBF03-110	CONTROL HORN	
12	1	DBF03-109	FLAPERON LINKAGE ASSEMBLY	
11	1	DBF03-108	FLAPERON HINGE TAPE	
10	2	DBF03-107	WING ADJUSTER	
9	1	NES-517	SERVO	NES
8	1	DBF03-114	SERVO MOUNTING BRACKET	
7	1	DBF03-106	WING ROOT RIB	
6	1	DBF03-105	WING LE	
5	1	DBF03-104	WING JOINER SOCKET	
4	1	DBF03-103	WING TIP	
3	1	DBF03-102	SPAR	
2	1	DBF03-101	WING SKIN TOP	
1	1	DBF03-100	WING FOAM	

PARTS LIST

-	ZEPHYR
NEXT ASSY	PROJECT

UNLESS OTHERWISE SPECIFIED
DIMENSIONS ARE IN INCHES
TOLERANCES ARE:
FRACTIONS ±1/16 DECIMALS .XX=±0.01 .XXX=±0.005 ANGLES ±0.1°
INTERPRET
FINISH
DO NOT SCALE DRAWING

CONTRACT NO

APPROVALS	DATE
DESIGN A. SPINNER	3/08/03
ENGINEERING W. GOODRICH	3/08/03
BUNDERSON	3/08/03
Q.A. N. ALLEY	3/08/03
RELEASED W. PHILLIPS	3/08/03

USU DBF
DESIGN BUILD FLY 2003
UTAH STATE UNIVERSITY
Logan, Utah

TITLE: LEFT WING ASSEMBLY

SIZE D | SCALE | DWG NO. DBF03-003 | REV

THIS DOCUMENT, WHEN PRINTED, IS FOR REFERENCE ONLY | SHEET 1 OF 1

DWG. NO. DBF03-009 | SH 1 | REV

REVISIONS

ZONE	REV	DESCRIPTION	RELEASED DATE	CHECKED BY

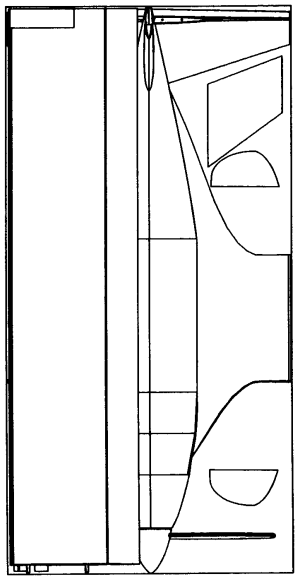

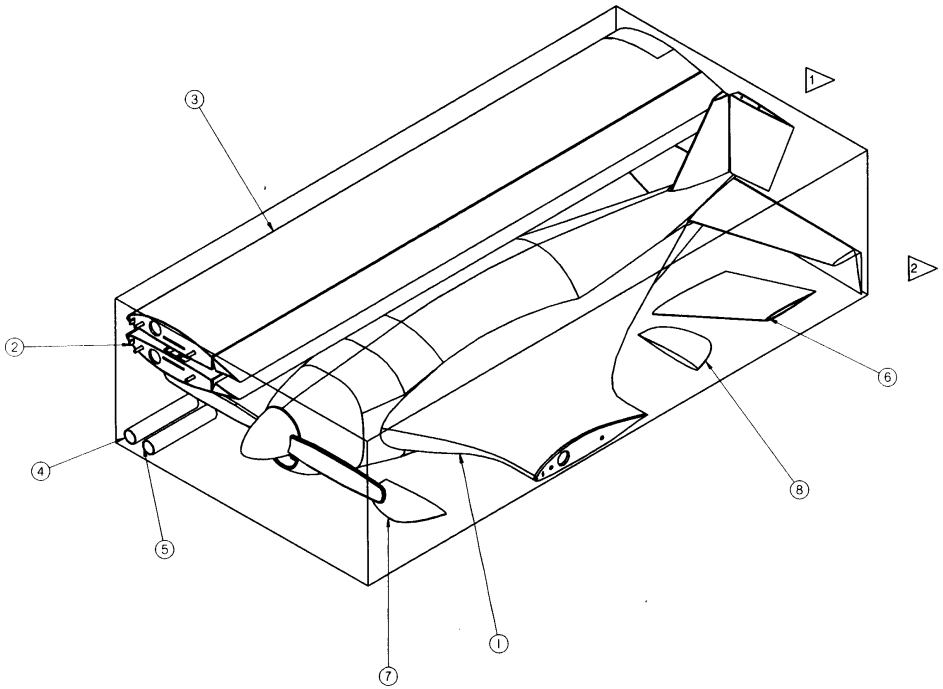

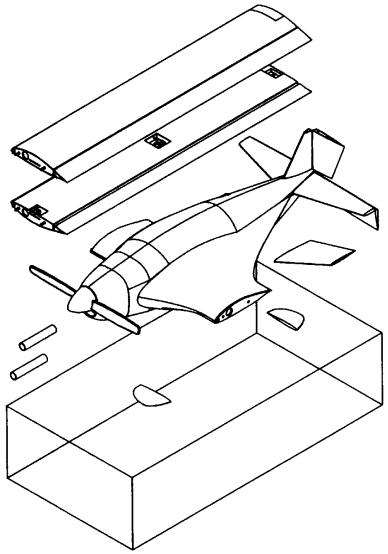

NOTES:

1. RUDDER DEFLECTED 90 DEGREES TO THE LEFT
2. ELEVATOR DEFLECTED 90 DEGREES DOWN

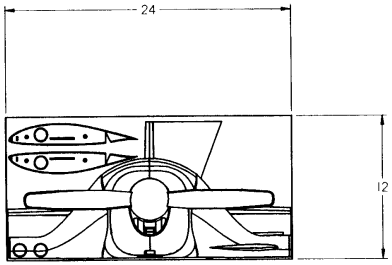

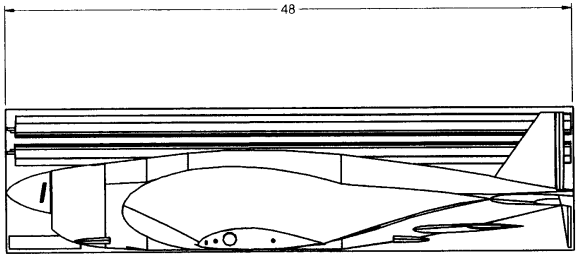

ITEM NO	QTY	PART OR IDENTIFYING NO	NOMENCLATURE OR DESCRIPTION	MATERIAL SPECIFICATION
8	1	DBF03-013	RIGHT ELEVATOR CAP ASSEMBLY	
7	1	DBF03-012	LEFT ELEVATOR CAP ASSEMBLY	
6	1	DBF03-011	RUDDER CAP ASSEMBLY	
5	1	DBF03-078	RIGHT WING JOINER TUBE	
4	1	DBF03-077	LEFT WING JOINER TUBE	
3	1	DBF03-004	RIGHT WING ASSEMBLY	
2	1	DBF03-003	LEFT WING ASSEMBLY	
1	1	DBF03-002	FUSELAGE ASSEMBLY	

PARTS LIST

UNLESS OTHERWISE SPECIFIED
DIMENSIONS ARE IN INCHES
TOLERANCES ARE:
FRACTIONS ±1/16 DECIMALS .XX±0.01 .XXX±0.005 ANGLES ±0.1°
TREATMENT
FINISH
DO NOT SCALE DRAWING

CONTRACT NO

APPROVALS	DATE
DESIGN A. SPINNER	3/08/03
ENGINEERING M. OKSNESS	3/08/03
M. ANDERSON	3/08/03
Q.A. N. ALLEY	3/08/03
RELEASED W. PHILLIPS	3/08/03

USU DBF
DESIGN BUILD FLY 2003
UTAH STATE UNIVERSITY
Logan, Utah

TITLE: STOWED CONFIGURATION

SIZE D | SCALE | DWG NO. DBF03-009 | REV

THIS DOCUMENT, WHEN PRINTED, IS FOR REFERENCE ONLY | SHEET 1 OF 1

-	ZEPHYR
NEXT ASSY	PROJECT

DWG. NO.	REV.
DBF03-001	1

REVISIONS

ZONE	REV.	DESCRIPTION	RELEASED DATE	CHECKED BY

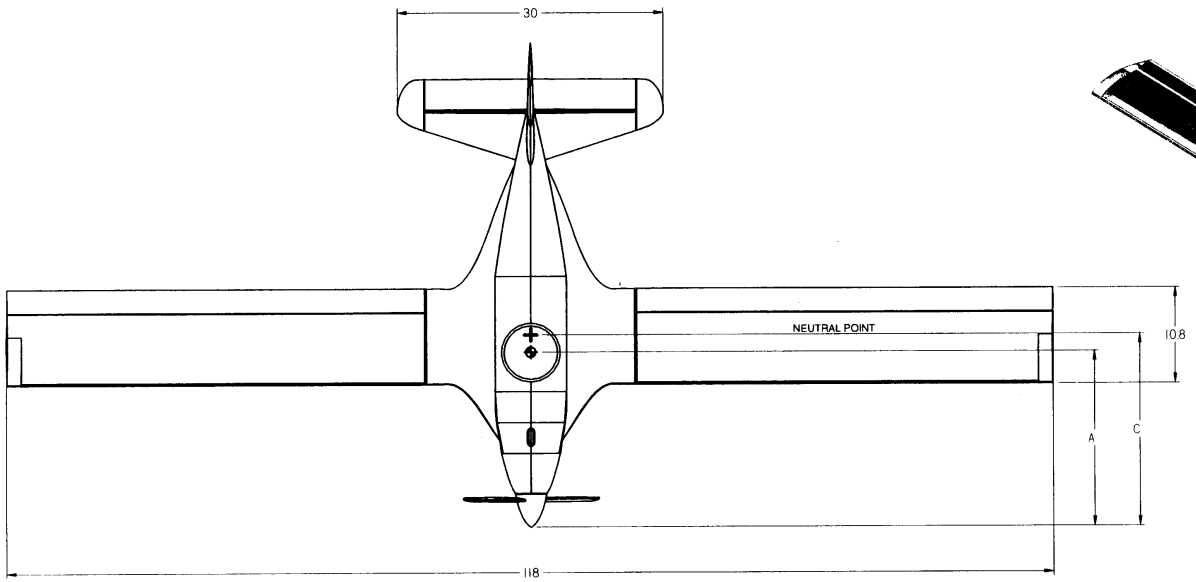

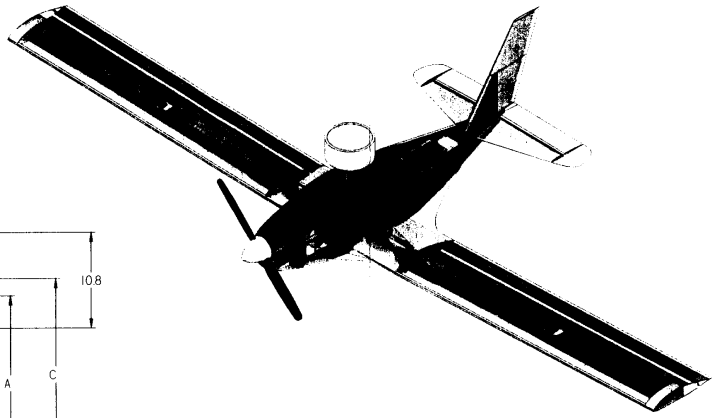

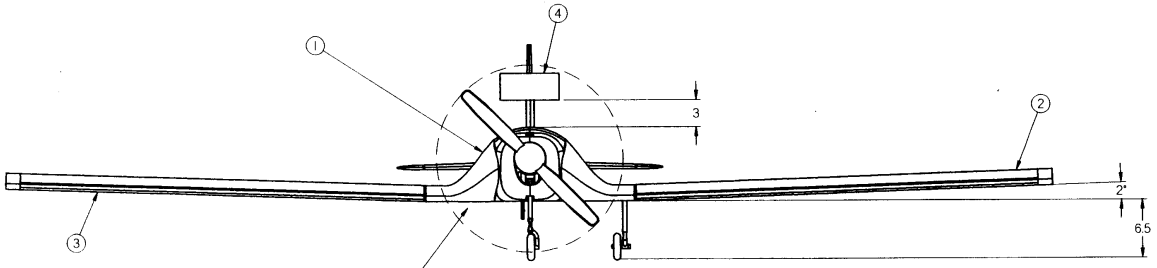

RIGHT MAIN LANDING GEAR IN RETRACTED POSITION

LEFT MAIN LANDING GEAR IN DOWN POSITION

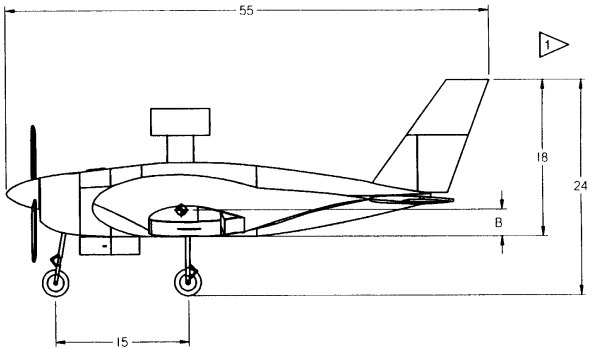

CENTER OF GRAVITY AND NEUTRAL POINT LOCATION DIMENSIONS

	A	B	C
WITH BOX AND ANTENNA	19.8	3.5	20.9
WITH BOX ONLY	19.8	3.0	20.9
UNLOADED	19.4	2.9	21.0

NOTES:

1. ESTIMATED TAIL HEIGHT. ACTUAL VALUE TO BE DETERMINED BY FLIGHT TESTING

ITEM NO	QTY	PART OR IDENTIFYING NO	NOMENCLATURE OR DESCRIPTION	MATERIAL SPECIFICATION
4	1	DBF03-005	ANTENNA ASSEMBLY	
3	1	DBF03-004	RIGHT WING ASSEMBLY	
2	1	DBF03-003	LEFT WING ASSEMBLY	
1	1	DBF03-002	FUSELAGE ASSEMBLY	

PARTS LIST

UNLESS OTHERWISE SPECIFIED
DIMENSIONS ARE IN INCHES
TOLERANCES ARE:
FRACTIONS ±1/16 DECIMALS .XX=±0.01 .XXX=±0.005 ANGLES ±0.1°
TREATMENT

APPROVALS		DATE
DESIGN	A. SPINNER	3/08/03
ENGINEERING	W. GOODRICH	3/08/03
Q.A.	N. ALLEY	3/08/03
RELEASED	W. PHILLIPS	3/08/03

CONTRACT NO.

USU DBF — DESIGN BUILD FLY 2003
UTAH STATE UNIVERSITY
Logan, Utah

TITLE: ZEPHYR TOP ASSEMBLY

SIZE	SCALE	DWG NO.	REV
D		DBF03-001	

THIS DOCUMENT, WHEN PRINTED, IS FOR REFERENCE ONLY — SHEET 1 OF 1

DO NOT SCALE DRAWING

NEXT ASSY	PROJECT
-	ZEPHYR

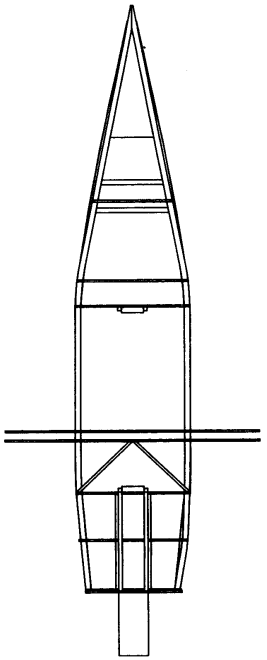

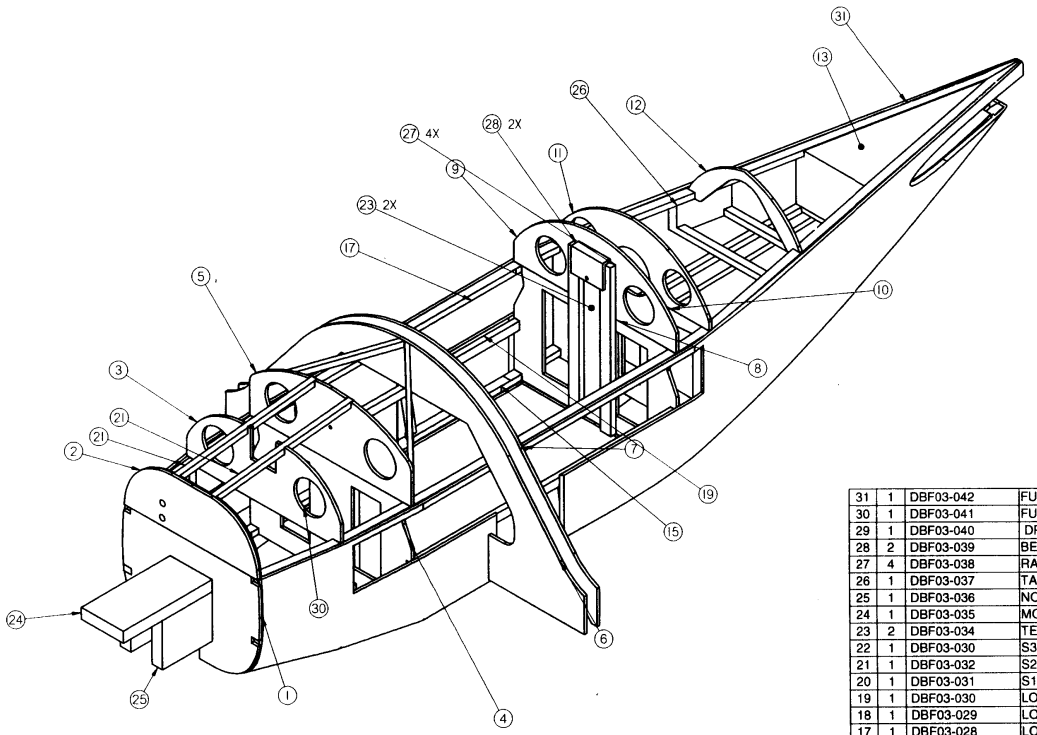

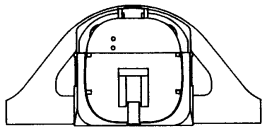

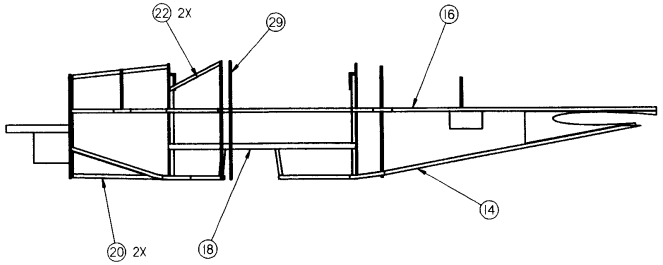

FUSELAGE SIDES HIDDEN FOR CLARITY

ITEM NO	QTY	PART OR IDENTIFYING NO	NOMENCLATURE OR DESCRIPTION	MATERIAL SPECIFICATION
31	1	DBF03-042	FUSELAGE SIDE RIGHT	1/8 BALSA
30	1	DBF03-041	FUSELAGE SIDE LEFT	1/8 BALSA
29	1	DBF03-040	DROP SERVO MOUNT	BALSA
28	2	DBF03-039	BEARING PLATE	STEEL
27	4	DBF03-038	RAIL	BALSA
26	1	DBF03-037	TAIL SERVO MOUNT	BALSA
25	1	DBF03-036	NOSE GEAR MOUNT	MAPLE
24	1	DBF03-035	MOTOR MOUNT	MAPLE
23	2	DBF03-034	TEFLON TAPE	TEFLON
22	1	DBF03-030	S3	BALSA
21	1	DBF03-032	S2	BALSA
20	1	DBF03-031	S1	BALSA
19	1	DBF03-030	LONGERON MIDDLE RIGHT	BALSA
18	1	DBF03-029	LONGERON MIDDLE LEFT	BALSA
17	1	DBF03-028	LONGERON TOP RIGHT	BALSA
16	1	DBF03-027	LONGERON TOP LEFT	BALSA
15	1	DBF03-026	LONGERON BOTTOM RIGHT	BALSA
14	1	DBF03-025	LONGERON BOTTOM LEFT	BALSA
13	1	DBF03-024	TAIL MOUNT	BALSA
12	1	DBF03-023	F7	1/8 PLY
11	1	DBF03-022	F6 TOP	1/8 PLY
10	1	DBF03-021	F6	1/8 PLY
9	1	DBF03-020	F5 TOP	1/8 PLY
8	1	DBF03-019	F5	1/8 PLY
7	1	DBF03-018	F4	1/8 PLY
6	1	DBF03-017	F3	1/8 PLY
5	1	DBF03-016	F2 TOP	1/8 PLY
4	1	DBF03-015	F2	1/8 PLY
3	1	DBF03-014	F1	1/8 PLY
2	1	DBF03-013	FIREWALL TOP	1/4 PLY
1	1	DBF03-012	FIREWALL BOTTOM	1/4 PLY

PARTS LIST

ENG. NO.	SH	REV
DBF03-005	1	

REVISIONS

ZONE	REV	DESCRIPTION	RELEASED DATE	CHECKED BY

UNLESS OTHERWISE SPECIFIED
DIMENSIONS ARE IN INCHES
TOLERANCES ARE:
FRACTIONS ±1/16 DECIMALS .XX=±0.01 .XXX=±0.005 ANGLES ±0.1°
TREATMENT
FINISH
DO NOT SCALE DRAWING

CONTRACT NO.		
APPROVALS		DATE
DESIGN	A. SPINNER	3/08/03
ENGINEERING	T. YOUNG	3/08/03
	K. BARTON	3/08/03
Q.A.	N. ALLEY	3/08/03
RELEASED	W. PHILLIPS	3/08/03

USU DBF
DESIGN BUILD FLY 2003
UTAH STATE UNIVERSITY
Logan, Utah

TITLE: FUSELAGE FRAME ASSEMBLY

SIZE	SCALE	DWG NO.	REV
D		DBF03-005	

THIS DOCUMENT, WHEN PRINTED, IS FOR REFERENCE ONLY — SHEET 1 OF 1

-	ZEPHYR
NEXT ASSY	PROJECT

DWG. NO. DBF03-002 | SH 1 | REV.

REVISIONS

ZONE	REV	DESCRIPTION	RELEASED DATE	CHECKED BY

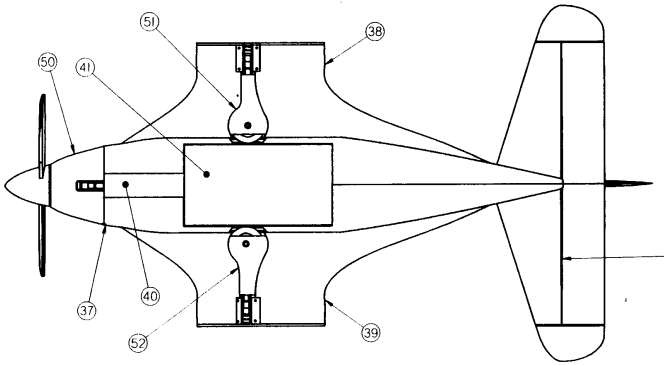

BOTTOM VIEW

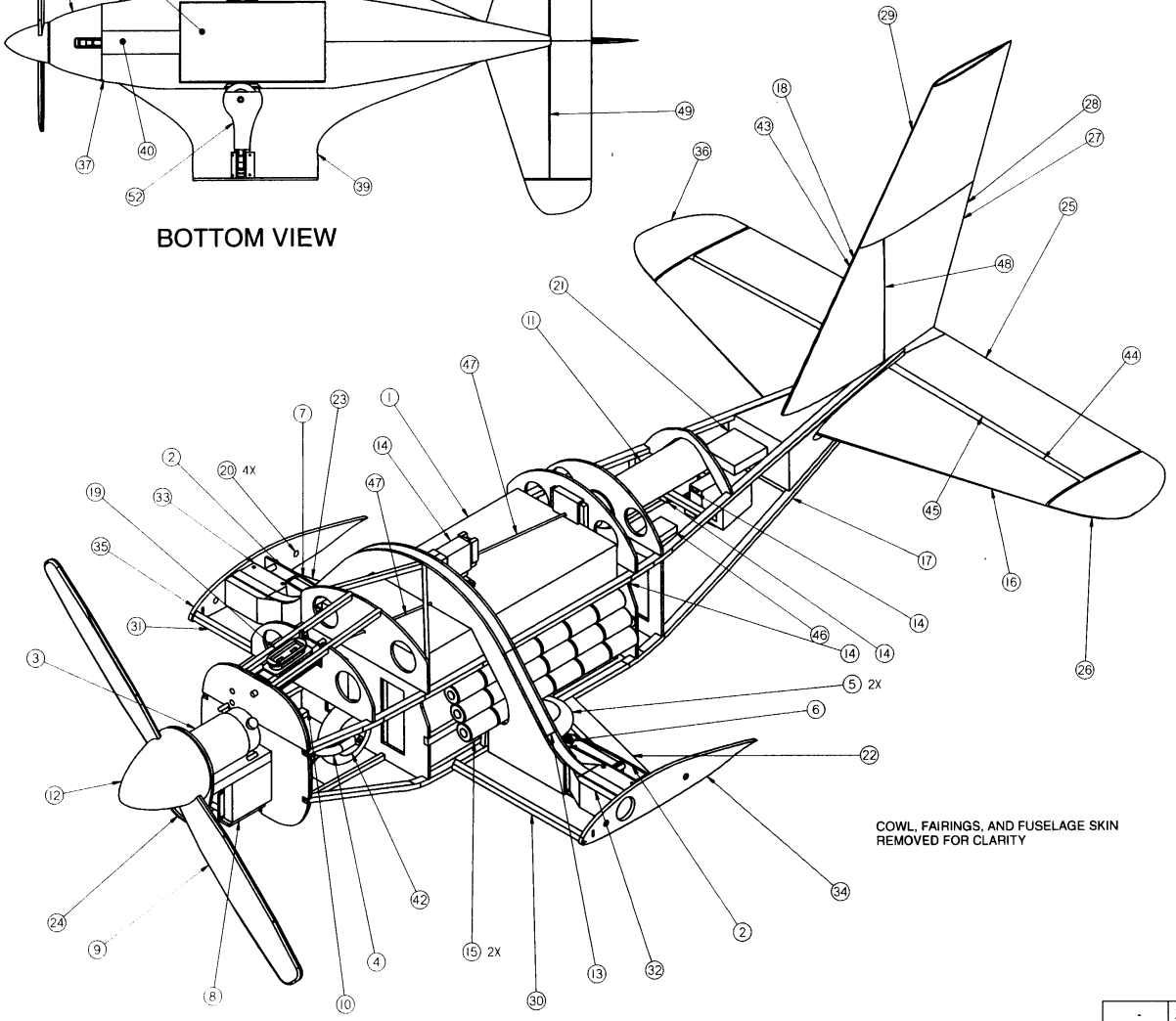

COWL, FAIRINGS, AND FUSELAGE SKIN REMOVED FOR CLARITY

ITEM NO	QTY	PART OR IDENTIFYING NO	NOMENCLATURE OR DESCRIPTION	MATERIAL SPECIFICATION
52	1	DBF03-081	MAIN GEAR DOOR RIGHT	
51	1	DBF03-080	MAIN GEAR DOOR LEFT	
50	1	DBF03-079	COWL	
49	1	DBF03-078	ELEVATOR GLASS TAPE HINGE	
48	1	DBF03-077	RUDDER PIANO WIRE HINGE	
47	1	DBF03-076	PAYLOAD RELEASE PUSHRODS	
46	1		RECEIVER	SR
45	1	DBF03-075	ELEVATOR CORE	
44	1	DBF03-074	HORIZONTAL STAB CORE	
43	1	DBF03-073	VERTICAL FIN CORE	
42	1	DBF03-072	NOSE WHEEL (3 IN)	ROBART
41	1	DBF03-071	BOMB BAY DOOR	
40	1	DBF03-070	NOSE GEAR DOOR	
39	1	DBF03-069	FAIRING RIGHT	
38	1	DBF03-068	FAIRING LEFT	
37	AR	DBF03-067	FUSELAGE SKIN	
36	1	DBF03-008	RIGHT ELEVATOR CAP ASSEMBLY	
35	1	DBF03-066	JOINER RIB RIGHT	
34	2	DBF03-065	JOINER RIB LEFT	
33	1	DBF03-064	FUSELAGE JOINER SOCKET RIGHT	
32	1	DBF03-063	FUSELAGE JOINER SOCKET LEFT	
31	1	DBF03-062	INBOARD LE RIGHT	
30	1	DBF03-061	INBOARD LE LEFT	
29	1	DBF03-006	RUDDER CAP ASSEMBLY	
28	1	DBF03-061	RUDDER CORE	
27	1	DBF03-060	RUDDER SKIN	
26	1	DBF03-007	LEFT ELEVATOR CAP ASSEMBLY	
25	1	DBF03-059	ELEVATOR SKIN	
24	1	DBF03-058	SPINNER RING	
23	1	DBF03-057	RIGHT GEAR SUPPORT	
22	1	DBF03-056	LEFT GEAR SUPPORT	
21	1		RECEIVER BATTERIES (6V)	SR
20	2	DBF03-055	WING ADJUSTER SOCKET	GATOR
19	1	114LF	FUSE SOCKET	DIGIKEY
18	1	DBF03-054	VERTICAL FIN SKIN	
17	1	DBF03-050	FUSELAGE FRAME ASSEMBLY	
16	1	DBF03-053	HORIZONTAL STAB SKIN	
15	2		BATTERY PACK (1700 mAhr)	DMA
14	4	NES-517	SERVO	NES
13	1	DBF03-052	FUSELAGE SPAR	
12	1	237158	SPINNER (3.5 INCH)	MAGNUM
11	1	172	AIR TANK (SMALL)	ROBART
10	1	204D	SPEED CONTROLER	ASTROFLIGHT
9	1		CARBON FIBER PROPELLER	BOLLY
8	1	63090	FRONT GEAR HINGE	ROBART
7	1	670	STRUT RIGHT	ROBART
6	1	670	STRUT LEFT	ROBART
5	3	5688	MAIN WHEEL (3IN WITH BRAKES)	BVM JETS
4	1	661	NOSE STRUT	ROBART
3	1	691	MOTOR	ASTROFLIGHT
2	2	63090	MAIN GEAR HINGE	ROBART
1	1	DBF03-051	PAYLOAD BOX	

PARTS LIST

UNLESS OTHERWISE SPECIFIED
DIMENSIONS ARE IN INCHES
TOLERANCES ARE:
FRACTIONS ±1/16 DECIMALS .XX±0.01 .XXX±0.005 ANGLES ±0.1°
TREATMENT

APPROVALS	DATE
A. SPINNER	3/08/03
M. ANDERSON	3/08/03
K. BARTON	3/08/03
N. ALLEY	3/08/03
W. PHILLIPS	3/08/03

DO NOT SCALE DRAWING

SPACE DYNAMICS LABORATORY
UTAH STATE UNIVERSITY RESEARCH FOUNDATION
North Logan, Utah

TITLE: FUSELAGE ASSEMBLY

SIZE D | SCALE | DWG NO. DBF03-002 | REV

THIS DOCUMENT, WHEN PRINTED, IS FOR REFERENCE ONLY | SHEET 1 OF 1

-	ZEPHYR
NEXT ASSY	PROJECT

5.3.2. Rated Aircraft Cost Calculation. As required by the contest rules, a detailed rated aircraft cost worksheet is included in Table 5.3.2. These values represent the design as presented in this report.

	Value	Computation		Cost (k$)
MEW	17.85 lbf	0.1 k$/lbf(MEW)		1.785
REP			**(lbf)**	
Number Engines (N_e)	1	$[1+.25(N_e-1)]W_b$	5.0	
Battery Weight (W_b)	5.0 lbf	1.5 k$/lbf(REP)		7.500
MFHR			**(hrs)**	
Wingspan (b_w)	9.83 ft	8 hrs/ft(b_w)	78.6	
Max Chord (c_{max})	0.9 ft	8 hrs/ft(c_{max})	7.2	
Wing Control Surfaces (N_{wcs})	2	3 hrs/surface(N_{wcs})	6.0	
Fuselage Length (l_{max})	4.58 ft	10 hrs/ft(l_{max})	45.8	
Vertical Surfaces (N_{vs})	0	5 hrs/surface(N_{vs})	0.0	
Vert. Control Surfaces (N_{vcs})	1	10 hrs/surface(N_{vcs})	10.0	
Horiz. Control Surfaces (N_{hcs})	1	10 hrs/surface(N_{hcs})	10.0	
Servo/Controllers (N_{sc})	7	5 hrs/servo(N_{sc})	35.0	
Number Engines (N_e)	1	5 hrs/engine(N_e)	5.0	
Number Propeller (N_p)	1	5 hrs/engine(N_p)	5.0	
Total MFHR		0.02 k$/hr(MFHR)	**202.7**	4.053
RAC				**13.338**

Table 5.3.2. Rated Aircraft Cost computations for the final aircraft, as designed.

5.4. Final Aircraft Performance Analysis

With a final aircraft geometry and weight determined and the flight speeds and maneuvers known, the method of Phillips and Snyder (2000) was used to determine the flight characteristics of the aircraft.

5.4.1. Aerodynamic Coefficients and Derivatives. Using the method of Phillips and Snyder (2000), all of the aircraft's stability, control, and damping derivatives were calculated for takeoff, cruise, and turning flight. Table 5.4.1 lists the derivates for cruising flight.

5.4.2. Static Stability. The most common measure of an aircraft's flight stability is static margin. For the design presented, the static margin over the lift coefficient range that will be encountered in level flight is shown in Fig. 5.4.1. These values include the influence of the propeller and fuselage.

5.4.3. Dynamic Stability. In order to characterize the flying qualities of the aircraft, a complete dynamic stability analysis was performed. This was done using the method of Phillips and Snyder (2000) to compute the stability and damping derivatives. An original code was used to compute the five dynamic stability modes as shown in Table 5.4.2. All calculations included the contribution of the propeller and fuselage. This analysis revealed a divergent spiral mode with a very short doubling time during takeoff. This is usually attributed to excessive yaw stability. The original vertical stabilizer was sized to have a yaw stiffness in the range of 0.06. With such a short aircraft and a large aspect ratio wing, these values were overly stiff. In order to alleviate this problem, the vertical stabilizer was reduced in size by over 25%. This design change increased the spiral mode doubling time, reduced weight and drag, and simplified the design.

Stability Derivatives		Control Derivatives		Damping Derivatives	
$C_{L.\alpha}$	5.8665	$C_{L.\delta_l}$	0.0000	$C_{L.\bar{p}}$	0.0000
$C_{D.\alpha}$	0.0349	$C_{D.\delta_l}$	0.0000	$C_{D.\bar{p}}$	0.0000
$C_{L.\alpha}$	0.0000	$C_{Y.\delta_l}$	-0.0284	$C_{Y.\bar{p}}$	-0.0613
$C_{\ell.\alpha}$	0.0000	$C_{\ell.\delta_l}$	-0.5349	$C_{\ell.\bar{p}}$	-0.6827
$C_{m.\alpha}$	-1.3394	$C_{m.\delta_l}$	0.0000	$C_{m.\bar{p}}$	0.0000
$C_{n.\alpha}$	-0.0034	$C_{n.\delta_l}$	0.0347	$C_{n.\bar{p}}$	0.0261
$C_{L.\beta}$	0.0000	$C_{L.\delta_e}$	0.5608	$C_{L.\bar{q}}$	4.0333
$C_{D.\beta}$	0.0000	$C_{D.\delta_e}$	-0.0145	$C_{D.\bar{q}}$	0.1122
$C_{Y.\beta}$	-0.2306	$C_{Y.\delta_e}$	0.0000	$C_{Y.\bar{q}}$	0.0000
$C_{\ell.\beta}$	-0.0350	$C_{\ell.\delta_e}$	0.0000	$C_{\ell.\bar{q}}$	0.0000
$C_{m.\beta}$	0.0000	$C_{m.\delta_e}$	-1.3207	$C_{m.\bar{q}}$	-8.5377
$C_{n.\beta}$	0.0421	$C_{n.\delta_e}$	0.0000	$C_{n.\bar{q}}$	0.0000
$C_{m.\dot{\alpha}}$	-2.7262	$C_{L.\delta_r}$	0.0000	$C_{L.\bar{r}}$	0.0000
$C_{L.\dot{\alpha}}$	-1.1483	$C_{D.\delta_r}$	0.0000	$C_{D.\bar{r}}$	0.0000
		$C_{Y.\delta_r}$	0.1471	$C_{Y.\bar{r}}$	0.0931
		$C_{\ell.\delta_r}$	0.0086	$C_{\ell.\bar{r}}$	0.0910
		$C_{m.\delta_r}$	0.0000	$C_{m.\bar{r}}$	0.0000
		$C_{n.\delta_r}$	-0.3500	$C_{n.\bar{r}}$	-0.0312

Table 5.4.1. Aircraft aerodynamic derivatives for cruising flight.

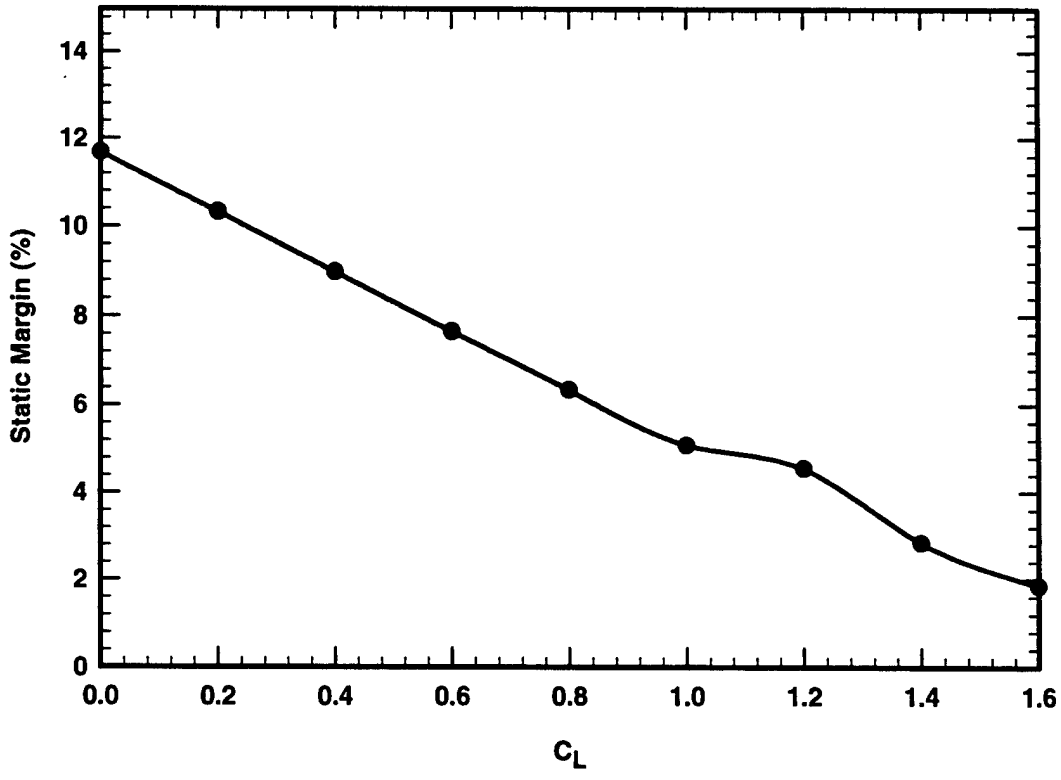

Figure 5.4.1. Aircraft static margin as a function of lift coefficient.

Short	Damping Rate (1/sec)	ωn (1/sec)	ωd (1/sec)	Period (sec)	ζ	99% Damping / Doubling Time (sec)
Takeoff	4.1661	6.3049	4.7324	1.3277	0.6608	1.1054
Cruise	12.7388	20.0834	15.5263	0.4047	0.6343	0.3615
Turn (5g)	12.7422	20.0501	15.4804	0.4059	0.6355	0.3614
Phugoid						
Takeoff	-0.0045					153.2080
Cruise	0.0451	0.3193	0.3161	19.8758	0.1414	102.0050
Turn (5g)	-0.0063					109.8680
Roll						
Takeoff	13.3633	2.232E-08			-4.11E-08	0.3446
Cruise	43.2992	8.212E-06			1.87E-04	0.1064
Turn (5g)	12.7422	20.0501			0.6355	0.3614
Spiral						
Takeoff	-0.2773					2.4992
Cruise	-0.0220					31.5224
Turn (5g)	-0.0063					109.8540
Dutch Roll						
Takeoff	0.8381	2.5219	2.3785	2.6417	0.3324	5.4945
Cruise	0.8322	6.8578	6.8071	0.9230	0.1214	5.5335
Turn (5g)	0.8091	6.8100	6.7618	0.9292	0.1188	5.6916

Table 5.4.2. Dynamic stability modes of final aircraft for critical operating conditions

5.4.4. Predicted Performance. The predicted performance of the aircraft for MDM and SDM are given in Table 5.4.3. Based on the flight model developed, MDM and SDM flight scores have a combined flight score of 0.90. Assuming an assembly time of 30 seconds and a generous report score of 100 the score for Utah State University's entry would be 6.748.

Aircraft Performance		MDM	SDM Loaded	SDM Empty
Takeoff	Distance (ft)	115.8	100.8	68.3
	Time (s)	4.7	4.1	2.9
Landing	Distance (ft)	165.5	161.6	124.0
	Time (s)	5.2	5.2	4.6
Maximum Climb	Rate (ft/min)	726	786	834
Turning	Load Factor (g's)	8.0	8.0	8.0
	Rate (deg/sec)	134.8	111.4	104.2
	Radius (ft)	46.1	67.6	77.3
Flight Speeds	Stall (ft/sec)	36.3	35.4	31.1
	Cruise (ft/sec)	108.5	131.4	140.5
Max Lift Coefficient		1.6	1.6	1.6
L/D	Max	18.1	27.3	27.3
	Cruise	4.4	6.1	5.5
Flight	Time (min)	1.81	1.97	
	Score	0.526	0.377	
Total Flight Score		0.903	**SCORE**	6.748

Table 5.4.3. Predicted aircraft performance for competition.

6. MANUFACTURING PLAN

A primary concern in the design process is the fact that the resulting aircraft must be manufactured in a relatively short period of time, with a limited amount of resources. Manufacturability was considered throughout the design process. To best meet design requirements, the aircraft must be constructed using the best combination of materials and manufacturing processes. To achieve these goals an outline was created to guide manufacturing decisions. This plan defines manufacturing figures of merit, analytical methods for comparison and lead-time prediction, and a schedule.

6.1. Figures of Merit

A list of FOM was prepared for the manufacturing plan. These factors were used to quantitatively compare the manufacturing options and provide a basis for the optimum selection of materials and processes. Decisions were made more objectively using the FOM when choosing the manufacturing processes for various components of the aircraft. The list was designed to aid in the elimination of construction techniques that would be too costly, too time consuming, too difficult to realize or adversely affect the competition score. The figures of merit are as follows:

6.1.1. Availability of Materials (AOM). An obvious limiting factor to the choice of any manufacturing process is the availability of the material or equipment required to carry out that process. If access could not be gained to necessary materials or machinery, the process received a –1. If lead times were long or access was difficult the process received a 0. If everything necessary was readily attainable the process received a 1.

6.1.2. Required Skill Level (RSL). Many manufacturing processes require extensive training and skill to execute effectively. If a process was beyond the expertise available, it received a –1. If the skills required to complete a process were available, but limited, it received a 0. If the expertise to carry out the process was readily available, it received a 1.

6.1.3. Time Required (TMR). A little more than a month is scheduled to build and test the aircraft. If a process required a time period of two weeks or more, it was given a –1. If a process could be completed within a four-day to two-week period, it was given a 0. Any process that could be realized in four days or less was given a 1.

6.1.4. Strength and Reliability (SAR). It was essential that each process reliably produce components that met the aircraft's design and strength requirements. If a process was undependable and thus unable to produce desirable components it was given a score of –1. If a process' reliability was questionable it was issued a 0. If a process could reliably produce quality components it was given a 1.

6.1.5. Actual Component Cost (ACC). A relatively tight budget limited the cost of the final aircraft and individual team members were required to raise the funds necessary for its construction. While the actual cost of manufacturing will not affect the final score, it will affect the team's ability to complete the project. Manufacturing processes that were beyond the financial means available received a –1. Any process considered costly but within the budget received a 0. If a process was inexpensive or donated free of charge it received a 1.

6.1.6. Estimated Component Weight (ECW). The weight that a component adds to the aircraft is detrimental in terms of performance and RAC. For purposes of optimization each process available was compared in terms of the estimate weight of the component built with that process. The processes were scored from lightest to heaviest with 1, 0, -1.

6.2 Manufacturing Processes Investigated

In a process parallel with the design of aircraft components, potential materials and construction methods were researched and analyzed. Though many manufacturing choices were immediately ruled out, some manufacturing options could not be finalized until the very end of detail design. Several of the most important choices were made concerning the wings, empennage, and fuselage.

6.2.1. Wings. The best initial option for the high load factor wing seemed to be the use of a carbon fiber structure and several full-scale wings were built and tested. A full-scale carbon fiber covered Rohacell foam wing and a carbon fiber covered built-up balsa wing were tested. Quality carbon fiber skin structures proved to be difficult to build without very costly tooling. Several designs utilizing a wing spar were also considered. Designs had to incorporate a non-permanent wing joiner mechanism. Mechanisms consisting of one or more plug-in spar pieces of varying cross-sectional shape were investigated. Materials analyzed for each joiner included carbon fiber composites, steels, titanium, and aluminum.

6.2.2. Empennage. Preliminary empennage designs consisted of several boom-mounted and plate-mounted detachable structures. Stability requirements and fuselage geometry made the use of an integral tail boom advantageous. The tail feathers themselves were to be either built-up balsa, balsa skinned foam, or composite skinned foam.

6.2.3. Fuselage. The primary fuselage structure had to be constructed of either built-up balsa, balsa sheeted foam, or glass sheeted foam due to limited resources and experience. Critical secondary structures such as the fuselage spar, the motor and landing gear mounts, and the drop mechanism could be manufactured by different methods. Various aluminum, steel, and carbon-fiber geometries were considered for use in the fuselage spar and landing gear mounts. Metallic designs requiring welding, heat-treating, machining, and/or casting operations were all examined and compared.

6.3 Analytic Methods Used

Materials and processes to be used in building an aircraft must be properly compared using quantifiable ratings. Each FOM was given a weighting value that was indicative of its importance. Scores were given to each process based on the FOM. The RSL scores were based on Table 6.3.1. This table lists the number of team members that have skills in each of the processes considered. Table 6.3.2. illustrates how the FOM chosen were used to determine the methods and materials to be used for the aircraft.

Available or Required Skills	CNC Milling	Lathe Work	Wood Working Skills	Carbon Filament Winding	Carbon Composite Lay-ups	Foam Hot-Wiring	Balsa/Plywood Framing	Balsa Sheeting	Fiberglass Sheeting	Model Painting	Monokote Application	R/C Aircraft Modeling
Number of Personnel	1	1	11	0	2	6	8	2	5	4	3	3
FOM Score	0	0	1	-1	0	1	1	0	1	1	0	0

Table 6.3.1. Skill matrix displaying the number of team members possessing required skills.

		AOM	RSL	TMR	SAR	CST	W 6	Total
	Weighting Factor	2	1	2	2	1	3	
Wings and Empennage	Foam Core w/ Composite Skin	0	-1	-1	1	-1	-1	**-5**
	Foam Wing w/Spar and Balsa Skin	1	0	1	0	1	1	**8**
	Ribbed Balsa Build-up w/ Composite Skin	0	0	0	1	-1	0	**1**
	Ribbed Spar Structure w/ Balsa Skin	1	-1	0	0	1	1	**5**
Wing Spar	Cylindrical Composite Spar	0	-1	0	1	0	0	**1**
	Composite I-beam	0	0	0	1	0	1	**5**
	Aluminum Tube	1	-1	1	1	0	-1	**2**
Fuselage Spar	Aluminum Truss	1	-1	0	1	-1	0	**2**
	Composite I-beam	0	0	0	0	1	1	**4**
	Composite Box Beam w/ Foam Core	0	0	0	-1	1	0	**-1**
Fuselage Frame	Balsa and Plywood Build-up	1	1	0	1	1	0	**6**
	Foam Core w/ Balsa Skin	1	-1	1	0	1	0	**4**
	Foam Core w/ Fiberglass Sheeting	1	-1	0	0	0	0	**1**
Fuselage/WingTransistion Section	Foam w/ Balsa Skin	1	0	-1	1	1	1	**6**
	Foam w/ Fiberglass Sheeting	1	0	-1	1	0	0	**2**
	Balsa Build-up w/ Balsa Strips for Skin	1	-1	-1	1	1	1	**5**
	Balsa Build-up w/ Composite Skin	0	-1	-1	1	1	1	**3**

Table 6.3.2. Manufacturing processes considered for each of the major components of the aircraft

6.3.1. Critical Path. During a production process, dependencies always exist between steps. Recognizing these dependencies is essential to minimizing the production time. The critical path method of Walker (1999) was used to determine these dependencies and estimate the time required to build the aircraft from start to finish. This method determines which processes must be done on time to not delay the end date. It also finds which processes have slack time and how much. It can find processes that can be done in parallel that may not have been obvious. An example of this method is shown in Fig. 6.3.1, which shows a spanning tree that contains all of the necessary processes to build the wings. The process description and dependencies are outlined in Table 6.3.3.

	Process Description	Dependencies	Time Est. (man-hr)
A	Hot-Wire the Foam Core.	-	3
B	Build Joiner Blocks.	-	4
C	Build Composite Spar	B	8
D	Assemble Spar and Wing Core	A, C	3
E	Place Control Linkages	D	3
F	Carve the Leading Edge	-	3
G	Glue Balsa Into Sheets	-	2
H	Carve Wing Tips	-	3
I	Glue Skin in Place	E, G	2
J	Carve openings and Place Servos	I	3
K	Attach Tips	H, I	1
L	Attach the Leading Edge	F, I	1
M	Sand and Apply Monokote to Skin	J, K, L	4

Table 6.3.3. Required processes for wing construction and dependencies for each step.

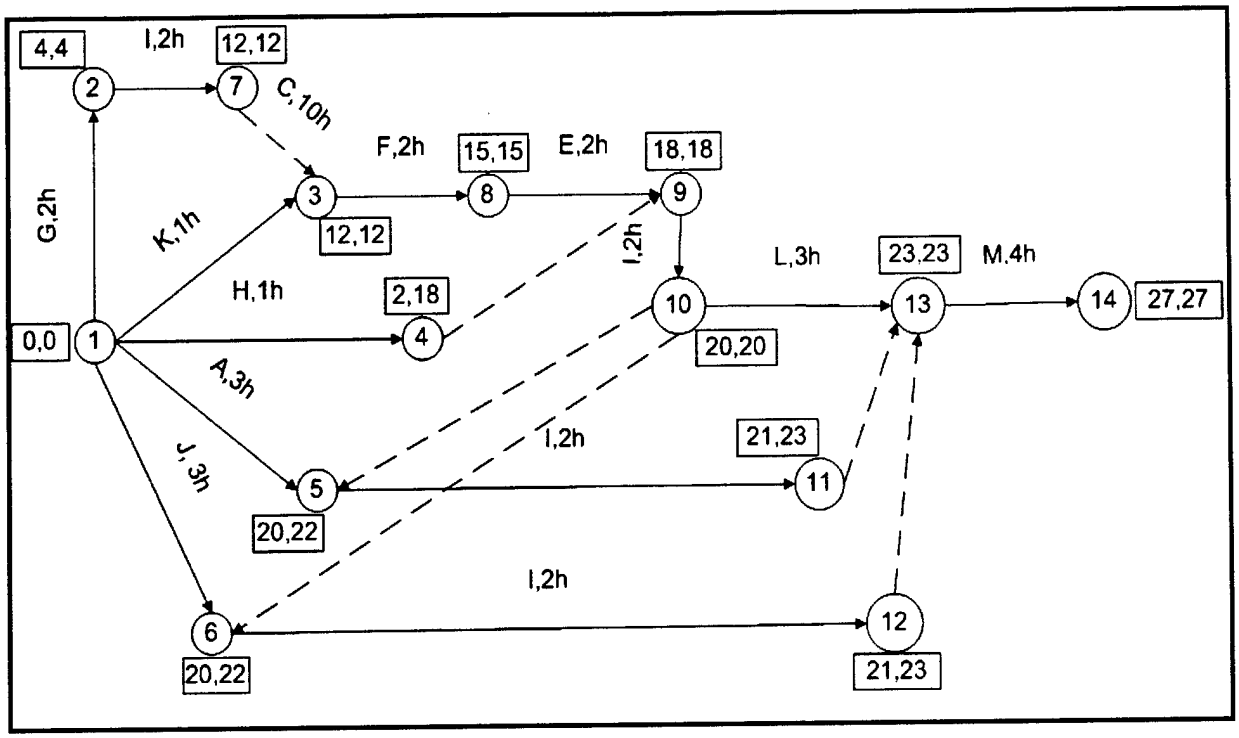

Figure 6.3.1. Critical path spanning tree, depicting necessary steps in the wing construction. Arrows indicate steps and circles mark start and end points. The critical path is marked in red. The values in the boxes indicate when the next step can be started and when the preceding step must be finished to not delay final completion. The dotted arrows indicate multiple dependencies preceding a step.

6.4 Processes Selected for Manufacture of Major Components

After selection of the optimum manufacturing processes, a detailed plan was prepared describing how these processes will be implemented in the construction of the major components of the aircraft.

6.4.1. Wing. The wings will be built of a foam core and a balsa skin. The process that will be used to build the wing was implemented by previous DBF teams. The foam is shaped using a "hot wire". The shape of the airfoil is cut using aluminum templates machined on a CNC mill. Channels in the foam made at this point and the linkages that control the twisterons will be placed. The skin is made from 4x48 in sheets of 1/16-in balsa. The sheets are trimmed to produce a flat edge and then a thin coat of CA glue is used to bond them edge-to-edge. The foam is then coated with a thin coat of slow cure epoxy and the skin is applied. Because the shape of the leading edge and the wingtips are critical to aerodynamic performance they will be carved from balsa and glued to the foam. Openings are then cut for the servos. The balsa is then lightly sanded before a layer of Monokote is applied. The control surfaces will then be cut out of the wing with a straight edge and a razor. They will be hinged on top with a strip of fiberglass tape bonded between the balsa and the foam.

A carbon fiber composite I-beam design was chosen to serve as the wing spar. 4 ft sections of 1 1/4-in square steel tubing will be used as molds. The forms will be wrapped with peel ply material to aid in the removal of the forms from the spar. A sheet will then be constructed consisting of four layers of 0.010-in unidirectional carbon composite (CC) laid at angles of 0, 90, 45 and -45 degrees. Two 1.75x48-in strips will be cut from this sheet. These two strips will then be placed face to face and then clamped between

the forms. The excess material in each sheet will then be folded back onto the top and bottom of the forms making the I-shaped web. The flanges, which are composed of a varying number of uni-directional lamina, will then be laid on the top and bottom of the web and clamped via two more steel molds.

A 1 1/8-in outer diameter 7075-T6 aluminum tube will be used to transfer the wing loads from the wing spar to the fuselage spar. The connection tube will be machined to precisely fit into spar end blocks of machined glass phenolic. The end blocks are 1 1/4 x 1 1/4 inches along the cross-section with a 1 1/8 inch diameter hole bored to a depth of 2.0 in. The blocks are tapered on the opposite end for transition into the web of the spar. The end blocks are sandwiched between the two strips of the web and the flanges. The assembled beam is then wrapped in a layer of shrink-tape and cured.

6.4.2. Empennage. The vertical and horizontal stabilizers will be hot-wired foam cores with balsa skins. The elliptic tips on the horizontal stabilizer will be carved from solid balsa. Both stabilizers will be built to their full span and covered with Monokote. Then the control surface hinges and removable sections will be cut out. Both control surface hinges must allow deflection of 90 degrees for storage. An aluminum piano style hinge will be used for the rudder to allow for equal deflection in both directions. The elevator will be hinged with tape on the bottom side. Here, the bottom surface must be smooth since the elevator deflections will usually be up.

6.4.3. Fuselage. The fuselage will be a classic built-up balsa construction. In a jig, balsa and plywood bulkheads will be glued to four full-length longerons and two full-length balsa sheets. The balsa sheets form the sides of the rectangular structure, which will later be blended into the wing with the fairing. The carbon fiber fuselage spar and other structural components will be joined to the bulkheads and the sheeted sides. Once landing gear, release mechanism, and control hardware are installed, the top and bottom of the fuselage box will be covered with balsa sheets. A portion of both the horizontal and vertical tail is permanently attached to the fuselage. After the fairing is attached the entire structure, except the tail feathers, will be covered with 2 oz. glass cloth, filled, polished, and painted.

A carbon fiber composite I-beam design was also chosen for the curved fuselage spar. This spar will be built in the same way as the wing spar with a few differences. The curved forms will be cut from particle board which will be broken if necessary to remove them from the spar after curing. The two sheets of the shear web will be cut from the four-lamina web sheet to the shape of the forms by laying the forms on the sheet and using a gauging block to keep the knife blade the correct distance from the forms. Relief cuts must be made in the flange attachments before it is folded back to accommodate the curves. The curved spar must be clamped between two molds and the end blocks must be fixed during cure to ensure proper alignment of the wings.

Making a smooth transition from the wing into the fuselage is critical to reducing drag. However the complex curves designed to accommodate this transition are difficult to build. It was this difficulty that necessitated the use of a foam core with a fiberglass skin. Table 6.3.2. shows that for other areas of the aircraft, the balsa skin has usually been chosen because of the ECW. But in this case the geometry is so complex that an easier and quicker method had to be used. The foam will be hand shaped using a hot wire. Then a layer of 2 oz fiberglass cloth will be applied and painted.

6.5 Manufacturing Milestones

An integral part of the manufacturing plan is the schedule. Figure 6.5.1 lists the major components of the aircraft and the time periods over which they are to be built and tested. Milestones and time allotted for the building and testing of the aircraft are outlined with horizontal bars. The blue bars represent the planned schedule while the pink bars show the time periods over which the events actually occurred.

ID	Task Name	Start	Finish
1	**Structural Testing**	**Sep 2**	**Mar 7**
2	Build & Test Composite Wings	Sep 12	Nov 8
3	-Actual-	Oct 23	Dec 3
4	Build & Test Composite Spars	Jan 21	Feb 18
5	-Actual-	Jan 21	Mar 7
6	**Manufacture Preparation**	**Jan 1**	**Feb 27**
7	Order & Receive Materials	Jan 30	Mar 16
8	Order & Receive Factory Components	Jan 20	Mar 16
19	**Build Aircraft**	**Mar 10**	**Apr 1**
20	Wing	Mar 10	Mar 22
9	Hot-Wire Core	Mar 10	Mar 10
10	Composite Spar	Mar 10	Mar 11
11	Empennage	Mar 10	Mar 20
12	Hot-Wire Cores	Mar 10	Mar 10
13	Fuselage	Mar 10	Mar 25
14	Fuselage Spar	Mar 26	Mar 26
15	Cut Bulkheads & Structure	Mar 10	Mar 13
16	Final Assembly	Mar 26	Mar 28
17	**Final Preparation**	**Mar 29**	**Mar 31**
18	Test Mounts and Linkages	Mar 31	Apr 1

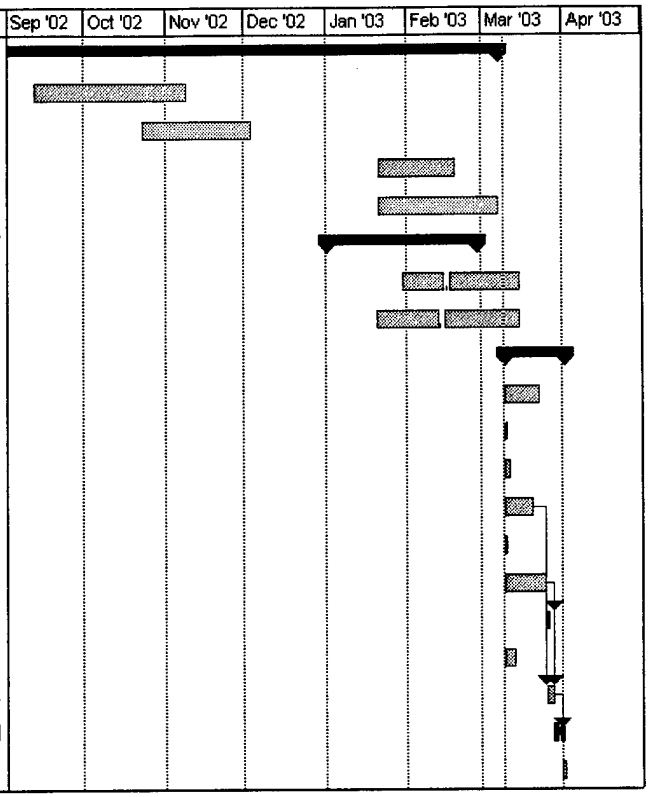

Figure 6.5.1 Manufacturing schedule.

7. TESTING PLAN

Testing is vital to the development of the design of the aircraft and to the formulation of the manufacturing plan. Questionable analytical data is either confirmed or refuted, and new designs are proven, or shown to be deficient. The following testing plan is devised to ensure that the overall analysis was as accurate as possible, to identify possible design flaws or manufacturing oversights, and to tweak the aircraft so as to make its performance as efficient as possible.

7.1 Test Objectives and Schedule

Components of the design requiring testing were identified and a schedule was set forth. Table 7.1.1 lists the various tests and their objectives, as well as the dates during which they occurred or will occur.

Test	Objective	Dates
Antenna Drag Test	Find drag created by the mock antenna used in MDM	9/02-11/02
Motor/Battery Test	Collect motor and battery performance data	9/02-12/02
Wing Structure Test	Investigate strengths and weights of various wing structures	9/02-1/03
Spar Test	Ascertain the strengths and weights of wing and fuselage spars	1/03-2/03
Final Motor/ Battery Test	Determine motor characteristics and optimize the motor and batteries to specific mission requirements	12/02-2/03
Flight Tests	Confirm or disprove the performance and stability predicted for the aircraft and fine-tune its performance	3/03-4/03

Table 7.1.1. Test objectives and schedule

7.2. Flight Testing Checklists

The success of the design depends on the thoroughness and careful execution of the flight tests. A pre-flight checklist (see Table 7.2.1) was developed to accompany the flight-testing checklist. The pre-flight tests are designed to identify structural fatigue or carelessness in assembly of the aircraft and are to be performed before each flight. The flight testing checklist was designed to methodically monitor the performance of the aircraft through a wide range of flight conditions and was divided into six segments; static thrust test, taxi test, first flight, first sortie, second sortie, and third sortie (see Table 7.2.2).

The static thrust test will be performed by attaching a spring scale to the rear of the aircraft while at full-throttle. This test will measure the static thrust generated by the propeller. The thrust data will serve to fine tune the analytical model and allow for more accurate propeller selection.

Low and high-speed taxi tests will demonstrate aircraft controllability on the ground, while the first flight will assess the controllability and stability of the aircraft through gentle maneuvers in the air.

During the first sortie, low to high-speed maneuvers, including stall and tight radius turning, will be used to assess the yaw stability of the aircraft. If the pilot feels that the aircraft has too much yaw-stability, one inch will be removed from the tip of the vertical stabilizer. Completion of the first sortie will occur once the shortest possible vertical tail span is found without compromising stability of the aircraft.

The second sortie will be used to test the total performance of the aircraft. A radar gun will be used to measure maximum and minimum flight velocities. Take-off distances and turning radii will be measured for both mission configurations and compared to predicted values. Wingspan, propeller selection, and battery packs might all be modified due to the results of these tests. This series of tests has been designed to improve the aerodynamic qualities and test the integrity of the aircraft.

The third sortie will consist of competition simulation. Competition tasks will be reproduced to provide practice and experience for the pilot and team. Areas of improvement will be identified and competition skills will be polished. The payload deployment mechanism will be tested extensively as well.

Weight and Balance-C.G. location (≤2" behind ¼ chord of main wing)				
Control Surfaces/Linkage	Flaperons	Elevator	Rudder	Nose Gear
-Linkages/Clevises properly attached?				
-Hinge integrity? (Tug firmly at control surface.)				
-Proper deflection direction and trim location?				
Motor Mount-18 lb longitudinal load?				
Landing Gear/Brake				
-Air Pressure at 60 psi?				
-Proper retract/deploy of gear and use of brakes?				
-Leak check?				
Wing Tip Test-Aircraft loaded +35 lb and lifted from wing tips w/o structural damage?				
Payload Security Test- Payload loaded to 30 lbs. w/o failure of mechanism?				
Range Test- W/ collapsed antennae, no chatter/interference at 50', w/ motor on and off?				
Fail-Safe- Tx off, elevator full up, flaperons/rudder full right, throttle off, payload in place?				
Miscellaneous-Verify all components secured to aircraft and fasteners tight w/ locktite.				

Table 7.2.1. Pre-flight checklist. All tests must be completed successfully before each flight.

(3/31) Static Thrust Test-Readings from spring scale at full throttle (lbf): _____, _____. *Concerns:*
(3/31) Taxi Tests-Sufficient control of aircraft while taxiing at low velocities? -Sufficient control of aircraft at speeds nearing the rotation velocity? *Concerns:*
(3/31) First Flight- Sufficient control of aircraft through majority of operating conditions? *Concerns:*
(4/1) First Sortie-Sufficient yaw stability throughout flight realm (including stall and high-g turns)? -If yes, remove 1" from vertical stabilizer. (Continue shortening vertical stabilizer until min. tail height is found without sacrificing yaw stability.) *Concerns:*
(4/2-4/4) Second Sortie-Test performance of aircraft: Take off distance: _____ Maximum Flight Velocity: _____ Stall Speed: _____. Take off velocity: _____ Turn Radius: _____ Landing Distance:_____. *Suggested Aerodynamic Improvements:*
(4/5-4/19) Third Sortie-Competition Simulation: MDM Flight Times:_____ SDM Flight Times:_____. *Setbacks and Suggested Improvements:*

Table 7.2.2. Flight testing checklist and schedule. Tests must be successfully completed sequentially.

7.3. Summary of Test Results and Lessons Learned

As each individual test was completed its results were analyzed and used to improve the design. The lessons learned through the testing plan thus far have been invaluable. Published values for cylinder drag and motor and battery performance were found to be highly idealized. Structural testing of mock wings and spars greatly influenced the evolution of the design of the wings and parts of the fuselage. Table 7.3.1 outlines the testing results and the knowledge gained through those tests.

Test	Test Results and Lessons Learned
Antennae Drag	Drag coefficient found to be 67% higher than published values (White 1999)
Motor/Battery Test	Battery resistance 300% higher than the manufacturer's listing. Battery capacity was 110% of the manufacturer's listing. Motor torque 85% of the manufacturer's listing. Peak motor efficiency was 70%, 9% below manufacturer's listing.
Wing Structure Test	All wings tested were strong enough to withstand flight loads. Composite skin wings were heavy and difficult to manufacture. Built-up balsa wings with composite spars were light but difficult to manufacture. Balsa/foam core wings with composite spars were light and easy to manufacture.
Spar Test	Fuselage and wing spars failed near loads predicted by F.E. analysis.
Final Motor/ Battery Test	Motor efficiency was independent of temperature, even after significant heating. Motor torque at max efficiency was found, and propellers were matched accordingly. 18x18 and 20x18 propellers were selected for use in MDM and SDM respectively. The 48 cell 1700 mAhr battery pack provided the best overall performance.

Table 7.3.1. Summary of test results and lessons learned.

REFERENCES

Abbot, I. H., and Von Doenhoff, A. E., (1959), *Theory of Wing Sections*, Dover, New York.

Boresi, A. P., Schmidt R. J., and Sidebottom O. M., (1993), *Advance Mechanics of Materials*, 5th ed., Wiley, New York.

Eppler, R., (1990), *Airfoil Design and Data*. Springer-Verlag, Berlin.

Greenberg, M.D. (1998), *Advanced Engineering Mathematics*, 2nd ed., Prentice Hall, Upper Saddle River.

Hepperle, M., *JavaFoil*, http://www.mh-aerotools.de/airfoils/javafoil.htm, Oct. 24, 2002.

Hoerner, S. F., (1965), *Fluid-Dynamic Drag*, Published by the Author, New York.

Phillips, W. F., and Snyder, D. O., (2000), Journal of Aircraft **37**, 4, pp. 662-670.

Phillips, W. F., (2003), *Lifting-Line Analysis for the Effects of Washout on Performance and Stability*, *AIAA-2003-0393*.

Phillips, W. F., Alley, N. R., and Goodrich, W. D., (2003), *Lifting-Line Analysis for Roll Control and the use of Twisterons*, *AIAA-2003-4061*.

Phillips, W. F., (2003), *Mechanics of Flight*, Wiley, New York.

Walker, R. C., (1999), *Introduction to Mathematical Programming*, Prentice-Hall, Upper Saddle River.

White, F. M., (1999), *Fluid Mechanics*, McGraw-Hill, Boston.

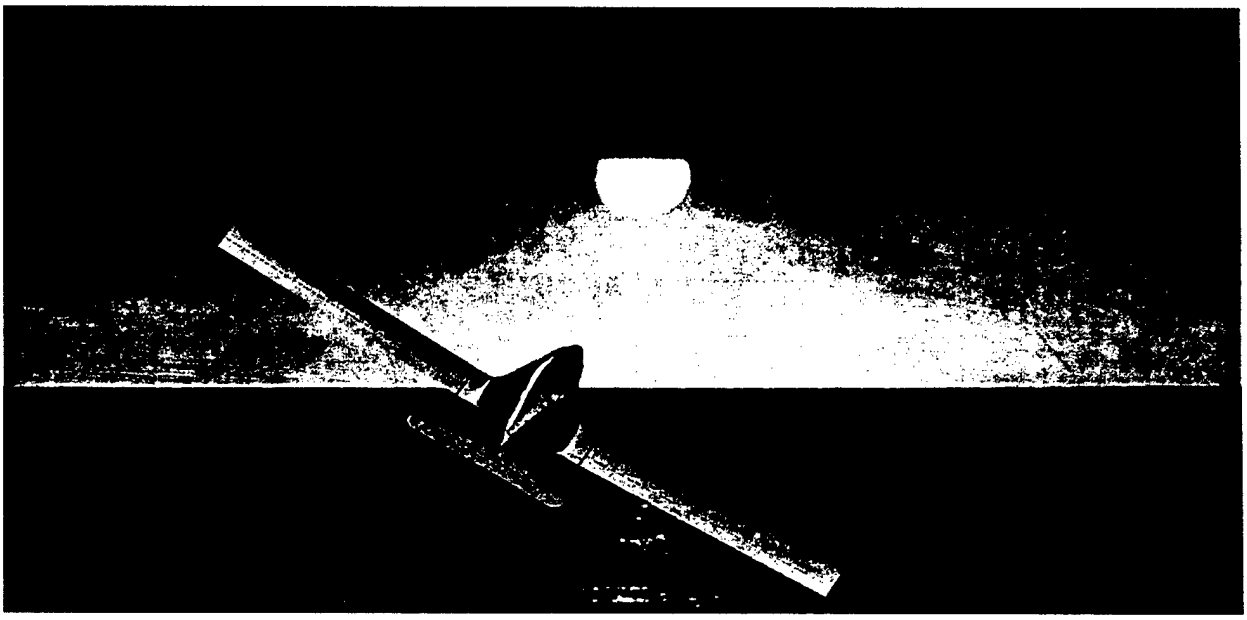

AIAA Student Design / Build / Fly Competition

7700

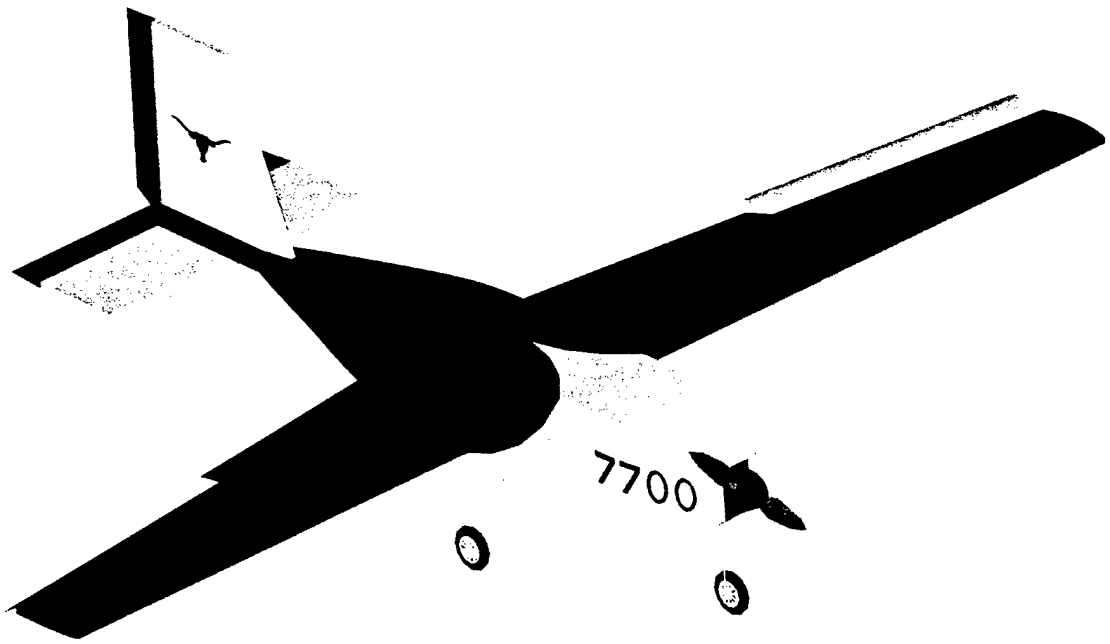

By:

The University of Texas at Austin
2002 / 2003 Design / Build / Fly Team

TABLE OF CONTENTS

1.0 EXECUTIVE SUMMARY 1
1.1 Conceptual Design 1
1.2 Preliminary Design 1
1.3 Detail Design 2
2.0 MANAGEMENT SUMMARY 3
3.0 CONCEPTUAL DESIGN 5
3.1 Figures of Merit 5
3.1.1 Required Time 5
3.1.2 Required Skill 5
3.1.3 Reliability/Assembly Time 6
3.1.4 Stability and Control 6
3.1.5 Effect on Rated Aircraft Cost 6
3.1.6 Effect on Drag 6
3.2 Assumptions Made 6
3.2 General Configurations 8
3.2.1 Monoplane 8
3.2.2 Biplane 8
3.2.3 Tandem 9
3.2.4 Flying Wing 9
3.3 Design Parameters 10
3.3.1 Wing Planform 11
3.3.2 Landing Gear Configuration 11
3.3.3 Empennage Configuration 11
3.3.4 Engine Configuration 12
3.5 Features that Produced Final Configuration 12
4.0 PRELIMINARY DESIGN 14
4.1 Figures of Merit 15
4.1.1 Required Time 15
4.1.2 Required Skill 15
4.1.3 Effect on Drag 15
4.1.1 Component Weight 15
4.2 Mission Choice 15
4.3 Design Parameters Investigated 17
4.3.1 Fuselage Shape and Assembly 17
4.3.2 Fuselage Materials 18
4.3.3 Spar Cross Section and Material 18
4.3.4 Wing Structure 21
4.3.5 Landing Gear Cross-Sections 22
4.3.6 Tail Assembly 22
4.4 Tail Sizing 23
4.5 Aircraft Performance Estimates 24
4.5.1 Weight Breakdown 24
4.5.2 Mission Performance 25
4.5.2 Stability Characteristics 28

5.0 DETAIL DESIGN **31**
5.1 Component Selection 31
5.1.1 Propulsion Configuration 31
5.1.2 Airfoil selection 33
5.1.3 Wing Placement 35
5.1.4 Control Surface Sizing 36
5.2 Systems Architecture 36
5.2.1 Connection of Wing / Fuselage / Tail Assembly 36
5.2.2 Wiring / Servos / Receiver Placement 37
5.2.3 Aircraft Assembly 37
5.3 Aircraft Configuration 37
5.3.1 Final Configuration 38
5.3.2 Weight and Balance Sheet 44
5.3.3 RAC Calculation 45
5.4 Ongoing Aircraft Optimization 46
5.4.1 Motor Optimization 46
5.4.2 Aircraft Wings 48
5.4.3 Tail Assembly 48
5.4.4 Tail Incidence 48
5.4.5 Number of Batteries 48
5.4.6 Assembly Time 49
5.4.7 Payload Deployment Mission 49
6.0 MANUFACTURING PLAN **50**
6.1 Figure of Merits 50
6.1.1 Performance 50
6.1.2 Weight Estimation 50
6.1.3 Construction Skill Required 50
6.1.4 Construction Time Required 50
6.2 Manufacturing Processes Investigated 51
6.2.1 Fuselage Construction 51
6.2.2 Wing Materials 52
6.2.3 Wing Sweep / Spar 52
6.2.4 Spar Material 52
6.2.5 Wing Attachment 53
6.2.6 Tail Design 53
6.2.7 Empennage Design 53
6.3 Final Manufacturing Process 53
6.3.1 Wings 53
6.3.2 Landing Gear 54
6.3.3 Empennage 54
6.3.4 Front Fuselage 55
6.3.5 Rear Fuselage 55
6.4 Manufacturing Timeline 56
7.0 TESTING PLAN **57**
7.1 Static Tests 57
7.2 Flight Test Check List 57

7.3 Flight Tests 57
7.3.1 February 1, 2003 57
7.3.2 February 9, 2003 58
7.3.3 March 8, 2003 58
8.0 REFERENCES 60

1.0 EXECUTIVE SUMMARY

Students at The University of Texas at Austin's Department of Aerospace Engineering and Engineering Mechanics have designed and built an electric RC airplane in order to compete in this year's Cessna/ONR Student Design Build Fly Competition. This year's mission profile involves flying two of three mission sorties: a missile mission in which laps are flown, a sensor deployment mission in which the payload must be remotely deployed, and a communications repeater mission in which the aircraft must fly with a simulated communications relay device. The aircraft is also required to fit inside of a four foot by two foot by one foot box and the assembly is timed. The aircraft was designed in three phases: conceptual design, preliminary design and detail design.

The design process began in conceptual design in which the team eliminated general configurations from consideration. Then in the preliminary design, the aircraft components were sized and optimized, stability analysis was performed, and performance analysis was performed. In the detail design process the aircraft's specific components were selected, the control surfaces were sized, and as the plane was built and tested, improvements were made to increase the performance of the aircraft. In addition, a manufacturing plan was created during the detail design phase to construct the aircraft. Both static tests and flight tests were performed to verify, and improve upon, the aircraft's performance.

1.1 Conceptual Design

The first step in conceptual design was to select figures of merit that would be used to judge the airplane configurations. The figures of merit selected were required skill to build, required time to build, reliability/assembly time, stability and control, rated aircraft cost effects, and effect on drag. Next, design concepts such as, monoplane, biplane, tandem wing, and flying wing were scored based on the figures of merit. The design parameters investigated for the design concepts were the motor configuration, wing planform, landing gear configuration, and empennage configuration. The conceptual design selected was a monoplane with a rectangular wing planform, a tricycle landing gear, and a conventional empennage.

1.2 Preliminary Design

The preliminary design started with creating figures of merit to judge the aircraft parameters. The figures of merit selected were component weight, required time, required skill, and effect on drag. The figures of merit were then used to decide which of the three mission sorties would be performed by the aircraft and to investigate several design parameters. The design parameters investigated were spar cross-section and material, wing/empennage structure, fuselage shape,

fuselage materials, landing gear cross-sections, and empennage structure. Once the aircraft's weight was more accurately determined, the static thrust and propeller pitch speed needed for takeoff were determined. Then, the aircraft's performance was predicted and an estimate of the aircraft's score was calculated.

1.3 Detail Design

The detail design phase began with selection of the propulsion configuration from the propulsion requirements determined in the preliminary phase. Then the airfoil was selected, the wing was positioned on the fuselage, and the control surfaces were sized. The details of the fuselage/wing connection and the servo wiring placement were also determined. Also, the overall aircraft performance was calculated with the most current parameters and weight. Finally, as an ongoing process, the overall aircraft will continue to be optimized until the week before the competition as test flights continue.

2.0 MANAGEMENT SUMMARY

In the summer of 2002, the 2003 UT DBF team began to prepare for this year's competition. By the beginning of the 2002 Fall Semester, the team was formed and new freshmen joined the team to aid in building an RC plane to compete in the 2003 Cessna/ONR Student Design Build Fly Competition. The team consisted of 4 seniors, 9 underclassman (who consisted of aerospace engineering majors) a student pilot, and one faculty advisor.

To keep the team motivated a Project Manager was chosen to oversee the project and the team was divided into three autonomous groups. The groups were Aerodynamics, Propulsion, and Structures. Table 2.1 shows the organizational structure of the team.

Table 2.1: Organizational Structure of the Team.

Project Manager: Chris Moore		
Aerodynamics ***Leader***: Chris Moore	**Propulsion** ***Leader:*** Clint Kam	**Structures** ***Leader:*** Bill Tandy
Zag Ahmadi Miranda Murdock Clint Kam	Khoi Duong Chris Moore Miranda Murdock	Khoi Duong Kyle Riggen Prasanna Weerakoon Ryan Zwerneman

The team leaders and project manager developed a production schedule with major and minor tasks. Table 2.2 is the original timeline with both the planned start and finish dates and the actual finish dates for the tasks. Whenever a deadline could not be met, the timeline was slightly altered and the team attempted to complete other tasks ahead of schedule.

Under the direction of the team leaders, each group was given tasks to complete over a certain amount of time. The workload was split among the group members as evenly as possible according to each member's abilities. Each building task was assigned to at least two people so that safety requirements were met and the task could be quickly completed.

Since this year's team was held to a very tight budget until a working aircraft was flown, it was decided that a conventional plane was better overall in order to compete and stay within the budget. The budget shortfall also forced the team to use the previous year's motor, controller, and batteries.

Table 2.2: Project Timeline.

TASK	START DATE	FINISH DATE	ACTUAL DATE COMPLETE
Start-Up Tasks	**7/15/2002**	**8/30/2002**	**9/6/2002**
Assemble Design Team	8/28/2002	8/30/2002	9/6/2002
Get Budget Approval	7/9/2002	7/13/2002	7/13/2002
Letter of Intent	7/6/2002	7/6/2002	7/9/2002
Conceptual Design	**8/28/2002**	**10/14/2002**	**10/14/2002**
Read and Discuss Contest	8/28/2002	9/6/2002	9/6/2002
Configuration Analysis	9/6/2002	9/30/2002	9/30/2002
Design Parameter Analysis	9/30/2002	10/14/2002	10/14/2002
Conceptual Design Written	9/30/2002	10/14/2002	10/14/2002
Preliminary Design	**10/14/2002**	**12/27/2002**	**12/31/2002**
Design Parameter Analysis	10/14/2002	11/8/2002	11/8/2002
Critical Dimension Sizing	11/8/2002	12/2/2002	12/2/2002
Stability Analysis	12/2/2002	12/20/2002	1/1/2003
Takeoff Velocity Code Written	12/10/2002	1/1/2003	1/10/2003
Preliminary Design Written	12/20/2003	1/14/2003	1/30/2003
Detail Design	**12/31/2002**	**2/1/2003**	**2/4/2003**
Propulsion Systems Selected	1/3/2003	1/10/2003	1/22/2003
Aerodynamic Analysis	1/3/2003	1/18/2003	1/21/2003
First Flight Analysis	1/21/2003	1/24/2003	2/2/2003
Design Iteration/Improvement	1/24/2003	4/19/2003	-
Detail Design Written	1/20/2003	2/1/2003	2/26/2003
Manufacturing Plan	**1/13/2003**	**1/21/2003**	**1/21/2003**
Final Airplane Construction	1/18/2003	1/21/2003	1/22/2003
Manufacturing Plan Written	2/14/2003	2/18/2003	2/20/2003
Initial Test Flight	**1/21/2003**	**1/21/2003**	**2/1/2003**
Flight Tests	**2/1/2003**	**4/19/2003**	**-**
Performance Modifications	**2/2/2003**	**4/19/2003**	**-**
Compile Paper	**3/1/2003**	**3/8/2003**	**3/10/2003**
Contest	**4/25/2003**	**4/27/2003**	**4/27/2003**

3.0 CONCEPTUAL DESIGN

The conceptual design process involved determining the general aircraft configuration and several design parameters. Each general design was scored by figures of merit and the winning design proceeded to preliminary design. In order to determine the overall shape of the aircraft for preliminary design, several design parameters were investigated.

The competition this year was to carry a five pound square box and perform two of three mission types. The missions were: A missile decoy mission in which the aircraft performs 360° turns over 4 laps, a payload deployment mission in which the five pound payload was deployed, and a communications repeater mission in which an antenna was placed on the aircraft. The score received for a given mission depended on the flight time, the time to assemble the aircraft, and the rated aircraft cost (RAC). Therefore, if any one of these factors were reduced, then this would result in an increased score.

3.1 Figures of Merit

The figures of merit were selected this year to minimize the design risks and maximize the overall score of the aircraft. In order to maximize the score while accounting for potential design setbacks or shortcomings, the figures of merit used were skill and time required to build, the design reliability, the inherent stability of the design, the design/parameter's expected Rated Aircraft Cost, and the overall effect of the design/parameter on the assembly speed of the aircraft and on the time to complete the mission. The complete conceptual design figure of merit table is shown in Table 3.2. The figure of merits and their relative weights are discussed below.

3.1.1 Required Time

Since the contest dictates a tight schedule, an important factor in the feasibility of each component's configuration was the time required to design and build the configuration. It would be unwise to choose a configuration that could potentially require more time to test and develop than was available before the contest date. Complicated configuration designs would increase the time required to build the component. This figure of merit was given a weight of 1.

3.1.2 Required Skill

An important factor in the feasibility of each component's configuration was the ability of the team to build the configuration. Complicated configuration designs would increase the skill, and material cost (due to mistakes) required to build the component because many of the members were new and inexperienced. This figure of merit was given a weight of 2.

3.1.3 Reliability/Assembly Time

Reliability of the configuration was a concern because in previous years, our aircraft have crashed the week before the competition. It was especially important that the plane be reliable this year due to the budget constraints. Also, this year the plane assembly is timed at the contest; the faster the better. Therefore, a configuration's complexity needs to be considered: the more complex the aircraft, the less reliable it will be and the longer it will take to build. This figure of merit favors designs that will be both modular and repairable. The reliability of a configuration or a parameter is a measure of its complexity and difficulty/strain on the pilot. This figure of merit was given a weight of 3.

3.1.4 Stability and Control

The inherent stability of a design concept/parameter was important because certain designs are more easily stable than others, lending to safer flight. Because of the budget constraints, a high degree of control was desirable for the aircraft. This figure of merit was given a weight of 3.

3.1.5 Effect on Rated Aircraft Cost

Each design parameter was evaluated by the team to have a certain effect on the overall Rated Aircraft Cost of the aircraft for a given payload. The lower the figure of merit score for a given parameter, the more that parameter would raise the Rated Aircraft Cost of a given design; that parameter being the only difference between aircraft concepts. This figure of merit was given a weight of 4.

3.1.6 Effect on Drag

Examination of the mission scoring reveals that the flight score a design could achieve is dependent on the design's total flight time. For a given thrust, one way to reduce the total flight time of the mission would be to reduce the aircraft's drag. This figure of merit was given a weight of 4.

3.2 Assumptions Made

Several assumptions were also made in the calculation of the Rated Aircraft Cost for each configuration. Ideally, a given aircraft design would maximize the amount of payload relative to the total aircraft weight. Thus it was assumed that the payload weight fractions from previous competitions would be similar to this year's aircraft. It was also assumed for the conceptual design phase, that each configuration would at least fly mission three. This was assumed

because the third mission was the most limiting in terms of payload weight. Therefore the payload weight was five pounds for the box and 0.9 pounds for the antenna.

Also, based on an RC rule of thumb, it was further assumed that 50 W of battery power would be required per pound of total aircraft weight. It was also assumed that last years batteries, which performed very well, would be used. They provide 1 V per cell at high amp loads and weigh 2.25 oz/cell. The motor configuration would run at 35 A so that the current would not be too close to 40 A, and yet still be large enough to allow for a low total battery weight. This allowed for the team to calculate the needed battery weight for the aircraft based on the loaded weight from the payload fraction calculation. Finally, it was assumed that each configuration would have one propeller and one motor.

The maximum wing loading was estimated using steady flight assumptions (L = W, T = D) for the landing approach phase, resulting in the equation:

$$\frac{W}{S} = \frac{1}{2}\rho\left(\frac{V_S}{1.2}\right)^2 C_{L,max} \qquad 3.1$$

where W/S is the wing loading, ρ is the density at sea level, V_s is the stall velocity of the aircraft, and $C_{L,max}$ is the maximum lift coefficient. The factor of 1.2 is a safety factor included to avoid stall on landing. The pilot requested that the stall speed be no greater than 30 mph so that his approach speed would not be too great; therefore a stall speed of 29 mph was assumed for each configuration. $C_{L,max}$ was assumed from previous team's efforts to be 1.3. With these assumptions, equation 3.1 can be used to find that a wing loading of 2 lbf/ft^2 is needed for each configuration. Using the wing loading found from equation 3.1, it was then possible to find the necessary wing area for a given configuration. It was further assumed, based on previous year's experience, that an aspect ratio of 8 would be a good balance between increasing structural weight and aerodynamic efficiency for single wing aircraft. For aircraft with two lifting surfaces, an aspect ratio of 9 would be viable because the lower wing loading each wing experiences would relieve some of the structural difficulties associated with a larger aspect ratio.

To calculate a Rated Aircraft Cost for some configurations, it was necessary to assume that each configuration would have a fuselage with a fineness ratio of 8, in order to reduce the parasite drag on the fuselage. A payload box positioned longitudinally along the fuselage would make the fuselage 7 inches wide and thus 4.6 feet long. This meant that the fuselage would have to come in two sections in order to fit in the required box.

3.2 General Configurations

The first step in designing an airplane is determining the general shape of the airplane. Four different airplanes configurations were chosen for analysis. These configurations are described below.

3.2.1 Monoplane

The monoplane configuration has one wing and a horizontal stabilizer. Its versatility in design as well as relative ease in manufacturability makes it very attractive. The reliability of this configuration was decided to be slightly less than a biplane because of the monoplane's generally higher wing loading, which requires faster landing velocities. The monoplane also had a higher build time than the flying wing because the fuselage had to come in two sections to fit in the box. The monoplane was considered by the team to have the most inherent stability and control; this style of aircraft is well documented in both design and performance which gave the DBF team a large database from which to draw. The monoplane was considered a relatively fast configuration owing to its lower parasite drag relative to the biplane or the tandem configurations.

Based on aircraft data from previous contests, the historical payload weight fraction for monoplanes was estimated to be 0.37. This led to an empty weight of 10.1 pounds and thus a wing area of 8 ft^2. For a wing with an aspect ratio of 8, the wingspan would be 8 ft and the chord would be 1 ft. The battery weight for a 16 pound loaded monoplane would be 3.1 pounds. For a monoplane, it was assumed that there would be 1 rudder, 1 elevator, 2 ailerons, 4 servos, and 1 motor controller. The monoplane's estimated RAC was 9.2 and the breakdown can be seen in Table 3.1.

3.2.2 Biplane

The biplane configuration is very similar to that of the monoplane, with the exception of a second wing above the main wing. In previous Design, Build, Fly competitions this design has done very well owing in part to both its high reliability and its good controllability. The skill and time required to build the aircraft would be the longest of the four configurations because of the need to build two wings and two pylons on the wings. Because of the large amount of surface area, the parasite drag of the biplane was considered large and therefore the configuration was considered slow.

Based on previous year's aircraft data, the historical payload weight fraction for biplanes was estimated to be ~0.35. This gives leads to an empty weight of 11 pounds. Since the biplane has two wings, the effective wing loading would be 4 lbf/ft^2 and thus each wing for the biplane had a

wing area of 4.3 ft^2. For a wing with an aspect ratio of 9, the wingspan would be 6.2 ft and the chord would be 0.7 ft. The battery weight for a 17 pound fully loaded biplane would be 3.4 pounds. For a biplane, it was assumed that there would be 1 rudder, 1 elevator, 2 ailerons, 4 servos, 1 motor controller, and two wing pylons (vertical surfaces) without control surfaces on them. The biplane's estimated RAC was 10.9.

3.2.3 Tandem

The tandem wing airplane consists of two similar sized wings, one in front and one in rear of the airplane. The tandem wing's horizontal stabilizer creates lift and controls the aircraft's pitch. The forward wing's downwash can make control difficult for the pilot and reduce the effective lift coefficient of the rear wing if not properly designed. Previous DBF teams have had direct experience with the design and implementation of the tandem wing configuration without much success leading the team to give the tandem design a low reliability score. This configuration also required the construction of two wings and therefore needed more time and skill in building it. Similar to the biplane, the tandem configuration has a large surface area, and therefore a large parasite drag resulting in slower flight speeds for a set amount of thrust.

Based on a previous year's design, the assumed payload weight fraction for the tandem was 0.35. This leads to an empty weight of 18.25 pounds. Since the tandem has two wings, the wing loading was approximately 4 lb/ft^2. Each wing on the tandem therefore had a wing area of 4.7 ft^2. For a wing with an aspect ratio of 7, the wingspan would be 5.7 ft and the chord approximately 0.82 ft. The battery weight for the tandem would need to be 4.3 pounds. For the tandem, it was assumed that there would be 1 rudder, 1 elevator, 2 ailerons, 4 servos, and 1 motor controller. The tandem's estimated RAC was 10.6.

3.2.4 Flying Wing

The flying wing is one of the most efficient designs for an airplane; however, stability is a strong limitation of the design. The flying wing can have substantially less drag because the lower aircraft weight translates into less induced drag, and the elimination of the horizontal tail reduces the parasite drag. Therefore the plane is able to fly at greater speeds given the same amount of thrust as other configurations. Difficulties arise, however, in the manufacturing of the plane since the airfoil requires special attention. Also, the flying wing is less suited for payloads that have large volumes compared to the other types of aircraft. Previous UT DBF teams have, however, had some success with the flying wing configuration, so this plane will be considered.

The flying wing aircraft built by a previous team at UT had a payload weight fraction of 0.39, corresponding to an empty weight of 9.2 pounds for this year's competition. The flying wing therefore needed a wing area of 7.6 ft^2, a wingspan of 7.8 ft and a chord of .95 ft. The battery weight for a 15.1 pound aircraft would be 3 pounds. For the flying wing, it was assumed that there would be 2 rudders, 0 elevators, 2 ailerons, 4 servos, and 1 motor controller and that the fuselage would only be 4 feet long. The flying wing's estimated RAC was 8.8.

Table 3.1: Configuration Rated Aircraft Cost Comparision.

Description	Monoplane	Biplane	Tandem	Flying Wing
MEW	**10.1**	**11**	**10.5**	**9.2**
REP	**3.100**	**3.400**	**3.400**	**3.000**
# of Engines	1	1	1	1
Total Battery Weight (lb)	3.1	3.4	3.4	3
MFHR	**179**	**233.4**	**221.32**	**171.4**
Wings	*78*	*122.4*	*120.32*	*76.4*
Wing Span (ft)	8	6.2	6.1	7.8
Max Chord (ft)	1	0.7	0.67	1
# of Control Surfaces	2	2	2	2
# of Wings	1	2	2	1
Fuselage	*46*	*46*	*46*	*40*
Fuselage Length (ft)	4.6	4.6	4.6	4
Empenage	*20*	*30*	*20*	*20*
Vertical Surfaces w/no control	0	2	0	0
Vertical Surfaces w/ control	1	1	1	2
Horizontal Surfaces	1	1	1	0
Flight Systems	*25*	*25*	*25*	*25*
# of Servos	4	4	4	4
# of Motor Controllers	1	1	1	1
Propulsion Systems	*10*	*10*	*10*	*10*
# Engines	1	1	1	1
# Propellers	1	1	1	1
TOTAL RATED AIRCRAFT COST	**9.2**	**10.9**	**10.6**	**8.8**

3.3 Design Parameters

For the initial stage of the conceptual design, several design parameters were investigated for their performance advantages and disadvantages. The design parameters that were chosen for further analysis were then considered in the preliminary design phase.

3.3.1 Wing Planform

The team considered three distinct planform shapes for the wing(s). The wing planforms considered were rectangular, tapered, and elliptical. The rectangular planform offers easy construction that the team was comfortable with from previous year's experience. However, the rectangular planform is the least efficient of the three planforms due to large tip-losses. The tapered wing planform has the advantage of more efficient production of lift while remaining relatively easy to construct; however, tapered wings can suffer tip stall due to the low Reynolds number and the thin airfoil at the wing tips. Tapered wings, while producing more lift per unit area than the rectangular wing, do not have a significant Rated Aircraft Cost advantage over the rectangular wings. This is because the manufacturing man-hours cost is calculated by adding eight dollars per foot of wing span and eight dollars per foot of maximum exposed chord, instead of charging per square-foot of wing area as in past years. A taper ratio of 0.6 gave the maximum increase in Oswald's efficiency, but the least chance of tip stall. The elliptical planform is the most efficient wing shape in that it minimizes the induced drag of the wing. Unfortunately the elliptical wing is also extremely difficult to construct. Therefore, a tapered planform was chosen for this year's aircraft.

3.3.2 Landing Gear Configuration

The team examined three landing gear configurations: tail dragger, tricycle, and retractable tricycle. The tail dragger configuration is inherently unstable, having the tendency to want to flip around such that the plane faces backwards. Neither tricycle configuration contains this instability; therefore they were both given scores of 1. A tail dragger would also be a short, lighter option (meaning less RAC) with less drag than a tricycle; however, the pilot felt uncomfortable with the tail dragger configuration. The tricycle configuration was simple and had been used by the design team in previous years, but would have relatively large amounts of drag even with fairings and would weigh more than the tail dragger. The retractable landing gear would have little to no drag; however, it would be the heaviest option and the most complicated and difficult to construct.

3.3.3 Empennage Configuration

The empennage configurations considered consisted of conventional, T-tail, canard, and V-tail. The conventional and T-tail are somewhat versatile, easily constructed, and well documented designs that have good stability and control characteristics. The T-Tail, with the extra structure required to place the horizontal tail on top of the vertical tail was more difficult and required more time to build. The V-tail, however, is much more difficult to build and not quite as controllable, but a little less expensive in rated aircraft cost as the conventional configuration. The canard, as discussed earlier, presents aerodynamic and control problems and has met with little success from previous UT DBF teams. It requires a little more skill than the conventional tail to build, but

still has the RAC disadvantage over the V-Tail. The canard design was also considered to be the fastest design because of the reduction in lift required from the wing.

3.3.4 Engine Configuration

The engine configuration was a decision between a pusher, puller or multiengine pusher/puller. The pusher configuration is better to resist aircraft crashes. The puller is more conventional and is sometimes required by the geometry of the aircraft. The multiengine configuration can allow propeller selection that results in a higher propeller pitch speed and thus a higher overall aircraft speed. It also has the advantage that if one engine fails, the plane could still possibly land safely. However, the use of two engines would increase the RAC. After much debate, it was decided that this year's aircraft would use the puller propeller configuration.

Table 3.2: Conceptual Design Figures of Merit.

	Component	Time Required (x1)	Skill Required (x2)	Reliability/ Build Time (x3)	Stability & Control (x3)	RAC effect (x4)	Speed (x4)	Final Score
General Configuration	**Monoplane**	1.00	1.00	0.95	1.00	0.95	0.90	**14.35**
	Biplane	0.80	0.85	1.00	0.95	0.76	0.80	12.59
	Tandem	0.85	0.85	0.80	0.80	0.80	0.85	12.35
	Flying Wing	0.90	0.75	0.80	0.75	1.00	1.00	13.45
Wing Planform	Rectangular	1.00	1.00	1.00	1.00	0.95	0.85	14.20
	Tapered	0.85	0.90	1.00	0.95	1.00	0.95	**14.30**
	Elliptical	0.50	0.50	1.00	0.90	1.00	1.00	13.20
Landing Gear Configuration	Tail Dragger	1.00	0.90	1.00	0.90	1.00	0.80	13.70
	Tricycle	0.95	1.00	1.00	1.00	0.95	0.75	**13.75**
	Retractable	0.50	0.60	0.80	1.00	0.90	1.00	13.10
Empennage Configuration	**Conventional**	1.00	1.00	1.00	1.00	0.90	0.90	**14.20**
	T-Tail	0.95	0.90	0.90	0.90	0.90	0.90	13.55
	V-Tail	0.90	0.75	0.80	0.95	1.00	0.95	13.85
	Canard	1.00	0.95	0.80	0.80	0.90	1.00	13.70
Engine Configuration	Pusher	1.00	1.00	0.90	1.00	1.00	0.95	14.70
	Puller	1.00	1.00	0.90	1.00	1.00	0.95	**14.70**
	Multi-Engine	0.95	1.00	1.00	1.00	0.90	1.00	14.55

3.5 Features that Produced Final Configuration

The winning general configuration was the monoplane. This was mainly due to the ease of construction and the stability and controllability of the design relative to the flying wing which came in second. While it did not have the best RAC or the best speed, it was competitive enough in those categories to warrant its selection. The wing planform selected for the monoplane was the tapered wing, because it had more efficient lift generation than the rectangular planform and was still simple and quick to build compared to the elliptic wing. The Tricycle gear was selected mainly due to the pilot's unease with the tail dragger and the unreliable nature of the retractable

gear. Finally the conventional tail was chosen because, while it wasn't the fastest or the cheapest (RAC) solution, it did have the overall best features.

4.0 PRELIMINARY DESIGN

Once the general configuration was selected in the conceptual design phase, the accuracy of the expected aircraft weight was further refined and optimized by sizing the structural components and determining the materials which gave just enough strength to carry the design loads. The tail surfaces were then sized with tail volume coefficients, stability analysis was performed on the design, and an estimate of the design's mission performance was obtained by equating the approximate thrust and drag of the aircraft over the course. The end goal of the preliminary design was therefore to analyze the effect of several design parameters so that the aircraft weight could be both optimized and determined with some accuracy, and to analyze the aircraft's general stability and expected mission performance.

The overall aircraft dimensions used for the analysis were those generated in the conceptual design phase. Last year's DBF team wrote and used an optimization code that iterated through various values for the aircraft's dimensions that were important to the performance of the aircraft (C_L, wingspan, chord, etc.); however, due to the difficulties imposed by the geometrical constraint (the box) the code was not utilized. Furthermore, last year's plane illuminated a potentially fatal flaw with such optimization: all of the aircraft components are at the brink of failure; despite individual component safety factors. In other words, the system as a whole has little to no safety factor built in; if one component fails (a wing stalls), then the whole system fails. This was illustrated several times during the testing of last year's aircraft in which the plane went out of control several times and crashed. It was also noted that the final optimized dimensions from last year's code were very similar to those designed during the conceptual phase. In fact, each component was no more than 1 or 2 percent different from their optimal counterpart and the overall configuration scored within 5% of the optimal design.

This year's competition emphasized the assembly time of the design as well as the flight time. This meant that the team would be equally served to reduce the assembly time of the aircraft as they would to reduce the flight time by the same amount. Therefore, instead of spending more time optimizing the aircraft dimensions to get the best mission time possible (since the dimension changes had negligible effect on the RAC), it was decided to instead build the aircraft designed in the conceptual phase and spend the additional time optimizing the assembly time by altering the physical aircraft. This also had the advantage that the team was able to empirically see the aircraft components that could be reduced in weight. If the team cut 10% from the aircraft's weight (non-battery) then the RAC from the conceptual phase would be reduced by ~2 percent and if the team cut 10% from the battery weight, then the RAC would decrease by ~6 percent. Building a conservative plane and then improving its weight and assembly time also had the

advantage that the aircraft would be much more likely to compete since the dimensions were conservative and the aircraft would be flight tested more than if the dimensions were optimized. The team concluded that the overall score could be more easily improved by optimizing the actual aircraft instead of the initial dimensions, given the assumption that the initial dimensions were 'close' to optimal.

4.1 Figures of Merit

In order to analyze/optimize certain design parameters, figures of merit were selected for the preliminary design phase. The complete preliminary design figure of merit table is shown in Table 4.4.

4.1.1 Required Time

Since the contest dictates a tight schedule, an important factor in the feasibility of each component's configuration was the time required to build the configuration. Complicated configuration designs would increase the time required to build the component. This figure of merit was given a weight of 1.

4.1.2 Required Skill

Another important factor in the feasibility of each component's configuration was the ability of the team to build the configuration. Complicated configuration designs would increase the skill, and material cost (due to mistakes) required to build the component. This figure of merit was given a weight of 1.

4.1.3 Effect on Drag

Examination of the mission scoring revealed that the flight score any given design could achieve was dependent on the design's total flight time and assembly time. For a given thrust, one way to reduce the total flight time of the mission would be to reduce the aircraft's drag. This figure of merit was given a weight of 3.

4.1.1 Component Weight

In order to compare the weight of each component's various possible configurations, the worst-case loading for each component was considered. The minimum weight for a given configuration that could withstand the worst-case load was then compared against other configurations of the same component. This figure of merit was given a weight of 3.

4.2 Mission Choice

In order to properly design and size the various aircraft components, it was necessary to decide which two mission sorties would be flown. It was decided to rank the three missions with the figures of merit described above and the assumption that the base mission (4 laps and 1 360°

turn) would take 300 seconds and that all assembly times were equal at 300 seconds. The scores were normalized such that the best of the three missions received a speed score of 1.

The first mission's difficulty factor was 1.0 and required the aircraft to perform three 360° turns each lap instead of just one, an increase of eight turns in total. At an estimated flight speed of 50 mph, this corresponds to an extra 45 seconds over the base time assuming a steady, constant altitude turn is performed. The speed figure of merit score was therefore equal to $330 * 1/(300+345) = .52$ where the factor of 330 is the normalization factor. The first mission required little time and skill to design because it was essentially just a timed course with a small payload which had been done in previous years. Finally, the weight of the aircraft for this mission would be the smallest of all the missions because it only required the structure needed to support the five pound payload.

The second mission's flight score would be multiplied by 1.5, but also required the aircraft to land, deploy the payload, and then takeoff again. This would add about 65 seconds to the base flight time; however, the aircraft would fly faster on the last two laps because of the significant decrease in weight. In the end the flight time was estimated as 350 seconds. The team decided that the second mission would require extensive design and testing to successfully deploy the payload. It would require the landing gear to be behind the payload and would require a hinge and a hatch with a servo attached. This would also increase the weight of the aircraft due to the extra structure and servo required.

The third mission had a multiplier of 2, but required a simulated communication antenna to be attached. This antenna would increase the aircraft's parasite drag by approximately 104%, increase the weight by 6%, and thus decrease the flight speed by ~20% assuming steady, level flight and a parabolic drag polar. Thus the flight time would increase from 300 seconds to about 360 seconds. The third mission also presented design difficulties, but they were largely thought by the team to be easier to overcome than the difficulties in the second mission. These difficulties included the induced moment on the aircraft due to the antenna, the effective vertical tail surface reduction due to the antenna's wake, and the increase in weight and drag. All of these factors affected the aircraft's ability to takeoff in 120 feet. The first and third missions were selected based on their figure of merit scores shown in Table 4.1.

Table 4.1: Mission Sortie Figures of Merit.

Mission Sortie	Time Required (x1)	Skill Required (x1)	Speed (x3)	Weight (x3)	Final Score
Missile Decoy (1)	1.00	1.00	0.52	1.00	6.56
Sensor Deployment (2)	0.70	0.75	0.76	0.90	6.43
Communications (3)	0.85	0.85	1.00	0.85	7.25

4.3 Design Parameters Investigated

4.3.1 Fuselage Shape and Assembly

The fuselage design, both its shape and assembly, was vital to success in this year's competition because the score is calculated by the difficulty factor divided by the total flight time of the mission plus the assembly time. The fuselage design affects the ability of a given aircraft configuration to carry the desired payload; the total mission time for that aircraft due to drag advantages or disadvantages; and the assembly time at the contest. The fuselage shapes considered were a horizontal extended symmetric airfoil, a vertical airfoil, and a streamlined box with filleted edges. In order for the symmetric airfoils to have a reasonable thickness (<15%) the airfoil would need to be ~4 feet long, though this was shorter than the streamlined fuselage which allowed easy assembly since no connection would be required. Also, airfoil shapes are extremely quick and easy for the team to manufacture. The main disadvantage to the vertical airfoil was that in crosswinds the airfoil would be at an angle of attack and, being a very low aspect ratio wing, it would generate a lot of drag making the vertical airfoil relatively slow. The horizontal airfoil fuselage was used for last year's plane and the stability issues created by the fuselage's quarter chord being in front of the cg were difficult to overcome since the cg could not be moved all the way up to the fuselage's quarter chord. Similar problems were expected if an airfoil were to be used for this year's aircraft and therefore a low skill score was given to the horizontal airfoil fuselage. Both airfoil shaped fuselages were potentially heavier than the streamlined fuselage due to the need for shear web structures inside the airfoil.

Previous years found it to be difficult and time consuming to manufacture light cylindrical shapes; therefore, this year streamlined fuselage with filleted edges was considered. This approximated the shape of the cylinder, but was much easier to build and had a smaller forward cross-section. This difficulty is reflected in the lower construction time and skill required scores given in the figure of merit matrix to the streamlined fuselage. The streamlined fuselage was also considered to have a slow assembly time because the fuselage would need to be 4.7 feet long to have a decent fineness ratio and thereby keep the drag low. Since the box that the plane must fit in was only 4 feet long, this required the streamlined fuselage to be made in two pieces that could then

be put together. An ingenious method of assembling the two pieces was decided upon and minimized the extra assembly time of the configuration. As can be seen in the design drawings, the rear fuselage had two longerons that protruded from the rear section and would fit tightly into two slots in the front section. The two sections were then secured together by putting several large rubber bands around two rods that protruded slightly from each section. These rubber bands also went over the wing spars and held the wing in place. While there were initial doubts if this method would be stiff enough, the rubber bands were found to meet the stiffness requirements easily through actual wingtip testing in which the aircraft was loaded in a cyclic manner. Table 4.4 shows the final ranking for the fuselage shapes and the streamlined shape was selected for the aircraft despite the difficulties involved in construction.

4.3.2 Fuselage Materials

Once the fuselage shape was determined to be streamlined/cylindrical, it was necessary to select the material to be used internally to support the payload and connect the tail section. The materials considered were balsa wood, a fiberglass/balsa composite, and poplar. Carbon fiber was not considered due to radio trouble experienced last year which was traced back to interference caused by carbon fiber structural members around the receiver. The fiberglass/balsa composite allowed the team to add strength only where it was needed such as to the wing carry-through or to the front shear web were the front gear attaches. Thus it was the lightest of the three options. The fiberglass/balsa option did take both more time and skill than the other options, but the team was relatively experienced with fiberglass and so this difficulty was limited. The poplar was constrained by both buckling and torsion because the longerons made from it could be made extremely thin and still theoretically support the bending load because of its large ultimate strength. The poplar, therefore, had to be made thicker to prevent buckling and was therefore the heaviest option. For these reasons, the material chosen was the fiberglass/balsa laminate.

4.3.3 Spar Cross Section and Material

In order to predict the weight of the spar, both the spar material and the spar geometry had to be chosen. The worst-case load on the spar's structural design was determined to be the "Wingtip test" stated in the competition rules. In this test point loads at each wingtip support the fully loaded plane, which was assumed to weigh 16 pounds. All spar designs considered must be at least strong enough to withstand this test. Also, the estimated maximum torque with ailerons fully deployed was considered as a constraint when necessary; however, in general it was less limiting than the bending case. The torque on the spar was estimated to be 15 ft-lbs.

The spar materials investigated included 2014-T6 aluminum, balsa wood, a fiberglass/balsa composite used last year, carbon-fiber, and a carbon-fiber/aluminum composite used in a

previous year. The aluminum spar cross-sections considered were a hollow circular geometry and box beam geometry. The balsa wood and fiberglass-balsa composite spar cross-sections considered were a rectangular box beam and a solid rectangular beam. The only carbon-fiber cross-section considered was a hollow circular cross-section. In order to properly design the spars, tapered cross-sections were needed because of the wing taper. The airfoil's maximum height at the root was 1.5 inches while at the tip it was only 1 inch. If the spar height was only 1 inch high over the entire wingspan, the spar would need to be excessively thick to support the bending load. Also, two spars were always assumed so that the rubber band attachment method could be used to secure the wing assembly to the fuselage without the wing twisting about the spar. The two spar assembly also had the advantage that the spars could be made straight since the quarter chord would always be between the two spars. The single spar would have to be angled along the quarter chord sweep so that the foam would not need to carry much of a load.

In order to find the minimum weight for a given material/cross-section combination, the following flexure formula was used

$$\sigma_u = \frac{M_{max}\, y}{I} \qquad 4.1$$

where σ_u is the ultimate stress, I is the moment of inertia and is determined by the spar geometry, y is the distance from the neutral axis, and M_{max} is the maximum moment the spar experiences from the load. Since the limiting load was a point load at the wing tip (equal to one-half of the plane's mass) and the maximum stress will occur at a height, y, equal to one-half of the spar's maximum height, (4.1) can be simplified into three different cases based on the spar's moment of inertia.

The following torsion formulas for (a) rectangular and (b) thin walled members were used to find the minimum weight:

$$\tau_{max} = \frac{T}{\alpha h w^2} \qquad 4.2a$$

$$\tau_{max} = \frac{T}{2tA_m} \qquad 4.2b$$

where, in (4.2a), τ_{max} is the maximum shear strength of the material, T is the applied torque from the deflection of the flaperons, h is the height of the spar, w is the width of the spar, and α is a dimensionless constant that depends on $^{h}/_{w}$ obtained from Table 4.3 in [1]. In (4.2b), A_m is the area enclosed by the median line, and t is the thickness of the spar.

For each of the materials, σ_u was obtained from previous year's test data in which three-point loads were applied until failure and, in the case of aluminum, the published ultimate stress value for 2014-T6 aluminum was used. Table 4.2 shows densities and ultimate stresses of the various materials

Table 4.2: Experimental Values for Material Properties.

	Al – 2014-T6	Balsa Wood	Fiberglass/Balsa	Carbon-Fiber	Carbon/Aluminum
σ_u (ksi)	60	1.7	3.1	7.5	6
τ_{max} (ksi)	4	0.3	~ 0.6	~ 2.5	4.5
ρ (lb/ft^3)	175	7.2	10.6	75	115

Two approaches were used to determine the spar dimensions for each configuration that gave the minimum weight and supported the wingtip load: one for rectangular cross sections and the other for the circular spar geometry. Both geometries were constrained by a maximum height/diameter that was based on the quarter chord thickness of the wing. For preliminary design purposes, this thickness of the airfoil was assumed to be 1.5 inches at the root and 1 inch at the tip. The hollow spars were also constrained by an estimated minimum thickness to avoid thin wall buckling. For the metal spars this was assumed to be 1/32 -inch, for the carbon-fiber and the balsa wood it was assumed to be 1/16 -inch. The last constraint on the spars was material availability. For the metal spars the aluminum is only readily available in discrete diameters leading to certain spar geometries being unattainable.

For the rectangular geometries, the torsion formula (4.2a) was solved for the minimum width assuming the height of the spar was equal to the maximum allowed height. The maximum stress the spar would experience was then calculated from the flexure formula for the wingtip load. If this exceeded the ultimate stress value shown in Table 4.2, the width was increased so that the maximum stress in the spar was less than the ultimate stress. The weight of the 4-foot long spar was then calculated from the dimensions found and is shown in Table 4.3.

For the hollow circular cross-section, the flexure formula was solved first. Assuming the wall thickness to be equal to the minimum thickness to avoid buckling, the minimum diameter required to satisfy the wingtip load was calculated. If this diameter exceeded the maximum allowed, the thickness was increased such that the diameter was equal to the maximum allowed. The maximum shear experienced in the spar was then found from formula (4.2b) based on the estimated pitching moments produced with full flaps down. If this shear exceeded known,

representative values, then the wall thickness was further increased until the spar could withstand the required loading. The weight of a 4 ft long spar was then calculated.

Table 4.3: Spar Material/Cross-Section Minimum Weights.

Material	Cross-Section	Weight (oz)
Al	Hollow-Circular	3.82
Al	Hollow-Rectangular	4.5
Al/Carbon	Hollow-Circular	7.23
Balsa	Hollow-Rectangular	3.89
Balsa	Solid	2.95
Carbon	Hollow-Circular	4.22
Fiberglass/Balsa	Solid	3.3
Fiberglass/Balsa	Hollow-Rectangular	3.2

The estimated time and skill required for each spar design was discussed in a group meeting. The aluminum spars would require machine shop access and skills that the team did not have, so they were scored correspondingly low. The composite laminate spars, such as the aluminum/carbon and the fiberglass/balsa designs, required skills with composites that several, but not all, of the team had from previous years. The hollow rectangular balsa wood spar designs required more time and slightly more skill than the solid balsa spar configurations, and were therefore scored slightly lower in both categories. The spar materials and cross-sections were assumed not to affect the speed of the flight. A solid balsa spar was selected initially based on its figure of merit score (see Table 4.4). However, after testing it was found that moderate torques caused unacceptable twisting of the spar and so the next best spar was chosen, the solid balsa spar with a fiberglass layer. The fiberglass was found to add sufficient resistance to twisting and prevented the balsa wood from warping.

4.3.4 Wing Structure

Four wing structures were considered: a solid foam core with a monokote surface, foam ribs covered by Econokote, balsa ribs with monokote, and foam ribs with birch sheeting. The solid foam core could be easily and quickly produced, but would weigh the most. The foam ribs would weigh the least, but take the longest to make and have higher drag than the solid foam wing because the Econokote tends to bow slightly in-between the ribs. The balsa ribs, since they are denser than foam, would need to be thinner in order to make the wing lighter; however, the Econokote was found to bow too much in-between the ribs as the thickness of the ribs decreased, and so the balsa rib wing was heavier and had more drag than the foam rib wing. Foam ribs with thin birch sheeting instead of a monokote surface eliminated the bowing of the Econokote, but added weight and significant time to the wing construction. The analysis of these considerations led to the foam rib wing with Econokote being chosen.

4.3.5 Landing Gear Cross-Sections

The team considered three different landing gear extension cross sections: a hollow circular beam, a solid circular beam, and a standard solid tapered rectangular beam. Both of the circular beams would require extra structure in the wing since the wheel base needed to be further apart for ground stability than the fuselage allowed. The standard solid tapered main gear commercially sold was bent such that the wheelbase was increased and yet the gear was still mounted on the fuselage. The aircraft drawings in the detail design show the standard gear more clearly. The hollow circular beam would be the lighter, but wider than the comparable solid circular beam and therefore, even after adding fairings, the hollow beam would have slightly more drag. Also, previous teams have already machined a connector between the landing gear strut and the extension for a solid cross section; however, this connector would not work for a hollow cross section and so new connectors would need to be machined, a skill the team did not have. Since properly sized tapered rectangular main gear were sold commercially, the time and skill required for them were minimal. The final landing gear are shown in the detail design drawing package and show that the team chose the solid tapered rectangular beam.

4.3.6 Tail Assembly

A conventional design warranted a tail structure that would provide both strength against vibration effects and adaptability for the construction portion of the competition, while remaining as light and easy to construct as possible. The dimensions of the control surfaces were determined from the preliminary design. However, the supporting structure was decided from several options. The first was to use two beams, which would be inserted into the back of the main fuselage and then slant towards the vertical tail structure. The beam design would provide strength against vibration due to the distance between the beams and the relatively solid structure of the beams. Additionally, this would make it relatively easy to construct in terms of the beam. The main drawback was that the angle precision required to perfectly align the tail section with the fuselage caused concern.

The next design feature was the use of balsa, or styrofoam ribs as a main structural component. This would satisfy the light weight requirement. By using longerons along the inner diameter of the ribs the vibration could be damped as well as providing a method of attachment to the main structure. While this design offered the most benefits, the construction skill required would prove to be its undoing. The third and chosen method was to create a version of the beam method, via a step approach. Instead of one beam slanting towards the tail, a beam would be divided and each piece would be attached to the other to create an extended, layered beam. While this beam design would weigh more than either of the previous solutions, it was determined that the vibration, and ease of construction benefits would outweigh the still relatively small drawbacks.

The final result was to build two stepped beams and use Styrofoam to shape the fuselage into its desired configuration.

Table 4.4: Preliminary Design Figures of Merit.

	Component	Time Required (x1)	Skill Required (x1)	Speed (x3)	Weight (x3)	Final Score
Fuselage Shape	Horizontal Symmetric Airfoil	1.00	0.80	1.00	0.90	7.50
	Vertical Symmetric Airfoil	1.00	1.00	0.90	0.90	7.40
	Streamlined/Cylindrical	0.90	0.95	0.95	1.00	**7.70**
Fuselage Shear Web Materials	Balsa Wood	1.00	1.00	0.00	0.88	4.64
	Fiberglass/Balsa	0.90	0.95	0.00	1.00	**4.85**
	Poplar	1.00	1.00	0.00	0.85	4.55
Spar Configuration	Al (H,C)	0.70	0.60	0.00	0.77	3.62
	Al (H,R)	0.50	0.40	0.00	0.66	2.87
	Al/Carbon (H,C)	0.75	0.70	0.00	0.41	2.67
	Balsa (H,R)	0.85	0.95	0.00	0.76	4.08
	Balsa (S,R)	1.00	1.00	0.00	1.00	5.00
	Carbon (H,C)	0.50	0.45	0.00	0.70	3.05
	Fiberglass/Balsa (H,R)	0.70	0.85	0.00	0.89	4.23
	Fiberglass/Balsa (S,R)	0.90	0.90	0.00	0.92	**4.57**
Wing Structure	Foam core w/monokote	1.00	1.00	1.00	0.74	7.22
	Foam ribs w/monokote	0.80	0.95	0.90	1.00	**7.45**
	Balsa ribs w/monokote	0.90	0.90	0.85	0.89	7.02
	Foam ribs w/birch sheeting	0.70	0.80	1.00	0.80	6.90
Landing Gear Cross-Sections	Hollow Circular Beam	0.90	0.90	0.98	0.95	7.59
	Solid Circular Beam	0.95	0.95	1.00	0.90	7.60
	Solid Rectangular Beam	1.00	1.00	0.90	1.00	**7.70**
Empennage Structure	Single Element Beam	0.85	0.80	0.00	0.90	4.35
	Balsa/Foam Ribs	0.65	0.80	0.00	1.00	4.45
	Stepped Beam	1.00	1.00	0.00	0.85	**4.55**

4.4 Tail Sizing

The vertical and horizontal tails were sized with the use of tail volume coefficients. The horizontal tail volume coefficient used was 1.2 and the vertical tail volume coefficient used was 0.08. These volume coefficients matched the previous pilot's personal RC plane volume coefficients and had been used the previous year with success. The horizontal tail volume coefficient is defined as

$$V_H \equiv \frac{S_H}{S}\frac{L_H}{\bar{c}} \qquad 4.3$$

where V_H is the horizontal tail coefficient, S_H is the horizontal tail planform area, S is the wing planform area, L_H is the distance from the wing aerodynamic center (ac) to the horizontal tail ac,

and $\bar{c}$ is the wing mean aerodynamic chord (MAC). The vertical tail volume coefficient is defined as

$$V_V \equiv \frac{S_V}{S}\frac{L_V}{b} \qquad 4.4$$

where V_V is the vertical tail coefficient, S_V is the vertical tail planform area, L_V is the distance from the wing ac to the vertical tail ac, and b is the wing span.

The distance from the tail's ac to the wing ac was set by the fuselage length of 4.7 feet. The horizontal tail's span was further constrained to be 2 feet, or, one quarter of the wingspan which was ~8 feet. The vertical tail needed to be tall in order to clear the wake of the antenna; however, it also needed a large base for attachment purposes. Therefore it was decided to taper the vertical tail by 70 percent. If it was assumed that the wing ac was a third of the way along the fuselage and that the trailing edge of the tails were at the end of the fuselage, it was possible to size the horizontal and vertical tails from (4.3) and (4.4). The calculated dimensions are shown in Table 4.5.

Table 4.5: Empennage Parameters (inches).

Horizontal Span	24
Horizontal Chord	10.5
Vertical Height	14.5
Vertical Root Chord	11
Vertical Tip Chord	16
L_H	39.5
H_H	4
L_V	37

4.5 Aircraft Performance Estimates

4.5.1 Weight Breakdown

It was necessary to determine the aircraft's weight more precisely to get a reasonable estimate for the aircraft performance. To this end it was assumed that each aircraft configuration would use 4 servos: 1 for the rudder and the front gear, 2 for the ailerons, and 1 for the elevator. For the Hobbico servos that the team used, the weight per servo was 1.1 oz. The receiver, battery, and controller that the team used weighed 1.1, 3.4 and 1.9 ounces respectively. The motor used in previous years was the Astroflight Cobalt 625 with a 3.1:1 gear ratio and it weighed 14.1 ounces. This year's team decided to use it as well due to budget constraints and the fact that the motor is a fairly common choice for the competition. It was assumed that a propeller of ~15 inches would be needed which weighs ~3.1 ounces while the corresponding spinner weighs 1.7 ounces. The battery weight used was estimated at 49.6 ounces which was the weight

determined in the conceptual design phase. The commercial main landing gear available weighed 9.7 ounces and the 3-inch diameter rubber wheels that the team selected weighed 1.7 oz. apiece, while the nose gear weighed 2.2 ounces. The other weights listed in Table 4.6 were calculated while investigating the design parameters for the aircraft.

Table 4.6: Preliminary Weight Estimate

Component	Weight [oz]
Wing and Spar	37.4
Vertical Tail	1.7
Horizontal Tail	2.4
Front Gear	2.2
Main Gear	9.7
Wheels	5.1
Longeron	17.0
Fuselage	12.0
Motor	14.1
Propeller	3.1
Spinner	1.7
Motor Controller	1.9
Radio Reciever	1.1
Propulsion Batteries	49.6
Servos and Wiring	11.0
Payload	80.0
Communications Antenna	14.4
MISSILE DECOY MISSION WEIGHT (lb)	**15.63**
COMMUNICATIONS RELAY MISSION WEIGHT (lb)	**16.53**

4.5.2 Mission Performance

In order to quantify the mission performance, several assumptions were necessary. The first aerodynamic assumption made was the flight plan. Since the flight score was dependent on the total flight time, the flight plan was designed to minimize the time while limiting the pilot difficulties. This was accomplished by limiting the flight plan such that the aircraft flew at full throttle for the entire course except for just before the landing approach turn. After the second 360-degree turn was completed, the throttle was set to zero, allowing the plane to glide until the velocity was 1.2 times the stall velocity of the aircraft. The plane was then flown at half throttle until landing. For calculating turn performance of the airplane, a quasi-steady, level turn was assumed. That is, the change in velocity in the direction of the flight path is assumed negligible as well as the component of thrust normal to the flight path and the turn takes place at constant altitude. Also, a coordinated turn is assumed. That is, the sideslip angle is zero so that the velocity is aligned with the flight path. This allowed the aircraft's flight time to be approximated as a takeoff segment, a landing segment, a cruise segment, and a turning segment. The aircraft's flight time in the cruise segment was determined by dividing the cruise distance as defined by the contest by the cruise

velocity. The cruise velocity was found by setting the thrust equal to drag and the lift equal to weight and solving the equations.

Before the analysis could be done the drag of the aircraft needed to be estimated. To estimate the drag of the aircraft, an empirical model was used; details of this model can be found in [2]. First, the model assumes a parabolic drag polar with constant coefficients of the form

$$C_D = C_{D_o}(M) + K(M)C_L^2 \qquad 4.5$$

where C_{Do} and K are assumed constant since the low speed of airplane removes the mach number dependence. To calculate C_{Do}, the equivalent parasite area method was used. That is, the contribution of drag from friction was summed according to

$$C_{Do} = C_{Df} = \sum_k \frac{1.1 f_k}{S_W} + \frac{S_{W_{CYL}}}{S_W} C_{D_{CYL}} \qquad 4.6$$

where f_k is the equivalent parasite for each component of the airplane, S_W is the exposed surface area of the wing, $S_{W_{CYL}}$ is the area of the cylinder, and $C_{D_{CYL}}$ is an empirical result equal to 0.64 for short cylinders. The cylinder term was not included for the drag estimate for the first mission. The equivalent parasite, f_k, is determined using the average skin friction coefficient, an interference factor accounting for imperfect connections between components (e.g. wing connection to the fuselage), and a form factor that accounts for thickness effects. The induced drag coefficient, K, was calculated using the standard form

$$K = \frac{1}{\pi A_W e} \qquad 4.7$$

where A_W is the aspect ratio of the wing and e is Oswald's efficiency estimated from the wing aspect ratio and taper ratio [3].

The propeller thrust as a function of velocity also needed to be determined in order to have a reliable performance estimate. According to Electricalc, a commercial propeller program, the pitch velocity corresponds to the speed at which the thrust deviates from a linear relation with the aircraft velocity. The thrust as a function of velocity up to the pitch velocity was

$$T(V) = T_0\left(1 - \frac{V}{2V_p}\right) \qquad 4.8$$

where T is the thrust for a given velocity, T_o is the static thrust, V is the velocity, and V_p is the pitch velocity of the propeller-motor combination. To ensure that the plane did not lose thrust and stall due to strong gusts, it was necessary to ensure that the stall velocity of the aircraft not approach the non-linear region of the thrust versus velocity curve. Therefore, the pitch velocity

was assumed to be at least 50 mph; which allowed for gusts up to 20 mph before the aircraft would lose thrust.

The takeoff time (and distance) was found by integrating the 1-D equations of motion numerically. Figure 4.1 shows the velocity of the plane at the end of the runway as a function of static thrust for several pitch speeds. The takeoff with the antenna attached was the most constraining requirement and was therefore used to determine the needed static thrust. A static thrust of ~5.25 pounds was needed in order to take off in 120 feet with the antenna attached and assuming a pitch speed of 60 mph, a $C_{L,TO}$ of 1.2 (~90 percent of assumed $C_{L,max}$), and airplane dimensions as designed in the conceptual phase. The time for the landing phase was estimated to take 30 seconds.

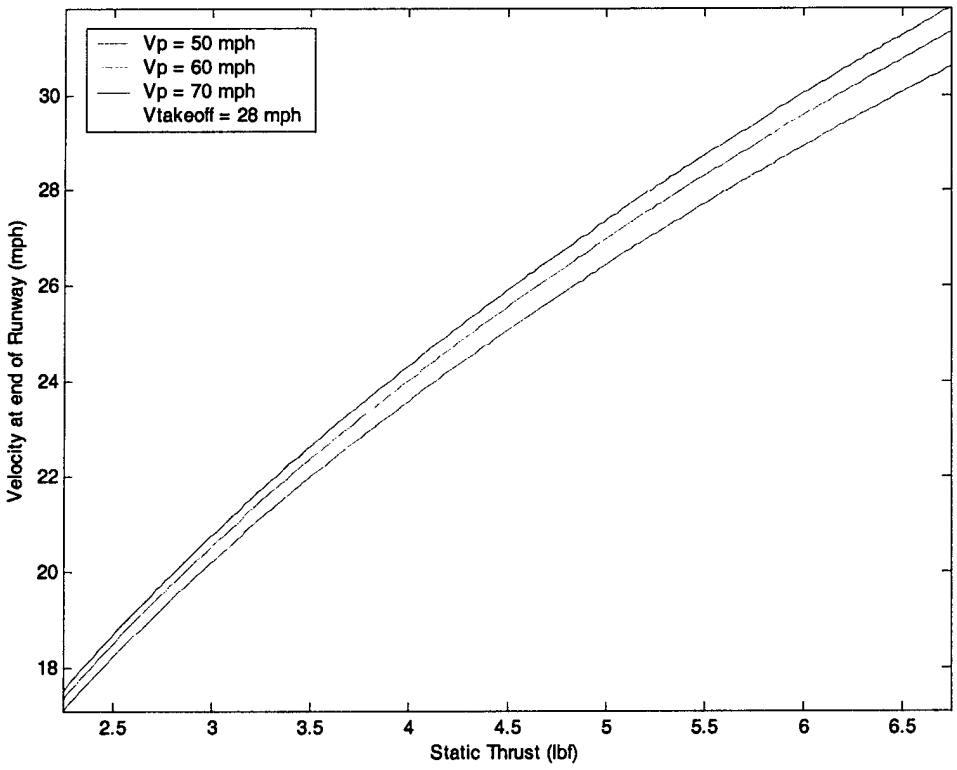

Figure 4.1: Velocity vs. Static Thrust at end of runway.

By setting the thrust equal to the drag and lift equal to weight at cruise, the following equation can be found

$$0 = \left(\frac{1}{2}\rho S_W C_{Do}\right)V^2 + \left(\frac{T_o}{2V_p}\right)V + \left(\frac{2kW^2}{\rho S_W}\right)\frac{1}{V^2} - T_o \qquad 4.9$$

where the variables are as defined earlier. Equation 4.9 can be solved with a Newton-Raphson technique for the cruise velocity. The values used for the aircraft are shown in Table 4.7; as are the cruise velocities determined from (4.9). Note that the static thrust used in the analysis is lower than that required for takeoff in the missile decoy mission. This is because the aircraft did not need to be at full throttle in order to obtain a velocity equal to the pitch velocity of the propeller.

Finally, in order to estimate the flight time of each mission, the time spent in turns must be accounted for. This was done by assuming quasi-steady, level turns as mentioned earlier. This allowed for the calculation of the turn time as

$$t = \frac{\theta * V_c}{g\sqrt{n^2 - 1}} \qquad 4.10$$

where t is the turn time, θ is the number of radians in the turn, V_c is the velocity at which the turn is taken, g is gravity, and n is the load factor of the turn. The velocity was assumed to be cruise velocity and the load factor was assumed to be 2.5 because the wingtip test simulates a 2.5g turn. Table 4.7 shows the time breakdown for the missions and the total estimated flight time. This estimate will have large errors if either the load factor assumed is not achievable or if the estimated value for the friction drag coefficient, C_{Do}, is wrong. A change of 10% in the load factor would change the time in the turns by ~13%, while a change in C_{Do} by 10% would change the time in the cruise segment by ~4%.

Table 4.7: Aircraft Performance Parameters.

Parameter	Missle Decoy	Communications Repeater
Wing Area (ft^2)	8.4	8.4
Static Thrust (lbf)	4	5.25
Pitch Velocity (mph)	60	60
Weight (lbf)	15.6	16.5
C_{Do}	0.0273	0.05726
k	0.0432	0.0432
Cruise Velocity (mph)	**57.9**	**49.0**
Takeoff & Landing	35	45
Turns	117	49
Cruise	94	111
Total Time (sec)	**246**	**205**

4.5.2 Stability Characteristics

Previous DBF teams experienced severe stability problems with the aircraft designed. Even though many of the difficulties lay in the aircraft configuration (i.e.: tandem wing), it was still

imperative that improvements be made in stability predictions of the aircraft. To perform stability calculations, a MATLAB stability code was written. This code took the aircraft parameters from the conceptual and preliminary design phases and calculated stability parameters.

The most important parameter in predicting the aerodynamic response, longitudinally, is the location of the aircraft aerodynamic center (X_{AC}) relative to this center of gravity (X_{CG}) as measured from the aircraft's nose. The difference X_{AC} - X_{CG} divided by the mean aerodynamic chord is termed the static margin. In order for the airplane to be statically stable, the static margin must be positive. Several geometric and aerodynamic properties must be taken into account in order to calculate the static margin.

First, the geometry of the airplane must be considered; that is, the location of the horizontal tail with respect to the wing. The horizontal and vertical dimensions of the horizontal tail aerodynamic center, L_h and H_h respectively, relative to the wing aerodynamic center are used to calculate the downwash from the wings and its effect on the horizontal tail. The downwash model used was empirical, and is given in [2]. Also, $C_{L_{\alpha,WB}}$ and $C_{L_{\alpha,HT}}$ were calculated from the wing aspect ratio (assuming the fuselage effect to be negligible) and the horizontal tail aspect ratio. Finally, $X_{ac,WB}$ was estimated and with all these quantities the X_{AC} of the whole aircraft could be calculated [2]. Using this method to calculate X_{AC}, the static margin was calculated as 0.21. Hence, the airplane was statically stable. While this value seemed high, the team decided a slightly sluggish response would be acceptable for the initial test flights.

As with longitudinal static stability, the airplane must also be stable laterally; that is, the plane must return to its original operating condition when perturbed by a gust of wind from the side or any sideslip angle. To ensure lateral static stability, the total yawing moment stability derivative, $C_{n\beta}$, must be positive. The two major contributions to yawing stability stem from the fuselage and the vertical tail. The fuselage tends to be destabilizing while the vertical tail is stabilizing. Thus, the vertical tail size must be such that lateral stability is maintained. Using empirical relations for the contribution of the fuselage and vertical tail to $C_{n\beta}$ from [4], the value of $C_{n\beta}$ was determined to be 0.18. Thus, the airplane is laterally stable.

With the airplane now sized to maintain static stability, both longitudinally and laterally, the dynamic performance of the airplane needed to be predicted. Using steady, level flight assumptions, the stability derivatives were approximated using relations from [2]. Table 4.8 shows the calculated non-zero stability derivatives for the aircraft. Correspondingly, the eigenvalues for the response of the airplane in steady, level flight at cruise velocities are shown in Table 4.9. Both modes display convergence. The short period mode is highly damped and will

be unobservable in flight, while the phugoid mode is lightly damped, but has a long oscillatory cycle and should be controllable even if it turns out to be slightly unstable.

Table 4.8: Longitudinal Stability Derivatives.

Derivative	Value	Derivative	Value	Derivative	Value
$C_{L\alpha}$	5.39	$C_{m\alpha}$	-1.12	$C_{z\alpha}$	-5.44
$C_{L\dot{\alpha}}$	0.99	$C_{m\dot{\alpha}}$	-2.98	$C_{z\dot{\alpha}}$	-.99
C_{Lq}	3.31	C_{mq}	-9.97	C_{zq}	-3.31
$C_{L\delta_E}$	0.613	$C_{m\delta_E}$	-1.74	$C_{z\delta_E}$	-.613

Table 4.9: Eigenvalues to Step Input at Cruise Velocity.

	Eigenvalues	**Natural Frequency (rad/sec)**	**Damping Ratio**
Short Period Mode	-6.83 ± 7.64i	10.24	0.67
Phugoid Mode	-0.017 ± 0.49i	0.49	0.035

The dynamic lateral stability was not calculated because the two references known to the team disagreed on some of the approximations used to find the lateral stability derivatives. Thus the team decided that, since the aircraft was a standard aircraft and had static lateral stability, the aircraft was at least controllable laterally, if not laterally dynamically stable. Flight tests later showed that this assumption was correct as no instabilities manifested themselves in ~10 mph crosswind gusts.

One of the major difficulties in determining the stability derivatives was the calculation of the moments of inertia for the airplane. The facilities to conduct a dynamic measurement to estimate the inertia characteristics of the aircraft were insufficient at the time. The team resorted to AUTOCAD. AUTOCAD provides inertia calculations based on a unit mass. The moments were found for the balsa, Styrofoam, and payload using AUTOCAD and then later scaled by the appropriate density and translated to the proper coordinate system. The materials are assumed homogeneous in this calculation. While this is not physically true, it was determined that the assumption should provide reasonable results in estimating the dynamic performance of the airplane. The contribution of the motor, batteries, and landing gear to the moments of inertia were approximated by using point masses at the specified locations of these components.

5.0 DETAIL DESIGN

Preliminary design chose several design parameters and made certain assumptions, and then the aircraft components were designed. The overall aircraft information is shown in Table 5.1. The purpose of detail design was to match components and systems that would allow the aircraft to achieve the desired characteristics given in the preliminary design.

Table 5.1: Preliminary Aircraft Parameters.

GENERAL PARAMETERS	
Empty Aircraft Weight	10.6 lb
Decoy Aircraft Weight	15.6 lb
Antenna Aircraft Weight	16.5 lb
Expected Total Flight Score	0.35
WING PARAMETERS	
Wing Span	8.17 ft
Mean Aerodynamin Chord	1.06 ft
Taper Ratio	0.6
Spar Height (root)	1.5 in
Spar Height (tip)	1 in
Spar Thickness	0.5 in
PROPULSION PARAMETERS	
# Motors	1
Static Thrust	5.25 lbf
Picth Velocity	60 mph
AERODYNAMIC PARAMETERS	
$C_{L,MAX}$	1.3
$C_{L,TO}$	1.2
$C_{L,CRUISE}$	0.23 - 0.32
C_{do}	0.273 - 0.573
k	0.043

5.1 Component Selection

5.1.1 Propulsion Configuration

It was decided in the conceptual design phase that the airplane would have 1 motor. Because of budget concerns, no motors could be purchased unless a competition-worthy plane was flying. Therefore, the team had to use the motor from the previous year's competition, the Astroflight Cobalt 625G with a 3.1:1 gear ratio. Further analysis into which motor would perform the best was done after the aircraft was shown to fly, and is presented in the ongoing improvements section. The previous year's batteries were also reused, though this was not a major limitation

because the SR 2400 Max batteries are fairly standard among the teams (unless more capacitance is needed and then it is SR 3000). The batteries were chosen last year by examining 177 different Ni-Cad batteries and ranking them based on their weight per battery cell, internal resistance, and total milliamp-hours. The SR 2400 Max batteries won the comparison due to their very low internal resistance, low weight, and decent capacitance.

The static thrust this motor needed to produce in order to takeoff in 120 feet was found in preliminary design to be 5.25 lbf and the desired pitch speed of the propeller was 60 mph. Propeller Tests were performed in order to determine the number of batteries, the diameter of the propeller, and the pitch of the propeller needed to meet the static thrust requirement. No experimental method for determining the pitch speed was available to the team, so the team relied on the commercial programs Electricalc and Motorcalc to estimate the pitch speed. Since the programs were fairly accurate (±10%) in their static thrust predictions, it was believed that the pitch speed estimates would be of similar error. Initial tests revealed that any propeller with a diameter smaller than 15 inches could not meet the 5.25 lbf static thrust requirement with 18 batteries. The pitch to diameter ratio also had to exceed ~0.7 in order to meet the desired pitch speed. Table 5.2 shows an abbreviated list of the propeller data collected. From this table, it can be seen that in order to meet the pitch speed requirement, 18 cells were needed. However, it was decided that meeting the static thrust requirement and reducing the battery weight was more important than exactly meeting the pitch speed. The propulsion configuration chosen was the 15x12 propeller with 16 batteries. While this did not have the desired pitch speed, it did produce more static thrust than needed and it reduced the RAC of the aircraft by 0.42 points (~5%). This reduction more than offset the slightly longer mission time that resulted from the slower cruise velocity. Finally, the takeoff distance remained the same due to the extra static thrust.

Table 5.2: Propeller Test Data (* indicates Electric Propeller).

Diameter (in)	Pitch	Static Thrust (lbf)	Pitch Speed (mph)	# Cells
14	10	4.250	51.9	18
14	12	4.700	53.5	18
15	**12**	**5.375**	**54.5**	**16**
15	12	5.375	62.4	18
15	10	4.625	59.4	14
15	10	5.500	42	16
16	11	2.875	46.8	12
16	11	5.000	38.9	14
16	11	5.500	43.9	16
16	11	6.250	48.4	18
16*	12	2.625	52.4	12
16*	12	4.000	41.9	14
16*	12	4.750	47.2	16

5.1.2 Airfoil selection

With the sizing parameters complete, the airfoil for the wing had to be selected. In order to select the airfoil, a search was done through the UIUC online catalog of airfoils [5]. The airfoils were then narrowed down with several constraints. The main constraint on the airfoil was that it must generate the desired lift coefficient for the airplane. This corresponded to a $C_{L,max}$ of 1.3 and a $C_{L,cruise}$ of ~0.3. Furthermore, the previous year's team experienced a great deal of trouble cutting the airfoil trailing edge, so the trailing edge must also be sufficiently thick so the shape could be cut with some uniformity. Finally, the airfoil was not considered if it was excessively thick/thin (>13% or <9%) or if it was highly cambered. Thick airfoils will generally have more drag, thin airfoils will present spar weight problems and highly cambered airfoils generally have a thin trailing edge making them difficult to construct.

Searching through the database and comparing to airfoil shapes, the list was narrowed to eight airfoils for detailed comparison. This airfoil was selected from this group by examining the drag coefficient properties of the airfoil around $C_{L,cruise}$, it's stall angle, and the airfoil's L/D_{max} ratio. The Eppler E214 airfoil and the SG 6042 airfoils had the best overall properties of the eight airfoils. Their polar curves are shown below and the data summed in Table 5.3. Though the SG 6042 has a larger stall angle and a higher $C_{L,max}$, the drag characteristics of the E214 are slightly better around the $C_{L,cruise}$ and the L/D_{max} is slightly higher for the E214. The E214 was also thicker, which would allow for a taller spar which would save weight by allowing a thinner spar. In the end, the E214 airfoil was selected based on its lower drag at cruise and its extra thickness.

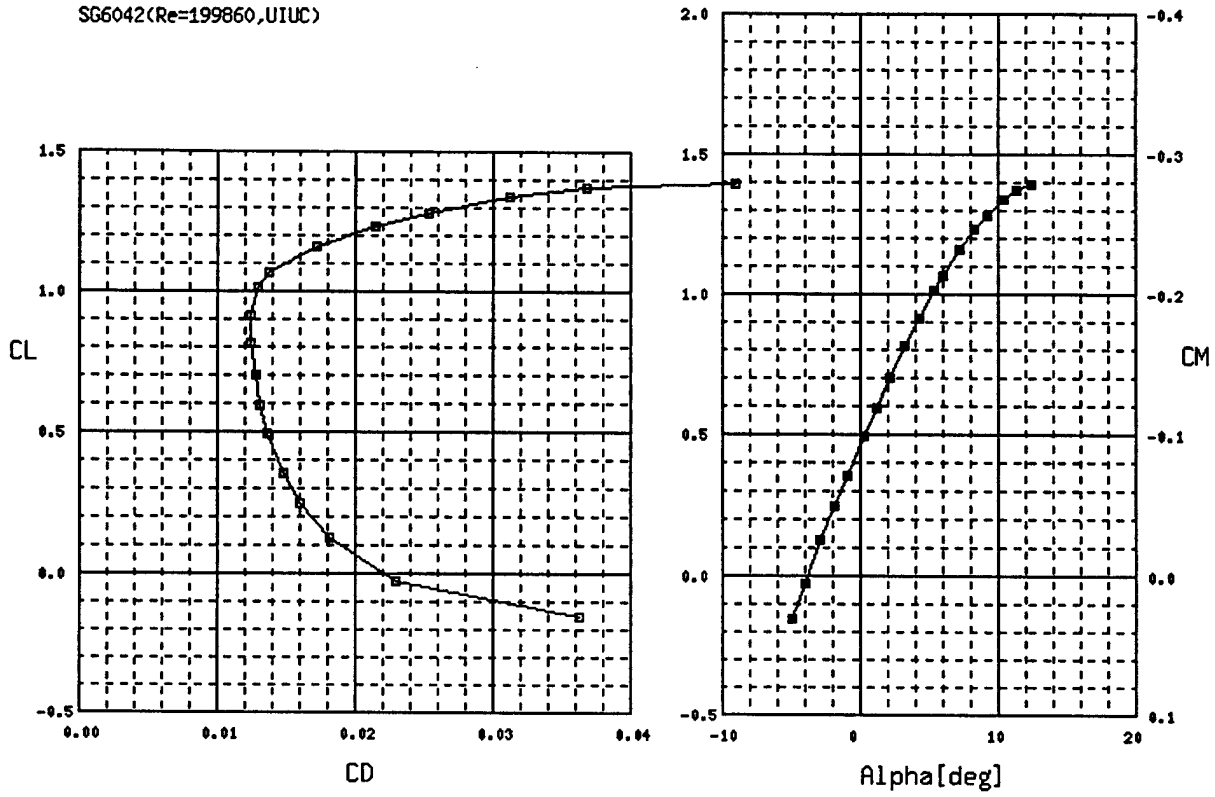

Figure 5.1a: SG6042 [5]

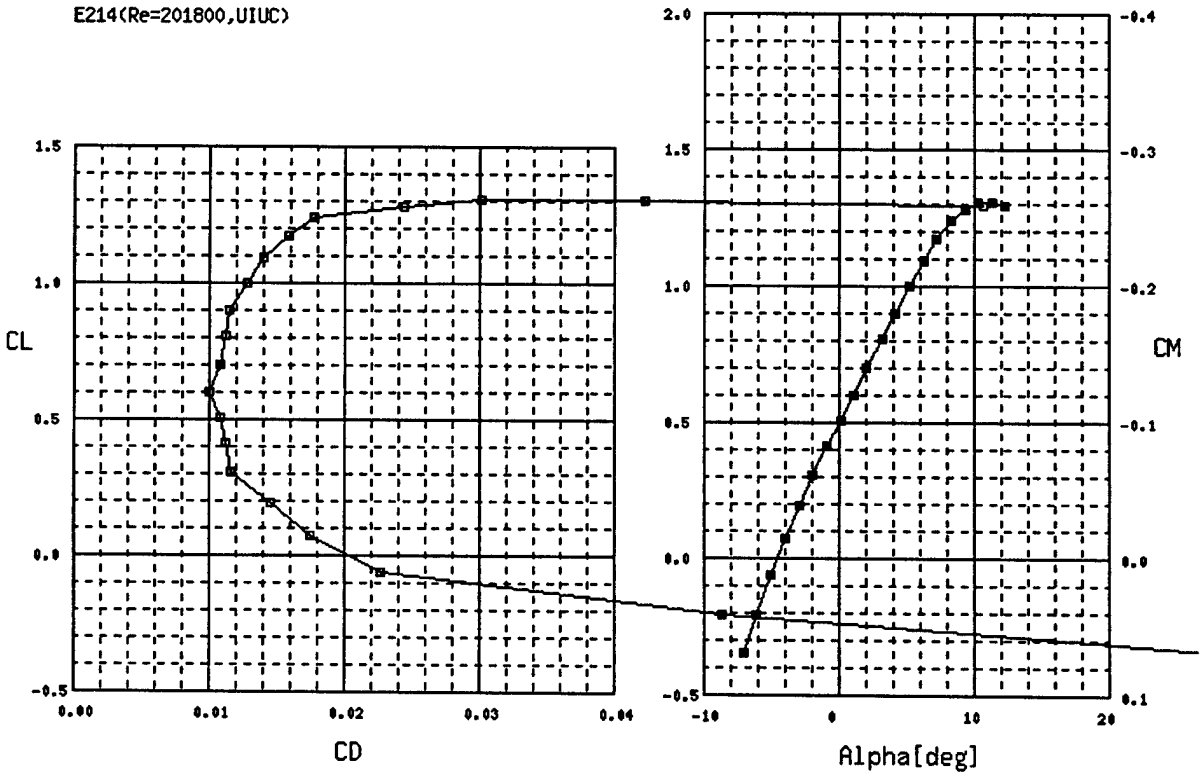

Figure 5.1b: E214 [5]

Table 5.3: Airfoil Property Comparision.

Property	SG 60423	E214
$C_{L,max}$	1.39	1.31
L/D_{max}	77.7	78.2
$C_{D,cruise}$	0.015	0.012
Thickness	0.1	0.11
Stall Angle (°)	12.5	11.4

5.1.3 Wing Placement

To more precisely place the wing, it was desirable to maximize ease of control for the pilot and to minimize trim drag. Hence, when in steady level flight, no elevator deflection should be required to maintain level flight. This meant that the aircraft's aerodynamic center should be placed relative to the aircraft's cg such that the moment from the aircraft's lift would exactly cancel the wing's nose down moment. This can be achieved by examining the equations of motion. Dividing the steady, level flight equations of motion by the dynamic pressure and substituting in the stability derivatives for the aerodynamic coefficients yields

$$\begin{aligned} C_T - C_{D0} - KC_L^2 - (W/\bar{q}S_W)\gamma = 0 \\ C_{Lo} + C_{L\alpha}\alpha + C_{L\delta E}\delta_E - W/\bar{q}S_W = 0 \\ C_m = C_{mo} + C_{m\alpha}\alpha + C_{m\delta E}\delta_E = 0 \end{aligned} \qquad 5.1$$

For level flight, $\gamma = 0$ and the equations can be solved for α and δ_E:

$$\begin{aligned} \alpha &= \frac{C_{m\delta E}\delta_E(C_L - C_{Lo}) + C_{L\delta E}C_{mo}}{C_{L\alpha}C_{m\delta E} - C_{m\alpha}C_{L\delta E}} \\ \delta_E &= \frac{-C_{L\alpha}C_{mo} - C_{m\alpha}(C_L - C_{Lo})}{C_{L\alpha}C_{m\delta E} - C_{m\alpha}C_{L\delta E}} \end{aligned} \qquad 5.2$$

where α equals the angle of attack in radians and δ_E equals the elevator deflection angle in radians. From these equations, the angle of attack for steady level flight and the elevator deflection can be calculated for each mission. Setting the $C_{m\alpha}$ equal to $-C_{L\alpha}$ times the static margin, the deflection angle of the elevator can be written as

$$\delta_E = -\frac{C_{mo} + (\bar{X}_{cg} - \bar{X}_{ac})(C_L - C_{Lo})}{C_{m\delta_E}} \qquad 5.3$$

This allows the placement of the aircraft ac relative to the cg. Since the position of the tail is known, the wing can therefore be placed on the fuselage such that $\delta_E = 0$. This requires a fairly precise determination of the moment coefficient of the airfoil; which the NASG or UIUC did not

have. Without a better alternative, the team used the software code Javafoil to predict the moment coefficient. To place the wing, the position first had to be estimated and put into the weight and balance cg sheet. Equation 5.3 could then be solved for the position of the wing so that the elevator deflection needed at cruise was zero. The new position of the wing was then put back into the cg spreadsheet to get the new cg. This process was iterated until convergence.

5.1.4 Control Surface Sizing

In order to allow the plane to rotate on takeoff, the elevator area needed to be relatively large because the fuselage was relatively short and the horizontal tail was smaller than ideal because of the contest restriction on the tail span. The elevator was made to span the entire horizontal tail in order to provide the necessary nose-up moment on takeoff. Even with the entire tail span elevator, the aircraft should not be overly sensitive to small elevator deflections due to the large static margin of the aircraft. This was verified during flight testing.

The rudder for the aircraft was designed to be along the entire span of the vertical tail because the interference caused by the antenna cylinder significantly reduced the effectiveness of the tail and our pilot preferred to fly with the rudder. The bottom of the rudder was cut at an angle so that even at maximum deflection, the elevator would not touch the rudder.

The ailerons were sized using aircraft from previous competitions for guidance so that the aircraft would have controllable roll response. If the ailerons were too big, then the aircraft would be overly sensitive to small deflections at cruise velocity, but if the ailerons were too small the aircraft would be in danger at the slower takeoff velocity. Therefore using history as a guide, the ailerons were made to span the outer half of the wing.

5.2 Systems Architecture

Most component analysis is discussed in the Manufacturing Plan, Section 6.0. Aspects of the aircraft warranting further detail in its operation and assembly of the aircraft are discussed below.

5.2.1 Connection of Wing / Fuselage / Tail Assembly

The connections of the wing and tail assemblies to the fuselage utilize a simple rubber-band technique. The rubber bands wrap around two brass rods that extend 1" from either side of the fuselage and are permanently fixed to the structure of the aircraft. The front brass rod is through the balsa support for the motor on the fuselage assembly slightly in front of the payload box. The rear brass rod is through the balsa support pieces for the tail assembly and is very near to the payload box. The wing rests on top of the fuselage between the two rods. Poplar "stoppers" were

added to prevent the wing from sliding forward or aft. By pulling a rubber band from the front rod over the wing carry-through structure and finally back to the rear rod, all three assemblies are held together at once. Three heavy-duty rubber bands on each side of the payload box were determined to be the minimum number to be able to properly hold the structure together.

5.2.2 Wiring / Servos / Receiver Placement

To minimize the lengths of the servo wires and to keep the center of gravity in an acceptable location, the receiver was placed in the tail assembly as far forward as possible. The rudder and elevator servos were also placed at this location and were directly connected to the receiver. Only the wing servos and motor controllers required wire extensions to reach the receiver. The motor controller wire extension and wing wire extensions fit easily between the payload box and overhead hatch to the receiver at the tail assembly of the aircraft. Nylon push rods were connected between the rudder and elevator servos and their corresponding control surfaces. The control horn for the rudder had two push rods connected to it. One push rod was linked to the servo while the other rod to the nose gear. Unfortunately, this extra push rod had to be connected when assembling the aircraft which increased the assembly time. On the other hand, utilizing one less servo decreased the rated aircraft cost and also decreased the complexity of the wiring and nose gear mount.

5.2.3 Aircraft Assembly

The contest scoring depended heavily on the assembly time of the aircraft. Component designs sometimes had to sacrifice strength and performance to meet this scoring demand. To begin the aircraft assembly, all components are pulled from the storage box. One team member immediately begins assembly of the wings. Each wing needs four bolts with wing nuts to be inserted into the carry-through box. During that time, the two other team members assemble the fuselage. On the fuselage assembly, first the nose gear and main gear are attached. After that, the tail assembly is slid into the fuselage assembly. At this point, the wings are assembled and ready to attach to the aircraft. Two team members wrap the rubber bands over the brass mounting rods now while the third person attaches the rudder push rod to the nose gear and completes connection of the wiring. Finally, the hatches are closed and any tape necessary for aerodynamics is added. Total assembly time is roughly three minutes. Several methods have already been discussed and are listed in section 5.5 to reduce this time. These new methods will be initiated before the competition date.

5.3 Aircraft Configuration

5.3.1 Final Configuration

The aircraft configuration as of writing the paper is shown in Table 5.4 and in the following drawing package. Updated performance estimates with the most recent weight and propulsion characteristics were calculated in the same manner as was done in the Preliminary stage. Several changes are being made in order to lighten the aircraft and lower its construction time. These are discussed in the future improvements section.

Table 5.4: Final Aircraft Data.

GEOMETRIC DIMENSIONS	
Fuselage Length	5.67 ft
Height	1.23 ft
Wing Span	8.17 ft
Mean Aerodynamic Chord	1.08 ft
Taper Ratio	0.6
Wing Area	8.8 ft^2
Aspect Ratio	7.6
Aileron Area (total)	3.25 ft^2
Elevator Area	1.75 ft^2
Rudder Area (total)	1.67 ft^2
PERFOMANCE	
Wing Airfoil	Eppler 214
$C_{L,max}$	1.31
L/D_{max}	14.6
Maximum Rate of Climb (missle decoy)	16.8 ft/sec
Stall Speed	24.2 mph
Maximum Speed	56 mph
Takoff Field Length (empty)	88 ft
Takoff Field Length (Missle Decoy)	104 ft
Takoff Field Length (Antenna)	120 ft
Total Predicted Flight Score	**0.422**
WEIGHT STATEMENT	
Airframe	6.97 lb
Propulsion System	3.38 lb
Control System	.98 lb
Payload System	0 lb
Payload	5.9 lb
Empty Weight	**11.33**
Missle Decoy Weight	**16.15**
Antenna Mission Weight	**17.05**
MISCELLANEOUS SYSTEMS	
Motor	Astro FlightCobalt 625G
Gear Ratio	3.1:1
Batteries	16 SR 2400 Max in series
Propeller	15 x 12 APC
Radio Used	Futaba PCM 1024
Servos	Hobbico CS-35MG

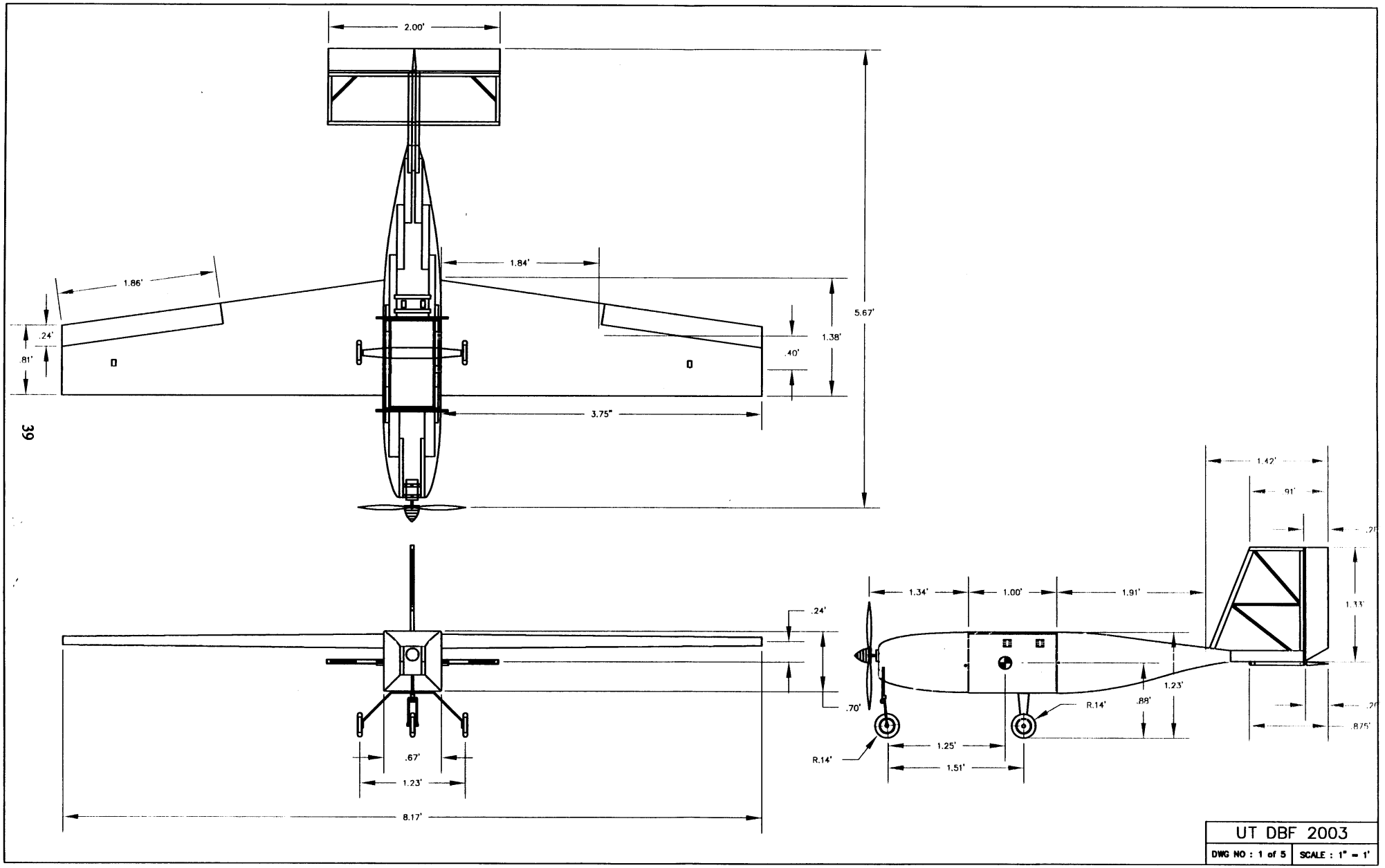

39

UT DBF 2003	
DWG NO : 1 of 5	SCALE : 1" = 1'

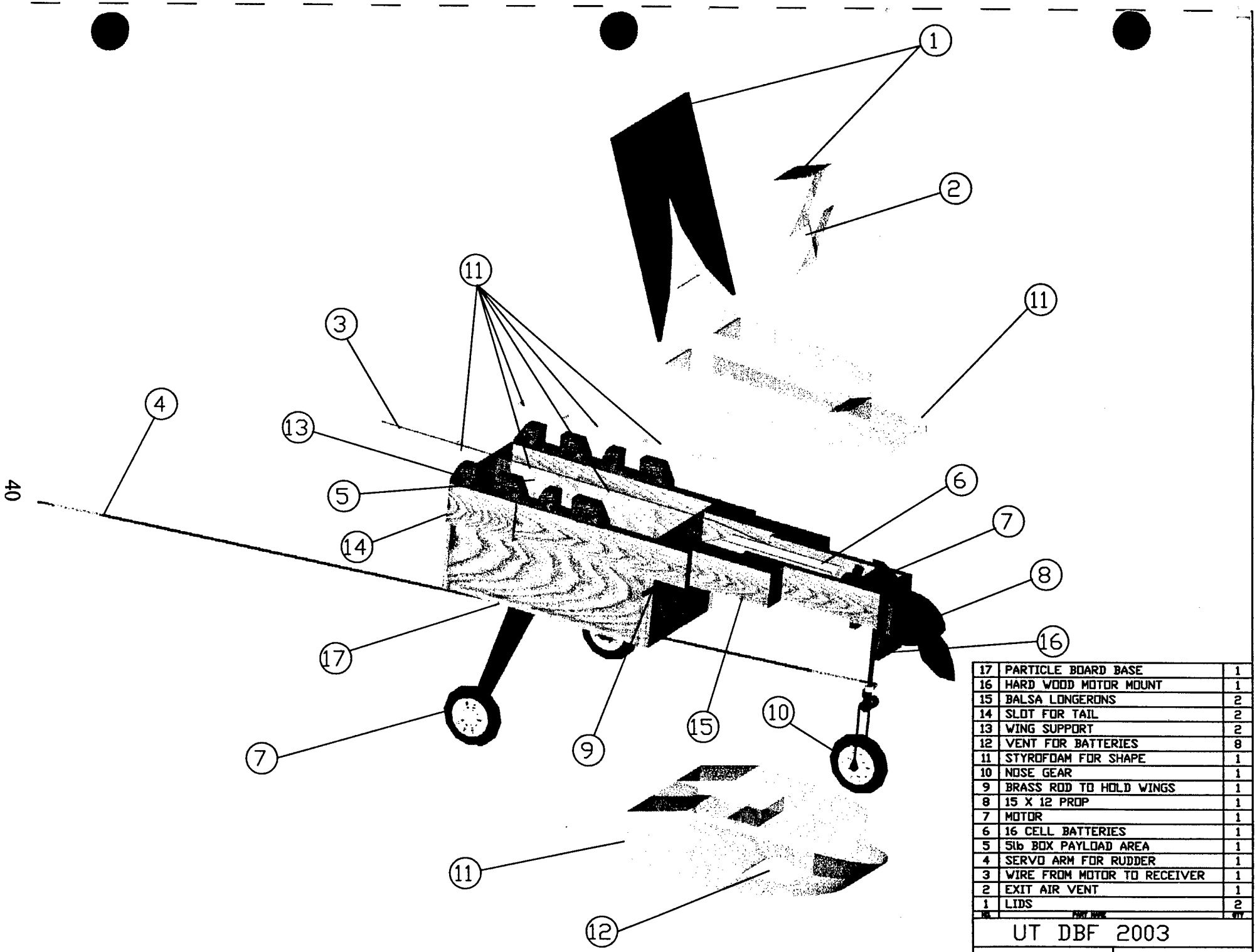

40

17	PARTICLE BOARD BASE	1
16	HARD WOOD MOTOR MOUNT	1
15	BALSA LONGERONS	2
14	SLOT FOR TAIL	2
13	WING SUPPORT	2
12	VENT FOR BATTERIES	8
11	STYROFOAM FOR SHAPE	1
10	NOSE GEAR	1
9	BRASS ROD TO HOLD WINGS	1
8	15 X 12 PROP	1
7	MOTOR	1
6	16 CELL BATTERIES	1
5	5lb BOX PAYLOAD AREA	1
4	SERVO ARM FOR RUDDER	1
3	WIRE FROM MOTOR TO RECEIVER	1
2	EXIT AIR VENT	1
1	LIDS	2
NO.	PART NAME	QTY

UT DBF 2003

DWG NO : 2 of 5 | SCALE : 1" = 1'

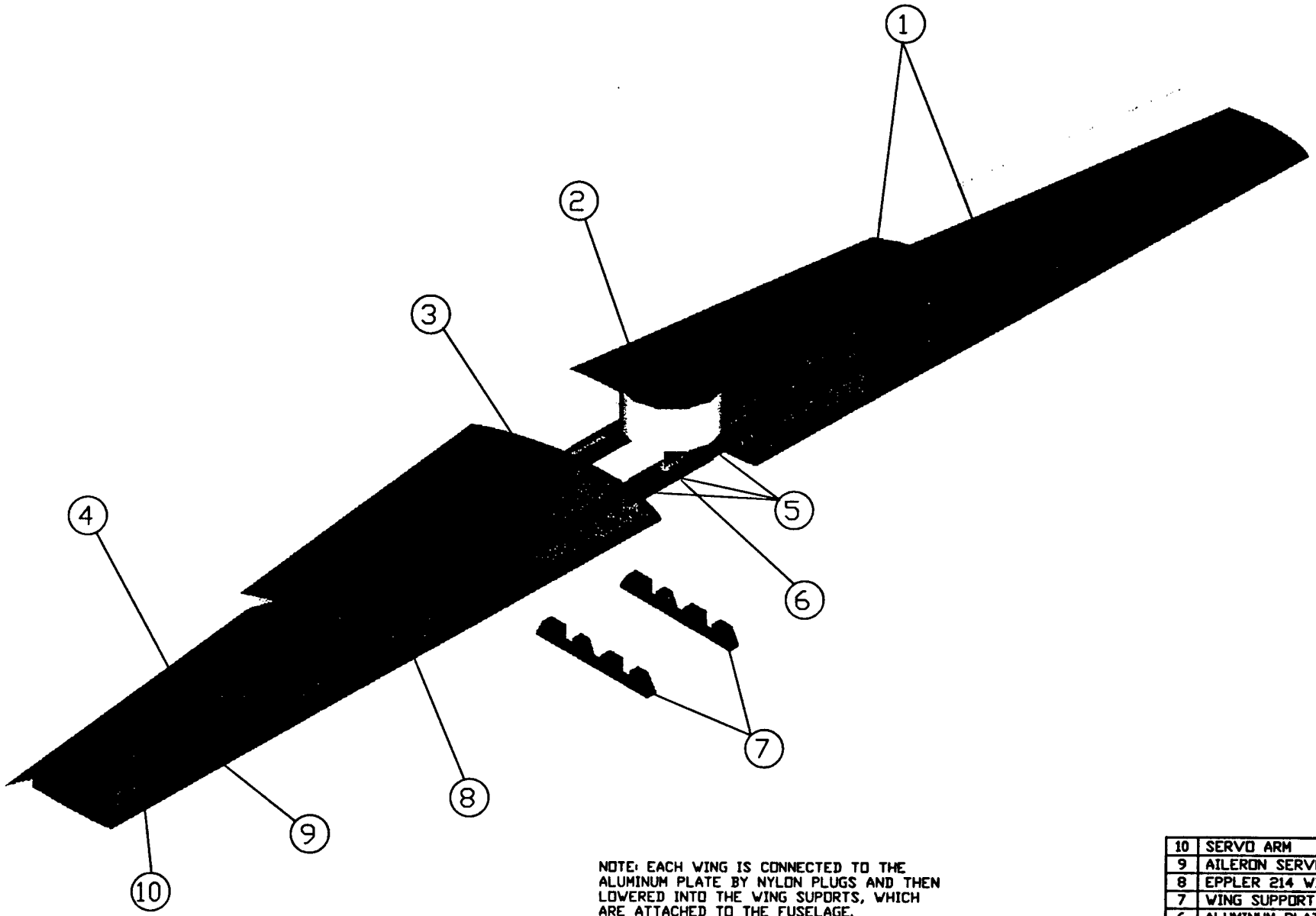

NOTE: EACH WING IS CONNECTED TO THE ALUMINUM PLATE BY NYLON PLUGS AND THEN LOWERED INTO THE WING SUPORTS, WHICH ARE ATTACHED TO THE FUSELAGE.
HARD WOOD ADDED TO PREVENT STRIPPING OF SPARS

NO.	PART NAME	QTY
10	SERVO ARM	2
9	AILERON SERVO	2
8	EPPLER 214 WING	2
7	WING SUPPORT	2
6	ALUMINUM PLATE	2
5	HARD WOOD	8
4	AILERONS	2
3	WIRE TO RECEIVER	2
2	ANTENNA	1
1	BALSA WING SPARS	4

UT D[illegible] 2003

DWG NO : 3 of 5 | SCALE : 1" = 1'

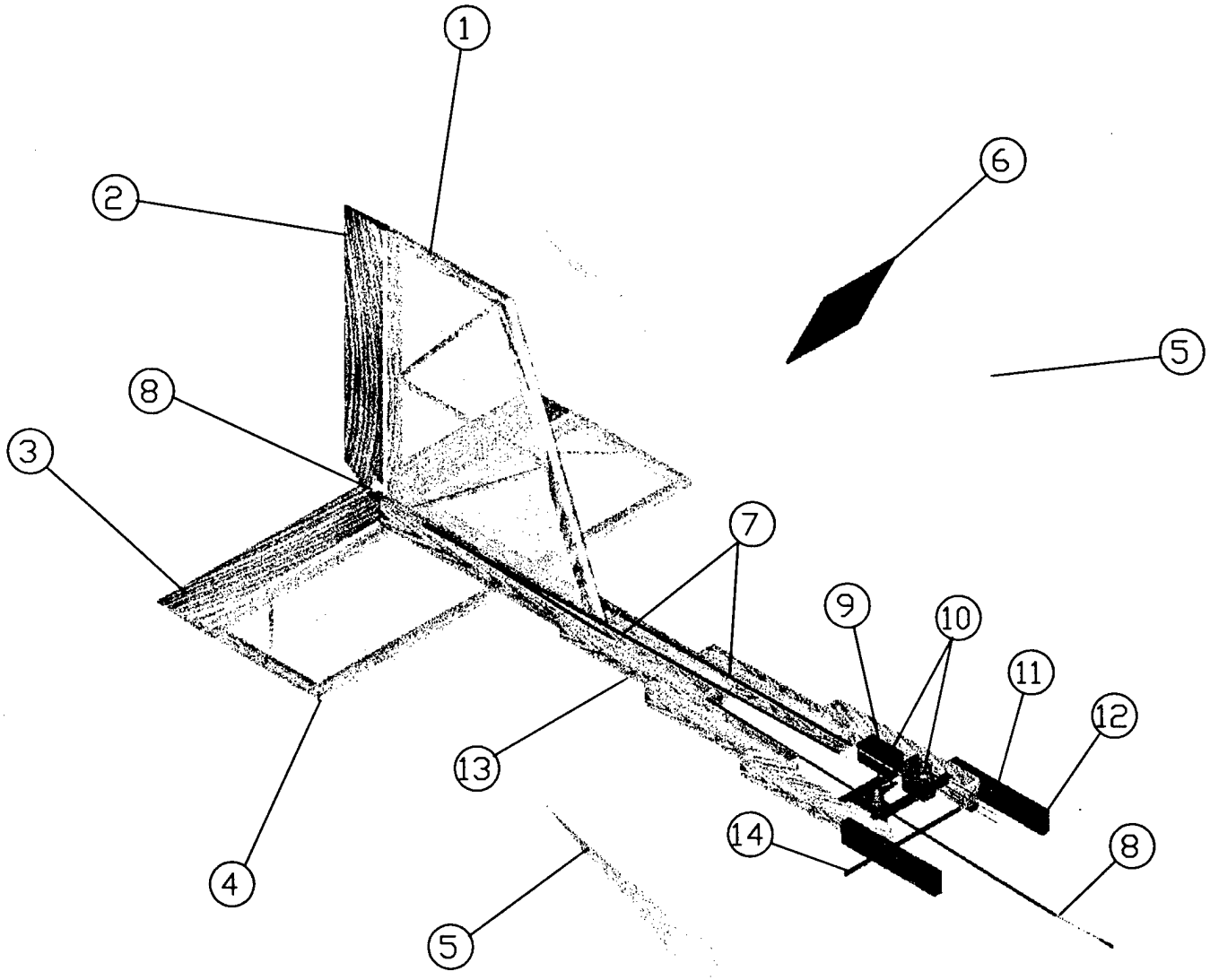

NOTE: HOLES CUT OUT IN STYROFOAM TO MINIMIZE WEIGHT. HARD WOOD PIECES SLIDE INTO ADJOINING SECTION ON FUSELAGE.

NO	PART NAME	QTY
14	BRASS RODS	1
13	BALSA	2
12	HARD WOOD	2
11	WIRES	5
10	SERVOS	2
9	RECEIVER	1
8	SERVO ARM CONNECTOR	2
7	SERVO ARMS	1
6	LID	1
5	STYROFOAM FOR SHAPE	2
4	HORIZONTAL TAIL	1
3	ELEVATOR	1
2	RUDDER	1
1	VERTICAL TAIL	1

UT DBF 2003

DWG NO : 4 of 5 | SCALE : 1" = 1'

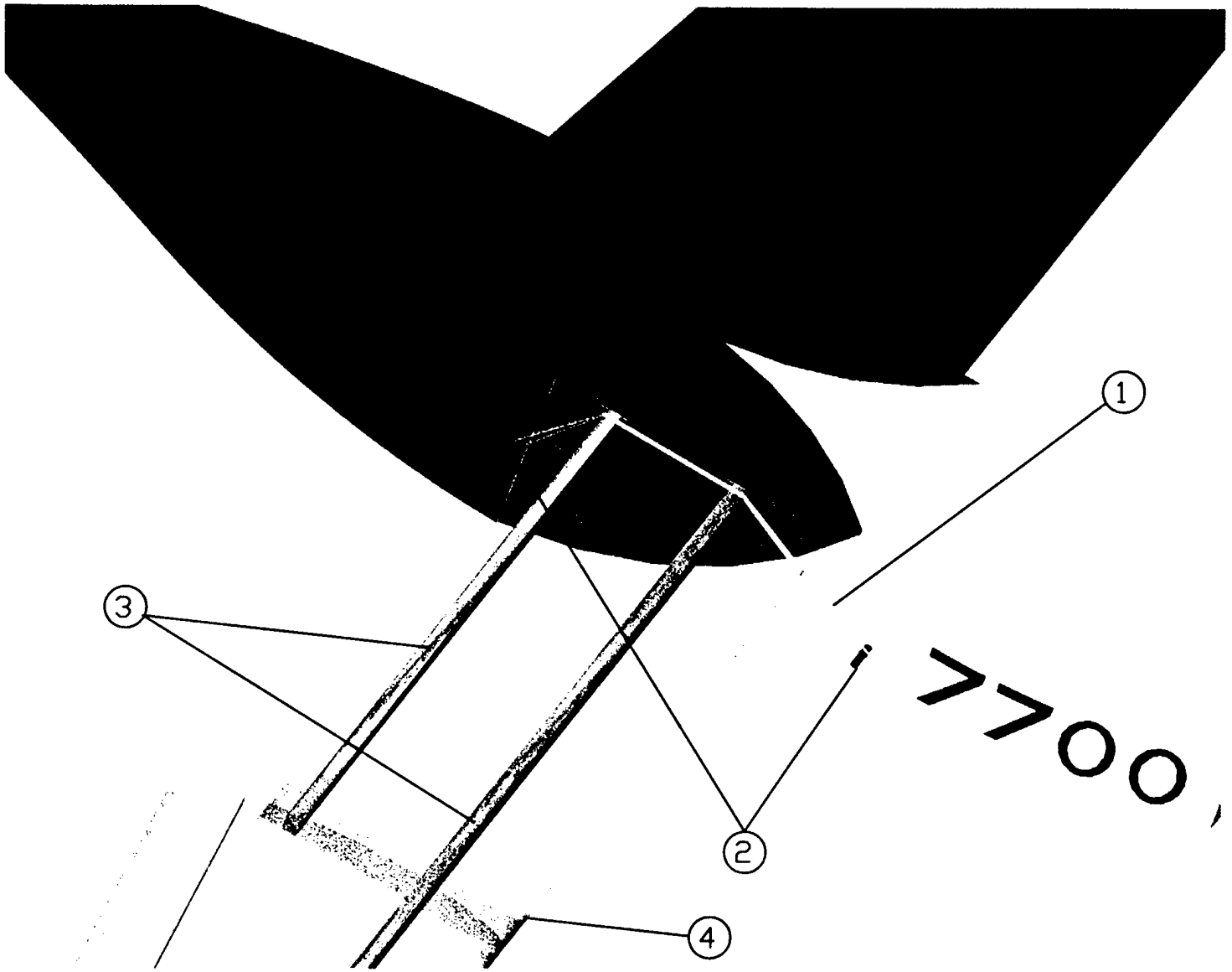

NOTE: WINGS ARE SECURED ONTO THE FUSELAGE WITH RUBBER BANDS BY THE BRASS RODS THAT ARE BUILT INTO THE FUSELAGE AND TAIL SECTION.
RUBBER BANDS ALSO KEEP THE TAIL IN PLACE.

NO.	PART NAME	QTY
4	FIBER GLASS	2
3	WING SPARS	4
2	BRASS ROD	2
1	RUBBER BAND	2

UT DBF 2003

DWG NO : 5 of 5

SCALE : 1" = 1'

5.3.2 Weight and Balance Sheet

In order to estimate the cg position of the plane, a weight and balance spreadsheet was created shown in Table 5.5. The total empty weight of the plane calculated from the individual parts was 11.05 pounds, in good agreement with the scale measurement for the entire plane, which was 11.18 pounds. The extra weight is most likely due to uncertainties in the weights measured. The missile decoy cg position found was 2.2 inches in front of the main gear and the antenna aircraft's cg position was 2.19 inches ahead of the gear. To more accurately determine the aircraft's cg, the load due to the aircraft on both the nose gear and main gear were measured with two scales so that the weight fraction on each could be measured. The cg found in this way contained little error and is reported in Table 5.5 as the actual cg position. The cg of the aircraft moves forward, towards the aircraft nose, when the antenna is placed on the aircraft. This has the advantage that some of the moment created by the antenna's drag is canceled out by the shift forward of the cg. Figure 5.2 shows the weight breakdown of the current aircraft in terms of percentages.

Table 5.5: Weight and Balance Spreadsheet.

	Weight (oz)	Position (in)
Empennage Assembly	31	-21
Front Fuselage Assembly	26	6
Wings	39.6	0
Propulsion Batteries	36.4	12.75
Motor Controller	2.2	17
Motor	14.1	19
Propeller/Spinner	5	21
Main Landing Gear	13	0
Nose Gear	5	19.5
Reciever Battery	3.4	-5.5
Reciever	1.1	-5
Payload	80	1.4
Antenna	14.4	2
MISSILE DECOY WEIGHT (lbf)	**16.05**	
MISSILE DECOY CG (in)	**2.20**	
ANTENNA WEIGHT (lbf)	**16.95**	
ANTENNA CG (in)	**2.19**	
ACTUAL MISSILE DECOY CG (in)	**2.51**	
ACTUAL ANTENNA CG (in)	**2.58**	

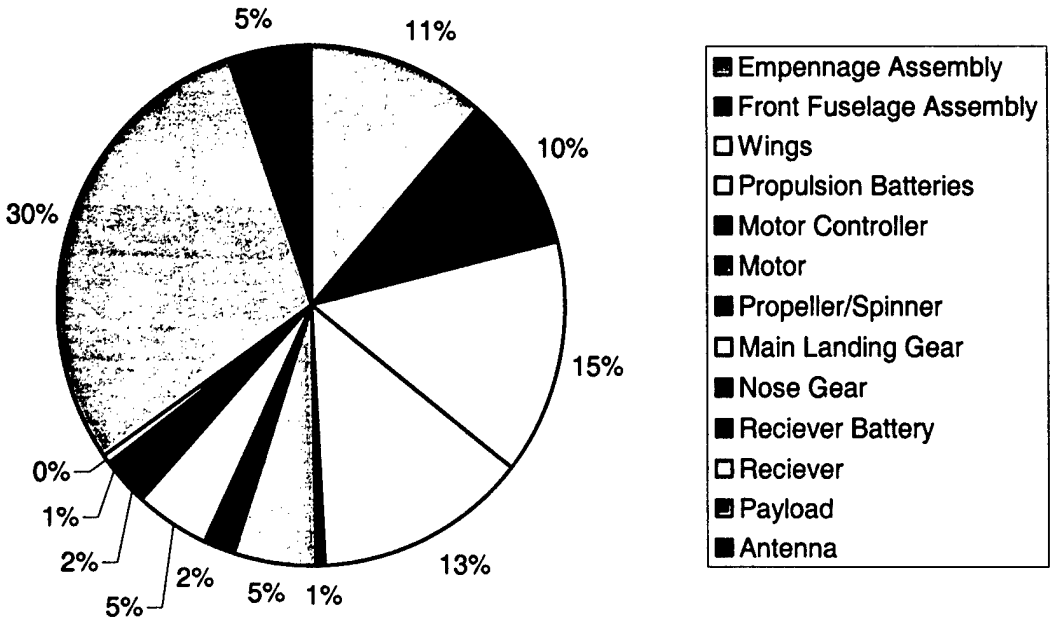

Figure 5.2: Component Weight Percentages.

5.3.3 RAC Calculation

An aircraft cost model is given in the contest rules in order to scale the aircraft. As stated in the rules the Rated Aircraft Cost, or RAC, is calculated by the following:

$$RAC = \frac{(100 * MEW + 1500 * REP + 20 * MFHR)}{1000} \qquad (5.1)$$

where MEW is the Manufacturers Empty Weight, REP is the Rated Engine Power, and MFHR is the Manufacturing Man Hours; all of which are defined in the contest rules. Table 5.6 shows the calculated RAC for the final aircraft design.

Table 5.6: RAC breakdown.

Description	Monoplane
MEW	**11.33**
REP	**2.275**
# of Engines	1
Total Battery Weight (lb)	2.275
MFHR	**191.7**
Wings	*80*
Wing Span (ft)	8.17
Max Chord (ft)	1.08
# of Control Surfaces	2
# of Wings	1
Fuselage	*56.7*
Fuselage Length (ft)	5.67
Empenage	*20*
Vertical Surfaces w/no control	0
Vertical Surfaces w/ control	1
Horizontal Surfaces	1
Flight Systems	*25*
# of Servos	4
# of Motor Controllers	1
Propulsion Systems	*10*
# Engines	1
# Propellers	1
TOTAL RATED AIRCRAFT COST	**8.38**

5.4 Ongoing Aircraft Optimization

Following the successful flights by the aircraft, the team began investigating ways to improve the aircraft's performance. Since the department was also willing to give more money to the team in order to improve the plane and guarantee that the aircraft could compete at the competition, we were able to investigate the use of a different motor.

5.4.1 Motor Optimization

The first area of improvement investigated was the purchase of a new motor. The rules of the competition require the motors be brushed Astroflight or Graupner motors; however, since the Graupner motors are difficult to obtain, they were not considered. The team investigated 15 different Astroflight motor/gearbox combinations. These motors with their respective gearboxes were examined with the aid of the commercial program Motorcalc.

The analysis was performed by iterating over many different combinations of propeller geometry and number of batteries. Propellers with diameters between 5 and 20 inches and pitches between 5 and 20 were entered into Motocalc. Next, the battery specifications and the number of cells (between 12 and 18) were entered into Motocalc. The choices that resulted in final motor temperature less than 250 ^{0}F were set aside for further examination. These motors were then analyzed to determine if they could provide a minimum 75% of ideal static thrust (3.9 lbf) and 90% of pitch velocity (54 mph). The thrust cutoff was 75% because when compared with propeller tests, Motocalc predictions were typically 10% or more below the actual value. The Table below shows properties of the motors able to provide 85% of the ideal pitch speed and ideal thrust while maintaining a motor temperature less than 350 ^{0}F. While this temperature seems high, propeller tests showed that the temperature predictions were off by ~50%.

The analysis showed significant promise in the Astroflight Cobalt 15 motor with 3.69:1 gearing. With several different configurations this motor should, in theory, provide the necessary thrust and pitch speed, but only weigh half of the Cobalt 25 motor that the plane currently uses. Table 5.7 shows the various possible configurations. The two most attractive propeller configurations are shown in bold which are the 16x13 propeller with 14 cells and the 15x11 propeller with 15 cells. The 14x16 propeller would be better, but the motor temperature is high. On the other hand, the 15x11 propeller provided the same static thrust and pitch speed, but was cooler because of the extra battery. Both combinations will be tested when the motor arrives.

Table 5.7: Astroflight Cobalt 15 Configurations Examined.

Number of Cells	Diam (in)	Pitch (in)	Temp (°F)	Thrust (lbf)	Pitch Speed
14	15	13	260	4.0	60.6
14	**16**	**13**	**312**	**4.5**	**56.2**
14	16	14	329	4.3	59.0
14	16	15	346	4.2	61.7
15	14	11	221	3.9	59.3
15	14	12	233	3.8	63.6
15	**15**	**11**	**265**	**4.6**	**55.7**
15	15	12	282	4.5	59.4
15	15	13	299	4.3	62.9
15	16	13	362	4.7	57.8
16	14	11	248	4.3	61.9
16	15	11	303	4.9	57.7
16	15	12	324	4.7	61.3

5.4.2 Aircraft Wings

The current wings on the plane are solid Styrofoam; however, they were originally supposed to be ribbed to save weight. By constructing the wings out of quarter-inch ribs every 3 inches, the wing could be made half a pound lighter. Also, the use of two spars was deemed unnecessary, except at the very root of the wing so that the rubber bands can have two points to secure the wing against rotation. The elimination of most of the second spar requires that the wing be slightly redesigned so that the quarter chord sweep is zero degrees. This allows the single spar to be built along the quarter chord and still be straight. The new wing design will have 3 inches of foam with a fiberglass skin to stiffen the foam at the root. The main spar will be made of a balsa and fiberglass, as well as light ply at the root for crush resistance and strength. The second spar will be made out of balsa and be present only in the first foam section. This new design should lighten the wing by ~0.7 pounds to a total weight of ~1.8 pounds.

5.4.3 Tail Assembly

The tail assembly longerons were thick in order to stiffen the tail to torsion; however, they were originally designed as an open-cell member. If the tail longerons were made as a closed cell member with a thin (3/16") layer of birch connecting the two longerons, the longerons could be made significantly thinner. This would lighten the aircraft by ~0.25 pounds.

5.4.4 Tail Incidence

After the first flight test (see section 7.2.1) the wing was put at a 4 degree angle of attack. This increased the downwash on the tail to 2.7°. With the tail's low aspect ratio, this resulted in a large amount of induced drag from the tail as well as an increase in the effective weight of the plane. Because the moment coefficient of the airfoil was not correct, the tail was now pushing down with ~1.7 lbf. This means that the wings must produce 1.7 lbf more to counter the tail and lift the aircraft. The wings therefore need to be restored to a zero degree angle of attack and moved forward by ~2 inches. The tail would also need to have a 1° angle of attack to further reduce the downwash. This would reduce the static margin, which was already too large, to a more reasonable 0.05. This will be accomplished over several test flights to ensure that the reduction in static margin is not too large. First it will be reduced to 0.17, then to 0.11, and then, if the pilot believes it is reasonable, to 0.05. Even without reducing the static margin to 0.05, significant performance gains can still be achieved.

5.4.5 Number of Batteries

The RAC of the aircraft is strongly influenced by the number of batteries that the aircraft requires. Therefore, propeller tests are still being run in an attempt to further reduce the number of batteries needed. Also, as the aircraft weight is reduced, the number of batteries needed will decrease in order for the aircraft to takeoff in 120 feet. If the aircraft weight reduction goals outlined above are met, then the aircraft will effectively weigh ~2.8 pounds lighter. This

corresponds to a reduction in the static thrust needed of 1.5 lbf to T_o = 3.75 lbf. It would then be possible to reduce the number of batteries to 12 and still meet the static thrust and pitch requirements.

5.4.6 Assembly Time

The current assembly time for the aircraft is unacceptabley long. This is due to the large number of bolts that must be tightened in order to assemble the aircraft. There are four to attach the wing, six to attach the landing gear, and two for the vertical tail. These bolts comprise most of the assembly time of the current aircraft. If they were replaced by nylon 'snap' bolts this time could be significantly reduced. The nylon 'snap' bolts would also save a small amount of weight.

5.4.7 Payload Deployment Mission

The final possible improvement to the flight score that the team is investigating is to perform the payload deployment mission. If done well, the mission has the possibility of scoring better than the missile decoy mission and so several team members are building another front fuselage section that will contain an extra servo to allow a hatch to open and the payload to drop out. The main difficulty that must be overcome is that the main gear is currently in the way.

6.0 MANUFACTURING PLAN

The design and construction of the UT-DBF aircraft was highly influenced by previous year's experience but also included several significant innovations for the team. For the initial aircraft, aspects such as simple construction and design were judged more importantly than other factors. After flight testing however, these pieces were redesigned to reduce weight and increase efficiency.

6.1 Figure of Merits

A figure of merits system was developed to determine how the aircraft's components would be designed and built. These merits included performance advantages, weight estimation, construction skill, and construction time. Although the cost of the materials is a concern, the variance of price for the designs was not significant enough to warrant a figure of merit. The figure of merits and the designs discussed are in Table 6.1.

6.1.1 Performance

The performance of the component was considered the most important figure of merit. How the component may affect the aircraft's drag and controllability is taken into account for performance. Also, performance is considered in how the design technique adversely affects and connects to other components of the aircraft. This figure of merit was given a weight of 3.

6.1.2 Weight Estimation

Due to the restrictive takeoff requirement, saving weight became a critical concern for the aircraft. Weight estimations were considered for the component designs and were given a figure of merit weight of 3.

6.1.3 Construction Skill Required

Most members of the team were previous DBF veterans and were thoroughly experienced in the typical construction techniques. New designs however were presented this year that warranted the need for a construction skill figure of merit. If the new design is too complicated, it may actually be less effective than the older proven techniques. This figure of merit was given a weight of 2.

6.1.4 Construction Time Required

As with any project, extensive amounts of time could not be devoted to minor components. However, the more time spent on an individual part typically corresponds with higher quality. A balance had to be found between the two when choosing component designs. For these reasons, a figure of merit with a weight of 1 was given to the construction time required.

6.2 Manufacturing Processes Investigated

Although all of the aircraft's components received design attention, some parts needed extra consideration and discussion. Those particular components are listed below and had the figure of merits system applied to them.

Table 6.1: Manufacturing Plan Figure of Merit.

	Option	Time Required (x1)	Skill Required (x2)	Performance (x3)	Weight Estimation (x3)	Final Score
Fuselage	Cylindrical - Foam	0.8	0.6	1	1	8
	Cylindrical - Balsa	0.7	0.6	1	0.9	7.6
	Streamlined Shape	0.9	0.9	0.9	1	**8.4**
Wing Materials	Full Foam	1	1	1	0.6	7.8
	Foam Ribbed	0.7	0.9	0.9	1	**8.2**
	Balsa Ribbed	0.6	0.8	0.8	0.4	5.8
Wing Sweep / Spar	Swept Forward - 1 Spar	1	1	0.7	0.9	7.8
	Swept Forward - 2 Spars	0.9	0.9	0.9	0.9	**8.1**
	Unswept	0.8	0.8	0.7	0.8	6.9
	Swept Back	0.6	0.7	0.4	0.4	4.4
Spar Materials	**Simple Balsa Sticks**	1	1	0.9	0.9	**8.4**
	Fiberglassed Balsa Sticks	0.7	0.8	1	1	8.3
	Aluminum Rods	0.7	0.7	0.7	0.5	5.7
	Carbon Rods	0.4	0.4	0.8	0.9	6.3
Wing Attachment	Wingbox /w Attachment Tabs	0.8	0.9	0.9	0.9	8
	Reinforced Connection	0.7	0.7	0.8	0.9	7.2
	Rubber-bands	1	1	1	1	**9**
Tail Design	Airfoil Shaped	0.8	0.7	1	0.9	7.9
	Balsa Frame	1	1	0.8	1	**8.4**
Empennage Design	Aluminum Rod	0.9	0.8	0.7	0.7	6.7
	Torsion Box	0.7	0.7	0.7	0.7	6.3
	Angled Balsa	0.8	0.5	0.9	0.9	7.2
	Step System Balsa	1	1	0.9	0.8	**8.1**

6.2.1 Fuselage Construction

The manufacturing of the fuselage for the desired shape and strength had to be analyzed. Shapes for the fuselage included an airfoil shape, a cylindrical shape, and also a general streamlined shape. The airfoil shape was dismissed because of aerodynamic reasons. The cylindrical shape could be constructed by two methods. One consisted of cutting styrofoam into the round shape and then sanding down the front and rear sections for a smooth transition. The second method involved creating many circular balsa ribs that would be wrapped with Econokote for a smooth shape. Since the cross-sectional area for the motor mount, payload box, and control surface attachment were all fixed, a general streamlined shape matching these dimensions would fit better than a set cylindrical shape. Styrofoam could easily be shaped to fit the transition

between these components. Therefore, the general streamlined shape was thought to be the easiest to construct.

6.2.2 Wing Materials

Several wing construction designs were investigated including a full foam wing, a foam ribbed wing, a balsa ribbed wing, and a built-up combination wing. The full foam wing was by far the easiest and quickest to construct but also potentially the heaviest. A foam-ribbed wing is very light but has a greater workload. A new idea for this year was the built-up combination wing that consisted of a foam leading edge and balsa sheets for the remaining area of the wing. The combination wing was believed to be the most complicated and also most time extensive design. Its promise of weight savings was debatable but very possible.

6.2.3 Wing Sweep / Spar

The spar through the wings was also a major factor in the design of the wing. The aircraft's wing could be swept forward, back, or unswept without a significant change in aerodynamics, but with major structural considerations. In the swept-forward arrangement of the wing, a primary heavy-duty spar could be located near or slightly forward of the average quarter-chord and a second smaller spar could be located closer to the rear. Since the aircraft's wings taper down, the smaller rear spar would not be able to continue through the entire length of the wing. The cross sectional area near the quarter chord of the wing closer to the tip would be sufficiently large for a single front spar to handle the load alone. The swept back arrangement of the wing would be the most difficult to handle structurally because the quarter-chord would be angled back and its cross-sectional area taper down substantially. Multiple spars, including possibly angled spars, would be needed to be able to support this structure, and the swept back arrangement would result in a wing spar to fuselage connection nightmare. The unswept wing would share some problems of the swept back wing because the leading edge of the wing still sweeps back, resulting in a shifting quarter-chord.

6.2.4 Spar Material

The considered materials for the spars included simple balsa sticks, fiberglassed balsa sticks, aluminum rods, and carbon rods. The simple balsa sticks were the easiest to buy and taper if necessary for the spar. Fiberglassing the spar greatly increases its strength but also the weight and construction time. Aluminum rods are the most restrictive in terms of design. Metal work cannot be machined easily so the wing would practically have to be designed around the spar. Carbon rods have the potential for great strength with low weight, but for the high quality of construction needed, the carbon is a questionable material to use successfully.

6.2.5 Wing Attachment

The method of attachment of the wings involved unique difficulties. To not affect the center of gravity of the aircraft, the payload box had to be placed underneath the location of the wings. A high wing was decided for stability, but a simple way to access the payload box was not an easy challenge. One idea investigated was a wingbox that the wings' spars slid into which had attachment tabs to hold the wingbox onto the fuselage. A second idea involved a technique in which part of the wing's spar would slide into a reinforced connection in the fuselage above and on either side of the payload. To stiffen the structure sufficiently, a removable carry-through box would be located over the payload that attached to both wings. The last idea was actually a method used by many radio-controlled modelers. High-strength rubber bands would be strapped over the wing spars and wrapped around pins forward and aft of the wings. A removable carry-through box connected to both wings would be necessary for the rubber bands to function properly.

6.2.6 Tail Design

Several techniques were studied for the vertical and horizontal surfaces. The traditional foam symmetrical airfoil over balsa spar technique was a proven UT-DBF method but required significant time. A rectangular balsa frame with Econokote covering resulted in a simple flat plate design. Although not aerodynamically the best solution, this idea was also considered.

6.2.7 Empennage Design

The only major manufacturing difficulty remaining was the design of the aircraft's empennage. The tail had to be removable to fit within the contest's required packaging box. Due to the long distance required for the light-weight support from the payload box to empennage, flutter became a concern in the design. A single aluminum rod extending back, a torsion box, angled balsa pieces, and lastly a step down system of balsa pieces were all considered. The aluminum rod and torsion box would not need to taper down but would be more difficult in attaching to the central fuselage. The angled balsa pieces would be able to taper from the required width of the payload box down to a reasonable area for the control surfaces to attach to, but creating a precise angle with the needed tolerances was considered very challenging. The step system would compose of balsa pieces epoxied one inside the other as it approached the rear end of the aircraft. At the wide payload box, the structure would be easy to connect, because it would be able to fit on either side of the box, but the step system would taper down for the control surfaces.

6.3 Final Manufacturing Process

6.3.1 Wings

The wings of the aircraft were the first pieces of the aircraft constructed. A double spar technique with a swept forward wing was determined to be the best solution. The spars were simple balsa

sticks with the front spar slightly larger than the rear spar and both tapering down through the wing. The front spar was continuous through the entire length of the wing but also extended an additional 3" at the root to be able to slide into the carry-through box. The rear spar also included the additional 3" at the root but ended halfway through the wing. To further strengthen the connection point between the wings and fuselage, fiberglass was added around the inner 6" of both the front and rear spars. West System 105 Epoxy Resin and 205 Fast Hardener was mixed and applied to 1.7 oz fiberglass as it was wrapped around the balsa. For the initial aircraft, the quick and simple solid foam wing technique was utilized to construct the wing. The competition version of the aircraft's wings, after the aerodynamics were proven, will instead have the lighter and more labor-intensive foam rib technique.

Templates were first designed using AutoCAD 2002 software to create an airfoil shape with slots for the inner two spars. Super 77, 3M spray adhesive glue, attached the paper template designs onto thin balsa sheets. These balsa sheets were cut out with a knife to complete the template. The templates were placed onto the appropriate width sheet of styrofoam and cut out using a hot-wire. With the wing shape created, the spars were then epoxied into the wing using the same West System's Resin and Hardener. Fiberglass, about 3" wide, was wrapped around the mid-section of the wing, where the rear spar ended, so the loads would transfer as required. After a 24 hour setting time, slits were cut into the foam for servo wiring and a hole was also cut to mount the servo inside the wing. Ailerons were created by simply cutting off the appropriate portion of the wing with the hot-wire. Top Flite's Econokote plastic covering was hot-ironed onto the wing to smooth its surface. The carry-through box was built out of 26-gauge zinc sheet metal. The zinc was bent into a U-shape with a clamp, and then holes were drilled for pins to hold the wing in place.

6.3.2 Landing Gear

The main landing gear was store-bought stock landing gear. Mounting holes were drilled at the top of the landing gear so that it may connect to the fuselage. The nose gear was also a stock gear bought commercially. The gear was allowed to pivot by utilizing the supplied plastic mounts, which were attached to the motor mount. A plastic steering attachment was also added to the nose gear to allow a push rod to be attached. This push rod would also be connected to the rudder so the nose gear could be steered in unison.

6.3.3 Empennage

Both the vertical and horizontal surfaces were built similarly. Balsa sticks were glued together with Elmer's glue to form the frame of each surface, and smaller crossways balsa sticks were glued to stiffen the frame. A half-cylindrical shaped balsa stick was added to the front of the frame as the leading edge. The actual control surfaces were thick balsa sheets that had been cut and

sanded into a trailing edge shape. Small, high strength paper tabs attached the control surfaces to the actual vertical and horizontal stabilizers. Nylon servo control horns were then mounted to the rudder and elevator to allow the push rods to be connected. To cover the vertical and horizontal surfaces, Econokote was ironed onto the frame after which a heat-gun was used to tighten the covering.

6.3.4 Front Fuselage

The fuselage was one of the more complex portions of the aircraft. First, a heavy-duty wood sheet was cut to shape and used as the base of the payload box. Thin balsa sheets were then epoxied and fiberglassed onto the edges of the base wood as walls for the payload. Holes were also drilled in the bottom of the box to mount the landing gear. A combination of balsa sticks with 1.7 oz fiberglass was used to create the mounting insert for the tail section to slide into. After that, poplar strips were cut and epoxied onto the top edges of the box to strengthen the frame, and additional poplar pieces were epoxied on the top of the box to act as "stoppers" so the wings would not slide forward or aft.

A step down system of balsa sticks was utilized as the motor support structure. Beginning on the side near the front of the payload box, sticks of balsa were epoxied one inside the other to extend out the nose of the aircraft. The step system tapered down to the appropriate size for the motor mount. Templates were then designed to create a smooth but blunt nose to the aircraft. Pieces of styrofoam were cut with these templates and after which positioned onto the front of the aircraft. Additional holes were cut out of this styrofoam to make room for the batteries and to add a cooling vent for the batteries. Next, hatches were created out of styrofoam to access both the batteries and motor and the payload box. Additional styrofoam was glued with Elmers as needed to create a uniform aerodynamic shape around the payload box. All parts were then covered with Econokote to finalize the streamline shape. Lastly, a brass tube was inserted slightly in front of the payload box through the motor support structure. This tube is used to wrap the rubber bands around when attaching the wings.

6.3.5 Rear Fuselage

A dual longeron step system was used connect the back portion of the payload box to the rear control surfaces of the aircraft. High strength wood was epoxied to the front of the step down system that would be able to insert into the mounts on either side of the payload box. Servo mountings were built with poplar and placed near the front of the rear fuselage support structure. Push rods connected these servos to the elevator and rudder. A second brass rod was installed near the front of the step down structure to assist in attaching the wings and also holding the empennage into place. The aft design of the step down system allowed the vertical tail to slide into place with screws to hold the vertical on. The horizontal tail was epoxied permanently to the

end of the step down structure to stiffen it further. Similarly to the front of the aircraft, templates were created and foam was cut to create a styrofoam aerodynamic covering. Lastly, Econokote was hot ironed and tightened with a heat gun to cover the entire structure.

6.4 Manufacturing Timeline

A manufacturing timeline was created in order to guide the construction of the aircraft. It is shown in Table 6.2.

Table 6.2: Manufacturing Timeline.

TASK	START DATE	FINISH DATE	ACTUAL DATE COMPLETE
Wings	**1/17/03**	**1/20/03**	**1/21/03**
Make Templates	1/17/03	1/17/03	1/17/03
Make Wing Spar	1/17/03	1/18/03	1/18/03
Cut Stryofoam	1/18/03	1/18/03	1/18/03
Cut Control Surfaces	1/18/03	1/18/03	1/19/03
Add Servos / Wiring	1/18/03	1/18/03	1/19/03
Attach Wing Spar	1/19/03	1/19/03	1/20/03
Monokote and Finish Wings	1/20/03	1/20/03	1/21/03
Empennage	**1/13/03**	**1/20/03**	**1/19/03**
Make Inner Support Structure	1/13/03	1/14/03	1/15/03
Build Frame for Stabilizers	1/13/03	1/14/03	1/15/03
Build and Attach Control Surfaces	1/14/03	1/15/03	1/16/03
Design Templates for Rear Fuselage	1/14/03	1/15/03	1/15/03
Econokote Stabilizers	1/15/03	1/16/03	1/16/03
Cut Styrofoam for Rear Fuselage	1/15/03	1/16/03	1/16/03
Mount Servos / Push Rods	1/16/03	1/17/03	1/18/03
Attach Styrofoam	1/17/03	1/18/03	1/18/03
Econokote Rear Fuselage	1/18/03	1/20/03	1/19/03
Fuselage	**1/13/03**	**1/20/03**	**1/20/03**
Build Payload Box Support	1/13/03	1/15/03	1/14/03
Build Motor Mount	1/13/03	1/14/03	1/16/03
Make Motor Support	1/15/03	1/16/03	1/15/03
Design Templates for Front Fuselage	1/15/03	1/16/03	1/15/03
Reinforce Box Components	1/16/03	1/17/03	1/15/03
Cut Styrofoam for Front Fuselage	1/16/03	1/17/03	1/17/03
Attach Landing Gear and Motor Mount	1/17/03	1/18/03	1/17/03
Attach Styrofoam	1/18/03	1/19/03	1/18/03
Econokote Front Fuselage	1/19/03	1/20/03	1/20/03
Build Carry-Through Structure	1/19/03	1/20/03	1/20/03

7.0 TESTING PLAN

7.1 Static Tests

Several static tests were performed before the first flight in order to verify theoretical expectations. The first was the propeller tests mentioned in the detail design phase to verify that the static thrust produced by the motor configuration would be sufficient. Second, the aircraft was dropped from 2 feet off the ground to verify that the landing gear could withstand a hard landing. The last major static test performed was the wingtip test, where the fully-loaded aircraft was lifted by the wingtips. All tests were successful and so the aircraft was cleared for its first flight.

7.2 Flight Test Check List

Prior to each flight, the following check list was completed to ensure the airworthiness of the aircraft.

1. Aircraft surfaces are undamaged and clean.
2. Check rubber bands tightness. Wing and tail components are securely fastened to the fuselage.
3. Check that landing gear is securely fastened. Vertical tail is properly secured. Propeller / spinner has been installed properly.
4. Check control surfaces (rudder, elevator, and ailerons) for deformations and excess play in their movement. Check for solid connection between servo arms, horns, and extension rods.
5. Servo and battery wires are snuggly fit. Receiver and transmitter battery power sufficient.
6. Hatches are completely closed and secured.
7. Switch on the receiver. The rudder, elevator, nose gear, and ailerons all rotate in the proper direction. Motor successfully engages / disengages. Controls continue to operate correctly with the motor on full power. Range check.
8. Check alignment of nose gear.

7.3 Flight Tests

7.3.1 February 1, 2003

The first flight test of the aircraft occurred on February First. The aircraft had actually been completed two weeks earlier; however, weather and pilot availability prevented an earlier flight. On the first flight the pilot tested the handling qualities and the glide capabilities of the aircraft without any payload. The main goal of the flight was to verify stability and prove the aircraft flight worthy. The flight was a success; however, the aircraft did initially pitch down on takeoff and the pilot noticed that the aircraft needed a large amount of trim in order to fly level at cruise. This

was attributed to the larger than expected moment coefficient of the airfoil used. As mentioned earlier, the moment coefficient was not given empirically on the UIUC website and so Javafoil was relied upon to give an estimate of the moment coefficient. Since the wings could not easily be moved forward to account for the extra nose down moment, the temporary solution was to raise the angle of attack of the wings by four degrees. This correspondingly increased the downwash angle on the horizontal tail and provided the appropriate nose up moment. This was not deemed a permanent solution since it solved the problem by making the airplane more inefficient. It effectively made the plane 1.7 pounds heavier by having the tail at a negative angle of attack and it increased the drag coefficient of the aircraft by ~0.004. The extra effective weight would make the takeoff distance larger and both would lower the cruise velocity. Cooling holes were also added for the motor since it was hotter than desired at the end of the 3 minute flight. Finally, the pilot felt that there was more play than was desirable in the elevator and rudder. This was because the push rods that connected the servos to the control surfaces were not securely fastened to the frame of the aircraft and were therefore buckling. This was resolved before the next flight.

7.3.2 February 9, 2003

The goal of the second flight test was to verify the correction to the level flight trim condition and to fly the aircraft with the five pound weight. The flights were successful on both accounts and the aircraft was flown for ~7 minutes with over 2 minutes of glide time. Also, this flight was performed in heavy crosswinds (~12 mph). The first takeoff was aborted when the aircraft tipped over onto its wings due to a strong gust. The next takeoff was uneventful and so the tipping problem was deemed acceptable.

7.3.3 March 8, 2003

Further flight tests were delayed until the weekend before the paper was due because the weather was poor and the aircraft was to be presented at Explore UT. The third flight test's goal was to fly the aircraft with the antenna and measure the cruise velocity and the takeoff distance. On the first takeoff attempt the aircraft lost motor control about 7 feet off the ground and the pilot was able to nose the plane down and land gently enough in the grass. It was discovered upon investigation that the battery packs used had a loose connection and that most likely it was responsible for the power loss. It was decided to fly the aircraft with the two 8-cell packs that the team had; however, the static thrust and pitch speed of the propeller were slightly lower with the 16 cell configuration. The takeoff distance was predicted at almost exactly 120 feet; however, the plane lifted off at around ~110 feet. The aircraft's predicted cruise velocity with the reduction in static thrust, pitch speed, extra drag, and 'weight' from the tail accounted for was 44 mph. The measured cruise velocity was 35 mph; however this was with a ~7 mph headwind. The aircraft also flew the entire course in 320 seconds; slightly longer than the predicted time. This was most

likely due to the slower cruise velocity and the larger than expected loops the aircraft made. Due to the success of this flight, 16 cells will be used for the competition as of the writing of the paper, instead of 18 cells.

8.0 REFERENCES

[1] Craig, Roy R. Jr., *Mechanics of Materials*, 1st ed., John Wiley & Sons, 1996.

[2] Hull, David G., *Introduction to Airplane Flight Mechanics*, Department of Aerospace and Engineering Mechanics , The University of Texas at Austin, Fall 2001.

[3] McCormick, Barnes W., *Aerodynamics, Aeronautics, and Flight Mechanics*, John Wiley & Sons, 1979.

[4] Nelson, Robert C., *Flight Stability and Automatic Control*, 1st ed., McGraw-Hill, 1989.

[5] 'UIUC Applied Aerodynamics Group' http://amber.aae.uiuc.edu/~m-selig/

UNIVERSITY OF CALIFORNIA, SAN DIEGO

Design Report

Furious Flier

March 11, 2003

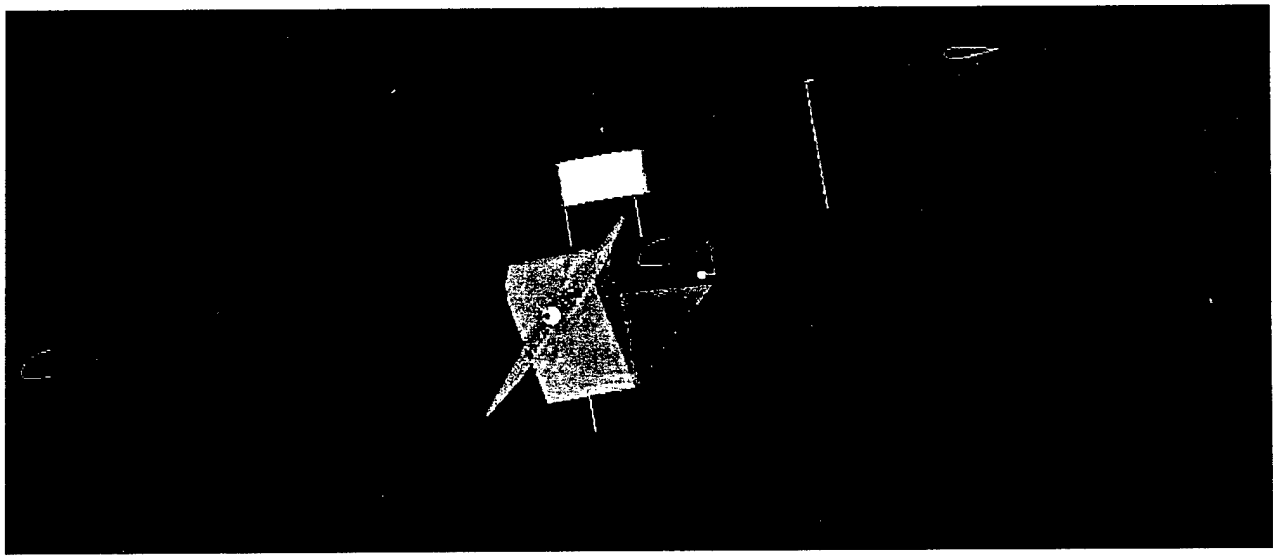

Table of Content

1.0 Executive Summary 4
1.1 Objective 4
1.2 Analytical Tools 4
1.3 Conceptual Design Phase 5
1.3.1 Goals 5
1.3.2 Methodology 5
1.4 Preliminary Design Phase 5
1.4.1 Goals 5
1.4.2 Methodology 6
1.5 Detailed Design Phase 6
2.0 Management Summary 7
2.1 Team Personnel 7
2.2 Sub-team Responsibilities 7
2.2.1 Propulsion 8
2.2.2 Structure 8
2.2.3 Aerodynamics 8
2.2.4 Stability/Controls 8
2.2.5 Performance 8
2.2.6 Construction 8
2.2.5 Task Scheduling 9
3.0 Conceptual Design 11
3.1 Design Parameters 11
3.1.1 Main Design Parameters 11
3.1.2 Rated Aircraft Cost 11
3.2 Aircraft Configuration 11
3.2.1 Fuselage and Tail Configuration 11
3.2.2 Wing Configuration 12
3.2.3 Landing Gear Configuration 13
3.2.4 Selecting a Payload Deployment System 14
3.3 Determining the Power Plant Configuration 15
4.0 Preliminary Design Phase 17
4.1 Determining the Optimum Number of Batteries 17
4.2 Motor Selection 18
4.3 Trade Study of Planform Area 19
4.4 Optimizing Tail Sizing 21
4.5 Payload Deployment System 21
4.6 Spar Analysis and Optimization 23
5.0 Detailed Design 25
5.1 Summary of Aircraft Geometry and Features 25
5.1.1 Fuselage Features 26
5.1.2 Wing Features 27
5.1.3 Tail Features 27
5.2 Assessing the Airfoil Properties 27
5.3 Properties o the Propulsion System 33
5.4 Static Stability 34
5.5 Mission Performance 36
5.6 Rated Aircraft Cost 38
5.7 Drawing 39
5.7.1 Overall Aircraft Design 39
5.7.2 Fuselage Structure with Payload Deployment System 40
5.7.3 Dimension of the Wing Assembly 41

5.7.4 Dimension of the Tail 42
6.0 Manufacturing Plan and Techniques for Furious Flier 43
6.1 Manufacturing Processes and Feasibility 43
6.2 Manufacturing Processes by Aircraft Component 43
6.2.1 Manufacturing FF's Wings and Empennage 43
6.2.2 The Spar and Spar Joiner Construction 44
6.2.3 Fuselage Construction 45
6.2.4 Boom 46
6.2.5 Landing Gear Manufacturing 46
6.3 Costs, Skills, and Schedules 46
6.3.1 Costs of Composites Materials 46
6.3.2 Skills and Tools Needed to Work with Composites 46
6.3.3 Manufacturing Schedule 46
7.0 Test Plan 48
7.1 Dynamic Testing: Graupner Motor 48
8.0 Work Cited 50

Table of Figures

Figure 2.1: Milestone Chart 10
Figure 3.1: Conceptual Design Considerations for the Payload Deployment Mechanism .. 14
Figure 3.2: Motor Configuration 16
Figure 4.1: Plot of the Number of Cells vs. Predicted Score 18
Figure 4.2: Planform Area vs. Predicted Score 19
Figure 4.3: Aspect Ratio vs. Predicted Score 20
Figure 4.4: The Payload Deployment System 22
Figure 4.5: Cross Section of the Spar 24
Figure 5.1: Coefficient of Lift C_L vs. Angle of Attack AOA 29
Figure 5.2: Coefficient of Lift C_L at Cruise Speed vs. Angle of Attack AOA 29
Figure 5.3: Coefficient of Pitching Moment at the Quarter Chord vs. Angle of Attack AOA .30
Figure 5.4: Lift to Drag Ratio vs. Angle of Attack AOA 31
Figure 5.5: Lift to Drag Ratio for Various Airfoils 31
Figure 5.6: Center Pressure vs. Angle of Attack 32
Figure 5.7: Angle of Climb Diagram 36
Figure 5.8: Rated Aircraft Cost 37
Figure 6.1: Gantt Chart 43
Figure 7.1: Dynamometer Plot 48

Table of Tables

Table 2.1: Structure of the Team 7
Table 3.1: Decision matrix of the payload deployment system 14
Table 3.2: Decision Matrix of the Motor Configuration 16
Table 4.4: Deployment Mechanisms Considered and Tested 22
Table 4.5: Relevant Dimensions to Estimate the Bending Moment 23
Table 5.1: Fuselage Sizing 25
Table 5.2: Wing Sizing with a S4022 Airfoil 26
Table 5.3: Empenage Sizing with a S9027 Airfoil 26
Table 5.4: Weight Estimation of Aircraft Parts 33
Table 5.5: Center of Gravity 34
Table 5.6: Predicted Performance of the Aircraft 36
Table 5.7: Estimated Rate of Climb Performance 37
Table 5.8: Rated Aircraft Cost 38

1.0 Executive Summary

This report summarizes what the student members of the American Institute of Aeronautics and Astronautics (AIAA) at the University of California, San Diego carried out in order to fulfill the objectives for the 2002/2003 AIAA Design/Build/Fly Competition.

The AIAA Design/Build/Fly (DBF) Competition emphasizes the importance of design, construction, and the actual flight performance of the final plane. Based on one of the Mission Tasks requiring the aircraft to self-deploy a simulated sensor package, the team designed the aircraft to carry a payload with the dimensions of 6 inches wide by 6 inches tall by 12 inches long and weighing at least 5 lbs., with a take-off distance less than 120 ft. The wingspan is approximately 7ft. in length, and the empty weight is 13.5 lbs. The final score given to the design is based upon a Written Report Score, Total Flight Score and the Rated Aircraft Cost.

1.1 Objectives

The objective of the contest is to design, fabricate, and demonstrate the flight capability of an unmanned, electric powered, radio controlled aircraft dubbed the "Furious Flier" to meet the best two of three required missions specified in the rules: Missile Decoy, Sensor Deployment, or Communications Repeater. The electric powered aircraft must possess good handling characteristics and has exceptional performance, while remaining practical and affordable to manufacture. The lowest RAC and the highest flight score were achieved through trade studies, comparing the properties of different motors, number of batteries, and the aerodynamic properties of various airfoils.

1.2 Analytical Tools

Several analytical tools were used throughout the entire design process. The most important was Microsoft Excel, which was used for estimating the flight conditions, flight performance, propulsion properties, and Rated Aircraft Cost. Visual Foil 3.0 allowed the team to analyze the aerodynamic properties of various airfoils under different flight speeds. The Electric Motor Calculator allowed the team to compare motors, propeller span and pitch, and battery cell configurations. The wind tunnel allowed the team to compare a scaled-down version of the team's selected airfoil, which is the Selig S4022, with the theoretical aerodynamics properties of the airfoil. Finally, the programs AutoCAD 2000 and PRO/ENGINEER 2001 were important tools to visualize and create two dimensional or three dimensional models.

1.3 Conceptual Design Phase

1.3.1 Goals

The operative goal for the Conceptual Design Phase (CDP) was to create a basic "outline" for the airplane. By the end of the phase, we intended to have a basic silhouette of the airplane showing its basic shape and configuration. This stage was dedicated to placing and fixing basic body, wing, and tail details. In order to determine a basic configuration for the aircraft, the team would also have to determine which of the three missions aircraft would perform.

1.3.2 Methodology

Before a task-specific airplane can be designed, its tasks must first be assigned. The team was divided up into three different groups, with each group being assigned a mission and given the responsibility for fully analyzing it and drawing up a list of pros and cons. The results were then input into a decision matrix or Figure of Merit (FOM) to determine which combination of missions would present the most empirical benefit. Utilizing the decision matrices, team members voted to pick the final conceptual design of the aircraft and the combination of missions to perform.

Each team member came up with several designs which they felt best met the mission goals while providing speed, stability, and the lowest Rated Aircraft Cost (RAC). The designs were presented and then evaluated for ideas and innovations. The designs were broken down into their key components: wing position, tail type, engine placement, basic body shape, and deployment mechanism. Variations for each design element were then analyzed and their merits were weighed till an ultimate winner in each category was established. Each of the elements was then pieced together into a final design. In terms of wing positioning, three different setups were evaluated: a low wing, high wing, and a canard system. Four separate tail setups were also considered, ranging from the traditional layout, to a T-Tail, V-Tail, as well as an H-Tail. Two different engine placements were also evaluated: a conventional puller configuration and a pusher. Six different fuselage types were evaluated, encapsulating three different drop mechanisms. Primary plane characteristics, such as body type, engine placement, and payload deployment system were evaluated for their strength, ease of construction, contribution to a low RAC and ease of combination with secondary plane characteristics such as wing location and tail type. Emphasis was placed on developing the most efficient and aerodynamic, yet simplest, structure possible.

1.4 Preliminary Design Phase

1.4.1 Goals

The purpose of the Preliminary Design Phase was to perform trade studies and optimizations analysis on the aircraft to achieve the highest flight score possible and the lowest RAC possible. Once the Conceptual Design Phase was complete, the properties of competing component configurations of

the aircraft were assessed in the Preliminary Design Phase. The best configurations were selected out of the competing the configurations.

1.4.2 Methodology

To optimize the aircraft, each sub-team performed analysis on components of the aircraft. The Aerodynamics sub-team used Visual Foil 3.0 to compare three competing airfoils before selecting the Selig S4022 airfoil that would provide the best lift under 120 feet. Alternative airfoils that were considered were Eppler E214 and the Selig S3002. They also analyzed the planform area that would give the lowest RAC while also providing the best flight performance score. The Propulsion sub-team used Motor Calculator to compare different motors, their efficiencies and the battery counts in selecting the motor that would give the best performance under the given constraints of having a 40A fuse. The motor selected was the Graupner 3300/5 over the Graupner 3300/6 and the Graupner 3300/7. The Structures sub-team analyzed the load on the wing joiner and optimized the spar to determine whether the component would fail under loads.

1.5 Detailed Design Phase

The Detailed Design Phase was less focused on actual aircraft configuration design as compared to the previous two phases. The focus in this section was to provide estimated performance, sizing, aerodynamics, and stability properties of the aircraft. The sub-teams worked to finalize the design of the aircraft in the Detailed Design Phase. The Propulsion sub-team finalized the power plant configuration, selecting the motor, the propeller span and pitch, and the battery configurations to be used. The Aerodynamics sub-team selected the airfoil after analyzing properties such as the pitching moment coefficient, the coefficient of drag, and the coefficient of lift, investigating the aerodynamics properties of the airfoil under different airspeeds. The Stability/Controls sub-team provided the estimated weight and the center of gravity of the aircraft through analyzing each component of the aircraft. The Structures sub-team provided the Drawing Packages and dimensions of the various components of the aircraft. The Performance sub-team provided the estimated turning radius, range, rate of climb, and cruise speed of the aircraft.

2.0 Management Summary

2.1 Team Personnel

The UCSD Furious Flier team is composed of five sub-teams where the team members ranged from Seniors to Freshmen and one project manager. The six sub-teams were Aerodynamics, Structures, Propulsion, Stability/Controls, Propulsion, and Construction. In every sub-team, one lead engineer is responsible for determining the overall direction of the sub-team and providing the individual members within the sub-teams proper tools and references to solve problems pertaining to the design of the Furious Flyer aircraft. Each member was not restricted to his sub-team as knowledge and expertise was shared within the various groups. The Construction sub-team had a lead engineer student but all members were able to contribute to the construction of the plane. It should be noted that most of the members on the Furious Flyer team have never competed in AIAA/ONR Design/Build/Fly and are learning from phases of construction. The criteria to be a lead engineer student in a sub-team were that the member must be a Junior or Senior who have taken the necessary courses pertaining to either Aerodynamics, Structures, Stability/Control, Propulsion, or Construction, and mentor underclassmen in the field that they are responsible for. Below is Table 2.1, showing the members within each sub-team and the lead engineer student in charge of the sub-team.

Table 2.1: Structure of the Team

Aerodynamics	Structures	Propulsion	Performance	Stability	Construction
Lead: Dana Pugh	Lead: Dan Dalton	Lead: Mann Chau	Lead: Patty Martinez	Lead: Andrew Fischer	Lead: Chad Valenzuela
Wings: Jeremy Bank	Fuselage/landing: Freddy Torrez Wendy Peterson Vladimir Guzaev	Current Analysis: Jeremy Bank	Predicted Performance: Jeremy Bank	Center grav.: Jeremy Bank	Wendy Peterson Mann Chau Vladimir Guzaev Brooke Mosely
Tail Sizing: Andrew Fischer	Payload: Amit Mulgonkar		RAC: Brooke Mosely		Freddy Torrez Amit Mulgonkar

2.2 Sub-team Responsibilities

The overall configuration of the aircraft was the combination of the design contribution of every sub-team members. Components were designed such that members collaborated about possible configurations. Often when collaborating among the lead engineers, compromises were made to fit the components together within the limited space.

2.2.1 Propulsion

The purpose of the Propulsion sub-team was to evaluate the properties of batteries, propellers, and motors on the overall thrust of the aircraft and Rated Aircraft Cost (RAC). The Propulsion sub-team was responsible for deciding on whether to configure the aircraft as a pusher or puller. Analysis was performed using the Electric Motor Calculator software to determine theoretical properties of different Graupner series motors.

2.2.2 Structures

The Structures team designed and analyzed the properties of the fuselage, landing gears, payload deployment system, skin, and tail under loads based on the mission requirements of the competition. The Structures team analyzed the optimum spar cross section configuration and determined the points at which the aircraft is most likely to fail. Among the tools used was Pro-Engineer, Pro-Mechanica, and AutoCAD.

2.2.3 Aerodynamics

Each member of the Aerodynamic group observed the use of Visual Foil software. From the results of the chosen airfoil, the coefficient of lift, the coefficient of drag, and the coefficient of the pitching moment at the quarter chord was collected for three different velocities. Each member was given a task in analyzing and understanding the data. The maximum coefficient of lift, the maximum lift to drag ratio, and finite wing analysis were the main calculations determined from the data.

2.2.4 Stability/Controls

The Stability and Controls sub-team assessed the center of gravity, center of lift, pitching moment and provided the tail sizing of the aircraft based on those properties. They collaborated with the Performance and Aerodynamics sub-team to optimize flight stability properties and handling of the aircraft.

2.2.5 Performance

The Performance sub-team assessed the flight characteristics of the aircraft. They were responsible for assessing the flight conditions during the competition, cruise speed, stall speed, take-off distance, rate of climb, turning radius and range. The Performance sub-team also collaborated with the Stability/Controls and Aerodynamics sub-team to assess the performance of the aircraft under various flight conditions.

2.2.6 Construction

The purpose of the Construction team was, simply put, to build a low weight, high strength, and high quality aircraft to submit into this year's Design/Build/Fly competition. It is their duty to ensure that component parts for the fuselage, empennage, and landing gear are made with precision and pride. Manufacturing was a team effort from the first brainstorm of a conceptual design, to placing the last

sponsor's sticker on the wing. Manufacturing an airplane takes time, patience and dedication. This team came together to exemplify that notion and has built a very strong plane.

2.2.5 Task Scheduling

In early November, the group decided upon a schedule of completion dates. Each subgroup was expected to complete tasks by a certain deadline. The chart below (Figure 2.1) depicts the milestones and actual dates of completion of each major event. Problems that were encountered completing these tasks were quickly resolved through teamwork and subgroup collaboration.

Figure 2.1: Milestone Chart

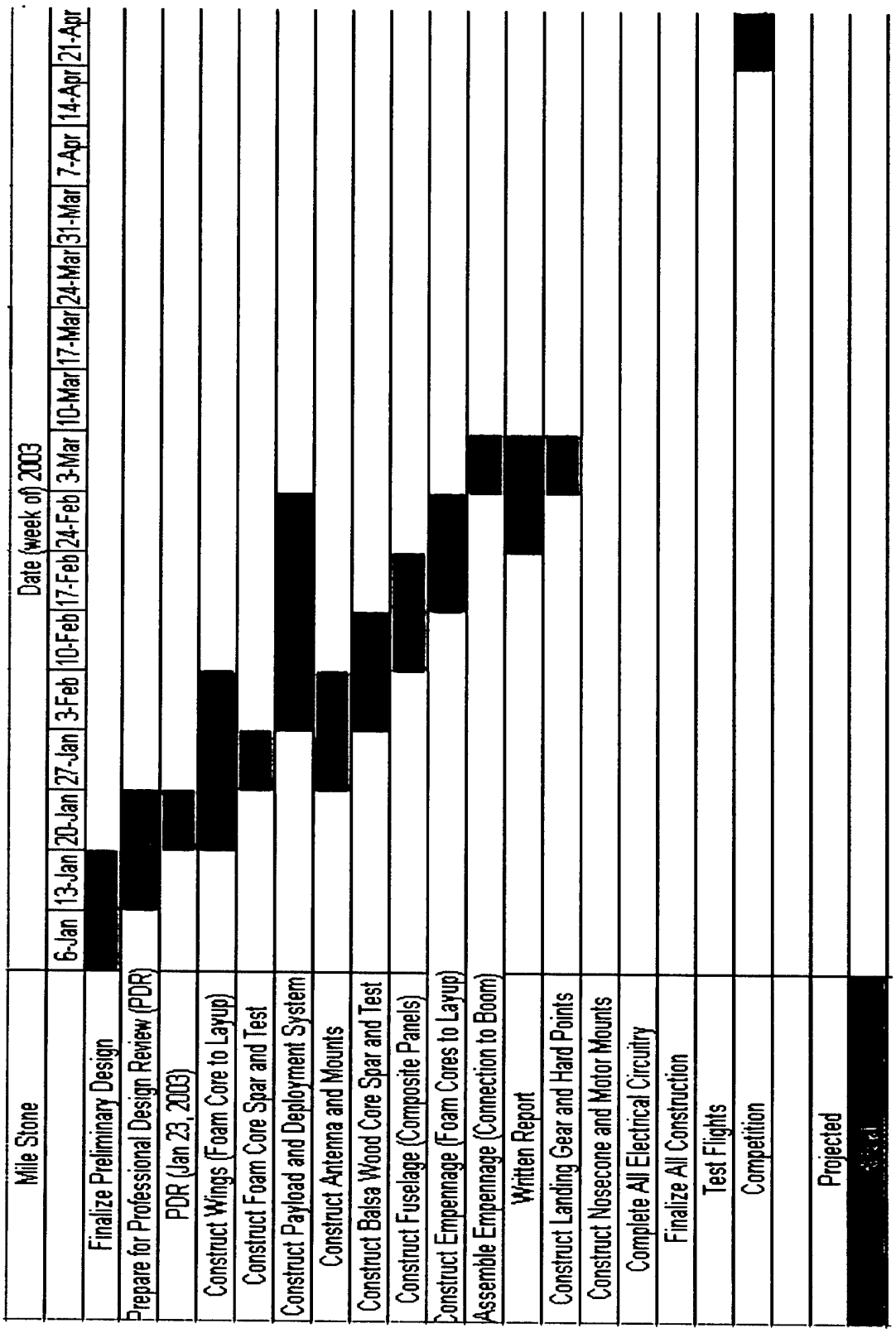

3.0 Conceptual Design

To first start the conceptual design process, the requirements for each mission were determined. Next, concepts for the aircraft were decided as to meet the requirements. Each design concept was thoroughly discussed and critiqued, and then the best aspects of each concept were found and compiled into one design. This concept was the basis for out final design.

3.1 Design Parameters

A design strategy was formulated based on the requirements of the aircraft during the mission.

3.1.1 Main Design Parameters

Certain specifications were deemed more important than others in order to maximize the point total in our aircraft development. Weight of the aircraft, number of engines, lift and drag of the wings, and wing sizing were the main factors we looked at to affect the aircraft.

Being able to take off in the allotted space was a major concern. In all of the initial calculations, the takeoff distance was too long for what was required. The sizing, lift, and drag of the wing reflected the need to take off in a short distance. Maximizing the performance of each did this.

The number of engines was lowered in order to lower the RAC of the aircraft, but this lessened the power of the aircraft, which limited its performance, but the reduced RAC outweighed the worse performance.

3.1.2 Rated Aircraft Cost

The RAC of the aircraft was a major factor in the design of the aircraft. Limits in aircraft design were created in order to minimize the RAC, while not limiting the aircraft to a point where it could not be made effectively. The RAC is based mainly on weight, battery weight, number of engines, fuselage size, wing sizing, control surfaces and servos. The weight of the batteries, the weight of the aircraft, and the number of engines are very large factors in the RAC. Knowing this, the weight and engines were reduced.

3.2 Aircraft Configuration

Once the initial specifications were decided, each aspect of the actual aircraft was looked at. Figures of Merit were used to rate each possibility for every aspect of the aircraft.

3.2.1 Fuselage and Tail Configuration

Figures of Merit were used to analyze the effect of the RAC, size specifications, performance, and handling of the aircraft on the fuselage and tail design. These analyzed figures of merit were used in

accordance with the design specifications created to decide upon the most effective and realistic alternatives for the fuselage and tail.

In regard to the fuselage, the main two alternatives were a flying wing, or a conventional body type. Based on the dimensions required to hold the payload, a flying wing type body was decided to be incompatible. This was because the body structure for the flying wing would have to be too large to fit the payload.

The tail however, took more analysis. A conventional tail, a V-tail, a H-Tail, and a T-tail were all considered. A conventional tail is fairly good all around, except the fact that disturbances from the body and antenna could affect the handling of the aircraft during flight. A V-tail would have a better RAC than the others because of fewer surfaces, but other than that, would be fairly similar. An H-tail, would reduce the effects of disturbances on the tail and increase handling, but would increase the RAC because of more control surfaces. A T-tail allows the horizontal stabilizers to clear the disturbances of the fuselage and antenna, while keeping the RAC relatively low. After rating each configuration concept, it was decided that the T-tail would suit the requirements the best, so it was chosen.

Fitting the boom of the tail inside the size constraints was a major concern, so it required a lot of decisions and analysis. To fit the boom inside the box, it had to move from its position for flight while inside the box. Possibilities were: a folding boom, a detachable boom, or a sliding boom. A folding boom would lessen the stability and strength of the boom, but would allow it to fight inside the box. A detachable boom would fix the size constrain problem, but adds to the assembly time. A sliding boom could create a problem with slight movements in flight. The strength of the boom was deemed and important aspect, as was the fact that slight movements in the tail create handling difficulty. These factors caused the decision for a detachable boom, even at the cost of an increased assembly time.

3.2.2 Wing Configuration

Payload deployment, flight stability, and construction all were analyzed figures of merit for the wing configuration.

- Deployment of the payload had a very large effect on the wing design because only certain deployment mechanisms would work for certain wing designs.
- The placement of the wings can create very stable or very unstable flight conditions.
- Certain wing types are more easily created than others; this must be taken into account because of time and material limitations.

There are three types of wing design possibilities that were compared: low, middle, and high wing designs.

- Low Wing: A low wing design provides a little less stability, but requires less structural support than other wing possibilities. It also creates problems in deploying the payload, forcing it to come out behind the aircraft, instead of below it.
- Middle Wing: A middle wing design is much harder to build than the other configurations and does not allow enough room for the payload to be attached to the aircraft in an efficient manner. It provides structural stability, and some flight stability.
- High Wing: A high wing design allows an easy way to deploy the payload, creates stability for flight and is relatively easy to build.

The high wing provides results that can meet the requirements for a wing design by ease of construction, stability, and proper payload deployment methods.

3.2.3 Landing Gear Configuration

The structural strength, payload clearance, drag, and weight were the figures of merit analyzed for the landing gear configuration.

- The structural strength of the lading gear is a very important factor because the landing gear must be strong enough to support the weight of the aircraft while landing.
- The landing gear must also be big enough to clear the payload while on the aircraft and when it is deployed.
- The amount of drag of the landing gear can affect the flight of the aircraft, so should be minimized.
- The weight of the landing gear is a major factor because more weight adds to our RAC, so any weight we can cut down on landing gear is very helpful.

The three types of landing gear considered were a tricycle, a quadracycle, and a tail-dragger. Having a continuous piece to support the landing gear creates a stronger support and increases its structural strength, so it was an advantageous design to use. It is assumed that each design could be made to clear the payload, and have a continuous piece for support of the landing gear.

- A tricycle design for the landing gear could reduce the weight and drag from the quardacycle because of a three-wheel design, instead of a four-wheel design.
- A quadracycle design creates a more stable wheelbase, but can create more weight and drag because of an extra wheel.

- A tail- dragger design has three wheels, as does the tricycle, but becomes unstable as wind conditions get high.

The tricycle design was not quite as stable as the quadracycle design, but the reduced weight and drag make it a better design for the requirements.

3.2.4 Selecting a Payload Deployment System

The Sensor Deployment mission requires that the aircraft fly two laps, land, release a 6"x6"x12" payload, and fly two more laps. Several conceptual design configurations were considered. In Figure 3.1, four design configurations were considered for the payload deployment systems. In System A, a solenoid pushes the payload from out of the fuselage; in System B, a servo pulls a trigger mechanism that would release the payload down; in System C, a motor pulls the belly of the fuselage open for the payload to drop; and in System D, a servo pulls a pin from a tab, which is a permanent part of the payload, causing the payload to drop directly down.

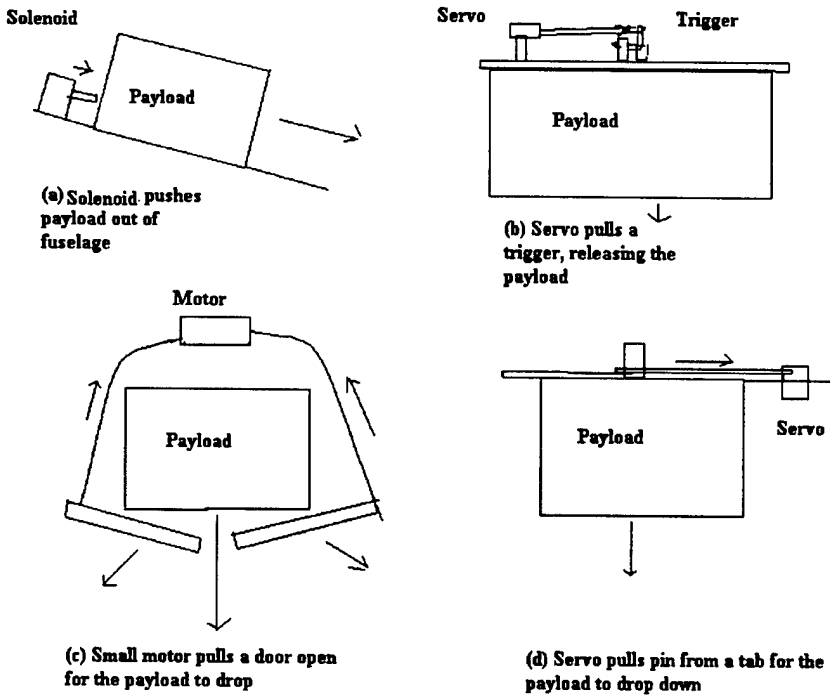

Figure 3.1: Conceptual design considerations for the payload deployment mechanism

The deployment mechanism designs were weighed against each other based on the ease of manufacturing, RAC concerns, and reliability. The mechanism itself must function with little or no technical difficulties, so reliability was given the most weight. Manufacturing the payload deployment

system could be a potential problem, so it was also weighed in. Because all of the deployment mechanisms require an extra servo, motor, or solenoid and because these devices add weight, the RAC concerns was also factored into the decision process. Below is a Figure of Merit study between the four competing designs (Table 3.1).

Table 3.1: Decision matrix of the payload deployment system.

Figures of Merit	Reliability (x50)	RAC (x30)	Ease of Manufacturing (x20)	Total Score	Decision
A	-1	-1	1	-30	Rejected
B	0	0	-1	-20	Rejected
C	-1	-1	-1	-100	Rejected
D	1	0	1	70	Kept

Based on weighing the concerns of the reliability, RAC score, and the ease of manufacturing, System D was chosen.

3.3 Determining the Power Plant Configuration

Several design configurations of the motors and batteries were considered. In Figure 3.2, three main design configurations of the propulsion systems were considered: (a) one motor with 18 nickel-cadmium cells, (b) two motors with 9 cells each, and (c) two motors connected in series to a total of 18 cells. When considering each configuration, the RAC was given the most weight, followed by the power, weight, and efficiency. Below is a Figure of Merit decision matrix between these options (Table 3.2).

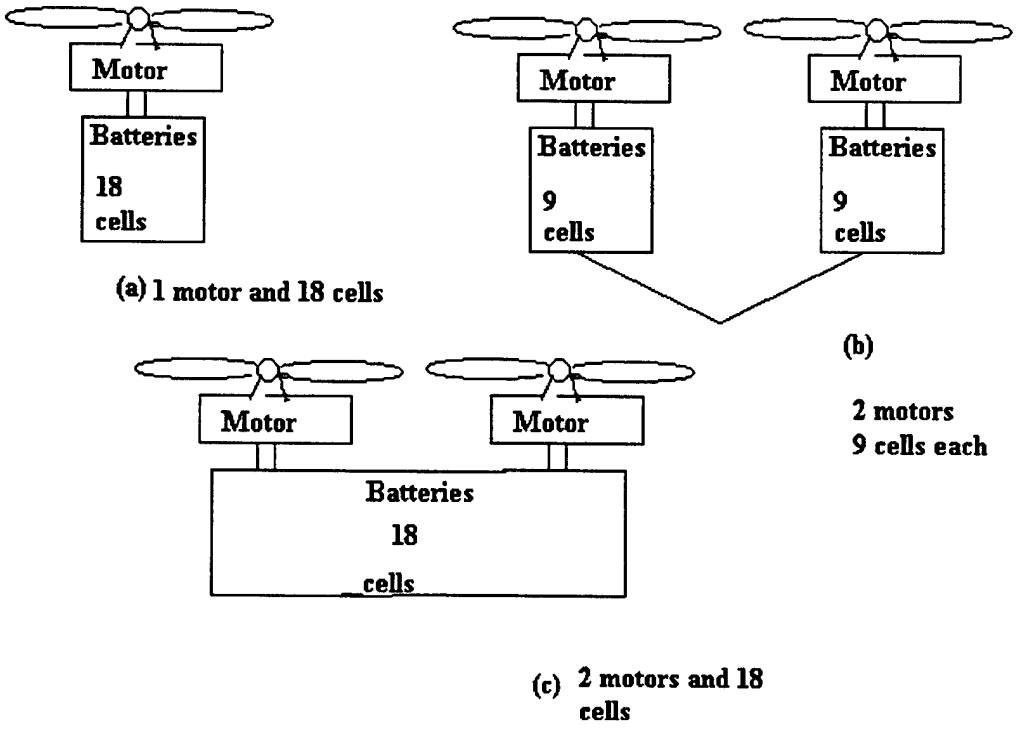

Figure 3.2: Motor configurations

Table 3.2: Decision Matrix of the Motor Configuration

Figures of Merit	RAC (x30)	Efficiency (x20)	Power (x25)	Weight (x25)	Total Score	Decision
1 motor 18 cells	1	1	0	1	80	Kept
2 motors 9 cells each	0	0	1	0	25	Rejected
2 motors 18 cells total	0	-1	1	0	5	Rejected

The final decision was with one motor with 18 cells. The RAC had the greatest weight because while it would be beneficial to have powerful thrust with two motors, having two motors would not be efficient while incurring unnecessary RAC cost, which makes the option less desirable. The three missions can be performed using just one motor with 18 cells. Anything that can be done to reduce RAC and raise efficiency is much more desirable.

4.0 Preliminary Design Phase

The preliminary design phase is a time to perform trade studies, calculate the best flight score results and ultimately optimize the performance of the aircraft based on the final conceptual design. For example, the characteristics of the airfoil were investigated, the tail sizing was selected, and the properties of motors were analyzed for their efficiencies.

4.1 Determining the Optimum Number of Batteries

Analysis was conducted on the number of batteries to be used in flight versus the Total Flight Score. Note that the Single Flight Score is proportional to the Difficulty Factor and inversely proportion to the Mission Flight time while the overall score is proportional to the Total Flight Score and inversely proportional to Rated Aircraft Cost (Eq. 4.1 - 4.2).

$$Single_Flight_Score = \frac{Difficulty_Factor}{(Mission_Flight_Time + Aircraft_Assembly_Time)} \quad (4.1)$$

$$Total_Flight_Score = \frac{\mathrm{Re}\,port_Score * Flight_Score}{Rated_Aircraft_Cost} \quad (4.2)$$

To find the predicted best number of batteries to produce the greatest overall score, certain assumptions had to be made. It was estimated that the Written Report Score would be roughly 85, the Aircraft Assembly Time approximately 1 min and 30 sec, and that the Difficulty Factor would level the performance gaps for each mission. The Electric Motor Calculator software was used to analyze the predicted pitch speed on a Graupner 3300/5 motor under several different numbers of batteries. The number of batteries considered was between 15 and 20 cells. These minimum and maximum cell counts were determined by the very minimum amp hours we could complete the course in and the maximum number of cells the motor could deplete if it were to be run at full power through the entire course. While having large quantities of batteries can provide extended full power to the motors, the weight of the batteries can severely reduce the aircraft's performance by adding substantial weight and by increasing the RAC due to the higher cell count. These two factors are heavily weighted in determining the final score. Figure 4.1 plots the number of batteries in use to the predicted total score.

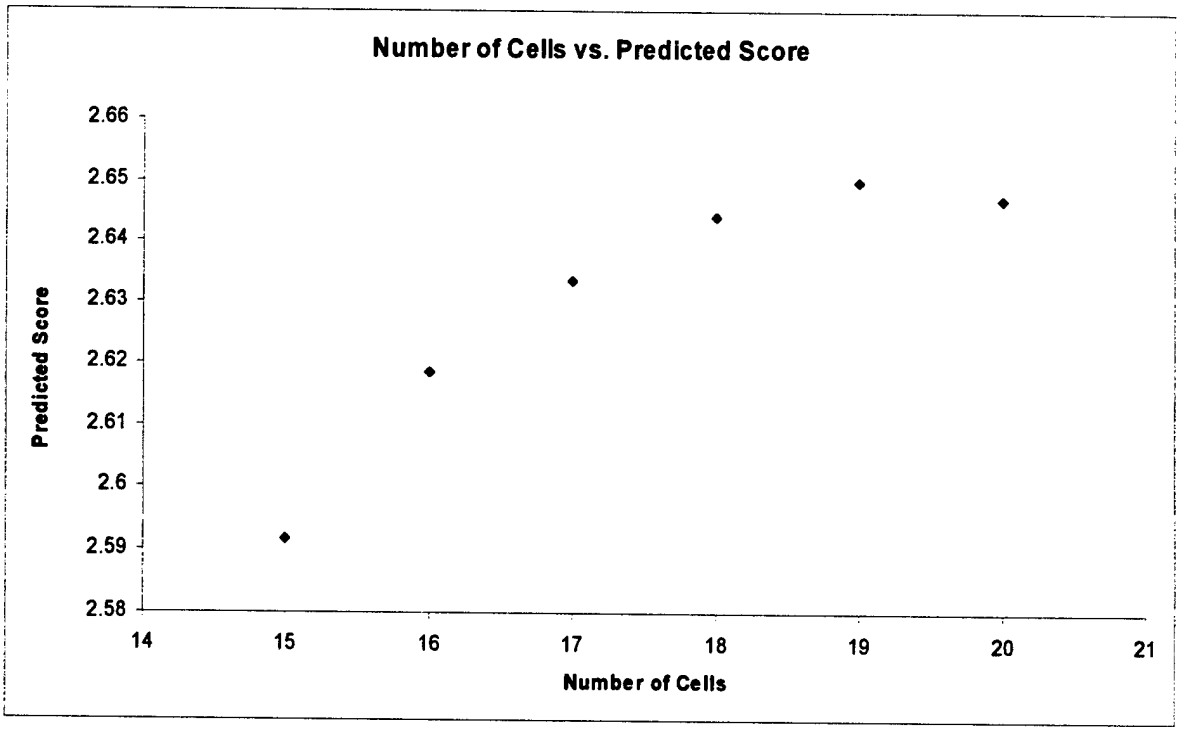

Figure 4.1: Plot of the Number of Cells vs. Predicted Score

By our predictions, the optimum number of batteries to provide the best score is 19 cells. Beyond 19 cells, the weight and number of the batteries becomes a larger factor into the RAC, reducing the overall score.

4.2 Motor Selection

Trade studies and data analysis were performed before selecting the motor that would power this years plane. Three motors were considered: Graupner 3300/5, Graupner 3300/6, and Graupner 3300/7. The motors were compared based on their maximum efficiencies, prop pitch speed, and the prop in-flight thrust. The rules state that there must be a 40 Amp (A) fuse to regulate the current draw of the motors. The three motors were analyzed in Electric Motor Calculator and were given 2:1 gear ratios based on the 40 A fuse limit. Below is a table of the properties of the motors using nineteen Sanyo 2400 mAh Ni-Cad cells (Table 4.1).

Table 4.1: Comparison of three Graupner Motors

Motors	Efficiency (%)	Prop Pitch Speed (mph)	Prop Flight Thrust (lb)
Graupner 3300/5	71.9	52.5	5.34
Graupner 3300/6	68.3	50.4	4.92
Graupner 3300/7	76.9	51.9	5.21

When the three motors were weighed against each other, the Graupner 3300/5 with a gear ratio of 2: 1 produced the most desirable values for the task at hand. It is predicted to produce more in-flight thrust

and prop pitch speed than the Graupner 3300/6 and Graupner 3300/7 models while the efficiency is only 5% less than that of the Graupner 3300/7, making the Graupner 3300/5 our motor of choice.

4.3 Trade Study of Planform Area

A trade study analysis was preformed in order to get a better idea of what the dimensions of the wing should be and how it would affect the team's overall score. A range of different wingspans and chord lengths were chosen to calculate a range of planform areas in a spreadsheet; both the wing span and the chord length gave a range of planform areas of 5 to 16 square feet. A range of estimated weights of the airplane based on components parts, the size of those components, and the material makeup of those components was ranged appropriately with the planform area in order to get truer results. Using the velocity equation for the endurance properties of a propeller aircraft, a range of velocities for each planform area was calculated (Eq. 4.3).

$$V = \sqrt{\frac{2 \times W}{\rho \times S \times C_L}} \quad \text{where} \quad \begin{aligned} W &= \text{instantaneous } weight \\ \rho &= density\ of\ air \\ S &= planform\ area \\ C_L &= \max imum\ coefficient\ of\ lift \end{aligned} \tag{4.3}$$

From the velocity and an approximated distance of 2300 feet, an estimated time was calculated. From this estimated time for each planform area, a single flight score was calculated for the Missile Decoy mission. It was assumed that the Difficulty Factor would level the scoring gap between the missions and the estimated Paper Score was to be 85. A plot was created for the single flight score versus planform area (Fig. 4.2).

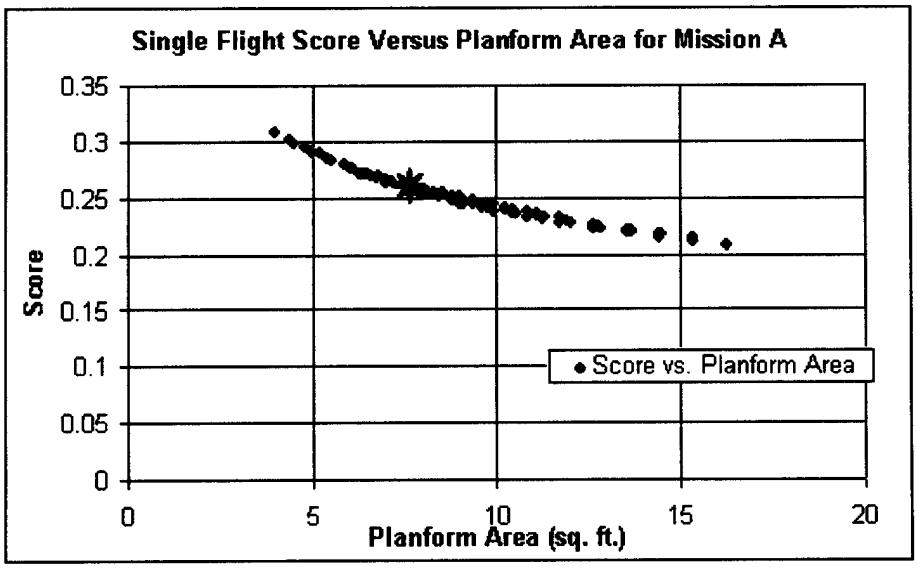

Fig. 4.2: Planform Area vs. Predicted Score

Even though the smallest planform area would raise the single flight score the most due to its decreased weight and RAC score, there is a minimum planform area that would make it unacceptable as flight would be unattainable. If the planform area is too small it will be unable to lift the airplane weight; therefore a planform area under 6 square feet can not be used. Also, with a smaller planform area there would not be enough lift for the airplane to take off in the limited runway length of 120 feet. Thus, anything less than a planform area of approximately 7 square feet could not be used. The team chose the minimum planform area that would give the proper amount of lift for the airplane to take off at 120 feet as well as correspond to the trade study of the aspect ratio (Fig. 4.3).

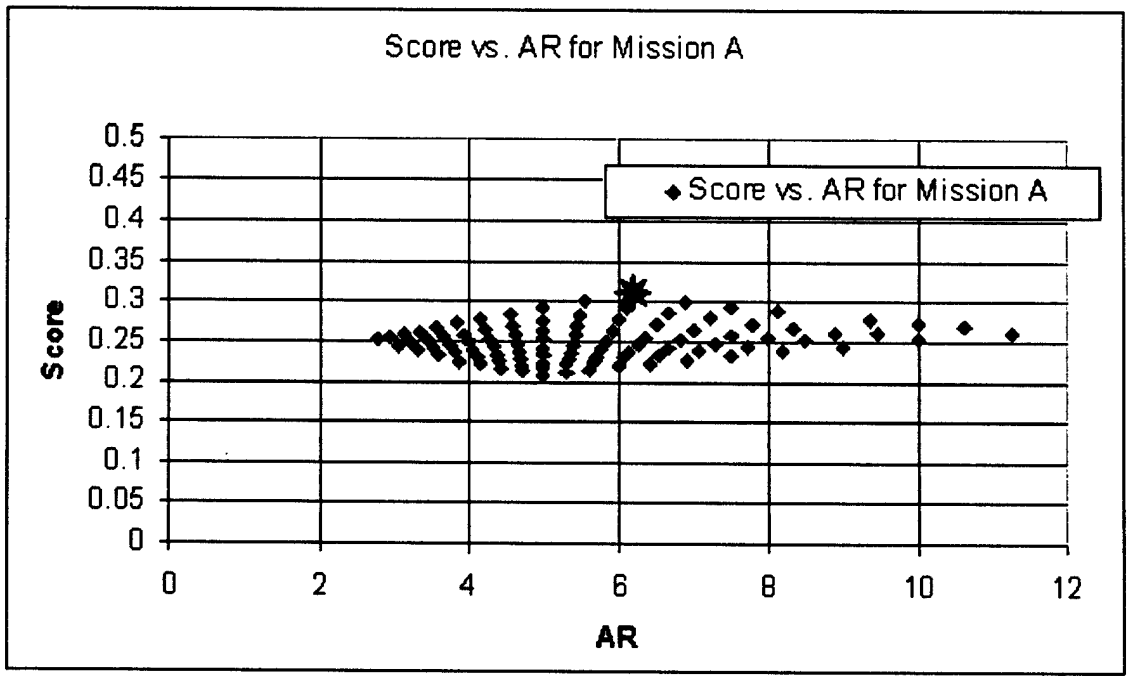

Fig. 4.3: Aspect Ratio vs. Predicted Score

The conclusion was to have the airfoil between 7.5-7.8 square feet which was in the range of a 6.2-6.3 aspect ratio.

The airfoil for this year's airplane, the S4022, showed that it has better lift properties than last year's airfoil, the Eppler 212 airfoil, which was as evident in the results of the lift to drag ratio plot (Fig. 5.4). Comparing the airplane properties of UCSD's 2002 Design/Build/Fly competition airplane, TLAR 3, the S4022 airfoil will fly equivalently, if not better. TLAR 3 had a wingspan of 8 feet and a chord length of 14 inches. From the comparison, the trade study data was reasonable and was therefore accepted. The chord was finalized at 1.1 feet or 13.2 inches, and the wingspan was finalized at 7 feet. The planform

area would then be 7.7 feet with an aspect ratio of 6.36. Further analysis on the lift and drag coefficients C_L and C_D can be found in Detailed Design 5.2.

4.4 Optimizing Tail Size

The sizing of the tail was determined by aerodynamic characteristics needed for stable flight. Initial design began with the sizing of the vertical and horizontal stabilizers. Next, the control surfaces and the placement of the tail from the center of gravity were considered. Below are Equations 4.4 and 4.5 used to calculate the planform areas of the horizontal and vertical stabilizers respectively.

$$Area_{HorizontalStabilizer} = \left(Coefficient_{HorizontalVolume}\right)\left(MAC_{MainWing}\right)\left(Area_{MainWing}\right)/\left(Arm_{HorizontalStabilizer}\right)$$

(4.4)

$$Area_{VerticalStabilizer} = \left(Coefficient_{VerticalVolume}\right)\left(Span_{MainWing}\right)\left(Area_{MainWing}\right)/\left(Arm_{VerticalStabilizer}\right)$$

(4.5)

The airfoil selected is the same for both the vertical and horizontal stabilizers. The Selig S9027-8 was chosen because it is symmetric and therefore its aerodynamic properties could be modified during flight by the aileron or rudder. The volume coefficients were mirrored after historical values for home built aircraft which were 0.50 and 0.04 for the horizontal and vertical stabilizers respectively. The tail arm is 31.5 inches which yielded an area of 232.3 in^2 and 88.7 in^2 for the horizontal and vertical stabilizers, respectively.

The horizontal stabilizer is not tapered and has an aspect ratio of 1.9. The span and tail chord are 21.0 and 11.1 inches, respectively. The vertical stabilizer is slightly tapered to strengthen the tail geometry. For low-speed aircraft very little taper is needed, if at all. The taper ratio for the tail is 0.80 with a sweep angle of 15.0 degrees. The vertical stabilizer's aspect ratio is 1.1 which is high via historical data for T-tails. The span of the vertical tail is 10.0 in. The calculated root and tip chord for the tapered vertical stabilizer is 11.1 and 8.9 in, respectively.

4.5 Payload Deployment System

The proposed payload deployment system requires a servo to pull a pin from a hole in the tab, causing the payload to drop directly down. Figure 4.10 depicts the side, top, and front view of the payload deployment system. When activated the servo pulls a pin from the tab releasing the payload. Two servo models and two solenoid models were tested to determine if they were able to reliably pull a pin from the tab of the payload. The servo or solenoid must overcome approximately 1 lbf of friction to be able to pull

the pin from the tab. A Hitec HS-55 servo with a torque of 15 / 18 oz-in. was first used, but it was not strong enough to perform the task. A Hitec HS 81MG servo with a torque of 36 / 42 oz.-in. was able to perform the task. Both of the solenoid models, however, were not able to pull the pin from the tab, and the masses of both of the solenoids were too large to even be considered in the deployment system design. Below is a table of the results of the testing (Table 4.4).

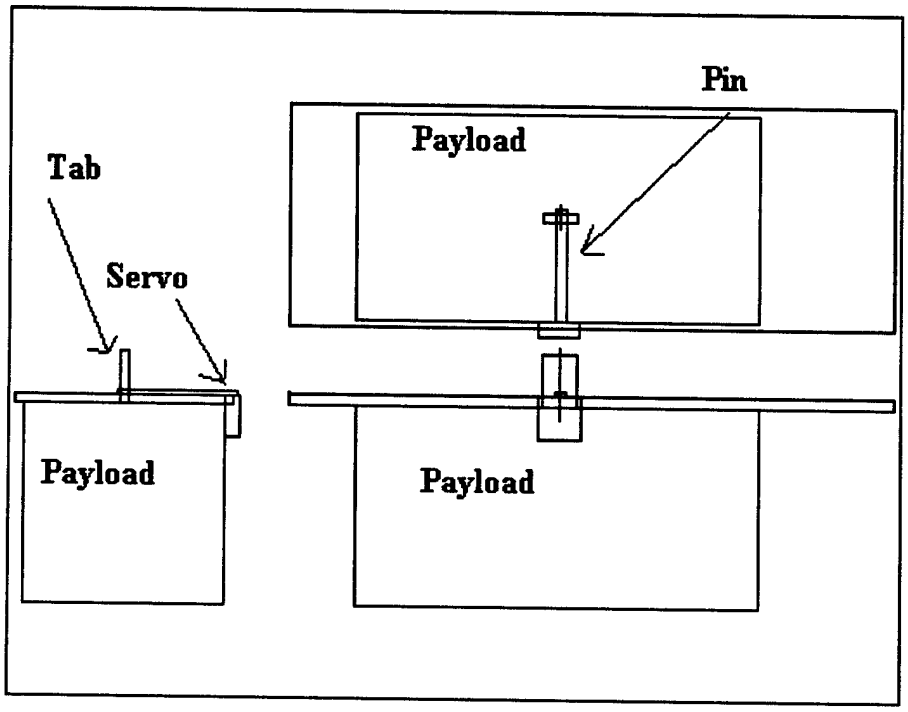

Figure 4.4: The payload deployment system.

Table 4.4: Deployment Mechanisms Considered and Tested

Model	Description	Result
Hitec HS-81MG	Torque = 36 / 42 oz.-in.	Successfully deployed.
Hitec HS-55	Torque = 15 / 18 oz.-in.	Torque was too low.
24 DC Solenoid	Force = 40 oz.	Payload jammed.
12 DC Solenoid	Force = 80 oz.	Too bulky to test.

After the risk reduction testing was performed, it was determined that Hitec HS-81MG or a servo with higher torque should be used to release the payload from the tab.

4.6 Spar Analysis and Optimization

The spar was analyzed based on the properties of balsa wood, which is the material to be used to construct the spar and wing joiner. Because the balsa wood will carry the load of the aircraft, the spar and wing joiner must be able to withstand the predicted maximum bending moment under the weight of the aircraft estimated at approximately 17 lb (75.7 N) with the payload and undergoing 3 g of acceleration. It can be assumed that the two spars are beams under constant upward load, bending moment, and torsion. The two spars are joined by a wing joiner. The point where the spar is most likely to fail under constant bending moment is at the center of the two joined spars. Equation 4.7 describes the maximum moment at the center of the spar located in the fuselage where F is the load and L is the total length of the two spars combined.

$$\text{Maximum Moment: } M = \tfrac{3}{4} * F * L \qquad (4.7)$$

Below are the relevant estimated dimensions for the aircraft to determine the bending moment M (Table 4.5).

Table 4.5: Relevant Dimensions to Estimate the Bending Moment

Description of Components	English Units	Metric Units
Total Length of Spars	84 in.	2.14 m
Estimated Weight with Payload	17 lbs	76 N
w (N/m)	0.202 lb/in	35.5 N/m
Bending Moment M	1,070 lb-in	122 N-m

To determine the optimal cross-section for the spar structure, stress and static analyses were conducted. Optimization of the spar cross section involved determining the maximum stresses during banked turns, which is estimated at 3 g of acceleration. Equations 4.8 and 4.9 were utilized to determine the values of stress and moment of inertia under the maximum bending moment respectively.

$$\text{Maximum Bending Stress: } \sigma = \frac{Mc}{I} \qquad (4.8)$$

$$\text{Moments of Inertia of a Rectangular Cross Section: } I = \tfrac{1}{12} bh^3 \qquad (4.9)$$

In optimizing the cross-section, a factor of safety of 1.5 was used to be able to withstand bending moments and torsions. The ultimate tensile strength of carbon fiber in 0, 45, and 90 degree orientations is approximately σy = 2900 MPa, and the ultimate tensile strength of medium density balsa is 19.2 MPa. The maximum tension and compression is located a length c from the axis (Fig. 4.5).

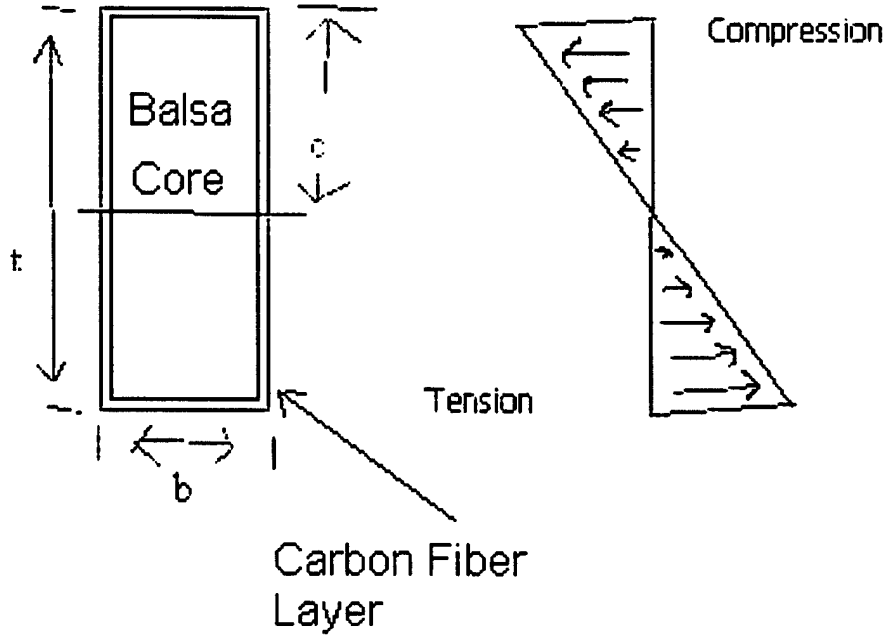

Figure 4.5: Cross section of the spar

The vertical length t of the cross section is 1.7" (43.2 mm). From the properties of balsa, a length b can be determined (Eq. 4.10).

$$b = \frac{12 * M * c * FS}{\sigma_y * t^3} \qquad (4.10)$$

where FS = 1.5, $c = t/2$, and σ_y is the yield strength of balsa

Based on Equation 4.8, the base length b of the cross section was found to be 1.34" (34.2 mm). Because the weights and bending moments are only estimates, it is probably more advisable to further strengthen the spar by glassing with a thin layer of uni-directional carbon fiber around the balsa core. Therefore, the final dimension of the cross section of the spar is 1.8" x 1.3" (45.7 mm x 33.0 mm) with the added layers of carbon fiber. The structural integrity of the spar and wing joiner is vital to the overall aircraft because the majority of the loads during flight is concentrated in the spar and wing joiner. Optimizing the spar and wing joiner can insure that the structure does not fail.

5.0 Detailed Design

Under the Detailed Design Phase, the vital statistics of the aircraft are given. The Aerodynamics sub-team evaluated the pitching moment coefficient C_M, coefficient of lift C_L and the coefficient of drag C_D under various angles of attack and velocities. The Propulsion sub-team selected the motor, propeller, and batteries to be used. The Controls/Stability sub-team analyzed the center of gravity of the aircraft when empty, with the payload, and fully loaded with the payload and antenna based on the weight estimates. The Structures sub-team provided a detailed geometric sizing of the aircraft, its payload deployment system, and the Rated Aircraft Cost (RAC).

5.1 Summary of Aircraft Geometry and Features

The Furious Flier aircraft was designed to fulfill the requirements and constraints of the 2003 Design/Build/Fly rules. It was designed to fit within a 4'x2'x1' storage container, to assemble with the quickest time possible while out of the container and to perform the Missile Decoy and Sensor Deployment Missions. Some distinct features of this aircraft include an externally mounted payload, high mounted wing, rear landing gears to allow clearance for the 6"x6"x12" payload when it is deployed, a detachable T-tail boom with a horizontal tail span of 21", vertical tail span of 10", a Graupner 3300/5, two propeller blades with a total span of 18" and 13" pitch. The payload is released by activating a high-torque servo which pulls a pin from a hole in the tab, causing the payload to drop directly down and a door-like structure to close the opening of the aircraft. The simulated antenna is made from a 6" Scheduled 40 PVC pipe that is 3" high with 1/16" thick birch plywood closing the simulated antenna as specified in the rules. Two polyurethane columns reinforced by uni-directional carbon fiber composites hold up the simulated antenna in place. Detailed descriptions of the dimensions of the fuselage, wings, tail, and weight estimates can be found further in the Detailed Design 5.1.1—5.1.4. Below are Tables 5.1 through 5.4 summarizing the basic dimensions of the fuselage, wings, tail, and weight estimates while a Three-View Drawing of the aircraft can be found in Drawing Package 5.7.1.

Table 5.1: Fuselage Sizing

Description	English	Metric
Length from nose to tail	53 in (4.42 ft)	1.346 m
Width	6.5 in (0.542 ft)	0.165 m
Total Height	12.5 in (1.04 ft)	0.318 m

Table 5.2: Wing Sizing with a S4022 Airfoil

Description	English	Metric
Chord Length	13.3 in (1.1 ft)	0.335 m
Total Span	84 in (7 ft)	2.134 m
Area	1108.8 in^2 (7.7 ft^2)	0.715 m^2
Aspect Ratio	6.36	6.36
Taper Ratio	1	1
Control Area per Wing	84 in^2 (0.583 ft^2)	0.054 m^2

Table 5.3: Empenage Sizing with a S9027 Airfoil

Description	English	Metric
Tail Arm	31.5 in (2.63 ft)	0.8 m
Horizontal Taper Ratio	1	1
Horizontal Area	232.3 in^2 (1.613 ft^2)	0.150 m^2
Horizontal Aspect Ratio	1.9	1.9
Horizontal Tail Span	21.0 in (1.75 ft)	0.533 m
Horizontal Tail Chord	11.0 in (9.21 ft)	0.281 m
Vertical Area	88.7 in^2 (0.616 ft^2)	0.0572 m^2
Vertical Aspect Ratio	1.127	1.127
Vertical Taper Ratio	0.8	0.8
Vertical Tail Span	10 in (0.833 ft)	0.254 m
Vertical Chord Tip	8.87 in (0.739 ft)	0.225 m
Vertical Chord Root	11.09 in (0.924 ft)	0.282 m
Vertical Tail Sweep	15°	15°

5.1.1 Fuselage Features

The fuselage consists of two compartments with specific functions. The top compartment, which is approximately 1.8" high, 6.5" wide, and 16" long is the "backbone" structure of the aircraft, containing the wing joiner and holding the tail's boom in place. Because the lower plate of the upper compartment has to undergo moment, torsion, and shock loads from the wings, tail boom, rear landing gears and motor, the plate of the lower floor is composed of dense polyurethane material reinforced by uni-directional carbon fiber at 0° and 90° orientations and bi-directional carbon fiber at 45° and 135° orientations. According to Matweb.com, polyurethane with carbon fiber reinforcement has an ultimate tensile strength of between 55—248 MPa. Because of the high density of polyurethane with carbon fiber reinforcement, which is between 0.0444—0.0495 lb/in^3 (1.23—1.37 g/cc), only one plate was used to provide structural support. Making all of the walls of the upper compartment out of this material would

add unnecessary weight to the aircraft. The side and upper plates of the upper compartment is composed of dense foam sandwiched by uni-directional and bi-directional carbon fiber which would provide support under shear stress. The purpose of the bottom compartment, which is 1.25" high, 6.5" wide, and 16" long, is to hold the nineteen nickel-cadmium cells, receivers, speed controllers, and payload tab in place. The payload is actually located below the bottom compartment while the tab of the payload protrudes into the bottom compartment secured by a pin fastened onto a high torque servo. Once activated, the servo pulls the pin from the hole in the tab allowing the payload to drop. Enough gap space between the cells to prevent the battery cells from interfering with the motion of the pin. The manufacturing process of the spar/wing joiner, fuselage, boom, and landing gears can be found in Manufacturing FF's Wings and Empennage 6.2.2, 6.2.3, 6.2.4, and 6.2.5 respectively while a detailed 3D model of the wings can be found in the Drawing Package 5.7.4.

5.1.2 Wing Features

The wings were designed to be quickly mounted onto the wing joiner of the fuselage once taken out of the 4'x2'x1' shipping container. The spars which are made from balsa reinforced by uni-directional carbon are secured by two pins inside of the wing joiners. The wing ribs and torsion pin provide stiffness under torsional loads while the cross section of the spar is optimized to perform under moment. The wings are cut from low density white foam and glassed with fiber glass and epoxy. The manufacturing process of the wings and empennage can be found in Manufacturing FF's Wings and Empennage 6.2.1 while a detailed 3D model of the wings can be found in the Drawing Package 5.7.4.

5.1.3 Tail Features

The main feature of the tail is that it is detachable from the fuselage and is held in place by balkheads while in the fuselage. The carbon fiber boom provides stiffness while undergoing bending and torsion. The vertical and horizontal stabilizers are cut from low density foam and glassed with fiber glass to give it structural support. The manufacturing process of the wings and empennage can be found in Manufacturing FF's Wings and Empennage 6.2.1 while a detailed 3D model of the wings can be found in the Drawing Package 5.7.5.

5.2 Assessing the Airfoil Properties

Assumptions were made based on medium properties and on theoretical software of VisualFoil version 4.0. VisualFoil is simulation software that can analyze and compare airfoils. The majority of the preliminary aerodynamic features of the aircraft came from the results of VisualFoil.

The environmental properties and flight conditions were the first assumptions determined. Air properties were taken at sea level. From the experience of flying previous design/build/fly airplanes and from the power of the batteries and motor, a predicted cruise velocity of the designed airplane was

estimated to be 50 miles per hour. The Reynold's number was calculated from the estimated flight conditions and the estimated cruise velocity (Eq. 5.1).

$$\mathrm{Re} = \frac{\rho_\infty \times V_\infty \times c}{\mu_\infty} \quad \text{where} \quad \begin{aligned} \rho_\infty &= \textit{freestream density} \\ V_\infty &= \textit{Velocity at the freestream velocity} \\ c &= \textit{chordlength} \\ \mu_\infty &= \textit{freestream viscousity} \end{aligned} \tag{5.1}$$

The Reynold's number calculation determined the airfoil the final airfoil. With VisualFoil, different airfoil properties were observed by the members of the aerodynamic group. The S4022 showed a low drag coefficient, a high maximum lift, and good stall characteristics for the predicted Reynold's number. Therefore, the aerodynamic group agreed the S4022 would give the best aerodynamic qualities in the airplane design.

The VisualFoil software produced data for the coefficient of lift, the coefficient of drag, and the coefficient of the pitching moment at the quarter chord at various speeds. To see changes in the coefficient properties from 50 miles per hour, 30 miles per hour and 40 miles per hour were the chosen speeds to take coefficients. Through Microsoft Excel 2002, data tables and plots were created for the coefficient of lift, the lift to drag ratio, and the center of pressure against each angle of attack (Fig. 5.1). In figure 5.1, maximum coefficient of lift was determined by the average of the point before the plots change directions. The angle of attack where the maximum coefficient of lift occurs shows the maximum angle of attack the airfoil can go to maintain the greatest lift. When the curve peaks stalling occurs. The maximum coefficient of lift for 30mph, 40mph and 50mph averages to 1.6 (5.1).

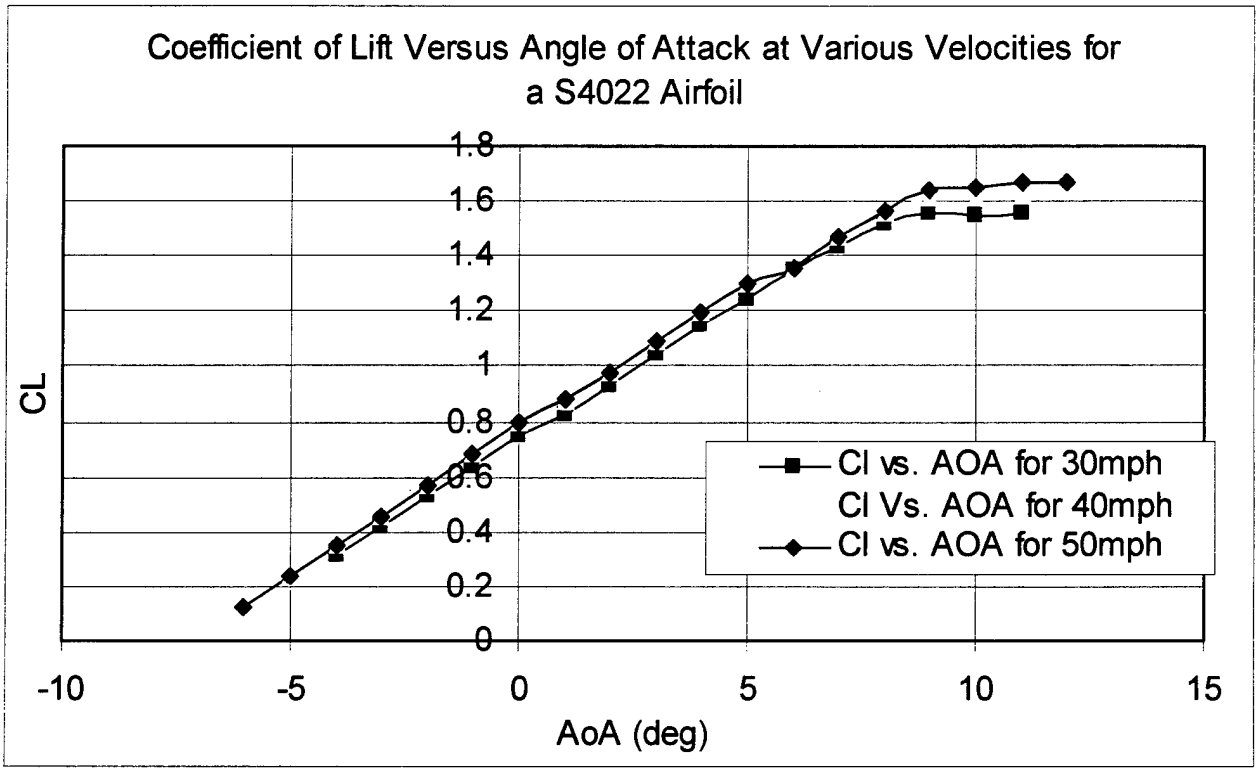

Figure 5.1: Coefficient of Lift C_L vs. Angle of Attack AOA

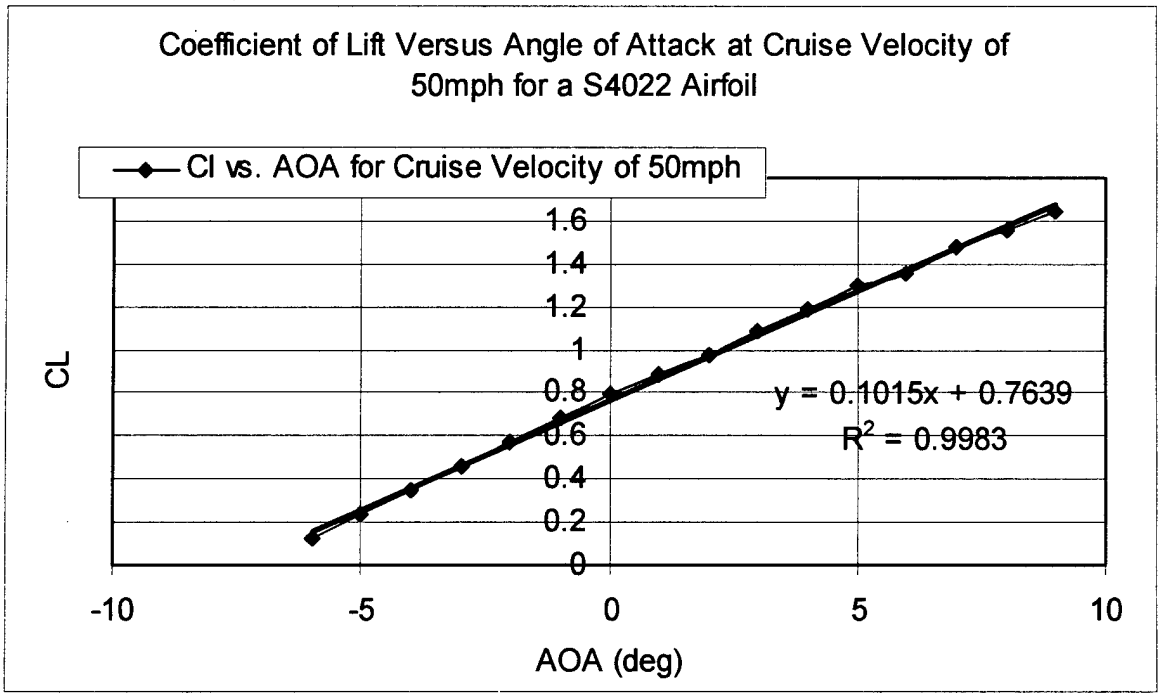

Figure 5.2: Coefficient of Lift C_L at Cruise Speed vs. Angle of Attack AOA

The coefficient of lift versus angle of attack at cruise velocity of 50 miles per hour is singled out to show the best fit line. The best fit line and equation is used in calculations of finite wing.

The pitching moment can essentially be anywhere on the chord line at different angles. The pitching moment taken from the VisualFoil was calculated at the quarter chord. The pitching moment coefficient has a gradual increase at each angle of attack for each of the velocities. The pitching moment is small compared to other airfoils as can be seen in the plot of Cm,c/4 versus angle of attack (Fig. 5.3).

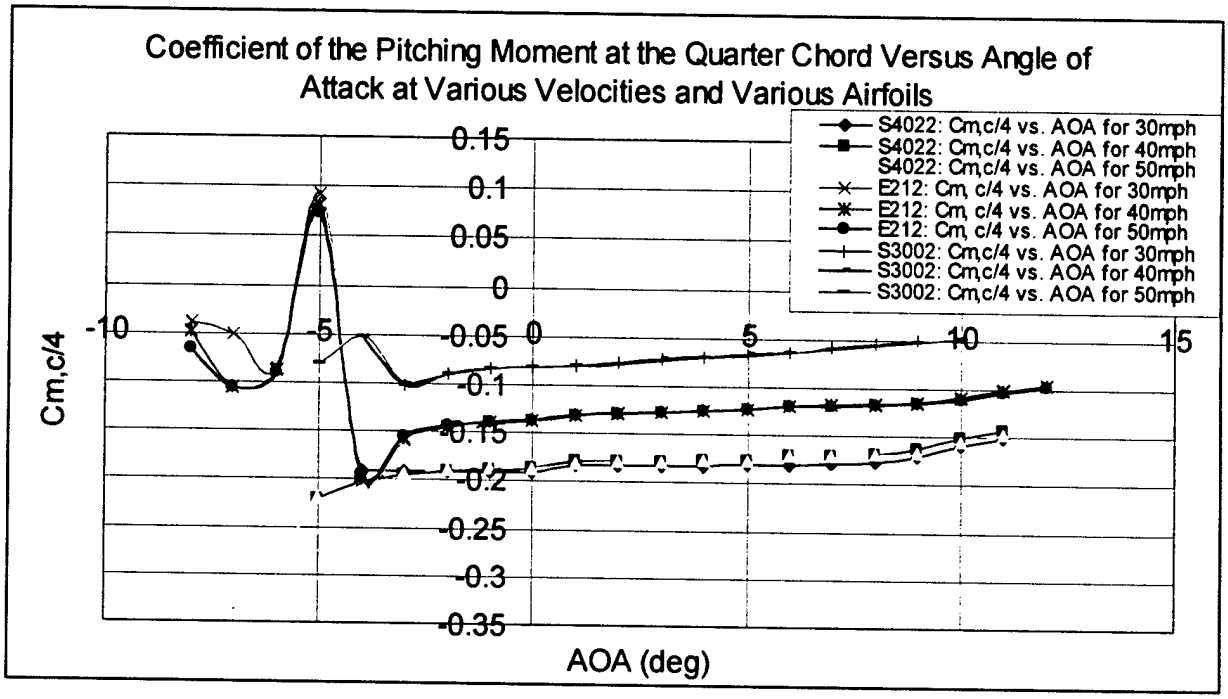

Figure 5.3: Coefficient of Pitching Moment at the Quarter Chord Cm,c/4 vs. Angle of Attack AOA

To plot the lift to drag ratio, an aerodynamic group member used the coefficient of lift and the coefficient of drag from the VisualFoil data. Below is a plot of the lift to drag ratio of the chosen airfoil S4022 (Fig. 5.4).

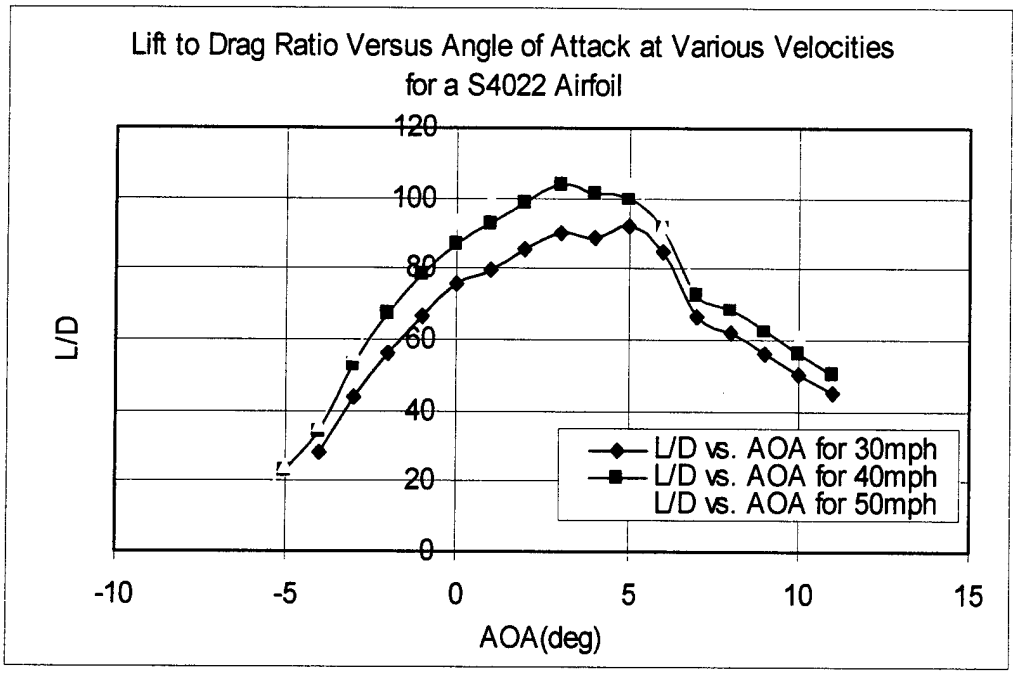

Figure 5.4: Lift to Drag Ratio vs. Angle of Attack AOA

From the lift to drag ratio versus angle of attack plot, a new plot of maximum lift to drag ratio versus velocity was created (Fig. 5.5).

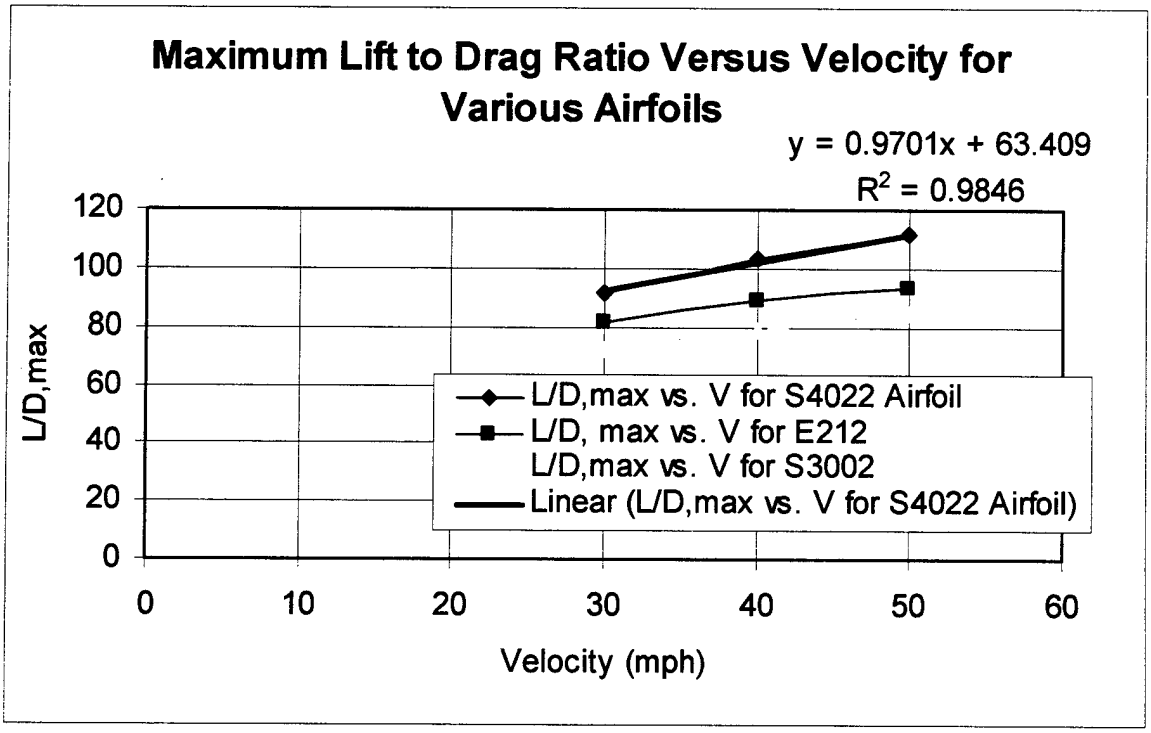

Figure 5.5: Lift to Drag Ratio for Various Airfoils

Other maximum lift to drag ratios for different velocities was done for the E212 airfoil and the S3002 airfoil to compare the better aerodynamic properties of the S4022 airfoil that was chosen. The lift to drag ratio is a true measure of the aerodynamic efficiency of a body shape. The higher $(L/D)_{max}$ for any given velocity, the more aerodynamically efficient is the body. This analysis of the lift to drag ratio only corresponds to the S4022 airfoil alone. The actual body of the airplane will cause the maximum lift to drag ratio to reduce for each speed.

The center of pressure was calculated for each angle of attack using the Equation 5.7.

$$X_{cp} = chord \times (\frac{1}{4} - \frac{C_{m,c/4}}{C_L}) \quad (5.7)$$

Below is a plot of the Center of Pressure vs. Angle of Attack AOA (Fig. 5.6).

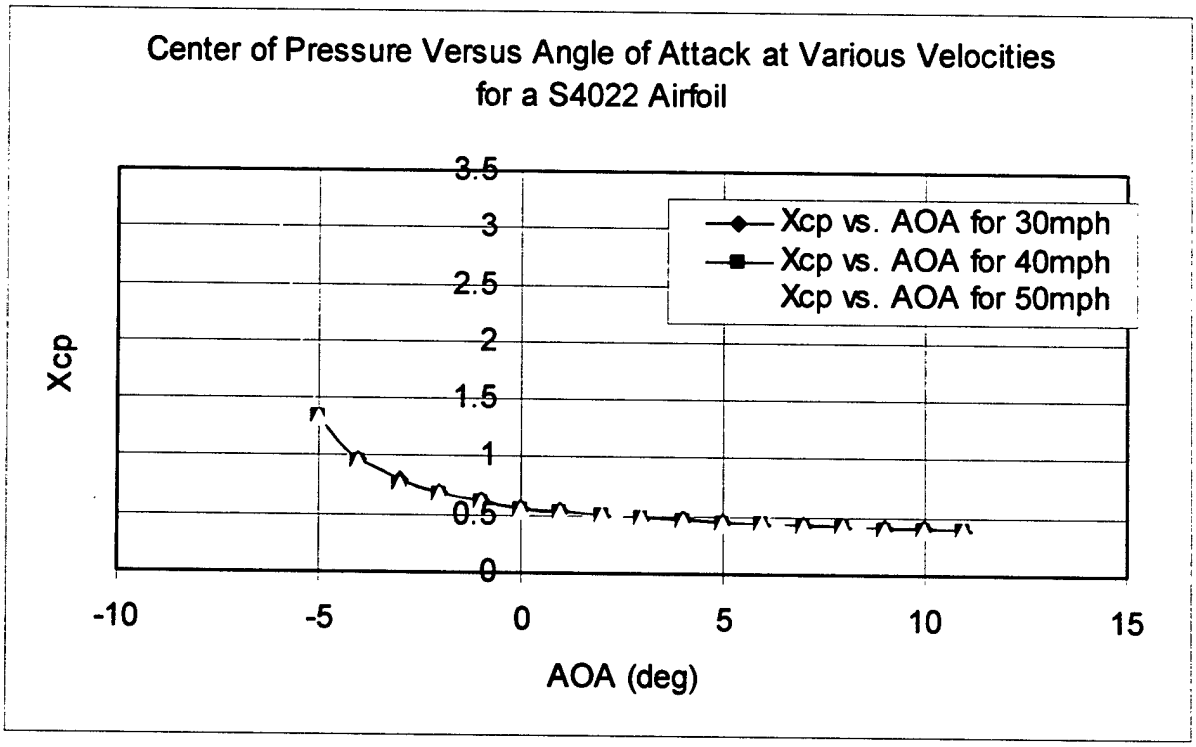

Figure 5.6: Center Pressure vs. Angle of Attack

The center of pressure is the location where the resultant of a distributed load effectively acts on the body. It is also a point on the body about which the aerodynamic moment is zero. The center of pressure changes with the angle of attack. In general, from the plot, the center of pressure moves closer to the leading edge as the angle of attack increase. The center of pressure seems to stabilize a certain distance from the leading edge before stalling, and the center of pressure never goes beyond the leading edge or trailing edge. From this interpretation and analysis, the airfoil is very stable in flight.

5.3 Properties of the Propulsion System

The configuration of the propulsion system was based on the power management, efficiency, and RAC concerns. The maximum propeller span of 18" was selected while the 13" pitch was selected based on achieving a 50 mph flight. The total power available to the Graupner 3300/5 is given by P = I*V = 731 Watts while the power out is approximately 540 W. The final thurst-to-weight ratio is 0.27. Nineteen Sanyo 2400 mAh batteries will be used to supply the power because of their high energy density of 1.11 Wh/oz. The maximum efficiency is achieved when the motor is at 12000 RPM.

5.4 Static Stability

The static stability of the aircraft, i.e. the ability of the aircraft to remain in stable flight after wind disturbances, is an important aspect of the design. The first step was to calculate the Center of Gravity (CG). To do so the masses and location of every part of the plane were measured and recorded in Table 5.4.

Table 5.4: Weight Estimation of Aircraft Parts

Weight Estimation					
Part	**Station**		**Weight**		**Moment**
Propulsion					
Propeller	0	In	8	oz	0 in-oz
Motor	2.5	In	21	oz	52.5 in-oz
Batteries	11	In	45	oz	495 in-oz
wiring harness	16	In	2	oz	32 in-oz
Fuselage					
fuselage shell	12	In	10	oz	120 in-oz
Backbone	12	In	20	oz	240 in-oz
landing gear	10	In	16	oz	160 in-oz
nose gear	5	In	5	oz	25 in-oz
Avionics					
speed controller	7	In	6	oz	42 in-oz
Receiver	7	In	1.65	oz	11.55 in-oz
wing servo	13	In	2	oz	26 in-oz
tail servo	47	In	1	oz	47 in-oz
payload servo	12	In	2	oz	24 in-oz
Payload					
Payload	12	In	80	oz	960 in-oz
antenna mount	12	In	2	oz	24 in-oz
Antenna	12	In	16	oz	192 in-oz
trap door	13.5	In	6	oz	81 in-oz
Aircraft Structures					
Wing	12	In	30	oz	360 in-oz
Boom	28.85	In	5	oz	144.25 in-oz
Empennage	47	In	10	oz	470 in-oz
Total Weight			287.65	oz	
			17.98	lbs	

The moment is calculated about the front tip of the aircraft. The sum of the moments about CG is zero. CG is calculated through Equation 5.8.

$$CG = \frac{\sum_{i=1}^{n} (Moment)_i}{\sum_{i=1}^{n} (mass)_i} \qquad (5.8)$$

Three different CG's were calculated—empty, with payload, and with payload and antenna—and are listed in Table 5.3.

Table 5.5 Center of Gravity

CG			
	Weight (oz)	weight (lbs)	CG (in)
empty	192.65	12.040625	12.22061
w/payload	272.65	17.040625	12.15588
w/payload & antenna	288.65	18.040625	12.14724

With CG calculated, the stability of the aircraft was analyzed. Stability was analyzed in 3 directions: rolling, pitching, and yawing.

The aircraft is completely symmetric about the x-z plane (x direction positive is from CG to the front of the aircraft, y direction positive is from CG out through the right wing, and z direction positive is from CG pointing downward normal to level flight), therefore roll stability is achieved without any aileron deflection provided there are no perturbations in wind or pressure. Since that is only a theoretical condition, the ailerons are deflected to offset the rolling moment created by changes in wind or pressure. The ailerons are placed near the ends of the wings so that little deflection is needed to get a large rolling moment on the aircraft.

The pitching stability is controlled through use of the horizontal tail and the elevators. Every lifting surface creates a moment about CG; the horizontal tail's function is to offset the moment created by the wing. The high lifting force on the wing is offset by the long moment arm set by the length of the tail boom: 37 in. This distance allows the range of the deflection of the elevators to remain small because not much lift is needed through the horizontal stabilizer. The horizontal tail surface is a symmetrical airfoil elevators are used to create camber, thus producing lift to offset the moment of the wing's lift. The elevators are also used in controlling flight against small wind disturbances and pressure fluctuations that create a pitching moment on the aircraft.

Yawing stability is maintained with the vertical stabilizer and tail rudder. The rudder and vertical stabilizer are used to avoid side slip. The rudder maintains the front of the aircraft pointing in the same

direction as the direction of flight. If there is a cross wind during flight the rudder helps to maintain a straight flight path. The deflections of the rudder, needed to produce desirable results, are small because of the long moment arm created by the tail boom. In steady level flight with no perturbations in wind or pressure, the yawing moment will be zero and there would be no use of the rudder. Unfortunately, for the ease of control and stability, this is not the case. Small deflections of the rudder are used to maintain yawing stability throughout flight.

5.5 Mission Performance

In order to evaluate and estimate our plane's performance; analysis of rate of climb, stall speed, and take-off and landing specifications was necessary. The performance calculations requires the relevant dynamic pressure taken at air properties at sea level and at the takeoff velocity. Below is the dynamic pressure (Eq. 5.9).

$$q_\infty = (1/2)*\rho_\infty*(V_{takeoff}^2) \quad (5.9)$$

The take-off and landing velocity calculations were based on the stall speed (Eq. 5.10—5.11).

$$V_{takeoff} = 1.2*V_{stall} \quad (5.12)$$

$$V_{landing} = 1.3*V_{stall} \quad (5.13)$$

where the level flight stalling velocity is found in Equation 5.14.

$$V_{stall} = \sqrt{((2*Weight)/(\rho_\infty*S*C_{L,max}))} \quad (5.14)$$

where S = planform area

From these takeoff /landing velocities and dynamic pressures, take-off and landing distances can be found. Takeoff distance is the sum of the ground run and airborne distance. The takeoff distance should be as minimal as possible for quick and efficient operation of the aircraft.
Table 5.4 shows the performance summary of the aircraft at various stages of the mission.

Table 5.6: Predicted Performance of the Aircraft

Performance Summary			
	Empty	With Payload	With Payload and Antenna
Stall Speed	22.0 ft/s	26.2.ft/s	27.0 ft/s
Take Off Speed	32.4 ft/s	32.4 ft/s	32.4 ft/s
Take Off Lift	5.34 lbf	5.34 lbf	5.34 lbf
Take Off Drag	0.27 lbf	0.27 lbf	0.27 lbf
Take Off Distance	4.18 ft	5.93 ft	6.29 ft
Take Off Time	0.26 s	0.36 s.	0.39 s
Landing Speed	28.7 ft/s	34.1 ft/s	35.1 ft/s
Landing Distance	3.27 ft	6.58 ft	7.39 ft

It should be noted that the estimated take off distance empty, with the payload, and with the payload and antenna is approximately 4.2 ft, 4.9 ft, and 6.3 ft respectively, which should allow the aircraft to clear the 120 ft range specified by the rules.

The rate of climb (V_y) is the vertical component of the plane's true airspeed. Below is Figure 5.5, showing the components of the angle of climb.

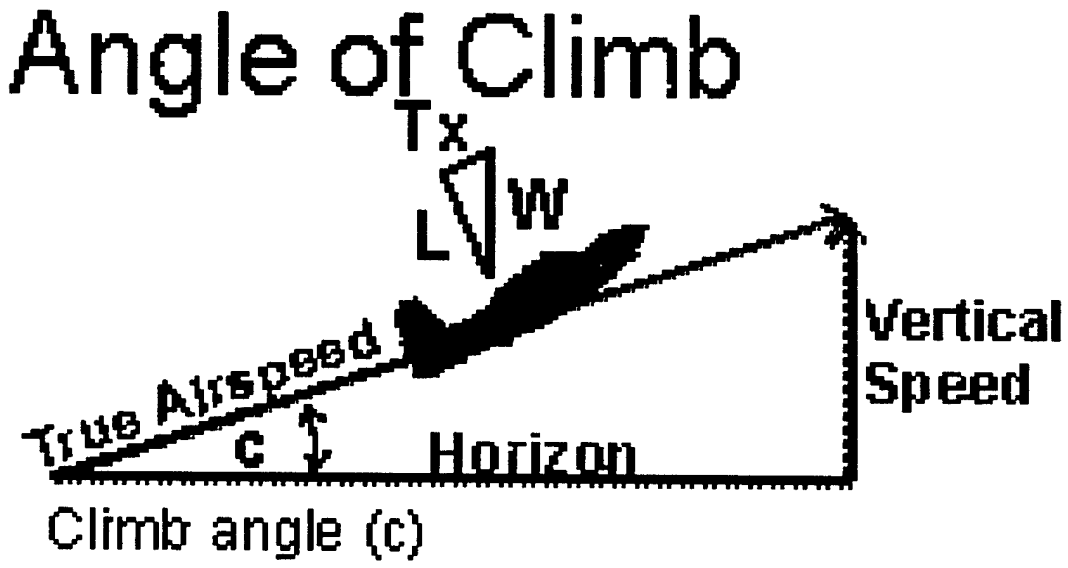

Figure 5.7: Rate of Climb Diagram

The climb angle (c) is the measured angle from the horizon to the flight path. The rate of climb can be expressed by Equation 5.15.

$$Vy = \frac{(Thrust - Drag) * True_Air_Speed}{Weight} \quad (5.15)$$

Utilizing Equation 5.15, the rate of climb was calculated for the empty weight plane, the plane with the payload, and the plane with the payload and antenna. The rate of climb performance can be seen in Table 5.5.

Table 5.7: Estimated Rate of Climb Performance

Rate of Climb Performance			
	Empty	With Payload	Fully Loaded
Rate of Climb	13.7 ft/s	9.7 ft/s	9.2 ft/s
Climbing Distance	144 ft	209 ft	222 ft
Climb Angle	19.2 deg	13.4 deg	12.7 deg
Climb Time	1.96 s	2.85s	3.03s
Turning Radius	81.4 ft	132.0 ft	145 ft

The performance of the aircraft is critical in how well the aircraft competes in the Design/Build/Fly Competition. For example, the turning radius when empty, with the payload, and fully loaded with the payload and antenna are 81.4 ft, 132 ft, and 145 ft respectively. The smaller the turning radius, the faster the aircraft can perform its mission. The numbers are only estimates, so the properties of the performance of the aircraft can further be verified through flight testing.

5.6 Rated Aircraft Cost

After the aircraft was designed, a more accurate value of the Rated Aircraft Cost of the design was given to be 9.774. Keeping the Rated Aircraft Cost low is essential to be competitive.

Table 5.8: Rated Aircraft Cost

Rated Aircraft Cost (RAC) = (A * MEW + B * REP + C * MFHR) / 1000 =					**9.655**
Manufacturers Empty Weight Multplier (MEW)	A = $ 100				
Total Weight w/o Payload =	15 lbs				
				MEW =	15
Rated Engine Power Multiplier (REP)	B = $ 1500				
# of engines =	1				
Battery Weight =	3.09 lbs				
				B * REP =	3.09
Manufacturing Cost Multiplier (MFHR)	C= $ 20				
WBS 1.0 Wings					
Wing Span=	7 ft	*	8 hrs/ft		
Max Chord=	1.125 ft	*	8 hrs/ft		
# of Control Surfaces =	2	*	3 hrs/c.s.		
				WBS 1.0 =	71.0 hrs
WBS 2.0 Fuselage					
Fuselage Length =	5 ft	*	10 hrs/ft		
				WBS 2.0 =	50.0 hrs
WBS 3.0 Empenage					
# of Vertical Surfaces w/o cntrl =	0 v.s.	*	5 hrs/v.s.		
# of Vertical Surfaces w cntrl =	1 v.s.	*	10 hrs/v.s.		
# of Horizontal Surfaces w cntrl =	1 v.s.	*	10 hrs/v.s.		
				WBS 3.0 =	20.0 hrs
WBS 4.0 Flight Systems					
# of Servo or Motor cntrler =	5 ser	*	5 hrs/ser		
				WBS 4.0 =	25.0 hrs
WBS 5.0 Propulsion Systems					
# of engines	1 eng	*	5 hrs/eng		
# of propellers	1 prop	*	5 hrs/prop		
				WBS 5.0 =	10.0 hrs
				MFHR	176
				RAC	**9.655**

5.7 Drawings

5.7.1 Overall aircraft

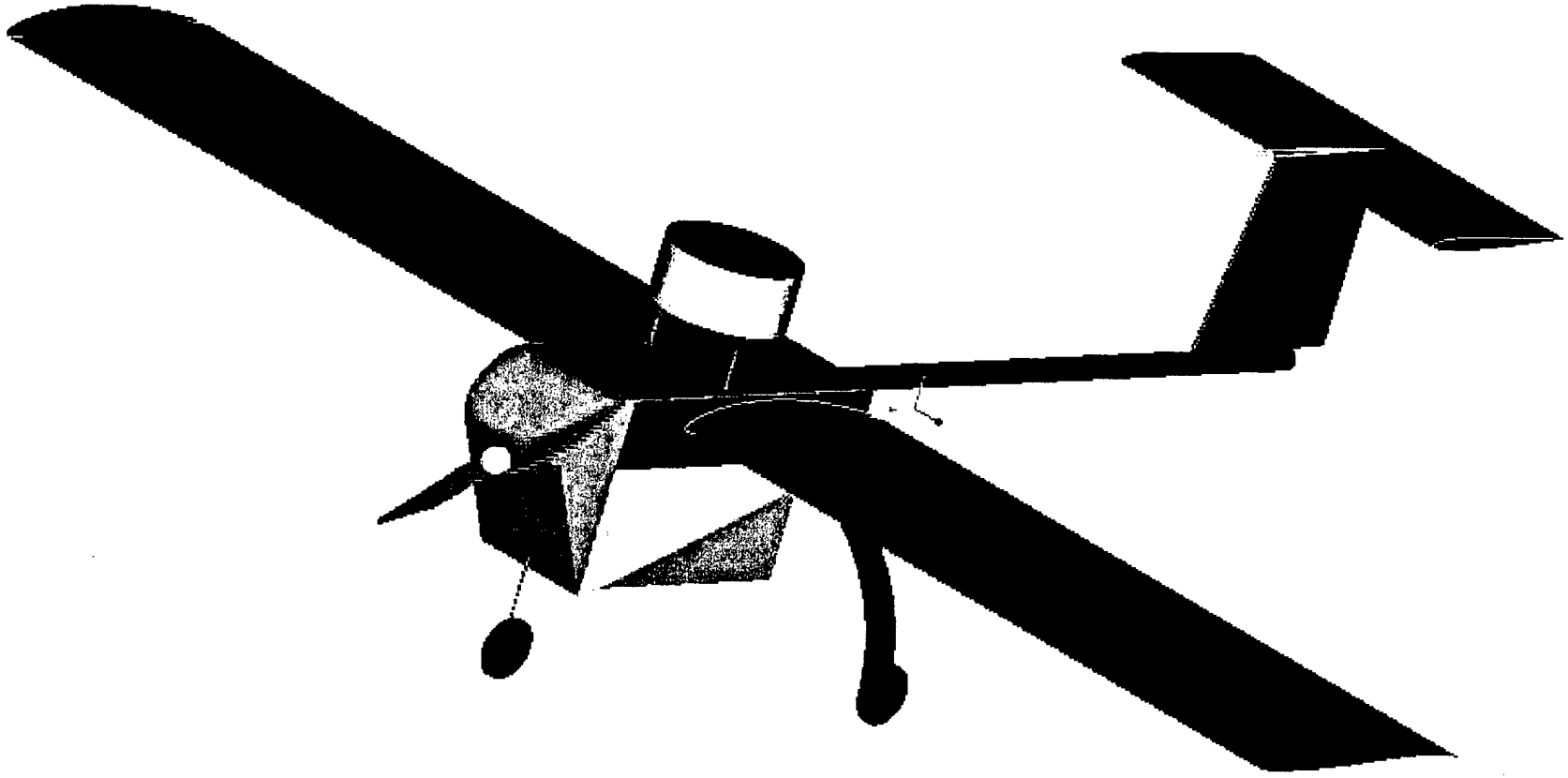

5.7.2 Fuselage Structure with Payload Deployment System

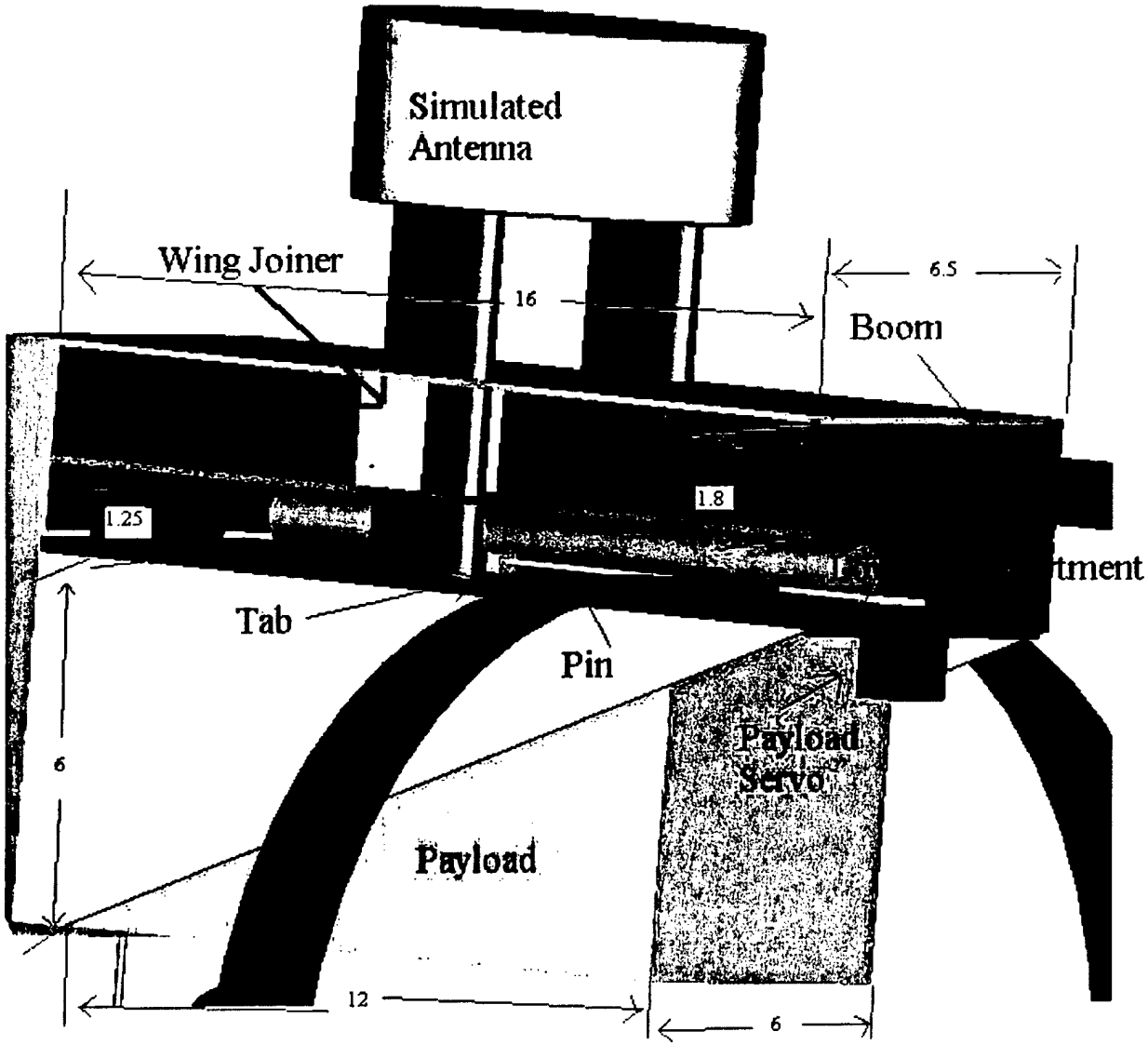

5.7.3 Dimensions of the Wing Assembly

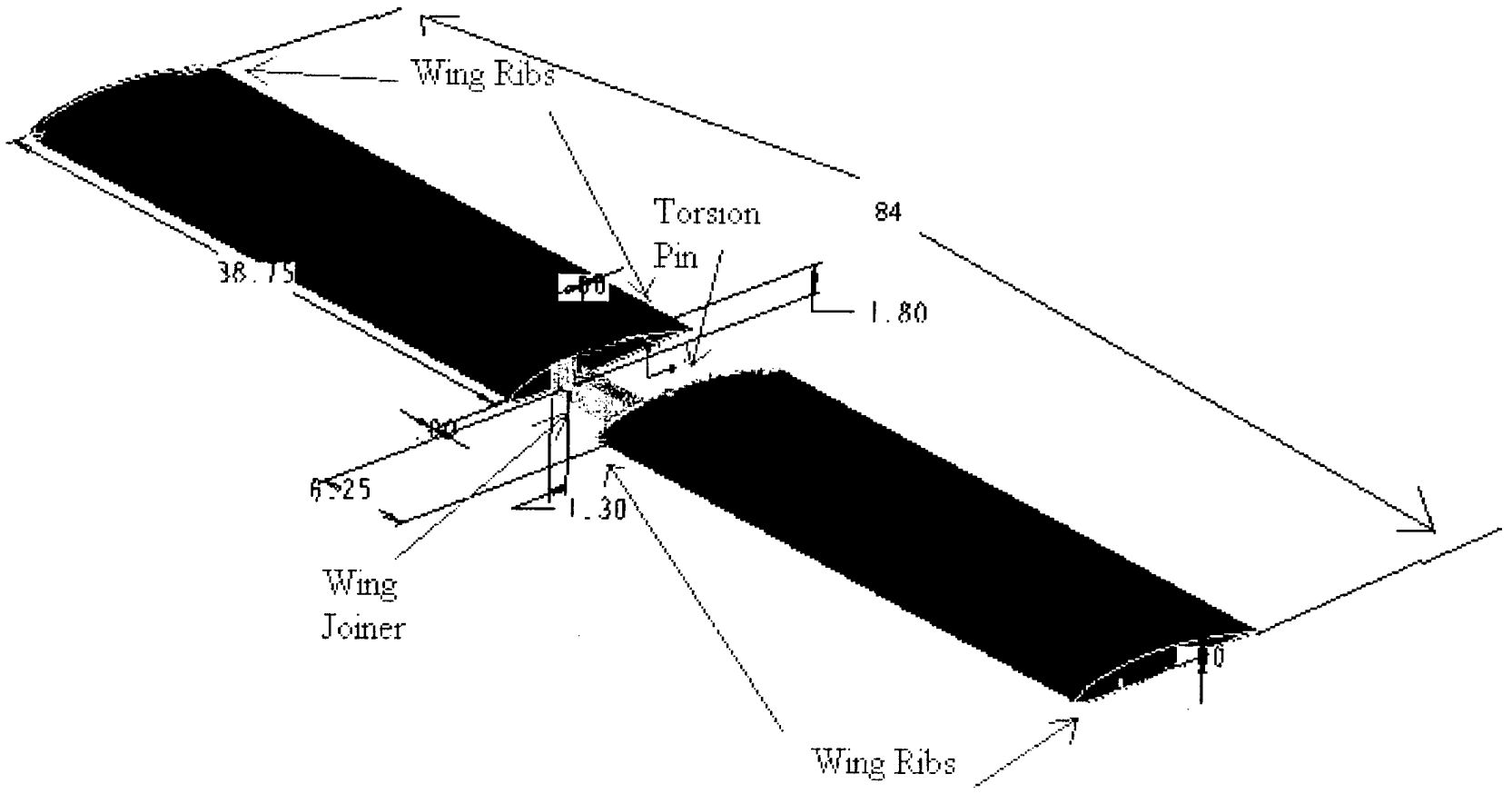

5.7.4Dimensions of the Tail

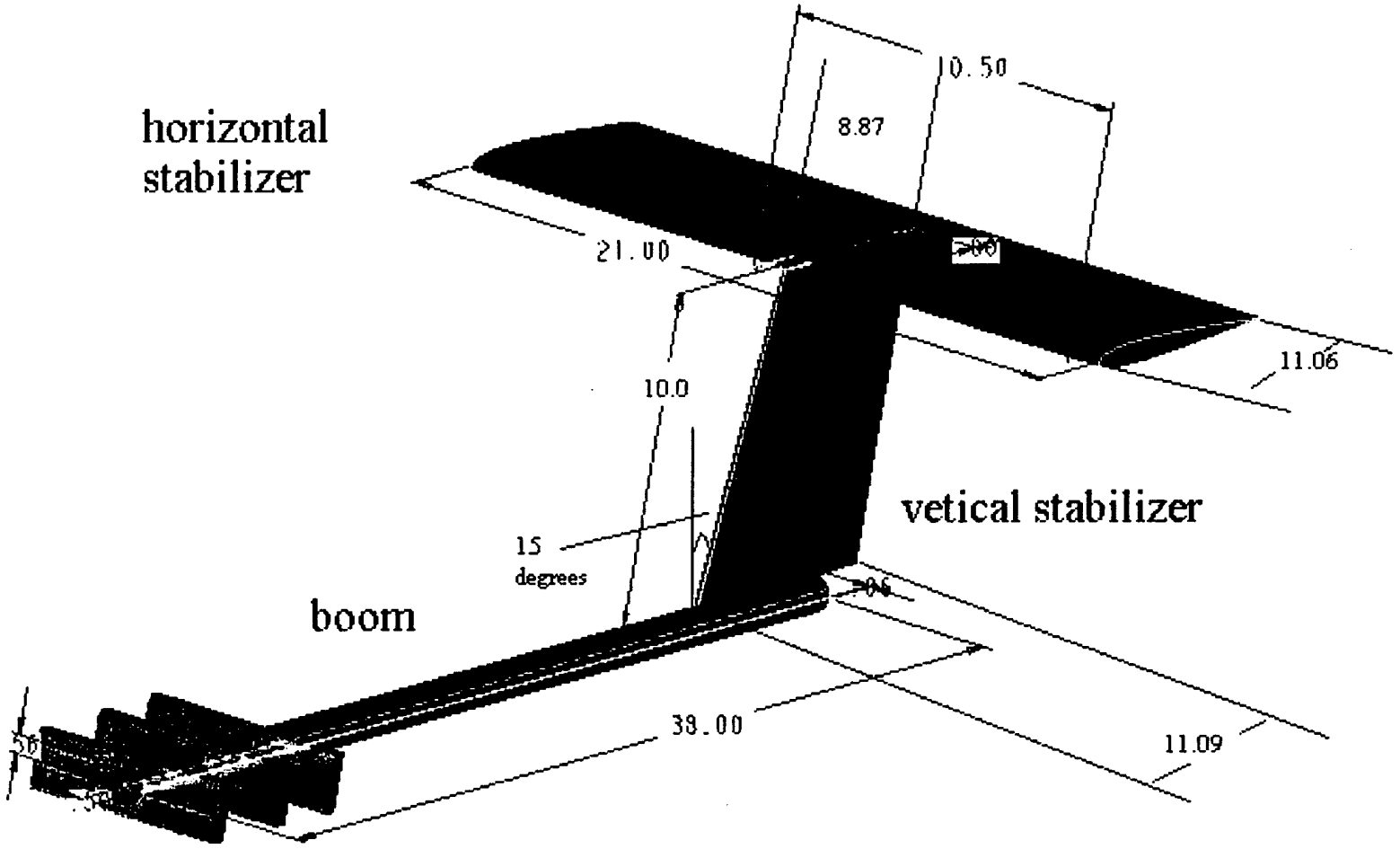

6 Manufacturing Plan and Techniques for Furious Flier

6.1 Manufacturing Processes and Feasibility

The necessary skills, tools, and materials needed to produce the Furious Flier (FF) this year were many. Manufacturing an aircraft predominantly of composite materials brought with it certain difficult yet unavoidable challenges. Some of these challenges included, but have not been limited to; ease of working with the materials, cost of these materials, experience or skills needed to work with these materials, the time involved in manufacturing component parts, reproducibility of these parts in both shape and strength, and having the necessary tools to work with these materials before, during and after they become components for our aircraft. Below is a Gantt Chart depicting the progress of the team (Fig. 6.1).

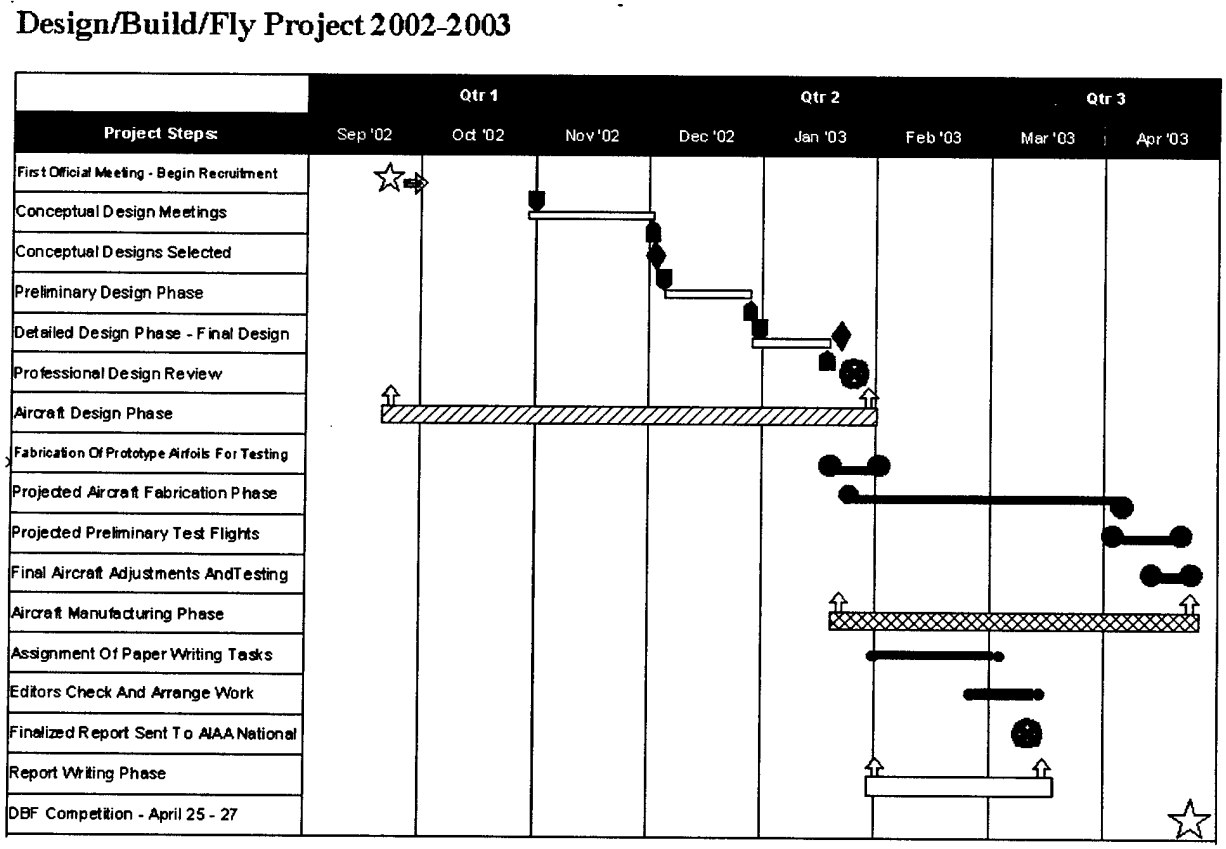

Figure 6.1: Gantt Chart

6.2 Manufacturing Processes by Aircraft Component

6.2.1 Manufacturing FF's Wings and Empennage

In order to create a wing structure that was strong yet light, we opted to construct a foam core that would be covered in a lightweight composite skin. To add structural strength to the wing, a spar (stringer) was inserted at its quarter cord. To create the wing's foam core, we used a data base of airfoils to get a set of (x,y) plane coordinates for our foil, the Selig 4022. Feeding these coordinates into a

computer program at school networked with a laser computer aided machining (Laser CAM) device, we were able to cut templates, or exact dimensioned replicas of our airfoil's cross section out of thin plywood. Attaching one of these templates on each end of large blocks of low-density white foam and using a hot wire (bow) cutter, we drew a heated wire over the wooden templates and were left with the foam cores of our wings. Very fine sand paper was then used to eliminate any waves or imperfections that may have resulted from the bow cutter, and to round the leading edge of the wing. Large pieces of fiberglass cloth were then cut and wetted with epoxy and laid onto the foam wing. Mylar, a thick but very smooth and pliable plastic, was then draped onto the wing and everything was placed onto a sealed bag which held a vacuum hose. Applying a vacuum to the bag (bagging/bagged) would eliminate the air inside and apply equal pressure to the core as it cured. The Mylar will give the skin of the wings a very smooth look and feel and will help to reduce drag during flight.

While the same hot wire process was used to cut out horizontal and vertical stabilizers for the aircraft, no spars were needed because the stabilizers are fairly small and the skins will acceptably take all of the loads encountered during flight. However, to error on the side of caution several strands of carbon tow were affixed to the leading and trailing edges of both of the stabilizers to ensure strength in flight and during transportation. Similarly to the main wing, the horizontal and vertical stabilizer foam cores were covered with a fiberglass skin and bagged to cure with Mylar to keep surfaces as smooth as possible.

6.2.2 The Spar and Spar Joiner Construction

The afore mentioned spar was made by first removing a section of the foam wing core 1 inch wide about the quarter cord length from the entire length of the wing. Using layers of epoxy wetted bidirectional carbon cloth, we placed six layers of the cloth (two each of three different lengths: one-third, two thirds, and full length) onto both the top and bottom of the excised piece of foam and bagged it overnight to cure. The inner third of the spar has been covered on each side by six layers of carbon cloth, the middle third by four, and the outer third by only two, in order to ensure enough wing strength to survive a 3 "G" load while keeping weight to a minimum. Excess carbon fibers were sanded off before proceeding to lay approximately 3 layers of epoxy wetted fiberglass cloth around the entire spar structure and bagging again.

At this point, we decided to test the strength of our spar by keeping four inches of the inner portion of the spar (root end) stationary in a bench vice and setting several small weights on the suspended end. We were disappointed to see a fair amount of deflection in the length of the spar after loading with less than 5 pounds. Had we continued with this design, the wings may have buckled during the "wingtip test" or worse, during flight. A stronger and stiffer design was needed for our spar application.

In our never-ending search for high strength with lightweight, we were turned to balsa wood to reconstruct the wing spar. Balsa, with its natural fiber structure and lightweight was as ideal for our application as we were going to find. A piece of balsa was trimmed to the exact dimensions of the now

broken foam core of our previous spar. We then subjected the wood the same rigorous layers of unidirectional carbon fibers, wraps of fiberglass, and finally two extra layers of unidirectional carbon on the three and a half inches of the spar nearest its root. After completely curing, we tested the new spar in the same fashion we had the last. With almost 10 pounds of weight near the spar's tip, there was very little deflection and the spar was deemed acceptable. Another balsa spar was made as described above for the other wing and the spars were then replaced and bonded into their respective wings. These processes made a sufficiently light yet very strong box-beam structure central to the wing helping to keep it rigid under all conditions.

The spar joiner was an engineering challenge from the start. All loads on the wings will be transferred through this joiner, necessitating that it be stout. While most machined metal joiners would have been sufficient strength wise, their weight was unacceptable. Our attention turned to carbon once again and a mold was made of aluminum to the exact dimension of where our joiner would sit when placed into the fuselage. The spars were temporarily attached together and placed into the mold. Epoxy wetted unidirectional carbon strands were then placed on all sides of the spar until the two sides and the top and bottom had equal amounts of carbon material between the spar and the mold. The mold was then closed and left to cure, making an exact female acceptor for the spars to slide into during assembly. Upon curing, the spars were removed from the joiner, and the joiner removed from the mold. The joiner was then sanded into the exact shape needed for its installation into the fuselage.

6.2.3 Fuselage Construction

Due to this year's different and fairly unique set of requirements, the fuselage took on a shape that directly resembled its payload, a box. While it is not the most aerodynamic of choices, it was necessary in order to comply with the "packing box" constraints. With exception of the plane's nose cone and main fuselage floor, the fuselage is made entirely of composite "sandwich material" which has proven to be strong and light in previous years' contests. Slices one-fourth inch thick of high-density "blue" foam were cut from larger blocks. These slices were then sandwiched by a layer each of epoxy wetted unidirectional and bidirectional carbon cloth on top and bottom, then vacuumed. After curing, marks were made on the material and panels were cut in the exact dimensions of fuselage secondary floors, walls, and fairings. The primary floor of the fuselage was produced from a one-fourth inch thick piece of aircraft grade birch plywood. This was necessary in order to have a very stiff, load and vibration absorbing central backbone of the aircraft. Although it was slightly heavier than the sandwich material, the extra strength it gained was well worth it.

The nose cone of the aircraft is a fiberglass shell with an internal rib structure of balsa wood that will act as a bulkhead for the motor. By cutting and sanding the blue foam to a desired shape made a male foam mold of the nose cone. The mold was then covered with four layers of epoxy wetted fiberglass and bagged until cured. The foam mold was then removed from its shell and internal measurements were taken. Using these measurements, ribs of balsa wood were cut out and placed in the nose cone

forward of the motor mount on the fuselage to act as bulkheads for the motor. A small hole was cut at the front of the nose cone for the propeller shaft to pass through and as a ventilation hole for motor cooling.

6.2.4 Boom

The boom attaching the fuselage body of the plane to the empennage is a pre-manufactured carbon composite spun tube with a one inch inner diameter. The tail section is attached to the boom with two nylon screws threaded through the boom from the bottom and into the vertical stabilizer. The boom attaches to the fuselage through three bulkheads internal of the body. There will be a notch on the boom that will allow the entire tail section to be locked into place when the boom turned a quarter of a revolution about its axis.

6.2.5 Landing Gear Manufacturing

The landing gear for the aircraft was made with prepreg carbon composite. A mold for our landing gear was made by rolling a sheet of aluminum that had been machined to the desired shape and curve of the gear. The carbon was then laid onto the machined piece and placed in an autoclave for curing. When the gear emerged, a hole was drilled at the bottom for the wheel axels, and at the top several holes were made in order to attach the gear to our fuselage.

6.3 Costs, Skills, and Schedules

6.3.1 Cost of Composite Materials

While the cost associated with using composite materials is greater than using non-composites the decrease in weight and increase in strength made composites the hands down choice for many manufacturing applications. From the start of the project, the team anticipated incurring the cost of these materials and therefore was budgeted for their purchase. Nonetheless, care was taken in purchasing materials like carbon cloth, fiberglass, and epoxies to reduce cost and waste.

6.3.2 Skills and Tools Needed to Work with Composites

Nearly half of this year's team is returning members from last year's team. This helped to create a group of students that were familiar with working on composite materials. This knowledge included not only the ability to manipulate these materials in the necessary fashion, but also being able and confident to use the tools associated with building composites such as sanders, heat guns, vacuum pumps, and rotary tools. Using epoxy resins is also a small science of its own in which attention to detail is essential. Of course safety is always a priority, so goggles, face masks, gloves, breathing filters and lab coats were supplied to those working in and around the shop to protect them from any lab associated dangers.

6.3.3 Manufacturing Schedule

Manufacturing began as soon as funds became available to purchase needed materials and tools. The team met Thursdays, Fridays and Saturdays in order to get 12 to 15 hours of work completed

each week for the first 4 weeks of the manufacturing phase. Goals were set for what needed to be completed by the end of each week in order to keep the team organized and motivated. At least 2 team members met to do construction at any given time. One "veteran" team member was present whenever any manufacturing was taking place to ensure safety, productivity and quality. The Furious Flier is planned to be fully completed by the last week of March 2003. Completing the manufacturing several weeks before the competition will enable the team to have plenty of time in which to do flight testing and make any last minute changes or amendments to the aircraft. This will also enable our pilot to become accustomed to the plane and its characteristics before arrival at the competition site.

7.0 Test Planning

7.1 Dynamic Test: Graupner Motor

The purpose of testing the Graupner Ultra 3300/5 is to help in determining what RPM gives the greatest efficiency for the motor used. The motor in question is a Grauper Ultra 3300/5 and operates at 18 volts with a gear ratio of 2:1. Figure 7.1 is arranged to use two relationships to best confirm how the motor should be operated for best efficiency in flight. The first relationship is that of power (watts) and RPM. The second relationship is that of current (amperes) and efficiency.

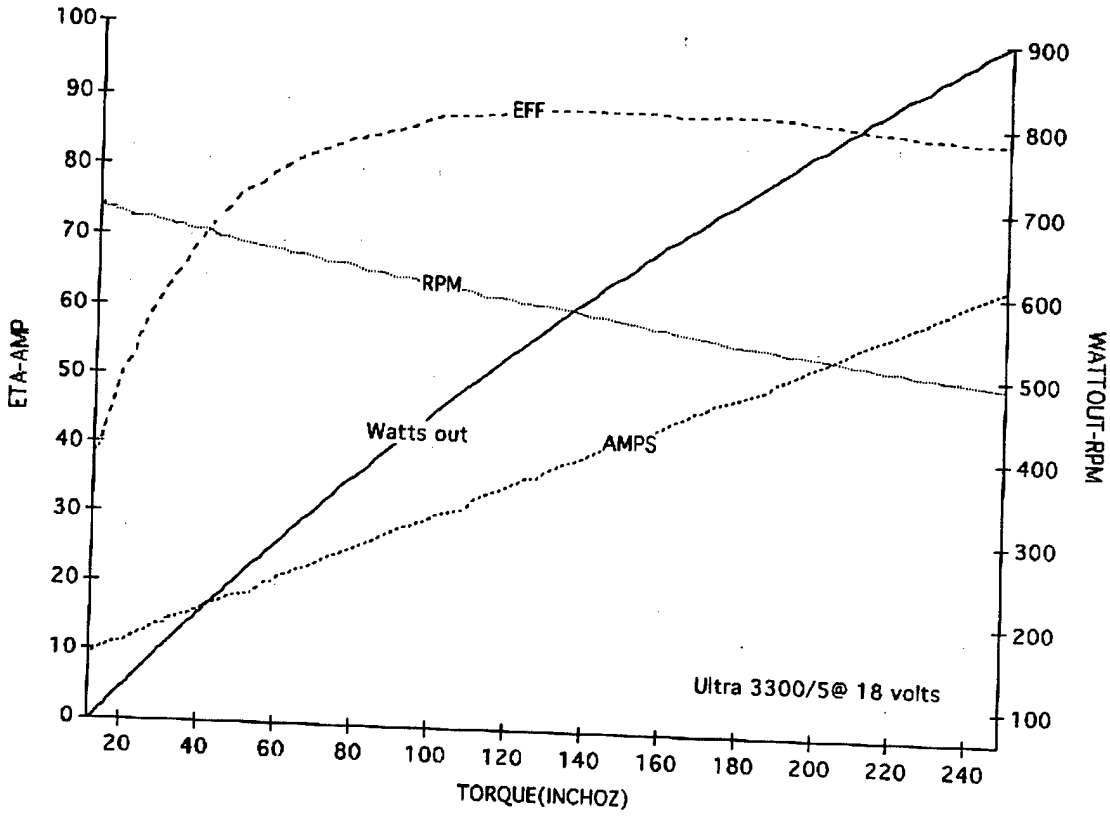

Figure 7.1: Dynamometer plot

An example of how the graph yields information is attained by examining the data for a specific efficiency. When the motor is performing at 60% efficiency, the current supplied to it is 15 amperes. At this efficiency the power from the motor is 8W. Also, the RPM exerted by the motor are 675.

The data on the graph indicates that the highest efficiency achievable by the motor is 89%. This occurs when the current supplied to the motor is 40 amperes. At 40 amperes, the power produced by the motor is 580. From this data it is determined that the RPM ideal for maximum efficiency is 560 RPM. Therefore the motor should ideally be operated at 560 RPM to achieve maximum efficiency.

The process of gathering the data represented in the graph took a total of one hour to complete by the UCSD D.B.F. team. The data serves to provide direction when deciding how the motor's performance should be integrated to the aircraft as a whole. For example, if it is not possible to operate the motor at 560 RPM during flight, the data represented in the graph will aid in choosing another suitable RPM setting for the aircraft's operation. One reason why the motor may not be able to be operated at 560 RPM during flight could be the interaction between the vibrations given off by the motor and the aircraft structure. In such a case the data in the graph would prove indispensable in deciding how the motor should be operated.

8.0 Reference:

1. Abbot I.H., Theory of Wing Sections, Dover Publications Inc, 1949.
2. Nelson, R., Flight Stability and Automatic Control, McGraw Hill, 1989.
3. Nicolia, L..M., Fundamentals of Aircraft Design, METS Inc, 1984.
4. Peery, D.P., Aircraft Structures, McGraw-Hill Inc., 1982.
5. Przemieniecki, J.S., Performance, Stability, Dynamics, and Control of Airplanes
6. Raymer, D.P., Aircraft Design: A Conceptual Approach, AIAA Education Series, 1989.

3 View Drawings

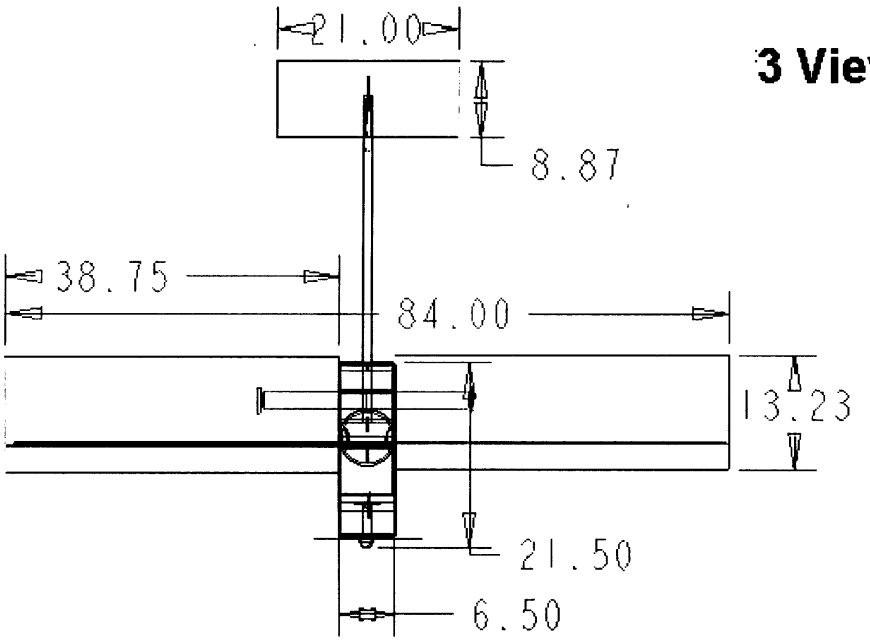

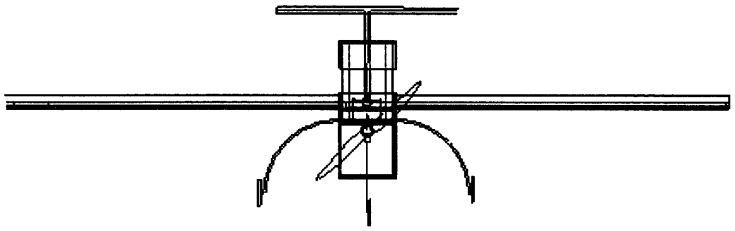

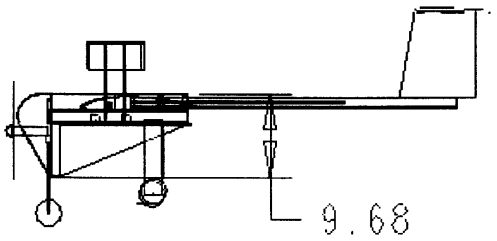

2003 AIAA Design / Build / Fly

Team Bellwether – University of Colorado

Prepared By:

Stephen Nauman/AE/JR
Gabe LoDolce/AE/JR
Cory Dixon/AE/GRAD
Christian Ehiem/AE/GRAD
Michael Sheek/AE/SR
Tom Bateman/AE/JR
Jake Hanft/AE/SR
Derek Lerner/AE/JR
Derrick Maestas/AE/SR
Jason Leiby/AE/JR

Submission Date: 3/10/03

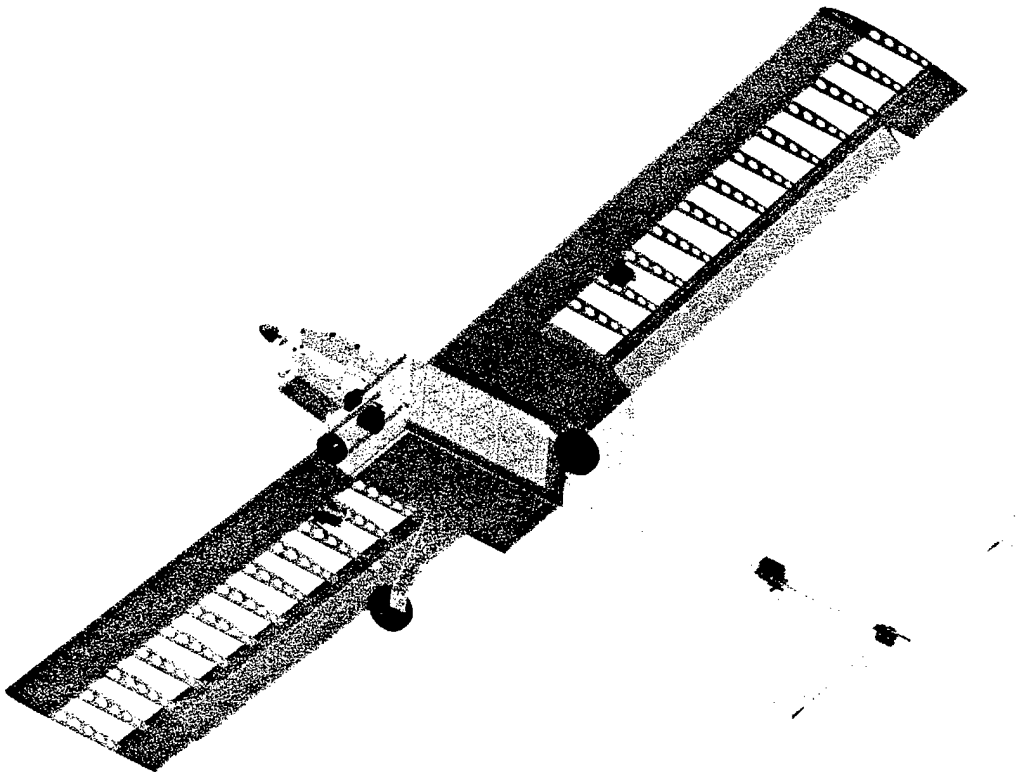

TABLE OF CONTENTS

1	**Executive Summary**	4
1.1	***Conceptual Design***	4
1.1.1	*Design Alternatives*	4
1.1.2	*Design Tools*	5
1.1.3	*Conceptual Design Results*	5
1.2	***Preliminary Design***	5
1.2.1	*Design Analysis*	5
1.2.2	*Design Tools*	6
1.2.3	*Preliminary Results*	6
1.3	***Detail Design***	6
1.3.1	*Design Analysis*	6
1.3.2	*Design Tools*	6
1.3.3	*Detail Results*	7
2	**Management Summary**	8
2.1	***Leadership Structure***	8
2.1.1	*Aerodynamics Team*	8
2.1.2	*Propulsion Team*	8
2.1.3	*Structures Team*	9
2.2	***Milestone Chart***	9
3	**Conceptual Design**	9
3.1	***Basic Mission Requirements***	9
3.2	***Deployable Payload Requirement***	10
3.3	***Antenna System***	10
3.4	***Basic Configuration***	11
3.5	***Trade Studies***	11
3.5.1	*Cost Model*	11
3.5.2	Alternative *Designs*	12
3.5.3	*Aircraft Fuselage and Tail Configuration*	13
3.5.4	*Wing Configuration*	13
3.5.5	*Structural Configuration*	14
3.5.6	*Propulsion*	14
4	**Preliminary Design**	15
4.1	***Design Parameters and Sizing Traits***	15
4.1.1	*Wing Design*	15
4.1.2	*Tail Design*	17
4.1.3	*Power & Propulsion*	19
4.1.4	*Fuselage Design*	21
4.1.5	*Antenna Design*	22
4.2	***Analysis Methods Used***	22
4.3	***Mission Model and Predicted Performance***	23
4.3.1	**Mission A – Missile Decoy**	25
4.3.2	**Mission B – Sensor Deployment**	25
4.4	***Lift, Drag, and Stability Estimates***	26
4.4.1	*Lift and Drag*	26
4.4.2	*Stability*	26
4.5	***Design Optimization and Trade Studies***	29
4.5.1	*Wing*	30
4.5.2	*Tail*	31
4.5.3	*Fuselage*	31
4.5.4	*Propulsion*	32

4.5.5 Antenna 32

5 Detail Design 33
5.1 Materials 33
5.2 Propulsion 34
5.3 Wing Design 35
5.4 Fuselage Structural Design 35
5.5 Wing Attachment 35
5.6 Tail Design 36
5.7 Tail Attachment 36
5.8 Weight and Balance 36
5.9 Drawing Package 38
5.10 Rated Aircraft Cost and Aircraft Sizing 39
5.10.1 Rated Aircraft Cost 39
5.10.2 Sized Aircraft Table 40

6 Manufacturing Plan and Processes 41
6.1 Manufacturing Processes Examined 41
6.2 Manufacturing Utilized for the Fuselage 41
6.3 Manufacturing Utilized for the Wing and Tail 42
6.4 Manufacturing Schedule 42

7 Testing Plan 43
7.1 Objectives and Schedule 43
7.2 Schedule 43
7.3 Test Descriptions 44
7.3.1 Antenna Flight Test 44
7.3.2 Motor and Propeller Tests 45
7.3.3 Taxi Test 45
7.3.4 HOP Test 45
7.3.5 Flight Test 46

8 References 46

9 Acknowledgements 46

Table of Figures

Figure 1: Leadership Structure 8

Figure 2: Cost Model Sensitivity 12

Figure 3: Wing Loading 17

Figure 4: Tail Volume in relation to Neutral Point Location 18

Figure 5: Motor Efficiencies as a Function of Current Draw 20

Figure 6: Representative Motor Parameter for 40 sized Astro-Flight Motors 21

Figure 7: Cruise Performance in relation to Weight 23

Figure 8: Cruise Performance Stall Speed with Full Flaps in relation to Weight 24

Figure 9: Stall Speed with Full Flaps in relation to Weight 25

Figure 10: C_L with respect to Angle of Attack....27

Figure 11: C_M with respect to Angle of Attack....28

Figure 12: C_L and Elevator Deflection....29

Figure 13: Drag Polar for a Selection of Airfoils [WEB XXX]....30

Figure 14: Movements in the Center of Gravity due to Payload and Antenna....38

Figure 15: Rated Aircraft Cost Breakdown....40

Figure 16: General Aircraft Sizing....40

Figure 17: Manufacturing Schedule....43

Figure 18: Testing Schedule....44

Table of Tables

Table 1: Project Milestone Chart....9

Table 2: Aircraft Configuration Figures of Merit....13

Table 3: Wing Configuration Figures of Merit....14

Table 4: Structural Configuration Figures of Merit....14

Table 5: Propulsion Configuration Figures of Merit....15

Table 6: Stability Coefficients....26

Table 7: Elevator Lift and Moment Coefficients....28

Table 8: Weight Estimation Chart....37

Table 9: Center of Gravity and Movements due to Payload and Antenna....37

1 EXECUTIVE SUMMARY

Def: bell·weth·er [n] - One that serves as a leader or as a leading indicator of future trends[1].

Team Bellwether, from the University of Colorado, Boulder, formed to compete in the 2002/2003 Cessna/ONR Student Design Build & Fly competition. The team name was chosen to represent the fact that this is CU's first year in the competition, and is representative of the growing student interest at CU in miniature aircraft. The team name also represents the fact that one of the team's goals is to establish the DBF competitions as on ongoing yearly project at CU.

The competition is based on designing, fabricating, and demonstrating a miniature sized [REF] electric powered radio controlled aircraft that is capable of performing two of the three specified missions. The competition score is determined by a combination of the Total Flight Score, Written Report, and Rated Aircraft Cost. Thus obtaining the highest score equates to designing an aircraft that can complete the most difficult missions in the shortest amount of time while minimizing the Rated Aircraft Cost and assembly time.

The design process followed by Team Bellwether is the standard three-step process consisting of three phases: the Conceptual Design, Preliminary Design, and the Detail Design. At the completion of each stage a design review is held to discuss the decisions made in each phase with the help of a review panel.

1.1 Conceptual Design

The first task of the conceptual design stage was to formulate and understand the problem at hand. This involved scrutinizing the competition requirements and rules to formulate the design requirements. It was during this phase, with the understanding of the design requirements, where the team set the initial project goals. The goals consisted of designing a standard configuration, standard structure, R/C aircraft capable of flying the most difficult mission. This initial choice was based on the desire to keep the design and construction as simple as possible, while having a high scoring aircraft.

With the project goals decided, the design team was split into subsystems consisting of Aerodynamics, Propulsion and Structures. It was the task of these teams to suggest various preliminary configurations of the system. These configurations were then rated based on several factors including construction, difficulty, time, Rated Aircraft Cost, and ability to satisfy the project goals. These factors were formed into figures of merit to enable a quantification of the design analysis. The end goal of the conceptual design phase was the suggestion of a systems level design based on the figure of merits of the competing designs.

1.1.1 Design Alternatives

[1] *The American Heritage® Dictionary of the English Language,* Fourth Edition. Copyright © 2000 by Houghton Mifflin Company.

The preliminary design alternatives focused on the propulsion system, wing planform, and fuselage layout and payload placement since it was decided in the beginning to design a standard configuration aircraft. This main configuration was varied with different wing planforms, tail configurations, propulsion system layouts, and payload placement. The wing planforms considered were tapered and rectangular. The tail configurations considered consisted of T-tail, H-tail, and conventional layouts. The power systems analyzed used single and multiple engines with assorted battery pack configurations. The standard configuration leads to certain, unavoidable, payload placement and structural design requirements.

1.1.2 Design Tools

Trade studies and Figures of Merit were the primary tools used during the conceptual design phase. The trade studies consist of historical and experiential data and were used to aid in initial design choices by suggesting trends. The FOM were used to quantify different design constraints and to suggest a best-choice configuration of those analyzed.

1.1.3 Conceptual Design Results

A standard configuration with a single engine, single power supply was chosen as the conceptual design. To minimize design complexity, a detachable two-piece wing was chosen, which due to shipping container constraints, gives a maximum wingspan of 7.5 ft. To minimize the effect of the antenna on the vertical tail and thus yaw control, an H-Tail configuration was chosen. The tail design was also chosen so that it is a single unit with the fuselage, fitting within the box in one piece to minimize assembly time. Finally, it was decided to carry the box below the aircraft, using a pin to release the box onto the runway. The design of the tail and fuselage was made to allow the airplane to have clearance to simply drive away from the dropped payload box.

1.2 Preliminary Design

The goal of the preliminary design phase was to generate aircraft specifications for the conceptual design. These aircraft specifications were used to analyze the conceptual design against the design constraints and for mission performance predictions, and when necessary changes were made to the design to meet mission and performance requirements.

1.2.1 Design Analysis

During the preliminary design, the major subsystems that were analyzed were aerodynamics and propulsion. These systems were varied in their designs to find a configuration that meets the mission requirements. The first step taken was to specify a wing loading, which directly relates to takeoff and flight performance. Since meeting the 120 feet takeoff distance is one of the hardest objectives, most of the analysis during this phase was related to takeoff performance.

1.2.2 Design Tools

The design tools used during the preliminary phase consisted of an Excel spreadsheet along with several MATLAB routines. The spreadsheet is the primary tool used by the team for the design analysis. It is broken into the major subsystems consisting of Propulsion, Aerodynamic, and Structures. The propulsion section takes as input motor, battery, and propeller parameters and outputs power and performance predictions. The aerodynamic section is quite extensive and consists of several major subsections. Of these, the more important ones consisted of wing analysis and drag predictions for the aircraft. The aerodynamics and propulsion sections were used to evaluate mission performance based on the predicted values.

1.2.3 Preliminary Results

From trade studies of R/C electric aircraft, a value of 30 oz/ft^2 was chosen as the target wing loading of the fully loaded aircraft. A rectangular wing with a wingspan of 7.5 ft and a 1 ft chord was chosen and gave a projected takeoff weight of 14 lb. The C_{Lmax} for the aircraft at takeoff was chosen to be 1.2, which with the wing loading gave a takeoff speed of 44 ft/s at 1.2 V_{stall}. With an estimate of drag, it was determined that a minimum of 5-lb static thrust was required to meet the takeoff distance. To accomplish this, an Astro Flight 40 electric motor was chosen as the preliminary propulsion system.

1.3 Detail Design

In the detail design phase, the final aircraft configuration was designed to maximize mission performance and meet specified project goals. This implied determining a final design with the fastest flight and assembly times while minimizing the RAC. During this phase, the aircraft was refined several times to obtain the best values possible from the preliminary design. The detail design also focused much more on the structural and mechanical aspects of the system. Emphasis was placed on simplicity when possible for construction and manufacturing purposes.

1.3.1 Design Analysis

The detail design finalized the several aspects of the aircraft including airfoil selection, tail size, cruise conditions, propulsion system, structures, weight, and finally stability. The wing configuration and propulsion system were analyzed in detail to obtain the best configuration for cruise conditions while meeting the takeoff requirement. The manufacturing process was also analyzed and set for the next phase of the project.

1.3.2 Design Tools

The detailed design analysis was performed using the Excel spreadsheet and MATLAB scripts mentioned above. The MATLAB scripts were heavily used during this phase to provide faster, more efficient numerical analysis of the different subsystems. MATLAB was also used to simulate some of the different subsystems to help in the final design choice. The structural and mechanical designs were implemented using AutoCAD. The 3D drawing of the aircraft aided in the placement of components and the layout of the structure.

1.3.3 Detail Results

The final aircraft configuration was designed to have a gross takeoff weight of 14 lb, including antenna and payload box. With a wing loading of 30 oz/ft^2, using an Astro Flight 40 motor geared to 1.63, and spinning a 14x10 propeller, the predicted takeoff distance was a little less than 100 ft at a speed of 44 ft/s. Cruise speed was set to be 66 ft/s based on the most efficient operating conditions of the propulsion system. The Clark-Y airfoil was chosen due to its excellent low speed qualities along with the fact that it is a flat bottom airfoil, which helps reduce construction and design difficulties.

2 MANAGEMENT SUMMARY

2.1 Leadership Structure

University of Colorado's "Team Bellwether" was comprised of four groups: structures, propulsion, aerodynamics, and documentation. A team lead was assigned to each of these groups and placed responsible for the productivity of each respective team as well as communication with the team systems engineer. All other members of the team were placed in one of the three aircraft specific groups i.e.: structures, propulsion and aerodynamics. The documentation team lead served as recorder and organizer of all activity during the entire design, build, and fly process. The systems engineer was responsible for not only the accountability of the team leads but the overall successful progression throughout the mission. Below is Figure 1 showing the team structure.

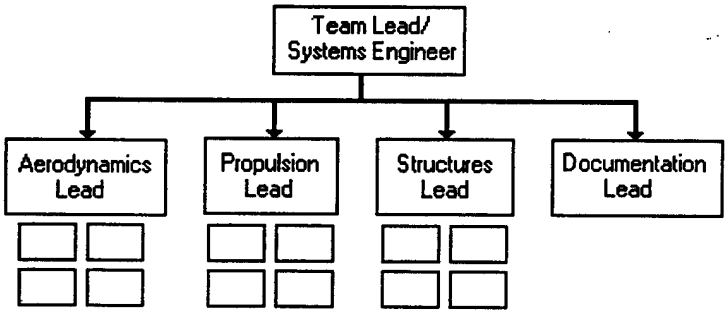

Figure 1: Leadership Structure

2.1.1 Aerodynamics Team

The aerodynamics team was responsible for considering the overall design of the aircraft from an aerodynamics point of view. This included but was not limited to the selection of an airfoil as well as conduction of the drag expected over the aircraft and antenna. The aerodynamics team also participated in the stability calculations of the center of gravity and aerodynamic center. During the flight-testing, stability and drag will be further tuned for efficient flight.

2.1.2 Propulsion Team

The propulsion team was responsible for attacking the design process from a propulsion standpoint. This team chose the motor, propeller, battery size, and configuration based on a trade study that was conducted to determine the propulsion configuration most efficient for the given design parameters. This team worked closely with the aerodynamics team to ensure proper stability and weight balance. During the building stage, the team was responsible for assembly and testing of the propulsion system. Flight tests are to be overseen by members of the propulsion team to ensure proper operation of the engine.

2.1.3 Structures Team

This team was responsible for all integration of the propulsion system as well as the design and structural analysis of the aircraft fuselage, wing, payload system, and antenna attachment system. During the design phase, the team had to examine such topics as material selection and overall aircraft structural design. During the building stage, the structures team explored various manufacturing techniques and completely machined and fabricated all structural components of the aircraft. Structures team members will be present during flight-testing in order to assess the structural performance of the aircraft as well as to make any modifications or repairs that may be needed.

2.2 Milestone Chart

At the beginning of the engineering process, the team planned out a schedule of all the primary steps that must be met to ensure the successful completion of the given mission. Below is a chart of these primary milestones.

Table 1: Project Milestone Chart

Date	Milestone
10/20/2002	Design Build Fly Team Assembled
10/20/2002	Begin Conceptual Design
11/2/2002	Present Design Suggestions
11/18/2002	Conceptual Design Review
12/19/2002	Concept Set
12/20/2002	Begin Detailed Design
3/4/2003	Complete Detailed Design
3/11/2003	Report Due
3/12/2003	Begin Manufacturing
4/11/2003	Complete Manufacturing
4/13/2003	Begin Flight Testing
4/18/2003	Complete Flight Testing
4/25/2003	Competition

3 Conceptual Design

3.1 Basic Mission Requirements

The basic mission requires that an electrically powered, miniature sized, remotely controlled aerial vehicle carry aloft a deployable five-pound sensor package and antenna/radome assembly. The aircraft must have a maximum takeoff run of 120 feet at maximum takeoff weight, and be able to fly a specific flight path, including two takeoffs and two landings, on one battery charge. The sensor package is to be remotely deployable when the aircraft is on the ground.

3.2 Deployable Payload Requirement

The dimensions of the payload to be carried directly affect the overall configuration of the aircraft. Of primary importance was the location of the payload and its effects on the center of gravity of the aircraft. Since the payload must be deployable, it must be positioned such that the center of gravity shift due to deployment (if any) will not exceed the requirements for longitudinal stability. The amount of shift is dependent upon the weight of the aircraft, the weight of the payload (fixed at 5 pounds), and the distance between the centers of gravity of the payload and aircraft. Zero shift occurs when the center of gravity of the box and aircraft are coincident. Since the aircraft gross weight could not be precisely determined prior to development of a detailed design, the initial design target was to place the center of gravity of the sensor package longitudinally coincident with that of the empty aircraft.

Two basic configurations on how the payload was to be carried were explored: an exposed payload and an enclosed payload. The initial drag estimates indicated that parasite drag would be dominant, so an enclosed payload was chosen in order to take advantage of drag reduction by streamlining. Since the payload must be ground-deployable, the cargo compartment must have some type of opening. In addition, since the obvious method of deployment was to drop the payload below the aircraft, there must also be some provision to allow the aircraft to taxi away from the package after deployment. Whereas employing long landing gear could provide sufficient ground clearance, the savings in weight from the shorter landing gear, and lack of rear fairing favors a payload compartment that is open to the rear as well. In the initial assessment, the aforementioned weight savings were determined to outweigh the drag reductions (if any) by streamlining the rear of the payload compartment.

Some attention was given to the effects on both drag and stability caused by payload deployment. The first conceptual design included retractable doors that would cover the bottom and rear of the payload compartment after deployment. The rear doors were discarded early after determining that a flat section downstream of the flow would have the same drag effect, regardless of whether it would be covered. The possibility of increased interference drag due to exposed payload compartment walls was determined to be inconsequential, since the significant weight reduction after payload deployment would greatly improve performance anyway. The concern over the possible effects of stability or trim changes due to payload deployment was determined to be less important than the function of the payload deployment system, so the doors were eliminated in favor of reliability.

3.3 Antenna System

The antenna's effect on the performance of the aircraft is manifold. Its size and cylindrical shape produces a significant amount of drag, and the drag potentially induces a moment that could affect trim and both longitudinal and yaw stability. The slipstream of the antenna could affect the flow over the vertical and/or horizontal stabilizers – this was a major influence in the design of the tail assembly. Lastly, there could be a center of gravity shift associated with configuration changes. The requirement for minimum separation from

structures and for horizontal mounting limits the possibilities for positioning. For alaterally symmetric design, the antenna must either be mounted above or below the centerline of the fuselage. In order to mount the antenna below, a minimum of six inches ground clearance would be required in order to meet the separation requirements. In addition, the landing gear might affect the visibility of the antenna. Furthermore, if mounted below the fuselage, the drag moment would contribute to an unstable pitch-velocity relationship. The most attractive configuration given these choices is above the fuselage centerline.

When mounted above the fuselage centerline, the antenna's slipstream would impinge directly upon a conventional vertical stabilizer. For this reason, a twin vertical stabilizer design was employed. The details of the stabilizer are discussed later in the report. The vertical position of the antenna is essentially fixed by the standoff requirement, however the longitudinal position could be placed anywhere between the propeller and stabilizer. If the antenna is placed forward of the aircraft center of gravity, the assembly would adversely affect the yaw stability of the aircraft. This suggests that the antenna should be placed either above the wing, or somewhere on the tail section. In order to minimize the center of gravity shift due to configuration changes (the aircraft is flown without the antenna installed on one mission), the antenna should be placed close to the aircraft center of gravity. The antenna weight is approximately eight ounces, so it's effect on the aircraft center of gravity is significant..In order to balance the yaw stability and center of gravity effects, the center of the antenna was placed about two inches aft of the trailing edge of the wing. This is consistent with existing aircraft, such as the E-2C Hawkeye airborne early warning platform. This configuration was successfully flight tested on a test aircraft (A Tower Hobbies Trainer Forty).

3.4 Basic Configuration

The conventional wing and tail design was chosen as the overall configuration. This is the predominant design of all aircraft due to a combination of factors, which, in the absence of special requirements is usually the best choice. The necessity for taxiing away from the sensor package eliminated the possibility of a pusher aircraft. Canard designs were also immediately eliminated due to their increase in complexity of the aerodynamic design and from the lack of success of the canard design in the competition.

The tail configuration was affected by both the sensor package requirements and the antenna location. To allow clearance to the rear during payload deployment, the tail section was configured as a high mounted tail boom. Twin vertical tails (H-tail) were employed, in order to place the vertical stabilizers outside the turbulent wake of the antenna, and to provide sufficient surface area within the box sizing requirements. This allows for a tail assembly that will fit in the specified shipping container as a single unit. The initial design of the vertical surfaces was such that the entire fuselage would fit into the shipping container without disassembly.

3.5 Trade Studies

3.5.1 Cost Model

Since the cost model was established as a major design influence, some emphasis was placed upon optimization of the design, with regards to modeled cost. The first step in this process was to determine the sensitivity of the cost model to certain design elements. A chart was developed which enabled some visualization of this sensitivity (Figure 2).

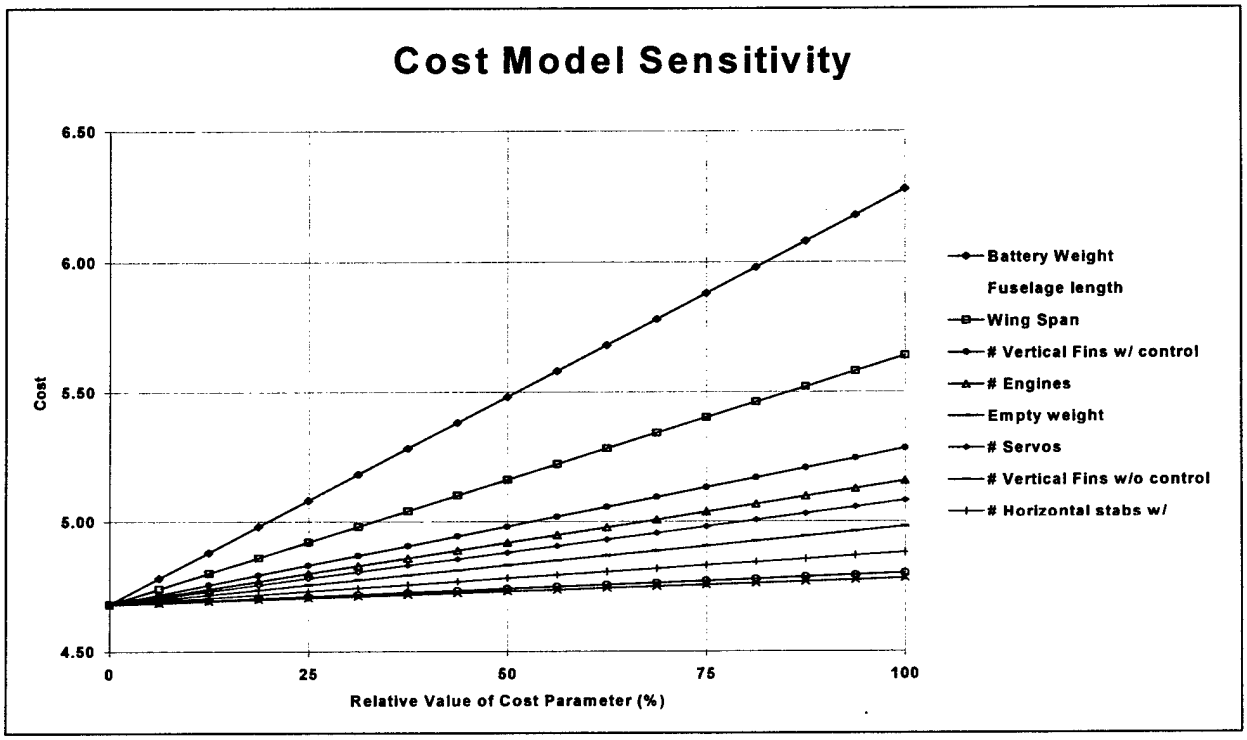

Figure 2: Cost Model Sensitivity

From this visualization, it became obvious that a primary concern was battery weight (which is also a function of overall weight), followed by the wingspan and fuselage length.

3.5.2 Alternative *Designs*

Figures of merit for different aspect of the aircraft were identified and examined. With the figures of merit, decision matrices were generated to aid in choosing a final design. Within the decision matrices each figure of merit was given a weight, signifying how it affects the outcome of the design. The figures of merit for each alternative design were given a score relative to a basic configuration (i.e. rectangular wing). Within each decision matrix the alternative design with the highest score was chosen.

3.5.3 Aircraft Fuselage and Tail Configuration

The configuration of the aircraft is dependent on the following figures of Merit (FOM).

- Aircraft Size: The aircraft is required to fit into a 4x2x1 ft (interior dimensions) box. This competition requirement limits the size and shape of the aircraft.
- Aircraft Cost: The RAC is one of the primary factors weighed when designing the aircraft since it has a significant affect on the overall score.
- Aircraft Control: Control of the aircraft is an important factor in any aircraft design. In order to compete effectively the aircraft must be stable and be relatively simple to fly.
- Drag Performance: Since the maximum takeoff distance is set at 120 ft, and for one mission an antenna will be attached, the power of the aircraft must be used efficiently.
- Construction: With resources available, the manufacturing of the aircraft plays a role in its configuration.

With the figures of merit that affect the aircraft configuration identified, different aircraft configurations where examined. The following table shows how each figure of merit affected the aircraft configuration in comparison to a standard configuration; the aircraft with the highest score was chosen.

Table 2: Aircraft Configuration Figures of Merit

		Configuration				
Figures of Merit	Weighting Factor	Standard	Canard	V-tail	H-tail	Delta Wing
Aircraft Size	0.25	0	-0.25	0	0	-1
Rated Aircraft Cost	0.3	0	0	-0.75	-0.75	0
Aircraft Control	0.2	0	-1	0	0	-1
Drag Performance	0.2	0	1	1.5	1.5	-1
Construction	0.5	0	0	-1	0	-1
Score		0	-0.0625	-0.425	0.075	-1.15

Of the configurations examined the H-tail configuration scored the highest. Although this configuration does not have the best RAC, it has drag advantages when the antenna is attached to the aircraft.

3.5.4 Wing Configuration

Once the fuselage and tail configuration were decided upon the configuration of the tail was considered. Figures of merit for the tail configuration are as follows.

- Loading: The wing must have a high enough wing loading to carry the payload.
- Construction: The group must be able to manufacture the wing with the resources available.

- Stability: The wing must provide a stable aircraft for control purposes.

Table 3 shows the wing alternative wing configurations considered and how they are affected by each figure of merit.

Table 3: Wing Configuration Figures of Merit

		Configuration		
Figures of Merit	Weighting Factor	Rectangular	Tapered	Swept-Tapered
Loading	0.5	0	0.5	0.5
Construction	0.3	0	-1	-1.5
Stability	0.2	0	0	0
Score			-0.05	-0.2

Because the advantages of having a swept or tapered wing are outweighed by the difficulty involved in manufacturing a wing of this type, a rectangular wing was chosen.

3.5.5 Structural Configuration

Several alternatives were examined for the structural configuration of the aircraft. The figures of merit considered in this decision are construction, strength to weight ratio, and cost. The alternative structural configurations and how they compare to a wood build up are shown in Table 4.

Table 4: Structural Configuration Figures of Merit

		Configuration			
Figures of Merit	Weighting Factor	Wood	Wood/Aluminum	Carbon Fiber	Foam Core
Construction	0.5	0	0	-1	-1
Strength to Weight Ratio	0.4	0	0.5	1	0.5
Cost	0.1	0	-0.5	-1	-1
Score		0		-0.2	-0.4

The structural configuration chosen is a conventional wood build up, with an aluminum spar, which acts as a backbone and ventilation shaft. This configuration with the aircraft best because of it is relatively simple to build and has a high strength to weight ratio.

3.5.6 Propulsion

From the given aircraft cost model, it was found that the most expensive aspect of the design is due to the battery weight. This in-turn drove the choice for an engine size. While it was desired to have the most power possible in order to complete the missions the fastest, more power equated to more battery weight and even possibly causes the power to be less efficient as well. Thus it was ultimately decided to choose the engine which would provide the minimum amount of power necessary to fly the aircraft while keeping the battery weight to a minimum.

Different engine configurations were examined using the following figures of merit.

- Rated Aircraft Cost: The power plant has a large affect on the rated aircraft cost, due to weight.
- Thrust to Weight Ratio: The amount of power generated must be met in order to successfully complete the missions.
- Propeller Diameter: The propeller must be adequately sized to provide the desired thrust, while still having ground clearance.

Table 5: Propulsion Configuration Figures of Merit

		Engine Type (gear ratio)		
Figures of Merit	Weighting Factor	Standard (1.68 to 1)	Direct (1 to 1)	SuperBox (3.1 to 1)
Rated Aircraft Cost	0.45	0	0	-0.5
Thrust to Weight Ratio	0.35	0	-1	1
Propeller Diameter	0.2	0	0.5	-1
Score	-		-0.25	-0.075

An engine with a standard gearbox was chosen over a direct drive gearbox engine or superbox gearbox engine because it provides the amount of thrust needed with a smaller propeller.

4 PRELIMINARY DESIGN

4.1 Design Parameters and Sizing Traits

The most important driving parameter behind the design was the size constraint put on the aircraft due to the requirement that the aircraft must fit within a 4x2x1 ft box. This constraint immediately placed an eight-foot maximum wingspan condition within the design because of the complexity involved with attaching a wing in 4 spots instead of two spots. It also brought up the notion that the tail may have to be designed to be detachable in order for all the components of the structure to fit inside the box. The possible adverse effect of the simulated antenna on the vertical stabilizer was another important design parameter. This led to the design of an H-Tail configuration, which would allow rudder control without

4.1.1 Wing Design

4.1.1.1 Planform

The preliminary design of the wing was based on a practical limit of a 90-inch wingspan, which would allow a two-piece wing to fit into the shipping container with a reasonable amount of clearance. With a set wingspan, the effects of different taper ratios and wing areas were explored. Increased wing area was found to improve performance, but at the cost of a larger or longer tail requirement. At this stage of the design, the target for tail length was such that the entire fuselage would fit into the container without disassembly. This meant that

a wing with minimum area to meet performance requirements was desired. Late in the preliminary design phase, it was discovered that the taper was undesirable. Whereas a 35 percent taper ratio would theoretically produce a nearly optimal elliptic lift distribution, at the relatively low flight Reynolds numbers, the tips will be in a regime in which most airfoils will perform poorly. The initial design specified a straight trailing edge to facilitate simple construction of the control surfaces. This required a 12-degree sweep at the quarter chord. The lift reduction due to sweep effectively cancelled any gain that would have been obtained from better efficiency. In addition, the choice of a rectangular wing over a tapered wing would reduce the wing's moment coefficient, reducing the tail size requirement. Another added benefit to a rectangular design is the simplified construction, requiring only one airfoil template for the entire wing.

4.1.1.2 Wing Loading

Figure 4The wing loading of an aircraft is directly related to the takeoff performance and the power required for flight. To this end, a trade study of wing loadings for various electric R/C models was used to help in the initial sizing. Figure 3 shows the takeoff weight and wing area for the data collected. It is seen from this plot that most electric R/C aircraft fall between 10 and 30 oz/ft^2. The estimated wing loading for the conceptual design was 30 ounces per square foot. Compared to similar radio-controlled aircraft, this wing loading places this design alongside high performance sport and aerobatic planes.

The wing loading of an aircraft is directly related to the takeoff performance and the power required for flight. To this end, a trade study of wing loadings for various electric R/C models was used to help in the initial sizing. Figure 3 shows the takeoff weight and wing area for the data collected. It is seen from this plot that most electric R/C aircraft fall between 10 and 30 oz/ft^2. The estimated wing loading for the conceptual design was 30 ounces per square foot. Compared to similar radio-controlled aircraft, this wing loading places this design alongside high performance sport and aerobatic planes.

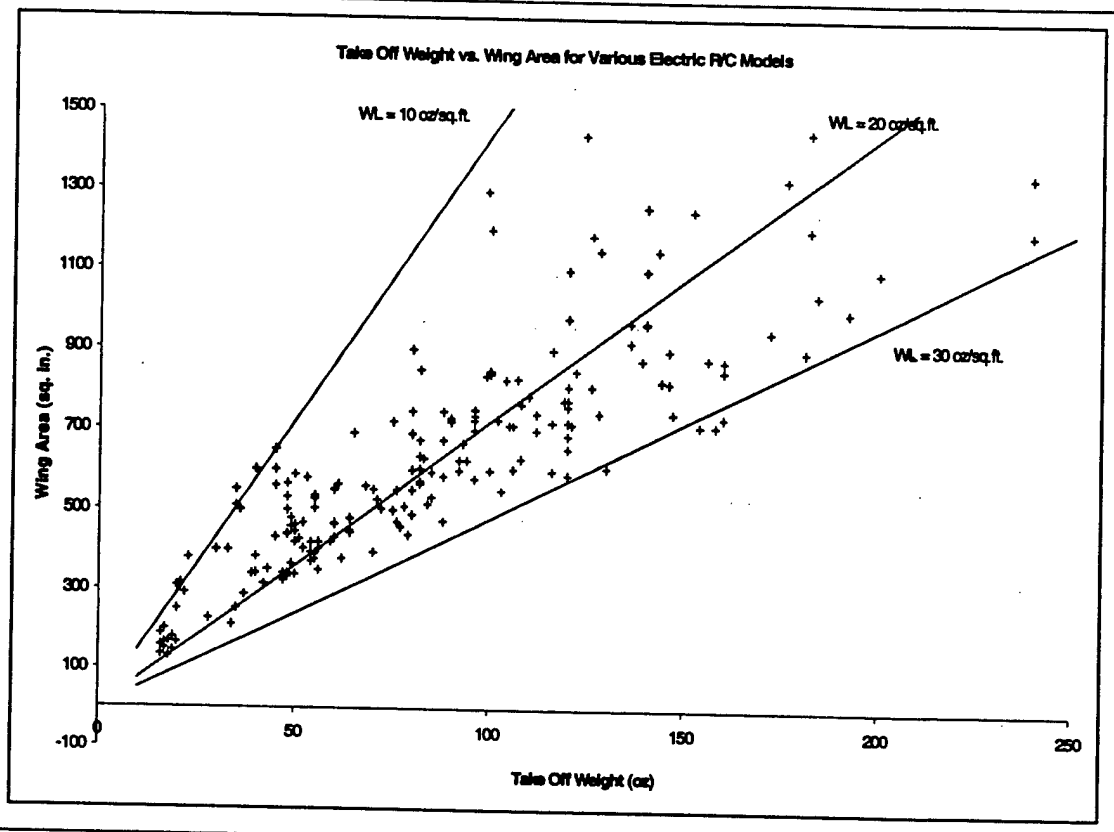

Figure 3: Wing Loading

4.1.2 Tail Design

With an H-tail configuration chosen based on the considerations voiced in the Conceptual Design *Basic Configuration* section the general parameters and construction deliberation could be made. Since the tail is directly responsible for the longitudinal stability, yaw stability, and pitch control it was a vital component of the stability characteristics of the aircraft. Rough sizing characteristics were defined based on the 4x2x1 ft box that the aircraft was to be shipped in. Based on this constraint the horizontal tail span was not to exceed 2 ft in width and the vertical tail were not to exceed 1ft in height so the detachable tail boom and tail could fit in the box in the desired configuration. The tail sizing is discussed in further depth in the following *Tail Volume* section.

For the horizontal stabilizer three different construction techniques were considered: simple flat plate, symmetric airfoil wood skeleton, and foam core with fiberglass sheeting. Due to time constraints the foam core construction technique was abandoned simply due the difficulty and time of construction. On the basis of time of construction the wood skeleton was abandoned as well, but not until after the consideration of the decreased efficiency with the flat plate design. Efficiency was a concern due the fact that the horizontal tail was mounted directly behind the wing and therefore directly in the wake. This was due to the mission constraints requiring the plane to taxi away from the payload box keeping the tail high relative to the wing.

Also, the tail could not obstruct the 360° non-obstructed view of the antenna. In the end it was decided that in order to compensate for the decreased efficiency, the chord of the horizontal tail could easily be increased. Again further tail sizing analysis is discussed in the following Tail Volume section.

4.1.2.1 Tail Volume

The aircraft horizontal tail volume is given by

$$V_H = \frac{S_H l_H}{S_W \bar{c}} \qquad (4.1.2.1.1)$$

where S_H is the horizontal tail area, l_H is the length between the tail quarter chord and wing quarter chord, S_W is the wing area and $\bar{c}$ is the mean aerodynamic chord. This quantity scales the tail lift coefficient in the moment calculations and is therefore of great importance to the engineer designing the aircraft. Along with the horizontal tail efficiency, the down wash angle, and the tail lift coefficient itself, the horizontal tail volume greatly affects the position of the neutral point of an aircraft.

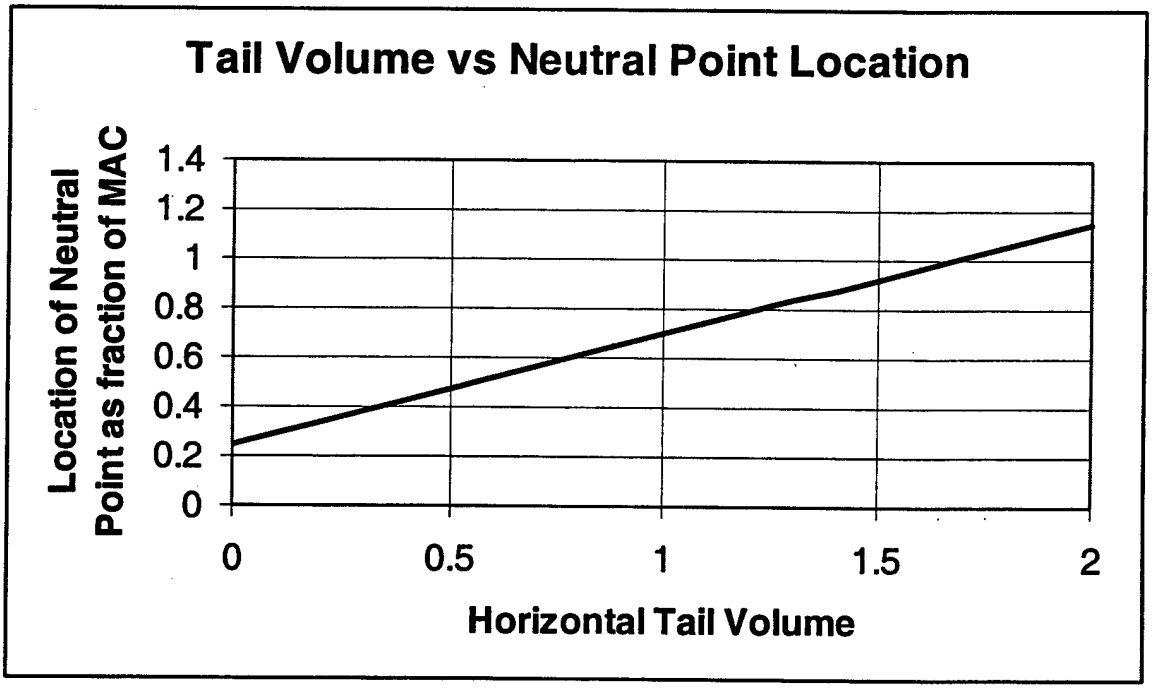

Figure 4: Tail Volume in relation to Neutral Point Location

As given by Simons (1999), the neutral point of an aircraft can be estimated by

$$h_n = h_0 + \eta_s V_s \frac{a1}{a}\left(1 - \frac{d\varepsilon}{d\alpha}\right) \qquad (4.1.2.1.2)$$

The position of the aerodynamic center of wing, ignoring the effects of the fuselage, can be roughly estimated to be at the quarter chord of the wing. The elevator efficiency factor and the downwash angle are conservatively approximated to be 0.8 and 0.3, respectively, for a normal configuration with an average tail length. As a first order approximation for the lift curve slope ratio, a Clark Y airfoil for the wing and a flat plate for the horizontal tail were chosen, which resulted in a lift slope ratio of 0.8. With this data Figure 4 was produced. The information found in the figure was kept in mind during the preliminary design phase. The decision was made by the design team that the tail volume needed to be at least 0.5, given that most conventional model aircraft report a c.g. location of 33% of the chord from the wing leading edge. With a tail volume of 0.5, the neutral point for the aircraft should lie at around 45% of the chord, which would result in a static margin of 12%. This static margin should provide enough stability for a pilot to be able to control the aircraft. However, during the preliminary design, the team decided that for yaw stability reason, the antenna would be mounted aft of the cg location behind the wing. Mounting the antenna half a foot behind the c.g. was computed to shift the cg location up to one half of an inch, roughly 5% of the desired mean aerodynamic chord. This would reduce the static margin to 7% and the aircraft might no longer be easy to fly due to the increased agility. A horizontal tail volume of 0.5 was therefore decided to be the minimum requirement and values of 0.7 or more should be achieved to guarantee stability with the antenna mounted on top of the aircraft behind the c.g.

4.1.3 Power & Propulsion

The power system was analyzed primarily based on the takeoff constraint of 120 feet while minimizing the overall weight of the motor and battery supply as well as maximizing the overall efficiency. Figure 5 shows the efficiency of three different sized Astro Flight motors as a function of current. In the plot on the left, the efficiency is of the motor alone, while on the right the efficiency is calculated for the entire power system including batteries, electronic speed controller, and motor.

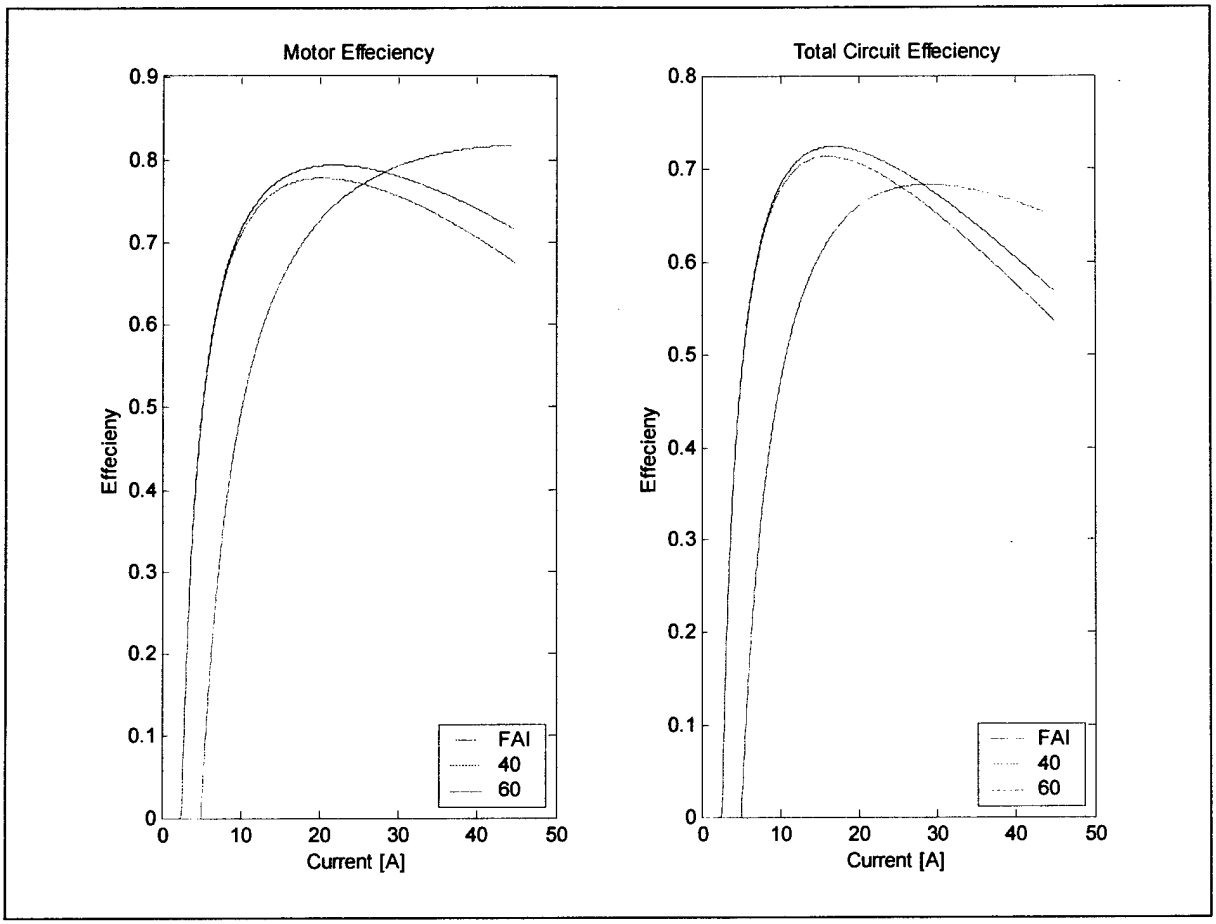

Figure 5: Motor Efficiencies as a Function of Current Draw

Even though this figure shows that the Astro Flight 60 sized motor is more efficient at mid-currents, it is 8 oz heavier than the 40 sized motor and also requires a higher voltage. The increase in weight due to the increase in the number of battery cells effectively cancels the gain in efficiency of the 60. For these reasons, the Astro Flight 40 sized motor is chosen. The 40-sized motor from Astro Flight comes in three different gear ratios: direct drive (g=1), geared (g=1.63) and superbox (g=3.1). These different gear ratios were analyzed for their mission performance. Figure 6 shows a representative comparison of the different systems with a single battery supply at a nominal voltage of 24 volts.

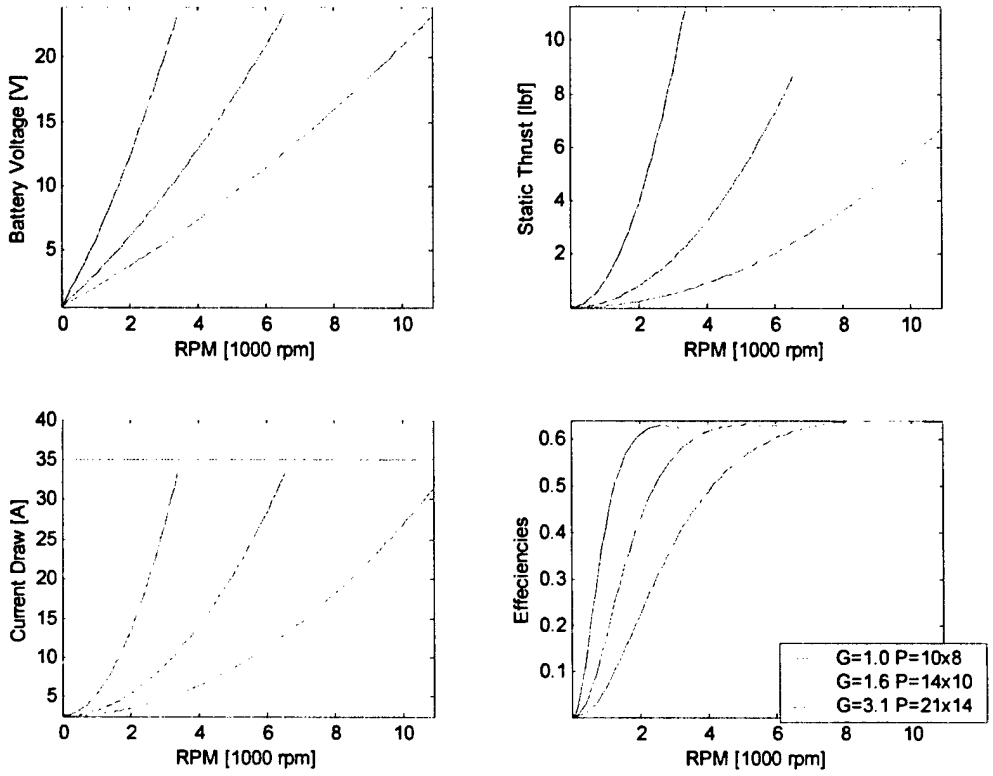

Figure 6: Representative Motor Parameter for 40 sized Astro-Flight Motors

It is seen that for a given voltage supply and properly chosen propellers, the performance of the motors is almost equivalent, except for the static thrust produced. The takeoff distance requirement suggest one to choose the configuration with the most thrust, however the propeller diameter needed for the higher thrust on the superbox motor (21 inch) is larger than the designed ground clearance. Also, with the low rotational speed of the superbox, a propeller with a large pitch is needed to achieve the desired speed. Large pitch propellers are less efficient at slow speeds, where the propeller airfoil may be in a stalled condition, and thus takeoff performance is affected. Thus, the geared motor (g=1.63) is chosen to obtain a large static thrust with a reasonable forward propellers speed.

4.1.4 Fuselage Design

The fuselage design matured through several iterations, until a discussion about the routing of cooling air for the motor and batteries gave rise to an innovative idea. The design of the fuselage was driven by the requirement to implement a simulated payload package. This resulted in a fuselage design that was designed around this payload package. The fuselage was created as a geometric configuration that would be able to incorporate the following requirements: the dimensions of the payload; an estimate on the amount of room

needed for the battery pack, engine, and other control devices; and the size of the wings that would attach to the top of the fuselage. It was decided that the payload be enclosed on the sides so that the aircraft would still have the same aerodynamic features that it would have before the deployment of the payload. Because of the design restraints mentioned before, the resulting fuselage was 20 1/4 in long, and 7 1/8 in high, and 6 5/8 in wide. In order to be able to deploy the payload and successfully taxi away from it, the landing gear was designed to allow a clearance of 3.25 inches from the ground to the bottom of the fuselage.

At this stage of the design process, it was determined that the batteries and engine would need to be cooled for better flight efficiency. This resulted in the discussion of incorporating an air scoop in the front of the fuselage and directing the air across the different components. In order to implement this scoop, it was considered to build the front section of the fuselage out of one solid structure using the rapid prototype machine in the CU Boulder machine shop. After several unsuccessful attempts to model this in AutoCAD along with the added cost of this method, this approach was abandoned. The next consideration taken into account was to incorporate an aluminum channel at the top of the fuselage in order to provide a single structure that would be a solid base that every component of the plane would be attached to as well as a tunnel through the aircraft to provide a heat sink for the batteries and the motor. With overall shape and size of the fuselage decided upon, it was ultimately decided to implement this aluminum channel within the fuselage.

4.1.5 Antenna Design

The design of the antenna was dictated by the competition rules for the antenna configuration. The rules required the antenna to be made out of 6-inch schedule 40 PVC pipe three inches tall, with the top and bottom sealed flush with sixteenth inch plywood sheets. The antenna was required to be completely exposed on the exterior of the aircraft and standoff from the nearest airframe structure by a minimum of three inches. In addition, the antenna could not be faired or altered in any manner. During preliminary design, it was decided to make the antenna mount out of single structure with an integrated airfoil section in order to reduce the amount of turbulent flow and therefore drag that it would create.

4.2 Analysis Methods Used

The aerodynamic design and analysis of the aircraft was completed in a design Excel spreadsheet that was implemented according to the theories and formulae presented in Shevell [1989], McCormick [1995], and Roskam [1998]. The spreadsheet offers an iterative design tool for airplanes that let's the users define a chosen design and computes the force and moment derivatives and then offers several optimization options. Several variations of the preliminary design were analyzed this way until the final, optimized design was found.

To verify the correctness of the implemented algorithms, the aircraft performance parameters and stability derivatives were compared to the output of commercially available software called Advanced Aircraft Analysis (AAA) by DARCorporation, which also implements the formulae given by Roskam (1998) The numbers

obtained from AAA compared very well to the numbers that were computed in the spreadsheet for the final configuration of the aircraft. Not only did this prove the validity of the numbers calculated in the spreadsheet, it also showed that our design seemed feasible.

The final aircraft configuration was also modeled in a flight simulator called X-Plane. The model seemed to perform as predicted and showed excellent flying qualities. Takeoff distance, climb and glide slope, as well as cruise speed and trim could also be verified with this program. Although the results from X-Plane should be taken with caution, since the exact aerodynamic analysis of the program is not known, the simulation seemed to be another indication for a successful design.

4.3 Mission Model and Predicted Performance

The following figures show the variation of aircraft parameters as a function of the takeoff weight. These show the variation of the conditions from the fully loaded payload, at 14 lb, to the unloaded clean configuration at 9 lb. The cruise performance chart was generated by first computing the optimum lift coefficient for cruise based on available power, endurance, and drag. These factors were weighed, to obtain a target cruise CL. The performance chart was then generated by computing the flight speed required to generate lift equal to the weight at the given CL. Curves for different altitudes up to 6000 feet were created because testing would be done in Boulder, CO (elev. 5340 ft). The takeoff and landing stall speed charts were developed using the same methodology, except the takeoff stall CL was estimated at 1.2, and the landing stall CL was estimated at 1.5.

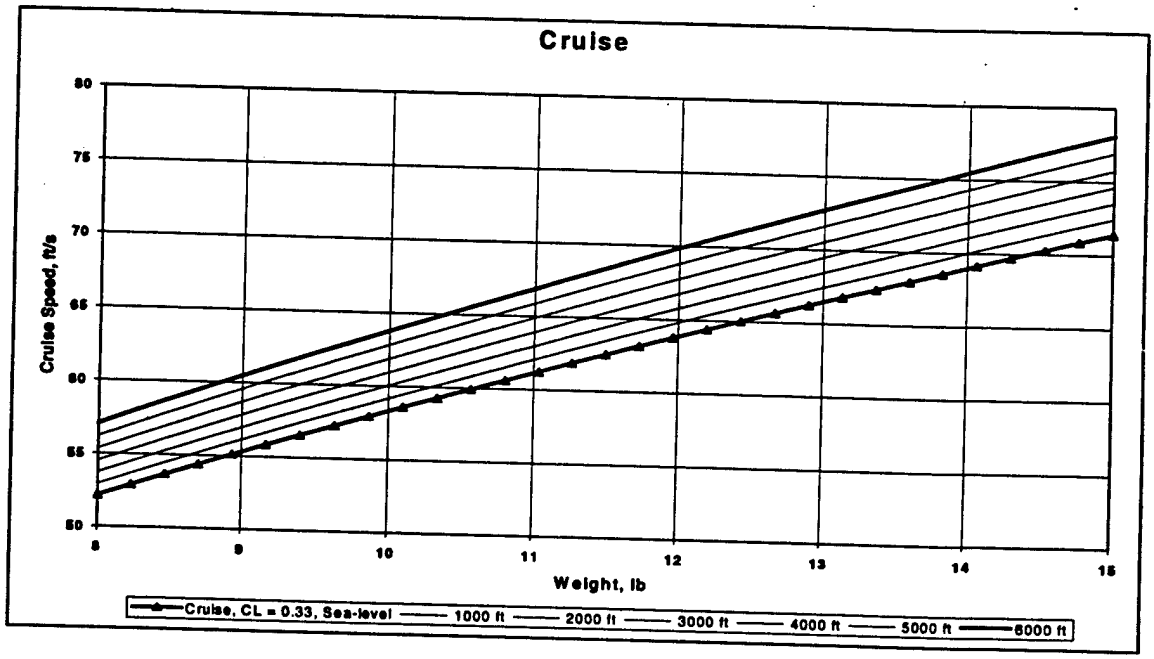

Figure 7: Cruise Performance in relation to Weight

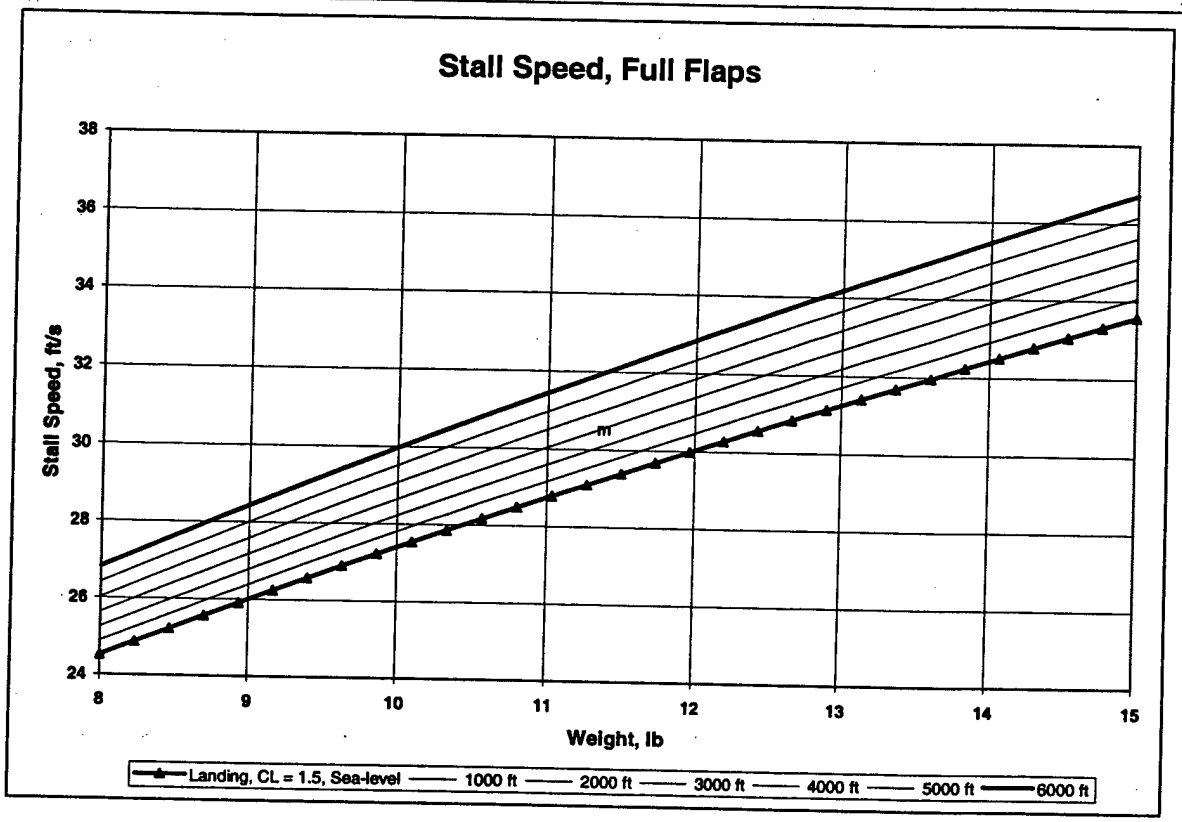

Figure 8: Cruise Performance Stall Speed with Full Flaps in relation to Weight

The takeoff distance chart was computed based on the predicted takeoff static thrust available, and estimates of rolling friction, parasite drag, and induced drag during the ground roll. The total aerodynamic drag was computed for the rotation point, and the average during the ground roll was estimated to be one-half this value. Using the equation of motion for the aircraft under the known forces, (Anderson, et. al.) the distance required to accelerate to takeoff speed was computed. The rotation speed used for the computation was based on takeoff stall speed multiplied by a standard safety factor of 1.2. This process was repeated to generate curves for different field elevations.

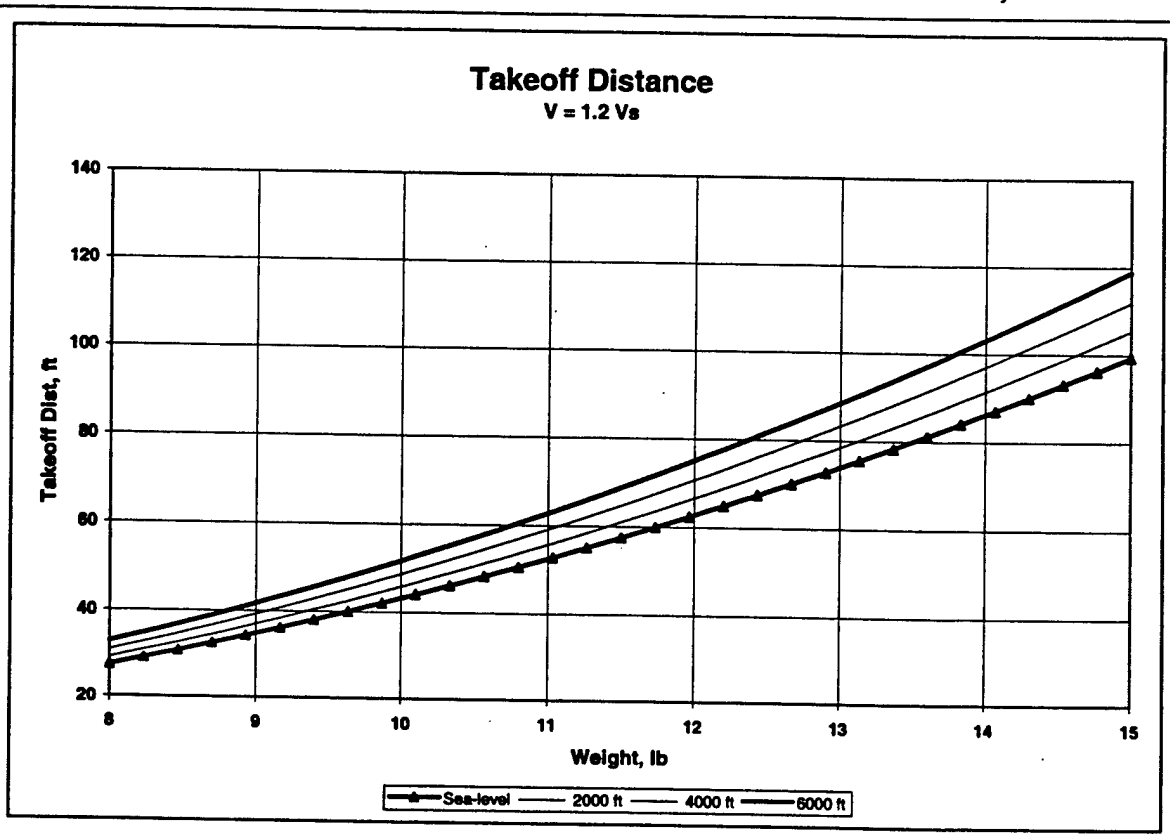

Figure 9: Stall Speed with Full Flaps in relation to Weight

4.3.1 Mission A – Missile Decoy

This mission led to the design parameters affected by the antenna simulation. Mission A, "Missile Decoy", required the aircraft to complete 4 laps and land within the 10 minutes allotted for mission completion. While doing so, the aircraft must have a simulated antenna and avionics payload attached and be able to takeoff within 120 ft. The preliminary design of the aircraft was performed taking this mission's requirements into consideration. The current design of the aircraft is expected to complete this mission under the 10 minute time limit with a takeoff distance under 120 ft. in the worst case scenario.

4.3.2 Mission B – Sensor Deployment

In addition to the 10 minute time frame for mission completion and the 120 foot takeoff distance, this mission required that the aircraft compete two laps, land, deploy the simulated relay device (the five pound payload), takeoff, compete two laps, and land again. The simulated antenna mount was not required. For this mission, two separate analyses were performed in order to predict the aircraft's performance. The first model included the 5 lb simulated relay device and its effect on performance for the first two laps, while the second model predicted the aircrafts optimal flight performance that did not include the simulated relay device, which

reduces the weigh considerably and increases the aircraft's flight speed. It is expected that the aircraft will be able to complete the mission in the ten-minute time limit as well as take off in the 120 feet. Using the initial estimates with the motor and batteries, the second takeoff and landing will use a lot of battery power shortening the total aircraft fly time. This was taken into account with the choice on the type and number of batteries and should not be a problem.

4.4 Lift, Drag, and Stability Estimates

4.4.1 Lift and Drag

Estimates of flight performance, including lift, drag, takeoff run, power required, stability, etc, were computed using a spreadsheet that implemented basic fundamentals of flight. The spreadsheet provided the flexibility to tailor the interface to best support the design process, and allowed some visualization of design trades. In order to estimate the takeoff performance, an estimate of the takeoff lift coefficient was required. The takeoff C_L used for the purpose of design was the maximum flaps-up C_L for the wing, reduced by a safety factor of 16 percent. The resulting takeoff C_L was 0.81 with a lift to drag ratio of 11.4. At these conditions, the parasite drag coefficient was computed to be 0.042, while the induced drag coefficient, just after rotation, was 0.029. The drag model was a composite based on known geometric shapes, which approximated the fuselage and other components, and established empirical models for the wing and tail.

4.4.2 Stability

Static longitudinal stability and control of the final aircraft design was analyzed in the Excel spreadsheet that was designed to yield the stability and control derivatives for a given aircraft configuration. Given the final aircraft design above, the longitudinal aerodynamic force and moment derivatives were computed and are tabulated in Table 6.

Table 6: Stability Coefficients

Lift Coefficient at zero angle of attack	**0.1535**
Lift Curve Slope	**0.0841**
Moment Coeff at zero angle of attack	**0.0228**
Moment Curve Slope	**-0.0088**

The analysis of the structural weight distribution predicts the location of the cg to be at 33% of the MAC from the leading edge of the wing. It was found that the neutral point of the final design is at 43% of the chord in the worst case analysis and with the antenna mounted 6 inches behind the cg location, which results in a static margin of 10%. Since the cg location of the payload box that will be deployed during one of the mission was placed at the same distance from the leading edge as the overall cg of the aircraft, the deployment of the box will not contribute to a cg shift and does not affect the static margin.

The lift and moment curves are given in Figure 10 and Figure 11, respectively. The negative slope of the moment curve confirms the stick-free stability of the design. The horizontal tail incidence angle of 3.6 degrees downward was chosen to result in a trim angle of attack of 2.6 degrees. This angle of attack corresponds to an aircraft lift coefficient of 0.36, which will produce the needed lift during cruise at 66 ft/s.

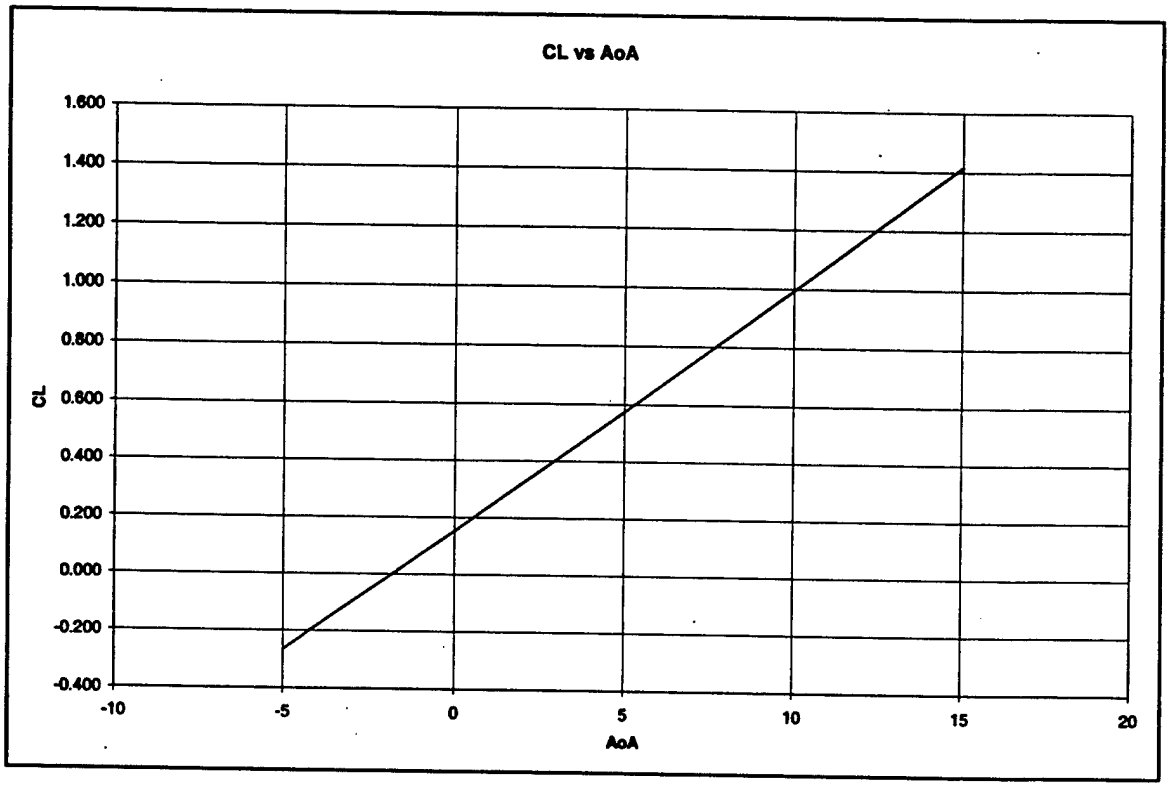

Figure 10: C_L with respect to Angle of Attack

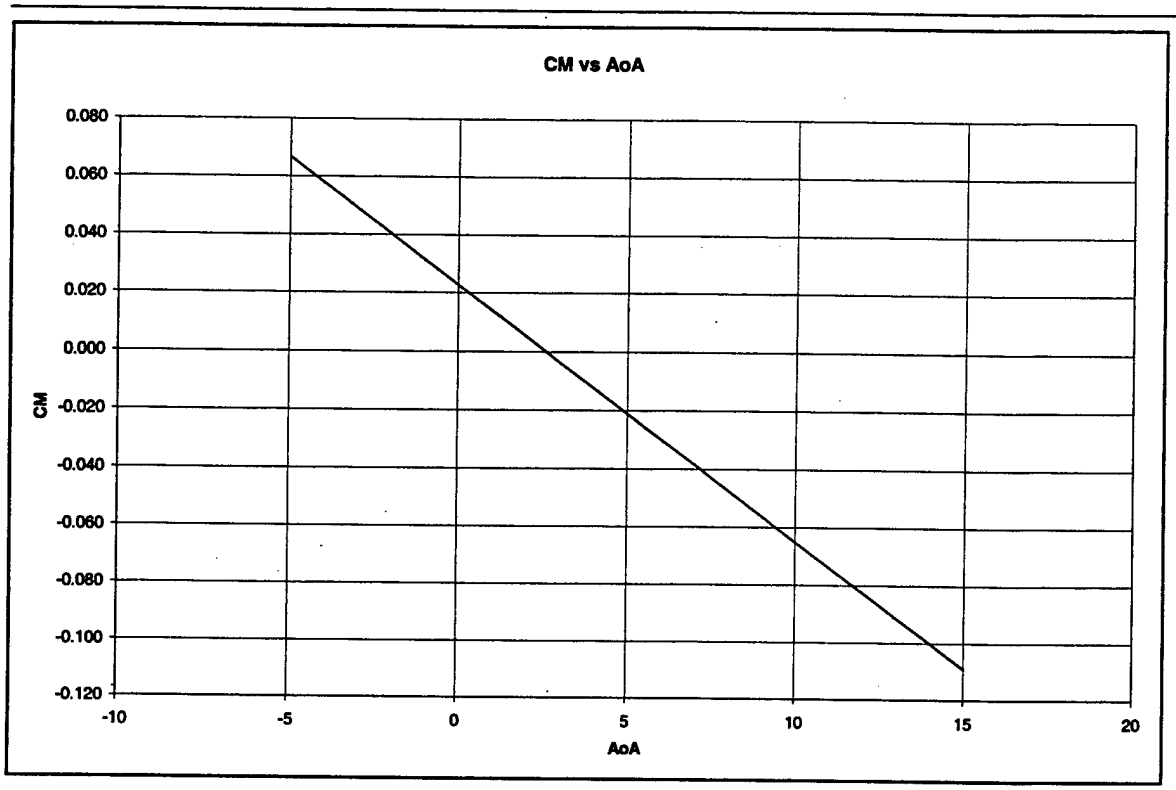

Figure 11: C_M with respect to Angle of Attack

The elevator lift and moment coefficients were also found and are given in Table 7.

Table 7: Elevator Lift and Moment Coefficients

Lift Curve Slope of Elevator angle	**0.00321**
Moment Curve Slope of Elevator	**-0.0104**

Given an elevator size of 20% of the tail chord, spanning the entire horizontal stabilizer, the elevator authority was computed and is shown in Figure 12.

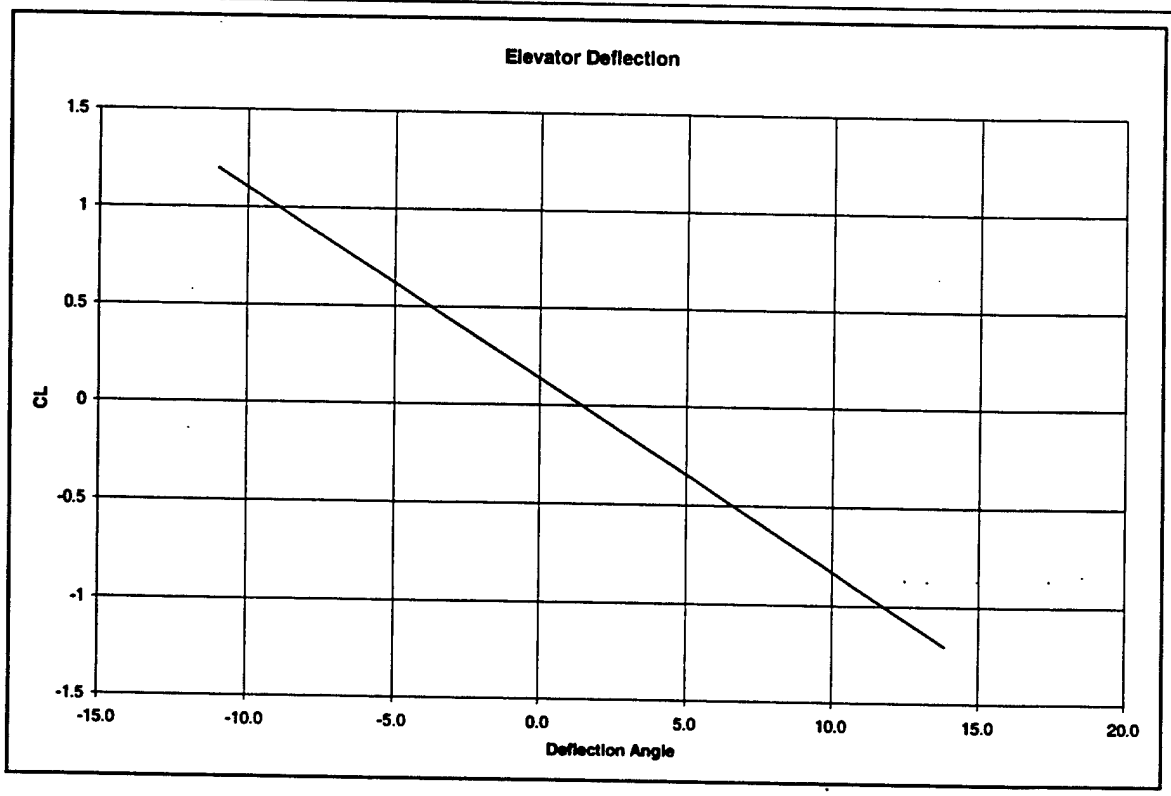

Figure 12: C_L and Elevator Deflection

From the above figure, it can be seen that the required takeoff lift coefficient of 1.0 can be achieved by an up elevator deflection of 9 degrees. As noted above, for drag optimization, the aircraft is trimmed during cruise condition and does not require any elevator deflection. The maximum deflection needed, which will define the control surface throw, was found to be 15 degrees up and down. This should give the pilot enough longitudinal authority far any coordinated maneuver.

4.5 Design Optimization and Trade Studies

The main driving force behind the preliminary design phase was the requirement that all components of the aircraft be able to fit within a 4x2x1 ft box. Next, the RAC model was considered; however, stability issues during flight outweighed the RAC considerations. In order to create the optimal design, trade studies for each major component of the aircraft were performed which dictated the final design. The design optimizations, trade studies performed, along with the resulting final configurations are summarized next by each major component.

4.5.1 Wing

The major consideration taken into account for the wing design was its stability characteristics during flight. Although the RAC would be increased as the wingspan and maximum chord were increased, it was decided to allow the wing area to be determined by takeoff considerations. This resulted in maximizing the wingspan that would fit into the box. This span was 8 feet long; however, it was also desired to have some extra room within the box so that it would be easier to fit the wings within it. This resulted in a final wingspan of 7.5 ft.

Whether to incorporate taper into the design of the wing was also considered. Initially, a 35% taper ratio was chosen to approach the optimal elliptical lift distribution. Later in the design process, it was found from Simons [1999] that due to the low Reynolds numbers involved, a taper ratio would lead to an increase in drag at the tips and is thus undesirable. Considering this and the fact that a rectangular wing is easier to construct, a wing size of 7.5 ft with a chord of 1 ft was decided upon.

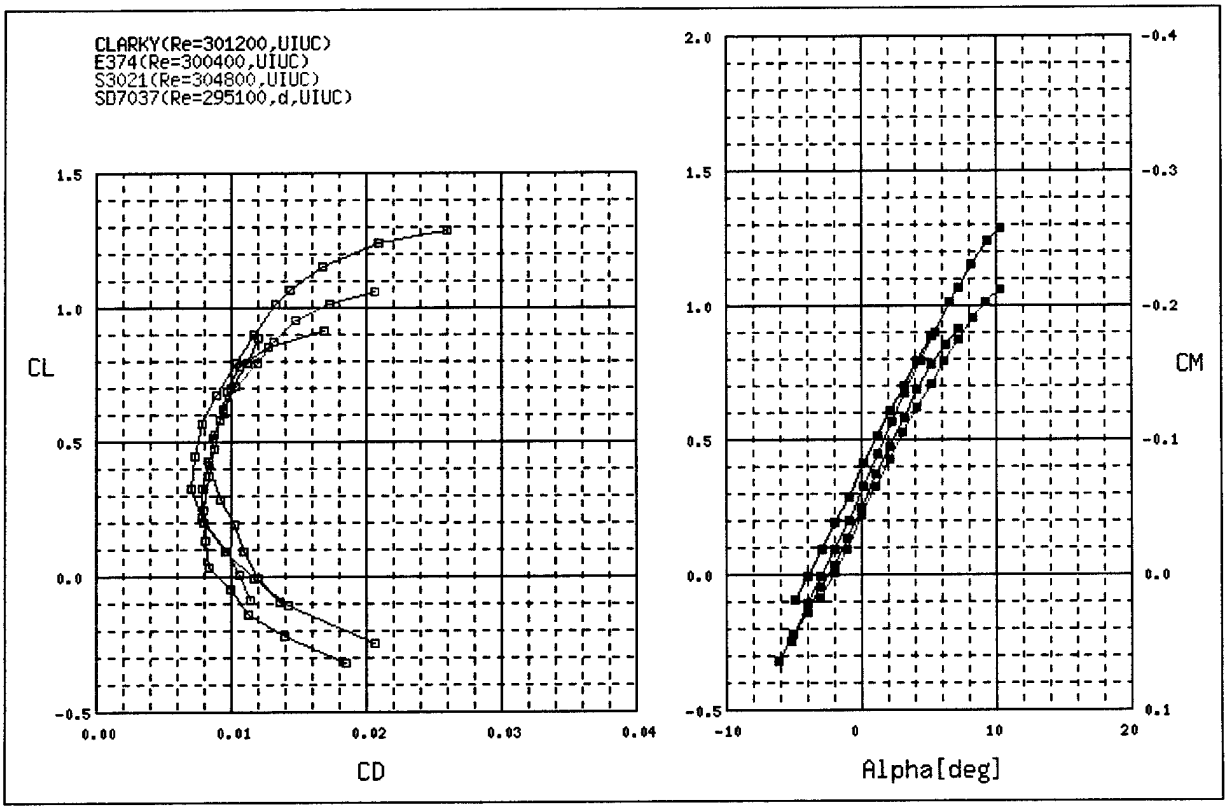

Figure 13: Drag Polar for a Selection of Airfoils [WEB XXX]

After determining the size of the wing and required lift parameters, the airfoil for the wing was chosen. This decision was based on the need for large c_l and low c_d at in the desired cruise range. Figure 13 shows the drag polar for various low speed airfoils. Other considerations were based on airfoil complexity (e.g., amount of under camber) and thickness. It is easily seen that the Clark-Y has a lower drag value in the range of c_l

greater than 0.2 and also has a much larger c_{lmax} than the other airfoils. Other considerations were based on airfoil complexity (e.g., amount of undercamber) and thickness. It ultimately came down to the selection between two airfoils; the Clark-Y and the Selig-Donovan 3037 (SD-3037) airfoils. While the data analyzed on both of these airfoils showed that they provided the required amount of lift, the SD-3037 showed to have a slightly better performance attributes. These small advantages, however, were outweighed by the Clark Y's flatter bottom section that would make the attachment of the wings to the top of the fuselage relatively simple compared to that of the cambered Selig airfoil, while still having a comparable minimum of c_d. With the large c_{lmax}, small c_d and being relatively thick (13.7%) and simple (flat bottom) airfoil leads to the choice of the Clark-Y. Thus, the final design of the wings was determined to be two rectangular 3.75x1 ft sections implementing the Clark-Y airfoil.

4.5.2 Tail

The first consideration in the design of the tail section was the rudder design configuration. The first aspect of this competition decided upon was that the two missions with the highest difficulty factors would be performed. This resulted in the design of the airplane that would accommodate an antenna structure attached to the aircraft. This immediately affected the design of the rudder control configuration. Due to the RAC model, it was desired to have the least amount of control surfaces possible, thus using the conventional method of a single vertical control surface. However, it was decided that the best place to attach the antenna would be on top of the fuselage over the c.g. location. When considering the effects of the antenna, it was determined that if the single vertical control surface was used, the turbulent flow created from the antenna could interfere with the airflow around vertical stabilizer. Therefore, once again, the performance of the aircraft was decided to outweigh the RAC model. This resulted in the final H-tail configuration.

4.5.3 Fuselage

The basic size of the fuselage was determined by the mission requirement of carrying a simulated payload. The only part of the structure left in question was whether or not to incorporate the unconventional design incorporating the aluminum channel at the top of the fuselage. The alternative to this design was to use the conventional method of balsa wood throughout the entire structure. The only disadvantages to using the aluminum structure was the added weight it would create along with the lack of experience of the team members in using aluminum within the design of a RC aircraft. The advantages of using the aluminum channel ultimately outweighed its disadvantages. The advantages were numerous. The first and foremost was that the amount of aluminum needed would not create a significant weight gain. By using the aluminum, a strong support at the top of the fuselage would be created that would be able to be used as the attachment for all the major components of the airplane: battery backs, engine, wings, and tail attachment. Along with these advantages, the aluminum channel could act as a funnel through which air could move and as a heat sink for the battery pack and engine. Considering the advantages of incorporating this design, a final fuselage structure was decided upon. The length would be approximately 20-1/4-inches long, and 7-1/8-inches high,

with an aluminum channel running along the centerline of the top of the structure for added support and to act as an air channel that would cool the engine and batteries.

4.5.4 Propulsion

Given the choice of the Astro Flight 40-sized motor, the propulsion system was analyzed for the available gear ratios, different battery pack configurations and finally propeller combinations. The battery packs considered were of a single pack with all cells in series and a pack with cells in parallel. Even though the parallel battery pack will significantly increase run time, it will also double the battery weight, which is a major cost of the RAC. Thus, a configuration with a single battery pack is desired. The propeller sizing is based on the consumed power, static thrust and diameter. The structural design of the aircraft placed restrictions on the propeller diameter to be less than 16 inches for ground clearance. Because of this, a gear ratio of 3.1 (Astro Flight Superbox) is not feasible since a very large diameter propeller is required.

4.5.5 Antenna

The first consideration taken into account for the antenna was where to mount it. Different locations along the aircraft were considered, such as underneath and on top of the fuselage and various placements along the tail-boom. Due to the requirement for the structure to stand off from the nearest airframe structure, and the 6-inch height of the completed structure, placing the antenna underneath the fuselage was ruled out due to the ground clearance that would be required and its proximity to the landing gear. This left open locations on top of the fuselage and along the tail-boom to mount the antenna. Since the antenna structure would add a significant amount of weight and therefore moment arm when removed, it was decided that it should be mounted along the centerline of the top of the fuselage and as close to the longitudinal location of the c.g. as possible.

Two options were considered when deciding on the material to make the mount out of. The first was simply by constructing it out of balsa wood. This would be a light, strong, inexpensive method for the mount creation. The second method considered was to create the antenna using the rapid prototype machine in the CU Boulder machine shop. This method involved creating the mount in an AutoCAD file, which would be created by the machine. It was considered that after the prototype was made, the mount would still have to be sanded down in order to create the smooth surface desired for laminar flow. Considering the time required and cost ($5 per cubic inch) of this method, it was decided to create the mount using balsa wood. These two trade studies resulted in an optimal design that placed the antenna on top of a balsa mount with an integrated airfoil section, all of which would be mounted on top of the fuselage over the longitudinal location of the c.g.

5 DETAIL DESIGN

5.1 Materials

Choice of materials throughout the design process plays an imperative role in the overall success of the aircraft. Every part of the aircraft had to be discussed thoroughly to utilize the positive features of the materials that could be applied to the part. Decisions were based off the strength, stiffness, weight, desired functionality, cost, and ease of construction.

The analysis started at the backbone of the aircraft where an aluminum channel was chosen. This is the best choice because this "backbone" will be absorbing the bulk of the load distributed throughout the aircraft because it will include landing gear mounts, a motor mount, a tail joint mount, an antenna mount, and wing mounts. Also, because the batteries and motor will produce a lot of heat during flight, the aluminum channel will act as a heat sink due to the fact it is a good conductor as well as it will be open to the air entering through the nose air intake. This will keep the batteries and motor cool and efficient. Since aluminum is a heavy material compared to most woods, it will have to be weight relieved in order to be practical.

The skin for the aircraft will have to be stiff yet light enough to be able to be structurally sound when the payload box is dropped on the second mission and also to withstand any shocks from any accidental mishaps that could happen on the airfield. This is accomplished using two thin balsa sheets separated by spacers for stiffness for the mid fuselage section and with three thirty-second inch balsa sheeting for the tail boom. The nose of the aircraft will be comprised of mainly plywood bulkheads and thin balsa sheeting to get the correct cone shape, while the air intake scoop will be carved and sanded out of block balsa wood. There will also be some plywood buildup inside the nose area for the nose gear and placement of the electronics in the front of the aircraft.

The inner structure of the aircraft is comprised of the bulkheads and joint strengtheners placed throughout the fuselage. The bulkheads in the fuselage had to be very stiff as well to absorb any loads applied through the fuselage. This led to the decision to use sixteenth and thirty-second inch plywood with lightening holes. Since the plywood will be very thin throughout the aircraft, it will need to have added strength along the joints. This can be accomplished using simple triangle stock balsa wood because balsa is very light per cubic inch so there can be a large area to bond without a large increase in weight. The triangle stock will be placed along the joints on the inside of the fuselage to ensure a good bond between every part of the aircraft.

When designing the wing, a classic approach was taken to ensure a quality wing with a small amount of weight. The majority of the wing will consist of sixteenth inch balsa ribs with two pine wing spars running the whole length of the wing on top and bottom. To keep the airfoil shape throughout the wing, some leading edge and trailing edge balsa stock was purchased and sanded to the correct shape as well as sheeting up to the quarter chord and behind the three quarter chord of the whole wing respectively. In order to strengthen the wing further, thin balsa airfoil caps were added to give a larger surface for the MonoKote to attach to and

better distribute the loads along the wing. The first four ribs on both halves of the wing will be fabricated out of sixteenth inch plywood for added strength in the section that will comprise of the dihedral braces and the wing attachment rods. Because the center section of the wing will experience the most loads, the wing attachment rods will have to be very strong. Thin aluminum rods will be used to account for this along with plywood dihedral braces.

Since the mount for the antenna must be removable between flights, it was decided to mount it directly to the aluminum "backbone" of the aircraft to prevent screw stripping through the wood. The antenna itself will be attached to an airfoil shaped balsa mount that will be mounted to the 'backbone' of the aircraft. The thick balsa midsection will provide enough strength and stiffness to keep the antenna from fluctuating or breaking during flight.

The horizontal and vertical stabilizers will be made of quarter inch balsa wood for many reasons. Although an airfoil based system is stronger, it was decided that for this section the added strength was not needed and it is much easier to construct this section out of a flat plate. For added stiffness through this section, carbon fiber tape will be used along with stock triangle balsa at the joints between the horizontal and vertical stabilizers.

For weight issues, a carbon fiber composite landing gear would be more desirable than an aluminum gear. Also, the weight to strength ratio for a carbon fiber gear is much higher than that of an aluminum landing gear. However, building a carbon fiber landing gear is extremely difficult with the resources available. For these reasons a commercial landing gear was purchased from TNT Landing Gear for this aircraft. The landing gear chosen was originally designed for the Dave Patrick Extra ARF RC aircraft.

5.2 Propulsion

The final configuration of the propulsion system is an Astro Flight 40-sized motor with a gear ratio of 1.63, spinning a 14x10 propeller. The battery pack is chosen to be a 20 cell battery pack consisting of Sanyo 1900 SCR cells. From this combination, a static thrust of 8.2 lbf is expected. The maximum output power is 578 W, which with the drag estimate gives a maximum airspeed of 94 ft/s. The most efficient cruise current and speed for the propulsion system are 16.1 A and 72 ft/s, respectively. At cruise conditions, the battery is expected to last for 7 minutes, 3 minutes at full throttle.

Takeoff performance was analyzed by numerically solving the differential equation of motion using MATLAB, taking into account rolling friction, thrust and drag. It was found that with a fully loaded aircraft, the takeoff distance is expected to be less than 100 feet. For the rate of climb, a small angle approximation is used and is given as:

$$RC = \frac{P_{available} - P_{required}}{W} \qquad (5.2.1)$$

where W is the aircraft weight, $P_{available}$ is the available motor power and $P_{required}$ is the required power due to drag. From this, a RC for the loaded and unloaded cases are found to be 15.6 and 25.7 ft/s respectively.

5.3 Wing Design

The final aerodynamic design of the wing is a rectangular planform with a 90-inch span and a 12-inch chord. This gives the initially chosen wing loading of 30 oz/ft^2 for the 14 lb aircraft. The Clark-Y airfoil was chosen for the wing due to the fact that it's a flat-bottom thick airfoil with a high c_l and comparable c_d values. From the wing parameters, the C_L of the finite wing is approximated with Shevel(1989)

$$C_L = \frac{a_o \alpha}{1 + a_o / (\pi \cdot AR)} \qquad (5.3.1)$$

where a_o is the section lift curve slope, α is the absolute angle of attack and AR is the aspect ratio of the wing. From this, the lift curve slope of the wing can be found and is given as $C_{L\alpha} = 0.098$.

5.4 Fuselage Structural Design

The structural design of the fuselage will incorporate an aluminum channel, measuring about 2 inches wide by one inch tall that will be used as a 'backbone' to which all flight and structural loads would be attached. This will potentially provide a strong, stiff, and lightweight structure, with benefits of simplicity, ease of construction, and efficient cooling. The cooling requirements were based upon analysis of the amount of power dissipated by the motor and battery that is not output to the shaft. This power is dissipated in the form of a significant amount of heat, which needs to be exhausted to avoid overheating of the power components and reducing efficiency. The design entails an air scoop under the propeller spinner, through which air is directed around the motor housing. From there, the air flows through the aluminum channel over the payload compartment, and overboard at the tail boom attachment. The main batteries would be firmly attached to the channel on either side, and would dissipate heat into the channel by conduction. The channel provides a common mounting frame to which the motor, landing gear, wing, cargo, fuselage, and tail-boom attach. Since the primary flight and landing loads are transmitted directly to the backbone, the fuselage can be of very lightweight construction, as it carries no significant loads. Because one of the missions require the payload box to be dropped in mid mission, the side walls of the mid-fuselage section had to be made very stiff to prevent buckling during flight. This can be accomplished by implementing a system with two balsa sheets separated by thin eighth inch balsa stock placed in a truss structure to provide the needed support.

5.5 Wing Attachment

The wings are joined at the center by a removable aluminum spar, which will fit tightly into pockets in each wing half. The center rib of each wing has a forward extension, which locks into a slot attached to the fuselage backbone. Each half of the wing is held to the channel by a quarter inch nylon bolt at approximately 30% forward of the trailing edge, while the bottom of each wing half rests in a cradle formed by the sidewalls of the fuselage. The primary flight loads are carried by the bolts and rib extensions in tension, by the

aluminum spar in bending, and rolling moments are absorbed by the cradles. The bottom of the wing has key extensions, which fit tightly into the fuselage cradle, to absorb moments produced by drag.

5.6 Tail Design

The twin vertical tail design is intended to provide sufficient yaw stability, while remaining clear of the wake produced by the antenna assembly. A modified flat plate airfoil was chosen for the horizontal and vertical tail surfaces for reasons of simplicity. The modified flat plate was chosen based on known radio control aircraft using similar designs. The horizontal surface will be constructed from a solid quarter inch plank, reinforced with carbon fiber tape for rigidity. The vertical surfaces, which are expected to be subjected light loads, will be constructed of fully sheeted built-up balsa plank and stringer construction, for lightweight and reasonable stiffness.

5.7 Tail Attachment

Initially a one-piece fuselage was desired for simplicity but in order to achieve this, the overall fuselage length would have to be less than 4ft, a constraint resulting due to the size of the box. Since the dynamic stability of the aircraft with such a short tail moment arm was questionable a longer and thus a detachable tail was opted for. The major component of the fuselage that created the needed moment strength for the tail attachment was the aluminum C-bar in the backbone of the fuselage. With a strong anchor point in hand a wood structure was designed with four evenly spaced bulkheads that would encase both the horizontal and vertical tail servos. This removable tail attachment not only allowed for a greater tail moment arm and thus a greater tail volume, but it also allowed for slight modification of the cg point if needed.

5.8 Weight and Balance

As with any aircraft, the weight and the center of gravity play imperative roles in the design and success of flight. First to be discussed is the weight of the aircraft. After finalizing the preliminary design of the aircraft and the materials needed, a spreadsheet was made to get an estimate of the final weight of the aircraft. As time progressed, the details of the aircraft were altered causing the weight estimate to be flawed. Because of the amount of changes to the aircraft design, it is emphasized that the weight spreadsheet is just an estimate. The final weight estimation of the major parts of the aircraft can be seen below in Table 8.

Table 8: Weight Estimation Chart

Weight Chart	
Aircraft Section	**Weight (lbs)**
Wing	1.129
Stabilizers	0.193
Forward Fuselage	2.515
Tail boom	0.240
Electronics	0.749
Powerplant	3.471
Payload	5.000
Antenna	0.750
TOTAL	**14.046**

Using the weights calculated from the weight estimate above, the next step was to find the center of gravity of the aircraft. Since this competition requires two different missions that both require the aircraft to have different configurations, three different center of gravity spreadsheets had to be created. Using the weights and placements of every specific part of this aircraft, an estimated center of gravity could be calculated using the equation:

$$x_{c.g.} = \frac{\sum Moments_{Nose}}{\sum Weight} \qquad (5.9.1)$$

This equation was used for both the longitudinal and vertical directions. The lateral direction was assumed to be symmetric about the centerline of the aircraft and therefore ignored. Table 9 and Figure 14 show the locations and the movement of the center of gravity for a fully loaded aircraft (payload and antenna), a payload only aircraft, and an empty aircraft.

Table 9: Center of Gravity and Movements due to Payload and Antenna

CG Locations for the Three Aircraft Configurations				
	X-Location From Nose (in)	X-CG Movement (in.)	Y-Location From Ground (in)	Y-CG Movement (in)
Fully Loaded CG Placement	14.876	0	8.015	0
CG Movement with No Antenna	14.418	-0.458	7.701	-0.315
CG Movement with No Payload or Antenna	14.441	0.023	8.651	0.950

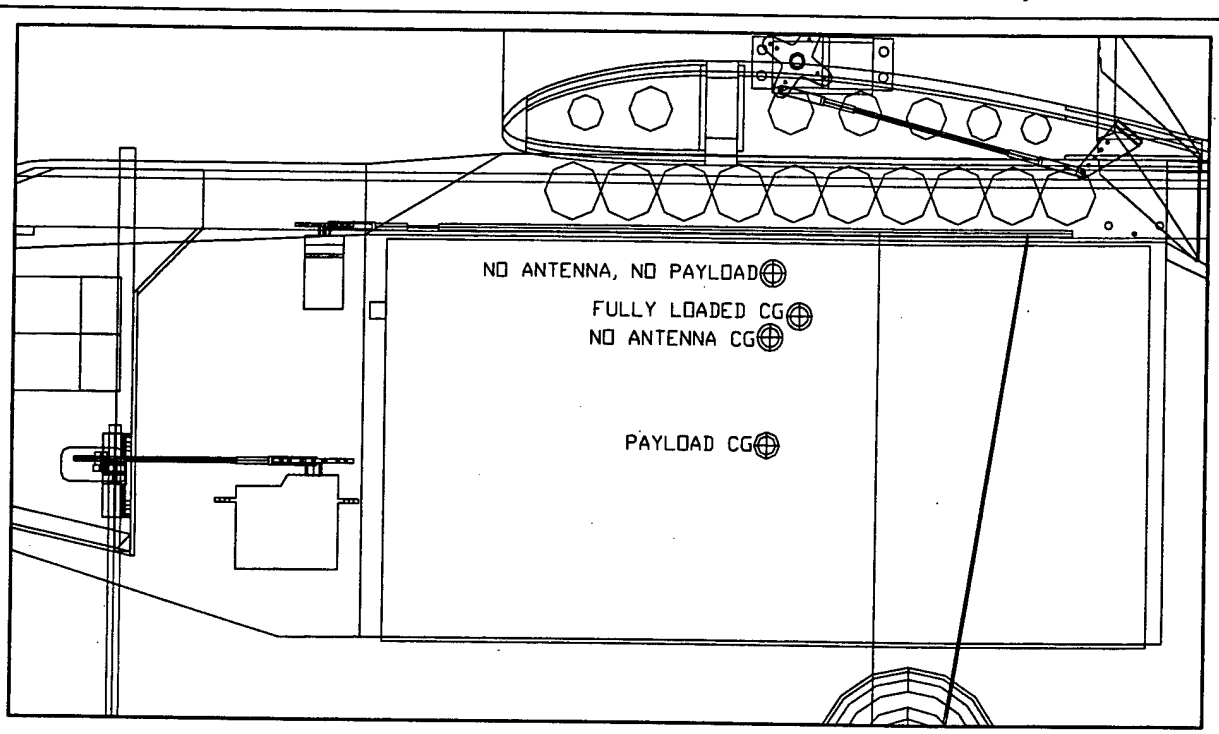

Figure 14: Movements in the Center of Gravity due to Payload and Antenna

5.9 Drawing Package

The drawing package can be found in Appendix A at the end of the report.

5.10 Rated Aircraft Cost and Aircraft Sizing

5.10.1 Rated Aircraft Cost

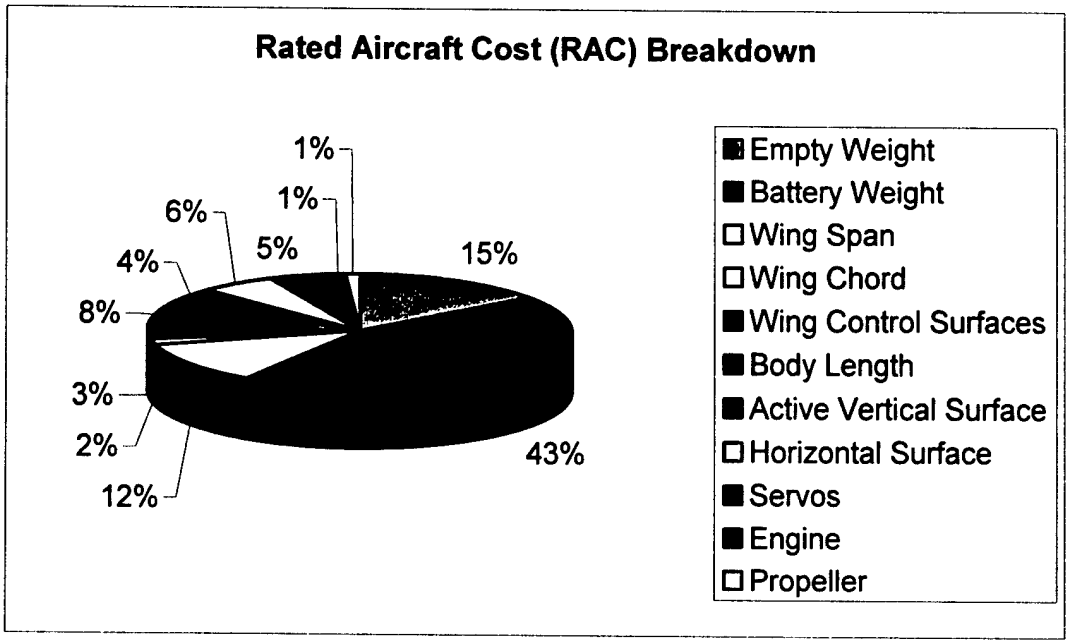

8 hr/ft	7.5	60
8 hr/ft	1	8
3 hr/control surface	2	6
10 hr/ft	4.25	42.5
5 hr/vertical surface	0	0
10 hr/vertical surface	2	20
10 hr/horizontal surface	1	10
5 hr/servo or motor control	7	35
5 hr/engine	1	5
5 hr/popeller or fan	1	5
Total Manufacturing Man Hours		**191.5**

	Actual airframe weight, lb., with all flight and propulsion batteries but without any payload.	$100	8.5	—	0.85
	Total battery weight defined as the weight of the propulsion batrtery pack	$1,500	2.5	—	3.75
	Prescribed assembly hours by work break down structure (WBS)	$20	—	191.5	3.83
			Rated Aircraft Cost		8.43

*Note: RAC = (A*MEW + B*REP + C*MFHR) / 1000

Figure 15: Rated Aircraft Cost Breakdown

5.10.2 Sized Aircraft Table

Geometry		
Aircraft Length	4.28	ft
Height	1.69	ft
Span	7.50	ft
Wing Area	7.50	ft
Aspect Ratio	7.50	

Radio System	
Radio	Futaba 9
Servos	Futaba: Standard and Mini

Performance	*Empty*	*Full*	
Cl max (with flaps)	1.5	1.5	
L/D Max	######	11.7	
Rate of Climb	0.0	0.0	ft/s
Stall Speed (without flaps)	######	###	ft/s
Maximum Speed	95.0	94.0	ft/s
Take-off Length	29.0	72.0	ft

Propulsion System		
Propellor	14x10	in x in
Static Thrust	7.5	lbf
Gear Ratio	1.63	
Battery Configuration	1900SCR: 20 cells in series	
Motor Used	Astro Flight 640G: Cobalt 40	

Weight		
Airframe	4.00	lbf
Propulsion System	3.47	lbf
Control System	0.75	lbf
Payload System	5.80	lbf
Empty Weight	8.22	lbf
Gross Weight	14.02	lbf

Control Volumes		
Ailerons	0.042	in/in
Rudder	0.039	in/in
Elevator	0.118	in/in

Figure 16: General Aircraft Sizing

6 Manufacturing Plan and Processes

6.1 Manufacturing Processes Examined

Due to the variance of materials and the different needs of every piece of the aircraft, many different manufacturing methods had to be employed. This including using an Epilog CNC (Computer Numerically Controlled) Laser Cutter, a milling machine, and hand cutting. The CNC laser cutter is an excellent tool because of its precise cutting abilities on many thin, lightweight woods. The milling machine is good for precisely cutting and shaping larger wood and metal pieces. Hand cutting and sanding will be optimized when using already cut stock wood or when cutting easy shapes with the thin balsa wood. The figures of merit used to assess these different methods include: ease of use, time required, preciseness, and materials used.

6.2 Manufacturing Utilized for the Fuselage

The fuselage section comprises of four main parts; the aluminum column; the nose, the mid-section, and the tail boom. Each of these sections performs different tasks requiring materials and therefore different manufacturing styles.

The first and most important section is the aluminum column that provides the backbone structure for the entire aircraft. This column must be thick enough to tap into for all the mounts that must be attached but yet light enough to not weigh down the aircraft. Thinning the sides of the structure that do not require the added structural support does this. Using the milling machine, a detailed AutoCAD drawing can be entered into the computer to output a final product that is at least 25 percent lighter. This allows an almost flawless product as well as saving time and the tedious effort involved in machining a part such as this. Attaching the braces for some of the wider mounts, such as the wing and landing gear, will be done with a spot welder and some lightweight brackets.

The nose section of the aircraft will have three basic parts: the internal structure for integrity, the external balsa sheeting for maintaining a curved shape, and the air intake for the engine cooling. The internal structure will be made of thin plywood that would be best manufactured on the CNC laser cutter allowing very precise cutting for the most accurate shape without sanding and therefore saving valuable construction time. The balsa sheeting over the exterior of the aircraft will be cut by hand. Since this thin sheeting is easy to cut and shape there is no need use the precise cutting of the CNC machines. The air intake for the engine and batteries will also be made from a block of balsa wood. Because of the lack of machines able to manufacture a complex three-dimensional shape such as this, the intake will be made from hand cutting and sanding.

The mid-section of the aircraft encompasses four parts: the outer skin, the internal bulkheads, the box release device and backbone mount, and the sidewall strengtheners. The outer skin of this section of the aircraft will be made of two thin balsa sheets with separators in the middle for structural support. Many of the parts for the skin do not need to be exact and they will be made from a soft easily cut material so the quickest manufacturing method would be to cut the parts by hand. The inner bulkheads and the payload release top

plate in this section will be made from thin plywood for strength. The use of the CNC laser cutter would be the quickest method because it is difficult to cut plywood to exact specifications and the laser cutter could easily insert the lightening holes. The remainder of the structure will be triangle balsa stock that can easily be cut by hand and sanded to the correct size.

Similar to the mid-fuselage section, the tail boom will consist of a balsa wood outer skin with plywood bulkheads and triangle balsa stock for reinforcement. Since the plywood will be thirty-second inch thin with a lightening hole, the CNC laser cutter would be the best choice for manufacturing. As for the triangle balsa wood, the easiest method would be to hand cut the wood and sand to the correct size.

6.3 Manufacturing Utilized for the Wing and Tail

The wing of the aircraft is the most critical part of the aircraft manufacturing. To achieve the expected flight characteristics, the airfoil shape must be maintained throughout the entire wing. Since the airfoil shape is so imperative to the success of the aircraft, the thin balsa and thin plywood will be cut using the CNC laser cutter. This will allow for the quickest and most precise manufacturing. The thin balsa wood sheeting and stringers along with the spars of the wing will all be stock wood, and it will be easy to cut and correctly shape the wood by hand. The leading and trailing edge stock will also be cut and sanded by hand to get the correct airfoil shape.

The horizontal and vertical stabilizers of the aircraft will be fairly simply made. They will be made from quarter inch balsa sheets with triangle stock and carbon fiber tape for added strength and stiffness. The triangle stock and the carbon fiber tape will be used for attaching the vertical stabilizers to the horizontal stabilizer as well as attaching the horizontal stabilizer to the tail boom. All of this section will be made by hand and then sanded to the required shape except for the carbon fiber tape, which will be purchased.

6.4 Manufacturing Schedule

Through the manufacturing of the aircraft, it will be very important to keep the group on task and ahead of schedule. To accomplish this, the schedule will be modified twice a week to ensure that people that need the help will get more help and people that are ahead of schedule are assigned to the next task. Figure 17 is an initial estimate at the time required to build the aircraft based on the assumptions that everyone can only work one hour a day.

ID	Task Name	Start	Finish	Duration
1	Finalize Manufacuring Drawings	3/10/2003	3/12/2003	3d
2	Cut Aluminum Column	3/12/2003	3/12/2003	1d
3	Precut tail boom	3/13/2003	3/13/2003	1d
4	Assemble tail boom	3/14/2003	3/20/2003	7d
5	Precut Mid-Fuselage Section	3/14/2003	3/19/2003	6d
6	Assemble Mid-Fuselage Section	3/21/2003	3/29/2003	9d
7	Precut nose section	3/20/2003	3/23/2003	4d
8	Assemble nose section	3/30/2003	4/6/2003	8d
9	Precut wing parts	3/24/2003	3/26/2003	3d
10	Assemble Wing	3/27/2003	4/7/2003	12d
11	Cut Horizontal and Vertical Stabs	4/7/2003	4/7/2003	1d
12	Sanding	4/7/2003	4/9/2003	3d
13	Attach Remaining Sections	4/8/2003	4/9/2003	2d
14	Cover final product	4/10/2003	4/11/2003	2d

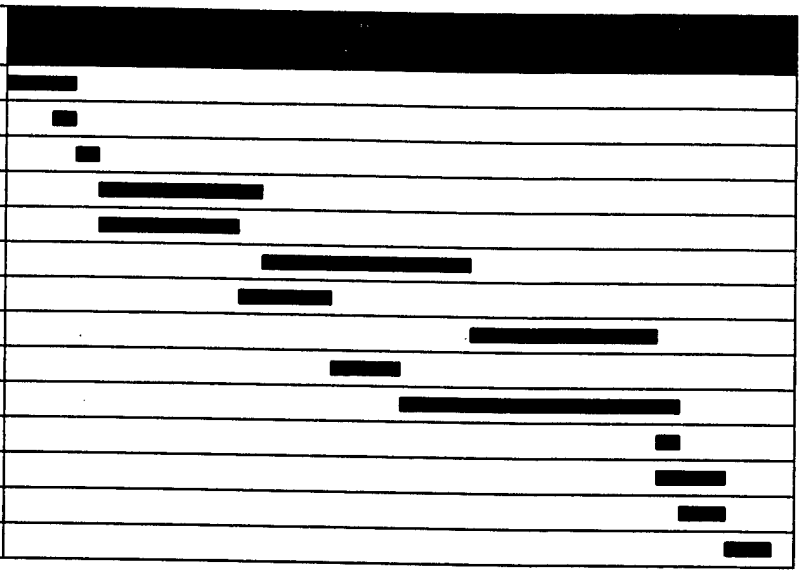

Figure 17: Manufacturing Schedule

7 Testing Plan

Once the aforementioned tests are successfully completed, the first attempt at a flight test will be made. Again, starting with an unloaded aircraft, the pilot will attempt to fly the aircraft through various gradual maneuvers careful to identify any handling problems. Progressively the payload and antenna will be added until a test run of each required mission is completed. After the airworthiness of the aircraft is fully proven certain aspects of the aircraft may be altered to optimize performance. For example, a few select propellers will be flown to find the best combination of maximum flight speed to minimize flight time and thrust required to meet the 120 ft takeoff distance.

7.1 Objectives and Schedule

During the design phase of an aircraft, every detail is critically analyzed to prevent unexpected problems and to ensure that the vehicle will perform as envisioned by the engineers. Often the complexity of an aircraft leads to uncertainties in the design that cannot be clarified solely by theory, and multiple levels of testing are required to develop the best possible design. In general the testing phase, similar to the design phase, is broken down to the component, subsystem, and system levels. The major objectives of the testing are to ensure the vehicle can satisfy the mission requirements, verify structural integrity, verify vehicle stability, and optimize the performance of the aircraft.

7.2 Schedule

Initially the group decided that testing and experimentation would occur throughout the duration of the project. During the design and fabrication phases component level tests would be performed as necessary to verify

functionality. Optimally a prototype would be built after the preliminary design was finished, and used for rigorous testing. It is often more desirable to use a prototype for the bulk of the tests to prevent damaging equipment that will be needed for the final product. The results from the experimentation would be used to identify and fix any problem areas and to make improvements during the critical design phase. After the construction of the competition aircraft, full system tests including flight tests would be performed to finalize the design. Unfortunately due to time and funding constraints a prototype was not built, and amount of scheduled testing was reduced. This meant that only small amounts of component and subsystem level testing took place, and a majority of the testing occurred at the system level. Figure 18 below depicts the schedule of testing for the aircraft.

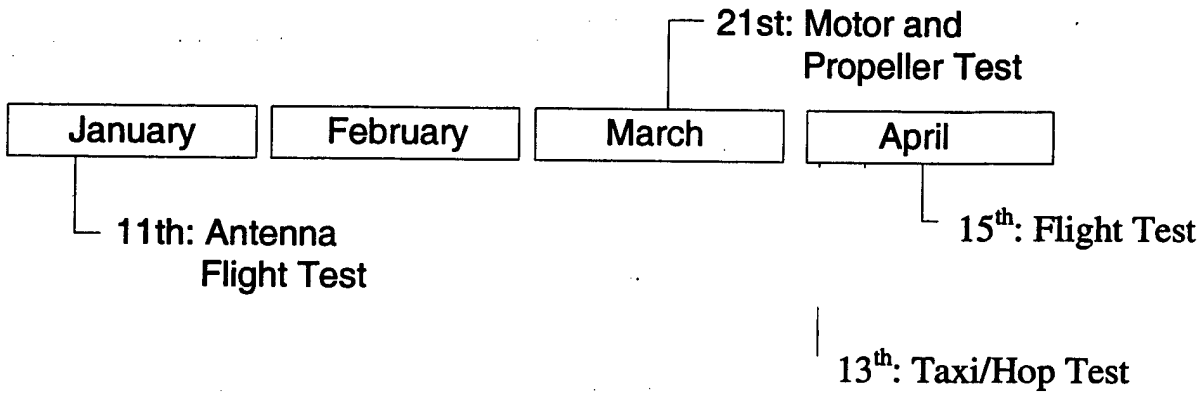

Figure 18: Testing Schedule

7.3 Test Descriptions

A total of five separate tests were planned for the project with the following breakdown: one component test, one subsystem test and three systems tests. Detailed descriptions of each test are given in the following sections.

7.3.1 Antenna Flight Test

The first test performed involved attaching the antenna to an existing RC aircraft to identify the effects the antenna had on an aircraft's performance. The aircraft used was a balsa construction trainer with a rectangular, high mounted wing with a forty-size engine. The test aircraft was similar in size and power to the competition aircraft to provide realistic results. The antenna was mounted slightly aft of the wing trailing edge, directly in the center of the fuselage. The experiment was used to obtain three major results: first to measure the difference in takeoff distance with and without the antenna attached, second to obtain the drop in maximum flight speed, third to observe the changes in flight characteristics with and without the antenna.

By running the experiment it was found that the takeoff distance with the antenna increased approximately 10% from the required takeoff distance without the antenna. Although the absolute speed of a model aircraft is difficult to measure, it was also found that the maximum flight speed decreased 10%. The results to the last objective were much more qualitative than the previously mentioned results. As noted by the pilot, the aircraft was more difficult to control with the antenna attached due to sluggish responses and the constant need to provide yaw correction with the rudder. It was found that the pilot needed to handle the aircraft conservatively by limiting maneuvers and that the aircraft needed constant attitude correction.

A few major conclusions could be made from the results of the test. First, the higher than expected static thrust would be required to accelerate the aircraft to takeoff speed. It was also decided that the control surfaces would need to be enlarged in order to counteract the random moment generation by the antenna. Lastly, this verified the use of an H-tail to help prevent the vertical stabilizer from residing in the antenna slipstream, therefore increasing the ability to control the aircraft.

7.3.2 Motor and Propeller Tests

This test will cover two aspects of the propulsion subsystem. During this experiment the motor will be attached to a mount and run with varying propeller pitches and sizes. The purpose of the test will be to measure the static thrust provided by varying propellers and to measure the rate of power consumption. This will help optimize the propeller used on the aircraft and to verify the batteries can supply power for the entire duration of each mission.

7.3.3 Taxi Test

The purpose of this test is to verify the stability of the aircraft while on the taxiway, and to verify correct deployment of the payload. Intended as the first full system test, it will be performed after final construction of the aircraft to determine the aircraft's on-ground stability, and ability to deploy the payload. The experiment will involve trial runs including taxiing without the payload, with the payload and deploying the payload onto the runway. If the aircraft is unable to deploy the payload, corrections and modifications will be made before continuing on to the next set of tests.

7.3.4 HOP Test

The HOP tests will be used to verify takeoff speed and distance of the aircraft and to identify potential problems with handling characteristics before the first flight test. These tests will be broken into trials starting by accelerating from rest to the predicted takeoff speed of 44 ft/s, and back to rest. If any issues with trim or handling occur, the aircraft will be modified and/or the control surfaces will be trimmed accordingly. Next the aircraft will accelerate from rest to takeoff speed and the pilot will attempt to raise the landing gear from the ground for a brief distance without gaining more than a few feet of altitude. This will help verify that the center of gravity is in the correct position for longitudinal stability and that the control surfaces are correctly sized to

provide the necessary moments without seriously risking the aircraft. A set of trials will be performed starting without the payload or antenna, progressing to a fully loaded aircraft with the payload and antenna.

7.3.5 Flight Test

Once the aforementioned tests are successfully completed, the first attempt at a flight test will be made. Again, starting with an unloaded aircraft, the pilot will attempt to fly the aircraft through various gradual maneuvers careful to identify any handling problems. Progressively the payload and antenna will be added until a test run of each required mission is completed. After the airworthiness of the aircraft is fully proven certain aspects of the aircraft may be altered to optimize performance. For example, a few select propellers will be flown to find the best combination of maximum flight speed to minimize flight time and thrust required to meet the 120 ft takeoff distance.

8 References

McCormick, Barnes W. *Aerodynamics, Aeronautics, and Flight Mechanics.* 2nd Edition. John Wiley & Sons., Inc. 1995

Shevell, Richard S. *Fundamentals of Flight.* 2nd Edition. Prentice Hall, Englewood Cliffs, New Jersey. 1989

Roskam, Jan. *Airplane Flight Dynamics and Automatic Flight Controls, Part 1.* 2nd Edition. DARCorporation. 1998

Advanced Aircraft Analysis. DARCorporation.

X-Plane. Laminar Research.

Simons, Martin. *Model Aircraft Aerodynamics.* 4th Edition. Biddles Ltd. Great Britain. 1999

WEB1XXX Nihon University Aero Student Group, Airfoil Comparison ToolDatabase Site, http://soaring.cnde.iastate.edu/calcs/frames.shtml.www.nasg.com/afdb Airfoil data taken from UIUC Applied Aerodynamics Group, Low Speed Airfoil Tests.

9 Acknowledgements

Team Bellwether would like to thank the following people. Without these contributors, this project would never have been completed.

The Engineering Excellence Fund

Thank you for contributing the necessary funds to the team.

Dr. Brian M. Argrow

Team Bellwether appreciates the funding and your support in this project.

The CU Aerospace Engineering Faculty

Thank you for the time and advice that you donated to the team.

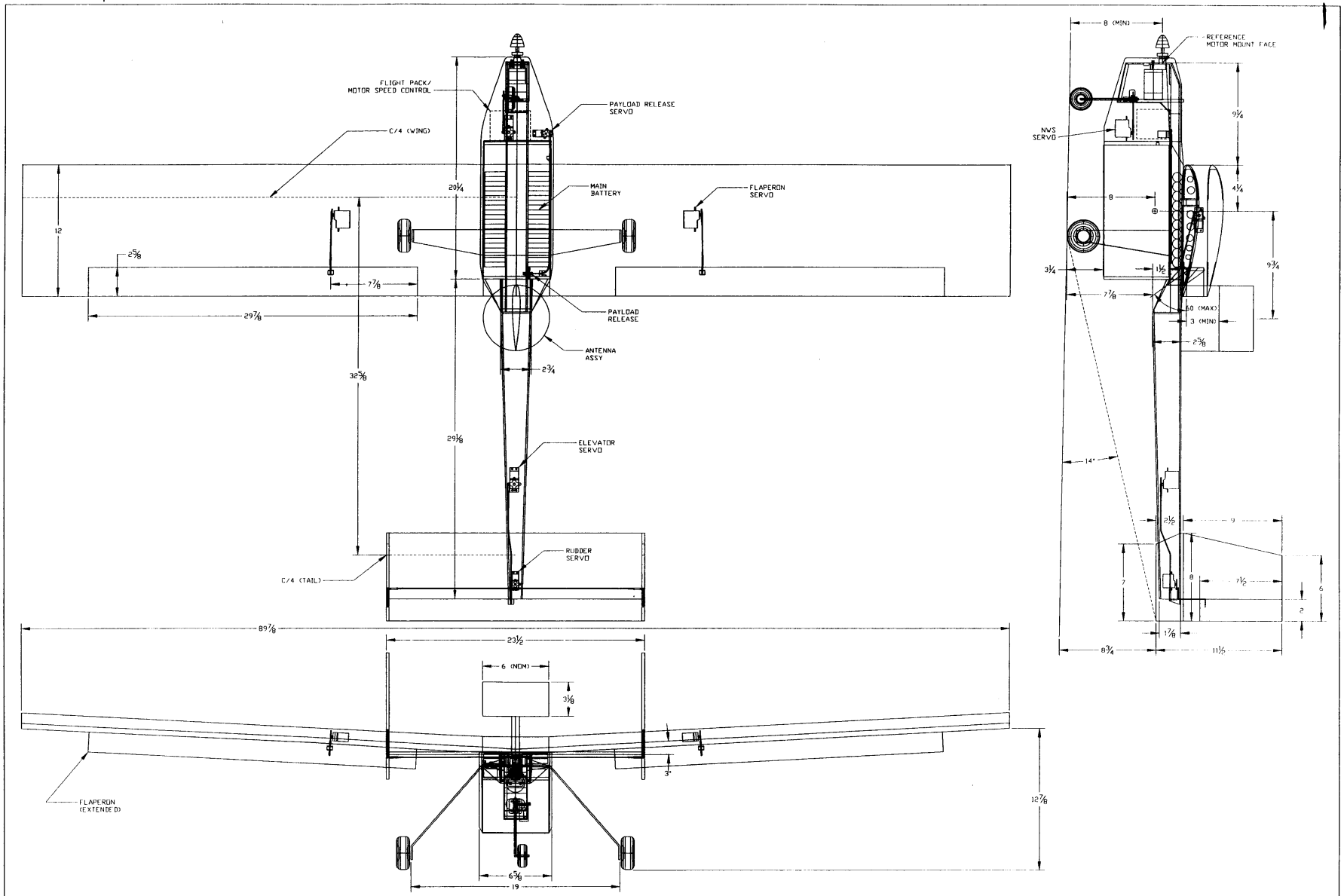

#	REVISIONS	DRWN BY	APP'D BY	DATE

DESIGNED BY: TB/CD/SN
DRAWN BY: TB
CHECKED BY:
APPROVED BY:
SCALE: NO SCALE
DATE: 3/8/03

DRAWING TITLE: GENERAL ARRANGEMENT

PROJECT: UNIVERSITY OF COLORADO
DBF TEAM BELLWETHER

DRAWING SET STATUS
- ☐ PROGRESS PRINT _____
- ☒ FINAL REVIEW _____
- ☐ NOT FOR CONSTRUCTION
- ☐ RELEASED FOR BIDDING OR CONSTRUCTION _____ / _____ (AUTHORIZED / DATE)

SHEET NUMBER
1 OF 1

DWG. NO.
001

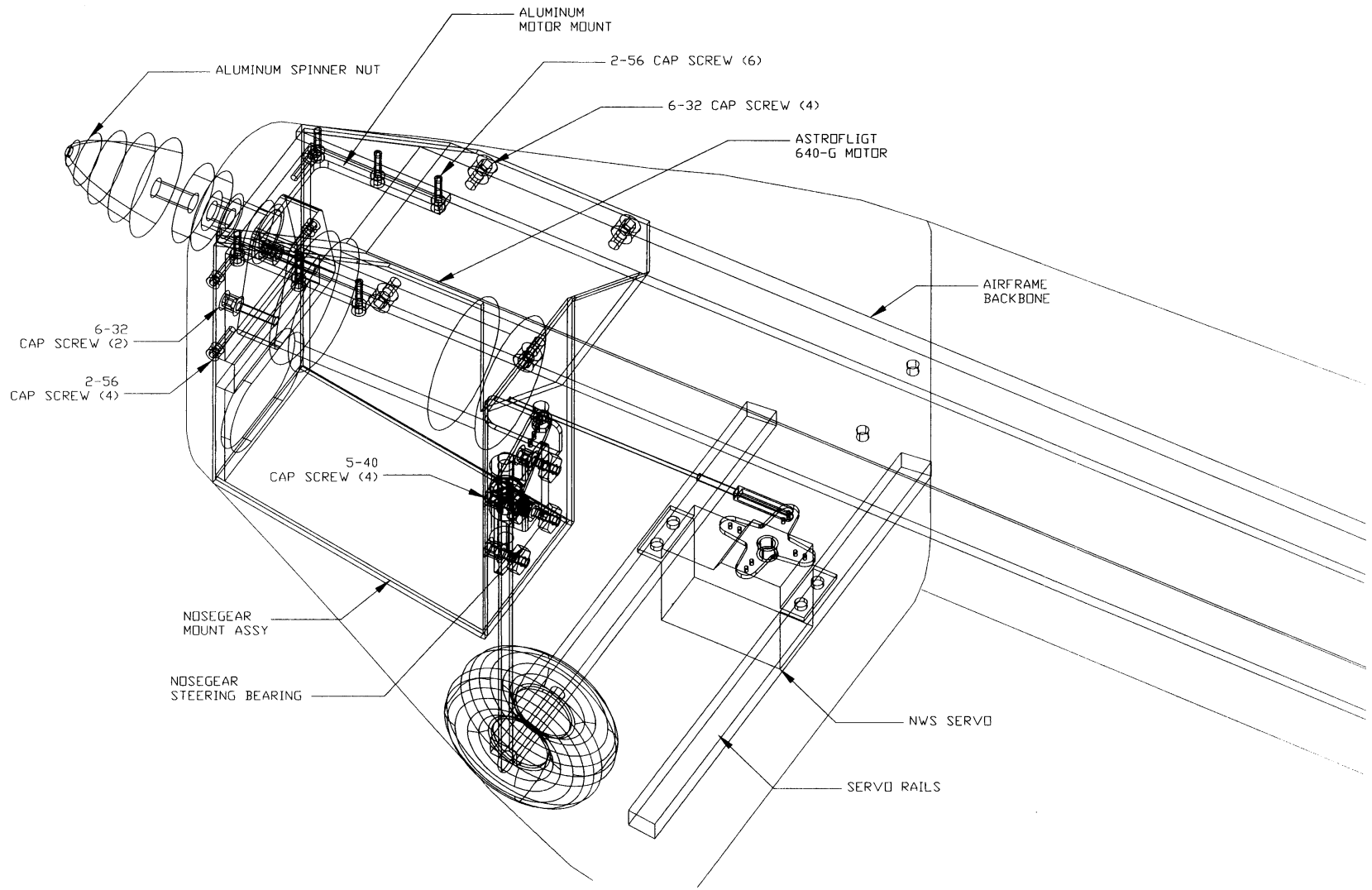

#	REVISIONS	DRWN BY	APP'D BY	DATE

DESIGNED BY: TB/CD/SN
DRAWN BY: TB
CHECKED BY:
APPROVED BY:
SCALE: NO SCALE
DATE: 3/8/03

DRAWING TITLE: NOSE SECTION

PROJECT: UNIVERSITY OF COLORADO
DBF TEAM BELLWETHER

DRAWING SET STATUS
- ☐ PROGRESS PRINT _____
- ☒ FINAL REVIEW _____
- ☐ NOT FOR CONSTRUCTION
- ☐ RELEASED FOR BIDDING OR CONSTRUCTION _____ AUTHORIZED / DATE

SHEET NUMBER
1 OF 1

DWG. NO.
002

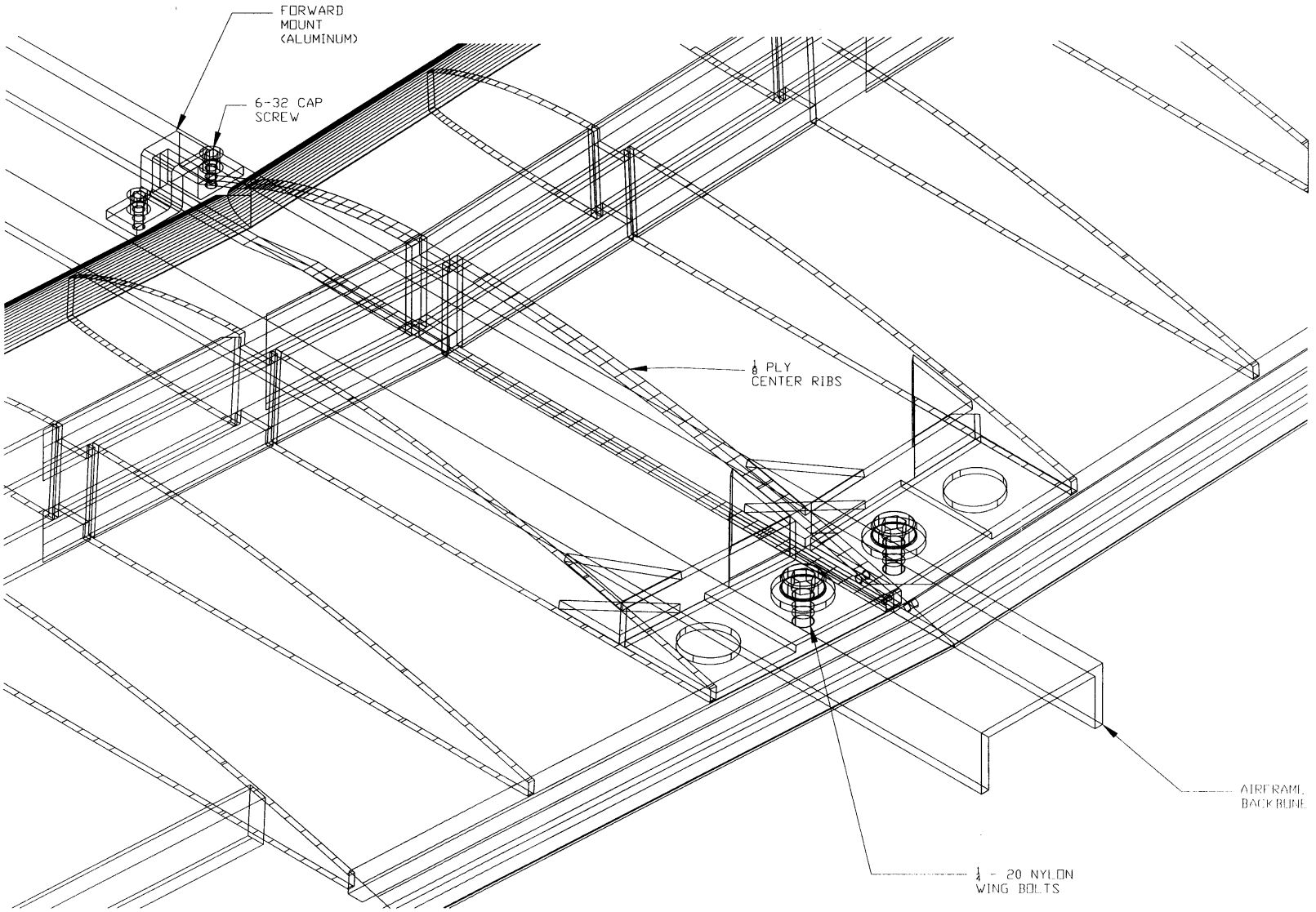

#	REVISIONS	DRWN BY	APP'D BY	DATE

DESIGNED BY: TB/CD/SN
DRAWN BY: TB
CHECKED BY:
APPROVED BY:
SCALE: NO SCALE
DATE: 3/8/03

DRAWING TITLE: WING MOUNT DETAILS

PROJECT: UNIVERSITY OF COLORADO
DBF TEAM BELLWETHER

DRAWING SET STATUS
- ☐ PROGRESS PRINT _____
- ☒ FINAL REVIEW _____
- ☐ NOT FOR CONSTRUCTION
- ☐ RELEASED FOR BIDDING OR CONSTRUCTION _____ AUTHORIZED / _____ DATE

SHEET NUMBER
1 OF 1

DWG. NO.
003

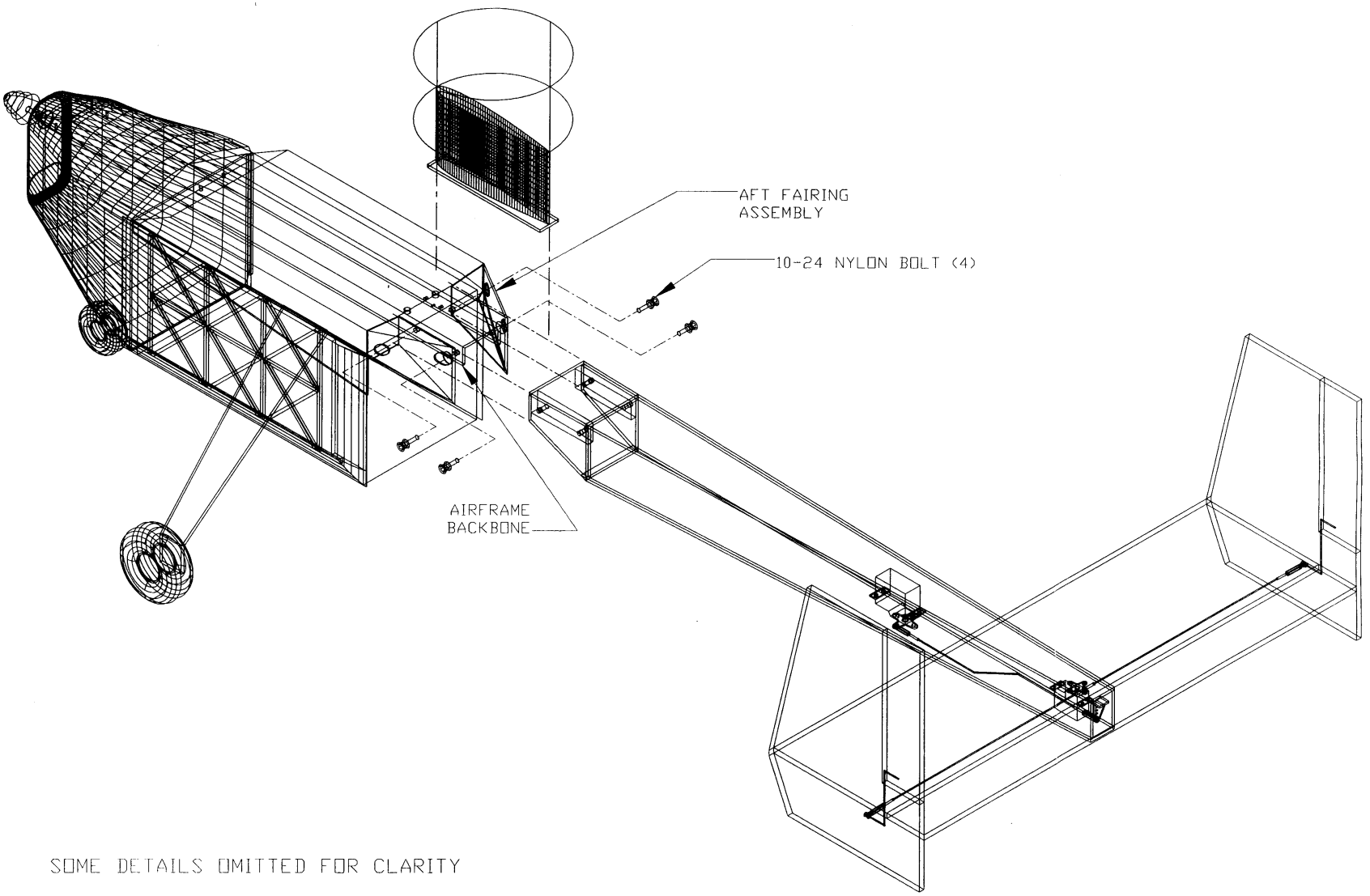

SOME DETAILS OMITTED FOR CLARITY

#	REVISIONS	DRWN BY	APP'D BY	DATE

DESIGNED BY: TB/CD/SN
DRAWN BY: TB
CHECKED BY:
APPROVED BY:
SCALE: NO SCALE
DATE: 3/8/03

DRAWING TITLE: TAILBOOM ATTACHMENT (EXPLODED)

PROJECT: UNIVERSITY OF COLORADO
DBF TEAM BELLWETHER

DRAWING SET STATUS
- ☐ PROGRESS PRINT _____
- ☒ FINAL REVIEW _____
- ☐ NOT FOR CONSTRUCTION
- ☐ RELEASED FOR BIDDING OR CONSTRUCTION AUTHORIZED / DATE

SHEET NUMBER
1 OF 1

DWG. NO.
004

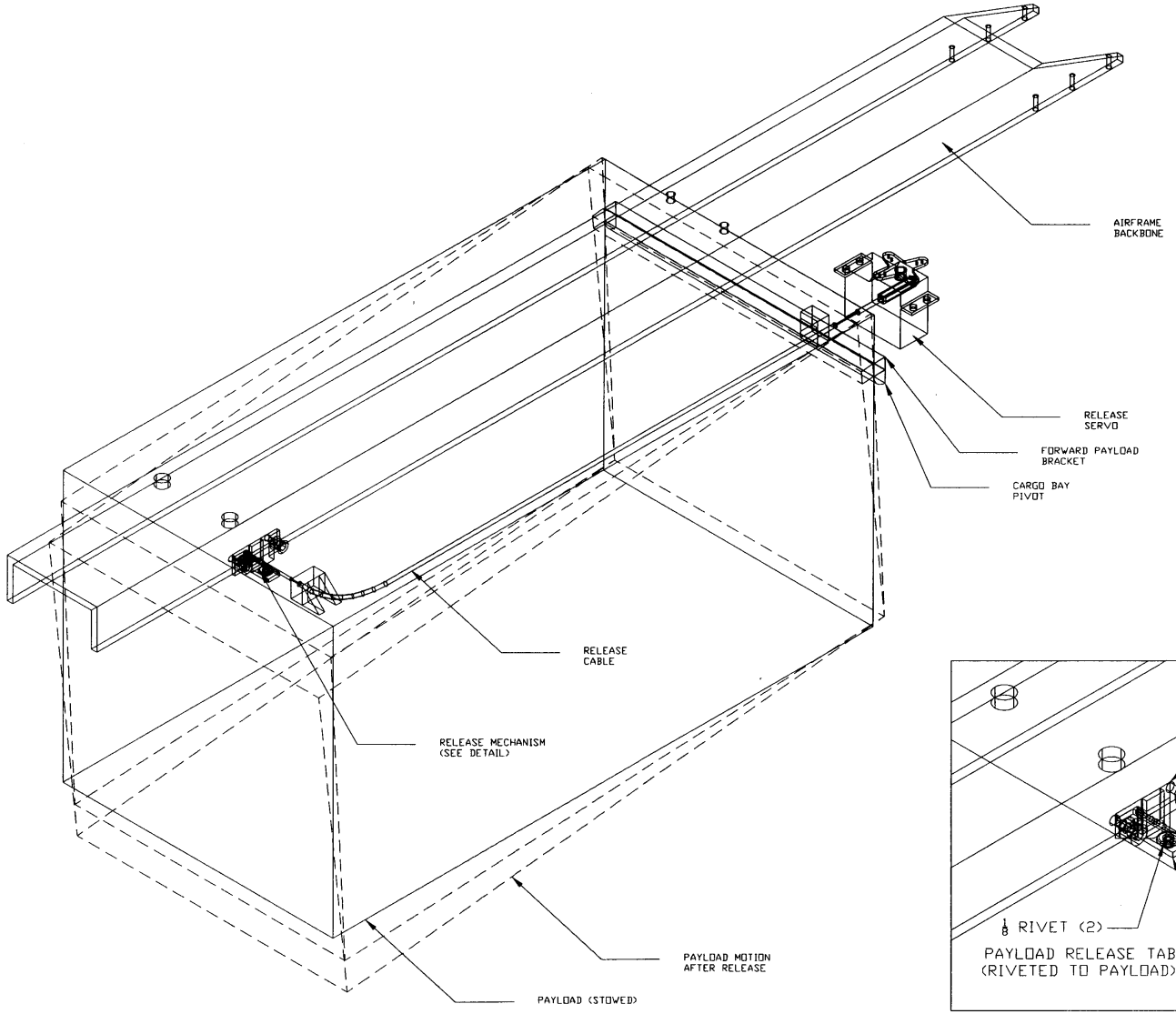

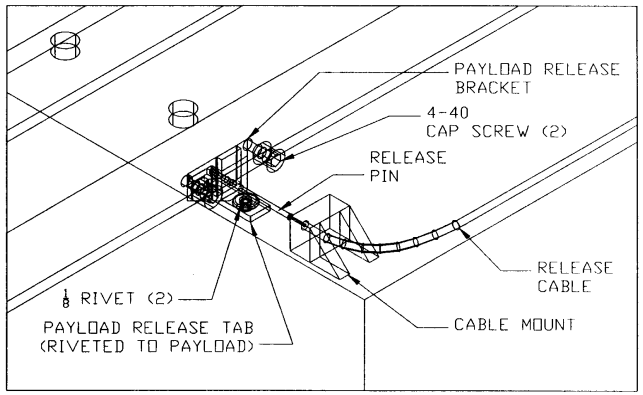

#	REVISIONS	DRWN BY	APP'D BY	DATE

DESIGNED BY: TB/CD/SN
DRAWN BY: TB
CHECKED BY:
APPROVED BY:
SCALE: NO SCALE
DATE: 3/8/03

DRAWING TITLE: PAYLOAD RELEASE SYSTEM

PROJECT: UNIVERSITY OF COLORADO DBF TEAM BELLWETHER

DRAWING SET STATUS
- ☐ PROGRESS PRINT _____
- ☒ FINAL REVIEW _____
- ☐ NOT FOR CONSTRUCTION
- ☐ RELEASED FOR BIDDING OR CONSTRUCTION _____ AUTHORIZED / _____ DATE

SHEET NUMBER: 1 OF 1

DWG. NO.: 005

UNIVERSITÄ La Sapienza di ROMA

FACOLTÄ DI INGENERIA

Leonardo

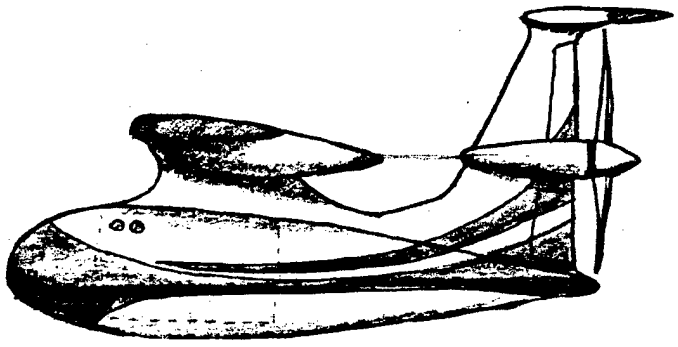

(Flight Centurions 3)

CESSNA / STUDENT
ONR / DESIGN / BUILD / FLY
COMPETITION
An AIAA Student Activity

Table of Contents

1.0 EXECUTIVE SUMMARY 1
1.1 CONCEPTUAL DESIGN 1
1.1.1 Valuable Conceptual Design 1
1.1.2 IPT Evaluation 2
1.1.3 Concept al Results 2
1.2 PRELIMINARY DESIGN 2
1.2.1 Preliminary Design Solutions 3
1.2.2 Preliminary Design Tools 3
1.2.3 Preliminary Results 3
1.3 DETAIL DESIGN 3
1.3.1 Detail Design Solutions 4
1.3.2 Detail Design Tools 4
1.3.3 Detail Design Result 4
1.4 MANUFACTURING AND PROTOTYPE TESTING 4

2.0 MANAGEMENT SUMMARY 5
2.1 TEAM ORGANIZATION AND PERSONNEL ASSIGNMENT WORKING AREAS 5
2.2 RESPONSIBILITIES OF EACH TECHNICAL GROUP 5
2.2.1 Aerodynamics and Flight Mechanics Groups 6
2.2.2 Propulsion Group 6
2.2.3 Structures and Systems Groups 6
2.3 SCHEDULING, DOCUMENT, AND CONFIGURATION CONTROL 8

3.0 CONCEPTUAL DESIGN 8
3.1 DESIGN PARAMETERS 9
3.1.1 Primary Design Parameters 9
3.1.2 Design Parameter Sensitivity Analysis 10
3.1.3 Rated Aircraft Cost Analysis 11
3.2 AIRCRAFT CONFIGURATION 12
3.2.1 Alternative Fuselage and Tail Configuration 12
3.2.2 Alternative Wing Configuration 15
3.3 STRUCTURAL CONFIGURATION 16
3.3.1 Figures of Merit 16
3.3.2 Assumptions Made and Design Parameters Investigated 17
3.3.3 Alternative Wing Structures 17
3.3.4 Alternative T-tail Structures 18
3.3.5 Alternative Fuselage Structures 18
3.3.6 Alternative Landing Gear Configurations 19
3.4 ALTERNATIVE POWER PLANT CONFIGURATIONS 21

3.5 ANALYTICAL TOOLS 22
3.5.1 Optimization Program Architecture 22
3.5.2 Other Methods Used 22
3.6 FINAL AIRCRAFT CONFIGURATIONS 23

4.0 PRELIMINARY DESIGN **24**
4.1 INITIAL TRADE STUDY RESULTS 24
4.1.1 Study of Model and Number of Batteries 24
4.1.2 Study of Take Off Battery Performances 25
4.1.3 Study of Cruise Battery Power Requirements 25
4.1.4 Study of Wing Planform Area Requirements 25
4.1.5 Study of Wingspan Requirements 26
4.1.6 Study of Aspect Ratio Requirements 26
4.1.7 Study of Plane Structural Weight Effects 26
4.1.8 Study of Rated Aircraft Cost Effects 26
4.2 AERODYNAMIC CONSIDERATIONS 26
4.2.1 Wing Figures of Merit, Assumptions, and Analysis 26
4.2.2 Fuselage Figures of Merit, Assumptions, and Analysis 28
4.2.3 Tail Figures of Merit, Assumptions, and Analysis 29
4.3 STRUCTURAL ANALYSIS 29
4.3.1 Figures of Merit 29
4.3.2 Design Parameters and Trade Studies Investigated 30
4.3.3 Wing Assumptions and Structural Analysis 30
4.3.4 Tail Assumptions and Structural Analysis 30
4.3.5 Structural Analysis 31
4.3.6 Main Gear Assumptions and Structural Analysis 32
4.4 PROPULSION ANALYSIS 32
4.4.1 Figures of Merit 32
4.4.2 Design Parameters and Trade Studies Investigated 33
4.4.3 Weighted Decision of Motors 33
4.4.4 Investigation of Graupner Motor 33
4.5 ANALYTICAL TOOLS 35
4.5.1 Optimization Program Architecture 35
4.5.2 Other Methods Used 35
4.6 FINAL AIRCRAFT CONFIGURATIONS 35
4.6.1 Wing and Power Loading 35

5.0 DETAIL DESIGN **36**
5.1 AERODYNAMIC PERFORMANCE ANALYSIS 36
5.1.1 Final Configuration Features 36
5.1.2 Estimated Mission Performance 37

5.1.3 Takeoff and Climb 38
5.1.4 Flight Conditions 38
5.2 PROPULSIVE PERFORMANCE ANALYSIS 39
5.3 STRUCTURAL CONSIDERATIONS 39
5.3.1 Fuselage Structural Details 39
5.3.2 Wing Structural Details 41
5.3.3 Tail Structural Details 42
5.4 DETAIL DESIGN ASSUMPTIONS AND COMPARISONS 42
5.5 DRAWING PACKAGE 43

6.0 MANUFACTURING PLAN **49**
6.1 MANUFACTURING PROCESS INVESTIGATED 49
6.2 PROCESSES SELECTED FOR COMPONENT MANUFACTURING 49
6.2.1 Fuselage Manufacturing Process and Tooling 49
6.2.2 Wing and Tail Manufacturing Process and Tooling 49
6.2.3 Landing Gear Manufacturing Process and Tooling 50
6.3 ANALYTIC METHODS INCLUDING COST, SCHEDULING AND SKILLS MATRIX 50
6.3.1 Manufacturing Cost 50
6.3.2 Skills Matrix 50
6.3.3 Manufacturing Scheduling 51

***7.0* TESTING** **51**
7.1 STATIC TESTS 51
7.2 FLIGHT TESTS 52
8.0 REFERENCES **56**

Table of Figures

Figure 1: Leonardo Team Organization tree with Design Personnel and Assignment Areas 5
Figure 2: Milestone Chart 7
Figure 3: Sensitivity Analysis Graphics 9
Figure 4: Velocity Field around Fuselage 10
Figure 5: Fuselage and Tail Configuration Weighted Decision Matrix 13
Figure 6: A Photo of Playboy Senior 14
Figure 7: Battery-Motor-Propeller Alternatives and Propulsion Weighted Decision Matrix 21
Figure 8: Final Plane Configuration 23
Figure 9: Tradeoff Analysis Results 25
Figure 10: Polar and Cm curve for Selected Airfoil 28
Figure 11: Tail Assembly 31
Figure 12: Graupner Ultra 920 Motor Performance Data 34
Figure 13: Pressure Field behind the Plane 38
Figure 14: Fuselage Structural Details 40
Figure 15: Wing Stress Analysis 41
Figure 16: Weight Balance Spreadsheet 42
Figure 17: 3-View Drawing 44
Figure 18: Payload, its Location and Restraint Method 45
Figure 19: Location of Propulsion and Flight Control System Components 46
Figure 20: Manufacturing Schedule 51
Figure 21: Simulation of Wing Load 52
Figure 22: Telemetry Instrumentation 53
Figure 23: Flight Tests Results 54
Figure 24: Longitudinal Stability 54
Figure 25: Prototype photos 55

Table of Tables

Table 1: Wing Configuration Weighted Decision Matrix 15
Table 2: Wing and Tail Structural Decision Matrix 18
Table 3: Fuselage Structural Concept Decision Matrix 19
Table 4: Landing Gear Concept Decision Matrix 20
Table 5: Main Landing Gear Conceptual Decision Matrix 20
Table 6: Batteries Rank 24
Table 7: Motor Weighted Decision Matrix 34
Table 8 : Final Aircraft Configuration Features 36
Table 9: Time Spent in Mission Phases 37
Table 10: Aircraft Data 47
Table 11: Rated Airacraft Cost Worksheet 48
Table 12: Skill Matrix for Leonardo Team 50

1.0 Executive Summary

This report has been redacted by Leonardo Team (University La Sapienza of Rome , Italy) in the sphere of the works performed for attending at the AIAA 2002/2003 Design/Build/Fly (DBF) Competition .Specifically in this paper we describe the mainlines followed by the group during several tasks of planning, design, construction and testing of an electric and propeller driven unmanned aircraft according to competition rules. At first glance, we want outline the main goal of the competition is to realize an optimized aircraft in terms of aerodynamic, propulsive, flight and structural characteristics, subjected to a continuum control of costs in order to minimize the Rated Aircraft Cost.

1.1 Conceptual Design

In first of all the group planned the whole operation defining two macrophases in their turn divided in a series of steps concerning several areas of work. First macrophase involves, in sequence:

- Planning
- Production
- Flight tests and model tuning ;

Second macrophase regards:

- Definition and organization of spare parts (and relative tools of installation);
- Managing of travel logistic;
- Planning of tasks for each team member during the competition.

As regards first macrophase, an IPT (Integrated Product Team) was formed to reach following goals:

- CPD (Concurrent Product Definition);
- DFMA (Design for Manufactoring and Assembly);
- DAT (Determinant Assembly Techniques).

IPT performed several studies in the areas of Aerodynamic, flight mechanics, propulsion, systems and structures during which the relative groups were in constant contact each other. CPD was obtained integrating the best design concept in each area of work where relatives groups performed sensitivity studies scrutinizing each rule of the competition to focus design specifics with the aim to maximize overall scoring. Each group proposed some design concepts in their respective technical areas to meet defined design requirements;then IPT performed a design optimization analysis which results were used to create figures of merit to compare various concepts and evaluate different approaches of aircraft definition to achieve the highest possible score in terms of RAC as regards design/building competition and best flight performances concerning flight competition. After several evaluations for each iteration of optimization process, an optimum region was determined according to whom each group tailored their respective ideas into their final concepts.

1.1.1 Valuable Conceptual Designs

The aerodynamic group conceived three degrees of analysis: analysis of wing airfoil according to low Reynolds number foreseen, definition of fuselage geometry subjected to propeller position and, at least, wing and horizontal tail position with respect to the fuselage keeping in count the location of cargo vane and encumbrances of respective opening mechanism and trajectory of cargo expulsion

during its discharging. Different combinations of fuselage shapes, discharging cargo ways, wing configurations and tail configurations were evaluated for the components that made up the different configurations. Concurrently structural evaluations was performed in order to select only viable alternatives in terms of feasibility of construction, RAC minimization, rapidity of assembly during competition, control of weight and piloting . Three propulsion system alternatives were defined evaluating several schemes generated combining number of engines, propeller characteristics and position, estimated weight and drags, length of flight and battery characteristics .

1.1.2 IPT Evaluation

A decision making process was performed after each group of IPT defined all possible schemes of solution concerning respective work ambits. Our process was split in two steps: during first one score sensitivities were determined using an optimization code where all aspects of the mission were keep in count; the code was developed employing models of weight and drag, aerodynamic and propulsive effects of various components and RAC. Time of construction and RAC was effected by each model which, moreover, in turn adjusted the overall score of a specific configuration. Subsequently, six parameters were selected. The performance program adjusted six parameters using random variables and found local maximums in the performance of the plane. Weighted decision matrices were constructed using the sensitivities studies produced from these models. Finally configurations were evaluated in the weighted decision matrices for scoring potential.

1.1.3 Conceptual Results

The result of the conceptual design work, with the highest scoring potential was a high-wing monoplane with a T-tail in which, moreover, is inserted a four-blade propeller (a single engine configuration with a pusher propeller resulted to be the optimum propulsive scheme). As this group was interested to pay homage to centenary of first Wright's flight, materials selected for all the airplane structures are wood and binding, except for control cables which are in metal and nose which is of resin. Cargo vane was allocated in center fuselage with discharge port on the right side; radar position had been defined over the tail.

1.2 Preliminary Design

After having frozen aircraft configuration the groups focused their attention to aircraft sizing and control surface sizing, structural design and propulsion components definition and configuration.In detail, aerodynamics and flight mechanics groups defined number, location and size of control surfaces, valuating ,concurrently, static stability of the aircraft versus manoeuvring necessities. The structures group, assumed use of wood and binding for structure, performed static and dynamic stress analysis of the aircraft enclosed therein simulations of drop test and aircraft lifting by tips. Propulsion group determined the best combination of motor, reducer, propeller and batteries to be tested.

1.2.1 Preliminary Design Solutions

During preliminary design work, aerodynamicists and flights mechanics evaluated wing, fuselage and tail sizing combinations , concurrently defining dimensions of surface controls. Then structurists began to work for a preliminary sizing of primary structure and definition of construction procedures; cargo vane geometry, place for engine and radio racks in addiction to space for control cables was determinant design ties. Meantime propulsion group evaluated different engine, reducer, batteries and propeller configurations in order to scale down number of system components and overall weight.

1.2.2 Preliminary Design Tools

Preliminary modelling of the aircraft was initiated by developing bi-dimensional and then three-dimensional models employing Studio 3-D program in a single computer work-station: in this way all members of the IPT developed a feel for initial component sizing and placement early in the design. Then this was exported in a F.E. program in order to allow aerodynamicists to perform their fluidodynamic studies whose results influenced both structurists work, in terms of geometries of each part of the airplane, and propulsion group activity finalized to evaluate the complete number of batteries to employ with the aid of a dedicated computer code. During the whole work, all group work stations were connected each other by a LAN in order to reduce transfer data times.

1.2.3 Preliminary Results

Once preliminary design phase was ended, type, sizes and construction procedures of aircraft components were finalized. The flight-mechanics group determined the static stability derivatives and provided geometries, dimensions and tolerances on wing, tail, fuselage and control surfaces to the structures group, while gave a propulsion mission profile to the propulsion group which so tailored own studies towards well-defined targets in terms of electricity consumption.
The structures group integrated aerodynamics data with forecasted mission loads in order to define primary structure. At the end of this step final dimensions and makeup of each primary structural component were available for the detail design phase.

1.3. Detail Design

The detail design was generated from components defined during preliminary design phase. This time aerodynamicists, with the help of CFD (Computational Fluid-dynamics), performed dynamic stability analysis valuating handling characteristics and control systems requirements. Meantime, the propulsion group finalized propulsion system characteristics in terms of engine model, batteries number (and model), propeller model. Instead the Structures group was able to complete a three dimensional model and detailed drawings of surfaces, structures and subsystems only after having received a report from aerodynamicist about the feasibility (luckily confirmed) of employing rotating (in a conjugated way) wings as large ailerons in order to eliminate apposite mobile surfaces for their purpose maximizing, in such way, the RAC. During whole work also pilot's requirements were considered.

1.3.1 Detail Design Solutions

Detail design alternatives in each group focused on secondary components and process used in the construction and operation of the aircraft. Once again figures of merit system was implemented to analyze the specific impact of each decision to score. Components system, like cargo handling, gears, electric wire and control cable routing, transmission power (between engine and propeller) mechanism, wings and elevator insertion mechanisms were finalized. Different methods and hardware alternatives for realizing the aircraft components were considered. Moreover manufacturing processes were examined for each component. The propulsion group tested the performance of different propellers in combination with different models and numbers of batteries and motor types during real test and computers simulations via dedicated software; this group also evaluated some different types of fuse holders and methods for charging batteries developing specific procedures to be followed during the competition. Flight mechanics group determined control system alternatives in the form of servo requirements and control characteristics.

1.3.2 Detail Design Tools

The aerodynamics group used Ansys (in which was imported 3-D Studio model) code for evaluation of the aerodynamic field around the fuselage and its modification due to propeller, wings and simulated communications relay device presence; airfoils were analyzed employing "Profili" code while stability derivatives was determined using "Fluent" code. The structure group also employed Ansys program for Finite Elements analysis while final design and details of each component was obtained under a CAD program. A scheduling program was implemented to develop a manufacturing process schedule. The Propulsion group used the "Motocalc" software to evaluate engine model, batteries and propeller possible combinations and a dynamometer to compare actual system performance to analytical predictions.

1.3.3 Detail Design Result

At the end of the detail design phase, all aircraft geometries and dimensions and system components (and their respective lay-out) had been selected while aircraft performance capabilities and control characteristics had been determined. It was, therefore, possible to develop a manufacturing process. Moreover, finally detailed production drawings had been prepared together with emanation of some recommendations for construction process, to be verified by apposite checks audits.

1.4.Manufacturing and Prototype Testing

As in all constructive process, the project was subjected to some refinements during works; audits were useful to control critical points of realization like lower side of wings near the trailing edge, high degree of smoothness of surfaces of wing roots and CWB (Center Wing Box) which had to be side by side without interference (pernicious for wing rotation) during flight, alignment of ribs holes in the tail for the exact insertion of the pin under the elevator and alignment of the tail with the fuselage nose. As regards flight test, it was determined the utility of providing wing tips with slim soft steel appendices working as skates to prevent wings from damages due to uncontrolled rolls during take-

off/landing manoeuvres due to relative short distance between wheels of main gear. On the other hand this solution is aerodynamically (and so in terms of energy consumption) better than the adoption of a larger distance between main gear wheels.

2.0 Management summary

2.1 Team Organization and Personnel Assignment Working Areas

The Leonardo team was divided in five technical groups: aerodynamics, flight mechanics, structures, propulsion and systems. Each technical group was comprised of a lead engineer; structures group was comprised of two component specialists. Figure 1 outlines the architectural structure of the team. The chief engineer was responsible for overall team direction and performance as well as ensuring that each group had the tools and information necessary to complete assigned tasks. The lead engineer of a group was responsible for coordinating the efforts of the underclassmen and, in the case of structures group, also the efforts of the component specialists to meet the overall goals of that technical group, as set forth by the chief engineer. Together, the chief and lead engineers assured that the design process followed a logical progression from day to day and ensured that every aspect was properly considered.

2.2 Responsabilities of Each Technical Group

According the aim of an IPT, we can affirm the aircraft conceived by Leonardo team was the result of interoperability of all groups each other. The effectiveness of such an integration is demonstrated by the fact that each decision made by one group affected the constraints placed on the conceptual design of the other groups. Each group agreed upon each single concept before further progress was made. Moreover, resposabilities of each group were shared among its members. Managers individual contributions are displayed in figure 1.

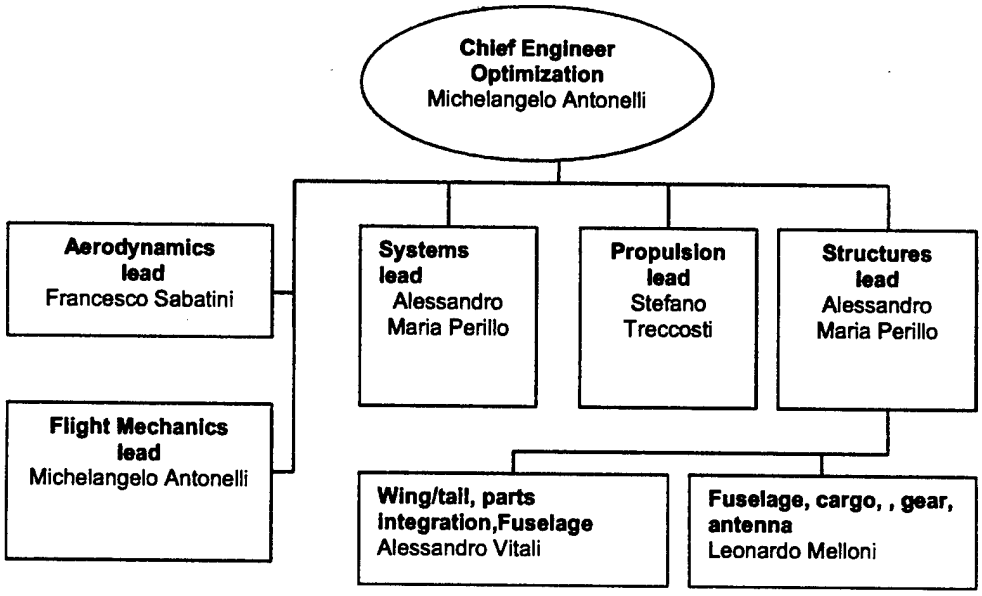

Figure 1: Leonardo Team Organization Tree with Design Personnel and Assignment Areas

2.2.1 Aerodynamics and Flight Mechanics groups

Aerodynamic group, after incorporated competition regulations, oversaw the mathematical modelling process as regards fluiddynamics field due to fuselage and propeller. Meantime propulsion group made some rough estimates of performance parameters involved during the flight. Then both groups combined their first evaluations and generated new and more refined estimates of performance parameters for themselves and the other groups as a base for conceptual studies. Subsequently aerodynamics group, in conjunction with flight mechanics group, progressed to analyzing different aircraft configurations by scoring potential. Figures of merit were defined to further rate the scoring potential of each concept. The final result of the aerodynamic conceptual study was the final aircraft configuration. However developing of mathematical model followed up through refinements in order to improve lift, reduce drag and interference between fuselage and wing, wing and equilibrator, this one and tail also evaluating spin prevention by an analysis concerning the TDPF (Tail Damping Power Factor) which, automatically conducted to a correct tail dimensioning . In this way was possible to estimate a first degree of stability and controllability of the aircraft .

2.2.2 Propulsion Group

The propulsion group was responsible for the design and evaluation of different motor, propeller, reducer and battery (in terms of number and models) combinations. Of course the concepts were judged on the effective use of available power, possible performances of each component and effect on Rated Aircraft Cost. During the conceptual phase, the propulsion group decided how many engine and propellers would be required to produce the thrusts (specially during take-off run) calculated by classic mathematical models. Moreover it was decided whether a pusher or a tractor configuration would have been implemented. At least the propulsion group developed analytical and experimental means by which the wide selection of motors and propellers was narrowed to a few combinations to be prototype tested. Also this group continued in during following steps an analysis more and more refined of the components checking validity of preliminary and historical data. Prototype analysis allowed the group to further refine the combination of propulsion components (especially in terms of type and number of batteries and selection of reducer once the motor was chosen) to best met the mission requirements and help minimize the Rated Aircraft Cost. Propulsion group was the only affected , in terms of scheduling, by typical delivery delays of parts.

2.2.3 Structures and Systems Groups

This group was responsible for the structural design, the integration of components and at least, but not last, c.g. position and weight controlling. It worked together with system group in order to keep in count storage and handling needs for cargo and defining spaces for wire and cables passage. In this way , during the conceptual phase, the structures group examined several different methods of building the general structures required. As kinds of materials was fixed, the structures group evaluated only few possible type of woods employable. An other task was the definition of a construction algorithm to be followed as regards definition of attaches of pieces each other. An other

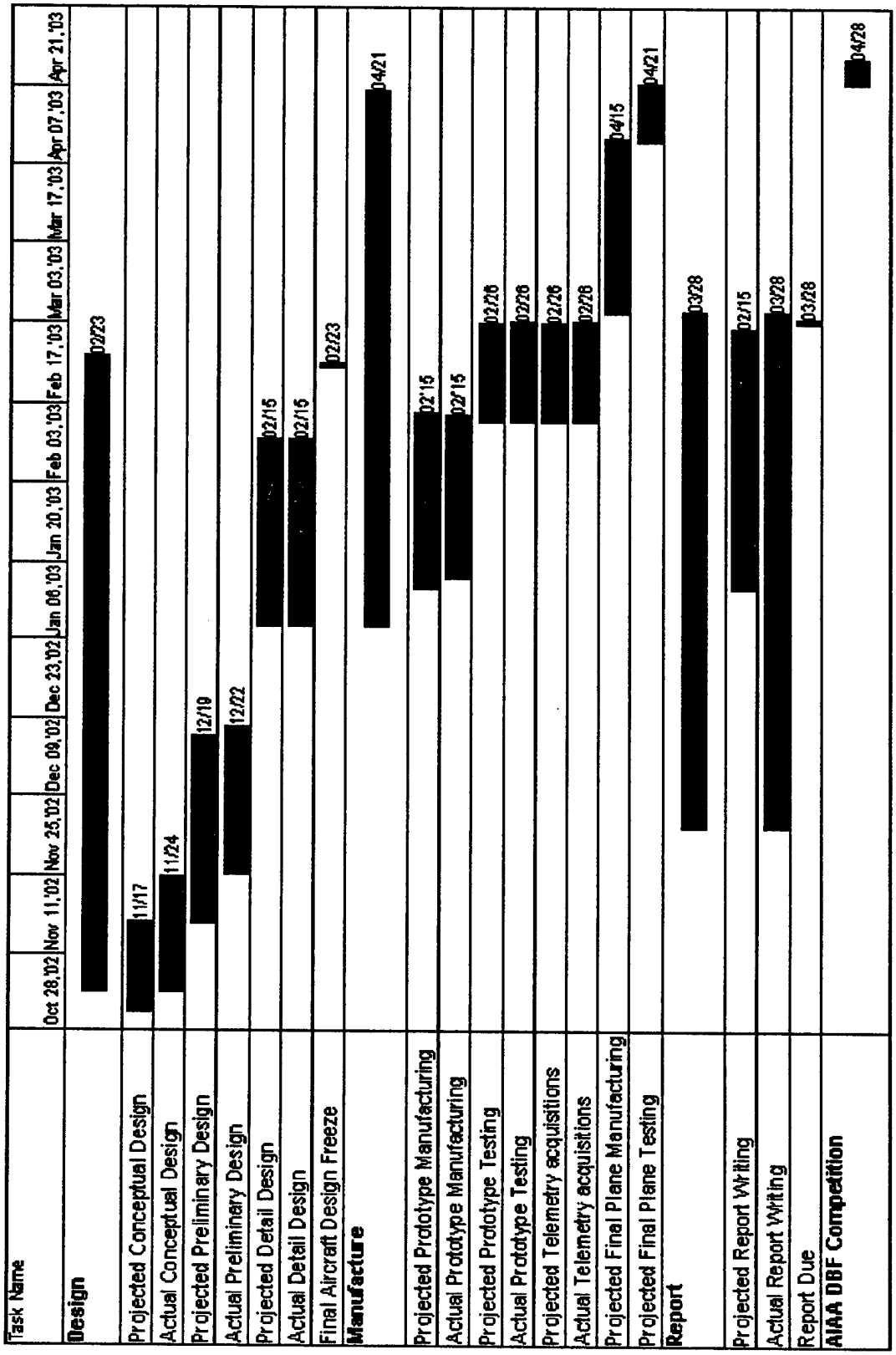

Figure 2: Milestone Chart

head-ache was the definition and integration of mechanism of cargo-vane opening, automatic complete expulsion of cargo and closing again of door vane minimizing servos quantities in order to affect as less as possible RAC. Finally it was clear from the beginning that it was necessary to reduce weight of the rear portion of fuselage without weaken resistance but also without adopting sharp boom (aesthetically not accepted from members of Leonardo team) threatening to preserve fluiddynamics field originated in the fore portion of fuselage. During the preliminary design phase, the structures group used loading parameters given by the aerodynamics and propulsion groups to decide on the quantity and size of primary structural components in the wing, fuselage and tail. Due to decision of mounting the propeller on the trailing edge of the tail, it was possible to adopt a short undercarriage, bypassing typical problems of form resistance. However this idea obliged to simulate drop test in order to evaluate the capability of the structures to absorb violent shocks (for example due to improvise gusts) during landing with low damping (due to rigid connection of wheels to fuselage). This problem was, besides, exacerbated by the fact that internal structures of the airplane presented a large discontinuity due to the presence of the cargo compartment . So It was necessary to conceive a box structure in order to absorb torsion and flexion. During the detail design phase, the landing gear and primary structures were tested for compliance to preliminary parameters. Further analysis resulted in the sizing of the secondary structures. Finally the structures group also considered all tooling and construction methods to be used during the manufacturing phase. Final drawings and implementation of the manufacturing processing were under the responsibility of structures group.

2.3 Scheduling, Document, and Configuration Control

In order to meet the competition deadline, the design process was performed through strict milestones, just identified, threatening to maintain correction margins for the structures and the systems eventually to overwork during tuning phase in the second macrophase. The design process was divided into the conceptual design, preliminary design, detail design and manufacturing phases. Dates were set for the completion of the ingredients for each of these phases. During design and manufacturing process several minutes were redacted at all steps: they were determinant for the realization of this report. Figure 2 is a milestone chart developed for the design process

3.0 Conceptual design

Above all during concept selection process there were performed sensitivity studies on the competition in the areas of aerodynamics, flight mechanics, aircraft systems, propulsion and structures. Then ideas for accomplishing all aspects of the competition were generated. Subsequently each concept was discussed to determine the benefits and penalties of implementation. Ideas were combined and evolved until a final concept was reached. The final configuration chosen was best suited for the contest rules and mission, allowing for the most scoring potential: moreover this one resulted compatible with our construction skills and general costs. Mission requirements were: the aircraft must fit in a 2 foot wide by 1 foot high by 4 foot long box; maximum take-off distance must be

120 ft, possibility to mount a simulated cylindrical antenna, and transporting a simulated avionics package of 5 lbs of weight.

3.1 Design Parameters

A performance program (excel sheet) was written to investigate the design parameters of the plane over the entire mission. The program was used to perform sensitivity to each design parameter was known, an overall strategy was developed and implemented during the three design phases.

3.1.1 Primary Design Parameters

The performance program considered all phases of competition flight and RAC. Six primary parameters were chosen as major contributing factors in the development of the plane: weight of batteries, weight of cargo box, power used in cruise, power used in takeoff, planform area of the wing and span of the wing; these ones were weighted by a global performance factor obtained combining single performances of each component.

The six factors were used to maximize the scoring potential of the design. The program found that the highest scoring plane configurations carried the limit of 5 lb of weight for the cargo box. Takeoff distance was limited to 108.26 ft. The full 120 ft feet was also used by every high scoring configuration . Another limiting factor was the number of batteries. Each high scoring configuration used 96% to 100% of the energy capacity of the batteries. These tendencies confirmed the plane needed to fly efficiently in cruise, while still taking off under the limit with a payload of 5 lbs. Figure 3 summarizes the sensitivity analysis results. Takeoff power was found to be between 455 and 530

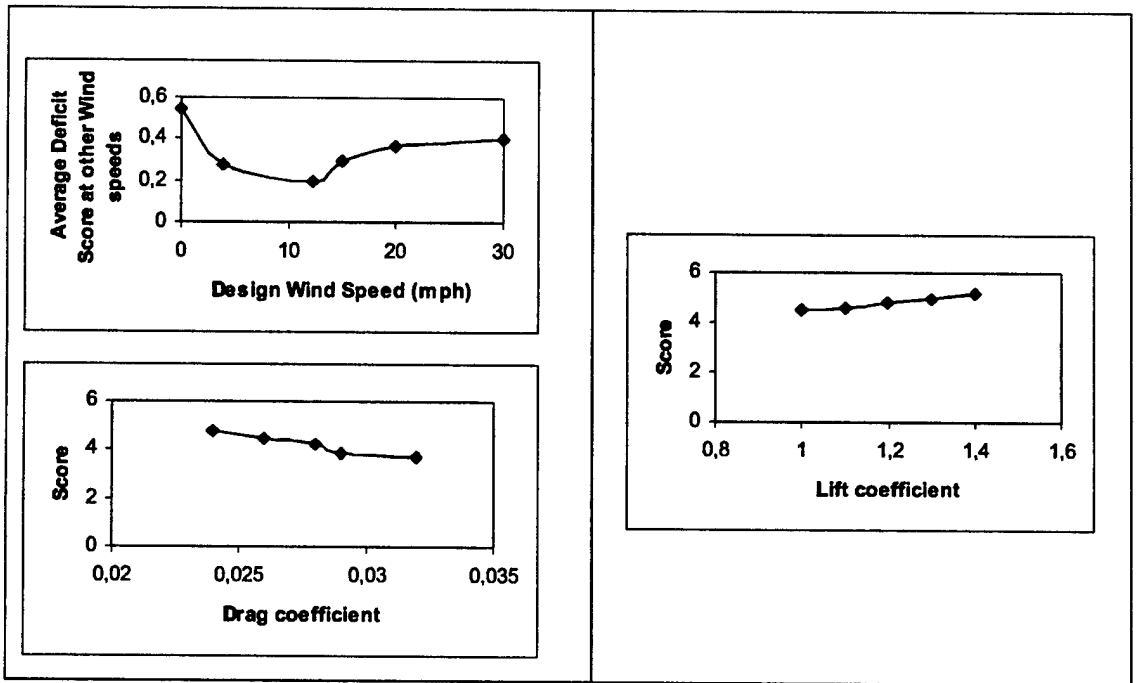

Figure 3: Sensitivity Analysis Graphics. From top left clockwise: sensitivity to wind, lift coefficient and drag coefficient

watts, while cruise power was between 270 and 310 watts. The wing planform ranged from 6.99 and 8.077 square feet with a span of 7.1 to 8.2 feet. The above parameters were given to the propulsion and structures group so that refined analysis could be made during the conceptual design phase.

3.1.2 Design Parameter Sensitivity Analysis

Sensitivity checks were made regarding other major parameters. The parameters consisted of the following: weight model of plane, lift and drag coefficients, aerodynamic effects of propeller , fuselage length and assembling time before race. The parameters were fixed within the program and therefore had to be used with care to avoid to affect the outcome with macroscopic errors. The sensitive of the major parameters helped to optimize the plane and determine the desired values of the parameters within the program.

- Weight model of the plane: weight models for the plane were developed from historical data. These models included different combinations of kind of woods and amounts of glue and rivets. Also composites were considered but only for curiosity as just wood use had been decided. The weight models, when analyzed through the optimization, showed that the performance of the plane was very sensitive to the overall structural weight. Definitive selection couldn't be done due to realization definition problems, but, at least, the weight model sensitivity did show that construction material selection would be very important to the final design.

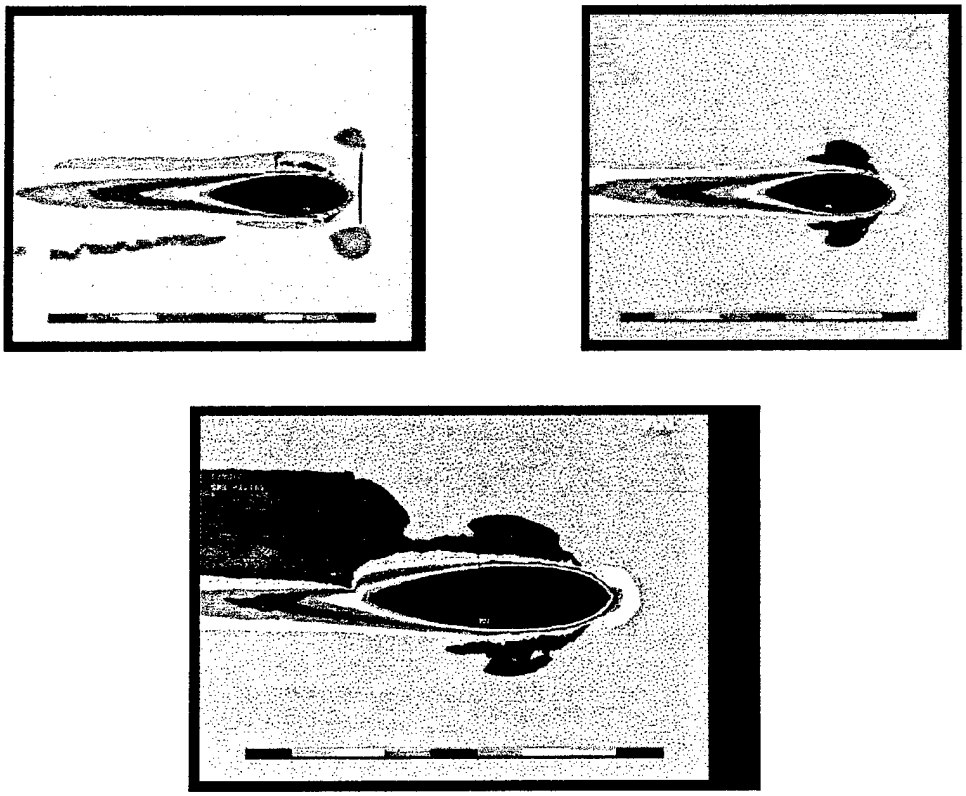

Figure 4: in clockwise direction: Velocity Field around Fuselage with fore propeller, no propeller and aft propeller.

- Lift and drag coefficients: analysis was accomplished by comparing the three optimal scoring capabilities of several lift and drag coefficients. Fewer batteries were required for higher coefficients of lift and lower coefficients of drag. The better performance prompted an airfoil study for maximum lift coefficients ranging from 1.1 to 1.5 (see figure 3)
- Aerodynamic effect of propeller: propeller position influenced heavily drag as you can see in CFD studies of figure 4. Simulate cylindrical antenna position was determined from propeller position (that is above the tail), so it wasn't take in count during studies.
- Fuselage length: it was investigated for sensitivity by dividing the length into spaces needed to carry the payload and additional length for the nose and tail structures. A constraint to this analysis was imposed by transportation box limited length. The results concluded that the fuselage needed to be slightly long than transportation box. The total length was analyzed using a combined aerodynamic and structural model.
- Wind sensitivity: it was investigated so that the performance could be optimized in preliminary design. To accomplish this goal, the six major parameters were optimized at various wind speeds and compared to other winds according to our historical data. Figure 3 shows an average score deficit for wind speeds from 0 to 30 mph. The plane optimized at 12 mph resulted to have the smallest average deficit.
- Time on ground (in terms of extraction from transportation box and mounting of the plane): this was the final sensitivity analysis. Resulted showed that time was a major factor and that decreasing ground time would drastically boost the score in terms of time of flight.

3.1.3 Rated Aircraft Cost Analysis

Another concern was the impact that Rated Aircraft Cost (RAC) had on the design. To evaluate the RAC, a computer program was written to calculate the effects of the RAC parameters from a few configuration inputs. One of the major factor limiting configurations through the RAC was the total battery weight: this one was counted in both the Rated Engine Power and in the Manufactures Empty Weight. Additionally, the Rated Engine Power Multiplier was the largest of the multiplier values. All three factors combined to give the weight of the batteries the greatest influenced over the design; in practice it was necessary to develop a high performing aircraft from an aerodynamic point of view in order to minimize drag that is energy dissipation translating in necessary number of batteries .Other important factors were the wingspan, empty weight of the aircraft and body length. To give an idea of the relative importance of these three components, the battery weight had a greater impact on RAC than all three of the other factors combined. Other factors, while not directly having a large effect on the RAC, greatly increased the importance of certain components. For example, the number of engines did not significantly increase the Manufacturing Man-Hours; however, when the power for the extra motors and the Rated Engine Power were considered, the impact of adding an additional motor became large. Number of servos and mobile surfaces was at least determining for the final configuration of the plane (for this reason rotating wings had been adopted); at beginning it was decided to connect unlocking mechanism of cargo door to a simultaneous movement of elevator and

rudder in the some direction; in this way it would have been possible to gain points versus RAC, but this idea had been abandoned after Greg's considerations about.
Using the RAC program, the rating of each configuration could be immediately evaluated.

3.2 Aircraft Configuration

Once the primary design parameters were identified and investigated, the various aircraft component alternatives were evaluated. For each major component, the Figures of Merit (FOM) were outlined and used to judge the various alternatives through a weighted decision matrix. The matrices determined the alternative that best meet the Figure of Merit.

3.2.1 Alternative Fuselage and Tail Configuration

Figures of Merit (FOM) in the analysis of the fuselage and tail configurations included:

- Rated Aircraft Cost: since RAC strongly affects the overall score of the aircraft, RAC was heavily weighted.
- Take off and landing: from the design parameter studies, the take off lift coefficient and take off roll were key to producing a high scoring airplane.
- Handling qualities: handling qualities in terms of smoothness of cargo discharging operation and following closure again of cargo vane door.
- Drag performance: with battery weight counting twice in the RAC, a successful design must make efficient use of the available power and complete the mission quickly.

Once the design parameters and figures of merit for the fuselage and tail were defined, numerous configurations and combinations of configurations were considered. After the concept generation phase, the most promising alternatives were evaluated further. For further analysis, several assumptions were made including: the fuselage could be sized to hold the cargo box; the propulsive efficiencies were approximately equivalent while the difference in structural weight was negligible. The parameters could be considered constant during conceptual configuration. Given the assumption and the figures of merit above, the alternatives were evaluated as follows:

1. Flying wing: the flying wing had an obvious advantage in the RAC by removing the tail and relative control surfaces. The flying wing had some problems, namely extended take off roll and poor handling qualities in gusty winds due to a lower wing loading.
2. Conventional A: the conventional fuselage with a standard cross tail was set as standard for comparing the various configurations. For A version we intend a plane with low wing and cross tail.
3. Canard: the canard configuration had excellent stall characteristics; however, by preventing the main wing from stalling, this design limits the maximum lift at take off. The canard configuration had the added benefit of flexible motor setups, both tractor and pusher.
4. Conventional, V tail: a conventional fuselage with a V-tail had the same performance as the conventional tail alternative, but had the RAC advantage previously mentioned

5. Conventional B: for B version we intend a plane with high wing and a T-tail: this design was relatively straightforward with well-documented performance characteristics.

In order to evaluate the Rated Aircraft Cost figure of merit for the various configurations, the RAC of each alternative was calculated. The results of the analysis are listed below with configuration, RAC value and then the RAC benefits of that configuration:

1. Flying wing (RAC of 8.3) does not have a horizontal tail surface or elevator servos
2. Conventional fuselages (RAC= 8.2) doesn't present any difference between A and B version.
3. Canard (RAC of 7.8) is slightly penalizing in terms of RAC
4. Conventional fuselage with V-tail (RAC 8) has passive vertical surface instead of active

A weighted decision matrix was used to evaluate the alternatives according to the figures of merit to determine the configuration with the highest scoring potential. Weighting factors were assigned with different magnitudes according to the defined mission sensitivities. While RAC is the dominating factor, it is not the only consideration. For instance, while the flying wing has the highest RAC, the poor performance of the design with regard to the other figures of merit limited its overall scoring potential. The results of the decision matrix can be seen in figure 5. The highest-ranking was that of conventional fuselage and cross tail (or T-tail). This arrangement best met the figures of merit because of an improved RAC advantage and average performance qualities. Due to short distance between wing and tail, a T-tail configuration was preferred.

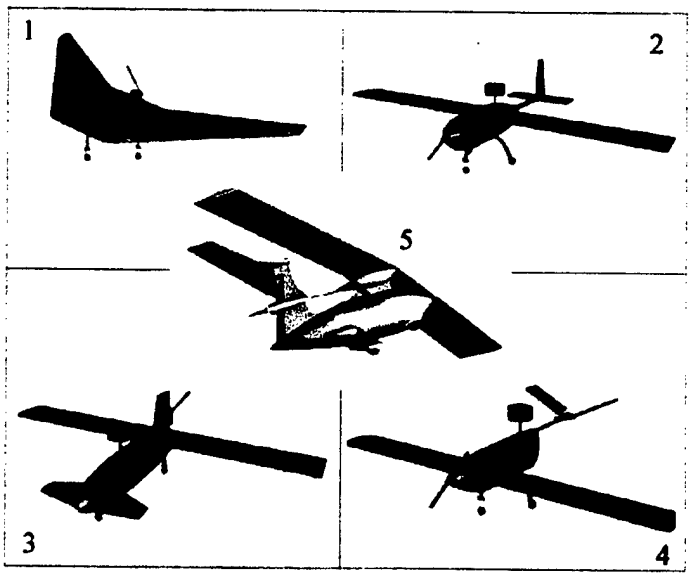

Figures of merit	Weigthing factor	Model 1	Model 2or5	Model 3	Model 4
RAC	0.4	8.3	8.2	7.8	8
Drag	0.15	2	1	2	4
Construction	0.25	6	8	7	6
Handling qualities	0.2	1	5	4	2
Score	-	5.32	6.43	5.97	5.7

Figure 5: Fuselage and Tail Configuration Weighted Decision Matrix

*Wing fuselage connection:*as regards wing-fuselage connection we considered the following idea. We decided to adopt a high wing, so we had to decid how realize this one avoiding to improve drag and preserving high wing stability characteristics.Generally high wing aircraft are realized with a wing which is also a part of ceiling fuselage: this way is the better to preserve stability but it isn't the most useful in terms of drag. Of course we were more concentrated to drag reduction than stability. Luckily there was our consultant, who took part during his career in airmodels competitions based on endurance: He suggested us to proceed to a sort of reconsideration of "Old Timers" aircraft of early 50's. These aircraft were characterized by having great stability together with a large endurance, and since these properties seemed apt for the competition, we decided to adopt such a configuration. These particular configuration is evident in the following image where it can be seen the large pylon on the upper fuselage, on which the wings had been bolted.

This particular configuration was known as "sunshade wing": it allows to minimize wing/fuselage interference and so improving drag reduction that is energy consumption reduction.

On the other hand, it seems clear that for commemoring Wright brothers first flight, there is no better thing than to rethink to Old timers with their architetures and materials.

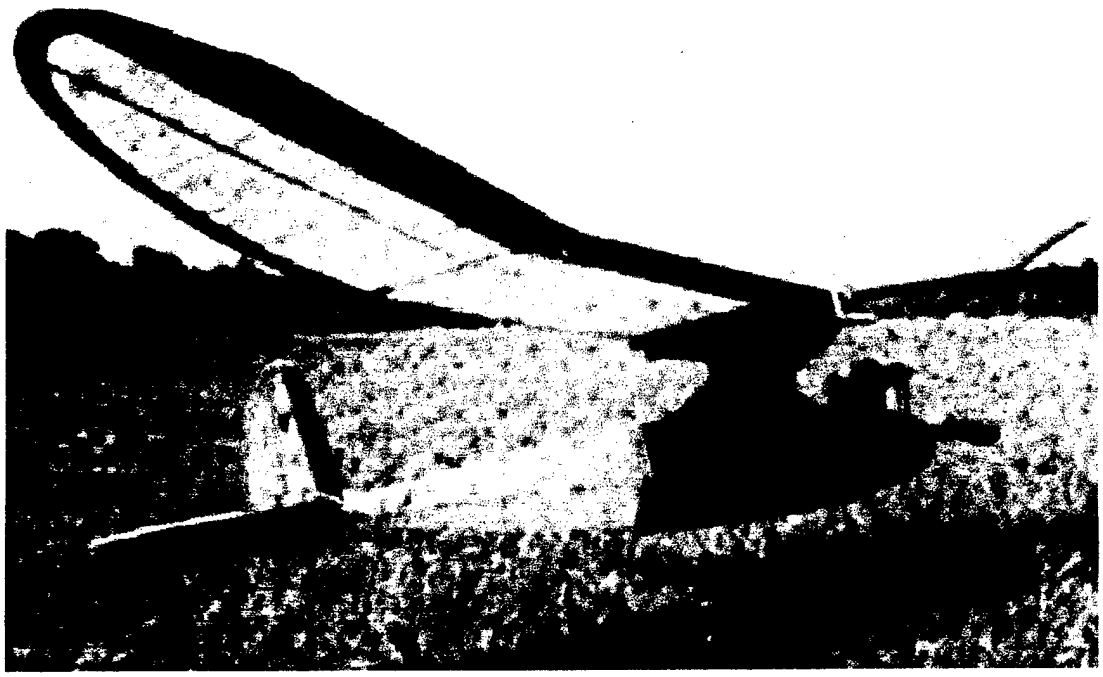

Figure 6: A Photo of Playboy Senior, the famous "sunshade" wing model actually is a great sailer and of very stable aircraft of 1956

3.2.2 Alternative Wing Configuration

Figures of merit in the analysis of the wing configurations included

- Payload interference: wing position had to be higher than maximum cargo box height from terrain. This need was accomplished, on the other hand, by the use of "sunshade" wing concept.
- Construction: the alternative selected must be as light as possible and, meantime, as resistant as possible. Moreover it must be within the team's construction abilities in order to be manufactured correctly and without spending too time.
- Stability: the stability contributions of the wing location were estimated from historical data. High mounted wings typically provide roll stability, while low mounted wings can produce instability.

The three basic alternatives for wing location were considered: low, middle and high wing attachment. For analysis the following assumptions were made: the taper ratio was one for better stall characteristics and ease of construction; the sweep angle was 7° for better c.g. positioning and also for aesthetic reasons, low Reynolds number effect and more efficient lift production.

- High wing: the high wing did not significantly interfere with cargo box expelling, produced roll stability without adding dihedral into the wings.
- Mid wing: the mid wing design would have proved to be difficult to construct and it would have obliged to adopt a vertical way of box discharging with consequently raising, and so weakening, of gear legs.
- Low wing: the low wing alternative has less roll stability, which might require dihedral. Moreover it presented the same problems of mid wing, in terms of cargo box handling.

Figure of merit	Weighting factor	High	MID	LOW
Stability	0.075	1	0	-1
Payload expulsion	0.35	1	0	0
Construction	0.15	0	-1	0
Payload interference	0.35	1	-1	1
Gear Interface	0.075	0	0	1
Score		0.775	-0.5	0.35

Table 1 : Wing Configuration Weighted Decision Matrix.

The weighting factors of the wing decision matrix in table 1 shows the relative importance of each figure of merit in the wing selection. While the payload and construction played a large part in the decision matrix, the stability and landing gear issues were secondary effects. Since the high mounted wing better addressed more of the important figures of merit than the other alternatives, the high wing rated the highest and was selected as the wing configuration for the aircraft.

3.3 Structural Configuration

3.3.1 Figures of Merit

A topic area of the structural conceptual design was the development of figures of merit to represent mission objectives for each component to perform. The mission objectives chosen were designed to represent crucial areas within the competition that were affected by different structural components. The figures of merit which were developed for the conceptual structural design were:

- Scoring Potential: each aircraft component had a direct effect on the ability the design to achieve a high score. Since the size, shape, and capability of each component can affect both aircraft performance and Rated Aircraft Cost, the design of each component is important to perform the mission in the most efficient way. In order to maximize scoring potential this figure of merit is the overall result of all figures of merit analyzed.
- Strength and Weight: the weight of each component influences both Rated Aircraft Cost and aircraft performance in every phase of flight. Therefore the proper balance between the strength of a component and the weight of the component was necessary to determine.
- Formability: the ability to produce the desired component shape with the least amount of manhours and components has an affect on the quality of the component, the overall weight of the structure, and the Rated Aircraft Cost
- Ease of construction: certain construction techniques required more time and skill to produce complex shapes such as high camber airfoils and streamlined bodies or smooth nose. The ability to produce such shapes directly affected the capabilities of the aircraft in all phases of flight
- Repairability: during the flight-testing phase and the competition, minor to moderate damage was expected. On site repair of the damage was desired to reduce amount of time.
- Cost: while a score efficient structure was desired, the cost of certain construction methods and materials have a drastic affect on the validity of some concepts. However this figure of merit had been attenuated by sponsorization.
- Durability: during flight operations, the aircraft was expected to experience hard landings. In order to be competitive, the aircraft had to withstand the conditions and operations of the competition through many cycles.

While the figures of merit were valid for all structures, several specialized figures of merit were developed for individual components. These figures included:

- Taxing: the landing gear must be capable of precise aircraft manoeuvring while the aircraft is on the ground. The mission advantage was to provide quick turnaround times between different phases of the mission sortie.

- Landing Performance: also contributing to the aircraft score was time spent in the landing phase of the sortie.
- The ability for the landing gear to both endure hard landings and damp out the landing force with out springing the aircraft back into the air was important to achieving a time efficient landing manoeuvre.

Moreover, the box had to be unloaded without interfering with the normal operations (i.e. taxing on the runway).

3.3.2 Assumptions Made and Design Parameters Investigated

During the conceptual design phase, assumptions were made to allow an unbiased look at different alternatives. For the four primary components analysed, loading conditions were assumed based on simple models produced from available material samples, such as were those of the weight.

Parameters that had the most influence on score were identified for each primary component. These influenced not only the structural design but also the conceptual studies of the aerodynamics and propulsion groups. The parameters investigated for each structural component included scoring potential, efficient use of structural weight, strength, dimensional alternatives of the component, different material and construction alternatives, and effects on Rated Aircraft Cost.

3.3.3 Alternative Wing Structures

The figures of merit used to investigate wing alternatives were strength to weight ratio, formability, ease of construction, durability, reparability, and cost. Additional constraints were imposed on the wing design as a result of the functions of the wing: to generate lift and transfer that lifting force to the rest of the aircraft. To create lift, the wing had to be capable of holding an airfoil shape. For the high aspect ratio indicated by the mathematical model, the wing was required to be rigid enough to prevent a decrease in the angle of attack at the wing tips due to the aerodynamic loads. Due to initial estimates, the wing design was expected have an area of approximately 7.5 feet square and to experience a 3 g-load during a turn at maximum gross weight. Both the functions of the wing must be met on a weight budget for the wing to be efficient. Material alternatives and construction methods were considered. The three types were conventional build-up of lightweight wood skeleton, conventional build-up of carbon fibre skeleton and skin (there were the possibility of employing stitched composites at our university), and composite skin with foam core. However even if we were conscious of the advantages related to the use of composite materials we remained focused on the original idea.

In addition to the structural build-up of the wing, conceptual alternatives for internal system components of the wing were generated. These included servos, wire and control cables routing, and how the wing will mate and transfer loads to the rest of the fuselage. A final conceptual sketch of the wing structure can be seen below.

Figures of Merit	Weighting Factor	Conventional Buildup with Wood	Conventional Buildup with Carbon Fiber	Composite Buildup with Foam Core
Strength to Weight Ratio	0.3	-1	1	0
Formability	0.25	-1	0	1
Ease of Construction	0.15	0	0	1
Durability	0.15	0	1	1
Repairability	0.1	-1	0	0
Cost	0.05	1	-1	-1
Score	I-	-0.6	0.4	0.5

Table 2: Wing and Tail Structural Decision Matrix

3.3.4 Alternative T-tail Structures

Similar considerations as those used on the wing were made for the tail. The figures of merit used to investigate wing alternatives were strength to weight ratio, ease of construction, durability, reparability and cost. The three types of tail construction alternatives were conventional build up of lightweight wood skeleton, conventional build up of carbon fibre skeleton and skin and composite skin with foam core.The function of horizontal tail was to apply longitudinal stabilizing moment to provide control in aircraft pith; the function of vertical tail was to apply laterally stabilizing moments to provide control in aircraft yaw. The tail unit needed to be lightweight, durable and able to adjust the incidence angle.

3.3.5 Alternative Fuselage Structures

The fuselage concept was developed as a combination of requirements. Figures of merit involved were: ease of construction, strength, formability, durability, reparability, and cost. The fuselage must be capable of handling the optimum amount of payload with the lowest drag possible while carrying all radio equipment, batteries, and the propulsion system. The fuselage also serves as the convergence point of all other aircraft components supporting the weight of the entire plane and transferring moments and loads between components. Several different construction techniques were evaluated, including conventional build-up with wood, conventional build up with carbon fibre, solid foam construction, and monocoque.Conventional build-up with wood had been evaluated first: it consisted of frames and stringers to carry loads and maintain shapes. The framework was covered with a cover that had no load bearing capability. The method featured very lightweight construction but had the

Figures of Merit	Factor	Conventional Buildup with Wood	Conventional Buildup with Carbon Fiber	Solid Foam Buildup	Monocoque
Strength to Weight Ratio	0.3	1	0	-1	0
Formability	0.25	0	1	-1	0
Ease of Construction	0.25	1	-1	1	-1
Durability	0.05	1	-1	1	1
Repairability	0.1	1	0	-1	1
Cost	0.05	1	-1	-1	0
Score	-	0.75	-0.15	-0.4	-0.1

Table 3: Fuselage Structural Concept Decision Matrix

potential to lose the advantage if the structure was required to be very rigid. Other techniques being evaluated were:

- Conventional build-up with carbon fibre; it was built up of the same frame work as conventional build up with wood however the use of carbon fibre skin allows loads to be transferred throughout the skin
- Solid foam construction; it consisted of a solid fuselage of foam coated with epoxy hollowed out for payload and equipment.
- Monocoque fuselage; it consisted of a fully load bearing outer shell made of composite material built up on foam molds. Monocoque provided a very lightweight rigid structure that can be formed into almost any shape.

However, in order to pay a tribute to the Wright brothers we finally choose conventional build-up with woods.

3.3.6 Alternative Landing Gear Configurations

The gear concept also was developed to satisfy mission requirements. Figures of merit involved: dimensions, weight, aerodynamic drag, ease of construction, rotation attitude and landing performance. Various configurations were available but we finally chose the low-tricycle configuration since this was the most robust and permitted the transport of the fuselage in the fixed-dimension box without disassembling, with all the advantages in terms of time. Once the landing gear configuration was determined, configurations of the main gear were considered. The primary function of the main gear was to absorb energy during landing; it had to be lightweight, durable, and have a low drag. Figures of merit involved: dimensions, weight, aerodynamic drag, ease of construction, landing

Figures of Merit	Weighting Factor	Tricycle	Quad	Bicycle	Tail Wheel
Ground Tracking	0.20	1	-1	-1	-1
Landing Performance	0.15	0	1	0	-1
Chaulked Fuselage Attitude	0.15	1	1	-1	-1
Braking	0.15	0	1	1	-1
Weight	0.10	0	-1	1	0
Ease of Construction	0.07	0	-1	-1	0
Drag	0.06	0	-1	1	0
Component Mating	0.06	1	-1	-1	1
Cost	0.06	0	0	0	0
Score	-	0.41	-0.04	-0.17	-0.59

Table 4: Landing Gear Concept Decision Matrix

Figures of Merit	Weighting Factor	Bow	Aluminium legs	Leaf Spring
Landing Performance	0.25	0	-1	0
Weight	0.25	0	-1	0
Realization	0.25	0	1	0
Damping	0.15	0	0	1
Ease of Construction	0.07	1	-1	0
Drag	0.03	0	1	0
Score	-	0.07	0.35	0.15

Table 5: Main Landing Gear Conceptual Decision Matrix

performance, and damping effects.

3.4 Alternative Power Plant Configurations

The propulsion system had three main components: batteries, motor, and propeller. Three major configuration ideas were considered: single stack, double stack, and shared electrical. Figures of merit (FOM) were developed to evaluate the three configurations. These included:

- Rated Aircraft Cost (RAC): the propulsion system is very influential in the RAC function.
- Score Effects: the propulsion system had influence in every variable of the score function.
- Power Produced: the power produced by the motor has direct effect on aircraft performance. Power also requires battery performance, which affects the weight of the aircraft and RAC.
- Weight: the battery weight was determined to consume the majority of the overall RAC.
- Efficiency: the ability to produce the required performance with the lowest number of batteries was important in both aircraft flight performance and Rated Aircraft Cost.
- Price: although the highest performance possible was important, the cost of components limited the level of components used.

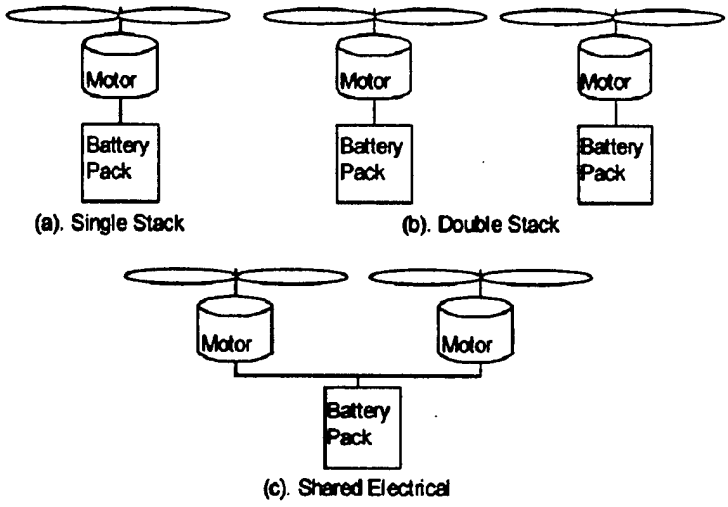

Figures of Merit	Weighting Factor	Single Stack	Double Stack	Shared Electric
RAC	0.35	1	-1	-1
Power Produced	0.25	-1	1	1
Weight	0.2	1	-1	0
Efficiency	0.15	1	-1	0
Total Number of Fuses	0.05	1	-1	1
Score	-	0.5	-0.5	-0.05

Figure 7: Battery-Motor-Propeller Alternatives and Propulsion Weighted Decision Matrix

The figure above shows the propulsion alternatives and decision matrix used to evaluate the different propulsion alternatives. From the decision matrix, the single stack was found to be the best option. The single stack had the lowest RAC and while meeting the required thrusts and speeds to achieve takeoff and climb. The single stack could provided enough power, thus eliminating the need for two motors. Anything that can be done to make the system more efficient was desirable. Another draw back to using two motors was the loss in efficiency. In the RAC equation, the battery weight was the most detrimental. In order to increase the efficiency of the engine, several cooling concepts were considered. The concepts investigated included air-cooled, water-cooled, and ice-cooled systems. An air-cooled system was chosen as the best concept based on cost, weight, and complexity.

3.5 Analytical Tools

3.5.1 Optimization Program Architecture

The performance program was written to help analyze each phase of the mission individually as a contribution to the overall score. The program contained mathematical models for the structural weight, propulsive efficiency, and aerodynamic characteristics. The models were written into the program so that refinement and expansion could be done quickly and simply. The structural weight and propulsive models were constructed from our historical data, as calculated from component build-up. The aerodynamic model was constructed using a simple drag build-up method suggested by Jensen (1990) and the coefficient of lift corrected for aspect ratio of the wing.

After the flight characteristics of the plane were calculated from the four models, the performance characteristics for each phase were calculated:

- The time and energy consumption required to takeoff under the 120 feet limit.
- Time, energy consumption, and power required to climb at a vertical speed of 2.5 fps.
- Time, distance and g-loading during turning were calculated from weight and stall characteristics.
- Time and distance to slow down from cruise velocity to stopping. Time in cruise given the selected power settings.

Finally, the times, distances, and energy consumption were summed and compared. The overall values of the three parameters were used to calculate total flight time, flight path distance, and total battery usage. Rated Aircraft Cost was further calculated, and the Flight Score was calculated using both flight time and RAC.

3.5.2 Other Methods Used

During the conceptual design phase, the various groups used weighted decision matrices to decide upon important decisions. Decision matrices were used so that the opinions of group members did not bias the decision, but rather the best configuration was chosen in a more numerical form. The graph of weight and volume effects along with RAC calculator were used to access parts of the factors input into the decision matrices.

3.6 Final Aircraft Configuration

When the final ranking phase was completed the design that stood out on top was the "drop-type" fuselage with "sunshade" wings and pushing propeller shown below. The configuration had good handling qualities and a reasonable take-off distance, one that fell within the prescribed 120 feet. A high mounted wing is a typical configuration of a cargo aircraft, the tail wing span fell within the 25% of the span of the greatest span horizontal surface while still providing adequate control of the plane. The propulsion system was composed of a single propeller tractor setup. The entire aircraft (apart from the antenna and the nose) was constructed of wood. The final configuration was the best compromise between all of the ranking factors.

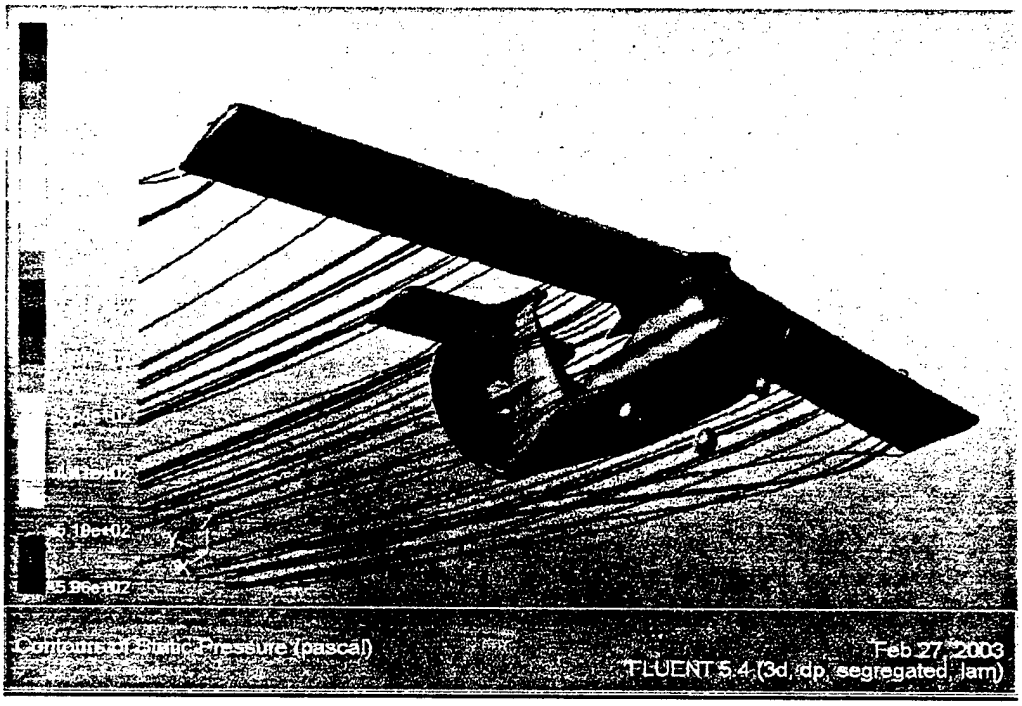

Figure 8: Final Plane Configuration (extracted from fluidynamics studies; contours of static pressure

4.0 Preliminary Design

Once conceptual design phase was over, each group began preliminary design phase. The optimization program was refined with preliminary models and used to find parameters to begin this phase: the last one were employed as in wing and fuselage aerodynamic and propulsive plant sizing. Then dimensions and tolerances for components were passed on the structures group so that trade studies and structural analysis could be performed on primary structures. At this point propulsion group was able to identify some possible combinations for testing in the detail design phase.

4.1 Initial Trade Study Results

After the conceptual phase was ended, the weight, drag, propulsive and RAC models in the optimization process were updated. The previous models were considered only as conceptual simulations because the previous versions were developed from the La Sapienza Aerospaceal Department, NACA and Sponsor historical database. The new program optimized features of the plane and helped to develop trade studies for each parameter in relationship to final score. The optimization program was only able to output the local maximums for plane performance; the global maximum was solved by graphical means.

4.1.1 Study of Model and Number of Batteries

As regards model, batteries were selected evaluating energetic characteristics versus weight: by the way it was redacted a classification involving batteries with not less then 60mOhm internal resistance (that is able to furnish high currents during discharge phase without overheating). So it was possible to obtain reliable batteries with the best energetic performances affecting as less as possible RAC in terms of batteries-pack weight. As it results from the reading of the following matrix, the best option is represented from Sanyo RC2400.

CAPACITY vs. WEIGHT	CELLNAME	CAPACITY	INERTANCE	WEIGHT	VOLTAGE
40.7	Sanyo RC2400	2400	0.0032	59	1.2
39.6	Sanyo 2300SCE	2300	0.0055	58	1.2
39.6	Sanyo CP-2400SCR	2300	0.0053	58	1.2
38.3	Sanyo 1800SCE	1800	0.0065	47	1.2
38.0	SR 2000 MAX	2000	0.0035	53	1.2
35.8	Sanyo 3000CR	3000	0.0032	84	1.2

Table 6: Batteries Rank

As regards the number of batteries, this one was assumed, in terms of energy requested, as a start point for the definition process of propeller and planform. A desirable number of batteries was twelve but it was almost impossible to go under 18.

4.1.2 Study of Take Off Battery Performances

Batteries system resulted good with respect to competition constraint of 40 A while enables the aircraft to take off in 108.26 ft granted by 7.05 lb of fixed point thrust and 4.188 lb at 39.37 ft/sec.

4.1.3 Study of Cruise Battery Power Requirements

Similar to take off power, the battery power required during cruise was also examined. The score comparison has maximums ranging from 455 to 530 watts and an optimal value of 480 watts. Again, the broad range gives a margin of safety for the propulsion group to work within. moreover it is possible to maintain a 1.54 lb of thrust at a cruise speed of 60.14 ft/s during 7.56 minutes (time equivalent to a flight of 29002.62 ft , i.e. a distance double longer than that of the competition).

4.1.4 Study of Wing Planform Area Requirements

The wing planform area was shown to have a direct relationship to score. The relationship existed on one side of the optimal value and dropped off on the other side; also in our opinion this is due to the added propulsive requirements to get the plane to take off under the limit of 120 feet (i.e. 108.26 ft): in

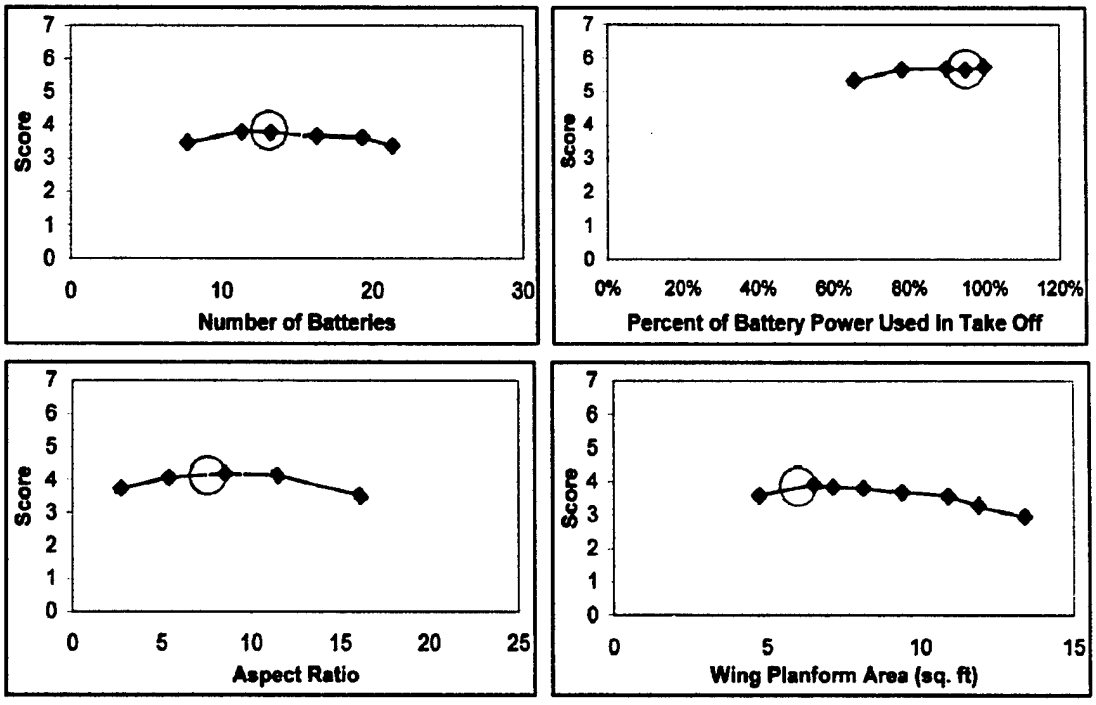

Figure 9: Tadeoff Analysis Results. From top left clockwise: number of batteries required, take off power required as a percent of available power, wing planform area requirement, aspect ratio requirement.Red circles represent the optimal value found by the program

such a way we had to trade-off number of battery (to be minimized in terms of RAC and airplane weight) versus maximum take-off length. As regard the relationship above mentioned, up to the optimal, this one appeared to well represent the aircraft because of the cruise efficiency decreases as planform increases. All of the above features of the linear trend can be seen in figure 9.

4.1.5 Study of Wing Span Requirements

Wingspan was shown to have a rectangular relationship with optimal score. Also in our opinion, rectangular scatter indicates that many different spans can be considered optimal. Really also in this step we traded off wingspan with chord length in order to complain with wing planform area previously fixed. The maximum length of airplane box transport was determinant in the decision process as it was preliminary decided to minimize assembling time avoiding to realize multi-pieces wings.The final value determined was 7.939

4.1.6 Study of Aspect Ratio Requirements

Due to the bent of the optimization process to an efficient propulsive system, the optimal scores were graphed versus corresponding aspect ratios in order to illustrate the aerodynamic trend toward efficient planes In this way the optimal range of aspect ratios was from 8 to 9.
The value chosen was 8.22 (see fig 9).

4.1.7 Study of Plane Structural Weight Effects

Plane structural weight was heavily take in account in the overall performance of the plane during the conceptual phase. Also weight revealed a linear relationship with score. Optimal weight was determined 17.63 lbs . As intuitable, a decrease in the overall structural weight of the plane increased the overall performance and score of the plane.

4.1.8 Study of RAC effects

In the idea of minimizing RAC, a final study of the effects of RAC on performance and score was completed during the preliminary phase; so it was possible to trade-off minimization RAC with keeping the plane within good performance parameters. The optimal plane had a RAC value of 11.25 within a range of 11 to 12 for the top 5 configurations.

4.2 Aerodynamic Considerations

Using the design parameters determined during the preliminary phase, it was possible to perform a further analysis in order to refine the design. The areas examined included: wing area, tail sizing, fuselage , wing/fuselage connection, stability and control.

4.2.1 Wing Figures of Merit: Assumptions and Analysis

Preliminary considerations have to be done are the following.
Airfoil selection is related to the following parameters: projected air-speed, Reynolds numbers corresponding to maximum and minimum airspeeds, construction technique and relative effective

feasibility, airfoil beahaviour at angle of attack in proximity of stall, and drag developed in the range of possible angle of flight.It is clear, at this point the airfoil to be selected must develop a minimum drag if it is desired to construct an airplane adapt to rapid flight without enhancing energy consumption. In fact, if an airfoil was characterized by an high C_d, it would have been requested an installation of a motor with necessary and adequate power in order to obtain aimed performances with consequent weight and consumption problems . From an analytical point of view, there are other considerations to be done in order to perform the optimization process.

Specifically it was necessary to define figures of merit that, for the wing analysis, included:

- Total Flight Score: since the score is used to rank the aircraft for the competition, total flight score was set as the primary figure of merit. The wing sizes that produced the greatest scoring potential ranked highest. The flight score included the RAC effects of the configuration.
- Performance: this one quantifies the effects not considered in the optimization; namely, tip strike, strength, and deflection. The performance merits tended to shorten the wing to ensure that the wing could realistically achieve the characteristic calculated in the optimization.

The wing was modelled in the optimization program to provide estimates of the flight score based on the wing area and span required for the mission profile. On the highest scoring configurations, the chord varied from 10.63 to 12.99 inches while the wingspan ranged between 7.14 and 8.723 feet. The optimization also included other factors involved in the analysis of the wing dimensions, such as the takeoff power and cruise power.The power necessary for takeoff and cruise was related to the wing area through calculations of lift and thrust. Therefore, a study of the motor performance was necessary in the analysis of the wing dimensions. Another aspect of sizing the wing was deciding whether a greater chord length or a longer wingspan best achieved an increase in planform area.

The wing span length was penalized heavily in the RAC calculations, while the chord was only a minor factor. Increasing the wing chord produced more wing area, but decreased the aspect ratio. Higher aspect ratios produced drag efficient lift production as predicted by the conceptual assumptions. The optimization program altered the constraints to find the best scoring configuration.

The optimized wing was then slightly oversized to allow for both construction and aerodynamic margins of safety. The wingspan and chord were 7.93 feet and 11.81 inches, giving a wing planform of 7.53 sq. ft. The coefficient of lift necessary for takeoff predicted by the optimization program was 1.5. Using the assumption of 80% of Cl_{max} at takeoff, the wing airfoil required a Cl_{max} around 1.2.

Employing preliminary consideration, taking in count the estimated low Reynolds numbers (nearly 200000) on the go, aerodynamicists identified , among optimization results, a family of airfoils (projected by Dr Richard Eppler) which is very efficient in the range of modelling Reynolds numbers (from 60000 to 200000); respective diagrams were determined during wing tunnel test at Stoccarda University. By the way, keeping in mind estimated structure weight and wing joint kind (realized inserting an aluminium pipe previously passed through upper fuselage), a 0.15 thickness was adopted. At least, as structurists wanted a ribbed and binded wing, the attention was focused on EPLER 793 airfoil (fig.10).

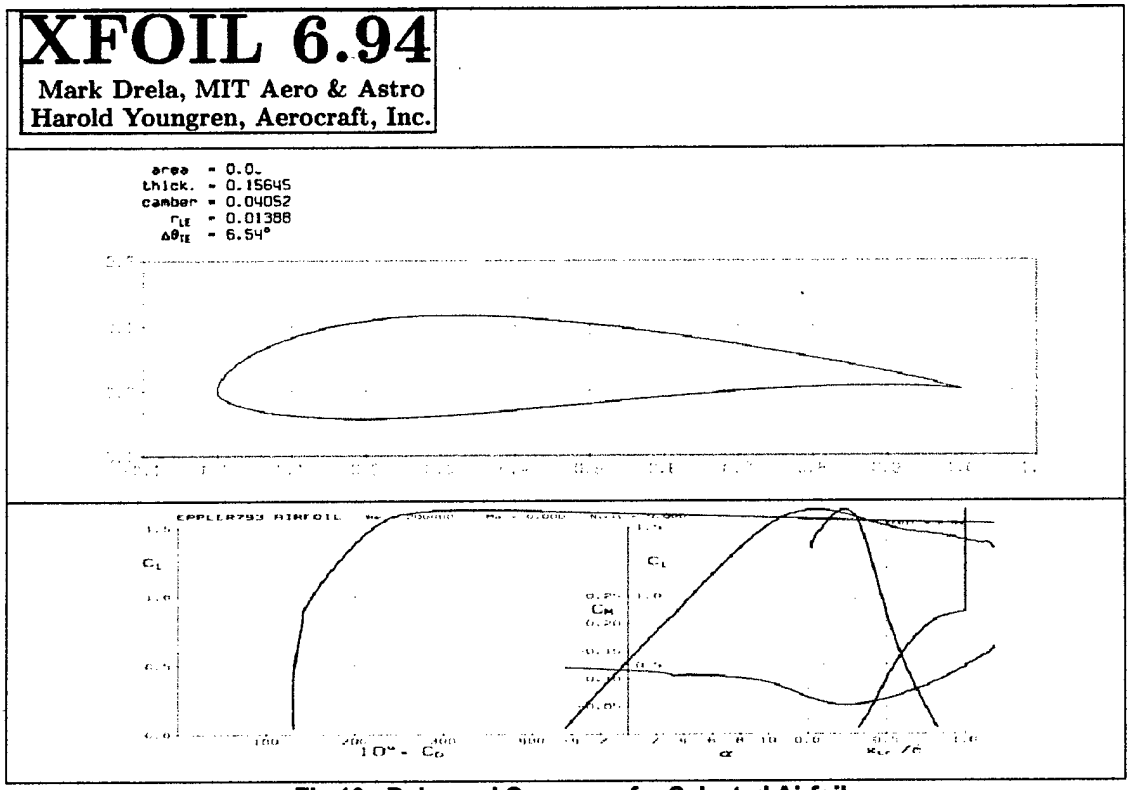

Fig.10 : Polar and Cm curve for Selected Airfoil

If characteristic curves trend was observed in the preceding diagram, it would be clear the chosen airfoil is characterized by a $Cl_{\max}$ value of 1.55 while $C_{M_{med}}$ is -0.1. So, according to the competition rule according to maximum take off run length is 120 ft and as the airplane wasn't provided of secondary control surfaces (as flaps and slats), it is clear how the obtaining of more and more high $Cl_{\max}$ values is determinant .

4.2.2 Fuselage Figures of Merit, Assumption and Analysis

The Figures of Merit for the fuselage analysis included:

- RAC: the main RAC affect of the fuselage was the body length. So, in order to reduce the RAC, the body length was minimized but still contained all components and , above all, was less length than maximum dimension of transportation box.
- Drag: this one, on the fuselage was minimized in order to reduce the thrust required ultimately decreasing the battery weight. The factors contribute to a higher score.

Further studies into effects of the fuselage were performed to obtain better drag models and stability characteristics. Cargo box dimensions governed the optimization of fuselage, in terms of both section and length. The fuselage was broken into three sections: the propulsion compartment, cargo bay and tail section. The necessary area for each portion was evaluated independently. Propulsion equipment, such as the motor and speed controller, needed to fit within the confines of the compartment existing in the pylon which joint fuselage to wing. The length of cargo bay was defined by the space necessary

to hold the box. The governing factor in the tail section dimensioning were propeller position (with relative mechanical transmission) and the T.P.D.F. (Tail damping Power Factor).
The three parts combine to form the total fuselage length of 4.59 ft. By designing fuselage around the components, rather than vice versa, the length of the fuselage was minimized.

4.2.3 Tail Figures of Merit, Assumption and Analysis

As in this work propeller position was fixed ab initio, tail positioning and dimensioning must be defined in a way such to not perturb air flux directed towards propeller.
The only two possible feasible solutions were the adoption of a conventional cross tail or a T-tail; after having determined fuselage length, we observed a reduced c.g –tail distance; so when we calculated TPDF it resulted so low that it was necessary to adopt a T-tail In order to guarantee the possibility to exit from a corkscrew dive.
(Final T.P.D.F was, so: 394 E-06).

$$TPDF = \frac{S_e l_e^2}{S(b/2)^2} \frac{S_1 l_1 + S_2 l_2}{Sb/2}$$

where

S_1, S_2 = tail surfaces not put in the shade by elevator at specifics angles of attack

l_1, l_2 = distances from c.g. and, respectively, tail areas S_1, S_2.

4.3 Structural analysis

4.3.1 Figures of merit

During the preliminary design phase several figures of merit were used to represent different mission features for structural design.

1. Scoring potential: every aspect of each component had the potential to influence score through the ability to efficiently perform a task.
2. Weight: the weight of each component played an important role in both aircraft performance and RAC.
3. Ease of construction: more than anything construction time was determinant each time it was necessary make a choice.
4. Aerodynamic considerations: the design of the fuselage, wing, tail, wing/tail coupling, power transmission and landing gear influenced lift, drag and aircraft stability.
5. Allows easy automatic unloading of payload: in order to allow the plane to take-off immediately after unloading, the structural design needed not interfere with payload handling operations.
6. Cost: as Leonardo construction was sponsorised, only pieces reconsidered too expensive weren't adopted.

4.3.2 Design Parameters and Trade Studies Investigated

During the preliminary design phase parameters for primary components were identified for structural analysis. The design parameters investigated included

- Weights for primary components
- The number of spars and ribs required for fuselage, tail and wing
- Landing gear dimensions

During the structural analysis, different approaches to the design of each parameter were investigated to identify tradeoffs. The trade studies compared structural alternatives in the areas of material selection for each component, strength vs. weight tradeoffs, component deformation and aerodynamics. Using information from the studies assisted in the design of each parameter to achieve each components highest scoring potential.

4.3.3 Wing Assumptions and Structural Analysis

The wing structure was constituted of two halfwings in which a rod had to be inserted: this one had to pass though the holes in the structure above the fuselage. Wing-rod insertion was modelled as a two DOF, degree of freedom system ,while wing/ fuselage section (realized by the rod) was modelled as a SDOF, single degree of freedom system (see fig.17): each halfwing (included the portion with the rod inserted) was considered as a cantilever . For simplicity of the analysis, the lift and drag loads were assumed evenly distributed along the lengths of the wing portion. Since the bending stresses in the wing caused by the lift will be the dominant factors contributing to failure, an evenly distributed load assumption will provide a more conservative analysis. When the distributed load was resolved into a resultant point load, the load was applied further out on the wing compared to a resolved elliptically distribution. Therefore the calculated bending moment will be larger. The same reasoning was used for justification for the drag load analysis. As a reinforced panels for wings was adopted, buckling analysis was easily conducted without surprises.

A trade study on three or two spar cross-sections, was analyzed in order to provide the needed structural integrity with the least amount of material and weight. The investigation included calculating the bending, shear and axially tensile and compressive stresses that spars would encounter under conditions of a fully loaded aircraft at 3g load. At gross weight, the conditions resulted in a vertical wing loading of 2.34 lbs per square inch. The results of spars analysis showed that two main spar located, respectively, at 10% and 30% of the airfoil chord would be sufficient to support the expected loads.The shear stress on the rib was calculated from the aerodynamic moment on the wing. The shear stress showed to be extremely low compared to the material properties of the wood.

As regards bending, statically safety factor adopted was 2.2. The wing structural assembly weight was estimated at 2.204 lbs.

4.3.4 Tail assumptions and Structural analysis.

The moments created by the tail for longitudinal stability were a function of both airfoil used for the cross-section and the control surface deflection angle. The loading cases assumed for the structural design of the tail was loads of a 10-degree elevator deflection at a flight speed of 63.79 fps. The

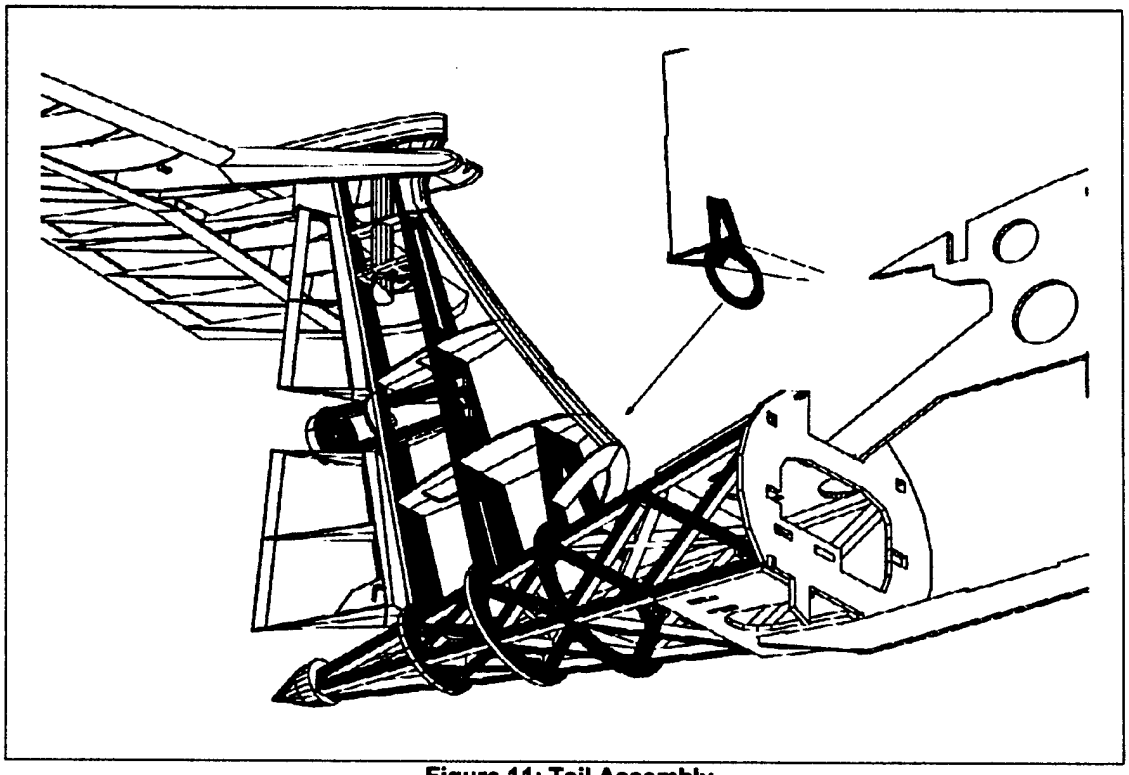

Figure 11: Tail Assembly

loading case corresponded to an emergency control reaction at high airspeeds. Loads were also modelled from the aerodynamic moments and forces created by the airfoil. The stress analysis was performed in a similar manner . Tail configuration is atypical T-tail. The horizontal plane is almost all mobile and has a single spar. Fin is high 1.279 in while span-elevator is 1.935 in and generates a maximum aerodynamic moment of 14.88 dyne per inc. Rudder was split in two section in order to allow passage of transmission shaft.

4.3.5 Structural Analysis

In order to simplify structural analysis, our calculusses were tailored by torsion considerations. Airplane structure (except tail cone which is a reticular assembly) is based on torque box configuration whose basament is able to support flexion thanks to under reiforcements. Wing swept and mass distribution were varied until c.g. location was at 6%of wing chord fore the neutral point.

The center of gravity was fixed such that no rotation or translation was allowed. Dynamic tail forces were not included in the fuselage strength analysis because the aircraft was assumed to be in level flight. When applying loads to the fuselage, the following assumptions were made. All loads where modelled as resultant point loads with a safety factor of 1.5. The loads were developed as if the aircraft was loaded with the transportation box and 18 batteries and experiencing a 3g loading. Engine torque was also analyzed at maximum power settings. These assumptions were based on information from the preliminary design aerodynamic and propulsive studios and historical data.

The fuselage was broken into two sections (tail cone section with reticular structure and the remaining part) in order to determine different inertia values at the relative location of the loads. Using singularity functions, the maximum shear stress due to torsion (elevator effect) was calculated at 0.49

psi; the maximum flexional stress was calculated at 15.36 psi (coverage wasn't taken in count because wasn't structural). In this way it was possible to obtain a margin safety of 71.3.

4.3.6 Main Gear Assumptions and Structural Analysis

Only main gear effect was modelled as concentrated forces applied under the basament edges of the fuselage . Tyres were considered as solid springs :in this way, reaction soil transmitted to fuselage can be considered not concentrated forces of infinite magnitude .

Raymer informations were considered sufficient to develop loading cases for the landing gear.

The analysis began establishing a wing tip scrape angle and a maximum gear height. The wing tip scrape angle was specified to be 21°, and the maximum gear height was set at 3.444 inches: this last decision was due to the need of employ strong gear-legs (in aluminium). The wing tip scrape angle was determined by a combination of historical data and experience.

According to these constraints and the lengths of the wing, the overall gear track width was calculated to be 8.79 inches: in order to have a better roll control during take off/landing/ taxying operations, a slim steel skate for each wing tip was adopted.

Good results was obtained during tests performed to verify fuselage strength in the cases of a two-wheel touchdown and a one-wheel touchdown (drop test) in MLW (Maximum Landing Weight). A gear load factor of 3 was assumed for ordinary two-wheel landings. The gear load factor caused the landing weight to increase by a multiple of 1.5 per wheel for two-wheel landing conditions. As regards drop test, the multiple was increases to 5.

4.4 Propulsion Analysis

For the preliminary design phase for the propulsion system we availed ourselves of Motocalc program for optimizing the major components: batteries, motor, and propeller. The program simulated the complete propulsion system from the power used by the batteries to the power produced by the propeller in flight. Components were allowed to vary in such a way as to match and/or exceed the output values estimated for thrust, current, power, and efficiency for the overall propulsion system. Estimated values were provided from the optimized aerodynamic aspects of the plane. Four propulsive components were varied in the optimization program: battery cell count, propeller dimensions, motor-size, and gearbox ratio. Six motor series were examined for the program: the Astro Cobalt 25, 40, and 60 and Astro FAI 25, 40 p/n 642, and 40 p/n 643 series. The gearbox is entirely self-built. See below for component's choice criteria.

4.4.1 Figures of Merit

Figures of merit were developed to evaluate the design parameters. The figures of merit represented the relation between efficient propulsion system and the competition goals and regulations. The figures of merit used were:

- Score: in all aspects of the design, score was the ultimate figure of merit. All aspects of every design decision had the potential to influence the overall scoring potential of the aircraft

- Efficiency: the propulsion system affected score in both flight performance and Rated Aircraft Cost. Efficiency of each part was optimized to offer good performance in both areas
- Weight: the weight of the propulsion system was determined to be a large player in the Rated Aircraft Cost because battery weight was heavily penalized. Therefore reducing the weight of the batteries as well as other propulsion system components can provide a dramatic score improvement
- Current: the current draw on the batteries was a limiting factor set forth by the competition regulations
- KV Values: the KV Value of a motor was a ratio that relates RPM to voltage. Selecting a motor with the proper KV Value allowed thrust to be produced at acceptable current levels
- Energy Density: the energy density of the batteries was crucial to determining which batteries provided the most energy with the lowest increase in battery weight.
- Historical Data: historical data was invaluable in predicting efficiencies and performance during the trade studies performed on the different propulsion components

4.4.2 Design Parameters and Trade Studies Investigated

Following are component's choice criteria of propulsive group. As said, we used Motocalc program.

- P/D ratios: by fine-tuning the ratio of propeller pitch to propeller diameter, it was possible to increase the efficiency of the motor and thereby reduce the number of batteries required.
- Propeller Diameters: the propeller diameter has a direct affect on the amount of current required to maintain an RPM setting. Since the propulsion system is limited to 40 amps of current the propeller diameter was a limiting design parameter.
- Number and type of batteries: overall aircraft efficiency was a crucial parameter on the competition. An efficient propulsion system would find the optimum balance between power produced and batteries required. Balance was crucial to reach the aircrafts maximum scoring potential.
- Size and type of motor: Different motors were optimized for operation in specific ranges. Motor selection was important with the most potential to operate efficiently under the predicted flight constraints

4.4.3 Weighted Decision of Motors

The results of a weighted decision matrix were analysed for the FAI motors and Graupner motors.From the decision matrix resulted FAI motor series score were all fairly close in relationship with each other. Apparently Graupner motor efficiency is generally lower than the FAI motor series, but to determine which motor was best for the design, other parameters must be considered.

4.4.4 Investigation of Graupner Motor

Following there is a numerical analysis of performance behaviour based on Motocalc program. From the first inset, left to right, top to bottom, we have total efficiency vs. airspeed (mph); power (W) vs. airspeed; thrust vs. airspeed; current vs. airspeed.

Figure of Merit (FOM)	Weight	FAI 25	FAI 40 / 642
Number of Batteries	0.3	0.9	1
Current	0.25	0.7	1
Takeoff Thrust	0.25	1	1
Cruise Power	0.1	1	1
Efficiency	0.1	0.9	0.8
Score		0.90	0.98

Table 7 : Motor Weighted Decision Matrix

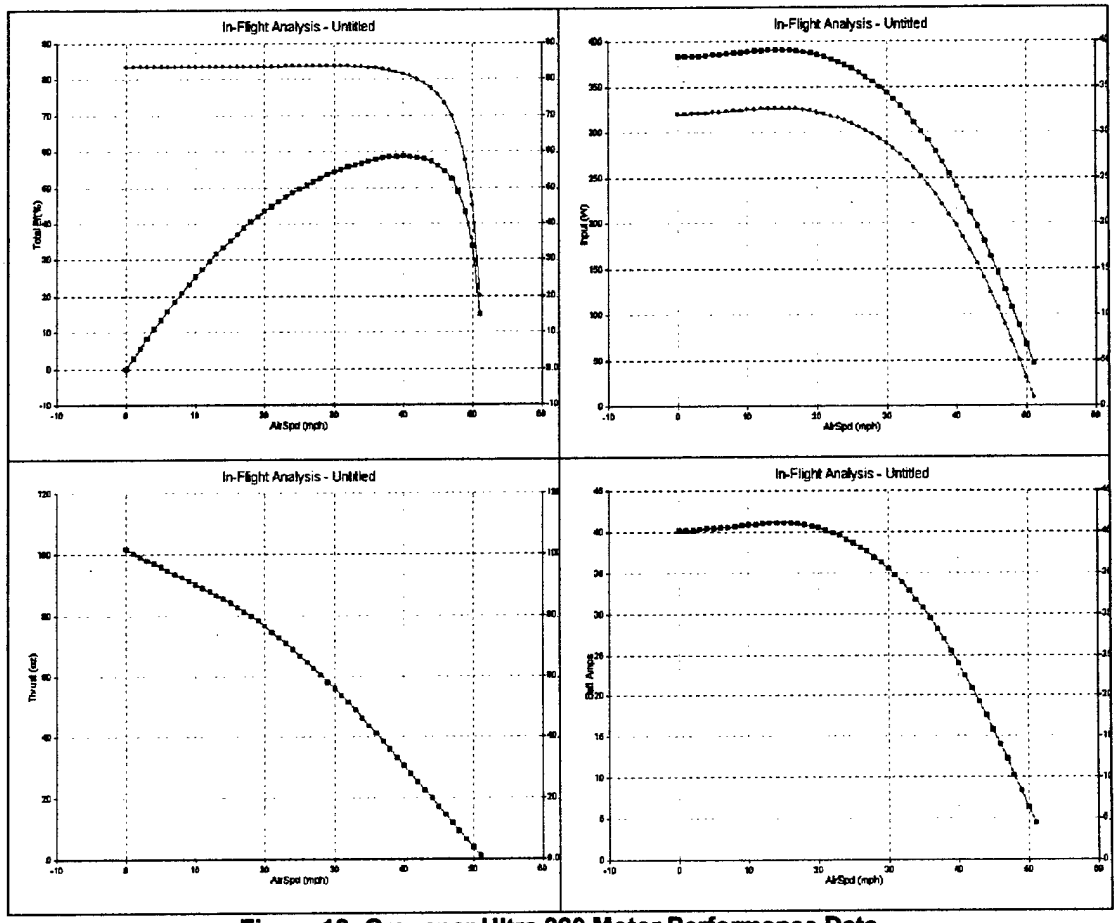

Figure 12: Graupner Ultra 920 Motor Performance Data.

4.5 Analytical tools

4.5.1 Optimization Program Architetture

After the conceptual phase was completed, the drag, weight, propulsive and RAC models were updated. The following models describe the updates to the program:

- Drag Model: the weight model was reconstructed according to the drag build-up method found in Raymer (1999). The method gave a closer estimate of drag without requiring the parameters developed in the preliminary and detail design phases. The drag model also included the drag polar and lift curve for the chosen airfoil. Different values were used for both cruise and take-off Reynolds numbers. Conservative margins of safety were also adopted.
- Weight Model: the weight model wass reconstructed according to the strcutural and propulsive assessments presented earlier in the conceptual design phase.
- Propulsive Model: the propulsive model was compared to the analytical model used by the propulsion group in its analysis. The model showed that the conceptual model was a little bit too conservative (it was probably due to the aerodynamics refinements).
- RAC Model: the RAC wasalso updated to meet all the RAC requirements, and better represented the features chosen in the conceptual design phase.

Drag, weight propulsive and RAC models were placed in the program along with the parameters that best support an optimal design. The program was adapted so that the scoring potential was maximized and trade studies occurred using the optimization process

4.5.2 Other Methods Used

Other than optimization, several other programs were used to calculate the various parameters of the design. First we started with 3D Studio MAX, then aerodynamics group used ANSYS for Computational Fluid Dynamics (CFD) and structures group for a structural analysis, while the flight mechanics group used Fluent to verify stability, then the layout was transferred to the CAD program for three-dimensional modelling.

4.6 Final Aircraft Configuration

At the end of preliminary, the primary components of the configuration were all sized and placed according to the figures of merit. The fuselage length was minimized using a "drop-type" fuselage to accommodate the payload and keeping the overall drag low. As said the wing configuration was "sunshade" type, mounted on a large fin. The tail was "tailored-made" so that the wing span was less than a quarter span of the wing. The spars and the ribs in the wing and the tail were sized, along with the makeup of the fuselage design.

4.6.1 Wing and Power Loading

Wing and power loading for the preliminary configuration was 2.34 lb/ft2 and 26.3 lb/hp. The two loading values were a compromise to achieve the correct mission balance and achieve the best scoring potential. Higher wing loading allowed the plane to penetrate through the wind better, achieve higher cruise velocities, and makes the configuration less susceptible to gusting conditions because

greater changes in pressure differential are required to disturb the plane. Drawbacks to high wing loading occurred at takeoff and climb. Higher wing loading was not helpful during the critical phases. To overcome the wing loading disadvantage, higher power loading was required to help the plane overcome takeoff and climb requirements. Therefore, a compromise was met between wing and power loading to result in the preliminary configuration.

5.0 Detail Design

After the primary components were sized in the preliminary phase, secondary components were sized and added. The aerodynamics group had the task of verify the preliminary design. As a model of analysis we preferred to use the Fluent program, so a 3D model within the simulator was created. This analysis granted a more global view of pressures acting on the aircraft with respect to experimental methods (i.e. wind tunnel). Moreover, it was able to verify that the downwash angles used for tail keying were correct; it has been used to determine the dynamic stability and verifying the initial hypothesis: the fact that besides not having a dihedral angle the fluxes interaction between fuselage and wing permitted a good behaviour on roll.

5.1 Aerodynamics Performance Analysis

The optimization code was modified to provide data on the flight performance of the final configurations. The use of an airfoil analysis program allowed the characteristics of the airfoils of the wing and tail to be included in the analysis. The following sections contain results from the two computer codes, representing how the plane would perform.

5.1.1 Final Configuration Features

The final aircraft configuration is a rather unconventional one. A "drop-type" fuselage with a

Fuselage		**Wing**	
Length (overall)	4.59 ft	Airfoil	Eppler 793
Maximum width	9.645 in	Span	7.93 ft
		Chord	11.81 in
Horizontal Tail Properties		Area	7.534 sq ft
Airfoil	Eppler	Incidence angle	2.6 °
Span	1.9 ft	Incidence angle (zero lift)	6.85 °
Chord	10.63 in	**Total aircraft**	
Vertical Tail Properties			
Airfoil	NACA 0012	Rated Aircraft Cost	11.25
Height	19.29 in		
Chord	9.44in		

Table 8 : Final Aircraft Configuration Features

"sunshade" wing, with a tail slightly less than a quarter of the wing span to avoid RAC penalty. The landing gear, which is 3.44 inches tall, provides a tail scrape angle of 12 degrees for a safe pitching at takeoff. The wings can rock 21 degrees on landing before scraping the runway. A more complete description of the aircraft configuration features is listed in the following table

5.1.2 Estimated Mission Performance

The estimated mission performance of the configuration was calculated from the performance code used in the optimization. Each stage of the mission was individually evaluated. The time consumed for each step was of particular interest. Table 9 shows the time spent in each portion of the mission profile. The time spent in cruise, both loaded and unloaded, was the total time at cruise velocity, including all turns and straight legs. Also included in Table 9 were the expected flight velocities and distance of each phase. The performance information was calculated assuming a wind speed of 5 mph. Accounting for all phases of the mission as well as the RAC, the aircraft was predicted to score 1.75 times the report score.

Mission Components	Time Spent	Distance	Velocity
Takeoff unloaded	2.5 sec	37.81 ft	15.124 fps
Climb unloaded	9 sec	—	29.25 fps
Cruise unloaded (all 4 laps included)	240 sec	—	70.13 fps
Slow down unloaded	8 sec	—	—
Ground time for cargo expelling	1 sec	—	—
Takeoff loaded	5.2 sec	108.26	20.82 fps
Climb loaded	15.1 sec	—	48.15 fps
Cruise loaded (both laps included)	280 sec	—	81.72 fps
Slow down loaded	7.2 sec	—	—
Ground time for antenna mounting	1 sec	—	—

Table 9: Time Spent in Mission Phases. Value predicted by performance program.

5.1.3 Takeoff and Climb

The takeoff distance for loaded conditions was 108.26 feet from the optimization code. Takeoff velocity was approximately 20.82 fps. The plane needed to accelerate after takeoff to a velocity of 60 fps to maintain the proper climb speed. For unloaded conditions, the takeoff decreased significantly to 37.81 feet, and takeoff velocity also decreased to a speed of 15.124 fps. When the plane accelerated to climb velocity at unloaded conditions, the plane moved at an airspeed of 29.25 fps. The time for takeoff and climb scenarios can be seen above in Table 9.

5.1.4 Flight Conditions

The aircraft was designed to perform best in a 5 mph wind. At this wind speed, the empty cruise speed was projected to be 85.1 fps while the loaded speed was projected at 79.6 fps.

In order to close aerodynamic considerations, we produced the following picture by fluent in which it is possible to appreciate the uniform pression field behind the propeller and wings. It is evident the low degree of perturbation .

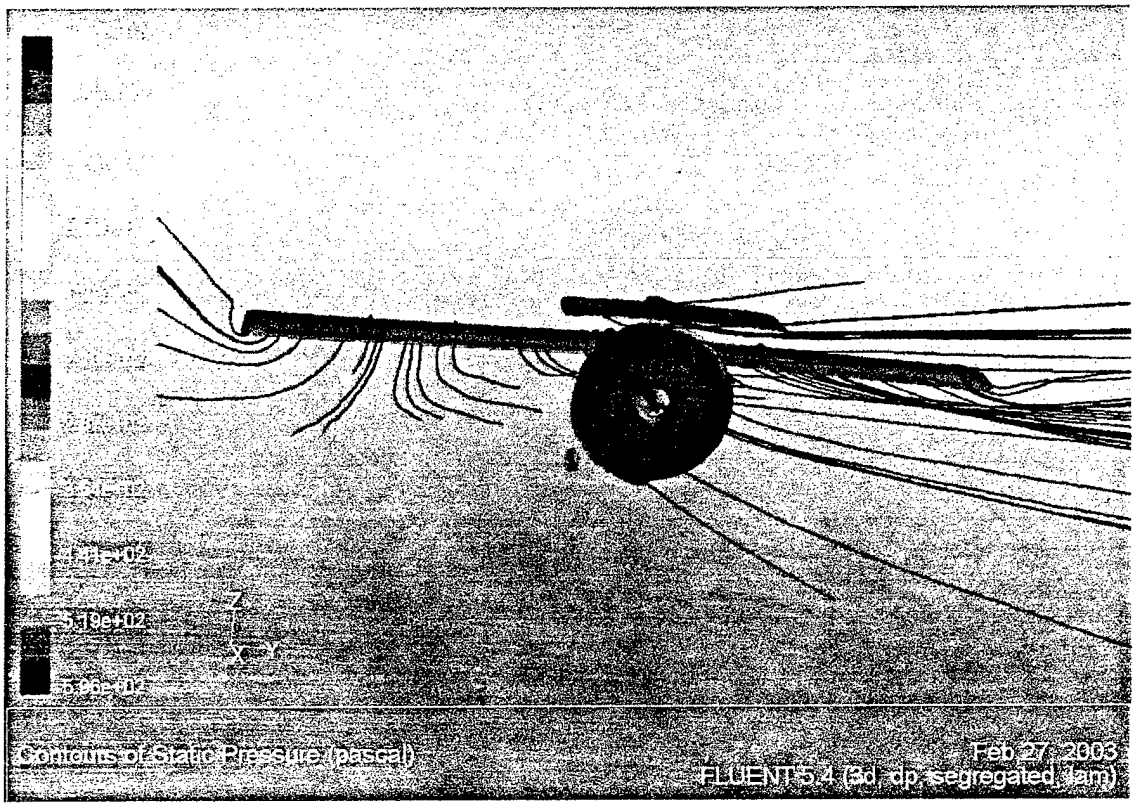

Figure 13: Pressure Field behind the Plane

5.2 Propulsive Performance Analysis

The final propulsion system was designed in the preliminary phase using analytical methods. Using a dynamometer, the propulsion group tested several of the top motors that remained at the end of the preliminary phase. The final motor and propeller combination was decided to be the Graupner with a 14.4 inch diameter propeller.18 batteries were needed to produce the thrust (they were of course NiCad batteries). The final output was 6.6 pounds at fixed point, using approximately 700 watts from the batteries; 4.4 pounds (with approximately 600 watts) at rotation; cruise thrust 1.7 pounds and drew 400 watts from the batteries. The values above were used for the construction of the prototype and refined the optimal results.

5.3 Structural Considerations

The focus of the detail design phase was the integration of the primary components with each other and the various systems comprising the aircraft as a whole. The details of the four major aircraft components, the fuselage, wing, tail, and gear, were designed to insure form, fit, and function of each component.

5.3.1 Fuselage Structural Details

The "drop-type" form of the fuselage was designed to accommodate the payload represented by a fixed-dimension box simulating an avionics package while exhibiting the lowest drag possible. Fuselage design was accomplished employing Studio 3D program and then importing the data in CAD to shape the fuselage around internal components while minimizing wetted surface area. The contours were also designed to blend from fore and aft portions of the fuselage to minimize drag between components. Functionally, the fuselage as a whole is made up of two sections: fore and aft.

The fore section must be able to absorb, transfer, and redistribute stresses coming from wings, gear (i.e. landing) and tail. The structure is made-up of the following pieces: a bridge-structure (in light blue, see fig.14) carrying the engine and the wing; a basement carrying gear and load (see fig.14, yellow picture); two bulkheads liking the bridge-structure to the basement (see fig.14, green picture); two connections bridge-structure / bulkhead / reticular truss (see fig.14, violet picture); front landing gear support (in brown). The bridge-structure tranfers lift-induced stresses to fuselage in the vertical direction; this transfer is realized by the means of the bulkheads. Due to the nature of the load to which is subject the bridge-structure, this has been dimensioned in order to support stresses caused by: flexion induced by the fact that the bridge-structure is fixed by the ends and loaded at the center by the lift; torsion due to sharp rolling manoeuvres; torsion due to an asymmetrical landing on a single gear, during which the wing, given its relevant inertial and aerodynamic characteristics, would tend to oppose to moment of a couple generating at touchdown.

The basement gear-carrier and load carrier has been dimensioned to support shear and axial stresses. Shear stresses are caused by the contribution of the reaction of the front landing gear and of that given by torsion. Shear stresses due to the reaction developed by the gear are absorbed by four spars (colored in red in figure 14), while those due to torsion would exist in case of an asymmetrical landing; for this reason it has been adopted a torsion box structure (colored in light blue

in the following figure), in correspondence of the zone that is more subject to solicitation comprised between the two bulkheads.

Axial stresses are due to the inflexion caused by the reaction of the wing (whose central part houses the engine) at the moment of touchdown, following the reaction of the front landing gear. Vertical bulkheads realize the connection bridge-structure –basement allowing the vertical load transfer (i.e. lift); moreover they realize the transfer of torsional moments between bridge-structure /basement. The two rear connections "seized" to the bridge-structure and basement transfer axial stresses due to flexion induced by drag generated by the horizontal empennage during pitching manoeuvres. Front gear support divides between the bridge-structure and the basement stresses of the front landing gear. Another function is to prevent the bridge-structure from sliding in the direction of the basement; such sliding would take place in case of a landing on the front gear.

The aft section was designed for purely aerodynamic reasons which made it preferred to a boom. It is made up of reticular truss able to absorb flexional, torsional and compression loads.

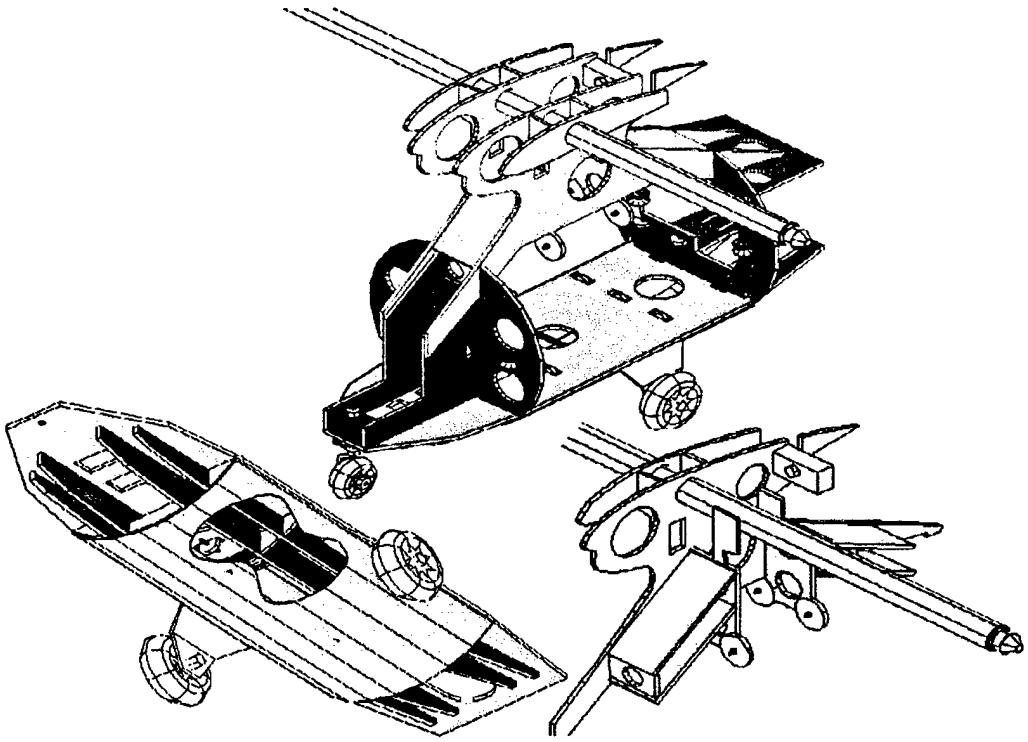

Fig.14 Fuselage Structure Details

5.3.2 Wing Structural Details

We have taken in consideration that the wings, in order to be transported inside a fixed-dimension box, had to be necessarily detached from the fuselage, implicating, of course, a series of troubles thus extending assembly time during competition. Those troubles have been resolved by adopting a systems made up of an aluminium tube to insert in proper holes in the upper part of the fuselage. On this tube wing -roots plug themselves. Since we have chosen an "all-mover" wing instead of a more classical wings + ailerons, we designed a system made up of a hinged pivot on a proper wing rotation system. Before we proceed in this study, we want to examine another critical load situation that is corresponding to the wing tip lift test, whose successful overcoming is necessary to be admitted to the fly-off. The load is a concentrated-type one and is 4.165Mdyne(41.65N). We verified that in order to have a structure that is able to absorb, in case of a lift load, axial stresses of 342.289 psi (2.36 MPa) and shear stresses of 72.51 psi (0.5 MPa; stresses given by wing tip loads are smaller), it was sufficient to adopt: spars with slabs having transversal section of 0.039 x 0.039 sq are inch, stringers having sections of 0.236 x 0.236 square inch; wing cover 0.059 in thick except for the sectors between the two spars where it has to be thicker (0.118 in). The reason for this solution appears clearly if we examine the following figure where it is shown with red arrows shear stress trend, almost entirely absorbed in the area comprised between the two spars. We determined at last that the value of the force acting on the wing rotation pivot is 12 Mdyne (12N), so it was necessary to adopt a pretty massive mechanism since a more slim junction would not be able to resist to such a load. To

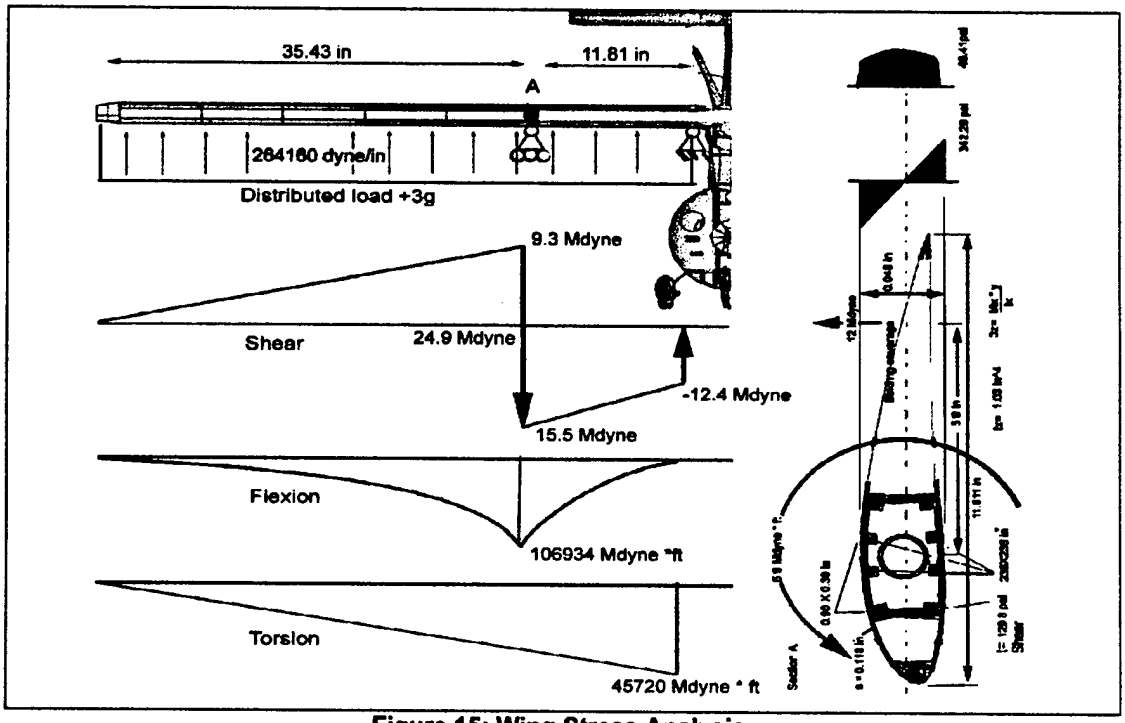

Figure 15: Wing Stress Analysis

determine the stresses to which is subject the aircraft during possible manoeuvres, once fixed maximum and minimum load factors, we made a preliminary study to define diagram of manoeuvring loads: in this way we have rapidly visualised aircraft structural limits. Then we proceeded to the stress analysis within the structure. Following are the results of shear, flexion and torsion trends.
As we can see, the sections to be studied are those in correspondence of the 'A' point in figure 15 and the wing root: in the 'A' point we have a shear discontinuity, while the maximum value of torsion is in proximity of wing root.

5.3.3 Tail Structure Details

The tail section was designed with similar goals to the wing (obviously, tail empennage is not lifting). Like the wing a single carry through spar was incorporated to transfer loads to the aft section of the fuselage. It is an "all-mover" just as the wing, but this time torsion is absorbed by cover.

5.4 Detail Design Assumptions and Comparisons

During detail design analytical assumptions made in preliminary design were reinforced by static structural testing, propulsion dynamometer testing and finally prototype flight-testing. The prototype aircraft, less payload and batteries weighted about 11.24 lbs during flight test number one. Luckily estimated total weight of 18.74 lbs in preliminary design became17.63 lbs.
Center of gravity resulted to be in the estimated position (30% of equivalent swept wing chord). In

Aircraft component	Station (inches)	Weight (pounds)	Moment (pound-in)
Brake battery	0	0	0
Propulsion battery	13	2.64	34.32
Servo batteries	12	0.55	6.6
Engine	5	0.52	2.6
Propeller	27	0.26	7.02
Watt-meter	0	0	0
Brake controller	0	0	0
Fuselage (with hatch)	9	2.87	25.83
Main gear	1	0.15	0.15
Nose gear	12	0.11	1.32
Tail	26	0.33	8.58
Wing	1	2.2	2.2
Box	0	5	0

Figure 16: Weight Balance Spreadsheet. Center of gravity located at 30% of equivalent swept wing chord

flight the aircraft proved to be stable in pitch, jaw and roll. Takeoff thrust and climb performance were better than expected mainly due to the number of cells, resulted generous.

5.5 Drawing Package

Detail drawings are provided in the next pages of this document.

Figure 17 contains a 3-view drawing of the design were aircraft sizes and configuration are indicated.
Figure 18 contains details of payload and relative location and restraint method (including sizes).
Figure 19 contains details about location of propulsion and flight control system components
Table 10 indicates:

- Geometry: lenght, span, height, wing area, Aspect Ratio, control volumes
- Performance: CL max, L/D max, maximum Rate of Climb, stall speed, maximum speed, take-off field length (two sets, empty and gross weight)
- Weight Statement (airframe, propulsion system, control system, payload system, empty weight, gross weight)
- Systems (radio used, servos used, battery configuration used, motor used, propeller (nominal), gear ratio.

Table 11 includes Rated Aircraft Cost Worksheet And Pie chart

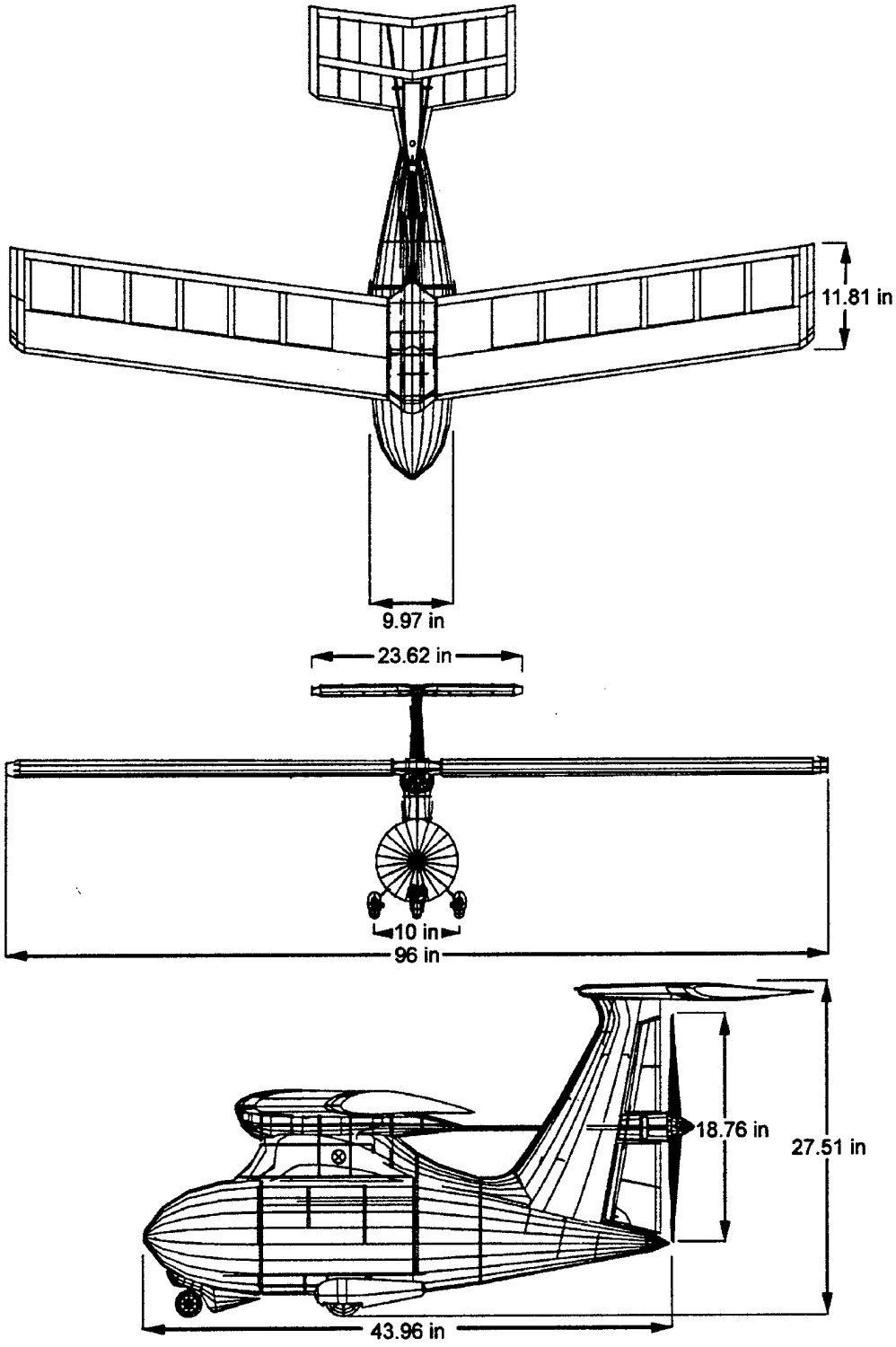

Figure 17: 3-View Drawing

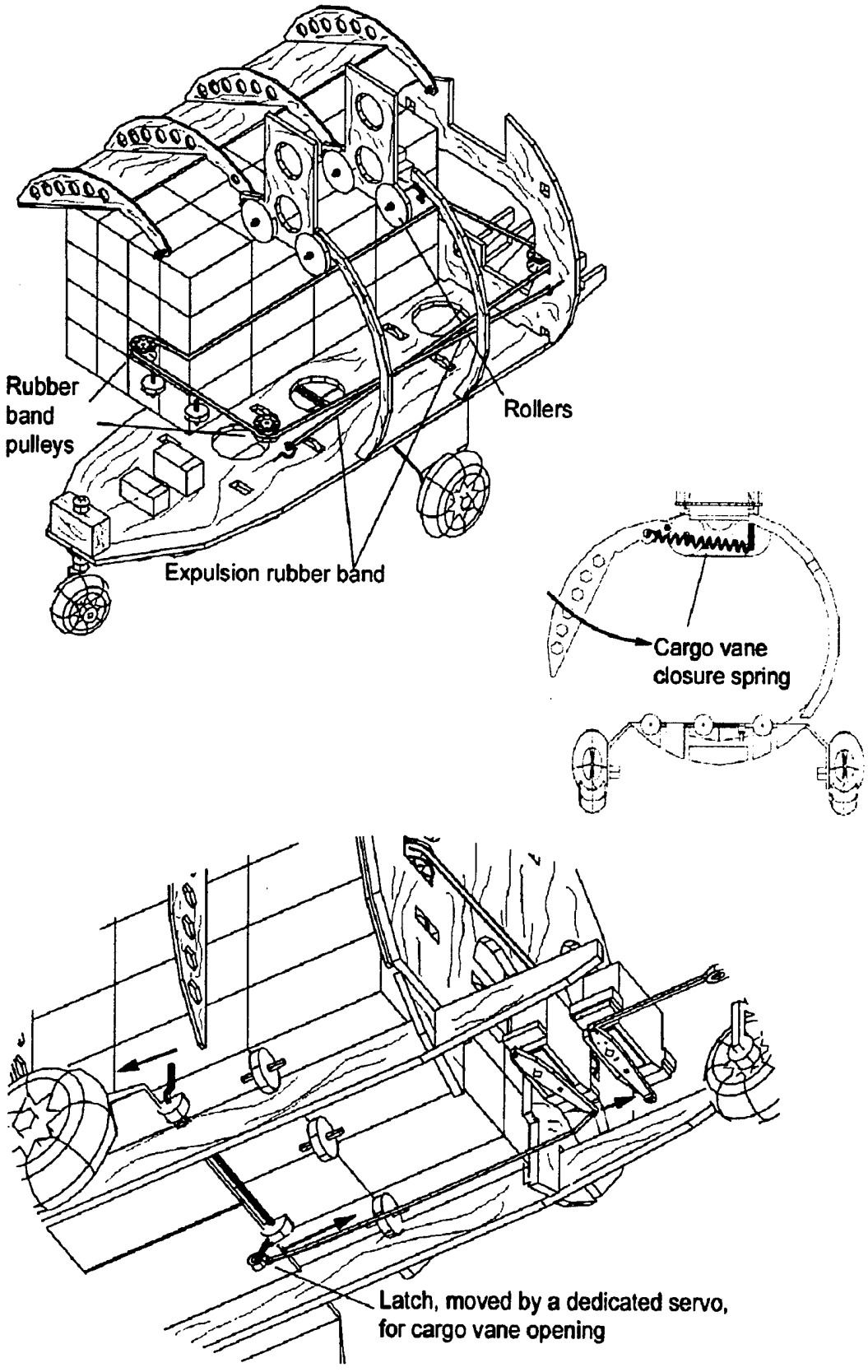

Figure 18: Payload, its location and Restraint Method

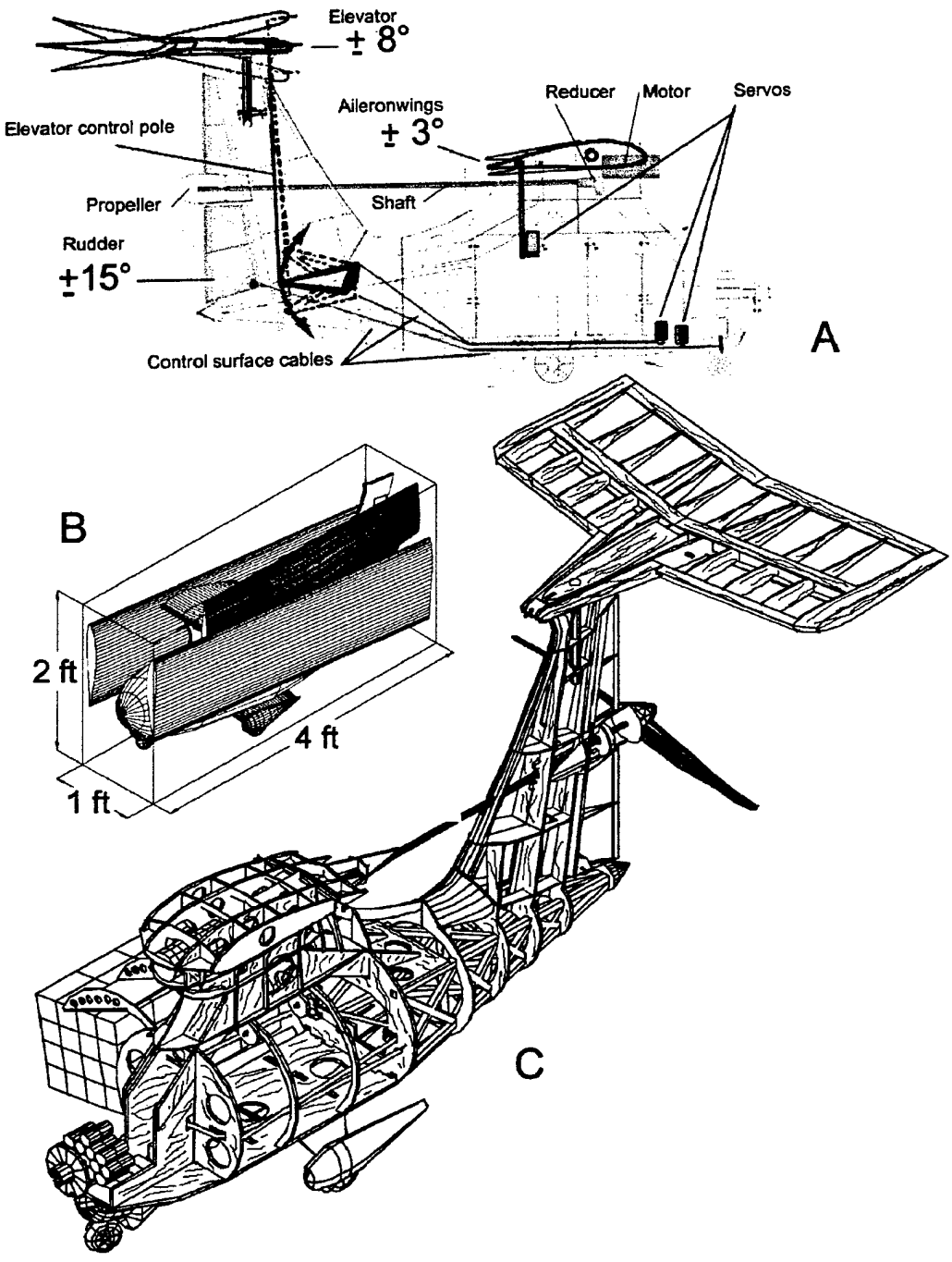

Figure 19/A: Location of Propulsion and Flight Control System Components

Figure 19/B:Lay-out of airplane components in the transport box defined by competition rules

Figure 19/C:Perspective of fuselage, cargo vane and shaft

Geometry	Datas	Measures
	Length	4.59 ft
	Wing Span	7.93 ft
	Height	27.56
	Wing Area	7.534 sq ft
	Aspect Ratio	8.34
	Control Volumes	2250 cubic ft
Performance		
	CL max	1.5
	L/D max	11
	Max Rate of Climb (ft/sec)	48.15
	Stall Speed (ft/sec)	36.45
	Max Speed (ft/sec)	61.05
	Take-off Field Length (empty)	37.81
	Take-off Field Length (gross weight)	108.26
Weight Statement		
	Whole Airframe (lbs.)	5.66
	Propulsion System (lbs.),batteries included	4.4
	Control System (lbs.)	1.41
	Payload System (lbs.)	0.2
	Empty Weight (lbs.)	11.67
	Payload (lbs.)	5
	Gross Weight (lbs.)	16.67
Systems		
	Radio Used	Graupner X-3810
	Servos Used	8
	Battery Configuration Used	Series
	Motor Used	Graupner Ultra 920
	Propeller (Nominal)	18/14 (4-bladed)
	Gear Ratio (Reducer)	1:9.8

Table 10: Aircraft Data

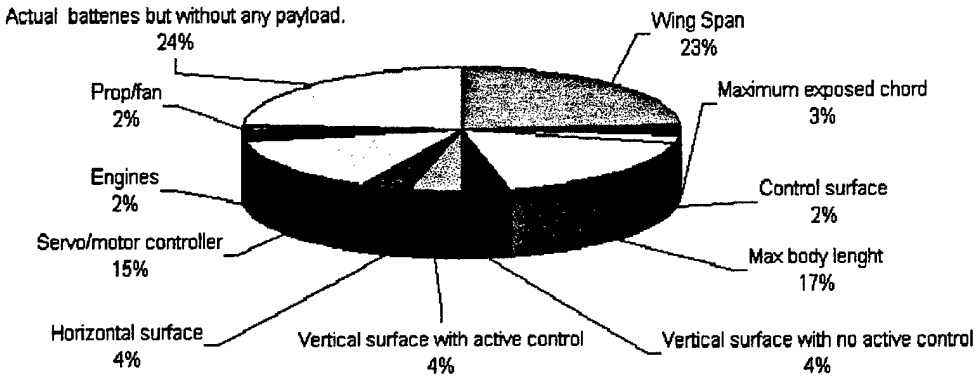

Manufacturing Man Hours: Work Breakdown Structures				
Aircraft Component	Man Hours/Unit	Aircraft Parameter	Individual Hours	Individual Contributions
Wing WBS				
Wing Span	8 hr/ft	7.94	63.5	1270
Maximum exposed chord	8 hr/ft	0.98	7.8	156
Control surface	3 hr/surface	2 surfaces	6	120
Fuselage WBS				
Max body length	10 hr/ft	4.59	45.9	918
Empenage WBS				
Vertical surface with no active control	5 hr/surface	2 surfaces	10	200
Vertical surface with active control	10 hr/surface	1 surface	10	200
Horizontal surface	10 hr/surface	1 surface	10	200
Flight Systems WBS				
Servo/motor controller	5 hr/servo	8 servos	40	800
Propulsion System WBS				
Engines	5 hr/engine	1 engine	5	100
Prop/fan	5 hr/prop	1 propeller	5	100
Total Manufacturing Man Hours				**4064**

Description	Value Definition	Multiplier	Aircraft Parameter	Man Hours	RAC
Manufactures Empty Weight (MEW)	Actual airframe weight, lb., with all flight and propulsion batteries but without any payload.	$100	12.63 lb.	NA	**1263**
Rated Engine Power (REP)	"Total Battery Weight" defined as weight of propulsion batteries.	$1,500	1 Engine 3.3 lb. Batteries	NA	**4950**
Manufacturing Man Hours (MMH)	Sum of assembly hours defined by Work Breakdown Structure (WBS).	$20/hour	-	190.25	**3964**
					10177

Predicted Rated Aircraft Cost = 10.177

Table 11: Rated Aircraft Cost Worksheet and, Pie chart. Predicted RAC of 10.177

6.0 Manufacturing plan

6.1 Manufactoring Process Investigated

In order to produce the aircraft, several different manufacturing techniques would have to be employed for the different components. Several different methods for obtaining the desired shapes (specially the wing airfoil) , the surface finishes (specially in terms of interfaces between mobile surfaces and fixed) and smoothness of mechanisms were investigated for each component. The figures of merit used to evaluate different manufacturing techniques included the ability to produce the desired shapes and finish, cost of tooling and manufacturing, build time, required materials (in terms of different woods and metal pieces), skill levels and process repeatability.

6.2 Processes Selected for Component Manufacturing

In order to produce the aircraft, some different manufacturing techniques were evaluated. The figures of merit used to evaluate different techniques included ability of wood cutting, cost of tooling and manufacturing, build time, skill levels, and process repeatability. Drawings in scale 1:1 were employed for cutting of pieces from woods. This technique resulted very useful as allowed to minimize errors during cutting, sizing and shaping of singular pieces. Mainly cyanoacrylic clue was used.

6.2.1 Fuselage Manufacturing Process and Tooling

In first of all, frame spaces for spars and reinforces alignment was determinant for the correct alignment of the tail with respect to the nose. Then it was necessary to reinforce each clutch of pieces (not jointed) with angular reinforces glued at respective edges. An other topic of primary importance was the exact conforming of cargo vane in order to guarantee a smooth discharging of the box. By the way it was also necessary to reinforce adequately insertion point of the pulleys (positioned in the perimeter of the cargo vane,: they had to support the elastic for the box expulsion) and the rollers on the basement of the cargo vane. Also cargo vane door was a critical point because had to present all sides aligned with the correspondent edge of the fuselage cut which had to close. Also the alignment of the holes through which rods (for wings, horizontal tail and radome) had to pass was realized carefully in order to avoid interferences during mounting with consequent losses of time and so total time flight extensions. Obviously, during structure mounting, control cables, shaft, then motor and wires and at least servos were positioned. Fuselage was covered after test (with the airplane fixed on the terrain, of correct working either of mobile surface either of engine and propeller. Aircraft nose was realized in resin modelled around a conformed pasteboard mandrel.

6.2.2 Wing and Tail Manufacturing Process and Tooling

The wing and the horizontal tail had an architecture of spars and ribs. As occurred for the fuselage, also for them alignment of ribs spaces for reinforcement passage was a topic problem. During construction also dimensions (as wing-span and horizontal tail span) was strictly controlled : as regards horizontal tail, it resulted slightly wider than projected, so it was necessary to shrink it by reducing tips thickness. Continuing with fuselage analogy, also alignment of holes for the passage of the rod for wing attachment was strictly controlled. We paid attention also to low side of wing in correspondence to trailing edge due to particular shape of airfoil and its relative difficulty of

conforming. As regards horizontal, it was necessary to realize smooth inner edges in order to ensure a smooth rotation of elevator without interfering with fin. Elevator structure was constructed with analogue technique used for wing. Also as regards vertical tail we have to say the some things: the only difference consisted in the presence of shaft which required a rudder split tin and the realization of a support for the roll bearing by which is supported in the fin. Control cable of rudder rotation, whose one end is on the rudder top side was arched in correspondence of shaft. Control cable of elevator was passed in the leading edge of the fin. Moreover this one was positioned slightly decentred with respect to horizontal fuselage axe in order to avoid interference with shaft.

6.2.3 Landing Gear Manufacturing Process and Tooling

Each wheel of main landing gear was connected to fuselage by an aluminium leg screwed to fuselage basement. They where also streamlined. Bow gear can steer .

6.3 Analytic Methods Including Cost, Scheduling and Skills Matrix

6.3.1 Manufacturing Cost

With the preliminary design study complete, manufacturing and tooling costs were estimated. Luckily our work was greatly sponsored by a modelling shop.

6.3.2 Skills Matrix

In order to assign tasks for the manufacturing process it was necessary to develop a matrix of the skills required for each task. Table 12 contains the skills matrix. In the matrix a component that requires a lot of skill in a certain area was rated two, a component that required average skill in an area was score with one and a component that required no skill in an area received a zero. The columns of the skill matrix represent required skills in the manufacturing process; the rows represent the major assemblies and system of the aircraft. Members were assigned to components matching their expertise. An external laboratory consultant observed our work.

Primary Aircraft Assemblies and Systems	Wood cutting	Wood clueing	Resin modelling	Radio Equipment Installation	Electrical work	CAD modelling
Wing	2	2	0	2	1	2
Fuselage	2	2	1	2	2	2
Landing gear	0	0	0	0	0	1
tail	2	2	0	2	2	2
Propulsion system	0	0	0	2	2	2

Table 12: Skills Matrix For Leonardo Team

6.3.3 Manufacturing Scheduling

The aircraft was constructed in three assemblies: the fuselage (included vertical tail and landing gear), wing, horizontal tail. The assemblies were constructed to allow components to be constructed simultaneously. Considerations such as material availability were of critical importance to maintaining a smooth manufacturing process. Figure 20 is the milestone chart developed for the manufacturing process.

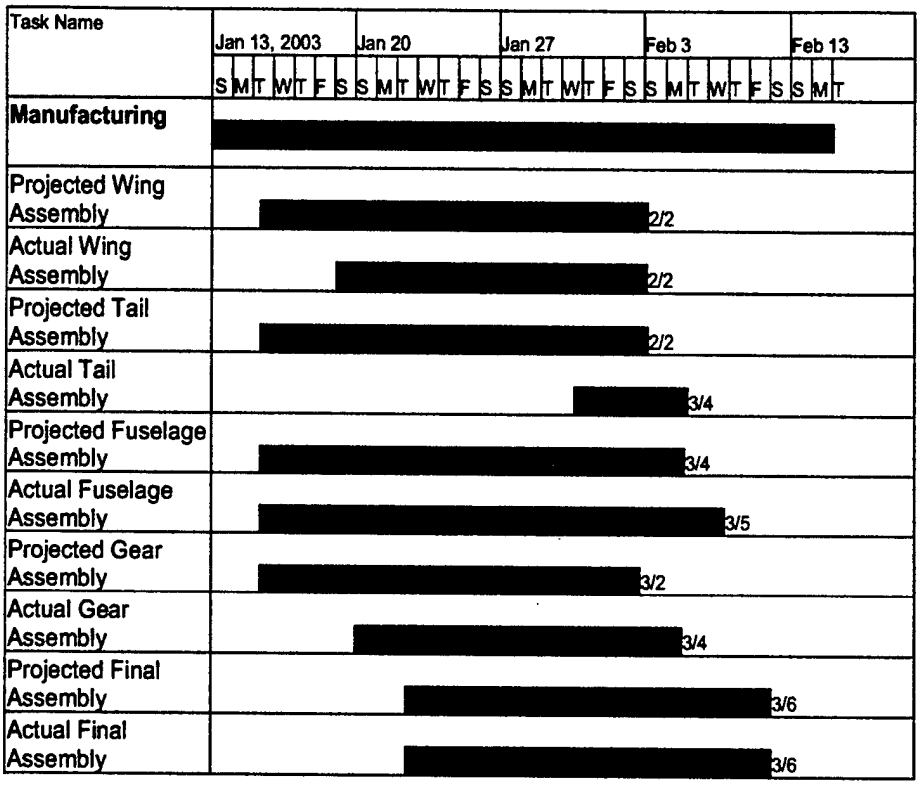

Fig.20 Manufacturing Schedule

7.0 Testing

7.1 Static Tests

To be sincere, our tests (static) began during airplane assembly. Of course wings were the main character of our tests. Mainly we verified their strenght when subjected to lift (that is to say airplane weight) supposed to be elliptic. In the following image (figure 22) we can see our static test.

An another test was to verifiy smoothness of wing connection to the fuselage in order to ensure a rapid and sharp assemblage of them during competition. This last operation resulted very useful as we had to refine several times all our plug-connections and in one case it was necessary to replace a spring of plug system. Moreover we tested also smoothness degree as regards shaft rotation. We observed it was necessary to insert two axle box (*in carbon, we apologize for this historical licence!*), one in the fin an the othe in the trailing edge of the "sunshine". We didn't considered fatigue tests as low values of static loads in a wood contest. Motor and propeller vibrations didn't manifested a serious risk for structural integrity. Another test repeated continuosly was the actioning of control cables

correct working in terms of degree of rotation of control surfaces. Last tests involved cargo vane opening mechanism. We had to reinforce repeatedly pulley's attachments.

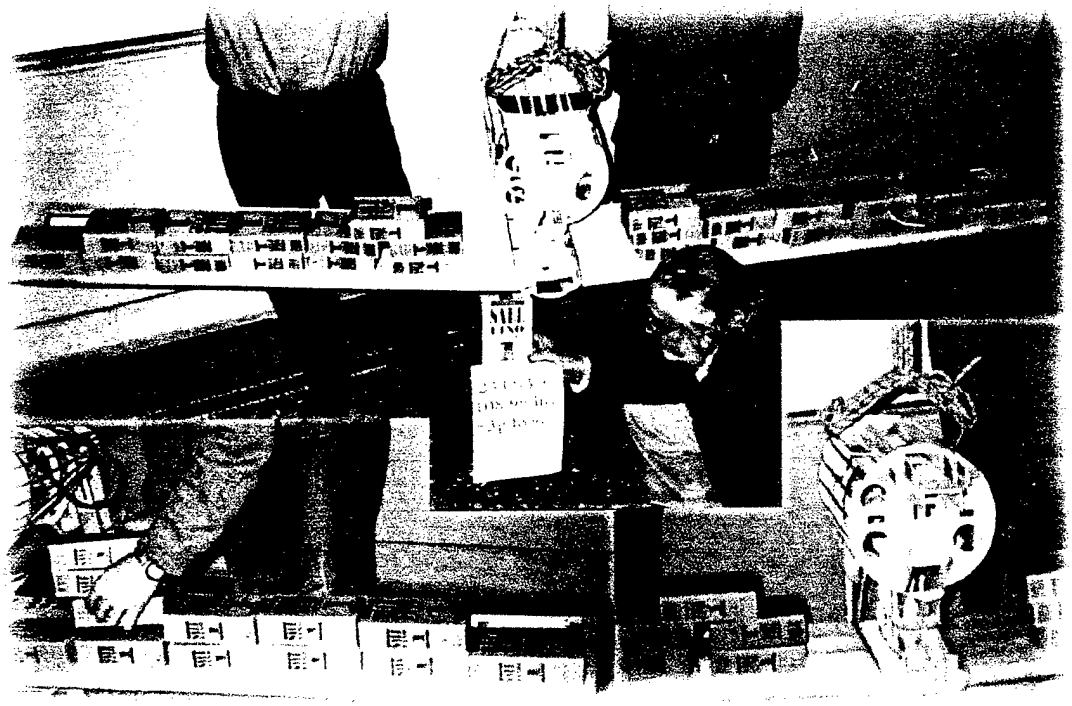

Fig.21 Simulation of Wing Load (the man in the photo is our consultant Enrico Nizzica) during Leonardo construction. Wings were loaded employing salt wrappings of 108.96 lbs each one(as declared in the sheet handled by our consultant in the photo), simulating an elliptical lift; the airplane was suspended overturned.

7.2 Flight Tests

An interesting item considered during tests was (and still is) the evaluation of batteries number. It seemed that we had an excess of batteries: but it is necessary time for evaluating a reduction in their number.

Moreover,flight tests have been conducted with the double goal of testing flight performance and aircraft endurance, obviously maintaining structural integrity. To this purpouse, we employed telemetry acquisition data instruments, used in the past by our sponsor, the RCR Club: this is self-made and is made up of a modelling radio for data transmission and a self-made PC card for data acquisition. To gather more details go to the web pages mentioned in references. On the model aircraft there have been assembled instruments for measuring:speed (free propeller), angle of attack (weathercock), angle of horizon (plumb-line), altitude (static port), propeller rounds (photoelectric cell). In addition to this parameters are besides being monitored all the commands the pilot sends to the aircraft (thrust, pitch-up/pitch-down angle, angle of ailerons, angle of rudder), for a total of 5+4 parameters being monitored.The speed sensor and the angle of attack sensor, and the static

Fig.22: Telemetry Instrumentation. In this photo we can see the instrumentation mounted inside the cargo vain and the appendix prominent to the nose bearing sensors and photoelectric cell.

pressure intake have been assembled on an appendix prominent to the nose in order not to influence too much the model aerodynamics, and for this reason a supplementary weight has been added on the tail to re-center the one. Some flight tests were performed at:

- Minimum stall speed planning (engine off) 23.61 – 24.85 mph
- Minimum stall speed (engine on) 24.85 – 26.09 mph
- First rate speed 26.09 – 27.96 mph
- Maximum speed 41.63 mph
- Paling at maximum efficiency (11 ~ 12) 31.06 mph

Moreover estimated drag during glide (in which the only force is weight) is 588399 dyne at 31.06 mph. The following figure 23 is a record of parameters during a stall in which we can notice CL max = 1.6. In the sphere of static stability, from flight tests it was confirmed the desired inverse relation between air speed and rotation angle, delta of 4 degrees for a speed variation between 37.28 (delta elevator = 0 degrees) and 24.85 mph.

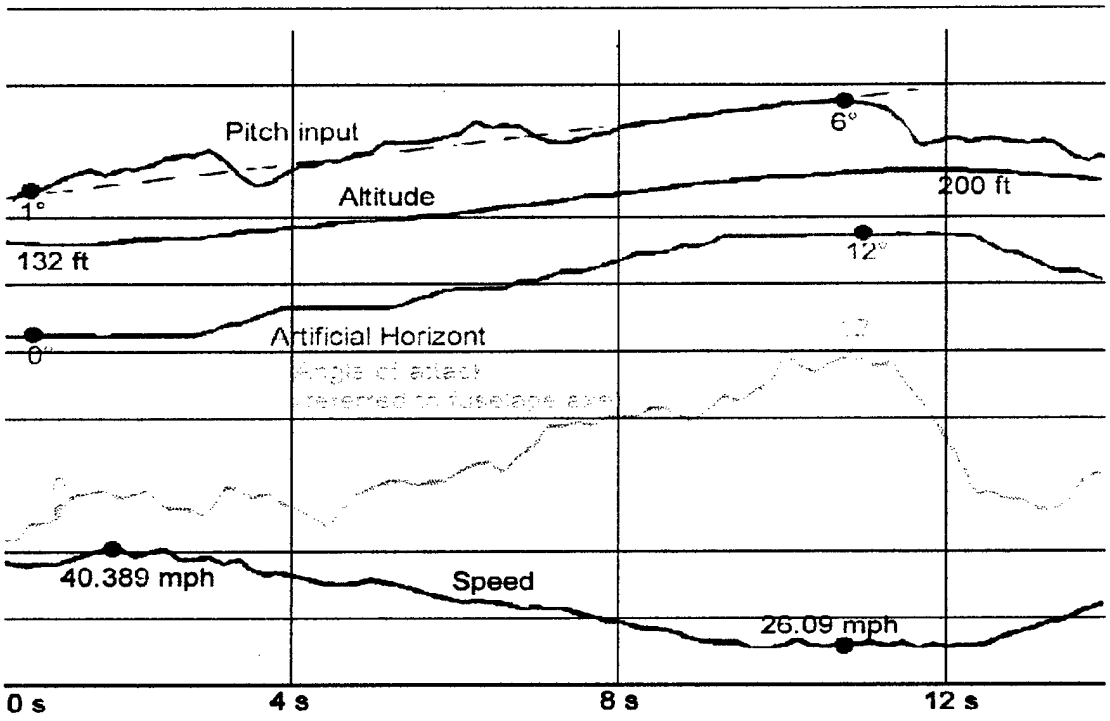

Fig.23: Flight Test Results; stall at Clmax=1.6

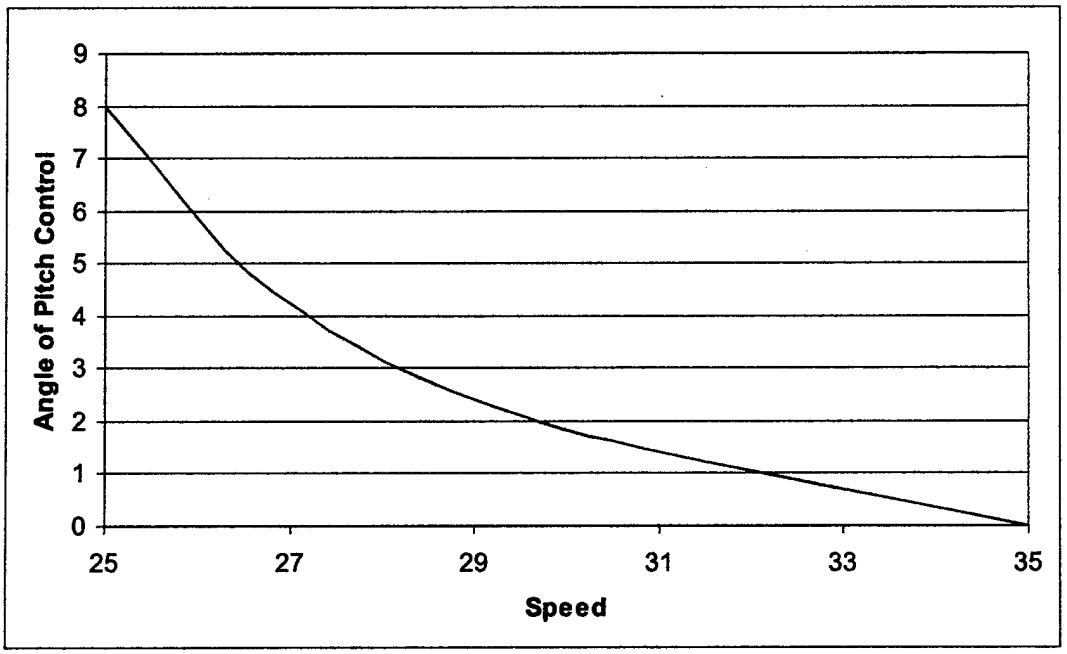

Figure 24: curve of longitudinal stability obtained from experimental data. It was verified the fact that when speed decreases, pitch angle increases.

Fig.25: Leonardo tests: it is possible to see in the photo above, pitot sensor and angle of attack weathrcock (mounted on the nose)

8.0 References

Michael C.Y.Niu, *Airframe Stress Analysis and Sizing*, Second Edition, Hong Kong Conmilit Press LTD

Michael C.Y.Niu, *Aircraft Structural Design,* Kong Conmilit Press LTD

Renato Barboni, *Costruzioni Aeronautiche*, ESAGRAFICA

Francesco Botta, *Robustezza del velivolo*, Editoriale Aeronautico, 1943 ROMA

Angelo Mori, *Manuale di tecnica Aeronautica*, Editoriale Aeronautica, 1940 ROMA

Bernard Etkin, Lloyd Duff Reid, *Dynamics of flight-stability and control*-3rd edition, John Wiley & Sons,INC

Attilio Lausetti, Federico Filippi, *Elementi di meccanica del volo*, Levrotto & Bella

Esteban Onate, *Estabilidad y control del avion,* Editorial Paraninfo

L.M.Milne Thomson, *Theoretical Aerodynamics*, Dover O-486-61980-X

NACA Report 540 pages 592, 593, 594

Oklahoma State Ubiversity Orange Team report presented during AIAA 2002

Raymer, D.P., *Aircraft design: a conceptual approach, 3rd edition, AIAA, Reston, VA, 1999.*

http://web.tiscali.it/rcrclub/telemetria/strumentazione/Strumentazione.htm

http://web.tiscali.it/rcrclub/telemetria/telemetria.htm

http://web.tiscali.it/fcenturions

Buzzweiser

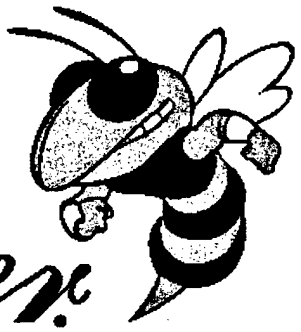

2002-2003 Georgia Tech DBF Design Report

ASDL

TABLE OF CONTENTS

Executive Summary **2**
Configuration Development Process 2
Range of Alternatives Investigated 3
Management Summary **6**
Organization of Team 6
Team Leaders 6
Personnel and Their Areas of Assignment 7
Milestones of Program Execution 8
Conceptual Design **11**
Problem Statement and Key Mission Requirements 11
Screening Methods 11
Configuration Selection Overview *11*
Mission Analysis *12*
RAC Sensitivity Analysis *14*
Figures of Merit *16*
Alternative Concepts Investigated 17
Configuration Discussion *17*
Previously Successful DBF Designs *19*
IPPD Process 20
Morphological Matrix *20*
Pugh Matrix *20*
Alternate Methodology *22*
Preliminary Design **25**
Mission Model 25
Analysis Methods Used 26
Early Sizing Studies *26*
Fuselage Parameters and Trades *27*
Propulsion System Parameters and Trades *29*
Wing Parameters and Trades *30*
Traditional Constraint Analysis *30*
Alternative Sizing Method *31*
The Optimization Routine 32
Empennage Sizing and Trades *33*
Landing Gear Sizing and Trades *33*
Predicted Mission Performance 33
Detail Design **35**
Systems Architecture 35
Component Selection 37
Mechanical: *37*
Electrical: *37*
Electromechanical: *37*
Pneumatic: *38*
Material Selection 38
Predicted Performance Parameters 38
Manufacturing Plan **46**
Component Manufacture 46
Manufaturing Processes Investigated 48
Figures of Merit for Manufacturing Plan *48*
Analytic Methods 49
Testing Plan **52**
Component testing 52
Flight Testing 53
Results and Lessons Learned *54*
References **56**

This report summarizes the major developments of Georgia Institute of Technology's entry into the 2002-2003 American Institute of Aeronautics and Astronautics' (AIAA) Design, Build, Fly (DBF) student design competition. This annual event is organized by the Office of Naval Research and Cessna Aircraft Company and is sanctioned by the rules set forth by the Academy of Model Aeronautics (AMA). Though a new rule set is released every year, the nature of the competition always involves designing and building an unmanned aerial vehicle to carry a specified payload for a specified mission. The total score for a school's entry is based on three components: the design report's score, manufacturing cost model rating, and total flight score.

CONFIGURATION DEVELOPMENT PROCESS

Upon release of the contest rules in the summer of 2002, a few veteran Design, Build, Fly (DBF) members under the direction of faculty and staff working for the Aerospace Systems Design Laboratory (ASDL) at Georgia Tech formulated a plan of action for the coming contest season. The rules were analyzed in detail for major implications and the group formulated a preliminary timeline for major deliverables in the project.

Previous entries into the competition exposed many challenges in applying formal design programs to light UAVs. These essentially disposable aircraft are built cheaply without rigorous quality control standards by craftsman skilled in manual (not machine) manufacturing processes under tight budget and time constraints. The installed components and flight performance of such vehicles is also unique. Quality historical documentation on these vehicles is nearly non-existent, making regression studies nearly impossible. Clearly, producing an aircraft that is optimal for a given set of flight requirements, with little knowledge, experience, skill, time, or money is a highly challenging task.

Recognizing these challenges, the team anticipated that validation of the design through building and testing were paramount to establishing the fit between the performance prediction models and achieved results. However, veteran DBF members did not want to create an environment promoting disjoints between design efforts and building efforts. They also did not want to spend excessive time building aircraft that were not backed by solid engineering design analysis. The blend between building and designing had to be seamless and highly efficient in order to produce a quality product in less than one year. The desired program called for the formation of new methods specific to disposable light UAVs and the integration of design methodologies based on empirical data rather than scaling and regression models from larger aircraft.

The project objectives and schedules were specified such that the methods and tools to handle design phases were in place in time to be used for the contest season's effort. A multidisciplinary project such as the AIAA DBF competition requires many areas of specialized expertise. Georgia Tech's DBF program involved not only traditional aerospace engineering studies, but also included electrical engineering, computer programming, statistical analysis, and advanced systems optimization methodologies. Knowledge and experience in these areas was extremely valuable to the team, and team

leaders wanted to ensure that new team members were given the opportunity to participate in as many areas as possible. This critically valuable investment in future capabilities was often at the expense of direct project progress.

The appropriate level of detail of analysis for configuration selection was heavily debated. Without an acceptable industry design standard for light UAVs, the task of screening competing concepts was handled rather subjectively with emphasis on qualitative assessment of uncertain variables. Some students believed that the process should be more quantitative and systematic, incorporating end-point performance predictions of competing concepts and arriving at one result at the close of Conceptual Design. The counter argument was that such end-point predictions were not comprehensive and did not give merit to interaction effects. Some felt that it was impossible to assign value with any level of fidelity with which to make comparisons and that prior data on configurations might not be comparable to the performance of similar alternatives.

The team agreed that configuration selection should be driven by a qualitative assessment of metrics as they pertain to relative success over competing concepts. For Conceptual Design, team leaders wanted to arrive at the optimal solution for a class of relative arrangement of aircraft components. The process for screening the arrangement combinations was roughly based on Integrated Product and Process Design (IPPD) methods. This method included documenting all geometric combinations, and eliminating the "worst" of these configurations using a Pugh matrix screening tool. Remaining configurations were scored against weighted Figures of Merit (FOMs) for their weight relative to a previously chosen baseline configuration.

The team augmented the process with a decision tree diagram, which attempted to document the logical processes deemed most important to configuration arguments. Throughout the process, discussion was guided by a mission analysis and score sensitivity study conducted at the beginning of the project. One of the major results of this study was identification of the very-high sensitivity of total score to propulsion battery weight.

RANGE OF ALTERNATIVES INVESTIGATED

The range of alternatives investigated included wing designs from straight to swept planform, low-wing to high-wing placement, and from single to multiple lifting surfaces. Various geometries of fuselages for packaging the payload were considered, including wing-body configurations. Propulsion systems were considered in fore and aft as well as multiple installations. Besides various propeller configuration options, tractor-fans, pusher fans, and ducted fan configurations were evaluated. Tricycle landing gear, tail-dragger landing gear, bicycle, unicycle and skate-type gear were evaluated. A range of stability and control surfaces were considered – from canards to conventional tails, and the many candidate morphs of empennage type, such as T-tails, H-tails, twin tails, and ring tails. All of the possible alternatives and combinations were enumerated and evaluated through use of a design morphological matrix.

After configuration selection, the team strategy was to begin parallel efforts in design and procurement. The range of alternatives investigated for Preliminary Design included all reasonable

combinations propulsive components and their corresponding optimal wing design. The performance profiles of these combinations were used to optimize the geometry of the wing in terms of aspect ratio and wing area from the range of all reasonable choices for definition of the wing. Detailed component weight breakdowns helped the team define the probable weight of all configurations, from the smallest, lightest vehicle to the largest, heaviest vehicle. Total scores were calculated for each, and the top scoring solutions were evaluated for final selection.

Preliminary sizing and synthesis studies included a number of combined efforts but primarily involved the development of modeling and simulation environments to generate performance predictions for variable combinations. Battery, motor, propeller, and aircraft performance models were matched to empirical data gathered by the team. This environment, along with statistically-based analysis tools, allowed the team to screen the entire design space for the optimal solution to the RFP.

Some of the analysis tools used during the course of the project included NASA's RAM modeling tool, which was used to generate the aircraft geometry and write the necessary files to VORLAX and BEDAP to obtain induced drag and skin friction estimates. This information, along with the MATLAB performance data, was integrated into a flight simulation tool to generate final score scenarios. This comprehensive tool was able make final, high fidelity performance predictions which included variability in total score due to such things as pilot error and weather conditions.

Three aircraft were constructed over the course of the project. The first prototype was a functional test-bed for installed components and never flew. The second prototype vehicle was designed to be modular, allowing the team to change components with minimal alteration. Detachable wings not only allowed the aircraft to fit inside the container box, but also provided a means by which to change to wings of an alternate design before final parameters were specified. Data-logging systems were installed on this aircraft, and it was used as the primary test vehicle for information about the chosen design point. This aircraft was fully compliant with the contest rules, and could serve as a back-up aircraft in the event of a catastrophic failure. Functional systems had been tested and approved, and the team was able to make final decisions about the definition of the final contest vehicle. At the time of this report, the final contest vehicle was nearly complete and being prepared for initial taxi-tests.

A small team of students simultaneously generated the CAD geometry with IronCAD as another group was procuring the final vehicle. Installed components were measured and drawn to scale in the CAD rendering. Excerpts of the drawing are included in this document.

Please refer to the Compliance Matrix, (Table 1, page 5) for a summary of the contest entry.

Table 1: Vehicle Compliance Matrix

RFP SPECIFICATIONS		BUZZWEISER
	Constraint Summary	Response
Team	1/3 of the Team must be underclassmen	73.9% of team is underclassmen
General	No rotary wing or lighter-than-air	Fixed-wing aircraft configuration
	No payload internal to wing	Payload internal to fuselage
	Propeller driven and electric powered, unmodified	Unmodified electric propeller propulsion employed
	Must be *Graupner* or *AstroFlight* brand motors	Graupner motor selected
	Must use commercially available propeller	Prop. manufactured by Mejzlik Modellbau, Czech Republic
	Current limited to 40 Amps by specified fuse	Design current < 40 Amps, specified fuse inline to motor
	Must use Nickel Cadmium batteries	Sanyo 2400 SCR NiCd batteries employed
	Maximum battery weight 5.0 lbs	Battery weight 1.9 lbs
	Aircraft and pilot AMA legal	Compliant in full
	Present completed and signed RAC worksheet	To be delivered April 25, 2003 at contest site
Safety	Proper construction and function	Built with proven methods and tested for functionality
	Must pass lift test from wingtip at max weight	Structural design to 10g max weight loading
	Radio Fail Safe check	Programmed, compliant operation verified
	Capable of disarming by specified fuse	RFP spec' fuse removable from aircraft exterior
Mission Profile	Aircraft must fit inside 1x2x4' box	Short fuselage and "plug-in" type wings compliant
	Teams must select from three missions	Two missions selected
	Takeoff distance must be less than 120ft	Takeoff distance approximately 100 ft
	Payload must be adequately secure	Positive mechanical locking employed
	Avionics Package 6x6x12", 5lbs about centroid	Compliant in full
	Missile Decoy clear 360 deg view, 3" from aircraft	Compliant in full
Design Report	10pt Arial font, 1" margins, 8.5x11", 3-view 11x17", etc...	Compliant in full
	60 page limit, no greater than 5pp for drawing package	Page count 58, 5 pages of drawing package
	All figures 1/2 page or full page	Compliant in full
	Seven report sections, requirements specified	Complete and presented in this document

ORGANIZATION OF TEAM

In past years, the approach of organizing student members into specific teams created an environment that fostered disjoints and muddled communication within the group. Individual tasks arose almost daily over the course of the project, and assigning tasks to people that were outside their designated field of study was inevitable. The team management had to sacrifice focused project studies for research diversity. It was clear a better approach was needed.

Team members were expected to multitask and participate wherever their knowledge or capabilities could be applied to the task at hand. However, team management recognized that cumulative disciplinary knowledge and manufacturing experience were precious resources that had to be invested in and managed just as rigorously as time and money. The organization of the team and areas of work of team members is illustrated in Table 2 (page 9). As long as the level of participation of the members was high and overall effort generally on schedule, the team leadership did not want to unnecessarily restrict themselves with deadlines that would freeze the evolution of the design before reaching a superior solution. In some cases, though, firm deadlines had to be imposed to encourage the completion of a key project.

For these reasons, team management focused on creating an atmosphere of accountability and organization within a broad framework of required tasks, with individual detailed tasks being delegated to team members as they were identified. Team management, which was composed of three aerospace engineering seniors, knew from previous years how long each design task should last, and these design tasks often had to overlap because of time constraints.

TEAM LEADERS

The team was organized under three senior aerospace engineering students; referred to in this report as "team management." These three team members were responsible for identifying necessary project tasks, and delegating these tasks to the team membership.

The roles of all three team leaders are worth discussion. One of the team leaders, Graham Clark, had a great deal of experience in shop activities and was a natural choice for leading construction efforts. These efforts included not only the production of the aircraft, but also the design and assembly of test apparatus, test pieces, and experimental assemblies. Few team members had any experience in shop activities, and the requirement of orienting inexperienced team members in building techniques and shop safety were additional responsibilities which Graham assumed.

The second team leader, Santiago Balestrini, was very proficient with programming, systems analysis, and advanced design methods. Santiago ensured that design and analysis methods were applied correctly. His primary activities were writing and integrating code, debugging others' code, and interpreting results. He also educated other members in complex material, and consulted as necessary with professors and research engineers to validate design analysis decisions.

The third team leader, Benjamin Poole, was the project coordinator. Although not a previous DBF member, his experience and good engineering intuition ensured that the best ideas were pursued and poor ideas eliminated in a timely manner. Benjamin was also diligent about screening design work for its application to the DBF project. He rapidly obtained a thorough grasp of the design project and was quick to identify when a traditional aerospace design practice was not applicable to the design of light UAVs. Benjamin was also responsible for schedule control: coordinating the timing of projects such that full synthesis could happen seamlessly.

PERSONNEL AND THEIR AREAS OF ASSIGNMENT

During the early stages of the project work all nineteen team members met together to brainstorm ideas. For Conceptual Design, experience was as valuable as fresh minds, because problems with "new" ideas were often raised that newer members had not considered. The early development period was used as a time to explore the implications of the rules and identify the implied constraints on configuration necessary for conformity to design requirements. The early design development period also set the pace of progress for individual work in later phases. While most students were studying the problem of configuration selection, a few were working on contest rule-driven sensitivity studies to identify which mission selection choices and performance metrics were most influential to final score.

Movement through the design process meant a dispersion of the team members from one large group to small groups and individuals. The need for coordination among efforts was facilitated by weekly status meetings conducted with one of Georgia Tech ASDL's research engineers, Adam Broughton. At these meetings, students gave updates on progress, discussed future developments, and received suggestions from Mr. Broughton. Progress made in the smaller groups and by individuals was continuously reviewed each day by the team leadership, creating a truly cohesive atmosphere and promoting the "team" environment needed for success.

The Georgia Tech DBF team web site facilitated communication between students and can be found at www.dbf.gatech.edu. The site provided a means for outside correspondence and also featured a private discussion forum. Full contact information, including phone numbers, e-mail addresses, and web-based messaging handles were provided so students could quickly communicate with each other. Other features of the web site included postings of special announcements, work schedules, progress updates, and links to information on previous Georgia Tech DBF entries.

Individual work groups were continuously changing as the project developed. As mentioned, all personnel were involved in brainstorming activities during Conceptual Design. Some of the individual work involved short studies needed to settle engineering disputes about alternative configurations or component arrangements and their relative impact on overall performance. For example, drag coefficient varies largely over a small range in Reynolds number for a cylinder in the flight regime of interest, and is highly sensitive to surface roughness, not to mention three dimensional effects. Two team members spent nearly two months studying these effects while attempting to quantify the drag around the radome and appropriately account for sensitivities in Reynolds Number effects. Other studies included

cost/benefit analysis for fixed and retractable landing gear, canard vs. conventional trim drag estimates (which later developed into multi-lifting surface studies), and studies of the tradeoffs involved with propulsion configuration.

Toward the end of Conceptual Design, efforts were focused on aircraft performance issues and basic aerodynamics. Sizing trade studies involved more analytical preparation than was involved in configuration selection. While one student compiled research on performance measures for light UAVs, three others began exploring design constraints and defining design space.

Shop activities started with the beginning of Conceptual Design and were fast-paced throughout the project. Team management recognized that some team members were more naturally inclined to shop activities than others, and to contribute to the configuration selection, these team members were asked to build full-scale concept models. Later, this group would begin work on an early prototype, and then a second prototype, and a final contest vehicle. There were also wing construction experimentation efforts and the procurement of a propulsion system test apparatus.

Material selection and structural analysis were two other significant areas of study. Three team members were dedicated to this task, and because of their work with developing finite element analysis (FEA) models in CATIA, were asked to draft the final CAD drawings required for this document.

In the later stages of development, two of the senior DBF members began working with some graduate students to draft the MATLAB propulsion model. This project involved writing mathematical models for batteries, motors, propellers, and aircraft performance to validate studies of the design space.

In support of this project, eight other students developed tests and gathered empirical data for the propulsion system components. The gathering of empirical data was one of the most time consuming and laborious tasks the team had to handle. Test equipment had a high failure rate, and consequently many tests had to be run multiple times. However, the benefits of the work were realized as the performance code neared completion and began to accurately predict the sub-system and system performance.

Final performance predictions were made with the use of a flight simulation tool. In order for the tool to be useful, the simulation of the performance of the aircraft had to be accurate. Three team members expended great effort on modeling the final design in the simulation environment and modifying parameters until the simulation gave an accurate representation of vehicle performance. The team pilot then flew the simulation, and the three team members post-processed performance information to generate final estimates of total score.

MILESTONES OF PROGRAM EXECUTION

A *chart of the major milestones* in the Georgia Tech DBF design program is shown in Figure 1 (page 10), illustrating the execution of the team's effort both as originally planned and as actually achieved.

Table 2: Organizational Chart – Personnel and Areas of Assignment

ADVISOR	Adam Broughton					
LEADERS FOCUS AREA	Graham Clark *Construction*		Santiago Balestrini *Analysis*		Benjamin Poole *Management*	
CONCEPTUAL DESIGN	*Historical Studies*	C Shaffer	*Sensitivity Analysis*	D Cooksey	*IPPD Process*	Z Zurita
		R Haynes		L Garza		C Ong
		E Matthews		B Wisler		R McGehee
		N Calvo	*Drag Studies*	D Cooksey		B Searcy
	Conceptual Mock-ups	L Garza		L Garza		B Crowell
		R Haynes		Z Zurita	*Alternate Method*	J Oubre
		R Reese		J Kinzer		A Anupkumpar
PRELIMINARY DESIGN	*Propulsion Testing*	E Matthews	*Propulsion Modeling*	B Wiesler	*Performance Estimation*	C Ong
		N Calvo		B Searcy		Z Zurita
		Z Zurita		A Anupkumpar		B Searcy
	Prototype Development	R Reese	*T/W vs Wing Loading*	D Cooksey		R Haynes
		Z Zurita		L Garza	*Structural Studies*	C Ong
		B Searcy		R McGehee		R Haynes
		E Matthews		R Reese		N Calvo
		C Shaffer	*Stability Estimation*	A Anupkumpar		B Searcy
				Z Zurita		
DETAIL DESIGN	*Aircraft Production*	Z Zurita	*Systems Optimization*	B Weisler	*Report Writing*	C Ong
		B Searcy		A Anupkumpar		D Cooksey
		R Reese		Z Zurita		B Crowell
		D Cooksey	*Flight Simulation*	A Anupkumpar		R McGehee
		J Kinzer		B Searcy	*CAD*	B Wisler
		J Oubre	*Installed Components*	N Calvo		C Ong
	Misc Components	Jay Kinzer		B Crowell		R Haynes
		B Searcy		J Kinzer		N Calvo
		D Cooksey		E Matthews		C Shaffer
		E Matthews		L Garza		B Searcy
		R Reese		C Ong		
FLIGHT TESTING	*Replacement Components*	R Reese	*Data Processing*	R McGehee	*Data Acquisition*	J Kinzer
		B Searcy		C Ong		N Calvo
		J Kinzer		D Cooksey		R Reese
		E Matthews		L Garza		

Personnel Key
Name/AIAA #/Year
Anupkum A, 223071, So
Balestrini S, 209511, Sr
Calvo N, 227669, So
Clark G, 210750, Sr
Cooksey D, 223103, So
Crowell B, 221792, So
Garza L, 221937, Jr
Haynes R, 223183, Fr
Kinzer J, 227305, So
Matthews E, 227353, So
McGehee R, 223931, So
Ong C, 223611, Fr
Oubre J, 227364, So
Poole B, 223182, Sr
Reese R, 205225, Sr
Searcy B, 223178, So
Shaffer C, 223656, Jr
Wisler B, 221799, Fr

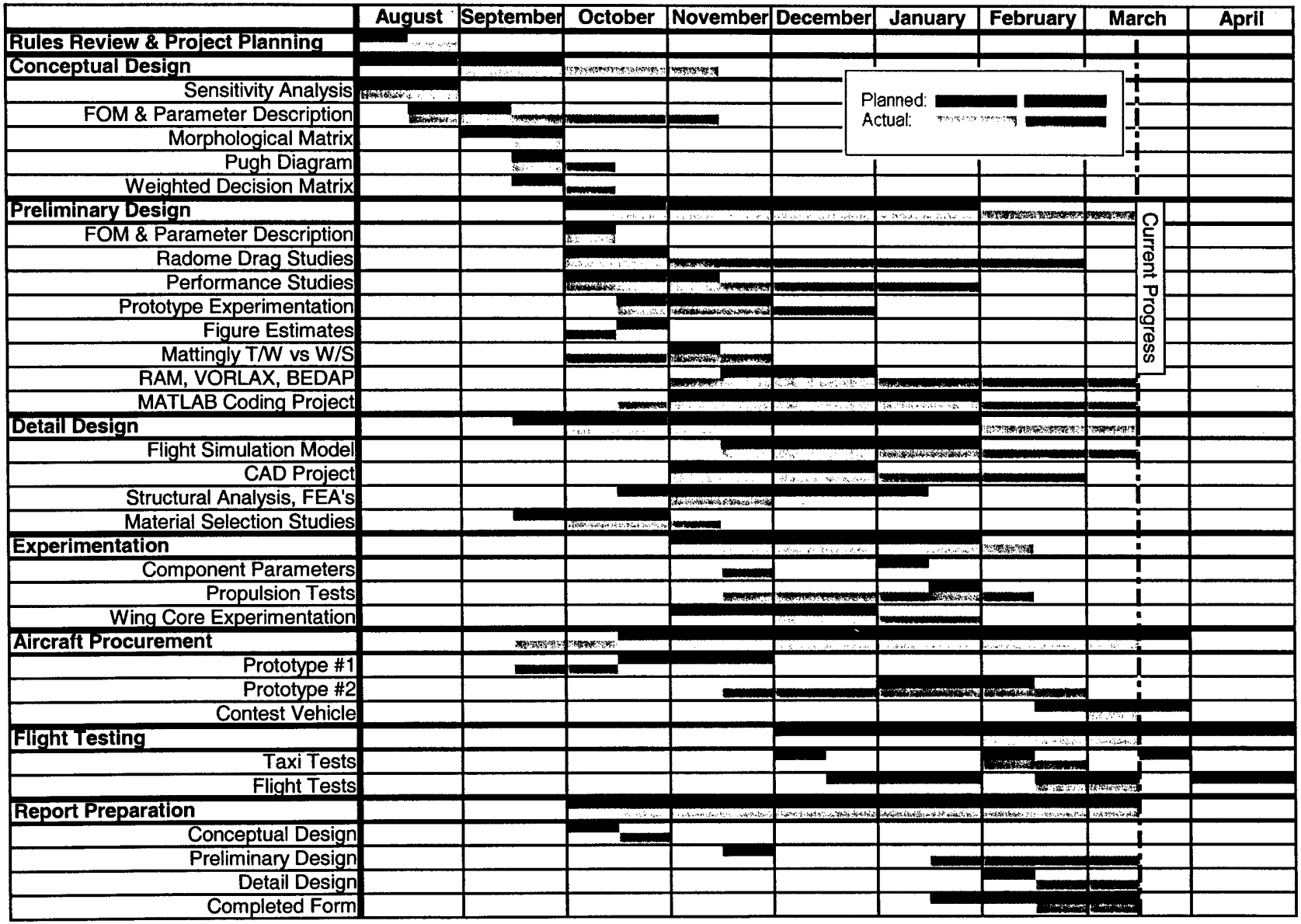

Figure 1: Design Milestones

The team decided "Conceptual Design" was synonymous with "configuration selection." The team goal in this phase was to select the most appropriate configuration for the given set of mission criteria. This configuration selection included specification of relative orientation of the payload, the flying surfaces, the landing gear, and the propulsion system. Each arrangement of these four components had implications relating to mechanical function, structural integrity, and aerodynamic performance. The most appropriate arrangement would be the one that fit inside the 1x2x4 foot container box, was able to carry the radome and the payload box could reliably deploy the payload box, and minimized mission times at low RAC.

PROBLEM STATEMENT AND KEY MISSION REQUIREMENTS

The RFP defined three missions and specified that two would be scored during the flight demonstration portion of the contest. These missions were called Mission "A", Mission "B", and Mission "C". The key elements of Mission "A" were that the aircraft would carry an unfaired 3 inch piece of PVC tubing, 6 inches in diameter, standing 3 inches away from the aircraft, and a box 6x6x12 inches weighing 5lbs balancing about its centroid. The team interpreted the rules to mean that the PVC tubing, or "radome," would be mounted on the aircraft with its circumference in the same plane as the horizontal and lateral axes of the aircraft. The aircraft would need to have all wheels off the ground in less than 120 feet from the start of ground roll. Five hundred feet away from its initial starting point, the aircraft would turn 180°. A 360° turn in the opposite direction would be initiated anytime after the completion of the 180° turn. At 1000ft from the point where the first 180° turn was initiated, the aircraft would then complete another 180° turn and fly to the starting point to complete one lap. In all, four laps would be completed before the aircraft would be landed after the last 180° turn. Upon landing, the aircraft would come to a complete stop some (small) distance beyond the starting line.

Mission "B" was interpreted as the same pattern as Mission "A", but the aircraft would not carry the radome or radome mount; it would land after two laps, come to a complete stop, self-deploy the payload box, and take off again to finish the remaining two laps unloaded.

Mission "C" was interpreted as the same pattern as Mission "A", but the aircraft would not carry the radome or radome mount and would complete three 360° turns on each "downwind" leg of the flight pattern.

In addition to the above flight performance requirements, the aircraft had to be capable of being packaged into a 1x2x4 foot container box and assembled in the minimum time to flight-ready status.

SCREENING METHODS

Configuration Selection Overview

Unlike previous DBF competitions, the nature of the 2002-2003 contest seasons requires greater attention to the configuration of the aircraft. The choice among missions had implications on which configurations were most appealing. For example, missions not including the simulated antenna (radome) would favor designs not requiring as much longitudinal stability, such as a flying wing. Missions which did

not require the deployment of the simulated avionics package (payload box) favored designs with fixed spring landing gear or one-piece wings. The fact that two of these missions had to be flown complicated decisions about an overall optimal configuration. It was found from the statistical analysis that attempting a higher difficulty factor would produce higher scores for the similar aircraft performance, but the variability in total score would be much greater.

Discussion such as this lead to the generation of a long list the major design considerations about the aircraft as they related to the contest rules. As the rules were discussed, similar design considerations were compiled into groups, forming a smaller and smaller list. The final list of five categories was called the Figures of Merit (FOMs) for Conceptual Design, and these FOMs were weighted on how important they were to maximizing total score.

Then a morphological matrix of feasible configurations was screened to eliminate configurations that had too many unfavorable characteristics as weighted by the FOMs. This process was documented in the "Pugh Diagram." The remaining configurations were investigated in more detail and scored, again by the FOMs, and ranked in order of their corresponding score. This process was documented as the "Weighted Decision Matrix." It will be shown that the highest scoring configuration was a mid-wing (see page 20), conventional tail, tractor fan, with retractable tricycle landing gear. This is the configuration that the team chose to carry into Preliminary Design for sizing and performance studies.

Mission Analysis

One of the very first studies conducted for selecting the aircraft configuration was a study of the impact of the components of the contest rules on total score. This study involved both a mission performance profile and a RAC sensitivity analysis. A generic contest entry was modeled using Rated Aircraft Cost (RAC) and this model was used to analyze the sensitivity of design components to total score. A generic mission model was used to generate statistics on the predictability of total score based on aircraft performance.

The mission performance profile is based on a catalog of times for each performance maneuver that the aircraft must do to complete a mission. These performance maneuvers were the takeoff ground roll, climb (1/2 leg), cruise (1 leg), turn 180°, descent (1/2 leg), and land to full stop. Since dynamic effects could not be captured at this early stage of analysis, the cruise velocity was used as an indicator of total aircraft performance. For example, if cruise velocity was set at 65 mph, the takeoff ground roll was 2.5 seconds, climb was 8.0 seconds, and so on. Performance degradation for carrying the payload box and both the payload box and radome were also variable inputs to the mission model. Initially, these numbers were set at 15 and 20 percent worse than without such payload. Also included was an estimate of the assembly task time and penalties for incomplete laps. Generic estimates for written report score (WRS) and RAC were included to capture the relative impact of the flight score on total score.

The mission model calculates total score by using the cataloged times for flight maneuvers in three possible combinations of missions. These combinations were missions "A" and "B", "A" and "C", or "B" and "C"; represented by AB, AC, and BC respectively. The team used a Monte Carlo Simulation to assign

a variable range to the assembly task, cruise speed, headwind speed, and the two increments of performance degradation. A Monte Carlo Simulation statistically simulates a system by using probability distributions for unknown variables as opposed to discrete values. Random number generators, created through Crystal Ball (an after-market addition to MS Excel) ran 100,000 cases at the 95% confidence level for values under each probability distribution and generated the score distributions shown in Figure 2 (page 14).

From Figure 2, flying mission combination AB will yield, on average, total score of 7.06. Correspondingly, mission combinations AC and BC yield scores of 5.99 and 5.01 respectively.

Quantitatively, the 25th percentile lies at 6.67 for combination AB, meaning that there is a 25% chance of obtaining a score of 6.67 or worse with that combination. However, the 90th percentile for combination AC lies at about the same point: 6.69. This means that there is a 90% chance of scoring 6.69 or worse with combination AC. The combination for BC yields even lower scores than AC. Although there is a higher level of uncertainty associated with choosing to fly "A" and "B" (variance of 0.40 versus 0.29 and 0.20) the distribution is not spread enough to merit consideration for flying another combination unless complications associated with carrying the radome could be identified. These complications were equated to the difficulty factors associated with each mission.

In order to validate the assumption that the mission model accurately predicts the choice to fly missions "A" and "B" (and carry the radome), the team raised the degradation in performance to extreme levels. This exercise would indicate whether complications associated with carrying the radome were a determining factor over the difficulty level associated with each mission. Carrying the payload box was set to 60% worse performance over empty, and carrying the box and radome was set at 90% worse than empty. Results confirmed suspicions. In fact, combination AB was on average 27% higher than the other two combinations. For configuration selection, the implications were that the aircraft would be required not only to carry the radome, but also necessitated the capability to deploy the internal payload box. Any configuration not favoring these capabilities was eliminated.

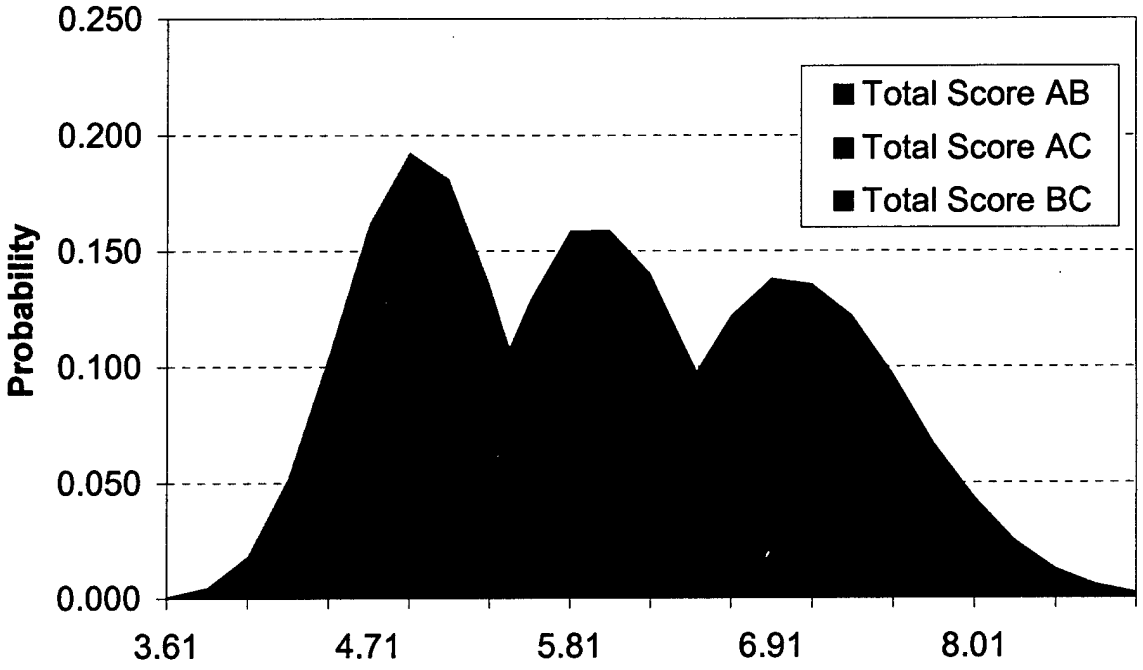

Figure 2: Rated Aircraft Cost Frequency Comparison

RAC Sensitivity Analysis

Some of the team members were familiar with the Pareto Principle, which is the principle that only a few factors are truly influential to the response of a complex system of variables. For configuration selection, the team was interested in the parameters (or variables) influencing RAC that were most influential on total score. For this screening test, the team developed a designed experiment (using DoE methodology) to vary the twelve input factors for RAC. The DoE reduced the number of possible combinations of input parameters to a much smaller (executable) set that should still indicate the response of the system. The response of RAC score to these parameters was specified from the contest rules, and the team modeled these calculations in a MS Excel spreadsheet. Instead of specifying specific values to the inputs of the RAC worksheet, the team assigned ranges to each variable (as listed below in Table 3) in combinations as defined in the DoE experimental design.

Table 3: Design Of Experiments Parameter Ranges

INPUT	#	LOW	HIGH
Empty Weight	1	10	18
# Motors	2	1	2
Battery Weight	3	2	5
Wing Span	4	2	10
Wing Chord	5	0.2	2
# Control Surfaces	6	2	7

INPUT *(CONTINUED)*	#	LOW	HIGH
Maximum Body Length	7	3	5
V Surfaces, No Active Control	8	0	2
V Surfaces, Active Control	9	0	2
Surfaces < 25% Wing-Span	10	0	2
Servos/Motor Controllers	11	3	10
# Propellers/Fans	12	1	2

Using the statistical analysis tool JMP, the team ran the DoE and computed the prediction profile for the twelve input variables. This profile is given in Figure 3 (page 15) and shows by the slope of the lines

that battery weight is by far the factor most "sensitive" to the overall RAC. None of the other factors, with the possible exception of the number of motors or wingspan, showed significant influence over any of the others. The red horizontal line in the figure indicates the overall level for the numbers shown, and the vertical red lines indicate the current condition. By moving these lines in JMP, the team could see the how relative sensitivities changed according to both individual parameters and parameter interaction effects.

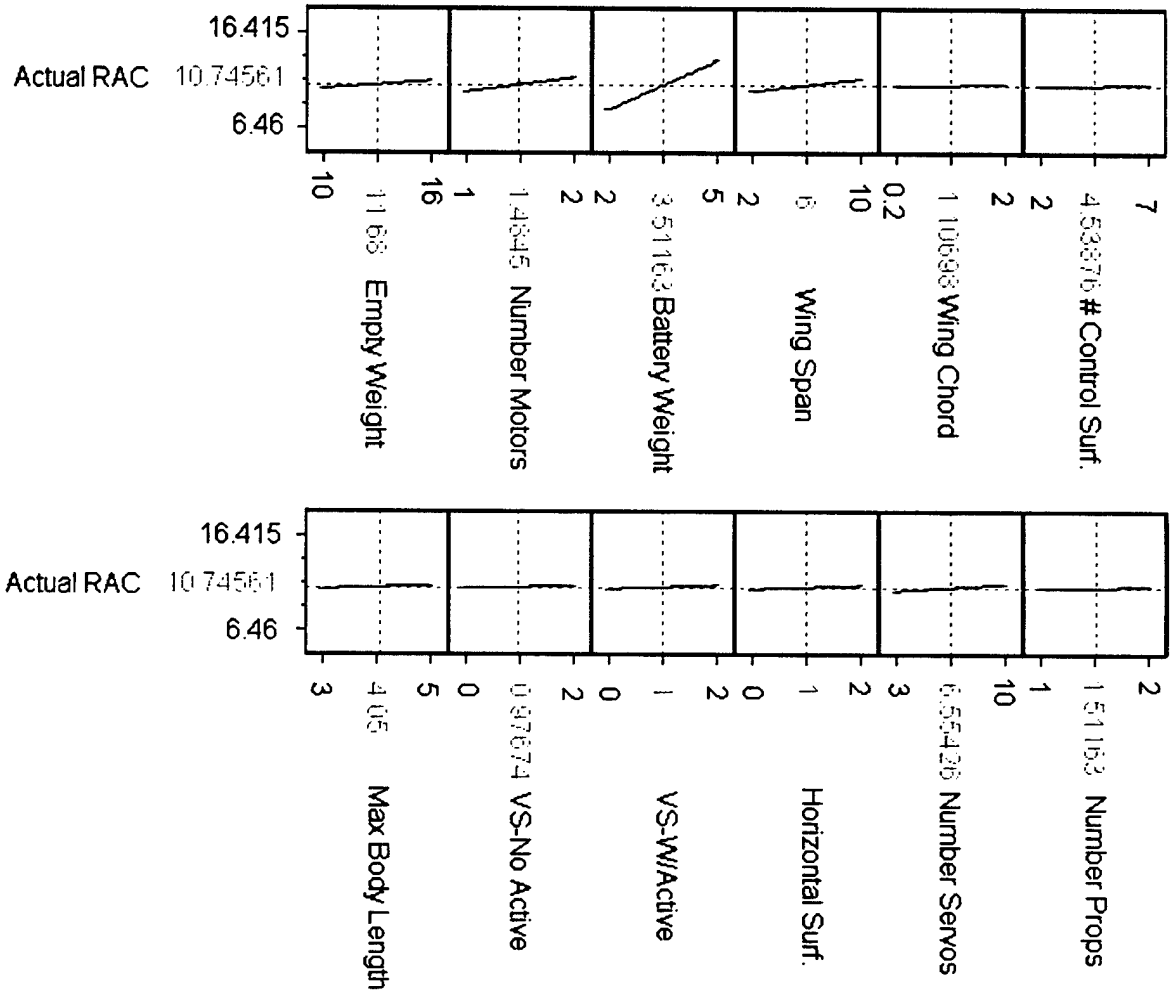

Figure 3: Prediction Profiler For Rated Aircraft Costs

Interpreting the results of the JMP file output, the team identified that the RAC favors wings of square planform rather than of rectangular planform. The same cost has been associated with the span as has been with the chord length, which means the product of the span and the chord, or wing area, is lowest when both are equal. For example, a wing measuring 2x2feet will have a wing area of 4sq. feet and a RAC score of (2x8hr +2x8hr) 32hrs. A wing of 1x4feet, also with a wing area of 4sq. feet, will have a RAC score of (1x8hrs + 4x8hrs) 40hrs. However, stability and control calculations in Preliminary Design showed that higher aspect ratios, although more expensive, were favored over lower aspect ratios.

Figures of Merit

Favorable design considerations were discussed among the group and recorded as design features that would contribute to success. Again by the Pareto principle, these design considerations were grouped into similar categories and scored based upon their contribution to the success of the design. This scored list became the Figures of Merit used to screen competing concepts in Conceptual Design. Table 4 shows the compiled list of the five FOMs as recorded during the team's discussions. The direction of improvement and contributing factors were recorded to consider the design characteristics that positively contributed to each FOM.

Table 4: Figures of Merit

FOM	POLAR / DESCRIPTION	WEIGHT
Speed	**INCREASE by:**	**9**
	DECREASE Frontal Area	
	DECREASE # of Surface Intersections	
	INCREASE Aspect Ratio	
	DECREASE Volume/Wetted Area	
Stability & Control	**INCREASE Stability by:**	**3**
	INCREASE Static Margin	
	INCREASE Size (Time Constants)	
	Improve Gust Response	
	Better Ground Stability	
	DECREASE P-factor	
Assembly Time	**DECREASE by:**	**9**
	DECREASE Complexity	
	INCREASE Design Modularity	
Structural Integrity	**INCREASE by:**	**3**
	INCREASE Material Strength	
	INCREASE Structure Thickness	
	DECREASE Empty Space	
RAC	**DECREASE by:**	**9**
	DECREASE Battery Weight	
	DECREASE # of Servos	
	DECREASE # of Control Surfaces	
	DECREASE # of Motors	
	etc.	

The available weights assigned for each FOM were only a 1, 3, or 9 based on the team's evaluation of their importance, 9 being most important. As opposed to more uniform distributions, these scores were chosen to give greater emphasis on favored FOMs than those which were less favored. The weighting exercise would later be used to score competing concepts.

"Speed" was given the highest weight of 9 because it directly related to total flight score. "Stability and Control" were important for overall mission success but (as long as generally acceptable) not directly related to maximizing total score. The team recognized that these aircraft have the luxury of programmable control inputs, channel mixing, and piezoelectric stability augmentation devices that their larger counterparts generally do not have. "Stability and Control" was therefore given a 3.

From the sensitivity analysis, the Timed Assembly Task did not seem to have a great effect on total score. Although there was the freedom to have longer assembly times without significant penalty, the team felt as though good engineering could reduce assembly times to just a few seconds and wanted to emphasize the opportunity for speed of assembly. Because the team was confident that a fast assembly time could be achieved, the "Timed Assembly Task" FOM was given a weight of 9.

"Structural Integrity" described the overall robustness of the design, and the team wanted to emphasize synergy and simplicity as much as possible. Again, because the FOM was favorable but did not directly result in increasing total score, this category was given a weight of 3. The last category seen in Table 4 is "RAC." This FOM is probably the most influential to configuration selection and also directly relates to total score. It was therefore also given a weight of 9.

ALTERNATIVE CONCEPTS INVESTIGATED

Configuration Discussion

The fact that the aircraft had to carry a large object three inches away from any aircraft member posed serious questions about aircraft stability. It was fairly clear from the rules that the radome had to be well away from the CG of the aircraft. At best, the centerline of the drag from the radome would be approximately 4.5 inches from the CG of the aircraft. It was likely that this measurement would be much larger. It was also anticipated that the aircraft would be designed to be as fast as possible, because higher flight times reduce total score. This meant that the pitching moment caused by the displaced radome would be a significant factor in evaluating candidate configurations. Understanding the magnitude of this pitching moment was recognized as a very important design consideration, and two students began to investigate the issue in detail.

The other payload component, the payload box, had to deploy from the aircraft somehow. This created wing placement problems in addition to trying to define the manner in which the payload should be deployed. Also of concern was the size of payload. Its size and shape did not lend itself to slim aerodynamic profiles under 48 inches in length. If oriented laterally, airfoil fuselage shapes started at about a 13% fineness ratio and became larger when components were rearranged. If oriented longitudinally, airfoil fuselage shapes began at about a 20% fineness ratio.

Although not explicitly forbidden as it had been in previous years, it was assumed that the payload box would be fully enclosed by the fuselage shape. Streamlining, important to obtain higher speeds, proved a difficult challenge for configuration decisions. Some team members supported the idea that an airfoil shaped fuselage with transverse payload box would provide good lifting effects in addition to fully streamlining the payload in a vehicle configuration which required no assembly. This configuration was given serious thought as a potential candidate. Eventually it was abandoned because of uncertainty in stability and control analysis, its large front profile area, and large wetted area.

Arguments about the type and orientation of landing gear directly correlated with discussions about payload deployment. The team favored the idea of dropping the payload box directly beneath the airplane. This meant that carry through structure for the wing or spring landing gear was not permitted. If

strut-type gear were going to be used, retracting them to reduce drag was a natural consideration. Tail-dragger configurations, although potentially lighter weight than tricycle, required extremely long main gear in order for the rear of the box to clear the bottom of the aircraft (assuming a 48 inch fuselage). The team also did not like the idea of the tail of the aircraft ramping up over the box when driving away.

Decisions about empennage did not make compelling arguments for discrimination between overall aircraft configurations unless a no-assembly design (with wings oriented with the long dimension of the container box) was selected. This option had previously been excluded (as discussed earlier) due to fairing issues for the payload box (a flying wing with lengthwise payload box orientation) or excessive forward profile/wetted areas (with transverse payload box).

The team generally agreed that the chosen tail configuration should favor a low RAC and give adequate control of the lifting plane. Before the rules about radome fairing were clarified, the twin boom-mounted tail looked attractive. Empennage of the inverted V-type configuration had a relatively low RAC as long as its projected span did not exceed 25% of the wing span (at which point it would be counted as another wing and incur a cost penalty). Using rough calculations for required wingspan, the team was concerned that the projected horizontal span of the inverted V-type tail would have to exceed 25% of the wingspan in order to give adequate pitching control for takeoff. Other arguments about mounting the empennage included discussions about employing a single long boom that tied into the structure of the wing, payload support system, and propulsion system.

The placement of the engine thrust lines was important for discussions of dynamic flight stability. In general, the team favored configurations that featured synergistic structural arrangements that could easily support the weight of the motor and placed the thrust line close to the CG. Basic motor theory suggested that multiple motors would be less efficient than using a single larger motor to produce the same power. Therefore, the idea of multiple motors was discarded until an analysis could credibly suggest some possible incentive.

Importance was given to the ability to successfully stow the completed aircraft and all its components in the 1x2x4 foot container box. Configurations that called for very large parts needing a high degree of rigidity were discarded due to the necessity of breakdown for storage. The V-tail configuration presented this problem. In addition, configurations that would allow components to simply "plug in" were favored. Preliminary calculations showed that a fuselage length of 48 inches would allow sufficient tail surface control authority. A single piece fuselage with detachable wings was therefore considered the primary candidate.

Other major discussions about aircraft configuration included discussions about multiple lifting planes and tailless aircraft. The canard configuration was abandoned because of arguments about inherent stability. Biplanes were also discarded early because the additional wing was considered unnecessary for the payload and turn-rates the RFP mission required and the extra wing increased RAC. The flying wing, although potentially favoring a low assembly time, was suspected to be relatively difficult to design or even fundamentally have inadequate pitch / yaw stability and control.

Previously Successful DBF Designs

Other sources for configuration decisions came from a study of the previous DBF contest entries. Several consistencies were identified, but due to the large changes in RFP from year to year, specific detail design ideas were inconclusive. The most overwhelming trend identified was the success of simplicity and robustness. Notably, canards and ducted fan units have always finished lower than aircraft with a more conventional design. In the previous competition, three of the top four planes were conventional single motor, low-wing, fixed gear, monoplane designs. The exception was the winner, UC.

The 2001-2002 contest season was the first year speed played a major role in the points system. Accordingly, the teams that finished with the fastest times chose higher wing loading; some claiming as much as 100 oz. per square foot. It was noted that higher wing loading proved catastrophic in several cases, causing tip stalls during turns.

Table 5: Past DBF Competition Results

		SCHOOL	PTS.	CONFIGURATION	RULE CHANGES
2002	1ST	U of Calif at San Diego #2	132	Single engine, lifting body, T-tail	No Wingspan Limit, Timed Mission
	2ND	USC	115	Single engine, low wing, T-tail	
	3RD	West Virginia Univ. #2	105	Single engine, low wing	
	4TH	U of Illinois, Champaign	85.9	Single engine, low wing	
2001	1ST	Oklahoma State Univ. #2	4976	Single engine, low wing	Wingspan Limit Increase, No Brushless Motors, Current Limit, Longer Takeoff
	2ND	Cal. Poly SLO	4864	Single engine, low wing	
	3RD	Oklahoma State Univ. #1	4243	Single engine, mid-wing, T-tail	
	4TH	U of Calif at San Diego	3927	Twin engine, low wing, T-tail	
2000	1ST	Utah State Univ.	672	Single engine biplane	Wingspan Limit Reduced, Battery Limit Imposed
	2ND	Oklahoma State Univ. #2	586	Single engine, hi-wing, T-tail	
	3RD	Illinois	522	Twin engine, mid-wing	
	4TH	Georgia Tech	475	Single engine biplane	
1999	1ST	Utah State Univ	9360	Tri-engine, biplane	No Battery Limit, Wingspan Limit (9ft).
	2ND	Oklahoma State Univ	6280	Single engine, low wing	
	3RD	USC	4203	Twin engine, high wing, T-tail	
	4TH	Georgia Tech	3901	Twin eng, high wing, twin boom tail	

Given these observations, the team was convinced that with a conventional design, and reasonable stability and control, the winning aircraft would be determined by the most effective propulsion system. As was demonstrated in the RAC sensitivity analysis conducted in conceptual design, RAC is most sensitive to elements of propulsion, particularly, the size of the propulsion battery pack. Given these compelling factors, the primary focus of the team's research and design for the Preliminary Design phase became optimizing the size of the vehicle with respect to a fully optimized battery, motor, and propeller combination.

IPPD PROCESS

Morphological Matrix

There were concerns that the team could possibly overlook some configurations that would have a competitive advantage over other competing concepts. Seven configuration categories describing the components of the aircraft were identified as most critical to configuration decisions (Table 6). All appropriate morphs of these categories were listed to the right of these categories forming the complete morphological matrix. The development of the Morph Matrix allowed the team to assign general types and locations of aircraft components, rather than biasing specific configurations. For example, *any* wing placement where the wing spar was in the same plane as the payload was called a "mid-wing", and implied a discontinuous spar.

In all, there were 40 options for configurations, and a total of 112,320 possible combinations. Representative candidate combinations were selected by choosing one option from each category; shown in the figure by the circles. Some combinations, such as a flying wing with a conventional tail, did not make sense. Other combinations, such as those of identical design but having different types of empennage, did not have significant differences over similar designs. In short, the team chose only those combinations that were necessary to adequately describe the design space.

Table 6: Morphological Matrix with Sample Configuration Selected

Wing	Low	Mid	High			
# Of Lifting Surfaces	1	2	3			
Wing Shape	Straight	Swept Aft	Swept Forward	Delta	Flying Wing	
Centerline Structure	Single	Double	Blended	None		
Tail Configuration	Conventional	T-tail	Cruciform	H-tail	Triple	V
	Inverted-V	Y	Twin	Boom-Inverted-V	Ring	Canard
Type Landing Gear	Tail-dragger	Tricycle	Unicycle	Skate		
Propeller Placement	Forward	Center-CG	Above-Wing	Aft	Ducted Fan	Tail

Pugh Matrix

The chosen combinations were listed in no particular order with the exception of the first entry. This first entry was the "baseline" configuration used to compare other competing designs. The team chose this configuration for the baseline as it was considered to be a reasonable choice for any light UAV. This configuration calls for a high wing of straight planform, with fixed tricycle gear and a tractor-fan type propulsion system.

Each of the 61 possible configurations was compared to the baseline and scored against it in each of the FOMs as being either better (+), worse (-), or the same/indeterminate (0). Any configuration with three or more negative marks was discarded. A sample excerpt of the Pugh Matrix that the team used is shown in Figure 4.

CONFIGURATION	FIGURES OF MERIT: Speed	Controlability and Stability	Assembly Time	Structural Integrity	Rated Aircraft Cost	Pass/Fail
High-Wing, Straight, Conventional, Fixed, Tricycle, Tractor	0	0	0	0	0	0
Low-Wing, Straight, Conventional, Fixed, Tricycle, Tractor	0	0	0	+	0	+
Low-Wing, Straight, Conventional, Retract, Tricycle, Tractor	+	0	0	+	0	+
Low-Wing, Straight, V-Tail, Fixed, Tricycle, Tractor	0	0	0	+	+	+
Low-Wing, Straight, V-Tail, Retract, Tricycle, Tractor	+	0	0	+	+	+
Low-Wing, Straight, Inv. V-Tail, Fixed, Tricycle, Tractor	0	-	+	+	+	+
Low-Wing, Straight, Inv. V-Tail, Retract, Tricycle, Tractor	+	-	+	+	+	+
Low-Wing, Straight, Twin Boom, Fixed, Tricycle, Tractor	0	0	0	+	-	0
Low-Wing, Straight, Twin Boom, Retract, Tricycle, Tractor	+	0	0	+	-	+
Low-Wing, Straight, Twin Boom I.V-Tail, Fixed, Tricycle, Tractor	0	0	+	+	+	+
Low-Wing, Straight, Twin Boom I.V-Tail, Retract, Tricycle, Tractor	+	0	+	+	+	+
Low-Wing, Swept Aft, Conventional, Fixed, Tricycle, Tractor	-	-	0	+	0	-
Low-Wing, Swept Aft, Conventional, Retract, Tricycle, Tractor	0	-	0	+	0	0
Low-Wing, Swept Aft, V-Tail, Fixed, Tricycle, Tractor	-	-	0	+	+	0
Low-Wing, Swept Aft, V-Tail, Retract, Tricycle, Tractor	0	-	0	+	+	+
Low-Wing, Swept Aft, Inv. V-Tail, Fixed, Tricycle, Tractor	-	-	+	+	+	+
Low-Wing, Swept Aft, Inv. V-Tail, Retract, Tricycle, Tractor	0	-	+	+	+	+
Low-Wing, Swept Aft, Twin Boom, Fixed, Tricycle, Tractor	-	-	0	+	-	-
Low-Wing, Swept Aft, Twin Twin Boom, Retract, Tricycle, Tractor	0	-	0	+	-	-
Low-Wing, Swept Aft, Twin Twin Boom I.V-Tail, Fixed, Tricycle, Tractor	-	-	+	+	+	+
Low-Wing, Swept Aft, Twin Twin Boom I.V-Tail, Retract, Tricycle, Tractor	0	-	+	+	+	+
High-Wing, Straight, Conventional, Fixed, Tricycle, Tractor	0	0	0	0	0	0
High-Wing, Straight, Conventional, Retract, Tricycle, Tractor	+	0	0	0	0	+
High-Wing, Straight, V-Tail, Fixed, Tricycle, Tractor	0	0	0	0	+	+
High-Wing, Straight, V-Tail, Retract, Tricycle, Tractor	+	0	0	0	+	+
High-Wing, Straight, Inv. V-Tail, Fixed, Tricycle, Tractor	0	-	+	0	+	+
High-Wing, Straight, Inv. V-Tail, Retract, Tricycle, Tractor	+	-	+	0	+	+
High-Wing, Straight, Twin Boom, Fixed, Tricycle, Tractor	0	0	0	0	-	-
High-Wing, Straight, Twin Boom, Retract, Tricycle, Tractor	+	0	0	0	-	0
High-Wing, Straight, Twin Boom I.V-Tail, Fixed, Tricycle, Tractor	0	0	+	0	+	+
High-Wing, Straight, Twin Boom I.V-Tail, Retract, Tricycle, Tractor	+	0	+	0	+	+
High-Wing, Straight, Conventional, Fixed, Tricycle, Tractor	-	-	0	0	0	-
High-Wing, Swept Aft, Conventional, Retract, Tricycle, Tractor	0	-	0	0	0	-
High-Wing, Swept Aft, V-Tail, Fixed, Tricycle, Tractor	-	-	0	0	+	-
High-Wing, Swept Aft, V-Tail, Retract, Tricycle, Tractor	0	-	0	0	+	0
High-Wing, Swept Aft, Inv. V-Tail, Fixed, Tricycle, Tractor	-	-	+	0	+	0
High-Wing, Swept Aft, Inv. V-Tail, Retract, Tricycle, Tractor	0	-	+	0	+	+
High-Wing, Swept Aft, Twin Boom, Fixed, Tricycle, Tractor	-	-	0	0	-	-
High-Wing, Swept Aft, Twin Boom, Retract, Tricycle, Tractor	0	-	0	0	-	-
High-Wing, Swept Aft, Twin Boom I.V-Tail, Fixed, Tricycle, Tractor	-	-	+	0	+	0
High-Wing, Swept Aft, Twin Boom I.V-Tail, Retract, Tricycle, Tractor	0	-	+	0	+	+
Mid-Wing, Straight, Conventional, Fixed, Tricycle, Tractor	0	0	0	-	0	0

Figure 4: Pugh Evaluation Matrix

Weighted Decision Matrix		Figures of Merit					
		Speed	Controllability & Stability	Assembly Time	Structual Integrety	Rated Aircraft Cost	Total
CONFIGURATIONS	Weights	9	3	9	3	9	
Low-Wing, Straight, Conventional, Retract, Tricycle, Tractor		8	7	7	8	6	234
Low-Wing, Straight, V-Tail, Retract, Tricycle, Tractor		8	5	6	8	7	228
Low-Wing, Straight, Inv. V-Tail, Retract, Tricycle, Tractor		8	2	7	7	7	225
High-Wing, Straight, Inv. V-Tail, Retract, Tricycle, Tractor		8	2	7	5	7	219
Low-Wing, Straight, Twin Boom Inv. V-Tail, Retract, Tricycle, Tractor		5	5	7	8	7	210
Low-Wing, Straight, Twin Boom Inv. V-Tail, Fixed, Tricycle, Tractor		5	5	7	8	7	210
High-Wing, Straight, Twin Boom Inv. V-Tail, Retract, Tricycle, Tractor		6	5	7	5	7	210
High-Wing, Straight, V-Tail, Retract, Tricycle, Tractor		8	5	5	5	7	210
Low-Wing, Straight, V-Tail, Fixed, Tricycle, Tractor		7	5	5	8	7	210
Low-Wing, Straight, Inv. V-Tail, Fixed, Tricycle, Tractor		6	2	7	7	7	207
Low-Wing, Swept Aft,Inv. V-Tail, Retract, Tricycle, Tractor		5	1	7	8	7	198
High-Wing, Swept Aft, Inv. V-Tail, Retract, Tricycle, Tractor		6	1	7	5	7	198
Low-Wing, Swept Aft, Twin Boom Inv. V-Tail, Retract, Tricycle, Tractor		4	2	7	8	7	192
High-Wing, Straight, Twin Boom Inv. V-Tail, Fixed, Tricycle, Tractor		4	5	7	5	7	192
High-Wing, Straight, Conventional, Retract, Tricycle, Tractor		8	5	5	5	5	192
Low-Wing, Straight, Conventional, Fixed, Tricycle, Tractor		7	5	5	8	5	192
Low-Wing, Swept Aft, Inv. V-Tail, Fixed, Tricycle, Tractor		4	1	7	8	7	189
Low-Wing, Swept Aft, Twin Boom Inv. V-Tail, Fixed, Tricycle, Tractor		3	2	7	8	7	183
High-Wing, Straight, Twin Boom Inv. V-Tail,Fixed Tricycle, Tractor		4	2	7	5	7	183
Low-Wing, Swept Aft, V-Tail, Retract, Tricycle, Tractor		5	2	5	8	7	183
High-Wing, Straight, V-Tail, Fixed, Tricycle, Tractor		5	5	5	5	7	183
Low-Wing, Straight, Boom, Retract, Tricycle, Tractor		5	5	5	8	3	156

Figure 5: Weighted Decision Matrix

The judgment used to assign a +, -, or 0 was intentionally superficial. More detailed arguments were made for the configurations which survived the down-select. As before, each of the 68 configurations was evaluated as it pertained to the corresponding FOM, but this time scores ranged from 1 to 10; 1 being the least influential. The scores assigned in each cell were multiplied by the weights assigned earlier to the FOMs. All weighted scores were summed to the right in Figure 5 to give the overall rank of that configuration. For this report, the configurations have been reorganized according to rank.

Alternate Methodology

The process of generating a morphological matrix, Pugh Matrix, and Weighted Decision Matrix works well when the engineering intuition and accumulated program experience of senior engineers ("grey beards") can be employed in the process. Most team members however, did not have the accumulated program or engineering experience to reliably apply sound engineering judgment to the engineering choices with which they were faced. Many team members were facing the design trades and choices they encountered for the first time.

Reviewing the process in detail, the team recognized that the FOMs chosen were done so by qualitative analysis of the contest rules. Weights for the selected FOMs were assigned based upon what the team believed important in the context of the discussion, not from experience or prior training.

Although numerical, these weights were assigned almost exclusively by qualitative analysis. The evaluation of the Pugh matrix and Weighted Decision Matrix were also subject to the same problems, which meant that any bias by the team before the process began would not be filtered out by the process.

Frustrated with the difficulties of implementing the IPPD process, the team formulated a supplementary exercise in order to gain greater insight into evaluation. This new process involved systematic documentation of the necessary decisions as they were understood by the general membership. This process was called the "decision tree" and is shown in Figure 7.

Major design considerations are outlined with a box in the figure. To the side are the primary considerations associated with that decision, and branching from it are the next logical decisions. The first branch occurs with the orientation of the payload box. The options are that it can be oriented with a 6x6inch face forward, or with a 6x12 inch face forward. If the 6x6 inch face is oriented forward, the next major decision is whether or not to have a continuous wing, or in some way go around it. Similar logic follows for the remainder of the figure.

The team was able to seek consultation about the each of the decision blocks shown in the figure. Fortunately, final decisions about the aircraft's configuration validated the previous process. Although there were subtle differences in some details, the basic configuration selected was a mid-wing aircraft with conventional empennage, retractable tricycle landing, and a tractor fan propulsion system. This configuration is shown in Figure 6.

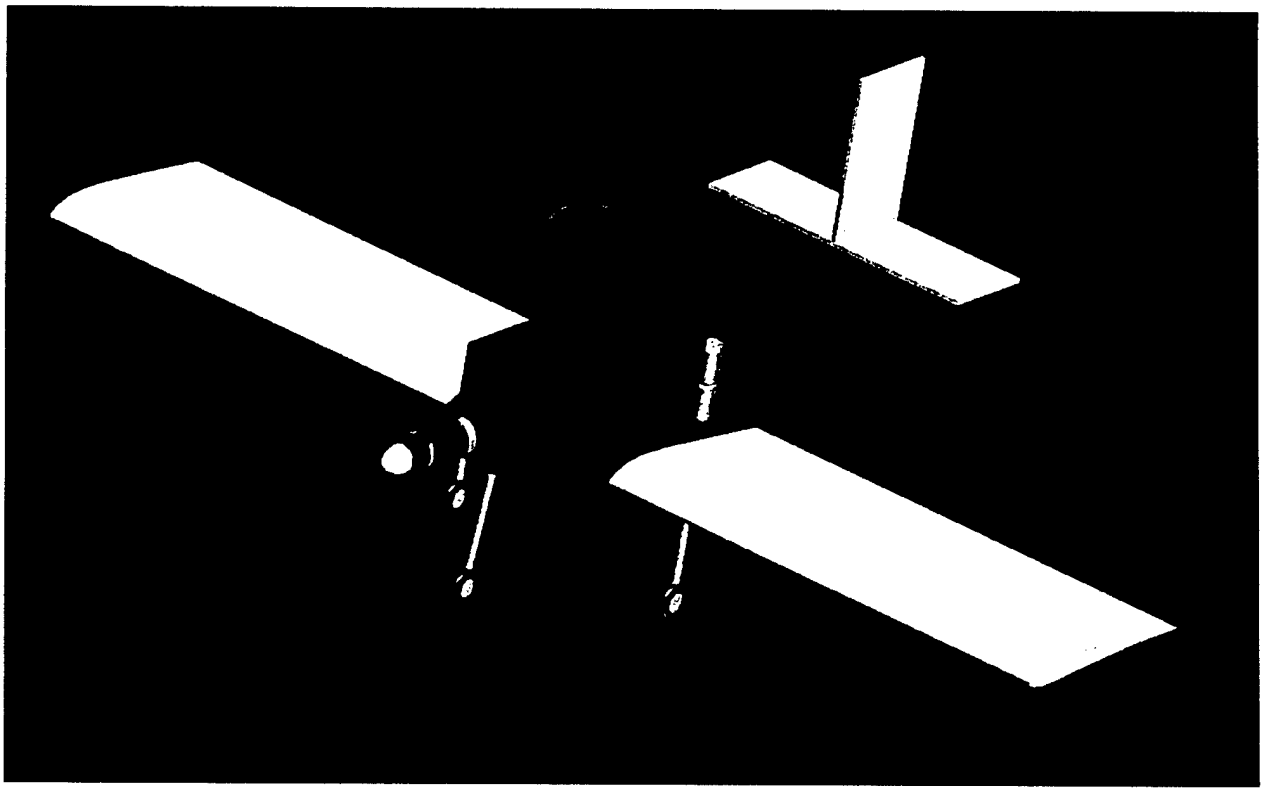

Figure 6: Component / Layout Configuration Selected

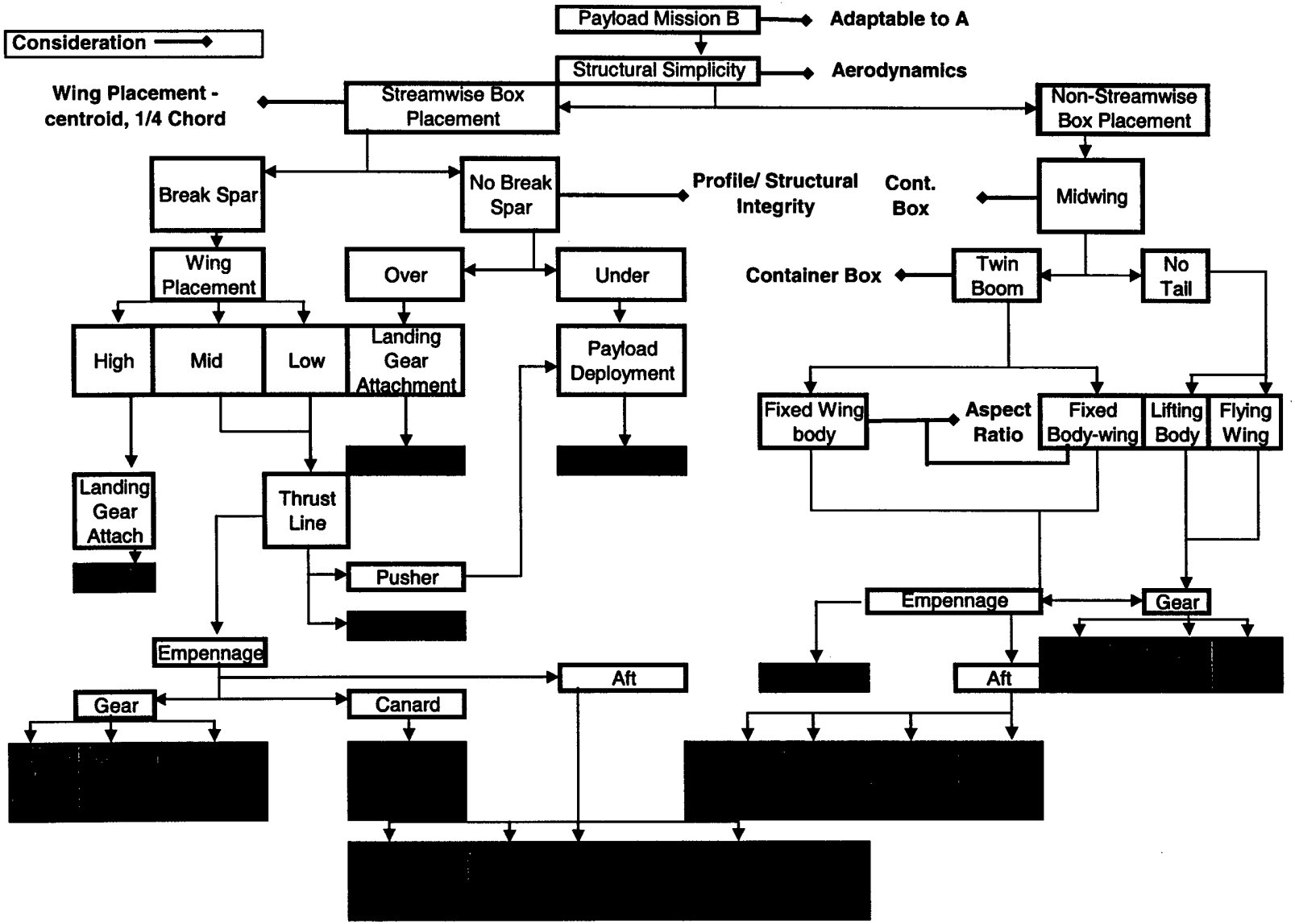

Figure 7: Decision Tree

The configuration selection process in Conceptual Design could not have been done without consideration of the relative size of the vehicle. The configuration chosen was based on preliminary sizing studies that suggested that the overall length of the fuselage could be made less than 48inches to fit inside the container box. This interdependence of aircraft size and overall configuration overlapped Conceptual and Preliminary Design studies. These early sizing studies were intended to give rough estimates of vehicle parameters and did not involve any optimization routines. After selecting the final configuration, the sizing studies were continued in greater detail to develop the optimization routines for the final design parameters of the vehicle. Conclusions before or after the selection of the aircraft configuration that lead to the selection of the final vehicle sizing parameters were the team's interpretation of "Preliminary Design" and are documented here.

MISSION MODEL

The three missions specified in the contest rules were segmented into the various required flight maneuvers. Shown in Figure 8 for Mission "A" and "B," these maneuvers included a takeoff ground roll,

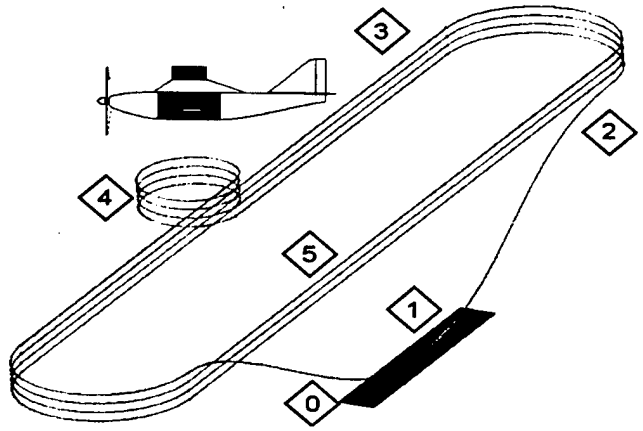

0-1 Takeoff Ground Roll
1-2 Climb
2-3 180ºTurn
3-4 360º Loiter
4-5 Cruise
5-0 Land
6 Deploy Payload, Repeat 0-5

Mission "A"

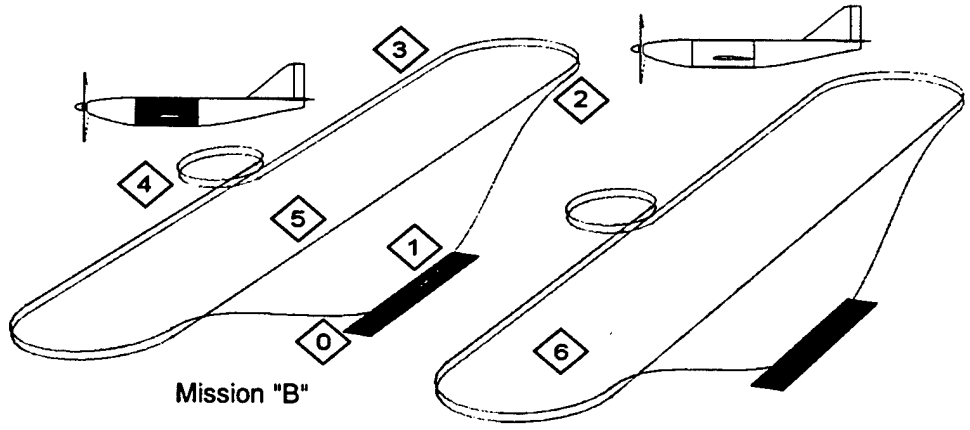

Mission "B"

Figure 8: Selected Mission Profiles

climb, turn, cruise, 360° loiter, and a descent to land. For the analysis conducted in Conceptual Design (page 11) these generic mission segments were compiled to define the individual requirements in Missions "A, B," and "C." This mission analysis told the team that flying Missions "A" and "B" would yield the highest score regardless of the degradation in flight performance due to the excess drag of the radome in Mission "A" or the extra time turning on the downwind legs of Mission "B."

For detailed sizing of the aircraft, this mission model was coded in MATLAB to figure the total score obtained from flying aircraft of various designs. This coded MATLAB model was much more detailed than the MS Excel model, and included a 30 ft. cruise altitude, turn radius of 50 feet, and individual aircraft performance. Performance was calculated every 1/10th of a second to figure the total score obtained for flying a given design on the specified mission.

The mission was modeled a third time in the simulation environment. Here, the team pilot was able to fly the course with the top design candidates, and the team could gather vital statistics on the performance of the aircraft including such high fidelity factors as human error and weather conditions.

ANALYSIS METHODS USED

Early Sizing Studies

The constraint of the design to fit inside the 1x2x4 foot container box was the largest concern of the team during configuration studies. It was not known whether or not a total fuselage under 48inches in length would provide sufficient stability and control for a successful design. It was also not known whether the empennage height would fit inside the payload box. Control volumes could not yet be calculated because the wing design had not yet been determined. To gauge the initial estimates of vehicle size, the team looked at the designs of teams for several previous DBF competitions.

The distribution of scores is given in Figure 9. It can be seen from the figure that only a few teams each year have generated successful scores. Conventionality of design was interesting for Conceptual Design, but for Preliminary Design, the aircraft size was proportional to the payload size and power available. Payload volume was lower and payload weight was slightly smaller for the new RFP than for the top scoring teams from the previous year, yet propulsion system constraints had not changed. Wing loading was over 100 ounces per foot in some cases, but these aircraft had a tendency to stall in turns (where wing loading increases due to centripetal forces). For contestant designs with significantly tapered wings, these stalls frequently resulted in tip-stalls followed by un-recovered spins. Historical wing areas and aircraft weights were estimated to determine that a wing loading of around 60-70 oz/sq. foot was more appropriate for success. Overall fuselage length was scaled for the new RFP to conclude that a fuselage of less than 48 inches was not only feasible, but most likely near optimal. Empennage height was also estimated to be under 12 inches and capable of fitting vertically inside the container box. It was noted that empennage size might have to be overly large to offset the pitching or yawing moments caused by the external radome.

Fuselage Parameters and Trades

The primary parameters for investigating the size of the fuselage were its wetted area and length. Overall size had to be as small as possible to minimize wetted area and other sources of drag, yet large enough to house the internal components. The length of the fuselage was a major determining factor of the overall length of the vehicle (scored in the RAC), and it was desirable to have it as short as possible. The tradeoff was that shorter fuselages would be more difficult to stabilize than longer ones. It was also noted that given the width of the payload box, 6 inches, it would be difficult to streamline the fuselage around the payload if the length was not significantly longer than the width.

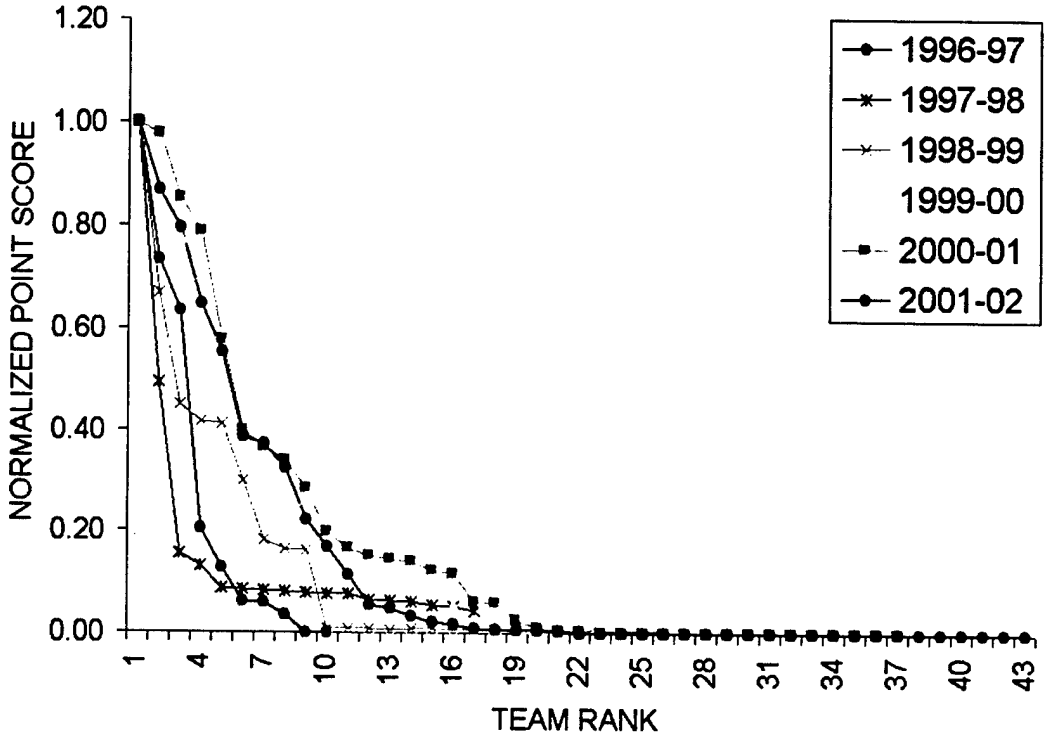

Figure 9: Past Team Rankings as Determined by Normalized Point Scores

The layout of fuselage components was one of the major developments of Conceptual Design. From the mission analyses conducted in Conceptual Design, the team knew that the aircraft would have to be able to deploy the 5lb payload box. This payload weight was a significant part of the gross weight of the vehicle, and it was clear that the payload must be positioned on the quarter chord of the wing such that the CG would not shift after deploying the payload.

The approximate position of the quarter chord of the wing on the fuselage was determined from scaling the proportions of general aviation aircraft (reference Roskam). This distance was approximately 3/4 of the distance from the empennage to the nose of the aircraft. The team favored having longer tail moment arms for stability and control, but the precise location of the quarter chord from the empennage was not yet known.

Other determining factors for placing the quarter chord on the fuselage were the arrangement of the propulsion system, the placement of the landing gear, and the *required* tail moment arm. It was argued that the motor and the propulsion battery would most likely not be placed on the same side of the payload, because both components are significant sources of weight and proper balance would be difficult. It was possible to place the propulsion battery laterally on either side of the payload, but initial estimates of the propulsion system (2.2lbs for AstroFlight Cobalt 90, and 3.3 lbs for propulsion battery) placed the propulsion battery behind the payload box, and the motor well forward of the box.

Probably the most significant argument for the placement of the wing quarter chord on the fuselage originated from discussions about retracting the landing gear. Tricycle retractable landing gear had been selected in Conceptual Design, and the height of the aircraft must be at least six inches to clear the payload once it is deployed. This height meant that the nose leg would be at least six inches long. The team discussed retracting the nose leg obliquely to one side or possibly retracting the gear in a telescoping or scissors-like fashion vertically; neither option was simple or robust. There was even discussion of fixing the nose leg with a fairing or wheel pant and only retracting the main gear. It was decided that the most practical method would be to retract the gear forward and provide enough room inside the nose of the fuselage to contain the gear in it's retracted position. This option allowed the nose leg to remain in one piece and promoted positive locking at touchdown. However, the tradeoff was that the extra room needed to retract the gear forward would push the wing position rearward, and make the tail moment shorter. Later calculations showed that the position of the tail at the rear extreme of the available space would be sufficient for stability and control.

The volume of the fuselage and its corresponding shape were determined from minimizing the wetted area in a streamlined shape around the payload box. The outside limits of the fuselage were set at one quarter inch around all corners of the payload box. The propulsion system was originally placed inline with the estimated vertical height of the CG, but it was later raised for better propeller clearance. The final placement was one inch above the centroid of the payload box. The empennage was set in line with the top of the fuselage (see Figure 10) and the bottom of the fuselage was tapered up to a point two inches below the empennage. Laterally, the fuselage was enhanced by large wing fairings, intended to give volume to the shape for landing gear and sub-systems while reducing interference drag around the wing root. The lateral extremes of the fuselage were set at eighteen inches across to take advantage of the rule on scoring the wing chord at nine inches away from the centerline for blended-wing bodies. The potential for lifting body effects in addition to reducing interference drag were the reasons behind the extremely large wing fairings.

The configuration called for a mid-wing type configuration, but it was understood that the wing would be placed as low as possible to take advantage of ground effect. Knowing that the wing loads would have to be transferred over the top of the fuselage, and favoring a less aggressive taper around the box, the wing was raised two inches up from the bottom of the fuselage to a point much closer to the anticipated aircraft centroid (Figure 10).

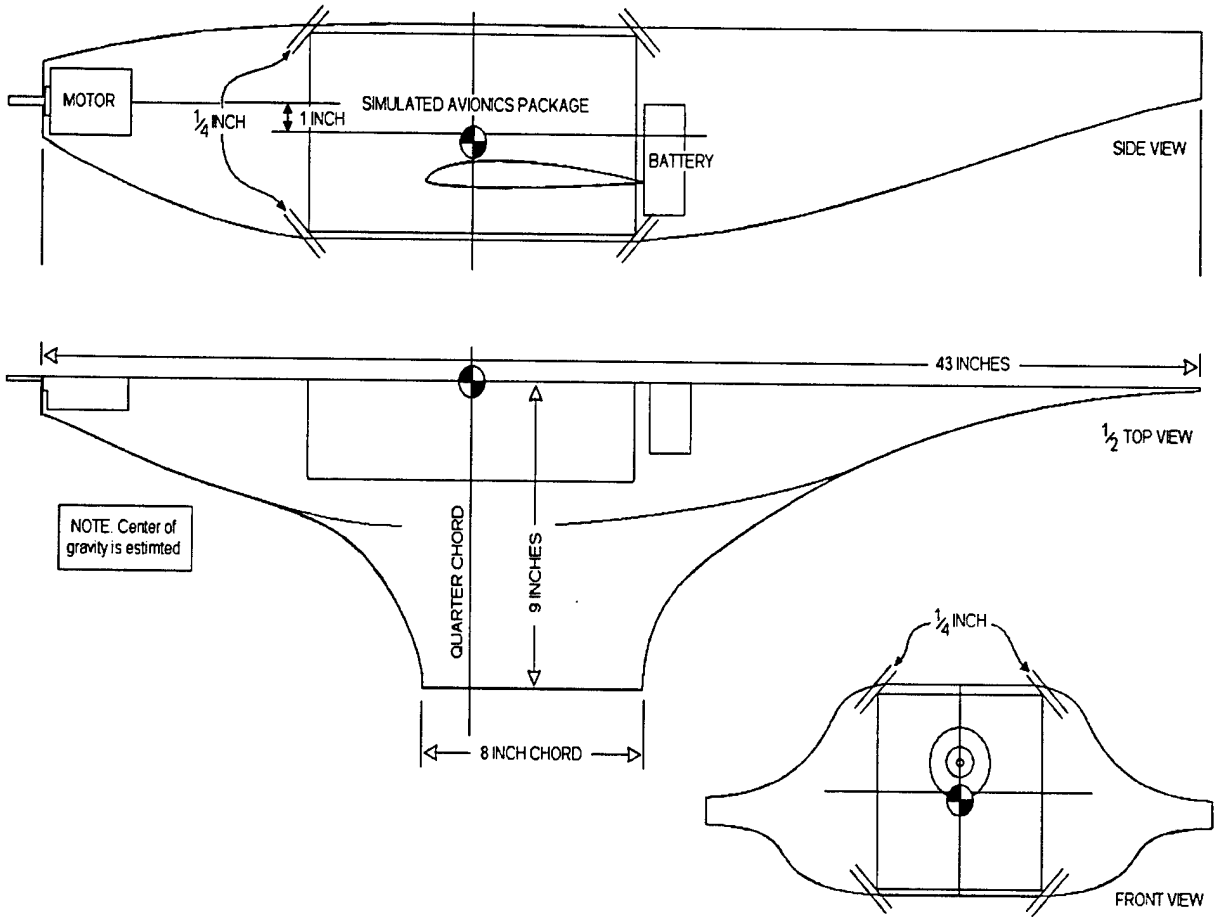

Figure 10: Fuselage Payload Packaging Layout

Propulsion System Parameters and Trades

The primary parameters for sizing the propulsion system were the battery weight, thrust, and overall propulsion system weight. Battery weight, as mentioned in Conceptual Design (page 11) was the single most influential component of calculating RAC. Increasing the number of cells in the pack did not necessarily translate to an increase in battery weight if the capacity of the cells was sacrificed. However, lower capacity meant that power available was lower (per cell) and mission completion became a concern. Increasing the number of cells was also not always favorable, as the total voltage of the battery pack may exceed the operating limits of some candidate motors. Increasing capacity meant better performance over the mission and ensured mission completion but translated into lower voltage potential to drive the motor, and output performance became a concern. In either case, an increase in battery weight due to a poorly designed propulsion system would significantly reduce the total score because of its impact on RAC.

The thrust of the propulsion system required that it accelerate the vehicle to takeoff speeds before it reached the 120 foot-takeoff line. Takeoff performance is enhanced by choosing propellers with lower pitch. However, the tradeoff is a reduction in cruise velocity (because pitch speeds are reached earlier

and prop-efficiency drops rapidly above optimum pitch speed). Larger diameter helps to improve thrust over the speed range of the propeller but increases total power required. Furthermore, the ideal operating conditions of the motor often did not match the ideal operating conditions for the propeller, and tradeoffs would have to be balanced in order to have the entire system optimized. Finally, overall propulsion system weight was an important consideration for reducing takeoff distance and RAC but meant, in some cases, that the power output of the system would be sacrificed. It was clear to the team that the RAC favored propulsion systems that were well designed for takeoff distance and maximum cruise velocity.

Wing Parameters and Trades

The primary sizing parameters for the wing were the wing area, planform shape, and aspect ratio. As discussed in Conceptual Design (page 11), the RAC favored planforms of square design. It was also desirable to have high wing loading for high cruise velocity. Unfortunately, the combination of the two would lead to a very unstable aircraft. Induced drag would be high, roll stability would be very poor, and takeoff distances would be comparatively long. Broadly speaking, simply choosing a design that had the lowest RAC would not optimize the aircraft for maximum performance for the mission. The lowest RAC lifting platforms would not score well in total flight time, and thus total score.

Increasing aspect ratio would reduce induced drag and improve roll stability and takeoff distance. However, there were diminishing returns because of increased skin friction, increased RAC, and structural requirements that increased overall weight for constant wing area. The optimal wing design was chosen by the team from calculations of flight performance and resulting flight score based on the choice of propulsion system.

The team combined flap and aileron functions to reduce the number of required control surfaces. The use of "flapperons" maximizes the benefit of the increased Cl from flap action at a minimal penalty in drag for the entire wing. During flight-testing, programmable mixing was used to slave the flapperons to the elevator for extremely tight turns, further reducing flight times.

Traditional Constraint Analysis

The basis for the initial vehicle sizing analysis was the plot of vehicle thrust-to-weight against wing loading (reference Mattingly), and is given by:

$$\frac{T_{SL}}{W_{TO}} = \frac{\beta}{a}\left\{\frac{qS}{\beta W_{TO}}\left[K_1\left(\frac{n\beta}{q}\frac{W_{TO}}{S}\right)^2 + K_2\left(\frac{n\beta}{q}\frac{W_{TO}}{S}\right) + C_{D_0} + \frac{R}{qS}\right] + \frac{1}{V}\frac{d}{dt}\left(h + \frac{V^2}{2g_0}\right)\right\}$$

where T_{SL}/W_{TO} is the thrust-to-weight ratio, W_{TO}/S is the wing loading, β is the mission segment weight fraction, a is the thrust lapse, K_1 is the induced drag factor, K_2 is the drag offset due to camber, n is the load factor, C_{D0} is the zero-lift drag coefficient, q is the dynamic pressure, R is the additional drag due to flaps or landing gear, h is the altitude, and g_0 is the acceleration at the Earth's surface due to gravity. In this form, this so-called "master equation" can be used to map point-performance constraints on a design plot as a visualization tool for investigation of the design space. These plots could be generated for each of the flight conditions associated with the mission segments shown in Figure 8. Its only requirements are

a generic mission model to determine the weight fractions, a thrust lapse model, a parabolic drag polar, and a flight condition.

This constraint analysis was simplified in a couple of ways for its application to the DBF project. Since the aircraft is not burning fuel, its mission segment weight fraction β will always be equal to 1.0 (except after payload deployment). Furthermore, the drag due to camber, K_2, is typically a very small negative number, so it is often ignored in first order analyses. Therefore, the drag polar and normalized thrust lapse are the only remaining information needed to complete the plots. The thrust lapse was assigned a distribution based on previously gathered empirical data, so a normalization of this equation to the system static thrust is sufficient. A physics based model would have been preferable at this point, but time constraints required a more immediate solution using available information.

The only inputs required for the drag polar are the zero-lift drag coefficient and induced drag factor – both functions of an unknown design. The zero-lift drag was assumed to be approximately 0.03 from past experience, but the team was cautioned that this value was a guess and would need later refinement. The induced drag factor, K_1, was a function of aspect ratio and Oswald efficiency factor, and it was a major component of the calculations. It was desirable for K_1 to be small, but this required higher aspect ratios. Unfortunately, this condition equates to a higher RAC as discussed in Conceptual Design (page 11). Furthermore, the same cost is associated per foot of *maximum* chord and maximum span. This means that the design is charged only for a rectangular planform, and any deviation from that (such as an elliptically shaped wing with an Oswald efficiency of one) would be sacrificing wing area for a better fit to an elliptically shaped wing. These conditions were significant and not captured in the T/W vs W/S plots.

The team was then keyed to the fact that the traditional methods for constraining design space in order to locate the optimal design point may not have been applicable to the DBF project. The only true constraint on the design space was the takeoff condition. Normally, these plots would include constraints for maximum cruise speed, minimum cruise speed, dash speeds, rate of climb, maneuver requirements, or landing requirements. None of these had a true application to this project. This meant that the T/W vs W/S plots favored higher and higher ratios without bound.

Alternative Sizing Method

Sufficiently convinced that the team needed to investigate an alternative to the prescribed design point determination, the team took inventory of critical metrics influencing total score. The team could very accurately predict the weight of a given design from the team's historical documentation. The number of candidate motors, and consequently the combinations for propulsion system components, was also known. Flight performance could be simulated, and given the mission model and RAC, total score could be calculated. By generating representative performance models of the aircraft and its propulsive components, the team could size the aircraft by finding the optimal wing area and aspect ratio that gave the best flight score for each propulsion system combination.

This new process was very attractive to the team because each of the performance models for the components in the system could matched to empirical data. Motor performance, battery performance, and

propeller performance were all modeled in MATLAB code, while test apparatus for these components were being designed and built. Once the empirical data was gathered, the performance models were calibrated to match actual performance. Predicted performance was consistently accurate, and the team felt comfortable about the capabilities for optimization. Later, similar models were created for aircraft performance and compared to data gathered from the prototype's flight data recorder.

THE OPTIMIZATION ROUTINE

The optimization routine for the synthesis of all components was done by the following:

1. A full factorial DoE of the propulsion design space was created and nested "for" loops for motors, propellers, cells (type) and number cells were written in the MATLAB code.
2. Each propulsion combination was then calculated to give a particular amount of static thrust. This thrust was a function of (1) the RPM at which the propeller is spun, and (2) the diameter and pitch of the propeller. The propeller RPM was a function of (1) the voltage input to the motor, (2) the voltage constant of the motor, and (3) the torque required to spin the propeller at that RPM. The voltage supplied to the motor was then a function of the energy available from the battery. The battery performance was a function of the current drawn, which in turn was a function of the torque applied by the motor.
3. The initial weight from propulsion system and airframe weight were estimated. It was agreed at the beginning of Preliminary Design that due to the complex curve for the blend of the fuselage and the wing, the shell of the aircraft would have to be made of fiberglass with carbon fiber reinforcements. This construction was extrapolated from the wing construction database for accurate weight estimations.
4. The T/W ratio was determined using the aircraft weight estimate and the thrust for that given configuration. For the 90^{th} percentile, the T/W vs. W/S takeoff slope (the inverse of thrust loading) would have to be 0.148 square feet per pound. The wing loading and estimated weight yielded a wing surface. This information was used to recalculate the weight fraction for wing panels from the average of the estimates for the top three wing construction candidates (again, referring to the database). This weight was added to the one found in step 2. This process was iterated until the two gave a area per unit thrust of .148. An empirical zero-lift drag calculation as a function of wing area was used to estimate the drag for each configuration (since the wing area was now known).
5. With that wing area and thrust, the aspect ratio of the design was varied to observe which aspect ratio yielded the maximum score. AR had the following effects: (1)reduced induced drag (C_{Di}) increasing cruise speed and therefore reducing flight time and (2) increased maximum score but, at the same time, increased RAC. This yielded an optimum aspect ratio for each propulsion combination. The average AR was around 7 with a standard deviation of 0.43.
6. Running steps 1 through 5 produced a total score for all possible propulsion systems. A script was written to identify the top scoring configurations. The complete sizing iteration then only required definition of the empennage and landing gear.

Empennage Sizing and Trades

The detailed definition of the tail geometry was derived from the empennage sizing methods outlined in (reference Roskam). At the time of detailed geometry definition, the following had been fixed: fuselage geometry; CG placement; wing placement; and wing geometry. Smaller tails were favored over larger ones for reducing drag. The tradeoff was a reduction in control authority. Tail volume coefficients were chosen to be similar to those found on fighter aircraft. For the horizontal tail, the tail volume coefficient was 0.54 (fighter is 0.6) and the vertical tail was 0.68 (fighter 0.7). The height of the tail had to be slightly reduced in order to fit easily in the container box. The horizontal tail was proportionally reduced to match.

Landing Gear Sizing and Trades

Typical tricycle landing gear installations call for placement of the mains at 15° away from the vertical plane passing laterally through the CG. However, because of the 120 foot-takeoff constraint, the main gear was placed 7° away from the CG in order to make the aircraft rotate with lighter empennage forces. A common distribution of load is 80% of aircraft total weight on the main gear, and 20% on the nose gear. The new distribution made the proportion of weight 91% on the mains and 9% on the nose gear. Some ground handling stability was sacrificed, but flight-testing proved that the condition was acceptable for an airplane that was intended to only fly only one weekend.

After the placement of the wing and the design of the wing fairings, there was not much room for the gear inside the fuselage when retracted. When placed closer to the root of the wing panel, there was insufficient room to mount the bulky retract unit. At the other extreme, near the payload box, there was insufficient room for the wheel at the trailing edge of the fairing.

The team had not fully decided on the exact placement of the gear until the fuselage of the second prototype was ready for component installation. With the components in hand, it was clear that if the gear were placed such that they pointed inboard when retracted, that the wheel would have to be slightly rotated and coincidentally fit the curvature of the inside of the fairing. Because of this angle, the gear point slightly outward when deployed (see 3-views). Although not part of the intended design, it was noted that this angle would help reduce side-loads when touching down slightly rolled to one side. It also widened the stance of the aircraft and helped ground handling. Later taxi tests showed that the plane had a slight tendency to tip when turned too sharply and at too high speed. It was suspected that this tendency would be much worse had the gear been placed vertically. On the final design, this angle was increased to 12° to enhance ground handling while maintaining the retracted rake.

PREDICTED MISSION PERFORMANCE

The final performance predictions for the vehicle are as follows: Mission "A" will be completed in just under four minutes, RAC will be 6.75, and total mission score will be 0.612. The aircraft will cruise at 48.3 MPH, stall speed will be approximately 33.4 MPH, and takeoff distance will be 117 feet with a Mejzlik 16x10 inch propeller, Graupner 930-6 motor geared 3.7:1, and on 14 cells of Sanyo 2400 SCRs. Aircraft gross weight will be 13.2 lbs and the maximum Cl will be 1.30, giving a maximum L/D of 10.4 and a maximum rate of climb of 6 ft/sec.

For Mission "B" the radome and radome mount will be removed, lowering the takeoff weight to 12.2 lbs for the first part of the mission. Takeoff distance will be 103 ft, maximum cruise will be 57.3 MPH, and maximum rate of climb will be approximately 7 ft/sec. After deploying the payload, the weight drops to 7.2 lbs, and with the projected remaining battery capacity, the takeoff distance is 36 ft. and the maximum rate of climb will be 12 ft/sec.

The static stability margin, nearly 18% (or equivalently 1.5 inches), suggests that the stability and control characteristics of the vehicle should be favorable. The limit load factor of 6.5 was figured from the design ultimate yield strength of the wing to withstand 10 g's. Minimum turn radius was estimated to be approximately 64 ft for Mission "A," 62 ft for the first segment of Mission "B", and without either radome or payload box, the turn radius was estimated to be 48 feet (assuming coordinated turns). These figures may be enhanced by programmable mixing of the flapperons to the elevator.

Assembly time for the vehicle has been recorded at a low of 3 seconds. Assuming a normalized report score of 100, the projected total score is 14.3. A summary of the final parameters of the vehicle is given in Table 8.

"Detail Design" developed and integrated all elements of aircraft definition necessary for the manufacture of the team's design, such as final analyses, geometry definition, and process definitions (discussed later in the manufacturing section). Higher fidelity estimates of performance metrics, such as estimated mission completion times and their associated confidence intervals were calculated during the detail design phase. Detail design also involved design and refinement of aircraft structural components and specification of the commercially purchased component integration.

Material selection and final definition for manufacturing were performed for the aircraft structures requiring custom fabrication. The commercially purchased components were integrated into the onboard subsystems, which included the mechanical, electrical, electromechanical, and pneumatic systems. The final detailed definition of all aircraft systems resulted from these efforts. As part of the process of Detail Design, engineering drawings were drafted and used to aid the manufacture the final aircraft. Final design parameter definitions are given at the end of this section.

SYSTEMS ARCHITECTURE

The installed components of the final contest entry include not only those basic systems required for flight, but also retractable landing gear, brakes, and payload release mechanisms. Flap action and aileron action have been combined to reduce RAC, enhance performance, and simplify construction.

The elevator servo is installed in the aft section of the fuselage. Both rudder and elevator servos are mounted such that they can be accessed for removal through the payload bay. In the event that either servo fails, it can be replaced quickly and easily without damage to the aircraft. Their proximity to corresponding control surfaces minimizes control linkage length, which reduces the possibility of linkages buckling under load.

Flapperon linkages are also very short. Mounted midway along the length of each wing panel, the flapperon servos not only minimize control linkage length, but also minimize the possibility of the control surface itself twisting under load. It was decided that the aircraft would feature "plug-in" type wings, but it wasn't until the construction of the final contest vehicle that the team solved the problem of how to retain the wing on the spar tube, prevent the wing from rotating on the spar tube, and connect the wing servo. Emphasizing synergy as much as possible, the team found a commercially available, three-conductor plug, about the size of a normal servo plug, which featured positive locking. The male side of the plug is rigidly installed in the wing, and the female side is rigidly installed in the fuselage. From the stowed position, assembly of the aircraft only requires that the wings be pushed in until they click into place. Wing spar tubes extend 6 inches beyond the wing root and fit inside a phenolic wing tube. The commercially available plug was slightly modified to be more self-guiding.

There was a great deal of discussion as to whether or not a rudder was needed, as this is considered a "finesse" item on most model aircraft. It was argued that a simple fin would be sufficient, and that the team could subtract a servo from the Rated Aircraft Cost. The counter argument to eliminating the servo was that the rudder servo only counts 5 hours in Rated Aircraft Cost, and does not have a significant

impact on total score as compared to other components. Furthermore, the aircraft configuration calls for a steerable nose leg, and rudder function could be combined with steering the nose leg such that only one servo was needed to perform both functions. At the time of the report, the rudder servo is installed and currently also being used to steer the nose leg.

For additional turn stability, a piezoelectric gyro was installed inline with the rudder servo. The device had negligible weight impact (.416 oz with servo lead) and there was no penalty in Rated Aircraft Cost for the addition of stability augmentation devices.

The fact that the nose leg retracts forward created some difficulty in connecting the steering linkage. The rudder servo is mounted in the upper rear of the aircraft. Two flexible cables are routed around the payload bay to the front of the aircraft near the motor. These cables then turn 180° back toward the nose strut control horns. When in the "down" position, the cables are tight and give accurate steering control of the aircraft. When retracted, the cables go limp and allow the strut to fold up into the fuselage

The gear retract mechanisms are pneumatically actuated, as are the braking mechanisms. Since space was very limited, both functions are powered by compressed air in a small tank on one side of the aircraft. Normal installation of these components calls for two separate tanks, but since the aircraft only has to brake once during Mission B in the flight sequence, adequate pressure to perform all functions is maintained. Additional pressure savings come from using air only to retract the gear. The retract mechanisms are spring loaded, such that in the event of pressure loss in the system, the gear spring down into the fully locked position for a safe landing.

The retract units, brake systems, and necessary pneumatic valves are commercially available and purchased from a local source. The spring loaded struts, however, were custom built. These struts feature a threaded retaining bolt, in which springs of different rates can be quickly exchanged for varying conditions. The struts were built to hold the aircraft 6.125 inches above the ground when fully loaded. Once the 5 lbs. payload is deployed, the aircraft only rises to 6.25 inches. This height gives minimal compensation for clearing the payload box once deployed. The tires chosen for the aircraft are extra-hard rubber to prevent the aircraft from sinking when fully loaded. These hard tires also provide a solid ride for takeoff acceleration.

The payload release mechanism is controlled by a separate servo to avoid the possibility of the payload being released in flight by another control input. The method of release is based on the box being mechanically locked into place by the airframe pocket in which it is housed. A small piston/cylinder type assembly at the rear of the box pushes it toward the front bay wall. A small tab glued to the box sits on top of the piston to prevent the box from dropping free. This tab is tapered at the lower end to prevent it catching on the airframe while the box drops free (Figure 14).

The antenna mount for Mission A is retained by two nylon ¼-20 bolts, and two #6 self-tapping wood (flat head) screws. The two self-tapping screws are spaced at the lateral extremes of the mount to support the antenna in side loads. It was recognized that side loads would probably originate on the ground by clumsy handling rather than from dynamic flight loads. The nylon bolts, which are much larger

than the #6 screws, support the mount just fore and aft of the payload bay. The long shape of the mount, and the corresponding placement of these bolts, was designed to make use of the available space just fore and aft of the payload box. The team also felt the long base of the mount, almost 18inches, would give a more secure mount than one that is simply 3inces long. The mount itself is glued permanently to the cylinder, since when the antenna comes off, the mounting mechanism must also come off.

COMPONENT SELECTION

Mechanical:

The mechanical systems of the vehicle include push-rods, hinges, and the payload release mechanism. The push rods for the flapperons were 4-40 threaded rods with high-quality clevises. The same clevises were used on all linkages because of their locking thread-housing and locking clevis pin. Flex cables were routed from the empennage controls to their corresponding servos. These cables allowed imprecise installation of the servos and routing of control linkages around irregular shapes. The rudder servo has steel cables routed around the payload box and up to the nose of the aircraft.

The hinges chosen were "CA" type flat hinges. These hinges were easily installed, and do not disrupt the hinge line. This allowed the wing covering to be installed over the joint and prevented pressure leakage from the bottom of the wing to the top while in flight.

The payload release mechanism is shown in Figure 14. The piston was made from Teflon-impregnated Delrin. This material was chosen because it was lightweight, machines easily, and has a very low coefficient of friction. The cylinder was made from a piece of phenolic tubing also because of its light weight and low coefficient of friction.

Electrical:

The electrical systems include the batteries, speed control, fuse, and receiver. The batteries chosen were Sanyo 2400SCR Nickel Cadmium cells. These batteries are the only batteries specifically made for the RC hobby industry, and were designed to handle high charge/discharge rates. They also have the highest energy density of any of the candidate cells investigated. The speed control used was a Jeti JES500 speed control. It was chosen because of its small size and low weight. The receiver used was a Futaba R149DP PCM receiver, and was on hand before the contest season began.

Electromechanical:

The electromechanical components are the motor and servos. The optimization code that the team developed suggested that the Graupner 930-6 motor was the best choice of all candidate motors. This motor used an Aveox 3.7:1 gearbox for flight testing.

The servo selection was based on the requirements of the physical controls, the available space to install the servo, its contribution to weight, and the purchase price. These metrics are shown below in Table 7.

Table 7: Actuator Mechanism Selection Metrics

COMPONENT	BRAND/MODEL	WEIGHT (OZ)	DIMENSIONS (INCH)	TORQUE (IN-OZ)	PRICE
Elevator	JR DS8411	2.03	0.75x0.54x1.36	115.0	$114.95
Rudder/Nose Gear	JR DS8411	2.03	0.75x0.54x1.36	115.0	$114.95
Flapperons (x2)	Hitec HS-5125	0.84	0.39x1.33x1.18	41.66	$64.95
P/L Release Mech.	JR 507 STD	1.47	0.73x1.52x1.32	40.30	$26.95
Brakes	JR DS321	0.77	0.58x1.30x1.30	29.20	$52.95
Retracts	JR DS321	0.77	0.28x1.26x0.98	29.20	$52.95

Pneumatic:

The retract mechanisms and brake system were both pneumatically operated. The retract units chosen were Spring Air brand retracts, and feature a piston/spring assembly that deploys the gear in the event of pressure loss. The brakes were supplied from Trim Aircraft Company, and were the cheapest brand available to the team that featured an expanding o-ring configuration for secure, reliable braking. Brakes were considered necessary to stop the vehicle quickly in the deployment segment of Mission "B."

MATERIAL SELECTION

The material selection process was probably the most important step toward the construction of the contest entry. This process began during Conceptual Design with discussions of how to support the weight of the aircraft around the payload box. The material selection process that followed involved researching materials, analyzing structures, and experimenting with construction techniques. The documentation of this process was extremely valuable for training new students for shop activities, and involved (1) generating a list of possible aircraft materials, (2) documenting the properties of the materials and evaluating the most appropriate application, and then (3) cataloging the materials into their most appropriate application.

Some of the major developments from materials research included documentation of estimated flight loads and the corresponding structural loads delivered to the airframe. The team was willing to sacrifice some structural integrity in order to lower aircraft weight as low as possible to complete the mission. Materials were selected for specific applications if they had high strength-to-weight ratio, sufficient ultimate yield strength, low cost, and were readily available.

PREDICTED PERFORMANCE PARAMETERS

A listing of the predicted performance parameters as defined at the time of this report is given in Table 8. Parameters have been given for the configuration of the vehicle in Mission "A" and when not carrying any payload, as in second half of Mission "B." Also shown are the aircraft dimensions, documentation of the aircraft system components, and a detailed weight component breakdown.

Table 8: Predicted Performance

Aircraft Dimensions	
Length (ft)	3.90
Span (ft)	5.00
Height (ft)	0.81
with Fin (ft)	1.28
Wing Area (sq. ft)	3.540
Aspect Ratio	7.07
Horizontal Tail Volume Coeff	0.540
Vertical Tail Volume Coeff	0.068

Aircraft Performance	W_E	W_{TOGW}
$(C_L)_{MAX}$	1.30	1.30
$(L/D)_{MAX}$	12.2	10.4
$(RC)_{MAX}$ (ft/sec)	12.0	6.0
V_{STALL} (MPH)	24.7	33.5
V_{MAX} (MPH)	63.4	48.3
s_{TO} (ft)	36	117

Aircraft Systems

Radio: *Futaba 9Z*

Servos: *JR DS8411, JR DS321, JR 507 STD*
HITEC HS-5125
JETI JES-500

Battery Configuration: *14 N-2400SCR NiCads*

Motor: *Graupner Ultra 930-6*

Propeller (nominal): *Mejzlik 16-12*

Gear Ratio: *3.7-to-1*

Aircraft Weight Statement	W (lbs)
Airframe	**3.6428**
Monocoq Fiberglass Shell	*1.0263*
Internal Structure	*0.5842*
Retract Unit (x3)	*0.5288*
Wheel and Strut (x3)	*0.1487*
Propulsion System	**2.6250**
Graupner Ultra 930-6	*0.6550*
Gear Box	*0.2200*
N-2400SCR NiCad (x14)	*0.1250*
Control System	**0.5404**
JR DS8411 (x2)	*0.1269*
JR DS321 (x2)	*0.0481*
HITEC HS-5125 (x2)	*0.0525*
JETI JES-500	*0.0594*
Gyro	*0.0260*
Payload Release System	**0.3919**
JR 507 STD	*0.0919*
Payload Securing Mech	*0.1063*
Door Springs (x2)	*0.0969*
Payload	**6.1875**
Payload Box	*5.0*
Radome	*1.0*
Radome Pylon	*0.188*
Empty Weight	**7.20**
Gross Weight	**13.39**

W_{TOGW} figures include Radome, Fin, and Payload Box; W_E figures are without ".

Georgia Tech - DBF 2002/2003 - Team Buzzwiser
Rated Aircraft Cost

Description	Inputs	Hour Multiplier	Number of Hours		Cost Multiplier	RAC
			Component	Total		
Manufacturer's Empty Weight (MEW)						
Empty Weight	7.200 lbs				$100.00	$720.00
Rated Engine Power (REP)						
Number of Motors	1 motor				$1,500.00	$2,812.50
Battery Weight	1.875 lbs					
Manufacuring Man Hours (MFHR)						
WBS Wing						
Span	5.00 feet	8	40			
Max Exposed Wing Chord	0.71	8	5.664	51.66	$20.00	$1,033.28
Number of Control Surfaces	2 surfaces	3	6			
WBS Fuselage						
Body Maximum Length	3.90 feet	10	39.00	39.00	$20.00	$780.00
WBS Empennage						
Number of vertical surfaces with no active control	0 surfaces	5	0			
Number of vertical surfaces with active control	1 surface	10	10	20.00	$20.00	$400.00
Number of horizontal surfaces (span <25% of wing span)	1 surface	10	10			
WBS Flight Systems						
# Servos/Controllers	8 servos	5	40	40.00	$20.00	$800.00
WBS Propulsion System						
Number of motors	1 motor	5	5			
Number of propellers or fans	1 propeller	5	5	10.00	$20.00	$200.00
			Rated Aircraft Cost, $ (Thousands)			**$6.75**

Figure 11: Rated Aircraft Cost

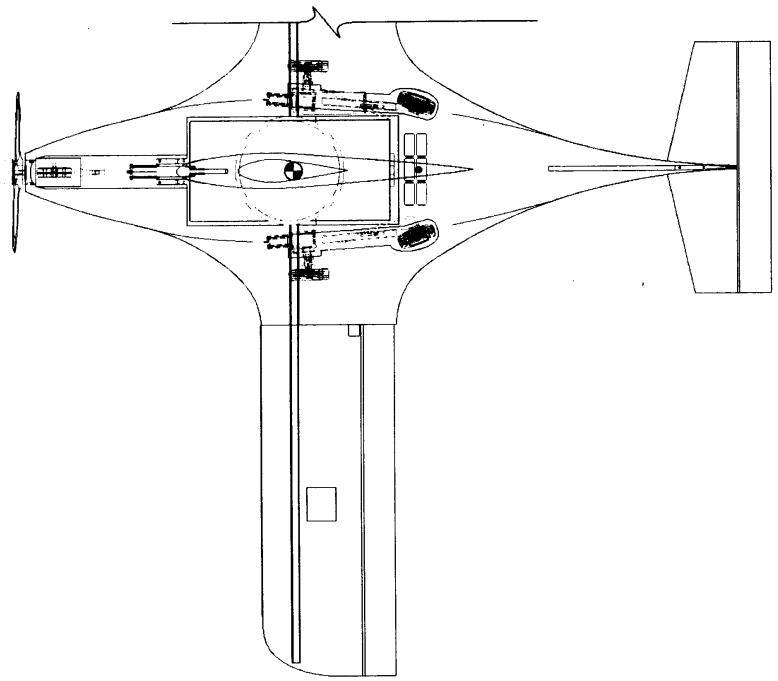

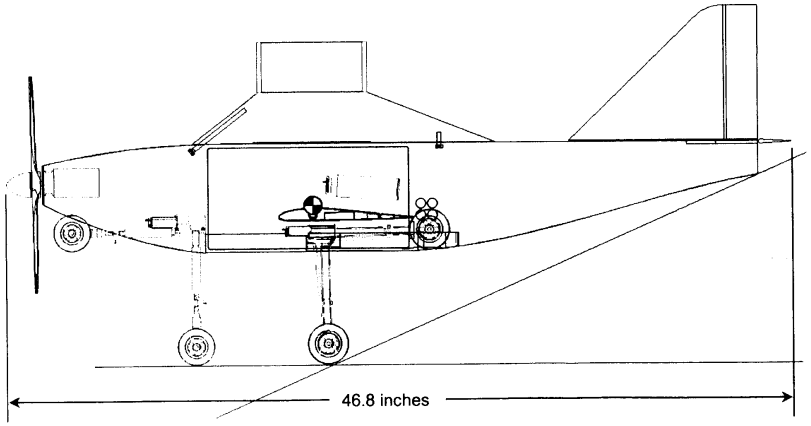

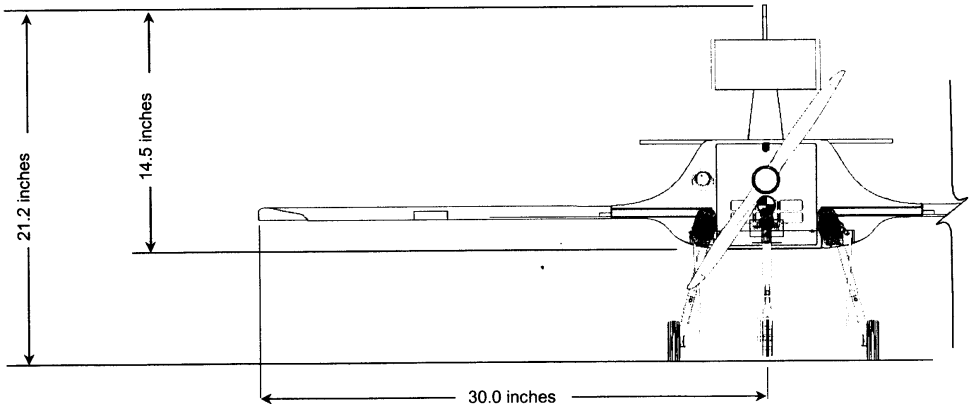

Buzzweiser

Missile Decoy Configuration for Georgia Tech Design, Build, Fly entry "Buzzweiser"

Gross Weight	13.2 lbs.
Takeoff Distance	117 ft.
Propeller Used	16 x 10 Mejzlik
Maximum Cruise Velocity	48.3 MPH
Rate of Climb	6 ft/sec
RAC	6.75
Projected Mission Time	00:03:52
Projected Mission Score	0.612

Figure 12: Missile Decoy 3-View

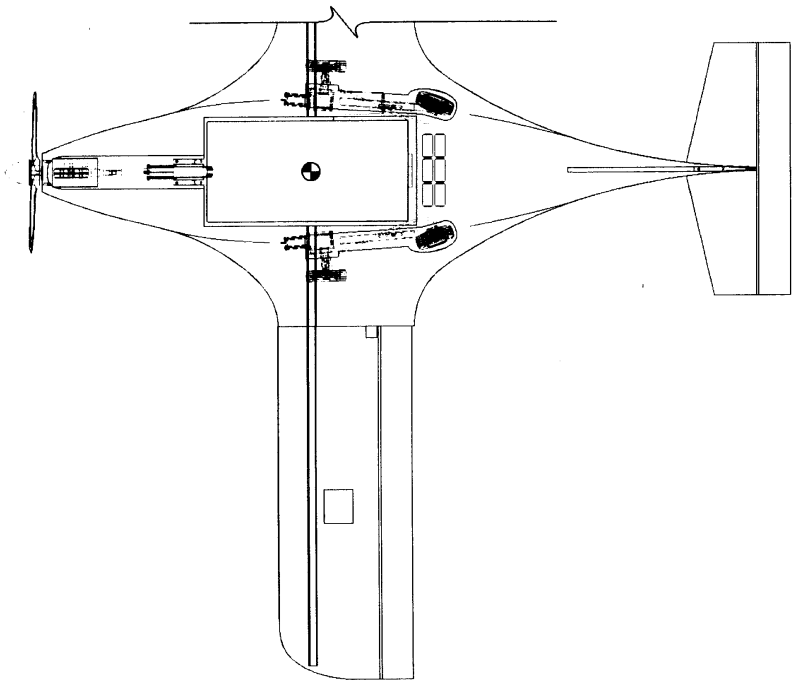

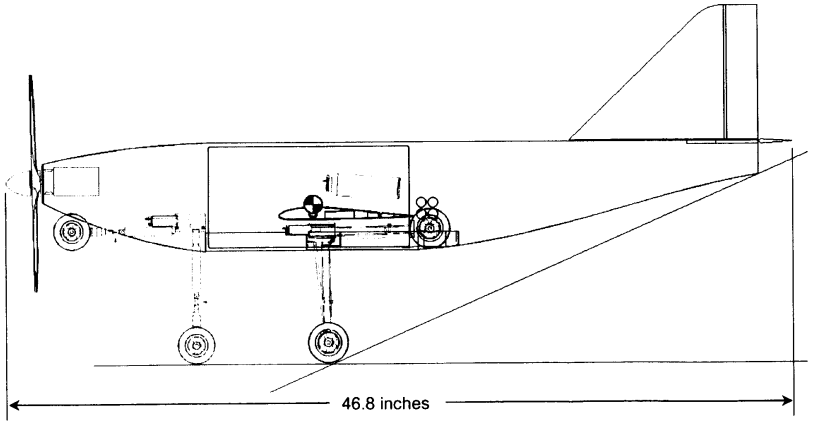

Buzzweiser

Sensor Deployment Configuration for Georgia Tech Design, Build, Fly entry "Buzzweiser"

	With Sensor Package	Without Sensor Package
Gross Weight	12.2 lbs.	7.2 lbs.
Takeoff Distance	103 ft.	36 ft.
Propeller Used	16 x14 Mejzlik	
Maximum Cruise Velocity	57.3 MPH	63.4 MPH
Rate of Climb (w /box)	7 ft./sec.	12 ft./sec.
RAC	6.75	
Mission Time	00:03:12	
Projected Mission Score	0.460	

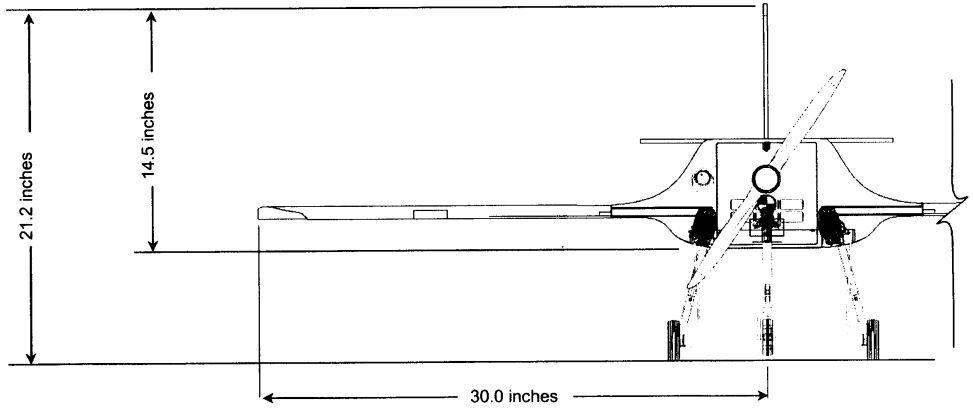

Figure 13: Sensor Deployment 3-View

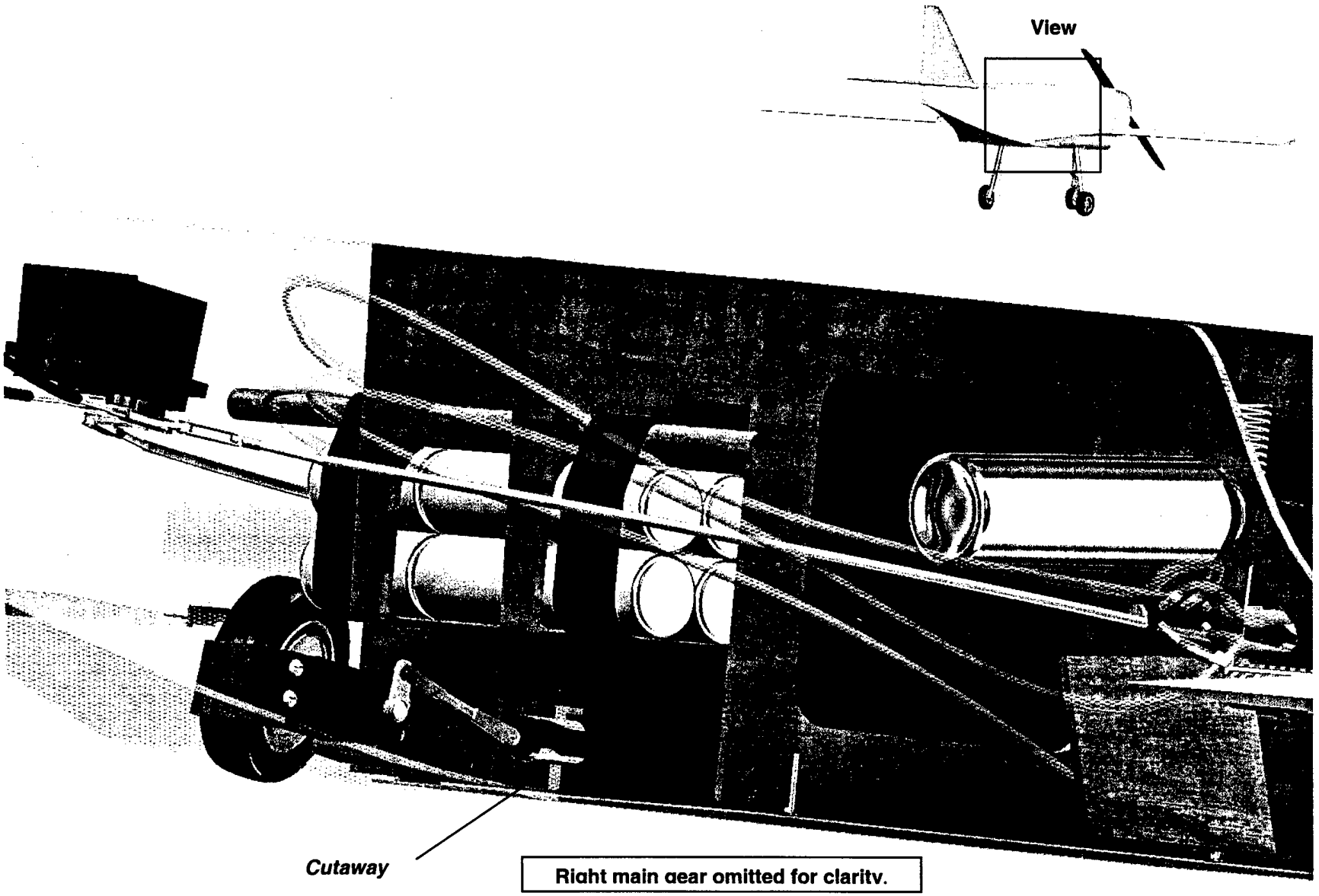

Figure 14: Payload Deployment Mechanism and Battery Restraint Method

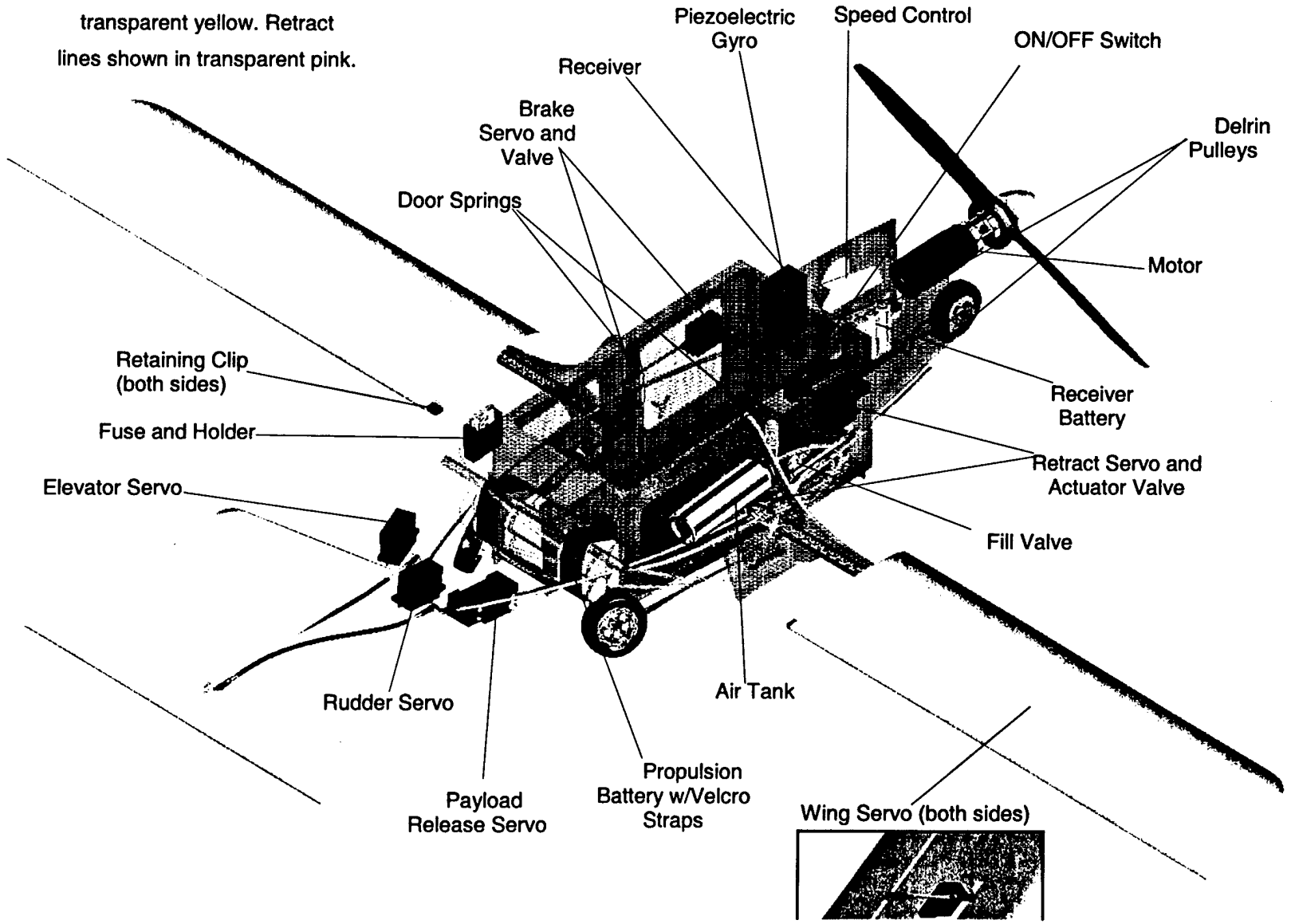

Figure 15: Systems Diagram

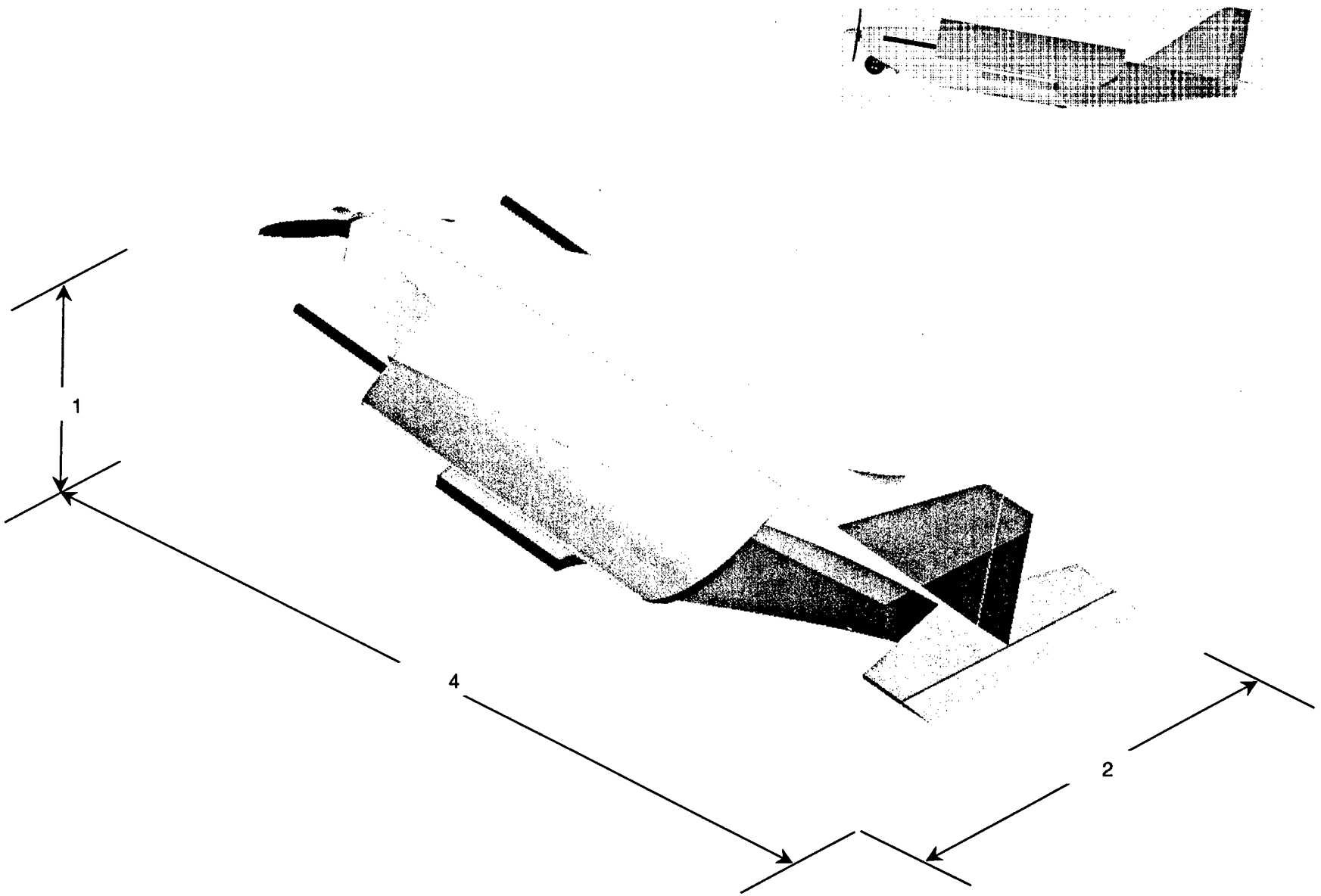

Figure 16: Aircraft Stowage Compatibility with Container Box

The Manufacturing Plan for the vehicle involved screening various methods of manufacture appropriate for constructing the components of the final design. The process selection was a culmination of experience, research, and experimentation and has been documented in this section of the report.

COMPONENT MANUFACTURE

There were four major assemblies to the final design. These were the fuselage, the landing gear, the empennage, and the wing panels. Their construction is described below. The planned and actual development times can be seen in Figure 18.

Fuselage:

Construction of the final vehicle began with the fuselage. The design requirements of the fuselage were that it had to support the components of the aircraft as well as streamline the package as much as possible. Traditional composites production involves building a solid plug, building a mold of the plug, then laying the final part inside the mold. This process is extremely time consuming, and every step must be done properly in order to ensure that the product of hundreds of committed hours is acceptable. Mold-making was considered inappropriate for a "disposable" DBF aircraft and more suited for industry production.

The alternative to this time consuming process is to skip the plug-making and mold-making processes, and begin construction directly on the fuselage. The team was able accomplish this by using a soft foam plug, laying composites on the outside of the plug, and then destroying the inner plug. The remaining steps were very similar to having a composite fuselage made by the traditional methods and included finishing the outer surface and installing internal components.

The front view, side view, and top view generated from CAD geometry were traced on a rectangular block of extruded polystyrene which fit the external dimensions of the fuselage. A hotwire cutting tool was used to trim the block along the lines drawn on the block. This shape was then smoothed with various grits of sandpaper until the desired shape was achieved.

The next steps involved laying fiberglass over the foam shape. As mentioned, aside from providing a streamlined shape, the other requirement of the fuselage was that it had to support the components of the aircraft. Primarily, the fuselage had to support the weight of the aircraft from one wing tip to the other without crossing through the payload bay. Carbon fiber tape placed laterally across the fuselage was intended to support this load. Carbon fiber tape was also applied in crossed patterns along the length of the fuselage to support torsion loads.

The lay-ups were also done over expanded polystyrene, and the team experimented with different methods of removing the foam from the cured fiberglass. Using heat to melt the foam away not only melted the epoxy resin (totally destroying the intended shape) but also left a crusty residue behind which added weight of the part and made adhesion difficult. Various chemicals were used to dissolve the foam, including gasoline, mineral spirits, lacquer thinner, acetone, and even cyanoacrylate accelerator but

results were either too slow or too destructive. Physical extraction of foam, although laborious, proved to be the most appropriate method. Sharp, penetrating tools were used on the core of the shape, and a much more gentle wire brush was used near the inside of the cured fiberglass.

A final layer of ¾oz cloth was applied to the outside of the fuselage. This layer was added not for strength, but to give the outside surface of the shell a smoother texture from which to sand and prime for finishing.

The fuselage was almost entirely of monocoque construction. However, installed components necessitated internal structure. Primarily, reinforcing formers were added to disperse the tremendous loads of the landing gear in the event of a hard landing, but an internal frame was also needed to adequately support the payload box. American yellow poplar light plywood was chosen as former material for its availability, workability, excellent strength, and low cost.

Landing Gear:

The team had initially chosen retractable landing gear because of drag considerations, but once construction considerations began for the aircraft struts, the team realized that they could predict the impulse response of the landing gear much better with piston/cylinder spring gear rather than a using a flex-beam fixed gear.

The standing height (preloaded gear) and travel of impulse response of the aircraft's landing gear would be dictated by the spring used inside the strut housing. The 7000 series of Aluminum alloys was used for the manufacture of the landing gear because of its superior strength over other Aluminum alloys. This material cuts easily on a lathe, and finishing requires little de-burring. Most components of the gear were cut with a small lathe, but finishing the angles of lower piston required the use of a milling machine.

Empennage:

For simplicity, the team chose to use a flat tail surfaces as opposed to airfoil shaped tail surfaces. It was not necessary to investigate alternate manufacturing alternatives, as there is really only one way to cut balsa frame members, glue them together, and cover them in polyvinyl heat-shrink skin. There were some finesse techniques used to ensure solid glue joints, square angles, and other such delicate intricacies, but these techniques are not considered significant discussion for this report. If the team had chosen an airfoil shape for the tail surfaces their construction would have been similar to that of the aircraft's wings, requiring more labor and care.

Wing Panels:

The wings of the final design are foam core, balsa sheeted with polyvinyl heat shrink covering. Carbon fiber tape was used to provide additional strength to the wing. A carbon fiber tube was installed as the main structural member of the wing, and served to guide the wing onto the fuselage during the assembly task.

Construction of the wing began with the foam core. The core had to be just slightly smaller than the intended shape so that the wing was the proper size after balsa sheeting had been applied. Two airfoil

templates were used to cut the entire span of the aircraft was cut at once (for uniformity). Once cut, Balsa sheeting was applied to the outside of the wing for surface preparation rather than for strength. Previous wing constructions showed that the polyvinyl heat shrink covering would be smoother with a well-prepared balsa surface than with bare foam. Balsa skin was applied with the use of a vacuum bag and vacuum pump.

Once the balsa skins had been applied, a hole was drilled through the entire length for the installation of the (round) wing spar, and the piece was cut into two 21 inch wing panels. The control surfaces were cut away, shaped, and reattached to the wing. The spar and wing servo were installed and the whole assembly was covered in polyvinyl heat-shrink covering.

MANUFATURING PROCESSES INVESTIGATED

The aircraft design called for a complex curvature of the wing to the fuselage, and the team investigated several manufacturing processes that favored complex curves. Specifically, these processes involved the use of composite materials. There were several methods of composite construction that were discussed among the team. The team eliminated the mold-making process or any process involving the use of an autoclave by the FOMs given on page 48. Successful results were obtained in most cases by applying composites on the outside of a core material, or just under the surface of a finishing material (such as a balsa skin).

Most of the lessons learned for selecting the manufacturing process came from the wing core construction experimentation described in the Testing Plan section of this report (see page 52). However, the team also sought training on advanced machining equipment such as a vertical milling machine and an engine lathe. The skills acquired from basic training on these machines opened many manufacturing opportunities to the team, because custom components could be tailored to fit the design better than similar components commercially available. For example, the team decided to build custom landing gear struts after not finding a suitable commercial product. Also, the payload release mechanism, a highly custom-tailored component was constructed using both a lathe and a milling machine.

Other process information came from the skills of the veteran DBF members. Previous experience in both conventional and unconventional construction techniques were carried into the 2002-2003 project efforts. Some of the experience carried over came from hot wire foam-cutting processes for long wing cores (straight and tapered), fiberglass molding techniques, wing covering techniques, soldering, gluing, cutting balsa and other light woods, and constructing custom control linkages. This experience was the primary driver in determining the FOMs for manufacturing before final manufacturing processes had been selected.

Figures of Merit for Manufacturing Plan

Careful attention had to be given to those processes that would yield favorable results without exhausting too many resources. For screening construction processes, the applicable FOMs are described below:

- Low complexity: The team could not afford to employ time-consuming processes which had a significant risk of failure. Processes not previously attempted and drastically different from the general experience of the team were avoided unless they were suspected of yielding a significant competitive advantage over competing alternatives.
- Availability: Availability of labor was a critical component of manufacturing success for timely parts yield. Team members were required to be full time students, and DBF activities often came after other studies were complete. Studying the intricacies of a process, experimenting with an unfamiliar process, and reworking mistakes all absorb tremendous amounts of precious time. Known processes that had proven results were almost invariably chosen over alternative processes for the construction of the final vehicle.
- High fidelity results: It was pointless to attempt to build a competition vehicle unless the design was known and understood. Conversely, it was pointless to build a vehicle unless the process could yield results that matched the intended design. Inability to produce intended results would nullify any previous design efforts. Structural or mechanical failures had to be understood in terms of their design and physical construction.
- Repeatable results: The predictability of future outcomes was dependent on the ability of team to produce results consistently. Consistent results could be directly interpreted as manufacturing capabilities, and thus managed as a valuable resource.
- Required skill level: Operator capability was also managed as a critical asset. The team had unrestricted access to such equipment as lathes, milling machines, routers, and saws, but the equipment was of little use if team members had not been properly trained on how to use the equipment. When such was the case, team members would take advantage of training opportunities when available and appropriate.
- Tools and equipment: Mechanical capability was also managed as a critical asset. Specialized tools opened the envelope of potential capabilities. For example, had a lathe and milling machine not been available to the team, manufacturing of aluminum landing gear would not have been considered.
- Safety: Safety was of primary concern to the team. Safe practices were of greater importance to the team than meeting deadlines or producing superior components. Team members were continually encouraged to look after themselves as well as each other.
- Low cost: The team was very limited on funds and had to closely manage the cost of materials and laboratory operating expenses.

By the time that construction had begun on the contest vehicle, the team had built two prototype vehicles, one of which was fully functional and could replace the contest vehicle in the event of a catastrophic failure.

ANALYTIC METHODS

The process selected for component manufacture was often inherent in the nature of the component

itself. For example, balsa-frame empennage surfaces were chosen as part of the results of material selection research and the analysis conducted during Preliminary Design. The "process" of cutting balsa and gluing the pieces together was a trivial decision. However, the means by which such decisions were made were not without consideration to the cost, skill capabilities of the team, the equipment capabilities of the team, adherence of final results to intended results, and the overall evaluation of associated risk; regardless of whether or not they were formally discussed.

The approach to this evaluation of process selection is represented by Figure 17: Process Selection Matrix. The financial expense of an operation may not appear to be a critical factor because the operation of most tools only require electrical power. However, there were operating expenses inherent in operating the machinery. Carbon fiber in particular would dull cutting blades very quickly, and in the case of the shop band saw, had the potential for becoming very expensive.

Skill capability of the team, previously discussed in the FOMs, played a vital role in the capabilities of the team to produce parts of high fidelity and in a timely manner. Acquired skills were of little use if the proper equipment was not available to the team. This situation was the primary reason that the use of an autoclave was ruled out for composites manufacturing. Other processes were screened in a similar manner, some of which have been illustrated in the figure.

-2	very unfavorable
-1	unfavorable
0	undetermined or N/A
1	favorable
2	very favorable

Component	Potential Processes Invetigated	Cost	Skill Capability Rating	Equipment Capability Rating	Design Fidelity	Associated Risk	Score	Chosen
Fuselage								
	Mold-making	-1	-2	1	0	-2	-4	no
	Wood frame	2	1	1	-2	-1	1	no
	Soft plug	1	1	1	1	1	5	yes
Landing gear								
	Custom Subcontracted	-2	0	0	-1	0	-3	no
	Commercially Purchased	-2	0	0	-1	-1	-4	no
	Team Manufactured	2	-1	2	2	-1	4	yes
Empennage								
	Fiberglass	-2	-1	0	1	0	-2	no
	Balsa Frame	2	2	2	-1	-1	4	yes
Wings								
	Polycarbonate Shell	2	2	2	1	-2	6	no
	Molded Composite Shell	-2	-2	1	0	-2	-5	no
	Reinforced B/F	2	1	2	1	1	6	yes
	Balsa and Foam (B/F)	2	1	2	1	-2	4	no
	Balsa Frame	2	-1	2	1	-1	3	no

Figure 17: Process Selection Matrix

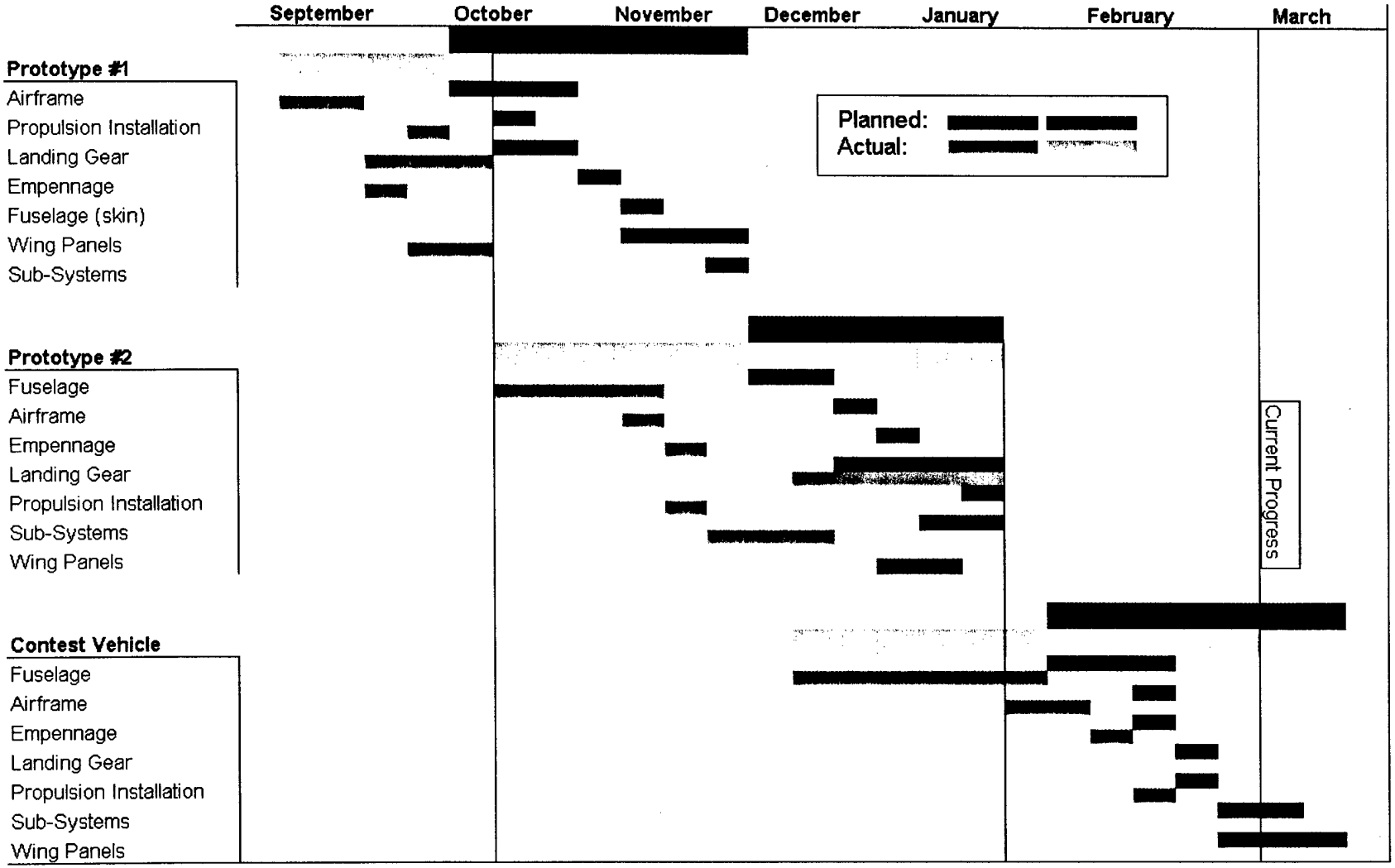

Figure 18: Manufacturing Milestone Chart

Team management recognized that most of the membership had little or no formal education in aircraft design. Only four team members had participated in previous years' DBF competitions, and no members had ever flown a remotely controlled aircraft without an instructor. The shortage of proper knowledge and experience made it clear that gathering empirical data was essential to taking inventory of team skills as well as for validation of design efforts. Early project planning had called for building two fully functional prototype vehicles for testing and evaluation in addition to individual component testing.

COMPONENT TESTING

The component test fields and their corresponding objectives are given below in Table 9: Test Objectives. Wing sections were built to gain experience in new construction methods. All sections were of a Clark-Y airfoil, 8 inches in chord, and 36 inches in span. All component weights were recorded during construction, including weight fractions due to adhesives. The cores were then clamped at one end and loaded at the leading edge, trailing edge, and quarter chord and deflections were recorded. The results were used in component manufacture.

The propulsion system components were each tested in order to calibrate the MATLAB performance code to empirical data. The pitch angle, thickness, chord, and distance from central axis were recorded at ten stations along the span of one propeller blade. Static tests were conducted for all J-Zinger propellers commercially available from 9 inches in diameter to 20 inches. Dynamic tests for only three propellers were necessary for performance calibration.

Battery cell performance was modeled from plots of individual cell performance published in the 1998 Sanyo catalog. However, the team needed to test the performance of an assembled battery pack in order to capture errors in the performance coding, interaction effects within an assembled battery pack, or difference in predicted and actual performance of a used battery pack. Discharge curves were plotted using a 26 cell battery pack on a string of 14 light bulbs. A variable potentiometer was used to regulate discharge current. Voltage and current was recorded every 5 seconds for the duration of the discharge. These discharge plots were consistent with the curves published in the Sanyo catalog, and only minor scaling factors were needed for accurate modeling.

Motor performance tests were conducted for the AstroFlight Cobalt 90, Cobalt 60, and Cobalt 40, as well as the Graupner 930-6, 930-7, 920-4, and the Speed 700 series of motors. No-load tests, stall tests, and dynamic tests were necessary for each motor in order to accurately catalog its performance.

Table 9: Test Objectives

TEST FIELD	COMPONENT DESCRIPTION	OBJECTIVES
Wing Sections	Team-manufactured wing test sections 12x36inch Clark-Y	1. Quantify the material weight fractions of all installed materials 2. Quantify the deflection for various loads. 3. Catalog results for future reference
Propellers	Brand: J-Zinger only D range: 9-20inches P range: 6-14	1. Measure physical metrics 2. Quantify static performance 3. Quantify dynamic performance 4. Catalog the results for performance modeling
Batteries	26 cells, 3000mAh I range: 12-40 Amperes	1. Document the entire discharge curve for multiple currents 2. Catalog the results for performance modeling
Motors-No Load	V range: 0-max opr. T range: zero	1. Document the RPM curves across voltage range 2. Catalog the results for performance modeling
Motors-Stalled	V range: 0-max opr. T range: stalled	1. Document the current at 3 voltage points 2. Catalog the results for performance modeling
Motors-Static	V range: 0-max opr. T range: all propellers	1.Document performance parameters at static conditions 2. Catalog the results for performance modeling
Motors-Dynamic	V range: 0-max opr. T range: all propellers	1.Document performance parameters at dynamic conditions 2. Catalog the results for performance modeling

FLIGHT TESTING

The flight testing schedule is shown below in Table 10. The team was prepared to complete a vehicle by the end of January. Flight data recording equipment was installed and used throughout flight testing. The dark blue shown below represents the actual development of flight tests. The light blue shows projected development of future flight tests and forecasted at the time of this report.

Table 10: Flight Test Schedule

	FEBRUARY				MARCH				APRIL		
Taxi Tests	■	■	■								
Systems Refinement		■	■	■							
Takeoff Tests				■	■						
Functional Assessment					■						
Augmentation and Re-Test											
Performance Evaluation			■	■	■						
Final Optimization											

Flight performance data was acquired using a commercially available flight data recorder. The eight metrics recorded during flight-testing were airspeed, propeller RPM, longitudinal (x-axis) acceleration, vertical (z-axis) acceleration, operating voltage, operating current, motor temperature, and battery temperature. Sampling rate was programmed to twenty-five samples per second, and the data was post processed for interpretations about not only the adequacy of the propulsion system but also to validate the aerodynamic performance of the design.

Flight testing came in three phases: taxi-testing, initial flights, and optimization flights. The objectives for each flight test are given in Table 11, and the preflight, flightline, and post flight checklists are given in Table 12.

Table 11: Flight Test Objectives

FLIGHT-TEST PHASE	OBJECTIVES
Taxi Tests	1. Ensure the aircraft tracks correctly 2. Evaluate control volumes and determine appropriate configuration 3. Evaluate acceleration and approve for flight 4. Identify unforeseen problems and apply contingency plans
Initial Flights	1. Trim the aircraft 2. Adjust the CG within static stability margin 3. Program control output ranges, dual rates, exponential rates, and channel mixing 4. Identify unforeseen problems and apply contingency plans
Optimization Flights	1. Evaluate takeoff performance and adjust as necessary 2. Record flight data for each remaining candidate component 3. Identify unforeseen problems and apply contingency plans

Results and Lessons Learned

Component test results used in the coded performance modeling were consistent with the theoretical models that were intended to describe them. However, the test apparatus needed refinement before test results would be repeatable with a high degree of accuracy. The team felt the component testing during the project was the single most influential activity in identifying the optimal design for the RFP.

Vehicle flight testing was critical for identifying unforeseen problems and for further development of the team's MATLAB performance code. Once working properly, the code was able to predict actual flight times and flight scores with a high degree of accuracy and was generally considered a great success. The team considers that the testing projects performed constituted an extremely valuable part of the design process and will use the lessons learned in these activities for future projects.

Table 12: Preflight & Flightline Checklists

Preflight Checklist

Propulsion battery	
Voltage	verify charged
Installation	verify security
Connection	disarmed
Transmitter	on
Receiver	on
Flapperon switch	set neutral
Flapperons	check neutral, level
Trims	set/verify
Left wing panel	
Retaining clip	locked
Control surface	tug for security
Clevises	secure
Control horns	secure
Position	verify neutral
Right wing panel	
Retaining clip	locked
Control surface	tug for security
Clevises	secure
Control horns	secure
Position	verify neutral
Elevator	
Installation	tug for security
Clevises	secure
Control horns	secure
Position	verify neutral
Rudder	
Installation	tug for security
Clevises	secure
Control horns	secure
Position	verify neutral
Wheel retaining collar	secure
Landing gear strut	secure, locked
Air tank	charge to 120psi
Propeller	correct size, secure
Center of gravity	verify location
Receiver	off
Transmitter	off
Receiver battery	verify charged

Flightline Checklist

Transmitter	on
Receiver	on
Elevator	correct movement
Rudder	correct movement
Ailerons	correct movement
Flaps	correct movement
Dual Rates	correct volume
Propulsion battery	arm
40 Amp fuse	Install
Throttle	10%
Brakes	check
**Ground crew hold aircraft*	
Throttle	0-100-0%
Range	check
Fail safes	verify

Postflight Checklist

40 Amp fuse	remove
Receiver	off
Transmitter	off

Borst, H. V., & Hoerner, S. F. (1985). Fluid-dynamic lift. Bakersfield, CA: Hoerner Fluid Dynamics.

Boucher, R. J. (1995). Electric motor handbook. Marina Del Rey, CA: AstroFlight, Inc.

Hoerner, S.F. (1965). Fluid-dynamic drag. Bakersfield, CA: Hoerner Fluid Dynamics.

Hoerner, S.F. (1965). Fluid-dynamic drag. Bakersfield, CA: Hoerner Fluid Dynamics.

Mattingly, D. P., et al. (1987). Aircraft engine design. Washington, DC: American Institute of Aeronautics and Astronautics, Inc.

Roskam, J. (1989). Airplane design part 1: Preliminary sizing of airplanes. Lawrence, KS: DAR Corporation.

Sanyo Electric Co., Ltd. (1998). Sanyo Cadnica engineering databook. Osaka: Author.

Special thanks to the Lockheed Martin Aeronautics Company, Boeing Aircraft Company, and the William R. T. Oakes Endowment for their generous financial support.

With Grateful Appreciation,

Georgia Tech DBF Team

ONR Student Design/Build/Fly Competition

THE STOP AND GO (SNG)

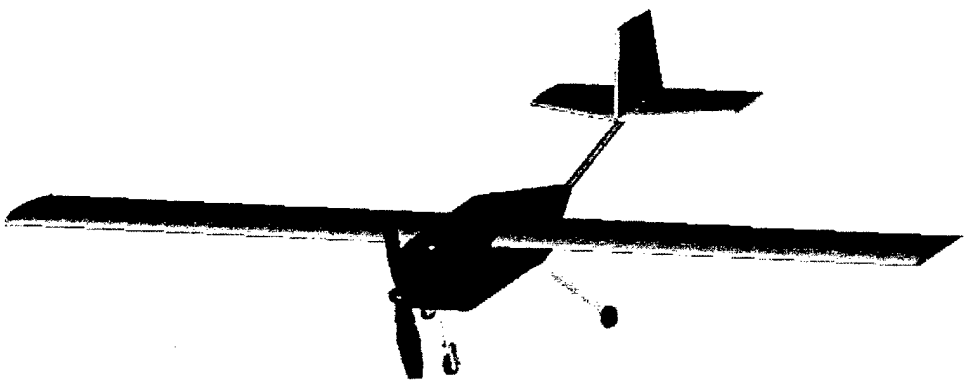

University of Maryland
Department of Aerospace Engineering
College Park, Maryland

1 EXECUTIVE SUMMARY 1

1.1 Mission Requirements and Objectives: 1

1.2 Selection of Conventional Aircraft Configuration 1

1.3 Design features of The STOP AND GO (SNG) Aircraft: 2

2 MANAGEMENT SUMMARY 5

2.1 Group Structure 5
2.1.1 Aerodynamics 6
2.1.2 Propulsion 6
2.1.3 Structures 6
2.1.4 Vehicle Integration 6
2.1.5 Information Management 6

2.2 Project Schedule 7

3 CONCEPTUAL DESIGN 7

3.1 Flight Score Assessment 8

3.2 Aerodynamics 13
3.2.1 Aircraft Layout 13
3.2.2 Wing Configuration 14
3.2.3 Tail Configuration 15

3.3 Propulsion 16
3.3.1 Motor Configuration 16
3.3.2 Landing Gear Configuration 17

3.4 Conceptual Design Results 18

4 PRELIMINARY DESIGN 18

4.1 Aerodynamics 19
4.1.1 Lift Needed for Takeoff 19
4.1.2 Effects of Wing Area on Performance 20
4.1.3 Analysis of Wingspan, Chord Length, and Aspect Ratio 21
4.1.4 Airfoil Selection 21
4.1.5 Tail Sizing 22

4.2 Propulsion 23

4.3 Structures 25

4.3.1 Wing Spars 25
4.3.2 Landing Gear Sizing 26

4.4 Vehicle Integration 26
4.4.1 Payload Deployment System 27
4.4.2 Fuselage Sizing 28
4.4.3 Antenna Mounting System 30

4.5 Preliminary Design Results 31

5 DETAIL DESIGN 31

5.1 Aerodynamics 31
5.1.1 Final Selection of Wing Design 31
5.1.2 Final Selection of Tail Design 31
5.1.3 Static Margin 32
5.1.4 Control Surface Sizing 32
5.1.5 Flap Analysis 32

5.2 Propulsion 33
5.2.1 Propulsion Analysis Software 33
5.2.2 System Configuration 34

5.3 Structures 37
5.3.1 Wing Spar Sizing 37
5.3.2 Landing Gear 37

5.4 Vehicle Integration 37
5.4.1 Payload Deployment System 37
5.4.2 Fuselage Sizing 38
5.4.3 Antenna Mounting System 39
5.4.4 Antenna Placement 40

5.5 Weight Statement 40

5.6 Rated Aircraft Cost 43

5.7 Detail Design Results 44

5.8 Drawing Package 45
5.8.1 Drawing Package: Three View 45
5.8.2 Drawing Package: Locations of Aircraft Components 46
5.8.3 Drawing Package: Detail views of select aircraft components 47
5.8.4 Drawing Package: Explode view 48
5.8.5 Drawing Package: Storage Box Configuration 49

5.9 Sized Aircraft Data 50

6 MANUFACTURING PLAN **51**

6.1 Aerodynamics 51
6.1.1 Wing and Tail Construction 51

6.2 Structures 52
6.2.1 Wing Spar Insertion 52
6.2.2 Landing Gear Construction 52

6.3 Vehicle Integration 53
6.3.1 Fuselage Construction 53

6.4 Manufacturing Results 54

7 AIRCRAFT TESTING **55**

8 BIBLIOGRAPHY **58**

List of Figures

Figure 1.	Mission Flight Pattern	3
Figure 2.	3 Dimensional View Drawing of The Stop and Go Aircraft	4
Figure 3.	Team Architecture Chart	5
Figure 4.	Team Milestones. Blue: Planned. Red: Actual. Black: Span of Task.	7
Figure 5.	Payload Deployment with Low and Mid Wing	15
Figure 6.	C_L vs Wing area	20
Figure 7.	Clark Y Drag Polar and Lift Curve Slope	22
Figure 8.	Thrust and Amperage vs. Velocity for AstroFlight Motors	25
Figure 9.	Power Calc: Calculates flight times and power usage	34
Figure 10.	Thrust/Power Available and Req. for 22-18 Prop with Cobalt 90	36
Figure 11.	Drag vs. velocity plot for antenna assembly across flight enveloper	39
Figure 12.	Breakout of MFHR and RAC	43
Figure 13.	Manufacturing Milestones Chart	51
Figure 14.	Testing Schedule	55
Figure 15.	Aerodynamic Performance of Clark-Y Airfoil	56
Figure 16.	Side View of Stop and Go aircraft in Wind Tunnel	57
Figure 17.	Isometric View of Stop and Go in Wind Tunnel	57

List of Tables

Table 1.	Approximate Maximum Values	10
Table 2.	Derivatives of Score Components	10
Table 3.	Figure of Merit Chart	12
Table 4.	Wing Configuration FOM	14
Table 5.	Tail Configuration FOM	16
Table 6.	Motor Configuration FOM	17
Table 7.	Motor and Battery Configuration FOM	24
Table 8.	Motor Selection FOM	24
Table 9.	Deployment System FOM	28
Table 10.	Cross Sectional Fuselage Shape FOM	29
Table 11.	Antenna Mounting System FOM	30
Table 12.	Lift Contribution of Plain Flap for $S_{flapped} / S_{ref}$	32
Table 13.	Chart of scores for various prop selections with the Cobalt 60 motor.	35
Table 14.	Comparison of scores for different cell counts on the Cobalt 90 motor.	35
Table 15.	Weight Statement	41
Table 16.	Center of Gravity Calculations	42
Table 17.	Geometry, Performance Weight Statement, and Systems	50
Table 18.	Control Volumes	50
Table 19.	Airfoil Manufacturing Methods FOM	52
Table 20.	Landing Manufacturing Methods FOM	53
Table 21.	Fuselage Manufacturing Methods FOM	54

1 Executive Summary

The STOP AND GO AIRCRAFT is a conventional fixed wing aircraft that has been designed in response to the 2003 Cessna/ONR Design-Build-Fly Competition. The vehicle has the ability to takeoff in less than 100 ft and cruise at speeds near 40 miles per hour.

1.1 Mission Requirements and Objectives:

The 2003 Design-Build-Fly Competition rules described a task matrix that consisted of a timed aircraft assembly, and three different missions with decreasing levels of difficulty. These missions included a Missile Decoy mission (Difficulty Factor of 2), a Sensor Decoy mission (Difficulty Factor of 1.5) and a Communication Repeater mission (Difficulty Factor of 1.0). The Missile Decoy mission required an aircraft to take-off, complete 4 laps, and land. The aircraft was required to carry a simulated avionics payload consisting of a box 12 in. x 6 in. x 6 in. In addition, a simulated antenna consisting of a 6 in diameter schedule 40 (white) pipe had to be flown external to the fuselage of the aircraft. The Sensor Deployment mission required the aircraft to takeoff, complete 2 laps, land, and release its avionics box payload. After releasing the payload box, the aircraft was required to complete two additional laps and land. Finally, the communications repeater mission required the aircraft to takeoff, complete 4 laps, and land. The aircraft was required to carry an avionics payload box that was ballasted to weigh at least 5 lbs. On all missions and on all laps flown the aircraft needed to complete a 360-degree turn in the direction opposite of the base and final turns on the downwind leg of each lap. The course for all missions flown is shown below (Figure 1). The rules required teams to design, fabricate, and demonstrate the flight capabilities of an unmanned, electric powered, radio controlled aircraft that could best meet the specified mission profiles. The goal was a balanced design possess, good demonstrated flight handling qualities, and a practical and affordable manufacturing process while providing a high vehicle performance.

1.2 Selection of Conventional Aircraft Configuration

During the conceptual design phase of this process, several single-engine configurations were considered including, conventional, canard, flying wing and a two-boom pusher aircraft. To evaluate each of these single-engine concepts, the team developed a unique set of performance criteria based on the following items:

- Ability to fly all missions
- Box containment & assembly
- Rated aircraft cost
- Handling & control
- L/D ratio
- Construction

After careful consideration, it was determined that a conventional forward wing/rear tail aircraft would offer the best solution for the suite of competition missions. The advantage of this configuration was that there was plenty of information available on manufacturing and performance of these types of aircraft. This reduced the rated aircraft cost since data for these types of aircraft was well known. Thus, The STOP AND GO aircraft design developed by the University of Maryland was selected to ensure maximum confidence in completing the two most difficult missions, i.e. the Missile Decoy and Sensor Decoy missions. In addition, the aircraft design was developed to meet competition storage and quick assembly requirements.

1.3 Design features of The STOP AND GO (SNG) Aircraft:

The SNG was designed to be a high aspect ratio, fixed wing, electric powered aircraft. The design was dominated by the goal to complete each of the mission requirements as quickly as possible. Thus, the vehicle was sized to have sufficient lift to meet all takeoff requirements and fly at cruise speeds of approximately 45 to 50 miles per hour. The Gross Takeoff Weight (GTOW) of the aircraft was approximately 20.4 lbs for the most demanding mission.

Some unique features of the aircraft included:

- A rapid payload release mechanism was utilized that relied on a lever mechanism controlled by turning the front landing gear to the left to release the payload quickly upon reaching a complete stop. A strap was used to secure the payload in place during flight. The landing gear mechanism was used to release the strap so that the payload would fall out of the aircraft.

- An all-movable tail was designed to provide rapid takeoff and landing to meet the 120 ft takeoff distance with ease. The all-movable tail provided a greater control moment capability for pitching the aircraft up as quickly as possible.

- A 22 in. diameter with 18-pitch propeller powered by an electric motor would be used to deliver optimum thrust to the aircraft during takeoff and landing as well as during cruise.

- An 8.5 ft wing with an aspect ratio of 9.9 positioned at the top of the fuselage maintained good center of gravity performance to ensure good handling and control characteristics of the aircraft. A Clark-Y airfoil was chosen because of its high lift coefficient and performance at low Reynolds numbers.

- Tricycle landing gear was chosen to support the aircraft during takeoff and landing for all missions. This landing gear configuration provided for an ease of payload deployment and enough clearance for the simulated antenna.

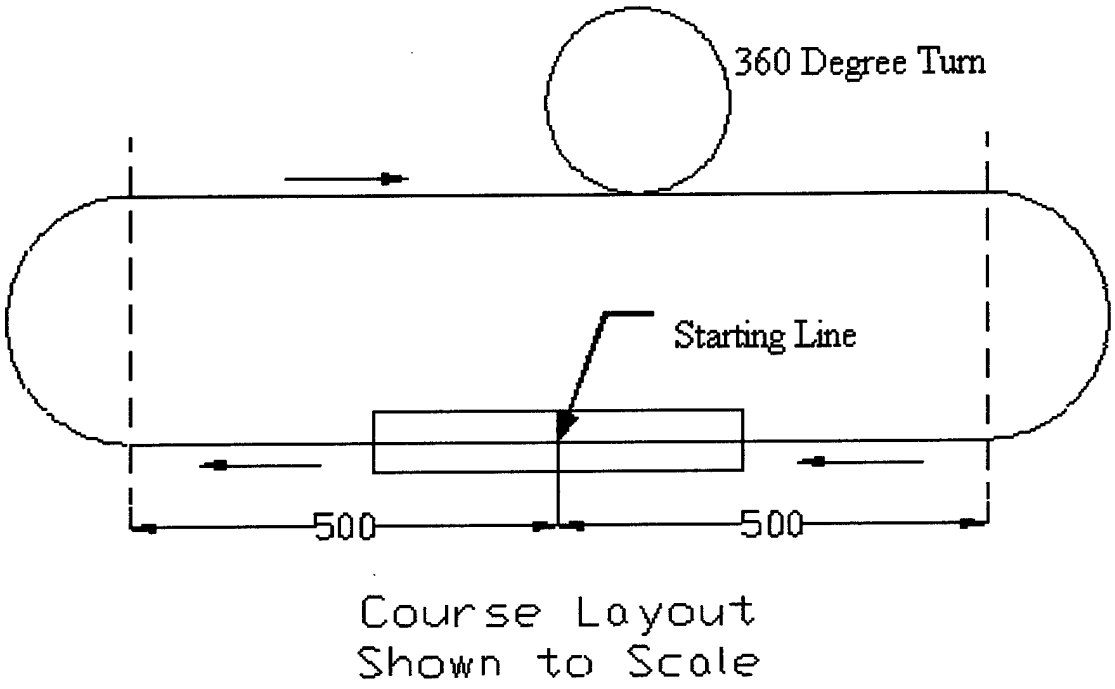

Figure 1. Mission Flight Pattern

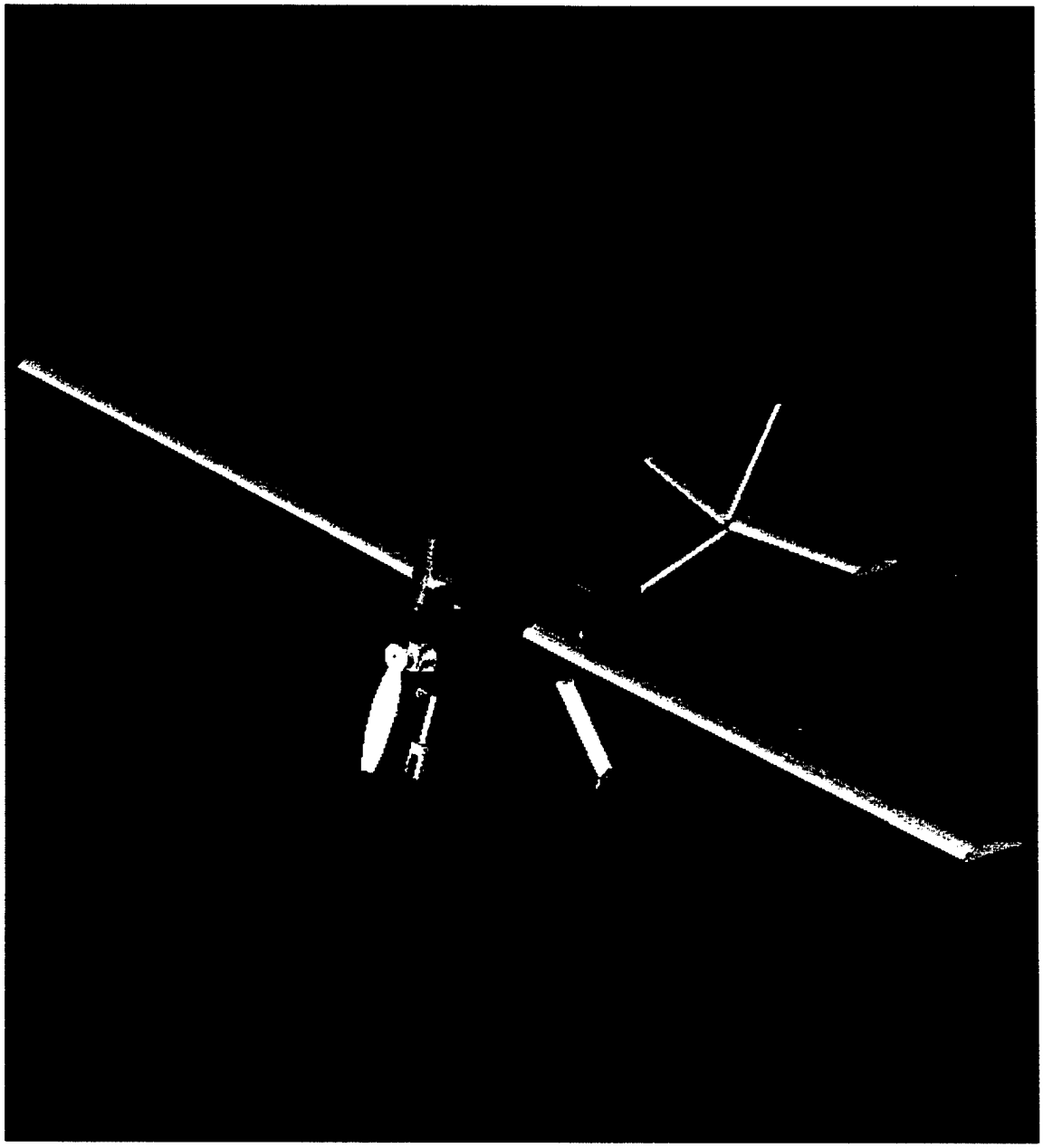

Figure 2. Three View Drawing of The Stop and Go Aircraft

2 Management Summary

The University of Maryland team was divided into five groups: aerodynamics, propulsion, structures, vehicle integration, and information management. Two team leaders oversaw the tasks of all groups through weekly team meetings. At the group level, a group lead was responsible for group organization. This organization including weekly group meetings, monthly timelines, and a designated work schedule. While each group member reported to the group lead, each group lead reported to the overall team leaders. In this manner, aircraft decisions were researched and calculations completed within each group and final choices were presented at weekly team meetings so that the team was kept informed and any concerns were shared within the team. These weekly team meetings ensured that a logical progression of the aircraft was taking place and that choices were made to best achieve the ONR/Cessna competition requirements.

2.1 Group Structure

The need for smaller groups within the team was apparent from the beginning of the Design-Build-Fly meetings. Groups were arranged so that a senior was the group leader. Areas of interest, areas of strength, and university status determined the members of each group. This can be seen on the organizational team chart that follows (Figure 3.).

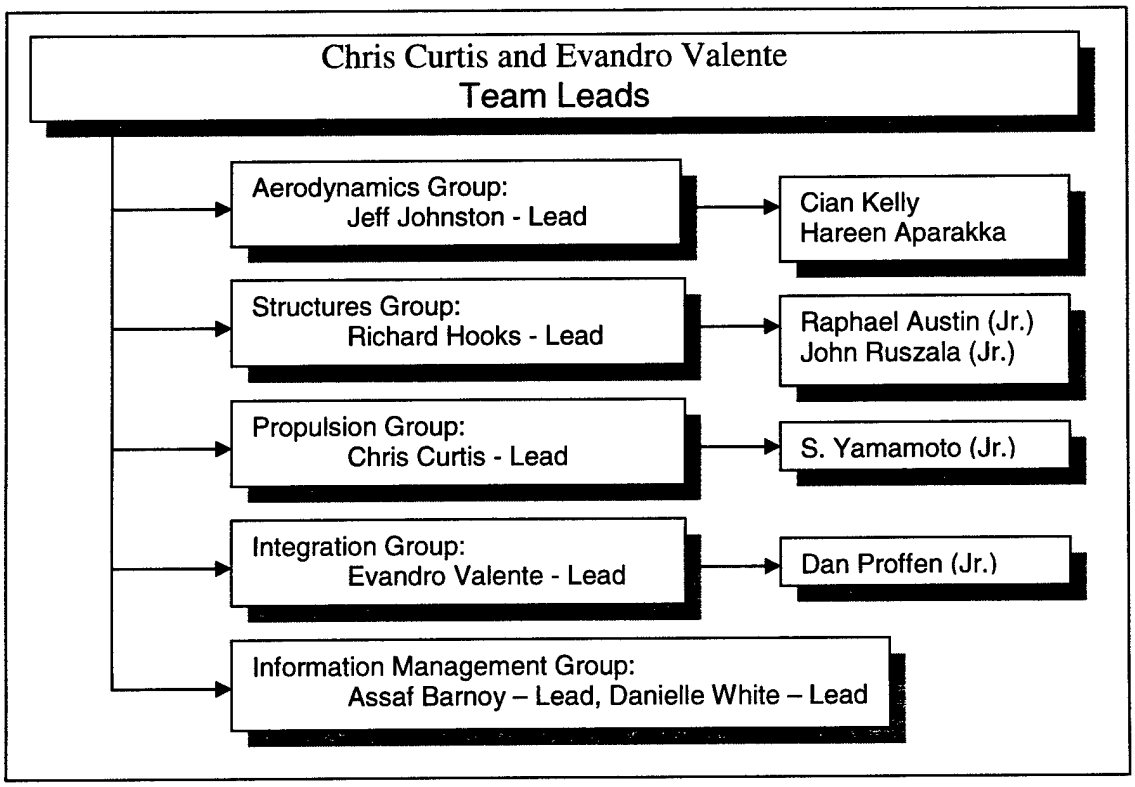

Figure 3. Team Architecture Chart

2.1.1 *Aerodynamics*

The aerodynamics group was responsible for completing the wing and tail trade studies. During the conceptual design phase, wing configurations and tail configurations that could best support the missions were analyzed. Preliminary design finalized wing and tail sizing, airfoil choices, control surface sizing, and manufacturing methods. In the detail design phase, final dimensions were determined for the wing and tail structures.

2.1.2 *Propulsion*

The propulsion group was responsible for choosing the combination of motor, propeller, and battery that would provide the fastest flight times with the least weight. During the conceptual design phase, research was completed in order to choose a group of propellers, motors, and batteries that may be able to meet these requirements. Preliminary design testing narrowed down the choices of combinations able to meet the propulsion efficiency needed. Through continued testing in the detail design phase, finalized choices were made for the motor, propeller and battery configuration that best suited the mission requirements.

2.1.3 *Structures*

The structures group was responsible for determining the best-suited spar material and landing gear configuration. During preliminary design, the group was responsible for analyzing material properties and strengths needed for the wing spars and the wing attachment system. The members also worked to size, design, and choose the proper manufacturing materials for the landing gear. Finalized choices for the wing attachment system and landing gear were made in the detail design phase.

2.1.4 *Vehicle Integration*

The vehicle integration group was responsible for sizing of the fuselage and the payload deployment system. Preliminary design challenged the group to properly size the fuselage in order to achieve the best overall aircraft design while still incorporating enough space for all the internal components. Most of the fuselage sizing was completed during preliminary design, but the payload deployment system required more attention to detail. Finalized choices for the payload deployment system were completed during the detail design phase.

2.1.5 *Information Management*

The information management group consisted of two group leads. One was responsible for the software development and organization, while the other was responsible for keeping detailed notes in order to compile the report. Both of these team functions were necessary from the start of the conceptual design phase. The responsibilities of this group continued to support the team with information management up to the competition date.

2.2 Project Schedule

Critical to the efficient success of the project was an outline depicting the schedule and manufacturing milestones. These milestones are summarized in Figure 4 below.

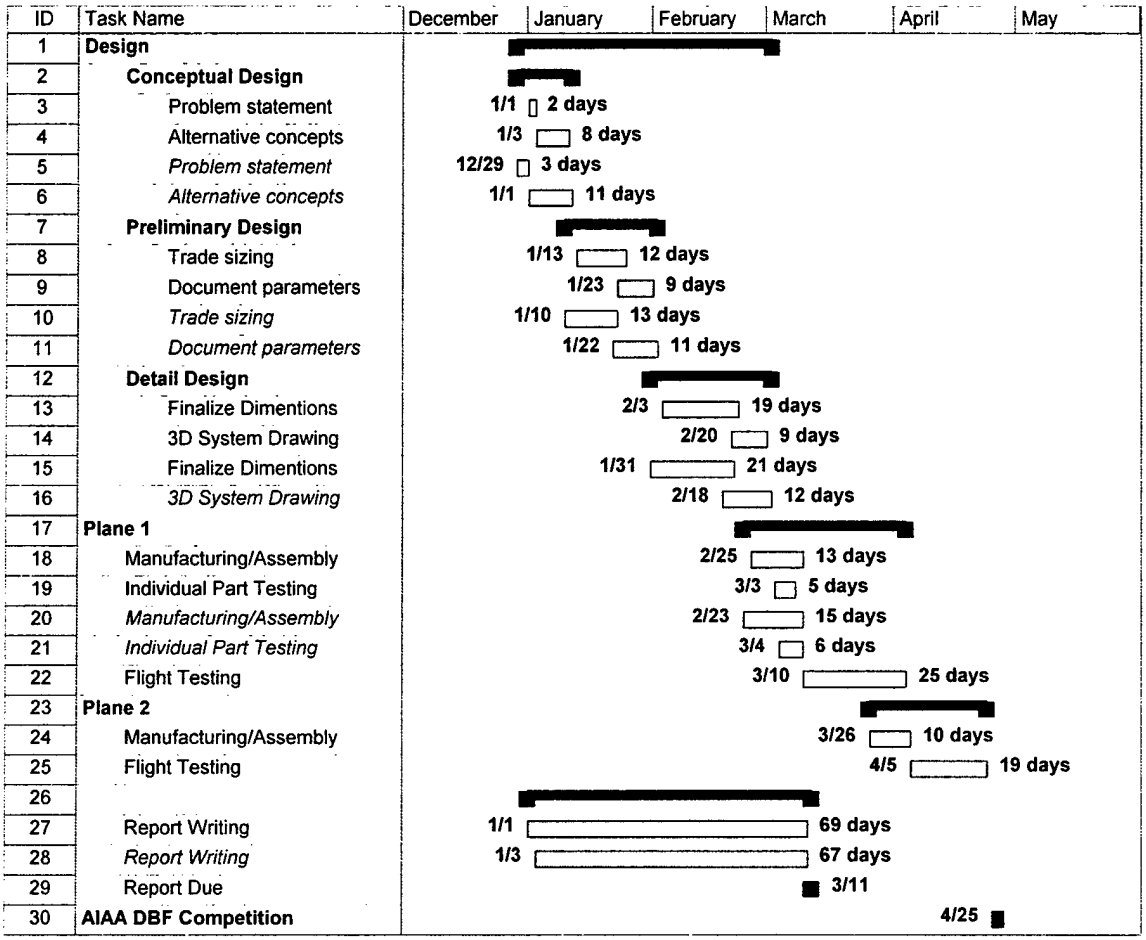

Figure 4. Team Milestones. Blue: Planned. Red: Actual. Black: Span of Task.

3 Conceptual Design

3 Conceptual Design

The design choices for the aircraft were dictated by the mission requirements in the competition guidelines. Competition rules stated that each team must complete two out of the three designated missions. Each mission required a propeller driven, unmanned aircraft under 55 lbs to takeoff in 120 ft. This aircraft was required to fit into a 4' x 2' x 1' box. In addition, assembly time was factored into the total flight score. During all missions, the aircraft had to carry a five pound payload with specified 12" x 6" x 6" dimensions. Each mission entailed a different flight pattern and degree of difficulty. Mission C, which corresponded to the lowest degree of difficulty, required the aircraft to fly four laps around the flight pattern. Mission B had the second highest degree of difficulty and required the aircraft to land halfway through the mission, deploy the payload, and take off a second time to complete the flight pattern. The highest degree of difficulty mission is Mission A where an antenna, mounted three inches from the airframe, would be carried during the entire mission. The Stop and Go Team opted to attempt the two higher difficulty missions. Completion of these two missions was key to achieving the best possible score. The highest overall score would be attained through a combination of the highest report score, the lowest rated aircraft cost, and the fastest flight times on the higher difficulty missions.

3.1 Flight Score Assessment

The ultimate goal for the Design-Build-Fly team was to maximize the score, which would be computed from the following equation:

$$SCORE = \frac{\text{Written Report Score} * \text{Total Flight Score}}{\text{Rated Aircraft Cost}} \quad \text{(Equation 1)}$$

The two parameters related to conceptual design were Total Flight Score (TFS) and Rated Aircraft Cost (RAC). The Total Flight Score (TFS) was the sum of Single Flight Scores (SFS) from two different missions where:

$$SFS = \frac{\text{Difficulty Factor}}{\text{Mission Flight Time} + \text{Aircraft Assembly Time}} \quad \text{(Equation 2)}$$

To achieve a high SFS the team needed to design an aircraft capable of accomplishing missions of high Difficulty Factor (DF) with minimal Mission Flight Time (MFT) and Aircraft Assembly Time (AAT). The three combinations of missions, in order of decreasing difficulty, were Missions 1 & 2, Missions 1 & 3 and Missions 2 & 3. In Table 1, Mission 1 corresponds to Mission C of the

competition, while Mission 2 corresponds to Mission B of the competition. One question posed by the team was: Do the benefits of a higher DF choice offset the possible increases in AAT, MFT and RA? The answer required estimates of mission profiles, including battery drain and MFT required, and complete RAC buildups for each mission combination choice. Minimizing MFTs required an aircraft that would fly at a high cruise speed, which required a low coefficient of drag, a high lift to drag ratio airfoil and a high thrust propulsion system. Minimizing AAT required the design to have the fewest number of aircraft sections that would be assembled and that would be completed in the smallest amount of time.

The equation for RAC was given by:

$$RAC = (A*MEW + B*REP + C*MFHR)/1000 \quad \text{(Equation 3)}$$

The Manufacturer Empty Weight Multiplier (MEW), the Rated Engine Power Multiplier (REP), and the Manufacturing Man Hours (MFHR) needed to be kept to a minimum. MFHR was defined as the sum of the Work Breakdown Structure (WBS) hours. A compact, lightweight airframe with one motor and a low weight battery configuration was desired.

There were five components to the WBS hours:

WBS 1.0 Wing(s):
8 hr / ft Wing Span
8 hr / ft Max exposed wing chord
3 hr / control surface

WBS 2.0 Fuselage
10 hr / ft body maximum length

WBS 3.0 Empennage
5 hr / Vertical Surface
10 hr / Vertical Surface with an active control
10 hr / Horizontal Surface.

WBS 4.0 Flight Systems
5 hr / servo or motor controller

WBS 5.0 Propulsion Systems
5 hr / engine
5 hr / propeller or fan

To analyze the overall sensitivity of Equation 1, an excel spreadsheet program was written that could calculate the total flight given all of the parameters. Very optimistic values were initially chosen to determine what the approximate highest score would be, assuming there were physical constraints. Aircraft dimensions were chosen to be small, and flight and assembly time chosen to be very low, while using the highest difficulty factors. Table 2 lists parameters of the aircraft design and competition requirements that affect the overall score.

Variable Name	Approximate Maximum Value
Report Score	100
Mission 1 Difficulty Factor	2
Mission 1 Flight Time	4
Aircraft Assembly Time	0.5
Mission 2 Difficulty Factor	1.5
Mission 2 Flight Time	5
Weight	10
Battery Weight	3.5
Number of Engines	1
Wing Span	6
Maximum Exposed Wing Chord	3
Number of Control Surfaces	4
Aircraft Length	4
Number of Vertical Surfaces (non-controlled)	0
Number of Vertical Surfaces (controlled)	1
Number of Servos	3
Numbers of Props	1

Table 1. Approximate Maximum Values

Using these values a score of 7.60521 was calculated and was assumed to be the highest possible total score. To continue the analysis, the derivatives with respect to each variable in the scoring function were calculated. Some of the derivative step sizes were larger than others because of the function constraints. For example, the smallest allowable step size for Difficulty Factor is 0.5 because this would be the next lowest value allowed by the project rules, whereas the step size for flight time was chosen to be around 0.001, since there would be no constraint on it. The table below showed the values of the derivatives at the highest score.

Variable Name	Approximate Maximum Value	Step Size	Value of Derivative
Report	100	1	0.0760521
Difficulty Factor 1	2	0.5	2.35655
Mission Flight Time 1	4	0.1	-1.02458
Aircraft assembly Time	0.5	0.1	-1.02458
Difficulty Factor 2	1.5	0.5	1.92808
Mission Flight Time 2	5	0.1	-0.516451
Weight	10	0.1	-0.0805637
Battery weight	3.5	0.1	-1.1908
Number of engines	1	1	-0.990765
Wing span	6	0.01	-0.129017
Maximum exposed wing chord	3	0.01	-0.129017
Number of control surfaces	4	1	-0.0480835
Aircraft Length	4	0.01	-0.161264
Number of vertical surfaces (non-controlled)	0	1	-0.0798029
Number of vertical surfaces (controlled)	1	1	-0.157948
Number of servos	3	1	-0.0798029
Number of props	1	1	-0.0798029

Table 2. Derivatives of Score Components

The derivatives illustrated how sensitive the scoring function would be to each competition variable, i.e., how fast each of the variables would cause the score to change. In other words, if a parameter was altered, how would that increase or decrease affect the overall competition score. Since the scoring function was by no means a linear function, the values of the derivatives would change when different design parameters were input, but the values were about the same trend-wise. This was verified by trying many different values for the variables. Plots of each variable versus score were made and sensitivity trends were obtained.

The reason that the derivative information was so useful was because it allowed the aircraft design choices to be traded against one another. When designing the aircraft, certain sacrifices needed to be made in order to accommodate the different missions. These derivatives showed which variables were most critical. As an example from the table above, the derivative value for the number of servos was –0.079 and the derivative for battery weight was –1.19. This implied that for one additional servo the score would be expected to drop by 0.079 points, while the score would be expected to drop by 1.19 for only 0.1 additional pounds of battery weight. This clearly showed that battery weight impacted the overall score more than the number of servos.

This analysis gave the team important information about the design of the aircraft. Based on this sensitivity analysis, the team could assess which parameters were more likely to affect the final total score.

All of the parameters discussed above would be coupled. For example: Minimizing RAC established a trend toward smaller motors and a reduction in battery cell count and weight, thus decreasing thrust and endurance. At some point the thrust available would be insufficient to get the aircraft in the air in the specified 120 ft, and the lowered flight speed and battery endurance would not be sufficient to complete the course. Similarly, low MFTs required maximum thrust, thus higher battery weight, raising RAC. This negated any bonus in SCORE from the low MFT. An iterative process was required to find a balance between the parameters to maximize the competition score, taking into account design restrictions.

3.1 Conceptual Design Figure of Merit Table

The team developed a unique set of performance metrics based on discussion about the aircraft configuration and the requirements/missions for the 2003 DBF Competition. These performance metrics consisted of the following items:

- Ability to fly all missions
- Box containment & assembly
- RAC
- Handling & control

- L/D ratio
- Construction

To evaluate each performance metric, a figure of merit scale (ranging from 1-worst to 10-best) was used to compare various aircraft configurations. Rated Aircraft Cost was calculated from an internally created program. The rated aircraft costs were calculated as actual RAC values and did not follow the 1 to 10 scaling used for other performance metrics. Results are summarized in Table 3. The most feasible design layouts for remote control aircraft were listed here for consideration. Design layouts such as those seen on the seaplane, the Twin Mustang (double fuselage), or other exotic prototypes were not listed because of the limited information available on such designs and their unnecessary specialization. All layouts were for single engine aircraft.

			Complete Missions	Boxability & Assembly	Construction	Handling & Control	Rated Aircraft Cost	
Configuration		Weight Factor	0.3	0.2	0.1	0.15	0.25	1
Conventional: Forward Wing/Rear Tail	Tail Dragger	V.	7.67	8	7.33	7.17	10.41	**8.3883**
		Conv.	7	9.33	9	8.5	10.51	**8.7086**
	Tri. Gear	V.	9.67	7	5.83	8	10.46	**8.7107**
		Conv.	9.67	8.33	7.5	9.33	10.56	**9.2186**
Twin Boom Pusher	Tail Dragger	V.	5	5.33	3.83	7.67	10.48	**6.7413**
		Conv.	5	5.67	5	9	10.61	**7.1364**
	Tri. Gear	V.	4	5	4.5	6.67	10.53	**6.3846**
		Conv.	2.33	5.33	5.67	8	10.66	**6.3104**
Canard Config.	Tail Dragger	Pusher	3	3	5	5	12.61	**6.0855**
		Tractor	6	5.67	5	5.67	12.61	**7.4835**
	Tri. Gear	Pusher	2.67	4.67	5	6.33	12.66	**6.5464**
		Tractor	9	4.33	5	6.67	12.66	**8.2212**
Flying Wing		Pusher	1.67	4.33	4.67	2.67	13.55	**5.9652**
		Puller	7	4	4.67	2.33	13.55	**7.3073**

Table 3. Figure of Merit Chart

It was assumed that no aircraft configuration was inherently lighter than the next simply by its geometry. Instead, it was more important to choose an aircraft configuration based on how well its geometry would fit the mission requirements and other competition scoring factors. It was assumed that no matter which aircraft configuration was selected, the team would be capable of constructing an aircraft that was as light as possible and as strong as necessary.

Each category was given a weight factor that indicated the importance of a given column to the preliminary design effort and future design stages. The merit table clearly rated the conventional, tricycle gear aircraft with a conventional tail as superior.

3.2 Aerodynamics

During the conceptual design phase, the aerodynamics group focused on three main areas of design for the aircraft. These areas included fuselage shape, wing configuration and tail configuration.

3.2.1 Aircraft Layout

The primary concern when choosing the aircraft layout was to ensure that all of the mission requirements could be fully satisfied with each configuration. It was also vital that the chosen configuration was able to give the Stop And Go team the highest score possible. For this project the major mission requirements were the capability of dropping the payload and the ability to fly with the PVC antenna protruding from the aircraft. After ensuring that the aircraft could conceivably complete a given mission the advantages and disadvantages of each could be evaluated. Four major configurations were initially considered: the traditional layout, a flying wing, a twin boom and a canard aircraft. All four of these options could conceivably carry the payload, drop it by some mechanism, and carry the PVC antenna.

The following advantages and disadvantages were considered for each of these layouts given the competition missions:

- Flying Wing:
  - Advantages:
    - High lift efficiency so that required takeoff distance would be achieved
    - Relatively low drag
  - Disadvantages:
    - Ineffective at carrying the payload
    - Thickness required in the central airfoil cross-section would be great compared to feasible chord length giving large flow separation and enormous drag result

- Twin Boom:
  - Advantages:
    - Better rotational support for tail because booms offered twice the support
    - Allowed for larger elevator
  - Disadvantages:
    - Two vertical surfaces increased RAC
    - Increased weight

- Canard layout:
  - Advantages:
    - Canard will stall before the wing, making a wing stall situation almost impossible
    - Overall lift efficiency is higher because there is more total lifting area
  - Disadvantages:
    - Canard wake disrupting flow over the wing A
    - An inability of the wing to fly at C_{Lmax} due to canards stalling

- Conventional Forward Wing / Rear Tail
  - Advantages:
    - Large amounts of information available on conventional aircraft performance
    - Team's pilot had more experience flying aircraft of this type
  - Disadvantages:
    - Landing gear had to be supported by the fuselage
    - Weight of the tail shifts the center of gravity of the aircraft rearward compared to other layouts

Due to these considerations and our conceptual scoring estimates, a conventional aircraft layout was chosen. It would be able to fulfill all mission requirements and would have the highest score potential.

3.2.2 Wing Configuration

The placement of the wing on the fuselage would affect the stability and maneuverability properties of an aircraft. It would also have an affect on the aircraft's ability to perform a given mission. Since there were three possible wing placement configurations: high, mid, and low, it was important to develop a set of criteria to evaluate the placement of the wing on the fuselage. These different criteria consisted of:

- Stability: The ability of the aircraft to return to its initial condition after being disturbed is highly desirable.
- Maneuverability: The only maneuvers to be performed are the turns in the pattern.
- Payload Dropping: The ability of a wing configuration to drop the payload would be essential to mission performance

	Weight	High	Mid	Low
Stability	0.3	3	2	1
Maneuverability	0.3	1	2	3
Payload Dropping	0.4	3	2	1
	1	**2.4**	**2**	**1.6**

Table 4. Wing Configuration FOM

Table 4 summarizes how each of the different wing placements compares to one another. A figure of merit scale was used to rate the different wing placement configurations. The main

reason low and mid wings were undesirable was due to their inability to drop the payload in a stable manner as shown in Figure 5. For aircraft stability the payload should be carried so that its center of gravity lines up with the center of lift. This prevented the pitch dynamics from being affected significantly by dropping the payload. Because this would not be possible with either the low or mid wing configurations, they could not be used for this aircraft.

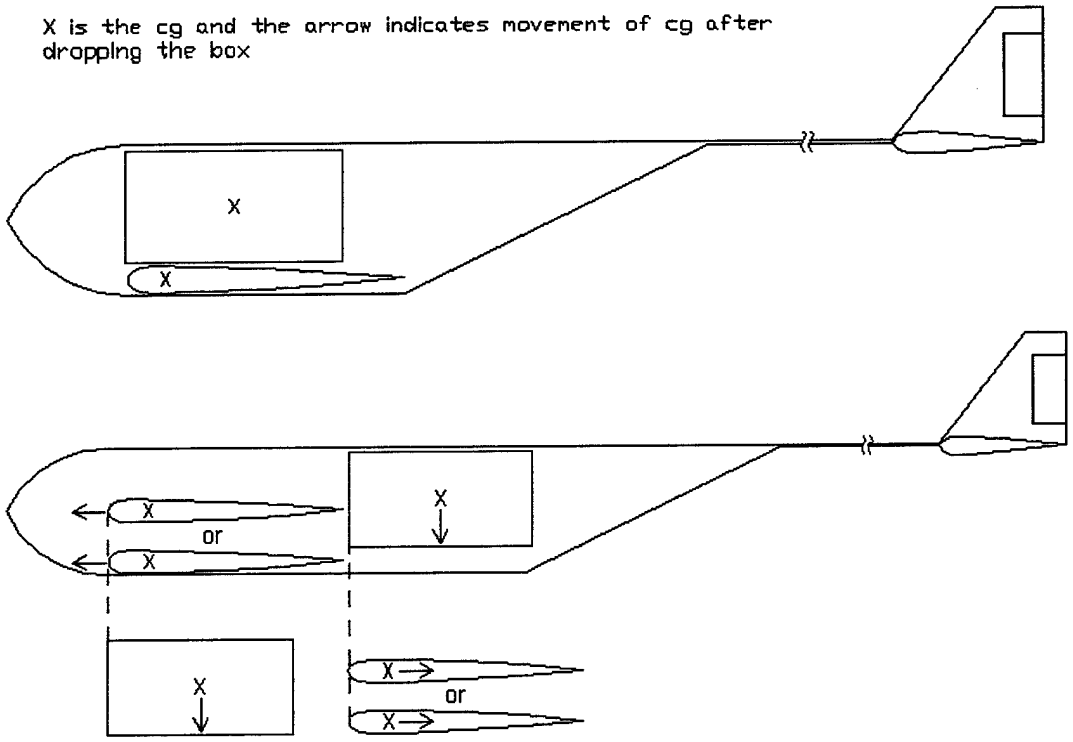

Figure 5. Payload Deployment with Low and Mid Wing

3.2.3 Tail Configuration

Three different tail configurations were examined for this project: conventional, T-tail, and V-tail. Although each of these tail configurations could function on the Stop and Go, the goal was to select the smallest, lightest one that would give the required trim, stability, and control. The following were the advantages and disadvantages considered for the aircraft relative to a conventional tail:

- T-tail
  - Advantages:
    - Vertical stabilizer can be smaller while still providing the necessary yawing moments
    - Ideal for meeting aircraft storage requirements
  - Disadvantages:
    - Requires a much stronger vertical stabilizer, which negates the weight savings
    - Blanketing of the horizontal stabilizer by flow from the wings during takeoff and landing, which reduces the effectiveness of the elevators during flight at high angle-of-attack

- V-tail
  - Advantages:
    - Weight savings over a conventional tail
    - Only requires two servos, which would reduce the RAC of our aircraft
  - Disadvantages:
    - Use of 'rudder-vators' is very complicated
    - Complexity makes a V-tail excessively difficult to develop

	Weight	Conventional	T-tail	V-tail
Stability	0.3	2	3	1
Construction	0.35	3	1	2
Stiffness	0.35	3	1	2
	1	**2.7**	**1.6**	**1.7**

Table 5. Tail Configuration FOM

Due to the aerodynamic disadvantages of the T-tail and V-tail designs, a conventional tail configuration was the most likely candidate (See Table 5). This would give the necessary trim, stability, and control properties, while also being relatively simple to construct.

3.3 Propulsion

The propulsion group concentrated on two areas during the conceptual design phase. These areas included motor configuration and landing gear configuration.

3.3.1 Motor Configuration

Three motor configurations were considered: tractor, pusher, and multi-motor. Choosing the best configuration was important to the mission not only for efficiency, but also for its effect on rated aircraft cost. The following advantages and disadvantages were considered for the motor configuration:

- Tractor
  - Advantages:
    - Helps keep the center of gravity near the quarter-chord of the wing
    - Keeps the propeller clear of the runway during takeoff and landing
  - Disadvantages:
    - Swirling flow from the propeller moves along the length of the aircraft
    - Some disruption of lift and a leftward yawing moment caused by flow hitting the vertical stabilizer
- Pusher
  - Advantages:
    - Undisturbed flow across its length because of the aft placement of the propeller
    - Larger upsweep angle on the tail boom because the pull of the propeller prevents the flow from separating

- Disadvantages:
  - Tends to move the center of gravity back from quarter chord
  - Incapable of achieving proper propeller clearance necessary to continue in Mission B once payload was deployed

- Multiple Motors
  - Advantages:
    - Can be wing mounted, pod mounted, or a pusher/tractor configuration
    - Theoretically, doubles the amount of thrust
  - Disadvantages:
    - Battery life is shortened with two motors drawing power
    - Added construction complexity

	Weight	Tractor	Pusher	Multi
Stability	0.25	2	3	1
Power	0.25	2	1	3
Structural Support	0.15	3	2	1
Weight	0.15	3	2	1
Payload Deployment	0.2	3	1	3
	1	**2.5**	**1.8**	**1.9**

Table 6. Motor Configuration FOM

Due to the results of this analysis, the Stop and Go was designed with a single engine, tractor motor (See Table 6). There were two factors in this decision. The first was the ease of payload deployment without interference from the propulsion system, and the second was the ease of controlling battery weight because only one motor would be drawing power.

3.3.2 Landing Gear Configuration

One of the main considerations in choosing the landing gear configuration was stability during takeoff and landing. Only two configurations, the tail-dragger and the tricycle, satisfied this parameter when considering the two higher difficulty missions. The following advantages and disadvantages were considered when selecting the landing gear configuration:

- Tail Dragger
  - Advantages:
    - Without nose gear, one less servo needed (lower RAC)
    - Increased propeller clearance
  - Disadvantages:
    - Difficulty maneuvering around deployed payload during Mission
    - Unstable control during landing
- Tricycle:
  - Advantages:
    - Maneuverability around dropped payload during Mission B
    - Ground stability due to center of gravity placement
  - Disadvantages:
    - Extra servo needed to control nose gear, increasing RAC

- Less than optimal placement of rear landing gear due to payload placement

After serious consideration of both of these options for landing gear configurations, the tricycle configuration was determined to provide the highest score potential. Its primary advantage was the ability to complete Mission B without the extra necessity to maneuver around the payload once it was deployed. Also, the additional servo would be used to deploy the payload, distributing the RAC over two aircraft systems.

3.4 Conceptual Design Results

After considering all factors that significantly affected overall mission completion and flight score, an aircraft layout, wing configuration, tail configuration, motor configuration, and landing gear configuration were selected. Using the figure of merit chart, it was determined that the Stop and Go aircraft would be a high wing aircraft with conventional forward wing/rear tail. The high wing was chosen due to its effective dihedral, which when combined with aspect ratio would contribute to increased lift, thus allowing the aircraft to takeoff in 120 ft. Also, the high wing was the only wing that allowed for stable, efficient payload deployment. The conventional tail was chosen because it was lighter than other configurations and easier to construct. The aircraft would have a single tractor engine and tricycle landing gear. The single engine was chosen because this configuration had the best overall efficiency while a tractor engine allowed ease of payload deployment and continued maneuverability after payload deployment. This aircraft configuration achieved the highest score on the Figure of Merit Chart and provided the best possible flight score when the two most difficult missions were considered.

4 Preliminary Design

After the conceptual design of the aircraft was completed, the preliminary design phase involved in-depth trade studies and component sizing and testing. The aerodynamics group chose parameters for wing and tail sizing and airfoil types. The vehicle integration group completed the fuselage sizing and the structures group focused on the necessary strength and sizing of the landing gear. The propulsion group tested to find the most efficient combination of motor, propeller, and battery. Several areas that had not been considered during the conceptual design phase, including spar sizing and payload deployment, were investigated. The next few sections summarize trade studies and component testing conducted for each subsystem area of the aircraft.

4.1 Aerodynamics

During preliminary design, the aerodynamics group focused on wing sizing, tail sizing, and selection of the airfoil type for the aircraft. Trade studies were completed to determine the airfoil that best met the performance needs of the missions. Utilizing the necessary C_{Lmax}, wing sizing was determined. After the airfoil shape and size were selected, tail sizing was completed and manufacturing begun.

4.1.1 Lift Needed for Takeoff

To commemorate the initial Wright Brothers flight, the competition mandated a maximum takeoff distance of 120 ft. It was imperative for the aircraft to meet this requirement. To ensure that this requirement is not violated, the aircraft was designed to take off within 100 ft. This provided some margin for imperfections in the aerodynamic calculations and unknown variables under real flight conditions (such as wind).

Due to the vital importance of meeting the takeoff distance requirement, this would be the foundation for selecting a wing design. A MATLAB script was created which had estimated weight, drag, and dynamic thrust. This script took an input parameter of wing area and returned the value of C_L required to get the aircraft off the ground in 100 ft. Results from this program allowed the team to determine the C_L versus wing area needed for takeoff (See Figure 6).

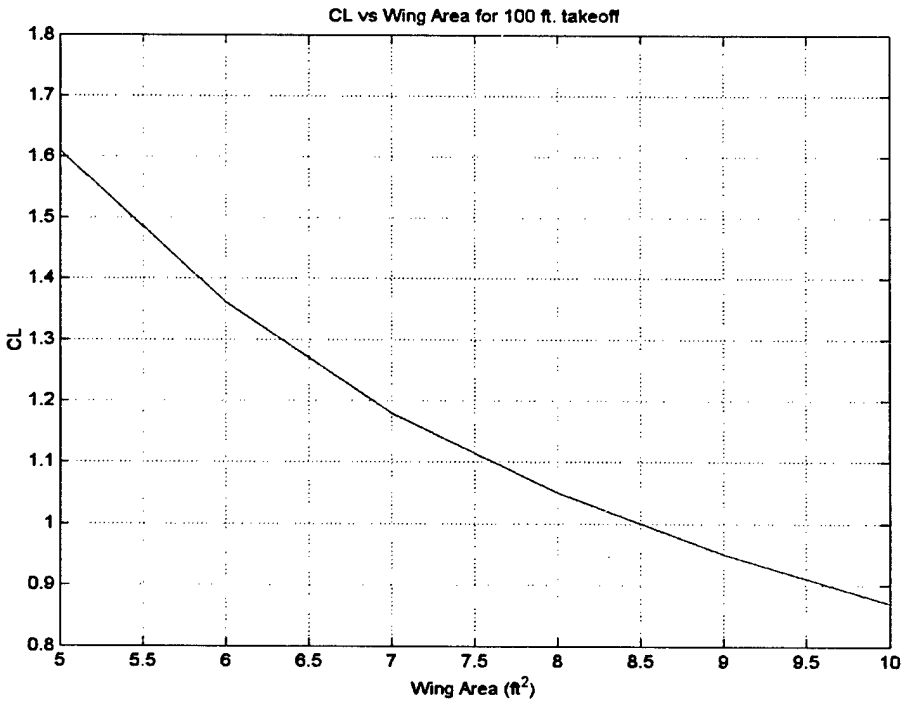

Figure 6. C_L vs Wing area

This graph showed that the wing would require at least 6 ft^2 of surface area. A smaller wing would require an unattainable value of C_L. To get off the ground the wing would require a value of C_L from 1.05 – 1.35. Further analysis would be performed to determine which wing area/C_L pair would result in the highest cruise speed.

4.1.2 Effects of Wing Area on Performance

Many analyses were done to determine the optimum planform area for the wing. Each analysis was done with the understanding that at least 6 ft^2 was necessary to get off the ground in the required takeoff distance. Options for the surface area were analyzed with respect to drag produced, weight, and stall speed. The results showed that a planform area from 6 to 8 ft^2 would perform admirably, but the aerodynamics group was reluctant to choose a planform area of only 6 ft^2 due to takeoff distance considerations. Due to the added drag from the antenna, which could not be accurately calculated, it was decided to slightly oversize the planform area. The effect on RAC for selecting a larger planform area was negligible compared to being disqualified for not meeting the 120 ft. takeoff distance requirement. Other analyses showed that the increase in drag on a 7 ft^2 planform would not have a large effect on maximum velocity. Therefore, the final planform area selected was 7 ft^2.

4.1.3 Analysis of Wingspan, Chord Length, and Aspect Ratio

The primary concern when selecting the wingspan was the ability to fit the wing into the box. Using the two-piece wing concept, it was decided that no wing section could be longer than 4 ft. A longer section would have to fit in the box diagonally, reducing the amount of space available for the fuselage, tail assembly, and landing gear. For simplicity of assembly the number of wing sections was restricted to two, otherwise the increased assembly time could have a significantly adverse effect on the score. Each of the wing sections would be 4 ft. long, giving the aircraft a wingspan (without taking the fuselage into consideration) of 8 ft.

The chord length of the wing had a significant effect on the drag characteristics. Studies showed that a chord length between 8 and 12 in. would be the optimum for our aircraft. A chord longer than 12 in. would have problems with flow separation at the aircraft's speeds while a chord shorter than 8 in. would not have sufficient thickness to accommodate its attachment to the fuselage. The other consideration was the necessary positioning of the wings inside the box. Final chord length selection was determined by dividing the selected planform area by the wingspan. The resulting 10.5 in. chord satisfied all of the selection criteria for chord length.

When designing the wing it was desirable to have a relatively high aspect ratio. This would give the wing high lift efficiency and excellent performance characteristics. The aspect ratio was not set before selecting other wing dimensions. It was instead decided that a long span and short chord should be selected and if the aspect ratio was not above 8, the design would be reconsidered. The final aspect ratio was calculated to be 9.92.

4.1.4 Airfoil Selection

The selection of the airfoil was based on the following parameters:

- C_{Lmax} – For a 7 ft^2 wing a C_L of 1.2 was needed at some angle of attack to meet the takeoff requirement
- L/D max – It was desirable to have a high L/D at cruise (low angle of attack) for efficient performance.
- C_L at cruise – The wing needed to have a C_L capable of supporting the aircraft during cruise flight.

Looking through numerous books with airfoil performance data the Clark Y airfoil was selected. It would provide ample lift during cruise flight, gave enough lift for takeoff well below stall speed, and had a high L/D maximum. Other airfoils (including the NACA 2312 and N22) had similar performance characteristics but slightly more drag at cruise or less lift at takeoff. The Clark Y provided the best combination of cruise and takeoff performance. (See Figure 7.)

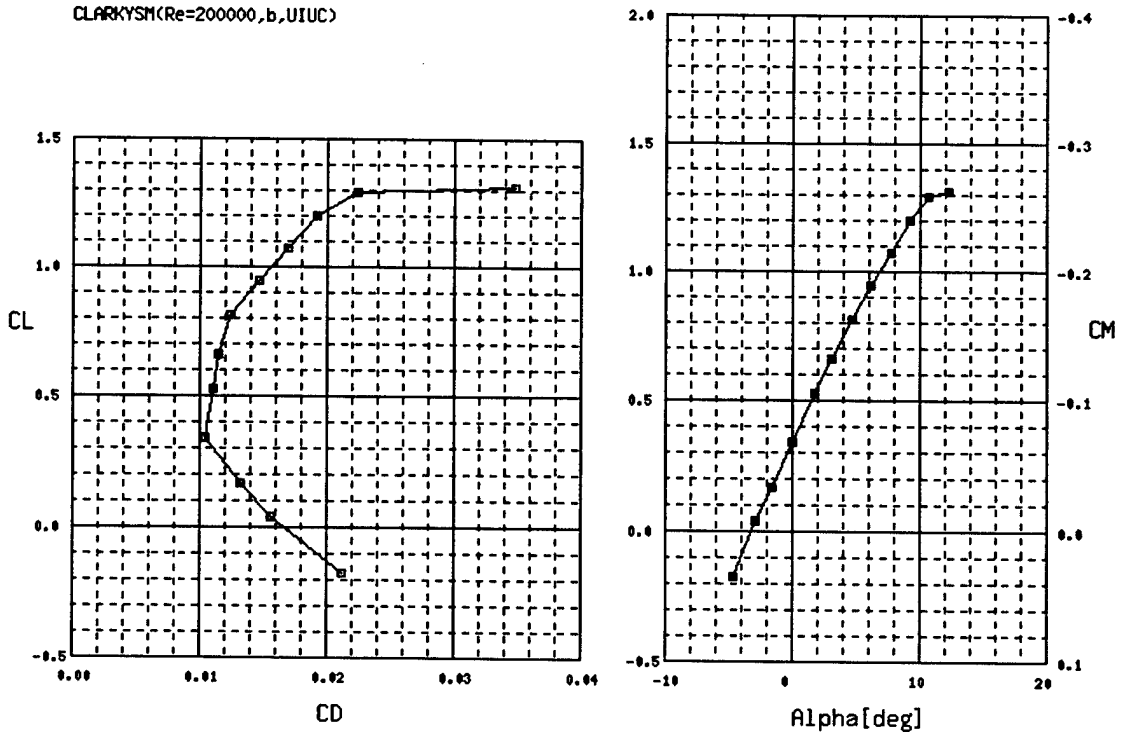

Figure 7. Clark Y Drag Polar and Lift Curve Slope

From the drag polar, lift and drag were expected to be 18 lb and 0.3 lb at takeoff, respectively. During cruise flight the lift was expected to be roughly the same and the drag to be 1.16 lb., although these numbers would change after the payload was deployed or the antenna attached.

4.1.5 Tail Sizing

During the conceptual design phase, the decision was made to use a conventional style tail. After determining the general tail configuration, the sizing of the tail and control surfaces and the moment arm distance had to be investigated. The material, construction method, and integration methods available also had to be explored.

Several basic parameters contributed to the initial estimate of the tail size. One of the major factors was the limitation that the tail span could not exceed 25% of the wingspan. Another major factor was the storage requirement for the disassembled aircraft. In order to have a single tail section, the horizontal tail span could not exceed two feet while the vertical tail height could not exceed one foot. This sizing was necessary in order to meet the "boxability" requirement.

Initially, the tail was to be manufactured from balsa wood. Later in the design stage, however, a composite airfoil similar in construction to the wing was selected to give the tail better torsional stiffness and less weight than the balsa. This decision became critical after deciding to design the tail with the maximum surface area possible. A larger tail area would increase its

effectiveness, thus decreasing the moment arm and allowing the boom to be shortened considerably. The larger tail surface would also help to compensate for the drag and instability created by adding the antenna assembly to the aircraft during Mission A. Considering all of these factors while including the "boxability" requirement, the maximum horizontal tail span could measure 23 in., and the vertical tail 11 in.

At the time of initial tail sizing, exact wing dimensions had not yet been chosen. Therefore it was necessary to make a spreadsheet that fixed the wing reference area while varying the span. Based on wing aspect ratio and chord length, the spreadsheet was used to find the appropriate tail dimensions, keeping the horizontal tail span at 25% of the wingspan. The moment arm was calculated using the tail volume coefficient equations from Raymer (pg. 123) as referenced in the bibliography.

4.2 Propulsion

The impact of the propulsion system on the aircraft design was of utmost significance. The choice of components for the propulsion system was determined by the ability to complete the missions in the lowest time possible, thus providing for the highest possible score. The battery weight must be kept to a minimum while obtaining the best propeller and motor configuration.

In addition to the competition requirements, a list of performance parameters for the propulsion system was compiled. Initially, a list of optimal velocities was established around which to configure the propulsion system. A stall speed range of 20 to 30 mph, a cruise speed range of 30 to 50 mph, and a maximum speed of 50 to 60 mph were established. In addition, battery endurance was specified to be 15% above that which would occur from the highest expected amperage draw.

The goal of the propulsion group was to select a configuration of propeller, motor, and battery that would maximize the score by minimizing flight times and component weights while adhering to the previously established system requirements.

Initially, three basic system configurations were considered: single motor with single battery, double motor with double battery, and double motor with single battery. In order to analyze the different options and identify the optimal configuration, several analysis categories were developed. A weight factor was assigned to the following elements: RAC effect, weight, boxability and assembly, construction complexity, and cost. The resulting analysis indicated that the single motor with single battery configuration was the optimal configuration. Table 7 is the merit chart through which each motor and battery configuration was analyzed.

	Weight Factor	Double motor/ Single battery	Double motor/ Double battery	Single motor/ Single battery
RAC	0.35	2	1	3
Power	0.2	2.5	2.5	1
Weight	0.15	2	1	3
Boxability & Assembly	0.15	1.5	1.5	3
Construction Complexity	0.1	1.5	1.5	3
Cost	0.05	1.5	1.5	3
	1	**1.95**	**1.45**	**2.6**

Table 7. Motor and Battery Configuration FOM

The first component within the propulsion system to be analyzed was the motor. Due to availability, the AstroFlight family of motors was chosen over the Graupner family. Of the motors offered by AstroFlight, the Cobalt 40, 60, and 90 size sport motors showed to be feasible and were chosen for further analysis. (See Table 8.) Historical data on these motors was scarce and their reliability was uncertain, so performance software was chosen to obtain propulsion performance estimates.

	Weight Factor	AstroFlight 40	AstroFlight 60	AstroFlight 90
Maximum Thrust	0.2	1	2	3
Maximum Velocity	0.2	1	2.5	2.5
Amperage at V_{max}	0.15	1	2	3
Amperage at V_{cruise} (~45 mph)	0.15	1	2	3
Number of Cells Required	0.15	3	1.5	1
Motor Weight	0.1	3	2	1
	1	**1.45**	**1.925**	**2.25**

Table 8. Motor Selection FOM

Of the airplane motor software packages on the market, Motocalc 6.05 proved to be the most comprehensive software available. Motocalc uses information from the manufacturers of different motors, speed controllers, propellers and battery cell types, along with aircraft geometry, to predict various propulsion parameters such as thrust at full throttle versus velocity, amperage at full throttle versus velocity, and amperage draw versus cruise velocity (Figure 8). To validate the predictions gained from Motocalc, static thrust and amperage tests were performed, and this data agreed with that obtained from the software. The amperage data showed some discrepancies but was consistent throughout all motor types tested, thus the incongruity was disregarded.

In order to identify the optimal motor, several analysis categories were developed. A weight factor was assigned to the following elements: maximum thrust, maximum velocity, amperage at maximum velocity and cruise velocity, required number of battery cells, and motor weight. The resulting analysis indicated that the AstroFlight 60 and 90 motors warranted further analysis. Provided is the merit chart through which each motor was analyzed.

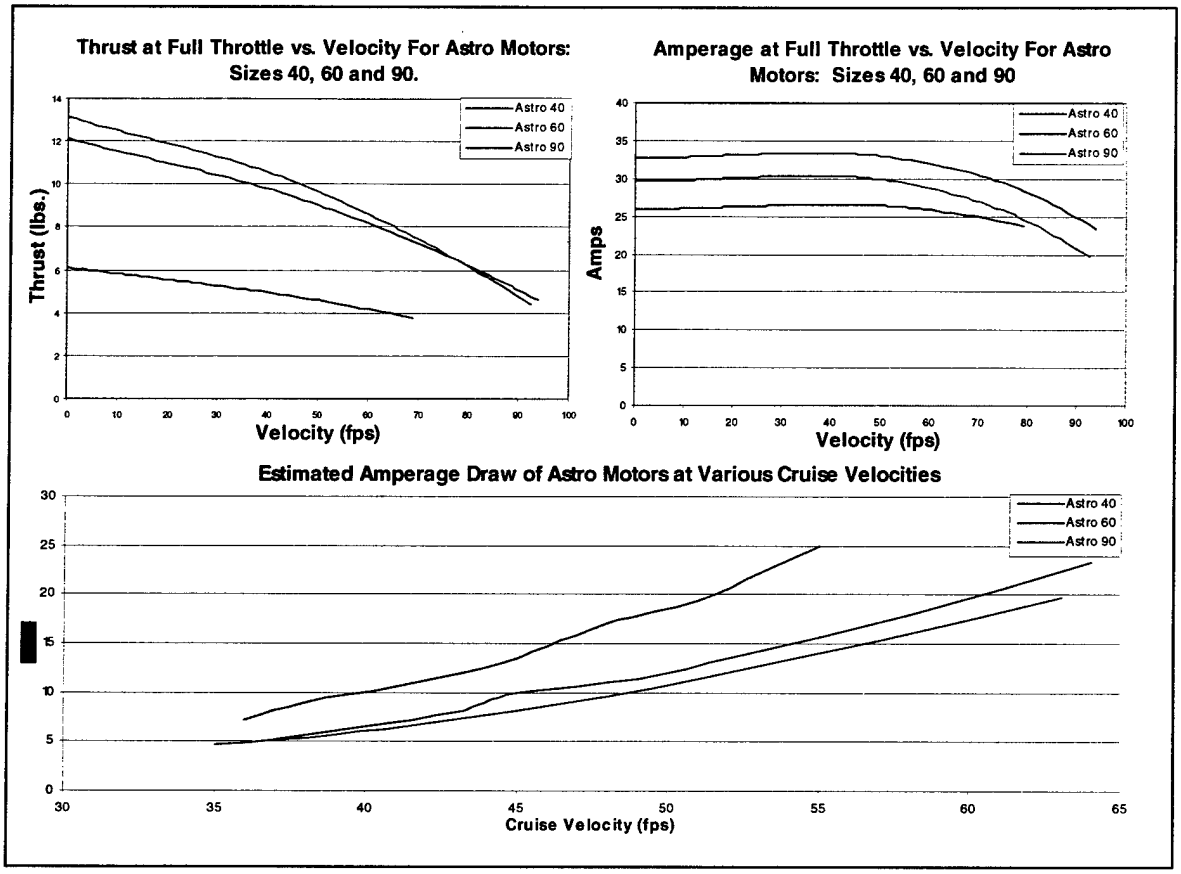

Figure 8. Thrust and Amperage vs. Velocity for AstroFlight Motors

4.3 Structures

The biggest challenge for the structures group was fitting aircraft components into the designated 4' x 2' x 1' box. The selection of the wing spar was determined by availability of appropriate products and sizing constraints. Wing spars were necessary to act as support and connection structures for the wings given the storage requirements ("boxability") for the aircraft. The landing gear configuration was determined by three main factors: payload deployment, 'boxability', and propeller diameter. With these factors in mind, specific measurements, manufacturing choices, and strength calculations were formulated.

4.3.1 Wing Spars

The spar structures in the aircraft were designed with the consideration for fitting the plane into the box. First, a combination of two 4 ft wing sections was selected because a continuous wing would not fit in the box. This design would call for some kind of support at the root of the wing. Therefore, the decision was made to use a spar to enable a snap-together configuration. Running the spar only partially through the wing was not possible due to our manufacturing capability, so it needed to run the full span of the wing. With this in mind, the spar would

distribute the load along with the composite skin. To select a material for the spar, a study was done to compare the relative strength to weight ratios between aluminum and carbon fiber tubing.

The analysis of the spar was completed by modeling each section of the wing (right and left) as a cantilever beam with elliptical loading. Each 4 ft spar was analyzed with an assumed 4g-load factor to simulate the absolute max load that the plane would exhibit in normal flight conditions during a quick turn. To make sure the calculations were within the expected margin of safety, a safety factor of 2 was used. Matlab code was developed to perform an iterative calculation of the diameter required vs. span for the two materials. It was found that the carbon fiber tubing outperformed the aluminum by far. The carbon fiber maximum outer diameter was calculated to be 0.3 in. with only a very thin wall needed to withstand the load, although a larger diameter of about 0.75 in. carbon tube was chosen because it was a more standard size. Therefore, the carbon fiber spar would be more than strong enough to survive any load it may see.

4.3.2 Landing Gear Sizing

The next structure that was analyzed was the landing gear. One of the early concerns of the team was to make the landing gear as strong and as light as possible. The gear was designed to provide sufficient propeller and payload deployment clearance. Also, the location of the main landing gear was important for aircraft rotation on takeoff, and it would bridge the bottom of the fuselage.

The first material considered was aluminum, but composite materials were considered because of their strength and low weight. After a simple bending, shear, and buckling analysis of the landing gear made with a piece of wood wrapped in composite (either carbon fiber or fiberglass), it was verified that the composite wrapped wood was going to outperform the aluminum.

The landing gear would be a necessary part of each mission. If the gear fails, then there would be a risk of losing the aircraft without completing the mission. Thus, it was important to over-design the landing gear to more than withstand the loads transferred to it in landing. A trade study would be conducted to determine the optimum cross-sectional dimensions of the wrapped wood material. Trade studies would also be completed on fuselage strength, the need for a rear bulkhead, and the strength of the tail connection.

4.4 Vehicle Integration

The payload deployment system was the highest priority project for the vehicle integration group along with fuselage sizing and antenna mounting. Payload deployment would be crucial in the successful completion of Mission B. With the payload acting as the fuselage bottom, there was also a door needed to cover the hole made in the fuselage after deployment of the payload. The

focus next shifted to Mission A, which required the aircraft to carry an antenna. The antenna was required to be offset three inches from the airframe into the airflow and, therefore, a mounting system was designed. During the invention of these systems, the vehicle integration group was working with other groups to make sure the fuselage was properly sized to perform well during the missions, but still be able to incorporate all the necessary internal components.

4.4.1 Payload Deployment System

The preliminary design requirements established for the payload deployment system were: its ability to efficiently secure the payload inside the fuselage, simplicity of design, minimal weight, lack of necessity for a dedicated servo, maintenance of fuselage aerodynamics once payload is deployed, and the use of minimal attachments to the payload box. An additional design allowance was that the payload deployment be an irreversible process, in that the mechanism for releasing the payload may be a single-fire action.

Two main sizing parameters were considered for the payload deployment system. First, the release and door systems were required to add minimal width to the fuselage. Second, the release mechanism was required to be clear of interference with any other system such as motor battery pack, wing spar carry-through, and nose-gear control mechanism.

The effect of the payload system on each mission was analyzed. The efficiency of all three missions requires confinement of the payload within the fuselage. During the box-release mission, the successful release of the payload is inherently crucial to the achievement of the mission. In addition, the proper seal of the fuselage after deployment is important to efficient completion of that mission, and a lightweight release system benefits the rated aircraft cost of the airplane. In order to prevent the mid-flight interference that could occur from an unexpected shift of the aircraft center of gravity, the fuselage housing of the box must ensure security of the payload.

In order to analyze different possible payload deployment systems, several methods of analysis were developed and implemented on each configuration. A weight factor was assigned to the following analysis categories: ease of construction and assembly, ease of integration into the fuselage, expected reliability, and compliance with the previously established preliminary requirements.

	Weight Factor	Spring-Hinged Doors	Bomb-Bay Style Doors	Box Exposed to the Flow
Ease of manufacturing and assembly	0.1	1	2	3
Ease of integration into fuselage	0.25	1	2	3
Reliability	0.35	3	1	2
Compliance with preliminary requirements	0.3	1	2	3
	1	**0.6625**	**0.975**	**1.725**

Table 9. Deployment System FOM

Three deployment systems were considered. Each consisted of an opening in the bottom of the fuselage through which the payload box would drop upon release. The figure of merit, given in Table 9, shows the highest scoring deployment system.

The first deployment system consisted of a set of spring-hinged doors that rested against the side of the box prior to release. The bottom of the payload would be exposed to the airflow and would serve to span the hole in the bottom of the fuselage. The payload release system would consist of a ring and pin contraption. Upon deployment, a servo-activated pin retracts from the ring attached to the top of the box, thus releasing the payload. The deployment of the box would cause the spring-loaded doors to close downward and seal the bottom of the fuselage.

The second deployment system involved a set of bomb-bay style doors that covered the fuselage opening before and after box deployment. The box would sit on the doors, which would be held shut via a ring and pin system. As the pin retracted through the rings, the spring-hinged doors would swing open under the weight of the box and then promptly return to the closed position to seal the fuselage.

Finally, a payload release system was considered that, similarly to the first system, consisted of a box exposed to the flow. However, the box would be held inside the fuselage via a longitudinal strap along its bottom surface and would not contain any attachments itself. The strap would be released by way of a ring-pin system, and the box would fall through the floor, guided by front and rear guide rails that would provide longitudinal constraint. A floor panel resting on top of the box would fall into place to fill the hole in the fuselage.

4.4.2 Fuselage Sizing

The preliminary design parameters for the fuselage sizing were a suitable fit in the aircraft assembly box, minimal cross-sectional area, minimal skin area, minimal internal volume, and lightweight design.

The primary fuselage-sizing objective was to provide the smallest fuselage possible that successfully holds the payload box and other internal components. The two available body shapes that were considered were the circular cross section and the rectangular cross section.

The effect of the fuselage sizing on each mission was analyzed. For all three missions, the fuselage must be large enough to house and support the payload, as well as to successfully integrate all components and control systems. The sizing of the fuselage was also required to provide for an internal component configuration such that the aircraft center of gravity would be located at the wing quarter-chord.

In order to analyze different fuselage sizing options, several methods of analysis were developed and implemented on each configuration. A weight factor was assigned to the following analysis categories: ease of construction and assembly, aerodynamic quality, ease of internal payload support, ease of integration with other components (such as the wing, empennage and landing gear), and compliance with the previously established preliminary requirements.

The two configurations considered were the circular cross section and the rectangular cross section. While the rectangular shape would allow for easier construction, its aerodynamic efficiency is less than that of the circular shape. However, a rectangular cross-section would facilitate construction of the payload support, provide easier integration with the other aircraft components, and complies more thoroughly with the preliminary design parameters. Table 10 is a merit chart through which each configuration was compared against the weighted analysis categories, with the highest-scoring configuration highlighted in yellow.

	Weight Factor	Circular Configuration	Rectangular Configuration
Ease of manufacturing and assembly	0.15	1	3
Aerodynamic quality	0.25	3	2
Ease of payload support	0.25	1	3
Ease of integration with other components	0.2	2	3
Compliance with preliminary requirements	0.15	2	3
	1	**1.3**	**1.85**

Table 10. Cross Sectional Fuselage Shape FOM

4.4.3 *Antenna Mounting System*

The preliminary design requirements established for the antenna mounting system were simplicity, maximum aerodynamic efficiency, sufficient strength to support the antenna and its associated drag, sufficient stiffness to minimize vibration, and minimal weight.

Two main sizing parameters were considered for the antenna mounting system. First, the shape of the mechanism needed to be selected such that the drag would be minimized. Second, as specified in the competition rules, the mounting system was required to provide the adequate distance between the PVC antenna and the fuselage.

In order to analyze different possible mounting mechanisms, several methods of analysis were developed and implemented on each configuration. A weight factor was assigned to the following analysis categories: ease of construction and assembly, ease of integration into the fuselage, aerodynamic effects, and compliance with the previously established preliminary requirements.

Three mounting systems were analyzed. The first configuration entailed a cylindrical connection directly between the top surface of the antenna and the bottom of the fuselage. The second system was similar to the first, but consisted of an airfoil-shaped connection. The third configuration consisted of two flat composite pieces connecting the fuselage walls to the sides of the antenna. While the airfoil-shaped connection offered the highest aerodynamic efficiency, the double-connection configuration provided for the highest scoring in every other category. Table 11 is a merit chart through which each configuration was compared against the weighted analysis categories, with the highest-scoring configuration highlighted in yellow.

	Weight Factor	Cylindrical Connection	Airfoil-Shaped Connection	Composite Pieces Connection
Ease of manufacturing and assembly	0.1	2	1	3
Ease of integration into fuselage	0.25	2	1	3
Aerodynamic efficiency of support struts	0.3	1	3	2
Compliance with preliminary requirements	0.35	2	1	3
	1	**1.05**	**0.675**	**1.8**

Table 11. Antenna Mounting System FOM

4.5 Preliminary Design Results

The figure of merit charts that had been considered during the conceptual design phase of the competition determined the direction of each group within the team at the beginning of the preliminary design phase. Each group evaluated the figures of merit in order to decide which parameters deserved closer attention. Larger considerations, like wing sizing and propulsion efficiency, required trade studies and testing. Wing sizing was determined such that the aircraft would achieve high lift at takeoff in order to meet the 120 ft takeoff distance requirement. Propulsion efficiency proved to be important not only for faster flight times, but also to reduce the aircraft RAC. As the coupling of each choice became clearer, more parameters were developed in new figure of merit charts in order to fine-tune each system and its components. The decisions made within the team concerning final configurations determined the approach each group would take during detail design.

5 Detail Design

As soon as the preliminary design phase was completed, the detail design phase began. The detail design phase consisted of final wing sizing, selection of an airfoil, and final tail sizing. Landing gear sizing and manufacturing techniques were finalized, while the payload deployment system and the antenna-mounting device continued to be investigated. The best combination of propeller, motor, and battery was chosen for the propulsion system. The aircraft specifications were completed and the team was ready to move on to the manufacturing process.

5.1 Aerodynamics

Based on the testing completed and trade studies performed in the preliminary phase, the aerodynamics group made selections for the wing and tail of the aircraft.

5.1.1 Final Selection of Wing Design

The wing consisted of two sections, each 4 ft long. With the inclusion of the fuselage, the wingspan totaled 8 ft, 7.125 in. The chord of the wing was selected to be 10.5 in. The wing was made of Cycom 919 Glass wrapped around a foam core. A carbon-fiber composite tube spar was installed through the length of the wing for increased rigidity. The inner diameter of the wing spar was slightly greater than a second tube that extended through the fuselage with 6 in. of tube exposed on either side. This allowed the wings to slide onto the tube extending from the fuselage and fastened with a pin.

5.1.2 Final Selection of Tail Design

The tail was composed of three identical tapered sections constructed using the same material as the wing. It was attached to the fuselage by a composite tube identical to the fuselage spar. At the rear tip another tube was attached in the perpendicular direction. The tail was mounted around this perpendicular tube, which allowed for rotation of the entire tail assembly to provide

pitch control. The entire empennage rotated with the horizontal stabilizer, allowing entire fuselage and tail to fit into the box without disassembly.

5.1.3 Static Margin

After the locations of the aircraft center of gravity, wing and tail aerodynamic centers, and airfoil stability derivatives were determined, a code was written to calculate the static margin of the aircraft. Historical values for some variables were used and variables determined to have little affect were ignored. The effects of propulsion moments and fuselage stability derivatives were unknown at the time of this report; therefore they were ignored as well. A current estimate of the static margin of the aircraft is 82.6%, which was found to be well above the safe value necessary to fly. This would give the integration team a wide margin for the positioning of internal components.

5.1.4 Control Surface Sizing

The control surfaces were sized using equations from Raymer as well. Ailerons were chosen to have a standard value of 20% wing chord. Based on graphical analysis of aileron historical guidelines, the aileron span was chosen to be 50% of the wingspan. The aileron dimensions, found to be 2.1 in. chord and 48 in. span, were calculated. Rudder sizing was less important because the aircraft pilot stated that extensive rudder use would not be required to fly the aircraft. Therefore the rudder size was selected to be on the lower end of the scale at 30% vertical tail chord. This also increased vertical stabilizer stiffness. For ease of construction, the rudder would run the vertical length of the tail. The incorporation of the stabilator made elevator sizing unnecessary.

5.1.5 Flap Analysis

Flaps could be used during takeoff by large aircraft, especially on short-field takeoffs. The flap deflection would increase the camber of the wing, which would increase C_L and C_D. The overall result was a shorter takeoff distance. Instead of adding separate flaps the high-rate signal to the ailerons could be used to deflect both ailerons in the same direction. Using the ailerons in this method would turn them into 'flaperons.' Even after this flaperon deflection, both control surfaces could be used as ailerons for roll control. Table 12 shows the increase in C_L for different sized flaperons.

$S_{flapped} / S_{ref}$	0.1	0.11111	0.125	0.14286	0.16667	0.2	0.25
ΔC_{Lmax}	0.0486	0.054	0.06075	0.069429	0.081	0.0972	0.1215

Table 12. Lift Contribution of Plain Flap for $S_{flapped} / S_{ref}$

The ability to use an airfoil with a smaller camber would reduce the drag on the aircraft. This would increase the top speed of the aircraft during cruise allowing for faster mission completion. The low camber also increased the stall speed making the approach speed very fast. The 'flaperon' deflection temporarily gave the necessary lift to the wing at low speeds in order to achieve a slow approach. It also would have the ability to decrease the takeoff distance. The contribution of the 'flaperon' during takeoff and the lowered approach speed should allow the aircraft to land, to deploy the payload, and to take off without any taxi-back necessary while meeting the 120 ft. runway distance requirement. This capability would significantly increase our score for the payload deployment mission.

5.2 Propulsion

The impact of the propulsion system on the overall aircraft design was critical, and care was taken to ensure all details were fine-tuned. The choice of components was centered on the ability to complete the missions in the lowest time possible with minimal battery weight, thus providing for the highest possible score.

5.2.1 Propulsion Analysis Software

In order to evaluate different system configurations, the Motocalc software was utilized to generate thrust plots for various propeller and motor combinations. Using a custom-designed software package titled PowerCalc (See Figure 8), functions of thrust versus velocity were developed. These functions provided for the calculation of flight times and amperage usage for various flight maneuvers, thus allowing overall flight times and battery weights to be estimated for each mission. Each propeller and motor configuration was evaluated by this method and assigned a score based on the calculated mission times and battery weight. The configurations producing the highest scores were considered the optimal choices for the propulsion system.

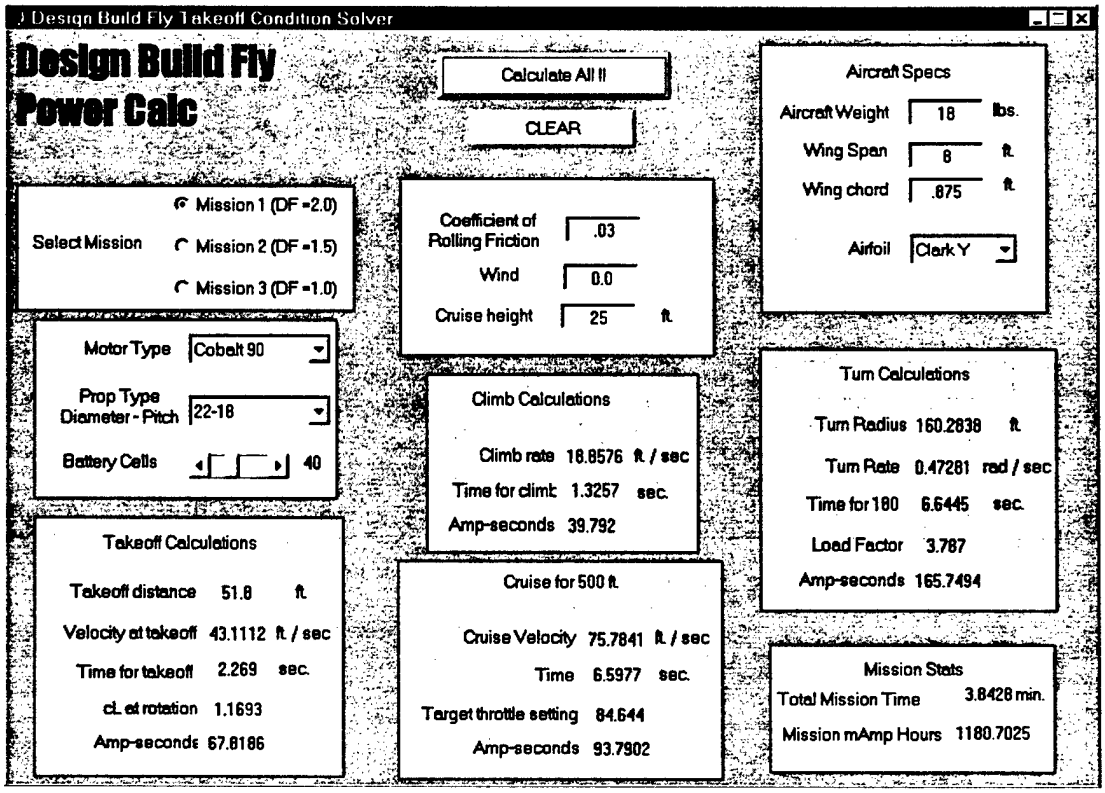

Figure 9. Power Calc program written in Matlab to solve flight times and power usage

5.2.2 System Configuration

Initially an analysis was performed on the AstroFlight Cobalt 60 motor with a 38-cell battery pack (See Table 1). After establishing a maximum motor heat of 250°F, it was determined that many of the propeller configurations with 38 cells would be operating in an overheated state. Although a decrease in the number of cells would provide for less severe motor heating, the consequent lack of power would cause the flight times to increase and the required milliamp-hours to increase. Therefore, decreasing the number of cells would result in an undesirable drop in score (See Table 13). Conversely, increasing the number of cells would provide for a lower score, under the limiting factors of motor heating effect and the maximum battery weight. Therefore, on the larger Cobalt 90 motor, the propeller analysis was performed under the effects of a 40-cell battery pack (See Table 14).

Mission 1						Mission 2						Overall
Diameter	Pitch	Time	mA hours	mA Hours (Safety)	Battery Weight	Diameter	Pitch	Time	mA hours	mA Hours (Safety)	Battery Weight	Score
18	12	N/A	N/A	N/A	N/A	18	12	N/A	N/A	N/A	N/A	**N/A**
	14	N/A	N/A	N/A	N/A		14	N/A	N/A	N/A	N/A	**N/A**
	16	3.712	1050.6	1208.1	2.9135		16	4.28	941.77	1083.0	2.5620	**6.307**
	18	3.617	1072.1	1232.9	2.9793		18	4.182	962.78	1107.2	2.6323	**6.367**
20	12	N/A	N/A	N/A	N/A	20	12	N/A	N/A	N/A	N/A	**N/A**
	14	3.79	1061.3	1220.5	2.9465		14	4.34	955.52	1098.8	2.6082	**6.185**
	16	3.53	1051.6	1209.4	2.9167		16	4.07	951.92	1094.7	2.5961	**6.562**
	18	3.46	1075.4	1236.7	2.9893		18	4.01	976.53	1123.0	2.6777	**6.567**
22	12	N/A	N/A	N/A	N/A	22	12	N/A	N/A	N/A	N/A	**N/A**
	14	3.78	1090.52	1254.1	3.0346		14	4.313	983.88	1131.5	2.7017	**6.113**
	16	3.47	1079.29	1241.2	3.0010		16	4.01	978.7	1125.6	2.6849	**6.548**
	18	3.43	1104.87	1270.6	3.0771		18	3.97	1006.3	1157.2	2.7741	**6.518**
24	12	N/A	N/A	N/A	N/A	24	12	N/A	N/A	N/A	N/A	**N/A**
	14	3.88	1124.57	1293.3	3.1346		14	4.42	1009.5	1160.9	2.7845	**5.893**
	16	3.49	1108.7	1275.0	3.0885		16	4.02	1012.0	1163.8	2.7925	**6.43**
	18	3.46	1139.3	1310.1	3.1767		18	4	1044.4	1201.1	2.8945	**6.373**

Cells = 38, wind = 30ft/s, Safety Factor 15%

Table 13. Chart of scores for various prop selections with the Cobalt 60 motor.

Mission 1						Mission 2						Overall
Diameter	Pitch	Time	mA Hours	mA Hours (Safety)	Battery Weight	Diameter	Pitch	Time	mA Hours	mA Hours (Safety)	Battery Weight	Score
18	12	N/A	N/A	N/A	N/A	18	12	N/A	N/A	N/A	N/A	**N/A**
	14	N/A	N/A	N/A	N/A		14	N/A	N/A	N/A	N/A	**N/A**
	16	N/A	N/A	N/A	N/A		16	5.72	1052.5	1210.3	2.9193	
	18	4.32	1049.7	1207.155	2.9108		18	4.93	941.22	1082.4	2.5602	**5.57**
20	12	N/A	N/A	N/A	N/A	20	12	N/A	N/A	N/A	N/A	**N/A**
	14	N/A	N/A	N/A	N/A		14	N/A	N/A	N/A	N/A	**N/A**
	16	4.352	1054.7	1212.9	2.9261		16	4.93	953.67	1096.7	2.6020	**5.54**
	18	3.84	985.02	1132.7	2.7055		18	4.41	888.52	1021.8	2.3786	**6.323**
22	12	N/A	N/A	N/A	N/A	22	12	N/A	N/A	N/A	N/A	**N/A**
	14	N/A	N/A	N/A	N/A		14	N/A	N/A	N/A	N/A	**N/A**
	16	4.15	1049.6	1207.0	2.9104		16	4.7	947.41	1089.5	2.5810	**5.768**
	18	3.63	977.79	1124.5	2.6818		18	4.17	886.09	1019.0	2.3700	**6.648**
24	12	N/A	N/A	N/A	N/A	24	12	N/A	N/A	N/A	N/A	**N/A**
	14	N/A	N/A	N/A	N/A		14	N/A	N/A	N/A	N/A	**N/A**
	16	4.22	1087.4	1250.5	3.0252		16	4.76	988.66	1137.0	2.7173	**5.586**
	18	3.53	997.27	1146.9	2.7452		18	4.07	908.15	1044.4	2.4471	**6.707**

Cells = 40, wind = 30ft/s, Safety Factor 15%

Table 14. Comparison of scores for different cell counts on the Cobalt 90 motor.

In each of the propulsion analyses a 30 ft/s steady wind was considered, providing for the worst-case scenario on competition day. In addition, a factor of safety of 15% was added to the maximum expected battery draw. Through the quantitative analyses represented in Tables 13 and 14, the highest score achievable through a Cobalt 60 motor was calculated to be 6.567, which resulted from a 20x18 propeller and 38 battery cells. The optimal configurations with the Cobalt 90 motor were the 22x18 propeller with 40 battery cells, which resulted in a score of 6.648, and the 24x18 propeller with 40 cells, which produced a score of 6.707. In consideration of necessary aircraft ground clearance, the 22x18 propeller was selected. For this configuration, 2 three-dimensional plots were generated. The first plot represented power available and power required vs. velocity and %throttle, while the second represented thrust available and thrust required vs. velocity and %throttle were generated (See Figure 9).

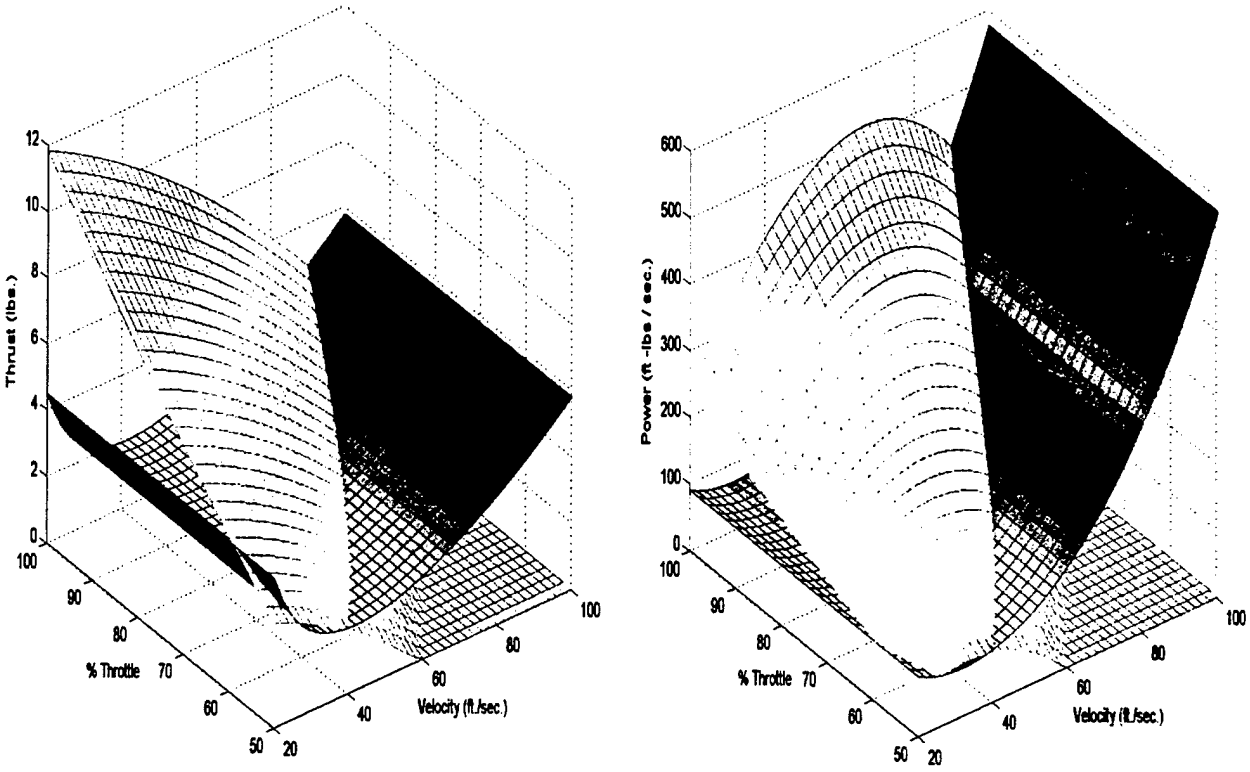

Figure 10. Thrust and Power Available and Required for 22-18 Prop with Cobalt 90

5.3 Structures

Two areas were finalized in the structures group during preliminary design. The first was the spar design, size and material choice. Second, the landing sizing was finalized and the manufacturing technique was chosen.

5.3.1 Wing Spar Sizing

The final dimensions of the two major structures were based on calculations from simple mechanics of materials problems made with load factors of 4 and safety factors of 2. From the numerical analysis of the wing spar, it was found that an outer spar diameter of 0.3 inches was needed. Realizing there was a maximum thickness of about 1.25 in, the wing was filled with the spar, thus making the spar larger and stronger by default. The next step was to look for a manufacturer where a spar that was approximately 0.75 in. in diameter could be purchased. This dimension would leave about 0.25 in. on the top and bottom of the wing between the spar and the skin. The spar that was purchased had a 0.71 in. outer diameter and a 0.625 in. inner diameter. Then the smaller tube that had to fit into the spar for the connection at the fuselage was determined by how closely the outer diameter matched the inner diameter of the larger spar. Measurements of 0.615 in. outer diameter and 0.555 in inner diameter were found to be the best choice for the smaller tube. With a difference of 0.01 in., the close fit necessary to make a solid connection was achieved

.

5.3.2 Landing Gear

The landing gear cross-section of wood wrapped in composite materials was determined to be 2 in. in depth and 1/4 in. in width. This would be the minimum cross-sectional area that would resist the loads applied when landing the aircraft during each mission. The gear was analyzed in bending, shear, and buckling to make sure that all loads were accounted for. The maximum height and width of the landing gear were determined by the strength requirement during landing and the necessary propeller clearance.

5.4 Vehicle Integration

During detail design, the vehicle integration team worked to finalize the fuselage sizing, the antenna placement and mounting, and the payload deployment designs. All the necessary choices that needed to be made by the vehicle integration group were completed.

5.4.1 Payload Deployment System

In order to analyze different possible payload deployment systems, several methods of analysis were developed and implemented on each configuration. The possible systems were weighed against these analysis parameters: ease of construction and assembly, ease of integration into the fuselage, expected reliability, and compliance with the previously established preliminary

requirements. The optimum payload deployment system was found to be the configuration in which the payload composed the bottom of the fuselage and was secured via a longitudinal strap along its bottom surface.

The chosen deployment system was selected for a myriad of reasons. First, it was selected because it would provide for easy manufacturing and integration into the fuselage. In this configuration, a taut fabric strap two inches in diameter would prevent the payload from falling prior to release. The forward end of the strap would contain a ring which would be fed through the bottom of the fuselage forward of the box, and a servo-activated pin would hold the ring in place until deployment. Upon release, a floor panel velcroed to the top of the box would fall into place to fill the hole in the fuselage. Guide-rails forward and aft of the box would prevent the box from shifting during flight. This configuration would require no complicated materials or hardware, thus providing easy manufacturing and assembly.

The configuration was also chosen because of its close adherence to the preliminary design requirements. First, the design was simple and would leave less room for error than a complicated system. The only components that would add weight to the aircraft would be the virtually weightless strap, the servo-activated rod, and the payload guide-rails. In addition, no dedicated servo would be needed because the system would utilize the nose wheel servo. In this configuration, the aerodynamic efficiency of the fuselage would be maintained after deployment because a floor panel would cover the payload hole. However, the free-hanging strap would add a nominal amount of drag. Finally, this system would not require any physical attachments to the payload box, therefore alleviating any concerns about guideline adherence with respect to attachments.

5.4.2 Fuselage Sizing

In order to analyze different possible fuselage sizing configurations, several methods of analysis were developed and implemented on each configuration. The possible configurations were weighed against the analysis categories of: ease of manufacturing and assembly, aerodynamic quality, ease of payload support, ease of integration with other components, and compliance with the previously established preliminary requirements. The optimum fuselage configuration was found to be the rectangular cross section.

The chosen configuration was selected for several reasons. First, it was selected because of its ease of construction. Simple composite panels would be autoclaved together around a rectangular plug. This design was also chosen because of its ease of payload support. The fuselage would be easily sized to hold the payload box and necessary components without wasting internal volume. In addition, the rectangular design would more easily accommodate

other aircraft components such as the wings, which would be fastened to the sides of the fuselage via spar construction, and the main landing gear. Finally, the rectangular cross-section would accommodate the preliminary requirements to efficiently fit within the assembly box and to make the most economical use of internal volume and external surface area.

5.4.3 Antenna Mounting System

In order to analyze different possible antenna mounting systems, several methods of analysis were developed and implemented on each configuration. The possible systems were weighed against the analysis categories of: ease of manufacturing and assembly, ease of integration into the fuselage, aerodynamic efficiency of support struts, and compliance with the previously established preliminary requirements. The optimum antenna mounting system was found to be the configuration in which the two flat composite pieces connected the sides of the antenna to the fuselage walls.

The chosen mounting system was selected for several reasons. First, it was selected for its ease of manufacturing, because it would only consist of two flat composite strips. This configuration was also chosen because of its simple integration into the fuselage, as it would be connected to the fuselage via simple bolt connections on either wall. As well, this system would not generate any significant drag.

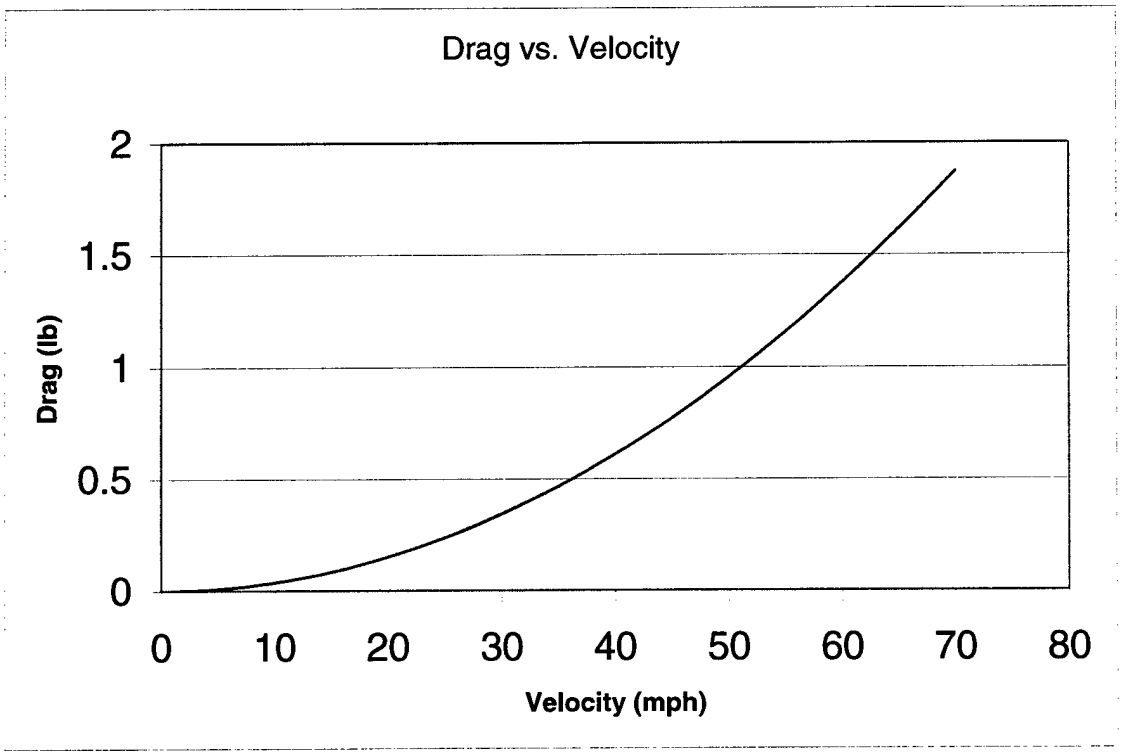

Figure 11. Drag vs. velocity plot for antenna assembly across flight enveloper

5.4.4 *Antenna Placement*

The placement of the antenna assembly on the aircraft has a large impact on the performance of the plane. The antenna must be visible to the flow, therefore it was decided to place it underneath the aircraft so any drag force incurred would result in a pitch down moment, making the aircraft more stable. The addition of the antenna must have as little affect as possible on the overall center of gravity of the aircraft. As for the vertical center of gravity, little could be done to adjust the distance from the aircraft because the antenna must stand 3 inches off from the nearest airframe structure. However, for the longitudinal center of gravity, the best placement for the antenna center of gravity is directly below the aircraft center of gravity. Therefore, the antenna center of gravity coincides with the wing quarter chord and the payload center of gravity. To reduce the drag created by the antenna, the end caps are mounted interior to the cylinder and flush with the ends. The struts used are miniature symmetrical airfoil type shapes with composite construction. Based on the dimensions of the antenna, a drag estimate calculation was performed for the entire flight envelope and the results are shown above in Figure 11.

5.5 Weight Statement

A weight statement would be necessary to evaluate the performance and stability of the aircraft. Each system of the aircraft was evaluated by component for weight, specific gravity, thickness (where applicable), surface area, and volume. The data was accumulated from three sources. It was either calculated by a team member, weighed by a team member, or published by a manufacturer. Two items included in Table 18 were required by the competition. The payload was required to be five pounds and the antenna, which did not have a specified weight, was required as a component of the aircraft to complete Mission A.

Evaluating each aircraft component using the parameters discussed above, an exact weight for each system was calculated by component. These weights along with longitudinal and vertical centers of gravity and their respective moment arms produced the data available in Table 19. This table verified the placement of each component within the aircraft. It showed that the longitudinal center of gravity was placed exactly at the quarter chord of the wing, which was the most preferred point. The vertical center of gravity was determined to be less than 0.01 in. away from the desirable location at the vertical centerline of the fuselage.

All distances in ft. All weights in lbs.	Surface Area (ft^2)	Thickness (ft)	Volume (ft^3)	Specific Gravity (lbs/ft^3)	Weight (lbs)	Source of Weight Figures*
Fuselage						
Main Fuselage (2 plies symmetric - no boom)	3.309	0.0027	0.0088	141.680	1.250	calculated
Main Fuselage (3/8 in. balsa core side panels)	1.936	0.0313	0.0605	4.500	0.272	calculated
Nose-cone (2 plies - no core material)	0.669	0.0013	0.0009	141.680	0.126	calculated
Rear-cone (2 plies - no core material)	1.428	0.0013	0.0019	141.680	0.270	calculated
Firewall (2 plies symmetric)	0.396	0.0027	0.0011	141.680	0.150	calculated
Firewall (1/4 in. balsa core)	0.396	0.0208	0.0082	4.500	0.037	calculated
Rear bulkhead (2 plies symmetric)	0.396	0.0027	0.0011	141.680	0.150	calculated
Rear bulkhead (1/4 in. balsa core)	0.396	0.0208	0.0082	4.500	0.037	calculated
Wing and Tail						
Wing - 4 ft , 10.5 in. chord	-	-	-	-	2.463	actual
Horizontal Tail - C_t = 7 in, C_r = 11 in, 23 in. span	-	-	-	-	0.425	actual
Vertical Tail - C_t = 7 in, C_r = 11 in, 10.5 in. span	-	-	-	-	0.231	actual
Structural Supports						
Wing Spar (4 ft. per wing)	0.741	0.0035	0.0026	144.000	0.374	calculated
Fuselage Carry Through Spar (19.125 in. long)	0.257	0.0024	0.0006	144.000	0.088	calculated
Tail Boom (19 in. long)	0.255	0.0024	0.0006	144.000	0.087	calculated
Tail hinge inner sleeve (4.615 in)	0.062	0.0024	0.0001	144.000	0.021	calculated
Tail hinge outer sleeve (3 in. per elevator half)	0.093	0.0035	0.0003	144.000	0.047	calculated
Boom to Fuselage sleeve connection (4 in)	0.062	0.0035	0.0002	144.000	0.031	calculated
Forward payload guard rails (2 plies symm, 2 rails)	0.333	0.0013	0.0004	141.680	0.063	calculated
Forward payload guard rails (1/4 in. balsa, 2 rails)	0.333	0.0208	0.0069	4.500	0.031	calculated
Rear payload guard rail (2 plies symmetric, 2 rails)	0.333	0.0013	0.0004	141.680	0.063	calculated
Rear payload guard rail (1/4 in. balsa, 2 rails)	0.333	0.0208	0.0069	4.500	0.031	calculated
Motor mount	-	-	-	-	0.375	estimated
Electronics						
Futaba FP- R148DP Receiver	-	-	-	-	0.069	manufacturer
Receiver battery 4 cell pack, 600mA	-	-	-	-	0.200	manufacturer
Astro Flight Cobalt 90 p/n 691s	-	-	-	-	2.188	manufacturer
Sanyo Max 1300mA, 40 cells, 1.4oz/cell	-	-	-	-	3.500	manufacturer
Astro Flight Speed Control Model 204D	-	-	-	-	0.066	manufacturer
Servos						
Rudder - Hitec HS - 225MG Mini Precision	-	-	-	-	0.062	manufacturer
Nose Gear - Hitec HS - 225MG Mini Precision	-	-	-	-	0.062	manufacturer
Elevator - JR NES - 4131	-	-	-	-	0.106	manufacturer
Aileron (2) - Hitec HS - 85MG+ Mighty Micro	-	-	-	-	0.100	manufacturer
Landing Gear						
Main Gear (Cycom Kevlar 49 Fiber, 2 plies symm.)	0.363	0.0160	0.0058	87.399	0.508	calculated
Main Gear (1/4in balsa core)	0.363	0.0208	0.0076	4.500	0.034	calculated
Nose Gear (15.25 in. spar shaft)	0.204	0.0035	0.0007	144.000	0.103	estimated
Dubro Light Foam Tires 2.5 in. diameter (3)	-	-	-	-	0.075	actual
Miscellaneous						
Zinger Propeller 22 in. x 18 pitch	-	-	-	-	0.369	actual
Payload Box	-	-	-	-	5.000	required
Payload Release Mechanism	-	-	-	-	0.125	estimated
Antenna (PVC Schedule 40)	-	-	-	3.5350	0.902	required
Servo Extension Wires - 16ft (0.6oz per 3 foot)	-	-	-	-	0.200	actual
Screws, Blind Nuts, etc.	-	-	-	-	0.125	estimated

Weight Result	**Airframe**	**7.591**
	Propulsion System	**6.056**
	Control System	**0.865**
	Payload System	**0.125**
	Aircraft Empty Weight (no payload, no antenna)	**14.512**
	Gross Weight	**20.414**
	Mission A Weight	**20.414**
	Mission B and C Weight (no antenna included)	**19.512**

Table 15. Weight Statement

Component and Weights in lbs.	C.G. Longitudinal (Nose of aircraft as datum) (ft)	Moment Arm about datum (lb-ft)	C.G. Vertical (ground as datum) (ft)	Moment Arm about datum (lb-ft)
Fuselage				
Main Fuselage (2 plies symmetric - no boom)	1.396	1.745	0.979	1.224
Main Fuselage (3/8 in. balsa core side panels)	1.396	0.380	0.979	0.267
Nose-cone (2 plies - no core material)	0.625	0.079	0.979	0.124
Rear-cone (2 plies - no core material)	2.432	0.656	0.979	0.264
Firewall (2 plies symmetric)	0.760	0.114	0.979	0.146
Firewall (1/4 in. balsa core)	0.760	0.028	0.979	0.036
Rear bulkhead (2 plies symmetric)	2.063	0.308	0.979	0.146
Rear bulkhead (1/4 in. balsa core)	2.063	0.077	0.979	0.036
Wing and Tail				
Wing - 4 ft , 10.5 in. chord	1.458	3.591	1.229	3.027
Horizontal Tail - C_t = 7 in, C_r = 11 in, 23 in. span	4.425	1.881	1.263	0.537
Vertical Tail - C_t = 7 in, C_r = 11 in, 10.5 in. span	4.425	1.023	1.575	0.364
Structural Supports				
Wing Spar (4 ft. per wing)	1.375	0.514	1.229	0.459
Fuselage Carry Through Spar (19.125 in. long)	1.375	0.121	1.229	0.108
Tail Boom (19 in. long)	3.671	0.320	1.099	0.096
Tail hinge inner sleeve (4.615 in)	4.363	0.092	1.263	0.027
Tail hinge outer sleeve (3 in. per elevator half)	4.363	0.204	1.263	0.059
Boom to Fuselage sleeve connection (4 in)	2.979	0.093		
Forward payload guard rails (2 plies symm, 2 rails)	0.865	0.054	0.979	0.062
Forward payload guard rails (1/4 in. balsa, 2 rails)	0.865	0.027	0.979	0.031
Rear payload guard rail (2 plies symmetric, 2 rails)	1.885	0.119	0.979	0.062
Rear payload guard rail (1/4 in. balsa, 2 rails)	1.885	0.059	0.979	0.031
Motor mount	0.646	0.242	0.979	0.367
Electronics				
Futaba FP- R148DP Receiver	0.771	0.053	0.938	0.064
Receiver battery 4 cell pack, 600mA	0.771	0.154	0.729	0.146
Astro Flight Cobalt 90 p/n 691s	0.375	0.820	0.979	2.142
Sanyo Max 1300mA, 40 cells, 1.4oz/cell	1.375	4.813	1.267	4.433
Astro Flight Speed Control Model 204D	0.771	0.051	1.115	0.074
Servos				
Rudder - Hitec HS - 225MG Mini Precision	4.279	0.265	1.346	0.083
Nose Gear - Hitec HS - 225MG Mini Precision	0.875	0.054	0.646	0.040
Elevator - JR NES - 4131	4.446	0.471	1.263	0.134
Aileron (2) - Hitec HS - 85MG+ Mighty Micro	1.594	0.159	1.229	0.123
Landing Gear				
Main Gear (Cycom Kevlar 49 Fiber, 2 plies symm.)	1.958	0.994	0.646	0.328
Main Gear (1/4in balsa core)	1.958	0.067	0.646	0.022
Nose Gear (15.25 in. spar shaft)	0.729	0.075	0.698	0.072
Dubro Light Foam Tires 2.5 in. diameter (3)	0.729	0.055	0.000	0.000
Miscellaneous				
Zinger Propeller 22 in. x 18 pitch	0.042	0.015	0.979	0.361
Payload Box	1.375	6.875	0.896	4.479
Payload Release Mechanism	1.375	0.172	0.646	0.081
Antenna (PVC Schedule 40)	1.375	1.240	0.313	0.282
Servo Extension Wires - 16ft (0.6oz per 3 foot)	n/a	n/a	n/a	n/a
Screws, Blind Nuts, etc.	n/a	n/a	n/a	n/a

		C.G. - X axis (ft)		C.G. - Z axis (ft)
Center of Gravity Results along the X and Z axes	**Calculated**	1.375	**Mission A**	0.996
			Mission B and C	1.028
	Desired	1.375	**Desired**	0.979
	Difference	0.000	**Diff. Mission A**	0.017
			Diff. Miss. A & B	0.049
Center of Thrust Results for Mission A and Mission B and C (without antenna)	**Center of Thrust**	n/a	**Center of Thrust**	1.042
	Diff. Mission A	n/a	**Diff. Mission A**	-0.046
	Diff. Miss. A & B	n/a	**Diff. Miss. A & B**	-0.014

Table 16. Center of Gravity Calculations

5.6 Rated Aircraft Cost

Using the model and equations supplied by the competition, the expected Rated Aircraft cost was determined as shown in Figure 12. The rated aircraft cost of the Stop and Go is 8.487.

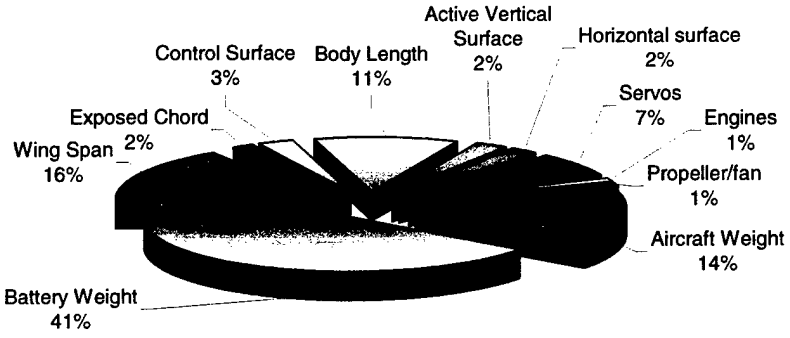

		Man Hours/Unit	Parameters	Individual Hours
Wing WBS - sum for multiple wings	Wing Span	8hr/ft	8.583ft	68.67
	Maximum exposed chord	8hr/ft	0.875ft	7
	Control Surface	3hr/surf	4surfaces	12
Fuselage WBS	Maximum body length	10hr/ft	4.687ft	46.87
Empennage WBS	Vertical surface with no active control	5hr/surface	0surfaces	0
	Vertical surface with active control	10hr/surface	1surfaces	10
	Horizontal surface	10hr/surface	1surfaces	10
Flight System WBS	Servo/motor controller	5hr/servo	6servos	30
Propulsion System WBS	Engines	5hr/engine	1engines	5
	Propeller/fan	5hr/prop	1props	5
			WBS	194.53

	Multipliers	Aircraft Parameter	Individual Hou
Manufacturers Empty Weight (MEW)			
Actual airframe weight, lb., with all flight and propu batteries but without any payload.	$100	12.2 lbs	1220
Rated Engine Power (REP)		1 engine,	
(1+.25*(# engines-1))*Total Battery Weight	$1,500		3375
The weight of the propulsion battery pack(s).		2.25 lbs weigh	
Manufacturing Man Hours (MFHR)			
MFHR = □ WBS hours → Prescribed assembly hc the Work Breakdown Structure (WBS).	$20 / hour	194.53 hours	3891
RAC			8.486

Figure 12. Breakout of MFHR and RAC

5.7 Detail Design Results

The results of the detail design were demonstrated with the final aircraft configuration. Within each group, dimensions were finalized and manufacturing methods chosen. All of the final configurations were selected with the intention of completing all missions, decreasing RAC, and lowering flight times. With these goals in mind, wing dimensions, tail dimensions, and control volumes were calculated. The wings were dimensioned to generate increased lift for takeoff and the tail was sized to increase the stability of the aircraft configuration. A final motor, propeller, and battery combination was selected in spite of its higher contribution to RAC than the other configurations. The apparent decrease in expected total competition score was offset by higher power and thrust available, which would allow the aircraft to complete the missions faster. Therefore, the lower flight times outweighed the increased RAC. With these final adjustments in place, the team was confident that the aircraft would perform efficiently and safely during the competition.

5.8 Drawing Package

5.8.1 Drawing Package: Three View

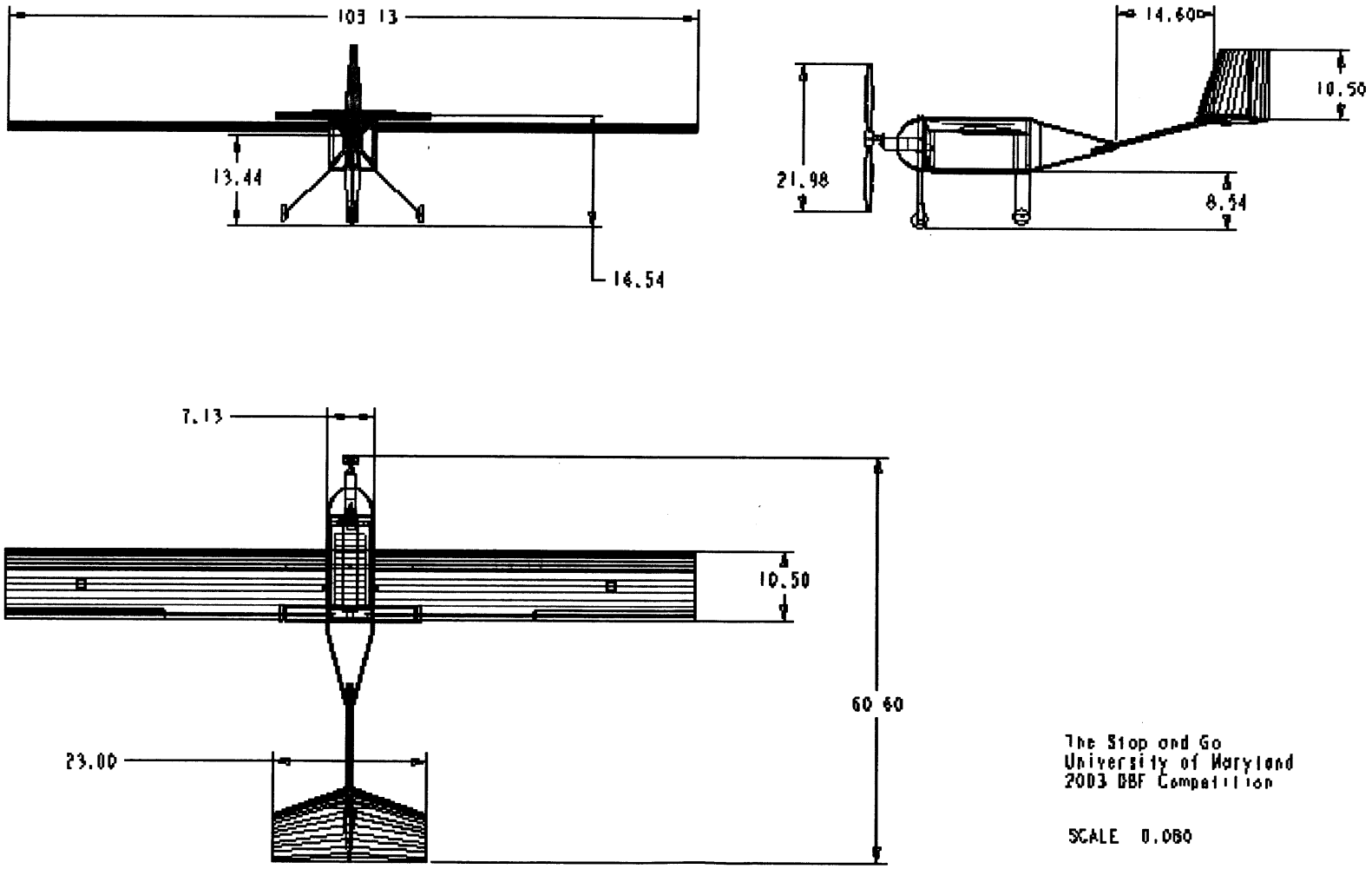

5.8.2 Drawing Package: Locations of Aircraft Components

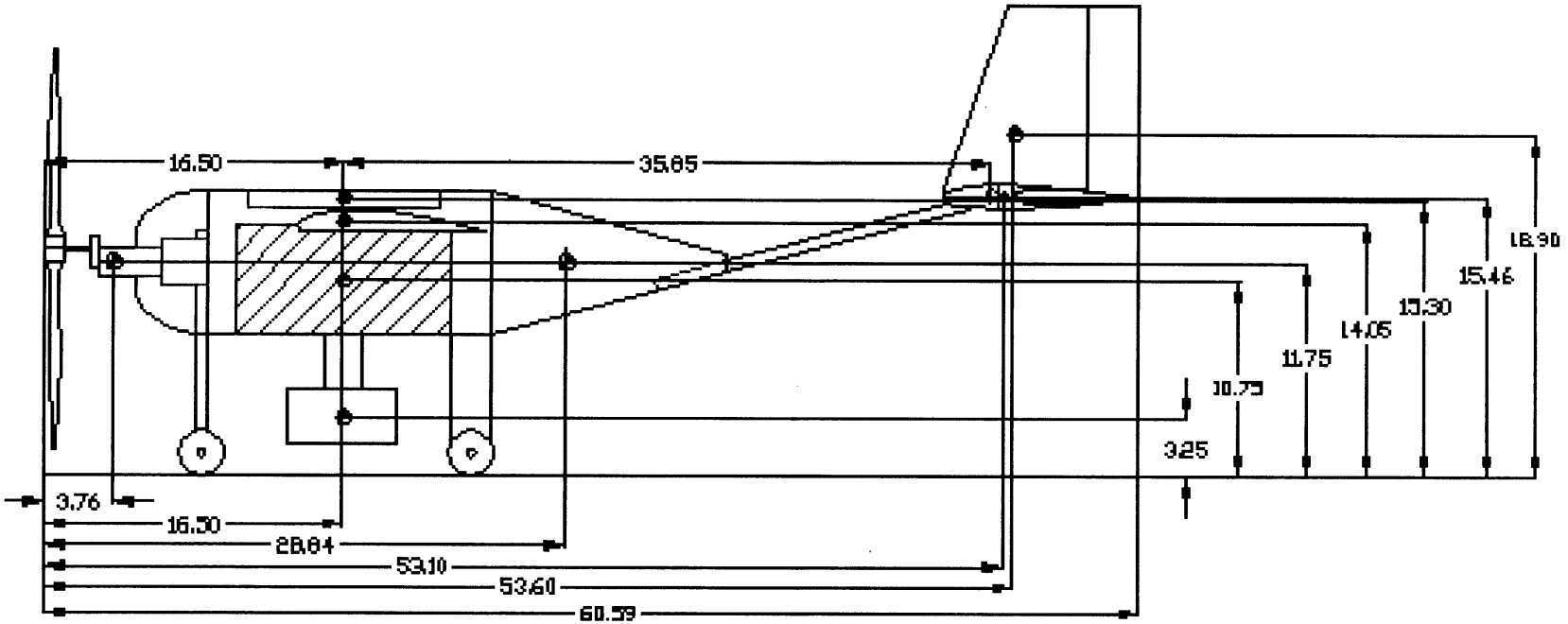

5.8.3 Drawing Package: Detail views of select aircraft components

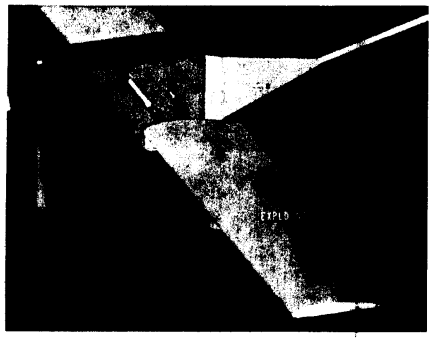

Wing support detail

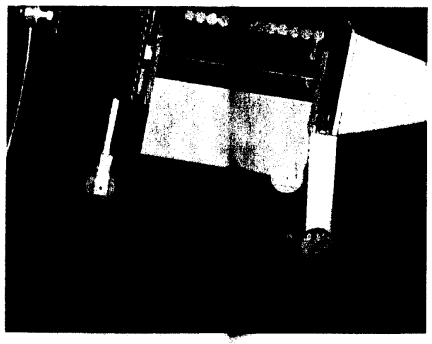

Payload deployment system detail

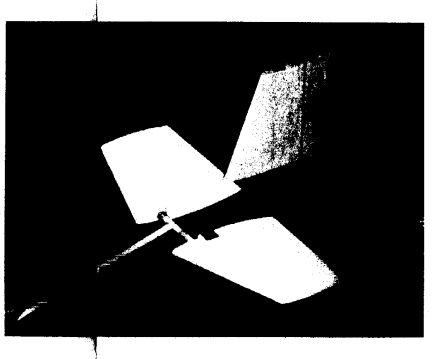

Horizontal and vertical stabilizer detail

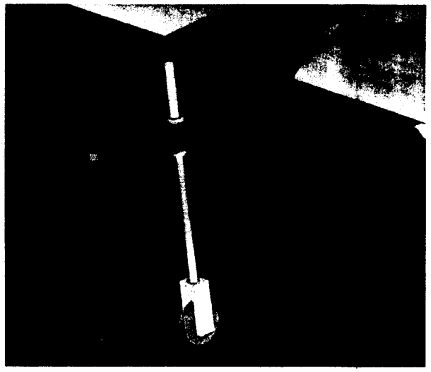

Nose gear and motor mount detail

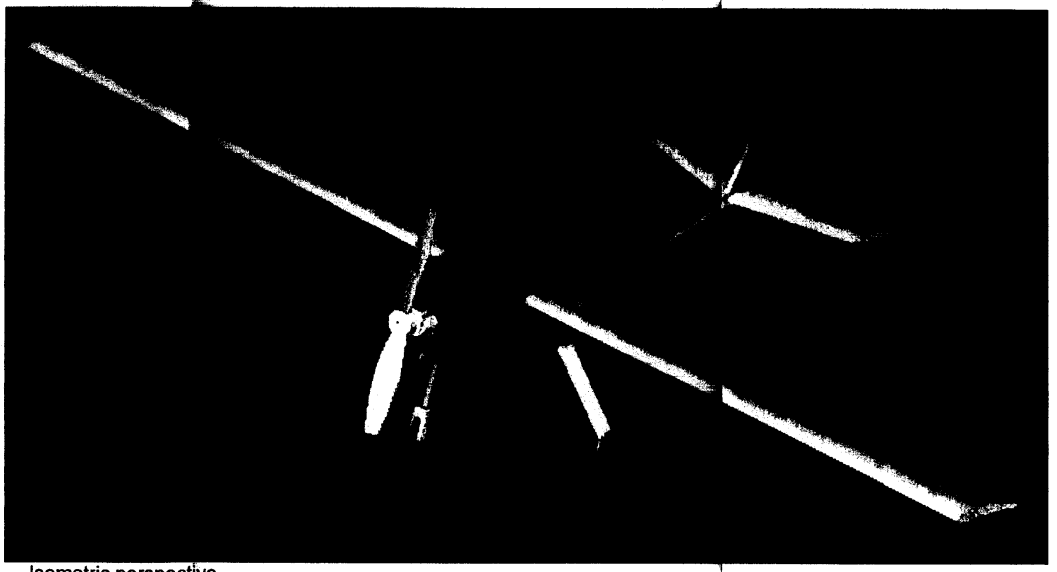

Isometric perspective

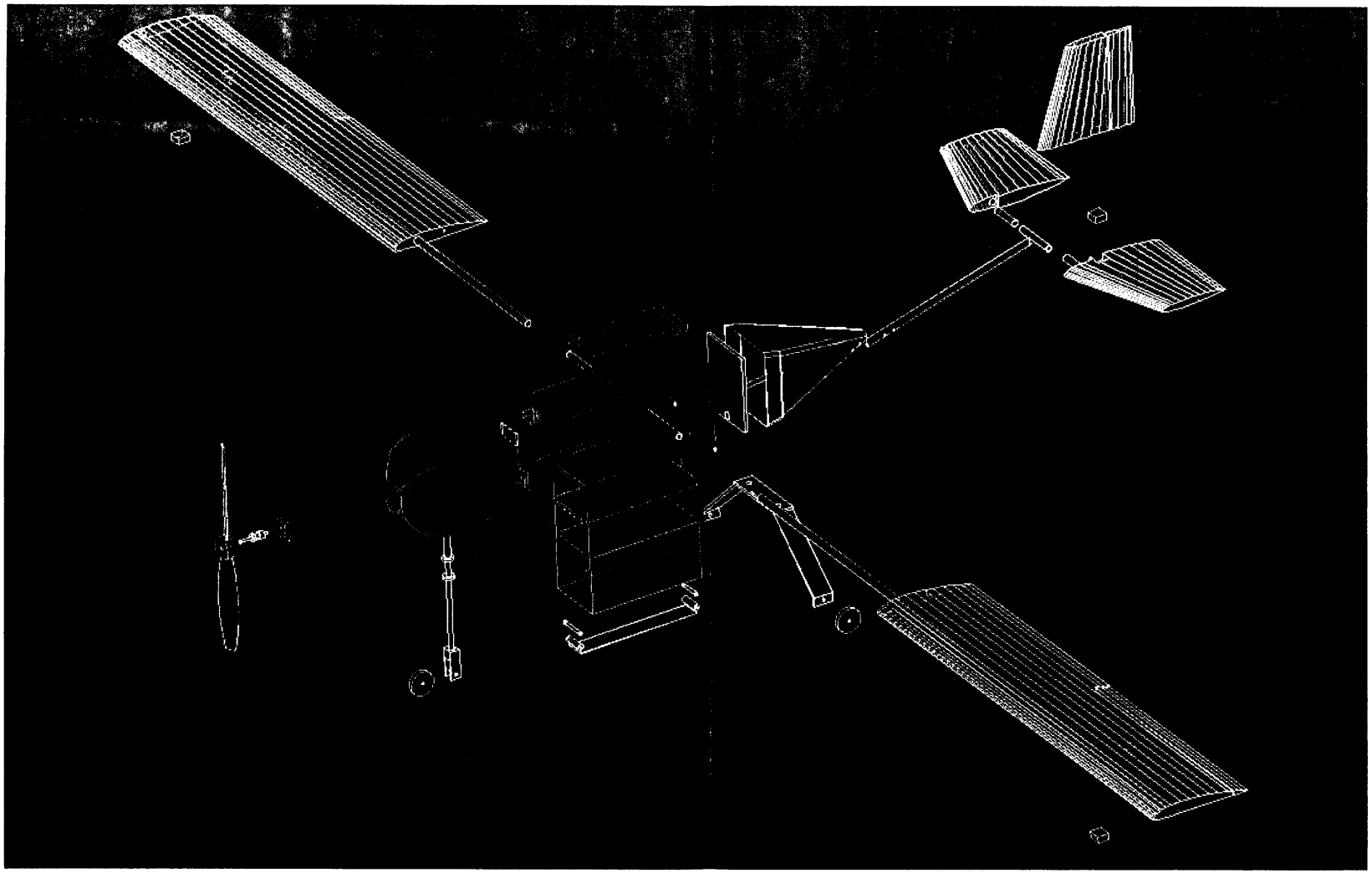

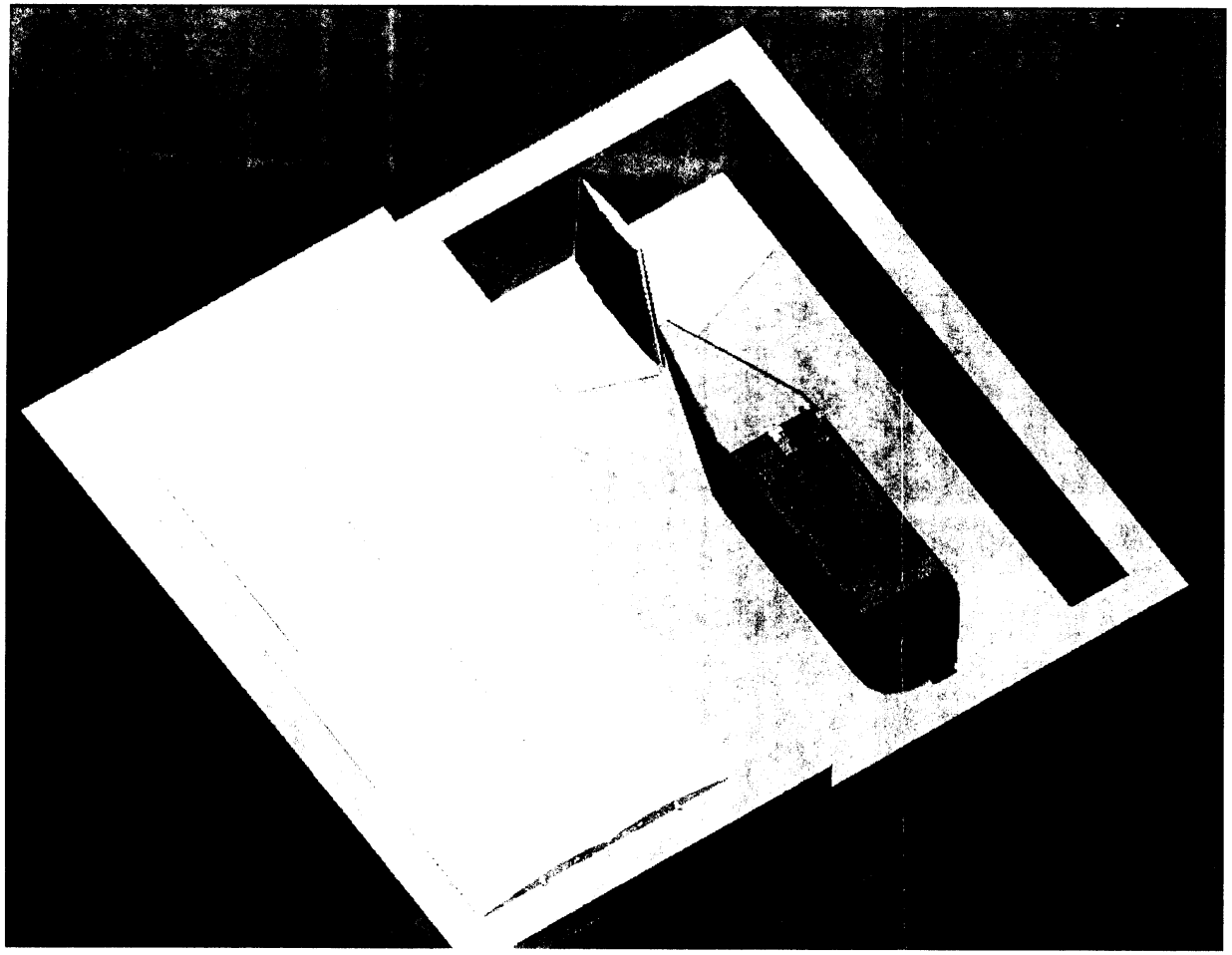

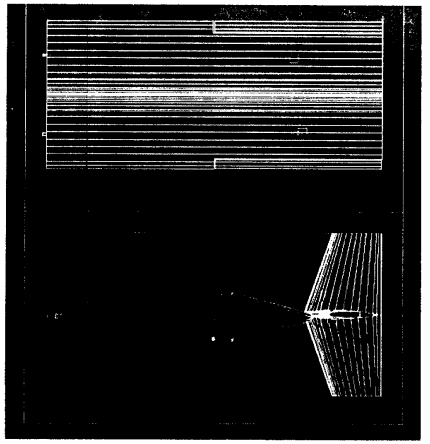

Top view

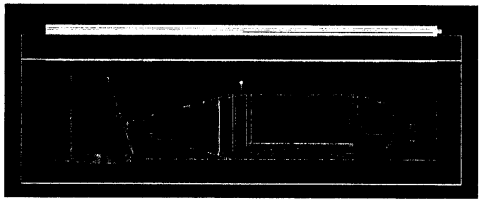

Side View

5.9 Sized Aircraft Data

Performance					
Gross Weight	C_{Lmax}	1.4	Empty Weight	C_{Lmax}	1.4
	L/D Max	22		L/D Max	22
	Max Rate of Climb	19.08 ft/s		Max Rate of Climb	25.19 ft/s
	Stall Speed	42.08 ft/s		Stall Speed	35.8 ft/s
	Max Speed	93.5 ft/s		Max Speed	93.5 ft/s
	Takeoff Length	51.4 ft		Takeoff Length	25.9 ft

Weight	Airframe	7.954 lbs	Geometry	Length	60.6 in
	Propulsion System	6.056 lbs		Span	103.13 in
	Control System	0.865 lbs		Height (Fuselage)	15.75 in
	Payload System	0.125 lbs		Height (Maximum)	25.65 in
	Payload Weight	5 lbs		Wing Area	1083 in^2
	Empty Weight	15 lbs		Aspect Ratio	9.8
	Gross Weight	20.902 lbs		Control Volume	Table 18

Systems	Radio	Transmitter	Futaba PCM 1024	- T8UAF
		Receiver	Futaba PCM 1024	- FP-R148DP
	Servos	Rudder	Hitec	- HS-225MG Mini Precision
		Elevator	JR Servo	- NES-4131
		Aileron	Hitec	- HS-85MG+ Mighty Micro
		Nose Gear	Hitec	- HS-225MG Mini Precision
		Speed Control	Astro Flight Speed Control	- Model 204D
	Battery	Model	Sanyo	- Max Series 1300 mAmp
		Configuration	5 sticks of 8 cells - 10.64in L x 4.5in W, 1.4oz/cell	
	Motor		Asto Flight	- Cobalt 90 Motor P/n 691S
	Propeller		Zinger Propeller	- 22in x 18 pitch
	Gear Ratio		Astro Flight Superbox	- 2.75 to 1

Table 17. Geometry, Performance Weight Statement, and Systems

	Surface Area (in^2)	Lever Arm (in)	Reference Length (in)	Control Volume
Aileron (2)	36	39.5	24	59.25
Rudder	31.5	42.6	10.5	127.8
Elevator (2)	103.5	42.6	11.5	383.4

Table 18. Control Volumes

6 Manufacturing Plan

The manufacturing plan was not really coordinated until the preliminary design phase was underway. As the best choices for each area of the aircraft were narrowed down, manufacturing choices became more important. Strength to weight ratio, ease of construction and availability of products started to place importance on the manner in which components could be constructed. The following section discusses the manufacturing processes investigated and finally chosen for several of the major aircraft components. Figure 13, below, shows the manufacturing schedule kept by the University of Maryland team for the prototype aircraft.

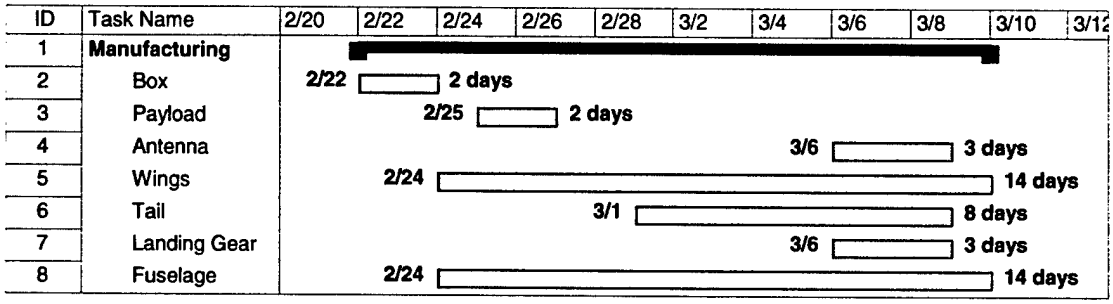

Figure 13. Manufacturing Milestones Chart

6.1 Aerodynamics

The aerodynamics group was responsible for manufacturing the wing sections and tail sections. Several manufacturing processes were investigated, but foam core composite construction was the best choice for wing and tail construction. Although foam core composite was chosen as the manufacturing process that would provide the best results, it was not without its problem areas during the construction phase, especially of the wing sections.

6.1.1 Wing and Tail Construction

A typical wing for RC aircraft is constructed by one of two methods. The most common method is to use balsa wood ribs and spars covered by a tight layer of fabric or plastic. A more advanced method is to use composite structures to provide a wing of similar weight but vastly superior strength. The factors considered in deciding between these options included stiffness, ease of construction, reparability, and others. The strength of the wing and the ease of its construction are of the utmost concern. The group's plan is to construct two aircraft so that very little can prevent the aircraft from flying in the competition. If the wing requires an incredible amount of time to build, an accident during testing could put the group out of the competition.

	Weight Factor	Balsa Monokote	Foam Core, Balsa Skin	Foam Composite
Stiffness	0.3	1	2	3
Ease of Construction	0.25	3	2	1
Reparability	0.2	1	2	3
Skill Level	0.15	2	1	3
Availability	0.05	3	2	1
Cost	0.05	3	2	1
	1	**1.85**	**1.85**	**2.3**

Table 19. Airfoil Manufacturing Methods FOM

Due to its high strength, durability, availability, and relatively low cost of construction as shown in Table 18, the decision was made to use a foam composite construction for the wing and tail. The process involves cutting the foam core with a hot wire, wrapping it in Cycom glass, wrapping it again in Teflon. Then wing is then placed in a vacuum bag and cured in the autoclave located at the Composites Research Lab here at the University of Maryland.

6.2 Structures

The structures group determined which manufacturing method would be best for the landing gear. Along with landing gear manufacturing, wing spar insertion was a concern during the manufacturing phase of the design.

6.2.1 Wing Spar Insertion

The wing spar was developed as a means of making the plane easy to assemble and "boxable." Many configurations were considered as to how the spar was going to be put in the wing, and also whether it would span the whole wing or just a fraction of the wing. The group considered cutting a hole in the foam core of the composite wing that only went partially through the wing, but decided against that design because it would be harder to construct and would leave room for oscillation within the foam. The team considered many other manufacturing possibilities, all of which had their significant pros and cons. The one the team settled on was to drill a hole through the entire wing using many guide supports to make sure the cut turned out pretty straight. Once the hole was finished then the wing spar could be slid inside the wing with some 20-minute epoxy to hold the spar in place. Then the wing would be connected to the fuselage via a smaller diameter tube fixed to the fuselage.

6.2.2 Landing Gear Construction

The landing gear structures are typically manufactured from composite skin with balsa core, shaped hardened aluminum or steel rods. The choice of materials for the landing gear system was dictated by spatial and weight requirements considered for the intended application. The

figures of merit chart shown in Table 19 below lists the analysis parameters considered for the three different landing gear materials. Different weight factors were applied to their respective merits figures and a result was found. The composite Kevlar skin and balsa construction was found to be favorable mostly by virtue of its superior expected strength to weight ratio. The design of both the nose and main landing gears are custom build assemblies manufactured to specifications requirements like airplane height, weight, propeller clearance, tip back angle and wheel base width. The results of these calculations can be found in the detailed landing gear structures portion of the report. The nose gear was assembled from the same composite spar rod found in the wing. The main landing gear was laid up on a wood plug. The composite/balsa/composite construction was made to take the shape of the plug then cured into the desired shape.

	Weight Factor	Composite Balsa	Aluminum	Steel Rods
Strength to Weight Ratio	0.35	3	1	2
Ease of Construction	0.1	1	3	2
Reparability	0.25	3	1	2
Skill Level to Manufacture	0.15	2	3	1
Availability	0.05	1	3	2
Cost	0.1	1	2	3
	1	**2.35**	**1.7**	**1.95**

Table 20. Landing Manufacturing Methods FOM

6.3 Vehicle Integration

The main concern of the vehicle integration group was the construction of the fuselage. Manufacturing methods, which were best for the fuselage, were implemented during the manufacturing phase of the design.

6.3.1 Fuselage Construction

The primary function of the fuselage would be to transfer static and dynamic loads and to house required components and payload in an aerodynamic shape. Manufacturing of the fuselage occurred in three sections: nose faring, main fuselage, and tapering boom. As shown in the figure of merit (Table 20), composite covered balsa was determined to be the best method to manufacture the fuselage. The primary materials needed were wooden plugs, balsa "core" panels, pre-impregnated Cycom 919 fiberglass fabric, Teflon sheeting and tape, thin-weave breather fabric, and plastic vacuum bag. Lay-up of the fuselage was sequenced over the plugs as follows: Teflon, two layers of composite, Teflon, breather, vacuum bag. The main fuselage section had fore and aft bulkheads and full length and height structural panels made of ¼ in. and 3/8 in. balsa respectively. Where a bulkhead or structural panel was needed, layers of

'composite, "core", 'composite' were substituted for the single section of 'composite' above. To minimize the wet lay-up process needed to join the three sections, the fiberglass wrap for the nose faring and tapering boom was extended ½ in. onto the main fuselage section, providing a 'tight fit' after the cure process. Instead of the fiberglass tape and epoxy technique used for joining sections, the wet lay-up process would require only epoxy. After completing the lay-up sequence, the fuselage was cured in an autoclave at 180 degrees Fahrenheit for 8 hours. All internal sub-structures were added to the fuselage after the main curing process.

	Weight Factor	Balsa Monokote	Balsa Monokote with Pre-molded Plastic	Composite Balsa
Stiffness	0.2	1	2	3
Weight	0.25	3	2	1
Ease of Construction	0.2	2	1	3
Reparability	0.15	1	2	3
Skill Level	0.1	2	1	3
Availability	0.05	3	1	2
Cost	0.05	3	2	1
	1	**2**	**1.65**	**2.35**

Table 21. Fuselage Manufacturing Methods FOM

6.4 Manufacturing Results

The procedure of manufacturing the major components of the aircraft was very detailed and carefully considered before construction. Some of the areas that required consideration before construction were stiffness, weight, ease of construction, reparability, skill level, availability of the material and cost of the fuselage. For each component, Cycom glass was used for manufacturing. The Cycom glass achieved high scores for each area considered in the figure of merit charts throughout the manufacturing section for the wing and tail construction, fuselage construction, and landing gear construction. Skill level needed for composite manufacturing received high scores throughout because several team members already had experience working in the CORE Lab at the University. The CORE Lab also contributed to the Cycom glass being easily available through the school. Although the cost of the composite was higher than other manufacturing options, the other benefits mentioned above outweighed this downfall. Therefore, the team chose to manufacture the aircraft components from composite material.

7 Aircraft Testing

The team conducted a number of small-scale experimental investigations to help finalize design decisions for the propulsion system, airfoil geometry and the payload and landing gear configurations. A brief discussion of some of the testing is detailed below. The schedule for the aircraft testing is presented in Figure 14

Propulsion System Testing

The initial testing performed was performed for the propulsion system. A test stand was created to record the static thrust of different motor-propeller combinations at various frequencies. An ammeter was used to record the current drawn at each frequency. This testing narrowed the choices for the propulsion system to two motors and eight propellers.

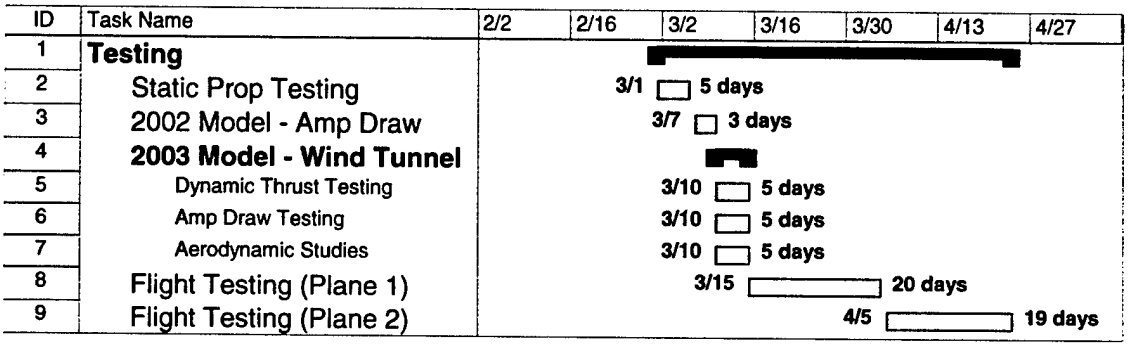

Figure 14. Testing Schedule

Airfoil Testing

Several candidate airfoil test sections were constructed with the intent to evaluate their aerodynamic performance in the aerospace department's free-jet wind tunnel. These sections consisted of 12" chord by 15" span geometries that were made using foam-core wrapped in fiberglass and gave the team experience in manufacturing before tackling the larger wing development. Unfortunately the large snowfall in the area around the University prevented the Stop and Go team from using the free-jet tunnel. Thus, it was not possible to obtain experimental results to support the team's airfoil trade studies. Nevertheless, the team found some experimental data in the literature and compared the lift properties of a Clark-Y airfoil to CFD calculations. These results are presented in Figure 15. Notice that the experimental Clark-Y airfoil had lower aerodynamic performance than the CFD and analytical predictions. The experimental results were still sufficient to allow the team to down select the Clark-Y for the final aircraft configuration.

Full-Scale Wind Tunnel Testing

The next of the airfcraft development involves full-scale wind tunnel testing of the assembled aircraft in the Glenn L. Martin Wind Tunnel. Fortunately, the director of the wind tunnel has

provided free time to obtain the aerodynamic stability derivatives of the fully integrated aircraft at no cost to the Stop and Go team. Thus, the team spent an enormous amount of effort to simulataneously manufacture the aircraft so as to prepare it for wind tunnel testing before actual flight testing. Because of scheduling constraints the team was offered free time in the GLM Wind Tunnel the same day the DBF report was to be submitted to AIAAA. Thus, the construction of the aircraft using the detailed design information in this report was initiated. Over a 72 hour period, the final aircraft was completed and prepared for wind tunnel testing. Figure 16 depicts the aircraft at different views in the Glenn L. Martin Wind Tunnel. Thus, the next few days will involve a complete slew of tests to determine the longitudinal and lateral stability derivatives of the aircraft. This will help the team obtain an understanding of the handling properties of the aircraft before actual flight testing. In addition, the team will be able to ascertain the effects of c.g. location and its novel all moving tail control performance

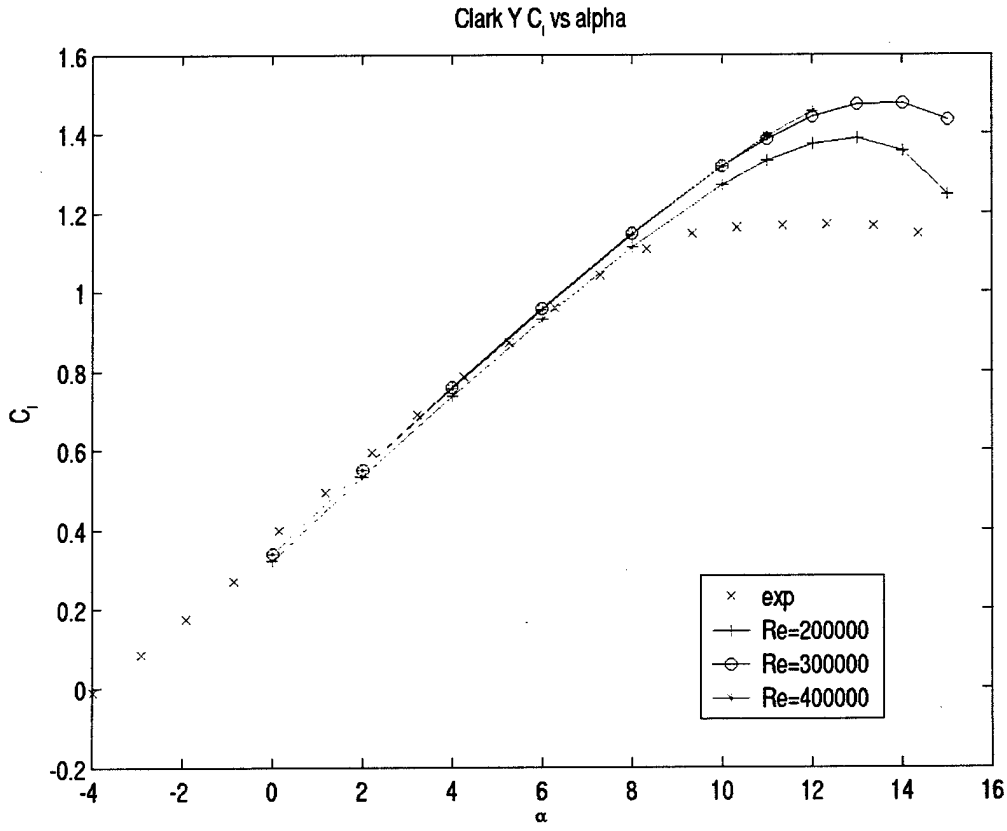

Figure 15. Aerodynamic Performance of Clark-Y Airfoil

Flight Testing

Once the stability derivatives from the wind tunnel testing have been computed and the effects of c.g. as well as the all movable tail are known, flight testing of the aircraft will begin during mid March and continue until the competition deadline. The team will attempt to fly all missions to work out any details that may help improve the vehicles flight performance.

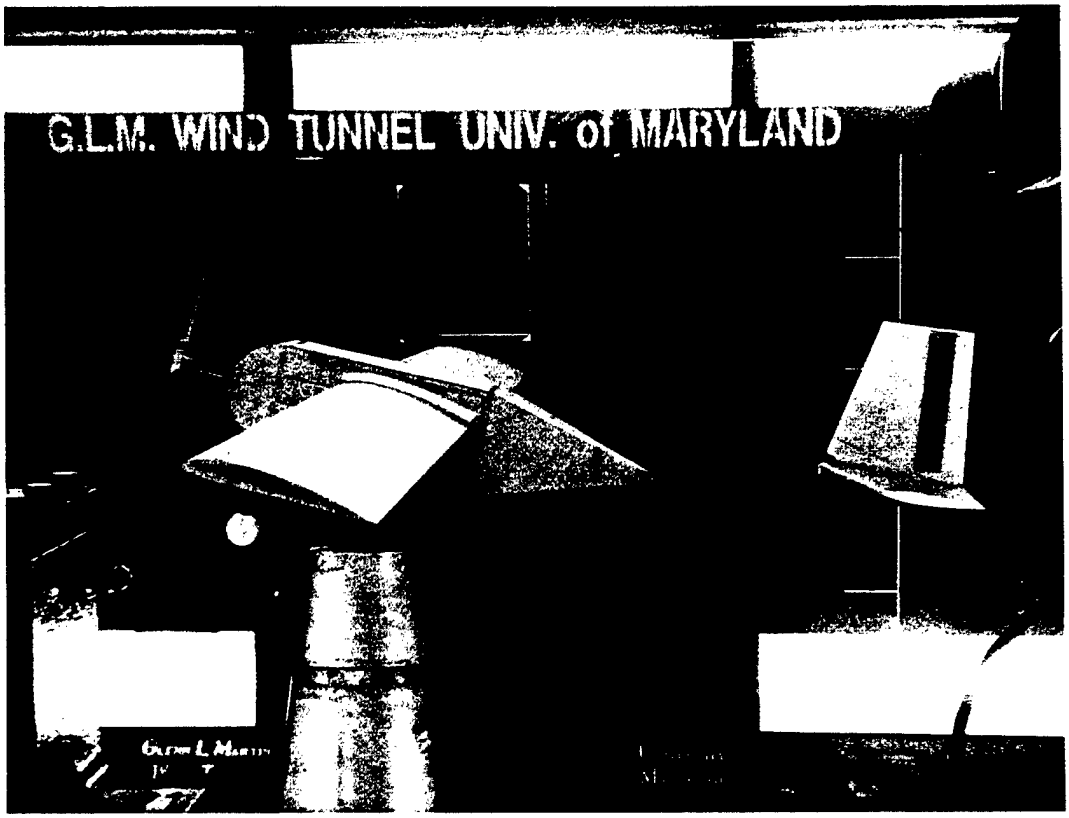

Figure 16. Side View of Stop and Go aircraft in Wind Tunnel

Figure 17. Isometric View of Stop and Go in Wind Tunnel

8 Bibliography

Websites:

"MacLean Quality Composites: Carbon Fiber Tubing."
URL: http://www.macqc.com/mqc1.html

"Motocalc Electric Flight Performance Prediction Software." April 2002.
URL: http://www.motocalc.com/index.html

"Nihon univ. Aero Student Group Airfoil Database." Nov. 2000.
URL: http://www.nasg.com/afdb/index-e.phtml

Selig, Michael."UIUC Airfoil Data Site." Sept. 2002
URL: http://www.aae.uiuc.edu/m-selig/ads.html

Books and Workbooks:

Anderson, John D, Jr. Aircraft Performance and Design. New York: McGraw-Hill, 1999.

Lee, Sung. "Lecture Notes for Aerospace Structures." University of Maryland Jan 2002.

Raymer, Daniel P. Aircraft Design: A Conceptual Approach. Reston, VA: American Institute of Aeronautics and Astronautics, 1999.

Rice, M.S. Handbook of Airfoil Sections for Light Aircraft. Milwaukee, WI: Aviation Publications, 1971.

CESSNA ONR / STUDENT DESIGN/BUILD/FLY COMPETITION

An AIAA Student Activity

2002/2003 AIAA Foundation

Cessna/ONR Student Design/Build/Fly Competition

Design Report

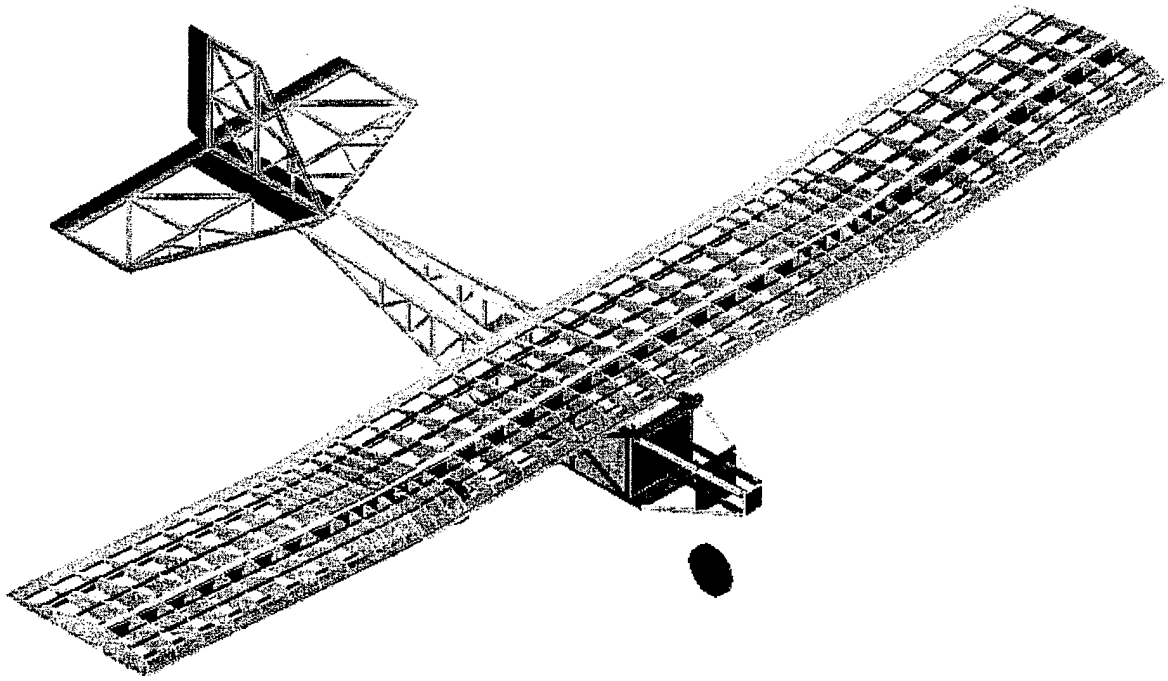

"It's Supposed To Fly?"

Ohio Northern University

March 2003

Table of Contents

Page #

1. Executive Summary....3
   - 1.1 Conceptual Design....3
   - 1.2 Preliminary Design....3
   - 1.3 Detail Design....4
   - 1.4 Maufacturing and Prototype Testing....4
2. Management Summary....6
   - 2.1 Architecture of the Design Team....6
   - 2.2 Schedule, configuration, and Documental Control....6
3. Conceptual Design....8
   - 3.1 Design Parameters and Aircraft Configurations....8
   - 3.2 Figures of Merit....12
   - 3.3 Final Aircraft configuration....14
4. Preliminary Design....16
   - 4.1 CFD Analysis of Ideal Final Design....16
   - 4.2 Initial Product Testing....17
   - 4.3 Final Preliminary Design....18
5. Detail Design....20
   - 5.1 Primary Components....20
   - 5.2 Secondary Components....20
   - 5.3 Performance Parameters....22
   - 5.4 Payload Deployment Mechanism....22
   - 5.5 Final Aircraft Dimensions....23
   - 5.6 Rated Aircraft Cost....23
6. Manufacturing Plan and Processes....25
   - 6.1 Order of Manufacturing Plan and Processes....25
   - 6.2 Wing Center Section Construction....25
   - 6.3 Wing Outer Section Construction....25
   - 6.4 Fuselage Construction....25
   - 6.5 Tail construction....26
   - 6.6 Miscellaneous Construction....26
7. Testing Plan....27
   - 7.1 Testing Objectives....27
   - 7.2 Testing Schedules....27
   - 7.3 Check-Lists....27

7.4 Results.....27
7.5 Conclusion.....28
8. References.....29

1.0 Executive Summary

The senior design team comprised of Jeff Clements, Brian Deily, and Joe Finfera has decided to compete in the 2002-03 AIAA Design/Build/Fly competition as their senior capstone project. The competition will require the students to design, fabricate, and demonstrate flight capabilities of an unmanned, electric powered, radio controlled aircraft that can complete the specified missions. The aircraft is to be designed around stable flight characteristics, cost, manufacturability, and mission performance. Jeff Clements fell seriously ill after fall quarter and was forced to leave both the university and the team. Helping to aid the team is freshman Matt Castellucci, junior Dan Avers, and junior Jeff Switzer (Pilot). Advising the team is Dr. Jed E. Marquart. The specific goal of the design team was to design, build, and compete with the first successful aircraft by Ohio Northern University students.

1.1 Conceptual Design

The conceptual design process began with breaking down the eight month timeline into four sections: Research, Design, Build, and Testing. The eight major aircraft components were then divided into the following groups; wings, fuselage, tail, airfoil, motor/prop, batteries, landing gear, and radio. A team member was assigned to each aircraft component group to research and design the various concepts and configurations. The group responsible for each component of the aircraft then generated 2-3 design concepts for further analysis in a decision matrix. Two decision matrices were then created, one for the *general aircraft configuration* and one for the *airfoil analysis*, to determine the top three aircraft configurations and top two airfoils. After reviewing manufacturability, cost, and flight performance, the final design concept was to be decided upon, and preliminary drawings and construction techniques were then to be analyzed for further revision.

1.1.1 Conceptual Design Alternatives

Different configurations were generated for evaluation based on combinations of components researched during the conceptual design. The different configurations consisted of combinations of four wing configurations, two fuselage shapes, three tail types, five airfoils, two different motors, and two landing gear setups. The *general aircraft configurations* matrix evaluated some of the above configurations using the following criteria: take-off distance, flight stability, competition flight performance, rated aircraft cost, drag, weight, lift, size, ease of repairs, responsiveness, rigidity/strength, flexibility, ease of construction, cost, and ground clearance.

1.1.2 Conceptual Design Tools

Several different computer programs were used for the analysis of design configurations, computational fluid dynamics (CFD) analysis, design drawings, and 3D modeling. Microsoft Excel and RC CAD were used for the analysis of the various design configurations. The decision matrices and rated aircraft cost (RAC) were constructed using Microsoft Excel to determine the leading designs and costs. RC CAD was used to generate basic 3D illustrations of the aircraft and to help evaluate their manufacturing feasibility and general flight responsiveness. The CFD analysis required the use of Solid Edge to generate the geometry model, Gridgen to generate the grid, Cobalt to solve the flow, and

FieldView to view the solution. AutoCAD 2002 was used to generate preliminary and final 2D design drawings, along with the 3D modeling drawings.

1.1.3 Conceptual Results

Following the evaluation of the decision matrices and excel spreadsheets, the top designs that best satisfied our design criteria were selected from the alternatives. The best aircraft configuration was predicted to be a conventional fuselage, with a conventional tail, and a three-piece wing. The second best configuration also used a conventional tail and three piece wing; however the fuselage would utilize a skeleton type of configuration. The third configuration would have been a skeleton fuselage, with a conventional tail, and a two piece wing. All three aircraft configurations were to utilize a tricycle landing gear, powered by a single Cobalt 40 geared motor in the tractor style configuration, with batteries connected in series.

1.2 Preliminary Design

Upon selecting the best configuration, the aircraft specifications were the next area of concentration. The aircraft specifications include basic dimensions of the fuselage, wing chord, control surface areas, wing and tail areas, and controls routing. The internal supporting structures were also analyzed further to ensure structural stability and rigidity. The motor/prop system was also specified around flight performance and speed.

1.2.1 Preliminary Design Alternatives

The preliminary design phase required the evaluation and decision on component types, sizes, costs, and quantities. Items that required analysis include; tires, control horns, servos, propellers, control surfaces, battery configurations, and deployment mechanisms. After selecting the ideal components for the given situation, the parts were both theoretical and experimentally tested against structural failure, performance, and robustness.

1.2.2 Preliminary Design Tools

Component location, controls routing, and control surfaces were determined and illustrated using RC CAD. The component testing was done through manual methods of exerting excessive forces to each of the components. A safety factor of about four was used to ensure the safety of the aircraft. Experimental data from http://www.nasg.com/afdb/show-airfoil-e.phtml?id=1080 was used to ensure that the airfoil would generate the required lift under the predicted flight performance.

1.2.3 Preliminary Results

The preliminary results yielded a 46 in. fuselage (without the propeller and motor shaft), a 292 $in.^2$ horizontal stabilizer, a 88 $in.^2$ vertical stabilizer, and a nine foot wing made up of a four foot center section with two 30 in. outer sections that covers 1620 $in.^2$ with the 15 in. chord. The Astroflight Cobalt 40 geared motor was selected to generate the required thrust when used with either a 14x7 or 13x10 propeller.

1.3 Detail Design

The detail design phase began with optimization of the aircraft configuration. This included refining the aerodynamics of the airframe, ensuring the power plant configuration would be adequate, and

testing the structural components of the aircraft. The optimization relied upon the components selected during the preliminary design phase.

1.3.1 Detail Design Alternatives

Detail design alternatives focused around varying locations of the components previously selected, mounting procedures and placement, and payload deployment mechanisms. Location analysis included locating the control horns on the control surfaces, location of the landing gear, and weight distribution control. The mounting procedures and placement included longitudinal placement of the wings on the fuselage, tail attachment points, and trailing distance from the propeller to the wing leading edge. Several payload deployment mechanisms were considered, and further testing would be performed to create the simplest, most robust actuation device.

1.3.2 Design Tools

A Microsoft Excel spreadsheet was used to generate weight distribution and summation so that the aircraft weight and center of gravity could be determined.

1.3.3 Detail Design Result

The detail design phase resulted in the selection of required aircraft construction equipment, system components, and final airframe optimization. The aircraft flight performance and control surfaces have been analyzed and the construction process laid out.

1.4 Manufacturing and Prototype Testing

The manufacturing construction process was first tested to see if the wing ribs could be mass produced and the 5° angle of dihedral could be accomplished using a 5° wing joiner. Having successfully created preliminary wing ribs, the predicted construction process proved to be successful.

2.0 Management Summary

The Ohio Northern University team was initiated by three senior mechanical engineers who were competing in the AIAA Design/Build/Fly competition for their senior capstone project. Each of the three seniors would take a turn as team leader for one quarter. After fall quarter, the next proposed team leader became seriously ill and was forced to withdraw from the project. In order to help assist the remaining two seniors, and to satisfy competition requirements, three underclassmen were recruited to help with the project.

2.1 Architecture of the Design Team

Each of the eight aircraft component groups was managed by one of the three seniors, with all three seniors performing the research and designing together, but with the respective senior being in charge of the overall decisions and construction in their specified area. With the loss of the third senior, the remaining areas were divided amongst the remaining two seniors and the underclassmen. The team leader position was allotted to each senior for a quarter, with the competition leader shown below in Table 2.1.

	Team Leader:	Joe Finfera (Fall + 1/2 Winter)	
Pilot: Jeff Switzer		Brian Deily (1/2 Winter + Spring)	
Dan Avers (Junior)	**Matt Castellucci (Freshman)**	**Brian Deily (Senior)**	**Joe Finfera (Senior)**
Tail PVC Payload	Assembly Box 6"x6"x12" Payload	Wings Landing Gear Radio CFD	Fuselage Airfoil Motor/Prop Batteries

Table 2.1 Architecture of the Design Team

Under the guidance of the team leader, the group leader of each of the aircraft component groups was responsible for dividing up the required tasks in order to research, design, build, and test the respective aircraft component.

2.2 Schedule, Configuration, and Documental Control

In order to complete the project within eight months, the team had to set forth a schedule that had a rapid pace from research, to design, to construction, all while accumulating the required documentation for submittal. The schedule contained many milestones which were implemented through time periods and deadlines (see Figure 2.1, Gantt Chart). The overall process was divided into conceptual research, conceptual design, specific research, preliminary design, detail design, and manufacturing processes. Each week the team met with faculty advisor Dr. Jed E. Marquart. During these meetings the team discussed progress, problems, and future plans. A weekly email was also sent out each Friday to update team members on accomplishments, completion percentages, problems, and future plans. The team also met throughout the week to address problems. The team remained on track with the Gantt chart and most milestones throughout the project.

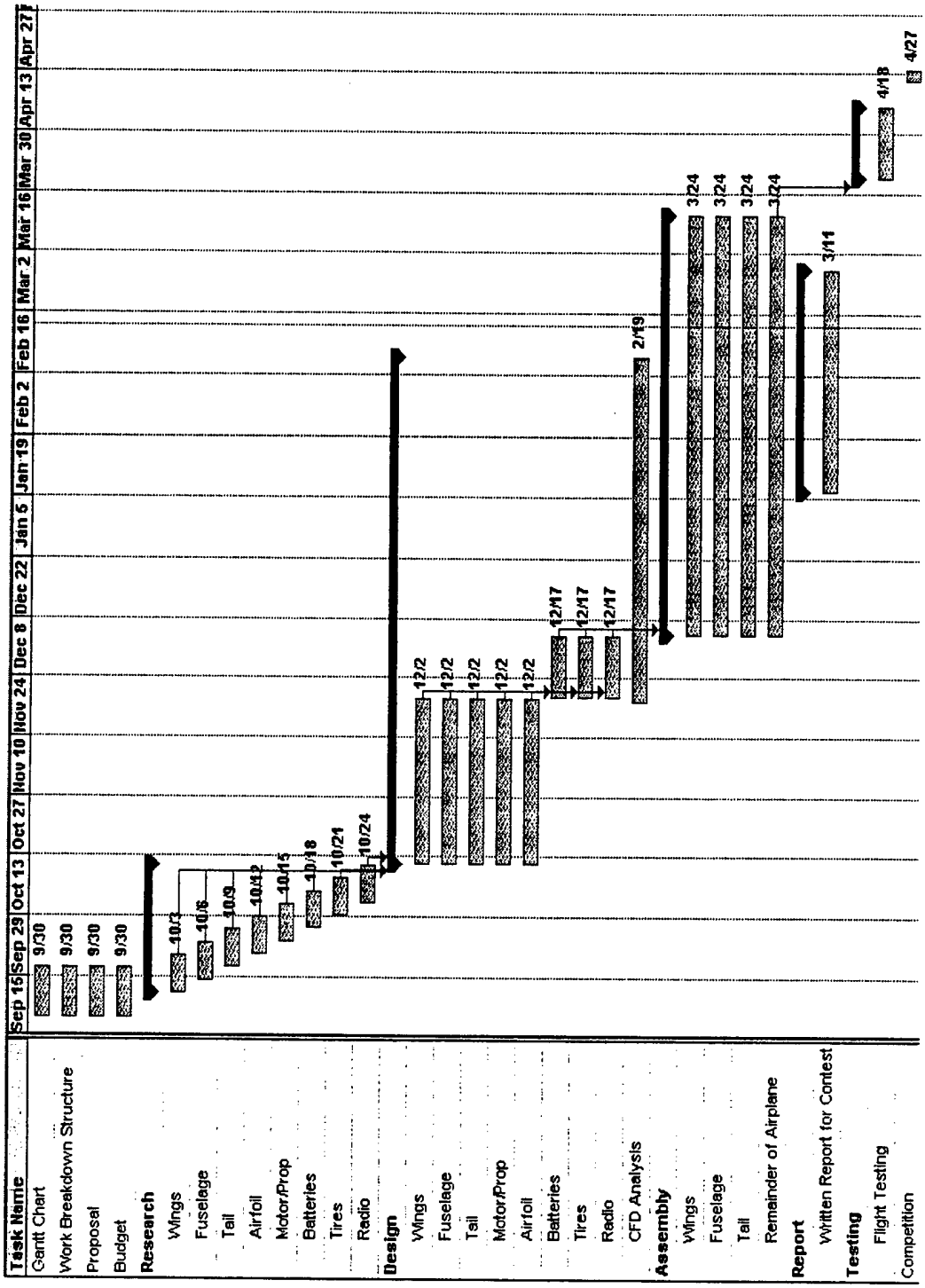

Figure 2.1 Gantt Chart

3.0 Conceptual Design

The conceptual design phase began following conceptual research. The team first considered all airplane design parameters that were found during research. After identifying all the available design parameters, the team reduced the parameters so that a student with no previous flight experience could build and fly the final design. The majority of the parameters that were focused upon are commonly found in trainer and beginner level aircraft.

3.1 Design Parameters and Aircraft Configurations

The design parameters and aircraft configurations that were identified in the conceptual design phase were now being evaluated with greater precision. Configurations that were difficult to construct, fly, or too expensive were eliminated The result yielded the slower, more stable trainer-type aircraft that are not intended for sport or aerobatic flying.

3.1.1 Wing Planform

A major focal point of the team was the wing type. Since the plane will be flown by an amateur pilot the stability is important. Also since the plane will be electric powered and carrying at least five pounds of dead-weight, the lift generated by the wings was another key factor. The six factors used in determining design parameters included: trainer-like flight performance, ease of construction, low wing loadings (20 oz/ft^2 $\pm$2), high lift coefficients, and low weight and drag.

Several basic wing shapes were analyzed, such as a swept wing, delta wing, bi-wing, and a conventional wing. The team decided upon a conventional wing to prevent the construction complexity of the other types of wing. The wing will be built in three pieces, with the outer two sections utilizing a 5° angle for dihedral. The wing will not include any form of taper, with the exception of the wing tips which will utilize the airfoil with a 45° slanted tip.

Due to the low airspeeds that the plane will be flying at, the Reynolds number will also be low and will require a low Reynolds number airfoil.

3.1.2 Wing Configuration and Location

The vertical positioning of the wing was considered when designing the wing and fuselage. In order to keep the center of gravity below the wing, maintain trainer-like stability, and have an aircraft that returns to level flight, the team unanimously agreed upon a high wing rather than a low or mid wing aircraft. With the center of gravity below the wing, the next focus was upon the longitudinal location of the center of gravity. Due to the potential of flying some laps with the payload, and some without, the center of gravity of the aircraft was designed so that it would remain in the same spot with or without the payload. Upon determining the center of gravity at the middle of the payload carriage, the wings were to be positioned directly above the center of gravity, such that the center of lift and the main spar would be located directly above the center of gravity.

3.1.3 Airfoil Selection and Configuration

The selection of the airfoil was an important consideration. The experimental data that was available on airfoil performance at the website http://www.nasg.com/afdb/show-airfoil-e.phtml?id=1080

was examined. Since the aircraft will not be flying at a high rate of speed, only the low Reynolds number type airfoils were examined. After the data had been researched there were five possible airfoils that were selected.

The five different airfoils that were selected for further analysis were the; FX63137, ClarkY, S2091, SG6043, and SD7062. All of these airfoils were selected for consideration because each had higher coefficients of lift than drag. A decision matrix was then constructed in order to evaluate the different types of configurations. This decision matrix rated the airfoils in several categories which included; low Reynolds number lift and drag, average Reynolds number lift and drag, manufacturability, and structural integrity. The low Reynolds number refers to when the aircraft is in flight, while the average Reynolds number refers to when the aircraft is taking off. Of the two of these Reynolds numbers, the average Reynolds number is higher. The decision matrix is shown below. As a result of the decision matrix the SD7062 airfoil was determined to be the best choice of the five.

3.1.4 Fuselage Configuration

The main purpose of the fuselage was to contain the payload carriage at the largest part of the fuselage. The square cross-sectional profile was designed around giving the payload the best aerodynamics possible. The structural integrity of the airframe must be strong enough to handle forces induced by the lift of the wings, torque from the tail, landing gear impacts, payload shifting, and motor vibrations. It must house the payload, motor, batteries, control equipment, and deployment mechanism. In addition to structural designing, the fuselage must also be designed for aerodynamics, weight conservation, manufacturability, and quick and easy assembly. It will need to be able to house and deploy the payload, through a servo actuated deployment mechanism that does not interfere with aerodynamics or weight criteria. The two basic shapes that were considered in the detail design phase were the skeleton fuselage and conventional fuselage.

Both fuselage designs would begin with the tractor type propeller and expand back towards the payload carriage. The skeleton fuselage would continue past the payload carriage, about three inches allotted for control equipment, and then abruptly end with a flat plate and a one inch square beam protruding out the flat plate until the tail attachment point. The advantages to this design were the construction simplicity, the ability of the beam to absorb any impact forces, and easy replacement of the beam in the result of a crash. The conventional fuselage design tapers from the payload carriage down to a rectangular profile that is three inches wide by half an inch tall. This rectangular profile will serves as the tail attachment point, using two nylon bolts to attach the two structures together. While this structure would be more difficult to build, repair, and design, the flight performance of this profile is the major reason that this design was selected for further revision.

3.1.5 Tail Configuration

The tail assembly used to correct the pitch and yaw of the aircraft was researched considering four different tail types. The conventional tail was the first tail considered. It provided a large surface for mounting to the fuselage, relatively easy construction, and familiar flight characteristics. The major

disadvantage to this design was the low ground clearance and possibility of turbulence from the wings. The mid-tail was the second tail considered. It had a small point of attachment to the fuselage, would require more construction time, and would experience large amounts of turbulence from the trailing edge of the wing. The benefit to this wing is its ground clearance, it was high enough to clear debris on the ground, but possibly not the deployed payload. The third design was the T-tail which would experience no turbulence from the wings, and had the highest ground clearance of the four designs. The major disadvantages to this design were its small area of attachment to the fuselage, the large construction necessary to build a stable T-tail, and our lack of experience with its flight performance. The fourth design was the consideration of the V-tail. This design was omitted rather early in the design phase, as the group had no experience with V-tails and it provided no major benefits.

The final design selection yielded a conventional tail. The disadvantage of low ground clearance was solved with the tricycle landing gear which was designed to keep the tail at least six inches off the ground, enough to clear ground debris and the deployed payload.

3.1.6 Landing Gear Configuration

The performance of the landing gear is important for several reasons, both when on the ground and in the air. The characteristics of "tail-dragger" and tricycle landing gears were researched to include: ground steering control, impact force dissipation, ground and payload clearance, drag characteristics, cost, and weight. The consideration of a retractable landing gear was not included due to budget constraints and lack of previous experience.

The bicycle landing gear provided low drag characteristics, less weight, and was more cost effective. However, the bicycle landing gear would not be difficult to steer, would have higher impact forces, and have minimal ground and payload clearance. Due to the possibility that payload deployment would be severely hindered, the bicycle landing gear was succeeded by the tricycle landing gear. The tricycle design allows ground steering control, better impact force dissipation, and exceptional ground and payload clearance.

3.1.7 Motor/Prop Configuration

The motor/prop configuration consisted of the motor, propeller, and batteries. The motor is required to accelerate the plane up past stall speed within 120 feet, maintain cruise speed for the time to complete all laps, and minimize weight. The motors considered for evaluation were brushed Astroflight motors (size 40, 60, 90). The main concern of motor selection was the power supply and consumption of the motor/prop/battery configuration. An analysis of the motors was completed to yield the thrust calculation results shown below in Table 3.1.

Model	Weight	Cells	Power	Thrust	Time	Model Weight
40	13 oz	20	550 W	4.4 lb	8 min	6-8 lbs
40 G	14.5	20	550 W	5.6 lb	8 min	8-10 lbs
60	22 oz	32	1100 W	6.9 lb	7 min	8-12 lbs
60 G	23.5 oz	32	1100 W	7.3 lb	7 min	10-14 lbs
90	30 oz	36	1450 W	9 lb	7 min	11-18 lbs
90 G	32 oz	36	1450 W	10 lb	7 min	15-20 lbs

Table 3.1: Thrust Calculation Results

The to minimize cost, power consumption, and weight, the Astroflight Cobalt 40 motor was selected with a 1.7:1 gear reduction. This motor should provide enough thrust to take-off within 120 feet, requires the least amount of power, and weighs the least. By reducing the rotation rate of the propeller, a larger propeller can be turned at a smaller RPM, resulting in more efficient thrust generation.

Several battery combinations were considered, using varying levels of 2400 mAh six cell battery packs. The number of battery packs was varied, along with arranging them in series or parallel. For the final design, the power for the Cobalt 40 motor will be stored in 2400 mAh NiCad sub-C battery packs. Three of the six cell packs will be used in series to yield an eight minute flight at the motor peak efficiency voltage.

3.1.8 Aircraft Configuration

The aircraft configuration was narrowed down to eight final designs. These designs consisted of various configurations of the type of fuselage, number of wing sections, and the type of tail. The eight configurations can be seen in Figure 3.1.8, with a description of each contained in the Figure 3.2.1: Aircraft Configuration Decision Matrix.

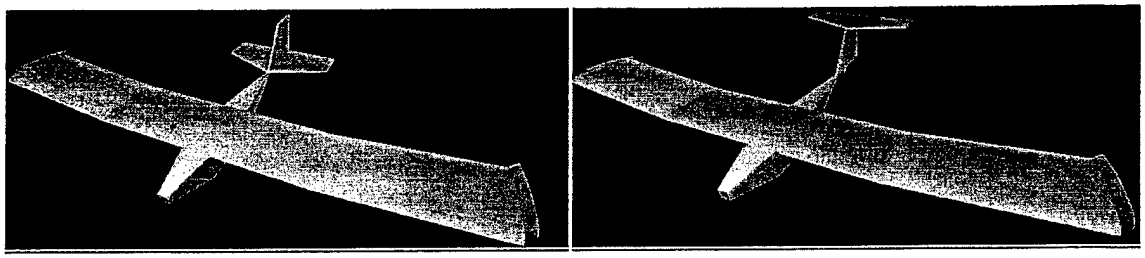

Option 1 Option 2

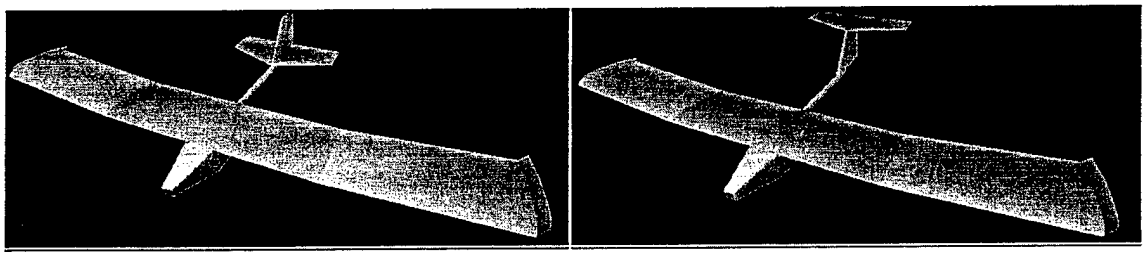

Option 3 Option 4

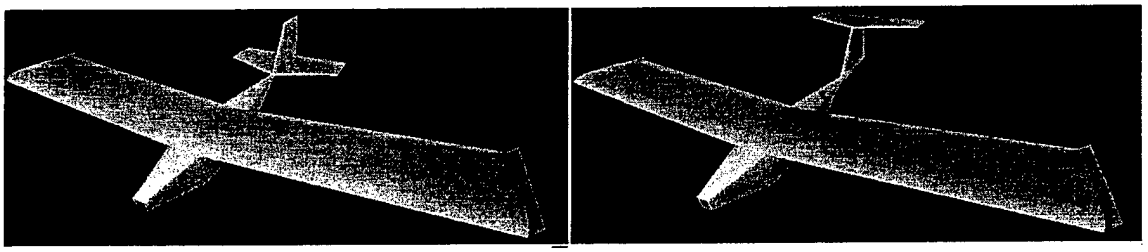

Option 5 Option 6

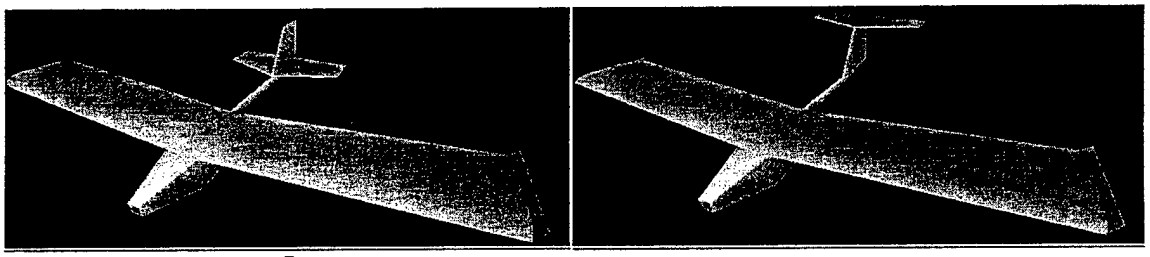

Option 7 Option 8

Figure 3.1.8: Final Eight Aircraft Configurations

3.2 Figures of Merit

Using various figures of merit to quantify and compare the benefits of various design configurations, the final designs can be assigned numerical values of preferential order. Two figures of merit were used for the analysis of final design, a decision matrix of the aircraft configuration and a decision matrix of the airfoil selection. The rated aircraft cost was not evaluated using a figure of merit due to the original goals of the teams design.

3.2.1 Aircraft Configuration

The aircraft configuration utilized a decision matrix to evaluate the final eight designs. The decision matrix was weighted on takeoff distance, flight stability, competition flight performance, rated aircraft cost, drag, weight, lift, size, ease of repair, responsiveness, rigidity/strength, flexibility, ease of construction, cost, and ground clearance. The results can be seen in Chart 3.2.1: Aircraft Configuration Decision Matrix.

3.2.2 Airfoil Selection

The airfoil selection also utilized a decision matrix to determine the final airfoil to be used. The weighted factors for this matrix include drag and lift at low (takeoff speed) and average (cruising speed) Reynolds numbers, manufacturability, and structural integrity.

				Alternate solutions									
		Ideal		FX63137		ClarkY		S2091		SG6043		SD7062	
Criteria	Weight	Max	Max	Rating	Score	Rating	Score	Rating	Score	Rating	Score	Rating	Score
Low Reynolds Drag	15	10	150	4	60	7	105	9	135	2	30	4	60
Avg. Reynolds Drag	10	10	100	3	30	7	70	7	70	3	30	5	50
Low Reynolds Lift	15	10	150	9	135	2	30	6	90	8	120	6	90
Avg. Reynolds Lift	10	10	100	7	70	4	40	4	40	8	80	4	40
Manufactuability	15	10	150	3	45	9	135	6	90	4	60	8	120
Structural Integrity	20	10	200	7	140	6	120	5	100	4	80	9	180
	Total	60	850		480		500		525		400		540
	Rank				4		3		2		5		1

Table 3.2.2: Airfoil Selection Decision Matrix

		Ideal		Option 1		Option 2		Option 3	
Criteria	Weight	Max	Max	Rating	Score	Rating	Score	Rating	Score
Takeoff Distance	25	10	250	7	175	8	200	7	175
Flight Stability	20	10	200	8	160	6	120	8	160
Competition Flight Performance	20	10	200	7	140	8	160	7	140
Rated Aircraft Cost	20	10	200	5	100	5	100	5	100
Drag	20	10	200	8	160	6	120	4	80
Weight	20	10	200	5	100	5	100	7	140
Lift	15	10	150	9	135	9	135	9	135
Size	10	10	100	6	60	6	60	6	60
Ease of Repair	10	10	100	6	60	4	40	9	90
Responsiveness	10	10	100	5	50	7	70	5	50
Rigidity/Strength	10	10	100	8	80	6	60	7	70
Flexibility	10	10	100	9	90	9	90	5	50
Ease of Construction	5	10	50	5	25	3	15	7	35
Cost	5	10	50	6	30	6	30	7	35
Ground Clearance	5	10	50	6	30	6	30	7	35
	Total	150	2050		1395		1330		1355
	Rank				1				2

Option 4		Option 5		Option 6		Option 7		Option 8	
Rating	Score	Rating	Score	Rating	Score	Rating	Score	Rating	Score
8	200	4	100	5	125	4	100	5	125
6	120	7	140	5	100	7	140	5	100
8	160	5	100	6	120	5	100	6	120
5	100	8	160	8	160	8	160	8	160
3	60	9	180	7	140	6	120	4	80
7	140	7	140	7	140	9	180	9	180
9	135	6	90	6	90	6	90	6	90
6	60	8	80	8	80	8	80	8	80
7	70	5	50	3	30	8	80	6	60
7	70	6	60	8	80	6	60	8	80
5	50	9	90	7	70	8	80	6	60
5	50	6	60	6	60	4	40	4	40
6	30	6	30	5	25	9	45	5	25
7	35	7	35	7	35	8	40	8	40
7	35	6	30	6	30	7	35	7	35
	1315		1345		1285		1350		1275
							3		

Table 3.2.1: Aircraft Configuration Decision Matrix

3.3 Final Aircraft Configuration

At the conclusion of the evaluation stage, the final design was a conventional fuselage that was supported by a three piece wing with a nine foot wingspan, and stabilized with a conventional tail. The aircraft will be powered by an Astroflight Cobalt 40 brushed motor with a 1.7:1 gear reduction and 14x7 propeller. The landing gear, tail, and wing will all be held on by nylon bolts so that the center of gravity of the plane is located at the center of lift of the wing and the main spar of the wing. The ground clearance shall be high enough to allow the aircraft to deploy the payload on the runway and take off without interference. The tricycle landing gear with steerable nose wheel shall extend six inches beyond the bottom of the fuselage.

4.0 Preliminary Design

With the conclusion of the conceptual design phase, the preliminary design phase quickly began with preliminary AutoCAD 2D and 3D drawings, RC CAD 3D simulations, final weight calculations, and a CFD analysis.

4.1 CFD Analysis of Ideal Final Design

In order to get a rough estimate of what kind of lift and drag the plane will generate a CFD analysis of the plane in three dimensions was performed. The first step in this process was to create a model of the plane. The solid modeling program Solid Edge was utilized for this task. Since the plane is symmetrical in nature, only the left of the plane was modeled. This was done to reduce the size of the file being created and also to keep the amount of computational time required to a minimum. The landing gear and the propeller were not added to the geometry.

After the geometry model had been created it was then imported into Gridgen. In Gridgen the database that made up the shape of the plane was then turned into connectors. From these connectors the domains were created over the surface of the airplane. These domains represent the surface mesh over a particular part of the aircraft. Large numbers of cells were created at the leading edge of the wing in order to keep the airfoil shape as smooth as possible. After the surface of the plane had been completely meshed, a control volume was created around the airplane. The surface of this volume was meshed so that a volumetric block could be created between the two. This block represented the flow domain around the aircraft.

After the block creation was complete, the boundary conditions had to be added to the mesh. The boundary conditions were set so that the surfaces of the plane were a solid wall, as was the symmetry plane, and the remaining boundaries were set as farfields. The two solid wall boundary conditions were set as separate patches so that they could be viewed separately.

Cobalt was used to solve the flow once the boundary condition file was completed. The solution took 1800 iterations, roughly eleven and a half hours, to converge. The Euler equations and ideal gas assumption were both used to solve the flow. This meant that inviscid conditions with air being treated as an ideal gas were assumed when the flow was being solved. An angle of attack of 0° and a Reynolds number which corresponded to the lower one used in the evaluation of the different configurations. This showed the aircraft as it would appear in flight. The coefficient of lift and drag were obtained from the output file generated by Cobalt. These coefficients had been calculated using a reference area of 1 square inch, so they had to then be changed to apply to the actual plane. After performing this calculation, the lift that was expected to be generated by the plane was estimated at 30 pounds. Using a similar technique the drag was estimated at slightly above 4 pounds.

After the output file from Cobalt was examined, FieldView was used to view the results. The pressure distributions over the surface of the airplane were the first result viewed. The results showed what was expected, a region of low pressure along the top of the airfoil and a higher one underneath. It was also noted that there was a region of high pressure on the tail at a point which was directly behind

where the wing and the fuselage meet. This region seemed to be the result of vortices coming off that region of the wing. Next, the velocity distributions and streamlines were analyzed. The streamlines showed that the flow over the wing was laminar.

4.2 Initial Product Testing

After generating a list of required items, several purchase orders were made to obtain the standard parts that would be used. These parts included controls equipment, power plant equipment, and construction equipment.

4.2.1 Controls Equipment Testing

One of the most important components of the aircraft was the mandatory Fail-Safe Radio. The radio to be used is the Futaba 6XAPS PCM programmable radio. The major test for the radio was to measure the torque provided by a Futaba S3004 servo, to determine if the torque could overcome the friction required to deploy the payload. With two synchronized servos, the radio was able to overcome the friction of the payload, and successfully deploy it without any major problems. The servos were also tested to verify that they could provide enough travel for the control surfaces to effectively control the aircraft.

4.2.2 Power Plant Equipment

The power plant equipment, consisting of motor, batteries, and propeller, was tested to verify that they could perform under the required specifications. The propellers were correctly balanced and free from any major defects, which ensures the safest operation possible. The motor was tested with the propeller to verify the generation of five pounds of thrust. Without any calibrated equipment, the thrust of the motor was estimated to be just under five pounds. The batteries were also tested to verify their 2400 mAh rating. This was done by running 10 $\pm$ 0.1 amps from them through a motor. A 2400 mAh power source should provide 14.4 minutes at 10 amps, however, the batteries were barely able to provide 10 minutes at 10 amps. The reduction in time signifies that the batteries should only be rated at 1800 mAh. This problem will be evaluated in later sections.

4.2.3 Construction Equipment

The construction equipment included balsa, plywood, spruce, and Monokote covering. The materials were acceptable, with the exception of the plywood. The plywood density had not been included in conceptual weight calculations and resulted in slightly heavier plywood wing joiner boxes.

4.2.4 Potential Problems and Solutions

The first preliminary problem was with the batteries which are rated at 2400 mAh. Upon receiving the batteries after their purchase, they were tested to verify how many milli-Ampere-hours they would produce. It was discovered that they could only store 1800 mAh. This will result in a serious reduction of the flight time, approximately 25% less. In order to correct this problem, a couple of options were evaluated. The first option was to cycle the NiCads several times through a series of charge and discharging steps in an effort to remove any cell memory that may have developed after remaining idle on

stock shelves. The second idea was to implement a third battery pack in series with the other two battery packs. It was determined that adding the additional pack of batteries to the plane was the best alternative.

The second preliminary problem was the added weight of using plywood wing joiner boxes. The additional weight of the plywood had not been considered in original aircraft weight calculations, and the plane is still just within the safety factor for airframe weight. As long as the weight remains within the airframe weight limit, no corrective steps will be taken.

4.3 Final Preliminary Design

The final preliminary design included minor modifications to the conceptualized final design.

4.3.1 Final Preliminary Design Parameters

The basic objective of the competition is to transport a six inch wide, by six inch tall, by six inch long wooden box that weighs five pounds. The fuselage is designed to aerodynamically route the thrust generated from the Cobalt 40 motor around the payload carriage, over the wings to generate lift, and back to the oversized tail for stability. The alternative fuselage designs were omitted due to cost, weight, building experience, flight experience, and overall performance. The fuselage shall incorporate a two servo actuator system to deploy the payload on the runway, and shall be activated through channel 6 of the PCM fail-safe radio. The wing design utilizes nine feet of wing, with 15 inches of chord, and flared wingtips, to generate the required lift. The wing is shaped around the Selig-Donovan 7062 airfoil, specifically designed for low speed flight. The outer sections of the three piece wing have a 5° dihedral incorporated into them to provide stability and level flight. The net surface area of the wing will be 1620 in^2 and shall be covered with transparent orange to allow observation of any incurred damages. The horizontal stabilizer is oversized, at 292 in^2, to cover approximately 18% of the wing area and provide gentle flight response. The vertical stabilizer constitutes 5% of the wing area, with its 88 in^2 of surface area.

4.3.2 Preliminary Performance Factors

The preliminary performance factors have been determined as illustrated in Chart 4.3.2 Preliminary Performance Factors.

Wing Loading	Airframe Weight	Empty Weight	Max. Weight	Center of Gravity	Center of Gravity
16.5 oz/ft^2	36 oz.	98 oz	178 oz	(W/ out Payload	(W/ Payload)
				5 in. from L.E.	5 in. from L.E.
				1 in. below wing	1.25 in below wing
Center of Lift	**Wing Area**	**Hor. Stab. Area**	**Vert. Stab. Area**		
5 in. from L.E.	1620 in^2	292 in^2	88 in^2		

Table 4.3.2: Preliminary Performance Factors

The overall dimensions of the aircraft shall be five feet long by nine feet wide by 15 inches tall, with an aspect ratio of 7.2. The shape will have a 1.5 lift coefficient with a maximum lift to drag ratio of 6.67. The predicted stall speed is just over 20 MPH with the average cruising speed of about 30 MPH. The controls will required six servos communicating with a six channel PCM radio. The power from 18 sub-C cells in series will power the Cobalt 40 geared electric motor which will turn the 14x7 propeller. The rated aircraft cost for this design will be 6.47. This is largely due to the oversized horizontal stabilizer that will help keep the aircraft on a level flight path. Due to the rated aircraft cost specifications, the horizontal stabilizer will be considered a second wing because its width is more than 25% of the wingspan. This aircraft configuration will provide the slow, stable, trainer-like performance that the team was designing for. It should be able to be built and flown by an amateur, and shall be within the allotted $1,000 budget.

5.0 Detail Design

After selecting and sizing the primary components in the initial order, the secondary components were sized and selected. A summary of primary and secondary components can be seen in charts 5.1 and 5.2.

5.1 Primary Components

The primary components consisted of basic building supplies that would be required for constructing any one of the eight conceptualized designs. This includes wood, glue, and radio.

5.2 Secondary Components

Upon selecting the final design, the aircraft specific components were purchased. These components included the Cobalt 40 motor, electronic speed, and landing gear equipment.

Primary Components

Component	Quantity	Cost
Futaba PCM Radio	1	$259.99
Small Hinges	1	$3.39
Large Nylon Control Horns	2	$1.70
Thin CA glue	1	$5.99
6-Minute Epoxy	1	$7.99
Thick CA glue	1	$5.99
Plywood 1/4 X 6 X 12"	3	$5.37
Semi-Flexible Pushrod	2	$8.98
Balsa 1/4 X 3/8 X 36"	1	$4.99
Wood Dowel 1/4 X 36"	1	$15.99
Balsa 1/8 X 1/8 X 36"	2	$6.58
Balsa 1/8 X 1/4 X 36"	1	$2.99
Balsa 3/8 X 1-1/2 X 36"	1	$4.99
Spruce 1/4 X 1/2 X 48"	1	$19.99
Balsa 1/8 X 4 X 36"	2	$15.98
Balsa 1/8 X 3 X36	1	$5.49
Balsa 2 X 2 X30"	2	$5.58
Monokote Transparant Orange	2	$23.98
Monokote Black	1	$10.99
Total Cost:		$416.95

Table 5.1: Primary Components

Secondary Components

Components	Quantity	Cost
Servo SYS3000 Standard	3	$27.97
Straight Nose Gear	1	$4.29
Futaba Y-Harness	2	$19.98
Futaba Extension 24"	3	$13.97
13X10 Electric Prop	2	$9.38
14X7 Electric Prop	3	$14.07
Rubber Bands	1	$1.59
Power-Maxx 2400 mAh	3	$113.97
Lite Wheel 4"	2	$18.98
Birch Plywood 1/8 X 6 X 12"	1	$20.19
Extra Landing Gear	1	$8.99
Speed Control	1	$89.99
Cobalt 40 Geared Motor	1	$188.99
Total:		$532.36

Table 5.2: Secondary Components

5.3 Performance Paramaters

The performance characteristics of the aircraft are shown in Chart 5.3.

Parameters		System	Weight (lb)
Length	5 ft	Airframe	2.500
Span	9 ft	Propulsion	2.706
Height	2 ft	Control	0.785
		Payload	
Wing Area	11.25 ft^2	System	0.08125
Aspect Ratio	7.2	Payload	5.625
C_L Max	1.5	Empty Weight	6.1
L/D Max	6.666666667	Gross Weight	11.8
Max Rate of Climb	14.7 ft/s		
		Control	
Stall Speed	24.8 mph	Volumes	
Max Speed	30 mph		
Take-Off Field Length Empty	23.4 ft	Ailerons	1.014 ft^3
Take-Off Field Length Gross	87.7 ft	Elevator	0.627 ft^3
Radio Used	Futaba 6XAPS	Rudder	0.209 ft^3
Servos Used	Futaba S3004 (6)		
Battery Configuration Used	18 Cells in Series		
Motor	Cobalt 40G		
Propellor	14X7		
Gear Ratio	1.7:1		

Table 5.3: Performance characteristics of the aircraft.

The maximum coefficient of lift was determined from the data given for the SD7062 airfoil found in NASG airfoil database. The L/D maximum was calculated by dividing the lift and drag forces found in the CFD analysis. The maximum rate of climb was determined from the maximum thrust to weight ratio. The arcsine of the thrust divided by the empty weight of the plane was used to find the maximum angle at which the plane could climb. This value was then multiplied by the maximum speed of the aircraft. The stall speed was calculated using an equation in reference 6. The take-off lengths were calculated using an equation in reference 3. It should be noted that this value for the take-off distance is slightly optimistic, by about 10-20%.

5.4 Payload Deployment Mechanism

The payload shall be deployed using two servos at the longitudinal ends of the payload box. They shall be synchronized so that when channel 6 is flipped from the closed to open position, they will rotate 90° and the payload will fall out of the bottom of the fuselage. The supplied servo arms will be extended to reach an additional 0.25 inches under the payload. This will require additional torque from the servos; however, it will prevent the accidental deployment of the payload during flight.

5.5 Final Aircraft Dimensions

The outer aircraft dimensions were designed to provide the payload carriage with basic aerodynamic qualities. The internal supports will handle most of the structural loadings, and have been designed to fail under crash situations, so as to absorb as much shock as possible and to protect the expensive control and motor equipment. See Figure 5.4 Final Aircraft Design for overall dimensions.

5.5.1 Fuselage Dimensions

The nose of the fuselage will house the Cobalt 40 motor. It will begin with a two inch square piece of eighth inch plywood that widens back to the six and a half inch square fuselage profile. The payload carriage will extend and additional 13 inches back, before tapering back down to the four inch wide, half inch tall rectangular tail attachment box. See Figure 5.4.1: Fuselage Design for additional dimensions.

5.5.2 Wing Dimensions

The three piece wing will span nine feet with 15 inches of chord. The outer sections will house the 24 inch ailerons with a single servo designated for each aileron. The wings will be joined together with a ¼ inch thick plywood wing joiner with a 5° bend to incorporate dihedral, and two ¼ inch O.D. steel tubes to align the leading and trailing edges. See Figure 5.4.2: Wing Design for additional dimensions.

5.5.3 Horizontal Stabilizer

The horizontal stabilizer will span 30 inches wide and just over 12 inches long. It will have a ¼ inch thickness, and will be followed by a 1 ½ inch thick elevator. The surface area of the horizontal stabilizer will be 292 in^2. See Figure 5.4.3: Horizontal Stabilizer and Elevator Design for additional dimensions.

5.5.4 Vertical Stabilizer

The vertical stabilizer has a height of 10 inches, and it is just over 12 inches long. It also has a ¼ inch thickness and is followed by a 1 ½ inch thick rudder. The surface area of the vertical stabilizer is 88 in^2. See Figure 5.4.4 Vertical Stabilizer and Rudder Design for additional dimensions.

5.5.5 Drawing Package

The drawing package is located on the last five pages of this report.

5.6 Rated Aircraft Cost

The rated aircraft cost was significantly lower than those of last years contest. This is to be expected since the payload size for this year is significantly smaller and the aircraft must be able to fit inside the assembly box. The rated aircraft cost for the final design is shown below in Chart 5.5: Rated Aircraft Cost.

A

Empty Weight	6.1	lb
Multiplier	100	
Total	$610.00	

B

REP	1	
Multiplier	1500	
Total	$1,500.00	

C

			Multiplier	Hours
MFHR	Wing Span	11.5 ft	8 hr/ft	92
	Chord	1.25 ft	8 hr/ft	10
	Control Surfaces	2	3 hr/surface	6
	Fuselage	5 ft	10 hr/ft	50
	Vertical, No Controls	1	5 hr/surface	5
	Vertical, with Controls	1	10 hr/surface	10
	Horizontal Surface	0	10 hr/surface	0
	Servo/Speed Control	7	5 hr/part	35
	Engine	1	5 hr/engine	5
	Propeller	1	5 hr/prop	5
			Total:	218
	Cost = $20/hr			
	Total Cost of MFHR:	**$4,360.00**		

Total Cost of Plane:	**$6,470.00**
RAC:	**6.47**

Table 5.5: Rated Aircraft Cost

6.0 Manufacturing Plan and Processes

The aircraft manufacturing process was first laid out to organize a plan that would begin with the most critical components, and end with the similar components. Several different methods were considered for various levels of manufacturing techniques. The components required varying levels of shape production, assembly order, and surface finish.

6.1 Order of Manufacturing Plan

The manufacturing process was to begin with the center section of the wing, followed by the outer two sections, then the payload carriage would be assembled, with the two spruce supports attached to the front of the payload carriage and spanning back to the tail point of attachment. The spruce supports were to then be supported with an internal supporting structure, while at the same time the horizontal and vertical stabilizers were being constructed. Upon receiving the motor, the front half of the fuselage would begin to form. Upon completion of the wooden structure, all control equipment would be mounted, and the final step would be to cover the aircraft with transparent orange Monokote.

6.2 Wing Center Section Construction

The center section of the wing began with the notching of the four feet long spruce beams. The ¼ inch by ½ inch spruce beams were notched starting 4.5 inches from the ended, and continuing with three inch spacing between the notches until reaching 4.5 inches from the opposite end. The wing ribs were cut by placing a tracing of the Selig-Donovan 7062 airfoil on eight layers of 1/8 inch thick balsa and cutting eight wing ribs at a time. After cutting 48 identical ribs, they were placed between the spruce I-beams. Strips of balsa 2-7/8 inches thick by 1 ½ inches tall were then placed between the spruce flanges and the wing ribs, to form an I-beam type of construction along the spar. The outer 4 ½ inches of the spruce flanges were then reinforced with 1/8 inch thick plywood to form the wing joiner boxes. Three of the remaining ribs were then placed at either end of the wing to support the plywood joiner boxes. The ribs, which contained notches, were then reinforced with 1/8 inch by 1/8 inch strips of balsa to help support the bending and flexing of the wing. The final steps of wing construction included notching and attaching the leading and trailing edges.

6.3 Wing Outer Section Construction

The wing outer sections were constructed in a very similar fashion as the center section. The trailing edges were modified to implement a 24 inch aileron on each section. The construction of the plywood joiner box also only appeared on one end of each section, with the opposite ended being blended with a balsa wing tip.

6.4 Fuselage Construction

The center of the entire fuselage concentration is upon the payload carriage. The payload carriage will house the payload, the center of gravity, and the least amount of structural support. The fuselage construction began with the support structure of the payload carriage. The support structure consists of ¼ inch thick, 3/8 inch wide balsa that is constructed around 1/8 inch balsa sheets. The backbone of the rear fuselage is made up of two spruce beams that run 36 inches back from the front of

the payload carriage. After attaching the spruce beam to the payload carriage, a support structure was constructed around the rear fuselage to provide aerodynamics characteristics. The rear portion of the fuselage tapers from the payload carriage down to the tail point of attachment. The tail point of attachment consists of two 1/8 plywood pieces that are sandwiched around the spruce beams, and will have blind nuts inserted into them to attach the tail. The front portion of the fuselage uses four internal support members to carry the load of the electric motor. The outer section of the front fuselage used four ¼ inch square balsa strips to direct airflow from the two inch square motor mount to the 6.5 inch square fuselage.

6.5 Tail Construction

The construction of the horizontal and vertical stabilizers was performed separately, after finishing construction of both surfaces they were attached to each other and fitted with their respective control surfaces. The horizontal stabilizer will house the nylon bolts for attachment to the fuselage.

6.6 Miscellaneous Construction

The final construction will conclude with the insertion of the motor firewall, landing gear, and Monokote covering. The control equipment will need to be installed, along with the necessary wire extensions, before applying the Monokote covering.

7.0 Testing Plan

The testing plan was based off of testing objectives, putting together a testing schedule, following a testing checklist, and summarizing and evaluating the results.

7.1 Testing Objectives

There are several objectives that are set for the testing portion of the project. The batteries and the motor were tested upon receiving them to verify their performance. The nylon wing bolts are going to be tested to see whether or not they will shear off before the wing structure. Next, the wing structure will be tested in order to make sure that it can hold the weight of the plane. Finally, the last objective in the testing phase of the project is to test the flight worthiness of the plane.

7.2 Testing Schedules

First the batteries were tested in order to determine how many millamp hours they were actually able to output. After this test was completed, the motor was tested in order to verify that it would turn and begin the breaking process. The next objective in the testing schedule is to check the nylon bolts. The bolt's tensile strength and also shear strength are going to be tested. This is to determine whether or not they will shear off before the wing is destroyed in a crashed. Next on the schedule is the testing of the wing structure. This test is being performed to ensure that the wing structure will support the weight of the plane with its payload. This will be done by balancing the plane on its wingtips. This will also provide information on the actual location of the center of gravity. The last item on the schedule is to test whether or not the aircraft is flight worthy. This will be done by test flying the aircraft once the construction has been completed.

7.3 Check-Lists

There are several parameters which must be tested under each objective. First on the check-list for the nylon bolts is making sure that they will shear before the wing. After this has been completed, the bolts will be tested in tension to make sure that they will adequately hold the wing. There is no check-list for the testing the structural integrity of the wings.

The check-list for testing the flight worthiness of the aircraft is extensive. First, the flaps will be tested in order to make sure the servos are working properly. After this has been completed the other servos will be checked to make sure that they will function as intended as well. After all of the servos have checked out the flight testing will begin. First, a check will be made to ensure that the plane will leave the ground, disregarding the distance required for it to do so. After it has been verified that the aircraft is capable of flight we will check to make it sure that it can do so within the distance specified by the contest. The performance of the aircraft, when subjected to varying wind and weather conditions, will also be examined. After all of these parameters have been examined and determined satisfactory the testing phase of the project will end.

7.4 Results

The batteries were tested in order to determine the exact amount of milliamp hours that could be received. The results of these tests indicated that only 1800 mAh could be received from the batteries,

which were rated at 2400 mAh. This caused a problem which was solved by adding a third pack of batteries to the design of the plane. Another test was performed on the motor to begin the breaking in process. This test was performed at half voltage in order to get the motor started and verify that it worked properly. This test was successful and the motor did begin to work.

7.5 Conclusion

Brian Deily, Joe Finfera, and Jeff Clements have entered the AIAA Design/Build/Fly competition for their senior project. The underclassmen Matt Castellucci, Dan Avers, and Jeff Switzer will be also be helping the team. A setback was suffered at the end of fall quarter when Jeff Clements fell seriously ill and was forced to leave the team. The contest was divided into four sections: research, design, build, and testing. These categories were broken down into the eight major components of the aircraft; wings, fuselage, tail, airfoil, motor/prop, batteries, landing gear, and radio. After completing research, general aircraft configurations were generated and evaluated using a decision matrix. The decision matrix revealed the three best designs according to the criteria that we set. These designs were then further evaluated.

One of these three configurations was selected as the best choice. Calculations were performed to determine various performance characteristics of the aircraft. A CFD analysis was performed on the aircraft as well to visualize what the airflow over the aircraft would be and also to approximate the lift and drag experienced by the aircraft in flight. Construction also began on the plane at this time. Tests were performed on the motor and batteries to verify that they worked correctly and to examine what kind of results they produced. Once construction has been completed, testing will begin on the aircraft. The tests planned include; testing the nylon bolts, testing the wing structure, and flight testing.

8.0 References

1. Boucher, Robert J. Electric Motor Handbook. United States: AstroFlight, Inc., 2001.
2. Design Guidelines for Electric Powered Model Aircraft. MaxCim Mototrs, Inc. 29 Sept. 2002 <http://www.maxcim.com/guide.html>.
3. Hale, Francis J. Introduction to Aircraft Performance, Selection, and Design. New York: John Wiley & Sons, 1984.
4. Higley, Harry. Entering Electrics. Illinois: Harry B. Higley & Sons, Inc., 1990.
5. NASG Airfoil Database. 10 Oct. 2002 <http://www.nasg.com/afdb/show-airfoil-e.phtml?id=1080>.
6. Raymer, Daniel P. Aircraft Design: A Conceptual Approach. Washington DC: American Institute of Aeronautics and Astronautics, Inc., 1992.
7. Smith, Timothy. Electric Model Aircraft Circuit Diagrams. 29 Sept. 2002 <http://www.vision.net.au/~timotsc/elecmod2.htm>.
8. Sullivan, Howard. Practical R/C Model Design. 29 Sept. 2002 <http://www.uoguelph.ca/~antoon/hobby/pmdesign.htm>.

REVISIONS				
ZONE	REV	DESCRIPTION	DATE	APPROVED

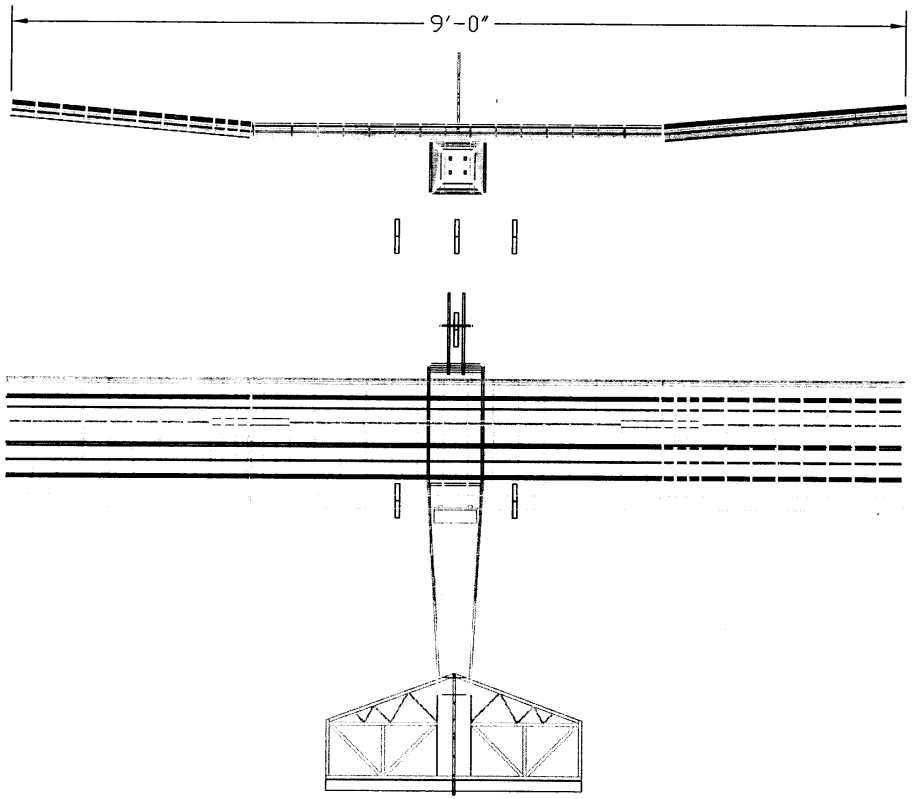

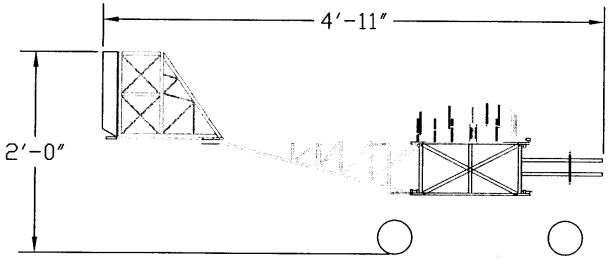

Figure 5.4: Final Aircraft Design

SIZE	FSCM NO.	DWG NO.	REV
B		0	
SCALE NTS		SHEET 1 of 1	

AIAA_DESIGN_BUILD_FLY-02_27-05_FINAL_DESIGN.DWG

FUSELAGE.DWG 2-1-03 AIAA_DESIGN/BUILD/FLY

REVISIONS				
ZONE	REV	DESCRIPTION	DATE	APPROVED

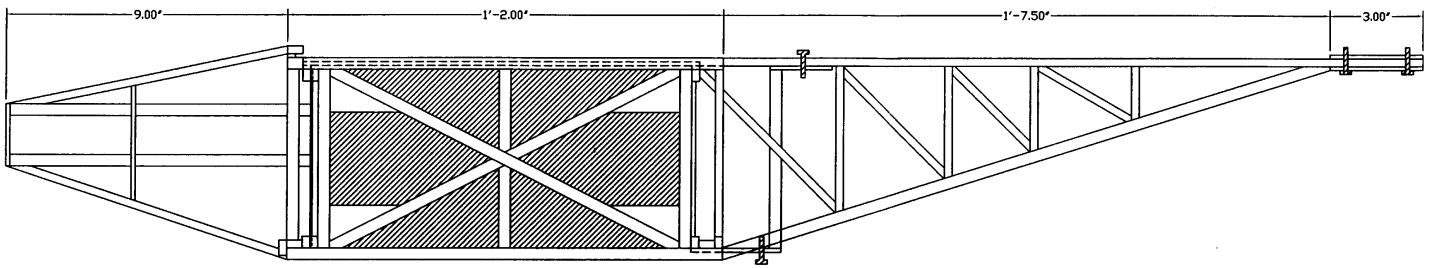

Side View

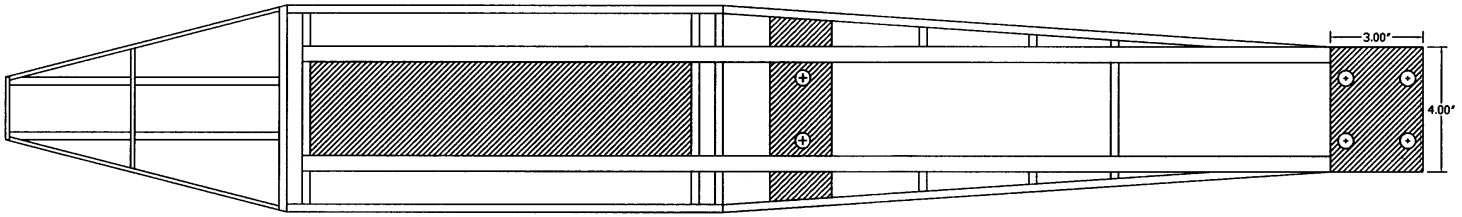

Top View

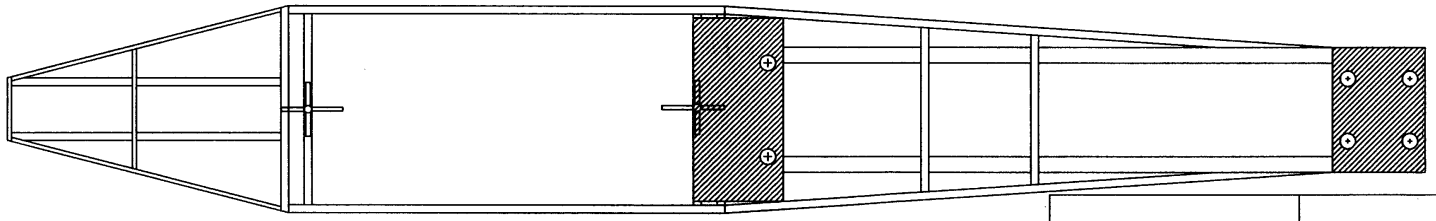

Bottom View

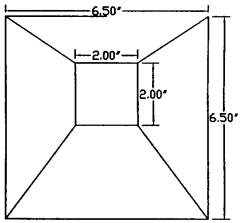

Figure 5.4.1: Fuselage Design

SIZE	FSCM NO.	DWG NO.	REV
B		1	
SCALE 1"=4"		SHEET 1 of 1	

AIAA_L_SIGN/BUILD/FLY 02/__/03 3PIECE_WING.DWG

REVISIONS				
ZONE	REV	DESCRIPTION	DATE	APPROVED

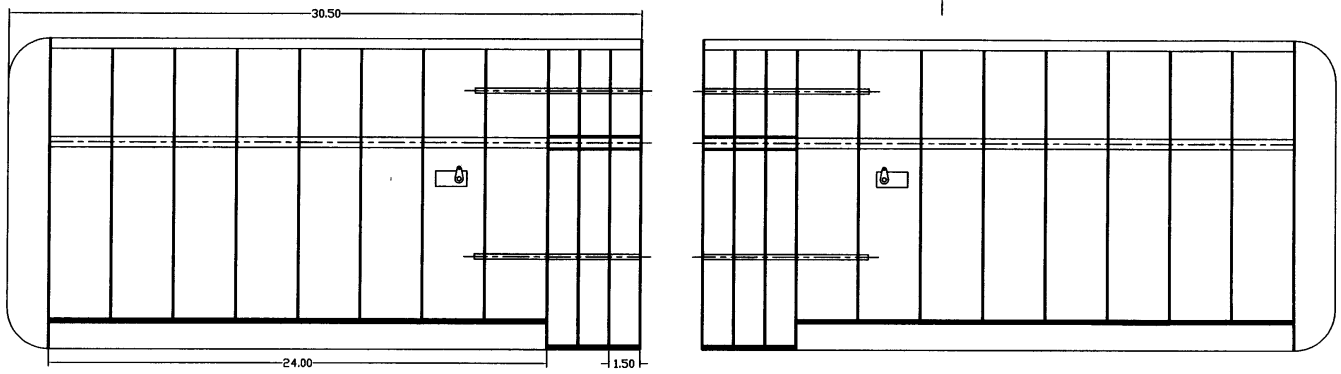

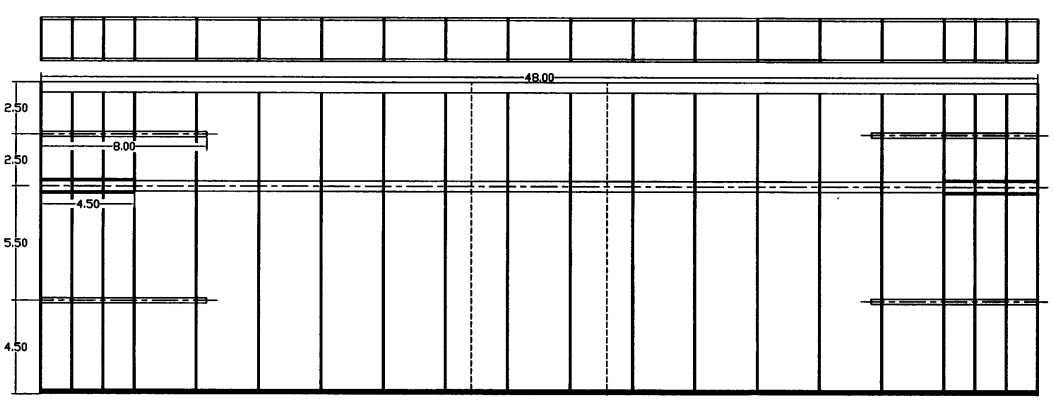

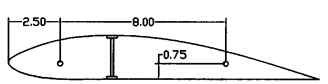

Figure 5.4.2: Wing Design

SIZE	FSCM NO.	DWG NO.	REV
11x17		1	
SCALE 1"=6"		SHEET 1 of 1	

AIAA_DESIGN/BUILD/FLY 01-06-03 HORIZONTAL_STABILIZER&ELEVATOR.DWG

REVISIONS				
ZONE	REV	DESCRIPTION	DATE	APPROVED

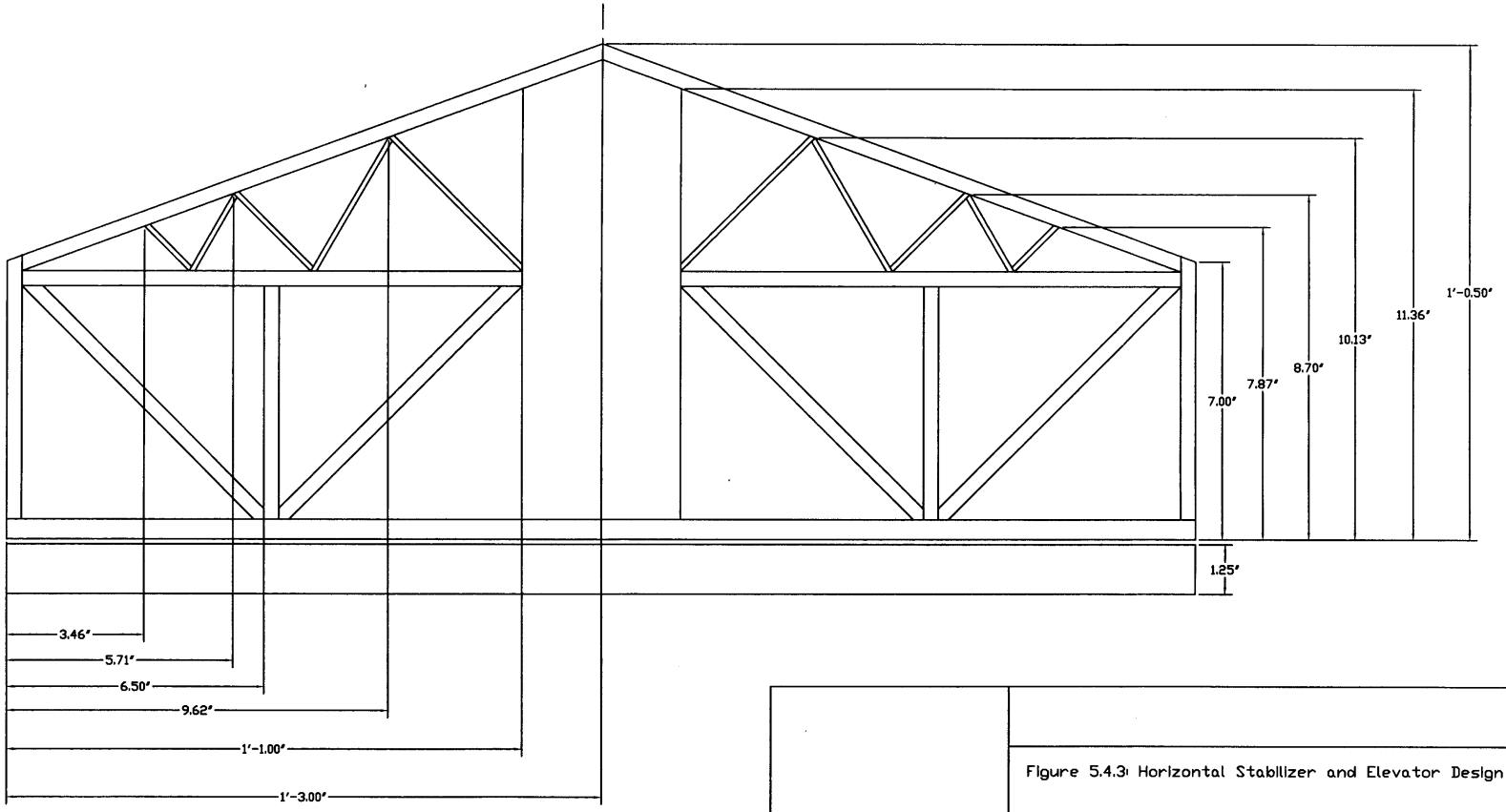

Figure 5.4.3: Horizontal Stabilizer and Elevator Design

SIZE	FSCM NO.	DWG NO.	REV
B		3	

SCALE 1"=3" SHEET 1 of 1

AIAA_ _'SIGN/BUILD/FLY 01- .6-03 FIN&RUDD=R2B.DWG

REVISIONS				
ZONE	REV	DESCRIPTION	DATE	APPROVED

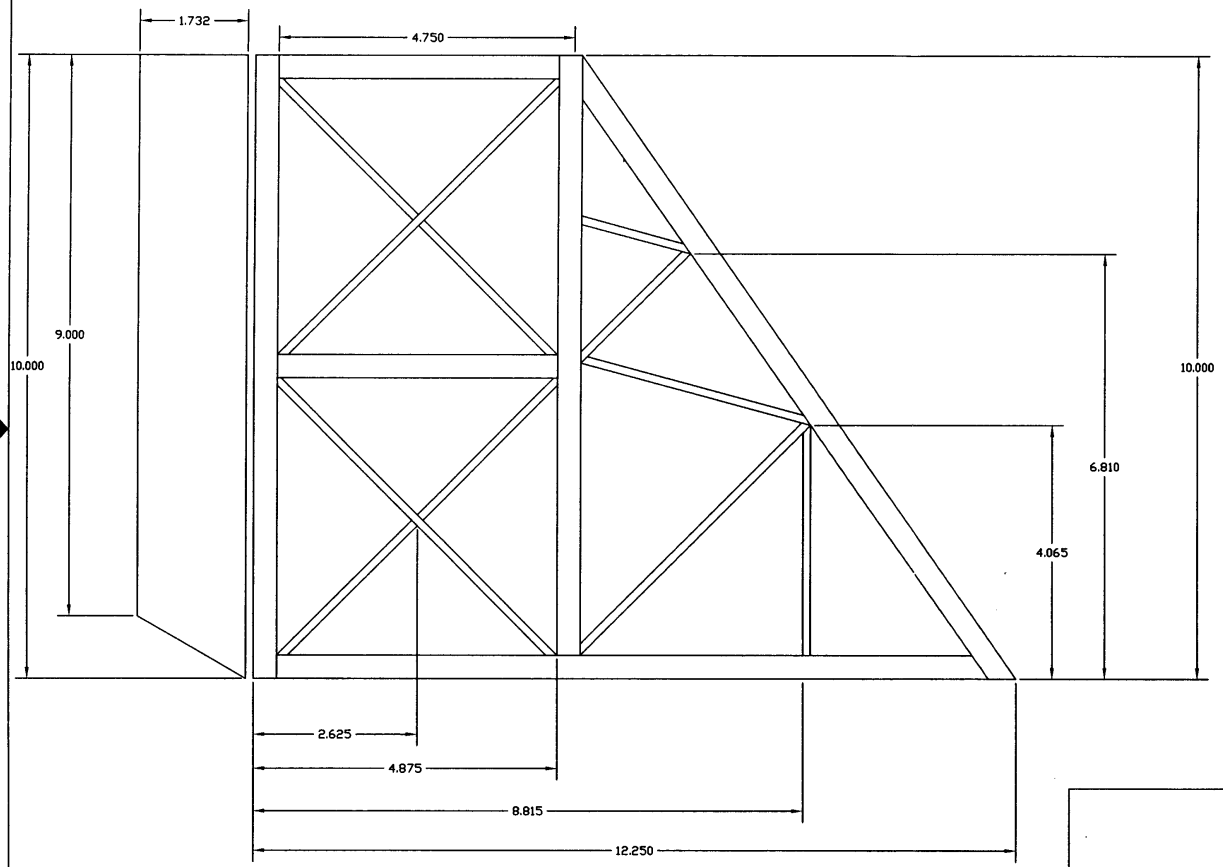

Figure 5.4.4: Vertical Stabilizer and Rudder Design

SIZE	FSCM NO.	DWG NO.	REV
B		4	

SCALE		SHEET
1"=2"		1 of 1

CWRU DBF 2003

2003 DESIGN / BUILD / FLY COMPETITION
CASE WESTERN RESERVE UNIVERSITY

MARSUPIAL FALCON X

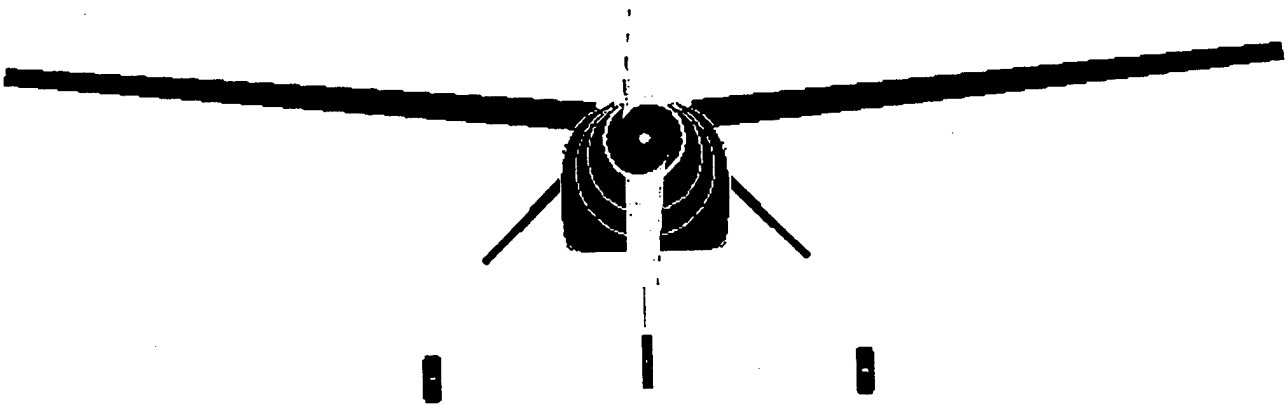

TABLE OF CONTENTS

1 EXECUTIVE SUMMARY 3
1.1 Summary of the Final Design 3
2 MANAGEMENT SUMMARY 5
3 CONCEPTUAL DESIGN 7
3.1 Design Parameters 7
3.2 Concept Generation and Selection 7
3.2.1 Antenna 8
3.2.2 Fuselage 8
3.3 Tail Configurations 14
3.4 Wing Configurations 14
4 PRELIMINARY DESIGN 17
4.1 Antenna Analysis 17
4.2 Fuselage Analysis 22
4.3 Wing Analysis 26
4.4 Tail Analysis 27
4.5 Landing Gear 28
4.6 Propeller 30
4.7 Batteries 31
4.8 Payload 31
4.9 Storage Container 31
5 DETAIL DESIGN 32
5.1 Antenna 32
5.2 Fuselage and Payload Bay 32
5.3 Wings 35
5.4 Tail Section 36
5.5 Final Aircraft Configuration 37
6 MANUFACTURING PLAN AND PROCESS 38
6.1 Fuselage Manufacturing Plan and Process 38
6.2 Wing and Tail Manufacturing Plan and Process 39
6.3 Landing Gear Manufacturing Plan and Process 39
6.4 Payload Bay and Payload Manufacturing Plan and Process 39
6.5 Systems Integration and Electronics Assembly 40
7 RATED AIRCRAFT COST 42
8 REFERENCES 44

1 EXECUTIVE SUMMARY

This report outlines the methodology that was taken by the team from the conceptual design phase to the manufacturing plans for the 2003 AIAA Design / Build / Fly competition. The goal is to design and fabricate an unmanned, electric powered, radio controlled aircraft that is both affordable and will be able to achieve the performance requirements of the three missions that the aircraft will be competing in. The three missions are (1) Missile Decoy, (2) Sensor Deployment and (3) Communications repeater.

1.1 Summary of the Final Design

The final design chosen for the tail was the inverted V-tail, with a 35 degree angle from the horizontal. This was chosen over a T-tail, conventional, or regular V-tail because of the need to fit the box's dimensions, and because this design juts into the air that is least affected by turbulence from the wings and the fuselage.

The final design chosen for the landing gear was gear attached at the front and back of the fuselage, near the bulkheads in front of and behind the cargo bay. The gear will be 3/16" thick to support the weight of the plane and give about 7" clearance from the ground. The landing gear will be made of T-6 aluminum and have 2-3" wheels. A little machining will have to be done on the gear to cut the desired holes for screws to attach the gear to the fuselage. The location of the landing gear on the fuselage was chosen because of the uneven distribution of weight in the plane. The thickness of the gear and the material to be used, and what size wheels to use, was decided upon based on the need to support the weight of the plane. It was decided to do the machining ourselves because then we can be sure the screw holes will be in the precise location that we need to attach the gear to the fuselage.

The final wing design was chosen based almost fully on the need for the wing to be light, strong, easy to attach to the fuselage, and fit inside the box. The design chosen was a foam wing reinforced with fiberglass cloth, with a strip of carbon fiber epoxied to an aluminum center spar through the middle center of the wing to give the wing increased strength. The wings will each be 36" long, with a surface area of 8.25 ft and panels tapering from 18" to 15" of chord. This was chosen because of upper constraint of the size of the box and lower constraint of wing area needed to provide enough lift to take off in the allotted runway distance for the weight of the plane. The load on the wings will be 39 oz/square foot if the

plane weighs as much as is allowed, but it should be lighter than that. If the plane weighs 15 lbs as planned, the wing load will be reduced to 29 oz/square foot. The rated aircraft cost is estimated to be 60 hours. The NACA 2412 airfoil was chosen because of versatility, and a dihedral of 5 degrees wing design was chosen because of the excellent maneuverability capabilities of dihedral wings without needing ailerons. The option of installing ailerons is left open in case they are found to be necessary while testing the plane. If ailerons are needed, the servos to control them will be flush mounted in the wing so that the control wires to the receiver will be the only part that needs to be connected when the wings are attached.

The final design propeller design for the propulsion system has not been chosen yet, but the batteries to be used are 18 N1700 SC RC batteries. These were chosen because they fit the Astroflight 40 geared (#640) motor. The batteries will be split up, with some in front of the payload and some behind the payload. There are several different propellers being considered. The APC 9.0 X 10.0 propeller would be ideal if the whole 10 minutes are to be taken up. The 11.0 X 12.0 propeller is a much faster option, but it may not last as long as desired. The APC 11.0 X 4.0 or the APC 10.0 X 6.0 propellers would be good for extra time or bad weather conditions. Lastly, the APC 9.0 X 9.0 propeller would last longer than others and has a good speed capability. The final decision on the propeller will be chosen as testing begins.

The final design of the antenna is chosen to be a circular PVC pipe mast under a main PVC disk. The PVC was chosen over the idea of a balsa ellipse because of ease of manufacturing, strength to withstand expected stress, and low weight. The balsa option had a lower drag coefficient, but the fact that it was so heavy and more difficult to manufacture than the PVC made it an easy choice.

We decided on a conventional cylindrical fuselage made of a variety of woods, some polycarbonate, and foam. The payload bay consists of a door hinged on one side and a spring-loaded latch on the other. There will be padding in the bay in case of a crash to provide resilience. The design was decided based on manufacturability, accommodation of payload, weight, durability, rated aircraft cost, aerodynamic streamlined structure, conservation of space to fit into the box, ability to mount wings, and environmental concerns such as weather. The aircraft will be covered in light balsa wood and shrink wrap mylar covering. This provides an aerodynamic and waterproof covering for the fuselage. This type of covering is also very easy to repair.

2 MANAGEMENT SUMMARY

The organization of the design team entailed one leader – in charge of assigning tasks, and making sure deadlines are met – and eight members, who worked under the leader.

Table 1: Assignment of Personnel

Name	Assignment Area
Chris Roberts	Wing and Tail design
Eric Braun	Landing Gear design
Tim Witushynsky	Propulsion design
Joel Scheuer	Antenna design
Mike Brescilli	Fuselage and Cargo Bay
Cory Theobald	Cargo Bay
Petrina Ee	Documentation
Lindsay Miller	Documentation

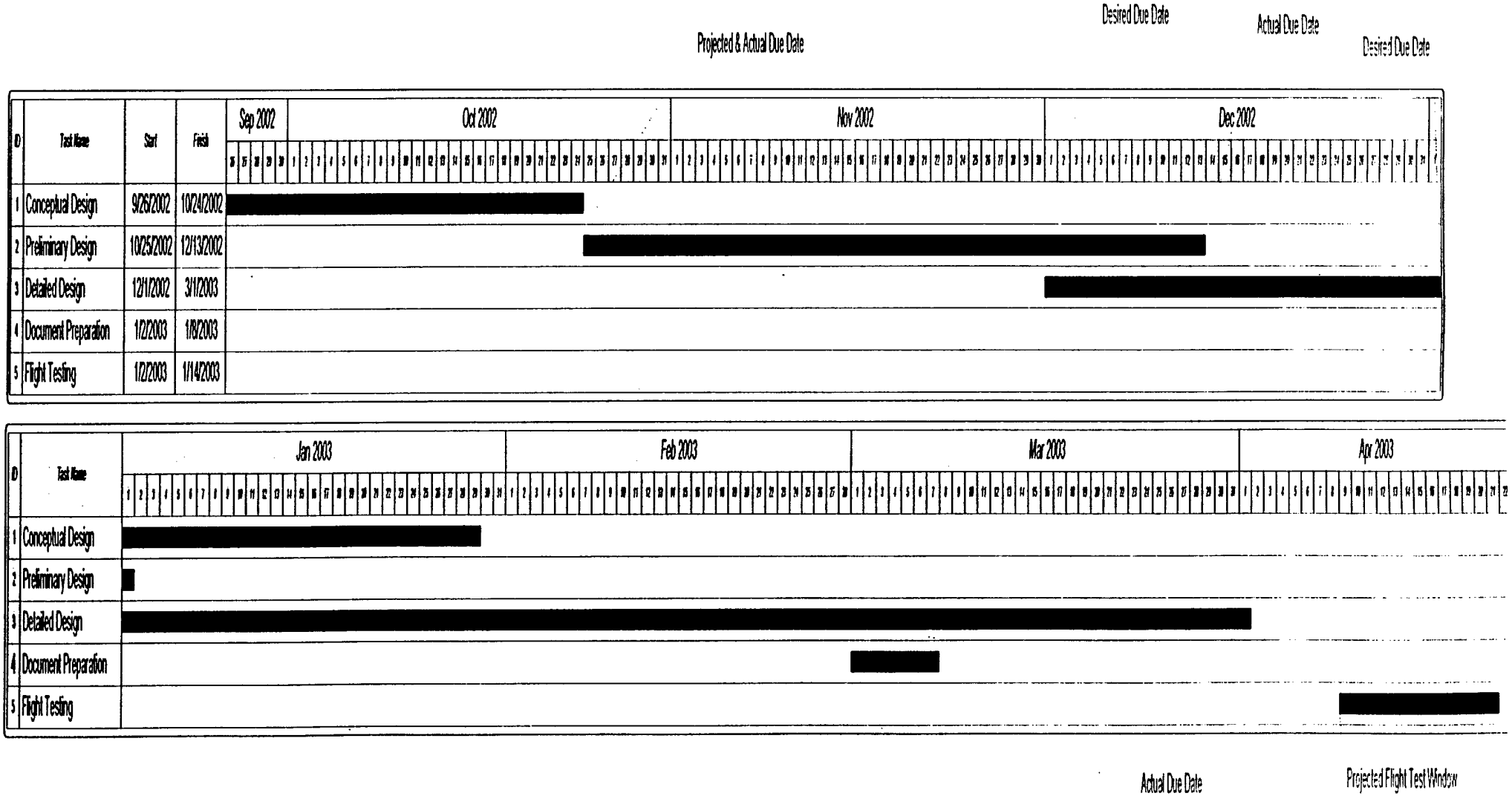

Figure 1: The Design Team's Milestone Chart

3 CONCEPTUAL DESIGN

The first step in the design process was the conceptual design phase. Each idea generated was evaluated to determine the advantages and disadvantages in itself and when integrated into the aircraft. The mission requirements were used as the design parameters and the concept that best fulfilled the design parameters was selected as the final aircraft configuration.

3.1 Design Parameters

The goal is to establish a balanced design that produces an aircraft with affordable manufacturing and high vehicle performance. The aircraft has to be able to compete in all three variants of the 2003 competition which are:

1) Missile Decoy (Difficulty 2.0)
   - lbs. (6in. x 6in. x 12in) simulated avionics package payload
   - Simulated 6" PVC antenna
2) Sensor deployment (Difficulty 1.5)
   - Self deploy sensor package (5 lbs., 6in. x 6in. x 12in) after landing on the runway
3) Communications repeater (Difficulty 1.0)
   - simulated communications relay device payload (5 lbs., 6in. x 6in. x 12in)

In addition, the aircraft must fulfill the following basic requirements:

- Fit into a 4x2x1 foot box
- Take-off must be within 120 feet
- Land on the prescribed runway
- Maximum mission time is 10 minutes
- Easily assembled for the Timed Assembly Task

3.2 Concept Generation and Selection

The following section describes the various concepts that were considered and the methods used to determine the final configuration that met the requirements of the mission requirements.

3.2.1 Antenna

The design of the antenna has to be optimized for minimizing drag and weight which are the top two priorities, followed by strength, manufacturability, and overall cost. The two main concepts to support the antenna as outlined by the rules were: 1) a balsa ellipse with a semi-major axis to semi-minor axis ratio of 2:1 with a section hollowed out for a long (around 3.5 inches) bolt, and 2) a three inch section of PVC pipe with a smaller diameter than the disk glued to the disk with a smaller screw on the bottom to attach the antenna to the fuselage. These two concepts are sketched out in the figure below:

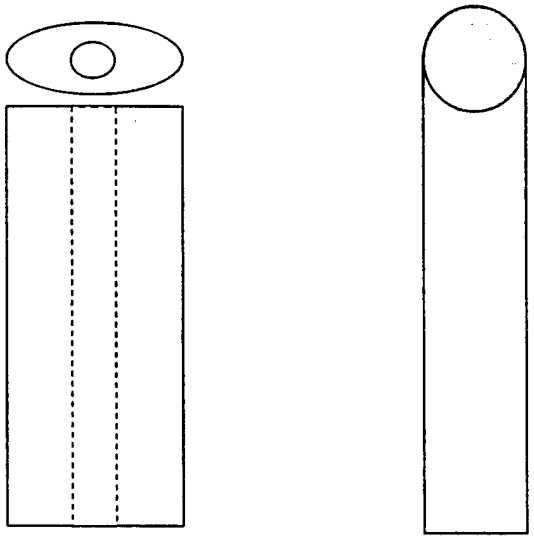

Concept 1:
Balsa Ellipse

Concept 2:
PVC mast

Figure 2: Antenna Concepts

3.2.2 Fuselage

This section describes the method used for determining the final concept to meet the need. The first step was to create simple sketches in which each sketch showed the general structure and any general mechanisms related to the structure. These sketches do not define dimensions, materials, or engineering properties but just pure concepts. Concept selection was conducted using a Pugh screening and scoring matrix.

According to the specifications established. each team member came up with several sketches of a possible fuselage concept. Each design is labeled below. The advantages and disadvantages of each design are also listed next to each sketch.

Datum Design

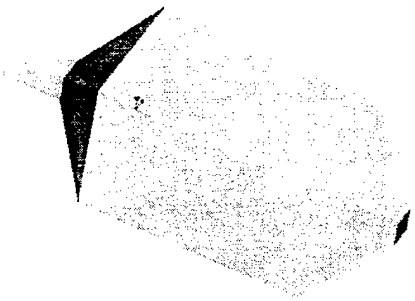

Idea:

- Box/square bulkheads.

Advantages:

- Easy to manufacture.
- Detachable tail.
- Fits in box.

Disadvantages:

- High drag because of box shape.
- Heavy.
- Not streamlined.

Design A

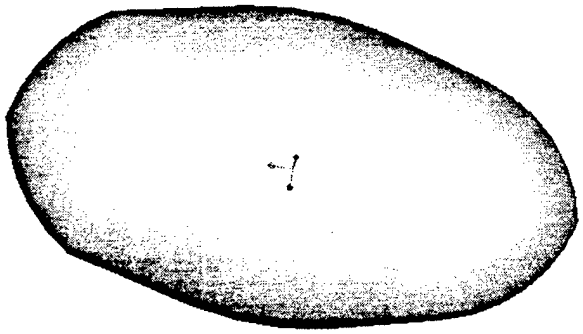

Idea:

- Flattened cylindrical shape

Advantages:

- Easy to manufacture
- Can fit payload and motor well
- Wings are fitted on top

Disadvantages:

- Not very aerodynamic
- No detachable tail
- May not fit in box effectively

Design B

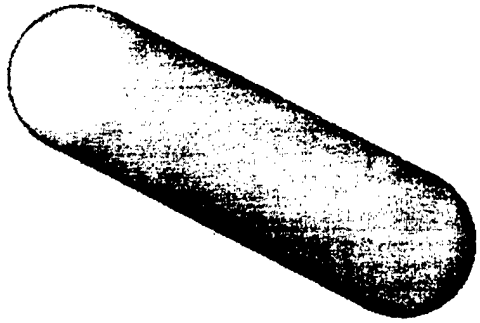

Idea:

- Plain cylinder with hemisphere nose and tail.

Advantages:

- Easier to manufacture due to circular cross-section.
- More storage space for payload, batteries, etc.

Disadvantages:

- Non-detachable tail.
- Higher drag with hemisphere front

Design C

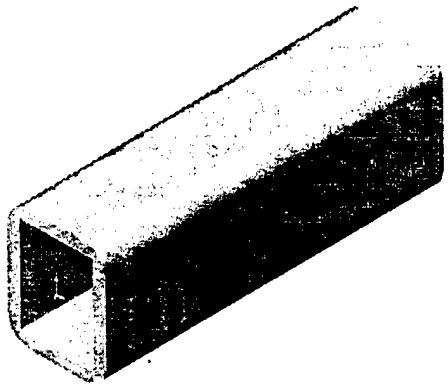

Idea:

- Box with fillets.

Advantages:

- Efficient use of space for box payload.

Disadvantages:

- High drag with big frontal area.
- Complicated mfg.
- No detachable tail.

Design D

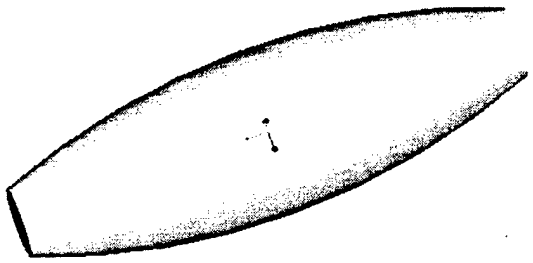

Idea:

- Similar to 747 fuselage.

Advantages:

- Non-detachable tail.
- Streamlined.
- Known it will fly because industry standard.

Disadvantages:

- Hard to fit everything inside.
- Hard to attach wings.
- Hard to manufacture

Design E

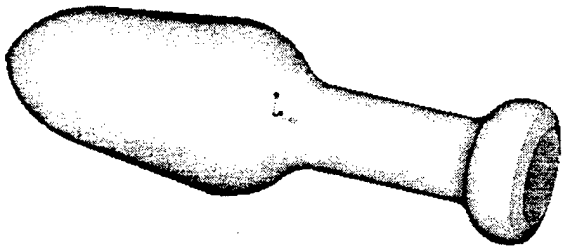

Idea:

- Bottle – shape.

Advantages:

- Lowest drag in front.
- Efficient use of space.

Disadvantages:

- Tail not detachable.
- Induced swirl of transitions.
- Hard to mfg.
- Wing and tail surface mounting is difficult

Design F

Ideas:

1. Flying wing.

Advantages:

2. High lift/low drag.
3. One piece.
4. Easy Assembly.

Disadvantages:

5. Hard to control.
6. Difficult mfg.

Concept Selection

The next step in the design process is to reduce the seven preliminary designs down to the best three design alternatives. A Pugh screening matrix will be used to select the three best designs. Below, is a list of the design criteria used in the screening matrix. These criteria are also known as the 'numerical figures of merit' (FOM's). The mission feature that each FOM is selected to support is listed next to each FOM in the list:

1. Manufacturability - Affects time and resources needed to complete aircraft
2. Accommodation of payload - 'Missile Decoy' mission
3. Lightweight - Directly affects speed of mission and the 120 feet of max. runway space
4. Durability - Ability to complete 360° turns and land safely
5. Rated aircraft cost - Directly affects the overall score
6. Aerodynamic/streamlined structure - Ability to complete 360° turns and land safely in the shortest time possible
7. Conservation of space - Ability to fit into a 2'x1'x4' box
8. Ability to mount wings - Timed assembly task
9. Environmental concerns - Affects time and resources needed to complete aircraft

The 'Datum Design' model is used as the datum in the Pugh Screening Matrix. Please see **Table 2** for the results of the matrix:

Table 2: Pugh Screening Matrix

	Design Alternatives					
Criteria	**A**	**B**	**C**	**D**	**E**	**F**
Manufacturability	-	+	-	-	-	-
Accommodation of payload	0	0	+	+	0	0
Lightweight	-	0	-	+	0	-
Durability	+	+	+	+	+	+
Rated aircraft cost	-	-	-	0	-	-
Aerodynamic/streamlined structure	+	+	+	+	+	+
Conservation of space	-	0	-	-	0	-
Ability to mount wings	0	0	-	0	-	+
Environmental concerns	-	-	-	0	-	-
Totals:	**-3**	**1**	**-3**	**2**	**-2**	**-3**

Using the data in the above screening matrix, it appears that the datum design and designs B and D are the best choices when considering the nine design criteria. The next step is to create a Pugh Scoring Matrix to determine the best design. The nine criteria are now sorted through and ordered from most important to least important. This order from most to least important is: (1) conservation of space, (2) aerodynamic/streamlined structure, (3) manufacturability, (4) durability, (5) accommodation of the payload, (6) rated aircraft cost, (7) lightweight, (8) ability to mount wings, and (9) environmental concerns. The criteria are weighted linearly, with the conservation of space criterion assigned a weight of 20% and the environmental concerns criterion assigned 3%. To determine the raw score, 1, 5, or 9 points were assigned to each design, with 9 being the best and 1 being the worst. The data from the scoring matrix appears in **Table 3**, below.

Table 3: Pugh Scoring Matrix

	Design Alternatives						
	Datum Design		Design D		Design B		
Design Criteria	Raw	Weighted	Raw	Weighted	Raw	Weighted	Weight
Manufacturability	1	0.2	5	1	9	1.8	20%
Accommodation of payload	5	0.85	9	1.53	5	0.85	17%
Lightweight	9	1.35	9	1.35	5	0.75	15%
Durability	1	0.13	5	0.65	9	1.17	13%
Rated aircraft cost	1	0.11	5	0.55	9	0.99	11%
Aerodynamic/streamlined structure	1	0.09	9	0.81	5	0.45	9%
Conservation of space	9	0.63	5	0.35	1	0.07	7%
Ability to mount wings	9	0.45	9	0.45	5	0.25	5%
Environmental concerns	5	0.15	5	0.15	9	0.27	3%
Totals:	**41**	**3.96**	**61**	**6.84**	**57**	**6.6**	

Using the data from the scoring matrix, it was decided that the final fuselage design should be a hybrid of designs D and B.

3.3 Tail Configurations

Four tail configurations were considered and a decision matrix was used in the selection of the final design to be used. The major factors influencing our design decision were the Rated Aircraft Cost and the compactness of the design. For a tail to work well, the stabilizing surfaces must be exposed to incoming air that is unaffected by the wings and the fuselage. The conventional tail has a higher RAC and the profile of it is rather large, because it sticks up about the fuselage. A T-Tail is almost identical to the conventional tail; only the horizontal surface is prone to handling damage in transportation, and the flight characteristics change at different engine speeds. The following are sketches of the configurations that were considered and the decision matrix used:

Design A

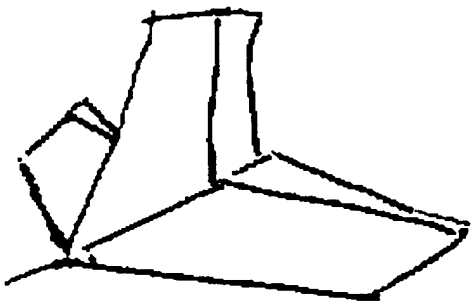

Configuration:

- Conventional Tail

Remarks:

- 2 servos
- 2 active controls surfaces
- 30 hours RAC
- High Profile

Design B

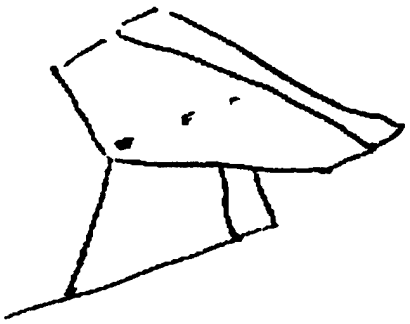

Configuration:

- T-Tail

Remarks:

- 2 servos
- 2 active control surfaces
- 30 hours RAC
- Extra high Profile

Design C

Configuration:

- V-Tail

Remarks:

- 2 surfaces
- 1 active control surface
- 25 hours RAC
- High Profile

Design D

Configuration:

- Inverted V-Tail

Remarks:

- 2 surfaces
- 1 active control surface
- 25 hours RAC
- Low Profile

Table 4: Tail Configuration Decision Matrix

Item	A	B	C	D
Rated Aircraft Cost	0	0	1	1
Clearance	0	0	0	1
Drag	0	0	1	-1
Space Efficiency	0	-1	-1	1
	0	-1	1	2

Therefore, as seen from the matrix, a V-tail offers a lowered RAC for the amount of control surface offered to the vehicle. It also juts out above the airframe. Inverting this V-tail allows the tail to project out beside the fuselage, creating a more compact profile to fit in the container.

3.4 Wing Configurations

The wings are a critical part of the design of the aircraft for obvious reasons. Due to the fact that the aircraft must be able to drop the payload and fly with equally well flight characteristics as before the payload was removed, it is immediately apparent that the wings be placed over the center of gravity.

The next decision we discussed was whether to have a high aspect ratio wing, or a mixed wing design for the aircraft. The fact that the entire aircraft must fit into a relatively small box quickly led to the decision that a conventional type wing may be constructed so that it can easily fit into the crate along with the other aircraft components. At this point it was also decided that the wings should be built in such a manner as to be quickly connectable to the fuselage.

The last wing configuration obstacle we discussed was whether to have a low wing, mid wing, or high wing design for our aircraft. Possible wing placements are shown below. The low and mid wing designs offered less stability, and presented a major problem: connecting them to the fuselage would be very difficult because the payload would be mounted inside directly where the wings will mate. We then settled upon the more stable and easier interfaced high wing design.

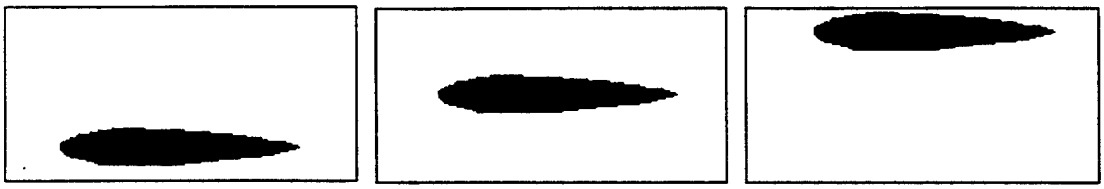

Possible Wing Mounting Locations

Design C

Configuration:

- V-Tail

Remarks:

- 2 surfaces
- 1 active control surface
- 25 hours RAC
- High Profile

Design D

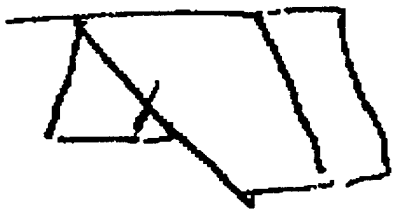

Configuration:

- Inverted V-Tail

Remarks:

- 2 surfaces
- 1 active control surface
- 25 hours RAC
- Low Profile

Table 4: Tail Configuration Decision Matrix

Item	A	B	C	D
Rated Aircraft Cost	0	0	1	1
Clearance	0	0	0	1
Drag	0	0	1	-1
Space Efficiency	0	-1	-1	1
	0	-1	1	2

Therefore, as seen from the matrix, a V-tail offers a lowered RAC for the amount of control surface offered to the vehicle. It also juts out above the airframe. Inverting this V-tail allows the tail to project out beside the fuselage, creating a more compact profile to fit in the container.

3.4 Wing Configurations

The wings are a critical part of the design of the aircraft for obvious reasons. Due to the fact that the aircraft must be able to drop the payload and fly with equally well flight characteristics as before the payload was removed, it is immediately apparent that the wings be placed over the center of gravity.

The next decision we discussed was whether to have a high aspect ratio wing, or a mixed wing design for the aircraft. The fact that the entire aircraft must fit into a relatively small box quickly led to the decision that a conventional type wing may be constructed so that it can easily fit into the crate along with the other aircraft components. At this point it was also decided that the wings should be built in such a manner as to be quickly connectable to the fuselage.

The last wing configuration obstacle we discussed was whether to have a low wing, mid wing, or high wing design for our aircraft. Possible wing placements are shown below. The low and mid wing designs offered less stability, and presented a major problem: connecting them to the fuselage would be very difficult because the payload would be mounted inside directly where the wings will mate. We then settled upon the more stable and easier interfaced high wing design.

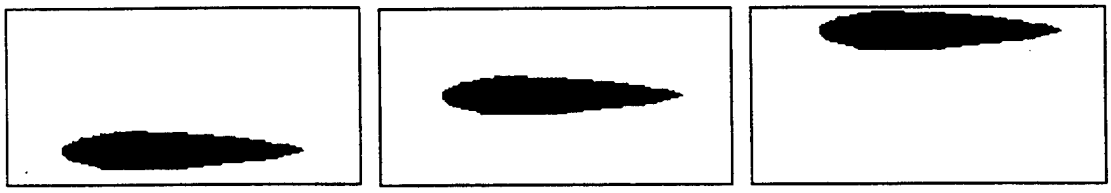

Possible Wing Mounting Locations

4 PRELIMINARY DESIGN

The preliminary design process started after selection for the best options for the various components were determined from the conceptual design phase. Based on the chosen options, a more detailed analysis was carried out on the various aircraft sections. The analysis was required to size the aircraft and its components and systems. The analysis also comprised of a search into commercial materials and parts that were available in the market that were compatible to the design and requirements of the aircraft.

4.1 Antenna Analysis

The following equations were used to analyze the drag of the entire antenna assembly:

(1) $$D = \frac{1}{2} C_D \rho v^2 A$$

(2) $$A = dh$$

The density of air at sea level, 2.38x10-3 slugs/ft3 (Anderson, 558) was used in the calculations. This was chosen because the competition site is very close to sea level. For the frontal area A, the value d was the diameter of the circles or the semi-major axis of the ellipse times the height. Since no numbers of the predicted flight speed were available at the time, the flight speed was calculated over a range from 25 ft/s to 50 ft/s, which were assumed to be reasonable flight speeds.

The following assumptions were made about the drag:

1. Due to the flight speeds on an order of 10^1 ft/s, airflow around the antenna would be invicid, isentropic, and incompressible.
2. The velocity profile would be uniform along the height of the antenna. This followed the invicid assumption.
3. The velocity would be in the x-direction (direction of flight path) only. This simplified analysis by making the drag in one direction.

The coefficient of drag for a cylinder and an ellipse is dependent on the Reynolds number. To calculate the Reynolds number the following equation was used:

$$\text{Re} = \frac{vd}{\nu} \quad (3)$$

The kinematic viscosity at sea level was 2.26x10-2 in2/s (Hill, 702), v was the flight speed converted into in/s, and d was the diameter or the semi-major axis. A Reynolds number above 10^7 was considered turbulent, and a number below that was considered laminar. The Reynolds number never exceeded this threshold at any velocity for the main antenna disk, the balsa ellipse, or the PVC mast. The laminar drag coefficient for an upright cylinder is 1.2 (Anderson 61) and a 2:1 ellipse is 0.6 (Çengel).

The main antenna disk had the height of 3.13 inches (3 inches plus the two .0625 inches plywood caps) and an outer diameter of 6.63 inches as outlined by the rules. The balsa ellipse had a semi-major axis of 1 inch and a semi-minor axis of 0.5 inches and a height of 3 inches. The PVC mast was a ¼ inch Section 40 PVC pipe with an inner diameter of 0.354 inches, an outer diameter of 0.54 inches, and a height of three inches. It also had 1/16 inch plywood end caps. These dimensions were chosen to minimize drag and weight yet provided more than sufficient strength.

The tables below show the drag calculations for all three components:

Table 5: Drag for the main antenna disk

Flight speed	Re	Cd	D
ft/s			lbf
20	7.02E+04	1.2	8.20E-02
25	8.78E+04	1.2	1.28E-01
30	1.05E+05	1.2	1.85E-01
35	1.23E+05	1.2	2.51E-01
40	1.40E+05	1.2	3.28E-01
45	1.58E+05	1.2	4.15E-01
50	1.76E+05	1.2	5.13E-01

Table 6: Drag for the PVC mast

Flight speed	Re	Cd	D	Total D
ft/s			lbf	lbf
20	5.72E+03	1.2	6.69E-03	8.87E-02
25	7.16E+03	1.2	1.04E-02	1.39E-01
30	8.59E+03	1.2	1.50E-02	2.00E-01
35	1.00E+04	1.2	2.05E-02	2.72E-01
40	1.14E+04	1.2	2.67E-02	3.55E-01
45	1.29E+04	1.2	3.38E-02	4.49E-01
50	1.43E+04	1.2	4.18E-02	5.54E-01

Table 7: Drag for the balsa ellipse

Flight speed	Re	Cd	D	Total D
ft/s			lbf	lbf
20	8.83E+02	0.6	9.90E-04	8.30E-02
25	1.10E+03	0.6	1.55E-03	1.30E-01
30	1.33E+03	0.6	2.23E-03	1.87E-01
35	1.55E+03	0.6	3.03E-03	2.54E-01
40	1.77E+03	0.6	3.96E-03	3.32E-01
45	1.99E+03	0.6	5.01E-03	4.20E-01
50	2.21E+03	0.6	6.19E-03	5.19E-01

The last column in Tables 6 and 7 show the total drag for the whole assembly. This shows that the balsa ellipse has lower drag than the PVC mast.

To determine the weight of the assembly in pounds force, the following equation was used:

(4) $W = \rho V g$

Density was in the units of lbm/in3, and for PVC it was 1.55x10-3 lbm/in3 (harvel.com), for plywood it was 0.0181 lbm/in3 (sres.anu.edu.au), and for balsa it was 0.00578 lbm/in3 (matweb.com). The bolt for the balsa ellipse concept was made of steel with a density of 3.35 lbm/in3 (Gere 888). Any glue or other adhesive used to attach the components together was assumed to have a negligible mass. The gravitational acceleration used was 32.2 ft/s, and the volume was calculated in cubic inches. The following tables show the calculated weight for the main antenna disk, the PVC mast, and the balsa ellipse:

Table 8: Weight calculations for the main antenna disk

PVC	
Volume	Weight
in3	lbf
1.77E+01	0.886

Plywood		
Volume	Weight	Weight for two
in3	lbf	lbf
2.15	1.26	2.51

Total Weight
Lbf
3.40

Table 9: Weight calculations for the PVC mast

PVC	
Volume	Weight
in3	lbf
3.92E-01	0.0196

Plywood caps

Volume	Weight	Weight for two
in3	lbf	lbf
0.0143	0.00834	0.0167

Total Weight
Lbf
0.0363

Table 10: Weight calculations for the balsa mast

Weight	
Balsa	
Volume	Weight
in3	lbf
1.03	0.192

Total Weight
lbf
1.69

Bolt	
Volume	Weight
in3	lbf
0.164	1.50

Based on the calculations above the PVC mast has a considerably large weight advantage over the balsa ellipse. The balsa ellipse was modified, removing the bolt and using adhesive in its place to reduce the weight. The new weight calculations were:

Table 11: New weight calculations for the balsa ellipse

Weight	
Balsa	
Volume	Weight
In3	lbf
1.18	0.219

Total Weight
lbf
0.219

Based on these new figures, the PVC mass was still six times lighter than the balsa ellipse. Combined with the main disk, the total antenna assembly weighs 3.43 lb_f.

For the strength calculations, normal stresses, shear stresses, and buckling were considered. For normal stresses at the top of the PVC mast, an axial stress due to the

weight of the main disk and a bending stress due to a moment caused by the drag were calculated. The equations used were:

$$\sigma_{axial} = \frac{W}{A} \quad (5)$$

$$\sigma_{bending} = \frac{Mc}{I} \quad (6)$$

The area was the cross-sectional area of the pipe, and the maximum moment was the maximum drag force on the main antenna disk multiplied by a moment arm of half the height, 1.56 inches. The moment of inertial of the PVC mast was calculated using the thin circular ring approximation (Gere 873):

$$I = \frac{\pi d^3 t}{8} \quad (7)$$

For the ¼ Section 40 pipe, the moment of inertia is 0.00617 in^4. The maximum normal stress is in the outer diameter, so c was the outer radius, 0.27 inches. Table 12 shows the normal stress calculations:

Table 12: Normal Stress calculations for the PVC mast

Normal				
	Axial Force	Area	Stress	
	lbf	in2	psi	
	3.40	0.229	14.8	
Bending Moment	c	I	Max stress	Total
lbf-in	in	in4	Psi	Psi
8.01E-01	0.27	0.00617	3.50E+01	4.99E+01

Based on these calculations, the normal stress the PVC mast would see is 49.9 psi. Although this is probably not a principle normal stress, the yield stress of PVC is on the order of thousands of pounds per square inch (matweb.com). Failure due to normal stress is therefore not a concern.

To calculate the shear stress on the PVC mast, the equation used was:

$$\tau = \frac{4D}{3A} \quad (8)$$

(Gere 342). This came out to be 2.98 psi at a flight speed of 50 ft/s.

Finally, a calculation was done to make sure the relatively thin support would not buckle under the weight of the larger disk. The equation for the buckling load in a column with both ends fixed is:

$$P_{cr} = \frac{4\pi^2 EI}{L^2} \quad (9)$$

(Gere 752). This bucking load for the ¼ inch Section 40 PVC with an elastic modulus E of 163,000 psi (matweb.com) is 4410 lb_f. Based on these results, it was concluded that the PVC mast, in spite of its size, would be more than strong enough to withstand failure from normal flight loads. No strength calculations were done for the balsa ellipse since it was assumed to be a trivial exercise.

The PVC mast would also be the easiest to manufacture. All that would be required would be to cut the two end caps from the same 1/16 inch think plywood sheet as the end caps of the main antenna disk and attach them to a 3 inch section of PVC pipe. The balsa ellipse would require careful cutting with a scroll saw and drilling out the hole. The PVC mast might cost more, but one PVC pipe of that grade should not be too expensive.

Therefore, based on the above analysis, the final design chosen for the antenna was a circular PVC mast under the main PVC disk.

4.2 Fuselage Analysis

The main goal of the radio controlled (RC) aircraft fuselage is to achieve optimum flight speed and maneuverability while carrying an avionics package payload. To meet these ends, the RC aircraft has the following qualitative specifications:

Demanded specifications (non-negotiable):

- Size – all components of the aircraft (including the wings) must fit into a 2x4x1 ft. box
- Payload bay – a payload bay must be built into the fuselage to house a 6x6x12 in. simulated avionics package. The package weighs at least 5 lbs.
- The plane must automatically deploy the package when it has landed.
- A simulated 6" PVC antenna closed at both ends with 1/16" plywood must stand off 3" from nearest airframe

- Must be able to take-off, fly 4 laps, and land. On the downwind leg of each lap, the plane must complete a 360 degree turn in the direction opposite of the base and final turns.

Desired specifications (negotiable):

- Functional Performance
  - Lightweight design to allow trouble-free flight with package
  - Durable – fuselage should remain intact after botched landing to protect payload
  - Aerodynamic fuselage with low air drag allowing maximum velocity
  - High strength fuselage that maintains structural integrity during flight
  - Enough ground clearance to allow bay doors to open beneath fuselage and deploy the package
  - Ability fly in adverse weather conditions – wind, rain, cold & hot temperatures
  - Detachable tail to fit in box with all components
- Manufacturing
  - Easy to assemble/construct
  - Modular Construction – aircraft built in sections making it easier to connect/disconnect for plane to meet size specifications
  - Quality control – high quality of construction with a minimal amount of defects
- Cost
  - Low material and manufacturing costs
  - Low amount of man-hours spent on construction (man-hours contribute to overall estimated cost for the competition)
- Human Factors
  - Aesthetics – sleek design

To achieve the required performance these qualitative specifications must be translated into quantitative specifications so that they may be realized in a practical manner:

Quantitative Specifications:

Units of Measurement: English Standard System

- Weight: pounds (lbs)
- Length, Width, Height, Radius: Inches (in)
- Area: Square Inches (in^2)
- Volume: Cubic Inches (in^3)
- Time: hours (hrs)
- Angle: Degree ($^\circ$)

- Density: Pounds/Cubic Inches (ρ)
- Drag Coefficient: C_d (dimensionless)

Possible Materials:

- Fiber Glass, aluminum, styrofoam, balsa wood, plywood (various sizes in thickness), carbon fiber

Fasteners:

- Mechanical Screws (various sizes), duct tape
- Adhesives: Super glue and/or Epoxy

Fuselage:

- Aesthetics – Design: CWRU logo
- Detachable tail section
- Number of Man Hours: Min: 10 hrs.; Max: 100 hrs.
- Quality Control: Due to print specifications (ex. tolerances)
- Durability: Based on materials that will be later chosen
- Costs: Within $500 budget given by Design Build Fly Team
- Bulkheads (separation distance): Min: 1 in.; Max: 4 in
- Modular: Must fit in a box dimensioned (12 X 48 X 24 in)
- Coefficient of Drag (dimensionless): Min: 0.1; Max: 0.5
- Weight of fuselage (without package): Min: 5 lbs.; Max: 10 lbs.
  (The target weight of the entire aircraft with all components including wings, landing gear, batteries, and motors, but without the package, given by the Design Build Fly team is 15 lbs.)
- Radius (referencing a cylinder): Min diameter: 6 in.; Max diameter: 10 in.
- Length: Min: 36 in.; Max: 48 in
- Volume (referencing a cylinder): Min: 670 in^3; Max: 3700 in^3

Analysis Models

There are three critical design parameters that must be analyzed for the ideal performance of the aircraft:

- Bending stresses on the entire structure
- Drag created by the fuselage
- Stresses in the wing mounting system

The entire system is modeled as a cylindrical hollow tube 42 inches long and subjected to a bending moment (See Fig). The bending moment is calculated to be 220 in-lbs by factoring the moment created by the batteries and the payload under a load factor of 10.0. According to this model, the maximum stress on the top portion of the structure (where most of the load will be carried) using pure bending theory is equal to 227 psi. This load will be carried by a number of different materials which are designed to be safety factors ranging from three to ten.

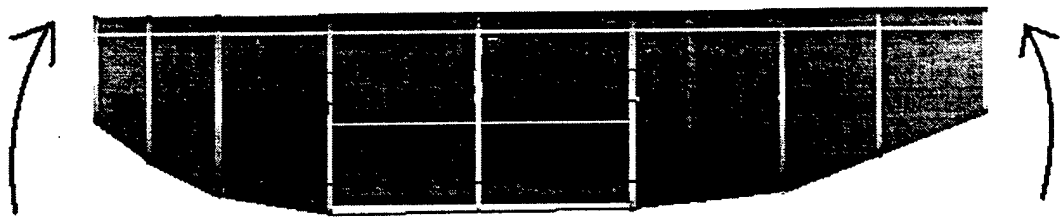

Figure 3: Bending Moment

The drag created by the fuselage is critical in for the flight characteristics of the entire aircraft, and the best way to estimate the contribution of the fuselage is to determine the coefficient of drag. The outer shape consists of three sections. The most critical is the payload section where the cross-sectional area is egg-shaped and it has a flat bottom payload door for stability and accommodation of the payload. The other two sections are the motor mounting section and the tail mounting section. These sections have a circular cross sectional shape because it provides the least amount of wetted surface with the largest amount of volumetric space. The fuselage is modeled as an ellipsoid with L/D=5.25. Thus for laminar flow C_d=0.32, and for turbulent flow C_d=0.1.

The wing mounting subsystem consists of a single bulkhead to which the aluminum L-channel wing spar is mounted through pre drilled ¼ inch holes making a 5 degree dihedral and connected with an attachment piece by wing nuts and bolts through the holes (see **Figure 3**). The bearing stresses on this single bulkhead at the 5 degree dihedral holes will be very high since most of the weight of the aircraft will be concentrated there and it will be undergoing fully reversing cyclic fatigue loading. When subjecting the aluminum spars to a 150 pound load (according to safety factor of 10) the bearing stress on the hole closest to the center of the fuselage is 2885.3 psi and the bearing stress on the hole farthest from the fuselage is 4085.3 psi. Not surprisingly, the material used for the wing mounting bulkhead

Looking over the various dimensions of wings that we could fit in shipping container, with a maximum wing area of 16 square feet, we calculated that the optimal wing area, with each wing being 36 inches long will have an area of a surface area of 8.25 square feet. The panels should taper from roughly 18" to 15" of chord. The wingspan gives an RAC of 48hours, and the maximum exposed chord gives an RAC of 12 hours. This gives the wing a total RAC of 60 hours.

If the plane weighs the maximum 20lbs, then the wing loading will be 39oz/square foot. After looking at the number, we should be able to keep this plane below 15 lbs. At 15lbs the wing loading is: 29oz/ square foot. This wing size should allow for the aircraft to take off in under the maximum runway distance allowed.

Looking at the various airfoils available, it was decided that the best airfoil for our purposes would be the versatile and friendly NACA 2412 airfoil. To aid in the stability of the aircraft, it was decided that dihedral should be applied to the wings. Consulting to many different model aircraft websites and dihedral of 5 degrees was finally settled upon. Ideally, the dihedral should allow for the aircraft to be very maneuverable without the use of ailerons. Initially the wings will be built without ailerons installed, but if the aircraft requires them after some flight testing, it has been decided that the servos controlling them will be flush mounted in the wing, and that the control wires to the receiver will be the only part of the ailerons that need to be connected during aircraft assembly. This setup would require 2 ailerons and 2 servos, increasing the RAC by 16, giving a total wing RAC of 76hours.

Many of these decisions were influenced by the model aircraft experience of some of our teams' members, as well as hobby shop owners and websites which we consulted.

4.4 Tail Analysis

Deciding upon the angles and size of the design posed many challenges. Major sources of information were the forums on www.ezonemag.com. Here we learned that the standard angle for a V-tail is 35 degrees off of horizontal. Many of the forums warned to keep the V-tail as large as possible to assure safe control capabilities, so we used basic trigonometry to find the maximum size tail we could fit in the box. We then scaled it down slightly so other aircraft components will be able to fit in the box.

must have high strength and fatigue properties as well as a light weight to keep the fully loaded airplane under 15 lbs.

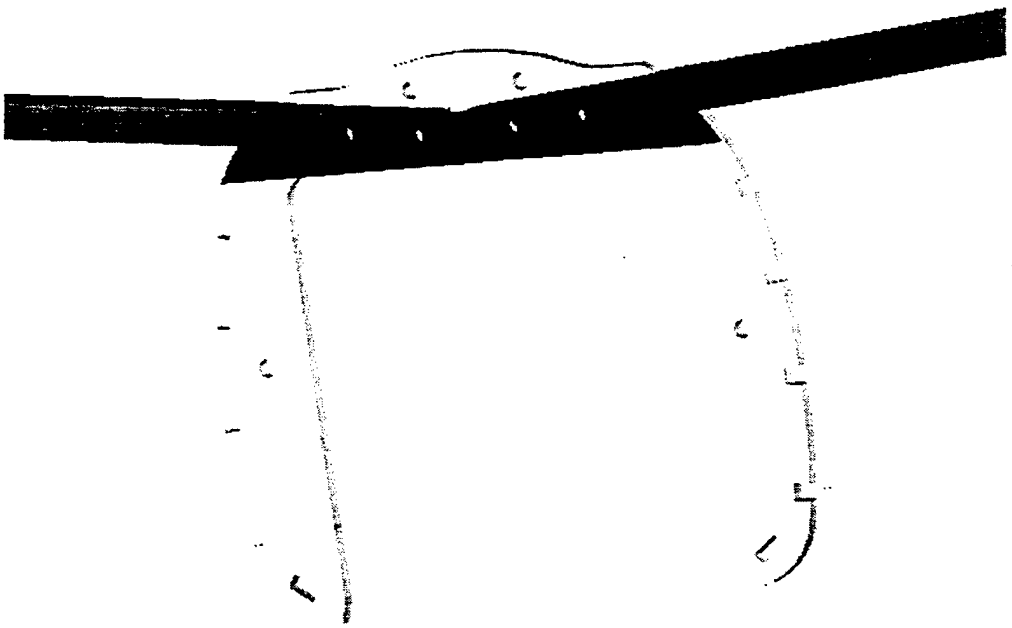

Figure 4: Wing Mounting System

4.3 Wing Analysis

The wing should be light, strong, and easy to attach to the fuselage. The wing needs to fit into the storage container, and support a weight of up to 18lbs. Examining the variety of construction techniques, we considered strength, weight, durability, rated aircraft cost, and ease of construction. The types of construction we considered were a typical wooden buildup of the wings, or a use of Styrofoam type wings. The major problems of a wooden wing over a reinforced foam wing are that it would be more fragile in transport, and would take much longer to build. We then decided to use a reinforced foam wing. The wing will be covered with a fiberglass cloth to give it strength and a smooth finish.

The wing must support the total weight of the aircraft when picked up by the wingtips, so an aluminum center spar was selected because it is very light and strong. To supplement the spar, a strip of carbon fiber cloth will be epoxied to the underside of the Styrofoam beneath the fiberglass to help support the weight of the aircraft in flight. The combination of these materials will make the wings extremely strong, easy to build, durable, and yet keep them relatively light.

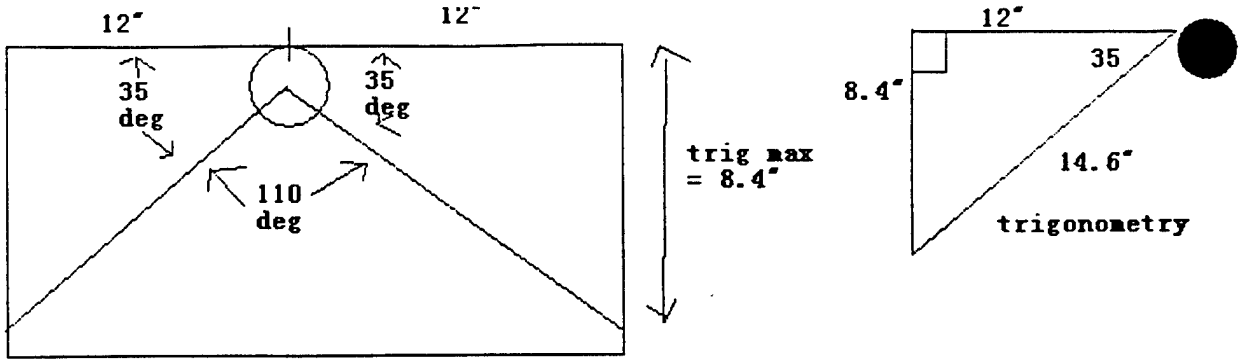

Figure 5: Tail Analysis

4.5 Landing Gear

Several criterions were used in the choice of the appropriate landing gear. For this plane, the landing gear has to be able to maneuver around a six inch tall box, withstand a weight of approximately fifteen pounds, and support a plane that will have a center of gravity more towards the front.

There are two common ways that landing gear is attached to a model airplane. First, for airplanes that have an even distribution of weight, a set of landing gears can be secured from the bottom of the nose and the tail. Second, for planes that have an uneven distribution of weight, the landing gears can be positioned at the front and back of the fuselage (assuming that the weight is in the fuselage, which it is). This second method will be the one used for this airplane. A sketch of the locations of the landing gear on the plane is shown in Figure 6. The shaded box in the center of the plane represents the box that the plane must carry for the mission. The landing gear will be attached near the bulkheads in front of and behind where the box sits in the fuselage of the plane.

In addition, the landing gear must be able to maneuver around a six inch box while being in the right size range to support fifteen pounds of weight. As such, a gear about 3/16" thick should hold fifteen pounds, and the gear should give about 7" of clearance to be safe.

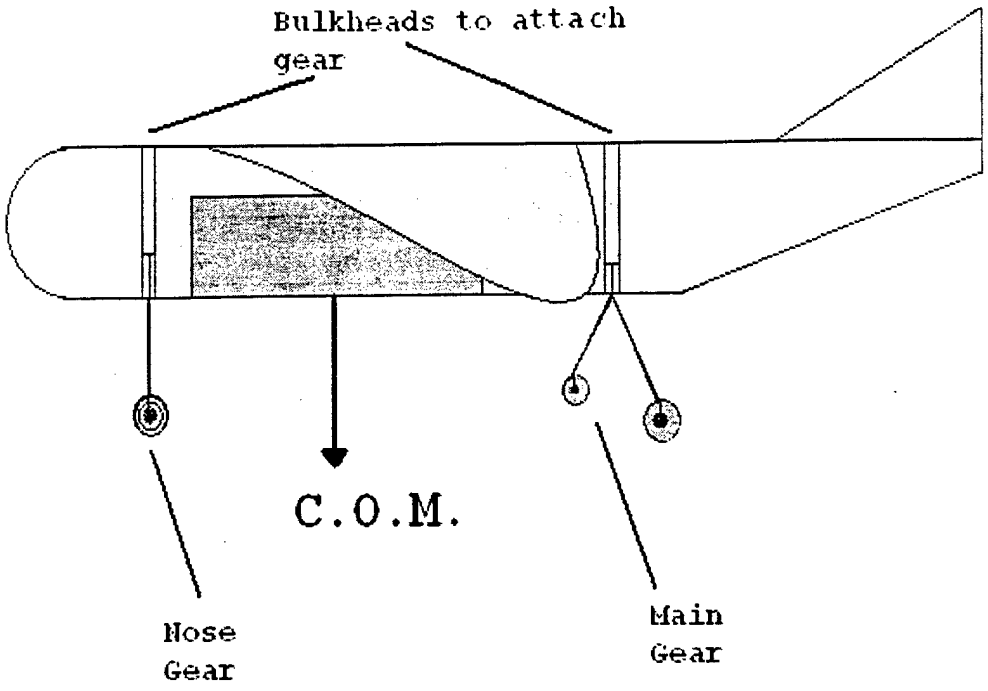

Figure 6: Placement of Landing Gears

During a parts inventory, a piece of nose gear was found to meet these requirements. It also had parts to attach it to a gear which could steer it around the box when it was dropped onto the ground. The length of the gear can be adjusted to give a suitable clearance.

After comparing the various landing gear options available from TnT Landing Gear Products, we found that we would be able to design a custom main landing gear that would meet the requirements. We simply had to specify the dimensions that we would need for the gear as well as the thickness (3/16") of the T-6 aluminum. The final dimensions appear in Figure 7. The width of the gear will gradually move from two inches near the fuselage to one and a half inches near the wheels. Lastly, looking at the various sizes of wheels and the corresponding weight loadings, it was determined that wheels from two to three inches shall are the most appropriate.

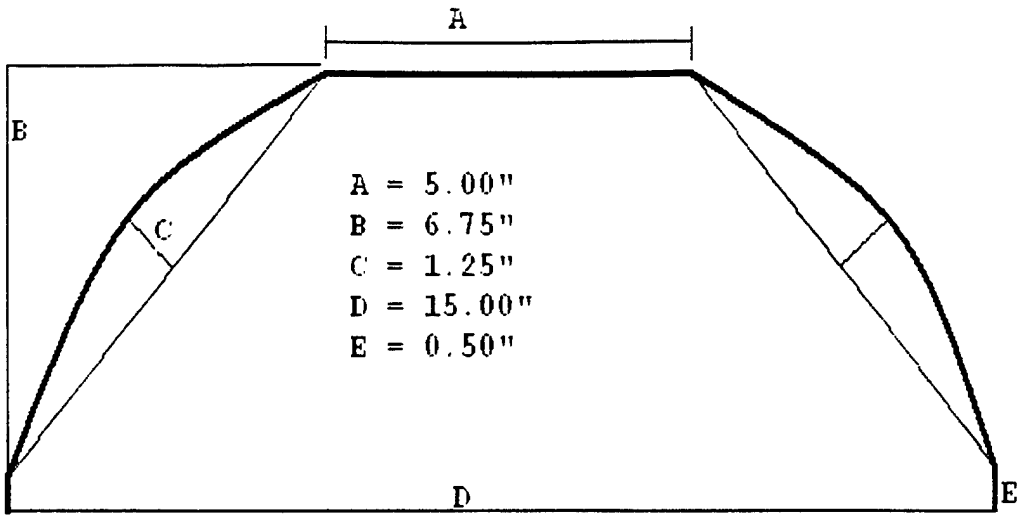

Figure 7: Dimensions of Landing Gear

4.6 Propulsion

The motor of choice was the Astroflight 40 Cobalt motor. The contest rules limit the choice of motors, and a vast amount of battery and propeller data assessing its flight characteristics could be found on www.ezonemag.com. These factors made the motor ideal for the purposes of the competition.

There were several factors in the choosing of the propeller type. The mission maximum time of ten minutes and the speed of the propeller were critical factors in the selection process. The choices are under the amperage maximum limit. Assuming that all ten minutes would be taken up, the APC 9.0x10.0 would be the best choice. However, the choice of the APC 9.0x10.0 excluded the factor of weather conditions that may be present at flight time. Assuming that our mission time is good, the APC 11.0x12.0 would be the prime choice. However, the propeller may not last as long as intended, with a maximum flight time of five minutes, this would be the fastest of all the propellers considered. Other propellers considered were the APC 11.0x4.0, and the APC 10.0x6.0, would be good for extra time, in the event that the flight does not run smoothly, or if the weather conditions are not favorable. If the plane were to hit a headwind, extra time from the propeller may be needed to land. This results in a considerable amount of speed that would be compromised at 31 and 46 mph. The last propeller under consideration was the APC 9.0x9.0. This model allows plenty of time to last the maximum time limit of ten minutes for the mission, and has an adequate speed of 70 mph. Our final choice for the propeller will be chosen at a later time as modifications are made to the aircraft.

4.7 Batteries

For the battery choice, we decided on packs of 18 N1700 SC RC batteries. Each of the batteries weighs approximately 55 grams. A pack of eighteen that we will use is then approximately 2 lbs. We chose these batteries since they would fit the Astroflight 40 geared (#640) motor. We will be using only one motor in the aircraft. The volume of each battery is 17.87 cm^3. The total pack will take up 321.7 cm^3 within the airplane. The batteries will be divided into two sections, one in front of the payload, and one behind the payload.

4.8 Payload

The Payload must weigh 5lbs and have external dimensions of 6" by 6" by 12". To facilitate ease of construction, we chose to build the payload of a plywood and then ad ballast to the payload using clay or a similar material to bring it up to the correct weight.

4.9 Storage Container

The storage container must have maximum internal dimensions of 4ft by 2ft by 1ft. We decided to use plywood and 2 x 4s to construct the crate to hold the aircraft together. The use of a wooden box allows for the team to easily added internal supports for aircraft components and padding. Handles can be added for easier handling, and latches can be added to hold the lid to the container securely to the container.

5 DETAIL DESIGN

On completion of the preliminary design of the various components of the aircraft. the final configuration of the aircraft had to be determined. This included the integration of other components such as the placement of batteries etc. Dimensional drawings were also created for the various structural components and material selections were made for the manufacturing process.

5.1 Antenna

Based on the design analysis of the antenna, a PVC mast and disk will be used. The final dimensions are shown in the figure below:

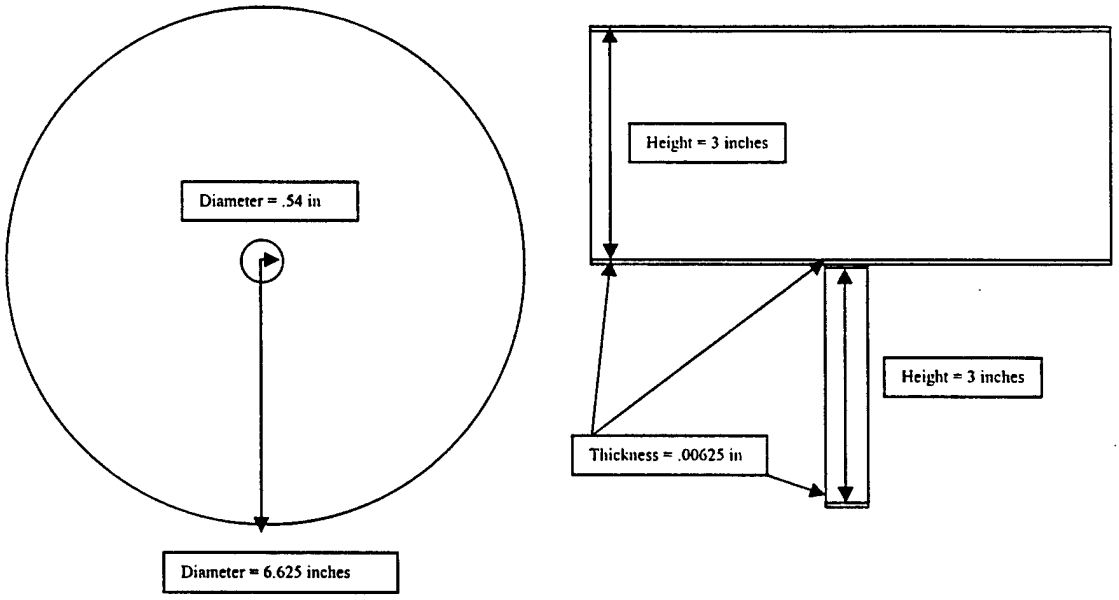

Figure 8: 2-D Drawing of the Antenna

5.2 Fuselage and Payload Bay

The fuselage is a traditional bulkhead skeleton design with rods running the entire length along the top section for alignment and reinforcement purposes. Reinforcing ribs will also be placed lengthwise along the fuselage to keep a streamlined shape between the bulkheads.

The fuselage was designed using *Pro/Engineer 2000i*^{2} and the skeleton with component placement is depicted below:

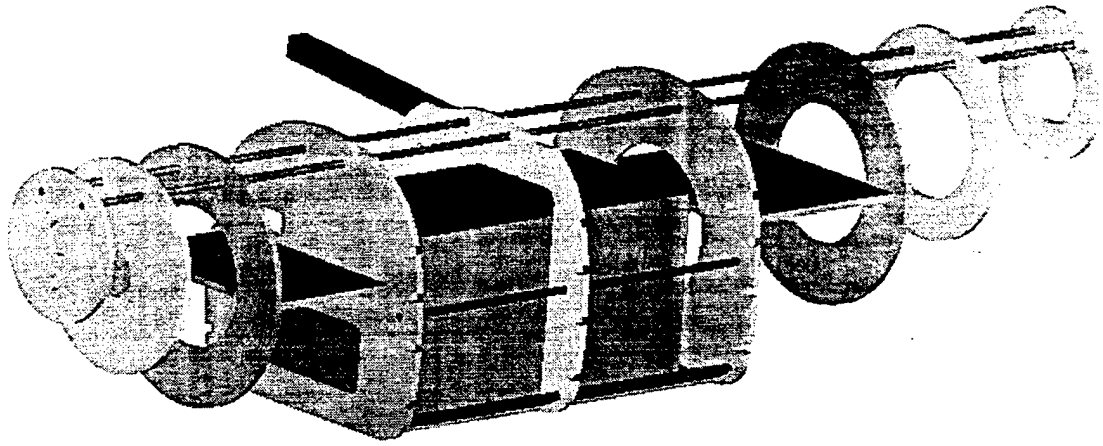

Figure 9: Fuselage skeleton

Decomposition into subsystems

Including the wing mounting subsystem, the fuselage has six other subsystems which are: motor mounting, payload bay and deployment, battery mounting, radar disk mounting, landing gear mounting, tail mounting, and control and electrical system mounting. The fuselage acts as the spine and 'brain' of the aircraft where all these subsystems meet, thus it must be constructed in such a way as to support the loads of all these components as well as promote their interaction in the most efficient manner.

The motor will be mounted high on the fuselage frame so that the propeller can grab the largest amount of air when it is at the top portion of its path and to give it as much ground clearance as possible. The motor being used is a 40 amp cobalt Astroflight motor with a gear reducer. There will be two bulkheads used to mount the motor, one in the front that mates with the motor mounting plate, and one in the rear that is mated with its cylindrical portion.

The payload bay and deployment system are critical for competing in the second most difficult variant of the 2003 competition. The bay was designed with the dimensions, 7"x7"x14", to give one inch clearance for the payload on all sides and for the payload to sit directly on the door. The front payload bulkhead has less surface area cut out of the middle because in event of a hard landing, the payload will be forced forward into this bulkhead. Therefore it needs more reinforcement than the aft payload bulkhead. Foam will be placed in

the spaces between it and the bulkheads during flight. The deployment system (see **Figure 9**) consists of a door hinged on one side on which the payload sits. Two servos, mounted forward and aft of the payload section, will pull a bar with pegs that disengages the door from the slots cut into it. Once the payload has dropped out, a spring mounted on the top of the payload section and connected to a wire will pull the payload door shut and the servos will re-latch the door.

The remaining subsystems mounting will be done by attaching plates and hatches in between the bulkheads and attaching those components to the plates. The radar disk will be mounted directly over the center of gravity onto a hatch that inserts into the top of the fuselage. The hatch will mount on a thin slot cut out of the front payload bulkhead and over the wing mounting bulkhead and then latched down on either side. The wing mounting bulkhead has the hatch shape cut out of it on top. The tail and tail servos will be mounted on plates between the rear shaper bulkhead and the two aft-most bulkheads (the tail bulkheads). The landing gear will be mounted on a four inch wide plate mounted on the back of the rear payload bulkhead and the front of the aft shaper bulkhead.

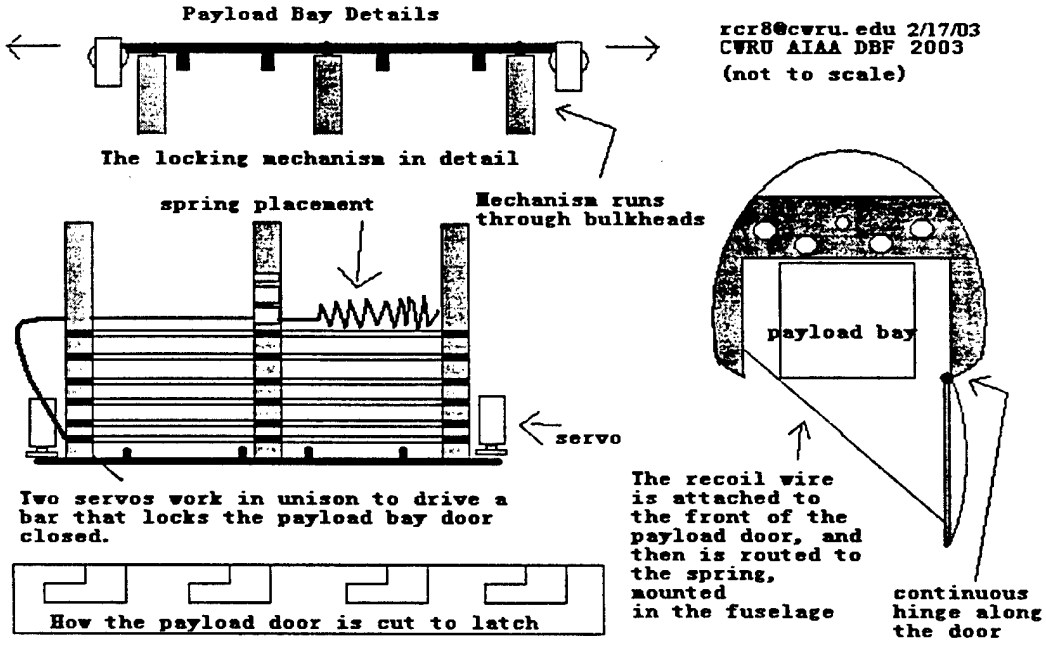

Figure. 10: Payload Deployment System

The batteries, control system , and electrical systems will be mounted on plates forward and aft of the payload bay. Front plates connect to a shaper bulkhead just behind the motor mount and to the front payload bulkhead. The rear plate connects to a shaper bulkhead in

front of the tail bulkhead and to the rear payload bulkhead. Holes are placed in the front payload bulkhead for wiring purposes.

5.3 Wings

The wing structure is comprised of a reinforced foam wing with an aluminum center spar to provide the strength required to support the fuselage and aircraft system components. A layer of fiberglass cloth will be used to provide the structure with additional strength and a smooth finish. The drawings below illustrate the wing design and its attachment to the fuselage.

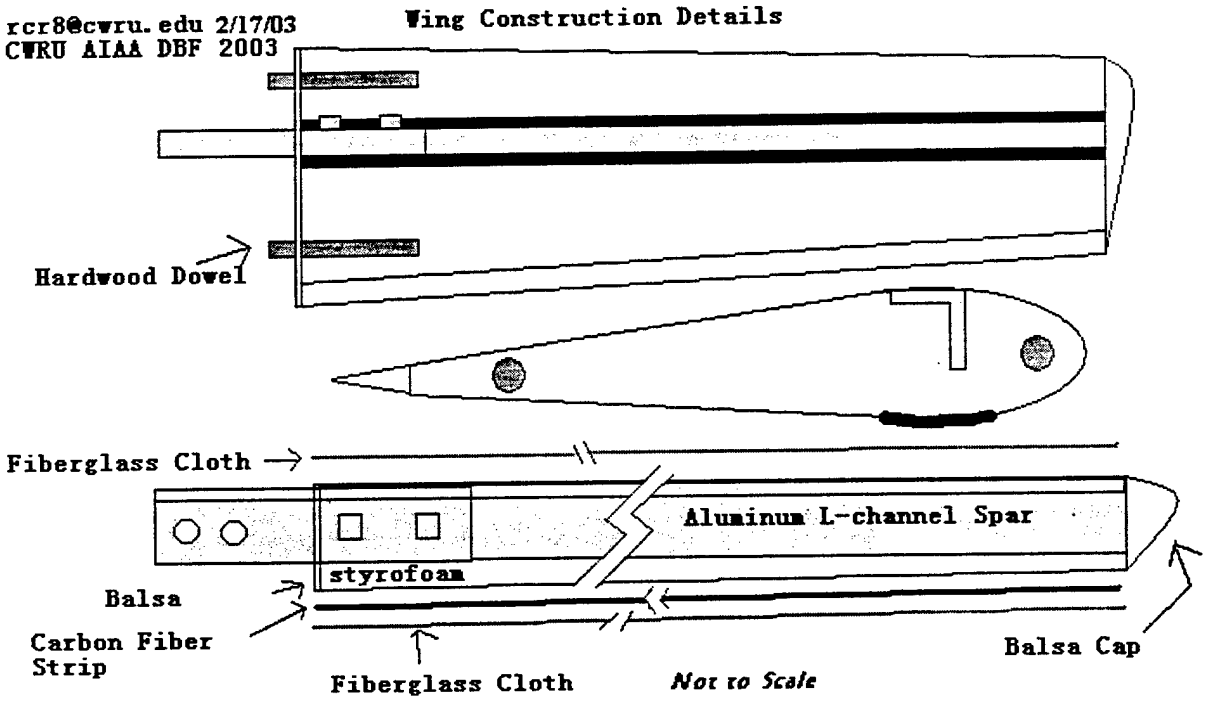

Figure 11: Wing Construction

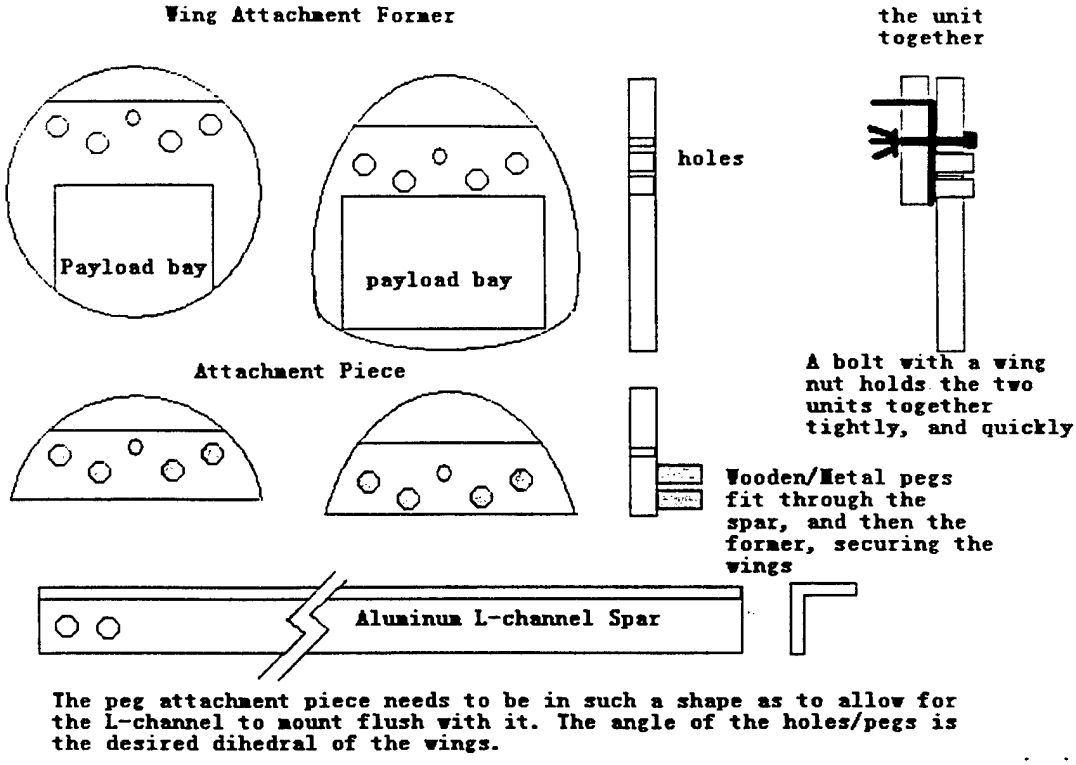

Figure 12: Wing Construction

5.4 Tail Section

To ensure that the tail will fit into the box together with the rest of the aircraft and its parts and yet meet the requirements for flight, the tail will be a maximum length of 14.6 inches. To control the tail we decided to use two flush mounted servos in the fuselage and the internal servo mixing capabilities of our transmitter. This allows for the flight controls to be modified easily so flight characteristics and be optimized during the testing phase. The dimensions of the tail are shown in the drawing below.

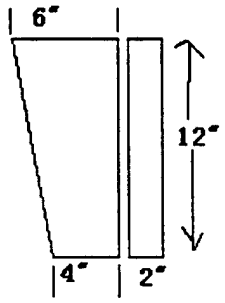

Figure 13: Tail Specifications

5.5 Final Aircraft Configuration

The final design of the aircraft will comprise of a conventional cylindrical fuselage of about 4ft in length with a NACA 2412 airfoil for the wing, with a span of 6ft and a wing loading of 39oz/ft^2. The tail is an inverted V-tail with a 35 degree angle from the horizontal. The aircraft will be supported with a landing gear that provides a 7inch clearance from the ground. Due to the uneven load distribution in the aircraft, the placement of the nose and body landing gear will be at the bulkheads in front of and behind the cargo bay respectively. Below is a summary of the final aircraft configuration.

Table 13: Aircraft Configuration

Description	Specification
Fuselage	
Maximum Length	48 in
Maximum Width	10 in
Wing	
Airfoil	NACA 2412
Span	72 in
Chord	18 in
Area	8.25 sq ft
Dihedral	5 degrees
Tail	
Span	14.6 in
Cord	6 in
Total Aircraft	
Maximum weight without payload	10 lb
Rated Aircraft Cost	7.46

6 MANUFACTURING PLAN AND PROCESS

Before fabrication of the aircraft, a manufacturing plan has to be formulated based on the preliminary and detailed design of the various parts of the aircraft. As such, the following sections describe the plans that were discussed for the production of the aircraft.

6.1 Fuselage Manufacturing Plan and Process

Before beginning construction, the manufacturing processes needed to be selected. The following is a list of possible manufacturing methods for the main body of the aircraft. The team decided to use the wings from last year's competition because they are in good condition and they will meet the design specifications of this year's aircraft.

Datum Main body: fiberglass with plywood bulkheads; nose & tail cone: fiberglass

1. Main body: Monokote with plywood ribs and bulkheads; nose & tail cone: fiberglass
2. Main body: balsa wood with plywood bulkheads; nose & tail cone: hard plastic
3. Main body: PVC or hard plastic; nose & tail cone: PVC or hard plastic
4. Main body: carbon fiber; nose & tail cone: carbon fiber

In order to evaluate these ideas and select the best one, Pugh Screening and Scoring matrices were used. In the screening matrix, the following criteria were used: availability, required skill levels, cost, extra equipment needed, and manufacturing time.

Table 14: Pugh Screening Matrix

	Manufacturing Processes				
Criteria	**Datum**	**1**	**2**	**3**	**4**
Availability		+	+	0	-
Required skill levels		+	+	+	0
Costs		0	+	0	-
Extra equipment needed		+	0	0	-
Manufacturing time		+	0	+	0
Totals:		**4**	**3**	**2**	**-3**

Based on the above matrix, the third and fourth manufacturing processes were eliminated. The next step is to create a Pugh Scoring Matrix to determine the best process. The five criteria are now sorted through and ordered from most important to least important. This

order from most to least important is: (1) required skill levels, (2) availability. (3) manufacturing time, (4) costs, and (5) extra equipment needed. The criteria are assigned weights ranging from 5% to 35%. To determine the raw score, 1, 5, or 9 points were assigned to each option, with 9 being the best and 1 being the worst. The data from the scoring matrix appears in **Table 15**, below.

Table 15: Pugh Scoring Matrix

	Manufacturing Processes						
	Datum		1		2		
Design Criteria	Raw	Weighted	Raw	Weighted	Raw	Weighted	Weight
Required skill levels	1	0.35	9	3.15	5	1.75	35%
Availability	5	1.25	5	1.25	9	2.25	25%
Manufacturing time	1	0.2	5	1	1	0.2	20%
Costs	1	0.15	9	1.35	9	1.35	15%
Extra equipment needed	1	0.05	9	0.45	5	0.25	5%
Totals:	**9**	**2**	**37**	**7.2**	**29**	**5.8**	

After analyzing the above data, manufacturing process #1 (with a weighted score of 7.2) was chosen over the other two options.

6.2 Wing and Tail Manufacturing Plan and Process

The wing and tail can be fabricated concurrently with the fuselage. The Styrofoam will have to be cut to size and the aluminum center spar integrated into the wing structure. This will be followed by the application of a carbon fiber cloth layer on the surface of wing.

6.3 Landing Gear Manufacturing Plan and Process

The main landing gear will require some simple machining. Two holes must be put on the top of the gear so it can be attached to the bottom of the fuselage. Two screws will be inserted from the fuselage where the main gear can be quickly attached. The wheel requirements of two to three inches will be taken from our current inventory.

6.4 Payload Bay and Payload Manufacturing Plan and Process

We anticipate that the most complex and detailed piece of the fuselage is the payload bay. This area of the fuselage should be started first so that problems that arise can be worked

out of it before other fuselage components are integrated, make accessing all areas more difficult.

6.5 Systems Integration and Electronics Assembly

After the bulkheads of the fuselage are in place, controls lines for the payload bay and steering can be run in the aircraft. When the fuselage has been assembled the tail, electronics, landing gear, and control lines can all be installed and configured on the aircraft.

The electronic components can be assembled and tested outside of the aircraft prior to installation. These tests will assure all components are in proper working order before installation.

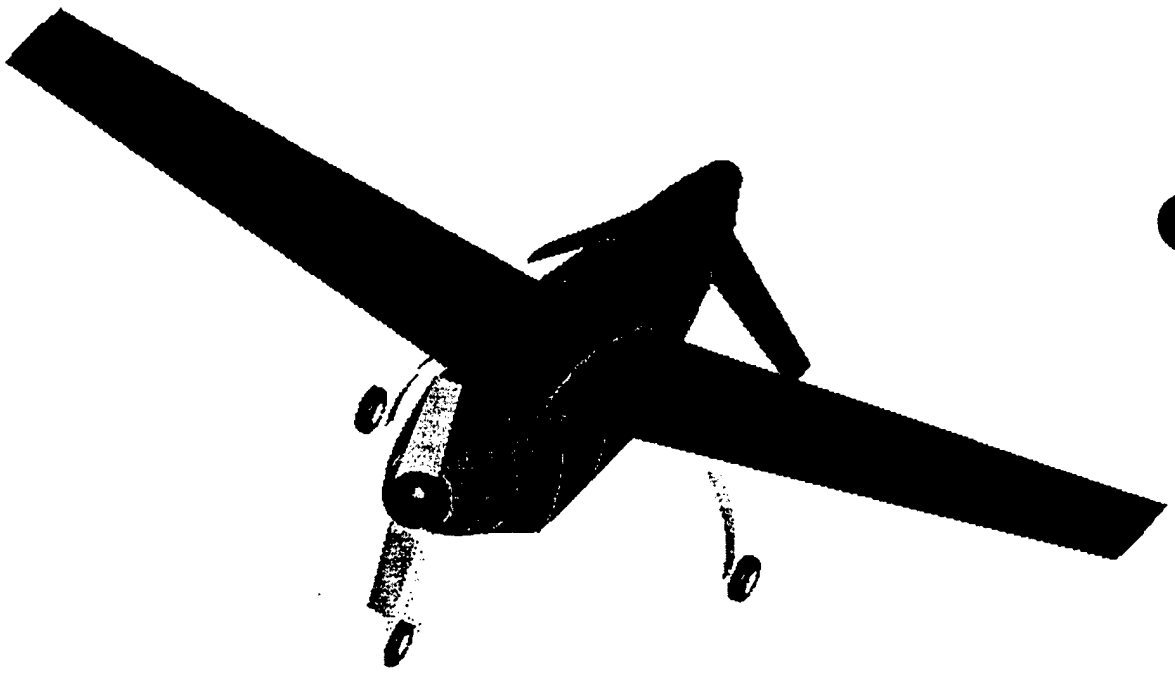

Figure 14: Design of the MFX

Construction Timeline

ID	Task Name	Start	Finish	Duration
1	Materials Acquisition	3/1/2003	3/17/2003	2w 2.5d
2	Component Fabrication	3/3/2003	3/21/2003	2w 5d
3	Container Construction	3/10/2003	3/14/2003	5d
4	Payload Bay construction	3/21/2003	3/27/2003	6.5d
5	Wing Construction	3/18/2003	3/24/2003	6d
6	Fuselage Assembly	3/24/2003	4/6/2003	1w 6d
7	Tail Construction	3/25/2003	4/1/2003	1w .5d
8	Control Systems Installation	4/1/2003	4/8/2003	1w 1d
9	Electronics assembly	3/18/2003	3/20/2003	2.5d
10	System integration	4/3/2003	4/8/2003	5.5d
11	Testing and modification	4/9/2003	4/24/2003	2w 1.5d

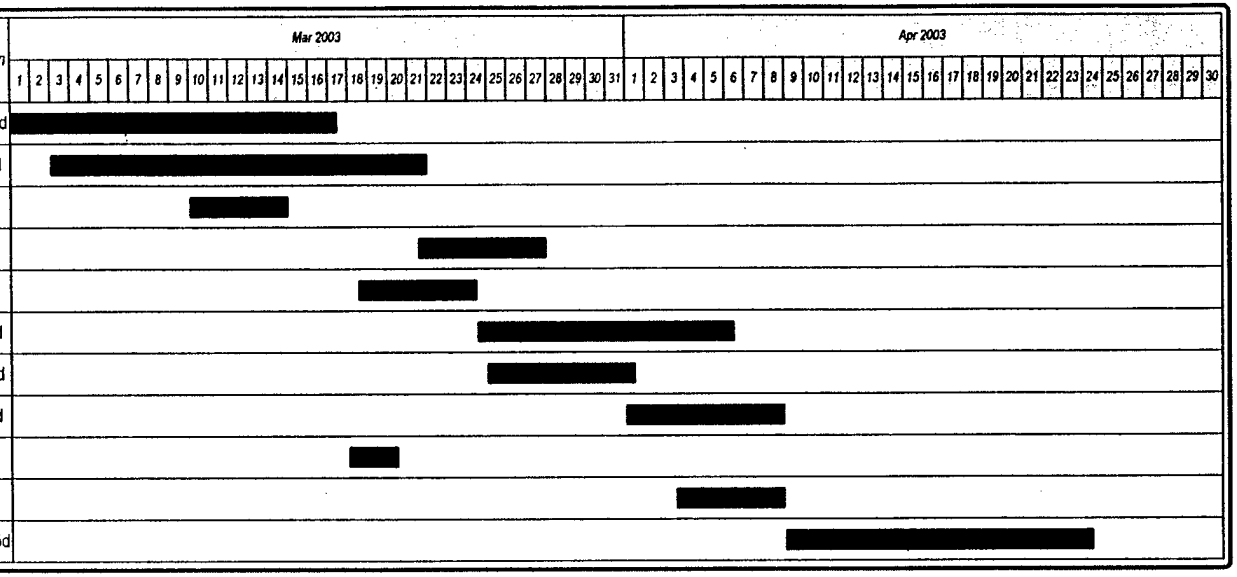

7 RATED AIRCRAFT COST

The rated aircraft cost of was computed after the final design parameters were determined. The predicted rated aircraft cost was 7.46. The breakdown of the calculations is shown in the tables below.

Table 16: Manufacturing Man Hours (MMH)

Manufacturing Man Hours (Work Breakdown Structure)			
Description	**Man Hours/Unit**	**Aircraft Parameter**	**Hours**
Wing			
Wingspan	8 hr/ft	6 ft	48
Wing cord	8 hr/ft	3 ft	24
Fuselage			
Maximum body length	10 hr/ft	4 ft	40
Empennage			
Vertical surface without control	5 hr/surface	1	5
Horizontal surface	10 hr/surface	1	5
Flight Systems			
Servo or motor controllers	5 hr/servo	6	30
Propulsion Systems			
Engines	5 hr/engine	1	5
Propellers	5 hr/propeller	1	5
		Total Hours	**173**

Table 17: Rated Aircraft Cost

Item	Description	Multiplier	Aircraft Parameter	Man Hours	Rated Aircraft Cost
Manufactures Empty Weight (MEW)	Actual airframe weight, lb with all flight and propulsion batteries but without any payload	$100	10 lb	Not Applicable	1,000
Rated Engine Power (REP)	"Total Battery Weight"	$1,500	1 Engine and 2lb batteries	Not Applicable	3,000
Manufacturing Man Hours (MMH)	Sum of hours from the Work Breakdown Structure	$20/hour	Not Applicable	173	3,460
				Rated Aircraft Cost	7,460
				Rated Aircraft Cost, (Thousands)	7.46

8 REFERENCES

Anderson, John D. Aircraft Performance and Design. Boston: WCB McGraw-Hill, 1999.

---. Fundamentals of Aerodynamics. 3rd ed. Boston: WCB McGraw-Hill, 2001.

Çengel, Yunus A. and Robert Turner. Fundamentals of Thermal-Fluid Sciences. Boston: WCB McGraw-Hill, 2000.

Gere, James M. and Stephen P. Timoshenko. Mechanics of Materials. 4th ed. Boston: PWS Publishing Company, 1997.

"Harvel PVC Pipe Schedule 40/80 Specifications." Web site. 27 Feb. 2003. <http://www.harvel.com/PVCpipe4080spec.html>

Hill, Philip and Carl Peterson. Mechanics and Thermodynamics of Propulsion. 2nd ed. Redding, Mass.: Addison-Wesley Publishing Company, 1992.

"Properties Affecting the Final Utility of Veneer and Plywood." Web site. 27 Feb. 2003. <http://sres.anu.edu.au/associated/fpt/plywood/finalutility.html>

"MatWeb – The Online Materials Information Resource." Web site. 27 Feb. 2003. <www.matweb.com>

2003 Cessna/ONR Student Design/Build/Fly Competition

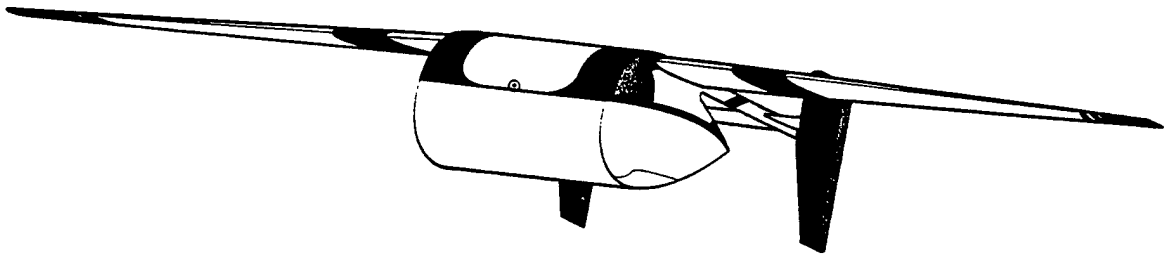

Draggin' Fly

Virginia Tech Design Build Fly Team

March 11, 2003

Table of Contents

	Page
1. Introduction	1
1.1 Executive Summary	1
1.1.1 Conceptual Design	1
1.1.2 Preliminary Design	1
1.1.3 Detailed Design	2
1.2 Management Summary	2
2. Conceptual Design	6
2.1 Conceptual Design Summary	6
2.2 Conceptual Payload Deployment Design	6
2.3 Conceptual Antenna Placement	7
2.4 Conceptual Fuselage Design	7
2.4.1 Box-wing Biplane	7
2.4.2 Airfoil Fuselage with Single Boom	8
2.4.3 Business Jet	8
2.4.4 Longitudinal Configuration	8
2.4.5 Lateral Configuration	8
2.4.6 FOM Analysis of Conceptual Fuselage Designs	9
2.5 Wing Conceptual Design	11
2.5.1 Wing Type Selection and FOM Analysis	11
2.5.1.1 Mono Low-wing	11
2.5.1.2 Mono Mid-wing	11
2.5.1.3 Mono High-wing	11
2.5.1.4 Flying Wing	11
2.5.2 Empennage Selection and FOM Analysis	12
2.5.2.1 Conventional Tail	12
2.5.2.2 Canard	12
2.5.2.3 T-tail	12
2.5.2.4 V-tail	13
2.5.2.5 Y-tail	13
2.5.2.6 H-tail	13
2.5.2.7 Inverted V-tail	13
2.5.2.8 Inverted Y-tail	13
2.6 Landing Gear Conceptual Design	14
2.6.1 Fixed Gear Designs	14
2.6.2 Fixed/retractable Composites	14
2.6.3 Fully Actuated Retractable Designs	15

2.6.4 Gear Selection and FOM Analysis 15
3. Preliminary Design 16
3.1 Preliminary Design Summary 16
3.2 Preliminary Wing Design 16
3.2.1 Wing Airfoil Selection 16
3.2.2 Wing Planform Area 17
3.2.3 Wingspan, Chord, and Taper Ratio 17
3.2.4 Aileron and Flapperon Sizing 18
3.2.5 Horizontal and Vertical Tail Foil Selection 18
3.2.6 Horizontal and Vertical Tail Sizing 18
3.3 Preliminary Fuselage Design 19
3.4 Landing Gear Preliminary Design 20
3.5 Payload Preliminary Design 25
3.6 Antenna Preliminary Design 26
3.7 Propulsion and Flight Mechanics Preliminary Design 27
4. Detailed Design 28
4.1 Detailed Design Summary 28
4.2 Detailed Wing Design 28
4.2.1 Wing Joints and Connections 28
4.2.2 Servos and Control Surfaces 29
4.2.3 Electrical Connections in the Wing 30
4.3 Detailed Fuselage Design 30
4.4 Detailed Landing Gear Design 32
4.5 Detailed Payload Deployment Design 33
4.6 Detailed Antenna Design 33
4.7 Detailed Propulsion and Flight Mechanics Design 34
4.7.1 Battery Layout 36
4.8 Stability and Control Analysis 37
4.9 Final Design Summary 38
4.10 Drawing Package 41
5. Manufacturing Plan 47
5.1 Manufacturing Summary 47
5.2 Wing and Empennage Manufacturing Process and Tooling 47
5.3 Fuselage Manufacturing Process and Tooling 47
5.4 Landing Gear Manufacturing Process and Tooling 48
5.5 Manufacturing Scheduling 48
6. Testing Plan 48

6.1 Materials Testing 48
6.2 Structural Testing of Wings 48
6.3 Structural Testing of Empennage 49
6.4 Structural Testing of Landing Gear 49
6.5 Propulsion Testing 50
6.6 Aerodynamic Testing 50
6.7 Ground Testing 51
6.8 Flight Testing 51
7. References 52

Table of Figures

Figure 1.1 Milestone Chart 4
Figure 1.2 Managerial Chart 5
Figure 2.1 Conceptual Designs 10
Figure 3.1 Graph of 2-D Drag based on Re and Planform Area 20
Figure 3.2 Landing Gear Concept Internal Components 22
Figure 3.3 Landing Gear Concept External View 23
Figure 3.4 Landing Gear Space Allocation 24
Figure 3.5 Preliminary Antenna Design 27
Figure 4.1 Detailed Fuselage Design, Internal Bracing 31
Figure 4.2 Sectional View of Radome 34
Figure 4.3 Battery Layout 36
Drawing Package 42

Table of Tables

Table 2.1 Conceptual Payload Ejection Methods FOM 6
Table 2.2 FOM for Radome Placement 7
Table 2.3 Conceptual Design FOM 9
Table 2.4 FOM for Wing Types 12
Table 2.5 Tail Design FOMs 14
Table 2.6 FOM for Landing Gear Configurations 15
Table 3.1 Airfoil Data 17
Table 4.1 Additional Motocalc™ Filters 35
Table 4.2 Validation of JKayVLM Code 37
Table 4.3 Draggin' Fly Stability Derivatives 37
Table 4.4 Draggin' Fly Final Specifications 38
Table 4.5 Rated Aircraft Cost Calculations 39

Symbols Appearing in Text

M	Mach number
μ	Viscosity
Re	Reynolds number
ρ	Density
t_{max}	Maximum thickness
V	Free stream velocity
C_L	Lift coefficient
C_D	Drag coefficient
C_{Lmax}	Maximum lift coefficient
L/D_{max}	Maximum lift to drag ratio
C_m	Moment coefficient
C_{Di}	Induced drag coefficient
CG	Center of gravity

1. Introduction

1.1 Executive Summary

The Virginia Tech Design Build Fly Team has decided to compete in the 2002-03 AIAA/Cessna/ONR Student Design/Build/Fly Competition with the Draggin' Fly aircraft. The three mission profiles are designed to simulate a military aircraft that carries a sensor package, possibly remotely deployable. Additionally, the aircraft may carry a simulated radar antenna to detect and track targets of interest. The team's goal is to not only meet these requirements, but to also design for optimum performance.

The team chose two of the three specified missions, and then conceptualized aircraft designs accordingly. The team set about accomplishing its goals by creating a schedule and setting deadlines to finish key aspects of the design.

1.1.1 Conceptual Design

The first process in accomplish these was to select the concept that would give the team the best chance to maximize its score. The concepts were separated into three different groups, fuselage concepts, wing concepts, payload deployment concepts, antenna concepts, and empennage concepts. Figures of Merit (FOMs) were applied to each of these concepts. The team selected the highest scoring FOMs of each of the concepts and applied them to an Excel file developed by past teams to analyze conceptual designs. At the end of the conceptual design phase, the team had found that a laterally mounted sensor package wrapped in a symmetrical airfoil, with an H-Tail, retractable landing gear, a gravity-induced payload deployment, and a radome mounted above the aircraft CG would provide the best competition performance.

1.1.2 Preliminary Design

With the concepts selected in the conceptual design phase the team needed to find the overall dimensions of the aircraft based on sizing methods. This was done through theoretical analysis and computation. The team used the Missile Decoy mission, and the 120 foot takeoff length as the worst-case scenarios for sizing the Draggin' Fly aircraft. Requirements during the preliminary design were selection of the motor and batteries, the wing dimensions and airfoil, the fuselage airfoil, payload deployment, and radome attachment.

By the end of the preliminary design phase, the overall dimensions of the Draggin' Fly had been defined. This resulted in an aircraft with an 81 inch wingspan, and a 43 inch overall length. The Astro Flight 60 motor was selected, along with Sanyo 2300SCE batteries. The team found that a NACA 0027 airfoil would have minimum drag during cruise. Finally the basic dimensions and design of the payload deployment, radome, and retractable landing gear were resolved.

1.1.3 Detailed Design

Once the general dimensions and component selection of the Draggin' Fly aircraft had been defined, the team selected final components and analyzed the aircraft's performance. Once the fuselage airfoil had been defined, the internal structural components and sizes were designed. The tail and aileron surfaces were sized during the detailed design, and the aircraft was analyzed for stable stability derivatives. Final component selection and design for methods of payload deployment and radome attachment were performed, and the team selected a propeller and battery configuration. Performance analysis was done through the use of a combination of codes. Some codes that were used were commercially developed, others developed by graduate research, and others were written specifically by the team to analyze the aircraft during competition conditions.

At the conclusion of the detailed design phase of the VT DBF's contest effort, the team had defined the system component selection and final dimensions of the aircraft. With this information, the team was able to calculate the stability and performance of the aircraft. This in depth design and analysis gave the team confidence that it would accomplish its goals for the 2002-03 AIAA/Cessna/ONR Student Design/Build/Fly Competition.

1.2 Management Summary

This year, the executive leadership of the team was composed of two Program Managers, a chief engineer, two consultants, and six component-team leaders. The six component-teams are the Finance Team, Propulsion / Flight Mechanics Team, Drafting Team, Fuselage Team, Payload / Radome team, and Wing Team.

The Program Managers have the primary function of guiding the team through the entire project, from conceptual design to competition. They were responsible for keeping the team on schedule, and integrating the efforts of each component team. The first challenge for the Program Managers was recruiting new team members by raising interest in students of all academic levels. As a result of recruiting efforts, the team size tripled from last year, expanding the team's vision for future competitions.

The Chief Engineer has the task of guiding the team's technical progress and assuring the validity of the results that are produced. This year's chief engineer is also team leader of the Propulsion / Flight Mechanics Team. The Propulsion / Flight Mechanics Team is responsible for selecting the motor and battery combination as well as designing maneuvers for optimal flight performance. The Finance Team has the task of raising the required funds for this year's competition team and future teams. This team also plans to improve the capital infrastructure facilities available to the team. The Drafting Team produces accurate and timely drawings of system components for prototyping and detail design work. This team also performs component testing to determine interoperability of the various systems. The Fuselage Team is responsible for determining the structural stability and integrity of the aircraft and designing the internal layout of the fuselage. This team also plays an integral role in material selection for major structural elements. The Wing Team designs the wing and tail portions of the aircraft for both

aerodynamic and structural criteria. This team also designs control surfaces to optimize stability and control. Methods of payload deployment and radome placement are determined by the Payload / Radome Team. The team is responsible for the design of the payload and radome such that drag from the radome and time to deploy the payload are minimized.

This organization style distributes the workload evenly, allowing the team to complete the design process in a timely fashion. Figure 1.1 shows the planned and actual timing of major elements of the design process. As an improvement from previous years, there is additional time allotted for flight-testing and report preparation. Figure 1.2 details the managerial layout and team organization.

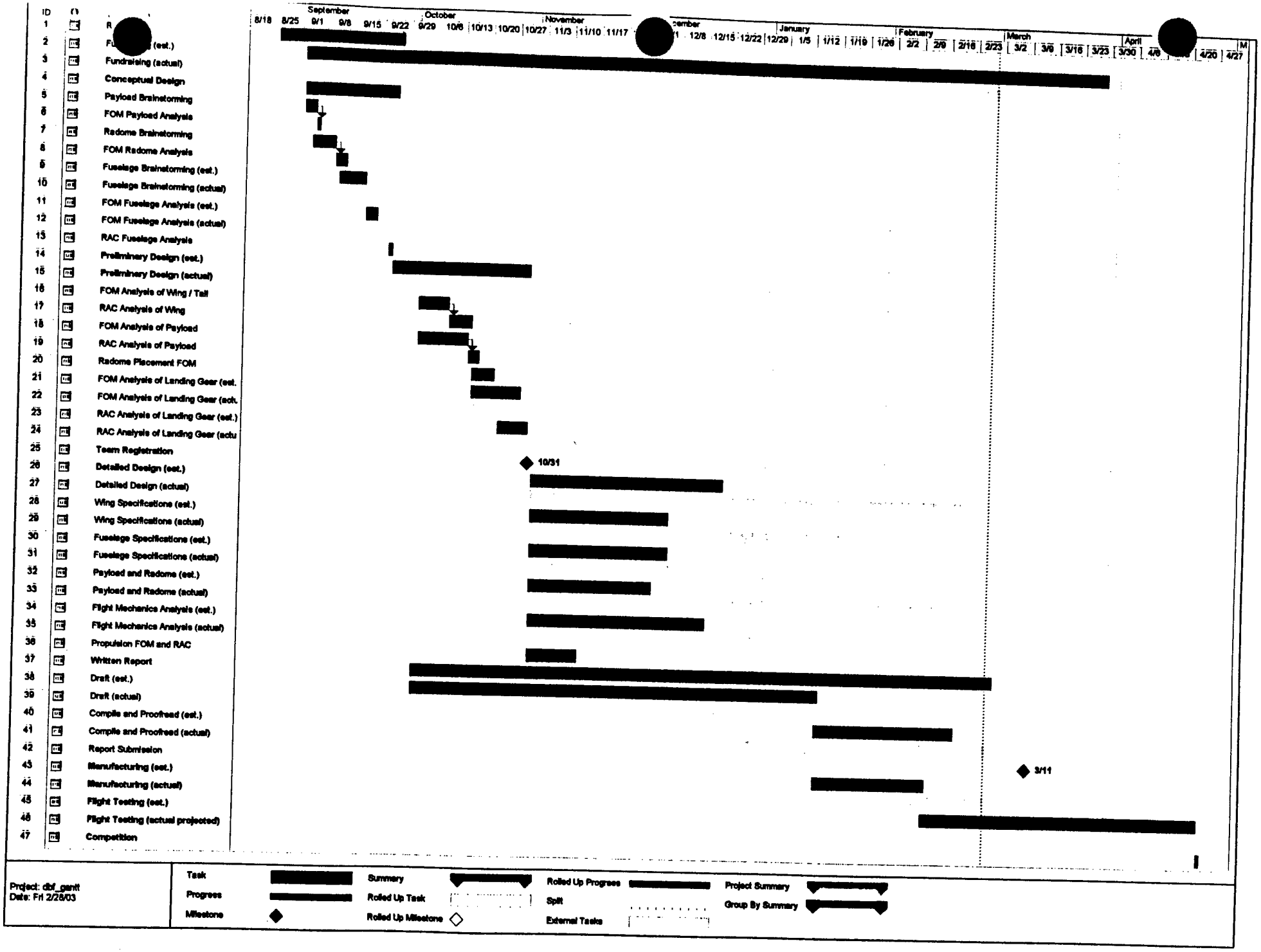
ID
1 R
2 Fu (est.)
3 Fundraising (actual)
4 Conceptual Design
5 Payload Brainstorming
6 FOM Payload Analysis
7 Radome Brainstorming
8 FOM Radome Analysis
9 Fuselage Brainstorming (est.)
10 Fuselage Brainstorming (actual)
11 FOM Fuselage Analysis (est.)
12 FOM Fuselage Analysis (actual)
13 RAC Fuselage Analysis
14 Preliminary Design (est.)
15 Preliminary Design (actual)
16 FOM Analysis of Wing / Tail
17 RAC Analysis of Wing
18 FOM Analysis of Payload
19 RAC Analysis of Payload
20 Radome Placement FOM
21 FOM Analysis of Landing Gear (est.
22 FOM Analysis of Landing Gear (act.
23 RAC Analysis of Landing Gear (est.)
24 RAC Analysis of Landing Gear (actu
25 Team Registration
26 Detailed Design (est.)
27 Detailed Design (actual)
28 Wing Specifications (est.)
29 Wing Specifications (actual)
30 Fuselage Specifications (est.)
31 Fuselage Specifications (actual)
32 Payload and Radome (est.)
33 Payload and Radome (actual)
34 Flight Mechanics Analysis (est.)
35 Flight Mechanics Analysis (actual)
36 Propulsion FOM and RAC
37 Written Report
38 Draft (est.)
39 Draft (actual)
40 Compile and Proofread (est.)
41 Compile and Proofread (actual)
42 Report Submission
43 Manufacturing (est.)
44 Manufacturing (actual)
45 Flight Testing (est.)
46 Flight Testing (actual projected)
47 Competition
8/18 8/25 9/1 9/8 9/15 9/22 9/29 10/6 10/13 10/20 10/27 11/3 11/10 11/17 12/1 12/8 12/15 12/22 12/29 1/5 1/12 1/19 1/26 2/2 2/9 2/16 2/23 3/2 3/9 3/16 3/23 3/30 4/6 4/13 4/20 4/27
September
October
November
January
February
March
April
10/31
3/11
Project: dbf_gantt
Date: Fri 2/28/03
Task
Progress
Milestone
Summary
Rolled Up Task
Rolled Up Milestone
Rolled Up Progress
Split
External Tasks
Project Summary
Group By Summary

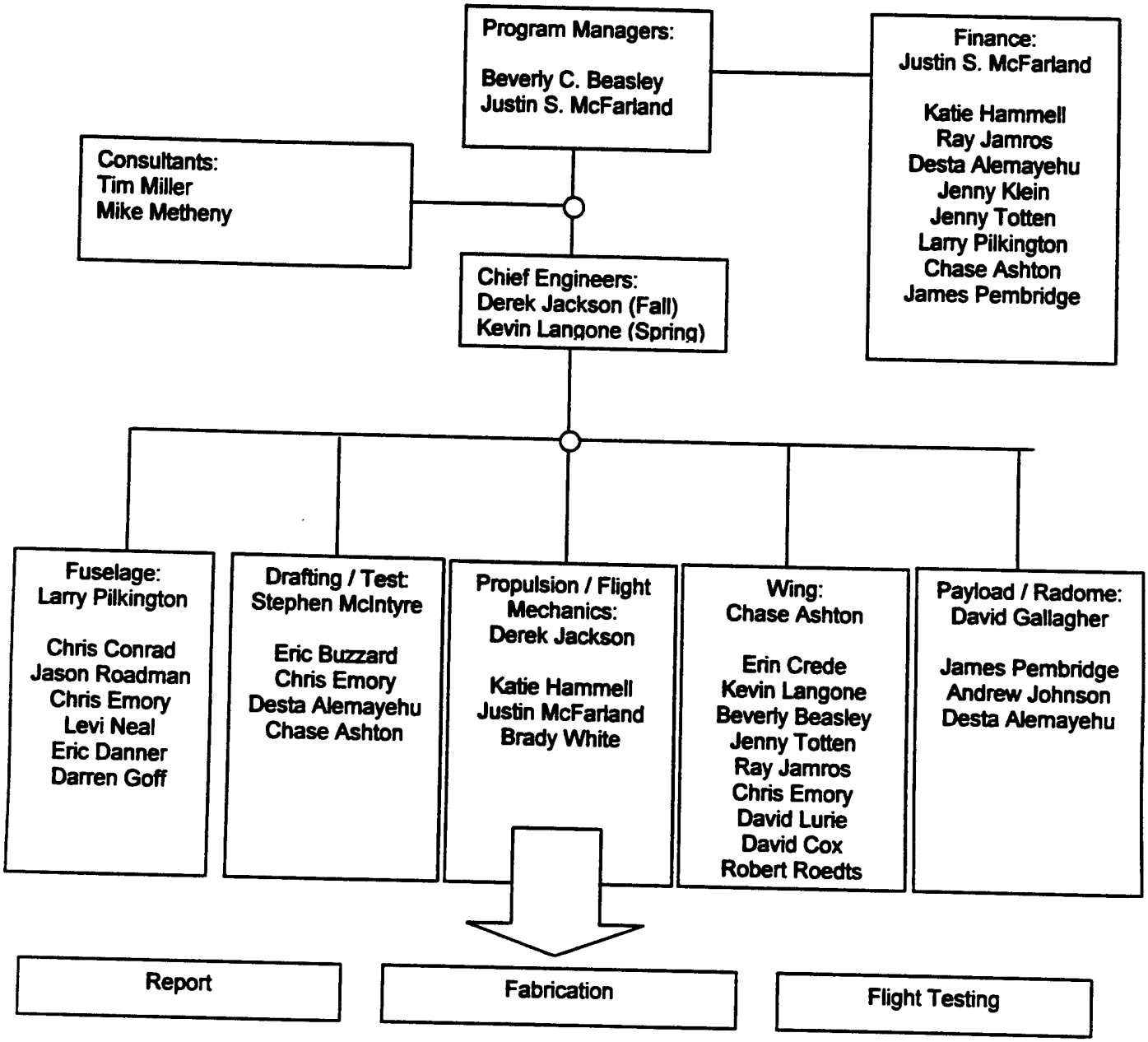

Figure 1.2 Managerial Chart

2. Conceptual Design

2.1 Conceptual Design Summary

The team began the conceptual design phase by studying the rules and mission requirements. Analysis of the stated missions led the group to decide to attempt the two most difficult missions: remote deployment of a simulated avionics payload weighing five pounds, and carrying a simulated cylindrical antenna of specified dimensions. The choice of these two missions will allow the team the best potential to score the maximum points. Based on the chosen missions, the goals set were to choose a viable method of payload deployment, choose a location for the antenna, and incorporate these components into a fuselage that would serve as the foundation for the remainder of the design process. These decisions were made after careful analysis of each design's figures of merit (FOMs), and analysis of effects on rated aircraft cost (RAC).

2.2 Conceptual Payload Deployment Design

First, payload deployment methods were brainstormed. The team considered dropping the payload from a cargo door using only gravity as one means of deployment. Another method consisted of a ramp or false back through which the payload would be deployed. Other ideas implemented the use of springs or gear to eject the payload from the aircraft. After discussion, the decision was narrowed down to four designs to compare in a Figure of Merit (FOM), Table 2.1.

Table 2.1 Conceptual Payload Ejection Methods FOM

	RAC	Weight	Lift and Drag	Manufacturing	Reliability	Total Out of 100
Importance:	**4**	**5**	**3**	**3**	**5**	
Cargo Door	4	3	3	3	4	**69**
Ramp	3	4	2	3	4	**67**
Gear	4	3	5	2	2	**62**
Springs	4	2	3	2	3	**56**

The FOMs in Table 2.1 convinced the team to pursue a payload deployment method involving the use of a cargo drop bay. This design was chosen because of its simplicity; the drop bay could implement gravity as its ejection means, provide easy storage of the payload, and the cargo doors are easily retracted.

2.3 Conceptual Antenna Placement

The team brainstormed unique ways of placing the antenna on the aircraft as to reduce drag. Some ideas considered were conventional placement on top of the aircraft, placing it below the tail, using the antenna as a tail structure or rudder, and sandwiching the antenna above and between two tail booms. After ruling out ideas that were against contest regulations, the team analyzed the remaining ideas in an FOM, Table 2.2.

The FOM in Table 2.2 revealed the conventional antenna placement to be optimal for design. Conventional antenna placement, while creating high drag, is easy to manufacture, reliable, and readily detachable.

Table 2.2 FOM for Radome Placement

	Structural Integrity	Weight Location	Lift and Drag	Manufacturing	Ease of Assembly	Total Out of 100
Importance:	**4**	**4**	**5**	**3**	**4**	
Between tail booms	2	3	4	3	3	**61**
Conventional	4	5	2	4	4	**74**
Below fuselage	4	4	2	4	3	**66**

2.4 Conceptual Fuselage Design

With general concepts for the payload deployment and antenna placement, the team began to incorporate these into a fuselage package. The team divided into smaller groups and each group conceptualized an aircraft, from wing configuration to landing gear. Each group analyzed their concept for aerodynamic characteristics, materials selection, weight, RAC, and manufacturability. The entire team rejoined and each group presented its concept and the benefits of their design. The entire team discussed the advantages and disadvantages of each concept. After this discussion, the team analyzed the FOMs of each concept and selected the concept with the highest score. The concepts explored are described below.

2.4.1 Box-wing Biplane

This conceptual design was a biplane with a 4 foot wingspan (see Figure 2.1a). The wings would be separated by 6 inches, sandwiching two collapsible booms that could be extended when brought out of the box. Two motors would be mounted in the front of each boom. This concept was designed with the intent of easy assembly. The entire plane would fit in the box except the tail, which could be pulled out by a telescoping track or folded to one side. The payload box would be placed in a center fuselage

running perpendicular to the wingspan, along with the flight batteries and radio gear. This design would have been very good at fulfilling the size requirement of the mission; however, the team decided that a 4 foot wingspan would make it difficult to take off in 120 feet and the biplane would produce too much drag. Additionally, the second engine and wing increased the RAC to unacceptable limits.

2.4.2 Airfoil Fuselage with Single Boom

This configuration had a main fuselage in the shape of an airfoil (see Figure 2.1b). It was wide enough to hold the payload box laterally. The wings could be mounted almost anywhere vertically along the fuselage. To balance the plane and provide stability, a single boom protruded from the rear of the main fuselage. Attached to the boom would be a single horizontal and vertical stabilizer. This tail design allows for a T-tail or conventional setup. It was determined that the single tail boom would not be able to support and transmit the torques and stress placed upon it, and was dismissed.

2.4.3 Business Jet

This design consisted of a long slender cylindrical fuselage, just large enough to enclose the payload (see Figure 2.1c). The motor would be mounted at the nose, while the batteries and radio gear would be evenly distributed on either side of the payload. The low wing would be mounted near the center of the fuselage. The tail would sit atop the tapered end of the fuselage. This design would be sleek and slender, giving it good aerodynamic characteristics. The low wing placement interfered with deployment of the payload requiring a heavier deployment system.

2.4.4 Longitudinal Configuration

This design held the payload box longitudinally within the fuselage (see Figure 2.1d). The fuselage is a long box, oriented at an angle of 45° from the horizontal. It is longer than the payload in order to store the motor, propulsion batteries, and the radio gear. Extended from the rear of the main fuselage is a single boom made of angle bracket, with an inverted V-tail at its end. The wing is pinned at the top corner of the fuselage with baffles for support. The landing gear extended from the top, angled side of the fuselage. Low scores for lift, drag, and RAC lowered this concept's FOM score.

2.4.5 Lateral Configuration

This design held the payload box laterally at the quarter-chord of a symmetrical airfoil fuselage, possibly based on a NACA 0030 airfoil (see Figure 2.1e). This design was favored for its historical success at previous DBF competitions. Two booms extended from the rear of the fuselage as extensions of side structural panels. At the end of the booms, two tail types were proposed. This design could have an inverted V-tail or a standard H-tail. The V-tail would have a lower RAC, but the H-tail would give more stability. The empennage would be decided upon during the preliminary design phase. The wing was mounted on the sides of the airfoil fuselage and had its quarter-chord aligned with the center of the

payload box to avoid CG changes during the mission. The wing was mounted midway from the bottom of the fuselage to allow for better maneuverability. Landing gear could be placed in the front of the aircraft and under the tail in either tricycle or quadricycle configuration.

2.4.6 FOM Analysis of Conceptual Fuselage Designs

The FOM chart in Table 2.3 quantifies the advantages and disadvantages of each design. The conceptual design FOMs resulted in the team's selection of the Lateral Configuration concept. Calculations of this concept showed that it would have less drag, produce more lift because of the airfoil fuselage, and have a total weight less than other concepts. This design was also desirable for its low RAC.

Table 2.3 Conceptual Design FOM

	RAC	Weight	Lift and Drag	Manufacturing	Assembly Time	Total Out of 100
Importance:	**4**	**5**	**3**	**5**	**3**	
Biplane	2	2	3	4	5	**62**
Single Boom	4	4	2	3	2	**63**
Business Jet	4	2	4	4	3	**67**
Longitudinal	4	4	3	4	4	**77**
Lateral	5	5	4	4	4	**89**

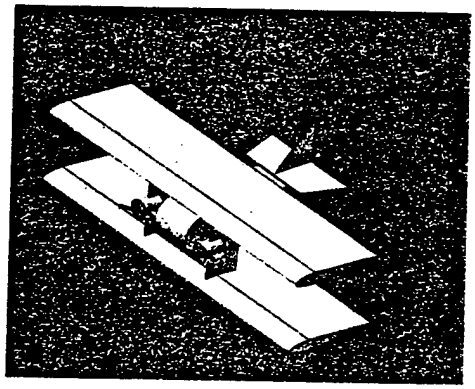

(a). Box-wing Biplane

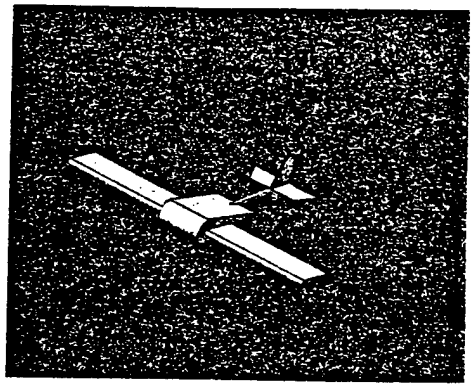

(b). Airfoil Fuselage with Single Boom

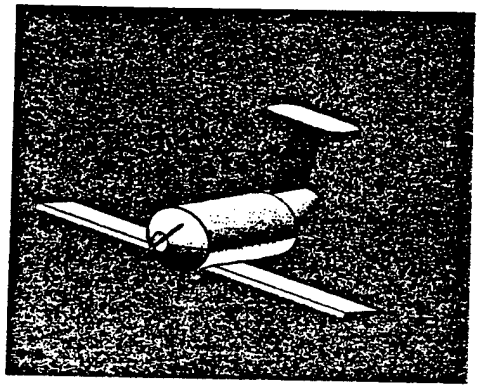

(c). Business Jet

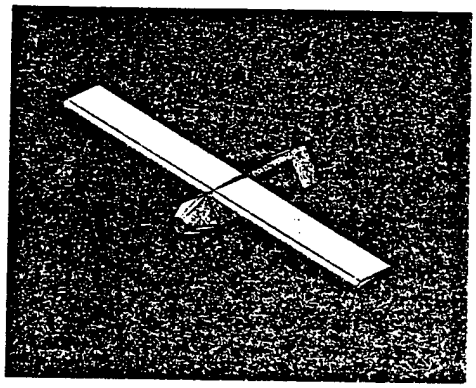

(d). Longitudinal Configuration

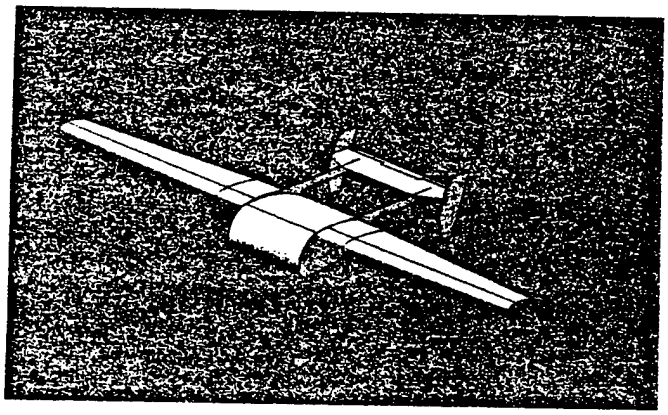

(e). Lateral Configuration

Figure 2.1 Conceptual Designs

2.5 Wing Conceptual Design

2.5.1 Wing Type Selection and FOM Analysis

Before designing a final wing configuration, several concepts were analyzed. Factors considered when deciding among different concepts were RAC, weight, lift and drag, ease of manufacturing, and assembly time. Table 2.4 shows the FOMs of the wing concepts considered.

2.5.1.1 Mono Low-wing

The mono low-wing setup provides for a stable aircraft with good handling characteristics. However, since the team decided to place the payload at the quarter chord of the wing and deploy it through the plane's bottom, the wing structure could not be joined through the fuselage. Although the configuration was ranked high, it was decided that this setup would not provide enough structural support for the aircraft to complete its mission.

2.5.1.2 Mono Mid-wing

This configuration is nearly the same as the mono low wing, except the wing is mounted midway between the top and bottom of the fuselage. Likewise in this setup, the wing structure would not be strong enough to support the craft in flight.

2.5.1.3 Mono High-wing

Similar to the mono mid-wing and mono low-wing, this configuration would consist of a single wing. It would be mounted at the top of the fuselage, with the quarter-chord aligned with the center of gravity. This configuration is structurally beneficial because the main wing spar could extend across the top of the fuselage, whereas this would not have been possible for a mid-wing, or a low-wing.

2.5.1.4 Flying Wing

This design has very good aerodynamic characteristics, but is not very stable in flight. The team had difficulty with this configuration in the past. Upon weighing these considerations, the configuration was rejected.

Table 2.4 FOM for Wing Types

	RAC	Weight	Lift and Drag	Manufacturing	Assembly Time	Total Out of 100
Importance:	**4**	**5**	**3**	**5**	**3**	
Mono Low	4	4	4	4	4	**80**
Mono Mid	4	4	4	4	4	**80**
Mono High	4	4	5	5	4	**88**
Flying Wing	4	5	4	4	4	**85**

2.5.2 Empennage Selection and FOM Analysis

Since the team ruled out the flying wing, it was decided that the plane would require a tail to be stable in flight. Several different configurations were considered. Table 2.5 shows the empennage configuration FOMs.

2.5.2.1 Conventional Tail

The conventional setup is defined as a vertical stabilizer at the center crossed with a horizontal stabilizer at its bottom. This setup is found on most aircraft today, and is thus stable and reliable. This design would be very easy to build and setup mechanically. Because the conventional tail reacted well to these project drivers, it had a high FOM ranking.

2.5.2.2 Canard

This configuration called for placing the main lifting wing towards the tail of the airplane and the horizontal stabilizer toward the nose. Historically, this configuration has good aerodynamic characteristics, but this configuration requires an unstable CG location for optimum aerodynamic performance. The main lifting wing would need to be larger than its conventional counterpart. This is because the wing has to be sized for takeoff without flaps, so that the canard always stalls before the main wing. In order for the canard to be efficient, it would have to have a high aspect ratio, which would require a heavy complicated structure. The possible instability, increase in RAC due to wing size, and increased horizontal tail weight caused this concept to have a low FOM rating.

2.5.2.3 T-Tail

The T-tail was inadequate because it had several problems. Blanketing of the horizontal tail was one of these problems. The team thought that the horizontal stabilizer would be blanketed by the wings at high angles of attack and the radome at lower angles of attack.

2.5.2.4 V-Tail

The V-tail has a lower comparative RAC, and would be relatively simple to construct. However, it was thought that it might not provide the amount of directional stability because of size limitations imposed by the travel box.

2.5.2.5 Y-Tail

The Y-tail has good directional stability. Unfortunately, this tail arrangement produces adverse yaw in turns due to the tail's anhedral. This would make the configuration have higher trim drag during turning flight, which is undesirable. The anhedral and servo mixing would make this configuration difficult to build and setup. The combined cost of a V-tail with an extra vertical surface would result in a high RAC. Finally, this tail configuration would be difficult to fit inside the travel box.

2.5.2.6 H-Tail

The H-tail was ranked highest because it would easily integrate with the two-boom fuselage structure. The two vertical stabilizers of the H-tail raise its RAC; however, the vertical tails have an endplate effect which lower the required horizontal tail area. These factors resulted in the H-tail having the highest empennage FOM ranking.

2.5.2.7 Inverted V-Tail

The inverted V-tail was rated very similarly to the regular V-tail. The inverted V-tail does not have the adverse yaw effects that the V-tail has. The inverted V-tail would have fit well between the two booms of the fuselage configuration; however, there were blanketing concerns, as well as concerns that the tail would be too tall to fit in the box. Because of these undesirable design elements, the inverted V-tail had a lower FOM score.

2.5.2.8 Inverted Y-Tail

The inverted Y-tail has good stability characteristics. However, it would have the same RAC score as the regular Y-tail, as well as an extra servo. It would also be more difficult to build and fit inside the box. Therefore this configuration was rated low.

Table 2.5 Tail Design FOMs

	RAC	Weight	Lift and Drag	Manufacturing	Assembly Time	Total Out of 100
Importance:	**4**	**5**	**3**	**5**	**3**	
Conventional	3	4	4	5	4	**81**
Canard	2	3	2	3	4	**56**
T-Tail	3	3	3	4	3	**65**
V-Tail	5	4	4	3	4	**79**
Y-Tail	4	3	2	3	3	**61**
H-Tail	4	3	4	5	5	**83**
Inverted V-Tail	5	4	4	3	4	**79**
Inverted Y-Tail	4	3	2	3	3	**61**

2.6 Landing Gear Conceptual Design

The team spent the first meetings compiling a list of basic design configurations that could be used. With the overall design of the aircraft requiring that the 5-lb payload box drop from the belly of the vehicle and the competition requirements calling for the aircraft to fit within the 1 x 2 x 4 foot box, the main gear would have to be tall, more than 10 inches in height, as well as collapsible. With this in mind, the initial concepts were divided into fixed, mixed, and fully actuated retractable designs.

2.6.1 Fixed Gear Designs

Fixed gear appeared very attractive because of its simplicity and inherent reliability. Most ideas featured a socket/plug design in which a loosely attached strut, linked to the fuselage with elastic or some other type of chord, could be quickly swiveled down and locked in place for flight. Other ideas evolved using hinged connections and various locking mechanisms. One of the final fixed gear designs featured a completely free set of struts sporting an expansion lock at the upper end. The strut would fit snugly into a deep well embedded in the fuselage that was integrated into the main structural trusses of the body.

2.6.2 Fixed/retractable Composites

A second approach involved installing pre-built, commercially available retractable gear assemblies into the aircraft. Instead of using these assemblies in their original form, however, the drive mechanisms were disabled. In this way, the team could use the already proven locking cams featured in these units to fix the main gear in the extended/down position, but without the added weight and complication of the servos or pneumatic equipment needed to actuate them in flight. On the ground, prior to flight preparations, the gear could be easily retracted manually to fit into the required space.

2.6.3 Fully Actuated Retractable Designs

The third approach investigated was a fully actuated retractable configuration. These designs offered a substantial savings in drag over fixed designs. Additionally, retracting the gear into the fuselage would serve to move the substantial mass of the struts, wheels, and dampers closer to the aircraft's center of gravity during flight, reducing the amount of energy spend performing aerial maneuvers. Unfortunately, conventional retracts would consume a large amount of fuselage volume bringing 10-inch struts and wheels inside and housing the servos or pneumatic equipment needed to operate them. Initially, commercially available retract units were considered with the intention of retracting the struts inboard and having them overlap in order to fit inside without further altering the width of the fuselage. Later in the design process, a more exotic concept was conceived.

Given the large, flat side panels afforded by the airfoil fuselage design, the team began to investigate the possibility of mounting retractable gear outboard of these panels and fairing them into the fuselage. This resulted in the introduction of a 'pull-pull' gear design. The proposal called for only one servo to drive both main gear struts, as opposed to the two needed for conventional mechanical retracts and could be constructed without a large amount of specialty machine work.

2.6.4 Gear Selection and FOM Analysis

Once a full list of configurations had been compiled, the team members took time to weigh each option against the others in terms of cost, weight, drag, ease of manufacturing, and ease of integration with the current fuselage configuration (Table 2.6). Based on research and personal experience, the team decided to take a calculated risk and continue on with the 'pull-pull' retractable design.

Table 2.6 FOM for Landing Gear Configurations

	RAC	Weight	Drag	Manufacturing	System Integration	Total Out of 100
Importance:	**2**	**5**	**5**	**5**	**3**	
Fixed Port	5	5	1	5	1	**68**
Fixed Hinge	5	3	1	5	5	**70**
Mix	1	5	1	3	3	**56**
Pre-built Pneu.	1	1	5	3	1	**50**
Pre-built Mech.	1	1	5	3	1	**50**
Pull-pull	5	3	5	5	5	**90**

3. Preliminary Design

3.1 Preliminary Design Summary

The team began preliminary design by dividing into component-teams. As discussed in section 1.2, each team was responsible for the preliminary and detailed design of some portion of the aircraft. Preliminary design consisted of individual team discussions, analysis using FOMs, and decision-making for critical components of the aircraft.

3.2 Preliminary Wing Design

The wing team first analyzed its two mission criteria: flight performance and assembly. By referencing past competition results, it was concluded that flight time was the primary factor, above RAC and report score, in deciding the outcome of the competition. To achieve a superior flight time during a sortie, a wing with high lift and low drag would be needed. To have a takeoff distance less than the maximum 120 feet at gross weight, the wing also needed enough lift to fly given the low thrust of the electric motor, and low weight of the payload. Also affecting flight time is the assembly time; the team must assemble the plane out of the 4 x 2 x 1 foot travel box to flight ready status. The assembly time is added to the flight time, the most influential factor of the competition, as determined by comparison calculations. To achieve the best flight score possible, the team needed to design a wing that was simple and quick to assemble. The wing team was also responsible for designing tail structures to provide enough stability for the Draggin' Fly to fly successfully. The tail structures also need to be assembled quickly and fit inside the specified box. The overall goal was to create a wing that had high lift in ground effect, low drag at cruise, and efficient assembly. The same criteria of high stability and low drag were considered when designing the horizontal and vertical stabilizers.

3.2.1 Wing Airfoil Selection

In order to fit the entire aircraft in the box with only detachable wings, an airfoil with a very low pitching moment would be required. The airfoil also needed to have a high C_{Lmax} and low C_D. Using this criteria, the wing team began its search for an airfoil. The wing team searched the low speed airfoil data from the m-selig, UIUC website[7]. From this database, the wing team selected three airfoils for consideration, the Eppler E387(c), the S7075, and the SG6043.

The driving factors of all three airfoils were collected and analyzed at a Reynolds number around 300,000. This Reynolds number correlates well to the Reynolds number 349,839 initially calculated by the team at cruise. Table 3.1 lists the C_{Lmax}, C_m, C_{Dmin}, and thickness to chord (t/c) ratio of all three airfoils. As can be seen from the table, the SG6043 had the largest value of C_{Lmax}, but also had the highest pitching moment. The E387(c) and the S7075 airfoils had very similar performance, though the E387(c) had the larger C_{Lmax} and the lowest C_m values. After comparing the data, the wing team chose the E387(c). The SG6043 was ruled out because it had the highest drag and moment coefficients,

despite its high C_{Lmax}. The team chose the E387(c) over the S7075 because it had a lower moment coefficient, a higher maximum lift coefficient, and comparable drag coefficients.

Table 3.1 Airfoil Data

Airfoil	Clmax	Cm	Cdmin	t/c (%)
E387(C)	1.33	-0.085	0.0147	9
SG 6043	1.4	-0.188	0.025	9
S 7075	1.26	-0.088	0.0143	10

3.2.2 Wing Planform Area

In order to approximate the takeoff performance of the airplane, an Excel code called "Takeoff" was used. This code has three primary variables: maximum gross weight, wing planform area, and static thrust. The output of the code is takeoff distance as a function of the aforementioned variables.

Using the known weight of the payload and approximated weights of the airplane components, the team calculated an estimated maximum weight of the aircraft to be 19 lbs. Next, the team used the computer program Motocalc™, to estimate the amount of static thrust that the motor could provide. Preliminary Propulsion/Flight Mechanics estimates predicted a static thrust of 10.5 lbs. The wing team decided to use a more conservative 9.75 lbs of static thrust to enter into the Excel "Takeoff" code. The team assumed an elliptical lift distribution over the wing. With a C_{Lmax} of 1.3, the team integrated to find the approximate C_{Lmax} along the wing to about 1.0. Abiding by competition rules, the aircraft must take off in one hundred twenty feet or less. Using this number as a reference and entering the above approximations into the Excel code "Takeoff," the team calculated a required planform area of 6.74 square feet.

3.2.3 Wingspan, Chord, and Taper Ratio

Though an elliptical lift distribution is desired aerodynamically, an elliptically shaped wing is very difficult to manufacture. This wing shape would either require a complex molding, or a significant amount of complicated wing ribs and spars to construct. Because of these production difficulties, the team decided not to use an elliptical wing. The wing team decided to explore tapered wings in order to maintain some of the desired characteristics of elliptical loading, while simplifying manufacturing. The wing team's research found that a taper ratio of 0.4 for a straight wing provides a nearly elliptical lift distribution[1].

A tapered wing has less area than a straight wing with the same span and chord dimensions. According to the rules, the wingspan and chord contribute to a large portion of the RAC. Thus, an optimal range of span and maximum chord had to be found. The wing team decided that the root chord must be greater than 12 inches for a taper ratio of 0.4. This would give a tip chord of about 4.5 inches, which

gives the wing a maximum thickness of less than ½ inch. The team decided this would be too thin to support the necessary loads. When the root chord was increased to compensate, resulting in an increase of the maximum thickness of the airfoil, cross sectional area, and parasite drag. Because of the drastic increases that occurred when the wingspan was lengthened or the maximum chord was increased, the wing team decided to increase the taper ratio to 0.6. The new taper ratio would also provide a near elliptical lift distribution; because of this and the improved structural characteristics, the team decided to use the higher taper ratio and larger root chord. The final dimensions called for a 6.75 foot wingspan, 14 inch root chord, and 8.4 inch tip chord. With this configuration, the wing root had a maximum thickness of 1.25 inches and a maximum thickness at the tip of 0.75 inch. This decision provided the team with the needed area, reduction of induced drag, and an RAC within acceptable limits.

3.2.4 Aileron and Flapperon Sizing

The size of the ailerons was determined with a graph of total aileron chord versus total wingspan and wing chord[6]. The team chose the largest possible area for the ailerons within limits. The final aileron dimensions were decided to have an 18-inch span and 2-inch chord. Each aileron was placed two inches inboard from the tip in order to decrease wing tip vortices and reduce induced drag caused by the ailerons.

Considering takeoff distance requirements, estimated total weight, and maximum static thrust, the ailerons were designed to also be used as flaps, called flapperons. Employing flapperons would increase maximum lift during the takeoff run without increasing the wing area. Flapperons can also increase drag, allowing the airplane to descend quicker and fly slower; this would ease the task of landing.

3.2.5 Horizontal and Vertical Tail Foil Selection

Ease of construction and strength for landing were the primary restraints for the tail surfaces. It was decided to use flat plates for both the vertical and horizontal stabilizers in order to decrease drag. This decision was supported by the fact that the team had calculated that the tails would be operating below the 140,000 Reynolds number threshold where flat plates are just as good as cambered airfoils.

3.2.6 Horizontal and Vertical Tail Sizing

According to the specifications of the fuselage team, the airfoil section of the fuselage was to be 13 inches wide and 27.375 inches long. Since the box is 48 inches long, this meant that the tail boom could be no longer than 22.2 inches. Other items to consider were the thickness of the propeller at the front of the aircraft and having extra room to be able to pick the plane out of the box without binding. Adding these two considerations into the formula, the wing team shortened the boom length to 15.2 inches, bringing the total fuselage length to 43 inches.

Using the moment arm specified above, required areas for the vertical and horizontal stabilizers were determined using Raymer's[6] method based on traditional composite kit airplanes. The total area

required for the vertical tail was 135.57 square inches and the area needed for the horizontal stabilizer was 195.5 square inches. Before proportioning the dimensions of the vertical tail, the total area was halved. This was done because of the H-tail. Since there were two vertical tails, the area of each could be added together for the total required area.

The RAC rules specify that any horizontal surface that is greater than 25% that of the total wingspan will be considered as a second wing, which increases the RAC. To avoid this penalty, the horizontal tail span was set at 20 inches, which is 24.69% of the total wingspan.

Due to box specifications, the vertical tail height is limited to a maximum of one foot. To allow for some extra room, the vertical tail height was set at 11 inches. To achieve the required area, a maximum chord was set at 7 inches. The corners of the vertical tails were swept and rounded for desired aerodynamic and aesthetic characteristics.

The tip chord of the horizontal tail was set at 7 inches, in accordance with the maximum chord of the vertical tails. This chord length however, did not provide enough area for proper stability. To compensate, the central chord of the horizontal stabilizer was increased to 10.5 inches. This inner section had a span of 13 inches between the two tail booms. The outward tips were tapered from 7 inches up to 10.5 inches.

Section 3.3 Preliminary Fuselage Design

The fuselage airfoil shape was an integral part of the preliminary design of the fuselage. Since the goal of the fuselage shape was to produce a minimum drag body, and not a lifting body, a symmetrical airfoil was chosen. The NACA 4-digit series symmetrical airfoils were then selected because of their well-known characteristics, and ease of manufacture. With the selection narrowed, the optimum thickness to chord (t/c) ratio was required. The team used the shareware program "Xfoil version 6.94[2]," developed by Mark Drela at MIT, to evaluate the drag of the different t/c ratios. The flight condition selected for inspection was cruise, using a $\rho = 0.002377$ sl/ft^3, $\mu = 3.737e\text{-}7$, maximum thickness (t_{max}) of 7", and V = 50 mph. The team used Xfoil's built-in NACA 4-digit series generator to define the airfoils, specifying the t/c by specifying the series number, i.e. t/c = 18% was entered as NACA 0018. The Reynolds number was computed for each airfoil because it varied with the t/c ratio used, and M was specified at 0.0657. Using the viscous routine, the characteristics of the airfoil were computed at an angle of attack, α, of 0°. With the drag coefficient from Xfoil recorded, the team wrote a Matlab script "fuse.m" that calculated the drag based on planform area of the fuselage. Figure 3.1 shows the output of this script file. Using this graph the team decided that a 27% thick NACA airfoil would be the shape of the fuselage.

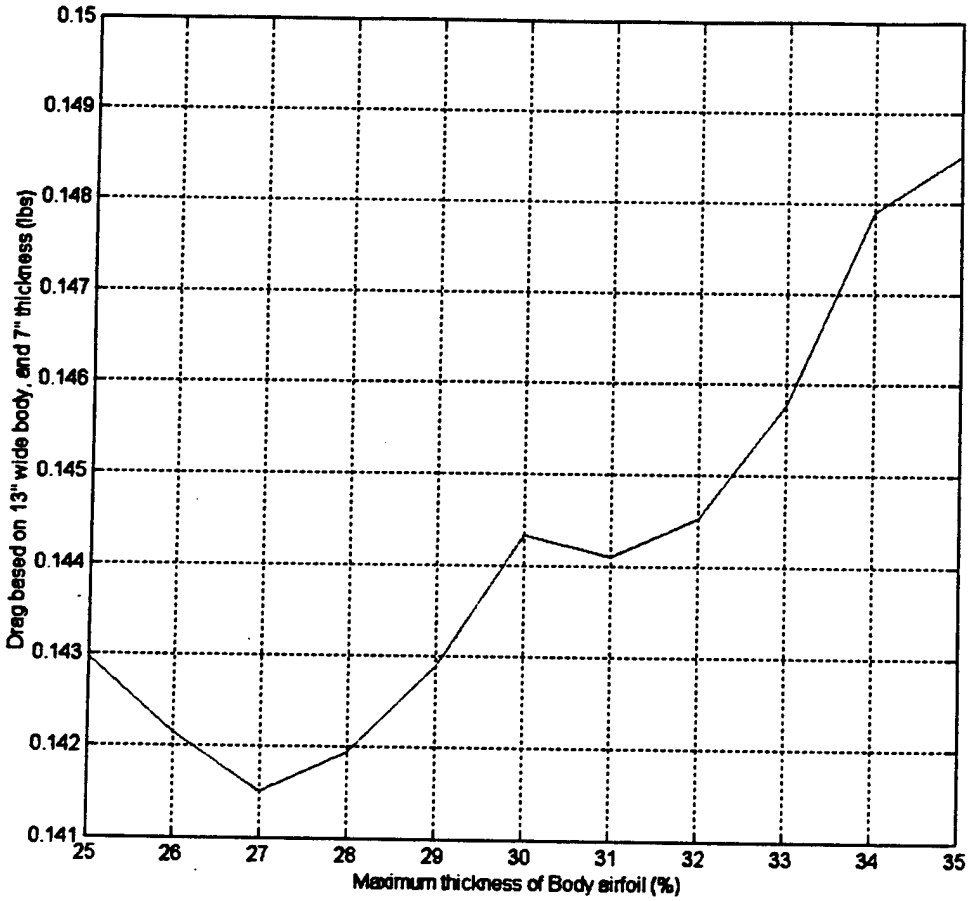

Figure 3.1 Graph of 2-D Drag based on Re and Planform Area

Section 3.4 Landing Gear Preliminary Design

Development of a viable, high-performance landing gear design became a priority out of necessity. Over the course of planning, landing gear configuration became one of the most discussed and fluid aspects of the overall craft design. In the opening stages of the team's conceptual design process, initial sketches of the airframe from the configuration chosen depicted a large fixed landing gear assembly mounted under the fuselage just ahead of the payload bay. These work in conjunction with a set of small tail wheels, one at the base of each of the vertical fins in the H-tail. This would form a four-point, four-wheel gear set with exceptional ground stability, good handling characteristics, plus, the ability to taxi "over" the payload box once it had been deployed on the runway. The exact positioning, attachment method, and specific design of the struts and wheel assemblies would be decided during detailed design. Final design of the gear was delegated to the Fuselage Team to ensure a problem-free integration with the main structural components of the airframe.

Due to the placement of the payload box within the fuselage, the landing gear could not be retracted inside the fuselage. Although retracting the gear on the outside of the fuselage provided a configuration with less drag compared to fixed gear, even more drag savings could be obtained if a fairing was placed overtop of the retracted gear. Many different fabrication techniques were considered for the fairings. An initial prototype was made out of molded two-liter PET bottles. When emptied and pressurized, these bottles can be stretched and formed using a heat gun. However, once cut, the plastic curled and formers were needed to make the parts conform to the necessary shape. These formers obstructed the motion of the landing gear, and the fabrication technique was abandoned. Additional fabrication techniques that were considered included: vacuum forming the fairing out of a single sheet of PET or similar plastic or molding the fairing out of fiberglass on top of a mold carved out of foam. Since the latter method required fewer tools, it was deemed more feasible.

To allow the gear to retract inside the fairing, a portion needed to be left open along the bottom of the fuselage. It was debated whether or not this opening should be covered when the gear was retracted. Covering this slot could be accomplished by attaching the section of the fairing cut out for the slot to the landing gear strut. However, it was debated if this design would increase the drag when the gear was in the extended position. A second method was suggested in which the entire fairing hinged away from the fuselage. Figures 3.2, 3.3, and 3.4 illustrate multiple views of the landing gear concept.

Single servo drives both landing gear struts

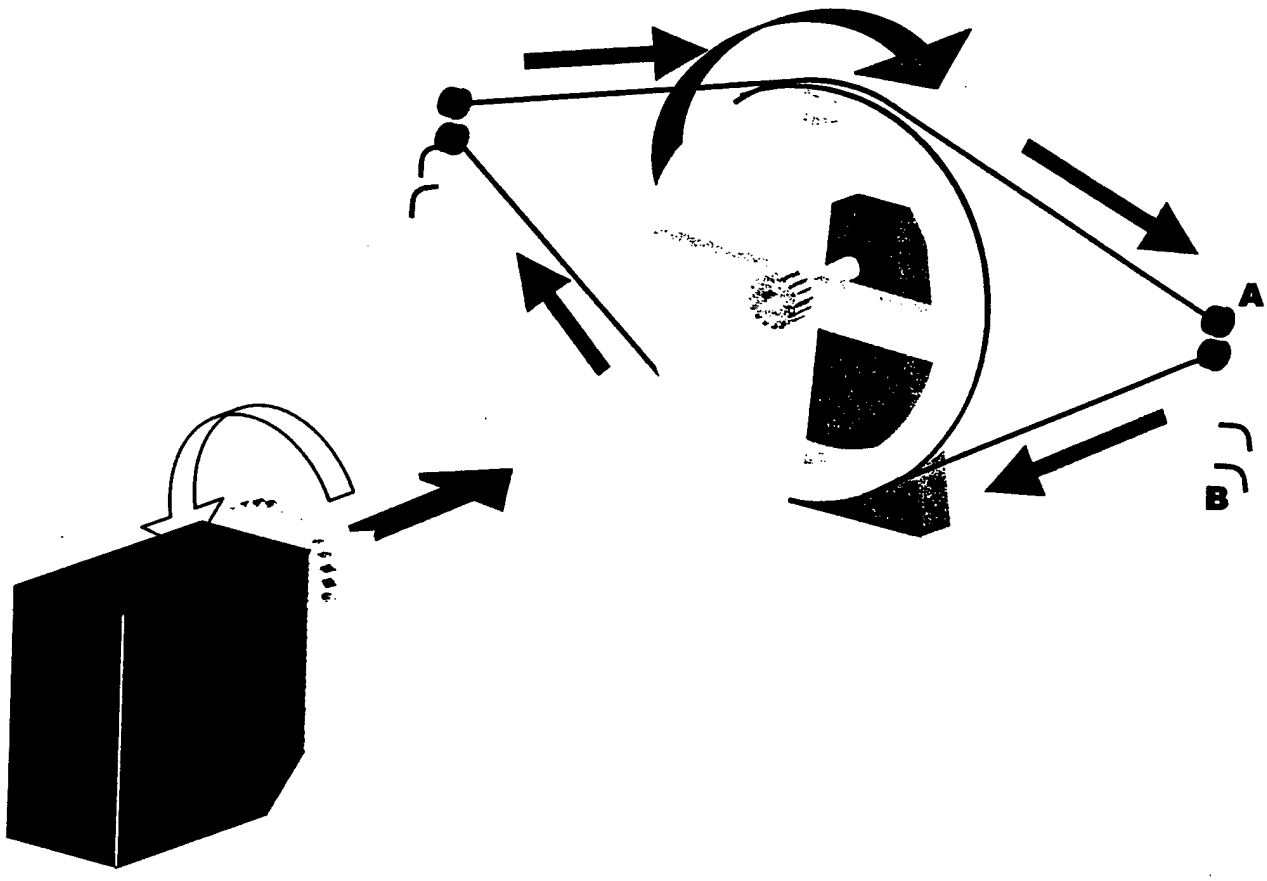

Dimensions: Servo: 1.54 x 0.79 x 1.38 inches
Main Drive Wheel: 2.5–3.0 inches x 1/8 inch
Gear Ratio: At least 1:2

-As Drive Wheel turns two control lines are retracted while the remaining two are given slack at an equal rate.

-Use of a retract servo w/ internal locking mechanism secures landing gear in the retracted or extended position.

Figure 3.2 Landing Gear Concept Internal Components

Side View

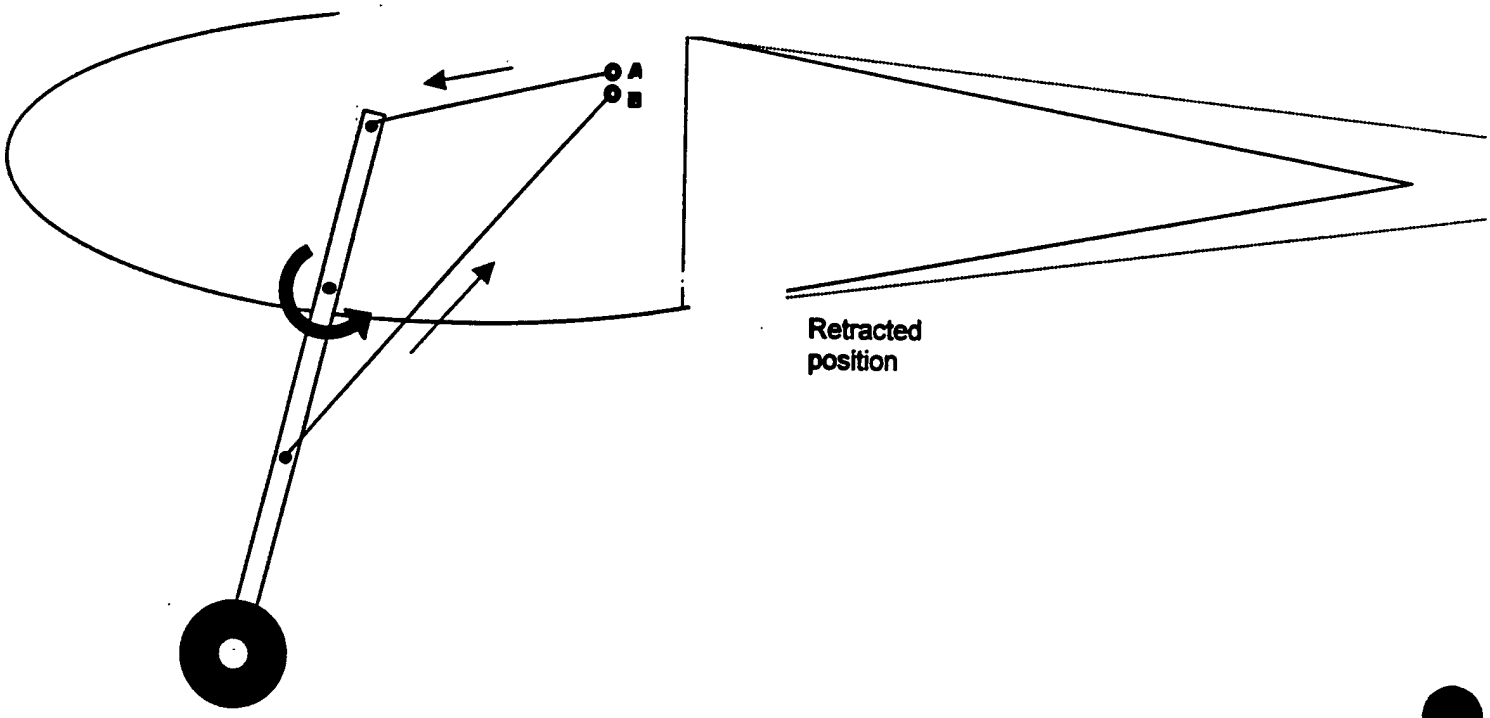

Front View

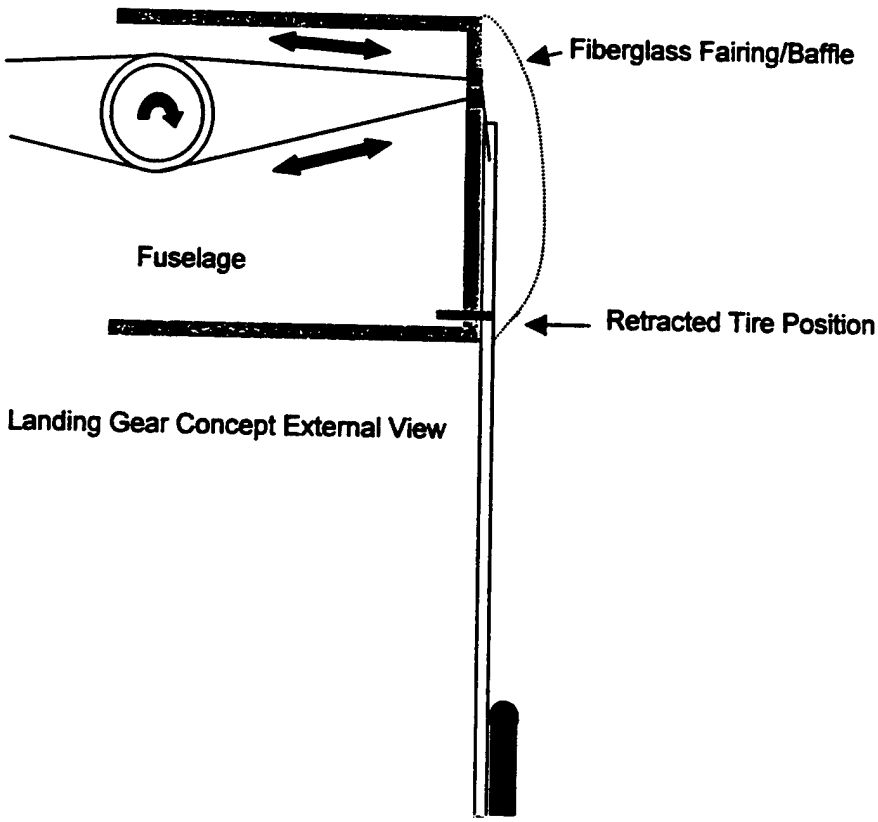

Figure 3.3 Landing Gear Concept External View

Side View

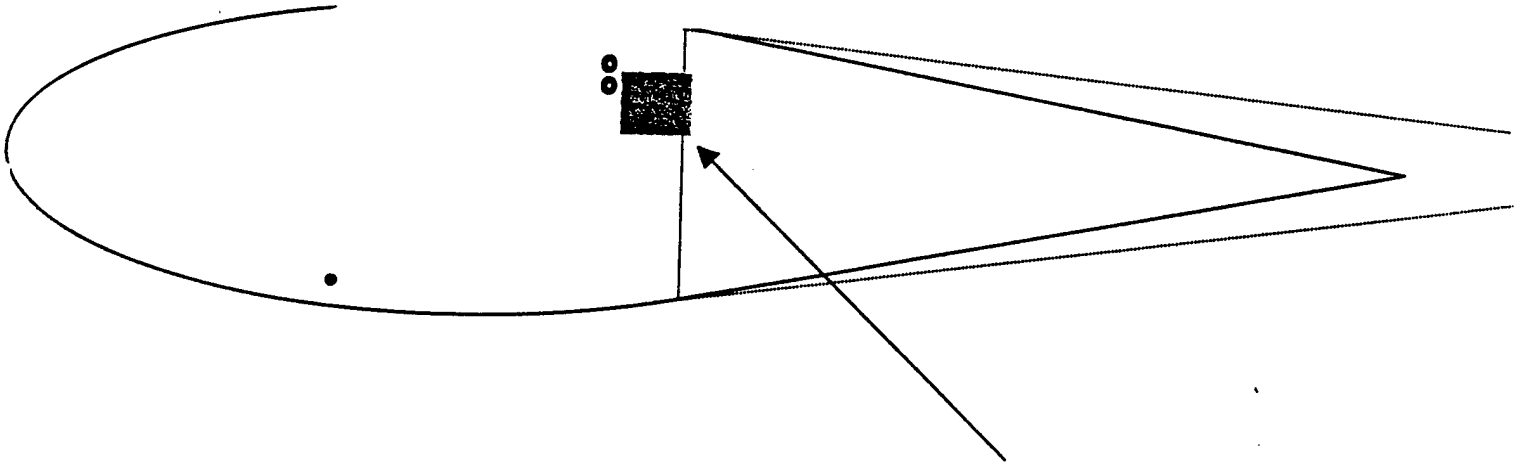

Top View:

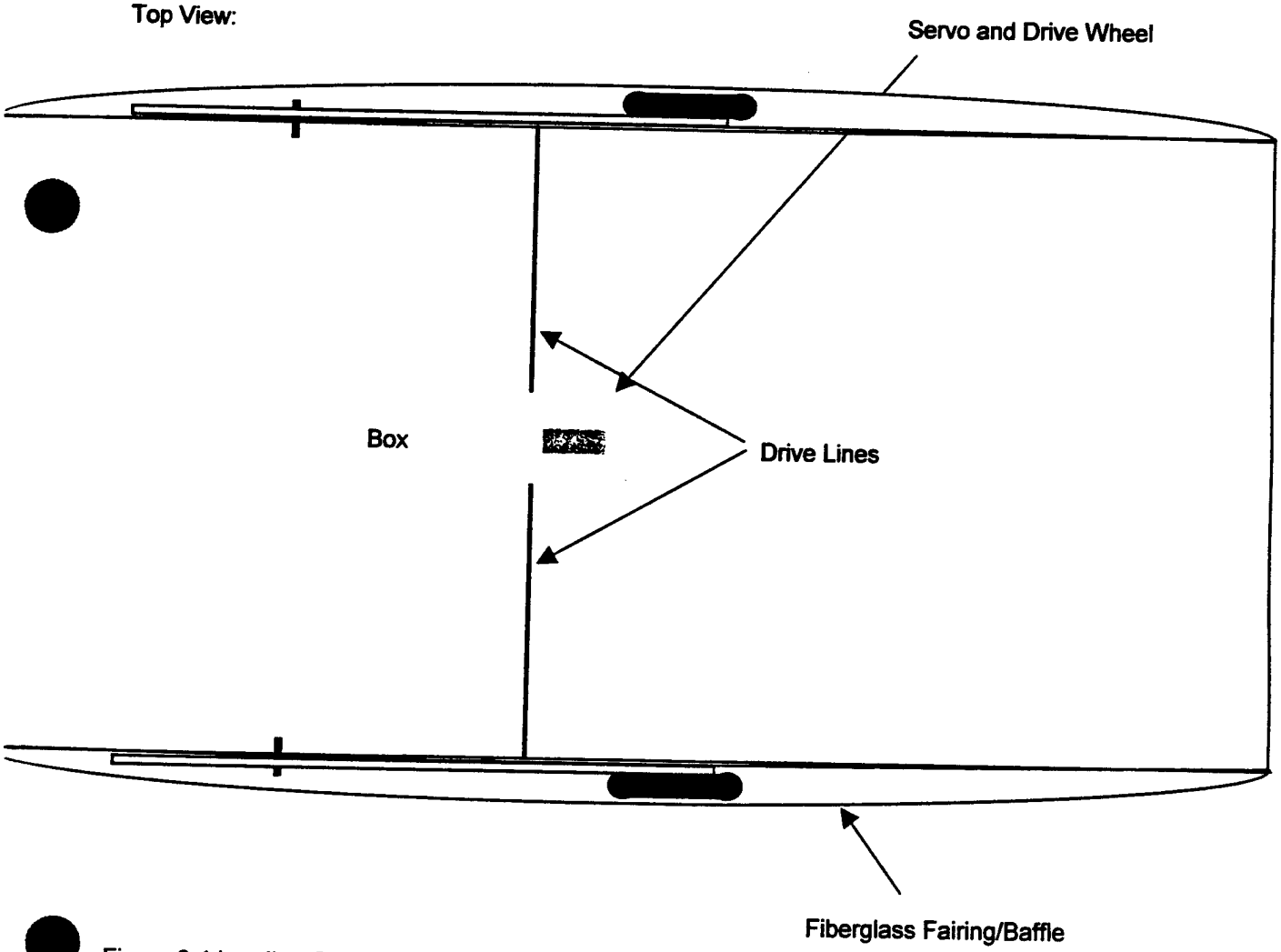

Figure 3.4 Landing Gear Space Allocation

Section 3.5 Payload Preliminary Design

The first payload concept began as a double door situated in such a way that a series of four clips attached to a cable could be pulled by a servo. When the servo pulled the clips to the open position, the door would open due to the weight of the payload. The clips would be spring-loaded and would be beveled such that when the payload was fully deployed and the door closed, it would be able to push the clip out of the way and return to its closed position. The door would have a receiving set of clips that would line up with the moving clips.

The second design utilized a single door that would have a hinge on one side and a series of clips on the other side. When the clips were opened, the payload would open the door due to the weight of the payload. A set of torsion springs would be attached to the hinge side to close the door once the payload was deployed. The clip system would consist of a series of moving and receiving clips. The moving clips would be attached to a rod and have their spring-loading action replaced by a servo that could turn them to either the open or closed position. The receiving clips would be attached to a frame and the fuselage fiberglass shell would then be glued on to the frame after. The clips would be L-shaped and have a bevel on the bottom so that the door could close.

The third payload deployment scheme involved a standard piece of angle iron that could be used to make the moving clips. The receiving clips on the door would be eliminated due to the fact that the payload would have to sit on top of them, thereby increasing the amount of space needed. The door would consist of a frame structure that would sit on the clips and would have a self-closing hinge assembly utilizing torsion springs.

On further thought, the team came up with three different types of torsion springs. They were: a standard torsion spring that would be mounted onto the main hinge pin, a self-closing piano hinge, and a turnbuckle that would be mounted between two supports and would have a bar integrated into the door that would also pass through the tightened cables. The payload would deploy automatically when the clips were turned to the open position due to the weight of the five-pound payload and would close once the weight was dropped due to the torsion mechanism.

Due to an inability to locate any self-closing piano hinges and the necessary strengthening of the turnbuckle in places that would not normally need strengthening, it was decided that a rod would form the hinge and that either a standard torsion spring would be set on the rod or a spring would be run form the clip side of the door to the main spar. Both would be designed to be weak enough to allow the payload to drop when the clip was opened, but strong enough to lift the door back to closed position.

A hinge consisting of a set of interlocking fingers with a rod running through them was decided upon. Two types of doors were considered: one made of wood with triangular holes and another made of a typical wire shelf frame.

A model of each door idea was built and weight was the deciding factor for which door to choose. The wood door was found to weigh one-quarter as much as the metal door. Thus, the wood door was chosen.

3.6 Antenna Preliminary Design

The team decided during conceptual design to place the radome on top of the aircraft. In preliminary design, the team considered several methods of attaching the antenna. The first method for attachment considered would be a bolt of some sort that ran through the central axis of the radome into a plate anchored to the main wing spars. It would be raised 3 inches above the aircraft by means of a symmetric airfoil or cylinder. For ease of assembly, the nut would be attached through the payload bay. The nut would be imbedded into the attachment plate. When attaching the radome, the bolt would be screwed on from the top.

The team considered cutting a hole into the top skin of the wing and having a receiving post that the antenna base could slide over to eliminate the long bolt that would be needed, thereby eliminating the weight of the bolt. A pin of some sort would have to be placed through the whole airfoil to keep it attached to the post. The team also considered buckles in lieu of a bolt or pin, but the buckles were considered undesirable because of low strength and difficulty in locating for purchase.

Instead of cutting a hole into the top of the aircraft, making a set of doors seemed more practical. However, this idea was later dropped because it would be too hard to close the doors when the radome was mounted, and on the missions without the radome there would be a hole in the skin.

The team discussed the first idea again, replacing the long bolt with two short bolts. A long screwdriver would be needed to reach the bolts, which would be permanently affixed to two nuts on the bottom of the radome. In order to attach the radome, it would be placed on top of the airfoil guided by a series of pins that would line up the bolts with their holes. Then the screwdriver would be used to screw the bolts into the aircraft. Figure 3.5 shows a preliminary drawing of the antenna.

Leftover angle iron could be used to make attachments for the internal mounting plate. Also, bolts were eliminated and replaced with threaded push rods that would screwed down from the top and anchored into the small nuts that are used normally with them. To distribute the forces on the small nuts, a series of larger washers would be used.

The team decided on the bolt idea, except with the bolts permanently attached inside the airfoil and the nuts screwed on through the payload opening. Two inside posts would be added to run from the bottom plate up to a top plate to help absorb any shock generated from landing.

After analysis, it was discovered that using the designated airfoil would have a Reynolds number close to the previously mentioned flat plate threshold. Thus, the team decided to use two angled, flat plates for support and stability. They would be joined into two different angled blocks inside the fuselage and into a beam internal to the PVC piece.

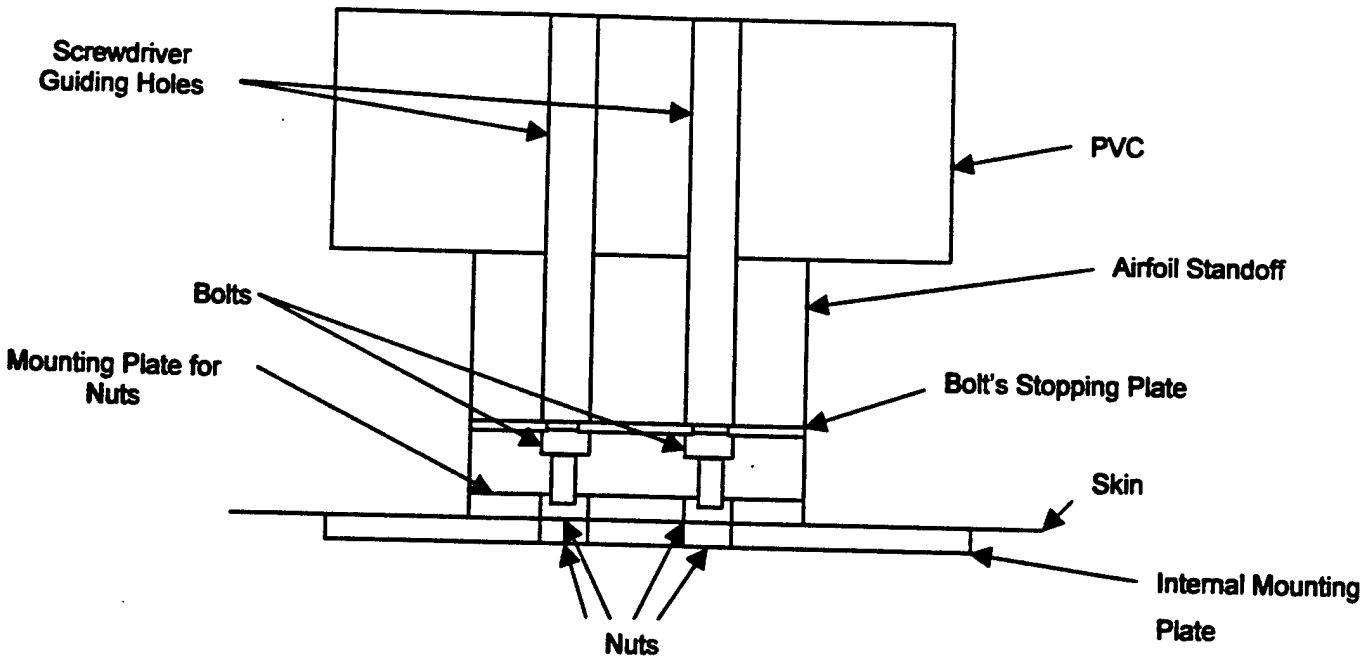

Figure 3.5 Preliminary Antenna Design

Section 3.7 Propulsion and Flight Mechanics Preliminary Design

The propulsion team had to choose the motor and batteries during the preliminary design. These choices were made from analysis of performance calculations estimated and updated from the wing and fuselage teams as their numbers became solidified. Parts were chosen based on the following criteria:

- Propeller diameter must be less than 24 inches to fit in the box.
- Battery pack must weigh less than 5 lbs.
- Battery endurance must exceed 5 minutes with changing throttle setting.
- Battery current must not exceed 40 amps.
- System static thrust must be at least 10 lbs to satisfy the takeoff distance.
- Steady state engine temperature should not exceed 350° F.
- Top speed should be greater than 45 mph to effectively compete.
- Components should be economically available.
- Configuration should have the minimum RAC to raise the total score.

Several engine configurations were tested and analyzed with propeller diameters ranging from 12 inches to 24 inches to fit in the required box and vary height above runway. There were three initial engine possibilities analyzed in both geared and direct drive configurations: dual Astro 40s, a single Astro 60, and a single Astro 90. Analysis was performed using Capable Computing's Motocalc Software Suite™. Inputs into Motocalc™ included many filters for analysis, several of these were provided by the

selection criteria. The team determined that dual Astro 40s would not provide sufficient additional performance to offset their high RAC and weight penalties. The Astro 60 was desirable for good performance to total cost ratio. The Astro 90 did not have sufficient RPM for top speed in a direct drive configuration. The engine was overpowered and inefficient using the available 2.75:1 gear ratio and the maximum diameter propeller. The optimum Astro 90 configuration required the use of a gearbox that was not commercially available. The team chose a configuration of the Astro 60, with a 2.75:1 Superbox gear box, and an Astro 204D speed control because of its performance levels and the team's current inventory.

The team conducted trade off studies with self-written computer scripts checking the performance of several battery amounts. The lightest battery found was the Sanyo KR-2300SCE with a weight of 2.05 oz per cell. This gave the team an upper cell count limit of 36, and the team calculated that 24 was the minimum number of cells required to complete the missions. These studies revealed that the use of 34 cells would optimize the RAC as well as provide ample thrust in the range of 210-248 oz. This amount of thrust allows for maneuvers while operating within required guidelines, and fit the flight time criteria. The battery type was selected as the Sanyo KR-2300SCE due to its high capacity to weight ratio.

The selection of the Astro 60 motor, and Sanyo KR-2300SCE batteries concluded the Propulsion / Flight Mechanics Team's duties during the preliminary design. This left the team with battery configuration and propeller selection to accomplish during detailed design. The team also had to analyze the Draggin' Fly aircraft's performance.

4. Detailed Design

4.1 Detailed Design Summary

With a clear vision of the final design, the component teams began the detailed design process. This included choosing materials and specific parts, integrating the various components of the aircraft, and analysis of the final design's performance.

4.2 Detailed Wing Design

4.2.1 Wing Joints and Connection

The midsection of the wing is 23 inches, and the quarter chord of the wing is mounted at 30% of the fuselage chord. Notches cut in the side panels of the fuselage 0.5 inches wide and 1.25 inches deep let the quarter chord spar pass through. Plywood tabs inserted between the I-beam caps against the shear web lock the spar into the fuselage. The whole assembly is bonded together with epoxy. The same setup is used to mount the rear spar to the fuselage.

The two outboard wing sections are 29 inches long. They plug into the 23 inch mid-section to create an 81 inch wingspan. The outboard wings have two 5 inch prongs that extend from the quarter-chord spar, and plug into sockets on the quarter chord spar of the inboard section. The rear spar has one plug on the outboard section that plugs into an opposite socket on the inboard section. Two plywood extensions on either side of the outer panel quarter-chord spars are for prongs that will guide the wing joining. Three prongs have holes at their ends into which slides a spring-loaded pin that is mounted on the inboard section. These pins lock the quarter-chord spar in place. The rear spar has a spring-loaded clip that holds it in place, and helps the prongs keep the wing in place.

The H-tail chosen in preliminary design was sized and designed for manufacturing. The tail boom is notched down 1/8 inch over the last 10.5 inches to facilitate horizontal stabilizer attachment. This will facilitate horizontal stabilizer attachment because both it and the vertical surfaces will be constructed out of 1/8 inch plywood. The horizontal stabilizer is glued with epoxy and supported by triangle blocks against the boom. The two vertical stabilizers are attached to the ends of the horizontal stabilizer. Triangle stock, carbon fiber strips, and epoxy attach the vertical stabilizers to the horizontal stabilizer.

4.2.2 Servos and Control Surfaces

During the final design, the team decided to place one aileron control surface on each wing. Analysis of the aircraft's takeoff performance showed a small margin of error. In order to increase the aircraft lift without increasing planform area, trailing-edge flaps were considered because of their simplicity and effectiveness. It was decided that the best way to incorporate both flaps and ailerons into the wing design was to provide the effects of each with a single control surface. During the landing phase, the ailerons will be deflected to act like flaps. Thus, the team named these control surfaces flapperons.

Once a single control mechanism had been decided on, it became necessary to design the exact dimensions for the flapperons. Typical trailing-edge flap systems span a large portion of the wingspan in order to increase the camber, and C_L, on as much of the span as possible. Raymer's historical data on aileron size versus percent chord length was used to get a rough dimension for the ailerons[6]. Further analysis showed that 18 inches of aileron per wing side would be optimum, leave room for the servo, and keep the aileron away from the wingtip, where it would be ineffective due to 3-D vortices created there. The servo was placed 9 inches outboard of the wing joint. Given this dimension and Raymer's method[6], the flapperon chord was determined to be 2 inches. In order to ease wing construction, the flapperon chord was kept constant despite the changing wing chord length. Another way to ease construction of the flapperon was to use a single plain flap. Generally trailing edge flaps work optimally when deflected 30°; this is the flapperon deflection during landing. In addition, the flapperon needs to move for roll control. 15° is sufficient to alter the lift on each wing and create enough rolling moment. Thus, the final flapperons will be able to deflect downward a maximum of 45° and upward a maximum of 15°.

Pitch and yaw control was necessary for the plane to complete its mission. Control surfaces were added to the horizontal and vertical tails. Upon review of Raymer[6], it was noted that both control surfaces typically make up about 90% of the tail span and from 25-50% of the tail chord. In the final design, the elevator will make up the entire horizontal tail span and have a constant chord equal to 1.5 inches. The elevator will be tapered inward so as not to conflict with rudder deflection. The rudder on each vertical tail will extend the height of the tails and have a constant chord of 1.5 inches. One servo is assigned to operate the elevator, with a maximum deflection of 15° in either direction. Another servo is dedicated to operating both rudders in unison, with a maximum 20° deflection permitted in each direction. Each tail control surface will be constructed as a single plain flap.

4.2.3 Electrical Connections in the Wing

The most important criteria for deciding what configuration the electrical connections to be used in the wing was time. The outboard sections of the wings were detachable, so the electrical connections had to allow fast and efficient assembly of the wing. Each wing has a stereo jack and a plug on it, and the stereo jack has three terminals. The servo to be used had three wires that correspond to the three terminals on the stereo jack. An extension is used to connect the receiver to the jack on each wing. Another set of extensions runs from the plugs to the servo. When the wings are attached, the servos are simply plugged in. This design of the electrical connections in the wing allows for a time efficient assembly.

4.3 Detailed Fuselage Design

After determining the airfoil for the shape of the fuselage as outlined in the Preliminary Design, the team created full size drawings to determine component placement and the internal structure of the fuselage. The airfoil was scaled up slightly to fit the increased height of the wing spar. To secure the cargo box and tie the fuselage to the wing spar, a simple truss system was designed. The truss consists of three sections, one on top of the cargo bay, and one in front of and behind the bay. Each member is made of ½ inch square balsa stock. A detailed picture of the internal bracing may be seen in Figure 4.1. Strips of carbon fiber reinforcement will be laminated to the truss members and wrapped around the fuselage sides, both to increase the stiffness of the truss, and to ensure that the truss will carry the loads incurred during landing without the fuselage sides separating from the truss. Gussets will also be utilized at the intersection of the truss and fuselage sides to ensure that the cargo will not shear the truss from the sides during a rough landing. The joint at the lower front of the truss will be reinforced with a thin plywood plate that will serve as a mount for the landing gear bearing block, and reinforcement for the door hinge mechanism.

Carbon fiber strips will also be laminated to the tail booms, and wrapped about the fuselage side at the intersection of the boom and the fuselage. Though each set of tail boom and fuselage side is cut from a single piece of plywood, the carbon reinforcement will ensure that the booms will carry the load of

a rough landing without separating from the fuselage. The reinforcement will also stiffen the booms against the side loads imposed during normal ground operations.

In addition to the main truss system, there will be a single ¼ x ½ inch hardwood stringer running across the front of the fuselage. The motor mount will be bolted to this stringer. An additional ½ inch balsa member will be mounted along the bottom of the motor and run between the front stringer and the front of the truss to provide support for the motor.

The section of the fuselage behind the truss will be used to mount the radio system. A single light balsa stringer will run between the fuselage sides at the very rear of the airfoil. The receiver and servos will be mounted to the inside of the fuselage sides.

A fiberglass skin will be laid up using the fuselage as a mold. The skin will be trimmed to allow for the motor gearbox protrusion, the tail booms, and the cargo bay door. A hatch will also be cut that will allow easy access to the motor batteries. The skin will be mounted to the fuselage utilizing a system of small balsa blocks and machine screws.

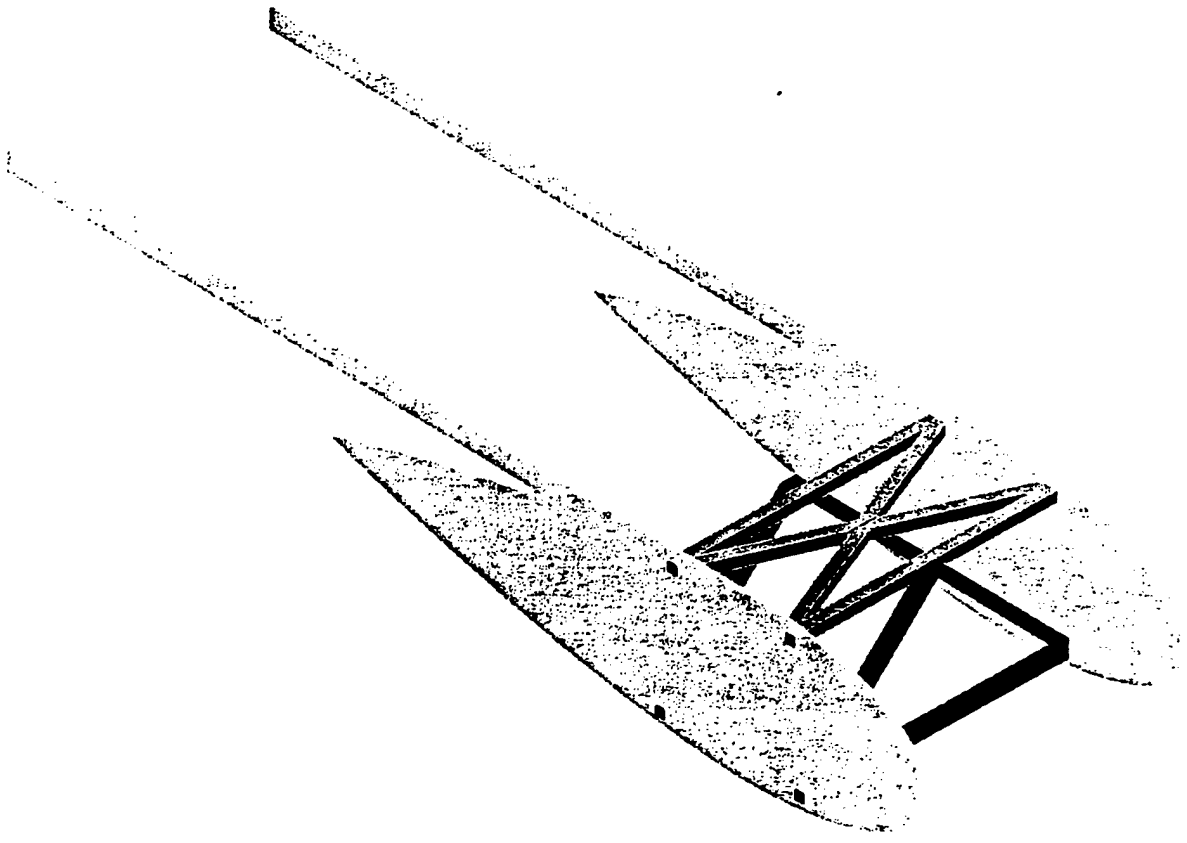

Figure 4.1 Detailed Fuselage Design, Internal Bracing

4.4 Detailed Landing Gear Design

Once the 'pull-pull' type landing gear had been chosen, a more detailed investigation and analysis was required before construction of the aircraft could begin. The next months saw the fuselage team devote large sums of time to developing a fine-tuned, well-designed final iteration of this hereto-untested configuration.

Early conceptual designs sported large, single piece struts with the pivot and driveline attachment points passing directly through their interiors. A single locking retract servo would be used to actuate the gear and fix the struts in the full-up or full-down positions. Four bumper-stops would transmit most of the forces at landing into the fuselage structure. Starting with the initial sketches produced during preliminary design, a full-scale fuselage mockup was created with the purpose of determining the correct geometry and orientation/placement of the gear systems. In later stages of the design's evolution, this mockup would serve as a test bed for failure trials of the final gear design. Construction of this mockup illuminated several major problems inherent to the team's initial design. First, despite the presence of the bumper-stops, even a small back-force on the lower end of the struts from wheel friction during landing would generate massive torques at the servo winch. These torques would easily destroy the comparatively fragile internal locking mechanism of the servo. A second problem materialized when the first struts were constructed. Passing the pivot and attachment holes for the drivelines through the struts' interior would invariably compromise the structural integrity of the system. A resolution to both of these problems came with a complete redesign of the struts.

In searching for a new way of locking the struts in the full-up and full-down positions without the addition of further power systems or unneeded complexity, the team was able to develop a simple and elegant solution that served to help solidify the validity of the entire gear concept. First, instead of passing the pivot and drivelines directly through the strut, they would be attached with aluminum collars. These would preserve the integrity of the strut and decentralize much of the force experienced at landing, spreading it over a much larger effective area. Next, instead of attaching the drivelines to these collars directly, they would be mated with a set of swiveling brackets. These brackets would in turn be connected with a simple mechanical linkage. As tension was transferred from one driveline to the other, the brackets would swivel to a small degree before allowing the strut to move. This swivel action was the basis for the whole locking system. A pin extending off of the upper bracket would ride along a newly cut slot in the fuselage as the whole strut assembly rotated up or down. At the upper- and lower-most extremes of its path, the slot made an abrupt 90° turn, continued for a short distance, and then terminated, forming small locking ports. As the strut approached the limits of its rotation, the tension on the driveline would pull/push the pin into one of the locking ports, fixing the entire assembly in either the full-up or full-down position. An additional benefit afforded by this new configuration was seen in the elimination of the locking retract servo. Instead, a much simpler and more powerful sailing winch servo could be substituted, removing the necessity of any complicated gearing needed to increase the number of rotations experienced by the drive wheel. This final change marked the end of major design changes

for the gear set. In its final iteration, the gear struts were constructed of 3/8 inch ID carbon fiber wrapped tubes and mounted Robostrut shock absorbers with 2.25 inch foam wheels.

4.5 Detailed Payload Deployment Design

The payload door is designed to carry the weight of the 5 lb payload and any load factors that may be incurred during a mission. It will be made of 1/8 inch plywood that has had fiberglass bonded to either side, and triangular holes cut into it to reduce its weight.

On the forward part of the door, there will be five glassed hinges, spaced evenly along the 13 inch width. The opposing side will be mounted to one of the beams in the fuselage. The aft portion of the door will sit on a set of Aluminum clips. These clips will be attached to a 1/8 inch diameter steel rod and the rod in turn will be attached to the fuselage. The rod will act as a pivot, which will be attached to a servo arm to allow the clips to swing out of the way of the door.

The door will open when the servo releases the clips open. When the clips are open, the door will fall open due to the weight of the payload. Once deployed, the plane will have to move forward so that the door can retract by means of a spring system that runs from the aft part of the door to one of the spars located at the top of the fuselage.

4.6 Detailed Antenna Design

Abiding contest rules, the radome will consist of a piece of 6 inch diameter PVC that is 3 inches tall. It will be attached to the top of the aircraft in such a way that the CG of the radome is at the wing quarter-chord, the CG location of the aircraft. The radome is sealed flush on both the top and the bottom by 1/16 inch thick plywood. It stands off of the fuselage skin 3 inches by means of two flat panels made of 1/8 inch plywood. The interior has a piece of 1/8 inch plywood glued to the bottom panel with two ½ inch plywood pieces glued to it. The ½ inch pieces are parallel to each other and have an inch between them. They are cut in such a way as to have the two supports enter into the radome and get glued to them. There are also other pieces of foam to add surface area that allows for more glue to be applied to the bottom/PVC joint. The two supports enter in at an approximate angle of 30°. The final design of the radome is illustrated in Figure 4.2.

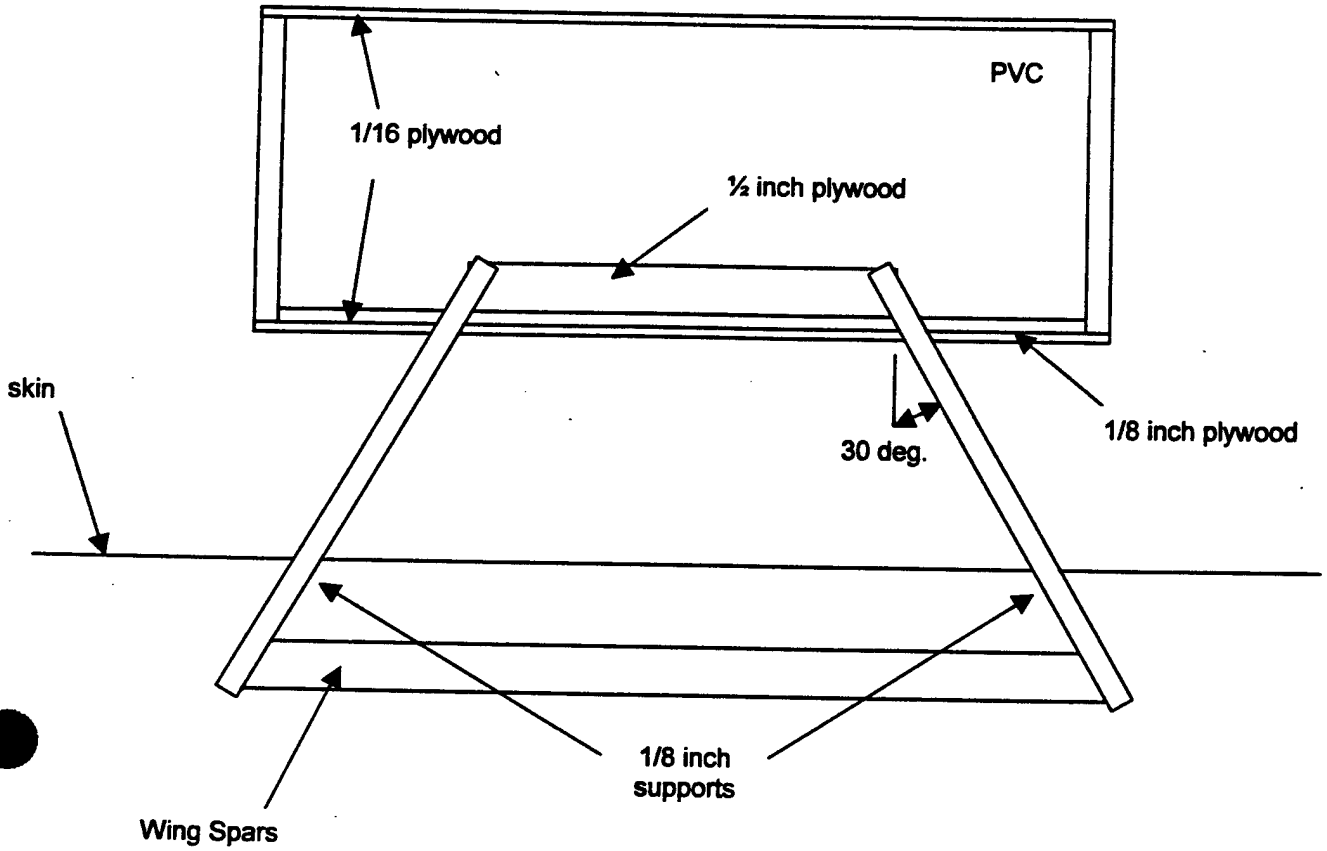

Figure 4.2 Sectional View of Radome

4.7 Detailed Propulsion and Flight Mechanics Design

In the Detailed Design the propulsion team needed to choose the propellers and the battery configuration, and analyze the final design's performance. The propulsion team developed multiple scripts to analyze the various performance aspects of the plane. One script mapped the flight course and estimated flight times based on average speeds for specific course sections. Another script took inputs from the flight time script, performed RAC calculations, and estimates on the report score and assembly time to predict the total score for various scenarios. This script was a major key in deciding which missions to attempt, and identified the dominant factors in the total score as the report, mission difficulty, and flight time. Lesser factors included the assembly time and RAC.

The first thing the team accomplished during detailed design was propeller sizing. Propeller sizes were limited to diameters between 12 and 24 inches, with a pitch range of 8 to 18 degrees. These constraints were chosen to satisfy box dimensions, runway clearance, and sufficient static thrust. The analysis was performed using Motocalc™. Inputs into the software suite included many filters to satisfy

the above constraints, based on the criteria outlined in the preliminary design and including the additions found in Table 4.1.

Table 4.1 Additional Motocalc™ Filters

Maximum current	40 amps
Maximum engine temperature	350° F
Minimum thrust	10 lbs
Minimum battery endurance	4 minutes at 100% throttle
Battery Pack	34 Sanyo KR2300SCE cells
Speed Control	Astro 204D
Gear Ratio	2.75:1
Propeller Diameter	Iterations of 12 to 24 inches
Propeller Pitch	Iterations of 8° - 18°
Wing Span	81 inches
Wing Area	971.6 square inches
Fuselage Weight*	96 oz, 176 oz, and 196 oz
Clmax	1.3
Cd	0.033 and 0.08
Clcr	0.84
*Depends on payload configuration, and does not include batteries, speed control, or motor.	

Motocalc™ included a wing airfoil profile that closely matched the E387(c); the team made slight modifications to the thickness and camber of the stored airfoil to match its C_{Lmax} of 1.3. According to Motocalc™, the Draggin' Fly should have a C_D of 0.075 at level flight. Motocalc™ predicted an L/D_{max} in the range of 8-12 depending on the presence of the radome. The two C_D values in Table 4.1 were used because of the changing drag of the aircraft between the Missle Decoy mission, and the Sensor Deployment mission.

When using Motocalc™ to select a propeller, the team implemented a few key ideas that would lead to optimum selection. In order to keep the motor at peak efficiency, reduce battery drain, maintain sufficient static thrust, and achieve high cruise speeds, the team would need to use a large diameter and highly pitched propeller. Using these filters initially resulted in Motocalc™ yielding optimum propeller pitches that were unavailable on the market. To keep parts selection limited to purchasable parts, a thorough Internet search was performed to determine the availability of propellers. As a result of cross-referencing the propeller availability, Motocalc™ results, and previous VT DBF experience, the team decided to use 22 x 14 and 22 x 16 propellers in high and low wind respectively. The team estimates that

both propellers will provide top speeds in excess of 50 mph. Both propellers also provide a very high static thrust to weight ratio, which will enable the Draggin' Fly to takeoff in a very short distance.

4.7.1 Battery Layout

Essential to this year's design is a compact battery layout because the airfoil shape of the fuselage and the volume of the sensor package caused system integration problems. The team realized that a balanced aircraft would need the batteries placed ahead of the sensor package, which meant that the batteries would interfere with the motor. To solve this problem one configuration was examined in detail. This 11 x 12 x 11 cell battery layout is depicted in Figure 4.3. It has maximum dimensions of 11.36 x 2.56 x 2 inches. A working cross section of the aircraft was used to position this configuration among the motor, payload deployment system, and speed controller.

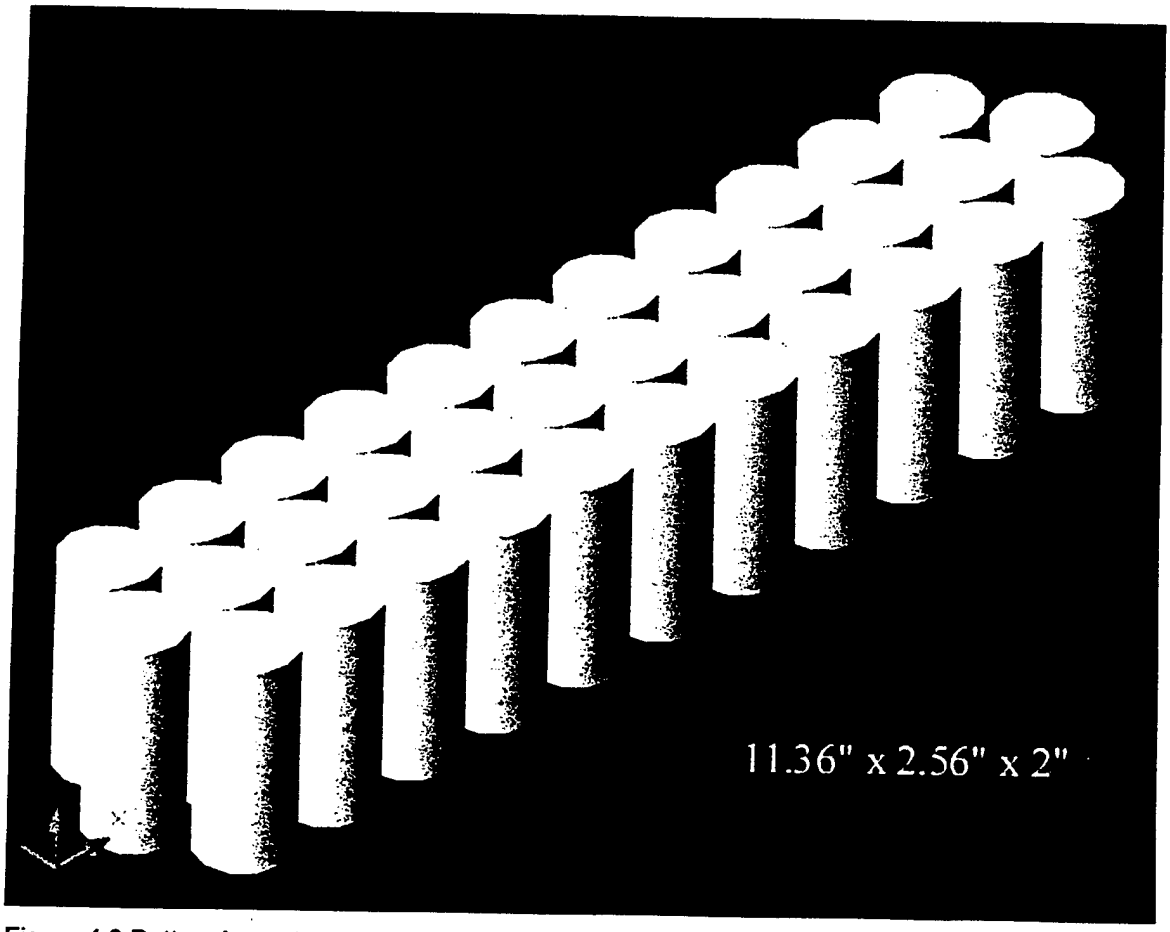

Figure 4.3 Battery Layout

4.8 Stability and Control Analysis

With the tail and wing sizing completed the handling quantities of the Draggin' Fly were calculated using two different Vortex Lattice Codes (VLM). JKayVLM was the first code used, and is only available to Seniors in the Virginia Tech Senior Design Lab. The other the program, Tornado[4], is freeware available to anyone who has the mathematical computation program Matlab. Initially the team had planned to just use the JKayVLM program, but ran into trouble calculating correct Lateral-Directional stability derivatives. Thus the Tornado code was brought in to complete the calculation of the stability derivatives. The JKayVLM program is based on flat plate assumptions, while the Tornado code relies on the slope of the camber line, as it has the equations for NACA 4 digit series airfoils as part of it's computation. Thus, the team found that the NACA 3310 airfoil approximated the camber line effects of the E387C airfoil that had been chosen.

The first thing that the team did in calculating the stability and control derivatives was to validate the JKayVLM code's performance in lateral directional response. In order to do this the team relied on the values posted by the 2001-2002 OSU Orange team in their winning report[5]. These values, the values calculated by JKayVLM and the corresponding error can be found in Table 4.2. Although, the computations from the JKayVLM will be considered the actual pitch stability derivatives of the Draggin' Fly because of previous validations available as part of the JKayVLM manual[3]. Table 4.3 has the control power derivatives calculated by JKayVLM and Tornado for the Draggin' Fly. An important thing to note from all these coefficients is that they show the plane is stable in all important flight conditions. The large static margin calculated by JKayVLM (32%) is important because it could help the team get around battery placement problems. Another solution that could be used is that the team might cut down the size of the horizontal tail to reduce drag. Although, this action will probably not be used since prior teams have found that increased stability is favorable over the course of flight conditions competition presents.

Table 4.2 Validation of JKayVLM Code

	JKayVLM	2001-2002 OSU "Orange"	Error (%)
$C_{M\alpha}/C_{L\alpha}$	-0.1636	-0.1772	-8.31296
H	0.25	0.25	
Neutral Point	0.4136	0.4272	-3.2882

Table 4.3 Draggin' Fly Stability Derivatives

Longitudinal		Lateral Directional	
Static Margin	32.42%	Cn_β	0.9980
$C_{L\alpha}$	4.1593	Cl_β	-0.0134
$C_{M\alpha}$	-1.3483	$Cn_{\delta r}$	-0.0401
$C_{M\delta e}$	-0.9982	$Cl_{\delta r}$	0.0120
		$Cn_{\delta a}$	-0.0070
		$Cl_{\delta a}$	0.2500

4.9 Final Design Summary

The final dimensions and performance characteristics of the Draggin' Fly are summarized in Table 4.4. With these final dimensions, the RAC of the Draggin' Fly could be calculated. The aircraft was designed to balance performance at a minimum RAC. This resulted in an 81 inch wing span with an aspect ratio of 6.76. One control surface per wing was used as both flaps and ailerons to keep a lower RAC. During the design process, the team decided that the higher RAC cost of two tails would be balanced by a significant decrease in assembly time. This also extends to the team's use of one servo per aileron, which would simplify and expedite the assembly of the removable wing panels. From these decisions the team broke down the individual component costs, which can be found in Table 4.5.

Table 4.4a Draggin' Fly Final Specifications - Geometry

Length	43 in
Span	81 in
Height	14 in
Aspect Ratio	6.76
Control Volumes	Elevator: 34.75 in^2
	Rudder: 33 in^2
	Aileron: 72 in^2

Table 4.4b Draggin' Fly Final Specifications – Performance Characteristics

C_{Lmax}	1.3
L/D_{max}	9.27 (fully loaded)
Maximum Rate of Climb	2045 fpm (fully loaded)
Stall Speed	24 mph (empty)
	29 mph (fully loaded)
Max Speed	53 mph
Take off Field Length:	
Empty	24 ft
Gross	56 ft

Table 4.4c Draggin' Fly Final Specifications – Weight Statement

Airframe	80 oz
Propulsion	96 oz
Control System	20 oz
Payload System	6 oz
Payload	100 oz
Empty Weight	202 oz
Gross Weight	302 oz

Table 4.4d Draggin' Fly Final Specifications – Systems

Radio	Futaba Fp-R309DPS
Servos	Futaba S9206
Battery Configuration	11 x 12 x 11
Motor	Astro 60
Propeller	22 x 14, 22 x 16
Gear ratio	2.5:1

Table 4.5a Rated Aircraft Cost Calculations - Prescribed Work Breakdown Structure (WBS)

WBS 1.0 Wing	**Value**	**Multiplier**	**Hours**
Span	81 inches	8 hr/ft.	54
Maximum Chord	14 inches	8 hr/ft.	9.33333
Number of Control Surfaces	2	3 hr/surface	6
		Total Hours	69.33333
WBS 2.0 Fuselage	**Value**	**Multiplier**	**Hours**
Body Maximum Length	47 inches	10 hr/ft.	39.167
		Total Hours	39.167
WBS 3.0 Empennage	**Value**	**Multiplier**	**Hours**
Horizontal Surfaces	1	10 hr/surface	10
Controlled Vertical Surfaces	2	10 hr/surface	20
Uncontrolled Vertical Surfaces	0	5 hr/surface	0
"V" Tail	0	15 hr	0
		Total Hours	30
WBS 4.0 Flight Systems	**Value**	**Multiplier**	**Hours**
Number of Servos in Wing	4	5 hr/servo	20
Number of Servos in Payload Bay	1	5 hr/servo	5
Number of Servos for Landing Gear	1	5 hr/servo	5
Number of Servos for Flight Control	1	5 hr/servo	5
		Total Hours	35
WBS 5.0 Propulsion Systems	**Value**	**Multiplier**	**Hours**
Number of Engines	1	5 hr/engine	5
Number of Propellers	1	5 hr/propeller	5
		Total Hours	10
WBS Manufacturing Hours	**Hours**	**Multiplier**	**RAC**
Total WBS Hours and Cost	183.5	20	$3,670

Table 4.5b Rated Aircraft Cost Calculations - Rated Engine Power (REP)

REP 1.0 Engine	**Value**	**Multiplier**	
Number of Engines	1	1	
REP 2.0 Batteries			
Weight of Batteries	4.375 lb	N/A	
REP	**Value**	**Multiplier**	**RAC**
Total REP and Cost	4.375	1500	$6,563

Table 4.5c Rated Aircraft Cost Calculations - Manufacturer's Empty Weight (MEW) and Gross Weight

MEW 1.0 Airframe	**Oz.**		
Wing/Tail, Fuselage, Gear	80		
		Total	80
MEW 2.0 Propulsion	**Oz.**		
Engine/Gearbox	25		
Speed Control	1		
Batteries	70		
		Total	96
MEW 3.0 Control System	**Oz.**		
Control horns, servos, receiver	20		
		Total	20
MEW 4.0 Payload System	**Oz.**		
Deployment System	6		
		Total	6
MEW	**Oz.**	**Multiplier**	**RAC**
Total MEW and Cost	202	6.25	$1,263
Payload:			
Box	80		
Radome	20		
		Total (oz.)	100
Gross Weight		**Total (oz.)**	**302**

Table 4.5d Rated Aircraft Cost Calculations - Total Rated Aircraft Cost (RAC)

Item	Cost
RAC 1.0 Manufacturing Hours	$3,670
RAC 2.0 Rated Engine Power	$6,563
RAC 3.0 Empty Weight	$1,263
Total RAC	**$11,495**

4.10 Drawing Package

The Drafting Team compiled data from the component-teams to produce accurate drawings of the Draggin' Fly aircraft. The drawing package consists of a dimensioned 3-view detailed design, an isometric layout of major components and their locations, a drawing of the payload deployment and restraint system, and a 3-view of the fuselage and its structural components.

5. Manufacturing Plan

5.1 Manufacturing Summary

Several different manufacturing methods would have to be used in order to produce the different parts of the aircraft. To produce the desired shapes, many different methods were researched to obtain unique qualities for each part. The different methods were ranked on a merit system to decide which would be suitable for the construction of the aircraft. The categories of the merit system were build time, required materials, difficulty, cost of the method, quality of produced component and repetition of the method.

5.2 Wing and Empennage Manufacturing Process and Tooling

The wing will have a foam core with a composite skin. To create the foam core, airfoil templates will be created using AutoCAD and cut using a LaserCAMM. The wing and spar will be constructed in two sections and joined on the sides of the fuselage. The foam core of the airfoil for each section will be cut using a high resistance wire cutter, and the section of the airfoil where the spar and ribs are placed will be removed from the foam. The places where the servos for the control surfaces are located will also be removed. The spar and ribs will then placed in the removed sections. The front and back sections of the airfoil will then be bonded to the spar. Fiberglass skins, with carbon fiber spar reinforcements will be attached, and the sections will be vacuum bagged and allowed to cure. The center sections of the wings will be built up in a similar fashion and attached to the sides of the fuselage.

The empennage will be constructed from plywood, and covered in a skin of carbon fiber. The wood components will be cut with a LaserCAMM from AutoCAD drawings. The two vertical and one horizontal pieces will have carbon fiber applied separately, then be vacuum bagged and allowed to cure. The pieces will be assembled and connected to the fuselage via the two extending booms and triangular stock reinforcement.

5.3 Fuselage Manufacturing Process and Tooling

Due to the relative complexity of the fuselage, it was decided to make use of the Virginia Tech Architectural LaserCAMM. The structure of the fuselage is drawn on AutoCAD and will cut with the LaserCAMM. Through this method, there is minimal error in parts manufacturing. This increases the performance of the aircraft by decreasing drag and weight.

After the side panels are cut out, the supporting frame structure will be built up between the side panels. With this constructed, the carbon fiber will be applied to the outside pieces of the fuselage at the locations specified in the detailed design. They will then be vacuum bagged and left to cure. The fuselage will be assembled and bonded through the use of adhesive. Next, the outer skin will be laved up and cured, then trimmed to the correct shape. With the skin and internal structure built, the motor mount and other system supporting structures will be installed. The radome and the bottom door will be attached and tested for operation. With this done, the individual radio systems will be installed.

5.4 Landing Gear Manufacturing Process and Tooling

The landing will be connected to the bottom of the fuselage and constructed to be retraceable. The struts of the gear are prefabricated, but the carbon fiber rods will have to be bonded to the Robostruts. Next, the pillow blocks and collars will be attached to the rods. The wheels will be connected to the gear, which then will be connected to the structure of the fuselage.

5.5 Manufacturing Scheduling

The aircraft will be constructed in four assemblies: the wing, fuselage, landing gear, and empennage. This will shorten the construction time. Projects will be coordinated so that the appropriate tools are available to the teams when needed; this will decrease the amount of hold ups and keep the construction going smoothly. The final product will be completed in a timely manner and be ready for testing with ample time remaining before competition.

6. Testing Plan

6.1 Materials Testing

Considerable time went in to determining what material the cargo door should be constructed from. To test materials a simply supported beam structure was assembled, in which a test section of the material supported at each end and loads applied in the middle. Weights were added until the structures ruptured. Based on these tests, it was decided to use plywood for the door cut $^1/_8$ inch thick and glass it on both sides.

6.2 Structural Testing of Wings

One of the most critical structural considerations for the airplane is the wing construction, particularly near the wing root where bending moments are maximum. For the Draggin' Fly, the joint connecting the main portion of the wing to the inboard section is perhaps equally important. The primary loading on the wings is not due to their own weight but the aerodynamic lift force that they generate. In steady, level flight this force is usually equal in magnitude to the weight of the aircraft. However, certain maneuvers increase this force to several times the weight. The wings must be able to withstand these high forces if the aircraft's mission is to be successful.

The aircraft's maximum service load factor was originally dictated by the performance team as 8 Gs. This is quite high and the airplane will most likely not approach this kind of loading in performing the maneuvers required of it. The final aircraft design will likely not be expected to accommodate this load in order to save weight. A load factor testing of 5 should be more than sufficient to test the aircraft's structural integrity.

In order to simulate these forces, the aircraft will be flipped upside down and sandbags placed on the bottom of the wings. For a load factor of 5, and given a total weight of about 20 lbs, the total loading should be about 50 lbs per wing. Since three-dimensional aerodynamic effects predict more of the lift will be produced near the root of the wing, the sandbag loading will be matched accordingly. If the wings can withstand this loading the structure should be safe for flight.

Also of interest is the deflection of the wings. If the lift forces bend the wings too much it will become difficult for the aircraft to fly and maneuver properly. The sandbag loading will also give insight into the deflection profile. However, it is expected that if the wings are strong enough to resist failure then severe deflection will not be an issue due to the stiffness of the wing materials.

6.3 Structural Testing of Empennage

The loading on the tail is in many ways coupled with that of the wing. With this in mind, the horizontal stabilizer will be tested in a manner similar to the wings. Most likely using the specified load factor, weight will be applied to the tail section to simulate the aerodynamic force generated there. The structure should be able to withstand this loading without failure or excessive deflection. Due to the design of the booms (high but thin) that attach the tail to the fuselage, it is not expected that either of these will be a problem due to the high moment of inertia about the pitch bending axis.

Perhaps of greater concern is the loading on the vertical tails and the corresponding bending of the booms. The thin width of the booms gives them a small moment of inertia that could present a deflection problem during rudder deflection, crosswinds, and other asymmetrical loading situations. In order to test this, a maximum loading will be calculated and this load will be applied to the vertical surfaces with the plane flipped on its side. If the deflection exceeds acceptable limits, the boom will require stiffening in that direction. This contingent has been prepared for and should not be difficult to implement.

6.4 Structural Testing of Landing Gear

During landing the plane typically undergoes a rapid acceleration to reduce its vertical velocity so as not to fly through the runway. Typically the aircraft's landing gear is responsible for damping this effect so that the rest of the vehicle does not endure such high load factors. In this case, the front gear includes a spring of known stiffness, while the rear gear is simply attached to the vertical tails.

The front gear will be tested by measuring its response to a given load factor, probably 3. Loading will be applied to the struts and the reaction assessed. Ideally the spring will shorten, but not to the point where it cannot be compressed farther. In this case, the strut will have the best possible effect in terms of reducing the acceleration undergone by the plane. Additionally, once the entire aircraft is assembled, a similar load factor will be applied to make sure that the gear does not break off or damage the airplane.

6.5 Propulsion Testing

It is desirable to know the static thrust characteristics of the propulsion system so that the theoretical data can be confirmed. The propulsive power must be great enough so that the aircraft can accelerate sufficiently quickly to reach takeoff velocity in the allotted runway distance. The test will begin by determining the elastic constant of a spring by applying known loads and measuring the displacement from static equilibrium. With this information in hand the spring will be attached to the motor and propeller assembly on a horizontal smooth surface. The throttle will be varied to different settings and the resultant spring displacement recorded. From this data the static thrust of the propulsion system can be determined. Using this information the aircraft design can be modified if necessary.

Knowing the operational limits of the batteries is essential to maximizing the performance of the aircraft. The batteries must be able to provide enough power for the aircraft to complete its mission with some reserve allowance, yet too many cells increases the weight unnecessarily. The number of batteries has been optimally designed for, but these estimates must be corroborated through testing. Initially, the batteries will be drained to determine their maximum energy output; this will likely be done several times in varying conditions to account for all possibilities. Based on this, the projection for the number of batteries built in to the aircraft can be modified. The power testing will be continued during flight testing. After each run the status of the battery system can be checked to make certain adequate reserve power is available if needed.

During flight testing, heat sinks stripped from a computer power supply will be tried for the purpose of reducing temperature on the propulsion system. It is hoped that the aluminum fins will dissipate heat to the ambient air much more effectively than a mere airflow tube through the fuselage. The lower temperature should reduce resistance of the system and increase lifespan and efficiency.

Additionally, a spinner cone configuration will be flight tested. Several years past VT DBF entries have not had a spinner cone. The propulsion team wants to see if this was a mistake or better judgment. The team intends on testing for speed enhancement to determine if the endeavor is indeed worthwhile.

Lastly the team will be looking at the trends of the thrust line. A thrust line approximately 1 inch above the mean chord of the NACA 0027 fuselage should be sufficient for use on the payload mission. Confirmation of this parameter will require several tests. All missions will use this same configuration with different trim setup. Each setup will require flight test for optimum use.

6.6 Aerodynamic Testing

During the time between the projected completion of construction of the aircraft and the competition, the Virginia Tech wind tunnel facilities will be booked fairly heavily. Thus another method of testing the aerodynamic characteristics of the aircraft is required. An idea, courtesy of an aerospace engineering professor, was to rig a mount to a pick up truck and use oil flow to measure the separation characteristics on various parts of the aircraft. Using lumber, a mounting post will be constructed and

affixed to the bed of the truck. The post will be long enough to extend the test piece at least three feet above the cab of the truck so that the body of the truck does not affect the local flow. The truck will be driven at speeds equivalent to those at which the airplane will operate; the tests will be conducted on a straight road on a calm day. These controls should provide a good simulation of actual flight conditions for the purpose of studying the stall characteristics of the airplane. Most desirable to know are the locations of separation on the wings, fuselage, tail assembly, and radome. In the case of the wings and tail the flow can be tested for different configurations of the control surfaces. Each of these can be tested separately and the design altered if need be before final construction.

6.7 Ground Testing

Once the entire aircraft is assembled, testing will be conducted to make certain that the aircraft is ready for the competition. Initial testing will be done on the ground. The first important thing is to check to make certain that the plane can roll straight and does not pull to either side. For obvious reasons, the ability to roll straight is nearly essential for a smooth takeoff. Also, the plane will be tested to ascertain the speeds it can reach in certain distances. Ideally, some of the tests will be conducted into the wind. Thus it can be determined if the aircraft can reach sufficient speeds for takeoff in the allotted runway distance, allowing for some margin of error as well.

In addition, the payload deployment system will be assessed. The door must be able to open, drop the box straight down, and close again for takeoff quickly and flawlessly. Given the small clearance between the box and the bottom of the plane incorporated in the design, it is crucial that the mechanisms work every time so that a potentially disastrous collision between the plane and the box do not occur during the competition.

6.8 Flight Testing

Once testing of all the systems is complete flight testing can begin. This is perhaps as much for the benefit of the pilot as anything else. Here the pilot will become accustomed to operating the aircraft. Also of interest is how the plane will react to different conditions, particularly high winds. In addition, these tests will give an indication as to the effectiveness of the control surfaces. Initially the tests will likely be done without the radome in place or the box in the cargo section, as these should be the easiest conditions to fly under. Assuming the plane performs successfully, the box and radome will be added individually, then simultaneously, and the results from the four cases will be compared. Most interesting should be the effect of the radome on the operation of the airplane. Before the competition, the entire mission will be run several times from assembling the plane to the end of the run to make certain that everything is ready for the contest.

7. References

1. Bertin, J.J., and Smith, M.L. Aerodynamics for Engineers, Third Edition. 1998 Prentice-Hall, Inc. Upper Saddle River, NJ, pg 286.

2. Drela, Mark. "Xfoil 6.94 Subsonic Airfoil Development System." http://raphael.mit.edu/xfoil/, Last updated December 18, 2001.

3. J. Kay, W. H. Mason, W. Durham, F. Lutze and A. Benoliel, "Control Authority Issues in Aircraft Conceptual Design: Critical Conditions, Estimation Methodology, Spreadsheet Assessment, Trim and Bibliography." November 1996.

4. Melin, Tomas. "Tornado 1.20" http://www.flyg.kth.se/divisions/aero/software/tornado/ Last updated February 11, 2001.

5. "Oklahoma State University Orange Team Report." Available http://www.aae.uiuc.edu/aiaadbf/01reports/osu_orange_2002.pdf

6. Raymer, Daniel P. Aircraft Design: A Conceptual Approach. 3rd Edition. AIAA: August 1999.

7. Selig, Michael. "UIUC Airfoil Data Site." http://www.aae.uiuc.edu/m-selig/ads.html. Last updated December 8, 2002.

PRODUCED BY AN AUTODESK EDUCATIONAL PRODUCT

DESCRIPTION:	DATE:	
DETAILED DRAWING OF INTERNAL STRUCTURE TOP, FRONT, RIGHT, AND ISOMETRIC VIEWS	02/28/2003	APPROVED

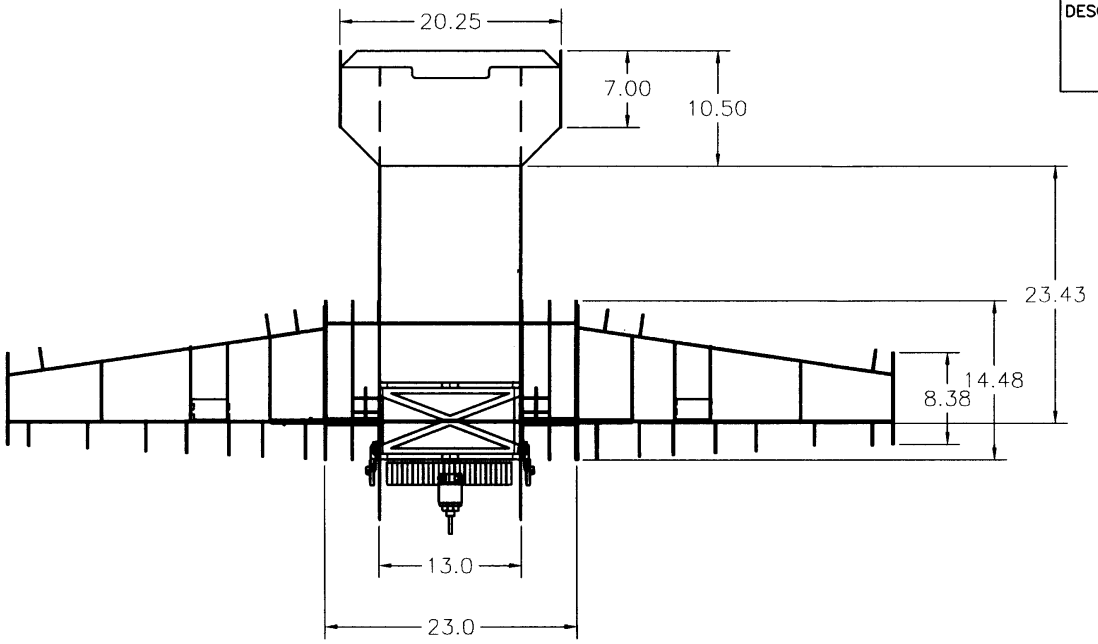

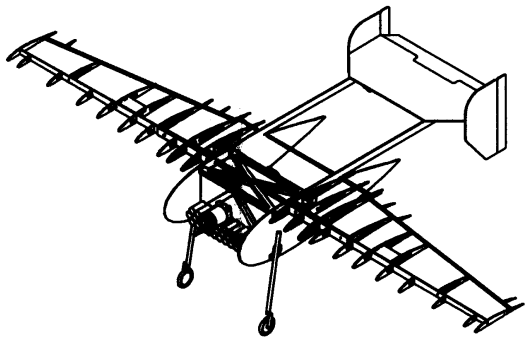

ISOMETRIC NOT TO SCALE

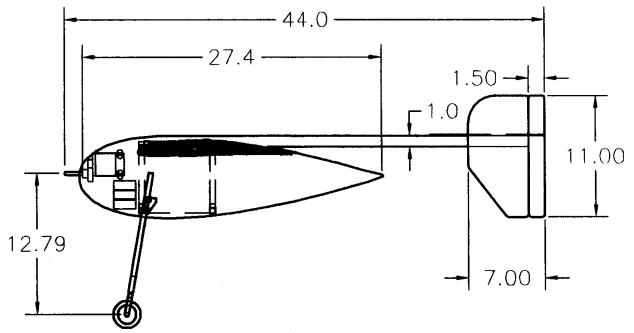

NOTE: FUSELAGE IS A NACA 0027
WING IS AN EPPLER E387(C) AIRFOIL

SCHOOL: VIRGINIA TECH	
NAME: DRAGGIN' FLY	
DRAWN BY: E. Buzzard, D. Alemayehu, & C. Ashton	
CHECKED BY: M. Metheny, T. Miller, S.D. McIntyre	
SCALE 1" = 0.09"	SHEET 1 of 5

PRODUCED BY AN AUTODESK EDUCATIONAL PRODUCT

PRODUCED BY AN AUTODESK EDUCATIONAL PRODUCT

PRODUCED BY AN AUTODESK EDUCATIONAL PRODUCT

PRODUCED BY AN AUTODESK EDUCATIONAL PRODUCT

DESCRIPTION:	DATE:	
DETAILED SYSTEMS ISOMETRIC	02/28/2003	APPROVED

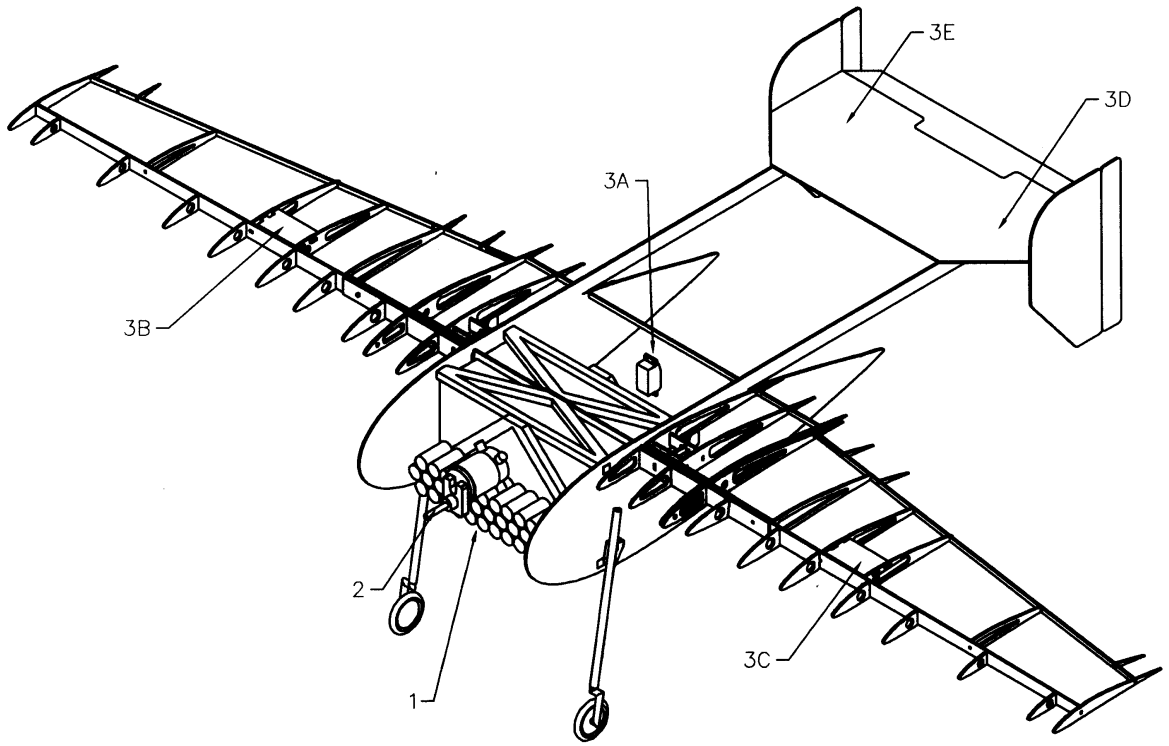

PART #	PART DESCRIPTION
1	34 CELL SANYO 2300SCE FLIGHT BATTERY PACK
2	ASTROFLIGHT COBALT 60 MOTOR WITH SUPERBOX
3A	PAYLOAD RELEASE SERVO
3B	RIGHT AILERON SERVO
3C	LEFT AILERON SERVO
3D	ELEVATOR SERVO (HIDDEN)
3E	RUDDER SERVO (HIDDEN)

SCHOOL: VIRGINIA TECH

NAME: DRAGGIN' FLY

DRAWN BY: E. Buzzard, D. Alemayehu, & C. Ashton

CHECKED BY: M. Metheny, T. Miller, S.D. McIntyre

SCALE: NOT TO SCALE

PRODUCED BY AN AUTODESK EDUCATIONAL PRODUCT

PRODUCED BY AN AUTODESK EDUCATIONAL PRODUCT

PRODUCED BY AN AUTODESK EDUCATIONAL PRODUCT

PRODUCED BY AN AUTODESK EDUCATIONAL PRODUCT

DESCRIPTION:	DATE:	
DETAILED DRAWING OF FUSELUGE STRUCTURE TOP, FRONT, RIGHT, AND ISOMETRIC VIEWS	02/28/2003	APPROVED

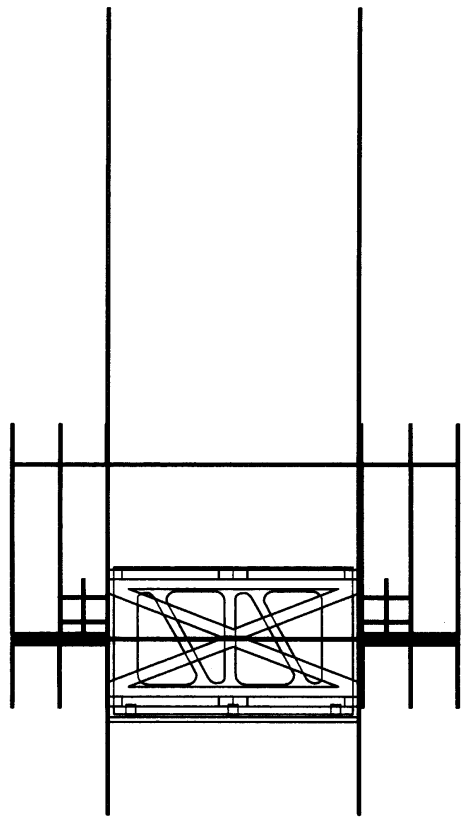

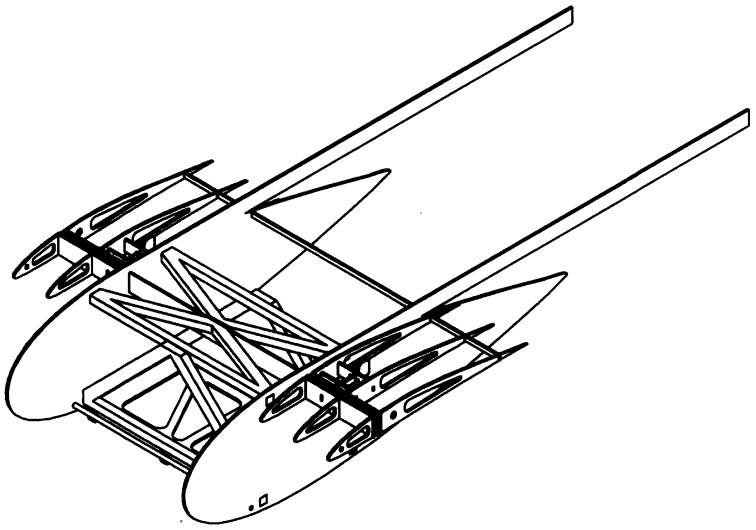

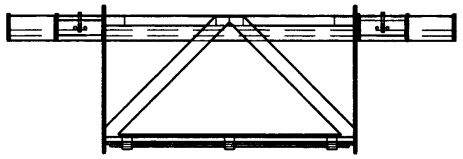

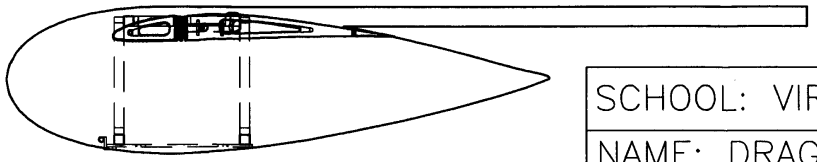

SCHOOL: VIRGINIA TECH

NAME: DRAGGIN' FLY

DRAWN BY: E. Buzzard, D. Alemayehu, & C. Ashton

CHECKED BY: M. Metheny, T. Miller, S.D. McIntyre

SCALE 1" = 0.16"

SHEET 3 of 5

PRODUCED BY AN AUTODESK EDUCATIONAL PRODUCT

PRODUCED BY AN AUTODESK EDUCATIONAL PRODUCT

PRODUCED BY AN AUTODESK EDUCATIONAL PRODUCT

PRODUCED BY AN AUTODESK EDUCATIONAL PRODUCT

DESCRIPTION:	DATE:	
ISOMETRIC DRAWING OF DRAGGIN'FLY DURING MISSION FLIGHT	02/28/2003	APPROVED

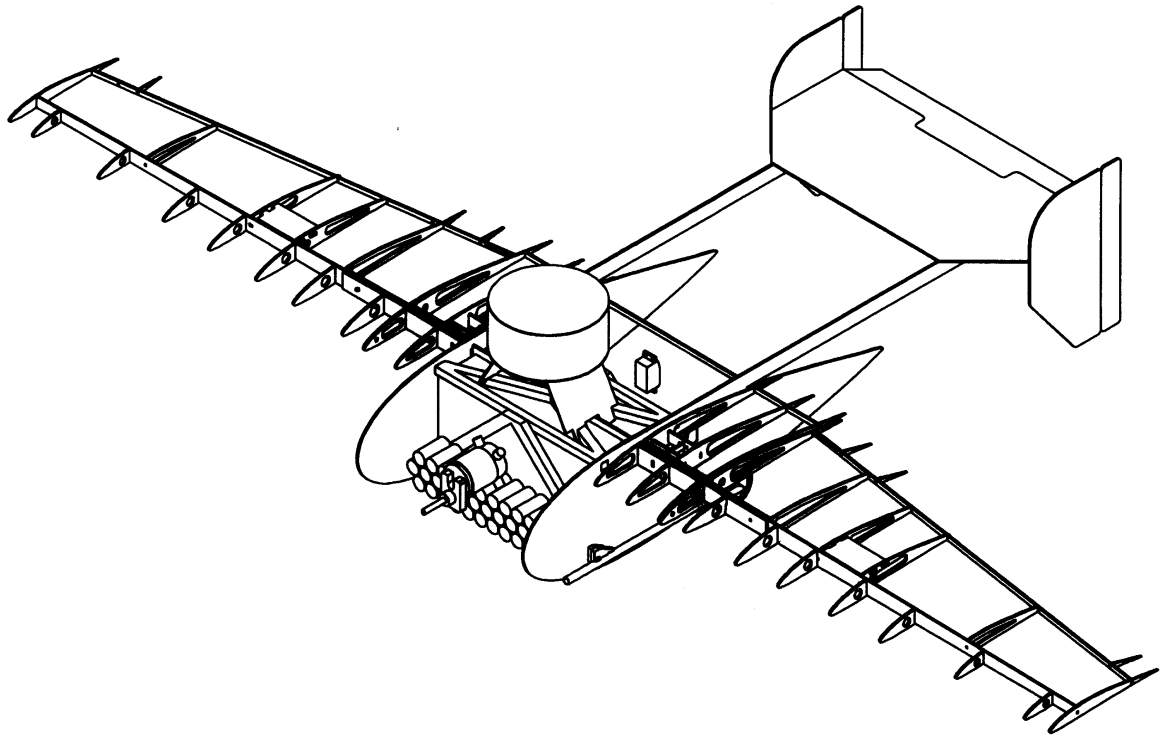

SCHOOL: VIRGINIA TECH	
NAME: DRAGGIN' FLY	
	DRAWN BY: E. Buzzard, D. Alemayehu, & C. Ashton
	CHECKED BY: M. Metheny, T. Miller, S.D. McIntyre
SCALE: NOT TO SCALE	SHEET 4 of 5

PRODUCED BY AN AUTODESK EDUCATIONAL PRODUCT

PRODUCED BY AN AUTODESK EDUCATIONAL PRODUCT

PRODUCED BY AN AUTODESK EDUCATIONAL PRODUCT

PRODUCED BY AN AUTODESK EDUCATIONAL PRODUCT

DESCRIPTION:	DATE:	
DETAILED DRAWING OF PAYLOAD DEPLOYMENT	02/28/2003	APPROVED

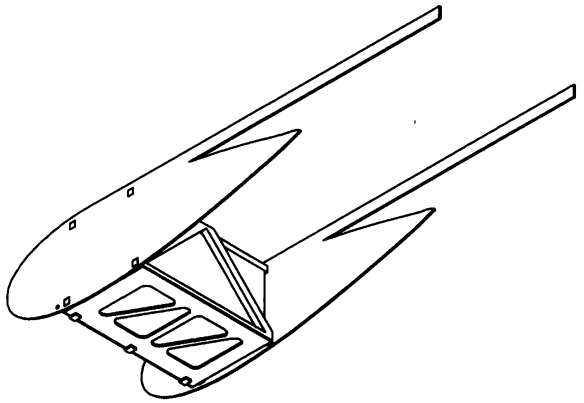

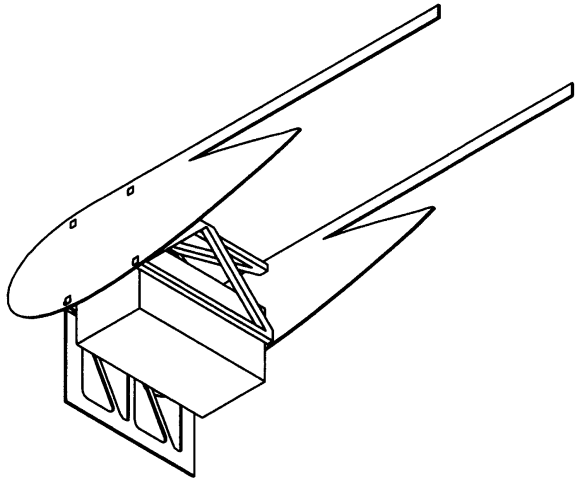

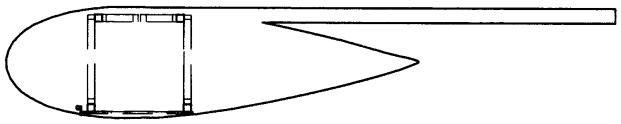

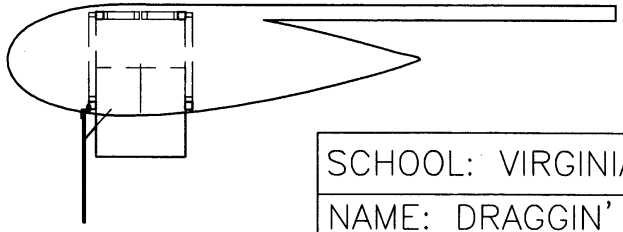

SCHOOL: VIRGINIA TECH

NAME: DRAGGIN' FLY

DRAWN BY: E. Buzzard, D. Alemayehu, & C. Ashton

CHECKED BY: M. Metheny, T. Miller, S.D. McIntyre

SCALE 1" = 0.125"

SHEET 5 of 5

PRODUCED BY AN AUTODESK EDUCATIONAL PRODUCT

PRODUCED BY AN AUTODESK EDUCATIONAL PRODUCT

Lock-N-Load

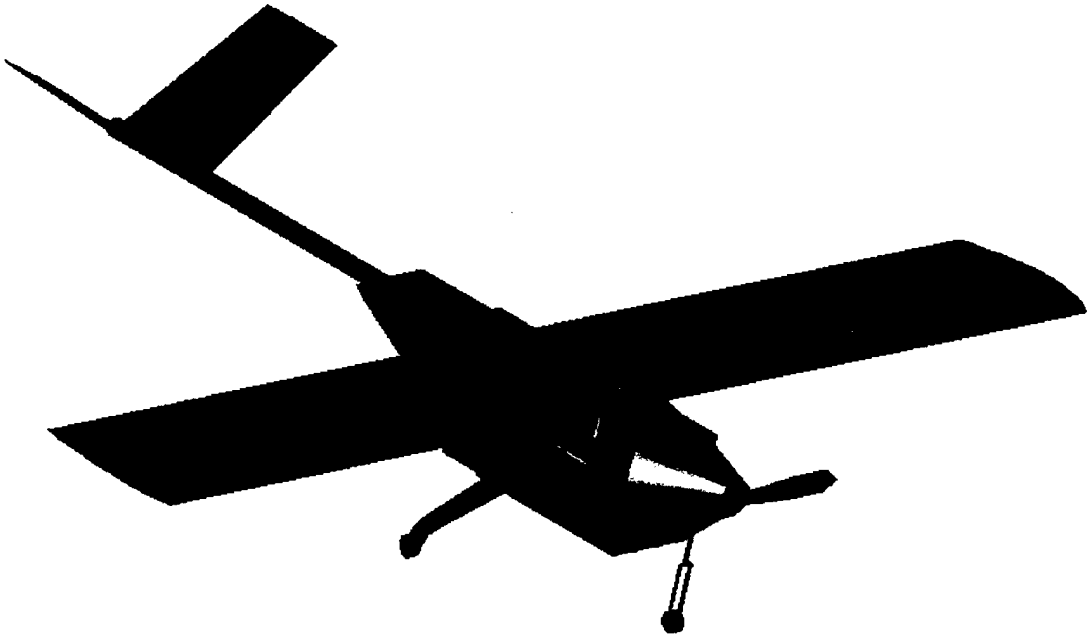

West Virginia University

2002-2003 AIAA Cessna/ONR
Design Build Fly Competition

Design Report

Table of Contents

1.0 Executive Summary 1
1.1 Conceptual Design 1
1.1.1 Conceptual Design Alternatives 1
1.1.2 Conceptual Design Tools 2
1.1.3 Conceptual Design Results 2
1.2 Preliminary Design 2
1.2.1 Preliminary Design Alternatives 2
1.2.2 Preliminary Design Tools 3
1.2.3 Preliminary Design Results 3
1.3 Detail Design 3
1.3.1 Detail Design Alternatives 4
1.3.2 Detail Design Tools 4
1.3.3 Detail Design Result 4
2.0 Management Summary 4
2.1 Team Architecture 4
2.2 Technical Group Responsibilities 5
2.2.1 Technical Group Leaders 5
2.2.2 Aerodynamics Group Responsibilities 6
2.2.3 Propulsion Group Responsibilities 6
2.2.4 Structures Group Responsibilities 7
2.2.5 Payload Deployment Group Responsibilities 7
2.3 Scheduling, Documentation, and Configuration Update 7
3.0 Conceptual Design 10
3.1 Design Parameters 10
3.1.1 Primary Design Parameters 11
3.1.2 Design Parameter Sensitivity Analysis 11
3.2 Aircraft Configuration 12
3.2.1 Alternative Fuselage and Tail Configuration 12
3.2.2 Alternative Wing Configurations 14
3.2.3 Alternative Payload Ejection Configurations 16
3.3 Structural Configurations 17
3.3.1 Figures of Merit 17
3.3.2 Assumptions Made and Design Parameters Investigated 18
3.3.3 Alternative Wing Structures 18
3.3.4 Alternative Tail Structures 19
3.3.5 Alternative Fuselage Structures 20
3.3.6 Alternative Landing Gear Configurations 21
3.4 Alternative Power Plant Configurations 22
3.5 Conceptual Aircraft Configuration 23
4.0 Preliminary Design 24
4.1 Flight Performance Objectives 24
4.1.1 Payload Ejection System Analysis 24
4.1.2 Carry – Through Analysis 25
4.1.3 Assembly Time 26
4.2 Aircraft Size Limitations 27
4.2.1 Wing Dimension Study 27
4.2.2 Tail Configuration Study 27
4.2.3 Battery Configuration Analysis 28
4.2.4 Aerodynamic considerations 29
4.2.5 Fuselage Study 29
4.2.6 Landing Gear Study 29
4.3.1 Airfoil selection 29
4.3.2 Wing sizing score optimization 30

4.3.4 Tail airfoil selection 30
4.3.5 Fuselage 30
4.4 Performance Estimates 31
5.0 Detail design 33
5.1 Component selection 33
5.1.1 Propulsion 33
5.1.2 Battery Pack 35
5.1.3 Control Actuation 35
5.1.4 Radio transmitter and receiver 36
5.1.5 Braking system 36
5.2 Fuselage Internal Schematics 37
5.3 Detailed Design from Drawing Package 38
5.4 Summary of Geometric Parameters 41
5.5 Summary of performance 41
6.0 Manufacturing Plan and Process 41
6.1 Manufacturing Processes Investigated 41
6.2 Figures of Merit Breakdown 42
6.3 Process Selected for Major Component Manufacture 43
6.3.1 Fuselage 43
6.3.2 Wing and Tail 44
6.3.3 Landing Gear 44
7.0 Testing Plan 44
7.1 Testing Objectives 44
7.2 Testing Schedule 45
7.3 Testing Checklist 45
7.4 Results and Lessons Learned 45
8.0 Rated Aircraft Cost (RAC) 46
8.1 Discussion of RAC 46
8.1.1 Breakdown of the RAC 46
8.1.2 Manufacturer's Empty Weight Multiplier 46
8.1.3 Rated Engine Power 46
8.1.4 Manufacturing Man Hours 46
8.1.5 WBS 1.0 Wing 46
8.1.6 WBS 2.0 Fuselage 46
8.1.7 WBS 3.0 Empennage 47
8.1.8 WBS 4.0 Flight System 47
8.1.9 WBS 5.0 Propulsion System 47
8.2 Features that Produced the Final Configuration 47
9.0 Bibliography 49

1.0 Executive Summary

This report is an account of the process taken by a team of engineering students from West Virginia University in entering the 2002/2003 AIAA Design Build Fly Competition. This competition challenges teams to design, build, and fly a remote controlled aircraft that must meet a specified set of goals and requirements. This competition requires each team to make design choices that create an optimum balance between speed, strength, propulsion efficiency, aircraft assembly time and a Rated Aircraft Cost (RAC). This year the teams may choose between three different missions, each consisting of a different number of laps as well as a different payload configuration. The total score awarded to each team is a function of a report score, flight score, and a RAC.

1.1 Conceptual Design

The first step in any design process is to investigate any and all concepts that are applicable to the given problem. It was determined that there were four main components of this aircraft that require intense investigation: aerodynamics, propulsion, structures, and payload ejection. Four groups were formed where each was given a component to investigate. Their job was to investigate all component configurations and how each would affect aircraft speed, strength, propulsion efficiency, and the RAC. The next step was to perform a design sensitivity analysis, which was accomplished by using figures of merit. These figures of merit compared each of the components effect on the overall score. The team then focused their attention on the components that obtained the highest score while also considering the effects on construction ease, construction time, and materials. This resulted in a narrowing of the design parameters.

1.1.1 Conceptual Design Alternatives

The aerodynamics group was responsible for setting the design concepts of the aircraft. Many design alternatives were evaluated for advantages and disadvantages for the major components including the fuselage, wings, and tail. Structural possibilities were also considered for each alternative. A very important characteristic considered for each alternative was the assembly time of the aircraft, once it was out of the box. The goal was to be able to assemble the aircraft to a flight ready status in under ten seconds. This feature was a dominant factor for consideration in almost all design choices. Each design alternative was evaluated for its effect on ease of construction, assembly time, strong lightweight structure, and RAC. Several propulsion schemes were considered based on battery selection, the type and number of motors, and propellers. It was determined that it was possible to come up with a propulsion system that would meet any endurance and thrust requirements that were generated by the aircraft alternatives under consideration.

1.1.2 Conceptual Design Tools

Several tools were used and developed to evaluate the scoring potential of many different design options. An excel spreadsheet was used to determine the effects of each design choice on the RAC. The RAC that was generated by this program was a function of every parameter that was set forth by the competition. The set of parameters that received the lowest RAC was then evaluated. An investigation was performed on the set of parameters to determine the feasibility of the design. It was important to determine:

1) If this set of parameters created a design that was easy to construct and assemble
2) If the propulsion requirements were within acceptable limits
3) If the design was aerodynamically feasible
4) If a payload ejection system could be designed

An Excel spreadsheet was created to model the aircraft's aerodynamics and propulsion system. This spreadsheet took into account the lift and drag of each major component and determined the required thrust needed. This spreadsheet then calculated the thrust and endurance produced by a chosen propulsion system and compared it with the needed thrust. If the propulsion system was not sufficient a new system was chosen and new calculations were made. The results of the excel spreadsheet and the spreadsheet were analyzed and a new score was calculated. In addition MotoCalc Electric Propulsion software was used for propulsion design optimization.

1.1.3 Conceptual Design Results

After many iterations involving both design tools the design with the highest scoring potential was selected. The selected aircraft was a high wing monoplane with a V-tail. The fuselage was a composite construction utilizing carbon and plywood. The wings and the tail were constructed of foam core with a balsa wood skin. The chosen propulsion system was a single engine configuration in series with the batteries.

1.2 Preliminary Design

With the conceptual design in place it was time to begin preliminary sizing of the aircraft. This included dimensions of the fuselage, wing, tail, and structures. With the preliminary sizing of structural components in place, the propulsion group began work on choosing the correct engine, battery, and propeller combination.

1.2.1 Preliminary Design Alternatives

The preliminary design phase was focused on validating results of the conceptual design. This entailed performing aerodynamic studies of the wing, tail, and fuselage. The goal of this study was to convince the team that the conceptual design did possess the best aerodynamic characteristics. After this study was performed any necessary aerodynamic changes were made. After the aerodynamic study

was performed a structures study was executed. This study determined the type of structure, the materials and the construction methods that would be used in the design. After the structure was established, a better estimation of the weight and drag of the aircraft could be determined. This was necessary for the propulsion team to conduct the analysis on the engines, batteries, and propellers.

1.2.2 Preliminary Design Tools

The first tool used in the preliminary design was CAD software. A three-dimensional drawing was developed including all portions of the aircraft. The model was used to demonstrate the relationship of all the components with each other in a much faster manner than could be achieved with a mach-up. From this model a more accurate set of dimensions could be determined. These dimensions were then used in the same Excel spreadsheet that was developed for the conceptual design, which facilitated iterations at all levels of design. After a good estimate of the necessary dimensions for the structure was obtained, test specimens were created as well as full-scale components. These test specimens made-up a second preliminary design tool. These test specimens and full-scale models were then subjected to many times the loading that could be expected to be experienced during the competition. A simple computer code was created using information gathered from motor and battery manufacturers to select the proper propulsion system.

1.2.3 Preliminary Design Results

The most important result of the preliminary design phase was the finalization of the major components type, size, and construction method. The aerodynamics group determined the static stability of the aircraft as well as dimensions for the fuselage, wing, and tail. The weight, lift, and drag of the aircraft was also determined and presented to the propulsion and structures teams. The propulsion team finalized the motor, battery, and propeller selection that could meet or exceed the thrust and endurance specifications. The structures team provided structural information that would most definitely survive any reasonable load that could be experienced during flight without too much additional weight, using the tools outlined in the Detailed Design Tools section 1.3.2. The final dimensions, materials, and construction methods for each component were available for the detail design phase.

1.3 Detail Design

This final phase of the design determined the exact type, size, and construction methods of the major components utilizing the information gathered in the preliminary design phase. The primary goal of the aerodynamics group in this design phase was to determine handling characteristics, dynamic stability, and the control system. The propulsion group determined the exact motor, type and number of batteries, and the type of propeller needed to meet all specifications. The structures group determined the exact structural components, including detailed drawings and a three-dimensional model. These drawings and model showed the exact location of all aircraft components.

1.3.1 Detail Design Alternatives

Detailed design alternatives were focused primarily on secondary systems and processes. This included aircraft construction, assembly, and operation. It was also important to run all the decisions made in the preliminary design phase through the codes previously utilized to verify that no mistakes were made. The only major component that needed to be finalized in this design phase was the payload ejection system. The propulsion group performed tests on the propulsion system to determine flight strategy in various flight conditions. The propulsion system was also investigated in its ability to perform flawlessly in the most adverse conditions. The structures group had the most difficult task in the detailed design phase. To them, it was important to determine all the primary and secondary components that would be present in the design. With this list of components, the structures team had to place each component in its proper location and the time it would take to assemble the aircraft. After this was completed, the complete structure was finalized. The goal was to create an aircraft where by each component was permanently attached to the aircraft and one person could assemble it in as little as ten seconds. The structures group also had the duty to produce a construction plan and schedule. The aerodynamics group had fewer responsibilities in this design phase that did the structures group. However, there duties could not be performed until the structures and propulsion groups were completed. The important task of the aerodynamics group was to validate the design choices of the other groups. It was also important to determine control surface sizes as well as the type number of servos to be used.

1.3.2 Detail Design Tools

The aerodynamics group used an aircraft simulation software package developed in an excel spreadsheet to model the aircrafts dynamic response. This code required the estimation of aerodynamic coefficients so that the software could determine the stability derivatives. The structures group made a final three-dimensional CAD model, which was used to determine the weight and center of gravity of the aircraft. A scheduling program was put in place to manage time and materials effectively.

1.3.3 Detail Design Result

This final design phase resulted in all finalized aircraft dimensions, components, and materials. The static and dynamic performance of the aircraft was determined. Detailed manufacturing plans and drawing were prepared. Construction was ready to commence.

2.0 Management Summary

2.1 Team Architecture

The West Virginia University team was divided into four technical groups each with individual responsibilities: aerodynamics, structures, propulsion, and payload deployment. This year's team

suffered from a severe lack of experience. There were only four returning veterans and two of them were only members until December. This required that all members to work cross-discipline duties. There were also a few additional tasks that were assigned to individual people such as computer programming and CAD work. Each group was assigned a lead engineer. The breakdown of accountability is as follows:

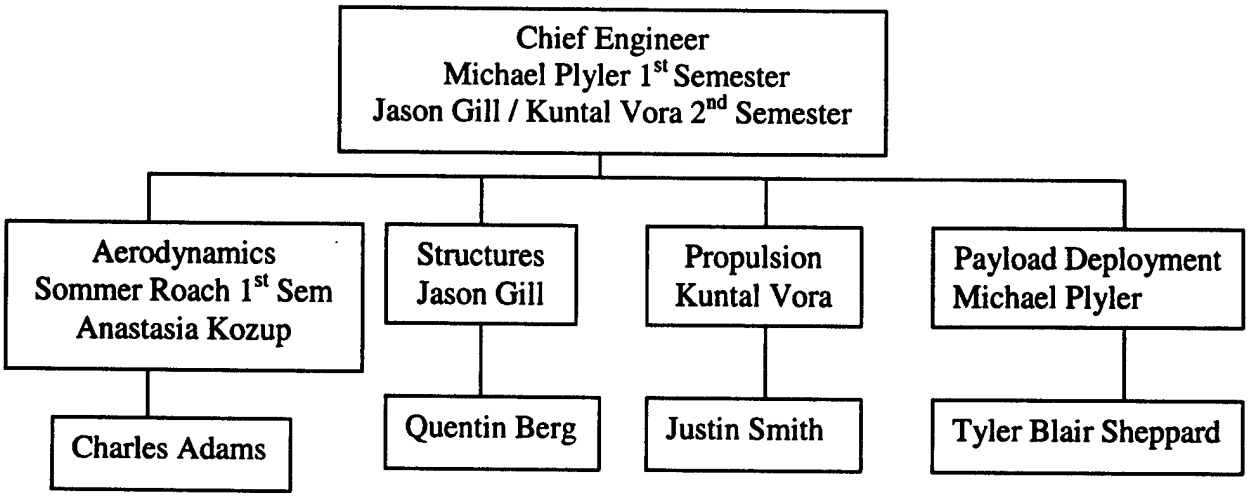

2.2 Technical Group Responsibilities

The ultimate success of the aircraft was dependent on the decisions made by each technical group. To ensure that each group considered all possibilities, each topic that required a significant decision was presented to the entire team. This allowed individuals to possibly present fresh ideas that may not have been considered. The entire team would then vote on each major decision. Minor decisions were left up to the group's lead engineer.

2.2.1 Technical Group Leaders

Jason Gill was chosen as the lead for the structures group for many reasons. The lead of this group would be expected to have the greatest commitment in time and energy over other group leads. The structures lead has to be familiar with all aspects of airplane construction and design. Jason has proven through prior team involvement that he possesses the necessary skills to perform this function.

Kuntal Vora's qualifications for the propulsion lead are many. As a member of the previous year's team, he was highly involved with the propulsion team and has demonstrated significant knowledge of the subject. He was also responsible for the wing design and fabrication. It was also important to find a person who would be with the team throughout the duration of the year.

Sommer Roach was chosen to head the aerodynamics group for the aircraft. As a member of last year's team, she was highly involved with the aerodynamic portion and demonstrated significant

abilities and knowledge in this area. However, Sommer Roach was a December (2002) graduate and it was determined that Anastasia Kozup, a senior level aerospace and mechanical engineering student, would take over the responsibilities of the head of the aerodynamics group. Although it was her first year on the team, Anastasia demonstrated the abilities and knowledge needed to be able to lead the aerodynamics group.

Michael Plyler was selected as the payload deployment lead for several reasons. He is a veteran and former team leader who possesses a great ability for innovation and original thinking. The new twist to the competition this year, automatic payload deployment required new ways of building aircraft of this type. Michael's qualifications are well suited for this requirement. Michael also possesses skills that are invaluable to the team such as CAD, programming, and aircraft modeling skills. However, Michael Plyler was a December (2002) graduate and it was found that we need another student to lead the group in his absence.

To fill Michael Plyler's absence, the two remaining students with previous experience were chosen to lead the group. Jason Gill and Kuntal Vora took on the responsibilities of leading the entire group and keeping their technical group leader positions. With such a lack of experience among the team, this was found to be the best solution, although it presented an extreme amount of work for each individual.

2.2.2 Aerodynamics Group Responsibilities

The first task of the aerodynamics group was to generate several feasible aircraft configurations incorporating the competition regulations. Concurrently to this and other tasks a computer software package was to be created to mathematically model and simulate the aircraft. The next task was to perform a conceptual study evaluating the different configurations according to scoring potential, construction ease, and assembly time. To further aide in the conceptual study, figures of merit were defined and applied to each configuration. The results of this study were applied in the preliminary design phase. In this phase of the design, more refined concepts were developed as well as better understanding as to the size and weight of the aircraft. A preliminary estimate of the wing, tail, control surfaces, and fuselage sizing was determined. The servo requirements were also determined.

2.2.3 Propulsion Group Responsibilities

The Primary responsibility of the propulsion group was to evaluate several designs of motor, battery, and propeller combinations. A major factor to be considered was the effect of each propulsion system on the RAC. It was also important to determine if the propulsion system with the best score provided the required thrust, enough available power, and enough endurance. The aerodynamic model provided the required thrust which the propulsion team used to determine the correct selection of motor number, type and propeller.

2.2.4 Structures Group Responsibilities

The main responsibility of the structures group was to design a strong and light structure while considering component integration, payload deployment, and material selection. The structural analysis during the conceptual design phase produced basic structural design for primary components. The preliminary design phase required loading parameters provided by the aerodynamics and propulsion groups. The loading conditions allowed for a more refined estimate of the structural components and for the landing gear to be designed. The detailed design phase allowed for the final dimensions of the structure to be defined. The final responsibility of the structures group was to produce detailed construction drawings as well as a final three-dimensional model.

2.2.5 Payload Deployment Group Responsibilities

The payload deployment group developed several methods for payload deployment and loading. It was important to consider the effects of each deployment method on structural components. The aerodynamics group posed restrictions on the placement of the payload due to static and dynamic characteristics. Each payload deployment scheme had the potential to drastically change the aircraft configuration.

2.3 Scheduling, Documentation, and Configuration Update

It was important to create a scheduling plan that allowed for unforeseen problems and setbacks. Several milestones were identified and deadlines were set in place. The design process was divided into three phases: conceptual, preliminary, and detailed as outlined previously. In order for the aircraft to progress in a timely manner, an order of construction was developed and dates wet assigned for each component. The design report was continuously written throughout the entire design, construction, and testing phases. Table 2.1 is a milestone chart developed for the design process.

Throughout the design and construction processes it was important to continuously record all design decisions and changes. When a major design decision was made a short write-up was posted in the Design Build Fly lab and e-mails were sent to all members the team. A list of aircraft components was continuously updated as was all drawings and three-dimensional models.

Table 2.1: Tabulated Milestone Summary

		Task Name	Duration	Start	Finish
1		⊞ **Design Report**	**20 days**	**Wed 1/22/03**	**Fri 3/7/03**
11		⊟ **Design**	**7 days**	**Wed 1/22/03**	**Wed 2/5/03**
12		Fuselage	1 day	Wed 1/22/03	Wed 1/22/03
13		Wing	7 days	Wed 1/22/03	Wed 2/5/03
14		Tail	4 days	Wed 1/22/03	Wed 1/29/03
15		Controls	7 days	Wed 1/22/03	Wed 2/5/03
16		Propulsion	5 days	Wed 1/22/03	Fri 1/31/03
17		Electronics	5 days	Wed 1/22/03	Fri 1/31/03
18					
19		⊟ **Fuselage**	**7 days**	**Wed 1/22/03**	**Wed 2/5/03**
20		Fuselage Plug	1 day	Wed 1/22/03	Wed 1/22/03
21		Basic Lay-up of Fuselage	3 days	Fri 1/24/03	Wed 1/29/03
22		Fuselage Internals	3 days	Fri 1/31/03	Wed 2/5/03
23		⊟ **Tail Construction**	**9 days**	**Wed 1/22/03**	**Mon 2/10/03**
24		Design	2 days	Wed 1/22/03	Fri 1/24/03
25		Tooling ie. Foam forms and jigs	2 days	Mon 1/27/03	Wed 1/29/03
26		Cover	2 days	Fri 1/31/03	Mon 2/3/03
27		Control Surfaces	3 days	Wed 2/5/03	Mon 2/10/03
28		⊟ **Payload/Ejection System Construction**	**15 days**	**Wed 1/22/03**	**Mon 2/24/03**
29		Design	10 days	Wed 1/22/03	Wed 2/12/03
30		Build	5 days	Fri 2/14/03	Mon 2/24/03
31					
32		⊟ **Electronics**	**4 days**	**Fri 2/7/03**	**Fri 2/14/03**
33		Batteries	2 days	Fri 2/7/03	Mon 2/10/03
34		Motor/Speed Controller	2 days	Fri 2/7/03	Mon 2/10/03
35		Motor/Prop/batery testing	2 days	Wed 2/12/03	Fri 2/14/03
36		Receiver Servos	3 days	Fri 2/7/03	Wed 2/12/03
37					
38		⊟ **Wing**	**10 days**	**Wed 1/22/03**	**Wed 2/12/03**
39		Design	4 days	Wed 1/22/03	Wed 1/29/03
40		Tooling ie. Foam forms and jigs	3 days	Fri 1/31/03	Wed 2/5/03
41		Cover	2 days	Fri 2/7/03	Mon 2/10/03
42		Control Surfaces	1 day	Wed 2/12/03	Wed 2/12/03
43		⊟ **Integration**	**8 days**	**Wed 2/12/03**	**Fri 2/28/03**
44		Wing to Fuselage	2 days	Wed 2/26/03	Fri 2/28/03
45		Tail to Fuselage	2 days	Wed 2/12/03	Fri 2/14/03
46		Sevos and Pushrods	2 days	Fri 2/14/03	Mon 2/17/03
47		Powerplant	1 day	Mon 2/17/03	Mon 2/17/03
48		Ground Testing	1 day	Mon 3/3/03	Mon 3/3/03
49		Flight Testing	3 days	Wed 3/5/03	Mon 3/10/03
50		Modification Phase	5 days	Wed 3/12/03	Fri 3/21/03
51		Phase 2 Flight Testing	1 day	Mon 3/24/03	Mon 3/24/03

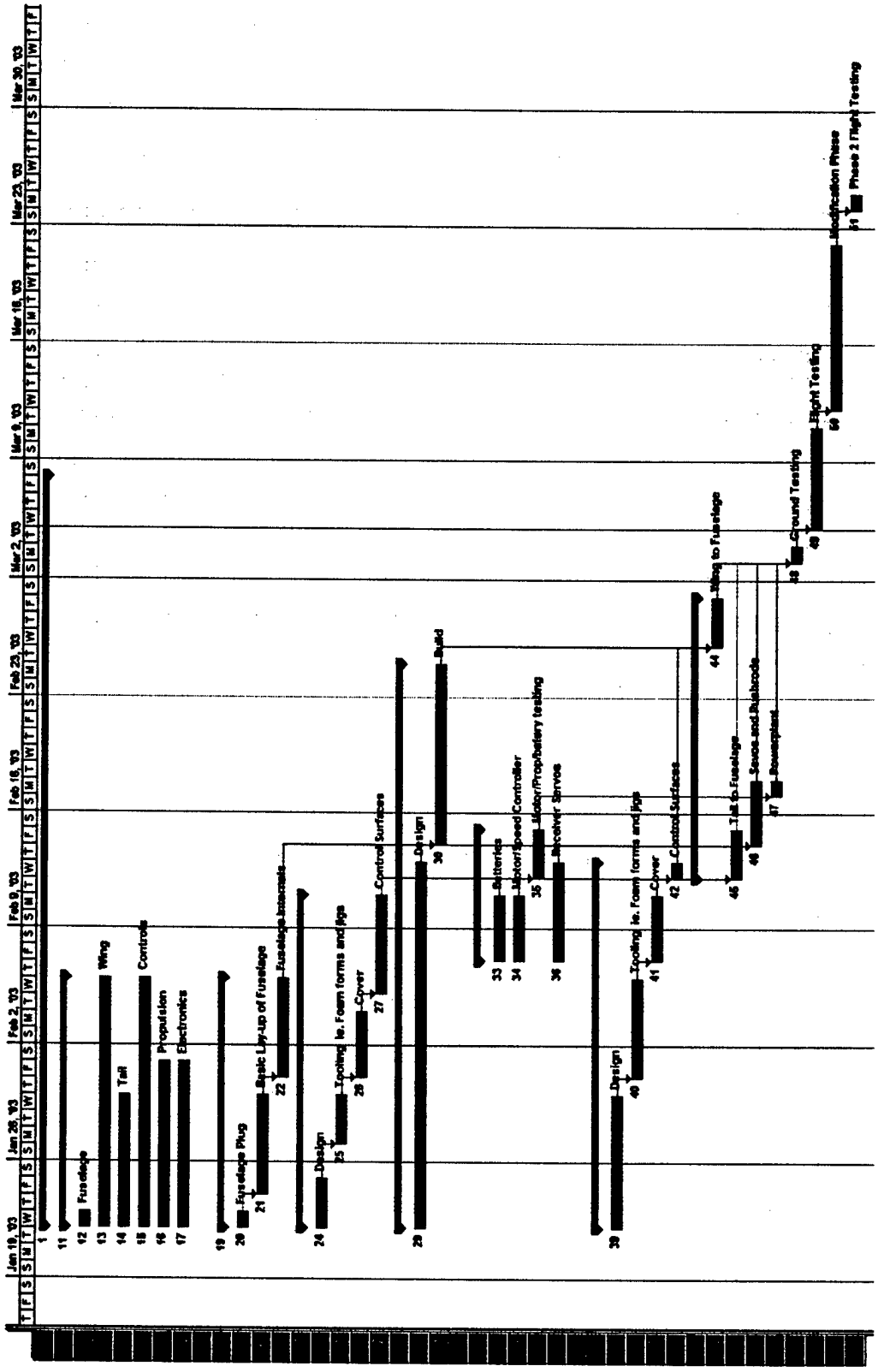

Figure 2.1: Graphical representation of Milestone data

3.0 Conceptual Design

3.1 Design Parameters

The first step in the design process was to identify the major parameters that were not previously determined by the competition committee. Parameters such as takeoff distance and payload weight and size were defined parameters that each team had to incorporate into their design along with the parameters for the two missions the team selected to perform for the competition. It was important to determine how each parameter would effect both the RAC as well as the total score. The mission selected for this aircraft were the ones with the highest difficulty factors, which were mission one and two. The objectives of the two missions were:

1. Missile Decoy – Difficulty Factor 2.0
   - Aircraft must take-off, complete 4 laps, and land.
   - Payload for this mission is a simulated avionics package. The payload is a box 6 inches wide by 6 inches tall by 12 inches long and must be ballasted about it's planform centroid to weigh at least 5 lbs. Payload weight will be verified on the judge's scale during technical inspection.
   - The aircraft must have a simulated cylindrical antenna, a section of (unmodified) "6-inch" Schedule 40 (white) PVC pipe three inches tall, with the top and bottom sealed flush with flat 1/16" Plywood sheets. The antenna must be completely exposed on the exterior of the aircraft and stand-off from the nearest airframe structure by a minimum of 3 inches. The antenna (cylinder) may not be faired in any manner.
   - On all laps flown the aircraft must complete a 360° turn in the direction opposite of the base and final turns on the downwind leg of each lap.
2. Sensor Deployment – Difficulty Factor 1.5
   - Aircraft must take-off, complete 2 laps, and land. When on the runway and stopped the aircraft will self-deploy the simulated sensor package. The aircraft will then take-off and complete 2 additional laps and land. The ground crew may not reposition the aircraft except to move it from off of the runway (if it runs off) to the nearest runway edge.
   - Payload for this mission is a simulated sensor package. The payload is a box 6 inches wide by 6 inches tall by 12 inches long and must be ballasted about it's planform centroid to weigh at least 5 lbs. Payload weight will be verified on the judge's scale during technical inspection.
   - On all laps flown the aircraft must complete a 360° turn in the direction opposite of the base and final turns on the downwind leg of each lap.

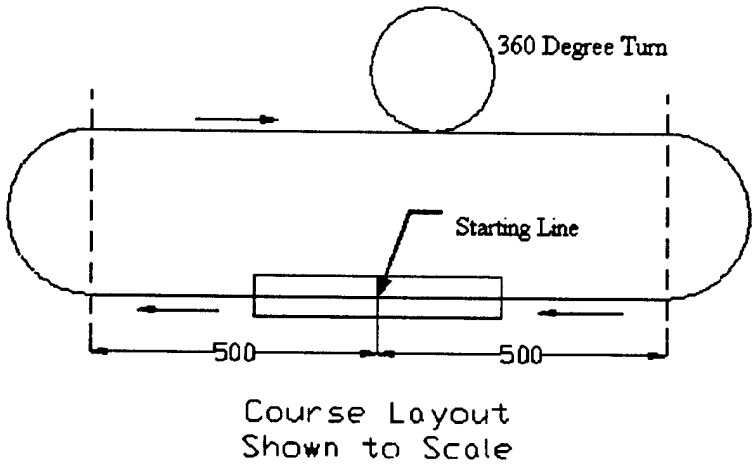

Figure 3.1: Course Layout

3.1.1 Primary Design Parameters

It was determined that there were seven separate primary design parameters. Each design parameter required that many components be considered. The major design parameters are: wings, fuselage, empennage, flight system, propulsion system, payload ejection system, and assembly. Many different configurations were investigated for each design parameter.

3.1.2 Design Parameter Sensitivity Analysis

A design parameter sensitivity analysis was performed to identify the effects of each design parameter had on the total competition score. Trends in the RAC and total score were identified for each component variable was modified. Each major component's defining value was increased and the effect on the RAC and total score was identified. The results of this study can be seen in Table 3.2. This study resulted in a simple and obvious conclusion. The key to a good score is to keep the plane small with as few parts as possible.

Table 3.2: Sensitivity Analysis Identifying Trends in the RAC and Total Score

Component	Effect on RAC	Effect on Total Score
Aircraft Weight	Increase	Decrease
Fuselage Length	Increase	Decrease
Number of Engines	Increase	Decrease
Number of Control Surfaces	Increase	Decrease
Wing Span	Increase	Decrease
Maximum Wing Chord	Increase	Decrease
Empennage Configuration	None	None
Payload Ejection System	None	Decrease

3.2 Aircraft Configuration

3.2.1 Alternative Fuselage and Tail Configuration

Figures of merit (FOM) were used to evaluate the different fuselage and tail configurations that were chosen. Each FOM was weighted according to the importance it exhibited in making design decisions and was rated on a scale of one to five based on each FOM criterion. For example, if a certain configuration offered stability that could not be improved on it received a five. However if another configuration resulted in instability that could only be overcome with a complex automatic control system, it received a one. There were five FOM's used in this investigation include:

- **Rated Aircraft Cost (RAC)**: Any effects on the RAC are directly seen in the overall score.
- **Assembly Time**: A very important factor was to design a plane that could easily be assembled in as little time as possible.
- **Stability**: The competition location posses interesting stability issues due to the tendency towards large wind gusts.
- **Power Requirements**: The drag that each configuration would induce because it is important to use as few batteries as possible.
- **Construction Ease**: Considering the techniques and time involved to construct each configuration was extremely important.

Several assumptions were made in this first analysis of fuselage and tail configurations. It was assumed that any configuration could be adapted to include any chosen payload ejection system and the difference in structural weight was negligible. With these assumptions six fuselage and tail configurations were identified for further consideration. Given the assumptions and the FOM above, the alternatives that were evaluated are as follows:

- **Canard**: This configuration offers excellent stall characteristics but creates a limit on the maximum lift for takeoff.
- **Conventional**: This configuration offers many benefits, which are the reason it has become known as the convention. The FOM's for this configuration were given a three.
- **Flying Wing**: The flying wing configuration offers many benefits in reducing the RAC by not having an empennage and reducing the number of control surfaces and servos. However, it possessed stability problems that are very difficult to overcome.
- **Bi-Wing**: This configuration allows for the wingspan to be reduced or for the aircraft to have increased weight. However, the RAC suffers greatly.
- **V-Tail**: A V-tail is beneficial because it has the same effect on the RAC as a conventional tail while at the same time requiring less space to store. It does require the addition of a servo.

- **Conventional Twin-Boom:** A conventional twin-boom tail configuration increases the number of tail surfaces thereby negatively affecting the RAC. If the two tail booms were made stiff, stability would increase but at the same increase overall weight.

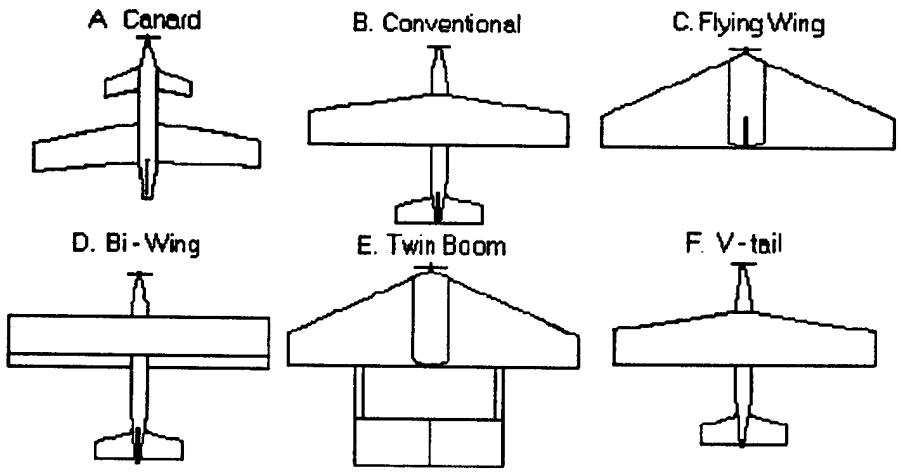

Figure 3.1: Various Aircraft Configurations

The first step in evaluating the FOM's was to calculate the RAC for each configuration. The RAC FOM was rated with configuration B being the conventional design receiving a three. Table 3.3 shows the RAC's and FOM's for the six different fuselage and tail configurations.

Table 3.3: RAC and FOM's for Different Configurations

Configuration	RAC	FOM Rate
A	11.92	3
B	11.92	3
C	11.47	5
D	13.08	1
E	12.02	2
F	12.22	2

To determine which configuration possessed the most benefits a weighted decision matrix was created. In this matrix all five figures of merit were considered and assigned a weight based on its importance in decision making for the aircraft. It was determined that for this competition the most important FOM was the RAC followed very closely by the assembly time. Assembly time was considered most important because its time must be added to every mission flight time during the competition. Therefore it has a significant effect on the overall score. The FOM that was considered to have the middle importance was construction ease. This is made possible because the team has access to

experienced aircraft builders who were willing to lend their skills and knowledge. The FOM that fell second to last in importance was the power requirements. This was because our initial study of propulsion and power systems showed that it was possible to produce a system that would match any requirements that may be required. The least important FOM was stability. Any stability problems that could arise with any of the configurations could be overcome. This is due in part to a very experienced pilot in charge of the flight of the aircraft. Figure 3.4 shows the weighted decision matrix with the highlighted final choice for the fuselage and tail configuration.

Table 3.4: FOM for Fuselage and Tail Configuration

		Configurations					
Figures of Merit	Weight	A	B	C	D	E	F
Rated Aircraft Cost	0.3	3	3	5	1	2	2
Assembly	0.25	2	3	4	1	5	1
Construction	0.2	2	3	3	2	4	3
Power	0.15	4	3	1	3	4	4
Stability	0.1	2	3	1	4	3	4
Score	-	2.6	3	3.35	1.8	3.55	2.45

The V-tail configuration proved to be the winning contender in the fuselage and tail configuration analysis. This configuration creates a RAC that is relatively high. However, the extremely low assembly time that can be obtained with this configuration more than compensates for the high RAC.

3.2.2 Alternative Wing Configurations

The analysis of alternative wing configurations was completed after the fuselage and tail configuration was determined. This decision could potentially add restraints to the choices for wing configuration. The five figures of merit used in this analysis are as follows:

- **Payload Deployment:** A very important task that the plane must perform is to automatically deploy the payload. The fuselage and landing gear configuration must be designed to allow for easy payload deployment.
- **Construction:** The wing itself must be easy to construct as well as any carry-through structure.
- **Landing Gear Placement:** The wing must have no interference with the placement of the landing gear.
- **Stability:** Historical data was used to analyze the stability of each configuration. High mounted wings provide the best stability.
- **Assembly Time:** The wing design must provide the fastest assembly time possible. Mid wings were to difficult to allow the pre-assembled plane to fold up in the box.

Several design decisions were made before analysis of the wing configurations could begin. The first decision made was to use a low taper ratio based on historical data of low Reynolds number flight. The second decision was to define the wing area as a constant based on wing loading needed during gusts. The three wing configurations that were considered were low, mid, and high wing attachment. The following are the factors that were considered for each configuration. Also follows the weighted decision matrix for the wing configuration analysis.

- **Low-Wing:** This wing configuration caused a great deal of interference with payload ejection. It proved to be very difficult to design a carry-through structure to accommodate the payload as well as a fast assembly time. It also possesses a great deal of instability.
- **Mid-Wing:** This configuration posed the most difficulty in the areas of payload deployment, construction, and assembly time. It was determined that it was not possible to design a carry-through structure for this configuration that would be feasible.
- **High-Wing:** This configuration allowed for the most flexibility of all the configurations. All carry-through structure possibilities were feasible and the assembly time was very low. This configuration also has the greatest stability.

Table 3.5: FOM for Various Wing Locations

		Configurations		
Figures of Merit	Weight	Low-Wing	Mid-Wing	High-Wing
Assembly Time	0.28	3	3	5
Payload Deployment	0.28	2	1	5
Construction	0.28	2	1	4
Landing Gear Placement	0.1	1	3	4
Stability	0.06	1	3	5
Score	-	2.12	1.88	4.62

The weighted decision matrix determined that the high-wing configuration gave the best results. This year's competition requires an interesting emphasis on the payload and assembly time. This causes the assembly time, payload deployment, and construction FOM's to be weighted the same. In this configuration, the landing gear placement could potentially cause problems but the design team felt that potential problems could be dealt with. The same was determined for the stability issues caused by any wing configuration. The only problems that could be foreseen with the high wing placement are a minor landing gear issue if the payload is ejected from the bottom of the aircraft and the construction of a strong carry-through structure that allowed for a fast assembly time.

3.2.3 Alternative Payload Ejection Configurations

An in depth analysis of payload ejection configurations could only be performed after the wing configuration was determined. The high-wing placement allowed for a great deal of flexibility in designing a payload ejection system. An ejection system that deployed the payload at the front of the aircraft was immediately dismissed because of major wiring and propulsion interference. There were three configurations that were considered: bottom, rear, and side. The figures of merit that were considered for the payload ejection system were as follows:

- **Construction:** It was very important to design a payload ejection system that would not be overly difficult to construct. This would add unnecessary construction time.
- **Assembly Time:** It was important to consider the effects of each ejection system on the mechanisms necessary to create a fast assembly time.
- **Rate Aircraft Cost:** The number of servos that are required for the payload ejection system can impact the RAC.
- **Ejection Time:** To keep the flight time as low as possible the payload ejection system must be as fast as possible.
- **Mechanical Ease:** It is imperative that the payload ejection system be as mechanically easy as possible. A mechanical failure during a flight could be disastrous.

The following are the factors that were considered for each of the three payload ejection configurations. Also following the payload ejection configurations is the weighted decision matrix.

- **Bottom:** This configuration would cause problems with constructing a solid structure for the fuselage as well as the wing carry-through. It also created mechanisms of a high degree of complexity. The main problem that this configuration caused was with the landing gear. The landing gear would not be able to be permanently attached to the plane. This would drastically increase the assembly time.
- **Side:** This configuration was almost completely unfeasible from the start. It would require a very complex mechanism that would impact every aspect of the aircraft.
- **Rear:** This configuration lent itself to a wide range of simple mechanisms that would be easy of construct and assemble. It would allow for a low RAC and assembly time.

Table 3.6: FOM for Payload Ejection Mechanism

		Configurations		
Figures of Merit	Weight	Bottom	Side	Rear
Mechanical Ease	0.3	3	1	5
Construction	0.25	3	1	5
Ejection Time	0.2	4	2	5
Assembly Time	0.15	2	4	5
Rated Aircraft Cost	0.1	4	4	5
Score	-	3.15	1.95	5

As can be seen from Table 3.6, the payload ejection configuration from the rear is the obvious choice. It lends itself to the widest range of mechanisms with very little effect on the aircraft.

3.3 Structural Configurations

3.3.1 Figures of Merit

The creation of figures of merit was a key component of the analysis of structural configurations. Six FOM's were considered for all components of the aircraft. The following are the six FOM's that were universally considered for each structural component.

- **Scoring Potential:** This figure of merit (FOM) considers the effect that each configuration has on scoring potential. It considers the effect of weight and assembly time, among all the other FOM's.
- **Strength vs. Weight:** A balance between strength and weight was important. The weight of the aircraft affects scoring potential as well as performance of the aircraft in flight. Every phase of flight is effected by the aircraft weight.
- **Ease of Construction:** The aircraft structure must be easy to construct requiring as few man-hours as possible. It was also important to consider the skill that would be required to construct each component.
- **Quality Assurance:** This was important in that each structural component must be easy to achieve the quality and accuracy required in the design. Some structural designs are very difficult to construct with the accuracy required by a design.
- **Repair:** If the aircraft were to experience a crash during flight, each structural component must be easily repaired.
- **Assembly Time:** Each structural component must require as little time to assemble as possible. Complex connection points requiring many tools and people would not be considered

3.3.2 Assumptions Made and Design Parameters Investigated

There were four structural components that were analyzed in the conceptual design phase. To complete this task several assumptions were required. When one component was analyzed all other components were ignored. Simple weight models were created based on a maximum aircraft weight of 18.5 pounds.

The parameters that were investigated in the conceptual design phase were those that affected scoring potential the most. The parameters that were investigated included scoring potential, weight, strength, materials, and construction techniques.

3.3.3 Alternative Wing Structures

The figures of merit that were investigated for wing structures were only the universal six. No special FOM's were necessary in this investigation. The other factors for consideration were the ability of the wing to hold an airfoil shape, the transfer of lifting force to the fuselage, and the wings resistance to torque causing the wing to have a varying angle of attack. The initial estimate of the wing planform area was determined to be 6.6 square feet. The wing must be strong enough to withstand a 4 g-load while at the same time not cause a high weight penalty. A weight allocation table was created to set an initial estimate at the weight each component could weight. The wings weight was determined to be two pounds. Material alternatives and construction methods were considered. Three concepts were analyzed: balsa buildup with monocote skin, carbon skin and struts, and foam core with balsa skin. The following is the weighted decision matrix used to determine the wing structure.

Table 3.7: FOM for Wing Material Composition

		Configurations		
Figures of Merit	Weight	Balsa Buildup	Carbon Skin and Struts	Foam Core and Balsa Skin
Scoring Potential	0.25	3	4	4
Assembly Time	0.2	3	3	5
Strength vs. Weight	0.2	3	5	4
Ease of Construction	0.15	4	2	4
Quality Assurance	0.1	3	4	5
Repair	0.1	1	3	5
Score	-	2.95	3.6	4.4

After the structural configuration for the wing was selected a basic concept for the internal structural components could be determined. This included placement of struts, carry-through structure, lift force transfer, and assembly mechanisms. A final conceptual drawing of the wing can be seen in Figure 3.2.

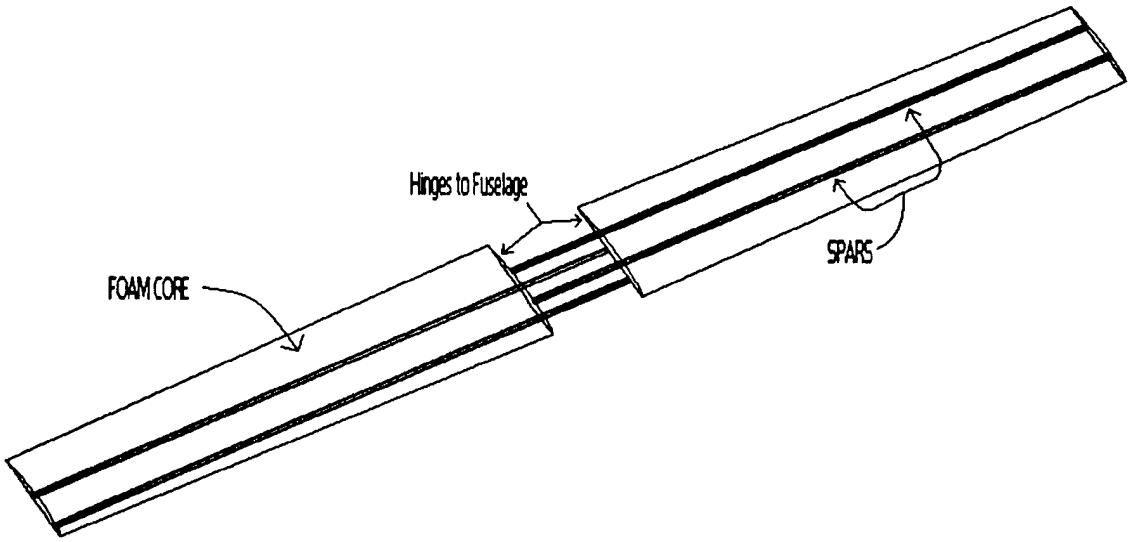

Figure 3.2: Final Wing Configuration

3.3.4 Alternative Tail Structures

The same factors that were considered for the wing structure were considered for the tail. The FOM's were the same for both the wing and the tail. The three concepts that were considered were: balsa buildup with monocote skin, carbon skin and struts, and foam core with balsa skin. The tail had to be light but at the same time strong enough to withstand the forces needed to maintain longitudinal and lateral stability. The weighted decision matrix used for the tail resulted in the same basic structure as the wing. The following is the conceptual drawing of the tail.

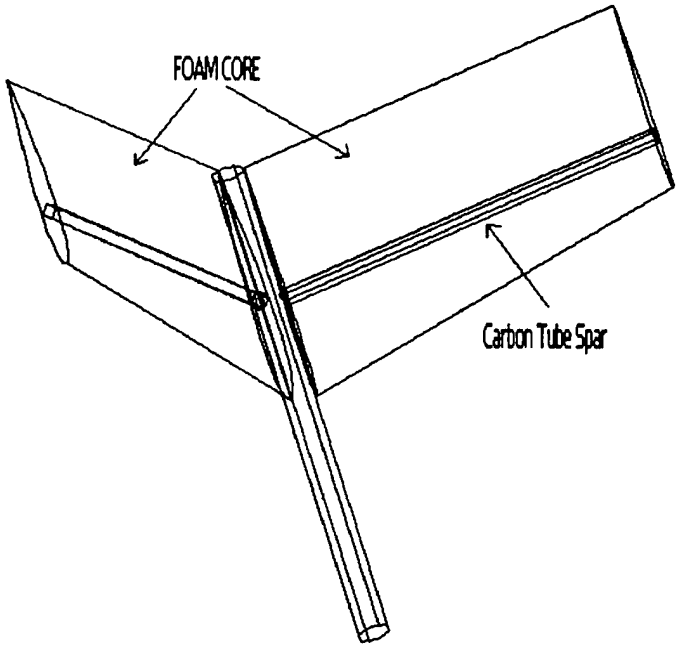

Figure 3.3: Final Tail configuration

3.3.5 Alternative Fuselage Structures

Analyzing the different structures for the fuselage required the consideration of all aspects of the airplane including all other components. It was important to consider how other components would be incorporated in the fuselage as well how different components would load the fuselage. The fuselage is the point on the aircraft where all forces and moments converge. This factor made strength and rigidity very important. The fuselage must also possess ample internal payload storage space without creating an excessive external surface area and cross-sectional area. In analyzing the four different fuselage structures, the six universal structures FOM's were considered. The four fuselage structures considered are as follows:

- **Wood Frame-Monocote Skin:** This structure relies solely on a wood frame with wood stringers to carry the loads and hold the shape. The monocote skin only covers the frame and does not supply any structural support. The size of the frame components needed to create a stiff fuselage would be much too large. This structure also suffers from a difficulty to create complex contours.
- **Carbon Frame-Carbon Skin:** this structure is almost identical to the wood frame with monocote skin. The difference is that the wood is replaced with carbon fiber as well as the monocote skin. This is advantageous because the skin can now carry loads. This fact as well as the fact that the strength to weight ratio of carbon is much lower than that of wood allows a smaller internal volume to be used with structure. The major disadvantage is that the frame components require immense amounts of man-hours to produce.
- **Carbon Monocoque:** This structure consists of fully load bearing outer shell constructed of carbon composite. This structure allows for the elimination of all internal frame components freeing all internal space for payload and other various components. This structure also has the added benefit of having the highest strength to weight ratio.
- **Plywood-Carbon Monocoque:** This structure is identical to the carbon monocoque; however there is an added layer of plywood added to the outer shell. This adds stiffness to the structure.

To determine which construction method to use a weighted decision matrix was created based on the six universal FOM's. The weighted decision matrix in table 3.8 shows that the best construction technique would be the plywood-carbon monocoque. This limited the types of materials that could be used to plywood, carbon, and fiberglass. This construction method allows for a very aerodynamic, strong, and light fuselage.

Table 3.8: FOM for Fuselage Structure

Figures of Merit	Weight	Configurations			
		Wood Frame-Monocote Skin	Carbon Frame-Carbon Skin	Carbon Monocoque	Plywood-Carbon Monocoque
Scoring Potential	0.25	4	4	5	5
Assembly Time	0.2	2	3	5	5
Strength vs. Weight	0.2	1	3	4	5
Ease of Construction	0.15	3	2	5	5
Quality Assurance	0.1	2	4	5	5
Repair	0.1	2	3	4	4
Score	-	2.45	3.2	4.7	4.9

3.3.6 Alternative Landing Gear Configurations

Landing gears play a vital part in almost all aspects of the aircraft. They have a strong effect on the drag of the aircraft as well as handling characteristics both on the ground and in the air. The three configurations considered were tricycle, tail dragger, and tail dragger with retractable gear. To analyze different landing gear configurations the six universal FOM's were considered along with a few additional specialized FOM's. The specialized FOM's are as follows along with the weighted decision matrix:

- **Ground Handling:** Landing gear can drastically affect the ability of the pilot to control the aircraft while on the ground. The landing gear can also affect the speed at which the plane can return to the air after the payload has been deployed.
- **Landing Performance:** It is important that the landing gear be strong enough to withstand the toughest of landings. It also must not be so strong as to transmit all the force of the landing to the fuselage. It must absorb some of the energy from impact.
- **Drag:** The type of landing chosen can increase the drag of aircraft significantly.
- **Cost:** Some landing gear systems are very expensive. The budget for this project was very tight.

The weighted decision matrix shows that the tricycle configuration would give the best results. This is also confirmed from experience. It was determined that there was no need to analyze different configurations of the nose and main gear. This is because the budget only allows for the use of materials already available to the team. This limits the nose gear to a conventional remote control aircraft configuration and the main gear to carbon composite bow gear. This was determined to be acceptable due to previous teams experience with these gear options.

Table 3.9: FOM for Landing Gear Configuration

		Configurations		
Figures of Merit	Weight	Tricycle	Tail Dragger	Tail Dragger with Retractable Gear
Scoring Potential	0.2	5	4	5
Assembly Time	0.15	5	5	3
Strength vs. Weight	0.15	4	5	3
Ease of Construction	0.12	4	5	1
Quality Assurance	0.1	5	4	2
Repair	0.1	4	4	1
Cost	0.07	4	5	1
Ground Handling	0.05	5	2	2
Landing Performance	0.05	5	4	3
Drag	0.05	3	4	5
Score	-	4.66	4.55	2.89

3.4 Alternative Power Plant Configurations

The components of the power plant required for design were the engine, batteries, and propeller. The propeller was not considered in this analysis because it could be changed depending on the flight conditions present during flight. There were three configurations chosen for analysis (figure 3.4). Also following is the weighted decision matrix for the propulsion system (Table 3.10).

The weighted decision matrix in table 3.10 shows that the single stack configuration is the best choice for the propulsion system. The goal was to find a system that would have the best balance between engine power, efficiency, and weight. The single stack had the correct balance that was desired. From experience from past competitions, the team decided to investigate methods to air-cool both the engine and the batteries. The decision was to expose the batteries to airflow by mounting them external to the fuselage under the wing. It was important to position the batteries such that the C.G. would move to the required location.

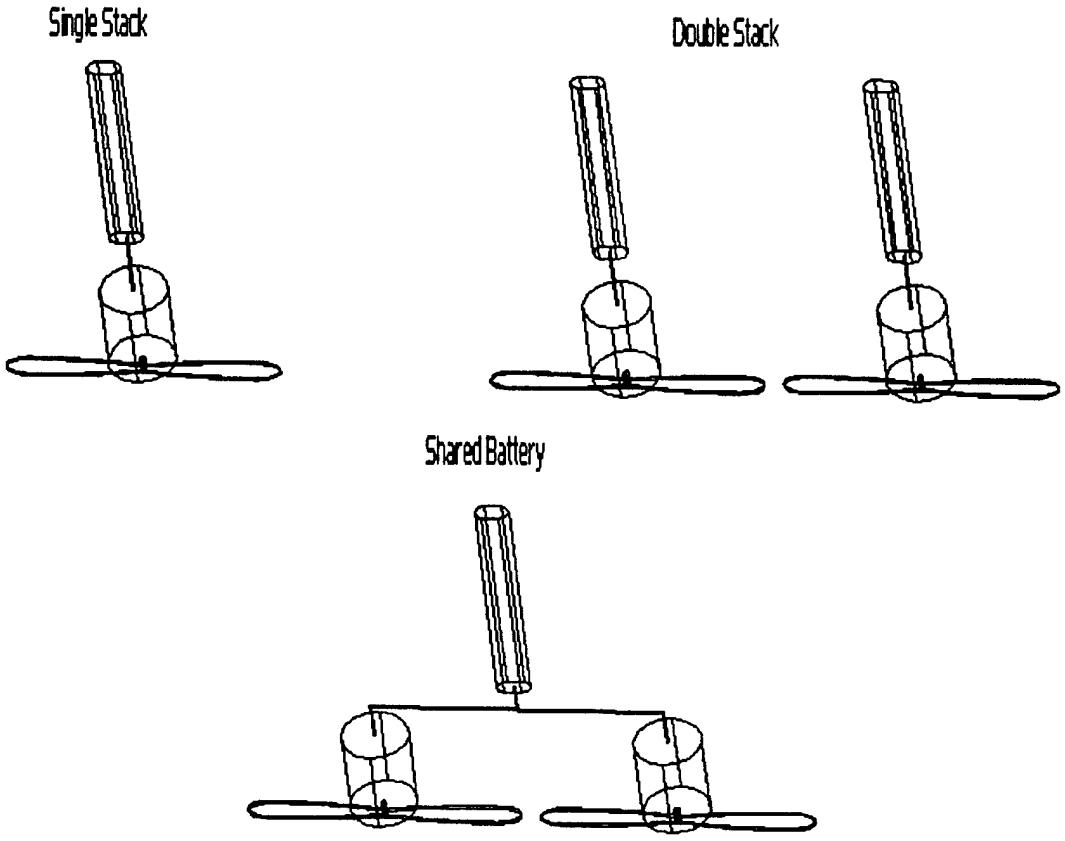

Figure 3.4: Various Power Plant and Battery Configurations

Table 3.10: FOM for Power Plant Configurations

		Configurations		
Figures of Merit	Weight	Single Stack	Double Stack	Shared Battery
RAC	0.3	5	1	3
Power	0.3	3	5	5
Weight	0.2	5	1	3
Efficiency	0.15	5	1	3
Number of Fuses	0.05	5	2	5
Score	-	4.4	2.25	3.7

3.5 Conceptual Aircraft Configuration

When the conceptual design phase was completed the optimum design was plywood-carbon monocoque fuselage, high wing, V-tail, and single stack propulsion. This design allows for fast deployment of the payload as well as a very fast assembly time. The high wing provides good stability while at the same time good strength. The monocoque fuselage allows for great strength, ample internal storage, and low drag. The V-tail provides stability and as little volume as possible. The single stack

propulsion unit provides ample thrust and efficiency. Every major component of the aircraft effects the RAC in the most favorable way possible.

Figure 3.5: Final Aircraft Configuration (Lateral View)

4.0 Preliminary Design

4.1 Flight Performance Objectives

4.1.1 Payload Ejection System Analysis

It was decided that the method of deploying the payload with the least chances of binding on the fuselage, would be the best. Also, due to the rule barring anything from being fixed on or drilled into the payload itself, it was decided that a carriage design was best.

The payload is suspended from two aluminum rails fixed to the top corners of the fuselage and moves about on wheels. A rubber band was stretched around the back of the payload and fixed to the rear of the fuselage on either side of the payload. A pin, inserted from the top of the fuselage, controlled by a servo is used to hold the payload in place. The rear of the fuselage is open.

The actual ejection process consists of the servo pulling the pin, releasing the payload. The rubber band then contracts, pushing the payload along the rails and out the back of the plane.

This assembly was chosen due to the speed of deployment, and insertion of the payload. A pin was used, instead of a servo arm, because the servo arm would constantly drain power, while a pin would use power only during payload ejection.

4.1.2 Carry – Through Analysis

The size restrictions imposed by the box made having a fixed wing nearly impossible. The weight of our plane required that some form of a folding wing was required. In order to make the hinged area of the wings as strong as possible, and to reduce assembly time, it was decided that the wings should fold at their roots, coming to lie along the fuselage sides in the box. This created an interesting setup in the carry-through area.

Carbon rods, which also act as wing spars were extended from the roots of the wings across the fuselage to the opposite side of the fuselage. Screen door latches were used to lock the carbon rods into deployed position. The locking mechanisms were placed on the opposite side to maximize the moment arm of the locking mechanism. Hinges were riveted to the fuselage and to the aluminum rails that carry the payload.

Due to the requirement for wing folding, the wing root bending moment required mathematical analysis. Also, the effect of the carbon rods puncturing through the top of the fuselage was another consideration. It was assumed that during the necessary wing-tip test, the carbon rods closest to the quarter chord suspends the entire weight of the airplane. Under these guidelines, the stress in the rod was found to be 6.26×10^3 psi. This results in a safety factor of 43, well within the design envelop.

The puncture analysis were done assuming that the carbon rod subjects a point force on the steel latches made of structural steel (ASTM A36), which intern applies a distributed load on the carbon-wood monocoque fuselage. The ultimate shear stress of the steel latches is given to be 21 Ksi and the calculated puncture force was 0.825 Ksi, assuming that a quarter inch of the carbon rod circumference is in contact with the latches. The safety factor for this was found to be 25.47. The next area of concern was the fuselage top in contact with the latches. Analysis of that section showed that the latches would exert a pressure force of 26.67 psi on the fuselage top. This is a very small load as the wood in the composite structure alone would be able to sustain that kind of loading. The wings are also hinged at the root cord and would put the hinge in tension and the fuselage under a shear loading. This scenario was ruled out as point of failure as the hinge is epoxied to the fuselage along with five rivets. This will allow a very nominal load distribution over that area. The equations used in these calculations were:

$$\sigma = \frac{Mc}{I};\ M = \frac{WL}{2};\ S.F. = \frac{Allowable}{Calculated};\ Ci = \pi\frac{D}{4};\ A = (Ci)t;\ F = A\sigma;\ A(l) = lb;\ R_a = \frac{WL}{L_d};$$

$$P = \frac{R_a}{A(l)}$$

Table 4.1: Carbon Spar Stress and Strain Calculations

Aircraft Weight	W	20 lbs
Length	L	40 in
Inertia	I	0.01598 in^4
Diameter	D	0.5 in
Latch Thickness	t	0.1 in
Latch Length	l	2 in

Latch Breadth	b	1	in
Distance Between Latch and Hinge	L_d	7.5	in
Safety Factor	S.F.	3	
Material Properties			
Carbon Rods			
Modulus of Elasticity	E	1.9E+10	psi
Allowable Stress	σ	270000	psi
Structural Steel (ASTM-A36)			
Allowable Shear	σ	21000	psi
Calculations			
Sigma	σ	6257.822	psi
Safety Factor	S.F.	43.146	in
Root Bending Moment			
Carbon Rod on Latch			
Length of rod under pressure	Ci	0.392699	in
Area under pressure	A	0.03927	in^2
Required Puncture Force	F	824.6681	lbs
Safety Factor	S.F.	25.46479	
Latch on Airframe			
Latch Area	A(l)	2	in^2
Reaction Force on Latch	R_a	53.33333	lbs
Pressure exerted on Airframe	P	26.66667	psi

4.1.3 Assembly Time

A fast assembly time was desired to keep the flight time short. The rules for the competition stipulate that the assembly time is added to the flight time. By working to reduce the assembly time, our team was potentially increasing our flight score months ahead of the actual flight. The assembly time could be reduced in many ways such as the way the wings, tail, batteries, and landing gear were attached to the fuselage. By creating a hinge design for the spars of the wings to lock into, many seconds were eliminated. To position the wings into place, lift the wings from the folded position. The landing gear is mounted such that it swivels and locks in place, with no need for any tools or additional connections. The batteries were also mounted so that they swing and lock into place and do not require separate connections or time to secure them into place. The final connection involved with the assembly of the aircraft is to secure the tail boom. This was another very simple connection, which was hinged into position. With the simplicity of all of the connections of the aircraft, a significant amount of assembly time was eliminated which will directly effect the overall flight time of the aircraft.

4.2 Aircraft Size Limitations

4.2.1 Wing Dimension Study

The wingspan of the aircraft is limited to the size of the box dimensions. Due to the orientation within the box, the span is limited to twice the largest dimension, which is set at eight feet long. The aircraft is placed diagonally in the box to achieve the largest wingspan possible. The wings are hinged and folded down so that the largest wingspan possible is utilized. Through careful measurement of the teams transport box, a final span was found to be 7.5 ft.

4.2.2 Tail Configuration Study

The tail, as with the wing, is limited to the dimensions of the box the aircraft is to be folded into. Stability requires the length of the tail boom to be a specified length, but due to the specifications of the box, the boom must be hinged to meet the length requirements. The V-tail is to be rotated on a hinge to fit within the box. The V-tail design was chosen because the volume it takes up is less than the more traditional designs. It also lowered the overall RAC.

Packaging the plane to fit into the box was the main issue faced when designing the tail of the plane. With the 4'x2'x1' dimensions required us to design the plane, namely the wings and tail to fit inside. There were three objectives that were in focus when designing the tail: speed of deployment, weight, and maneuverability.

The overall goal was to have a plane that can be prepared to fly as soon as quickly as possible. The plane's design is to be completely attached together, using hinges to transform to a ready-to-fly plane. The tail utilizes a two hinges attached on parallel planes, with the upper hinge rotated ninety degrees counterclockwise. This upper hinge allows the tail boom to rotate along the fuselage. The reasoning for the upper hinge was to rotate the surface areas on the tail. This allows the tail to fit in the box. The lower hinge allows the tail spar to fold down toward the landing gear.

The tail spar is attached to the upper hinge. These hinges allow the spar to rotate about the rear of the fuselage, as well as rotate axially.

The V-tail used in this design was an attractive option mainly due to its ability to fit in a smaller area and yet retain sufficient area for control. This smaller surface area induces less drag as well. Overall the V-tail was the best fit for the general concept. With the tail boom's ability to rotate, the V-tail is able to rotate, and fit into the box.

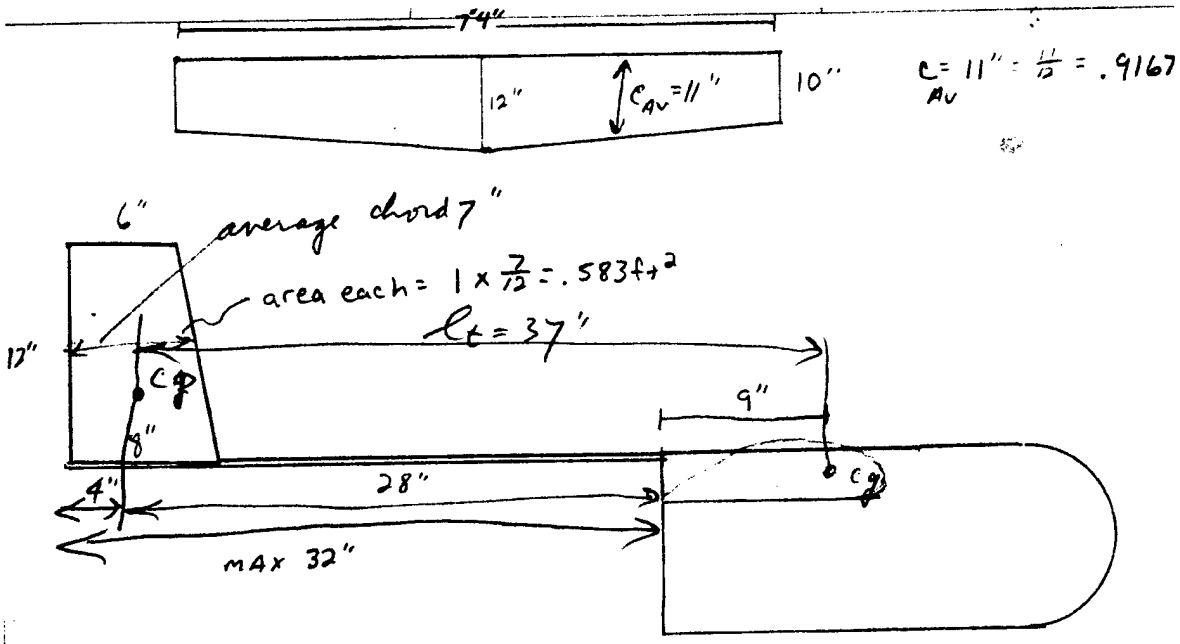

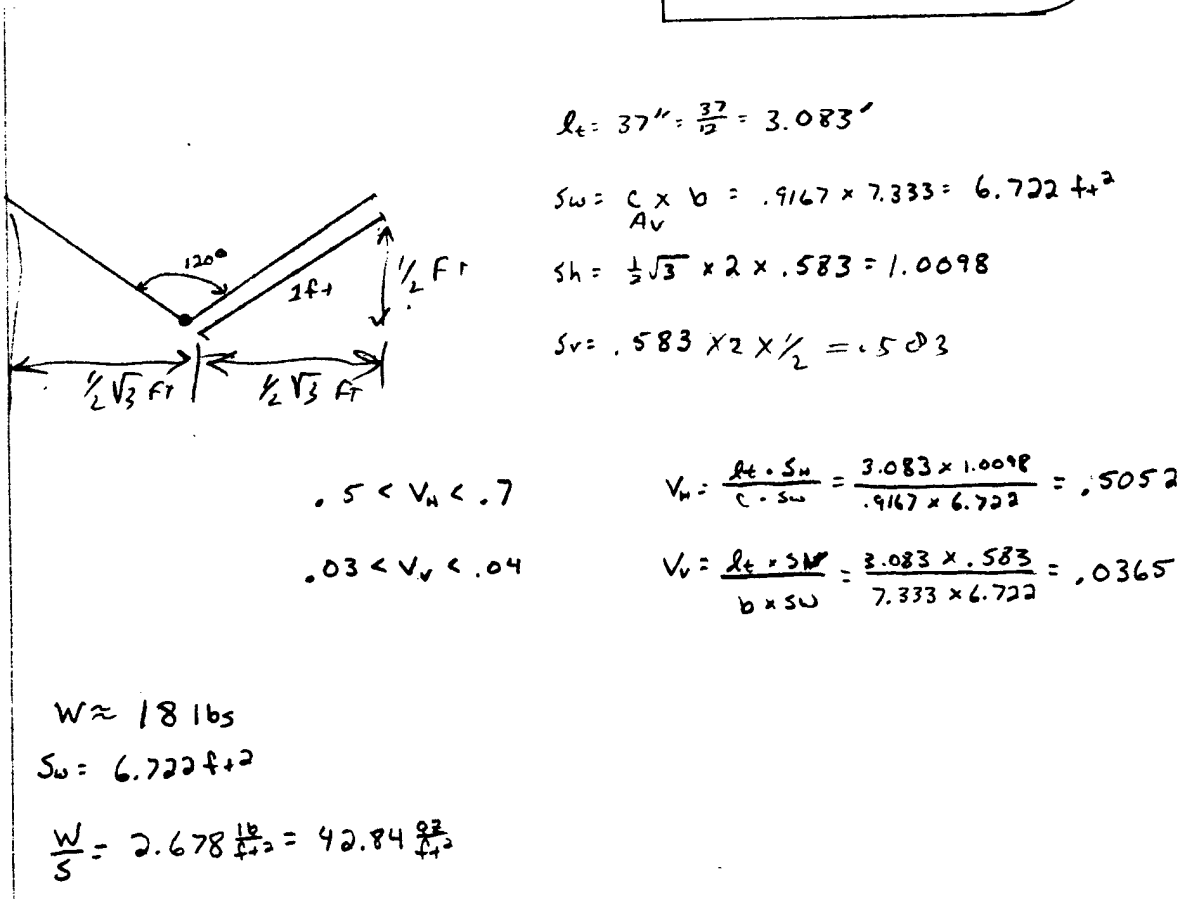

Figure 4.1: Hand Calculations of Tail Volume Sizing

4.2.3 Battery Configuration Analysis

Due to the design of the fuselage in relation to the payload, the batteries must be carried outside of the plane. During flight the batteries are suspended under the wing, next to the fuselage. Half of the

batteries are on each side of the fuselage, while parallel. This placement was chosen because there is a pocket of turbulence in that area. Putting an oddly shaped object there does not induce much drag; therefore it had a negligible effect on the L/D of the aircraft. Due to the wing/hinge design, the batteries must be able to move to and from the lower base of the wing quickly. This was achieved by hinging the end of the batteries that is at the front of the fuselage. The battery packs can now rotate to and from the base of the wings.

This is a quick method to get the batteries in place, and attributes to the space saving measures needed when dealing with the storage box.

4.2.4 Aerodynamic considerations

Generally, aerodynamic considerations include the estimation of lift, drag, and stability of the aircraft. A basic analysis of the aerodynamics of the craft allows for these estimations along with optimization of design. The main tool for analysis was a Microsoft Excel spreadsheet. Using this spreadsheet, various aerodynamic coefficients and performance data were obtained. The data was then used to design the basic dimensions of aerodynamic surfaces and to begin specifying the propulsion components.

4.2.5 Fuselage Study

The main limiting factor in the design of the fuselage was the rectangular payload that is to be stored within. Due to the size and shape of the payload, the fuselage was formed into the rectangular shape where the payload is to be located, and then rounded in the front to be more aerodynamic. The length of the fuselage is limited by the dimensions of the box, which is placed at an angle to achieve the largest length.

4.2.6 Landing Gear Study

The design of the landing gear was limited to the dimensions of the box and the needed dimensions and stiffness to support the aircraft. The size of the box limits the design of the landing gear to two distinct possibilities. The first possibility is that the landing gear could be detachable, sized to dimensions needed to support the aircraft. The second possibility, which is the design the team decided upon, is that the landing gear be mounted such that it could swivel beneath the aircraft such that the assembly fit within the box.

4.3.1 Airfoil selection

The wings must create the required lift for all stages of flight. This can present challenges as the airfoil selection for maximum lift at takeoff varies greatly from the airfoil with the best cruising capabilities or stall characteristics. Generally, a compromise must be made while keeping in mind the mission profile and worst-case scenarios.

A selection of low Reynolds number airfoils were found and evaluated, including the NACA 4415 and the Selig 7710. Both airfoils had similar lift to drag ratios and stall characteristics. The Selig was chosen due to the smaller thickness to chord ratio and therefore reduced drag at cruise. Although the stall characteristics were a bit worse for the Selig, the addition of flapperons to the wings would aid this problem.

4.3.2 Wing sizing score optimization

The overall RAC score reduction due to aircraft wing size was calculated and found to be relatively small and unimportant. There is a lower weight limit that an aircraft can safely reach and be structurally adequate. For a given minimal aircraft weight, you must have adequate wing surface area to perform within specifications regardless of the penalties. By building the lightest possible plane, you reduce the surface area required.

Wing loading must be taken into account as well. An aircraft with lower wing loading tends to be more stable and have better low speed flight characteristics. For the competition however, this low wing loading leads to slower aircraft. Since the flight time is a multiplier in the overall score, it is best that the plane be able to fly as fast as possible and therefore have a higher wing loading. This means that the surface area of the wing must be reduced to within certain aerodynamic and structural limits.

In the model aircraft industry, it is unusual to see wing loadings above 35oz per square foot. From our estimated aircraft weight and wing surface area, a loading of 46.7 oz per square foot was found. Although this is far from "normal" according to the industry, this loading is indicative of a larger, high-speed aircraft.

4.3.4 Tail airfoil selection

For the V-tail, the classic symmetric airfoil, NACA 0009, was chosen. These symmetric airfoils are generally the industry standard when applied to control surfaces such as the tail. The main reason is that the symmetric airfoil produces no lift or moment at zero angle of attack. Therefore, any lift or moments created are due strictly to the deflection of the control surface on the tail. It would be a nuisance to say the least if your control surface continually created lift or moments, necessitating one to deflect control surfaces in the proper direction to counteract this. The drag penalties alone are convincing.

4.3.5 Fuselage

At last year's competition, the softball payload could be configured in ways that were quite aerodynamic, such as stretching the softball distribution over the length of the fuselage. Aircraft with fuselage lengths near seven feet were seen because it is better to add length than width to help reduce the drag. This year, the shape of the payload and the size and shape of the storage box limits the shape of the fuselage to few options. Unfortunately, all of them have relatively large rectangular cross-section.

The fuselage was reduced in cross-section as much as possible to reduce drag. It closely resembles the payload in shape and dimension with the exception that there is a contoured nose. The payload protrudes from the rear of the fuselage, which facilitates quick payload deployment, but generally does not affect the aerodynamics due to turbulence and flow separation near the rear of the fuselage.

4.4 Performance Estimates

Table 4.2: Performance Calculations

AIRCRAFT CHARACTERISTICS INPUT

Wing Area Sw	**Sw**	6.76389	**ft^2**
Fuselage frontal area Sf	**Sf**	0.36502	ft^2
Horizontal tail St	**St**	1.5	ft^2
Vertical tail Sv	**Sv**	0	ft^2
Frontal area of three tires or Stires	**Stires**	0.03125	ft^2
Frontal area of landing gear structure	**Sstrut**	0.01389	ft^2
Gross weight W=lift L in level flight (Loaded)	**L=W**	18	lbf
Sealevel density rho	**r**	0.00238	slug/ft^3
pi=4*ATAN(1)	**p**	3.14159	
WING LOADING		2.66119	

Wing characteristics:

Span b	**b**	7.25	ft
Aspect ratio AR=b^2/Sw	**AR**	7.77105	
Average chord c=Sw/b	**Cavg**	0.93295	ft
2D lift curve slope Clalpha per degree	**Clα/deg**	0.1	per degree
α_0 at zero lift in degrees	**α_0**	-4	degree
3D slope CLalpha=Clalpha/(1+57.3*Clalpha/(pi*e*AR))	**CLa3D**	0.07732	
CLstall	**Clstall**	1.6	with Flaps
Drag coefficient of wing airfoil CDo=0.008+0.002*Cl(.6)^2	**Cdo**	0.00872	
Drag coefficient of vertical tail Cdv	**Cdv**	0.007	
Drag coefficient of fuselage Cdf	**Cdf**	1	
Drag coefficient of horizontal tail Cdh	**Cdh**	0.007	
Drag coefficient of tires Cdt	**Cdt**	1	
Drag coefficient of strut Cds	**Cds**	0.8	
Span wise loading coefficient e	**e**	0.8	

Calculations

Additional drag coeff. relative to wing area:CDadd=Cdf*Sf/Sw+Cdh*Sh/Sw+Cdv*Sv/Sw+Cdt*St/Sw+Cds*Ss/Sw	**Cdadd**		
Total parasite drag coefficient, proportional to q is: CDpara=CDadd+CDo	**Cdpara**		
Dynamic pressure q=0.5*rho*V^2	**q(ft^3/s)**		
Wing lift coefficient CL=L/(q*Sw)=W/(q*Sw)	**CL**		
Wing induced drag coefficient CDi=CL^2/(pi*e*AR). *Note -CDi is inversily proportional to q^2	**Cdi**		
Induced drag Di=CDi*q*Sw	**Di(lb)**	Fig. 4.1	
Parasite drag Dpara=CDpara*q*Sw	**Dpara(lb)**	Fig. 4.1	
Total drag D=Di+Dpara	**Dtotal(lb)**	Fig. 4.1	
CDadd=	**Cdadd**	0.06178	
qstall =W/(CLstall*Sw)=	**qstall(ft^3/s)**	1.66324	
	Vstall(ft/s)	37.4092	

2.5 lbf is 19 cells of 1.2 Volt, under motor load 1.1Volt or 19*1.1=20.9 Volt, with endurance spec: 2000 mAm/hr

max energy:1.2*19*(2000/1000)*3600=164160 Watt-s, for 2 packs or 5 lbs have 328320 Watt-s=242124ftlbf

Only able to fly level at V>Vstall, thus start at Vmin=INT(Vstall)

(1.2V*19)*(25Amps) rated motor, at 550 ftlbf/s/HP	**((1.2V*19)*(25 Amps))*.738 {ftlbf/s / W}**	420.66	ftlbf/s
Static Thrust (measured from AstroCobalt 601S Motor with 16 x 15 Propeller) at 75% eta prop., thrust Tavail=power*0.75/V	**Tstatic**	7.6	lbf

Takeoff Performance One Motor and 16 x 15 prop

Vrotation=Vstall*1.20	**Vrotation=Vstall*1.20 (ft/s)**	44.891
Rolling Resistance Force measured (Uk=.08) (lbf)	**Ffr=Fn*Uk (lbf)**	1.44
Ground Acceleration	**(Tstatic-Fdrag)/m=a (ft/s2)**	11.0196
Time to Vrotation	**t=(Vrotation-Vo)/a (sec)**	4.07376
Takeoff Distance	**x=1/2*a*t^2 (ft)**	91.4377

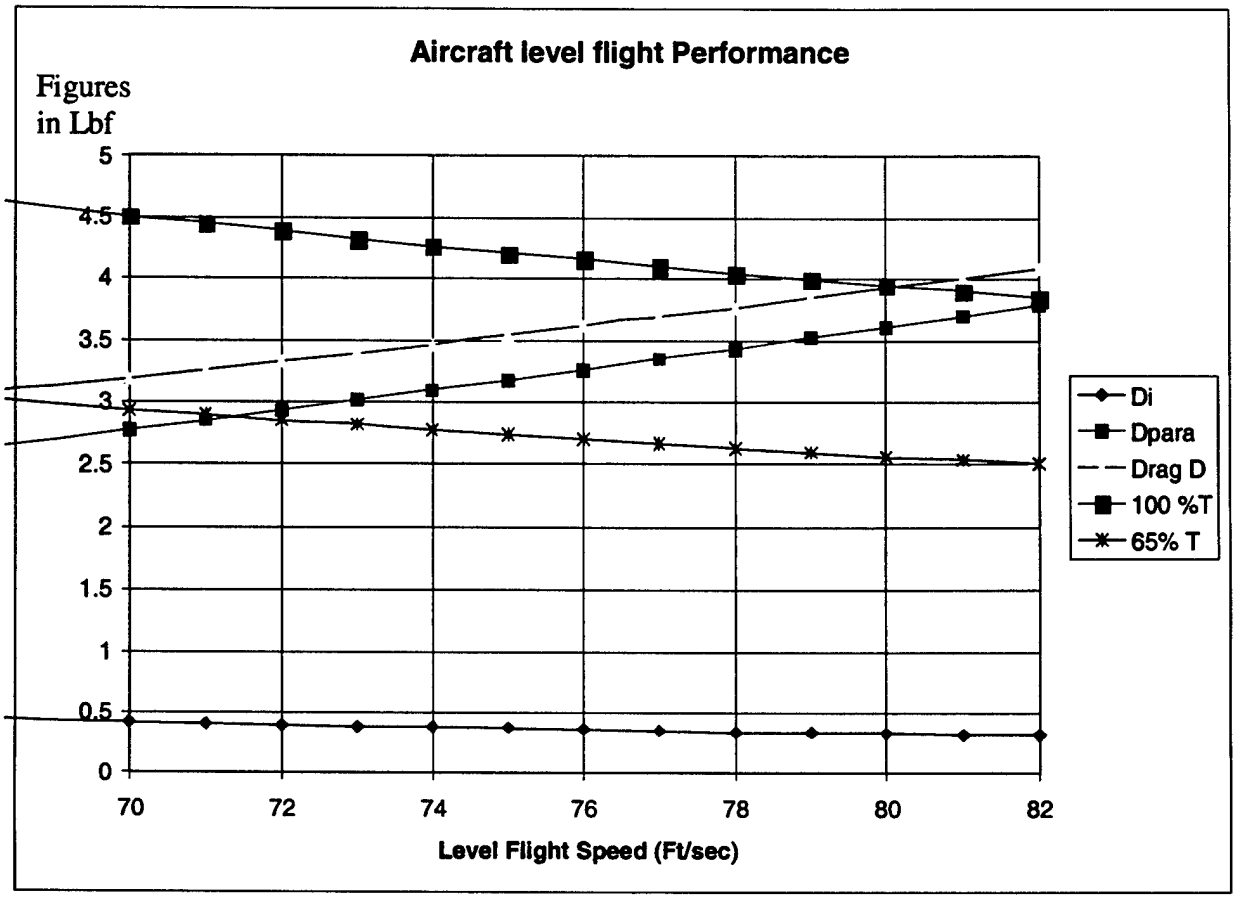

Figure 4.1: Flight Performance Graph

5.0 Detail design

From previous experience with the competition, it was found that in order to succeed; a team must purchase the highest quality components possible to ensure performance and reliability. Also, there is a trade off involved in the budget allowed for these components. In this light, critical components such as propulsion and batteries received the most attention, as they had the greatest impact on flight performance and therefore flight score.

5.1 Component selection

5.1.1 Propulsion

The rules specify that the motors available for the competition can be bought from one of two companies, Astro Flight or Graupner and the motors must be of brushed design. It is assumed that requiring brushed motors was done to keep the cost of the propulsion system down, as brushless motor systems can lead to thousands of dollars in expense. Using MotoCalc software, the propulsion group was able to iterate through various motor and propeller combinations using estimated final weights, dimensions of the aircraft, required thrust, and mission endurance.

From the MotoCalc software, it was found that Graupner motors tend to have overall better efficiency than the Astro Flights albeit at greater expense. The team has had extensive experience with the Astro Flight series in the past with reasonable results. This year, the team decided to give the Graupner motor series a chance. Eventually, the motor of choice became the Graupner 3450-7 with a 2:1 reduction gearbox and a folding 16x9 prop. This combination gives the greatest balance between maximum thrust and cruising efficiency. Also, one must remember that props are changed to fit flight conditions, the 16x9 was merely the best with the flight conditions specified to MotoCalc. Also, in the event of a crash, an Astro Flight 60 series motor and prop combination can be substituted. Below is the screen shot from the MotoCalc interface with the current design parameters entered.

Table 5.1: Propulsion System Analysis

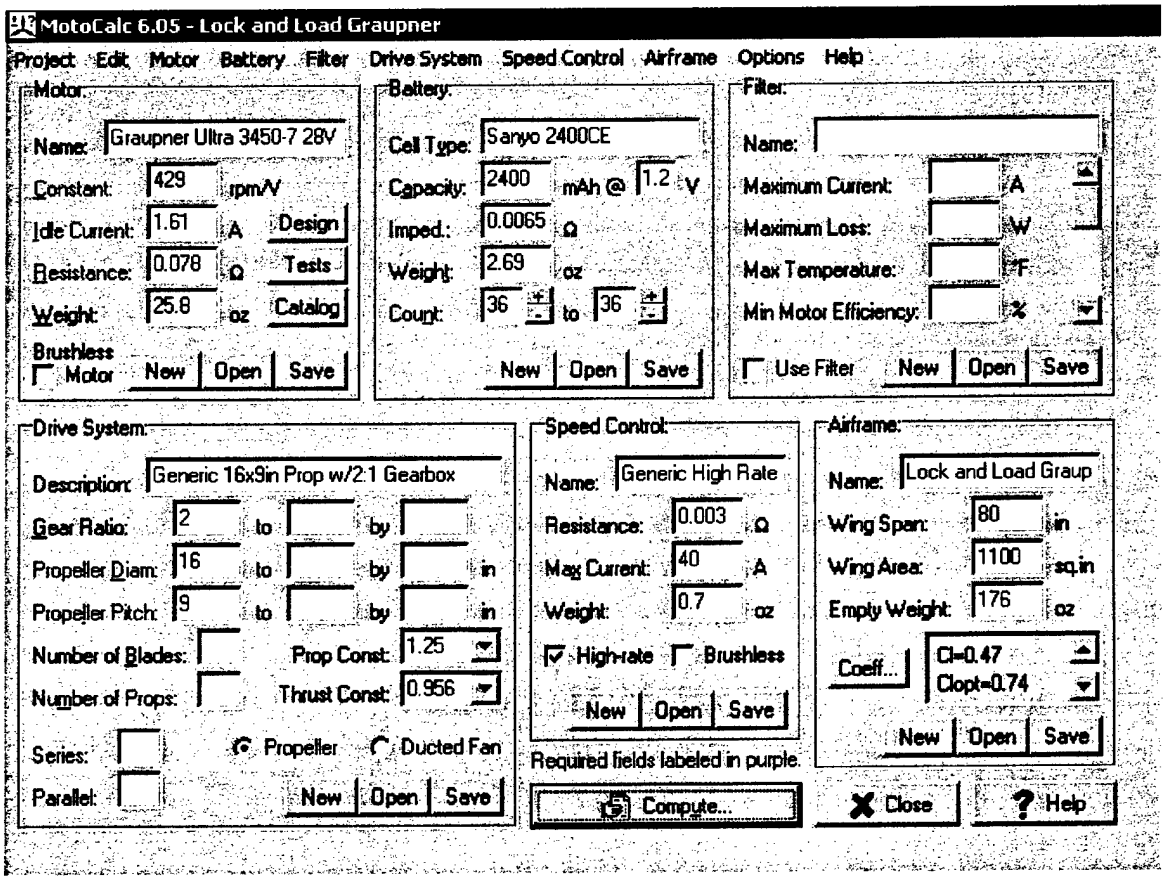

The following is the graphical representation of the calculations done in MotoCalc indicating motor efficiency compared to prop speed and airspeed. The software allowed for easy optimization outside of repeated flight-testing.

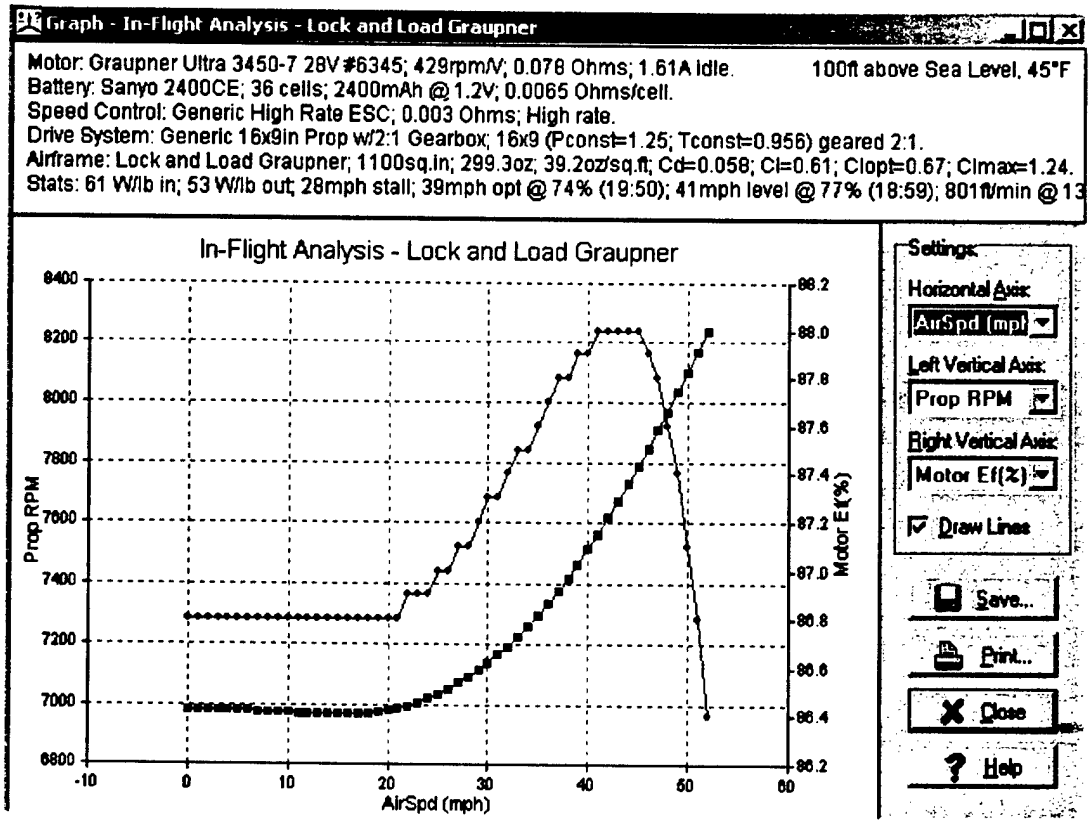

Figure 5.1: Propulsive Efficiency

5.1.2 Battery Pack

Again, to speed through the design process, MotoCalc was used to determine the number and power rating of the cells required. Through the iteration process involving estimated required mission endurance, a 36 cell, 2400 mAh pack was required. This results in a battery pack weighing near 4.5lbs, which is under the maximum of 5 lbs specified by the competition rules. The pack consists of Sanyo cells, as they are the most common found in the model aircraft industry.

For motor control, an Astro Flight Model 204 speed controller was used due to its lightweight and 50 Amp power limit, which keeps the ESC operating even if there is an initial power spike from the battery pack. More expensive speed controllers exist but this was found to be an excellent tradeoff between cutting edge technology and "bare bones" functionality.

5.1.3 Control Actuation

The team has chosen to use Hi-Tec and Futaba servos throughout the aircraft. The wing flapperons undergo the greatest loading so it was decided that "mini" Hi-Tec servos would be sufficient due to their robust nature along with generally good holding power consumption. Micro servos were chosen for the steering mechanism and the payload release mechanism, as both mechanisms required little torque and energy use. The V-tail required two mini servos.

In all, the aircraft requires six servos for proper operation. To keep RAC to a minimum, it is best to incorporate as few servos as possible. However, the use of the V-tail does not allow us to couple the steering to the rudder as in a conventional configuration, hence the need for a separate steering servo. Again, it would be difficult to incorporate the payload ejection within the control scheme, so it requires its separate servo. Finally according to the RAC, due to the classification of an electronic speed control as a servo we have a total of 7.

5.1.4 Radio transmitter and receiver

The use of an 8-channel Futaba radio with supplied receiver has provided great results in past. Most any radio system with sufficient channels will suffice, but the Futaba has several pilot amenities that make flying the aircraft easier.

5.1.5 Braking system

From previous experience, to reduce flight time, it is best to reduce the rolling time of the aircraft once it has reached the ground. To accomplish this goal, a pneumatic brake system from Bob Violett Models was chosen due to its reliability and simplicity. The system essentially uses a small compressed air canister to actuate drum-style brakes located on the two rear landing gear wheels. At full flaps down, the pressure valve is opened, sending air to the brakes, effectively stopping the aircraft.

Table 5.2: Summaries of Control Actuation Components

Location	Manufacturer	Designation	Number
Wing	Hi-Tec	HS225	2
Tail	Hi-Tec	HS225	2
Payload Release	Hi-Tec	HS225	1
Steering	Hi-Tec	HS225	1

Table 5.3: Summaries of Propulsion Components

Component	Manufacturer	Designation	Number of Components
Motor	Graupner	3450-7	1
Electronic Speed Control	Astro Flight	Model 204	1
Prop	Graupner		1
Gearbox	Graupner		1

Table 5.4: Summaries of Radio Components

Component	Manufacturer	Designation	Number of Components
Transmitter	Futaba	8UAP	1
Receiver	Futaba	R148	1

5.2 Fuselage Internal Schematics

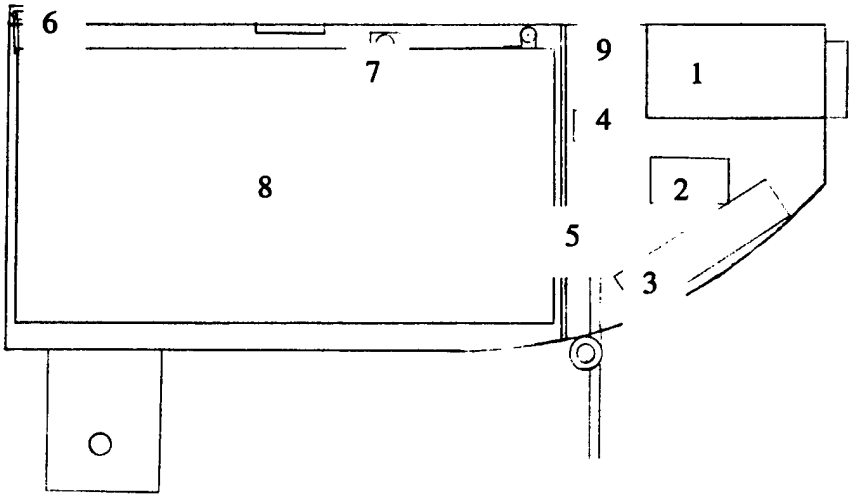

Figure 5.2: Fuselage Side View (see table 5.5)

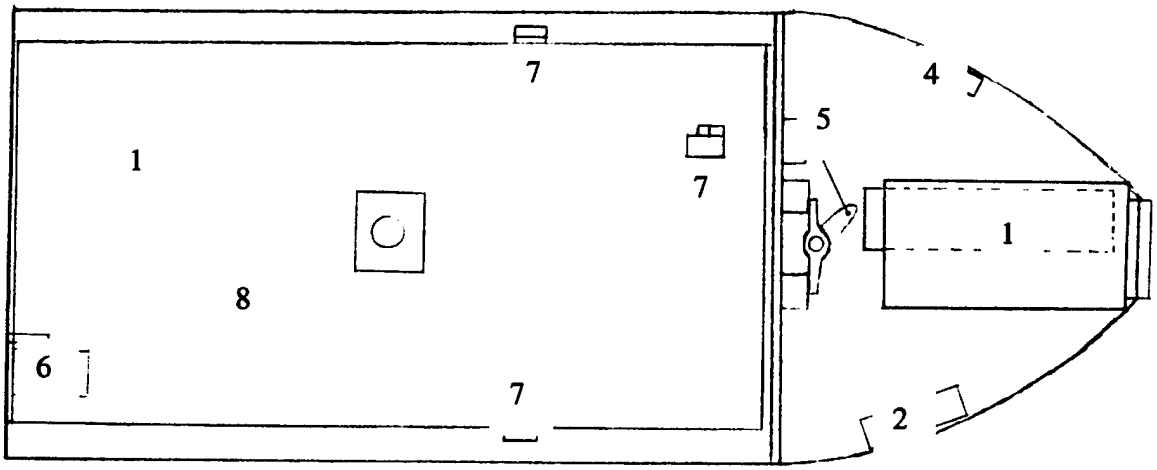

Figure 5.3: Fuselage Top View

Table 5.5: Legend

1	Electric Motor
2	Electronic Speed Controller (ESC)
3	Air Tank
4	Receiver
5	Steering Servo
6	Payload Release Servo
7	Guide Wheel
8	Payload
9	Fuse Holder

5.3 Detailed Design from Drawing Package

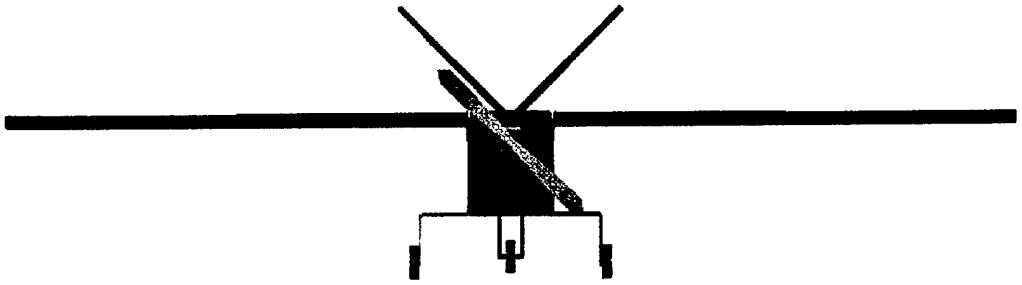

Figure 5.4: Front View of Aircraft

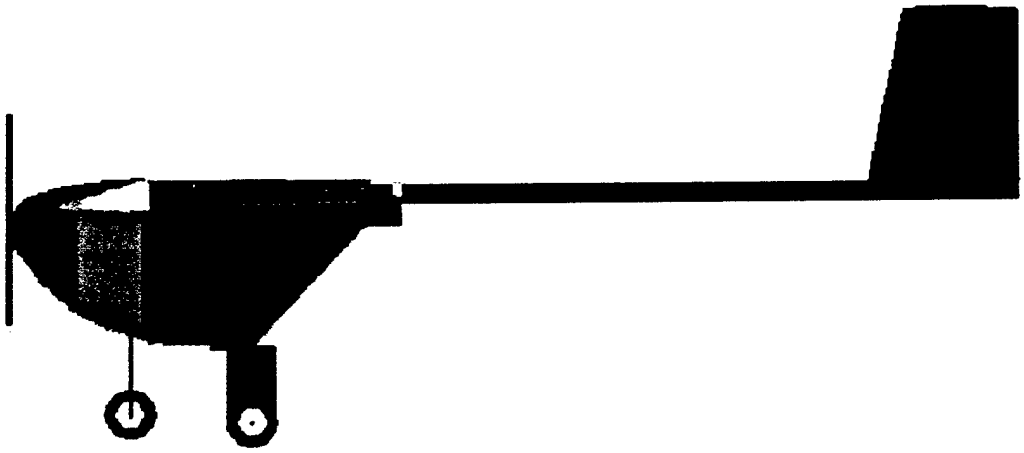

Figure 5.5: Side View of Aircraft

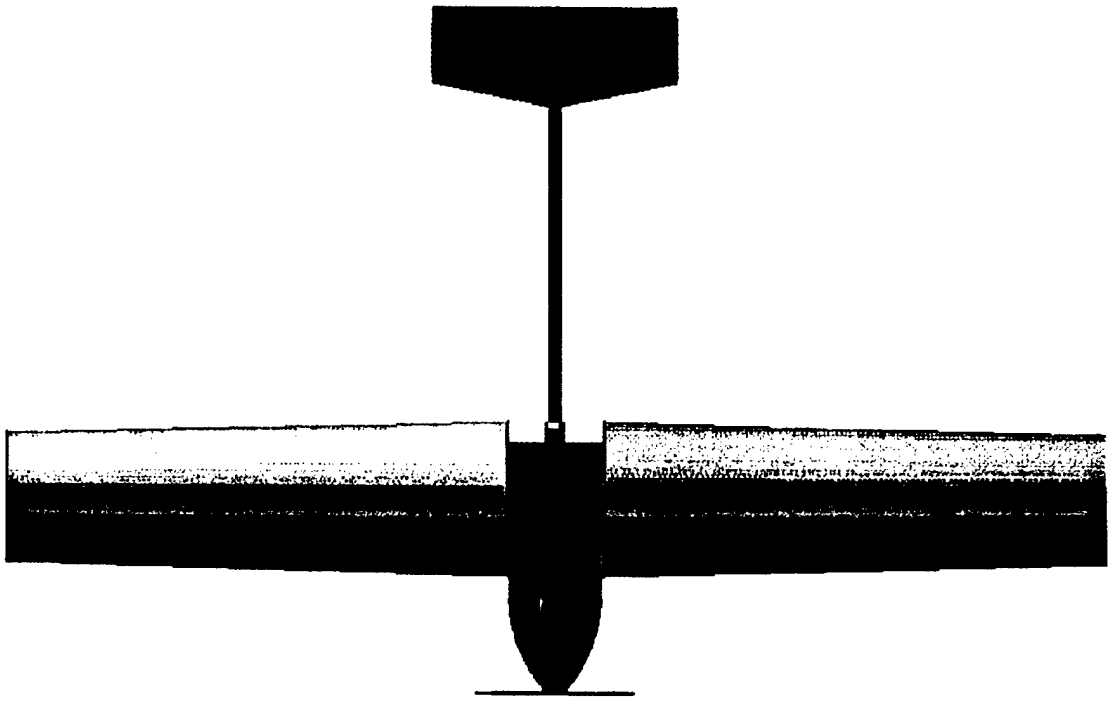

Figure 5.6: Top View of Aircraft

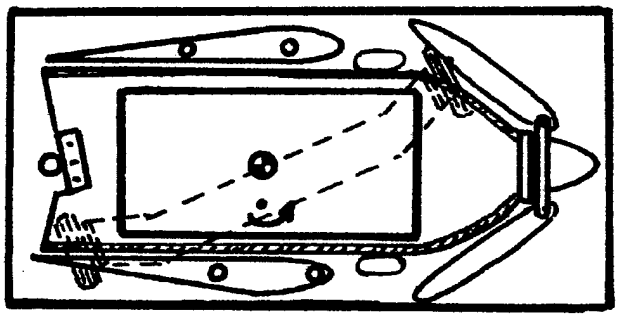

2 FT End View

WVU "Lock-N-Load", spring 2003
AIAA Design-Build-Fly entry
Designed to assemble within 10 seconds from box to flight ready

1 FT

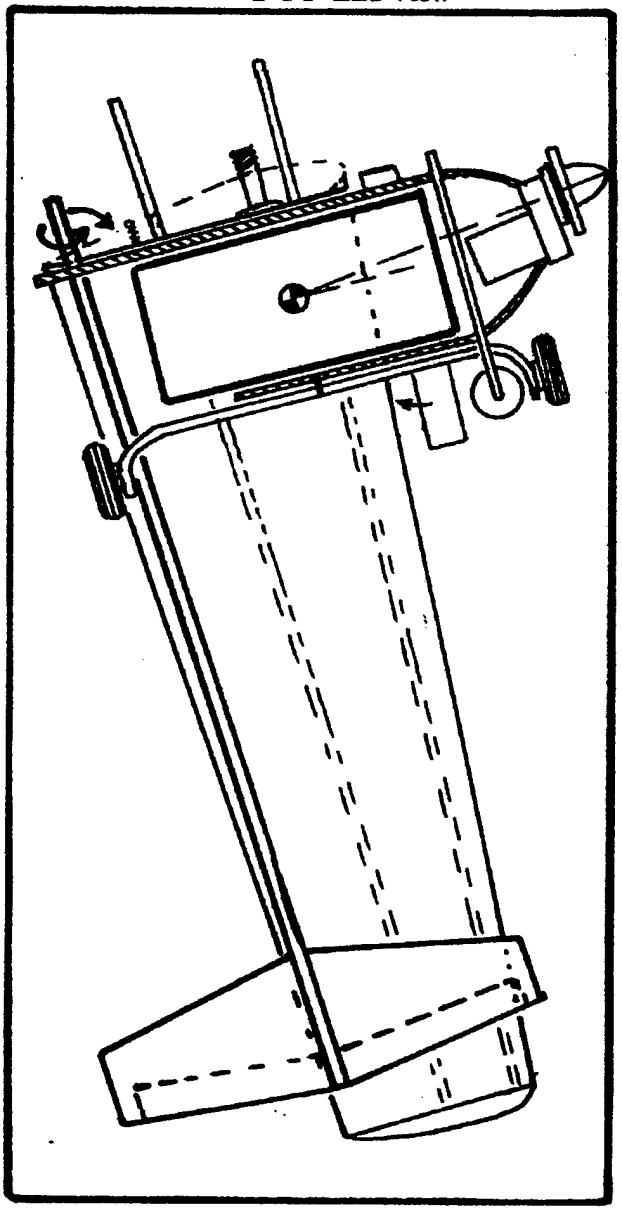

4 FT

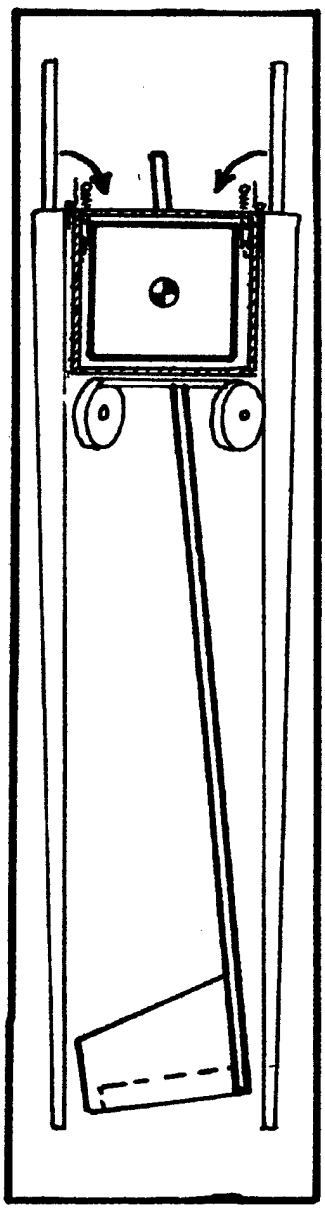

Top view

Side view

Figure 5.7: Aircraft in Transport Configuration

5.4 Summary of Geometric Parameters

The following is a table summarizing the geometric parameters of the aircraft.

Table 5.6: Geometric Parameters

Geometric Parameter	Dimension
Total Length (ft)	4.3
Wing Span (ft)	7.2
Height (ft)	1.0
Wing Area (ft^2)	6.6
Aspect ratio	7.86
Flapperon to Wing Chord Fraction	0.3
Tail Control Volume	.505

5.5 Summary of performance

Below is the summarized list of performance parameters for the aircraft.

Figure 5.7: Performance Parameters

Performance Parameter	Mission 1	Mission 2
C_{Lmax}	1.24	1.24
L/D max	9.87	10.44
Maximum Rate of Climb (ft/min)	695	795
Stall Speed (mph)	34	29
Maximum Speed (mph)	45	52
Takeoff Length Loaded (ft)	110	86
Takeoff Length Unloaded (ft)	75	75

6.0 Manufacturing Plan and Process

6.1 Manufacturing Processes Investigated

Speed and ease of construction were the main factors for the fabrication and assembly of the aircraft components. The WVU team is small with a few returning RC aircraft building experience. A schedule was developed with these limitations in mind. To meet the schedule, materials and techniques which were comfortable with the team members were comfortable with were chosen. The preliminary manufacturing plan was then evaluated using the following FOM shown in Table 6.1.

Table 6.1: FOM breakdown of manufacturing processes

		Simplicity (x5)	Cost (x1)	Strength to Weight (x6)	Time Required (x1)	Availability (x5)	Results
Wings and Empenage	Build Up (balsa wood ribs, hardwood spars)	3	4	3	2	4	59
	Foam Core with Balsa Wood Sheeting	*4*	*4*	*4*	*5*	*4*	*73*
	Composite Materials	2	1	5	2	2	53
	Balsa Wood Build up	3	5	4	3	4	67
Tail	*Foam core with Balsa Sheeting*	*4*	*4*	*4*	*5*	*4*	*73*
	All Composite	2	1	5	2	2	53
Fuselage	Build Up (balsa wood bulkheads, hardwood spars)	3	3	3	3	4	59
	All Composite	*2*	*1*	*6*	*2*	*4*	*69*
Landing Gear	Purchase	5	5	3	5	2	63
	Aluminum	3	3	3	3	4	59
	Composite Materials	*4*	*3*	*5*	*3*	*4*	*76*

6.2 Figures of Merit Breakdown

The purpose of the figures of merit is to give guidance in determining the pros and cons of each possible alterative in the construction of this aircraft. Using this process, various construction alternatives were evaluated to maximize production and efficiency. The figures of merit that were considered to be most influential in the final design were simplicity, time required, cost, strength to weight, and availability.

Simplicity

It was determined that there had to be some limitations as to the overall complexity of the aircraft to make it both producible and maintainable. If the construction of a single part was easily done, it was given a 5. If it was tedious or took skills not available by team members, it was given a 1.

Time required

Time was a large contributing factor as to the feasibility of construction for the aircraft. In order to complete construction on all the components of the aircraft, the team had little forgiveness in missed deadlines. For each process, the time required to produce the part was compared to the overall

advantage of making the part. If a part was time consuming, it was given a 1, if it could be completed quickly, it was given a 5.

Cost

The cost of the project was a very significant parameter that was non-negotiable. An estimation of materials needed and salvageable materials from past projects was done from conception to minimize new purchases and thus overall aircraft cost. With a limited budget, the selected parts and materials were first compared on a pros and cons basis for optimal results. Parts and materials with a low cost or donations were given a 5, high cost parts and materials were given a 1.

Weight

As in all aircraft, weight is a critical factor. It was the intention of this years team to build a lightweight aircraft with a low profile. The weight consideration of this years plane was one of the most critical aspects and most all decisions were based from it. Bulky and heavy parts and materials were given a 1, whereas light and slim parts and materials were given a 5.

Availability

The availability of materials needed to complete the manufacturing process was of important concern. If the material was donated or easily obtained, it was given a 1. If the material was expensive or needed special ordering and obtaining procedures, it was given a 5.

6.3 Process Selected for Major Component Manufacture

6.3.1 Fuselage

A combination of plywood, balsa and composite materials were used in the construction the fuselage. The construction of the fuselage began by first producing a male plug that was identical to the interior dimensions final fuselage. The plug was constructed out of foam that was cut to shape using a hot wire. Once the foam was cut it was then covered with a layer of 3 mm polyethylene sheet. The polyethylene gives a smooth finish and has good mold release qualities. Once the male mold was constructed, the fuselage shell was constructed. Poly Vinyl Alcohol was used as a release agent to the mold before the lay-up process began. The laminate decided upon for the final fuselage was one layer of 3/4oz fiberglass, one layer of 3k x 1k carbon fiber and 1 layer of 1/32" aircraft plywood. This combination was chosen to combine the high strength to weight ratio of graphite / epoxy and the ease of construction for plywood. One inch wide, 1 ply, 5.8oz unidirectional carbon tapes were placed at the landing gear attachment points and the wing attachment points to provide improved rigidity to the fuselage. The epoxy used was 'system 2000 w/20xx' for all carbon composite layups. Plywood bulkheads (1/16" thick) were added for the motor attachment area and the separation of the servo-compartment and the payload bay.

6.3.2 Wing and Tail

The wing and tail were constructed out of 1lb density Styrofoam that was then sheeted with 1/16" balsa wood. First, blocks of Styrofoam were cut to the wing planform. Next, the spar and tube holes were cut into the entire wing. The wing was then cut into sections corresponding to the breaks in the wing planform. Next, templates were made for each section. The airfoil shape was then cut of each section using a hot wire. Each section was then glued together with epoxy and the entire wing was sanded smooth. Next, the spars and alignment tubes were glued into place. Then 4" x 48" x 1/16" sheets of balsa wood were then glued together with CA glue to form large panels. These panels were then adhered to the foam core using Elmer's Pro Bond Polyurethane Adhesive. The wings panels were then trimmed to match that of the foam core and leading edge stock was applied. Next the wings were sanded smooth. Flaperons were then cut out of the wing and the hinges were installed and the flaperons were reattached. The wings were then covered in monocoat.

6.3.3 Landing Gear

The landing gear was constructed out of carbon fiber and Nomex honeycomb. Various laminate samples were fabricated to determine which had the best weight, strength and rigidity. The laminate chosen was as follows

a). 2 plys +-45 degrees 5.8 oz graphite

b) 1 layer 1/8" thick, 3/16" cell size Nomex Honeycomb

c). 2 plys +-45 degrees 5.8 oz graphite

The mold for the landing gear was constructed by cutting the shape out of foam, which was then laminated with a thin layer of mylar. Hand lay-up and vacuum bagging were then used to produce the final part.

7.0 Testing Plan

7.1 Testing Objectives

The testing phase of the aircrafts flight worthiness involved four stages. The first component to be tested was the landing gear. The carbon-honeycomb composite landing gear was subjected to a 3G impact loading, applied downward to the center of the landing gear, for worst case landing scenario. Deflection and noise that is cracking and damage were used as judgment criterion. The next component was the fuselage, which was tested for airframe integrity to resist torque and lateral compression. The wings also were tested for a 2.5G loading by a simple load test of hanging loads from the wing tips. This is the expected maximum loading of the aircraft. The aircraft was brought to flight ready status with the wings; landing gear and empennage connected to the fuselage; and then the propulsion system and flight control system were installed. A five pound weight was temporarily installed to simulate the cargo. A tip

deflection test was performed and the aircraft was rolled on the runway for a single lap flight test. The flight test had to be aborted and postponed to a latter date due to bad winter weather conditions.

7.2 Testing Schedule

Flight testing was scheduled between March 1, 2003 and April 20, 2003. Flight testing will be conducted on every weekend for the duration of the testing period or until acceptable optimization is reached, which ever date arrives first. Following is the tentative test schedule

- Weekend 1: Basic flight worthiness without payload and five pounds battery weight.
- Weekend 2: Basic flight test with standard banking maneuvers and performance evaluation for flaps effect on take off and landing.
- Weekend 3: Flight worthiness with simulated avionics payload and five pounds battery weight.
- Weekend 4: Full flight test with simulated avionics payload and five pounds battery weight (competition regulations enforced).
- Weekend 5: Full flight test with all missions and reduced battery weight (to be determined between weekend 4 and weekend 5 of flight testing).
- Weekends 6-8: Left open for delays, problem fixing and pilot training.

7.3 Testing Checklist

The testing of the aircraft was done based on the outline in Table 7.1 listed below.

Table 7.1: Testing Checklist

1	Structural integrity and tip deflection	Passed
2	Flight Worthiness	Pending
3	Maneuverability and Handling	Pending
4	Flight test with max payload	Pending
5	Flight test with modified battery weight	Pending

7.4 Results and Lessons Learned

The aircraft passed the structural integrity and tip deflection test without any problems. The wings were strong enough to withstand the 2.5G loading simulated by the tip deflection test without much deflection. It was concluded that the spars were sufficient for the wing loading and the shortening of the main spar to span only three-quarters of the span of the wing in case a new set of wings are needed to be fabricated. This result was based on comparison of previous years wing loading and design to our current design. Pending further flight testing, more data will be analyzed and possible modifications made to optimize the performance of the aircraft in relation to flight characteristics and the RAC.

8.0 Rated Aircraft Cost (RAC)

8.1 Discussion of RAC

The RAC can basically be described as the simplicity of the aircraft. It is a way for the competition to reward a team who can design an aircraft with the defined missions such as fitting in the box, short space to takeoff, assembling time, flight time, and the number of laps. This model is provided by the competition rules each year and is explained in the sections below.

8.1.1 Breakdown of the RAC

The overall RAC (RAC) is calculated by the equation:

$$RAC,(\$thousands) = \frac{A \times MEW + B \times REP + C \times MFHR}{1000} \quad (8.1)$$

In the above equation, A, B, and C represent values of multipliers used to convert aircraft characteristics into manufacturing hours. The Manufacturer's Empty Weight Multiplier (MEW), Rated Engine Power (REP), and the Manufacturing Man Hours (MFHR) are a breakdown of the different aircraft components to be converted to man-hours. A more detailed explanation of these parameters is described below.

8.1.2 Manufacturer's Empty Weight Multiplier

The manufacturer's empty weight multiplier, MEW, is comprised of the weight of the aircraft without payload. In equation 8.1'A' represents the manufacturer's empty weight multiplier and was given a value of $100/lb.

8.1.3 Rated Engine Power

The rated engine power, REP, was calculated using the following equation:

$$REP = battery \quad weight(1 + 0.25 * \#motors) \quad (8.2)$$

In equation 8.1 'B' represents the rated engine power multiplier and was given a value of $1500.

8.1.4 Manufacturing Man Hours

The manufacturing man hours, MFHR, further breaks down the components of the aircraft into the work breakdown structure, (WBS), and takes into account the number of wings and their size, the number of fuselages/pods, and their size, the number of horizontal and vertical surfaces, the number of servos used, and the number of motors and propellers used. In equation, 8.1 C represents the manufacturing cost multiplier and was assigned a value of $20/hr.

8.1.5 WBS 1.0 Wing

The rules state that 8hrs/ft of wing span, 8hrs/ft of max exposed wing chord, and 3hrs per control surface are to be used in the calculation of WBS 1.0.

8.1.6 WBS 2.0 Fuselage

WBS 2.0 consists of the length of the fuselage. 10hr/ft are used to calculate WBS 2.0.

8.1.7 WBS 3.0 Empennage

WBS 3.0 is the number of vertical and horizontal surfaces. For any vertical surface (winglets, struts, end plates, etc.) a penalty of 5hr per surface is to be assessed. For any vertical surface with an active control 10hr per surface is assessed. Any horizontal surface that is less than 25% of the span of the greatest span is assessed 10hr per surface.

8.1.8 WBS 4.0 Flight System

WBS 4.0 is the number of servos and controllers used on the aircraft. 5hrs was assigned per servo or controller.

8.1.9 WBS 5.0 Propulsion System

WBS 5.0 is the number of motors and propellers or fans used on the aircraft. 5hrs per motor, propeller, and fan was assigned.

8.2 Features that Produced the Final Configuration

After the figures of merit were assessed, the calculated design was scrutinized by asking several key questions. First, do we think this will work and can we construct it? How does this affect the RAC was also asked. As described above adding another servo or changing the aspect ratio of the wing greatly affects the RAC.

The RAC is a numerical rating system designed to estimate the actual cost of the aircraft after production. It includes nearly all aircraft dimensions along with provisions for electronics and vehicle weight. Using various multipliers, the estimated cost can be found. The following is the overview of the inputs for the RAC model and RAC calculation as specified by the competition guidelines for the aircrafts current configuration.

Table 8.1 Detailed Rated Aircraft Cost Breakdown

Input Parameters			
	Empty Weight	12.6	lbs
	Battery Weight	4.5	lbs
Wings			
	Wing Span	7.2	ft
	Max Wing Chord	1	ft
	Control Surfaces	2	
Fuselage			
	Body Max Length	4.3	ft
Empennage			
	Vertical Surface (no active control)	1	
	Vertical Surface (Active control)	0	
	Horizontal Surface	1	
Flight System			
	servo/motor controlers	7	
Propulsion system			
	engines	1	
	propeller or fans	1	

Rated Aircraft Cost, $ (Thousands)	(A*MEW + B*REP + C*MFHR)/1000	

Coef.	Description	Value	Value
A	Manufacturers Empty Weight Multiplier	$100.00	$100.00
B	Rated Engine Power Multiplier	$1,500.00	$1,500.00
C	Manufacturing Cost Multiplier	$20.00	$20.00
MEW	Manufacturers Empty Weight	Actual airframe weight, lb., with all flight and propulsion batteries but without any payload	12.6
REP	Rated Engine Power	(1+.25*(# engines-1)) * ***Total Battery Weight***	4.5
MFHR	Manufacturing Man Hours	Prescribed assembly hours by WBS (Work Breakdown Structure).	
		MFHR = S WBS hours	174.6
		WBS 1.0 Wing(s):	
		8 hr/ft. Wing Span	57.6
		8 hr/ft Max exposed wing chord	8
		3 hr/control surface	6
		WBS 2.0 Fuselage	
		10 hr/ft body maximum length	43
		WBS 3.0 Empenage	
		5 hr./Vertical Surface with no active control	5
		10 hr/Vertical Surface (Any vertical surface) with an active control	0
		10 hr./Horizontal Surface	10
		WBS 4.0 Flight Systems	
		5 hr./servo or motor controller	35
		WBS 5.0 Propulsion Systems	
		5 hr./engine	5
		5 hr./propeller or fan	5

9.0 Bibliography

Bertin and Smith, Aerodynamics for Engineers 3rd Edition, Prentice-Hall Inc. 1998

Raymer and Przemieniecki, Aircraft Design: A Conceptual Approach 3rd Edition, AIAA Education Series, 1999

Abbot and Von Doenhoff, Theory of Wing Sections, Dover Publications, 1980

Dr. Jan Roskam, Aircraft Design, DARcorporation 1997

Richard G. Budynas, Advanced Strengths and Applied Stress Analysis 2nd Edition, McGraw-Hill, 1999

http://www.aviasport.net/composites/graphlite.htm

http://www.nasg.org/

MotoCalc 6.05, Capable Computing, Inc. 2001

American Institute of Aeronautics and Astronautics

State University of New York at Buffalo Chapter

2002-2003 Cessna/ONR Student Design/Build/Fly Competition

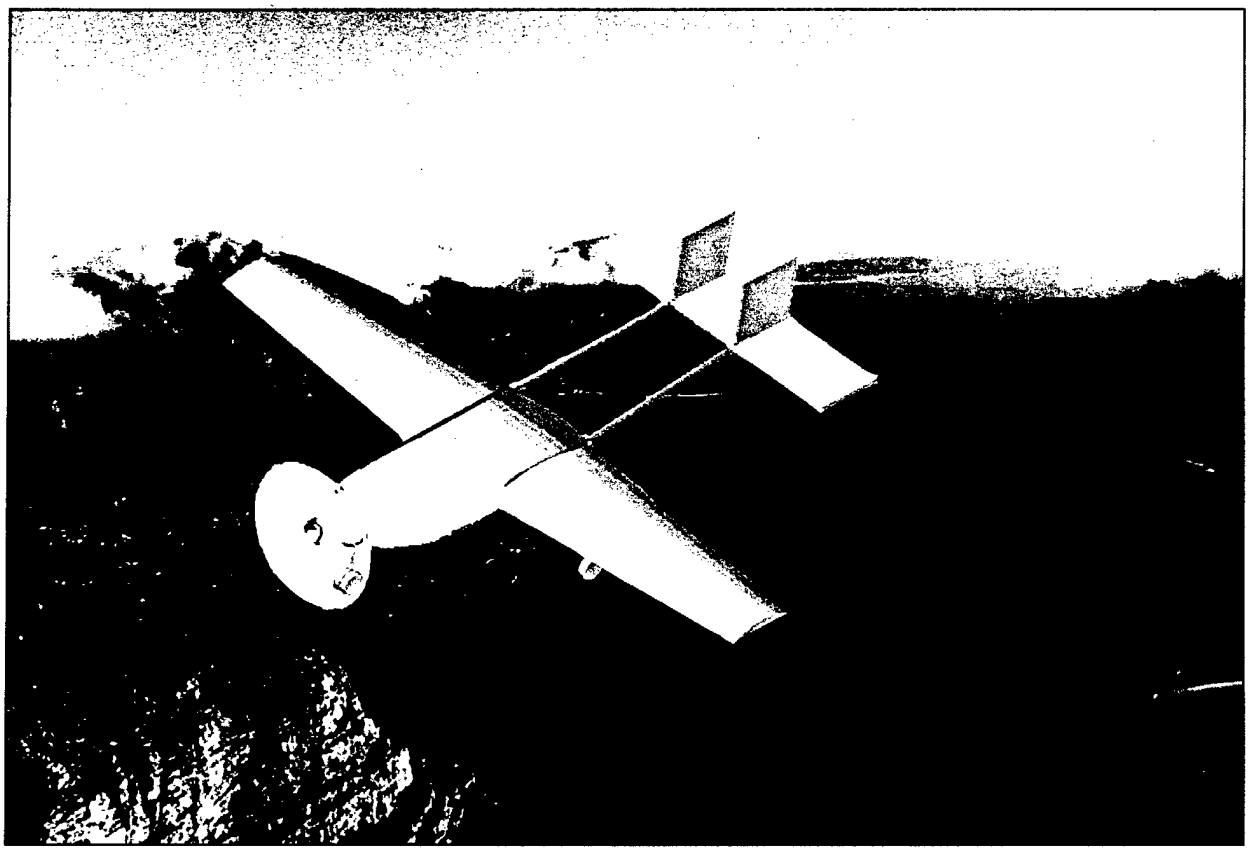

UB "Bull Ship"

Design Report

Table of Contents

1.0 Executive Summary **2**
- 1.1 Conceptual Design 2
- 1.2 Preliminary Design 2
- 1.3 Detailed Design 3

2.0 Management Summary **4**
- 2.1 Architecture of Design Team 4
- 2.2 Configuration and Schedule Control 6

3.0 Conceptual Design **8**
- 3.1 Wing 10
- 3.2 Tail 10
- 3.3 Fuselage 11
- 3.4 Propulsion 11

4.0 Preliminary Design **12**
- 4.1 Wing 13
- 4.2 Tail 16
- 4.3 Fuselage 17
- 4.4 Propulsion 18
  - 4.3.1 Motor 18
  - 4.3.2 Batteries 19
  - 4.3.3 Propeller 19
  - 4.3.4 Motor Test Stand 20

5.0 Detailed Design **22**
- 5.1 Wing 23
- 5.2 Tail 24
- 5.3 Fuselage 25
- 5.4 Propulsion 28

6.0 Manufacturing Plan **29**
- 6.1 Wing 29
- 6.2 Tail 30
- 6.3 Fuselage 30
- 6.4 Engine Mount 31
- 6.5 Landing Gear 31
- 6.6 Material Selection 32
  - 6.6.1 Availability 32
  - 6.6.2 Cost 32
  - 6.6.3 Skill Level 32
  - 6.6.4 Time 32
  - 6.6.5 Strength 32

7.0 Testing Plan **35**

1.0 Executive Summary

A team of students at The University at Buffalo decided to design and build a remote control airplane to compete in this year's Cessna/ONR Student Design Build Fly Competition (DBF). The AIAA sponsored competition will be held on Webster Field in St. Inigos Maryland, on April 25-27, 2003.

The competition involves designing and building a propeller driven, electric powered, unmanned radio controlled airplane capable of flying with and without a simulated avionics package payload as well as a simulated cylindrical antenna. The aircraft must fly a specified number of laps around a designated course in the shortest time possible. The airplane must be able to fly the designated course in at least three different ten-minute time periods, or sorties, in order for the scores to count.

The goal of the team was to design and build an airplane that would achieve the greatest score. The total score achievable at the competition is based on the product of the written report score and the total flight score for the three best sorties, divided by the rated aircraft cost. The written report will be judged and assigned a score by AIAA officials. The total flight score is based on the total number of laps flown, the number of softballs carried, and the total mission time. The rated aircraft cost is a measure of the complexity and size of the aircraft.

1.1 Conceptual Design

The goal of the conceptual design phase was to evaluate the imposed design constraints as well as the experience of previous design teams to generate several possible aircraft configurations. Configurations were selected that could score highly and were manageable by the design team. The team utilized hand sketches and simple spreadsheet programs to compare different configurations and evaluate how changes in them would affect the final score. The major design constraints evaluated when generating the configurations were maximum takeoff length, battery weight, payload configuration, and total aircraft weight. The team's desire to build a smaller, faster aircraft compared to the previous years also influenced the configuration decision. The analysis resulted in a single engine monoplane configuration with a twin tail and a tapered wing. The full five pounds of batteries would be utilized.

1.2 Preliminary Design

The goal of the preliminary design phase was to further develop the single engine monoplane configuration. The basic structure was developed and major components and materials were selected. The team utilized design software programs such as WinFoil, Pro/E and ThrustHP as well as spreadsheets to generate approximate dimensions and weights, and select possible components. Spar test sections were constructed and tested to validate the use of carbon fiber rods in the wings. Test sections of the rod connections were also made in order to determine the best way to fit the rods together for increased strength as well as fast assembly during the timed assembly task.

The weight of the loaded aircraft was estimated at 32 pounds. The wing loading was desired to be about 32 ounces per square foot, based on practical experience. The wing loading was used to select a

wingspan of 9.5 feet, a root chord of 22.67 inches and a tip chord of 1 foot. The tail volume was selected based on the size of the wing. The basic structure of the wings, tail, and fuselage were designed using carbon fiber rods and foam. The overall aircraft design revolves around the ability to use a basic structure of easy-to-assemble carbon rods which would take on the main loads, and carbon-fibered foam to keep the external shape of the plane. The required output of the motor was calculated to be 1400 Watts, therefore the motor selected was the only one that fit in this power range, the Astroflight Cobalt 90. The batteries were selected from a selection of virtually every commercial NiCd cell available, and the BYD DSC2100P was selected because of its high capacity to weight ratio as well as its ability to handle the high current discharge associated with the Cobalt 90. Finally, a motor test stand was designed and constructed to test different propellers and validate the preliminary choices made using the ThrustHP program.

1.3 Detailed Design

The goal of the detailed design phase was to refine the design so that manufacturing could begin. The final dimensions and structure were developed and all components and materials were selected. The team further utilized design programs such as Pro/E for 3D design as well as AutoCAD for 2D design. The motor test stand was used to test different propellers in order to select the best propeller based on real world performance data.

2.0 Management Summary

In the fall of 2002, a group of engineering students from the University at Buffalo assembled with the intent of designing and building an aircraft that would successfully compete in this year's Cessna/ONR AIAA Student Design/Build/Fly competition. The team consisted of 4 seniors, 3 graduate students, 2 sophomores, 6 freshmen, and was advised by two faculty members.

2.1 Architecture of Design Team

The team was designed and formed as a self-managed, interdisciplinary, dynamic group. This form was necessary due to the scope of the project and the number of people involved. The team's project managers were responsible for coordinating the administrative and technical efforts of the group. The development of the aircraft's design was divided into four teams as shown in Table 2.1. Each team concentrated in tasks relating to one area of the overall design. Membership in these individual design teams was based on expertise, interest, and team need.

Project Manager: Alexey Ouzounov & Gilbert Romanowski **Treasurer: Lindsay Volaski; Procurement: Nick Leone**			
Aerodynamics	**Power Plant**	**Structures**	**Control Systems**
Alexey Ouzounov	Brian O'Leary	Alexey Ouzounov	Gilbert Romanowski
John Fudella	Shu Ting Goh	Nick Leone	Ashish Shah
Danelle Schrader	William O'Meara	Koji Noguchi	Marie Roedger
Aditya Sachan	Dan Hallenback	Aditya Sachan	Koji Noguchi
Aditya s. Vaze	Danelle Schrader	Aditya s. Vaze	Shu Ting Goh
Amardeep Dugal	John Fudella	Amardeep Dugal	Nick Leone

Table 2.1: Team Concentration Break Up

Individual effort and expected individual effort in each area of design and manufacturing is detailed in Table 2.2. A rating of 3 indicates maximum involvement by the team member, and a rating of 0 indicates no involvement.

	Alexey Ouzounov	Brian O'Leary	Koji Noguchi	John Fudella	Danelle Schrader	Aditya Sachan	Romanowksi	Nick Leone	Aditya s. Vaze	Shu Ting Goh	Ashish Shah	William O'Meara	Marie Roedger	Dan Hallenback	Amardeep Dugal
Conceptual Design	2	2	3	1	1	1	3	3	3	1	1	1	1	1	3
Design Parameters - Initial Phase	3	1	1	0	0	0	3	3	2	0	0	2	0	0	2
Figures of Merit - Initial Phase	3	1	0	2	2	1	2	3	2	1	1	0	1	1	2
Quantitative Analysis	3	2	1	0	0	1	3	2	2	0	0	0	0	0	1
Wing Analysis	3	1	1	0	0	2	2	0	1	1	1	1	1	1	1
Empennage Analysis	0	2	2	0	1	1	1	3	1	2	2	1	2	2	2
Fuselage Analysis	2	2	3	2	2	2	1	3	2	1	0	2	1	2	2
Power Plant Analysis	0	0	1	1	0	0	2	0	2	0	0	2	0	1	3
Numerical Analysis	3	1	1	1	2	0	1	0	1	0	0	1	1	0	2
Configuration Selection	3	0	0	1	2	2	2	2	1	1	1	0	1	0	0
Preliminary Design	2	3	3	2	3	1	2	3	3	2	1	2	1	1	2
Prototype construction and testing	3	3	3	1	2	2	2	3	0	1	1	1	1	1	1
Figures of Merit	2	3	1	2	2	2	1	3	2	0	0	0	0	1	0
Refinement of Design Parameters	3	2	3	3	2	2	2	2	1	1	3	0	2	0	2
Refined Numerical Analysis	3	0	3	3	3	0	0	1	2	2	2	0	0	1	3
Configuration Selection	3	2	3	2	2	2	1	2	1	2	0	1	1	0	1
Engineering Requirement Selection	3	1	3	2	3	2	2	2	0	2	1	1	1	1	3
Detailed Design	3	1	3	2	3	3	3	3	2	1	3	2	1	3	2
Configuration Optimization	2	2	3	2	2	2	1	2	2	1	2	2	2	3	0
Airframe	0	2	2	0	2	1	0	2	1	1	3	1	2	2	0
Propulsion Systems	0	2	1	3	0	0	2	0	0	2	2	3	1	2	1
Structural Systems	0	2	3	0	2	1	0	2	2	3	2	2	0	0	2
Control Systems	1	3	3	3	2	2	0	1	1	1	2	1	1	2	2
Final Configuration	2	1	2	2	2	2	2	2	0	0	1	1	2	2	3
Assembly Drawings	0	2	3	0	0	3	0	0	0	0	2	0	1	2	3
Performance Analysis/Optimization	1	1	2	1	3	1	1	1	1	0	1	3	0	3	2
Take-off and Clime	0	2	2	3	2	1	0	2	2	0	1	1	0	2	3
Range, Endurance, and Payload	1	2	2	3	2	1	1	0	3	1	1	2	0	1	3
Handling Qualities	1	1	3	1	3	0	1	0	1	0	1	1	0	0	3

Table 2.2: Team Personnel Assignment

	Alexey Ouzounov	Brian O'Leary	Koji Noguchi	John Fudella	Danelle Schrader	Aditya Sachan	G. D. Romanowksi	Nick Leone	Aditya s. Vaze	Shu Ting Goh	Ashish Shah	William O'Meara	Marie Roedger	Dan Hallenback	Amardeep Dugal
Manufacturing Plan	3	3	3	2	2	3	1	2	2	3	3	3	3	3	3
Figures of Merit	1	1	2	1	1	2	1	3	0	1	2	1	2	3	3
Manufacturing Process Selection	2	2	3	1	2	3	0	2	1	1	3	2	1	1	1
Detail Manufacturing Plan	1	2	3	2	1	3	0	2	2	3	2	3	3	3	2
Final Airplane Construction	3	1	3	3	3	3	3	3	3	3	3	3	3	3	2
CAD Design	3	3	3	0	1	3	1	2	1	2	3	3	1	1	2
Project Management	2	0	3	1	0	3	0	0	1	2	1	3	2	0	2
Documentation	1	1	3	0	0	3	0	1	2	0	0	2	1	2	3
Journal	0	0	2	0	2	3	0	0	1	1	0	3	1	1	2
Letter of intent	0	0	1	0	0	1	0	3	0	1	1	1	1	0	1
Project Report	3	0	3	3	3	3	0	3	0	0	1	0	0	0	0

Table 2.2: Team Personnel Assignment (Cont'd)

2.2 Configuration and Schedule Control

The team implemented a schedule to help visualize the project milestones and the time periods in which they were to be realized. The project managers were responsible for maintaining the schedule and ensuring that the milestones were being met.

Each week the entire design team met twice. During these meetings each individual team reported their progress. This provided a forum for the discussion of interdisciplinary problems, overall status, task assignment, and general administrative concerns. The majority of team productivity took place at other times during the week when groups met individually to discuss designs and ways that they could be improved.

Task Name	Start	Finish
UB AIAA DBF Team	Tue 8/27/02	Sun 2/27/03
Conceptual Design Phase	Tue 8/27/02	Sat 11/30/02
Component Analysis	Tue 8/27/02	Tue 9/24/02
Analytical Analysis	Mon 9/25/02	Tue 11/19/02
Preliminary Design Phase	Sat 11/2/02	Sat 1/18/03
Prototype Construction/Testing	Sat 11/2/02	Sat 12/14/02
Refined Analysis	Tue 12/17/02	Tue 1/21/03
Detailed Design Phase	Tue 1/21/03	Sat 2/15/03
Aerodynamic Refinement	Tue 1/21/03	Sat 2/15/03
Structural Design & Analysis	Tue 1/21/03	Sat 2/15/03
Manufacturing Plan	Wed 2/19/03	Sat 3/29/03
Final Airplane Construction	Wed 2/19/03	Sat 3/29/03
Initial Test Flight	Sun 3/30/03	Sun 3/30/03
Flight Evaluation & Modification	Tue 4/1/03	Sat 4/19/03
Administrative	Tue 8/27/02	Sun 4/27/03
Journal	Tue 8/27/02	Sat 4/19/03
Preliminary Bugdet	Sun 9/24/02	Sat 10/5/02
Letter of Intent	Thu 10/31/02	Thu 10/31/02
Budget Finalization	Tue 10/8/02	Sat 11/16/02
Proposal Preparation	Tue 1/21/03	Mon 3/8/03
Proposal Submission to AIAA	Tue 3/11/03	Tue 3/11/03
DBF Contest	Fri 4/25/03	Sun 27/4/03

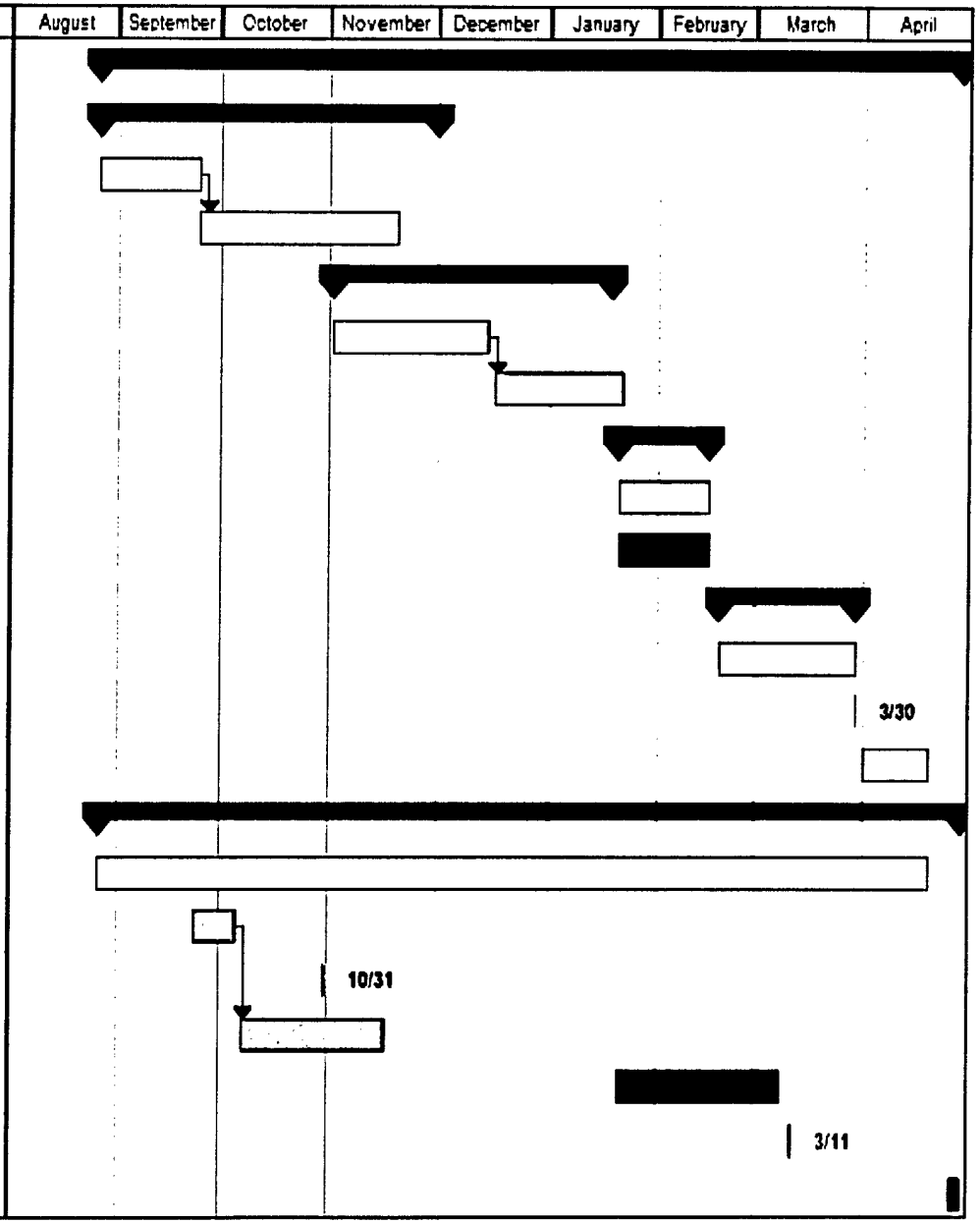

Table 2.3 Gantt chart showing timeline for project

3.0 Conceptual Design

The conceptual design process began with the forming of small teams of people to research different components of the airplane as seen in Table 2.1. The most important factor in this part is to stay within the competition guidelines, which are as follows:

- Wingspan is unlimited, but the whole airplane must be able to fit inside a 4x2x1 foot box.
- Battery weight is limited to 5 lbs.
- Gross takeoff weight must be less than 55 lbs.
- Motors must be brushed, from Astroflight or Graupner.
- A single motor can draw no more than 40 amps.
- Airplane must take off within 120 ft.

A Figures of Merit chart (Table 3.1) was used to determine an optimized configuration for this stage of the design process. The factors that were taken into account were aerodynamics, performance, manufacturing, and structural integrity. A single engine monoplane with a twin tail and tapered wing was selected. This configuration coincided well with what the team had in mind for a simple, fast plane, that would be able to complete any of the three possible missions within the allotted time.

		Aerodynamics		Manufacturing			Performance		Stucture		Total
		Lift	Drag	Time	Cost	Ease	Stability	Control	Strength	Weight	
	Weighting Factors	8	5	7	5	9	8	6	7	9	
Propulsion	Single	N/A	N/A	10	10	10	10	10	N/A	10	440
	Double	N/A	N/A	7	4	6	10	8	N/A	5	296
Wing	Mono plane	7	10	10	10	10	10	10	10	10	614
	Biplane	10	6	7	5	7	10	10	8	5	414
	Flying Wing	7	9	8	9	8	7	6	10	8	493
Tail	T-Tail	N/A	10	9	10	9	10	10	8	8	510
	V-Tail	N/A	10	7	8	7	9	7	7	7	428
	Twin Tail	N/A	10	8	8	10	10	10	10	10	536
	Conventional	N/A	10	10	10	10	7	9	9	8	505
Fuselage	Cylindrical	N/A	8	7	7	4	10	N/A	10	8	382
	Blended wing	N/A	10	8	9	7	8	N/A	10	10	436
	Box shaped	N/A	4	10	10	10	10	N/A	7	8	431
Landing gear	Tricycle	N/A	10	8	9	8	N/A	10	10	9	424
	Tail dragger	N/A	10	8	10	10	N/A	6	8	10	423
Wing Configuration	Straight	10	5	10	10	10	10	10	7	8	574
	Swept	7	10	7	7	6	7	9	9	9	494
	Taper	8	9	8	9	8	10	10	10	10	580
Empannage	Single Boom	N/A	7	10	10	6	8	N/A	6	10	405
	Twin Boom	N/A	9	9	9	8	10	N/A	10	9	454
	Fuselage blended	N/A	8	8	8	7	10	N/A	10	6	406

Table 3.1: Figures of Merit Chart for Conceptual Design phase

3.1 Wing

The goal of the wing design is to find the best wing and airfoil configuration to meet the airplane's needs and be within reasonable construction restrictions. These include a wingspan of no more than 10 feet, and an airfoil thickness around 12% for structural strength. The total loaded airplane weight was estimated to be around 32-pounds, therefore the minimum lift provided by the wing in level flight must be equal to that amount. This would require a significant lift coefficient at close-to-0 angle of attack, which eliminates symmetrical airfoils from consideration.

A tapered, single wing design was determined to be necessary due to its structural strength and low induced drag. Due to this choice, the airfoil used would have to be efficient at a large range of Reynolds numbers, averaging at around 700,000. The airfoil must also be of a relatively easily manufactured shape, which would provide enough thickness at all points of the airfoil so as to not require any special structural materials other than the foam core and carbon-rod spars. Any other material requirements would increase production cost, and could also result in greater overall weight.

From that point on, the choices for the wing configuration were basically restricted to the degree of the taper, the aspect ratio, and the dimensions of the wing root and tip chord lengths.

3.2 Tail

The main function of the tail is to provide pitch and yaw stability for the aircraft. Several configurations were considered in an effort to minimize cost, weight and construction time. Conventional tail, V-tail, T-tail, twin tail, and tailless designs were considered. The tailless design was the first to be eliminated because the amount of analysis and fine-tuning required for such a design would be excessive for our team considering the design timeframe as well as computational requirements. It would provide very significant weight savings, however all control of the aircraft would have to be done through the ailerons, which would require software control in order for the flight to be stable. The T-tail design is an aerodynamically efficient design because the control surfaces are outside the wake region of the wing, however it results in a heavier tail since the vertical stabilizer has to be reinforced in order to support the horizontal one on top of it. The V-tail was discarded as well in favor of simpler construction, alignment and analysis of the more conventional designs. Finally the twin tail design was selected over the conventional tail, due to the fact that both vertical surfaces would be outside of the propeller wake, as well as the simulated antenna, which creates a very significant wake. Since the attachment to the fuselage is in the form of two rods going to the tail, the two vertical surfaces can be attached directly to those rods, thereby not requiring any extra structural reinforcement of the horizontal stabilizer in order to support them.

3.3 Fuselage

The word fuselage is based on the French word 'fuseler', which means, "to streamline." The fuselage is the main body of an airplane, customarily streamlined in form. A plane can do without a fuselage like earlier planes did. However, since we need to carry the battery packs, the cargo, and control instruments like servos, a fuselage is an essential part of our design.

The fuselage needs to be designed in such a way that minimizes construction time and is also highly optimized in a sense that creates drag values as low as possible without violating the rules of the mission. To meet the above-mentioned criteria, a sleek shape of fuselage is needed. The fuselage has to be designed with enough strength to withstand torque generated at the center of gravity by ailerons, rudder and elevator. Also the construction of the fuselage should be within the allotted budget. Strength is also a major area of concern. The fuselage acts as the main connection for the wings, tail, and landing gear. In addition, it carries the payloads, electronics and other various items. Composites will be used to great degree in this area in order to optimize the strength to weight ratio. Last but definitely not least, the fuselage has to either be able to fit completely inside of the box, or it has to be able to be disassembled in order for everything to fit inside the box.

3.4 Propulsion

The goal of the power plant design team is to select a configuration of motor, batteries, and propeller that best meet the needs of the airplane while meeting the design constraints. These constraints include required use of Nickel-Cadmium batteries, a choice of two specified motor manufacturers, a maximum battery pack weight of 5 pounds, a maximum current of 40 amps through a single motor, and a maximum takeoff distance of 120 ft.

The power plant design basically consists of deciding on several parameters relating to the motor, batteries, and propeller. The decisions relating to the motor include the manufacturer, size, and number of motors to be used, and additional gearing. These choices must be made while taking into consideration the estimated overall aircraft weight, the maximum takeoff distance of 120 feet, and the 40 amp current limit through a single motor.

The decisions relating to the batteries include the manufacturer, type, number, and configuration of the battery packs (such as series or parallel). These choices must be made while taking into consideration the maximum battery pack weight of 5 pounds, the voltage required by the motor selected, and the maximum current draw the motor will need.

The decisions relating to the propeller include the manufacturer, propeller diameter, pitch, and material. These choices must be made while taking into consideration the power output of the motor, and the desired top speed of the airplane.

After computing the figures of merit chart shown in figure 3.1 the design was simplified to a single motor. However, this still left many parameters to decide upon.

4.0 Preliminary Design

The design parameters, which were of lesser consideration earlier, now play a vital role in determining the configuration of the airplane. Ideas discussed in the conceptual phase must be refined to obtain solid data on predicted airplane performance.

		Aerodynamics		Manufacturing			Performance		Structure		Total
		Lift	Drag	Time	Cost	Ease	Stability	Control	Strength	Weight	
	Weighing	8	4	7	5	9	8	6	7	9	
Propulsion	Single	N/A	N/A	10	10	10	10	10	N/A	10	440
	Double	N/A	N/A	7	4	6	10	8	N/A	5	296
Wing	Mono plane	7	10	10	10	10	10	10	10	10	604
	Biplane	10	6	7	5	7	10	10	8	5	408
	Flying Wing	7	9	8	9	8	7	6	10	8	484
Tail	T-Tail	N/A	9	9	10	9	10	10	8	8	500
	V-Tail	N/A	9	7	8	7	7	7	7	7	400
	Tailless	N/A	10	10	7	6	4	4	8	10	408
	Conventional	N/A	9	9	10	10	8	9	10	10	544
	Twin Tail	N/A	9	10	10	10	10	10	10	10	546
Fuselage	Airfoil	N/A	9	7	7	8	10	N/A	10	10	436
	Trapezoid	N/A	10	8	9	7	8	N/A	10	10	426
	Box shaped	N/A	4	10	10	10	10	N/A	7	8	427
Landing gear	Tricycle	N/A	10	8	7	8	N/A	10	10	10	421
	Tail dragger	N/A	10	8	10	10	N/A	6	8	10	413
Wing Config.	Straight	10	5	10	10	10	10	10	8	8	576
	Swept	7	10	7	7	6	7	9	10	10	500
	Taper	9	9	8	9	9	10	10	10	9	579
Empennage	Single Boom	N/A	7	10	10	6	8	N/A	6	10	398
	Twin Boom	N/A	6	9	9	10	8	N/A	10	9	435
	Tapered	N/A	10	8	8	9	10	N/A	10	7	433

Table 4.1 Preliminary Figures of Merit

4.1 Wing

The tapered wing was chosen because it provides greater strength at the wing root where the twisting and bending moments due to the lift and drag on the wing are greatest. The majority of the lift generated by the wing would also be toward the center, creating a smaller moment about the center section of the wing, thereby reducing the amount of stress it would have to be able to withstand. Tapered wings also have a much lower induced drag, due to the smaller tip chord length, which is where the tip vortices occur. The main disadvantage of this design was the varying Reynolds number along the length of the wing, due to which the wing tips would have a lower Reynolds number and would therefore stall at a lower angle of attack by a few degrees. This is highly undesirable since it would be impossible to make the airfoil shape of both tips exactly the same, so one would inadvertently stall before the other, and due to the large moment arm the tip has with respect to the fuselage, this would immediately result in a rather strong roll.

To avoid this, there were two choices, either have a wing twist so as to have the wing tips at a lower angle of attack by a few degrees compared to the root, or increase the wing tip's leading edge radius, which results in more drag, but increases the stall angle of the tip. It was determined that the manufacturing of the wing twist would be easier, especially since the basic shape could be easily cut out from foam, and also there was no exact way of determining the magnitude of the leading edge radius required to increase the stall angle by the desired amount.

The search for the optimal airfoil involved looking up a large number of different airfoils designed for a Reynolds number of the same magnitude as the range applicable to our aircraft, then testing it virtually for the full range of Reynolds numbers applicable to the wing design. The polar graphs of the lift coefficient vs. the drag coefficient were then compared with the Clark Y airfoil since it was the airfoil used in our previous designs, and a proven performer for small aircraft. Airfoils with difficult to manufacture shapes or insufficient thickness for structural strength were discarded from consideration.

The Eppler 387 airfoil was determined to be optimal for our needs, since it provides the same or greater lift coefficient as all other candidates, while at the same time retains a very low drag coefficient of under 0.01 over a rather large range of angles of attack. The profile of this airfoil and its polar graph are shown in figures 4.2 and 4.3 respectively. Its' lift coefficient at 0-angle of attack was 0.4, and the drag was 0.0061, which is very good for cruising conditions, although it might still be required to have a small angle of attack at cruising speed, depending on the final weight of the plane, in order to provide sufficient lift.

The stalling characteristics of this airfoil were average, and stall occurred at around 14-degrees at the wing root, and 12-degrees at the wing tip. The stall was not too abrupt since maximum lift occurs at around 10-degrees angle of attack, thereby providing somewhat of a feedback to the pilot about the aircraft's proximity to the stall angle. The thickness of the airfoil was 12%, which is sufficient for structural strength by providing enough room for the spars. The camber was 3.78%, and with the profile being of a rather simple shape, there should not be much manufacturing difficulty, with the exception of the wing

twist. However the wing twist would have been required for pretty much any airfoil since there is no airfoil that would retain the same stall angle over the required range of Reynolds numbers.

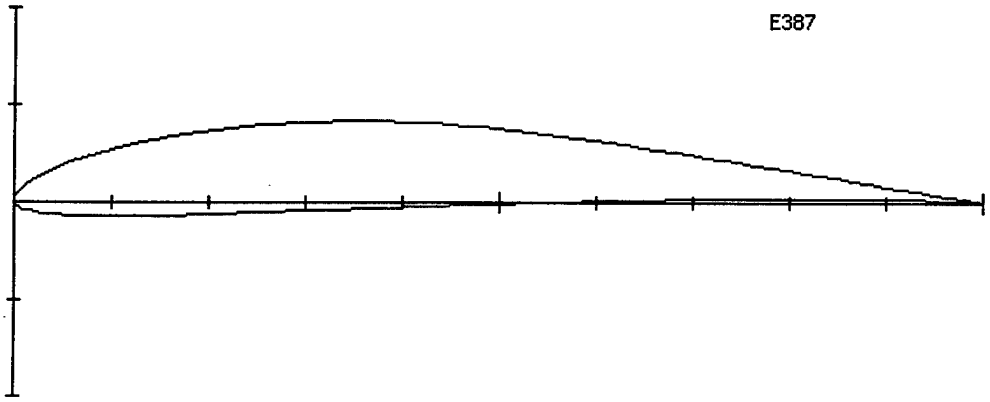

Figure 4.2 Eppler 387 airfoil [6]

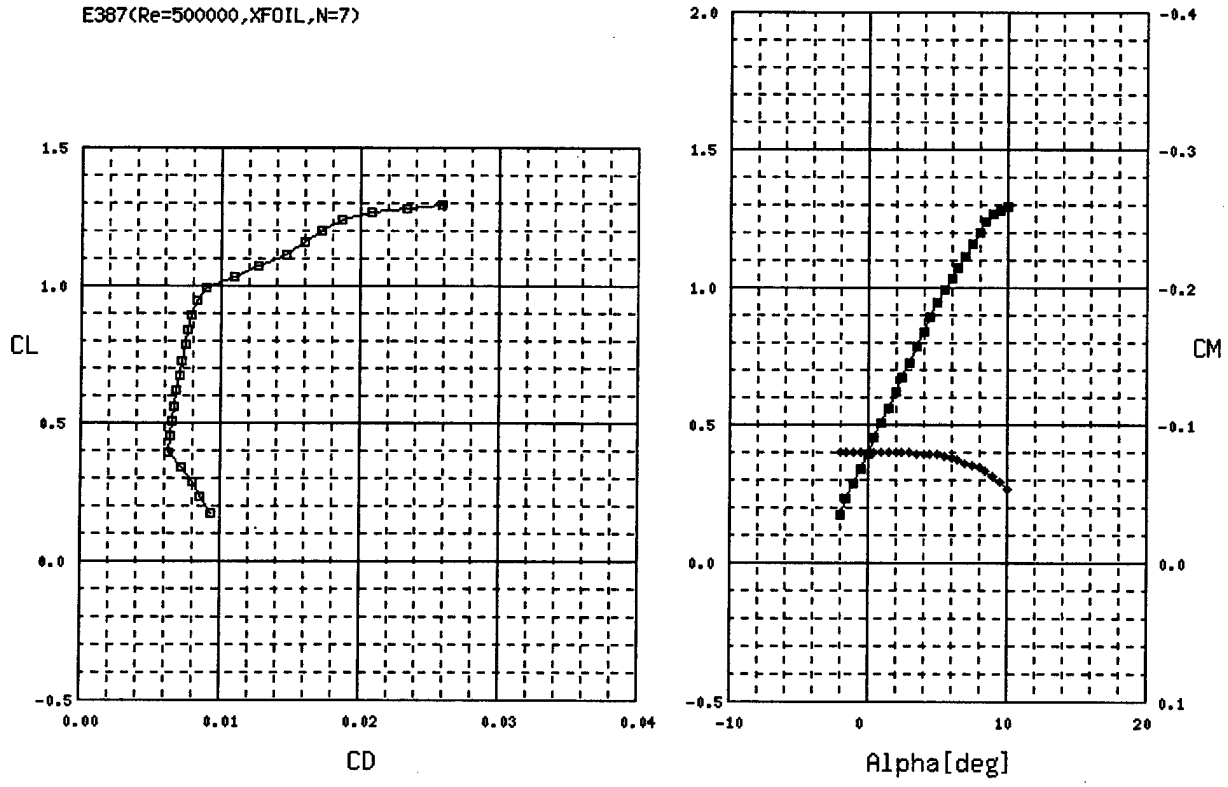

Figure 4.3: Eppler 387 lift coefficient vs. drag coefficient polar graph [6]

When compared to the Clark Y airfoil, the Eppler 387 was a definite improvement as can be seen by comparing their polar graphs in figures 4.3 and 4.4. It retains a larger lift coefficient over the full range of angles of attack, while keeping a considerably smaller drag coefficient at all times. The only disadvantage is the Eppler's rather abrupt changes in drag when it goes into a negative angle of attack as well as at around 6-degrees angle of attack. However this was determined not to have too great of an

effect in terms of control, and since the drag coefficient still remains lower than that of the other airfoils, it does not result in any relative performance losses. Also, for the most part, the plane should never require going into a negative angle of attack, unless an emergency occurs.

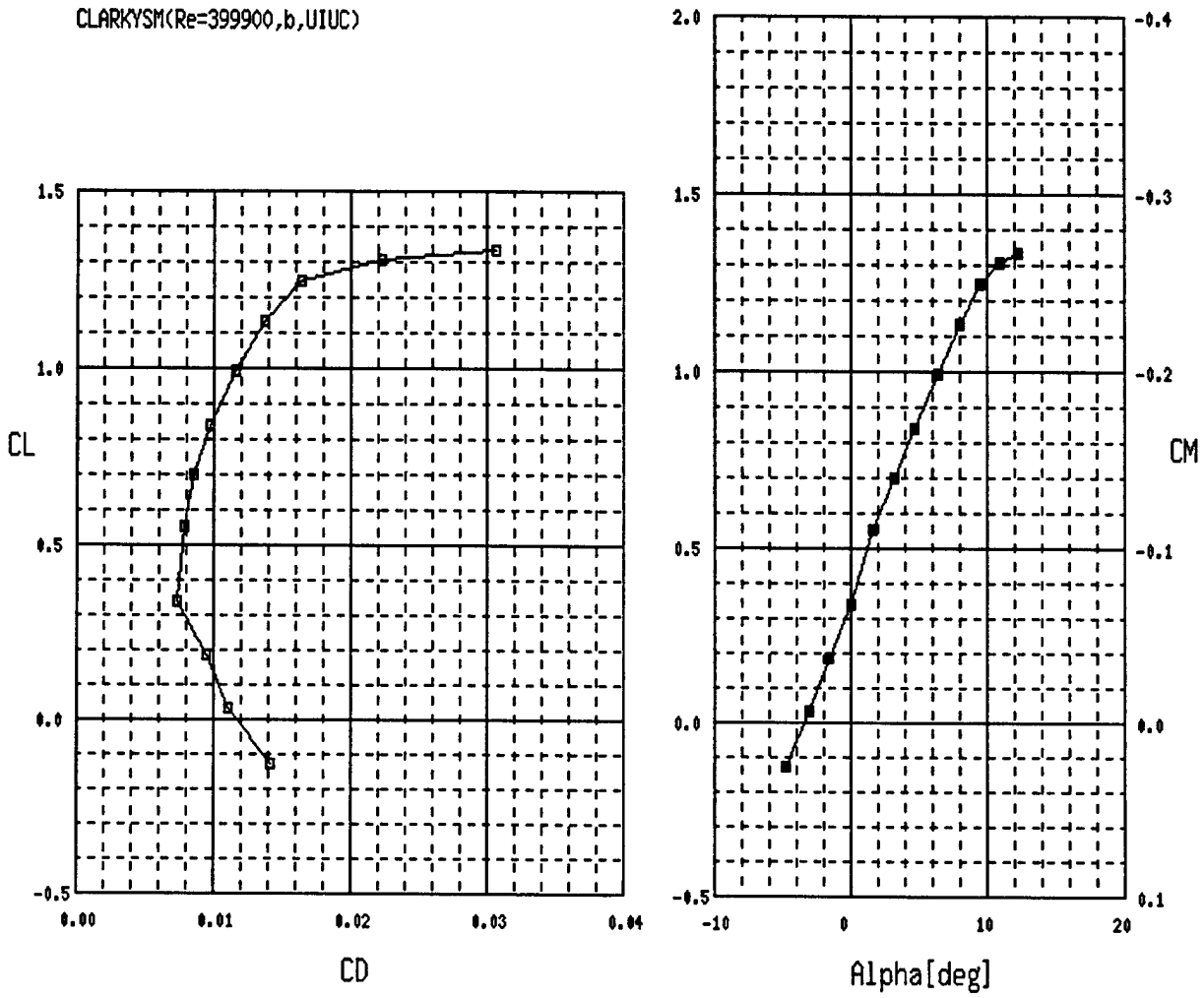

Figure 4.4: Clark Y lift vs. drag coefficient polar graph [6]

Since all of the data used for comparison of the airfoil performance was from virtual sources, it was necessary to determine the validity of this data when compared to real-world results. This was done by comparing the virtual polar graphs to those determined experimentally in the Langley Low-Turbulence Pressure Tunnel[6]. The experimental graphs matched almost perfectly the virtual graphs up to a Reynolds number of 460,000, and it was also stated in the technical report used that for larger Reynolds numbers, the experimental results match perfectly the theoretical, i.e. virtually determined, results.

The optimal wing configuration was determined to be: a wingspan of 9.5ft; root chord length of 22.67 inches (so as to have a taper ratio of 0.5); and a tip chord length of 12 inches. This results in a wing area of 13.5ft^2, which means an estimated wing loading of 36 ounces/ft^2. This number is easily

achievable, however exact lift calculations for this wing design are still underway. The taper ratio for this configuration is 0.5, which is a decent amount of taper, and results in a significant amount of drag reduction. A very good taper ratio would have been 0.2 or 0.3, however there was no way of achieving such a ratio without either decreasing significantly the aspect ratio, having an impossibly large root chord length, or a structurally very weak and small tip chord. Since the aspect ratio has a greater influence on total drag, it was determined to be much more desirable to have it at 5.7 compared to a slightly smaller taper ratio.

4.2 Tail

Once the configuration of the tail is decided, the next step is to find the shape, area, and location of the vertical and horizontal surfaces. The size and location of the tail can be related to the dimensions of the wing to give the tail moment volumes, which in turn can be used to calculate stability. The range of vertical and horizontal tail coefficients are chosen by comparison with similar planes with similar configurations. While staying in this range, the higher end of the spectrum corresponds to higher stability and greater flexibility for the placement of the center of gravity, whereas the lower end of the spectrum corresponds to lower stability and gives smaller margin of error in the placement of the center of gravity. A higher stability value is desirable, especially in heavy wind conditions, however it also makes the aircraft less maneuverable, thereby making the determination of the moment volumes an optimization problem.

In order to reduce the induced drag, the tail's aspect ratio should be quite large, but no greater than one quarter of the wingspan, since then it would count as a second wing, and seriously increase the cost of the airplane. For a wingspan of 114-inches, the horizontal stabilizer would have to be 28.5-inches. The surface areas of the horizontal and vertical stabilizers were determined using the following equations, which use volume coefficients that are typical for most existing aircraft of this size:

$S_h=V_h*S*c/x_h$ and $S_v=V_v*S*b/x_v$

Where S_h and S_v are the horizontal and vertical stabilizer areas respectively; V_h and V_b are the volume coefficients; c is the mean chord length of the wing equal to 19-inches; b is the wingspan at 108-inches; and x_h and x_v are the horizontal distances from the wing's aerodynamic centerline to the tail surfaces' aerodynamic centerlines, both of which are equal to 54.5-inches; finally, S is the wing area at 1944 square inches. The volume moment coefficients were picked to be the average of a series of 13 homebuilt aircraft, since homebuilts are of similar proportions as this airplane, even though this one is not designed for any passengers. The V_h used was 0.47, and V_v was 0.036. From the above equations, the required horizontal surface area was determined to be 316 square inches and the vertical one was 140 square inches. If the span of the horizontal stabilizer were to be kept under 28.5 inches, then the chord length would have to be about 11 inches in order to meet the 316 square inches area requirement. For ease of construction, the vertical stabilizers will be half of the tail span, and the half the chord length and profile for reduced drag, thereby meeting its' 140 square inches area requirement.

The profile of the tail surfaces was chosen to be symmetrical, since even though extra lift is usually desirable, it would require the center of gravity at a location further back than its current one. Since the tail is in the wake of the wing, the flow over it is quite turbulent, which would cause the lifting force from the tail to vary, thereby varying the center of gravity's moment on the plane, and therefore resulting in an unstable flight. The NACA 0012 airfoil was chosen as the tail profile due to its low drag coefficient, and the fact that it provides sufficient room for structural strength with its' 12% thickness.

4.3 Fuselage

Since the construction of the fuselage should be possible with the available resources, simple geometric shapes were studied. The cylinder was found to be most optimized option for fuselage shape. The idea was discarded due to the accuracy and skills needed for construction.

The team members didn't want to spend time on constructing something that they weren't sure how accurate it will turn out. A rough cylinder shape would have contributed significantly to the drag due to irregularities on the surface. Therefore circular shapes were eliminated as a possibility for our design.

The team then decided to investigate quadrilateral shapes due to the ease of construction. Square, rectangles and trapezium shapes were analyzed using simple mathematical skills. Trapezium was found to be aerodynamically better than square and rectangle shapes on the bases of aerodynamics and on past experience of some of the members of the team who were involved in airplane modeling. There were some tradeoffs with that particular shape. It was difficult to taper the fuselage on the end. It was important to taper at the end because the back part wasn't really needed as it contributed to weight and drag and thus putting load on the engine, which resulted in lower thrust. The empennage should be tapered to provide enough surface area for the horizontal and vertical stabilizers. Also with the slant sides, the part of the wing that gets attached to the fuselage needed a smooth slant. That meant spending more time on the construction.

The problem of fitting the fuselage inside the rectangular box was then considered, and it was decided that the fuselage should be no more than 4 feet long, with only the two carbon rods, that would make up the fuselage's structure, extending all the way back to the tail. Such a design would reduce the weight and drag of the fuselage. This meant that the fuselage would have to taper off rather quickly from a considerable thickness at the center of gravity, where the payload would have to be able to fit, especially since there is no way to have the payload between the wing rods, which must run through the fuselage unbroken. Therefore room for the payload would have to be made underneath the wing rods, extending the fuselage a minimum of 6 inches below that point. It was therefore decided that the fuselage would be of an airfoil-like shape made up of foam, with the carbon rods as its' structure. This would significantly reduce the drag, as well as resulting in some more lift, especially around the areas where it would taper-off into the wing airfoil. This design provides significant manufacturing difficulty, however the team feels confident enough in their skills to be able to at least sand down the foam to the right shape. The gains in aerodynamics would definitely be worth the effort required to manufacture this design.

The antenna attachment would be directly on top of the wing spars, which go through the fuselage, and provide a solid support for the aerodynamic loads generated by the antenna. The areas of the fuselage that would hold the payload, batteries and other control and power devices would be cut out from the foam very easily using an electric hot-knife. To counter the sheer stresses on the surface of the fuselage, it would be covered by a single layer of carbon fiber, which will also give the whole carbon rod structure significant torsion resistance.

4.4 Propulsion

The propulsion system consists of motor, propellers and battery pack. Selection of each was based on competition rules and considerations listed in the conceptual design section.

In addition, an issue was raised in regards to properly testing the static force output of the motor. This was resolved by designing a new motor test stand, which was machined and assembled by the team.

4.4.1 Motor

The motor selection starts with the estimated required motor power. From practical experience, we decided that 40 watts per pound of total aircraft weight would give the power we needed to takeoff within 120 feet. For a conservative estimated aircraft weight of 35 pounds, this results in a motor power output of 1400 watts. We also wanted a single engine configuration because of its low rated aircraft cost contribution, and the success of single engine teams in previous competitions. These considerations resulted in the selection of the largest motor allowed, the Astroflight Cobalt 90. The motor performance specifications are listed in Table 4.1

Model	**690**	**691S**
Name	CO-90 Direct	CO-90 Geared
Gear Ratio	Direct	2.75 to 1
Arm Winding	10 turns #22	10 turns #22
Resistance	0.111 ohms	0.111 ohms
Speed	256 rpm/volt	93 rpm/volt
No Load	3.0 amps	3.0 amps
Best Battery	32 to 36 cells	36 to 40 cells
Max Amps	35 amps	35 amps
Prop Rpm	8,000/10,000	3,500 to 4,500
Best Props	13x8 to 16x8	20x14 to24x12
Power Watts	1100 to 1200	1200 to 1400

Table 4.1 Manufacturer's Specifications

This motor has a maximum power output of 1400 watts when connected to 40 cells. This motor was the only one selected from the two manufacturers with a power output in the range that we needed. However, the motor comes with or without a 2.75 to 1 gear ratio, so this aspect needs to be taken into consideration when selecting the propeller.

4.4.2 Batteries

The most important factor in the selection of the batteries is the capacity to weight ratio. Because of the 5-pound weight limit on the batteries, we must make the most use of that weight as possible. Weight and capacity specifications were obtained for every battery from every major Nickel Cadmium battery manufacturer. This resulted in a list of 341 different Ni-Cd cells. This data was entered into a spreadsheet program and the cells were sorted according to capacity to weight ratio.

Next, the cells that are manufactured specifically for high current discharge use were identified. This resulted it the selection of the DSC2100P cell manufactured by BYD. It can handle the current expected in our power plant system while still having a high capacity to weight ratio of 42 mAh/g. This cell is also an excellent choice because 42 cells result in a weight of slightly less than 5 pounds and a voltage output of 50. This is the best voltage for high motor power output.

4.4.3 Propeller

With the motor and battery fixed, a suitable propeller must be selected that satisfies the power output of the motor and the needs of the mission. A useful computer program called "ThrustHP" was utilized in the selection of a range of propellers to be evaluated for further testing. The motor manufacturer suggests several propeller sizes for both the geared and direct drive versions of the motor (see table). An estimate of 1200 watts of max power output for both versions of the motor was used in the program and resulting rpms, static thrust, and speed values were calculated for propellers of varying diameters and pitches. Another factor taken into consideration was the aerodynamic effect of a small propeller diameter spinning in front of a fuselage of almost the same area, which would be the case of the direct drive motor. This analysis led to the conclusion that the geared version of the motor would be used along with a propeller with a pitch of 24. This resulted in acceptable speed, rpm, and thrust values over a range of propeller diameters. The diameter can then be varied to increase the thrust and decrease the speed, or vice versa. Since the program is just a tool and the actual rpm and thrust values had to be determined experimentally, several propellers with diameters between 20 and 24 inches were purchased for testing. The final balance of thrust and speed can then be selected to ensure that the aircraft takes off within 120 ft. APC was selected as the propeller manufacturer because of the amount of positive opinions of other modelers as to their performance and strength.

4.4.4 Motor Test Stand

An important aspect of our design process is being able to determine the thrust of our motor with the use of different propellers. In order to maximize this element in our design, we must be able to get accurate test results in the convenience of our own labs. Therefore, we needed to design a motor test stand to work with many different motor and propeller characteristics. Throughout the design of the test stand, many structures were considered and were finally narrowed down to one universal design. The following page illustrates the metamorphosis of the design from its conceptual phase to the final product.

The design of the stand was based on the two main functions it needed to allow for: unique motors (sizes, weights, etc.) and different diameter propellers. We needed a stand that could be used with many different formats and that would be durable enough to last for years to come. In order to measure the thrust results from each type of propeller, the stand is on wheels and is attached to a scale by a string. When the motor is powered up, we can see how much pull the scale receives and take our measurements from that.

The first design (Figure 4.2a) was intended for a specific motor and an overall propeller diameter. We then realized the value in making the stand capable of adapting to different motors. The original structure was then altered to the specifications in (Figure 4.2b). This stand has an adjustable upright portion, a sliding track-rod-system that can fit any size motor we might require for competition. With a few more changes we arrived at the design shown in (Figure 4.2c). This was brought about in the interest of simplicity. A single plate design with angled support seemed to be much easier than the rigid system of part (b). With this design we headed to the machine shop to consult with the shop attendants. The main concern brought up with our design was stability and weight. With the motor loaded, there was a concern that the stand would tip forward and become a safety hazard. Also, with a single plate system, the overall design may be too heavy to get accurate thrust results. Therefore, we retorted back to a form of design (b) as seen in the three-view drawing on page 14. This system is composed of angled aluminum beams, as opposed to single sheets, over the entire structure. The track with horizontally adjustable rods to hold the motor in place is simply attached between the two upright beams. This track in turn is capable of moving vertically up and down to get better results for smaller propellers.

After the motor test stand is completed, the motor will be tested using the chosen battery pack and various configurations of propeller diameter and pitch, as well as with or without the gearbox. From this data the best configuration resulting in desired thrust and speed can be chosen.

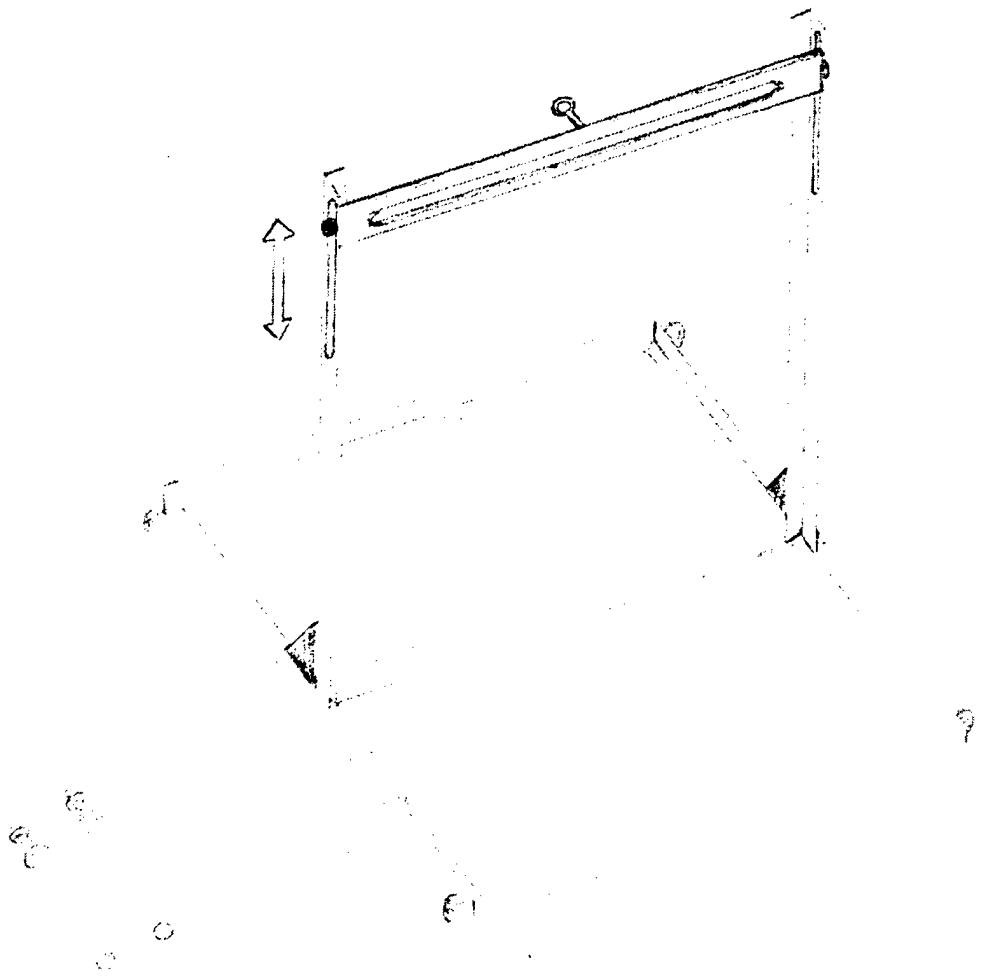

Figure 4.3 Final Motor Test stand design

5.0 Detailed Design

The results from the preliminary design phase are now refined and final dimensions and structure are generated. Figure 5.1 shows the final configuration of the aircraft. Table 5.1 shows the final rated aircraft cost.

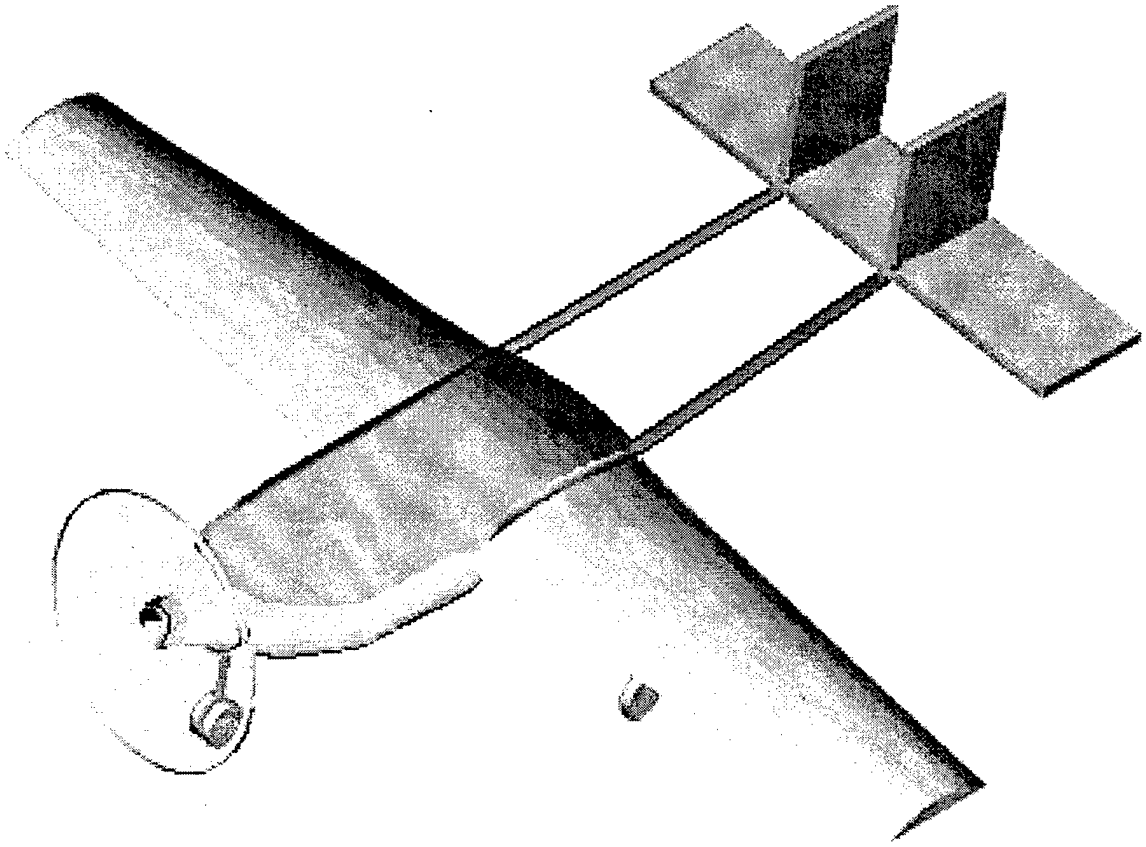

Figure 5.1 Exterior View of Final Design

Rated Aircraft Cost	15.78	
Airframe Weight (lbs)	32	
Batteries Weight (lbs)	5	
Rated Engine Power	5	
Man Hours	254	
Wing Span (ft)		9.5
Max Wing Chord (ft)		1.9
Control Surfaces		5
Body Length (ft)		8
Vertical Surfaces (no active control)		0
Vertical Surfaces (active control)		2
Horizontal Surfaces		1
Servos and Controllers		6
Engines		1
Propellers		1

Table 5.1 Rated Aircraft Cost

5.1 Wing

The structure of the wing is comprised of a foam mould, in the shape of the desired wing size and profile stated in the preliminary design, which is covered in carbon fiber at key stress areas, which is basically the bottom surface of the wing, and has a spar going along its lower part, which is to take the main load of the wing. The spar consists of two carbon-fiber rods, which go the length of the wing, and are epoxied inside pre-cut holes in the foam of the wing. The rods are 7 inches apart, 4 foot long, and are joined to the rods in the other wing by means of two 22 inch long rods that go through the fuselage. These attachment rods are exposed 4 inches on each side outside of the fuselage and attach to the other rods using bolts that are epoxied at each end, and screw into nuts that are epoxied 2 inches deep inside the wing rods. The bolts and nuts on one side of the fuselage are counterclockwise, so that when being assembled, the crew only has to turn the rod clockwise with respect to the left wing for two turns, which will be more than enough to hold the wings tightly to the fuselage. This joint has been tested up to 25lb/ft length of rod loading without failure. The joining rods themselves are able to move freely inside round tubes of carbon fiber attached at the ends of the fuselage. The outside of the wing is only covered with carbon fiber at the bottom surface. This is so as to save weight, since the epoxy used as the matrix for

the carbon fibers is extremely heavy, and the smaller the area covered with it, the better. In terms of strength, this configuration will be about as strong as when the whole wing is covered, as long as the loads applied are aerodynamic and landing gear-applied loads, since these loads act mostly on the bottom surface of the wing. This should be the case most of the time, unless the plane crashes. When these loads are applied, the bottom surface will be in tension, and since carbon fiber is good in tension and not compression, as would be the case for the top surface, this configuration is about the same strength as when the top is covered, except it is about half the weight.

The wing thickness at the end of the wings is much smaller than at the root, and therefore cannot fit the larger size rods used in the middle of the wing. Therefore a telescoping design is used, where the larger, 0.68 inch rods extend up to 3 feet into the wing on each side, at which point a smaller, 0.635 inch-diameter, rod extends the structure. The extension is made by covering a 6-inch end section of the smaller rod with a carbon dust/epoxy mixture, and then placing that section of the rod inside the larger rod, creating a bond area stronger than any of the rods by themselves.

Since the fuselage is a variable airfoil shape, the wing meshes smoothly into the fuselage, while the spar rods go through it using the extensions, thereby creating a very strong, but easily assemblable structure, without the need for extra weight in the form of a connecting surface, and reduces the frontal profile area of the plane. The wing structure is being designed to withstand a 5-g load.

The ailerons start at the fuselage, and extend only 40-inches into the wing, since the wing becomes structurally weak at the tips and cannot support the moment created by the aileron. The servos controlling the ailerons are located 20 inches into the wing, and are directly connected to the wing spar rods, thereby not requiring any extra structure, or extra long push rods extending from the fuselage that would increase weight significantly.

The rear landing wheels are located 4 inches behind the center of gravity, attached directly to the wing spar, 1.5 feet from the centerline on each side. This configuration provides reasonable stability against roll during landing, and prevents the risk of the plane tipping back at landing, since the angle pitch required to accomplish that would have to be greater than 15 degrees, which is rare, and the tail would also touch the ground at that angle. This distance is optimal since if the rear wheels were to be placed further back, it would result in the center of gravity applying too great a moment about them, and requiring a large amount of horizontal stabilizer deflection in order to achieve liftoff, which would create unnecessary drag.

5.2 Tail

The tail is constructed out of a balsa wood rib structure, covered with monokote plastic fabric, and balsa sheeting at the higher stress area where the tail attaches to the rods from the fuselage. The ribs are connected by two balsa wood spars, one on the bottom of the rib and another on the top, and leading and trailing edge balsa wood pieces. Both the vertical and horizontal stabilizers are constructed the same way, except for the vertical stabilizers being 14-inches high, and half the chord, compared to 27 for the

horizontal one. The connection of the tail to the fuselage is made by the use of two more junctions rods, which are 4 foot long , with the same design of bolts and nuts epoxied inside them as the wing connection rods. These attach to two other rods at the tail end, which are epoxied inside the tail under each vertical stabilizer, and two others epoxied inside the wing section. The vertical stabilizers are attached to the rods by simply epoxying them together, with the horizontal stabilizer running between the rods.

The rib structure of the horizontal stabilizer is only 8-inches long, at which point the carbon rods, to which it is connected, end, and the elevator control surface starts. The elevator runs the length of the horizontal stabilizer and is 4 inches wide, which can provide a very large moment about the center of gravity, for greater control. The rudders and vertical stabilizers are constructed the same way and with the same dimensions. The servos controlling the horizontal and vertical stabilizers are located in the rear, at the base of the vertical stabilizers, attached directly to the carbon rods, and with pushrods extending through the structure, to the control surfaces themselves.

5.3 Fuselage

The dimensions of fuselage were calculated on the basis of space needed for the payload as well as for control instruments and the carbon fiber rods. The total length of the plane was found to be 98 inches, with the fuselage only accounting for roughly the front 4, feet, which includes the propeller shaft. The width along the centerline of the fuselage is 18 inches. The wing is placed at a distance of 22.8 inches from the front. The center of gravity of the airplane lies about 26 inches from the front. The front landing gear is 13 inches high and connected at 3 inches from the front. The rear landing gear is a pair and fixed under the wing at a distance of 31 inches behind the front one. The first landing gear retracts between the carbon fiber rods in the fuselage and the second one between the spars of the wing. Aluminum is used to connect the motor to the carbon fiber rods. The motor is placed at 3.7 inches from the front end and in the middle of the rods. The length of the motor is about 4.7 inches. The fuselage front tapers off into the motor, while the back tapers off to the wing edge. The batteries will be placed on the bottom surface of the fuselage near the motor. They can be adjusted along the length of the fuselage in order to have location of center of gravity at 26 inches from the front, which is the optimal location for a relatively stable flight on a tapered wing of this size. The antenna is placed right on top of the wing connection rods on the fuselage, inside a circular cut into the foam, so as to transmit the forces due to the significant drag directly to the plane structure.

The communications package payload is held right under the fuselage, by a set of collapsible doors, made of balsa wood laminate, controlled by a servo that pulls their top surfaces in, thereby releasing the payload during the second mission. The payload's friction due to its aerodynamically inefficient shape is reduced by two latches one in front of it and the other behind it, which serve to guide the airflow around it, and after it is release, get pulled in by the same servo that pulls in the two holding doors. The ability for all of the latches to retract into the fuselage reduces the fuselage thickness, so as to be able to fit it inside the one foot height of the box, along with all the other components of the plane.

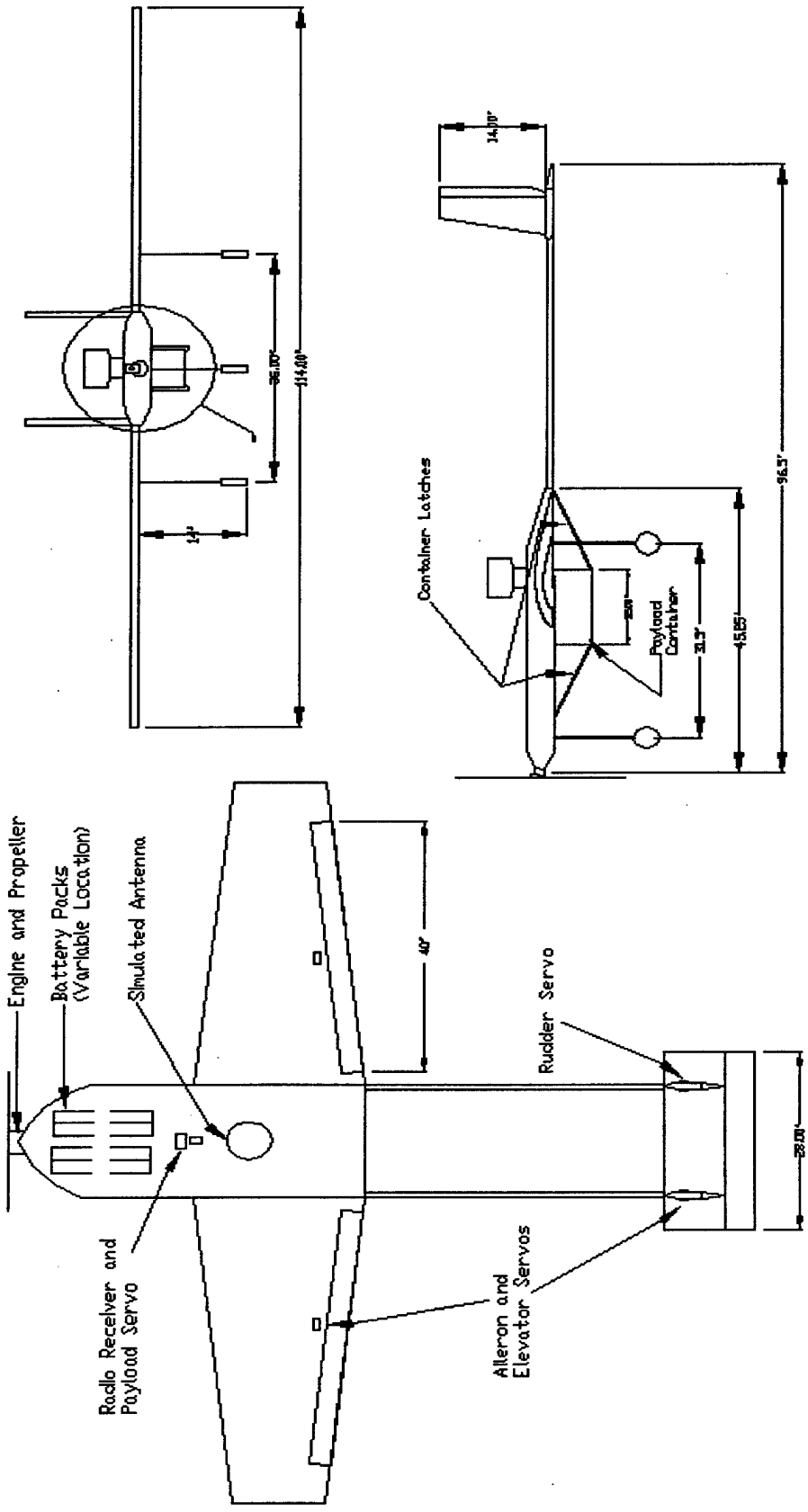

Figure 5.2: 3-View Drawing

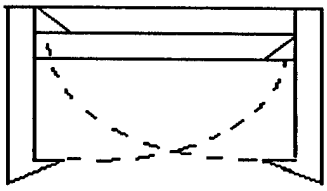

FRONT VIEW

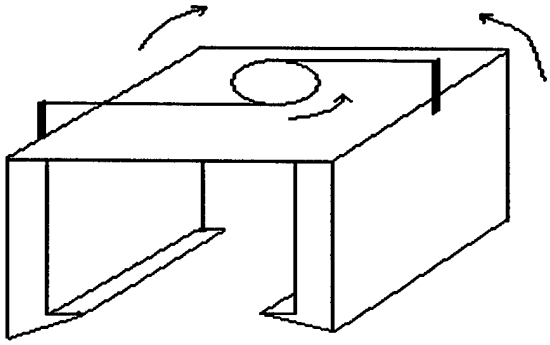

ISOMETRIC VIEW

Figure 5.3 Payload Catch Doors Design

5.4 Propulsion

Proceeding into the detailed design phase the motor and batteries were selected and a range of suitable propeller sizes were determined and purchased. With the motor test stand built the actual performance of these propellers was determined to aid in selecting the one with the best balance between high takeoff thrust and high cruise speed. The best propeller was determined to be 20 inches in diameter and a pitch of 14. At maximum power the propeller spins at 4700 rpm, which is a little beyond what the motor manufacturer suggests but is still acceptable. The static thrust was about 11 pounds, which results in an estimated power to weight ration of .3 for a 32-pound aircraft. This should be enough for takeoff within 120 ft, but if it is insufficient we can simply switch to a larger diameter. Estimated cruising speed using this propeller is 40 mph.

The battery packs will consist of two shrink-wrapped sets of 20 cells connected in series which will result in a combined weight of just under 5 pounds. The pack is split up to maximize in use as a counterweight, two rows of 20 pushed all the way forward in the fuselage will push the center of gravity further forward than one long pack.

With all elements of the propulsion system selected the total operating time can be estimated. The batteries have an estimated capacity of 2100 mAh at a discharge current of about 30 amps. The expected power draw is about 1200 watts, which results in 4.5 minutes of full powered flight, which is never the case for an actual flight, which rarely requires full power other than at takeoff or emergencies.

Geometry:		**Performance:**	
Length	8ft	CL max	1.3
Span	9.5ft	L/D max(wing)	65
Height	1.25ft	max RoC	4.5fps
Wing Area	13.5ft^2	Stall Speed	18mph
Aspect Ratio	5.7	Max Speed	40mph
Control Volumes		T/O length	
horizontal	179inch^2	empty	90ft
vertical	79.5inch^2	gross weight	110ft

Weight Statement:		**Systems:**	
Airframe	17lb	Radio Used	Futaba 8-channel
Propulsion System	7lb	Servos Used	6 servos rated at 11kg.cm
Control System	2lb	Battery Config	2x20 cells
Payload System	1lb	Motor	Cobalt-90
Payload	5lb	Propeller	20x14
Empty Weight	27lb	Gear Ratio	2.75/1
Gross Weight	32lb		

Table 5.2: Aircraft Specifications

6.0 Manufacturing Plan

The design and numerical analysis of an airplane is only half of the task in this project. There is still the actual production of a working airplane. Many different methods of manufacture exist for the different components of this airplane; however, there is a certain degree of expense and skill required for some of these processes. In order to determine the best methods for constructing a lightweight, structurally sound, high performance aircraft, each part of the airplane is compiled along with the figures of merit in Figure 6.1

6.1 Wing

The process of deciding a construction method for the wing was the most time consuming in the project. This was due in part to the critical importance of a lightweight wing that could support the entire airframe in flight. There were three methods discussed in the conceptual design section for the wing: a traditional spar and balsa wood rib wing, a hollow carbon fiber shell, and a foam core with a spar. Through numerical analysis of the particular figures of merit, it was decided to construct a wing with a foam core and spar.

The first step in the manufacture of the wings was cutting the foam to the shape of the chosen airfoil. The foam that was used in construction had to be low density, for weight savings, but had to be strong enough to resist being crushed when it was placed in a vacuum bag for laminating, a procedure that will be discussed later. A polystyrene foam block measuring 9' x 2' x 1' is used to cut the shape of the airfoil. This block provides enough volume to create a one-piece foam core for each wing.

Next, airfoil coordinates are entered into AutoCAD to produce a three-dimensional model of the wing. A computer-guided machine with the hot wire attachment is used for the cutting of the foam blocks. This machine provides more accuracy and a smoother surface for applying a laminate. Though this method costs more, the time savings are significant due to the lack of sanding and surface preparation needed.

However, the block must first be cut in half to form two 4-foot blocks. The hot wire attachment used to cut the wing can only cut from the root to tip and not from tip to tip. This is due to the taper in the wing. The foam wing is then cut into two span wise sections and circular channels are dug out for placement of the spars. The detail of the cuts can be seen in Figure 6...

The next step is to combine the two sections of the foam core to produce a one-piece wing section. A thin bead of five-minute epoxy is applied between each section and they are pressed together to form a foam core with a carbon fiber spar. However, before the wing is laminated, all hard points and other internal structures must be built into the wing. This will provide secure mounting for the fuselage and the landing gear.

For mounting the ailerons, two 4 foot long pieces of ½-inch balsa is glued to the ends of the third section of the foam core. This provides a secure place to attach the hinges for the ailerons. After that,

pairs of 1/8-inch diameter carbon tubes are mounted on the front and back of the spar and fuselage mounting locations. These provide sockets into which the mounting pins are inserted.

After all of the internal structure are in place, the wing is laminated in carbon fiber and vacuum bagged. The carbon fiber fabric is placed on the wing and a sufficient layer of epoxy is applied. Next, a sheet of peel ply is placed over the wing before it is placed in the vacuum bag. The peel ply is fiberglass cloth coated with Teflon, which allows excess epoxy to be lifted away from the carbon fiber leaving a lightweight, smooth surface wing. The whole wing is left in the bag for twelve hours before it is opened. The wing is at maximum strength in approximately three days. The long curing time is due to the use of extra slow hardener in the epoxy, which provides higher strength than the quick cure hardener. This was chosen over Monokote and balsa laminate because it is lighter weight and provides increased structural rigidity for the wing. Also, the addition of team members with experience in laminating carbon fiber made this a useful method of construction.

6.2 Tail

The two main designs for the tail involved either foam cores with carbon laminates or balsa frame with Monokote covering. After building test sections for each design, it was decided that a balsa frame would be the best solution. The foam core section was much stronger than the balsa wood section, but it was twice as heavy. Also, the strength exhibited by both was more than adequate for our needs and the balsa wood design was less expensive.

The first step in designing both the horizontal and vertical stabilizers is cutting out the ribs. A template, machined out of aluminum, is placed on a stack of $1/8^{th}$ in balsa wood and a band saw is used to cut out the ribs. This method is used to reduce the variance in the shape of the ribs. Even a small amount of deviation can severely decrease the control of the airplane. The details of each rib can be seen in Figure 6...

Pieces of $1/8^{th}$ inch balsa, acting as the spars, are then run across the top and bottom of the evenly spaced ribs. After that, the leading edges and trailing edges of the stabilizers are glued on with CA. Next, before the Monokote is put on, carbon rods, which are the main connections to the fuselage, are mounted inside the horizontal stabilizer.

6.3 Fuselage

The construction of the fuselage is the most elaborate and unique part of the UB Bullship. Originally, a balsa frame with Monokote covering was thought to be the simplest and strongest design. However, the aerodynamic qualities are not good. So, the decision was to use a foam core with a carbon fiber laminate. This provided high strength and the ability to produce more complex curves.

The foam core, which serves as the frame, is cut by the same method used in the wing construction. Various cuts are made in the foam with a hot wire and hot knife to form a groove for the wing mounts, an opening for cargo loading and batteries, and channels for the servos and control rods.

Additional grooves are cut for balsa wood strips that act as reinforcements, which run around the outside of the fuselage at high stress areas.

The opening for the cargo is cut using a hot knife, which allows us to make a tight fit perfectly shaped for the payload. The channels for the batteries are not cut as tight as the payload bay, so more air can flow over the packs for cooling. In addition, scoops are cut on each side of the fuselage so air can easily make it to the batteries.

The grooves for the servos are cut to fit the servos exactly. Three layers of fiberglass are then laminated on the inside of the grooves to provide secure mounting points. Also, channels are cut, so that the control rods may move the separate control surfaces with relative ease.

After the internal structures are in place, the whole foam core is laminated with a layer of carbon fiber and epoxy, and placed in a vacuum bag for a minimum of eight hours. Markers are left on the surface so that the various openings can be found and the excess carbon fiber cut out after curing.

6.4 Engine Mount

It was determined in the Preliminary design that the UB Bullship is a single engine airplane, which made the decision to mount the engine in the nose of the airplane trivial. Therefore a design was needed that would mount the engine securely to the fuselage. The design team thought it would be possible to secure a firewall directly to carbon rods, which run in the middle of the fuselage starting from the wing connection rods to the front.

For firewall construction, $1/8^{th}$ inch plywood is laminated with three layers of carbon fiber on each side. A template is made using AutoCAD, printed on a 1:1 scale, and then cut out. The paper template, with the mounting holes included, is glued to the carbon/plywood composite and the proper shape is cut out with a band saw.

High strength epoxy is used to attach the firewall directly to the carbon rods on the fuselage. For added security, screws are fastened from the shell of the fuselage to top of the firewall.

6.5 Landing Gear

The final landing gear design for this airplane is based on the tricycle style. However, the rear landing gear is mounted to the wing and not the fuselage for extra stability. The gear is attached to the hard points on the wing spar ensuring that the shock from landing is not transmitted to the fuselage. This design is more stable and fairly lightweight compared to using a hinge design that attached to the sides of the fuselage.

The nose wheel assembly used is commercially available and is rated for model aircraft of this size. It is controlled by a separate servo connected to the same channel as the rudder. This provides good ground handling and allows for easier hookup than routing a control rod from the rudder servo.

6.6 Material Selection

The following figures of merit provide the design team with the manufacturing characteristics of each component of the airplane. This was important in deciding how to go about construction the airplane outlined in the Detail Design section. The merit parameters are as follows: availability, cost, required skill level, time required, and strength.

6.6.1 Availability

This was extremely important to the design team when deciding what materials to use. There had to be material vendors available that could supply the team with the proper dimensioned and cost effective materials. A score of 0 was given if the product was not available and a score of 4 was given if the product was easily attainable.

6.6.2 Cost

The airplane built had to be cost effective. The team raised enough money to purchase some fairly exotic materials, but these had to be used in only the most essential components. A score of 0 is for and extremely expensive material and a score of 4 is for a relatively inexpensive material.

6.6.3 Skill Level

This year's team was fortunate to have the advice of many experienced builders. This allowed looking into processes that are somewhat more advanced. However, it was still important to stay within the scope of reality because reading a book on carbon lay-ups is different from actually doing it. A score of 0 is for expert skill level and a score of 4 is for beginner skill level.

6.6.4 Time

Time is always against a team in a design competition of this magnitude. The plan is to have the airplane built at least two weeks before competition. This allows enough time for testing the plane as a whole. All of the manufacturing has to be done relatively quickly in time for the competition. A score of 0 is for a very time consuming method and a score of 4 is for a fast manufacturing method

6.6.5 Strength

A strong plane is critical to surviving the sorties in the competition. This is where choice of material can make or break an airplane. A score of 0 is for a weak structure and a score of 4 is for structurally sound component.

		Availability	Cost	Skill Level	Time Required	Strength	**Total**
	Weighting	3	1	2	3	2	
Wing Structure	Balsa Wood Frame	4	4	3	2	3	34
	Foam Core/Carbon Laminate	4	3	4	3	4	40
Spar	Balsa Wood Core	4	3	3	3	4	38
	Carbon Rods	4	3	3	4	4	39
Fuselage	Balsa Frame w/ Monokote	4	4	4	2	3	36
	Foam Core/Carbon Laminate	3	3	3	4	4	38
Landing Gear	Spring Steel	4	4	4	3	4	41
	Carbon Fiber	2	1	4	4	4	35
Horiz. and Vert. Stabilizers	Balsa Frame w/ Monokote	4	4	3	4	4	42
	Foam Core/Carbon Laminate	4	3	3	2	3	33
Motor Firewall	Aluminum	4	4	4	3	3	38
	Steel	4	3	4	3	4	40
	Plywood/Carbon	4	4	4	4	4	44

Table 4.1 Manufacturing Figures of Merit

	Date Start	Date Finish
Fuselage		
Foam cutting	1/19/2002	1/20/2002
Engine mount	2/6/2002	2/12/2002
Hardware placement	2/1/2002	2/8/2002
Laminating	2/14/2002	2/15/2002
Tail		
Vertical Stabilizers	2/15/2002	2/17/2002
Horizontal Stabilizer	2/15/2002	2/17/2002
Wing		
Foam cutting	2/18/2002	2/19/2002
Spar construction	2/20/2002	2/23/2002
Hard point mounts	2/24/2002	3/1/2002
Laminating	3/3/2002	3/4/2002
Landing Gear	3/8/2002	3/10/2002

Table 6.2 Manufacturing Milestones

7. Testing Plan

The major testing objectives would be to determine the actual aircraft flying characteristics, so as for the pilot to know what to expect when applying various controls to the plane. This will include testing the actual maximum rate of climb, takeoff distances, carrying capacity, and possibly, if time permits, training by performing the actual missions on a model aircraft-dedicated airfield. These tests, however would have to wait until the basic static tests are performed to make sure the plane is relatively ready to even go on the runway. The main one of these would be whether or not the aircraft would be able to fit inside the 4x2x1 foot box. The wings have already been constructed and tested to fit inside this box. Determining the actual center of gravity, would also be an integral part of testing, once construction is finished, since the placement of the battery packs depends its' location, so as to bring it to the design specifications. A wing-tip stress test would also be very crucial, since it would be better if the plane fails this test early instead of at competition. Also the final gross weight would have to be determined in order to make sure that the wing loading is not excessive, in which case serious modifications would be required.

Static testing has already been performed on the majority of the aircraft components. The strength of the rods in terms of what kind of moment they can withstand has already been performed, and they have been deemed to provide more than adequate strength considering the loads experienced in typical flights. The rod junctions have also been tested and deemed adequate. The motor/gear/propeller setup has also been tested in order to ascertain whether it would perform to the theoretical expectations. This was done using the motor test stand and a scale to measure the resulting output thrust.

Testing Schedule		
Item/Parameter	**Start**	**Finish**
Carbon Rod Strength	Sat 02/15/03	Sat 02/15/03
Rod Junctions	Sat 02/16/03	Sun 02/17/03
Propulsion Setup Testing	Sun 02/23/03	Wed 02/26/03
Completing Construction		**Sat 03/29/03**
Overall Volume Test	Sun 03/30/03	Sun 03/30/03
Final Gross-Weight Check		
Center of Gravitation Determination and Adjustment	Wed 04/02/03	Wed 04/02/03
Wing-Tip Stress Tests		
Functioning of Control Surfaces	Sat 04/06/03	Sun 04/07/03
Takeoff Distance	Sun 04/07/03	Sun 04/07/03
Rate Of Climb	Fri 04/11/03	Sat 04/12/03
Maximum Payload Weight	Sat 04/12/03	Sun 04/13/03
Maneuverability	Thu 04/17/03	Sat 04/19/03
Mission Requirements	Sat 04/19/03	Sun 04/20/03

Table 6.1 – Tentative Testing Schedule

2003 AIAA DBF Competition Design Report

Queen's University at Kingston
"*Some Assembly Required"

Department of Mechanical Engineering
Department of Engineering Physics

March 7, 2003

1.0 Executive Summary 1
1.1 Major Development Areas 1
1.2 Design Tool Overview 2
2.0 Management Summary 3
2.1 Personnel and Organizational Structure 4
2.2 Scheduling 5
3.0 Conceptual Design 7
3.1 Initial Figure of Merit 8
3.2 Examined Designs 10
3.3 Screening the Three Designs 11
3.4 Analysis of the Rated Aircraft Cost 12
3.5 Design Summary 13
4.0 Preliminary Design 15
4.1 Take-off Gross Weight (TOGW) Estimation 15
4.2 Propulsion Systems Selection 15
4.3 Wing Area and Airfoil Selection 17
4.4 Aspect Ratio (AR) 19
4.5 Wing Platform 19
4.6 Horizontal Stabilizer Sizing 20
4.7 Vertical Stabilizer Sizing 21
4.8 Fuselage Design and Sizing 21
4.9 Undercarriage Design 23
5.0 Detail Design 24
5.1 Weight 24
5.2 Payload Fraction 25
5.3 Drag 26
5.4 Wing Sizing and Performance 28
5.5 Tail Sizing and Performance 29
5.6 Propulsion 31
5.7 G-loading 31
5.8 Take-off Performance 33
5.9 Endurance and Range 34
5.10 Stability 35
5.11 Control Systems 37
5.12 Aircraft Safety 38
5.13 Estimated Mission Performance 39
5.14 Weight and Balances 41
5.15 Rated Aircraft Cost 42
5.16 Sized Aircraft Data 44
6.0 Manufacturing Plan 48
6.1 Wing Construction 48
6.2 Fuselage Construction 49
6.3 Tail Construction 50
6.4 Figure of Merit 50
6.5 Evaluation and Selection 52
6.6 Description of Construction Techniques Employed 53
7.0 Testing 56
7.1 Materials Testing 56
7.2 Full Scale Modeling 58
7.3 Overall Impression 59
References 60

List of Nomenclature

A	Parasite drag coefficient	T	Thrust
A_{wetted}	Wetted area	TOGW	Takeoff gross weight
AOA	Angle of attack	T	Maximum airfoil thickness
AR	Aspect ratio	V	Velocity
a_m	Average acceleration on ground roll	V_{max}	Maximum cruise speed
Ac	Aerodynamic centre	V_{min}	Minimum cruise speed (stall speed)
B	Induced drag coefficient	V_{mean}	Mean velocity on takeoff roll
C	Chord	V_{stall}	Stall speed
C_D	Coefficient of drag	V_{TO}	Takeoff speed
C_{Dpara}	Coefficient of parasite drag	W	Fuselage Width
$C_{Dinduced}$	Coefficient of induced drag	W	Weight
C_f	Skin friction drag coefficient	X_{CG}	Position of CG
CG	Center of gravity	X_{ACW}	Position of wing aerodynamic center
C_L	Coefficient of lift of wing	X_{ACH}	Position of stabilator aerodynamic center
C_{Lh}	Coefficient of lift of stabilator	X_{NP}	Position of stability neutral point
$C_{L\alpha}$	Derivative of C_L with respect to AOA	α	Angle of attack
C_{Lmax}	Maximum coefficient of lift	β	Angle of bank
C_M	Coefficient of pitching moment	ρ	Air mass density
c_p	Power coeffienct	σ	Maximum stress
c_t	Thrust coefficient	ε	Downwash angle
D	Propeller diameter	η	Efficiency
D	Drag	θ	Pitch Angle
d_c	Climb-out distance	μ	Dynamic viscosity
d_r	Ground roll distance	γ	Kinematic viscosity
d_{TO}	Take-off distance		
E	Wing efficiency factor		
G	Acceleration due to gravity		
FOM	Figure of merit		
H	Altitude		
I	Mass moment of inertia		
K	Form factor		
L	Lift		
M	Mass		
M	Pitching moment		
R	Turning radius		
Re	Reynold's number		
S_h	Stabilator planform area		
S_w	Wing planform area		

1.0 Executive Summary

The Queen's 2003 entry to the Cessna/ONR student Design/Build/Fly (DBF) competition marks an application and extension of sound engineering fundamentals. With a wingspan of 2.66 m (8.48 feet), overall length of 1.35m (4.33 ft) and an sleek, aerodynamic design, *Some Assembly Required will prove to be a very competitive aircraft in this years competition. A significant departure was made from the traditional modeling techniques that had been used the last two years. However, the new designs and modeling techniques used have proven themselves lighter and more efficient than those in years past. Combining these new, innovative techniques with a more efficient power system gives us confidence that the 2003 competition will be our most successful competition to date.

1.1 Major Development Areas

*Some Assembly Required is a plane designed to be compact and efficient. In complying with the rule changes introduced this year, new construction techniques were researched and developed. These new techniques allowed the use of contours and profiles which would have been impossible in previous years. In order to perfect our new design features, full scale test sections were constructed on every major component of the aircraft, allowing us to test connection mechanisms, power systems, and perform volumetric analysis on full scale sections to ensure that our design was perfectly adapted to the rules set down for this year's competition.

Early in the conceptual design phase the team studied the volume restriction, payload criteria, time dependency factors, and issues pertaining to the rated aircraft cost (RAC). After preliminary consultation and the help of a simple spreadsheet the team concluded that a small, fast airplane with minimal assembly time would be the most competitive for this year's competition. Due to the inclusion of three different mission scenarios in this year's competition, preliminary spreadsheets were also used to determine the optimal combination of missions in order to guide the design effort.

Due to the height of the payload being six inches of the total allowed twelve inches, a small plane had to be designed that would enclose the payload and still fit in the cargo box. The shortening of the takeoff distance from 200 ft to 120 ft. also played a major role in the determination of our power system and wing configuration. Initially, a shrouded propeller was considered as they had been used successfully in the past. However, given the size requirement of the shroud itself, it was determined that it would not be feasible in this year's design. Due to the failure of our Astro 60 motor during last year's competition, a new motor was needed. After consultation with our contacts in the electric flight community and simulation on motor calculators, it was decided that the team would switch to a single, Graupner ULTRA 3500-8 motor for this year's competition. A larger motor was chosen in order to ensure that the shorter takeoff distance would not be a limiting factor in this year's design. Also, having only a single motor allows for a more streamline design, in keeping with the philosophy of this year's airplane. The motor will on two 18-cell packs of 2400 mAh cells. These cells were chosen due to their superior energy density

and efficiency. Unlike the past, in which we have used 2 cell by 9 cell "stick" packs, we altered the cell configuration to conserve space on the interior of the plane. This resulted in the use of two 2 cell by 3 cell by 3 cell cubes. These battery cubes allow us to confine the batteries to a single location, ultimately leading to a smaller fuselage.

A traditional tractor configuration with tricycle landing gear was also chosen. This was due to the fact that the sensor deployment mission profile demands that the payload is jettisoned from the plane, while the plane then has to continue down the runway and takeoff again, demanding adequate ground clearance at the back of the plane. Also heavily influenced by the volumetric restriction of our various modules was the selection the overall plane configuration. After preliminary estimates, design work began by building up the a low-wing, conventional tail aircraft with teardrop shaped fuselage around the payload. By designing the aircraft around the payload, we were able to restrict the size of the fuselage to an absolute minimum, providing benefits in both drag reduction and volume. These design features were incorporated into a full-scale prototype test section. Testing and modification of this section revealed a plane which satisfied the criteria the team set out resulting in *Some Assembly Required, a small, light, low-wing, airplane with a tailored power system.

1.2 Design Tool Overview

1.2.1 Conceptual Design

Throughout the conceptual design phase of *Some Assembly Required's development, a variety of tools were used to develop and evaluate different aspects of the aircraft's design. These ranged from researching old documents and studies on various components, to using solid modeling in Solid Edge to look in 3D at various designs, to actually building a full scale test section. This research and investigation allowed the team to compare a variety of different designs with proven theory from several respected sources. Testing was used to determine whether or not the technology could be applied to our design with the use of the team's limited resources. This allowed us to narrow down the permutations in design in preparation for the preliminary design stage.

1.2.2 Preliminary Design

Once the team entered this portion of the design process, the techniques used became more analytical than the qualitative methods used in the conceptual design. The *rated aircraft cost* spreadsheet was still used, but in a modified form to screen slight variations of *Some Assembly Required's design rather than the large structural variations examined in the previous section. Component weight was measured, estimated, or obtained from manufacturing specification sheets to allow for some first iteration values to be generated. Simple aerodynamic formulae were also used to determine such things as the coefficient of lift and tail sizing, and to determine areas that needed further development.

Computer software in the form of ElectriCalc and MotoCalc were used to obtain an estimation of how much thrust the chosen electric motors would produce across their given flight envelope. These figures were used to determine the battery pack weight and propeller sizing for the 40 Ampere current limit.

1.2.3 Detail Design

The final stage of the design process meant a transition to purely analytical methods. Classical aeronautical theory was used to determine such things as drag, stall speeds, takeoff rolls, and turning radii. The use of a master aerodynamic spreadsheet reduced the hours of number crunching, and helped the team quickly see the effect of slight design changes.

The final values obtained from this analysis were used to produce the drawing package and blueprints for the construction of the plane. AutoCAD 14 was the drafting package used to produce the required drawings and ensure that the calculated component sizes would mate correctly.

2.0 Management Summary

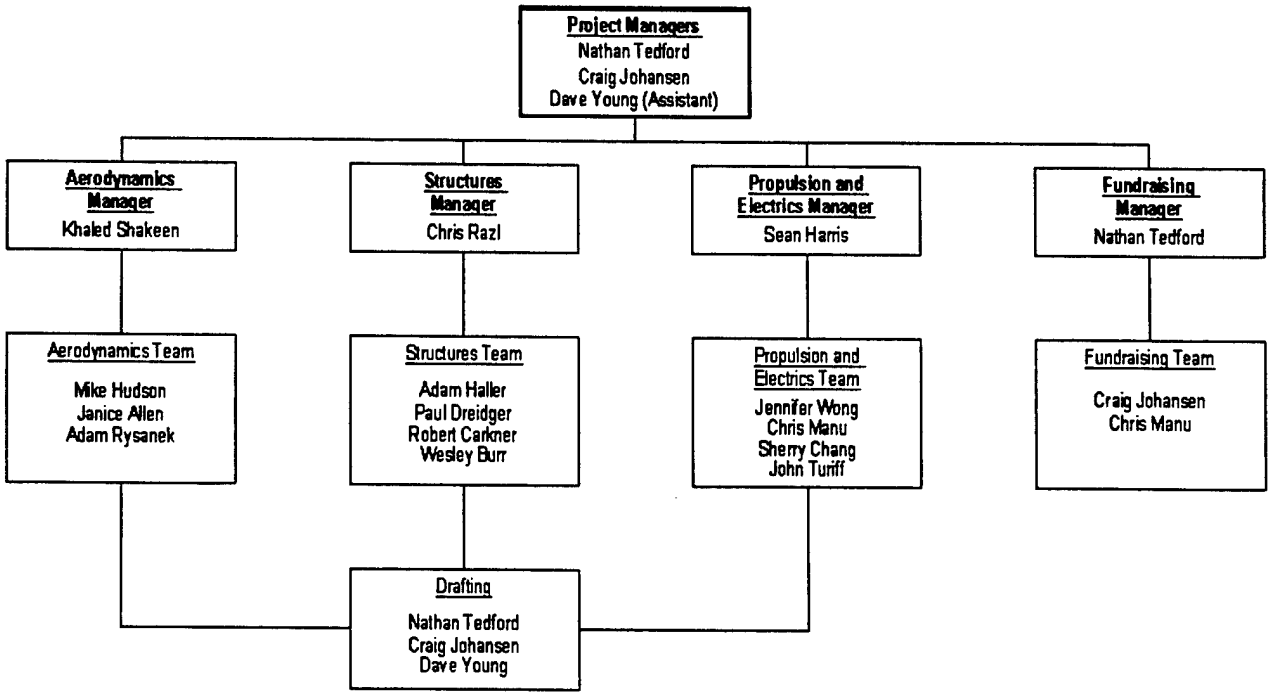

FIGURE 2.1 - Organizational structure

2.1 Personnel and Organizational Structure

The organizational structure chosen for this year's team was based on the functional matrix plan. The design tasks during the initial portion of the year were broken down into three subgroups, with fundraising and finances added as a fourth group. All team members were expected to be members of at least two of the subgroups, allowing each member of the team to contribute to multiple design stages while in turn increasing their knowledge of each. Figure 2.1 shows the team's subgroup structure. Note that only the primary subgroup of each member was listed.

The three design subgroups were tasked with the research, development and design of one of the major systems of the aircraft. The fundraising group was responsible for approaching outside companies to secure donations in the form of monetary donations, product discounts, and access to tooling. Rough sketches of each subgroups efforts were submitted to either Craig Johansen or Nathan Tedford who were responsible for drafting the working drawings of the aircraft into AutoCAD.

During the initial phases of the project, the entire team was assembled for a meeting once a week with the project managers, Nathan Tedford and Craig Johansen. The purpose of these full team meetings was to assemble all of the subgroups in one location, facilitating the integration of the systems. Each team gave a report on their progress and any problems encountered. Effort was made to ensure that viable solutions to each problem were generated by the team to allow the subgroup to continue with their design effort the following week. These meetings also helped ensure that there was adequate communication between the subgroups and ensure that each component would mate properly with the aircraft.

Also during this initial phase, separate meetings were held by the various subgroups. These meetings were scheduled by the respective subgroup managers to ensure that there were no conflicts with any of the subgroup members. These meetings were announced to the project managers, so that either Nathan or Craig could attend to help guide the component design. It should be noted that during these meetings, the project managers functioned as subgroup members, and were not responsible for leading the discussion or design. It was felt that the final aircraft configuration would benefit by leaving the younger students in charge of the various components, as this would ensure that everyone on the team had a chance to be an active participant in the design process. This process also helped develop some innovative ideas and techniques that would not have been thought of by the veteran members, as they were not "conventional" modeling techniques. Also, by ensuring that everyone was involved with the design process, the construction of *Some Assembly Required would progress much more rapidly.

After the design of each system had been finalized, the subgroups were disbanded to allow for the construction phase of the project. Shop hours were set by the project managers, with a schedule being given to each member of the team. This allowed individual team members to work around their own schedules and decide when they would be able to devote a time to construction. Shop hours were set in

order to ensure that there would be a senior member of the team present at each session to help guide the effort and to teach the newer members the construction techniques required for *Some Assembly Required. This system ensured that every team member, regardless of prior building experience, was able to contribute to the assembly of *Some Assembly Required.

2.2 Scheduling

To ensure that the project would be completed before the date of the actual competition, a timeline was produced during the team's second general meeting. Based on our veteran member's previous experience in the Design/Build/Fly Competition, the project managers were able to make reasonable assumptions as to the length of time required to complete each stage of the project. As can be see in the Gantt chart, most estimates were very close to the actual completion time. Figure 2.2 shows the Gantt Chart timeline that was generated during this meeting. It should be noted that during the construction of the timeline, slack was included in the projecting deadlines in an effort to prepare for any unaccounted for difficulties that the team would face.

ID	Task Name	Duration	Start	Finish
1	First Team Meeting	0 d	9/26/02	9/26/02
2	Background	26 d	9/26/02	10/31/02
3	Background - Actual	35 d	9/9/02	10/25/02
4	Conceptual Design	36 d	10/11/02	12/1/02
5	Conceptual Design - Actual	41 d	10/11/02	12/6/02
6	Entry Form Due	0 d	10/31/02	10/31/02
7	Wing Prototype Testing	19 d	11/5/02	11/29/02
8	Fuselage Prototype Testing	15 d	11/18/02	12/6/02
9	Fundraising	52 d	9/26/02	12/6/02
10	Fundraising - Actual	50 d	10/14/02	12/20/02
11	Preliminary Design	15 d	12/2/02	12/20/02
12	Prelimary Design - Actual	26 d	12/9/02	1/10/03
13	Christmas Break	11 d	12/23/02	1/5/03
14	Detail Design	10 d	1/6/03	1/17/03
15	Detail Design - Actual	15 d	1/6/03	1/24/03
16	Airframe Construction	20 d	1/27/03	2/21/03
17	Airframe Construction - Actual	30 d	2/3/03	3/14/03
18	Report Writing	10 d	2/24/03	3/7/03
19	Report Writing - Actual	5 d	3/3/03	3/7/03
20	Flight Testing	12 d	3/22/03	4/7/03
21	DBF Competition	3 d	4/24/03	4/28/03

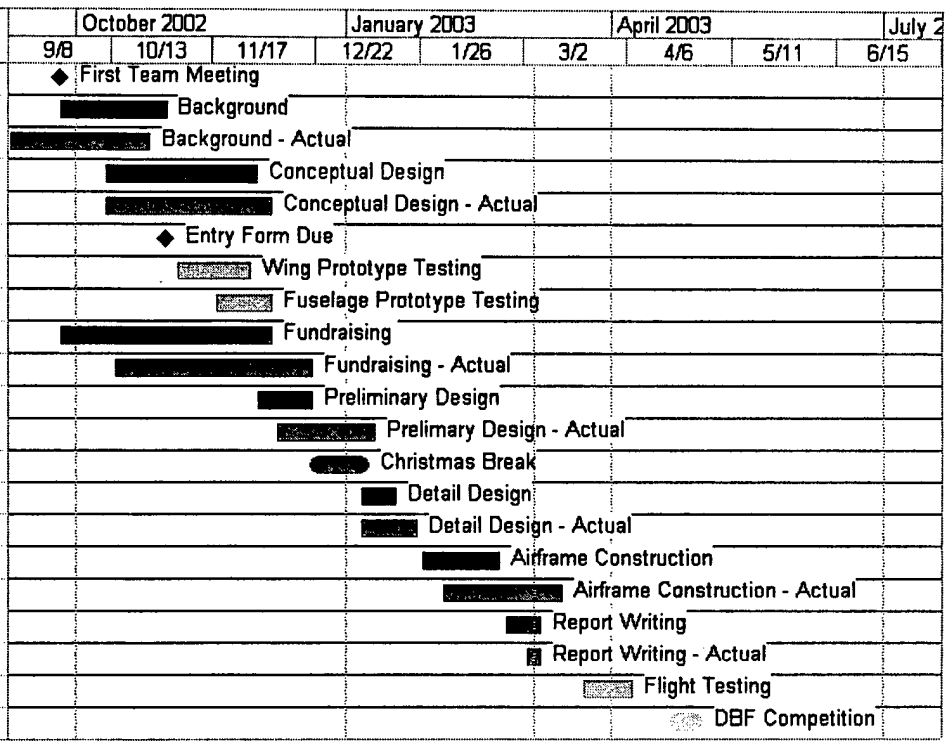

FIGURE 2.2 – Gantt Chart of 2002 / 2003 Scheduling

3.0 Conceptual Design

This year's competition requires a radically new design from previous years. The task of completing two of three available missions continues the evolution of the event from one that is dominated by raw power to one that forces adaptability in aircraft design. The limitations on aircraft dimensions, assembly time, and the choice of mission objectives have guided the team towards a design that is the most competitive for the given criteria.

Before any airframe design was started, the team examined the benefits and drawbacks of the different mission profiles. Some assumptions were made in order to accurately compare the three different missions. Each mission required the aircraft to carry a five pound payload and therefore the rated aircraft cost of each design would only differ in weight and number of standard servos. An estimated cruise velocity, take-off time, landing time, and turning radius were used to estimate each mission flight time. The estimated rated aircraft cost for an aircraft with and without opening bay doors was approximately 12.5. From Table 3.1, flying the two most difficult missions was shown to yield the highest total score. This initial analysis directed the team to create an aircraft designed for the missile decoy and sensor deployment missions. Table 3.1 was generated using the following scoring formula as stated in the competition rules.

$$\text{SCORE} = \frac{\text{Written Report Score} * \text{Total Flight Score}}{\text{Rated Aircraft Cost}}$$

TABLE 3.1 – Mission Profile Comparison based on Aircraft Performance

Mission Analysis	Missile Decoy	Sensor Deployment	Communications Repeater	Total Flight Score	Total Score
1	X	0.53	0.28	0.81	9.54
2	0.88	X	0.28	1.16	13.59
3	**0.88**	**0.53**	**X**	**1.41**	**16.50**

With the decision made to design for the two harder mission objectives, the team then turned to a figure of merit (FOM) to help narrow down the number of aircraft criteria. By examining wing position, tail configuration, payload release mechanism, and undercarriage design, the team was able to narrow the field down to three competing designs.

3.1 Initial Figure of Merit

3.1.0 Figures of Merit

Wing Position:

The position of the wing on the aircraft was the first criterion examined. Packaging restraints were considered in the selection of the wing. All components of the aircraft must fit within the flight box as specified in the competition rules. Arranging two wing sections along the length of the box would allow for a total wing span of eight feet. The team decided that having more than two wing sections would increase assembly time, lower total wing strength, and decrease the wing's efficiency. A bi-plane or tandem wing was not considered because the team felt that this would result in an unacceptable assembly time. A monoplane could be built to have sufficient wing area and would take up less volume in the flight box than other configurations. This left the location of the wing to be determined through the FOM. A high-wing design offers a dual advantage of good stability and an undisturbed cargo area. A mid-wing provides less parasitic drag, but the cargo compartment must be designed carefully around the structural components of the wing. The third design examined, a low-wing, provides slightly less stability, necessitating dihedral to be built into the wing. However, it allows an undisturbed cargo bay and provides a mount for a wider, more stable undercarriage.

Tail Configuration:

The tail configuration of the aircraft was also considered. The conventional tail is light, yet less efficient, resulting in a requirement for more area, which increases drag. A V-tail is light, yet has been known to create control problems in violent flight maneuvers. A T-tail is heavier, yet more efficient, producing less drag.

Release Mechanism:

Initial analysis (Table 3.1) suggests that the aircraft be designed to undertake the sensors deployment mission. This mission requires the aircraft to fly a circuit with a payload, land, drop the payload, take-off, and then fly another circuit. Dropping or unloading the payload must be performed by an unaided remotely controlled mechanism. Various methods of payload deployment were considered at this stage. The first mechanism considered was a spring loaded release mechanism that forces the payload out of the rear of the aircraft. Advantages of this method of deployment are its deployment speed and the ability to release the payload behind the aircraft avoiding contact with the undercarriage of the plane. A second mechanism considered was ejecting the payload from the top of the aircraft using a similar spring mechanism. Although it would be designed to propel the payload a safe distance from the aircraft, the spring mechanism will be bulky and could possess reliability issues. Finally, the payload can

be deployed from bay doors at the bottom of the fuselage. The force due to gravity will allow the payload to be released from the aircraft, however a mechanism will be needed to open and close the doors. Note that each of the systems considered does not interfere with the firewall mount, motor or nose gear systems.

Undercarriage Design:

The three types of undercarriage examined are tricycle, bicycle, and tail-dragger. The tricycle gear produces the most drag, yet offers the best ground handling. The bicycle gear is more complex as it requires out-riggers in the wings to give ground stability. The advantage of this design is that it produces a very low drag airframe for flight. A tail-dragger possesses better drag characteristics than a tricycle gear configuration, but has poor ground handling characteristics in windy conditions.

3.1.1 Figure of Merit Criteria

The following criteria were selected by the team to help identify the most promising aircraft configuration, with each design being assigned a score from 0-5, which is then multiplied by the weight of the specific criterion:

Drag: The drag of the component in question is important as it adds to the drag of the total airframe. In high wind situations, valuable battery power is lost fighting for headway, when a sleeker plane would have no trouble. This FOM was given a weight of 4.

Weight: Similar to drag, the weight of each component is added to produce the total plane weight. A wise man once said, "it's easier to take one gram from 100 parts than to take 100 grams from one part." The same principle applies here. This FOM was given a weight of 5

Performance: The design of the part is crucial to producing the best aircraft. If one option performs the same task a little better than the competition, then it receives a higher score. This FOM was given a weight of 4.

Ease of Manufacture: The best design in the world is useless if we can't build it. A higher rating indicates its relative ease of producing it. This FOM was given a weight of 4.

TABLE 3.2 –Initial Figure of Merit

		Drag (4)	Weight (5)	Performance (4)	Ease of Manufacture (4)	Total
Wing Position	High	4	5	4	5	77
	Mid	5	4	3	3	64
	Low	4	5	5	5	81
Tail Configuration	Conventional	3	5	5	5	77
	V-Tail	5	5	2	2	61
	T-Tail	4	3	5	4	67
Release Mechanism	Rear Ejector	5	3	2	4	59
	Top Ejector	5	4	2	3	60
	Bottom Release	4	5	4	5	82
Undercarriage	Tricycle	3	4	5	5	72
	Bicycle	5	3	2	2	51
	Tail-Dragger	4	5	2	4	65

3.2 Examined Designs

3.2.1 Flying Wing

The first possible design chosen by the team was a radical departure from anything Queen's has ever built. A flying wing with an oversized center section would house the 5 pound payload. The wing would require an airfoil with a very small pitching moment, but this means that the center section must be very long to accommodate the reflexed trailing edge. To keep the wing loading to a reasonable level and the aspect ratio high to minimize drag, the outboard wing sections would have a reduced chord. A higher aspect ratio can be achieved by increasing the wing span, but unfortunately the wing span is limited to the dimensions of the flight box. The outer wing panels would also feature some dihedral to improve flight stability.

3.2.2 Blended Fuselage

The second design selected is very similar to the flying wing but it includes a conventional tail for more predictable flight characteristics. The wing would not require the reflexed trailing edge profile that produced such a large chord on the flying wing; instead a conventional flat-bottomed wing could be used. The tail would be mounted on a light boom structure to minimize weight and drag.

3.2.3 Conventional

The final design considered was a more conventional aircraft design. The fuselage is engineered to accommodate the payload. The wing and tail sections attach into the fuselage with reliable clipping mechanisms. The fuselage has foam fairings around it in order to reduce drag while adding minimal weight. The chosen wing will have a high aspect ratio with a constant chord. The tail is located outside of the downwash produced by the wing on light, strong boom. The fuselage will be the main structural component, house all necessary electronic equipment, and will be fitted with an appropriate payload release mechanism.

3.3 Screening the Three Designs

Once the team had selected three designs to study further, another FOM was set up that studied how the various airframes compared with respect to drag, weight, performance, ease of manufacture, and their respective *Rated Aircraft Cost (RAC –see Figure 3.1)*. The weighting of the respective criteria remained the same as it was for the component selection process in Section 3.1. The FOM Rated Aircraft Cost was calculated by dividing 5 by the RAC, then multiplying by 10. This is a heavy rating as it was felt that this criterion had a huge effect on the team's final score and standing at the competition.

TABLE 3.3 – Screening the three designs

Aircraft Concept	Drag (4)	Weight (5)	Performance (4)	Ease of Manufacture (4)	Rated Aircraft Cost (5)	Total
Flying Wing	5	3	4	3	4.02	83.1
Blended Wing	5	4	4	3	3.60	86
Conventional	3	5	4	5	3.77	87.9

The manufacturability of both the a flying and blended wing were low due to the restrictions imposed by the flight box. Both of these aircraft would be extremely difficult to manufacture as there would have to be multiple sections which would require many joining mechanisms.

3.4 Analysis of the Rated Aircraft Cost

Once the decision had been made to build the conventional wing design as indicated by the FOM in Table 3.3, the team analyzed the RAC of the design by components (See Table 3.4). As the RAC has a direct bearing on the team's final score, reducing this would improve the team's final standings.

As the competition rules have been modified for the 2003 season, a shorter takeoff distance demands a plane with a large power system. Through preliminary modeling, it was discovered that a plane loaded with less than the maximum battery capacity runs an unacceptable risk of not acquiring sufficient velocity for takeoff in 120 feet. For this reason, it was decided that *Some Assembly Required would fly with the maximum battery weight.

FIGURE 3.1 –Rated Aircraft Cost Breakdown

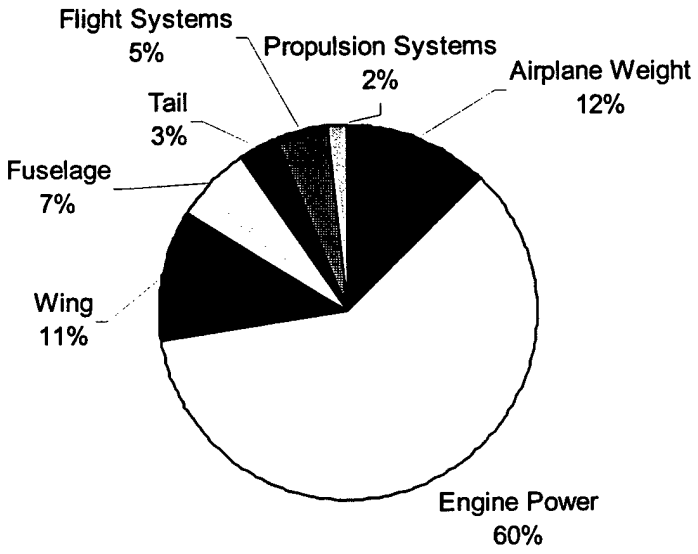

3.5 Design Summary

The final aircraft *Some Assembly Required (see Figure 3.2 –Conventional) has the following specifications:

- Cargo hold with a 6" x 6" x 12", 5 pound payload capacity
- Payload release mechanism through the bottom of aircraft
- Structural member at top of fuselage to attach simulated antenna during missile decoy mission
- Low-wing configuration, utilizing a high-lift airfoil
- Tricycle undercarriage with a wide stance for excellent ground handling
- A single motor with a five pound battery pack
- A RAC of 12.5 based on preliminary weight estimates

FIGURE 3.2 –Various Designs Examined

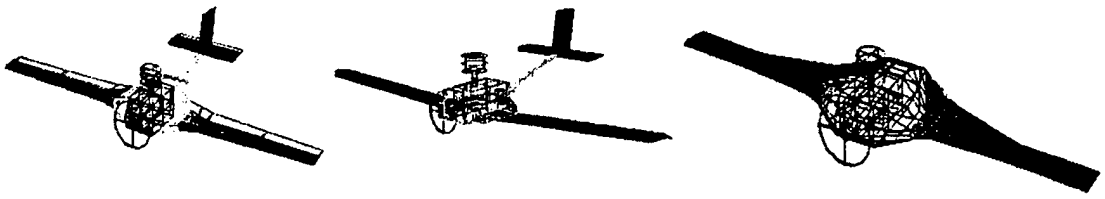

Blended Wing Conventional Flying Wing

TABLE 3.4 –Rated Aircraft Cost of the Three Designs Considered

AIAA Design/Build/Fly 2002/2003				
	Rated Aircraft Cost Spreadsheet	Flying Wing	Blended Wing	Conventional
Coeff.	**Description**			
A	Manuf. Empty Weight Multiplier ($/lb)	100	100	100
MEW	airplane weight (incl. batteries) (lbs.)	16	14	12
	Sum A*MEW ($)	**1600**	**1400**	**1200**
B	Rated Engine Power Multiplier ($/Watt)	1500	1500	1500
	number of engines	1	1	1
	total battery weight (lbs.)	5.15	5.15	5.15
REP	Rated Engine Power (Watt)	5.15	5.15	5.15
	Sum B*REP ($)	**7725**	**7725**	**7725**
C	Manufacturing Cost Multiplier ($/hour)	20	20	20
	number of wings	1	1	1
	wingspan (ft.)	8	8	8
	maximum chord (ft.)	4	2.3	0.833
	number of control surfaces	2	2	2
	WBS 1.0 Wing:	**102**	**88.4**	**76.664**
	length (ft.)	0	1.4	1.58
	WBS 2.0 Fuselage:	**0**	**14**	**15.8**
	number of vertical surfaces	0	0	0
	number of vertical surfaces with control	0	1	1
	number of horizontal surfaces	0	1	2
	WBS 3.0 Empennage:	**0**	**20**	**30**
	number of servos or controllers	5	7	7
	WBS 4.0 Flight Systems:	**25**	**35**	**35**
	number of propellers or fans	1	1	1
	WBS 5.0 Propulsion Systems:	**10**	**10**	**10**
MFHR	Manufacturing Man Hours	137	167.4	167.464
	Sum C*MFHR ($)	**2740**	**3348**	**3349.28**
	Total ($1,000s)	**12.07**	**12.47**	**12.27**

4.0 Preliminary Design

4.1 Take-off Gross Weight (TOGW) Estimation

The first step in the preliminary design phase was estimating the gross weight of the aircraft, as this parameter is crucial in determining the aircraft size and performance. To determine the TOGW, it was necessary to compile the individual weights of all known components and estimate the weight of various airframe structures.

A cargo capacity including a 5 pound payload and a 1 pound simulated antenna yields a total cargo weight of 2.72 Kg (6.0 lbs.). The three different mission profiles allowed for three optimized designs. The aircraft performance design was based on the missile decoy mission with a payload of 6.0 pounds. A small airframe is required to accommodate the volume that the payload occupies, and research was done investigating previous competition aircraft weights. With careful material selection, new construction techniques and engineered weight management, an empty airframe weight of 5.13 kg (11.28 lbs.) was expected. Adding a 2.27 kg (5.0 lb) battery pack and payload, a **TOGW of 9.63 kg (21.18 lbs.)** seemed reasonable.

4.2 Propulsion Systems Selection

4.2.1 Motor Selection

Regulations stating that brushed motors must be selected from the AstroFlight or Graupner lines remained in effect for the 2002 / 2003 season. After having an AstroFlight Cobalt 60 motor fail in flight during last year's competition, the decision was made to switch to the Graupner line of motors. These motors have a solid reputation, capable of handling the voltages and high currents present in this competition.

A rule of thumb used in the electric flight community is that a minimum of 120 Watts/kg be used in rise of ground (ROG) flight. This approximation is marginal for smaller sport airplanes but with the large aircraft considered here this performance is adequate. Previous competition experience has verified this suggestion and provides an excellent staring point for motor selection. Using this information and knowing the approximate TOGW *Some Assembly Required requires approximately **1150 Watts** of power.

MotoCalc and ElectriCalc, commercial software packages, were used to compare various combinations of motors, gearbox, propellers and batteries. The software would produce information regarding each configuration's efficiency, thrust, propeller pitch speed, duration and current draw. In the conceptual design phase it was chosen that a single motor would be used. This decision limited the choice of motors to the Graupner ULTRA family of motors. Utilizing our contacts within the electric flight community, the team was able to converse with Ulf Herder, who is an employee of Graupner specializing in brushed motor selection. After having analyzed our power system needs and aircraft configuration, he advised the team that the ULTRA 3500-8 would be the most suitable motor. This selection was justified as Electricalc had returned similar results during our power system optimization routines. In accordance with this advice, the Graupner ULTRA 3500-8 was used as the motor for *Some Assembly Required.

4.2.2 Battery Selection

The power output of the propulsion system is directly proportional to the voltage and current supplied to the motor. With the maximum current draw of 40 Amperes, the only feasible way to increase power output is to increase the number of cells used. The Graupner ULTRA 3500-8 is rated for operation on 30-40 cells which falls within the regulation weight limits (approximately 36 cells). Continued optimization led to the selection of batteries possessing the highest power density available. Research indicated that 2400 mAh cells fulfilled this criterion. In order to approach the maximum battery weight limit, 36 cells were purchased and arranged in two distinct battery packs. Each pack contains 18 batteries arranged in a 2x3x3 configuration.

4.2.3 Propeller and Gearing Selections

To maximize the efficiency of the power system, one must carefully balance the thrust produced and the propeller pitch speed. Adjustments to this balance may be made by gearing the motor to throw propellers of various sizes. Based on previous experience and preliminary calculations an initial pitch speed of **31.3 m/s (70 mph)** was chosen. Using this information an initial propeller diameter was selected considering various factors such as gear ratios and pitch. It was found that operating the Graupner motor on a direct drive system with a **14" by 8"** propeller would produce a pitch speed of **29.8 m/s (67 mph)** and static thrust of **47.7 N (10.68 lbs)**. This results in a thrust to weight ratio of approximately 1:2 and maximum aircraft velocity of **38.2 m/s (86 mph)**. These estimations have been made assuming a drag coefficient of 0.025 which was obtained from our preliminary spreadsheet values.

4.3 Wing Area and Airfoil Selection

The main characteristics driving wing area and airfoil specification were stall characteristics, drag estimation and lift requirements. An FOM was used in selecting the desired wing attributes. All criteria are explained below, on a rating scale of zero to five, with five being the most desirable.

C_l at Best Lift to Drag (L/D) Angle of Attack (AoA): The coefficient of lift at the best L/D was used to examine the amount of lift the airfoil would produce operating at peak efficiency. Inspecting the airfoil at this point is important as the airfoil's coefficient of lift is inversely proportional to weight and parasitic drag.

Maximum C_l: Maximum C_l was scrutinized as it is the key factor in stall speeds, take-off speeds and the maximum g-loading for a fixed area wing. Due to the limit on take-off distance and the energy advantages obtained by minimizing the amount of time in climb, a high C_l was considered advantageous. However, it should be noted that airfoils containing excessively high C_l's can create undesired induced drag.

Stall Characteristics: This FOM arises from the past experiences of too many modelers. An airfoil possessing a gentler stall increases the time available to react and increases the likelihood of recovery. The stalling characteristic scores were compared using published lift, drag and pitching moment data.

Induced C_d at Expected Cruise AoA: Due to the restrictions on battery power, drag reduction is of prime importance. All airfoils were compared at expected cruise C_l, where the drag will have the most influence on performance.

Ease of Manufacturing: The complexity of an airfoil shape has a direct effect on its ease of manufacturing and inherent structural integrity. Many intricate high lift airfoils possess thin trailing edges and concave undersides which are harder to build and sometimes require additional structure to maintain structural strength.

TABLE 4.1: Airfoil Figure of Merit

Airfoil Name	C_l at best L/D AoA	Maximum C_l	Stall Characteristics	Induced C_d at Cruise	Manufacturing Ease	**Total**
FX 63-137	4	4	5	4	4	**21**
FX 74-CL5-140 MOD	5	5	3	3	3	**19**
S1223 Clean	5	5	3	3	3	**19**
S1210	4	4	5	4	4	**21**
GEMINI	3	2	5	5	5	**20**

4.3.2 Airfoil Section and Wing Area

When sizing for wing area; wing loading, surface drag and induced drag must be considered, in addition to the parameters mentioned above. A larger wing area has higher parasitic drag, but lower induced drag. This arises from the fact that a large area does not require an airfoil with as high a coefficient of lift to produce the desired performance. The drawback of a large wing area is the added structure necessary, resulting in a slight increase in weight. It was decided that a desired wing loading under full payload conditions should be approximately **1485g/dec^2 (45 oz/ft^2)**. As the preliminary estimate of the TOGW was approximately 20 lbs, an wing area of about 0.6 m^2 (930in^2) would be required. A high lift airfoil would be necessary in order to provide the necessary C_L due to the shorter take off distance stipulated in this year's rules. Wing area is also restricted due to the dimensions of the flight box. From this, the C_L at cruise was determined from the standard lift equation.

$$C_{L\min} = \frac{2L}{\eta \rho S_w V_{\max}^{\ 2}}$$

Where η is the efficiency of the wing, assumed to be 0.9, and L is the total lift required, equal to the TOGW of 9.29 kg (20 lbs.).

This gives a required C_L of **0.2** at max a velocity **38.2 m/s (86 mph)** and a C_L of **0.25** at a of cruise speed of **34.6 m/s (77.9 mph)**. The stall speed would be determined by the maximum coefficient of lift obtainable from the airfoil. The Wortman FX 63-137 has a maximum C_l at approximately 1.7±0.1 with a well designed wing being able to achieve 90% of this maximum C_l. With these values, a stall speed of approximately **13.2 m/s (29.4 mph)** can be achieved. It was also desired to have an aircraft capable of maneuvering with a G loading of at least 2.5 at cruise speed, which gives a required C_L of 1.2±0.1, well within that of the high lift airfoils. Three-dimensional effects reducing the overall lift of the wing will be more thoroughly examined in the detailed design when the final wing configuration has been selected.

Maximum takeoff distance is one of the primary design considerations in determining the airfoils maximum C_l. If the C_l of the airfoil were not high enough to allow takeoff within the set distance, high lift devices would need to be incorporated. With the preliminary weight, thrust, and wing area known, for a set takeoff distance of 36.6 m (120 ft), a minimum C_l for take off was determined to be 0.72±0.1, achievable by high lift airfoils.

With all of the above preliminary calculations completed, the wing was required to have a **$C_{L\min}$ of 0.2 and $C_{L\max}$ of 0.72**. Airfoil and drag data were obtained from the UIUC Low-Speed Airfoil Test program and the Summary of Low-Speed Airfoil Data. Their performance was examined with regard to the parameters and the desired values calculated above. The final selection made was the **Wortman FX 63-137** with a C_L of 0.5 and a C_D of 0.013 at a minimum drag angle of -2°, and a maximum C_L of 1.7 at the

critical angle of attack of approximately 12°. The Wortman FX 63-137 has slightly more drag than last year's Eppler 197 airfoil but significantly more lift. The decision was made to use the high lift airfoil due to the slightly undersized wing area imposed by the geometry of the flight box. The extra lift would also help to ensure that the shorter takeoff distance could be met in adverse wind conditions.

4.4 Aspect Ratio (AR)

A higher aspect ratio reduces the induced drag of the aircraft (ie. Gliders), thus allowing for a faster cruise velocity for equal power output. The wingspan this year is limited to less than 8 feet (2.438 m), which is twice the length of the flight box. Aside from the RAC advantages of having a smaller span and the restrictions imposed by the flight box, the team felt that a smaller span would also allow sufficient speed and mobility during the competition. With the wing area previously estimated at 0.6 m^2 (930 in^2), an average chord of 0.254 m (10 in) would be required for a constant chord wing as discussed in the conceptual design section. The final wing set at 2.286 m (90 in) in span with a 0.254 m (10 in) chord resulting in a wing area of .581 m^2 (900 in^2). The subsequent aspect ratio was **9**, which is respectable for high lift aircraft with moderate speed and maneuverability.

4.5 Wing Platform

There are many choices of wing platform including rectangular, taper, double taper and elliptical. The main consideration of the wing platform this year was the restrictions imposed by the flight box. Also, the RAC imposes a penalty as the wing span increases. In efforts to keep the RAC as low as possible a shorter wing was desired. The "ideal" wing planform is an elliptical shape as it has the lowest induced AoA, induced drag and stalls evenly across the span (reduced tip stalling). The major drawback of an elliptical wing is the structural complexity of it. They are very hard to manufacture and repair if need be. A rectangular wing with an AR of 9 requires an induced AoA approximately 17% higher with a 5% greater induced drag than a similar elliptical wing. The major advantages of the constant chord wing are that they are easy to build, maintain constant Re across the span, and require the shortest span to produce the required wing area. The latter of concerns is the most important in minimizing the RAC. A double taper wing was also considered; but because of the span required and the danger of tip stalling at low Rn's it was not pursued. For this competition, the main concern was maximizing wing area with the restrictions imposed by the flight box. This took precedence over the efficiency of the wing.

4.6 Horizontal Stabilizer Sizing

The design considerations used to determine the required tail surface dimensions are stability and control authority. The wing is capable of approximately 2.5g before stalling (see Section 4.3.2), and the Wortman FX 63-137 has a moment coefficient of approximately -0.14 for a cruise angle approximated at -2°. The stabilizer must be capable of overcoming both the pitching moment of the wing and the moment caused by a finite separation between the center of gravity and the center of pressure on the wing (assumed for now to be within 0.0254 m or 1 in. of each other). The tail must then still provide enough torque for efficient control maneuvers. This leads to the inequality:

$$X_{ach}\,\tfrac{1}{2}C_{Lh}\rho S_h V^2 \geq \tfrac{1}{2}C_M \rho S_W V^2 c + 2.4X_{acw}W + I\ddot{\theta}$$

Using this expression, the product of stabilizer maximum coefficient of lift, surface area, and distance from the center of gravity ($X_{ach}C_{Lh}S_h$) can be found. In order to minimize its size and reduce drag, the tail is placed as far aft as feasible to give it a large moment arm on which to act. On this year's aircraft this placement is achieved through adjusting the length of the tail boom. It is common practice to use a stabilizer that is approximately 20 to 22% percent of the wing area. Furthermore, the accepted and recommended elevator size is 40% of the stabilizer area. It has been found that a **0.098 m^2 (152 in^2)** stabilizer located **0.826 m (32.5 in.)** from the CG would require a C_l of approximately -0.3±0.1. To provide extra stability and maneuverability a larger tail area of .121 m^2 (188^2) was used. This coefficient of lift would be easily provided by a **NACA 0009 airfoil** (C_{Lmax} of 1.3) (ref. 7), which has the desired horizontal stabilizer qualities of low drag and zero pitching moment. These will be further quantified in the detailed design section.

The horizontal stabilizer platform is again designed in a rectangular fashion to minimize span. An aspect ratio close to 4 was also desired in order to decrease induced drag. This resulted in a constant chord of **0.203 m (8 in)** and a **0.597 m (23.5 in)** span with a **3.0** aspect ratio. This is slightly smaller than the advised limits by Lennon (Ref 10), who recommends an AR of 4 or 5 on a horizontal stabilizer with a constant chord.

As decided upon in the conceptual design section, a conventional tail configuration would be used. Construction of this design is lighter than a T-tail but less efficient. However, having a low wing configuration and an angled boom, it was felt that the tail would be sufficiently out of the downwash of the wing.

4.7 Vertical Stabilizer Sizing

With the use of a conventional tail, no extra structure had to be added to the vertical stabilizer to support the loading of a T-tail. This allowed the team to produce a very lightweight vertical stabilizer, which provides yaw control and roll stability to the aircraft. For an airplane to be stable in yaw, the Center of Lateral Area should be about 25% back from the center of gravity. In the preliminary AutoCAD design, quick area moment calculations were done to show that the area selected was adequate for yaw control. A vertical fin area of approximately 35% of the horizontal tail area was decided upon therefore the vertical tail area **0.042 m^2 (65.33 in^2)** would be employed, resulting in a root chord of **0.203 m (8 in)**. The vertical fin was swept for aesthetics. Further analysis of the vertical fin height and width is completed in the detail design section.

4.8 Fuselage Design and Sizing

4.8.1 Fuselage Design Considerations

During the preliminary design stage, several design parameter and sizing trades were considered. While innovative design and construction methods were investigated, ease of manufacture, functionality and cost were considered. The decision of airframe design depended on compromises between simplicity of construction, strength, weight and reduction of drag. The following aspects of performance were considered in the proposals of fuselage geometry.

Efficiency: The layout of the fuselage should optimize the space required for the airframe structure and payload while limiting the fuselage's overall size. The payload size was the main factor in determining the most efficient airframe.

Manufacturing Ease: The preliminary design of the fuselage should limit the cost and time required for its construction. The goal this year was to produce the easiest and cheapest airframe to manufacture in light of previous year's experiences. Another aspect to consider at this point is the shop tooling and the facilities available to the team.

Functionality: The fuselage must act as the cargo-carrying portion of the aircraft. The design feature used for access to the cargo will also be used as the release mechanism for the Sensor Deployment mission. This release mechanism must be quick, rugged and reliable due to the rushed nature of the mission. It must also include provisions to support the payload under varying flight loading conditions. The weight of the simulated antenna and the dynamic forces it imposes on the fuselage during flight must also be considered.

Structural Rigidity: The airframe structure must be strong enough to hold and reliably release the cargo during all aspects of the mission including take-offs and landings. It must also be rigid enough to prevent flexing, resulting in reduced effectiveness of the vertical and horizontal stabilizers. The types of materials and structures used for the primary components would depend on the ability to withstand the expected loading.

Drag Penalty: The design of the airframe should minimize the amount of parasitic and interference drag created by the fuselage. This will reduce the power required for cruise and increase overall top speed and motor run time. All junctions between airframe components should be smoothly faired in order to reduce interference drag. Any fuselage upsweep should be less than 15° to prevent separation drag.

Weight: The weight of the fuselage is of prime importance because of the reduced wing area. The materials and structures must all be designed to minimize the weight required

4.8.2 Fuselage Sizing

The design of the fuselage was based on the figure of merit parameters listed above. The length of the fuselage was dictated by the size of the cargo bay and the volume required for the housing of the motor, batteries, and electrical equipment. A portion of the tail moment arm would also include the length of the fuselage located aft of the CG. The payload bay is 12" in length in order to accommodate the payload. An extra 2" in length are added aft of the payload bay to house the tail mounting mechanism, receiver pack, receiver battery, and the payload release servo. The fuselage is centered about 30% of the wing chord to minimize its pitching moment and effect on CG location. Having a rectangular cross-section with angled side panels also allows drag-reducing fairings to be applied to the fuselage. The motor is mounted on a rigid firewall at the nose of the aircraft. The final dimensions of the fuselage proper result in an overall length of **0.660 m (26 in)** with a frontal cross-sectional area of **0.0272 m^2 (42.19 in^2)**.

4.8.3 Cargo Access & Release Mechanism

Access to the cargo hold is facilitated through two bay doors mounted on the bottom of the fuselage and hinged on the outside. The doors are constrained by elastic bands and rare earth magnets. The doors provide no structural strength to the fuselage and do not support the payload in any matter. The payload has a small L-bracket through which a metal rod is placed. When the payload is released, a servo disengages the metal rod from the L-bracket causing the doors to be forced opened due to gravity. They are returned to the closed position by the restoring force provided by the elastic bands. Rare earth magnets ensure that vibration during flight is minimal.

4.9 Undercarriage Design

The tricycle landing gear design used for this year's aircraft must be able to absorb the landing shock and provide excellent ground handling capabilities. The main wheel stance is slightly wider than 1/5 of the wingspan, chosen to prevent upset in high crosswinds. The nose gear is located as far forward on the fuselage as possible, also increasing the stability of the aircraft. The propeller is mounted at the top of the firewall, which measures approximately 3 inches in height, located 10 inches above the ground. As the maximum propeller size that will be used is 14 inches in diameter, ground clearance will not be an issue. The length of the landing gear was based on providing adequate clearance for the payload release. The main landing gear was positioned 0.05 m (2 in) behind the center of gravity so that when the aircraft rotates on takeoff, the wheels remain behind the center of gravity.

Dual ball bearing supported aluminum wheels, 0.089 m (3.5 in) in diameter, are used for the main gear. Because the aluminum does not deform, the rolling resistance is very low. However, these wheels are prone to sliding sideways in crosswinds, necessitating a rubber coating to increase friction. A plastic rubber has been found which coats the running surface of the wheel and provides sufficient friction to prevent sideways motion without adding to the low rolling resistance of the wheel. The nose gear supports less weight, so a standard 0.063 m (2.5 in) model aircraft wheel was used. The higher friction of this wheel provides better directional control on takeoff.

The gear struts are formed from bent ¼ in diameter music wire. The main gear uses a torsion bar design for shock absorption, where as the nose gear uses a single coil design.

5.0 Detail Design

Drawings of the final aircraft configuration are presented at the end of this section. These drawings include detailed two-dimensional views of the airplane along with a three-dimensional isometric view.

The design of any airplane is a highly iterative process which involves making many modifications to the initial aircraft design before the final configuration is reached. In an effort to refine this process an aerodynamics spreadsheet was developed to perform all of the necessary calculations. Through the use of this tool, small variations in the overall design could instantly be reviewed for their effect on the properties of the final airplane. By entering the main geometrical and design parameters of the desired configuration, the appropriate parameters would be delivered, allowing large or small design changes to be analyzed much more quickly then by manual calculation.

5.1 Weight

The final weights of all of the electrical, control equipment and hardware was measured or calculated in order to obtain a reliable estimation of the final aircraft weight. As the vast majority of the plane is constructed from three materials, plywood, SM insulating foam, and a balsa-aluminum composite, the weight of the various key components could be estimated through the use of tabulated material properties and volumetric data acquired from the solid model of the aircraft. Extensive testing of each section also allowed the physical measurement of many of the components, which in almost every case correlated well with the theoretical estimate that had been made earlier in the design process. Though many of the component weights were known accurately, care was taken not to underestimate the weight of any particular component as all of the primary design features of the aircraft require an accurate weight estimate. A summary of the component weights is presented in Table 5.1 below.

TABLE 5.1 – Breakdown of Aircraft Component Weights

Description	Weight (lbs)	Weight (N)	Number	Subtotal (lbs)	Subtotal (N)
Payload	5.000	22.249	1	5.000	22.249
Antenna	1.000	4.450	1	1.000	4.450
Battery Pack	2.450	10.902	2	4.900	21.804
Receiver	0.125	0.556	1	0.125	0.556
Standard Servos	0.125	0.556	7	0.875	3.894
Landing gear	0.750	3.337	1	0.750	3.337
Wheels	0.125	0.556	3	0.375	1.669
Wing	1.500	6.675	2	3.000	13.349
Tail	1.000	4.450	1	1.000	4.450
Fuselage	3.000	13.349	1	3.000	13.349
Motors	1.375	6.118	1	1.375	6.118
Speed Controllers	0.075	0.334	1	0.075	0.334
Receiver Battery	0.250	1.112	1	0.250	1.112
Hardware	0.250	1.112	1	0.250	1.112
Props	0.200	0.890	1	0.200	0.890
TOGW with Payload				**21.175**	**94.223**
TOGW with Payload & Antenna				**22.175**	**98.672**
Empty Flying Weight				**16.175**	**71.974**
Airframe Weight				**11.275**	**50.171**

5.2 Payload Fraction

The payload fraction is a measure of the payload's contribution to the take-off gross weight (TOGW) of the aircraft. The calculated payload fraction of *Some Assembly Required is **0.270** which is well below previous year's entries. Much of this is due to the fact that *Some Assembly Required has a predominantly modular design. The requirement that the aircraft must disassembly to fit inside the flight box emphasized the importance of strong connections between the different modules when assembled. Thus, the connections present between mating modules on this aircraft are significantly heavier than in the past. Also, the payload jettison from underneath the airplane necessitates the fuselage having a higher structural strength than in previous years in which a one-piece wing was used. Both of these factors contribute to the below average payload fraction of this aircraft.

5.3 Drag

In order to make accurate predictions of flight speed, power requirements and in-flight accelerations, an accurate model of the aircraft must be generated in order to accurately estimate the drag of the aircraft. In the model used for *Some Assembly Required, the total drag is considered to be the sum of the parasitic drag and the induced drag of the aircraft. This model does not take into account the interference drag caused by the junction of various modules. This shortcoming is dealt with further in Section 5.3.3.

5.3.1 Parasitic Drag Coefficient

The parasitic drag of the aircraft was estimated using the "component build-up" method. A flat-plate skin friction drag coefficient (C_f) for a fully developed turbulent flow was calculated for each major component of the aircraft and then multiplied by a form factor (k) that estimates losses due to form drag:

$$C_{dPara} = \sum \left[\frac{k \times C_f \times A_{wetted}}{S_w} \right]_{componet}$$

$$\mathrm{Re} = \frac{V \times L}{\gamma} \qquad C_f = \frac{0.455}{(\log_{10}\mathrm{Re})^{2.56}}$$

TABLE 5.2 – Parasitic Drag Estimation

Component	A_{wetted} (m^2)	Re	C_f	Thickness Ratio	k	$C_{dParasitic}$
Wing	1.161	427523	0.005425	0.0343	1.22	0.013236
Fuselage	0.436	1111560	0.004525	3.8519	1.08	0.003671
Wheels	0.036	171009	0.006539	0.0625	1.13	0.000464
Gear Struts	0.002	10688	0.012739	1.0000	1.80	0.000074
Horizontal Stab.	0.243	342018	0.005670	0.0319	1.10	0.002606
Vertical Stab.	0.115	266014	0.005966	0.0254	1.03	0.001221
Antenna	0.044	283234	0.005890	0.4528	1.13	0.000510
Total						0.021272

Therefore, from our model, the total parasitic drag estimate is 0.021, which seems reasonable for an aircraft of this geometry and size. In order to enhance drag reduction, the foam / fiberglass shell that was present around the entire airframe was sanded to create a smooth surface finish and blend transitions between components. Cavities constructed to house servos and other control instruments were covered with Monokote, a commercial covering material.

5.3.2 Induced Drag Coefficient

The induced drag coefficient is dependent on a proportionality factor "K" and the square of the C_L (for moderate angles of attack). K is dependent on an Oswald efficiency factor "e" and the aspect ratio of the wing. In order to reduce induced drag, *Some Assembly Required was designed to increase the aspect ratio to a satisfactory number, given the span restriction imposed by the cargo carrying box. Given the indirect span restriction, a higher aspect ratio was required in order to obtain the necessary wing area for the aircraft.

The following equations govern the induced drag of the aircraft:

$$e = 1.78\left(1 - 0.045 \times AR^{0.68}\right) - 0.64 \qquad K = \frac{1}{\pi A e}$$
$$e = 0.783 \qquad K = 0.0452$$

Therefore, utilizing these two calculated variables;

$$C_{DInduced} = KC_L^2 = 0.0452C_L^2$$

The induced drag is $0.0452C_L^2$ and varies with the angle of attack of the airfoil.

5.3.3 Interference Drag

Interference drag arises from the inconsistencies in various geometries created by the mating of aircraft components. At these junctions, sharp edges or overlaps cause turbulence and add to the overall drag of the aircraft. However, by utilizing proper drag reduction techniques this form drag may be reduced to a point where it can be considered negligible. Some of the techniques employed on *Some Assembly Required are wing-fuselage fairings, a molded tail interface, and wheel pants. With these measures in place, the interference drag contribution to the total drag of the aircraft should be negligible. Due to this fact, the interference drag was excluded from the total drag calculation of Section 5.3.4.

5.3.4 Total Drag

The total drag on an aircraft is proportional to the square of the aircraft velocity. While the parasitic drag equation does include a Reynolds number term, which varies with velocity, its effects are negligible. However, as noted earlier, the induced drag is dependent on the square of the aircraft coefficient of lift (C_L^2). Thus the coefficient of drag at a known airspeed and C_L is given by the equation:

$$\mathbf{C_D = 0.022 + 0.0452C_L^2.}$$

Utilizing the calculated drag coefficient at a given velocity, the total drag force experienced by the airplane is given by $\mathbf{D = 0.5C_D\rho V^2 S_w}$.

5.4 Wing Sizing and Performance

5.4.1 Wing Planform

The wing dimensions proposed in the preliminary design phase were further refined in an attempt to increase the accuracy of the wing performance calculations. The wing area was recalculated through the use of detailed AutoCAD solid modeling giving a final sizing while taking into account any fuselage carry-over. The span of each wing section was finalized at **1.143 m (45.0 in)** and a constant chord of **0.254 m (10 in)**. This provides a total wing span **2.286 m (90 in.)** with a constant chord as noted above. The span remained unchanged in order to accommodate its position in the cargo box. Though tapering the wing had been considered to increase the efficiency of the wing planform, the reduction in wing area was deemed to great. Noting these dimensions, the final wing area is **0.58 m^2 (900 in^2)**. The maximum wing loading with the payload and antenna attached is **1754 g/dec^2 (56.8 oz/ft^2)**.

5.4.2 Aileron Sizing

The ailerons were sized based on historical data for the effective control of an aircraft. The ailerons were designed to utilize a 50% semi-span and 25% wing chord. The ailerons do not extend completely to the wing tips, helping to prevent flutter caused by wing-tip vortices. *Some Assembly Required possesses Frise type ailerons, which are designed to create drag when deflected upward causing the aircraft to yaw into the turns. The area of each aileron is **0.036 m^2 (56.25 in^2)**.

5.4.3 Stall Velocity

In order to relate two dimensional airfoil data to a three dimensional wing core, an appropriate airfoil efficiency factor must be chosen. For this year's entry, the airfoil was assumed to have an efficiency factor (η) of 0.9. This efficiency accounts for lift losses that occur at each wingtip as well as any inaccuracies in the airfoil profile that may have occurred during construction. This reduces the max coefficient of lift from 1.7 to approximately 1.53. From this data, the stall speed of the aircraft can be calculated as follows:

$$V_{STALL} = \sqrt{\frac{2Mg}{\eta C_{l\max} p S_w}} = 13.2 m/s$$

This results in a stall speed of 13.2 m/s (29 mph) assuming that the plane is flying with the payload box. This stall velocity is slightly faster than desired, but not unmanageable.

5.4.4 C_L at Cruise Velocity and Maximum Velocity

In order to determine the maximum velocity and resulting C_L, several mathematical iterations must be undertaken. By iterating different values of velocity and C_L, a final cruise velocity and maximum velocity can be found. Table 5.3 presents the results of these iterations. It should be noted that the cruise velocity of the aircraft was assumed to be 90% of the maximum velocity.

TABLE 5.3 – Maximum and Cruse Velocities

	Velocity	Velocity	C_L
V_{CRUISE}	34.4 m/s	77.4 mph	0.25
V_{MAX}	38.2 m/s	86 mph	0.20

5.4.5 Wing Incidence

With the desired cruise velocity having been calculated in order to conserve battery power, the angle of incidence for the wing at this cruise velocity was determined. This angle of incidence provides the aircraft with the correct line for level flight at the cruise velocity. The correct angle of incidence can be calculated by the following equation, which takes into account the aspect ratio and planform of the wing.

$$a = \frac{a_0 + 18.24 \times C_{Lcruise} \times (1.0 + T)}{AR}$$

$$\alpha = -1.38^{\circ}$$

Where, a_0 is the angle of attack of the wing at $C_{Lcruise}$ and T is the planform adjustment factor for the wing's aspect ratio (Fig 4., pg 6, Lennon, Andy, "Basics of Model Aircraft Design"). The negative angle of incidence is due to the fact that a high lift airfoil was employed this year to help compensate for the reduced takeoff distance. Using the calculated cruise velocity and angle of incidence at cruise, the pitching moment of the wing at cruise velocity can be calculated. For our chosen airfoil and calculated cruise velocity, the pitching moment at cruise was calculated to be **-17.5 N m (-1109 oz in).**

5.5 Tail Sizing and Performance

5.5.1 Horizontal Stabilizer Platform

The horizontal tail has an area of **0.121 m^2 (188 in^2),** which is 21% of the wing area. The horizontal stabilizer was designed with a rectangular planform, a span of **0.60 m (23.5 in)** and a chord of **0.203 m (8 in)** resulting in an aspect ratio of **2.9**. Historical guidelines were again consulted during the determination of the elevator area. For effective pitch control on sports style airplanes, an elevator area of between 30 and 40 percent of the tail area is suggested. An elevator area of **0.039 m^2 (60.0 in^2)** was used, representing 32% of the stabilizer area which is within the acceptable guidelines suggested for a sport plane.

5.5.2 Horizontal Stabilizer Lift

Aircraft modeling guidelines commonly state that the horizontal tail be placed at two and a half times the MAC of the wing, from neutral point to neutral point. For the purposes of this design, the neutral point of both wings was considered to be located at the ¼ chord line. For the geometry of our plane, this guideline would suggest a separation distance of 0.635 m (25 in) for the tail moment arm. However, due to the restriction on the span of the horizontal stabilizer because of its chosen orientation in the cargo box, the tail moment arm was lengthened to **0.83 m (32.5 in)** to compensate for the reduced stabilizer span. Though this provides a slight penalty in the RAC, the increased stability due to the lengthened moment arm is an adequate tradeoff. With a calculated pitching moment at cruise velocity of **-17.5 N/m (-1109 oz/in)** and a tail moment arm of **0.83 m (32.5 in)** the horizontal tail must produce a downward force of **22.4 N (40 oz)**, assuming that the conventional tail employed is 85% efficient. This down force must be provided by the negative lift of the stabilizer airfoil thus requiring a $\mathbf{C_{Lstab} = -0.31}$.

5.5.3 Horizontal Stabilizer Incidence

The angle of incidence required to provide the C_{Lstab} for our chosen airfoil was taken from published airfoil data and was determined to be -3.4° for standard two-dimensional flow. Using the equation introduced in Section 5.4.5 for the angle of wing incidence, and accounting for the stabilizer aspect ration of **2.9,** the required incidence angle becomes -5.54°. However, another factor that must be considered in the calculation of the angle of incidence is the effect of downwash from the wing on the horizontal stabilizer. The horizontal moment arm and the vertical distance between the stabilizer and wing were calculated and compared to charts (Figure 2, pg 40, Lennon, Andy; "Basics of RC Model Aircraft Design" ref 10.) in order to determine the proper stabilizer incidence. Interpolation from these tables gives a final angle of incidence of **–3.82 °** for the horizontal stabilizer, which was incorporated into the final design of the aircraft.

5.5.3 Vertical Stabilizer Platform

The vertical stabilizer remained relatively unchanged from the preliminary design. Problems were encountered during the initial fitting of the aircraft components in the cargo box. Due to these complications, the vertical stabilizer was shortened to **0.267 m (10.5 in)** and was swept from a **0.203 m (8 in)** root chord to a **0.102 m (4 in)** tip chord. These modifications allowed the space issues to be resolved without adversely affecting the performance of the aircraft. .A rudder area of 35% of the vertical tail area was decided upon. This is slightly higher than historical recommendations of approximately 25% of vertical tail area, but was desired to provide added stability to the plane in high banking turns. The resultant rudder area was **0.015 m^2 (24 in^2)**.

5.6 Propulsion

Motor and propeller selection did not change during this phase of the design. A single Graupner ULTRA 3500-8 motor will provide the aircraft with adequate power both during takeoff and in flight. The motor is large enough to turn a 13" x 8 propeller with an approximate pitch speed of **28.8 m/s (65 mph)**, providing approximately **48.7 N (10.9 lb.)** of static thrust. At a predicted current draw of **41 Amperes**, full throttle duration from the 36 cell battery pack is approximately **3.2 minutes**. The computer radio will control the current draw to below 40.0 amps to prevent a fuse blowing under static conditions. As the propeller unloads in the air, the current draw will be reduced. Also, due to the fact that the majority of each mission will be flown at cruise velocity, which has been calculated earlier, the endurance of the aircraft will be greater than calculated under full throttle conditions.

5.7 G-loading

Two major parameters were considered in order to predicting the maximum g-loading experienced by the airframe. Firstly, the aircraft's structural capabilities were estimated with a calculation of the wing spar's maximum allowable bending stress. Once calculated, this led to predictions of the accelerated stall characteristics of the wing, aided by published lift data on the FX 63-137 airfoil.

5.7.1 Structural Loading

It was decided that the aircraft would not experience loading conditions exceeding 4 G. Therefore, a **G-load rating of 4** was assigned as a design parameter representitive of the maximum loading the airplane would experience under normal flying conditions, while at the maximum TOGW. From this assumption, the size and strength of the wing spar, and thus the wing, can be determined.

For the purpose of these calculations, it was assumed that the wing spar carried all the wing loads, and also that the wing spar would experience heavier loading than any other aircraft part. Thus, the maximum bending stresses the spar can handle will determine the G-load capability of the plane. However, as the wing spar terminates upon junction with the main fuselage side panel, the side panel itself was structurally reinforced in order to withstand the same theoretical loading as the wing spar.

The traditional wing manufacturing plan employed by the team has been an "I" beam spar with a carbon laminate for each flange and a vertical grain balsa shear web. However, as the wing material was changed to foam / fibreglass for this competition, this configuration was modified. It was found during initial testing that the carbon laminate used for the "I" beam flanges was impinging on the underlying foam while under load, causing buckling in the wing. To remedy this, the carbon laminate was only applied directly on top of the balsa shear web. The balsa has a substantially higher compressive strength than the foam, ensuring that the carbon laminate would function as intended. This resulted in the recalculation

and redistribution of carbon laminate used in order to maintain the same strength as the original "I" beam structure.

The maximum bending stresses the composite beam can handle is the determining factor for the G-load capability of the plane. As nearly all loadings placed on the airframe are positive, the upper flange is mainly in compression whereas the lower flange is held in tension. As the carbon laminate used is much stronger in tension than in compression, this arrangement of forces requires the number of carbon fiber laminates to vary between the top and bottom flange. From these assumptions, the required cross-sectional area of the respective materials can be calculated.

The maximum bending moment experience by the wing spar was calculated using basic force and moment analysis and found to be **333.8 kN m (1905 lb_f in)** at the root. The moment varies along the length of the spar, decreasing from root to wing tip. The second moment of inertia (I_y) was then calculated to determine the area of the carbon fiber cross section. As the distance to the neutral plane (z) is known, the bending stress was be calculated using the equation:

$$\sigma_x = \frac{M \cdot z}{I}$$

The dimensions of the upper spars (stock sizes) were then iterated to achieve a safety factor of approximately 1.5 (to account for lamination defects) with positive 4 G loading. It was found that **14** layers of carbon fiber applied to the 0.635 cm (0.25 in) wide carbon shear web was required for the bottom spar. Due to the material properties of carbon fiber, **24** layers were necessary for the top spar in order to achieve the same safety factor. As noted earlier, a vertical grain balsa shear web was used to support the carbon spars and prevent shear failure in the wing.

5.7.2 Accelerated Stall Characteristics

The controlled level turning radius of an airplane is determined by the maximum radial acceleration the wing can sustain before and accelerated stall condition occurs. Also, the maximum G-load that can be placed on an aircraft given by the ratio between maximum lift available from the airfoil and the lift generated in steady level flight. It is necessary to determine the angle of bank at which the wing can still produce the required lift for the airplane. It is calculated using the equation below:

$$Cos\beta = \frac{C_{Lcruise}}{C_{L\max}}$$

Using the coefficient of lift data for our particular airfoil, the **maximum angle of bank is 80.1°.** The maximum radial acceleration before an accelerated stall sets in is given by:

$$Tan\beta = \frac{a_{stall}}{1 \cdot g}$$

This gives a loading of **5.7G's.** Hence, if the aircraft sustains a load more than 5.7 G in lateral acceleration, the maximum lift of the wing will be exceeded and an accelerated stall will ensue.

Using this data, the minimum radius of turn with no loss of altitude was calculated to be **19.9 m (65.2 ft)** through the use of the following equation:

$$R = \frac{V_{cruise}^2}{a_{stall}}$$

5.8 Take-off Performance

The take-off performance of any aircraft is composed of three segments: the ground roll, rotation and climb-out distance. Due to the high lift nature of *Some Assembly Required, the rotation distance is assumed to be negligible.

5.8.1 Ground Roll

The ground roll distance is given by: $d_g = \frac{V_{TO}^2}{2 \cdot a_{mean}}$

Where, $M \cdot a_{mean} = \left[T_{mean} - \left(A + B \cdot C_{Lcruise}^2\right) 1/4\, pV_{Mean}^2 S_w - \mu\left(W - C_{Lcruise}\, 1/4\, \rho V_{Meam}^2 S_w\right)\right]$

Take-off speed (V_{TO}) is assumed to be 15% above the stall speed, that is: $V_{TO} = 1.15 \cdot V_{stall}$

C_L and C_D used in this equation are the values at cruising speed. This assumption is valid due to the fact that the plane can be considered in level flight while on the ground, with its angle of incidence relative to the runway. The static thrust term is estimated from ElectriCalc and is used to yield a ground roll acceleration of **4.97 m/s^2 (16.32 ft/s^2).** This acceleration leads to a ground roll distance of **21.0 m (69.0 ft).** This calculated ground roll distance is more than acceptable given that the allowed take off distance is 37.7 m (120 ft). Note that these values have been calculated assuming a zero wind take-off condition.

5.8.2 Climb Out Distance

The following equation governs the climb-out angle of the aircraft: $Tan\vartheta = \frac{T}{W} - \frac{D}{L}$

By substituting the appropriate values into this equation, a **climb angle of 19.4°** is achieved. If this climb angle was sustained as to keep velocity constant in flight, a distance of **28.3 m (93.0 ft)** would be required to reach an altitude of 10 m (32.8 ft). This climb out angle is acceptable and all calculations have been presented for a loaded aircraft.

5.9 Endurance and Range

5.9.1 Minimum Drag Velocity

Both induced drag and parasitic drag are directly related to the velocity of the aircraft, with both increasing as velocity increases. Therefore, there is a velocity at which a minimum drag force is achieved on the airframe as a whole. This minimum drag velocity also corresponds to the velocity with the minimum required thrust. The minimum drag velocity is given by:

$$V_{\min drag} = \left(\frac{B}{A}\right)^{1/4}\left(\frac{2Mg}{\rho S_w}\right)^{1/2}$$

In this equation A and B refer to the parasitic and induced drag respectively. The minimum drag velocity for *Some Assembly Required is **19.6 m/s (44 mph)** at which only **5.84 N (1.31 lbs)** of thrust are needed.

5.9.2 Endurance

An airplane achieves its maximum endurance when it is flying at its minimum drag velocity. The ElectriCalc software package was used to estimate the endurance of the plane with the selected power plant. It was found that the velocity at which drag is minimized occurs at a throttle setting of **47% maximum** throttle. At this setting there is an estimated running time of **22.1 minutes** for the aircraft. However, due to losses present in the wires, leads, speed controller, motors and the inherent difficulty in maintaining a constant velocity, a conservative estimate of 90% system efficiency was assumed. With a 90% system efficiency, the endurance of *Some Assembly Required was found to be **19.9 minutes** at the minimum drag velocity. Note that this estimate does not account for the energy drawn on take-offs, ground roll, climb out, maneuvers and landing. All of these factors significantly reduce the total endurance of the power system.

5.9.3 Range

The maximum range characteristics of an electrically powered aircraft differ from those of a gas-powered plane, as motor efficiency drops at increased throttle settings. To calculate the range, the endurance prediction of 19.9 minutes is multiplied by the endurance velocity of 19.6 m/s (44 mph). This method produces a maximum range of **23.4 km (14.6 miles).** This estimated maximum range value assumes a zero wind condition and also neglects the power needed for takeoff, climb, landing and energy loss maneuvers.

5.10 Stability

Static stability is achieved when the forces on the aircraft created by a disturbance to the flight path push the aircraft back in the **direction** of its original state. Dynamic stability is achieved when the dynamic motions of the aircraft will eventually return the aircraft to its original state (motions are damped). As the software to perform a dynamic stability analysis was not available to the team, the stability analysis presented is limited to static stability. However, for most modes of flight, static stability analysis is sufficient for an aircraft with a conventional layout such as *Some Assembly Required.

5.10.1 Longitudinal Stability

The maximum allowable distance between the center of gravity of the aircraft and the location of the ¼ chord neutral point of the wing was determined using the following stability criterion:

$$\frac{dC_{M(CoG)}}{dL} = \frac{x}{c} - \eta_H \left(\frac{S_H}{S_W}\right)\left(\frac{l_H}{c}\right)\left(\frac{a_H}{a}\right)\left(1 - \frac{d\varepsilon}{d\alpha}\right) + \frac{dC_{Mf}}{dC_L} \leq 0$$

The marginally stable case value of x, the distance from the ¼ chord, was found by setting the above inequality to zero and evaluating. This yielded a value of **43.6%**, which means that for the aircraft to be longitudinally stable, the center of gravity can be located at no more than 43.6% of the wing chord from the leading edge. The difference between the actual center of gravity and the maximum allowable center of gravity is termed the static margin. With the predicted center of gravity at 30% of the mean aerodynamic chord, a **static margin of 0.136** is achieved. This is a sufficient value to obtain an acceptable longitudinal stability.

5.10.2 Lateral-Directional Stability

In order to provide directional stability, the moments about the center of gravity must be such that the derivative of the yawing moment is less than zero. In order to determine the yawing moment derivative about the center of gravity, the pitching moment derivative of the fuselage and vertical fin must be evaluated. The derivative of the pitching moment of the fuselage in the case of *Some Assembly Required will be negligible because the fuselage areas ahead of and behind the center of gravity are equal. The derivative of the vertical fin pitching moment can be expressed by:

$$\frac{dC_{mfin}}{d\theta} = \left(\frac{dC_{Lfin}}{d\alpha}\right)\left(\frac{S_{fin}}{Sw}\right)\left(\frac{I_H}{c}\right)$$

Where $dC_{Lfin}/d\alpha$ is the slope of the lift curve of the vertical fin, S_{fin} is the vertical fin area, S_w is the wing area, I_H is the tail moment arm and c is the mean aerodynamic chord of the wing. The value of the vertical fin pitching moment derivative was evaluated to be 1.4. This value is subtracted from the fuselage pitching moment derivative to determine stability as follows:

$$\frac{dC_{mCG}}{d\theta} = \frac{dC_{mFuselage}}{d\theta} - \frac{dC_{mfin}}{d\theta}$$

The evaluated derivative was found to be positive 1.4, which indicates that the aircraft is directionally stable as the value is greater than zero.

This results in a **lateral-directional pitching moment derivative of –1.4**, meaning that the aircraft will exert a restoring force in the direction opposite any disturbance which is the criterion for static stability.

5.10.3 Roll Stability

Based on historical data, **6° of wing dihedral** provides sufficient roll stability for an unswept, low-wing aircraft. As an aircraft with dihedral banks, it begins to slide slip towards the lowered wing, effectively increasing the lowered wing's angle of attack and increasing its lift. This provides a restoring force to level the wings. As this approach has been utilized with great success in previous competitions, the wing dihedral angle of *Some Assembly Required was set at 6°.

5.11 Control Systems

5.11.1 Receiver and Programming

Control of the aircraft is provided by a **Futaba 8 channel PCM** transmitter and receiver with failsafe programmed as per competition rules. Each control surface has its own servo and receiver channel, allowing programmable mixing to be incorporated. Ailerons are programmed to provide differential control for more up throw than down throw due to the style of ailerons employed. Slight rudder application is also programmed to operate in conjunction with the ailerons to provide coordinated turns. In addition, as no flaps were incorporated into the design, if more lift or drag is needed during take-off or landing the ailerons may be drooped to give the effect of flaps.

5.11.2 Flight Pack Battery

A five cell, **600mAh, NiMh** battery pack is used to power the receiver and servos. The pack size was chosen to be large enough to complete several missions, but will peak charged again after each mission is completed to ensure a control power failure is not encountered. The **6.0V** power system is slightly overpowered for its application; however it increases the power available to the servos which is advantageous enough to justify the small weight gain.

5.11.3 Servo Selection

All servos must provide quick, accurate and strong control authority to the flight surfaces. Any slop in the control set-up could lead to flutter, and possible departure of that control surface. To reduce this risk, all servos are dual ball bearing supported. While many mini servos have static load torques capable of actuating the flight surfaces, their fragile gear sets are unable to handle sudden dynamic loads. For this reason, standard sized servos with metal gears are used. In order to select the proper servo, the load on each control surface must be calculated. The torque experienced by each servo can be calculated using the following equation:

$$T = 8.5 \times 10^6 (C^2 V_{max}{}^2 L \sin(S_1) \tan(S_1) / \tan(S_2)) = oz \cdot in$$

Where T is the torque in oz in, C is the control surface chord, L is the control surface length, S_1 is the max control surface deflection (assumed to be 20°), and S_2 is the maximum servo deflection from center (30° each way for most servos). In this manner, the maximum torque experienced by each flight surface was calculated and recorded. As the aileron servos were shown to experience the highest flight loading of any component at **49.5 N cm (69 oz in)**, it was decided that this loading would be used to select the servos necessary for the aircraft. After viewing many servos and comparing their torque, weight, speed

and price, the **Hitec 645 MG Super Torque Metal Servo** was selected. At 6.0V, this servo provides 94.2 N cm (133 oz in) at a speed of 20°/sec in 57.5 g (2.1 oz) package. While the power output of this servo may seem excessive in overcoming only static loads, the extra torque generated provides a factor of safety against the dynamic loading experienced in flight. It was decided to use this servo exclusively as control for each surface as there was a negligible weight difference between servo brands. By using only one type of servo, it also meant that only one type of replacement servo is needed for the entire aircraft in the event that the aircraft encountered difficulties.

5.12 Aircraft Safety

5.12.1 Fuses

In compliance with the contest rules, a fuse will be placed on the motor power line in order to restrict the steady state current to below 40 Amperes. This in turn prevents the motor and speed controller from drawing too much current in the event that a propeller jams or the motor fails. Blade type fuses are being used and will be removed from the aircraft to disarm the motors while not in actual flight.

5.12.2 Data Acquisition System

One of the difficulties in flying electric powered RPV's is the monitoring of remaining battery capacity. Expended batteries can result in an airplane losing power suddenly in the air causing a costly crash. In order to prevent this, an AstroFlight Whatt® meter has been incorporated into the aircraft design. This device will measure the voltage of the battery pack, the current draw and the amount of charge left in the battery packs. By recording the amount of charge each battery pack received before flight, the capacity left in the batteries can be quickly determined. This tool was used extensively during the testing of our propulsion system as it allowed us to generate actual run times of the active system. Though the missions do not require a ground crew this year, the Whatt® meter will be present in the aircraft during the competition to determine the effect of various competition wind conditions on the battery pack. Figure 5.1 provides *Some Assembly Required's wiring diagram.

FIGURE 5.1 – Wiring Diagram of *Some Assembly Required

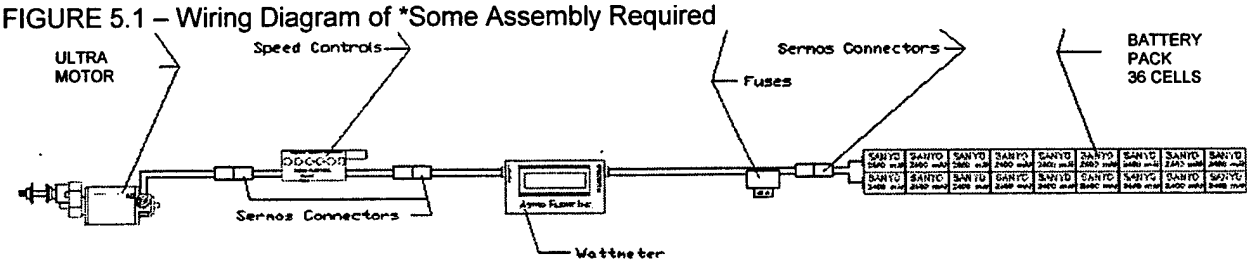

5.13 Estimated Mission Performance

Having finalized the design, the estimated mission performance of the aircraft was considered for each of the three mission profiles This will be looked at in three sections: Assembly Time, Flight Time and Overall Performance.

5.13.1 Assembly Time

The inclusion of an aircraft assembly time along with a volumetric restriction via the flight box required the development of many innovative connection designs. Well designed connection mechanisms should allow the plane to be assembled in 15 seconds or less with no loss in structural strength. As this assembly time is added to the total flight time in order to determine the final flight score, it is necessary to reduce the assembly time to an absolute minimum to remain competitive. This lead to the inclusion of simple male / female backpack clips at each structural joint. The electrical connections were also streamlined with the inclusion of a 9-pin unidirectional connector in the tail mount. This reduces the time spend attaching individual servo wires together and prevents the possibility of incorrectly wiring a control surface, which carries a 1 minute time penalty. Due to the well designed connections present on *Some Assembly Required, it should have one of the fastest assembly times at the competition

5.13.2 Mission Performance

Early in the design of the aircraft, relative scores of the various mission profiles were generated to help guide the design process, as only two of the three missions would be counted towards the final competition score. Given that a powerful power system was required in order to ensure adequate take off distance, *Some Assembly Required was designed to be a fast, aerodynamic plane in order to utilize its power system to provide the fastest possible flight times. With the takeoff and cruise values having been calculated, the various flight scores for different mission profiles were calculated based on the layout of the flight course. The actual flight time estimates for the sensor deployment mission is presented in Table 5.4 as representative of the estimation process. Table 5.5 gives a breakdown of the expected flight scores for each mission profile assuming a constant assembly time. As flight times tend to be underestimated, each estimated mission time was increased by 25% during the calculation of the flight scores.

TABLE 5.4: Time Estimations for Missile Decoy

Missile Decoy Mission	**Units**	**Value**
Difficulty Factor (F)		2
Aircraft Weight (M)	N	98.67249443
Turn Radius (TR)	m	21.784621
180 Length (180L)	m	68.43840529
360 Length (360L)	m	136.8768106
Take-Off Distance (TD)	m	30.98
Take-Off Velocity (TV)	m/s	14.475
Cruise Velocity (CV)	m/s	24.58652778
Lap Distance (LD)	ft	2000
Lap Distance (LD)	m	609.600
Take Off Time (TT)	s	2.140592857
Cruise Time with Takeoff (CwT)	s	26.55476905
Cruise Time without Takeoff (CoT)	s	24.79406631
180 Time (180T)	s	2.783573423
360 Time (360T)	s	5.567146846
# of Laps (NL)		4
# of 180/Lap (N180)		2
# of 360/Lap (N360)		1
# of Takeoff (NT)		1
Estimated Mission Time (EMT)	s	*145.4741427*
Estimated Mission Time (EMT)	min	*2.424569046*

TABLE 5.5 – Flight Score Estimates for each Mission Profile

Mission	**Difficulty**	**Estimated Mission Time (EMT)**	**Estimated Flight Score**
Missile Decoy	2.0	3.031	0.610
Sensor Deployment	1.5	2.715	0.506
Communications Repeater	1.0	3.862	0.243

As is shown in Table 5.5, the highest flight score is obtained flying the missile decoy mission, followed closely by the sensor deployment mission. The fastest flight time was calculated to be 2.7 minutes for the sensor deployment mission, mainly due to the fact that half of the sortie involves flying without the five pound payload. Using this data, single flight scores of 0.5 or greater should be possible for both of these two missions. Also, based on these estimates, the communications repeater mission profile will not be attempted by the team during the competition due to the gap in flight score between it and the other two missions.

5.13.3 Overall Performance

*Some Assembly Required is a very competitive aircraft. The team feels that it has the ability to finish within the top rankings of the competition. With a sleek design and a powerful propulsion system enabling very fast lap times and well designed connection mechanisms designed to minimize assembly times, the flight scores for each mission should reflect well with those being posted by other competitors. Also, due to the takeoff distance restriction and nature of the payload, the team feels that the *RAC* of *Some Assembly Required should also provide a very competitive aircraft, as it is unlikely that a competitors plane would be able to takeoff inside the required distance with less than the maximum battery capacity.

5.14 Weight and Balances

The center of gravity (CG) is considered to be at the spar of the wing, or located at 30% of the wing chord. Using this assumption, the component weights and their location relative to the CG were used to determine the balance of the airplane. Many components had a fixed location on the airframe and were thus restricted from moving in order to balance the aircraft. Unlike previous competition years in which the battery packs were centered around the CG, this was not possible in the design of *Some Assembly Required due to the volume restriction placed on the fuselage. The batteries are therefore located directly ahead of the payload (approximately 3.5" ahead of the CG) in an effort to minimize their effect on the balance of the plane. Due to the imbalance created by the location of the battery packs, the tail moment arm was increased slightly to compensate. Any fine tuning can be accomplished by the shifting of either the propulsion batteries forward, or the receiver and receiver pack backwards. The payload and the fuselage are designed to be centered on the CG location of the plane at approximately 30% of the wing chord. Table 5.6 shows the balance calculations performed for *Some Assembly Required.

TABLE 5.6: Calculation of Moments about CG

Description	Weight (lbs)	Weight (N)	Distance to CG (m)	Moment About CG (Nm)
Battery Pack	4.900	21.850	0.1143	2.497
Servos Fore of Spar	0.125	0.557	0.2974	0.166
Servos Aft of Spar (Tail)	0.375	1.672	-0.6953	-1.163
Servos Aft of Spar (Payload Release)	0.125	0.557	-0.1588	-0.088
Landing Gear Fore of Spar	0.250	1.115	0.2974	0.332
Landing Gear Aft of Spar	0.500	2.230	-0.0546	-0.122
Tail	1.000	4.459	-0.6953	-3.101
Motor	1.375	6.131	0.3175	1.947
Speed Controller	0.075	0.334	0.3048	0.102
Receiver Battery	0.250	1.115	-0.2096	-0.234
Prop	0.200	0.892	0.3556	0.317
Receiver	0.250	1.115	-0.2096	-0.234
Tail Mount	0.400	1.784	-0.1842	-0.328
Totals:	9.825	43.811		***0.009***

As can be seen from the above table, the total moment about the CG is 0.009 Nm which is negligible. Therefore, there is no moment about the center of gravity. Note that the sections of the airframe that were built to balance around the CG were not listed in Table 5.6 as their designed moments about the CG are zero. These systems include the wings, fuselage, payload and antenna.

5.15 Rated Aircraft Cost

The Rated Aircraft Cost is a model used to approximate the cost of the finished aircraft in financial terms. It provides an easy method of comparing various design costs within the competition, as the procurement costs associated with each team will undoubtedly differ. It also provides an efficiency rating as a plane with a lower RAC that can complete the required tasks in the same given time as a plane with a high RAC has been more efficiently planned. The Rated Aircraft Cost is given by the formula below, with the variables being described in subsequent sections.

$$\textit{Rated Aircraft Cost, \$ (Thousands)} = (A*MEW + B*REP + C*MFHR)/1000$$

5.15.1 Manufacturers Empty Weight (MEW)

The Manufacturers Empty Weight is the weight of the airframe in pounds, including all flight and propulsion batteries but no payload. In order to convert this weight to a dollar value, the coefficient "A", which has a value of $100, is multiplied by the MEW. The Manufacturers Empty Weight of *Some Assembly Required is **16.175 lbs**.

5.15.2 Rated Engine Power (REP)

The Rated Engine Power is a measure of the amount of battery power being used. It takes into account the amount of number of engines used and the total weight of the batteries used to power them. This is given by the equation:

$$REP = (1+0.25*(\#\ engines-1)) * Total\ Battery\ Weight$$

For *Some Assembly Required this calculation is:

$$REP = (1 + 0.25*(1-1)) * 4.9\ lbs = \mathbf{4.9}$$

The REP is then multiplied by the coefficient "B" which has the value of $1500.

5.15.3 Manufacturing Man Hours (MFHR)

The Manufacturing Man Hours value is used to approximate the number of hours it takes to construct the airframe based on its size and complexity. The MFHR is broken down into several sections as dictated by the Work Breakdown Structure (WBS). The sum of all the hours from the WBS is noted as the total MFHR. The coefficient "C" is used to assign the value of $20 per manufacturing hour. Table 5.7 gives the breakdown of the MFHR for *Some Assembly Required.

TABLE 5.7 – Rated Aircraft Cost - MFHR

WBS	Assigned Hours	Aircraft Dependant Parameter	Hours Subtotal
1. Wings	8 hr / ft wing span	101.75 in (8.48 ft) span	67.84
	8 hr / ft max exposed chord	10 in (0.833 ft) chord	6.67
	3 hr / control surface	2 control surfaces	6.00
WBS Wing Total			80.507
2. Fuselage	10 hr / ft body	52.0 in (4.333 ft)	43.33
WBS Fuselage Total			43.33
3. Empenage	5 hr / Vertical surface (n/control)	0 Vert. surface (No Control)	0
	10 hr / Vertical surface (control)	1 Vert. Surface (Control)	10
	10 hr / horizontal surface	1 Horizontal surface (Control)	10
WBS Empenage Total			20
4. Flight Systems	5 hr / servo	7 servos	35
	5 hr / motor controller	1 motor controller	5
WBS Flight Systems Total			40
5.Propulsion Systems	5 hr / motor	1 motor	5
	5 hr / propeller	1 propeller	5
WBS Propulsions Systems Total			10
TOTAL MFHR			**193.837**

5.15.4 Final Rated Aircraft Cost

The Total Rated Aircraft Cost for *Some Assembly Required was calculated to be:

*Rated Aircraft Cost, $ (Thousands) = ($100/lb * 16.175 lb + $1500/lb * 4.9 lbs + $20/hr * 193.8 hrs) / 1000*

Rated Aircraft Cost, $ (Thousands) = 12.84

5.16 Sized Aircraft Data

Final values regarding the geometry and performance variables for *Some Assembly Required have been assembled in Table's 5.8 and 5.9. A detailed component weight breakdown was presented in Table 5.1.

TABLE 5.8 – Performance Variables of *Some Assembly Required

Item	Loaded		Unloaded	
	Imperial	*Metric*	*Imperial*	*Metric*
Clmax	1.7	1.7	1.7	1.7
L/D Max	75	75	75	75
Climb out Angle [°]	19.5	19.5	28.5	28.5
Stall Speed [mph]-[m/s]	28.0	12.44	24.0	10.67
Max. Speed [mph]-[m/s]	86.0	38.22	89.0	39.56
Take-off Distance [ft]-[m]	92.7	28.26	60.3	18.38

TABLE .5.9 - Summary of Aircraft Geometry based on preliminary and detail design calculations

Item	Imperial	Metric
Propulsion		
Motor	Graupner ULTRA 3500-8	
Servos	Hitec 645 MG Super Torque Metal Servo	
Radio System	Futaba 8 channel PCM	
Cells	2 x 18 cells, 2400mAh	
Speed Controller	Astro 204D	
Propeller	13 by 8	
Static Prop Thrust	10.9 lbf	48.7 N
Run Time (100%)	3.2 min	3.2min
Motor Efficiency	89%	89%
Wing		
Airfoil	FX 63-137	
Wing Area	900 in^2	0.581 m^2
Span	90 in	2.286 m
Chord	10.0 in	0.254 m
MAC	10.0 in	0.254 m
Wing Thickness	1.367 in	0.035 m
Aspect Ratio	9	9
Taper	None	None
Aileron Area	71in^2	0.046 m^2
Aileron Length	28.44 in	0.722 m
Aileron MAC	2.5 in	0.064 m
Fuselage		
Length	26.0 in	0.660 m
Max Height	6.25 in	0.159 m
Width	6.75 in	0.171 m

Item	Imperial	Metric
Horizontal Stabilizer		
Airfoil	NACA 0009	
Area	188 in^2	0.121 m^2
Span	23.5 in	0.597 m
Chord	8 in	0.203 m
MAC	8 in	0.203 m
Thickness	1.07 in	0.027 m
Aspect Ratio	2.97	2.97
Taper	None	
Elevator Area	90 in^2	0.058 m^2
Elevator Span	21 in	0.533 m
Elevator MAC	3.00 in	0.076 m
Tail Moment Arm	32.5 in	0.826 m
Vertical Stabilizer		
Airfoil	NACA 0009	
Area	65.3 in^2	0.042 m^2
Root Chord	8.0 in	0.203 m
Tip Chord	4.0 in	0.102 m
MAC	6.22 in	0.158 m
Height	10.5 in	0.267 m
Rudder Height	9.5 in	0.241 m
Rudder MAC	2.53 in	0.064 m
Rudder Area	24.1 in^2	0.016 m^2
Velocities		
V_{max}	86 mph	38.1 m/s
V_{cruise}	78 mph	34.6 m/s
V_{stall}	29 mph	13.2 m/s

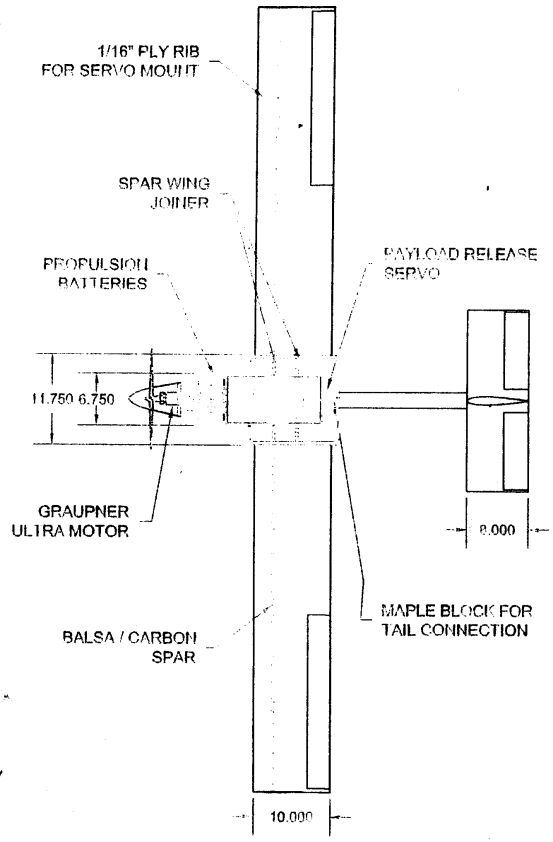

A **PLAN VIEW**
SCALE 1:16

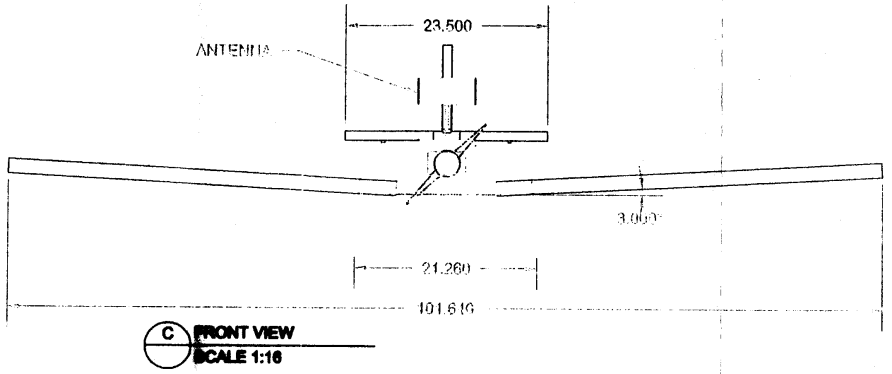

C **FRONT VIEW**
SCALE 1:16

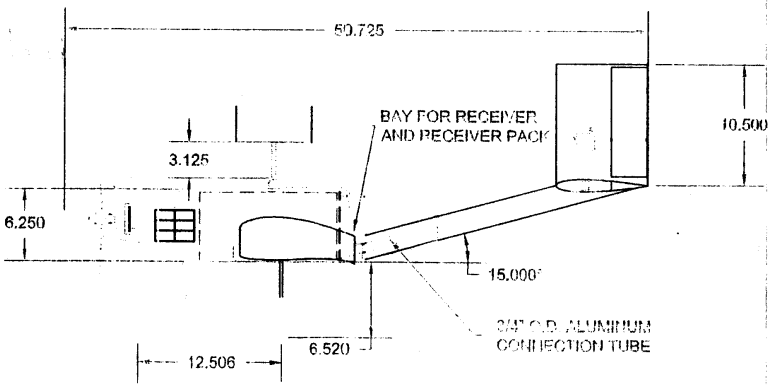

B **ELEVATION**
SCALE 1:10

Notes:

1.) All Dimensions are in inches.

2.) All surfaces composed of SM foam have been covered with a minimum of two layers of fibreglass to enhance their structural rigidity.

3.) Foam / fibreglass mouldings are present around the exterior of the fuselage to reduce drag. These have been omitted for clarity.

- PAYLOAD
- THIN PLYWOOD
- SM INSULATING FOAM
- AIRCRAFT PLYWOOD
- HARDWARE
- BALSA WOOD
- CARBON FIBER
- ALUMINUM BALSA
- PVC

Some Assembly Required

QUEEN'S AERO DESIGN TEAM
2003 CESSNA/OCR DBF COMPETITION

FINAL AIRCRAFT LAYOUT - 3 VIEW

6.0 Manufacturing Plan

*Some Assembly Required's design can be broken down into three separate components, each of which employs a different construction technique. Various methods of building the wing, fuselage, and tail appendage were analyzed and the best choices were determined with a figure of merit matrix. The timing of the construction process is documented in a Gantt chart (see Figure 6.4) presented at the end of the section.

6.1 Wing Construction

6.1.1 Foam and Fiberglass

This technique involves cutting a wing from low density foam using a hot-wire cutting apparatus. The wing cores are then strengthened by adding balsa or carbon fiber spars along the top and bottom surfaces. Provision is then made for flap and aileron actuation installation, and then the entire surface is coated with one or two layers of fiberglass. This results in a structurally strong wing without too much effort. The chief disadvantage of this technique is that the weight can become prohibitive.

6.1.2 Built-up Construction

Built-up construction is the oldest and most traditional form of building a wing; unfortunately, it is also the most time consuming. Ribs are cut in an airfoil shape from thin balsa or aircraft plywood and are then positioned on a jig so that there are 4 to 6 inches between each one. The spars, made of balsa, spruce, carbon fiber, or of some combination, are glued in and a shear web of cross-grained balsa is positioned to form the web of the I-beam structure. Gluing balsa to the front and back of the ribs forms leading and trailing edges, and the whole structure is then sanded to ensure a streamlined shape. Thin balsa sheeting is applied from the leading edge back to the spar on both the top and bottom of the wing, forming a strong D-tube structure, which is good in torsion. The whole structure is then covered with a thin plastic film to form an airfoil. This technique forms a light, rigid structure.

6.1.3 Carbon Fiber Monocoque

This technique is the most technically demanding of the three choices presented here. An airfoil is drawn up in a 3-D modeling computer program and is transmitted to a computer controlled milling machine. The machine must mill two female molds, one for the top of the wing, the other for the bottom of the wing, from a temperature stable material. The molds are then prepared and pre-impregnated carbon fiber is laid up into the cavity. The mold is then placed under vacuum in an autoclave and baked at approximately 120 degrees Celsius for three hours. Once cooled, the wing halves are released from their molds and are carefully sanded and glued together. This technique requires very complex and expensive facilities, materials, and expertise; however, it results in a very light, strong wing.

6.2 Fuselage Construction

6.2.1 Foam and Fiberglass

This form of construction requires that a foam block is shaped and hollowed with a hot-wire foam cutter. Layers of fiberglass cloth are then applied to the exterior to provide strength. This structure is tough, light, and produces an excellent surface finish. Unfortunately, weight can be a problem on larger structures.

6.2.1 Built-up Construction

This form of construction stretches back to the first days of both full-sized and model aircraft flight. Many thin strips of wood (balsa on model planes) connect several wooden formers to produce the fuselage frame. This frame is then covered by doped paper or silk, or in more recent times, by a shrinkable plastic film. This method is labor intensive, yet produces good results. This type of structure requires extensive repair after a crash, yet can be repaired quickly if necessary.

6.2.2 Carbon Fiber Monocoque

This technique makes use of expensive composite materials to produce a very strong and lightweight fuselage. A mold of the required fuselage shape is made up of a heat resistant material. Several layers of pre-impregnated carbon fiber are laid up onto the mold, a sheet of thin structural honeycomb (which acts as a shear web for the carbon) is placed into the lay-up, and then more carbon fiber is laid up on top. The assembly is vacuum bagged and then heated until the epoxy cures. This technique requires access to expensive materials, equipment, and expertise, but can produce excellent results. The chief disadvantage is that it is nearly impossible to repair after a mishap.

6.3 Tail Construction

6.3.1 Foam and Fiberglass

A strong and smooth airfoil can be manufactured quickly by cutting the required shape from medium density foam and then adding a single layer of fiberglass. The fiber glassed surface is then covered by a sheet of mylar and the whole assembly is placed in a vacuum until the epoxy has hardened. The mylar sheets can then be peeled away, leaving a perfect tail surface. While this method of construction can result in a perfectly sculpted complex airfoil, it tends to be slightly heavier than the other options available.

6.3.2 Sheet Balsa

A simple way to construct a tail is by cutting the required planform from a thick sheet balsa and then sanding the edges with a sanding block. Although the construction is relatively easy, the tail does not take a proper streamlined shape. This method of construction is durable, but is heavy and prone to warping with changes in temperature and humidity.

6.3.3 Built-up Construction

A built-up tail is the lightest, but most fragile option under consideration. Construction is very similar to a built-up wing, with a set of evenly spaced ribs joined by a double spar and shear web, and the leading and trailing edges. Sheeting is sometimes extended right to the trailing edge to give a slight increase in torsional stiffness. The chief disadvantage of this design is that it is very time consuming to construct. Also worth considering is that the tiny balsa structure that makes up a built-up surface is vulnerable to damage, especially as the tail is a portion of the plane that is often accidentally banged and knocked during storage and transportation.

6.4 Figure of Merit

To choose the best combination of manufacturing processes for this year's aircraft, a qualitative figure of merit was conceived to evaluate each technique's merits and weaknesses in an easily interpreted chart. Five criteria were selected, weight, structure, time, skill, and expense, and each construction method was given a qualitative score that illustrates its performance in each category. The separate categories are described in detail below.

Weight: Building weight is the one element that can seriously affect every aspect of the flight envelope. Wherever possible, a builder should always strive to make the components as light and efficient as possible. Thus, this was selected as the first criterion in the FOM.

Strength: Structural failure is expensive and can be dangerous under the wrong conditions. To ensure that the aircraft will be able to withstand the loads experienced in flight and on the ground, structural integrity was chosen as the second criterion in the FOM.

Skill: To produce the required components of the aircraft, the selected construction technique must either be known to the team or it must be easy to learn. Also worth considering is that more experience with the specified building technique produces a more accurate final product and less waste, thus it is desirable to choose methods that are familiar to a larger number of team members. Skill was selected as the third criterion in the FOM.

Expense: Among the various construction techniques discussed, there is a huge difference in cost. This is because some techniques use exotic materials or machining, while the more mundane and traditional techniques make use of the builder's individual skill rather than a complex mould or machine. As this year's aircraft was built with our meager budget in mind, the cheaper option is often worth pursuing due to fiscal necessity. As such, the expense of the construction technique was chosen as the fourth entry into the FOM.

Time: The final item worth considering when evaluating the construction choices is the length of time that the method requires. *Some Assembly Required was designed and built on a 100% volunteer basis as Queen's University does not offer course credit towards participation in a design competition. As all design and construction must be made around the demands of a full engineering course load, time is a precious commodity and was given the final place in the FOM.

6.5 Evaluation and Selection

6.5.1 Analytical Method

Each construction technique was evaluated in terms of the five criteria listed above. Total scores were tabulated with the following equation, which weights the relative importance of each of the criterion.

Total = 200 / weight + strength / 2+ 20 / skill + 200 / expense + 100 / time

TABLE 6.1 - Manufacturing Process Evaluations

	Weight (oz)	Strength	Skill	Expense		Time	Total
				Can$	US$		
Wing							
Foam and Fiberglass	64	6	5	180	113.21	30	13.07
Built-up Construction	56	5	6	150	94.34	35	12.35
Carbon Fiber Monocoque	40	5	10	3000	1886.79	100	9.32
Fuselage							
Foam and Fiberglass	160	6	5	150	94.34	35	10.94
Built-up Construction	48	5	6	200	125.79	42	12.13
Carbon Fiber Monocoque	72	5	10	2000	1257.86	60	7.79
Tail							
Foam and Fiberglass	18	6	3	6	3.77	3	87.44
Sheet Balsa	24	7	3	6	3.77	3	85.17
Built-up Construction	16	5	6	5	3.14	4	83.33

6.5.2 Selection

The Figure of Merit (Table 6.1) indicated that foam and fiberglass techniques would be suitable for the flight surfaces (wing and tail), and that built-up construction would be the best choice for the fuselage. The methods we employed during the construction of these components are described below.

6.6 Description of Construction Techniques Employed

6.6.1 Flying Surfaces

Once the Figure of Merit indicated that both the wing and the tail surfaces would utilize foam and fiberglass construction techniques, work began with drafting software to produce the set of working drawings necessary for this type of construction. With foam cutting techniques the airfoil shape is created by cutting cores of foam with a hot wire cutter which passes cleanly through the foam leaving an airfoil shaped core.

The templates were constructed using a vertical milling machine. The CNC machine follows a MasterCAM program to cut out a set of templates from a sheet of aluminum. Once the foam cores were prepared, the shear webs were then inserted. ¼ inch balsa was chosen for the shear web material due to its high shear strength/weight ratio. Airfoil shaped plywood ribs are then added at the root of the wing and at the location of the servo. These ribs serve to strengthen the base material in these critical areas.

With the ribs in place, the wing is ready for the vacuum bagging process. Kevlar strips were introduced this year to function as the hinges for the ailerons, elevator, and rudder.

The entire assembly is then covered in fiberglass and placed in a vacuum bag while the epoxy cures. Once the wing is removed from the vacuum bag, the resulting panel can be handled to install servo and landing gear mounts. *Some Assembly Required features a wing built with 3 degrees of washout to improve the aircraft's stall characteristics.

6.6.2 Tail & Boom Construction

The tail structure includes a vertical fin, horizontal stabilizer, and a boom. The fin and stabilizer were created using the same techniques detailed in Section 6.6.1. Likewise, the boom was cut out of blue foam using a hot wire cutter. However, the inner diameter of the boom was cut in order to match an aluminum pipe mounted to the back of the fuselage. This inner diameter hole also allows the servo wires from the fin and stabilizer to run to the fuselage unobstructed. Backpacking clips were then applied to the end of the tail boom which connects to the fuselage to allow for a quick assembly time.

6.6.3 Fuselage Construction

The fuselage design was drafted into AutoCAD at an early stage to allow precise dimensions to be determined. By constructing the fuselage around the payload geometry, a tapered boxlike structure was designed to enclose the payload while maintaining a low drag profile. Testing was conducted on multiple fuselage materials before ¼" 5-ply Birch plywood was decided upon. High stress regions, such as the firewall and wing mounting panels were constructed from a balsa-aluminum composite for extra rigidity. Each structural joint on the fuselage was constructed using a finger joint method. Though time consuming, these joints provide exceptional strength and increase the overall rigidity of the structure. In

efforts to conserve weight, low stress regions of the fuselage were removed from the structure. This allows significant weight reduction on the entire aircraft with a modest loss in strength. Foam / fiberglass fairings were designed to fit around the boxlike structure of the fuselage to form it into a more aerodynamic teardrop shape. The foremost of these fairings is removable to provide access to the propulsion batteries.

As the various aircraft components must all mate properly to the fuselage, great care was taken to ensure that the alignment of each joint was perfect. Very little error was allowed as all of the connection surfaces involved anywhere from 3 to 5 individual connections, each with little tolerance to play. To achieve this degree of precision, the mating pieces were built simultaneously with all connections in place. This ensures that once separated, each component will be able to mate with little to no play.

In order to provide adequate cooling to the motor and maintain the teardrop shape of the fuselage, a moulded cowl was designed. This cowl was built using a incremental forming aluminum mill which allows very precise shapes to be formed with relative ease.

FIGURE 6.4 – Gantt chart detailing construction schedule

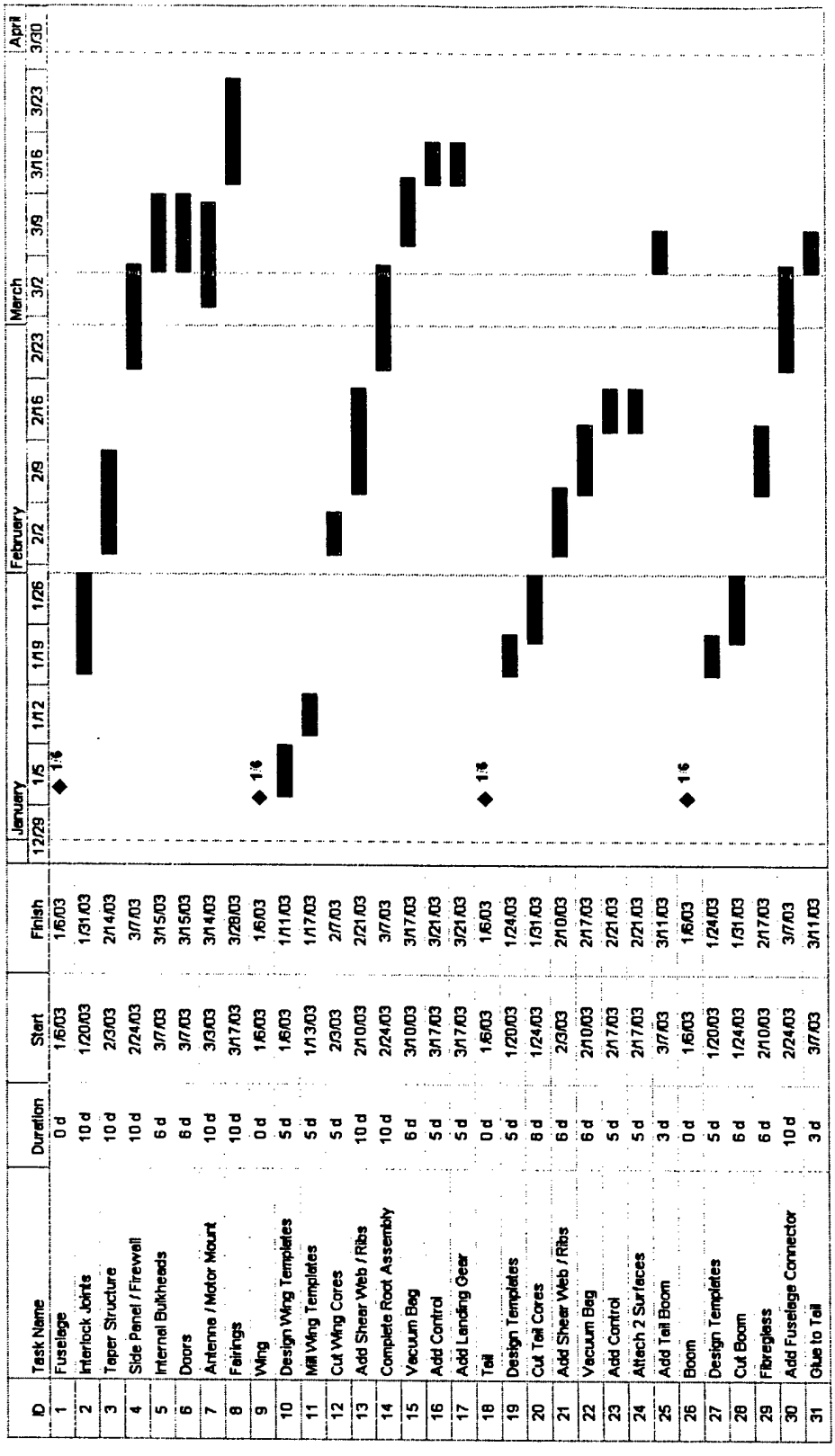

ID	Task Name	Duration	Start	Finish
1	Fuselage	0 d	1/5/03	1/5/03
2	Interlock Joints	10 d	1/20/03	1/31/03
3	Taper Structure	10 d	2/3/03	2/14/03
4	Side Panel / Firewall	10 d	2/24/03	3/7/03
5	Internal Bulkheads	6 d	3/7/03	3/15/03
6	Doors	6 d	3/7/03	3/15/03
7	Antenna / Motor Mount	10 d	3/3/03	3/14/03
8	Fairings	10 d	3/17/03	3/28/03
9	Wing	0 d	1/5/03	1/5/03
10	Design Wing Templates	5 d	1/5/03	1/11/03
11	Mill Wing Templates	5 d	1/13/03	1/17/03
12	Cut Wing Cores	5 d	2/3/03	2/7/03
13	Add Shear Web / Ribs	10 d	2/10/03	2/21/03
14	Complete Root Assembly	10 d	2/24/03	3/7/03
15	Vacuum Bag	6 d	3/10/03	3/17/03
16	Add Control	5 d	3/17/03	3/21/03
17	Add Landing Gear	5 d	3/17/03	3/21/03
18	Tail	0 d	1/5/03	1/5/03
19	Design Templates	5 d	1/20/03	1/24/03
20	Cut Tail Cores	8 d	1/24/03	1/31/03
21	Add Sheer Web / Ribs	6 d	2/3/03	2/10/03
22	Vacuum Bag	6 d	2/10/03	2/17/03
23	Add Control	5 d	2/17/03	2/21/03
24	Attach 2 Surfaces	5 d	2/17/03	2/21/03
25	Add Tail Boom	3 d	3/7/03	3/11/03
26	Boom	0 d	1/5/03	1/5/03
27	Design Templates	5 d	1/20/03	1/24/03
28	Cut Boom	6 d	1/24/03	1/31/03
29	Fibreglass	6 d	2/10/03	2/17/03
30	Add Fuselage Connector	10 d	2/24/03	3/7/03
31	Glue to Tail	3 d	3/7/03	3/11/03

7.0 Testing

The purpose of component, full aircraft, static, and dynamic testing is to produce the most efficient aircraft possible. The two main testing programs that were implemented were material testing and full scale modeling. The material testing program was aimed at determining the strongest materials for each of the aircraft components. The full scale modeling program was directed towards the integration of various and their overall effect on the aircraft. In flight testing falls under the full scale modeling program. Unfortunately, due to seasonal weather conditions in Canada, flight testing was not an option as our testing runway was not available.

7.1 Materials Testing

7.1.1 Foam Core Testing

Once the decision was made to use fiberglass for the control surfaces a series of tests were conducted to determine the optimum strength to weight ratio. The accuracy, weight, and strength of foam with varying density were factors analyzed.

The team prepared small single foot test sections that were compared using the above criteria. Although the white and pink allowed for reasonably high accuracy during the hotwire procedure, they became deformed during handling, sanding, and vacuum bagging. Blue foam, the densest foam available to the team, provided the best accuracy. Blue foam is relatively heavy but has the necessary strength needed for high wing loading conditions.

7.1.2 Fuselage Material Testing

The weight and strength of the fuselage is determined by the design and the materials utilized. Early tests were required to determine strength properties of a series of construction materials. The materials considered were: Balsa / Aluminum with holes, Plywood / Balsa, Plywood / Foam, Balsa / Aluminum without holes, and Nomex / Epoxy. A 10 inch (0.254 m) by 0.875 inch (0.022 m) test sample was manufactured from each material. An Instron® test was performed by applying a progressively increasing load to the sample. The material's behavior was observed through a three point bending system, shown in Figure 7.1 below.

FIGURE 7.1 – Instron® Test of Nomex/Epoxy sample

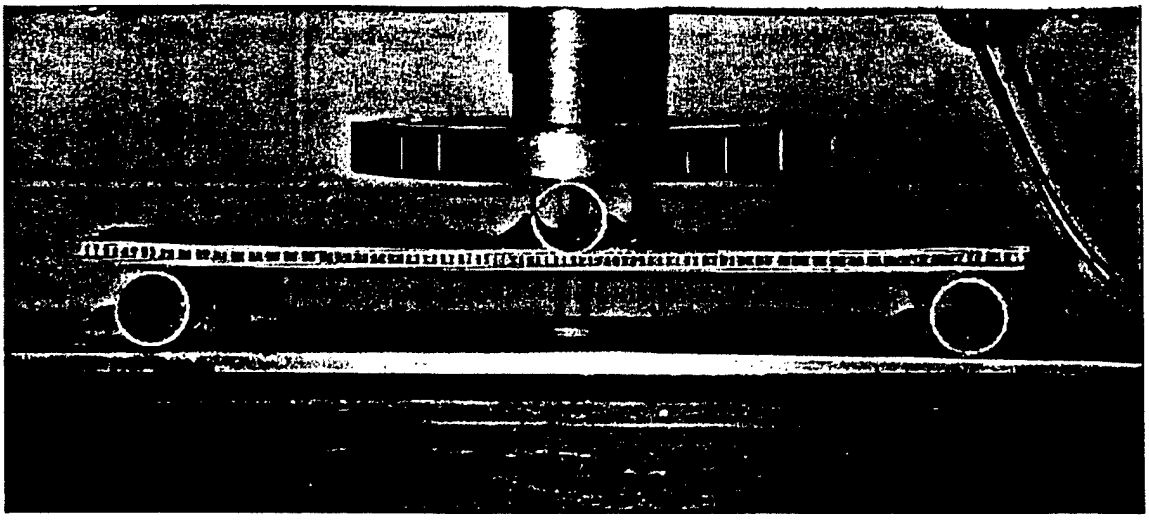

The recorded data from all of the materials was combined in a single graph of deflection and applied load shown in Figure 7.2 below:

FIGURE 7.2 – Material Comparisons

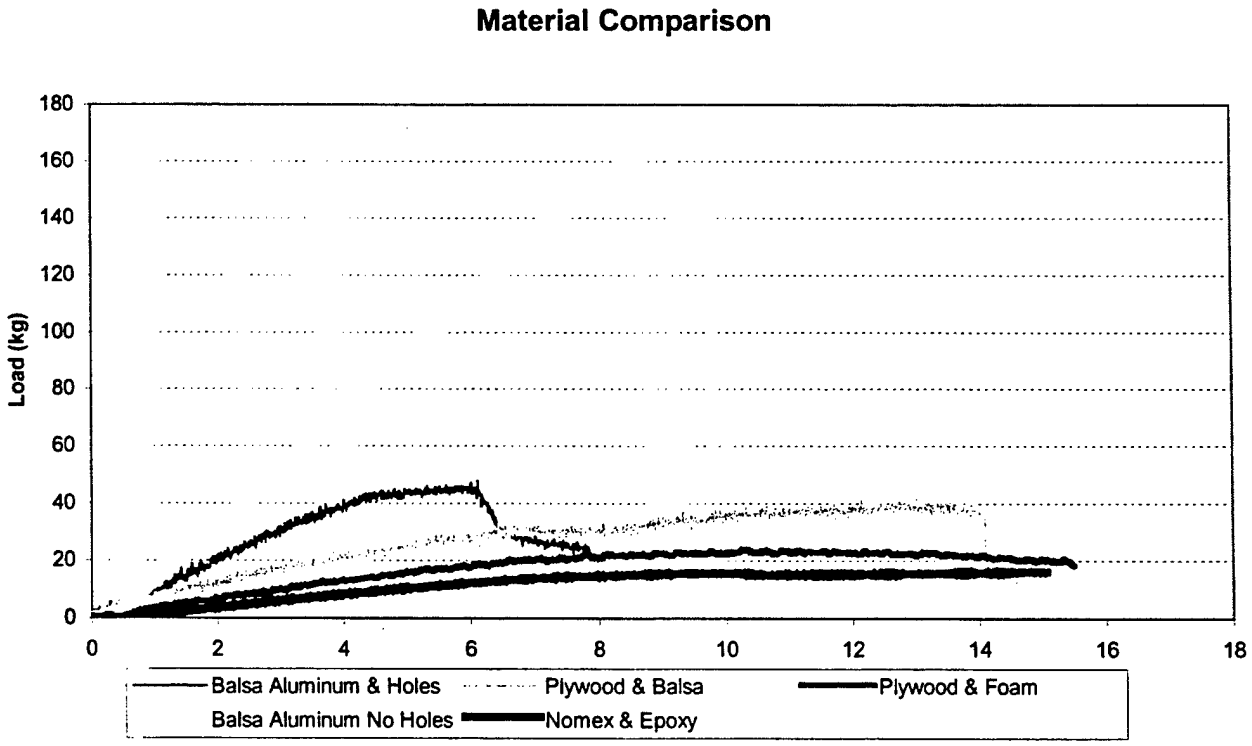

As can be seen from the results, the Balsa/Aluminum without holes undergoes the least deflection with increasing load; however, it fails at a deflection less than 1cm. The Nomex/Epoxy does not fail for the loads applied in this experiment, but it undergoes large deflection for relatively small loads. The Plywood/Balsa is a good intermediate material since it undergoes a relatively small deflection for a high load.

7.2 Full Scale Modeling

In this testing program, various full scale test sections were constructed and integrated to replicate the final airplane configuration. Full scale sections were constructed of the wing, fuselage and tail in order to determine the required strengths of the connection mechanisms, and the amount of play present in each connection. Each section was then stressed to see the final result on the structure of the fuselage.

Full scale testing of the wing sections resulted in the determination that SM insulating foam be used as the base material. During an early test in which a full length wing panel was mated to the fuselage, weight was applied along the length of the wing to simulate a flight load. The test was designed to determine the strength of the wing – fuselage connector, but instead caused the wing to buckle as it had been composed of lighter, white foam. Though a failure from a materials standpoint, the structure of the wing – fuselage connection was shown to be sound. A Wing test section can be seen below in Figure 7.3.

FIGURE 7.3 – Modular Wing Test Sections

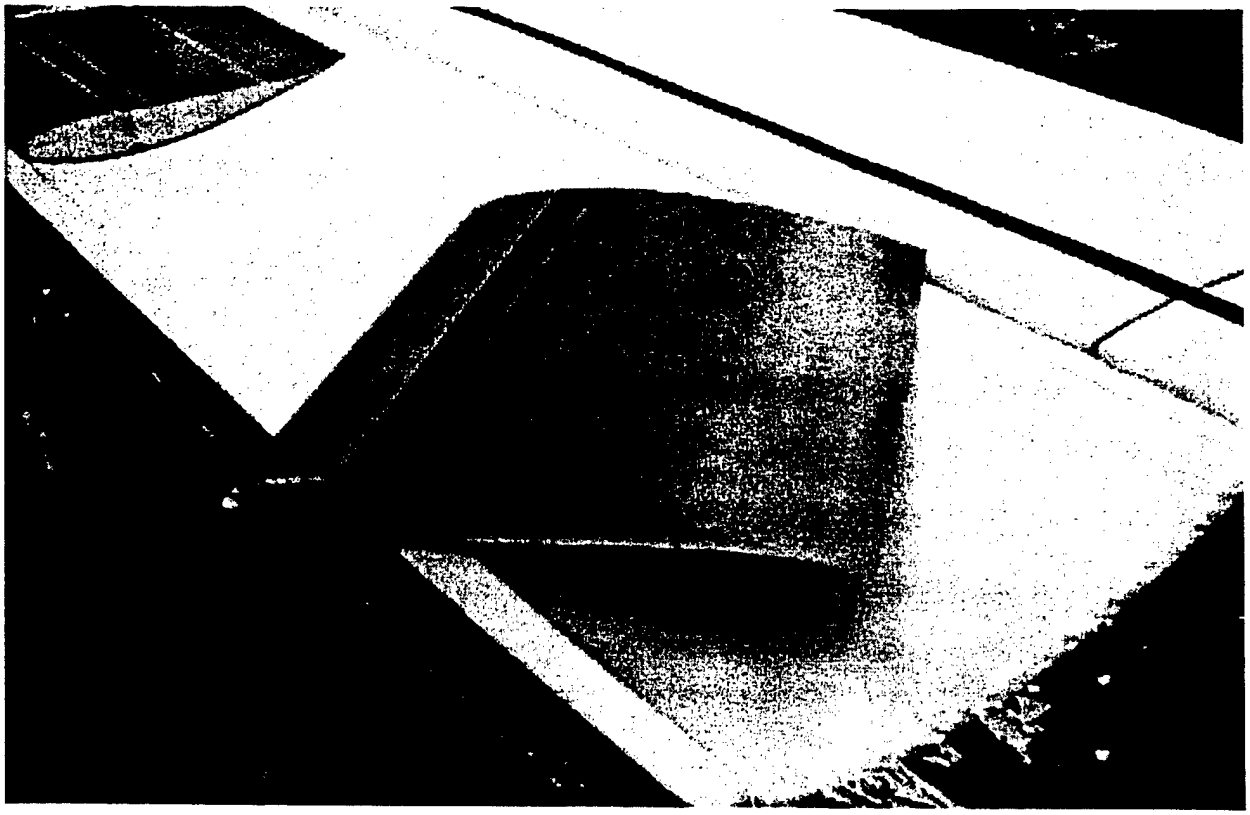

As a continuation of the same series of tests, the tail was joined to the fuselage using the connection mechanism that had been designed at the time. After mounting the tail to the fuselage, a small amount of pressure was applied to the horizontal stabilizer. It was noted that this small amount of pressure, corresponding to forces generated by elevator actuation, generated noticeable deflection in the fuselage and in the connection itself. This led to the redesign of both the exterior fuselage panel and the tail mount. After subsequent design and mock-up testing, this deflection had been reduced to acceptable levels.

7.3 Overall Impression

After an extensive testing phase, *Some Assembly Required is ready for flight testing as soon as the weather permits. With our two testing programs having been great successes, flight performance is expected to be impressive. Part of the success of our extensive test program is due to the nature of the construction materials used. As both the SM insulating foam and plywood used to construct the testing sections are relatively inexpensive and available in bulk, this allowed many iterations of various designs to be tested and compared to both each other and to theoretical predictions. With solid theoretical performance, sound construction techniques, and extensive testing, *Some Assembly Required will be able to challenge for the overall title at this year's DBF competition.

References

1. Eppler, Richard. Airfoil Design and Data. Springer-Verlad: Germany. 1990.
2. Easton, Matt; McCracken, David; Splinter, Joe; Young, Dave. "*Design of a Variable Geometry Propeller Shroud*" Undergraduate Design Project, Department of Mechanical Engineering. December, 2000.
3. Foster, Steve. *"Undercarriage Design for Queen's Cargo Aircraft."* Undergraduate Thesis Project, Department of Mechanical Engineering. March, 1994.
4. Horton, Johanna Lisa. *"Cargo Aircraft Stability Analysis."* Undergraduate Thesis Project, Department of Mathematics and Engineering. April, 1993.
5. McCormick, Barnes. Aerodynamics, Aeronautics, and Flight Mechanics, second edition. John Wiley & Sons, Inc.: New York. 1995.
6. Munson, Young, and Okiishi. Fundamentals of Fluid Mechanics, second edition. John Wiley & Sons, Inc.: New York. 1994.
7. Raymer, Daniel. Aircraft Design: A Conceptual Approach. AIAA Education Series. American Institute of Aeronautics and Astronautics, Inc.: Washington, D.C. 1989.
8. Abbott, Ira. Theory of Wing Sections. McGraw-Hill Book Company Inc.: Toronto. 1949.
9. White, Frank M. Fluid Mechanics, 4th Edition. McGraw-Hill Book Company Inc.: Toronto. 1999.
10. Lennon, Andy. Basics of R/C Model Aircraft Design. Y. DeFrancesco: Ridgefield, CT. 1999.

Notes:

1.) Colour scheme does not correspond to actual building material. It is presented for visual aid only. Refer to the 3 - View drawing provided for construction materials.

2.) Foam / fibreglass moulding are present around the exterior of the fuselage. These have been omitted to allow a more detailed view of the fuselage.

3.) The motor and propeller shown are similar in size and geometry to the ones employed for this year's model but are meant as a representation only.

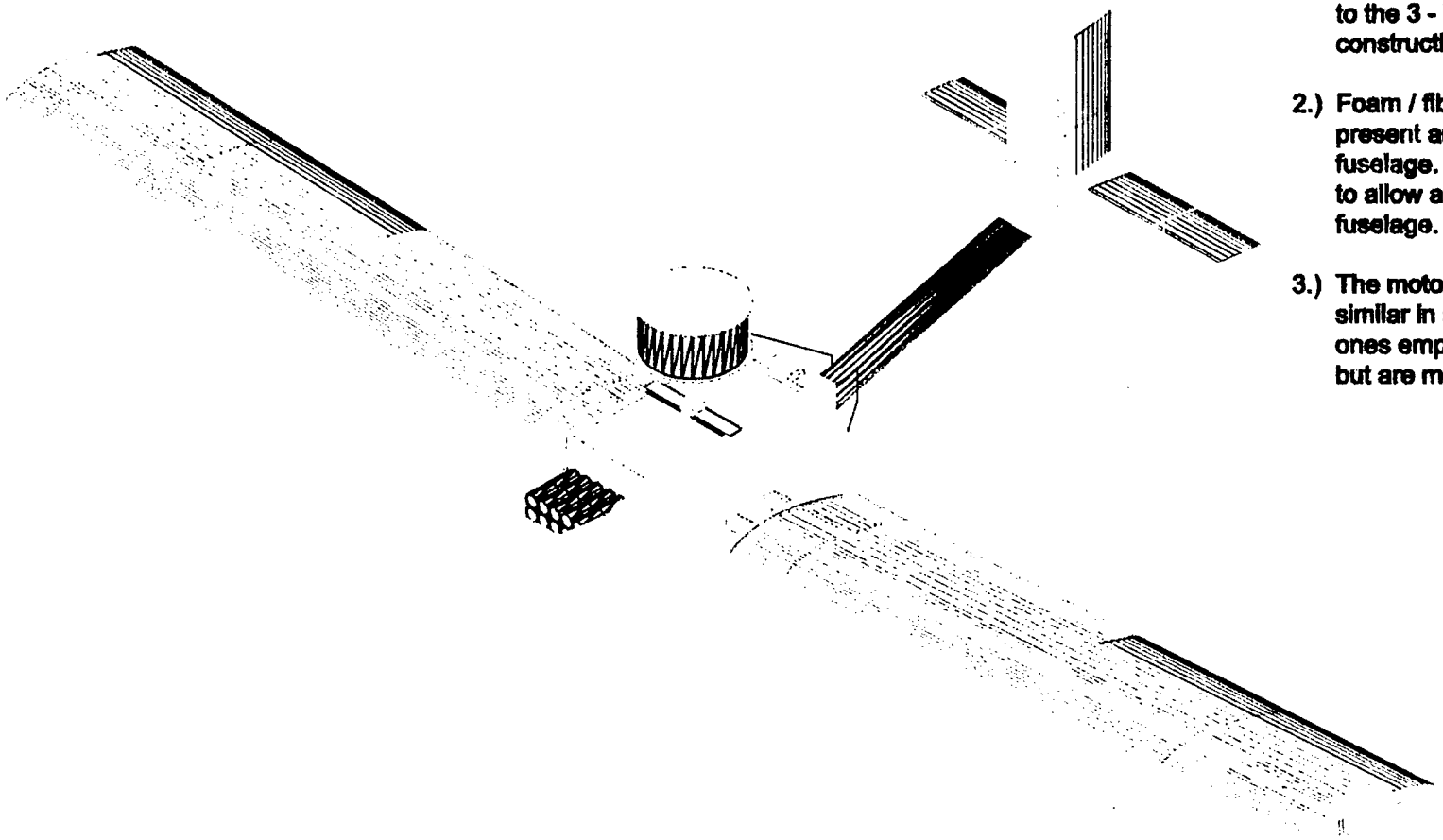

A ISOMETRIC
SCALE 1:10

Some Assembly Required

QUEEN'S AERO DESIGN TEAM
2003 CESSNA/OCR DBF COMPETITION

FINAL AIRCRAFT LAYOUT - ISOMETRIC

College of Engineering

Department of Aerospace Engineering
Wichita State University
Wichita, Kansas
U. S. A.

AIAA/Cessna/ONR Student Design/Build/Fly Competition

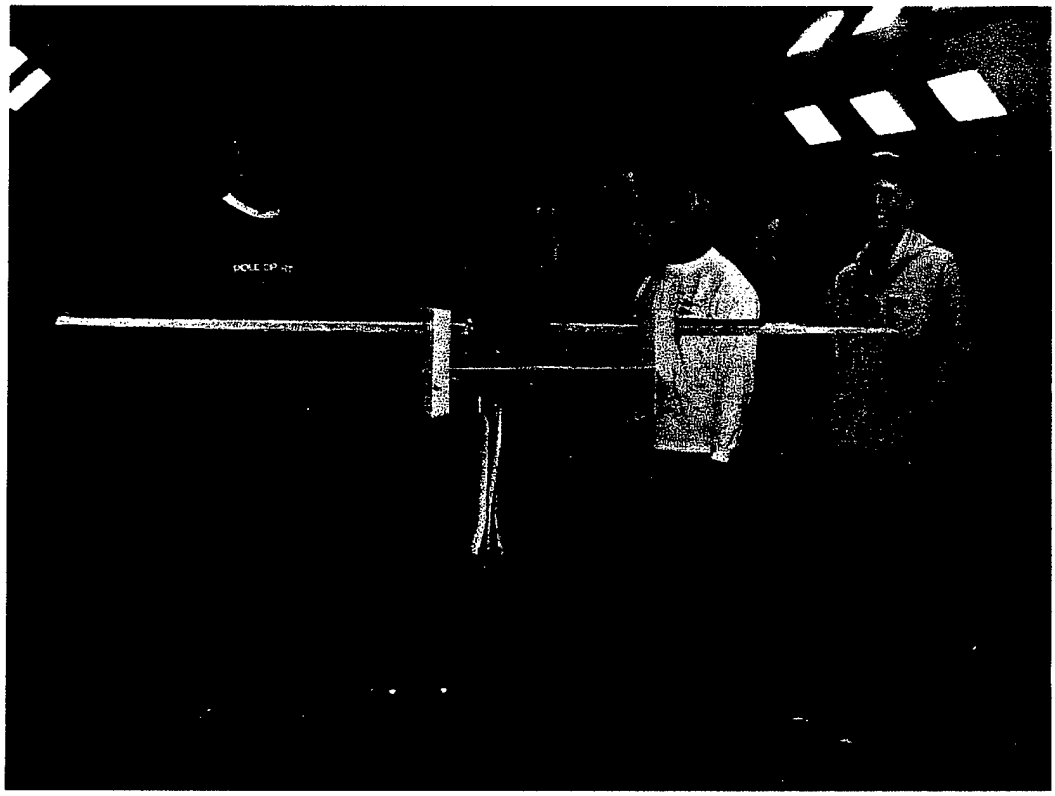

The WSU DBF Team and the WU Flyer

DESIGN REPORT
March 11, 2003

APPROVED **Curtis Farnham**
APPROVED **Joshua Koehn**
APPROVED **Kevin Pfeiffer**
APPROVED **Philip Butler**
APPROVED **Nick Denault**
APPROVED **Levi Palsmeier**
APPROVED **James McCall**
APPROVED **Matthew McCarthy**
APPROVED **Loren Strahm**

APPROVED **Tom Farrell**
APPROVED **Matthew Morgan**
APPROVED **Matthew Tran**
APPROVED **David Jeager**
APPROVED **Monal Merchant**
APPROVED **Tyler Rempel**
APPROVED **Lillian Cabrejos**
APPROVED **Seth Lambert**

FACULTY ADVISOR **Dr. L Scott Miller**

Table of Contents

Title Page i
Table of Contents ii
Figures and Tables iii
Symbols and Characters iv
1. EXECUTIVE SUMMARY 1
  1.1. Conceptual Design Phase 1
  1.2. Preliminary Design 1
  1.3. Detailed Design 2
2. MANAGEMENT SUMMARY 2
  2.1. Team Architecture 2
  2.2. Configuration Management and Accountability 5
  2.3. Advisory Board 6
  2.4. Schedule 6
3. CONCEPTUAL DESIGN 8
  3.1. Contest Rules and Mission Familiarization 8
  3.2. Requirements and Constraints 10
  3.3. Aircraft Configuration Studies 10
  3.4. Final Concept Selection 13
4. PRELIMINARY DESIGN 14
  4.1. Aerodynamics 14
  4.2. Stability and Control 18
  4.3. Propulsion 22
  4.4. Structures 27
5. DETAIL DESIGN 29
  5.1. Aerodynamics 29
  5.2. Propulsion 31
  5.3. Stability and Control 32
  5.4. Weight and Balance Worksheet 36
  5.5. Structures 36
  5.6. Rated Aircraft Cost Worksheet 40
  5.7. Drawing Package 42
6. MANUFACTURING PLAN AND PROCESSES 48
  6.1. Manufacturing Processes Investigated and Figures of Merit 48
  6.2. Manufacture of Major Components and Assemblies 49
  6.3. Manufacturing Milestones 50
7. Testing 51
8. Conclusions 54
9. References 55

Figures and Tables

Name *Page*

Table 2.1.1: WSU DBF Team Composition....3
Figure 2.4.1: Project Schedule....7
Figure 3.3.1: Individual Conventional and Flying Wing Designs....12
Figure 3.3.2: The Two Final Candidates....13
Figure 4.1.1: NACA 4415 Airfoil Data....15
Table 4.1.1: Flap Size Optimization Table....16
Table 4.1.2: WU Flyer Wing Parameters....17
Figure 4.1.2: Aircraft Drag Polar....18
Figure 4.2.1 Payload Center of Gravities....20
Table 4.2.1 Stability and Control Characteristics....21
Figure 4.2.1: Elevator Trim Crossplot at Cruise With Antenna....21
Figure 4.3.1: Scoring Ratio = (Mission Score/RAC)*1,000,000 vs Flight Speed....25
Table 4.3.1 – Mark 6 Scoring Performance....26
Figure 4.4.1: V-n Diagram – Unloaded....28
Table 4.4.1: Material Properties....29
Figure 5.1.1 WU Flyer VS-Aero Model....29
Figure 5.1.2: C_L & C_D vs Alpha Wind Tunnel Data....30
Figure 5.3.1: Elevator Trim Crossplot....33
Figure 5.3.2: $C_{M\,CG}$ vs Alpha....34
Figure 5.3.3: $C_{N\,CG}$ vs Beta....35
Figure 5.3.4: $C_{L\,CG}$ vs Beta....35
Figure 5.4.1: Weight and Balance Chart....36
Table 5.5.1: Force/Moment Equations....37
Table 5.5.2: Wing Shear Flow Properties....38
Figure 5.5.1: Bending Stress vs Span Location....38
Table 5.5.3: Spar Sleeve Properties....39
Table 5.6.1: Rated Aircraft Cost Worksheet....41
Figure 5.6.1: Contributions to Rated Aircraft Cost....41
Figure 3.6.1: Manufacturing Milestones and Scheduled Event Times....50

Symbols and Characters

Symbol	Description
AR	Aspect Ratio
b	Airplane wingspan
C_l	Airfoil lift coefficient
C_{lmax}	Airfoil maximum lift coefficient
C_L	Aircraft lift coefficient
$C_{L\alpha}$	Variation of airplane lift coefficient with angle of attack
$C_{L\beta}$	Variation of airplane rolling moment coefficient with angle of sideslip
$C_{L\,CG}$	Airplane rolling moment coefficient
C_d	Airfoil total drag coefficient
C_{do}	Airfoil parasite drag coefficient
C_D	Aircraft total drag coefficient
C_m	Airfoil pitching moment coefficient
$C_{M\,CG}$	Airplane pitching moment coefficient
$C_{M\alpha}$	Variation of airplane pitching moment coefficient with angle of attack
$C_{N\beta}$	Variation of airplane yawing moment coefficient with angle of sideslip
$C_{N\,CG}$	Airplane yawing moment coefficient
de	Upward elevator deflection in degrees
Δf	Flap deflection angle in degrees
ft	Feet
I	Moment of Inertia
in	Inches
I_{xx}	Moment of inertia about the pitch axis in the x direction
I_{yy}	Moment of inertia about the y axis in the y direction
I_{yz}	Moment of inertia about the y axis in the z direction
λ	Wing taper ratio
Λ	Wing quarter chord sweep back angle
lbs	Pounds
M	Moment
M_x	Moment about the pitch axis
M_y	Moment about the yaw axis
M_z	Moment about the roll axis
msl	Mean sea level
n	Load factor
Psi	Pounds per square inch
Rad	Radians
pcf	Pounds per cubic foot
Sec	Second
Sigma	Stress
S_{ref}	Wing reference area or planform area
S_{wet}	Wing wetted area
V	Velocity
V_c	Cruise Velocity

1. EXECUTIVE SUMMARY

The AIAA/Cessna/ONR Design Build Fly Competition is an annual collegiate design competition. Teams from around the world design, build and fly aircraft to complete a contest-defined mission. Payloads, missions, and aircraft restrictions are revised every year to encourage development of new aircraft designs. This year's task emphasizes mission planning as a part of the design process. The aircraft will be scored on its ability to complete two out of three optional missions. The missions are scored on the basis of time elapsed for the mission and a mission difficulty handicap. Selection of the best mission profiles to fly can greatly affect scores.

The team's primary design goal was to maximize total score. The best total score is a result of maximizing score in the written report segment of the contest, and maximizing the ratio of flight score to rated cost. The complexity of the task forced a large number of trade studies in the aircraft design. The design process was carried out according to the principles outlined in Raymer, Aircraft Design: A Conceptual Approach.[17] Due to time constraints for aircraft completion and testing before the contest, most of the design effort was carried out in the fall of 2002. The spring 2003 semester focused on construction and testing aspects of the effort.

1.1. Conceptual Design Phase

To achieve our goal, we first familiarized ourselves with this year's revised rules and missions. The team defined a set of requirements and constraints for our aircraft, and we began analyzing competing configuration choices. Five individuals on the team conducted individual configuration studies and the results of these studies were used to develop two promising aircraft designs, one a conventional monoplane, the other a flying wing. Taking advantage of local industry expertise, we called in an advisory board of experienced engineers and modelers to give feedback on our two design concepts and to point out issues that could arise. A week of further development to address design issues led to a final down-select when the team chose to proceed with a conventional aircraft design.

1.2. Preliminary Design

In preliminary design, the goal was to refine the design and finalize major sizing parameters. Major design concerns were settled to allow detail design to begin with a high degree of confidence in success. Six senior team members took leadership roles in the areas of Aerodynamics, Stability & Control, Structures, Propulsion, Manufacturing, and Testing. With good communications and analysis, we began making aircraft changes.

The tail was lengthened and the nose shortened, airfoils were changed, and propulsion systems were nailed down more closely. Feedback was provided from department leads and incorporated into a single Microsoft Excel™-based performance analysis spreadsheet carried over from the conceptual design phase. The design tool allowed fast turn-around and development from new data and aircraft changes. The tool also evolved, to follow the increase in sophistication necessary as a design grows closer to a final configuration. The design saw two major revisions up to the final accepted configuration, known as the Mark 8 WU Flyer. The Mark 8 met all the team-defined requirements and constraints, so with agreement, we began detail design drawings and aerodynamic lofts.

1.3. Detailed Design

Full-scale hand drawings were used to flesh out the aircraft shape, lofts, and structures to connect all the components. Structural analysis was done concurrent to aircraft detail layout to ensure that designs placed on paper were viable and would not pose problems later in the design. The fuselage loft was analyzed using a CFD code, in a tutorial with an advisory board member, and the flap deflections analyzed with several codes. The propulsion system wiring diagrams were finalized and tail sizing verified. Due to time constraints, construction began before the last design details were finished. As it worked out, manufacturing concerns pushed design changes in several areas, so a slightly delayed design completion turned out not to be a major issue.

2. MANAGEMENT SUMMARY

2.1. Team Architecture

The team is composed of 7 seniors and 10 underclassmen overseen by 1 faculty advisor. Efficient division of labor and task leadership required an organized team structure. Six students in the senior design class were made leads in the individual areas of Aerodynamics, Stability & Control, Structures, Systems & Manufacturing, and Testing. The remaining seniors and underclassmen were brought in voluntarily to assist individual disciplines in design, and later in manufacturing. The team list and assigned design responsibilities are shown below in Table 2.1.1.

Table 2.1.1: WSU DBF Team Composition			
Name	**Primary Discipline (lead*)**	**Secondary Disciplines**	**Class Status**
Curtis Farnham	Systems & Manufacturing*	Structures	Sr
Thomas Farrell	Aerodynamics*	Propulsion	Sr
Joshua Koehn	Testing*	Stability & Control	Sr
Matthew Morgan	Structures*	Testing	Sr
Kevin Pfeiffer	Propulsion*	Structures & Manufacturing	Sr
Matthew Tran	Stability & Control*	Aerodynamics	Sr
Philip Butler	Systems & Manufacturing	Testing	Jr
David Jaeger	Manufacturing	Testing	Fr
Nick Denault	Manufacturing		Fr
Monal Merchant	Propulsion	Testing	Jr
Levi Palsemeier	Manufacturing		Sr
Tyler Rempel	Manufacturing		Fr
James McCall	Manufacturing		Fr
Lillian Cabrejos	Structures		So
Matthew McCarthy	Structures		Jr
Seth Lambert	Aerodynamics		So
Loren Strahm	Structures		Jr

The following are brief biographies of the discipline leads and the first two underclassmen on the team roster who have contributed significantly above and beyond that which was asked. In addition, Dr. L Scott Miller, our faculty advisor is given a short bio.

Curtis Farnham

A senior in the Aerospace engineering program, Curtis' primary interests were in vehicle integration and overall design. Spacecraft have been his particular interest for some time. He has worked at NASA through a cooperative program through Wichita State University, been employed at the 7 by 10 foot wind tunnel at the university, and now works for Ken Razac (the first Dean of engineering at WSU) at his private engineering firm. Curtis will graduate in May 2003 and is applying to pre-med programs to become a doctor.

Thomas Farrell

With two years of experience in WSU's Aero-Design team and three semester internships at Cessna Aircraft Company, most recently in the Aerodynamics group, Tom brought a good body of experience in manufacturing and practical design to the team. The SAE Aero-Design team has experimented with

wood and composite sheeted foam wings, experience valuable to a start-up design effort. Tom will graduate in May 2003 and plans to attend Graduate School in engineering the next fall.

Joshua Koehn

One of the seniors in the design class, Josh took a role organizing wind tunnel testing for the aircraft. One of his first major experiences in design, he developed and began manufacture of the wind tunnel mount used to test the aircraft. He will graduate in May 2003.

Matthew Morgan

A radio control aircraft modeler and pilot, Matt is quite familiar with typical RC equipment and practices. Matt attends Wichita State full time and also worked hours approaching full-time at Cessna Aircraft Company as a flight-test and planning engineer. Matt is also a student pilot in light aircraft. He looks forward to completing his license when time and money permit. Matt will return next year to wrap up general education requirements and graduate in May 2004. Matt plans to work following graduation.

Kevin Pfeiffer

The only returning member of last year's Design/Build/Fly team, Kevin has experience in design and construction of a variety of aircraft types. He was been a bicycle mechanic before being hired to work at the Beech 7 by 10 foot wind tunnel at Wichita State University. During the summer, he works at a composites shop in New Mexico producing carbon fiber propellers and other composite aircraft parts. He is a licensed glider pilot, and a low time student in light single engine aircraft. Kevin will return to wrap up general education requirements before graduating in May 2004. He plans to attend graduate school in engineering the next fall.

Matthew Tran

The final student on the team in Senior Design, Matt has also worked on the SAE Aero-Design team for three years. He has wide-ranging interests, but has worked in structures, testing, and is our stability and control lead. He has worked at NASA through WSU's cooperative education program, and was assigned to an F-15 experimental flight test group. Matt will graduate in May 2003 and has applied to graduate schools for the fall semester.

Philip Butler

An experienced private pilot and mechanic on light aircraft, Philip has been a major asset to the team. Although he is not a discipline lead, he will make a good area lead in years to come. He has contributed to control and systems design as well as manufacturing methods. Philip is in the midst of the aerospace engineering program and will graduate in spring 2005.

David Jaeger

One of the youngest members of the team, David has not yet taken a large number of engineering courses, but he has shown a good aptitude for problem solving and strong motivation. He was one of the most regular people to attend and contribute during construction of the serial number 1 aircraft. He will make a good design leader in coming years.

Dr. L Scott Miller

Our faculty advisor, Dr. Miller is a graduate of Texas A&M. His specialty is experimental aerodynamics, but he teaches the senior design classes in addition to his aerodynamics courses. He emphasizes simplicity and coordinated thought in design. Aircraft work best when a feature can be made to serve a number of necessary purposes. He has also been named an AIAA Distinguished Lecturer for his studies of classified military aircraft. Dr. Miller has taught at Wichita State University for 15 years.

2.2. Configuration Management and Accountability

Lessons learned from last year's team indicated a stronger need for a leadership chain within the team and a single person appointed the team leader. This becomes absolutely critical in a team with an even number of regularly attending members. In decision-making, the discipline lead speaks for their section, and carries a single vote on issues that greatly impact the entire team. These six area leads are essentially responsible for their product and its success or failure. To break ties and to encourage good cooperation and communication between all disciplines, one area lead was nominated overall team leader and held responsibilities to mediate disputes and or to settle tie votes. In the fall semester, Curtis Farnham held the team lead position. In the current spring semester, Matt Morgan has assumed this responsibility. When the team lead is absent, he may delegate his duties. While the team lead is very important to success of the project, there is no official accountability or reward for the position beyond the esteem in which the position is held and the desire of the team that the project proceeds well.

The structure of primary and secondary design responsibilities outlined in the team roster was created to ensure that every team member would have a second engineer's opinion for their design discipline. The six team leads would serve to review another area's work and either approve or disapprove and suggest improvements. There is simply too much to be done, and too much risk involved in such a large project to leave a single person accountable for an entire design discipline without some assistance.

To assist in communication between team members, a website was set up to allow team e-mails and file uploads. Besides this website, most key team files are kept on CD at the senior design lab so they are available to anyone on the team who needs them. Revision control was a major difficulty early in the design process because design changes were very frequent, but this issue has nearly evaporated as the

design has come to completion. Most of our detail-design files have been smaller documents or hand-made scale drawings.

2.3. Advisory Board

Outside the typical human resources of the team, we realized that it would be very valuable to consult engineers with model design experience. With local Wichita aircraft industry, there was a large pool of people to select from. From last year's effort, we had become familiar with several pilots and modelers, so we turned to them again in a more formal fashion this year to provide insight and reviews as we developed our designs. Because of team associations, all of these advisory board members were employees at Raytheon Aircraft Company. Several of these people are modelers, but every one of them are engineers. Model experience can be valuable, but we cannot lose sight of the engineering emphasis of this effort.

Among the advisory board are two potential pilots for the aircraft. Dan Walton and Jerry Salter are both high-time radio control pilots familiar with large-scale models and complex radios. Another experienced modeler and engineer, David Aronstien, is a member of the Raytheon Aircraft Advanced Design Group. In aerodynamics, Neal Pfeiffer was able to assist in methods and texts for performance and drag estimation. Robert Steuver, Corey Hagemeister and Noel Deurksen have also attended design reviews for the aircraft.

The advisory board has been particularly valuable pointing out common pitfalls and indicating resources that we can use to develop our designs. The team appreciates the time that they have contributed, and the lessons that we've learned from conversation and the questions that they have answered.

2.4. Schedule

One of the largest problems that last year's effort faced was a poorly kept schedule. The gates for design completion and construction were in roughly the correct places, but since those deadlines were not met or enforced, the effort came to a poor end from a lack of time to test. For this reason, the schedule gates that we have defined have been very strictly enforced. We met our design dates, the aircraft completion date, and completed a valuable wind tunnel test in short order. The following sections outline the process used for design and construction of the vehicle with Figure 2.4.1 displaying, graphically, an overall project schedule. Detailed construction schedules are in the manufacturing portion of the report.

Figure 2.4.1: Project Schedule

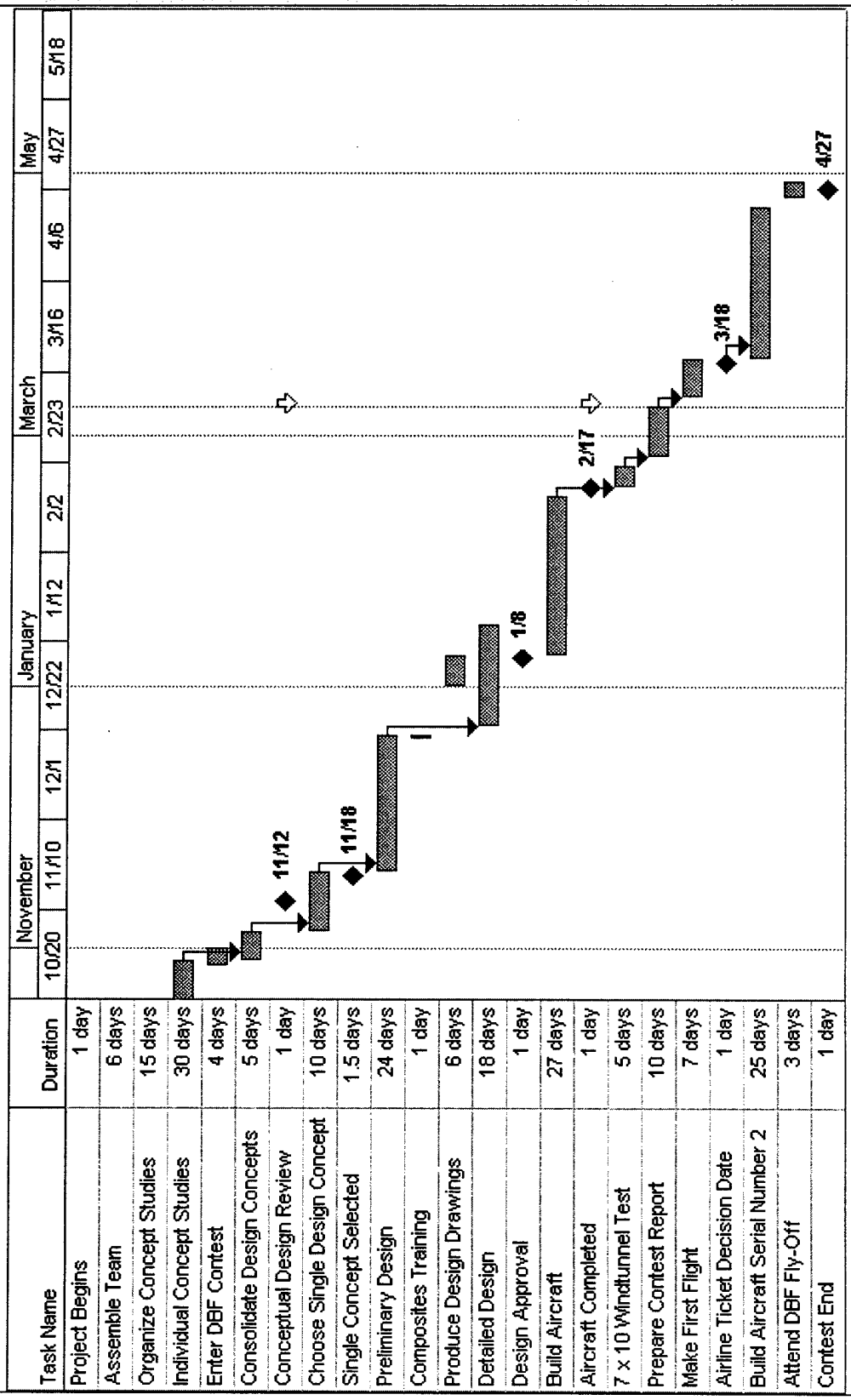

Task Name	Duration
Project Begins	1 day
Assemble Team	6 days
Organize Concept Studies	15 days
Individual Concept Studies	30 days
Enter DBF Contest	4 days
Consolidate Design Concepts	5 days
Conceptual Design Review	1 day
Choose Single Design Concept	10 days
Single Concept Selected	1.5 days
Preliminary Design	24 days
Composites Training	1 day
Produce Design Drawings	6 days
Detailed Design	18 days
Design Approval	1 day
Build Aircraft	27 days
Aircraft Completed	1 day
7 x 10 Windtunnel Test	5 days
Prepare Contest Report	10 days
Make First Flight	7 days
Airline Ticket Decision Date	1 day
Build Aircraft Serial Number 2	25 days
Attend DBF Fly-Off	3 days
Contest End	1 day

3. CONCEPTUAL DESIGN

3.1. Contest Rules and Mission Familiarization

In conceptual design, the team's objective was to select an aircraft class and configuration appropriate for the contest missions. To make this selection, the first step was to become familiar with the contest rules. It is only when you understand the requirements and constraints on an aircraft that it can be properly designed. With an understanding of the requirements to be faced, the team looked at a range of configurations, and decided on five worth of further study. Individuals took these five aircraft, and conducted studies to develop each into a viable aircraft. From these five concepts, a down-selection process led to two designs. At that stage, we consulted an advisory board for a design review of our competing concepts, before the team selected the single configuration that proceeded into preliminary design.

Rules Summary

The rules of the contest serve several critical purposes. They set some standards for safety in the design of a vehicle. They help to establish a level field of competition and hold costs within approachable bounds. The rules also define a clear criterion by which aircraft will be scored.

In the interest of a level playing field, the rules dictate that aircraft must be powered by electric motors with nickel cadmium (Ni-Cad) batteries for a power supply. Electric current through the power system is limited by a 40 amp maxi-sized slow-blow fuse. These restrictions greatly limit range and power available. Aircraft must disassemble into a shipping box 4 ft x 2 ft x 1 ft, a restriction already faced by teams that must travel long distances to compete. The aircraft must also be AMA legal, a requirement that will allow teams to fly their aircraft legally at many radio control airstrips.

For safety the airframe must be capable of holding its gross weight when lifted at the wingtips, and the radio system must put the aircraft into a configuration to promote immediate stall-spin if radio contact is lost. The aircraft propulsion system must also be disabled by the removal of in-line current limiting fuses so the planes can be made safe for handling between missions.

Scoring of the contest is governed by the three components already mentioned: the Written Report Score, Flight Mission Score, and Rated Aircraft Cost. The total score for the competition based on these components is scored as follows:

$$\text{Overall Score} = \frac{\text{Written Report Score} \times \text{Total Flight Score}}{\text{Rated Aircraft Cost}}$$

While the aircraft engineering will clearly affect the quality of the vehicle produced, the quality of the written report will not directly influence the performance of an aircraft. From this standpoint, the report should be written as well as possible. The report carries equal weight to aircraft performance in the score, so a large loss in score from a poor report can remove a team from contention as easily as a poor flight performance.

The second major term in the scoring equation is the ratio of Flight Mission Score to Rated Aircraft Cost. This term is entirely determined by the physical characteristics and performance of the aircraft produced. The Rated Aircraft Cost is based on increased cost corresponding to increased size, weight, and complexity in the aircraft. If an aircraft can be produced with a significantly reduced Rated Aircraft Cost and minimal penalty in flight performance, the overall score will improve. The flight performance is entirely based on two factors, mission completion time, and the handicap ("Difficulty Factor" in the rules) for the missions flown. Handicap number divided by mission time provides the Flight Mission Score. Included in the mission completion times is the time required to assemble the aircraft from packaged condition in the shipping crate to flight-worthy condition. In this way, an aircraft designed for fast assembly gains a scoring advantage over those less friendly to put together.

The implication of all these scoring terms is that the highest performance vehicle at the contest will not necessarily win overall. A good balance must be struck through careful thought and trade studies. A final twist in the rules allows for aircraft repairs after damage from flight missions. If the vehicle can be returned to air-worthy condition in half an hour or less, the mission score can be kept even if the aircraft was damaged in the flight. This makes an incentive for a repair-friendly design.

Initial Mission Analysis

Because a mission determines the challenges that an aircraft must face, configurations were considered only after an initial survey of the performance requirements inherent in the 3 contest-defined missions for this year.

Mission A, the Missile Decoy Mission, poses the greatest performance challenges that the aircraft will face. The vehicle must take off within the defined field length at maximum payload weight. The total payload weight is roughly 6.5 pounds. 5.0 pounds is associated with a box-shaped simulated avionics package. 1.5 pounds are from a large simulated external antenna. The antenna adds a significant amount of drag to the aircraft, and depending on mounting position, a large pitching or yawing moment. Use of the antenna requires a 3 inch separation between the main airframe and the antenna as well as a requirement for a 360 degree horizontal field of view (exceptions being made for the propeller disc, vertical tails, and landing gear struts). These requirements make positions above or below the aircraft the only viable options. The aircraft must fly 4 laps around the contest course in this configuration before

landing. The challenges to be faced then are the field length requirement at gross weight, range with the vehicle's increased drag, and stability trim changes associated with the antenna installation. These significant challenges give the mission a handicap of 2.0 points.

Mission B, the Sensor Deployment, requires the aircraft to carry 5 pounds of payload for two laps around the contest course before landing. The aircraft must come to a complete stop, drop the 5 pounds of payload, and takeoff again to fly another couple laps before landing again to conclude the mission. The payload drop must be made without physical intervention on the aircraft. The takeoff and range requirements are less strenuous because of the reduced weight and drag carried, but the payload drop makes new challenges. The aircraft must remain within CG limits with or without the payload, and the physical size of the payload requires that the aircraft have a means to clear the payload before taking off on the un-laden portion of the mission. Payload clearance can affect propulsion configuration, ground clearance requirements, and landing gear design. This mission carries a handicap of 1.5 points.

Mission C, the Communications Repeater mission, requires the aircraft to carry the same 5 pounds of payload as mission B, but there is no requirement for payload release. The aircraft must takeoff and fly four extended length laps before landing to complete the mission. The handicap is 1.0 points.

3.2. Requirements and Constraints

Examining the rules and the missions available for scoring, the team established some basic rules for comparison of competing aircraft designs. The requirements imposed on the design were intended to ensure contest legality and performance sufficient to place well. The basic requirements were as follows:

-The aircraft must comply with all AIAA Design/Build/Fly Rules for 2002-2003
-The aircraft must be able to complete all three of the mission profiles
-Takeoff must be made in 100 feet at gross weight, 1500 ft msl
-Range calculations will be made at Sea Level
-The aircraft would be assembled in less than a minute
-The aircraft must withstand a 6G ultimate load (later revised to 9G)

3.3. Aircraft Configuration Studies

Broad Aircraft Configuration Classes

With basic guidelines established, the team began configuration studies. Four major classes of aircraft were initially considered: conventional tailed aircraft, flying wings, tandem wings, and canard aircraft. Examination of these aircraft classes revealed trends that allowed us to focus on designs of interest.

Canard and tandem wing aircraft offer theoretical benefits because their surfaces are all lifting rather than a traditional down-loaded tail surface, but the stability and control challenges associated with trim and CG location were daunting. A Wichita-produced example of a canard design, the Starship, required articulation to move the canard fore and aft for trim conditions at different speeds. On a smaller scale, the Rutan-designed Vari-Eze and Long-Eze don't require a configuration change for trim, but they have a CG problem that they cannot stand on their landing gear without a pilot aboard, the equivalent of our payload. On the sensor deployment mission, this would be a major problem for takeoff. In addition, a single large pusher propeller at the aft of the aircraft would have clearance issues with the payload after deployment to the runway under the aircraft. For these reasons canard aircraft were eliminated from consideration. Tandem wing aircraft were similarly eliminated from consideration because they suffer many of the ailments of the canard, and takeoff rotation becomes a major problem. In support of our position on these aircraft, canards and tandem wings have rarely been flown successfully in the DBF fly-off.

Flying wing designs seemed more promising. The flying wing advantage is that wetted area is reduced to a minimum and the airframe structure is simplified. If the aircraft can be made with lower drag, less fuel is required, and the aircraft can be made smaller. The key challenges with flying wing designs are stability & control, CG management, and packaging layout. There is no clear standard for flying wing design in these areas. Flying wings have been flown successfully in the DBF contest before, but several have had noticeable short period pitch oscillation problems.

Conventional designs have the benefit that they are common and in widespread service. They fulfill many missions admirably; including missions similar to all those defined in the contest rules. These aircraft with conventional tails have good static margins and a large moment arm for pitch and yaw control. These characteristics allow stable and forgiving flying qualities, a critical trait for survival of an aircraft through prototype testing and contest flight. The last several years, conventional aircraft have dominated the DBF contest.

Individual Configuration studies

After narrowing the field of interesting configurations to conventional and flying wing designs, five members of the team each took a configuration to develop individually. There were two conventional aircraft, and three flying wing designs. Each had several unique characteristics for study. One aggressive flying wing design would rely on actuators for CG shift flight control. An overview of individual concepts is shown in Figure 3.3.1.

Figure 3.3.1: Individual Conventional and Flying Wing Designs

	Conventional – single tractor, antenna overhead	**Conventional** – single tractor, antenna between twin tail booms
	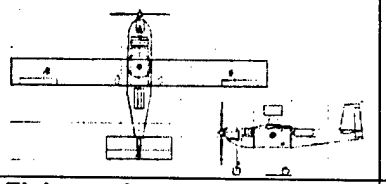	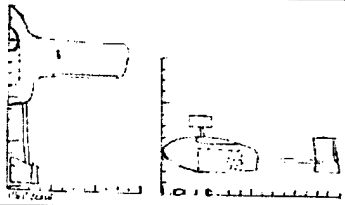
Tailless – high aspect ratio, high sweep, single tractor, vertical on fuselage, antenna overhead	**Flying wing** – high aspect ratio, low sweep, twin pusher, antenna in front	**Flying wing** – low aspect ratio, high sweep, single tractor, winglets, antenna behind
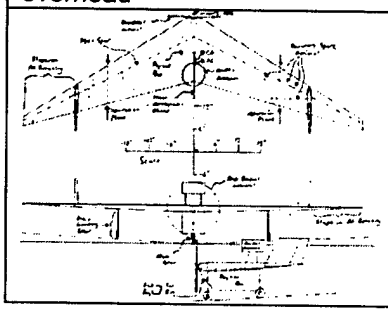	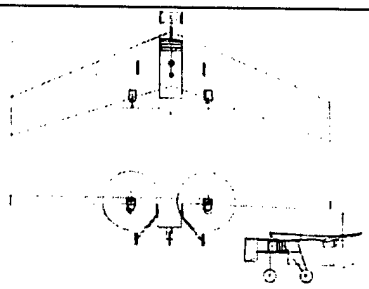	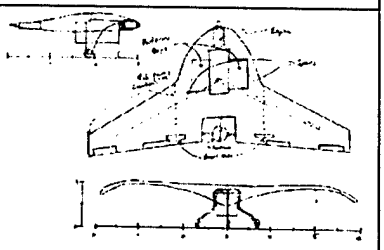

These five individual concepts were refined and developed with estimates of component sizes, weights, basic performance parameters like zero-lift drag, and takeoff performance. As the designs developed, key problems and benefits became clear. Capitalizing on lessons learned, the five individuals involved consolidated their designs to a single conventional aircraft and a single flying wing design. A week was spent analyzing these two refined aircraft before the team held a design review with the advisory board of engineers with model aircraft experience. The two aircraft presented were designated the Mark 6 Conventional Monoplane and the CTM-1 Flying Wing. At this stage, our design spreadsheets were advanced enough to begin incorporating more complex drawing tools for output, and proficient in automating a large number of calculations when geometry changes were made to each aircraft.

CTM-1

The CTM-1 design, shown in Figure 3.3.2, was an attempt to make a good performance aircraft at a minimum rated aircraft cost. The fuselage and tail components removal reduced weight and rated aircraft cost significantly compared to the team's conventional aircraft designs. Performance was good, but pitch stability and CG control were major points of concern. The plane was designed to fit into the contest shipping crate with the span fitting the long axis of the box, the chord being less than the width of the box to fit cleanly. The wing outer panels fold under the aircraft, and the landing gear remains attached to the aircraft in the box. This packaging design did not require any control disconnects for the wing surfaces.

Mark 6 Conventional Monoplane

The Mark 6 Conventional Monoplane, also shown in Figure 3.3.2, was a very typical design. It used a standard sized horizontal tail as defined in the radio control book by Lennon[13]. The most distinguishing characteristics of the design are the propeller, landing gear, and H-tail. The propeller is a monstrous 20 inch diameter to maximize static thrust. The landing gear is a split design that does not pass below the payload bay. Landing loads are transferred to the fuselage side structure. The H-tail alleviated stability concerns with yaw control with the antenna payload installed. It also allowed easier packaging within the contest shipping crate. The fuselage and tails are a single assembly in the shipping crate. The wings and gear sit beside the aircraft in the shipping crate. They assemble with quick-connect hardware.

Figure 3.3.2: The Two Final Candidates

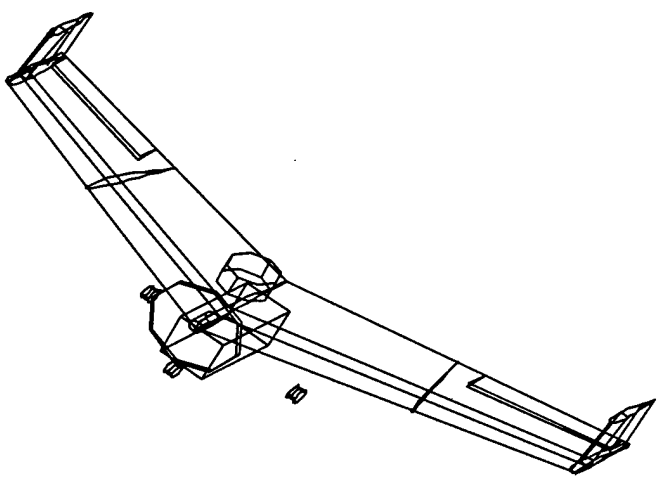

CTM-1 Flying Wing

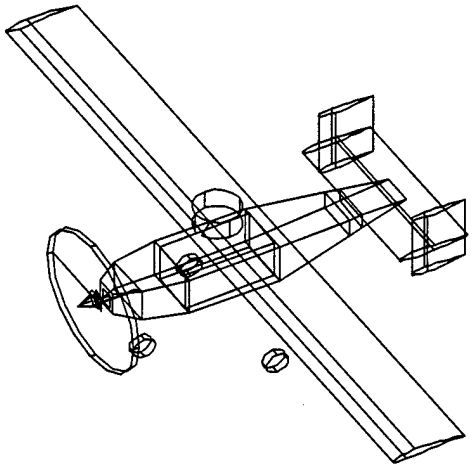

Mark 6 Conventional Monoplane

3.4. Final Concept Selection

With constructive criticism from our advisory board on the two aircraft designs at hand, we spent one week reviewing appropriate changes to both designs and decided, as a team, on a single concept to move forward. There were few confidence issues with the conventional design. The large propeller was seen as a distinct advantage over the short-gear flying wing. The landing gear design itself though was less desirable. Serious concerns were voiced over payload box drag and propeller slipstream blockage on the flying wing. The limited length allowed for the wing center section did not permit a nicely faired shape fore or aft of the payload box, and control could be a major problem with the antenna installed. Calculations showed that the flying wing could score 13 to 20% higher than the conventional design, but a failure to fly at all would mean a loss of all points. With all our data in hand, the team turned to its configuration Figures of Merit. The flying wing held an advantage in scoring potential, but the deciding factors were handling qualities, reliability, and confidence in success of the concept. Last year, 43 teams

entered the contest. Roughly 25 attended the fly-off. Less than 10 teams completed an entire mission sortie. Most of the battle is to show up with an airworthy design. The Mark 6 Conventional Monoplane concept was adopted as the WU Flyer and taken immediately into preliminary design.

4. PRELIMINARY DESIGN

4.1. Aerodynamics

Airfoil Selections

The first preliminary design task faced in the area of aerodynamics was selection of the wing, horizontal, and vertical tail airfoils. For this competition the low Reynolds Number requirement the aircraft must perform at, estimated to be 300,000 for all calculations, made airfoil selection a critical part of the design process. Research of published experimental data, such as that from Selig[20], and utilization of airfoil performance codes, like Xfoil[28] and DesignFoil[4], provided useful information that empirical data from full-scale aircraft could not. Some of the other airfoil requirements considered during this process were a high C_{lmax} required for takeoff, ease of manufacturing, gentle stall characteristics, and a well behaved drag polar. After extensive research several candidates for the wing airfoil began to emerge including the Wortmann FX63-137, Wayman, Eppler 214, NACA 4412, and 4415 airfoils. Performance parameters such as a C_{lmax} greater than 1.4 and a drag polar with a pronounced "drag bucket" were typically necessary to perform competitively at the competition. Ease of manufacturing is another crucial parameter, simply because if the airfoil cannot be manufactured within a reasonable tolerance to its actual shape the performance analyzed will not be reached. Finally, potential handling qualities like gentle stall performance must be taken into account especially if we are forced to use a pilot who is not familiar with our particular aircraft. With these considerations in mind, the NACA 4415 was chosen as the wing airfoil for the 2003 WSU DBF entry. This airfoil demonstrated the best resilience to manufacturing imperfections, while providing sufficient room for internal structure and other components. The only imperfection in this particular airfoil was the slight parasite drag increase due to the 15% thickness needed to obtain the required C_{lmax} performance. However, compared to the nearly impossible to manufacture trailing edge cusps present on many of the other airfoils studied, a slight increase in thickness was preferred. Published data from experimental analysis of the NACA 4415 airfoil in the NACA Variable Density Tunnel (VDT)[14] is shown in Figure 4.1.1.

Figure 4.1.1: NACA 4415 Airfoil Data

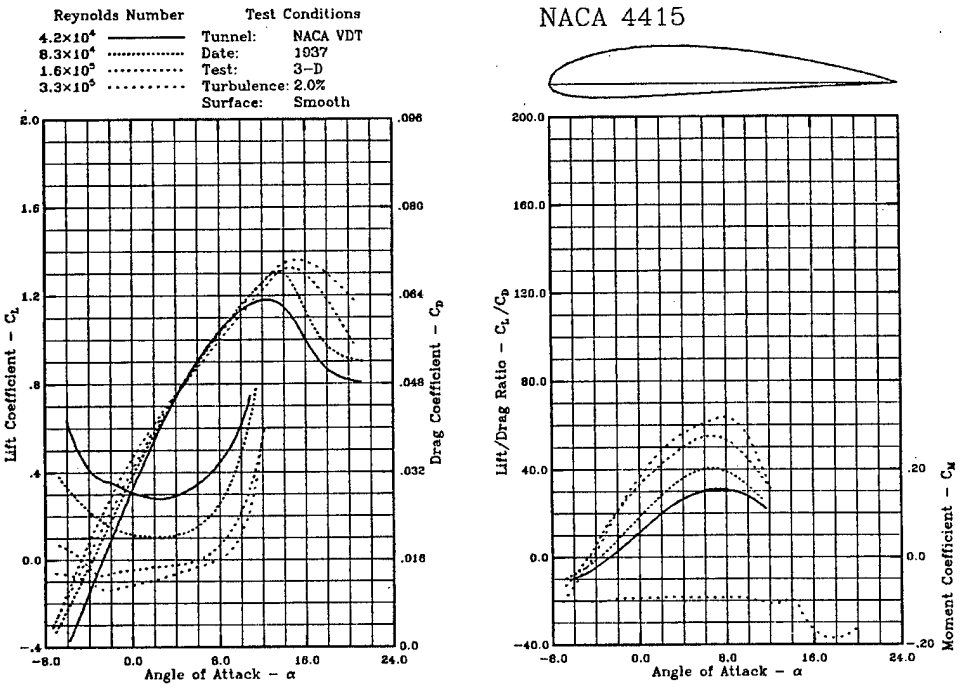

The stability and control specifications for the horizontal and vertical tail airfoils included airfoils with low drag at the resulting Reynolds numbers and ones with a C_{lmax} of around 1.0 for trim at very low drag. Also added were the constraints that they must be easy to build, thick enough to be robust in structure, and have, if possible, a drag "bucket" about the lower C_l range.

With the same techniques used to select the wing airfoil, the horizontal and vertical tail airfoils were quickly narrowed to a select few. For the horizontal the Clark Y, Selig/Donovan 7012, and NACA 0012 all presented favorable characteristics. However, the Clark Y was chosen as the final selection because of its moderate thickness of 11.7% to provide adequate structure, as well as its ease of manufacture and long reputation as one of the best low-speed airfoils ever created. Furthermore, the use of a cambered airfoil was considered a benefit in that it would require less incidence angle for cruising trim. The use of cambered versus symmetric was also addressed in the vertical airfoil selection process. The cambered Selig 8052 airfoil and the symmetric NACA 0009 and 0010 were considered for the vertical tails. While Raymer[17] showed the end-plate effects present, especially for an H-Tail configuration, could help reduce vertical tail size by as much as 5% for a full scale aircraft, the benefits of using a cambered airfoil to energize that area of flow were debatable. In the end the parabolic drag polar faced by the NACA 0009 at lower Reynolds numbers and added complexity of the Selig 8052 airfoils led to the selection of the

NACA 0010 as the vertical tail airfoil. This airfoil possesses a slightly higher C_{do} value than the previous two, 0.01 compared with 0.009. However, its flat drag curve emulates the qualities deemed necessary.

Wing Sizing

The next pertinent aerodynamic consideration for preliminary analysis was final wing sizing. Taking into consideration certain competition rules and requirements, there were several hard constraints. The half span of each wing could not exceed four feet, per interior box size specifications, however the wingspan must exceed four times the span of the horizontal tail for Rated Aircraft Cost considerations. Reynolds number effects were also considered, however since the NACA 4415 is widely used in turbo-machinery, the performance hit occurs well below the estimated, operational Reynolds number regime. Further restrictions were encountered in the team defined takeoff distance of 100 feet that, in effect, sized the wing area as a function of engine performance and airfoil C_{lmax}. Through our initial analysis we used a rectangular wing planform area that, from the given restrictions and assumed consistent engine performance, would have an average chord of 0.92 feet (11 inches) and a total area of 7.25 square feet.

Although satisfactory, the wing layout went through many more optimization cycles in order to account for a more elliptic lift distribution and provide additional weight savings during construction. After several iterations through an Excel based design tool, a takeoff distance change of 7 feet could be accomplished through an increase in C_{lmax} = 0.1 or an increase in wing area, S_{ref} = 0.5 square feet. After careful consideration it was determined, through Xfoil[28] predictions, addition of a flap could provide the increased C_{lmax} required to give a significant reduction in wing area. This significant change would allow for more flexibility in the design of the final wing layout at a cost of added complexity in the construction process. After some deliberation, the decision was made that a flapped wing would not only be beneficial, but essential to account for any possible weight growth during the construction phase. Plotting the results after several Xfoil[28] iterations of flap size and settings showed a 1.6 C_{lmax} value could be obtained through several different combinations, as summarized in Table 4.1.1.

Table 4.1.1: Flap Size Optimization Table

Flap (% Chord)	Δf (deg.)	C_{lmax}	C_{do}	Takeoff Dist. (ft)
0	0	1.4	0.0096	124
10	10	1.58	0.0112	103
10	15	1.63	0.0125	98
10	20	1.66	0.0145	95
20	10	1.62	0.0130	100
20	15	1.68	0.0183	94
20	20	1.71	0.0262	91
30	10	1.61	0.0159	101
30	15	1.65	0.0260	97
30	20	1.71	0.0452	92

By considering manufacturing constraints, such as foam and hot wire constructed parts must be greater than 0.25 inches in thickness, the size of the flap should not be less than 11% of the wing chord. Further analysis shows a sharp drag increase between the 15° and 20° flap deflection angles as well as the 20% to 30% chord sizes. For these reasons, a 20% flap with a 15° deflection was chosen to achieve the takeoff distance by giving the best performance at C_{lmax}. Taking into consideration the Rated Aircraft Cost dependence on additional servos, the flap needed for takeoff performance would extend full span and be used as a flap and aileron, or flaperon configuration. This would allow for a single servo per side, to accomplish the task of both the flap and aileron through the radio mixer functions. Taper ratio was also thought to prove beneficial in more than one way. Besides benefits associated with improving the lift distribution, the taper ratio could actually assist the ease of wing construction. Using two machined aluminum plugs, the carbon-fiber skin of the wings could be manufactured to the exact tolerances (± 0.005 inches) of the airfoil and then removed for installation of the interior rib and spar structure. A wing with a modest taper would promote easy skin removal from the plug. Typical modeler techniques for radio-controlled aircraft showed a taper ratio less than 0.5 produces undesirable stall characteristics due to the decreased Reynolds Numbers faced, and full-scale aircraft like the Cessna 172 were designed to a taper ratio of 0.7. After considering these aspects and iterating through several different wing area, span, and chord size combinations using the excel based design tool the wing dimensions shown in Table 4.1.2 were set as the WU Flyer final configuration.

Table 4.1.2: WU Flyer Wing Parameters

Span (b)	7.67 ft
Area (S_{ref})	6.5 ft^2
Aspect Ratio (AR)	9.04
Taper Ratio (λ)	0.7
¼ Chord Sweep (Λ)	0 deg
Mean Chord	0.848 ft
Root Chord	0.971 ft
Tip Chord	0.698 ft
Wetted Area (S_{wet})	13.0 ft^2
Wing Loading	3.30 lb/ft^2

Aircraft Drag Buildup

An initial piecewise drag buildup was performed on the final design configuration using the methods outlined in Roskam's text[19]. This drag estimation method uses an area buildup method, whereby each component's contribution to the total aircraft drag are added together to form the final drag polar of the aircraft. Several assumptions were made in this analysis that may affect the final results including: assumption of fully turbulent flow, normal aircraft configurations excluding low aspect ratio and highly swept wings, and empirical estimations from full scale aircraft. Conservative assumptions like fully

turbulent flow were thought to help equalize uncertainties in the full-scale empirical data used. Utilizing design drawings the results of the initial drag analysis, shown in Figure 4.1.2, an aircraft parasite drag coefficient, C_{Do}, calculated to be 0.033 excluding the antenna and 0.056 with the addition of the antenna for mission 2. By utilizing a payload carry technique that completely encloses the simulated avionics package internal to the fuselage and furthermore seals the cavity with internal bay doors after release, no significant drag increment is incurred either when the payload bay is full or empty.

Figure 4.1.2: Aircraft Drag Polar

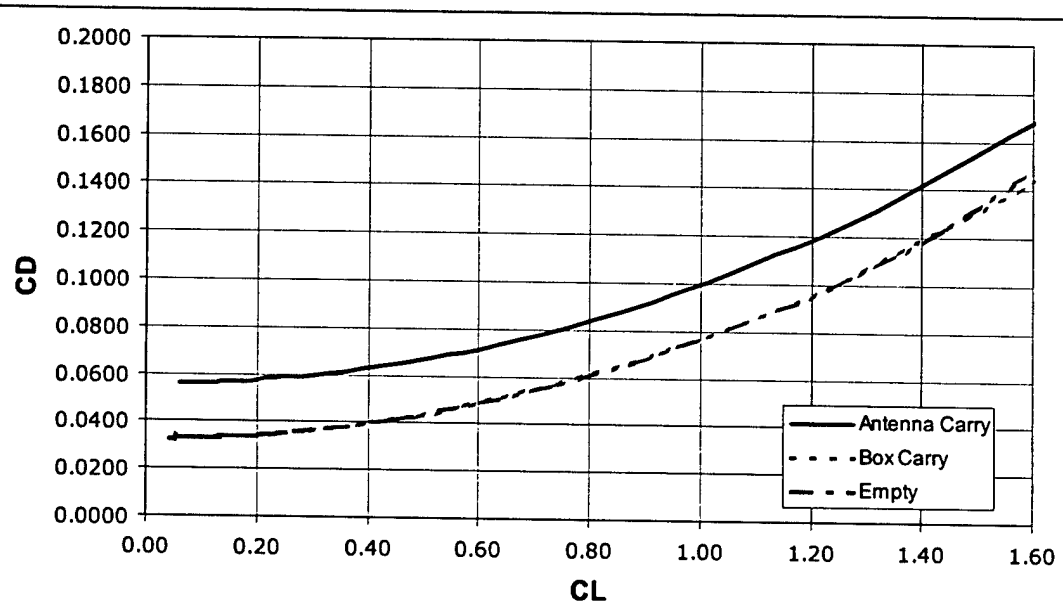

4.2. Stability and Control

The different missions, flight locations, and unpredictable weather conditions will require the aircraft to operate in a wide variety of conditions. In order to complete the two most difficult missions, the airplane must be trimmable in three different configurations: 1) with the cylindrical antenna and payload box, 2) with just the payload box, and 3) empty. Also, the airplane must be able to perform at the competition site, approximately sea level, as well as the test site near Wichita State University, approximately 1500 ft. msl. Weather conditions will also affect the aircraft performance, particularly the maximum allowable wind speed of the competition, 30-mph (close the aircraft's stall speed). Maximum allowable wind gusts will need to be determined to ensure the aircraft can be trimmed. The ultimate goal is to design an aircraft that complies with our design requirements and constraints while ensuring safety and performance.

Static and dynamic derivatives required for longitudinal and lateral-directional analysis were first estimated using Raymer[17], Roskam[18], and Etkin and Reid[5]. Trim analysis was performed using an Excel spreadsheet, and was verified through full scale wind tunnel testing.

Horizontal Tail

This year's packaging requirements set many limits on the aircrafts dimensions. Since the team chose a one-piece fuselage to simplify assembly, the fuselage could be no longer than 4 feet. In order to maximize tail length, the main wing was placed as far forward while maintaining room for components in the front bays. In order to package the empennage without disconnecting, the horizontal tail span had to be less than 2 feet. Also the rules limit the horizontal tail span to 25% of the wingspan to be counted as a horizontal tail and not as a second wing, which would lead to 2.5% increase in total score. To satisfy these two restrictions, the horizontal tail span was set for 22 inches. Finally, the necessary chord length was calculated using a horizontal tail volume coefficient of 0.475. A typical tail volume for RC airplanes is 0.5 according to Raymer[17] and past successful DBF entries.[24] With an H-tail design, the vertical surfaces act as endplates for the horizontal surface which can increase the effective tail volume by 5%.[17] The elevator is 35% of the chord, which is a typical ratio and provides over 50% of the effectiveness of an all-moving tail.[17]

Vertical Tail

An H-tail configuration was chosen for our design, mainly to avoid blanketing the vertical surfaces when the cylindrical antenna is mounted. This approach is similar to the modified 747 used to transport the space shuttle. An additional benefit is that using two vertical surfaces reduces the height of the vertical tail making packaging easier. The span of the vertical tail was limited to 10 inches to avoid disconnecting the verticals for packaging. The cost of using an H-tail compared to a standard tail is 1% in the total score, which was deemed acceptable given the benefits. Using the tail length mentioned previously and a vertical tail volume of 0.045, the chord of the vertical tail was determined. The rudders are also 35% of the chord. In order for the rudder to deflect inboard, a 20-degree chamfer had to be cut into the elevator. The horizontal chord was slightly increased to account for this loss in tail area. The verticals were set with a little over a degree of incidence to counteract the p-effect, which will cause the nose to yaw left.

Center of Gravity

The center of gravity (CG) was analyzed for the three payload configurations: empty, payload box, and payload box with cylindrical antenna. The 5 lbs payload box CG was placed on the empty airplane's CG, so that the fuselage station of the CG would not shift for these two configurations. The CG was first placed under the wing quarter chord. Combined with the horizontal tail described earlier, the aircraft's aerodynamic center was found to be at 0.41 MAC, making the static margin 0.16. This is comparable to a Cessna 182.[17]

Since the cylindrical antenna could not be mounted internally, it would cause an aerodynamic moment as well as a moment due to its weight. Therefore, the location of the antenna was carefully chosen so that these moments would counteract each other, reducing the pitching moment due to the antenna. The

antenna was mounted on the centerline, to avoid lateral-directional moments, and on the top, to avoid rotation interference and payload drop mechanisms. Since the antenna was mounted above the aircraft CG, its drag would cause a nose up pitching moment. Mounting the antenna forward of the CG would result in nose down pitching moment, but it would also increase the static margin and elevator authority necessary. Using an antenna and mounting weight of 1.5 lbs and the previously described horizontal tail design, the furthest forward the antenna could be mounted allowing for takeoff trim was 6.2 inches. The cylindrical aerodynamic forces of the antenna were estimated using Hoerner[8] then found experimentally through wind tunnel testing. Since the aerodynamic forces rely on dynamic pressure, the moments could only be balance at one condition. Since the controls would have the least amount of power at take off, the antenna location, 3 inches forward of the aircraft CG, was optimized for this condition.

Figure 4.2.1 Payload Center of Gravities

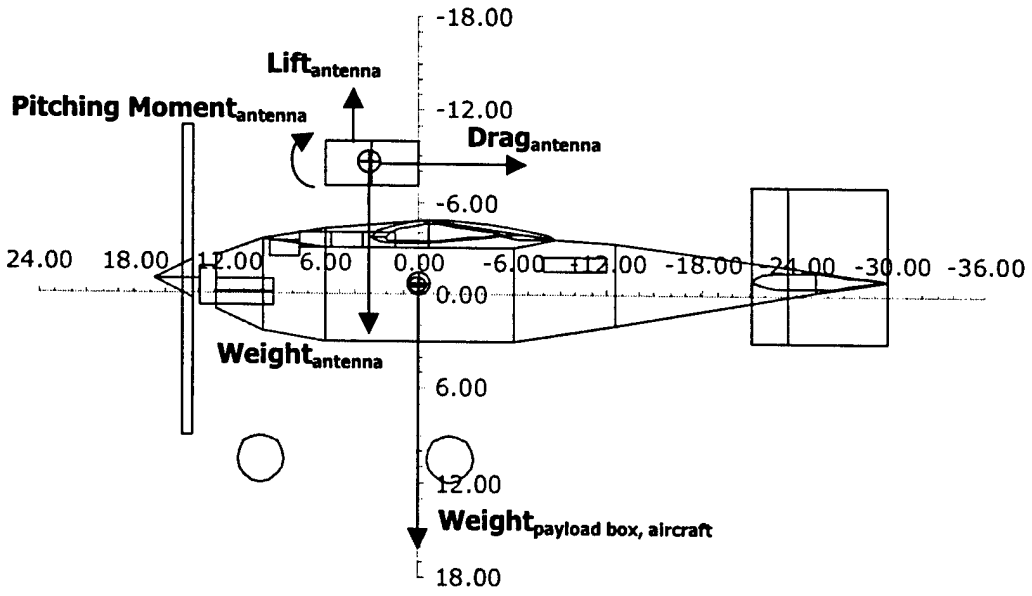

Cylindrcal antenna CG located 3 inches fwd of aircraft CG

Flaperons

In order to ensure takeoff C_L flaps were required. These flaps are 20% of the wing chord and would be deflected 15 degrees during takeoff. In order to minimize RAC the design has full span flaperons. The additional control surface area increased hinge moments, but typical RC servos provided sufficient torque. Concerns of wing tip stall led to a flaperon design with washout. Typically 2-3 degrees of washout is sufficient, but since our main wing structure was untwisted, the flaperon twist would effectively provide aerodynamic as well a slight geometric twist. Using X-foil[28], we found that the change in C_l from two degrees of flap deflection was about equal to one degree of angle of attack. Therefore, the flaperons were twisted 5 degrees at 65% span.

Table 4.2.1 Stability and Control Characteristics	
Horizontal Tail Volume	0.475
Horizontal Tail Span	1.88 ft
Horizontal Tail Chord	0.75 ft
Static Margin	0.16
$C_{M\alpha}$	-0.90
Vertical Tail Volume	0.045
Vertical Tail Height	0.83 ft
Vertical Tail Chord	0.71 ft
Flaperon Chord	20% chord
Elevator Chord	35% chord
Rudder Chord	35% chord

Wing and Tail Incidence

Wing and tail incidence were established for minimum drag in cruise condition. The wing incidence was set for cruise C_L, and the tail incidence was set so that no elevator deflection is required to trim in cruise. The wing incidence was found to be zero, due to the camber of the airfoil; and the tail, which has a negative camber, has an incidence of –3 degrees. With this configuration and the airfoil characteristics discussed earlier, the following trim plots were produced. The airplane's cruise C_L is 0.56 and the takeoff C_L is 1.4. Elevator effectiveness was estimated using empirical corrections from USAF DATCOM[8].

Figure 4.2.1: Elevator Trim Crossplot at Cruise With Antenna

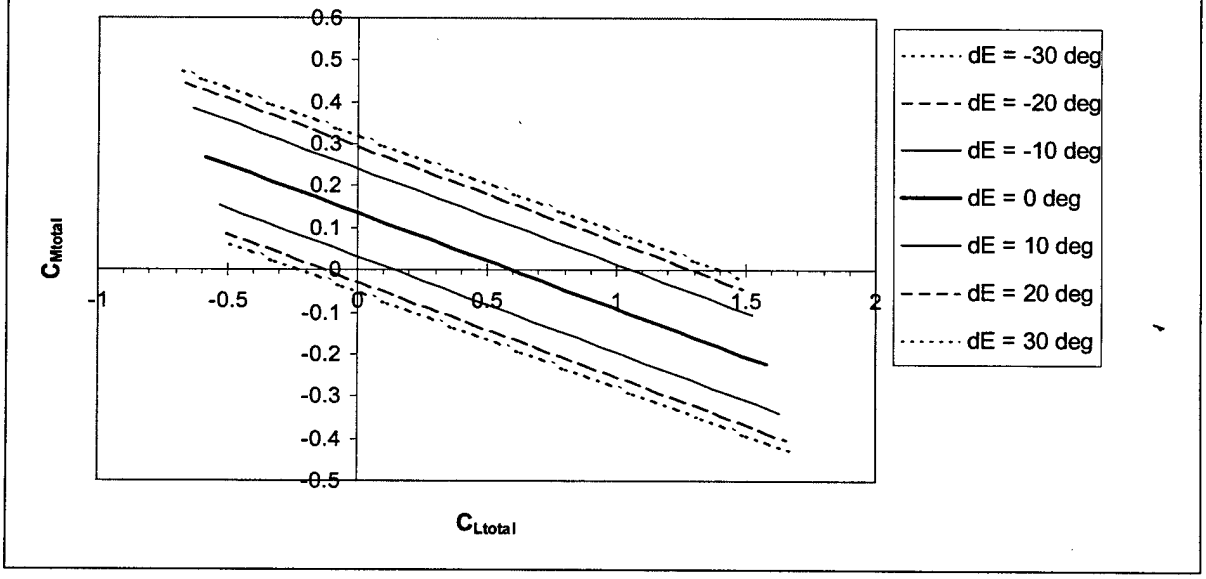

Stall/Spin Recovery

The vertical tail also plays a key role in spin recovery. During spins, a turbulent wake extends upward from the horizontal tail at approximately a 45° angle. As a rule of thumb 1/3 of the rudder area should remain un-blanketed in a spin. Since the vertical surfaces are endplates, one complete rudder will remain un-blanketed in a spin. The vertical location of the horizontal tail was also made in order to avoid the main wing wake during a stall. This location also determines the tail cone location and fuselage aerodynamic shape. The fuselage is shaped as a 17% thick airfoil with no camber.

Take-Off

Tail area was sized to ensure there was enough authority for take-off rotation, but the airplane must also have sufficient rotation angle to ensure take-off C_L can be achieved. The height of the landing gear was set in order for the airplane to roll over the payload box after being deployed. The vertical placement of the vertical tail was set partly due to packaging and also to reduce the adverse roll due to rudder deflections. With this configuration the rotation angle was found to be 18 degrees, which is sufficient for, take off rotation. To make sure the airplane could not sit on its tail, the main landing gear were set 4.0 inches aft of the CG so for the maximum rotation angle, the CG is still forward of the main gears. In order to protect the rudder during high angle-of-attack approaches and take offs, a 20 degree chamfer was cut in the bottom corner of the rudder. The vertical tail chord was increased to compensate for the area loss.

4.3. Propulsion

In the preliminary design phase, it was found that propulsion requirements would greatly affect many aspects of the aircraft's performance. Several key figures of merit were found by which the propulsion system would be judged. The key factors were maximum power output, battery endurance, flight speeds, mission scoring, and simplicity of the system. Looking through the key equations for the propulsion system it can be found that different requirements will size different components of the system, and certain requirements will take precedence and force the size of other parts.

If we begin by looking at the contest rules, electric propulsion requirements are very closely linked to scoring analysis in the Design/Build/Fly contest[23]. Score is determined by the following formulas:

Total Score = (Report Score * Mission Score) / Rated Aircraft Cost
Mission Score = Mission Difficulty Factor / (Mission Flight Time + Aircraft Assembly Time)

Rated Aircraft Cost is heavily dependent on the weight of the propulsion battery pack carried by the plane. The speed that the aircraft can fly and still complete a mission is also dependent on the battery weight carried. This means that battery analysis holds a major contribution in the scoring formula.

To analyze the propulsion requirements for this year's effort, spreadsheets were built to determine how much power would be required for successful takeoff, current and voltage requirements to avoid motor or fuse burnout, and three mission profile models to determine which missions would score highest. These tools were tied into the geometric and aerodynamic properties of the aircraft. This direct link allowed fast re-iteration of scoring numbers following configuration changes. The approach to the effort was that a highly capable design tool that takes a large amount of time to develop will reward the designer down the road with fast turnaround times for new data.

Analysis shows that different mission phases size different parts of the propulsion system. Takeoff power requirements determine the motor size required. Without a motor of sufficient output for a configuration, takeoff is not possible within the distance specified in the rules. The motor has a published set of allowable voltage and current ranges. The electric equations that govern system performance are the following:

Power (watt) = Current (amp) * Voltage (Volt)
Battery Pack Voltage (Volt) = Voltage per Cell (Volt) * Number of Cells in Series

To keep current below the motor's rated maximums, batteries are arranged in series to increase the voltage of the battery pack. The power required and the current limit set the minimum number of 1.2Volt cells that can be used. The contest dictates that a slow blow 40 amp fuse must be included in the propulsion system. This was intended to limit the current that teams would utilize and to reduce the odds of damage to the propulsion system. All the motors examined had current limits below 40 amp. These current limits are for steady state operation, so short duration over-capacity operation could be made, but serious damage could be done to the battery packs if current discharge rates get too high. All design efforts have been aimed at keeping current below the rated limits though to increase reliability and reduce the risk of component damage.

Battery pack capacity requirements are determined by the total energy drawn during the duration of each of the three missions. Takeoff calculations showed that power drawn in that mode is a small portion of the total battery capacity. The power draw rate during takeoff is high, but takeoff roll lasts only 5 to 6 seconds. The most energy is consumed during cruise and turning flight flying laps around the course. Power draw is relatively low, but the duration of each lap is large. Since power consumption is largely determined by the speed flown, the battery capacity required was determined as a function of flight speed. To model the course to be flown, a spreadsheet calculated the total distance flown on straight-aways, turns, and the effect of a crosswind as a function of airspeed flown. Increased speed requires increased battery capacity. The optimum speed for maximum score is determined for each mission, as well as the maximum and minimum allowable speeds. All of this is done assuming that 20% of the

battery pack is left for emergency reserve. That gives an available range 25% larger than that anticipated for a given mission including crosswind effects. Crosswind was assumed to be 30mph, the maximum that might be encountered before the contest is postponed or canceled according to the published rules. Scoring plots are included in the performance analysis section of the paper.

Using the design spreadsheets that were developed, it became clear that certain requirements would take precedence over others. Since takeoff field length is critical to being eligible to compete at all, the propulsion system would have to be capable of producing the necessary power. Aircraft packaging within the contest shipping crate made a small airframe and small wings desirable, holding wing loading relatively high and encouraging the use of flaps for high lift. With the payload weight fixed and the rough airframe weight known, it was clear that a high output motor would be required. The largest part of the motor's power would be needed just to accelerate the mass of the aircraft up to sufficient speed for flight in 100 feet. The portion used to counteract aerodynamic drag was relatively small. Takeoff analysis plots showed that a reduction in wing loading or aircraft mass would reduce the power required significantly. Comparing the two motor suppliers specified in the rules, the large power requirement and packaging concerns pushed us toward one answer.

The motor selected is the most powerful produced by Astro Flight, the sole domestic supplier of electric motors for the DBF contest. It is the Cobalt 90 model with Superbox gear reduction unit. Advertised output falls in the 1200 to 1500watt range (1.6 to 2.0 horsepower). Motor power output data is available, but not entirely clear on the website[26]. Ambiguity in manufacturer's data is a fairly common problem, so we made an independent analysis for a better design estimate. Motor efficiency is typically around 80%. The manufacturer's website indicated that the Cobalt 90 can use packs with 36 to 41 cells. Sales materials don't indicate a range, but give 36 cells as a typical number. To account for internal resistance in the batteries and wiring, the voltage of each cell was handicapped to 1.05Volt rather than the standard advertised 1.2Volt. Calculations based on 41 cells and the 35 amp maximum current limit suggests that the motor can accept 1506 watt of power (2.0 hp). With a motor efficiency of 80%, this gives an output of 1205 watt (1.62 hp) to the gearbox reduction unit and propeller without exceeding maximum current capacity. Running 36 cells, maximum useful output is reduced to 1058 watt.

Forty-one is not a standard number of cells for a battery pack, but 42 is a convenient multiple of both 6 and 7. Six and seven cell packs are commercially available to build our large pack. Eight cell packs could be used to make a 40 cell pack, but this route was declined because 8 cell chargers are more difficult to find and the packs are less common. There was some initial concern with using more battery cells than suggested in manufacturer literature, but it was decided that a slight voltage increase would not greatly affect the odds of electrical arcing, the main threat for damage from voltage increases. We

decided then to assume a main propulsion pack assembled from 6 packs of 7 cells each for a total of 42 cells.

With the motor and battery pack configuration set, flight mission analysis began. With the computer mission model available, it could be determined what flight speeds and scores are viable given the energy density of typical nickel cadmium battery packs. The data shows a clear optimum battery load for best score, and reduced score beyond. The scoring data though neglects the issue of safety. At optimum score, the aircraft has only a slight margin in speed above stall.

To prevent a catastrophic stall-spin accident, a full battery load of 5 pounds was considered in comparison to an optimum-scoring load. The change in battery load increases the margin above stall speed from roughly 26% on Mission A to 83%. For safety then, the decision was to carry the maximum legal battery load. The maximum load case will still be expected to score 75% as high as the optimum-scoring case. Observation of last year's contest also indicates that the fastest aircraft tend to do best in high wind conditions. Figure 4.3.1 and Table 4.3.1 show scoring and flight speed data for the optimum-scoring and maximum battery load, maximum speed battery loading cases. Scoring ratios of Mission Score over Rated Aircraft Cost are multiplied by one million so the numbers are easier to interpret.

Figure 4.3.1: Scoring Ratio = (Mission Score/RAC)*1,000,000 vs Flight Speed

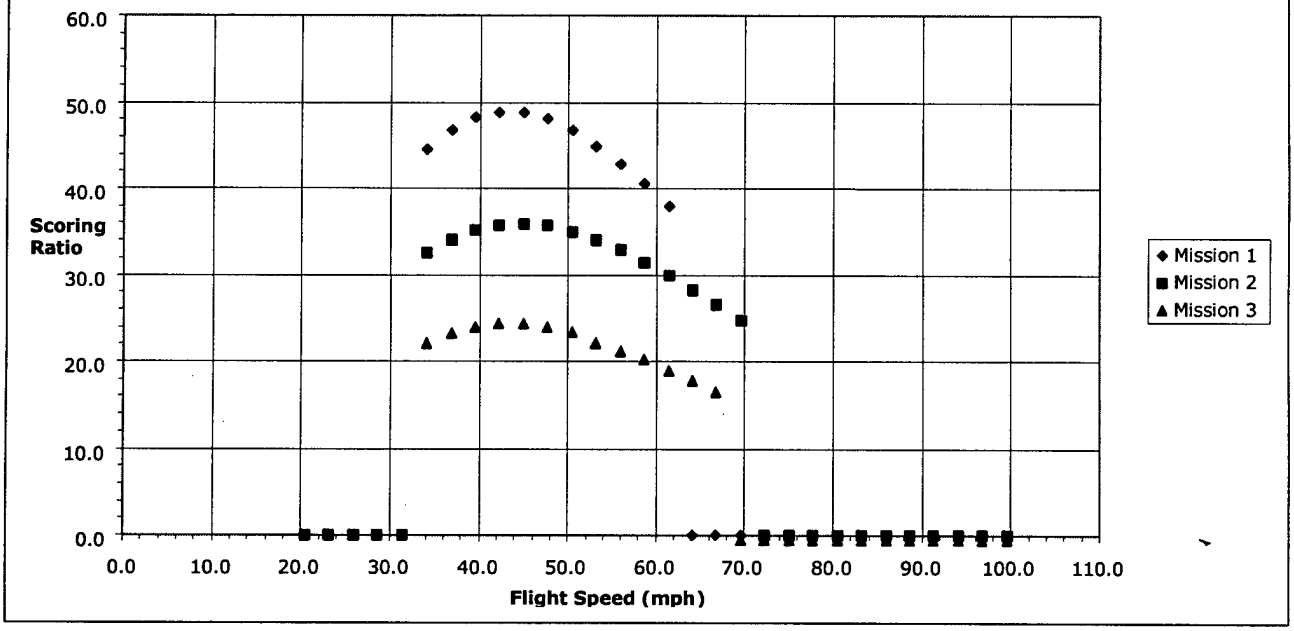

Table 4.3.1 – Mark 6 Scoring Performance

Times (min)			**RAC Data**	**RAC**	**% Total**
Assembly	0.5		Airframe	5128	41%
Takeoff	0.2		5lb Batt.	7500	59%
Land/Takeoff	0.8				
Criteria	**Mission A**	**Mission B**	**Mission C**		
Optimum Score (Mission Score/RAC)*1,000,000				**2.09**	**(lb) Batteries**
Speed	42.3	45.0	45.0	(mph)	
V/Vstall	1.26	1.39	1.61		
Score	0.40	0.28	0.19		
Time	5.0	5.4	5.2	(min)	
RAC	8261				2 Mission Max
Total Score	48.8	33.3	23.2		**82.2**
Maximum Speed(Mission Score/RAC)*1,000,000				**5.00**	**(lb) Batteries**
Speed	61.4	69.5	66.8	(mph)	
V/Vstall	1.83	2.15	2.38		% Max Score
Score	0.47	0.31	0.21		**75.7%**
Time	4.24	4.78	4.74	(min)	
RAC	12628				2 Mission Max
Total Score	37.4	24.8	16.7		**62.2**

The other clear trend shown in the data is that Mission A has the highest scoring potential followed by Mission B and Mission C. A single successful sortie of any should place the aircraft well in the contest standings, but ideally, the plane would fly Missions A and B for maximum score. This could be a point of concern if takeoff field length calculations were off because Mission A has a gross-weight, high-drag takeoff. Shortcomings in takeoff performance could make Mission A a "weather permitting" task only.

To maximize takeoff performance with the given motor, a large diameter propeller size was chosen. The propeller has a 20 inch diameter, as long as 43% of the aircraft's total length. Combined Blade Element/Momentum theory calculations showed an ideal efficiency of 67% for takeoff condition requirements. Takeoff performance estimates used 55% efficiency, allowing 12% for airfoil and lift distribution losses. For reference, one inch in diameter reduction reduced efficiency by roughly 1.5%.

To allow for a large propeller, the motor has a gear reduction unit with a reduction ratio of 2.75 to 1. It reduces propeller rpm from the motor's regular operation range around 9000 down to 3300rpm. The motor would not have enough power to swing the large propeller without this reduction in rpm. The result is improvement in static thrust with a minimum detriment in cruise.

Following single-point takeoff approximations, Combined Blade Element/Momentum theory was used to build a lookup table of propeller performance estimates from static condition to cruise speeds. The lookup table was fed into a graphical integration scheme for a better field length estimate. These calculations were less optimistic than the single point approximations by about 13 feet, but the aircraft

was revised until the integral method calculations indicated a field length of exactly 100 feet (per our requirement). In the case of an unfortunate vehicle weight gain, field length increased 6 to 7 feet for every pound of weight gained. Our design requirement leaves us a margin of 20 feet before rules violation assuming our calculations are exactly correct.

4.4. Structures

Load Paths

During preliminary design it was necessary to start looking at the load paths through the vehicle to determine proper placement of structural members. Since a mission requirement exists to drop a payload element from the aircraft, no structural members will be allowed to protrude through the payload bay area. Based on this assumption and having a high wing aircraft, the wing spar will be placed at the quarter chord of the airfoil and run over the top of the payload box. This means a method will need to be developed to attach the wing to the aircraft fuselage. The horizontal and vertical tails will also need to have spars to take bending loads produced, similar to the need for the spar in the wing. The landing gear poses unique issues to the WU Flyer aircraft. Due to the need to drop the payload from the bottom of the aircraft, landing loads cannot be transferred through traditional landing gear that pass below the aircraft. This method would block the payload from being dropped. This means the landing gear load paths must run up the sides of the payload bay and terminate or extend across the top of the payload bay like the wing spar load paths.

Load Factor

The next task for preliminary design was to determine a max load factor for the aircraft. Radio controlled aircraft are unique from traditional aircraft in that the pilot is unable to feel the loading on the airplane since he is flying from outside the aircraft. We have chosen a 6g load factor to design to with a 1.5 factor of safety. A 6g loading should give the pilot adequate margin to maneuver the aircraft in turning flight. Gust loading must be taken into account to ensure that any gusts seen by the aircraft during maneuvering flight do not stress the aircraft beyond its structural limits.

Figure 4.4.1: V-n Diagram – Unloaded

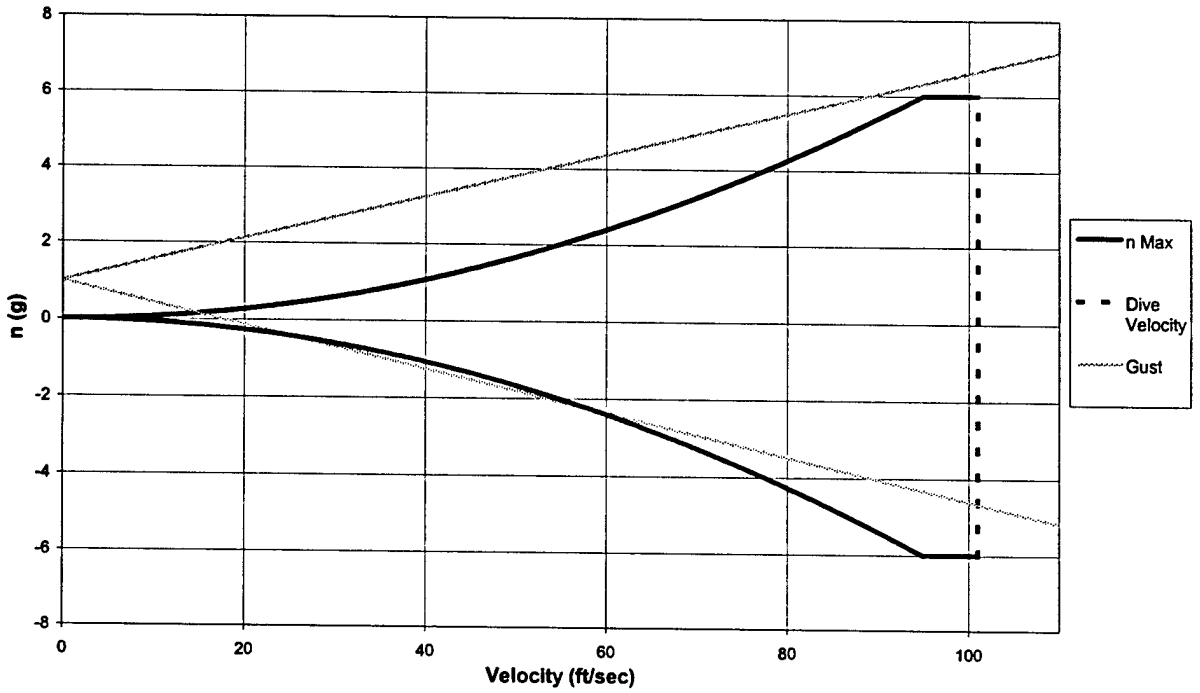

Gust loading was analyzed utilizing recommendations from Raymer[17] wherein a mass ratio is defined and a vertical upset speed of 30 ft/sec is used. Dive velocity was decided utilizing 14 FAR 23.335(b)(2)(i)[29] which states that design dive speed must be a minimum of $1.4V_c$. Utilizing this information dive speed comes out to 101 ft/sec. If we look at the V-n diagram we see that the upper limit of our design should be designed to near 6.5 g to account for gust loading during flight. The V-n diagram shown is for the lightweight vehicle flying without the payload. The gust loading is more severe on a light aircraft since it takes less upset gust to overload the aircraft, this is therefore the worst case scenario. A heavy weight V-n diagram was also created

Spar Material Selection

The final item considered during preliminary design was definition of material selection for the spar. Based on an approximation of weight a rectangular lift distribution was assumed across the wing. A bending moment was then determined at the root of the wing. Density and yield stresses were then found for a variety of materials. Utilizing the flexure formula of $\sigma=M*Y/I$ we can determine the cross-section required for each material to handle the generated moment by making a few simple assumptions. It is assumed that the cross section is simply loaded with only a lifting load and that the spar is a solid square cross-section. Based on results of our analysis the best material to build the spar out of is fir. Since past experience with fir has resulted in splitting of the material the second choice of Carbon fiber

was utilized. Material properties used for carbon fiber are the common material strengths used by homebuilt aircraft builders. Properties for other materials selected were obtained from MATWEB.com[13], a material property database.

Table 4.4.1: Material Properties

Material Name	Density (lb/in3)	Cross Section Area	Weight (lb)	Bending Strength (psi)
Fir	0.017	1.70	0.029	3,780
Carbon Fiber	0.061	0.57	0.034	100,000
Aluminum	0.101	0.65	0.065	68,000
Spruce	0.13	1.53	0.20	5,180

5. DETAIL DESIGN

5.1. Aerodynamics

Pressure Distribution and Contour Optimization

During the design process the aerodynamics analysis was assisted through a computational fluid dynamics (CFD) tutorial in VS-Aero, a three-dimensional paneling method used to predict the pressure distribution and aerodynamic coefficients of our aircraft design configuration. In order to identify potential problem areas in geometry or flow instabilities a model was created using various cross-sectional positions that could then be shaped and smoothed to a more desirable contour. Final results were a smooth transition from a 3 inch circular nose radius, to a rectangular payload bay cross-section with ¼ inch radius corners, to finally a 1/16 inch trailing edge elevator thickness. The final model is shown, top and bottom, in Figure 5.1.1.

Figure 5.1.1 WU Flyer VS-Aero Model

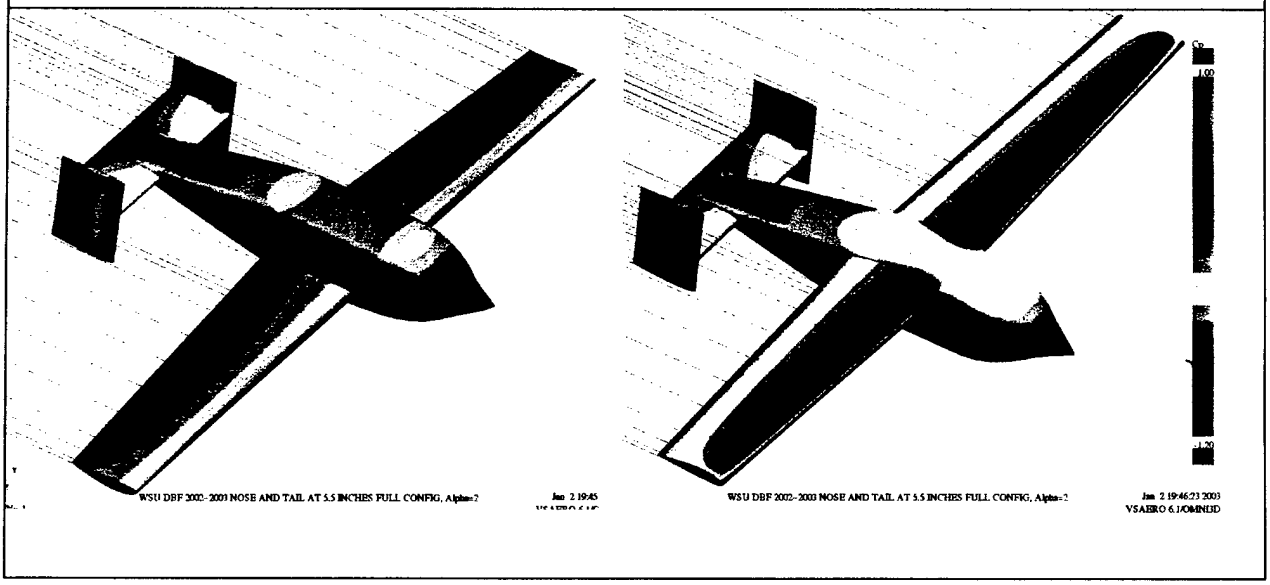

Final Drag Analysis and Reduction

In the preliminary design phase, area drag analysis was performed to the known aircraft specifications at the time. In order to verify the accuracy of these predictions several wind tunnel angle-of-attack sweeps were performed and the data gathered showed a significant difference in drag performance, particularly in the parasite drag coefficient, C_{DO}, which swelled to 0.050 from the calculated value of 0.033. The cause of this dramatic drag spike is still under investigation, however with some careful use of flow visualization and drag cleanup techniques during the testing phase the number was reduced to 0.047. Further changes to lower the overall drag may include wing root fillets, gear connection fairings, and low profile wheel selections. Analysis of the cylindrical antenna itself through a separate wind tunnel test showed the flow to be very near the range of transition from laminar to turbulent flow. So crucial was this aspect that the difference between 40 mph and 60 mph airflow gave a range of cylinder drag coefficients of 3.0 to 0.15 corresponding to drag values of approximately 2.9 and 0.48 pounds respectively. Further drag reduction could be accomplished through carefully directed airflow to trip the boundary layer into fully turbulent flow to avoid the separation drag at the lower flight speeds. Figure 5.1.2 documents the lift and drag polar for takeoff and cruise flap settings obtained through wind tunnel testing. Beyond just the drag differences, the lift curve displayed notable attributes like an increased C_{Lmax} and stall angle of 1.7 at 18° respectively compared to the predicted values of 1.6 at 12° as well as the possible presence of a small separation bubble. A slight increase in manufactured wing thickness was determined to cause both of these phenomenon, however they were not considered severe problems.

Figure 5.1.2: C_L & C_D vs Alpha Wind Tunnel Data

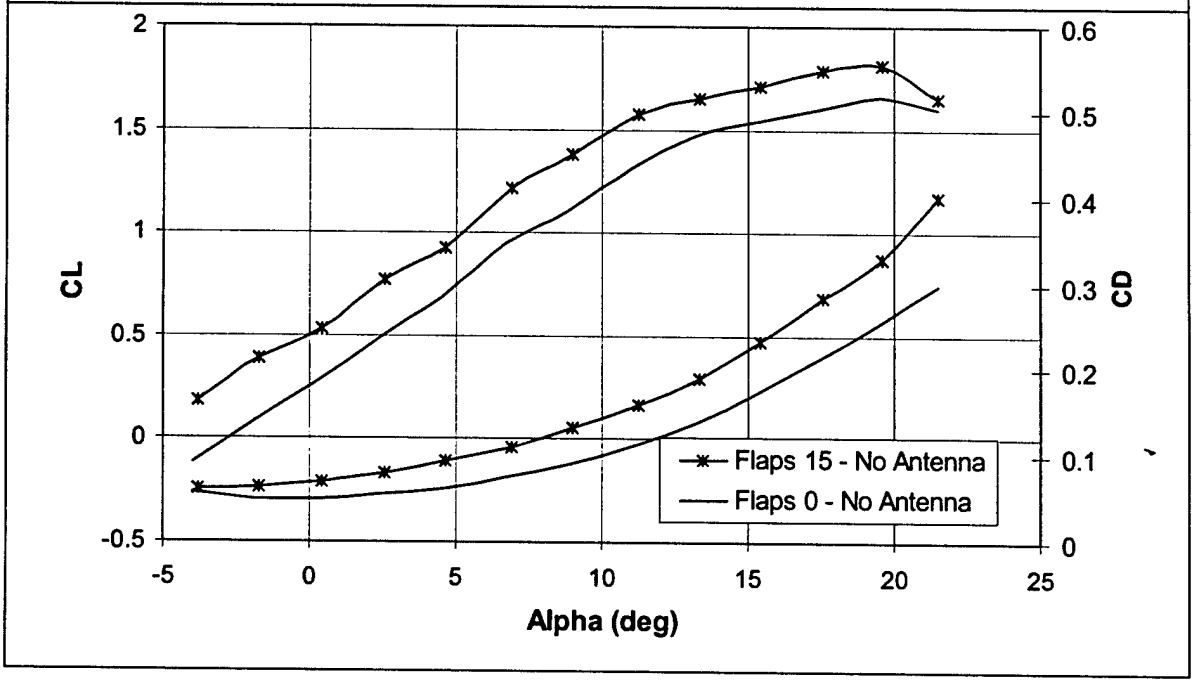

Final Aerodynamic Configuration Layout

The WU Flyer's final configuration was designed and built to make it as clean as possible, not including the addition of the antenna. This was critical for reducing our parasite drag to ensure enough power available to complete the specified missions. Since we are not allowed to fair the antenna in any way, per rules specifications, the drag produced by the remainder of the airframe must be minimized to ensure optimum performance. For this conventional aircraft, enclosing the payload entirely and having a very shallow angle for the aft fuselage to avoid laminar separation were used as the primary means of drag reduction. This design also has an added feature of an airfoil shaped fuselage that may provide a limited amount lifting body effect to the aircraft performance. However, a byproduct of this streamline philosophy was dropping the payload required the landing gear clearance to be at least 6 inches from fuselage belly to the ground. This problem was solved through detachable gear that allow the airframe to fit the required packaging limits. Other design complexities that were managed throughout this process include gap seal on all control surfaces using Monokote to prevent cross-flow and the C_L losses associated with that type of flow and a battery and motor cooling system designed utilizing an inlet located 3 inches aft of the propeller and an exit that corresponds to a specifically placed access panel according to the pressure distributions found using the VS-Aero model.

5.2. Propulsion

In detailed design, many of the critical propulsion system parameters were already set. The motor, speed control, and fuse holder were already in hand. The battery pack specifications were defined, and there were a few good ideas for wire paths through the aircraft. All of these characteristics were important to proper design of the rest of the aircraft, so much of the broad work was ready to go. Detail design served to refine the propulsion system though and allow the purchase of a last few parts necessary before testing could begin.

Component Wiring

Design of the wiring diagram saw some major design decisions. From contest rules, the fuse must go in between the battery pack positive lead and the speed controller input. For CG control and systems packaging, the six propulsion battery packs were split between two battery bays. One bay sat forward of the main wing spar. The other was just behind the payload bay. This left a choice of where to place the fuse holder and speed control. For safety of the team, we decided to place the fuse holder in the rear bay. That way, nobody needs to be near the propeller disc to remove the fuse and disable the motor. With the fuse in the rear portion of the aircraft, the speed control could be placed in the aft bay also, or it could be placed forward with the motor. The trade between these two options was one of weight and convenience versus some passed down knowledge. If the speed control went in the nose, only two wires would run past the payload bay. With the speed control at the rear, four lines would cross the length of the payload bay. Discussion though with Blaine Rawdon, an advisor for several years to the USC team,

indicated that long wire runs before the speed control can allow surge problems. Electric motors seem more tolerant of the power pulses, but a large pulse can damage a speed control's electronics. The nose position for the speed control left a long wire run from the positive side of the battery to the controller. It wasn't clear how much affect the power pulsing might have in practice for our particular design, but we decided to err on the safe side to protect our speed controller. The speed control was placed in the rear bay to minimize the wire run on the positive side of the battery. There was some weight increase for the wire, but that was deemed better than a damaged speed control.

Battery Selection

Battery selection was a matter of shopping around for a set of battery packs that would be under the legal weight restriction with the desired number of cells and the maximum capacity per cell. Four catalogs were examined, and two sets of viable packs were found. Hobby-Lobby and Great Planes each had 1700mah 7 cell packs worth considering. One set of packs would be well under the legal weight limit. The other set of packs would be very close to the limit, possibly just over. If that were the case, a couple batteries might have to be removed from packs to make the legal weight limit. Both types were ordered in the interest of testing to determine the better type to buy for the contest. Battery testing is not done yet, so the best packs have not been selected.

Propeller Selection

Propeller selection, often difficult on full sized aircraft, is nearly impossible to predict well on model aircraft. There is no reliable source at the current time for propeller selection or propeller performance. Our target design propeller has a 20 inch diameter, flat bottom, and 10 inches of pitch. We plan to test and investigate larger and smaller props with a couple higher and lower pitches. Final selection will be much like battery selection, using test data to pick the preferred size and type.

Detail design continues to some degree with the propulsion system. The system has been assembled and tested, but difficulties have delayed in depth testing. The team is de-bugging problems associated with a lack of power. Motor tuning was first suspected, but we wonder if some of the packs that we bought had dead cells. At high discharge rates, a dead cell may have caused damage to the rest of the packs. We plan to sort this issue out in the next couple weeks.

5.3. Stability and Control

In the detail design phase of stability and control, full scale wind tunnel testing was used to verify trim plots and stability coefficients calculated earlier. Using the actual aircraft data reduced assumptions made previously and accounted for differences in the designed model to what was actually manufactured. Any problems could then be identified and solved prior to first flight.

Elevator Trim Plots

The first priority was to determine whether the airplane could be trimmed for the take off C_L. The trim plot, Figure 5.3.1, was obtained by running alpha sweeps between –4 to 16 degrees with different elevator deflections. The pitching moments were resolved about the designed CG point. The change in slope between the last two data points (angle-of-attack equal to 12 and 16 degrees) signaled the flow had separated somewhere on the aircraft. Even with this separation, the airplane is just under the designed 1.4 C_L for take off. The zero elevator trim is also slightly under the designed cruise C_L of 0.56. This was most likely caused by the wing or tail incidence was manufactured slightly off. This was anticipated in the design phase so the wing and tail were designed so that the incidence could be changed. The small change in wing incidence will increase $C_{M\ CG}$ for all the points, shifting the plots up. This will then allow for take off C_L.

Figure 5.3.1: Elevator Trim Crossplot

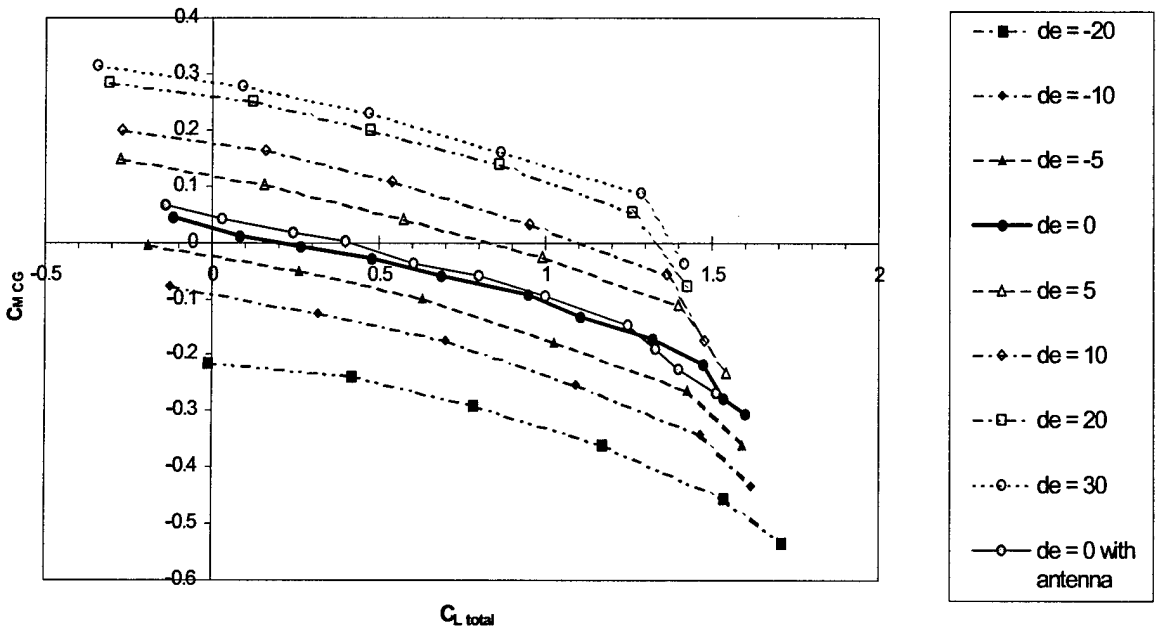

Pitch Stiffness

Pitch stiffness is mainly determined by the pitching moment due to angle-of-attack derivative, $C_{m\alpha}$. Typical values for general aviation and transporters range from –0.6 and –1.0[17]. Since the pilot will fly this airplane remotely and the mission calls for a stable aircraft, the airplane was designed with a $C_{m\alpha}$ value of –0.9, comparable to a Cessna 182. The wind tunnel analysis showed the aircraft had a power-off $C_{m\alpha}$ of –0.96 clean and –0.94 with the antenna. According to Raymer[17], power-on will reduce static margin by about 4-10%, so pitch stiffness is within desired range for power-on and off conditions. A plot showing the pitch stiffness of the WU Flyer is shown in Figure 5.3.2 (Page 33).

Yaw Stiffness

Yaw stiffness is measured by the rolling moment due to sideslip derivative, $C_{N\beta}$. Suggested goal values range from 0.05 to 0.1[17]. The airplane must be directionally stable to reduce pilot workload and for the safety of the audience. The aircraft was designed to a $C_{N\beta}$ of 0.8, similar to a Cessna 182. Wind tunnel results confirm the aircraft's actual $C_{N\beta}$ is 0.78, clean, and 0.086 with the antenna. A plot showing the yaw stiffness of the WU Flyer is shown in Figure 5.3.3 (Page 34).

Roll Stiffness

Roll stiffness is measured by rolling moment due to sideslip derivative, $C_{L\beta}$. At subsonic speeds, $C_{L\beta}$ should be negative and about half the magnitude of $C_{N\beta}$. This makes the desired range from 0.25 to 0.5. The wind tunnel analysis shows that $C_{L\beta}$ is –0.43, clean, and -.028, with the antenna. Both values are within range, but with the antenna the airplane may prove to be less stable in roll than desired. If this is the case, roll stability can be increased by adding a small amount of dihedral, which would require a change in the spar center section, or the vertical tail height could be adjusted a small amount. Alternatively, a gyro in the roll axis can be used to augment the roll stability. A plot showing the roll stiffness of the WU Flyer is shown in Figure 5.3.4 (Page 34).

Figure 5.3.2: $C_{M\,CG}$ vs Alpha

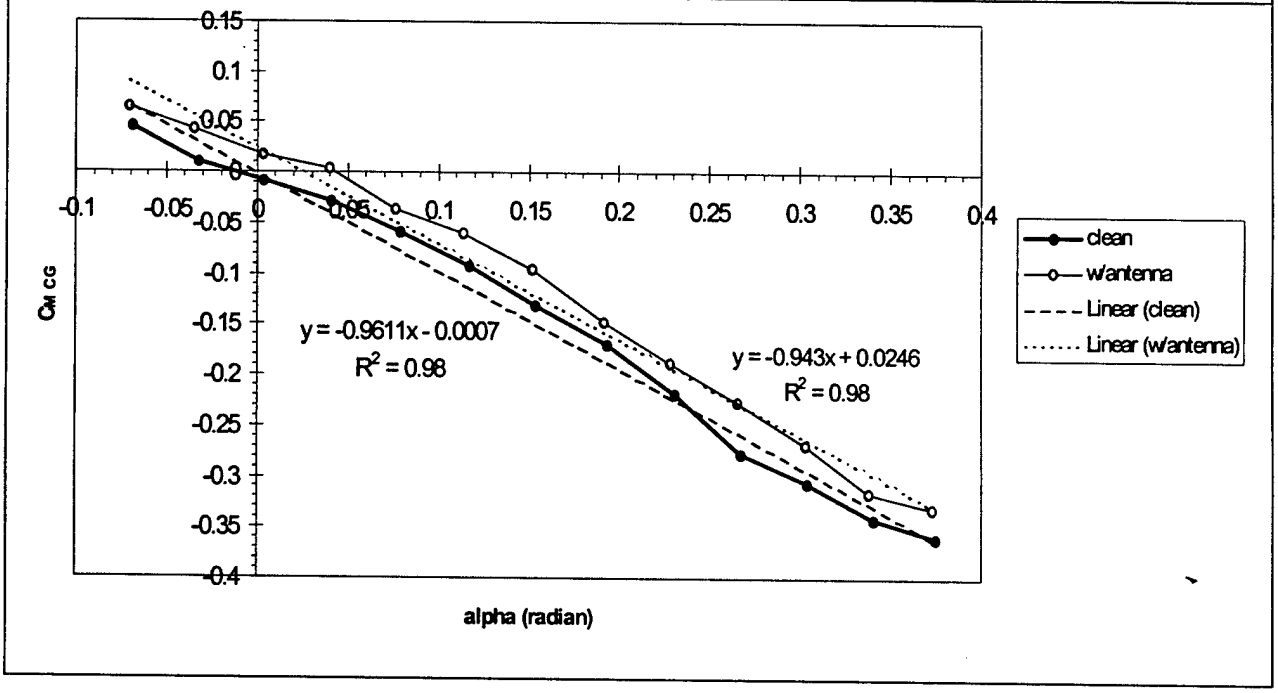

Figure 5.3.3: $C_{N\,CG}$ vs Beta

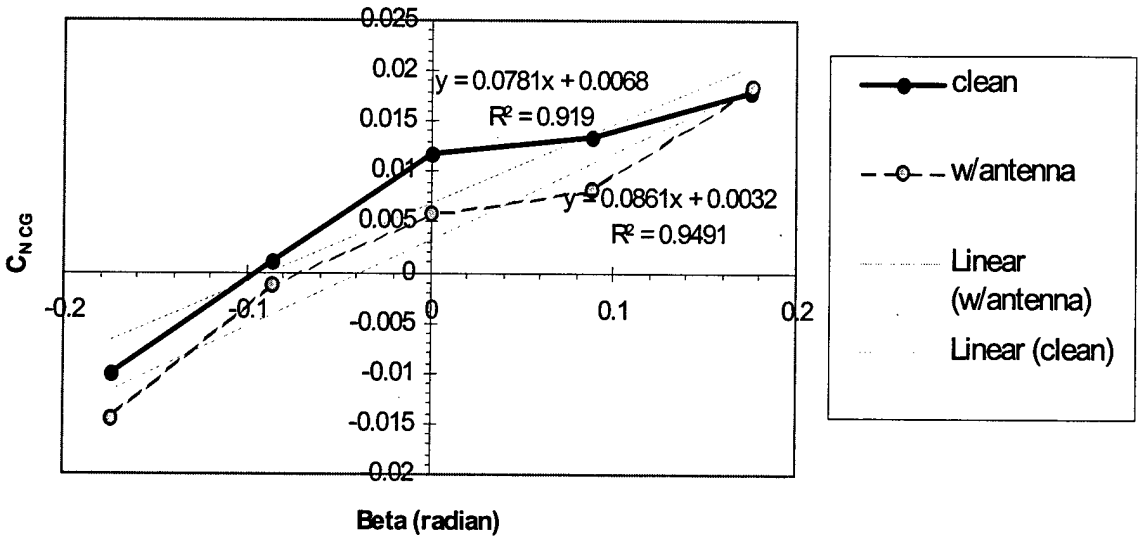

Figure 5.3.4: $C_{L\,CG}$ vs Beta

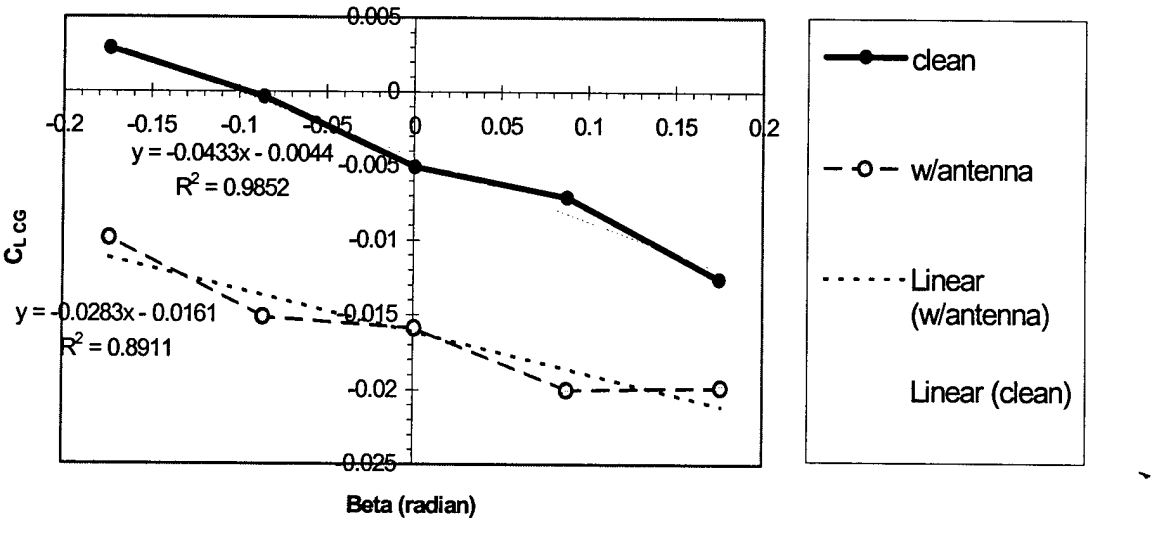

5.4. Weight and Balance Worksheet

Weight and Balance

The airplane must be properly loaded in order to ensure proper handling qualities. The chart below shows the CG envelope for the aircraft. CG locations are measured in %MAC. Aft CG's are limited by the pitch stability of the aircraft, the absolute aft limit would provide neutral stability and the suggested aft limit would provide a static margin of 5%[9]. The forward limit is limited by the elevator's ability to trim for take off C_L. The max gross weight is limited by C_{Lmax} of the airplane and the take off velocity. Extra room in the battery bays allow for the aircraft CG to be adjusted by shifting the batteries.

Figure 5.4.1: Weight and Balance Chart

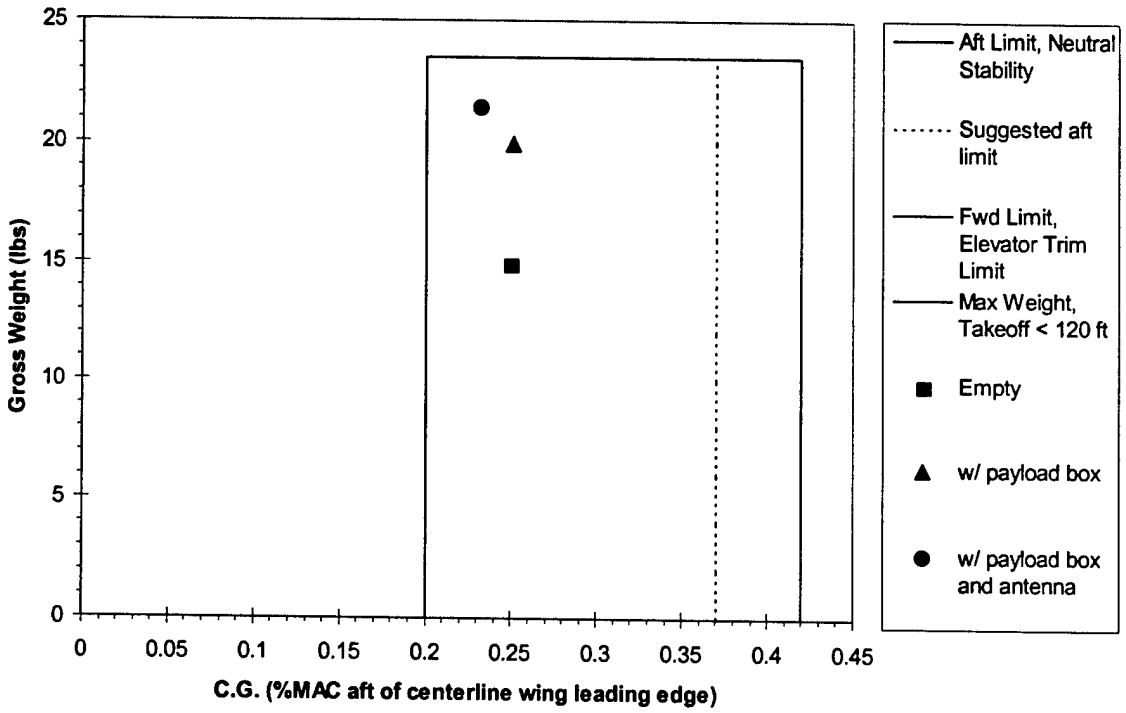

5.5. Structures

Wing Design

The WU Flyer employs a multi-piece wing spar consisting of the center section, left wing, and right wing. During spar design many aspects were taken into account: ease of building, ability to assemble spar sections quickly, and of course weight. The spar of the aircraft must be designed in such a way that it can easily be assembled. Since we are sliding the left and right wing spars onto the center section, we require that the spar slides on easily. Since we are limited in height by the maximum thickness of the wing, and the best way to ensure ease of assembly is to use a large cross section. Spar height at the root will be the height of the wing. The spar will continue as a constant cross section for the first 11", this

length was determined since we want to significantly overlap the wing spar with the center section spar to easily transfer loads between the two. If we make a wing spar center section of 22" it will fit inside the box as one piece, this allows 11" of spar per wing side actual wing overlap will be 4 inches since wings will be placed as close to the fuselage as possible.

To determine the thickness of the spar material we must look into the loads that are acting on the wing. Two load sets were considered for design. The first load set on the wing are caused by the lift distribution, drag on the wing, and the pitching moment. Utilizing equations from *Introduction to Aerospace Structural Analysis*[2] by D. H. Allen, aerodynamic coefficients for the wing, aircraft velocity, wing taper, and air density equations were developed for wing shear loadings and wing moments. For structural analysis a coordinate system was defined where the x-axis runs from fuselage center along the wing centerline (beam axis). The y-axis is in the lift direction and the z-axis runs parallel and opposite drag. We will also assume that we are flying at sea level since areas of low altitude are associated with higher density resulting in larger air loads. Utilizing boundary conditions that all loads and moments are zero at the tip and resolving all loads through the centroid of the spar we develop equations for shear created by lift and drag as well as moments created by lift, drag and pitching moment for a 6.5 g case with a 1.5 factor of safety. To determine loads created by the second case the wing was analyzed as a half weight load at the tip and fixed at the opposite end where the fuselage is attached.

Table 5.5.1: Force/Moment Equations

Force/Moment	Equation
Vy(lb) flight	$0.009x^2-2.74x+107.26$
Vz(lb) flight	$-0.001x^2+0.33x-12.82$
Mx (lb-in) flight	$-0.00035x^3-0.16x^2+24.50x-822.94$
My (lb-in) flight	$-0.00036x^3+0.16x^2-12.82x+277.53$
Mz (lb-in) flight	$-0.00298x^3+1.37x^2-107.26x+2321.86$
Vy (lb) static	11
Mz (lb-in) static	-506+11x

If we further our assumptions to include a homogenous advanced beam at a constant temperature we can determine the bending stress created by the complex loading.

$$\sigma_{xx} := -\frac{M_z}{I_{zz}} \cdot y + \frac{M_y}{I_{yy}} \cdot z$$

We can then analyze multiple span locations along the top and bottom of the spar where the stresses will be the highest to define the bending stress in the spar. Since we now have defined loads and a method for calculating stress we can optimize the thickness of the spar walls to help reduce weight.

Skin thickness was designed to handle the largest shear load. For this analysis the wing was split into two cells one forward and one behind the spar. Utilizing shear flow methods found in Introduction to Aerospace Structural Analysis shear flows, shear stress, and angle of rotation were calculated.

Table 5.5.2: Wing Shear Flow Properties		
Property	**Fwd. Cell**	**Aft Cell**
Shear Flow (lb/in)	26.14	36.7
Shear Stress (psi)	4753.72	6679.05
Angle of Rotation per Unit Length (rad/in)	0.0021	0.0021

Uni-directional fiber spar caps were utilized to handle bending loads. The minimum material required for the spar is determined so that the stress seen in the wing is near the upper limit of material strength. This method will make each cross-section out of the least amount of material as possible. Final stresses are shown in the following bending stress diagram.

Figure 5.5.1: Bending Stress vs Span Location

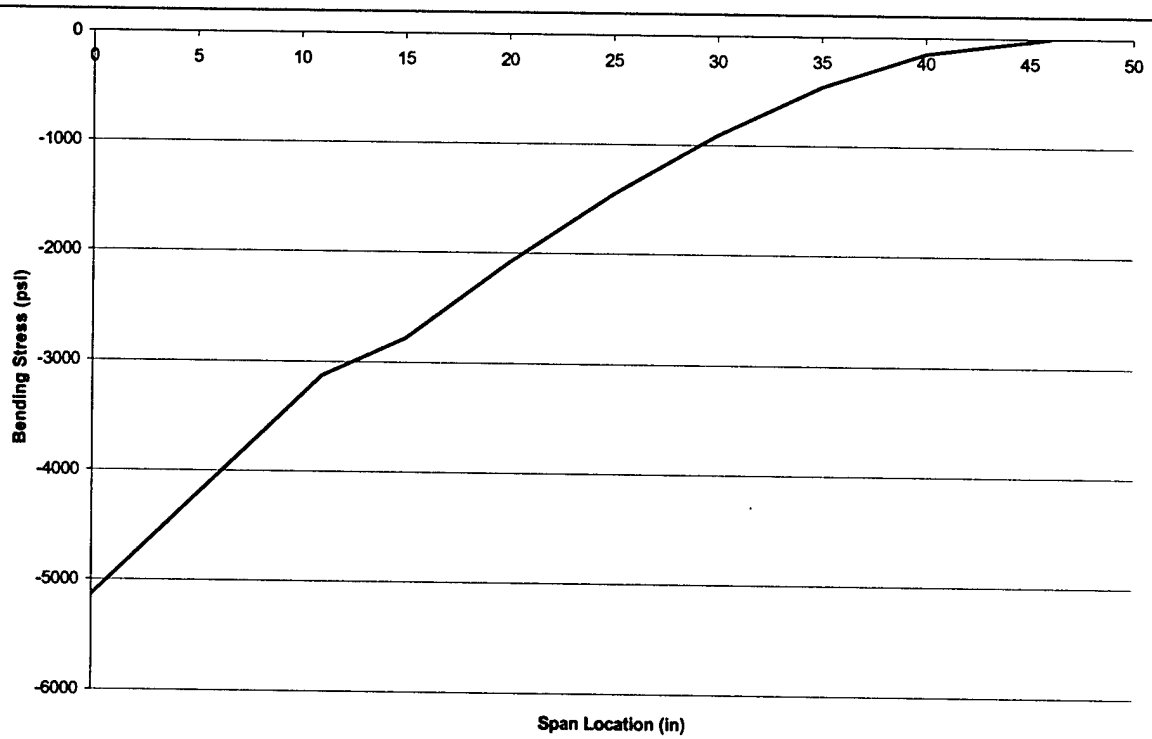

Since our wing cross-section changes from the root to tip, spar taper is required. To define taper a few key aspects were used. First we looked at the ability to build the spar once designed. Since our spar is a hollow square cross-section made from carbon fiber we must have a mold that is easy to build parts on. It was determined that a rectangular cross-section 3/4 inch by 3/4 inch is the minimum size that we can easily manufacture. The upper size of the tip cross-section is defined by the tip airfoil profile, which is 1.26 inches tall. We also considered the magnitude of taper on the cross-section. If it is too drastic we

may not be able to produce a high quality carbon part. For these reasons the wing spar tapers from 1.6 inches by 1 inch to 1.26 inches by 1 inch.

The wing center section spar sleeve will match into the wing spar, this means that it too will be the entire height of the wing and one inch in width. Calculations were also done to determine the minimum thickness of the sidewalls. It has been determined that 6 plies of the 3k carbon cloth will be adequate to take both maximum bending due to lift and drag as well as the shear loads. Spar center sleeve section properties can be seen in the table listed below.

Table 5.5.3: Spar Sleeve Properties

Material Property	Value
Ixx(in^4)	0.122
Izz(in^4)	0.087
Width (in)	1
Length (in)	22
Height (in)	1.6
Thickness (in)	0.022

To complete wing structure design is a method to transfer loads from the wing skin to the spar. The spar is designed to carry all bending loads and the wing skin can handle shear loads as determined by shear flow analysis. Based on these two assumptions two basic methods were evaluated. The primary goals of the ribbing structure is to hold aerodynamic shape of the wing and to transfer loads from the skin to the spar. The first structure analyzed was a wing filled with foam. Since the spar can handle the aerodynamic loads, lightweight foam can be used in the wing. This method will have an effect of infinite number of ribs from root to tip and airfoil shape will easily be maintained. The weight for foam cores for the wing using foam with a density of 0.75 pounds per cubic foot will weigh an approximate 0.375 lbs for both wings. The second method analyzed was the use of ribs. Since maximum deflection of the wing is determined to near 1" total under maximum loads, skin buckling will not be an issue therefore the ribs will be utilized to preserve aerodynamic shape. A final spacing of 5" was determined utilizing average scaled rib spacing numbers from general aviation aircraft. Based on this analysis we have chosen to go with a conventional wing building approach with ribs. By choosing a conventional wing structure we can minimize the weight of the wing as much as possible and still maintain the aerodynamic profile of the wing.

Fuselage

The fuselage design for this year is a complex shape. In order to reduce part count and weight it was decided to build the fuselage in as few pieces as possible. Since carbon fiber has high strength and is easily formed around complex molds, we have chosen to build the fuselage out of 3k cloth +/- 45° orientation. This orientation on the cloth will give a minimum strength of 8.3ksi. Maximum loads for the fuselage section are seen in the sidewalls of the fuselage during landing and the top of the fuselage

where the wing center section is attached during flight. Landing gear is assumed to translate the landing loads that the fuselage sees as bending and vertical loads. Wooden blocks were placed near the top and bottom of the payload bay to handle the bending loads seen in payload bay walls during landing. When the assumption is made that the upper leg of the landing gear is stiff and no bending or deformation will occur, the bending loads seen in the fuselage will be maximum. Lifting loads are carried by two horizontal oak pins and two vertical nylon bolts. The bolts and nut plate padding in the fuselage are designed to handle the pitching moment created by the wing at maximum flaperon deflection at cruise velocity in a 6g load scenario. The nut plates are backed with additional layers of carbon cloth to reduce possibility of tear out and nylon bolts were tested in tension to determine ultimate tensile strength.

Landing Gear

Each main gear will be a separate piece made of uni-directional carbon fiber with an outer carbon fiber skin cloth. The main gear strut leg will be 2 inches in width and have a thickness of 0.25 inches at the body-gear strut interface. The main landing gear will then fit into a sleeve, similar to the wing spar sleeve. With the fuselage skin made up of a +/-45° cloth orientation for a 3k cloth, the fuselage will have adequate strength to resist the torsional loads produced. The landing gear was designed for a vertical descent rate of 3.69 feet per second. This is .75 times the power off descent rate at stall. These numbers were backed out of a comparison to light business jet certification rules and drop test velocities. We assumed that all of the landing load would be taken by one main gear. Using kinetic energy formulas under the assumption that all landing energy is absorbed immediately on impact with ground, landing loads are equated to 57.6 in*lb. Utilizing a calculated spring constant of 31.15 lb/in for the landing gear strut we calculated a maximum deflection in the main gear of 1.92 inches. The maximum vertical load calculated in the landing gear system is 59.9 lbs and the compressive load on the strut is determined to be 33.8 lbs for this loading case.

5.6. Rated Aircraft Cost Worksheet

The following table shows the breakdown of Rated Aircraft Cost, and the figure following shows the breakdown in percentages. The required aircraft parameters are multiplied by their rates and formulae, as designated in the DBF Rules[23]. These are summed up as necessary to calculate the Manufacturer's Empty Weight, Rated Engine Power, and Manufacturing Man Hours, as shown in bold text in the table. These three values were then inserted into the final Rated Aircraft Cost formula. The final column in the table lists the contribution of each component to the final RAC score.

Table 5.6.1: Rated Aircraft Cost Worksheet

Manufacturer's Empty Weight			**Total MEW =**	**15.00 lb**	**11.75%**
Aircraft Empty Weight	15.00 lb		=	15.00 lb	11.75%
Rated Engine Power			**Total REP =**	**5.00 lb**	**58.76%**
No. of Engines	1				
Total Battery Weight	5.00 lb				
(1+0.25*(#eng-1))*batt_wt			=	5.00	58.76%
Manufacturing Man Hours			**Total MFHR =**	**188.2 hr**	**29.49%**
WBS 1.0 Wings					
Wing Span	7.67 ft	x	8 hr/ft =	61.3 hr	9.61%
Max Exposed Wing Chord	0.85 ft	x	8 hr/ft =	6.8 hr	1.06%
No. Control Surfaces	2	x	3 hr/surf =	6.0 hr	0.94%
WBS 2.0 Fuselage					
Body Maximum Length	3.91 ft	x	10 hr/ft =	39.1 hr	6.12%
WBS 3.0 Empennage					
No. Vertical Surfaces, inactive	0	x	5 hr/surf =	0.0 hr	0.00%
No. Vertical Surfaces, active	2	x	10 hr/surf =	20.0 hr	3.13%
No. Horizontal Surfaces	1	x	10 hr/surf =	10.0 hr	1.57%
WBS 4.0 Flight Systems					
No. Servo's and Motor Controllers	7	x	5 hr/item =	35.0 hr	5.48%
WBS 5.0 Propulsion Systems					
No. Engines	1	x	5 hr/item =	5.0 hr	0.78%
No. Propellers or Fans	1	x	5 hr/item =	5.0 hr	0.78%
Rated Aircraft Cost					
Manufacturer's Empty Weight	15.0 lb	x	$100 /lb =	$1,500	11.75%
Rated Engine Power	5.0 lb	x	$1,500 /lb =	$7,500	58.76%
Manufacturing Man Hours	188.2 hr	x	$20 /hr =	$3,764	29.49%
			Sub-total =	$12,765	100.00%
			Total RAC =	**12.76 k$**	**100.00%**

Figure 5.6.1: Contributions to Rated Aircraft Cost

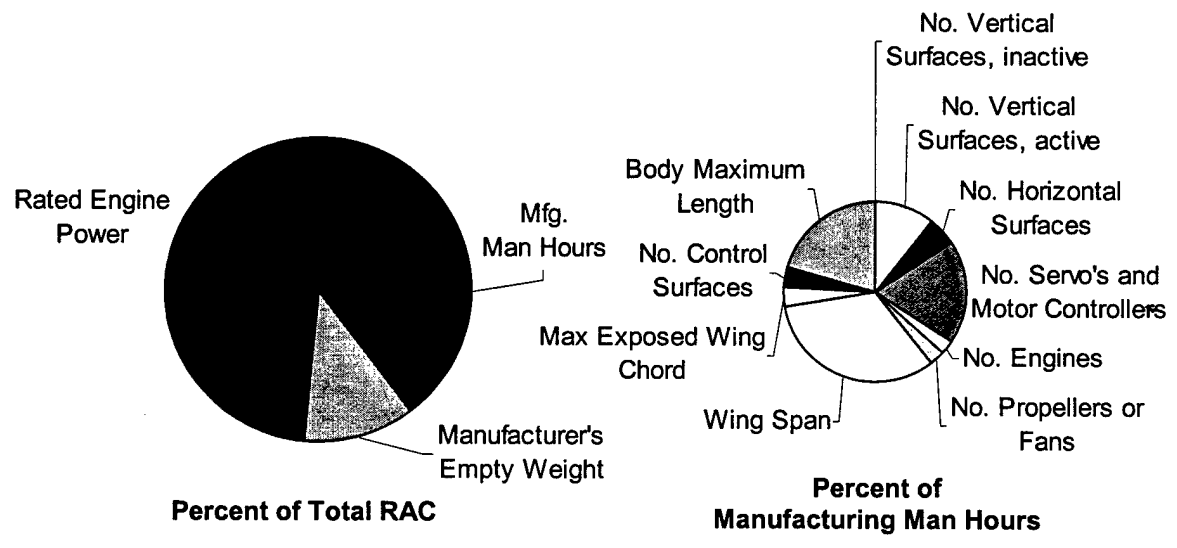

In the preceding figure, two pie charts are shown. The larger chart, on the left, gives the breakdown in terms of the three major RAC categories: Rated Engine Power, Manufacturer's Empty Weight, and Manufacturing Man Hours. The smaller chart on the right gives the breakdown of the Manufacturing Man Hours. Calculations show that the contribution of Rated Engine Power is significant. The equation given for accounting for multiple engines yields unity for single-engine aircraft. Therefore, the weights of the propulsion batteries become the single most significant factor in overall RAC. In this case, it is nearly 60%. In the design process for this aircraft, concern was originally manifested about reducing the number of servos in order to minimize Rated Aircraft Cost. However, when it was realized that the contribution of propulsion battery weight was an order of magnitude higher, the concern about the number of servos diminished.

5.7. Drawing Package

The following pages provide a computer aided drawings (CAD) package of the WU Flyer including:

1.) Exterior Three-View With Basic Dimensions
2.) Side View Detailed
3.) Top View Detailed
4.) Antenna Mounting System
5.) Microsoft Excel Isometric Views

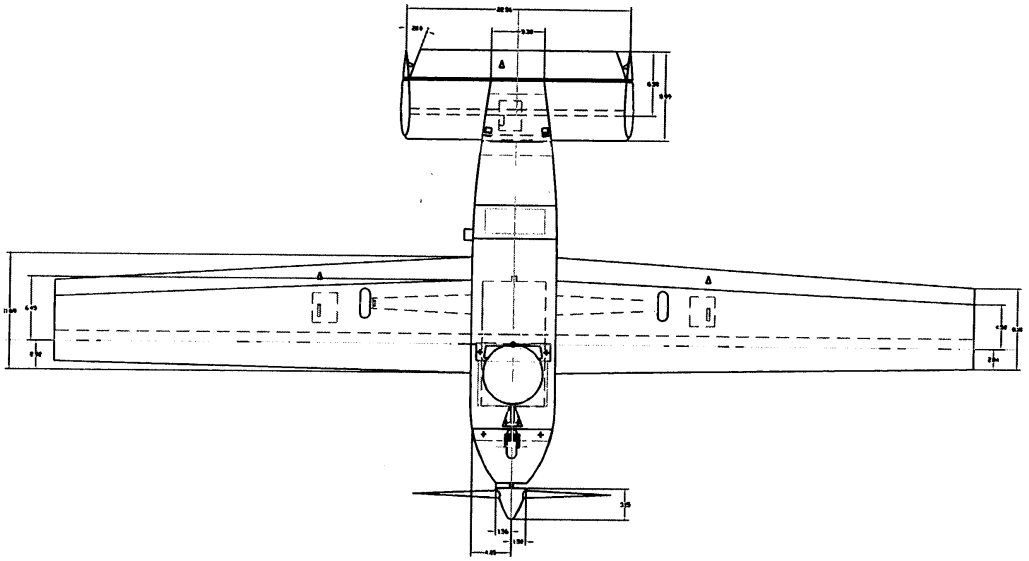

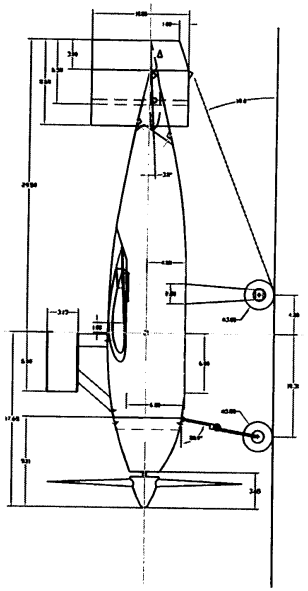

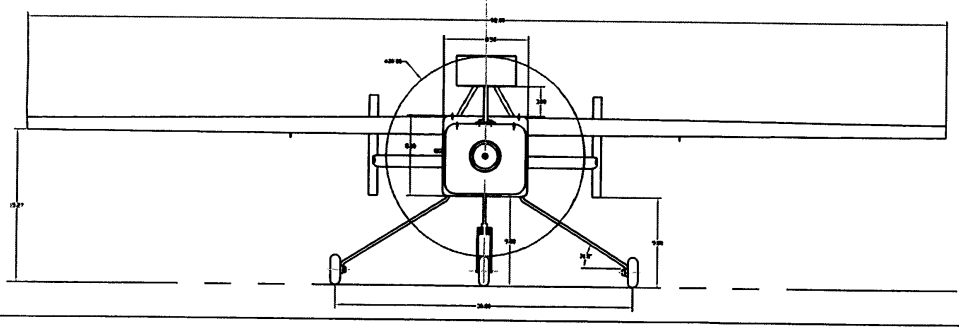

WSU DBF 2003 WU FLYER

BASIC ASSEMBLY 3-VIEW

SIZE	DRAWN	DWG NO.	REV
B	JPK	0001	–
SCALE NTS	DATE 03-08-03	SHEET 1 OF 5	

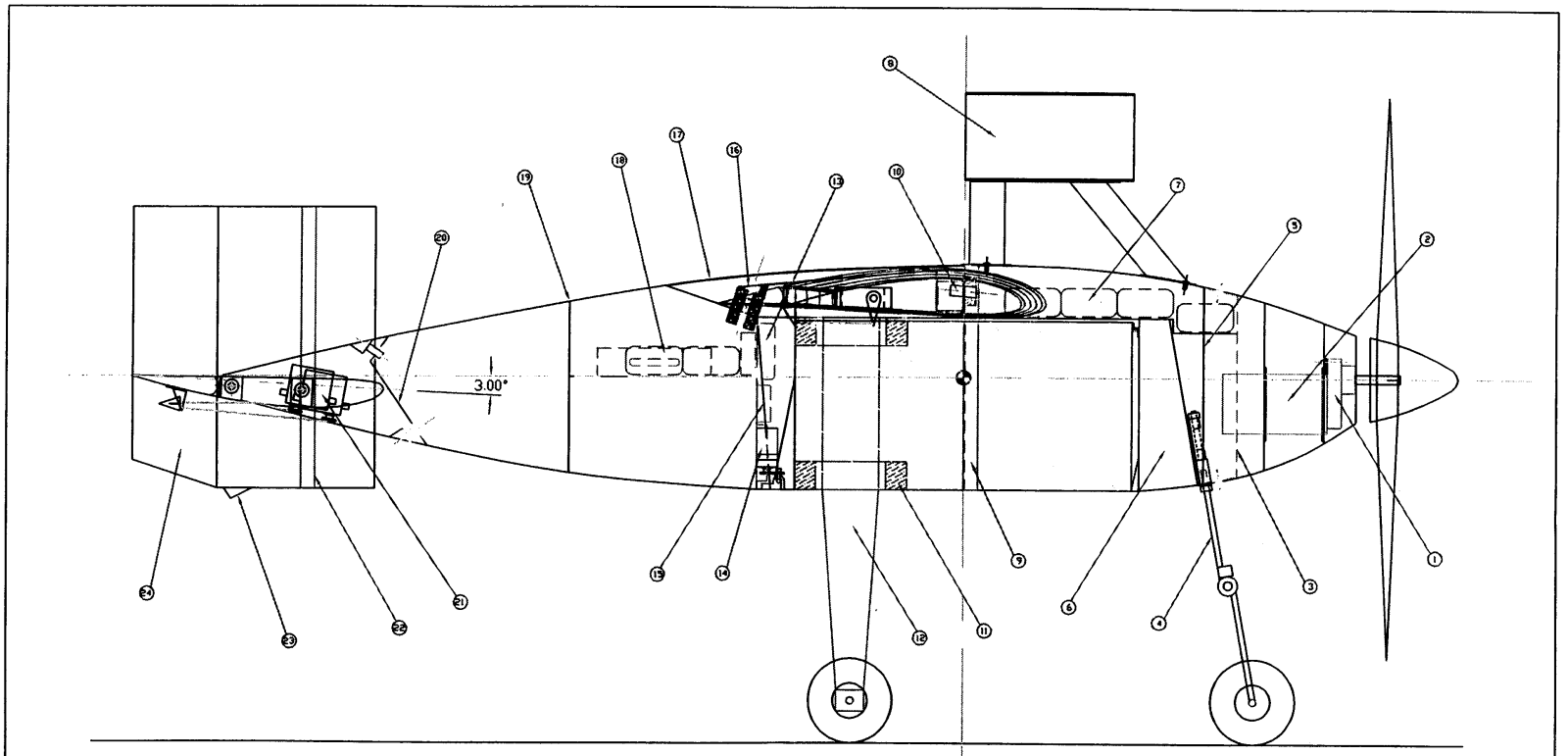

1	MOTOR GEAR REDUCTION	9	PAYLOAD BAY	17	CENTER SECT. FAIRING
2	ASTRO 90 MOTOR	10	FWD WING PITCH PIN	18	FUSE HOLDER & FUSE
3	NOSE CONE FLANGE	11	GEAR SUPPORT BLOCK	19	MAIN TAILCONE BLKHD
4	NOSE GEAR STRUT	12	MAIN GEAR STRUT	20	TAIL DETACH BLKHD
5	NOSE CONE DETACH	13	RECEIVER BATTERY	21	RUDDER/ELEV SERVOS
6	CRASH ABSORB BLOCK	14	RADIO RECEIVER	22	VERTICAL TAIL SPAR
7	7 CELL BATTERY PACK	15	PITCH GYRO	24	TAIL SKID PAD
8	CYLINDRICAL ANTENNA	16	AFT PITCH PIN	23	RUDDER

WSU DBF 2003 WU FLYER

DETAILED SIDE VIEW

SIZE	DRAWN	DWG NO.	REV
B	JPK	2003-8-0002	–
SCALE NTS	DATE 03-08-03	SHEET 2 OF 5	

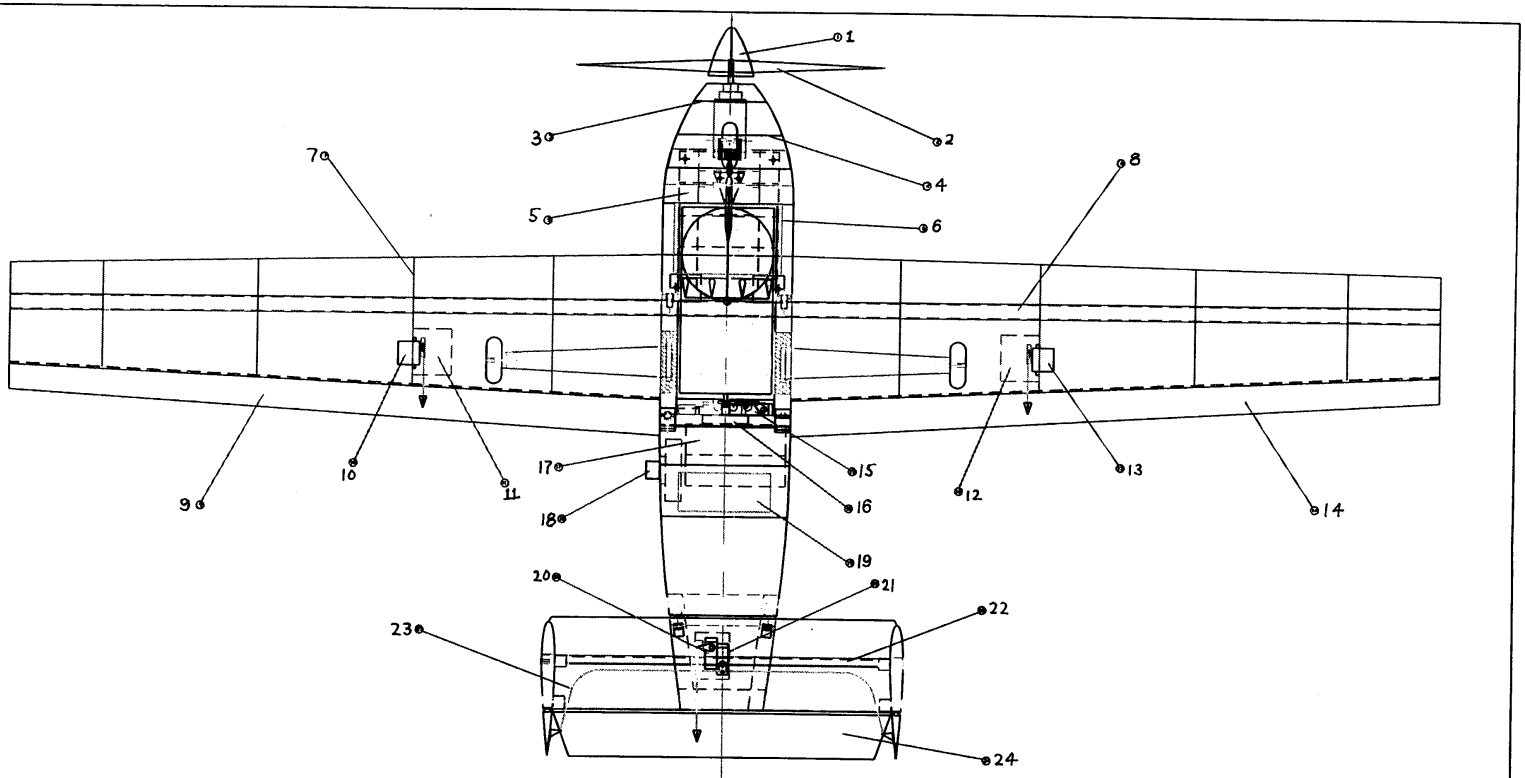

1	SPINNER	9	L FLAPERON	17	REAR BATTERY PACKS
2	PROPELLER	10	L FLAPERON SERVO	18	FUSE
3	FWD MOTOR MOUNT	11	L SERVO ACCESS PNL	19	BATT ACCESS PANEL
4	AFT MOTOR MOUNT	12	R SERVO ACCESS PNL	20	ELEVATOR SERVO
5	FWD BATTERY BAY	13	R FLAPERON SERVO	21	RUDDER SERVO
6	BATT ACCESS PANEL	14	R FLAPERON	22	HORIZ TAIL SPAR
7	WING RIBS	15	PAYLOAD DROP SERVO	23	RUDDER CONTROL ROD
8	WING SPAR	16	SPEED CONTROLLER	24	ELEVATOR

WSU DBF 2003 WU FLYER

DETAILED SIDE VIEW

SIZE	DRAWN	DWG NO.	REV
B	JPK	0003	–
SCALE NTS	DATE 03-08-03	SHEET 3 OF 5	

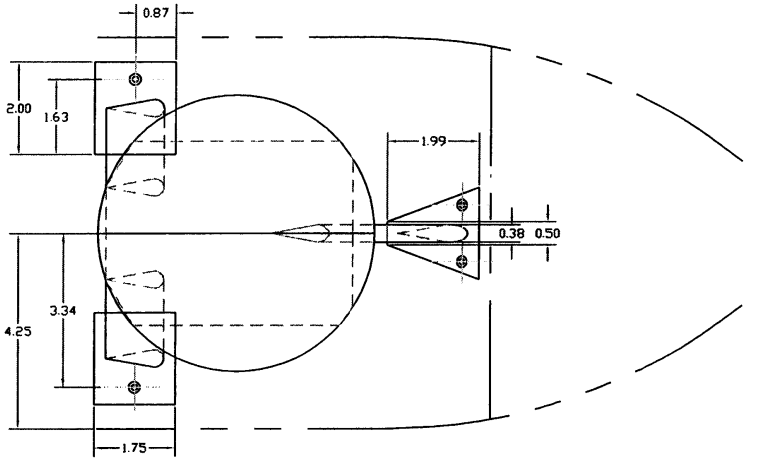

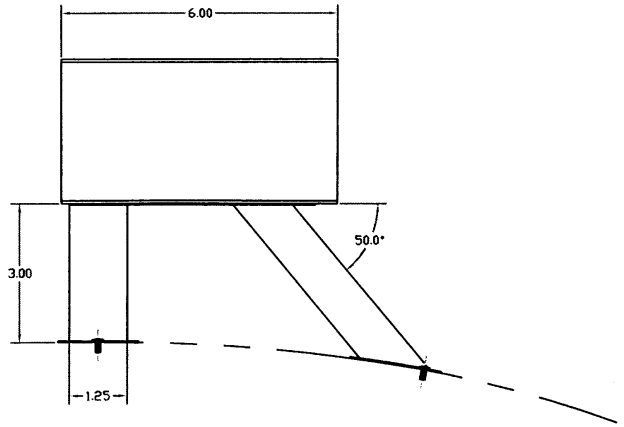

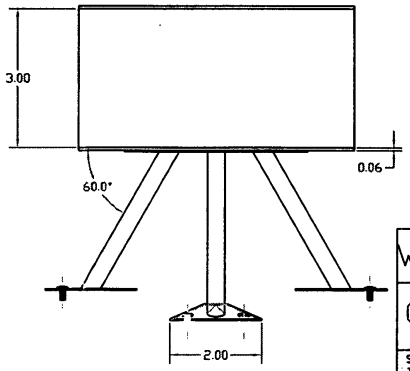

WSU DBF 2003 WU FLYER

CYLINDRICAL ANTENNA INST.

SIZE	DRAWN	DWG NO.	REV
B	JPK	0004	–

SCALE	DATE	SHEET
NTS	03-08-03	4 OF 5

Top View

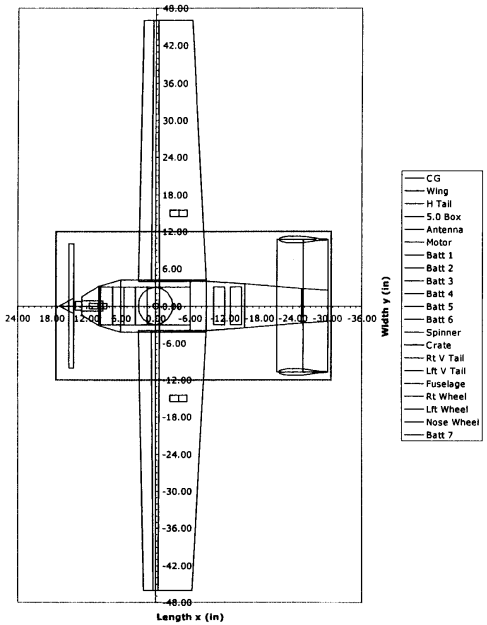

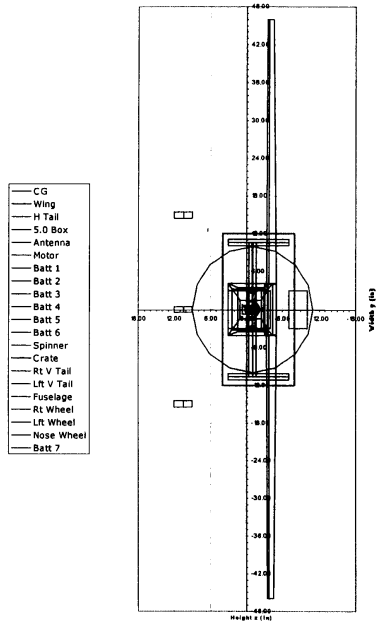

Front View

Side View

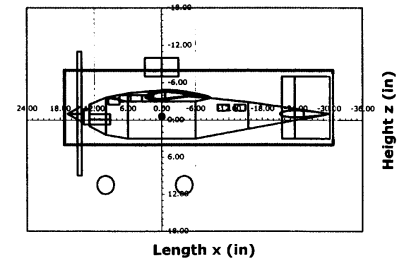

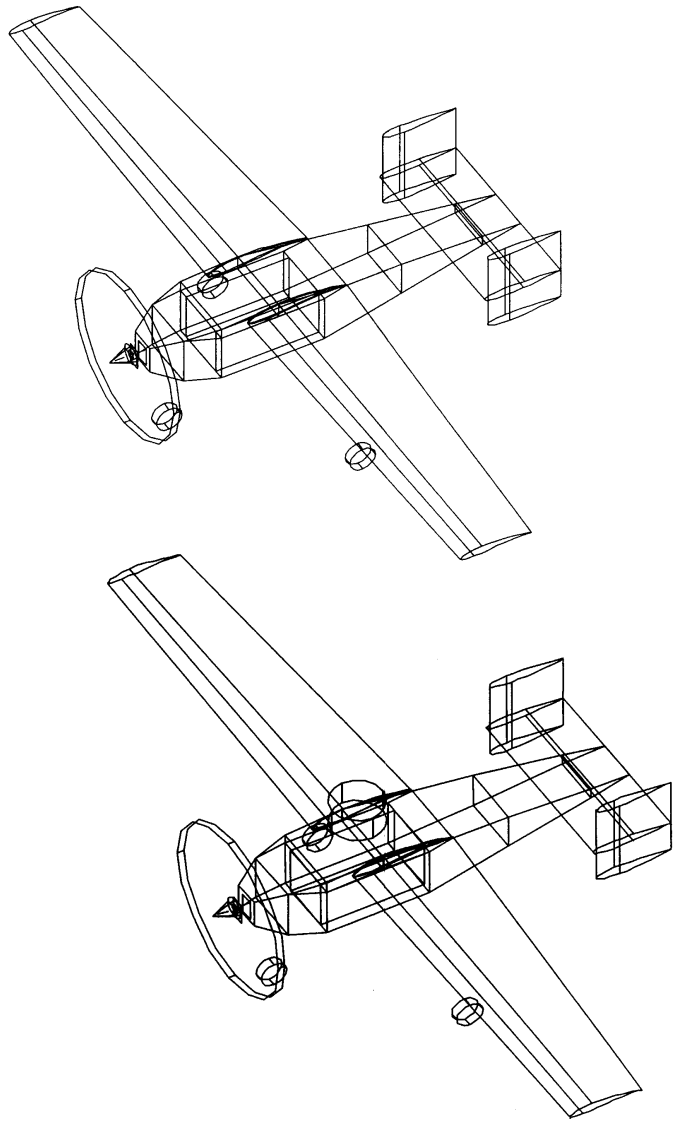

6. MANUFACTURING PLAN AND PROCESSES

6.1. Manufacturing Processes Investigated and Figures of Merit

General Description

Sharing a close tie to structural design, manufacturing design held an important place in the design process from the beginning of the design effort. Several key construction concepts were considered and screened based on a combined criterion of aircraft weight, manufacturing methods availability, and aerodynamic implications. These figures of merit eventually led to the structural design described earlier in the report.

From the beginning of the project, three primary construction methods were given a significant amount of attention. These three methods of construction were a skeletal wood structure with Monokote covering, a plywood based semi-monocoque construction, or composite semi-monocoque structure.

Skeletal structures with a Monokote skin are often the lightest structures possible at the model scale. The physical size of parts and the low loads applied to them in flight make conventional materials undesirable. An aluminum aircraft at model scale would be made of aluminum so thin that it would be dangerous to work with due to sharp edges. Composites, although less dense than metals, are still much heavier than necessary for most loads. Balsa or spruce wood though, assembled in trusses can be made exceedingly light, and Monokote is much less weight per square foot of coverage area than composites or plywood. Truss construction is the simplest method considered, cutting small simple parts and gluing them together. Lightweight wood structures though suffer several key difficulties. They are made of a huge number of small parts. Glue cure cycles for sequential construction consume large amounts of time. This becomes an issue in both construction and damage repair. External aerodynamic contours also suffer from faceting.

Wood-based semi-monocoque construction is a step between truss frame mono-cote structures and composite methods. This method avoids the aerodynamic faceting problem, but there is a large weight gain, relatively comparable to composite construction. The main difficulty with the method is in complex contours. Although fairings are generally better than with truss and Monokote, compound curves and tight radiuses are very difficult to make.

The final method, composite construction suffers some weight penalty, but it offers strong advantages in external shape and parts count. Tight leading edge radiuses are easy to make, and compound curves are possible without faceting. Carbon fiber is three times the density of wood, but it can be obtained a third as thick, so the weight trade is negligible compared with a wood sheeted structure.

The advantages of composite construction over plywood make composites a clear leader. The decision then becomes a choice between composites and Monokote covered wood truss structures. The team decided that the benefits in aerodynamic contour and composite damage tolerance outweighed the investment in tooling and weight gain. In addition, many of the aircraft's primary loads are concentrated in localized areas, making composites more desirable than low density wood construction. For these reasons, the aircraft is carbon fiber with a stressed outer skin and internal frames and ribs to prevent buckling. Foam cores were considered to improve damage tolerance but were not used in most areas due to the weight the foam adds.

6.2. Manufacture of Major Components and Assemblies

Wings

The aircraft's wing skins were laid up on aluminum male molds machined by the Wichita State University experimental research machine shop. Carbon fiber ribs were vacuum bagged over forms. The main wing spar was laid up as a pair of C-channels over a form. Uni-directional carbon fiber spar caps were bonded into one C-channel, and a second was used to close the cross section of the spar, making it a closed box to resist torsion. These parts were prepared with sandpaper and post-cure bonded to form a closed D-tube forward wing structure. The trailing edge was closed out by a balsa strip used to mount flaperon hinges. The wing center section spar was laid-up in a female mold machined on campus. The spar was bonded to a foam core structure used to restrain the wing in pitch.

Refinements for construction of the serial number 2 aircraft (SN 2) will include the use of a caul, a female mold with no structural reinforcement. The wing skins will be laid up between the aluminum plugs and the caul, ensuring a good interior and exterior surface finish.

Fuselage

For fuselage skins, plug was built to mimic the external contours, and skins were pulled directly from the surface of the tool. Internal bulkheads were laid-up in place. Wax-paper covered cardboard backings were taped in position, and the layups made against them. Following cure, the cardboard is removed leaving a carbon fiber frame.

To improve the skins for the SN 2 aircraft, we will likely make female molds for the second fuselage. Time constraints prevented the construction of female molds for the original aircraft.

Empennage

The empennage was laid up wet over foam cores. C-channel carbon spars carried the tail's bending loads. The vertical tails were skinned with very thin fiberglass while the horizontal tail used light carbon

fiber cloth. 1/32 inch plywood was used to reinforce hard points for removal of the vertical tails from the horizontal.

Gear

Each main gear strut is made with a prepared core and a single carbon fiber lay-up. The carbon fiber structure uses uni-tape on either side of the core material for bending strength and spring stiffness. These caps are encircled with a layer of carbon cloth to prevent splitting, torsional failure, and abrasion damage.

6.3. Manufacturing Milestones

Figure 6.3.1. shows key manufacturing milestones and scheduled event timings. The upper of each pair of bars shows the original scheduling for that item. The lower shows the actual scheduling. Note that this chart shows the completion of each item to a readiness for wind tunnel testing only, which commenced immediately after final assembly. At the time of writing, the fuselage and the landing gear both had further work before being ready for flight testing.

Figure 3.6.1: Manufacturing Milestones and Scheduled Event Times

		Fuselage	Wing	Tails	Gear	Testing
January	Thurs 23					
	Fri 24	Plug	Plugs			Windtunnel Mount
	Sat 25			Plugs		
	Sun 26					
	Mon 27	Forms	Forms	Forms	Forms	
	Tues 28					
	Wed 29	Skins, Blkds	Skins, Ribs, Spars	Skins, Ribs, Spars	Struts	
	Thurs 30					
	Fri 31		Assemble Structure			
February	Sat 1					
	Sun 2	Assemble Structure		Assemble Structure		
	Mon 3					
	Tues 4					
	Wed 5		Controls	Controls	Wheels, Locks	
	Thurs 6					
	Fri 7					
	Sat 8					
	Sun 9	Hardware and Power	Servo Install	Servo Install		Final Test Plan
	Mon 10					
	Tues 11					
	Wed 12		Locks			
	Thurs 13	Servo Install				
	Fri 14					
	Sat 15					
	Sun 16					
	Mon 17	7 x 10 Test				
	Tues 18	"				
	Wed 19	"				
	Thurs 20	"				
	Fri 21	"				
	Sat 22					

7. Testing

Safety in flight and in our wind tunnel test phase dictated a need for certain tests. Structural tests verify the integrity of our vehicle while wind tunnel and propulsion tests allow us to better predict performance and control characteristics. Aircraft testing is not yet complete, but the following tests have been conducted to date.

Spar Testing

The spar consists of two half spars which are joined to the fuselage by a shorter center spar that remains in the fuselage. Before each half spar was assembled into the wing structure and the center spar into the fuselage, they were tested to ensure they could withstand a 6g limit load. Each half spar was slipped onto a center spar mandrel, which was secured to a table with clamps. The half spar hung off the edge of the table as a cantilever beam. The spar was loaded at half span with 67 lbs, equivalent to a 6g load. Both half spar supported the load successfully. The center spar was tested by clamping half the spar to the table and loading the other half hanging over the edge. The spar was loaded similarly, but because of its short length, it could not be loaded to the full 6g limit load before shear load failure. Analysis and examination of the center section though showed that the spar caps were correctly placed and that the strength of the materials already verified in the outer spar sections would be more than strong enough to sustain limit loads.

Landing Gear Testing

The landing gear is a complex structure, consisting of two struts that are inserted into the fuselage sidewalls, which must resist compound loads, making the landing gear tests critical. The landing gear testing was divided into two tests to minimize loading the fuselage. First the struts were clamped to a table leg and loaded as a cantilever beam to a simulated 4g load on a single strut landing. After completing this test successfully, the struts will be attached to the fuselage and the entire assembly will be dropped from a height to simulate a 6g load spread between both struts. To date, three landing gear struts have been tested. The first was made of 2 lb foam core laminated with structural carbon fiber. This strut failed at the gear's upper corner on the compression side. The second strut was then made with a corkboard core rather than foam, but failed from the same buckling mode as the core material was crushed by compression loads. The third and current design uses laminated 1/32" plywood to form a pre-bent wood core for the carbon structural material. The harder core material prevented failure up to half the design failure load. The gear has not been tested to higher loads yet because completion for first flight is a critical concern right now. We hope to have a third strut soon to take to failure for comparison with our design numbers. Gear design was rather conservative though, so a half-design load would be equivalent to conducting the gear drop test with both struts rather than just one side as in the design case. An aircraft drop test was planned initially, but static loadings way be used instead. We believe our

design landing load case was very conservative, so we don't plan to take the aircraft near failure loads before first flight.

Nylon Bolt Tension Tests

Quarter inch nylon bolts are being used to secure the wing. In this test the bolts were loaded in tension to failure. The nylon bolt was inserted through a hole in a board clamped to a table. A wood block was threaded to the bottom of the bolt under the board, and weights were hung from the block. The bolt was then loaded in 1lb increments until the bolt failed. The bolt failed at a tensile load of 160lbs. This single bolt held more than 7 times the weight of the aircraft, so we are not worried about premature failure using these bolts to restrain our wing.

2.5g Wingtip Lift Test

Competition rules state that the structural integrity of all entries will be tested through with a roughly 2.5g load case. This structural verification consists of the aircraft being completely supported by one point on each wingtip. After manufacturing and assembly was complete, WU Flyer was successfully supported by the wingtips.

Payload Drop Mockup

To ensure the payload drop mechanisms, a mockup was built. The mockup was made of foam boards simulating the cargo bay. The servos, rails, and other components in the cargo bay were located in the mockup. The mockup was then supported on each side tables and the servo was activated. The payload was consistently deployed from the mockup with no binding.

Thrust Test

Static tests were performed on a workbench to break-in the motor and condition the batteries. The engine was mounted into the fuselage, set on dowels to serve as bearings. The empennage was tied by rope to a scale that was secured to the table on its side, to measure the horizontal force. An AstroFlight Whattmeter was used to measure current and voltage drawn while a strobe light was used to measure propeller RPM. The tests showed that the propulsion system is not performing even within an order of magnitude of what is required for takeoff.

Troubleshooting in the propulsion system is the next step here. Individual battery packs are in testing with a small motor now. A motor that runs on 7 cells is strapped vertically to a food scale ballasted to 5lb. The difference in lift is measured as the difference from 5lb on the scale. Initial comparisons to borrowed packs that we obtained indicate that the batteries are probably not our main problem. The bulk of data reduction is just beginning though, so detailed data is not ready for publication. Following battery check-out, motor tuning and speed control health will be our next concerns. Wiring might be an issue as well,

but the fact that the power system operates at all indicates that we do have a complete circuit, and the lack of melted connectors suggests reasonable connections have been made.

It is hoped that we will be able to resume thrust testing later using the 3 by 4 foot wind tunnel on campus to get both static and flight condition thrust data.

Wind tunnel testing

Cylindrical Antenna in the 3 by 4 foot Tunnel

Wind tunnel tests were conducted on the cylindrical antenna to determine the aerodynamic forces and moments acting on it. The antenna was attached to the test mount using the screws for the airplane mount. The wind tunnel was run 20, 40, and 60 mph. For each speed, the antenna was swept through angle-of-attacks from -5° to 20° in 5° increments. The data from the 20 mph run, Re 104,000, proved unreliable. The drag coefficient from the 40 mph run—approximately take off condition Re 208,000—was about 3. At 60 mph—about cruise speed 312,000—the drag coefficient dropped to about 0.6. This verified research that the cylinder was near critical Reynolds numbers.

Aircraft 7 ft X 10 ft Wind Tunnel Test

The completed airplane was tested in WSU's 7' X 10' wind tunnel to verify aerodynamic numbers, stability coefficients, and control effectiveness. The airplane was mounted to the tunnel's external balance on a two point harness. The tunnel was run at a dynamic pressure of 9, roughly equivalent to maximum cruise velocity. The test was run at this dynamic pressure to stay within the aircraft's structural capabilities while maximizing the forces generated on the balance to increase accuracy in our data. The balance was designed for large metal models that are run fast, so data resolution is not very good at low speeds. The first series of runs were conducted without the antenna. Alpha sweeps generated lift curves and drag polars. Psi sweeps provided yaw stiffness data. Following collection of basic clean configuration data, the aircraft radio was used to control flap, elevator, rudder, and aileron deflections for control authority verification. Runs with the external antenna provided data for comparison with the clean configuration and numbers for updated mission performance calculations.

Force data indicated that our lift predictions were very close to actual. Drag estimates were too optimistic, but there were several features on the model and mounting system that may have made the readings artificially high. Analysis of all the stability and control coefficients is nearly complete, but not ready for any sort of publication. The numbers indicate that the design is trimmable in the cruise range though.

Flow visualization tufts indicated good flow behavior on the aircraft. The wing stall was gradual and symmetric with an inboard wing stall initially, slowly moving outboard to the wingtips. Tufts on the fuselage didn't indicate any obvious separated regions despite a hump-back at the point of maximum

thickness caused by last-minute wing incidence adjustments. If there are separation bubbles present, we have not found them. Flow visualization oil would be a more guaranteed way to find such problems, but this method should only be used when there is confidence that no new parts will be bonded to the aircraft because the oil would be difficult to remove and only a clean surface will make a good bond joint.

8. Conclusions

With the notes on the testing conducted to date, the body of the report is complete. By our team assessments, the project is going well. We have kept our major deadlines, we have a finished airframe in ground test, and we have a week and a half before the decision date for the purchase of airline tickets. It is hoped that we will make first flight before that date. Propulsion issues are the only major barriers that remain to delay first flight. We hope to diagnose and solve these problems in the next week.

Following first flight and the go, no-go decision for the purchase of airline tickets for the contest, the team effort will focus on preparation for the fly-off. We will build our second aircraft, and catch up on sleep. The team would like to thank the advisory board: David Aronstien, Dan Walton, Jerry Salter, and Neal Pfeiffer. We appreciate the support of the Raytheon Aircraft Company through Robert Steuver, Corey Hagemeister, and Noel Deurksen. Thanks to Steve Hill of Twisted Composites (Moriarty, New Mexico) for advice concerning production methods and for donating the carbon fiber used to build the airframes. Thanks also to the Aerospace Engineering Department of Wichita State University for their financial and technical support. We look forward to the contest fly-off, and we hope to place well representing our school.

9. References

1. Abbott, Ira H. and Von Doenhoff, Albert E. "Theory of Wing Sections." Dover Publications Inc. 1959.
2. Allen, D.H. and Haisler, W.E., Introduction to Aerospace Structural Analysis, John Wiley & Sons, New York, 1985.
3. Anderson, John D. Jr., Introduction to Flight. 3rd Ed., 1989, McGraw Hill Book Co., New York.
4. "DesignFoil", Version 5.32, The DreeseCode Software Company, 2001.
5. Etkin B. and Reid, L.D., Dynamics of Flight: Stability and Control 3rd ed., John Wiley & Sons, Inc., 1996.
6. Hibbeler, R.C., Mechanics of Materials, Prentice Hall, Upper Saddle River, New Jersey, 1997.Janna.
7. Hoak, D., Ellison, D., et al., "USAF DATCOM," Air Force Flight Dynamics Lab., Wright-Patterson AFB, OH.
8. Hoerner, S., Fluid Dynamic Drag, Published by Author , 1958.
9. Lennon, Andy, R/C Model Aircraft Design, AirAGE Inc., 1996.
10. "LinAir", Version 1.4, Desktop Aeronautics, 1994.
11. "LinAir Pro", Version 3.4, Desktop Aeronautics, 1994.
12. "MATLAB", Version 6, MathWorks Inc., 2000.
13. MatWeb Material Property Data, http://www.matweb.com/ Copyright 1996-2002 Automation Creations.
14. Miley, S.J., "A Catalog of Low Reynolds Number Airfoil Data for Wind Turbine Applications," RFP-3387, UC-60, Department of energy, Feb. 1982.
15. Munson, Young and Okiishi, Fundamentals of Fluid Mechanics, 3rd Ed., John Wiley & Sons, Inc., 1998.
16. Nihon University Aero Student Group Airfoil Data, www.nasg.com/afdb/list-airfoil-e.phtml, Last modified 11/11/00.
17. Raymer, D. P., Aircraft Design: A Conceptual Approach 3rd ed., AIAA, 1999.
18. Roskam, Jan, Airplane Flight Dynamics and Automatic Flight Controls Part I, DARcorporation, 1995.
19. Roskam, Jan, Methods for Estimating Drag Polars of Subsonic Airplanes, University of Kansas, Lawerence, Kansas, 1971.
20. Selig, M., Summary of Low Speed Airfoil Data, Virginia Beach, Va., SoarTech Publications, 1995
21. Simons, M., Model Aircraft Aerodynamics, London, England, 1978.
22. Smith, K.L., Design & Build Your Own R/C Aircraft, Edmonton, Alberta, Canada, 1984.
23. UIUC AIAA Cessna/ONR, Student Design Build Fly 2002/03 Contest Year Homepage, http://aae.uiuc.edu/aiaadbf/index.html, February 13, 2003.
24. U.S. Naval Academy DBF Website, http://web.usna.navy.mil/~hallberg/briefs/TeamTango_files/frame.htm.
25. William S., Introduction to Fluid Mechanics. 3rd Ed., 1993, PWS Publishing, Boston.

26. www.astroflight.com , Motor Statistics, Sept. 10, 2002.
27. www.sanyo.com, Battery statistics, Sept. 10, 2002.
28. "Xfoil", Version 6.94, Mark Drela, MIT 2001.
29. 14 CFR, U.S. Department of Transportation, Federal Aviation Regulations for Aviation Maintenance Technicians, ASA Inc. 2001

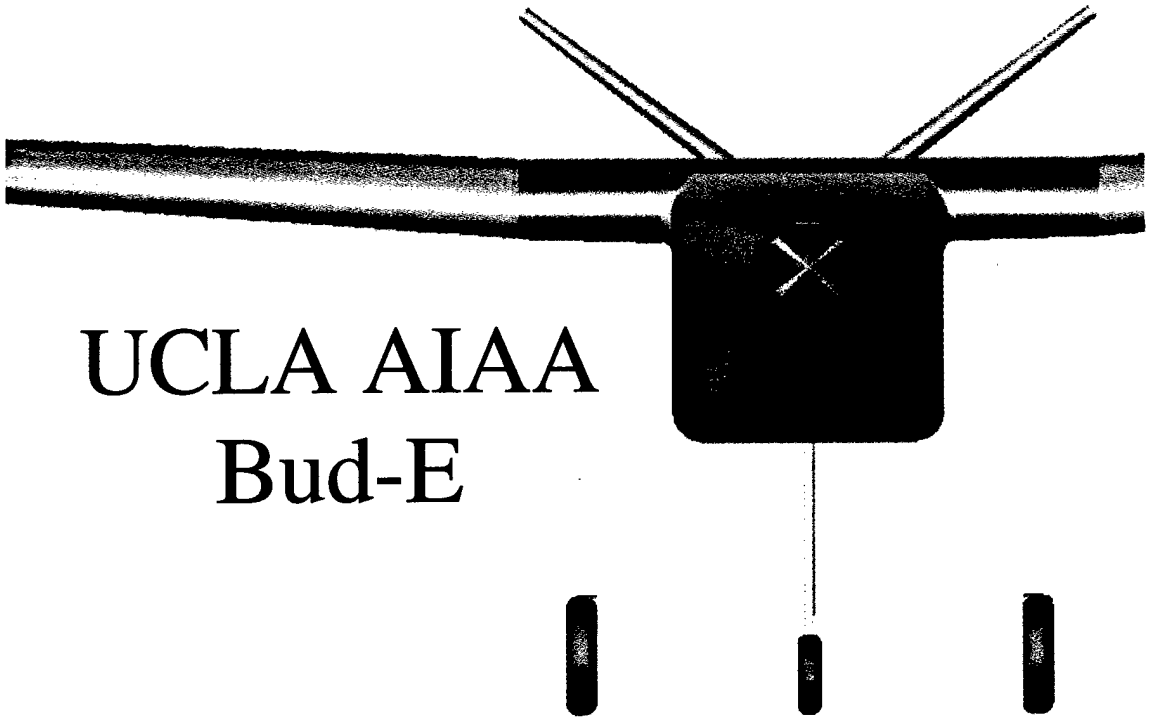

UCLA AIAA
Bud-E

AIAA Cessna / ONR
Design / Build / Fly Competition
2003

Table of Contents

Executive Summary 1
- Conceptual Design 1
  - Conceptual Candidates 1
  - Payload Concept 1
- Preliminary Design 1
- Detailed Design 2
- Manufacturing Plan and Processes 2
- Testing Plan 2

Management Summary 3
- Management Breakdown 3
  - Aerodynamics Team 3
  - Propulsion Team 3
  - Payload Team 4
  - Structures Team 4
- Scheduling and Documentation 4

Conceptual Design 6
- Problem Statement 6
- Conceptual Candidates 6
- Conceptual Evaluation and Selection 7
- Tail Conceptual Evaluation 8
- Payload Conceptual Design 9
  - Payload Design Considerations 9
  - Deployment Schemes 10
- External Payload 12
- Landing Gear Configuration 12
- Landing Gear Design 13

Preliminary Design 15
- Preliminary Wing Design 15
  - Initial Sizing and Planform Shape 15
  - Airfoil Selection 17
- Fuselage Design 23

Detailed Design 26
- Final Wing Sizing 26
- Power Plant Configuration 30

Design Package 31
Final Sized Aircraft Data 32
Rated Aircraft Cost 33
Manufacturing Plan and Processes 34
Structure and Manufacturing of Wings 34
Engine Mount 36
Tail Construction 37
Landing Gear Construction 37
Personnel Breakdown 38
Manufacturing Schedule 38
Testing Plan and Initial Results 39
Static Tests 39
Dynamic Tests (Flight Testing) 39
Initial Results 40
Wing Box Modifications 40
References 41

Table of Figures

Figure 1: Management Overview
Figure 2: UCLA AIAA Milestone Chart
Table 1: Conceptual Selection Figures of Merit
Figure 3: Conceptual Sketch of Design
Table 2: Tail Selection Matrix
Figure 4: Conceptual Payload Systems
Table 3: Payload Systems Figures of Merit
Figure 5: Landing Gear Concepts
Table 4: Landing Gear Selection Matrix
Figure 6: Airfoil Packing Possibilities
Figure 7: Selig S1223 and Goettingen GOE431 Airfoils
Figure 8: Eppler E205 Drag Polars and Lift Curves
Figure 9: Selig S3021 Drag Polars and Lift Curves
Figure 10: Selig / Donovan SD7062 Drag Polars and Lift Curves
Table 5: Afterbody Contraction Figures
Figure 11: Sizing of Afterbody Structure
Table 6: Rear Fuselage Selection Matrix
Figure 12: Final Tail-Boom Dimensions
Figure 13: Wing Section with Spars
Table 7: Manufacturer's Specification for Propulsion Components
Table 8: UCLA AIAA Bud-E Data Specifications
Table 9: Rated Aircraft Cost using Design Specifications
Figure 14: Wing Center Section.
Figure 15: Exploded View of Right Outboard Section
Figure 16: Wing Assembly.
Table 10: Skill Matrix
Table 11: Manufacturing Schedule

Executive Summary

This report outlines the design and manufacturing of the University of California, Los Angeles AIAA chapter's submission to the 2003 Cessna/ONR Student Design/Build/Fly Competition. This year's mission requires an unmanned portable air vehicle be developed which is capable of performing three distinct missions. The aircraft has the option of flying with an attached cylindrical antenna, performing a payload drop, or simply flying laps. The entry's total score is a combination of scores based on three criteria: report score, flight score, and rated aircraft cost.

Conceptual Design

This year's contest differs greatly from previous years. The addition of a standardized non-fared payload, timed assembly, and portability requirements creates numerous design challenges. Assembly requirements dictate a design that can be quickly connected from pieces that must fit into a 4' x 2' x 1' box. The payload box, which measures 12" x 6" x 6", also had to be taken into account for the design.

Conceptual Candidates

The general configuration of the plane was the first to be decided on. Several choices were scrutinized. Each offered strengths and weaknesses for this competition. A conventional plane would be difficult to fit into the box. A flying wing would also have this weakness. Some designs offered a unique advantage. A swivel wing design would allow the plane to be quickly assembled from a simple folded form. Comparing estimated Rated Aircraft Cost, ease of construction, and aircraft performance, it was ultimately concluded that the boomed design offered a slightly more feasible approach to meet the competition specifications.

Payload Concept

The shear size of the required payload demanded that it be taken into account from the earliest stages of development. Deployment methods included a simple drop, sideway deployment, or a rolling out the back method. From a rated cost standpoint, it was determined that the deployment system should use at most one servo. Our goal became to find the simplest system possible. The dropping mechanism was deemed the most efficient as it used gravity to our advantage. From several brainstorming sessions, different designs emerged. A small team was tasked with construction and testing of the most promising design.

Preliminary Design

The team was now broken into respective sub-groups. Airfoil, fuselage, electronics, internal payload, and external payload (simulated antenna), and propulsion all had to be properly selected and implemented. Concepts were continually streamlined and actual construction was considered. Structures for the fuselage and tail were given preliminary designs.

Most of the design work focused on the wing. The need for portability and good take-off performance required a careful balancing of wing area with space limitations. The SD 7062 airfooil was selected for the wing because of its relatively high lift coefficient, good drag characteristics and large volume.

Detailed Design

Final flight and performance data was calculated and final sizing was done to the wing. Taper and aspect ratio were varied to reduce induced drag and improve cruise performance and battery duration. Combining data with aspects such as propulsion, and structures, the aircraft specifications were set and finalized.

Detail Engine requirements were calculated using a common R/C motor software package. Using this data, the proper engine, propeller, and gearbox were chosen from the available models. The fuselage would house the internal payload and thus was primarily designed around its dimensions. Surface area was minimized to reduce drag. After successful testing of prototypes for the payload systems, work began on implementing them into the aircraft and integrating it with the fuselage. With all of this work done, construction of the aircraft could begin.

Manufacturing Plan and Processes

Manufacturing of the vehicle was scheduled to begin at the start of the year. Completion was planned for late February. This would give the flight team enough time to test and modify the competition plane. Most of the fuselage would be built using a combination of balsa, spruce, and plywood. The use of wood allowed for high flexibility in component placing and ease of manufacturing and repair. Wings were constructed of foam and fiberglass; this allowed for precise wing shaping. Carbon fiber spars would provide the necessary rigidity. Wire EMD cutting of foam allows flexibility in design of airfoils and is also relatively fast compared with alternatives. Construction of the UAV was completed in the last week of February and flight-testing began on March 1st.

Testing Plan

A series of static and dynamic tests are planned for the aircraft. The first of these have already been successfully run on the payload system. Wing loading and harsh landing testing is planned for immediate analysis. Dynamic tests will be performed in the future to determine flight characteristics and to uncover areas of necessary improvement or reinforcement.

Management Summary

Management Breakdown

Initial concept selection and preliminary trade studies were undertaken as a group. This led to a greater understanding of the challenges and design criteria amongst all members. The payload development, in particular, profited from the massive feedback. However, after the initial conceptual phase, the team was broken up into focused groups. The chief engineer/project manager oversaw the entire project and ensured that the design and building processes proceeding according to plan. The rest of the team was broken down into in aerodynamics, propulsion, payload, and structures sub-groups.

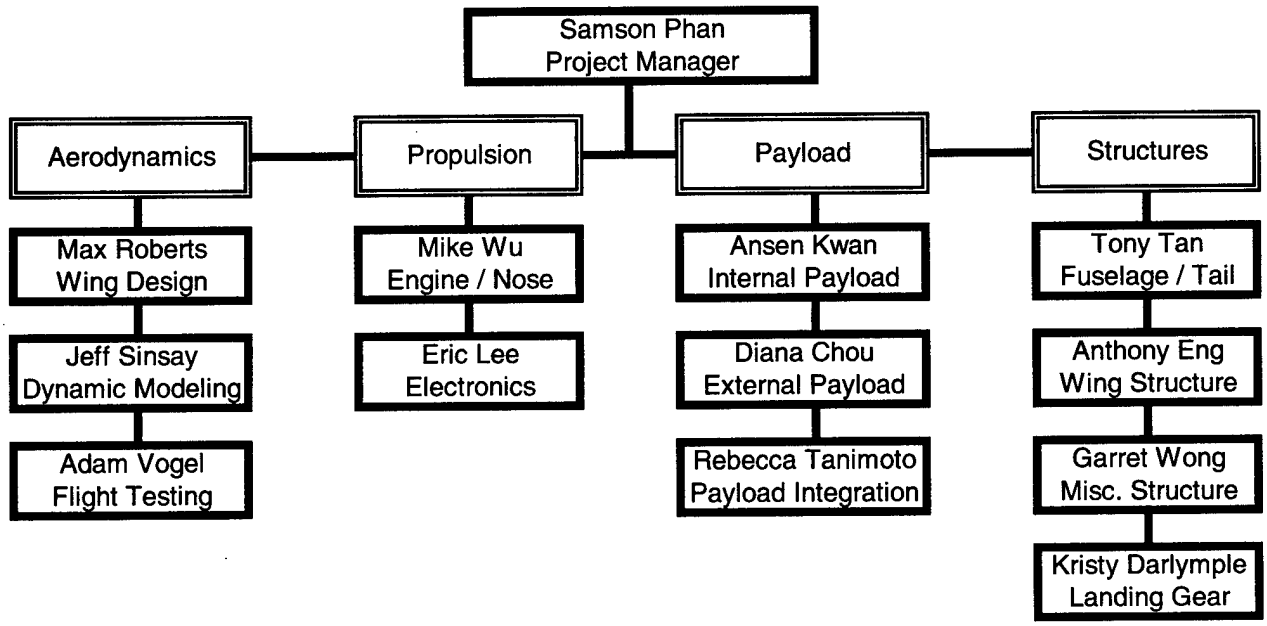

Figure 1: Management Overview.

Aerodynamics Team

The aerodynamics team developed mathematical models to evaluate the conceptual aircraft designs. Contest requirements and scoring were taken into account. A variety of planforms and taper ratios were considered. After deciding on the general layout of the aircraft, development moved on to the airfoils. Airfoil selection took into account aerodynamic and structural considerations. It was highly desirable to place the batteries in the wing, which placed constraints on airfoil selection. With the completion of the UAV, the aerodynamics teams became the primary flight-testing group. Their input will be used to improve the actual performance of the aircraft.

Propulsion Team

The propulsion team initially worked in conjunction with the aerodynamics team to determine the number and placement of engines. They then focused on optimizing the performance of the engine in conjunction with the batteries, propeller, gearbox, and speed control. After selecting a suitable

combination of components, the team began testing systems to ensure physical requirements for current draw and thrust were met. The team also worked on the various servo and wiring requirements of the aircraft.

Payload Team

The payload team used the conceptual designs to build and test two payload devices. Prototypes were constructed to test and optimize the payload deployment and attachment schemes. Several different versions of the external payload (the cylindrical antenna) were built in order to test its attachment and structure. The internal payload box was immediately built along with the corresponding deployment system around it. Since initial testing of the internal payload was successful, the team moved on to integrating the system into the rest of the plane.

Structures Team

The structures team was responsible for the fuselage and landing gear. The fuselage, above all, had to house the internal payload. They worked to minimize the size and weight of the sections while still maintaining their integrity. Materials selection and manufacturing fell within the realm of the structures team. The group also completed the final drawings of the aircraft. The team ultimately developed a central fuselage that matched the compactness requirements determined during the conceptual phase of the design process.

Scheduling and Documentation

It was decided early on that the UAV should be completed relatively early to allow for extensive flight-testing. As a result, design and construction had to take place at a quick pace. Milestones were set for every aspect of the project. Conceptual and preliminary design phases were scheduled to be finish by late December. Detail design and construction would be done by February. The design report would be completed along side the actual development of the design. Sections of the report were to be written shortly after the completion of the corresponding component. Figure 2 is a diagram of the predicted schedule and the actual completion dates.

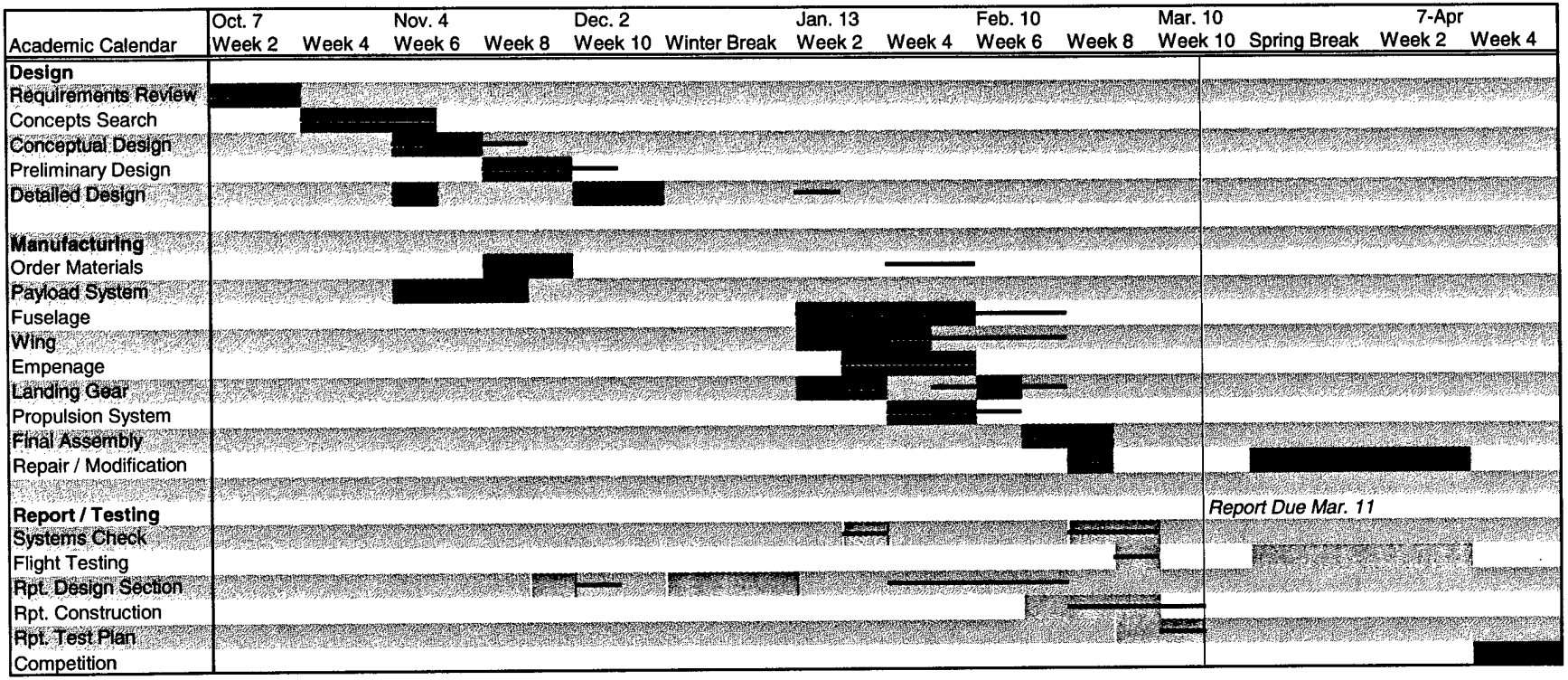

Figure 2: UCLA AIAA Milestone Chart. Green blocks designate projected design dates, blue blocks designate manufacturing dates, and orange blocks designate report writing and testing periods. The black bars indicate the actual development periods.

Conceptual Design

Problem Statement

The goal of the 2003 Cessna/ONR Design Build Fly competition is to build a UAV that quickly assembles out of a 4' x 2' x 1' inner dimensional box. The aircraft must carry a 5 lb. payload box with dimensions 12" x 6" x 6". The aircraft will fly one of three rated missions over a 1000-foot long course with a 360-degree turn in the opposing direction. And, in honor of the 100th Anniversary of the Wright Brother's flight, the aircraft must take off in under 120 feet. Mission type A requires the aircraft to attach an additional non-fared 6" diameter cylindrical payload with a clear field of vision. The UAV must complete 4 laps and land. Mission type B requires the aircraft to fly 2 laps and automatically deploy the payload box while at a full stop. The aircraft must then takeoff and fly an additional 2 laps. Mission type C simply requires the aircraft to fly 4 laps with the payload box, but with 2 additional 360-degree turns. The missions are scored on a combination of assembly time, flight time, and difficulty. The total score is the product of the report score and the highest flight score divided by the Rated Aircraft Cost.

Conceptual Candidates

Conventional Aircraft

A conventional configuration employs a long central fuselage that connects to both the wings and the tail. Aircraft of this type have been proven in the field and is by far the most popular configuration for modern airplanes. The major disadvantage would be its portability. The large fuselage could be difficult the fit in the required box. It was considered the baseline of what could be built.

Tail-Boomed Aircraft

This configuration is similar to the conventional aircraft except the tail is connected using one or two booms. The advantage of this configuration is that the tail can be designed to be removable and the structure of a full fuselage is not needed. This allows the design to save a significant amount of weight.

Swivel Wing Aircraft

Due to the new timed assembly, a large consideration would be ease of assembly. The swivel wing concept was an attempt to cut down manual labor in the assembly process. It incorporated one or two wings that would be permanently attacked to the body and only needed to pivot into place. Its main disadvantage would be that the wingspan was limited. In order to fit in the box, the span had to be under 8' with a cord less than 1'. Dual wings were also considered in the configuration, which would double the wing area.

Blended Wing Aircraft

A blended or flying wing design, which eliminates the need for a fuselage, would have several advantages. Its high lift and low drag were obviously in its favor. Another plus was its lowered Rated

Aircraft Cost due to the limited number of control surfaces. On the other hand, there would be difficulties in carrying the payload internally as a blended wing design lacks sheer volume. It would also be more difficult to pack into the required box and more difficult to balance for stability.

Faceted Body Aircraft

The final concept considered was a faceted body, similar to the popular F-117 Stealth Fighter. The faceted shape, as opposed to the smooth surface of the blended wing, allows for the increased volume for the payload. It would require very little assembly and its flight would be very stable and hard to stall. Its disadvantages included a high induced drag and a high flare angle. Ultimately, a faceted body design would also have a low cruise speed and presented too many design challenges.

Conceptual Evaluation and Selection

Conceptual designs were evaluated using 6 criteria. They were selected to provide a quantitative comparison of the possible aircraft choices. The criteria reflect what was felt to be the most important aspects of an aircraft corresponding to the competition rules.

Aircraft Weight

A common model was used to estimate weight build-up of the wing, fuselage, avionics, and payload system. The model focused on the structural differences between the designs. Materials were approximated by using construction methods based on previous UCLA entries in the competition.

Takeoff Airspeed

An approximation was used to determine the airspeed required for the sized wing to provide the lift for takeoff. This is especially important because of the 120' takeoff requirement (80' shorter than previous competitions).

Estimated Cruise Speed / Mission Time

A first order approximation of cruise speed was used to estimate the total mission time. Mission time is the primary component of the total score. A high cruise speed / low mission time was a definite necessity.

Drag at Cruise Speed

Drag was approximated because of its effect on cruise speed and power requirements. It varied significantly because of the different body types of the concepts.

Ease of Assembly

A qualitative judgment was made to approximate the ease and timeframe of the assembly. Number of pieces and their complexity played roles in this figure of merit.

Rated Aircraft Cost

The Rated Aircraft Cost is a figure specified by contest rules. It is a cost associated with the empty weight, rated engine power, and rated manufacturing hours. Manufacturing hours is determined by a set basis for rating surfaces and components.

Configuration	Baseline	Conventional Boom Tail	Swivel Wing	Blended Wing	Faceted Body
W/W'	1.0000	0.9238	0.9505	1.0842	1.0396
VLo / VLo'	1.0000	1.0152	1.1364	0.9242	0.9848
VC' / VC	1.0000	0.9780	0.8990	1.0988	1.0230
D40 / D40'	1.0000	0.8353	1.1176	1.1588	1.0000
RAC	1.0000	0.9410	0.9619	1.0038	0.9990
Assembly	1.0000	0.9500	0.7500	1.0500	1.0000
Final Score	**1.0000**	**0.9405**	**0.9692**	**1.0533**	**1.0077**

Table 1: Conceptual Selection Figures of Merit. Scores were normalized using the baseline configuration of the conventional aircraft. Lower final scores are better.

Based on the figures determined, the conventional design with a boom tail best satisfied the requirements of the competition. It was also determined that a high wing was preferable, due to conflicts with the payload system.

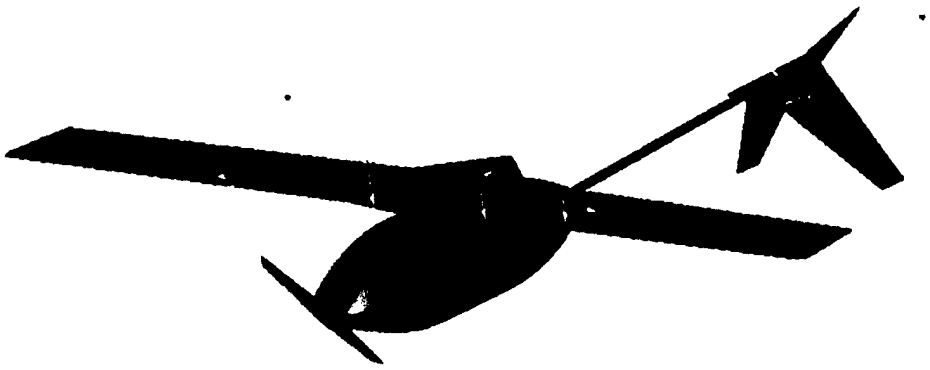

Figure 3: Conceptual Sketch of Design.

Tail Conceptual Evaluation

Three basic tail types were considered. They are conventional tail without controllable rudder, conventional tail with controllable rudder, and a V-tail. The following matrix was developed to quantify the advantages and disadvantages of each choice.

Type	Rated Aircraft Cost	Advantage	Disadvantage	Score
Conventional with Rudder	20	Low Risk	High RAC	1
Conventional without Rudder	15	Simplicity	Less Control	2
V-tail	15	Lowest RAC with Highest Control	Yaw-Roll Coupling	3

Table 2: Tail Selection Matrix. Rated Aircraft Cost is based on the number of surfaces. A v-tail is considered to be a vertical surface without control (5 hrs) and a horizontal surface with control (10 hrs).

The key benefit of a V-tail is the ability to control both yaw and pitch with the same control surface, maximizing our control authority over the aircraft while minimizing our RAC score. Concerns with this design include yaw-roll coupling. Radio control aircraft literature suggests that very little rudder input is required to control an aircraft during flight. While yaw-roll coupling can not be avoided, the second concern can be addressed. Increasing the angle between the two control surfaces will induce less yaw during maneuvering. Instead of the more conventional 90 degree angle, we increased ours to 112.6.

Our idea of the v-tail was taken from the Beachcraft Bonanza airplane. This type of tail has a taper ratio which is the ratio of the width of the wing rooted at the plane, and the width of the wing at the outside tip of the wing, C_{root} / C_{tip}. Each wing has a span of 9 inches and is 33.7 degrees above the horizon (112.6 degrees between the wings) when attached. These dimensions were determined in order to fit the box requirement.

The airfoil that was chosen is the NACA 0012. This symmetric airfoil provides lower drag than a flat plate while increasing control. The lack of camber ensures equal deflection translates into equal force imparted onto the moment arm.

The v-tail has all-moving wings, which eliminates the need for control surfaces on the tail planes. During design, a great concern was the short moment arm associated with our decision to have a one-piece fuselage. Deflecting the entire surface ensures enough control authority to maneuver the aircraft safely.

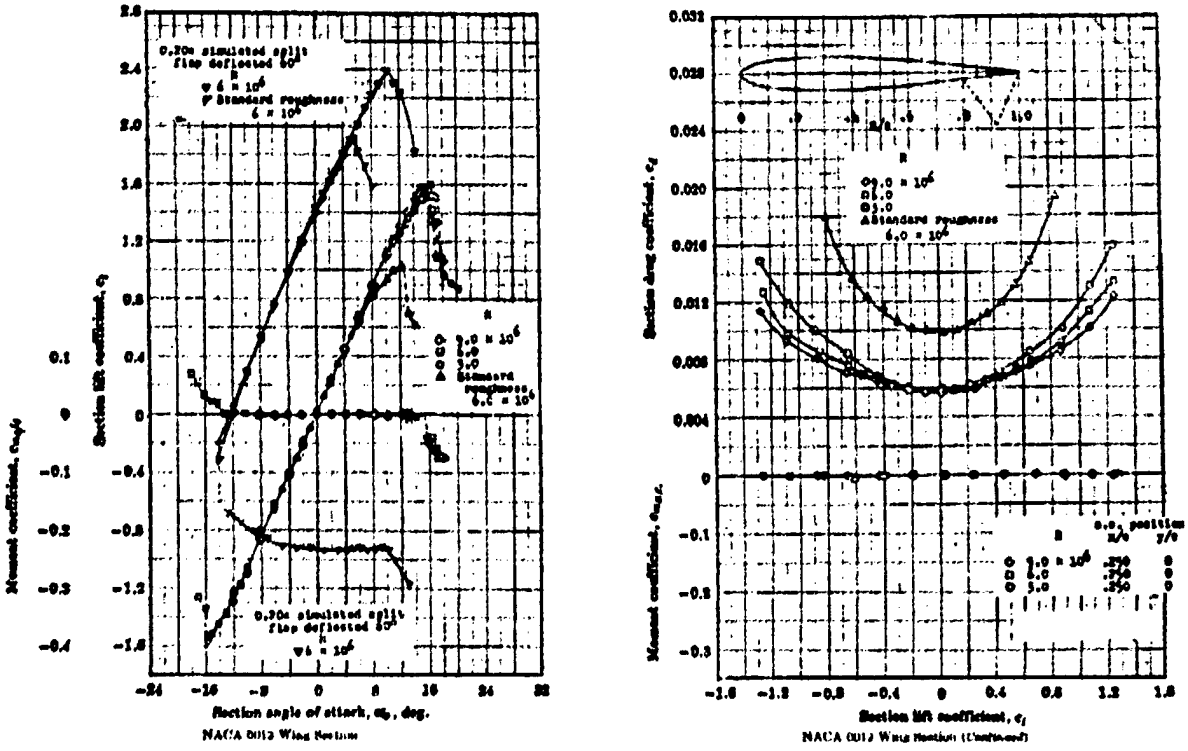

Figure 3a: Characteristics of NACA 0012 Airfoil.

Payload Conceptual Design

A major hurdle to this year's competition is the incorporation of a 5 lb. payload with fixed dimensions. The shear size of the required payload demanded that it be taken into account from the earliest stages of development.

Payload Design Considerations

1.) Payload should be secured and does not move/wiggle during takeoff, flight, and landing. While the payload is within the confines of the plane, it should not move, be loosely attached. Any such movement even if minor can affect flight. The 5 lbs. of weight should be placed in such a way not change the center of gravity of the plane during takeoff, flight and landings.

2.) Payload deployment should be as clean as possible. There should be minimal complications regarding the deployment of the payload. The edges should be smooth and have no protrusions. The payload front end and rear edges should fall at exactly the same rate to prevent the box from hitting any sides of the plane.

3.) Aerodynamics should not be affected by the presence of the payload. Aerodynamic

characteristics need to be consistent before and after payload deployment. Leaving a gapping hole in the frame of the plane would surely cause unwanted effects if the plane is traveling at 30+ mph. Carrying a large box on the exterior would also greatly hinder the performance of the aircraft.

5.) Take off and landing is not hindered with payload detached. Attention to center of gravity is critical to a plane that flies and flies well. Since the payload makes up 5 pounds of the plane's total weight, it will definitely have an effect on plane acceleration, speed, maneuverability and stability. The released payload should also not hinder the landing gears or clearance issues when it is to take off again.

Deployment Schemes

In all these issues needed to be address early in the design stages and not as a subsystem needing to be integrated. We started by looking at how the payload is inserted and removed. Two ways seemed most appropriate: deployment from the bottom of the aircraft or from the rear. An underside deployment system would use gravity to its advantage but would also require at least a 6-inch clearance of the fuselage with the ground. A rear deployment system would not have the height requirement and would not have a large hole in the underside, making the fuselage a much stronger section.

In conjunction with these, three deployment systems were conceived. The first, Type A, used a servo to hold the payload in place. Activating the servo would release the payload and a spring-loaded hatch would seal the opening. Type B required the use of two servos. The first actuated the payload doors and the second released the payload. The final scheme, Type C, relied solely on the payload doors to secure the payload.

Payload System

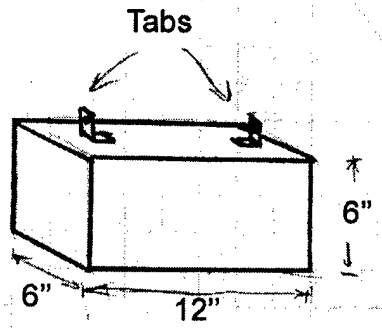

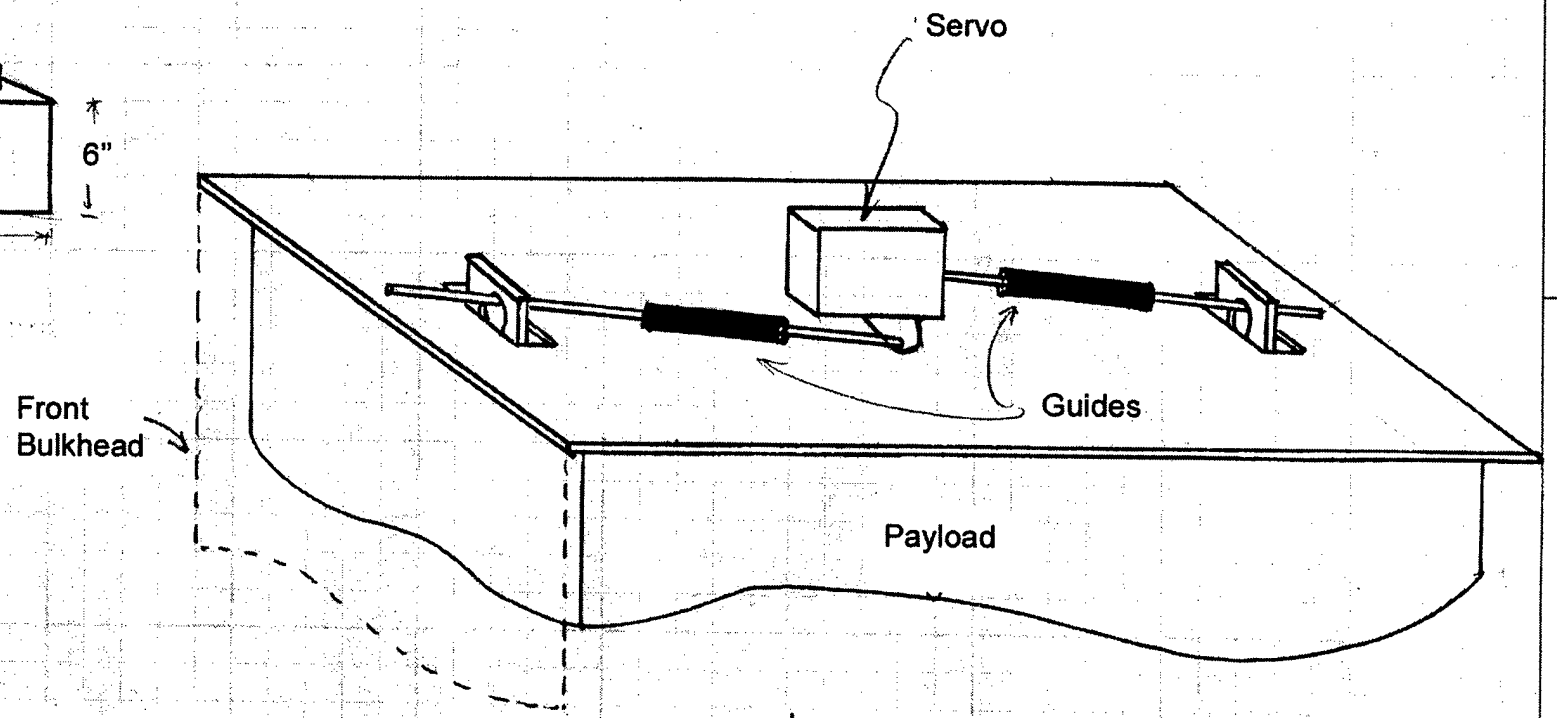

Secured (Payload Not Shown)

Release

Dropped

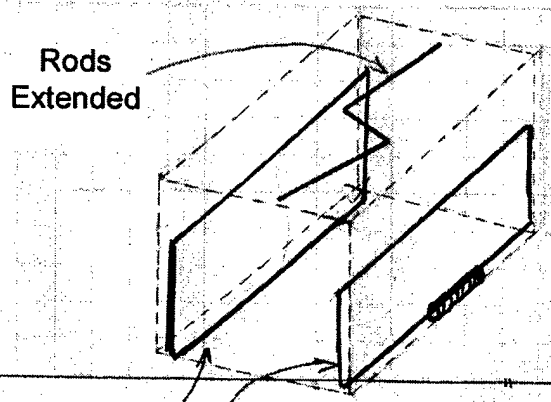

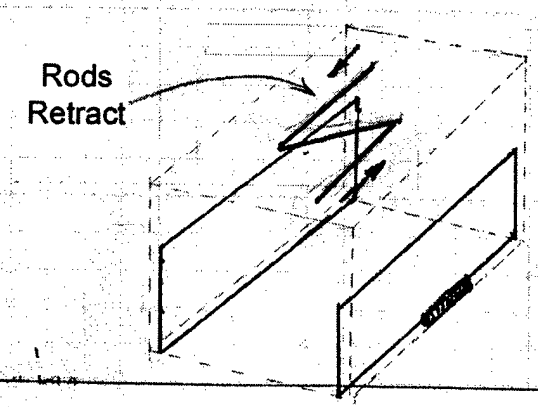

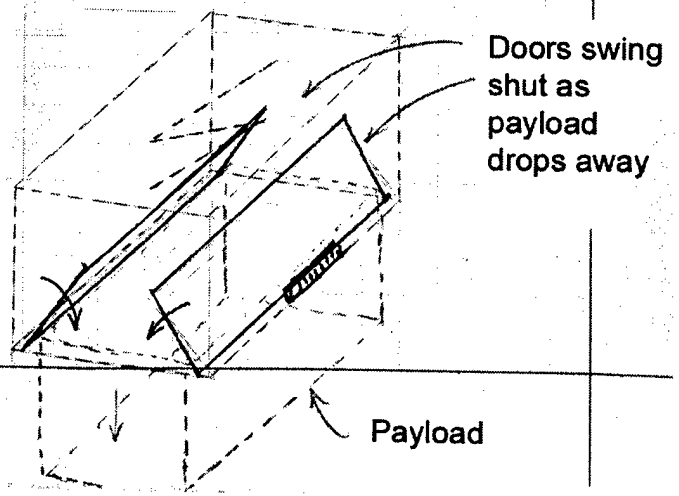

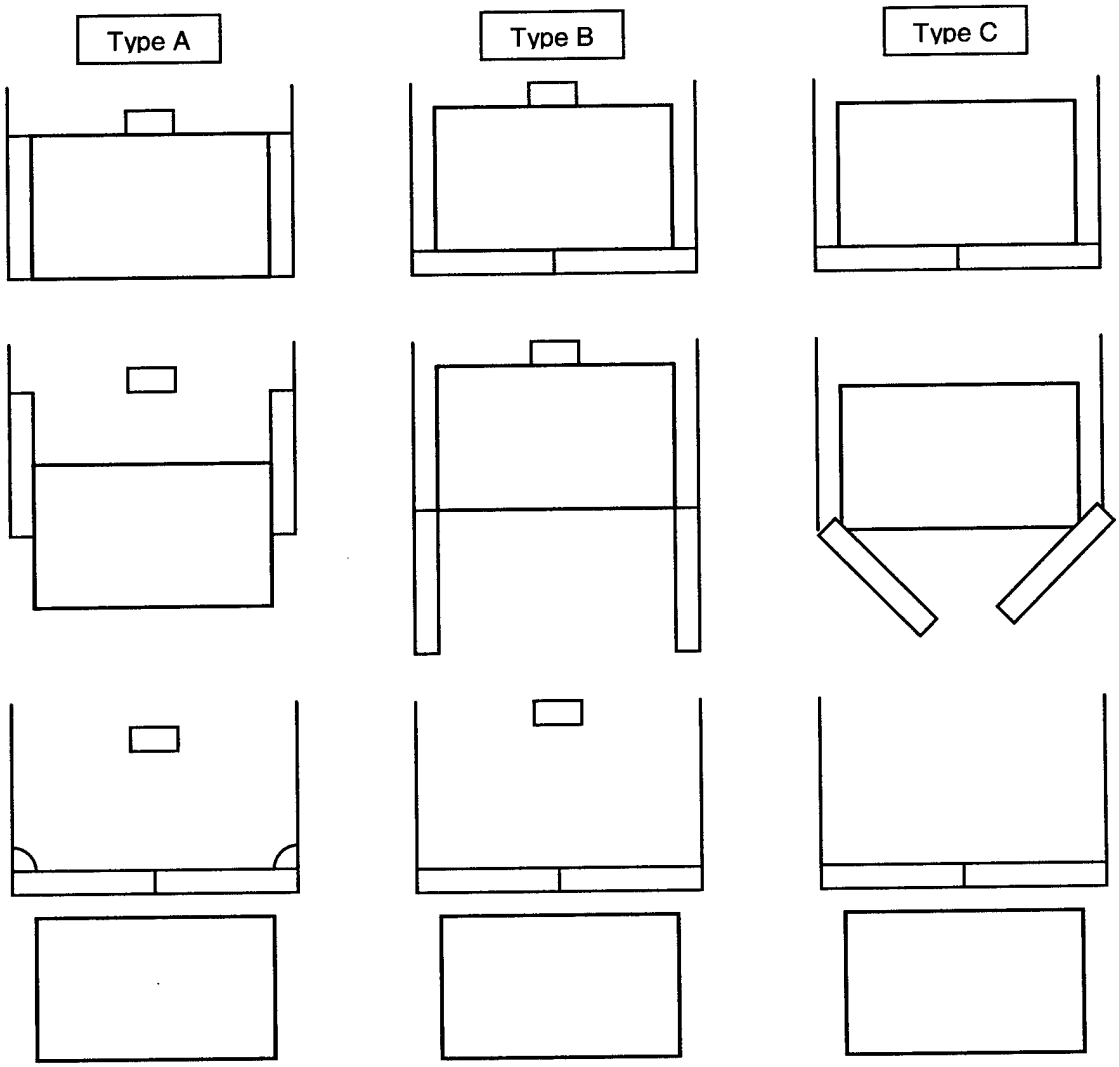

Figure 4: Conceptual Payload Systems. System types A, B, and C are shown as they would be implemented with a bottom loading / deployment method.

Design	Bottom Type A	Bottom Type B	Bottom Type C	Rear Type A	Rear Type B	Rear Type C
RAC	1	0	1	1	0	1
Height Restriction	-1	-1	-1	0	0	0
Ease of Construction	2	0	1	-2	-1	-1
Effect on Takeoff	0	1	1	0	1	1
Structural Integrity	-1	-1	-2	0	0	-1
Total	**1**	**-1**	**0**	**-1**	**0**	**0**

Table 3: Payload System Figures of Merit. Higher scores indicate an advantage.

External Payload

In mid-October, initial proposals were submitted as to how and where the external payload was to be placed. First, the idea of placing two screws and a rod between the external payload was suggested. It seemed like a good idea at the time because it was simple and convenient. The rod and payload would simply be screwed onto the airplane. It was also suggested that a hinge type mechanism would work. Somehow, the hinge would attach and detach the external payload.

During the final stages of the preliminary design, a final proposal was made. A rod would be placed inside of the 3-inch radius PVC pipe. Holes would be drilled in one piece of the plywood and stick out to be placed somehow onto the airplane. After long consideration, an idea came to mind that required foam to be placed inside of the PVC pipe and to surround the rod to hold it in place. Work was done almost immediately after this idea came about. Foam from a tube was placed inside of the PVC pipe and was sealed on both sides with plywood drilled with holes. A rod was inserted into the foam while it was still wet so the foam would wrap around the rod and secure it in place. After a few days when the foam was completely dry, it was found that the external payload was quite heavy. Wishing for the airplane to be as light as possible, another idea to attach the external payload had to be made.

A plan was made about attaching two 2 x 2 x 1 inch pieces of wood to the sections of plywood. Both pieces of 2 x 2 x 1 inch plywood would have a drilled hole through the center of it. One would be attached to the top of the payload. The second piece would be attached to the bottom of the payload with a drilled hole through the base piece of plywood. A rod would be inserted and glued to the base and top pieces of wood and plywood. Immediately, this idea was made into a product.

The external payload would be placed near the center of gravity on top of the airplane. This would reduce drag and minimize any changes in weight distribution.

Landing Gear Configuration

Like all aircraft, the landing gear configuration on this aircraft was chosen in accordance with its missions. The requirement of having the aircraft to fit inside a 4' X 2' X 1' box dictates that the gear would have to retractable. And as the result of the payload deployment requirement, this aircraft would need a set of gears that is compatible with the deployment system. With these in mind, we immediately ruled out the chance of having a tail dragger: the tail wheel would have got in the way of the released payload as the aircraft taxis away. We were left with the bicycle or the tricycle gear types as the practical choices. The bicycle type gear required having the center of gravity of the aircraft to be place approximately half way between the front and the back gear. This arrangement would have made takeoff more difficult since no rotation could be attained. Furthermore, the almost equal distribution of the weight on the wheels would have required both the front and back wheels to be steerable. This not only complicates the construction process, but also requires a higher level of calibration to make sure all parts are lined up straight. For these reasons, the tricycle gear configuration was chosen. This type offers great stability

during taxiing, ease of retraction and relative ease of construction. We determined the tricycle gear is the best compromise for this design.

Landing Gear Design

The purpose of the main landing gear is to support the weight of the plane during takeoff and to withstand the force produced during landing which will be about 3Gs of force. Due to the need of deploying the payload, the landing gear must provide a 7-inch clearance from the bottom of the fuselage to the ground. Due to this large distance, the landing gear must be attached prior to takeoff since it does not fit into the specified box when attached.

A number of designs were considered that consisted of landing gear that folded onto the fuselage, screwed into the fuselage, and landing gear that attached using pins. Below are preliminary sketches of these three ideas.

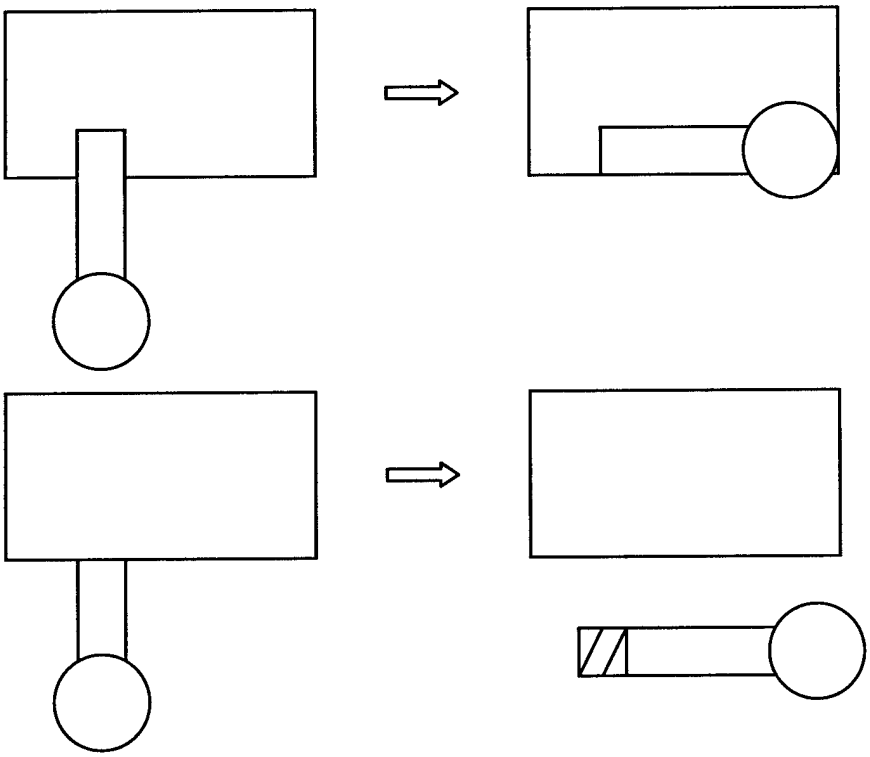

Figure 5: Landing Gear Concepts. Folding and screwing breakdown concepts are depicted above. The folding method pivots about a screw and uses a pin to lock in place. The pinned method is not depicted, but is similar to the screwing method.

Design	Advantages	Disadvantages	Score
Folding and Secured with Pins	Most Easily Assembled	Weakened Attachment	1
Screwed into Fuselage	Secure Attachment	Difficult Wheel Alignment, Complicated Construction, and Longer Assembly	-2
Attached with Pins	Quick Assembly	Insecure Attachment	0

Table 4: Landing Gear Selection Matrix.

Since the folding design obtained the highest score, it was selected for use on the airplane. It met both the portability and structural requirements.

Preliminary Design

Preliminary Wing Design

In the development of the wing for the UAV a large number of issues had to be considered in order to achieve an efficient and overall balanced design. These issues could be assigned to one of three broad categories:

1.) Wing sizing and planform considerations,

2.) Airfoil selection/optimization considerations, and

3.) Structural and manufacturing considerations.

These categories are presented above in roughly descending order of importance and sequence in the wing design process and we will thus address each in turn. Of course it should be noted that none of these categories exist in a vacuum. While wing sizing was treated as mostly independent from specific airfoil selection and structural layout, no wing could be appropriately sized without some knowledge of airfoils and structure. For example the lift characteristics of plausible airfoils that could be used, the structural loads the wing would have to withstand, and the manufacturing methods which could be employed to build the wing are all important aspects to sizing. Wing sizing was actually performed in two steps, initial and final sizing. In initial sizing the general wing size and shape was determined so that the wing would certainly perform the functions it needed to do before an airfoil was chosen for the wing and some structural concepts defined. Final wing sizing was performed after airfoil selection and represented an optimization of the wing developed in initial sizing.

There were also two important inputs that provided the genesis of the wing design process, the estimated final weight of the aircraft and the achievable thrust of the engine. Considering the relative experience of the design team and the available time to design and build the aircraft conservative estimates of weight and thrust were employed to avoid iterations and attempts to push the envelope. The fully loaded weight of the aircraft was set at the 'high' estimate of 13 lbs and the thrust was set at 4 lbs. even though many in the design team believed nearer to 5 lbs of thrust was possible. If anything these numbers would make our wing slightly large. But it was hoped that instead of being a hindrance these conservative assumptions would buy us some margin to change the wing design when actual construction began and some margin in the safe operation of the UAV as well.

Initial Sizing and Planform Shape

The first consideration used to shrink the 'design space' that was investigated for the wing was sizing and planform shape. A myriad of design issues are generally inherent to this category, amongst them the ability of the wing to provide enough cruise lift, meet the takeoff distance requirement and do so at minimum drag. In addition to these, the critical criteria that the wing sections fit into the 4' x 2' x 1' box was added. Common sense dictated that the wing be fairly large and have as high an aspect ratio as possible. A larger wing would be more likely to achieve the takeoff requirement, have less wing loading,

and would cruise at a lower lift coefficient and thus, in general, at a lower wing form drag coefficient. A larger aspect ratio would achieve a lower induced drag and result in a higher speed aircraft.

In initial sizing maximum span and root chord values were set. Optimization of taper ratio and aspect ratio were left to final sizing. It was decided that in order to maximize the general wing area the wing should be broken into three sections for carrying in the box, a center section and two outboard sections. The center section would be built integral with the fuselage and was hence limited to no more than two feet of span since the fuselage would sit lengthwise in the box. Not all of this span would be taken up by wing however. It was recognized early on that some amount had to be reserved for exposed structure that the outboard sections could mate with. The left and right outboard sections were mirror images of each other and would attach to the center section after removal from the box. Packing of the two outboard sections and the fuselage into the box was the driving factor in determining total wingspan and root chord. The span of each outboard section had to of course be 4' or less and for some breathing room in the box so a 47" span was chosen for each outboard.

The root chord of the wing was a much more delicate issue however as it depended very much on the specific airfoil selection. The fuselage was designed to be about 8.5" tall including the integral center wing section. This left a 3.5" x 24" x 48" section of empty space in the box for the two outboard sections which would lay side by side. Too large a root chord and the outboard sections would exceed the 24" packing restriction. A thicker airfoil reduced the allowable root chord. Thicker airfoils would impinge on the 3.5" vertical restriction perhaps even before the 24" restriction was reached. Airfoil shape also had an impact. Although no specific airfoil was selected until after initial wing sizing, a host of potential airfoils had already been picked, including the Seligs S1223 and S3021, the Selig / Donovan SD 7062, the Eppler 205, the Goettingen GOE431 and the NACA 23012. For the highly cambered airfoils with thin trailing edges such as the S1223 a 'yin and yang' packing approach seemed to work best. This allowed root chords higher than just 12". One of these sections would be a wing root and the other a tip. Thus an even higher root chord is actually allowed when there is a taper ratio and the tip chord shrinks. For less cambered airfoils the root chord was highly dependent on thickness when packed. As depicted in Figure 6, this was clearly the more efficient packing scheme. The SD7062, which was our final choice, the employed this method.

Selig S1223

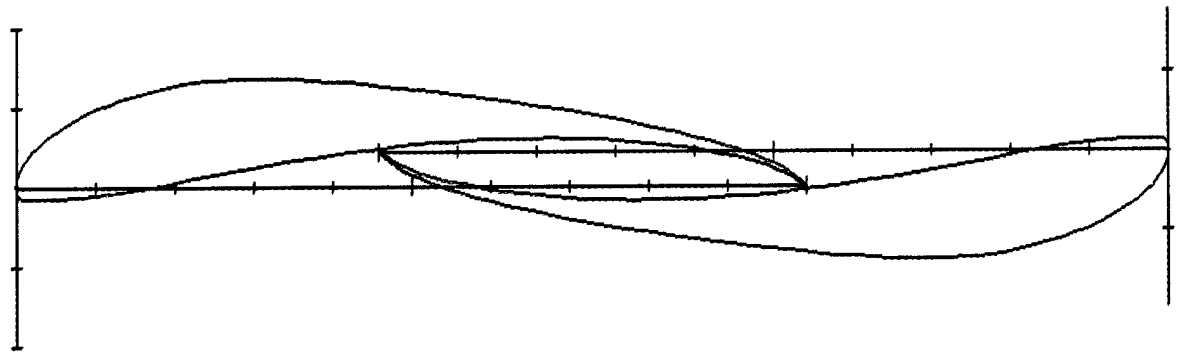

Selig S3021

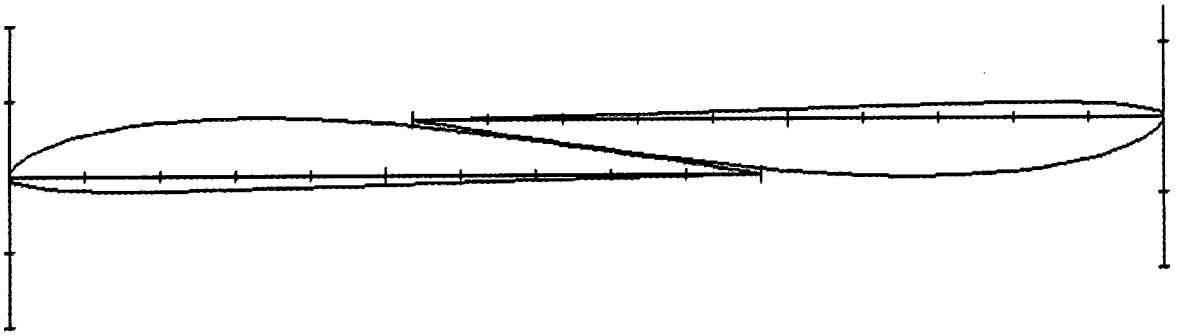

Selig / Donovan SD7062

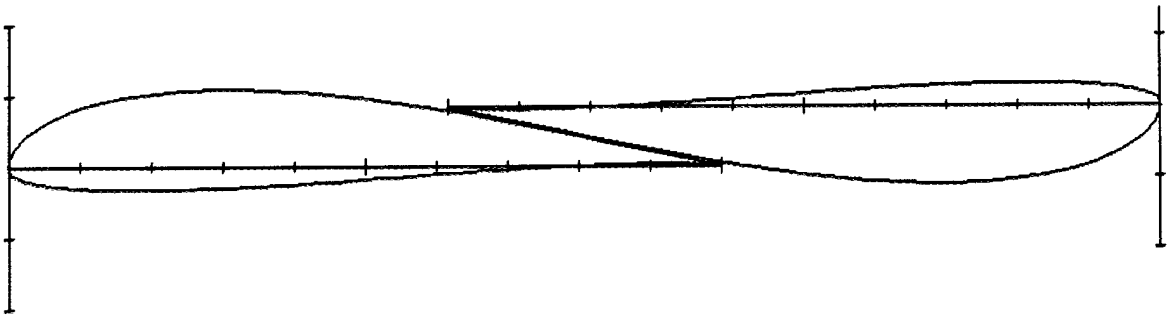

Figure 6: Airfoil Packing Possibilities. The S1223 demonstrates the yin and yang concept, while the S3021 and SD7062 use more efficient packing schemes.

Airfoil Selection

Once the overall wing size was roughly defined a good starting point for airfoil selection existed. Wing size, aircraft weight and expected cruise velocity gave an estimation of the cruise lift coefficient. Airfoil selection was then primarily driven by which airfoil had the minimum profile drag at or near the cruise lift coefficient. Airfoil shape was also important for two reasons. First the wing was supposed to hold the batteries and needed to have a thick enough section to stow the cells. Second manufacturability had to be taken into account. Although some very good lift characteristics were achieved by the highly cambered wings with sharp trailing edges, this trailing edge posed not only daunting manufacturing challenges but was unsuited to accommodate flaps or ailerons. As a result the S1223 and GOE431 airfoils from our preliminary consideration list were eliminated. Last the airfoil maximum lift coefficient should be as high as possible to generate large amounts of takeoff lift and thus reduce takeoff distance.

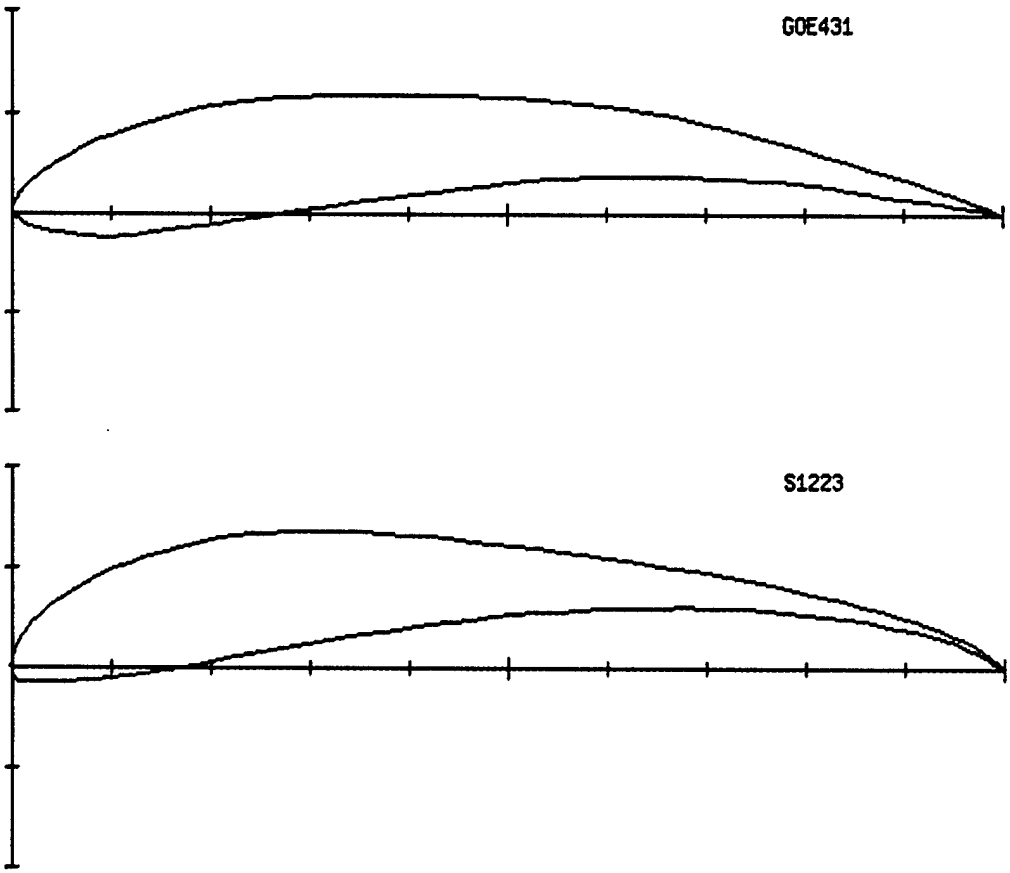

Figure 7: Selig S1223 and Goettingen GOE431 Airfoils.

One of the most important parts of selecting the 'optimal' airfoil for the aircraft was the need for accurate low Reynolds number data. Lift curves and drag polars were obtained from the NASG database online at http://www.nasg.com/afdb/index-e.phtml. The NACA 23012 airfoil was summarily eliminated due to the fact that it was designed for high Reynolds number, albeit subsonic, applications and plenty of other airfoils in the list were designed for R/C aircraft purposes.

From initial wing sizing the aircraft was known to have a wing with slightly less than a 10' span and a 13" root chord. Knowing that in the final design some taper ratio, probably near 0.4 for near elliptic lift distribution, overall wing size was estimated as being somewhere slightly less than 7 sq. ft. from the following formula and assumptions:

$$S = 2*\left(\frac{b}{2}\right)*\left(\frac{C_{Root}+C_{Tip}}{2}\right)$$

b = 9.5 ft.

C_{Root} = 1.0833 ft.

C_{Tip} = 0.3333 ft.

$$S = 9.5*\left(\frac{1.0833+0.3333}{2}\right) = 6.7\,ft^2$$

From previous drag models developed during the conceptual design phase, a cruise thrust of 3 lbs. yielded a cruise velocity of about 45 feet per second. Thus the expected cruise lift coefficient was determined as follows:

$$C_L = \frac{2W}{S\rho V^2}$$

W = 13 lbs

S = 6.7 sq. ft.

P = 0.0023769 slugs / ft^3

V = 45 fps

$$C_L = \frac{2*13}{6.7*0.0023769*45^2} = 0.8$$

The drag polars and lift curves of the remaining three airfoils, the Eppler 205, the Selig S3021 and the Selig/Donovan SD7062, were used to make the final selection.

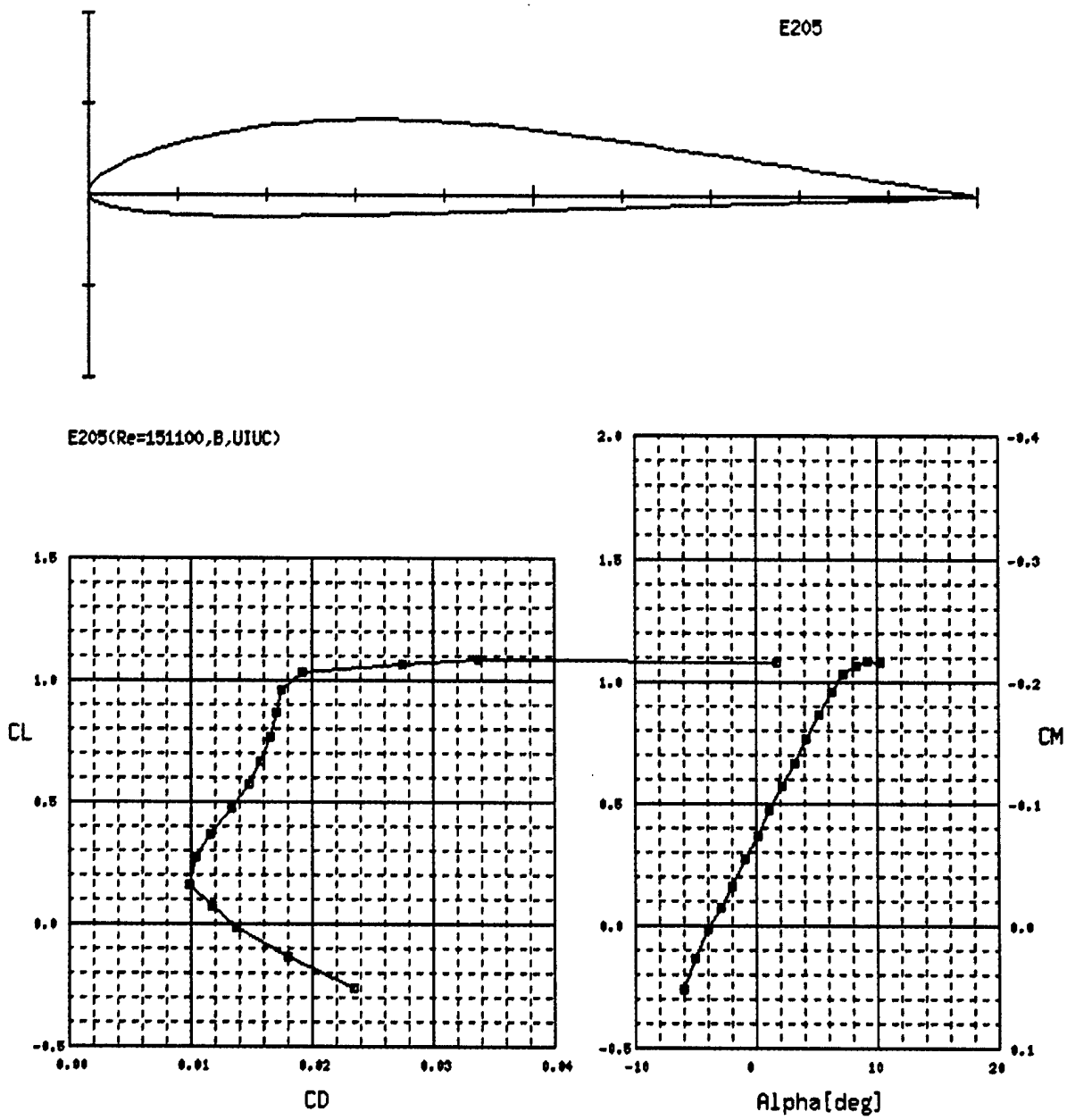

Figure 8: Eppler E205 Drag Polars and Lift Curves.

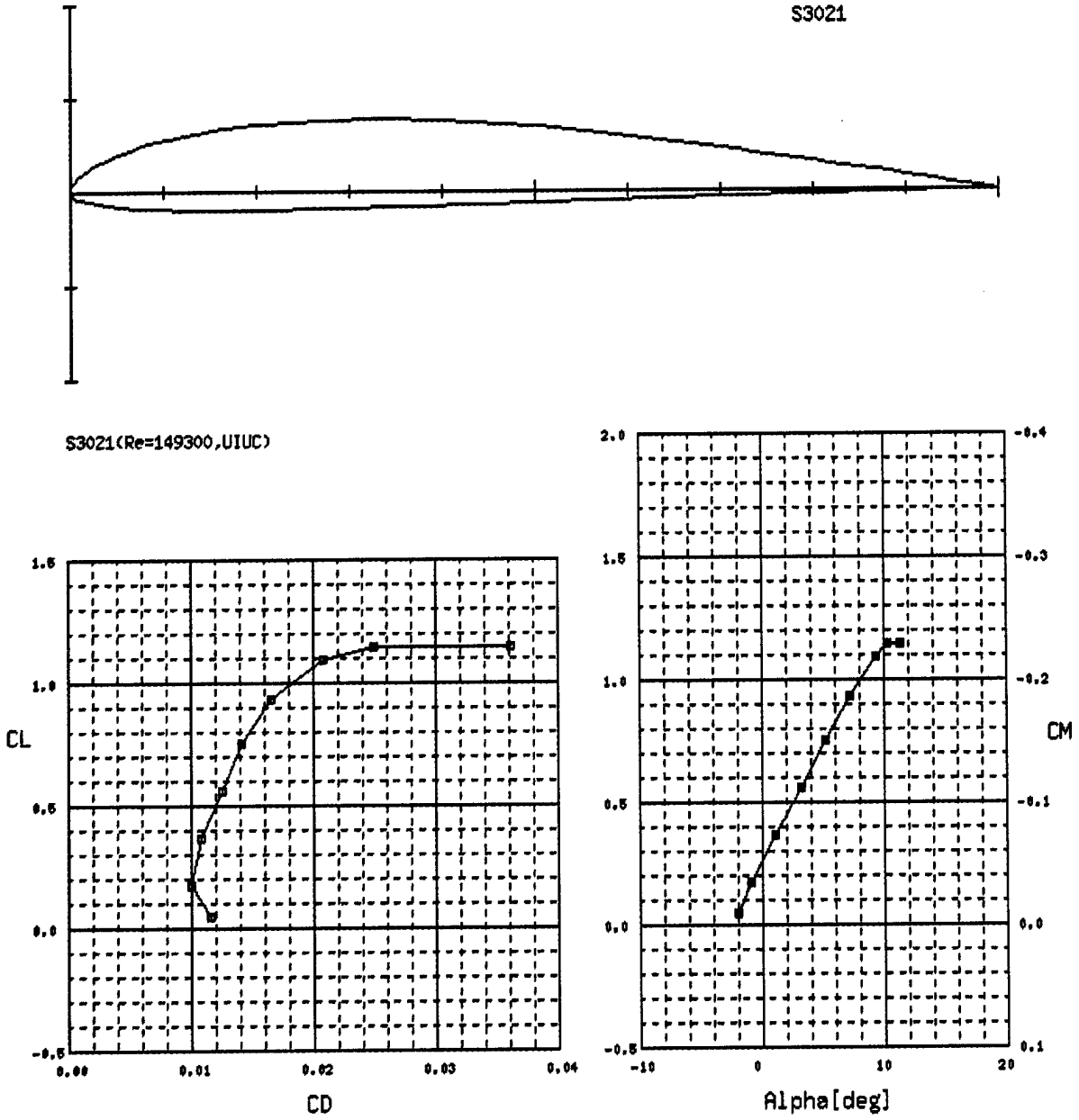

Figure 9: Selig S3021 Drag Polars and Lift Curves.

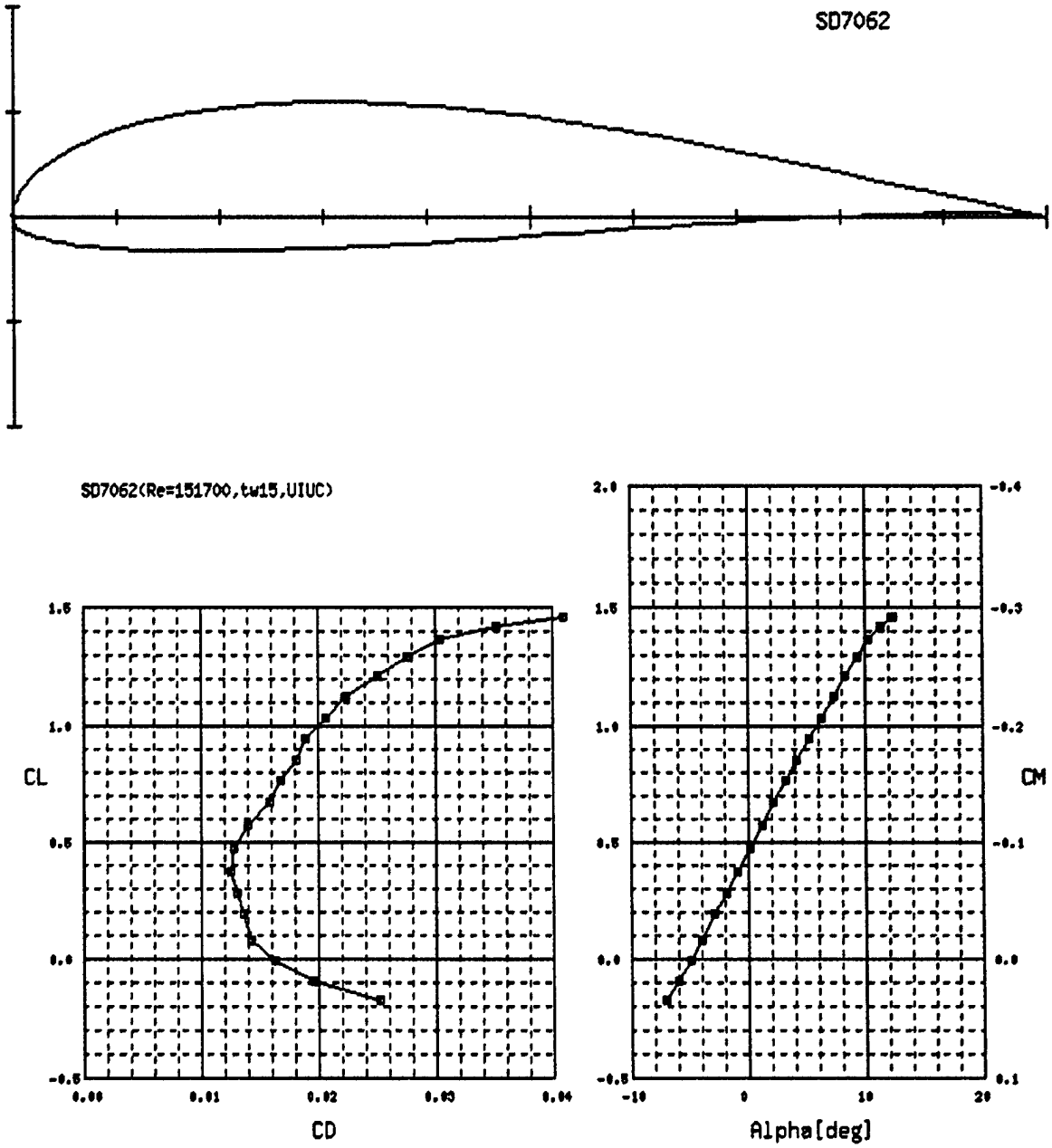

Figure 10: Selig / Donovan SD7062 Drag Polars and Lift Curves.

Of these three the S3021had the lowest drag at a C_l of 0.8, but it's lackluster $C_{l,max}$ relative to the SD7062 and the SD7062's thicker airfoil section tipped the balance in favor of the SD7062. This airfoil was thus selected for our aircraft. It balanced the needs for good drag performance, high C_{lmax} and, wing volume.

Fuselage design

Minimization of wetted area greatly affects friction drag, therefore tight internal packaging and a low fineness ratio would be the driving requirements for the fuselage (Raymer, 1999). Since RAC depends only on length of fuselage, it would be prudent to follow a low fineness ratio profile. To minimize pressure drag, a constant cross section fuselage was immediately ruled out. While it would greatly ease construction, the associated form drag from the increased equivalent frontal area and high boat tail drag would result in high power requirements and/or lower performance.

Knowing that a teardrop shape would offer the least drag penalty, it was now question of how close an approximation one should use. The only driving requirement is the need to fit the payload, engine and electronics in the structure. Profile drag is referenced to the maximum cross sectional area (Raymer, 1999). To fit the payload inside, the cross-sectional area of a teardrop must be larger than that of a square. Therefore, to decrease profile drag, the fuselage should be shaped to fit the payload and no more. The Shorts Company produced a long line of aircraft with square cross-sections, including the Skyvan. In addition to increasing the profile drag, the acute angle formed between the high wing and the circular fuselage would impose an interference drag penalty greater than a high wing/square fuselage interface (McCormick, 1995). Interference drag effectively doubles as the angle decreases from 90 degrees to 60 degrees (Hoerner, 1965).

To give the V-tail clean airflow, they were placed high above the fuselage. A low or mid-fuselage placement would allow turbulent airflow to impinge upon the tail, possibly resulting in a lessening of control authority. Instead of a symmetrical afterbody contraction, the contraction would be upwards. An afterbody contraction ratio of 2.0 would be ideal for a symmetric afterbody (McCormick, 1995). One that is longer would result in increased skin friction while a lower contraction ratio would increase profile drag. However because of our asymmetry, a compromise must be found between the varying ideal lengths. To determine the best compromise, a simple average weighted by area was used.

Height (in)	Ideal Contraction Length (in)	Contraction Area (in^2)	C. Area * Ideal Contraction (in^3)
1	2	7	14
6	12	36	432

Compromise Contraction Length (in) 10.37209302

Table 5: Afterbody Contraction Figures.

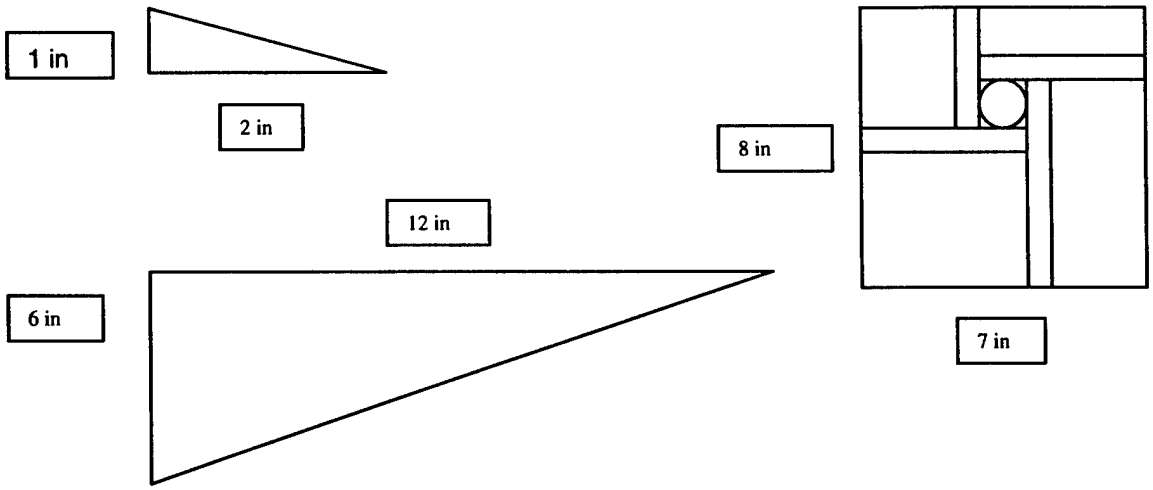

Figure 11: Sizing of Afterbody Structure. Shown above are the ideal streamlining measurements and the rear view of the tail-boom and webbing.

The only function of the rear fuselage is to provide a greater moment arm for the tail force to act upon. Placement of batteries and other objects would serve only to bring the center of gravity behind the quarter chord point. The front fuselage has more than adequate room for all electronics and batteries. The three choices for a rear fuselage along with associated scores are as follows:

Type	Advantage	Ad. Score	Disadvantage	Disad. Score	Total
Conventional	Built in Streamlining	1	Time Consuming Construction	-3	-2
Twin Boom	Greater Torsional Rigidity	2	Wetted Area	-2	0
Single Boom	Ease of Construction	3	Streamlining Required	-1	2

Table 6: Rear Fuselage Selection Matrix.

As stated before, CG concerns dictate the necessity for front fuselage room, the internal volume provided by a conventional type construction would not be used and only serve to increase the wetted area. In addition, the need for bulkheads of varying sizes makes construction more time consuming and difficult.

Twin boom designs allow for greater torsional rigidity as it provides more structure farther away from the axis of rotation. The key advantage for a twin boom design is to allow the placement of a pusher propeller. This benefit is negated by our tractor design. However, this design has the greatest wetted area. In addition to the booms, streamlining is still required for the fuselage. Why not combine the two and decrease the drag?

From this reasoning, the single boom was selected as the best choice for a rear fuselage. It's greatest benefit is its ease of construction, something very important for beginning aircraft builders. The addition of a streamlined afterbody would be relatively simple as it need not carry any forces; many difficult to manufacture bulkheads may be eliminated.

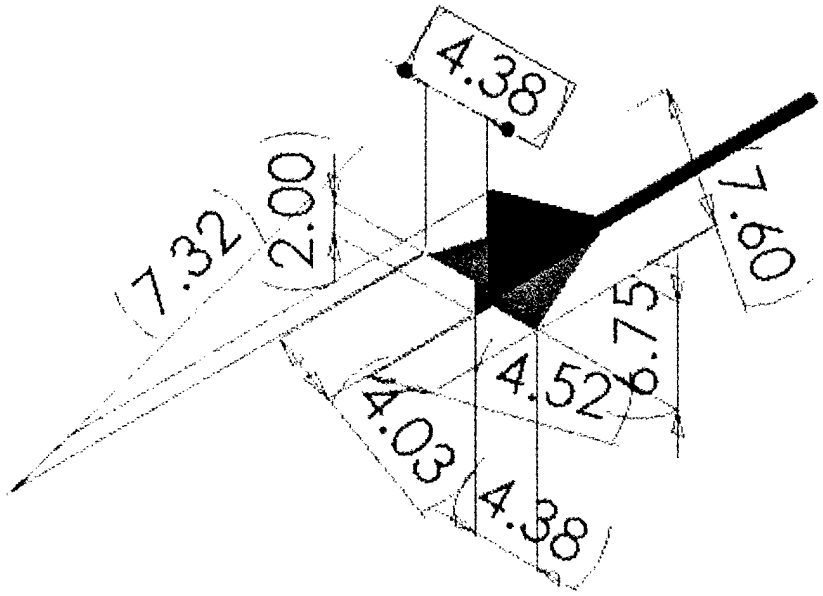

Figure 12: Final Tail-Boom Dimensions. Numbers are in inches.

Detailed Design

Final Wing Sizing

For final wing sizing, issues such as how the outboard sections would attach to the center section and what the taper ratio should be were analyzed. The center section was sized first. For simplest manufacturing and structural integration with the fuselage it was left as a straight section of 13" chord with 2' span. As previously mentioned however not all this span would be taken up by wing, it was decided that part of the spar would be exposed so that the outboard sections could plug into it by means of concentric tubes.

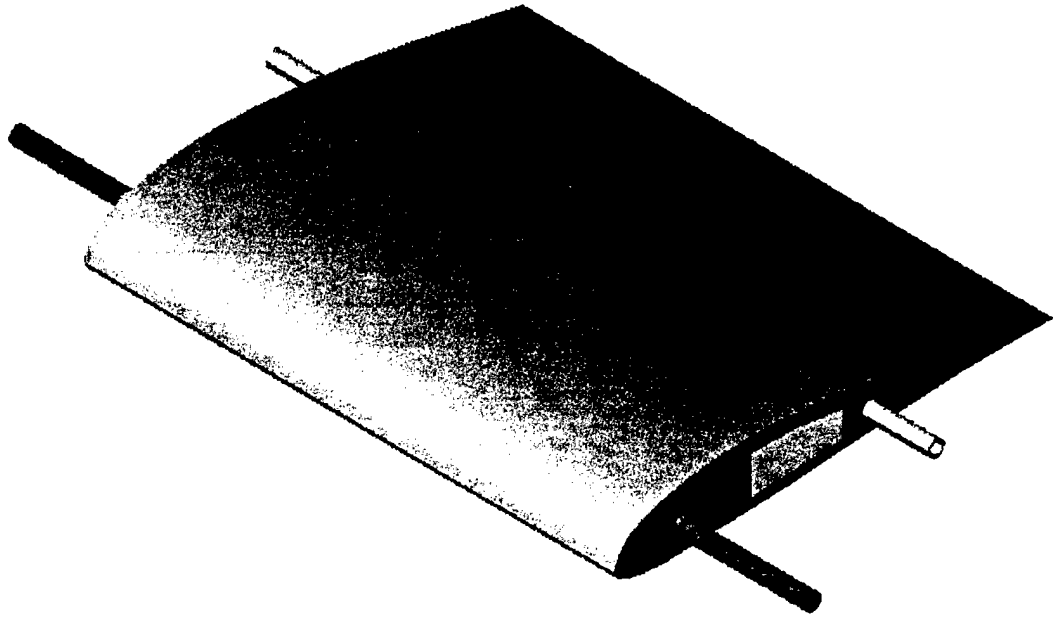

Figure 13: Wing Section with Spars.

The spar is shown above in green and structurally there had to be enough overlap between the center section spar and the outboard section spars. This is to efficiently transfer the bulk of the bending load developed in the outboard sections. However, too much overlap would reduce the overall span of the wing, increasing wing loading, and increasing induced drag by reducing aspect ratio. An overlap of 4" on each side was picked. This overlap may seem almost trivial, but consider that this decision reduces the maximum wingspan 8" from 120" to 112", or nearly 7%. It reduces the wing area considerably more by reducing the amount of straight wing. This left 16" of span for the center wing.

Since the root chord and span of the outboard sections were already determined the only part left to size was the tip chord, which would decide the aspect ratio. An MS Excel model was constructed to determine the effect the tip chord had on the total wing drag and takeoff distance. The idea was to choose the minimum drag result that still had a large enough wing area to meet the takeoff distance. The final result was that a 4" tip chord, the minimum stipulated, provided the aerodynamically most efficient result.

To verify the results the workings of the model will be explained step by step. The Excel model first calculated the wing area and aspect ratio based on a wing span of 110" (47" per outboard x 2 outboards + 16" for the center section) for tip chords ranging from 4", which was felt to be the minimum that could be produced and still leave enough room for ailerons in the trailing edge near the tips, to 10". Based on the aspect ratio and taper ratio a value of delta, δ, which is used to multiply the induced drag coefficient by (1+δ) to account for a non-elliptical lift distribution was determined from Figure 4.21 on page 172 of McCormick's *Aerodynamics, Aeronautics and Flight Mechanics 2nd Ed.* This value was also used for tau, τ, which accounts for the non-elliptical lift distribution in knocking down the actual 3D wing lift slope from the theoretical 2D airfoil lift slope.

For the 4" tip chord the overall area of the wing became:

$$S = S_{CenterSection} + 2 * S_{Outboard}$$

$$S_{CenterSection} = C_{Root} * b_{CenterSection}$$

$$S_{Outboard} = b_{Outboard} * \left(\frac{C_{Root} + C_{Tip}}{2} \right)$$

C_{Root} = 1.0833 ft.

C_{Tip} = 0.3333 ft.

$b_{CenterSection}$ = 1.3333 ft.

$b_{Outboard}$ = 3.9167 ft.

$$S = 6.99\, ft^2$$

The aspect ratio became:

$$AR = \frac{b^2}{S}$$

b = 9.1667 ft.

S = 6.99 sq. ft.

$$AR = 12.02$$

The taper ratio was taken to be an area weighted average of the taper ratio of 1 for the center section and the taper ratio of 0.307 for the 2 outboards yielding an effective taper ratio of 0.45. For this configuration tau and delta were read off the chart to be 0.014.

Next the model predicted the lift slope of the actual wing. From SD7062 lift curve data from the NASG database the airfoil lift slope a_0 and the $\acute{\alpha}_{L=0}$ were determined to be:

a_0 = 5.098 rad^{-1}

$\acute{\alpha}_{L=0}$ = -0.0891 rad

The wing lift slope was calculated according to the formula

$$a = \frac{a_0}{1 + \frac{a_0}{\pi AR} * (1 + \tau)}$$

τ = 0.014

AR = 12.02

$$a = 4.48 rad^{-1}$$

The next step was to calculate the takeoff lift coefficient, which was considered to be at the maximum angle of attack, $\acute{\alpha}_{max}$, the airfoil could sustain before stalling and was thus the same as the maximum lift coefficient C_{Lmax}. The $\acute{\alpha}_{max}$ appeared to be about 12° or 0.2094 rad for the SD7062 yielding:

$$C_{L,\max} = a(\alpha_{\max} - \alpha_{L=0})$$

a = 4.48 rad^{-1}

$\acute{\alpha}_{max}$ = 0.2094 rad

$$C_{L,\max} = 1.34 = "T/OC_L"$$

With this value determined the takeoff speed could be calculated for as follows:

$$V_{Stall} = \sqrt{\frac{2W}{\rho S C_{L,\max}}}$$

$$V_{T/O} = 1.1 V_{Stall}$$

W =13 lbs

ρ = 0.0023769 slugs / ft^3

S = 6.99 sq. ft.

$$V_{T/O} = 37.63 fps$$

After calculating this value the excel model derived takeoff drag and lift values. Drag is usually a very intricate and difficult thing to estimate so the drag was broken into three main categories: wing induced drag (reduced by ground effect on takeoff), wing parasite drag and fuselage parasite drag.

$$D = qS_{Wing}\left(C_{D,i} + C_{D,Para,Wing} + \frac{S_{Front}}{S_{Wing}} C_{D,Para,Fus}\right)$$

For the takeoff distance equation drag and lift are calculated at roughly 0.707 times the takeoff velocity, so the dynamic pressure was set to the appropriate value as follows:

$$q = \frac{1}{2}\rho\left(\frac{V_{T/O}}{\sqrt{2}}\right)^2$$

$$q = 0.84 psi$$

Induced drag on the takeoff role was reduced by a factor of 0.4 to account for ground effect.

$$C_{D,i} = 0.4 * \left(\frac{C_{L,\max}^2}{\pi AR} \right) * (1+\delta)$$

$$C_{D,i} = 0.0193$$

Wing parasite drag data was attained from the NASG Database and a regression analysis was used to determine the following equation for the parasite drag coefficient as a function of alpha in radians:

$$C_{D,Para,Wing} = 0.5964\alpha^2 - 0.0011\alpha + 0.0135$$

As airfoil drag data is obtained for optimistically smooth wings it was decided to add an additional skin friction drag coefficient of 0.006 to this. Since the reference area of the wing drag coefficient is the planform area and the reference area for the skin friction coefficient is taken to be the wetted area which is usually about twice the planform area a value of 2x0.006=0.012 was added to the overall wing drag coefficient to accurately account for the assumed increase in skin roughness. Thus:

$$C_{D,Para,Wing} = 0.5964\alpha^2 - 0.0011\alpha + 0.0255$$

ά=12°=0.2094 rad

$$C_{D,Para,Wing} = 0.0514$$

The fuselage parasite drag coefficient is where significant uncertainty arises. Based on examination of historical data and adding a conservative margin it was decided that a value of 0.12 when referenced to the frontal area was 'good' but there was little data or mathematical analysis involved in the derivation of this number. The frontal area was taken to be equal to 8"x8" or 0.5625 sq. ft. In the model the product of the fuselage drag coefficient and this frontal area was rounded up to 0.07 for extra margin. This drag was assumed to account for the additional drag of the external payload for the particular mission which required its use as this would be the most severe takeoff condition the UAV would face. Thus the takeoff drag model became:

$$D = 0.84 S_{Wing} \left(0.0193 + 0.0514 + \frac{0.07}{S_{Wing}} \right)$$

For our example with S_{wing} = 6.99 sq. ft.

$$D = 0.47 lbs$$

Lift on the other hand simply equals:

$$L = qS_{Wing} C_{L,\max}$$

$$L = 7.86 lbs$$

With these values accounted for the takeoff ground roll could finally be estimated. The equation used for this task was:

$$S_G = \frac{mV_{L/O}^2}{2[T - D - \mu(W - L)]_{0.707V_{L/O}}}$$

T = 4 lbs

D = 0.47 lbs

μ = 0.02 – Field Roughness accounting for friction between landing gear and runway

$$S_G = 83.5ft$$

Thus it is clear that the wing design should, if the assumptions hold in the actual design, enable the UAV to meet its takeoff requirements and achieve a low drag by virtue of its high aspect ratio. The final wing dimensions became:

Root Chord = 13"

Tip Chord = 4"

Wingspan = 114"

Wing Area = 6.99 sq. ft.

Aspect Ratio = 12.02

Effective Taper Ratio = 0.45

Power Plant Configuration

The power plant is an essential part of the aircraft. In any powered aircraft the power plant is a dominant factor in determining the performance of the aircraft. The energy consumption of the motor is a major concern when calculation the range and performance of the aircraft. To obtain a suitable motor, a simple program called MotoCalc was used. The program provides an accurate model of flight characteristics based on aircraft parameters such as weight, wing span, and battery type. By using MotoCalc we settled upon an AstroFlight Cobalt 40 #640 engine with a 3.1:1 gearbox.

Data from the preliminary design was used to size the motors. A conservative approach to airframe weight was used. The total aircraft empty weight was estimated at 5 lbs. Adding 5 lbs. of batteries and 5 lbs. of payload weight provided an initial weight estimate of 15 lbs.

Initially a wing CL and CC were estimated, but with the selection of the SD7062 by the aerodynamics group, the model was updated and a more accurate propulsion estimate was made.

A mission duration of 10 minutes was deemed optimal. Using data gathered from MotoCalc, a battery was selected. The Sanyo 2400 SCR was determined to have sufficient power and minimized weight. The motor sizing also allowed us to estimate peak current draw and a 40 Amp speed control was selected to provide adequate safety margin.

Manufacturer's Specifications	
Motor	
Constant	682 rpm/V
Idle Current	2 Amps
Resistance	0.121 Ohms
Weight	13 oz
Battery Specifications	
Capacity	2400 mAh
Impedence	0.0032 Ohms
Weight	2.08 oz
Gearbox	Superbox
Gear Ratio	3.1

Table 7: Manufacturer's Specification for Propulsion Components.

Using MotoCalc, we fine tuned the components of our aircraft's propulsion system. The diameter of the aircraft is about 8 inches. Therefore the propeller size has to be about 12 inches since a good rule of thumb is that the propeller size has to be at least 2 inches all around beyond the width of the aircraft. This ensures sufficient thrust past the fuselage. Optimizing flight performance, a 15 in. propeller with a 10 in. pitch was chosen. This configuration provides excellent thrust and cruise speed.

Design Package

A detailed design package is included at the end of this report.

UCLA AIAA Bud-E

Geometry

Length	Span	Height	Wing Area
47.97"	114"	11.1"	6.99 sq. ft.

Control Volumes		Aspect Ratio
0.01264 (Vertical)	0.2066 (Horizontal)	12.02

Performance

$C_{L\,max}$	L/D_{max}	Max Rate of Climb	Stall Speed	Max Speed
1.34	13.93	4.98 ft/s	37.63 ft/s	53.05 ft/s

Takeoff Length (empty weight)	Takeoff Length (gross weight)
29.7 ft	83.5 ft

Weight

Airframe	Propulsion System	Control System	Payload System	Payload
4 lbs	4.26 lbs	8.85 oz	3 oz	5 lbs

Empty Weight	Gross Weight
9 lbs	14 lbs

Systems

Radio Used	Servos Used
Futaba T6XHS (controller) Futaba FP-127DF (reciever)	Hitec HS-81MG (aileron) Hitec HS-300BB (v-tail)

Propeller Used	Battery Config	Gear Ratio
15/10	26 cell Sanyo 2400	3.1:1

Motor Used
AstroFlight Cobalt 40 #640

Table 8: UCLA AIAA Bud-E Data Specifications.

Rated Aircraft Cost

	Value	Multiplier	Total
Manufacturer's Empty Weight			
Aircraft Weight without Payload	9 lbs	$100	$900
Rated Engine Power			
Total Battery Weight	3.38 lbs		
Number of Engines	1		
REP	3.38	$1,500	$5,070
Manufacturing Man Hours			
Wing Span	9.5 ft	8 hr/ft	76 hr
Max Wing Chord	1.08 ft	8 hr/ft	8.64 hr
Number of Control Surfaces	2	3 hr	6 hr
WBS Wing			90.64 hr
Fuselage Length	4 ft	10 hr/ft	40 hr
WBS Fuselage			40 hr
Vertical Surfaces	0.5	10 hr	5 hr
Horizontal Surfaces	1	10 hr	10 hr
WBS Empenage			15 hr
Number of Servos	5	5 hr	25 hr
Number of Speed Controllers	1	5 hr	5 hr
WBS Flight Systems			30 hr
Number of Engines	1	5 hr	5 hr
Number of Propellers	1	5 hr	5 hr
WBS Propulsion Systems			10 hr
MFHR	185.64 hr	$20/hr	$3,712.80
Rated Aircraft Cost Total	**$9,682.80**	**1/$1000**	**9.6828**

Table 9: Rated Aircraft Cost using Design Specifications.

Manufacturing Plan and Processes

Structure and Manufacturing

Wing Construction

It now became critical that an efficient structure and manufacturing method be devised for the wing so that it would be light, easy to build and quick to assemble out of the box. Materials selection primarily drove the manufacturing methods available to us. The construction of carbon fiber or Kevlar ribs was initially considered. However it was rejected as being too labor and time intensive for initial wing fabrication while purchasing little structural improvement over more conventional methods. Indeed a composite wing would likely be far stronger than a non-composite wing, but as non-composite wings were seen to be strong enough this advantage was essentially negated. The remaining two manufacturing methods available were plywood frame with balsa skin, and spider foam cut into shape with hot wire EMD. Wood construction offered the advantages of having lighter weight and good geometric accuracy between design and finished product, but again came at the cost of long fabrication times and labor intensiveness. It was however the only manufacturing method which would allow placement of batteries and avionics in the wing as planned. Wood construction was therefore necessary for at least part of the wing. Hot wire EMD of foam was quick and relatively easy but as the wire frequently assumed some curvature during the cutting process it would alter the airfoil geometry a small degree. This deformation was deemed small enough to be acceptable and the quick manufacturing time argued nicely for this method. It was also quicker to fit control surfaces to a foam wing section.

A hybrid wing structure was designed based on the comparative advantages of the different manufacturing methods. The entire center section of the wing would be built out of wood with ribs 4" apart to stow the batteries. This kept the batteries close to the centerline of the UAV to ease balancing for roll stability. The outboard sections were initially planned to have the inner 8" made out of wood for lighter weight and the remaining 39" cut out of foam.

From a structures standpoint some provision for a wing spar had to be made. The mating method determined in the final wing sizing section already dictated that each of the three wing sections have their own spars which would interlock on final assembly, effectively producing a single load bearing spar. This load bearing spar was placed near the aerodynamic center of the root chord where the airfoil was thickest. Our design solution was to use concentric carbon fiber tubes and rods to facilitate mating. Carbon fiber represented a higher specific strength than brass tubing as was the material of choice. The center section was designed with a 0.5" outer diameter by 24" long rod for increased bending resistance, while each outboard section had a 0.5" inner diameter by 30" long tube which slipped over the center section rod. To secure the connection from pullout kotter pins would be inserted into the spar. Also an additional smaller spar was deemed necessary to resist any torsion about the main spar's axis from wing flutter. This 'guide' spar as it was called was placed near the trailing edge of the airfoil. It employed the same design philosophy as the main spar, with a 0.5" outer diameter by 20" tube in the center section to save weight and a 0.5" inner diameter by just 8" tube in each outboard section. This guide spar would

also feature kotter pins to connect the outboard sections with the center section. Since this spar resisted torsion primarily it did not need to go through much of the wing's span like the main spar which primarily resisted bending. Conceptual drawings of the center section, outboard sections and mating are provided below.

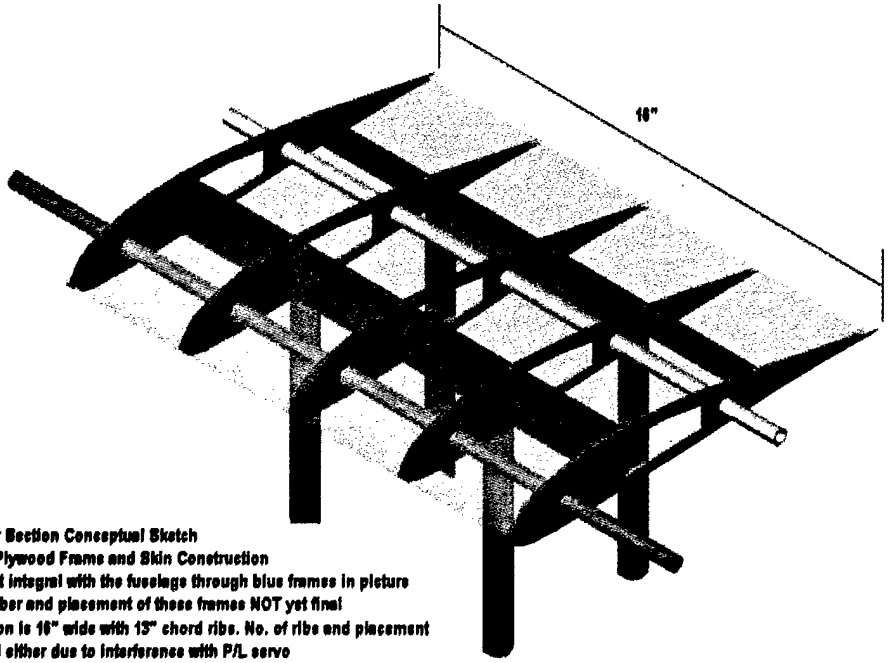

Figure 14: Wing center section. Main structural spar is shown in green and guide spar in gold.

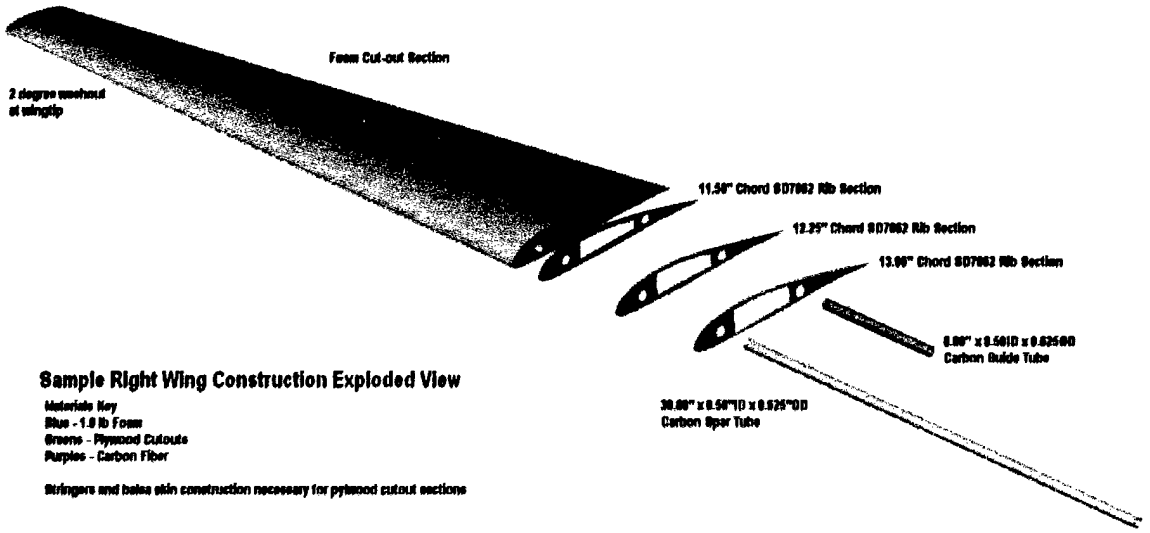

Figure 15: Exploded View of Right Outboard Section. Foam construction shown in blue, wood construction in green, main spar in light purple and guide spar in magenta.

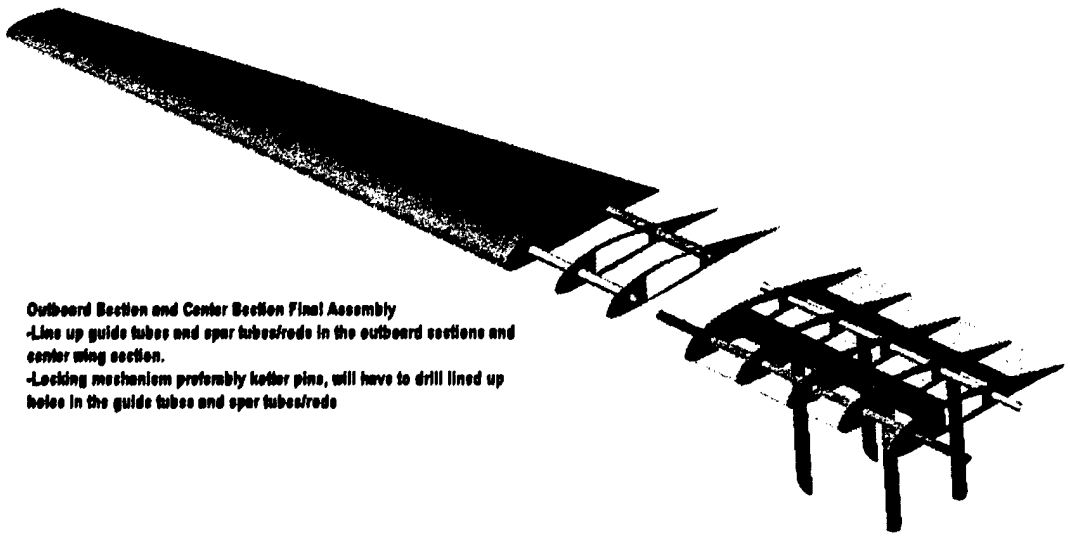

Figure 16: Wing Assembly.

To meet construction deadlines and speed construction of the wing section, the outer balsa wing sections were removed in favor of an all foam outer wing section. This reduced the total wing area slightly but was acceptable because of the initially conservative design approach.

Engine Mount

The aircraft has a front mounted motor. The short, stubby nose of the aircraft that contains the engine mount is attached to the rest of the airframe via the front bulkhead. The motor is secured by its front end to the inside of the front plate of the nose. The front plate is attached to the front bulkhead by a system of triangular lattice members, made of 3/16" circular dowels trusses. The trusses are joined to the front plate at the midpoint of each of its edges, and to the front bulkhead at the corners. The function of this lattice is to absorb the torsion produced by the motor.

Since the dowels have very little gluing surfaces to provide axial strength, a supplement would be needed. Considering the axial stress present would the tensile as the engine pulls the aircraft forwards, a system tensile members would be in order. We found ideal material for this application would be nylon wire. Nylon wire is extremely strong in tension (40lb, for beyond our motor thrust level) while having negligible mass. The wires would be tired between the front plate and the front bulkhead in a couple of loops. The wires would be pre-tensioned, so that as soon as the motor starts running, the tensile load would be immediately be taken up by them. While the engine is off, the dowel trusses would support the

tension in the nylon wires. The stress in the dowels would be compression, which is the ideal type of load for the dowels.

To further address the issue of lack of gluing surface of the dowel, measures would have to be taken strengthen the attachments. The solution would be aimed to increase the surface area. To achieve so, the dowels would not be directly glue to either the front plate or the bulkhead. Instead, holes would be drilled in the attachment point on the plate and the bulkhead. Then the dowel would be made just long enough to pass through these holes. To secure the dowels in place, wooden washers would be mounted onto the dowel heads, both ahead and behind the attachments points. The washers would sandwich the plate/bulkhead, thereby creating a extraordinary vast amount of gluing surface to epoxy the dowels in place.

This system of dowels and nylon wires is displayed in the drawings package. They provided a light structure that has excellent strength in both torsion and tension, which is the ideal.

Tail Construction

Attaching the two wings onto the rod in a v-shape surprisingly was quite a difficult task. Our idea of attaching the wings to the rod was to use a small wooden stick and insert one end into the wing and the other end into the rod. The problem we encountered was that the wing would fall out and flutter because of air resistance. We also could not glue both ends of the stick because we needed the wings to pivot. Our solution to this problem was to glue the stick on the end that goes into the rod (this prevented the fluttering). Then drilling a deep hold into the wings so that the stick could have a longer "grip" on the wings. The insurance that the wings would not fall all the way out of the stick's reach was our pivot device which prevented it from moving that far out.

All in all, the v-tail design gives an ultimate control authority for its RAC. Its all-moving tail deflects a lot of air just a little bit which lessens the force from air resistance, conserving the planes momentum and giving the design greater efficiency.

Landing Gear Construction

A stainless steel metal with 1/16" thickness was chosen for the material due to its high strength and mediocre flexibility to aid in absorbing the shock from landing. Upon constructing the main landing gear, two holes needed to be drilled at the specified locations for both legs. A great deal of care was taken to ensure that the holes were drilled in the precise location, however the holes were not exact due to the slipping of the metal while it was drilled. Also, the metal could not be bent exactly to the specified angle. However, it is close enough that the difference is negligible.

After attaching the landing gear to the fuselage of the plane, it was observed that the steel bent under the weight of the plane more than anticipated. Since not all of the weight was added to the aircraft, it was certain that some reinforcement needed to be added to the stainless steel. Some possibilities to fix this problem include: running a support rod between the two wheels or increasing the thickness of the

stainless steel to 1/8inch thickness. Until a more solid folding landing gear can be built, a solid non-detachable landing gear was attached in order to continue with testing of flight systems.

Personnel Breakdown

Construction of the aircraft required a broad range of skills. In order to minimize manufacturing errors and maximize productivity, personnel were assigned tasks according to their experience. Skill levels were assigned to specific tasks in order to facilitate this process.

	Wing	Fuselage	Landing Gear	Tail	Propulsion
Structure	2	1	1	2	1
Control Surfaces	2	0	0	1	0
Sheeting	1	1	0	0	0
Electrical	1	1	1	1	2

Table 10: Skill Matrix. Construction assignments are rated by required skill. Higher figures indicate higher complexity.

Manufacturing Schedule

The manufacturing schedule was design to create systems as quickly as possible. Simpler components such as the payload system were constructed early in the process. Other more complex components such as the wings were delayed. Building times were also scheduled around available time frames for the personnel. The earlier periods during the academic calendar, such as weeks 2 through 4, are times when class requirements are less constricting. Intense building was thus planned for those periods.

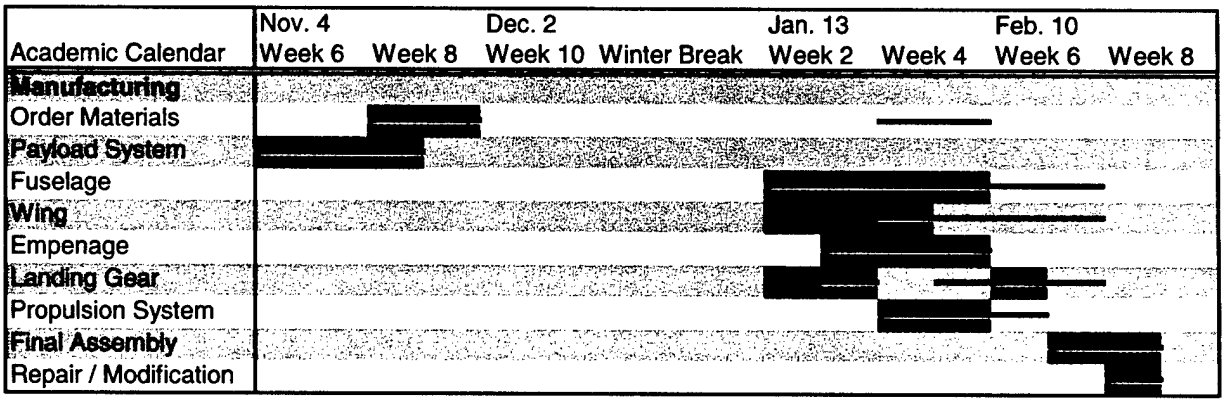

Table 11: Manufacturing Schedule. Blue blocks represent estimated dates and black bars represent actual manufacturing.

Testing Plan and Initial Results

With the completion of the aircraft nearing in late February, testing of components began. Among the first of the completed components was the payload system. Respective components underwent static testing. Propulsion components underwent duration and thrust testing. With the actual aircraft completion, it would undergo a series of dynamic flight testing.

Static Tests

1.) Payload Deployment Test

Payload deployment system is tested for both servo torque requirements and its ability to hold the payload securely. Expanded testing includes the attachment of the spring-loaded payload doors.

2.) Wing Tip Lift Test

The full size wings would be tested for structural integrity. Initially, the outboard sections are given tested on their ability to hold weight. With the completion of the aircraft, the fully loaded plane would be lifted by the tips of the wings. This simulates approximately 2.5Gs of force on the wing structure.

3.) Landing Gear Test

Landing gears were first tested on ability to hold the full weight of the aircraft. A drop test would be initiated afterwards from gradually increasing heights to a maximum of 3 feet to ensure structural strength and shock absorption.

4.) Motor / Battery Duration Test

The propulsion system would be put through a duration test. The motor is run at expected cruise power to determine the expected maximum flight time.

5.) Motor / Propeller Thrust Test

6.) Fuselage / Nose Torque Test

Dynamic Tests

1.) Fully Loaded Taxiing Test
2.) Unloaded Flight Test (Takeoff and Landing)
3.) Unloaded Flight Test (Turning and Rate of Climb)
4.) Loaded Flight Test (Takeoff and Landing)
5.) Loaded Flight Test (Turning and Rate of Climb)
6.) Unloaded Flight Test (Flight Duration / Full Course)
7.) Loaded Flight Test (Flight Duration / Full Course)
8.) Loaded Mission Flight Test (Type A: External Payload)
9.) Loaded Mission Flight Test (Type B: Internal Payload Deployment)

Initial Testing Results

Wing Box Modification

The original wing structure was carried on two spars. The forward spar was the only spar of the all through type. The back spar was cut to accommodate the servo used in the payload release mechanism. It was decided that the back spar could be cut in the middle because the forward spar was designed as the main load carrying spar. The function of the back spar was there to secure the incidence angle of the wings. This design, however, was change after the wing tip test. The test required having the aircraft be lifted by its wing tips. The test showed that the back spar also acted as a major load-bearing member. Without it being a solid piece, the wing box collapsed during the first wing tip test.

Changes were made to reinforce the wing box. One obvious change was replacing the back spar with a solid all through member. Bending moment increases at the wing roots when the aircraft was lifted by its wing tips. This results in the top surface of the wing box experiencing tremendous compression stress. A form of support would be required to prevent the wing box from deformation under this stress. A thin layer of plywood sheet was used to serve this purpose. The flexible plywood sheet covered the top surface the wing box with its grain point from wing tip to wing tip. This covering was firmly held to the each of the wind box ribs with an ample amount of epoxy. The thin plywood was the ideal material due to its lightweight. And because it was secured to each of the individual ribs with its grain run along the direction of the stress, it provided as an excellent compression member.

This new construction proved to be a major improvement in the repeat of the wing tip test. However, the upper surface still displayed inadequacy in dealing with the compression. The plywood sheeting displayed buckling extending from the leading edge to the quarter chord point. The solution to this problem was found in 3/64" steel rods. We discovered the stiffness of the rod would be sufficient to prevent the buckling in the plywood. Three rods with length that matched the width of the wing box were attached to the upper surface running from wing tip to wing tip. The rods were placed at stations located between 1" and 3" behind the leading edge. These rods were also fixed in place with plenty of epoxy. This gave an effect of having the rods being embedded in the surface of the plywood covering. The buckling effect was completely removed as the result of the addition of these rod stiffeners. With these modifications in place, the aircraft finally passed the wing tip test.

References

1. McCormick, B., *Aerodynamics, Aeronautics and Flight Dynamics,* John Wiley & Sons, New York, NY, USA, 1995
2. Raymer, D., *Aircraft Design: A Conceptual Approach,* American Institute of Aeronautics and Astronautics, Inc., Reston, VA 1999

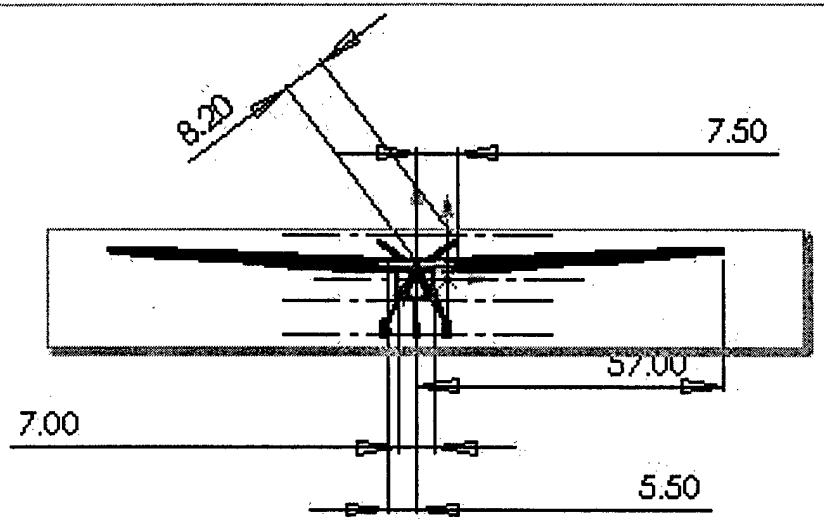

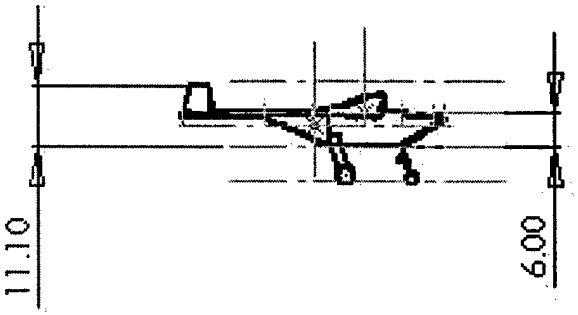

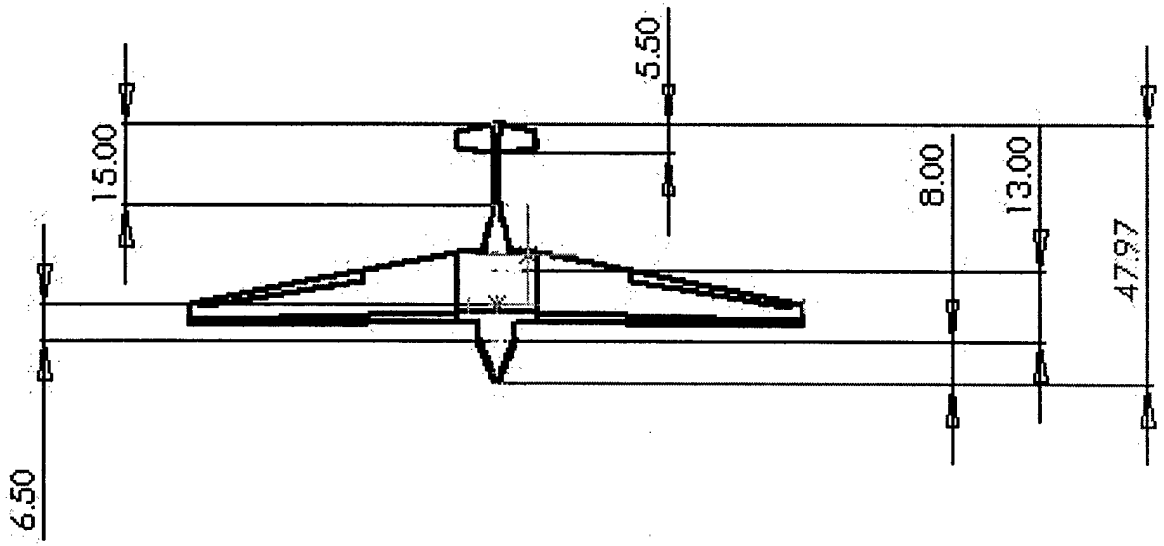

PROPRIETARY AND CONFIDENTIAL

UCLA AIAA

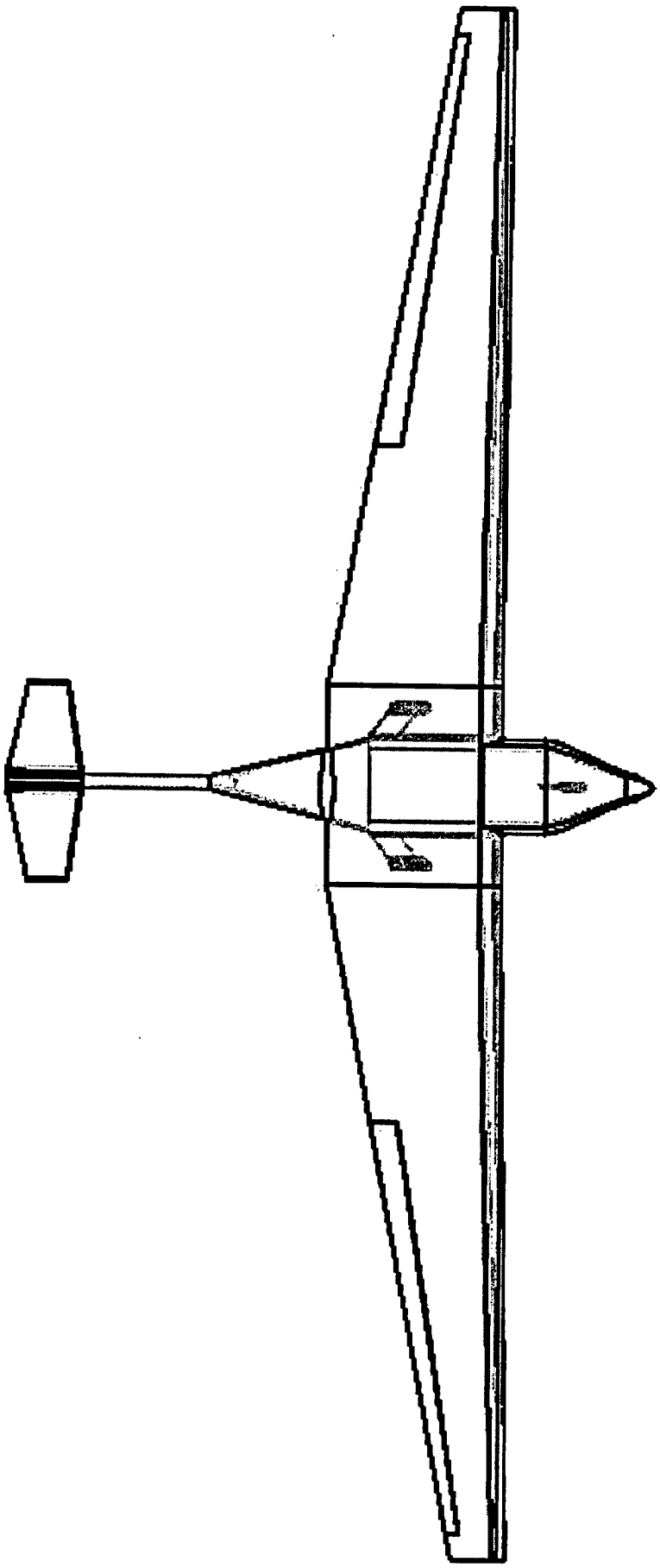

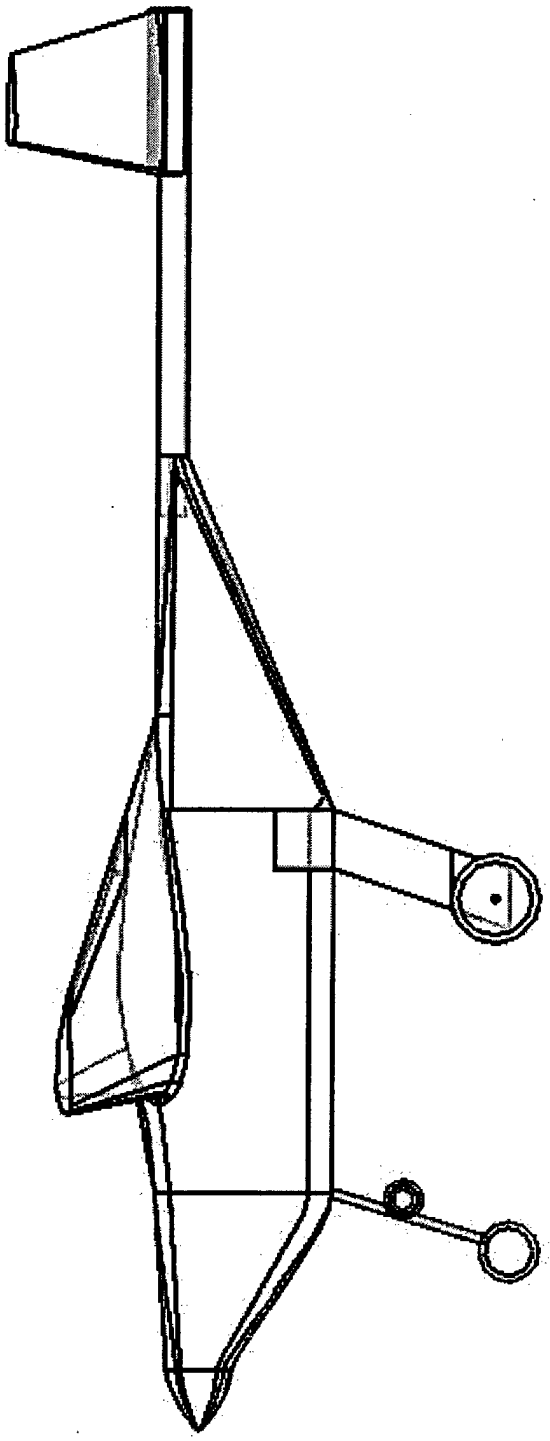

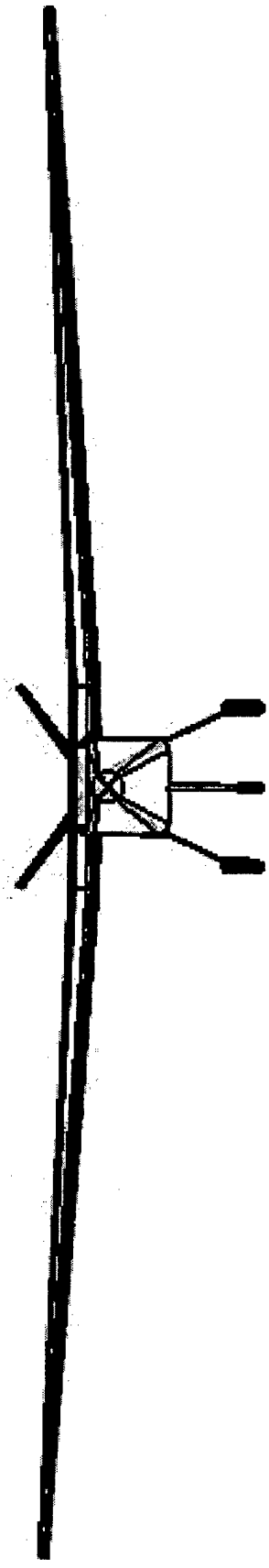

Engine Mount (Nose)

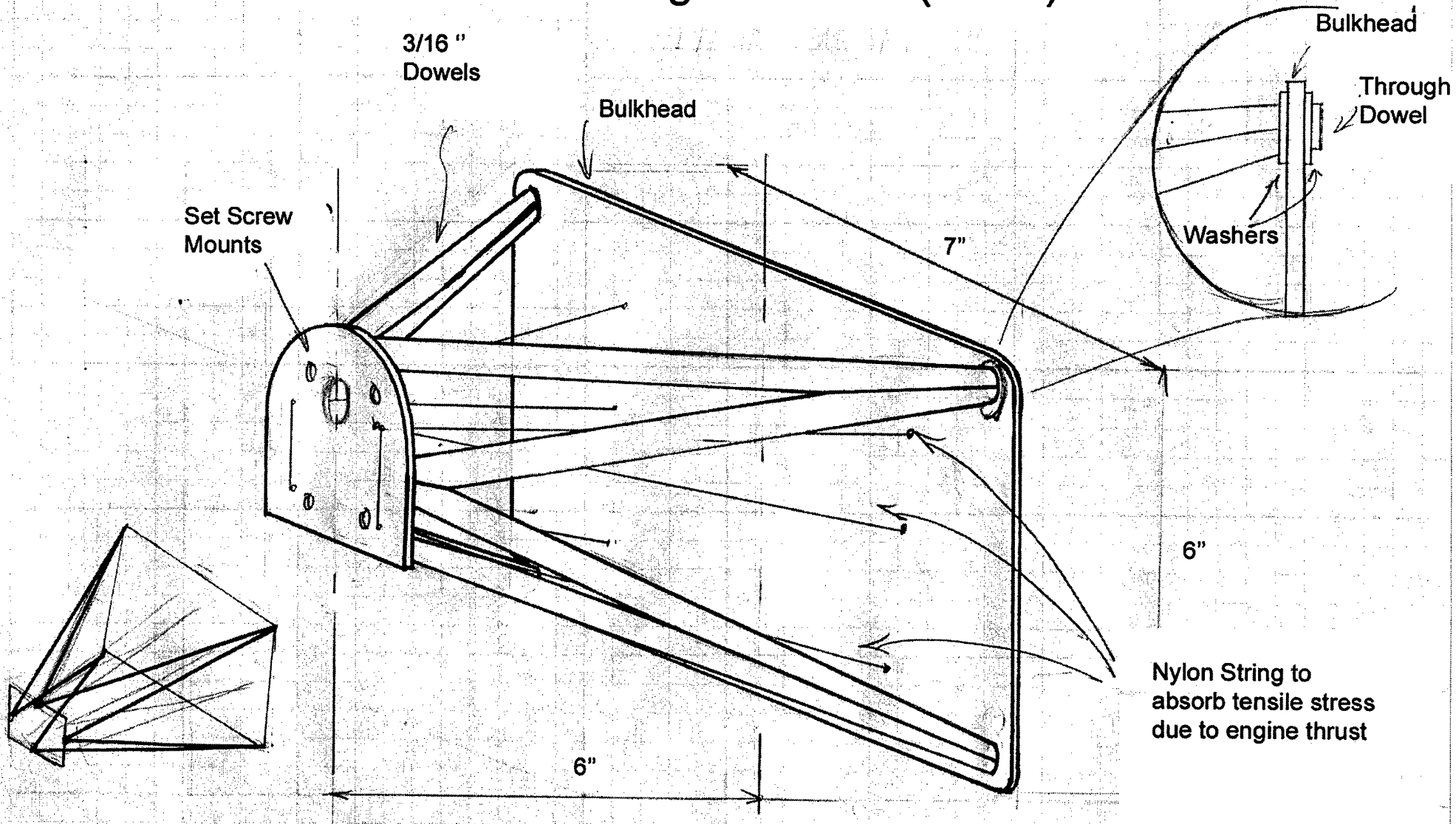

California State Polytechnic University, Pomona

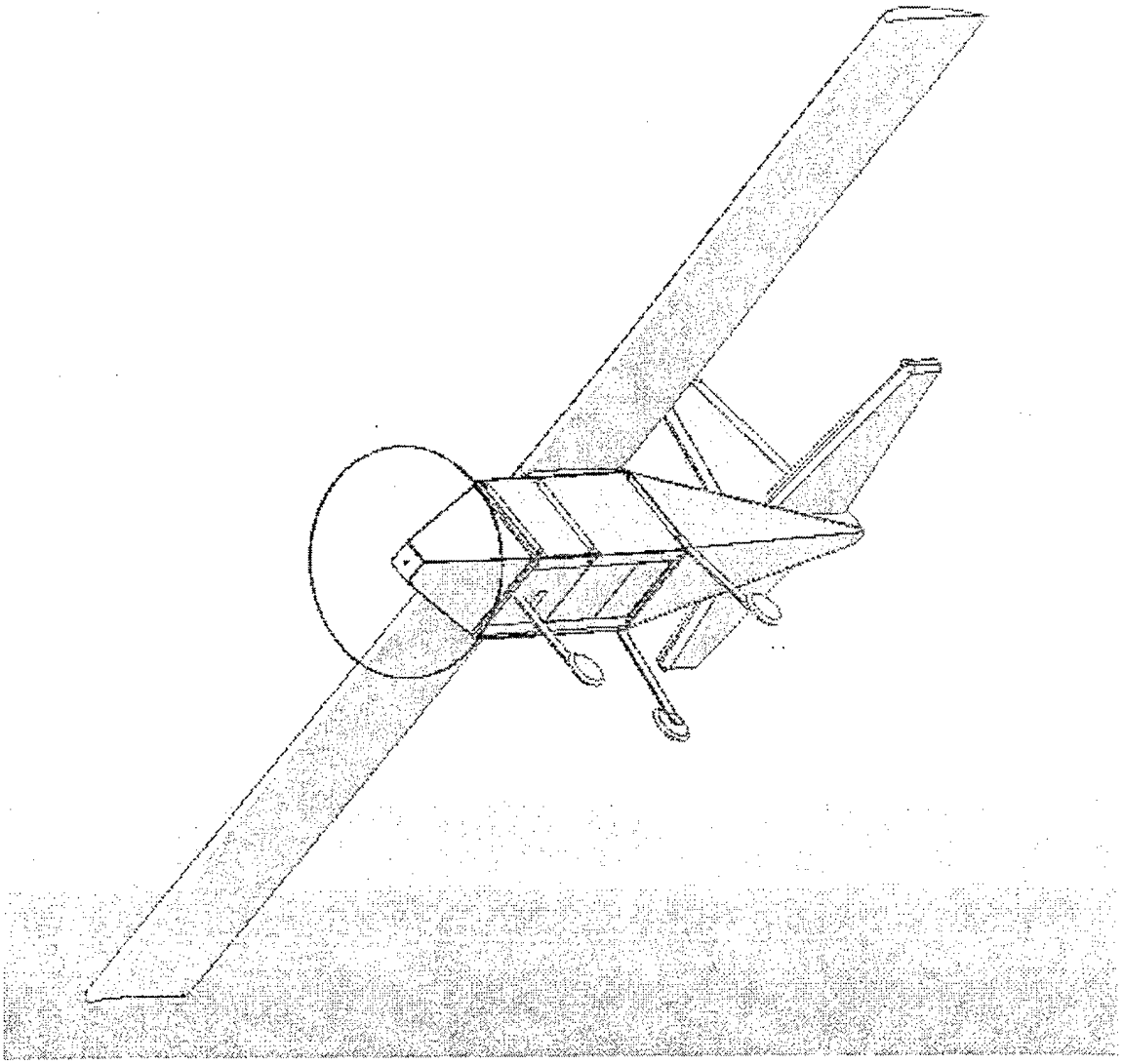

Aircraft: Pegasus

TABLE OF CONTENTS

1.0 **EXECUTIVE SUMMARY**.....1

1.1 CONCEPTUAL DESIGN.....1

1.2 PRELIMINARY DESIGN.....2

1.3 DETAIL DESIGN.....3

2.0 **MANAGEMENT SUMMARY**.....5

2.1 TEAM ORGANIZATION.....4

2.2 TEAM ASSIGNMENTS AND RESPONSIBILITIES.....5

2.3 SCHEDULING.....6

3.0 **CONCEPTUAL DESIGN**.....7

3.1 DESIGN PARAMETERS.....7

3.2 AIRCRAFT CONFIGURATION.....9

3.3 STRUCTURAL CONFIGURATION.....11

4.0 **PRELIMINARY DESIGN**.....15

4.1 PROPOLSION DESIGN PARAMETERS.....15

4.2 AERODYNAMIC DESIGN PARAMEERS.....15

4.3 STRUCTURAL ANALYSIS.....16

4.4 PROPULTION ANALYSIS.....19

5.0 **DETAIL DESIGN**.....22

5.1 PERFORMANCE ANALYSIS.....22

5.2 PROPULSIVE PERFORMANCE ANALYSIS.....23

5.3 STRUCTURAL CONSIDERATIONS.....23

6.0 **MANUFACTURING PLAN**.....25

6.1 PROCESS SELECTED FOR COMPONENT MANUFACTURING.....24

6.2 FINAL ASSEMBLY.....27

7.0 **REFERENCES**.....28

8.0 **TABLES AND FIGURES**.....29

1.0 Executive Summary

This paper will show the process taken to design, build and fly a remotely controlled electric powered airplane by the Cal Poly Pomona Pegasus team. As a first year entry to the AIAA Design/Build/Fly competition, it is the goal of the Pegasus team to design, build and fly an airplane that would accomplish mission goals in the least amount of time and minimize the rated aircraft cost model, as outlined in the rules for the competition. In doing so, the team went through three main phases of design and building, which resulted in the final aircraft.

1.1 Conceptual Design

The team first met to determine the goals of the competition. In order to maximize our score, we determined that our flight and assembly times should be minimized, along with our rated aircraft cost. This led to the team braking into three groups: aerodynamics, electronics/propulsion and structures. Throughout the process each group would report to the entire team about how certain parameters would affect our score.

1.1.1 Conceptual Design Overview

The team as a whole met to determine the aircraft configuration. We chose the model that had the lowest rated aircraft cost and was easiest to construct. The electronics and propulsion team began to compare engines and servos, while the structures team worked on determining the weight of the plane and the materials to build with. The aerodynamics team began to analyze airfoils and wing configurations.

1.1.2 Conceptual Design Methods

Methods used for calculations included decision matrices were to compare aircraft configurations and spreadsheets to compare engines and wing configurations. Some computer programs such as Visual Foil and X-foil and experimental data from wind tunnel testing were implemented to compare airfoils.

1.1.3 Conceptual Design Results

The plane configuration chosen was a conventional style because it would be the easiest

to construct, fly quickly and have a low rated aircraft cost. The wings would be made of foam core with fiberglass and sandwich structure. The fuselage would have a wooden frame with a fiberglass or carbon fiber skin. The airfoil was chosen to provide a high lift, but minimal drag as the plane would be carrying a five-pound payload. A single engine with a single prop was chosen because it would give us the required power to operate the plane, with the least added weight and rated A/C cost.

1.2 Preliminary Design

During the preliminary design, further analysis was done on the plane. The team broke into groups and each of the three groups worked on calculations in their respective areas. Weekly meetings were held as a large team so the entire team was kept up to date on what each individual group was working on. The efficiency of inter-group communication was critical to the design of the plane. Preliminary construction was done on the payload box, along with some test runs of building the fuselage.

1.2.1 Preliminary Design Overview

Each group worked independently while reporting to the team as a whole weekly. The aerodynamics team redesigned the wing to fly faster and the propulsion/electronics team compared propellers and servos. The structures group began analyzing landing gear and payload drop configurations, along with determining the strength of the wing and a more accurate weight. The team as a whole debated the number of control surfaces, including the use of a rudder.

1.2.2 Preliminary Design Methods

Spreadsheets were essential to the development of the plane. They provided quick analysis of multiple options for wing configurations along with thrust and strength calculations. Research from multiple textbooks made sure our formulas were correct. Internet research and communication through email produced potential sponsors. A three-dimensional computer model was also created so a more visual representation of the craft could be shown to possible sponsors and during our review presentations.

1.2.3 Preliminary Design Results

At the end of the preliminary design stage, the plane had a small wingspan and a short payload bay with a boom for the tail in order to minimize the drag and weight. The goal was to fly quickly.

1.3 Detail Design

Detail design came after we presented our plane to faculty members and industry representatives. Their input was used in a redesign of the wing and fuselage. This is also when the main construction phase began.

1.3.1 Detail Design Overview

Two major changes occurred during the detail design. First, the aerodynamics team increased the aspect ratio of the wing and changed the airfoil to allow for more lift. Next the structures team lengthened the payload bay to extend all the way to the empennage. The propulsion group did testing of the motor to analyze endurance of battery packs and the motor.

1.3.2 Detail Design Methods

Again, spreadsheets were very helpful when quick calculations were needed. Much of the work done during this stage was hands on, constructing test and practice runs of our wing and fuselage. Many first drafts of the plane's parts were created and used for physical testing of the plane.

1.3.3 Detail Design Results

The final product of the plane had a medium sized wingspan and a long fuselage. The fuselage structure was exchanged to a more rigid design, which brought a penalty to overall weight. However, the motor, along with a large propeller and our wing airfoil, then produced enough thrust and lift combined to compensate for the weight.

2.0 Management Summary

2.1 Team Organization

Cal Poly Pomona's Pegasus team was split into three subdivisions, which included aerodynamics, propulsion and structures. A leader headed each team of engineers. The team manager and systems engineer then superintended all subdivisions. An outline of the team organization and their assignment area is provided below in figure 1.

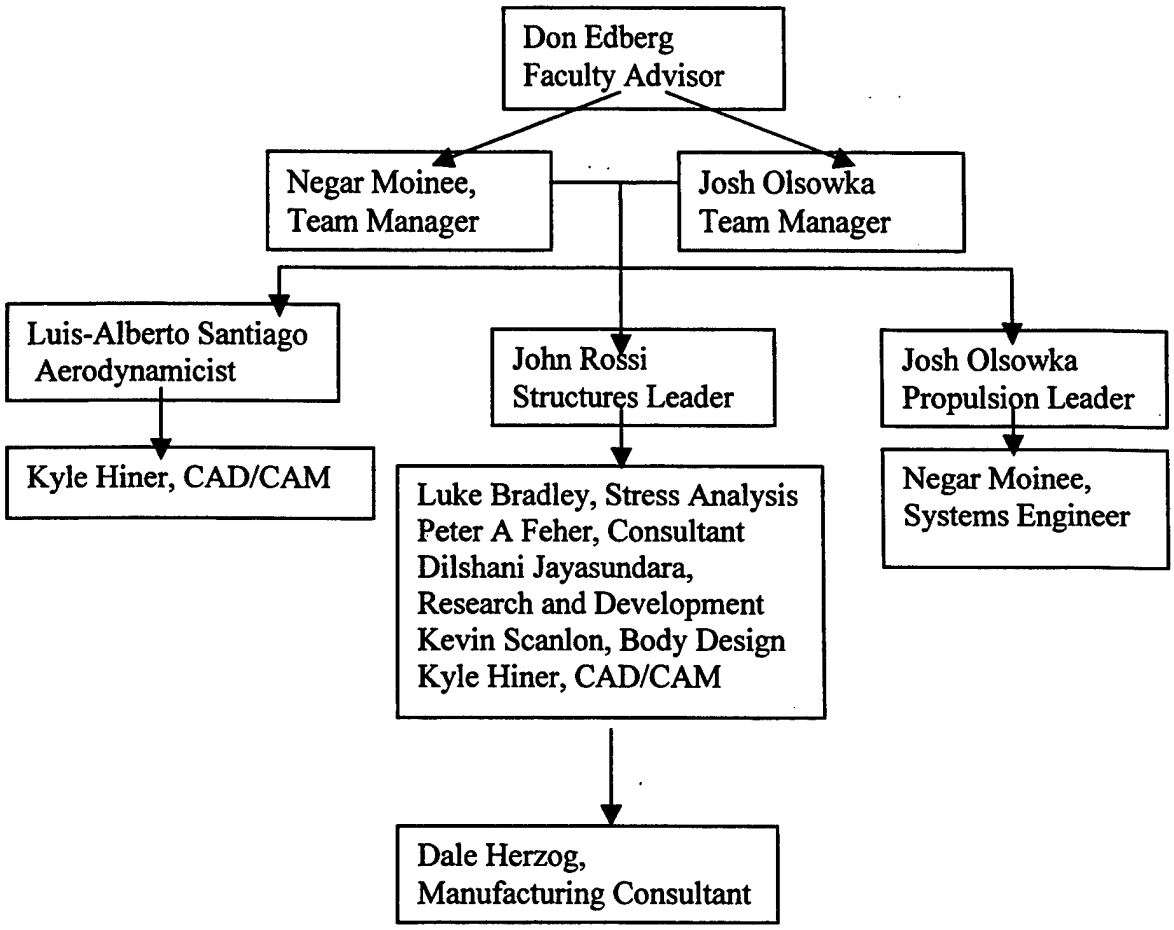

Figure 1. Cal Poly Team's Architecture Chart

2.2 Team Assignments and Responsibilities

The team leader's responsibilities were to manage and organize each subdivision, assure that all design requirements were met and provide the necessary equipment and parts needed for construction. The team manager and systems engineers assigned each team their tasks and supervised or planned each of the processes to ensure that all design requirements were met. Each team's design decisions were interrelated to the other; therefore all teams would meet regularly to discuss and share all decisions made to ensure a well-balanced design. Amongst the teams the leaders then assigned the tasks to each team member and those engineers would then report back to their leaders. Our faculty advisor, whom also was our pilot, also overlooked most of the design processes and commented on the design decisions made in each stage. A further detailed description of each subdivisions tasks are outlined below.

2.2.1 Aerodynamics Group

This team performed all the aerodynamic studies from the conceptual design up to the detailed design, which was our final configuration. They began by trade studies and configuring the figures of merit laid out according to the given design requirements for various aircraft. All of the analysis was done using mathematical modeling, computer software and programs written to incorporate the design provisions. This team was assigned to select an airfoil, wing and tail size, lift, drag, take off and cruise performance and analysis.

2.2.2 Propulsion Group

The propulsion group was assigned the selection of the motor, batteries, servos and all other electrical devices installed in the plane. Analysis on these components was done using the rated aircraft cost(RAC), which was formulated using the competition rules. Once the RAC was determined figures of merit were obtained and used to select the proper engine that was to provide the sufficient thrust and efficiency. All the tabulated values (which included required thrust and power) were given using the computer programs and mathematical modeling processes by the aerodynamicist. During the preliminary design phase this group was assigned to also test all

the propulsive parts to ensure their performance. Once all testing was complete this team was assigned to do all flight-testing along with the aerodynamicist.

2.2.3 Structures Group

The Structure of an airplane has to be able to resist the applied aerodynamic and inertial loads. The Structures group was responsible in designing the structure accordingly to withstand the applied loads. Weight of an aircraft is an essential quality in aircraft performance, thus the design process was started, by employing structural load analysis.

The structures team, scrutinized several methods of building aircraft structures using the past design parameters. Then, the group conducted researched on all possible available construction materials, providing figures of merit to make a decision as to what materials should be used in constructing the airplane. At the introductory design stage the wing, fuselage, tail and the landing gear were designed using the loading parameters given by the aerodynamic and propulsion teams. Once the structure was designed it was tested for compliance according to the introductory parameters. Furthermore, the structures team was also responsible in completing the final design drafts.

2.3 Scheduling

In order to comply with the given deadlines of the competition the team had to progress rapidly. Certain milestones and deadlines were set for the various design stages, which included the conceptual design, preliminary design, detailed design, and the manufacturing and testing phase. The design report was completed alongside each design phase and compiled at the end of the design phase. Figure 2 outlines the milestone chart for the design process.

3.0 Conceptual Design

3.1 Design Parameters

3.1.1 Design Parameters

A sensitivity analysis was performed encompassing all major flight parameters including:

Aircraft Weight: This parameter consisted of the empty and gross weights for the model and was analyzed base on publicly published data.

The original design for the fuselage included a plywood frame with hard wood reinforcements. A plywood design was the groups initial decision as the strength of plywood seemed appealing being the main structure of the aircraft. An experimental frame was constructed; although the frame sustained loads much greater than those the aircraft was designed to, it was abandoned in favor of a lighter balsa frame. After consideration of the plywood into the aircraft weight it proved that a balsa wood frame would give a weaker structure but benefit by making the aircraft weigh less, which came out to be a much more important. Following that, the original design of the fuselage would not be possible with the balsa wood alone. It became necessary to reinforce the balsa design to resist the flight loads. The design of the fuselage was then altered to add supports to the balsa frame. This was necessary in order to allow the stricture to resist higher load without significantly increasing weight.

While weight was the primary consideration for the fuselage design, its dimensions were The determination was governed primarily through the size of the payload. The fuselage structure had to be large enough to contain the payload box inside of it and be able to deploy the box either in the rear or the bottom of the fuselage. The fuselage was also designed so that the payload would coincide as much as possible with the center of gravity of the aircraft. The reasoning for this was to try to keep the moment about the center of gravity unaffected by the payload so the plane would fly similarly if the payload were on board or absent from the aircraft. Calculating the necessary volume for all internal components and adding them to the volume of the payload determined the final dimensions of the fuselage.

The antenna placed on the top of the fuselage creates a large amount of drag due to its

blunt face. Since the design of the antenna was set by the rules of the competition it could not be altered in any way. This left the group with the problem of accounting for the extra aerodynamic loads introduced by this structure. Taking this into consideration, the frame of the aircraft must be able to withstand the moment created by the aerodynamic forces acting on it. Since there will be a good amount of drag on the structure the group has to make sure that the structure can withstand the loads. By placing the cylinder at the beginning of the tail, it can be attached to the rear bulkhead, one of the stronger sections of the frame. The bulkheads will be one of the strongest and most reinforced parts of the fuselage so the drag moment on the antenna will be absorbed into the fuselage through the bulkhead.

During flight the aircraft will be exposed to various flight loads such as wind gusts and inertial loads. Design of the attachment of the wing to fuselage, is especially sensitive to inertial loads. In attaching the wings to the fuselage, hard points were created on the wings. The wing would be attached to similarly reinforced sections of the fuselage. The entire fuselage will be capable of resisting three times its own weight. The extra strength of the fuselage structure will then be used to resist the bending, shearing, and combined loading that the wing would undergo and transfer to the fuselage at the connection points.

3.1.2 Rated Aircraft Cost

The spreadsheet application program previously mentioned was designed so that it would output the RAC values for particular a aircraft configuration inputs. These values incorporate those values with performance parameters to estimate an overall project score. The RAC point value was listed next to each component of the RAC to show how many points per unit the component was worth. The highest rated RAC component was the engine at a value of 1.97 per engine with the batteries rating second at a value of 1.5. This meant that for every engine used the RAC value would increase by 1.97 and for every pound of battery used the RAC value would increase by 1.5. Since both items are counted multiple times for different sections of the RAC at any one time, it was easy to determine that these items should be minimized whenever

possible. See figure 4.

3.2 Aircraft Configuration

In choosing an aircraft configuration, a figure of merit analysis was conducted. Several different types of aircraft configurations were examined. The examined aircraft configurations were the following, canard, bi-plane, flying wing, conventional, v-tail, and twin boom. All non-conventional aircraft were compared to the conventional design in the figure of merit chart. When compared to the conventional design the canard was judged to have favorable rated aircraft cost, lift to drag ratio, and stability. Its negative characteristics were seen to be its maneuverability, ease of construction, ease of assembly, take-off and landing characteristics. Its figure of merit total score was -1/10th, meaning that its characteristics were less favorable then the conventional design.

The bi-plane was evaluated to have favorable qualities of maneuverability, and stability and high lift. The take-off and landing characteristics were viewed as being approximately equal to that of the conventional design. Unfavorable characteristics were seen to be the rated aircraft cost, lift to drag ratio, ease of construction, and ease of assembly. This gave the bi-plane a figure of merit score of -3/10th. Other unfavorable characteristics of the bi-plane are that it produces more drag, than the conventional design, it would also be more difficult to store within the transport box. The bi-plane scored achieved a score lower than the canard design, making it and even less desirable configuration that the canard.

The third configuration examined involved a flying wing. Favorable characteristics of the flying wing were the rated aircraft cost, the lift to drag ratio, and ease of construction. The take off and landing characteristics were also seen as being approximately equal to that of a conventional design. Negative characteristics of the flying wing were seen as its maneuverability, stability, and ease of assembly. Maneuverability and stability are mush more difficult for a flying wing. For practical purposes it would be ineffective, since the craft would have to be constructed thick enough to hold the payload. This gave the flying wing a score of -1/10th, equivalent to the canard,

and a better score than the bi-plane.

Due to the fact that all the aircraft configurations considered were calculated to have negative figures of merit when compared to the conventional design, this left the conventional design as being the most favorable over the other designs considered. As a result a conventional design was chosen as the type of plane to be constructed.

3.2.1 Fuselage Configuration

The fuselage configuration was designed to accommodate the payload deployment and radar transmitter missions. The fuselage sizing was estimated to be only a few inches longer over the height and width of the payload box. The length of the fuselage was set at the maximum length of the storage box. These estimates were chosen in compliance with the maximum storage box size requirement.

3.2.2 Wing Configuration

The design of the wing was conservative due to the sensitive nature of the take-off performance and size requirements. The following considerations were analyzed for lift loss reduction of the wing:

Low Wing: Such a configuration would cause interference with the lift distribution over the wing surface and payload deployment. The assembly of such a configuration would be painstaking and lengthy during the time assembly phase of the mission. In addition, the integration of the landing gear to the fuselage would cause a complexity in construction and assemply. Furthermore, in case of a landing gear failure, a belly landing would cause extensive damage to the wing.

Mid Wing: Such a configuration offers complex construction and assembly techniques, which would lead to a longer production time. Structurally, this configuration also comprises the strength over simple assembly. Furthermore, this configuration interferes with the lift distribution of the wing surface.

High Wing: Such a configuration offers stability and minimal low of lift distribution over the wing surface.

3.2.3 Tail Configuration

Since the PVC disk antenna would be the major contributor to the total drag of the aircraft, it was concluded that drag reduction would a primary design consideration. According to Hoerner (reference 3), the tail configuration with the minimal coefficient of drag was tail configuration a, the V-type tail configuration. Although the V-type offers a minimal drag coefficient of 0.20 and a interference drag of 3%, it will render control complication. Since the conventional tail is utilized widely as a tail configuration for 70% of aircraft in service because of its reliability and stability and control qualities. In addition, according to Hoerner, the conventional tail configuration offers a drag coefficient of 0.24 and an interference drag of 4%, which differs slightly from that of the V-type configuration. Finally, the conventional configuration also minimizes the rated aircraft cost since less surfaces are utilized in the tail configuration compared with the other configurations.

3.2.4 Aircraft Sizing Estimates

The proper sizing of the aircraft configuration the required the structures group to formulate detailed weight estimates of the aircraft configuration. The structures group estimated an empty weight and take-off weight of 8 and 13 pounds, respectively. These estimates were studied to determine the lifting surface areas and design velocities. The determined lifting surface areas and design velocities were then studied carefully to obtain the optimal take-off, and cruise performances utilizing various methods obtained from the references 1and 2.

3.3 Structural Configuration

3.3.1 Assumptions made and design parameters investigated

Preliminary aircraft weight estimates were based on a 4-foot fuselage made of wood and fiberglass, and an 8-foot by 1-foot rectangular wing (see figure 11).

3.3.2 Alternative wing structures

Preliminary ideas for wing structures included: foam-core covered with fiberglass, foam-core covered in fiberglass and carbon fiber, built-up balsa and spruce skeleton structure. A

decision matrix based on strength to weight ratio, ease of construction, and cost, was used to make our decision of a foam-core wing covered in fiberglass and carbon fiber. Strength was the most important factor in the wing materials decision matrix. No consideration to spar structure was given at this time. This means our preliminary wing design was an entirely monokote structure (given the low strength of foam) that relied entirely on the strength and rigidity of its composite skin for support of all loads.

Some wing planform alternatives included the delta wing, flying wing, rectangular, rear swept and the tapered wing. We chose a rectangular wing planform based on the following figures of merit:

- Ease of wing structural analysis.
- Simplicity of construction.
- Ease of disassembly and reassembly.

No dihedral angle was included in the preliminary wing designs which made design of wing structure easier.

3.3.3 Alternative tail structures

Several considerations for tail shape and design included the following:

- V-tail
- T-tail
- No-tail (delta wing aircraft)
- Canard

In effort to limit the number of control surfaces, the V-tail option was briefly considered then discarded due to its added complexity. The T-tail option also afforded merit due to its beneficial poisoning of the horizontal stabilizer out of propeller wake and turbulent cylinder wake. However, a standard tail configuration was chosen based on ease of construction and simplicity.

The tail surfaces must be rigid enough to hold their shape under torsional and bending loads primarily. Some options for tail construction included:

- Built-up balsa skeleton with plastic covering

- Built -up balsa with balsa sheeting

Foam-core covered in fiberglass was chosen since it offers the needed rigidity and holds its shape. The balsa skeleton with sheeting could possibly offer the same merit but with higher complexity and building time.

3.3.4 Alternative Fuselage Structures

The design of fuselage structure did not take place until later in the aircraft design process. Consideration was given to structural rigidity, bending and torsional strength, as well as low weight, and positioning of the payload. A simple box frame, which housed the payload, was supposed to form the core of the fuselage. The wing would rest above this frame and the nose and empennage would cantilever from its ends.

Preliminary concepts for fuselage structural design included:

- Full-Length semi-monocoque structure with thin plywood skin.
- Full-Length truss structure with built up plywood frames and stringers.
- Carbon or fiberglass monocoque pod with tail boom.

Options for construction materials were:

- Wood truss structure covered in monocot
- Metal frame covered in fiberglass
- Wood frame with fiberglass covering

A decision matrix based on strength, ease of construction, and price yielded a preferred semi-monocoque wood structure with fiberglass fabric skin.

3.3.6 Alternative Landing Gear configurations

The function of landing gear in this case is primarily to support the load of our estimated 13-pound aircraft at through take-off and a severe (4-g) landing. In addition it must be capable of maneuvering the aircraft while on the ground without severely hindering the aircraft's performance in the air.

Some configurations considered were:

- Tricycle
- Quad
- Tail dragger

The Tricycle gear was chosen by process of elimination. Firstl, the Tail dragger was eliminated because its tail wheel would interfere with payload deployment. Secondly, The quad configuration would provide too much aerodynamic drag and provide unnecessary amount of steering control complexity.

Payload clearance was of primary importance in landing gear design. Six inches was a bare minimum for fuselage clearance and seven inches was chosen to account for landing gear deflection and margin of safety.

4.0 PRELIMINARY DESIGN

4.1 Propulsion Design Parameters

4.1.1 Trade Study – Number of Batteries Required

To determine the number of batteries required, a scoring spreadsheet was created which related total score to airplane performance based on cell count. The range of cells examined varied from 10 to 30 batteries. The optimal number of cells was 21 with a weight of 2.73 pounds.

4.1.2 Trade Study – Takeoff Power

To determine the optimal takeoff power requirements of the propulsive system, power produced by the batteries was examined at the maximum current of 40 amps and the base voltage produced by 21 cells. The most promising values ranged from 555 to 710 watts with the optimal value being 645 watts.

4.0.3Trade Study – Power at Cruise

Repeating the steps to find the takeoff power requirement, the maximum scoring values for cruise power requirements of the propulsive system were found to be between 415 to 510 watts. The optimal value was found to be 462 watts.

4.2 Aerodynamic Design Parameters

4.2.1 Take-off Performance

Since the aircraft had to negotiate, the main design parameter focused on efficient lifting surfaces that would generate the necessary lift required for the aircraft to take-off at maximum take-off distance of 120 feet. From equation 5.53 (Reference 1)

$$S_{TO} = \frac{1.44W_{TO}^2}{\rho S C_{L_{max}} g[T - D - \mu(W_{TO} - L)]_{0.7V_{TO}}},$$

it can be shown that the take-off distance is a function of weight, the take-off velocity, wing planform area, drag and maximum lift coefficient, coefficient of friction, and thrust. Thus, a study of the aforementioned parameters was studied to determine the optimal planform area. Furthermore, a restriction of the wingspan and chord length was also considered to comply with the maximum storage box size requirement.

The lift and velocity required for take-off were obtained by transforming the aforementioned equation as lift as a function of take-off velocity. A plot of lift versus take-off velocity was then generated to obtain an estimate of the lift and take-off velocity to negotiate the 120 feet take-off distance. The minimum and maximum achievable take-off velocities were assumed to be, from figure 5, 20 and 35 mph, respectively. Thus comparing these two velocities with figure 5, it was concluded that the minimum and maximum lift coefficient for take-off were 2.00 and 0.9, respectively.

4.2.2 Wing Sizing

The wing planform area was then obtained by balancing performance and rated aircraft cost. By comparing figures 5-8, it was concluded that the most effective wing planform area with the lowest rated rated aircraft cost based on wing span, chord length yielded a wing surface of 8 ft^2.

4.3 Structural Analysis

4.3.1 Figures of merit

During preliminary design of the structure, several factors were evaluated. Construction materials were the first part considered. Figures of merit used were strength to weight ratio, cost, and ease of construction. Heavier materials reduce the score, but some heavier materials are required in some locations to resist loads. Due to the internal bending moments, it was determined that a fiberglass skin on its own would not be able to handle the loading the wing was expected to undergo during flight, so a spar would be needed for additional strength to the wing to resist the expected loads.

4.3.2 Fuselage Assumptions and Structural Analysis

It was also decided to build the fuselage frame out of balsa wood, in order to keep the weight low. Originally the frame was designed out of thin plywood members. This frame proved to be capable of resisting much greater loads than the aircraft is expected to be subjected to. The plywood structure proved to add to much weight to the plane and a lighter structure was

more desirable to help meet the mission goals. A balsa frame was chosen in order to reduce the weight of the fuselage. However, balsa wood is not the strongest of materials, so reinforcements were decided upon to be constructed out of a stronger spruce wood. Shear webs would be added to the sides of the frame, and small amounts of plywood would be used to reinforce the frame only in places necessary for increased strength such as the wing and landing gear attachments. Using other types of wood than balsa will make the plane heavier, which is not desirable, however the gain from using other wood for reinforcement alone will allow the fuselage to gain strength only where needed without much of a weight cost. Iron on plastic covering was chosen as lightweight easy to apply skin to cover the fuselage. Monokote is smooth and will help to reduce the skin friction drag, and being light it does not affect our weight.

4.3.3 Wing Assumptions and Structural Analysis

Conceptual design of the wing structure differed slightly from preliminary design and included stress analysis due to bending loads. The basic construction of foam-core covered with fiberglass and carbon fiber skin was kept. The center section that mates to the fuselage via nylon bolts was reinforced with plywood sheeting. The revised wing consisted of a six-foot span by 0.8-foot chord rectangular planform with an SD-6060 airfoil. The wing bending load distribution due to lift was calculated assuming the following:

- Uniform lift distribution
- A/C gross weight (13 lbs)
- Load factor (4.5)
- Margin of Safety (30%)

The uniform lift distribution assumption was made for simplicity and added margin of safety since it was a conservative estimate. After our preliminary design review, a decision was made to increase the number of wing spars from 0 to 2. One main spar was placed at the ¼ chord to resist maximum bending moment of 570 in-lbs. One smaller spar was placed near the trailing edge to reduce twisting of the wing structure. No consideration to aerodynamic drag was

given in the design of the wing structure. No buckling analysis was considered for the upper wing skin since the compression loads would be minimized by an overcompensating spar structure and supporting foam core.

4.3.4 Main Gear Assumptions and Structural Analysis

Conceptual design of the main landing gear was based on the original tricycle configuration. The idea of shock absorbers were briefly considered but soon discarded for reasons of extra weight and unnecessary complexity. One possible alternative for the main gear design, which received serious consideration, was a two-piece main gear. This would be which attached to either side of the fuselage. This implementation would have ideally suited our take-off rotation requirements since it would be able to be positioned at an optimum location relative to the center of gravity. The main disadvantage to the two-piece main gear was it relied upon the rigidity of the fuselage, which probably would not be sufficient to provide stable ground tracking. Therefore, the solution was a single piece, carry-through metal bracket type main gear. Advantages to this type of structure were that it carries all bending load and transfers only vertical loads to the fuselage. Furthermore, the load can be distributed over the entire fuselage-mating surface of 16 sq. in. In addition, the one-piece plate eliminated the possibility of a toe-out or toe-in condition since it was more rigid than a two-piece design. Finally, the one-piece gear offered symmetry of load distribution, natural shock absorption, and lightweight. Bending analysis was carried out using cantilever beam deflection and slope analysis for homogeneous material. See figure 3.

4.4 Propulsion Analysis

The preliminary design of the propulsion system required theoretical analysis of the main components, which included the propeller, motor and batteries. This was done through the use of an spread sheet program, which incorporated the values provided by the aerodynamics group. Starting with the minimum values and varying them in a positive direction, values for efficiency,

thrust, power and current were determined. Motor dimensions, number of batteries, propeller dimensions, and gear ratio values were input into the program to evaluate the optimal configurations.

Determination of the battery cell model was achieved through a multi-cell comparison chart of the available current to weight ratio. All non-NiCad cells were eliminated leaving the Sanyo RC2400 cells with the largest value for energy density. A motor comparison was based on six Astro Flight motors: the Astro Cobalt 25, 40 and 60 and the Astro FAI 25, 40 (642), and 40 (643). The Graupner model of motors was eliminated due to lack of availability and higher cost. Three gear ratios were chosen for analysis: 1:1, 1:1.68 and 1:3.1. The second two ratios were chosen based on Astro Flight gearboxes designed for the motors previously described. A range of values for the propeller pitch and diameter were chosen based on published historical data for the Astro Flight motors.

4.4.1 Figures of Merit

In order to narrow down the parameter choices for the propulsion system, figures of merit were used. Weighting the parameters allowed a visual confirmation of design requirements and their related values. The merits analyzed included:

Total Score: This was the greatest factor considered in analyzing any parameter due to the nature of the competition.

Weight: Reduction of weight was detrimental not only to the airplane performance but to the total score due to its value in the RAC.

Efficiency: Increasing the efficiency of the propulsion system improved the total score by reducing the weight of the components needed to complete the mission and by improving flight performance.

Current: This was a limiting factor specified by the competition rules.

Energy Density: The energy density determined which cell provided the largest energy output for the lowest weight thus improving the total score.

4.4.2 Trade Studies Examined

To analyze the optimal configurations for the propulsion system, tradeoffs had to be considered for the main component parameters. These parameters included: motor design and size, available battery energy density and weight, propeller pitch and diameter. Motor Design and Size: Motor selection was based on its ability to convert electrical energy to kinetic energy efficiently at the required aircraft performance level.

Battery Quantity/Quality: A balance between the number of batteries and its available current production helps to maximize the propulsion system efficiency and score.

Propeller Pitch/Diameter: Manipulation of the propeller's pitch and diameter allowed for the propulsion system efficiency to increase while reducing the number of batteries required. One drawback was the current limitation, which left a sizing constraint.

4.4.3 Motor Selection

Of the six motors chosen for analysis, the three Astro Flight FAI motors were eliminated due to the imposed current limitation. The cobalt 25 motor was eliminated due to thrust requirements imposed by the simulated antenna mission. The remaining two motors, the Cobalt 40 and 60, were left to be evaluated. The optimum flight performance values for each motor were evaluated through the spread sheet program to produce a maximum estimated total flight score. The Cobalt 40 motor received a higher score due to a lower number of batteries even though the efficiency was less than that of the Cobalt 60.

5.0 DETAILED DESIGN

5.1 Performance analysis

Great care was taken in calculating and determining the projected possible aircraft performance. The airplane operates at a very mission specific environment with a well defined requirement profile. This requirement profile was projected within a computer program to calculate and evaluate all primary and secondary performance parameters. The software was developed in-house with the collaboration of the aerodynamics and structure teams. The results were evaluated and cross-referenced with existing aircraft performance data.

5.1.1 Take-off Velocity

Referring to figure 5, this estimated wing planform area would require a minimum and maximum take-off velocity of 22 and 36 mph, respectively. Since it was estimated that the engine would allow the aircraft to fly at a maximum velocity of 35 mph, the 36 mph take-off was eliminated. The take-off velocity had to be lowered to a value between 20-30 mph due to the fact that he engine would not accelerate the aircraft to such a high take-off velocity. To accomplish the reduction of take-off velocity, a lift coefficient was searched that would yield the reduction of the take-off velocity. For a safety of margin, the maximum lift coefficient that could be acquired from any airfoil was determined to be 1.2. Referring to figure 5, this lift coefficient yielded a take-off velocity of 28 mph.

5.1.2 Airfoil Determination

Low Reynolds number wind tunnel airfoil data (Reference 4) was studied from various airfoils to determine the most adequate lift coefficient required to render a take-off velocity of 28 mph.

The airfoils analyzed for the wing configuration were:

SD 6060, WASP (smoothed), SD 7003, SD 8000, E 231, SD 7037, Clark-Y, SD 7032

5.1.3 Selected Airfoil

The Clark-Y airfoil generated a higher C_l from the airfoils listed above. The maximum

coefficient of lift of the Clark-Y airfoil is 1.35 from figure 9. Due to the take-off distance requirement, it was concluded that flaps would be needed to ensure proper take-off before 120 ft. The coefficient of lift due to a flap yielded a coefficient of lift of 1.69 at a flap deflection angle of 20° and a $C_f/C=0.21$.

5.1.4 Tail Volume

From the tail volume method prescribed in (see Aircraft Design pg. 111), the sizing of the tail configuration yielded the values shown in figure 14.

5.1.5 Aerodynamics Performance Parameters

The performance values are shown in figure 8 for the aircraft configuration.

5.2 Propulsive Performance Analysis

Using a Rapala ProGuide 50lb. digital scale, the thrust was measured to determine the optimal motor and propeller configuration. The final combination was determined to be an Astro Flight Cobalt 40 motor with a 1:1.63 ratio gearbox and a 14 inch diameter propeller.

5.3 Structural considerations

5.3.1 Fuselage structural Details

The design of the aircraft was an ongoing process throughout the project. The design was continuously modified as theoretical designs were modified for real world applications. This process affected every component of the aircraft at some point during construction. The final fuselage design involved the construction of a balsa and spruce frame. The primary shape of the fuselage was constructed of balsa wood. The balsa was joined together using epoxy and triangularly cut sections of balsa at the joints. The spruce was used as a shear webs around the sides of the frame, lighting holes were cut into the spruce to reduce weight. The bulkheads of the aircraft were also constructed of spruce wood. Plywood hard points were added at specific locations on the fuselage to accommodate special requirements. Hard points were necessary to attach the wing to the fuselage and to attach the landing gear; these hard points were necessary

to resist areas of greater stress.

5.3.2 Tail Structural Details

The final design settled upon for the tail involved a truss structure. This structure was constructed in the shape of a square base pyramid. The tail was constructed using balsa wood, reinforced with spruce shear webs, supplemented with lightning holes, similar to the fuselage. The base of the truss attached to the rear bulkhead of the frame. The tail flight control surfaces were then attached to the end of the truss using specially cut balsa members to keep the horizontal stabilizers at a zero angle of attack. The tail and fuselage were then covered in monokote.

5.3.3 Wing Structural Details

During the course of the project, three sets of wings were produced. All three wings were constructed in a similar manner. The final set of wings differed in the type of materials used. The first two wings constructed were constructed of fiberglass and epoxy. While the last wing constructed was made using carbon fiber. The manufacturing process greatly improved once better quality materials were used. The initial set wings were produced using the incorrect type of epoxy, producing poor quality wings. Once proper materials were obtained the quality of the third wing was greatly improved. The final wing also incorporated an improved leading edge reinforcer made of balsa. The balsa was added to protect the wings in the event of a crash. The final set of wings incorporated tapered Carbon spars that were added internally to the wings to resist the necessary bending loads. The wings were then attached with nylon screws through the hard points for ease of construction.

6.0 Manufacturing Plan

6.1 Process Selected for Component Manufacturing

6.1.1 Fuselage Manufacturing Process and Tooling

Construction of the craft began with the fuselage. Plywood sheets were cut into appropriate shapes and assembled into the designed frame structure. The first frame structure was used as a test model. The frame was placed under bending and torsional loading to determine its rigidity and maximum loading. Due to the rectangular shape of the fuselage, the frame was capable of resisting significant amounts of bending, but could only resist a small amount of torsional loading. It became clear from these tests that bulkheads would need to be added to help resist the torsional loading. In the event of a crash, it was desired that the structure survive with minimal damage. Simulating this occurrence the test structure was thrown off the roof of a building numerous times, and was found to be capable of surviving with minimal amount of damage.

During the construction of the wings it was found that they would be heavier than originally planned, as a result of this weight from other parts of the craft needed to be reduced. The plywood frame was replaced with a balsa and spruce frame of similar design. The main components of the frame were constructed of balsa strips reinforced with spruce shear webs, and spruce bulkheads. The connecting points between the main wing and the landing gear were reinforced with plywood. This reduced the weight of the frame from 2 lb to 1 lb, but also reduced the loading the structure was capable of resisting.

6.1.2 Nose Cone Manufacturing Process and Tooling

The nose cone of the craft was constructed of Styrofoam covered in fiberglass. The shape of the cone was made using a hot wire cutter, and was cut in the shape of a square base pyramid with a flat top. The edges of the pyramid were then sanded down to give the nose cone a more streamlined look. Afterwards the Styrofoam was coated in fiberglass and sealed with

epoxy. The Styrofoam was melted out using acetone, so that a solid hollow piece of fiberglass was produced. A new Styrofoam cone was constructed and a molding was made of the shape using plaster. The smooth surface of the plaster mold allowed a new fiberglass nose to be constructed of higher quality and with a much smoother surface.

6.1.3 Tail Manufacturing Process and Tooling

The empennage was constructed of spruce wood. The original design of the empennage consisted of only a carbon rod boom. After consultation with aerospace professors, it was suggested that a more traditional design would aid in helping the plane rotate faster during takeoff, although this would be at the cost of some more weight. The empennage was constructed of a hollow truss design, reinforced by a spruce skin. To reduce weight lighting holes were added to the design. The tail horizontal and vertical stabilizers were attached to the truss with small bolts. The empennage was attached to the frame using rails. Rails were selected to attach the empennage to the frame in order to facilitate assembly at the competition.

6.1.4 Landing Gear Manufacturing Process and Tooling

The landing gear of the plane was constructed of aluminum. Originally the gear was to be constructed of fared aluminum tubes, reinforced internally with rectangular tubes. During testing these proved unable to withstand the required loading. The gear was then replaced with larger flat aluminum plates. The plates were bent out from the fuselage at a 45-degree angle to give the aircraft a large more stable base. Due to the payload being released from the underside of the aircraft, the landing gear will support the bottom of the aircraft from 7 inches off the ground. The plates were attached to the bottom of the frame at a reinforced plywood section of the frame. The nose landing gear consists of an aluminum bar mounted to the forward bulkhead. The front gear is capable of turning and is linked to the same servo as the rudder, providing one less servo and allowing the aircraft to taxi on the tarmac.

6.1.5 Wings Manufacturing Process and Tooling

The wings of the plane were constructed of foam coated in fiberglass, reinforced with carbon spars. Once an airfoil had been selected, the foam cores were purchased in the shape of

the desired airfoil. The wings were then coated in fiberglass with epoxy and vacuum bagged so that the fiberglass would take on the desired airfoil shape. Due to lack of experience in the process the wings produced were of unsatisfactory quality. It was also discovered that the size of the wings were too small for our aircraft. A new airfoil was chosen with an increased chord and wingspan. This increase in the weight of the wings resulted in the conversion of the frame from plywood to balsa. A new set of foam cores was purchased, and the new set of wings was bagged. In the first set of wings the spars were added to the wing before bagging by using a soldering iron to cut a groove in the foam and inset the spar, which was sealed with bondo. This approach added more weight to the wings than necessary, due to the weight of the bondo; it also warped the skin of the wing due to the roughness of the bondo on the surface of the wing. The second sets of wings were packed without adding the spars. This eliminated the weight of the bondo and the roughness created by the un-smooth surface. The spars were then added after bagging by melting a channel for the spars to be inserted in.

6.2 Final Assembly

The final assembly of the aircraft involved mostly adjusting the constructed pieces to fit together. Discrepancies in the construction of the aircraft led to larger discrepancies in the final product and appropriate adjustments were critical to the success of the aircraft. Such as the base of the empennage was constructed with a larger base than designed for and had to be adjusted to fit the rear section of the frame. The nose cone was constructed with dimensions appropriate for the original plywood frame, and also required adjustment. The wing was attached to the reinforced sections of the frame to the hard points of the wing. The internal components such as the receiver, batteries, engine and servos were also added. The servos were connected to their respective components to complete the assembly of the aircraft.

7.0 REFERENCES

1. Steven A Brandt...[et al.], Introduction to Aeronautics: A Design Perspective, American Institute of Aeronautics and Astronautics, Inc., 1801 Alexander Bell Drive, Reston, VA 20 191, 1997.

2. Daniel P. Raymer, *Aircraft Design: A Conceptual Approach*, American Institute of Aeronautics and Astronautics Inc., Washington D.C., 1989.

3. Hoerner, *Fluid Dynamic Drag*, 1965

4. Selig, M, Summary of Airfoil Data Volume

8.0 TABLES AND FIGURES

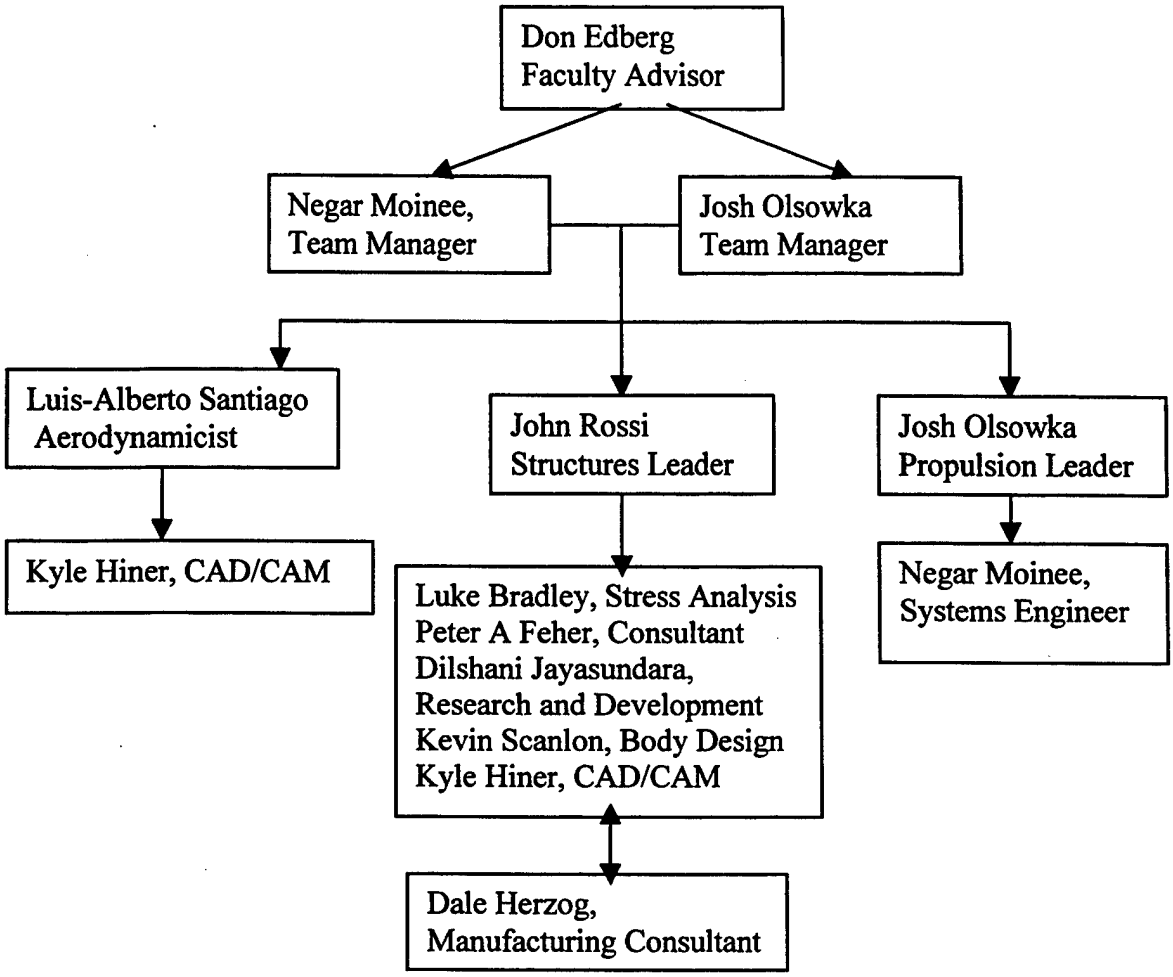

Figure 1. Cal Poly Team's Architecture Chart

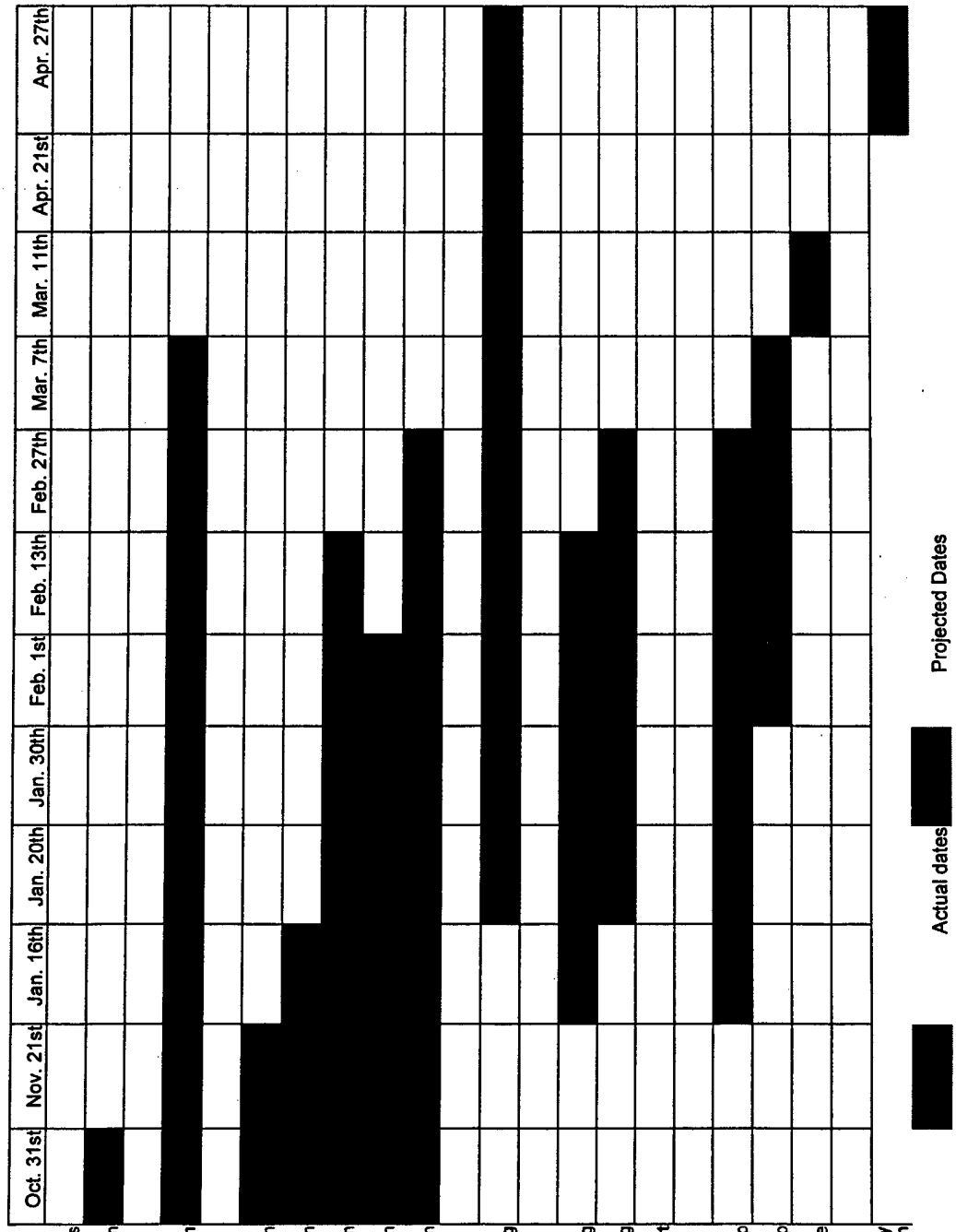

Figure 2: Milestone Chart

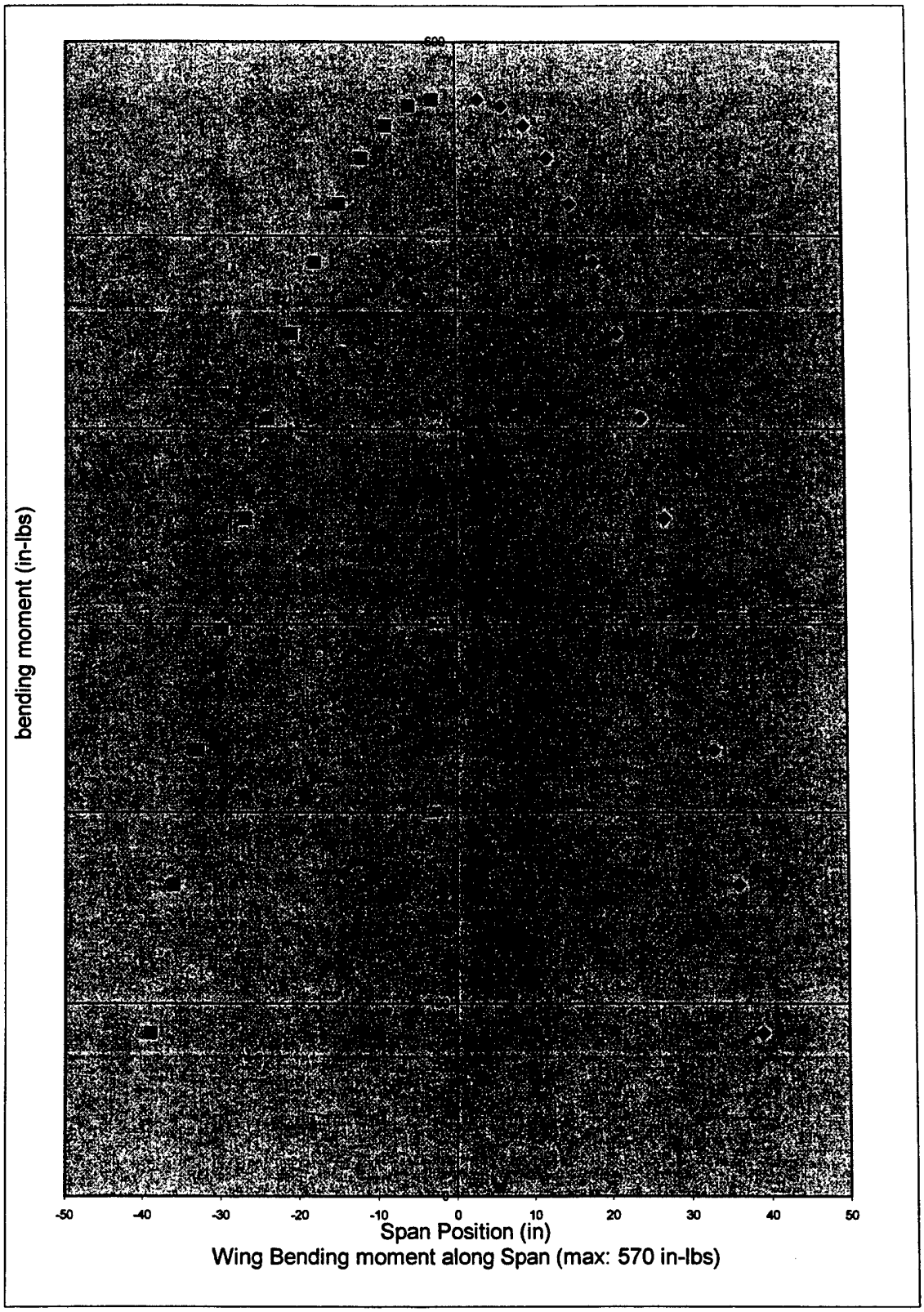

Figure 3: Wing Bending Moment

Figure 4: Ratted Aircraft Cost

Coefficient	Description	Canard	Bi-Plane	Flying Wing	Conventional	Bi-Wing w/V-tail	V-tail	Twin-Boom	Change in RAC per unit
A	Manufacturers Empty Weight Multiplier ($)	100	100	100	100	100	100	100	
B	Rated Engine Power Multiplier ($)	1500	1500	1500	1500	1500	1500	1500	
C	Manufacturing Cost Multiplier ($/hr)	20	20	20	20	20	20	20	
MEW	Manufacturers Empty Weight (lb.)	9	9	9	9	9	9	9	
REP	Rated Engine Power								
BAT	Battery Weight (lb.)	1	1	1	1	1	1	1	1.5
WBS									
Wing 1	Span (ft.)	6	6	7	6.5	6	7	7	0.16
	Chord (ft.)	1	1	3	0.8	1	1	3	0.16
Wing 2	Span (ft.)								
	Chord (ft.)								
	Wing Control Surfaces (# of)	2	2	2	2	2	2	2	0.06
Fuselage	Max Body Length (ft.)	4	4	5	4	4	4	6	0.2
Empenage	Vertical Surface, Non-active (# of)	0	0	0	1	0	0	1	0.1
	Vertical Surface, Active (# of)	1	1	0	0	0	0	1	0.2
	Horizontal Surface (# of)	1	1	0	1	0	0	0	0.2
	"V" Tail (# of)	0	0	0	0	1	1	0	0.3
Flight Systems	Servo/Motor (# of)	4	5	3	4	5	3	3	0.1
Propulsion Systems	Engine (# of)	1	1	1	1	1	1	1	1.97
	Propeller/Fan (# of)	1	1	1	1	1	1	1	0.1

MFHR	Manufacturing Man Hours	162	157	151	149	162	150	166
Total RAC	In Thousands Of Dollars	5.13	5.64	5.62	5.0840	5.441	5.24	6.124

Yellow = Inputs Orange = Outputs

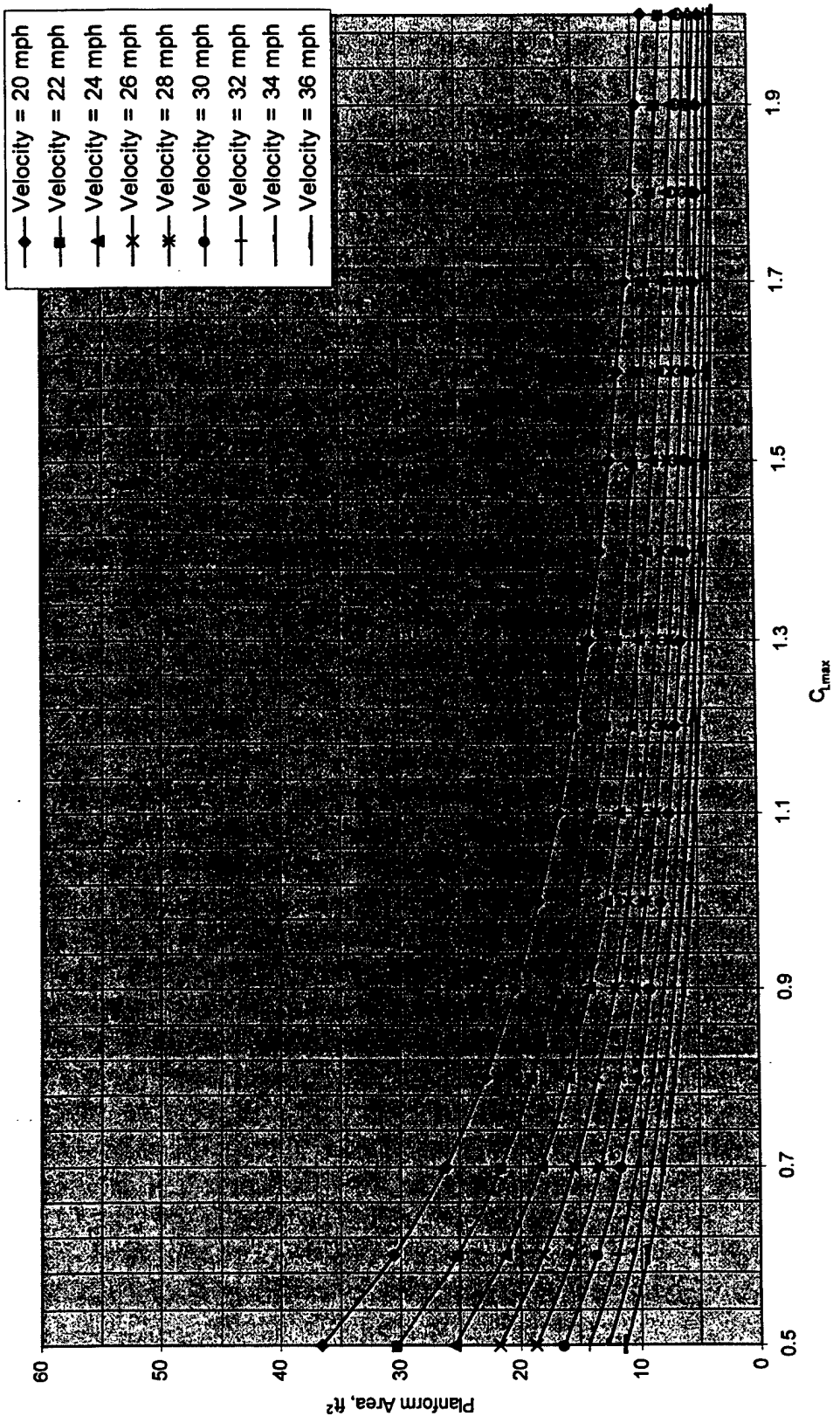

Figure 5: Wing Platform Area vs. Max Lift Coefficient. Take-off Performance

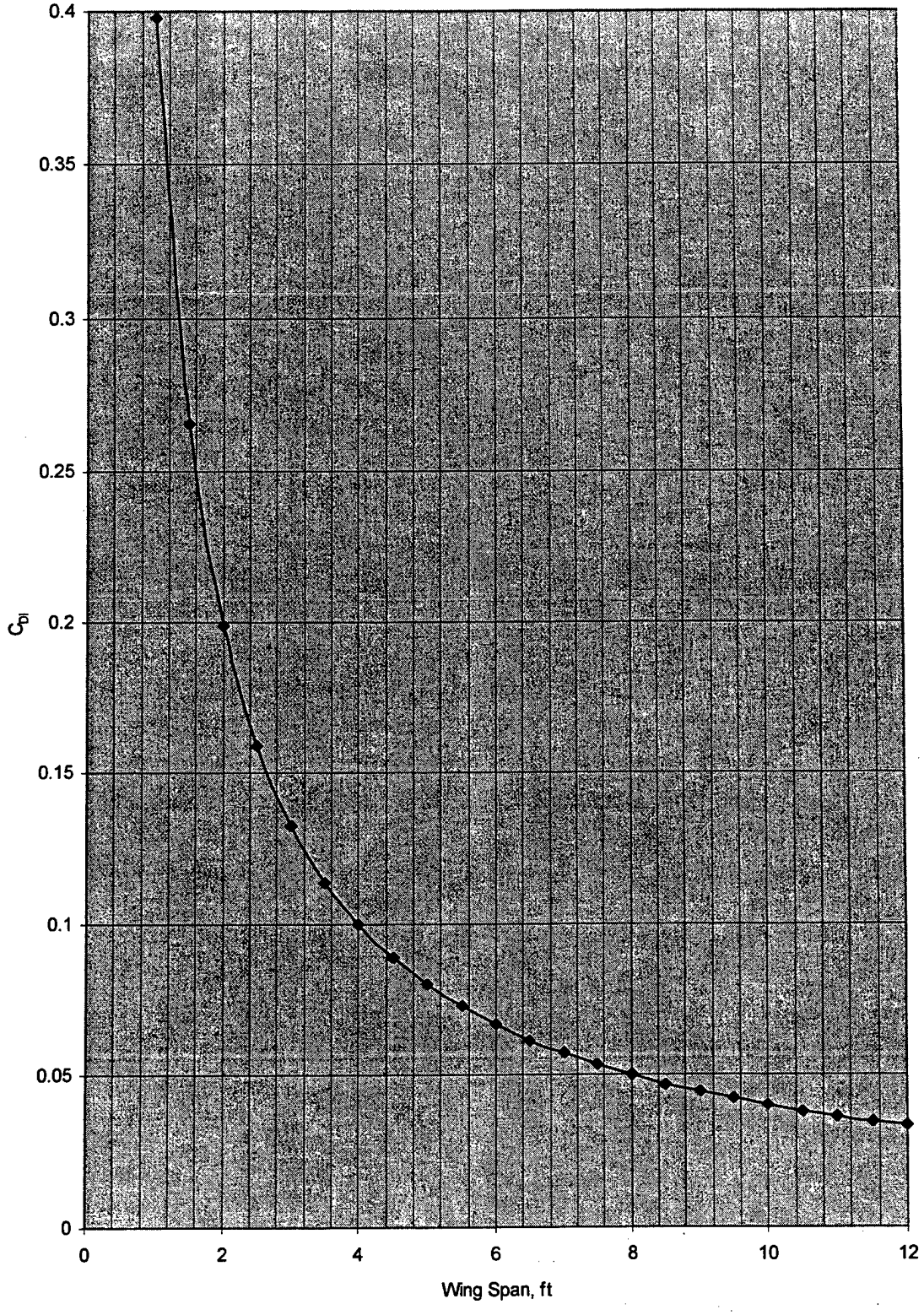

Figure 6: Coefficient of Induced Drag versus Wing Span

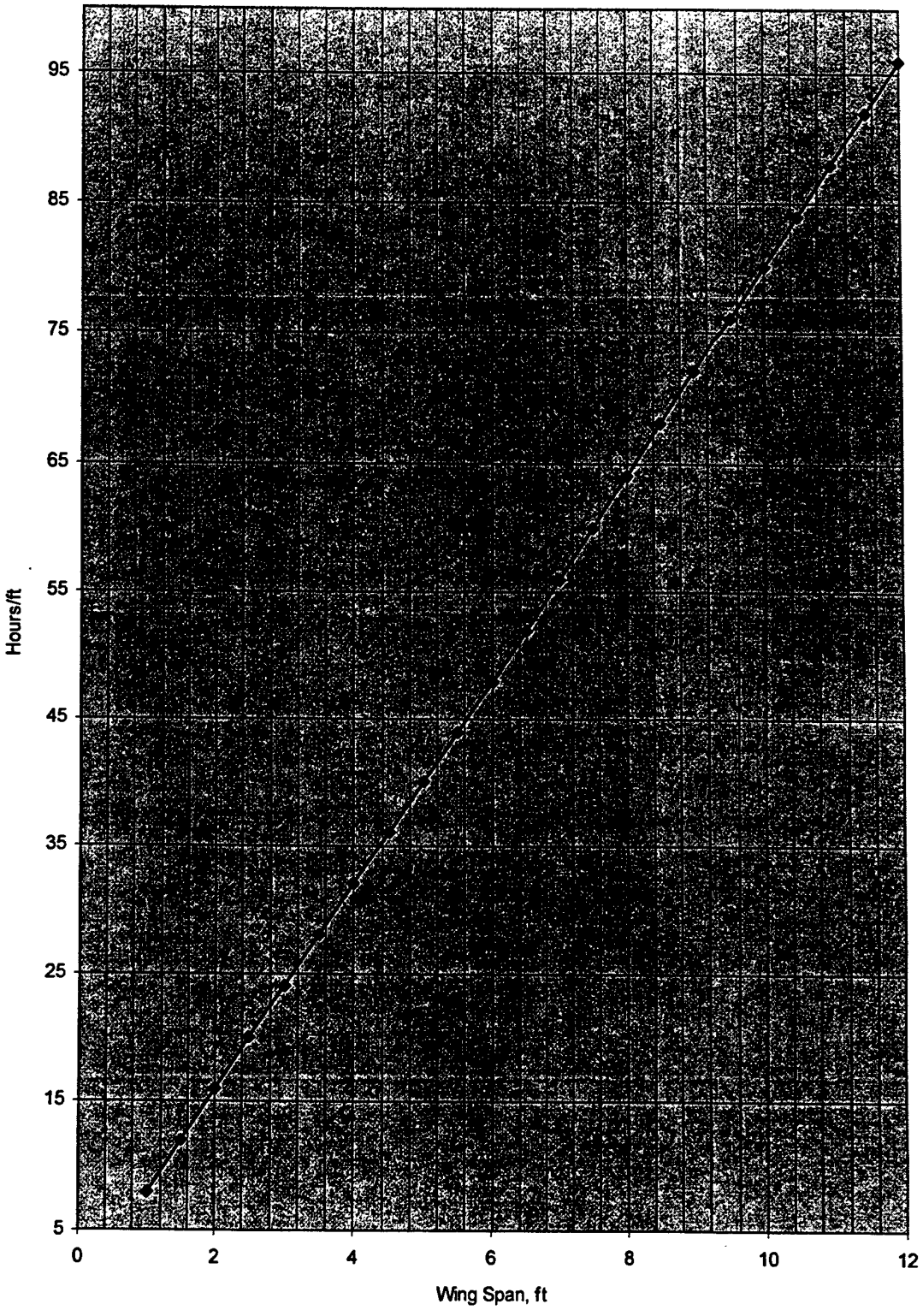

Figure 7: RAC Hours versus Wing Span

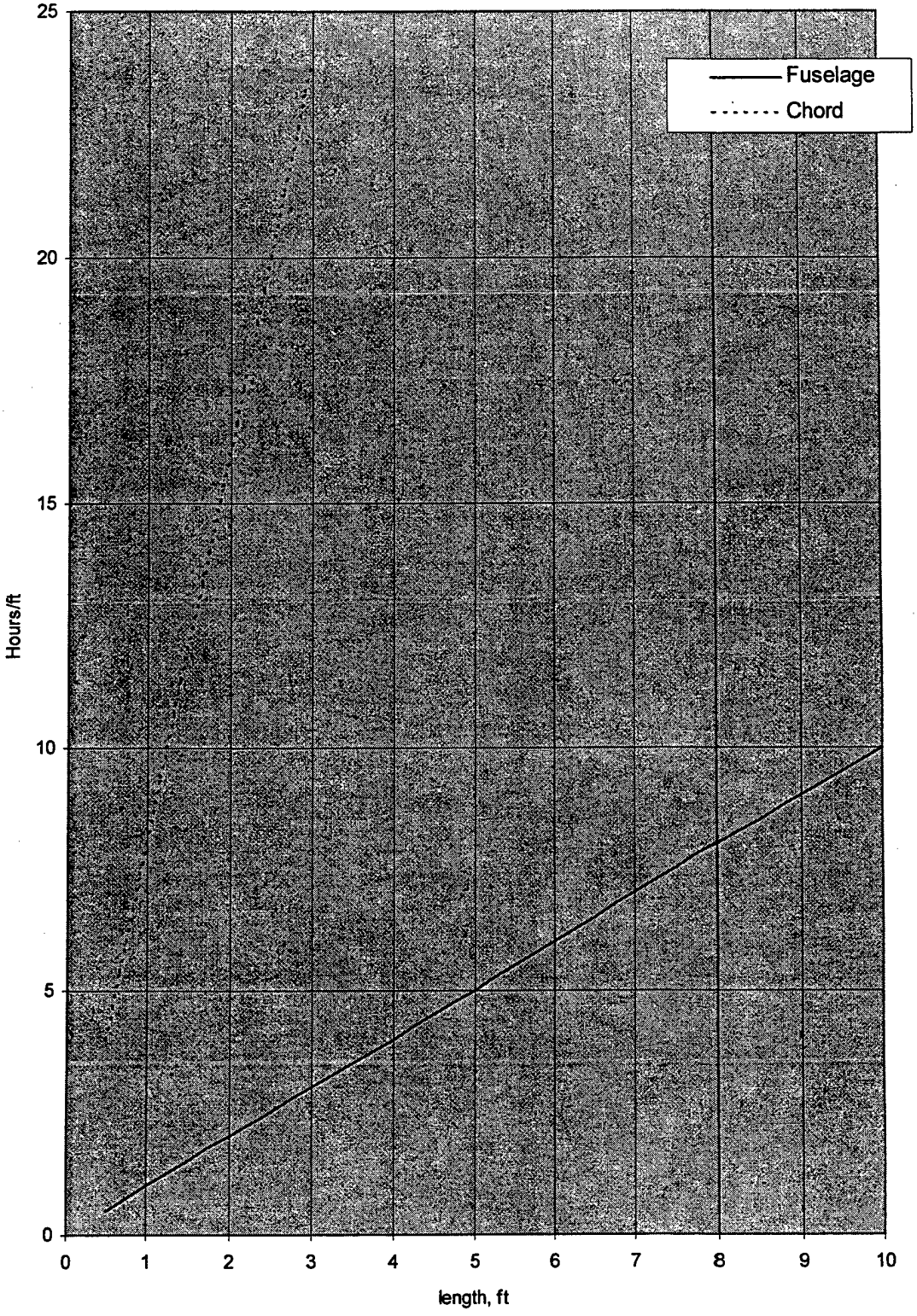

Figure 8: RAC Hours versus fuselage and chord length

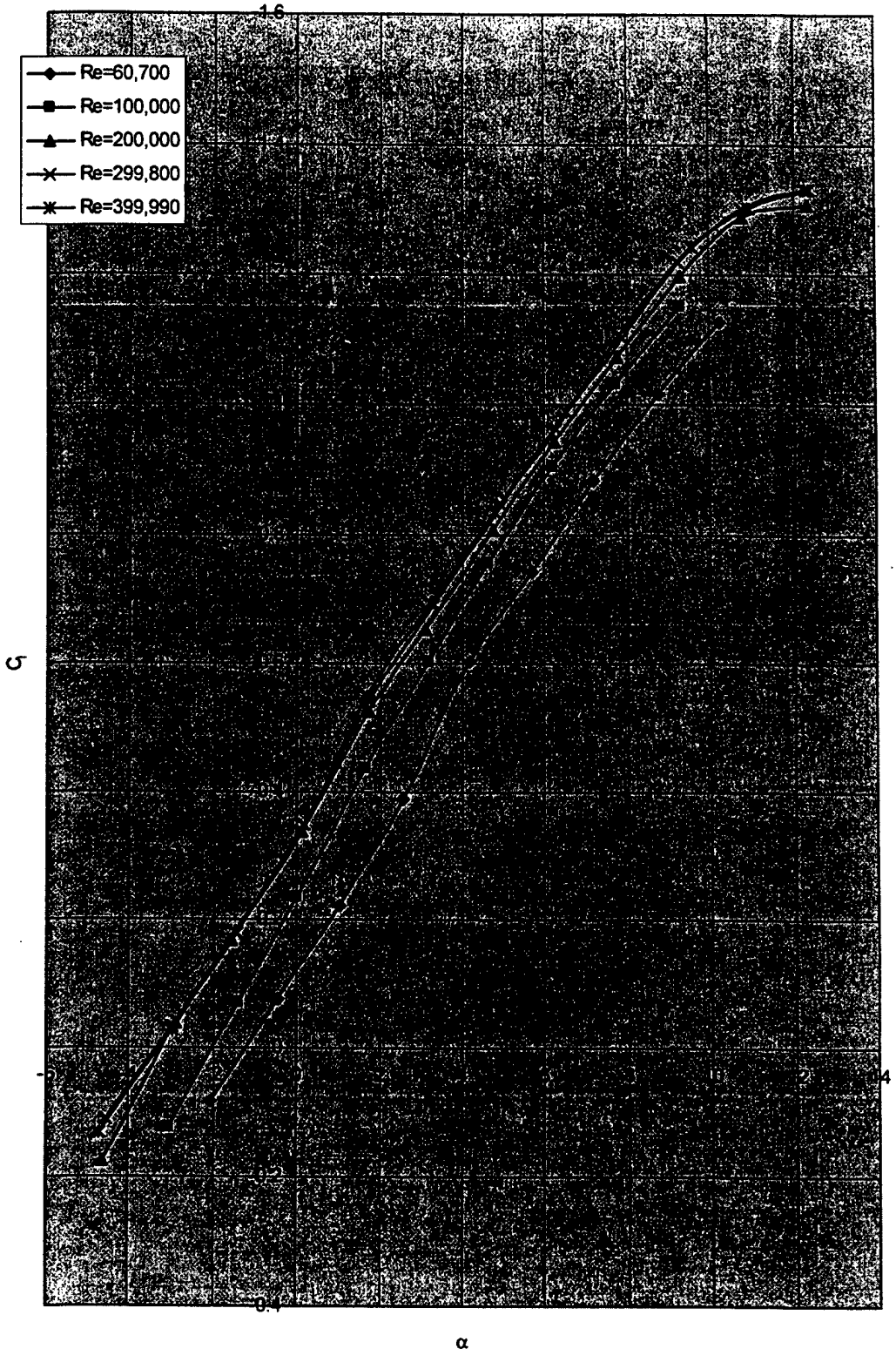

Figure 9a: Clark Y: Coefficient of lift versus Angle of attack

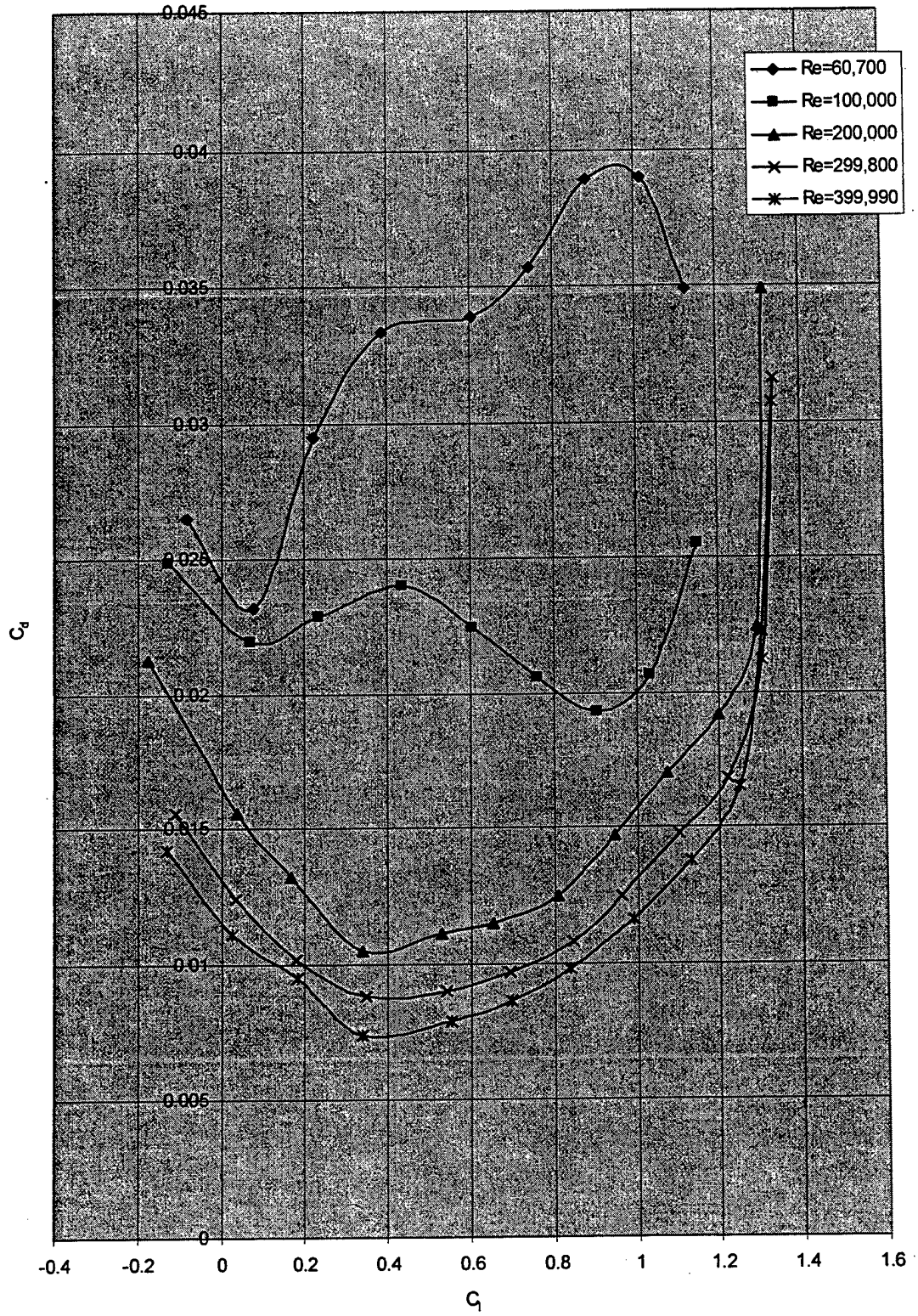

Figure 9b: ClarkY: Drag Polar

Manufacturing

Week of Construction	Jan. 19-25	Jan. 26-Feb. 1	Feb. 2-8	Feb. 9-15	Feb. 16-22	Feb. 23-Mar 1	Mar. 2-8
Projected Wing Assembly							
Actual Wing Assembly							
Projected Tail Assembly							
Actual Tail Assembly							
Projected Fuselage Assembly							
Actual Fuselage Assembly							
Projected Gear Assembly							
Actual Gear Assembly							
Projected Final Assembly							
Actual Final Assembly							
Projected Payload and Box Assmbly							
Actual Payload and Box Assmbly							

Figure 10: Manufacturing scheduling

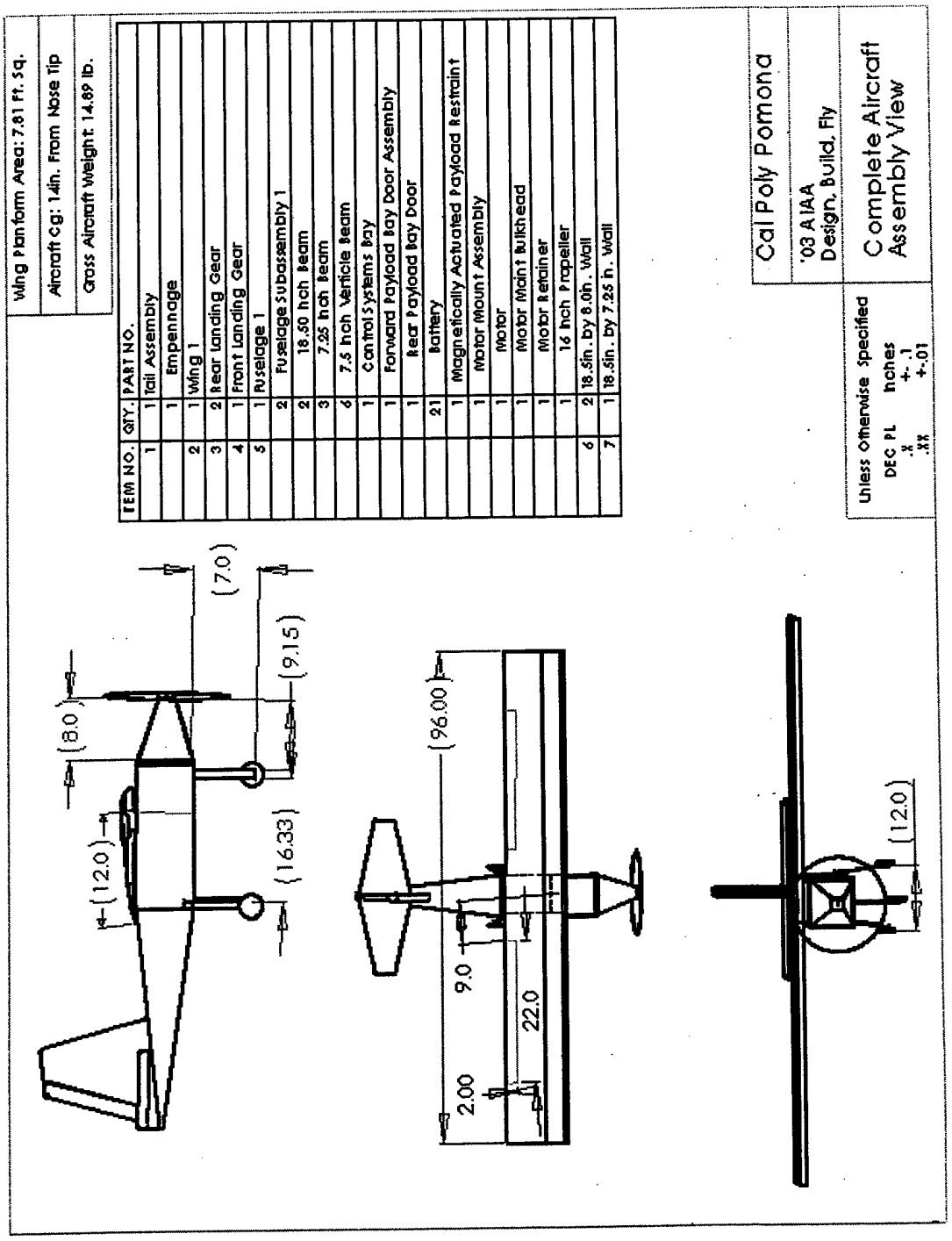

Figure 11: 3 View Drawing

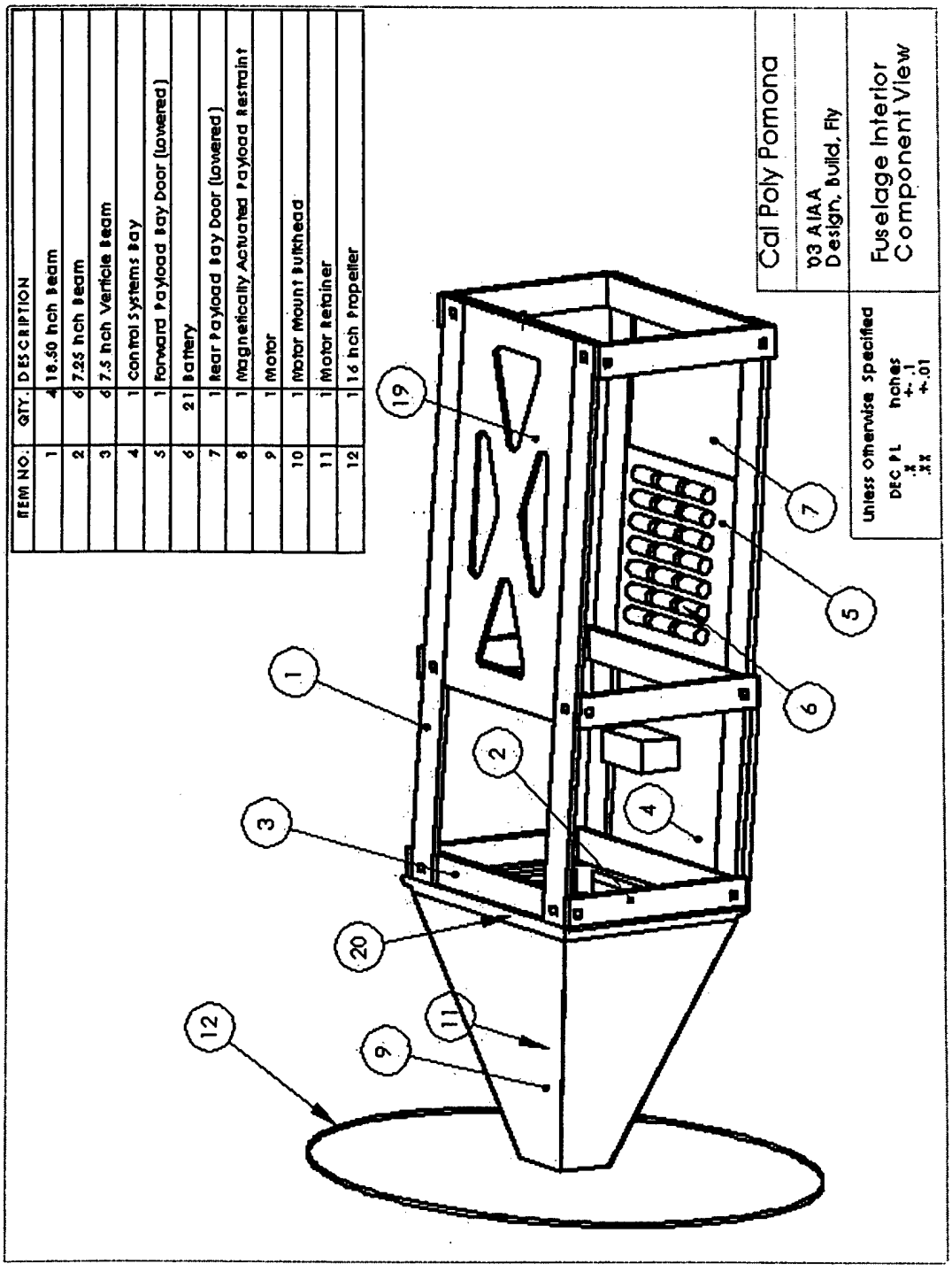

Figure 12: Fuselage and Nose Cone

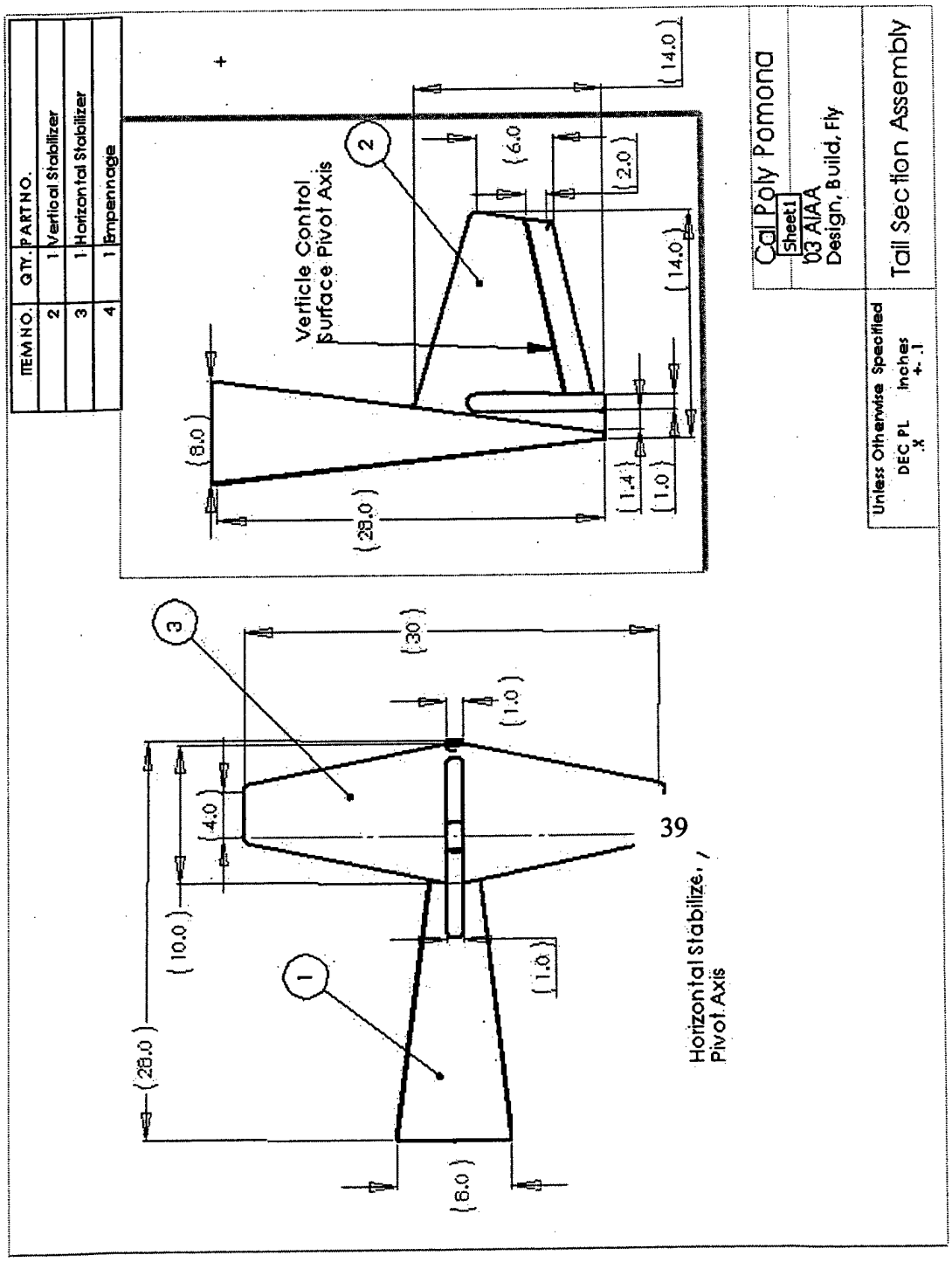

Figure 13: Tail Section Assembly

Pegasus Aircraft Configuration	
Cl_{max}	1.15
L/D_{max}	5.33
R/C_{max}	0.233
V_{stall}	33.8 mph
V_{max}	40 mph
Take off length	108 ft
Dimensions	
Wing span	8 ft
Chord Length	1 ft
Wing planfrom Area	7.83 ft^2
Fuselage length	2.7 ft
Height	15 in
Aspect Ratio	8.2
Control Volumes	
Vertical Stabilizer	
Span	14 in
Area	0.948 ft^2
Aspect Ratio	1.47
Taper Ratio	0.4
Horizontal Stabilizer	
Span	29 in
Area	1.48 ft^2
Aspect Ratio	4
Taper Ratio	0.4
Airframe	
Propulsion system	
Control system	
Payload system	
Payload	5 lbs
Empty weight	8 lbs
Gross weight	13 lbs
Systems	
Radio used	
Servos used	5
Battery configuration	11
Motor used	Astro Cobalt 40
Propeller	
Gear ratio	

Figure 14: Aircraft Configuration and Performance

Cessna ONR/Student Design/Build/Fly Competition

Western Michigan University
"Western Flyer"

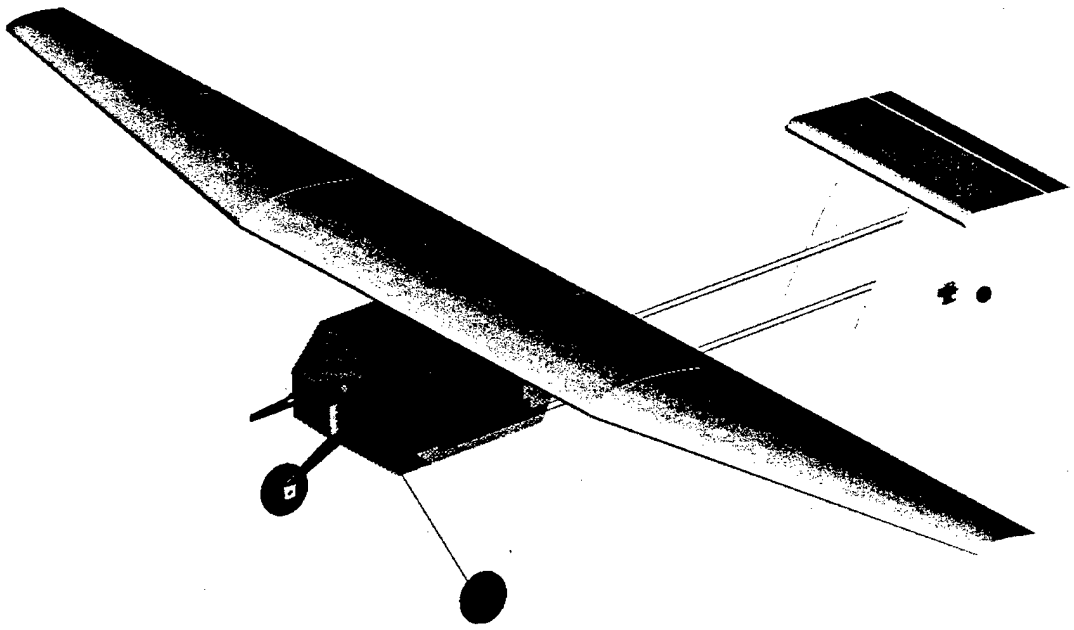

2002/2003 Contest Year
7th Annual Event

Table of Contents

EXECUTIVE SUMMARY 5

BACKGROUND 5
CONCEPTUAL DESIGN 5
Conceptual Design Alternatives 5
Conceptual Design Tools 5
Conceptual Results 5
PRELIMINARY DESIGN 6
Preliminary Design Alternatives 6
Preliminary Design Tools 6
Preliminary Results 6
DETAIL DESIGN 6
Detail Design Alternatives 7
Detail Design Tools 7
Detail Design Results 7

MANAGEMENT SUMMARY 7

ORGANIZATIONAL STRUCTURE 7
TECHNICAL GROUP RESPONSIBILITIES 8
Aerodynamics Team 8
Mechanical Team 9
Structures Team 9
Funding Team 9
ASSESSMENT OF ORGANIZATION 9

CONCEPTUAL DESIGN 11

DESIGN ALTERNATIVES 11
Aircraft Configuration Alternatives 11
Wing Placement Alternatives 12
STRUCTURAL CONFIGURATION 14
Fuselage Structure Alternatives 14

PRELIMINARY DESIGN 15

INITIAL STUDY 15
Batteries 15
Wing dimensions 16
Structural Weight 16
Rated Aircraft Cost 16
AERODYNAMIC CONSIDERATIONS 16
Wing 16
Fuselage 18
Tail 18
STRUCTURAL ANALYSIS 19
Wing 20
Fuselage 20
Tail 21
PROPULSION SYSTEM 21
Motor 21
Batteries 22
PAYLOAD DEPLOYMENT MECHANISM 22

DETAIL DESIGN 22

AERODYNAMICS 23
Wing 23

Tail 23
Fuselage 24
CONTROL SURFACES 24
Wing 24
Tail 24
STRUCTURAL 25
Wing 25
Tail 25
Fuselage 25
Landing Gear 25
INTERNAL COMPONENTS 26
Launching Mechanism 26
Servo placement 27
PROPULSION SYSTEM 27
Motor 27
Batteries 28
DRAWING PACKAGE 28
RATED AIRCRAFT COST 33

MANUFACTURING PROCESS **35**

MANUFACTURING 35
Wing and Flaperon Fabrication 35
Fuselage Manufacturing Process 36
Tail Fabrication 36
Landing Gear fabrication 37

TESTING PLAN **38**

TESTING OBJECTIVES 38
STATIC 38
Aircraft Assembly 38
Load Testing 38
Battery Testing 38
Control Deflection 39
Ejection Mechanism Testing 39
DYNAMIC 39
Advanced Wind Tunnel Testing 39
In Flight Trim 39
Load Variation 39
Time Trials 40
Contest Simulation 40
RESULTS AND LESSONS LEARNED 40

REFERENCES **42**

Table of Figures

Figure 1. Flow chart of team members and their positions. 8
Figure 2. The Western Flyer Milestone Chart. 10
Figure 3. Design matrix for aircraft configuration. 12
Figure 4. Design matrix for wing configuration. 13
Figure 5. Design matrix for structural configuration. 15
Figure 6. NACA 4312 airfoil characteristics. 17
Figure 7. Lift of wing and tail versus weight. 19
Figure 8. Fuselage stress analysis. 21
Figure 9. Aircraft specification chart. 23
Figure 10. Three-dimensional view of tail. 24
Figure 11. Landing gear analysis using Pro/ENGINEER. 26
Figure 12. Three-dimensional view of landing gear 26
Figure 13. Three-dimensional view of launching mechanism 27
Figure 14. Front View of "Western Flyer" 29
Figure 15. Side view of "Western Flyer". 30
Figure 16. Top View of "Western Flyer". 31
Figure 17. Three-dimensional transparent view of the entire aircraft. 32
Figure 18. Three-dimensional transparent view of the fuselage and internal components 32
Figure 19. Side transparent view of the fuselage with internal component description. 33
Figure 20. Rated Aircraft Cost and pie chart analysis. 34
Figure 21. Manufacturing process schedule. 37
Figure 22. The testing plan schedule for the static and dynamic tests. 40
Figure 23. Static testing check list 41
Figure 24. Dynamic Testing Check List. 41

Executive Summary

Background

The objective of the Design Build Fly project as set forth by the AIAA is the conceptualization, design, and fabrication of a Remote Controlled (RC) aircraft that is capable of carrying out a specified set of missions. For the year 2002-2003 the competition requires a battery powered propeller aircraft to carry out three specific missions of varying complexity. The design will be judged based on the aircraft's ability to complete the selected missions.

Conceptual Design

The conceptual design process began with several considerations for achieving the specified design requirements. After a brainstorming session, several initial sketches were made with space considerations and approximate locations for the different components that were deemed essential for the successful flight of this aircraft. Once these sketches were laid the team proceeded to a more refined analysis of the design considerations. This helped eliminate certain design alternatives, and narrowed down the possibilities to more feasible and practical options for further consideration.

Conceptual Design Alternatives

A variety of combinations were selected for design consideration at this stage of the design process. High wing and low wing designs were considered while a mid-section wing as determined to be inappropriate for the purposes of this project. These wing configurations in conjunction with several possible horizontal and vertical tail configurations were proposed for further examination. Possible locations for battery packs, power plant configurations and other major components were suggested. All these were considered bearing in mind the weight of components, ease of construction, and resources available for the on time fabrication of the aircraft.

Conceptual Design Tools

As part of the conceptual design process, rough 2D sketches were drawn up to put in perspective the relative locations of the various components of the aircraft. Mathematical Software tools helped in predicting a first estimate of performance capabilities and relative sizes of components. Initial weight estimates helped determine deciding factors such as range and cruise performance for the specified mission requirements. Decisions as to the number of power plants to be used on the aircraft were obtained from Balanced Field Length (BFL) calculations. A database was setup with a listing of all possible alternatives and results obtained from different estimates.

Conceptual Results

The conceptual design process resulted in first estimates for the performance characteristics of the aircraft for a variety of configurations. Based on trade off studies, it was determined that a single engine, high wing figuration with a twin boom design for the tail supports would be ideal to meet the specified design requirements while bearing in mind performance and construction

issues. It was decided that a non-retractable landing would meet requirements while being cheap and of relatively simple design.

Preliminary design

The next step in the design process was detailed research into the different aspects of the aircraft. For this purpose, the team was broken down into three design groups and a second group was setup to pursue sponsorship related concerns. Each team made a detailed listing of possible alternatives for materials and components and each of these were weighted against each other to determine the configuration that represented the most promising design for the purposes of the competition.

Preliminary Design Alternatives

As a first step in the preliminary design of the aircraft, detailed information regarding the components that were to be used in the aircraft was collected. A thorough study of the fabrication processes and material options were conducted. Options for battery sizes, and number of cells were laid out. From a wide-ranging list of prospective engines, design matrices helped narrow down the search to a select few.

Preliminary Design Tools

Much emphasis was placed on the used of CAD modeling software at the preliminary stage of the aircraft design. It was believed that an accurate model of the various components would help in understanding the spatial relationships and thereby ensure that no interference issues arose at the fabrication phase of the project. Detailed models of components were created and positioned at appropriate locations along the span of the aircraft. Detailed programs were developed to help incorporate the interdependency that existed between the several variables that determined the performance and handling characteristics of the aircraft. This ensured that modifications made to key parameters would automatically determine all the desired information ranging from takeoff performance, to cruise and all the way to landing. Information collected from various sources was cataloged to help in providing data essential for design and analysis.

Preliminary Results

The detailed research into the different aspects of the design at this stage helped determine the makeup of the majority of the aircraft. A monocoque design of carbon fiber and nomex honeycomb was chosen over a conventional space frame approach, for the major structural components of the aircraft. Number of control surfaces and relative positions were determined. The mechanism for the launching mechanism was decided upon as well as the landing gear design. Calculations for the power requirements of the aircraft led to the selection of a power plant for the aircraft and the number of cells

Detail Design

At the detailed design stage, all that remained was accurate placement of all the major components to help in determining the stability and control characteristics of the aircraft. Sizing

and placement of control surfaces and structural components were determined and design studies were constructed to optimize the weight and placement of all components to help locate the CG.

Detail Design Alternatives

The major focus of the structural team was detail considerations relating to the material properties, analyses and fabrication procedures for the structure of the aircraft. Wing and tail sizing coupled with extensive design studies to help in achieving desirable handling characteristics were performed, for the aircraft. Details relating to fasteners for components and accessibility issues were considered. Possible battery placement alternatives and routing of wires were studied and clearance between the launching mechanism and the battery casing were calculated. Different methods of assembling components into the specified box size were setup.

Detail Design Tools

Sensitivity studies constructed using CAD software helped optimize weight and maximize structural characteristics of the components that were designed. Motion simulations were conducted in CAD to ensure desirable deployment of the avionics package. The modeling software was used to setup a virtual mock-up of the aircraft and the interior components to guarantee sufficient clearance between parts and help accurately determine CG location. Through the use of fluid flow analysis software, desirable lift and drag properties were determined as well as Aerodynamic Center calculations. All this coupled with the mathematical software tools helped optimize performance and provided a level of confidence to move on to fabrication and testing of the aircraft.

Detail Design Results

At the conclusion of the detailed design phase, the aircraft was accurately modeled. Component placement and part fabrication had been determined. Analysis tools provided sufficient information to justify a stable aircraft with all the desirable characteristics. All design requirements had been met and the aircraft was deemed functional.

Management Summary

Organizational Structure

Team Western Flyer was divided into four technical groups: aerodynamics, mechanics, structures, and funding. A flow chart of the team members and their position is shown in ***Figure 1***. The advisors duty consists of maintaining proper direction throughout the projects life by corresponding with the team leaders. To minimize miscommunication throughout the project a team leader was specified to communicate between the advisor and the other group leaders. The specialists are responsible for the duties given by the team leader. Weekly meetings have been mandatory for the advisor and team leaders, which the team specialists are welcome to

attend as well. Here everyone presents their progress up to that point and input is given from every team member in order to idealize and optimize the overall aircrafts design.

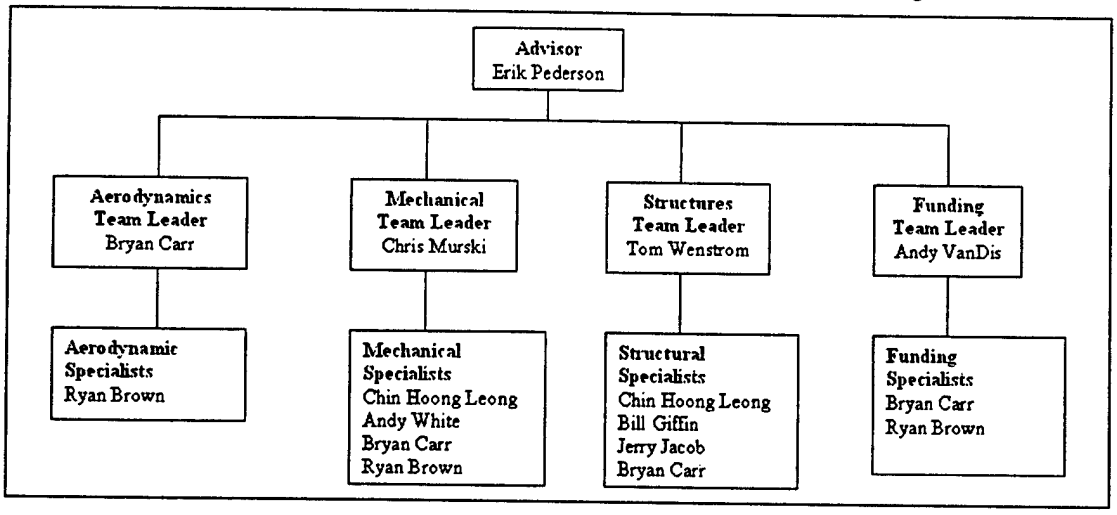

Figure 1. Flow chart of team members and their positions.

Technical Group Responsibilities

The technical groups responsibilities are to communicate with each other at all times throughout the design process to come up with an optimal design that will be easy to manufacture and meet all the required design specifications. Once a rough idea of a design of the aircraft was decided on the team leaders divided up tasks for the specialist in their specific department to work on. Each technical group is responsible for manufacturing their specified component of the aircraft. In ***Figure 1*** only the members are listed that have contributed immensely in each department. Other members including underclassman assisted as much as possible but was minimal in the design process compared to the listed members in the flow chart.

Aerodynamics Team

The main objective for the aerodynamic team was to focus on the design of the wing and tail. This team started out by reviewing the competition requirements. Once an understanding of the type of missions the aircraft would need to fly, the aerodynamics department proceeded with the brainstorming process. The results from the brainstorming are then discussed with the other team leads and the advisor to allow for any new ideas. Then only the initial ideas that have been agreed upon by everyone where taken into further consideration. The aerodynamics team is responsible for implementing the mounting points on the wings in order to mesh with the fuselage. The control surface sizing and stability characteristics will be another aspect that this team is responsible for. Throughout the design process this department will be interacting with the structural team and the mechanical team.

Mechanical Team

The mechanical team is in charge of the batteries, the engine, the propeller, the electrical, the ejection mechanism and the landing gear. After reviewing the competition requirements and understanding the aircrafts mission profile, the team proceeded through the brainstorming process. Once initial ideas where produced collectively for each specific portion of the mechanical team, further consideration was achieved. The mechanical team will need to interact with both the aerodynamics and structural teams in order to have a successful outcome.

Structures Team

The structures team was responsible for designing and manufacturing the fuselage. This involved intense interaction with the mechanical team in conjunction with having all the components mesh together flawlessly. The aerodynamics team corresponded with the structures team on placement of their finial design. After the competition requirements were reviewed, the initial idea was to have a brainstorming session in order to establish their starting point. Once some ideas had been produced, the team then used initial sizing estimates for components such as the engine and batteries that was furnished by the mechanical team to fabricate an idea of the over size of the fuselage. After more discrete decisions had been produced the structures team optimized their initial design to accommodate the other components. The structures team is responsible for the final drawings of the overall aircraft.

Funding Team

As a combined result of governor Engler's cut on the education tax just prior to the ending of his term and now the new appointed governor cutting away on the education tax, the university did choose to support this project. With this huge set back a funding team had to be formulated in order to solicit for financial support. The funding team initially corresponded with all of the groups including the advisor in order to generate an idea of the overall project cost. This is considering material cost and any tools needed to manufacture the aircraft. In conjunction with this cost an estimate on the funding needed to make the trip to Maryland had to be considered. This teams approach consists of soliciting door-to-door to local business, holding a carwash, implementing a pub-crawl, selling t-shirts and approaching the student senate to reach the project estimated financial goal.

Assessment of Organization

With time being a crucial component in this project, a competition schedule had to be produced. The design process was broken up into three main components: conceptual design, preliminary design, and detail design. The construction dates and deadlines of the aircraft had to be established along with obtaining a schedule to follow for the design report. A milestone chart showing planned and actual timing of major elements of the design process, including as a minimum the conceptual design stage, preliminary design stage, detailed design stage, flight testing and report preparation periods can be viewed in ***Figure 2***.

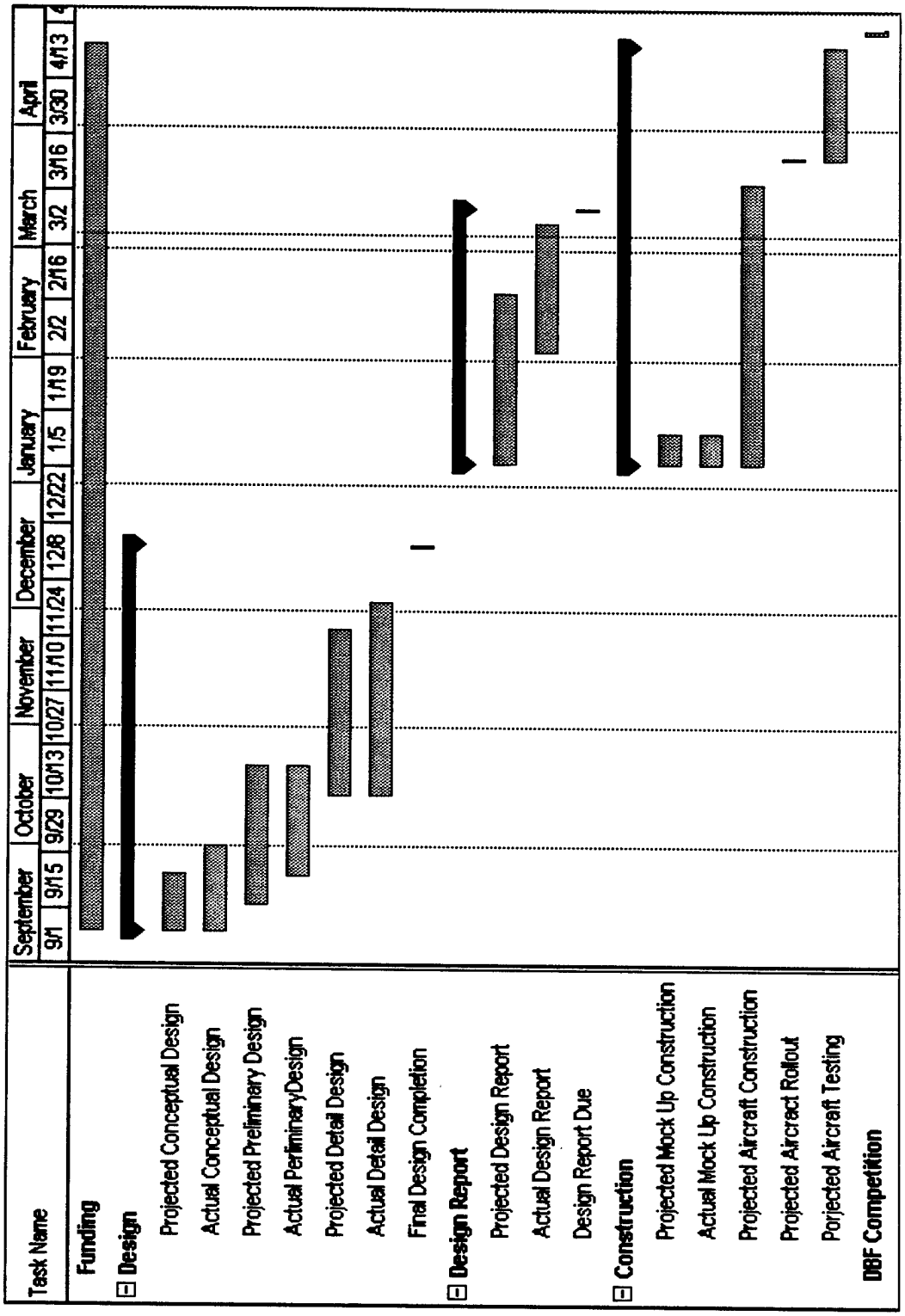

Figure 2. The Western Flyer Milestone Chart.

(Red and black represents beginning and completion milestones. Blue lines indicate projected dates. Green lines represent actual dates.)

Conceptual Design

The conceptual design process of the aircraft began by examining the rules for the competition and determining which would be the most important. The importance of each rule was based on how much of a change in the aircraft design would occur due to a different solution to the challenge presented by that rule. Rules that would have a greater impact on overall aircraft design were deemed more important than rules that had less of an impact. The two most important rules identified were to make sure that the disassembled plane would fit in the specified box size and that it could be swiftly put together out of the box. It was then also decided that the aircraft should have the ability to complete all three mission types available for the competition. Other important features included being able to lift off in the specified distance and making the fuselage large enough to carry a payload that is 6" x 6" x 12". These were the main rules governing the conceptual design of the aircraft, the rest of the rules were observed later on in the design process.

Design Alternatives

Aircraft Configuration Alternatives

To determine the configuration of the aircraft figures of merit were determined to provide the best possible configuration. The figures of Merit used in analyzing the fuselage included the following

- Payload Configuration: The payload will factor highly into the overall scoring, including the aircraft's ability to self unload, sufficient volume to carry the payload and unloading mechanism, and prevent change of flying qualities with the removal of the payload.
- Aircraft Stability: A stable and controllable aircraft will be able to complete the circuit in a shorter time resulting in a better score.
- Aircraft Performance and Efficiency: Performance and efficiency will be a determining factor in mission score.
- Construction Complexity: The complexity of the design will determine the timetable for construction and ultimately the construction quality of the aircraft.
- Aircraft Assembly/Storage: The mission requirement for timed assembly and defined storage volume will be a key factor in completing the given mission
- Rated Aircraft Cost: An important factor in the final score of the aircraft.

Several aircraft configurations were chosen for analysis using the design parameters and the figures of merit. Each configuration and the factors affecting them are listed below:

1. Conventional: The conventional configuration is of low complexity, good efficiency, high stability, and a fair aircraft cost. The Payload configuration is poor due to problems with ejecting it form a long fuselage. The long fuselage could also pose problems in assembly and storage. RAC will be good.

2. Canard: Payload configuration with a shorter fuselage and the canard will be lightweight. Aircraft stability is not as good as other designs and the control system could become complex. RAC should be average.
3. Boom tail: The boom configuration is excellent in the areas of stability, performance, and assembly/storage. The configuration will be negatively affected by construction complexity and RAC.
4. Flying Wing: The flying wing will be very efficient and have a low RAC. The configuration will have negative attributes in stability and construction complexity. This configuration will also be difficult to configure for payload.

These configurations were analyzed using a weighted design matrix, which is given in ***Figure 3*** shown below. The Payload configuration and RAC were given the highest weighting though the other factors were also given appropriate weighted values. It is determined from the design matrix that the boom tail will be the configuration to continue in development. The boom tail provides very good payload properties and will provide a very stable aircraft. Efficiency and construction properties are average while the aircraft assembly and storage rates very high. The factor of most likely having a twin tail will add to the RAC of the design.

Figure of Merit	Weighting Factor	Conventional	Canard	Boom Tail	Flying Wing
Payload Configuration	0.35	0	1	1	0
Aircarft Stabiliy	0.1	1	-1	1	-1
Aircarft Performance and Efficiency	0.1	0	0	0	1
Construction Complexity	0.1	1	-1	0	-1
Aircraft Assembly/Strorage	0.15	-1	1	1	0
Rated Aricraft Cost	0.25	0	0	-1	1
Total	1	0.05	0.25	0.3	0.15

Figure 3. Design matrix for aircraft configuration.

Wing Placement Alternatives

With the general aircraft configuration decided the following figures of merit were determined for the wing placement:

- Payload interference: Minimal interference with the payload and payload device will be necessary to minimize fuselage size.
- Stability: Wing placement will have an effect on the stability of the aircraft.

- Construction: How complex the wing will be to construct and integrate with the rest of the fuselage structure.

The placement of the wing was limited to three alternatives:

- High Wing: The high wing provides minimum payload interference and inherent stability. It is also poses few problems in construction though a large span wing may need to be supported with struts
- Mid Wing: Payload interference is very high with wing structure running through the fuselage. Construction will be complex to avoid payload interference.
- Low Wing: Low wing payload interference will be minimal but will require the payload to be elevated with respect to the ground. Stability will be low and will require a dihedral in the wing. Construction will be very good allowing for simple integration into the fuselage structure.

The factors were analyzed with a weighted design matrix given in ***Figure 4*** below. The payload interference was assigned the highest weighted factor with construction also being an important aspect. From the matrix the high wing position will be the best configuration.

Figures of Merit	Weighting Factor	High	Mid	Low
Payload Interference	0	1	-1	-1
Stability	0.2	1	0	1
Construction	0.2	0	-1	0
Total	1	0.8	-0.8	0.2

Figure 4. Design matrix for wing configuration.

Engine Configuration Alternatives

It was discussed early in the conceptual stage whether the aircraft should have single or twin engines. Because this is the team's first attempt at competition and due to the complexity and added weight of the twin configuration it was decided that a single engine would be best. In addition while both a pusher and tractor configuration were examined, a tractor engine placement will allow a rear cargo ejection. With a rear cargo door: cargo ejection will be quick, the door will not interfere with wing and fuselage structure, and will minimize drag in flight.

Structural Configuration

In order to chose the best configuration for the aircraft's structural components several design alternatives were analyzed. These alternatives were analyzed using the following figures of merit:

- Strength and weight: Strength and weight will affect the aircraft's performance as well as influence the aircrafts RAC. This will be the key structural figure of merit.
- Ease of construction: Each design alternative will require different skills with some being much harder to master than others.
- Formability: The ability to form smooth and complex shapes will be necessary for certain components.
- Modular Construction: To meet mission requirements the aircraft must be assembled in modules, thus structures must be able to transfer loads effectively.
- Cost: Cost will determine the time and effort need to raise appropriate funds.
- Durability/Reparability: Accidents do happen and the ability to repair the aircraft may be necessary in competition.

Fuselage Structure Alternatives

The fuselage is the largest structural component of the aircraft and has numerous design requirements. Its size must be minimized to reduce drag but also have sufficient volume to hold the payload, batteries, servos, engine, etc. The fuselage is also the convergence point of forces from the landing gear, wings, and tail and must be built to withstand these forces. To create the fuselage three design alternatives were considered and then analyzed in a weighted design matrix. These factors were analyzed with a weighted design matrix given in ***Figure 5*** below.

- Wood structure with monocote: This structure would consist of a wooden frame covered with a non-load bearing monocote skin. While being cheap and easy to construct, this method lacks rigidity, and could become heavy to meet the modular requirement.
- Wood structure with carbon fiber: Similar to the above method a wooden frame would be constructed and then covered with a carbon fiber skin. This skin would bear some load and increase strength.
- Monocoque structure: This structure consists of using a sandwich of carbon skins enclosing an aluminum honeycomb structure.

Figure of Merit	Weighting Factor	Wood with Monocote	Wood and Carbon	Monocoque
Strength and Weight	0.4	0	0	1
Ease of Construction	0.2	1	0	0
Formablity	0.2	-1	1	1
Modular Construction	0.1	-1	1	0
Cost	0.05	1	0	-1
Durabiltiy/Reparability	0.05	-1	1	0
Total	1	-0.1	0.35	0.55

Figure 5. Design matrix for structural configuration.

From the matrix it is apparent that the monocoque fuselage will meet the given figures of merit. This buildup has the greatest benefit in its high strength and low weight and also has very good formability to precise shapes.

Preliminary Design

As soon as the conceptual configuration was determined the preliminary design phase began. A preliminary design calculation model program was setup and implemented to give instant results on any design changes. This helped to explore how the design parameters affected the size of aerodynamic and propulsive systems. The required wing size was used to determine the width and length of the fuselage was set. The length of the tail booms was then determined so that the tail sizing could be determined. These parameters were then passed on the other groups to determine all other aircraft component sizing.

Initial Study

The weight, drag, propulsive, and rated aircraft cost characteristic were estimated for initial calculations. Each of the design group performed optimization analysis for every design parameter to obtain the highest score. Due to the fact that all design parameters had to be taken into consideration, it was found that an optimized design change in a single area of the aircraft was not always beneficial to the aircrafts scoring potential. Each group had to interact continuously to optimize the aircraft as a whole. Many of the optimization parameter must be verified through flight-testing.

Batteries

The number of batteries affected many aspects of the aircraft. The less batteries that are used in the aircraft decrease the rated aircraft cost and the takeoff gross weight. This also decreases the maximum payload capacity and the available power for takeoff and cruise. The batteries stored energy is drained faster with fewer batteries, which decrease the available flight time. If number of batteries used maximizes the allowable weight requirements, the rated aircraft cost will

increase. The available power would then be adequate to increase the weight of the payload to increase flight score.

Wing dimensions

When determining the optimal wing dimensions, analysis must be performed on wing area with its respective chord and span and the aspect ratio. These factors affect the power required for takeoff and cruise, rated aircraft cost, maximum payload, and the amount of space required to pack into the 4 x 2 x 1 foot box. The type of airfoil used for the wing will be a key factor in determining the necessary dimensions for peak aircraft performance.

The wing area primarily affects to the maximum weight of the aircraft and the power required for takeoff and cruise. The greater the wing area, the less power is required for takeoff and payload can increase if more power is add for takeoff. However, the large wing area increases the rated aircraft cost and the power required for cruise. Once the required wing area is determined, the wingspan and chord can then be varied to find optimal dimensions. The length of the wingspan determines the number of sections that the wing must be divided into to fit in the box. The more sections that are needed increases aircraft assembly time. The longer the wingspan is the shorter the chord will be; this increases the aspect ratio of the wing. High aspect ratio wings increase the efficiency of the aircraft by decreasing the drag produced by the wings in flight. High aspect ratio wings also need to be strengthened because of the large moment force applied to the wing.

Structural Weight

The aircrafts overall weight affect many aspects of the overall final score. The way the aircraft performs and the rated aircraft cost are largely affected by the weight. The aircraft must be as light as possible while maintaining structural integrity to achieve the best overall score. Through initial component estimate the over empty weight with out batteries is approximately 19 pounds.

Rated Aircraft Cost

Rated aircraft cost was a considerable factor in final score potential. It is crucial to find a balance between aircraft cost and performance. The two largest contributors to rated aircraft cost is battery and aircraft weight. These two factors must be minimized while aircraft performance is maintained to achieve the highest score potential.

Aerodynamic Considerations

Once design parameters were determined and basic configurations were selected, the aircraft was analyzed to further detail. The aircraft was examined for optimal aerodynamics in three major areas: wings, fuselage, and tail. Stability and control for the aircraft was then examined.

Wing

The factors that were used in analysis and final design of the wing were:

- Performance: The aerodynamic performance of the wing must be able to fulfill all competitions requirements. The wings must lift the aircraft off within the 120 feet and

carry its weight plus the minimum payload weight. The wings must be able to fit into the 4 x 2 x 1 foot box disassembled. Some other important performance characteristics include the deflection or twist of the wing and if tip strike is a concern in the final design.

- Total Score: The wings must produce the highest flight score possible by lifting large payload weights and decreasing the total mission flight time. The rated aircraft cost must also be reduced to maximize the total score.
- Assembly: The wing area and chord of the wings will determine the number of sections that the wing must be constructed in to ensure that the assembly fits into the box. When the sections are assembled, it is beneficial to the aerodynamics of the aircraft that all joints are free from gaps or large protruding fasteners.

Before the wing area could be determined, the type of airfoil had to be selected. Studies were conducted on various airfoil types to find one that had ideal characteristic. The airfoil would have to be one that was easy to construct and plot the x/c positions. The search was limited to NACA 4 and 5 digit types using Sub 2-D software. Any airfoil that had a high lift to drag ratio and had a high lift coefficient before its stall angle was reached was sought. The NACA 4312 airfoil was selected for the wing. The Clmax is 2.1 before stall and the L/D is 95. Lift and drag performance can be seen in ***Figure 6***.

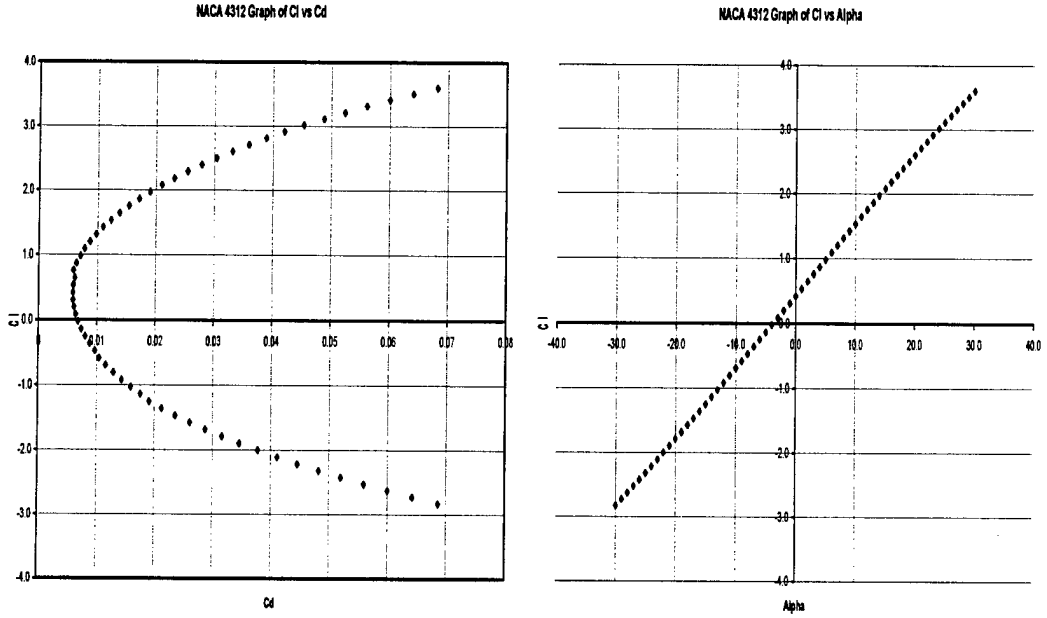

Figure 6. NACA 4312 airfoil characteristics.

With the information of the Clmax for this airfoil it was determined that for a takeoff at a velocity of 40 to 45 feet per second the wing area needed to be within 10.00 to 10.50 sq. ft. to takeoff within 120 feet. Keeping in mind that the wing had to fit in the box with the fuselage and all other aircraft components, the chord of the wing could not exceed 15 inches. The wingspan could be between

10 to 11 feet; this would require that the wing be separated into three sections disassembled to fit in the box. The wing loading is estimated to be 2.7 pounds per foot squared. The projected aspect ratio would be around 10 with these dimension limits. If the chord is much shorter then 15 inches, this would require that the span increase. The span of the wing has a greater influence on the rated aircraft cost then the chord. A large span would bring the overall aircraft score down to a larger scale then an increased chord.

Fuselage

The important factors that were considered for fuselage aerodynamic are:

- Drag: The drag that the fuselage produces must be at a minimum to decrease the power needed for takeoff and cruise. This will increase cruise velocity and flight score. It will also decrease the number of batteries needed, lowering the rated aircraft cost.
- Length: The length of the fuselage will determine the distance that the distance that the horizontal and vertical stabilizer are from the wing. The longer the fuselage is the small the tail areas need to be to counter act the moment of the wing.

The fuselage must be wide enough to carry the avionics package and the mechanism used to eject it out of the fuselage. If the chord of the wing is 15 inches and the sections are stacked on top of each other in the box this leaves a 9 by 12 inch area to put the fuselage. Due to the fact that the box is only 4 feet long the fuselage can be either 4 feet long maximum or the fuselage must be in sections also. The double boom option allows the fuselage length to extend beyond the 4 foot limit. This also degreases the wetted area of the fuselage, degreasing the total skin friction. The fuselage will have to maintain a box configuration with rounded corners to ensure that the avionics package will fit inside and have the fuselage stay within the given area in the box. The propulsion system must also fit inside the fuselage along with the payload.

Tail

Important factors that were considered for the tail:

- Performance: The tail must keep the aircraft in trimmed flight. The aircraft will fly with different factors in each of the various mission levels, the tail and its control must be able to keep the aircraft stable with these changes.
- Positioning: The positioning of the tail is critical so that it will not interfere with the avionics package when it is ejected from the fuselage. The tail must also be in a position to maintain controlled flight when the radar antenna is attached.

The length of the fuselage will set the size of the rear stabilizes. With an approximate length of 5 feet, the vertical stabilizer area needed is 150 sq. ft. The horizontal stabilizer must be 235 sq. ft. These sizing will help to ensure that the aircraft is stable in flight. These tail surfaces must be placed to clear the avionics package when the aircraft positions for takeoff after automatic deployment. The horizontal stabilizer must be more then 6 inches up off of the ground. The horizontal must also be out of the turbulent air flow caused by the radar antenna. The stabilizer

can either be place above or below the turbulent flow. The vertical stabilizer must also be placed to clear the avionics package. This can be done by place the vertical on top of the horizontal or using two vertical surfaces underneath the horizontal to straddle the avionics package. Since a double boom tail is used, it is best to use a double vertical tail surface. This will also keep the vertical stabilizer out of the turbulent flow produced by the radar antenna. A tail dragger landing gear configuration could be used with the double vertical stabilizer formation.

A NACA 4311 airfoil is used for the horizontal stabilizer. This will give the aircraft a lifting tail. The wing will not have to produce extra lift as it would for a no lift horizontal. The neutral point of the aircraft will be set further back on a lifting tail aircraft then on other aircraft. The lifting assistance of the tail will help the aircraft takeoff in a shorter distance. The CL of the wing compared with the CL of the tail vs. weight of the aircraft is compared in ***Figure 7***.

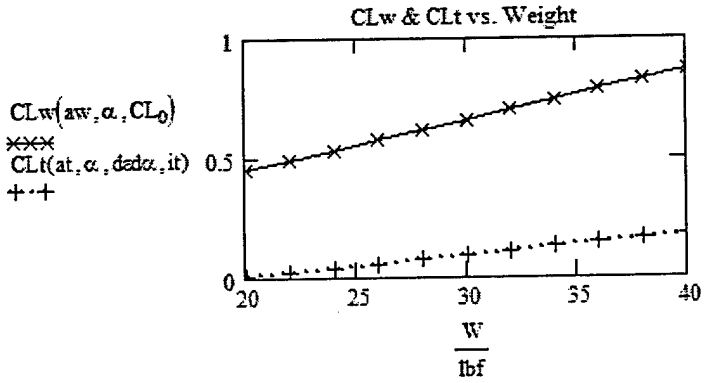

Figure 7. Lift of wing and tail versus weight.

Structural Analysis

Some of the deciding factors for the materials and thickness used in structural design are:

- Weight: The weight of each component on the aircraft has the potential to affect its performance.
- Ease of construction: The materials used should be easy to work with and manufacture to ensure that the aircraft can be constructed and repaired.
- Aerodynamics: The finished surface of any component should have a smooth surface to reduce the drag forces on the aircraft.
- Strength: The material used must be able withstand the applied forces. An ideal material would have high strength and be light weight.

Different materials and lay-ups were analyzed for structural analysis. Material selection for each component was based on the properties of the material and the easy of manufacturing for a

particular component. Characteristics such as strength to weight, lay-up orientation, and deformation were examined for the optimum aircraft performance.

Wing

The wing is an assembly of three sections that are connected with dowel inserts and pins into the fuselage. For simple analysis the drag and lift on the wing were assumed to be evenly distributed across the span. This will give a conservative analysis of wing stress. Since the lifting forces are at a greater magnitude then the drag forces, the lift force will be used for structural analysis. If the total lift forces are resolved to two single forces, one at each wing tip, the calculated stresses will be larger then the actual stresses.

A connecting spar is used to carry the wing loading trough the joints to the mid-section of the wing. The spars are located at the quarter chord of the mid-section of the wings. The spar is .5 inches wide and 1 inch high. The spar is connected to the outboard section of the wing and will be inserted and pinned six inches into the min-section of the wing. The spar is made out of foam raped in carbon fiber.

The wing is made of four layers of carbon fiber with a 1/8 inch thick piece of foam sandwiched between the layers of carbon fiber. The two middle layers of carbon fiber are laid 45 degrees from the other two layers. The wing was simplified into a cantilever beam with the weight force at the wing tips multiplied by a 2.5 g loading. The maximum bend stress in the wing was calculated to 550 psi. The weight of the wing is 7 pounds.

Fuselage

The fuselage is constructed of carbon fiber and honeycomb sandwich skin. The ¼ inch honeycomb will be placed between 4 layers of carbon fiber. The cabin fiber is laid at 90 degrees of one another. The forces from the wing, tail, and landing gear were placed in their perspective locations and analysis of stress was conducted. It was found that the maximum stress was 847 psi located at the tail boom mounting locations. This is within the strength of the material. Hard mounting points will be used at the locations that the wing and tail are mounted to the fuselage to ensure that the structure holds together. The hard points can be seen by the indicated red areas in ***Figure 8***.

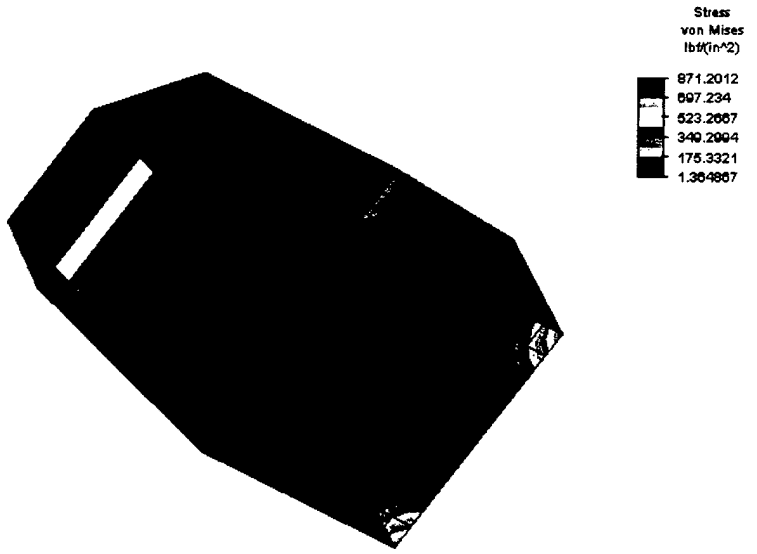

Figure 8. Fuselage stress analysis.

Tail

The tail is constructed of balsa wood build up. The forces on the horizontal tail are not as large as the wing so there was not a need to use carbon fiber for the tail. The factor that influences the structural performance of the tail is the deflection of the two tail booms that the tail is mounted to. It was found that with the forces of the tail, an aluminum 6061-t6 tube with a 7/16 inch outer diameter and a .065 inch wall thickness is used. The deflection of the tail boom was determined to be .424 inches. This deflection will not have a major impact on the aircraft performance. The vertical two vertical stabilizers will be permanently mounted to the tail booms. The horizontal stabilizer will then be mounted to the top of the verticals. The placement of to two vertical stabilizers is 9 inches apart and the horizontal is 9 inches from the ground. The deployed avionics package will be able to fit under and between the tail components.

Propulsion System

The propulsion system must be able to get the aircraft off the ground in less than 120 feet and provide enough battery life to complete each mission. The larger the payload is the more powerful the propulsion system must be. The speed at which the mission is completed also affects the propulsion system.

Motor

An Astro Cobalt 40 aircraft motor was selected for use. The CO-40 Superbox with a gear ratio of 3.1 to 1 is the name of the motor. Two different props were selected to do perform further testing. These props are a 15 x 8 and 16 x 8 props. After the testing is conducted, the prop that gives the best performance will be used for competition.

Batteries

The motor selected has a maximum current draw of 25 amps at 25 volts. In order to be conservative, the battery pack calculations were based on the assumption that the motor would draw this much power for the entire flight time. Every individual battery cell is rated at 1.2 volts. This means that every sub-pack must be made up of at least 21 cells, connected in series, in order to create 25 volts. The actual voltage across any given sub-pack is therefore 25.2 volts. In order to produce 25 amps, 2 or more sub-packs must be connected in parallel.

Different number of battery pack with different payload weights will be test and the optimal battery pack size and payload weight will be determine for competition flight. With a payload weight at the minimum of 5 pounds, the battery pack will only need to contain 2 sub-packs. The needed flight times for each payload weight will be tested to help determine the final battery pack configuration

Payload Deployment Mechanism

The payload deployment mechanism will be mounted inside the fuselage so that the payload will exit out the rear of the aircraft. The mechanism will be constructed of aluminum and will use elastic force to eject to package. The force needed to eject the package was 10 pounds force. A servo operated latch will hold the package in the mechanism until the latch is released.

Detail Design

Once the preliminary design phase was successfully completed, the final detailed design for the aircraft was decided on. The aerodynamics team determined the best airfoil considering all the necessary parameters (i.e. stability, performance, and control). The mechanical team made a decision on each component for an optimal aircraft configuration. The structural team made a decision on a final design for the fuselage by fine-tuning the results from the preliminary design stage. Each team has the responsibility of manufacturing and/or ordering their components. A chart of the final aircraft specifications can be viewed in ***Figure 9***.

Geometry	
Length	5.5 ft
Span	11 ft
Height	21 in
Wing Area	10.45 ft^2
Aspect Ratio	11.5
Control Volumes	N/A

Systems	
Radio	Futaba 9CHP
Servos	3 CS-5; 3 TS-35
Battery Configuration	70 KR-1400 AE
Motor	Astro-40 Cobalt
Propeller (nominal)	15 x 8
Gear Ratio	3.11:1

Performance	
Clmax	2.2
L/D max	95
Maximum Rate of Climb	15 ft/s
Stall Speed	32 ft/s
Maximum Speed	70 ft/s
Take-off Field Length (empty)	80 ft
Take-off Field Length (gross)	100 ft

Weight Statement	
Airframe	18.0 lbs
Propulsion System	1.0 lbs
Control System	0.5 lbs
Payload System	1.23 lbs
Payload	5.0 lbs
Empty Weight	22.0 lbs
Gross Weight	27.0 lbs

Figure 9. Aircraft specification chart.

Aerodynamics

The aerodynamics team had the responsibility of designing and manufacturing both the wing and tail of the aircraft. The structures team strived to have a fuselage with minimal air disruption while being capable of holding the desired payload and other components necessary for flight. Complying with the specified rules for the competition, the best aerodynamic design was achieved. The final design has a mean aerodynamic chord of 1.005 feet. The non-dimensional neutral point is 1.423. The reference point used was the firewall and the distance from the firewall to the neutral point is 1.43 feet. From the firewall to the center of gravity of the aircraft the distance is 1.375 feet with a static margin of 0.073 or that is 7.3 %. See ***Figure 17*** for an overall three dimensional view of the aircraft.

Wing

For the final design of the wing a NACA 4312 configuration was used. With this airfoil shape it produced a relatively flat lower surface. This is ideal for manufacturing purposes. The final design of the wing has a span of 11 feet, divided into three sections. The mid section spans 47 inches with a chord of 14 inches. A dihedral of 2 degrees was used and begins at the fuselage reference line. The two outboard sections have a span of 42 inches with an inboard chord of 14 inches and an outboard chord of 6 inches. Both outboard sections have a leading edge taper. This 4312 airfoil produces a lift to drag ratio of 95 and has a maximum lift coefficient of 2.2. The overall wing area is approximately 10.5 feet squared, which produced an aspect ratio of 11.5.

Tail

The final design for the tail was a pie configuration. The horizontal stabilizer consists of a NACA 4311 airfoil. A lifting tail was decided on to assure the aircraft takes off under the maximum allowed distance of 120 feet. With a span of 24 inches and a chord of 10 inches, the horizontal stabilizer has an area of 1.67 feet squared. The vertical stabilizer consists of two sections

located 4.5 inches out, both ways, from the fuselage reference line. Both of the vertical sections have a top chord of 10 inches and a bottom chord was 16 inches. See ***Figure 10*** for a three-dimensional view of the tail section.

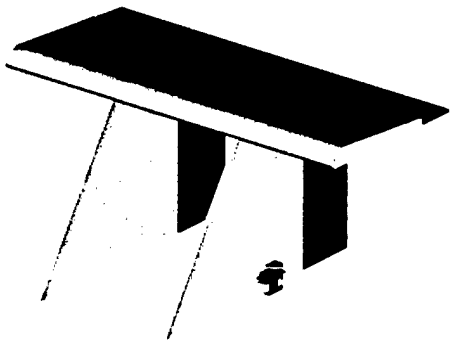

Figure 10. Three-dimensional view of tail.

Fuselage

The fuselage is going to produce the most drag compared to the rest of the components on the aircraft. Its rectangular base shape with dimensions of 10 inches wide by 10.5 inches tall by 25 inches long contains the propulsion system and the payload of the aircraft. The front of the fuselage tapers in to accommodate the motor while the back of the fuselage has less of a taper for payload ejection purposes. A transparent side view of the fuselage can be seen in ***Figure 19***.

Control Surfaces

Wing

The final wing design is equipped with a flaperon configuration oppose to the conventional flap-aileron design. The flaperons span on both sides of the fuselage reference line 5.5 inches out. The chord of the flaperon is 2.25 inches and has a span of 29 inches. The maximum deflection angle is 20 degrees in both directions. This design produces a 57.06 degree/second roll rate with a 20-degree flaperon deflection.

Tail

The tail is equipped with an elevator and two rudders. The elevator spans the entire distance of the horizontal stab, which is 24 inches and has a chord of 2.25 inches. The rudder size is 4 inches long by 8.5 inches tall on each vertical stabilizer. The yaw moment produced with respect to rudder deflection is -0.011. With this lifting tail design and the twin vertical stabs this configuration will have an outstanding flight performance.

Structural

Wing

The wing is made up of three sections (one mid section and two outboard sections). The wing joins to the fuselage by a male/female connection attached to the leading edge and is also fastened three-fourths of the way back on the wing by two vinyl-threaded bolts. A spar located just aft quarter chord of the wing is used to strengthen this design. The outboard sections of the wing attach to the mid section by the spars. The midsection spars a fraction of the size smaller than the outboard section spars. The inboard edges of the outboard sections are indented to slide into the outboard edge of the mid section. It is predicted a piece of duct tape will be laid over the connection to reassure the wing components don't come apart. A NACA 4312 was selected for the wing because of its impressive lift to drag ratio of 95, which will be more than enough to support a payload/cargo carrying mission. Carbon fiber was used to construct the wing due to its high strength and lightweight.

Tail

The tail is a pie configuration that is fastened to the aircrafts cylindrical booms by "U" clips. The two vertical stabilizers slide into position on the bottom surface of the horizontal stabilizer. Two plates, one on both sides of the each vertical stabilizer secure their connection between both surfaces by means of a pin joint. With this method used for the connection between the vertical and horizontal stabilizers the assembly time will be reduced. The tail section will be constructed out of balsa wood

Fuselage

The fuselage will carry the payload, the launching mechanism, the batteries, and the motor, which including all of the necessary components for operation. The final design is a boom tail configuration where the booms will slide into and out of the fuselage for storage purposes. This method will also decrease the assembly time. The booms where estimated to see a deflection of 0.217 inches with a 5 lb load on each boom in the negative direction, that is down being in the negative direction and up being in the positive direction.

Landing Gear

A landing gear shape had been determined and can be seen in ***Figure 12***. The design consists of a flat plat with two angled sections to accommodate the wheels. The wheels are 3.5 inches in diameter and made of hard foam. The landing gear span is approximately 25 inches. Sheet metal is used for this design. The sheet metal will act as a spring for the aircraft upon landings and takeoffs as a result of the metals properties to stretch/bend. An analysis was conducted (using the Pro/ENGINEER software package) on the landing gear with an applied force of 50 lbs. The magnitude of displacement and the maximum stress can be viewed in ***Figure 11***.

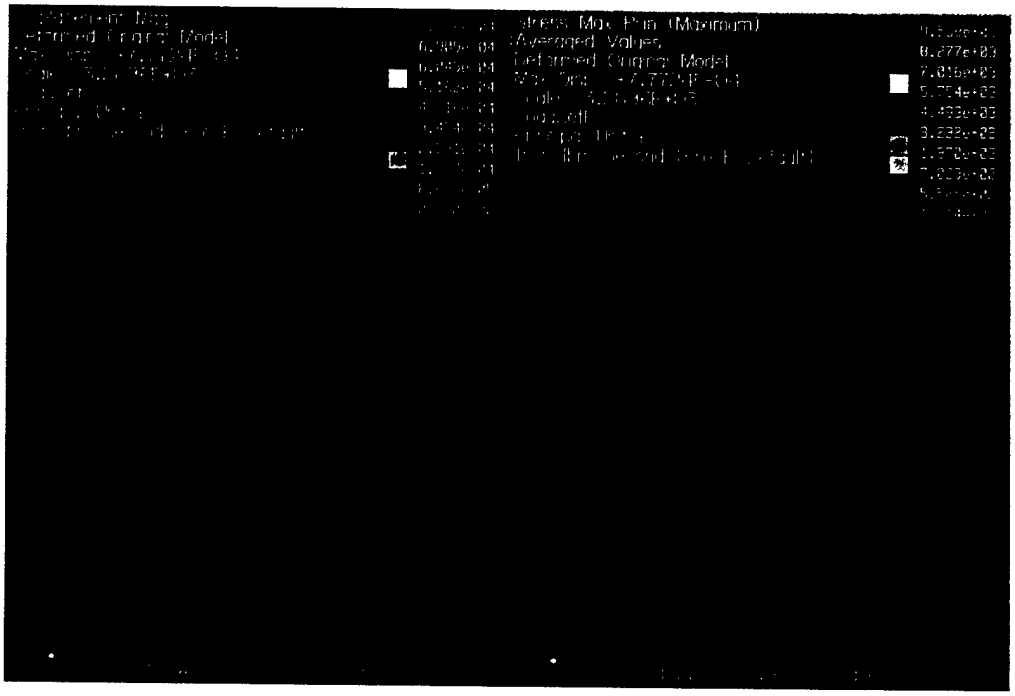

Figure 11. Landing gear analysis using Pro/ENGINEER.

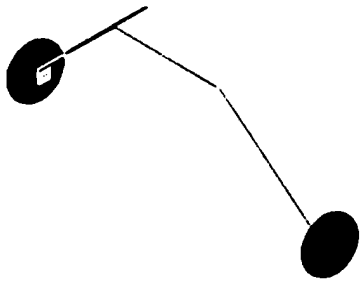

Figure 12. Three-dimensional view of landing gear.

Internal Components

Launching Mechanism

The main objective of this mechanism is to deploy a 6in by 6in by 12 in simulated avionics package from the cargo compartment from the aircraft. With increasingly limited amount of cargo space for the whole unloading mechanism and the specified dimensions of the simulated avionics package, the height of the top slider mechanism has to be minimal. A rocker system has been design for that purpose and the servo can be mounted flat to minimize the overall height of the mechanism. A thinner spring band was considered for weight reduction. The simulated avionic box slides into the launching mechanism parallel to the guiding rails on each side. By pushing the

box correctly in from the front, which is through the lock on the top, it will then catch on to the spring band. Continue on loading the spring band until the stopper catches the box. Put the stopper in the lock position in order to prevent the box from ejecting. By moving the stopper to the release position, the box will then be sprung from the fuselage as a result of the potential energy changing to kinetic energy on the band. See ***Figure 13*** for a three-dimensional view of the launching mechanism.

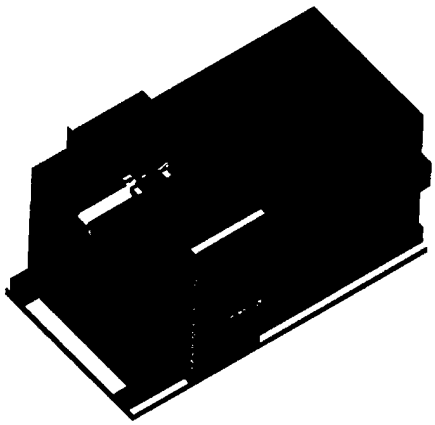

Figure 13. Three-dimensional view of launching mechanism.

Servo placement

There are two types of servos used on this aircraft. Two of the three CS-5 servos are used to control the flaperons on the wing. The other CS-5 servo is used to deploy the avionics package. The servos on the wing are located outboard the center wing section and are recessed into the bottom of the wing on each side. The other types of servos are the TS-35's, which are a little more weight but can produce the power needed to control the aircraft. The TS-35's servos are used on the tail of he aircraft. Two of the servos are mounted on the vertical stabs; each one is located on the outside of the vertical sections. A balsa wood nacelle housing was produced over these servos to reduce any possible aerodynamic deficiencies. The other TS-35 servo is located on the lower skin section of the horizontal stab. This servo is also recessed into the wing.

Propulsion System

Motor

In order to takeoff in the required runway distance of 120 ft, based on the weight calculations, it was determined that the motor would have to be a 1000 W output motor. Since the selection was limited to a single company, the best engine for the application was determined to be the CO-40 Superbox (p/n 640S). This engine weighs 16oz. (1 lb) and has a gear ratio of 3.1:1. Two props were selected for this particular engine, a (15 X 8) in and a (16 X 8) in. Testing on the engine will determine the propeller that would best suit the application.

Batteries

The battery pack that would best suit this application was rated at 1.2 Volts and could produce 0.4 amps. To meet the requirements of the motor and to span the entire mission, it was determined that three packs with 21 cells in each pack would be more than sufficient to complete a mission. The cells were arranged in a configuration of 7 X 3 cells. Three such packs were stacked in a box, which was placed in front of the deploying mechanism and behind the motor. The battery pack was estimated to be around 4.5 lbs, which in addition to all the wires and connectors, should come close to the battery pack weight limit of 5 lbs.

Drawing Package

The drawing package includes front, side and top two-dimensional views (***Figures 14, 15 and 16***) of the aircraft along with a three-dimensional view of the entire aircraft. A three-dimensional view of just the fuselage is also included and is shown in ***Figure 18***. In ***Figure 19*** a transparent two dimensional side view of the fuselage is depicted to show the internal layout of all the components with in. The drawing package represents the aircraft's final design.

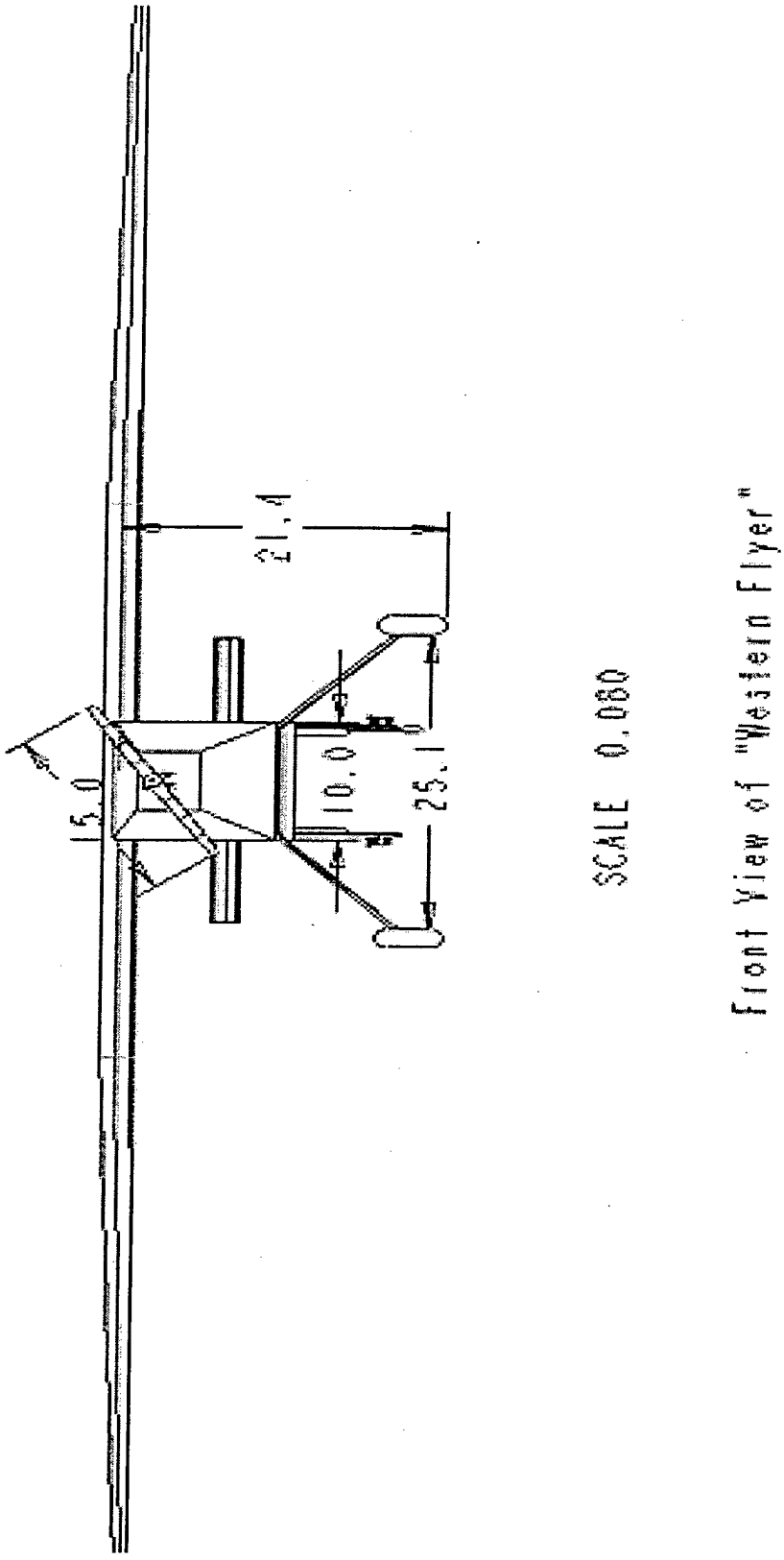

Figure 14. Front View of "Western Flyer"

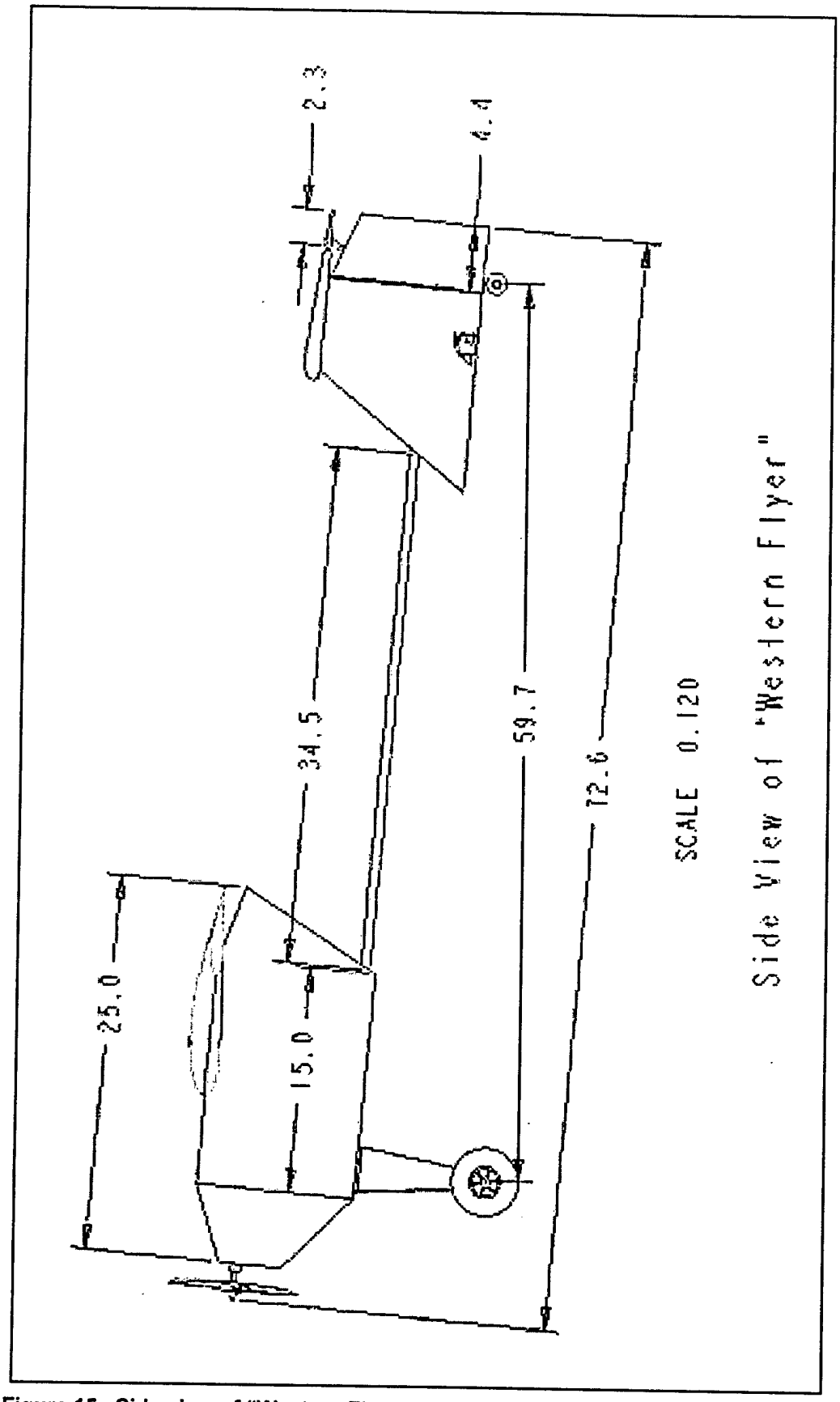

Figure 15. Side view of "Western Flyer".

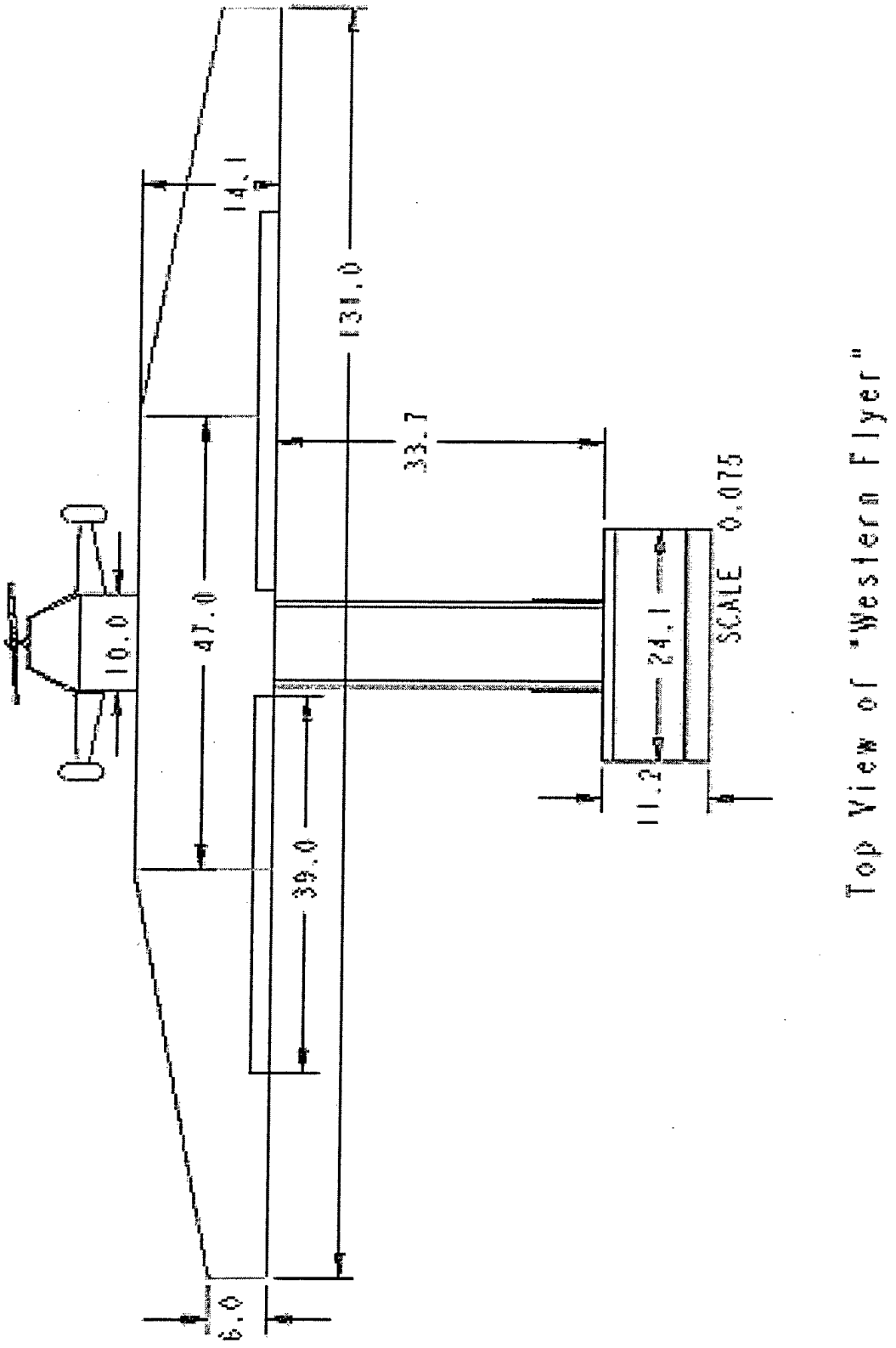

Figure 16. Top View of "Western Flyer".

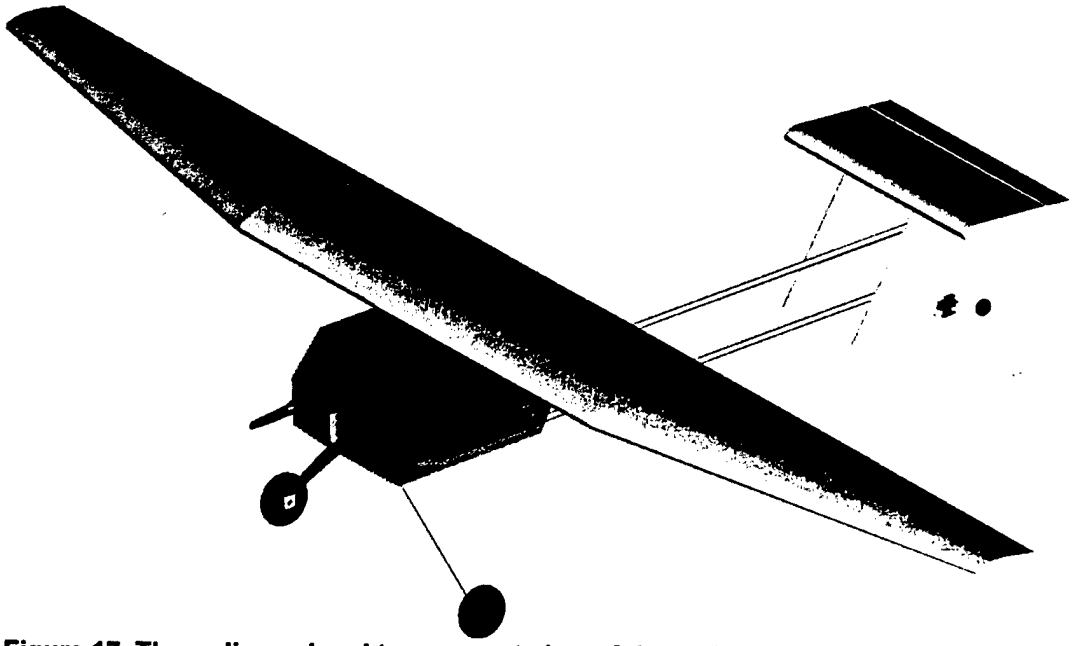

Figure 17. Three-dimensional transparent view of the entire aircraft.

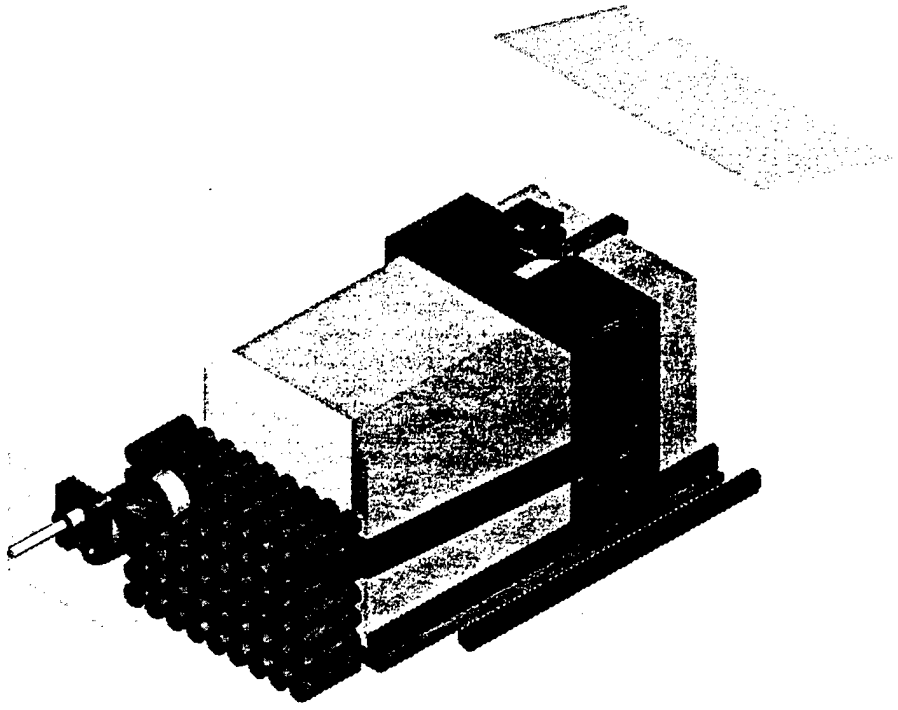

Figure 18. Three-dimensional transparent view of the fuselage and internal components.

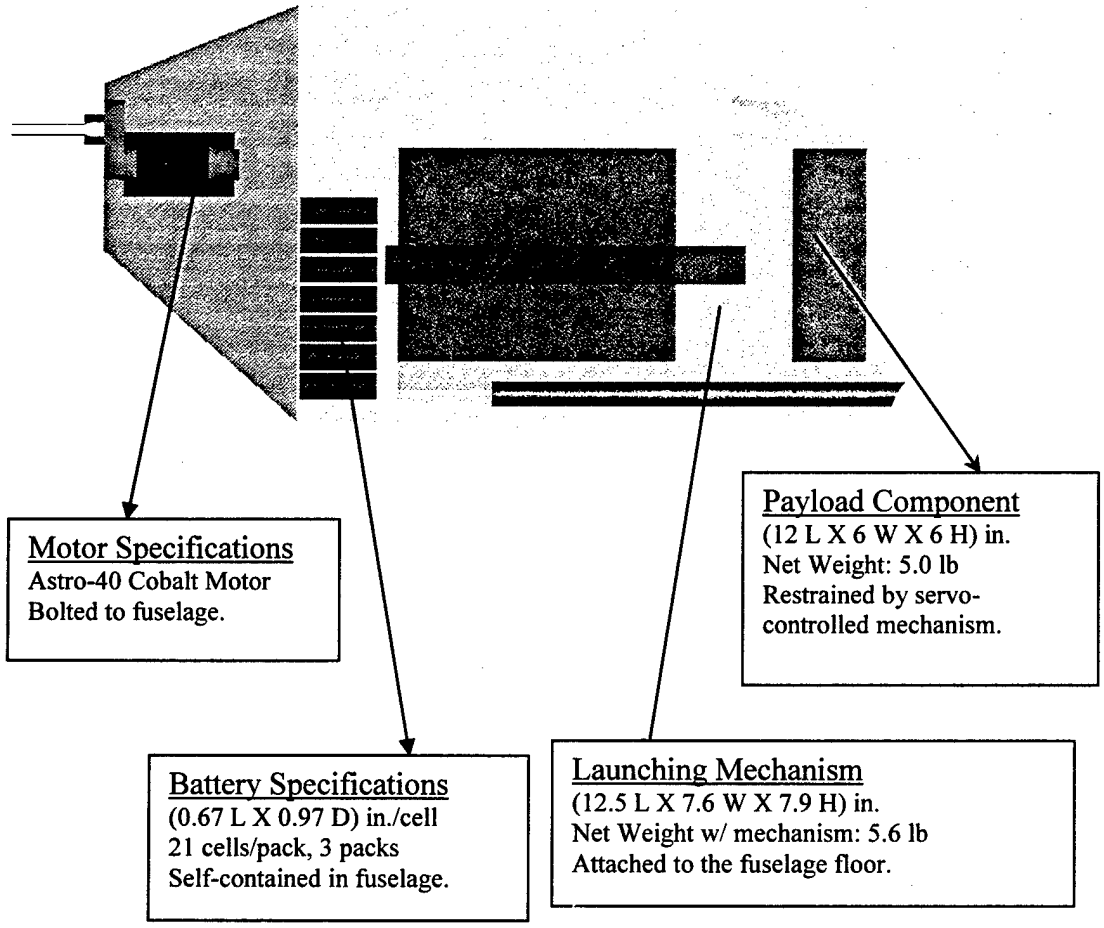

Figure 19. Side transparent view of the fuselage with internal component description.

Rated Aircraft Cost

Once the sizing of the components was determined the required Rated Aircraft Cost was calculated. A pie chart and worksheet can be viewed in ***Figure 20***. The estimated Rated Aircraft Cost was roughly 14.307.

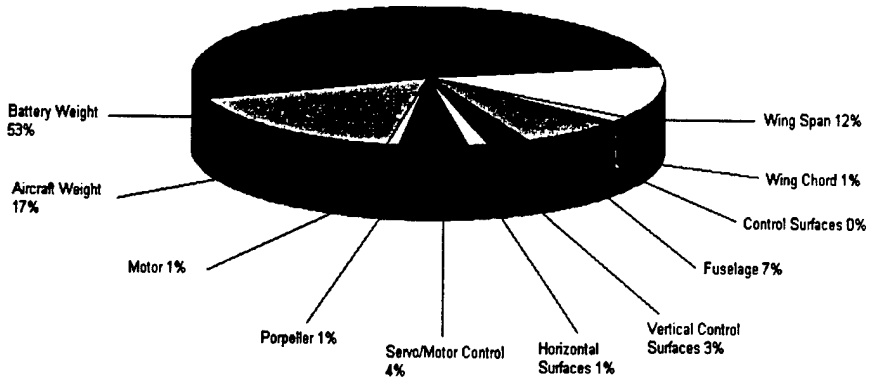

	Value	Weight lbs	Hours	Feet	Number	Cost
Wing WBS						
Wing Span	$20	88	11			$1,760
Wing Chord	$20	9.33333333	1.166667			$186.67
Wing Control Surfaces	$20	3			1	$60
Fuselage WBS						
Fuselage	$20	50	5			$1,000
Fuselage WBS						
Vertical Surface with Control	$20	20			2	$400
Horizontal Surface	$20	10			1	$200
Flight Systems WBS						
Servos an Motor Controller	$20	30			6	$600
Propulsion System WBS						
Engines	$20	5			1	$100
Propeller	$20	5			1	$100
	Totals	220.333333				$4,407

	Value	Weight lbs	Hours	Cost
Manufacturers Empty Weight	$100	24	N/A	$2,400.00
Rated Engine Power Multiplier One Engine	$1,500	5	N/A	$7,500
Manufacurturing Man Hours	$20/hour	N/A	220.3333	$4,407
		Rated Aircraft Cost		$14,307.00

Figure 20. Rated Aircraft Cost and pie chart analysis.

Manufacturing Process

Manufacturing

Several different methods are going to be used in manufacturing the aircraft. Each of the components will have a different method for construction. This will allow the aircraft to accomplish the shape and surface finish for a successful aircraft. Varying the methods used for construction also allows the weight to stay with in the desired range while maintaining structural integrity. The fuselage construction is out of carbon fiber and honeycomb. The Wing is built using carbon fiber. The Tail was made out of balsa wood while the landing gears manufacturing process is out of sheet metal. Each process will be explained in detail below and the manufacturing schedule can be viewed in ***Figure 21***.

Wing and Flaperon Fabrication

The wing was the first composite structure that was fabricated. The design of the wing comprised of a three sections. The mid-section was a Hershey bar wing while the two outboard sections either sides of it were tapered. Both an upper mold and a lower one had to be fabricated separately but essentially involved the same procedure as outlined below. The mold was to be fabricated out of fiberglass to reduce costs while the wing was to be made out of carbon fiber for structural reasons.

The fabrication began with the construction of a foam plug. First the airfoil sections at the tip and at the root of the outboard sections were water jet cut out of metal. These were used as braces and mounted onto a board. Liquid foam was poured into the board and was then sanded down to a rough shape after it had solidified. Following this, the foam was fine sanded, down to a smooth finish. A layer of PVC (Poly Vinyl Chloride) was sprayed onto the smooth surface followed by painting a layer of PVA (Poly Vinyl Alcohol). These were the release agents, so as to help the carbon fiber to come off the surface of the plug after it had cured. Once the release agents had dried, the surface was waxed and was ready for the fiberglass.

Six layers of fiberglass were used in the fabrication of each mold. The layers were laid onto the surface of the plug with resin, smoothed down to remove excess resin and the whole setup was vacuum bagged and left to cure. Once the resin had cured, the molds were taken and again sanded down and waxed to a gloss finish. Once again after the release agent had been applied and left to dry, layers of carbon fiber were laid onto the surface of the mold. Four layers of carbon fiber were used for the actual wing structure. Following the vacuum bagging and the curing process, the outboard wing sections were complete. A similar approach was adopted in the fabrication of the center section of the wing.

The flaperons were also manufactured from carbon fiber and it was connected to the wing section using Kevlar as a hinging mechanism.

Fuselage Manufacturing Process

Once again the use of a mold was considered beneficial since damage to the fuselage was anticipated during the testing phase of the design. As such the first step was the fabrication of a plug. Different cross-sections of the fuselage were sketched onto thin pieces of wood and the profiles were cut out. These were then positioned at a specified distance apart and the gaps were filled with solid blocks of Styrofoam. The foam was sanded down until a rough shape of the fuselage was obtained. Filler was used to even the surfaces followed by sanding to smooth the surface. A layer of PVA (Poly Vinyl Alcohol) was applied to ensure that the mold could be detached from the plug after the resin had cured. After polishing the surface, a couple of layers of fiberglass fabric, of different densities were laid, vacuum bagged and left to cure. As a result of the complex geometry it was required that the mold be separated into two parts, an upper and a lower one. Provisions had been made to ensure that the mold could be mated after separating them following the cure period. Once the mold was cured, the surface was polished to ensure a glass finish to the surface.

The next step in the fabrication process was laying the inner layers of carbon fiber and honeycomb. Pieces of honeycomb and carbon fiber were cut to meet the contours of the mold. A single layer of nomex honeycomb was sandwiched between two layers of carbon fiber and resin on either side. The vacuum bagged setup was let to dry and was ready for the reinforcements for the fixtures.

Aluminum sheets with holes drilled in specified locations were situated at pre-determined positions of the fuselage to help in reinforcing the structure where items such as the power plant, landing gear and loading/unloading door had to be mounted. The use of the CAD package greatly aided the manufacturing process to ensure that the parts came together correctly. However, lack of experience in the fabrication process led to certain imperfections in the fuselage.

Tail Fabrication

The tail was fabricated from balsa wood since it wasn't to be a major structural component of the aircraft. In order to ensure that the part could be fabricated quickly in case of damage during testing, a simple design was adopted for the tail section.

For the horizontal stabilizer, the airfoil sections were drawn up and laid out onto thin pieces of balsa wood. The individual sections were carefully cut out and set on a strip of wood which had their predetermined positions marked out. Strips were also made for the leading and trailing sections of the stabilizer, followed by thin rectangular pieces to help reinforce the structure at requisite locations.

The elevator was made from a single piece of balsa wood that was cut out to rough dimensions and was then sanded down to the right size. The leading edge of the wedge shaped piece was rounded to acquire the desired geometry. The servo mechanism was mounted to the center of the horizontal stabilizer.

The vertical stabilizer was more of a flat piece of wood that was cut to the right spec, than actual airfoil geometry. The rudder was fabricated from a similar piece of balsa wood. The leading edge of the rudder and the trailing edge of stabilizer were rounded to provided rotational clearance for the rudder. The rudder section was attached to the tail with the help of an adhesive piece of fabric. The servo mechanism was mounted to the outer facing side of the tail section in order to ensure that the boom section or the deploying mechanism did not interfere with the functioning of the actuating servos. A single tail wheel was attached to the left vertical stabilizer, as this was adequate to achieve the desired turning radius.

The boom section was affixed to the horizontal stabilizer using a U-clamp. The opposite end of the boom went into tubular mount in the fuselage.

Landing Gear fabrication

The landing gear was the only structural component of the aircraft that was made from sheet metal. A quarter inch thick piece of aluminum sheet metal was required for this purpose. Using the sheet metal package in the CAD software, the required bent section of the landing gear was drawn with the required bend radii and was optimized to meet design requirements. The sheet metal piece was then unbent in the software and the flat section was plotted and traced onto the aluminum stock. The part was cut out as per the design and once the lines were drawn, along which to bend the piece, the aluminum was bent to the desired shape. The wheels were attached to the mechanism using shafts and the cotter pins were used to ensure that the wheels stayed in place. The landing gear was to be bolted on to hard points on the fuselage.

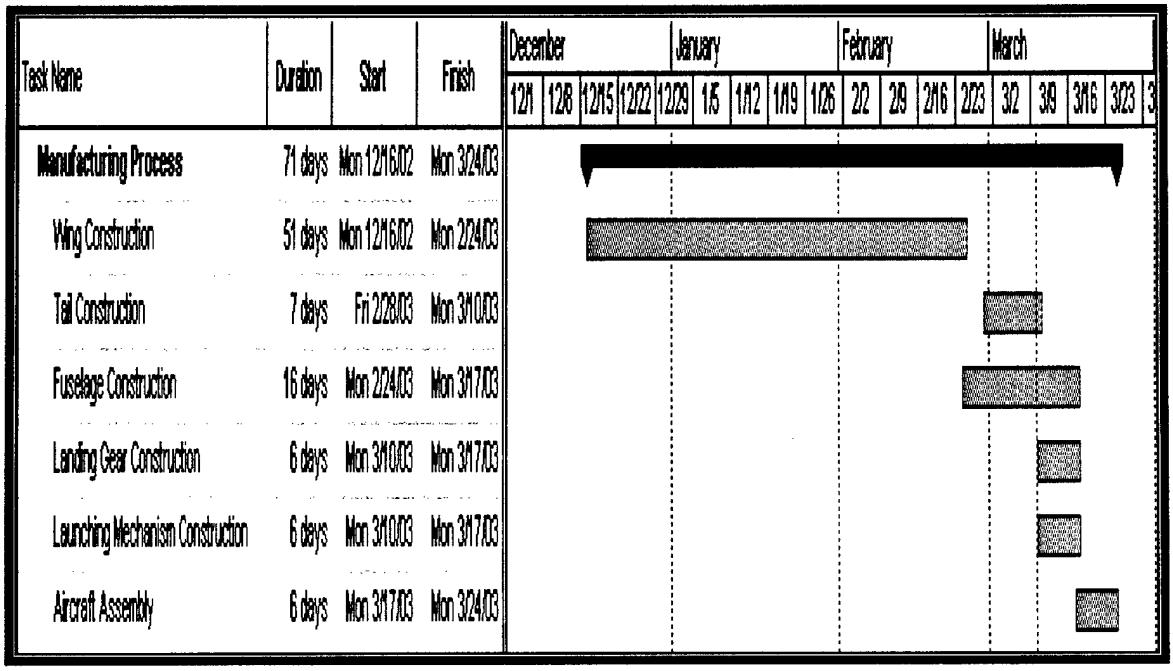

Figure 21. Manufacturing process schedule.

Testing Plan

Testing Objectives

Static testing will be a way of discovering, by questions or practical activities, what the aircraft is capable of in equilibrium. This is the initial stage of generating a foundation of reassurance on the aircraft prior to flight testing. The static testing will cover the assembly of the aircraft, load testing, battery testing, proper deflection of the control surfaces, and the testing of the ejection mechanism. A checklist of the static testing can be viewed in ***Figure 23***. A successful static test will be possible if every test on the checklist passes safely.

Dynamic testing will be a way of discovering, by questions or practical activities, what the aircraft is capable of relative to its energy or motion. The dynamic testing will consist of wind tunnel testing, in flight trim, payload variation, optimizing the time flight time, and a contest simulation. A checklist of the dynamic testing can be viewed in ***Figure 24***. A successful dynamic test will be possible if there is minimal time spent and safe results on each test while no set backs occur (i.e. aircraft crashes). Thus far the aircraft is still in the construction phase. The static and dynamic tests will follow the completion of the construction phase of the aircraft. An overview of the testing plan schedule can be seen in ***Figure 22***.

Static

Aircraft Assembly

One of the specified requirements for the competition is that the aircraft has to fit into a 2 foot wide by 1 foot high by 4-foot long (interior dimensions) box. With this the aircraft has to be equipped with removable parts. Once all of the components of the aircraft have been manufactured the next step will be assuring that every piece joins properly. A successful assembly will consist of fast and easy connections with minimal gaps between joints.

Load Testing

The load testing will help in assuring the structural integrity of the aircraft. This test will consist of analyzing the wing, tail, fuselage, booms, and landing gear. Lifting the aircraft from the wing tips will be the method used for testing the wing strength, which would roughly equate to a 2.5 gravitational load force. The aircraft is predicated to see a gravitational loading of no more than 1 to 1.5 g's. With a successful wing loading test, the wing structure would be capable of handling the loads acquired during its flight mission.

Battery Testing

To assure that each cell is dependable during flight, testing every cell will be necessary. This test consists of checking that every cell holds a charge using a voltage meter. A simple physical check for any damaged or possible punctured areas on each cell will also take place. Once the battery cells have been tested a static run with the motor, varying rpm's, will be used to verify how long the batteries will last. This will be a physical solution to how many batteries the aircraft will

need for the flight missions. A wire check will ensure that every point is safe from any possible outside force or interaction that would cut, burn or damage an electrical connection or wire.

Control Deflection

A control deflection test will consist of connecting all the servos to the batteries and their mounting position on the aircraft to see if each control surface deflects in the desired direction. The servo arm will be adjusted accordingly to maximize the deflection in the control surfaces.

Ejection Mechanism Testing

The ejection mechanism test is designed to optimize the mechanisms overall performance and give a better understanding of what it's capable of. The varying factors involved in this test will be the tension on the band, the payload weight, the ejection pin, and placement of the servo. By varying the tension in the band, this will affect the size of the force acting on the payload along with the rate at which it is ejected from the fuselage. The weight of the payload will affect the rate of ejection as a result of the tension force having more or less weight to act upon. As for the ejection pin, the shape and size will have an affect on whether the ejection rate is decreased or not. With the placement of the servo the throw on the ejection pin will be affected. A controlled ejection with in a sure cleared distance from the aircraft is the over goal of the mechanism.

Dynamic

Advanced Wind Tunnel Testing

Western Michigan University has an advanced wind tunnel available for use by the students, which data will be obtained from certain components of the aircraft. These components include the radar, the tail and fuselage. With the radar and the fuselage in the wind tunnel individually, the lift and drag coefficients and information on the wake produced can be determined. As for the tail, the lift and drag coefficients are obtainable along with its stall characteristics. Having this information is beneficial towards having a better understanding of what to expect from the aircraft's actual flight performance.

In Flight Trim

The control surfaces will most likely not be in an optimal position for the best controlled flight. Upon the first few flights in the flight test portion the pilot will trim the aircraft to his liking. It is expected to take two to three flight test runs to trim the aircraft.

Load Variation

Varying the load will determine what the aircraft is capable of carrying during flight. The test will be conducted by adjusting the weight in increasingly small increments in order to determine the best flight performance. The maximum weight that the aircraft should be capable of carrying is around 10 lbs. It is estimated that the best versus performance would be some were in the range of 6 to 6.5 lbs.

Time Trials

Once the best weight has been determined and the aircraft is trimmed, time trials will be conducted. Some initial calculations on how long the aircraft should take to complete each mission had been formulated but are not accurate. The time trials will give a more realistic idea of how long each mission will take. To achieve the best results the exact course needs to be simulated. The time trials will give the pilot the opportunity to have a better feel for what to expect while flying the missions.

Contest Simulation

Similar to the time trials, the contest simulation will consist of simulating the flight missions along with practicing the assembly of the aircraft. The assembly process will be conducted as many times as necessary in order to achieve the fastest possible time. The contest simulation will not only allow the three-man crew to get comfortable with the assembly process but also give the pilot more flight time.

Results And Lessons Learned

At this point in time the aircraft is under construction so no results under the aircraft testing can be obtained. The expected results would be a flawless aircraft that has exceptional flight handling characteristics with the radar attached while carrying the maximum rated payload. Completion of the assembly and flight mission under the 10-minute time limit would be expected as well. As a result of not going through the testing procedures, no lessons have been learned.

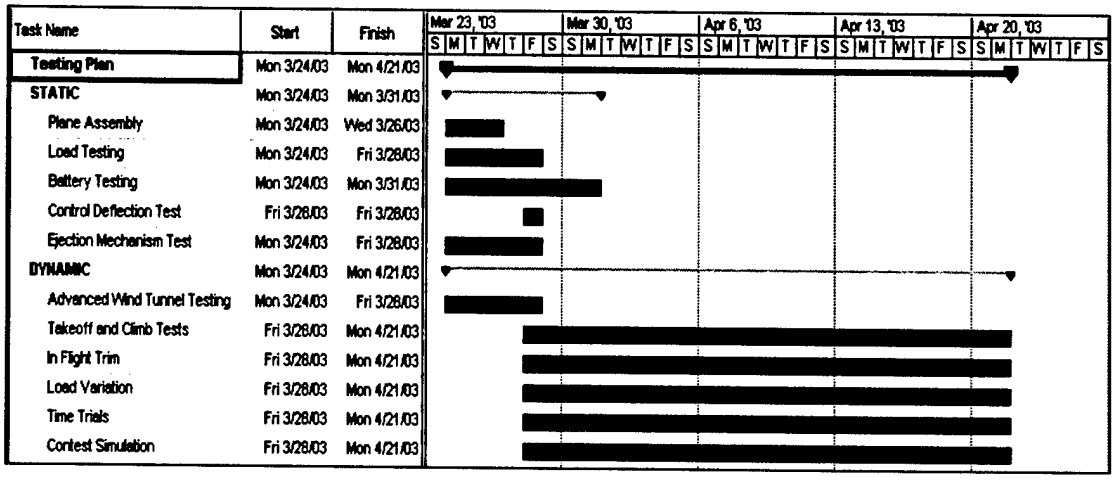

Figure 22. The testing plan schedule for the static and dynamic tests.

Static Testing Check List					
Task	Specific Testing Objective				
Plane Assembly	Test Run #1	Test Run #2	Test Run #3	Test Run #4	Test Run #5
	Test Run #6	Test Run #7	Tet Run#8	Test Run #9	Test Run #10
Load Testing	Wing	Tail	Booms	Fuselage	Landing Gear
Battery Testing	Physical Appeance	Voltage Check			
	Static Motor Run For Battery Life				
Control Deflection	Flapperons	Rudder			
	Elevator				
Ejection Mechanis	Tesnion Band	Payload Weight			
	Ejection Pin	Servo Placement			

Figure 23. Static testing check list.

Dynamic Testing Check List					
Task	Specific Testing Objective				
Advanced Wind Tunnel Testing	Radar	Fuselage			
	Tail				
In Flight Trim	Elevator	Rudders			
	Flaperons				
Load Variation	5 lbs	6 lbs	7 lbs	8 lbs	9 lbs
	10 lbs	11 lbs	12 lbs	13 lbs	14 lbs
Timed Trials	Trial Attempts	Mission 1	Mission 2	Mission 3	
	1				
	2				
	3				
Contest Simulation	Trial Attempts	AircraftAssembly	Mission 1	Mission 2	Mission 3
	1				
	2				
	3				

Figure 24. Dynamic Testing Check List.

References

Allen, H. D., Introduction to Aerospace Structural Analysis. John Wiley and Sons, Inc., New York, 1985.

Hibbeler, R. C., Mechanics of Materials, 4th Edition. Prentice Hall, Upper Saddle River, New Jersey, 2000.

McCormick, W. B., Aerodynamics Aeronautics and Flight Mechanics, 2nd Edition. John Wiley and Sons, Inc., New York, 1995.

Raymer, P. D., Aircraft Design: A Conceptual Approach, 3rd Edition. AIAA Education Series, Reston, VA, 1999.

Sudiku, A. Fundamentals of Electric Circuits. McGraw-Hill Higher Education, Boston, 2000.

Design Build Fly Senior Design Team

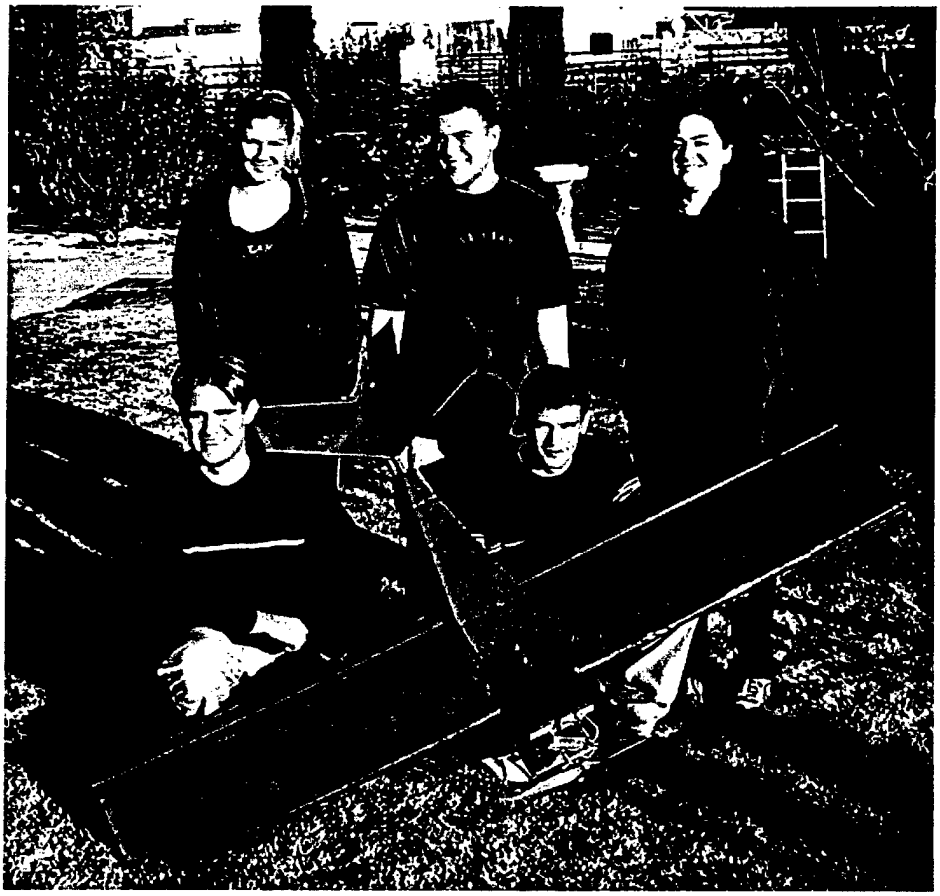

By

Brent Hampton

Leslie Watson

Sam Moreland

Jennifer Beaman

Burton Waite III

The University of Arizona
Aircat 2003

Table of Contents

TABLE OF CONTENTS 2

EXECUTIVE SUMMARY 4

CONCEPTUAL DESIGN 4

MANAGEMENT 4

TEAM MEMBER ROLES 4

Fuselage Design Team 4

Tail Design Team 5

Wing Design Team 5

Landing Gear and Nose Cone Design Team 5

Power Design Team 5

FINANCIAL CONCERNS 6

CONCEPTUAL DESIGN 8

DESIGN DRIVERS 8

Fuselage 8

Wing 11

Tail 12

Power 12

BASIC DESIGN POSSIBILITIES 13

Fuselage 13

Wing 14

Attachment 14

Vertical Wing Location 15

Airfoil Selection 15

Wing Shape 15

Control Surfaces 15

Tail 16

Power 16

STRUCTURAL CONCERNS 17

Fuselage 17

Wing 18

Tail 19

Power 19

DESIGN ANALYSIS 20

Fuselage 20

Wings 22

Attachment 22

Wing Arrangement 22

Airfoil Analysis 23

Wing Sizing 23

Wings with Flaps 24

Wing Shape 25

Tail 25

Power 26

Batteries 27

PROTOTYPE PRODUCTION 29

FUSELAGE 29

Specify Determined Structure 29

Outline Procedure to Construction 29

WINGS 33

Specify Determined Structure 33

Materials 33

Manufacturing *34*
Attachment *34*
Materials 34
Manufacture 34
Control Servos *35*
TAIL 35
Specified Design Structure *35*
Manufacture *35*
MOTOR MOUNT 36
Specified Design Structure *36*

DETAILS AND COMPLETION 37

FUSELAGE 37
WINGS 38
Wing/Fuselage Pins *38*
Tail *38*
Structure Reinforcement *39*
Attachment *39*
Securing Tail *39*
Servos *39*

AIRCRAFT CONTROL SYSTEMS 42

DESIGN DRIVERS 42
IMPLEMENTED SYSTEM 42
PROGRAMMING 42
SIGNAL 42
WIRING 42

MISSION 42

PAYLOAD BOX 42
STORAGE BOX 43

AIRCRAFT TESTING (PRE-FLIGHT TESTS) 43

STATIC THRUST 43
TAXI TESTS 43
SPRUCE GOOSE TEST 43
FLIGHT TEST EASEMENTS 43
SUMMATION 44

Figure 1 6
Figure 2 6
Figure 3 9
Figure 4 9
Figure 5 24
Figure 6 26
Figure 7 27
Figure 8 39

Executive Summary

This report is the basic outline for the procedure taken by the team to design and build the plane while complying with the rules for the 2002/2003 Design/Build/Fly (DBF) competition. The aircraft for competition needed to be propeller driven and unmanned. It also needed to be optimized for the rated aircraft cost. There are three possible missions that the plane was designed to complete. Mission one is to fly four laps with a "radar dish," PVC pipe, on top of the aircraft; mission two is to fly two laps, land and drop the payload, and take off and fly two more laps; mission three is to fly four laps. All missions are timed. The total score for the competition is based on the score of the flight, the score of the report and the rated aircraft cost.

Conceptual Design

In order to begin the conceptual design all of the competition requirements had to be recognized and discussed. Each team was able to see what aspect of the design they were in charge of and how they related to each other. Each team was responsible for researching their part and making sure that the plane could be optimized due to the competition restraints. Each team worked to find the constraints that optimized design. The teams then put everything together in order to test the configurations obtained. Using figures of merit various components were compared to find the best possible overall score. Using this information each team was then able to optimize their respective part of the aircraft. This allowed the most costly parts to be optimized so that the rated aircraft cost was the least.

Management

Team Member Roles

The team split into five different groups to begin production of the aircraft. The groups each contained design and stability. There was a team for the fuselage, tail, wings, landing gear/nose cone, and power. There was also someone in charge of funding but worked within a design team as well. The team leader was in charge of making sure each part of the plane was taken care of and that each member was meeting the deadlines. Each team member was in charge of making sure they had the materials needed to complete their task. Each member stayed in contact with the team leader to make sure that all aspects were taken care of and that everyone was following the scheduled table.

Fuselage Design Team

The fuselage team was in charge of making sure that the mission requirements matched the design. They had to make sure that the payload box had enough room within the fuselage and that the internal structure fit the motor and batteries without altering the center of gravity too much. The parameters were based off of an initial design and possible materials that would be durable but lightweight. They checked to make sure that all parts of the fuselage that would have pieces mounted to it were strong and able to hold the force that would be on it.

Tail Design Team

The tail design team had many decisions to make. The first was to decide if a t-tail or v-tail design should be used. Considerations for both were looked at and the main deciding factor was the "radar dish" or PVC pipe that would be on the plane for the first mission. After the v-tail was decided stability decisions had to be taken into account. The position of the tail needed to be decided as well as the size. In order for the team to figure out what was best they researched many different t-tail and v-tail configurations to check how stability was concerned.

Wing Design Team

The major decision in wing design was the shape of the airfoil. It was important to have an airfoil that provided plenty of lift. Many of airfoils were looked at and tested in the program VisualFoil. This enabled the team to choose an airfoil that optimized lift while minimizing drag. Once the airfoil was chosen the next decision was to decide on a material. Initially foam was desired but it was found that balsa wings provided the kind of strength and stability that was desired by the team. The balsa was also significantly lighter than the foam. This was ideal as one of the team goals was to have as light a plane as possible in order to make the most of the power from the motor.

Landing Gear and Nose Cone Design Team

The landing gear team worked closely with the fuselage team to decide on the best placement and what kind of support the landing gears would need. The decisions that this team needed to make also depended highly on material. The two materials focused on were aluminum and carbon fiber. The carbon fiber gears were stronger and lighter and so were chosen. The spacing of the landing gear was governed mostly by the fuselage width. It was determined that extra blocks would need to be placed into the fuselage so that the landing gear would have a wider base thus producing more stability overall for the aircraft. The nose cone was also made by the landing gear team. A general shape was decided on and the mold was made. They also talked closely with the fuselage team to work on placement and size.

Power Design Team

The power design team concerned themselves with the questions of what it would take to get the plane in the air. They worked with every design team to make sure that all numbers matched and that the constraints of the motor were taken into account. The power team also made the decisions on what propeller would work best with both the motor and the plane. They looked at what properties governed how the motor would respond to many different changes and the designs teams worked to make sure that their designs were optimized to ensure the plane would handle well with the chosen motor and propeller combination.

Figure 1

Fall 2002 Schedule

	Milestones	9/15	9/22	9/29	10/6	10/13	10/20	10/27	11/3	11/10	11/17	11/24	12/1	12/8
	Design/Build/Fly													
A	Gather Pertinent Information	Δ	Δ											
B	Design Main Wings		Δ	—	—	Δ								
C	Design Tail		Δ	—	—	Δ								
D	Design Thrust Supply		Δ	—	—	—	Δ							
E	Design Payload Relese		Δ	—	Δ									
F	Design Fuselage				Δ	—	Δ							
G	Static Force/Failure Analysis				Δ	—	—	Δ						
H	Design Landing Gear					Δ	Δ							
I	Design Motor Mount					Δ	Δ							
J	Stability Analysis					Δ	—	Δ						
K	Manufacture Test Model					Δ	—	—	—	—	Δ			
L	Solid Model					Δ	—	—	—	—	Δ			
M	Estimate Rated Aircraft Cost						Δ	Δ						
N	Dynamic Model							Δ	—	—	—	Δ		
O	Flight Test Design										Δ	Δ		
P	Optimize Design										Δ	Δ		
Q	Release Final Design with Model											Δ	—	Δ

Figure 2

Spring 2003 Schedule

	Milestones	1/29	2/5	2/12	2/19	2/26	3/5	3/12	3/19	3/26	4/2	4/9	4/16	4/23
	Design/Build/Fly													
A	Final Component Construction	Δ	—	Δ										
B	Component Static Tests		Δ	—	—	Δ								
C	Preliminary Flight Test			Δ	—	—	Δ							
D	Stability Analysis		Δ	—	—	—	Δ							
E	Flight Evaluation		Δ	—	—	—	Δ							
F	Design Report		Δ	—	—	—	—	Δ						
G	ProE Model		Δ	—	—	—	—	Δ						
H	Design assessment					Δ	—	Δ						
I	Design Refinement						Δ	—	Δ					
J	Rebuilding							Δ	—	—	—	Δ		
K	Train A Pilot	Δ	—	—	—	—	—	—	—	—	—	—	—	Δ
L	Mock Competition Test								Δ	—	Δ			
M	Spare Component Construction						Δ	—	—	—	—	—	—	Δ
N	Assembly Drilling											Δ	Δ	
O	Final Flight Test											Δ	Δ	
P	Calculate Rated Aircraft Cost											Δ	Δ	
Q	Design Report Addendum											Δ	—	Δ

Financial Concerns

There were many financial concerns that governed the manufacturing of the airplane. First, in order to start manufacturing, the team had to pay for everything out of pocket. After the initial construction was finished the club decided that the team was on the right track and began to reimburse and help pay for the continued costs of working on the plane. Also, a sponsorship letter was written and sent to different companies asking for donations to help with the cost of the plane and for travel costs to the competition. A CD was made with a power point presentation and distributed to different companies to let them see what we have been doing and also asking them for financial support.

CONCEPTUAL DESIGN

Design Drivers

Fuselage

The fuselage design of the aircraft is governed by the mission requirements, rated aircraft costs, and stability requirements. The main factors from the mission requirements stems from the necessary features that the fuselage design needs to posses in order to be able to complete each mission. Similarly, the rated aircraft costs provided a constraint system that set rules and consequences for different design features. Thirdly, the aircraft needs to be inherently stable allowing for reliable controllability. Taking everything into account the design drivers began to take shape.

The mission requirements demanded that the fuselage contain the payload box, be able to release the box via radio controls, and mount a "radar dish" to the aircraft. There were certain chices for the payload box that needed to be decided. It could be mounted internally or externally to the fuselage. Its location in regards to the aircrafts center of gravity, CG, was also a factor that went into the design.

The benefits and consequences of an internal and external payload were examined. The external payload would provide the simplest release mechanism along with easy and quick loading capabilities. On the other hand it would alter the aerodynamics of the aircraft after it was dropped, resulting in more complications. Also, the payload would leave a blunt non-streamline end of the fuselage, assuming height and length limitations of the fuselage would prevent the ability to provide a positive aerodynamic shape. However, an internal configuration grants aerodynamic similarity before and after the drop, and would allow for a streamlined shape to be incorporated into the fuselage. This allows for less drag, and a simpler design consideration due to the fact that the aircraft will not have to be trimmed differently due to aerodynamic similarity. The down side would be slightly more complicated internal structure that would have to incorporate the dimensions of the payload, and a more difficult loading procedure that would cost time to perform.

The payload's location to the aircraft's center of gravity was considered. It was desired to place the payload box's center of gravity as close to the aircraft's center of gravity so the static and dynamic stability of the aircraft would change very little reducing the complexity of the design. The downside would be an increase in the complexity of the design to ensure that the conditions were met while still taking into account other factors from the rated aircraft cost and general stability requirements, which will be discussed later. Something to consider was that, having a significant difference in the two CG locations would promote many stability and control complications that we would prefer to avoid.

The second major mission requirements on the fuselage design was how the payload box was to be released. It had to be capable of being remotely deployable, which meant that the release mechanism

would involve at least one servo. The simplest release mechanism was preferred to minimize the possibility of malfunctions resulting in an inability to complete the second mission. The idea of having a servo pull a rod through eyelets, one on the payload box that would be in between two on the fuselage, would provide the least complex system in comparison to straps that would encompass the payload and a pin insertion into the box that was considered. If the payload box was to be

Figure 3

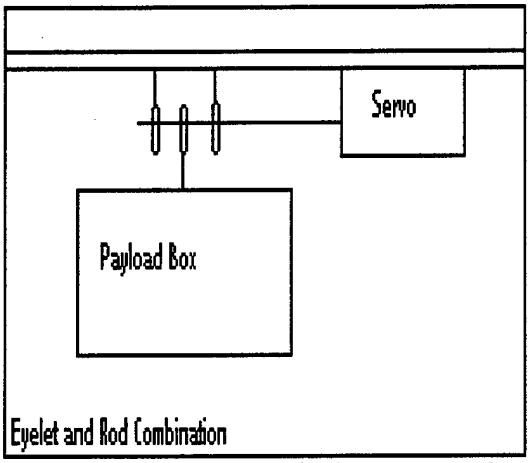

Figure 4

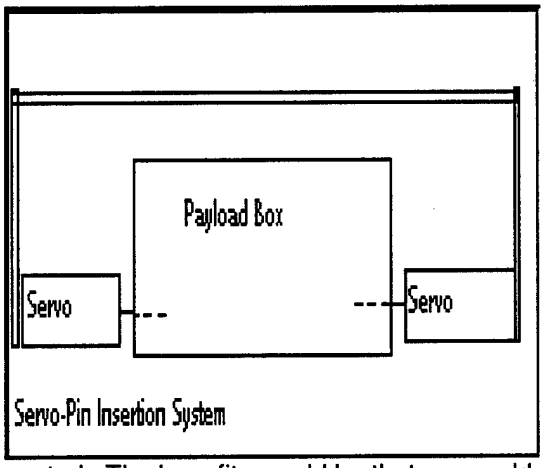

carried internally the idea of release cargo doors was presented. The benefits would be that we would avoid increased drag after the payload's release with the doors than having a large empty space without them. However, they would increase the difficult of the design's release mechanism while adding weight to the aircraft. Adding to the complexity would be deciding if the doors would be actuated by a servo, or more simply by the weight of the box and springs to provide a closing force. In any case since the box needs to be dropped, the motor will need to be a puller to avoid propeller collisions with the payload box and the landing gear would need to be a tricycle gear instead of a tail dragger.

The radar dish made it necessary for the aircraft to incorporate mounting hard points at a location on the fuselage that would comply with standoff distance of 3 inches from any other aircraft structure. The radar dish had the choice of being mounted on the upper side of the fuselage, or on the bottom. However, the bottom option was dismissed due to interference it would have with the payload box release. Similar to the payload's CG, the radar dish's CG could be mounted close to the aircraft's CG. Again, the benefits would be a similarity in mass qualities along with hard points that would already be present if the payload box's CG is located there also. However, it was also examined that the pitching moment caused by the drag of the radar dish could be cancelled by placing the radar dish's CG in front the aircraft's CG during cruise conditions. The negative side effects of this configuration would be that it would only be balanced at a set speed, like cruise speed, but on takeoff it would make it more difficult to pitch.

The rated aircraft cost introduced its own design drivers. It described the penalties for the constraints on the design. In the case of the fuselage the longer the fuselage the higher Manufacturing Man Hours, MFMH would be. The higher the MFMH the higher the aircraft rated cost will be. This provided a design driver to make the fuselage as short as possible. Well for a given wing area, CG location, and tail area the length of the aerodynamic center of the wing to the aerodynamic center of the tail is set. That leaves the parts of the fuselage in front of the wing's aerodynamic center as the focus to shorten up its length as much as possible.

Basic aerodynamic stability requirements played in the design drivers. Mainly, the location of the aircraft's CG and how the wing was to be mounted played became massive design drivers. The aircraft's CG could be mounted forward or aft of the wing's aerodynamic center. Having it in front would provide a pitching moment acting nose down if the aircraft became stalled or disturbed, making the aircraft stable. On the other hand, if the aircraft's CG was located aft of the wing's aerodynamic center the opposite would happen. The plane would become unstable to disturbances and would not be easily recovered from a stall. Having a forward aircraft CG seems the smart way to go, but it had its down side. It would make it very difficult to design arrangement of the heavy items like the motor, batteries, and the payload box all in a short length of the fuselage in front of the wing's aerodynamic center, especially if the payload box's CG was desired to coincide with the aircraft's CG. However, having a more unstable design would allow for easier balancing of components and a shorter fuselage from the fact that not so many parts would have to be located in the area in front of the wing's aerodynamic center and could be placed in the relatively empty space aft of it. Also, a consideration was if we where going to have a low, mid, or high wing aircraft configuration. The low and mid location would provide interference with the payload box, since we wanted to use a single spar set up that goes through the fuselage for superior strength and assembly advantages. That left a high wing configuration that would be able to provide clearance, but would lead to difficulty and weight problems later when it came time to design a landing gear that could mount to a hard point and still be wide enough apart so the aircraft would be less top heavy. That left us with a choice to develop a new low or mid wing attachment set up, so that we would be able to incorporate the low or mid wing, or settle with the negative consequences of a high wing. Another factor that came into the wing debate was the inherent stability that would be gained from the different configurations. A high wing would have the aircraft's CG located underneath the wing providing a pendulum effect that would help keep it level, while to accomplish that in a low or mid wing setup would require a dihedral to be introduced resulting in some of the net lift not contributing to overcoming the weight.

The design drivers come from the mission requirements, aircraft rated cost, and basic stability requirements. Some of the design drivers conflicted with design drivers from other areas. The result for our team was to choose which design drivers would be most beneficial. That lead us to examine which

combination of design possibilities provided the results that we wanted, while minimizing those that would contribute negatively to the fuselage.

Wing

The basic requirements of the competition were the main drivers of the wing design. Since the aircraft needed to be capable of carrying a five pound payload within the fuselage, not including the additional weight of the electrical motor and other aircraft power components, (which are responsible for most of the weight) it was determined that for the size and ensuing weight of the craft that more than four feet of wingspan would be needed. Within the bounds of the contest, the longest part of our aircraft that could remain intact would be four feet long, and therefore dictated that our wings be removable from the body of the craft (while having a total wing span of eight feet or less). The airfoil selection process was driven by the need to find an optimal performing airfoil that would create the greatest lift with the lowest drag while possessing a total wing span of 8 feet (four feet for each side) at Reynolds Numbers between 400,000 and 500,000 derived from assumed cruise speed, chord, and at sea level conditions. The airfoil that was chosen would be required to facilitate take-off within the allowable distance of 120 feet (and at a speed attainable from power available supplied from the engine), but that would also allow for higher flight speeds for the timed flight speed mission. The airfoil eventually chosen must also be capable of producing enough lift to maintain flight under the potentially adverse effects of the simulated radar dish. The overall weight of the wings was to be kept at a minimum while still maintaining the strength to hold its shape under a 4-G turn (a basic design parameter that we set). There was also the question of where to orient the wing on the fuselage with respect to the payload. One of the missions required that the payload be deployed with resumed flight after deployment. The plane needed to be designed to ensure the quickest payload storage and deployment. And, as always, the overall goal was to create a wing that had the greatest lift and the lowest drag while being as narrow and as short as possible for the optimization of the rated aircraft cost.

Wing FOM

		Wing Configuration		
Figures of Merit	Weighting Factor	High	Low	Mid
Rated Aircraft Cost	0.3	1	0	0
Lift Coefficient, C_L	0.2	1	0	0
Payload Deployment	0.3	1	-1	-1
Landing Gear Interface	0.1	-1	1	0
Spar Loading	0.1	1	0	0
Score	-	0.9	-0.2	-0.3

Table 1

Tail

Due to mission number three, which demanded the attachment of a simulated radar dish to the surface of our airfoil, concern was expressed with regards to the effect of the turbulent wake caused by the PVC pipe across the control surfaces of the tail. It was also noted that to keep the stability and control issues of the aircraft simple and effective with respect to other mission flights, the tail need only be used for trim of the aircraft during flight. For deconstruction purposes, the tail needed to be capable of detachment from the fuselage while leaving no question as to the maintenance of its desired shape and orientation with respect to the aircraft when fully assembled. The overall length of the aircraft, the overall weight of the aircraft, and the vertical and horizontal components (with or without control surfaces) all contributed to the final score of the plane within the rated aircraft cost guidelines.

Tail FOM

		Tail Configuration		
Figures of Merit	Weighting Factor	High T-Tail	Mid T-Tail	V-Tail
Rated Aircraft Cost	0.2	1	1	1
Stability	0.5	1	-1	1
Mission Capability	0.3	-1	-1	1
Score	-	0.4	-0.6	1

Table 2

Power

The Power system consists of the motor, batteries, speed controller and propellers. The motor and batteries are a part of the mission that are critical components. In fact they are the core of the power system. This system requires more of a focus and added attention to detail in order to perform at its maximum. The motor battery combination is governed by its performance, and limited by the Rated Aircraft Cost. The required performance of the motor is set based on the mission requirements and the operational conditions the plane will experience. The propeller type and sizing are governed by the desired speed and duration. The batteries are selected based on the power output, capacity and availability.

Power FOM

		Astroglide Cobalt Motor Possibilities			
Figures of Merit	Weighting Factor	60 Geared	60	90 Geared	90
Motor Weight	0.2	0	1	-1	-1
Batteries Required	0.4	0	1	-1	-1
Power	0.2	0	0	1	1
Endurance	0.3	1	0	1	-1
Torque/Propeller Size	0.1	1	0	1	0
Score	-	0.4	0.6	0	-0.7

Table 3

Basic Design Possibilities

Fuselage

Knowing the benefits and consequences of the main design drivers of the fuselage it came time to start deciding which combination of design possibilities we wished to incorporate. This led to different theoretical design structures for the fuselage that we could examine to see which would provide the most benefit for the least cost. Some of the design drivers had greater importance than others and that caused us to focus our attention mainly on the following design drivers: external vs. internal payload box, location of aircraft CG and payload CG, the release mechanism that we would wish to incorporate, and how the wing would attach to the fuselage. The remaining design driver options would be decided upon after the preliminary fuselage design was determined, since it was felt that they were independent of the above options. Upon examining the main design driver options three possible basic designs took form.

All three of the possible designs shared some basic design driver principles. In fact most aircraft that are required to store a large heavy payload that must be releasable share similar features. This legacy class of aircraft is called the heavy bombers, and for subsonic flight they do share many design similarities. Therefore, the basic design possibilities will resemble each other as well as full-scale bombers. Here are the shared basic design principles.

First, all the possible designs incorporated the high wing configuration versus the low or mid wing configurations. Next, the aircraft's CG was chosen to be located in front of the wing's aerodynamic center instead of locating further aft. Thirdly, the payload box's CG location was chosen to be located at the aircraft's CG rather than way from it, making the assumption to only consider longitudinal location and ignore lateral location of the CG. Also, the radar dish CG location was placed on top of the aircraft's CG. The next shared design driver was that the payload box release mechanism was chosen to be the eyelet and rod combination system. Finally, all the basic designs have a puller motor and tricycle landing gear instead of a pusher motor and a traditional (tail dragger) landing gear. All the remaining design drivers are expressed in the three possible designs that resulted.

Design Configuration 1:

The first basic possible design that was developed used an external payload location. The fuselage would be wide enough to provide an aerodynamic leading edge shape, and would be able to store all the key components of the aircraft. The payload box would hang from behind this leading edge shape. Once the box drops it would leave an empty space, where the backside of the fuselage would be a flat plane that the box would be flush to. The box

would be suspended from a body spar that would extend to connect to the tail. The basic fuselage design would actually look similar to the Sikorsky CH-54 seen in the picture.

Design Configuration 2:

The second basic design would have an internal payload. The fuselage would encompass the payload box in side of the outer shape. Aft of the payload area the fuselage would taper to the intersection with the tail. This design would also be lower to the ground. In this case the payload box would have payload doors stored up against the side of the box and sides of the fuselage while the box was in the fuselage so that when the box is gone the doors drop down. Once the box was dropped to the ground it would fall about 2-3 inches, and the aircraft would pull forward. The friction on the ground would hold the box stationary, forcing a hinged rear door system to swing open allowing the box to pass through the back of the fuselage. This door would only extend far enough up to allow the box to clear the fuselage.

Design Configuration 3:

The final basic possible design also has an internal payload storage system. The main difference between it and the second basic design is that it would have a higher landing gear to lift the bottom of the fuselage at least 6 inches off the ground. The box would be able to drop clear of the fuselage, where the aircraft would be able to taxi away. Payload doors would be hinged underneath the payload box, and held closed with springs. When the box drops it would push the doors open, and once the box is clear of the doors they would spring back up.

Fuselage FOM (General)

		Design Configurations		
Figures of Merit	Weighting Factor	1	2	3
Rated Aircraft Cost	0.1	1	1	1
Landing Gear	0.05	-1	1	0
Payload Loading	0.15	1	-1	-1
Stability	0.1	-1	1	1
Complexity	0.3	1	-1	0
Performance	0.2	-1	1	1
Score	-	0.2	0	0.25

Table 4

Wing

Since it had been predetermined that the wings be capable of detaching from the fuselage, it became a design parameter rather than a design possibility.

Attachment

The attachment of these wings became the focus of some concern. The options considered for wing attachment were:

-A leading edge spar, which would run some length of the wings and through the fuselage.

-A quarter chord spar that would run some length of the wing and through the fuselage

-A quarter chord spar that would run some length of the wing and be attached atop the fuselage with bolts or other fixtures and would essentially "sit" on the top of the fuselage

-A leading edge or quarter chord spar that would run the length of only half the wing, and be attached to the fuselage by pins or through hard points.

Vertical Wing Location

Then, the use of a high wing or a low wing was questioned. A high wing would allow for greater lift and ground clearance, as well as enable a single spar to be run from one wing to the other though the fuselage above the payload. A low wing would require that the payload ride over the wing spar, or that the spar not be continuous through the span of the wings

Airfoil Selection

The diversity of available airfoils is daunting. The catalogue of recorded data on countless NACA, Clark, and Eppler designs is extensive. For our purposes, a program named Visualfoil would be used to insert determined design constraints and apply this information to narrow down the countless airfoils for final design determination.

Wing Shape

For our specific mission types, the need to implement a swept back wing was immediately disregarded. There was no situation which would require that we use swept wings for the range of speeds in which the plane would operate. This dictated that our wing shape be rectangular or tapered.

Control Surfaces

The plane had the option of possessing flaps and ailerons if necessary, but these design characteristics could be added as needed to whatever general configuration was determined based on the more important factors of lift generation. Conversely, there was the option of leaving the control surfaces off entirety should the chosen design be capable of operating without them.

Tail

Two design configurations were readily apparent upon analysis of the design drivers of the aircraft:

Conventional T-Tail

V-Tail

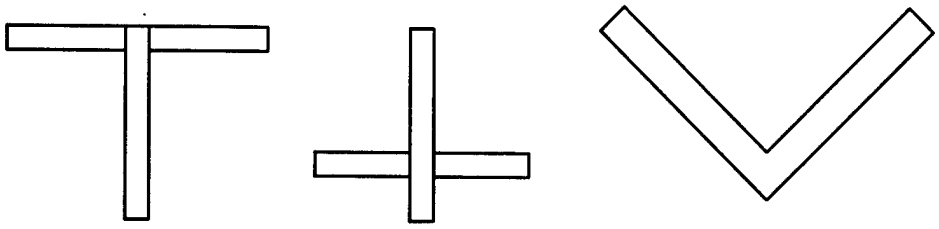

High T-tail Low T-tail V-tail

Within the conventional t-tail design, there were options of a high t-tail and a low t-tail configuration. No other design possibilities were considered.

Power

The power system had many possible configurations ranging from multiple motors to inducted fans. The choice of the motor was narrowed down to four combinations of Astroflight motors, A 90 Direct drive, 90 geared, 60 direct drive and 60 geared. The propeller selection was narrowed down to a range of sizes for a two blade propeller of 14 to 18 inches by 10 to 12 degrees pitch. The feasibility of a three bade propeller versus a two blade propeller was also looked at for increased performance. The NiCad batteries are the only source of power for the motor. The batteries are configured based on the motor selection and their competence to operate as needed. The batteries were measured by their ability to retain charge and discharge at a rate to maintain maximum power over the duration of the flights. To make the final selection of the power system the combination of motor with propellers and batteries was analyzed simultaneously.

Structural Concerns

Fuselage

Having the basic design of the fuselage that we wanted, we needed to decide on the possible construction solutions that our team would be capable of using. The method chosen to construct the fuselage would affect different areas such as weight, strength, and repair ability in case of damage. The possible construction methods that our team was capable of manufacturing the fuselage out of includes balsa wood and composite honeycomb structure members, Styrofoam shape covered in fiberglass, and a carbon fiber shell.

The first possible construction method incorporated the use of balsa wood and composite honeycomb structure members to produce a load bearing structure as well as required shape. The balsa wood would be used mainly to form a basic aerodynamic shape and for areas that would not experience much

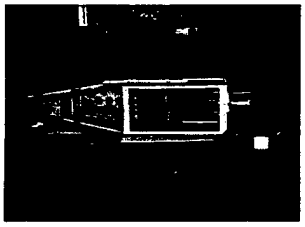

loading, while the composite parts would be used in high load bearing components. It was contemplated using a carbon fiber rod to support the payload box from in conjunction with the composite material. The fuselage would then be either covered in Monokote or sheeted in balsa wood, or it could have combination of each. It is principally a semi-monocoque design. This is a lightweight method of construction that would provide good strength. It would be more difficult to repair depending on what parts failed, but could potentially be reasonably achievable. Its main potential down fall would be that if the fuselage sustained a server impact, such as a bad crash, it would quite literally break into a million pieces, which would effectively eliminate the team from the competition if a mishap occurred.

Next, the Styrofoam shape covered in fiberglass was the construction method that previous teams had employed previous years. Basically, the shape of the fuselage is cut out of a solid block of Styrofoam, and then wrapped in a few layers of fiberglass. The result is true composite load bearing structure. It would be quick and easy to manufacture such a construction possibility. Foam is cut out for internal components. However, it is extremely heavy for its strength due to all the foam and fiberglass. It would provide good strength since load and moments are primarily accepted in the strong outer fiberglass. The ability to repair damage is low for such a construction method. If the fiberglass or foam breaks, it can not simply be glued back together. Serious damage sustained would not be repairable in a short period of time.

Thirdly, a carbon fiber outer shell construction possibility has been performed in the past. The carbon fiber outer shell contain internal structure framework, either balsa wood or composite honeycomb, to reinforce critical areas. The carbon fiber outer shell is constructed with large sheets of carbon fiber and a vacuum mold. It would be another light weight, good strength construction possibility. It posses the same

advantage as the pervious possibility, however it removes all the heavy foam from the fuselage and replaces it with light weight frame materials or a combination of wing and fuselage spars. This possibility would also provide fairly decent repair capabilities since the outer carbon fiber shell is near unbreakable for our applications, and if it does it can be fixed with tape since the shell mainly exists for aerodynamic shape. The internal components are few, and would be replaceable.

Comparing the three possible construction solutions the first one was picked. It was light weight, still strong, and had a reasonable ability to be repaired. The second choice was strong, but was going to be too heavy and not very repairable. The third choice had the optimum characteristics that were sought, but its downfall came with the large quantity of carbon fiber required. It would have been far too expensive of a cost for out team to have absorbed. So in the end, the fuselage was to be constructed of balsa wood and composite honeycomb for low and high load areas respectively.

Fuselage FOM (Materials)

		Construction Methods		
Figures of Merit	Weighting Factor	1	2	3
Weight	0.5	1	-1	0
Strength	0.2	1	1	1
Repair ability	0.2	0	-1	0
Monetary Cost	0.1	1	1	-1
Score	-	0.8	-0.4	0.1

1=Balsa Composite 2=Foam/Fiberglass 3=Carbon Fiber

Table 5

Wing

It was determined that since the aircraft must pass a wing tip test, that the arrangement joining the wings to the fuselage be extremely strong. This importance is underlined when it is considered that if a 4g force is to be supported, that the wings must sustain this force without alteration of function or orientation with respect to the rest of the aircraft. Carbon fiber spars were considered, as well as aluminum, fiberglass and wood. Three possibilities where examined for the actual wing construction:

-A balsa sheeted Foam core,

-A carbon-fiber and fiberglass shell,

-A balsa sheeted aircraft ply ribbed wing.

In all the above cases some load bearing structure would have to be incorporated that would allow for the wings to be easily detached for mission purposes. As with any wing, it was required that the final structure withstand deformation and extreme flex, and it was desirable that the plane be capable of sustaining mild jarring or short jolts. A concern was expressed over the possible construction of a wing with balsa wood due to its frailty, and inversely it was a concern that a wing constructed of foam not be

strong enough to withstand the stress of regular flight without specific reinforcement. As with manufacturing of all portions of the aircraft, finances and repeatability of constructed parts was important. In addition, it was noted that the more advanced the shape of the airfoil was, the more difficult it would be for the construction of the wing to remain true to the intended shape. It was also noted that for optimal performance, that the entire craft be kept as light as possible, and therefore light-weight materials would be preferable.

Tail

The tail, since designed for only trim purposes, did not need to be exceptionally strong. The desire to keep the aircraft as light as possible allowed for formability and weight of material to be the selection design drivers. Construction using balsa wood, molded carbon fiber, foam core, and Monokote were all potential material selections to be determined due to ease of construction.

Power

The motor mount attachment needs to be durable enough to retain the motor during flight as well as in any extreme circumstances. Heat generation by the motor and speed controller will directly affect the strength of the motor mount. If the temperature due to the heat transfer from the motor to the mount exceeds the thermal limit of the material, a catastrophic failure will occur. The ability of the motor mount to retain its structural integrity if there was a failure in flight, and the following impact of the aircraft, is essential to the survival of the motor. The weight of the motor mount is governed by the material used and the strength needed to prevent failure. The attachment of the motor must allow for removal, without adversely affecting the structural integrity of the motor mount and the fire wall.

DESIGN ANALYSIS

Fuselage

The choices for the shared design driver principles came about by weighing the benefits and consequences of each option and picking the best one. Here are the reasons for the shared design drivers being chosen:

The high wing was picked for its benefits of allowing for a strong, safe, and a fast means of attaching the wings while promoting stability, and allowing for the box to be fit in the fuselage. It was felt that the benefits out weighed the negative side of having to build new hard points for a heavy longer landing gear that would be necessary. Also, it was determined that trying to adapt a low or mid wing design of equal strength as a high wing would add more weight to the aircraft than the added hard points for the larger landing gear would.

Next, the aircraft CG located in front of the wing's aerodynamic center would provide static and dynamic stability. Considering the different conditions that the aircraft would have to fly with (i.e. with or with out the radar dish or payload box), the most stable platform was highly desired. Also, during takeoff the aircraft will be near or at the max coefficient of lift brings it to the verge of stalling. We would like the aircraft to be able to recover automatically if it does stall, instead of continuing to pitch nose up catastrophically. The downside of having an inherently longer fuselage from having to push the wings and tail farther back to allow this was determined to be minor in comparison, and therefore acceptable.

The payload box's CG was placed at the aircraft's CG for the simple fact of making the stability of the aircraft to remain as close to what it was before the drop, thus eliminating a need to trim the controls out again. At this stage in design we made the assumption to only consider the CG in regard to the longitudinal axis, effectively ignoring the lateral change in the CG along with the change in moment of inertia. Safe controllability would be retained after the box is dropped due to the similarity. Also, it was felt that a creative compact design would allow us to still be able to fit the large heavy components, like the batteries, motor, and payload box that close together to achieve our aircraft's CG location with only a slight increase in the fuselage cross sectional area.

Along with the payload box's CG the radar dish's CG was placed in line with the aircraft's CG. The main reason is that with the payload box's CG being located there a very strong hard point would already be present for attaching the radar dish. This would save weight by not having to build a new hard point. Complications due to the nose up pitching moment that would result in flight were determined to be of minimal consequence compared to the loose in weight.

The eyelet and rod combination was employed because it is simpler than the multiple servo-pin combination and easier to use than the strap and rod combination. The multiple servo-pin idea is very complex, needing all the servos to work properly, it added unnecessary weight, and penalize the aircraft rated cost by adding additional servos. The strap and rod concept is similar to the eyelet and rod combination, but it had a higher probability of unreliability or strap failure or having the strap snag on the aircraft on the way out. Also, loading a loose strap would be more difficult and time consuming than simply sliding the servo rod through a fixed circle.

The puller motor was necessary to avoid propeller collisions with the box after it was dropped. A pusher motor configuration would not be feasible, since it would require the motor to be located very high off the ground to avoid the box. Similarly a tricycle landing gear is needed to allow the box to pass under the fuselage, due to the fact that a traditional landing gear would result in the box hitting the aft part of the fuselage.

For the three basic design possibilities each configuration's advantages and disadvantages were compared showing the reason for the design being the way it is.

For the first design configuration the external payload location would allow for easy and quick loading of the payload as well as an extremely simple release system. There would be only a very low chance of the box failing to drop as long as the servo pulls the rod properly. Since the payload box would not have clearance problem due to the lack of an aft fuselage the aircraft could be low to the ground saving landing gear weight, drag from the landing gear, and lowering the aircraft's CG closer to the ground promoting taxiing stability. The most negative aspect of this design is that it would have horrible drag characteristics due to the lack of an aerodynamic shape.

The second design configuration has an internal payload storage, which provides a streamline shape for the entire length of the fuselage resulting in a significantly lower coefficient of drag by one to two orders of magnitude less compared to the hemisphere shape of the first case. Also, it would allow for aerodynamic similarity after the drop, resulting in simpler control abilities. Having internal payload is a beneficial characteristic that is an important design quality to posses. Heavy bomber design incorporates the same internal payload storage today as it did during World War II. I felt it safe to make the assumption that this was an important design feature for performance. The payload doors would prevent airflow from entering the bay causing in drag. Having the box drop and then force open rear doors would provide the benefit of a short landing gear presented in the first basic design combined with the aerodynamic advantages of having a

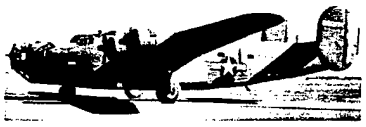

streamline shape. The down side is that the fuselage would be very complex with all the moving parts, assumption that the ground surface would provide enough friction on the box to force the rear doors open, and lowered structural integrity by having a "three sided" fuselage where the fourth, the bottom, is not a load supporting side. The last case would cause the rest of the structure to be beefed up, adding weight, to compensate for the loss of strength. This lacking would be very important since the main landing gear would need to be attached to the sides of the fuselage. A hard landing may produce a great bending moment on the fuselage ripping it apart.
providing better propeller clearance.

The third design configuration is similar to the second except that it had a higher landing gear. This allowed for better propeller clearance with the ground along with the simplicity of having the box clear of the fuselage entirely once it was dropped. It will allow a fuselage structure box to be formed allowing all sides to support loads providing a solid frame. It eliminates the need for rear doors, which added weight and complexity to the design. This design provides the simpler more reliable aspect of the first design, and combines it with the aerodynamic advantages of the second design. The largest consequence of this design is that it needs larger heavier landing gear causing more drag and weight, and will be more likely to tip over during taxi from its higher center of gravity.

Wings

Attachment

Since the aircraft was going to be designed to carry a payload from a high wing configuration, it was decided that the spar be located at the aerodynamic center of the wing (quarter chord) simply to ensure that the center of gravity of the plane be located close to this point. This quarter chord location made this parameter easier to measure and check, in addition to being a logical place to place the spar. As to the leading edge spar location, there was little or no need to support the wing from that point of the wing structure. The option of having a spar that ran through the fuselage and into both wings, or the configuration of two small semi-spars was then analyzed. For the sake of integrity of structure and reliability of reconstruction, a single spar was chosen. Structurally, it would ensure that the wings remain attached to the fuselage without being tempted to detach themselves from the high stress area at the root of the fuselage in shear. The spar would either run through the fuselage through hard points created to resist failure of structure or something similar to ensure that the arrangement of the wings and fuselage remain rigid.

Wing Arrangement

It was noted that though there were two possible wing attachment arrangements, only one of them seemed logical. There was no need for the payload to be located above the wing spar when one of the missions expressly indicated that the payload was to be deployed, and that the easiest way to accomplish

that would be to drop it out of the bottom of the plane. That could not be accomplished if there was a wing spar in the way. This dictated that the plane poses a high wing arrangement. The nature of that mission is similar to that of a cargo carrier, all of which aircraft are designed with high wing configurations as well. The high wing will generate slightly more lift than a low wing by bringing the lifting surface more inline with the thrust generated from the propeller. The high will be attached above the vertical Cg, thus the plane will have greater horizontal stability than a low wing. In conjunction to the analysis done on the fuselage, the high wing configuration was desirable because it allowed the use of the single spar and sheath, and the trade off for the heavier landing gear was negligible.

Airfoil Analysis

The correct airfoil choice is crucial to the success of the flight of the plane. The program visual foil was used to analyze the lift and drag produced by differing airfoils at the assumed Reynolds number while implementing the dimensional constraints determined by the confines of the storage box, the assumed weight of the plane, and the speed of the plane necessary for takeoff within the 120 foot distance. The airfoil chosen was a NACA 4412 with a 15% flap operating at a Reynolds number of 429,300. The airfoil needed to have high lift, low drag and operate efficiently at a low Reynolds number. From the power required analysis and the ground roll limiting factor of 120ft, the theoretical Cl_{min} for lift-off was calculated to be 1.2. The airfoils where narrowed down to two different NACA series airfoils, NACA 2212 and 4412. Employing calculations, manufactured charts, and a computer aided airfoil analysis, the most efficient airfoil was determined to be the NACA 4412 due to its produced enough lift at cruise conditions and less drag than the other airfoil. This airfoil produces a theoretical maximum lift coefficient (Cl_{max}) of 1.4 at an angle of attack of 14 degrees; this will generate over 15 pounds of lift.

Wing Sizing

The distance in which the plane has to take off with the motor/propeller combination dictated the size of the wing. From the power required analysis and the allotted ground roll distance of 120 ft the plane needed a wing area (S_w) equal too or greater than 6 square feet. Operating under the assumption that theoretical performance can never be achieved in real world situations the wings were intentionally over designed. The major limiting factor of takeoff distance was the wing area, which was increased by 12 percent to allow for real world conditions. The aspect ratio (AR), wing cord (C_o), and taper ratio, were all determined by comparative equations, yielding an AR of 5.33 giving a lift curve slope of the wing of 5.72, a Co of 1.125 ft, a S_w of 6.75 square feet, a span of 3 ft, and a taper ratio of one. The wing derived from comparative calculations was tested in VisualFoil. The results of this test are a wing that will allow the plane to takeoff in the allotted distance. The plane would need to reach a speed of 55 feet per second (37.5 mph) before it could take off. Given the limitations of the power available, this speed will be unachievable in less than 120 feet. Hence, the airfoil needs to be modified to generate more lift for takeoff at lower speeds.

Wings with Flaps

Since the plane was not producing the lift needed to achieve take off in the distance required by any airfoil that we analyzed, the addition of flaps became necessary. The lift coefficient possible from an airfoil is directly influenced by the addition of flaps. The following chart produced with Visual Foil design software, showed the relation of the coefficient of the lift C_l and coefficient of drag C_d with respect to the angle of attack for different size flaps.

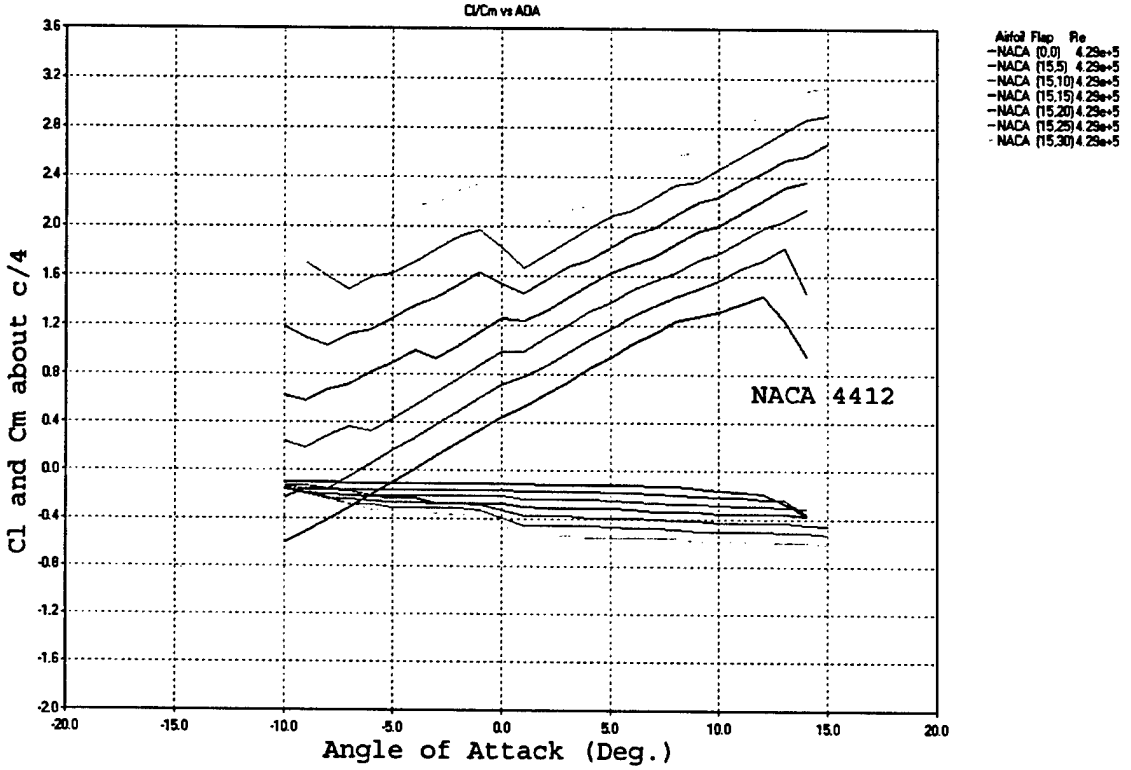

Figure 5- C_l and C_m vs. Angle of Attack

Due to the fact that multiple flaps added to our wing would drastically increase our rated aircraft cost and was not necessary for the increased lift coefficient of the aircraft, the flap implemented in the design was a simple hinged flap that ran the entire span of the wing and theoretically tripled the Cl_{max} of the wing to 3.2. With the addition of the flap, the wing will be able to lift the estimated 18-pound plane in 100 feet at 35 feet per second (24 mph). Applying the theoretical analysis to real world applications, the design allows for a 20 foot leeway for pilot and mechanical error. This safety margin will be critical in allowing the plane to perform mission 3 without the need for modifications to the aircrafts design due to the increased drag upon takeoff. The implementation of a full length flap left no room to or need to install ailerons. The solution to the lift production was the incorporation of the flaps and ailerons into one control surface. The flaporone allowed for a minimization of the number of servos required to control the flaps and ailerons while still maximizing the area for flap deflection.

Wing Shape

For the sake of construction, rectangular wings were designed. The unreliability of tapered wing construction was deterring, while the complexity of construction was not representative of the gain that would be acquired in flight. Therefore, rectangular wings were the choice of the team.

Tail

A sketch of each tail configuration was created to provide a visual representation of each design possibility. The concern relating to the effect of the wake caused by the PVC pipe became the focus of the sketch analysis. It was apparent that for each design accept for the v-tail that one or more control surfaces would be in direct line for turbulent airflow from the "radar." It was determined that reliability on the performance of the control surfaces within this turbulent wake could not be guaranteed. A book on aerodynamics was consulted to confirm our suspicion that the backflow caused by the radar might be detrimental to smooth laminar flow across the wing, and our assumptions were correct. The distance from the radar to the tail control surfaces could not be made great enough within our predetermined design drivers for the air flow which had been disturbed by the radar to return to laminar flow. The v-tail design could be manipulated to provide that all control surfaces would be outside the direct wake caused by the radar and gave us the advantage of better theoretical control surface use.

This led to a launch of some in depth research on the effectiveness of v-tail use. Practice alone indicates the reliability of the t-tail design (in both configurations), but our design of a v-tail would demand a direct conversion from known design reliability of the t-tail to a less known design (v-tail) without loss of stability or control. Direct calculations from an assumed t-tail design to a v-tail design of equal stability and control characteristics were provided within the NACA Report 823. These calculations were referenced further within an aero-modeling article specializing in the conversion between t-tail and v-tail configurations while also supporting the conjecture that within the conversion between the designs, there was little to no exchange of control characteristics.

This led us to believe that there was little to no difference in the overall performance of either design (regardless of high or low t-tail). Having determined that a reliable v-tail configuration could be constructed without loss of aircraft handling and control, the rated aircraft cost was analyzed. With respect to overall length, either design would require the same distance between the aerodynamic centers of the wing and tail for equitable control. Either configuration could be constructed of various materials, so the goal of lightweight construction was not problematic. And, either design could be manipulated to be consistently deconstructed. However, while a t-tail design would consist of two vertical

control surfaces (10 hours each) and one horizontal control surface (10 hours each) for a total of thirty hours, the v-tail design only demanded 15 hours total, half of that of the t-tail design.
Since the function of each tail design was to be the same, material selection and construction was of no consequence, and was not a factor in the design selection.

Power

The competition rules require that the teams to use only a stock brushed electric motors. The Astroflight Cobalt 60 Direct Drive brushed motor, (see picture the on the right), was incorporated into the design because it is the lightest motor rated for 1.5 horsepower. After calculating the thrust and acceleration verse velocity it was determined that the motor will need to peak 1.6 horsepower for a very short duration during takeoff. The AIAA has used the Astroflight motors for the last two years and has consistently pushed them passed their rated power limit without any problems. The motor, when matched with a 15x10x2 inch propeller, produces 8 pounds of static thrust at 8,675 RPM giving the 16 pound aircraft a power-to-weight ratio of .5. Assuming non-linear propeller efficiency, this combination should reach a calculated speed of 73 miles-per-hour and take off in a distance of 98 feet. This is 12 feet short of the 120-foot limit in order to take in account the unexpected parameters that show up during the first flight test. If the aircraft performs as expected in vary conditions we will decrease the propeller diameter and increase the pitch in order to increase the flight speed. The faster flight speed will decrease the overall mission completion time.

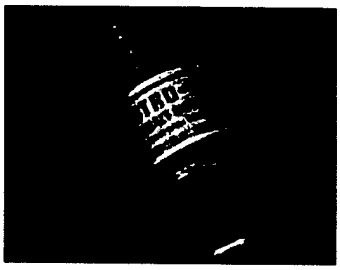

Figure 6
Power required and power available curves

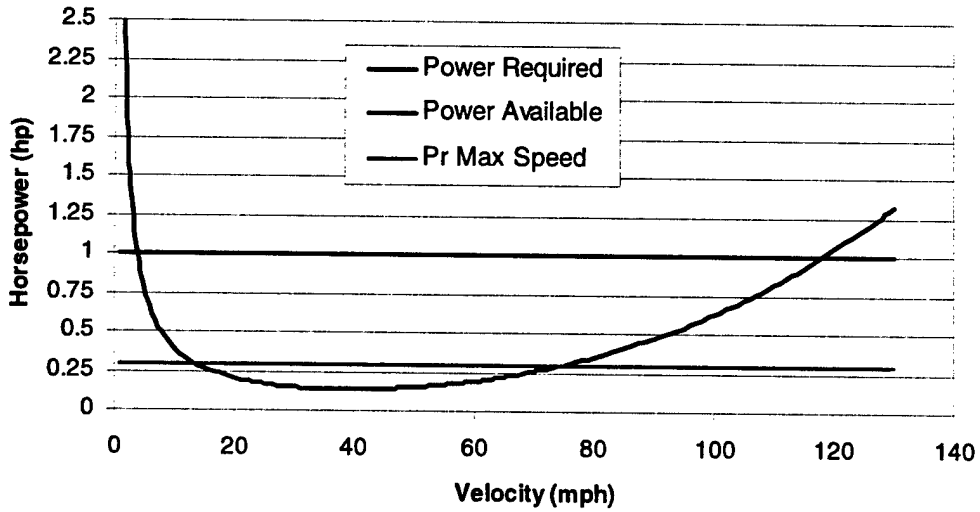

The power curves, shown above in Figure 6, show that the motor is capable of providing enough thrust to fly at 118 miles-per-hour. There are two main reasons why the aircraft was designed to fly at 70 miles-per-hour. The first is that the batteries are only 2400 milliamp hours. To fly at 118 miles-per-hour the motor would draw 40 amps. At this rate the batteries could only supply 3 minutes of flight time, Figure 7. This is to short of a time to successfully complete a mission. The second reason is that the aircraft was designed to take off in 120 feet. In order to do so, the propeller must not stall at low speeds. Smaller pitch propellers will accelerate harder, but will give you a slower top speed. The key is to find the exact balance during testing.

Figure 7

Battery Duration

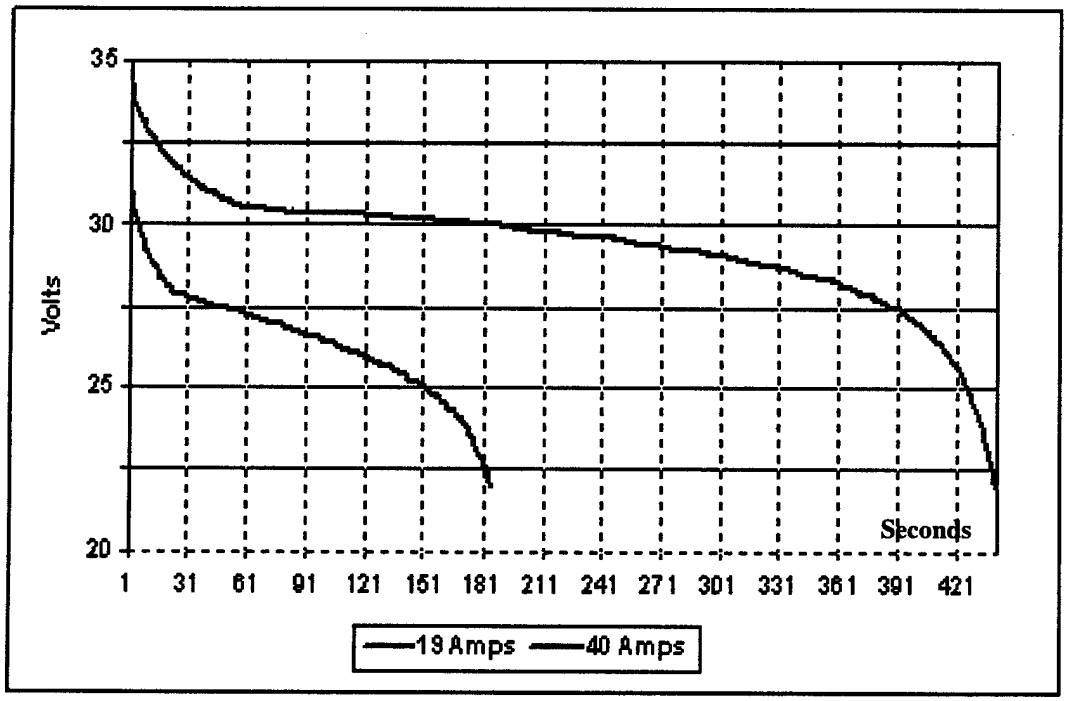

Batteries

The competition rules require all teams to use nickel cadmium or NiCad batteries. The Sanyo RC2400 NiCad batteries have one of the highest milliamp ratings with a relatively low weight, which is the reason they were chosen. Connecting 28 battery cells in series supplies the motor with an average 32 volts for takeoff and 26.5 volts for the entire mission. In order not to blow the 40-amp fuse, 32 volts are necessary for first few seconds of takeoff with a full payload

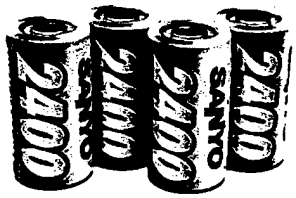

because during this time the motor draws just over 1200 watts. The estimated flight duration is 8 minutes with a full charge.

For the past three years the AIAA has not optimized the power for the type of aircraft they designed. The batteries can weigh no more than 5 pounds as stated by the competition rules. Previous battery packs weighed 4.95 pounds and the motor weighed 2.2 pounds not including the motor mount. By optimizing the power the new battery weight is only 3.83 pounds and the smaller motor only weighs 1.4 pounds. This is a total weight savings of 1.92 pounds or 12 percent of our total aircraft weight. This decreases the overall rated aircraft cost by 16 percent.

PROTOTYPE PRODUCTION

Fuselage

Specify Determined Structure

With the conceptual design of the fuselage complete it became time to go into a more in depth design. Knowing the shape of the fuselage along with the construction materials that we would use the design of the internal placement of components began. Consulting with different team members to determine the results of their conceptual design of their area of responsibility determined what needs and components that the fuselage has to provide or support. It was determined by the propulsion member that the aircraft would need an Astroglide Cobalt 60 motor with 28 NiCad batteries. The tail became a V-tail design, which requires two servos located in the very aft end of the fuselage. That information provided dimensions and weight of internal fuselage components not associate with the conceptual design of the fuselage. It became time to determine how all the internal components of the fuselage would be located inside of the shape.

Outline Procedure to Construction

To perform that task the longitudinal location of the CG of the aircraft needed to be determined, and then setting that location as a fulcrum point determines the location of all the parts so that the resultant moment at the aircraft's CG would be zero. To locate the aircraft's CG it was necessary to estimate how forward it could be located without interfering with necessary components that must be located in front. Taking an estimate on the total length of the propeller, motor, motor mount, and front firewall the aircraft's CG was placed 12 in from the most forward location of the fuselage. This would provide room for the payload box to be hung from the aircraft's CG. However, one of the heaviest parts, the motor batteries, needed to be located near the aircraft's CG due to its weight because a large moment is produced even if the battery pack's CG is located 4 in away from the aircraft's CG such that all the other components could not balance it in the dimensions of the fuselage. Therefore it was decided to locate the batteries somewhere above the payload box so that a balance could be achieved. Using Microsoft Excel a table of every part on the plane was created. That table, in conjunction with a preliminary blue print were internal components could be laid out, placed the CG of each individual component along with its weight in different locations so that the moment at the aircraft's CG was zero. Not all the weight or dimensions of some of the components were not at this point, so reasonable guesses were made for there values. Therefore a value close to zero moment was acceptable.

Weight & Balance

item	force down (oz)	Dist from CG (in)	M-CG (in-oz)	location (in)	Location CG (in)
propeller	5	-12	-60	0	12
motor	22	-9	-198	3	12
speed control	1.1	-7	-7.7	5	12
nose gear	5	-7.6	-38	4.4	12
motor mount	8	-7	-56	5	12
payload servo	1.6	3	4.8	15	12
batteries	64	-3.5	-224	8.5	12
payload	80	0	0	12	12
wing weight	24	0.25	6	12.25	12
alerion servos	3.2	5	16	17	12
rear mount	3	7	21	19	12
rear gear	10	1	10	13	12
receiver pack	2.1	20	42	32	12
receiver	1.4	20	28	32	12
elevator/rudder servo	3.2	15	48	27	12
tail weight	10	28	280	40	12
rest of plane	32	4	128	16	12
totals w/out radar	275.6 oz		0.1 in-oz		
	17.225 lb		0.00052083 ft-lb		

Table 6- CG Location Information

Using this iteration of possible location of parts with the moment that they would produce let the components being located generally where they are. At this time it the cross section of the fuselage needed for the payload area was found to be about 7 in by 8.5 in. By drawing out a detailed blueprint of the internal location of the parts it became possible to start designing the framework that would support all of the loads. The internal framework is divided into three areas: the payload area, the nose, and the tail of the fuselage.

The basic driving force for how the internal structure would be made was the payload box and it release mechanism. All the other parts of the fuselage where built to accommodate this area. As noted before the payload box needed to be hung from a beam of some kind that would allow for eyelets to be inserted and that a servo could be attached to. It was preferred that a high strength low weight rod be used to perform this task. Such materials as wood, aluminum, and a carbon fiber rod were possible choices. It was decided to use a ½ in diameter carbon fiber rod 14 in long to perform this task. The extra 2 in of length provides extra room for items like the nose wheel servo.

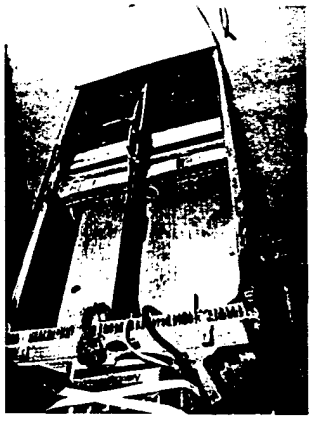

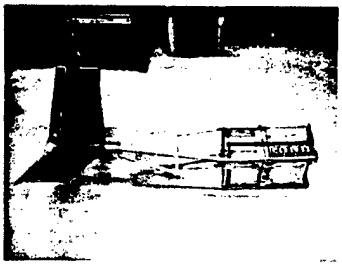

This rod would be attached to two mounts, the firewall in the front and the rear mount in the back. These mounts would support the majority of the structural loading and therefore the composite honeycomb material was selected for its strength. The firewall in the front carried exceptional

loads, since it needed to be able to support the weight of the motor and motor mount, the thrust, part of

the payload weight, and the nose gear. The rear mount only would take on the rest of the payload weight and the moments and torques produced by the tail. Holes were therefore drilled out of the rear mount to lower its weight. The firewall and rear mounts are connected at their four corners to provide strength as well as the aerodynamic shape. Balsa wood was used for the top two corners since the loading would mainly light tension and compression. Most of the heavy loading would be absorbed by the carbon fiber rod. The bottom corners had a 1 inch wide composite honeycomb stringer. The reason for that will be discussed shortly. During this design stage it was decided to put the 7/8 inch fiberglass sleeve for the wing spar directly underneath the ½ inch carbon fiber rod. This was done so that the upward force of the wings could be directly transmitted to the heaviest part of the fuselage, the payload box. In this case the eyelets were lengthened about 1 inch to allow for passage of the sleeve between the rod and the payload box without structural conflict with the release rod. In addition, the eyelet bolt could now extend up out of the upper surface of the fuselage to provide a mounting surface for the radar dish. A 2 inch wide composite honeycomb piece ran down from the top balsa stringers down to the bottom composite honeycomb stringers. In addition two ½ inch wide composite honeycomb pieces spanned the distance of the two side pieces along side the fiberglass sleeve and directly underneath the carbon fiber rod to reinforce the points where the eyelet bolts ran through the carbon fiber rod. These side pieces had a hole drilled through it for the fiberglass sleeve, and notches cut out so that the ½ inch wide reinforcing beams could fit in and be physically supported instead of just glued on. The point of this piece is to be the hard point for attaching the landing gear to. The landing gear was chosen to be located at that hard point so it would be about 2 inches behind the aircraft's CG so that the aircraft would be able to pitch easier on takeoff. The side piece and the bottom stringer were chosen to be made of the composite honeycomb in order to help provide strength and rigidity to that area. The landing gear has a tendency to pull outwards on the bottom stringers, that is why they are chosen not to be made of balsa wood. This framework effectively creates a box around the payload box that supports the main load transfer of the aircraft. The CG of the battery pack for the motor still needed to be fit into the area above the payload box and in between the firewall and the aircraft's CG. There existed a sufficient volume in that area to house the 28 batteries, but the carbon fiber rod ran right down the middle of that volume. Instead of just placing the batteries above the rod, which would increase the cross sectional area, we decided to break the pack into two and place them on either side of the rod. With the batteries being laid side ways and being glued together in a staggered fashion it was found that one side of the battery pack could rest on top of the front ½ in reinforcement beam while the other would be flush with the back of the firewall. Therefore a hole on each side of the firewall was drilled out and a wooden dowel inserted to support the

front of the battery packs. In order to keep the packs linked together two wire rods were glued to each pack and bent upwards to go over the carbon fiber rod.

The nose area of the fuselage is less complex than the payload area. The motor mount is aluminum frame that holds the motor in place. It directly mounts to the firewall. In this case it was mounted about 5.5 in above the bottom surface of the fuselage. This was done for two reasons. It would eliminate propulsive moments by putting the line of thrust near the CG in the z-axis direction. The other reason is that the higher up the motor the better the propeller clearance with the ground will be. Another nose component is the nose gear. This gear mounts to the firewall, and is angles forward to provide more taxing stability since the landing gear will have a narrow stance and the aircraft's CG is located high up. This helps prevent the aircraft from flipping forward during ground roll. The nose gear servo was placed to the side of the nose gear and mounted at an angle that matches that of the nose gear to make turning the nose gear smooth. Also, a nose cone needed to be manufactured. To do this a mold was made of the shape that was needed to cover all the components of the nose area and still be aerodynamic. A type of plastic was used that once heated can by formed into shapes. The plastic was heated and then using a vacuum box placed on top of the mold to suck the plastic down to the shape that we wanted. Finally, the speed controller is located above the motor, so that it will be cooled by the same airflow that enters through a hole in the nose cone for the propeller that cools the engine.

Lastly, the internal framework of the tail could be designed. The tail's shape is tapered from the square shape of the payload area to the narrow spar for the tail. It is shaped that way to so that flow separation could be minimized and thus lowering the pressure drag on the fuselage significantly. The tail's shape does not slope down on the top, in other words it stays straight with the top of the payload area. This means that the bottom slope of the tail is greater than the 6° to 7° necessary to keep the flow attached. This was done to provide better tail clearance for pitching for takeoff or landing. The tail is made primarily out of balsa wood. Four stingers run from the corners of the payload area to the end of the fuselage 32 inches away. The four balsa wood ribs were inserted about half way of the length of the tail to provide support. As well as two stringers on the side that run from the top of the payload area to the bottom of the side ribs. This provided torsional resistance and stiffness. The tail was made to be detachable, so it used a tail spar that could be inserted into the rear of the fuselage. For the spar to be able to attach to the fuselage we decided to use two plates of the composite honeycomb with a hole drilled through them so that the spar could slide in. One of these plates is located at the very end of the fuselage, while the other is located 4 inches in front of it. Another piece of composite honeycomb material was place on top and on bottom of the length of the in between the two

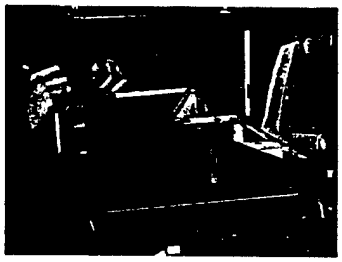

plates. A hole was drilled through from the top that goes through the tail spar. A bolt is then inserted to secure the tail spar to the fuselage.

Wings

Specify Determined Structure

Due to the analysis above, it was determined that high wing, single spar at quarter chord, balsa construction with single flaps with the delineated dimensions was optimal.

Airfoil: NACA 4412 with a 15% flap

Area: 6.75 square feet

Cord: 1.125 feet

Aspect Ratio: 5.33

Materials

The foam versus balsa debate was a major issue during the designing and manufacturing of the wing. However, the basic structure remained the same. A foam wing was implemented, with varying degrees of success. The speed by which a foam wing could be constructed was exchanged for width-wise strength and the ease (or lack thereof) by which a spar could be implemented. The wing was created with the NACA 4412 airfoil, using a foam cutting bow. The resulting shape did not exactly match the airfoil along the entire length of the wing; this was due to the size of the wire used during construction and the speed at which the bow was pulled though the foam. In later trials with a thinner wire and a new bow the wings that were cut where much more accurate to the intended shape of the wing. More problems were encountered when the foam was sheeted. The application of the sheeting had warped the wing so that it no longer resembled a NACA 4412 airfoil. Additionally, when the ribs where inserted in order to hold the spar in the wing, the holes for the spar did not match along the length of the wing, and therefore the wing could not be made to match the profile of the ribs. When the wing was finally finished it was tested for strength, it failed during the wing tip test. The reasons for the failure included the inability for the foam to support the load without a full length spar. The additional ribs inserted across the entire cord of the wing severely weekend the foam structure without enhancing the over all strength of the wing. The foam wings where abandoned due to the inability to make the system work. To accommodate the partial spar a different type of structure had to be created. The partial spar was employed because it was desired that the wings share the same spar while being capable of disassembly. The decision was made to design a balsa wing which would allow more flexibility in the layout of the internal structure. A balsa wing was selected based on advice from experienced RC constructors and the consecutive failures of the foam wing.

The wing is composed of a partial carbon fiber spar, 1/32 balsa sheeting, 3 equidistant aircraft plywwod ribs, and an aircraft plywood I-beam (as a continuation of the partial spar for structural enforcement). This structure allowed for maximum load transfer from the lifting area to the main carbon fiber spar while still

allowing the wings to be detached quickly. The completed balsa wings weighed in as one pound each and demonstrated no measurable deflection when a wing tip test was conducted. The resulting wings are both strong and reasonably light, while very accurately reproducing the NACA 4412 airfoil over the entire span.

Manufacturing

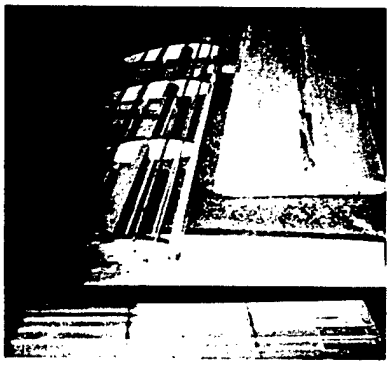

The method for wing construction was first to create eight identical ribs, then cutting ½ inch holes at the quarter cord in four of the ribs to account for the removable spar. The two wings where laid out simultaneously so that the four foot spar could pass through the fuse and be distributed evenly between the wings. This allowed about thirty percent of the wing to be supported by the carbon-fiber spar. The remaining length of the wing was reinforced with an I-beam made of aircraft plywood running longitudinally along the quarter cord. The entire structure was then sheeted with 1/32 inch balsa plywood. This resulting structure is a combination of a shell and formers with a partial spar that maintains its shape and position during the wing tip test.

Attachment

Materials

The spar used is a 3 foot circular carbon-fiber spar, running though a fiberglass sheath. The sheath is meant to guide the spar into the correct alignment when the plane is assembled as well as enhance the distribution of the wing loading along the length of the spar. The spar is most prone to fatigue failure at the root of the wing so by creating the spar of one continuous piece would create a more structurally sound design. Within the fuselage the wing spar travels below the body spar, which maintains structural stability. This allows for a direct transfer of loads from the strongest part of the wings to the strongest part of the fuselage. Thus the points of possible failure are able to be constructed with stronger and more rigid materials without affecting the overall weight, the rest of the structure only has to hold its shape while the spars hold the load.

Using one spar that only goes part of the way down the wings allowed for the point where the load is transferred from the wings to the fuselage to be at the midpoint of the spar and not at one of the ends. Thus, the maximum shear stress on the spar is at the midpoint not at an end. This allows the spar to be shorter and lighter while still being able to hold a greater load without deforming.

Manufacture

Within the wings, the spar travels up the wing to the second rib so that the end of the spar can be anchored in a solid piece of aircraft plywood and not just in the sheath. This allows for the seemingly

smooth transfer of loads from the shell of the wing to the formers, and then to the spar where it can be transmitted along to the spar to the fuselage.

Control Servos

The servos in the wing are mounted to hardwood and positioned at the end of the partial wing spar. This point was chosen for its inherent need for strength to hold the end of the spar, and thus is able to double as a mounting point for the servo. The wing servos were chosen to be stronger than the servos used for the tail due to the need to move more area of control surface

Tail

Specified Design Structure

Based on the superior rated aircraft cost contribution and the removal of control surfaces from the turbulent flow combined with the provision of equitable stability and control characteristics to that of a t-tail, the v-tail design was chosen.

The calculations used for dimensionalization (reference NACA Report and Article as well as Model book) yielded a tail with an eight inch root chord, and a six inch tip chord with an actual length (b/2, half of the tail) of 13 inches. The horizontal angle between the ground and the tail was determined to be 30 degrees, and the flap size was calculated from a recommended control surface percentage which yielded a flap of two inches wide.

Manufacture

Construction of the tail out of balsa wood was the easiest, simplest, most reproducible and most cost efficient. Two methods of balsa wood construction were attempted.

1) Two ¼ inch thick sheets (4x12 inch) were glued together, cut to shape, and hollowed out using a dremel tool and an exacto knife.

2) Balsa wood ¼ inch square rods were used to form a truss like structure using raw carbon fiber and CA at all weak joints for fortification.

The former of these two structures proved to be stronger while weighing less and was chosen as our final design. It was covered in Monokote for aerodynamic purposes.

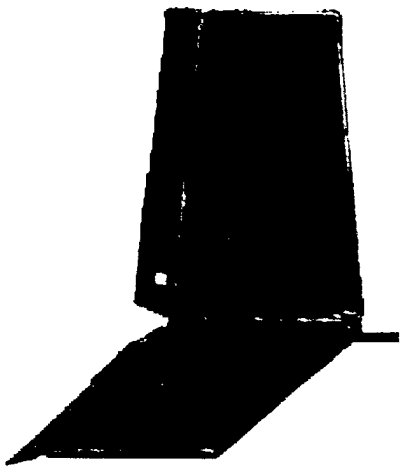

Motor Mount

Specified Design Structure

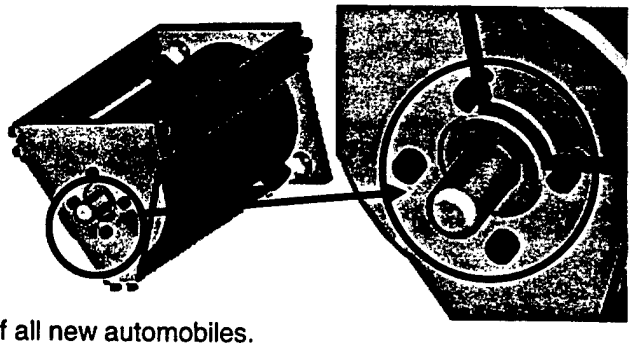

The motor mount is constructed from 6061-T6 aluminum because of it is relatively inexpensive, lightweight and simple to machine. The motor mount was designed to use the motor as a structural member to increase rigidity and save unnecessary weight. This idea stems from the uni-body construction of all new automobiles.

The front and rear plates of the motor mount were machined to fit exactly over the bearing hubs in the front and rear of the motor. The above picture shows a cut away view of the front plate. Then the two plates are held together with a slight compression in three places by thin ½ inch wide 1/32-inch aluminum strips. The sidepieces can be very thin because they not supporting all of the weight of the motor like most off the self motor mounts. They only need to hold the front and rear plate together and add protection for an unfortunate crash. This uni-construction system reduces the weight of the motor mount by 50 percent.

The motor will also make more power more efficiently the cooler it is, therefore, it is necessary to dissipate as much heat as possible. The aluminum motor mount was designed as a heat sink as well. The mount extracts heat from the motor through the front and rear plates. The tension between the two plates increases the overall rate of heat transfer between the motor and mount, which increases the rate in which the motor can dissipate heat through conduction. Using the motor mount as a heat sink increases the area in which the motor can dissipate heat through convection, thus the motor will run much cooler and more efficiently. The rear motor mount plate has 8 lightening holes, 4 of which line up with the vents in the rear of the motor. These holes reduce weight and vent the case of the motor. The mount is fastened to the firewall of the plane through the four holes in the rear mount plate. The mount can be either screwed or bolted to a firewall. You can see the 8 lightening holes and 4 fastening holes in the above picture.

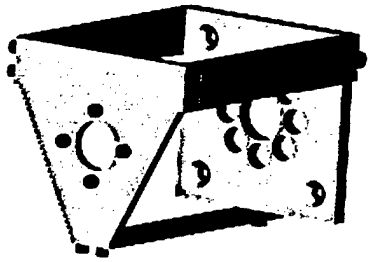

DETAILS AND COMPLETION

Fuselage

With main design of the fuselage completed and the location of all the components set it became time to start designing the details and smaller components. These details and smaller components are secondary designs that mainly have to deal with improving the main design, or are necessary due to the main design.

One smaller component that was necessary to incorporate was the air scope. The air scope was necessary to cool the batteries. Since the batteries are located above the payload box and behind the firewall they are effectively blocked of cooling airflow. If they are not cooled then they can heat up to extreme temperature where power is lost due to a rise in impedance within the batteries. The air scope

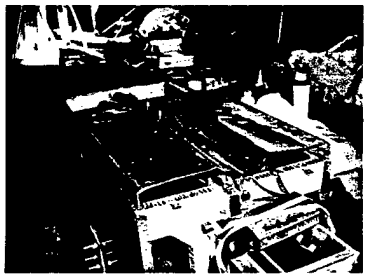

was designed to extend about ¼ inch above each battery pack which is about ½ inch above the top of the fuselage. It was manufactured by first cutting a foam shape of the air scope out of a block of foam. The foam was then sheeted in 1/32 inch balsa wood to protect the foam from the fiberglass resin that the air scope would eventually be covered in. Once the fiberglass was laid on the foam was removed. This scope was then glued to a plywood plate that covered the top of the fuselage. The plywood plate had two holes drilled in it to allow the eyebolt to extend through, and nuts were used to keep the air scope attached. It is quickly removable for loading and unloading of the battery packs. In addition to the air scope an exit hole was create in the bottom part of the tail area to allow the cooling airflow a way to exit.

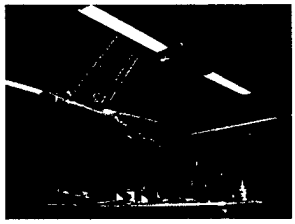

Another secondary design that needed to be installed on the fuselage was two access panels on top of the fuselage. The first panel was need above the receiver pack and the receiver. Since for weight and balance purposes both of these components needed to be placed in front of the forward plate that the tail spar goes through. The panel was placed on top of the fuselage and extended from that forward plate towards the nose by 6 inch, which is about the size need to fit a hand into the fuselage so work could be performed and the components accessed. This plate was made of a plywood sheet, with two tabs glued underneath the front and back of it. It is put in place by arching the plate so that the tabs could fit underneath the structure inside of the fuselage. Once the plate straightens out it can not be pulled off. This method was used because it adds negligible weight and is simple and fast. The second panel needed to be placed above the payload box release mechanism. In order to ensure that the box was loaded securely and quickly visual access to the eyelets along with the ability to guide the release rod was vital. This panel extended from the rear mount up to the plate that the air scope is attached to. Once again it is about 5 inches length, which in this case give good hand access to the necessary components

while also providing good line of sight to the eyelets. It is constructed exactly like the first panel and held into place the same too.

An addition that was added to the payload area was to drill holes in the firewall and the rear mount and insert wooden dowel pins through. The purpose of this was to hold the payload box in place so that it was not bouncing around during flight, which could have caused damage to the structure. Two dowels were put in the front and two in the back. This prevented limited twisting motion of the box.

One smaller design that improved the overall main design was to use gussets and or carbon fiber hair to strengthen joint areas. The gussets were triangles of balsa wood that could be inserted to fit into the joints and then glued. The carbon fiber hair would be used in the same manner, and then glued to form a hard strong joint. By doing this the joint became stronger and less likely to break.

After the main design was complete an analysis was performed on the payload doors. It was found that the doors that were created were not long enough, and therefore the box was catching up the springs that were being used to close them. A redesign was performed. The solution was found to add a small tab to the side of the door close to the hinges in the forward area where the springs are located. Similarly, spaces for the tabs were cut out from the bottom of the fuselage next to the doors where the tabs would fit in. The springs were then attached to the new tabs, and were clear of the payload box during drops.

Wings

Wing/Fuselage Pins

Due to the single spare design the wings would be free to rotate around the spar, hence wing pins where installed at the trailing edge of the wing. These pins restrict the wings ability to rotate and double as anchors to hold the wings to the fuse. The attachment of the wings to the fuse is done by wing nuts that are screwed into place during the planes assembly on the ground.

Tail

*Note: After each detail was completed, the plane was re-measured and analyzed to ensure no alteration of intended angles or dimensions

Structure Reinforcement

Once the two halves of the v-tail were complete, a balsa wood wedge was placed between them at the angle at which they were to be constrained. This wedge was glued and then reinforced with carbon fiber to ensure that it would not change configuration.

Attachment

A hexagonal aluminum pipe was cut to fit the base of the v-tail to provide a means to attach the tail to the plane upon demand. The pipe and v-tail attachment was facilitated by adhesive foam and three screws which went through the aforementioned balsa wedge and the pipe. The end of the fuselage was constructed with two honeycomb composite hard-points which were cut to allow the pipe to fit the through them, thereby attaching the tail securely.

Securing Tail

A sheet of 1/16 inch plywood was attached to the fuselage at the top and bottom around the tail-pipe. A vertical hole was drilled through each plywood sheet as well as the hexagonal aluminum pipe to fit a .25 inch bolt with an eye. After attaching the tail, the eye bolt was then screwed securely through the pipe and plywood sheets, ensuring not only that the tail resist twisting, but that it not slide out of its housing.

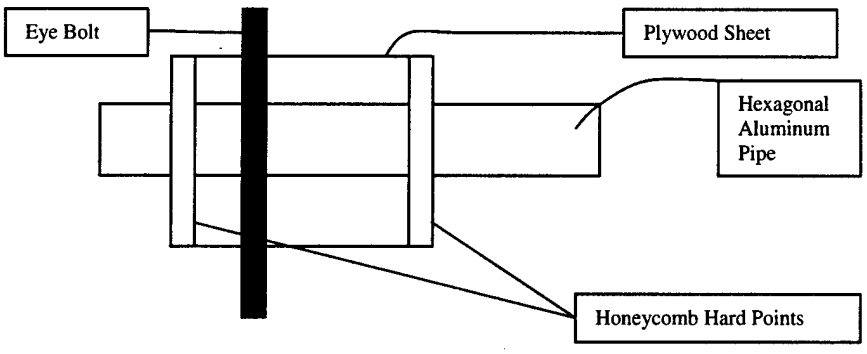

Figure 8-Tail Pin

Servos

The tail servos were attached at the base of the tail closest to the fuselage. The wires ran through the aluminum pipe to the interior of the fuselage where they remained attached to the receiver.

Sized Aircraft Data:

Aircraft Geometry	
Length	4.25 ft
Span	6.58 ft
Fuselage	1.25 ft
Hight	2 ft
Wing Area	6.25 ft^2
Aspect Ratio	5.33
Aircraft Performance	
CL max	3.2
L/D max	15
Maximum Rate of Climb	16 ft/s
Stall Speed	33 ft/s
Maximum Speed	103 ft/s
Takeoff Filed Length Empty	90 ft
Takeoff Field Length Loaded	120 ft
Aircraft Weights	
Airframe	2 Lb
Propulsion System	6.25 Lb
Control System	0.82 Lb
Payload	5.1 Lb
Empty Weight	13 Lb
Gross Weight	17.2 Lb
Aircraft Systems	
Radio	Hitec Prsum 7X
Servos	Curris
Battery Configuration	Sanyo 2400 serries 28 Cell Pack
Motor	Astorflight Cobalt 60 Direct Drive
Propeller	APC 16X12 Two Blade

Table 7- Sized Aircraft Data

Rated Aircraft Cost				
A	Multiplier	$100		
B	Multiplier	$1,500		
C	Multiplier	$20		
MEW	Weight (no payload)	(lb)	12.66	
	Battery Weight	(lb)	3.83	
REP	(1 + .25 * (# Motor - 1)) * Battery Weight		3.83	
MFHR				
	WSB 1.0			
	Wing	8 hr/ft	5.70	45.60
	Cord	8 hr/ft	1.00	8.00
	Control Surface (CS)	3 hr/CS	2.00	6.00
	WSB 2.0			
	Fuselage Length	10 hr/ft	4.00	40.00
	WSB 3.0			
	Vertical Surface	5 hr/ft	0.00	0.00
	Vertical CS	10 hr/ft	0.00	0.00
	Horizontal	10 hr/ft	0.00	0.00
	V-Tail	5 hr/ft	1.25	18.75
	WSB 4.0			
	Servo	5 hr/Servo	6.00	30.00
	WSB 5.0			
	Motor	5 hr/Motor	1.00	5.00
	Propeller	5 hr/Propeller	1.00	5.00
			SUM	158.35
Rated Aircraft Cost	$ (thousands) = (A * MEW + B * REP + C * MFHR)/1000		**10.18**	
		Total Aircraft Cost	**$10,180.00**	

Table 8- Recent Rated Aircraft Cost

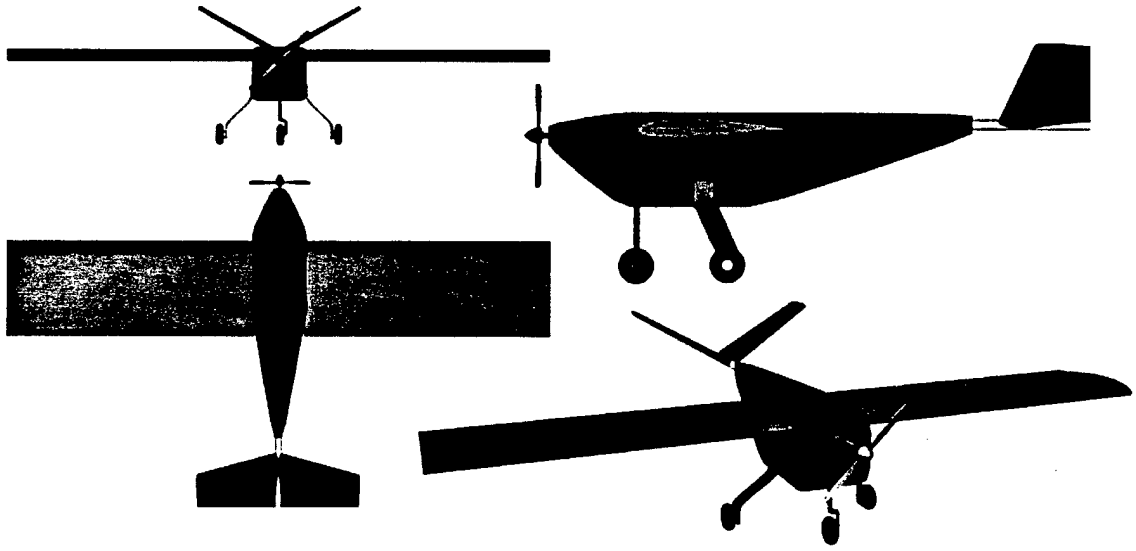

Figure 9- 3 View Drawings

The following images are of the aircraft in its prefabrication condition, an artistic impression of engineering concepts used to visualize the final design before the all of the dimensions and analysis is completed

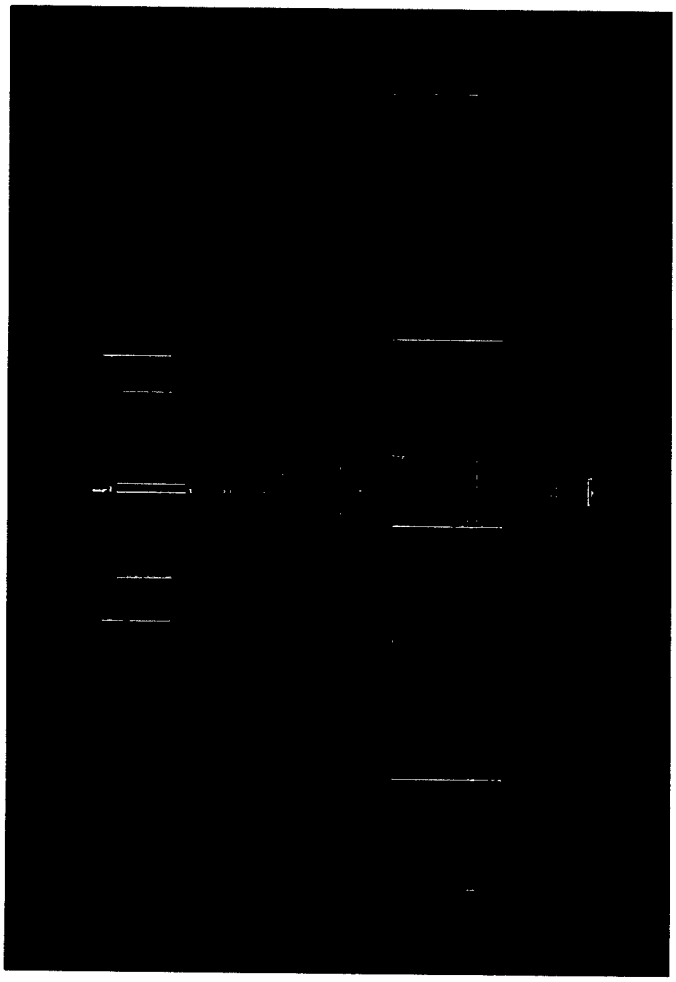

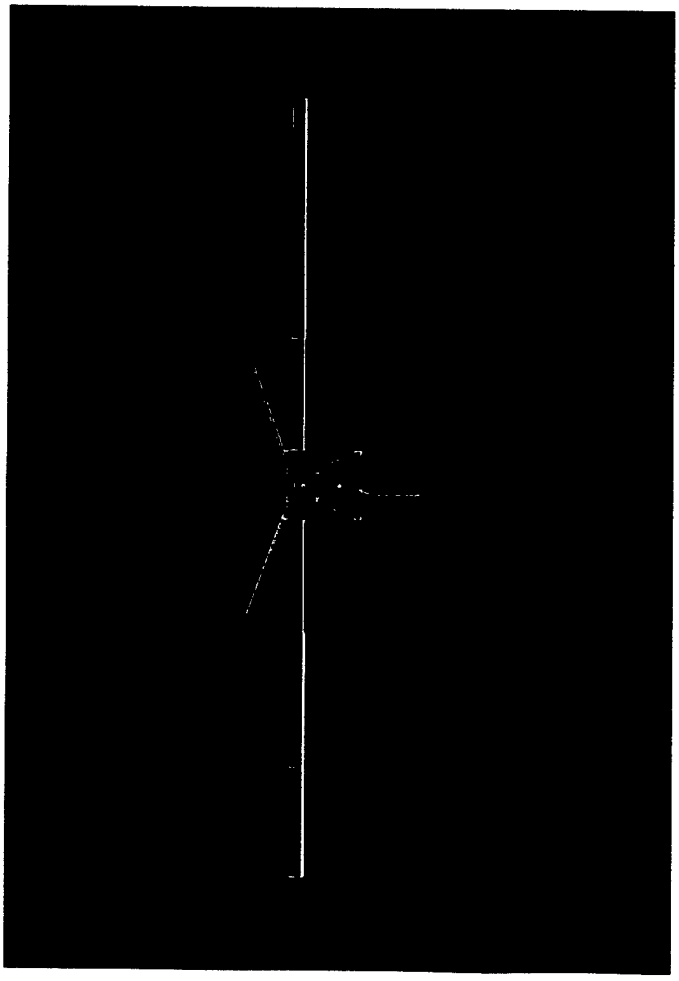

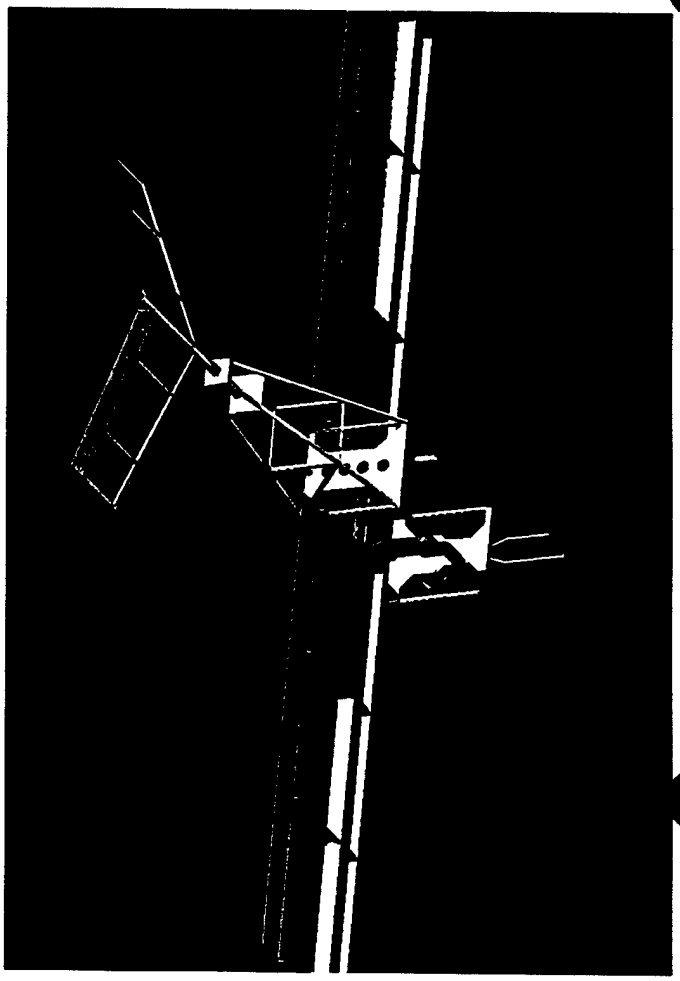

Aircraft Control Systems

Design Drivers

They control system for this aircraft has to be able to handle the complex nature of the plane. The plane does not have standard RC configuration; it requires a control system more complex than the typical RC trainer. This plane needs to have the control of more complicated RC planes, such as an aerobatic plane. This is due to the need to implement a V-Tail mixing, and flaperon controls, as well as payload deployment control. Additionally the method of communication between the pilot on the ground and the airborne plane needs to be as secure as possible, as to avoid any interference that could cause failure.

Implemented System

The system that has been implemented in the plane is one based on the needs of the plane and the availability of components. Due to funding restrictions the team was unable to purchase a new control package; instead we implemented a mix of components. The transmitter is an older Hitec Prism 7X capable of both PCM and PPM modes. This transmitter meets the requirements of features and programmability. Using this transmitter proved to be a stumbling block for the team has yet to find a Hitec PCM receiver. The team has been using a new Super Slim FM receiver from Hitec as an interim 8chanel receiver.

Programming

The transmitter was programmed to enable V-Tail mixing so that the two independent servos would work simultaneously as rudder and elevator. The transmitter was also programmed to enable simultaneous flap deflection while still retain the independent aileron control. Lastly the payload servo was programmed to remain fully rotated, until the payload was deployed.

Signal

The transmitter operates on a frequency of 72MHz with a range of channels from 11-60, in either PPM or PCM mode. For the competition the plane will by using channel 14. The use of PCM is warranted do to the ability to program a fail safe is necessary for the competition.

Wiring

The wiring used to connect the servos to the receiver is custom built to allow for quick and easy assembly of the plane. The wires are tagged and bundled in order to restrict their movement, and minimize the chance they might be damaged.

Mission Requirement Additions

Payload box

A prototype payload box was created out of oak with an eyelet bolted into the top for simulated payload release. A permanent payload was in the middle of construction at the time of the report, but its design

would consist of a permanently welded eyelet to a sheet of metal which would be permanently attached to the wooden payload box by adhesive and nails.

Storage box

The storage box was also created out of wood (oak) with the inner dimensions specified by the contest rules. The inside of the box was padded to soften the jolts that the disassembled aircraft would receive on traveling.

Aircraft Testing (Pre-Flight Tests)

Static Thrust

The static thrust was tested to insure the true performance would closely match the theoretical performance. Using a spring scale, the plane was throttled up to max power using a 16X11 prop the thrust was measured to be between 6-8 lbs.

Taxi Tests

Before the plane was taken up for its first flight test, a taxi test was preformed to asses the grown handling capability. It was observed that the nose gear was not maintaining its position, this dew in combination from the soft ground as well as an extremely soft tire. To solve this problem a hard rubber tire will be used in all fallowing tests.

During ground roll test the acceleration plane lagged a bit when throttled up. It was discovered later that the motor was out of phase, this was due to the repairs that where made to the motor fallowing the discovery that the driveshaft was wobbling when the motor was running. When the motor was reassembled the magnets where turned out of alignment. This was corrected and the timing on the motor was reset.

Spruce Goose Test

For the fist flight test a Spruce Goose style test was preformed to asses the planes flight worthiness. The results where promising until the plane touched back down, the nose wheel dug into the ground and the plane flipped head over heals.

Flight Test Easements

Results from the flight test where analyzed, and the problems where solved.

The tail was creating enough additional lift that the plane needed to have full up elevator in order not to nose over. Upon further inspection the tail set angle was positive instead of negative. This caused the tail to become airborne before the wings and lift the plane nose over.

The nose wheel needed to be adjusted; it was angled forward to increase the ground roll stability. By moving the nose wheel forward more then weight was shifted back more towards the rear gear.

The plane was known to be top heavy during the design phase; this was found to source of instability on the ground. The planes eagerness to roll nose down during any turning maneuver shows that the weighting of the plane was not refined enough for ground roll control. The optimizations in the design of the plane did place enough emphases on ground roll stability. This is not a mission critical failure, for the instability can be compensated for by the pilot.

Summation

The end results of the flight test show conclusively that the conceptual design was successful, the plane flies. It was critical for the pilot to get a feel for the handling of the airplane before the competition. Flight tests will continue up until the competition so that the plane can be refined and its optimal performance attained.

REFERENCE

McCormick, Barnes Warnock, 1926. Aerodynamics, aeronautics, and flight mechanics / Barnes W. McCormick – 2nd ed. 1995

Anderson, John David. Fundamentals of aerodynamics / John D Anderson, Jr. – 3rd ed. 2001

Tail References

*Report No. 823 NACA, Experimental Verification of a Simplified Vee-Tail Theory and Analysis of Available Data on Complete Models With Vee Tails; Paul E. Purser and John P. Campbell

*Online reference V-tails for Aeromodels: Yet Another Attempt at Explaining Them: www.fmsg-alling.de/vtail.htm

VisualFoil

VisualFoil was used as basis for all computational aerodynamics, this program has proven to be accurate and an effective tool in expiating the design process.

VisualFoil 4.1. Hanley Innovations 1997-2001
Written by, Dr Patrick E. Hanley Ph.D.

University of Texas at Arlington

The Spirit of Arlington

American Institute of Aeronautics and Astronautics

Office of Naval Research

Design-Build-Fly Competition 2003

1 Executive Summary

This report summarizes the techniques and methods used by The University of Texas at Arlington to construct a propeller driven, electrically powered, unmanned aircraft that carries out the mission profiles found in the Request for Proposal (RFP). The payload, a 5lb simulated avionics/sensor package, is carried onboard, with one mission requiring the deployment of the package onto the runway. Another mission requirement involves the attachment of a simulated AWACS-style radar antenna to the aircraft. Each team is ranked based upon their total compiled score. The total score is proportional to the product of the written report score and the total flight score, and inversely proportional to the Rated Aircraft Cost (RAC).

The team began the design process by examining the competition results from 2002. Last year's entry was deemed to have been overly large and heavy, and exhibited relatively sluggish response. Given that experience, a clean sheet of paper design began to unfold. This exercise ultimately led to the design philosophy: *Simplify, simplify, simplify.*

The major design challenges identified were:

- Short Takeoff 100ft
- Rapid Assembly
- Clean, Simple Design
- Low Dollar Cost
- Rugged Structure

Although the rules allow a takeoff roll of 120 ft, a 20% safety factor was deducted to ensure compliance. After considering canard, blended wing-body, conventional, and twin-boom fuselage arrangements, the conventional layout was deemed to be the most cost-effective (in terms of RAC), and simplest to construct. Because of the cargo drop requirement, a high-mounted wing was selected. This minimized the structural complexity of the wing carry-through structure, and was considered a very attractive tradeoff, since no major advantages to the low or mid wing location were identified.

The team then decided to discard the previous year's construction technique of fabric-covered balsa structures, and build the airframe from carbon fiber. The team members believed that although carbon fiber will present a challenging build, the performance benefits and the practical experience make it an attractive choice.

For power, the team selected the largest available electric motor, and planned for the maximum battery complement, primarily due to the short takeoff requirement. Plans were made to flight test with smaller battery packs in order to evaluate the feasibility of a lighter, but perhaps slower, aircraft.

In order to rapidly evaluate aircraft sizing parameters, a Microsoft Excel spreadsheet (the Sizing Worksheet) was designed using equations from Raymer (Ref. 1). This worksheet enabled the team to change dimensions and immediately recalculate expected takeoff roll distances. Although the model used to estimate takeoff roll was relatively crude, it was believed to be sufficient to select a conceptual sizing of the aircraft.

Discussions with members of the UTA Formula SAE racing car team resulted in the conclusion that a very rapid assembly time could be a significant strategic advantage. Therefore, the entire design was focused on minimizing the number of assembly tasks. The three-person assembly team plans to train intensively in order to meet a goal of a sub-20 second assembly time.

The aircraft as designed is quite powerful, and is expected to be among the faster aircraft competing. This conclusion is based on the assumption that last year, few (if any) teams specified the largest available motors and battery packs, coupled with a clean, lightweight airframe. Taking a motto from the fighter pilot community, it was determined that "speed is life".

2 Design Team Architecture

The team was structured into functional groups. The intention was not to lock members into one and only one function, but rather to foster a sense of ownership and responsibility for the major subsystems. A strong emphasis was placed on making certain that lower division students were paired with upper division students. It was very important that each team member saw their own contribution to the project, and had the opportunity to learn new skills and concepts. Each group was required to report back to the entire team on a weekly basis.

		Assignment Areas						
Design Personnel	**Class**	Aerodynamic Dimensions	Wing Systems	Tail & Fuselage Systems	Payload Systems	Battery & Wiring Systems	Propulsion & Control Systems	Paper
Tatsunori Aoki	Soph.		X					
Matt Burris	Sen.	X				X		X
Cesar Carrillo	Sen				X			
Nathan Christiansen	Jun.		X	X				
Michelle Craig	Fresh.		X					
David Fullmer	Soph.		X					
Lee Gibson	Sen.	X	X					X
Noah Hicks	Jun.		X	X			X	
Cindy Hollingshead	Sen.	X		X				X
Hisashi Inoue	Soph.				X			
Jason Lee	Sen.	X				X	X	
Caleb Leung	Sen.	X			X			X
Linda Phonaharath	Fresh.							X
Jenny Roetzel	Soph.							X
Nemu Shirota	Soph.		X					
Kevin Worrell	Jun.				X	X		

Table 2.1: Team Member Responsibilities

2.1 Aerodynamic Dimensions

The Aerodynamic Dimensions functional group was comprised of five seniors who had completed courses such as Flight Vehicle Design and Flight Dynamics. This was the only group that included only upperclassmen, due to the complicated and detailed nature of the required calculations. The entire team was briefed on the decisions made here, and at several points the team as a whole selected one design feature over another.

2.2 Wing Systems

The Wing Systems group was responsible for designing the structure and control systems contained within the wing panels and the wing box. The group also had the responsibility of rationalizing the configuration and aerodynamic characteristics of the wing.

2.3 Tail & Fuselage Systems

The Tail and Fuselage Systems group was responsible for structure, empennage control surfaces, and integration of tail to fuselage.

2.4 Payload Systems

The Payload Systems group had the responsibility of arranging the payload, which consisted of a 5lb. 6" x 6" x 12" simulated avionics/sensor package, into the fuselage, deploying the payload when required, and adjusting the structure to accommodate the payload. The following two missions were the obstacles the group would be faced with, with regards to payload. All missions require a takeoff roll of less than 120ft.

The team elected to design for Missions A and B.

Mission A (Difficulty factor 2.0)
In mission A, the 5lb simulated sensor payload and the simulated AWACS antenna are both to be carried through the course of four laps around the field.

Mission B (Difficulty factor 1.5)
In mission B, a payload drop is required. The aircraft will take off, perform two laps of the course, and land. The payload will then be deployed by the pilot via servo actuation. The sensor package will be deployed from the bottom of the aircraft's fuselage. The aircraft will then take off again, perform two more laps of the course, and land.

Mission C (Difficulty factor 1.0)
Mission C requires only that the aircraft take off in 120 feet, fly four laps, and land. Payload consists of the 5lb sensor box.

2.5 Battery Systems & Wiring

The Battery Systems and Wiring group was in charge of specifying and ordering electrical parts. The group was also responsible for presenting a rationale on choosing one power configuration (batteries and motor) over another. The group would to come up with schematics for the power and control system wiring.

2.6 Propulsion & Control

The Propulsion and Control group ensured that the proper motor was specified and ordered. The group reported to the entire team on aerodynamic and electrical characteristics of the motor, to include

characteristics with various prop sizes. The group also researched how to improve flight manners of the aircraft.

2.7 Paper

The Paper group was responsible ensuring that notes were being recorded at all group meetings. The paper group compiled team ideas and incorporated them into the rough draft paper then onto the final draft paper.

3 Conceptual Design Phase

3.1 Configuration Concepts

The wing/body layout was the first major design choice analyzed. As a brainstorming exercise, each team member was asked to sketch out concepts for each of the configurations discussed below. The resulting sketches were then presented to the group, and strengths and weaknesses both of the overall concept, and each team member's specific designs, were discussed.

Figure 3.1: Wing/Body Layouts

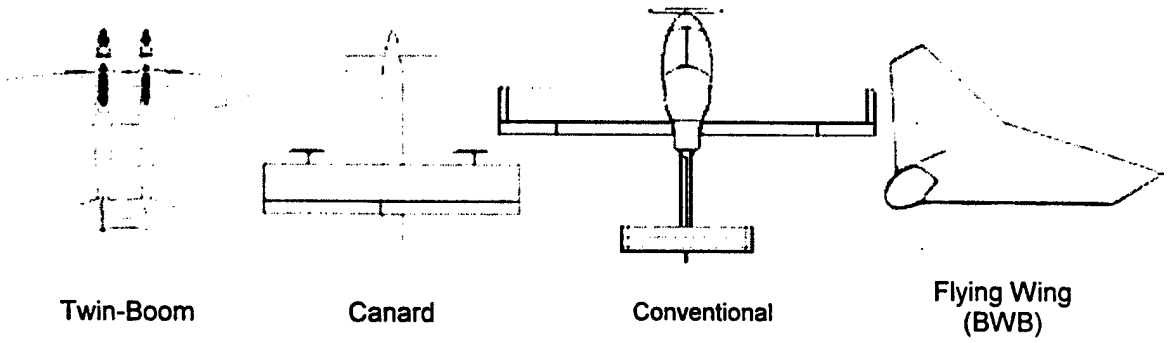

Twin-Boom | Canard | Conventional | Flying Wing (BWB)

3.1.1 Twin-Boom Design

The twin-boom configuration permits the structural members to be quite small, relative to a design with a full fuselage tube. On the unladen leg, the frontal area (and, hence, drag) would be minimized. If two motors are specified, this fuselage arrangement also allows for a simple thrust-bearing structure, since one motor can be located at the nose of each fuselage boom. With the twin boom arrangement, a payload fairing or pod would be desirable for the mission segments involving the sensor box. Unless the pod could be dropped along with the sensor box, the frontal area advantage of the twin boom design is lost.

3.1.2 Canard Design

A canard wing layout permits the use of an upward-lifting horizontal stabilizer. This allows the use of a smaller main wing, assuming equivalent weights. Because the payload section will not need be located near a spar, the canard design allows for more flexible design of center of gravity (CG) location. The frontal area of the aircraft may also be smaller, again since the spar need not be located above the payload. Canard designs can also be extremely resistant to stalling.

3.1.3 Conventional Design

The conventional layout, although pedestrian, is very well understood. The conventional configuration works very well in a wide variety of flight regimes.

3.1.4 Flying Wing (Blended Wing-Body)

Theoretically the BWB design will have extremely low parasitic drag. However, flying wing designs are notoriously sensitive to CG location, making the payload deployment mission difficult to perform reliably. This design would also be difficult to package in the shipping container.

3.2 Conceptual Design Parameters Investigated

3.2.1 Wing Placement

Because of the requirement to deploy the sensor payload, low and mid-fuselage wing locations were not considered feasible. By locating the wing high, the wing spar could be a continuous structure resulting in much sturdier construction. Low- or mid-wing designs would require stress bearing fuselage formers, or very strong stressed skin structures in order to bear the wing bending loads in flight. Since no major advantages to low- or mid-wing designs were identified, these alternatives were discarded.

3.2.2 Landing Gear Styles

The landing gear was identified as a major potential mission-failure point. Consequently, the landing gear selection process focused on ruggedness.

Retractable landing gear are available for model aircraft, but due to unforeseen circumstances seen at last year's competition the idea, in its complexity, was withdrawn. Although retracts are preferable for aerodynamic reasons, its cost (both in terms of actual budget and RAC) and fragility were less desirable.

Although taildragger style landing gear is popular both in model aircraft and general aviation aircraft, it was deemed unsuitable to the payload deployment requirement as stated in mission B.

Tricycle landing gear, with aerodynamic strut sections and faired wheels, was determined to be the most cost effective, rugged, simple solution.

3.2.3 Tail Configurations

Figure 3.2: Tail Configurations

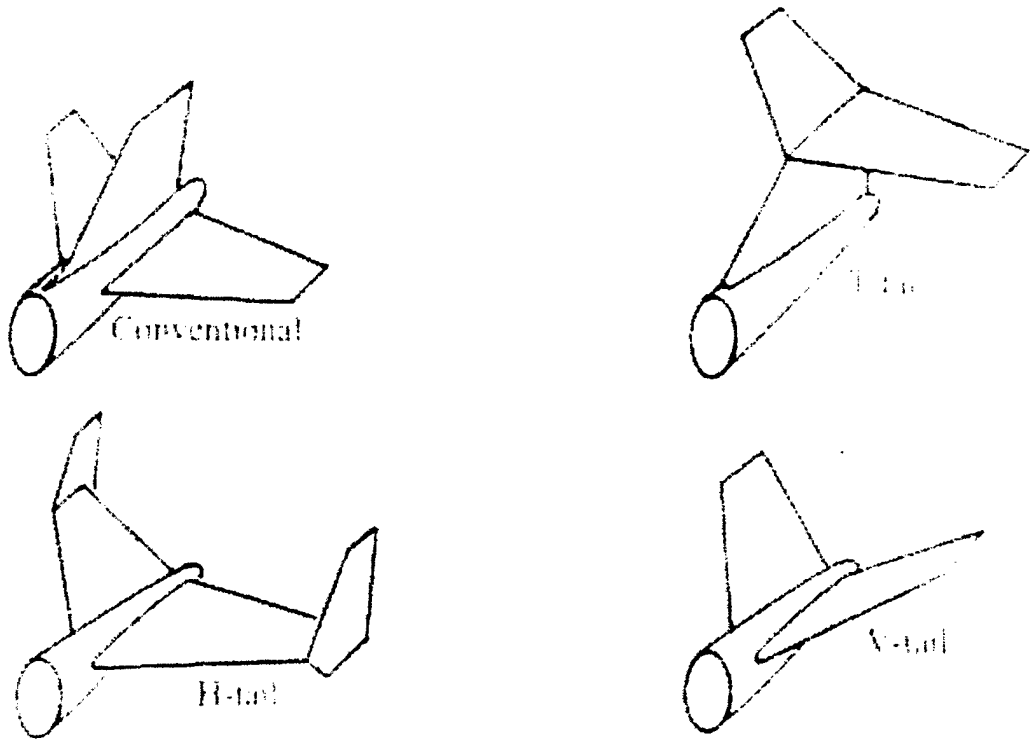

(Raymer Fig. 4.3)

3.2.3.1 Conventional

This configuration is the most popular of the four tails (hence 'conventional'), mainly because of its weight, it will provide enough stability and will work, simply put. The drawback to the conventional tail is that at high AoA, the rudder can be blanketed by the horizontal tail, which decreases rudder effectiveness. The wake of the AWACS antenna would cause a similar blanketing effect during cruise.

3.2.3.2 T-Tail

The T-tail is also used quite often for R/C aircraft. With the horizontal tail mounted high on the vertical, the horizontal is kept clear of downwash from the wing. However, the vertical tail will suffer from the same blanketing effect from the AWACS antenna mount. Also, for the vertical to support the horizontal tail, it will have to be heavier than in the conventional or V-tail configurations.

3.2.3.3 V-tail

The V-tail was considered for several reasons; One, because it would reduce the RAC with only two control surfaces rather than the three surfaces in the configurations discussed prior. Two, the control

surfaces would no longer be in the direct wash from the AWACS. Theoretically, the V-tail has lower drag than other configurations, since the overall wetted length of the surfaces is smaller. The V-tail would also have a very sturdy fuselage joint, and be relatively easy to fabricate. The coupling between the roll and the yaw control axes is also of concern with this design.

3.2.3.4 H-Tail

With the H-tail, the downwash on the vertical tails is almost negligible from the AWACS antenna. One downside is that the RAC will increase due the addition of a vertical surface, but with the addition tail the area/surface is lowered such that the vertical tails should not be any taller than the fuselage. This would dramatically decrease the assembly time, since the tail could fit in the space allowed without disassembly.

3.2.4 Motors

Two motor configurations were considered. The first is to have a large, single motor in the middle. This configuration decreases the RAC, but if a sufficiently powerful motor is not available, would make the short takeoff constraint difficult to meet. The second alternative is to have two smaller motors located in the wings. There are many disadvantages for the two motor design. First is the difficulty of manufacture. Additional motors are penalized in the RAC calculation, and two motors of modest power will be heavier than one large motor. Also, since the two motors has to be attached into the wing, the wing must be designed to bear the thrust and weight loads of the motors. Finally, buying one large motor costs less than buying two smaller ones. The final decision was to purchase one AstroFlight© Cobalt 90 motor. This is the largest motor available from the manufacturers specified by the competition rulebook. With a 24x10 propeller, thrust is estimated by the manufacturer to be 100 ounces.

3.2.5 Fuselage

A one-piece fuselage would be ideal from a timed-assembly perspective. If the fuselage, motor, propeller, and tail could be placed together into the shipping container, the number of assembly tasks will be minimized. The one-piece design will also exhibit lower drag than the other alternatives. The major disadvantage to this design is that the fuselage is quite short considering the wing area, necessitating a very large tail area to compensate.

A two-piece monocoque fuselage would be nearly as aerodynamically clean as the one-piece design, yet the aircraft can be longer to maintain proper CG location relative to the neutral point. The drawback to this alternative is fabrication difficulty of the fuselage joint mechanism.

A pod-boom arrangement, while not as aerodynamically clean as the other alternatives, is easy to fabricate and provides flexible sizing for balancing the aircraft. Assembly of the boom to the fuselage was planned to include a quick-attach feature.

3.3 Conceptual Numerical Figures of Merit

To compare various configuration options, Figures of Merit were assigned to various design parameters. This analysis was performed twice, once to select the wing/body layout, and a second time to select a tail layout.

Each figure of merit was scored from 1-10, and then that point score was multiplied by the weighting factor. The weighted scores were summed and compared to one another.

Definition of Figures of Merit for Wing/Body Selection

Real Cost: The dollar cost to manufacture the aircraft.

RAC (Rated Aircraft Cost): Cost breakdown as specified in the rules.

Aero. Performance: Lower estimated drag provides a higher score.

Manufacture: Difficulty of actual construction.

Assembly Time: How fast the aircraft can be assembled during the timed assembly task.

Flight Manners: How easy the aircraft is to fly.

CG Flexibility: How sensitive the aircraft will be to CG location.

Item	Weight	Twin Boom	Canard	Conventional	BWB
Real Cost	10%	5%	7%	7%	3%
RAC	20%	6%	10%	14%	14%
Aero. Performance	18%	11%	14%	12%	7%
Manufacture	15%	8%	9%	11%	3%
Assembly Time	20%	14%	14%	14%	8%
Flight Manners	10%	7%	3%	7%	4%
CG Flexibility	8%	5%	6%	5%	1%
Total:	**100%**	**56%**	**63%**	**69%**	**40%**

Table 3.1: Wing Layout Figures of Merit

As indicated in Table 3.1, the conventional layout will perform slightly better than the other options, and was therefore selected.

Initially a 4 foot long, one-piece fuselage was designed to fit into the shipping box with no assembly. After further analysis, the data reported complications between the neutral point (NP) and the CG. The CG was estimated to be 3 to 4 inches aft of the NP, resulting in a statically unstable aircraft. Although a piezoelectric gyro attached to the rudder servo would improve stability, it was decided that relying on active stability would require more familiarity and confidence in the flight envelope of the piezo system. After careful consideration and more data analysis, the choice was made to manufacture a two-piece fuselage. The forward part of the fuselage was reconfigured as a pod carrying payload, motor, and batteries. The aft portion was simply a hollow carbon rod supporting the tail. The battery pack was placed under the motor in the forward fuselage bay. Immediately aft, the payload bay will be located. Aft of the payload, the fuselage will taper down to the boom mount. The radio receiver will be located in this region, to minimize electrical interference from the power system.

Definition of Figures of Merit for Tail Selection

Real Cost: The dollar cost to manufacture the aircraft.

Aero. Performance: Lower estimated drag provides a higher score. Since the tail is located downstream of the AWACS antenna fixture, its wake is considered when rating the expected performance of the tail.

Fuselage Integration: Difficulty of affixing the tail to the fuselage.

Manufacture: Difficulty of constructing tail airfoils (More sections yields a lower score).

Assembly Time: How fast the aircraft can be assembled during the timed assembly task.

Flight Manners: How easy the aircraft is to fly.

CG Flexibility: How sensitive the aircraft will be to CG location.

Item	Weight	H-Tail	V-Tail	Conventional	T-Tail
Real Cost	10%	4%	7%	6%	5%
Aero. Performance	10%	7%	8%	7%	6%
Fuslage Integration	25%	20%	18%	20%	13%
Manufacture	15%	9%	12%	11%	11%
Assembly Time	25%	25%	13%	18%	8%
Flight Manners	15%	11%	6%	11%	12%
Total:	**100%**	**76%**	**63%**	**72%**	**54%**

Table 3.2: Tail Layout Figures of Merit

Primarily because it could fit into the shipping container intact, the H-tail was deemed the best choice. This configuration is slightly more difficult to construct, but the team elected to use this method to locate the vertical tails outside the wake of the AWACS antenna.

4 Preliminary Design

4.1 Preliminary Design Parameters and Sizing Trades

4.1.1 Initial Layout and Weight Estimate

The team began by assuming the largest wingspan that could reasonably fit into the shipping container would measure approximately 7 feet. This span would permit each wing panel to be built with a sturdy spar protruding from the wing root to join with the fuselage.

Item	Weight (lb)
Motor	2.5
Batteries	5
Payload	5
Wing	2.5
Fuselage	3
Tail	1.5
Landing Gear	1
Electronics	1.5
Total:	22

Table 4.1: Weight Estimates

Based on the weight of the known components, the team estimated a conservative gross take-off weight of 22 lbs. By comparing the estimate of size and weight from the preliminary design with large, commercially available model aircraft, the team was confident in its initial sizing.

	Top Flite Giant Series			UTA DBF
	Corsair	Thunderbolt	Mustang	Design
Span (in)	86.5	85.0	84.5	84.0
Chord (in)	16.0	15.6	14.7	15.0
Area (ft^2)	9.6	9.2	8.6	8.8
Aspect Ratio	5.4	5.4	5.7	5.6
Weight (oz)	384.0	320.0	272.0	368.0
Wing Loading (oz/ft^2)	40.0	34.7	33.0	40.2

Table 4.2: Sizing Comparison with Similar Aircraft

4.2 Preliminary Figures of Merit

4.2.1 Airfoil Selection

One of the most important choices for the aircraft is the airfoil, it needs to be chosen to fit exact needs of the mission, while still being flexible to changes that might arise. The danger when selecting an airfoil is to become bewildered by the array of options. For this design project several properties were identified

as being of particular. First, the airfoil should have low drag characteristics, which is crucial in these missions because they are timed, so the faster the aircraft completes the mission, the better the overall score. Also the airfoil, for this aircraft, should be thick enough towards the trailing edge chord to support a sizable control surface, e.g. flaperons for the wing, rudder for the tail. The maximum available Cl must be greater than 1.1 without flaps in order to satisfy the short takeoff requirement. Finally, the airfoil must be somewhat easy to fabricate, even with computer-aided tooling a heavily cambered airfoil is quite difficult to build. An airfoil with little to no camber would be an attractive option.

4.2.1.1 Eppler Airfoil Sections

Due to the experience that the team had with analyzing airfoils, initial preference was given to NACA four-digit series airfoils. Throughout the selection process other airfoils were being considered, including the Eppler E-series and the Lissaman 7769. After some research into airfoil selection for an aircraft with a low Reynolds number, the NACA airfoils that were considered (24xx, 44xx and 64xx series) did not seem suitable. The team's study of model aircraft design yielded the conclusion that Eppler airfoil sections are more optimal for the low-speed flight regime. The Eppler airfoils were developed by Dr. Richard Eppler for the sole purpose of small-scale aircraft. Upon examination of the drag polars, it was clear that this family of airfoils would meet our goals.

4.2.1.2 Wing Airfoil Section

For the wing, the Eppler E197 airfoil was chosen due to its good drag performance and that it maintains thickness along the chord, which is advantageous for packaging the servos and also for structural rigidity. This airfoil can be described as moderately cambered, which makes for ease in manufacturing while still providing enough lift at high angles of attack, up to 18 degrees. The stall characteristic of the E197 is described as "gentle", which is an excellent quality for any model aircraft. Aside from the stall, the E197 is a low drag airfoil with a moderate pitching moment, which has been determined by the team to have the ideal performance necessary for the mission scenarios.

Figure 4.1: Eppler 197 Airfoil Schematic and Drag Polar

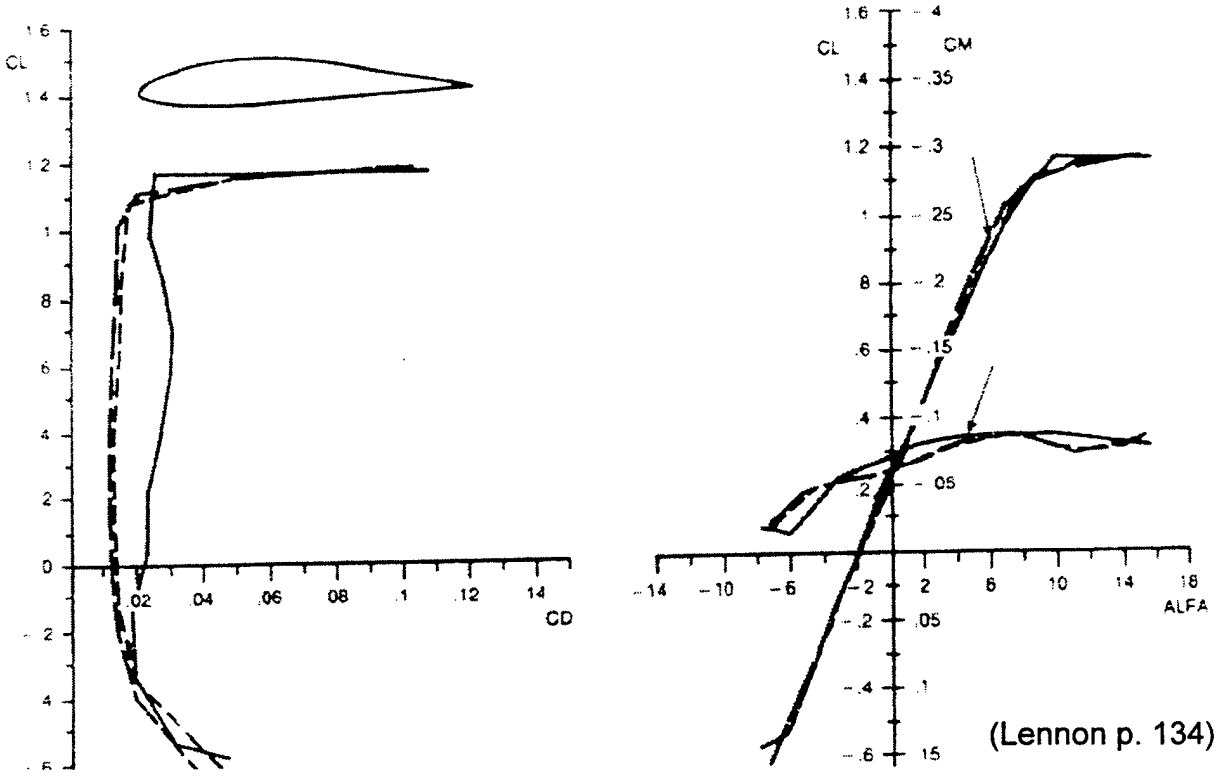

4.2.1.3 Tail Airfoil Section

For the tail airfoil selection, the factors that based our decision on that of the wing were all considered but weighed differently. Mainly, the Eppler E168 was chosen due to its symmetrical shape for ease of manufacturing and producing. Since the tail is not being used as a lifting device, the airfoil is simply being used for its low drag characteristics while being thick enough to provide ample room for a good sized control surface.

Figure 4.2: Eppler 168 Airfoil Schematic and Drag Polar

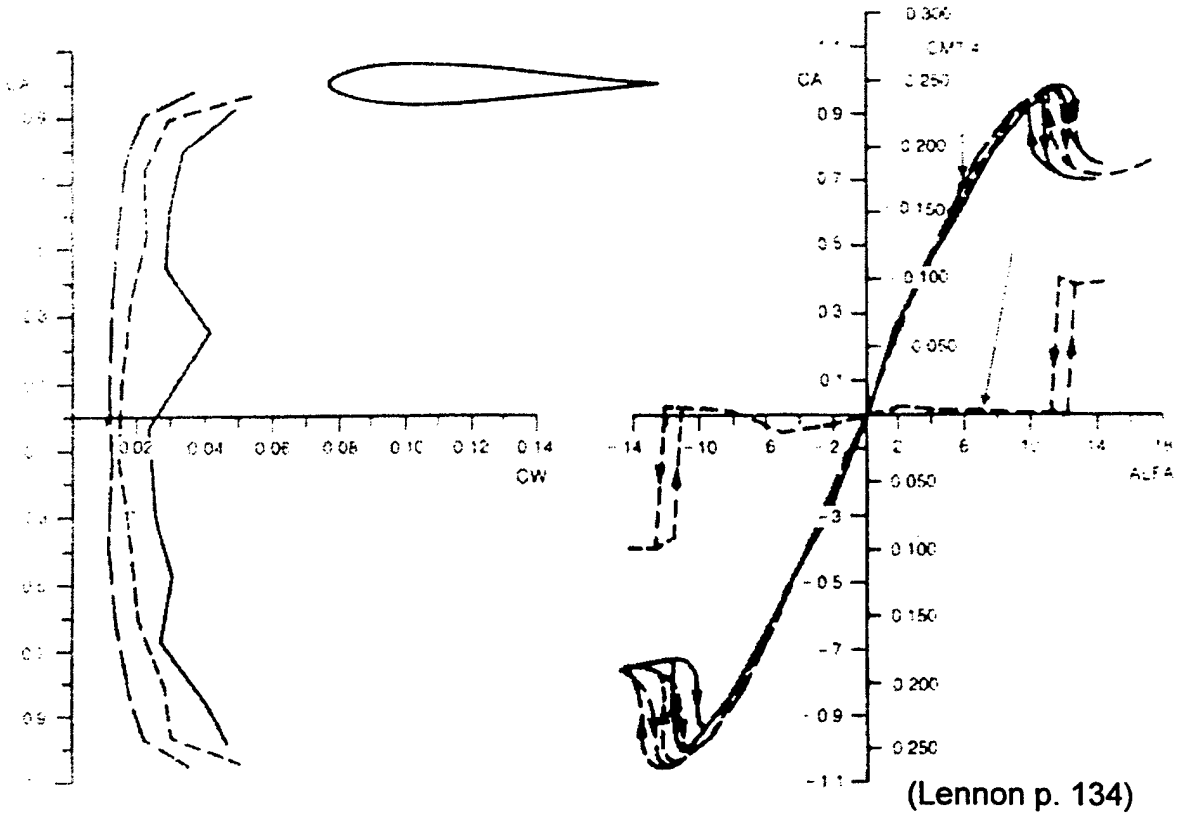

(Lennon p. 134)

4.2.2 Wing Planforms

For the different planforms, the wing is expected to exhibit different stall behavior, and different lift distributions in the spanwise direction. Unfortunately, the most efficient planforms are the most difficult to manufacture. The decision was made that manufacturing would be the major factor in determining the right planform, including wing sections, spars/ribs and building experience within the team.

Figure 4.3: Planforms, Area Distributions, Load Distributions, and Stall Characteristics

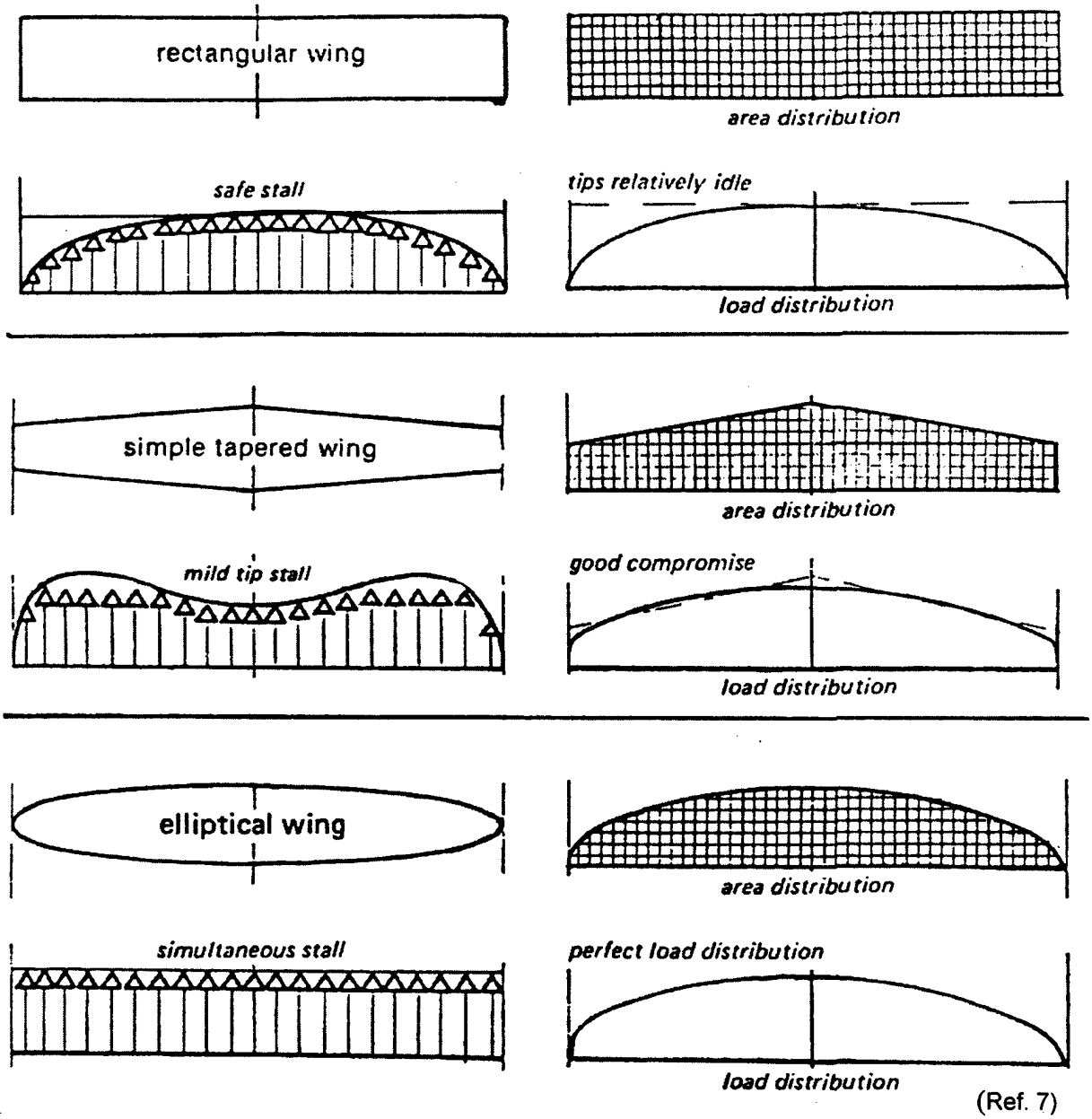

(Ref. 7)

4.2.2.1 Rectangular

The rectangular wing ("Hershey Bar") is the easiest to design and build because the chord remains constant along the span. This planform is well suited to low speed flight. However, relatively high induced drag is the main weakness of this planform. The major attraction for the Hershey bar wing is the ability to use one tool to form both wings. This dramatically reduces the time required to fabricate the aircraft.

4.2.2.2 Tapered

To simulate the benefits from the elliptical wing but without the level of difficulty with fabrication, a taper on the wing of about 45% can be designed along the span. This is used to some extent on most modern aircraft but for smaller aircraft (e.g. model r/c aircraft) the taper causes some problems with the tip chord being too thin, and would be inefficient at lower speeds. Because the downside of the taper for our purposes would equal more fabrication and inefficiency, the wing will not have any taper.

4.2.2.3 Elliptical

The elliptical planform is the ideal wing planform, because the induced drag is at a minimum and stalls occur evenly along the span. From a manufacturing standpoint, the elliptical wing is quite challenging. The tool would require two complex curves, both in the spanwise and thickness directions. Since simplicity of manufacture is a key factor in the decision, the elliptical wing will not be used.

4.2.2.4 NASA Safe Wing Feature

By adding this feature to the outboard third of the leading edge, research has shown that this will improve the stall/spin characteristics at high AoA (increasing by almost 10 degrees) by lowering the aspect ratio (AR) at the tip. When the root chord stalls, a cornered notch at the start of the drooped edge creates a vortex that separates the two areas and delays the stall. For manufacturing, the droop will be shaped from foam and will be bonded directly to the wing's surface. The NASA Safe Wing provides the advantages of washout, but with fewer performance penalties. The wing extension will be molded from foam, and bonded to the outboard wing panels.

Figure 4.4: NASA Safe Wing Schematic

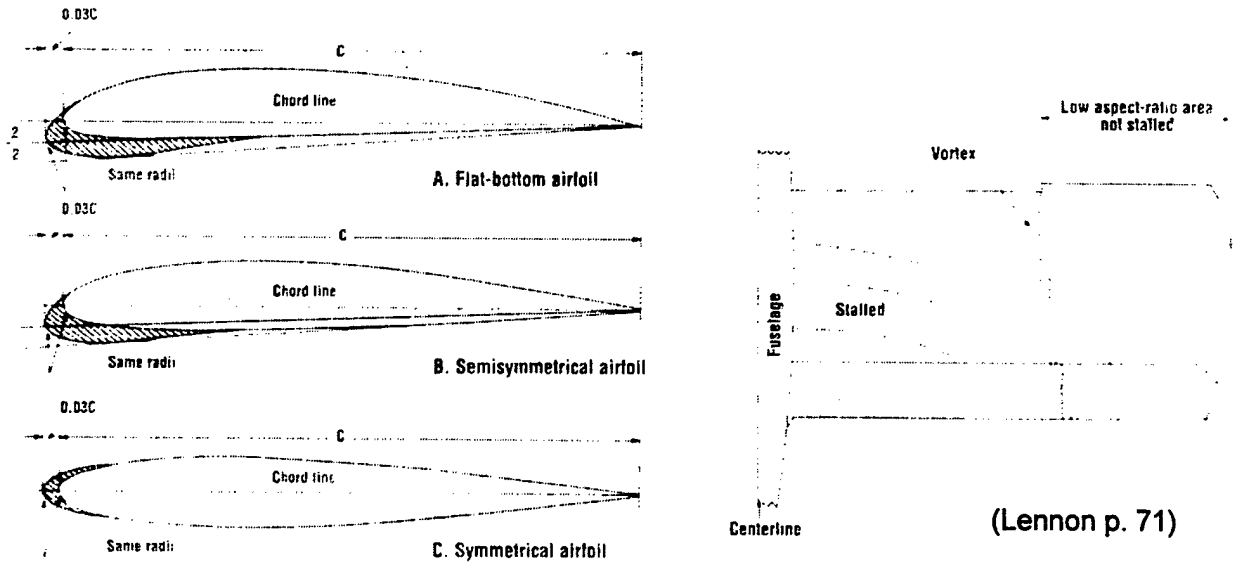

(Lennon p. 71)

4.2.3 Dimensions

	Item	Symbol	Value	Unit
Wing	Wing Span	B_w	84.0	in
	Wing Chord	C_w	15.0	in
	Wing Area	S_w	1260.0	in^2
H. Tail	Horizontal Tail Area	S_{ht}	225.1	in^2
	Horizontal Tail Root Chord	B_{ht}	22.0	in
	Horizontal Tail Tip Chord	C_{ht}	10.2	in
V. Tail	Vertical Tail Area	S_{vt}	100.8	in^2
	Vertical Tail Root Chord	B_{vt}	21.6	in
	Vertical Tail Tip Chord	C_{vt}	4.7	in
	Length of Aircraft	L	70.7	in
	Length of Fuselage Pod	L_{pod}	36.0	in

Table 4.3: Major Dimensions

4.2.4 Payload Configuration

The payload is retained by an L-shaped steel pin supported in the fuselage by two 1/8" aluminum ribs running between the wing spars. The pin is driven by a small servo motor. On top of the payload package, a 1/8" aluminum flange with a hole is installed. By retracting the pin and lifting the payload into the fuselage, the payload is supported by the extended pin. In order to prevent the payload from rocking inside the bay, open cell foam strips are located in the top of the payload bay. These strips are slightly compressed when the payload is fully stowed. The bottom surface of the payload forms the lower fuselage skin. When the payload is deployed, a spring-loaded door folds downward from the long edge of the bay, retaining aerodynamic performance without the payload element.

Figure 4.5: Payload Retention Mechanism

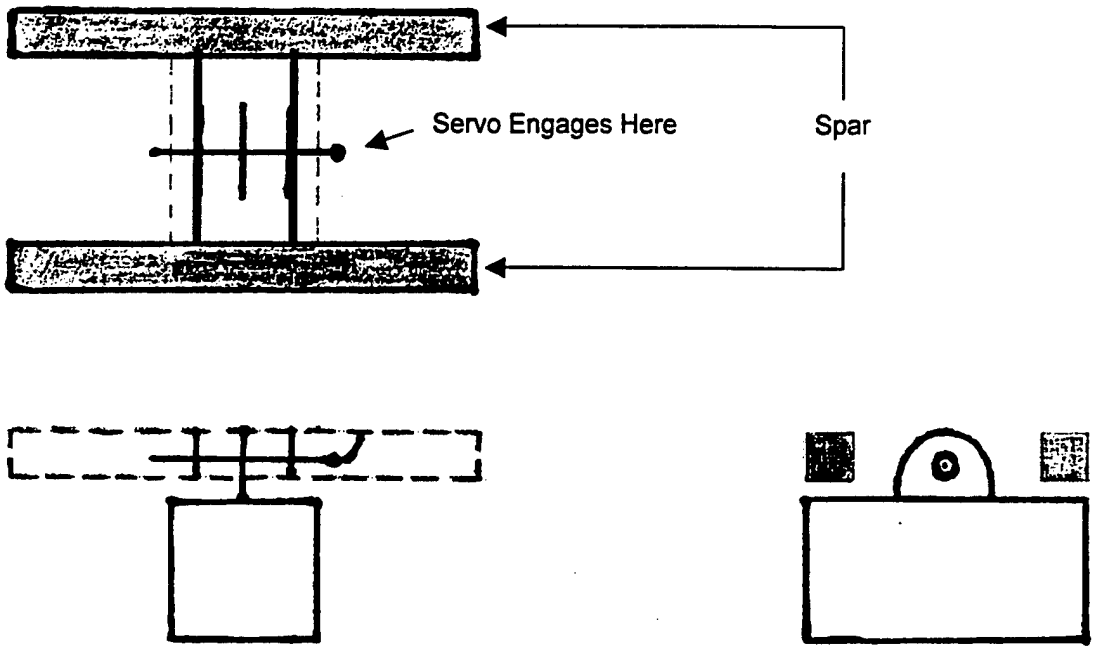

4.3 Preliminary Wing Loading

The wing loading is the primary factor in determining takeoff and landing performance. The requirement to stow the aircraft in the shipping container constrains both maximum allowable span and chord. With the preliminary weight estimate of 22lbs, a wing area of 8.75 ft^2 yields a wing loading of 2.51 lb/ft^2 (40.2 oz/ ft^2). See Table 4.1 for comparisons with other, similar aircraft.

4.4 Preliminary Power Loading

Because the motor vendors were constrained by the rules of the competition, and the team had opted to use one motor, the largest available electric motor was specified. The AstroFlight Cobalt 90 motor has a rated peak power of 1400 Watts, and a static thrust of greater than 6.25lb with a 24x12 propeller. For purposes of modeling the takeoff roll, the thrust was assumed to be constant.

4.5 Assumptions of the Preliminary Phase

- Cl and Cd of the 3-D wing are approximately equal to the values for the airfoil sections
- 6.25lbs constant thrust available from power system throughout takeoff roll
- 5lb battery pack desirable for takeoff power

5 Detailed Design Phase

5.1 Detailed Component Selection

5.1.1 Power System

The battery selected was the Sanyo RC-2400. The each cell measures 0.9" in diameter and 1.7" in height. Each cell weighs 2.0oz. After comparing the Nickel-Cadmium batteries that were commercially available, these cells had the highest power density. To fit within the 5lb battery pack constraint, 36 1.2V cells will generate a peak voltage of 43.2V. The motor is rated to turn at 93 RPM/V, for a peak of 4010 RPM (unloaded). The batteries were placed in the forward fuselage below the motor. In order to improve battery performance, the forward fuselage was equipped with a duct to capture prop wash air and route it between the batteries and the motor.

Figure 5.1: Battery Layout

5.2 Detailed Systems Architecture

5.2.1 Predicted Mission Performance

The primary performance requirement for all missions was determined to be the short take-off constraint. The team designed to a requirement of a 100ft take-off roll with no flaps. In order to estimate the take-off roll, the component buildup method (Raymer Ch. 12) was employed to calculate a parasitic drag coefficient for the airframe.

$C_{d0}=2.62*10^{-2}$

Knowing the parasitic drag coefficient, and estimating the wing lift coefficient, the drag on the airframe was calculated iteratively by considering a free body diagram. The Sizing Worksheet was used to perform numerical integration of the net force on the aircraft to determine acceleration, instantaneous velocity, and current position. Given the instantaneous velocity, the lift is calculated.

When the lift force (as a function of velocity) is calculated to be greater than the weight of the aircraft, the takeoff roll is finished and the aircraft is considered to be airborne. The estimated length of the takeoff roll using this method is 80 feet. The takeoff speed is estimated at 43ft/s.

5.2.2 Weight and Balance Worksheets

The weights and locations for all available components were tabulated. By summing the tail-down moments about the nose, the location of the CG was estimated. The location of the neutral point of the airframe was estimated at 35% of the wing chord. These estimates yield a static margin of 3", or 20% of the chord.

Component	CG distance from nose (in)	Weight (lb)	Moment (in-lb)
Motor	4	2.5	10
Battery Pack	8	5	40
Fuselage	18	3	54
Wing	24	2.5	60
Tail	64	1.5	96
Electronics	29	1.5	43.5
Landing gear	27	1	27
Total		17	330.5
CG	19.44		
NP (.35C)	22.50		

Table 5.1: Weight and Balance

5.2.3 Assumptions in the Performance Predictions

- 100oz constant thrust from motor
- Frictional coefficient of runway=0.03
- Cl constant during takeoff roll at 1.17 (maximum unflapped Cl from Eppler 197 airfoil)

5.3 Detailed Drawing package

Figure 5.2: Three-View Sketch

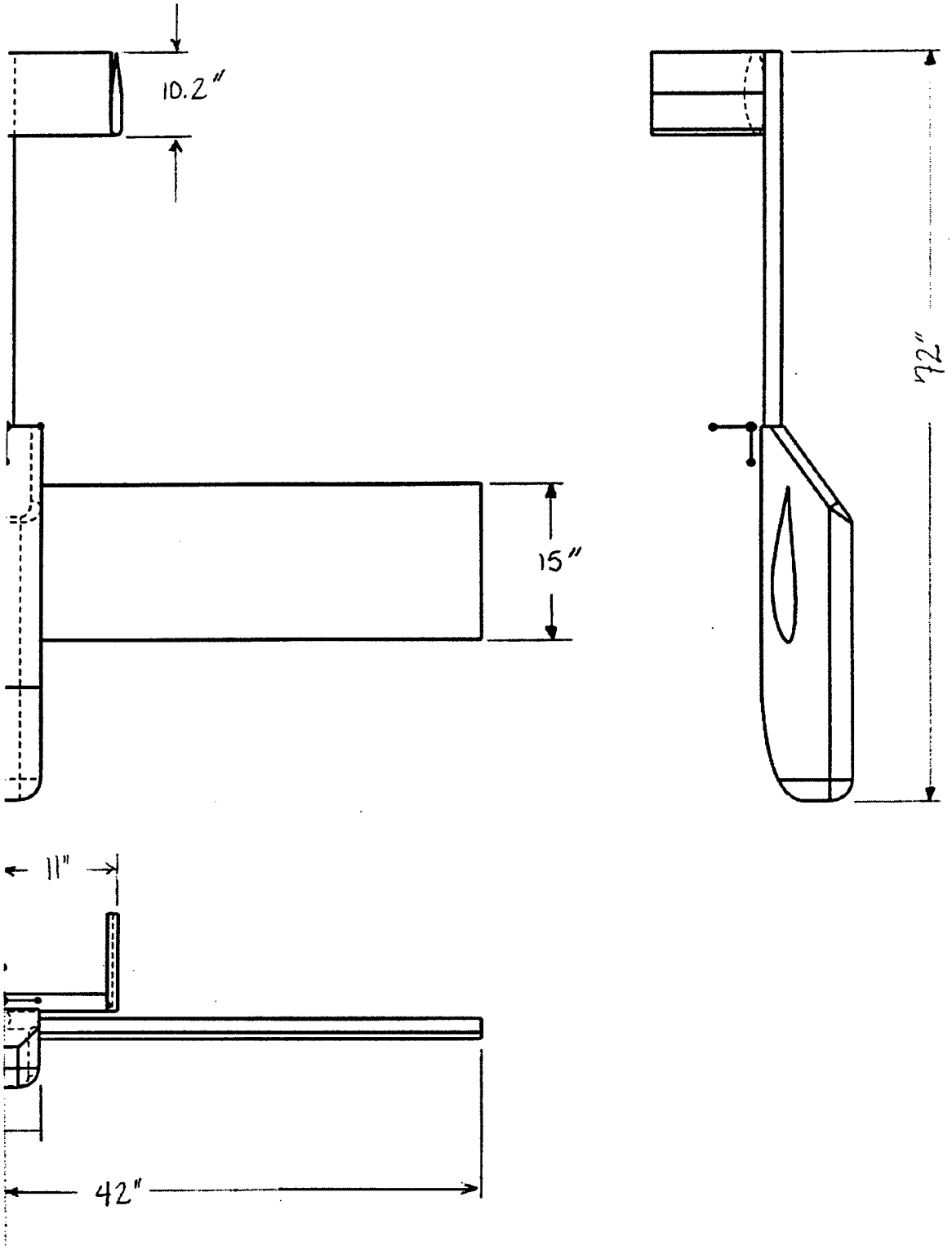

5.4 Rated Aircraft Cost Analysis

The RAC formula was programmed into the Microsoft Excel design spreadsheet. As various layouts and configurations were considered, it was a simple matter to evaluate the impact on RAC.

Since the RAC rewarded simplicity, all extraneous control surfaces and servos were discarded. Since the Futaba 6XAS radio selected for the competition had the facility to perform "mixing" of aileron and flap controls, it was decided that flaperons would be a low-cost way to dramatically improve the takeoff and landing performance of the aircraft. Because of the electronic mixing feature of the radio, each servo was attached to one flaperon, without requiring the design of a mechanical mixing device.

By specifying high-torque servos for the flaperons, only one servo was required for each surface, for a total of five servos (including one to actuate the payload release). Although the selection of the H-tail configuration requires two rudders, this was regarded as an acceptable trade-off (the addition of one control surface) relative to the benefit of moving the rudders far from the wake of the AWACS antenna.

Although the battery weight is penalized twice in the RAC calculation, the team determined that maximum power would be required in order to take off in the allotted 120ft. During flight test, a lighter battery pack will be installed to see whether additional weight savings can be realized and maintain short-field capability. At the end of the conceptual design phase, the RAC was calculated to be $13,300.

		Multiplier	Hrs	Extension
	Empty Weight	$100.00	17	$1,700.00
	Rated Motor Power	$1,500.00	5	$7,500.00
	Manufacturing Cost	$20.00	201	$4,017.84
	RAC=			**$13,217.84**
	Battery Weight (lbs)	5		
		Hrs/Item	**# Items**	**Extension**
WBS Detail	Span	8	7	56.00
	Chord	8	1.25	10.00
	Control Surfaces	3	2	6.00
	Wing Subtotal:			72.00
	Fuselage Length	10	5.89	58.89
	Vertical Surface	10	2	20.00
	Horizontal Surface	10	1	10.00
	Tail Subtotal:			30.00
	Flight Systems	5	6	30.00
	Motors	5	1	5.00
	Propellers	5	1	5.00
	Propulsion Subtotal:			10.00
	TOTAL HOURS=			200.89

Table 5.2: Rated Aircraft Cost

6 Manufacturing Plan and Process

6.1 Manufacture Process and Selection of Materials

6.1.1 Composite Construction

The aerospace industry has long enjoyed the benefits of carbon fiber composite construction. Carbon fiber is particularly well suited to stressed skin (monocoque) construction methods. Its high strength-to-weight ratio makes it a good choice for wing spars even on airframes constructed from other materials.

6.1.2 Wood Construction

This is the classic method for constructing model aircraft. Thin ribs of balsa wood are cut into the cross-sectional shapes of the wing and fuselage, and glued together onto structural spars. By adding thin balsa stringers perpendicular to the ribs, the fuselage and wing shapes are formed. The resulting wire-frame structure is sheeted in balsa wood and wrapped with a thin tissue paper or plastic material to form a smooth surface.

6.1.3 Foam Core Construction

In the model aircraft community, foam shapes formed by cutting blocks with a heated wire are a common structural component, particularly for airfoil sections. Foam cores are typically wrapped in a thin ply of balsa, fiberglass, or carbon fiber for additional strength and rigidity.

6.2 Manufacturing Figures of Merit

Item	Weight	Carbon	Balsa/Foamcore	Balsa Stringer/Rib
Real Cost	20%	14%	14%	16%
Weight	25%	25%	18%	18%
Manufacture	25%	15%	20%	20%
Educational Value	10%	10%	8%	7%
Available Expertise	20%	16%	16%	18%
Total:	**100%**	**80%**	**76%**	**79%**

Table 6.1: Manufacturing Figures of Merit

6.3 Selection of Processes for Major Components and Assemblies

With unlimited budget and manufacturing time, fabricating the entire aircraft from carbon fiber would be ideal. With the exception of the tail, this was the selection made by the team. For the major structural elements (wing, fuselage, tail boom), carbon fiber's light weight and high strength made it a very attractive option. The team also selected carbon fiber as a learning exercise, as it was perceived that experience with carbon fiber layup would be a valuable job skill.

In order to simplify construction, the vertical and horizontal tail elements were formed from hot-wired foam. Balsa and carbon fiber reinforcement on the horizontal stabilizer will provide the structural rigidity necessary to mount the vertical tails.

7 Testing Plan

In order to have successful predictable flights, lots of flight-testing is involved both statically and dynamically. The following section will describe the group's intentions from testing. Before the team can confidently take the aircraft to compete it has to satisfy our own requirements.

7.1 Testing Objectives

The objectives we hope to meet at flight-testing are those set in the RFP. These include, but are limited to, the following:

- Takeoff Distance (100 feet)
- Payload Deployment
- Takeoff w/Payload
- Takeoff w/Payload and AWACS
- AWACS Performance
- 360° Turning
- Estimate Good Turning Radius
- Time Trial
- Assembly Time
- Measure Top Speed
- Tail – Size and Incidence

7.2 Test Schedule

The aircraft is currently in production. Materials testing began mid-February and structural integrity testing begins at the latter part of March. Flight-testing is currently scheduled for the beginning of April and lasts until the competition.

7.3 Test Flight Checklist

A testing checklist is required for each flight (completed or attempted). The checklist will serve as a logbook page for future reference and will be available at the competition. The pilot and crew chief are required to sign on each checklist after test. If a line item isn't checked, the flight will be postponed until corrective action is taken.

Testing Checklist

Pre- Flight

Crew Chief: _____

- [ ] Radio Checks
- [ ] Check for Loose Parts
- [ ] Install Fuse
- [ ] Payload
- [ ] Control Surfaces
- [ ] Secure Assembly
- [ ] Clear Obstructions/Debris from Runway

Pilot: _____

Date: _____

In-flight

- [ ] Radio Check
- [ ] Control Surfaces
- [ ] Time Checks
- [ ] Maneuverability

Post- Flight

- [ ] Pull Fuse
- [ ] Check for Loose Parts
- [ ] Stress/Fracture Analysis
- [ ] Payload Release

Time: _____ (mins/sec)

Takeoff Distance: _____ (ft)

Top Speed: _____ (ft/s)

Assembly Time: _____ (secs)

Weather Conditions: _____

Mission:

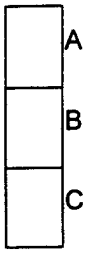

Comments: _____

_____

_____

_____

_____

7.4 Results and Lessons Learned

Our results are fairly limited, as no significant testing has occurred. Our only results are hypothetical as of now and are represented in our data analysis worksheet. The lessons learned have been to order parts early, solicit industry for donations and expertise early, and although designs may change throughout the project keep focused and remind the team of the common goal and philosophy.

8 References

1. Raymer, Daniel P., Aircraft Design: A Conceptual Approach, 3rd Edition, American Institute of Aeronautics and Astronautics, Inc., Reston, VA, 1999.
2. Anderson, John D., Jr., Fundamentals of Aerodynamics, 3rd Edition, McGraw Hill, New York, NY, 2001.
3. Etkin, Bernard & Reid, Lloyd D., Dynamics of Flight, Stability and Control, 3rd Edition, John Wiley & Sons, Inc., New York, NY, 1996.
4. Hibbeler, R. C., Mechanics of Materials, 3rd Edition, Prentice Hall, Upper Saddle River, NJ, 1997.
5. Lund, Thomas S., Lifting Line Program, The University of Texas at Arlington, Arlington, TX. Compiled 2001.
6. Lennon, Andy, Basics of RC Model Aircraft Design, Motorbooks International, 1996.
7. Simmons, Martin, Model Aircraft Aerodynamics, Transatlantic Publications, Philadelphia, PA, 1999.
8. Aircraft Design, http://www.dpa.unina.it/adag/eng/aircraft-design.htm, accessed 3-2003

9 Appendices

9.1 Nomenclature

Cd – drag coefficient

Cl – lift coefficient

BWB - Blended Wing Body

AWACS – Airborne Warning and Control System

RFP – Request for Proposal

RAC – Rated Aircraft Cost

AoA – Angle of Attack

CG – Center of Gravity

NP – Neutral Point

9.2 Sizing Worksheet Details

The Sizing Worksheet allowed rapid comparison of different configurations.

CVT and CHT are selected according to historical data found in Raymer Table 6.4. The values chosen reflect those of a homebuilt aircraft, which the team evaluated as having the most similar construction method to this design. The tail areas were compared to a similar analysis method found in Lennon, and the results were similar. Lvt and Lht are the distance between the quarter chord point of the wing, and the quarter chord points of the vertical and horizontal tails respectively.

Wing Area: $S_{ref} = b_w c_w$

Vertical Tail Area: $S_{vt} = \frac{CVT * b_w * S_{ref}}{L_{vt}}$ (Raymer Eq. 6.28)

Horizontal Tail Area: $S_{ht} = \frac{CHT * c_w * S_{ref}}{L_{ht}}$ (Raymer Eq. 6.29)

Tail Chords (Vertical and Horizontal): $c = \frac{S}{b}$

Turkish Air Force Academy

2003 AIAA Foundation
Cessna/ONR Student Design Build Fly Competition

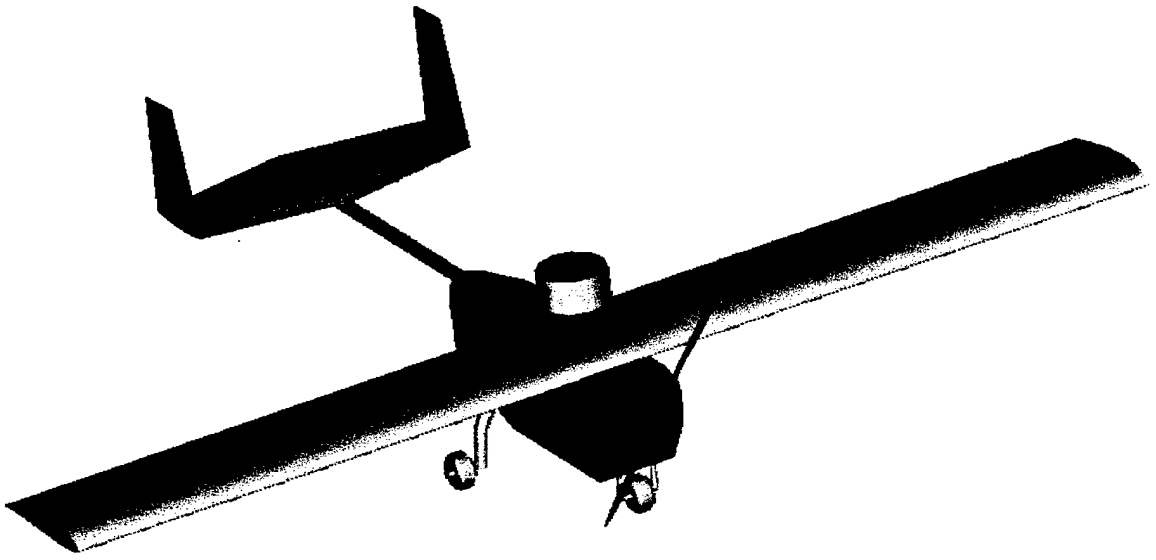

Haberci Aircraft Design Report

Table of Contents

1. Executive Summary 1
    1.1. Conceptual Design 1
        1.1.1. Design Alternatives 1
        1.1.2. Conceptual Design Results 2
    1.2. Preliminary Design 2
        1.2.1. Preliminary Design Alternatives 2
        1.2.2. Preliminary Design Results 2
    1.3. Detail Design 3
        1.3.1. Design Alternatives 3
        1.3.2. Detail Design Results 3
2. Management Summary 4
3. Conceptual Design 8
    3.1. Statement of Problem 8
    3.2. Quantitative Design Parameters 9
    3.3. Special Case: Antenna 13
        3.3.1. Theoretical Studies 13
        3.3.2. Flight Test 14
        3.3.3. Results 15
    3.4. Qualitative Analysis of Design Parameters 15
        3.4.1. Wing Configuration 16
        3.4.2. Wing Planform 17
        3.4.3. Fuselage Configuration 18
        3.4.4. Empennage Configuration 19
        3.4.5. Power Plant 20
        3.4.6. Landing Gear 21
    3.5. Configuration Selection 22
4. Preliminary Design 25
    4.1. Propulsion System Selection 25
        4.1.1. Motor Selection 25
        4.1.2. Battery Selection 27
        4.1.3. Propeller Selection 28
    4.2. Mission Selection, Performance Analysis 30
    4.3. Sizing Trades Investigated 33
        4.3.1. Airfoil Selection 33
        4.3.2. Wing 34
        4.3.3. Fuselage 34
        4.3.4. Empennage 37
        4.3.5. Landing Gear 37

4.4. Structure Analysis 38
4.4.1. Component Attachment and Integration 38
4.4.2. Assembly Firmness Analyses 38
4.5. Stability Analysis and Handling Qualities 39
4.8. Analysis Methods Used 41
5. Detail Design 41
5.1. Component and Systems Architecture Selection 41
5.1.1. Control Surfaces Sizing 41
5.1.2. Propulsive Considerations 42
5.1.2.1. Battery Durability 42
5.1.2.2. Motor Efficiency in Producing Required Output Power 42
5.1.2.3. Propeller Efficiency in Converting Shaft Power into Thrust 42
5.1.3. Structural Refinements 43
5.1.3.1. Wing 43
5.1.3.2. Tail Boom 44
5.1.3.3. Fuselage 45
5.1.3.3. Empennage 45
5.1.3.4. Landing Gear 46
5.2. Weight and Balance 46
5.3. Rated Aircraft Cost 47
5.4. Design Summary 47
5.5. Drawing Package 48
6. Manufacturing Plan and Processes 54
6.1. Manufacturing Processes Investigated and FOM 55
6.2. Results 56
6.3. Overview of the Actual Manufacturing Progress 56
6.4. Assembly Strategy 56
7. Testing Plan 58
7.1. Testing Objectives 58
7.2. Testing Schedules and Check-lists 58
7.2.1. Preflight Testing 58
7.2.1.1. Static Testing 58
7.2.1.2. Dynamic Testing 58
7.2.2. Flight Testing 59
7.3. Testing Results and Lessons Learned 59
8. References 60

Table of Figures

Figure 2.1. Timetable for design of Haberci aircraft 5
Figure 2.2. Personnel assignments 6
Figure 3.1. Design parameters' affect on score 11
Figure 3.2. Drag coefficient of a circular cylinder with its axis normal to the stream 13
Figure 3.3. Tested model aircraft and safety mechanism of the antenna 14
Figure 3.4. Alternative fuselage configurations 18
Figure 3.5. Alternative tail arrangements 19
Figure 3.6. Alternative aircraft configurations 24
Figure 4.1. Thrust, speed and current change with pitch of the propeller 30
Figure 4.2. Drag change with velocity 31
Figure 4.3. Coefficient of lift vs. coefficient of drag polar graph 34
Figure 4.4. Side view of the fuselage 35
Figure 4.5. Pitching moment contributions of components 40
Figure 5.1. Propulsive performance analyses results 43
Figure 5.2. Stress distribution according to Von misses criteria 44
Figure 5.3. Stress distribution according to Von misses criteria 44
Figure 5.4. W&B diagram 47
Figure 5.5. Poster reflecting all inclusive data about Haberci aircraft 48
Figure 6.1. Manufacturing milestone chart 57
Figure 7.1. The checklist allowed to examine the activities applied 59

Table of Tables

Table 2.1. Architecture of the design team 4
Table 3.1. Design parameters, figures of merit and configuration selection 24
Table 4.1. The best applicable choice of gear ratio for each motor 26
Table 4.2. Alternative motors' comparison 27
Table 4.3. Battery comparison 28
Table 4.4. Estimated aircraft performance 32
Table 4.5. Estimated completion times for each mission 33
Table 4.6. Static Stability derivatives 40
Table 5.1. Battery milliamp consumption for each segment of missions 42
Table 5.2. Weight Breakup 46
Table 5.3. RAC 47
Table 6.1. FOM were used to screen alternative manufacturing processes' advantages 55

1. EXECUTIVE SUMMARY

The AIAA Foundation annually arranges Cessna/ONR Student Design/Build/Fly Competition. The contest provides a real-world aircraft design experience for engineering students by giving them the opportunity to validate their analytic studies.

A student team in Turkish Air Force Academy, **Haberci** team, came together to accomplish the mission of designing and fabricating an unmanned, electric powered, radio controlled aircraft to compete in 2003 DBF competition. The aircraft should meet the specified mission profile while demonstrating the flight capabilities of a balanced design providing a high vehicle performance.

A variety of constraints were updated each of which received consideration during the entire design process. The major design constraints are as follows: the airplane is required to takeoff within 120 feet, the battery weight cannot exceed five pounds, team must select two missions out of three alternatives, payload for each mission is a box 6 inches wide by 6 inches tall by 12 inches long to weigh at least 5 lb. and aircraft must fit in a 2 foot wide by 1 foot high by 4 foot long box.

The missions include Missile Decoy, Sensor Deployment and Communications Repeater. In Missile Decoy mission, the aircraft must have a simulated cylindrical antenna, "6-inch" pipe by three inches tall, with the top and bottom sealed flush with flat plywood sheets. In Sensor Deployment mission the aircraft must self-deploy the simulated sensor package after two designated sorties. In Communications Repeater mission, the aircraft must carry simulated communications relay device. Designated course for this mission include three 360° turns in the direction opposite of the base for each lap. Each mission is assigned with a difficulty factor, which will affect the flight score.

The aircraft must be removed from the defined box that it will fit in, and assembled to flight ready condition by the ground crew before the competition. The assembly time will be added to flight time.

The score is a function of Written Report Score, Total Flight Score and Rated Aircraft Cost. Total flight score is the sum of the best Single Flight Scores from each of 2 different mission types.

Below is presented the summary of the design phases, alternatives and the development of the final design.

1.1 Conceptual Design

Because the design requirements and performance objectives are updated, a succinct depiction of the problem was the first thing to be done. Description of the key elements of the mission requirements were made, specifically, the limits of the "scope" of the effort was drawn in order to use the limited time efficiently. As the problems were defined, the aircraft's performance objectives were evaluated. Team wrote a Microsoft Visual Basic program to define quantitative design parameters' impact on the overall score. This helped the team to eliminate low scoring potential mission out of three choices and enabled rapid generation of alternative concepts. In order to arrive at empirical relations applicable to Missile Decoy mission, a flight test was held. Then qualitative analysis of the design parameters were made in order to narrow down the design alternatives to a certain limit and nine competing design options were re-evaluated and considerations continued until an aircraft, which met the design constraints, arose with a high scoring potential.

1.1.1 Design Alternatives: In Conceptual Design phase, the design team investigated several possible airplane configurations. The alternatives covered six major areas: wing configuration, wing

planform, fuselage shape, empennage configuration, landing gear configuration and power plant. There were four wing configurations considered that are mono-wing, bi-wing, flying-wing and wings in tandem configurations each of which has its own advantages and disadvantages. Considered wing planform alternatives during prescreening process were elliptical, rectangular, moderate tapered and high tapered planforms. The team generated six types of shapes for fuselage by taking into consideration the basis of structure and aerodynamics. Seven empennage types, ranging from conventional type to canard configuration, were considered to stabilize the aircraft efficiently. Three types of landing gear configurations were evaluated in conceptual design: fixed tricycle, retractable tricycle and tail dragger from all aspects. The team also examined four types of motor installation on the aircraft that were single tractor, single pusher, twin tractor and twin pusher types.

1.1.2 Conceptual Design Results: Initially defined qualitative design parameters narrowed down the configuration alternatives to nine competing concepts. Discriminating figures of merit were determined reflecting aircraft's scoring-potential from all aspects: complexity, aerodynamic and propulsive efficiency, assembly ease, effective volume usage and safety. Defined figures of merit enabled selection of the best choice: a high mono wing with single tractor motor, H tail with single boom and tricycle landing gear configuration. DBF-03 program was utilized and some performance ranges were derived. Weighing around 18 pounds, the aircraft would fly with a cruise speed of 38 mph to 48 mph. Wing loading value was predicted to range between 28 and 34 oz/ft^2. Alternative missions were AB or AC missions. Selection of the mission types from 2 remaining alternatives was left to be the study of preliminary design phase.

1.2 Preliminary Design

Preliminary design phase started as soon as conceptual design resulted with aircraft configuration determination. In this phase, selected configuration was optimized via enhanced DBF-03 program with analytical and numerical models. Design parameters were defined and propulsion system selection was initially held in order to generate mission performance models for AB and AC missions. Aerodynamic and propulsive parameters demonstrated that the best score for determined aircraft configuration and performance objectives was obtainable with AB mission selection. Then sizing trades were investigated for wing, fuselage, empennage and landing gear. Special cases, that were deployment system, components attachment and integration, payload and propulsion system access and assembly problem, were considered in structures analysis. Stability of the aircraft was then investigated. These studies resulted in optimization of the final aircraft dimensions and performance.

1.2.1 Preliminary Design Alternatives: All alternative motor, battery and propeller combinations were analyzed bearing in mind the initially determined performance parameters. After analyzing design parameters for motor, Figures of Merit were determined in order to find the right propulsion package. Determining the motor type, battery type and number and propeller geometry and material, attachment alternatives to fit the aircraft in defined box, alternative mechanical systems to deploy to payload, assembly styles and alternative structures were considered. Also one of the most important parts of the contest, mission selection, was finalized in this phase.

1.2.2 Preliminary Design Results: Studies revealed the geometry of the aircraft and this formed the basis for material selection in detail design. Propulsion and aerodynamic studies were conducted and

their combination finalized the mission performance of the aircraft. Predicted score for Haberci aircraft to compete in A and B missions was found to be 6.297. Mechanical systems to suffice mission requirements were designed with minimum weight and maximum simplicity. After stability of the aircraft was determined, everything to conduct detail analyses of aircraft was prepared.

1.3 Detail Design

Initially carried out work in detail design was to size the control and lifting surfaces. Then, knowing the geometry and performance of the design, propulsive and aerodynamic considerations were concluded. Required refinements were made and material considerations for each component was carried out considering the strength of alternatives. Detailed analysis of structure was conducted and structural refinements were made. Weight and balance of the design was then investigated. Freezing the design at that point, design summary was made and detailed structural, dimensional and propulsive drawing package was prepared.

1.3.1 Design Alternatives: As more approximate weight of the airframe was predicted, balance of the aircraft was maintained with alternative placements of mechanical systems and electronic equipment placement. Control system of the aircraft was then scrutinized. Overall design geometry, performance and control summary was made and detailed drawings were generated. Strength of materials was analyzed by modeling the aircraft in ANSYS program and structurally critical parts' refinements were made. Basic production of the aircraft was then considered and basis for manufacturing of the aircraft was formed.

1.3.2 Detail Design Results: Detailed design's result was an optimized aircraft from both aerodynamic and propulsive aspects. Primary sizing trades were conducted in preliminary phase and detail design phase caused refinements in basic components of the aircraft. By conducting detailed sizing trades and structural analysis, the design was finalized and materials to produce the major components of the aircraft were determined.

2. MANAGEMENT SUMMARY

Past year's senior DBF contest attendees made an appointment to familiarize the aeronautical and electronics engineering students with DBF contest before the graduation. Seven desirous cadets met after that meeting in order to attend this year's DBF contest in name of Turkish Air Force Academy. The team is formed of four senior aeronautical engineering students, one junior electronic engineering student, one junior and one sophomore aeronautical engineering student.

Not long after the project was initiated and timetable was prepared, it was realized that to compete the task in projected time, the team had to be well organized and be composed of dynamic groups. And in order to maintain the dynamism with rather small number of attendees, it was determined that tasks should have been delegated to individuals rather than groups. This would enable rapid proceeding in design phases and the control mechanism for individuals was maintained at weekly appointments, held on every Sunday. Design process had not begun until every member of the team got more familiar with design concept and this process continued after the contest rules were released, until November of 2002. Conceptual design was carried out by all the team members' participation and entrusting everyone voluntarily with a special part of the design. Every member investigated the design from all aspects however each member controlled concepts from their entrusted aspect. Because Conceptual Design is rather group work, a diversity of ideas was required and this was maintained with all members' equal attendance. This gathered everyone's focus on the design and all team members contributed with different creative ideas to various sides of design. This part of the effort was commonly carried out in meetings and these meetings were generally concluded with different ideas conflicts. Conflicts resulted in more analysis to be conducted and problem solutions led the optimized concept design. As team proceeded to Preliminary Design, jobs became more specific. All team members got familiarized with all aspect of phases of design and efficiently contributed to basic formation of the aircraft. In the beginning of preliminary phase, the entrustment was more efficiently rearranged. As structure-based courses are taken before 4^{th} grade, underclassmen efficiently participated in all design phases.

Haberci team was divided into 5 sub-groups: Aerodynamics, Structures, Performance and Optimization, Propulsion and Stability and Control (Table 2.1).

Every member participated in at least two groups and this enabled easier control of tasks. Task were delivered to groups however members equally shared the tasks and after each member finished his own task, he represented it to the sub-group and after the task was put in order, it was represented at weekly meetings to all group.

Project Manager: Okan Arslan				
Aerodynamics	**Structures**	**Propulsion**	**Performance & Optimization**	**Stability & Control**
Çağlar Utku Güler	Serkan Çalışkan	Okan Arslan	Okan Arslan	Şükrü Muştu
Şükrü Muştu	Erkan Benli	Erkan Benli	Serkan Çalışkan	Çağlar Utku Güler
Okan Arslan	Aytuğ Akkor	Barış Süzen	Aytuğ Akkor	
	Barış Süzen			

Table 2.1 Architecture of the Design Team

In these meetings, every member represented his finished task. Overall situation of the design was discussed and the new tasks for the next meeting were arranged. These meetings became so useful for following the overall state of design. Notes from all finished tasks were taken in these meetings and these notes became invaluable sources in report preparation. Report preparation was given a lot of importance and started with the first meeting. Report preparation work was carried out as team progressed through phases of the design and the report for each phase was prepared as team progressed into next phase. So there happened to be no difficulty in report preparation. Each sub-group's responsibilities are as follows:

Aerodynamics Group: Focusing on especially wing and antenna analysis, group was responsible of maximizing all components' aerodynamic performances. Their tasks generally required analytical studies. For especially antenna study, they have made an extensive search via Internet and library. Most of the effort was spent for airfoil selection for wing and tail. And further in design, group made sizing for control and lifting surfaces. Their studies formed the basis for performance studies.

Structures Group: Group generally participated in sizing all components of the aircraft except wing and empennage. Group was also in charge of landing gear, which is a critic part of the aircraft. In conceptual design they have made basic sizing trades for all alternative configurations and defined RAC for each concept. Further in design phases, they have made analysis of all components' structural endurances and have participated in testing of the aircraft. They analyzed most important parts of selected missions that are Component Attachment and Integration, Material Selection and Aircraft Assembly and Disassembly. Their main effort, as the design progressed, was these three main jobs.

Performance and Optimization Group: Group initiated the design by examining the rules and made a brief summary of possible problems that team could face in design phases. Then they have made elimination of one mission out of three choices by writing the program, DBF-03, to make performance analysis of three missions. Group determined figures of merit and they were responsible for configuration selection. They always worked in cooperation with propulsion and aerodynamic groups. This group enhanced the program in further phases of design and provided optimization between aerodynamic and propulsive aspects.

Propulsion Group: Propulsion group's main job was to define the proper motor-battery-propeller package. Beside analytical studies, they have extensively utilized Internet. Determination of power requirement depended upon thrust need. So they speeded up their studies after aerodynamics group finished the task of antenna thrust requirement. Basic types of motor locations were studied in conceptual design and further in studies, efficiency was the main concept that they have tried to maximize.

Stability and Control Group: As stability and control courses are taken in last term of school, the group had not taken these courses when they have started the project. So analytical studies took most of their time. Since basic geometries of the aircraft is needed for examining the stability of the aircraft, they have caught up with the team in late times of preliminary design and made the basic stability and control calculations. Their calculations resulted in optimized tail geometry determination and their study resulted in reconsideration and rearrangement of design.

Figure 2.1 Timetable for design of Haberci aircraft. Blue bars represent projected time and red bars show the actual time. Diamonds symbolize the major milestones.

	Okan	Şükrü	Çağlar	Serkan	Erkan	Aytuğ	Barış
Conceptual Design							
Quantitative Design Parameters	X	X	X	X	X	X	X
Qualitative Analysis of Design Parameters	X	X	X	X	X	X	X
Configuration Selection	X	X		X	X		
Preliminary Design							
Propulsion System Selection	X				X		X
Performance Analysis	X			X		X	
Sizing Trades		X	X			X	
Structure Analysis				X	X	X	X
Stability and Control		X	X				
Control System	X	X	X			X	
Detail Design							
Component and Systems Architecture Selection				X	X		X
Conrol Surfaces Sizing		X	X				
Propulsive Considerations	X				X		X
Structural Refinements					X		X
Drawing Package	X	X		X		X	X
Manufacturing Plan and Processes							
Manufacturing Processes Investigation	X			X	X		
Actual Manufacturing Process	X	X	X	X	X	X	X
Testing Plan							
Preflight Testing	X		X	X	X	X	
Flight Testing			X	X	X		
Documantation							
Report Preparation	X	X	X	X	X		
Executive Correspondence	X		X				

Figure 2.2. Personnel Assignments. "X" stands for participation in that section of design phase.

3. CONCEPTUAL DESIGN

Conceptual design phase is composed of 4 stages. First stage was an overview of the problem. As the problems were defined, quantitative design parameters' impact on the score was evaluated. This helped the team to eliminate low scoring potential mission and enabled rapid generation of alternative concepts. In third stage, qualitative design parameters were studied. Nine competing design concepts out of this study were re-evaluated based on selected figures of merit in fourth stage. Considerations continued until an aircraft, which met the design constraints, arose with a high scoring potential.

3.1. Statement of Problem

This part of the report contains a broad description of the mission requirements. Detailed mission characteristics should have been studied in order to supply discriminating information on each mission's individual requirements. Because statement of the problem formed half way to solution, team had to focus on the constraints in deep. This section of the report outlines the general problems that team would most probably encounter in design phases.

The score is a function of written report score, total flight score and rated aircraft cost. In order to maximize the score, RAC should be as low as possible while maintaining enough performance to complete the designated missions within least possible time. There are 3 types of mission alternatives two of which must be selected. The payload for all three alternatives of missions is a box 6 inches wide by 6 inches tall by 12 inches long and must weigh at least 5 lbs. In all missions, aircraft must complete 4 laps. And on all laps flown in A and B missions, the aircraft must complete a 360° turn in the direction opposite of the base and final turns on the downwind leg of each lap. In C mission the number of 360° turns is three. These missions are as follows:

A Missile Decoy – Difficulty Factor 2.0: A type of mission included an antenna, 6-inch diameter pipe with three inches tall, to be carried throughout the mission. The antenna must be completely exposed on the exterior of the aircraft and standoff from the nearest airframe structure by a minimum of 3 inches. The antenna may not be faired in any manner. Aircrafts that carry antenna were studied. Antenna placements were either over the fuselage or on the vertical tail. However the requirements pertaining the antenna forced the configuration to place the antenna either on or below the fuselage. Placing the antenna below the fuselage would lengthen the landing gear and aircraft's fitting in transportation box would be more difficult with this configuration. Below placement option could be better than above placement however analyses to stabilize this configuration would require more than theoretical studies. Evidently, testing would be mandatory in either wind tunnel or by prototype manufacturing. Studies in conceptual design showed that most influential possible advantage of placing the antenna below would be to prevent stall tendency of the aircraft by causing pitch down moment. Considering the history of aviation, generally this kind of surfaces is not placed below. So, for the ease of design, this configuration is not considered and if A mission would be selected, the only option to place the antenna would be above.

Antenna would have a mass and more importantly this unmodified section of PVC pipe would drastically increase pressure drag due to flow separation, which is a major factor in aerodynamic efficiency of the aircraft. Also moment, it creates, and horizontal placement should be analysis

concern. If not properly placed power need would increase. Here the question arose "How could the drag, that the antenna would cause, be determined?" and special effort is spent to cover this question.

B Sensor Deployment – Difficulty Factor 1.5: In B type of mission, aircraft must take-off, complete 2 laps, and land. When on the runway and stopped the aircraft will self-deploy the simulated sensor package. The aircraft will then take-off and complete 2 additional laps and land.

B type of mission required a self-deployment mechanism that would increase takeoff gross weight. This mechanism would depend upon extra servos, which is a factor in RAC calculation. Also this type of mission's effect on the total flight time was one of the major concern as this mission required a "deployment on ground" segment which would demand one more takeoff and landing times to complete the mission. Deployment mechanism should be such that the aircraft gets the package on ground immediately and takes off as soon as possible. Obviously this would cause an increase in total flight time consequently a decrease in total flight score. Difficulty factor of this mission could eliminate the deficiency of flight time. So detailed quantitative analysis should be made in order to determine the positive or negative aspects of this mission.

C Communications Repeater – Difficulty Factor 1.0: C type mission required high turn and roll rates as this mission included three 360° turns on each lap.

Two of the three alternative missions should be selected. So designing the aircraft, possessing a high performance of a single mission and not completing other missions, seemed to be an probable problem and integrity of an aircraft, competing in a mission, to one another mission was determined to be a study concern too. For example if A and C missions were selected then the aircraft must be able to fly the designated course both with and without the antenna.

Next thing to be defined was the assembly problem. The aircraft should be such that it could both fit in the aforementioned box and establish enough structural strength to stand the forces in flight as well. Volume of the aircraft should be kept minimum. Hence team should have determined if aircraft needed to fold to fit in the box or not. This would also lead to an integrity styles examination. Among the styles best one should be selected for the determined aircraft configuration.

Another thing to be defined was the fact that past competitors encountered wind problems on the contest date. Although their designs established itself with good performance in windless conditions, under windy conditions the model's performance decreased. One another problem was the battery usage. As power was a design driving factor and this year's rules apparently demanded more power that past, power plant, battery and propeller package should be studied deeply. Having described the key elements of the mission requirements, next thing was the design parameters' evolution.

3.2. Quantitative Design Parameters

A program was written in Microsoft Visual Basic, namely "DBF-03", which made sensitivity analysis of the missions (including all segments of three types), propulsive parameters, sizing parameters and RAC. After a number of iterations DBF-03 showed the sensitivity results both in numerical and graphical ways. DBF-03 helped the team to search different parameters in detail. The program enabled analysis of individual parameters interference on the score as well as two and three parameters effect at the same time. The database, that program used, extensively depended upon historical trends. Analytical studies created different means of arriving the conclusion among which

team members selected the most efficient to drive results in the easiest and quickest way. These methods also included some crude estimates and rule of thumb data. Motor and battery suppliers provided catalogues among which propulsion group could analyze and select the proper propulsion package. Internet also provided extensive data on different subjects. Sensitivity analysis showed that parameters that are affecting the score most, concentrated on the performance parameters of the aircraft that were wing loading, maximum lift coefficient and cruise speed. Also empty weight affected the weight of the batteries, resultant to a significant difference in total score. Because the heavier the weight of the airframe, the more power required, resulting the number of batteries to increase. The parameters that affect the aircraft configuration and size were analyzed by selecting 2 missions out of three and this created 3 types of mission selection. These are: A and B missions, A and C missions, B and C missions. But propulsive parameters were individually analyzed. Because if the aircraft could complete a mission, which require more power than the other selected mission then it would complete the "requiring less power" mission as well.

Wing Loading: Because wing loading affects the performance of the aircraft on all segments of flight, it is quite affective on score. Takeoff distance is limited with 120 feet, which meant that power loading and wing loading should well be optimized to takeoff in assigned distance. These two parameters are interconnected and have large affect on the performance of the aircraft. Higher wing loading was desired because average wind speed in Webster Field was 12 mph in April, which meant good wind penetration was excessively needed. Another advantage of higher wing loading is that it allows higher cruise speeds. However 120 feet was a short distance and studies on wing loading showed that the aircraft could not perform 120 feet takeoff in higher wing loading values than ~2.81 lb/ft^2 (45 oz/ft^2) assuming an average maximum lift coefficient and average thrust value, obtained from DBF historical database. Also its affect on the score showed different trends for three alternative missions (Figure 3.1-a). To maximize the score, DBF-03 gave an average value of 32 oz/ft^2 considering all segments of missions. This value was reliable considering historical trends and takeoff distance. So for initial studies a range of 28-34 oz/ft^2 was adopted for further analysis.

Cruise Speed: Cruise speed directly affects the score by changing the flight time. However it indirectly affects score by changing drag and lift. Drag and lift changes proportionally with square velocity. When velocity exceeded some limits, power need increases such that overall score decreases. DBF-03 made sensitivity analysis and found high scoring potential averages for all three types of missions. These values ranged from 38 mph to 48 mph. (Figure 3.1-b).

Empty Weight: Although not directly affecting RAC in great deal, its affect on total battery weight is quite more (Figure 3.1-c). Empirical fractions were obtained from historical trends and quantitative studies, and it was seen that battery weight showed linear change with empty weight. Battery weight is the most influencing component of RAC and therefore score is highly decreased by empty weight increase. Although it is a general rule in design process to minimize the empty weight as much as possible, this output showed that not only the flight capabilities but also the score is highly affected by empty weight. Therefore this has direct impact on configuration selection. DBF historical database showed that an aircraft, carrying 5 pounds, would weigh around 18 pounds. But if good techniques for weight reduction could be made, both power usage and battery weight would decrease.

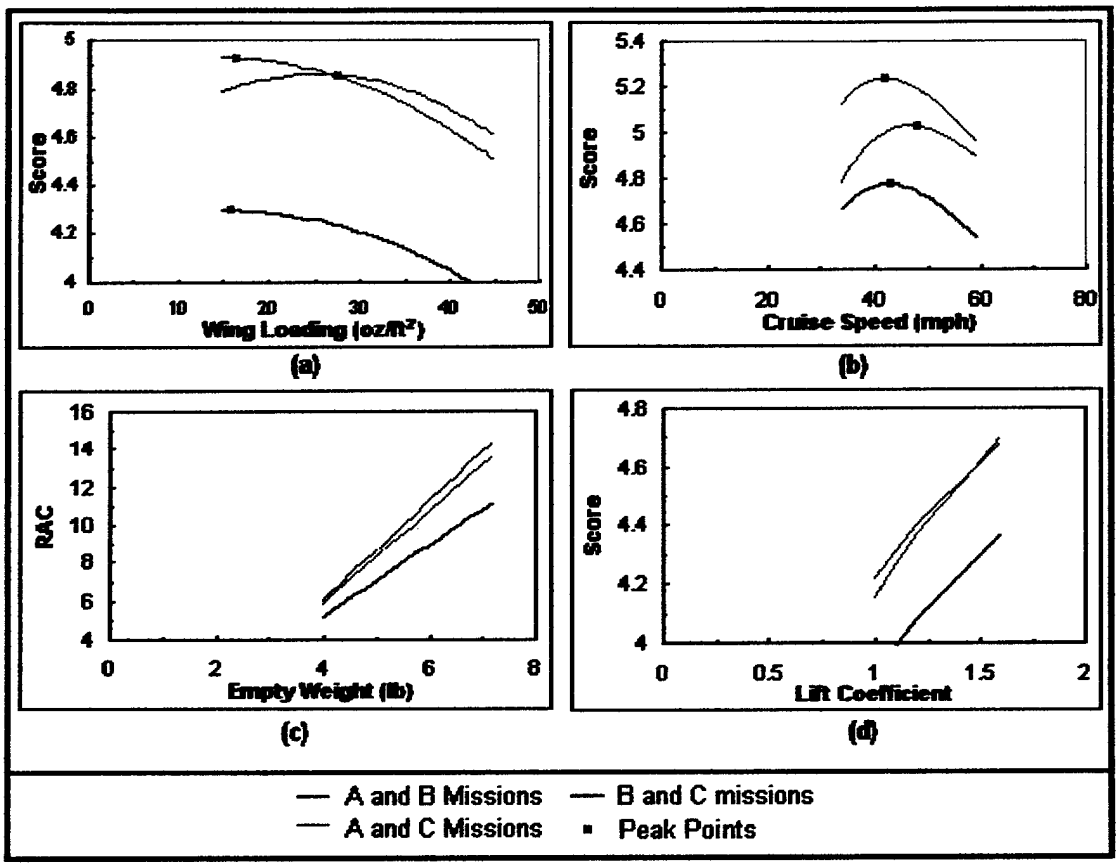

Figure 3.1 Design parameters' affect on score

CL_{max}: Maximum lift coefficient is affecting takeoff and landing that are the most important parts of the designated missions. Its affect on score is highly determined by the time spent for takeoff, descent and landing. Higher lift coefficients proposed less power to fly the aircraft and as a result, less battery usage. However risk of higher lift coefficients was stall tendency. As pitch up moment would be created in flight due to existence of the antenna, stall characteristics of the aircraft were very important. DBF-03 helped to determine Cl_{max}'s affect on the score (Figure 3.1-d). When calculating this, DBF-03 program considered flight time but not stall characteristics so more detailed analyses were needed and the data given at the figure was subject to change. There were a large library of airfoils giving high lift coefficient values with less drag coefficients and pitch up moments. So it was considered by team to evaluate a large range of 1.3 to 1.8 for maximum lift coefficients.

Power requirement: Although not being able to define power requirement for each mission exactly, some limits were derived in an effort to define which mission would require more power. It was seen that in this initial studies power requirement would not be sensitive. DBF-03 considered power loading range from 44.5 watts/lb to 62.7 watts/lb. This was quite a large range however determination only depended upon experiences and historical trends. Aircrafts with different performances were powered with different ratios. As determination of power requirement was one of the most important segments of the competition, it was evaluated that consideration of a round number could lead to misunderstandings at both mission and configuration selection. At this stage, it was better to define as to which mission would require more power in regard to other missions. DBF-03 gave some

approximate mission completion times for all three types. These completion times were obtained via iterating the above-mentioned wing loading values. When doing this, DBF-03 considered that for all three types, the performance parameters were the same. That is, if it defined a cruise speed of 40 mph, then whether with or without antenna, the cruise speed would be the same. Under same performance parameters, A mission would be completed in 5 minutes, B mission in 6.44 minutes (not considering the deployment time) and C mission in 6.74 minutes. Considering the deployment time B and C type of missions would be completed in almost same time. "A" mission type showed rather shorter time however completing the mission with the same performance as B and C mission type was difficult with the antenna. Also as B mission type included two takeoff and landings it was apparent that B mission's power requirement was greater that C mission type. Antenna in A type of mission causes both skin-friction and pressure drags. Some crude estimations were made in an effort to determine whether A or B type of mission would require more power than the other. But it was soon realized that this special case needed more than "crude estimates" and special effort is spent for determining the thrust increase for A type of mission. As will be mentioned in **"3.3 Special Cases: Antenna"** section of the report, thrust and therefore power demand for A type of mission is more than B mission type. So estimated power requirement sequence was A, B and C. C type would be achieved with high performance whether A or B was the mission, selected with it.

RAC Analysis: Rated aircraft cost is one of the primary parameters of the score function in negative relation. It is compromised of three components: manufacturer's empty weight, reflecting the weight of the airframe, rated engine power, reflecting the power consumption and effective power usage, and manufacturing man hours reflecting the aircraft's size and complexity of the mechanisms. All three components have multipliers, rated engine power multiplier being the most affecting one. To decrease RAC, aircraft should be lightweight with no more than required power. Among these three components the one with high decrease potential is the rated engine power. Manufacturers empty weight should be as low as possible but its affect on total RAC is quite low. 5 pounds of decrease in total weight of the airframe decreases RAC only 0.5. And if initial estimates are proper, it's almost impossible to reduce the empty weight by that ratio however as stated above its indirect effect is on the consumed power. Rated engine power is the primary influence on RAC. With single motor configuration, 1 pound battery decrease causes 1.5 of RAC reduction. Extra motor usage provokes this number to 1.875 of RAC change. Aircraft's dimensional values affect RAC but these are secondary. Main limiting factor on aircraft dimensions is the transportation box and therefore when deciding the aircraft configuration the box was the dominant factor affecting the geometry.

Mission Factor: Mission factor stands for alternative mission types' individual characteristics. Initial design parameters allowed discrimination between three types. As seen on figure 3.1 selecting B and C mission is establishing itself with the least scoring potential. At any given wing loading, any cruise speed or lift coefficient, score obtained from the third mission selection could not reach other two type's scoring potential. So a crucial decision should be made at this point both to narrow down the choices and to eliminate the low-scoring-potential alternatives. This investigation of the initial design parameters showed that selection of BC mission type, even though properly balanced and flown

perfectly, would not provide high score that the team assumes to get from other types of missions. Difficulty factor was a penalty for this type of mission and caused the elimination from further studies.

3.3 Special Cases: Antenna

As two important factors in design process, aerodynamic efficiency and power requirement, are dependent on antenna in A type of mission, this special case should be studied individually. Antenna placement is determined to be over the fuselage, however the increase in drag was still unknown and the team was not still sure what antenna existence over the aircraft could result and how it would change the performance parameters of an aircraft. So, this section outlines the means of answering the question: "How could the drag, that the antenna would cause, be determined?".

3.3.1. Theoretical Studies: Form drag is roughly proportional to the size of the wake behind the antenna. Therefore turbulent flow will create less form drag than laminar flow because making the free stream turbulent will move the separation point backward and wake region will be smaller. However turbulent flow will create more skin friction drag than laminar flow. Considering the rather small Reynolds number of antenna, around 200,000 in cruise flight, increase in skin friction drag due to turbulent flow will not be as high as form drag rise due to laminar flow. So forcing the oncoming laminar flow to turbulent flow is advantageous from drag reduction aspect. And the way to do it, is the propeller. Placing the propeller in front will speed up air particles and the particles will gain more energy. This energy increase will make the air turbulent and drag reduction will be provided. However there are some other factors for placing the propeller whether in front of the fuselage or on the wings. This analysis is done in **"3.4.5 Power Plant"** section of the report using the output of antenna study.

An important graph from reference 1 helped to find out the C_d of the antenna (Figure 3.2). Total drag, calculated by this C_d, included both skin friction and form drag. This graph gave a C_d of 1 for cruise flight and a C_d of 1.2 for takeoff conditions. These values corresponded 20 ounces drag increase in cruise flight and 16 ounces in takeoff conditions. However a better estimation of drag increase should be made, because antenna is one of the most important parameters of the mission, which could lead to significant performance reduction or even a crash. Therefore these reasons led to a flight test.

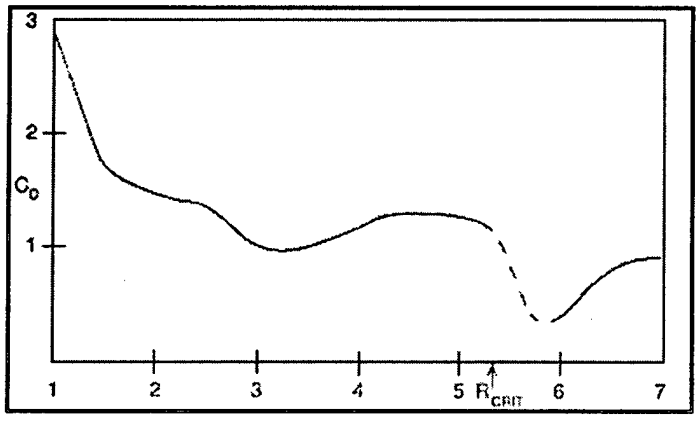

$$\text{Log}_{10} R = \text{Log}_{10} (u_o.d/v)$$

Figure 3.2 Drag coefficient of a circular cylinder with its axis normal to the stream.

(d = cylinder diameter, u_o = Stream Velocity)

3.3.2. Flight Test: The most effective method to determine the drag of the antenna is the wind tunnel tests however considering the current troublesome state of the academy's wind tunnel in drag measurement and the time to arrange the balance of the tunnel lead to a different method of finding the drag of the antenna: Flight-testing of the antenna was done on an aircraft for which the flight properties (maximum rate of climb at a given wing loading, handling qualities, etc.) are already well known. This ensured that when different conditions were tested on the aircraft, the only independent parameter was the antenna and any change occurred in flight, would be a cause of it. On absolutely calm morning, which was to make sure that the only performance dependent parameter of the aircraft was antenna, "Paragon" was sent aloft to compare the differences it would face (Figure 3.3). The model tested was a trainer aircraft, which was already being flown in model aircraft club in the academy. Paragon aircraft was all balsa and plywood with a 62.2 inches wingspan, a wing surface of 635.5 in^2 and 12 $ounces/ft^2$ wing loading. The weight of the model was 3.3 lb.

The way to learn the thrust increase, was considered before test was held: Aircraft would be flown 100 meters without the antenna with fixed throttle settings for five sorties and the average time of five sorties would be noted on the transmitter by a dot. Then, aircraft would be send aloft with the antenna and it would be flown until it flew the same distance of 100 meters in the same time. This would make sure that the velocity and therefore the Reynolds numbers for two different flights are the same. Again the throttle settings would be fixed but this time at a higher throttle setting, therefore at a higher RPM. The increase in the throttle would be noted when the pilot managed to fly the same distance in the same time. And when the aircraft landed, the team would learn the exact thrust increase by the help of a tachometer. The same throttle settings as noted in flight, would be applied on ground and team would calculate the RPM increase by tachometer. RPM change between two different cruise flights would be known and as the diameter of the propeller is already known, thrust would be calculated. Because thrust is proportional with RPM and the diameter of the propeller.

The aircraft was first tested without the antenna. The performance parameters were as follows: 31.83 mph (100 meters in 7.03 seconds-average of 5 tests) with enough thrust takeoff in 25 feet. Handling qualities were sufficient enough. It could easily make a loop from level flight.

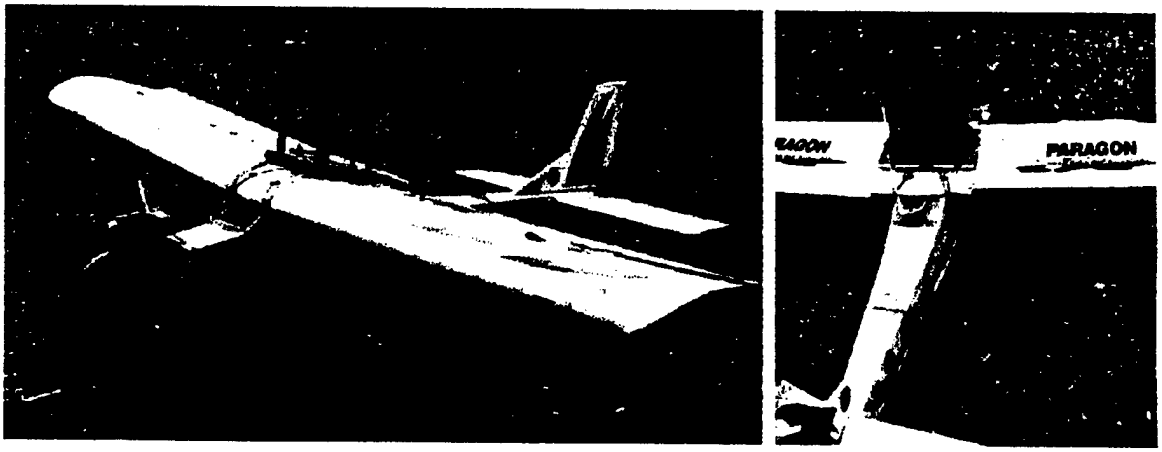

Figure 3.3 Antenna was tested on a model airplane. Safety mechanism of the antenna consisted of a servo, a plate and two pushrods.

The model established tight turns. And for the next step, flight with antenna, it was decided by the team to take some precautions in case something unexpected happens. Without having enough safety, the aircraft could not be sent to test the influences of the antenna. So a mechanism was settled to deploy the antenna whenever needed (Figure 3.3). The deployment mechanism consisted of a servo and a plate on which the antenna was settled. The antenna's dimensions were that of the one defined by the rules. When the pilot felt it to be deployed, he would activate the servo and the antenna would drop on the ground.

Hopefully there happened to be no need to use the safety mechanism. The decrease in performance was more than expected. First, takeoff distance was one and a half times more, 37 feet, which showed that drag increase at takeoff conditions were significant and aircraft had difficulty in accelerating. Then it was observed that rate of climb was not the same as the first flight but the decrease was not significant. And when the model came to the flight altitude it was seen that the aircraft was flying near-stall speeds. The responses were quicker. However the team estimated it as a result of the model's flying in less speed and therefore the torque applied to servos was less than before. And this was approved when the model flew almost at the same velocity of 31.83 mph. This time the responses were more or less the same as the first flight. Analysis showed that to get the same performance, thrust increase was 26 ounces. This output was more than analytical studies estimated it to be and the cause of it, is the mutual influence of the fuselage and the antenna.

3.3.3. Results: Model's operating Reynolds Number was around 300,000. And Haberci aircraft was intended to fly at around 45 mph with a Reynolds number of 420,000, which meant at a higher Reynolds number. In this test what the team wanted to learn was the extra thrust need for antenna. The drag, caused by the antenna, is the sum of the skin friction drag and form drag. Both skin friction drag and form drag can vary with Reynolds number, but in different measure. A high Reynolds number will reduce form drag by causing the boundary layer laminar flow to transition earlier to turbulent flow, thus delaying boundary layer flow separation. As both flights were in low-speed region and form drag was predicted to be more than skin friction drag for a circular shape in low speed the result of 26 ounces increase in thrust was adopted for further performance studies.

3.4 Qualitative Analysis of Design Parameters

Initial studies showed that B and C types of missions together was not to be selected and a mission selection method should be determined at this stage. Instead of individually examining AB and AC mission types; as both included A mission, it was accurate to go on to configuration selection section as if the design process was being for A mission type, and then on 2^{nd} stage determining the next mission seemed the proper way to follow. Also power requirement investigation showed that A mission was demanding more power than other two types. So configuration selection consisted of 2 stages one of which was to determine the configuration for A type of mission and then examining the configuration as to which type of mission it would better provide higher performance and score. When determining of the configuration, qualitative design parameters were investigated by taking into account the initial performance parameters.

Based on design constraints stated by rules, key elements of aircrafts were selected in an effort to

narrow down the choices and select the optimum balanced design with good performance capabilities while still maintaining high score. At this stage, configurations that were behind the scope of this study and the ones without the manufacturability with the tools the team had in hand and could obtain, were disregarded from selection. These predefined design parameters and various configurations were considered and rated based on selected figures of merit. The synthesis of the initial design parameters also helped when generating configurations and finally an aircraft configuration was drawn out of various alternatives.

3.4.1 Wing Configuration: The wing of an aircraft is its most important component, its only means of support in flight. Although not being able to define every parameter of wing at this stage, it was quite credible to decide the type of the wing, planform and vertical location. There were four wing types considered that are mono-wing, bi-wing, flying-wing and wings in tandem configurations. The wing parameters that influence RAC are wingspan, maximum exposed wind chord, number of control surfaces and the number of the wings. Driving factors for wing configuration selection were aerodynamic efficiency, structural weight and rapid assembly. As the configuration was intended to fly with the antenna, wings interaction with the antenna was also a matter of concern.

A monoplane with either high or low wing was considered. The team, because of design constraints, chose not to analyze mid-wing configuration in detail. The payload and the batteries covered a great deal of volume in the fuselage that there could not be a place for a carry-through mid wing. If the mid wing were not of a carry-through structure than required structural strength would increase significantly resultant to an increase in weight. Therefore monoplane configuration with low and high wing types were the subjects of concern. Low wing configuration would enable rather shorter landing gears if gears were mounted on wings. Although this type enables access to payload in the fuselage easier, access to payload is not the main concern for the design. Because the payload and batteries will not be installed during the timed assembly task. And the team will have enough time installing the payload inside the fuselage. So a high wing would not represent a problem from this aspect. Another drawback for low wing is that when taking off the ground and landing, in case something unexpected happens, wing tips are likely to hit the ground and cause a crash. On the other side, an advantage of a high wing is that it enables satisfactory stability without dihedral. As the payload access is not the concern for design constraints, high wing would not constitute a problem. A biplane has two sets of wings, one above the other. The main reasons for usage of biplane are due to span limitations and total increase in lift. The span of the wing was not limited by the rules but considering the transportation box, the span is projected to be between 8 and 12 feet. A biplane configuration has its advantages such as decrease in induced drag and low structural weight due to shorter span proportional to a monoplane but considering a biplanes mutual-interference on overall configuration, a biplane established itself as a drawback. Because commonly biplanes require strut usage, which is a factor both in rated aircraft cost and total skin-friction drag. Another drawback for this type is its assembly problem. Needing more space in the required box, the antenna mounting is rising as a problem too. The affect of two wings on the RAC is quite disadvantageous when the advantages of a biplane are taken into account. Considering the effort, spent last year to design a biplane to carry softballs, the biplane configuration soon established itself as shortcoming for design requirements from most aspects of design

constraints. Flying wing is different from all other types, having no tail and fuselage. A flying wing is the most aerodynamically efficient of aircrafts both with its lesser-wetted area and light weight, causing from all aspect, in low rated aircraft cost. But the control of flying wing was becoming more evident. Stability being a major concern of this configuration, a detailed analysis of yaw control, roll and pitch stability should be made. Center of gravity should exactly be calculated so that the antenna could be placed where it would cause no pitching moments because of its weight. If not perfectly analyzed, this configuration would be a big penalty. A tandem wing was also considered proposing advantages like a biplane. Tandem wing was also a good alternative for reducing the induced drag but the efficiency was reducing proportionally. The aft-wing, being in the wake region of the front-wing, creates a need to separate the two wings as much as possible. Efficiency is a major concern due to limited battery capacity. This and transportation box limitation reasons caused elimination of tandem wing from consideration. Winglets were not considered for none of the four types because its effect on RAC could not equal to its performance advantages.

3.4.2 Wing Planform: Wing planform is a major parameter of the wing, forming the basis for aircraft performance. It does not have direct effect on RAC however stall characteristics, lift distribution, induced drag are some of the dependant factors that wing planform directly affects. The types that are considered during prescreening process were elliptical, rectangular, moderate tapered and high tapered including delta wing configuration planforms. Prandtl's lifting-line theory shows that most efficient planform is the elliptical planform, having a uniform lift distribution span-wise and equal downwash speeds at the trailing edges. This creates good stall characteristics. An elliptical wing stalls evenly across the span. However manufacturability of the elliptical wing was one of the factors for elimination of this type. Even if properly built and flown, the team should have thought of pilot's handling quality that in case a crush happens, wing should be repaired in a time period in terms of minutes and this is the major factor why elliptical wing planform is eliminated from consideration. Rectangular planform offered less aerodynamic effectiveness, approximately 10% of induced drag increase, however it's the easiest to build among the investigated wing planforms. Stall pattern was better according to other types except elliptical planform such that it stalls at the root first allowing the tips and ailerons effective well into the stall. This also helps pilot to take precaution before the whole wing is stalled. This feature of rectangular wing was very important as stall characteristics became very important due to antenna existence. Moderate taper of 0.4 to 0.6 was a way of likening the lift distribution to that of an elliptical planform's. Its manufacturability is fair considering the elliptical wing's and stall pattern is confidential to warn the pilot before the whole wing is stalled. High taper or delta wing configurations are poor in tip stall conditions. Because of low Reynolds numbers occurring at the tips, tips are likely to stall in a small change in flight conditions. This would create problems in the most important parts of the flight, which are takeoff and landing. As safety was a major factor in all phases of design this planform was rated considering these deficiencies. Another disadvantage of small Reynolds numbers occurrence at tips was poor lift distribution. Twist may be applied to the wings to improve the lift distribution of tapered or rectangular wings. But this is considered to be negligible at this stage. Detailed analysis of wing shall be done in preliminary design.

The monoplane configuration with high wing was selected for further analysis. Considering the

superior stall characteristics of rectangular planform, its induced drag increase of around %10 was not taken into account and this type of planform was selected with high mono-wing configuration.

3.4.3 Fuselage Configuration: The fuselage is the central body portion, the integral part of the aircraft, designed to accommodate the payload, mechanical mechanisms, batteries, motor and flight control equipment. It should structurally maintain strength to withstand the static and dynamic forces acting the fuselage during the mission profiles. Body maximum length is the parameter affecting RAC. Main concern on fuselage configuration determination was the drag it created. A well-streamlined fuselage was needed as the antenna increased parasite drag already. So while allowing enough space for the payload and batteries, it should be well designed and lofted, creating the least drag possible. As the aircraft was to fit in the transportation box, volume should be effectively used. Effective volume usage would decrease both RAC and weight of the airframe. Another advantage of shortening the fuselage was maintained by wetted area reduction. This was the result of fineness ratio optimization. Several references advise a fineness ratio of 3 to 5 for drag reduction in low Reynolds numbers. Considering these parameters' affect, the team generated six types of fuselage shapes (Figure 3.4)

First shape is a box with fillets. Among other considered types it has least aerodynamic efficiency. However production of it is easier relative to other types and it promotes to place the cargo and electronic equipment in a compact form. Another advantage of a box shape is its connection with the wing. In case wing and fuselage are detached to fit in the defined box, it would be difficult to place fillets at the intersections, which seemed to be mandatory to increase aerodynamic efficiency. With this type of a fuselage, fillets would not be required to exist. Also, as the wing is a high mono-wing, separation of place for the wing to pass through from the upper end of the fuselage like a carry-through structure, allows rapid assembly and a good method for fitting the aircraft components in the defined box. Second shape has better aerodynamic efficiency relative to first one however "dead" volume, defined as having no use but still existing, would be quite much. As the box that will be carried in the fuselage is in rectangular form, the outer parts of the cylindrical shape could not be used productive. And this shape of fuselage would need fillet at the wing intersection parts and assembly, as stated before, would not allow this shape of a fuselage. Considering third shape, this problem is relatively solved. However still remains the problem of production for second and third shapes. Also the bottom part is in circular form, so if B type of mission selected, deploying the payload is getting difficult for deployment from the bottom of the fuselage. Following on to fourth shape, aerodynamic efficiency is showing itself. This shape shall be thought as modified form of box. Mainly compact placement of the cargo and equipments is provided with credible aerodynamic efficiency.

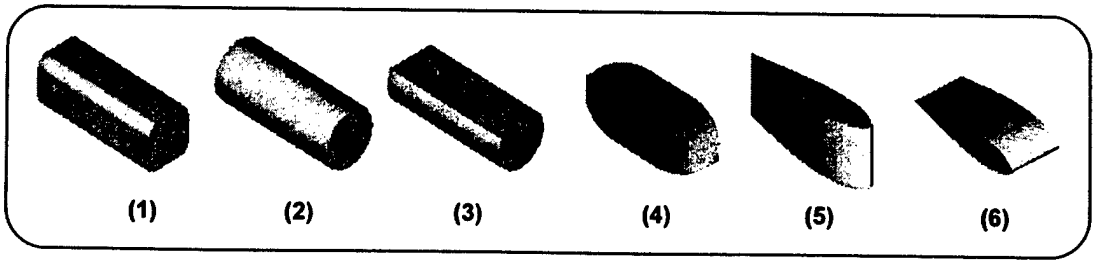

Figure 3.4 Alternative Fuselage Configurations

Production is less complicated relative to circular shapes and providing strength is easier. Also the pressure drag in the back of the fuselage could be prevented with a smooth fairing from the back part of the fuselage. Fifth and sixth shapes are horizontal and vertical symmetrical airfoils. These shapes are creating least drag however placement problem arises. To be able to place the defined box into these shapes, airfoils should be cut from maximum thickness. This lengthens the fuselage quite much, resulting an increase in RAC and also weight of the airframe increases. But the main deficiency of longer fuselage is rising when transportation box subject comes into scene. Defined box has the longest value of 4 feet and if fuselage exceeds this value, the fuselage should be cut into two or should fold to fit in the box and this reduce both strength and volume. Cutting into two would require some extra parts to attach and detach which would increase the weight of the airframe.

So 4^{th} type, "modified-box" shape, was considered for further analysis.

3.4.4 Empennage Configuration: Empennage is the main component to maintain the aircraft's control and stability. Empennage is contributing to RAC with number of horizontal and vertical tails and active control presence in vertical tail. Because the payload is rather small in dimensions, and transportation box size is defined by the rules, fuselage configuration is selected providing least available volume so approximate fuselage length will not be long enough to allow the horizontal tail span to be 25% of the span of the wing. If the horizontal tail is greater than 25% of the wingspan it is counted to be a wing and RAC increases. So empennage configurations without boom(s) were not considered. To achieve the goal of stabilizing the aircraft, seven empennage types were considered at this stage as seen in Figure 3.5. When deciding on the empennage configuration main thought was that: Tail should be out of the wake of any component to effectively perform its task. First option, a conventional tail, is the basis of tail configurations. This configuration is frequently used because it provides adequate control and stability; and stall characteristic at high angles of attack is able to fulfill the mission requirements. However as antenna would be carried on the fuselage, the conventional tail would be blanket by the antenna and lose its benefit. Next configuration consideration was a T tail. This configuration provides favor by removing the horizontal tail out of the wake region of the antenna, and increase in weight due to requirement to strength the vertical tail was considered to be so small and is thought to have no effect on weight. Nevertheless, because the wing blankets the vertical tail at high angles of attack, its high angle of attack performance is poor. However increasing vertical tail height could eliminate this deficiency. But this would cause increase in RAC. Third option is H tail with single boom. This type has a negative affect on RAC due to possessing two vertical tails with active controls. But it removes the vertical tails out of the wake region. Horizontal tail is partially in the wake of the antenna and fuselage.

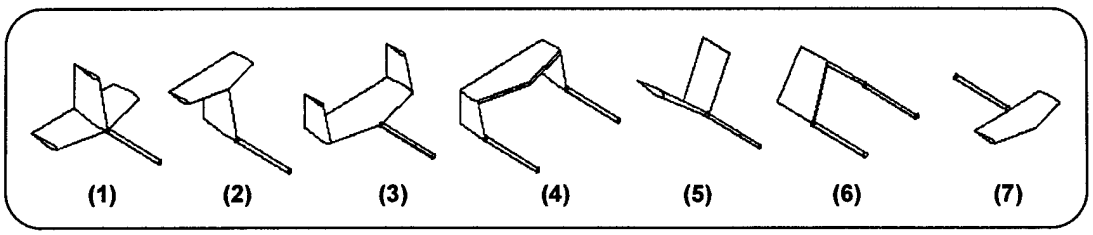

Figure 3.5 Alternative Tail Arrangements

However due to end-plate effect of the vertical tails, horizontal tail operates more efficiently and therefore eliminates the drawback. Fourth type, two vertical tails with horizontal tail over them proposed effectiveness of removing both horizontal and vertical tails out of the wake region of any component. However to provide enough structural strength it would be heavier than H tail which is already heavy. Beside its weight penalty, its RAC contribution is more than other considered configurations. A V tail is good for reduced wetted area and reduced RAC, which is the dominant factor on configuration selection because of its highly effect on the overall score. The problem with a V tail configuration is the control difficulty. Team had constructed other types of tail before however none of the team members had ever experienced V or inverted V tail arrangements. Although V and inverted V tail configurations serve well with aerodynamic efficiencies and RAC effects, they were disregarded from consideration because of difficulties in control of them. Seventh and the last type of empennage was canard type. When working on aft-tail configurations the main concern was the antenna and fuselage effects on the tail however a canard configuration establishes the task of stability in front part of the aircraft. RAC decrease is quite noticeable. But canard style suffered from insufficient stability, which is the main task of empennage. It also requires perfect calculations of stability. The aircraft already had an extra surface, the antenna, which would create extra moments. So in order to maintain good handling characteristics and control, flight-testing would be mandatory. And performing a flight-test task would require a lot of steps such as sizing the aircraft and selection of propulsion system etc. So after performing these tasks, if V-tail establishes itself with less performance than other types, returning to the beginning of the design would require a lot of effort and time. Considering the limited time and scope of the study, this configuration would be a high risk.

Vertical tail configuration without active control was not considered, because the pilot advised that effective rudder usage would be tremendously advantageous in turns to provide constant velocity coordinated turn. So for further analysis 2^{nd}: T tail with single boom, 3^{rd}: H tail with twin boom and 4^{th}: n tail with twin boom empennage types were considered for configuration selection.

3.4.5 Power Plant: Power plant is one of the main components of the aircraft composed of motor, propeller, and batteries. It should provide enough power to takeoff, fly the designated mission profile and make a safe landing. RAC contributions of these components are the most affective of all other contributors. RAC increases by multiple motor usage, battery weight and number of propellers. As determined at the first stage, power need to fly the mission would be excessive. 40 amps, being the highest current from single motor, led to extensive analysis of multiple motors. Although multiple motor usage has RAC drawback, to have the performance of the aircraft as defined in initial studies, this alternative has attracted team's attention. Main concern was that either antenna would be in propeller's wake region in tractor configuration, or propeller would operate in antenna's wake region in pusher configuration. The tractor location has been standard for most of the history of aviation. However fuselage, being in the disturbed air, increased skin friction drag. Pusher configuration didn't have this problem however suffered from reduced propeller efficiency. Because the propeller operated in the turbulent flow of the fuselage or wing.

The exposure of the antenna to turbulent is more favorable than exposure to laminar flow. Also motor placement affected the aircraft's fitting in the defined box. Consequently investigations extensively

concentrated on propulsion system. Taking these mutual affects of antenna and propeller into account, the team examined 4 types of power plant. These are: single tractor motor, single pusher motor, twin tractor motors and twin pusher motors.

Single tractor motor is generally used type. Although this type leaves the fuselage in the turbulent flow, propeller is operating in laminar flow therefore increased efficiency is maintained. As initially defined, antenna would be carried over the fuselage. This means that not only fuselage but also the antenna is going to be in turbulent flow. However, as determined in **"3.2 Special Case: Antenna"** section of the report, antenna causes less drag in turbulent flow. The separation point moves backward, therefore reduces the drag. Therefore this type was advantageous for both antenna drag reduction and for propeller efficiency. Single pusher motor is good for removing the fuselage from disturbed air. On the other hand the propeller effectiveness reduces therefore requires more powerful motor and therefore more batteries to fly in the same period of time with the same performance. Another disadvantage is its requirement for a longer landing gear for safety in takeoff. When the nose lifts off the ground, propeller may hit the ground and may cause damages that cannot be repaired. Another drawback for pusher configuration is that motor moves the center of gravity backwards and causes either weight increase in fuselage's front part or horizontal tail surface increase. RAC for tractor and pusher configurations are the same. Twin tractor motor configuration is good for exposing both propellers to laminar flow. However antenna is exposed to laminar flow too. Also it requires more power for the intended level of performance. Motor current is increased as a result of increasing the applied voltage or resizing the prop. This will involve more input power and will result in a corresponding increase in mechanical output power. However drawing the maximum limit of 40 amps from a single motor requires batteries with higher internal resistance therefore loses which is proportional with square current increases drastically. So cutting the current in half reduces resistance losses to 1/4 from what it was with single motor. Twin motor usage enables rather smaller motors and the drawn current therefore decreases. However losses are still higher than single motor configuration. The main advantage of twin motor usage is that it enables more input power applicability. Nevertheless it has its drawback of RAC increase. Another aspect is that if the motors are mounted on the wings then significant dihedral need arises which may result dutch roll. Twin pusher motor configuration is carrying all advantages of above-mentioned single pusher motor. However the antenna is completely exposed to laminar flow and this time the propellers are in wing's wake region causing a loss of efficiency. Its main drawback is RAC increase.

3.4.6 Landing Gear: Three types of landing gear configurations were evaluated in conceptual design: fixed tricycle, retractable tricycle and taildragger. Parameters affecting the score were the drag of the gears, ground handling capabilities and weight.

Fixed tricycle landing gear creates excessive drag, however it is a widely used because of its good ground handling performance and support at landing. And structural strength is adequate. It's lightweight in regard to retractable tricycle landing gear. But past experiences showed that drag of a fixed landing gear could be as high as some 30% of the total drag. So in an effort to eliminate this deficiency, retractable tricycle landing gear configuration was analyzed. There are 2 main systems of retracts in radio controlled aircrafts that are mechanical and air operated retract systems. While totally

diminishing the drag, weight of the airframe increased. Also additional servo usage increases RAC. However the increased power consumption affect to the score due to weight penalty cannot equalize the drag reduction affect of this type. Other problem with retractable landing gear was reliability. In case it stuck because of some mechanical problems at landing, whole effort of design would be wasted. A tail dragger offered less drag and weight than a tricycle however its ground handling was difficult and landing performance was poor. Because, a taildragger configuration's nose could hit the ground as happened before in previous DBF contest when landing.

It was soon found out that, differences between these two types, tricycle and taildragger, are not to be put forward at this stage. It was negligible to comment on one of the types. So tricycle and taildragger types were selected for further detailed analysis.

3.5 Configuration Selection

The best aircraft design practice is when the components of the aircraft serve multiple functions and when they work together in an interconnected fashion. For example a pusher configuration evidently demands twin boom usage. Selected design parameters narrowed down configuration alternatives, and nine leading configurations were selected for analysis (Figure 3.6). According to selected figures of merit, configurations were rated and a final concept with the highest scoring potential was selected for further analysis.

3.5.1 Figures of Merit: Benefits and drawbacks of each design were compared by means of defining discriminating figures of merit in an effort to select the configuration to produce highest acquirable score. Selected figures of merit at this stage were rated aircraft cost, effective volume usage, aerodynamic efficiency, assembly ease and power consumption. These parameters reflected the mission features, possible performance of the configuration and score. For each figure of merit, evaluation criteria was defined to see how each configuration affected score and let to see which configuration would prove itself as the best alternative out of competing concepts.

Many other features of both the mission and that specific configuration were thought but it was soon discovered that parameters just like stability and control could not be defined at this stage. Because those analysis involved many parameters of the configuration and required data was not available at this stage.

RAC: Rated aircraft cost is one of the most affective parameters of the score function. According to historical trends, fractions were obtained and some initial sizing trades were made. This study enabled RAC definition for each configuration. When doing this, battery weight was assumed to be the same, 5 lb., for all configurations. Because not many quantities were defined for power plant requirement, development of a method for defining battery differences between alternative configurations could lead to erroneous evaluation of configurations. Also one of the figures of merit: power consumption, reflected how battery need would change between configurations. Team has determined criteria for evaluation of configurations and each configuration is given a rate between 1 and 10 according to defined RAC (refer to Figure 3.6 for RAC for each configuration)

Effective Volume Usage: Effective volume usage was important as rules specified a volume, which aircraft should fit in. So effective volume usage became one of the discriminating figures of merit in configuration selection. All configurations were given "10" rate and some factors caused this rate to

lessen with different ratios. These affecting parameters were extra vertical surface, extra boom or extra motor existence.

Aerodynamic Efficiency: This figure of merit is one of the primary parameters of the aircraft reflecting the performance of the aircraft from all aspects. Its main components are lift and drag. Drag has direct effect on required thrust. So a high L/D would provide reduction in both required power and RAC. Again a rate of 10 was given to all alternative concepts and stall patterns, existence of a component in wake region of another component, tricycle landing gear configuration and extra vertical tail existence decreased the given rate with different ratios.

Assembly Ease: The configuration should be assembled rapidly. This was a parameter in flight score function, so easier assembly would shorten the time, therefore increase score. Again some parameters were defined which affect assembly such as twin boom existence or having T tail, and each configuration was rated according to these defined factors.

Power Consumption: Power consumption was highly affecting the score by changing the required cell number, which is the most effective factor in RAC function. Each configuration was rated according to some defined parameters that would increase required thrust. Empty weight again played a vital role in power consumption determination. Instead of defining a round number for all configurations it was thought to rate them as to which would need more power than others. Selected parameters, such as wake region existence, pusher configuration and twin motor usage, affected the power consumption rate.

Handling Qualities: As stated before, analytical studies could not be applied for handling qualities differences determination at this stage however experiences and pilot advice helped select some parameters that most likely would prevent effective handling of the aircraft. As already mentioned in statement of the problem, antenna would create positive pitching moment and handling qualities arose as the primary need for the aircraft. So four main affecting parameters were defined that most likely affect the handling qualities: performance at high angles of attack, control loss recovery, fuselage nose length and pilot advice. Each configuration was rated according to the criteria determined by the team. Handling qualities of each configuration also reflected the safety of configurations.

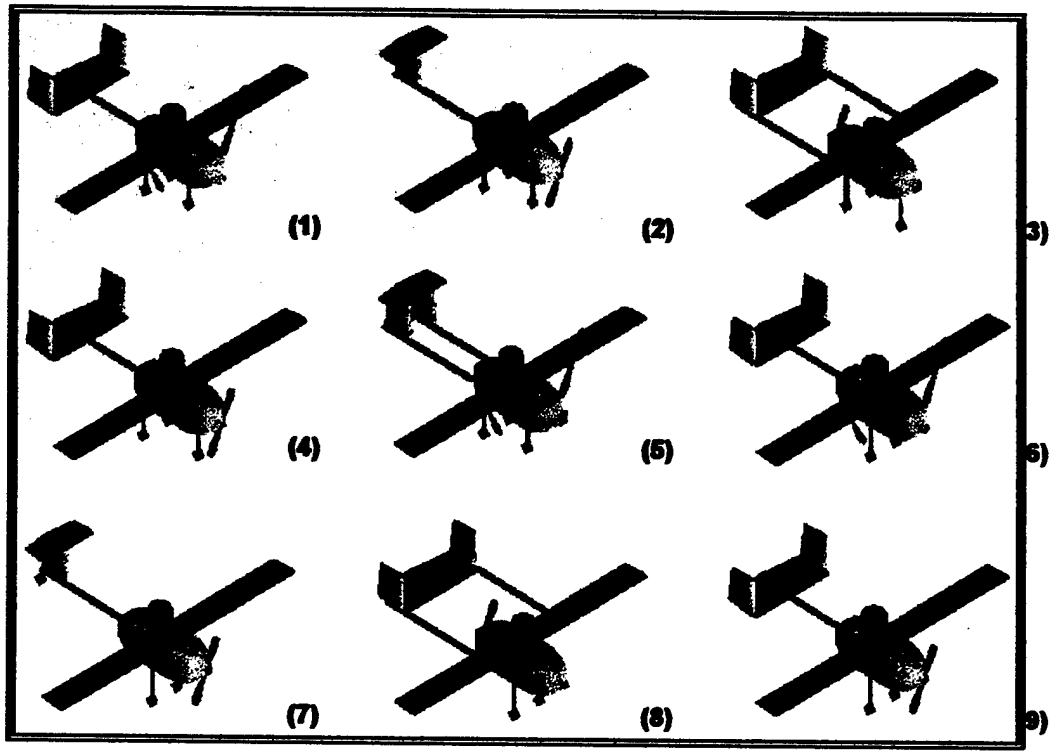

Figure 3.6 Alternative Aircraft Configurations

		Design Parameters					FOM						
		Landing Gear	Empennage		Motor								
Configuration	RAC	Tc : Tricycle Td : Taildragger	Tail H : H tail T : T tail n : n tail	Boom S : Singleboom T : Twinboom	Number T : Twin S : Single	Type T : Tractor P : Pusher	RAC 5	Effective Volume Usage 3	Aerodynamic Efficiency 5	Assembly Ease 3.5	Power Consumption 3	Handling Qualities 4	TOTAL
1	15.135	Tc	H	S	T	T	5	5	6	7	7	8	147.5
2	12.81	Tc	T	S	S	T	9	9	5	6	8	7	170
3	12.925	Tc	H	T	S	P	8	6	6	6	7	7	158
4	12.91	Tc	H	S	S	T	8	7	7	8	8	9	**184**
5	15.135	Tc	n	T	T	T	6	5	6	5	6	6	134.5
6	15.125	Td	H	S	T	T	7	5	7	7	7	6	154.5
7	12.8	Td	T	S	S	T	10	9	6	6	8	5	172
8	12.91	Td	H	T	S	P	9	6	7	6	7	5	160
9	12.9	Td	H	S	S	T	8	7	6	8	8	7	171

Table 3.1 Using six discriminating Figures of Merit, configuration with the greatest score, Highlighted red, **is selected for further analysis.** Blue numbers **are the weight of each Figure of Merit.**

4. PRELIMINARY DESIGN

The preliminary design started with determination of design parameters to further analyze the selected configuration's performance, geometry, structure, stability and mechanical systems. Enhancing DBF-03 program with wider analytical and numerical models, initially determined parameters were refined to obtain solid data on aircraft capability to compete in Missile Decoy mission. Defining aerodynamic and propulsive performances of the aircraft, the task of mission selection was carried out. This was the finalization of the mission selection method determined in conceptual design. But before performance studies could be carried out, propulsion system of the aircraft should have been investigated, as mission performance is dependent on propulsive efficiency. After determining the propulsion system and missions to be selected, sizing trades were investigated and preliminary design phase was concluded by static stability analysis.

4.1. Propulsion System Selection

Flight performance of the aircraft is proportional with propulsive performance. Therefore in order to gain the intended level of flight performance, aerodynamics group studied thrust requirement for each segment of flight and results of that study became the requirements for propulsion system selection. Considering the thrust requirements, determination of propulsion system was done by keeping the propulsive package's weight the least and efficiency the most. Keeping the weight of the batteries to a certain level limited both the available power and the duration of that power. However maximizing the power and therefore thrust was not the subject of concern. Because minimum required level of power was determined and keeping the produced power in that range with the least battery weight was the main idea of the propulsion group. However studies showed that sufficient thrust to power the aircraft is only available when the batteries weigh 5 lb. This section of the report is composed of three sections. After determining the design parameters for motor, figures of merit were defined as to which motor would compete the best, considering mission requirements. Then batteries were investigated and on the last step the propeller was selected to suffice the mission performance.

4.1.1. Motor Selection: The first step in selection of the motor was to examine the requirement of the power. Aerodynamics group's study showed that to complete the selected A mission, which was the most power demanding of mission alternatives, excessive thrust was required. Considering the flight speeds and thrust requirements of each segment, power requirements were obtained. Maximum power requirement was in takeoff segment of A mission, 1050 watts. For cruise conditions this value reduces to 892 watts. If these power ranges were achieved, resultant thrust would be sufficient for both B and C type of mission. Before starting the analysis for alternative motors, it was accurate to narrow down the choices by some assumptions. Design parameters provided focus on certain number of alternatives.

4.1.1.1. Design Parameters: Design parameters of propulsive characteristics were defined to discriminate between different power plants. These parameters illustrated the initial motor features and enabled rapid generation of figures of merit to select the proper motor.

Thrust: As thrust is the prime need, gearing usage is mandatory. The gearing increases thrust and decreases forward velocity. The geared motor turns a bigger prop more slowly. More thrust is delivered but at lower speed. This results in larger than average sized propeller selection.

Motor Amperes: Power is current times voltage into motor. The highest current that might be drawn is set by the rules as 40 amps. However, to get a determined amount of input power, lower voltage and higher currents are less efficient than higher voltage and lower currents. Because, terminal resistance (defined as internal losses inside the motor due to wiring in the armature) losses due to resistances (internal resistance of the cells, resistance of connectors, wires, speed control) are all proportional to the square of the current. The only voltage dependent losses of the motor are the iron loses which is applied voltage times the no-load-current (Io). Io is defined to be the minimum current required to turn the motor itself without prop loads. So as losses decrease, efficiency increases.

The motor's turns and windings, and the mechanical load (propeller), will determine the current draw at any given source voltage. Increase in voltage will involve more input power and will result in a corresponding increase in mechanical output power. In other words, the motor's "performance" will improve. The problem to avoid is overheating the drive system when the source voltage is abused.

K_v : Voltage constant gives the RPM produced by the motor per volt applied. A motor with a higher K_v will be able to turn the propeller faster but it will require more current to do so, or the propeller will be smaller. So for the defined specifications, motors with rather low K_v values will be selected.

So initially selected motor features are as follows: Gear will be used. Motor current will be low (25-33 amps range) while allowing the motor to produce enough power. Thrust will be the primary factor in selection. Motors with low K_v constants will be selected.

4.1.1.2. Figures of Merit: When choosing the motor, motors of similar voltage constants, for a range, which is known to work well with defined large propellers, are compared for their weight, efficiency, mounting ease, cost and score based on criteria determined by the propulsion group. Then the motor that efficiently accomplishes to meet the predefined requirements is selected.

K_v: Selected range for K_v value is 75 to 125 (rpm/V). The important thing in comparing voltage constants was to divide the motor K_v by the gear ratio for geared motors to arrive at effective K_v. This gives a wider range of motors to analyze. Keeping the voltage constant between these values keeps losses as low as possible and provides high efficiencies. Motor's overall efficiency is directly proportional with the performance of the aircraft and therefore score. To attain the stated K_v values, all Astro and Graupner motors were applied four commercially available gears (Table 4.1). The K_v, I_o, R_m values and weight of each motor are obtained from the manufacturer's Internet databases. Four columns on the right of the table are the effective K_v values of motor and gear combinations.

	Kv	Io	Rm	Weight		Gear Ratio			
Motor Name	(RPM/V)	(Amp)	(Ohm)	(Oz)		4.36	3.69	3.1	2.75
Astro Cobalt 60 11T#23 [1]	347	2.5	0.103	22	Effective Kv	79.59	94.04	111.9	**126.2**
Astro Cobalt 60 13T#24 [1]	293	2	0.15	22		67.2	79.4	94.52	**106.5**
Astro Cobalt 90 11T#23 [1]	230	2.5	0.15	30		52.75	62.33	74.19	83.64
Astro Cobalt 90 FAI 10T#22 [1]	256	3	0.111	28		58.72	69.38	**82.58**	93.09
Graupner Ultra 3600-8 30V	328	1.73	0.107	26.1		**75.23**	88.89	**105.8**	**119.3**

Table 4.1. Highlighted and Red K_v values are between the selected range of K_v for least loss and optimum performance. Red values represent the best applicable choice of gear ratio for each motor.

[1] aT#b - "a" stands for turns and "b" for winding

Mounting ease: In order not to encounter any problems such as extra surfaces usage in manufacturing of the aircraft, mounting ease became one of the FOM for selection of the motor.

Score: The performance of the aircraft, and therefore score, is directly proportional with the motor. Since score is the sole parameter that team tried to maximize, it is the most influencing parameter in power plant selection.

Static thrust: For high static thrust values in regard to the weight of the aircraft, the required level of performance such as takeoff distance or climb rate, is easily maintained. All alternative motors were not in hand to test however static trust values for these motors with the propeller advised by the manufacturer were available from Internet. According to those values, the motors are rated.

According to defined figures of merit, Astro Cobalt 90 FAI 10T#22 with a gear ratio of 2.75 to 1, established itself as the best out of other choices (Table 4.2). Weight of the motor is 35 ounces.

		Astro				Graupner
	Weighing	Cobalt 60 11T#23	Cobalt 60 13T#24	Cobalt 90 11T#23	**Cobalt 90 FAI 10T#22**	Ultra 3500-8
Weight	0.6	1	1	-1	**-1**	0
Score	1	-1	-1	1	**1**	0
Mounting Ease	0.25	1	1	0	**0**	-1
Static Thrust	0.8	0	1	0	**1**	1
Total Score		-0.15	0.65	0.4	**1.2**	0.55

Table 4.2 Alternative motors' comparison. Astro Cobalt 90 FAI 10T#22 is selected for Haberci aircraft.

4.1.2. Battery Selection: A battery, in the simplest terms, is described by two parameters: voltage and capacity. Each Nicad cell will on average produce 1.2 volts at full charge and has a fixed capacity. However, because of a cell's internal resistance, the actual available voltage is slightly lower; more like 1.1 volts per cell or even down to 1 volt per cell in the higher current installations. The capacity or how much charge a pack can hold is usually measured in milliamp-hours and tells how long the pack can produce a fixed voltage. Applied voltage adjusts how fast the motor will run and milliamp-hour capacity adjusts total run time.

Initial performance studies showed that 5 minutes of flight was required to complete the missions. So to get the determined range of 25 to 33 amperes, batteries, which are rated between 2000 milliamps to 3300 milliamps, will be the subjects of further analysis.

It is considered that batteries should take a compact form in the fuselage both to have ability to move it in the fuselage wider to stabilize the aircraft as guess limitation to stability studies and not to increase weight. So the batteries are thought to be at most C sized, which means a case diameter of 26 mm. and a length of 46 mm. Eight leading Sanyo battery types, that is in the determined region of 2000 to 3300 amps were analyzed. By dividing 5 lb. to the weight of each battery, number of available batteries is obtained. How much current should the batteries provide for the maximum total run of 5 minutes, is then found. That is, if a cell has 2400 milliamps capacity, which means it can provide 2,4 amps for 60 minutes, 28,8 amps is the value that it can provide for 5 minutes of flight. So power into the motor is found by multiplying voltage and current (Table 4.3). 3 batteries out of 8 provided enough power for defined flight time. Other 5 types could provide the same amount of power by increasing current into the motor however as aforementioned, increasing current is undesirable since efficiency of the propulsion system is reducing.

Cell Type	Capacity	Resistance	Unit Weight	Energy Density	Battery Number	Current (A)	Power In (watts)
Sanyo 2300SCE	2300	0.0055	2.05	1.122	39	27.6	1076.4
Sanyo 2400CE	2400	0.0065	2.69	0.892	29	28.8	835.2
Sanyo 2500CR	2500	0.0034	2.84	0.88	28	30	840
Sanyo 2800CE	2800	0.007	2.76	1.014	28	33.6	940.8
Sanyo 3000CR	3000	0.0032	2.96	1.014	27	36	972
Sanyo CP-2400SCR	2300	0.0053	2.05	1.122	39	27.6	1076.4
Sanyo RC2000	2000	0.0035	1.99	1.005	40	24	960
Sanyo RC2400	**2400**	**0.0032**	**2.08**	**1.154**	**38**	**28.8**	**1094.4**

Table 4.3 Each of Red written batteries provides enough power for defined flight time within defined current range. **Highlighted** battery is selected to supply energy to motor.

Sanyo RC2400 batteries are the same batteries as Sanyo CP-2400SCR but with less internal resistance. Therefore Sanyo CP-2400SCR battery was eliminated from consideration. Also RC2400 battery type has higher energy density and less resistance than Sanyo 2300SCE battery type. Therefore RC2400 batteries were selected for Haberci aircraft. Analysis for RC2400 batteries showed that between 27 and 34 amperes it efficiently provides sufficient current and voltage into the motor. Knowing that best performance of the selected motor is at 32 amperes, it established itself as the proper choice for selected motor.

4.1.3. Propeller Selection: Propeller converts the power of the motor into thrust. This makes the choice of propeller vital for the performance of the aircraft. A propeller in model aircraft industry is defined by two parameters: diameter and pitch values, generally in inches. Propeller pitch is the distance a propeller advances in one revolution assuming no slip. Propeller diameter is the diameter of the rotating propeller disc. As cruise speed, required thrust, motor and battery types are known, the rest of the work is to select the appropriate pitch and diameter values to convert the power, produced by selected motor, into defined requirements of thrust.

Performance studies showed that thrust is more needed than speed. DBF-03 program was enhanced using Blade Element Theory and Freude Propeller Theory and dynamic situation of the propeller and static thrust values are estimated. Diameter and pitch values should be such optimized that required static thrust is maintained while air speed is as predetermined. Static thrust is highly determined by propeller diameter while air speed is proportional with pitch and RPM values. How much current a motor "pulls" is set by the propeller's diameter, pitch and design. Using a larger diameter or higher pitched propeller increases current of the motor. Increasing the diameter of the propeller will increase static thrust however motor current will increase as well. Diameter is more affective on the motor load than the pitch value. So diameter of the propeller will be determined considering the 25 to 33 amps values of motor current.

Both diameter and pitch values affect factors such as the performance of the aircraft, static thrust and motor load. So to reflect the affects of both terms, diameter to pitch ratio is used. Historical trends reveal that d/p ratios between 1.5:1 and 2.0:1 give both average speeds and thrust. Greater d/p ratios result in reduced propeller efficiency at cruise speed, and lower p/d ratios result in stall occurrence on propeller blades at low speeds and efficiency again reduces. Although flying characteristics are not affected much, reduced efficiency in low speeds increases takeoff run. The reason for this reduced

efficiency is that thrust is traded for speed and slower acceleration provoked longer takeoff runs. So keeping d/p ratio around 1.5:1 will result in higher speed values and keeping the value around 2.0:1 will result in higher thrust values at the expense of speed.

The main limiting factor of the diameter of the propeller is the clearance from propeller tip to the ground. Because of the main limiting factor in design, the box that the aircraft should fit in, structural group designed the fuselage such that maximum distance from the top of the fuselage to the ground is 13.5 inches. As it has been already considered to keep the propeller diameter as much as possible, the main focus became on the pitch value. With a 1.5 inches of propeller clearance, diameter is determined as maximum 24 inches. For this value pitch is iterated between 8 and 24 values to find the proper combination.

Analysis showed that optimum pitch value between motor voltage and current is 16 inches. In battery selection, it was found out that RC2400 batteries efficiently supplied 28.8 ampere current for 5 minutes and a 24x16 propeller pulled 32 amperes at full throttle working conditions (Figure 4-1-a). However the airplane will not fly at full throttle settings for whole mission and the battery pack could supply 32 amps for 4.5 minutes at full throttle. So battery pack provided enough energy for propeller to work in determined region of RPM values for intended duration. For 16 inches pitch value static and cruise velocity available thrust values sufficed performance requirements (figure 4.1-b, 4.1-c) and maximum aircraft velocity is calculated as 57 mph (figure 4.1-d).

Propellers transform power to thrust and transformation ratios vary with the material of the propeller. Geometric definition (diameter and pitch values) of the propeller is done however material and manufacturer of the propeller played an affective role in power transforming into thrust. Although there are a lot of vital factors for the performance of the propeller such as blade shape, airfoil and tip shape, commercial propellers are being sold by only defining the diameter and pitch values. For the ease of design, experienced modelers were consulted instead of calculating the propellers performances via investigating the commercially sold propellers' airfoils or tip shapes. Modelers have defined some multipliers by experimental studies for propellers that are commercially sold. The constants reflect the airfoil's, tip shape's, blade angles' and these kind of parameters' effect on the performance. There are two main multipliers: thrust and prop constants. The team investigated 10 different manufacturers' propellers. None of the propellers suited for all segments of flight because if thrust constant is higher than prop constant, then the propeller transforms more of the power into thrust instead of RPM and therefore speed. And if the prop constant is higher than thrust constant, then the propeller converts the power into RPM and therefore speed more than thrust. So in segments such as climb, thrust is more needed than speed, in contrary for cruise conditions speed becomes the prime need and thrust is secondary. So propellers are not effective for all segments of flight however given the multipliers of each propeller, DBF-03 made mission analysis and showed the most appropriate propeller for each mission. Studies showed that wood APC propeller with a prop constant of 1.11 and thrust constant of 1.0 is the proper alternative.

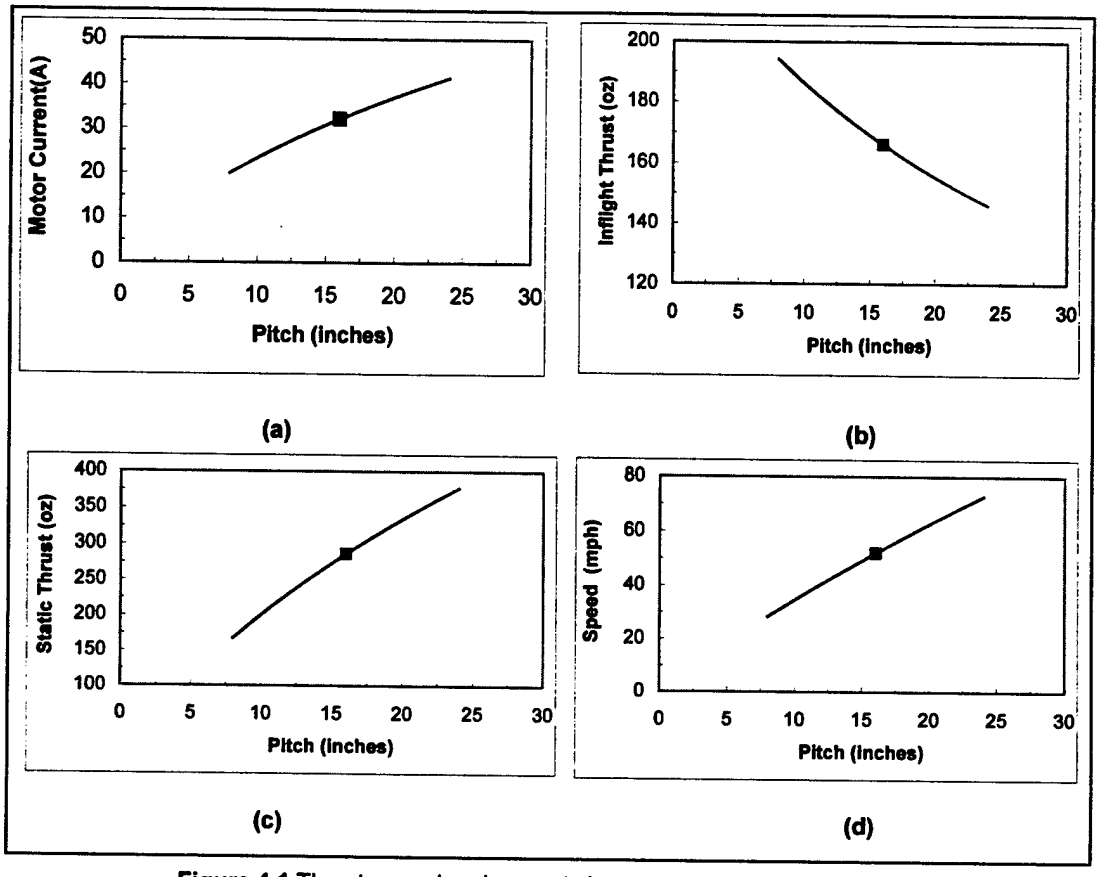

Figure 4.1 Thrust, speed and current change with pitch of the propeller

4.2. Mission Selection, Performance Analysis

Initial studies showed that A mission was selected and configuration selection was concluded as if the design process was done for A mission type. Following on the 2nd stage of determined mission selection method, selected configuration's mission performances for B and C types of missions was examined as to which type of mission it would better provide higher performance and score.

In order to develop the overall performance of the aircraft for A, B and C types of missions, first each mission segment was analyzed individually. Harmony between aerodynamic and propulsive performances gave optimized cruise and turn velocities for alternative missions. Propulsive studies showed the efficiency of the selected propulsion system.

Before starting the performance analysis, some basic parameters should be derived and assumptions should be made. The very basic parameter of an aircraft is the zero-lift coefficient known also as parasite drag coefficient. Considering the initial sizing trades investigated in conceptual design, historical trends and Component Buildup Method in Reference 2 helped the estimation of C_{Do}. Another basic parameter is Oswald span efficiency factor (e), which reflects the similarity of the lift distribution of a wing to the most efficient, elliptical, wing. e of the rectangular wing with aspect ratio of approximate 8.5 is assumed to be 0.72.

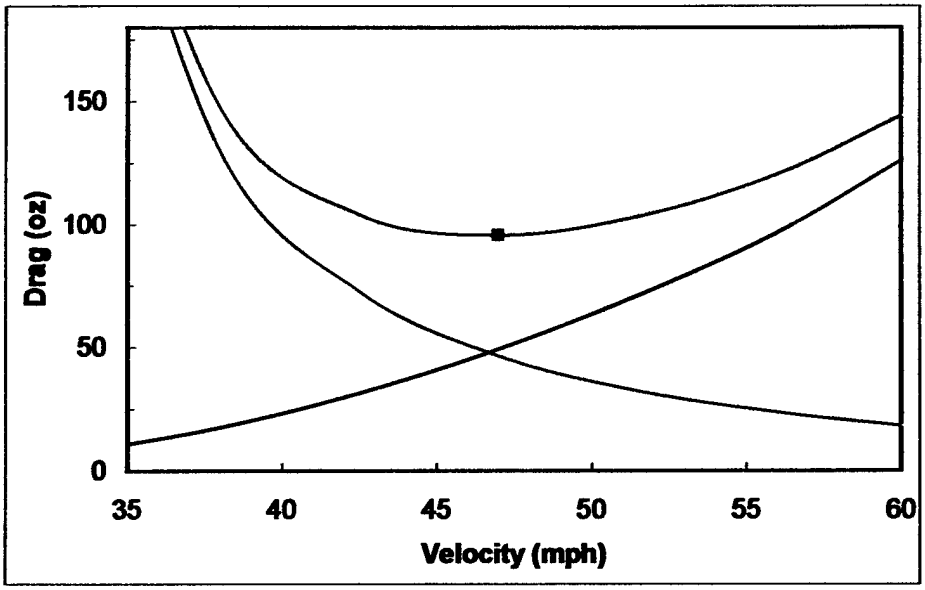

Figure 4.2 Red Drag change with velocity.Black curve is induced drag and blue curve is parasite drag

Cruise Performance: In order to spend the limited energy useful, cruise velocity was projected to be at minimum drag. With optimized wing loading value of 32.8 oz/ft^2 and lift coefficient of 0.36, the aircraft was intended to fly at 47 mph where minimum drag occurs (figure 4.2). Thrust value does not change with mission and as drag increases with the existence of antenna, 40 mph velocity is obtained with the same thrust value.

Takeoff Analysis: Takeoff ground roll is proportional with takeoff speed, available thrust, total drag and rolling friction of the wheels. The aircraft is intended to takeoff at full throttle settings and continue in the same manner until it climbs to its flight altitude. The most thrust demanding takeoff type is in A mission as both antenna and payload are on the aircraft. Propulsive studies showed that static thrust is around 218 ounces and thrust reduces down to 150 ounces until it reaches to takeoff velocity. The value of 150 ounces was adopted as takeoff thrust and the excess thrust will be the safety margin. Assuming the rolling friction coefficient of 0,04 for asphalt runway, ground roll and takeoff time were calculated for three types of missions.

Climb and Descend Analysis: In order to complete the mission in the least time, climb and descend times should be minimized and iterations in propulsive performance studies resulted in with full throttle climb and 25% throttle descend. The 25% descend will take more time however Haberci aircraft is designed without flaps and in order to come to a full stop before the start-line, power should be cut before landing. This will eliminate the risk of passing the start line and returning back. Brakes could be used however extra weight carriage throughout the mission was disadvantageous and as a general rule in designing Haberci aircraft, all possible weight reduction was the aim of the team. Inclusive data about climb and descend of three types of flights is in table 4.4.

			I	II	III
	Antenna		☑	☐	☐
	Payload		☑	☑	☐
Takeoff	Ground Roll	(ft)	110.3	72.83	52
	Takeoff Time	(s)	4.6	3.5	3
Climb	Climb Angle	(degrees)	18	21	23
	Rate of Climb	(fps)	12.36	14.33	15.63
	Climb Time	(s)	9.7	8.37	7.68
Descend	Descend Angle	(degrees)	-5	-6.5	-7.4
	Rate of Descend	(fps)	8.17	9.42	10.17
	Descend Time	(s)	8	6.65	6.1
Turn	Bank Angle	(degrees)	38.6	51.32	58.6
	Turn Radius	(ft)	134.6	86	65.62
	Load Factor (n)	(g)	1.28	1.6	1.92
	360 degree turn time	(s)	14.4	9.2	7.12
	Weight	(lb)	17.8	17.5	12.5
	L/Dmax		8.86	10.75	10.75
	Cruise Velocity	(mph)	40	40	46
	Stall Velocity	(mph)	26	26	22
	Maximum Velocity	(mph)	50	57	57
	W/S	(oz/ft2)	33.38	32.82	23.45
	P/W	(watt/lb)	68	68	77

Table 4.4 Estimated aircraft performance.

A - Missile Decoy mission consists of **I**

B - Sensor Deployment consists of **II** and **III**

C - Communications Repeater consists of **II**

Turn Optimization: Turn is another important segment of the missions. The goal is set to minimize the turn time. Important thing to consider while analyzing turn was the stall velocity in turn. Stall velocity increases with the square root of load factor. Therefore there is an upper limit for load factor not to stall the aircraft. When load factor increases to 2g, the stall speed passes the cruise speed. Optimization studies showed that turn at 1.6g minimizes the turn time at 40 mph. So the pilot will not need to lessen the throttle because 40 mph is also the cruise speed with antenna. For missions without antenna, pilot will cut down the throttle to 70% before entering the turn and the aircraft will again turn at 40 mph. Vital static about turn is in table 4.4. After optimizing all segments' completion times, single flight scores were analyzed. As seen in table 4.5, estimated completion times for each segment of flight in second was found using the output of aerodynamic performance study. Single flight score is the difficulty factor divided by flight and assembly times in seconds. Assembly time is not considered in this study, as the aim was to find out which of the missions would be selected. Single flight scores for each mission are found as 0.426, 0.384 and 0.253 in sequence with A, B and C. Therefore A and B missions were selected for Haberci aircraft for further studies. Especially this output will affect sizing trades because mechanism to settle the payload will be considered when sizing the fuselage.

	Missions			
	A	B		C
Segment	Total 4 laps	2 laps with payload	2 laps without payload	Total 4 laps
takeoff	4.6	3.5	3	3.5
climb	9.7	8.37	7.68	8.37
turn *	115.2	36.8	28.48	147.2
descend	8	6.65	6.1	6.65
landing	6.2	5.1	4.7	5.1
Cruise	138.3	66.14	57.52	66.14
Total (sec)	282	126.56	107.48	236.96
Total (min)	4.7	2.11	1.8	3.95
Completion Time	04:42	03:54		03:57
Difficulty Factor	2	1.5		1
Flight Score	0.426	0.384		0.253

Table 4.5 Estimated completion times for each mission (in seconds)

4.3. Sizing Trades Investigated

4.3.1. Airfoil Selection: Utilizing enhanced DBF-03 program, maximum lift coefficient of 1.6 was found to assure a safe take-off in the required distance. As antenna provoked stall tendency of the aircraft by increasing drag and reducing velocity, stall characteristic of the airfoil was the most important factor that was sensitively investigated. For the best stall characteristics, high stall angle and quickest stall recovery were desired. An abrupt stall meant unsecured flight, which is totally unacceptable. Since the aircraft would operate for majority of the time at cruise flight, airfoils that provided required level of stall characteristics were examined for maximizing efficiency during steady level flight. Therefore the airfoils that provided a lift coefficient capable of maintaining steady level flight near the airfoil's minimum drag angle of attack were desired. Based on an estimated design weight of 17.5 lbs, airfoils with minimum drag characteristics corresponding to lift coefficients in the range of 0.3-0.6 provided maximum aerodynamic efficiency. Therefore the parameters affecting the airfoil selection were primarily high lift coefficient and good stall characteristics, secondarily low drag coefficient and efficiency. Internet was widely utilized to find airfoils that are designed for Reynolds numbers of the same estimated magnitude of 400,000 for cruise and 250,000 for takeoff.

Among many airfoils, DAE11, DAE21 and SD7062 were the most promising airfoils for their efficiency in providing initially determined requirements of stall characteristics and maximum lift coefficient. Therefore secondary parameters showed the differences between three alternatives and the lift characteristics of each airfoil were the primary concern in consideration. While DAE11 and DAE21 offered higher lift coefficients than SD7062, lift coefficients for DAE series airfoils where minimum drag occurs were 0.72 and 0.9 in sequence (Figure 4.3). As the predicted cruise flight lift coefficient values ranged between 0.3 and 0.6 for the best aerodynamic performance, two alternatives' drag in cruise flight would be higher that optimum values. SD7062 offered a maximum lift coefficient of 1.62, which sufficed mission requirements. And providing a lift coefficient of 0.5 at zero degree angle of attack with 0.008 drag coefficient, SD7062 established itself as the optimum choice for Haberci aircraft.

* Turn includes both 360° turns and two 180° turns on each leg.

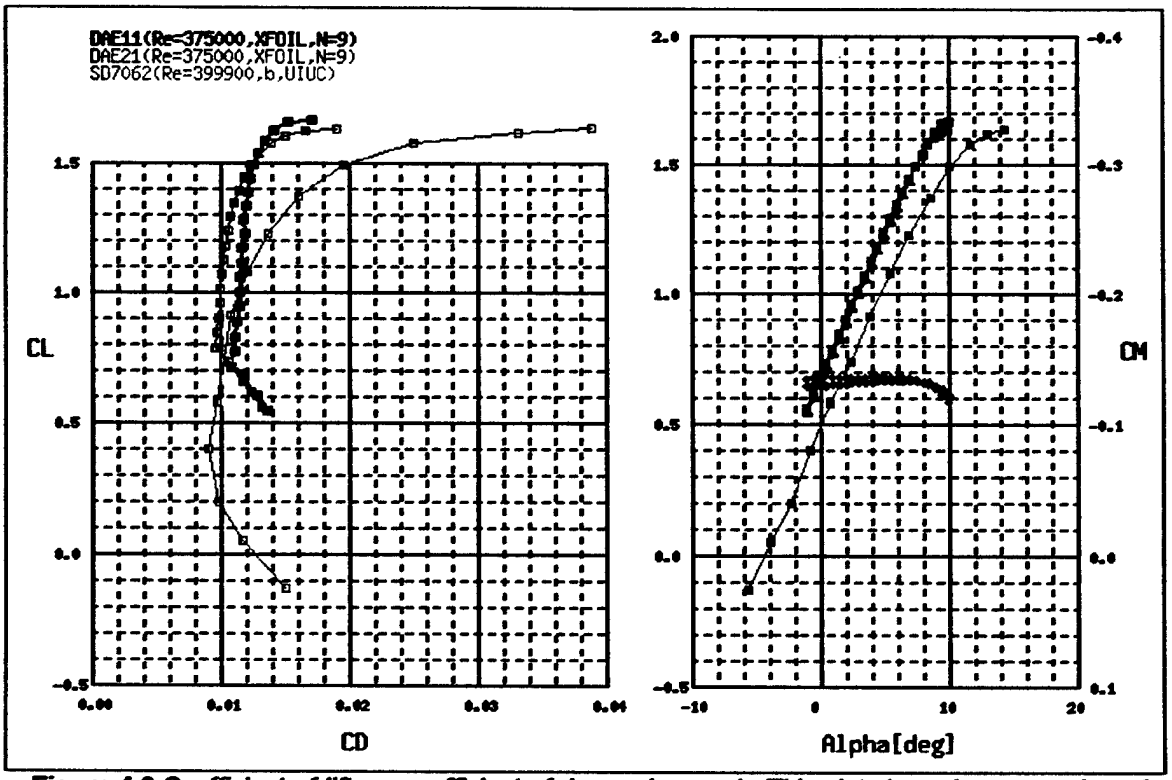

Figure 4.3 Coefficient of lift vs. coefficient of drag polar graph. This plot shows how a number of different airfoils compared with each other. An airfoil with a high lift coefficient and minimum drag at cruise lift coefficients was desired.

With SD7062 airfoil, stall occurred at around 15-degrees and loss of lift was gradual therefore takeoff in 120 feet and safe flight was assured. As aircraft would be assembled, detachment and attachment of wing to other parts was required. This would be achieved by a finite spar only at the connection parts and enough room for this material was required. The thickness of the airfoil was 14%, which was sufficient for structural strength and room for spar material. The camber was 3.97% and the profile was of a rather simple shape, therefore it would not constitute any manufacturing difficulty.

The profile of the tail surfaces was chosen to be symmetrical. SD8020 airfoil was chosen as the tail profile due to its low drag coefficient, and the fact that it provides sufficient room for structural strength with its 10% thickness.

4.3.2 Wing: Considering the estimated weight of the aircraft, the wing area was found 8.53 ft^2 to produce required lift. Utilizing DBF-03 with Prandtl's improved lifting line theory, the size of the wing was optimized to create the least drag with an aspect ratio of 8.53 and constant chord of 1 feet.

4.3.3. Fuselage: The fuselage should structurally maintain strength to withstand the static and dynamic forces during the mission profiles. Another factor to consider is the weight of the airframe. The less the weight of the airframe, the better performance the aircraft establishes in flight. However, besides these secondary factors in sizing of the fuselage, the centerpiece was the box that the aircraft will fit in and the payload deployment system. To have more handling over the fuselage, it was divided into three parts: nacelle section, main structure section and aft-fuselage section. (Figure 4.4)

Motor placement is determined to be in front of the fuselage in conceptual design and as the dimensions of motor were known, the front part of the fuselage would be sized considering the best aerodynamic efficiency, least airframe weight and volume. In order not to create excessive pressure drag in aft part of the fuselage, this part could be smoothly faired and control system components were thought to be placed in this aft part of the fuselage. So it was predicted that approximate sizes of aft and front parts would not change in great deal. The main part of the fuselage is the middle part that will carry both payload and deployment mechanism.

Nacelle section: The motor dimensions and weight are constant. In this case the main concern was to have enough strength to withstand thrust and weight forces. The main constants that will guide this section dimensions are: engine length, enough structural strength, aerodynamic efficiency, and engine mount attachment. Propulsive studies' resulted in 24 inches propeller selection and enough propeller clearance was obtained by mounting the motor in upper part of the nacelle. This also provides ventilation cooling, and reaching ease. And aerodynamic studies showed that the most effective way to minimize the drag of this section is an ellipsoid shape. Considering motor length, the shaft of the motor and hub of the propeller, the front part of the fuselage is determined to be 5.9 inches. The width of this section would be determined considering the main section width to have an aerodynamic continuity surface at the connection points. The approximated width for the nacelle section was 7.48 inches. The height of engine section was decided with the structural strength and aerodynamic counter continuity with the payload section. This led to an approximately height of 8.66 inches. Nacelle section will be constructed to accommodate the engine mounting and battery cables. In addition to this, servo for the deploy mechanism was going to be connected to the firewall to have structural strength. Firewall, the key structure of nacelle section, is related to the loads of thrust and weight from motor mount, load of payload weight and other structural loads of lift and weight from payload section. Firewall was considered to be manufactured of 0.2 inches plywood plate.

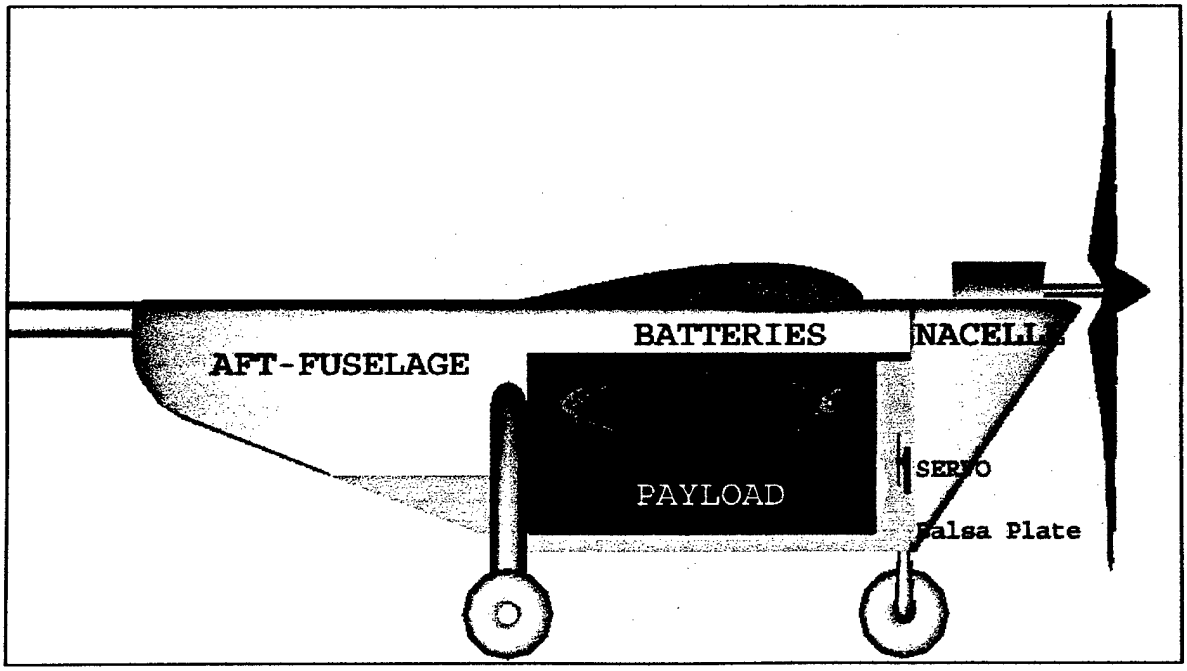

Figure 4.4 Side view of the fuselage. Side surface is removed to see the mechanical systems.

Main structure section: This section is the aircraft's main structural unit that will combine the other parts. The probable loads on main structure are from: payload, batteries pack, deploy mechanism, landing gear, wing, and boom connection part. The constant dimensions for main structure section are the payload and battery pack.

First consideration on this part was about location of center of gravity. As the aircraft was intended to fly three different sorties (with antenna and payload, without antenna with payload and without antenna and without payload) center of gravity is a major parameter for control of the aircraft. In order to control the aircraft easily by small trim adjustment in elevator and rudder in three different sorties, the center of gravity of aircraft was assumed to be at the cg of payload. This caused no extra study for mission flight without the payload. By intersecting the cg of payload with cg of the aircraft, the same cg location is obtained for mission profiles with and without payload. Another thing to consider was the battery placement and formation. They cover a great deal of volume in the fuselage and they form almost 30% of the weight. So for the ease of design, the batteries were thought to be placed in such a way that their cg almost equalizes the moment of the motor and eccentricity of thrust from longitudinal axis. This would constitute almost the same cg of the aircraft. This means that the best way to solve this problem was to place them over the payload, below the surface of the upper part of the aircraft (Figure 4.4). Also battery section has a great importance with its structural construction. Under sudden loadings its structure must withstand loads for a safe flight. Such a structure will be assembled with thicker balsa panels. This part has same duties like spine structure, obtaining homogenous load distribution between nacelle section (thrust) and aft section (loads from boom). Spine structure is main load carrying assemble between nacelle, aft-fuselage and wing groups.

At this stage, the deployment mechanism should be analyzed: Deployment mechanism should be so simple that there shouldn't be any problem during the flight. The drop mechanism included three main parts that are projecting parts located around the payload, sliding mechanisms at the inferior of the fuselage, shaped like an ear, and deploy mechanism. (Figure 4.4) Projector parts, located around the payload, were used to keep the payload stable and carried most of the weight. This tool would be fitted on to the sliding mechanism. This part should have been designed by an element that would allow the payload projecting parts to slide easily. This part could be made of a core element wrapped with nylon. Sliding mechanisms at the inferior of the fuselage were used to slide the payload and drop it. The ear shaped parts were thought to be located with an angle respect to the x-axis, to facilitate the sliding. Ears were to be constructed united with the fuselage to have a rigid structure. Deploy mechanism consisted of a balsa plate and a servo. Plate would keep the payload stable in flight, and on the ground it would be pulled by the servo. Then the payload would slide and then drop. Payload drop mechanism's driving force would be the servo, located in fuselage-side of the firewall. A spring or an elastic rubber could be attached to servo, by which enough moment force could be obtained. The below part of the fuselage would not be "closed" like the side parts however the payload and the plate on which the payload was settled, would fair the fuselage and behave to be a surface in that area. A balsa plate would be placed over the payload to close the gap after deployment. Cover could be made below the fuselage for deployment however simpler alternative of deployment enabled not to investigate complicated mechanisms to "open" and "close" the cover.

Aft Section: The key factor for determining the rear part of the plane was the aerodynamic efficiency. The aerodynamic group gave an approximate value of 30 degrees angle to fair aft fuselage. The aft fuselage section should resist the moment that the boom and empennage causes. To have such strength this part was lengthened. The boom holding structure at the aft section had to be connected with the payload section. The maximum distance available from boom-aft fuselage connection part to the main fuselage section would make a tougher structure. Because of deploying the payload just beneath the aircraft aft section's height was considered to be shorter than the payload section's height (Figure 4.4). Constructing such a shape enhanced the plane to run over the payload easily, and enabled the landing gears to become shorter than normal aerodynamic counter surface. This absolutely had negative affect of the gap existence when flying with the payload. However the mission requirements demanded generation of such concept. And when flying without payload, the below fuselage part would be closed by a balsa plate and this plate would be connected to the leading point of the aft part. So gap would not exist when flying without payload and les than 30 degrees of fairing would exist, which was efficient enough not to create excessive form drag.

These first structural and volume related approximations for the aft section has lead to 9.85 inches length. But this would be steep for aerodynamic effects so this part was lengthened to approximately 13.38 inches. The difference of 3.54 inches would be the boom in the aft section. So by this structure the boom load would scatter to a wider area.

4.3.4. Empennage: The main function of the tail was to provide trim, control, and pitch and yaw stability for the aircraft. H-tail configuration was selected amongst the others and this facilitated the fitting of the aircraft into the transportation box by lowering the tail height. Once H-tail configuration was decided, the next step was to find the shape, area and location of the horizontal and vertical stabilizers. These evaluations were made based on performance and stability.

Horizontal Tail: Horizontal tail size and location were determined by running simple stability calculations in order to reach a 20% static margin. To keep the aircraft in that stable position, required horizontal area was estimated using tail moment coefficient (V_H). Horizontal stabilizer area was found to be 245.67 in^2, and tail moment arm was 22.44 inch from the cg of the aircraft to the mean aerodynamic center of the horizontal tail. Wingspan of horizontal tail was equal to quarter of the wingspan of the wing, 25.59 inch. C_{root} and C_{tip} were 12 inch and 7.2 inch respectively with a taper ratio of 0.6. Also stability calculations resulted in one degree of incidence angle.

Vertical Tail: Vertical stabilizers were sized based on determining the yaw stability derivative. In order to have good yawing characteristics vertical tail moment coefficient (V_V) was used and total area was found. Since it was a H-tail configuration, the area of each vertical surface was estimated as 59.9 in^2. Wingspan of each vertical surface was 10.24 inch. C_{root} and C_{tip} were 7.07 inch and 3.94 inch respectively. SD8020 symmetrical airfoil was used on both horizontal and vertical surfaces.

Tailboom: A hollow cylinder was determined for tailboom geometry. It provided enough stiffness to ensure that the aircraft would not experience elevator control reversal. The tail moment arm of horizontal stabilizer was 22.44 inches from cg of aircraft to aerodynamic center of horizontal stabilizer. 1.181 inches of diameter of the tailboom was estimated to structurally suffice the loads.

4.3.5. Landing Gear: Transportation box regulation led the team to design a plane with the shortest height. As described in fuselage sizing, little changes could be made to the payload section because of the fixed dimensions of the payload and the batteries. Under this situation landing gear determined the height in relation with the propeller. Landing gear's limiting subjects were box dimensions, propeller diameter, payload deploy mechanism and boom clearance from the ground when landing and taking off. Payload section's approximate 8.66 inches height has left only 0.2 inches for the landing gear. This dimension should be used effectively to have a ground clearance enough for the propeller. To allow the aircraft go over the payload, the landing gear must pass through the upper part of the aft section. Because of this configuration, the payload section would get the landing loads by its upper sections, which were the main framework of the aircraft. By this connection there projected to be no need for any other strengthening structure and this would result in lighter aircraft (Figure 4.4).

4.4. Structure Analysis

4.4.1. Component Attachment and Integration: Haberci aircraft has 4 fundamental component groups: wing, fuselage, empennage and landing gear. These basic component groups could be classified as fixed and detachable parts. Because detachable parts require more space and weight, their size were kept as minimum as possible.

Fixed Components: Most of the components were designed to attach each other constantly. It was considered to attach these fixed components with advanced adhesive bonding techniques. These methods include both the same and different materials' bonding. Rather than mechanical fasteners, bonding technique has superiorities in load distribution. Distributing the load to wider area, it does not cause notch effect. Probable sections that carry critical loads were laid out with fixed components. During the design, butt joints were avoided and tee and lap joints were preferred. Most of the fixed components were bonded to the fuselage so that these components would have enough stiffness to support the wing and the empennage against aerodynamic forces and weight.

Detachable Components: Transportation box size limitation required detachable components. Aircraft was thought with three main attachable parts, which were fuselage, wing and empennage to fit in the determined box. Tee and lap joints were again selected for detachable components. All detachable parts were thought with discrete fasteners. These fasteners are easy to install and remove however they condense load distributions. Cross sectional areas of places where load distributions are getting higher should be expanded or their numbers should be increased. Main structure around these connection parts should be supported with materials that have better resistance.

According to approximation about load distributions, connection points between fuselage-wing and fuselage-boom was very critical. Wing platform was divided into three main parts to lessen the load distribution on connection parts. Tip parts of wing were relatively longer than the middle wing part, which is constantly attached to fuselage. Fuselage-boom attachment section should have enough stiffness to carry the moment forces applied by the empennage.

4.4.2. Assembly Firmness Analyses: Because of attachment and detachment requirements to fit in transportation box, connection parts were sensitive in structure and should be analyzed. Three main connection parts were analyzed:

Wing Fuselage Connection: In flight, aircraft's whole weight is carried at this joint. This critical part was considered to be connected with epoxy and nut. And over this structure, fiberglass composite would be applied. The main concern in applying epoxy was that it could damage the foam. To prevent this, the epoxy curing time will be scheduled and obeyed very strictly. At the combining sections if air remained, that section would have no more strength.

When combining foam and the balsa with nut, nut can damage the foam. If the torque applied to the nut is excessive, the foam crushes. Also in composite structures, if the composite is drilled in some place, it looses its superior features at that point. To avoid this, a screw would be united to the composite structure as it was constructed and cured. By embedding screw into composite it was considered not to damage it to cause undesirable results. Since foam and nuts were covered with fiberglass, the structure would be more stiff and tough. The fiberglass was projected to be wrapped in longitude and lateral axis. The main problem here was the discontinuity counters at the boundaries of the connections. The fiberglass would be cut to match the shape of the structure and than be plastered. This would cause discontinuity of fiber at the connection parts. So the strength of the construction would lessen but was still estimated to carry loads sufficiently and help to form the main structure of the aircraft.

Fuselage-Boom connection: The moment that boom transmits to the fuselage was the main concern. This moment would cause deformations both in the boom and the boom-fuselage joint. But here in this discussion the boom is negligible. Because the deformation at the connection could be prevented by using two nuts located tandem far enough from the edge not to cause any cracks. The overall structure was wrapped with fiberglass and epoxy mixture. Furthermore mechanical fitting was considered to be applied. The boom's extension to the main section of the fuselage would be advantageous for providing strength against moments. So boom extension part into the fuselage was determined to be kept as long as possible. However this had some disadvantages like keeping volume in the fuselage and increasing the weight. Optimum extension distance into the fuselage was determined to be approximately 11.81 inches.

Fuselage-Landing Gear Connection: The sudden loading at the landing gear is transmitted to the fuselage at the joints. At this stage, a general landing gear shape could be approximated. To transmit the loading without any damage to the fuselage, the landing gear would pass through the fuselage. At the touch points between the landing gear and the fuselage, epoxy would be used to combine these two parts. At the top section of the landing gear, fuselage structure would be strengthened.

4.5. Stability Analysis and Handling Qualities

From the beginning of design, stability and control analysis of the aircraft were given much importance, because it was thought that the antenna and the payload would remarkably affect the stability characteristics of the aircraft. While optimizing the dimensions of the aircraft, stability requirements were considered attentively. During preliminary design phase, both static and dynamic stability conditions were examined. Static stability refers to the tendency of an aircraft to return to a trimmed condition after having a disturbance or following a small perturbation. After all dimensions of the aircraft were known, pitching moment contributions of the antenna, wing, fuselage and tail were examined to determine if they were in the direction to force the aircraft back into equilibrium.

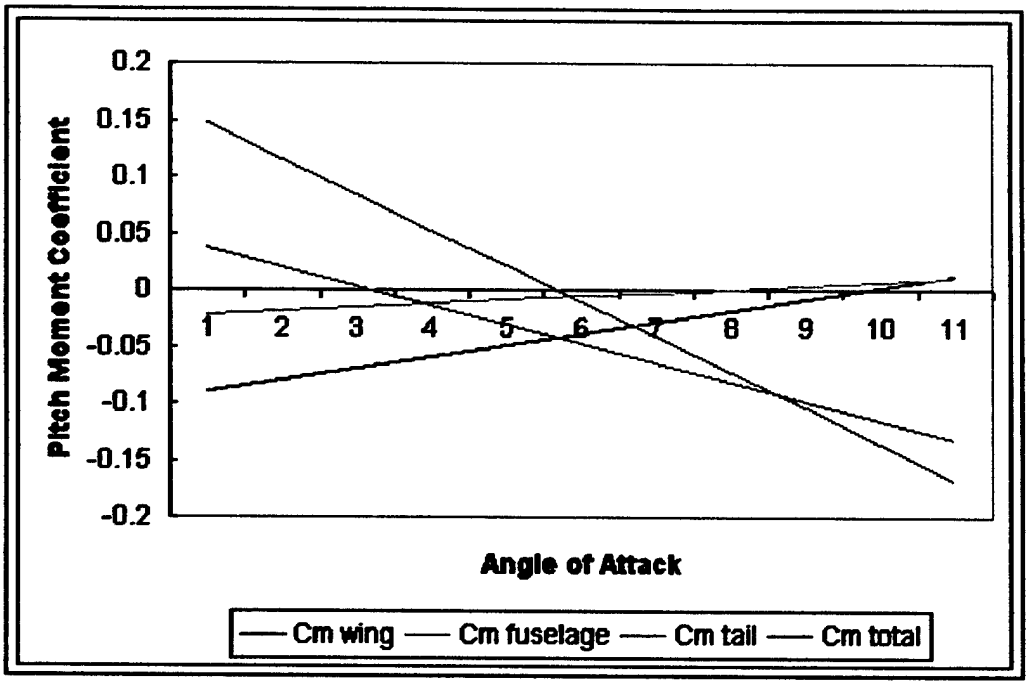

Figure 4.5 Pitching moment contributions of components.

CMα total stability derivative was found and pitching moment characteristics are shown on the Figure 4.5. Pitching moment contribution of the antenna was investigated with fuselage. Static margin was found to be 20% and the aircraft was trimmed at 2,75 degrees angle of attack in cruise. A static margin of 20% would be enough to let the pilot control the aircraft in safe flight conditions and also it was decided that a static margin of 20% would provide sufficient stability giving the pilot the feeling that the aircraft is handled well or not. One of the main problems was the longitudinal control of the aircraft. The aircraft should be trimmable at different values of C_L, cg location, and airframe configuration. The tail and elevator areas were determined in order to meet these requirements. Control power derivative, which shows change in pitching moment due to elevator deflection, was determined.

In addition to this, lateral-directional stability characteristics were examined. Control power derivatives were investigated. H-tail configuration gave a yaw stability derivative of 0,153 per radian. It was provided to be slightly roll stable in order to avoid from sideslipping that could occur from a roll moment, and also effects of the wing and configuration of the aircraft were taken into consideration. The other control power derivatives were determined and the results were shown on the table 4.6.

$C_{L\alpha}$	5.74	$Cm_{\delta e}$	-1.856
Cm_o	0.036	$Cl_{\delta a}$	0.473
Cm_α	-0.968	$Cn_{\delta a}$	-0.0317
Cn_β	0.103	$Cn_{\delta r}$	-0.101
Cl_β	-0.029	$Cl_{\delta r}$	0.035

Table 4.6 Static Stability Derivatives

In dynamic stability analysis, two major values were the subject of concern to determine. These were damping ratio (ζ) and undamped natural frequency (ω_n). They were determined 0,925 and 3,52 rad/s respectively, which meant that Haberci aircraft had acceptable stability characteristics.

4.7. Analysis Methods Used

In structural considerations, numerical methods were used for crude estimates. However for sensitive components' structural analysis such as wing tips or boom, Finite Element Methods were used and utilizing ANSYS software, analyses were made in sensitive parts to investigate the tensions and displacements that are presented in detailed design. According to Von-Misses criteria, a safety margin of 1.25 was determined to accommodate in all design phases. For aerodynamic considerations, initial studies depended upon classical lifting-line theory but further in design phases extended methods, including approximate solution of wake momentum integral equation, were used especially for determination of overall drag. Propulsive studies were generally based on experiments, estimates and assumptions. Theoretical basis of propulsive studies was founded upon classical electronics calculations. Propeller subroutine of DBF-03 was enhanced with Blade Element Theory and Freude Propeller Theory. Results from two theories were then compared. Also classical stability and performance studies were carried out. DBF-03 program was enhanced in preliminary design by these methods and was extensively used in all design phases.

5. DETAIL DESIGN

Major components sizing in preliminary design phase required subsystems' examination and component selection. Component attachment and integration was also a subject of concern. Therefore central premises in detail design phase were to increase the various sides of the components. Propulsive efficiency, control and lifting surfaces sizing and structural refinements were made. A good weight & balance calculation is the keystone of flight-testing. Therefore after structural refinements were concluded, balance of the aircraft was inspected. Minor components could cause serious problems if they are disregarded from consideration. Therefore detailed drawings were developed and every component was sized. The drawings were then used in manufacturing process.

5.1 Component selection and systems architecture selection

5.1.1. Control Surfaces Sizing: The ailerons were sized to give satisfactory roll control at angles of attack above the stall. The chord-wise aileron length was determined to be 3 inches with the span-wise length of 1.7 ft. And because the wing with the selected airfoil SD7062 assured required lift at takeoff and landing, the team decided not to use flaps. Once the tail was sized, the elevators were considered in order to provide enough stability during cruise. Elevator effectiveness is related to the percentage of elevator area to tail surface area. The determination of the chord-wise elevator length was based on experimental data. Since no flap was used on the aircraft, 25% ratio of elevator to total tail area was considered to be adequate for trim adjustment between different sorties. The full up-elevator travel was 35 degrees, while a down elevator of 20 degrees was adequate. Therefore, the area of elevator is 61.4 in^2 with root chord length of 3 in. and tip chord length of 1.8 in.

Since for adequate rudder effectiveness to recover from spins, for sideslipping and to control slipstream effects at high rpm and low speed in climb, a rudder area of 32 percent of total vertical tail

area was determined. Angular travel was 30-degrees on either side of neutral. The rudder area was determined as 30% of vertical tail area. Since an H-tail configuration was used, two vertical tails and rudders appeared. Therefore, fitting the rudder came up with a span of 20.83 inches and a chord of 0.87 inches.

5.1.2. Propulsive Considerations: After performance parameters were determined, propulsive efficiency for the determined combination of specific motor, gearbox, battery and propeller was investigated. DBF-03 program was enhanced via mathematical models and applicability of aerodynamic performance was confirmed. 3 main abilities of propulsion system were analyzed.

5.1.2.1. Battery Durability: After durations of all segments of flight were determined, batteries' durability for missions was analyzed. DBF-03 program iterated over mission segments in order to find the optimum throttle settings for each segment of flight. Motor amperes and therefore battery amperes change with throttle setting. So for each throttle setting, consumed milliamps of battery capacity changes. RC2400 batteries provide 2,4 amps for 60 minutes and as the ampere to the motor increases, the duration of batteries reduce. Given the inputs of all segments completion times, DBF-03 gave the optimum throttle settings for each segment. The analysis showed that with a throttle setting of 80%, the aircraft both gives the thrust required for 40 mph cruise flight with antenna and batteries long until mission completion. The consumed milliamps for A type of mission is 2355 and for B type 2050. Thus batteries are used effectively. The results can be seen in table 5.1.

		Consumed milliamps		
Segment	**Throttle**	**A**	**B**	
takeoff	100%	42.17	35.97	27.5
climb	100%	88.92	76.725	70.4
turn	80%	960	368	284.8
descend	25%	33.33	27.7	25.41
landing	0%	0	0	0
Cruise	80%	1230.92	606.2	527.2
Total		2355.33	1114.6	935.3
Total comsumed mamps		2355.33	2050.07	

Table 5.1. Battery milliamp consumption for each segment of missions

5.1.2.2. Motor efficiency in producing required output power: As required thrust values for all segments of flight was determined, motor's efficiency in producing the required power was investigated. Motor volts and amperes was known, therefore the input power and motor's efficiency in transferring the input power to the shaft was calculated considering the losses of the motor (Figure 5.1-a). The maximized efficiency at cruise was 80%.

5.1.2.3. Propeller efficiency in converting the shaft power to thrust: The last segment of conversion of battery energy into thrust is the propeller. Determining diameter, pitch, material and the manufacturer of the propeller, efficiency of transformation shaft power into thrust was analyzed for different airspeeds. (Figure 5.1-b). This plot showed that estimated values in aerodynamic performance analyses were sufficed by propulsion system for takeoff, climb and cruise conditions.

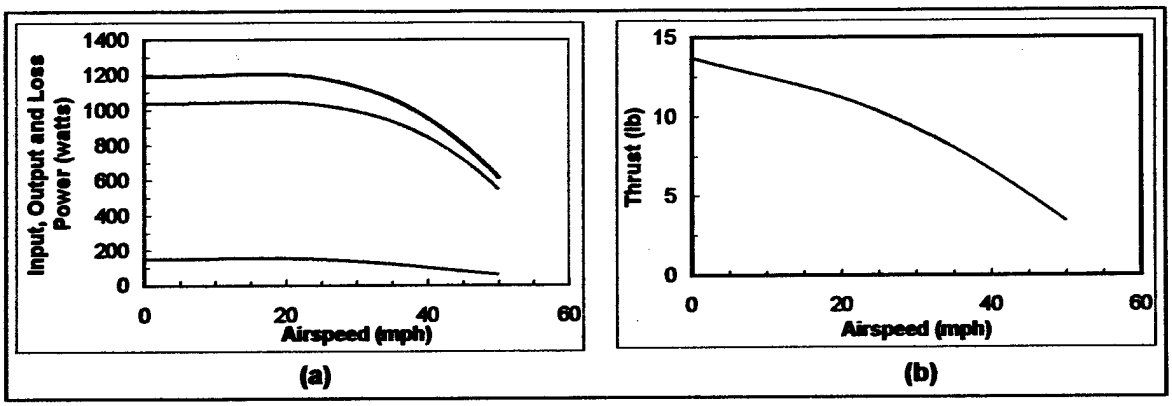

Figure 5.1 Propulsive Performance Analyses Results

(a) - Black input, Red output, Blue loss power **(b)** - Red Thrust

5.1.3. Structural Refinements

5.1.3.1. Wing: Loads that act on the wing are aerodynamic loads, gravity, and maneuvers g-loads. To withstand these forces the sensitive sections that are fuselage-wing and main wing - outer wing, have been modified by the results of the ANSYS analyzes. First, the main wing part and outer wing part connection was modeled. The sensitive part was the outer section, so only this part has been investigated. Because the wing is composed of foam core and fiberglass cover, an average value for Modulus of Elasticity (*E*) was needed. Reference 4 helped to guess the *E* of foam. The foam's *E* depends on the density and is around 0.14Gpa. The fiberglass's *E* is 68.9 GPa. Because the fiberglass's *E* is much greater than the foam's, the average value for the whole wing construction will be likely the fiberglass's *E*. The foam's mass is excessive when compared with the fiberglass but its portion in the overall *E* will be smaller. Under these assumptions the overall *E* is accepted 70 GPa.

To obtain the load distributions and deformation spectrum over the surface, the wing was modeled in the ANSYS-GUI. The whole wing was thought as a uniform and homogeny material. From the material library "structural solid > Brick 8 node 45" element was selected. Because the main wing-outer wing connection point was accepted to face no deformation zone, the model was fixed from this part. The aerodynamic lift distribution curve was modeled as a linear load, and it was equalized to the weight of the aircraft. By these assumptions, the aerodynamic load acts on the outer wing part was 98.1 Pa. For the maneuvers g-loads, n = 1.92, was applied. After the solution phase, applying the postprocessor, the deformation and load distribution, according to von misses criteria, was obtained.

The wing tips deformation was as predicted, greater than the other sections. And the maximum deformation at the wing tip was 0.239 10^{-4} meters. This deformation was so small that the wing could be supposed as a rigid bar. In the Von misses stress distribution figure 5.2, root sections' trailing edge part was one of the most stressed regions. This was because, the aerodynamic lift distribution was applied as a linear function, but in reality it is elliptical. This region was not supposed to be analyzed in this solution, so results for other sections were still applicable. Under this situation, the maximum stress distribution was seen in the root part that vindicates the predicted approximations. The maximum stress was 642686 Pa, which is much lesser than the yielding strength of the even foam. Foam's yielding strength is approximately 12 MPa. After analyzing the wing outer section, it was observed that the structure was strong enough to withstand the acting forces.

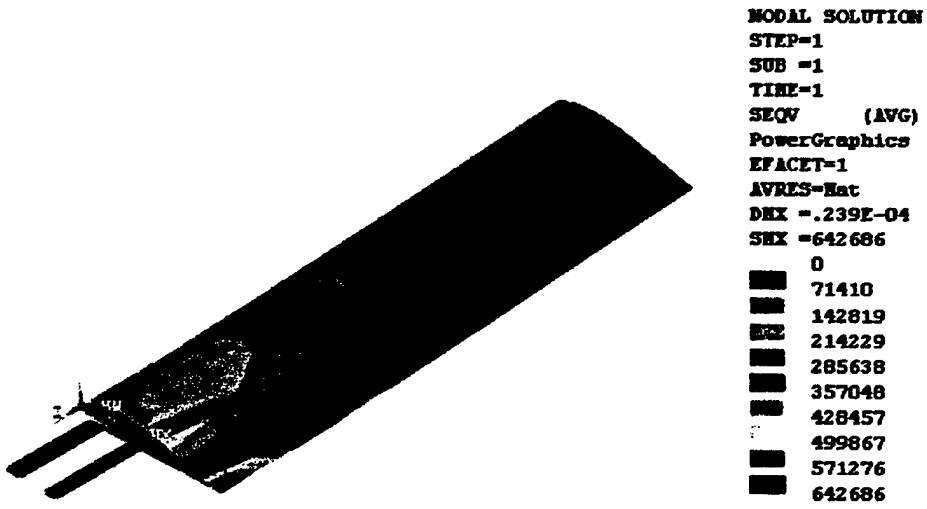

Figure 5.2 Stress distribution according to Von misses criteria.

Figure 5.3 Stress distribution according to Von misses criteria.

5.1.3.2. Tail Boom: For the tail boom, a balsa bar core and a fiberglass covering would be used. The fiberglass was dominant part here and the assumptions made for the wing could be used for an sufficient approximation of the stress distribution. So the elasticity of modulus was taken as 70 GPa. The loads here is the moment that empennage created under aerodynamic forces, and the mass of the boom. The boom was 22.44 inches. To have rigid connection at the fuselage-boom connection point, the bar was thought to go into the fuselage until it reaches 7.88 inches depth. By this construction structure the boom's overall length would be 30.32 inches in total. Empennage created a -0.7 foot-pound moment at the tip of the boom. Under this loadings and boundary conditions the result is shown in figure 5.3. The deflection at the tip was 0.641 10^{-4} m. The maximum stress was at the singular attachment points, so they can be omitted. The yield strength of the material was much greater that the stress value in the bar. As it was stated for the wing, the boom had enough strength for the loadings. It has been approved that the composite configuration satisfied the n = 1.92 safety coefficient.

5.1.3.3. Fuselage: Loads acting on the fuselage are wing's aerodynamic loading, engine's thrust force, landing gear loads, and empennage moment transmitted with the boom. To endure these forces structural improvements have been made. By the wing and boom analyze results it can be stated that the construction with fiberglass is strong enough to resist stated loads. Under this assumption the general model aircraft construction experiences was used. To resist the loading of the wing at the fuselage-wing connection, an 8 mm balsa sheet was determined to be used. The connection would be made with nuts and fiberglass was thought to cover the fuselage. By experimental data, fiberglass would give enough strength to the structure.

At the landing gear-fuselage connection, it will be tried to scatter the load to a wider area. The load that would be applied to the landing gear will be about 1.53 times the aircraft weight. To achieve a safe landing, the landing gear is thought to go through the fuselage. At the connection area epoxy is determined to be used to fix the landing gear.

The nacelle would transmit engine's thrust load to the fuselage. Epoxy and fiberglass covering would be used in the connection of fuselage and nacelle. The engine mount would ease this connection but its first task is to fix the engine.

To have a stable connection at the boom-fuselage part the balsa sheets was decided to be used. The main thought here was to spread the moment and this would expand the load to a wider area.

5.1.3.3. Empennage: The empennage was decided to be constructed with balsa profiles. The number of the balsa profile was estimated from experimental. The main loading on the empennage would be caused by the moment. Because the horizontal stabilizer, and vertical stabilizer have a symmetric profile, there is no lift but when the elevator and rudder is turned, moment occurs at the 0.25 of the chord. To resist such a moment, two tandem spars will be used. The thickness of these spars is 5mm.

5.1.3.3. Landing Gear: Landing gear was examined in two parts, which were main landing gears and nose landing gear. Both of them have different features because of the main configuration of the modal aircraft. Nose landing gear was designed for strain bending abilities because of the propeller dimension. Main landing gear carries most of the static load of the structure during the taxi and landing. As stated in fuselage section the approximated load that acts on the landing gear is 1.53

times the aircraft weight. To resist such a force, the core of the landing gear would be cut from the balsa sheets using templates. Three layers of balsa sheet would be attached to each other with epoxy. Fiberglass would cover this balsa sheet structure.

5.2.Weight and Balance

Accurately determining the aircraft's take-off weight (Table 5.2) and ensuring that the cg is within the aircraft's design for each flight is critical conducting safe flight test. More accurate weight breakup of the aircraft was prepared and this helped to conduct the balance study (Figure 5.4). As the batteries, payload, wing, main fuselage section and antenna, weighing 199 ounces in total, were placed at the cg of the aircraft, the balance of the aircraft was easily provided. The result of balance studies showed that cg was accurately determined and the aircraft was safe for test flights.

Weight Breakup

Propulsion And Control System	
Motor	35
Batteries	79.04
Shrink Wrap and End caps	0.9
ECS	1.060
Rx and Rx Batteries	4.5
Propeller and nut	3.43
Servos	12.1
Total	**136.03**

Wing	
Outer	7x2
Inner	6
Fitting Mechamism	1.47

Empennage	
Horizontal Tail	3.53
Veritical Tail	1.24
Boom	1.6
Total	**6.37**

Fuselage	
Nacelle section	
Foam	4
Motor mount	3
Firewall Plywood	1.76
Main Section	
Foam	3.2
Balsa	7.04
Payload	80
Aft-Section	
Foam	4.2
Total	**103.2**

Landing Gear	
Nose	4.9
Main	9.2
Total	**14.1**

Total Airframe weight	65.14
Control System Weight	17.660
Propulsion System	118.37

Payload	80
Empty weight	201.17
Total Weight	281.17

Table 5.2. Weight Breakup

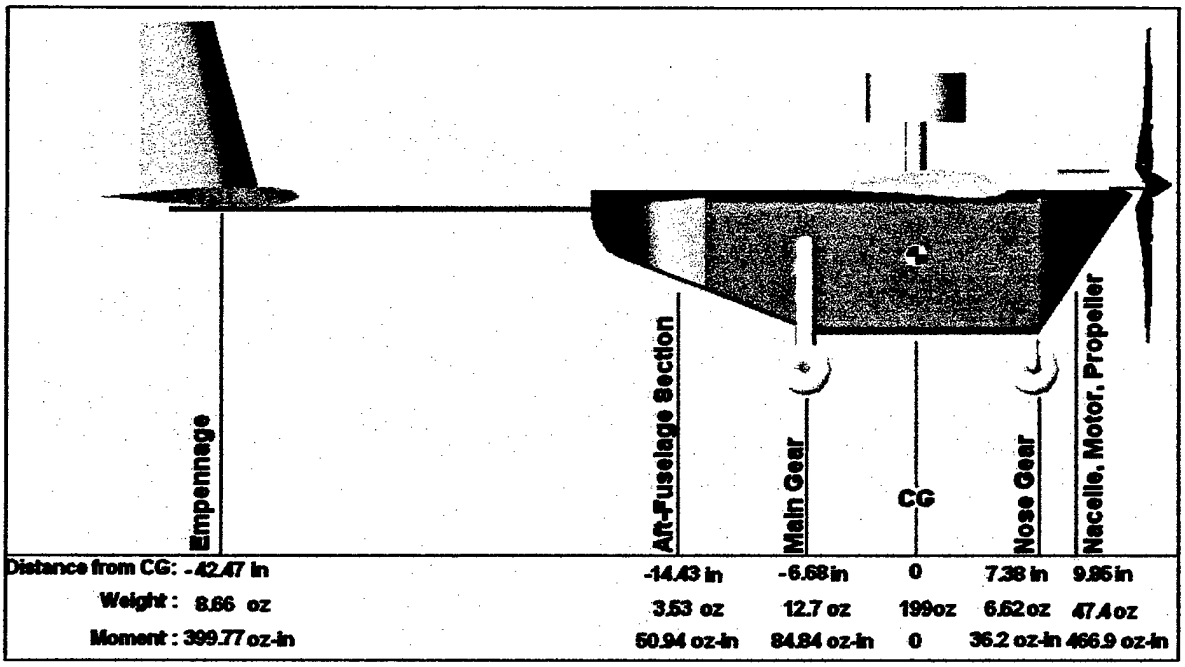

Figure 5.4. Weight & Balance Diagram

5.3. Rated Aircraft Cost

WBS	Man hours/Unit	Aircraft Parameter	Hours
WBS Wing			
Wing Span	8 hr/ft.	8.53 ft.	68.24
Max exposed wing chord	8 hr/ft.	1 ft.	8
Control Surface number	3 hr/ft.	2 unit	6
WBS Fuselage			
Body Maximum Length	10 hr/ft.	5.418 ft.	54.18
WBS Empennage			
Vertical Surface with active control	10 hr./vertical surface	2 unit	20
Horizontal Surface	10 hr./horizontal surface	1 unit	10
WBS Flight Systems			
Number of servo or motor controller	5 hr./servo + motor controller	7 unit	35
WBS Propulsion Systems			
Number of engine	5 hr./engine	1 unit	5
Number of propeller or fan	5 hr./propeller or fan	1 unit	5
		MFHR = Σ WBS hours =	211.42

	Multiplier	Aircraft Parameter	RAC Contribution
MEW	$100	12.57 lb	1257
REP	$1500	4.94 lb	7410
Σ WBS hours	$20	211.42 hours	4228.4

RAC	12895.4
RAC (Thousands)	12.8954

Table 5.3 RAC of the aircraft is 12.8954

5.4. Design Summary

Figure 5.5 is the summary of Haberci aircraft. More detailed info about geometry is in drawing package, performance is in table 4.4, weight statement is in table 5.2.

All Inclusive Data - Haberci Aircraft

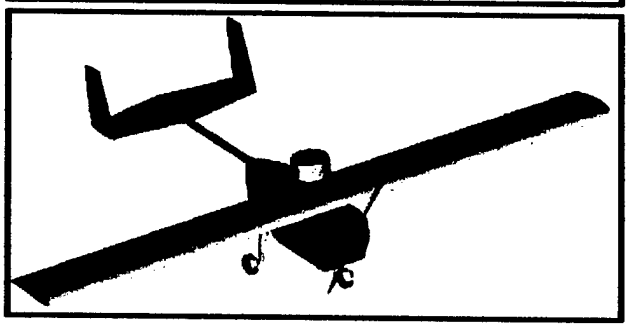

Geometry	
Length	5.41
Wingspan	8.53
Height	1.95
Wing Area	8.53
AR	8.53

Performance	w/ Payload		w/o Payload
	w/ Antenna	w/o Antenna	w/o Antenna
Clmax	1.486	1.486	1.486
L/D max	10.75 @4.5	8.86 @ 6	10.75 @4.5
R/Cmax	12.36	14.33	15.63
Stall Speed	26	26	22
Max Speed	50	57	57
Takeoff Length	110.3	72.83	52
W/S	33.38	32.82	23.45
P/W	68	68	77

Weight Statement	(ounces)
Airframe Weight	65.14
Propulsion System	118.37
Control System	17.66
Payload System	9.2
Payload	80
Empty Weight	201.17
Gross weight	281.17

Systems	
Radio	Futaba 9-Channel PCM aircraft radio
Servos	Futaba - 4 x S3001 + 2 x S3101micro
Battery	38 x RC2400
Motor	Astro 90
Propeller	24x16 wood APC
Gear ratio	2.75:1

Figure 5.5. Poster reflecting all inclusive data about Haberci Aircraft

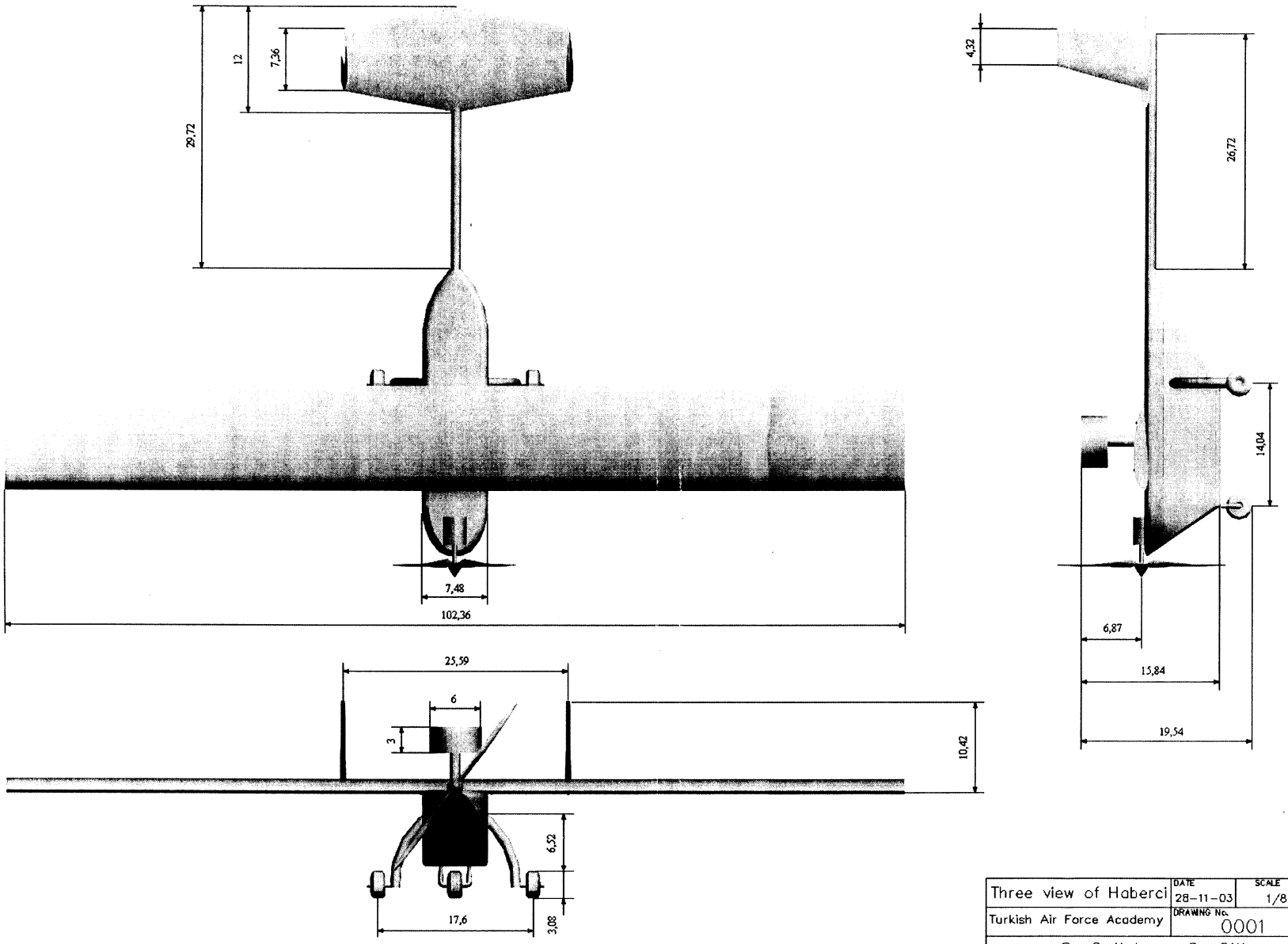

Three view of Haberci	DATE 28-11-03	SCALE 1/8
Turkish Air Force Academy	DRAWING No. 0001	
S. Çaliskan, Ç. Güler		

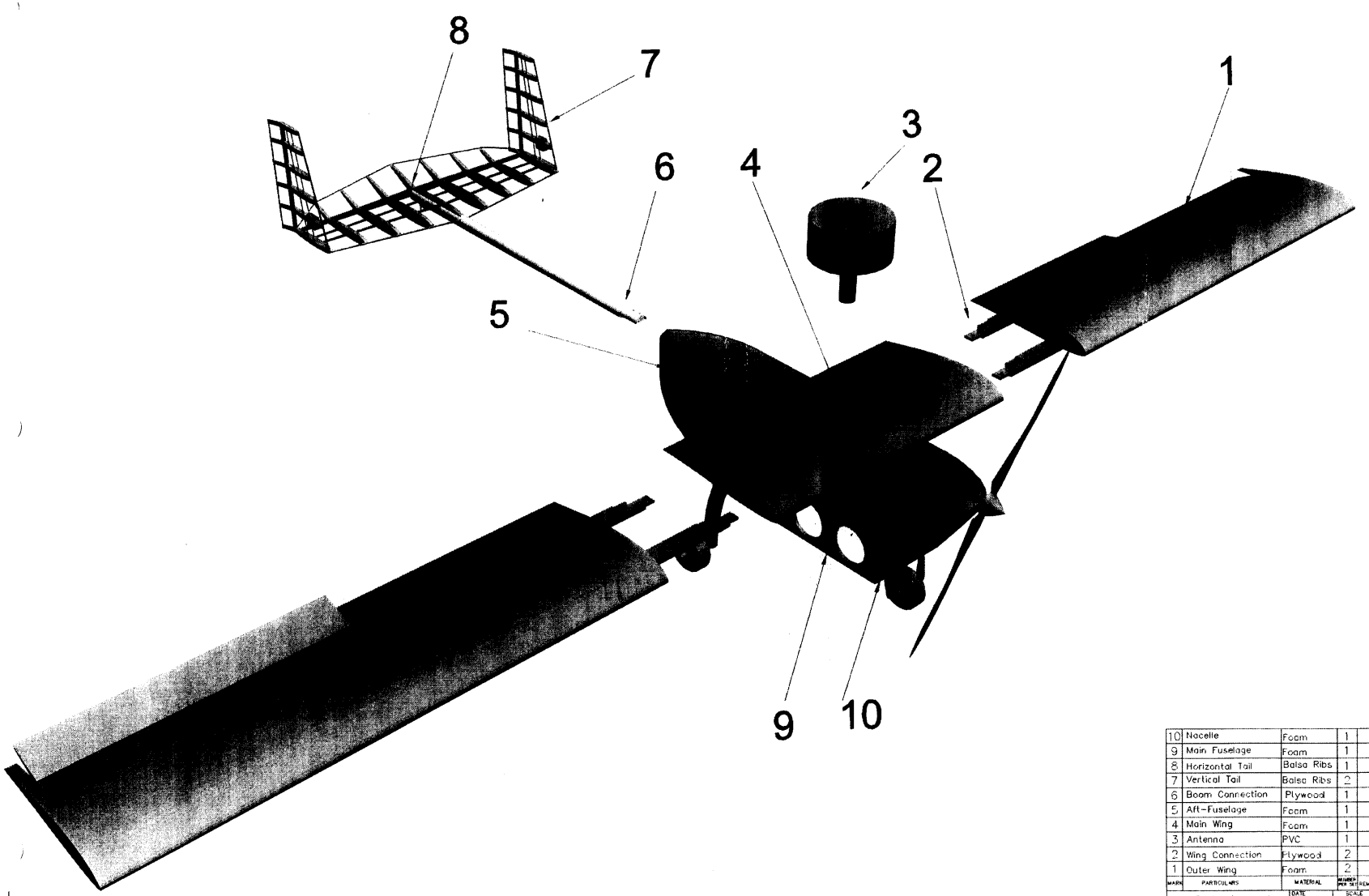

10	Nacelle	Foam	1	
9	Main Fuselage	Foam	1	
8	Horizontal Tail	Balsa Ribs	1	
7	Vertical Tail	Balsa Ribs	2	
6	Boom Connection	Plywood	1	
5	Aft-Fuselage	Foam	1	
4	Main Wing	Foam	1	
3	Antenna	PVC	1	
2	Wing Connection	Plywood	2	
1	Outer Wing	Foam	2	
MARK	PARTICULARS	MATERIAL	NUMBER PER SET	REMARKS

Detachment	DATE 01-10-03	SCALE 1/8
Turkish Air Force Academy	DRAWING No. 0002	
S. Çaliskan, Ç. Güler		

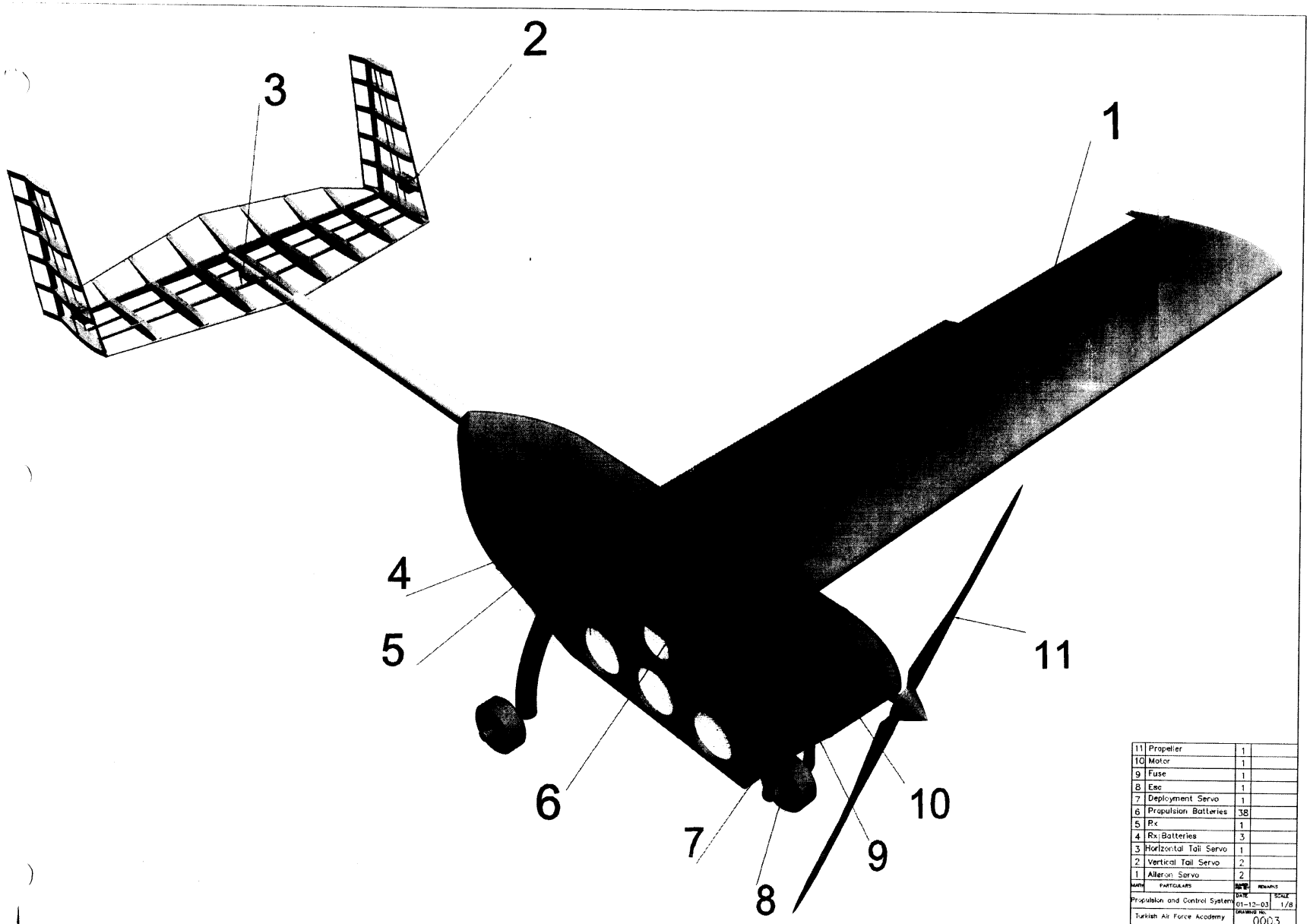

11	Propeller	1	
10	Motor	1	
9	Fuse	1	
8	Esc	1	
7	Deployment Servo	1	
6	Propulsion Batteries	38	
5	Rx	1	
4	Rx Batteries	3	
3	Horizontal Tail Servo	1	
2	Vertical Tail Servo	2	
1	Aileron Servo	2	
MARK	PARTICULARS	NO. REQ'D	REMARKS

Propulsion and Control System	DATE 01-12-03 / SCALE 1/8
Turkish Air Force Academy	DRAWING NO. 0003
O.Arslan, E. Benli	

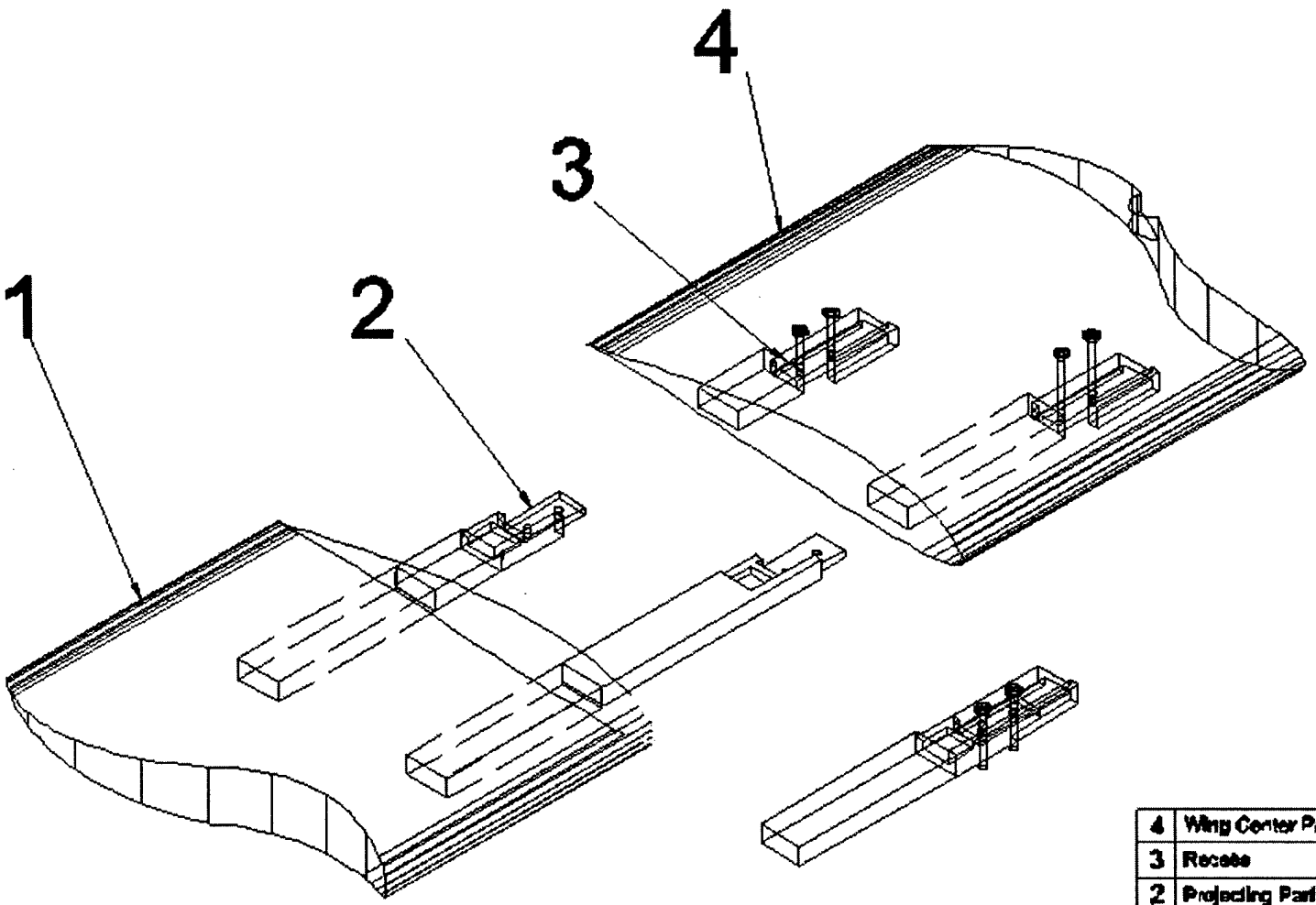

Two tandem nuts hold the seperate parts in one.
In the smaller illustration, the projecting part and recess are united to form the wing.

MARK	PARTICULARS	MATERIAL	NUMBER PER DEF	REMARKS
4	Wing Center Part	Foam	1	
3	Recess	Plywood	2	
2	Projecting Part	Plywood	2	
1	Outer Wing	Foam	2	

Detachment of Wing	DATE 01-01-09	SCALE 1/8
Turkish Air Force Academy	DRAWING No. 0002-01	
A. Akkor		

6. MANUFACTURING PLAN AND PROCESSES

6.1. Manufacturing Processes Investigated and FOM

Manufacturing plan has been taken into account in every phase of design. This greatly facilitated the producing of the aircraft and overall design layout was obtained with much proximity at the end of the manufacturing. Team's experiences also played a vital role in manufacturing process. Vital considerations in manufacturing were obtaining the projected level of surface features for aerodynamic efficiency and keeping aircraft weight the least. Detailed drawing package was generated and although many different manufacturing processes were considered in this phase, some factors caused some methods elimination. For example during the investigation of manufacturing processes, paper honeycombs were thought for using in the wing core section, but the difficulties in construction and lack of experience for the honeycomb lead us to the conventional model aircraft wing construction. These factors are reflected by figures of merit. To have more handling over the manufacturing process the aircraft was divided into 4 modular components that are wing, empennage, landing gear and fuselage. Each of these components were divided into subgroups. The FOM selected were the availability of the materials, simplicity, required technical knowledge, structural strength, cost and weight:

Availability of Material: A comprehensive market research has been done for the available materials. Materials that can be found within Turkey and Europe will lessen our construction time and cost. If the material can be found easily within the country it was scored 1, if it would be shipped and reception of the material would take more than a week, it was scored -1.

Required Technical Knowledge and Skill: Some construction methods required technical knowledge and specific skill. If the technical knowledge and experience at that specialization lacks it was scored -1, if it is easy to achieve and needs no further technical knowledge it was scored 1.

Required Man-Hour: Some tasks take too many man-hours, which leads to longer production time. In all parts, less time production should be taken for a fast construction phase. By this way, probable problems in flight-testing, if occurred, could be refined before the due date. If too much man-hour needs for a production type, it was scored -1, if the production type can be done with few man-hour, it was scored 1.

Structural Strength: The aircraft should withstand the aerodynamic and landing loads without any damage. To have such strength, the materials that will resist the loads should be selected. For example at the wing's attachment point, hard balsa wood could be used to cover the aerodynamic loads. If a material covers the loads without damage, it was scored 1. If there exists problems or damages during the ANSYS analyses or the experiments the team has made, it was scored -1.

Cost: The team's limited funds should be used effectively to construct the aircraft and join the contest. So the selected materials' cost should not overcome budget. The materials that exist in the country could be obtained cheaper as there existed no shipping charge. So if a material can be obtained from the country and has a bearable cost it was scored 1. If the material should be bought from another country or it will cost too much it was scored -1.

Weight: In all phases of design, the team tried to keep the weight of the airframe the least and manufacturing process was the only part that these thoughts were to be put into practice. The work,

carried out up to manufacturing process, consisted of assumptions and general sizing trades. However in selection of the material, same amount of strength could be provided with totally different weighing materials. So, if the material extensively decreased the aircraft weight in regard to other options, it is scored 1. If the material increased the weight in great deal, it is scored –1.

According to selected figures of merit, materials to produce the Haberci aircraft were selected.

		Figures of Merit						
		Availability	Required Technical Knowledge and Skill	Required Man-Hour	Structural Strength	Cost	Weight	Results
	Weighing Factor	2	1	2	2	1	2	
Wing	Ribbed Spar Structure	1	1	-1	0	1	1	4
	Foam Core and Composite Covering	1	1	0	1	0	0	5
	Foam wing with Spar and Balsa sheet	1	1	-1	0	1	0	2
	Paper Honeycombs	0	-1	-1	1	-1	1	0
	Carbon Composite (no core)	0	-1	-1	1	-1	1	0
Motor Mount	Foam Core and Composite Covering	1	1	0	1	0	0	5
	Plywood framing	1	0	0	1	-1	0	3
Landing Gear	Balsa Core and Fiberglass covering	1	0	0	1	1	0	5
	Outsource Aluminum Landing Gear	-1	-1	1	0	-1	-1	-4
Horizontal and Vertical Stabilizers	Ribbed Spar Structure	1	1	-1	1	1	1	5
	Foam Core and Composite Covering	1	1	0	0	0	0	3
	Foam wing with Spar and Balsa sheet	1	1	-1	0	1	0	2
	Carbon Composite (no core)	0	-1	-1	1	-1	1	0
Tail Boom	Balsa Core and Fiberglass covering	1	1	1	1	1	0	6
	Foam Core and Composite Covering	1	0	1	1	0	0	6
Fuselage	Balsa / Plywood Framing	1	0	0	1	0	-1	2
	Carbon Fiber Composite	0	0	-1	1	-1	1	1
	Foam Sheeted with Balsa	1	1	-1	1	1	1	5
	Balsa Framing and Fiberglass Covering	1	1	0	1	1	0	6

Table 6.1 FOM were used to screen alternative manufacturing processes' advantages.

6.2. Results

The result of figures of merit table was a conventional manufacturing process in almost every part of design. Balsa and foam forming the most of the aircraft, fiberglass was selected to cover the aircraft. Main reason for this kind of a result was that these selected conventional methods were cheap and easy to build. And team members were familiar with these materials. Experiences proved these materials' sufficient strength and rather less weight. Balsa is strong in tension and reasonably strong in compression. Although substitutions of balsa such as carbon fiber or composites served better in fuselage construction, the experiments and manufacturing technology to build the fuselage with carbon fiber was not satisfactory. Plywood is another example. It is stiff and rigid in all directions and ideal for heavily stressed areas. Different materials could result in a less weighing and structurally more strong aircraft however manufacturing process time was projected to finish in 2 weeks in order

to test and have the possibility to refine the aircraft if required. With the existent tools and capacity, the conventional method established itself ideal from every aspect. Therefore wing and motor mount was projected to be produced from foam core and composite covering. Balsa core and fiberglass covering was decided to be the method to build the landing gear and tailboom. Horizontal and vertical stabilizers were from balsa ribs and fiberglass covering. For the fuselage, balsa framing and fiberglass covering would be used to produce the main fuselage while foam sheeted with balsa is used to produce the nacelle and aft fuselage section parts as these sections. Below is presented the progress of manufacturing of major components of the aircraft.

6.3. Overview of the Actual Manufacturing Progress

Figure 6.1 illustrates the scheduled milestones of manufacturing. As seen on the figure, the tasks were synchronized and almost all task were finished in the same time. The initial work carried out was foam cutting for wing, nacelle and aft part of the fuselage. When this process was in progress, balsa ribs for tail were prepared. Tail boom and landing gear were then produced as they both were of balsa core with fiberglass covering. As the main components were shaped, their integrity was maintained. Since the highly stressed places were examined in detail design by ANSYS results, these areas were strengthened with either balsa or plywood plates. Aileron was cut out of the wing and prepared hinges were located to the wing. Then cut out aileron was straightened and attached to the hinges. Elevator and rudder were of balsa ribs therefore they were separately manufactured and hinging them became easier than aileron surface preparation. Detachment parts were produced of plywood and they were firmly bonded to the main components. As these parts were so sensitive for design success, manufacturing was carefully carried out. Especially attachment of connection parts to the main structures was given much of the importance and rivets were used to maintain the firmness. The detachment parts were designed to minimize the assembly time and screws and nuts enabled rapid assembly. A different adhesive was used to attach components to each other this year. CU25, which is used to attach faiences to each other, weighed less than epoxy and more importantly it is stronger. Epoxy was again used to attach small components. Deployment mechanism, motor and antenna mounts were then prepared. After confirming the electrical installations applicability, the whole aircraft was covered with fiberglass and composites. Completing the installation of electrical components, the transportation box was produced of foam blocks and testing of the aircraft was initiated.

6.4. Assembly Strategy

The aircraft will be removed from the transportation box in 4 main parts: the main section formed of whole fuselage and middle wing part, 2 outer portions of wings, empennage and landing gear wheels. As soon as the components are taken out of the box, electrical equipment to the tail and wings will be connected. When two competitors are attaching the wheels to landing gear by nuts, the other competitor will attach empennage to the fuselage by an electric screwdriver. When his work is finished, the other two will take the screwdriver and attach wings together. As all mechanical systems and payload will already be in the fuselage, the assembly will be over by 5 seconds of control of main components integration and electrical systems correction approval.

ID	Task Name	Start	Finish
1	**Wing**	**28 Jan '03**	**17 Feb '03**
2	Foam Cutting	28 Jan '03	03 Feb '03
3	Build Joint Supporters	03 Feb '03	03 Feb '03
4	Fiberglass Covering	11 Feb '03	17 Feb '03
5	**Fuselage**	**04 Feb '03**	**17 Feb '03**
6	Foam Cutting for Nacelle and Aft Fuselage	04 Feb '03	04 Feb '03
7	Main Structure of The Fuselage	04 Feb '03	11 Feb '03
8	Fuselage Covering	13 Feb '03	17 Feb '03
9	**Empennage**	**30 Jan '03**	**14 Feb '03**
10	Balsa Rib Cutting for Horizontal and Vertical Stabilizers	30 Jan '03	03 Feb '03
11	Tailboom Balsa Preparation	04 Feb '03	04 Feb '03
12	Fiberglass Covering of Tail and Boom	11 Feb '03	14 Feb '03
13	**Landing Gear**	**11 Feb '03**	**14 Feb '03**
14	**Components and Control Systems**	**04 Feb '03**	**11 Feb '03**
15	Antenna Mount Preparation	04 Feb '03	05 Feb '03
16	Deployment Mechanism Preparation	05 Feb '03	07 Feb '03
17	Motor Mount and Electrical Accessories Installation	07 Feb '03	11 Feb '03
18	**Final Integration of All Components**	**18 Feb '03**	**18 Feb '03**

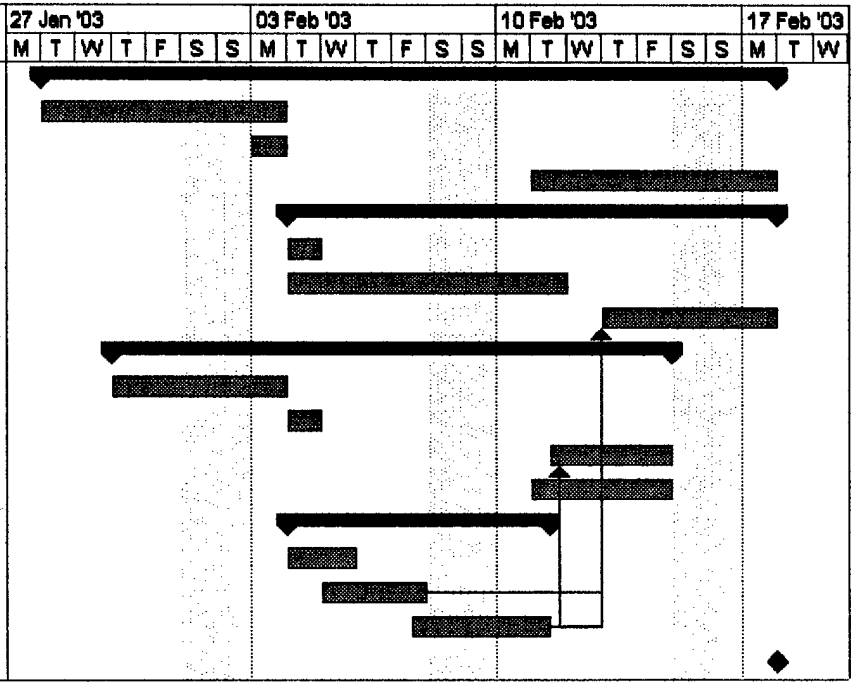

Figure 6.1. Manufacturing Milestone Chart

7. TESTING PLAN

As soon as manufacturing process is concluded, flight-testing of the aircraft is conducted. Defining the objectives of testing, schedule and checklist were prepared. With the static and dynamic tests, the aircraft is prepared for free flight testing and free flight showed the capabilities of aircraft. On the last stage missions are flown and basic refinements were made.

7.1. Testing Objectives

The test activity has been performed to compare static, dynamic and stability behavior of aircraft and effectiveness of active control in flight with those predicted by analysis. Also, as mechanical part usage has increased in number in regard to past years' designs, test is held to illustrate the limitations of flight caused by possible mechanical malfunctions. Finally some researches were directed towards improving basic elements for aircraft performance and development of new designs in future.

7.2. Testing Schedules and Check List

Schedules for testing is illustrated in figure 2.1. Testing of the aircraft was divided into three tasks. The first task was the identification of critical design parameters for both static and dynamic situations of the aircraft. Critical information needed to assess, validate or refine the design was noted in this task and experimental test program is developed. Then, using the defined test parameters, assessment of the identified parameters is carried out (Figure 7.1 Left column). After final critical evolution parameters were characterized, the second task of performing the tests was carried out. Figure 7.1 is the prepared checklist for tests. It is structured to encompass all of the critical activities that may change the performance and structure of the aircraft. It reflects the tasks carried out, results and comments about each test. These tests revealed that one component refinement was necessary. So, on the last task, required refinements to increase performance are conducted.

7.2.1. Preflight Testing

7.2.1.1. Static Testing: Static testing of the aircraft was reflected in checklist as "preflight tests". The important parameters that constraints of the contest demand are initially investigated. Compulsory subjects of aircraft fitting in the defined box and performing assembly are initially carried out. It took 82 seconds to assemble the aircraft to flight-ready condition. The attached parts structural integrity is then verified. Wing tip test, defined as holding the aircraft from two tips of wing, is held and boom structural sufficiency is verified by holding from tail and nose of the aircraft. Boom was stiff enough not to bend from any portion or from attachment sections.

7.2.1.2. Dynamic Testing: On the next stage, mission requirements feasibility is investigated. Leaving the aircraft from 3 feet to free-fall, payload mechanism safety, landing gear shock absorption and propeller safety is investigated. Possible mechanical malfunctions or instrumentation could lead to payload dropping in landing segment of flight. In order not to leave any dilemma for free flight test, this dynamic test is held. Another investigation by this free-fall test is the landing gear shock absorption. Landing gear is designed not to stretch more than 1.6 inches due to propeller probability to hit the ground. And by leaving the aircraft from 3 feet, it was tested if landing gear was stiff enough not to violate propeller safety and flexible enough not to come off loose from the fuselage. So it transmits optimum forces to the body of the aircraft. And results of this dynamic test verified that on the worst

kind of landing, payload mechanism safety, the propeller safety and landing gear safety would not be violated.

7.2.2. Flight Testing

Flight-testing is another part of dynamic testing of the aircraft. Tasks to complete in this section were free flights with and without antenna and completion of all three missions. 120 feet takeoff constraint, stability of the aircraft and performance of the aircraft in cruise, climb and turn were investigated in free flights. The aircraft took off in designated distance both with antenna and without antenna. For stability analysis, pilot artificially disturbed the aircraft's equilibrium and the airplane managed to stabilize itself in cruise flight. Cruise performance was as predicted however turns took more time than predicted. The reason for this deficiency was that the aircraft responded slowly and large control motion to maneuver was needed. As aircraft came to its turn bank angle very slowly, turn radius increased and this concluded turn time increase. The easiest way to solve this problem is found to make the aileron bigger. Team is currently in this progress. And when the aircraft successfully accomplished these constraints, all three missions are flown. Flights showed that aircraft performed higher scores in initially selected A and B missions.

7.3. Testing Results and Lessons Learned

Testing of the aircraft resulted in verification of analytical studies and safety of the aircraft. Initially predicted performance level and handing qualities are closely gained. The only change in aircraft was aileron area. Team has learned the approximate level of analytical studies' closeness to that of the real conditions and capabilities of the aircraft.

HABERCI AIRCRAFT CHECKLIST

TASKS	RESULT	COMMENTS
Preflight		
Aircraft fitting in defined box	✓	
Assembly	✓	B2 screws
Payload deployment mechanism	✓	
Structural verification	✓	
Wing tip test		Connecting parts moving must be tightly screwed
Verify boom structural sufficiency	✓	
Verify landing gear shock absorption	✓	
Verify propeller safety	✓	SAFE
Flight		
Takeoff in 120 ft	✓	T.M.
Complete free flight without antenna	✓	
Verify responses adequacy	✓	
Verify static and dynamic stability	✓	
Complete free flight with antenna	✓	
Verify responses adequacy	✓	
Verify static and dynamic stability	✓	
Complete Sensor Deployment mission	✓	Completed in 04:02.
Complete Missile Decoy mission	✓	Completed in 04:45
Complete Communications Repeater mission	✓	Completed in 03:52

HABERCI TEAM

Figure 7.1 The checklist allowed to examine the activities applied.

8. REFERENCES

1. Young, A. D., *Boundary Layers*, AIAA Education Series, AIAA 1989
2. Raymer, Daniel P., *Aircraft Design: A Conceptual Approach*, AIAA Education Series, AIAA 1989
3. NASG Airfoil Database. http://www.nasg.com/index-e.html
4. Hoskins, Brian C., Baker, Alan A., *Composite Materials*, AIAA Education Series, AIAA 1986
5. Yükselen, Adil, *Aerodinamik Ders Notları*, Hv.H.O. Yayınları, Hv.H.O. 1995
6. Materials Information Resource. http://www.matweb.com/
7. Motocalc Homepage. http://www.motocalc.com/
8. Schmidt, Louis V., *Introduction to Aircraft Flight Dynamics*, AIAA Education Series, AIAA 1998

2002/2003

Syracuse University

Design/Build/Fly Team

"The Judge Chaser"

Acknowledgements

The Syracuse University Design Build Fly team would like to acknowledge the following individuals.

Dr.Higuch

Dr.Davidson

Dr.Murphy

Reid Thomas

Tori Garnier

Table of Contents

Acknowledgements i
Table of Contents ii
1.0 Executive Summary 1
1.1 Rules and Requirements Analysis 1
1.2 Conceptual Design 1
1.3 Preliminary Design 1
1.4 Detailed Design 2
1.5 Manufacturing and Testing 2
2.0 Management Summary 2
Actual Completion Date 4
3.0 Conceptual Design 4
3.1 Rules and Requirements Analysis 5
3.2 Morphological Matrix 5
3.2.1 Initial Downselect 6
3.2.1.1 Configuration Downselect 6
3.2.1.2 Propulsion System Downselect 7
3.2.1.3 Empennage Downselect 7
3.2.1.4 Landing Gear Downselect 7
3.2.2 Preliminary Comparisons 8
3.2.2.1 Concept 1 8
3.2.2.2 Concept 2 9
3.2.2.3 Concept 3 9
3.2.2.4 Concept 4 10
3.2.2.5 Concept 5 11
3.2.2.6 Concept 6 12
3.2.2.7 Concept 7 13
3.3 Pugh Matrix Comparison 14
3.3.1 Figures of Merit for Pugh Matrix Comparison 15
3.3.1.1 Rated aircraft cost 15
3.3.1.2 Speed 15
3.3.1.3 Assembly Time 15
3.3.1.4 Stability 15
3.3.1.5 Manufacturability 15
3.3.1.6 Payload Capacity 16

3.3.2 Subjective Pugh Matrix 16
3.3.3 Weighted Pugh Matrix 16
3.4 Conclusions From Conceptual Design 17
4.0 Preliminary Design 17
4.1 Initial Sizing 17
4.1.1 Constraint Analysis 17
4.1.2 Initial Vehicle Sizing 19
4.1.3 Initial Weight Estimate 19
4.2 Propulsion Analysis 20
4.2.1 Trade Study of Number of Batteries Required 20
4.2.2 Take-Off Battery Power Requirements 21
4.2.3 Cruise Battery Power Requirements 21
4.2.5 Motor Investigation 21
4.4 Preliminary Aerodynamics 21
4.4.1 Airfoil Selection 21
4.4.1.1 Figures of Merit 21
4.4.1.2 Airfoil Comparison 22
4.4.2 Drag Polar 27
4.6 Preliminary Design Conclusions 28
5.0 Detailed Design 28
5.1 Final Configuration Features 29
5.2 Weight and Balance 29
5.2.1 Final Weight Estimation 29
5.2.2 Center of Gravity 30
5.3 Aircraft Performance 30
5.3.1 Takeoff and Climb Performance 30
5.3.2 Flight Performance 31
5.3.3 Stability and Control 31
5.3.4 Mission Performance 31
5.4 Propulsion System 32
5.5 Structural Design 32
5.5.1 Load Factor 32
5.5.2 Wing Structure 33
5.5.3 Fuselage Structure 34
5.6 Rated aircraft cost 34
5.7 Final Aircraft Parameters 35
5.8 Drawing Package 37

6.0 Manufacturing Plan 42
6.1 Process Investigation and Figures of Merit 42
6.2 Wing and Empennage Manufacturing and Process and Tooling 42
6.3 Fuselage Manufacturing Process and Tooling 43
6.4 Landing Gear Manufacturing Process and Tooling 45
6.5 Analytical Methods 45
6.5.1 Manufacturing Cost 45
6.5.2 Skills Matrix 45
Component 46
7.0 Testing Plan 46
7.1 Manufacturing Testing 46
7.1.1 Testing Goals 46
7.1.2 Testing Results 46
7.2 Static Testing 47
7.2.1 Testing Goals 47
7.2.2 Testing Results 47
References 48

1.0 Executive Summary

This document contains the efforts of the 2002/2003 Syracuse University Design/Build/Fly team. Included is a summary of the complete effort: starting from an analysis of the current rules, moving into a requirements analysis, continuing through the conceptual, preliminary, and detailed design stages. Also included are detailed drawings of the aircraft, a manufacturing outline, and a testing and results section. The following is a brief description and overview of the path taken by the team for this competition.

1.1 Rules and Requirements Analysis

The initiation of this year's aircraft began with a requirements and rules analysis. The team initiated an analysis of the rules by comparing and contrasting the rules with previous years. Particular attention was paid to the difference for the 2002/2003 competition and the possible implications of the changes.

The team also began to analyze the requirements for this competition. Of particular interest were the new flight missions and the box assembly compatibility. The main conclusions from this initial step were that the concept would need the flexibility to handle the multiply missions, and that a smaller aircraft, as compact as possible would be desirable in order to minimize the assembly time of the aircraft.

1.2 Conceptual Design

After completion of the rules and requirements analysis, the team began formulating possible configurations to best tackle the requirements. In order to capture the largest number of combinations, the team began by formulating a morphological matrix. The morphological matrix was comprised of the main design parameters, such as the number of engines, the type of tail, the placement of the wing, and other critical characteristics. With the morphological matrix, the team was able to begin downselecting the main features of the concept. Utilizing several figures of merit the team selected a box fuselage with a single tractor motor, a high wing, tricycle gear and a conventional tail as the design that would best fit the requirements. From further expansion of the morphological matrix, the team selected eight promising concepts based upon the requirements analysis, and the overall concept selected.

1.3 Preliminary Design

With the selection of a concept in the previous design phase, the initial sizing and preliminary design of the aircraft could begin. The initial sizing began with a constraint analysis to determine the thrust to weight and wing loading requirements for the aircraft. To complete this analysis, an initial upper limit for weight was estimated, as well as a maximum thrust. This threshold (maximum thrust to weight ratio) provided the upper bounds of the design space. The rules for the competition provide one other

main constraint for this analysis: takeoff field length. With the combination of thrust to weight threshhold, and takeoff field length constraint, the design point which maximizes wing loading and minimizes thrust loading was chosen. This point, plus the initial weight estimate are enough to determine the other main parameters for the aircraft, starting with wing area. With these estimates, a more precise weight estimate can be obtained, and the process repeated. After several iterations, when the initial and final weight estimates converge, the design point can be fixed, and the aircraft sized from that point. The sized aircraft can then be passed into the detailed design phase for final optimization and mission performance predictions.

1.4 Detailed Design

With the sized concept from the preliminary design phase, the overall vehicle optimization, structural analysis, and detailed internal layout can be determined. One of the major accomplishments of the detailed design section was the determination that a V-tail could adequately meet the performance requirements, while providing a lower total Rated Aircraft Cost. Additionally detailed mission performance data was calculated, and over all mission performance determined. In order for construction to begin the final design of all parts for the aircraft were completed, as well as detailed drawings to aid in construction. Last, a final rated aircraft cost was computed for the finalized design.

1.5 Manufacturing and Testing

In order to test manufacturing and design possibilities, different test models were built. A full-scale payload compartment section was build and used to investigate different door mechanisms. To obtain better properties of laminated composites, the team investigated different lay-up techniques. Carbon fiber and fiberglass lay-ups were tested for weight and tensile strength. Results showed that fiberglass was ideal for the wing construction, and carbon fiber for the fuselage construction. Two half-scale wing sections were built to test the manufacturing techniques. To reduce possible delamination of the fiberglass, one of the two test sections was stitched with fiberglass tow at the trailing edge. Comparing both sections, it was discovered that delamination was not a problem. Several carbon fiber landing gear struts were manufactured, and each was tested under a static load. Delamination of fiberglass at the base of the strut was observed. To correct the problem, adjustments were made in the amount of epoxy used in the lay-up.

2.0 Management Summary

This year's design team consisted of 6 Syracuse University students with Michael Czabaj as the team leader. The students and their main responsibilities are listed in Table 1.

Table 1: Team Breakdown

Team Member	Responsibilities	Year
Michael Czabaj	Preliminary and Detail Design, Structures, Manufacturing	Junior
Ben Nesmith	Propulsion, Manufacturing	Junior
Chris Corbin	Aerodynamics, Stability and Control	Senior
Brian Foo	Manufacturing	Junior
Carlos Perez	Manufacturing, Research	Freshman
Vasco Burgos	Manufacturing, Research	Freshman

The main contributors to this year's design were Czabaj and Nesmith. Czabaj was the team captain and chief design engineer on the project. Using his experience from past competitions and personal model aircraft he has built, he was able to coordinate and direct the design and construction of the airplane. Besides leading the team, Czabaj contributed a great deal to the project; he was widely involved in all design stages and his responsibilities included research of new technologies, preliminary design and detail design, structural analysis, and manufacturing. Nesmith was the primary propulsion system expert for this year's design. Nesmith conducted trade studies, and overall optimization of the propulsion systems within the framework of the design.

Corbin, the only senior on the team, was responsible for aerodynamics and stability and control optimization. At meetings he kept minutes and took notes of all sketches and ideas. He also helped plan the transportation and accommodations for the trip to the competition at Maryland.

The rest of the group consisted of Foo, Perez and Burgos. Foo helped with initial design stages, worked countless hours on the final aircraft assembly, and helped write the final report. Perez and Burgos took an active role in development of new ideas, helped with initial research, and contributed significant amounts of time in the fabrication and assembly of the aircraft: Perez was in charge of making the landing gear, and Burgos developed and manufactured the payload door compartment.

Table 2 lists the team milestone chart. Included on the chart are both estimated and actual completion dates. The goal of this year's team was to complete the aircraft a month before the competition and have ample time for test flights and problem debugging.

Table 2: Milestone Chart

FALL SEMESTER		
Task	**Projected Completion Date**	**Actual Completion Date**
Rules and Requirement Analysis	9/01/02	9/01/02
Configuration Downselect	9/13/02	9/13/02
Initial Sizing	9/22/02	9/22/02
Initial Weight Estimate	10/01/02	10/04/02
Propulsion Analysis	10/01/02	10/02/02
Airfoil Selection	10/18/02	10/18/02
Drag Polar Estimation	10/25/02	10/25/02
Entry Form Due	10/31/02	10/31/02
Power Configuration	11/05/02	11/08/02
Detailed Weight Estimation	11/15/02	11/14/02
CG Location	11/22/02	11/22/02
Aircraft Performance	12/11/02	12/12/02
SPRING SEMESTER		
Structural Design	01/10/03	01/12/03
Begin drafting report	01/10/03	01/12/03
Rough Draft of Report Complete	01/25/03	01/25/03
Begin manufacturing	02/01/03	02/01/03
Fuselage complete	02/15/03	02/15/03
Empennage Complete	02/20/03	02/20/03
Wing Complete	02/26/03	02/26/03
Aircraft Assembled	02/28/03	02/28/03
Components placed	02/28/03	03/01/03
Presentation to Faculty	03/04/03	03/04/03
Hand report to faculty	03/07/03	03/07/03
Report Due	03/11/03	03/11/03
Aircraft Complete	03/15/03	TBD
Flight testing	03/22/03	TBD
Final Modifications	04/11/03	TBD
Competition	04/25/03	04/25/03

3.0 Conceptual Design

The Conceptual Design phase began with an analysis of the requirements for this year's rules. Once it was determined what was required of the aircraft, possible configurations were brainstormed. Of

these configurations, a morphological matrix was created to compare the different designs. From this comparison, the optimal configuration and propulsion system were selected. Also during this stage, the optimal landing gear, empennage, and structural approach were chosen. This process allowed the team to debate the plusses and minuses of many different designs, and come up with a unanimously agreed upon design.

3.1 Rules and Requirements Analysis

The rules for this year's competition were examined carefully. Every step of the design stage was performed within the guidelines specified by the competition rules. The aircraft had to be an electrically powered, fixed-wing aircraft with up to five pounds of batteries, pulling no more than forty amps.

The mission outline was also critical in the design stages. There are three possible missions, two of which were chosen for the team's aircraft. The two hardest missions were chosen, as they result in the highest flight scores. One mission is to carry a five-pound payload in flight, land, deploy the payload, and fly again. The second mission is to carry the five-pound payload, as well as a simulated cylindrical antenna on top of the aircraft, in flight. These missions will be test flown prior to the competition to ensure stable flight is possible.

3.2 Morphological Matrix

In order to capture the full extent of the design space, the team constructed a morphological matrix. A morphological matrix is a tool that helps visualize the breakdown of the different system components, as well as the main features of the design. The team's morphological matrix is shown in Table 1.

Table 1: Morphological Matrix

Wing	Planform	rectangular	eliptical	delta	tapared	
	Number	1	2	3		
	Placement	low	mid	high		
	Sweep	none	backward	forward		
	Wingtips	rounded	sharp	cut-off	hoerner	winglet
	Dihedral	none	positive	negative		
Fuselage	Number	0	1	2		
	Shape	Box	Cylinder	BWB	Airfoil	Eliptical
Propulsion	Number	1	2	3	4	
	Type	propeller - tractor	propeller - pusher	ducted fan		
	Placement	wing	fuse	pod		
Empennage		none	conventional	v-tail	t-tail	inverted v
Landing Gear		tricycle - fixed	tricycle retrac	tail-dragger fixed	tail-dragger retrac	

The creation of this morphological matrix allowed the team to rapidly create, contrast and compare different designs and different design features. From this comparison the initial downselect of the vehicle was completed.

3.2.1 Initial Downselect

The morphological matrix provided the team with many different design possibilities. In order to narrow down the possible choices, an initial downselect was performed. This initial effort used three figures of merit to compare different configurations: rated aircraft cost, manufacturability, and payload compatibility. With these three figures of merit the team looked at the overall configuration, the propulsion system the empennage, the landing gear and also began to look at initial possibilities for the structural design of the aircraft.

3.2.1.1 Configuration Downselect

The configuration downselect examined different possibilities for the overall layout of the aircraft. Possibilities included a traditional configuration, a biplane, a canard, a joined wing, a blended wing body and a flying wing. For the first figure of merit, rated aircraft cost, both the biplane and joined with concepts showed dramatic increases, with the other three configurations all at the same relative level. The second figure of merit, manufacturability favored the conventional (traditional) concept. This is because the remaining concepts required either extra manufacturing sections (biplane), or more precision

in manufacturing (flying wing). For the final figure of merit, payload compatibility, only two concepts stand out. The biplane concept has a negative relationship here due to the multiple wings, while the blended wing body has a positive relationship due to the increased interior volume.

Based upon this initial comparison the team selected both the conventional and blended wing body concepts for further investigation.

3.2.1.2 Propulsion System Downselect

For the initial propulsion system assessment, the three main features identified in the morphological matrix each accounted for one of the figures of merit. The number of motors selected has a very strong impact upon the rated aircraft cost. The added cost of an additional motor was shown to be very high, and so a single motor was selected.

The placement of the engine had a strong correlation with the Payload compatibility. In order to drop the payload package in mission 2, the engine must be in a tractor configuration. With a single engine this would indicate either mounting at the front of the aircraft, or in a pod above the aircraft. However, a podded nacelle above the aircraft would interfere with the Raydome in mission 3.

The final figure of merit, for manufacturability, eliminates ducted fans due to their much higher time and precision requirement.

3.2.1.3 Empennage Downselect

There were four different empennage configurations considered for the aircraft. The conventional tail, T-tail, V-tail, and inverted V-tail were the possibilities. The conventional tail is relatively simple to manufacture, and requires three control surfaces. The T-tail is harder to manufacture, as well as not being as structurally rigid as the conventional tail. The V-tail is slightly harder to manufacture than a conventional tail, due to the fact that all angles are not orthogonal. However, the V-tail only requires two control surfaces, and has less material, thus less drag. The inverted V-tail has the traits of the regular V-tail, except that it is inverted. Due to the mission requirements, the inverted V-tail was decided against, because the aircraft must be able to freely roll over the payload once it is deployed. The regular V-tail was seen to be the optimal configuration for the empennage. It will require less material to build, and will produce less drag than a conventional or T-tail configuration.

3.2.1.4 Landing Gear Downselect

There were four different landing gear configurations considered. Tricycle gear and tail-dragger gear were considered, as well as retractable gear of the same setup. It was decided that retractable gear, while it would save considerable drag during flight, added too much weight to be beneficial. The tail-dragger was not feasible, as the mission requires that the aircraft be able to clear the payload once it is deployed. Thus by process of elimination, tricycle gear was chosen as the landing gear of choice.

Having three main wheels will add to the drag of the aircraft, but it will be stable during takeoff and landing, and will be able to clear the payload once deployed.

3.2.2 Preliminary Comparisons

With an initial overall configuration selected, the team began looking at perturbations around that concept. Going back to the morphological matrix, the team was able to create seven possible designs to try and best complete the selected missions.

3.2.2.1 Concept 1

This is the first design that was analyzed. This aircraft employs a box-type fuselage together with a zero-taper, mid-wing configuration. The benefit of this design is primarily the ease of manufacturability. The fuselage has a square cross-section with minimal curves, thus lessoning the complexity of the manufacturing process. The wing is also simple to manufacture: there are no curves or tapers to manufacture.

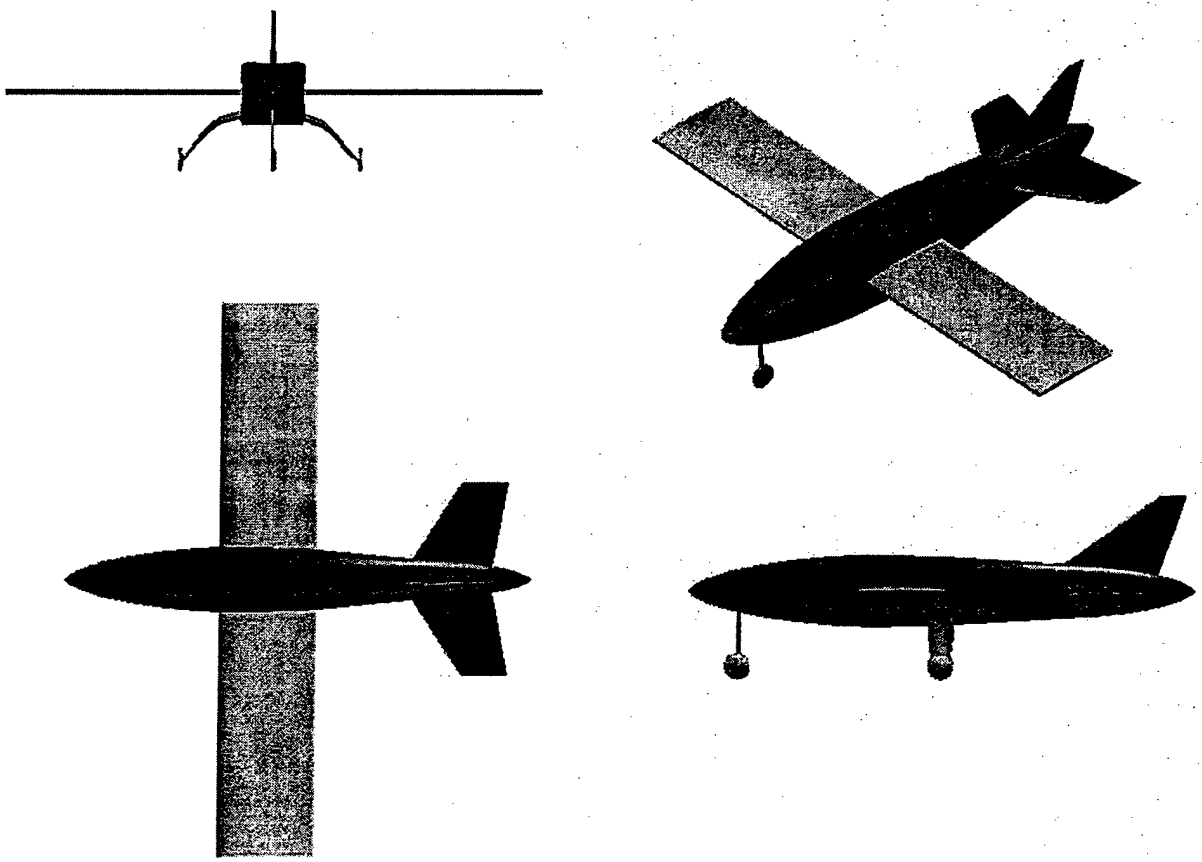

Figure 1: Three View Drawing for Concept 1

3.2.2.2 Concept 2

The second design that was considered was again a traditional configuration. In this design, a high-mount wing is used. High mounted wings provide better roll stability during flight. In the event of excessive roll, the high-wing will out perform a low or mid wing. This design has a square fuselage and zero-taper wings. The ease of manufacturability is essentially equal to that of the first design.

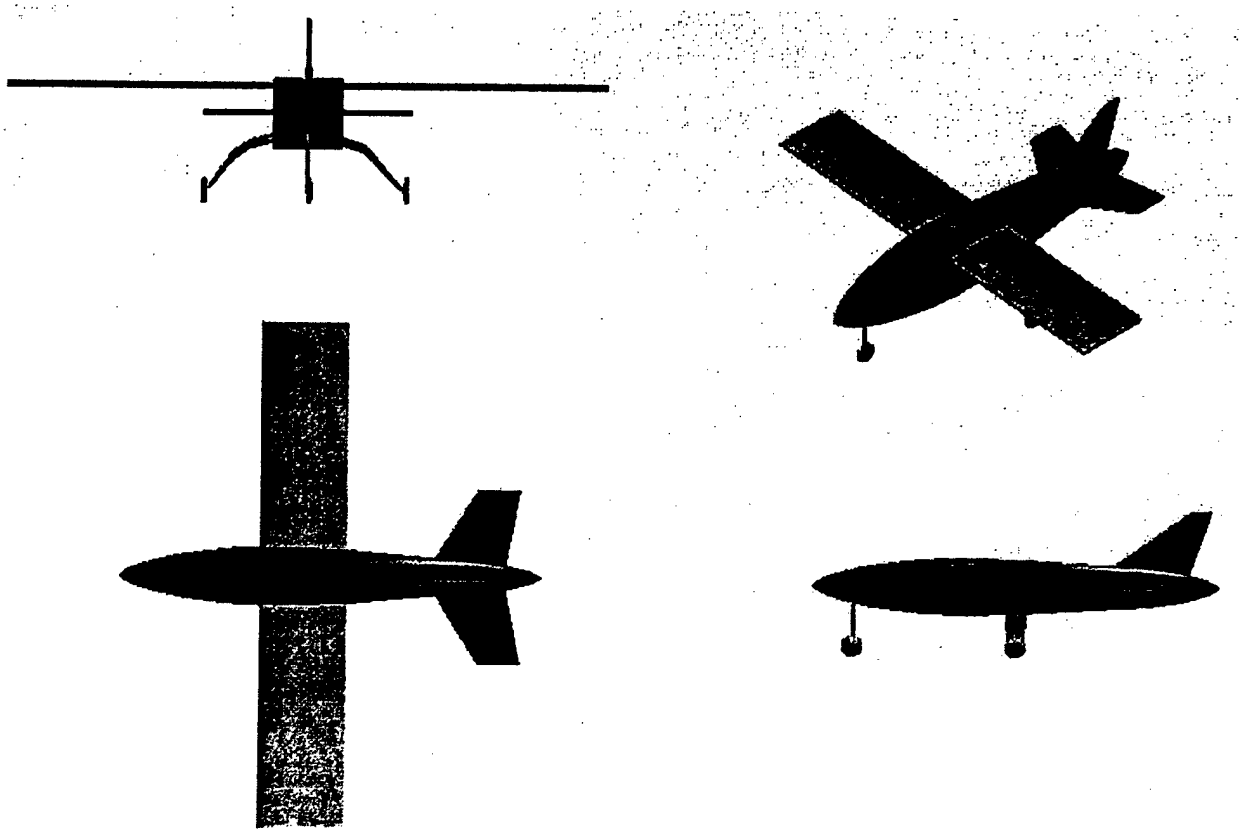

Figure 2: Three View Drawing for Concept 2

3.2.2.3 Concept 3

The third design that was considered was a square-type fuselage with high-mount tapered wings. The tapered wings serve to reduce induced drag, thus improving the overall efficiency of the aircraft. Along with the improved efficiency, however, comes a large increase in the complexity of manufacturing. The high wing mount increases overall stability of the aircraft. The square-type fuselage allows for ease of manufacturing.

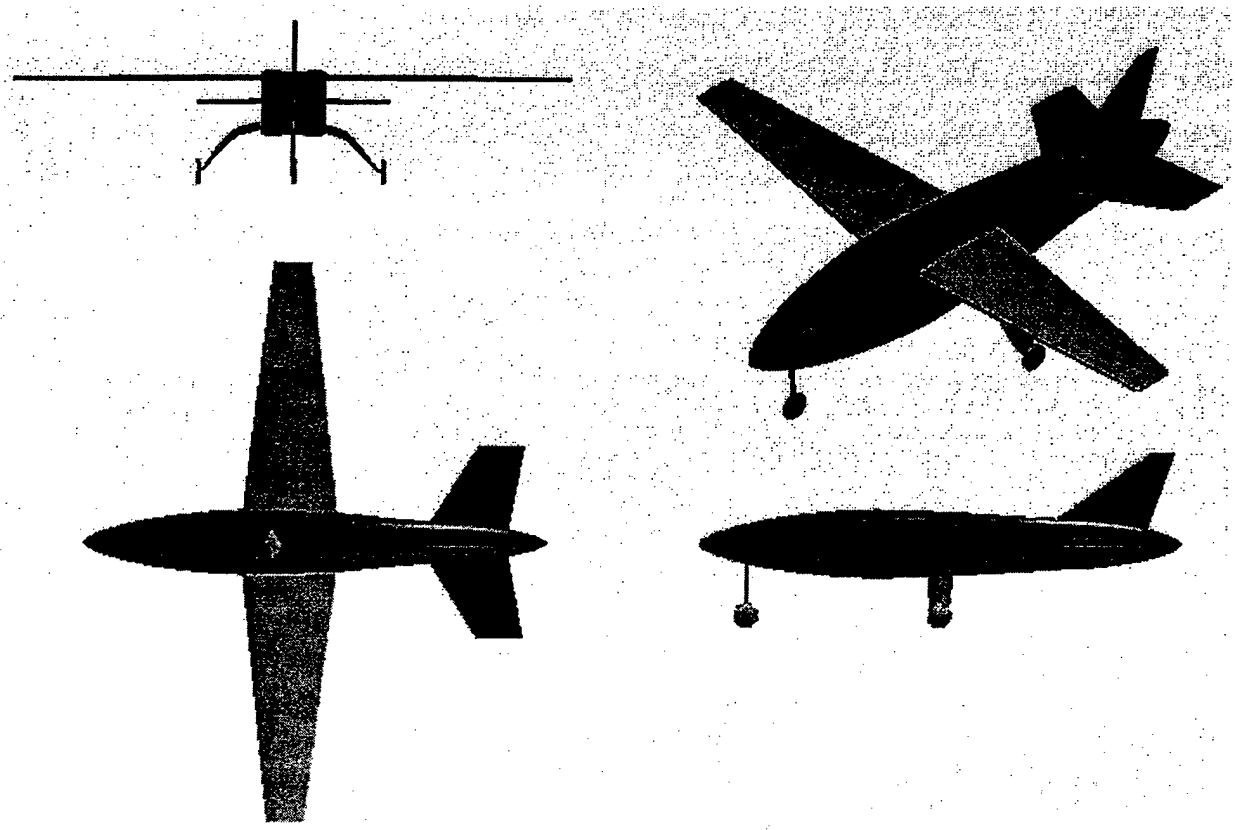

Figure 3: Three View Drawing for Concept 3

3.2.2.4 Concept 4

The fourth design considered was an aircraft with a cylindrical fuselage. The purpose of the cylindrical shape is to reduce the drag that would be incurred from a square shaped fuselage. The streamlining of the fuselage will serve to reduce drag, as well as reduce the overall weight of the aircraft. This type of fuselage will, however, be significantly harder to manufacture. The wings are mounted high on the fuselage, so as to increase stability. The tapering of the wings will reduce weight and induced drag.

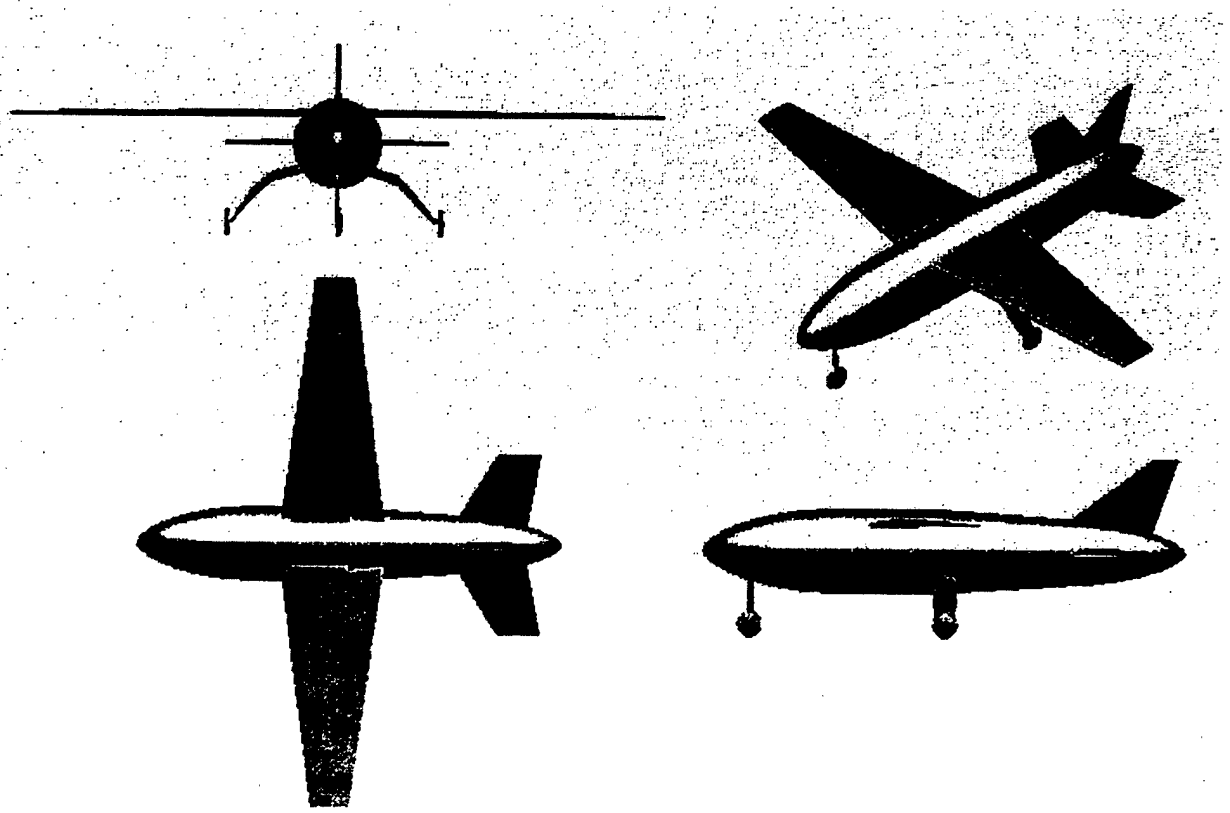

Figure 4: Three View Drawing for Concept 4

3.2.2.5 Concept 5

The design shown above utilizes a blended wing body. The elliptical cross section is much more efficient than the square crossection. There is less material, and the body is streamlined to reduce drag. The shape also serves to blend well with the wing. With a smooth transition from the wing to the body, drag will be significantly reduced. The high-mounted wing will better stabilize the aircraft in flight. This design would be very complicated to manufacture. The elliptical fuselage, as well as the blended wing, would require much planning and design expertise.

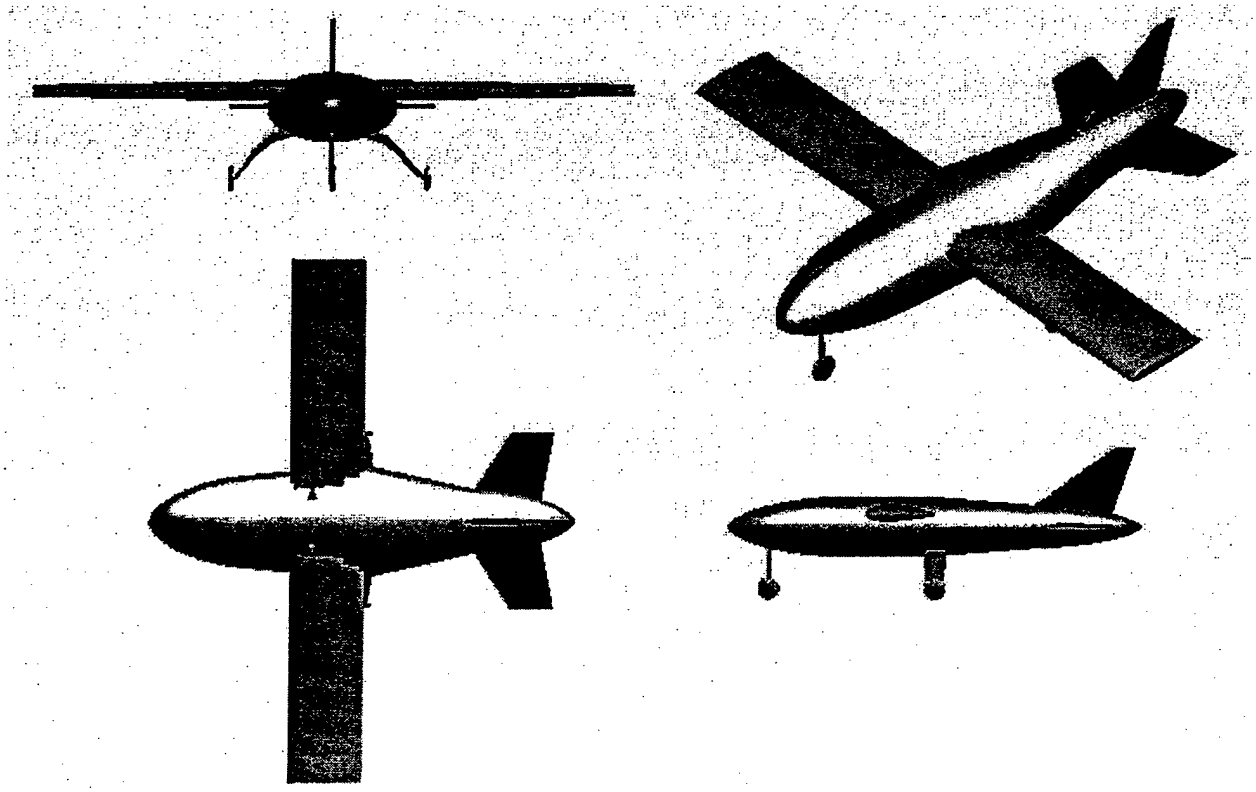

Figure 5: Three View Drawing for Concept 5

3.2.2.6 Concept 6

Another possible design is the cylindrical fuselage with a tapered wing blended into the body. This design is very aerodynamically efficient as compared to the other possible designs. The blended wing and cylindrical body serve to reduce all sharp corners, thus greatly reducing the induced drag of the aircraft. The tapering of the wing serves to further economize the aircraft. The tapered shape reduces induced drag, as well as aircraft weight.

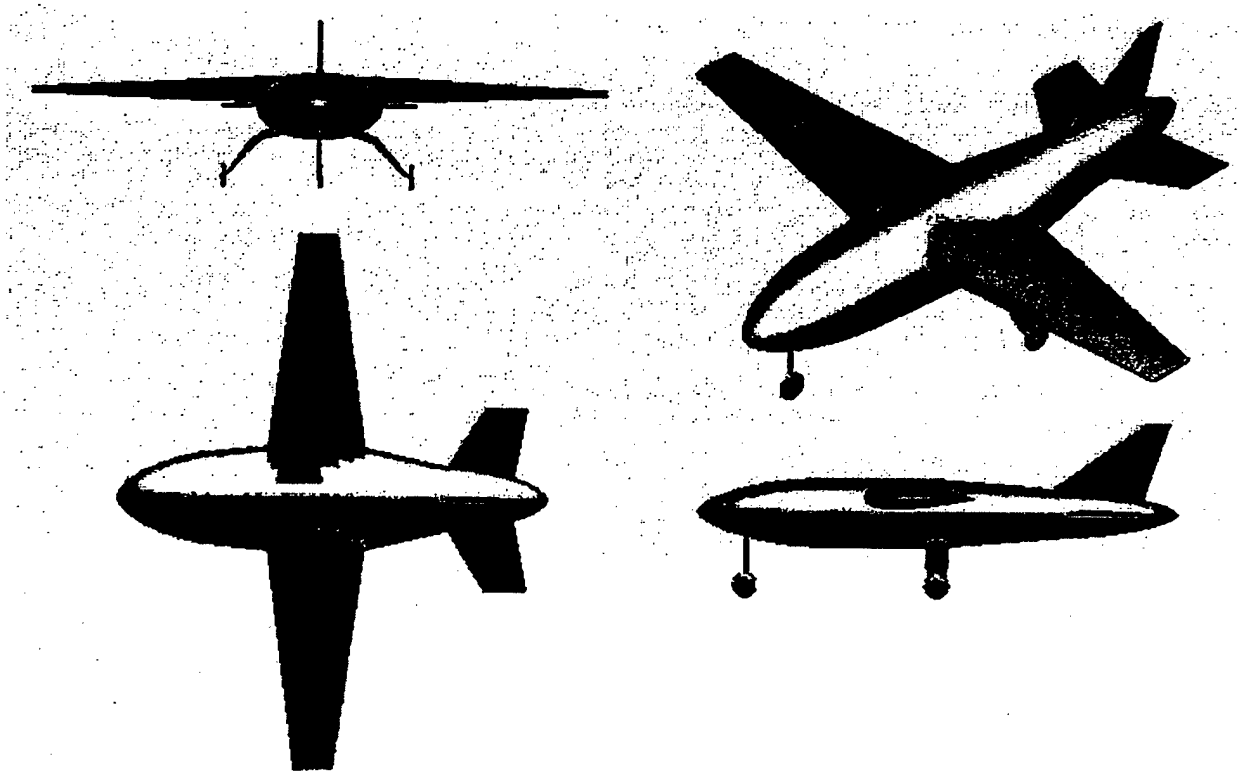

Figure 6: Three View Drawing for Concept 6

3.2.2.7 Concept 7

The design pictured above incorporates the use of a V-tail instead of the conventional rudder and horizontal stabilizer. The V-tail reduces the number of stabilizing surfaces from three (conventional) down to two. This reduces weight and manufacturing time. The added complexity comes with programming the two control surfaces to perform the same as a traditional tail performs. The design also encompasses a high mount, tapered wing, with a box-type fuselage. The high-mount and taper of the wings will lead to better stabilization and reduced drag. The box-type fuselage will provide ease of manufacturability.

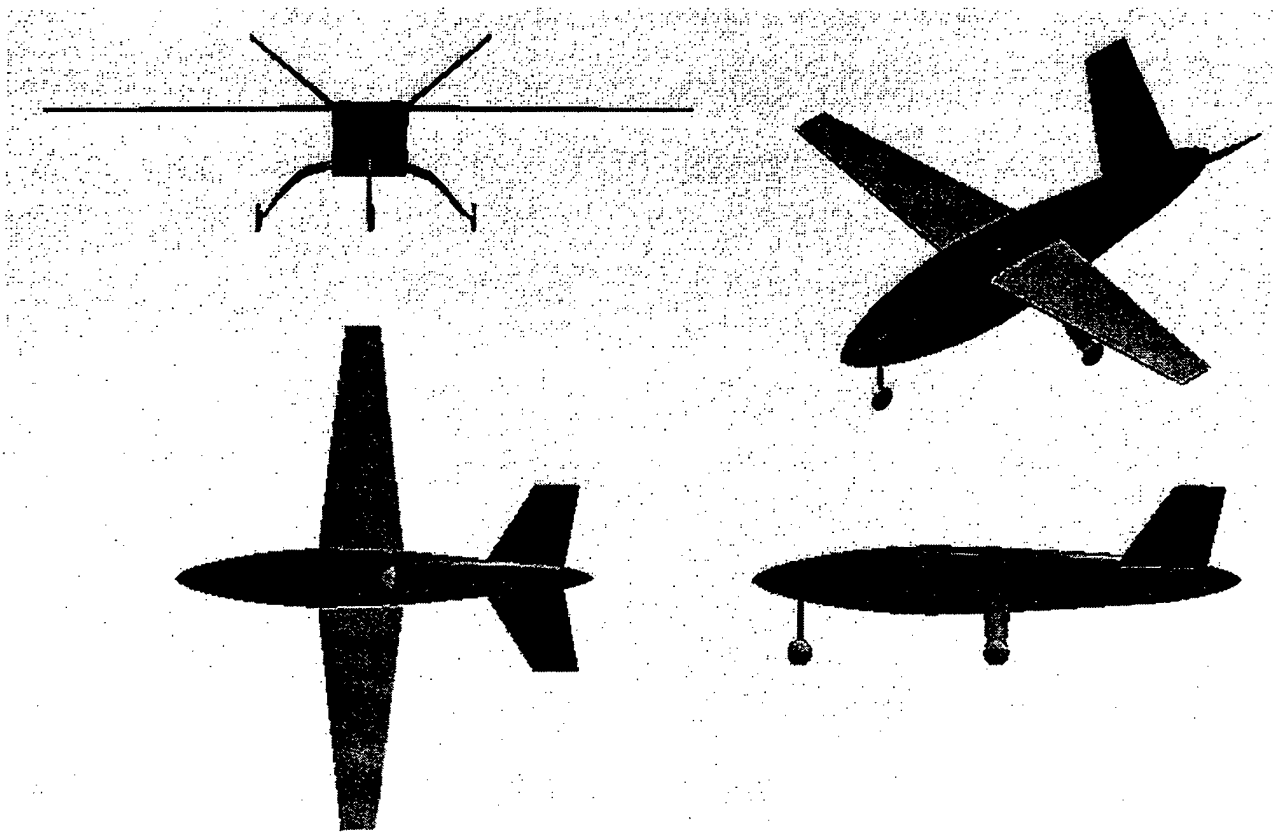

Figure 7: Three View Drawing for Concept 7

3.3 Pugh Matrix Comparison

The Pugh Concept Selection Method is a powerful tool with a mix of qualitative and quantitative techniques used to eliminate, combine, and compare various ideas and concepts based on a set of figures of merit. Each concept is listed out with various figures of merit and then compared qualitatively to a baseline concept. After the concepts are scored, the scores are tabulated for each concept and score differences yield an overall total score for each concept. The overall total is used to see where an individual concept is lacking or where its strong points lie. In order to rank the concepts they must be rated against a baseline design. This design is either a previous design or a concept that is a solution to the problem. The concepts are usually scored relative to the standard baseline using a symbolic approach. The concepts are rated to be either better than (+), equal to (0), or less than (-) the baseline concept. It is also possible to rank concepts numerically to determine an overall numerical score from that ranking. Ranking concepts numerically has the potential to yield a more objective comparison. Because each concept has a numerical score, it is easily determined which concept is better according to the Pugh Matrix. Also, with a numerical scale it is possible to weight each figure of merit and determine

solutions. The ability to weight each figure of merit is important if some figures of merit are more important than others.

3.3.1 Figures of Merit for Pugh Matrix Comparison

Six figures of merit were chosen for the Pugh selection matrices. The figures if merit selected were: Rated aircraft cost, Speed, Assembly Time, Stability, Manufacturability and Payload Capacity.

3.3.1.1 Rated aircraft cost

Rated aircraft cost is a measure of the "cost" of the designed aircraft. It takes into account such items as the number of engines, the number of wing and tail surfaces and wing and tail areas. Rated aircraft cost is a divisor in the total competition score; therefore, the team wants to minimize rated aircraft cost. Because of its role in scoring, the rated aircraft cost was chosen as a figure of merit for the Pugh Matrix.

3.3.1.2 Speed

Aircraft speed to complete the mission is another figure of merit that is used in the Pugh Matrix. Completion of each mission is timed and this time is used in the calculation of the overall score. The team wants to complete each mission in the shortest amount of time possible, and therefore, by extension, have the fastest aircraft possible.

3.3.1.3 Assembly Time

Before each flight, the aircraft assembly is timed. Aircraft assembly does not include payload installation. Assembly time is added to flight time in order to calculate a total mission time. It is in the best interest of the team's score to have as short an assembly time as possible. In order to have a short assembly time, the assembly must be as simple as possible with few mechanical hookups.

3.3.1.4 Stability

Aircraft stability is an important aspect for any aircraft, but the mission requirements for this year's competition made stability even more important. Because of the large changes in mission requirements, such as a dramatic decrease in weight (mission 2) and the addition of a large weight and drag source high above the vehicle centerline (mission 3), any potential design would need the flexibility to handle these vastly different flight conditions.

3.3.1.5 Manufacturability

Manufacturability refers to the team's ability to manufacture the aircraft. An aircraft that is more difficult and/or time consuming to manufacture will decrease the amount of time available for design and testing of the aircraft and parts. An aircraft that is more complicated to manufacture also increases the

chance that a part will not be completed as planned or will not work in its intended manner. The team intends to keep manufacturability within the realm of what can be reasonably accomplished. The team does not want to need to try out new manufacturing techniques on the aircraft final product; instead, the team would prefer to manufacture full size mock-ups of any part that requires a manufacturing process the team is unfamiliar with.

3.3.1.6 Payload Capacity

The amount of payload carried during flight is a direct multiplier in the total score. Therefore it is beneficial to carry as much payload as possible.

3.3.2 Subjective Pugh Matrix

The subjective Pugh Matrix is shown in Table 2 below. All concepts are compared against concept 6, which is the baseline concept. There is no concept that is significantly better or worse than all other concepts in this ranking; however, concept 5 is slightly worse than average while concepts 3 and 7 are slightly better than average. At this point, no concepts are deleted and a weighted Pugh Matrix is computed.

Table 2: Subjective Pugh Matrix

	RAC	SPEED	ASSEMBLY TIME	STABILITY	MANUFACTURABILITY	PAYLOAD CAPACITY	SUM OF S	SUM OF +	SUM OF -
Concept 1	-	-	+	-	+	+	0	3	3
Concept 2	-	-	S	S	+	+	2	2	2
Concept 3	S	-	S	S		+	3	2	1
Concept 4	S	S	S	S	S	S	6	0	0
Concept 5	-	S	S	S	-	S	4	0	2
Concept 6	-	+	S	S	-	S	3	1	2
Concept 7	S	-	S	S	+	+	3	2	1

3.3.3 Quantitative Pugh Matrix

After completion of the subjective Pugh matrix, a second, quantitative Pugh matrix was computed. While the subjective Pugh is a very useful tool, it does not possess the ability to quantify how much better or worse a design is from some datum concept. The seven design concepts were all entered into the quantitative Pugh on a scale of one to ten, with five being the datum reference point.

Table 3: Quantitative Pugh Matrix

	RAC	Speed	Assembly Time	Stability	Manufacturability	Payload Capacity	Sum
Concept 1	3	3	6	4	6	6	28
Concept 2	4	4	5	5	7	7	32
Concept 3	5	4	5	5	6	6	31
Concept 4	5	5	5	5	5	5	30
Concept 5	3	5	5	5	4	5	27
Concept 6	3	6	5	5	3	5	27
Concept 7	5	3	5	5	6	7	31

3.4 Conclusions From Conceptual Design

With the selection of a concept, the conceptual phase of the design process is concluded, and the team moved forward into the preliminary design phase. Passed forward were all of the qualitative and quantitative decisions leading up to the selection of the second concept.

4.0 Preliminary Design

The goal of the preliminary design phase includes the initial and secondary sizing of the vehicle, a second order understanding of the propulsion system and an initial understanding of aircraft performance. Starting from the configuration selection in the conceptual design phase, the first task was the initial sizing of the vehicle.

4.1 Initial Sizing

The initial sizing of the aircraft began with an initial estimate for weight and thrust based upon the payload size and weight requirements. These estimates were then combined with a constraint analysis to determine the design point which maximized wing loading and minimized thrust to weight requirements for the aircraft. From this design point the wing area could then be found, and the rest of the vehicle sized from there. From the sized aircraft a more detailed weight estimation could then be made, and the entire process iterated. The process was repeated three times, until the initial and final weight estimates converged.

With the preliminary sizing of the vehicle completed, the aircraft could be matched with a motor and battery combination. With this data, the preliminary structural and aerodynamic data could also be calculated.

4.1.1 Constraint Analysis

The basis for this analysis comes from Mattingly [1], and utilizes an energy constraint analysis for initially sizing an aircraft based upon wing and thrust loading. This constraint analysis begins with the balance of the rate of mechanical energy input and the storage rates of potential and kinetic energy. From these properties, Equation 1 can be derived for any generic constraint.

$$\frac{T_{SL}}{W_{TO}} = \frac{\beta}{\alpha}\left[\frac{q\cdot S}{\beta\cdot W_{TO}}\left[K_1\left(\frac{n\beta}{q}\cdot\frac{W_{TO}}{S}\right)^2 + K_2\left(\frac{n\beta}{q}\cdot\frac{W_{TO}}{S}\right) + C_{Do} + \frac{R}{qS}\right] + \frac{1}{V}\cdot\frac{d}{dt}\left(h + \frac{V^2}{2g_o}\right)\right]\right| \quad (1)$$

Equation 1 is referred to as Mattingly's Master Equation, or simply the Master Equation, where the terms are:

T_{SL}	Sea level thrust
W_{TO}	Takeoff gross weight
B	Instantaneous weight fraction
A	Installed thrust lapse rate
q	Dynamics Pressure
S	Wing area
K_1	Induced drag coefficient
N	Load Factor
K_2	Non-zero lift, minimum drag term
C_{Do}	Zero lift drag coefficient
R	Additional drag (landing gear, friction, drag chute, etc.)
V	Velocity
h	Height of the aircraft
g_o	Gravity

Different design missions will then dictate the assumptions for the unknowns in Equation 1, which can then be used to find all of the constraint performance conditions for a given aircraft and map them all back onto a single plot of wing loading and thrust to weight ratio. This can then be used to see which mission requirements are driving the design, and where the design point should be.

The initial weight estimate and maximum thrust estimate from the conceptual design stage provided one constraint for the aircraft design point and the takeoff ground roll provided another. The intersection of these two constraints provides the feasible design space for the vehicle. To achieve the best results the vehicle should try and maximize wing loading and minimize thrust to weight ratio. After several iterations, the results will look like Figure 8.

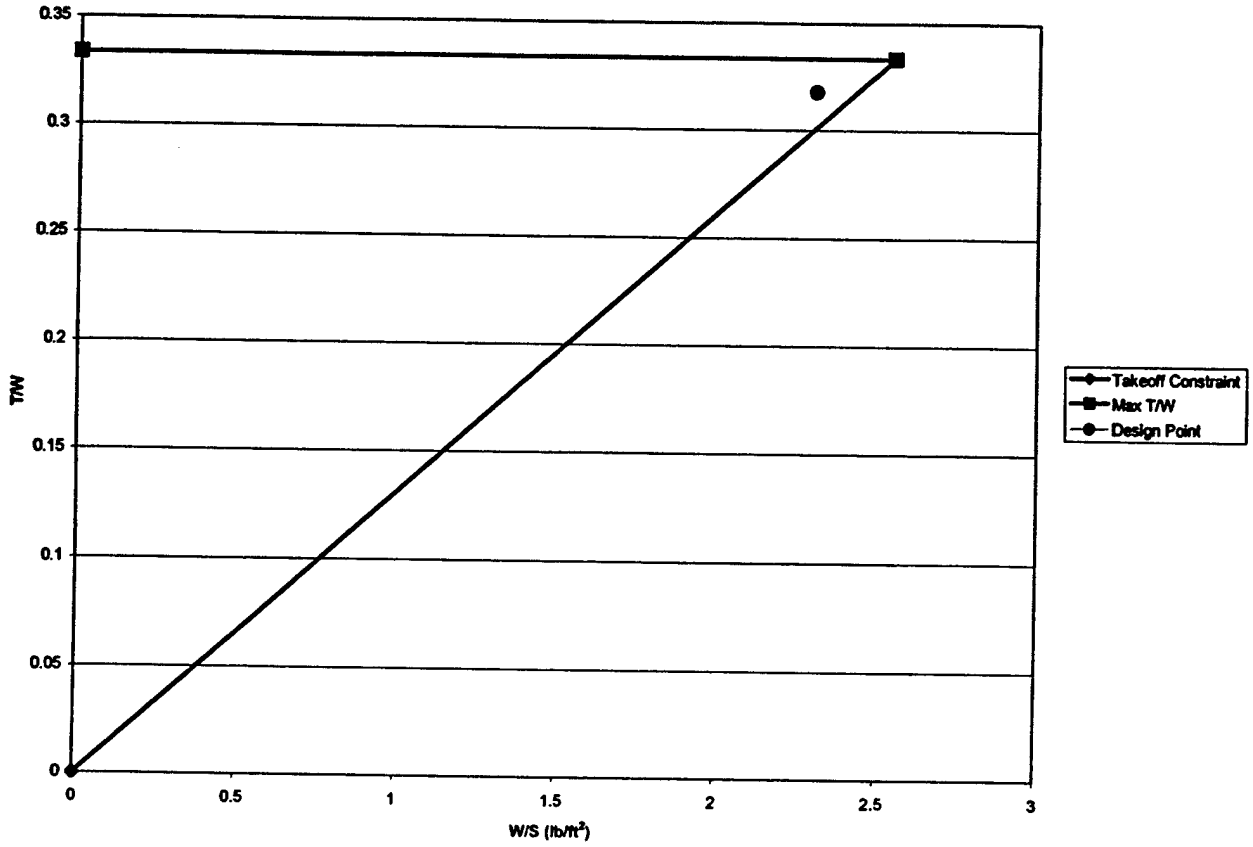

Figure 8: Thrust to Weight vs. Wing Loading

Because this is the preliminary sizing, the design point was taken at ninety-five percent of the maximum case at the intersection of the constraints. This point allowed for the complete sizing of the vehicle at the preliminary stage.

4.1.2 Initial Vehicle Sizing

With the design point set in place, and the total weight of the airplane roughly estimated, the wing area was determined. Wingspan and the fuselage length were defined based on size of the box in which the plane had to be stored. Wing chord was simply determined by dividing the wing area by the wingspan. Based on size of the payload that the airplane must carry, an approximate fuselage width and height were determined. With all major components of the airplane defined, a historical approach presented in Raymer [6] was used to estimate the tail size.

4.1.3 Initial Weight Estimate

With the aircraft sizing completed, a more detailed weight estimation was performed. Since the plane was to be manufactured almost entirely out of laminated composites, the team investigated weight of different carbon fiber and fiberglass lay-ups. For the initial weight estimation, assumption was made

that the wings were made out of 2 plies of fiberglass, and fuselage made out of 4 plies of carbon fiber. For each lay-up, weight per unit area was obtained experimentally. To obtain the total weight of the airframe, an approximate surface area of the wings and the fuselage was calculated, and multiplied by the weight of fiberglass and carbon fiber respectively. Also, based on historical data gathered by the team over the years, overall weight of the servos, batteries, engine and landing gear were estimated. With the weight of the payload described in the rules, an initial weight of the airplane was found.

4.2 Propulsion Analysis

Several possibilities for aircraft propulsion were examined. Assuming a traditional motor and propeller assembly, the major design choices were between a single or multiple motor configuration, and a tractor or pusher system. In previous years the team has used a tractor type propulsion system. A tractor system seemed appropriate for this aircraft design, since a motor in the back of the aircraft would have led to stability problems. Also, from past years, the team was familiar with the manufacturing process involved in a tractor design. A single motor was chosen as opposed to a dual, or multiple, motor system. A single motor had the advantage of less weight than multiple motors, and that the thrust loss was an allowable sacrifice.

Another possibility for propulsion would have been to use a ducted fan system. This system was chosen for the team aircraft three years ago. The ducted fan proved to be difficult to manufacture and was otherwise problematic. For these reasons, a ducted fan was not chosen for this year's aircraft.

The competition guidelines require the use of either Astroflight or Graupner brushed electric motors. This requirement immediately limited the number of available engines. Since the aircraft weight was estimated at eighteen pounds with payload, either one large motor or two smaller motors were required. Since additional motors increase weight and rated aircraft cost, the team chose to pursue configurations with only a single motor. This further reduced the possible engine combinations, and allowed for a more detailed look at the remaining candidates.

4.2.1 Trade Study of Number of Batteries Required

The Program MotoCalc 6.05® was used to determine the optimal number and best type of batteries to be used in the aircraft. It had already been determined that the motor to be used was the Astroflight Cobalt 60. Also determined were estimated aircraft parameters including weight, length and span. Using this information, MotoCalc 6.05® was used to analyze the pros and cons of different numbers of batteries. It was found that the optimal number of batteries to be used with the selected motor was twenty-four: twenty-four batteries will give maximum run time and power without overheating. Twenty-four batteries weigh less than four pounds; this is within competition guidelines requiring less than five pounds of batteries.

4.2.2 Take-Off Battery Power Requirements

The nominal goal of the batteries was determined from information in an article by Robert Benjamin. He writes that fifty watts of input power from the batteries per pound of aircraft take-off-weight will allow for take off and steady flight [3]. With twenty-four batteries (see previous paragraph), rated at 1.2 volts each, and assuming the maximum current draw of forty amps, the motor should have 1152 watts of input power. This works out to be sixty-four watts per pound, assuming a take-off-weight of eighteen pounds. Thus the optimal configuration of twenty-four batteries will be used for this aircraft.

4.2.3 Cruise Battery Power Requirements

Using MotoCalc® 6.05, it was found that the battery power requirements during cruise will be between six hundred and seven hundred watts. As shown in the previous paragraph, this amount of power will be achievable by the motor/battery configuration that has been chosen.

4.2.5 Motor Investigation

The program MotoCalc 6.05® was used to compare different motors for use on the aircraft. Using estimated parameters for aircraft weight, length, wing span and area the program calculated the amount of thrust required for flight. The program also provided a first-order guess at a motor/battery combination to achieve the desired results. The top choices for motors were determined to be an Astroflight Cobalt 60 or an Astroflight Cobalt 90. These two motors were then analyzed more extensively using the MotoCalc 6.05® program. It was determined that the Astroflight Cobalt 90 was overpowered for the needs of the aircraft, and would also add unnecessary weight and significantly reduce run time. The best motor for the competition requirements, as well as the parameters of this specific plane design, was determined to be the Astroflight Cobalt 60.

4.4 Preliminary Aerodynamics

The initial aerodynamics work in the preliminary design phase centered primarily around the selection of the best airfoil for the given configuration, and a better estimate of the aircraft drag.

4.4.1 Airfoil Selection

Airfoil selection is a critical step in aircraft design. Many different factors go into the design of an airfoil and a "good" airfoil can only be determined with a specific flight regime in mind.

4.4.1.1 Figures of Merit

As with aircraft sizing, several figures of merit were established to help determine airfoil selection. These figures of merit served as the initial criteria for airfoil selection.

- C_{lmax}

- Stall Angle
- C_d
- L/D

The maximum lift coefficient, C_{lmax}, is an important airfoil characteristic used in take-off performance as related to the stall speed of the aircraft. Shorter take-off field lengths are attained with higher values of C_{lmax}, due to the lower stall speeds attainable. Stall angle is an important characteristic for handling qualities. A higher stall angle allows for larger tolerances in flight. Aircraft with higher stall angles are also more maneuverable than those with lower stall angles. This proves important in this application, as pilots for small UAV's have fewer stall indications than pilots situated in the aircraft. The drag of the airfoil is another important characteristic of airfoils. Lower values of C_d mean that the airfoil creates less drag in flight. This is directly tied into the next figure or merit. The L/D is the ratio of lift to drag. This provides a good indication of the efficiency of an airfoil. This was weighted slightly more in overall considerations than the other figures of merit.

4.4.1.2 Airfoil Comparison

The flight characteristics of the competition allowed for several assumptions. The flight envelope of the plane would be at most 300 feet above sea level, and flying at very low subsonic speeds, making an assumption of incompressible flow very accurate. Airfoil data gathered from previous year's competition was used. Airfoils from the UIUC Airfoil Coordinates Database [7] were compared with the figures of merit defined above, and those that best fit the figures of merit were compared further. Comparisons were made using airfoil analysis program titled Calcfoil. Calcfoil utilized conformal mapping, with the Reynold's Number and airfoil coordinates as inputs. Comparisons of Calcfoil outputs and data published in Reference 7 were made, and the difference was negligible.

Upon review, the following nine airfoils were considered further:

- LS-413 Modified
- LS-417 Modified
- CLARK Y
- DAE51
- DEFCND2
- Eppler 1230
- Wortman FX 62-k-131
- Wortman FX 62-k-153/20
- Wortman FX 63-100

These were compared at Reynold's numbers of 200,000, 600,000, and 1,200,000. A comparison of the figures of merit is show in Figures 9, 10, and 11 below.

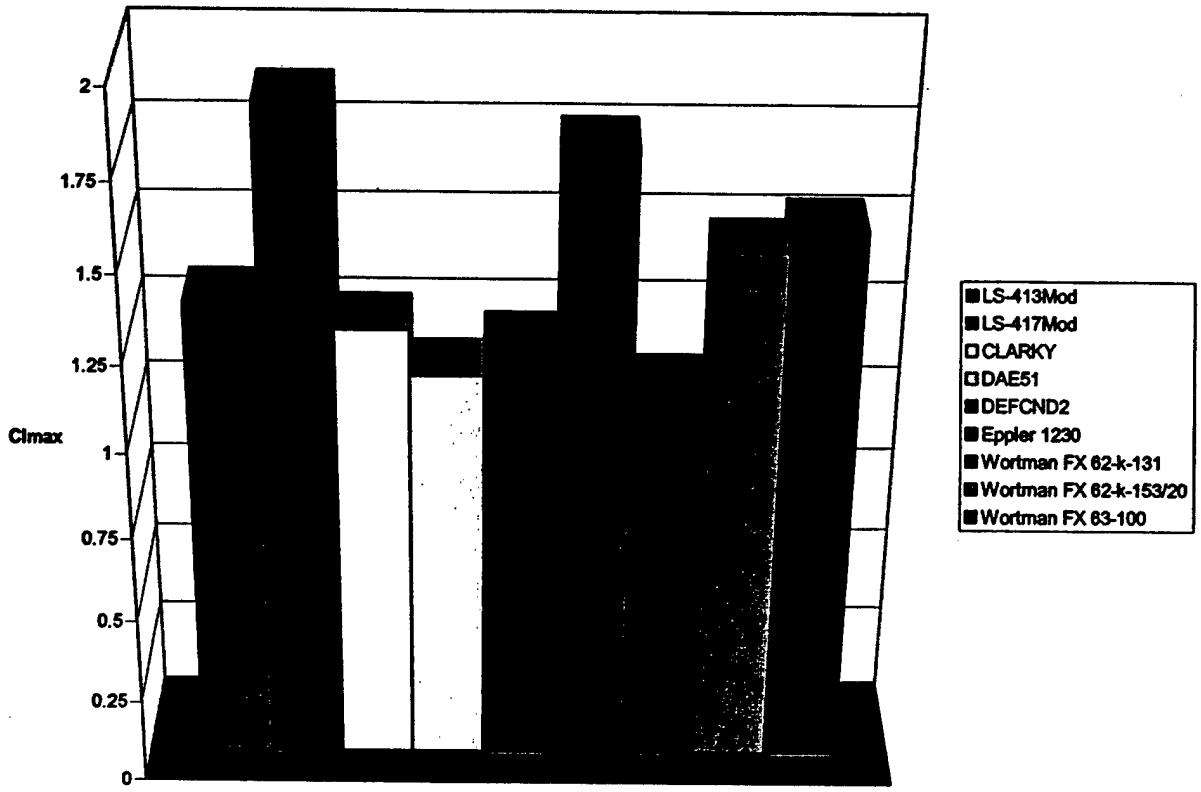

Figure 9: C_{lmax} Comparison Re=200000

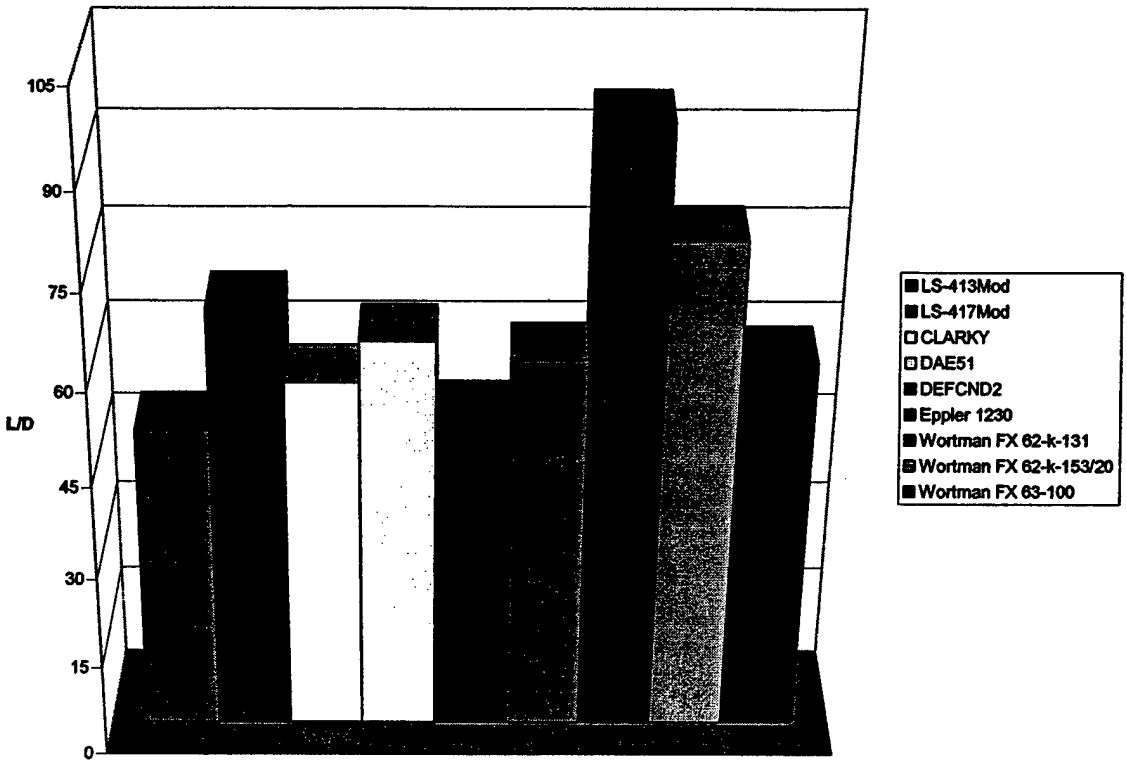

Figure 10: L/D Comparison Re=200000

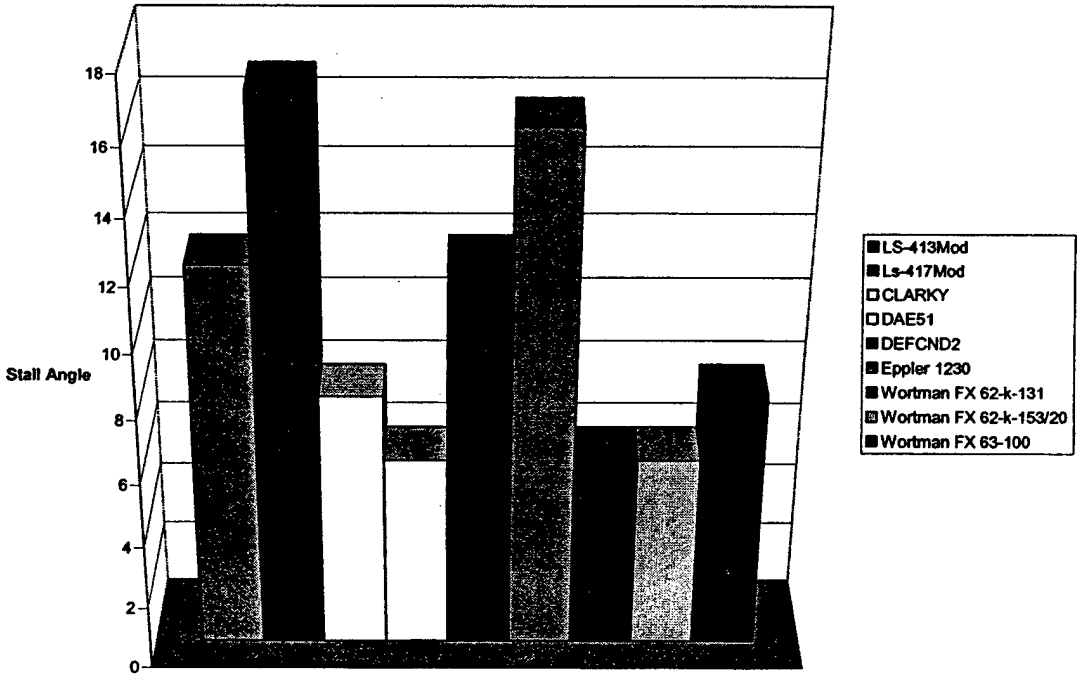

Figure 11: Stall Angle Comparison Re=200000

Based on figures 10-12, the LS-417 Modified airfoil was selected. This was due to the high C_{lmax}, high stall angle, and above average L/D ratio. The characteristics of the LS-417 Modified airfoil were further compared at an estimated aircraft Reynold's number of 2,700,000 for the aircraft. This data is shown below in Figures 12, 13, and 14.

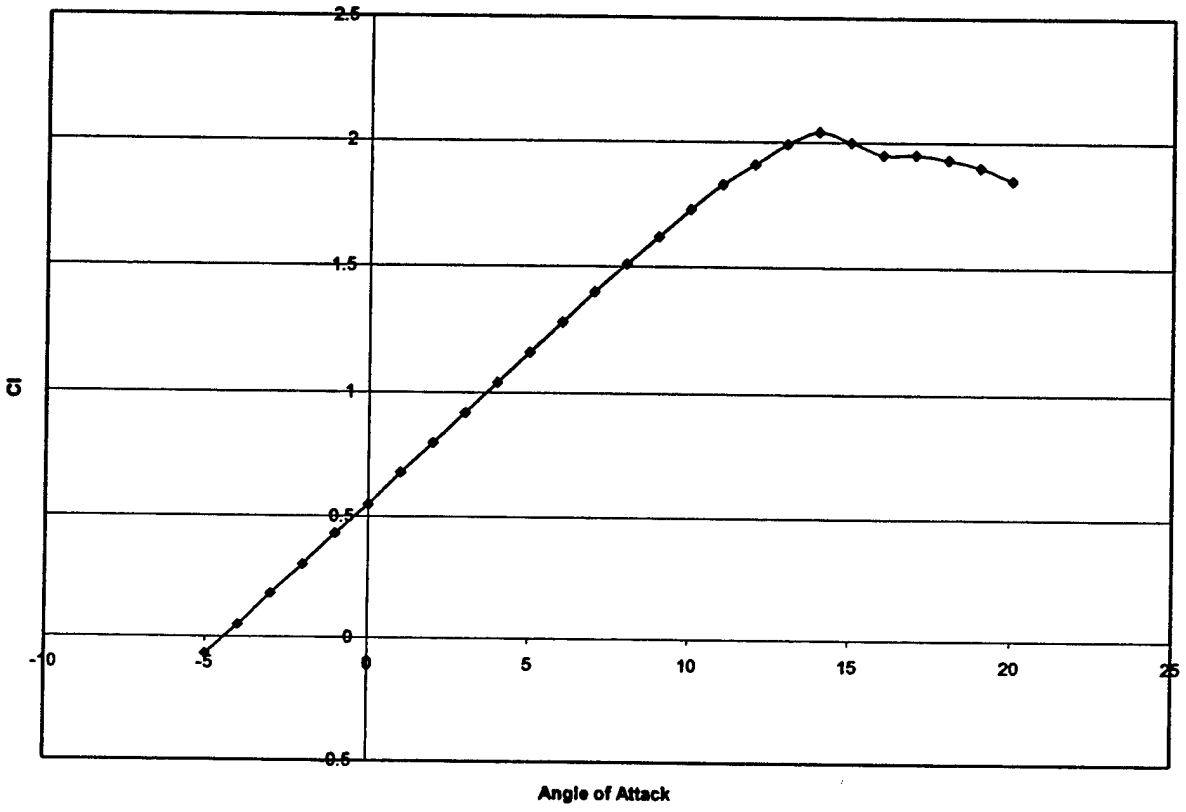

Figure 12: Cl vs AOA

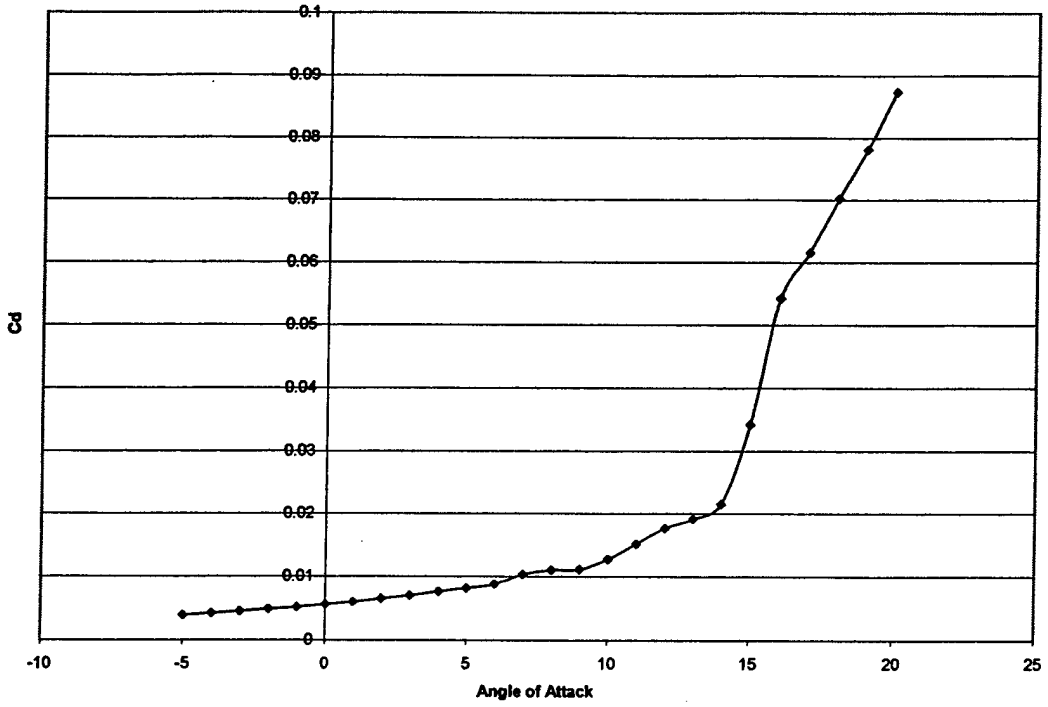

Figure 13: Cd vs AOA

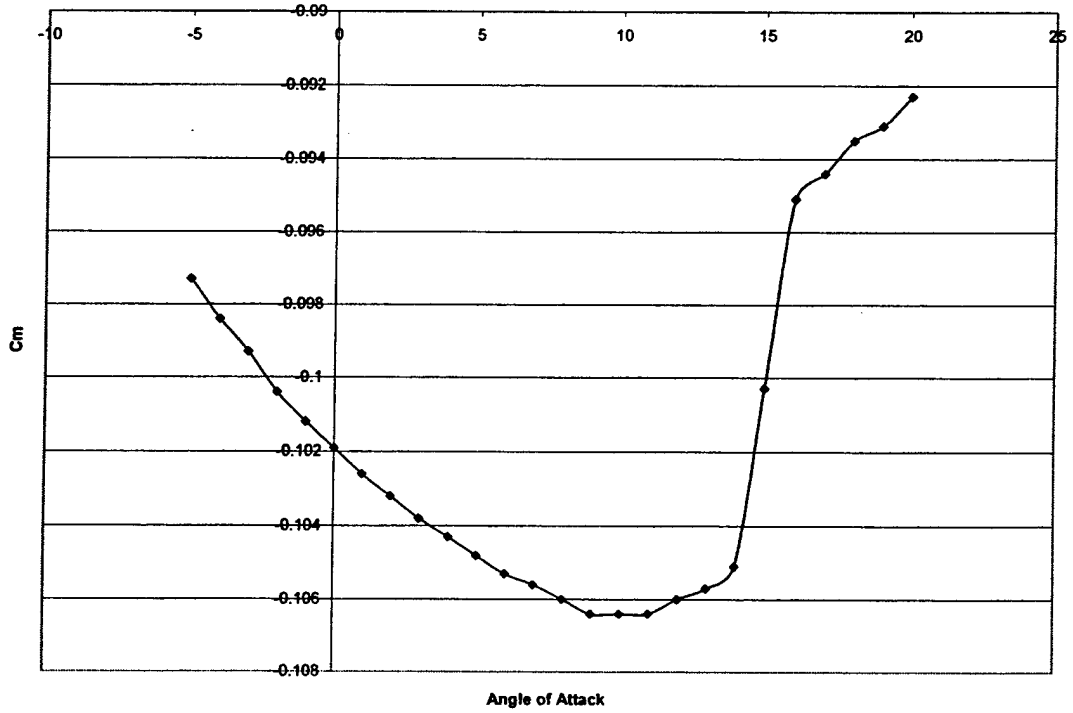

Figure 14: Cm vs AOA

4.4.2 Drag Polar

In order to determine the range and endurance of the aircraft, an accurate measure of the drag was needed. With these range and endurance calculations the mission performance can be found. A level one estimation was used for drag calculations; this was expected to provide an accurate drag prediction, with a slight tendency for over-prediction. Drag is comprised of three main components: induced, compressibility, and skin friction drag. Because of the low Mach numbers of the flight, drag do to compressibility effects was neglected. At this stage the drag polar could be evaluated by Equation 2.

	$C_D = C_{Do} + KC_L^2$	(2)

Here C_D is the total drag, C_{Do} is the zero-lift drag, K is the induced drag constant, and C_L is the aircraft lift coefficient. Part of C_{Do} is the skin friction drag. This can be found after computing the skin friction coefficient for each body. Assuming a turbulent boundary layer, the skin friction coefficient is found with Equation 3.

	$C_f := \frac{0.455}{(\log(Re))^{2.58}}$	(3)

C_f is the skin friction coefficient, and Re is the Reynold's number based upon body length. Reynold's numbers were found at the stall speed of the aircraft. C_f values were found for the fuselage, the wing, and both the horizontal and vertical tail and their total drag was found with Equation 4.

	$C_{Do} := \frac{1.2 \cdot \left(\sum_n C_{fbody} \cdot S_{wetbody} \right)}{S}$	(4)

In Equation 4, the C_{fbody} is the skin friction coefficient of the specific body, and $S_{wetbody}$ is the wetted area of that body. Here S is the reference wing area.

This left the calculation of induced drag to finalize the aircraft drag polar. The induced drag coefficient was found using Equation 5

	$K = 1/\pi Ae$	(5)

A is the aspect ratio of the wing and e is Oswald's span efficiency factor. With unswept wings this value is estimated using Equation 6.

	$e = 1.78(1 - 0.045A^{0.68}) - 0.64$	(6)

The resulting drag polar is shown in Figure 15.

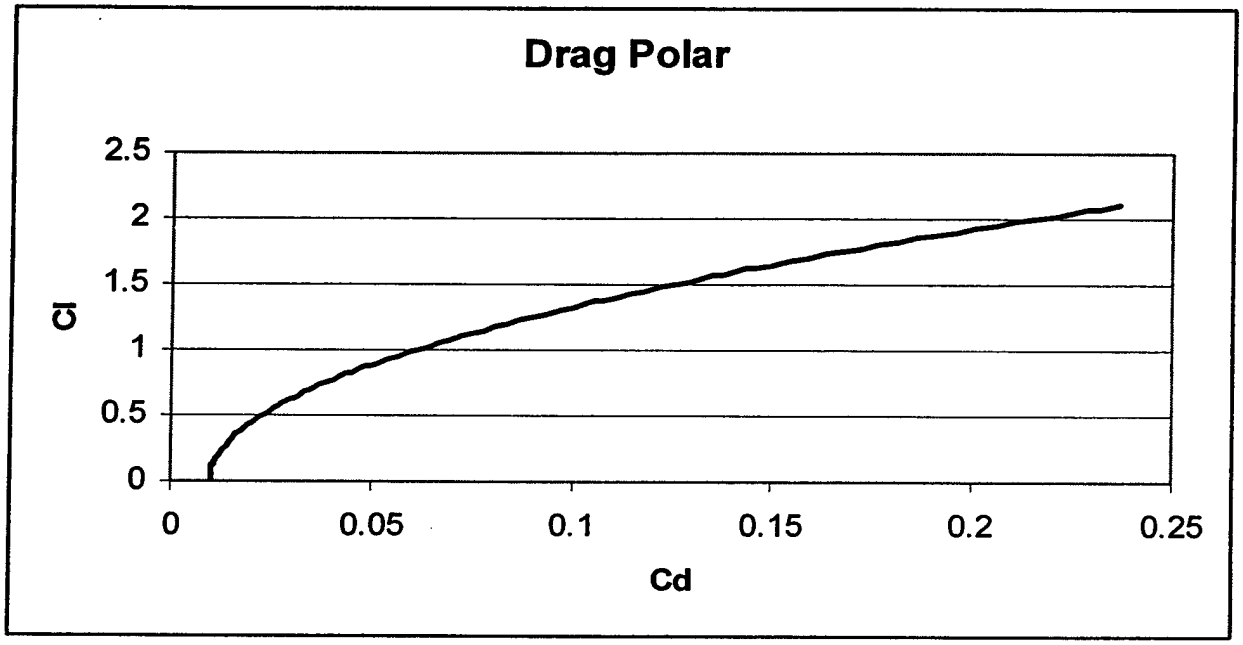

Figure 15: Aircraft Drag Polar

4.6 Preliminary Design Conclusions

This provides the team with enough data to finish the preliminary design phase, and allows for the detailed design phase to begin.

5.0 Detailed Design

With the completion of Preliminary design final component selection can be completed. With the final selection of all aircraft components the final performance calculations are made and the final optimization of the aircraft occurs. Additionally with the selection of final components the structural design of all components can be finalized and the aircraft's final weight calculated.

5.1 Final Configuration Features

5.2 Weight and Balance

5.2.1 Final Weight Estimation

The final weight of the aircraft was estimated from individual component weights. The aircraft structures, now sized, could be re-evaluated for the final weight estimation. The value was important as it determined the aircraft performance and handling qualities. The weight of each component as well as total weight is presented in the Table 4.

Table 4: Final Weight Estimation

Components	Weight (lb)
Wing	1.481
Fuselage	0.619
V-Tail	0.283
Tail Arm	0.150
Engine	1.700
Batteries	3.280
Servos (5)	0.500
Speed Controller	0.116
Receiver	0.088
Receiver Battery	0.250
Payload	6.000
Landing Gear	1.000
Wheels	0.500
Hardware	2.000
Cables	0.125
Wing Mounting	0.500
Total	**18.59**

5.2.2 Center of Gravity

All entries are expected to demonstrate adequate handing qualities for both maximum and ferry loading conditions. T herefore, the C G of the payload was to be located right at the C G of the entire aircraft. This would result in little change in the static margin for either load case.

The CG calculations involved a simple static analysis. The weight estimation carried out previously indicated each component's weight. The location of each component's centroid was then found from the nose of the aircraft. The moments about the nose of the aircraft due to each component were then summed, and this sum was subsequently divided by the total weight of the aircraft. This indicated the aircraft CG location from the nose. Some components, such as the radio control equipment, could be moved within the airplane.

The values for the necessary and actual CG location of both the ferry and maximum load cases converged to within one hundred of an inch after iteration of the component locations. The locations after construction will likely vary from this range, so the actual location of the components may differ slightly after the aircraft is built.

5.3 Aircraft Performance

5.3.1 Takeoff and Climb Performance

Take off was a critical design parameter this year because the plane was required to take of in 120 feet. Climb performance is also important because it is best to get to cruising altitude as quickly as possible. These two parameters were calculated for the final design using the methods from reference (4) and can be seen in Table 5.

Table 5: Flight Performance Characteristics

Performance Characteristic	Empty	Payload
Take off field length (ft)	54	105
Max Rate of Climb (ft/s)	34.3	33.6
$C_{l,max}$	1.05	1.05
L/D_{max}	10.85	10.85
V_{stall} (ft/s)	39.6	46.6
V_{max} (ft/s)	106.9	107.5

5.3.2 Flight Performance

Though take off and climb are two important parameters, they are not the only important performance parameters. Other important performance characteristics for this plane include maximum lift coefficient, maximum lift to drag ratio, stall speed, and maximum speed. Again, these parameters were calculated using the methods from Pamadi [4] and can be seen in Table 5.

5.3.3 Stability and Control

Aircraft stability is often demonstrated through the use of dimensionless stability derivatives. Roskam [8], states that the following must be true to demonstrate basic stability:

- $C_{l_\alpha} > 0$ – aircraft lift curve slope
- $C_{m_\alpha} < 0$ – pitching moment curve slope
- $C_{m_q} < 0$ – variation of pitching moment coefficient with pitch rate
- $C_{D_u} > 0$ – variation of drag coefficient with speed
- $C_{m_u} > 0$ – variation of moment coefficient with speed
- $C_{y_\beta} < 0$ – variation of moment coefficient with sideslip angle

The derivatives were found per the methods from Roskam [9]. Two assumptions were made for the calculation of these derivatives; first, that compressibility effects could be ignored due to the low flight speeds, and second, that the aircraft was flying at small angles of attack in normal flight. This design met all of the requirements laid out for stability. The results of this analysis are displayed in Table 6.

Table 6: Stability Derivatives

C_{l_α}	1.113 rad^{-1}
C_{m_α}	-0.1116 rad^{-1}
C_{m_q}	-1.027 rad^{-1}
C_{D_u}	0.00
C_{m_u}	0.00
C_{y_β}	-0.2543 rad^{-1}

5.3.4 Mission Performance

In order to determine the time it will take to perform the different missions the times were broken down into four separate segments and found using the methods from Pamadi [4]. These can be seen in Table 7.

Table 7: Mission Time Segments

Segment	Empty	Payload
Time for one Lap (sec)	40.7	40.7
Time for a 360 turn (sec)	6.3	6.3
Time for one Lap w/Takeoff (sec)	56.7	61.2
Time for one Lap w/Landing (sec)	60.3	67.7

An approximate time for each mission under zero gust conditions are shown in Table 8.

Table 8: Total Mission Time

	Total Time (sec)
Mission A	235
Mission B	271
Mission C	286

5.4 Propulsion System

The Astroflight Cobalt 60 motor will be used as the propulsion system for the aircraft. This motor weighs twenty-seven ounces. It will produce 347 rpm per volt. The motor will be geared down with a 2.75 to one ratio gearbox (by Astroflight). A twenty-two inch propeller with a pitch of eighteen will be used.

5.5 Structural Design

5.5.1 Load Factor

For the wings, the limit load factor was determined from the worst case scenario of a fully loaded airplane supported by the wingtips. This resulted in a limit load factor of 2.0. This was multiplied by 1.5, the standard factor for aerospace vehicles as specified by the Federal Aviation Regulations, resulting in an ultimate load factor of 3.0. The team wished to keep the wing ultimate load factor low, based on past experiences. The use of a high load factor results in a strong, yet very heavy wing.

For the fuselage, the limit load factor was determined from the worst case zero-gust flight condition of an instantaneous turn at the maximum lift coefficient and maximum velocity. This resulted in an approximate ultimate load factor of 6.0. Initially, this value may seem needlessly high for anything other then a high-performance fighter aircraft. However, in provided a nice cushion in the event of a hard landing or even for a moderate crash.

5.5.2 Wing Structure

The team wished to assemble the wing from a foam core wrapped in fiberglass cloth. This would result in a wing structure that would be stronger and lighter then one made of wood build for the same loads. The design was considered a bending-critical application.

The wing was approximated as a cantilever beam for structural analysis. For simplicity, the lift was approximated as a point load at the tip of the wing, and was calculated for 2.5 times 1-g flight load. The resulting bending moment was greatest at the wing root.

Since the foam cores would carry substantially less load then the fiberglass, they were neglected entirely for bending analysis. As the wing skin would be much thinner then the thickness of the wing, the loads in the upper skin were treated as pure axial compression, while the lower skin was assumed to be under axial tension. Each of these loads was approximated to act at the center of each skin. As both forces acted in opposite direction, this resulted in a couple equal to the distance between the two axial forces times the magnitude of this force. The magnitude of this couple would equal the magnitude of the root bending moment. Since the root bending moment and distance between wing skins were known, the magnitude of the axial forces in the wing skins was found by dividing the root bending moment by the distance between the skins. These forces were found for skins with two to nine plies of fiberglass. The resulting average ply stress could be found by dividing this force by the cross-sectional area of the skins.

The fiberglass cloth that was to be used had fibers running at right angles to each other. As such, each ply of material would effectively behave like two piles of unidirectional material at right angles to each other, with the only major difference being the Poisson ratio of the material (due to the weave of the fabric). Therefore, the qualities for a singe unidirectional ply of fiberglass could be used in the calculation of the material properties of the upper and lower wing skins. These properties (longitudinal Young's modulus, ultimate tensile strength, and ultimate compressive strength) were estimated from Kaw [10].

It is desirable to construct laminates that are balanced and symmetric; that is, laminates have the same number of plies running at the angle $+\theta$ as at the angle $-\theta$, and that are symmetric about their thickness centerline. It has been shown that laminates that are especially resistant to impact damage have plies at ±45 degree orientation on the outermost layer. Therefore, the ply orientation of the wing was chosen such that the outer layer of cloth would be at ±45 degree orientation. These plies would also provide the best torsional rigidity. The fabric in the middle layers would need to have a 0/90 degree orientation to carry the bending loads of the wing.

Skin thicknesses of two and three layers of fabric were chosen for further analysis. The first had an orientation of [±45/0/90], and second [±45/0/90/±45] (note that each layer of fabric consisted of two plies of material). Three test sections of each lay-up were then manufactured and tested under pure tension with a standard load frame, as described in section 7.2. The average stress to failure of each lay-up was obtained and compared with the stress in each wing skin and the factor of safety was determined.

The three-layer laminate exhibited a factor of safety of approximately 1.7, giving it the capability to withstand 5.1 g's. The two-layer laminate exhibited a factor of safety of approximately 1.25, with capability to withstand 3.75 g's.

Finally, the entire wing structure underwent a deflection analysis. The wing was assumed to be a cantilever beam with a force acting on the tip, and the deflection found from Gere [11]. The result of this analysis was a 3 inch tip deflection during a 3.0-g loading condition.

5.5.3 Fuselage Structure

The fuselage also underwent a simple bending structural analysis. It differed from the wing analysis in that the fuselage was modeled as a beam supported at its CG. Each component was represented by a point mass located at their respective centroid locations, as specified in section 5.2.2. The moments of each of these points times the limit load factor was taken about the aircraft CG. Since the aircraft was balanced about this point, the moment ahead and behind the CG were equal and opposite. Therefore, only one side was considered, so the fuselage could be analyzed as a cantilever beam.

The fuselage is characterized by two rectangular plywood bulkheads stiffened by the carbon fiber skin. The bulkheads merely provide torsional stiffness, while the skin carries the fuselage bending loads. The stress in the skin was found utilizing the same methods described for the stresses in the wing skins. These stresses were compared to ultimate tensile stress of a four ply carbon fiber lay-up obtained from experimental testing described in section 7.2.

The ultimate tensile stress was divided by the actual stress in the skins to determine the factor of safety. This was found to be approximately 4.2, giving a maximum load capability of 25.2 g's. Again, while this may seem excessive, the benefits of increased crashworthiness and lack of considerable deflections were of prime importance.

5.6 Rated aircraft cost

Rated aircraft cost is one of the most important parameters of the competition as it is a direct score multiplier. The performance parameter of the code was based upon mission performance, as well as Rated aircraft cost. The equation for Rated aircraft cost is shown in equation 7.

$$RAC := \frac{(A \cdot MEW + B \cdot REP + C \cdot MFHR)}{1000} \qquad (7)$$

A description of these variables, as well at the actual rated aircraft cost, is shown in Table 9.

Table 9: Rated Aircraft Cost

Coefficient	Description	Value
A	Manufacturers Empty Weight Multiplier	100
B	Rated Engine Power Multiplier	1500
C	Manufacturers Cost Multiplier	20
MEW	Manufacturers Empty Weight	14
REP	Rated Engine Power	4.1
MFHR	Manufacturing Man Hours	171.00
	RAC	**10.97**
	REP:	4.1
	Number of Engines	1
	Total Battery Weight	3.28
	MFHR:	171.00
	Wing Span	7.41
	Max Exposed Chord	0.93
	Control Surfaces	2
	Fuselage Length	4.33
	Vertical Surface, without control	1
	Horizontal Surface, with controls	1
	Servos and Controllers	6
	Engines	1
	Propellers	1

5.7 Final Aircraft Parameters

The results of the detailed design phase are shown in Table 10. This is the data that has been used to construct the competition aircraft.

Table 10: Final Aircraft Parameters

Configuration	Conventional, aft tail
Wing Location	High
Wing Airfoil	LS-417
Engines	1
Motors	Astro Flight 661S
Batteries	Sanyo RC-2400
Landing gear	Tricycle – fixed
Wing Span	7.41 ft
Wing Chord	0.927 ft
Wing Area	6.87 ft^2
Fuselage Length	4.33 ft
V-Tail Span	2.5 ft
V-Tail Chord at root	1.08 ft
V-Tail Chord at tip	0.58 ft
V-Tail Projected Horizontal Area	1.46ft^2
V-Tail Projected Vertical Area	1.46ft^2
V-Tail Angle to Horizontal	45 deg
Maximum Take Off Weight	20 Lbs
Take Off, Empty	54 ft
Take Off, Full	105 ft

5.8 Drawing Package

With all drawings in Section 5.8, the units are inches

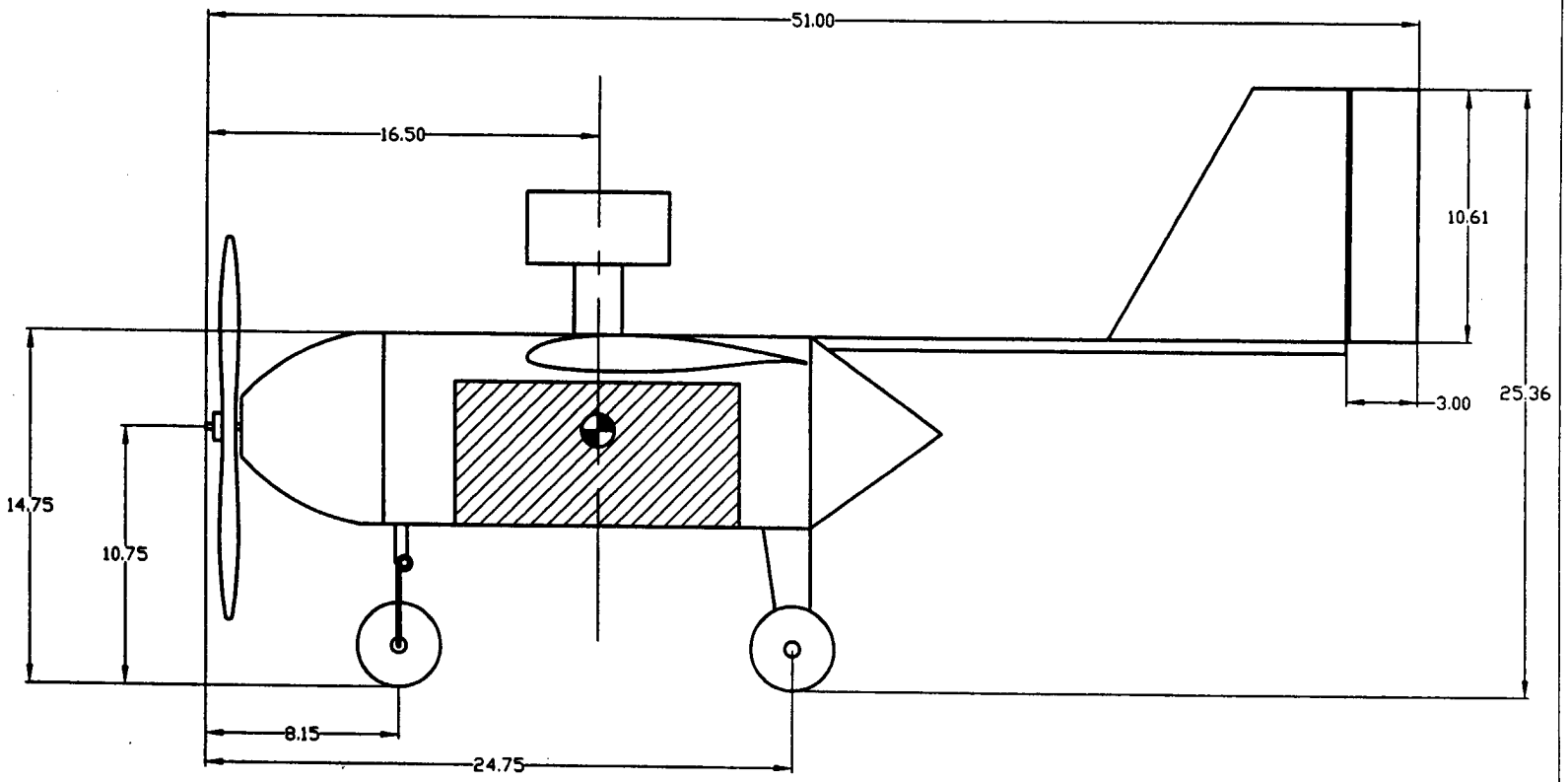

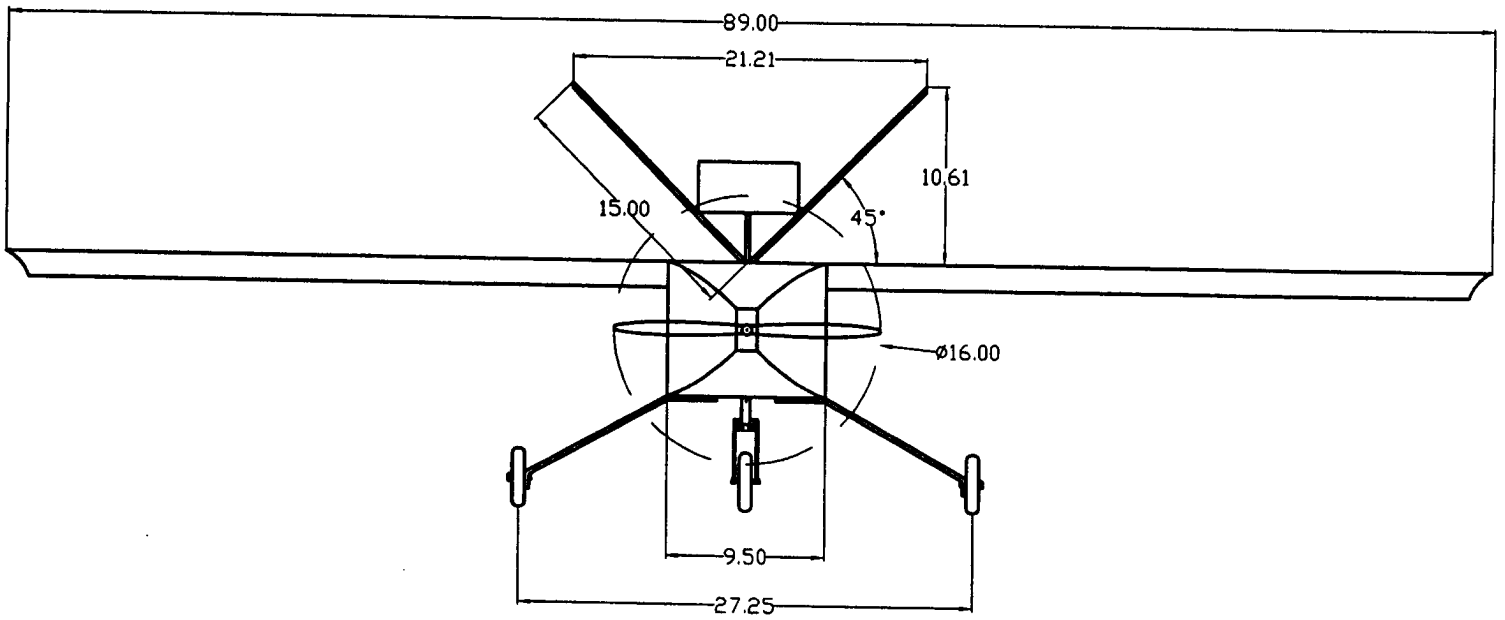
89.00
21.21
10.61
15.00
45°
Ø16.00
9.50
27.25

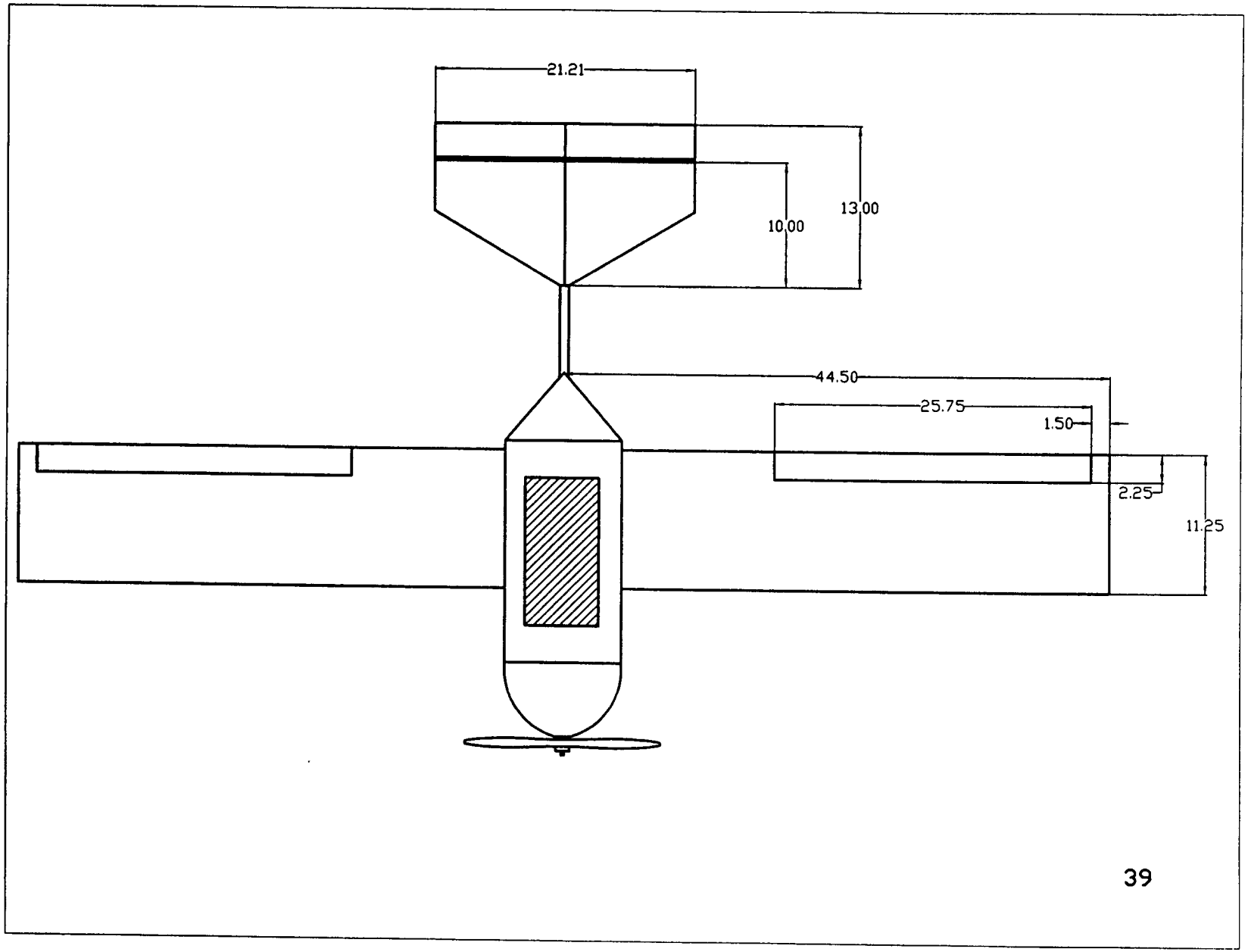
21.21
13.00
10.00
44.50
25.75
1.50
2.25
11.25

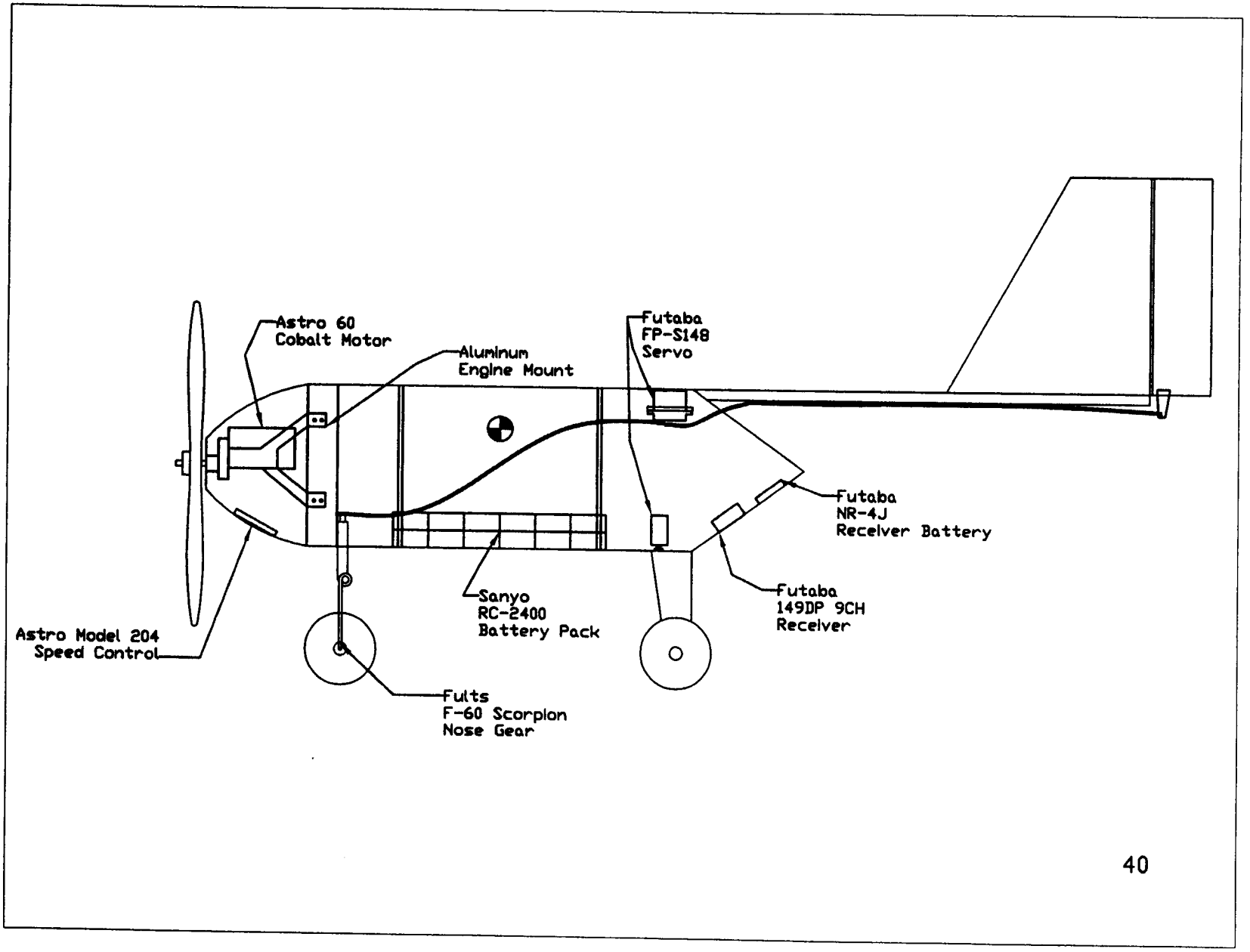
Astro 60
Cobalt Motor
Aluminum
Engine Mount
Futaba
FP-S148
Servo
Futaba
NR-4J
Receiver Battery
Sanyo
RC-2400
Battery Pack
Futaba
149DP 9CH
Receiver
Astro Model 204
Speed Control
Fults
F-60 Scorpion
Nose Gear

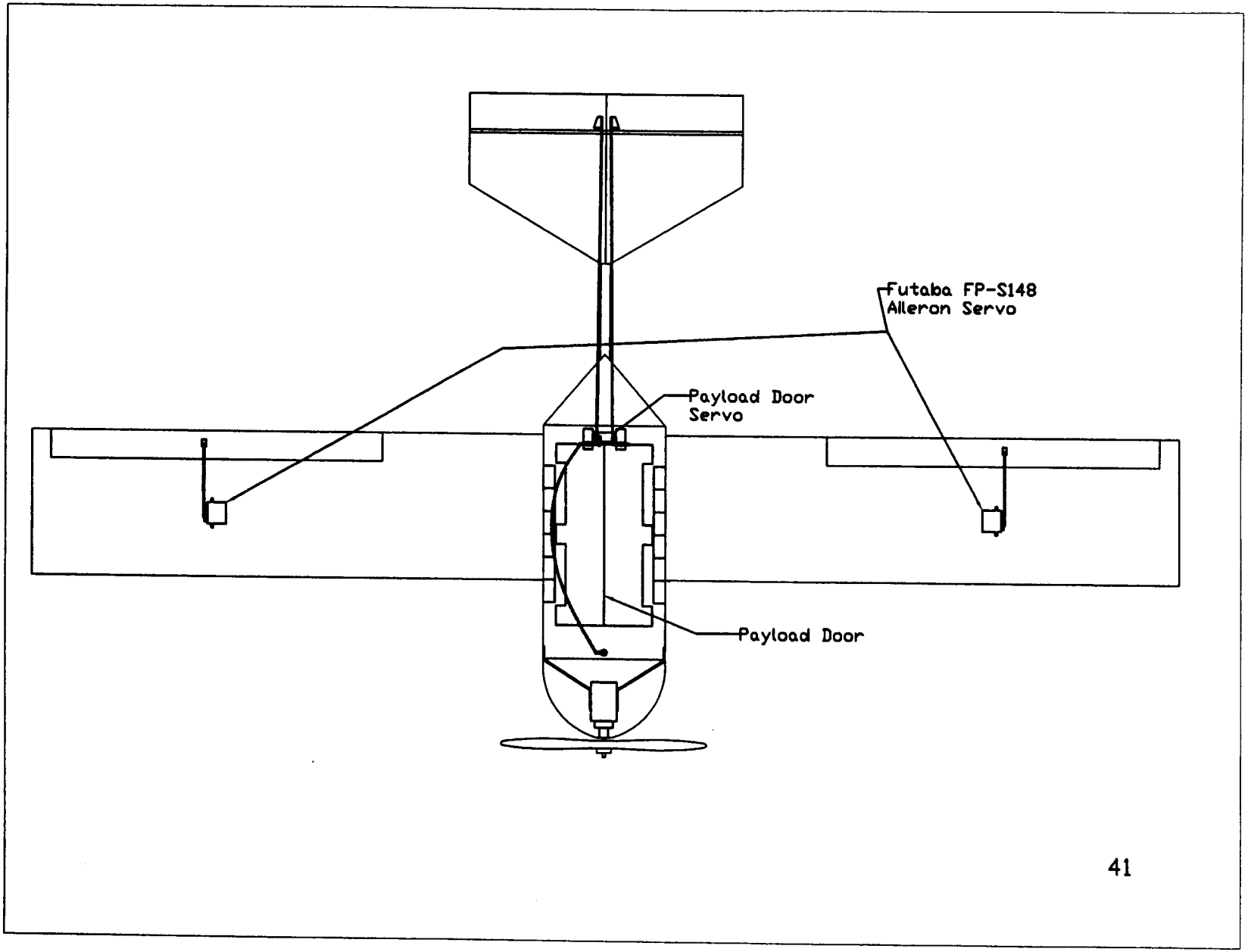
Futaba FP-S148
Aileron Servo
Payload Door
Servo
Payload Door

6.0 Manufacturing Plan

6.1 Process Investigation and Figures of Merit

The team used seven figures of merit (FOM) when considering manufacturing materials and plans:

- Availability
- Reparability
- Strength/Weight Ratio
- Necessary Skills
- Past Experience
- Monetary Cost
- Man Hour Cost

The team placed heaviest consideration on the Strength/Weight Ratio and Past Experience categories. Strength/Weight Ratio is an important consideration due to the compact size of this year's plane; the team needs high-strength materials to carry the payload and assure crashworthiness, but the limiting power requires light materials to get off the ground. Past experience is also an important consideration because it allows the team to make decisions based on what has and has not worked instead of relying purely on theory.

6.2 Wing and Empennage Manufacturing and Process and Tooling

From the experience standpoint, wood is the best material for wing construction. It is easy to work with, inexpensive, common in radio-controlled aircraft. However, balsa has a low strength/weight ratio and the team decided that a wood wing, when build to withstand design loads, was too heavy. Instead it was determined that a foam core covered in a continuous fiber composite material is preferable. Fiber composite materials have higher strength/weight ratios than wood and the team has an extensive experience with composite parts manufacturing. The team looked at covering the wing in carbon fiber and fiberglass. Fiberglass was chosen because it is significantly less expensive and easier to work with then carbon fiber. A summation of the wing material is presented in Table 11.

Table 11: Figures of Merit

Material	*Availability*	*Reparability*	*Strength/ Weight*	*Skills Needed*	*Past Experience*	*Time*	*Cost*
Wood	5	5	2	1	5	2	2
Fiberglass	4	2	4	4	4	4	3
Carbon Fiber	2	2	5	4	2	4	5
Foam Core	2	3	2	5	4	2	3

In order to cut the foam wing cores, the team designed and manufactured a hot wire foam cutter. A stainless steel wire was attached to an adjustable span wooden bow, and powered by a DC current source. Two thin aluminum templates of wing cross-sections were constructed: one of the tip and one of the root. The templates are then placed on the end of expanded polypropylene foam and a stainless steel wire is stretched the length of the foam blocks. A current is run through the wire, which then follows the templates and cuts the foam to the correct shape.

The wing cores were manufactured in two semi-span segments. In order to attach the aluminum spar, two 6" segments were cut off at the root of the wing. Each segment was reinforced with 1/16" plywood ribs, and channel for the spar was cut out. Both segments were then glued back on to the wing, and the 1" aluminum tube spar was epoxied into the wing. Servo compartments and wire channels were cut. Long servo wires were placed in the channels and covered with thin foam strips. Any imperfections were eliminated with use of microballons and careful sending.

Fiberglassing the wing was a three stage process. Two plies of fiberglass were used for the skin. First, each skin was pre-wetted away from the wing, and all excess epoxy was removed. Wet skins were then placed over the cores at the leading edge, and worked down to meet at the trailing edges. Next, all wrinkles and air bubbles were removed, and a nylon release cloth was applied. The whole lay-up was then covered with a bleeder/breather cloth and placed in a vacuum bag. Finally, vacuum was applied and was held constant at 25 in. of Hg. Vacuum bag was placed in a specially designed curing oven, and left to cure for 24 hours.

With the epoxy completely cured, excess fiberglass was trimmed and the wing was sanded. Aileron slots were cut out, and balsa ailerons were installed. Servo actuators were installed in previously cut compartments, and connected to the ailerons with steel push rods. Finally the wing was primed and painted.

6.3 Fuselage Manufacturing Process and Tooling

The fuselage was also built using composite materials. As with the wing, the composites will reduce the weight of the fuselage. The main body of the fuselage was built using plywood bulkheads and a carbon fiber skin. The nose and the rear of the fuselage were constructed with fiberglass.

To begin the fuselage, a foam core mold was assembled, having the dimensions of the main part of the fuselage. This rectangular shaped foam core was then cut into three separate pieces. Plywood bulkheads, as shown in Figure 16 were made to fit in between each cut of the foam.

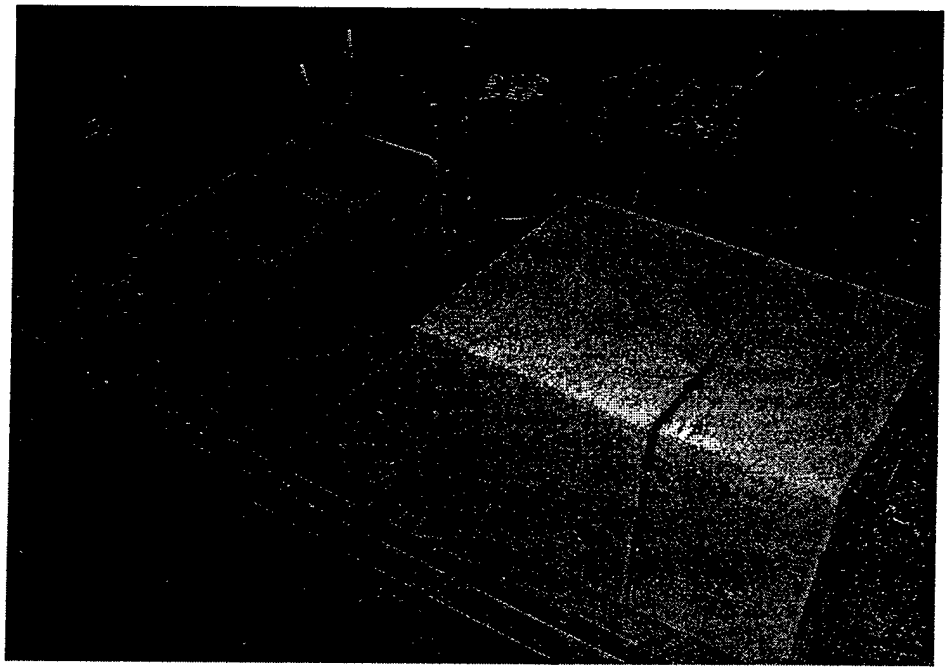

Figure 16: Fuselage Mold

The foam core was then glued together with the bulkheads in place. Final sanding was done to ensure a smooth finish. The core was then covered with epoxy-soaked carbon fiber and vacuum bagged until the epoxy cured. The next step was to get the foam out of the piece. The foam was chipped away from inside the carbon fiber using chisels. The result was a rectangular tube of carbon fiber, supported by two bulkheads. A hole was then drilled on both sides of the body to allow the wings to be attached by means of an aluminum tube.

The nose cone was assembled by first creating a foam core in the desired shape. The foam was cut to approximate size and then finish-sanded until the cone shape was sized correctly. The core was then covered with epoxy-soaked fiberglass and vacuum bagged. Fiberglass was used because it was assumed that the nose cone would not be supporting much load, except for housing the motor. To use carbon fiber would have been unnecessary weight. The cone was sized to slide over the carbon fiber body. This was seen as preferable to it fitting inside the body, as that would create more drag.

The tail is attached to the fuselage by means of a channel-shaped aluminum rod. This rod allows for structural integrity while adding minimal weight. The aluminum rod slides into the fuselage and is secured using two screws.

To account for the large opening at the back of the fuselage (where the rod is attached), a rear section was added. This section was added to change the body into a slightly more streamlined shape. This section was manufactured the same way the nose section was. A foam core was created in the

desired shape, then the core was covered with fiberglass. The team chose a pyramid shape for the rear section, as it was assumed that this shape would create less flow separation than a rear facing cone shape. Contrary to the nose cone, the rear section was made to slide into the fuselage. This was again done because the other option (sliding over the fuselage) would provide more drag.

6.4 Landing Gear Manufacturing Process and Tooling

Landing gear was manufactured based on the process outlined in Reference 5, with each strut manufactured separately. First, a matching face mold was constructed out of 1/16" aluminum sheet supported by foam block. The mold was then sprayed with a PVA mold release, and left to dry. Next, the carbon fiber tow and bi-directional fabric were cut to length, pre-wetted with epoxy resin, and laid out on the mold. Finally, nylon release cloth was applied along with the breathe-bleeder cloth, and the entire lay up was vacuum bagged. After curing, the strut was removed from the mold, sanded and predrilled for attachment.

6.5 Analytical Methods

6.5.1 Manufacturing Cost

The majority of the manufacturing cost came from the propulsion system and the composite materials. A single engine was purchased, along with twenty-four battery cells and a speed controller. The majority of the aircraft was made with carbon fiber or fiberglass. This all had to be purchased, as the team has historically used balsa wood. All other manufacturing components were of minimal cost. The team had many materials left over from previous years, including the radio, wheels, epoxy, and tools. Saving funds by reusing materials allowed the team to build a more composite-based aircraft, whereas in past years funds have dictated that a balsa aircraft was the only plausible approach.

6.5.2 Skills Matrix

The skills matrix was used to assess the difficulty of producing each aircraft component. The ratings range from zero to three, with three being the most difficult. This assessment was used to aid in the choice of manufacturing method for the aircraft. It can be seen from Table 12 that the wing is assumed to be very challenging to manufacture. With this knowledge the team knew to focus more heavily on the design and manufacture of the wing. The skills matrix gave the team a good idea of what parts of the plane required more, or less, preparation and man-power. In this way, the manufacturing process went smoother and more efficiently.

Table 12: Skill Matrix

Component	Foam Cutting	Molding	Finishing	Carbon Fiber	Fiberglass	Computer Model
Wing	3	2	2	3	2	3
Fuselage	2	3	2	2	2	2
Tail	0	0	1	1	1	1
Landing Gear	0	1	1	1	1	1

7.0 Testing Plan

7.1 Manufacturing Testing

7.1.1 Testing Goals

The majority of component manufacturing was done prior to the final manufacture. This was to ensure that the team was familiar with the process before working on the final components, as well as identifying any improvements that could be made. It was the goal of the team to assemble a half-scale wing and payload door compartment and test different methods of curing composites.

7.1.2 Testing Results

The team constructed a half-scale section of the wing for testing. It was found by comparison that fiberglass was sufficient for covering the wing, as opposed to using carbon fiber. It was also found that stitching the trailing edge of the fiberglassed wing to prevent delamination was unnecessary and time consuming.

A full scale payload door compartment was built and tested with different door mechanisms. It was experimentally determined that the most efficient way of releasing the payload is by using spring actuated doors. The springs were designed to be flexible enough to open under the weight of the payload, yet stiff enough to close the payload door after the payload was released.

For curing the fiberglass and carbon fiber, two methods were evaluated and tried. The first method used a nylon-release peel cloth. The wing section that was made using this cloth came out light but with a rough finish. The second curing method used high-gloss perforated release cloth. This resulted in a slightly heavier wing, but with a much smoother finish. It was determined that the smoother finish was more desirable than the reduced weight, so the high-gloss perforated release cloth was used in the final wing manufacture.

7.2 Static Testing

7.2.1 Testing Goals

The goal of the static testing was to evaluate the strength of the carbon fiber and fiberglass. The team needed to know where carbon fiber was necessary and where fiberglass could be used to conserve weight.

7.2.2 Testing Results

Series of carbon fiber and fiberglass specimens were tested in tension by a standard load frame, as shown in Figure 17.

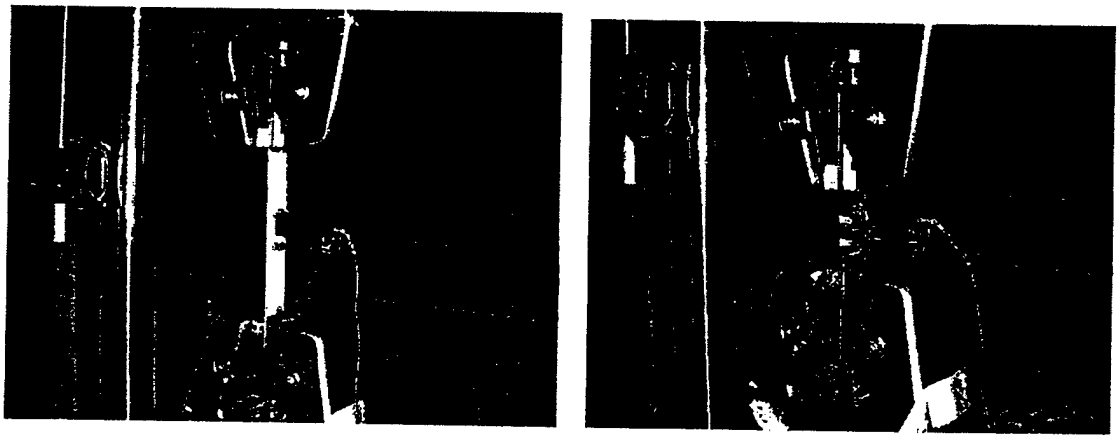

Figure 17: Tensile Test of a Laminated Composite

Each specimen consisting of 10 plies of laminated bi-directional fabric was loaded until failure. The elongation was monitored with an extensometer, and ultimate failure load was recorded. From that, elastic modulus was determined, as well as ultimate stress for a single ply of laminated carbon fiber and fiberglass.

Since the landing gear were to be constructed from carbon fiber, a test section was made. A test section was clamped at the point were it was to attach with the fuselage, and statically loaded to failure. Fracture at the strut occurred under a load of thirty-three pounds. This was more than sufficient for the estimated aircraft weight of eighteen pounds.

References

1.) Mattingly, Jack D., "Aircraft Engine Design (AIAA Education Series)", 2nd Edition. American Institute of Aeronautics and Astronautics, October 2002.

2.) MotoCalc 6.05. Capable Computing Inc.

3.) Benjamin, Robert. "Which Motor Should I Use?" http://www.rcmodel.com/whatmotor.html 1/13/2003

4.) Pamadi, Bandu N., "Performace, Stability, Dynamics, and Control of Airplanes (AIAA Education Series)", American Institute of Aeronautics and Astronautics, 1998

5.) http://winshiprc.tripod.com/carbon_fiber_composites.htm

6.) Raymer, Daniel P., "Aircraft Design: A Conceptual Design (AIAA Educational Series)", 3rd Edition. American Institute of Aeronautics and Astronautics, 1999.

7.) Selig, M.; "UIUC Airfoil Coordinates Database"; http://amber.aae.uiuc.edu/~m-selig/ads/coord_database.html; University of Illinois, Urbana,1995

8.) Roskam, J.; "Flight Dynamics of Rigid and Elastic Airplanes"; published by the author; Lawrence, 1972

9.) Roskam, J.; "Methods for Estimating Stability and Control Derivatives of Conventional Subsonic Airplanes"; published by the author; Lawrence, 1971

10.)Kaw, A. K.; "Mechanics of Composite Materials"; CRC Press; Boca Raton, 1997

11.)Gere, James M., "Mechanics of Materials"; 5th Edition. Brooks/Cole, 2001

2002/2003 AIAA Foundation Cessna/ONR Student Design Build Fly Competition

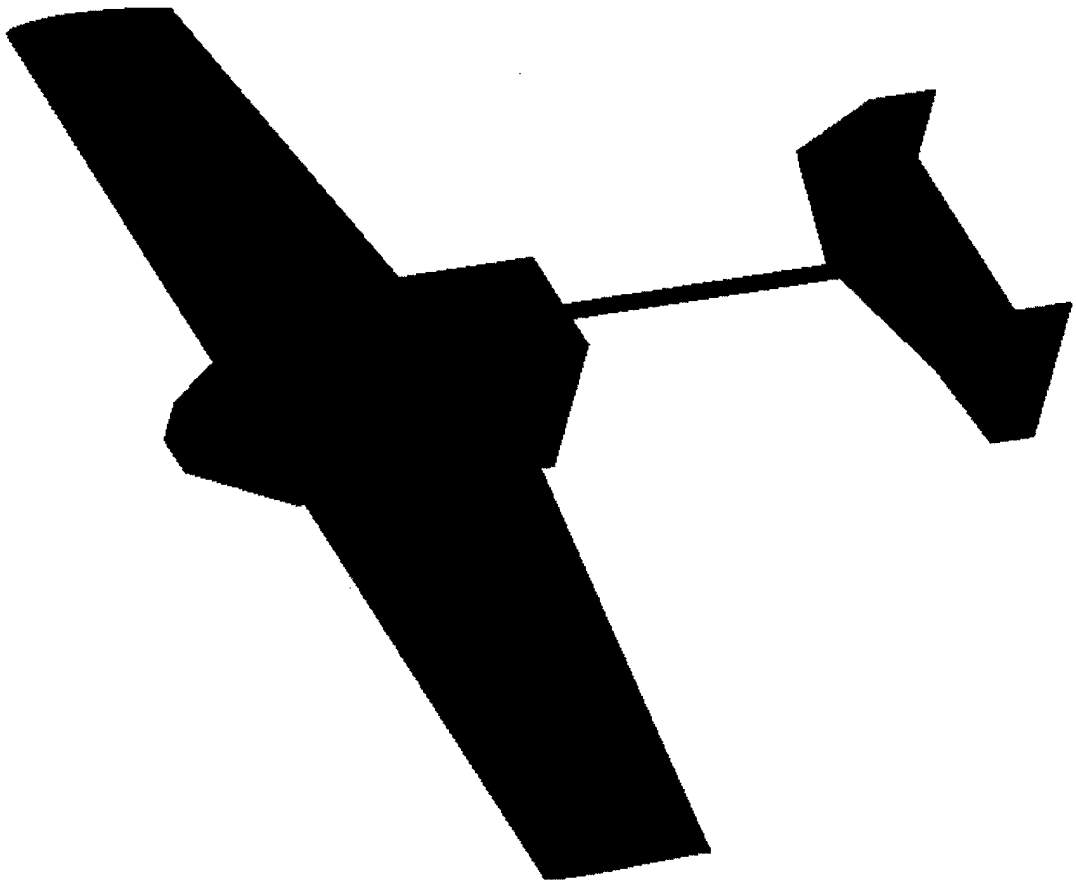

Clarkson University

March 2003

Table of Contents

Table of Contents 2

1.0 EXECUTIVE SUMMARY **5**

1.1. CONCEPTUAL DESIGN 5
1.1.1. CONFIGURATIONS CONSIDERED 5
1.1.2. CONCEPTUAL DESIGN RESULTS 5
1.2. PRELIMINARY DESIGN 6
1.3. DETAIL DESIGN 6
1.4. 1.4 MANUFACTURING AND TESTING 6

2.0 DESIGN TEAM CONFIGURATION **8**

2.1. SCHEDULING 8

3.0 CONCEPTUAL DESIGN **10**

3.1. MISSION PROFILE 10
3.1.1. MISSION SPECIFICATIONS FOR A UAV 10
3.2. CONFIGURATIONS CONSIDERED 10
3.2.1.1. WING CONSIDERATIONS 10
3.2.1.2. WING PLACEMENT 11
3.2.1.3. PLANFORM SHAPE 11
3.2.1.4. WINGLETS AND WING TIPS 11
3.2.1.5. WING FLAPS 11
3.2.2. TAIL CONFIGURATIONS 12
3.2.3. FUSELAGE CONFIGURATION 12
3.2.3.1. NUMBER OF FUSELAGES 12
3.2.3.2. TYPES OF FUSELAGES 13
3.2.3.3. BOOMED –VS- CONVENTIONAL FUSELAGE 13
3.2.3.4. OPEN VERSUS CLOSED FUSELAGE 13
3.2.4. PROPULSION 14
3.2.4.1. NUMBER OF MOTORS/ PROPULSIVE DEVICES 14
3.2.4.2. TYPE OF PROPULSIVE DEVICE 14
3.2.4.3. PROPULSION INTEGRATION 14
3.2.5. LANDING GEAR CONFIGURATIONS 15
3.2.6. PAYLOAD PLACEMENT AND DEPLOYMENT 15
3.3. FIGURES OF MERIT FOR EACH CANDIDATE DESIGN 16

4.0 PRELIMINARY DESIGN **18**

4.1. COMPARATIVE STUDIES 18

4.1.1. AIRFOIL SELECTION (WING) 18
4.1.2. AIRFOIL SELECTION (TAIL) 19
4.1.3. WING- LOADING 19
4.2. AIRCRAFT WEIGHTS 20
4.3. PERFORMANCE ANALYSES 21
4.3.1. WING PLANFORM 21
4.3.1.1. TAPERING 22
4.3.1.2. 4.3.1.2 ASPECT RATIO 23
4.3.2. AIRCRAFT'S PERFORMANCE 26
4.3.3. FUSELAGE CONSIDERATIONS 26
4.4. STABILITY AND CONTROL 27
4.4.1. LONGITUDINAL STATIC STABILITY 27
4.4.2. LONGITUDINAL CONTROL 30
4.4.3. 4.4.3 DIRECTIONAL STATIC STABILITY 33
4.4.4. DIRECTIONAL CONTROL 34
4.4.5. ROLL STATIC STABILITY 36
4.4.6. STATIC ROLL CONTROL 38
4.4.7. DYNAMIC STABILITY DERIVATIVES 38
4.4.8. DYNAMIC STABILITY OF LONGITUDINAL MOTION 41
4.4.9. DYNAMIC STABILITY OF LATERAL MOTION 43
4.5. PROPULSION 44
4.5.1. PROPULSION INTEGRATION 44
4.5.2. POWER REQUIRED 44
4.5.3. POWER-PLANT SELECTION 46
4.5.4. BATTERY SELECTION 46
4.5.5. PROPELLER SELECTION 47

5.0 DETAIL DESIGN 48

5.1. CONFIGURATION DETAIL DESIGN 48
5.2. STRUCTURAL COMPONENT SELECTION 48
5.2.1. FUSELAGE 48
5.2.2. WING 49
5.2.3. EMPENNAGE 49
5.3. SECONDARY COMPONENT SELECTION 49
5.3.1. PROPULSION AND CONTROLS 49
5.3.2. AVIONICS PACKAGE DEPLOYMENT SYSTEM 50
5.3.3. SIMULATED CYLINDRICAL ANTENNA 50

6.0 MANUFACTURING PROCESS 56

6.1. FUSELAGE 56
6.1.1. FORMERS (BULKHEADS) 56
6.1.2. ENGINE MOUNT 56
6.1.3. BASE 56
6.2. WING 56
6.2.1. AIRFOIL 56
6.2.2. RIBS 57
6.2.3. ASSEMBLY 57
6.3. TAIL 57
6.3.1. VERTICAL SURFACES 57
6.3.2. HORIZONTAL SURFACE 57
6.4. ANALYTICAL METHODS: COST, SKILL MATRIX AND SCHEDULING TIME LINES 58
6.4.1. MANUFACTURING COSTS 58
6.4.2. SKILL MATRIX 58
6.4.3. MANUFACTURING SCHEDULING 58

7.0 TESTING PLAN 59

7.1. STATIC 59
7.1.1. WIND TUNNEL TESTING 59
7.1.2. WING SPAR LOAD TESTING 59
7.1.3. LANDING GEAR LOAD TEST 59
7.1.4. PAYLOAD DEPLOYMENTS SYSTEM 60
7.2. DYNAMIC: 60

1.0 Executive Summary

Outlined in this report are the methodologies utilized by the Clarkson University "Knight Riders" Team throughout the process of designing and constructing an aircraft capable of fitting inside of a 1'x2'x4' box. This aircraft must be able to complete 2 of the three missions specified by the 2002/2003 AIAA Design Build and Fly Competition. This year's competition consists of three different mission profiles, each with a different difficulty multiplier. Of these, the plane must complete two. The first mission option (mission A), known as "missile decoy" requires the aircraft to complete 4 laps while carrying a five-pound payload meeting a set 6"x6"x12" dimension requirement. Additionally, a simulated antenna constructed from 6" diameter PVC pipe must be attached to the aircraft. The difficulty multiplier assigned this mission was 2.0. The second mission option (mission B), named "sensor deployment", with a multiplier of 1.5, requires the aircraft to complete two laps, land and deploy the five pound payload. The aircraft must then complete two more laps without the payload. The last mission (mission C), difficulty multiplier of 1.0, is known as "communications repeater" and requires the aircraft to complete 4 laps carrying only the "communications equipment" payload. The overall team score depends upon the aircraft's assembly time, report score, flight score, and Rated Aircraft Cost.

1.1. Conceptual Design

This portion of the report addresses the initial idea generation associated with this year's aircraft. The team, along with its respective mission requirements, explored each mission profile. Possible aircraft, wing, tail, fuselage, propulsion, and landing gear configurations, as well as payload placement and deployment, were all individually examined and investigated. This was accomplished using Figures of Merit (FOM) tables to weigh each variable and compare it to other proposed alternatives.

1.1.1. Configurations considered

The configurations considered found different ways to meet the specifications listed above. Among the wing configurations considered were, wing placement, planform shape (elliptical, tapered, etc.), winglets and wing tips, flap type, and dihedral. To choose the appropriate tail configuration, the advantages and disadvantages of t-tails, v-tails, double vertical tails, and conventional tails were weighed. In deciding upon a fuselage design the configurations considered were the number of fuselages, types of fuselages, boomed vs. conventional fuselages, and open vs. closed fuselage. For propulsion, the number of motors, types of propulsive devices, and propulsion integration were all investigated. Retractable and fixed landing gear configurations, as well as tail dragger and tricycle gear were compared. Also investigated were methods of payload placement and deployment.

1.1.2. Conceptual Design Results

Upon completion of the conceptual design phase, the team had reached the conclusion that a tail-dragging, tapered-wing aircraft with a double vertical tail would be utilized for the task. This aircraft would

employ a closed, single-boomed fuselage, a traditional propeller, and slotted flaps to perform missions A and B. This combination was chosen, along with a rising cargo door in the rear of the fuselage, to give us the best performing, most cost-effective aircraft possible.

1.2. Preliminary Design

In the preliminary stage, teams were formed to begin a more detailed analysis of the chosen aspects of the aircraft design. Trade studies were completed for five major portions of the design, comparative studies, performance, weights, stability and control, and propulsions. The performance team investigated the ability of different materials, dihedrals, and skins to reduce drag, while increasing lift, speed, drag, and stability. The team studying weight scrutinized the market for various motors, servos, woods, and other parts and materials to discern which would meet our needs with the least possible weight. Stability and control was principally accomplished by calculating and experimenting with various surface areas, proportions, and angles for any lift-generating or control surface. The propulsion team searched to find a motor that was both lightweight and powerful enough for our needs. Additionally, the team investigated propeller size and construction towards the end of getting the most speed an power from the chosen motor possible. Given the results of each team's investigation, a revised and finalized CAD drawing was made of the aircraft, and the design went into construction.

1.3. Detail Design

With a general layout of the airplane in place it was necessary to select the components which would make up the plane along with choosing the inside architecture. Comparisons were completed to the 2001 Clarkson University entry and decisions were made accordingly.

The 2001 entry suffered from over-engineering therefore, materials and architecture were selected to combat these problems. A conventional former or rib and skin system was utilized to guarantee strength, but avoid extra material. Some pieces such as landing gear, motor mounts and servos were purchased to avoid functional and application problems. Finally a conventional wing construction was selected for its ease, strength and relatively light weight.

1.4 Manufacturing and Testing

As soon as the material arrived, construction began. For the fuselage/payload team this largely included cutting, sanding, and gluing sheets of balsa and plywood to achieve the appropriate size and shape. These pieces were based on the CAD drawing for our most refined and promising aircraft. The wing team also based construction on the same drawing. An additional part of the building process for the wing team included finding the appropriate size for the spar, and ordering it in time to finish the wing in a timely manner. Other parts that had to be ordered include the Cobalt 60 motor, and multiple servos and mini-servos.

For the purpose of testing the aircraft the location of Clarkson University is rather poor. With temperatures hovering between -30° and 10° Fahrenheit and high winds, the weather is nothing new

here. Unfortunately this prevents actual flight testing until the last week in March at earliest. To compensate for this lack of testing time, has tested pre-construction models in the available wind tunnel facility found on campus.

2.0 Design Team Configuration

This year's design team took on a new set up as well as new additions to help with management of the team. Two program managers were added to the team in addition to the Team Leader and managers of the wing and fuselage team. The program managers are to help with budget analysis, inventory, design report as well as tracking the progress of the team.

The entire team meet together at the beginning of the project once a week, to brainstorm and do the preliminary designs of the aircraft. Once a design was decided upon and the tasks of the completing the aircraft were determined the team divided up. Each member chose which team they would like to participate with, either wing or fuselage. Many made their choice based on pure interest, and others on what they may not have worked on previously. Notices were sent out through e-mail to make aware to the other team members when someone will be in shop working on the aircraft. They could work as a team or if an individual felt it is possible they could work on their own. Everyone who worked on the aircraft signed in on a log sheet telling when, who, and for how long they worked on the aircraft.

Another side group was formed for the design project. Anyone that had interest in learning how to write the design report was welcome to participate. This team met once a week to work on, as well as review all other sections that have been completed. Anyone who could attend was welcome and the work was divided up evenly among those who did.

2.1. Scheduling

To follow the progress of the team and to stay on track with our deadlines a team timeline was created. The project managers, using Microsoft Project, put together are the beginning of the project deadlines that each team manager wished to follow. To accomplish this each manager of the wing and fuselage team made a list of their desired completion dates for different aspects of their project. These dates and tasks were placed into the timeline along with desired scheduling of the design report to create the entire timeline for the DBF team.

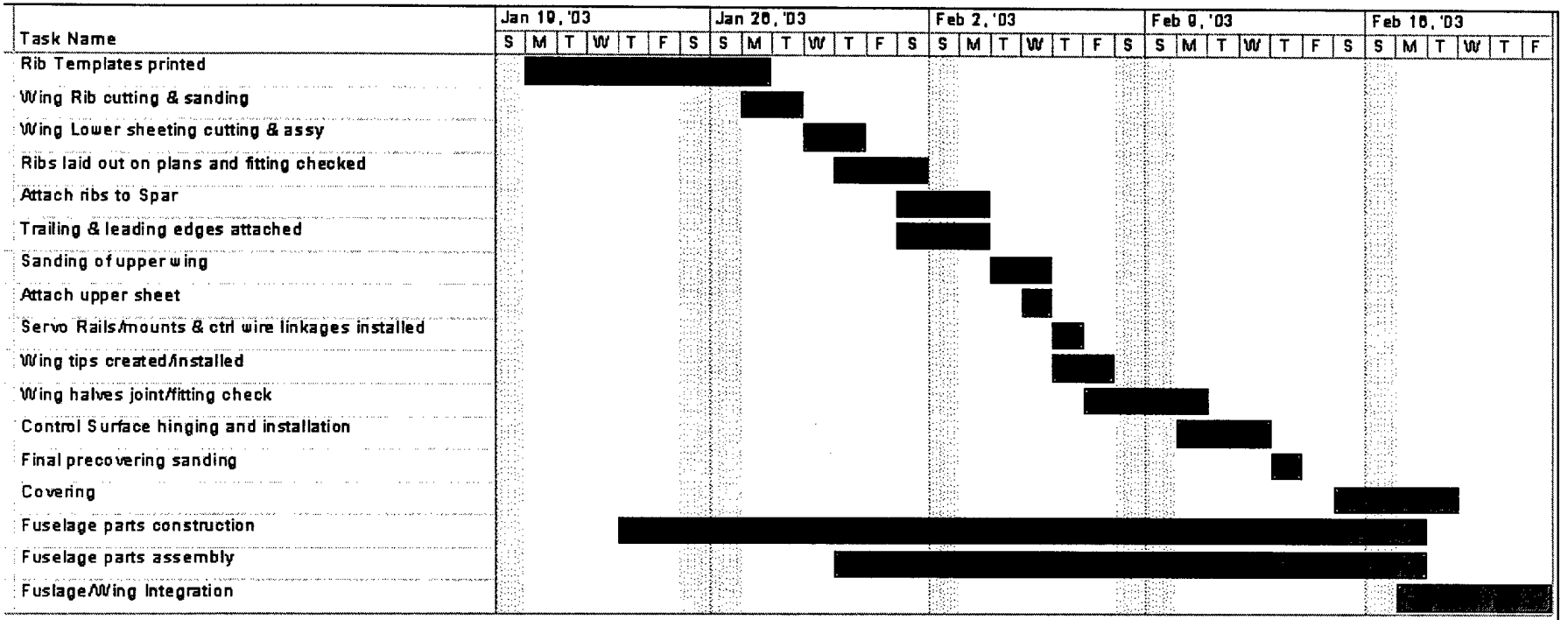
Task Name
Jan 19, '03
Jan 26, '03
Feb 2, '03
Feb 9, '03
Feb 16, '03
S M T W T F S
Rib Templates printed
Wing Rib cutting & sanding
Wing Lower sheeting cutting & assy
Ribs laid out on plans and fitting checked
Attach ribs to Spar
Trailing & leading edges attached
Sanding of upper wing
Attach upper sheet
Servo Rails/mounts & ctrl wire linkages installed
Wing tips created/installed
Wing halves joint/fitting check
Control Surface hinging and installation
Final precovering sanding
Covering
Fuselage parts construction
Fuselage parts assembly
Fuslage/Wing Integration

Figure 2.1

3.0 Conceptual Design

This year the aircraft mission profile was to complete two of three possible missions that were each assigned a multiplier based on their degree of difficulty. These missions required the aircraft to carry/deploy a payload and or an added drag surface. The first conceptual decision made was to complete mission A. This decision was based strictly on the merit of the high difficulty multiplier. After exploring the design requirements for all three missions, it was decided that mission B (the next most difficult) would be attainable without insurmountable design complications. The decision to proceed with missions A and B provided a guideline to the conceptual designs considered, and had a heavy hand in narrowing the design possibilities.

3.1. Mission Profile

3.1.1. Mission Specifications for a UAV

Payload: A Simulated Avionics package, 6"x 6" x 12", 5 pound box ballasted around the centroid with the option of a gauge 40, 6" diameter, 3" tall section of PVC pipe that must be 3" from and aircraft surface

Range: 4 laps around a designated course with a payload.

Cruise Speed: 50 MPH

Take-off/Land: Balanced field length of 120'

Power plant: Astroflight Cobalt 60 Electric Motor, 40 Amp fuse, maximum of 5 pounds of batteries

3.2. Configurations Considered

With payload and speed being the governing design factors on the aircraft, reducing weight during construction and streamlining of the design were top priority while considering various configurations. Since the aircraft had no aerobatic or pattern flying requirements, design requirements such as long tail moments for better tracking and precise control were immediately discarded. Hence all unneeded sections of the aircraft could be done away with to conserve weight, reduce drag and mass. This led to the immediate conclusion of using a carbon fiber tail boom, as the aft section of the fuselage is not required for any payload. Were it to be of a built up nature as the rest of the payload carrying section of the fuselage, it would simply add unnecessary bulk, drag and weight to the design.

3.2.1.1. Wing Considerations

As the competition calls for the fastest design possible, the ideal wing shape would call for a degree of sweep incorporated into it, however from the payload aspect of the competition, having a swept wing would seriously limit such lifting capabilities. This led to the implementation of the tapered wing, which is

generally considered the "ideal wing planform". Such a planform not only provided generous amounts of lift, but also made the aircraft maneuverable as opposed to a constant chord wing.

3.2.1.2. Wing Placement

A major consideration was where the wing was to be placed. The three suggested configurations were a high wing, a mid-wing, and a low-wing. Various aspects of each are displayed in Table 3.1.

Table 3.1: FOM Chart for Wing Placement

Wing Placement	Stability	Ease of Construction	Time Assembly Task	Sturdiness of Gear	Total
High	8	8	8	3	27
Mid	7	6	5	5	23
Low	5	8	8	8	29

A low wing mounting was determined to be optimal. It provided a more maneuverable aircraft and solved the issue of landing gear mounts.

3.2.1.3. Planform Shape

The shapes considered were an ideal elliptical planform, tapered, and constant chord. The advantages and disadvantages are displayed in Table 3.2.

Table 3.2: FOM Chart for Wing Planform

Wing Planform	Stability	Ease of Construction	Aerodynamic Performance	Total
Elliptical	6	3	10	19
Tapered	7	7	9	23
Swept	8	5	5	18
Constant chord	6	10	6	22

The tapered planform was decided upon because of its consummate balance between simplicity of construction and stability, while still maintaining an excellent capacity for aerodynamic performance.

3.2.1.4. Winglets and Wing Tips

The usage of winglets was considered to increase the aerodynamic aspect ratio, which, in effect, increases the performance by decreasing the induced drag on the aircraft. After careful consideration, it was found that the performances increases were not comparable to the increase in RAC (5 hr./Vertical Surface). In comparison, an efficient raked tip design was found to increase performance without any change in RAC.

3.2.1.5. Wing Flaps

Various types of wing flaps were considered based on their ability to increase takeoff and landing performance without sacrificing cruise speed. These options were explored in Table 3.3.

Table 3.3: FOM Chart for Wing Flaps

Wing Flaps	Ease of Construction	Aerodynamic Performance	Total
Split	8	6	14
Slotted	7	9	16
Double-Slotted	3	10	13
Conventional	5	5	10

The slotted flap configuration was chosen due to the combination of simple construction and excellent performance. Though the performance of the double-slotted flap was slightly superior; the difference was negligible for the mission requirements, and its simpler construction made the slotted flap a far more attractive option.

3.2.2. Tail Configurations

The types of configurations considered were t-tails, v-tails, double vertical tails, or a conventional tail. Each type was evaluated in Table 3.4.

Table 3.4: FOM Chart for Tail Configuration

Tail Configuration	Stability	Ease of Construction	Additional RAC	Interference during Payload deployment	Total
T-tail	6	5	10	5	26
V-tail	3	4	10	6	23
Double inverted verticals	10	7	5	9	31
Conventional	6	7	10	5	28

The somewhat unconventional tail setup called for two vertical tails mounted at each tip of the horizontal tail. While causing an increase in the RAC, the design provided further stability and ensured that the empennage would clear the sensor package after deployment by passing right over it.

3.2.3. Fuselage Configuration

3.2.3.1. Number of Fuselages

A single fuselage –Vs- dual fuselages was discussed. Advantages and disadvantages for each were evaluated using Table 3.5.

Table 3.5: FOM Chart for Number of Fuselages

Number of Fuselages	Ease of Construction	Weight	Payload capabilities	Aerodynamic Performance	Total
Single	8	8	7	8	31
Double	6	4	9	5	24

The mission requirements called for a single sensor package. A double fuselage therefore held no advantages over a single, as with only one effective piece of payload, the load cannot be spit up between two fuselages. Also, the double fuselage would increase the rated aircraft cost significantly as well as double the weight. The single fuselage was therefore the obvious choice.

3.2.3.2. Types of Fuselages

The types discussed were blended wing bodies, lifting bodies, and a standard configuration. Advantages and Disadvantages are as shown in Table 3.6.

Table 3.6: FOM Chart for Fuselage Type

Fuselage Type	Ease of Construction	Aerodynamic Performance	Stability	Total
Blended Wing Body	3	8	1	12
Lifting Body	5	6	3	14
Standard Configuration	8	3	9	20

The most practical design for the stability and construction needs was the standard fuselage. Though it suffered in the performance category it is still most suited to the necessary missions based on stability.

3.2.3.3. Boomed –Vs- Conventional Fuselage

Tail booms were considered for their reduction of weight and skin friction drag. The advantages and disadvantages were weighted and evaluated using Table 3.7.

Table 3.7: FOM Chart for Boom Configuration

Booms	Weight	Stability	Aerodynamic Performance	Ease of Construction	Time Assembly Task	Total
Single	8	6	8	7	6	35
Double	5	8	6	6	3	28
None	3	7	7	6	8	31

As discussed earlier, the single tail boom was selected as the most practical design. As a light and low-drag way to attach the tail, the single boom cuts unnecessary weight and construction time.

3.2.3.4. Open versus Closed Fuselage

An open fuselage was considered to cool the batteries as well as reduce weight. A closed fuselage was considered to reduce the drag on the payload and the amount of skin friction due to the increased exposure of surface area. It quickly became clear that the reduction in drag on the closed fuselage was far more effective than the small weight increase generated by the open fuselage. Therefore we chose the closed design.

3.2.4. Propulsion

3.2.4.1. Number of Motors/ Propulsive Devices

The usage of one or two motors was debated. The advantages and disadvantages for each were found and inserted into Table 3.8 to decide which would be used.

Table 3.8: FOM Chart for Number of Motors

Number of Motors	Weight	Power	Ease of Construction	Total
Single	8	4	6	20
Double	4	7	5	16

The single motor was chosen because it was capable of meeting the necessary power needs, and drastically reduced the weight of the aircraft.

3.2.4.2. Type of Propulsive Device

The usage of a conventional prop configuration –Vs- a ducted fan was considered. The advantages and disadvantages for each were put into Table 3.9.

Table 3.9: FOM for Ducted Fan

Ducted Fan	Aerodynamic Performance	Weight	Battery Power Needs	Ease of Construction	Thrust	Total
Ducted Fan	8	5	2	5	6	26
Conventional Propeller	6	7	8	8	8	37

The conventional propeller was selected due to the exorbitant battery-power cost of a ducted fan, as well as the added unnecessary weight of a ducted fan.

3.2.4.3. Propulsion Integration

How the propulsive device was to be integrated was considered as well as whether a pusher or a tractor propeller should be used, if not both. The characteristic differences were evaluated using Table 3.10.

Table 3.10: FOM Chart for Propulsive Integration

Propulsive Integration	Aerodynamic Performance	Weight	Cooling	Ease of Construction	Total
Wing Root	7	6	6	6	25
Inside Fuselage	8	8	7	8	31
Tail Mounted	5	5	8	7	25
Wing Tips	7	6	8	5	26
Outside Fuselage	8	7	8	4	27

The decision was made to house the propulsive device within the fuselage for the significant reduction in drag that this option offers, as well as its low weight requirement.

3.2.5. Landing Gear Configurations

The types of landing gear considered were the tail dragger and the tricycle landing gear with a controllable nose wheel. Both configurations were also considered using retractable landing gear and fixed landing gear. The benefits and disadvantages of these designs were explored in table 3.11.

Table 3.11: FOM Chart for Landing Gear

Wing Planform	Weight	Ease of Construction	Drag Performance	Total
Retractable Dragger	5	3	10	18
Tail Dragger	9	8	5	22
Retractable Tricycle	4	3	10	17
Tricycle	7	7	3	17

The non-retractable tail-dragger was chosen for its moderate drag performance and low weight. Additionally, the tail dragger proved to be the simplest design, saving valuable construction time.

3.2.6. Payload Placement and Deployment

It was decided that the payload (the box and the cylindrical antenna) be placed at the center of gravity of the aircraft for stability and control. Two types of deployment were discussed. The usage of bomb-bay doors versus a rear door was considered. The bomb-bay door would need a high ground clearance, but offered an easy deployment, whereas a rear door would need little to no ground clearance, but would be more complex to automate.

3.3. Figures of Merit for Each Candidate Design

Standard			Lifting Body		
		Penalty			Penalty
Weight	12 lbs	$1,200.00	Weight	12 lbs	$ 1,200.00
Engine(s)	2 engines/4 lbs batteries	$6,000.00	Engine(s)	1 engine /4 lbs batteries	$ 6,000.00
Wing	6 ft	$ 960.00	Wing	6 ft	$ 960.00
Chord	1.5 ft	$ 240.00	Chord	1.8 ft	$ 288.00
Ailerons		$ 60.00	Ailerons		$ 60.00
Elevators		$ 60.00	Elevators		$ 60.00
Flaps		$ 60.00	Flaps		$ 60.00
Rudder	2	$ 120.00	Rudder		$ 60.00
Fuselage	10 hr/surface	$ 400.00	Fuselage	10 hr/surface	$ 360.00
Empennage	2	$ 200.00	Empennage	1	$ 100.00
Horizontal	1	$ 300.00	Horizontal	2	$ 300.00
Flight systems		$ 120.00	Flight systems		$ 100.00
Propulsion	5hr/engine	$ 100.00	Propulsion	5hr/engine	$ 100.00
		$9,820.00			$ 9,648.00

Dual Fuselage			"Spitfire"		
		Penalty			Penalty
Weight	12 lbs	$1,200.00	Weight	12 lbs	$ 1,200.00
Engine(s)		$3,000.00	Engine(s)		$ 3,000.00
Wing		$ 960.00	Wing	6 x 8hr/foot	$ 960.00
Chord		$ 240.00	Chord	1.5 x 8hr	$ 240.00
Ailerons		$ 60.00	Ailerons		$ 60.00
Elevators		$ 60.00	Elevators		$ 60.00
Flaps		$ 120.00	Flaps		$ 60.00
Rudder		$ 120.00	Rudder		$ 60.00
Fuselage	10 hr/surface	$ 800.00	Fuselage	10hr/surface	$ 400.00
Empennage	2	$ 200.00	Empennage	1	$ 100.00
Horizontal	2	$ 200.00	Horizontal	3	$ 300.00
Flight systems	5 hr/engine	$ 80.00	Flight systems	5 hr/ servo	$ 100.00
Propulsion	5 hr/engine	$ 80.00	Propulsion	5 hr/engine	$ 100.00
		$7,120.00			$ 6,640.00

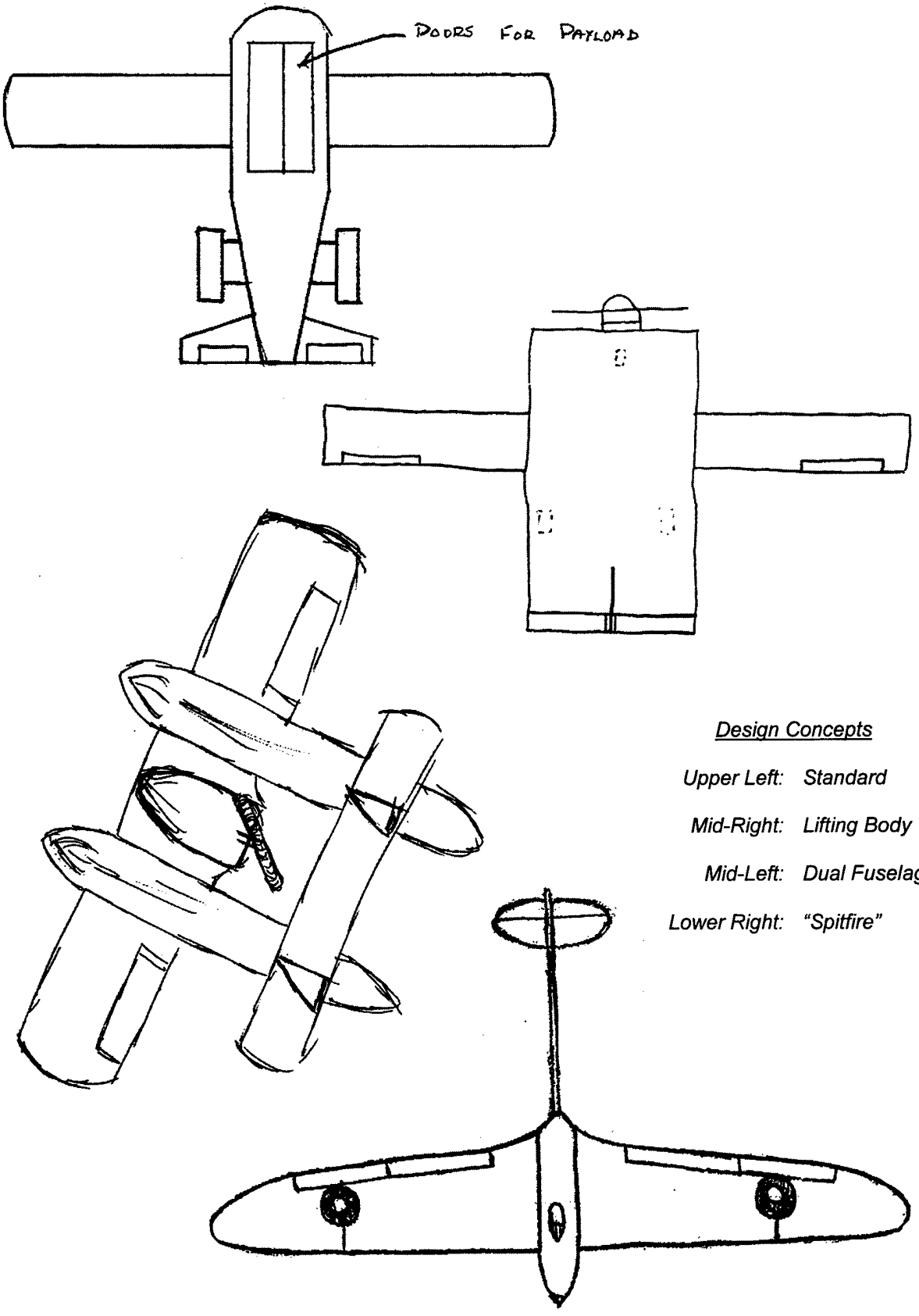

Design Concepts

Upper Left: *Standard*

Mid-Right: *Lifting Body*

Mid-Left: *Dual Fuselage*

Lower Right: *"Spitfire"*

4.0 Preliminary Design

The Preliminary Design Phase commenced once the Conceptual Design Phase was complete. A comparative study of airplanes with similar mission performances was conducted yielding approximate parameters. Trade studies of four disciplines: Weight, Performance, Stability and Control, and Propulsion were also initiated. The Performance group sized the wing and fuselage accordingly and passed their parameters to the Weight and Stability and Control Groups. The design's parameters were optimized and given to the propulsions group. The propulsions group used the sizes and developed the necessary drag calculations and propulsion unit.

4.1. Comparative Studies

The comparative study yielded a wing and tail airfoil type and an approximate wing loading and take-off weight.

4.1.1. Airfoil Selection (Wing)

Three characteristics were considered when the airfoil was picked. The first was the maximum lift coefficient. The higher the lift coefficient on the airfoil the less planform area is needed on the wing. The second consideration is its' stall characteristics, thinner airfoils generally stall more abruptly compared to thicker ones. The third is the associated drag of the airfoil. Several airfoils were considered, all of which are currently being used on model aircraft. It was in best interest that the aircraft contain a moderate stall behavior with low drag and a moderate lift coefficient. Since the aircraft will be flying at very low Reynolds numbers < 700,000 only 11 airfoils were considered due to their exceptional performance at low Reynolds numbers. Table 4.1 demonstrates the characteristics of each of the airfoils.

Table 4.1: Candidate Airfoils

Airfoil	C_{Lmax}	AOA°@ C_{Lmax}	C_D @ C_{Lmax}	Stall Behavior
NACA 2412	1.1	12	.015	Gentle
NACA 0012	0.9	12	.014	Moderate
NACA 6412	1.4	12	.025	Gentle
NACA-64-412	1.3	12	.01	Abrupt
E197	1.17	10	.015	Gentle
E168	1.0	12	.03	Abrupt
E214	1.2	10	.03	Moderate
E211	1.1	12	.035	Abrupt
E205	1.2	13	.03	Moderate
E222	1.1	12	.03	Moderate
E230	0.8	8	.02	Moderate

The E197 was the airfoil of choice; it demonstrated a low drag coefficient coupled with a moderate coefficient of lift and a gentle stall. The airfoil also contains a moderate moment coefficient allowing less material to strengthen the wing for torsional rigidity. Figure 4.1 illustrates the airfoil's performance at several Reynolds numbers.

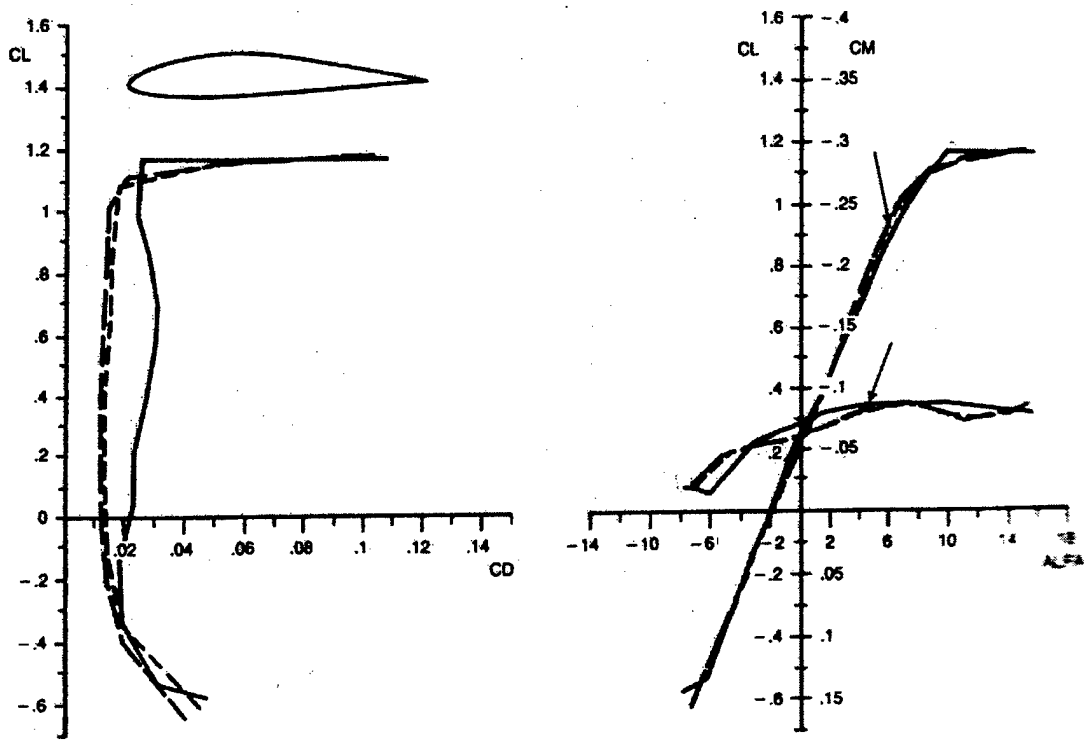

Figure 4.1: Eppler 197 lift curve.

4.1.2. Airfoil Selection (Tail)

For the selection of the tail it was noted that the section must be symmetrical. The section must also stall after the wing section, for control and stability. An airfoil section was desired over a flat plate for its structural strength and lower drag coefficient. The polar curve of the flat plate has a lower coefficient of lift and higher drag coefficient than the E168. The E168 stalls 2 degrees later than the wing section and has a relatively high C_{Lmax} of 1.0 compared to the 0.8 of the flat plate.

4.1.3. Wing- Loading

The wing loading was estimated by comparing fourteen different model aircraft all of which did not have payloads. Due to the size restriction on the wings the wing loading that will be picked will not incorporate the payload. This will result in a higher wing loading when the payload is placed in the aircraft. The wings

will need additional structural support for the additional stress/strain placed on the aircraft. Table 4.2 illustrates the fourteen model aircraft types and designs.

Table 4.2: Wing Loadings of Fourteen Aircraft

Name	Type	Gross Weight (oz.)	Wing Area (sq. in.)	Wing Loading (oz./sq.ft.)
SEAHAWK	Amphibious	121	655	26.6
CANADA GOOSE	Canard	75	444	24.3
SWIFT	Sport	92	600	22
WILD GOOSE	Three-surface	97	787	20.7
CROW	STOL	88	500	25.4
OSPREY	Sport	143	768	26.5
WASP	Tandem-wing biplane	36.25	300	17.42
SWAN	Canard	115	669	24.75
SNOWY OWL	Sport	98	643	22
FLAMINGO	Flying boat	74	500	21.3
SPARROW HAWK	Sport	38	250	22
SEA LOON	Amphibious	40	250	23
SEAGULL II	Flying boat	112	694	23.3
DOVE	Powered glider	55.375	602	13.16

All types of aircraft were compared. Amphibious were chosen due to their large empennage and blunt bodies, empennage that are similar to the empennage that will be found on the design. The sport type was chosen for a look at high performance wing loading figures and the glider was picked to see wing loadings values found on an efficient aircraft. An average was taken for all three types; a wing loading of 24.2 oz./ft^2 was resolved.

4.2. Aircraft Weights

The weight of the aircraft was estimated using an average weight for each component of the aircraft. After totaling each of the above aircrafts' components an average of each of the components was placed below:

Power:	Spinner Prop, engine nuts and bolts	36.07 %
Control:	receiver five servos, switch foam rubber protection	7.86 %
Landing Gear:	3-inch diameter wheels music-wire-legs, fairings nuts and bolts.	6.50 %

Wing:	1/16-inch thick balsa skin, two spars, ailerons, slotted flaps (0.039 oz./sq. in.)	26.23 %
Horizontal Tail:	1/16-inch thick balsa skin and elevators (0.028 oz./sq. in.)	1.43 %
Vertical Tail:	1/16-inch thick balsa skin, one spar and rudder (0.030 oz./sq. in.)	0.50 %
Fuselage:	Complete volume of the fuselage containing 3/32-inch thick balsa skins and 3/16-inch thick balsa corners control cables included. (0.017 oz./in.^{3})	21.41 %

The first three components are fixed weight and encompass 52 % of the take-off weight, it can be found by weighing each component. The total fixed weight was found to be 4.8125 lbs.; the total projected take-off weight of the aircraft is 9.528 lbs without the 5 lb payload and missile decoy. Table 4.3 illustrates the projected weights of each component of the aircraft. Note the power plant and the wing have the highest percentage of the aircraft's weight; steps will be taken to reduce the weight of each of the components.

Table 4.3: Aircraft Components.

Component	Average (%)	Projected Weight (lbs)
Power Plant	36.07	3.437
Control	7.86	0.750
Landing Gear	6.50	0.625
Wing	26.23	2.500
Horizontal Tail	1.43	0.136
Vertical Tail	0.50	0.048
Fuselage	21.41	2.040

4.3. Performance Analyses

4.3.1. Wing Planform

The wing planform area can be estimated using the required wing loading and the maximum take-off weight. The wing planform was found to be 7.2 ft^2 or 1040.5 in.^{2}. From the conceptual design a tapered planform was selected due to its reduced weight over a rectangular planform and its aerodynamic efficiency. Due to geometric restrictions, it was decided that the wing be composed of two pieces with a span of no more than eight feet.

4.3.1.1. Tapering

Taper effects the distribution of the lift along the span of the wing. Induced drag is minimized when the load distribution has an elliptical shape. Having taper allows the distribution to "mimic" this elliptical shape. Figure 4.2 illustrates the effect of taper ratio on the load distribution along the wingspan.

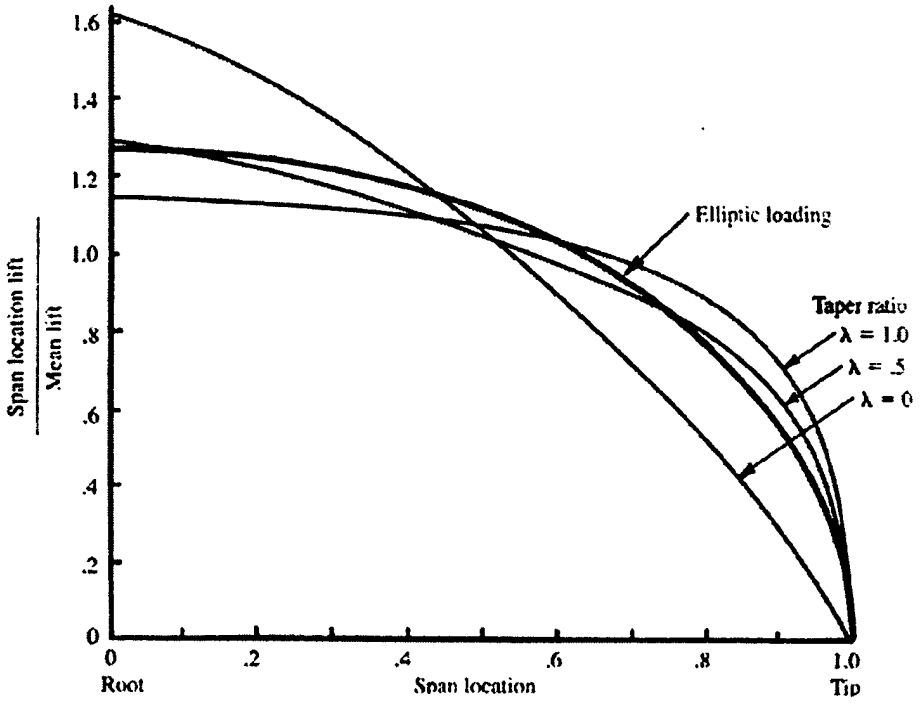

Figure 4.2: Effect of taper on lift distribution

Using a software program called Advanced Aircraft Analysis the load distribution was optimized. Figure 4.3 demonstrates the optimal lift distribution, yielding a taper ratio of 0.699.

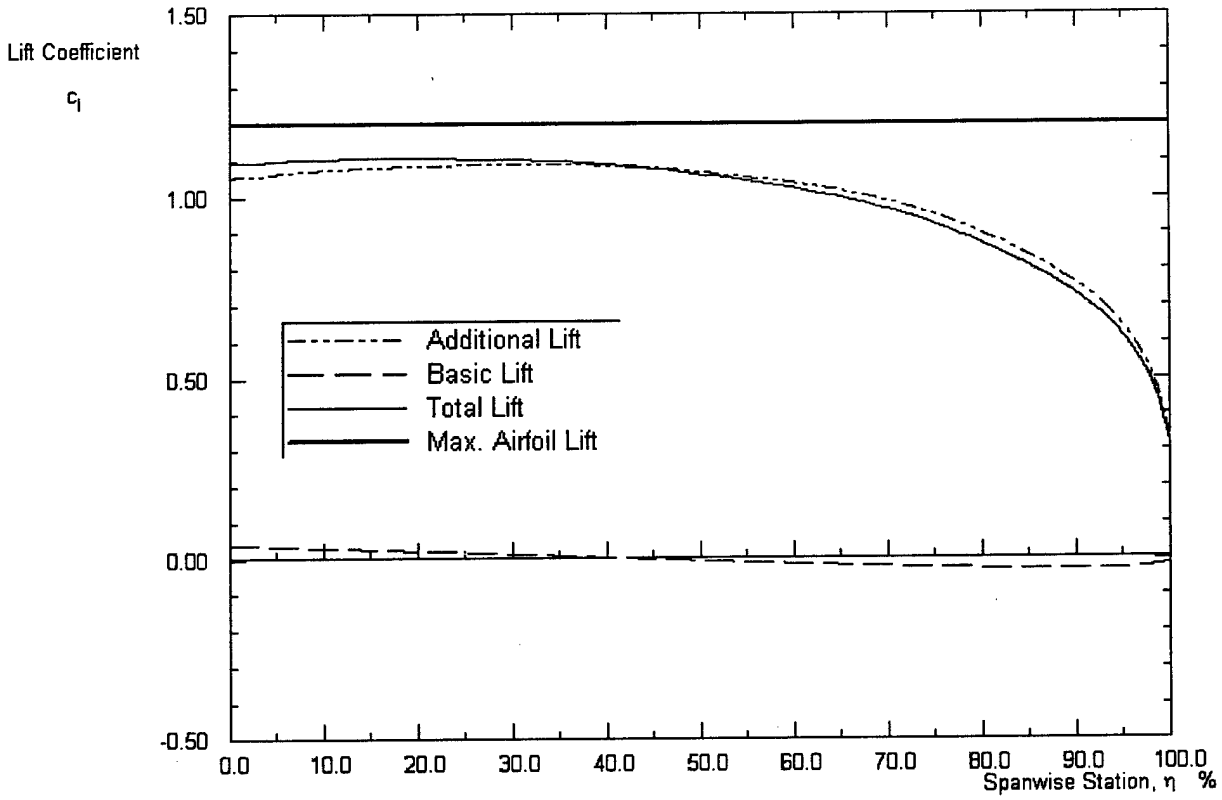

Figure 4.3: Optimal lift distribution

4.3.1.2. 4.3.1.2 Aspect Ratio

Aspect ratio is another geometric consideration in reducing induced drag. It was desired to have the largest aspect ratio for the given geometric constraints. Figure 4.4 illustrates the importance of a high aspect ratio in wing design.

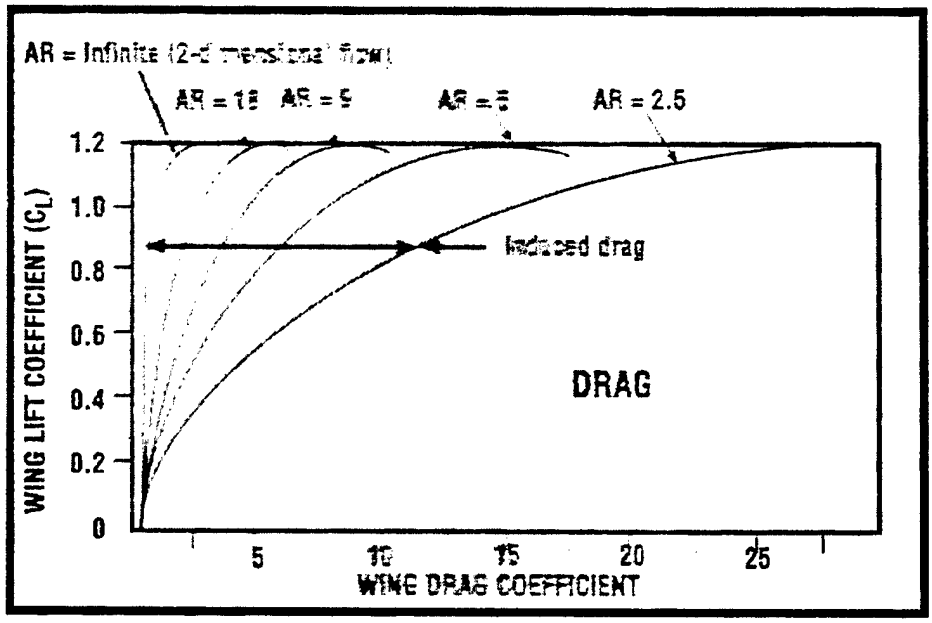

Figure 4.4: How aspect ratio effects drag at a given lift

For a given root chord length the greatest increase in aspect ratio was found to be from a chord of 1.25 ft to 1.00 ft. To distinguish the most optimal root chord length the total man-hours for each chord was plotted in Figure 4.6. Figure 4.5 illustrates that the optimal chord is 1.345 ft. in length with an aspect ratio of 5.6.

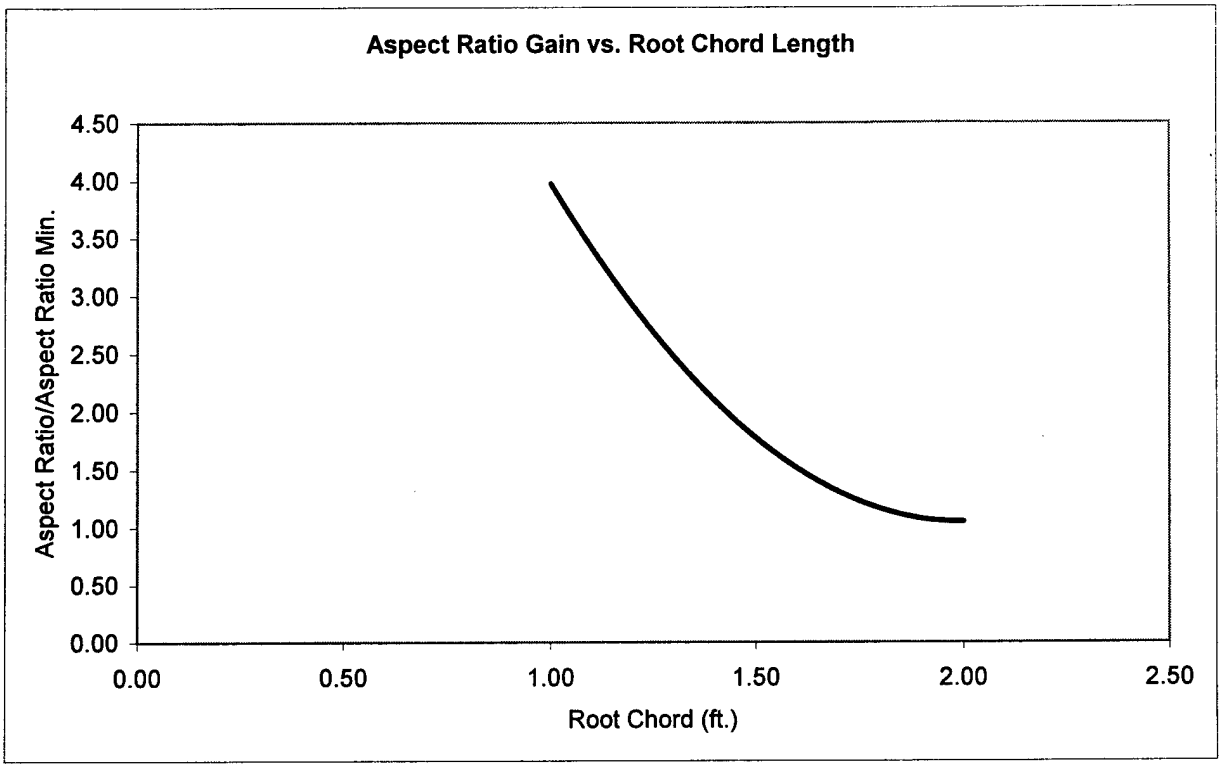

Figure 4.5: Aspect ratio gain vs. root chord length

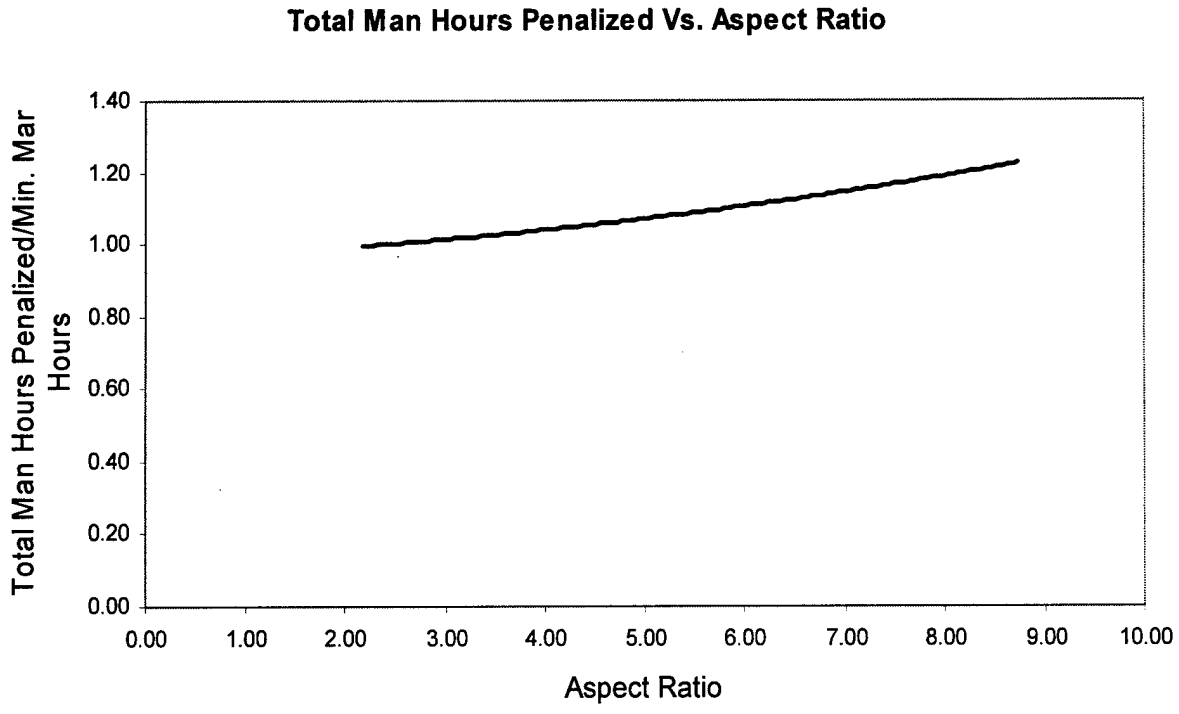

Figure 4.6: Increase in man-hours for a given aspect ratio.

4.3.2. Aircraft's Performance

For an aircraft to be efficient it must fly at an attitude that is the most efficient and desirable for a given mission. The aircraft being evaluated must have a relatively high speed due to the time requirement but maintain a desirable drag count. Figure 4.16 yields a minimum drag velocity of 28 mph. This velocity is very low and is only a few miles per hour faster than the stall speed; the value also does not incorporate the efficiency of the aircraft but only the minimum drag. A second evaluation of an aircraft's efficiency is the lift to drag ratio. The lift to drag ratio is determined from Figure 4.7.

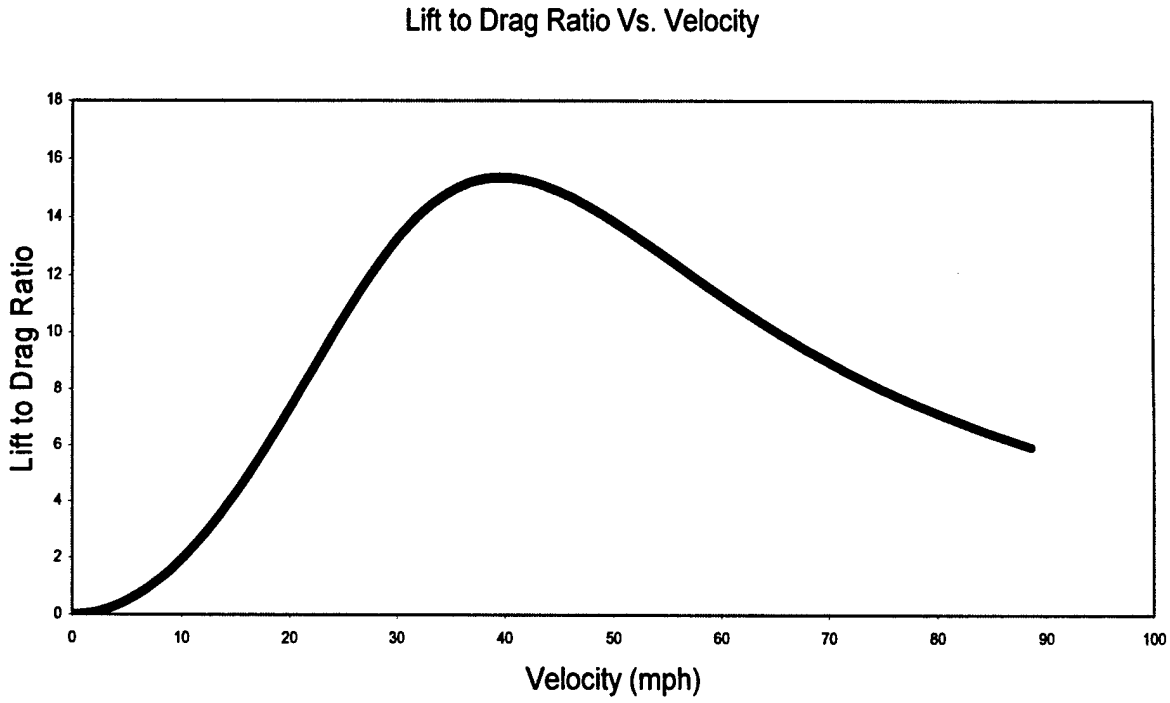

Figure 4.7: Lift to drag ratio vs. velocity.

From Figure 4.7 it is easy to see that the maximum L/D value for the plane is 15.35 at a velocity of 40 mph. If the aircraft was to fly at a higher velocity it would be still efficient up to ~55 mph where the L/D values begin to drop dramatically. To save time the aircraft will be designed to fly at 50 mph. The L/D value for 50 mph is 14, ~ 8 % less than the maximum L/D value.

4.3.3. Fuselage Considerations

The fuselage has the largest drag component on the aircraft. To reduce the drag on the fuselage, several aspects of its design were explored. The first aspect was the aft cone. To decide on the size and geometry of the cone, three different fuselage configurations were made. The three types included were as follows:

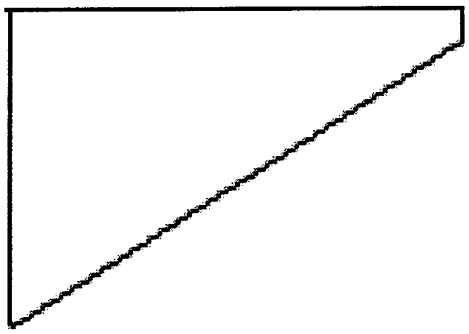

Long aft cone

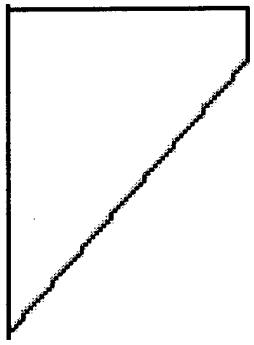

Short aft cone

Figure 4.8

The third configuration did not include an aft cone. The fuselage was placed in the wind tunnel and ran at 43 mph, the maximum velocity the tunnel would reach. The temperature of the tunnel was 22° C and had an average total pressure of 996.508 (mbar). The long aft cone had an average drag of 6.09 N. The smaller aft cone was also placed in the wind tunnel with very similar conditions having an average of 6.25 N of drag. The configuration having no aft cone was then placed into the tunnel and displayed an average drag of 5.92 N. It was plausible to state that the aft cone created more skin friction drag than it saved on form drag. The fuselage was to be built with no aft cone. The propulsions group had another concern with the fuselage; the interference factor with the wing was very high, 1.2, compared to the tail's interference factor of 1.04. To lower the interference drag a foam filet was placed between the fuselage and the wing.

4.4. Stability and Control

It is of great importance to evaluate the stability of the aircraft in flight. This section provides the necessary calculations to demonstrate the stability of the aircraft statically and dynamically.

4.4.1. Longitudinal Static Stability

Longitudinal static stability demonstrates that the aircraft is stable in the longitudinal direction, yields the C.G. travel of the aircraft and the necessary trim needed in level flight.

The pitching moment curves C_{mo} and $C_{m\alpha}$ can be found using equations 1-7.

$$C_{mo\,(wing)} = C_{m\,ac\,(wing)} + C_{L\,0\,(wing)}\left(\frac{X_{cg}}{\overline{C}} - \frac{X_{ac}}{\overline{C}}\right) \quad (1)$$

Where $C_{m\,ac\,(wing)}$ of the wing is suggested to be approximately –0.15. The aerodynamic center of the wing can be found by equation 2.

$$X_{ac} = X_{c/4} + \Delta X_{ac}\sqrt{S_{wing}} \quad (2)$$

Where $X_{c/4}$ is $0.25 * C_{root\,(wing)}$ and ΔX_{ac} can be found by equation 3.

$$\Delta X_{ac} = 0.26(M-0.4)^{2.5} \quad (3)$$

the value of $C_{mo\,(wing)} = -0.1200$.

For the tail an efficiency factor as well as a tail volume ratio must be considered. The efficiency factor is assumed to be 1. The tail volume ratio can be found from equation 4.

$$V_H = \frac{l_{HT} S_{HT}}{\overline{C} S} \quad (4)$$

The l_{HT} is approximately 2.197 ft. The volume ratio for the horizontal tail is 1.036.

The equation for $C_{mo\,(tail)}$ can be found below:

$$C_{mo\,(tail)} = \eta V_H C_{L\alpha t}\left(\varepsilon + i_w - i_t\right) \quad (5)$$

$C_{mo\,(tail)} = 0.2827$.

$C_{m\alpha\,(wing)}$ can be found from equation 6. The value is 0.859 rad^{-1}

$$C_{m\alpha\,(wing)} = C_{L\alpha\,(wing)}\left(\frac{X_{cg}}{\overline{C}} - \frac{X_{ac}}{\overline{C}}\right) \quad (6)$$

The tail contribution is found in equation 7.

$$C_{m\alpha\,(tail)} = -\eta V_H C_{L\alpha t}\left(1 - \frac{d\varepsilon}{d\alpha}\right) \quad (7)$$

Where $\frac{d\varepsilon}{d\alpha}$ is found from equation 8.

$$\frac{d\varepsilon}{d\alpha} = \frac{2C_{L\alpha w}}{\pi A_w} \tag{8}$$

The tail contribution is -2.066 rad.$^{-1}$. The two pitching moment curves (C_{mo} and $C_{m\alpha}$) describe the aircraft's stability in flight. A positive $C_{m\alpha}$ value will result in an unstable aircraft; a negative value will result in a stable aircraft. The wing contains a positive value contributing to an unstable aircraft as seen in Figure 4.9, the larger negative value of the tail contributes stability to the plane, that's its function. The overall pitching moment in relation to the AOA can be found from equation 6. The negative value of $C_{m\alpha}$ demonstrates that the aircraft has static longitudinal stability in flight. The C_{mo} value also has importance in that it provides a positive y-intercept allowing the use of trim at a positive angle of attack.

$C_{m\square} \square C_{m\square wing} C_{m\square tail}$. I□

$C_{m\square} \square 1.207 rad^{-1}$

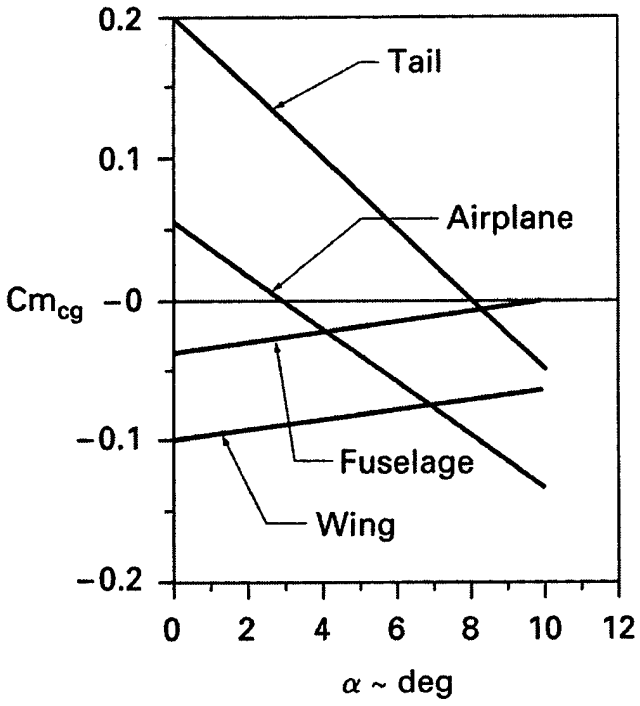

Figure 4.9: Component contributions to pitching moment.

To ensure static longitudinal stability the aircraft's neutral point needs to be located allowing to know their limits as to the movement of the center of gravity (C.G.). If the C.G. is in front of the aerodynamic center the plane is stable, if it is behind the aerodynamic center it is unstable. At the neutral point $C_{m\alpha} = 0$. Equation 9 yields the value of the neutral point. If the C.G. moves to the value found from equation 9 the plane will be neutrally stable if it moves further the aircraft will become unstable.

$$\frac{X_{NP}}{\bar{C}} = \frac{X_{ac}}{\bar{C}} + \eta V_H \frac{C_{L\alpha t}}{C_{L\alpha w}}\left(1 - \frac{d\varepsilon}{d\alpha}\right) \quad (9)$$

The neutral point is $\frac{X_{NP}}{\bar{C}} =$ 0.6811. The C.G. of the aircraft lies approximately .0833 ft. forward of the neutral point with the maximum payload. The C.G. position makes the aircraft 5% statically stable.

4.4.2. Longitudinal Control

The aircraft's elevator is used to control the longitudinal motion of the aircraft it contains a control surface of 0.225 ft^2. The elevator moves through an arc deflection of +/- 10 degrees. The elevator effectiveness for the aircraft can be derived from equation 10.

$$C_{m\delta e} = -V_H \eta C_{L\alpha t} \tau \quad (10)$$

Where τ is the flap effectiveness factor found to be 0.3. The $C_{m\delta e} = -1.636\ rad^{-1}$

$$C_{L\delta e} = \frac{S_t}{S} \eta C_{L\alpha t} \tau \quad (11)$$

From equation 11 $C_{L\delta e}$ is 0.381 rad^{-1}. Using this equation a plot of C_{Lt} vs. AOA with elevator deflection can be found in Figure 4.10.

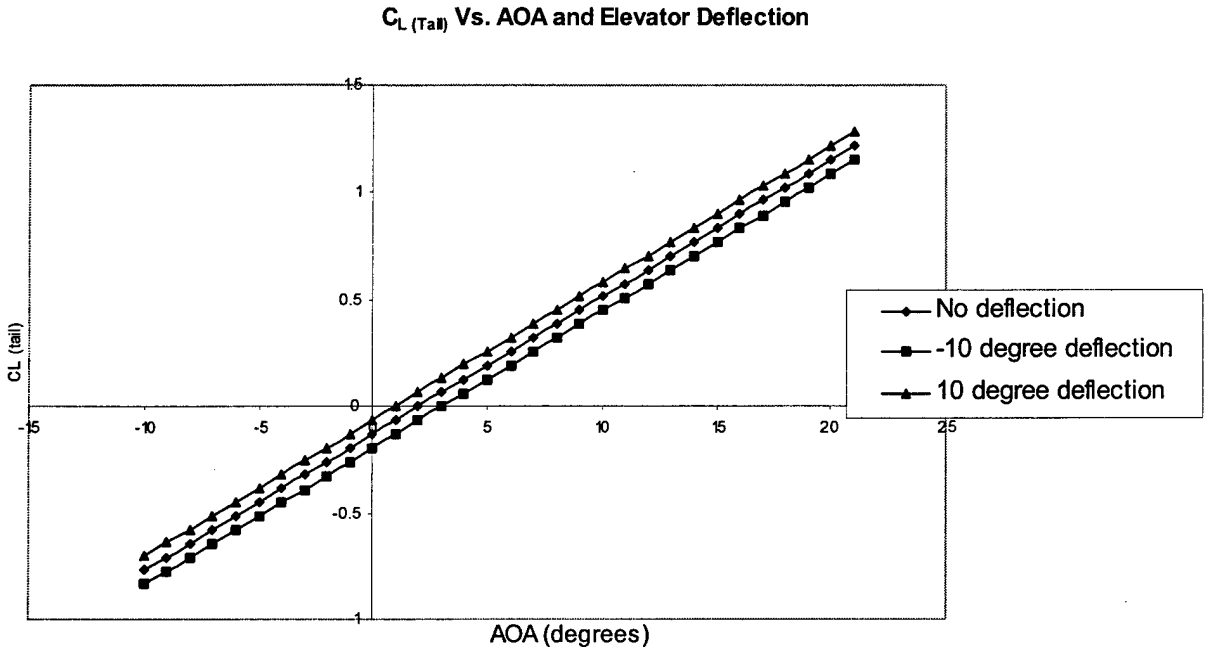

Figure 4.10: Elevator effect on coefficient of lift of tail.

Figure 4.10 demonstrates a positively deflected elevator yields a positive change in lift and a decrease in lift with a negative deflection. The change in the lift coefficient is 0.0066 per degree of elevator deflection. The elevator deflection also changes the moment of the aircraft; Figure 4.11 illustrates the change in the moment as the elevator is deflected.

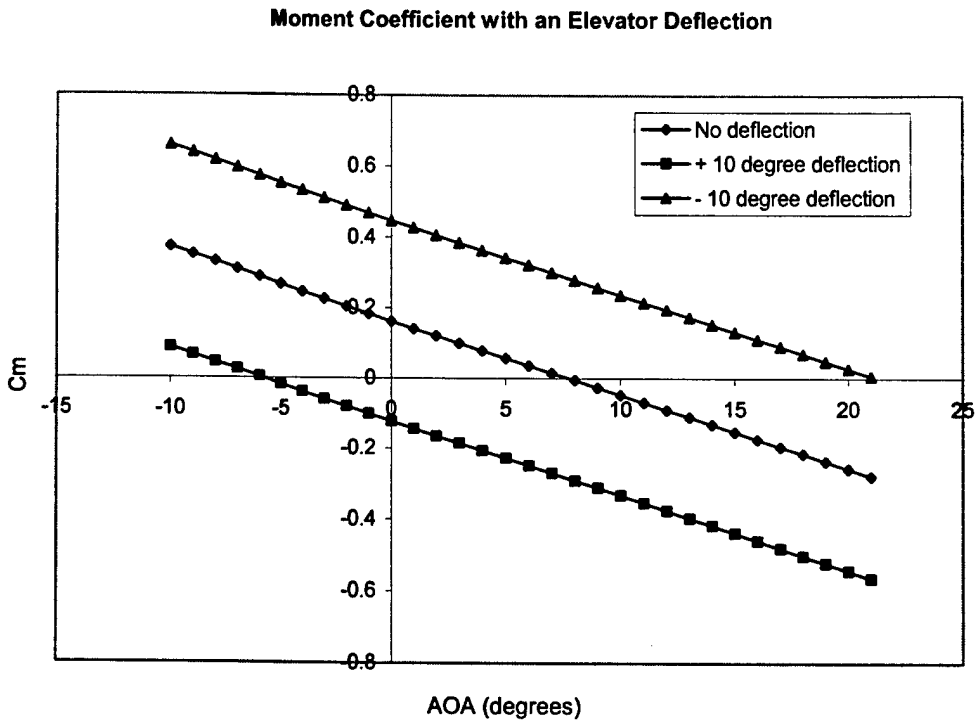

Figure 4.11: Moment coefficient with elevator deflection.

From Figure 4.11 the moment decreases with a positive deflection and increases with a negative deflection. The change in the moment coefficient is 0.02855 per degree of elevator deflection.
The trim of the aircraft will vary with the AOA of the aircraft. In Figure 4.12 the necessary trim can be found for a given AOA. Equation 12 gives the necessary elevator trim to make the longitudinal moment zero.

$$\delta_{trim} = -\frac{C_{m0} + C_{m_\alpha}\alpha_{trim}}{C_{m\delta e}} \tag{12}$$

Where α_{trim} is the AOA at which the trim will be assessed.

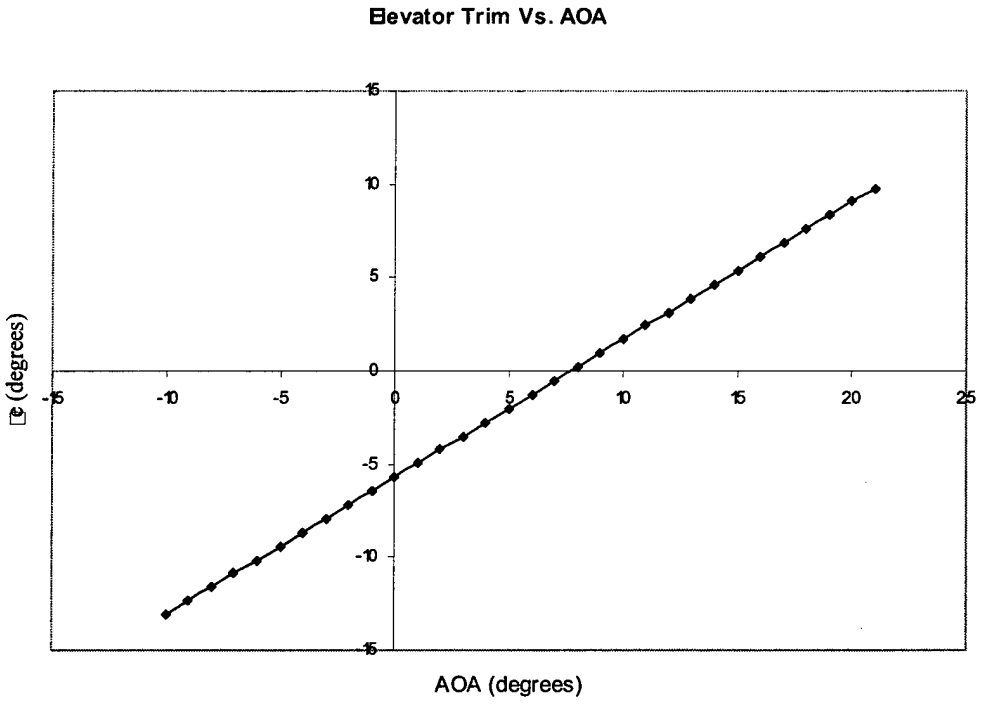

Figure 4.12: Necessary elevator-trim vs. AOA.

4.4.3. 4.4.3 Directional Static Stability

Directional static stability is concerned with the static stability of the airplane about the z-axis. It is desirable that the airplane should tend to return to an equilibrium condition when subjected to some form of yawing disturbance. For static directional stability an aircraft must contain a positive yawing moment curve ($C_{n\beta} > 0$). The contribution of the wing to directional stability is minimal compared to the fuselage. The fuselage creates a negative contribution to directional stability. The wing-fuselage contribution can be found in equation 13.

$$C_{n\beta_{wf}} = -k_n k_{rl} \frac{S_{fs} l_f}{S_w b} \tag{13}$$

Where $\mathbf{k_n}$, $\mathbf{k_{rl}}$ can be found from Figure 2.29 and 2.30 in Reference 1. The two values of k_n, k_{rl} are 0.0024 and 2.0 respectively. $\mathbf{S_{fs}}$ is the body side area, which is approximately 1.833 ft. 2 and lf, is the length of the fuselage. The wing-fuselage contribution is –0.3367 rad^{-1}. The vertical tail contributes a large positive value, making the aircraft stable directionally. Equation 14-15 yields the vertical tail component.

$$C_{n\beta_v} = V_v \eta_v C_{L_{\alpha_v}} (1 + \frac{d\sigma}{d\beta}) \tag{14}$$

Where η_v is assumed a value of 1, and V_v is the vertical tail volume ratio having a value of 0.10693.

$$\eta_v(1+\frac{d\sigma}{d\beta}) = 0.724 + 3.06\frac{S_v/S}{1+\cos\Lambda_{c/4w}} + .4\frac{z_w}{d} + .009AR_w \quad (15)$$

The constant **d** is the depth of the fuselage having a value of 0.66 ft. and $\mathbf{z_w}$ is the distance parallel to the z-axis, from the wing root quarter chord point to the fuselage centerline, having a value of 2.16 ft. The complete directional stability derivative is 0.2769 rad^{-1}. The value is positive making the aircraft statically stable in the directional region. Figure 4.13 shows a plot of C_n at β values ranging from –10 deg to +10 deg.

4.4.4. Directional Control

Directional control can be achieved by the deflection of a rudder on a vertical stabilizer. By deflecting the flap to either side the lift force created on the vertical surface will create a moment along the z-axis. The effectiveness of the rudder can be found in equation 16.

$$C_{n_{\delta_r}} = -\eta_v V_v \frac{dC_{L_v}}{d\delta_r} \quad (16)$$

Where $\frac{dC_{L_v}}{d\delta_r} = C_{L_{\alpha_v}}\tau$ and τ is the effectiveness factor which can be found from Figure 2.21 in Reference 1; the factor has a value of 0.35. The rudder control effectiveness has a value of –0.144596 rad^{-1}. Another value that needs consideration is the rudder control effectiveness without the means of a moment arm. Equation 17 yields a control effectiveness coefficient without taking the moment arm into consideration. Figure 4.14 is a plot of C_n versus rudder deflection from –20 deg to +20 deg.

$$C_{Y_{\delta_r}} = -\eta_v \frac{V_v dC_{Lv}}{l_v d\delta_r} \quad (17)$$

From equation 17 a value of -.016512 / rad.-ft is obtained for the rudder effectiveness.

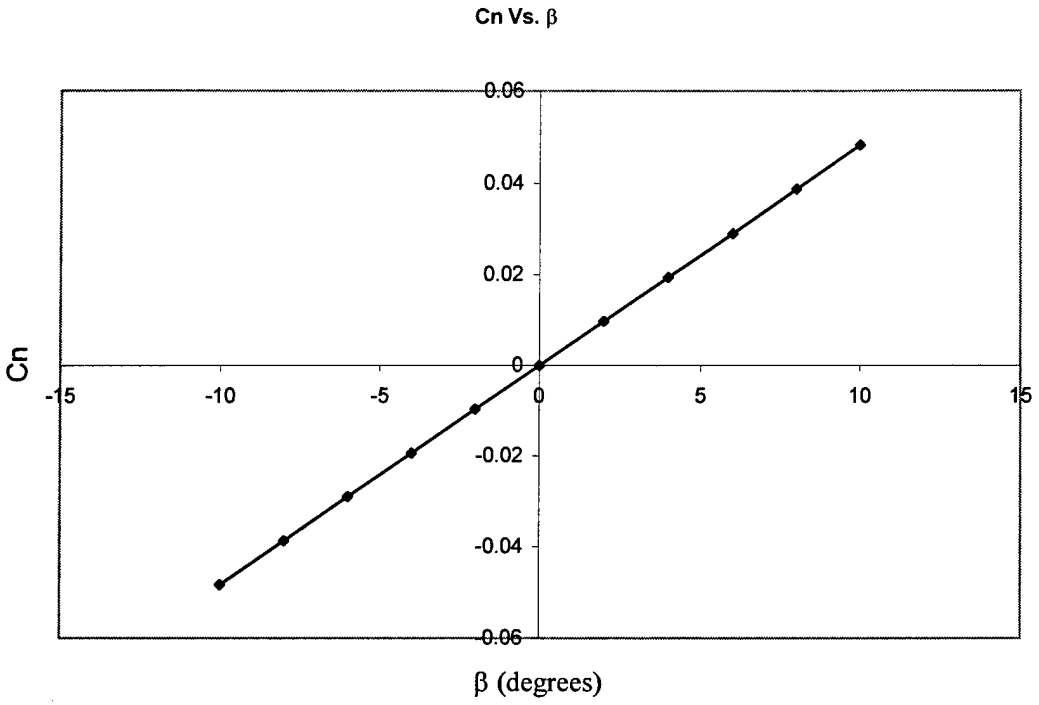

Figure 4.13: C_n vs. Beta.

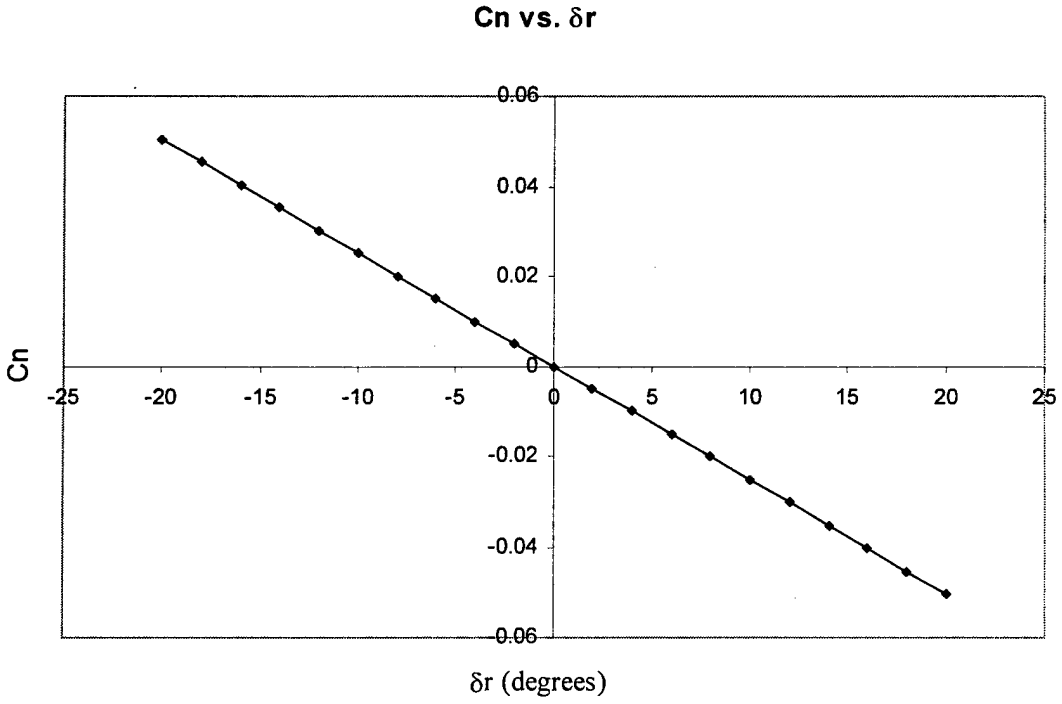

Figure 4.14: Cn vs. rudder deflection.

From Figures 4.13 and 4.14 it is plausible to say the rudder is limited by its effectiveness. From Reference 1, Table 2.1 are lists of requirements presented for directional control. The lists explain what the rudder must accomplish to be a successful aircraft. Below is a similar table.

Table 4.4: Rudder Requirements

Rudder Requirements	Implication for rudder design
Adverse Yaw	When an airplane is banked for a turning maneuver the ailerons may create a yawing moment that opposes the turn, the rudder must overcome the adverse yaw when the airplane is flying slow.
Crosswind Landings	To maintain alignment with the runway during a crosswind landing.
Asymmetric power condition	The critical asymmetric power condition is when one or more engines fail on one side of the aircraft creating a moment along the z-axis. The rudder must be able to overcome the induced moment to fly in a straight flight path.
Spin Recovery	The primary control for spin control in many planes is the rudder. The rudder must be powerful enough to oppose a spin rotation.

From Table 1 and Figures 4.13 and 4.14 equation 18 has been created for a maximum sideslip angle for a given rudder deflection

$$\beta_{max} = ((\delta_r)^*(C_{n\delta r}))/C_{n\beta} \tag{18}$$

From equation 27 and a rudder deflection of + 20 degrees the maximum steady sideslip is –10.4427 deg. The sideslip angle is acceptable with the aircraft's pilot therefore the vertical tail and rudder assembly is sufficient for the aircraft's mission requirements in the static stability region.

4.4.5. Roll Static Stability

An aircraft will have static roll stability if it restores to level flight conditions when it is disturbed from a wings-level attitude. The requirement for stability is $C_{l\beta} < 0$. The roll moment depends on the wing dihedral, wing sweep, vertical tail and the position of the wing i.e. high, low, mid-wing. The major contributor to roll stability is the wing dihedral. It was decided that the aircraft was not to contain dihedral do to complexity and the added structural weight to the wing. The only contributor comes from the vertical tail. Equation 19 gives the value for the vertical tail.

$$C_{l_\beta} = -\frac{S_v Z_v}{Sb}\eta_v C_{L_{\alpha v}}\left(1+\frac{d\varepsilon}{d\beta}\right) \tag{19}$$

The contribution from the vertical tail is -.0937 rad^{-1}. Z_v is the distance from the aerodynamic center of the vertical tail and the x-axis, having a value of 0.333 ft., and $\frac{d\varepsilon}{d\beta}$ has been assumed a value of 0.3 rad. The total static roll stability derivative is -0.1874 rad^{-1}, due to the two vertical tails. The static roll stability derivative is negative making the aircraft stable along the x-axis. Figure 4.13 is a plot of the stability derivative versus a range of beta values from –10 to +10 deg.

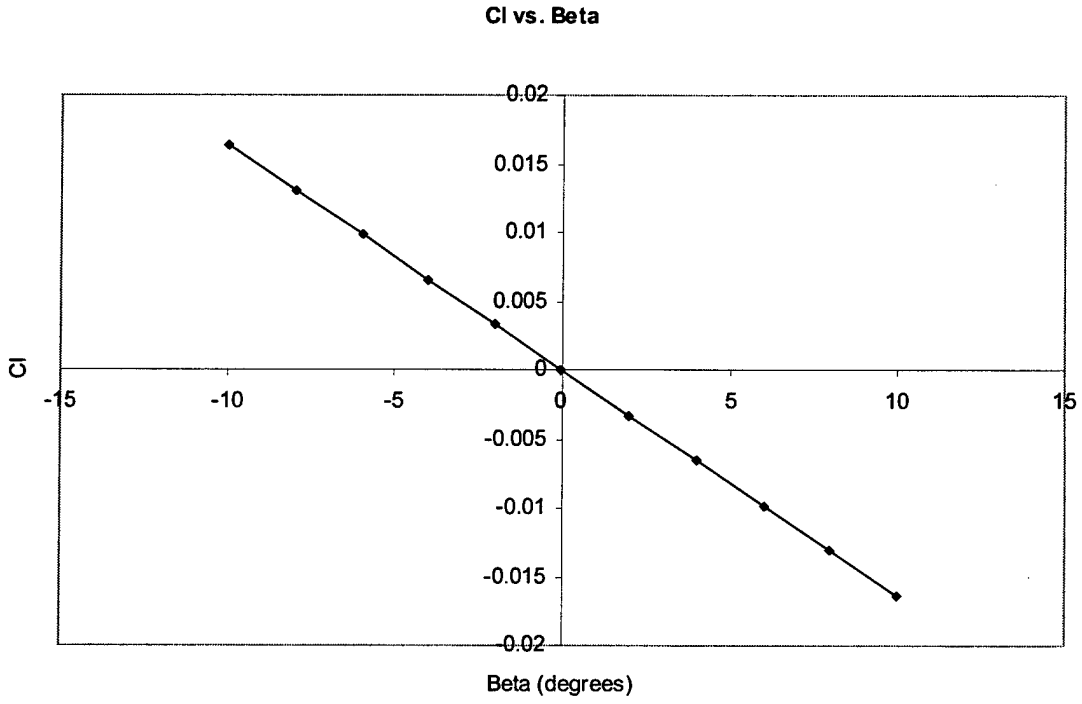

Figure 4.13: Roll derivative vs. beta.

Note from Figure 4.13 the reduction of the rolling moment with a positive beta and the production of a rolling moment with a negative beta, creating roll stability.

4.4.6. Static Roll Control

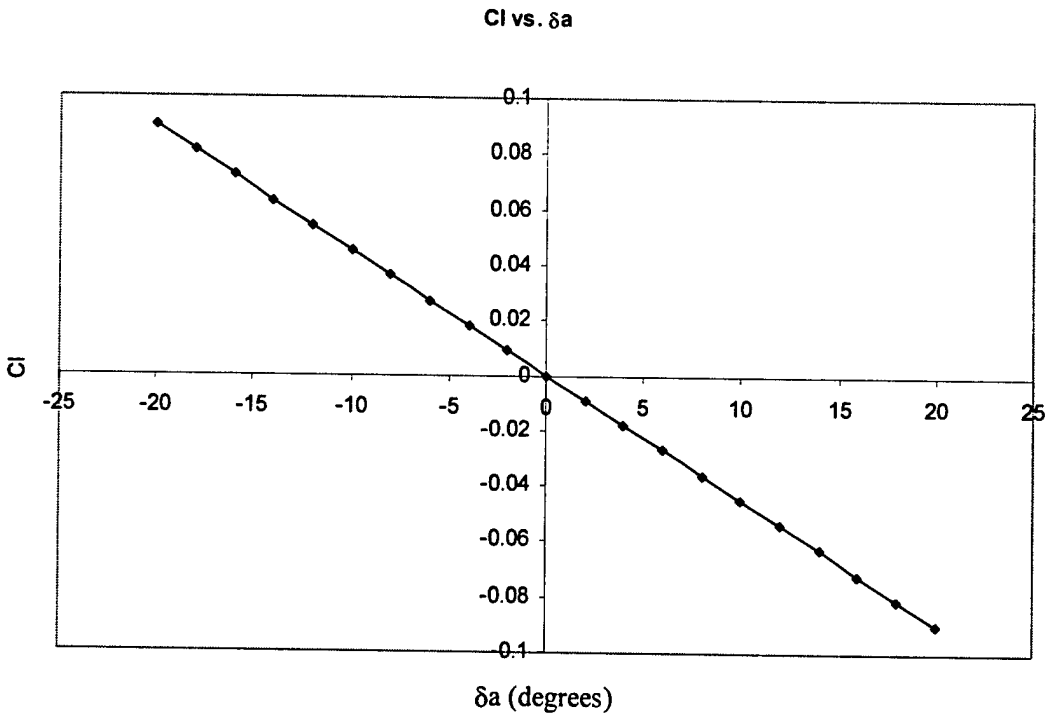

Figure 4.14: Cl vs. aileron deflection

Figure 4.14 is a plot of the incremental change 0.0044 deg^{-1} in roll moment due to a change in aileron deflection. The plot indicates that the ailerons are affective in controlling the static stability of the aircraft sufficiently.

4.4.7. Dynamic Stability Derivatives

Dynamic stability derivatives are necessary for the examination of how an aircraft will handle in flight conditions. The three different axis of motion the x, y, and z directions and can involve movement and pitching around each axis. The first of these to be examined are the speed derivatives or Xu, Zu, and Mu, these are all related to a change in forward speed, due to the effects from drag, lift and pitching moments. To solve for these speed derivatives it is first required to solve for the longitudinal stability coefficients. Using equations 20 and 21 it is possible to solve for these coefficient which when plugged into equations 22 and 23 give the values for the speed derivatives.

$$C_{X_u} = -(C_{D_u} + 2C_{D_0}) + C_{T_u} \approx -2C_{D_0} \tag{20}$$

$$C_{z_u} = -\frac{M^2}{1-M^2} C_{L_0} - 2C_{L_0} \tag{21}$$

Which yields $C_{X_u} = -.031276$ and $C_{z_u} = -1.3882$

$$X_u = \frac{C_{x_u} QS}{u_0 m} \tag{22}$$

$$Z_u = \frac{C_{z_u} QS}{u_0 m} \tag{23}$$

Giving values for X_u = -2.1548e^{-4} /s, Z_u = -0.0064/s, with M_u assumed to be equal to 0 for the aircraft. Next under analysis is the pitch rate and "rate of change of AOA" derivatives, the pitch rate derivatives are M_q and Z_q while the "rate of change of AOA" derivatives are M_α and Z_α. Again to solve for these variables it is required to first solve for the longitudinal stability coefficients, and then use those values to solve for the respective derivatives. This is done by solving equations 24 through 27 seen below.

$$C_{m_q} = -2\eta C_{L_{\alpha_t}} V_H \frac{l_t}{c} \tag{24}$$

$$C_{m_\alpha} = C_{L_{\alpha_w}} \left(\frac{X_{cg}}{\bar{c}} - \frac{X_{ac}}{\bar{c}}\right) - \eta V_H C_{L_{\alpha_t}} \left(1 - \frac{d\varepsilon}{d\alpha}\right) \tag{25}$$

$$M_q = C_{m_q} \frac{\bar{c}^2 QS}{2u_o I_y} \tag{26}$$

$$M_\alpha = C_{m_\alpha} \frac{\bar{c} QS}{I_y} \tag{27}$$

Where equations 26 and 27 give values for M_q = 0.0216/s and M_α = -0.7094 /s^2 with Zq and Z_α both assumed to be equal to 0.

The roll rate derivatives show the effectiveness of the plane in rolling. There are three roll rate derivatives which are L_p, N_p, and Y_p in the X, Z, and Y directions respectively. Y_p is assumed to be zero while L_p and N_p can be solved for using equations 28 through 31. This is done by first solving for the lateral stability coefficients and then using these values to solve for the roll rate derivatives.

$$C_{l_p} = -\frac{C_{L_\alpha}}{12} \frac{1+3\lambda}{1+\lambda} \tag{28}$$

$$C_{n_p} = -\frac{C_L}{8} \tag{29}$$

$$L_p = \frac{QSb^2 C_{l_p}}{2I_x u_0} \tag{30}$$

$$N_p = \frac{QSb^2 C_{n_p}}{2I_z u_0} \tag{31}$$

Solving these four equations leads to L_p=0.0841 /s and N_p= -0.0037 /s

The last of the dynamic stability derivatives is due to the Yaw Rate, which is solved for by first solving for the lateral stability coefficients, then using these values in equations 35 though 37. This leads to an approximate value for the dynamic stability derivatives.

$$C_{y_r} = -2(\frac{l_v}{b})(C_{y_\beta})_{tail} \tag{32}$$

$$C_{l_r} = \frac{C_L}{4} - 2\frac{l_v z_v}{bb}(C_{y\beta})_{tail} \tag{33}$$

$$C_{n_r} = -2\eta_v V_v (\frac{l_v}{b}) C_{L_{a_v}} \tag{34}$$

$$Y_r = \frac{QSbC_{y_r}}{2mu_0} \tag{35}$$

$$L_r = \frac{QSb^2 C_{l_r}}{2I_x u_0} \tag{36}$$

$$N_r = \frac{QSb^2 C_{n_r}}{2I_z u_0} \tag{37}$$

The values from the equations above are Y_r = -0.0412 /s, L_r = 0.0165 /s, and N_r = -0.0081 /s respectively.

With the use of the dynamic stability derivatives it was then possible to approximate an approximate calculation of the overall stability of the longitudinal and lateral motion of the aircraft.

4.4.8. Dynamic Stability of Longitudinal Motion

The equations of longitudinal motion for an aircraft can be written in state-space format, which allows for a quick examination of the flight characteristics and flying qualities of the airplane, in a compact and easy to understand form.

$$\begin{bmatrix} \Delta\dot{u} \\ \Delta\dot{w} \\ \Delta\dot{q} \\ \Delta\dot{\theta} \end{bmatrix} = \begin{bmatrix} X_u & X_w & 0 & -g \\ Z_u & Z_w & u_0 & 0 \\ M_u+M_{\dot{w}}Z_u & M_w+M_{\dot{w}}Z_w & M_q+M_{\dot{w}}u_0 & 0 \\ 0 & 0 & 1 & 0 \end{bmatrix} \begin{bmatrix} \Delta u \\ \Delta w \\ \Delta q \\ \Delta\theta \end{bmatrix} + \begin{bmatrix} X_\delta & X_{\delta_T} \\ Z_\delta & Z_{\delta_T} \\ M_\delta+M_{\dot{w}}Z_\delta & M_{\delta_1}+M_{\dot{w}}Z_{\delta_T} \\ 0 & 0 \end{bmatrix} \begin{bmatrix} \Delta\delta \\ \Delta\delta_T \end{bmatrix} \tag{38}$$

Placing values found earlier from the dynamic stability derivatives while ignoring the control surfaces portion of the equation for our analysis yields equation 39 below. This equation can then be used to solve for the longitudinal flight characteristics of the plane.

$$\begin{bmatrix} \Delta\dot{u} \\ \Delta\dot{w} \\ \Delta\dot{q} \\ \Delta\dot{\theta} \end{bmatrix} = \begin{bmatrix} -2.1548e004/s & 8.1410e004/s & 0 & -9.8m/s \\ -0.0064/s & -3.40/s & 22.352m/s & 0 \\ 8.4648e005[1/(m*s)] & -0.0524[1/(m*s)] & -3.8140[1/(m*s)] & 0 \\ 0 & 0 & 1 & 0 \end{bmatrix} \begin{bmatrix} \Delta u \\ \Delta w \\ \Delta q \\ \Delta\theta \end{bmatrix} \tag{39}$$

The matrix above is written in the format $\dot{x} = Ax$ and to solve for the longitudinal flight characteristics, the eigenvalues of the matrix must be calculated (setting $|\lambda I - A| = 0$). Solving for the eigenvalues gives four roots, two for the long period or phugoid solution and the other two roots for the short period solution. The aircraft being discussed falls within a category B flight phase which incorporates gradual maneuvers without precision tracking it also includes climb, cruise, loiter, descent, emergency descent and emergency deceleration.

An aircraft falls within 3-levels of flying quality. Level 1 is clearly adequate for the mission flight phase. Level 2 flying qualities are adequate to accomplish the mission flight phase but with some increase in pilot workload and/or degradation in mission effectiveness or both. The Level 3 flying qualities are such that the airplane can be controlled safely but pilot workload is excessive and/or inadequate or both. Table 4.5 illustrates the required phugoid and short-period damping coefficients for each level.

Table 4.5: Longitudinal flying qualities

Longitudinal flying qualities

Phugoid mode				
	Level 1	$\zeta > 0.04$		
	Level 2	$\zeta > 0$		
	Level 3	$T_2 > 55$ s		
Short-period mode				
	Categories A and C		**Category B**	
Level	ζ_{sp} min	ζ_{sp} max	ζ_{sp} min	ζ_{sp} max
1	0.35	1.30	0.3	2.0
2	0.25	2.00	0.2	2.0
3	0.15	—	0.15	—

Table 4.6 demonstrates the roots and characteristics for each mode of the longitudinal motion

Table 4.6: Longitudinal Flying Characteristics.

Root	Mode	$T_{1/2}$	$N_{cycles(double)}$	Period	ζ	Flying Qualities
$\lambda=\eta\pm i\omega$	-	$=0.69/\lvert\eta\rvert$	$=0.110\lvert\omega\rvert/\lvert\eta\rvert$	$=2\pi/\lvert\omega\rvert$	$=\sqrt{\frac{1}{\omega/\eta - 1}}$	Level 1,2, or 3
-0.2055 ± 0.8603i	Short Period	3.372s	0.460501	7.303	0.3574	Level 1
-0.0006 ± 0.0140i	Phugoid	115s	2.566	448.8	0.0424	Level 1

From Table 4.6 it is plausible to state that the aircraft is dynamically stable in the longitudinal motion containing level one flying qualities. From the static and dynamic longitudinal data it is safe to state that all geometric tail sizing is complete.

4.4.9. Dynamic Stability of Lateral Motion

The lateral motion of an aircraft can be examined and the equations of motion can be summarized in the state space format, similar to the equations for longitudinal motion. The lateral equations of motion have been provided below as equation 40.

$$\begin{bmatrix} \Delta\dot{v} \\ \Delta\dot{p} \\ \Delta\dot{r} \\ \Delta\dot{\phi} \end{bmatrix} = \begin{bmatrix} Y_v & Y_p & -(u_0 - Y_r) & g\cos(\theta_0) \\ L_v & L_p & L_r & 0 \\ N_v & N_p & N_r & 0 \\ 0 & 1 & 0 & 0 \end{bmatrix} \begin{bmatrix} \Delta v \\ \Delta p \\ \Delta r \\ \Delta\phi \end{bmatrix} + \begin{bmatrix} 0 & Y_{\delta_T} \\ L_{\delta_a} & L_{\delta_r} \\ N_{\delta_a} & N_{\delta_r} \\ 0 & 0 \end{bmatrix} \begin{bmatrix} \Delta\delta_a \\ \Delta\delta_r \end{bmatrix} \tag{40}$$

Equation 41 can be created with the use of the dynamic derivatives and equation 40. Similar to what was completed for the longitudinal motion, equation 41 allows for a rough examination of the lateral flight characteristics and the flying qualities of the aircraft.

$$\begin{bmatrix} \Delta\dot{v} \\ \Delta\dot{p} \\ \Delta\dot{r} \\ \Delta\dot{\phi} \end{bmatrix} = \begin{bmatrix} -0.0025 & 0 & -(290+0.0412) & 9.81 \\ -16.0200 & 0.0841 & 0.0165 & 0 \\ 3.9698e004 & -0.0037 & -0.0081 & 0 \\ 0 & 1 & 0 & 0 \end{bmatrix} \begin{bmatrix} \Delta v \\ \Delta p \\ \Delta r \\ \Delta\phi \end{bmatrix} \tag{41}$$

Equation 41 is written in the format of $\dot{x} = Ax$ where the flight characteristics can be solved for by solving for the eigenvalues of matrix A ($|\lambda I - A| = 0$). Solving this leads to 4 roots, which can be used to solve for the different lateral flight characteristics.

Table 4.7 Lateral Flying Characteristics

Root	Mode	$T_{1/2}$	$N_{cycles(double)}$	Period	Flying Qualities
5.2115	Rolling	0.1330	-	-	Level 1
-0.0091	Spiral	76.1538	-	-	Level 1
-2.5645 ±4.5020i	Dutch Roll	0.2702	0.1931	1.3949	Level 1

The data in Table 4.7 demonstrates the lateral flying characteristics of the aircraft including the time to half or double, the number of cycles to half, the time period of the motion, and the mode of motion. Using this data the aircraft can be placed into one of three levels. The aircraft demonstrated all level 1 flying qualities proving that the aircraft geometries are acceptable for dynamic lateral stability.

4.5. Propulsion

4.5.1. Propulsion Integration

The aircraft's power-plant will be placed in the nose of the aircraft. This was decided due to the reduced parasitic drag found on this power-plant in contrast to power-plants found outside the fuselage. The second consideration was the cooling of the motor during flight. A convective method was chosen over conduction methods for the lack of necessary weight. Figure 4.15 illustrates the use of air convection cooling for the motor. The air flows from two inlets across the motor and out the two nozzle exits. The airflows efficiently due to the higher pressures found at the inlet and the lower pressures found at the nozzle exits. The pressure difference is caused by an increase in air velocity found at the nozzle exit in comparison to the stagnant air found at the inlets.

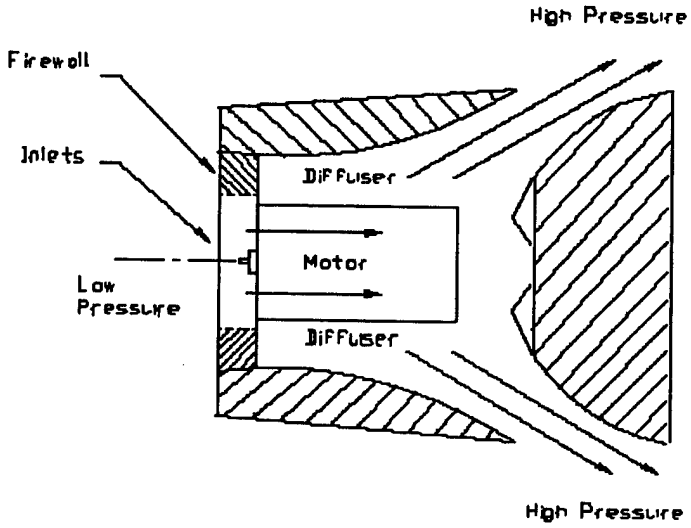

Figure 4.15: Convection cooling by air.

4.5.2. Power Required

To select the appropriate power-plant for the aircraft the required power was necessary. Figure 4.16 illustrates the required power for the aircraft at different free-stream velocities in steady level flight at an altitude of 500 ft. The curve was found using the drag polar for the aircraft. The parasitic drag for each component, except the fuselage, was found by the use of equation 42. Table 4.8 yields the values for each component.

$$CD_o = \frac{\Sigma\left(C_f FF_c Q_c S_{wet}\right)}{S_{ref}} + CD_{misc} + CD_{l\&p} \quad (42)$$

Where C_f is the drag coefficient, FF_c is the form factor, Q_c is the interference drag, S_{wet} is the wetted area and CD_{misc} and $CD_{l\&p}$ are miscellaneous and leakage drag for each component. The reference area for the evaluation was the planform of the wing at 1040 in.^{2}.

Table 4.8: Drag coefficients for each aircraft component

Aircraft Components	CD_o
Wing	0.0034
Tail	0.00142
Boom	0.000105
Fuselage (found from wind tunnel data)	0.00758

Table 4.8 demonstrates the largest parasite drag originates from the fuselage. Special interest was placed on aerodynamically optimizing the fuselage in areas such as the aft cone as stated in the performance section.

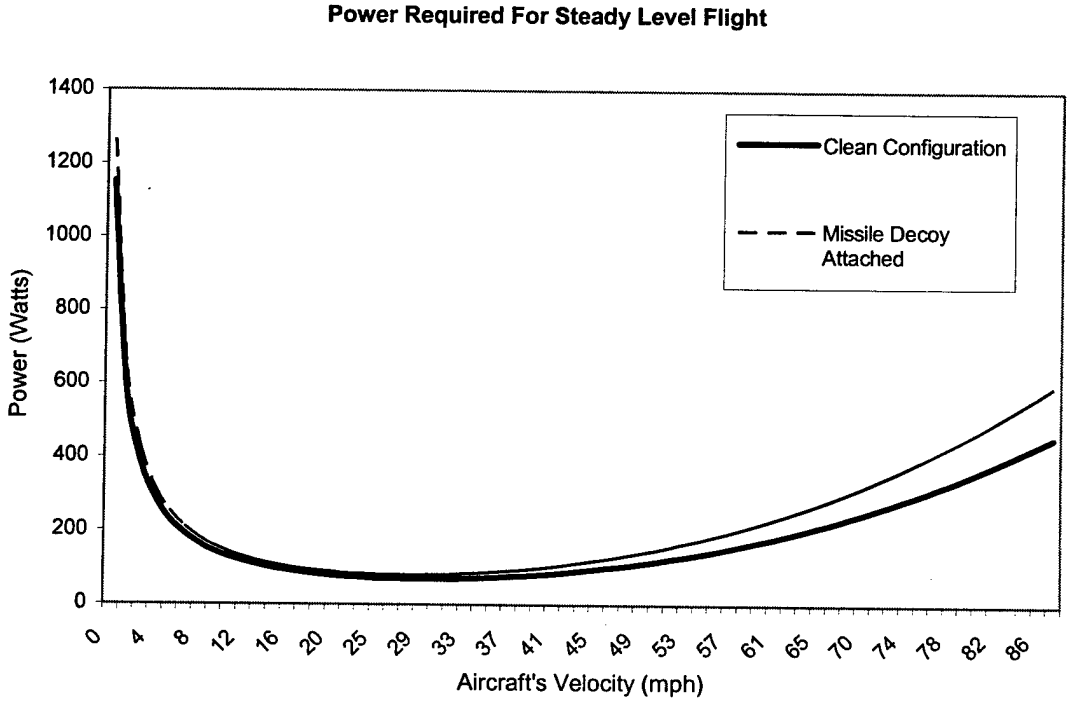

Figure 4.16: Power required at steady level flight.

Figure 4.16 demonstrates the aircraft will need a minimum of 70 watts at its take-off speed of 29 mph in the flap down configuration carrying the missile decoy. To have the aircraft accelerate at a static position and take-off with a required field length of 120 ft., the aircraft must contain a $(W/P)_{TO}$ of 10 with a wing

loading of 32 oz./ft^2. The $(W/P)_{TO}$ value can be seen from Figure 4.17, the figure was developed using the Advanced Aircraft Performance software. The W/P ratio correlates to a minimum required power level of 1146 watts. Figure 4.17 demonstrates W/P values for three separate flap deflections: 0°, 20° and 40°.

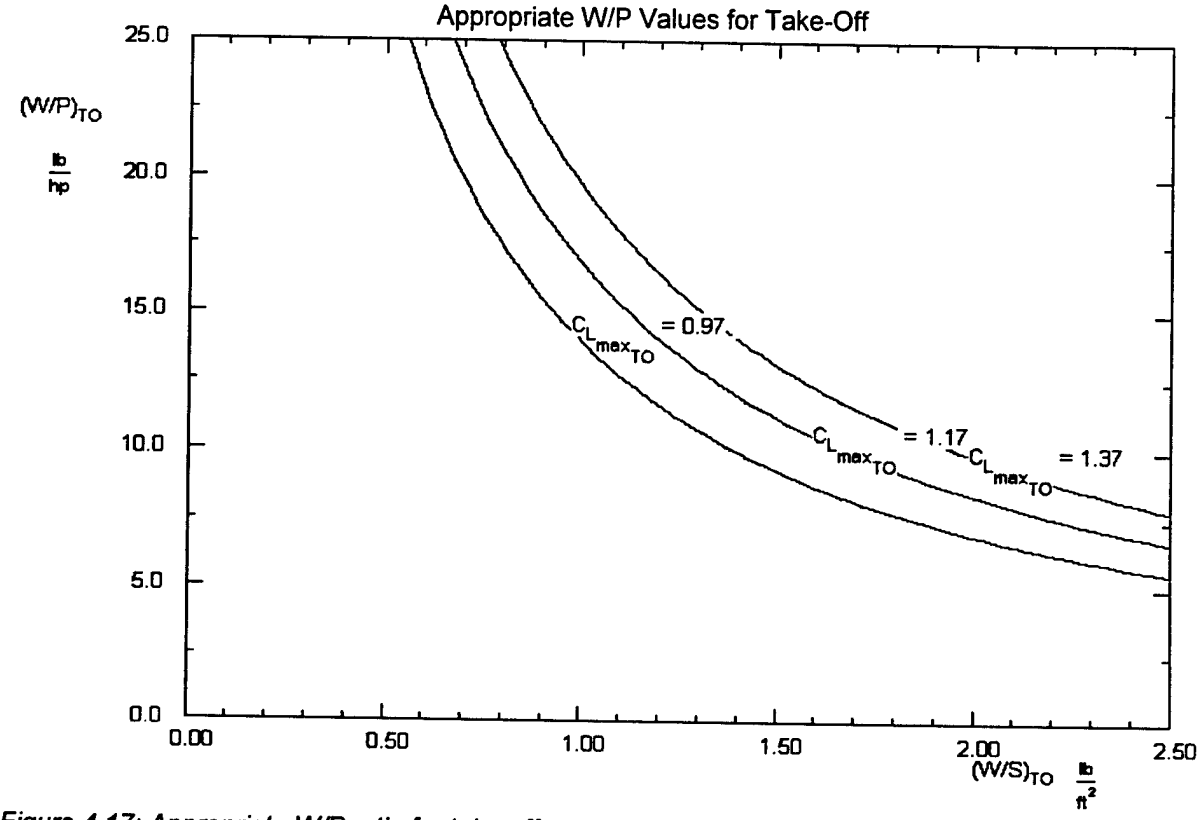

Figure 4.17: Appropriate W/P ratio for take-off.

4.5.3. Power-Plant Selection

The Astro Flight motor was the motor of choice due to past experiences with them. Astro Flight carries several sizes, all of which had to be cobalt and contain a fuse of 40 amps. From the selection only two motors developed enough power for the aircraft, the p/n 661 and the p/n 690. The p/n 661 develops 1100 watts and the p/n 690 develops 1400 watts. Both motors have a gear box option that reduces the rpm ratings but increases their total power by ~12 %. From a P/W aspect the gearbox is efficient. The P/W rating increases 6.83 % but the aircraft must carry 11.8 oz. of additional motor and batteries. The Astro Flight p/n 661 was selected to keep the aircraft at the target weight of 14.669 lbs. and to reduce any excess thrust that may be created with a p/n 661 (geared) and a p/n 690. Excess thrust demands more amperage and batteries and will reduce a given flight time.

4.5.4. Battery Selection

The suggested number of batteries for the p/n 661 is between 28 and 32 cells. Due to the power demand placed on the motor 28 cells will be used with a cell capacity of 2300 milliamps.

4.5.5. Propeller Selection

AstroFlight also suggests two different propellers for the motor. They suggest a 2-blade 12x8 and a 13x8 propeller. The two propellers suggested yield static rpm's of 9,000 and 11,000 respectively. Data for the available thrust on each propeller was not found. Several propellers having 2, 3 and 4 blades were ordered and will be placed on a force balance in the Clarkson University Wind tunnel. A thrust available curve will be generated with the data for each of the propellers. Also an amp-meter will be used to evaluate the required amps for each propeller/motor configuration. The configuration with the greatest thrust/amp will be used.

5.0 Detail Design

After completing preliminary design it was necessary to size and select both primary and secondary components. By comparing previously collected data, a motor size was selected, along with primary building materials. Methods of component construction were weighed and investigated along with component make up. Finally a mockup fuselage was constructed in order to gauge internal component meshing.

5.1. Configuration detail design

The final configuration resembled a somewhat cross breed. A high performance, low mounted elliptical wing planform with raked wingtip and slotted flaps seemed somewhat out of place when mated with the overly bulky mass of the fuselage. To keep weight to a minimum fuselage dimensions were cut close to those of the box leaving little room for streamlining, which in turn was found somewhat ineffective at the low Reynolds numbers the vehicle operates at. The unusual twin inverted tail added a Cessna Skymaster look to the aircraft and showed to perform well both aerodynamically and structurally.

5.2. Structural Component Selection

5.2.1. Fuselage

Due to struggles in the past with engineering the fuselage, a new approach was taken towards component selection. The 2001 fuselage consisted of fiberglass and basswood as its major construction components, which resulted in a total weight of 9 pounds. Preliminary calculations suggested an estimated fuselage weight of 2 pounds for this year's design. In order to achieve structural durability while staying under the weight limit, basswood was compared to existing building materials. It was found that 1/8" thick plywood, which weighed much less, would provide the necessary rigidity for the fuselage. However, to achieve this it was necessary to stack pieces of plywood to obtain necessary strength. It was completely unnecessary to use fiberglass as the skin component for the 2001 plane. In order to keep weight down, 1/16" balsa wood was selected to sheet this year's design. In 2000, two aluminum beams were used as a boom and wing spar for the aircraft, with a weight of over two pounds. With this in mind the boom for this year's plane was chosen to be a carbon fiber tube of 60 grams in weight. By using a conventional method to construct the fuselage, excess components, and therefore weight, were eliminated. Three formers [bulkheads] were connected by a balsa skin, which covers the entire fuselage, with a baseboard running the length of the fuselage to support the payload. A section of the fuselage floor was removed to reduce weight and allow easy access to the interior. The formers were made in a rectangular fashion, so as to better fit the payload, and ease the construction process.

5.2.2. Wing

To keep the wing light and simple, a regular balsa spar and rib method of construction augmented with a carbon fiber spar that doubled as a plug in spar wing joiner was selected. R/C aircraft in the 15lb category regularly employ 1/16' balsa ribs and were therefore chosen. The wing design was sheeted at the center section and till the quarter chord span-wise. 1/8" upper and lower spars were slotted into the wing at the quarter chord and webbing was designed to transfer the load off the balsa spars and onto the main carbon fiber spar.

To ensure a fit into the 4' long box, the maximum wingspan for a single piece wing was limited to 4 feet. For this reason, the wing was designed in 2 halves that employ a plug-in spar to join them. A dowel and bolt method was designed to attach the wing to the fuselage. This consists of two dowels that protrude from the central leading edge of wing and slot into two matching holes drilled in the 3rd former of the fuselage. At the rear of the wing, two bolts running vertically through the trailing edge into tapped blocks mounted inside the fuselage ensure a tight fit. This method is a tried and tested method employed regularly on most R/C aircraft.

5.2.3. Empennage

Horizontal tail span was limited severally by the 25% of wing area rule in the competition rules. This rule states "a horizontal surface is a "wing" if it is more than 25% of the span of the greatest span horizontal surface." With this consideration, the maximum horizontal tail span was a somewhat small 19inches (78" x 25%). A twin vertical tail was chosen for two primary reasons. Firstly, the simulated cylindrical antenna mounted above the fuselage, created a wake of turbulent air that would render a central vertical tail less effective and more susceptible to flutter. By mounting the vertical tails on the tips of the Horizontal tail, this problem was easily surpassed. Taking this design to the next step called for inverting the vertical tails. There was a huge advantage here in that with a tail dragger design, inverting the tails and mounting the tail wheel at their lower tips increased the height of the empennage by several inches when on the ground. Thus by taxing forward after package deployment, and passing its tail right over the package, the aircraft was provided with a simple and effective method of vacating the deployment area.

5.3. Secondary Component selection

5.3.1. Propulsion and Controls

As a result of a relatively large aircraft weight of 16 pounds, a larger motor was required for the 2001 plane. The Astroflight Cobalt 90, weighing 32 ounces, was eventually decided upon. With an estimated aircraft weight of 9 pounds for the current design, the Astroflight Cobalt 60, with overall weight 22 ounces, was selected for propulsion. This motor requires fewer cells, 32 as compared to 36. Additionally, the motor requires fewer amps, 2.5 as compared to 3.0; and can attain a higher top speed of 347(rpm/volt) as compared to 256(rpm/volt). Due to previous mounting difficulties, a Great Planes 60-120 motor mount was purchased for reliable configuration.

Radio selected for this year's aircraft was a top of the line JR PCM-10X. This provided the aircraft and the pilot with nearly infinite degrees of flexibility and precision and will be able to handle any sort of competition design it is used to control. As the model is not a precision, high performance pattern aircraft, standard ball bearing brushless JR 517 servos were once again selected for this year's plane because of previous outstanding performance, reliability, and cost effectiveness. A Hobbico CS-35 mini servo was selected for sensor package deployment.

5.3.2. Avionics package deployment system

With the low wing configuration already chosen placing the wing under the fuselage, the obvious remaining method for package deployment was a rear cargo door system as employed on full-scale cargo aircraft such as the C-130 etc. A spring-loaded system between the avionics package and the 3rd former was designed to propel the package out of the fuselage. A latching mechanism with a rotating arm holds the package in place until the deployment switch is actuated at which point a single micro servo sequentially actuates the rear cargo door and the package latching mechanism. To ensure that the package deploys straight out of the fuselage without scraping and damaging the fuselage on its exit path, a system of dual guide rails of 1/32 steel rod was devised. The package was provided with a friction free ramp by running on ½' wheels.

5.3.3. Simulated cylindrical antenna

A tripod-like mounting system was designed for the simulated cylindrical antenna. Tripod legs consisted of ¼' streamline aluminum tubing to reduce drag. The tripod mounts onto predrilled blocks mounted to the formers within the fuselages creating a clean gapless finish.

Table 5.1 Aircraft Specifications

Performance	
CL max(clean)	0.971
L/D max	15.35
Max Rate of Climb	2300 ft/min
Stall Speed	34.76 ft/s
Max Speed	130.53 ft/s
T/o length (empty)	60 ft
T/o length (gross)	100 ft

Weight Statement	
Airframe	5.475 lbs
Propulsion System	3.9375 lbs
Control System	.75 lbs
Payload System	0.2 lbs
Payload	5 lbs
Empty Weight	10.362 lbs
Gross Weight	15.362 lbs

Wing Geometry	
Length	3.7 ft
Span	6.375 ft
Height	1.073 ft
Wing Area	7.82 ft^2
Aspect Ratio	5.56
Aileron Area Per Side	0.21 ft^2
Flap Area Per Side	0.34 ft^2
Root Chord	1.4 ft
Tip Chord	0.947 ft

Systems	
Radio Used	JR PCM-10x
Servos Used	JR 517 & HOBBICO CS-35
Battery Config	Yet to be determined
Motor	AstroFlight Cobalt 60
Propeller	13x9
Gear Ratio	Direct Drive

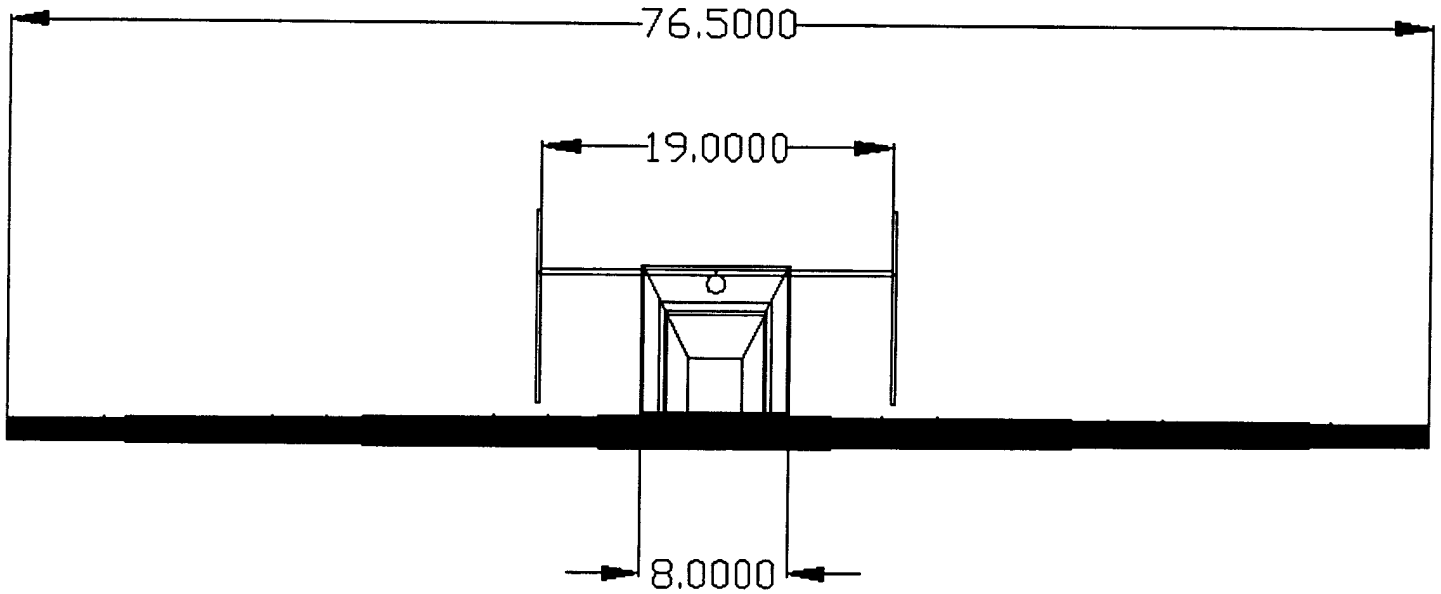

Figure 5.1 : Front View

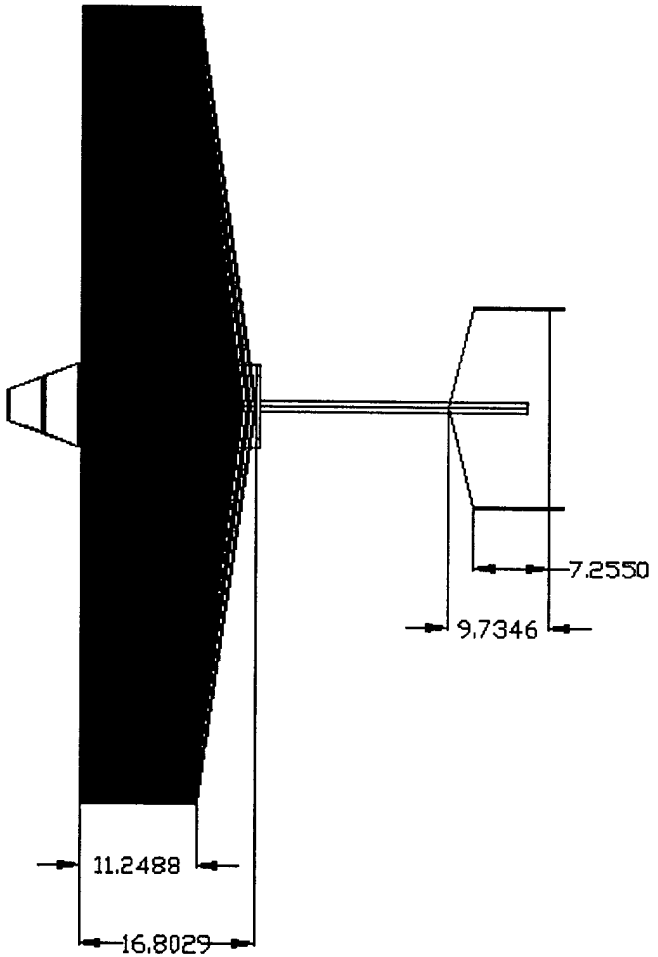

Figure 5.2 : Top View

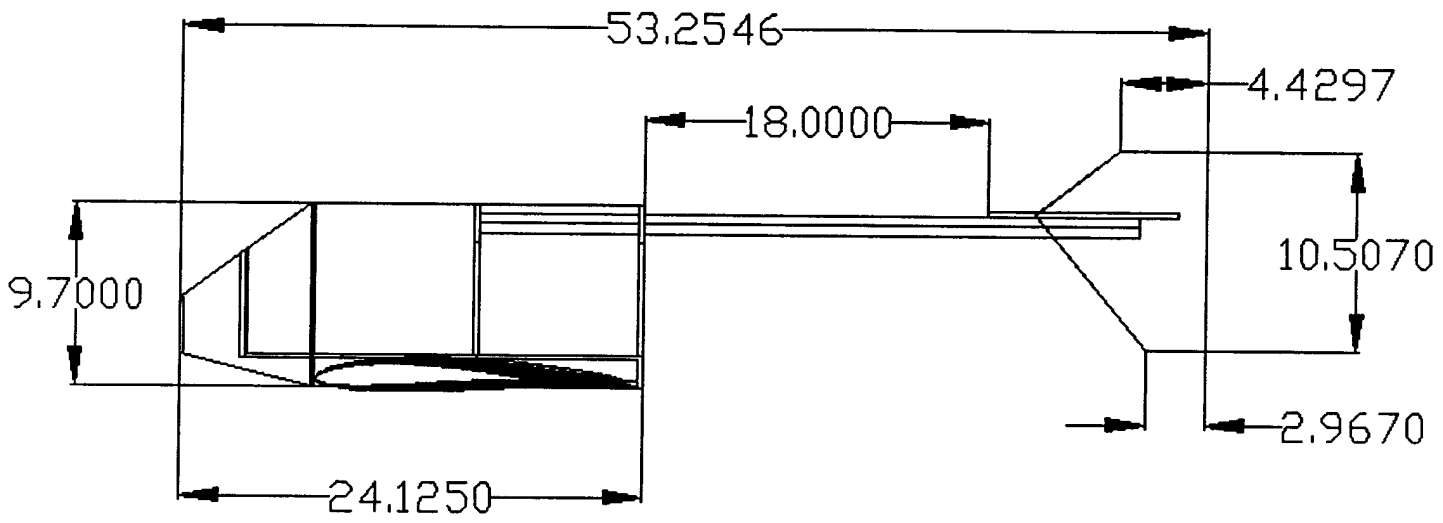

Figure 5.3 : Right-Side View

Table 5.2: RAC for final configuration

Final Configuration			
		Penalty	
Weight	12 lbs	$	1,200.00
Engine(s)		$	3,000.00
Wing	6 x 8hr/foot	$	960.00
Chord	1.5 x 8hr	$	240.00
Ailerons		$	60.00
Elevators		$	60.00
Flaps		$	60.00
Rudder		$	60.00
Fuselage	10hr/surface	$	400.00
Empennage	1	$	100.00
Horizontal	3	$	300.00
Flight systems	5 hr/ servo	$	100.00
Propulsion	5 hr/engine	$	100.00
		$	6,640.00

6.0 Manufacturing Process

All manufacturing took place in Clarkson University's Center for Advanced Materials Processing Student Projects Lab. All wooden parts were cut and sanded in the woodshop. Layout and final assembly was accomplished in an area designated for the Design Build and Fly Team.

6.1. Fuselage

The fuselage was constructed using standard model aircraft construction methodology. Sections, consisting of three bulkheads, an engine mount and a base were constructed in this fashion to maximize strength while minimizing the weight of the aircraft

6.1.1. Formers (Bulkheads)

Each Bulkhead is exclusive to its' position in the fuselage. The forward bulkhead and aft bulkhead were laminated with two sheets of 1/8' plywood, as they are the load-bearing members. The middle bulkhead is a single sheet of 1/8" plywood. Each bulkhead has the middle cut out leaving hollow fuselage to reduce weight and create space for cargo.

6.1.2. Engine Mount

The firewall (F1) is constructed of triple laminated plywood. Three sheets were used in order to support the weight of the engine. It was also reinforced to withstand the forces of the package ejection system.

6.1.3. Base

The base was cut of a single sheet of plywood and notched to receive the bulkheads and engine mount. This was done in order to make the entire fuselage one unit, as opposed to several pieces bonded together with adhesive. There is an opening in the center of the base to allow access to the inside of the aircraft for installation of batteries and maintenance/repair.

6.2. Wing

A wing jig was constructed to ensure accurate construction. It consisted of predetermined slots for rib, trailing and leading edge placement. The wings consisted of thirteen ribs on a side. In accordance with a tapered elliptical wing, each rib tapers off as it diverges from the fuselage at λ=. 59. The wings are tapered to obtain a more elliptical lift distribution.

6.2.1. Airfoil

An eppler-197 airfoil was chosen for it's low Reynolds number; it has a slight camber.

6.2.2. Ribs

The cutout by hand from balsa sheets and then stacked and drilled for spars and then sanded down to a near perfect finish. The first three ribs on either side of the fuselage are constructed from one sheet of 1/8" ply wood and reinforced on either side with a sheet of 1/8" balsa in order to provide the necessary strength. The fourth and fifth ribs were also constructed from 1/8" ply wood sheets to reinforce the landing gear blocks. The remaining ribs were constructed from 1/8" balsa sheets and were not reinforced.

6.2.3. Assembly

Lower wing sheeting was laid down on the planned jig and the lower spar, leading and trailing edges over that. The ribs were then slotted onto the lower spar and the main carbon fiber spar was run through them and glued into place. Top spar and sheeting was then added and the leading edge was sanded down to shape. Flap and Aileron construction went on simultaneously with the wing, using the trailing ends of the ribs cut out for the wings. A hardwood block was mounted in the wing between ribs 3 and 5 to provide a solid base for the landing gear to mount to.

To achieve the highest level of pre covering finish, approximately 10 hours of sanding were put into the wing.

6.3. Tail

The tail is constructed of two vertical surfaces at each tip of a horizontal surface. The tail is connected to the fuselage by a single carbon-fiber boom with extremely high strength to weight characteristics. To keep assembly times down, the tail control servos were mounted directly to the horizontal surface, just behind the tail boom and wiring for the servos was run through the boom. Tail construction was kept simple with a sheeted framework construction.

6.3.1. Vertical Surfaces

Each of the vertical surfaces is constructed of ¼" balsa framework sheeted with 1/8" balsa sheets. The rudders were constructed from tapered 1/2" balsa sheets. The rudders are fixed to hinges to facilitate movement and a long pushrod links the rudders to one another as well as to their control servo. Each rudder incorporates a tail gear at its lower tip for steering while on the ground.

6.3.2. Horizontal Surface

The horizontal surface was constructed using ¼" balsa sheets used to construct the framework. It was then covered with 1/8" balsa sheeting. Both Control servos for the tail assembly were placed in the horizontal surface.

6.4. Analytical Methods: Cost, skill matrix and scheduling time lines

6.4.1. Manufacturing Costs

Based on the design of our aircraft manufacturing and tooling costs were estimated. The design called for a substantial portion of the aircraft to be composed of balsa wood. A new radio was also required and used a large portion of the budget. This left for a less substantial portion of the budget to be used for carbon fiber tubes, servos, wiring, and the drive motor.

6.4.2. Skill Matrix

For the aircraft to be built the team needed to be divided and assigned to certain aspects of the aircraft. To accomplish this a skill matrix was derived to produce the best aircraft possible. Table 6.1 contains the skill matrix for the how the team was divided. A scale of one to five was used; one being requiring no skill up to five requiring the most skill. The columns represent manufacturing process; the rows show the major components of the aircraft. Members of the team were then assigned to processes according to their experience.

Table 6.1 Skill Matrix

Primary Aircraft Assemblies and Systems	Wood Cutting	Layout Preparation	Gluing and Jointing	Electrical Work	Radio Equipment Installation	CAD Modeling
Fuselage	4	5	3	4	5	3
Landing Gear	NA	3	2	2	2	2
Tail	4	4	4	3	3	4
Wing	4	5	4	3	3	5
Propulsion	3	3	5	5	3	2

6.4.3. Manufacturing Scheduling

The aircraft was constructed in five different sections; fuselage, landing gear, tail, wing and propulsion. With team members divided all sections were worked on simultaneously.

7.0 Testing Plan

The initial design phase involved intensive testing to optimize the airflow over the entire aircraft. Results obtained from testing were the primary figures used to finalize the design. Testing was conducted in the following areas:

7.1. Static

7.1.1. Wind Tunnel Testing

The initial design phase called for several wind tunnel tests of the fuselage to determine most favorable dimensions. Testing was conducted to establish the lowest drag nose and aft cone profiles. The Clarkson University subsonic wind tunnel was used and data was collected using a 2-point beam balance supplying drags and lift forces.

Extensive testing was performed after which it was determined that at the low Reynolds numbers (650 – 700) at which the aircraft would fly, the shape of the aft cone did not make a significant difference and in fact not having an aft cone at all produced less drag over even the longest aft cone that was tested. Three tail cones of different lengths were tested at constant condition. Results of the aft cone tests can be seen in Table 7.1.

Table 7.1

Experimental Section	Velocity (mph)	Drag (Newtons)	Cd
No aft cone	43.8	6.31	0.038
Small aft cone	43.8	6.31	0.04
Large aft cone	43.8	6.16	0.039

Results showed that parasite drag for the aft cones caused their overall drag to supersede that of the fuselage without and aft cone.

7.1.2. Wing Spar Load Testing

Never having used a circular carbon fiber wing spar, a 3-point bending test was provided to determine the maximum load. The spar was loaded with 400 lbs of weight on each end simulating a 30g test, before it was destroyed. Such high loads however were deemed unattainable for an aircraft of this nature and the spar was found more then sufficient for the required 10g wingtip test.

7.1.3. Landing Gear Load test

Previous experiences with insufficient landing gear led to testing the current setup. Each landing gear leg was loaded statically to twice the aircraft weight. The landing gear oleos retracted half of their entire distance. Dynamic tests were incurred by dropping the landing gear with a weight of 14lbs from a height

of 6 inches simulating a rough landing. The oleo struts still did not bottom out were in fact adequate for a pilot with even basic landing abilities.

7.1.4. Payload deployments system

The payload (simulated avionics package) deployment system was tested intensively to find the ideal method. A number of various deployment linkages were swapped into the mockup fuselage and it was found that a system which provided rails to ensure the box tracked straight out of the fuselage on the under-box roller wheels similar to those found on a regular cargo aircraft.

7.2. Dynamic

At the time of report compilation, outside air temperatures varied between –5F and –30F complemented by 2 – 9 inches of snow. These conditions are standard for this time period and always render dynamic testing impossible till end of March.

University of Central Florida

College of Engineering & Computer Science

AIAA Electric Airplane

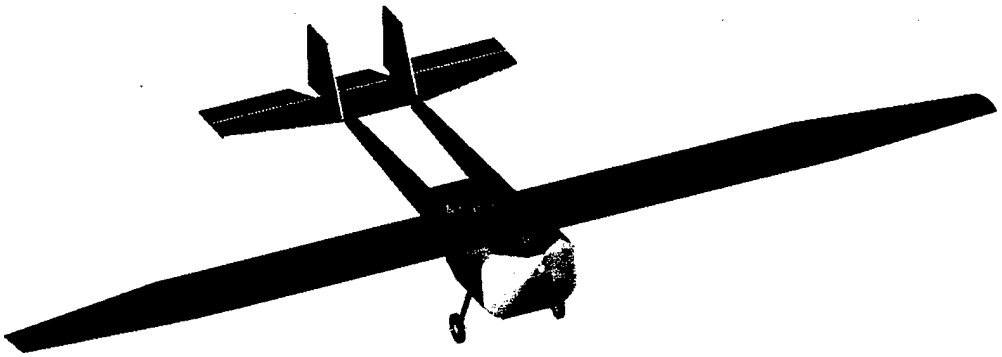

K-03 Pegasus

Team Members

Gary Ballmann
Paula Bejarano
Aaron Brueckman
Michael Denton
Ryan Holmes
Jonathan Langley
Bruno Michilli
Kristina Morace
Nick Novack
Bernardo Sam
Shawn Schembri
Schuyler Smith
Matthew Stephens
Ia Whiteley

Mentor

Dr. Eric Petersen
petersen@mail.ucf.edu

March 11, 2003

Table Of Contents

1.0 EXECUTIVE SUMMARY 1
1.1 Conceptual Design Summary 1
1.1.1 Conceptual Design Alternatives 1
1.1.2 Conceptual Design Tools 1
1.1.3 Conceptual Results 1
1.2 Preliminary Design Summary 2
1.2.1 Preliminary Design Alternatives 2
1.2.2 Preliminary Design Tools 2
1.2.3 Preliminary Results 2
1.3 Detail Design Summary 2
1.3.1 Detail Design Tools 2
1.3.2 Detail Design Result 2
2.0 MANAGEMENT SUMMARY 3
2.1 Management Architecture Analysis 3
2.2 Division Responsibilities 4
2.2.1 Power Plant 4
2.2.2 Aerodynamics 4
2.2.3 Payload 4
2.2.4 Fuselage 4
2.3 Scheduling and Information Management 5
3.0 CONCEPTUAL DESIGN 7
3.1 Rated Aircraft Cost (RAC) Analysis 7
3.2 Aircraft Transportation System (ATS) 7
3.3 Alternative Landing Gear and Payload Drop Configuration 7
3.3.1 CAGE (Cargo Alignment and Grappling Endoskeleton) Configuration 8
3.3.2 Landing Gear Configuration 10
3.3.3 CAGE (Cargo Alignment and Grappling Endoskeleton) Configuration Figures of Merit 10
3.4 Alternative Fuselage Configuration 12
3.4.1 Fuselage Material Figures of Merit 12
3.4.2 Fuselage Design Shape Figures of Merit 14
3.5 Alternative Wing Configuration 17
3.5.1 Wing Structure Figures of Merit 18

3.6 Alternative Empennage Configuration 20
3.6.1 Alternative Empennage Structure 20
3.7 Alternative Power Plant Configuration 21
3.8 Further Analysis Tools 21
3.8.1 Past Team Experience 21
3.8.2 Testing Methods 22
3.9 Final Aircraft Configuration 22
4.0 PRELIMINARY DESIGN 23
4.1 Trade Study of Previous Results 23
4.1.1 Study of Previous Motor Performance 23
4.1.2 Study of Previous Battery Power Requirements 23
4.1.3 Study of Previous Wing Designs 24
4.1.4 Study of Previous Fuselage Designs 24
4.2 Initial Trade Study Results 24
4.2.1 Study of Type of Batteries Required for the Cobalt 661s Motor 24
4.2.2 Study of Wing Planform Area Requirements 25
4.2.3 Study of Wingspan Requirements 25
4.2.4 Study of Fuselage CAGE and Landing Gear Requirements 26
4.3 Aerodynamic Analysis 26
4.3.1 Wing Analysis 30
4.3.2 Empennage Analysis 30
4.4 Structural Analysis 30
4.4.1 Wing Structure 30
4.4.2 Empennage Structure 31
4.4.3 Fuselage and Landing Gear Structure 32
4.5 Final Aircraft Configurations 32
5.0 DETAIL DESIGN 33
5.1 Rated Aircraft Cost 33
5.2 Aerodynamic Analysis 34
5.2.1 Wing Design Details 34
5.2.2 Flight Performance 35
5.2.3 Empennage Design Details 37
5.3 Motor and Propeller Analysis 38
5.4 Fuselage Analysis 39
5.4.1 Rib Design 39
5.4.2 Tail cone design 40
5.4.3 CAGE design 41

5.4.4 Landing gear final design 41
5.5 Sized Aircraft Data and Drawing Package 42
6.0 MANUFACTURING PLAN 46
6.1 Component Manufacturing Process 46
6.1.1 Fuselage, CAGE, and Landing Gear 46
6.1.2 Wing 46
6.1.3 Empennage 46
6.2 Analytic Methods Including Cost, Scheduling and Skills 47
6.2.1 Tabulated Manufacturing Cost 47
6.2.2 Required Skill Level 48
6.2.3 Manufacturing Milestone Chart 49
7.0 TESTING 50
7.1 Static Wing Test 50
7.2 Dynamic Fuselage design testing 50
7.3 3-Dimensional Testing 55
7.4 Scaled Model Testing 55
8.0 REFERENCES 56

1.0 EXECUTIVE SUMMARY

This report outlines the approach taken by the University of Central Florida K-03 Pegasus Team. The goal of the Design Build Fly competition is to construct an unmanned electric powered aircraft, complete mission profiles, and obtain the best overall flight score. This year's mission profiles include a missile decoy, a sensor deployment, and a communications repeater. The difficulty factors of each mission are 2.0, 1.5, and 1.0, respectively. The K-03 Pegasus team chose mission difficulties 1.5 and 1.0. The first mission, sensor deployment, requires the aircraft to fly two laps, land, self-deploy a simulated sensor package, and take off again completing 2 additional laps. The second mission requires the aircraft to take-off, complete four laps, and land carrying a simulated communications relay device. The simulated payloads for both missions are five pound 6x6x12 inch boxes. Finally, in honor of the Wright Brothers' first flight K-03 Pegasus will take-off in 120 feet.

1.1 Conceptual Design Summary

The conceptual summary outlines the first part of the design process. It highlights special considerations and final decisions that transferred to the preliminary design phase.

1.1.1 Conceptual Design Alternatives

The conceptual design phase highlights each aircraft component and selects several design alternatives for comparison. It also introduces the Rated Aircraft Cost (RAC) as an important scoring factor in the competition. The aerodynamics team analyzed combinations of four wing types, four wing geometries, and 3 wing structures. It also looked at empennage boom configurations and the benefits of a high or low tail. The fuselage team analyzed four different body shapes and four different body materials, while the payload team analyzed different methods of payload deployment. Finally, the power plant team examined three different AstroFlight motors, and all teams met together to decide on the final conceptual design.

1.1.2 Conceptual Design Tools

Decision matrices were the prime conceptual design tools. Figures of merit were chosen for each component and weighted according to importance. These matrices helped organize ideas and come to a reasonable final result.

1.1.3 Conceptual Results

At the end of the conceptual design phase, K-03 Pegasus contained a Cargo Alignment Grappling Endoskeleton or CAGE for payload deployment, a two piece rectangular tapered wing made from foam and light ply, a double boom empennage, and an AstroFlight Cobalt 60 motor.

1.2 Preliminary Design Summary

The preliminary design phase takes the conceptual design alternatives and further investigates their strengths and weaknesses.

1.2.1 Preliminary Design Alternatives

The preliminary design started with trade studies of previous UCF design/build/fly aircrafts. Since rules change from year to year, aircrafts differ in size, configuration, and RAC. It helped to learn from past mistakes and incorporate prior triumphs into the K-03 Pegasus design.

1.2.2 Preliminary Design Tools

For the preliminary design, the team wanted to get an idea of how the aircraft would look. AutoCad 2002, Pro-Engineer 2000, and MathCad 2000i were employed to construct possible airfoils, calculate dynamic and static analysis of the landing gear, produced graphs of lift, drag, and angle of attack and display a three-dimensional drawing of the empennage ribs.

1.2.3 Preliminary Results

After the completion of the preliminary stage, the wingspan was determined to be 8.5 feet with an Eppler 214 airfoil and a mid-sized 8.8 aspect ratio. The chosen batteries for the AstroFlight Cobalt 60 were Sanyo RC 2400 cells in a 32 cell series.

1.3 Detail Design Summary

The detail design aims to provide the final configuration for all aircraft components. A drawing package at the end of the detail section displays the final configuration.

1.3.1 Detail Design Tools

The tools used for the detail design were the same used in the preliminary design. MathCad 2002 was used for detailed flight performance calculations, AutoCad 2000i produced the drawing package, and Pro-Engineer charted a three dimensional picture of the aircraft.

1.3.2 Detail Design Result

Based on the decisions from the preliminary design stage, the RAC was calculated to be 12.79. Flight performance was examined, and all aircraft components were finalized.

2.0 MANAGEMENT SUMMARY

2.1 Management Architecture Analysis

In order to increase group efficiency, Team K-03 Pegasus was divided into four specialty divisions under a managerial chain of command (Figure 2.1). The divisions consisted of: Power Plant, Aerodynamics, Payload, and Fuselage. Each division included a head engineer and multiple specialty engineers. The head engineers were to, within their division, oversee all progress, make final design decisions, and report statuses periodically to the Co-Captains. The Co-Captains managed the team through their head engineers to ensure clear communications and steady progress. The team pilot was outside of these groupings having only one job, to fly the aircraft for testing and competition. The Pilot was positioned directly under the Co-Captains but, however, did not have the same responsibilities/authorities as the head engineers. Even though this structure was put in place, each member was involved at some point in each of the areas. This was partly to ensure that all members would be familiar with each part of the design for future projects.

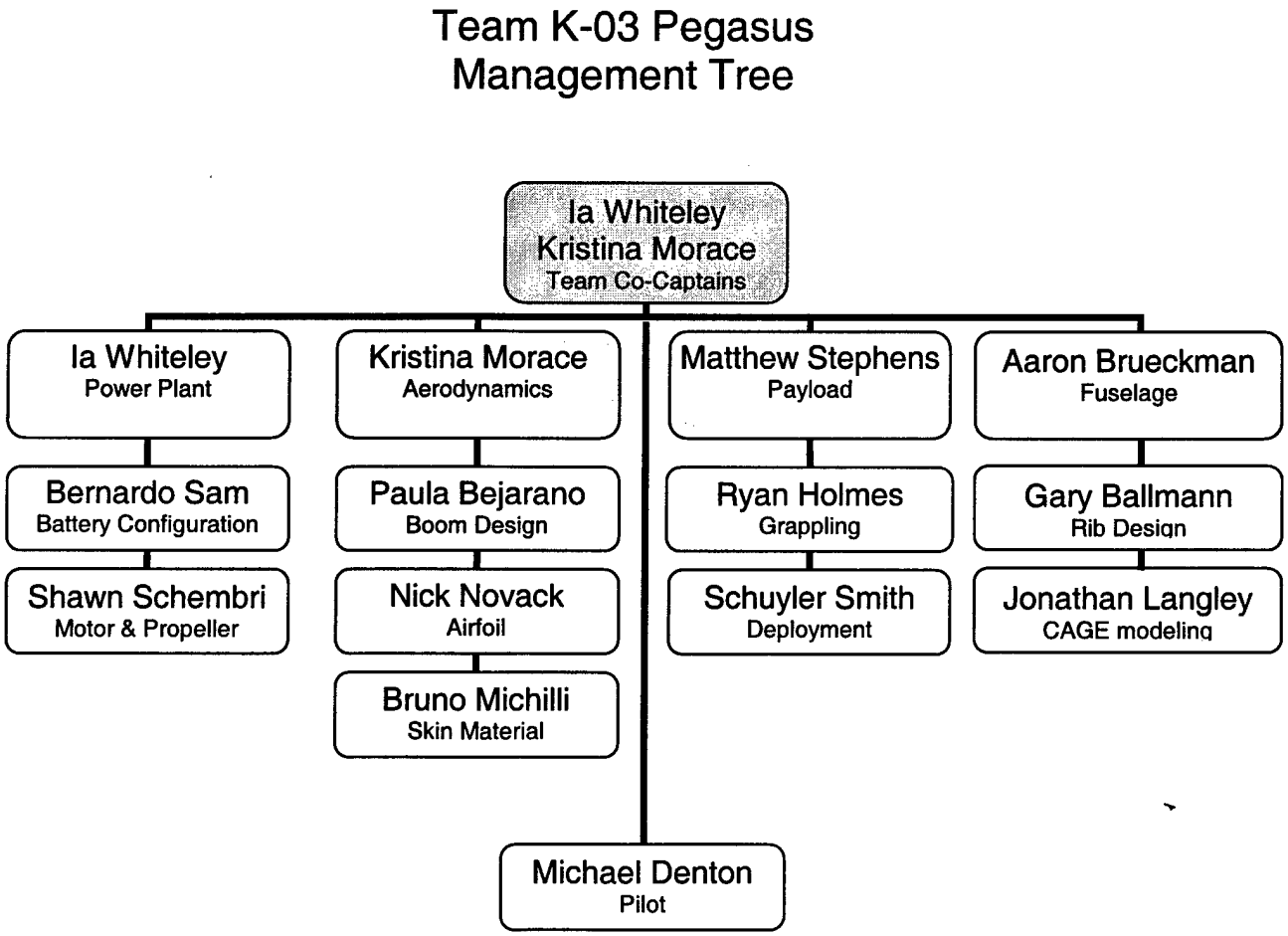

Figure 2.1 Management Tree for K-03 Pegasus

2.2 Division Responsibilities

Each division was given certain aspects of the airplane to study, design, and construct. While most of the work was conducted individually, some interdivision cooperation was needed to settle disputes over large design aspects of the airplane. Each division included specialty engineers who would further narrow their concentration down to specific details of the division's main part. Each individual division is also responsible for the repair of their individual components during test flights and competition.

2.2.1 Power Plant

This group focused on all of the project's electronics. This included choosing which model motor to use for the aircraft and which, if any, gearbox with which to supplement it. Once a motor was selected the division's next job was to determine the most efficient battery configuration considering power output, weight, and cost. Then the division had to procure all necessary radio control materials which included receiver, fail-safe, throttle control, transceiver, RC battery, and servos. The division was also responsible for testing the flight-readiness of all of these systems.

2.2.2 Aerodynamics

The main responsibility of this group was studying and designing all aspects of the airplane that was affected by any aerodynamic forces. This included choosing the airfoil type, wing and control surface dimensions, and any method of tapering. Also, this division was responsible for the empennage design. They were to study and test different possibilities and choose the best design based on stability, drag, and fuselage integration. They also had to cooperate with Fuselage in analyzing the aerodynamics of the airplane's main body and its overall effects. Once Power Plant selected a motor, Aerodynamics was in charge of deciding which of the suggested manufacturer's propellers to use. Aerodynamics was also in charge of selecting skin materials for the airplane.

2.2.3 Payload

The rules of this competition entailed specific tasks for the airplane to carry out; ensuring that the airplane could fulfill these tasks was the responsibility of the Payload division. Conceptualizing numerous deployment methods and concluding which to use was their biggest task. They also were in charge of building and testing a deployment model. In addition, Payload was responsible for ensuring that all other divisions incorporated sufficient clearance for the airplane to move after the payload was deployed. Payload, with advice from Aerodynamics, was to investigate the possibilities for connecting the instrument pod riding above the airplane.

2.2.4 Fuselage

This division was influential in combining the plans of all the other divisions. This included designing the Cargo Alignment and Grappling Endoskeleton (CAGE). The CAGE was then altered by Fuselage to

connect all the other systems to one centralized infrastructure. This division was in charge of selecting materials for both CAGE construction and other structures within the fuselage. As well, all support structures such as ribs were designed and placed by Fuselage.

2.3 Scheduling and Information Management

To ensure project progress a timeline was made for individual tasks and was broken up into three phases: design, construction, testing, and report. Each task had a planned timeframe and was given a deadline for completion. These deadlines and the AIAA Design/Build/Fly competition were added to the end of Figure 2.3 as milestones.

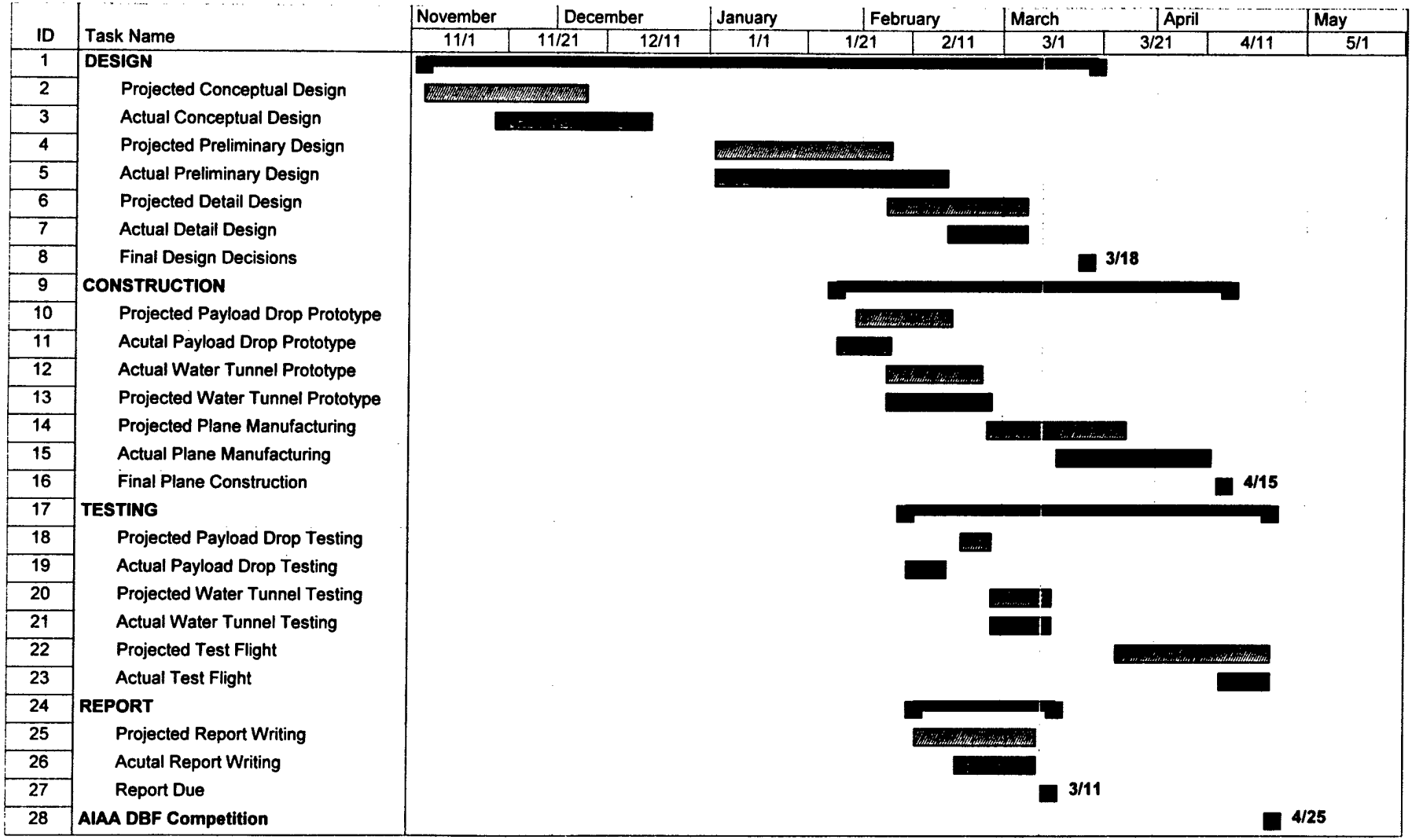

Figure 2.3 UCF Project Timeline. Green bars represent proposed timeframes. Red bars represent actual timeframes. Black Diamonds represent milestone marker

3.0 CONCEPTUAL DESIGN

The conceptual design phase began by collecting and organizing ideas important to the competition. Many solutions exist but not all could be synthesized into a functional aircraft. By introducing weighting factors and comparing available choices, the best compromise was found to meet mission requirements and increase scoring potential. Provided in this section are details from the conceptual design pertaining to the competition rules, the payload, the landing gear, the fuselage, the wing, the empennage, and the power plant.

3.1 Rated Aircraft Cost (RAC) Analysis

In each step of the conceptual process, the team analyzed design alternatives against the Rated Aircraft Cost (RAC). The RAC's purpose is to provide a numerical value for the physical size and complexity of the designed aircraft. It is advantageous to keep the RAC low for a higher total score. To evaluate the RAC, the team calculated parameters such as Manufacturer's Empty Weight (MEW), Rated Engine Power (REP) and Manufacturing Cost (MC) by changing different factors and exploring the RAC's limiting factors. The biggest limiting factor is battery weight. The battery weight gets counted twice in the RAC – once in the REP and again in the MEW. The multiplier for the REP is very high and the battery weight is multiplied directly to that multiplier. The MEW directly multiplies the battery weight as well but with a multiplier 15 times smaller than the REP. In short, the battery weight impacts the RAC more than all the other factors combined. Detailed RAC calculations can be found in section 5.1. Other important factors were wingspan, total body length, and total body weight. Although their effects were small compared to the battery weight, they made the most impact compared to the other aircraft parameters.

3.2 Aircraft Transportation System (ATS)

Many conceptual design configurations refer back to the Aircraft Transportation System (ATS). According to competition rules, the ATS must have interior dimensions of 2 foot wide by 1 foot high by 4 foot long. All aircraft components must fit within those dimensions and be carried to the flight line for assembly. Satisfying constraints for the ATS becomes a major design concern and appears as a factor in several figures of merit.

3.3 Alternative Landing Gear and Payload Drop Configuration

In past years, teams from the University of Central Florida found a recurring problem in their designs. This problem was landing gear stability upon impact. This year the mission of dropping the aircraft's payload was given as an option. From both of these, an idea came forth of using a structural center for the plane to support all of the forces encountered. This structural system would be stronger than the fuselage itself and all systems would attach to it as their back support. The payload drop system, empennage, motor, wing, and landing gear will all transfer their loads to this base system. This system,

over time, came to be known as the Cargo Alignment and Grappling Endoskeleton, also known as the CAGE. The CAGE underwent a long process for analysis, which started at the Conceptual level.

3.3.1 CAGE (Cargo Alignment and Grappling Endoskeleton) Configuration

A second problem arose during early stages of Conceptual design. This problem was due to the size of the box the aircraft must fit in. This size constraint requires the CAGE with landing gear to be a height of 12 inches. For the payload to drop with clearance there must be a total of 6 inches for the payload storage and an extra inch for a deployment device making a total of 7 inches. Another 7 inches is needed for clearance once the payload is dropped so that the aircraft can pass over it and proceed to begin the next sortie. This hindrance requires the payload to be in the angular configuration as seen in Figure 3.3.1.

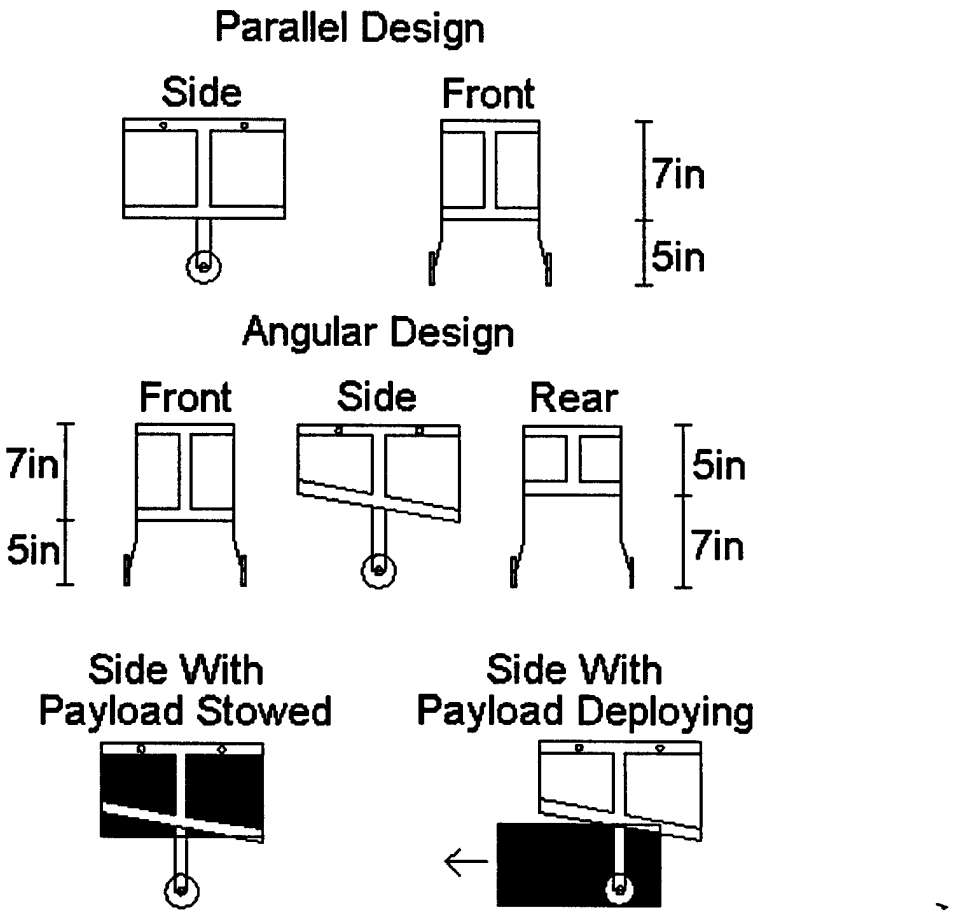

Figure 3.3.1 Parallel Design versus the Angular CAGE Design.

After a basic cage design was chosen, potential CAGE materials were compared. The variables for manufacturing comparison are as follows:

- Strength – The strength for the material is a measure of how long it will take the material to break, how susceptible the material is to breakage, and the chance for buildup of cracks and micro fractures over time.
- Weight – The weight of the CAGE factors into the total weight of the aircraft and is dependent upon the manufacturing material.
- Reparability – The reparability is how easy the material can be fixed. Chances are that if the CAGE undergoes enough stress to cause a break, the CAGE will not last through further flights.
- Cost – The Cost includes the materials, manufacturing processes and any outside services.
- Manufacturability – The manufacturability includes the amount of effort required from the team to manufacture the CAGE from the given substance.
- Material Equivalence – The Material Equivalence is a factor added in to make up the difference between materials so that they can be compared equally. This means that one material weighing less than another may require more material to have equal strength, and in the end, weigh more.

Five types of Materials were analyzed for construction of the CAGE. These materials, described below, were: Balsa, Plywood with Carbon fiber support, Sheet Aluminum, Composites, and Balsa Plywood. Table 3.3.1 shows the values given to each type according to certain characteristics and their totals that represent their levels of desirability for use. These values are described as good (1), indifferent (0), and bad (-1) and are used throughout the Conceptual Design. Table 3.3.1 shows Aluminum to be the best.

- Balsa – A Balsa construction would consist of many layers of Balsa strips glued with CA adherent.
- Plywood with Carbon fiber support – The Plywood and Carbon construction is made of Plywood reinforced with strips of carbon fiber sheeting.
- Sheet Aluminum – This consists of large sheets of Aluminum cut, bent, and welded to shape.
- Composites – The composites in this comparison are very similar to those mentioned in the fuselage section (3.4.1) consisting of a foam core with fiberglass or carbon fiber cloth cured over it with Epoxy.
- Balsa Plywood – The type of Plywood being compared in this matrix consists of layers of balsa adhered together with CA. The Balsa Ply is much denser than plain Balsa and much stronger.

Table 3.3.1 Cage Material Decision Matrix

Materials	Weighting factor	Aluminum	Balsa	Plywood / carbon	Composite	Plywood
Strength	0.5	1	-1	0	1	-1
Weight	0.2	0	1	1	-1	1
Reparability	0.05	-1	1	0	-1	-1

Cost	0.05	-1	1	0	-1	1
Manufacturability	0.1	1	1	0	-1	1
Material equivalence	0.1	1	-1	0	-1	-1
Totals	1	0.55	-0.35	0.2	0.15	-0.45

3.3.2 Landing Gear Configuration

Five types of landing gear configurations were compared in a matrix for the K-03 Pegasus. These five were Tricycle, Quad, Bicycle, Tail wheel, and Wing tip. The Tricycle consists of one wheel at the nose of the plane, and two on the body of the plane. The Quad requires two sets of two wheels along the fuselage. The bicycle consists of two wheels along the center of the fuselage and one on each wing tip for stabilization. The tail wheel is a reverse design from the Tricycle because the third wheel is at the end of the tail and not at the nose of the aircraft. The wing tip design requires the greatest quantity of wheels - one at the nose, two at the internal body, and one on each wing tip.

These designs were compared through five different criteria. The Landing performance, Braking ability, Drag in flight, and Cost of design were all common variables used in this analysis, however a fifth variable was added. This variable, feasibility in the CAGE design, represents the ability of the design to be implemented with the design of the CAGE and allow for the payload to be dropped. The Matrix analysis is seen in Table 3.3.2. Base on the results of Table 3.3.2, the tricycle configuration was selected.

Table 3.3.2 Landing Gear Concept Decision Matrix

Figures of Merit	Weighing factor	Tricycle	Quad	Bicycle	Tail wheel	Wing tip
Landing	0.2	0	1	0	-1	0
Feasibility in cage design	0.3	1	-1	-1	-1	1
Braking	0.2	0	1	1	-1	0
Drag	0.2	0	-1	1	0	1
Cost	0.1	1	0	0	0	-1
Totals	1	0.6	-0.1	0.1	-0.7	0.4

3.3.3 CAGE (Cargo Alignment and Grappling Endoskeleton) Configuration Figures of Merit

Assuming simple designs for the fuselage, the decision matrix compares only the landing gear and does not analyze the fuselage structure. The design for the CAGE body was assumed to be a simple angular shape as mentioned previously in section 3.3.1. The specific designs are seen and described in Figure 3.3.3.

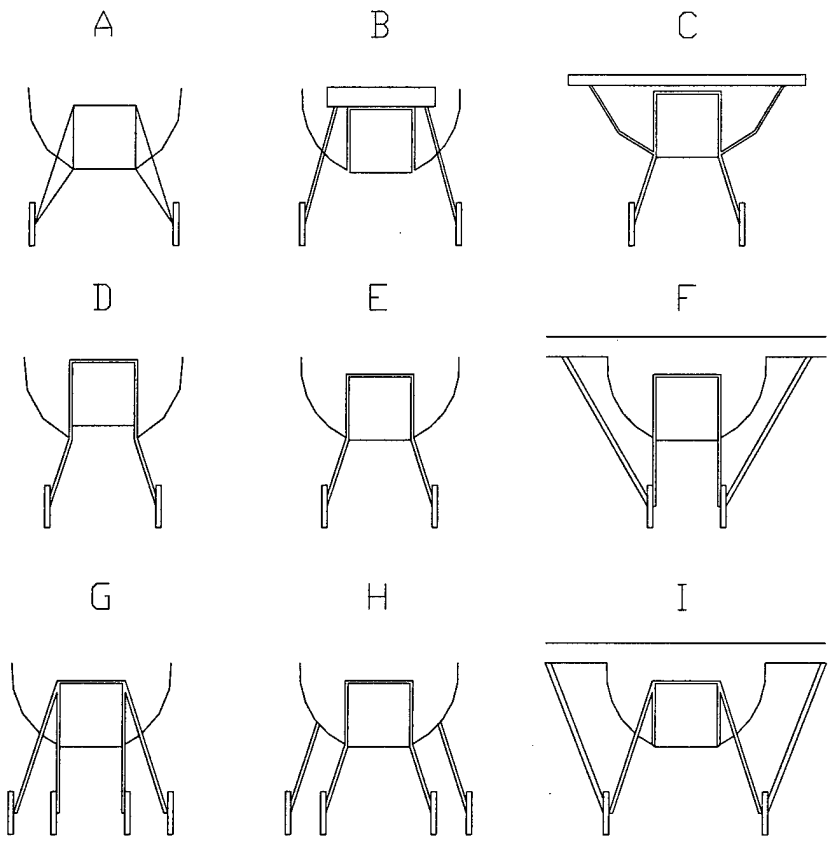

Figure 3.3.3 CAGE and landing gear Conceptual Design Options A-I (see text for details)

- Design A – This design consists of landing gear bars protruding from the cage at both the top and bottom of the CAGE. The top bar comes out of the fuselage and meets the bottom bar at the wheel.
- Design B – Design B incorporates a structural bar that goes out of the top of the CAGE and the landing gear protrude down form that bar.
- Design C – Design C involves a structural bar at the top of the CAGE connected into the wings, internal struts to the wing, and the typical landing gear design from the bottom.
- Design D – In this design the landing gear and fuselage hang below the payload about an inch.
- Design E – In design E, the basic design, the fuselage lines up with the bottom of the cage
- Design F – Simply put, this is the design for E but with external struts that extend upward to support the wing.
- Design G – Design G is the basic CAGE design with a second set of landing gear coming from the top of the CAGE on each side.
- Design H – This design differs from design G in that the main wheels angle out away from the CAGE and the second set are parallel.

- Design I – In design I, the landing gear angle outward from the CAGE, and struts run from the wheels to the wings in a W-shaped manner.

The areas of interest for the landing gear on the CAGE are the force distribution on each wheel, the weight of the design, the support given to the wing, the drag created in flight, the cost, and the result of the RAC due to the design. Values assigned to these and the results of each design can be seen in Table 3.3.3. According to this table two designs tied as the most desirable: designs D and E.

Table 3.3.3 CAGE and Landing Gear Decision Matrix

Figures of Merit	Weighting Factor	A	B	C	D	E	F	G	H	I
Force distribution on each wheel	0.1	0	0	0	0	0	0	1	1	0
Weight	0.35	0	0	0	1	1	-1	-1	-1	-1
Wing support	0.1	0	0	1	0	0	1	0	0	1
Drag	0.15	0	1	1	1	1	-1	-1	-1	-1
Cost	0.05	0	0	0	1	1	-1	-1	-1	-1
RAC	0.25	0	0	0	0	0	-1	0	0	-1
Totals	1	0.25	0.4	0.5	0.8	0.8	-1.2	-0.2	-0.2	-1.2

3.4 Alternative Fuselage Configuration

To begin the conceptual design process for the fuselage, figures of merit involving materials, structure, and aerodynamic properties were assigned values of importance in order to determine both the ideal design shape and material for the K-03 Pegasus fuselage. Two areas of the fuselage were focused on during this design process. These two areas were the manufactured design material and the basic structural analysis of the design shape (regardless of material composition).

3.4.1 Fuselage Material Figures of Merit

Figures of merit in determining the ideal material for construction of the aircraft fuselage have been chosen as follows:

- Manufacturability – Manufacturability can be defined as a sum of all the variables included in the ease of manufacturing a fuselage out of each specific material being analyzed. The two variables that are focused on the most highly are the amount of time required to manufacture any design out of the material and the amount of skill required to do so in a timely manner without error.
- Ease of Design – The ability to take a design from a conceptual idea to a design stage is referred to as the ease of design. Therefore, this variable analyzes the ease of bringing a design from "thought to paper".

- Design Predictability – This variable measures and compares the ease of use of each material to follow the original design. This variable answers the question, "how easy will it be to model the real fuselage after the actual engineered design". The design predictability of a material tends to directly relate to the manufacturability of that same structural method. If the end result does not match the original design it is immensely difficult to predict its performance by previously calculated and tested results.
- Weight – The weight, having the second highest impact in a material selection, has been ranked highly due to the simple idea that the more the final design of K-03 weighs, the more lift that is needed. If the weight can be minimized a heavier payload can be lifted and the end score will be higher.
- Cost – Cost includes the price of all materials to produce the fuselage out of the particular material or method. The cost does not include the price of labor.
- Durability and Structure – The durability and structure of the design is the highest-ranking figure of merit and the most important. If the fuselage will not repeatedly withstand the forces and stresses of take-off, flight, and landing then the design cannot be considered. If a design ranks low in this figure it can only make up for it by its reparability value.
- Reparability – The competition rules clearly state that a plane must be repaired within a certain interval of time if it is to become injured during flight or upon landing and inspected after repair for the team to receive point value for the sorties. If the durability of a design is to fail, it will be the reparability of that design that determines whether the plane will be able to continue in the competition. However, if a design can be easily damaged and easily repaired continual repair will gradually degrade its structural stability.

Four Materials were chosen for the structure of the aircraft's fuselage. These four methods were analyzed under the assumption that the force from a centered-single-wheeled landing gear impact is directly distributed into the sides of the aircraft and that upon landing the landing gear will press outward and against the sides of the fuselage. All methods are compared as assembled by the team and not an outside source. The building methods and materials compared are as follows:

- Carbon Fiber with Epoxy over foam – This method is accomplished by carving the fuselage shape out of foam and then using Epoxy to bond carbon fabric over the foam. A second layer of Epoxy is then added later to create a smooth surface.
- Fiberglass with Epoxy over foam – Applying fiberglass cloth to foam is done in the same manner as the carbon fiber cloth. The look of both methods from a distance would appear the same.
- Monokote skin over Ply Ribs – This method consists of ribs made of very thin plywood balsa, which is denser than plain balsa wood. Next, square stringers of balsa are glued along the

edges of the ribs to add a structure for the Monokote skin to be applied. The Monokote skin is a thin, clear, plastic that is applied with a heat iron and fully seals the fuselage.

- Balsa and Ply – The balsa in this method of construction replaces the Monokote in the previous method. Typically the Monokote will still be applied to the outside of the balsa skin. The Balsa skin in this method still covers balsa stringers attached to balsa ply ribs.

The final values given to these materials according to the above-described characteristics can be viewed in Table 3.4.1. According to these ratings Balsa and Ply were determined to be the most desirable material to use for the fuselage.

Table 3.4.1 Fuselage Material Decision Matrix

Fuselage Materials	Weighting factor	Carbon Fiber w/ Epoxy over Foam	Fiberglass w/ Epoxy over Foam	Monokote skin over Ply Ribs	Balsa /Ply
Manufacturability	0.15	-1	-1	1	1
Ease of Design	0.05	-1	-1	1	1
Design predictability	0.05	0	0	1	1
Weight	0.2	0	-1	1	0
Cost	0.1	0	-1	1	1
Durability/Structure	0.3	1	1	-1	0
Reparability	0.15	-1	-1	1	1
Total	1	-0.05	-0.35	0.4	0.5

3.4.2 Fuselage Design Shape Figures of Merit

Many of the figures of merit in determining the shape of fuselage are the same but directed in a different manner as follows:

- Ease of design and Predictability – The ease and predictability of design for the fuselage shapes is a comparison of the ability to take a design as seen in Figure 3.4.2 and make detailed structural drawings and take those designs to the next step, manufacturing.
- Manufacturability – The Manufacturability value for each shape is a measure of the skill to assemble the design. The time required for this is not a factor in assigning values.
- Drag – during the conceptual design process a relational assumption of the drag for the different shapes was assumed. Due to the low speeds the aircraft will be attaining, drag will be a minimal factor and is therefore given little value for merit
- Efficiency of design – The efficiency of each design is a factor of weight and space. How efficient is the design's use of space? How much extra weight has been added to keep this design shape? These are the two questions that led to a value for this figure.
- Structural Stability – The structural stability value was given the highest weight. The most important factor in choosing a design for the fuselage is the stability. If the fuselage fails upon landing impact the plane will have to be repaired. Repairs can gradually degrade the structure. If a structure has a weak point in its design an unexpected accident could cause damage beyond repair.

- Reparability – As mentioned in the material analysis, the competition rules clearly state that a plane must be repaired with a certain interval of time if a break or injury occurs. Some designs allow for repairs that are easy to fix. A plane that is not may allow for uneven areas causing a pull to one direction or a weak point for the next landing. The reparability is not dependant on material in this section and is only analyzed by means of the shape of the design.

In Section 3.4.1, four types of material methods were analyzed. For the variable of manufacturing, there is a direct dependence on the type of material used. A clarification of this figure is as follows:

- Manufacturability for a ribbed structure – A ribbed structure includes both the Balsa and Monokote covered designs. The manufacturability for a ribbed structure is based on the ability for designs of these means to be constructed. During construction ribs are typically lined up and made parallel to each other with a square, and stringers are glued in place between them.
- Manufacturability for a composite structure – A composite structure includes both the fiberglass and carbon covered foam designs. A patch or repair to a foam covered design would typically be repaired by means of balsa and glue. Quick dry Epoxy could be used to smooth out the surface.

The design shapes analyzed in this matrix are the rectangle, "D" shape, cylinder, and the Tapered cylinder, the four designs for comparison are seen in Figure 3.4.2. Each design contains the 6-inch by 6-inch by 12-inch box with no clearance around it. This was done simply for the analysis of the variables previously listed. For all designs the batteries would remain in the areas outside of the payload box.

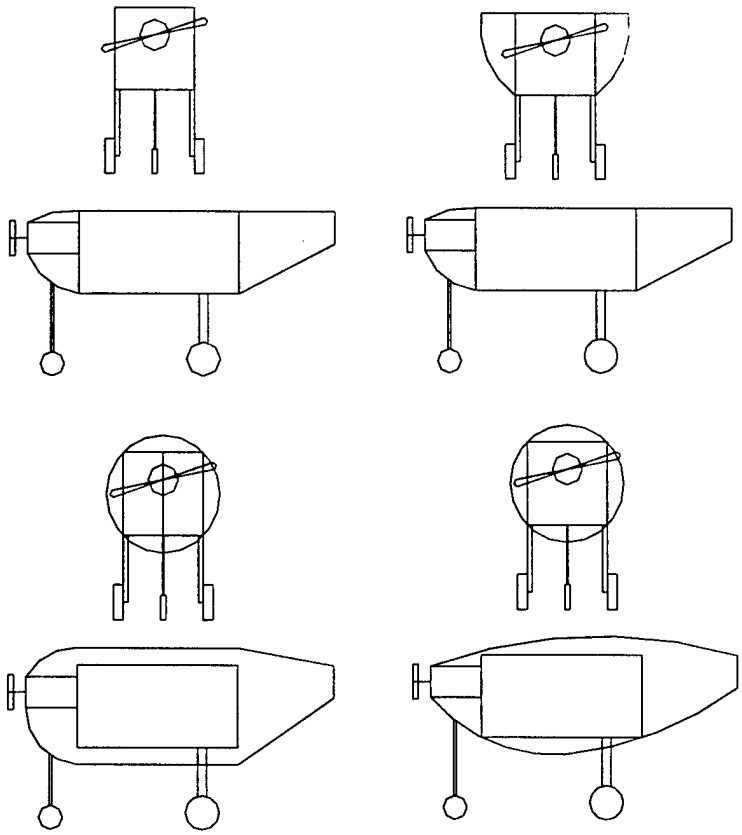

Figure 3.4.2 Possible fuselage design shapes. From top left to right: Rectangular, "D" Shape, Cylinder, and Tapered Cylinder.

Table 3.4.2 Fuselage Design Shapes Decision Matrix

Design Type	Weighting factor	Rectangular	The "D" Shape	Cylindrical	Tapered Cylinder
Ease and Predictability	0.2	1	0	1	-1
Drag	0.05	-1	1	1	1
Efficiency of design	0.2	-1	1	-1	-1
Structure Stability	0.25	1	0	1	-1
Reparability	0.2	1	1	-1	-1
Totals	0.9	0.4	0.45	0.1	-0.8
Manufacturability for a ribbed structure	0.1	1	1	0	-1
Ribbed total	1	0.5	0.55	0.1	-0.9
Manufacturability for a composite structure	0.1	0	-1	1	-1
Composite total	1	0.4	0.35	0.2	-0.9

These designs were compared in Table 3.4.2 according to the stated design characteristics. According to the table's totals the Rectangular and "D" Shape designs tied as the most desirable. Comparing the designs according to their material is extremely important. Continuing into the Preliminary stage will cause many new problems to be encountered, and a decision chosen now, in the conceptual stage, can change. Therefore, with the ribbed and composite structures equally compared, analyzing a new change can be done with ease.

3.5 Alternative Wing Configuration

Figures of merit in the analysis of the wing configuration include:

- Manufacturability – The selected wing configuration must be within the team's range of manufacturability. Relative time and effort factors were addressed and compared.
- Strength – The strength of the wing weighs more heavily than the manufacturability. The team must manufacture a wing that will take the load of the plane
- RAC – The Rated Aircraft Cost drives the competition and is always an important consideration.
- ATS – The wing can be both strong and desirable according to the RAC, but if it does not fit in the box, it will not make it to the flight line. This constraint weighs most heavily.

Four basic wing alternatives were considered: two piece, one piece, bi-plane, and hinged. The one-piece wing fairs well for strength and fairs equally well as the rest for the RAC, but its limiting factor is the ATS. Given the box's largest dimension, the longest possible one-piece wingspan is only four feet – not a large lifting surface. The bi-plane yields a similar limitation but also increases the manufacturing effort and the RAC. The hinged and two-piece wing designs fair best for K-03 Pegasus, but due to the manufacturability and the increased strength of the solid two pieces, the latter is shown to be best.

Table 3.5 **Number of Wings Decision Matrix**

Number of Wings	Weighting factor	Two-piece	One-piece	Bi-plane	Hinged
Manufacturability	0.15	0	0	-1	-1
Strength	0.25	0	1	1	0
RAC	0.25	1	1	-1	1
ATS	0.35	1	-1	-1	1
Totals	-	0.6	0.15	-0.5	0.45

Given the chosen mission profiles, the wing can neither pass through the payload nor obstruct the payload from dropping. Coupling this constraint with the size constraint of the Plane Box, the wing cannot be low, along Pegasus's underbelly, or mid, passing through the middle of the Pegasus's fuselage. Referring to Table 3.5, note that a two-piece wing best fits the parameters important to the aerodynamic

team. A low two-piece wing requires a spar to pass just above the Bombay doors, obstructing the payload drop area, and a mid two-piece wing presents a similar problem. However, a high wing configuration yields an area just above the payload drop system for spar connection; the payload and the path of the payload are unobstructed making this the best configuration for K-03 Pegasus.

3.5.1 Wing Structure Figures of Merit

Figures of merit in the analysis of the wing structure include:

- Manufacturability - The selected wing configuration must be within the team's range of manufacturability. Relative time and effort factors were addressed and compared.
- Reparability – With the nature of the competition, there are foreseen occurrences where the wing may need repair. Conceptually, reparability is not weighted heavily but is still important enough to consider.
- Durability – The structure of the wing must support the wing load and do so for numerous flights.
- Weight – Factored into the total weight of the aircraft, the weight of the wing affects RAC and in this case is most heavily weighted.
- Cost – The actual monetary value of the wing did not factor into the RAC but was still considered due to the team's budget.

The three structure types considered were: a foam core covered in light ply sheeting, a foam core covered with carbon fiber, and a skeleton design consisting of ribs covered with Monokote. The comparison of these different types can be seen in Table 3.5.1a. As recorded on the table the skeleton design scored poorly due to low reparability and durability. From previous experience, it has been shown that this method cannot survive a possible tumble landing and is irreparable. A foam core fairs well in durability and is easier to repair than a rib configuration. The deciding factors between light ply and carbon fiber were cost and manufacturability. By comparison, carbon fiber covering is much more expensive than the light ply, but from experience, it has shown to be more cumbersome to manufacture. The light ply will allow the best durability and strength and will satisfy the other design considerations adequately; Table 3.5.1a shows it's total to be superior to the alternatives.

Table 3.5.1a Wing Structure Decision Matrix

Wing Structure	Weighting factor	Foam core/light ply	Foam core/carbon fiber	Ribs/Monokote
Manufacturability	0.25	1	-1	0
Reparability	0.1	0	0	-1
Durability	0.25	1	1	-1
Weight	0.3	0	0	1
Cost	0.1	0	-1	0
Totals	-	0.5	0	-0.05

Figures of merit in the analysis of the wing geometry include:

- Manufacturability – Again, the manufacturability is a key factor in the wing structure. This factor weighs heavily in wing geometry because of the team's skill level. Relative time and effort factors were addressed and compared.
- Root Chord – The root chord length factors into the RAC making it an important consideration.
- Weight – Again, the weight of the wing affects the RAC and in this case is weighted as heavily as manufacturability.
- Handling – Because the flight plan is not a straight line, handling is important in considering wing geometry.

The four geometric wing configurations considered were: Tapered, Elliptical, Rectangular, and Rectangular tapered. A qualitative comparison of these types can be seen in Table 3.5.1b. The tapered and elliptical wings faired the same in all geometry considerations. Both are difficult to build because of their consistent decrease in chord length from the root chord. However, they are superior to the rectangular wing in weight and handling. The rectangular wing is best in manufacturability due to its constant chord length. The rectangular tapered design is a compromise between the elliptical/tapered wings and rectangular. With the rectangular tapered wing the handling and weight parameters are preserved and in is also easy to manufacture. Past UCF teams determined it superior to the rest as well.

Table 3.5.1b Wing Geometry Decision Matrix

Wing Geometry	Weighting factor	Rectangular tapered	Rectangular	Elliptical	Tapered
Manufacturability	0.3	0	1	-1	-1
Root Chord	0.2	0	0	0	0
Weight	0.3	1	-1	1	1
Handling	0.2	1	0	1	1
Totals	1.0	0.5	0	0.2	0.2

3.6 Alternative Empennage Configuration

The empennage configuration limitations were similar to the wing configuration limitations. Just like the wing, the empennage cannot interfere with the payload or the payload drop area. Ideally the payload will drop from its ballasted position in the fuselage to the ground and Pegasus will pass over the payload. For Pegasus to clear the payload, the tail must be high and slope away from the ground. (Refer to Figure 3.3.1) A low tail causes too much interference. A typical single boom configuration potentially causes interference too. By implementing a double boom configuration with booms connecting to either side of the fuselage, Pegasus passes clearly over the payload and is ready for take off again. Further figures of merit in the tail structure analysis included:

- Manufacturability - The selected tail structure must be within the team's range of manufacturability. Relative time and effort factors were addressed and compared.
- Stability – The tail must be stable in terms of elevator and rudder control.
- Weight – Factored into the total weight of the aircraft, the weight of the empennage affects RAC and in this case is considered one of the more important figures of merit.
- Length – The plane's length contributes to the MFHR of the RAC - not as considerable as the weight but considerable enough for comparison's sake.
- ATS – Coupling with length, the tail must not exceed the maximum dimension of the box in order to make it to the flight line.

At this point, there was no foreseeable trouble that would distinguish the double boom from the single boom configuration in terms of manufacturability. Both configurations fell within the team's skill level. However, a double boom configuration increases the control and stability of the plane while decreasing its weight. It also yields an empty area between the booms for storage in the ATS and can be made a desirable length according to both the box and the RAC parameters.

3.6.1 Alternative Empennage Structure

Figures of merit in the analysis of the empennage structure were similar to the tail configurations but eliminated the box and length merits. The "rib and runner" structure faired best for the team. Weighing heavily on manufacturability, the rib and stringer idea fell within the team's building knowledge and time constraints. Building the tail booms from carbon fiber would be costly, only adding what is believed to be unnecessary strength. Conceptually, there is no need to manufacture the vertical and horizontal

stabilizers from foam and ply like the wing. From past experience, both stabilizers can be made from a truss and Monokote combination, which reduces weight but still endures flight conditions.

3.7 Alternative Power Plant Configuration

According to specifications in the competition rules, the motors must be brushless and of the Graupner or AstroFlight families. AstroFlight has been tested by the UCF team in the past and is most trusted. The RAC, which will be discussed later in the detail description, has the heaviest weight of all factors. However, it becomes a trade-off between having the best RAC score and having enough power to fly the aircraft. These figures of merit, which were used in the analysis of the power plant configuration, are described below in detail and can be seen with ratings according to motor models in Table 3.7.

- RAC – The RAC was the most important weighting factor for the power plant. The weight of the motor and the weight of the batteries used to power the motor have the most impact on the RAC and the team's final score.
- Liftoff– The power plant must supply enough power for speed of takeoff.
- Flight Time– Total flight time is factored into the final score and carries as much weight as the RAC.
- Cost– Although the monetary amount of the power plant does not factor into the final team score, it is still an important merit due to budget constraints.

Table 3.7 Power Plant Decision Matrix

Power Plant	Weighting factor	AstroFlight 40	AstroFlight 60	AstroFlight 90
RAC	0.35	1	0	-1
Lift off	0.2	-1	0	1
Flight Time	0.35	-1	1	0
Cost	0.2	1	0	-1
Totals	-	0	0.35	-0.35

In previous competitions, using the AstroFlight 40 motor, power for liftoff and flight time were compromised for a better RAC. However, by giving flight time and lift off more merit, the AstroFlight 60 motor appears best as shown in Table 3.7. It finds a middle ground between the, RAC friendly but weakly powered, AstroFlight 40 and the, high powered yet extremely costly, AstroFlight 90.

3.8 Further Analysis Tools

3.8.1 Past Team Experience

Knowledge gained from UCF's electric airplane team is passed down from senior members to underclassmen at the end of every year. Many of the team members begin working on the electric airplane when they begin attendance of their freshman year. As a result, many members develop detailed building skills and knowledge of possible mishaps, increasing their engineering analysis abilities.

Such variables are the conditions at competition: uneven landing strips, unpredictable motors, and the quick discharge rate of servo batteries. One of the most useful items of knowledge passed down through teams is the efficiency and actual performance of the AstroFlight motors and the need for an adequately powered motor.

3.8.2 Testing Methods

A vast array of testing occurred (explained in detail within the testing section of the report) throughout the entire conceptual design. Some testing was as simple as seeing if typical servos can drop a 5 lb payload. Other testing was detailed including visual analysis of fuselage and tail sections in a water tunnel. Different thicknesses of balsa and ply were purchased and both visually and physically analyzed. In a design team, testing is a continual process. During the conceptual stage, decisions are not directly based on testing but, rather, on questions that need to be further explored.

3.9 Final Aircraft Configuration

The components of the K-03 Pegasus to pass on to the preliminary stage were a double boom, AstroFlight 60 motor, a rectangular to tapered wing configuration, tricycle landing gear with a simple angular CAGE design, and a "d" shaped fuselage. The plane consists of balsa, birch plywood, and aluminum, with a foam wing.

4.0 PRELIMINARY DESIGN

Only those items that survived the rigorous conceptual design phase analysis saw the preliminary design phase. This phase took the best conceptual designs and found their weaknesses, means of implementation, and further areas of correction. During the Preliminary phase the K-03 Pegasus team looked for errors and discrepancies in conceptual design and analyzed how preliminary phase components would integrate into the final design.

4.1 Trade Study of Previous Results

As mentioned in the conceptual design phase, many assumptions made for this year's design were based on past UCF Design/Build/Fly performances. This section researches those assumptions for previous motor performance, wing designs, and fuselage designs.

4.1.1 Study of Previous Motor Performance

Previous design teams found their motors to be highly underpowered and unreliable. The typical motors used by those teams were the direct and geared AstroFlight Cobalt 40 series. All previous UCF teams stated that they would have used a motor of the Cobalt 60 series if they had the budget available to do so. Therefore, their only reason for refusing the 60 series was the cost. It was later found that lack of battery power was to blame for the underpowered motors. Table 4.1.1 lists the specifications for each AstroFlight motor.

Table 4.1.1 AstroFlight Motor Specifications

Model	p/n 640	p/n 640G	p/n 640S	p/n 661	p/n 661S	p/n 691
Gear	Direct	Geared	Superbox	Direct	Superbox	Direct
Speed (rpm/volt)	682	406	220	347	126	256
Best Battery (cells)	18 to 21	18 to 21	21 to 24	28 to 32	32 to 36	32 to 36
Max Amps	35	35	35	35	35	35
Prop RPM max	1500	7000	6000	11000	4500	10000
Voltage max	2.20	17.24	27.27	31.70	35.71	39.06
Prop Min	10x5	13x8	14x10	12x8	18x12	13x8
Power (watts)	600	750	1000	900 to 1100	1100 to 1200	1100 to 1200
Length (in.)	2.75	3.75	3.75	3.00	4.00	3.70
Weight (oz.)	13.5	15	16	22	25	32
Price	$149.95	$199.95	$209.95	$249.95	$319.95	$299.95

4.1.2 Study of Previous Battery Power Requirements

In the past, design teams chose AA batteries to power their 40 series motors. After contacting both the Motor Manufacturer and the Battery Suppliers, it was found that the AA battery was not the best choice and that a C battery configuration would power both the 40 and 60 series motors, however, more would be required for the 60 series motor.

4.1.3 Study of Previous Wing Designs

Much of the team's knowledge of wing design and construction was handed down from previous UCF aircraft team members. In past competitions, the wing was constructed from a Selig 1223 airfoil – an airfoil known for its camber and high lift at low speeds. Although the Selig creates high lift, it also creates high drag. In past competitions, the flight time was not a scoring factor but this year, it is factored into the team's total score. Also, because of its characteristic ultra-thin trailing edge, the Selig 1223 has never been easy to construct. When cut with a hot wire from blue foam, the Selig's trailing edge tends to break and tear. With this in mind, the aerodynamic team was hesitant to use the Selig 1223 again.

4.1.4 Study of Previous Fuselage Designs

In past years UCF teams have used a construction of ply ribs for the fuselage. This was chosen as the same method by this team. The ribs have shown to have a good amount of structural support in all areas except for the landing gear impact force surrounding areas. The current cage design eliminates this problem. Most landing impacts proved the landing gear to distribute all of its force to the ply ribs and as a result the ribs would fracture. This fracture occurred at almost every landing, proving that either the landing gear should absorb more of the impact and not transfer impact forces to the ribs, or the fuselage design should be able to withstand more force.

4.2 Initial Trade Study Results

This section takes the knowledge gained from the trade studies of previous results and delivers new study results for this year's competition. It explains how each piece of knowledge is applied to the battery requirements, wing requirements, and fuselage and CAGE requirements. It also includes the calculation for this year's Rated Aircraft Cost.

4.2.1 Study of Type of Batteries Required for the Cobalt 661s Motor

The specifications for the Cobalt 661Superbox Motor, as stated by Astroflight, recommend 32 to 36 cells for proper operation. According to the rules for this competition a maximum of 5 lbs of NiCad batteries are allowed to power the motor. It was discovered that using C batteries instead of the usual AA batteries would improve the power to the plane and still remain within the weight limits. It is believed that teams overlooked this in the past because both battery sizes typically have the same Voltage of 1.2V

The C size batteries compared were the Sanyo CP-2400CR, the Sanyo CP-1700SCR, the Sanyo RC-2000, and the Sanyo RC-2400. The Sanyo RC-2400 was the final choice for the Motor battery. The batteries were designed in a configuration of 4 sets of 8 cells in series. This value is at the lower limit of what is recommended for our motor. If any more cells were added, however, the weight limit for battery

power would be exceeded, and it would be difficult to fit a configuration any larger into the fuselage. Table 4.2.1 compares the specifications of each battery.

Table 4.2.1 Sanyo Battery Specifications

Battery	Volts	Milli-Amp Hours	Weight (oz)	Height (in)	Diameter (in)
Sanyo CP-2400CR	1.2	2400	2.11	1.673	0.866
Sanyo RC-2000	1.2	1900	2.05	1.693	0.906
Sanyo CP-1700SCR	1.2	1700	1.62	1.299	0.866
Sanyo RC-2400	1.2	2400	2.09	1.65	0.84

4.2.2 Study of Wing Planform Area Requirements

Past studies of wing planform area show that an elliptical planform produces the ideal lift distribution for a wing. However, an elliptical wing planform is very difficult to build and the option has been to taper the wing. When a rectangular wing is tapered, the tip chords become shorter, alleviating the undesired induced drag effects of the constant-chord rectangular wing. Past wings began rectangular and started to taper at a distance that was more than half way down the length of the wing from the root chord. Previous wings also kept a taper ratio of 0.45 and were expected to produce a lift distribution very close to the elliptical planform. According to Fundamentals of Aerodynamics by John D. Anderson, a taper ratio between 0.4 and 0.5 creates the best lift distribution. The aerodynamics team kept this in mind when making a final decision and produced a wing similar in shape to previous competitions but with a taper ratio of 0.458.

4.2.3 Study of Wingspan Requirements

From prior knowledge, the wing itself can have a small span and a large chord (small aspect ratio), a very long span and small chord (large aspect ratio), or be somewhere in between. As the aspect ratio increases, the lift produced increases, and the induced drag decreases. Due to its high aspect ratio, a large wingspan appears ideal, but with weight and wingspan penalties it becomes a trade-off in competition parameters. In past years, teams took the high aspect ratio approach and found other methods of reducing weight and wingspan penalties. The aerodynamic team took that into consideration but was constrained by the internal dimensions of the Aircraft Transportation System. The longest wingspan possible (without segmenting the wing more than once) is 8 feet plus the width of the fuselage.

4.2.4 Study of Fuselage CAGE and Landing Gear Requirements

During the preliminary design phase it was decided that the fuselage would not undergo any force of impact. About 95 percent of the force of impact would be spread evenly through the CAGE structure. As mentioned in the study of previous designs, the danger of a broken landing plate is obsolete due to the design of the cage. All forces are absorbed into the CAGE from the landing gear. As also mentioned in section 4.1.4, the landing gear needed to absorb more of the impact or the fuselage needed to be made stronger. As a compromise, in this design the CAGE, stronger than the outer ribs, will absorb the impact and transfer it more evenly and to a lesser extent than a rib and landing plate design.

4.3 Aerodynamic Analysis

4.3.1 Wing Analysis

To find the optimal wing configuration in terms of RAC, the aerodynamic team compared possible wingspan and chord length combinations. The ATS limited each wing to a maximum length of 4 feet making the total possible wingspan 8 feet plus the width of the fuselage. Both chord length and wingspan add into the MFHR with a multiplier of 8 hr/ft. Therefore, increasing the chord length is more beneficial than increasing the wingspan in terms of RAC. However, in terms of aircraft performance, increasing the chord increases drag and lowers the aspect ratio. To maximize the planform area while keeping the aspect ratio high and the RAC low, the aerodynamic team chose a root chord length of 12 inches and the maximum wingspan of 8 feet. The wing will taper 2.5 feet from the root chord with a taper ratio of 0.458. The taper will supply a better lift distribution and will compensate for increased induced drag due to the large chord length. The planform area and aspect ratio for K-03 Pegasus are 7.225 square feet and 8.85, respectively.

Then, four airfoils underwent comparison for the K-03 Pegasus team. The airfoils compared were the NACA 4412, Selig 1223, FX 60-100, and Eppler 214, shown in Figure 4.3.1. All but the NACA airfoil were found to be ideal for low-speed performance. The NACA airfoil did not continue in the analysis because it was not designed for lower speeds and would not provide enough lift for the speeds available.

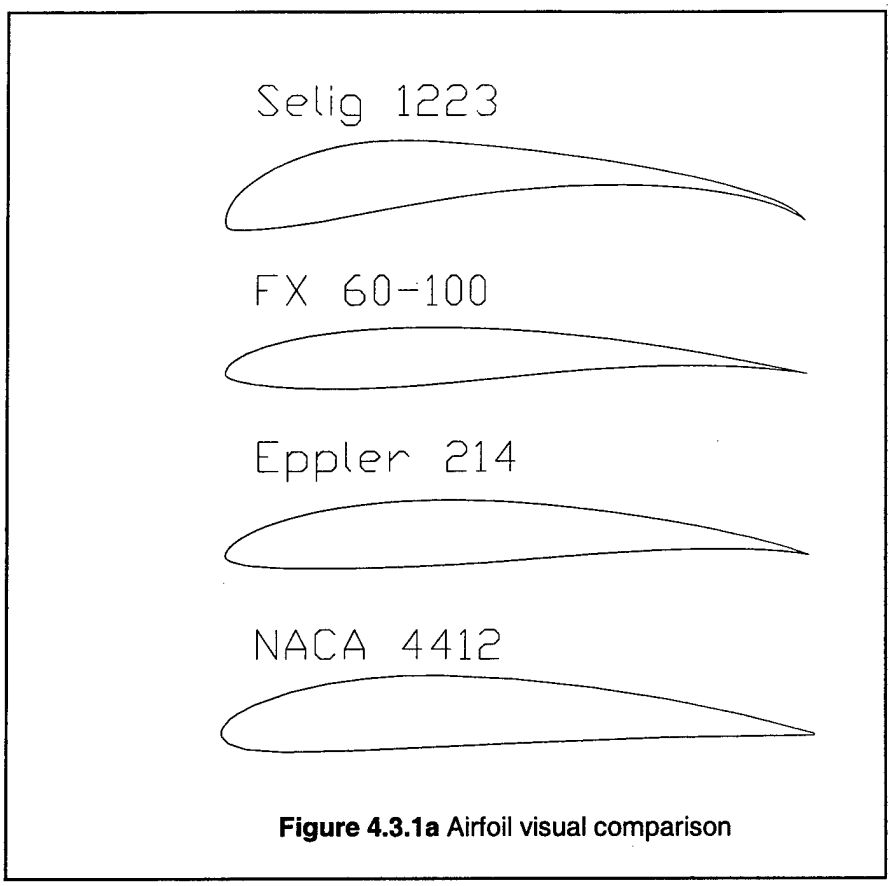

Figure 4.3.1a Airfoil visual comparison

Using a density of 1.225 kg /m^3, a velocity of 32mi/hr (our proposed max velocity), air viscosity at about 290K of 1.7894 x 10^{-5} kg/ms and a chord length of 12 inches, a Reynolds number of 298800 was used to compare the three remaining airfoils. Data was obtained for the airfoils from the NASG Database as contained in Table 4.3.1a.

Table 4.3.1a Airfoil Coefficient Data Comparison chart

Eppler 214			FX 60-100			Selig 1223		
Alpha	C_l	C_d	Alpha	C_l	C_d	Alpha	C_l	C_d
-3.91	0.025	0.0139	-2.92	0.012	0.0123	0.48	1.131	0.0164
-2.39	0.172	0.0117	-1.88	0.128	0.0104	2.05	1.282	0.0187
-0.86	0.33	0.011	-0.86	0.236	0.0093	3.6	1.429	0.02
0.68	0.484	0.0108	0.17	0.34	0.0093	5.1	1.548	0.0212
2.2	0.626	0.0112	1.18	0.441	0.0093	6.61	1.671	0.0232
3.7	0.774	0.0124	2.21	0.541	0.0095	8.21	1.8	0.0257
5.24	0.923	0.0133	3.21	0.635	0.0097	9.7	1.91	0.0281
6.78	1.062	0.0151	4.22	0.721	0.0098	11.22	2.016	0.0307
8.32	1.184	0.0178	5.26	0.812	0.0112	12.84	2.116	0.0336
9.84	1.243	0.0257	6.27	0.9	0.0129	14.74	2.175	0.0371
11.36	1.254	0.04	7.28	0.982	0.0148	16.38	2.217	0.0454

Figure 4.3.1b graphically compares angle of attack, coefficient of lift, and coefficient of drag for each airfoil. Notice the similarity between the Eppler and the FX airfoils both visually and graphically.

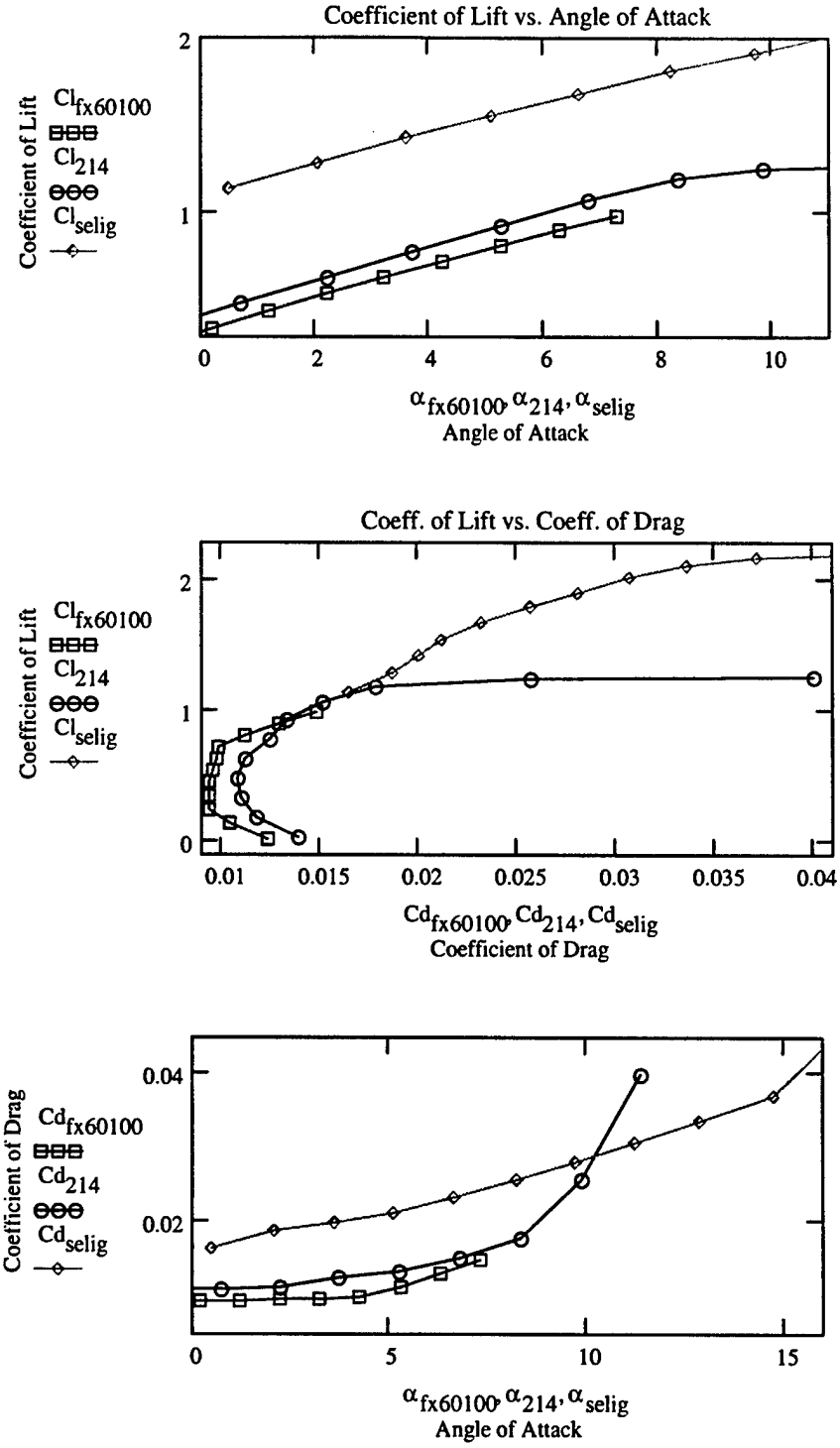

Figure 4.3.1b Coefficient and Angle of Attack Comparison Graphs

Concluded from the graphs, the Selig airfoil gives the most amount of lift all three airfoils. However, this airfoil also gives the most amount of drag. Due to the original goal of only lifting 5 lbs of weight, and a

plan to compromise the payload weight for speed, the Selig will not be sufficient for this design team's goals. The drag and lift of the Eppler and FX airfoils are further compared in Figure 4.3.1c using a planform area of 7.225 ft^2 as follows:

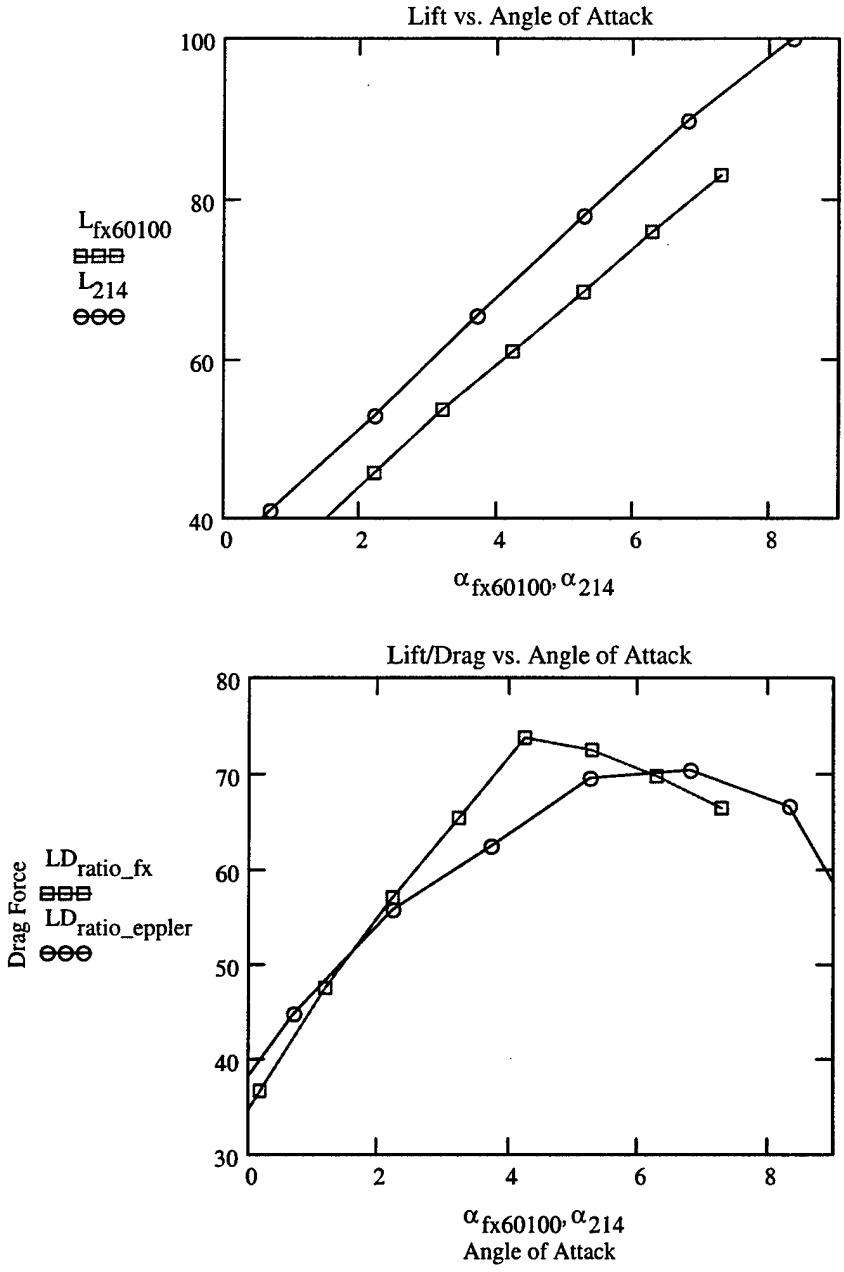

Figure 4.3.1c Eppler 412 and FX 60-100 Comparison Graphs

From this analysis of the lift, drag, and lift/drag ratio the Eppler 214 airfoil was chosen. The lift and drag graphs showed the values for both lift and drag to be the same factor larger than the FX airfoil. Visually between the two graphs, it appeared that the lift for both was the same ratio larger than the drag. From this the Eppler was chosen, however, the lift over drag graph raised question. At about 4.22 degrees the

FX showed a larger lift to drag ratio, however, at this value the FX only produces about 13.665 lbs of lift. Estimating the plane's empty weight to be 15 lbs, there will not be enough lift for take-off. Therefore, an amount of 8 degrees of angle of attack has been chosen. This value allows enough room for the tail boom structure and batteries. It also gives about 22 lbs of lift in the Eppler airfoil. This value leaves room for 7 lbs for payload and lifting force. See Table 4.3.1b.

Table 4.3.1b

Eppler 214			FX 60-100		
Alpha	L (lbf)	L/D	Alpha	L (lbf)	L/D
-3.91	0.474	1.802	-2.92	0.227	0.974
-2.39	3.26	14.685	-1.88	2.426	12.315
-0.86	6.254	30.067	-0.86	4.473	25.415
0.68	9.173	44.746	0.17	6.444	36.614
2.2	11.864	55.962	1.18	8.358	47.489
3.7	14.669	62.421	2.21	10.253	56.961
5.24	17.493	69.417	3.21	12.035	65.408
6.78	20.127	70.374	4.22	13.665	73.489
8.32	22.439	66.585	5.26	15.389	72.59
9.84	23.558	48.374	6.27	17.057	69.906
11.36	23.766	31.354	7.28	18.611	66.468

4.3.2 Empennage Analysis

A twin boom empennage configuration allows an aircraft to sport a dual vertical stabilizer system. This is beneficial aerodynamically, adding increased stability, but it increases the RAC. A dual vertical stabilizer system allows the empennage to have a smaller profile area. That smaller area gives the tail better control in crosswind conditions; conditions that tend to produce greater yaw effects on large vertical surfaces. Comparing the two, the aerodynamic team judged that the increased stability out-weighed the minimal RAC affects. The second control surface only adds 0.2 points to the RAC.

4.4 Structural Analysis

4.4.1 Wing Structure

The aircraft's wing will be made from light ply sheeting with a foam core. In order to find the best core structure for the wing, an analysis was performed on different types of foam. For the best performance, the wing must be strong and light. The densities for each foam type are listed in Table 4.4.1. Note that the densities are given in terms of weight, not mass.

Table 4.4.1 Foam Density Comparison Chart

Foam Types	Foam Density (lbf/cubic foot)	Total Wing Weight (lbf)
Light Green	2.3	2.176

2 lb	2	2.029
Blue	1.748	1.905
Green	1.7	1.882
Pink	1.5	1.784

The total weight of the wing given in the table includes the total weight of the foam plus the total weight of the light ply sheeting. Since the range of the total weight from Light Green to Pink is only 0.392 lbs, it is difficult to judge which foam is best. Blue foam was used in previous competitions and proved trustworthy in both construction and in flight. It is also the median value in the comparison and was chosen as K-03 Pegasus' wing core structure.

4.4.2 Empennage Structure

The chosen empennage structure is a double boom configuration using the rib and stringer method. Ribs, made from 3/32-inch balsa, take the shape of a pointed ellipse and project out from the sides of the fuselage. The pointed ellipse shape, seen in Figure 4.4.2, allows the booms to blend into the shape of the fuselage's body.

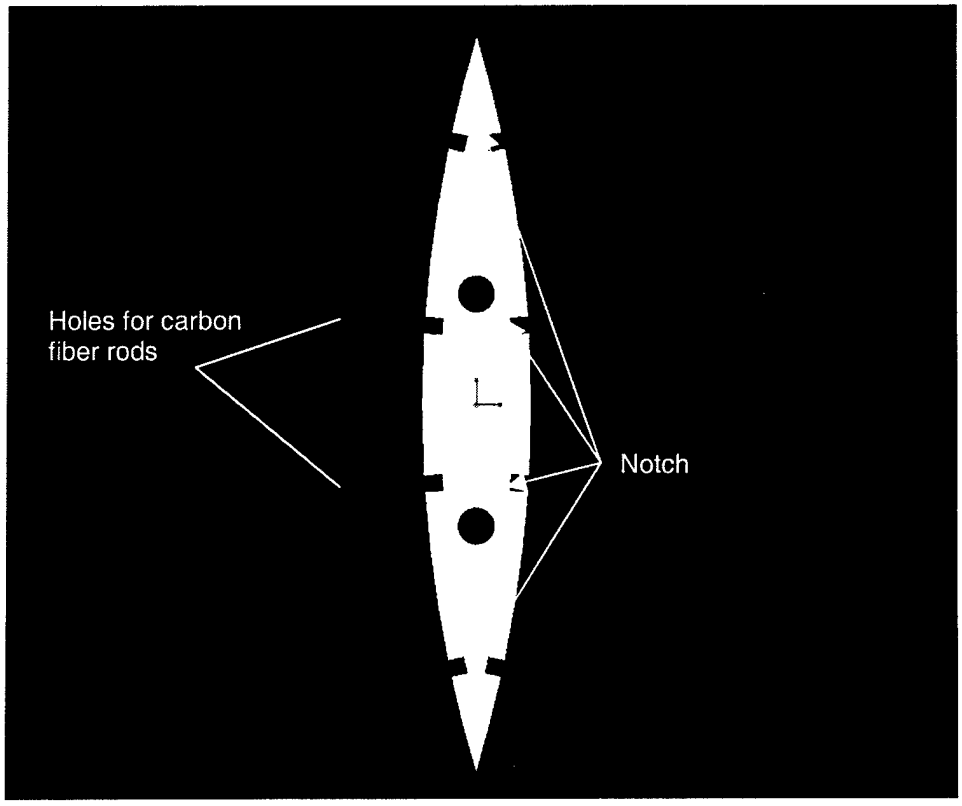

Figure 4.4.2 Empennage Rib Shape

Stringers notch into groves located around the perimeter of each rib, and ribs reduce in size from the fuselage to the tail tip. For added strength, two carbon fiber rods run through the center of each rib and attach to the central CAGE structure. This prevents the tail from twisting in possible windy flight

conditions and contributes to stability upon landing impact. Each boom is covered in light balsa sheeting and measures a distance of 2.5 feet. The boom configuration is permanently attached to the fuselage and will fit within the constraints of the ATS; it will not need to be assembled on the flight line. The horizontal and vertical stabilizers are removable to meet ATS constraints and are stored in between the booms until flight line assembly.

4.4.3 Fuselage and Landing Gear Structure

Once an aluminum landing gear design was chosen, analysis of the CAGE landing gear impact reassured the decision. Assuming the aircraft, fully loaded, weighs 20lbs (9.065 kg), and an impulse time of 1 second, the maximum conditions for impact were analyzed. Those maximum conditions were an angle of 25 degrees, an approach velocity of 20 mi/hr and a landing velocity of 10 mi/hr.

The results of these calculations were a horizontal impulse force of 8.9 lbs and a vertical force of 2.4 lbs. It is believed that in the past the horizontal force caused a twisting to occur at the base of the landing gear. The moment created was about 6.1 N-m per 6 inches of landing gear. This calculation explains why the landing plates in the past have failed. The result of the dynamic analysis proves the need for a structure such as the CAGE, which was a good decision made by the K-03 Pegasus team.

The team's decision was to have a landing gear design that angles outward about 15 degrees away from the fuselage. Continuing with the previous calculations, dividing the force between the two main landing gears (the front landing gear has been excluded to analyze the maximum or worse case scenarios) a force of 1.2 lbs is exerted on each in the vertical direction. The result is a force running along the landing gear towards the cage of 1.6 lbs and a force pushing the landing gear away from the plane of 1.0 lbs. The force pushing outward creates a moment of 0.7 N-m where the landing gear attaches to the base of the CAGE, an amount the aluminum CAGE structure can handle.

4.5 Final Aircraft Configurations

The preliminary design phase determined the general shape and performance of K-03 Pegasus. The aircraft wing has an 8.5 ft span with an Eppler 214 airfoil and a mid-sized 8.89 aspect ratio. Analysis shows that the plane will lift its own weight plus the weight of the payload and additional forces encountered on take-off and landing. For optimal power plant performance, the aircraft uses an AstroFlight Cobalt 60 motor with a configuration of 32 Sanyo RC-2400 batteries. The CAGE shapes the body of the fuselage and carries the impact from the landing gear. All this combined gives K-03 Pegasus an RAC of 12.79.

5.0 DETAIL DESIGN

5.1 Rated Aircraft Cost

The coefficients for calculating the Rated Aircraft Cost are: Manufacturers Empty Weight multiplier (A), Rated Engine Power multiplier (B), and Manufacturing Cost Multiplier (C). The coefficients are multiplied by the Manufacturers Empty Weight (MEW), Rated Engine Power (REP), and Manufacturing Man Hours (MFHR), respectively. This yields the total RAC equation in thousands of dollars.

$$RAC = (A*MEW + B*REP + C*MFHR)/1000$$

Values for the UCF K-03 Pegasus team can be found in Table 5.1.The quantity column includes the number of items or the length of certain items on the aircraft. The WBS multiplier is used only for the MFHR and is specified in the competition guidelines. The final calculated RAC for K-03 Pegasus is 12.79.

Table 5.1 Rated Aircraft Cost

MFHR	Quantity	WBS Multiplier	WBS Total
Wingspan =	8.5	8	68
Chord Length =	1	8	8
Control Surfaces =	2	3	6
Maximum Length =	4.25	10	42.5
Verticals =	0	5	0
Verticals/cntrl =	2	10	20
Horizontals =	1	10	10
Servos =	5	5	25
Motors =	1	5	5
Propeller =	1	5	5
		MFHR Total	189.5
REP			
		32 Battery cells =	5
		REP Total	5
MEW			
		Empty Weight =	15
		MEW Total	15
Coefficients			
		A =	100
		B =	1500
		C =	20
		RAC Total	**12.79**

5.2 Aerodynamic Analysis

5.2.1 Wing Design Details

From the preliminary design, the taper ratio of the wing is .458 with a wingspan of 8.5 feet and a root chord length of 12 inches. A combination of a rectangular and tapered wing geometry generates the desired lift distribution while decreasing wing weight and easing the manufacturing process for a full tapered wing.

Important wing details not previously mentioned are the control surfaces and the spar. On a wing, a flap is used to provide additional lift at takeoff while providing additional drag to slow down the aircraft upon landing. While in flight, an aileron is used to provide roll for the airplane. Having both flaps and ailerons would mean having four servos on the wing adding weight and servo cost in the RAC. For this reason, the aerodynamic team decided to use flaperons – a combination of flaps and ailerons. The flaperon will provide the necessary lift and drag for takeoff and landing and will require only two servos. From past experience, the flaperon can range from 50-90% of the wingspan but for construction purposes, it will only extend the length of the wing's rectangular section. Both flaperons will extend 27 inches consuming 53% of the wing and falling within the suitable range. The wing and flaperons are shown in Figure 5.2.1.

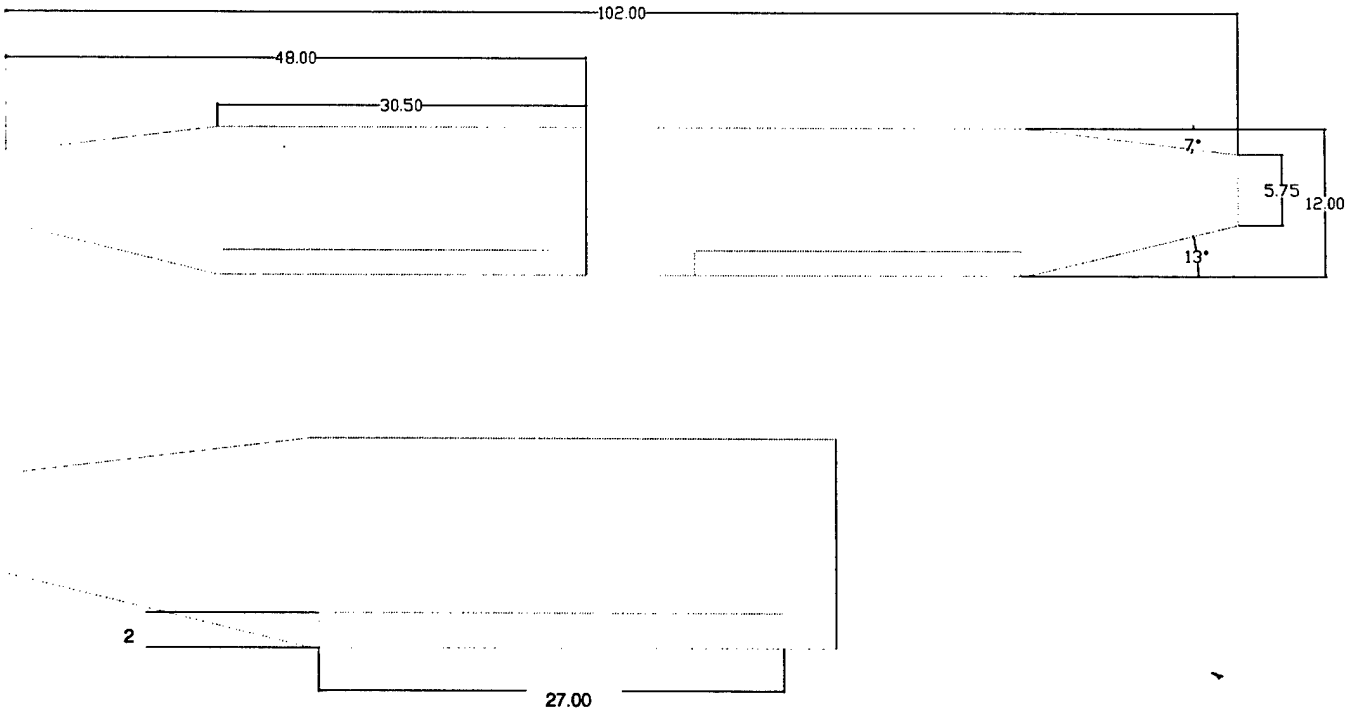

Figure 5.2.1 Wing and Flaperon Dimensions

The spar of the wing increases its structural integrity. Since the wing of K-03 Pegasus is two-piece, it is important to have a strong joining member between each wing and the plane. To avoid obstructing the

payload drop area, two carbon fiber rods protrude from each side of the aircraft's fuselage. The spar, internal to each wing, is a hallow carbon fiber tube which will fit snug around the protruding carbon fiber rods. This will make the wing easy to attach on the flight line and add additional strength to the aircraft. According to an acceptable rule of thumb, the spar is located 1/3 the distance of the root chord from the leading edge.

5.2.2 Flight Performance

In order to analyze the performance of the aircraft, data was gathered for the Eppler 214 airfoil at many Reynolds numbers. From the Reynolds number, velocity, angle of attack, Coefficient of lift, and drag coefficient data was gained. The data is provided in Table 5.2.2.

Table 5.2.2 Flight Performance Data

Re	V (mi/hr)	Alpha	Cl	Cd
298800	32.032	8	1.159	0.017
202600	21.719	8	1.213	0.019
150200	16.102	8	1.14	0.017
104200	11.171	8	1.136	0.02
59700	6.4	8	1.124	0.028

The data originally received was not in terms that fit the aircraft. The data in the previous table was linearly interpolated from the original data for an angle of attack of 8 degrees. From the Cl, Cd, and velocity, the lift drag, and L/D were calculated for this aircraft. Figure 5.2.2a shows the final data.

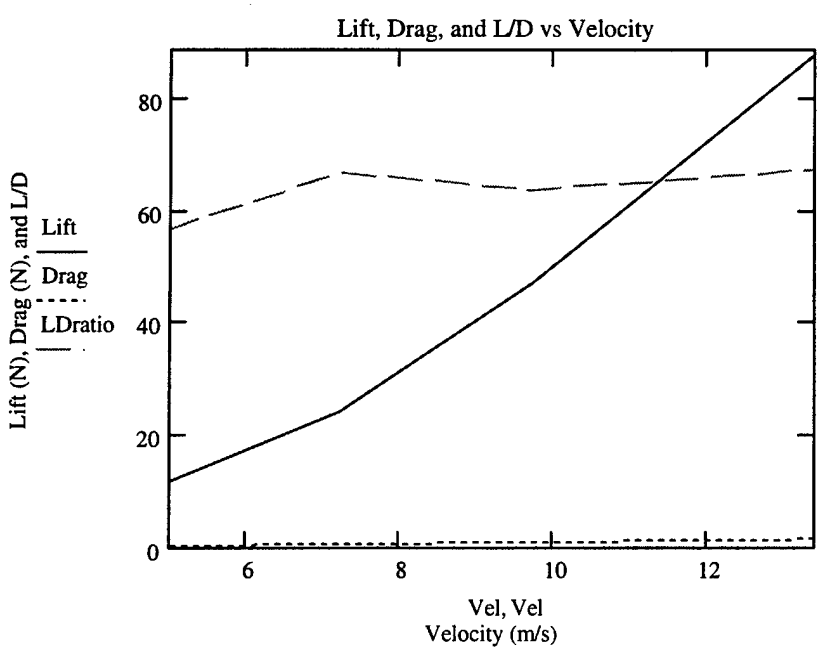

$$\text{Lift} = \begin{pmatrix} 21.965 \\ 10.569 \\ 5.459 \\ 2.618 \\ 0.85 \end{pmatrix} \text{lbf}$$

$$\text{Drag} = \begin{pmatrix} 0.322 \\ 0.166 \\ 0.081 \\ 0.046 \\ 0.021 \end{pmatrix} \text{lbf}$$

$$\text{LDratio} = \begin{pmatrix} 68.176 \\ 63.842 \\ 67.059 \\ 56.8 \\ 40.143 \end{pmatrix}$$

Figure 5.2.2a Lift, Drag, and L/D verses velocity

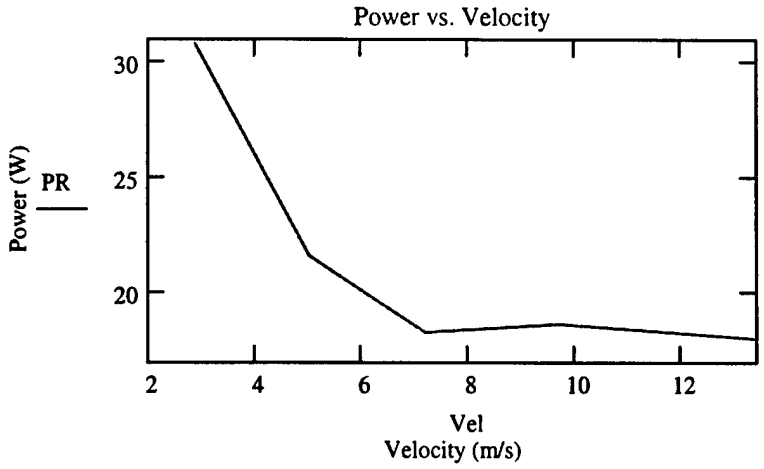

$$PR = \begin{pmatrix} 17.83 \\ 18.612 \\ 18.278 \\ 21.617 \\ 30.75 \end{pmatrix} W$$

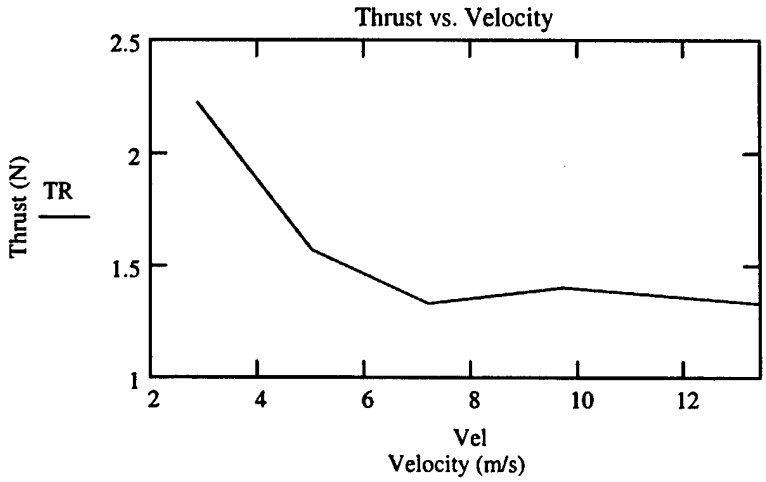

$$TR = \begin{pmatrix} 1.305 \\ 1.394 \\ 1.327 \\ 1.566 \\ 2.216 \end{pmatrix} N$$

Figure 5.2.2b Power and Thrust versus velocity

The turning radius calculated for a max cruise velocity of 50 mi/hr was 37.821 feet. This value shows that about 76 feet will be needed for the aircraft to make a complete 180-degree turn.

The velocity required to take off has been determined to be a value of 35 mph with a take off distance of about 30 feet, which is well within the requirement of 120 feet. The Stall velocity was figured to be 29.878 mph, which is only 6 mph below the take-off velocity. This value means that while in flight if the plane velocity lowers to a value near 39.9 mph the flow will be lost and the plane will lose lifting capabilities and crash. On a lighter note, the landing velocity was calculated as 38.8 mph with a landing distance of 162.7 feet. All values were calculated with an average coefficient of friction for a paved runway of .04.

The aircraft as seen in this section is satisfactory for the competition. The values gained through flight mechanics equations are estimates and the actual aircraft performance is much different and unpredictable.

5.2.3 Empennage Design Details

Recall that the twin-boom empennage design yields ease of payload drop and increased stability from dual vertical stabilizers. It is also reinforced with carbon fiber rods and built through a rib and stringer method. The length of the tail was determined by ATS dimensions and later checked using equilibrium equations with the expected lift from the wing, the weight acting at the center of gravity, the expected lift from the tail, and the distance between each boom. The length of the tail was found to be 2.5 feet.

The horizontal and vertical stabilizers are sized from reasonable rules of thumb and modeled after a combination of two previous UCF electric aircraft. An acceptable horizontal stabilizer should be 15-20% of the wing area or an aspect ratio of 3-4. The vertical stabilizer should be 8-10% of the wing area with an aspect ratio of 2-3 and the rudder should be approximately half that area. With this in mind, the final dimensions of the vertical stabilizer are 8 inches high, 5.1 inches wide at its tip, and 9 inches wide at its base. The final horizontal stabilizer dimensions are 31 inches in length, 6 inches in width, and 3 inches wide at the most tapered point. The elevator is 3 inches wide and sectioned 3 times. Stabilizer dimensions are shown in Figure 5.2.3. The dual rudders are controlled in unison by one servo, and the horizontal stabilizer is controlled by one additional servo.

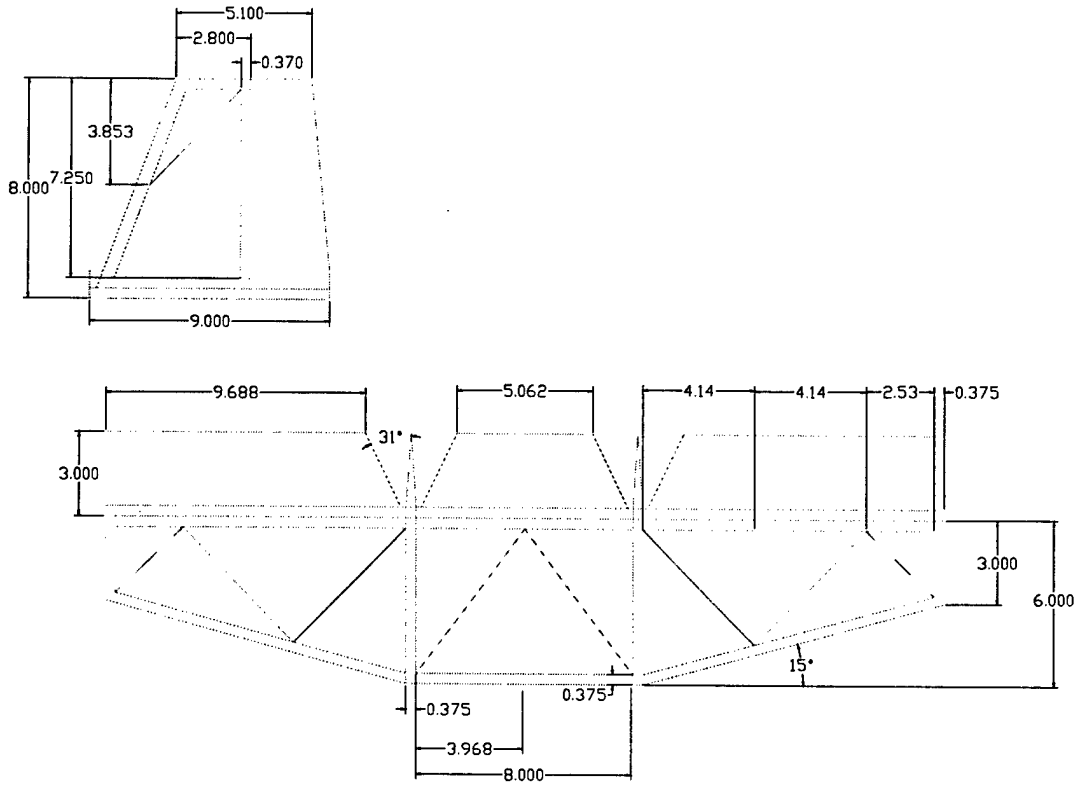

Figure 5.2.3 Horizontal and Vertical Stabilizer Dimensions

5.3 Motor and Propeller Analysis

As previously stated, the AstroFlight Cobalt 60 motor powers the K-03 Pegasus. This motor provides adequate thrust needed for a minimal mission time. According to AstoFlight specifications, a propeller for this motor should be within the range of 18x12 to 20x10. The first number represents the length of the propeller and the second number represents the pitch. Since this range of propeller is large in length, the smallest recommended propeller was chosen. Possible propeller types include: wood, plastic, and composite. In the past, plastic propellers were known to loose their shape. As it spins, the tips go forward and the propeller looses its efficiency. Wooden propellers are light and keep their shape but shatter upon minimal impact. If landing is imprecise, the wooden propeller tip could nick the ground and ruin the mission. APC propellers made from composite materials are known as the most efficient propellers on the market. They keep their shape and have strong tips that do not give in the event of impact. The final decision was an 18x20 APC composite propeller.

In the past, motors were attached to the front of the fuselage with a firewall and a motor mount. With the design of the CAGE, a firewall and motor mount are no longer necessary. The aluminum structure of the CAGE will support the motor and keep the payload from damaging the motor on landing.

5.4 Fuselage Analysis

5.4.1 Rib Design

Seen in Figure 5.4.1 is a diagram of the CAGE, fuselage ribs, battery, and tail cone sections. Originally an air scoop was part of the design of the fuselage due to past experience of the aircraft heating up. This idea was taken out of the design due to many constraints including the fitting of the wing, batteries, and tail boom supports.

With an angle attack of 8 degrees the trailing edge of the wing did not allow the batteries to be easily loaded from the back of the plane. Therefore, the batteries are loaded out of the front of the plane allowing the wing to be attached when loading or unloading the batteries.

The tail boom structure depends on the support of two carbon fiber rods. These rods extend into the fuselage parallel to the CAGE. Both the batteries and the carbon fiber rods must run through the ribs. The batteries, CAGE, Payload, and wing have all been centered about the CG with the aerodynamic center of lift of the wing at the CG as well.

The rib design does not allow the batteries to slide past the 5^{th} rib, and the carbon fiber tail supports do not extend forward past the landing gear bar. A plug will keep the batteries from shifting forward, and the carbon rods will be glued into place within the ribs.

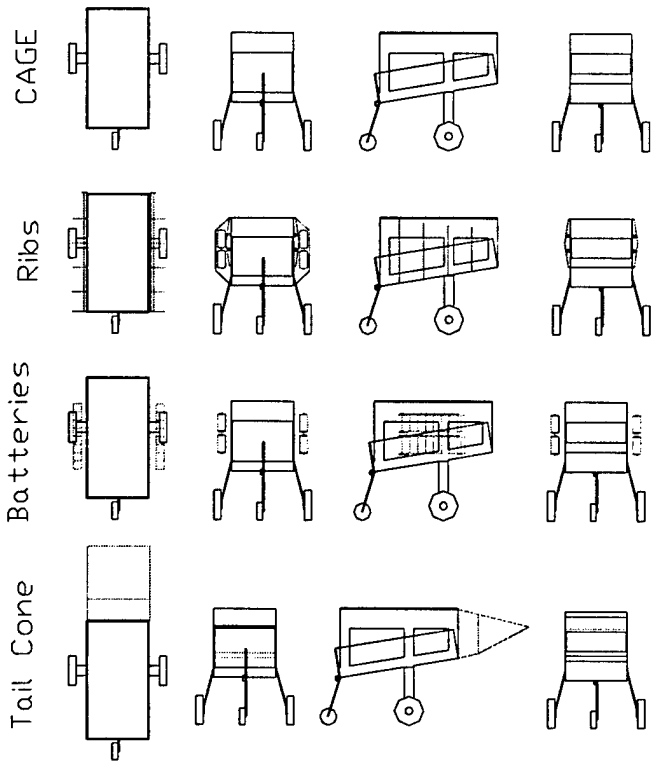

Figure 5.4.1a Detail Fuselage Configuration

The design of the ribs (seen in Figure 5.4.1b) decreases in size due to the slope of the CAGE and the placement of the wing. The air scoop could not be added to the design because there was not enough clearance to add one. Taking out more area from the ribs would reduce the structural stability of the ribs. Therefore, to cool the batteries the sides of the fuselage by the batteries will be covered in Monokote to allow all of the heat to dissipate to the outside air.

5.4.2 Tail Cone Design

A tail cone has been added to reduce drag in the back of the aircraft. The tail cone is a triangular shape and the top and bottom meet at a point higher than the CAGE's back middle. This is done in hopes that the flow will remain attached once it flows out from the fuselage. The flow will be directed up and over the horizontal stabilizer. This is extremely important because the large propeller will cause turbulent flow in its wake. When testing designs for the tail cone in the water tunnel the double boom design with a tail cone showed results to reassure these conclusions

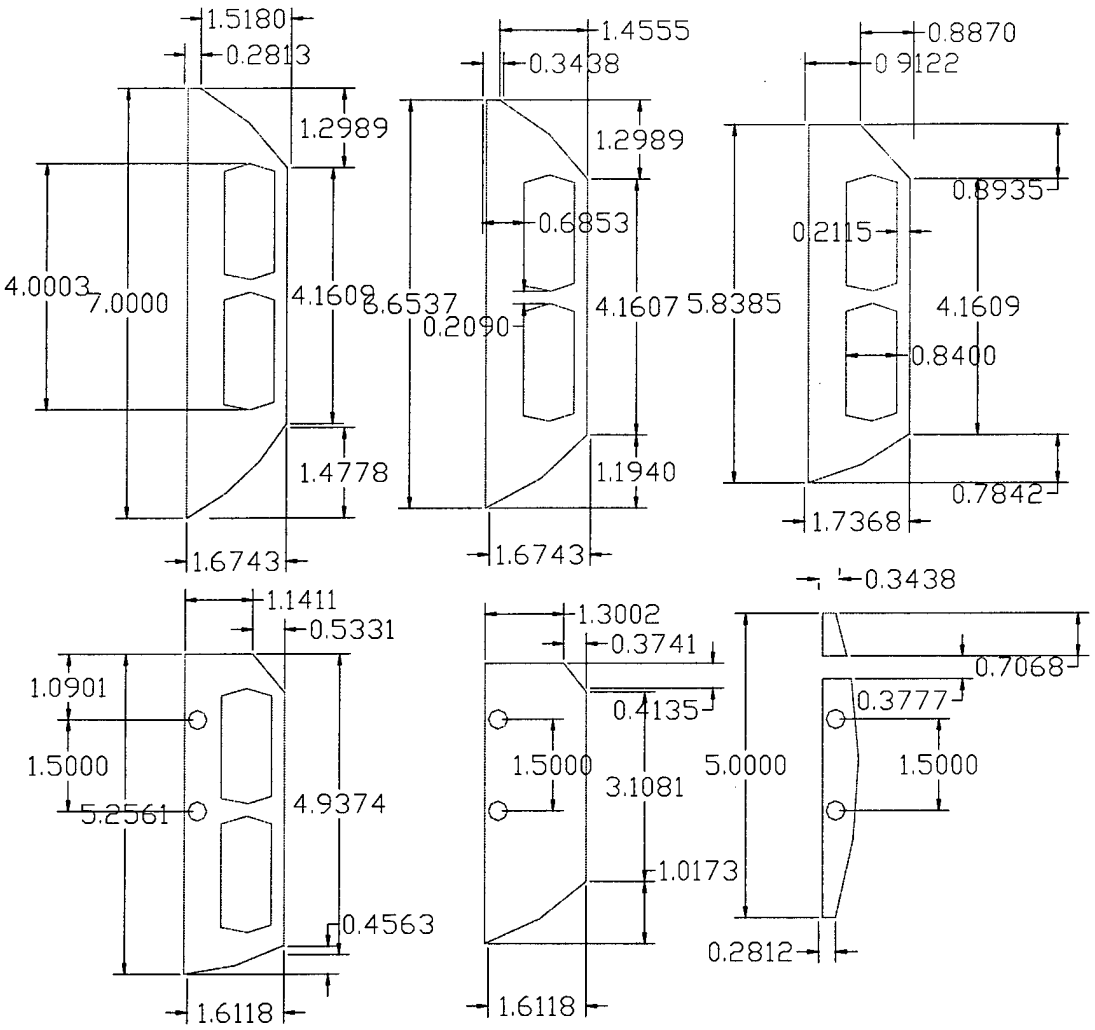

Figure 5.4.1b Rib Components

5.4.3 CAGE Design

The final design for the CAGE can be seen in figure 5.4.1a. Aluminum sheet metal will be used to form the shape of the cage. Having the CAGE milled out of a solid block would be too expensive, and using a method of bars welded together will allow weak points at the welds. The figure does not show the holes that will be drilled out of the CAGE to reduce its weight. The motor will be directly attached to the CAGE along with the ribs structure.

5.4.4 Landing Gear Final Design

The front landing gear and the main gear will include rollerblade wheels that have been shaved down to a thinner size. The roller blade wheels will not allow the plane to bounce and have shown to absorb the shock of landing well in previous competitions. The front landing gear will be connected to the rudder servo for steering on the ground. Our team believes that while in flight the angle of the landing gear when the rudder is moved will not cause a considerable amount of drag.

5.5 Sized Aircraft Data and Drawing Package

The following tables list the sized aircraft data for K-03 Pegasus.

Geometry	
Length	4.25 ft
Span	8.5 ft
Height	17.65 in
Wing Area	7.225 ft^2
Aspect Ratio	8.8

Performance	Loaded	Unloaded
CL max	1.213	1.213
CD max	0.019	0.019
Stall Speed	29.878 mi/hr	25.875 mi/hr
Rate of Climb	27.149 mi/hr	36.198 mi/hr
Take-off length	30 ft	16.3 ft

Weight Statement	
Airframe	8 lbs
Propulsion System	25 oz
Payload System	5 lbs
Empty Weight	15 lbs
Gross Weight	20 lbs

Systems	
Radio	9 Channel Futaba
Servos	Futaba Low Torque
Batteries	Sanyo RC 2400
Motor	AstroFlight Cobalt 60 Superbox
Propeller	APC 18x12
Gear Ratio	2.75 to 1

The next three pages include the drawing package for K-03 Pegasus.

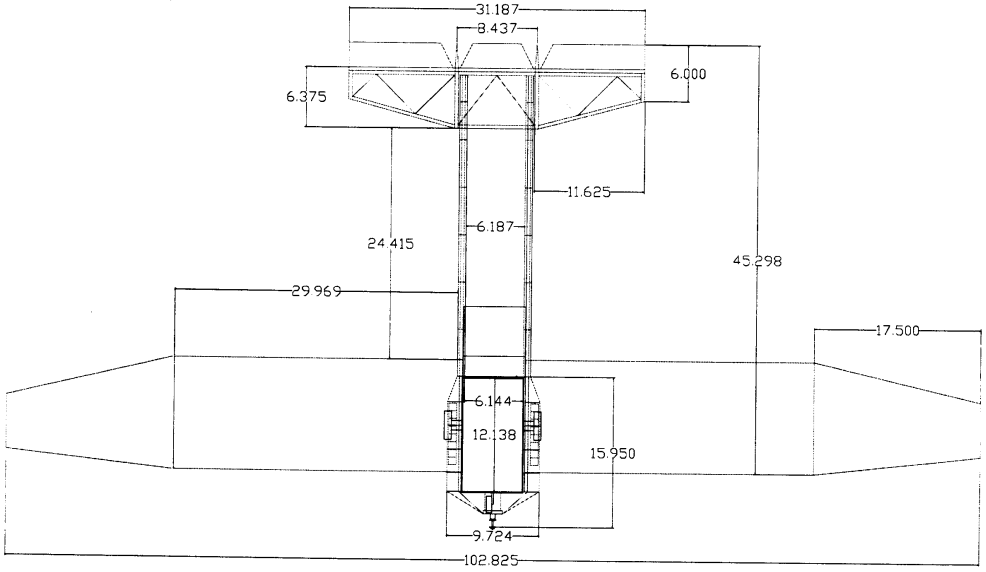
31.187
8.437
6.000
6.375
11.625
6.187
24.415
45.298
29.969
17.500
6.144
12.138
15.950
9.724
102.825

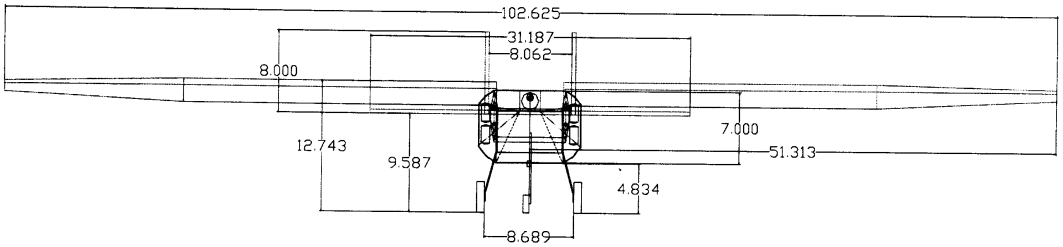
102.625
31.187
8.062
8.000
7.000
12.743
9.587
51.313
4.834
8.689

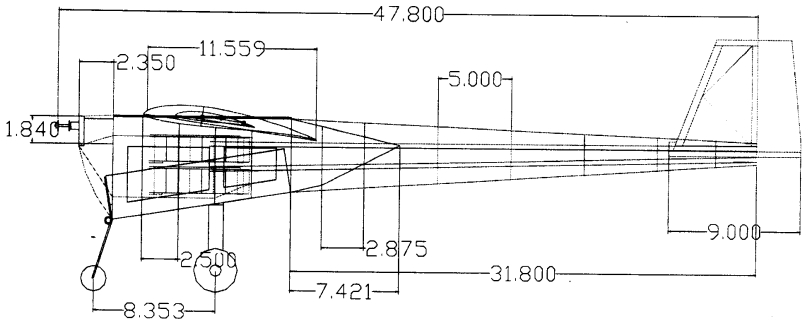
47.800
11.559
2.350
5.000
1.840
9.000
2.875
2.500
31.800
7.421
8.353

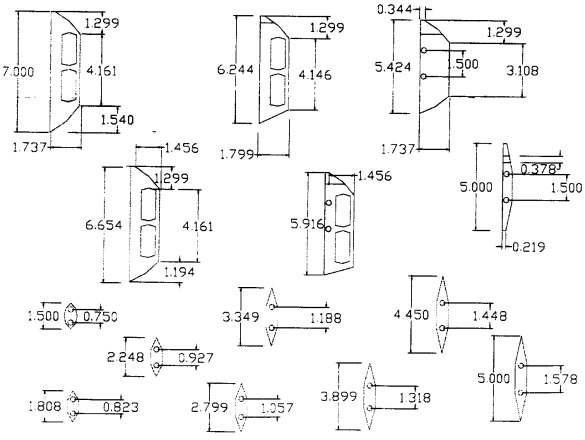
1.299
7.000
4.161
1.540
1.737
1.299
6.244
4.146
1.799
0.344
1.299
5.424
1.500
3.108
1.737
1.456
1.299
6.654
4.161
1.194
1.456
5.916
0.378
5.000
1.500
0.219
1.500
0.750
3.349
1.188
4.450
1.448
2.248
0.927
5.000
1.578
1.808
0.823
2.799
1.057
3.899
1.318

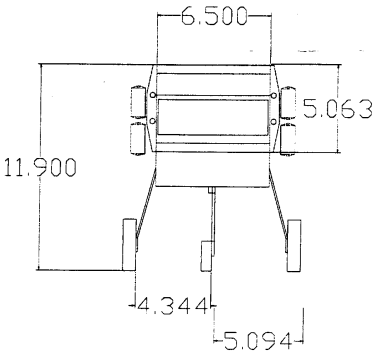
6.500
5.063
11.900
4.344
5.094

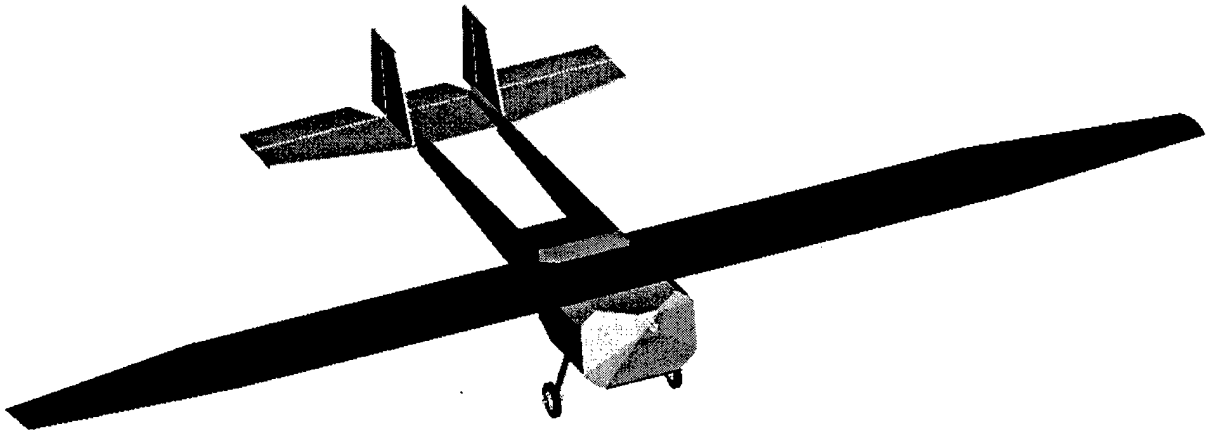

Isometric view of final plane design

Front view of final plane design

Left side view of final plane design

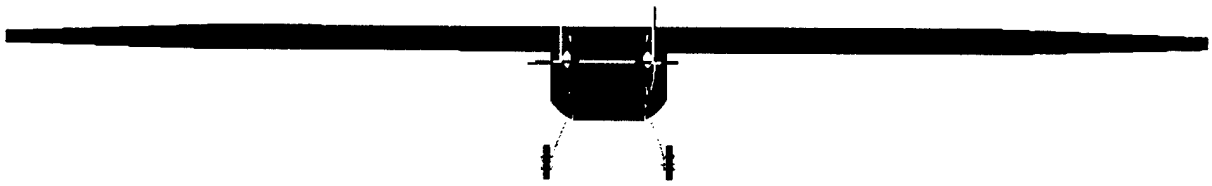

Rear view of final plane design

6.0 MANUFACTURING PLAN

6.1 Component Manufacturing Process

Manufacturing was a recurring concern in each stage of K-03 Pegasus' design. In this section, the manufacturing process for each component is summarized.

6.1.1 Fuselage, CAGE, and Landing Gear

The CAGE is the prime component of the fuselage. As stated throughout the design process, the CAGE supports the load of all the other components as well as the payload. With this in mind, it needs to be strong but light enough to keep the total aircraft weight low. Making the CAGE out of aluminum provides both strength and low weight. Since no team members were skilled in working with aluminum, the design of the CAGE was sent to the automotive shop on UCF's campus. Members of the Society of Automotive Engineers (SAE) were eager to help construct the CAGE. After forming the aluminum shell, they drilled holes throughout the structure to reduce weight. After the CAGE was finished, the aluminum landing gear was welded into place and the payload dropping mechanism was installed.

To create the shape of the fuselage, plywood ribs will be attached to the CAGE structure to make the fuselage more streamline. It is easier to have the ribs laser cut than cut by hand. Knowing this, the rib drawings and specifications will be sent to Full Spectrum for professional laser cutting. Full Spectrum will cut notches into the rib's perimeter for stringer attachment and will cut larger notches inside the ribs to support the battery packs. The stringers will connect each rib and will then be covered in light ply sheeting to make the full shape of the fuselage.

6.1.2 Wing

In order to ease the wing's manufacturing process, the aerodynamic team searched for a skilled foam cutter. The search ended with a company named Compu-Foam. With an AutoCad drawing of the wing and the wing's specifications, Compu-Foam carved the core section of the aircraft's wing. After the wing was carved, the aerodynamic team carved another section for the spars, covered the wing with light ply and epoxy, and attached the control surfaces. As mentioned in the detail design, the spar of the wing is a hollow carbon fiber tube and will attach to the fuselage by protruding carbon fiber rods.

6.1.3 Empennage

The empennage boom sections were constructed of balsa ribs and stringers with two carbon fiber rods running through the center of each rib. To complete the structure light ply sheeting was used to cover the booms. The horizontal and vertical stabilizers were constructed from balsa and covered with the same light ply sheeting making a complete empennage structure with detachable control surfaces.

6.2 Analytic Methods Including Cost, Scheduling and Skills

6.2.1 Tabulated Manufacturing Cost

The major costs for manufacturing K-03 Pegasus can be seen in Table 6.2.1.

Table 6.2.1 Manufacturing Cost Breakdown

AstroFlight

Product #	Description	Unit Price	Quantity	Total
661S	AstroFlight Cobalt 661s motor with super box	$319.95	1	$319.95
			Total	$319.95

TNR Technical

Product #	Description	Unit Price	Quantity	Total
RC-2400	Sanyo RC 2400 high rate	$6.00	32	$192.00
	Battery "zap"	$1.00	32	$32.00
	Labor (shrink wrap and wires)	$20.00	1	$20.00
			Total	$244.00

Colonial Photo and Hobby

Product #	Description	Unit Price	Quantity	Total
-	Speed Controller Astroflight 212D	$109.99	1	$109.99
-	9 Channel Futaba Computerized PCM Radio	$380.00	1	$380.00
-	6 Volt Battery Pack 1000mA	$35.99	1	$35.99
-	Pearl Yellow Monokote	$13.49	1	$13.49
-	Black Monokote	$11.99	1	$11.99
-	Light ply	$5.00	20	$100.00
			Total	$651.46

Tower Hobbies

Product #	Description	Unit Price	Quantity	Total
LXK320	sand paper 80	$4.99	1	$4.99
LXK321	sand paper 150	$4.99	1	$4.99
LXK323	sand paper 220	$4.99	1	$4.99
			Total	$14.97

Balsa USA

Product #	Description	Unit Price	Quantity	Total
	Adhesives			
708	2 oz. Quik-Shot w/sprayer	$3.25	1	$3.25
710	2 oz. Un-Stick-It Debonder	$3.95	2	$7.90
712	Replacement Bottle Tips	$1.19	4	$4.76
A702	2 oz. Tin	$10.95	3	$32.85
A705	2 oz. Thick	$10.95	5	$54.75
	Epoxy			
544	5 Minute	$5.49	2	$10.98
545	12 Minute	$5.49	2	$10.98
546	30 Minute	$5.49	1	$5.49
	Balsa Sheets			
81	1/16	$0.54	5	$2.70
82	3/32	$0.65	5	$3.25
			Total	$136.91

Compu-Foam

Product #	Description	Unit Price	Quantity	Total
-	Foam Wing	$45.00	2	$90.00
			Total	$90.00

The total for the manufacturing cost breakdown is roughly $1,500.00.

6.2.2 Required Skill Level

The manufacturing ability changes from team member to team member. Different backgrounds bring different skills to the team but not all manufacturing aspects are covered. Table 6.2.2 highlights the most comfortable manufacturing levels for the team. By choosing a familiar manufacturing process or a process that can be learned with ease, the aircraft can be constructed more efficiently. The plus signs symbolize where each process is desirable, while negative signs symbolize where the process is undesirable. Zeros symbolize indifference.

Table 6.2.2 Skill Level Matrix

		Cost	Availability	Skill Level	Time Required	Total
Component	**Process**					
Wing	Foam/ Carbon Fiber	-	0	-	-	-3
	Foam/Light Ply	0	+	+	+	3
	Ribs/Monokote	+	+	0	+	3
Vertical/Horizontal Stabilizers	Airfoil & Foam	+	+	+	-	3
	Balsa Ribs & Flat Plate	+	+	+	+	4
Empennage	Ribs & Stringers	+	+	+	+	4
	Truss	-	+	-	-	-2
Fuselage	Ribs & Stringers	+	+	+	+	4
	Box Beam	+	+	+	-	3

6.2.3 Manufacturing Milestone Chart

A milestone chart including scheduled event timings is described in Figure 6.2.3.

ID	Task Name	December	January	February	March	April
1	**Manufacturing**					
2	Find and order supplies					
3	Construct CAGE					
4	Get wing cut					
5	Put spar in wing					
6	Light ply over wing					
7	Construct fuselage around CAGE					
8	Construct horiz and vert stabilizers					
9	Finish double boom tail					
10	Mount motor to CAGE					
11	Mount landing gear to CAGE					
12	Mount tail to fuselage					
13	Mount wing to CAGE					
14	Build box					
15	Take apart and put in box					4/10

Figure 6.2.3 Schedule and Milestones for K-03 Pegasus

7.0 TESTING

In past years the electric airplane team at UCF has done minimal testing for their aircraft design. Much of this was due to lack of facilities at the university. Within the last year our team has become very familiar with many ways to test our design. The first method of testing was done with wings; in particular, different manufactured types of wings. The second step in testing was to use a water tunnel to test conceptual designs for the tail and fuselage configuration. The last step was to test models in virtual 3-D programs, a step which is currently going on. Another step that will be explored is prototyping small models of the entire plane to test in the water tunnel.

7.1 Static Wing Test

A static test was performed to test the rigidity of different types of wing construction. Of the four sections tested, one was constructed with balsa ribs and covered with Monokote, one with balsa ribs and balsa ply covering, one with a foam core and balsa and carbon fiber covering, and one with a foam core and only carbon fiber covering. Each wing was two feet and two inches in length, and the load was applied at one foot from the clamped end. The deflection of each wing section was measured in inches and the results can be found in Table 7.1.1.

Table 7.1.1 Static Wing Test Results

Wing type	Deflections for 4.81 N-m moment (in)	Deflections for 12.20 N-m moment (in)
Balsa ribs, Monokote covering	0.75	1
Balsa ribs, balsa covering	0.5	0.75
Foam core, balsa and carbon fiber covering	0.0625	0.1875
Foam core, carbon fiber covering	0.0625	0.375

7.2 Dynamic Fuselage design testing

The second phase of testing was a water tunnel test of three fuselage designs. Deciphering between the results was difficult in the end. The method of comparing the results from the water tunnel to what would actually happen in the air is as follows

In water

$$\mu_{water} := .000891\frac{(N\cdot s)}{m^2} \qquad \rho_{water} := 62\frac{lbf}{ft^3} \qquad x_w := 6in \qquad V_w := 3\frac{in}{s}$$

$$R_{ew} := \frac{\rho_{water}\cdot V_w\cdot x_w}{\mu_{water}\cdot g} \qquad R_{ew} = 1.294\times 10^4$$

In air:

$$\mu_{air} := 1.894\,10^{-5}\cdot\frac{kg}{m\cdot s} \qquad \rho_{air} := 1.225\frac{kg}{m^3} \qquad X_{air} := 1ft$$

$$V_{air} := \frac{R_{ew}\cdot\mu_{air}}{\rho_{air}\cdot X_{air}} \qquad V_{air} = 0.657\frac{m}{s}$$

Figure 7.2a Velocity scaling calculations

As seen above in Figure 7.2a, the research done in the water tunnel represents performance that would occur at a velocity in air of .657m/s or 1.469 mi/hr.

In the Figure 7.2b you can see the boundary layer occurring between the flow and the objects. The visualization of this process is done with ink being injected into the flow. The models, made of balsa and ply, were painted white to aid in the visualization of this test.

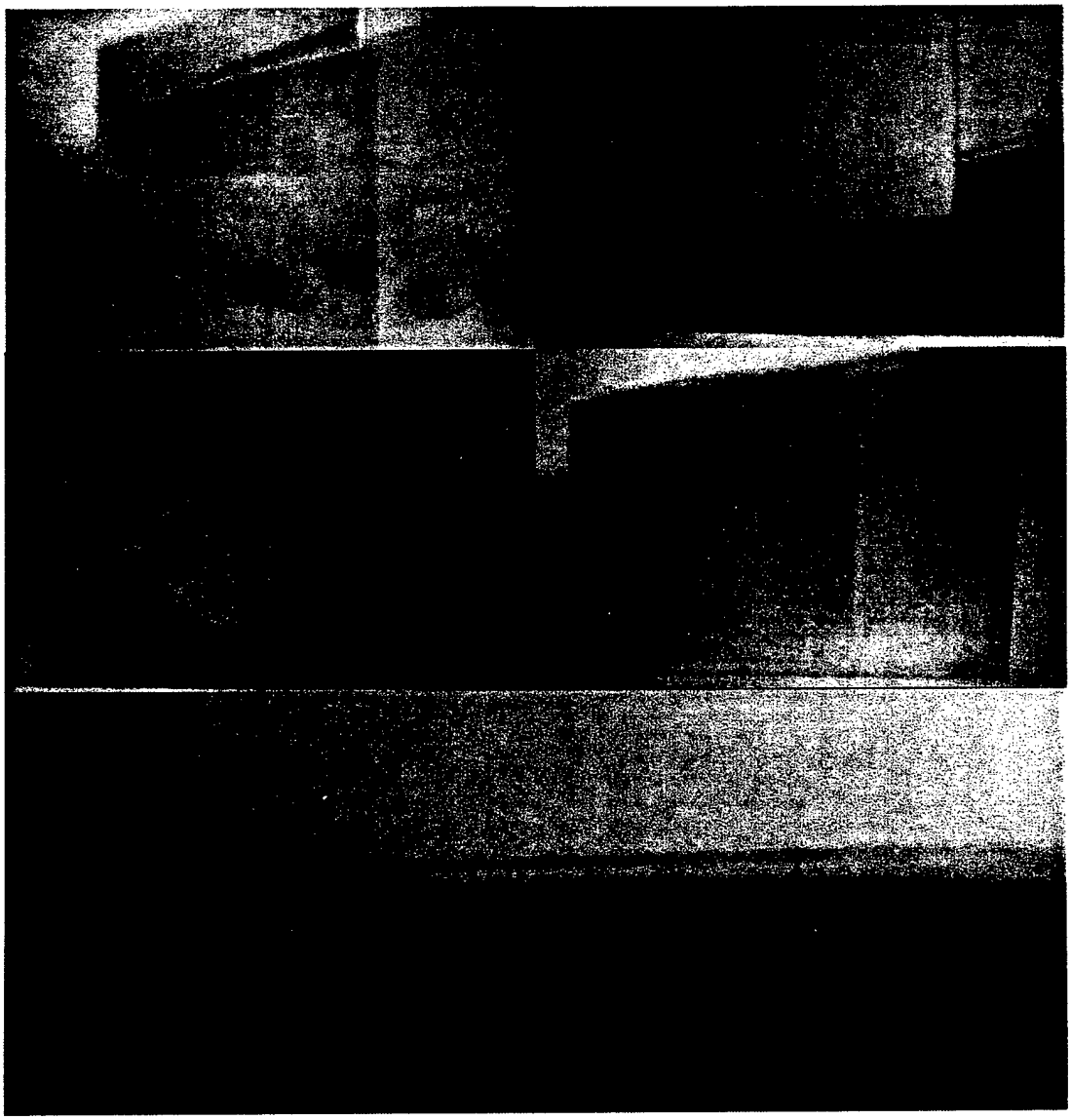

Figure 7.2b Observations of boundary layer in water tunnel testing

On the next page, Figure 7.2c shows three examples of flow separation that were visually observed. In the pictures the dark areas are vortices carrying the ink. The further away the flow got from the test object the larger the vortices became.

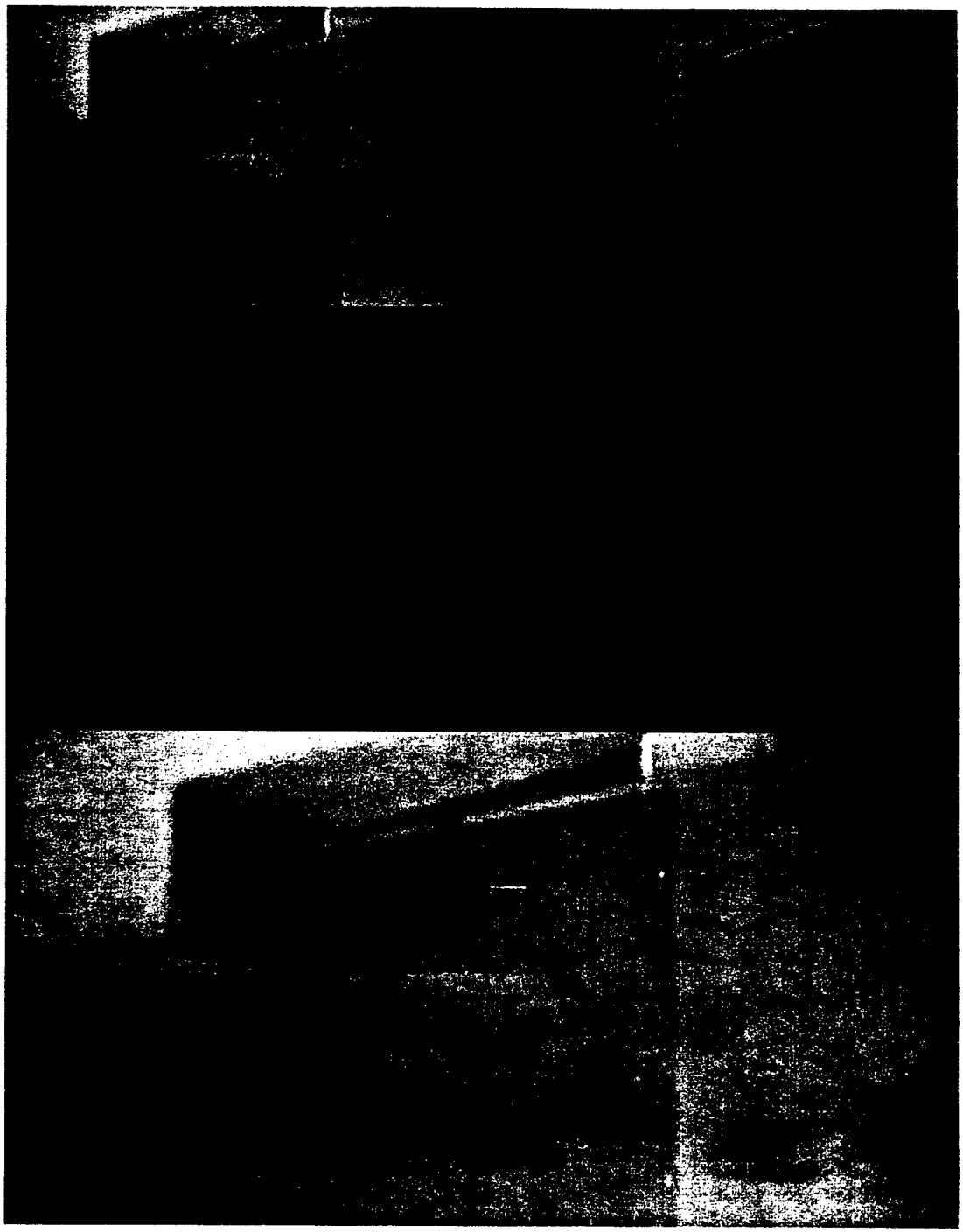

Figure 7.2c Close up of prototype's rear vortices

This test was the main deciding factor in the choice of a double boom empennage for our design. As seen in the Figure 7.2d and Figure 7.2e, the double boom allowed for the flow to become laminar again, beyond the area of the fuselage. The ink in the fluid can be seen flowing back into one single streamline; this is best shown in Figure 7.2e.

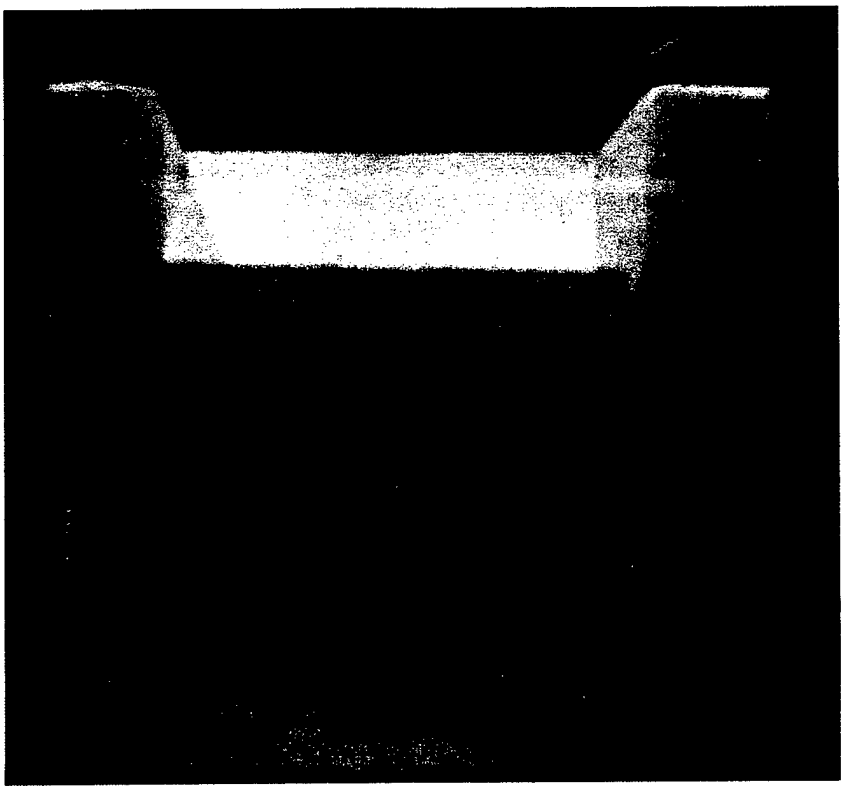

Figure 7.2d Rear view of double boom water tunnel test

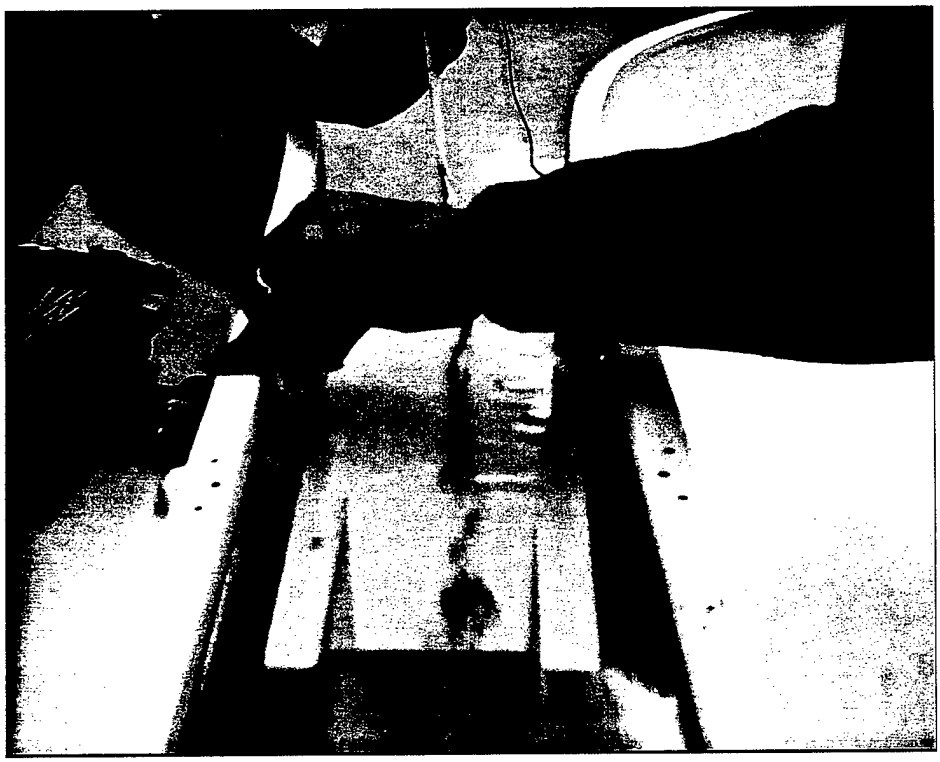

Figure 7.2e Top/rear diagonal view of double boom water tunnel test

7.3 3-Dimensional Testing

Currently testing is in progress to model the aircraft in a virtual 3-D manner. Two programs were the main focus for this process. These two programs were I-DEAS and Fluent. I-DEAS is a program in which forces can be placed on a 3-D design and their stress distribution analyzed. The main item that underwent analysis was the CAGE design. The results of the CAGE analysis were positive and reassured us that our design would not fail upon impact. Fluent will be used to map the aerodynamics of the virtual 3-D model. This will help show air behavior not only around the wing area but also the aircraft as a whole.

7.4 Scaled Model Testing

The final step in the process of testing the plane was to model the aircraft in a scaled manner. Two ideas for making such a model were either by method of balsa or by a resin rapid prototype model. An attempt to continue with this track is still ongoing.

The rapid prototype method is done using an ultra violet laser to mold a resin layer by layer. This method is expensive and the process of developing funds to afford a model of this nature is not currently within the team's grasp.

The second method, balsa, was found to not be strong enough for the water tunnel. The model was six inches long and incredibly delicate. The model never could be tested in the water tunnel. Small ribs were cut from balsa and covered with paper. The paper was sealed with paint but was found to not be water tight enough to give sufficient data in a test. In conclusion, the plane will be modeled with the rapid prototyping method and tested in the water tunnel for final analysis.

8.0 REFERENCES

Abbot, I. H. and A. E. von Doenhoff. Theory Of Wing Sections. New York: Dover Publications, Inc., 1959.

Beer, F. P. and E. R. Johnston Jr.. Vector Mechanics for Engineers. Boston: McGraw-Hill, 1997.

Anderson, John D., Jr.,. Introduction to Flight. Boston: McGraw-Hill, 2000.

"Astro Flight Inc.." Cobalt Airplane Motors. 2000. AstroFlight, Inc.. September 19, 2002 <www.astroflight.com>.

"TNR Technical." Nicad / NiMH Batteries. 2002. TNR Technical, Inc.. September 19, 2002 <www.tnrtechnical.com>.

"NASG Airfoil Database." All Airfoils. NASG January 24, 2003. <http://wwww.masg.com/afdb/list-airfoil-e.phtml>.

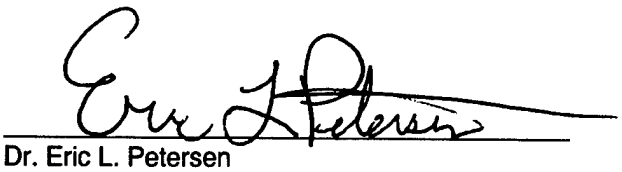

Dr. Eric L. Petersen

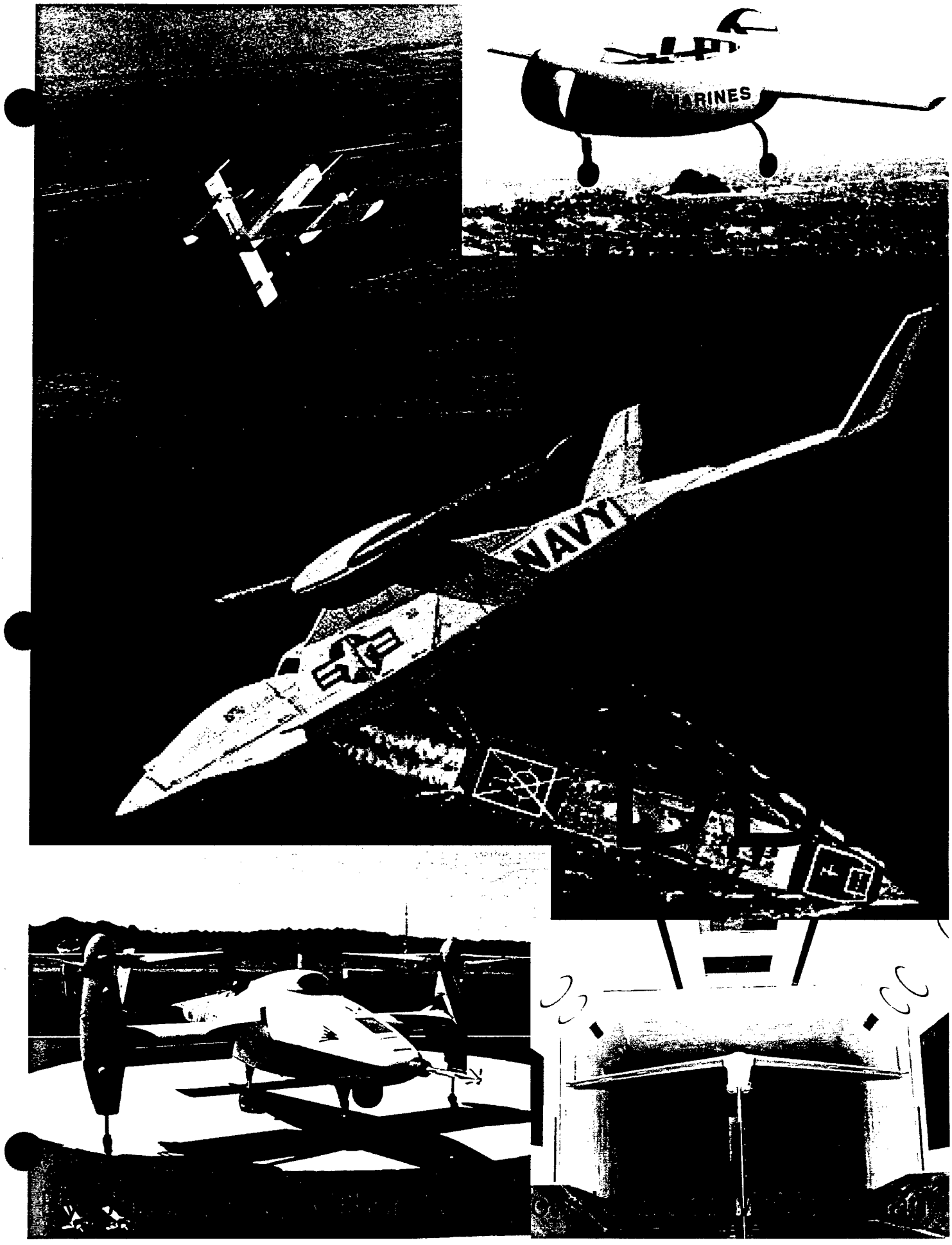
MARINES
NAVY

American Institute of Aeronautics and Astronautics

State University of New York at Buffalo

2002-2003 Cessna/ONR Student Design/Build/Fly Competition

UB "Firer Fly"

Design Report

Presented by: Jason Reiter, Gilbert Romanowski & Joe McManaman

Table of Contents

1.0 Executive Summary	2
2.0 Management Summary	2
3.0 Conceptual Design	4
4.0 Preliminary Design	13
5.0 Detailed Design	22
6.0 Manufacturing Plan	27
7.0 Testing Plan	32

1.0 Executive Summary

The AIAA club at the State University of New York at Buffalo, is participating in this years Cessna/ONR Student Design Build Fly Competition (DBF). Hosted by the Office of Naval Research, the competition will be held at Webster Field part of the NAVY Patuxent River Flight Test Center complex. The UB AIAA design team is responsible for designing, building, and flying an aircraft, at the competition, that meets the restrictions and specifications set forth in the competition guidelines.

The first stage in the development of the design was the conceptual design stage. During this stage various aircraft configurations were looked at. This included configurations for the fuselage, wing, and tail. The configuration was decided on by using a Figure of Merit (FOM). The FOM is a system by which we rate a configuration based on certain characteristics. This chart can be seen in the *Conceptual Design* of the report. For this stage of the design we researched all aspects of the fuselage, wing, and tail configurations. We looked at the advantages and the disadvantages; this also factored into the decision making process.

Preliminary design was the second phase of the development process to be completed. For this phase we conducted basic calculations for weight, and sizing the aircraft (i.e. Wing Loading, Wing Area, etc.). Also included in this section was investigation of lift, drag and stability characteristics of the configuration. The major factors concentrated on for the preliminary design stage was sizing the aircraft to fit in the box requirement.

The stage that followed preliminary design was detailed design. This is the phase of design where we concentrated on the material to be used for each component, the selection of electrical components and finalizing the configuration with scaled drawings. This stage was the focus of making sure everything was worked out so that the manufacturing process could begin.

Manufacturing of the aircraft was where the team began to see their design come to life. This phase of design was carried out by following all of the research and plans that were laid out prior to the manufacturing process. This phase of the design is still in progress and will lead to the testing stage.

2.0 Management Summary

The design team was composed of three individuals, Joe McManaman, Jason Reiter, and Gilbert Romanowski, all seniors in Aerospace Engineering at UB. The rest of the UB AIAA club will participate in the manufacturing process and the competition. During each stage of the design process, the team discussed each of the tasks they faced and then once an attack plan was figured out the team equally divided the tasks. Each individual was responsible for their own task. Once each had completed their task, the team got together to go through the information and decide the proper steps to take.

		Joe McManaman	Jason Reiter	Gil Romanowski	AIAA Club
Conceptual Design	Fuselage			X	
	Wing		X		
	Tail	X			
	Propulsion	X			
	Drawings	X	X	X	
Preliminary Design	Fuselage			X	
	Wing		X	X	
	Tail			X	
Detailed Design	Material	X	X	X	
	Fuselage	X	X	X	
	Wing	X	X	X	
	Tail	X	X	X	
	Propulsion	X	X	X	
	Configuration	X	X	X	
Testing	Static		X		
	Weights			X	
	Volume	X			
	Dynamic	X	X	X	
Report	Executive Summary		X		
	Management Summary		X		
	Conceptual Design		X		
	Preliminary Design	X			
	Detailed Design	X	X	X	
	Manufacturing Plan			X	
	Testing Plan		X	X	
	CADD Drawing	X			
	Manufacturing	X	X	X	X

Figure 2.1 – Team Task List

The figure above is a breakdown of the tasks carried out. As can be seen in the figure, many of the tasks were worked on collectively.

Planned Schedule of Operations			
		Date	Series
Conceptual Design	Start	9/16/2002	1
	End	10/4/2002	1
Preliminary Design	Start	10/7/2002	2
	End	11/15/2002	2
Detailed Design	Start	11/1/2002	3
	End	12/17/2002	3
Manufacturing	Start	1/15/2003	4
	End	3/27/2003	4
Report	Start	2/19/2003	5
	End	3/7/2003	5
Testing	Start	3/3/2003	6
	End	4/8/2003	6
Test Flights	Start	4/9/2003	7
	End	4/22/2003	7

Actual Schedule of Operations			
		Date	Series
Conceptual Design	Start	9/16/2002	1.25
	End	10/10/2002	1.25
Preliminary Design	Start	10/9/2002	2.25
	End	11/18/2002	2.25
Detailed Design	Start	11/15/2002	3.25
	Temp End	12/18/2002	3.25
	Resume	1/15/2003	3.25
	End	1/17/2003	3.25
Manufacturing	Start	1/15/2003	4.25
	In Progress		4.25
Report	Start	2/25/2003	5.25
	End	3/8/2003	5.25
Testing	Delayed		
Test Flights	Delayed		

Figure 2.2

Milestone Chart
Figure 2.3

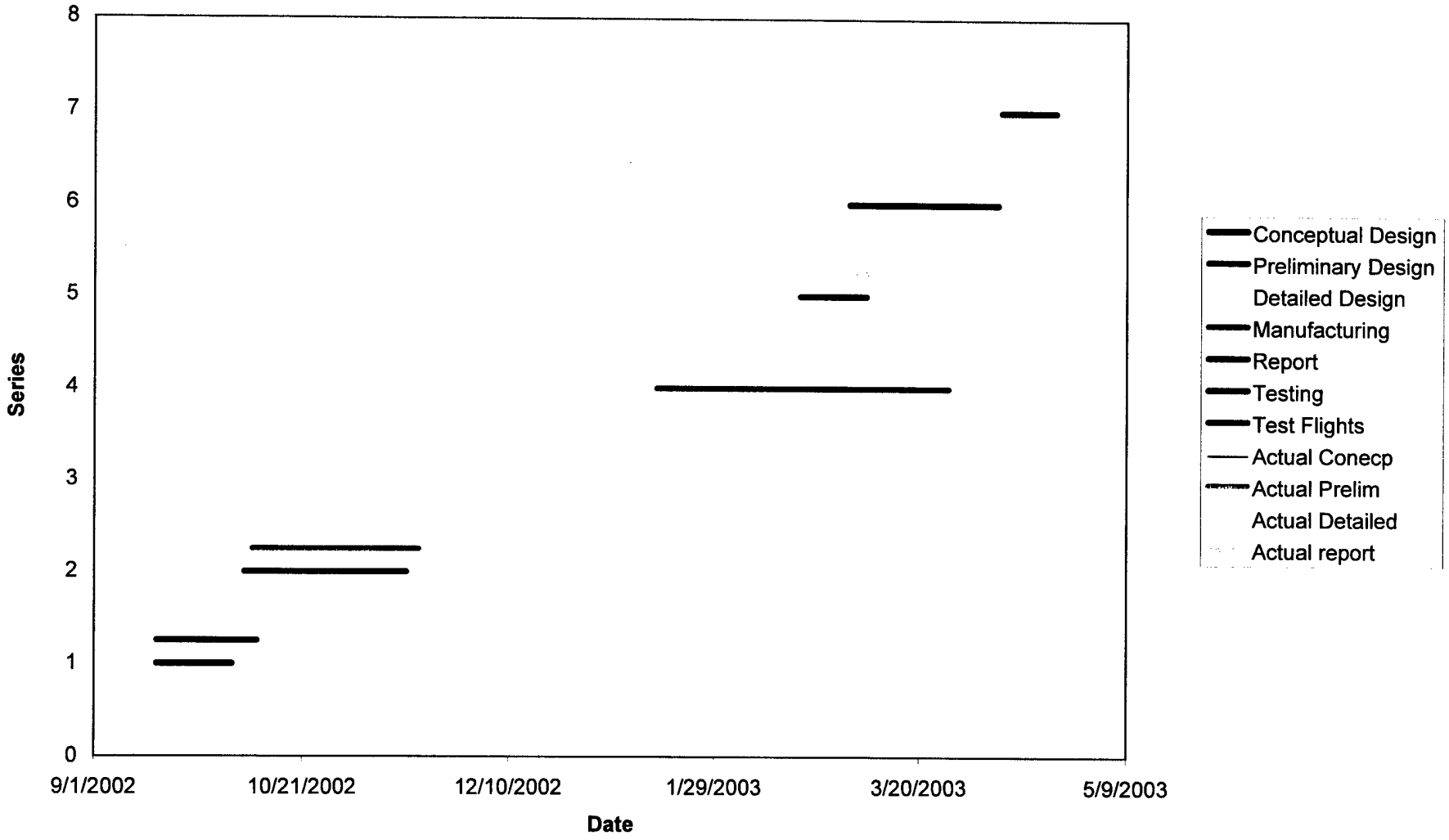

Figure 2.2 depicts a schedule of the development process. One set of data is for the planned schedule. At the beginning of the UB fall school semester, the design team discussed and came up with goals of when they wanted to start and have things finished by. As can be seen in the chart (Figure 2.3) the team's actual schedule follows the planned one quite closely. Reasons for deviation in the plan come from complications within the design process as well as the amount of class work each of the members had to handle. Note: Winter break started December 18th and the spring semester started up again on January 12th. During this time period no work was completed in the development process of the aircraft. This was due to the fact that the design team was spread out throughout the State of New York.

3.0 Conceptual Design

The goal of the conceptual design phase was to analyze the strengths and weaknesses of all aspects of aircraft configurations for the fuselage, wings, and tail. This analysis was based on the constraints in the mission specifications imposed by the rules of the competition.
The first and foremost constraint is that the aircraft has to fit in a 4' x 2' x 1' box (interior dimensions). During each of our flight attempts we will be completing one of three missions. One of the missions we can choose to do is *Missile Decoy*. For this mission the payload is a 12" x 6" x 6" box weighing a minimum of 5.0 lbs. The aircraft must also have a simulated cylindrical antenna made of PVC pipe 6" diameter, and 3" in height. The ends will be sealed with flat 1/16" plywood sheets. Another mission we can opt to do is the *Sensor Deployment* mission. For this mission the aircraft has to self-deploy a simulated sensor package. The package once again will be a 12" x 6" x 6" box weighing a minimum of 5.0 lbs. The third and final mission we could choose from is the *Communications Repeater*. This mission consists of a single payload, once again a 12" x 6" x 6" box weighing a minimum of 5.0 lbs.

Figure 3.1 exemplifies the Figures of Merit used to determine the configuration of each component of the aircraft. A weighting system, scale, and strength of preferences were used to determine the values that would be assigned.

The design process started off with the selection of the overall configuration, many configurations were designed by the team members. They were all influenced by the mission requirements, technical consideration (i.e. weight, flight stability and relative ease of construction) and by styling considerations. These configurations are presented in Appendix A. They are of a wide variety of configurations with: one to two engines, propellers or ducted fans, various wing configurations and various engine placements.

The configuration we decided to use is a bi-plane wing, a twin fin tail, tricycle landing gear and an aerodynamic fuselage. It is propeller driven by a single electric motor. This configuration was chosen because of its ease of construction and its flight stability qualities, plus everyone liked its persona.

Fuselage

To fulfill the two missions that the team chose to do, a fuselage configuration for the plane had to be decided on. This decision was limited by the mission constraints. Early on in the design process the fuselage configuration of the radio controlled model aircraft shown in figure 3.2 decided on. As it can be seen the fuselage has to contain a small storage compartment represented by the striped area of the fuselage and a mock-up radio antenna seen in the figure as a cylinder on top of the aircraft. Due to these limitations, two configurations were looked at more closely. These were traditional configurations of cargo/passenger aircrafts and single engine fighter aircrafts.

The cargo/passenger configuration does have a benefit; it has a large storage volume. This allows the aircraft to hold a large payload. The mission objectives are to haul a missile decoy (a disc similar to the one on the AWAC) and a communication repeater, not to haul the most cargo. Therefore, this attribute is not as preferable to the attributes of the fighter configuration.

The main attribute of the fighter aircraft configuration's fuselage, is its low drag. Unlike the cargo/passenger aircraft fuselage configuration, which has a large drag coefficient, the fighter aircraft fuselage configuration has a much lower drag coefficient. This is preferable since the drag due to the missile decoy mission is going to be large itself, the drag of the rest of the aircraft should be minimized. And since the internal cargo is limited to a 6" x 6" x 12" volume, the fighter aircraft fuselage configuration with a limited cargo capacity would be sufficient.

Wing

When designing an airplane's wing and airfoil configuration, there are many parameters to take into consideration. Depending on the scope of the missions, (what the plane is used for), the parameters will vary.

When dealing with airfoils there are two parameters to take into consideration, the thickness and the camber. Thicker airfoils are used for low flight speed planes because it allows for more stability and they stall more gradually. By having a thicker airfoil the separation of the boundary layer occurs at the trailing edge. As the angle of attack is increased the turbulent boundary layer increases and gradually moves towards the leading edge. This causes the loss of lift to also be gradual, allowing for a higher angle of attack for stall. The trade off for having a thicker airfoil is that it adds weight to the plane. This means that more thrust and/ or lift needs to be generated. For moderate to thin airfoils, there is an abrupt change in lift and pitching moment when a certain angle of attack is reached. This is because the airflow separates from the leading edge. For small angles of attack the flow will reattach itself. As the angle of attack is increased the flow reattaches itself further and further back on the airfoil, until a certain angle of attack is reached where the flow does not reattach itself, causing the airfoil to stall. Thinner airfoils are generally used for high flight speed aircrafts because they allow for high maneuverability and are lighter.

		Overall Weighting									Total
		0.25		0.1			0.4		0.25		
		Aerodynamics		Manufacturing			Performance		Structure		
		Lift	Drag	Time	Cost	Ease	Stability	Control	Strength	Weight	
Wing	*Weighting*	*0.5*	*0.5*	*0.5*	*0.1*	*0.4*	*0.5*	*0.5*	*0.4*	*0.6*	
	Mono plane	6	8	7	6	7	6	5	7	6	6.24
	Biplane	8	5	5	4	5	9	9	9	5	7.365
	Flying Wing	9	9	8	8	9	1	2	8	7	5.54
Tail	T-Tail	3	5	6	7	5	8	8	4	7	6.22
	V-Tail	1	8	3	9	1	3	3	5	9	4.455
	Tailless	0	10	10	10	10	0	0	0	0	2.25
	Twin Fin	2	5	6	6	7	9	9	8	4	6.515
	Conventional	2	7	8	7	8	7	7	7	6	6.315
Fuselage	Fighter Config	5	9	6	8	7	6	0	7	9	5.66
	Cargo/ Pass Config	8	3	9	4	9	8	0	9	5	5.475
	Private Aircraft Config	4	5	5	6	6	6	0	8	8	4.875
Landing gear	Tricycle	0	1	8	8	8	7	9	8	9	6.275
	Tail dragger	0	2	8	8	8	6	5	6	9	5.2
Wing Config.	Not considered because of Biplane Configuration										
Other Empannages	Not considered because of Fuselage Configuration										

Figure 3.1 - Figures of Merit (FOM)

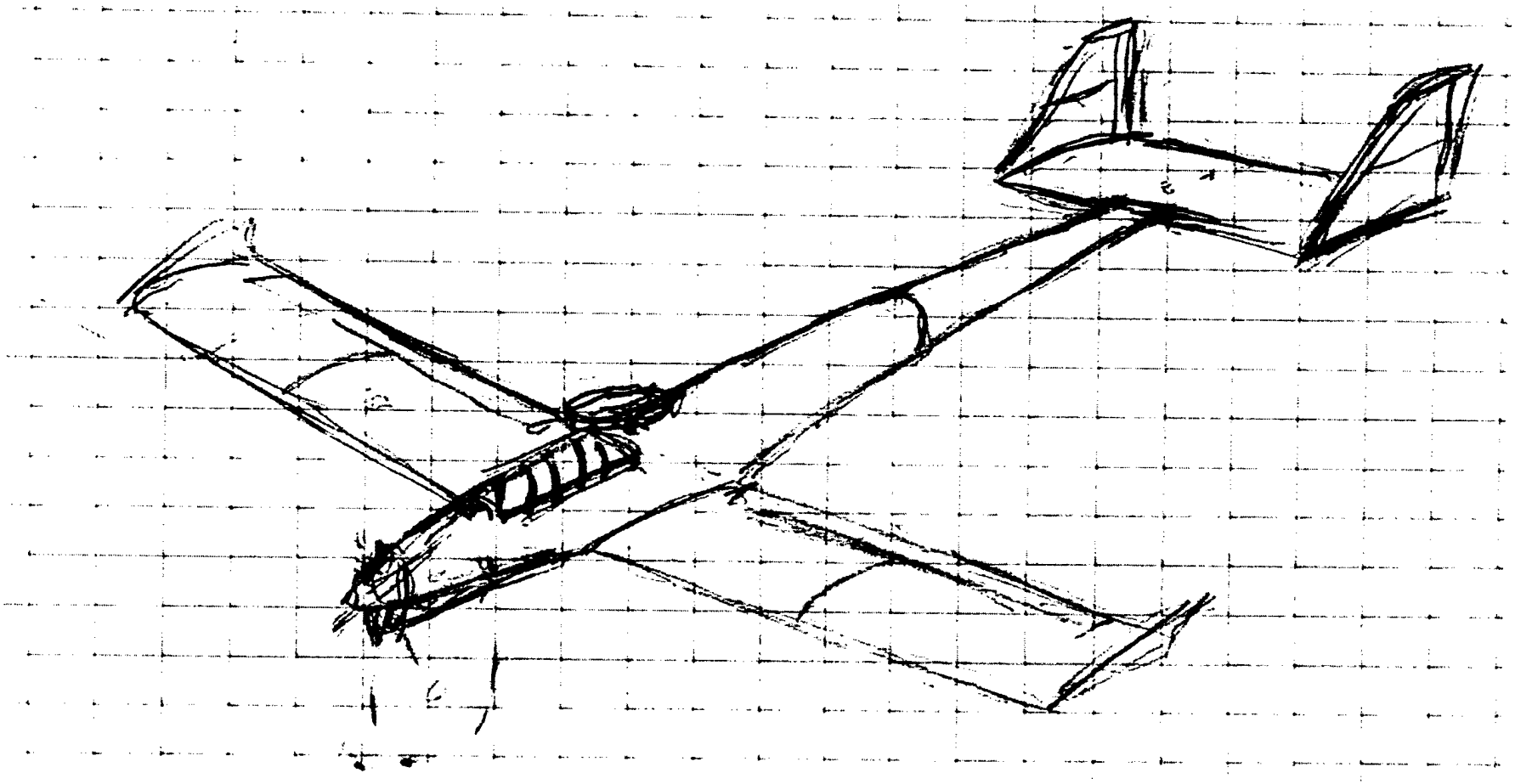

Figure 3.2

They are used on high flight speed airplanes because faster airplanes have more thrust which compensates for the way that the flow separates from the airfoil.

The other major parameter concerning airfoils is the camber. Camber allows for the airflow to remain attached to the airfoil. This increases the lift and simultaneously reduces the drag; the lift to drag ratio is one of the overall parameters that a designer needs to optimize. From graphical data obtained from our Aerodynamics project, it was shown that the camber and the location of the maximum camber contribute a good deal to the change in the aerodynamic characteristics: C_l, C_{mLE}, and X_{cp}. However, since we are dealing with low speed, radio controlled aircrafts, the aerodynamic characteristics do not change drastically with great changes in the camber and its location. This is because of the scale (size) of the plane.

The wing, which is a three-dimensional airfoil, has many parameters itself, not including the airfoil. The first is the aspect ratio of the wing. Larger aspect ratios are preferred for wings because they reduce the effect of wingtip vortices, which are the main contributor to induced drag. Since the bottom of the wing has a higher pressure than the top part of the wing, there tends to be airflow from the bottom to the top. This causes a circulatory flow around the wingtip called a vortex. As the aspect ratio of the wing is increased, the wing comes closer to extending to "infinity". This causes the strength of the vortices to be reduced, and as the wing goes to infinity the vortex strength approaches zero. There is a penalty for increasing the aspect ratio, that is it adds more weight to the plane, and it also lowers the angle of attack for stall. Lower aspect ratios are used for very maneuverable airplanes, where as high aspect ratios are used for airplanes that need greater lift (i.e. gliders, transports).

Associated with reducing induced drag is the configuration of the wingtip. Sharp wingtips make it more difficult for the flow to go from the under-side to the upper-side. A smoothly rounded tip allows the air to flow with relative ease. Another configuration to take into account is the endplate, or the winglet. These types of wingtips block the flow from going from the lower to the upper surface. However, the wetted area of the endplate itself creates drag. Also, by taking the endplates' height and adding it to the span, only 80% of the actual span increase contributes to the effective span increase. When wingspan is limited, endplates and winglets are useful.

Wing twist is a way of preventing tip stall and to revise the lift distribution to approximate an ellipse. By preventing tip stall and having the wing stall at the root, before the tip, it increases control during stall and helps to reduce wing rock. On the other hand, by having wing twist, the wing will be optimized for one lift coefficient, and other lift coefficients will not benefit from the twist as much.

Tapered wings affect the lift distribution. By tapering a wing it starts to act more like an elliptical wing. An elliptical wing is more desired because it minimizes the induced drag. So by tapering the wing more, it takes on the form of the elliptical wing. The wing only needs to have a taper ratio of 0.45 for it to eliminate the effects of an unswept wing, and will produce a lift distribution very close to that of an elliptical wing. By not having a tapered wing, the wingtips produce more lift than is ideal and along with it, generates more drag due to lift.

Dihedral wings help the stability of the plane. With dihedral (when the wingtips are higher than the root), the wings will tend to roll the plane level when it is banked. The dihedral effect also relates to the sweep of the wing and the placement of the wing. For a 10 degree angle of sweep it produces about 1 degree of effective dihedral. In relation to the placement of the wing, an excessive dihedral (if the wing is mounted on the bottom of the fuselage) creates a Dutch roll. However, if the wing is mounted on the top side of the fuselage, for sideslip on the fuselage the flow follows a path that flows over and under the fuselage which causes the flow to push up on the wing increasing the dihedral effect. This is why many high-mounted wings have a negative dihedral effect.

Wing incidence is chosen for an angle to minimize drag at some operating condition, usually cruise. It is chosen so that when the wing is at the correct angle of attack for the selected design condition, the fuselage is at the angle of attack for minimum total drag.

Swept wings are primarily used for transonic and supersonic planes. Swept wings help to delay the effect of shocks, hence our justification for not considering swept wing.

Essentially there are three locations for the wings to be mounted, the top, middle, and bottom of fuselage. Wings that are mounted in the middle of the fuselage are primarily for fighter aircrafts because it does not restrict the pilot's view and allows ground clearance for weapons. The major benefits for having high mounted wings are having the fuselage lower to the ground, engines will have some ground clearance, and the wingtips will not hit the ground for nose-high rolled attitude. The benefit for having the fuselage closer to the ground is for loading and unloading of cargo. By having the fuselage closer to the ground, excess equipment is not needed to raise the cargo to a desired height to load. The reason for clearance of the engines, and wingtips, are pretty obvious. You do not want them to strike the ground because this would cause some major problems. Another advantage to mounting the wing on top is that it allows for larger flaps to be implemented to increase the lift coefficient for STOL aircrafts (Short Takeoff and Landing). Debris, as well as rocks, are not easily accessible to hitting the propellers and the wings. In correlation with our missions, the disadvantages of having a high-mounted wing is that it interferes with our placement of the antenna (a disc along the lines of the AWAC) and the radio package that has to be carried. In correlation with our missions, the low mounted wing has one major advantage, that is the trunnion about which the gear is retracted can be attached directly to the wing box which, being strong already, will not need much extra strengthening to absorb the gear loads. This will allow the landing gear to be stored in the wing itself. A disadvantage to having the low mounted wing is that the fuselage has to be mounted at an incidence angle.

Based on the facts that have been previously stated, we have chosen the following wing and airfoil configuration. An Eppler 387 airfoil is being implemented. As seen in Figure 1, the airfoil has a slight camber to it and it also has some thickness to it. The camber and the thickness give the plane stability and it allows the flow to separate at the trailing edge and it also allows for a gradual loss in lift. For the wing we have decided to go with a bi-plane configuration. The team arrived upon this decision because a high aspect ratio was needed. If a single wing was utilized it would have had to be a 16 ft wingspan which would result in having to bulk up the middle part of the wing for structural support. This

then results in extra weight being added to the plane. By using the bi-plane configuration the same amount of lift is generated with half the wingspan and extra weight due to structural support would not be added.

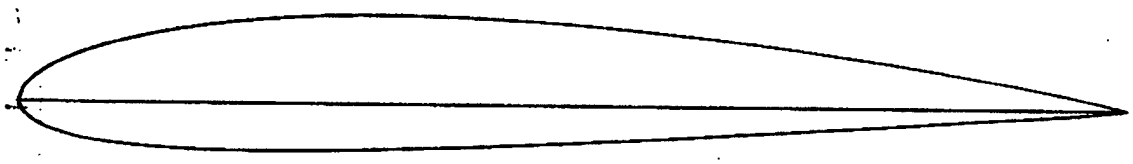

Figure 1: Eppler 387 Profile

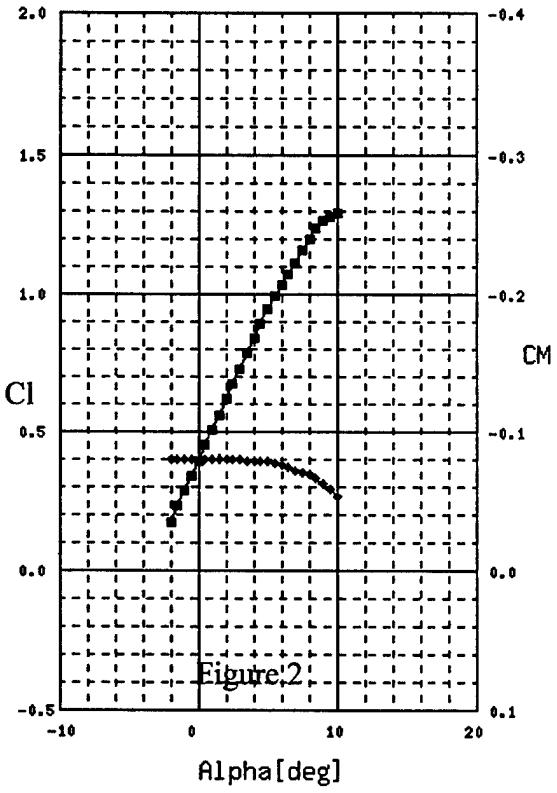

Figure 2

The plot of the lift and moment coefficients versus the angle of attack for the Eppler 387 airfoil is shown to the left:

Compared to other airfoils, as seen in the C_l vs. C_d plots (Figures 3 and 4), the Eppler 387 performs better than most airfoils. In other plots of C_l vs. C_d, Figures 5, the Eppler 387 is plotted for different Reynold's Numbers. As you can see, there is a fairly high C_l range with nearly a constant drag. Figure 6, shows the L/D ratio versus the lift coefficient for various Reynolds numbers.

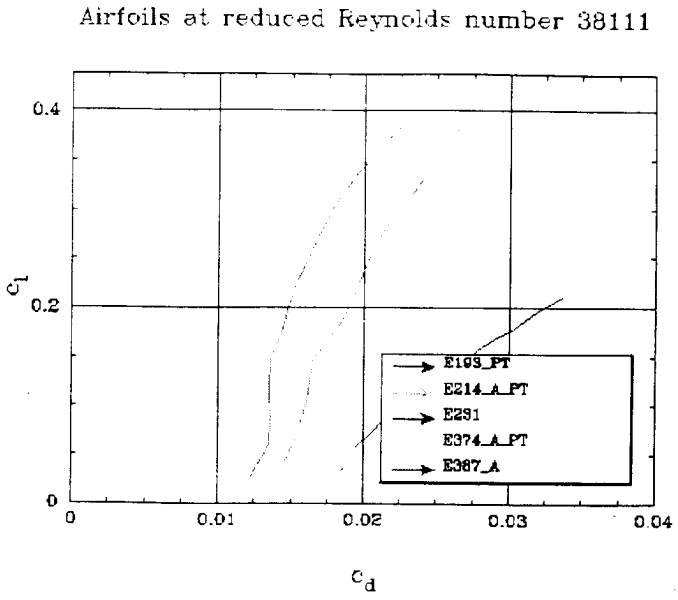

Figure 3

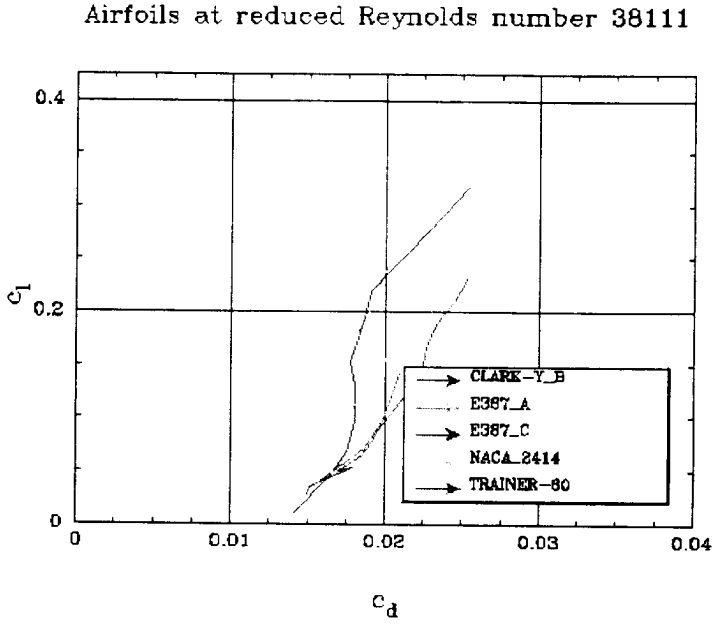

Figure 4

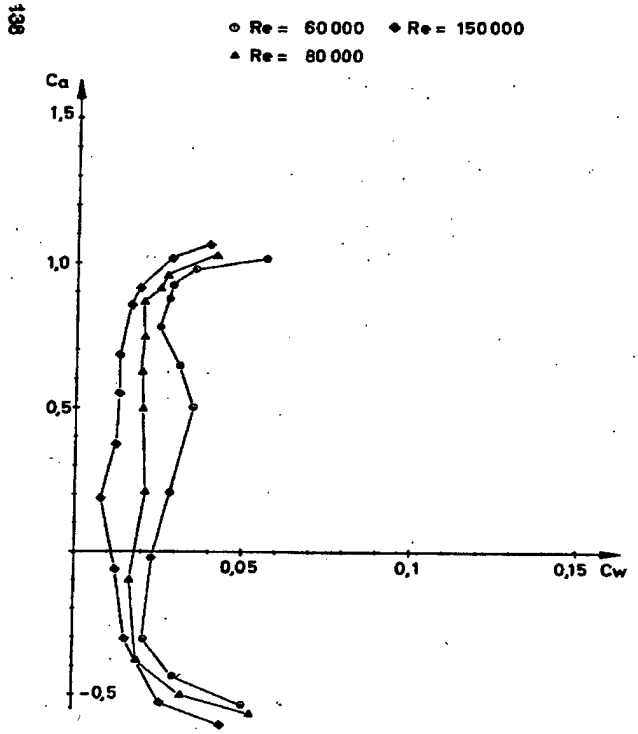

Figure 5: E-87 Drag Polars for various Reynold's Numbers

$C_a = C_l$, $C_w = C_d$

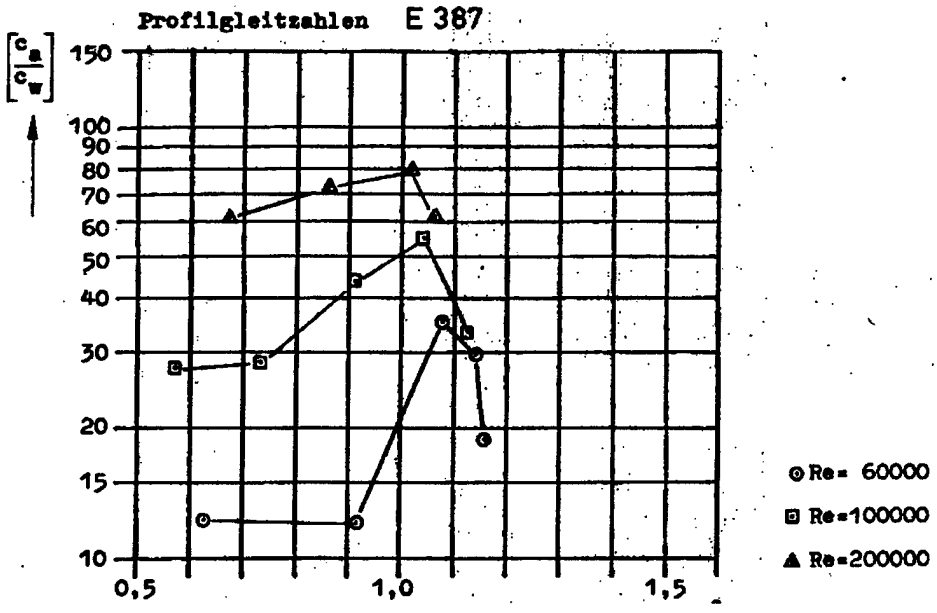

Figure 6: L/D vs. C_l for E-387

Tail

The primary function of a tail is to provide for trim, stability and control for pitch and yaw. As a group, we have chosen a twin tail configuration for a couple of reasons, despite some of the obvious concerns. The twin tails will be located on the outside of the horizontal tail, making the aircraft left-right symmetric. This will eliminate the unbalanced aerodynamic yawing moments requiring trim during normal flight. But, propeller aircraft do produce a yawing moment called "p-effect", when the disk of the propeller is at an angle, such as during climb, the blade going downward has a higher angle of attack and is also at a slightly higher forward velocity. This condition produces higher thrust on the downward-moving side and hence a yawing moment away from that side. Also, the propeller tends to "drag" the air into a rotational corkscrew motion. There is also a sideways force on the vertical tail caused by the rotating prop-wash, which creates a yawing moment adding to the p-effect. For this reason, the vertical tails are often offset from the centerline several degrees. For our model aircraft, this will be a concern, and once we reach the final design stage, we will be testing to determine the importance of this effect and if an offset tail is necessary.

Since one of the main functions of the tail is control, the tail must be sized to provide the adequate control power at all critical conditions. For the horizontal tail, these include nose-wheel lift off and low speed flight with the ailerons down. For the vertical tail, these include maximum roll rate and spin recovery. For our nearly straight-winged propeller driven airplane, the vertical tail will be between half and two-thirds the area of the horizontal tail. Twin tail configurations are usually a higher proportion of the horizontal wing due to the nature of the twin tail configuration. The tail volume required for all types of tails are directly proportional to the aircraft's wing area, using the formula: $V_T = \frac{l_t S_T}{\bar{c} S}$, where l_t is the tail moment arm, S_T is the tail area, $\bar{c}$ is the mean wing chord length and S is the main wing area. The larger the surface of the tail, the larger the tail moment and the further aft the center of gravity might be arranged to lie with out the airplane becoming neutrally stable. Since our load locations will be fixed for the missions, we do not need a large static margin. (The static margin is the distance through which the center of gravity might be arranged to move before the neutral point is reached) For positive stability, the tail must be rigged so that any departure from the desired main angle of attack will result in a corrective moment being applied by the other lifting surface. For a wing and tail arranged in tandem, there will be a point between the two which is in effect the aerodynamic center of the pair, which depends on their areas and distance apart.

For most aircraft designs, the conventional tail will usually provide adequate stability and control at the lightest weight. But due to the mission requirements for the competition, the group has decided on an unconventional tail configuration, the twin tail. The only way to understand the strengths and weaknesses of this design is by understanding the strengths and weaknesses of other design possibilities. One of the mission statements requires a Communications Repeater, a type of antennae, which is idealized as a 6-inch diameter piece of PVC pipe placed on top of the fuselage. Because of the

turbulent flow, vortices and overall unpredictable plow patterns that will be trailing the antenna, the conventional tail did not seem to be the ideal tail configuration.

The first option besides the conventional tail would be the tailless airplane. It is not common to design tailless planes for low speed flight, such as we would have, except in an effort to reduce drag. This design would also necessitate a larger wing area to increase lift for landing, which often generates more drag than a separate tail or wing stabilizer would. Although we are always looking to reduce drag, the antennae will create the most drag, and the proper tail configuration could be used to counteract this.

The T-tail configuration is one which could potentially get the horizontal lifting surface outside of the turbulent wake from the antennae. Placing the horizontal tail above the vertical height of the antennae is not practical since the antennae will be placed at a minimum of six inches above the fuselage. But even with a short vertical tail section, the horizontal tail could extend well beyond the wake of the antennae, main wings and prop-wash, making the elevator more efficient for control purposes while also reducing the buffet. The disadvantage being that the rudder will have a reduced and unpredictable affect on the control of the airplane. Furthermore, in some circumstances the T-tail leads to "deep stalling". When the main wing approaches stall, the wake becomes broader and at the same time the tail, because the nose of the model is rising, comes down into the wake and loses efficiency. When the main wing is stalled, the wake tends to strike the whole tail-plane. So, although the low mounted tail will be out of the wake and more efficient than usual, the strong downwash caused by the vortices may strike a high tail and keep it down.

The next option to consider is the V-tail, which can theoretically reduce drag. However, the construction precision necessary to connect the fins at proper and identical angles, along with the construction of the control surface movements is very demanding. And, the total area required is no less, and might actually be slightly more in practice to achieve the same stability as a conventional tail-plane. Furthermore, since the elevator and rudder control effects are obtained by coupling only two hinged surfaces, there are some situations where full control is not available such as full spins. The biggest advantage probably comes from the reduction in a radar profile, which obviously is unnecessary for our model aircraft.

The H-tail configuration is another attractive option for our model aircraft because of the way it positions the vertical tails outside of the undisturbed air, especially during high angles of attack. The disadvantage is that this is heavier than the conventional tail, but its endplate effect allows a smaller horizontal tail. This is the most similar option to the twin tail which will be used for this particular model aircraft. With this design, the rudders can be positioned away from the aircraft centerline, which may become blanketed by the wing or forward fuselage at high angles of attack. Also, twin tails are used to reduce the height required with a single tail. Twin tails are usually heavier then an equal-area centerline-mounted single tail, but are often more effective. This configuration is also apparent on most large modern fighters such as the F-14, F-15, F-18 and MiG-25.

The twin tail configuration chosen for this project will certainly challenge our construction precision more than a conventional tail would have. But this will result in better control due to the

placement of the antennae, while also providing more lifting surfaces and stability from the rudders and elevator.

Propulsion

The propulsion system is fixed for the airplane design, based on manufacturer specifications and competition rules. We will begin by calculating the power needed for the aircraft, which will then dictate our motor of based on required power and weight.

4.0 Preliminary Design

Wing

The Eppler 387 airfoil was determined to be optimal for our needs, since it provides the same or greater lift coefficient as all other candidates, while at the same time retains a very low drag coefficient of under 0.01 over a rather large range of angles of attack. The profile of this airfoil and its polar graph are shown in figures 4.2 and 4.3 respectively. Its' lift coefficient at 0-angle of attack was 0.4, and the drag was 0.0061, which is very good for cruising conditions, although it might still be required to have a small angle of attack at cruising speed, depending on the final weight of the plane, in order to provide sufficient lift.

The stalling characteristics of this airfoil were average, and stall occurred at around 14-degrees at the wing root, and 12-degrees at the wing tip. The stall was not too abrupt since maximum lift occurs at around 10-degrees angle of attack, thereby providing somewhat of a feedback to the pilot about the aircraft's proximity to the stall angle. The thickness of the airfoil was 12%, which is sufficient for structural strength by providing enough room for the spars. The camber was 3.78%, and with the profile being of a rather simple shape, there should not be much manufacturing difficulty, with the exception of the wing twist. However the wing twist would have been required for pretty much any airfoil since there is no airfoil that would retain the same stall angle over the required range of Reynolds numbers.

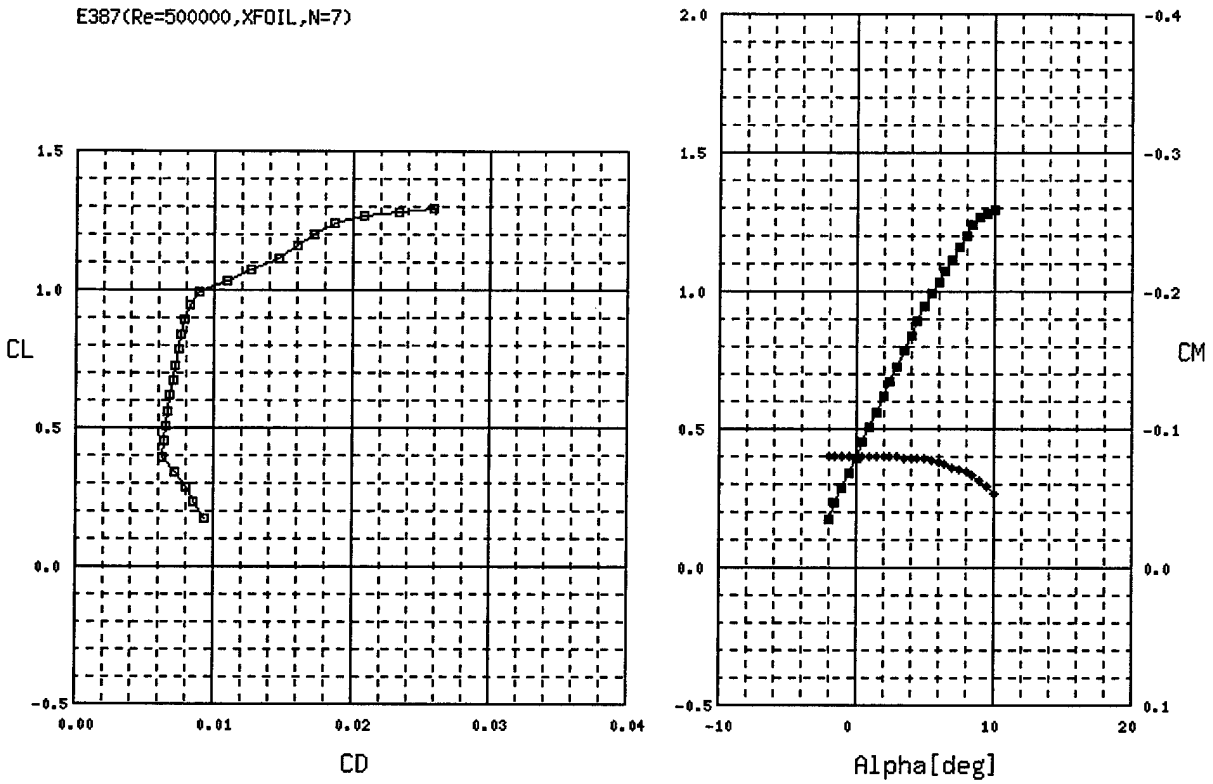

Figure 4.3: Eppler 387 lift coefficient vs. drag coefficient polar graph

When compared to the Clark Y airfoil, the Eppler 387 was a definite improvement as can be seen by comparing their polar graphs in figures 4.3 and 4.4. It retains a larger lift coefficient over the full range of angles of attack, while keeping a considerably smaller drag coefficient at all times. The only disadvantage is the Eppler's rather abrupt changes in drag when it goes into a negative angle of attack as well as at around 6-degrees angle of attack. However this was determined not to have too great of an effect in terms of control, and since the drag coefficient still remains lower than that of the other airfoils, it does not result in any relative performance losses. Also, for the most part, the plane should never require going into a negative angle of attack, unless an emergency occurs.

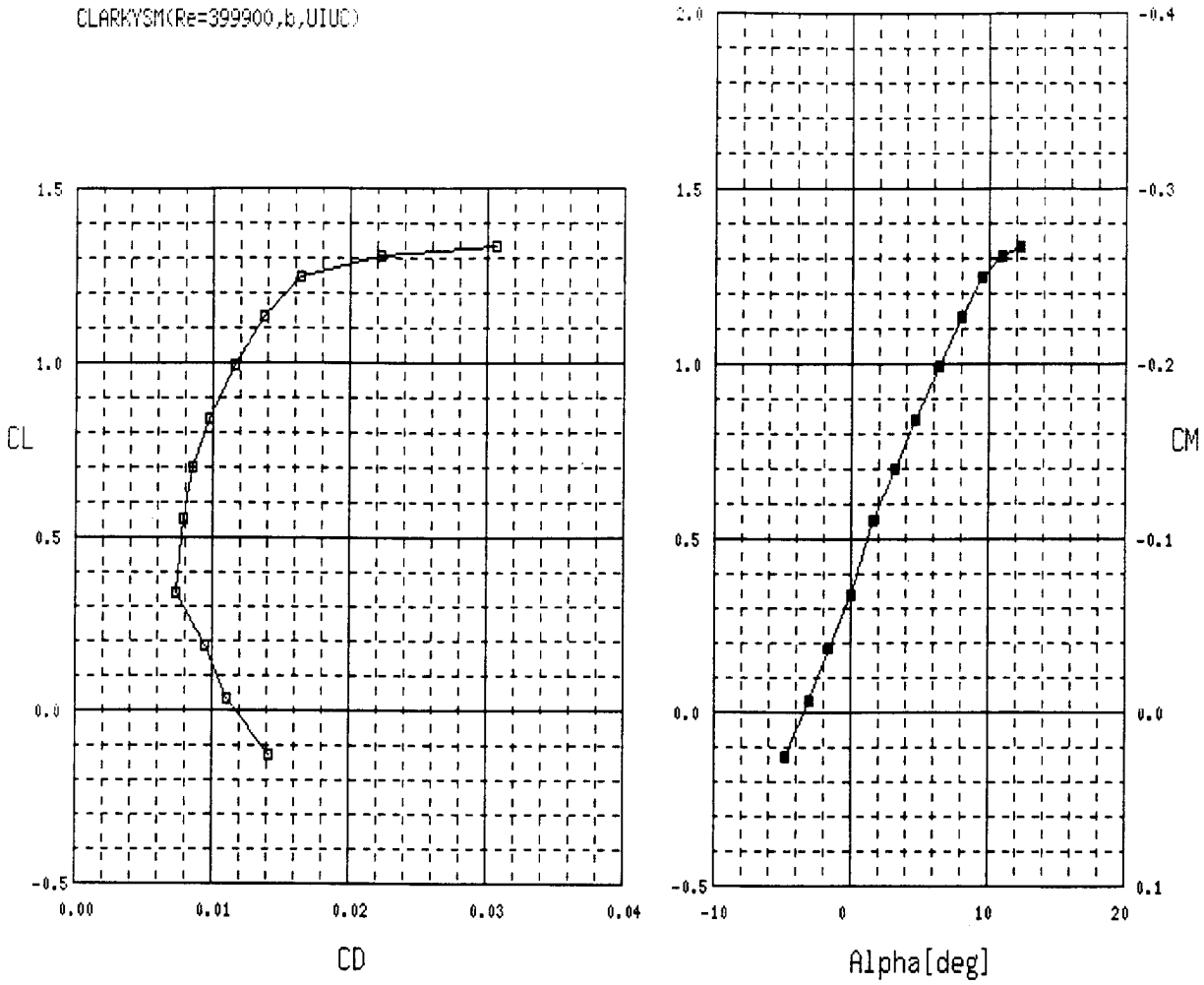

Figure 4.4: Clark Y lift vs. drag coefficient polar graph

Since all of the data used for comparison of the airfoil performance was from virtual sources, it was necessary to determine the validity of this data when compared to real-world results. This was done by comparing the virtual polar graphs to those determined experimentally in the Langley Low-Turbulence Pressure Tunnel[6]. The experimental graphs matched almost perfectly the virtual graphs up to a Reynolds number of 460,000, and it was also stated in the technical report used that for larger Reynolds numbers, the experimental results match perfectly the theoretical, i.e. virtually determined, results.

The optimal wing configuration was determined to be: a wingspan of 9.5ft; root chord length of 22.67 inches (so as to have a taper ratio of 0.5); and a tip chord length of 12 inches. This results in a wing area of 13.5ft^2, which means an estimated wing loading of 36 ounces/ft^2. This number is easily achievable; however exact lift calculations for this wing design are still underway. The taper ratio for this configuration is 0.5, which is a decent amount of taper, and results in a significant amount of drag reduction. A very good taper ratio would have been 0.2 or 0.3, however there was no way of achieving such a ratio without either decreasing significantly the aspect ratio, having an impossibly large root chord

length, or a structurally very weak and small tip chord. Since the aspect ratio has a greater influence on total drag, it was determined to be much more desirable to have it at 5.7 compared to a slightly smaller taper ratio. The sizing of the wing was calculated with the following equation:

$$S = W_{TO} / (W / S)$$

where W_{TO} is the Take – off weight (32 lbs) and W/S is the wing loading (2lb/in^2). This gave the wing an area (S) of 16 ft^2, with a chord of 1 ft and a wing configuration of a bi-plane the wing span if 8 ft long.

Tail

Once the configuration of the tail is decided, the next step is to find the shape, area, and location of the vertical and horizontal surfaces. The size and location of the tail can be related to the dimensions of the wing to give the tail moment volumes, which in turn can be used to calculate stability. The range of vertical and horizontal tail coefficients are chosen by comparison with similar planes with similar configurations. While staying in this range, the higher end of the spectrum corresponds to higher stability and greater flexibility for the placement of the center of gravity, whereas the lower end of the spectrum corresponds to lower stability and gives smaller margin of error in the placement of the center of gravity. A higher stability value is desirable, especially in heavy wind conditions, however it also makes the aircraft less maneuverable, thereby making the determination of the moment volumes an optimization problem.

In order to reduce the induced drag, the tail's aspect ratio should be quite large, but no greater than one quarter of the wingspan, since then it would count as a second wing, and seriously increase the cost of the airplane. For a wingspan of 114-inches, the horizontal stabilizer would have to be 28.5-inches. The surface areas of the horizontal and vertical stabilizers were determined using the following equations, which use volume coefficients that are typical for most existing aircraft of this size:

$$S_h = V_h * S * c / x_h \quad \text{and} \quad S_v = V_v * S * b / x_v$$

Where S_h and S_v are the horizontal and vertical stabilizer areas respectively; V_h and V_b are the volume coefficients; c is the mean chord length of the wing equal to 19-inches; b is the wingspan at 108-inches; and x_h and x_v are the horizontal distances from the wing's aerodynamic centerline to the tail surfaces' aerodynamic centerlines, both of which are equal to 54.5-inches; finally, S is the wing area at 1944 square inches. The volume moment coefficients were picked to be the average of a series of 13 homebuilt aircraft, since homebuilts are of similar proportions as this airplane, even though this one is not designed for any passengers. The V_h used was 0.47, and V_v was 0.036. From the above equations, the required horizontal surface area was determined to be 316 square inches and the vertical one was 140 square inches. If the span of the horizontal stabilizer were to be kept under 28.5 inches, then the chord length would have to be about 11 inches in order to meet the 316 square inches area requirement. For ease of construction, the vertical stabilizers will be half of the tail span, and the half the chord length and profile for reduced drag, thereby meeting its' 140 square inches area requirement.

The profile of the tail surfaces was chosen to be symmetrical, since even though extra lift is usually desirable, it would require the center of gravity at a location further back than its current one. Since the tail is in the wake of the wing, the flow over it is quite turbulent, which would cause the lifting force from the tail to vary, thereby varying the center of gravity's moment on the plane, and therefore resulting in an unstable flight. The NACA 0012 airfoil was chosen as the tail profile due to its low drag coefficient, and the fact that it provides sufficient room for structural strength with its' 12% thickness.

Fuselage

Since the construction of the fuselage should be possible with the available resources, simple geometric shapes were studied. The cylinder was found to be most optimized option for fuselage shape. The idea was discarded due to the accuracy and skills needed for construction.

The team members didn't wanted to spend time on constructing something that they weren't sure how accurate it will turn out. A rough cylinder shape would have contributed significantly to the drag due to irregularities on the surface. Therefore circular shapes were eliminated as possibility for our design.

The team then decided to investigate quadrilateral shapes due to the ease of construction. Square, rectangles and trapezium shapes were analyzed using simple mathematical skills. Trapezium was found to be aerodynamically better than square and rectangle shape on bases of aerodynamics and on past experience of some of the members of the team who were involved in airplane modeling. There were some trade offs with that particular shape. It was difficult to taper the fuselage on the end. It was important to taper at the end because the back part wasn't really needed as it contributed to weight and drag and thus putting load on the engine, which resulted in lower thrust. The empennage should be tapered to provide enough surface area for the horizontal and vertical stabilizers. Also with the slant sides, the part of the wing that gets attached to the fuselage needed a smooth slant. That meant spending more time on the construction.

The team decided to go with rectangle shape fuselage initially. The dimensions were calculated on the basis of space required by the cargo i.e. 8.5" x 7" cross section. Once having the dimensions and the shape for the fuselage, the team discussed the materials to be used. Most likely candidates were balsa wood and carbon fiber. Most of the plane will be made of balsa wood but some parts of the airplane where high stress exists, the team decided to use carbon fiber to add additional strength.

For increased aerodynamics, fillets constructed of balsa wood can be added to the edges of the fuselage. In addition, the fillets will add a significant amount of strength to the joints. The amount of weight added to the fuselage will be three or four ounces, which is considerable, but the integrity of the structure is essential.

The third option for the fuselage design was a combination of circular shape and rectangle. Such a design will help us reducing drag due to circular smooth areas and secondly it will also ease construction as we have rectangular shape. Foam will be used as a mould for the fuselage. Once the

foam is made in the desired shape, the foam would be cut off using a hot wire foam cutter at areas where cargo space is required as well as for saving weight. This would result in a weaker structure. But we have to make the inner surface hollow because that's where the cargo is to be carried. So in order to make the fuselage strong enough to bear various stresses due to different forces that it will be subjected to, the foam will be covered with a single layer of carbon fiber around the outer surface. Multi layered carbon fiber would make the fuselage stronger but it will be over designing for our purpose. To have a slightly better safety margin, the team came up with the idea of using two pre-manufactured carbon fiber rods, which will run along the length of the fuselage. They will be connected to the front and the end of the structure and will take the main stress applied to the fuselage. Thus we will have additional tolerance without addition of much extra weight.

The first two designs were on the extreme sides of the spectrum. One end being the ease of construction and the other being aerodynamic qualities. The third option is midway on the spectrum. Thus it was the optimized design to go with for our mission profile.

Propulsion

The propulsion system consists of motor, propellers and battery pack. Selection of each was based on competition rules and considerations listed in the conceptual design section.

In addition, an issue was raised in regards to properly testing the static force output of the motor. This was resolved by designing a new motor test stand, which was machined and assembled by the team.

Motor

The motor selection starts with the estimated required motor power. From practical experience, we decided that 40 watts per pound of total aircraft weight would give the power we needed to takeoff within 120 feet. For a conservative estimated aircraft weight of 35 pounds, this results in a motor power output of 1400 watts. We also wanted a single engine configuration because of its low rated aircraft cost contribution, and the success of single engine teams in previous competitions. These considerations resulted in the selection of the largest motor allowed, the Astroflight Cobalt 90. The motor performance specifications are listed in Table 4.1

Model	690	691S
Name	CO-90 Direct	CO-90 Geared
Gear Ratio	Direct	2.75 to 1
Arm Winding	10 turns #22	10 turns #22
Resistance	0.111 ohms	0.111 ohms
Speed	256 rpm/volt	93 rpm/volt
No Load	3.0 amps	3.0 amps
Best Battery	32 to 36 cells	36 to 40 cells
Max Amps	35 amps	35 amps
Prop Rpm	8,000/10,000	3,500 to 4,500
Best Props	13x8 to 16x8	20x14 to24x12
Power Watts	1100 to 1200	1200 to 1400

Table 4.1 Manufacturer's Specifications

This motor has a maximum power output of 1400 watts when connected to 40 cells. This motor was the only one selected from the two manufacturers with a power output in the range that we needed. However, the motor comes with or without a 2.75 to 1 gear ratio, so this aspect needs to be taken into consideration when selecting the propeller.

Batteries

The most important factor in the selection of the batteries is the capacity to weight ratio. Because of the 5-pound weight limit on the batteries, we must make the most use of that weight as possible. Weight and capacity specifications were obtained for every battery from every major Nickel Cadmium battery manufacturer. This resulted in a list of 341 different Ni-Cd cells. This data was entered into a spreadsheet program and the cells were sorted according to capacity to weight ratio.

Next, the cells that are manufactured specifically for high current discharge use were identified. This resulted it the selection of the DSC2100P cell manufactured by BYD. It can handle the current expected in our power plant system while still having a high capacity to weight ratio of 42 mAh/g. This cell is also an excellent choice because 42 cells result in a weight of slightly less than 5 pounds and a voltage output of 50. This is the best voltage for high motor power output.

Propeller

With the motor and battery fixed, a suitable propeller must be selected that satisfies the power output of the motor and the needs of the mission. A useful computer program called "ThrustHP" was utilized in the selection of a range of propellers to be evaluated for further testing. The motor manufacturer suggests several propeller sizes for both the geared and direct drive versions of the motor (see table). An estimate of 1200 watts of max power output for both versions of the motor was used in the program and resulting rpms, static thrust, and speed values were calculated for propellers of varying diameters and pitches. Another factor taken into consideration was the aerodynamic effect of a small propeller diameter spinning in front of a fuselage of almost the same area, which would be the case of the direct drive motor. This analysis led to the conclusion that the geared version of the motor would be used along with a propeller with a pitch of 24. This resulted in acceptable speed, rpm, and thrust values over a range of propeller diameters. The diameter can then be varied to increase the thrust and decrease the speed, or vice versa. Since the program is just a tool and the actual rpm and thrust values had to be determined experimentally, several propellers with diameters between 20 and 24 inches were purchased for testing. The final balance of thrust and speed can then be selected to ensure that the aircraft takes off within 120 ft. APC was selected as the propeller manufacturer because of the amount of positive opinions of other modelers as to their performance and strength.

Motor Test Stand

An important aspect of our design process is being able to determine the thrust of our motor with the use of different propellers. In order to maximize this element in our design, we must be able to get accurate test results in the convenience of our own labs. Therefore, we needed to design a motor test stand to work with many different motor and propeller characteristics. Throughout the design of the test stand, many structures were considered and were finally narrowed down to one universal design. The following page illustrates the metamorphosis of the design from its conceptual phase to the final product.

The design of the stand was based on the two main functions it needed to allow for: unique motors (sizes, weights, etc.) and different diameter propellers. We needed a stand that could be used with many different formats and that would be durable enough to last for years to come. In order to measure the thrust results from each type of propeller, the stand is on wheels and is attached to a scale by a string. When the motor is powered up, we can see how much pull the scale receives and take our measurements from that.

The first design (Figure 4.2a) was intended for a specific motor and an overall propeller diameter. We then realized the value in making the stand capable of adapting to different motors. The original structure was then altered to the specifications in (Figure 4.2b). This stand has an adjustable upright portion, a sliding track-rod-system that can fit any size motor we might require for competition. With a few more changes we arrived at the design shown in (Figure 4.2c). This was brought about in the interest of simplicity. A single plate design with angled support seemed to be much easier than the rigid system of part (b). With this design we headed to the machine shop to consult with the shop attendants. The main concern brought up with our design was stability and weight. With the motor loaded, there was a concern that the stand would tip forward and become a safety hazard. Also, with a single plate system, the overall design may be too heavy to get accurate thrust results. Therefore, we retorted back to a form of design (b) as seen in the three-view drawing on page 14. This system is composed of angled aluminum beams, as opposed to single sheets, over the entire structure. The track with horizontally adjustable rods to hold the motor in place is simply attached between the two upright beams. This track in turn is capable of moving vertically up and down to get better results for smaller propellers.

After the motor test stand is completed, the motor will be tested using the chosen battery pack and various configurations of propeller diameter and pitch, as well as with or without the gearbox. From this data the best configuration resulting in desired thrust and speed can be chosen.

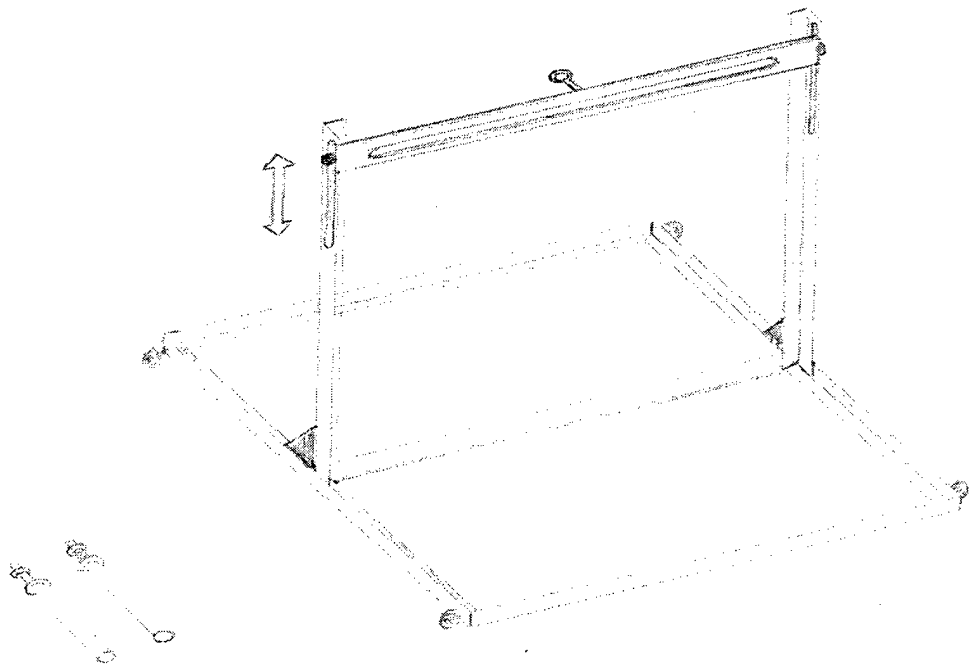

Figure 4.3 Final Motor Test stand design

5.0 Detailed Design

From the Preliminary Design phase it was decided that the Firer Fly would be a single engine bi-plane with a twin fin tail. This configuration was gave the most control with the most stability This was very important considering that for the Missile Decoy mission, the simulated antenna creates a large amount of drag and causes stability problems. The following is a disruption of the Firer Fly's final configuration, with a detailed list of its dimensions, weights and performance parameters. The rated aircraft cost is also included in this section.

Configuration

The single engine bi-plane, twin fin tail configuration was chosen because of its stability and control qualities as stated before. The single engine provides enough power to pull the aircraft through the air, is impossible of causing a yawing moment which a multi-engine design may cause if missed aligned. The bi-wing gives the pilot an extra pair of control surfaces, enhancing the handling of the Firer Fly's rolling characteristics and during landing and/or take-off provides more effective lifting area compared to a mono-wing configuration. The twin fin tail provides more effective yaw and pitch control compared to a more traditional tail design considering the air moving over it will be dirtied by the simulated antenna. The following is the dimensions of each component. The final configuration is shown in figure 5.1

Wing

The bi-wing is straight winged, has a chord of 1ft, a wing span of 8 ft and is staggered by 50%. The top wing of the bi-plane is placed a foot above the bottom wing, this prevent the lower wing from inferring with the performance of the top wing. To reduce induced drag end plates are mounted at the wing tips, these also provide structural strength to wings and enhance the Firer Fly's stability. Because of the required strength of the end plates they are a ¼ inch thick 12 inches wide and 14 inches tall.

Fuselage

The fuselage is where all and payload, propulsion system and control system are located. It has a length of 7.26ft at its longest point and has a width of 7 inches at its widest point. It is mounted to bottom wing so that its center of gravity sits 3 inches in front of the quarter chord. The engine is mounted in the front of the fuselage in puller configuration. The simulated radio package it centered at the fuselage center of gravity and is restrained with a bolt and nut this can be seen figure 5.2. The payload itself is 6x6x12 box following the rules of the competition. The simulated antenna sits on two stoats on the fuselage 3 inches above and 6 inches (from the center of the antenna) behind the top wing. The tail is mounted 2.4 ft behind the lower wing.

Tail

The twin fin tail has a single horizontal stabilizer that is 2 ft long and 1ft wide. It connects to tail boom section of the fuselage at the center of the horizontal stabilizer. The two vertical tails are mounted to the tips of the horizontal stabilizer and are 1 ft tall with a base of 1ft.

Geometry:	
Length	7.26ft
Span	8ft
Height	2.7ft
Wing Area	16ft^2
Aspect Ratio	8
Control Volumes	
horizontal	2ft^2
vertical	1.067ft^2

Performance:	
CL max	1.3
L/D max(wing)	65
max RoC	4ft/s
Stall Speed	18mph
Max Speed	40mph
T/O length	
empty	90ft
gross weight	100ft

Weight Statement:	
Airframe	17lb
Propulsion System	7.5lb
Control System	1lb
Payload System	1lb
Payload	5lb
Empty Weight	27lb
Gross Weight	32lb

Systems:	
Radio Used	Futaba 8-channel
Servos Used	4 servos rated at 11kg.cm
Battery Config	2x20 cells
Motor	Cobalt-90
Propeller	20x14
Gear Ratio	2.75/1

Geometry, Weight Statements, Performance Qualities, Systems

Rated Aircraft Cost Tables

Coeff	value	units
A =	100	dollars
B =	1500	dollars
C =	20	dollars/hr
MEW =	27	lbs
REP =	5	lbs
MFHR =	202	hr

RAC =	10204.04	dollars

MFHR table

item	multiplier	value	hours	
wing(s)	8	8	64	hr
Fuselage	10	7.3	73	hr
end plates	5	2	10	hr
rudder	10	1	10	hr
elevator	10	1	10	hr
servo	5	5	25	hr
engine	5	1	5	hr
propeller	5	1	5	hr
		MFHR =	202	hr

RAC Tables

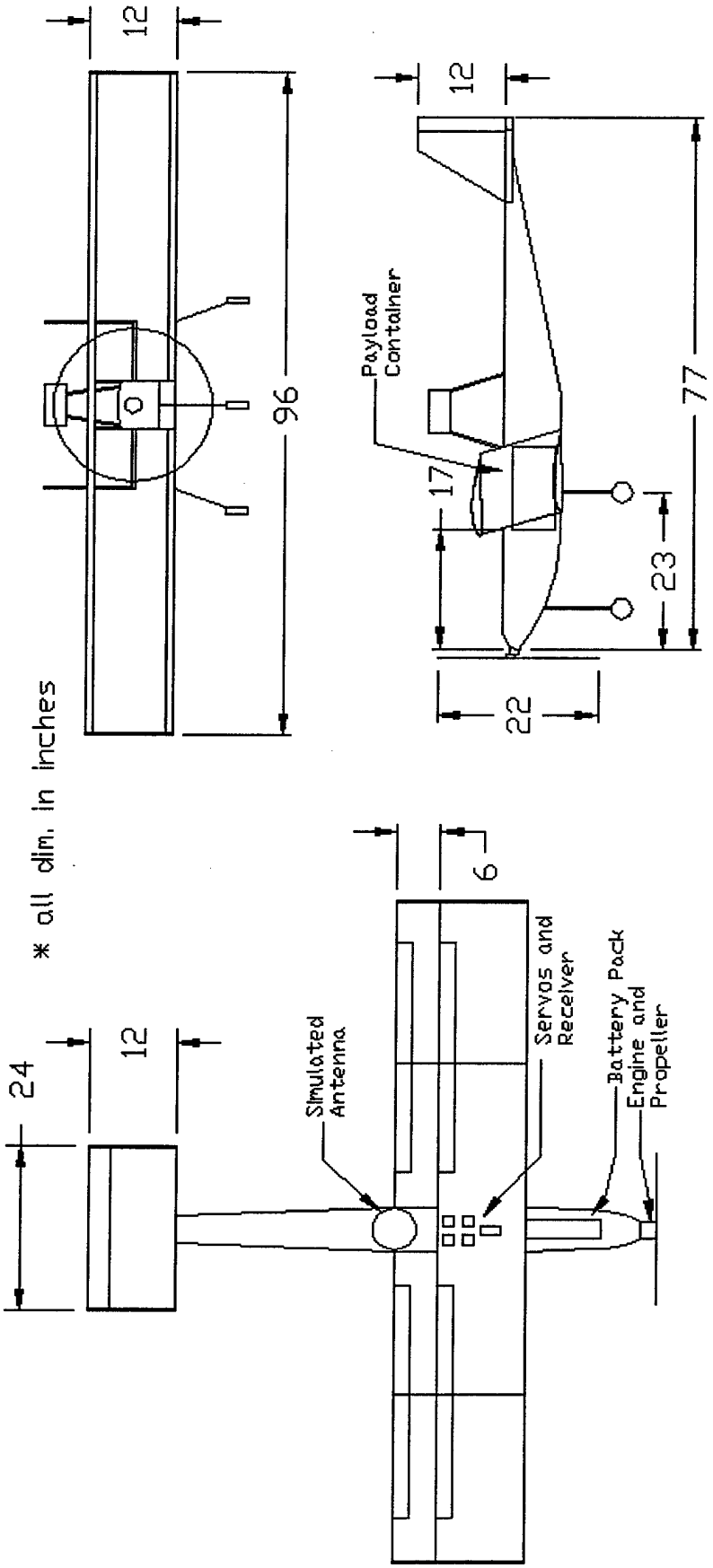
12
96
12
Payload
Container
77
17
23
22
* all dim. in inches
6
24
12
Simulated
Antenna
Servos and
Receiver
Battery Pack
Engine and
Propeller

Figure 5.1

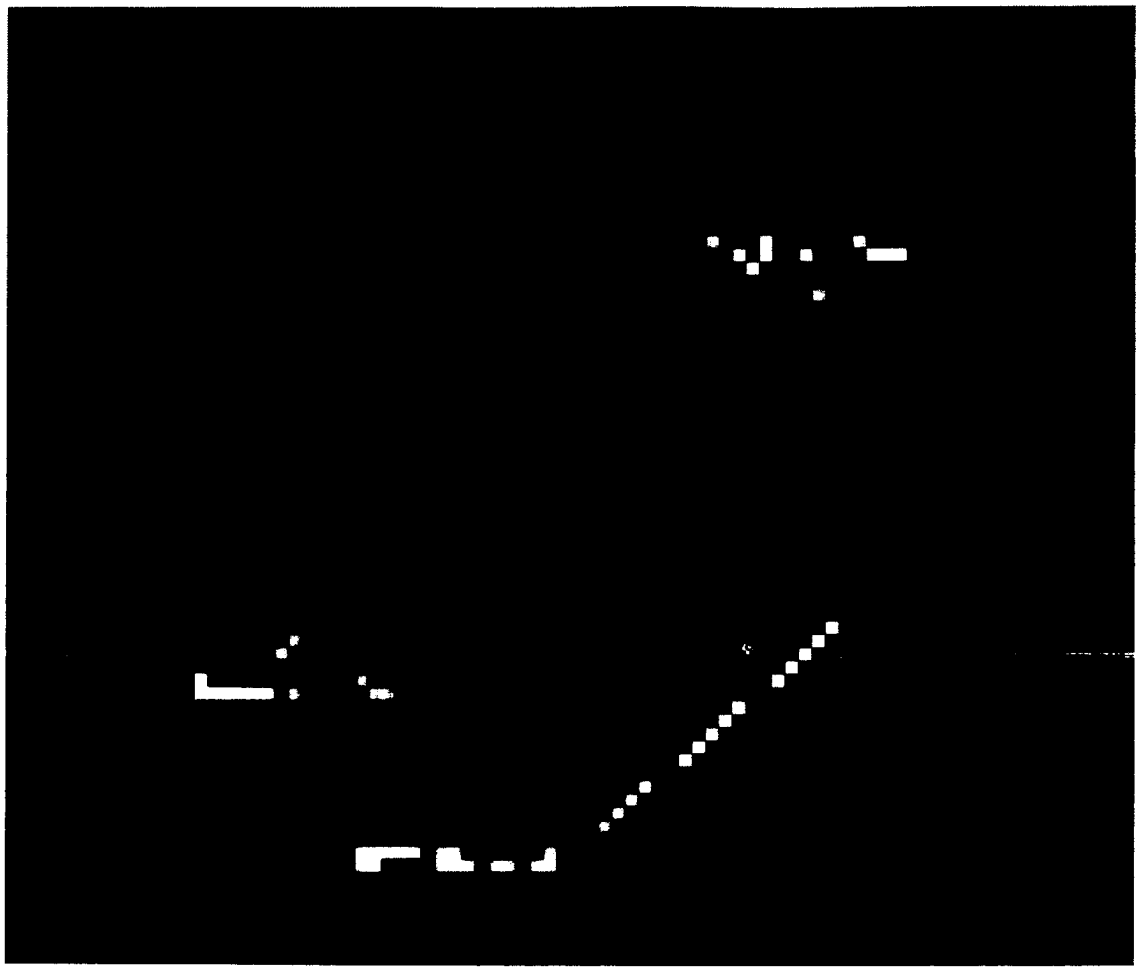

Figure 5.2

6.0 Manufacturing Plan

The manufacturing plan of the "Firer Fly" was conceived from past years experience and new ideas. Many construction methods were considered and are still being considered. For each component of the plane a separate construction method was considered. Different materials were considered and were chosen based on availability, cost and easy of application. Finally a tentative schedule was made up that was dependent, in large part, on procurement of building materials. What follows is a discussion of the manufacturing plan for the Firer Fly's components, the materials used for each component and the schedule that will be followed during construction.

Fuselage

The construction of the fuselage for the Firer Fly is fairly easy and does not take up too much time. Originally, a foam core with a carbon fiber laminate was considered, it would be easy to construct and very strong. It does have a fault however; it makes the placement of hard points difficult. Next a balsa-wood frame with Monokote covering was considered, it is very simple and is easy to construct. However, in order to make the fuselage strong enough the balsa wood frame would have to be built in a way that it make the structure heavy. Based on these facts the decision was made to use a combination of the foam core with a carbon fiber laminate and the balsa wood frame with Monokote covering. This provided high strength, the ability to have hard points and the ability to produce more complex curves for aerodynamic proposes.

The foam core of the fuselage is cut with a hot wire and hot knife to form the grooves for the aerodynamic shaping, and channels for the balsa-wood stoats that make up the frame of the fuselage.

Hard points for the attachment of the wings, tail, landing gear and antenna are made of carbon fiber laminated balsa wood. The carbon fiber laminate reinforces the balsa-wood so that it can take the loads that are required of it.

The opening for the cargo, battery and servo compartments are covered by hatches that are constructed of balsa-wood and monokote covering. They are constructed with a light balsa-wood frame glued by CA super adhesive glue, then covered with monokote to create a smooth surface.

After the internal frame of balsa-wood is built the foam with the pre-cut channels is placed around the frame. To insure its strength, the foam and balsa-wood is then carbon fibered in a vacuum bagging process. This process involves taking the component to be carbon fibered, and then wrapping it in a release film and another layer of breather material. This is done after the object and carbon fiber have been adequately covered in epoxy. The object, with the two layers of film and breather material, gets placed in a bag that gets sealed and a vacuum pump is inserted. The pump is used for removing the excess epoxy out of the carbon fiber and into the breather material. This leaves just enough epoxy for the epoxy to harden and laminate the carbon fiber to the object.
This process is used in the construction of all major components of the "Firer Fly".

Wing

The process of deciding a construction method for the wing was based on past experience and some new ideas. Considering the rules of this year's competition the construction of the wing was decided to be a combination of construction methods. The center section of the wing is made of foam with a carbon fiber laminate structure with carbon rods for spars. On the rest of the wing will be constructed of a balsa-wood rib structure with carbon rods for spars. The carbon rods, in the balsa-wood section of the wing, are of a smaller diameter than the carbon rods of the center section of the wing. This allows for the spars in the balsa-wood sections to be able to slide in to the center section, transferring the moment from the outer section to the center section.

The first step in the manufacturing process of the wings was cutting the foam to the shape of the chosen airfoil, for the center section of the wings. This was done by a local supplier, Thermo-foam. The foam that was used in construction had to be low density, to save weight, but had to be strong enough to resist being crushed when it was placed in a vacuum bag for laminating. An airfoil was cut out of a polystyrene foam block measuring 4'x 1'x 3". This block provides enough volume to create a one-piece foam core for each wing. After the pre-cut foam is received from Thermo-Foams, the rods are then epoxied into place and then the foam is laminated with carbon fiber using the method of vacuum bagging previously described.

For the outer sections of the wings, ribs are cut in the shape of the airfoil out of a 1/8 inch balsa-wood sheet. The ribs are not cut to exactly the shape of the airfoil, a rough cut is made then once all the ribs are made they are all sanded together to make sure they are virtually identical. To place them on the carbon rods a jig is made that holds the rods in place while the ribs slid into position. Once all the ribs are placed correctly they are glued into position. After the glue has dried monokote is laminated to the sections creating a smooth, uniform shape.

For mounting the wings to the fuselage, hard points are placed in the center section of the wings. These hard points are made of laminated balsa-wood similar to the hard points in the fuselage. The same kind of hard points are placed in the center section of the lower wing for mounting the landing gear.

Tail

The two main designs for the tail involved either foam cores with carbon laminates or a balsa-wood frame with Monokote covering. After building test sections for each design, it was decided that a balsa-wood frame would be the best solution. The foam core section was much stronger than the balsa wood section, but it was twice as heavy. Also, the strength exhibited by both was more than adequate for the needs of the "Firer Fly" and the balsa-wood design was less expensive.

The first step in constructing both the horizontal and vertical stabilizers is cutting out the ribs. A template, machined out of aluminum, is placed on 1/8 inch balsa-wood sheets and a band saw is used to

cut out the ribs. This method is used to reduce the variance in the shape of the ribs. Even a small amount of deviation can severely decrease the control of the airplane. This is the same method used for the construction of the ribs of the wings.

Pieces of 1/8 inch balsa-wood, acting as the spars, are then run across the top and bottom of the evenly spaced ribs. After that, the leading edges and trailing edges of the stabilizers are glued on with CA. Next, before the Monokote is laminated on, control wires and control horns are mounted in the horizontal and vertical tails.

Engine Mount

It was determined in the Preliminary Design that the "Firer Fly" would be a single engine airplane, which made the decision to mount the engine in the nose of the airplane trivial. Therefore a design was needed that would mount the engine securely to the fuselage. The firewall is mounted to hard points in the nose of the fuselage. .

For firewall construction, $1/8^{th}$ inch Aluminum plate is cut to a length of 7" and a width of 2". After the Aluminum is cut, the piece is bent so that 2" on each side of the plate is flush with the hard points of the fuselage. To secure the firewall to the fuselage, the firewall is bolted to the hard points.

Landing Gear

The final landing gear design for this airplane is based on the tricycle configuration. However, the rear landing gear is mounted to the wing and not the fuselage for extra strength and stability. The gear is attached to the hard points on the wing spar ensuring that the shock from landing is not transmitted to the fuselage. This design is more stable and fairly lightweight compared to using a hinge design that attached to the sides of the fuselage, and a tail-dragger configuration.

The nose wheel assembly used is commercially available and is rated for model aircraft of this size. It is controlled by a separate servo connected to the same channel as the rudder. This provides good ground handling and allows for easier hookup than routing a control rod from the rudder servo.

Material Selection

The following figures of merit provide the design team with the manufacturing characteristics of each component of the airplane. This was important in deciding how to go about constructing the airplane outlined in the *Detail Design*. The merit parameters are as follows: availability, cost, required skill level, time required, and strength.

Availability

This was extremely important to the design team when deciding what materials to use. There had to be material vendors available that could supply the team with the proper dimensioned and cost effective materials. A rating from 0-4, with zero being the product is unavailable and 4 is easily obtainable, was used to determine the availability of the products.

Cost

The airplane built had to be cost effective. The team raised enough money to purchase some fairly exotic materials, and since the club has two planes going cost was a huge issue. These materials had to be used in only the most essential components, to limit the amount that was spent on the quantity of exotic materials. A scale from 0-4 was used once again, with 0 being extremely expensive and 4 being the least expensive.

Skill Level

This year's team was fortunate to have the advice of many experienced builders. This allowed looking into processes that are somewhat more advanced. However, it was still important to stay within the scope of reality because reading a book on carbon lay-ups is different from actually doing it. A score of 0 is for expert skill level and the scale ranges to a score of 4 for beginner skill level.

Time

Time is always against a team in a design competition of this magnitude. The plan is to have the airplane built at least two weeks before competition. This allows enough time for testing the plane as a whole. All of the manufacturing has to be done relatively quickly in time for the competition. A score of 0 is for a very time consuming method and the scale ranges to a score of 4 for a fast manufacturing method.

Strength

Strength is very important, after all if the plane is not strong enough to hold itself together it can't fly. A score of 0 is for a weak structure and the scale ranges to a score of 4 for structurally sound components.

		Availability	Cost	Skill Level	Time Required	Strength	Total
	Weighting	***0.1***	***0.1***	***0.2***	***0.4***	***0.2***	
Wing Structure	*Balsa Wood Frame*	8	5	9	5	4	5.9
	Foam Core/Carbon Laminate	5	2	5	3	7	4.3
	Combo of Balsa-Wood & Foam	7	4	8	4	9	6.1
Spar	*Balsa Wood Core*	8	5	9	5	4	5.9
	Carbon Rods	5	2	10	10	10	8.7
Fuselage	*Balsa-Wood Frame w/ Monokote*	8	5	9	5	4	5.9
	Foam Core/Carbon Laminate	5	2	5	7	8	6.1
	Combo of Balsa-Wood & Foam	7	4	8	8	9	7.7
Landing Gear	*Piano Wire*	10	10	10	7	10	8.8
	Carbon Fiber	5	2	4	5	10	5.5
Horiz. and Vert. Stabilizers	*Balsa Frame w/ Monokote*	8	5	9	7	6	7.1
	Foam Core/Carbon Laminate	5	2	5	8	7	6.3
Motor Firewall	*Aluminum*	9	5	8	8	8	7.8
	Steel	5	5	6	8	10	7.4
	Plywood/Carbon	10	7	7	6	8	7.1

7.0 Testing Plan

Two types of tests will be performed on the "Firer Fly", a component test and a fully assembled aircraft test. The fully assembled aircraft test, itself, will have two tests; a static test and a dynamic test. Due to the whether in Buffalo an alternate testing method will be implemented.

Component Testing

Each component of the aircraft (i.e. wings, fuselage, tail, etc.) will be put through a series of tests to determine their strengths and their weight & volume.

Strength tests are done to determine whether or not the components will be able to sustain the loads they will experience during flight.

The weight test is done to mainly to verify the size of the wing. If the weight, of the aircraft, is over its estimated weight then the wing has to be re-sized so that enough lift will be generated to support the weight of the plane. Another reason for the weight test is so that the design team can get an accurate weight for calculations of moments and stresses that will affect certain components due to other components' weights. An example of this is the calculation of the moments on the fuselage due to the weight of the tail.

Volume will of the aircraft will be tested to verify that the aircraft structure will be able to fit in the 4' x 2' x 1' box, specified in the mission specs of the competition rules. If the aircraft does not fit then the design team will modify the aircraft.

The strength of the components will be tested by applying weights to critical points on each of the components to simulate the forces and moments that they will undergo during flight, as well as the static loads of being motionless.

Full aircraft testing

The fully assembled aircraft test will be used to test the control surfaces, static stability and dynamic stability. The static stability of the aircraft will be tested first. The first part of the static stability, and the easiest test to perform, is letting the plane sit motionless to see if the landing gear can support the weight of the structure and each of the attached components support the forces exerted on them. The second part of the static stability is to locate the center of gravity (C.G), and after calculations of forces and moments due to the wing and tail, the plane will be pivoted at its C.G. If the aircraft pitches, up or down, or there is any roll, the structure is statically unstable, and adjustments need to be made. If there is no movement in the aircraft then it is statically stable and no adjustments need to be made. The third part to testing the static stability of the aircraft will be to lift the structure by its wings. This simulates

the force of lift that the wings will feel. If the wings do not deflect drastically then the aircraft was designed and built properly. If there are signs of failure in the structure and there is a significant amount of deflection in the wing, then the design team will have to go back and make the proper modifications. The structure will then be raised to a height of approximately 2 ft, where the team will then proceed to drop the aircraft to see if the landing gear can support the forces exerted on them during landing.

Once the static stability tests are complete then the weight of the aircraft will be measured by placing the landing gear on scales. Once again this is to determine if the weight is above or below what the design team calculated. If the weight is more than projected two things can be done. The first measure that could be taken would be to find ways of lightening the weight of the structure. If this can not be done then the wings will have to be modified so that enough lift will be generated to support the weight. After measuring the weight, the aircraft will be broken down and the design team will place all of the components in the box. This is done to see if the aircraft meets the specifications of the competition. If all of the aircraft does not fit then modifications to the size of the components need to be made; these modifications will have to be made so that they do not jeopardize the structural integrity or the stability of the aircraft.

Dynamic tests of the fully assembled aircraft are the second to last tests to be completed. These tests will be carried out at Veridian (a flight research center), by the design team with the aide of one of UB's professors. To test the dynamic stability of the aircraft, a series of springs will be connected to the structure. The location of these springs will be in key places where the pitch, roll and yaw are experienced the most. These locations would be the bottom of the fuselage at the tip and tail, the sides of the tip and tail of the aircraft, and at the very tips of the bottom wings. The aircraft will be "tweaked in a certain degree of freedom. Then the oscillation induced by the "tweak" will be timed, using a stopwatch, to measure the time to damp. From here moments of inertia can be calculated, and then with values, more calculations can be done to determine the various characteristics of the aircraft. This test will also determine part of the static stability, because for the structure to be statically stable, it will want to go back to its original position once "tweaked".

After the static and dynamic tests are completed the testing of the avionics will commence. This testing will involve the testing of the control surfaces to see if they have adequate movement with minimal resistance for flight conditions. If the control surfaces do not have enough movement or, on the flip side of the coin, have too much resistance then the control rods will need to be adjusted. For throttle control the plane will be fixed in one location and the throttle will be set to its maximum and the thrust will be measured. If the thrust is the maximum thrust of the motor then no adjustment will be made if it is not the maximum thrust then adjustments will be made by changing the propeller or by adjusting the voltage/current of the batteries.

The final test of the aircraft is to fly it. Ultimately, this is the most beneficial tests. That is because the team will be able to witness how the aircraft will actually perform and not just go by calculations from previous tests. Unfortunately the team will not be able to do this until close to the competition. This is due to the inclement weather in Buffalo.